11.1 Groundwater and Air Contamination: Risk, Toxicity, Exposure Assessment, Policy, and Regulation

RJ Watts and AL Teel, Washington State University, Pullman, WA, USA

This article is reproduced from the previous edition, volume 9, pp. 1–16, © 2003, Elsevier Ltd.

11.1.1 Introduction

The improper disposal of hazardous wastes and subsequent contamination of surface and groundwaters has exposed the public and ecosystems to toxic chemicals that have detrimental consequences. The cost of cleaning up the thousands of hazardous waste sites throughout the world is daunting, and the effort to do so is economically impractical. As a result, some level of contamination will always remain, both locally and globally. The presence of a residual level of contamination carries with it the probability of negative impacts on the world's population; e.g., enhanced risk of cancer or the onset of neurological disorders. Risk is the probability of such events. Risk assessments are routinely performed at contaminated sites

and in areas of widespread environmental contamination, such as an entire aquifer, as a means of quantifying the potential threats to public health and to ecosystems.

11.1.2 Principles, Definitions, and Perspectives of Hazardous Waste Risk Assessments

Risk assessment is the attempt to measure the potential for harm. It is a process that aids in site assessments, determining end points in remediation, and evaluating the danger of engaging in potentially hazardous acts such as drinking contaminated groundwater. The use of risk assessment has become commonplace since the promulgation of Comprehensive Environmental Response, Compensation, and Liability Act (CERCLA), or Superfund, and has been important in assessing hazards such as the occurrence of earthquakes, hurricanes, and floods.

Hazardous waste risk assessments are systematic and quantitative; there is a well-established algorithm for conducting the process. However, a significant amount of uncertainty and data gaps are inherent in making risk assessments of contaminated sites and contaminated groundwaters; therefore, the quantitative methodologies are constrained by uncertainty limits. Furthermore, input data for many of the calculations (e.g., the volume of groundwater ingested per individual per day) may be difficult to obtain, or totally unavailable. Because of this, risk assessment teams must have sufficient risk assessment experience to accurately evaluate the inevitable data gaps.

11.1.2.1 Definitions of Hazard and Risk

Risk is the probability of harm or loss and can be considered to be a product of the probability and the severity of specific consequences. Risk, as it relates to hazardous wastes and groundwater contamination, may be defined as the chance that humans or other organisms will sustain adverse effects from exposure to these environmental hazards. Risk is inherent in the life of all organisms – humans, animals, and plants. Tornadoes, landslides, hurricanes, earthquakes, and other natural disasters carry a risk of injury or death to any living thing in their path. Similarly, human-caused risks such as automobile accidents, plane crashes, and nuclear disasters occur with varying levels of severity.

Specific definitions apply to different aspects of risk assessment in hazardous waste management. *Background risk* is the risk to which a population is normally exposed, excluding risks from hazardous chemicals or groundwater contamination. *Incremental risk* is the additional risk caused by hazardous chemicals or the contaminated groundwater. *Total risk* is the background risk plus the incremental risk. For example, the background risk of cancer for the average US citizen is one in four, or 0.25 (Guidotti, 1988). The target incremental risk at Superfund sites for carcinogen exposure to the 'most exposed individual,' proposed by the Environmental Protection Agency (EPA), is 1×10^{-6}. The target for total lifetime risk for exposure to carcinogenic contaminants at Superfund sites is then 0.25 plus 1×10^{-6}. Analysis of the total risk often involves critical evaluation of the quantitative risk assessment itself, including analysis of the uncertainties of the assessment and the acceptable risk of the hazardous waste.

Hazard is different from risk; it is a descriptive term that characterizes the intrinsic ability of an event or a substance to cause harm. Hazard is one source of risk and is a function of the persistence, mobility, and toxicity of the contaminants.

11.1.2.2 Typical Risks Encountered – Natural and Anthropogenic

Risk assessment and risk management are used widely in scientific, engineering, medical, economic, and even sociological evaluations. Risk from natural hazards, such as storms, floods, hurricanes, tornadoes, and even insect and animal attacks have been studied in detail to evaluate the potential for disaster and economic effects. Structural engineers often evaluate the risk of bridge failures, building failures during earthquakes, and other damage that can result from natural disasters and the aging of structural materials. Epidemiologists often determine risk from disease outbreaks, and other health effects. Many insurance companies and investment firms have risk management departments that use risk models for quantifying economic risks.

11.1.2.3 Risks Associated with Contaminated Sites and Groundwater

More than 600 chemicals have been discovered at Superfund sites. The contaminants that are found most frequently at National Priorities List (NPL) sites are lead (43% of sites), trichloroethylene (42%), chromium (35%), benzene (34%), perchloroethylene (28%), arsenic (28%), and toluene (27%) (ATSDR, 1989). Although chemicals regulated as hazardous wastes are often classified as corrosive, flammable, explosive, or toxic, toxicity is the most common concern in regard to groundwater contaminants. Toxicity, in turn, is classified as acute or chronic. Acute toxicity results from short-term exposure to relatively high contaminant dosages. Chronic toxicity occurs as the result of drinking low contaminant concentrations over decades. The most common concern resulting from the improper disposal of hazardous chemicals and subsequent groundwater contamination is chronic toxicity and resulting effects such as cancer and neurological diseases.

11.1.3 Regulatory and Policy Basis for Risk Assessment

11.1.3.1 Examples of Contaminated Sites and Potential Risk Exposure Pathways

Before strict regulatory measures were passed that prevented the improper land disposal of hazardous wastes, numerous disposal practices were used that produced thousands of contaminated sites requiring cleanup activities that have lasted for decades. A common disposal practice was to spread waste liquids, especially lubricating oils and other petroleum residues, on soils and unpaved roads. Many industries disposed of waste chemicals by placing them in unlined soil pits and lagoons. Workers simply dug pits into which wastes were poured; the wastes then disappeared by seeping into and through the soil. Many large industries constructed landfills

that were used primarily for the land disposal of industrial by-products, such as building materials or out-of-date equipment. Unfortunately, these landfills were also used for the disposal of chemical wastes. Sanitary landfills that were designed to accept newspapers, cans, bottles, and other household wastes also received waste petroleum products, solvents, pesticides, transformer oils, etc. Though liquid hazardous wastes were often disposed of in drums, in some cases they were poured directly into the landfills. Since these sanitary landfills were unlined, the wastes often migrated to surface and groundwater. Waste chemicals stored in 55-gallon drums were often placed on loading docks, concrete pads, or other temporary storage areas awaiting disposal. The drums often accumulated, sometimes to the point where thousands were stored and stacked. Drums stored in this manner eventually corrode and leak, resulting in chemical releases into the underlying soil and groundwater. Underground storage tanks (USTs) that had been buried for decades began to leak in the 1970s resulting in the saturation of soil with leaking chemicals, and the eventual contamination of groundwater.

As a result of these improper disposal practices, sites contaminated with hazardous wastes came to public attention throughout the 1970s and 1980s. The effects of improper hazardous waste disposal may persist for decades or even centuries when the contaminants have low degradation rates and migrate slowly through the subsurface.

The US EPA summarized the results of studies of potential pathways for the release of chemicals from Superfund sites (US EPA, 1988). Migration to groundwater was cited as the primary pathway of contaminants at these hazardous waste sites, a trend confirmed by the data in **Table 1**; 37% of sites involved releases to groundwater and 23% were responsible for releases to both groundwater and surface water. Other studies document the potential hazards of hazardous waste disposal. The EPA, in a survey of 466 public water supply wells, found that one or more volatile organic compounds (VOCs) were detected in 16.8% of small water systems and 28% of large water systems. The VOCs found most often were trichloroethylene and perchloroethylene (Westrick et al., 1983). A survey of 7000 wells conducted in California from 1984 through 1988 showed that 1500 contained detectable concentrations of organic chemicals and 400 contained these in concentrations exceeding the state's regulatory requirement or the maximum contaminant level (MCL) prescribed by the Safe Drinking Water Act (SDWA) (MacKay and Smith, 1990). The most common chemicals detected were perchloroethylene, trichloroethylene, chloroform, 1,1,1-trichloroethane, and carbon tetrachloride. The impact of hazardous wastes is serious because of our dependence on groundwater resources; 48% of the US population as a whole receives its drinking water from groundwater; 95% of the rural US population relies on groundwater for domestic use (Patrick, 1983).

Table 1 Pathways of releases of hazardous chemicals from NPL landfills

Observed releases from NPL landfills to water and air	*Percent*
Groundwater only	37
Groundwater and surface water	23
None observed	15
Surface water only	9
Groundwater, surface water, air	8
Groundwater and air	3
Surface water and air	3
Air only	2

Source: US EPA (1988).

11.1.3.2 Risk-Based Nature of CERCLA

CERCLA was passed in 1980 to provide a federally supervised system for the mitigation of chronic environmental damage, particularly the cleanup of sites contaminated with hazardous waste. In 1986, CERCLA was amended by the Superfund Amendments and Reauthorization Act (SARA). Each Superfund site has been assessed, characterized, and prioritized based on risk. Potential sites are first screened using a preliminary assessment (PA); sites deemed a significant threat are then evaluated using a hazard ranking system (HRS) to measure the risk of the site relative to that of other potential sites. The most hazardous sites are then placed on the NPL in the order of their potential risk.

Hundreds of chemicals are regulated under CERCLA; they are classified as (1) hazardous substances and (2) pollutants or contaminants. The definition of a hazardous substance under CERCLA is broad and is based on other environmental regulations. A CERCLA hazardous substance does not need to be a waste or waste material. It can be a commercial chemical, formulation, or product. A CERCLA *hazardous substance* is defined as any chemical regulated under the Clean Water Act, the Clean Air Act, the Toxic Substances Control Act (TSCA), or the Resource Conservation and Recovery Act (RCRA). However, two materials that are excluded from the hazardous substances list are petroleum and natural gas. A CERCLA *pollutant or contaminant* is defined as any other chemical or substance that "will or may reasonably be anticipated to cause harmful effects to human or ecological health." Together, these two categories encompass a broad range of chemicals.

A primary directive of CERCLA is the protection of public health. Because the hazards that exist at Superfund sites tend to be quite variable, it has not been possible to establish specific cleanup criteria for the hazardous substances regulated under CERCLA; potential human health effects must be evaluated by quantitative risk assessment on a site-by-site basis. Each Superfund site is assessed individually to determine *how clean is clean*. The rationale is that the hazard of a contaminant is a function of its potential to reach a receptor (e.g., groundwater, population) and the potential harm to the exposed receptor. The ability of a contaminant to migrate, its potential to degrade, and its distance to a receptor of concern (i.e., the risk), all are site-specific. Only on the basis of such individualized risk assessment is it possible to achieve efficient and cost-effective cleanup of the thousands of hazardous waste sites throughout the US.

11.1.3.3 Risk-Based Corrective Actions

Throughout the 1980s, tens of thousands of USTs began to leak due to corrosion. By October 1994, more than 270 000 leaking USTs had been discovered in the United States. Until that time,

absolute standards for various petroleum indicators were used as cleanup standards. Although cleanup levels varied from state to state, the most common standard was a soil concentration of 100 mg kg^{-1} of total petroleum hydrocarbons (TPH). Such absolute guidelines were thought to streamline corrective action at UST sites, because minimal exposure and toxicity assessments were required. However, as UST cleanups proceeded, it became apparent to owners and operators of USTs, as well as regulators, that site cleanup to an absolute standard sometimes displaced thousands of cubic meters of soil that posed no risk to human health or to the environment.

Although absolute cleanup standards have been used for a number of contamination problems in addition to those related to leaking USTs, the trend in managing these releases has been toward risk-based decision making. State and local agencies are implementing a process that is based on risk and exposure assessments to evaluate the extent and urgency of needed cleanup actions. The risk-based decision process for the UST corrective action process is called risk-based corrective action (RBCA). The first approach to RBCAs was developed by the American Society of Testing and Materials (ASTM); this has since been implemented by the EPA and state and local agencies.

11.1.3.4 Use of Applicable or Relevant and Appropriate Requirements

The passage of SARA in 1986 resulted in the development of *applicable or relevant and appropriate requirements* (ARARs), which are used as *de facto* values for cleanup end points. The ARARs are usually based on other environmental laws, such as the SDWA or the RCRA.

One of the more common ARARs is the use of SDW A MCLs as an action level for contaminated groundwater. As part of the SDWA, MCLs were established for many contaminants to protect the health of the public over a lifetime of drinking water. The MCLs of many of these common hazardous chemicals are in the low μg l^{-1} range; this makes analytical sensitivity and quality control a necessity in the chemical analyses of drinking water. The MCLs are based on MCL goals (MCLGs), which are nonenforceable goals based on extremely low risk. The EPA has been given the directive to set MCLs as close to MCLGs as possible. In many cases, MCLs do not correspond to the MCLG level for a cancer risk of 1×10^{-6} (based on an intake of 2 l (0.53 gal) of water per day). Instead, they are set at a pragmatic level dictated by water treatment technologies and analytical detection limits (Travis et al., 1987). Many state and local regulatory authorities use MCLs as *de facto* cleanup criteria for contaminated groundwater.

11.1.3.5 Limited Uses of Absolute Standards

Universal across-the-board cleanup criteria are not commonly used as end points for soil and groundwater cleanup, because of the wide range of risks found at these sites. However, two classes of contaminants have been subject to universal action levels for cleanup: petroleum and polychlorinated biphenyls (PCBs). Most petroleum hydrocarbon action levels are regulated by state and local agencies; the parameters used and their corresponding action levels vary widely from state to state. The specific petroleum parameters that are regulated include total petroleum hydrocarbon–gasoline fraction (TPH-G); total petroleum hydrocarbon–diesel component (TPH-D); benzene, toluene, ethylbenzene, and xylenes (BTEX); and benzene alone. Common regulatory levels include concentrations in soil of 100 mg kg^{-1} for TPH-G, 200 mg kg^{-1} for TPH-D, and 1 mg kg^{-1} for benzene. A state-by-state listing of petroleum standards has been reported by the Association for Environmental Health and Science (Nascarella et al., 2002).

In the United States, PCBs are regulated under the TSCA. The universal standard for total PCBs (i.e., the total of all 209 congeners) in commercial products such as electrical transformers is 50 mg kg^{-1}. The same regulatory standard is applied to soils and other media contaminated by PCB spills and other environmental releases of PCBs.

11.1.4 The Risk Assessment Process

11.1.4.1 Sources, Pathways, and Receptors: The Fundamental Algorithm for Risk Assessments

Hazardous waste problems are frequently generated by mixtures of complex wastes that have been disposed of on land and that have migrated through the subsurface. One approach to assessing the risks of contaminated sites has been to divide the problem into three elements: sources, pathways, and receptors (Watts, 1998) as noted in Table 2. The first step in assessing the risk at a hazardous waste site is to identify the waste components at the *source*, including their concentrations

Table 2 Elements of sources, pathways, and receptors algorithm used in hazardous waste risk assessments

Sources
Time since environmental release
Contaminants potentially present
Sampling
Contaminant concentrations
Contaminant locations
Contaminant properties
Water solubility
Octanol-water partition coefficient
Vapor pressure
Henry's law constant
Pathways
Rate of release from the source
Air
Groundwater
Atmospheric transport
Wind speed
Dispersion
Groundwater transport
Advection-dispersion
Sorption
Distance to receptors
Receptors
Characteristics of receptor population
Acute toxicity
Chronic toxicity
Noncarcinogenic
Carcinogenic

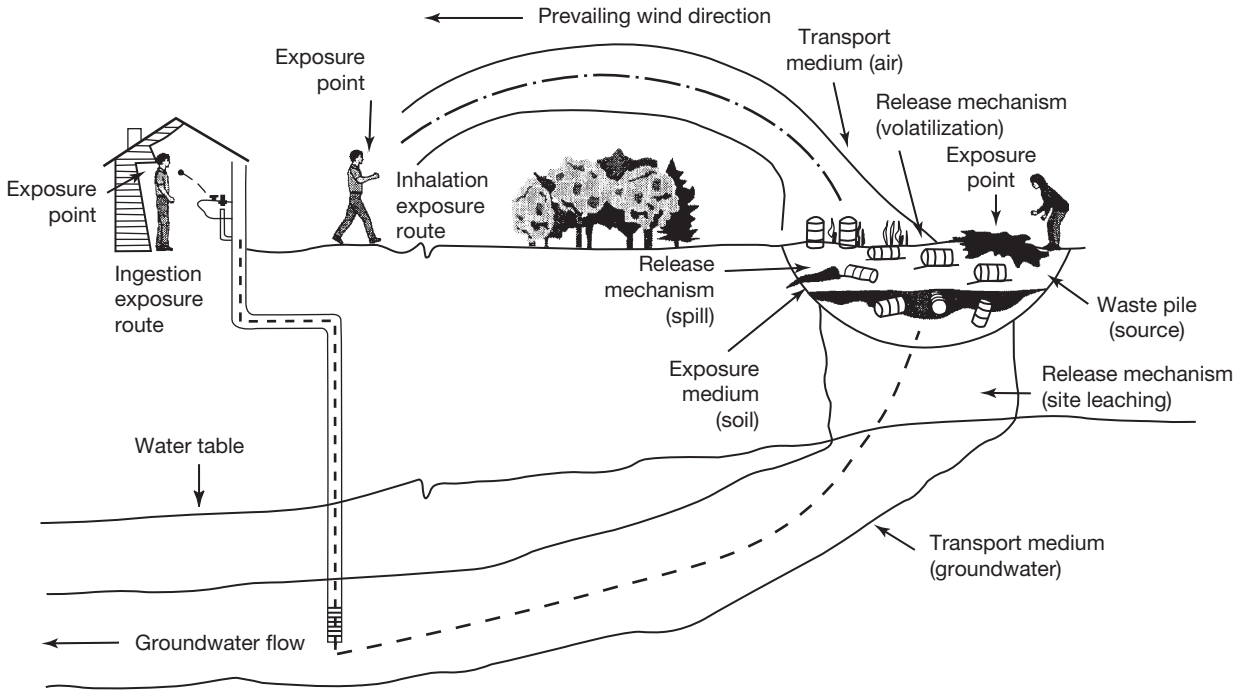

Figure 1 Common pathways for contaminant migration from a hazardous waste source.

and physical properties such as density, water solubility, and flash point. After the source has been characterized, the *pathways* of the hazardous chemicals are analyzed by quantifying the rates at which the waste compounds volatilize, degrade, and migrate from the source (Figure 1). Pathway analysis is built on source information – the identity and nature of the source chemicals must be known in order to quantify their potential to migrate, degrade, or be treated. Pathway analyses may show that the contaminant will be transformed within weeks and cease to be a problem, or they may show that the contaminant persists in the environment and will reach a receptor (such as a drinking water well) long before it is degraded. Finally, if the pathway analysis shows that the contaminant will come into contact with *receptors* (humans, endangered species, etc.), the hazard must be assessed with the aid of toxicological data.

11.1.4.2 The Four-Step Risk Assessment Process

The National Academy of Sciences and the EPA have defined four steps in the assessment of risk from hazardous wastes (US EPA, 1989a; NAS, 1983):

1. *hazard identification* (source analysis; investigating the chemicals present at the site and their characteristics),
2. *exposure assessment* (pathway analysis; estimating the potential transport of the chemicals to receptors and levels of intake),
3. *toxicity assessment* including the determination of numerical indices of toxicity (receptor analysis), and
4. *risk characterization* involving the determination of a number that expresses risk quantitatively, such as one in one hundred (0.01) or one in one million (1×10^{-6}).

11.1.5 Hazard Identification

11.1.5.1 Determining Contaminant Identity, Concentration, and Distribution

The first step in risk assessment is the evaluation of the identity and properties of the contaminants, their potential for release from the source, and their rate of release. Specific tasks in hazard identification include sampling, installation of monitoring wells, chemical analysis, creating quality assurance/quality control plans, and data analysis. Sampling is usually conducted so as to assess both the identity and the concentration and distribution of contaminants at the source. Based on the sampling and their analyses, a data set is developed (subdivided by type of media – soil, sludge, standing surface water, etc.) for input into exposure assessment models. Hazard identification is usually focused more on contaminants of concern, i.e., those presenting the highest hazard. For example, more detailed source characterization is required for 2,3,7,8-TCDD than for dodecane.

11.1.5.2 Contaminant Surrogate Analysis

Most hazardous waste sites and facilities contain tens to hundreds of chemicals. The process of collecting data can therefore be overwhelming and is sometimes unrealistic. However, risk at a hazardous waste site is often dictated by a few contaminants or one or two pathways; these are the risk drivers. The most common practice in assessing the risks of Superfund sites is to screen the contaminants and pathways using surrogate analysis. The use of surrogates reduces the numbers used in pathway studies and streamlines the computing efforts significantly.

The two most important source characteristics used in screening a large number of contaminants at a hazardous waste site or facility are their concentrations and toxicities. Screening for surrogates has been called *concentration–toxicity screening* by the EPA (US EPA, 1989a). A risk factor or *chemical score* is determined for each chemical based on its concentration and toxicity, and the scores are reported by medium. The units for the chemical score (R) are a function of the medium that is evaluated. The units do not usually matter, as long as they are consistent. If toxicity data are available for both oral and inhalation routes, the most conservative number (i.e., the most toxic) is used in concentration–toxicity screening. After Rs are determined for all of the chemicals, surrogates are chosen that account for 99% of the potential risk.

11.1.6 Exposure Assessment

Exposure is the contact of an organism with a toxic substance; *exposure assessment* is the estimation of the magnitude, frequency, duration, and route of exposure (Patton, 1993). The primary tasks of exposure assessments include (1) identifying the populations that may be exposed, (2) identifying the possible exposure pathways, (3) estimating the concentrations to which the populations are exposed, and (4) estimating chemical intakes.

11.1.6.1 Potential Exposure Pathways

The rate at which a contaminant is released from a source is a critical parameter in quantifying risk at contaminated sites. Picture two different extremes of release from the source: In the first case, 1000 kg of benzene (a confirmed human carcinogen) exists in a lined surface impoundment and is volatilizing at a rate of 0.5 kg d^{-1} and is potentially inhaled by a nearby population. In the second case, the same mass of benzene is strongly sorbed to a clay soil rich in organic matter 1 m below the soil surface, from which the volatilization rate is 10^{-7} kg d^{-1}. Obviously, the risk of hazardous chemicals depends on the rate of contaminant release.

Quantifying contaminant release rate is an integral part of source release assessment. Because release rates may vary over space and time, a spatial- and temporal-dependent emission rate is often obtained. Most analytical contaminant transport models are based on simple or constant spatial and temporal release rates; however, actual release rates are often very complex, varying significantly with time and space. Nevertheless, release rates are often approximated using constant rates in space and time.

When the effects of time variations in release rates are included, pulse (or instantaneous) and continuous (plume) emissions are the two most common time-variant inputs in transport models. The classic example of a pulse release is a hazardous waste spill. The steady release of contaminants into groundwater from a subsurface contaminant and the continuous release of volatile solvents from an air-stripping tower are examples of plume emissions.

Environmental releases of hazardous waste from contaminated sites can result in transport through several media. The most common pathways include (1) transport through the subsurface to groundwater and (2) atmospheric transport after release into the air. Other less common pathways after release include surface waters, and plant and animal uptake.

11.1.6.2 Estimating Exposure Concentrations

The goal of exposure assessment is to determine the concentration of contaminant to which the receptor organism is exposed. This procedure involves two steps: (1) determining the concentration of the contaminant to which the population is exposed, and (2) quantifying contaminant intake at the point of exposure.

In some cases, direct measurements of contaminant exposure may be made, such as in the assessment of the steady-state release of an established hazardous waste source. Groundwater monitoring wells or air-sampling devices can be used to determine current exposure concentrations for exposed populations. Commonly, however, air, surface water, and groundwater sampling is neither a logical nor a practical choice. Typical situations in which sampling is not feasible include (1) the evaluation of future exposure and risk to potentially exposed populations and (2) the potential risk from an event that has yet to occur (e.g., a hazardous waste spill).

Contaminant transport models are most commonly used for determining the concentrations of contaminants that reach the exposed population. Such models for the atmosphere, surface waters, and the subsurface have developed substantially; their use has been described by Anderson and Woessner (1992), Watts (1998), and Zheng and Bennett (2002).

11.1.6.3 Identifying Potentially Exposed Populations

An important part of exposure assessment is the identification of the population that may be exposed to hazardous chemicals. Characterizing potentially exposed populations is often an intricate and difficult process (Van Leeuwen and Hermens, 1995). It involves visiting sites, screening populations near the sites, evaluating land use and housing maps, and surveying recreational data. Prospective land use patterns must be considered as hazardous chemical exposures may occur in the future. The daily and seasonal activity patterns of the population must also be evaluated, though these are often difficult to quantify. The demographics of the receptor population may include the total population of a residential area, the identification of sensitive populations (e.g., children, elderly, infirm), or site workers and personnel. In complex systems, the aid of a geographer and geographic information systems (GIS) may be necessary. In the end, however, identifying potential receptor populations is often a qualitative exercise requiring the use of professional judgment.

11.1.6.4 Estimating Chemical Intake

After the receptor population is identified, data about population behavior are gathered. These include duration of exposure, frequency of exposure, mean body weight, and probable future demographics such as population increases or decreases. Intake (I) is estimated using equations consisting of three types of variables: (1) contaminant-related (exposure concentration), (2) exposed population (contact rate, exposure frequency,

duration, and body weight), and (3) assessment-determined (averaging time). Exposure concentration (C) is the arithmetic mean of the contaminant concentration over the period of exposure. The contact rate (CR) is the amount of contaminant encountered per unit time. The time of exposure is estimated using the site- and population-specific terms, exposure frequency (EF) and exposure duration (ED). Conservative assumptions are normally used for each variable, such as the 95th percentile value for exposure time (US EPA, 1989a). The body weight (BW) value is the average weight of a member of the receptor population over the exposure period. If children are the primary individuals exposed, this value should be the average child's body weight; a BW of 70 kg is commonly used for adult exposures. The averaging time (AT) is a value that is based on the mechanism of toxicity. The most commonly used averaging time for carcinogens is 70 yr × 365 d yr^{-1}; a pathway-specific period of exposure is generally used for noncarcinogenic effects (i.e., the ED × 365 d yr^{-1}).

Contaminant intake may be estimated by using the mean exposure concentration of contaminants in conjunction with the exposed population variables and the assessment-determined variables. The general equation for chemical intake is

$$I = \frac{C \times \mathrm{CR} \times \mathrm{EFD}}{\mathrm{BW}} \times \frac{1}{\mathrm{AT}} \quad [1]$$

where I is the intake (the amount of chemical at the exchange boundary) (mg kg^{-1} d^{-1}); C the average exposure concentration over the period (e.g., mg l^{-1} for water or mg m^{-3} for air); CR the contact rate, the amount of contaminated medium contacted per unit time (l d^{-1} or m^3 d^{-1}); and EFD the exposure frequency and duration. EFD is usually divided into two terms: EF the exposure frequency (d yr^{-1}) and ED, the exposure duration (yr). BW is average body mass over the exposure period (kg) and AT the averaging time (the time period over which the exposure is averaged; d).

Accurate intake data are sometimes difficult to obtain; because exposure frequency and duration vary among individuals, these variables must often be estimated using professional judgment. Daily contamination intake rates from air, contaminated food, drinking water, and through dermal exposure to water while swimming may be estimated by other equations reported by the US EPA (1989b). Drinking contaminated water and breathing contaminated air are two of the most common exposure routes. The intake for ingestion of waterborne chemicals is estimated by the following equation:

$$\mathrm{Intake}\left(\mathrm{mg\,kg^{-1}d^{-1}}\right) = \frac{\mathrm{CW} \times \mathrm{IR} \times \mathrm{EF} \times \mathrm{ED}}{\mathrm{BW} \times \mathrm{AT}} \quad [2]$$

where CW is the chemical concentration in water (mg l^{-1}), IR is the ingestion rate (l d^{-1}), and EF, ED, BW, and AT have the same meaning as in Equation (1).

Some of the values used for the variables in Equation (2) include:

- CW: site-specific measured or modeled value;
- IR: 2 l d^{-1} (adult, 90th percentile) (US EPA, 1989b), 1.4 l d^{-1} (adult, average) (US EPA, 1989b);
- EF: pathway-specific value (dependent on frequency of exposure-related activities);
- ED: 70 yr (lifetime; by convention), 30 yr (national upper-bound time (90th percentile) at one residence) (US EPA, 1989b), and 9 yr (national median time (50th percentile) at one residence) (US EPA, 1989b);
- BW: 70 kg (adult, average) (US EPA, 1989b), age-specific values (US EPA, 1985, 1989b); and
- AT: pathway-specific period of exposure for noncarcinogenic effects (i.e., ED × 365 d yr^{-1}), and 70 year lifetime for carcinogenic effects (i.e., 70 yr × 365 d yr^{-1}).

The intake for inhalation of airborne contaminants is

$$\mathrm{Intake}\left(\mathrm{mg\,kg^{-1}d^{-1}}\right) = \frac{\mathrm{CA} \times \mathrm{IR} \times \mathrm{ET} \times \mathrm{EF} \times \mathrm{ED}}{\mathrm{BW} \times \mathrm{AT}} \quad [3]$$

where CA is contaminant concentration in air (mg m^{-3}), IR the inhalation rate (m^3 h^{-1}), ET the exposure time (h d^{-1}), and other symbols have the same meaning as before.

Some of the values used in Equation (3) include:

- CA: site-specific measured or modeled value;
- IR: 30 m^3 d^{-1} (adult, suggested upper bound value) (US EPA, 1989b); 20 m^3 d^{-1} (adult, average) (US EPA, 1989b);
- ET: pathway-specific values (dependent on duration of exposure-related activities);
- EF: pathway-specific value (dependent on frequency of exposure-related activities);
- ED: 70 yr (lifetime; by convention); 30 yr (national upper-bound time (90th percentile) at one residence) (US EPA, 1985); 9 yr (national median time (50th percentile) at on residence) (US EPA, 1989b);
- BW: 70 kg (adult, average) (US EPA, 1989b); age-specific values (US EPA, 1985, 1989b);
- AT: pathway-specific period of exposure for noncarcinogenic effects (i.e., ED × 365 d yr^{-1}), and 70 yr lifetime for carcinogenic effects (i.e., 70 yr × 365 d yr^{-1}).

11.1.7 Toxicity Assessment

11.1.7.1 Overview of Human Health Toxicology

Most health effects from environmental toxins are due to a detrimental change in the structure or function of biological molecules in the organism, which lead to a disruption of biochemical and physiological function. Two basic categories of cytological damage are recognized: (1) binding to an enzyme or energy-carrying molecule, resulting in cellular dysfunction or cell death (necrosis); and (2) binding to or modification of the cell's genetic material (deoxyribonucleic acid; DNA), resulting in abnormal changes in the cell's rate of reproduction and other cellular behavior. Genetic damage to somatic cells may result in cancer, and genetic damage to germ cells can result in teratogenesis (i.e., birth defects). Cellular injury is a detrimental effect in which the extent of toxicity is frequently a function of contaminant dose, while genetic toxicity is classified as stochastic without a safety threshold.

A fundamental principle of hazardous waste risk assessments is the concept of dose response. Except for genetic toxins (e.g., carcinogens, in which the exposure to one molecule can potentially cause a toxic response), every chemical is toxic at some level, and the toxicity is usually directly proportional to

the mass ingested. For example, 210 g of table salt is toxic to the average adult, as is 2080 g of sugar. Hazardous chemicals are, of course, significantly more toxic than sugar. Most exhibit no toxicity below certain concentrations or exposure levels. Furthermore, elements such as chromium, iron, selenium, iodine, and compounds such as vitamins are toxic at high concentrations, but are vital nutrients at lower concentrations.

Toxicity data, which are determined experimentally in studies with laboratory animals, may not be generally applicable due to biological variability. Susceptibility to toxicological effects within a population of organisms is described by a Gaussian distribution. Individuals at one end of the spectrum may be highly susceptible to toxicity, whereas individuals at the other end of the spectrum exhibit more tolerance of the toxic effect. The dose representing the midpoint of the curve is the LD_{50}: the lethal dose to 50% of the population. The values of the LD_{50} vary with the animal species tested, and are generally unavailable for humans; however, data for closely related species, such as monkeys, are considered a close approximation to human responses. The LD_{50} is only useful in cases of acute toxicity. In hazardous waste risk assessment it is applied where a nearby population may be exposed to a toxic cloud or plume.

11.1.7.1.1 Classification of toxic responses

The most important factor that influences toxicity is the dose: it has been said that the dose makes the poison. A second important factor is the time period of exposure. Toxicity is often classified by the number and/or the duration of exposures. For example, a worker exposed to a mixture of sulfuric acid and sodium cyanide might receive a one-time, high dose of this toxic substance that can cause death through the binding of cyanide to energy-transferring molecules known as cytochromes. Repeated exposures are most simply classified as *chronic*. A common chronic exposure to hazardous chemicals is the ingestion drinking water contaminated with trace levels of hazardous chemicals.

Many chemicals that are acutely toxic are not chronically toxic, and vice versa. For example, pure vitamin D exhibits high acute toxicity. However, low repeated doses (such as in the normal intake of milk) are not only nontoxic but also essential to good health. For chemicals that are both acutely and chronically toxic, the mechanisms of the two types of toxicity are often different. For example, acute toxicity from a large dose of chloroform is caused by effects on the central nervous system that cause dizziness and narcosis. However, ingesting water containing trace concentrations of chloroform over a lifetime results in liver damage and cancer (Stewart, 1971).

11.1.7.1.2 Quantifying reversible toxic effects

In hazardous waste management, chronic toxicity is often caused by long-term, low-level exposure to hazardous chemicals. Chronic toxicity is difficult to quantify, because less is known about the long-term effects of chemicals than about their acute toxicity. The lack of toxic response from zero dose to the threshold dose is the result of a biochemical or physiological defense (e.g., detoxification or excretion) that prevents the occurrence of toxicological effects. Toxicity first appears at the threshold dose. As the exposure to the chemical is increased, the detoxification mechanisms are overwhelmed and the effects increase as a function of dose. Eventually, all of the toxicological effects are exhibited. Animal studies are used to evaluate the effects of chronic toxicity. Feeding or inhalation evaluations are carried out for most of the animals' lives. Upon completion of the study, the animals are sacrificed and pathological evaluations are conducted. The results are then extrapolated to humans using biochemically based models for carcinogens and a series of safety factors for noncarcinogens.

11.1.7.2 Quantifying Noncarcinogenic Risk: Reference Dosages

Noncarcinogenic toxicities are detrimental effects caused by chemicals that do not induce cancer. The most common effects are due to interactions between the chemical and the biological molecules in the receptor, especially enzymes. Toxic chemicals can bind to an important enzyme and reduce or eliminate its function. Some of the most important noncarcinogenic interactions between toxic chemicals and biological molecules include the inhibition of acetylcholinesterase by organophosphate ester and carbamate insecticides, the binding of carbon monoxide to hemoglobin, and the binding of cyanide to cytochromes.

Estimates of the toxicity of noncarcinogens are based on the concept of their threshold: the dose below which there are no short- or long-term effects on the organism. The lack of effect below the threshold dose can be understood in terms of its molecular basis. If millions of receptor biomolecules are available for a given function (e.g., nerve transmission, transport of oxygen), the binding of a toxic chemical to a small number of these receptor molecules does not produce a measurable toxic effect. A good example is the inactivation of a very small number of molecules of acetylcholinesterase by an insecticide such as parathion.

11.1.7.2.1 The no observed adverse effect level

An important parameter in the risk assessment of hazardous wastes is the no-effect level to which a population may be exposed. This level, defined as the *no observed effect level* (NOEL), is difficult to measure and also difficult to define accurately. Its values are based on epidemiological data and controlled animal experiments designed to determine the highest dose that will not produce an adverse effect. The *no observed adverse effect level* (NOAEL) is a variant of the NOEL in that it classifies only toxicological effects. Other measures related to the NOEL and the NOAEL are the LOEL *(lowest observed effect level)* and LOAEL (*lowest observed adverse effect level*), a stricter version of the LOEL.

11.1.7.2.2 Acceptable daily intakes and reference doses

The *acceptable daily intake* (ADI) is the level of daily intake of a toxic substance that does not produce an adverse health effect. ADIs are based on NOAELs, but are not considered an absolute physiological threshold; they are based on safety factors that reflect variations in the population. Therefore, values for ADIs are significantly lower than values of corresponding NOAELs (US EPA, 1986, pp. 33992–34003).

Reference doses (RfDs) are a regulatory parameter also based on NOAELs. The RfD is used by the EPA in place of the ADI (which sometimes results in lower values for acceptable

intakes). Safety factors are used in the derivation of RfDs to account for hypersensitivity reactions. RfDs usually incorporate two safety factors: (1) a factor of 10 for variation among individuals and (2) another factor of 10 for extrapolation from experimental animal data to humans (Barnes and Dourson, 1988). Another safety factor that may be used with the RfD is a 'modifying factor' ranging from 1 to 10, which is based on professional judgment. The procedure for establishing RfDs is somewhat more detailed than for ADI development, and includes use of the most sensitive species, the appropriate route of exposure, and the most sensitive end point (US EPA, 1986, pp. 34028–34040). RfDs have become a widely used indicator of chronic toxicity, and have been established for oral and inhalation routes. RfDs for the most common hazardous compounds are listed in **Table 3**.

Table 3 Reference doses of some common hazardous compounds

Compound	*Oral RfD* ($mg\ kg^{-1}\ d^{-1}$)	*Inhalation RfD* ($mg\ kg^{-1}\ d^{-1}$)
Monocyclic aromatic hydrocarbons		
Benzene	0.029	0.029
Toluene	0.2	
Ethylbenzene	0.1	0.286
Xylenes	2.0	
Polycyclic aromatic hydrocarbons		
Anthracene	0.3	
Fluorene	0.04	
Pyrene	0.03	
Nonhalogenated solvents		
Acetone	0.1	
Methyl ethyl ketone	0.6	0.286
Chlorinated solvents		
Carbon tetrachloride	7.0×10^{-4}	
Chloroform	0.01	
PCE	0.01	
Insecticides		
Aldrin	3.0×10^{-5}	
Carbaryl	0.1	
Dieldrin	5.0×10^{-5}	
DDT	5.0×10^{-4}	
Lindane	3.0×10^{-4}	
Malathion	0.02	
Herbicides		
Atrazine	0.035	
2,4-D	0.01	
2,4,5-T	0.01	
Trifluralin	0.0075	
Fungicides		
Pentachlorophenol	0.03	
Industrial intermediates		
Chlorobenzene	0.02	
2,4-Dichlorophenol	0.003	
Hexachlorocyclopentadiene	0.007	
Phenol	0.6	
Explosives		
2,4,6-Trinitrotoluene	5.0×10^{-4}	
Polychlorinated biphenyls		
Aroclor 1016	7.0×10^{-5}	
Aroclor 1254	2.0×10^{-5}	

11.1.7.3 Quantifying Carcinogenic Risk: Slope Factors

Two methods have been used to estimate carcinogenicity in humans: epidemiological studies and animal studies. Of the two, the use of animals is considered more reliable among toxicologists because epidemiological studies are usually based on random data (i.e., without experimental design) and yield a less secure basis for establishing cause–effect relationships. Because of the difficulty of measuring human carcinogenicity, the International Agency for Research on Cancer (IARC), an organization that is part of the World Health Organization (WHO) of the United Nations, has developed three categories for evidence of carcinogenicity. These include: (1) sufficient evidence of human cancer definitely caused by exposure, (2) limited evidence due to inadequate data, and (3) inadequate evidence (i.e., no data available) (IARC, 1987).

A significant question in the quantification of carcinogen risk is the hazard imposed by exposure to very low concentrations of chemicals. To quantify potential carcinogenesis using the low contaminant concentrations to which the public is typically exposed would require chronic toxicity studies with an enormously large number of test animals. Dose–response relationships can be determined experimentally at higher doses, and these high-dose data can be extrapolated to the lower doses to which populations are typically exposed. Therefore, most animal studies use higher doses than commonly found in the environment. Other guidelines include the use of lifetime studies on at least 50 animals × two sexes × two species × at least three doses (a control and two doses) (IRLG, 1979). A phenomenon that must be considered is the background cancer level, which may be a function of the environment and the genetic makeup of the population being evaluated.

The extrapolation of empirical data requires a careful assessment of the assumptions regarding the mechanisms of carcinogenesis at the lower dosages. Two classes of models have been developed to quantify the probability of cancer as a function of dose, including the extrapolation from higher doses to lower doses. *Tolerance models* (e.g., log-probit, log-logistic) are based on statistics. *Mechanistic models* (e.g., one-hit, gamma, multihit, and Weibull) are based on known biochemical and physiological processes. Mechanistic models are usually favored over tolerance models. Information regarding carcinogenic dose–response models is available in Rai and Van Ryzin (1979) and Gaylor and Kodell (1980).

Two criteria must be considered when evaluating the carcinogenicity of hazardous chemicals: (1) the carcinogenic potential and (2) the availability of data on the carcinogens. As in all toxicological evaluations, a dose–response relationship is the basis for quantifying a toxicological response. Dose–response evaluations are usually based on animal studies and provide a quantitative relationship between tumor incidence and dose. The procedures for such assays involve giving test animals a dose according to body weight per day ($mg\ kg^{-1}\ d^{-1}$). The response (y-axis) is the incidence of cancer corrected for background cancer rates. The cancer incidence in the test animals must then be extrapolated to humans. In linking animal data to humans it is assumed that there is no threshold dose for cancer-causing chemicals because even one molecule can initiate cancer. Therefore, any concentration of a

Table 4 Slope factors of some common hazardous compounds

Compound	*Oral SF* $(mg\ kg^{-1}\ d^{-1})^{-1}$	*Inhalation SF* $(mg\ kg^{-1}\ d^{-1})^{-1}$
Monocyclic aromatic hydrocarbons		
Benzene	0.029	0.029
Chlorinated Solvents		
Carbon tetrachloride	0.13	0.13
Chloroform	0.0061	0.081
1,1,2-TCA	0.057	0.057
Insecticides		
Aldrin	17	17
Dieldrin	16	16
DDT	0.34	0.34
Hexachlorobenzene	1.6	1.6
Herbicides		
Trifluralin	0.0077	
Fungicides		
Pentachlorophenol	0.12	0.12
Industrial intermediates		
2,4,6-Trichlorophenol	0.011	0.011
Explosives		
2,4,6-Trinitrotoluene	0.03	

carcinogen carries some degree of risk. The most common value of acceptable risk used in hazardous waste assessments is 1×10^{-6}, or one in one million. However, bioassays for cancer cannot evaluate doses for such a low response by any currently known method. The data collected from animal studies are therefore extrapolated to a 1×10^{-6} risk. Such extrapolation of carcinogen risk uses a *carcinogen potency factor* (CPF), which is the slope of dose–response curves at low exposures. The EPA has adopted the use of carcinogenic dose-response relationship slopes and these have become commonly known as *slope factors* (SFs) with units of $(mg\ kg^{-1}\ d^{-1})^{-1}$. As with RfDs, oral and inhalation slope factors have been reported by the EPA (US EPA, 1995). SFs for the most common hazardous chemicals are listed in Table 4.

11.1.8 Risk Characterization

Risk characterization is the calculation of risk for all potential receptors that may be exposed to hazardous wastes. It includes calculating risk for different exposure routes to both noncarcinogenic and carcinogenic hazardous chemicals. Often this requires the use of toxicological data derived from animal studies. Furst (1994) discussed issues in the interpretation of this data, and suggested that animal toxicity data should only be used for risk calculation when experiments employ routes that mimic human exposure (i.e., oral, inhalation, or dermal).

11.1.8.1 Determination of Noncarcinogenic Risk

Noncarcinogenic risk is represented by the hazard index (HI), which is the ratio of the chronic daily intake to the RfD:

$$\mathrm{HI} = \frac{I}{\mathrm{RfD}} \qquad [4]$$

where HI, the hazard index, is dimensionless, I is the intake $(mg\ kg^{-1}\ d^{-1})$, and RfD is the reference dose $(mg\ kg^{-1}\ d^{-1})$.

A hazard index of <1.0 represents an acceptable cumulative risk for all contaminants and routes of exposure. In other words, if the hazard index is <1.0, the receptors are exposed to concentrations that do not present a hazard because detoxification and other mechanisms forestall toxic effects that could result from exposure to the contaminant. The quantitative value obtained for the HI is not a value of risk; it does not indicate the probability of harm as the result of exposure.The hazard index only provides an indication of the probable presence or absence of effects from exposure to noncarcinogens.

11.1.8.2 Determination of Carcinogenic Risk

Carcinogenic risk is a function of the chronic daily intake (calculated using Equation (1) and the slope factor (SF)):

$$\mathrm{Risk} = \mathrm{CDI} \times \mathrm{SF} \qquad [5]$$

where Risk is the probability of carcinogenic risks (fraction), CDI the chronic daily intake $(mg\ kg^{-1}\ d^{-1})$, and SF the carcinogenic slope factor $(mg\ kg^{-1}\ d^{-1})^{-1}$.

The value for risk is the quantitative end point determined in risk assessment calculations; it is commonly used in regulatory and management decisions regarding hazardous wastes. As with noncarcinogens, the risk term is calculated for each contaminant, each route of exposure, and for all sets of receptor populations; each element of risk is then summed to provide the value of cumulative risk.

11.1.9 Sources of Uncertainties in Risk Assessment

A limitation of both human health and ecological risk assessments is the uncertainty inherent in almost every level of the calculations. Although the risk assessment process results in a relatively straightforward numerical value for the probability of hazard, a significant degree of uncertainty is inherent in that value.

Suter (1990) emphasized that at our current level of knowledge, the detrimental effects of hazardous chemicals on ecosystems cannot be adequately predicted. The current methods can only assess risks in a simplified manner by providing a relative ranking of risk – from chemical-to-chemical or site-to-site. Nonetheless, such relative-risk ranking provides a useful basis for prioritizing environmental hazards, particularly if data are analyzed by qualified risk assessors.

Most risk assessments use data based on assumptions and extrapolations. These generate uncertainties due to the lack of knowledge or data. A degree of caution is used by risk assessors in assigning absolute numbers to risk values and hazard indices because a significant degree of uncertainty is inherent in each of the four steps of risk assessment, which is then compounded into the final risk value.

11.1.9.1 Source Characterization

Uncertainties in source characterization include imprecise source sampling, limitations of the analytical results, and

selection of the contaminants used to calculate risk. For example, priority pollutant analyses are often used to screen chemicals at hazardous waste sites. However, contaminants other than the 129 priority pollutants, as well as their metabolites, may be found at these sites, and are not detected by Methods 624, 625, or other standard analytical schemes. The problems of including nondetected chemicals in a health risk assessment were discussed by Seigneur et al. (1995). They noted that this practice may lead to estimated risks that exceed regulatory thresholds, because the detection limit or half of the detection limit must be used in risk calculations.

11.1.9.2 Lack of Available Data

Lack of data is often a significant source of uncertainty in risk assessments. Unavailable data may include source concentrations or source contaminants such as those not quantified by standard analyses such as EPA methods 624 and 625. RfDs and SFs are currently only available for fewer than two hundred chemicals; however, since thousands of chemicals are potentially present at contaminated sites and hazardous waste facilities, the paucity of available data may be responsible for a significant amount of uncertainty.

11.1.9.3 Exposure Assessment Models and Methods

Whether predictive models or sampling and analysis of the media are used to determine contaminant concentrations to which receptor organisms are exposed, uncertainties are inevitable. Many risk assessments use exposure assessment models to predict possible future contaminant concentrations at a point of exposure. The uncertainty of such modeling of contaminant concentrations projected into the future is obvious. The possible occurrence of hazardous waste spills and traffic accidents involving hazardous materials is also predicted using stochastic modeling. These predictive models also contain a significant degree of inherent uncertainty. Although most hazardous waste sampling is conducted using strict quality control and quality assurance measures some uncertainty in sampling is inevitable. Furthermore, some standard analytical procedures are subject to false positive and false negative results; for example, natural soil organic matter appears in TPH analyses in the same manner as hydrocarbons, resulting in a false positive error. Some contaminants are not efficiently extracted into organic solvents for analysis from soils and sludge, resulting in a false negative error.

11.1.9.4 Quality of Toxicological Data

ADIs, NOAELs, RfDs, and SFs are based on extrapolation of animal toxicity data to humans using accepted safety factors. These parameters incorporate a degree of variability of up to several orders of magnitude (1000–10 000), which significantly affects the outcome of any risk assessment. Toxicity data for ecological risk assessments are often subject to even greater uncertainty than human health toxicity data. Furthermore, the toxicological effects on communities via disruption of predator–prey relationships and changes in species diversity and community structure are unknown, and estimates of their magnitude are likely to be very uncertain.

11.1.9.5 Evaluating Uncertainty

One approach to evaluating uncertainty is the use of stochastic modeling. Ünlü (1994) used Monte Carlo, first-order, and point estimate methods to evaluate uncertainties in contaminant concentrations downgradient from a waste pit. A comparison analysis showed that for conservative contaminants, the accuracy of the first-order method is comparable with that of the Monte Carlo method and can be used as an alternative to Monte Carlo analyses. In general, the accuracy of the first-order and point-estimate methods was sensitive to the fate and transport of the contaminants. Uncertainties in groundwater contamination risk have also been evaluated with a model that addressed the effects of source-, chemical-, and aquifer-related uncertainties (Hamed et al., 1995). The application of the method was demonstrated with a nonreactive solute and with oxylene as a reactive contaminant in groundwater. The model results were checked against those from a Monte Carlo simulation method, and were found to be in good agreement except for low probability events. Shevenell and Hoffman (1993) used uncertainty analyses to improve the reliability of risk assessment modeling, a procedure that helps to moderate the sometimes unknown model assumptions and the uncertainty associated with some model parameters. Finally, Doyle and Young (1993) recommended that conclusions about whether the uncertainty in the risk assessment over- or underestimates risk should be included in the assessment report. In most cases, the effect of uncertainties in the potential negative public health effects are addressed by the use of conservative assumptions. For example, conservative estimates of attenuation and lower natural degradation rates than normal may be used to counter the uncertainty of exposure assessment models.

11.1.10 Risk Management and Risk Communication

Risk assessment in itself provides a quantitative value for potential hazards from hazardous waste sites and facilities; however, risk evaluation is usually carried further with risk management. *Risk management* is a decision-making process that uses the quantitative values obtained from risk assessment models along with the insight, experience, and judgment of professionals. Risk assessment and risk management are multifaceted methodologies that require the consideration of quantitative values, qualitative assessments, and professional judgment. The lines between science, engineering, economics, and policy become blurred, and, therefore, the ultimate decisions based on risk analysis have to be balanced by professional judgment.

Scientists and engineers involved in hazardous waste risk assessment often have an innate appreciation of the risks associated with hazardous wastes. However, the public, especially those who live near a hazardous waste site or facility, require information regarding the risk assessment process, its uncertainties, and the value judgments that have been made. This information is conveyed through *risk communication*, an integral part of the risk assessment process.

A hazardous waste risk assessment team must be able to communicate effectively with the public about the risk

assessment process and the results of the risk assessment at the site that is of concern to the local population. Some of the specific elements of risk communication include (1) the steps of the risk assessment process, (2) acceptable levels of risk, and (3) the uncertainties and value judgments that are inherent in the risk assessment process. The four fundamental steps in the risk assessment process for hazardous wastes (source characterization, exposure assessment, toxicity assessment, and risk estimation) can easily be presented in outline form at citizens' meetings and hearings. Typical acceptable levels of risk, such as the typical Superfund level of 1×10^{-6}, are often discussed in relation to other natural and anthropogenic risks that are part of the world in which we live. In addition to communicating the risk assessment procedure and commonly used levels of risk, the public must be made aware of the uncertainties at the different stages of the risk assessment process, and must know that the quantitative value of risk that is obtained is bounded above and below that number by a range of uncertainties. Furthermore, the public must be aware that these uncertainties are part of quantifying such complex processes, and absolute certainty in such assessments will probably never be realized. The public should also be aware that the experience and value judgments of the risk assessment team are an important and necessary part of the risk assessment process, and that the use of such qualitative tools is a common and effective procedure.

References

Anderson MP and Woessner WW (1992) *Applied Groundwater Modeling*. San Diego, CA: Academic Press.

ATSDR (1989) *ATSDR Biannual Report to Congress: October 17-September 30, 1986*. *Agency for Toxic Substances and Disease Registry*. Atlanta, GA: US Public Health Service.

Barnes DG and Dourson M (1988) Reference dose (RfD): Description and use in health risk assessments. *Regulatory Toxicology and Pharmacology* 8: 471–486.

Doyle ME and Young JC (1993) Human health risk assessments. In: Maughan JT (ed.) *Ecological Assessment of Hazardous Waste Sites*, ch. 5. New York: Van Nostrand Reinhold.

Furst A (1994) Issues in interpretation of toxicological data for use in risk assessment. *Journal of Hazardous Materials* 39: 143–148.

Gaylor DW and Kodell RL (1980) Linear interpolation algorithm for low dose risk assessment of toxic substances. *Journal of Environmental Pathology and Toxicology* 4: 305–312.

Guidotti TL (1988) Exposure to hazard and individual risk: When occupational medicine gets personal. *Journal of Occupational Medicine* 30: 571–577.

Hamed MM, Conte JP, and Bedient PB (1995) Probabilistic screening tool for ground-water contamination assessment. *Journal of Environmental Engineering* 121: 767–775.

Interagency Regulator Liaison Group (IRLG) (1979) Scientific bases for identification of potential carcinogens and estimation of risks. *Journal of the National Cancer Institute* 63: 241–268.

International Agency on Research of Cancer (IARC) (1987) Overall evaluations of carcinogenicity. *IARC Monographs on the Evaluation of Carcinogenic Risks to Humans. An Updating of International Agency on Research of Cancer Monographs* 1–42 (supplement 7).

MacKay DM and Smith LA (1990) Agricultural chemicals in groundwater: Monitoring and management in California. *Journal of Soil and Water Conservation* 45: 253–255.

Nascarella MA, Kostecki P, Calabrese E, and Click D (2002) AEHS's 2001 survey of states' soil and groundwater cleanup standards. *Contaminated Soil Sediment and Water* 15–68 Jan./Feb.

National Academy of Sciences (NAS) (1983) *Risk Assessment in the Federal Government: Managing the Process*. Washington, DC: National Academy Press.

Patrick R (1983) *Groundwater Contamination in the United States*. Washington, DC: National Academy Press.

Patton DE (1993) The ABCs of risk assessment. *EPA Journal* 19: 10–15.

Rai K and Van Ryzin J (1979) Risk assessment of toxic environmental substances using a generalized multi-hit dose response model. In: Breslow NE and Whittemore AS (eds.) *Energy and Health*. Philadelphia, PA: Society for Industrial and Applied Mathematics.

Seigneur C, Constantinou E, Fencl M, Levin L, Gratt L, and Whipple C (1995) The use of health risk assessment to estimate desirable sampling detection limits. *Journal of the Air & Waste Management Association* 45: 823–830.

Shevenell L and Hoffman FO (1993) Necessity of uncertainty analyses in risk assessment. *Journal of Hazardous Materials* 35: 369–386.

Stewart RD (1971) Methyl chloroform intoxication: Diagnosis and treatment. *JAMA* 215: 1789–1792.

Suter FW II (1990) Endpoints for regional ecological risk assessments. *Environmental Management* 14: 9–23.

Travis CC, Crouch EAC, Wilson R, and Klema ED (1987) Cancer risk management: A review of 132 federal regulatory cases. *Environmental Science & Technology* 21: 415–420.

Ünlü K (1994) Assessing risk of ground-water pollution from land-disposed wastes. *Journal of Environmental Engineering* 120: 1578–1597.

US EPA (1985) *Development of Statistical Distributions or Ranges of Standard Factors used in Exposure Assessments. US Environmental Protection Agency Office of Health and Environmental Assesment*. Washington, DC: US Government Printing Office.

US EPA (1986) *Guidelines for Carcinogen Risk Assessment*. US Environmental Protection Agency, Federal Register, 51, pp. 33992–34003. Washington, DC: US Government Printing Office 34028–34040.

US EPA (1988) *Report to Congress: Solid Waste Disposal in the United States, Vol. II*, EPA/530-SW-88–011B. US Environmental Protection Agency. Washington, DC: US Government Printing Office.

US EPA (1989a) *Risk Assessment Guidance for Superfund: Environmental Evaluation Manual* (EPA/540/1–69/001A, OSWER Directive 9285.7–01). US Environmental Protection Agency. Washington, DC: US Government Printing Office.

US EPA (1989b) *Exposure Factors Handbook*. (Publication EPA/600/8–89/043).US Environmental Protection Agency. Washington, DC: US Government Printing Office.

US EPA (1995) *Integrated Risk Information System (IRIS)*. US Environmental Protection Agency. Washington, DC: US Government Printing Office.

Van Leeuwen CJ and Hermens JLM (1995) *Risk Assessment of Chemicals: An Introduction*. Dordrecht, The Netherlands: Kluwer.

Watts RJ (1998) *Hazardous Wastes: Sources, Pathways, Receptors*. New York: Wiley.

Westrick JJ, Mills JW, and Thomas RF (1983) *The Ground Water Supply Survey: Summary of Volatile Organic Contaminant Occurrence Data*. Cincinnati, OH: US EPA, Office of Drinking Water.

Zheng C and Bennett GD (2002) *Applied Contaminant Transport Modeling*. New York: Wiley.

11.2 Arsenic and Selenium

JA Plant, Centre for Environmental Policy/Earth Science & Engineering, Imperial College London, London, UK
J Bone and N Voulvoulis, Centre for Environmental Policy, Imperial College London, London, UK
DG Kinniburgh and PL Smedley, British Geological Survey, Wallingford, UK
FM Fordyce, British Geological Survey, Edinburgh, UK
B Klinck, British Geological Survey, Nottingham, UK

This article is a revision of the previous edition article by J.A. Plant, D.G. Kinniburgh, P.L. Smedley, F.M. Fordyce, B.A. Klinck, volume 9, pp. 17–66, © 2003, Elsevier Ltd.

11.2.1 Introduction

Arsenic (As) and selenium (Se) have become increasingly important in environmental geochemistry because of their significance to human health. Their concentrations vary markedly in the environment, partly in relation to geology and partly as a result of human activity. Some of the contamination evident today probably dates back to the first settled civilizations that used metals.

Arsenic is in Group 15 of the Periodic Table (**Table 1**) and is usually described as a metalloid. It has only one isotope, ^{75}As. It can exist in the −III, −I, 0, III, or V oxidation states (**Table 2**).

Selenium is in Group 16 of the Periodic Table and although it has chemical and physical properties intermediate between metals and nonmetals (**Table 1**), it is usually described as a nonmetal. The chemical behavior of selenium has some similarities to that of sulfur. Formally, selenium can exist in the −II, 0, IV, and VI oxidation states (**Table 2**). Selenium has six natural stable isotopes, the most important being ^{78}Se and ^{80}Se. Although ^{82}Se is generally regarded as a stable isotope, it is a β-emitter with a very long half-life (1.4×10^{20} years). Both arsenic and selenium tend to be covalently bonded in all their compounds.

Arsenic is 47th and selenium 70th in abundance of the 88 naturally occurring elements. Much more has become known about the distribution and behavior of arsenic and selenium in the environment since the 1980s because of the increased application of improved analytical methods such as inductively coupled plasma-mass spectrometry (ICP-MS), inductively coupled plasma-atomic emission spectrometry (ICP-AES), and hydride generation-atomic fluorescence spectrometry (HG-AFS). These methods can detect the low concentrations of arsenic and, generally, selenium found in environmental and biological media accurately, and as a result, arsenic and selenium are increasingly included in determinand suites during systematic geochemical mapping and monitoring campaigns (Plant et al., 2003).

Arsenic is highly toxic and can lead to a wide range of health problems in humans. Arsenic has become increasingly important in considering environmental quality because of its high toxicity (Bodénan et al., 2004) and recent evidence of severe health impacts at the population level, especially in Bangladesh. It is carcinogenic, mutagenic, and teratogenic (National Research Council, 2001). Symptoms of arsenicosis include skin lesions (melanosis, keratosis) and skin cancer. Internal cancers, notably bladder and lung cancer, have also been associated with arsenic poisoning. Other problems include cardiovascular disease, respiratory problems, and diabetes mellitus. There is no evidence of a beneficial role for arsenic (IOM (Institute of Medicine), 2001; National Research Council, 2001) and it is unclear whether there is any safe dose for humans. Indeed, the precise nature of the relationship between arsenic dose and carcinogenic effect at low arsenic concentrations remains a matter of much debate (Clewell et al., 1999; Smith et al., 2002). It has been shown that normal cells can become cancerous when treated with inorganic arsenic (Waalkes et al., 2007). When cancer cells are placed near normal stem cells, the normal stem cells very rapidly acquire

Table 1 Physical properties of arsenic and selenium

Name	Arsenic	Selenium
Symbol	As	Se
Atomic number	33	34
Periodic table group	15	16
Atomic mass	74.9216	78.96
Classification	Metalloid	Nonmetal
Pauling electronegativity	2.18	2.55
Density (kg m^{-3})	5727	4808
Melting point (°C)	817 (at high pressure)	220
Boiling point (°C)	614 (sublimes)	685
Natural isotopes and abundance	^{75}As	100%
		^{74}Se 0.87%
		^{76}Se 9.02%
		^{77}Se 7.58%
		^{78}Se 23.52%
		^{80}Se 49.82%
		^{82}Se 9.19%

Table 2 Chemical forms of arsenic and selenium

Element and formal oxidation state	*Major chemical forms*
As(–III)	Arsine (H_3As)
As(−I)	Arsenopyrite (FeAsS), loellingite ($FeAs_2$)
As(0)	Elemental arsenic (As)
As(III)	Arsenite ($H_2AsO_3^-$, H_3AsO_3)
As(V)	Arsenate (AsO_4^{3-}, $HAsO_4^{2-}$, $H_2AsO_4^-$, H_3AsO_4)
Organic As (V and III)	Dimethylarsinate (DMA, $(CH_3)_2AsO(OH)$), monomethylarsonate (MMA(V), $CH_3AsO(OH)_2$ or MMA(III), $CH_3As(OH)_2$), arsenobetaine (AsB, $(CH_3)_3As^+{\cdot}CH_2COO^-$), arsenocholine (AsC, $(CH_3)_3As^+{\cdot}CH_2CH_2OH$)
Se(–II)	Selenide (Se^{2-}, HSe^-, H_2Se)
Se(0)	Elemental selenium (Se)
Se(IV)	Selenite (SeO_3^{2-}, $HSeO_3^-$, H_2SeO_3)
Se(VI)	Selenate (SeO_4^{2-}, $HSeO_4^-$, H_2SeO_4)
Organic Se	Dimethylselenide (DMSe, CH_3SeCH_3); dimethyldiselinide (DMDSe, $CH_3SeSeCH_3$), selenomethionine ($H_3N^+CHCOO^-{\cdot}CH_2CH_2SeMe$), selenocysteine ($H_2N^+CHCOO^-{\cdot}CHSeH$)

the characteristics of cancer stem cells (Xu et al., 2012). This finding may explain observations that arsenic often causes multiple tumors of many types to form on the skin or inside the body. Arsenic ranked first on each of the hazardous substances priority lists compiled for the Comprehensive Environmental Response, Compensation, and Liability Act (CERCLA) between 1997 and 2007 due to its frequency, toxicity, and potential for human exposure at National Priorities List sites (ATSDR, 2010).

The principal public health concern with arsenic is from the development of naturally high-arsenic groundwater resources (Smedley and Kinniburgh, 2002). Extensive arsenicosis from such sources has been reported from Argentina, Bangladesh, Chile, China, Mexico, India, Thailand, and Taiwan. 'Blackfoot disease,' a form of gangrene arising from excessive arsenic intake, was first described in Taiwan by Tseng et al. (1968).

In contrast to arsenic, trace concentrations of selenium are essential for human and animal health. Until the late 1980s, the only known metabolic role for selenium in mammals was as a component of the enzyme glutathione peroxidase (GSH-Px), a selenoenzyme that plays an important role in the immune system (Johnson et al., 2010; Rotruck et al., 1972). There is now growing evidence, however, that the selenoenzyme is involved in the synthesis of thyroid hormones (Arthur and Beckett, 1989; Combs and Combs, 1986). In the body, selenium is used as part of a group of molecules known as selenoproteins, which contain the amino acid selenocysteine. These selenoproteins have a variety of functions, including acting as components of glutathione peroxidase, selenoprotein SEPS1, selenoprotein P, and thioredoxin reductase, antioxidant defense, cell redox control, and selenium transport in the plasma; they are also anti-inflammatory (Papp et al., 2007). Selenium deficiency has been linked to cancer, Acquired Immune Deficiency Syndrome (AIDS), heart disease, muscular dystrophy, multiple sclerosis, osteoarthropathy, immune system and reproductive disorders in humans, and white muscle disease in animals (Clark et al., 1996; Johnson et al., 2010; Levander, 1986; Rayman, 2008; WHO, 1987, 1996, 2011). A review of selenium in the food chain (Rayman, 2008) and its role in human health and disease was carried out recently (Fairweather-Tait et al., 2011). Selenium deficiency in humans has been implicated in the incidence of a type of heart disease (Keshan disease (KD)) and an osteoarthropathic condition (Kashin–Beck disease (KBD)) over extensive regions of China. Domestic animals also suffer from 'white muscle disease' in these areas (Tan, 1989). In the 1970s and 1980s, the diet of people in the affected regions of China was supplemented with selenium, and sodium selenite was used to treat growing crops. This has resulted in a decline in the incidence of selenium deficiency disease (Liu et al., 2002). Selenium deficiency has been reported from New Zealand and Finland and falling concentrations of selenium in the diet are of increasing concern in many western countries (Oldfield, 1999). In Europe, this trend may have been exacerbated by the increasing use of native low-selenium grains rather than the imported selenium-rich grains of North America (Rayman, 2002). Selenium supplementation of livestock is common. On a global scale, overt selenium toxicity in human subjects is far less widespread than deficiency (Fordyce, 2005), with between 0.5 and 1 billion people estimated to have an insufficient intake of selenium (Combs, 2001).

Despite the essentiality of selenium, the range of intake between the quantities leading to selenium deficiency (<40 μg day^{-1}) and toxicity (selenosis) (>400 μg day^{-1}) is very narrow in humans (WHO, 1996, 2011). Investigations of the relationships between selenium in the environment and animal health were pioneered by Moxon (1938) in the western United States, where selenium accumulator plants are found and both selenium toxicity and deficiency are of concern. It has since been investigated extensively with regard to toxicity and deficiencies in humans and livestock (Environment Agency, 2009; Kabata-Pendias and Mukherjee, 2007). Long-term exposure to high levels of selenium (1270 μg, 10–20 times higher than normal exposure) can cause selenosis associated with numbness, paralysis, and occasional hemiplegia (ATSDR, 2003). Listlessness and lack of mental alertness were reported in a family who drank well water containing 9 mg l^{-1} selenium for about 3 months, but their symptoms disappeared when they ceased drinking well water (ATSDR, 2003). Human

selenosis at the population level is rare and is generally related to excesses from food rather than from drinking water. It has been reported from China and Venezuela, where selenium-rich food is grown and consumed locally (Tan, 1989; WHO, 1996, 2011). Cancers of the skin and pancreas have been attributed to high selenium intakes (Vinceti et al., 1998). Selenium sulfide is used in antidandruff shampoos and is potentially carcinogenic, but is not absorbed through the skin unless there are lesions (WHO, 1987). Selenium toxicity can lead to hair and nail loss and disruption of the nervous and digestive systems in humans and to 'alkali' disease in animals. Chronic selenosis in animals is not common, but has been reported from parts of Australia, China, Ireland, Israel, Russia, South Africa, the United States, and Venezuela (Oldfield, 1999). Liver damage is a feature of chronic selenosis in animals (WHO, 1987). Selenium was number 147 on the US 2007 CERCLA hazardous substances priority list (ATSDR, 2010).

It is now recognized that arsenic and selenium interact with each other in various metabolic functions and animal models indicate that each element can substitute for the other to some extent (Davis et al., 2000). This could partly explain the reported protective effect of selenium against some diseases, including some cancers (Shamberger and Frost, 1969). Arsenic was also shown long ago to protect against selenium poisoning in experimental studies with rats (Moxon, 1938). Following the relatively recent discovery of dissimilatory As(V) reduction and the various mechanisms that organisms have evolved to deal with the toxicity of As(V) and As(III), there has been a rapid increase in the understanding of the microbial chemistry of arsenic (see Frankenberger, 2002 and the individual chapters therein) and its consequences for the broader environment. Selenium chemistry is also closely linked to microbial processes but these are less well understood.

Contamination as a result of human activity is of increasing concern for both elements, but especially for arsenic. In the past, the problem was exacerbated by an absence of waste management strategies.

Arsenic concentrations in the natural environment have increased as a result of a number of activities, including mining and smelting, the combustion of arsenical coals, petroleum recovery (involving the release of production waters), refining, chemical production and use, the use of biocides including wood preservatives, the use of fertilizers, the manufacture and use of animal feed additives, and the development of high-arsenic groundwater for drinking water and irrigation. Such activities have progressively transferred arsenic from the geosphere into the surface environment and have distributed it through the biosphere, where it poses a potential risk to humans and the wider environment. Endemic arsenic poisoning is associated mostly with naturally high concentrations of arsenic in drinking water, although in China it is a result of burning coal rich in arsenic (Ng et al., 2003; Sun, 2004). In certain occupational settings, the principal pathway of arsenic to humans can be through inhalation. Arsenicosis caused by the indoor combustion of arsenic-rich coals has also been reported from Guizhou province, China (Aihua et al., 2000; Ding et al., 2000; Finkelman et al., 2003), where open coal burning stoves are used to dry chili peppers, increasing arsenic levels from 1 to 500 mg kg^{-1} (Kapaj et al., 2006; Zheng et al., 1996).

Human activities that have increased the concentrations of selenium in the environment include the mining and processing of base metal, gold, coal, and phosphate deposits, the use of rock phosphate as fertilizer, the manufacture of detergents and shampoos, and the application of sewage sludge to land. The increased use of selenium in the pharmaceutical, glazing, photocopying, ceramic, paint, and electronics industries may also be increasing the amount of selenium entering the environment.

In the following sections, the source and occurrence of arsenic in the environment are first reviewed and then its pathways are considered as a basis for an improved understanding of exposure and risk assessment. This should lead to better risk management. A similar format is followed for selenium. In discussing the two elements, and in line with the threats outlined earlier, the emphasis on arsenic is on the behavior of arsenic in water, whereas in the case of selenium it is on the soil–water–plant relationships.

11.2.2 Sampling

Selenium and arsenic have been measured in a wide range of environmental media. Here sampling procedures for rocks, soils, sediments, and natural waters are described.

11.2.2.1 Rocks, Soils, and Sediments

In the case of rocks, soils, and sediments, sufficient material representative of the medium to be analyzed should be collected. Soil and sediment samples should be dried at temperatures <35 °C to avoid volatilization losses of arsenic or selenium (Rowell, 1994) and ideally freeze-dried (BGS, 1978–2006). Sampling, analysis, and quality control should be carried out by recognized procedures wherever possible (Darnley, 1995; Salminen and Gregorauskiene, 2000).

11.2.2.2 Water

11.2.2.2.1 Techniques

As with other solutes, sampling natural waters for arsenic and selenium requires (1) the sample to represent the water body under investigation, and (2) that no artifacts are introduced during sampling or storage. Sampling methods vary according to whether 'dissolved,' 'particulate,' or 'total' concentrations are to be determined and whether speciation studies are to be undertaken. Water samples are most commonly analyzed for 'total' concentrations of arsenic and selenium. Speciation measurements require additional precautions to ensure preservation of the in situ species until separation or measurement.

As arsenic and selenium are normally present in natural waters at only trace concentrations (<10 μg l^{-1} and frequently much lower), considerable care is required to perform reliable trace analyses. Marine chemists were the first to undertake reliable low-level trace analyses of natural waters and develop 'clean/ultraclean' sampling procedures (Horowitz et al., 1996). Probably the most thorough accounts of sampling procedures for surface water and groundwaters are those given by the US Geological Survey (USGS) (Wilde and Radtke, 2008). Specific procedures for sampling rainwater, lake water, and seawater are also given. The precautions required in sampling for arsenic and selenium are the same as those for other trace elements

present in water at micrograms per liter concentrations. For example, there should be minimal contact between the sample and metallic substances. Sample bottles should be tested first by analyzing deionized water stored in them to ensure that they do not contaminate the sample. They should also be rinsed thoroughly with the sample water before collection.

Ideally, groundwater should be sampled from purpose-built water quality monitoring boreholes or piezometers. In practice, existing wells or boreholes are frequently used. As far as practically possible, it is important to purge the borehole by pumping at least three borehole volumes to remove standing water before sampling. Low-flow ($<4\ l\ min^{-1}$) pumping is preferred to minimize resuspension of colloidal material.

Several procedures have been devised to obtain water quality depth profiles in wells and aquifers. These include depth samplers, nested piezometers, strings of diffusion cells, multilevel samplers, and multiple packers. Each method has its advantages and disadvantages, with very different costs and sampling logistics. As yet, few methods have been devised for arsenic and selenium profiling specifically; probably the most detailed profiling has been carried out in ocean sediments (Sullivan and Aller, 1996). Pore water, including from the unsaturated zone, can be obtained using a high-pressure squeezer or high-speed centrifugation (Kinniburgh and Miles, 1983; Sullivan and Aller, 1996).

There are as yet no methods for the in situ determination or continuous monitoring of arsenic and selenium. However, the diffusive gradient thin-films (DGT) method is a novel sampling method that has been used mainly for cationic metals, but may be adaptable for measuring arsenic and selenium, as it has been for phosphorus (Zhang et al., 1998). In this case, the normal cation exchange resin is replaced by an iron oxide (ferrihydrite) gel. Solutes sorbed by the resin or gel are displaced and subsequently analyzed in the laboratory. In principle, the DGT approach is sensitive with detection limits of the order of nanograms per liter. The method also has the advantage that it can measure a wide range of solutes simultaneously with high spatial resolution (at the mm scale) and determine the average water quality over relatively long timescales (days or longer).

Most water samples do not require pretreatment for a total elemental analysis, but where organic arsenic or selenium compounds are suspected, pretreatment by digestion with a strong acid mixture, for example, a 3-min sulfuric acid–potassium persulfate digestion or a nitric acid digestion is necessary. Where preconcentration is required, cold-trapping of the hydrides or liquid–solid extraction has been used, but this is very labor intensive when performed off-line. Groundwater samples usually need no pretreatment.

11.2.2.2.2 Filtered or unfiltered samples

Studies of the behavior of arsenic and selenium usually require the proportions of their dissolved and particulate components to be identified as this affects their biological availability, toxicity, and transport. It also affects the interpretation of their mineral solubility, adsorption, and redox behavior. Specifications for compliance testing vary with regulatory authority; for example, the US Environmental Protection Agency (US EPA) specifies a 0.45-μm filter while most authorities in developing countries specify (or assume) that water samples are unfiltered. If the water is reducing, it should be filtered before any oxidation occurs. Geochemists typically filter water samples using membrane filters in the range 0.1–0.45 μm, but the effective size of the filter can change as it becomes clogged. There continues to be much discussion about the merits of various filtering strategies (Hinkle and Polette, 1999; Horowitz et al., 1996; Shiller and Taylor, 1996). Small iron-rich particles with adsorbed arsenic, selenium, and other trace elements can pass through traditional filters (Chen et al., 1994; Litaor and Keigley, 1991) and subsequently dissolve when the sample is acidified.

Colloids tend to be most abundant in reducing groundwaters and turbid surface waters. In clear groundwater samples that have usually been filtered naturally by movement through an aquifer, differences between concentrations in filtered and unfiltered aliquots are often relatively small. Filtered and unfiltered groundwater samples from high-arsenic areas in Bangladesh were found to have broadly similar arsenic concentrations (within ±10%) although larger differences were found occasionally (Smedley et al., 2001b). Similarly, 9 out of 10 groundwater samples from arsenic-affected wells in Oregon showed little difference (mostly <10%) between filtered and unfiltered samples (Hinkle and Polette, 1999).

Some studies have reported larger differences. A survey of 49 unfiltered groundwater sources in the United States found that particulate arsenic accounted for more than half of the total arsenic in 30% of the sources (Chen et al., 1999) although arsenic concentrations were all relatively small.

11.2.2.2.3 Sample preservation and redox stability

For analysis of total arsenic and selenium, samples are normally preserved by adding ultrapure acid (1 or 2 vol.%), with the choice of acid depending on the analytical procedures to be used. HCl is used before hydride generation-atomic absorption spectrometry (HG-AAS), hydride generation-atomic emission spectrometry (HG-AES), HG-AFS, and HNO_3 before ICP-MS, graphite furnace-atomic absorption spectrometry (GF-AAS), and anodic stripping voltammetry (ASV). Acidification also helps to stabilize the speciation (see later discussions) although Hall et al. (1999) recommended that nitric acid should not be used for acidifying samples collected for speciation. Organic arsenic species are relatively stable and inorganic As(III) species are the least stable (National Research Council, 1999). There are as yet no well-established methods for preserving water samples for arsenic or selenium speciation analysis, although methods are being investigated for arsenic (Kumar and Riyazuddin, 2010; National Research Council, 1999; Rasmussen and Andersen, 2002).

Laboratory observations indicate that the oxidation of As(III) and Se(IV) by air is slow and is often associated with microbial activity. $MnO_2(s)$, which can precipitate following atmospheric oxidation of manganese-rich water, is also known to be a very efficient catalyst for the chemical oxidation of As(III) (Daus et al., 2000; Driehaus et al., 1995; Oscarson et al., 1983). Iron oxides have also been implicated in increasing the abiotic rate of oxidation of As(III) although the evidence for this is somewhat equivocal and it probably does not occur in minutes or hours unless some H_2O_2 is present (Voegelin and Hug, 2003). Precipitation of manganese and iron oxides can be minimized by ensuring sufficient acidity (pH 2 or less) and/or adding a reducing/complexing agent such as ascorbic acid, Ethylenediaminetetraacetic acid (EDTA), or phosphate. Recent studies have demonstrated the efficacy of

EDTA (Bednar et al., 2002; Gallagher et al., 2001) and phosphate (Daus et al., 2002) for preserving arsenic speciation.

Arsenic speciation in urine is stable for at least 2 months without additives at 4 °C (National Research Council, 1999), though the stability of arsenic species has been found to be dependent on urine matrices (Feldmann et al., 1999). It is reasonable to conclude that natural water samples probably behave in a similar way. As(III) in samples of Ottawa river water survived oxidation for at least 3 days at ambient temperature and without preservatives (Hall et al., 1999). The lowest rates of oxidation occur under slightly acidic conditions (Driehaus and Jekel, 1992) and acidification to pH 3–5 has been found to help stabilize As(III), although it is not always successful (Cabon and Cabon, 2000). HCl normally prevents reduction of As(V) to As(III) and arsenic speciation has recently been shown to be preserved for many months, even in the presence of high Fe(II) concentrations, if water samples are filtered and acidified in the usual way (1 or 2% HCl) (McCleskey et al., 2004). Traces of chlorine in HCl can lead to some long-term oxidation of As(III). One of the critical factors enhancing the oxidation of As(III) is the presence of dissolved Fe(III). On the other hand, the presence of Fe^{2+} or SO_4^{2-}, two species often found in arsenic-rich acid mine drainage (AMD) waters, inhibits the oxidation (McCleskey et al., 2004).

Reduction of As(V) can occur in the presence of air if samples contain dissolved organic carbon (DOC), arsenate-reducing bacteria, and no preservatives (Bednar et al., 2002; Hall et al., 1999; Inskeep et al., 2002). Arsenic(V) can then be reduced rapidly, within a few days. Storage at 3–5 °C and in the dark helps to preserve the speciation (Hall et al., 1999; Lindemann et al., 2000). Ideally, speciation studies for either arsenic or selenium should involve the minimum of time between sampling and analysis.

An alternative approach to the determination of As(III)/As(V) speciation is to separate the As(V) species in the field, using an anion exchange column (Bednar et al., 2002; Vagliasindi and Benjamin, 2001; Wilkie and Hering, 1998; Yalcin and Le, 1998). At near-neutral to acidic pH, typical of most natural waters, uncharged As(III) is not retained by the resin and the retained As(V) can be eluted subsequently with high-purity acid. Providing that total arsenic is known, As(III) can be estimated by difference. Bednar et al. (2002) favored an acetate resin because of its high pH-buffering capacity. Such anion exchange methods do not work for selenium speciation as both the Se(IV) and Se(VI) species are negatively charged and retained by the column.

11.2.3 Analytical Methods

11.2.3.1 Arsenic

11.2.3.1.1 Total arsenic in aqueous samples

11.2.3.1.1.1 Laboratory methods

Methods for arsenic analysis in water, food, and biological samples have been reviewed in detail elsewhere (ATSDR, 2007; Irgolic, 1994; National Research Council, 1999; Rasmussen and Andersen, 2002) (**Table 3**).

Early colorimetric methods for arsenic analysis used the reaction of arsine gas with either mercuric bromide captured on filter paper to produce a yellow–brown stain (Gutzeit method) or with silver diethyldithiocarbamate (SDDC) to produce a red dye. The SDDC method is still widely used in developing countries. The molybdate blue spectrophotometric method that is widely used for phosphate determination can be used for As(V), but the correction for P interference is difficult. Methods based on atomic absorption spectrometry (AAS) linked to hydride generation (HG) or a graphite furnace (GF) have become widely used. Other sensitive and specific arsenic detectors (e.g., AFS, ICP-MS, and ICP-AES) are becoming increasingly available. The accuracy is much better using atomic absorption methods than ICP (Nathanail and Bardos, 2004). HG-AFS in particular is now widely used for routine arsenic determinations because of its sensitivity, reliability, and relatively low capital cost.

Table 3 Recognized methods of arsenic analysis

Technique	*LoD ($\mu g\ l^{-1}$)*	*Sample size (ml)*	*Equipment cost (US$)*	*Analytical throughput per day*	*Comments*	*Accredited procedure*
HG-AAS	0.05	50	20–100 000	30–60	Single element	ISO 11969 SM 3114
GF-AAS	1–5	1–2	40–100 000	50–100		ISO/CD 15586 SM 3113
ICP-AES	35–50	10–20	60–100 000	50–100	Multielement; requires Ar gas supply. Can reduce LoD with HG	ISO/CD 11885 SM 3120
ICP-MS	0.02–1	10–20	150–400 000	20–100	Multielement	SM 3125 US EPA 1638
HG-AFS	0.01	40–50	20–25 000	30–60	Single element but can be adapted for Se and Hg	
ASV	0.1	25–50	10–20 000	25–50	Only free dissolved As	US EPA 7063
SDDC	1–10	100	2–10 000	20–30	Simple instrumentation	SM 3500 ISO 6595

HG, hydride generation; AAS, atomic absorption spectrometry; GF, graphite furnace; AES, atomic emission spectrometry; MS, mass spectrometry; AFS, atomic fluorescence spectrometry; ASV, anodic stripping voltammetry; SDDC, silver diethyldithiocarbamate. ISO, International Standards Organization; ISO/CD, ISO Committee Draft; SM, 'Standard Methods'; US EPA, US Environmental Protection Agency; LoD, limit of detection.

Source: Rasmussen L and Andersen K (2002) Environmental health and human exposure assessment (draft). *United Nations Synthesis Report on Arsenic in Drinking Water*, ch. 2. Geneva: World Health Organization.

Conventional ICP-MS has great sensitivity but suffers from serious interferences. Cl interference leads to the formation of $^{40}Ar^{35}Cl^{+}$ which has the same mass/charge ratio as the monoisotopic ^{75}As ($m/z = 75$). Hence, HCl and $HClO_4$ should not be used for preservation or dissolution if ICP-MS is to be used. There may also be significant interference in samples with naturally high Cl/As ratios. A Cl concentration of 1000 mg l^{-1} gives an arsenic signal equivalent to about 3–10 μg l^{-1}. The use of a high-resolution magnetic sector mass spectrometer, which can resolve the small difference in m/z for $^{75}As^{+}$ at 74.922 from that of $^{40}Ar^{35}Cl^{+}$ at 74.931, eliminates the Cl interference. New collision-cell techniques, in which the atomized samples are mixed with a second gas (usually H_2) in a reaction cell, also minimize this interference. Arsenic detection limits of a few nanograms per liter have been reported in matrices containing 1000 mg l^{-1} NaCl. The Cl interference can also be avoided by preseparation using HG, GF, or chromatography.

The American Society for Testing and Materials (ASTM) D 2972-08 standard test methods for arsenic in water cover the photometric and atomic absorption determination of arsenic in most waters and wastewaters. Three test methods are detailed in the standard; that is, silver diethyldithiocarbamate colorimetric; atomic absorption hydride generation; and atomic absorption, graphite furnace (American Society for Testing and Materials, 2010).

Recently, the use of carbon nanotubes has been proposed in several analytical methods, including use as solid-phase extraction adsorbents for arsenic pretreatment and enrichment from water samples (Li et al., 2009a), and in ASV (Xiao et al., 2008).

11.2.3.1.1.2 Field-test kits

A detailed study of field measurement and sensors for arsenic has been carried out by Melamed (2004). A large number of wells need to be tested (and retested) for arsenic worldwide. Hence, there is a need for reliable field-test kits that can measure arsenic concentrations down to 10 μg l^{-1}, the World Health Organization (WHO) guideline value for arsenic in drinking water. Test kits offer the advantage of being relatively inexpensive, portable, and effective for indicating the presence of arsenic. Some of the more recently developed kits based on the Gutzeit method are semiquantitative (Kinniburgh and Kosmus, 2002). Several field-test kits based on this method are available commercially, but their performance is variable (Spear, 2006).

The main limitations of test kits for arsenic in water are that other chemical reactions may interfere; the sensitivity and accuracy of the kits fluctuate depending on the model used and there are differences between field workers, especially as many kits rely on comparison of a test strip to a color chart (Petrusevski et al., 2007).

11.2.3.1.2 Total arsenic in solid samples

X-ray fluorescence spectrometry (XRF) and instrumental neutron activation analysis (INAA) are commonly used for multielement analysis of rock, soil, and sediment samples as they do not require chemical dissolution. However, the detection limit for arsenic using XRF, for example, is of the order of 5 mg kg^{-1} and is too high for many environmental purposes. Once dissolved, arsenic can be determined using many of the methods described earlier for aqueous samples, although the method of digestion must be capable of destroying all solids containing arsenic.

11.2.3.1.3 Arsenic speciation

11.2.3.1.3.1 Aqueous speciation

At its simplest, speciation of arsenic consists of separating it into its two major oxidation states, As(III) and As(V). This can be achieved on unacidified samples by ion chromatography. More detailed speciation involves determining organic species and less common inorganic species such as sulfide (thio), carbonate, and cyanide complexes, as well as less common oxidation states such as As(III) and As(0). There is increasing interest in the bioavailability of arsenic. Organic speciation usually involves quantifying the two or three major (mainly the methylated) species present. The oxidation state of arsenic in these organic species can be either As(III) or As(V). Generally, such studies are carried out in research rather than water-testing laboratories.

A two-stage approach to speciation is often used: this involves preseparation by high-performance liquid chromatography (HPLC) or ion chromatography followed by arsenic detection. The detection methods must be highly sensitive and capable of quantifying inorganic and organic species at the nanograms per liter to micrograms per liter level (Yalcin and Le, 1998). Many combinations of separation and detection methods have been used (Bohari et al., 2001; Ipolyi and Fodor, 2000; Lindemann et al., 2000; Martinez-Bravo et al., 2001; National Research Council, 1999; Taniguchi et al., 1999). All of them require expensive instrumentation and highly skilled operators and none has acquired 'routine' or accredited status.

A widely used but indirect method of As(III)/As(V) speciation involves no preseparation but involves two separate determinations, with and without prereduction. The rate of AsH_3 production by sodium borohydride ($NaBH_4$) reduction depends primarily on the initial oxidation state of the arsenic in solution and the solution pH. Under typical operating conditions of about pH 6 where the neutral As(III) species, H_3AsO_3, predominates, only As(III) is converted to the hydride (Anderson et al., 1986; Driehaus and Jekel, 1992). For the most part, the negatively charged As(V) species are not converted. For the determination of total arsenic, As(V) to As(III) prereduction can be achieved by adding a mixture of HCl, KI, and ascorbic acid ideally at pH < 1 to ensure full protonation and efficient hydride generation. High concentrations of HCl are particularly effective at this. As(V) can then be estimated by difference. AFS or AAS provide sensitive and fairly robust detectors for the arsine gas produced. High concentrations of some metal ions, particularly Fe^{3+} and Cu^{2+}, can interfere with the hydride generation, but this can be overcome by adding masking agents such as thiourea (Anderson et al., 1986) or by their prior removal with a cation-exchange resin.

11.2.3.1.3.2 Solid-phase speciation

While most speciation studies have been concerned with redox speciation in solution, speciation in the solid phase is also of interest. Both reduced and oxidized arsenic and selenium species can be adsorbed on minerals, soils, and sediments, albeit with differing affinities (see **Sections 11.2.5.3** and **11.2.7.2**). Such adsorption has been demonstrated on metal oxides and clays and also probably takes place to some extent on

carbonates, phosphates, sulfides, and perhaps organic matter. Structural arsenic and selenium may also be characterized.

Solid-phase speciation has been measured both by wet chemical extraction and, for arsenic, by instrumental methods, principally X-ray absorption near edge structure spectroscopy (XANES) (Brown et al., 1999). La Force et al. (2000) used XANES and selective extractions to determine the likely speciation of arsenic in a wetland affected by mine wastes: they identified seasonal effects with As(III) and As(V) thought to be associated with carbonates in the summer, with iron oxides in the autumn and winter, and with silicates in the spring. Extended X-ray absorption fine structure spectroscopy (EXAFS) has been used to determine the oxidation state of arsenic in arsenic-rich Californian mine wastes (Foster et al., 1998b). Typical concentrations of arsenic in soils and sediments (As $<20\ mg\ kg^{-1}$) are often too low for EXAFS measurements, but as more powerful photon beams become available, the use of such techniques should increase. A method for on-site separation and preservation of arsenic species from water using solid-phase extraction cartridges in series, followed by elution and measurement of eluted fractions by ICP-MS for 'total' arsenic, has recently been presented (Watts et al., 2010). Classical wet chemical extraction procedures have also been used to assess the solid-phase speciation of arsenic, but care must be taken not to oxidize As(III) during extraction (Demesmay and Olle, 1997). Extractions should be carried out in the dark to minimize photochemical oxidation.

11.2.3.1.3.3 EPA TCLP test

The US EPA's 'toxicity characteristics leaching procedure' (TCLP) is the most commonly used test for determining the long-term stability of arsenic precipitates. The procedure involves first reacting the solid with a pH-buffered acetate solution (pH 4.93) at a solid-to-liquid ratio of 2:1 to determine solubility. The slurry is agitated for 20 h, and if the concentration of certain toxic elements is found to be above specified thresholds, the material is classified as toxic. The current limit for arsenic is $5\ mg\ l^{-1}$ (Monhemius and Swash, 1999).

Most researchers in the field agree that this test gives only a poor indication of the long-term storage problems that may arise in the case of arsenic (Ghosh et al., 2004, 2006, US EPA, 1999). Moreover, the $5\ mg\ l^{-1}$ limit for arsenic is too high for current and likely future legislation. Arsenic compounds such as scorodite, which are used to immobilize arsenic, often pass the US EPA's TCLP test limit of $5\ mg\ l^{-1}$ arsenic because the lowest solubility for both scorodite and arsenical ferrihydrite is in the weakly acid pH range of 3–4.

11.2.3.2 Selenium

11.2.3.2.1 Total selenium in aqueous samples

Historically, analysis of selenium has been difficult, partly because environmental concentrations are naturally low. Indeed, selenium analysis still remains problematic for many laboratories at concentrations below $0.01\ mg\ l^{-1}$, a relatively high concentration in many environments (Steinhoff et al., 1999). Hence, selenium has often been omitted from multielement geochemical surveys, despite its importance (Darnley, 1995). Recent improvements in analytical methods, however, mean that even low levels of selenium can be determined routinely in geological and environmental samples (Johnson et al., 2010). Analytical methods with limits of detection of $<0.01\ mg\ l^{-1}$ include colorimetry, total reflectance-XRF, HG-AFS, gas chromatography (GC) of organic species, ICP-MS, and HG-ICP-AES. Of these, HG-AFS and ICP-MS are probably now the most widely used methods. Like arsenic, there are no generally accepted ways of preserving selenium speciation in water samples, and even fewer studies of the factors controlling the stability of the various species. Many of the precautions for arsenic-preserved species (**Section 11.2.2.2.3**) are also likely to apply to selenium species preservation.

The ASTM D 3859-08 standard test methods for selenium in water include the determination of dissolved and total recoverable selenium in waters and wastewaters. Two of the test methods are atomic absorption procedures, namely gaseous hydride AAS and GF-AAS (American Society for Testing and Materials, 2010).

11.2.3.2.1.1 Pretreatment to destroy organic matter

Organic selenium species are more widespread in the environment than comparable arsenic species. The determination of total selenium by most analytical methods requires samples to be pretreated to remove organic matter, release selenium, and change its oxidation state.

Wet digestion using mixtures of nitric, sulfuric, phosphoric, and perchloric acids, with or without the addition of hydrogen peroxide, has been used for organic samples and natural waters. Nitric acid reduces foaming and/or charring. The trimethylselenonium ion is resistant to decomposition by wet digestion, so a long period of digestion is required for urine and plant materials that may contain the ion.

11.2.3.2.1.2 Laboratory methods

Fluorimetry has been used widely for selenium analysis in environmental samples, but is being superseded by more sensitive instrumental methods. Some of the instrumental methods used for arsenic speciation and analysis can also be used for selenium. In particular, HPLC and HG can separate selenium into forms suitable for detection by AAS, AFS (Ipolyi and Fodor, 2000), or ICP-AES (Adkins et al., 1995). Only Se(IV) forms the hydride and so Se(VI) must be prereduced to Se(IV) if total selenium is to be determined. This is normally achieved using warm HCl/KBr followed by coprecipitation with $La(OH)_3$ if necessary (Adkins et al., 1995). KI is not used as it tends to produce some Se(0) which is not reduced by HG. $La(OH)_3$ collects only Se(IV) so the prereduction step to include the contribution from Se(VI) is required before coprecipitation. Other methods of preconcentration include coprecipitation of Se(IV) with hydrous iron oxide or adsorption onto Amberlite IRA-743 resin (Bueno and Potin-Gautier, 2002).

ICP-MS detection of selenium is now favored because of its sensitivity even without HG or other forms of preconcentration. However, selenium can be seriously affected by matrix interferences when using ICP-MS. The polyatomic Ar^{2+}, with a mass of 80, overlaps with the most abundant isotope of selenium (^{80}Se). Even using hydrogen as a collision gas results in the formation of 2–5% of selenium hydride for which a correction must be applied. For routine analysis of selenium, the hydride-free but less abundant isotopes, ^{76}Se and ^{82}Se, are usually determined; however, this results in lower sensitivities and higher detection limits. Detection limits for ICP-MS are around $2–20\ \mu g\ l^{-1}$ because of the argon plasma background and interferences. The use

of reaction or collision cells or dynamic collision cells can reduce detection limits greatly (Nelms, 2005).

11.2.3.2.2 Selenium in solid samples

Direct analysis of solids for selenium by XRF has a detection limit of about 0.5 mg kg^{-1} and so is often insufficiently sensitive. Rock, sediment, and soil samples can be dissolved using wet chemical methods (HF, HCl, etc.) followed by $La(OH)_3$ coprecipitation to separate hydride-forming elements including selenium. This is present as Se(IV), following acid dissolution (Hall and Pelchat, 1997). The methods described earlier for aqueous samples can then be used.

Modern thermal ionization mass spectrometry (TIMS) is now sensitive and precise enough to measure individual selenium isotope abundances (e.g., $^{80}Se/^{76}Se$) in solid samples or residues so that it can be used to study environmental cycling/distributions (Johnson et al., 1999). Microbial reduction leads to isotopically lighter products, that is, selenate to selenite reduction has a $^{80/76}Se$ fractionation factor, ε, of about −5.5‰ (Johnson et al., 1999). INAA has been used to determine different selenium isotopes, especially ^{75}Se in plant tracer studies, and foodstuffs (Combs, 2001; Diaz-Alarcon et al., 1996; Noda et al., 1983; Ventura et al., 2007).

11.2.3.2.3 Selenium speciation

Selenium speciation in waters is poorly understood, although in principle it can be determined using HG with and without a prereduction step (see **Section 11.2.3.2.1**). Ion-exchange chromatography is used extensively to determine selenium species in plant extracts, and gas chromatography can measure volatile selenium compounds. Recent developments in anion exchange HPLC and MS techniques (ICP-dynamic reaction cell-MS, TIMS, and multiple collector-MS) mean that it is now possible to determine selenium isotope abundances and concentrations in selenamino acids including selenocysteine and selenomethionine (Gomez-Ariza et al., 2000; Sloth and Larsen, 2000; Wang et al., 2007). Electrochemical methods such as cathodic stripping voltammetry (CSV) are highly sensitive and in principle can be used for speciation because only Se(IV) species are electroactive (Lange and van den Berg, 2000). Due to the important role that selenium plays in human nutrition, there is increasing interest in measuring the 'bioavailable' amounts, especially in foodstuffs, using various bioassays (Casgrain et al., 2010; Fairweather-Tait et al., 2010).

11.2.3.3 Quality Control and Standard Reference Materials

Although analysts usually determine the precision of their analyses using replicate determinations, the analysis of arsenic and selenium can be affected seriously by contamination and matrix interferences during sampling and analysis. These can be difficult to identify and are best found by sample randomization and the collection of duplicate samples as part of an objective, independent quality-control system (Plant et al., 1975).

The measurement of standard reference materials (SRMs) provides the best method of ensuring that an analytical procedure is producing accurate results in realistic matrices. Many SRMs are now available (Govindaraju, 1994; Rasmussen and Andersen, 2002) but the most widely used are those supplied by the National Institute of Standards and Technology (NIST). Arsenic and selenium concentrations have been certified in a range of natural waters, sediments, and soils (Tables 4 and 5). The certified standards from the National Research Council of Canada (NRC) also include river waters with much lower arsenic concentrations than the NIST standards (~0.2–1 μg l^{-1}). Certified standards for As(III)/As(V) and Se(IV)/Se(VI) speciation are available commercially (e.g., SPEX Certiprep® speciation standards).

The Canadian Certified Reference Materials Project (CCRMP) also provides reference materials for lake sediments, stream sediments, and soils (tills) for arsenic, but not for selenium. However, the Institute for Reference Materials and Measurements (IRMM), Geel, Belgium, provides reference materials for estuarine sediments, lake sediments, and channel sediments for arsenic and selenium.

Table 4 Standard reference materials for natural waters from various suppliers

SRM	*Supplier*	*Medium*	*Arsenic (μg l^{-1})*	*Selenium (μg l^{-1})*
TMRAIN-04	NWRI	Rainwater	1.14	0.83
SLRS-5	NRC	River water	0.413[a]	–
CASS-5	NRC	Seawater	1.24	
NASS-6	NRC	Seawater	1.43	
SLEW-3	NRC	Estuarine water	1.36	
SRM 1640a	NIST	Natural water	8.075	20.13
SRM 1643e	NIST	Fresh water	60.45	11.9
BCR-609	IRMM	Groundwater	1.20[a]	–
BCR-610	IRMM	Groundwater	10.8[a]	
CRM 403	IRMM	Seawater	9.9[a]	–
CASS-4	NRC	Seawater	1.1	–

NWRI, National Water Research Institute, Environment Canada; NIST, National Institute of Standards and Technology, Gaithersburg, MD, USA; IRMM, Institute for Reference Materials and Measurements; NRC, National Research Council of Canada.
[a]Expressed in μg kg^{-1}.

Table 5 Standard reference materials for soils, sediments, and sludges from the National Institute of Standards and Technology (NIST)

SRM	*Medium*	*As (mg kg^{-1})*	*Se (mg kg^{-1})*
1646a	Estuarine sediment	6.23	0.193
1648a	Urban particulate matter	115.5	28.4
1944	New York/New Jersey waterway sediment	18.9	1.4
2586	Trace elements in soil (contains lead from paint)	8.7	0.6
2587	Trace elements in soil (contains lead from paint)	13.7	
2702	Inorganics in marine sediment	45.3	4.95
2703	Sediment for solid sampling (small sample) analytical techniques	45.5	4.9
2709a	San Joaquin soil	10.5	1.5
2710a	Montana I soil	0.15%	1
2711a	Montana II soil	107	2
2780	Hard Rock mine waste	48.8	5
2781	Domestic sludge	7.82	16
2782	Industrial sludge	166	0.44
8704	Buffalo River sediment	17	

Concentrations are in mass fractions (mg kg^{-1}) unless noted as %

The Geological Survey of Japan (GSJ) provides a wide range of rock SRMs along with 'recommended' arsenic and selenium concentrations. The USGS issues 17 SRMs for which it provides 'recommended' and 'information' (when less than three independent methods have been used) concentrations. Nine of these include data for arsenic and two for both arsenic and selenium (the SGR-1 shale and CLB-1 coal samples). Hall and Pelchat (1997) have analyzed 55 geological SRMs for As, Bi, Sb, Se, and Te, including SRMs from the USGS, Institute of Geophysical and Geochemical Exploration (IGGE; China), GSJ, CCRMP, and NRC programs. Methods have been developed recently for the determination of selenium in geological materials at nanograms per gram and lower levels (Forrest et al., 2009).

11.2.4 Abundance and Forms of Arsenic in the Natural Environment

11.2.4.1 Abundance in Rocks, Soils, and Sediments

The average crustal abundance of arsenic is 1.5 mg kg^{-1} and it is strongly chalocophile. Approximately 60% of natural arsenic minerals are arsenates, 20% sulfides and sulfosalts, and the remaining 20% are arsenides, arsenites, oxides, alloys, and polymorphs of elemental arsenic. Arsenic concentrations of more than 100 000 mg kg^{-1} have been reported in sulfide minerals and up to 76 000 mg kg^{-1} in iron oxides (Smedley and Kinniburgh, 2002). However, concentrations are typically much lower. Arsenic is incorporated into primary rock-forming minerals only to a limited extent, for example, by the substitution of As^{3+} for Fe^{3+} or Al^{3+}. Therefore arsenic concentrations in silicate minerals are typically of the order of 1 mg kg^{-1} or less (Smedley and Kinniburgh, 2002). Consequently, many igneous and metamorphic rocks have average arsenic concentrations of 1–10 mg kg^{-1}. Similar concentrations are found in carbonate minerals and rocks.

Arsenic concentrations in sedimentary rocks can be more variable. The highest arsenic concentrations (20–200 mg kg^{-1}) are typically found in organic-rich and sulfide-rich shales, sedimentary ironstones, phosphatic rocks, and some coals (Smedley and Kinniburgh, 2002).

Although arsenic concentrations in coals can range up to 35 000 mg kg^{-1} in some parts of China, concentrations in the range <1–17 mg kg^{-1} are more typical (Gluskoter et al., 1977; Palmer and Klizas, 1997; Sun, 2004). Evidence for arsenic enrichment in peat is equivocal. Shotyk (1996) found a maximum of 9 mg kg^{-1} arsenic in two 5000–10 000-year-old Swiss peat profiles and in the profile with the lower ash content, the arsenic content was 1 mg kg^{-1} or lower.

In sedimentary rocks, arsenic is concentrated in clays and other fine-grained sediments, especially those rich in sulfide minerals, organic matter, secondary iron oxides, and phosphates. The average concentration of arsenic in shale is an order of magnitude greater than in sandstones, limestones, and carbonate rocks. Arsenic is strongly sorbed by oxides of iron, aluminum, and manganese as well as some clays, leading to its enrichment in ferromanganese nodules and manganiferous deposits.

Alluvial sands, glacial till, and lake sediments typically contain <1–15 mg kg^{-1} arsenic although higher concentrations are found occasionally (Farmer and Lovell, 1986). Based on a survey of 747 flood-plain sediment samples and 852 stream sediment samples over Europe, median arsenic concentrations of 6.00 and 6.00 mg kg^{-1}, respectively, were reported (FOREGS, 2005). Sediments from Qinghai Lake on the Tibetan Plateau have been shown to have arsenic enrichment factors of up to 2× pre-1900 levels; this has been suggested to reflect the burning of arsenical coal for industrial development in western China (Wang et al., 2010).

Stream sediments from England and Wales had a median arsenic concentration of 10 mg kg^{-1} (Webb, 1978). A more detailed survey of stream sediments in Wales gave a median concentration of 14 mg kg^{-1} (BGS, 1978–2006). Black et al. (2004) state that one grain of arsenopyrite ~200 μm across in a 5-g stream sediment sample is equivalent to approximately 1 mg kg^{-1} arsenic in the sample. The median arsenic concentration in stream sediments from 20 study areas across the United States collected as part of the National Water-Quality Assessment (NAWQA) program was 6.3 mg kg^{-1} (Rice, 1999).

The arsenic concentration in soils shows a similar range to that found in sediments, except where they are contaminated by industrial or agricultural activity. Organic-rich soils tend to have higher concentrations of arsenic due to the presence of sulfide minerals; for example, peaty and boggy soils have an average concentration of 13 mg kg^{-1} (Dissanayake and Chandrajith, 2009; Smedley and Kinniburgh, 2002). A survey of 2600 soils from the Welsh borders had a median arsenic concentration of 11 mg kg^{-1} (BGS, 1978–2006). A survey of the concentrations of arsenic in rural soils, thought to reflect 'background' conditions in the United Kingdom, reported a range of 0.50–143 mg kg^{-1} (Ross et al., 2007). A survey of soil profiles covering 26 countries in Europe gave a median arsenic concentration of 7.03 mg kg^{-1} in topsoils (840 samples) and 6.02 mg kg^{-1} in subsoils (783 samples) (FOREGS, 2005). Concentrations of 1000 mg kg^{-1} or more have been found at contaminated sites close to smelters or industrial sites (Lumsdon et al., 2001). Arsenic and its compounds are used as pesticides, especially herbicides and insecticides, and high arsenic levels in soils over the cotton-growing areas of the United States reflect the past use of such pesticides (US EPA, 2006; see **Chapter 11.15**). Comparison of soil samples taken following the 2005 flooding of New Orleans with archived soil samples collected in 1998–1999 suggests that the flooding resulted in the deposition of arsenic-contaminated sediments (Rotkin-Ellman et al., 2010).

11.2.4.2 National and International Standards for Drinking Water

National standards for maximum concentrations of arsenic in drinking water have been declining over the last few decades as the toxicity of arsenic has become apparent. The 1903 report of the Royal Commission on Arsenic Poisoning in the United Kingdom set a standard of 150 μg l^{-1}. In 1942, the US Public Health Service set a drinking-water standard of 50 μg l^{-1} for interstate water carriers and this was adopted nationally by the US EPA in 1975.

The WHO guideline value for arsenic in drinking water was reduced from 50 μg l^{-1} to a provisional value of 10 μg l^{-1} in 1993, based on a 6×10^4 excess skin cancer risk, 60 times higher than the factor normally used to protect human health (Kapaj et al., 2006). In most western countries, the limit for arsenic in

Table 6 Concentration ranges of arsenic in various water bodies

Water body and location	*Arsenic concentration: average or range ($\mu g\ l^{-1}$)*
Rainwater	
Maritime	0.02
Terrestrial (western USA)	0.013–0.032
Coastal (Mid-Atlantic, USA)	0.1 (<0.005–1.1)
Snow (Arizona)	0.14 (0.02–0.42)
Terrestrial rain	0.46
Seattle rain, impacted by copper smelter	16
River water	
Various	0.83 (0.13–2.1)
Norway	0.25 (<0.02–1.1)
Southeast USA	0.15–0.45
USA	2.1
Dordogne, France	0.7
Po River, Italy	1.3
Polluted European rivers	4.5–45
River Danube, Bavaria	3 (1–8)
Schelde catchment, Belgium	0.75–3.8 (up to 30)
High-As groundwater influenced	
Northern Chile	400–450
Northern Chile	190–21 800
Córdoba, Argentina	7–114
Geothermally influenced	
Sierra Nevada, USA	0.20–264
Waikato, New Zealand	44 (19–67): 32 (28–36)
Madison and Missouri Rivers, USA	10–370
Mining influenced	
Ron Phibun, Thailand	218 (4.8–583)
Ashanti, Ghana	284 (<2–7900)
British Columbia, Canada	17.5 (<0.2–556)
Lake water	
British Columbia	0.28 (<0.2–0.42)
Ontario	0.7
France	0.73–9.2 (high Fe)
Japan	0.38–1.9
Sweden	0.06–1.2
Geothermally influenced	
Western USA	0.38–1000
Mining influenced	
Northwest Territories, Canada	270 (64–530)
Ontario, Canada	35–100
Estuarine water	
Oslofjord, Norway	0.7–2.0
Saanich Inlet, British Columbia	1.2–2.5
Rhône Estuary, France	2.2 (1.1–3.8)
Krka Estuary, Croatia	0.13–1.8
Mining and industry influenced	
Loire Estuary, France	up to 16
Tamar Estuary, UK	2.7–8.8
Schelde Estuary, Belgium	1.8–4.9
Seawater	
Deep Pacific and Atlantic	1.0–1.8
Coastal Malaysia	1.0 (0.7–1.8)
Coastal Spain	1.5 (0.5–3.7)
Coastal Australia	1.3 (1.1–1.6)
Groundwater	
Various USA aquifers	<1–2600
Various UK aquifers	<0.5–57
Bengal Basin, West Bengal, Bangladesh	<0.5–3200
Chaco-Pampean Plain, Argentina	<1–5300
Lagunera, northern Mexico	8–620
Inner Mongolia, China	<1–2400
Taiwan	<10 to 1820
Great Hungarian Plain, Hungary, Romania	<2–176
Red River Delta, Vietnam	1–3050
Mining-contaminated groundwaters	50–10 000
Geothermal water	<10–50 000
Mineralized area, Bavaria, Germany	<10–150
Herbicide-contaminated groundwater, Texas	408 000
Mine drainage	
Various, USA	<1–850 000
Ural Mountains	400 000
Sediment pore water	
Baseline, Swedish estuary	1.3–166
Baseline, clays, Saskatchewan, Canada	3.2–99
Baseline, Amazon shelf sediments	up to 300
Mining-contam'd, British Columbia	50–360
Tailings impoundment, Ontario, Canada	300–100 000

Modified from a compilation by Smedley and Kinniburgh (2002).

drinking water is now also 10 $\mu g\ l^{-1}$ (Yamamura, 2003). This includes the European Union (EU) and the United States. The standard in Switzerland remains at 50 $\mu g\ l^{-1}$. While the US EPA maximum contaminant level (MCL) is now 10 $\mu g\ l^{-1}$, they have also set an MCL goal of zero for arsenic in drinking water, reflecting the risk to human health.

11.2.4.3 Abundance and Distribution in Natural Waters

Concentrations of arsenic in natural waters vary by more than four orders of magnitude and depend on the source of the arsenic and the local geochemical conditions (Smedley and Kinniburgh, 2002). The greatest range and highest concentrations of arsenic are found in groundwaters, soil solutions, and sediment pore waters because of the presence of favorable conditions for arsenic release and accumulation. Arsenic is mobilized at pH values normally found in groundwaters (pH 6.5–8.5) and under both oxidizing and reducing conditions (Dissanayake and Chandrajith, 2009). Because the range in concentrations of arsenic in water is large, 'typical' values are difficult to derive. Concentrations can also vary significantly with time. Oil spills and leakages increase concentrations of arsenic in both fresh and marine water. Moreover, oil prevents underlying sediments from adsorbing the arsenic, which would remove it from the water column (Wainipee et al., 2010).

11.2.4.3.1 Atmospheric precipitation

Arsenic enters the atmosphere as a result of wind erosion, volcanic emissions, low-temperature volatilization from soils, marine aerosols, and pollution. It is returned to the Earth's surface by wet and dry deposition. The most important pollutant inputs are from smelter operations and fossil-fuel combustion. Concentrations of arsenic in rainfall and snow in rural areas are typically <0.03 $\mu g\ l^{-1}$ (**Table 6**), although they are

generally higher in areas affected by smelters, coal burning, and volcanic emissions. Andreae (1980) found arsenic concentrations of about 0.5 $\mu g\,l^{-1}$ in rainfall from areas affected by smelting and coal burning. Higher concentrations (average 16 $\mu g\,l^{-1}$) have been reported in rainfall 35 km downwind of a copper smelter in Seattle, USA (Crecelius, 1975). Values for Arizona snowpacks (Barbaris and Betterton, 1996) are also slightly above baseline concentrations, probably because of inputs from smelters, power plants, and soil dust. A study of sediments in Canada found that profiles of arsenic reflected its deposition as a result of past coal combustion and historical measurements of arsenic in dry and wet atmospheric deposition in rural areas of North America (Couture et al., 2008). In most industrialized countries, sources of airborne arsenic are limited as a result of air pollution-control measures. Unless significantly contaminated, atmospheric precipitation contributes little arsenic to surface waters.

11.2.4.3.2 River water

Concentrations of arsenic in river waters are also low (typically in the range 0.1–2.0 $\mu g\,l^{-1}$; **Table 6**; see **Chapter 7.7**). They vary according to bedrock lithology, river flow, the composition of the surface recharge, and the contribution from baseflow. The lowest concentrations have been found in rivers draining arsenic-poor bedrocks. Seyler and Martin (1991) reported average concentrations as low as 0.13 $\mu g\,l^{-1}$ in rivers flowing over karstic limestone in the Krka region of Yugoslavia. Lenvik et al. (1978) also reported average concentrations of about 0.25 $\mu g\,l^{-1}$ arsenic in rivers draining basement rocks in Norway.

Relatively high concentrations of naturally occurring arsenic in rivers can occur as a result of geothermal activity or the influx of high-arsenic groundwaters. Arsenic concentrations of 10–70 $\mu g\,l^{-1}$ have been reported in river waters from geothermal areas, including the western United States and New Zealand (McLaren and Kim, 1995; Nimick et al., 1998; Robinson et al., 1995). Higher concentrations, up to 370 $\mu g\,l^{-1}$, from the Yellowstone geothermal system have been reported in the Madison River in Wyoming and Montana as a result of geothermal influence. Wilkie and Hering (1998) also found concentrations in the range of 85–153 $\mu g\,l^{-1}$ in Hot Creek, a tributary of the Owens River, California. Values higher than 27 $\mu g\,l^{-1}$ are reported over the volcanic area of Naples, Italy (FOREGS, 2005). Some river waters affected by geothermal activity show distinct seasonal variations in arsenic concentration. Concentrations in the Madison River are highest during low-flow conditions, reflecting the increased proportion of geothermal water (Nimick et al., 1998). In the Waikato river system of New Zealand, arsenic maxima occur in the summer months, reflecting temperature-controlled microbial reduction of As(V) to the more mobile As(III) species (McLaren and Kim, 1995).

Increased arsenic concentrations are also found in some river waters dominated by baseflow in arid areas. Such waters often have a high pH and alkalinity. For example, surface waters from the Loa River Basin of northern Chile (Atacama desert) contain naturally occurring arsenic in the range 190–21 800 $\mu g\,l^{-1}$ (Cáceres et al., 1992). The high arsenic concentrations correlate with high salinity. While geothermal inputs of arsenic are likely to be important, evaporative concentration of the baseflow-dominated river water is also likely to concentrate arsenic in the prevailing arid conditions. Increased arsenic concentrations (up to 114 $\mu g\,l^{-1}$) have also been reported in alkaline river waters from central Argentina where regional groundwater arsenic concentrations are high (Lerda and Prosperi, 1996).

Although bedrock influences river water arsenic concentrations, rivers with typical pH and alkalinity values (~pH 5–7, $HCO_3 < 100\ mg\,l^{-1}$) generally contain lower concentrations of arsenic, even where groundwater concentrations are high, because of oxidation and adsorption of arsenic onto particulate matter in the stream bed and dilution by surface runoff. Arsenic concentrations in the range of 0.5–2.7 $\mu g\,l^{-1}$ have been reported for seven river water samples from Bangladesh, with one sample containing 29 $\mu g\,l^{-1}$ (BGS and DPHE, 2001).

High arsenic concentrations in river waters can also reflect pollution from industrial or sewage effluents. Andreae and Andreae (1989) reported arsenic concentrations up to 30 $\mu g\,l^{-1}$ in water from the River Zenne, Belgium, which is affected by urban and industrial waste, particularly sewage. The background arsenic concentration was in the range 0.75–3.8 $\mu g\,l^{-1}$. Durum et al. (1971) found that 79% of surface waters from the United States had arsenic concentrations below the detection limit of 10 $\mu g\,l^{-1}$. The highest concentration, 1100 $\mu g\,l^{-1}$, was reported from Sugar Creek, South Carolina, downstream of an industrial complex.

Arsenic can also be derived from mine wastes and tailings. Azcue and Nriagu (1995) reported baseline concentrations of 0.7 $\mu g\,l^{-1}$ in the Moira River, Ontario, upstream of gold mine tailings, with concentrations up to 23 $\mu g\,l^{-1}$ downstream. Azcue et al. (1994) reported concentrations up to 556 $\mu g\,l^{-1}$ (average 17.5 $\mu g\,l^{-1}$) in streams draining mine tailings in British Columbia. Williams et al. (1996) and Smedley (1996) noted high arsenic concentrations (typically around 200–300 $\mu g\,l^{-1}$) in surface waters from areas of tin and gold mining, respectively. Such anomalies tend to be localized because of the strong adsorption of arsenic by oxide minerals, especially iron oxide, under oxidizing and neutral to acidic conditions typical of many surface waters. Arsenic concentrations are therefore not always very high even in mining areas. For example, stream water arsenic concentrations from the Dalsung Cu–W mining area of Korea ranged from 0.8 to 19.1 $\mu g\,l^{-1}$ (Jung et al., 2002).

11.2.4.3.3 Lake water

Arsenic concentrations in lake waters are typically close to or lower than those of river waters. Baseline concentrations of $<1\ \mu g\,l^{-1}$ have been reported from Canada (**Table 6**) (Azcue and Nriagu, 1995; Azcue et al., 1995). Higher concentrations in lake waters may reflect geothermal sources or mining activity. Concentrations of 100–500 $\mu g\,l^{-1}$ have been reported in some mining areas and up to 1000 $\mu g\,l^{-1}$ in geothermal areas. However, arsenic concentrations can be much lower in mining-affected lake waters as a result of adsorption onto iron oxides under neutral to mildly acidic conditions. For example, Azcue et al. (1994) reported concentrations in lake waters affected by mining activity in Canada of about 0.3 $\mu g\,l^{-1}$, close to background values.

High arsenic concentrations can also occur in alkaline, closed-basin lakes. Mono Lake, CA, has dissolved arsenic concentrations of 10 000–20 000 $\mu g\,l^{-1}$ with pH values in the range 9.5–10 as a result of the combined influences of

geothermal activity, weathering of mineralized volcanic rocks, evaporation of water at the lake surface, and a thriving population of arsenate-respiring bacteria (Maest et al., 1992; Oremland et al., 2000).

Arsenic concentrations show considerable variations in stratified lakes because of changes in redox conditions or biological activity (Aggett and O'Brien, 1985; Hering and Kneebone, 2002). Arsenic concentrations increase with depth in lake waters in Ontario, probably because of an increasing ratio of As(III) to As(V) and an influx of mining-contaminated sediment pore waters at the sediment–water interface (Azcue and Nriagu, 1995). In other cases, seasonal depletion at the surface parallels that of nutrients such as silicate (Kuhn and Sigg, 1993). Concentrations are higher at depth in summer when the proportion of As(III) is greatest, probably reflecting lower oxygen concentrations as a result of biological productivity.

11.2.4.3.4 Seawater and estuaries

Average arsenic concentrations in open seawater are typically around 1.5 $\mu g\,l^{-1}$ (**Table 6**; see **Chapter 8.2**). Surface depletion, as with nutrients such as silicate, has been observed in some seawater samples, but not others. Concentrations in estuarine water are more variable because of different river inputs and salinity or redox gradients, but they typically contain less than 4 $\mu g\,l^{-1}$. Peterson and Carpenter (1983) found arsenic concentrations of between 1.2 and 2.5 $\mu g\,l^{-1}$ in waters from Saanich Inlet, British Columbia. Concentrations of less than 2 $\mu g\,l^{-1}$ were found in Oslofjord, Norway (Abdullah et al., 1995). Higher concentrations reflect industrial or mining effluents (e.g., Tamar, Schelde, Loire Estuaries) or inputs of geothermal water.

Some studies have reported conservative behavior during estuarine mixing. In the unpolluted Krka Estuary of Yugoslavia, Seyler and Martin (1991) observed a linear increase in total arsenic with increasing salinity, ranging from 0.13 $\mu g\,l^{-1}$ in freshwaters to 1.8 $\mu g\,l^{-1}$ offshore. Other studies, however, have observed nonconservative behavior in estuaries due to processes such as diffusion from sediment pore waters and coprecipitation with iron oxides or anthropogenic inputs (Andreae and Andreae, 1989; Andreae et al., 1983). The flocculation of iron oxides at the freshwater–saline interface as a result of increases in pH and salinity can lead to major decreases in the arsenic flux to the oceans (Cullen and Reimer, 1989).

11.2.4.3.5 Groundwater

The concentration of arsenic in most groundwater is $<10\ \mu g\,l^{-1}$ (Edmunds et al., 1989; Welch et al., 2000; see **Chapter 11.1**) and often below the detection limits of routine analytical methods. An analysis of groundwaters used for public supply in the United States showed that only 7.6% exceeded 10 $\mu g\,l^{-1}$ with 64% containing $<1\ \mu g\,l^{-1}$ (Focazio et al., 1999). Nonetheless, naturally high-arsenic groundwaters are found in aquifers in some areas of the world and concentrations occasionally reach the milligram per liter range (Smedley and Kinniburgh, 2002). Arsenic levels are naturally high in groundwaters in Bangladesh, Hungary (Smedley and Kinniburgh, 2002), and Holland (Van der Veer, 2006), associated with subsiding Holocene deltaic sediments near recently emergent Himalayan or Alpine mountain ranges. Industrially contaminated groundwater can also give rise to very high dissolved arsenic concentrations, but areas affected are usually localized. For example, Kuhlmeier (1997) found concentrations of arsenic up to 408 000 $\mu g\,l^{-1}$ in groundwater close to a herbicide plant in Texas.

The physicochemical conditions favoring arsenic mobilization in aquifers are variable, complex, and poorly understood, although some of the key factors leading to high groundwater arsenic concentrations are now known. Mobilization can occur under strongly reducing conditions where arsenic, mainly as As(III), is released by desorption from, and/or dissolution of, iron oxides. Many such aquifers are sufficiently reducing for sulfate reduction, and in some cases for methane generation, to occur (Ahmed et al., 1998). Immobilization under reducing conditions is also possible: some sulfate-reducing microorganisms can respire As(V) leading to the formation of an As_2S_3 precipitate (Newman et al., 1997a,b). Some immobilization of arsenic may also occur if iron sulfides are formed.

Reducing conditions favorable for arsenic mobilization have been reported most frequently from young (Quaternary) alluvial, deltaic sediments, where the interplay of tectonic, isostatic, and eustatic factors have resulted in complex patterns of sedimentation and the rapid burial of large amounts of sediment together with fresh organic matter during delta progradation. Thick sequences of young sediments are quite often the sites of high groundwater arsenic concentrations. The most notable example of these conditions is the Bengal Basin which incorporates Bangladesh and West Bengal (BGS and DPHE, 2001). Other examples include Nepal, Myanmar, Cambodia, parts of northern China (Luo et al., 1997; Smedley et al., 2003; Wang and Huang, 1994), the Great Hungarian Plain of Hungary and Romania (Gurzau and Gurzau, 2001; Varsányi et al., 1991), the Red River Delta of Vietnam (Berg et al., 2001), Mekong River Delta, Vietnam (Hoang et al., 2010), and parts of western United States (Korte, 1991; Welch et al., 2000). Recent groundwater extraction in many of these areas, either for public supply or for irrigation, will have induced increased groundwater flow and this could induce further transport of the arsenic (Harvey et al., 2002). Probability modeling and measured arsenic concentrations in the Red River Delta, Vietnam, indicate drawdown of arsenical waters from Holocene aquifers to previously uncontaminated Pleistocene aquifers as a result of >100 years of groundwater abstraction (Winkel et al., 2011).

High concentrations of naturally occurring arsenic are also found in oxidizing conditions where groundwater pH values are high ($\sim$>8) (Smedley and Kinniburgh, 2002). In such environments, inorganic As(V) predominates and arsenic concentrations are positively correlated with those of other anion-forming species such as HCO_3^-, F^-, H_3BO_3, and $H_2VO_4^-$. Examples include parts of western United States, for example, the San Joaquin Valley, California (Fujii and Swain, 1995), Lagunera region of Mexico (Del Razo et al., 1990), Antofagasta area of Chile (Cáceres et al., 1992; Sancha and Castro, 2001), and the Chaco-Pampean Plain of Argentina (Nicolli et al., 1989; Smedley et al., 2002) (**Table 6**). These high-arsenic groundwater provinces are usually in arid or semi-arid regions where groundwater salinity is also high. Evaporation has been suggested to be an important additional cause of arsenic accumulation in some arid areas (Welch and Lico, 1998).

High concentrations of arsenic have also been found in groundwater from areas of bedrock and placer mineralization, which are often the sites of mining activities. Arsenic

concentrations of up to 5000 μg l^{-1} have been found in groundwater associated with former tin-mining activity in the Ron Phibun area of Peninsular Thailand, the source most likely being oxidized arsenopyrite. Many cases have also been reported from other parts of the world, including the United States, Canada, Poland, and Austria. Examples include the Fairbanks mining district of Alaska, where arsenic concentrations up to 10 000 μg l^{-1} have been found in groundwater (Welch et al., 1988), and the Coeur d'Alene district of Idaho, where groundwater arsenic concentrations of up to 1400 μg l^{-1} have been reported (Mok and Wai, 1990).

Groundwater arsenic problems in nonmined mineralized areas are less common, but Boyle et al. (1998) found concentrations up to 580 μg l^{-1} in groundwater from the sulfide mineralized areas of Bowen Island, British Columbia. Heinrichs and Udluft (1999) also found arsenic concentrations up to 150 μg l^{-1} in groundwater from a mineralized sandstone aquifer in Bavaria.

11.2.4.3.6 Sediment pore water

Much higher concentrations of arsenic frequently occur in pore waters extracted from unconsolidated sediments than in overlying surface waters. Widerlund and Ingri (1995) reported concentrations in the range 1.3–166 μg l^{-1} in pore waters from the Kalix River estuary, northern Sweden. Yan et al. (2000) found concentrations in the range 3.2–99 μg l^{-1} in pore waters from clay sediments in Saskatchewan, Canada.

High concentrations are frequently found in pore waters from geothermal areas. Aggett and Kriegman (1988) reported arsenic concentrations up to 6430 μg l^{-1} in anoxic pore waters from Lake Ohakuri, New Zealand. Even higher concentrations have been found in pore waters from sediments contaminated with mine tailings or draining ore deposits. McCreadie et al. (2000) reported concentrations up to 100 000 μg l^{-1} in pore waters extracted from mine tailings in Ontario, Canada. High pore water-arsenic concentrations probably reflect the strong redox gradients that often occur over a few centimeters below the sediment–water interface. Burial of fresh organic matter and the slow diffusion of oxygen through the sediment lead to reducing conditions with the consequent reduction of As(V) to As(III) and the desorption and dissolution of arsenic from iron and manganese oxides.

There is much evidence of arsenic being released into shallow sediment pore waters and overlying surface waters in response to temporal variations in redox conditions. Sullivan and Aller (1996) investigated arsenic cycling in shallow sediments from an unpolluted area of the Amazonian offshore shelf. They found pore water-arsenic concentrations of up to 300 μg l^{-1} in anaerobic sediments with nearly coincident peaks of dissolved arsenic and iron. The peaks for iron concentration were often slightly above those of arsenic (**Figure 1**). The magnitude of the peaks and their depths varied from place to place and possibly seasonally, but were typically between 50 and 150 cm beneath the sediment–water interface (Sullivan and Aller, 1996). There was no correlation between pore water-arsenic concentrations and sediment-arsenic concentrations (**Figure 1**).

11.2.4.3.7 Acid mine drainage

Acid mine drainage (AMD), which can have pH values as low as −3.6 (Nordstrom et al., 2000), can contain high

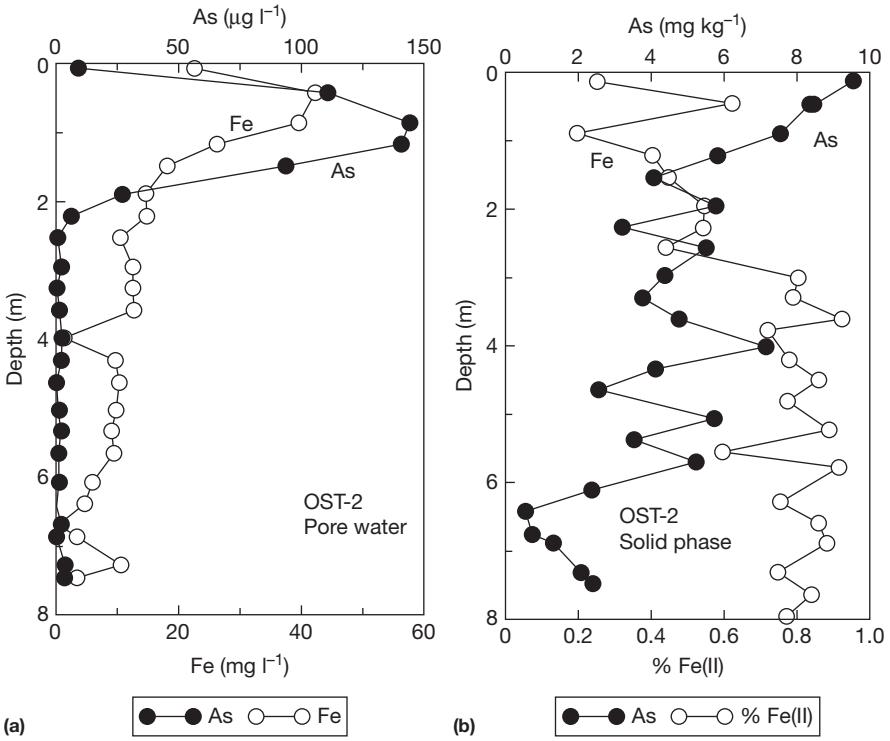

Figure 1 (a) Pore water and (b) cold 6 M HCl-extractable element concentrations in marine sediments from a pristine environment on the River Amazon shelf some 120 km off the coast of Brazil. Reproduced from Sullivan KA and Aller RC (1996) Diagenetic cycling of arsenic in Amazon shelf sediments. *Geochimica et Cosmochimica Acta* 60: 1465–1477.

concentrations of many solutes, including iron and arsenic (see **Chapter 11.5**). The highest reported arsenic concentration, 850 000 μg l^{-1}, was found in an acid seep in Richmond mine, California (Nordstrom and Alpers, 1999). Plumlee et al. (1999) reported concentrations ranging from <1 to 340 000 μg l^{-1} in 180 samples of mine drainage from the United States, with the highest values from Richmond mine. Gelova (1977) also reported arsenic concentrations of 400 000 μg l^{-1} in the Ural Mountains. Dissolved arsenic in AMD is rapidly removed as the pH increases and as iron is oxidized and precipitated as hydrous ferric oxide (HFO), coprecipitating large amounts of arsenic.

11.2.4.4 Arsenic Species in Natural Waters

The speciation of arsenic in natural waters is controlled by reduction, oxidation, and methylation reactions that affect its solubility, transport, bioavailability, and toxicity (Hering and Kneebone, 2002). The relatively small amount of arsenic released into stream waters during weathering is mobile only if the pH and E_h are sufficiently low to favor its persistence in trivalent form. Otherwise, dissolved arsenic is rapidly oxidized to insoluble As^{5+} and it becomes sorbed as the arsenate ion (AsO_4^{3-}) by hydrous iron and manganese oxides, clays, and organic matter (Cheng et al., 2009). Inorganic speciation is important because the varying protonation and charge of the arsenic species present at different oxidation states has a strong effect on their behavior, for example, their adsorption. While the concentrations of organic arsenic species are low in most natural environments, the methylated and dimethylated As(III) species are now of considerable interest as they have recently been found to be more cytotoxic, genotoxic, and potent enzyme inhibitors than inorganic As(III) (Thomas et al., 2001).

11.2.4.4.1 Inorganic species

Redox potential (E_h) and pH are the most important factors governing inorganic arsenic speciation. The redox behavior of inorganic arsenic species is complex and is mediated by chemical reactions such as ligand exchange, precipitation with iron and sulfide, adsorption to clay and metals, and biotic and abiotic oxidation–reduction reactions (Cullen and Reimer, 1989; Ferguson and Gavis, 1972; Fisher et al., 2007). Under oxidizing conditions, and pH less than about 6.9, $H_2AsO_4^-$ is dominant, while at higher pH, $HAsO_4^{2-}$ is dominant ($H_3AsO_4^0$ and AsO_4^{3-} may be present in extremely acid and alkaline conditions, respectively) (**Figure 2**) (Nordstrom and Archer, 2003; Yan et al., 2000). Under reducing conditions where the pH is less than about 9.2, the uncharged arsenite species, H_3AsO_3, predominates. Native arsenic is stable under strongly reducing conditions.

In the presence of high concentrations of reduced sulfur and low pH, dissolved As(III)-sulfide species can be formed rapidly by reduction of arsenate by H_2S. There is now strong evidence for the existence of the trimer, $As_3S_4(SH)_2^-$, under strongly reducing, acidic and sulfur-rich conditions with the thioarsenite species, $AsO(SH)_2^-$, appearing at higher pHs (Helz et al., 1995; Nordstrom and Archer, 2003; Rochette et al., 2000; Schwedt and Rieckhoff, 1996). Reducing, acidic and sulfur-rich conditions also favor precipitation of orpiment (As_2S_3), realgar (AsS), or other arsenic sulfide minerals (Cullen and Reimer, 1989). High concentrations of arsenic are unlikely in acidic waters containing high concentrations of free sulfide (Moore et al., 1988). In more alkaline waters, As(III) sulfides are more soluble and higher dissolved arsenic concentrations could persist. There is some evidence for the existence of As(V)–carbonate species (Kim et al., 2000), but their environmental significance has not yet been understood. Examination of the effects of sulfide on aerobic arsenite oxidation in alkaline lake water samples and in laboratory enrichment culture showed that arsenite oxidation occurred only in treatments with bacteria present; production of arsenate was greatly enhanced by the addition of sulfide or thiosulfate (Fisher et al., 2007). Like dissolved hydrogen, arsine is only expected under extremely reducing conditions. Green rusts, complex Fe(II)–Fe(III) hydroxide minerals that form under reducing conditions, have been shown to be able to reduce selenate to selenite abiotically but not arsenate to arsenite (Randall et al., 2001).

The E_h–pH diagram for the As–O–S system is shown in **Figure 3**. While such diagrams are useful, they necessarily simplify highly complex natural systems. For example, iron is not included despite its strong influence on arsenic speciation. Hence, scorodite ($FeAsO_4 \cdot 2H_2O$), an important arsenic-bearing mineral found under a wide range of near-neutral, oxidizing conditions, is not represented; neither is the coprecipitation of arsenic with pyrite, nor the formation of arsenopyrite (FeAsS) under reducing conditions. The relative stability of

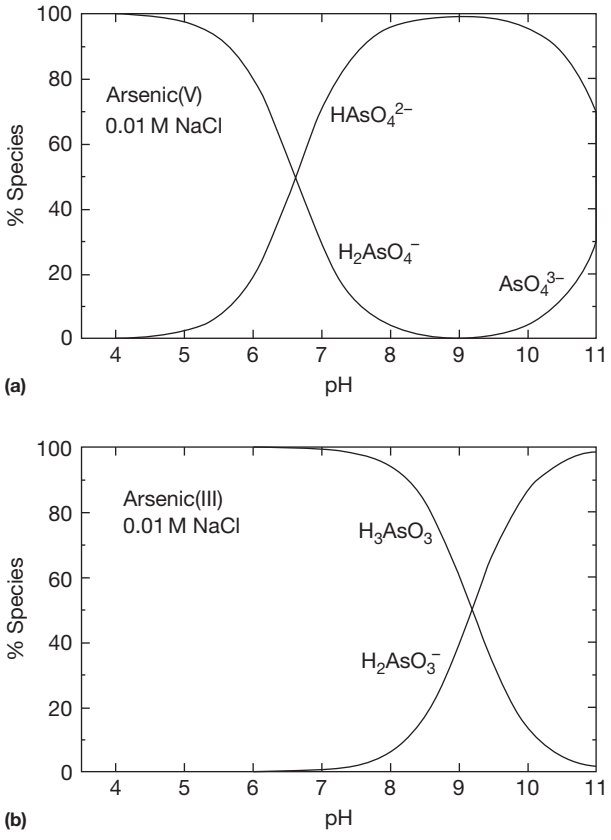

Figure 2 Speciation of As(V) and As(III) in a 0.01 M NaCl medium as a function of pH at 25 °C. Reproduced from Smedley PL and Kinniburgh DG (2002) A review of the source, behaviour and distribution of arsenic in natural waters. *Applied Geochemistry* 17: 517–568.

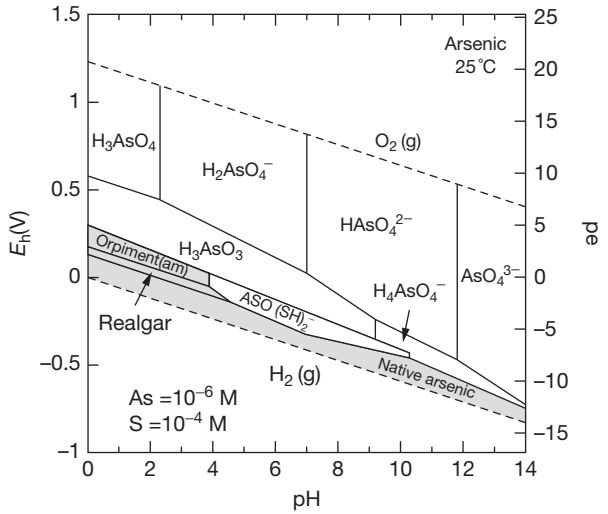

Figure 3 E_h–pH stability diagram for arsenic in the presence of sulfur at 25 °C, 1 bar total pressure. The stability field for water is shown by the dashed lines. The gray area represents a solid phase.

the various As–S minerals is very sensitive to their assumed free energies of formation and the stability of the various soluble As–S species. The E_h–pH diagram can vary significantly depending on the chosen forms of realgar and orpiment, including their crystallinity.

The extent of redox equilibrium in natural waters has been the cause of considerable discussion. In the case of arsenic, Cherry et al. (1979) suggested that redox equilibrium was sufficiently rapid for As(V)/As(III) ratios to be useful indicators of redox status. Subsequent findings have been somewhat equivocal (Welch et al., 1988) although some recent data for pore water As(V)/As(III) ratios and E_h measurements have indicated substantial consistency (Yan et al., 2000). While observations of the rate of oxidation of As(III) in groundwater are difficult under field conditions, the rates are believed to be slow. However, biological activity in these waters is also generally low, making redox equilibrium easier to attain than in more productive environments.

11.2.4.4.2 Organic species

Organic arsenic species are important in food, especially fish and marine invertebrates such as lobsters (AsB and arsenosugars), and in blood and urine (monomethylarsonate (MMA) and dimethylarsinate (DMA)), although they usually form only a minor component of arsenic in natural waters (Francesconi and Kuehnelt, 2002; National Research Council, 1999). Their concentrations are greatest in organic-rich waters such as soil and sediment pore waters and productive lake waters and least in groundwaters. The concentrations of organic species are increased by methylation reactions catalyzed by microbial activity, including bacteria, yeasts, and algae. The dominant organic forms found are DMA and MMA in which arsenic occurs in the pentavalent state. Proportions of these two species are reported to increase in summer as a result of increased microbial activity (Hasegawa, 1997). Organic species may also be more abundant close to the sediment–water interface (Hasegawa et al., 1999).

Small concentrations of trimethylarsonate, AsB, AsC, and phenylarsonate have been observed occasionally (Florencio et al., 1997). Arsenic can also be bound to humic material, but this has not been well characterized and may involve ternary complexes with strongly bound cations such as Fe^{3+}.

There have been reports of 'hidden' arsenic species in natural waters. These are organic species that do not form arsine gas with $NaBH_4$ and were therefore undetected in early speciation studies. Some, though not all, such arsenic species are detected after UV irradiation of samples (Hasegawa et al., 1999; National Research Council, 1999).

11.2.4.4.3 Observed speciation in different water types

The oxidation states of arsenic in rainwater vary according to source, but are likely to occur dominantly as As(III) when derived from smelters, coal burning, or volcanic sources. Organic arsenic species may be derived by volatilization from soils, and arsine ($As(-III)H_3$) may be produced from landfills and reducing soils such as paddy soils and peats. Arsenate may be derived from marine aerosols. Reduced forms will undergo oxidation in the atmosphere and reactions with atmospheric SO_2 or O_3 are likely (Cullen and Reimer, 1989).

In oxic seawater, the As(V) species predominates, though some As(III) is invariably present, especially in anoxic bottom waters. As(V) should exist mainly as $HAsO_4^{2-}$ and $H_2AsO_4^-$ in the pH range of seawater (pH around 8.2; **Figures 2** and **3**) and As(III) mainly as the neutral species H_3AsO_3. In fact, relatively high proportions of H_3AsO_3 occur in surface ocean waters (Cullen and Reimer, 1989) where primary productivity is high, often with increased concentrations of organic arsenic species as a result of methylation reactions by phytoplankton.

The relative proportions of arsenic species in estuarine waters are more variable because of changes in redox, salinity, and terrestrial inputs (Abdullah et al., 1995; Howard et al., 1988). As(V) tends to dominate, although Andreae and Andreae (1989) found increased proportions of As(III) in the Schelde Estuary of Belgium, with the highest values in anoxic zones near sources of industrial effluent. Increased proportions of As(III) also occur near sources of mine effluent (Andreae and Andreae, 1989). Seasonal variations in concentration and speciation have been reported in seasonally anoxic waters (Riedel, 1993). Peterson and Carpenter (1983) reported a clear crossover in the proportions of the two species with increasing depth in the Saanich Inlet of British Columbia. As(III) represented only 5% (0.10 μg l^{-1}) of the dissolved arsenic above the redox front but 87% (1.58 μg l^{-1}) below it. In marine and estuarine waters, organic forms of arsenic are usually less abundant but are often detected (Howard et al., 1999; Riedel, 1993). Their concentrations depend on the abundance and species of biota present and on temperature.

In lake and river waters, As(V) is generally dominant (Pettine et al., 1992; Seyler and Martin, 1990), although concentrations and relative proportions of As(V) and As(III) vary seasonally according to changes in input sources, redox conditions, and biological activity. The presence of As(III) may be maintained in oxic waters by biological reduction of As(V), particularly during summer months. Higher proportions of As(III) occur in rivers close to sources of As(III)-dominated

industrial effluent (Andreae and Andreae, 1989) or where there is a component of geothermal water.

Proportions of As(III) and As(V) are particularly variable in stratified lakes with seasonally variable redox gradients (Kuhn and Sigg, 1993). In the stratified, hypersaline, hyperalkaline Mono Lake (California, USA), As(V) predominates in the upper oxic layer and As(III) in the reducing layer (Maest et al., 1992; Oremland et al., 2000). Oremland et al. (2000) measured in situ rates of dissimilatory As(V) reduction in the lake and found that this could potentially mineralize 8–14% of the annual pelagic primary productivity during meromixis, a significant amount for a trace element, and about one-third of the amount of sulphate reduction. Such reduction does not occur in the presence of NO_3. In fact, NO_3 leads to the rapid, microbial reoxidation of As(III) to As(V) (Hoeft et al., 2002). Fe(III) acts similarly.

The speciation of arsenic in lakes does not always follow thermodynamic predictions. Recent studies have shown that arsenite predominates in the oxidized epilimnion of some stratified lakes while arsenate may persist in the anoxic hypolimnion (Kuhn and Sigg, 1993; Newman et al., 1998; Seyler and Martin, 1989). Proportions of arsenic species can also vary according to the availability of particulate iron and manganese oxides (Kuhn and Sigg, 1993; Pettine et al., 1992). Sunlight could promote oxidation in surface waters (Voegelin and Hug, 2003).

In groundwaters, the ratio of As(III) to As(V) can vary greatly in relation to changes in the abundance of redox-active solids, especially organic carbon, the activity of microorganisms, and the extent of convection and diffusion of oxygen from the atmosphere. As(III) typically dominates in strongly reducing aquifers in which Fe(III) and sulfate reduction is taking place. Reducing high-arsenic groundwaters from Bangladesh have As(III)/AsT ratios varying between 0.1 and 0.9 but are typically around 0.5–0.6 (Smedley et al., 2001a). Ratios in reducing groundwaters from Inner Mongolia are typically 0.6–0.9 (Smedley et al., 2003). Concentrations of organic forms of arsenic are generally small or negligible in groundwaters (e.g., Chen et al., 1995; Del Razo et al., 1990).

11.2.4.5 Microbial Controls

The toxicity of arsenic results from its ability to interfere with a number of key biochemical processes. Arsenate can interfere with phosphate biochemistry (oxidative phosphorylation) as a result of their chemical similarity. Arsenite tends to inactivate sulfhydryl groups of cysteine residues in proteins (Oremland et al., 2002; Santini et al., 2002). Microbes have evolved various detoxification strategies for dealing with this (Frankenberger, 2002; Mukhopadhyay et al., 2002; Rosen, 2002). Some microbes have also evolved to use arsenic as an energy source. Certain chemoautotrophs oxidize As(III) by using O_2, nitrate, or Fe(III) as a terminal electron acceptor and CO_2 as their sole carbon source. A select group of other organisms grows in anaerobic environments by using As(V) for the oxidation of organic matter or H_2 gas (Newman et al., 1998; Oremland and Stolz, 2003; Oremland et al., 2002, 2000; Stolz and Oremland, 1999). Such so-called dissimilatory arsenate reduction (DAsR) was discovered only relatively recently (Ahmann et al., 1994). Fourteen species of Eubacteria, including *Sulfurospirullum* species, have so far been shown to be capable of DAsR (Herbel et al., 2002a) as well as two species of hyperthermophiles from the domain Archaea. Laboratory studies indicate that microbial processes involved in As(V) reduction and mobilization are many times faster than inorganic chemical transformations and that microorganisms play an important role in subsurface arsenic cycling (Ahmann et al., 1997; Bhattacharya et al., 2007; Islam et al., 2004; Jones et al., 2000). In Mono Lake, eastern California, a hypersaline and alkaline water body bacterium strain GFAJ-1 of the Halomonadaceae has been reported, which substitutes arsenic for phosphorus to sustain its growth (Wolfe-Simon et al., 2011).

The bacterium *Thiobacillus* has been shown to have a direct role in precipitating ferric arsenate sulfate (Leblanc et al., 1996). Temporal variations between the proportions of arsenate and arsenite have been observed in the Waikato River, New Zealand, and may reflect the reduction of As(V) to As(III) by epiphytic bacteria associated with the alga *Anabaena oscillaroides*. Arsenate reduction does not necessarily take place as an energy-providing (dissimilatory) process (Hoeft et al., 2002). Detoxifying arsenate reductases in the cytoplasm does not provide a means of energy generation. Macur et al. (2001) found active As(V) to As(III) reduction under oxic conditions in limed mine tailings, which they ascribed to a detoxification rather than an energy-producing, respiratory process. This is often combined with an As(III) efflux pump to expel the toxic As(III) from the cell. Purely chemical (abiotic) reduction of As(V) to As(III) has not been documented.

Arsenic can also be released indirectly as a result of other microbially induced redox reactions. For example, the dissimilatory iron-reducing bacterium *Shewanella alga* (strain BrY) reduces Fe(III) to Fe(II) in scorodite ($FeAsO_4 \cdot 2H_2O$), releasing As(V) but not As(III) (Cummings et al., 1999). This process can be rapid (Langner and Inskeep, 2000).

The rapid oxidation of As(III) has also been observed in the geothermally fed Hot Creek in California (Wilkie and Hering, 1998). Oxidation with a pseudo-first-order half-life of approximately 0.3 h was found to be controlled by bacteria attached to macrophytes. Where microbial activity is high, there is frequently a lack of equilibrium between the various redox couples, including that of arsenic (**Section 11.2.4.4**). This is especially true of soils (Masscheleyn et al., 1991).

11.2.5 Pathways and Behavior of Arsenic in the Natural Environment

Most high-arsenic natural waters are groundwaters from particular settings such as mineralized, mined, and geothermal areas, young alluvial deltaic basins, and inland semiarid basins (Smedley and Kinniburgh, 2002). The most extensive areas of affected groundwater are found in the low-lying deltaic areas of Southeast Asia, especially the Bengal Basin, and in the large plains ('pampas') of South America. The sediments of these areas typically have 'average' total arsenic concentrations although concentrations may increase in iron oxide-rich sediments. The chemical, microbiological, and hydrogeological processes involved in the mobilization of arsenic in such groundwaters are poorly understood, but

probably involve early diagenetic reactions driven by redox and/or pH changes.

11.2.5.1 Release from Primary Minerals

The arsenic in many natural waters is likely to have been derived naturally from the dissolution of a mineral phase. The most important primary sources are sulfide minerals, particularly arsenic-rich pyrite, which can contain up to 10% arsenic, and arsenopyrite (FeAsS). In one study, the greatest concentrations of arsenic were found in fine-grained (<2 μm) pyrite formed at relatively low temperatures (120–200 °C) (Simon et al., 1999). A variety of other sulfide minerals such as orpiment As_2S_3 and realgar As_2S_2 also occur in association with gold and base metal deposits. Arsenic is a component of some complex copper sulfides such as enargite (Cu_3As_4) and tennantite ($(Cu, Fe)_{12}As_4S_{13}$). Rare arsenides are also found in mineralized areas. All of these minerals oxidize rapidly on exposure to the atmosphere, releasing the arsenic to partition between water and various secondary minerals, particularly iron oxides. Both microbially mediated redox reactions (**Section 11.2.4.5**) and abiotic processes are involved. Bacteria can influence the oxidation state of arsenic in aquatic environments (Oremland and Stolz, 2003). The microbial oxidation of arsenic minerals such as arsenopyrite, enargite, and orpiment has been discussed by Ehrlich (2002).

Oxidation of sulfide minerals can occur naturally or as a result of mining activity. Arsenic-rich minerals around mines may therefore produce arsenic-rich drainage locally, but this tends to be attenuated rapidly as a result of adsorption of various arsenic species by secondary minerals. Some of the best-documented cases of arsenic contamination therefore occur in areas of sulfide mineralization, particularly those associated with gold deposits.

Oxidation is enhanced by mining excavations, mine dewatering, ore roasting, and the redistribution of tailings in ponds and heaps. In the past, this has been the cause of serious environmental damage leading to high arsenic concentrations in soils, stream sediments, surface waters and some groundwaters, and even the local atmosphere. Although these activities have often had a severe impact on the local environment, the arsenic contamination in surface water and groundwater tends to be restricted to within a few kilometers of the mine site.

Oxidation of arsenopyrite can be described by the reaction:

$$4FeAsS + 13O_2 + 6H_2O = 4Fe^{2+} + 4AsO_4^{3-} + 4SO_4^{2-} + 12H^+$$

which involves the release of acid, arsenic, and sulfate as AMD (see **Chapter 11.5**). Further acidity is released by oxidation of the Fe^{2+} and precipitation of HFO or schwertmannite. These minerals readsorb some of the released arsenic, reducing dissolved arsenic concentrations, and may eventually lead to the formation of scorodite ($FeAsO_4 \cdot 2H_2O$).

Experience from bioleaching of arsenic-rich gold ores has shown that the ratio of pyrite to arsenopyrite is an important factor controlling the speciation of the arsenic released (Nyashanu et al., 1999). In the absence of pyrite, about 72% of the arsenic released was As(III) whereas in the presence of pyrite and Fe(III), 99% of the arsenic was As(V). It appears that pyrite catalyzed the oxidation of As(III) by Fe(III) as Fe(III) alone did not oxidize the arsenic (Nyashanu et al., 1999).

11.2.5.1.1 Examples of mining-related arsenic problems

Mining and mineral processing can cause arsenic contamination of the atmosphere (in the form of airborne dust), sediment, soil, and water. The contamination can be long-lasting and remain in the environment long after the activities have ceased (Camm et al., 2003). Recent estimates suggest that there are approximately 11 million tonnes of arsenic associated with copper and lead reserves globally (USGS, 2005). In developing mines containing significant amounts of arsenic, careful consideration is now given to treatment of wastes and effluents to ensure compliance with legislation on permitted levels of arsenic that can be emitted to the environment. Such legislation is becoming increasingly stringent. Arsenic contamination from former mining activities has been identified in many areas of the world including the United States (Plumlee et al., 1999; Welch et al., 1999, 1988, 2000), Canada, Thailand, Korea, Ghana, Greece, Austria, Poland, and the United Kingdom (Smedley and Kinniburgh, 2002). Groundwater in some of these areas has been found with arsenic concentrations as high as 48 000 $\mu g\,l^{-1}$. Elevated arsenic concentrations have been reported in soils of various mining regions around the world (Kreidie et al., 2011). Some mining areas have AMD with such low pH values that the iron released by oxidation of the iron sulfide minerals remains in solution and therefore does not scavenge arsenic. Well-documented cases of arsenic contamination in the United States include the Fairbanks gold-mining district of Alaska (Welch et al., 1988; Wilson and Hawkins, 1978), the Coeur d'Alene Pb–Zn–Ag mining area of Idaho (Mok and Wai, 1990), the Leviathan Mine (S), California (Webster et al., 1994), Mother Lode (Au), California (Savage et al., 2000), Summitville (Au), Colorado (Pendleton et al., 1995), Kelly Creek Valley (Au), Nevada (Grimes et al., 1995), Clark Fork river (Cu), Montana (Welch et al., 2000), Lake Oahe (Au), South Dakota (Ficklin and Callender, 1989), and Richmond Mine (Fe, Ag, Au, Cu, Zn), Iron Mountain, California (Nordstrom et al., 2000).

Phytotoxic effects attributed to high concentrations of arsenic have also been reported around the Mina Turmalina copper mine in the Andes, northeast of Chiclayo, Peru (Bech et al., 1997). The main ore minerals involved are chalcopyrite, arsenopyrite, and pyrite. Arsenic-contaminated groundwater in the Zimapan Valley, Mexico, has also been attributed to interaction with Ag–Pb–Zn, carbonate-hosted mineralization (Armienta et al., 1997). Arsenopyrite, scorodite, and tennantite were identified as probable source minerals in this area. Increased concentrations of arsenic have been found as a result of arsenopyrite occurring naturally in Cambro–Ordovician lode gold deposits in Nova Scotia, Canada. Tailings and stream sediment samples show high concentrations of arsenic (39 ppm), and dissolved arsenic concentrations in surface waters and tailing pore waters indicate that the tailings continue to release significant quantities of arsenic. Biological sampling demonstrated that both arsenic and mercury have bioaccumulated to various degrees in terrestrial and marine biota, including eels, clams, and mussels (Parsons et al., 2006).

Data for 34 mining localities of different metallogenic types in different climatic settings were reviewed by Williams (2001). He proposed that arsenopyrite is the principal source of arsenic released in such environments and concluded that in situ oxidation generally resulted in the formation of poorly soluble

scorodite, which limited the mobility and ecotoxicity of arsenic. The Ron Phibun tin-mining district of Thailand is an exception (Williams et al., 1996). In this area, arsenopyrite oxidation products were suggested to have formed in the alluvial placer gravels during the mining phase. Following cessation of mining activity and pumping, groundwater rebound caused dissolution of the oxidation products. The role of scorodite in the immobilization of arsenic from mine workings has been questioned by Roussel et al. (2000), who point out that the solubility of this mineral exceeds drinking water standards irrespective of pH.

11.2.5.1.2 Modern practice in mine-waste stabilization

Although large international mining companies now generally work to high environmental standards, mineral working by uncontrolled and disorganized groups (especially for gold) continues to cause environmental problems in a number of developing countries.

Modern mining practices including waste storage and treatment are designed to minimize the risk of environmental impacts (Johnson, 1995). In most countries, environmental impact assessments and environmental management plans are now a statutory requirement of the mining approval process. Such plans include criteria for siting and management of waste heaps and for effluent control. Closure plans involving waste stabilization and capping to limit AMD generation are also required to reduce any legacy of environmental damage (Lima and Wathern, 1999).

Treatment of AMD includes the use of liming, coagulation, and flocculation (Kuyucak, 1998). Other passive technologies include constructing wetlands that rely on sulfate reduction, alkali generation, and the precipitation of metal sulfides. These are often used as the final step in treating discharged water. More recently, permeable reactive barriers (PRBs) have been advocated. For example, Harris and Ragusa (2001) have demonstrated that sulfate-reducing bacteria can be stimulated to precipitate arsenic sulfides by the addition of rapidly decomposing plant material. Monhemius and Swash (1999) investigated the addition of iron to copper- and arsenic-rich liquors to form scorodite. The arsenic is immobilized by incorporation into a crystalline, poorly soluble compound (Sides, 1995). Swash and Monhemius (1996) have also investigated the stabilization of arsenic as calcium arsenate.

11.2.5.2 Role of Secondary Minerals

11.2.5.2.1 The importance of arsenic cycling and diagenesis

The close association between arsenic and iron in minerals is frequently reflected by their strong correlation in soils and sediments. Iron oxides play a crucial role in adsorbing arsenic species, especially As(V), thereby lowering the concentration of arsenic in natural waters. O'Reilly et al. (2001) suggested that arsenic is specifically sorbed onto goethite through an inner-sphere complex through a ligand-exchange process. Manganese oxides play a role in the oxidation of As(III) to As(V) and also adsorb significant quantities, although to a much lesser degree than the more abundant iron oxides. HFO is a very fine-grained, high surface area form of iron oxide that is often formed in iron-rich environments in response to rapid changes in redox or pH. It is frequently involved in the cycling of As(III) and As(V). Significant As(V) desorption occurs at pH values of approximately pH 8 and higher (Lumsdon et al., 2001) and this process has been suggested to be important in generating high-arsenic groundwaters (Smedley, 2003; Welch et al., 2000). Arsenic can also be released under reducing conditions (**Section 11.2.5.5**).

The mobility of arsenic can also be limited in sulfur-rich, anaerobic environments by its coprecipitation with secondary sulfide minerals, and more generally by clays. The precise behavior of arsenic in sediments is poorly understood, but it is likely that important changes occur during sediment diagenesis. Arsenic adsorbed on mineral surfaces is likely to be sensitive to changes in the mineral properties such as surface charge and surface area. A very small mass transfer from solid to solution can lead to a large change in dissolved arsenic concentration. For example, sediments with average arsenic concentrations of less than 5–10 mg kg^{-1} can generate milligram per liter concentrations of arsenic when only a small fraction (<1%) of the total arsenic is partitioned into the water.

11.2.5.2.2 Redox behavior

Solid surfaces of many minerals, especially redox-sensitive minerals like iron and manganese oxides, also play an important role in redox reactions and interactions with microbes (Brown et al., 1999; Grenthe et al., 1992). Solid $Mn(IV)O_2$, notably birnessite (δ-MnO_2), assists in the oxidation of As(III) to As(V) while being partially reduced to Mn(II) (Oscarson et al., 1983; Scott and Morgan, 1995). The rate of oxidation depends on the surface area and surface charge of the MnO_2 and is slightly greater at low pH (pH 4). The Mn(II) and As(V) produced are partially retained or readsorbed by the MnO_2 surface, which may lead in turn to a deceleration in the rate of As(III) oxidation (Manning et al., 2002). Reactions with birnessite at very high initial As(III) concentrations may lead to the insoluble mineral krautite ($MnHAsO_4 \cdot H_2O$) being formed on the birnessite surface (Tournassat et al., 2002). The catalytic role of solid MnO_2 in removing As(III) is used to advantage in water treatment (Daus et al., 2000; Driehaus et al., 1995). TiO_2 minerals and Ti-containing clays may also be able to oxidize As(III).

HFO and other iron oxides may also play a significant role in the oxidation of As(III) in natural waters, as the oxidation of As(III) adsorbed by HFO is catalyzed by H_2O_2 (Voegelin and Hug, 2003). This reaction may be significant in natural environments, with high H_2O_2 concentrations (1–10 μM) and alkaline pHs, or in water treatment systems where H_2O_2 is used. Similar surface-catalyzed reactions do not occur with aluminum oxides (Voegelin and Hug, 2003).

The reductive dissolution of Fe(III) oxides in reducing sediments and soils (McGeehan et al., 1998) can also lead to the release of adsorbed and coprecipitated arsenic. Reduction and release of arsenic can precede any dissolution of the iron oxides themselves (Masscheleyn et al., 1991). These processes are likely to be the same as those responsible for the development of high-arsenic groundwaters in the Bengal Basin (Bhattacharya et al., 1997; Kinniburgh et al., 2003; Nickson et al., 2000) and other reducing alluvial aquifers (Korte and Fernando, 1991). The release of sorbed arsenic during diagenetic changes of iron oxides, including loss of surface area, changes in

surface structure, and charge following burial, may also be important under both reducing and oxidizing conditions.

The photocatalytic activity of anatase (TiO_2) has been shown to catalyze the oxidation of As(III) in the presence of light and oxygen (Foster et al., 1998a). Unlike the role of manganese oxides in As(III) oxidation, there is no change in the oxidation state of the surface Ti(IV) atoms.

11.2.5.3 Adsorption of Arsenic by Oxides and Clays

Metal ion oxides are often important in minimizing the solubility of arsenic in the environment in general and more specifically for localizing the impact of arsenic contamination near contaminated sites, especially old mines (La Force et al., 2000; Plumlee et al., 1999; Roussel et al., 2000; Webster et al., 1994). Organic arsenic species tend to be less strongly sorbed by minerals than inorganic species.

There have been many laboratory studies of the adsorption of arsenic species by pure minerals, especially iron and aluminum oxides and clays (Goldberg, 1986; Inskeep et al., 2002). The general features of the processes involved are now established. Dzombak and Morel (1990) critically reviewed the available laboratory data for the adsorption of a wide range of inorganic species, including those for arsenic, by HFO and fitted the most reliable data to a surface complexation model – the diffuse double-layer model. This model, and the accompanying thermodynamic database, is now incorporated into several general-purpose geochemical speciation and transport models, including PHREEQC2 (Parkhurst and Appelo, 1999) and The Geochemist's Workbench (Bethke, 2002). These software packages enable rapid calculations of the possible role of arsenic adsorption by HFO to be made. Critically, in PHREEQC2, this adsorption behavior can also be automatically linked to the dissolution/precipitation of HFO. The results of such calculations demonstrate the important role of both oxidation states (arsenate vs. arsenite) and pH (**Figure 4**).

The oxidized and reduced species of arsenic behave very differently on HFO (**Figure 4**) and this along with the pH dependence of adsorption accounts, at least in part, for their different behavior with oxides and clays and hence their behavior in natural waters. As(V) is very strongly adsorbed by HFO especially at low pH and low concentrations, but is desorbed as the pH increases as a result of the increasingly strong electrostatic repulsion on the negatively charged HFO surface. The adsorption isotherm for arsenate is consequently highly nonlinear and can be approximated by a pH-dependent Freundlich isotherm; that is, the slope of the adsorption decreases markedly with increasing arsenic concentration (the K_d varies with concentration). In contrast, As(III) in the pH range 4–9 is present mainly in solution as the neutral $As(OH)_3$ species and so electrostatic interactions are not nearly so important. Therefore, arsenite is adsorbed over a wide range of pH and because the adsorbed species is uncharged, arsenite adsorption tends to follow a Langmuir isotherm; that is, the isotherm has an adsorption maximum and approaches linearity at low concentrations. It is also almost independent of pH. Organic arsenic species are weakly adsorbed by oxides, so their formation can increase arsenic mobility.

In oxidizing environments, arsenate is more strongly adsorbed than arsenite in neutral to acidic conditions, and especially at low concentrations. Arsenate tends to be much less strongly adsorbed at high pH and this has important environmental consequences. The precise pH where this occurs depends on several other factors (e.g., the total arsenic concentration and the concentrations of other competing anions) but it is in the region pH 8–9. Under these conditions, arsenite may be more strongly bound.

The adsorption of arsenic species also depends to some extent on competition from other anions, which in reducing groundwaters include phosphate, silicate, bicarbonate, and fulvic acids (Appelo et al., 2002; Hiemstra and van Riemsdijk, 1999; Jain and Loeppert, 2000; Meng et al., 2002; Wang et al., 2001; Wijnja and Schulthess, 2000). As(V) and P sorption on HFO are broadly similar although there is usually a slight preference for P (Jain and Loeppert, 2000). Not surprisingly, As(V) is much more strongly affected by P competition than As(III) (Jain and Loeppert, 2000). Cations, such as Ca^{2+} and Fe^{2+}, may increase arsenic adsorption (Appelo et al., 2002). Once the oxides have an adsorbed load, any change to their surface chemistry or the solution chemistry can lead to the release of adsorbed arsenic, thereby increasing groundwater concentrations. The extremely high solid/solution ratio of soils and aquifers makes them very sensitive to such changes and redox changes are likely to be particularly important (Meng et al., 2001; Zobrist et al., 2000).

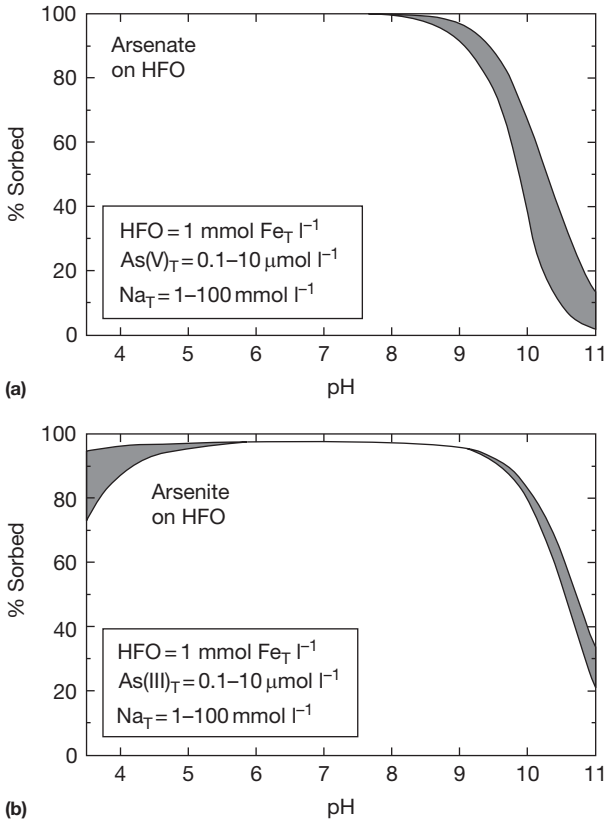

Figure 4 Calculated percent adsorption of (a) oxidized and (b) reduced arsenic species by hydrous ferric oxide (HFO). Infilled areas show the adsorption for a range of total As concentrations (0.1–10 μmol l^{-1}) and ionic strengths (1–100 mmol l^{-1}).

Adsorption by aluminum and manganese oxides and clays has not been studied much (Inskeep et al., 2002). As(III) binds strongly to amorphous $Al(OH)_3$ over pH range 6–9.5, a somewhat greater range than found for HFO. It also binds significantly but somewhat less strongly to montmorillonitic and kaolinitic clays (Manning and Goldberg, 1997). As(V) shows the same declining affinity for clays at high pH as shown by HFO, but in the case of the clays, this decline may begin to occur above pH 7.

11.2.5.4 Arsenic Transport

There are few observations of arsenic transport in aquifers and its rate of movement under a range of conditions is poorly understood. The transport of arsenic, as with many other chemicals, is closely related to adsorption–desorption reactions (Appelo and Postma, 1993). Arsenate and arsenite have different adsorption isotherms and would be predicted therefore to travel through aquifers at different velocities, leading to their separation along the flow path.

Gulens et al. (1979) used breakthrough experiments with columns of sand (containing 0.6% iron and 0.01% manganese) and various groundwaters pumped continuously from piezometers to study As(III) and As(V) mobility over a range of E_h and pH conditions. Radioactive ^{74}As (half-life = 17.7 days) and ^{76}As (half-life = 26.4 h) were used to monitor the breakthrough of arsenic. The results showed that (1) As(III) moved 5–6 times faster than As(V) under oxidizing conditions with pH in the range 5.7–6.9; (2) As(V) moved much faster at the lowest pH but was still slower than As(III) under reducing groundwater conditions; and (3) with a pH of 8.3, both As(III) and As(V) moved rapidly through the column but when the amount of arsenic injected was substantially reduced, the mobility of the As(III) and As(V) was greatly reduced. This chromatographic effect (used to advantage in analytical chemistry to speciate arsenic) may account in part for the highly variable As(III)/As(V) ratios found in many reducing aquifers. Chromatographic separation of arsenic and other species during transport would also destroy the original source characteristics, for example, between arsenic and iron, further complicating interpretation of well water analyses.

Few field-based investigations, which allow the partition coefficient (K_d) or retardation factor of arsenic species to be determined directly, have been carried out on natural systems. However, the work of Sullivan and Aller (1996) indicates that K_d values calculated for sediment profiles from the Amazon Shelf are in the approximate range of 11–5000 $l kg^{-1}$. High-arsenic pore waters were mostly found in zones with low K_d values (typically $<100\ l kg^{-1}$). Evidence from various studies also suggests low K_d values ($<10\ l kg^{-1}$) for arsenic in aquifers in which there are high arsenic concentrations (Smedley and Kinniburgh, 2002). Factors controlling the partition coefficients are poorly understood and involve the chemistry of the groundwater and the surface chemistry and stability of solid phases present.

11.2.5.5 Impact of Changing Environmental Conditions

Arsenic moves between different environmental compartments (rock–soil–water–air–biota) from the local to the global scale partly as a result of pH and redox changes. Being a minor component in the natural environment, arsenic responds to such changes rather than creates them. These changes are driven by the major (bio)geochemical cycles.

11.2.5.5.1 Release of arsenic at high pH

High arsenic concentrations can develop in groundwaters as As(V) is released from oxide minerals and clays at high pH. High pH conditions frequently develop in arid areas as a result of extensive mineral weathering with proton uptake. This is especially true in environments dominated by sodium rather than by calcium, as $CaCO_3$ minerals restrict the development of high pHs.

11.2.5.5.2 Release of arsenic on reduction

Flooding of soils generates anaerobic conditions and can lead to the rapid release of arsenic (and phosphate) to the soil solution (Deuel and Swoboda, 1972; Reynolds et al., 1999). Similarly, arsenic can be released to pore water in buried sediments. The concentration of dissolved arsenic in some north Atlantic pore waters varies inversely with the concentration of easily leachable arsenic in the solid phase and directly with increasing concentrations of solid phase Fe(II) (Sullivan and Aller, 1996). This reflects a strong redox coupling between arsenic and iron whereby oxidized arsenic is associated with iron oxides in surface sediments and is subsequently reduced and released into pore water with burial. Upward diffusion and reworking of sediment releases the dissolved arsenic to the water column or releases it for readsorption in surface sediments as HFO is formed (Petersen et al., 1995). Some reducing, iron-rich aquifers also contain high concentrations of arsenic (Korte, 1991), but there are also many iron-rich groundwaters with low arsenic concentrations.

11.2.5.6 Case Studies

11.2.5.6.1 The Bengal Basin, Bangladesh, and India

In terms of the number of people at risk, the high-arsenic groundwaters from the alluvial and deltaic aquifers of Bangladesh and West Bengal represent the most serious threat to public health from arsenic yet identified. Health problems from this source were first identified in West Bengal in the 1980s but remained unrecognized in Bangladesh until 1993. In fact, the scale of this disaster in Bangladesh is greater than any such previous incident, including the accidents at Bhopal, India, in 1984, and Chernobyl, Ukraine, in 1986 (Smith et al., 2000). Concentrations of arsenic in groundwaters from the affected areas have a very large range from <0.5 to $\sim 3200\ \mu g\ l^{-1}$ (Kinniburgh et al., 2003). In a survey of Bangladesh groundwater by BGS and DPHE (2001), 27% of shallow (<150 m) tubewells in Bangladesh were found to contain more than the national standard of $50\ \mu g\ l^{-1}$ for arsenic in drinking water.

Groundwater surveys indicate that the worst-affected area is in southeast Bangladesh (**Figure 5**) where more than 60% of the wells in some districts are affected. It is estimated that approximately 30–35 million people in Bangladesh and 6 million in West Bengal are at risk from arsenic concentrations of more than $50\ \mu g\ l^{-1}$ in their drinking water (BGS and DPHE, 2001). A study of the data collected by the DPHE–UNICEF (Bangladesh Department of Public Health Engineering–United Nations International Children's Emergency Fund) arsenic

mitigation programme found a prevalence rate of arsenicosis (keratosis, melanosis, and depigmentation) of 0.78 per 1000 people exposed to arsenic levels above 50 $\mu g\,l^{-1}$ in 15 heavily affected administrative units in Bangladesh (Rosenboom et al., 2004). The authors state that the data were difficult to interpret as the exposure period has been relatively short and the prevalence rate could increase (Howard et al., 2006). Drinking water is widely accepted as the main exposure route; however, recent studies have reported that rice can be a significant route of exposure to arsenic (Kile et al., 2007; Meharg et al., 2009; Mondal and Polya, 2008), which can be more important than drinking water in the Midnapur area of West Bengal (Mondal et al., 2010).

The affected aquifers of the Bengal Basin are generally shallow (less than 100–150 m deep) and consist mainly of Holocene micaceous sands, silts, and clays associated with the Ganges, Brahmaputra, and Meghna river systems. In West Bengal, the area east of the Hoogli River is affected. The sediments are derived from the Himalayan highlands and Precambrian basement complexes in northern and western West Bengal. In most of the areas with high-arsenic groundwater, alluvial and deltaic aquifer sediments are covered by surface horizons of fine-grained overbank deposits. These restrict the entry of air to underlying aquifers and together with the presence of reducing agents such as organic matter facilitate the development of strongly reducing conditions in the affected aquifers. Mobilization of arsenic probably reflects a complex combination of redox changes in the aquifers, resulting from the rapid burial of the alluvial and deltaic sediments, reduction of the solid-phase arsenic to As(III), desorption of arsenic from iron oxides, reductive dissolution of the oxides, and changes in iron oxide structure and surface properties in the ambient reducing conditions (BGS and DPHE, 2001). Some researchers have also suggested that, in parts of Bangladesh at least, enhanced groundwater flow and redox changes may have been imposed on the shallow aquifer as a result of recent irrigation pumping (Harvey et al., 2002).

Deep tubewells (>150–200 m), mainly from the southern coastal region, and wells in older Plio–Pleistocene sediments from the Barind and Madhupur Tracts of northern Bangladesh almost invariably have arsenic concentrations of less than 5 $\mu g\,l^{-1}$ and usually less than 0.5 $\mu g\,l^{-1}$ (BGS and DPHE, 2001). It is fortunate that in Calcutta and Dhaka people draw their water from these older sediments and do not face the problem of high arsenic concentrations in drinking water. Dhaka is sited at the southern tip of the Madhupur Tract (**Figure 5**). Shallow open dug wells also generally have low arsenic concentrations, usually <10 $\mu g\,l^{-1}$ (BGS and DPHE, 2001).

The high-arsenic groundwaters of the Bengal Basin typically have near-neutral pH values and are strongly reducing with measured redox potentials usually less than 100 mV (BGS and

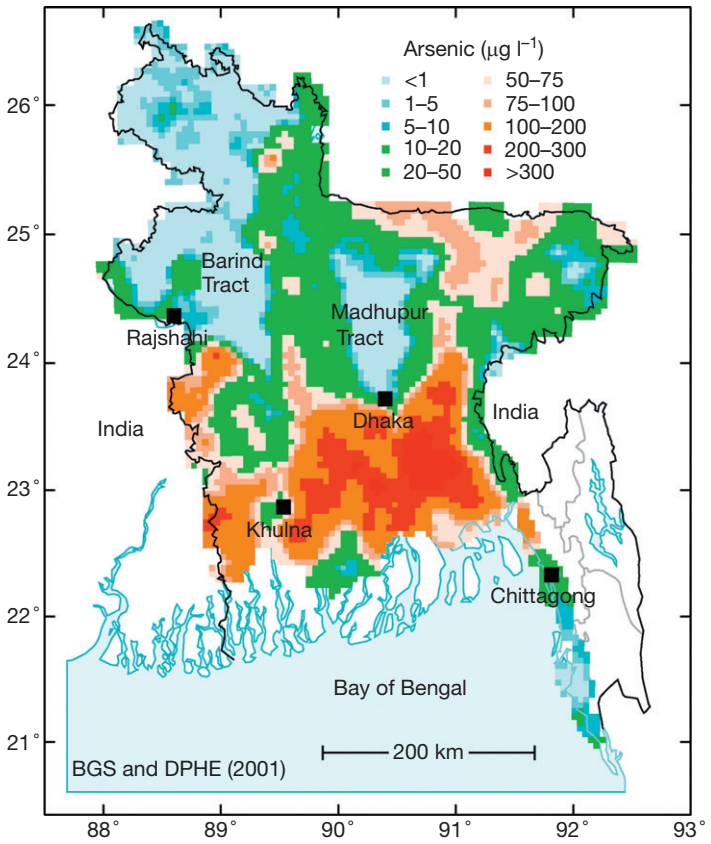

Figure 5 Map showing the distribution of arsenic in shallow (<150 m) Bangladesh groundwaters based on some 3200 groundwater samples. Reproduced from BGS and DPHE (2001) Arsenic contamination of groundwater in Bangladesh. In Kinniburgh DG and Smedley PL (eds.) *BGS Technical Report WC/00/19*. Nottingham: British Geological Survey (see http://www.bgs.ac.uk/Arsenic/bphase2/home.html).

DPHE, 2001). The source of the organic C responsible for the reducing conditions has been variously attributed to dispersed sediment C (BGS and DPHE, 2001), peat (McArthur et al., 2001), or soluble C brought down by a combination of surface pollution and irrigation (Harvey et al., 2002). High concentrations of iron (>0.2 mg l^{-1}), manganese (>0.5 mg l^{-1}), bicarbonate (>500 mg l^{-1}), ammonium (>1 mg l^{-1}), and phosphorus (>0.5 mg l^{-1}) and low concentrations of nitrate (<0.5 mg l^{-1}) and sulfate (<1 mg l^{-1}) are also typical of the high-arsenic areas. Some Bangladesh groundwaters are so reducing that methane production has been observed (Ahmed et al., 1998; Harvey et al., 2002). Positive correlations between arsenic and iron in the groundwaters have been reported in some studies at the local scale (e.g., Nag et al., 1996), although the correlations are generally poor on a national scale (Kinniburgh et al., 2003). As(III) typically dominates the dissolved arsenic load, although As(III)/As(V) ratios are variable (BGS and DPHE, 2001).

The arsenic-affected groundwaters in the Bengal Basin are associated with alluvial and deltaic sediments with total arsenic concentrations in the range <2–20 mg kg^{-1}. These values are close to world average concentrations for such sediments. However, even though the arsenic concentrations are low, there is a significant variation both regionally and locally and the sediment iron and arsenic concentrations appear to be indicators of the concentration of dissolved arsenic (BGS and DPHE, 2001). The mineral source or sources of the arsenic are still not well established. Various researchers have postulated the most likely mineral sources as iron oxides (BGS and DPHE, 2001; Bhattacharya et al., 1997; Nickson et al., 1998), but pyrite or arsenopyrite (Das et al., 1996) and phyllosilicates (Foster et al., 2000) have also been cited as possible sources. High-arsenic groundwaters tend to be associated with relatively arsenic-rich and iron-rich sediments. The solid–solution mass transfers involved are so small that it is difficult to identify, or even eliminate, any particular sources using mass balance considerations alone.

The reasons for the differing arsenic concentrations in the shallow and deep groundwaters of the Bengal Basin are not yet completely understood. They could reflect differing absolute arsenic concentrations in the aquifer sediments, differing oxidation states, or differences in the arsenic-binding properties of the sediments. The history of groundwater movement and aquifer flushing in the Bengal Basin may also have contributed to the differences. Older, deeper sediments will have been subjected to longer periods of groundwater flow, aided by greater hydraulic heads during the Pleistocene period when glacial sea levels were regionally up to 130 m lower than today (Umitsu, 1993). These will therefore have undergone a greater degree of flushing and removal of labile solutes than Holocene sediments at shallower depths.

Isotopic evidence suggests that groundwater in some parts of the Bengal Basin has had a variable residence time. At a site in western Bangladesh (Chapai Nawabganj), tritium was found to be present at 2.5–5.9 TU (tritium units) in two shallow piezometer samples (10 m or less), indicating that they contained an appreciable component of post-1960s recharge (Smedley et al., 2001b). At this site and two others in south and central Bangladesh (Lakshmipur and Faridpur, respectively), groundwater from piezometers between 10 and 30 m depth had tritium concentrations ranging between 0.1 and 9.6 TU, indicating a variable proportion of post-1960s recharge. Some of the low-tritium wells contained high arsenic concentrations suggesting that the arsenic was released before the 1960s; that is, before the recent rapid increase in groundwater abstraction for irrigation and water supply. Groundwater from piezometers at 150 m depth in central and south Bangladesh contained <1 TU, also indicating pre-1960s water.

Radiocarbon dating has a longer time frame than tritium and provides evidence for water with ages on the scale of hundreds of years or more. Radiocarbon dating of groundwater sampled from the above piezometers in the 10–40 m depth range typically contained 65–90 percent modern carbon (pmc) while below 150 m the groundwater contained 51 pmc or less (Smedley et al., 2001b). The lowest observed ^{14}C activities were in water from deep (>150 m) piezometers in southern Bangladesh. Here, activities of 28 pmc or less suggested the presence of paleowaters with ages of the order of 2000–12 000 years.

Taken together with the tritium data, these results indicated that water below 31 m or so tended to have ages between 50–2000 years. Broadly similar results and conclusions were reported by Aggarwal (2000). However, Harvey et al. (2002) drew the opposite conclusion from data from their field site just south of Dhaka. They found that a water sample from 19 m depth contained dissolved inorganic carbon (DIC) with a ^{14}C composition at bomb concentrations and was therefore less than 50 years old. This sample contained about 200 μg l^{-1} arsenic and they postulated that the rapid expansion of pumping for irrigation water has led to an enhanced inflow of organic carbon and that this has either produced enhanced reduction and release of arsenic or displacement of arsenic by carbonate. However, a sample from 31 m depth that had a lower ^{14}C DIC activity and an estimated age of 700 years also contained a high arsenic concentration (about 300 μg l^{-1}). This predates modern irrigation activity. Whether, in general, irrigation has had a major impact on arsenic mobilization in the Bengal aquifers is a matter of current debate.

11.2.5.6.2 Chaco-Pampean Plain, Argentina

The Chaco-Pampean Plain of central Argentina covers around 1 million km^2 and constitutes one of the largest regions of high-arsenic groundwaters known. High concentrations of arsenic have been documented from Córdoba, La Pampa, Santa Fe, Buenos Aires, and Tucumán provinces. Symptoms typical of chronic arsenic poisoning, including skin lesions and some internal cancers, have been recorded in these areas (Hopenhayn-Rich et al., 1996). The climate is temperate with increasing aridity toward the west. The high-arsenic groundwaters are from Quaternary deposits of loess (mainly silt) with intermixed rhyolitic or dacitic volcanic ash (Nicolli et al., 1989; Smedley et al., 2002), often situated in closed basins. The sediments display abundant evidence of post-depositional diagenetic changes under semiarid conditions, with common occurrences of calcrete.

Many investigations of groundwater quality have identified variable and often extremely high arsenic concentrations. Nicolli et al. (1989) found arsenic concentrations in groundwaters from Córdoba in the range of 6–11 500 μg l^{-1} (median 255 μg l^{-1}). Smedley et al. (2002) found concentrations for groundwaters in La Pampa Province in the range of

<4–5280 μg l^{-1} (median 145 μg l^{-1}), and Nicolli et al. (2001) found concentrations in groundwaters from Tucumán province in the range of 12–1660 μg l^{-1} (median 46 μg l^{-1}). A map showing the distribution of arsenic in groundwaters from northern La Pampa is given in Figure 6.

The geochemistry of the high-arsenic groundwaters of the Chaco-Pampean Plain is quite distinct from that of the deltaic areas typified by the Bengal Basin. The Argentine groundwaters often have high salinity and the arsenic concentrations are generally highly correlated with other anionic and oxyanionic species such as fluorine, vanadium, HCO_3, boron, and molybdenum. The WHO guideline value for fluorine in drinking water (1.5 mg l^{-1}), as well as that for arsenic, boron, and uranium, is exceeded in many areas. Arsenic is predominantly present as As(V) (Smedley et al., 2002). The groundwaters are also predominantly oxidizing with low dissolved iron and manganese concentrations. There is no indication of reductive dissolution of iron oxides or pyrite oxidation. Under arid conditions, silicate and carbonate weathering reactions are pronounced and the groundwaters often have high pH values. Smedley et al. (2002) found pH values typically of 7.0–8.7.

While the reasons for these high arsenic concentrations are unclear, metal oxides in the sediments (especially iron and manganese oxides and hydroxides) are thought to be the main source of dissolved arsenic, although the direct dissolution of volcanic glass has also been cited as a potential source (Nicolli et al., 1989). The arsenic is believed to be desorbed under high pH conditions (Smedley et al., 2002). A change in the surface chemistry of the iron oxides during early diagenesis may also be an important factor in arsenic desorption.

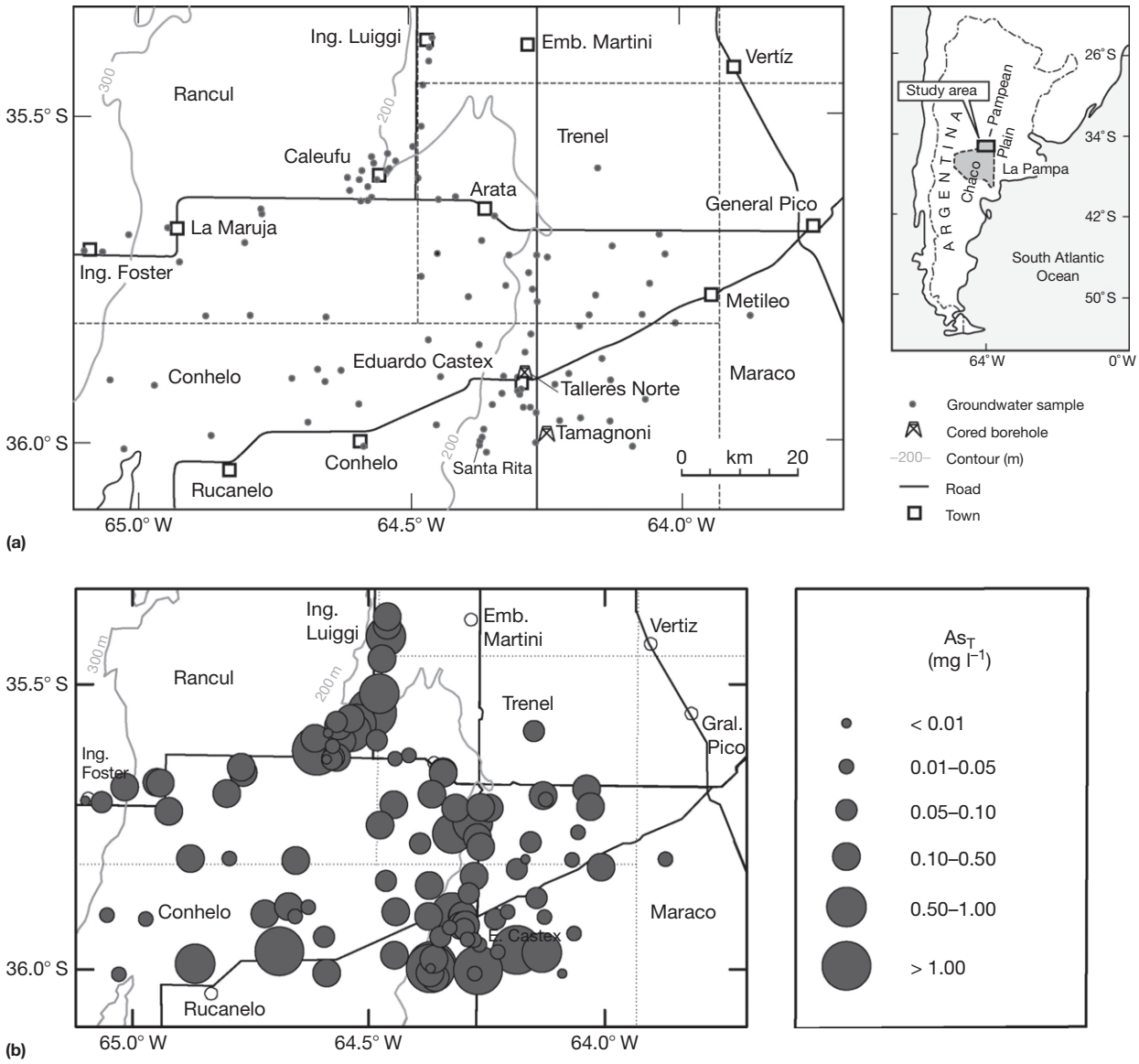

Figure 6 Map showing (a) groundwater sampling locations and (b) observed arsenic concentrations in the Chaco-Pampean Plain of central Argentina. Reproduced from Smedley PL, Nicolli HB, Macdonald DMJ, Barros AJ, and Tullio JO (2002) Hydrogeochemistry of arsenic and other inorganic constituents in groundwaters from La Pampa, Argentina. *Applied Geochemistry* 17: 259–284.

The released arsenic tends to accumulate where natural groundwater movement is slow, especially in low-lying discharge areas. Evaporative concentration is also a factor, but the lack of correlation between arsenic and chlorine concentrations in the groundwaters suggests that it is not the dominant control (Smedley et al., 2002).

11.2.5.6.3 Eastern Wisconsin, USA

The analysis of some 31 350 groundwaters throughout the United States indicates that about 10% exceed the current 10 $\mu g\,l^{-1}$ drinking water MCL (Welch et al., 2000). At a broad regional scale (**Figure 7**), arsenic concentrations exceeding 10 $\mu g\,l^{-1}$ are more frequently observed in the western United States than in the east. The Mississippi delta shows a locally high pattern but is not exceptional, when viewed nationally. Arsenic concentrations in groundwater from the Appalachian Highlands and the Atlantic Plain are generally very low (<1 $\mu g\,l^{-1}$). Concentrations are somewhat greater in the Interior Plains and the Rocky Mountains and within the last decade, areas in New England, Michigan, Minnesota, South Dakota, Oklahoma, and Wisconsin have been shown to have groundwaters with arsenic concentrations exceeding 10 $\mu g\,l^{-1}$, sometimes appreciably so. Eastern Wisconsin is one such area.

The St. Peter Sandstone (Ordovician) aquifer of eastern Wisconsin (Brown, Outagamie, Winnebago Counties) is a locally important source of water for private supplies. Arsenic contamination was first identified at two locations in 1987 and subsequent investigations showed that 18 out of 76 sources (24%) in Brown County, 45 out of 1116 sources (4.0%) in Outagamie County, and 23 out of 827 sources (2.8%) in Winnebago County exceeded the then current MCL for arsenic of 50 $\mu g\,l^{-1}$ (Burkel and Stoll, 1999). The highest arsenic concentration found was 1200 $\mu g\,l^{-1}$. A depth profile in one of the affected wells showed that most of the groundwater was slightly acidic (pH 5.2–6.6) and in some places very acidic (pH < 4). There were also high concentrations of iron, cadmium, zinc, manganese, copper, and sulfate, and it was concluded that the arsenic and other elements were released following the oxidation of sulfide minerals (pyrite and marcasite) present in a cement horizon at the boundary of the Ordovician Sinnipee Group and the underlying unit, either the St. Peter Sandstone or the Prairie du Chien Group depending on the location. The low pH values are consistent with iron sulfide mineral oxidation.

Subsequent detailed studies in the Fox River valley towns of Algoma and Hobart confirmed the importance of the sulfide-rich cement horizon as a probable source of the arsenic (Schreiber et al., 2000) (**Figure 8**). In the town of Algoma, one well contained 12 000 $\mu g\,l^{-1}$ arsenic. There was, however, much apparently random spatial variation. Two wells close to the high-arsenic well contained much lower arsenic concentrations (12 and 34 $\mu g\,l^{-1}$). The highest arsenic concentration found in wells from the town of Hobart was 790 $\mu g\,l^{-1}$.

Oxidation of sulfide minerals appears to have been promoted by groundwater abstraction, which has led to the lowering of the piezometric surface at a rate of around 0.6 m $year^{-1}$ since the 1950s, leading to partial dewatering of the confined aquifer. The high arsenic concentrations occur where the piezometric surface intersects, or lies close to, the sulfide cement horizon (Schreiber et al., 2000).

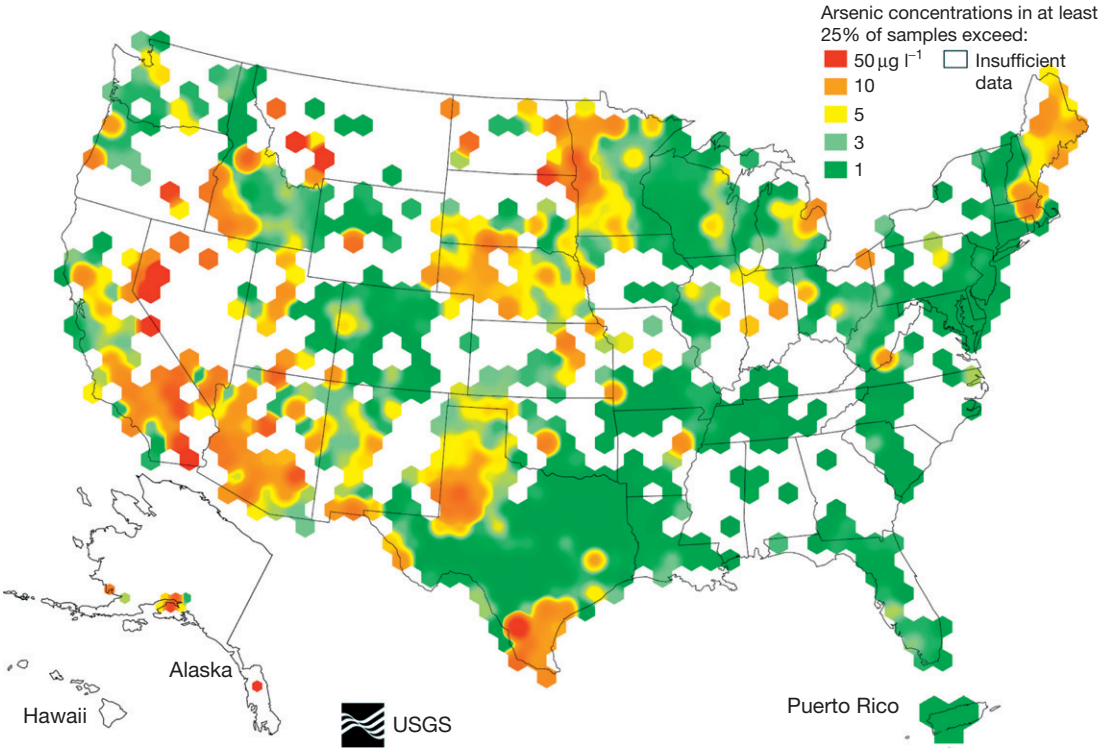

Figure 7 Map of the United States showing the regional distribution of arsenic in wells (from http://water.usgs.gov/nawqa/trace/pubs/geo_v46n11/fig3.html after Ryker, 2001). This shows where 25% of water samples within a moving 50-km radius exceed a certain arsenic concentration. It is computed from 31 350 water samples and updated from the results presented by Welch et al. (2000).

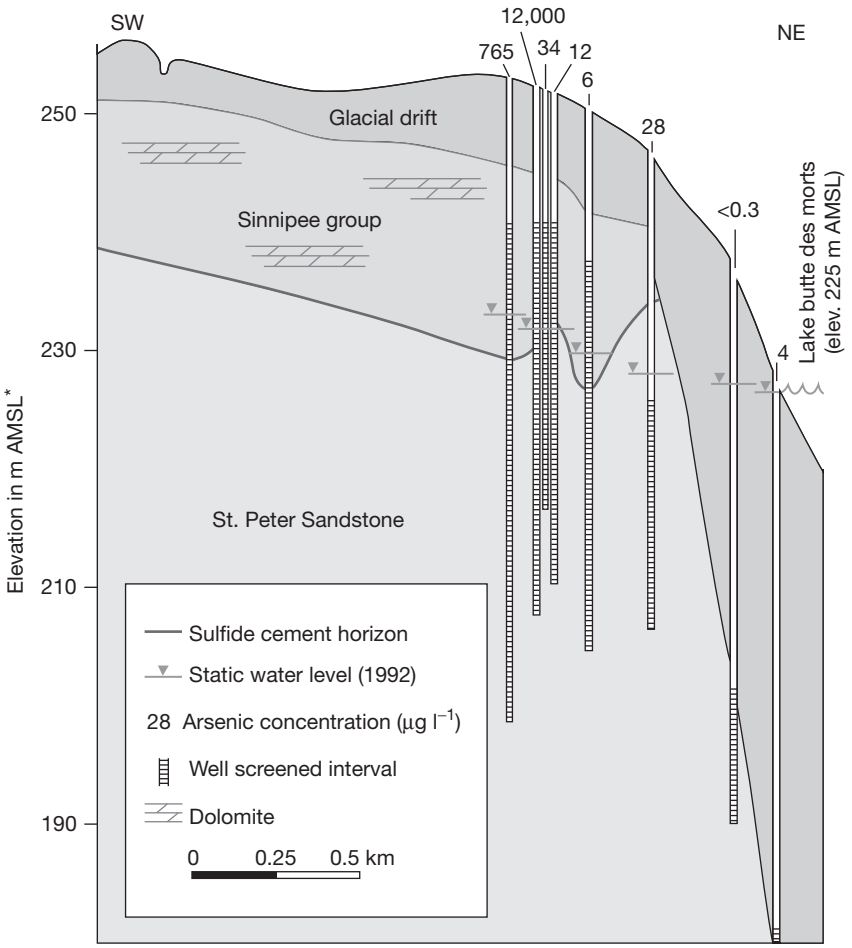

Figure 8 Hydrogeological section through part of Algoma, Winnebago County, Wisconsin, showing the arsenic concentration in various wells in relation to the cemented sulfide-rich horizon and the static water level. Reproduced from Schreiber ME, Simo JA, and Freiberg PG (2000) Stratigraphic and geochemical controls on naturally occurring arsenic in groundwater, eastern Wisconsin, USA. *Hydrogeology Journal* 8: 161–176.
*AMSL: above mean sea level.

11.2.6 Abundance and Forms of Selenium in the Natural Environment

11.2.6.1 Abundance in Rocks, Soils, and Sediments

The average crustal abundance of selenium is 0.05 mg kg^{-1} (Jacobs, 1989) and like arsenic, selenium is strongly chalcophile and is partitioned into sulfides and rare selenides, such as crooksite and clausthalite. Selenium generally substitutes for sulfur in sulfide minerals but elemental (native) selenium has also been reported (Alloway, 1995; Davies, 1980; Tokunaga et al., 1996).

Selenium concentrations in coal and other organic-rich deposits can be high and typically range from 1 to 20 mg kg^{-1}. The average selenium concentration in coals from the United States is 4.1 mg kg^{-1} (Swanson et al., 1976). Large concentrations of selenium, like arsenic, are often associated with the clay fraction of sediments because of the abundance of free iron oxides and other strong sorbents. The main source to humans is thought to be from bedrock, which affects soil concentrations and availability for plant uptake (Fordyce, 2005). Intrusive igneous and volcanic rocks generally have low concentrations, although the ash and gases from volcanic activity can contain high concentrations (Fergusson, 1990). Selenium concentrations are generally larger in shales than in limestones or sandstones (Neal, 1995) (**Table 7**). Selenium concentrations of over 600 mg kg^{-1} are found in some black shales. Selenium is present in these shales as organoselenium compounds or adsorbed species (Jacobs, 1989). Concentrations exceeding 300 mg selenium per kilogram have also been reported in some phosphatic rocks (Jacobs, 1989). In an area with diverse geology, it is likely that the geographical distribution of selenium will be quite variable due to the occurrence of different rock types or sulfide mineral deposits (Johnson et al., 2010).

There are no selenium mines, but selenium is produced as a by-product of refining other metals such as lead or copper and from sulfuric acid manufacture (Johnson et al., 2010). Soil is a fundamental control on selenium concentrations in the food chain and is a major control of the selenium status of crops and livestock (Fordyce, 2005). Except where there is contamination, there is generally a strong correlation between the selenium content of rocks and the sediments and soils derived from them. Soil selenium concentrations are typically in the range of 0.01–2 mg kg^{-1} with a world average of 0.4 mg kg^{-1} (Fergusson, 1990; Fordyce, 2005). The selenium concentration

Table 7 Selenium concentrations in selected rock types

Material	*Selenium (mg kg^{-1})*
Earth's crust	0.05
Igneous rocks	
Ultramafic rocks	0.05
Mafic rocks	0.05
Granite	0.01–0.05
Volcanic rocks	0.35
Volcanic rocks, USA	<0.1
Volcanic rocks, Hawaii	<2.0
Volcanic tuffs	9.15
Sedimentary rocks	
Marine carbonates	0.17
Limestone	0.03–0.08
Sandstone	<0.05
Western USA shale	1–675
Wyoming shale	2.3–52
S Korean shale	0.1–41
Carbon-shale China	206–280
Mudstone	0.1–1500
Phosphate	1–300
USA Coal	0.46–10.7
Australian coal	0.21–2.5
Chinese stone-coal	<6500
Oil	0.01–1.4

Sources: Jacobs LW (1989) *Selenium in Agriculture and the Environment*. Madison, WI: Soil Science Society of America. SSSA Special Publication 23; Fordyce FM, Zhang G, Green K, and Liu X (2000) Soil, grain, and water chemistry in relation to human selenium-responsive diseases in Enshi District, China. *Applied Geochemistry* 15: 117–132; WHO (1987) *Environmental Health Criterion 58 – Selenium*. Geneva: World Health Organization; Oldfield JE (1999) *Selenium World Atlas*. Cavite, Philippines: Selenium-Tellurium Development Association; Alloway BJ (1995) *Heavy Metals in Soils*. London: Blackie; Davies BE (1980) *Applied Soil Trace Elements*. Chichester: Wiley.

Table 8 Selenium concentrations in soils

Soil	*Total Se (mg kg^{-1})*	*Water-soluble Se (mg kg^{-1})*
World general	0.4	
World seleniferous	1–5000	
USA general	<0.1–4.3	
USA seleniferous	1–10	
England/Wales general	<0.01–4.7	0.05–0.39
Ireland seleniferous	1–1200	
China general	0.02–3.8	
China Se deficient	0.004–0.48	0.00003–0.005
China Se adequate	0.73–5.7	
China seleniferous	1.49–59	0.001–0.25
Finland	0.005–1.25	
India Se deficient	0.025–0.71	0.019–0.066
India seleniferous	1–20	0.05–0.62
Sri Lanka Se deficient	0.11–5.2	0.005–0.043
Norway	3–6	
Greece Se deficient	0.05–0.10	
Greece Se adequate	>0.2	
New Zealand	0.1–4	

Sources: Davies BE (1980) *Applied Soil Trace Elements*. Chichester: Wiley; Thornton I, Kinniburgh DG, Pullen G, and Smith CA (1983) Geochemical aspects of selenium in British soils and implications to animal health. In: Hemphill DD (ed.) *Trace Substances in Environmental Health*, vol. XVII, pp. 391–398. Columbia, MO: University of Missouri.; Jacobs LW (1989) *Selenium in Agriculture and the Environment*. Madison, WI: Soil Science Society of America. SSSA Special Publication 23; WHO (1987) *Environmental Health Criterion 58 – Selenium*. Geneva: World Health Organization; Alloway BJ (1995) *Heavy Metals in Soils*. London: Blackie; Oldfield JE (1999) *Selenium World Atlas*. Cavite, Philippines: Selenium-Tellurium Development Association; Fordyce FM, Johnson CC, Navaratna URB, Appleton JD, and Dissanayake CB (2000) Selenium and iodine in soil, rice and drinking water in relation to endemic goitre in Sri Lanka. *Science of the Total Environment* 263: 127–141; Fordyce FM, Zhang G, Green K, and Liu X (2000) Soil, grain and water chemistry in relation to human selenium-responsive diseases in Enshi District, China. *Applied Geochemistry* 15: 117–132.

in soils rarely exceeds 0.1 mg kg^{-1} (Moreno Rodriguez et al., 2005). The geographical distribution of selenium in soils is, however, extremely varied (Wang and Gao, 2001). Extremely high concentrations (up to 1200 mg kg^{-1}) have been found in some organic-rich soils derived from black shales in Ireland (**Table 8**). Soils from England derived from black shales had an average concentration of 3.1 mg kg^{-1} compared with an overall average of 0.48 mg kg^{-1}for a range of more typical English soils (Thornton et al., 1983). Concentrations of 6–15 mg kg^{-1} have been reported in volcanic soils such as those of Hawaii (Jacobs, 1989). High concentrations tend to be found in soils from mineralized areas and in poorly drained soils.

The median selenium concentration in stream sediments from 20 study areas across the United States was 0.7 mg kg^{-1} (Rice, 1999) and 0.5 mg kg^{-1} in 19 000 stream sediments in Wales (BGS, 1978–2006). Selenium levels in sediments of the Lewis and Clark Lake near the Missouri River are in the range of 0.012–9.62 mg kg^{-1}, far higher than the toxic-effect threshold of 2 mg kg^{-1}. The selenium is thought to be derived from the erosion of shale bluffs containing high levels of the element (Johnson et al., 2010; Lemly, 2002; Pracheil et al., 2010). Relatively low selenium concentrations are found in well-drained soils derived from limestones and coarse sands.

Selenium-rich vegetation, including the selenium-indicating vetches (*Astragalus* sp.), is widespread in South Dakota and Wyoming, USA. It grows on soils developed over black shales and sandstones with high selenium concentrations (Moxon, 1937). Tuffs are also a source of high Se soils in these areas of the United States. Selenium toxicity was first documented in 1856 near Fort Randall, where a physician in the US Cavalry reported horses experiencing hair, mane, and tail loss and sloughing of hooves. Forage that contains 2–5 mg kg^{-1} selenium poses a marginal threat to livestock, and acute effects are likely to occur above 5 mg selenium per kilogram.

Although geology is the primary control on the selenium concentration of soil, the bioavailability of selenium to plants and animals is determined by other factors including pH and redox conditions, speciation, soil texture and mineralogy, organic matter content, and the presence of competing ions (Fordyce, 2005). Even soils with relatively high total selenium concentrations can give rise to selenium deficiency if the selenium is not bioavailable. The first map of the selenium status of soil and vegetation in relation to animal deficiency and toxicity was prepared by Muth and Allaway (1963).

Several techniques are available to assess selenium bioavailability in soils but the most widely used is the water-soluble concentration (Fordyce et al., 2000b; Jacobs, 1989; Tan, 1989). In most soils, only a small proportion of the total selenium is dissolved in solution (0.3–7%) and water-soluble selenium contents are generally <0.1 mg kg^{-1} (**Table 8**).

Selenium is also added to soils as a trace constituent of phosphate fertilizers and in selenium-containing pesticides and fungicides, as well as by the application of sewage sludge and manure (Alloway, 1995; Frankenberger and Benson, 1994; Jacobs, 1989; see **Chapter 11.15**). Sewage sludge typically contains about 1 mg selenium per kilogram dry weight. Precautionary limits are set for several chemical elements likely to be increased by the application of sewage sludge to land. In the European Union (EU), for example, the banning of the discharge of sewage sludge into the sea since 1999 has increased its application to land. The maximum admissible concentration of selenium in sewage sludge in the United Kingdom is 25 mg kg^{-1}, and in soil after application is 3 mg kg^{-1} in the United Kingdom and 10 mg kg^{-1} in France and Germany (Fordyce 2005; ICRCL, 1987; Reimann and Caritat, 1998). In the United States, the limit is 100 mg kg^{-1}.

11.2.6.2 National and International Standards in Drinking Water

The WHO guideline value for selenium in drinking water is currently 40 μg l^{-1}. The standard adopted by the EC, Australia, Japan, and Canada is 10 μg l^{-1}. The US EPA primary drinking water standard is 50 μg l^{-1}. In California, the MCL for selenium is also 50 μg l^{-1}, but a public health goal of 30 μg l^{-1} for water-soluble and bioavailable selenium compounds in drinking water has been set (California Environmental Protection Agency, 2010).

11.2.6.3 Abundance and Distribution in Natural Waters

The selenium concentration in most natural waters is very low, often less than 1 μg l^{-1} and frequently just a few nanograms per liter. Typical levels of selenium in groundwater and surface water range from 0.00006 to 0.400 mg l^{-1}, with some areas having as much as 6 mg l^{-1} (Fordyce, 2005; WHO, 1996, 2011) Hence, selenium from drinking water only constitutes a health hazard in exceptional circumstances (Fordyce et al., 2000a; Vinceti et al., 2000). However, occasionally, much greater concentrations are found. Groundwaters containing up to 275 μg l^{-1} have been reported from aquifers in China and 1000 μg l^{-1} selenium from seleniferous aquifers in Montana, USA (**Table 9**). Selenium concentrations of up to 2000 μg l^{-1} or more have also been reported in lakes from saline, seleniferous areas. Such areas are rare but include some arid parts of the United States, China, Pakistan, and Venezuela. In general, data on selenium concentrations in water are scarce. The mining and processing of gold, base metal, and coal deposits can be an important source of selenium. For example, contamination of the Chayanta River by mine water leached from the nearby Potosi mine in Bolivia resulted in water concentrations of 0.005–0.020 mg l^{-1} selenium, which exceed the guideline value for freshwater aquatic organisms (0.001 mg l^{-1}) (Rojas and Vandecasteele, 2007).

Reported ranges from the literature are summarized in **Table 9**.

Waters containing 10–25 μg l^{-1} selenium may have a garlic odor, while waters containing 100–200 μg l^{-1} have an unpleasant taste. Groundwaters generally contain higher

Table 9 Concentration ranges of Se in various water bodies

Water body and location	*Se concentration and range (μg l^{-1})*	*References*
Rainwater		
Various	0.04–1.4	Hashimoto and Winchester (1967)
Polar ice	0.02	Frankenberger and Benson (1994)
River and lake water		
Jordan River, Jordan	0.25	Nishri et al. (1999)
River Amazon, Brazil	0. 21	Jacobs (1989)
Colorado River, USA	<1–400	NAS (1976); Engberg (1999)
Mississippi River, USA	0.14	Jacobs (1989)
Lake Michigan, USA	0.8–10	Jacobs (1989)
Gunnison River, USA	10	Jacobs (1989)
Cienaga de Santa Clara wetland, Mexico	5–19	García-Hernández et al. (2000)
Seawater and estuaries		
Seawater	0.09; 0.17	Hem (1992); Thomson et al. (2001)
San Francisco Bay, USA	0.1–0.2	Cutter (1989)
Carquinez Strait, San Francisco Bay, USA	0.07–0.35	Zawislanski et al. (2001a)
Groundwater		
East Midlands Triassic Sandstone, UK	<0.06–0.86	Smedley and Edmunds (2002)
Chaco-Pampean Plain, loess aquifer, Argentina	<2–40	Nicolli et al.(1989); Smedley et al. (2002)
Bengal Basin alluvial aquifer, Bangladesh	<0.5	BGS and DPHE (2001)
Soan-Sakesar Valley alluvial aquifer, Punjab, Pakistan	Avg 62	Afzal et al. (2000)
Colorado River catchment, USA	up to 1300	Engberg (1999)
Coast Range alluvial aquifer, San Joaquin Valley, California, USA	<1–2000	Deverel et al. (1994)
Sierra Nevada alluvial aquifer, San Joaquin Valley, California	<1	Deverel et al.(1994)
Central Barents groundwater, Norway	0.01–4.82	Reimann et al. (1998)
Slovakian groundwater	0.5–45	Rapant et al. (1996)
Pore water		
Baseline, estuarine Lake Macquarie, Australia	<0.2	Peters et al. (1999)
Smelter and power-station-impacted, Lake Macquarie, Australia	0.3–5.0	Peters et al. (1999)

selenium concentrations than surface waters because of more extensive water–rock interactions (Frankenberger and Benson, 1994; Jacobs, 1989).

11.2.6.3.1 Atmospheric precipitation

Selenium in rainfall is derived principally from earth-surface volatilization, volcanic sources, fossil-fuel combustion (especially coal), and the incineration of municipal wastes. Few determinations of selenium in atmospheric precipitation have been reported, but concentrations are usually very low. Hashimoto and Winchester (1967) found concentrations in the range 0.04–1.4 $\mu g\,l^{-1}$ (**Table 9**).

11.2.6.3.2 River and lake water

Selenate (Se(VI)) is only weakly adsorbed by oxides and clays at near-neutral pH. Hence, oxidation of Se(IV) to Se(VI) enhances selenium mobility and persistence in natural waters (see **Chapter 7.7**). High concentrations of selenate can occur in agricultural drainage waters in arid areas. Seleniferous soils, especially those derived from black shales, are common in central and western United States and irrigation can give rise to concentrations of selenate of several hundred micrograms per liter in drainage water. In water, it exists as selenic and selenious acids (Barceloux, 1999). Further concentration can occur in lakes by evapotranspiration. Well-documented cases of such situations include California (Kesterson Reservoir, Richmond Marsh, Tulare Basin, and Salton Sea), North Carolina (Belews Lake and Hyco Reservoir), Texas (Martin Reservoir), and Wyoming (Kendrick Reclamation Project) in the United States. Problems of selenium toxicity are also found in other semiarid areas. In the Soan-Sakesar Valley of Punjab, Pakistan, average selenium concentrations were 302 $\mu g\,l^{-1}$ ($n=13$) in streams and springs and 297–2100 $\mu g\,l^{-1}$ in lake water (three lakes) (Afzal et al., 2000). The highest concentrations were reported from low-lying, salinized areas.

The Colorado River catchment, Utah, USA, is also a seleniferous area. Median selenium concentrations in the Colorado River and its major tributaries are in the range of 1–4 $\mu g\,l^{-1}$ (Engberg, 1999), although values up to 400 $\mu g\,l^{-1}$ have been reported (NAS, 1976). Water samples from the Republican River Basin of Colorado in the United States indicated that nine sites contained concentrations above 0.005 $mg\,l^{-1}$ selenium, which is considered a high hazard for selenium accumulation in the planktonic food chain (May et al., 2001). Irrigation is believed to have been responsible for about 70% of the selenium reaching Lake Powell (Engberg, 1999). Selenium concentrations in the Cienega de Santa Clara wetlands on the east side of the Colorado River delta, Mexico, are also in the range of 5–19 $\mu g\,l^{-1}$ (García-Hernández et al., 2000). However, high selenium concentrations do not occur in all rivers in arid areas. For example, concentrations in the Jordan River average only 0.25 $\mu g\,l^{-1}$ (Nishri et al., 1999). Selenium concentrations in surface waters may be increased locally near sources of waste, including sewage effluent.

11.2.6.3.3 Seawater and estuaries

The main natural flux for selenium is via the marine system. Despite this, selenium concentrations in estuarine water and seawater are generally low. An average concentration of 0.17 $\mu g\,l^{-1}$ was estimated for seawater by Thomson et al. (2001). Dissolved concentrations in the range of 0.1–0.2 $\mu g\,l^{-1}$ have been reported in San Francisco Bay (Cutter, 1989). Zawislanski et al. (2001b) reported concentrations of 0.07–0.35 $\mu g\,l^{-1}$ in the nearby Carquinez Strait. Much of the selenium is thought to have been derived from industrial sources, including historical releases from oil refineries. During low-flow conditions, oil refineries contribute up to 75% of the total selenium load entering San Francisco Bay. Refineries processing oil derived from the neighboring San Joaquin Valley, California, produce effluent-containing selenium concentrations an order of magnitude greater than those in refinery effluent from Alaskan North Slope crude oil (Zawislanski and Zavarin, 1996).

11.2.6.3.4 Groundwater

As in the case of surface waters, the concentrations of selenium in groundwater are usually low and commonly below analytical detection limits (see **Chapter 11.10**). Concentrations tend to be higher in oxidizing groundwaters because the dominant form present, Se(VI), is less prone to adsorption by metal oxides than Se(IV). Elemental selenium is also unstable under oxidizing conditions. High selenium concentrations have been found under oxidizing conditions in groundwaters in some arid and semiarid areas as a result of evaporation. Extremely high concentrations (up to 1300 $\mu g\,l^{-1}$) have been reported from shallow wells in the upper reaches of the Colorado River catchment, Utah (Engberg, 1999).

Deverel and Fujii (1988) also reported concentrations in the range of <1–2000 $\mu g\,l^{-1}$ (**Table 9**) in shallow groundwater from Coast Range alluvial fan sediments near Kesterson Reservoir, California. Concentrations of <20 $\mu g\,l^{-1}$ were found in the middle fan deposits, but reached several hundreds of micrograms per liter in the lower fan deposits. Concentrations increased with groundwater salinity, probably as a result of leaching of soil salts by irrigation and subsequent evaporation. Deverel and Fujii (1988) found low concentrations of selenium in groundwater from the eastern side of the San Joaquin valley in alluvial sediments of the Sierra Nevada Formation. Values were generally less than 1 $\mu g\,l^{-1}$, probably as a result of reducing conditions in which selenium occurred in less mobile forms, notably Se(IV).

Selenium-rich groundwaters are also found in the semiarid regions of Argentina (**Table 9**). Nicolli et al. (1989) found concentrations up to 24 $\mu g\,l^{-1}$ in oxidizing groundwater from Córdoba province. Concentrations were correlated positively with salinity. Smedley et al. (2002) also found selenium concentrations in the range of <2–40 $\mu g\,l^{-1}$ ($n=34$) in oxidizing groundwaters from the neighboring province of La Pampa, with the highest concentrations in high-salinity shallow groundwaters in which selenium was concentrated by evaporation. No speciation studies were carried out, although selenate is likely to dominate. None of the groundwater samples in the Smedley et al. (2002) study exceeded the WHO guideline value of 40 $\mu g\,l^{-1}$ for selenium in drinking water.

In the Soan-Sakesar Valley of Punjab, Pakistan, the average selenium concentration in groundwater was 62 $\mu g\,l^{-1}$ ($n=29$) (Afzal et al., 2000). Again there was a positive correlation between salinity and selenium concentration. Most of the selenium in the groundwater was present as Se(VI).

Selenium concentrations in reducing groundwaters are very low or undetectable as a result of reduction to Se(IV). Concentrations in samples of the strongly reducing high-arsenic groundwaters of Bangladesh were $<0.5\ \mu g\ l^{-1}$ (BGS and DPHE, 2001). In the Triassic Sandstone aquifer of the English East Midlands, selenium concentrations varied from less than 0.06 to 0.86 $\mu g\ l^{-1}$ (**Table 9**). Concentrations were highest in the unconfined oxidizing part of the sandstone aquifer and fell abruptly to less than 0.06 $\mu g\ l^{-1}$ at and beyond the redox boundary (Smedley and Edmunds, 2002).

11.2.6.3.5 Sediment pore water

Few data are available for the selenium content of pore waters. However, Peters et al. (1999) reported concentrations of up to 5 $\mu g\ l^{-1}$ in estuarine pore waters from Mannering Bay (Lake Macquarie), New South Wales, Australia. Investigations followed concerns during the 1990s about high selenium concentrations in marine organisms from the area. Concentrations were highest in the upper 5 mm of the profile and were substantially higher throughout the profile than from nearby Nord's Wharf where concentrations were typically $<0.2\ \mu g\ l^{-1}$ selenium (i.e., below the detection limit). Although redox controls influenced the trends with depth, the high selenium concentrations in the uppermost sediments were thought to reflect contamination from smelter and power station inputs.

11.2.6.3.6 Mine drainage

Since selenium substitutes for sulfur in the structure of sulfide minerals, drainage from mineralized and mined areas may have high dissolved selenium concentrations (see **Chapter 11.5**). Acid seeps derived from oxidation of sulfide minerals draining the Moreno Shale in the Coast Ranges, USA, have selenium concentrations up to 420 $\mu g\ l^{-1}$ with concentrations of aluminum, manganese, zinc, and nickel in the milligram per liter range (Presser, 1994).

11.2.6.4 Selenium Species in Water, Sediment, and Soil

The behavior of selenium in the environment is similar in many respects to that of arsenic. Importantly, it also occurs naturally in several oxidation states and is therefore redox sensitive. Methylation and hydride formation are important, and sulfur and iron compounds play an important role in the cycling of selenium. Microbiological volatilization of organic selenium, particularly dimethylselenide, is known to be an important factor in the loss of selenium from some selenium-rich soils and waters (Frankenberger and Arshad, 2001; Oremland, 1994; Wu, 2004). Phytoplankton can also promote the production of gaseous selenium compounds in the marine environment (Amouroux et al., 2001).

Selenium occurs in natural waters principally in two oxidation states, Se(IV) and Se(VI). Elemental selenium, Se(0) (red and black forms), and selenide, Se(–II), are essentially insoluble in water and so selenate and selenite are the dominant aqueous forms. $Se(VI)O_4^{2-}$ occurs mainly in oxidizing waters while $HSe(IV)O_3^-$ and $Se(IV)O_3^{2-}$ dominate under reducing conditions (**Figure 9**). The concentration ratio of Se(IV) to Se(VI) species in natural waters does not necessarily follow that of other redox couples (e.g., Fe^{2+}/Fe^{3+}). This reflects the slow kinetics involved (White and Dubrovsky, 1994).

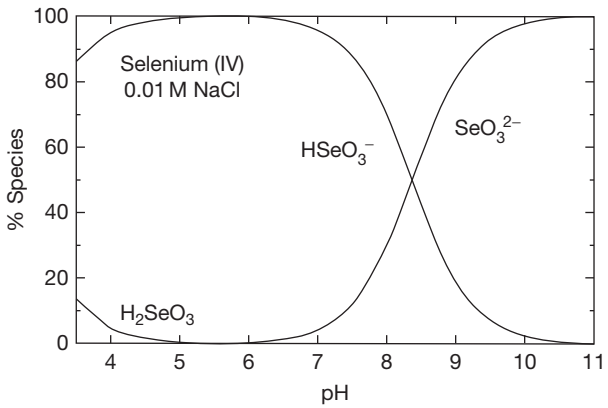

Figure 9 Speciation of selenium in a 0.01 M NaCl medium as a function of pH at 25 °C. The plot for Se(VI) is not shown as this is always dominated by SeO_4^{2-}.

Elemental selenium, selenides, and selenium sulfide salts are stable only in reducing acidic conditions and are largely unavailable to plants and animals. Zawislanski et al. (2001b) found a strong positive correlation between selenium and organic carbon in suspended particulate matter from San Francisco Bay, possibly reflecting reduction of selenium by organic matter. Strong positive correlations of particulate selenium with particulate iron and aluminum were also noted. The oxidation and reduction of selenium is related to microbial activity. For example, the bacterium *Bacillus megaterium* can oxidize elemental selenium to selenite.

It has been estimated that up to 50% of the selenium in some soils may be present as organic compounds, although few such compounds have been isolated and identified (Jacobs, 1989). In acidic and neutral soils, inorganic selenium occurs as insoluble Se(IV) compounds, and in neutral and alkaline soils as soluble and hence more bioavailable Se(VI) compounds (Allaway, 1968). Se(IV) is absorbed on to soil particle surfaces with a greater affinity than Se(VI) (Johnson et al., 2000). Selenomethionine has been extracted from soils and is 2–4 times more bioavailable to plants than inorganic selenite, although selenocysteine is less bioavailable than selenomethionine (Alloway, 1995; Davies, 1980; Frankenberger and Benson, 1994; Jacobs, 1989). The bioavailability of the different selenium species in soils can be summarized as:

$$\text{selenate} > \text{selenomethionine} > \text{selenocysteine} > \text{selenite} > \text{selenium metal}$$

In general, selenate is more available and more mobile than selenite in the environment, so selenium is much more bioavailable under oxidizing alkaline conditions.

An E_h–pH diagram for the system Se–O–S is given in **Figure 10** as a guide but, as in the case of arsenic, it is necessarily an oversimplification of a complex natural system. Se_2S_3 is not shown as no thermodynamic data are available for this species. It would probably displace native selenium (black) as the dominant phase under strongly reducing sulfur-rich conditions. The stability of Fe–Se minerals and the effects of selenium adsorption by metal oxides are not represented in the diagram.

Selenium is more readily reduced than arsenic. In the solid phase, elemental selenium dominates under strongly reducing

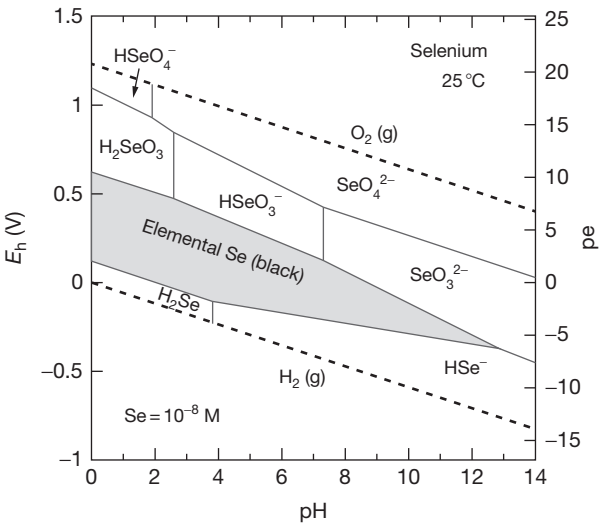

Figure 10 E_h–pH stability diagram for selenium at 25 °C, 1 bar total pressure. The stability field for water is shown by the dashed lines.

conditions with the gaseous H_2Se becoming important under acid, strongly reducing conditions. Organic selenides occur in biological materials. Some of these selenides are highly volatile.

The most detailed studies of selenium distribution and speciation have been carried out for seawater. Cutter and Cutter (2001) found that selenate had generally higher concentrations in marine waters from the southern (0.019 $\mu g\,l^{-1}$) than the northern hemisphere (0.014 $\mu g\,l^{-1}$). In contrast, selenite had low concentrations in seawater from the southern hemisphere (0.005 $\mu g\,l^{-1}$) with the highest concentrations in the equatorial region and below the Intertropical Convergence Zone (0.009 $\mu g\,l^{-1}$). Depth profiles of total dissolved selenium, selenite, and selenate in Atlantic seawater all showed surface-water depletion and deepwater enrichment, characteristic of nutrient-like behavior. In North Atlantic Deep Water, the Se(IV)/Se(VI) ratios were generally similar to those found in the eastern Atlantic and North Pacific (0.7), but waters originating in the southern polar regions were enriched in selenate and had low Se(IV)/Se(VI) ratios (~0.4). Organic selenide was found in surface ocean waters but was not detected in mid- or deepwaters.

Selenium profiles in sediments from the northeast Atlantic Ocean indicate concentrations of around 0.2–0.3 mg kg^{-1} in the oxic zone, and typically 0.3–0.5 mg kg^{-1} below the redox boundary, reflecting immobilization under reduced conditions (Thomson et al., 2001). Similar increases for cadmium, uranium, and rhenium have also been observed in the suboxic zone.

As with arsenic, microbiological processes are important in the reduction of selenium, principally through the microbial reduction of Se(IV) and Se(VI) (Oremland et al., 1990). Oremland (1994) found that the areal rate of dissimilatory selenium reduction in sediments from an agricultural evaporation pond in the San Joaquin Valley was about 3 times lower than for denitrification and 30 times lower than for sulfate reduction. Stable-isotope studies of water in the Tulare Lake Drainage District wetland, California, indicated little selenium isotope fractionation (Herbel et al., 2002b). This suggested that the primary source of reduced selenium was selenium assimilation by plants and algae, followed by deposition and mineralization rather than the direct bacterial reduction of Se(VI) or Se(IV).

11.2.7 Pathways and Behavior of Selenium in the Natural Environment

11.2.7.1 Release from Primary Minerals

As noted earlier, the principal natural sources of selenium in water are likely to be sulfides or metal oxides containing adsorbed selenium, especially Se(IV). Coal can be an additional primary source of selenium either directly through oxidation or indirectly via atmospheric precipitation following combustion. Selenium is readily oxidized during the weathering of minerals. Seleniferous groundwater areas such as those occurring in the United States and Pakistan are most common where underlain by selenium- and organic-rich shales that release selenium on weathering. Selenium-rich groundwaters tend to be found in semiarid areas under irrigation. Examples are central and western United States (Deverel et al., 1994) and parts of Pakistan (Afzal et al., 2000).

11.2.7.2 Adsorption of Selenium by Oxides and Clays

High soil organic matter, iron oxyhydroxide (HFO) and clay mineral content can all absorb or bind selenium to the soil, with the main control on selenium concentration in many soils being the organic matter content. Selenium can become concentrated in organic matter and organic-rich sediments (Fordyce et al., 2010; Shand et al., 2010). In contrast to arsenic, the reduced form of selenium, Se(IV), is very strongly adsorbed by HFO. This may account in part for the very low selenium concentrations in many strongly reducing environments. Furthermore, also in contrast with arsenic, the oxidized form of selenium, Se(VI), is less strongly adsorbed to HFO than the reduced species. These differences, also reflected by other oxide-based sorbents including clays, account for the markedly different behavior of arsenic and selenium in natural waters.

The behavior of soils mirrors that of pure oxides (Goldberg, 1985). In acidic soils, selenium is likely to occur mainly as Se(IV) strongly adsorbed to iron oxides. Less commonly, Se(IV) may form highly insoluble iron compounds such as ferric selenite ($Fe_2(OH)_4SeO_3$) or iron selenide (FeSe). In alkaline, oxidized, and selenium-rich soils, most of the selenium is likely to be present as Se(VI), which is very weakly adsorbed. Furthermore, there are no common insoluble selenate minerals. Hence, selenate accumulates in soluble form, particularly in arid and semiarid areas where evaporation tends to concentrate selenium along with other soluble salts (Deverel et al., 1994).

The strong affinity of iron oxides for Se(IV) has been well documented (Dzombak and Morel, 1990) and calculations based on the Dzombak and Morel (1990) diffuse double-layer model and default HFO database show the principal response to pH and redox speciation changes (**Figure 11**). The selenate species is less strongly adsorbed by iron oxides at near-neutral pH than the selenite species (**Figure 11**). Clay minerals (Bar-Yosef and Meek, 1987) also adsorb Se(IV).

The iron oxide and clay content of soils and sediments can affect the bioavailability of selenium markedly. The strong pH

dependence of adsorption is an important control. Maximum adsorption occurs between pH 3–5 and decreases as the pH rises. Organic matter also removes selenium from soil solution, possibly as a result of the formation of organometallic complexes. Addition of phosphate to soils increases selenium uptake by plants because the PO_4^{3-} ion displaces selenite from soil particles, making it more bioavailable. Conversely, increasing the concentrations of phosphate in soils can dilute the selenium content of vegetation by inducing increased plant growth (Frankenberger and Benson, 1994; Jacobs, 1989)

11.2.7.3 Selenium Transport

The transport of selenium is related strongly to its speciation. The weak adsorption of selenate by soil and aquifer materials, especially in the presence of high SO_4^{2-} concentrations, means that it is relatively unretarded by groundwater flow (Kent et al., 1995). There is also little likelihood that insoluble metal selenates, such as $CaSe(VI)O_4 \cdot 2H_2O$, will limit Se(VI) solubility under oxidizing conditions (White and Dubrovsky, 1994). By contrast, the strong adsorption tendency of Se(IV) and low solubility of Se(0) and Se(–II) species mean that transport of selenium is strictly limited under reducing conditions.

The strong contrast in selenium mobility between reducing and oxidizing conditions means that changes in redox conditions in soils, sediments, or aquifers can result in significant changes in selenium concentrations in water and crops.

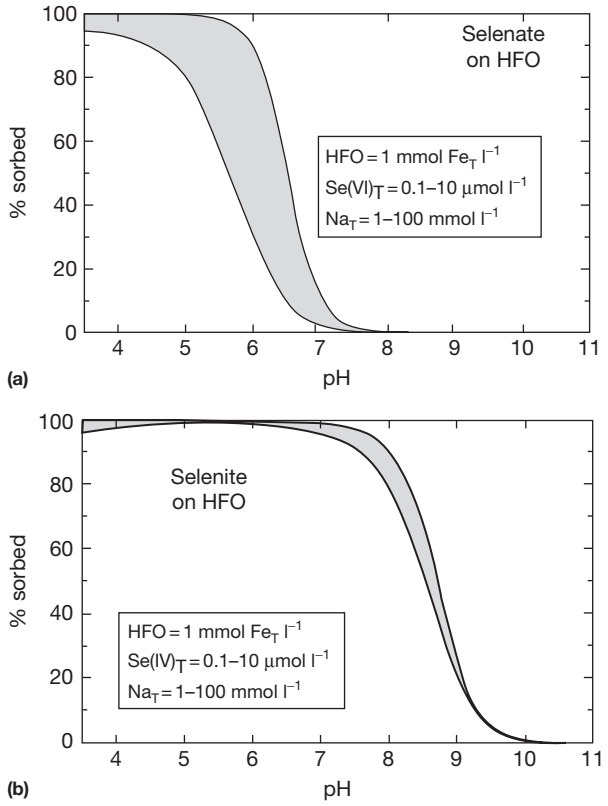

Figure 11 Calculated % adsorption of (a) oxidized and (b) reduced selenium species by hydrous ferric oxide (HFO). Infilled areas show the adsorption for a range of total Se concentrations (0.1–10 μmol l^{-1}) and ionic strengths (1–100 mmol l^{-1}).

For example, the accumulation of selenium in the reduced bottom sediments of the Salton Sea, California, could be mobilized if engineered changes to transfer water out of the Salton Sea Basin lead to oxidation of the sediments (Schroeder et al., 2002). Such a process has already occurred at Kesterson Reservoir (**Section 11.2.7.4.1**). The change of land use, for example, from wet paddy soils to dryland agriculture, could also lead to an increase in the uptake of selenium by crops (Yang et al., 1983).

11.2.7.3.1 Global fluxes

Selenium is dispersed through the environment and is cycled by biogeochemical processes involving rock weathering, rock–water interactions, and microbiological activity. Estimates of the selenium fluxes through the atmosphere, land, and oceans indicate that the anthropogenic flux now exceeds the marine flux, the principal natural pathway (**Table 10**).

The global flux of selenium from land to the oceans via rivers has been estimated as 15 380 tonnes per year (Haygarth, 1994). The cycling of selenium from land to water is poorly understood, but approximately 85% of the selenium in rivers is thought to be in particulate rather than dissolved form.

Typical concentrations of selenium in seawater are around 0.1–0.2 μg l^{-1} (**Table 9**) with an estimated mean residence time of 70 years in the mixed layer and 1100 years in the deep ocean. The oceans are therefore an important sink for selenium (Haygarth, 1994; Jacobs, 1989). Biogenic volatilization of selenium from seawater to the atmosphere is estimated to be 5000–8000 tonnes per year. Amouroux et al. (2001) have demonstrated that biotransformation of dissolved selenium in seawater by blooms of phytoplankton in the spring is a major pathway for the emission of gaseous selenium to the atmosphere. Hence, oceans are an important part of the selenium cycle.

11.2.7.3.2 Selenium fluxes in air

In air, selenium is mostly bound to particles with volatilization of selenium from volcanoes, soils, sediments, the oceans, microorganisms, plants, animals, and industrial activity, all contributing to selenium in the atmosphere. Natural background concentrations of selenium in nonvolcanic areas are only around 0.01–1 ng m^{-3}, but the short residence time, usually

Table 10 Global selenium fluxes

Source	*Pathways*	*Se flux (tonne year^{-1})*
Anthropogenic releases	Mining, anthropogenic releases to atmosphere, water, land, and oceans	76 000–88 000
Marine loss	Volatilization, sea salt suspension, into marine biota, sediment transfer to land	38 250
Terrestrial loss	Volatilization, particle resuspension, dissolved and suspended load to oceans	15 380
Atmospheric loss	Wet and dry deposition to the oceans and land	15 300

Source: Haygarth PM (1994) Global importance and cycling of selenium. In: Frankenberger WT and Benson S (eds.) *Selenium in the Environment*, pp. 1–28. New York: Marcel Dekker.

a matter of weeks, makes the atmosphere a rapid transport route for selenium. Most urban air has concentrations of 0.1–10 ng m^{-3} (WHO, 1996, 2011). Higher levels may be found in the vicinity of coal-fired thermal power stations (90 ng m^{-3}; background level, 10 ng m^{-3}) with selenium in an amorphous state (Giere et al., 2006; Jayasekher, 2009). For example, in the United Kingdom, soil samples collected between 1861 and 1990 by the Rothamstead Agricultural Experimental Station show that the highest concentrations of selenium were between 1940 and 1970, coinciding with a period of intensive coal use. The decline in selenium in herbage more recently is thought to reflect a switch to fuel sources such as nuclear, oil, and gas (Haygarth, 1994).

Volatilization of selenium into the atmosphere results from microbial methylation of selenium from soil, plant, and water and is affected by the availability of selenium, the presence of an adequate carbon source, oxygen availability, and temperature (Frankenberger and Benson, 1994; Jacobs, 1989).

Most gaseous selenium is thought to be in the dimethylselenide (DMSe) form and it is estimated that terrestrial biogenic sources contribute 1200 tonnes per year of selenium to the atmosphere. Atmospheric dust derived from volcanoes and wind erosion of the Earth's surface (180 tonnes per year) and suspended sea salts (550 tonnes per year) from the oceans are also significant sources of atmospheric selenium. Particle-bound selenium can be transported several thousands of kilometers before deposition. Wet deposition from rain, snow, and other types of precipitation is thought to contribute 5610 tonnes per hectare per year of selenium to the terrestrial environment. In the United Kingdom, for example, wet deposition has been shown to account for 76–93% of the total with >70% in soluble form. Near-to-point sources of selenium, for example, from industry and atmospheric deposition, can account for 33–82% of the selenium present on the leaves of plants (Frankenberger and Benson, 1994; Jacobs, 1989). A study of selenium in plant rings near a village close to coal-fired power stations burning seleniferous coal in China reported much higher concentrations than in plants collected away from the source (Liu et al., 2007).

11.2.7.3.3 Soil–water–plant relationships

Despite selenium being essential for some green algae such as *Chlamydomonas*, it has not been shown to be essential for higher plants (Novoselov et al., 2002; Pilon-Smits and LeDuc, 2009). The selenium concentrations in plants generally reflect those of the soils in which they are grown. An important factor which may determine whether or not selenium-related health problems affect man and animals is the variable capacity of different plant species to accumulate selenium (Alloway, 1995; Frankenberger and Benson, 1994; Jacobs, 1989; Oldfield, 1999). Plants with ≥25 mg kg^{-1} selenium may cause acute poisoning of animals, but these plants are generally distasteful and not eaten unless the animals are especially hungry (Knight and Walter, 2001).

Rosenfield and Beath (1964) classified plants into three groups based on their selenium uptake from seleniferous soils. They are: (1) selenium accumulator plants which can contain >1000 mg kg^{-1} selenium and grow well on high-selenium soils; (2) secondary selenium absorbers with concentrations in the range of 50–100 mg kg^{-1}; and (3) others which include grains and grasses that can contain up to 50 mg kg^{-1} selenium. Selenium concentrations can range from 0.005 to 5500 mg kg^{-1} in selenium accumulators, with most plants containing less than 10 mg kg^{-1}.

Plants that require selenium for growth are called obligate accumulators; they are capable of accumulating 10 times the amount of selenium present in soil and include *Astragalus*, *Conopsis*, *Xylorhiza*, and *Stanleya*. Plants known as facultative accumulators do not require selenium for growth, but will bind selenium in its organic forms if it is present in the soil; these plants belong to the genera *Acacia*, *Artemisia*, *Aster*, *Atriplex*, *Castilleja*, *Penstemon*, and *Grindelia* (Knight and Walter, 2001). Accumulators belonging to the plant genera *Astragalus*, *Haplopappus*, and *Stanleya* are commonly found in the semiarid seleniferous environments of the western United States and elsewhere and are used as indicators of high-selenium environments, although other species of these genera are non-accumulators (Alloway, 1995; Jacobs, 1989).

The exclusion of selenium from the proteins of accumulator plants is thought to be the basis for their selenium tolerance with selenium metabolism based mainly on water-soluble, nonprotein forms such as selenium–methylselenomethionine (Jacobs, 1989). The 'garlic' odor characteristic of selenium-accumulating plants reflects the volatile organic compounds DMSe and dimethyldiselenide. Plants can suffer selenium toxicity as a result of selenium competition with essential metabolites for biochemical sites, replacement of essential ions by selenium, mainly major cations, selenate occupation of the sites of essential groups such as phosphate and nitrate, or selenium substitution in essential sulfur compounds.

Experimental evidence suggests that there is a negative correlation between very high soil selenium concentrations and plant growth. Alfalfa yields have been shown to decline when extractable selenium in soil exceeds 500 mg kg^{-1}. Yellowing, black spots, and chlorosis of plant leaves and pink root tissue can occur (Frankenberger and Benson, 1994; Jacobs, 1989). Phytotoxicity in nature has been reported only from China, where high selenium concentrations in soil caused discoloration of maize corn-head embryos and also affected the growth and yield of wheat and pea crops, respectively (Yang et al., 1983).

In alkaline soils, selenium is often present as selenite, which is bioavailable to plants and may prevent selenium deficiency in people who eat them. The oxidation state of selenium is critical in determining its availability in the food chain. For example, in neutral to alkaline soils, Se^{6+} (selenate) is the dominant state. This form of selenium is generally more soluble and mobile in soils and is readily available for plant uptake than selenite (Se^{4+}), which has lower solubility and greater affinity for adsorption on soil particle surfaces (Mikkelsen et al., 1989).

Food crops generally have a low selenium tolerance but most crops have the potential to accumulate selenium in quantities toxic to animals and humans (Jacobs, 1989). In general, root crops contain the highest selenium concentrations (**Table 11**) with plant leaves containing a higher concentration than the tuber. For example, Yang et al. (1983) noted that selenium concentrations in vegetables (0.3–81.4 mg kg^{-1}) were generally higher than in cereal crops (0.3–28.5 mg kg^{-1} in rice and maize) in seleniferous regions of China. Brassicas

Table 11 Examples of Se contents in various crops grown in the United States

US crop type	*Average Se (mg kg^{-1} dry wt)*
Roots and bulbs	0.407
Grains	0.297
Leafy vegetables	0.110
Seed vegetables	0.066
Vegetable fruits	0.054
Tree fruits	0.015

Source: Jacobs LW (1989) *Selenium in Agriculture and the Environment*. Madison, WI: Soil Science Society of America. SSSA Special Publication 23.

are unable to distinguish selenium from S and so tend to accumulate selenium. Turnip leaves can have particularly high concentrations with an average of 460 mg kg^{-1} ranging up to 25 000 mg kg^{-1} compared to an average of 12 mg kg^{-1} in the tuber. *Boletus pinicola* and *Boletus edulis* species of edible mushroom collected in Galicia, Spain, were found to have mean selenium concentrations in the hymenophore of 74.93 and 52.7 mg kg^{-1} dry weight, resulting in a recommendation to consume in moderation (Melgar et al., 2009).

In moderate to low selenium environments, alfalfa (*Medicago* sp) has been shown to take up more selenium than other forage crops. Crop species grown in low-selenium soils generally show little difference in selenium uptake, so changing the type of crop grown makes little impact. An exception has been reported from New Zealand, where changing from white clover to the grass *Agrostis tenuis* increased the selenium content of fodder (Davies and Watkinson, 1966).

11.2.7.4 Case Studies

11.2.7.4.1 Kesterson Reservoir, USA

One of the best-documented cases of selenium toxicity in animals occurred at Kesterson Reservoir, California, USA (Jacobs, 1989; Wu et al., 2000). Soil irrigation in the western San Joaquin valley of California began in the late 1800s and accelerated particularly in the 1930s–1940s. Irrigation water was taken from both surface water and groundwater (Deverel and Fujii, 1988). During the 1970s, flow into the reservoir was mainly surface water, but over the period 1981–1986 almost all the inflow was from shallow agricultural drainage for which the reservoir acted as a set of evaporation ponds. This inflow contained 250–350 μg l^{-1} selenium, mostly present as bioavailable selenate (Se(VI)).

The primary source of the Se is believed to have been pyrite in shales, particularly the Upper Cretaceous–Paleocene Moreno Shale and the Eocene–Oligocene Kreyenhagen Shale. Concentrations of selenium in these formations range up to 45 mg kg^{-1} with median concentrations of 6.5 and 8.7 mg kg^{-1}, respectively (Presser, 1994). The concentration of selenium in the surface sediments (0–0.3 m depth) of the old playas is in the range 1–20 mg kg^{-1}, reflecting the historical accumulation of selenium from the selenium-rich drain water. Deeper sediments typically contain much lower selenium concentrations of 0.1–1 mg kg^{-1} (Tokunaga et al., 1994).

Between 1983 and 1985, the US Wildlife Service compared the biological impact of the high selenium in the Kesterson Reservoir region to that of the adjacent Volta Wildlife area, which was supplied with water containing normal selenium concentrations. The research showed that the high concentrations of selenium in the irrigation waters were having a detrimental effect on the health of fish and wildlife (Tokunaga et al., 1994). Health effects on birds in the Kesterson Reservoir area were very marked, with 22% of eggs containing dead or deformed embryos. The developmental deformities included missing or abnormal eyes, beaks, wings, legs, and feet, as well as hydrocephaly. It has been estimated that at least 1000 adult and young birds died between 1983 and 1985 as a result of consuming plants and fish containing 12–120 times the normal amount of selenium. No overt adverse health effects were noted in reptile or mammalian species, but the concentrations of selenium present were of concern in terms of bioaccumulation through the food chain.

These findings led the US Bureau of Reclamation to halt the discharge of agricultural drainage to the reservoir. The reservoir was also dewatered and the lower parts were infilled to prevent groundwater rising to the soil surface. Bioremediation based on microbial reduction of selenite and selenate to insoluble Se(0) or methylation of these species to DMSe was used to immobilize the selenium. Field trials demonstrated that microorganisms, particularly *Enterobacter cloacea*, were effective in reducing selenium to insoluble Se(0) and that the process was stimulated by the addition of organic matter (Wu et al., 2000). The area was planted with upland grass. Biological monitoring has demonstrated that selenium concentrations in the water and vegetation at Kesterson are now much lower and largely within safe limits. By 1992, concentrations of selenium in surface pools that formed after periods of rainfall were in the range 3–13 μg l^{-1}.

11.2.7.4.2 Enshi, China

Human selenosis has been reported from Enshi district, Hubei province, China. Between 1923 and 1988, 477 cases of human selenosis were reported, 338 resulting in hair and nail loss and disorders of the nervous system. In one small village, the population was evacuated after 19 out of 23 people suffered nail and hair loss and all the livestock had died from selenium poisoning. Cases of selenosis in pigs reached a peak between 1979 and 1987, when 280 out of 2238 pigs were affected in one village.

No human cases of selenium toxicity have been reported in recent years, but animals continue to show health problems as a result of the high concentrations of selenium in the environment (Fordyce et al., 2000b; Yang et al., 1983). Yang et al. (1983) were the first to compare concentrations of selenium in soil, crops, drinking water, human urine, blood, nail, and hair samples from the Enshi area with other regions of China. They demonstrated that the endemic selenium poisoning was related to the occurrence of selenium-enriched Permian coal deposits. These contained selenium concentrations of up to 6470 mg kg^{-1}. Selenium concentrations in the soil, food, and human samples from areas underlain by these rocks were up to 1000 times higher than in samples from nearby low-selenium areas and dietary intakes of selenium greatly exceeded the recommended international and Chinese

Table 12 Deficiency and toxicity thresholds for selenium in various media

Medium	*Units*	*Deficient*	*Marginal*	*Moderate*	*Adequate*	*Toxic*	*Criterion*	*References*
Soils								
Worldwide	mg kg^{-1}	0.1– 0.6					Animal health	Various
Chinese soils	mg kg^{-1}	0.125	0.175	0.400		>3	Human health	Tan (1989)
Chinese soil water-soluble	mg kg^{-1}	0.003	0.006	0.008		0.020	Human health	Tan (1989)
Vegetation								
Worldwide	mg kg^{-1}	<0.1			0.1–1.0	3–5	Animal health	Jacobs (1989), Levander (1986)
Chinese cereals	mg kg^{-1}	0.025	0.040	0.070		>1	Human health	Tan (1989)
Animals								
Food, chronic exposure	mg kg^{-1}	<0.04			0.1–3	3–15	Animal health	Jacobs (1989), Mayland (1994)
Cattle and sheep liver	mg kg^{-1}	0.21					Animal health	WHO (1986)
Cattle and sheep blood	mg kg^{-1}	<0.04	0.05–0.06		0.07–0.10		Animal health	Mayland (1994)
Humans								
Chinese human hair	mg kg^{-1}	0.200	0.250	0.500		>3	Human health	Tan (1989)
Urinary excretion rate	μg day^{-1}				10–200		Human health	Oldfield (1999)
Food	mg kg^{-1}	<0.05				2–5	Human health	WHO (1996, 2011)
Ref. dose US EPA	mg kg^{-1} day^{-1}				0.005		Human health	US EPA (2011)
Human diet (WHO)	μg day^{-1}	<40			55–75	>400	Human health	WHO (1996, 2011)
Drinking water (WHO)	μg l^{-1}					>40	Maximum admissible concentration	WHO (2011)

thresholds (Table 12). Locally grown crops constituted 90% of the diet in the Enshi area with cereal crops (rice and maize) accounting for 65–85% of the selenium intake. In addition to exposure through the food chain, villagers also mined the coal for fuel and used the residues as a soil conditioner.

Concentrations of selenium in the soils and foodstuffs can vary markedly from deficient to toxic in the same village, depending on the outcrop of the coal-bearing strata (Fordyce et al., 2000b). Villagers were therefore advised to avoid cultivating areas underlain by the coal or using coal ash to condition the soil. The outbreaks of human selenosis in the late 1950s and early 1960s coincided with drought and failure of the rice crop, leading to an increased dependence on locally produced vegetables and maize. As the source of food crops diversified, incidence of the disease diminished.

11.2.7.4.3 Soan-Sakesar Valley, Pakistan

The Soan-Sakesar valley is situated in the center of the Salt Range mountains in Punjab, northeast Pakistan. The geochemistry of the waters in the area has been studied extensively by Afzal et al. (1999, 2000). The average altitude of the Soan-Sakesar valley is 762 m and the mean annual rainfall (1984–1994) is 613 mm. The average summer temperature is 33 °C and average winter temperature 3 °C, with periods below freezing. Average evaporation is estimated to be about 950 mm $year^{-1}$. The area is essentially a closed basin, although ephemeral streams and rivers, including the River Soan, flow seasonally westwards toward the River Indus.

The area is covered by sedimentary rocks mainly of Tertiary age. The valley lies between two parallel east–west ridge systems. Wheat and maize are grown in the area. Three quite large brackish-saline lakes (3–14 km^2) occur within synclinal structures formed by the folding of Eocene rocks. The largest and most saline lake, Lake Uchhali, has a TDS (total dissolved solids) of about 36 g l^{-1}, a nitrate concentration of 28 mg l^{-1}, and a boron concentration of nearly 1 mg l^{-1}. It also contains a selenium concentration of 2.1 mg l^{-1}. The major-element chemistry is dominated by Na–Mg–Cl–SO_4. The majority of surface waters in the region exceeded the WHO guideline value of 40 μg l^{-1} for selenium in drinking water, with an observed mean concentration in streams and springs of 302 μg l^{-1} (Table 13).

The Soan-Sakesar aquifer consists of two major formations, a freshwater Sakesar limestone (Chharat Group) of the Eocene age and a brackish formation (Rawalpindi Group). Groundwater recharge is mainly from infiltration through the alluvial fans during times of stream flow. Groundwater has been used extensively for irrigation and has led to substantially altered groundwater flow patterns. The water table is generally 4–7 m bgl and varies by 1–2 m seasonally.

The groundwaters of the area also contain a high salt content with a large majority of selenium concentrations in excess of the WHO guideline value for drinking water and the FAO (Food and Agriculture Organization) guideline value for irrigation water (20 μg l^{-1}). The median concentrations of NO_3 and boron in groundwaters from the area were 27.5 and 0.52 mg l^{-1}, respectively. The Sakesar Formation is dominated by shale. This probably forms the ultimate source of selenium. Selenium concentrations, as well as the overall dissolved salt concentration, were greatest in low-lying areas where a shallow water table existed and where intense evaporation of soil water had occurred.

Table 13 Average concentrations (mg l^{-1}) in groundwater and stream/spring samples from the Soan-Sakesar valley, Pakistan

Parameter	*Lake Uchhali (n = 3)*	*Groundwaters (n = 29)*	*Streams/springs (n = 13)*
Ca	159	22	64
Mg	1770	62	104
Na	9890	130	323
K	254	14	25
Alkalinity	584	234	577
Cl	9530	89	216
SO_4	14300	243	551
NO_3	28	30	20
Li	2.86	0.3	0.65
B	0.96	0.61	0.36
P	0.48	0.17	0.52
SiO_2	5.1	3.7	5.2
Se	2.10	0.062	0.302
Mo	0.02	0.021	0.019

Source: Afzal S, Younas M, and Ali K (2000) Selenium speciation studies from Soan-Sakesar valley, Salt Range, Pakistan. *Water International* 25: 425–436.

Selenium speciation confirmed that all the waters were dominated by selenate with 10–20% selenite (Afzal et al., 2000). A small percentage of the selenium was present as organic selenium in the surface waters but this was absent from the groundwaters. Volatilization of selenium from the lakes was suspected but not proven. It is likely that selenate was reduced to selenite or elemental selenium in the anoxic sediments.

11.2.7.4.4 Selenium deficiency, China

In contrast, selenium deficiency has been implicated in several human diseases, most notably KD and KBD. KD is an endemic selenium-responsive cardiomyopathy that mainly affects children and women of child-bearing age and is named after Keshan County in northeast China (Wang and Gao, 2001). During the years of peak KD prevalence (1959–70), 8000 cases and up to 3000 deaths were reported annually (Tan, 1989). The disease occurred in a broad belt from northeast to southwest China where subsistence farmers depended on local food supplies. White muscle disease in animals occurred in the same areas. In areas with KD in China, selenium levels in the soil are around 0.112 mg kg^{-1} compared to an average of 0.234 mg kg^{-1} in nonendemic areas of the world (WHO, 1986) where selenium may occur in its inorganic form as selenide, selenate, and selenite. Grain crops in the affected areas contained <0.04 mg kg^{-1} selenium, which led to extremely low dietary intakes (10–15 μg selenium per day) in the local population. A very low selenium status in the affected population was indicated by selenium concentrations in hair of <0.12 mg kg^{-1} (Tan, 1989; Xu and Jiang, 1986; Yang and Xia, 1995). In Tibet, soil selenium concentrations in KBD areas were lower than those in nondisease areas, and the mean concentrations of soil selenium in Tibet were lower than the average of China (0.29 mg kg^{-1}), with a close relationship between soil selenium concentrations and KBD in Tibet (Li et al., 2009b). Supplementation with 50 μg selenium per day prevented the condition, but had no effect on those already showing signs of disease.

The precise biological function of selenium in KD is unclear and seasonal variations in prevalence suggested the involvement of a virus. High levels of the Coxsackie B virus were found in KD patients (Li et al., 2000). Work by Beck (1999) showed that a normally benign strain of the Coxsackie B3 virus becomes virulent in selenium- or vitamin E-deficiency conditions.

The incidence of the disease has fallen in recent years as a result of selenium supplementation and improved economic conditions in China generally (Burk, 1994). The evidence of viral mutogeny in the presence of selenium deficiency has important implications for many infections. Selenium deficiency may increase the likelihood of dying from Human Immunodeficiency Virus (HIV)-related diseases (Baum et al., 1997) and may have exacerbated the incidence of AIDS in parts of Africa.

The relation between selenium deficiency and KD in Zhangjiakou District, China, has been described in detail by Johnson et al. (2000). Soils in the villages with a high prevalence of KD were found to be black or dark brown, with a high organic matter content and lower pH than other soils in the region. Although the soil in the KD-affected areas contained a high total selenium concentration, the selenium was strongly bound by soil organic matter and it was not in a bioavailable form (Johnson et al., 2010). Water-soluble selenium concentrations in the villages with a high prevalence of KD were lower than deficiency threshold values (geometric mean, 0.06 μg l^{-1}; threshold, 3 μg l^{-1}).

The study concluded that when the bioavailability of selenium is low, any factor that further reduces its bioavailability and mobility may be critical. Adding selenium fertilizer to crops rather than to soils was recommended to increase the selenium concentrations in local diets. No cases of KD have been reported since 1996 as the diet has become more diversified as a result of improvements in economic conditions and transport.

KBD, named after the two Russian scientists who first described it in the late 1800s, is an endemic osteoarthropathy which causes deformity of joints. It is characterized by impaired movement, commonly with shortened fingers and toes and in extreme cases, dwarfism (Levander, 1986; Tan, 1989; WHO, 1993). In China, the distribution of the disease is similar to KD in the north, but the links with selenium deficiency are less clear. Iodine supplementation of the diets of children and nursing mothers, together with 0.5–2.0 mg sodium selenite a week for 6 years, reduced the disease prevalence from 42% to 4% in children aged 3–10 years (WHO, 1987). As with KD, other factors have been implicated in the pathogenesis of KBD. These include drinking water high in humic acids, greater fungal (mycotoxin) contamination of grain, and iodine deficiency (Peng et al., 1999; Suetens et al., 2001). KBD also occurs in Siberia, North Korea, and, possibly, parts of Africa.

11.2.8 Concluding Remarks

The recent surge of research on the behavior of arsenic in the environment has followed the discovery of human health problems linked to high concentrations of the element in some groundwaters, soils, and contaminated land. Fewer studies of selenium have been undertaken , although serious health

problems related to selenium toxicity or deficiency have been reported. There have also been many studies on the distribution of arsenic, and more recently selenium, for metalliferous, especially gold, exploration.

This chapter has outlined the main effects of arsenic and selenium on human and animal health, their abundance and distribution in the environment, sampling and analysis, and the main factors controlling their speciation and cycling. Such information should help to identify aquifers, water resources, and soils at risk from high concentrations of arsenic and selenium, and areas of selenium deficiency. Human activity has had, and is likely to continue to have, a major role in releasing arsenic and selenium from the geosphere and in perturbing the natural distribution of these and other elements over the Earth's surface.

Arsenic and selenium demonstrate many similarities in their behavior in the environment. Both are redox-sensitive and occur in several oxidation states under different environmental conditions. Both partition preferentially into sulfide minerals and metal oxides and are concentrated naturally in areas of mineralization and geothermal activity. Also, both elements occur as oxyanions in solution and, depending on redox status, are potentially mobile in the near-neutral to alkaline pH conditions that typify many natural waters. However, some major differences also exist. Selenium is immobile under reducing conditions, while the mobility of arsenic is less predictable and depends on a range of other factors. Selenium also appears to partition more strongly with organic matter than does arsenic.

While concern with arsenic in the environment relates principally to toxicity conditions, concerns with selenium relate to both deficiency and toxicity conditions. The optimum range of selenium concentrations for health is narrow. In certain environments, high intakes of arsenic or selenium, or very low intakes of selenium, can occur, potentially leading to a wide range of disease conditions, not all of which are well understood and some of which may not yet have been recognized.

Many of the health and environmental problems caused by arsenic and selenium were not predicted until recently because of a lack of knowledge of the distribution and behavior of arsenic and selenium in the environment. Recent improvements in understanding have been aided by improved and cost-effective analytical techniques and more powerful data processing, which have made it easier to prepare high-resolution geochemical maps. Also, modern digital datasets of geochemical and hydrochemical data are used increasingly in modeling studies to estimate element speciation, bioavailability, and risk.

The discovery of high concentrations of arsenic in groundwater from parts of the Bengal Basin of Bangladesh and West Bengal and elsewhere after several years of groundwater development has highlighted the need to analyze for a wide range of water-quality parameters before using such water sources. With the advent of modern multielement analytical techniques capable of measuring arsenic and selenium at environmentally relevant concentrations on an almost routine basis, it should be possible to include arsenic and selenium in more geochemical and hydrochemical surveys and thereby acquire a much better picture of their distribution, behavior, and role in the environment.

Acknowledgments

The authors would like to thank Kirk Nordstrom for an early copy of his review of the thermodynamics of the As–O–S system and also an anonymous reviewer for constructive comments about the microbiology of arsenate reduction. The contribution of David Kinniburgh, Pauline Smedley, Fiona Fordyce, and Ben Klinck to the chapter is published with the permission of the Executive Director of the British Geological Survey (Natural Environment Research Council).

References

Abdullah MI, Shiyu Z, and Mosgren K (1995) Arsenic and selenium species in the oxic and anoxic waters of the Oslofjord, Norway. *Marine Pollution Bulletin* 31: 116–126.

Adkins R, Walsh N, Edmunds W, and Trafford JM (1995) Inductively coupled plasma atomic emission spectrometric analysis of low levels of selenium in natural waters. *Analyst* 120: 1433–1436.

Afzal S, Younas M, and Ali K (2000) Selenium speciation studies from Soan-Sakesar valley, Salt Range, Pakistan. *Water International* 25: 425–436.

Afzal S, Younas M, and Hussain K (1999) Selenium speciation of surface sediments from saline lakes of the Soan-Sakesar Valley Salt-Range, Pakistan. *Water Quality Research Journal of Canada* 34: 575–588.

Aggarwal PK (2000) *Preliminary Report of Investigations – Isotope Hydrology of Groundwater in Bangladesh: Implications for Characterization and Mitigation of Arsenic in Groundwater*. Vienna: International Atomic Energy Agency.

Aggett J and O'Brien GA (1985) Detailed model for the mobility of arsenic in lacustrine sediments based on measurements in Lake Ohakuri. *Environmental Science & Technology* 19: 231–238.

Aggett J and Kriegman MR (1988) The extent of formation of arsenic (III) in sediment interstitial waters and its release to hypolimnetic waters in Lake Ohakuri. *Water Research* 4: 407–411.

Ahmann D, Krumholz LR, Hemond HF, Lovley DR, and Morel FMM (1997) Microbial mobilization of arsenic from sediments of the Aberjona watershed. *Environmental Science & Technology* 31: 2923–2930.

Ahmann D, Roberts AL, Krumholz LR, and Morel FMM (1994) Microbe grows by reducing arsenic. *Nature* 371: 750.

Ahmed KM, Hoque M, Hasan MK, Ravenscroft P, and Chowdhury LR (1998) Occurrence and origin of water well methane gas in Bangladesh. *Journal of the Geological Society of India* 51: 697–708.

Aihua Z, Xiaoxin H, Xianyao J, Peng L, Yucheng G, and Shouzheng X (2000) The progress of study on endemic arsenism due to burning arsenic containing coal in Guizhou province. *Metal Ions in Biology and Medicine* 6: 53–55.

Allaway WH (1968) Control of environmental levels of selenium. *Trace Substances in Environmental Health* 2: 181–206.

Alloway BJ (1995) *Heavy Metals in Soils*. London: Blackie Academic.

American Society for Testing and Materials (2010) *Annual Book of ASTM Standards*. West Conshohocken, PA: American Society for Testing and Materials.

Amouroux D, Liss PS, Tessier E, Hamren-Larsson M, and Donard OFX (2001) Role of oceans as biogenic sources of selenium. *Earth and Planetary Science Letters* 189: 277–283.

Anderson RK, Thompson M, and Culbard E (1986) Selective reduction of arsenic species by continuous hydride generation. Part II. Validation of methods for application to natural waters. *Analyst* 111: 1153–1157.

Andreae MO (1980) Arsenic in rain and the atmospheric mass balance of arsenic. *Journal of Geophysical Research* 85: 4512–4518.

Andreae MO and Andreae TW (1989) Dissolved arsenic species in the Schelde estuary and watershed, Belgium. *Estuarine, Coastal and Shelf Science* 29: 421–433.

Andreae MO, Byrd TJ, and Froelich ON (1983) Arsenic, antimony, germanium and tin in the Tejo estuary, Portugal: Modelling of a polluted estuary. *Environmental Science & Technology* 17: 731–737.

Appelo CAJ and Postma D (1993) *Geochemistry Groundwater and Pollution*. The Netherlands: AA Balkema.

Appelo CAJ, Van der Weiden MJJ, Tournassat C, and Charlet L (2002) Surface complexation of ferrous iron and carbonate on ferrihydrite and the mobilization of arsenic. *Environmental Science & Technology* 36: 3096–3103.

Armienta MA, Rodriguez R, Aguayo A, Ceniceros N, Villasenor G, and Cruz O (1997) Arsenic contamination of groundwater at Zimapan, Mexico. *Hydrogeology Journal* 5: 39–46.

Arthur JR and Beckett GT (1989) Selenium deficiency and thyroid hormone metabolism. In: Wendell A (ed.) *Selenium in Biology and Medicine*, pp. 90–95. New York: Springer.

ATSDR (2003) *Toxicological Profile for Selenium*. Atlanta, GA: US Department of Health and Human Services, Public Health Service.

ATSDR (2007) *Toxicological Profile for Arsenic*. Atlanta, GA: US Department of Health and Human Services, Public Health Service.

ATSDR (2010) *CERCLA Priority List of Hazardous Substances*. Atlanta, GA: Agency for Toxic Substances & Disease Registry. http://www.atsdr.cdc.gov/cercla/, Accessed 25 January 2011.

Azcue JM, Mudroch A, Rosa F, and Hall GEM (1994) Effects of abandoned gold mine tailings on the arsenic concentrations in water and sediments of Jack of Clubs Lake, BC. *Environmental Technology* 15: 669–678.

Azcue JM, Mudroch A, Rosa F, Hall GEM, Jackson TA, and Reynoldson T (1995) Trace elements in water, sediments, porewater, and biota polluted by tailings from an abandoned gold mine in British Columbia, Canada. *Journal of Geochemical Exploration* 52: 25–34.

Azcue JM and Nriagu JO (1995) Impact of abandoned mine tailings on the arsenic concentrations in Moira Lake, Ontario. *Journal of Geochemical Exploration* 52: 81–89.

Barbaris B and Betterton EA (1996) Initial snow chemistry survey of the Mogollon Rim in Arizona. *Atmospheric Environment* 30: 3093–3103.

Barceloux DG (1999) Selenium. *Clinical Toxicology* 37(2): 145–172.

Bar-Yosef B and Meek D (1987) Selenium sorption by kaolinite and montmorillonite. *Soil Science* 144: 12–19.

Baum MK, Shor-Posner G, Lai SH, et al. (1997) High risk of HIV-related mortality is associated with selenium deficiency. *Journal of Acquired Immune Deficiency Syndromes and Human Retrovirology* 15: 370–374.

Bech J, Poschenreider C, Llugany M, et al. (1997) Arsenic and heavy metal contamination of soil and vegetation around a copper mine in Northern Peru. *The Science of the Total Environment* 203: 83–91.

Beck MA (1999) Selenium and host defense towards viruses. *Proceedings of the Nutrition Society* 58: 707–711.

Bednar AJ, Garbarino JR, Ranville JF, and Wildeman TR (2002) Preserving the distribution of inorganic arsenic species in groundwater and acid mine drainage samples. *Environmental Science & Technology* 36: 2213–2218.

Berg M, Tran HC, Nguyen TC, Pham HV, Schertenleib R, and Giger W (2001) Arsenic contamination of groundwater and drinking water in Vietnam: A human health threat. *Environmental Science & Technology* 35: 2621–2626.

Bethke C (2002) *The Geochemist's Workbench: User Guide*. Urbana: University of Illinois.

BGS (1978–2006) *Regional Geochemical Atlas Series*. Nottingham: British Geological Survey (formerly Institute of Geological Sciences).

BGS and DPHE (2001) Arsenic contamination of groundwater in Bangladesh (four volumes). In: Kinniburgh DG and Smedley PL (eds.) *BGS Technical Report WC/00/19*. Nottingham: British Geological Survey.

Bhattacharya P, Chatterjee D, and Jacks G (1997) Occurrence of arsenic-contaminated groundwater in alluvial aquifers from delta plains, Eastern India: Options for safe drinking water supply. *Water Resources Development* 13: 79–92.

Bhattacharya P, Welch AH, Stollenwerk KG, McLaughlin MJ, Bundschuh J, and Panaullah G (2007) Arsenic in the environment: Biology and chemistry. *The Science of the Total Environment* 379: 109–120. http://dx.doi.org/10.1016/j.scitotenv.2007.02.037.

Black A, Craw D, Youngson JH, and Karubaba J (2004) Natural recovery rates of a river system impacted by mine tailing discharge: Shag River, East Otago, New Zealand. *Journal of Geochemical Exploration* 84(1): 21–34.

Bodénan F, Baranger P, Piantone A, et al. (2004) Arsenic behaviour in gold-ore mill tailings, Massif Central, France: Hydrogeochemical study and investigation of in situ redox signatures. *Applied Geochemistry* 19(11): 1785–1800.

Bohari Y, Astruc A, Astruc M, and Cloud J (2001) Improvements of hydride generation for the speciation of arsenic in natural freshwater samples by HPLC-HG-AFS. *Journal of Analytical Atomic Spectrometry* 16: 774–778.

Boyle DR, Turner RJW, and Hall GEM (1998) Anomalous arsenic concentrations in groundwaters of an island community, Bowen Island, British Columbia. *Environmental Geochemistry and Health* 20: 199–212.

Brown GE, Henrich VE, Casey WH, et al. (1999) Metal oxide surfaces and their interactions with aqueous solutions and microbial organisms. *Chemical Reviews* 77–174.

Bueno M and Potin-Gautier M (2002) Solid-phase extraction for the simultaneous preconcentration of organic (selenocystine) and inorganic Se(IV), Se(VI) selenium in natural waters. *Journal of Chromatography A* 963: 185–193.

Burk RF (1994) *Selenium in Biology and Human Health*. New York: Springer.

Burkel RS and Stoll RC (1999) Naturally occurring arsenic in sandstone aquifer water supply wells of north-eastern Wisconsin. *Ground Water Monitoring and Remediation* 19: 114–121.

Cabon JY and Cabon N (2000) Determination of arsenic species in seawater by flow injection hydride generation in situ collection followed by graphite furnace atomic absorption spectrometry – Stability of As(III). *Analytica Chimica Acta* 418: 19–31.

Cáceres L, Gruttner E, and Contreras R (1992) Water recycling in arid regions – Chilean case. *Ambio* 21: 138–144.

California Environmental Protection Agency (2010) *Public Health Goals for Chemicals in Drinking Water; Selenium*. Sacramento, CA: California Environmental Protection Agency.

Camm GS, Butcher AR, Pirrie D, Hughes PK, and Glass HJ (2003) Secondary mineral phases associated with a historic arsenic calciner identified using automated scanning electron microscopy: A pilot study from Cornwall, UK. *Minerals Engineering* 16(12): 1269–1277.

Casgrain A, Collings R, Harvey LJ, Boza JJ, and Fairweather-Tait SJ (2010) Micronutrient bioavailability research priorities. *The American Journal of Clinical Nutrition* 91: 14235–14295.

Chen SL, Dzeng SR, Yang MH, Chlu KH, Shieh GM, and Wal CM (1994) Arsenic species in groundwaters of the Blackfoot disease areas, Taiwan. *Environmental Science & Technology* 28: 877–881.

Chen HW, Frey MM, Clifford D, McNeill LS, and Edwards M (1999) Arsenic treatment considerations. *Journal of American Water Works Association* 91: 74–85.

Chen SL, Yeh SJ, Yang MH, and Lin TH (1995) Trace element concentration and arsenic speciation in the well water of a Taiwan area with endemic Blackfoot disease. *Biological Trace Element Research* 48: 263–274.

Cheng H, Hu Y, Luo J, Xu B, and Zhao J (2009) Geochemical processes controlling fate and transport of arsenic in acid mine drainage (AMD) and natural systems. *Journal of Hazardous Materials* 165: 13–26.

Cherry JA, Shaikh AU, Tallman DE, and Nicholson RV (1979) Arsenic species as an indicator of redox conditions in groundwater. *Journal of Hydrology* 43: 373–392.

Clark LC, Combs GF Jr, Turnbull BW, et al. (1996) Effects of selenium supplementation for cancer prevention in patients with carcinoma of the skin. *Journal of the American Medical Association* 276(24): 1957–1963.

Clewell HJ, Gentry PR, Barton HA, Shipp AM, Yager JW, and Andersen ME (1999) Requirements for a biologically realistic cancer risk assessment for inorganic arsenic. *International Journal of Toxicology* 18: 131–147.

Combs GF (2001) Selenium in global food systems. *British Journal of Nutrition* 85: 517–547.

Combs GF and Combs SB (1986) *The Role of Selenium in Nutrition*. Orlando, FL: Academic Press.

Couture RM, Gobeil C, and Tessier A (2008) Chronology of atmospheric deposition of arsenic inferred from reconstructed sedimentary records. *Environmental Science & Technology* 42: 6508–6513.

Crecelius EA (1975) The geochemical cycle of arsenic in Lake Washington and its relation to other elements. *Limnology and Oceanography* 20: 441–451.

Cullen WR and Reimer KJ (1989) Arsenic speciation in the environment. *Chemical Reviews* 89: 713–764.

Cummings DE, Caccavo F, Fendorf S, and Rosenzweig RF (1999) Arsenic mobilization by the dissimilatory Fe(III)-reducing bacterium *Shewanella alga* BrY. *Environmental Science & Technology* 33: 723–729.

Cutter GA (1989) The estuarine behavior of selenium in San Francisco Bay (California, USA). *Estuarine, Coastal and Shelf Science* 28: 13–34.

Cutter GA and Cutter LS (2001) Sources and cycling of selenium in the western and equatorial Atlantic Ocean. *Deep Sea Research Part II: Topical Studies in Oceanography* 48: 2917–2931.

Darnley AG (1995) International geochemical mapping – A review. *Journal of Geochemical Exploration* 55: 5–10.

Das D, Samanta G, Mandal BK, et al. (1996) Arsenic in groundwater in six districts of West Bengal, India. *Environmental Geochemistry and Health* 18: 5–15.

Daus B, Mattusch J, Paschke A, Wennrich R, and Weiss H (2000) Kinetics of the arsenite oxidation in seepage water from a tin mill tailings pond. *Talanta* 51: 1087–1095.

Daus B, Mattusch J, Wennrich R, and Weiss H (2002) Investigation on stability and preservation of arsenic species in iron rich water samples. *Talanta* 58: 57–65.

Davies BE (1980) *Applied Soil Trace Elements*. Chichester: Wiley.

Davies E and Watkinson J (1966) Uptake of native and applied Se by pasture species. *New Zealand Journal of Agricultural Research* 9: 317–324.

Davis C, Uthus E, and Finley J (2000) Dietary selenium and arsenic affect DNA methylation in vitro in Caco-2 cells and in vivo in rat liver and colon. *Journal of Nutrition* 130: 2903–2909.

Del Razo LM, Arellano MA, and Cebrian ME (1990) The oxidation states of arsenic in well-water from a chronic arsenicism area of northern Mexico. *Environmental Pollution* 64: 143–153.
Demesmay C and Olle M (1997) Application of microwave digestion to the preparation of sediment samples for arsenic speciation. *Fresenius' Journal of Analytical Chemistry* 357: 1116–1121.
Deuel LE and Swoboda AR (1972) Arsenic solubility in a reduced environment. *Soil Science Society of America Proceedings* 36: 276–278.
Deverel S, Fio J, and Dubrovsky N (1994) Distribution and mobility of selenium in groundwater in the western San Joaquin valley of California. In: Benson S (ed.) *Selenium in the Environment*, ch. 7, pp. 157–183. New York: Marcel Dekker.
Deverel SJ and Fujii R (1988) Processes affecting the distribution of selenium in shallow groundwater in agricultural areas, western San Josquin Valley, California. *Water Resources Research* 24: 516–524.
Diaz-Alarcon JP, Navarro-Alarcon M, de la Serrana HLG, and Lopez-Martinez MC (1996) Determination of selenium in meat products by hydride generation atomic absorption spectrometry: Selenium levels in meat, organ meats, and sausages in Spain. *Journal of Agricultural and Food Chemistry* 44: 1494–1497.
Ding Z, Finkelman R, Belkin H, Aheng B, Hu T, and Xie U (2000) The mode of occurrence of arsenic in high arsenic coals from endemic arsenosis areas in Southwest Guizhou province, China. *Metal Ions in Biology and Medicine* 6: 56–58.
Dissanayake CB and Chandrajith R (2009) Medical geology of arsenic. *Introduction to Medical Geology*, pp. 157–189. Berlin: Springer.
Driehaus W and Jekel M (1992) Determination of As(III) and total inorganic arsenic by on-line pretreatment in hydride generation atomic absorption spectrometry. *Fresenius' Journal of Analytical Chemistry* 343: 352–356.
Driehaus W, Seith R, and Jekel M (1995) Oxidation of arsenate(III) with manganese oxides in water-treatment. *Water Research* 29: 297–305.
Durum WH, Hem JD, and Heidel SG (1971) Reconnaissance of selected minor elements in surface waters of the United States. *US Geological Survey Circular* 64, pp. 1–49. Menlo Park, CA: US Geological Survey.
Dzombak DA and Morel FMM (1990) *Surface Complexation Modelling – Hydrous Ferric Oxide*. New York: Wiley.
Edmunds WM, Cook JM, Kinniburgh DG, Miles DL, and Trafford JM (1989) Trace-element occurrence in British groundwaters. *British Geological Survey Research Report SD/89/3*. Keyworth: British Geological Survey.
Ehrlich H (2002) Bacterial oxidation of As(III) compounds. In: Frankenberger W (ed.) *Environmental Chemistry of Arsenic*, ch. 7, pp. 313–342. New York: Marcel Dekker.
Engberg RA (1999) Selenium budgets for Lake Powell and the upper Colorado River Basin. *Journal of the American Water Resources Association* 35: 771–786.
Environment Agency (2009) Contaminants in soil: Updated collation of toxicological data and intake values for humans. Selenium. *Environment Agency Science Report SC050021*. Bristol: Environment Agency.
Fairweather-Tait S, Bao Y, Broadley M, et al. (2011) Selenium in human health and disease. *Antioxidants & Redox Signalling* 14(7): 1337–1383. http://dx.doi.org/10.1089/ars.2010.3275.
Fairweather-Tait SJ, Collings R, and Hurst R (2010) Selenium bioavailability: Current knowledge and future research requirements. *The American Journal of Clinical Nutrition* 91: 1484S–1491S.
Farmer JG and Lovell MA (1986) Natural enrichment of arsenic in Loch Lomond sediments. *Geochimica et Cosmochimica Acta* 50: 2059–2067.
Feldmann J, Lai VWM, Cullen WR, Ma M, Lu X, and Le XC (1999) Sample preparation and storage can change arsenic speciation in human urine. *Clinical Chemistry* 45: 1988.
Ferguson JF and Gavis J (1972) A review of the arsenic cycle in natural waters. *Water Research* 6(11): 1259–1274.
Fergusson JE (1990) *The Heavy Elements: Chemistry, Environmental Impact and Health Effects*. London: Pergamon Press.
Ficklin WH and Callender E (1989) Arsenic geochemistry of rapidly accumulating sediments, Lake Oahe, South Dakota. In: Mallard GE and Ragone SE (eds.) *US Geological Survey Water-Resources Investigations Report 88-4420*. US Geological Survey Toxic Substances Hydrology Program – Proceedings of the Technical Meeting, Phoenix, Arizona, 26–30 Sept 1988, pp. 217–222. Menlo Park, CA: US Geological Survey.
Finkelman RB, Belkin HE, Centeno JA, and Baoshan Z (2003) Geological epidemiology: Coal combustion in china. In: Skinner HC and Berger AR (eds.) *Geology and Health: Closing the Gap*, p. 45. Oxford: Oxford University Press.
Fisher JC, Wallschläger D, Planer-Friedrich B, and Hollibaugh JT (2007) A new role for sulfur in arsenic cycling. *Environmental Science & Technology* 42(1): 81–85.
Florencio MH, Duarte MF, Facchetti S, et al. (1997) Identification of inorganic, methylated and hydride-refractory arsenic species in estuarine waters. Advances by electrospray, ES-MS, pyrolysis-GC-MS and HPLC-ICP/MS. *Analysis* 25: 226–229.
Focazio MJ, Welch AH, Watkins SA, Helsel DR, and Horng MA (1999) A retrospective analysis on the occurrence of arsenic in ground-water resources of the United States and limitations in drinking-water-supply characterizations. *US Geological Survey Water-Resources Investigations Report 99-4279*. Menlo Park, CA: US Geological Survey.
Fordyce FM (2005) Selenium deficiency and toxicity in the environment. In: Selinus O, Alloway B, Centeno JA, Finkelman RB, Fuge R, Lindh U, and Smedley P (eds.) *Essentials of Medical Geology*, pp. 373–415. London: Elsevier.
Fordyce FM, Brereton N, Hughes J, Luo W, and Lewis J (2010) An initial study to assess the use of geological parent materials to predict the Se concentration in overlying soils and in five staple foodstuffs produced on them in Scotland. *Science of the Total Environment* 408(22): 5295–5305.
Fordyce FM, Johnson CC, Navaratna URB, Appleton JD, and Dissanayake CB (2000a) Selenium and iodine in soil, rice and drinking water in relation to endemic goitre in Sri Lanka. *The Science of the Total Environment* 263: 127–141.
Fordyce FM, Zhang G, Green K, and Liu X (2000b) Soil, grain and water chemistry in relation to human selenium-responsive diseases in Enshi District, China. *Applied Geochemistry* 15: 117–132.
FOREGS (2005) *Geochemical Atlas of Europe: Part 1 – Background Information, Methodology, and Maps*. Espoo, Finland: Geological Survey of Finland.
Forrest A, Kingsley R, and Schilling JG (2009) Determination of selenium and tellurium in basalt rock reference materials by isotope dilution hydride generation-inductively coupled plasma-mass spectrometry (ID-HG-ICP-MS). *Geostandards and Geoanalytical Research* 33(2): 261–269.
Foster AL, Brown GE, and Parks GA (1998a) X-ray absorption fine-structure spectroscopy study of photocatalyzed, heterogeneous As(III) oxidation on kaolin and anatase. *Environmental Science & Technology* 32: 1444–1452.
Foster AL, Brown GE, Tingle TN, and Parks GA (1998b) Quantitative arsenic speciation in mine tailings using X-ray absorption spectroscopy. *American Mineralogist* 83: 553–568.
Foster AL, Breit GN, Whitney JW, et al. (2000) X-ray absorption fine structure spectroscopic investigation of arsenic species in soil and aquifer sediments from Brahmanbaria, Bangladesh. 4th Annual Arsenic Conference, San Diego, 18–22 Jun.
Francesconi KA and Kuehnelt D (2002) Arsenic compounds in the environment. In: Frankenberger W (ed.) *Environmental Chemistry of Arsenic*, ch. 3, pp. 51–94. New York: Marcel Dekker.
Frankenberger WT (2002) *Environmental Chemistry of Arsenic*, pp. 391. New York: Marcel Dekker.
Frankenberger WT and Arshad M (2001) Bioremediation of selenium-contaminated sediments and water. *Biofactors* 14: 241–254.
Frankenberger WT and Benson S (1994) *Selenium in the Environment*, pp. 456. New York: Marcel Dekker.
Fujii R and Swain WC (1995) Areal distribution of selected trace elements, salinity, and major ions in shallow ground water, Tulare Basin, Southern San Joaquin Valley, California. *US Geological Survey Water-Resources Investigations Report 95-4048*. Menlo Park, CA: US Geological Survey.
Gallagher PA, Schwegel CA, Wei XY, and Creed JT (2001) Speciation and preservation of inorganic arsenic in drinking water sources using EDTA with IC separation and ICP-MS detection. *Journal of Environmental Monitoring* 3: 371–376.
García-Hernández J, Glenn EP, Artiola J, and Baumgartner DJ (2000) Bioaccumulation of selenium (Se) in the Cienega de Santa Clara wetland, Sonora, Mexico. *Ecotoxicology and Environmental Safety* 46: 298–304.
Gelova GA (1977) *Hydrogeochemistry of Ore Elements*. Moscow: Nedra.
Ghosh A, Mukiibi M, and Ela W (2004) TCLP underestimates leaching of arsenic from solid residuals under landfill conditions. *Environmental Science & Technology* 38: 4677–4682.
Ghosh A, Mukiibi M, Sáez AE, and Ela WP (2006) Leaching of arsenic from granular ferric hydroxide residuals under mature landfill conditions. *Environmental Science & Technology* 40: 6070–6075.
Giere R, Blackford M, and Smith K (2006) TEM Study of PM2.5 emitted from coal and tire combustion in a thermal power station. *Enivronmental Science & Technology* 40: 6235–6240.
Gluskoter HJ, Ruch RR, Miller WG, Cahill RA, Dreher GB, and Kuhn JK (1977) *Trace Elements in Coal – Occurrence and Distribution*, p. 154. Champaign, IL: Illinois State Geological Survey.
Goldberg S (1985) Chemical modeling of anion competition on goethite using the constant capacitance model. *Soil Science Society of America Journal* 49(4): 851–856.
Goldberg S (1986) Chemical modeling of arsenate adsorption on aluminum and iron oxide minerals. *Soil Science Society of America Journal* 50: 1154–1157.
Gomez-Ariza JL, Velasco-Arjona A, Giraldez I, Sanchez-Rodas D, and Morales E (2000) Coupling pervaporation-gas chromatography for speciation of volatile forms of

selenium in sediments. *International Journal of Environmental Analytical Chemistry* 78: 427–440.
Govindaraju K (1994) Compilation of working values and description for 383 geostandards. *Geostandards Newsletter* 18: 1–158.
Grenthe I, Stumm W, Laaksuharju M, Nilsson AC, and Wikberg P (1992) Redox potentials and redox reactions in deep groundwater systems. *Chemical Geology* 98: 131–150.
Grimes DJ, Ficklin WH, Meier AL, and McHugh JB (1995) Anomalous gold, antimony, arsenic, and tungsten in ground water and alluvium around disseminated gold deposits along the Getchell Trend, Humboldt County, Nevada. *Journal of Geochemical Exploration* 52: 351–371.
Gulens J, Champ DR, and Jackson RE (1979) Influence of redox environments on the mobility of arsenic in ground water. In: Jenne EA (ed.) *Chemical Modeling in Aqueous Systems*, vol. 93, pp. 81–95. Washington, DC: American Chemical Society.
Gurzau ES and Gurzau AE (2001) Arsenic exposure from drinking groundwater in Transylvania, Romania: An overview. In: Chappell WR, Abernathy CO, and Calderon RL (eds.) *Arsenic Exposure and Health Effects*, vol. IV, pp. 181–184. Amsterdam: Elsevier.
Hall G and Pelchat J-C (1997) Determination of As, Bi, Sb, Se and Te in fifty five reference materials by hydride generation ICP-MS. *Geostandards Newsletter* 21: 85–91.
Hall GEM, Pelchat JC, and Gauthier G (1999) Stability of inorganic arsenic(III) and arsenic(V) in water samples. *Journal of Analytical Atomic Spectrometry* 14: 205–213.
Harris MA and Ragusa S (2001) Bioremediation of acid mine drainage using decomposable plant material in a constant flow bioreactor. *Environmental Geology* 40: 1192–1204.
Harvey CF, Swartz CH, Badruzzaman ABM, et al. (2002) Arsenic mobility and groundwater extraction in Bangladesh. *Science* 298: 1602–1606.
Hasegawa H (1997) The behavior of trivalent and pentavalent methylarsenicals in Lake Biwa. *Applied Organometallic Chemistry* 11: 305–311.
Hasegawa H, Matsui M, Okamura S, Hojo M, Iwasaki N, and Sohrin Y (1999) Arsenic speciation including 'hidden' arsenic in natural waters. *Applied Organometallic Chemistry* 13: 113–119.
Hashimoto Y and Winchester JW (1967) Selenium in the atmosphere. *Environmental Science & Technology* 1: 338–340.
Haygarth PM (1994) Global importance and cycling of selenium. In: Frankenberger WT and Benson S (eds.) *Selenium in the Environment*, ch. 1, pp. 1–28. New York: Marcel Dekker.
Heinrichs G and Udluft P (1999) Natural arsenic in Triassic rocks: A source of drinking-water contamination in Bavaria, Germany. *Hydrogeology Journal* 7: 468–476.
Helz GR, Tossell JA, Charnock JM, Pattrick RAD, Vaughan DJ, and Garner CD (1995) Oligomerization in As(III) sulfide solutions – Theoretical constraints and spectroscopic evidence. *Geochimica et Cosmochimica Acta* 59: 4591–4604.
Hem J (1992) *Study and Interpretation of Chemical Characteristics of Natural Water*, 3rd edn. Menlo Park, CA: US Geological Survey.
Herbel MJ, Blum JS, Hoeft SE, et al. (2002a) Dissimilatory arsenate reductase activity and arsenate-respiring bacteria in bovine rumen fluid, hamster feces, and the termite hindgut. *FEMS Microbiology Ecology* 41: 59–67.
Herbel MJ, Johnson TM, Tanji KK, Gao SD, and Bullen TD (2002b) Selenium stable isotope ratios in California agricultural drainage water management systems. *Journal of Environmental Quality* 31: 1146–1156.
Hering J and Kneebone PE (2002) Biogeochemical controls on arsenic occurrence and mobility in water supplies. In: Frankenberger W (ed.) *Environmental Chemistry of Arsenic*, ch. 7, pp. 155–181. New York: Marcel Dekker.
Hiemstra T and van Riemsdijk WH (1999) Surface structural ion adsorption modeling of competitive binding of oxyanions by metal (hydr)oxides. *Journal of Colloid and Interface Science* 210: 182–193.
Hinkle S and Polette D (1999) Arsenic in groundwater of the Willamette Basin, Oregon. *US Geological Survey Water Resources Investigations Report 98-4205*. Menlo Park, CA: US Geological Survey.
Hoang TH, Bang S, Kim K, Nguyen MH, and Dang DM (2010) Arsenic in groundwater and sediment in the Mekong River delta, Vietnam. *Environmental Pollution* 158(8): 2648–2658.
Hoeft SE, Lucas F, Hollibaugh JT, and Oremland RS (2002) Characterization of microbial arsenate reduction in the anoxic bottom waters of Mono Lake, California. *Geomicrobiology Journal* 19: 23–40.
Hopenhayn-Rich C, Biggs ML, Fuchs A, et al. (1996) Bladder-cancer mortality associated with arsenic in drinking water in Argentina. *Epidemiology* 7: 117–124.
Horowitz A, Lum K, Garbarino J, Hall G, Lemieux C, and Demas C (1996) Problems associated with using filtration to define dissolved trace element concentrations in natural water samples. *Environmental Science & Technology* 30: 954–963.
Howard AG, Apte SC, Comber SDW, and Morris RJ (1988) Biogeochemical control of the summer distribution and speciation of arsenic in the Tamar estuary. *Estuarine, Coastal and Shelf Science* 27: 427–443.
Howard G, Bartram J, Pedley S, Schmoll O, Chorus I, and Berger P (2006) Groundwater and public health. In: Schmoll O, Howard G, Chilton J, and Chorus I (eds.) *Protecting Groundwater for Health: Managing the Quality of Drinking-Water Sources*, pp. 3–19. London: IWA Publishing.
Howard AG, Hunt LE, and Salou C (1999) Evidence supporting the presence of dissolved dimethylarsinate in the marine environment. *Applied Organometallic Chemistry* 13: 39–46.
ICRCL (Interdepartmental Committee on the Redevelopment of Contaminated Land) (1987) Guidance on the assessment and redevelopment of contaminated land. *ICRCL Guidance Note 59/83*. London: Department of the Environment.
Inskeep WP, McDermott T, and Fendorf S (2002) Arsenic(V)/(III) cycling in soils and natural waters: Chemical and microbiological processes. In: Frankenberger W (ed.) *Environmental Chemistry of Arsenic*, ch. 8, pp. 183–215. New York: Marcel Dekker.
IOM (Institute of Medicine) (2001) *Dietary Reference Intakes for Vitamin A, Vitamin K, Arsenic, Boron, Chromium, Copper, Iodine, Iron, Manganese, Molybdenum, Nickel, Silicon, Vanadium, and Zinc*. Washington, DC: National Academy of Sciences.
Ipolyi I and Fodor P (2000) Development of analytical systems for the simultaneous determination of the speciation of arsenic As(III), methylarsonic acid, dimethylarsinic acid, As(V) and selenium Se(IV), Se(VI). *Analytica Chimica Acta* 413: 13–23.
Irgolic K (1994) Determination of total arsenic and arsenic compounds in drinking water. In: Chappell WR, Abernathy CO, and Cothern CR (eds.) *Arsenic: Exposure and Health*, pp. 51–60. Northwood: Science and Technology Letters.
Islam FS, Gault AG, Boothman C, et al. (2004) Role of metal-reducing bacteria in arsenic release from Bengal delta sediments. *Nature* 430: 68–71.
Jacobs LW (1989) *Selenium in Agriculture and the Environment*. Madison, WI: Soil Science Society of America. SSSA Special Publication 23.
Jain A and Loeppert RH (2000) Effect of competing anions on the adsorption of arsenate and arsenite by ferrihydrite. *Journal of Environmental Quality* 29: 1422–1430.
Jayasekher T (2009) Aerosols near by a coal fired thermal power plant: Chemical composition and toxic evaluation. *Chemosphere* 75: 1525–1530.
Johnson MS (1995) Environmental management in metalliferous mining: The past, present and future. In: Zak K (ed.) *Mineral Deposits: From Their Origin to Their Environmental Impact*, pp. 655–658. Rotterdam: Balkema.
Johnson CC, Fordyce FM, and Rayman MP (2010) Factors controlling the distribution of selenium in the environment and their impact on health and nutrition. *Proceedings of the Nutrition Society* 69: 119–132.
Johnson CC, Ge X, Green KA, and Liu X (2000) Selenium distribution in the local environment of selected villages of the Keshan Disease belt, Zhangjiakou District, Hebei Province, People's Republic of China. *Applied Geochemistry* 15: 385–401.
Johnson TM, Herbel MJ, Bullen TD, and Zawislanski PT (1999) Selenium isotope ratios as indicators of selenium sources and oxyanion reduction. *Geochimica et Cosmochimica Acta* 63: 2775–2783.
Jones CA, Anderson HW, McDermott K, and Inskeep TR (2000) Rates of microbially mediated arsenate reduction and solubilization. *Soil Science Society of America Journal* 64: 600–608.
Jung MC, Thornton I, and Chon HT (2002) Arsenic, Sb and Bi contamination of soils, plants, waters and sediments in the vicinity of the Dalsung Cu–W mine in Korea. *The Science of the Total Environment* 295: 81–89.
Kabata-Pendias A and Mukherjee AB (2007) *Trace Elements from Soil to Human*. Berlin: Springer.
Kapaj S, Peterson H, Liber K, and Bhattacharya P (2006) Human health effects from chronic arsenic poisoning – A review. *Journal of Environmental Science and Health, Part A* 41: 2399–2428.
Kent DB, Davies JA, Anderson LCD, and Rea BA (1995) Transport of chromium and selenium in a pristine sand and gravel aquifer: Role of adsorption processes. *Water Resources Research* 31: 1041–1050.
Kile ML, Houseman EA, Breton CV, et al. (2007) Dietary arsenic exposure in Bangladesh. *Environmental Health Perspectives* 115: 889–893.
Kim MJ, Nriagu J, and Haack S (2000) Carbonate ions and arsenic dissolution by groundwater. *Environmental Science & Technology* 34: 3094–3100.
Kinniburgh DG and Kosmus W (2002) Arsenic contamination in groundwater: Some analytical considerations. *Talanta* 58: 165–180.
Kinniburgh DG and Miles DL (1983) Extraction and chemical analysis of interstitial water from soils and rocks. *Environmental Science & Technology* 17: 362–368.
Kinniburgh DG, Smedley PL, Davies J, et al. (2003) The scale and causes of the ground water arsenic problem in Bangladesh. In: Welch AH and Stollenwerk KG (eds.) *Arsenic in Groundwater: Occurrence and Geochemistry*, pp. 211–257. Boston, MA: Kluwer Academic.
Knight AP and Walter RG (2001) *A Guide to Plant Poisoning of Animals in North America*. Jackson, WY: Teton New Media.

Korte N (1991) Naturally occurring arsenic in groundwaters of the midwestern United States. *Environmental Geology and Water Sciences* 18: 137–141.
Korte NE and Fernando Q (1991) A review of arsenic(III) in groundwater. *Critical Reviews in Environmental Control* 21: 1–39.
Kreidie N, Armiento G, Cibin G, et al. (2011) An integrated geochemical and mineralogical approach for the evaluation of arsenic mobility in mining soils. *Journal of Soils and Sediments* 11: 1–16.
Kuhlmeier PD (1997) Partitioning of arsenic species in fine-grained soils. *Journal of the Air & Waste Management Association* 47: 481–490.
Kuhn A and Sigg L (1993) Arsenic cycling in eutrophic Lake Greifen, Switzerland – Influence of seasonal redox processes. *Limnology and Oceanography* 38: 1052–1059.
Kumar AR and Riyazuddin P (2010) Preservation of inorganic arsenic species in environmental water samples for reliable speciation analysis. *Trends in Analytical Chemistry* 29(10): 1212–1223.
Kuyucak N (1998) Mining, the environment and the treatment of mine effluents. *International Journal of Environment and Pollution* 10: 315–325.
La Force MJ, Hansel CM, and Fendorf S (2000) Arsenic speciation, seasonal transformations, and co-distribution with iron in a mine waste-influence palustrine emergent wetland. *Environmental Science & Technology* 34: 3937–3943.
Lange B and van den Berg CMG (2000) Determination of selenium by catalytic cathodic stripping voltammetry. *Analytica Chimica Acta* 418: 33–42.
Langner HW and Inskeep WP (2000) Microbial reduction of arsenate in the presence of ferrihydrite. *Environmental Science & Technology* 34: 3131–3136.
Leblanc M, Achard B, Othman DB, Luck JM, Bertrand-Sarfati J, and Personne JC (1996) Accumulation of arsenic from acidic mine waters by ferruginous bacterial accretions (stromatolites). *Applied Geochemistry* 11: 541–554.
Lemly AD (2002) *Selenium Assessment in Aquatic Ecosystems: A Guide for Hazard Evaluation and Water Quality Criteria*. New York: Springer.
Lenvik K, Steinnes E, and Pappas AC (1978) Contents of some heavy metals in Norwegian rivers. *Nordic Hydrology* 9: 197–206.
Lerda DE and Prosperi CH (1996) Water mutagenicity and toxicology in Rio Tercero (Cordoba, Argentina). *Water Research* 30: 819–824.
Levander OA (1986) Selenium. In: Mertz W (ed.) *Trace Elements in Human and Animal Nutrition*, pp. 209–266. New York: Academic Press.
Li L, Huang Y, Wang Y, and Wang W (2009a) Hemimicelle capped functionalized carbon nanotubes-based nanosized solid-phase extraction of arsenic from environmental water samples. *Analytica Chimica Acta* 631: 182–188. http://dx.doi.org/10.1016/j.aca.2008.10.043.
Li S, Li W, Hu X, Yang L, and Xirao R (2009b) Soil selenium concentration and Kashin–Beck disease prevalence in Tibet, China. *Frontiers of Environmental Science & Engineering in China* 3(1): 62–68.
Li Y, Peng T, Yang Y, Niu C, Archard LC, and Zhang H (2000) High prevalence of enteroviral genomic sequences in myocardium from cases of endemic cardiomyopathy (Keshan disease) in China. *Heart* 83: 696–701.
Lima HM and Wathern P (1999) Mine closure: A conceptual review. *Mining Engineering* 51: 41–45.
Lindemann T, Prange A, Dannecker W, and Neidhart B (2000) Stability studies of arsenic, selenium, antimony and tellurium species in water, urine, fish and soil extracts using HPLC/ICP- MS. *Fresenius' Journal of Analytical Chemistry* 368: 214–220.
Litaor MI and Keigley RB (1991) Geochemical equilibria of iron in sediments of the Roaring river alluvial fan, Rocky Mountain National Park, Colorado. *Earth Surface Processes and Landforms* 16: 533–546.
Liu Y, Chiba M, Inaba Y, and Kondo M (2002) Keshan disease – A review from the aspect of history and etiology. *Nippon Eiseigaku Zasshi* 56(4): 641–648.
Liu G, Zhang Y, Qi C, Zheng L, Chen Y, and Peng Z (2007) Comparative on causes and accumulation of selenium in the tree-rings ambient high-selenium coal combustion area from Yutangba, Hubei, China. *Environmental Monitoring and Assessment* 133(1): 99–103.
Lumsdon DG, Meeussen JCL, Paterson E, Garden LM, and Anderson P (2001) Use of solid phase characterisation and chemical modelling for assessing the behaviour of arsenic in contaminated soils. *Applied Geochemistry* 16: 571–581.
Luo ZD, Zhang YM, Ma L, et al. (1997) Chronic arsenicism and cancer in Inner Mongolia – Consequences of well-water arsenic levels greater than 50 mg l^{-1}. In: Abernathy CO, Calderon RL, and Chappell WR (eds.) *Arsenic Exposure and Health Effects*, pp. 55–68. London: Chapman and Hall.
Macur RE, Wheeler JT, McDermott TR, and Inskeep WP (2001) Microbial populations associated with the reduction and enhanced mobilization of arsenic in mine tailings. *Environmental Science & Technology* 35: 3676–3682.
Maest AS, Pasilis SP, Miller LG, and Nordstrom DK (1992) Redox geochemistry of arsenic and iron in Mono Lake, California, USA. In: *Proceedings of the Seventh International Symposium on Water–Rock Interaction*, pp. 507–511.
Manning BA, Fendorf SE, Bostick B, and Suarez DL (2002) Arsenic(III) oxidation and arsenic(V) adsorption reactions on synthetic birnessite. *Environmental Science & Technology* 36: 976–981.
Manning BA and Goldberg S (1997) Adsorption and stability of arsenic(III) at the clay mineral–water interface. *Environmental Science & Technology* 31: 2005–2011.
Martinez-Bravo Y, Roig-Navarro AF, Lopez FJ, and Hernandez F (2001) Multielemental determination of arsenic, selenium and chromium(VI) species in water by high-performance liquid chromatography-inductively coupled plasma mass spectrometry. *Journal of Chromatography*. A 926: 265–274.
Masscheleyn PH, DeLaune RD, and Patrick WH (1991) Effect of redox potential and pH on arsenic speciation and solubility in a contaminated soil. *Environmental Science & Technology* 25: 1414–1419.
May TW, Walther MJ, Petty JD, et al. (2001) An evaluation of selenium concentrations in water, sediment, invertebrates, and fish from the Republican River Basin: 1997–1999. *Environmental Monitoring and Assessment* 72: 179–206.
Mayland H (1994) Selenium in plant and animal nutrition. In: Frankenberger WT and Benson S (eds.) *Selenium in the Environment*, ch. 2, pp. 29–45. New York: Marcel Dekker.
McArthur JM, Ravenscroft P, Safiulla S, and Thirwall MF (2001) Arsenic in groundwater: Testing pollution mechanisms for sedimentary aquifers in Bangladesh. *Water Resources Research* 37: 109–117.
McCleskey RB, Nordstrom DK, and Maest AS (2004) Preservation of water samples for arsenic(III/V) determinations: An evaluation of the literature and new analytical results. *Applied Geochemistry* 19: 995–1009.
McCreadie H, Blowes DW, Ptacek CJ, and Jambor JL (2000) Influence of reduction reactions and solid phase composition on porewater concentrations of arsenic. *Environmental Science & Technology* 34: 3159–3166.
McGeehan SL, Fendorf SE, and Naylor DV (1998) Alteration of arsenic sorption in flooded-dried soils. *Soil Science Society of America Journal* 62: 828–833.
McLaren SJ and Kim ND (1995) Evidence for a seasonal fluctuation of arsenic in New Zealand's longest river and the effect of treatment on concentrations in drinking water. *Environmental Pollution* 90: 67–73.
Meharg AA, Williams PN, Adomako E, et al. (2009) Geographical variation in total and inorganic arsenic content of polished (white) rice. *Environmental Science & Technology* 43: 1612–1617.
Melamed D (2004) Monitoring Arsenic in the Environment: A Review of Science and Technologies for Field Measurements and Sensors. *US EPA Report 542-R-04-002*. Washington, DC: US Environmental Protection Agency.
Melgar MJ, Alonso J, and García MA (2009) Selenium accumulation in wild edible mushrooms: Uptake and toxicity. *CyTA – Journal of Food* 7(3): 217–223.
Meng XG, Korfiatis GP, Bang SB, and Bang KW (2002) Combined effects of anions on arsenic removal by iron hydroxides. *Toxicology Letters* 133: 103–111.
Meng XG, Korfiatis GP, Jing CY, and Christodoulatos C (2001) Redox transformations of arsenic and iron in water treatment sludge during aging and TCLP extraction. *Environmental Science & Technology* 35: 3476–3481.
Mikkelsen RL, Page AL, and Bingham FT (1989) Factors affecting selenium accumulation by agricultural crops. In: Jacobs LW (ed.) *Selenium in Agriculture and the Environment*, pp. 65–94. Madison, WI: Soil Science Society of America. SSSA Special Publication 23.
Mok W and Wai CM (1990) Distribution and mobilization of arsenic and antimony species in the Coeur D'Alene River, Idaho. *Environmental Science & Technology* 24: 102–108.
Mondal D, Banerjee M, Kundu M, et al. (2010) Comparison of drinking water, raw rice and cooking of rice as arsenic exposure routes in three contrasting areas of West Bengal, India. *Environmental Geochemistry and Health* 32: 463–477.
Mondal D and Polya DA (2008) Rice is a major exposure route for arsenic in Chakdaha block, Nadia district, West Bengal, India: A probabilistic risk assessment. *Applied Geochemistry* 23: 2987–2998.
Monhemius AJ and Swash PM (1999) Removing and stabilising arsenic from copper refining circuits by hydrothermal processing. *Journal of the Minerals, Metals & Materials Society* 51(9): 30–33.
Moore JN, Ficklin WH, and Johns C (1988) Partitioning of arsenic and metals in reducing sulfidic sediments. *Environmental Science & Technology* 22: 432–437.
Moreno Rodriguez MJ, Cala Rivero V, and Jiménez Ballesta R (2005) Selenium distribution in topsoils and plants of a semi-arid Mediterranean environment. *Environmental Geochemistry and Health* 27: 513–519.
Moxon AL (1937) Alkali disease or selenium poisoning. *South Dakota State College Bulletin* 311: 99.
Moxon AL (1938) The effect of arsenic on the toxicity of seleniferous grains. *Science* 88: 81.
Mukhopadhyay R, Rosen BP, Pung LT, and Silver S (2002) Microbial arsenic: From geocycles to genes and enzymes. *FEMS Microbiology Reviews* 26: 311–325.

Muth OH and Allaway WH (1963) The relationship of white muscle disease to the distribution of naturally occurring selenium. *Journal of the American Veterinary Medical Association* 142: 1379–1384.

Nag JK, Balaram V, Rubio R, Alberti J, and Das AK (1996) Inorganic arsenic species in groundwater: A case study from Purbasthali (Burdwan), India. *Journal of Trace Elements in Medicine and Biology* 10: 20–24.

NAS (1976) *Selenium*. USA: National Academy of Sciences.

Nathanail CP and Bardos P (2004) *Reclamation of Contaminated Land*. Chichester: Wiley.

National Research Council (1999) *Arsenic in Drinking Water*. Washington, DC: National Academy Press.

National Research Council (2001) *Arsenic in Drinking Water: 2001 Update*. Washington, DC: National Academy Press.

Neal RH (1995) Selenium. In: Alloway BJ (ed.) *Heavy Metals in Soils*, pp. 260–283. London: Blackie Academic.

Nelms S (2005) *Inductively Coupled Plasma Mass Spectrometry Handbook*. Oxford: Blackwell.

Newman DK, Ahmann D, and Morel FMM (1998) A brief review of microbial arsenate respiration. *Geomicrobiology Journal* 15: 255–268.

Newman DK, Beveridge TJ, and Morel FMM (1997a) Precipitation of arsenic trisulfide by *Desulfotomaculum auripigmentum*. *Applied and Environmental Microbiology* 63: 2022–2028.

Newman DK, Kennedy EK, Coates JD, et al. (1997b) Dissimilatory arsenate and sulfate reduction in *Desulfotomaculum auripigmentum* sp. nov. *Archives of Microbiology* 168: 380–388.

Ng JC, Wang J, and Shraim A (2003) A global health problem caused by arsenic from natural sources. *Chemosphere* 52: 1353–1359.

Nickson R, McArthur J, Burgess W, Ahmed KM, Ravenscroft P, and Rahman M (1998) Arsenic poisoning of Bangladesh groundwater. *Nature* 395: 338.

Nickson RT, McArthur JM, Ravenscroft P, Burgess WG, and Ahmed KM (2000) Mechanism of arsenic release to groundwater, Bangladesh and West Bengal. *Applied Geochemistry* 15: 403–413.

Nicolli HB, Suriano JM, Peral MAG, Ferpozzi LH, and Baleani OA (1989) Groundwater contamination with arsenic and other trace-elements in an area of the Pampa, province of Cordoba, Argentina. *Environmental Geology and Water Sciences* 14: 3–16.

Nicolli HB, Tineo A, García J, Falcón C, and Merino M (2001) Trace-element quality problems in groundwater from Tucumán, Argentina. In: Cidu R (ed.) *Water-Rock Interaction,* pp. 993–996. Lisse: Balkema.

Nimick DA, Moore JN, Dalby CE, and Savka MW (1998) The fate of geothermal arsenic in the Madison and Missouri Rivers, Montana and Wyoming. *Water Resources Research* 34: 3051–3067.

Nishri A, Brenner IB, Hall GEM, and Taylor HE (1999) Temporal variations in dissolved selenium in Lake Kinneret (Israel). *Aquatic Sciences* 61: 215–233.

Noda K, Taniguchi H, Suzuki S, and Hirai S (1983) Comparison of the selenium contents of vegetables of the Genus Allium measured by fluorometry and neutron activation analysis. *Agricultural and Biological Chemistry* 47: 613–615.

Nordstrom DK and Alpers CN (1999) Negative pH, efflorescent mineralogy, and consequences for environmental restoration at the Iron Mountain superfund site, California. *Proceedings of the National Academy of Sciences of the United States of America* 96: 3455–3462.

Nordstrom DK, Alpers CN, Ptacek CJ, and Blowes DW (2000) Negative pH and extremely acidic mine waters from Iron Mountain, California. *Environmental Science & Technology* 34: 254–258.

Nordstrom DK and Archer DG (2003) Arsenic thermodynamic data and environmental geochemistry. In: Stollenwerk KG (ed.) *Arsenic in Ground Water: Geochemistry and Occurrence*, pp. 1–25. Boston, MA: Kluwer Academic.

Novoselov SV, Rao M, Onoshko NV, et al. (2002) Selenoproteins and selenocysteine insertion system in the model plant cell system, *Chlamydomonas reinhardtii*. *The EMBO Journal* 21(14): 3681–3693.

Nyashanu R, Monhemius A, and Buchanan D (1999) The effect of ore mineralogy on the speciation of arsenic in bacterial oxidation of refractory arsenical gold ores. *Biohydrometallurgy and the Environment* 431–441.

Oldfield JE (1999) *Selenium World Atlas*. Cavite, Philippines: Selenium-Tellurium Development Association.

O'Reilly SE, Strawn DG, and Sparks DL (2001) Residence time effects on arsenate adsorption/desorption mechanisms on goethite. *Soil Science Society of America Journal* 65(1): 67–77.

Oremland RS (1994) Biogeochemical transformations of selenium in anoxic environments. In: Frankenberger WT and Benson S (eds.) *Selenium in the Environment*, ch. 16, pp. 389–419. New York: Marcel Dekker.

Oremland RS, Dowdle PR, Hoeft S, et al. (2000) Bacterial dissimilatory reduction of arsenate and sulphate in meromictic Mono Lake, California. *Geochimica et Cosmochimica Acta* 64: 3073–3084.

Oremland R, Newman D, Kail B, and Stolz J (2002) Bacterial respiration of arsenate and its significance in the environment. In: Frankenberger W (ed.) *Environmental Chemistry of Arsenic*, ch. 11, pp. 273–295. New York: Marcel Dekker.

Oremland RS, Steinberg NA, Maest AS, Miller LG, and Hollibaugh JT (1990) Measurement of in situ rates of selenate removal by dissimilatory bacterial reduction in sediments. *Environmental Science & Technology* 24: 1157–1164.

Oremland RS and Stolz JF (2003) The ecology of arsenic. *Science* 300 (5621): 939–944.

Oscarson DW, Huang PM, Liaw WK, and Hammer UT (1983) Kinetics of oxidation of arsenite by various manganese dioxides. *Soil Science Society of America Journal* 47: 644–648.

Palmer CA and Klizas SA (1997) *The Chemical Analysis of Argonne Premium Coal Samples*. US Geological Survey Bulletin 2144. Menlo Park, CA: US Geological Survey.

Papp LV, Lu J, Holmgren A, and Khanna KK (2007) From selenium to selenoproteins: Synthesis, identity, and their role in human health. *Antioxidants & Redox Signaling* 7: 775–806.

Parkhurst D and Appelo C (1999) User's guide to PHREEQC (Version 2) – A computer program for speciation, batch-reaction, one-dimensional transport, and inverse geochemical calculations. *US Geological Survey Water-Resources Investigations Report 99-4259*. Menlo Park, CA: US Geological Survey.

Parsons MB, Hall GEM, Daniels C, et al. (2006) Speciation, transport, and fate of arsenic in the Seal Harbour gold districts, Nova Scotia, Canada. Geological Society of America Annual Meeting, Philadelphia, 22-25 October 2006.

Pendleton JA, Posey HH, and Long MB (1995) Characterizing Summitville and its impacts: Setting and scene. In: Posey HH, Pendleton JA, and Van Zyl D (eds.) *Proceedings: Summitville Forum '95*. *Colorado Geological Survey Special Publication 38,* pp. 1–12. Denver, CO: US Geological Survey.

Peng A, Wang WH, Wang CX, et al. (1999) The role of humic substances in drinking water in Kashin–Beck disease in China. *Environmental Health Perspectives* 107: 293–296.

Peters GM, Maher WA, Krikowa F, et al. (1999) Selenium in sediments, pore waters and benthic infauna of Lake Macquarie, New South Wales, Australia. *Marine Environmental Research* 47: 491–508.

Petersen W, Wallmann K, Li PL, Schroeder F, and Knauth HD (1995) Exchange of trace-elements at the sediment–water interface during early diagenesis processes. *Marine and Freshwater Research* 46: 19–26.

Peterson ML and Carpenter R (1983) Biogeochemical processes affecting total arsenic and arsenic species distributions in an intermittently anoxic fjord. *Marine Chemistry* 12: 295–321.

Petrusevski B, Sharma S, Schippers JC, and Shordt K (2007) *Arsenic in Drinking Water*. Netherlands: IRC International Water and Sanitation Centre.

Pettine M, Camusso M, and Martinotti W (1992) Dissolved and particulate transport of arsenic and chromium in the Po River (Italy). *The Science of the Total Environment* 119: 253–280.

Pilon-Smits EAH and LeDuc DL (2009) Phytoremediation of selenium using transgenic plants. *Current Opinion in Biotechnology* 20(2): 207–212.

Plant JA, Jeffery K, Gill E, and Fage C (1975) The systematic determination of accuracy and precision in geochemical exploration data. *Journal of Geochemical Exploration* 4: 467–486.

Plant J, Smith DB, Smith B, and Reeder S (2003) Environmental geochemistry on a global scale. In: Skinner HCW and Berger AR (eds.) *Geology and Health: Closing the Gap*, ch. 20. Oxford and New York: Oxford University Press.

Plumlee GS, Smith KS, Montour MR, Ficklin WH, and Mosier EL (1999) Geologic controls on the composition of natural waters and mine waters draining diverse mineral-deposit types. *Environmental Geochemistry of Mineral Deposits*. *Part B: Case Studies*. *Reviews in Economic Geology*, vol. 6B, ch. 19, pp. 373–432. Denver, CO: Society of Economic Geologists.

Pracheil BM, Snow DD, and Pegg MA (2010) Distribution of selenium, mercury, and methylmercury in surficial Missouri River sediments. *Bulletin of Environmental Contamination and Toxicology* 84: 331–335.

Presser T (1994) Geologic origin and pathways of selenium from the California coast ranges to the West-Central San Joaquin Valley. In: Frankenberger WT and Benson S (eds.) *Selenium in the Environment*, ch. 6, pp. 139–155. New York: Marcel Dekker.

Randall SR, Sherman DM, and Ragnarsdottir KV (2001) Sorption of As(V) on green rust ($Fe_4(II)Fe_2(III)(OH)_{12}SO_4{\cdot}3H_2O$) and lepidocrocite (gamma-FeOOH): Surface complexes from EXAFS spectroscopy. *Geochimica et Cosmochimica Acta* 65: 1015–1023.

Rapant S, Vrana K, and Bodis D (1996) *Geochemical Atlas of Slovakia. Part 1. Groundwater*. Bratislava: Geological Survey of Slovak Republic.

Rasmussen L and Andersen K (2002) Environmental health and human exposure assessment (draft). *United Nations Synthesis Report on Arsenic in Drinking Water*, ch. 2. Geneva: World Health Organization.

Rayman MP (2002) The argument for increasing selenium intake. *Proceedings of the Nutrition Society* 61: 203–215.
Rayman MP (2008) Food-chain selenium and human health: Emphasis on intake. *British Journal of Nutrition* 100(2): 254–268.
Reimann C and Caritat P (1998) *Chemical Elements in the Environment*. Berlin: Springer.
Reimann C, Äyräs M, and Chekushin V (1998) *Environmental Geochemical Atlas of the Central Barents Region*. Trondheim: Geological Survey of Norway.
Reynolds JG, Naylor DV, and Fendorf SE (1999) Arsenic sorption in phosphate-amended soils during flooding and subsequent aeration. *Soil Science Society of America Journal* 63: 1149–1156.
Rice KC (1999) Trace-element concentrations in streambed sediment across the conterminous United States. *Environmental Science & Technology* 33: 2499–2504.
Riedel GF (1993) The annual cycle of arsenic in a temperate estuary. *Estuaries* 16: 533–540.
Robinson B, Outred H, Brooks R, and Kirkman J (1995) The distribution and fate of arsenic in the Waikato River System, North Island, New Zealand. *Chemical Speciation and Bioavailability* 7: 89–96.
Rochette EA, Bostick BC, Li GC, and Fendorf S (2000) Kinetics of arsenate reduction by dissolved sulfide. *Environmental Science & Technology* 34: 4714–4720.
Rojas JC and Vandecasteele C (2007) Influence of mining activities in the north of Potosi, Bolivia on the water quality of Chayanta River, and its consequences. *Environmental Monitoring and Assessment* 132: 321–330.
Rosen BP (2002) Biochemistry of arsenic detoxification. *FEBS Letters* 529: 86–92.
Rosenboom JW, Ahmed KM, Pfaff A, and Madajewicz M (2004) Arsenic in 15 upazilas of Bangladesh: Water supplies, health and behaviour. Report prepared for APSU.
Rosenfield I and Beath OA (1964) *Selenium; Geobotany, Biochemistry, Toxicity and Nutrition*. New York: Academic Press.
Ross SM, Wood MD, Copplestone D, Warriner M, and Crook P (2007) Environmental concentrations of heavy metals in UK soil and herbage. *UK Soil and Herbage Pollutant Survey UKSHS Report No. 7*. Rotherham: Environment Agency.
Rotkin-Ellman M, Solomon G, Gonzales CR, Agwaramgbo L, and Mielke HW (2010) Arsenic contamination in New Orleans soil: Temporal changes associated with flooding. *Environmental Research* 110(1): 19–25.
Rotruck JT, Pope AL, Ganther HE, and Hoekstra WG (1972) Prevention of oxidative damage to rat erythrocytes by dietary selenium. *Journal of the American Chemical Society* 79: 3292–3293.
Roussel C, Bril H, and Fernandez A (2000) Arsenic speciation: Involvement in evaluation of environmental impact caused by mine wastes. *Journal of Environmental Quality* 29: 182–188.
Rowell DL (1994) *Soil Science Methods and Applications*. Harlow: Longman Scientific and Technical.
Ryker SJ (2001) Mapping arsenic in groundwater: A real need, but a hard problem – Why was the map created? *Geotimes* 46: 34–36.
Salminen R and Gregorauskiene V (2000) Considerations regarding the definition of a geochemical baseline of elements in the surficial materials in areas differing in basic geology. *Applied Geochemistry* 15: 647–653.
Sancha AM and Castro M (2001) Arsenic in Latin America: Occurrence, exposure, health effects and remediation. In: Chappell WR, Abernathy CO, and Calderon RL (eds.) *Arsenic Exposure and Health Effects*, vol. IV, pp. 87–96. Amsterdam: Elsevier.
Santini JM, Vanden Hoven RN, and Macy JM (2002) Characteristics of newly discovered arsenite-oxidizing bacteria. In: Frankenberger W (ed.) *Environmental Chemistry of Arsenic*, ch. 14, pp. 329–342. New York: Marcel Dekker.
Savage KS, Bird DK, and Ashley RP (2000) Legacy of the California Gold Rush: Environmental geochemistry of arsenic in the southern Mother Lode Gold District. *International Geology Review* 42: 385–415.
Schreiber ME, Simo JA, and Freiberg PG (2000) Stratigraphic and geochemical controls on naturally occurring arsenic in groundwater, eastern Wisconsin, USA. *Hydrogeology Journal* 8: 161–176.
Schroeder RA, Orem WH, and Kharaka YK (2002) Chemical evolution of the Salton Sea, California: Nutrient and selenium dynamics. *Hydrobiologia* 473: 23–45.
Schwedt G and Rieckhoff M (1996) Analysis of oxothio arsenic species in soil and water. *Journal Fur Praktische Chemie-Chemiker-Zeitung* 338: 55–59.
Scott MJ and Morgan JJ (1995) Reactions at oxide surfaces. 1. Oxidation of As(III) by synthetic birnessite. *Environmental Science & Technology* 29: 1898–1905.
Seyler P and Martin J-M (1989) Biogeochemical processes affecting arsenic species distribution in a permanently stratified lake. *Environmental Science & Technology* 23: 1258–1263.
Seyler P and Martin JM (1990) Distribution of arsenite and total dissolved arsenic in major French estuaries: Dependence on biogeochemical processes and anthropogenic inputs. *Marine Chemistry* 29: 277–294.
Seyler P and Martin JM (1991) Arsenic and selenium in a pristine river-estuarine system: The Krka (Yugoslavia). *Marine Chemistry* 34: 137–151.
Shamberger R and Frost D (1969) Possible inhibitory effect of selenium on human cancer. *Canadian Medical Association Journal* 100: 682.
Shand CA, Balsam M, Hillier SJ, et al. (2010) Aqua regia extractable selenium concentrations of some Scottish topsoils measured by ICP-MS and the relationship with mineral and organic soil components. *Journal of the Science of Food and Agriculture* 90: 972–980.
Shiller A and Taylor H (1996) Comment on 'Problems associated with using filtration to define dissolved trace element concentrations in natural water samples'. *Environmental Science & Technology* 30: 3397–3398.
Shotyk W (1996) Natural and anthropogenic enrichments of As, Cu, Pb, Sb, and Zn in ombrotrophic versus minerotrophic peat bog profiles, Jura Mountains, Switzerland. *Water, Air, and Soil Pollution* 90: 375–405.
Sides AD (1995) Can gold mining at Mokrsko (Czech Republic) be environmentally acceptable? In: Pasava J, Kribek B, and Zak K (eds.) *Mineral Deposits: From Their Origin to Their Environmental Impact*, pp. 701–703. Rotterdam: Balkema.
Simon G, Kesler SE, and Chryssoulis S (1999) Geochemistry and textures of gold-bearing arsenian pyrite, Twin Creeks, Nevada: Implications for deposition of gold in Carlin-type deposits. *Economic Geology and the Bulletin of the Society of Economic Geologists* 94: 405–421.
Sloth JJ and Larsen EH (2000) The application of inductively coupled plasma dynamic reaction cell mass spectrometry for measurement of selenium isotopes, isotope ratios and chromatographic detection of selenoamino acids. *Journal of Analytical Atomic Spectrometry* 15: 669–672.
Smedley PL (1996) Arsenic in rural groundwater in Ghana. *Journal of African Earth Sciences* 22: 459–470.
Smedley PL (2003) Arsenic in groundwater – South and east Asia. In: Welch AH and Stollenwerk KG (eds.) *Arsenic in Ground Water: Geochemistry and Occurrence*, pp. 179–209. Boston, MA: Kluwer Academic.
Smedley PL and Edmunds WM (2002) Redox patterns and trace-element behavior in the East Midlands Triassic sandstone aquifer, UK. *Ground Water* 40: 44–58.
Smedley PL and Kinniburgh DG (2002) A review of the source, behaviour and distribution of arsenic in natural waters. *Applied Geochemistry* 17: 517–568.
Smedley PL, Kinniburgh DG, Huq I, Luo ZD, and Nicolli HB (2001a) International perspective on arsenic problems in groundwater. In: Chappell WR, Abernathy CO, and Calderon RL (eds.) *Arsenic Exposure and Health Effects*, vol. IV, pp. 9–26. Amsterdam: Elsevier.
Smedley PL, Kinniburgh DG, Milne C, Trafford JM, Huq SI, and Ahmed KM (2001b) Hydrogeochemistry of three special study areas. In: Kinniburgh DG and Smedley PL (eds.) *Arsenic Contamination of Groundwater in Bangladesh, Final Report, BGS Report WC/00/19*, vol. 2, ch. 7, pp. 105–149. Keyworth: British Geological Survey.
Smedley PL, Nicolli HB, Macdonald DMJ, Barros AJ, and Tullio JO (2002) Hydrogeochemistry of arsenic and other inorganic constituents in groundwaters from La Pampa, Argentina. *Applied Geochemistry* 17: 259–284.
Smedley PL, Zhang M-Y, Zhang G-Y, and Luo Z-D (2003) Mobilisation of arsenic and other trace elements in fluviolacustrine aquifers of the Huhhot Basin, Inner Mongolia. *Applied Geochemistry* 18(9): 1453–1477.
Smith AH, Lingas EO, and Rahman M (2000) Contamination of drinking-water by arsenic in Bangladesh: A public health emergency. *Bulletin of the World Health Organization* 78: 1093–1103.
Smith A, Lopipero P, Bates M, and Steinmaus C (2002) Arsenic epidemiology and drinking water standards. *Science* 296: 2145–2146.
Spear JM (2006) Evaluation of arsenic field test: Kits for drinking water analysis. *Journal of American Water Works Association* 98(12): 97–105.
Steinhoff PJ, Smith BW, Warner DW, and Moller G (1999) Analysis of interlaboratory performance in the determination of total selenium in water. *Journal of AOAC International* 82: 1466–1473.
Stolz JF and Oremland RS (1999) Bacterial respiration of arsenic and selenium. *FEMS Microbiology Reviews* 23: 615–627.
Suetens C, Moreno-Reyes R, Chasseur C, et al. (2001) Epidemiological support for a multifactorial aetiology of Kashin–Beck disease in Tibet. *International Orthopaedics* 25: 180–187.
Sullivan KA and Aller RC (1996) Diagenetic cycling of arsenic in Amazon shelf sediments. *Geochimica et Cosmochimica Acta* 60: 1465–1477.
Sun G (2004) Arsenic Contamination and Arsenicosis in China. *Toxicology and Applied Pharmacology* 198(3): 268–271.
Swanson VE, Medlin JH, Hatch JR, Coleman SL, Woodruff SD, and Hildebrand RT (1976) Collection, chemical analysis and evaluation of 799 coal samples in 1975. *US Geological Survey Open-File Report 76–468*, pp. 503. Menlo Park, CA: US Geological Survey.
Swash PM and Monhemius AJ (1996) Characeristics of calcium arsenate compounds relevant to disposal of arsenic from industrial processes. Minerals, Metals and the

Environment II, Prague, Czech Republic, 3–6 September 1996, IMM, London. pp. 353–361.
Tan J (1989) *The Atlas of Endemic Diseases and Their Environments in the People's Republic of China*. Beijing: Science Press.
Taniguchi T, Tao H, Tominaga M, and Miyazaki A (1999) Sensitive determination of three arsenic species in water by ion exclusion chromatography-hydride generation inductively coupled plasma mass spectrometry. *Journal of Analytical Atomic Spectrometry* 14: 651–655.
Thomas DJ, Styblo M, and Lin S (2001) The cellular metabolism and systemic toxicity of arsenic. *Toxicology and Applied Pharmacology* 176: 127–144.
Thomson J, Nixon S, Croudace IW, et al. (2001) Redox-sensitive element uptake in north-east Atlantic Ocean sediments (Benthic Boundary Layer Experiment sites). *Earth and Planetary Science Letters* 184: 535–547.
Thornton I, Kinniburgh DG, Pullen G, and Smith CA (1983) Geochemical aspects of selenium in British soils and implications to animal health. In: Hemphill DD (ed.) *Trace Substances in Environmental Health*, vol. XVII, pp. 391–398. Columbia, MO: University of Missouri.
Tokunaga T, Pickering I, and Brown G (1996) Selenium transformations in ponded sediments. *Soil Science Society of America Journal* 60: 781–790.
Tokunaga T, Zawislanski P, Johannis P, Lipton D, and Benson S (1994) Field investigations of selenium speciation, transformation, and transport in soils from Kesterson Reservoir and Lahontan valley. In: Frankenberger T and Benson S (eds.) *Selenium in the Environment*, ch. 5, pp. 119–138. New York: Marcel Dekker.
Tournassat C, Charlet L, Bosbach D, and Manceau A (2002) Arsenic(III) oxidation by birnessite and precipitation of manganese(II) arsenate. *Environmental Science & Technology* 36: 493–500.
Tseng WP, Chu HM, How SW, Fong JM, Lin CS, and Yeh S (1968) Prevalence of skin cancer in an endemic area of chronic arsenicism in Taiwan. *Journal of the National Cancer Institute* 40: 453–463.
Umitsu M (1993) Late quaternary sedimentary environments and landforms in the Ganges Delta. *Sedimentary Geology* 83: 177–186.
US EPA (1999) Waste leachability: The need for review of current agency procedures. *US EPA Report EPA-SAB-EEC-COM-99-002*. Washington, DC: US Environmental Protection Agency.
US EPA (2006) *Revised Reregistration Eligibility Decision for MSMA, DSMA, CAMA and Cacodylic Acid*. Washington, DC: US Environmental Protection Agency.
US EPA (2011) *Air Toxics Web-site: Selenium and Compounds*. Washington, DC: US Environmental Protection Agency. http://www.epa.gov/ttn/atw/hlthef/selenium.html.
USGS (2005) *Mineral Commodity Summaries*. Washington, DC: US Geological Survey.
Vagliasindi FGA and Benjamin MM (2001) Redox reactions of arsenic in As-spiked lake water and their effects on As adsorption. *Journal of Water Supply Research and Technology – AQUA* 50: 173–186.
Van der Veer, G. (2006) *Geochemical Soil Survey of the Netherlands. Atlas of Major and Trace Elements in Topsoil and Parent Material: Assessment of Natural and Anthropogenic Enrichment Factors*. PhD Thesis, Utrecht University.
Varsányi I, Fodr Z, and Bartha A (1991) Arsenic in drinking water and mortality in the southern Great Plain, Hungary. *Environmental Geochemistry and Health* 13: 14–22.
Ventura MG, do Carmo Freitas M, Pacheco A, and Wolterbeek HT (2007) Selenium content in selected Portuguese foodstuffs. *European Food Research and Technology* 224: 395–401.
Vinceti M, Nacci G, Rocchi E, et al. (2000) Mortality in a population with long-term exposure to inorganic selenium via drinking water. *Journal of Clinical Epidemiology* 53: 1062–1068.
Vinceti M, Rothman KJ, Bergomi M, Borciani N, Serra L, and Vivoli G (1998) Excess melanoma incidence in a cohort exposed to high levels of environmental selenium. *Cancer Epidemiology, Biomarkers & Prevention* 7: 853–856.
Voegelin A and Hug S (2003) Catalyzed oxidation of arsenic(III) by hydrogen peroxide on the surface of ferrihydrite: An in situ ATR-FTIR study. *Environmental Science & Technology* 37(5): 972–978.
Wainipee W, Weiss DJ, Sephton MA, Coles BJ, Unsworth C, and Court R (2010) The effect of crude oil on arsenate adsorption on goethite. *Water Research* 44(19): 5673–5683. http://dx.doi.org/10.1016/j.watres.2010.05.056.
Waalkes MP, Liu J, and Diwan BA (2007) Transplacental arsenic carcinogenesis in mice. *Toxicology and Applied Pharmacology* 222: 271–280.
Wang ZJ and Gao YX (2001) Biogeochemical cycling of selenium in Chinese environments. *Applied Geochemistry* 16: 1345–1351.
Wang R, Hsu Y, Chang L, and Jiang S (2007) Speciation analysis of arsenic and selenium compounds in environmental and biological samples by ion chromatography–inductively coupled plasma dynamic reaction cell mass spectrometer. *Analytica Chimica Acta* 590: 239–244. http://dx.doi.org/10.1016/j.aca.2007.03.045.
Wang L and Huang J (1994) Chronic arsenism from drinking water in some areas of Xinjiang, China. In: Nriagu JO (ed.) *Arsenic in the Environment, Part II: Human Health and Ecosystem Effects*, pp. 159–172. New York: Wiley.
Wang HC, Wang PH, Peng CY, Liu SH, and Wang YW (2001) Speciation of As in the blackfoot disease endemic area. *Journal of Synchrotron Radiation* 8: 961–962.
Wang X, Yang H, Gong P, et al. (2010) One century sedimentary records of polycyclic aromatic hydrocarbons, mercury and trace elements in the Qinghai Lake, Tibetan Plateau. *Environmental Pollution* 158: 3065–3070. http://dx.doi.org/10.1016/j.envpol.2010.06.034.
Watts MJ, O'Reilly J, Marcilla AL, Shaw RA, and Ward NI (2010) Field based speciation of arsenic in UK and Argentinean water samples. *Environmental Geochemistry and Health* 32(6): 479–490.
Webb J (1978) *The Wolfson Geochemical Atlas of England and Wales*. Oxford: Clarendon Press.
Webster JG, Nordstrom DK, and Smith KS (1994) Transport and natural attenuation of Cu, Zn, As, and Fe in the acid mine drainage of Leviathan and Bryant creeks. *ACS Symposium Series* 550: 244–260.
Welch AH, Helsel DR, Focazio MJ, and Watkins SA (1999) Arsenic in ground water supplies of the United States. In: Chappell WR, Abernathy CO, and Calderon RL (eds.) *Arsenic Exposure and Health Effects*, pp. 9–17. Amsterdam: Elsevier.
Welch AH and Lico MS (1998) Factors controlling As and U in shallow ground water, southern Carson Desert, Nevada. *Applied Geochemistry* 13: 521–539.
Welch AH, Lico MS, and Hughes JL (1988) Arsenic in ground-water of the Western United States. *Ground Water* 26: 333–347.
Welch AH, Westjohn DB, Helsel DR, and Wanty RB (2000) Arsenic in ground water of the United States: Occurrence and geochemistry. *Ground Water* 38: 589–604.
White A and Dubrovsky N (1994) Chemical oxidation–reduction controls on selenium mobility in groundwater systems. In: Frankenberger WT and Benson S (eds.) *Selenium in the Environment*, ch. 8, pp. 185–221. New York: Marcel Dekker.
WHO (1986) *Selenium – Environmental Aspects*. Geneva: World Health Organization. vol. 58.
WHO (1987) *Environmental Health Criterion – Selenium*. Geneva: World Health Organization. vol. 58.
WHO (1993) *Guidelines for Drinking-Water Quality*. Geneva: World Health Organisation.
WHO (1996) *Trace Elements in Human Nutrition and Health*. Geneva: World Health Organization.
WHO (2011) Guidelines for Drinking-Water Quality, 4th Edition. Geneva: World Health Organization.
Widerlund A and Ingri J (1995) Early diagenesis of arsenic in sediments of the Kalix River estuary, Northern Sweden. *Chemical Geology* 125: 185–196.
Wijnja H and Schulthess CP (2000) Interaction of carbonate and organic anions with sulfate and selenate adsorption on an aluminum oxide. *Soil Science Society of America Journal* 64: 898–908.
Wilde F and Radtke D (2008) Field measurements. In: *Handbooks for Water-Resources Investigations. National Field Manual for the Collection of Water-Quality Data*, ch. A6, Book 9. Menlo Park, CA: US Geological Survey.
Wilkie JA and Hering JG (1998) Rapid oxidation of geothermal arsenic(III) in streamwaters of the eastern Sierra Nevada. *Environmental Science & Technology* 32: 657–662.
Williams M (2001) Arsenic in mine waters: An international study. *Environmental Geology* 40: 267–279.
Williams M, Fordyce F, Paijitprapapon A, and Charoenchaisri P (1996) Arsenic contamination in surface drainage and groundwater in part of the southeast Asian tin belt, Nakhon Si Thammarat Province, southern Thailand. *Environmental Geology* 27: 16–33.
Wilson FH and Hawkins DB (1978) Arsenic in streams, stream sediments and ground water, Fairbanks area, Alaska. *Environmental Geology* 2: 195–202.
Winkel LHE, Trang PKT, Lan VM, et al. (2011) Arsenic pollution of groundwater in Vietnam exacerbated by deep aquifer exploitation for more than a century. *Proceedings of the National Academy of Sciences of the United States of America* 108(4): 1246–1251.
Wolfe-Simon F, Blum JS, Kulp TR, et al. (2011) A bacterium that can grow by using arsenic instead of phosphorus. *Science* 332(6034): 1163–1166.
Wu L (2004) Review of 15 years of research on ecotoxicology and remediation of land contaminated by agricultural drainage sediment rich in selenium. *Ecotoxicology and Environmental Safety* 57: 257–269.
Wu L, Banuelos G, and Guo X (2000) Changes of soil and plant tissue selenium status in an upland grassland contaminated by selenium-rich agricultural drainage sediment after ten years transformed from a wetland habitat. *Ecotoxicology and Environmental Safety* 47: 201–209.
Xiao L, Wildgoose GG, and Compton RG (2008) Sensitive electrochemical detection of arsenic (III) using gold nanoparticle modified carbon nanotubes via anodic stripping voltammetry. *Analytica Chimica Acta* 620: 44–49. http://dx.doi.org/10.1016/j.aca.2008.05.015.

Xu G and Jiang Y (1986) Se and the prevalence of Keshan and Kaschin-Beck diseases in China. In: Thornton I (ed.) *Proceedings of the First International Symposium on Geochemistry and Health*, pp. 192–205. Northampton: Science Reviews.

Xu Y, Tokar EJ, Sun Y, and Waalkes MP (2012) Arsenic-Transformed Malignant Prostate Epithelia Can Convert Noncontiguous Normal Stem Cells into an Oncogenic Phenotype. *Environmental Health Perspectives*. 120: 865–871.

Yalcin S and Le XC (1998) Low pressure chromatographic separation of inorganic arsenic species using solid phase extraction cartridges. *Talanta* 47: 787–796.

Yamamura S (2003) Drinking water guidelines and standards. In: Hashizume H and Yamamura S (eds.) *Arsenic, Water and Health: The State of the Art*, ch. 5. Geneva: World Health Organization.

Yan XP, Kerrich R, and Hendry MJ (2000) Distribution of arsenic(III), arsenic(V) and total inorganic arsenic in porewaters from a thick till and clay-rich aquitard sequence, Saskatchewan, Canada. *Geochimica et Cosmochimica Acta* 64: 2637–2648.

Yang G, Wang S, Zhou R, and Sun S (1983) Endemic selenium intoxication of humans in China. *The American Journal of Clinical Nutrition* 37: 872–881.

Yang G and Xia M (1995) Studies on human dietary requirements and safe range of dietary intakes of selenium in China and their application to the prevention of related endemic diseases. *Biomedical and Environmental Sciences* 8: 187–201.

Zawislanski PT, Chau S, Mountford H, Wong HC, and Sears TC (2001a) Accumulation of selenium and trace metals on plant litter in a tidal marsh. *Estuarine, Coastal and Shelf Science* 52: 589–603.

Zawislanski PT, Mountford HS, Gabet EJ, McGrath AE, and Wong HC (2001b) Selenium distribution and fluxes in intertidal wetlands, San Francisco Bay, California. *Journal of Environmental Quality* 30: 1080–1091.

Zawislanski PT and Zavarin M (1996) Nature and rates of selenium transformations in Kesterson Reservoir soils: A laboratory study. *Soil Science Society of America Journal* 60: 791–800.

Zhang H, Davison W, Gadi R, and Kobayashi T (1998) In situ measurement of dissolved phosphorus in natural waters using DGT. *Analytica Chemica Acta* 370: 29–38.

Zheng B, Yu X, Zhand J, Zhou D (1996) Environmental geochemistry of coal and endemic arsenism in southwest Guizhou, P.R. China, 30th International Geologic Congress, vol. 3, Abstracts p. 410.

Zobrist J, Dowdle PR, Davis JA, and Oremland RS (2000) Mobilization of arsenite by dissimilatory reduction of adsorbed arsenate. *Environmental Science & Technology* 34: 4747–4753.

11.3 Heavy Metals in the Environment – Historical Trends

E Callender, US Geological Survey, Westerly, RI, USA

Published by Elsevier Ltd.

This article is reproduced from the previous edition, volume 9, pp. 67–105, Published by Elsevier Ltd.

11.3.1 Introduction

11.3.1.1 Metals: Pb, Zn, Cd, Cr, Cu, Ni

These six metals, commonly classified as heavy metals, are a subset of a larger group of trace elements that occur in low concentration in the Earth's crust. These heavy metals were mined extensively for use in the twentieth century Industrial Society. Nriagu (1988a) estimated that between 0.5 (Cd) and 310 (Cu) million metric tons of these metals were mined and ultimately deposited in the biosphere. In many instances, the inputs of these metals from anthropogenic sources exceed the contributions from natural sources (weathering, volcanic eruptions, forest fires) by several times (Adriano, 1986). In this chapter, heavy metals (elements having densities greater than 5) and trace elements (elements present in the lithosphere in concentrations less than 0.1%) are considered synonymous.

It has been observed in the past that the rate of emission of these trace metals into the atmosphere is low due to their low volatility. However, with the advent of large-scale metal mining and smelting as well as fossil-fuel combustion in the twentieth century, the emission rate of these metals has increased dramatically. As most of these emissions are released into the atmosphere where the mammals live and breathe, we see a great increase in the occurrence of health problems such as lead (Pb) poisoning, cadmium (Cd) Itai-itai disease, chromium (Cr), and nickel (Ni) carcinogenesis.

In this chapter, the author has attempted to present a synopsis of the importance of these metals in the hydrocycle, their natural and anthropogenic emissions into the environment, their prevalent geochemical form incorporated into lacustrine sediments, and their time-trend distributions in watersheds that have been impacted by urbanization, mining and smelting, and

other anthropogenic activities. These time trends are reconstructed from major–minor–trace–element distributions in age-dated sediment cores, mainly from reservoirs where the mass sedimentation rates (MSRs) are orders of magnitude greater than those in natural lakes, the consequences of which tend to preserve the heavy-metal signatures and minimize the metal diagenesis (Callender, 2000). This chapter focuses mainly on the heavy metals in the terrestrial and freshwater environments whilst the environmental chemistry of trace metals in the marine environment is discussed in Nightingale and Liss (2003).

The data presented in **Tables 2–5** are updated as much as possible, with many of the references postdate the late 1980s. Notable exceptions are riverine particulate matter chemistry (**Table 2**), some references in **Table 3**, and references concerning the geochemical properties of the six heavy metals discussed in this chapter. There appears to be no recent publication that updates the worldwide average for riverine particulate matter trace metal chemistry (Martin and Whitfield, 1981; Martin and Windom, 1991).This is supported by the fact that two recent references (Li, 2000; Chester, 2000) concerning marine chemistry still refer to this 1981 publication. As for references in **Table 3**, there is a very limited data available concerning the pathways of heavy-metal transport to lakes. Some of the important works have been considered and reviewed in this chapter. In addition, the analytical chemistry of the sedimentary materials has changed little over the past 30 years until the advent and use of inductively coupled plasma/mass spectrometry (ICP/MS) in the late 1990s. Extensive works concerning the geochemical properties of heavy metals have been published during the past 40 years and to the author's knowledge these have survived the test of time.

11.3.1.2 Sources of Metals

There are a variety of natural and anthropogenic sources of these heavy metals (Pb, Zn, Cd, Cr, Cu, Ni) in the environment.

11.3.1.2.1 Natural

The principal natural source of heavy metals in the environment is from crustal material that is either weathered on (dissolved) and eroded from (particulate) the Earth's surface or injected into the Earth's atmosphere by volcanic activity. These two sources account for 80% of all the natural sources; forest fires and biogenic sources, account for 10% each (Nriagu, 1990b). Particles released by erosion appear in the atmosphere as windblown dust. In addition, some particles are released by vegetation. The natural emissions of the six heavy metals are 12 000 (Pb); 45 000 (Zn); 1400 (Cd); 43 000 (Cr); 28 000 (Cu); and 29 000 (Ni) metric tons per year, respectively (Nriagu 1990b). Thus, we can conclude that an abundant quantity of metals are emitted into the atmosphere from natural sources. The quantity of anthropogenic emissions of these metals is given in the next section.

11.3.1.2.2 Anthropogenic

There are a multitude of anthropogenic emissions in the environment. The major source of these metals is from mining and smelting. Mining releases metals to the fluvial environment as tailings and to the atmosphere as metal-enriched dust whereas smelting releases metals to the atmosphere as a result of high-temperature refining processes. In the lead industry, Pb–Cu–Zn–Cd are released in substantial quantities; during Cu and Ni smelting, Co–Zn–Pb–Mn as well as Cu–Ni are released; and in the Zn industry, sizeable releases of Zn–Cd–Cu–Pb occur (Adriano, 1986). **Table 1** shows that the world metal production during the 1970s and the 1980s has remained relatively constant except for Cr production that substantially increased during the 1980s due to the technological advances and increased importance (Faust and Aly, 1981).

Much of the demand for Cr was due to steel and iron manufacturing and the use of Cr in pressure-treated lumber (Alloway, 1995). **Table 1** also shows that anthropogenic emissions to the atmosphere, to which mining and smelting are major contributors, are in the interval of two times (Cu, Ni), five times (Zn, Cd), and 33 times (Pb) greater than the natural emissions of metals to the atmosphere. Anthropogenic atmospheric emissions decreased substantially from the 1970s to the 1980s for Pb, Zn, and Cu (**Table 1**). On the other hand, Cd and Cr have remained the same and Ni emissions have increased in the 1980s. In addition, anthropogenic emissions of Cr are only about one-half of those from the natural sources. The major contributor of Cr to natural atmospheric emissions is windblown dust (Nriagu and Pacyna, 1988).

Other important sources of metals to the atmosphere include fossil-fuel combustion (primarily coal), municipal waste incineration, cement production, and phosphate mining (Nriagu and Pacyna, 1988). Important sources of metals to the terrestrial and aquatic environment include discharge of sewage sludges, use of commercial fertilizers and pesticides,

Table 1 Global primary production and emissions of six heavy metals during the 1970s and the 1980s

Metal	*Metal production*		*Emissions to air*		*Emissions to soil*	*Emissions to water*
	1970s	*1980s*	*1970s*	*1980s*	*1980s*	*1980s*
Pb	3400	3100	449	332	796	138
Zn	5500	5200	314	132	1372	226
Cd	17	15	7.3	7.6	22	9.4
Cr	6000	11 250	24	30	896	142
Cu	6000	7700	56	35	954	112
Ni	630	760	47	56	325	113

All values are thousand metric tons.
Source: Nriagu (1980a), Pacyna (1986), and Nriagu and Pacyna (1988).

animal waste and waste-water discharge (Nriagu and Pacyna, 1988). Table 1 shows that metal emissions to soil are several times those to air, suggesting that land disposal of mining wastes, chemical wastes, combustion slags, municipal wastes, and sewage sludges are the major contributors of these emissions. Emissions to water are only about twice those relative to air (except for Pb and Cd) suggesting that direct chemical and wastewater releases to the aquatic environment are the only additional inputs besides the atmospheric emissions (Table 1).

Table 2 gives a comparison of the six heavy-metal contents of a variety of natural earth materials that annually impact atmospheric, terrestrial, and aquatic environments. The primary data of metals are also normalized with respect to titanium (Ti). Titanium is a very conservative element that is associated with crustal rock sources. Normalization with respect to Ti compensates for the relative percentage of various diluents (non-crustal rock sources) and allows one to see more clearly metal enrichment due to anthropogenic inputs. For instance, in Table 2, recent lacustrine sediment is clearly enriched in metal content relative to pre-Industrial lacustrine sediment.

It is obvious that there is a progressive enrichment in the metal content of the earth materials as one migrates from the Earth's upper crust to the soils to river mud to lacustrine sediments, and finally to the river particulate matter. This is especially true for Zn and Cd. If we consider the recent lacustrine sediments, then Pb, Zn, Cd, and Cu are all highly enriched compared to the upper crust and soils. Chromium and Ni, on the other hand, are not especially enriched when compared to the crust and soils (Table 2). The metal content of the river particulate matter is also highly enriched in relation to the crust and soils. It is obvious that anthropogenic activities have a pronounced effect on the particulate matter chemistry of lakes and rivers. It is also obvious that much of the enriched portion of the riverine particulates are deposited near river mouths and in the coastal zone (continental shelf) as the Ti-normalized metals for estuarine sediments and hemipelagic mud are less enriched than riverine particulates but still enriched relative to the crust and soils. Table 2 also shows the effect of diagenetic remobilization and reprecipitation of ferromanganese oxides in surficial pelagic clays as both Cu and Ni (major accessory elements in ferromanganese nodules) are significantly enriched in these marine deposits relative to the precursor earth materials. Finally, Table 2 shows the effects of high-temperature combustion on the enrichment of metals in coals as they are concentrated in fly ash. This is especially true for Pb, Zn, Cr, Cu, and Ni.

11.3.1.3 Source and Pathways

The two main pathways for heavy metals to become incorporated into air–soil–sediment–water are transport by air (atmospheric) and water (fluvial). In the previous section it was shown that heavy-metal emissions to air and water (Table 1) are a significant percentage of the amounts of metals that are extracted from the Earth's crust by mining. Ores are refined by smelting thus releasing large amounts of metal waste to the environment (primary source). Relatively pure metals are incorporated into a multitude of technological products which, when discarded, produce a secondary, but important, source of metals to the environment. Metals are also incorporated naturally and technologically into foodstuffs which, when consumed and discarded by man, result in an important metal source to the aquatic environment (sewage wastewater), soils, and sediments (sewage sludge).

We can see from Table 3 that except for Pb in the terrestrial environment and Cd in the marine environment, metal transport to the lakes and to the oceans via water (fluvial) is many times greater (2–10) than that by air (atmospheric). This undoubtedly reflects the prevalence of wastewater discharges from sewage–municipal–industrial inputs that are so common in our industrialized society. The prevalence of Pb atmospheric emissions is probably due to the burning of leaded gasoline which was phased out in North America and Western Europe by the early 1990s but is still occurring in the Third World countries. Natural atmospheric emissions of Cd (volcanoes) are most likely the cause of substantial atmospheric Cd fluxes to the marine environment (Nriagu, 1990b).

11.3.2 Occurrence, Speciation, and Phase Associations

11.3.2.1 Geochemical Properties and Major Solute Species

11.3.2.1.1 Lead

Lead (atomic no. 82) is a bluish-white metal of bright luster, is soft, very malleable, ductile, and a poor conductor of electricity. Because of these properties and its low melting point (327 °C), and resistance to corrosion, Pb has been used in the manufacture of metal products for thousands of years. In fact, the ancient world technology for smelting Pb–Ag alloys from PbS ores was developed 5000 years ago (Settle and Patterson, 1980). Lead has a density of 11.342 g cm^{-3}, hence finds extensive use as a shield for radiation; its atomic weight is 207.2. Lead has two oxidation states, +2 and +4. The tetravalent state is a powerful oxidizing agent but is not common in the Earth's surficial environment; the divalent state, on the other hand, is the most stable oxidation level and most Pb^{2+} salts with naturally-occurring common anions are only slightly soluble. It is composed of four stable isotopes ($^{208}Pb = 52\%$) and several radioisotopes whose longest half-life is 15 Myr (Reimann and de Caritat, 1998). Lead belongs to group IVa of the periodic table which classifies it as a heavy metal whose geochemical affinity is chalcophilic (associated with sulfur).

In a simple freshwater system, exposed to atmospheric CO_2 and containing 10^{-3} M Cl^-, 10^{-4} M SO_4^{-2}, and 10^{-6} M HPO_4^{-2}, it is predicted that Pb will be complexed by the carbonate species $Pb(CO_3)_2^{-2}$ in the pH range of 6–8 (Hem and Durum, 1973). The complex $PbSO_4^0$ is stable below pH 6 (or in low sulfate waters Pb^{2+}) and the complex $Pb(OH)_2$ is stable above pH 8 (Hem, 1976). In oxygenated stream and lake environments the concentration of dissolved Pb is less than 1 μg l^{-1} over the pH range of 6–8 (Reimann and de Caritat, 1998) while its average concentration in world river water is 0.08 μg l^{-1} (see Chapter 7.7). The dissolved Pb concentration in ocean water (0.002 μg l^{-1}) is an order of magnitude lower than that in river water (Chester, 2000).

Adsorption and aggregation-complexation with organic matter appear to be the most important processes that transform dissolved Pb to particulate forms in freshwater systems.

Table 2 Average concentration of six heavy metals in natural earth materials

Material	*Pb (ppm)*	*Zn (ppm)*	*Cd (ppm)*	*Cr (ppm)*	*Cu (ppm)*	*Ni (ppm)*	*Ti wt%*	*References*
Upper crust	17(52)	67(203)	0.1(0.30)	69(209)	39(118)	55(167)	0.33	Li (2000)
Average soils	26(68)	74(195)	0.1(0.26)	61(160)	23(60)	27(71)	0.38	Li (2000)
River mud	23(42)	78(142)	0.6(2.0)	85(155)	32(58)	32(58)	0.55	Govindaraju (1989)
Pre-industrial, baseline lacustrine sediment	22(69)	97(303)	0.3(0.55)	48(150)	34(106)	40(125)	0.32	Shafer and Armstrong (1991); Forstner (1981); Heit et al. (1984); Mudroch et al. (1988); Eisenreich (1980); Kemp et al. (1976, 1978); Wren et al. (1983); Wahlen and Thompson (1980)
Recent lacustrine sediment	102(316)	207(640)	2.2(6.8)	63(195)	60(186)	39(121)	0.32	Above references plus: Dominik et al. (1984); Rowell (1996); Mecray et al. (2001)
River particulate matter	68(120)	250(446)	1.2(2.1)	100(178)	100(178)	90(161)	0.56	Martin and Windom (1991); Martin and Whitfield (1981)
Estuarine sediment	54(108)	136(272)	1.2(2.4)	94(188)	52(104)	35(70)	0.50	Alexander et al. (1993); Coakley and Poulton (1993); Anikiyev et al. (1994); Hanson (1997)
Hemipelagic mud	23(49)	111(236)	0.2(0.44)	79(168)	43(91)	44(94)	0.47	Li (2000); Chester (2000)
Pelagic clay	80(174)	170(370)	0.4(0.9)	90(196)	250(543)	230(500)	0.46	Li (2000)
Coal	15(24)	53(84)	0.4(0.6)	27(43)	16(25)	17(27)	0.63	Tillman (1994); Adriano (1986)
Fly ash	43(70)	149(245)	0.5(0.8)	115(189)	56(92)	84(137)	0.61	Hower et al. (1999); Adriano (1986)

Values in parentheses are Ti-normalized.

Table 3 Relative percentage of atmospheric (%A) and fluvial (%F) inputs of six heavy metals to lakes, a coastal zone, and the ocean

Lake/Ocean	Metal												References
	Pb		Zn		Cd		Cr		Cu		Ni		
	%A	%F	%A	%F	%A	%F	%A	%F	%A	%F	%A	%F	
Lake IJsselmeer	NA	NA	7	93	2	98	0.1	99.9	6	94	1	99	Salomons (1983)
Southern Lake Michigan	47	53	22	78	NA	NA	NA	NA	13	87	NA	NA	Dolske and Sievering (1979)
Lake Michigan	60	40	35	65	10	90	41	59	15	85	NA	NA	Eisenreich (1980)
Lake Erie	40	60	12	88	NA	NA	NA	NA	9	91	NA	NA	Nriagu et al. (1979)
South Atlantic Bight	2	98	1	99	41	59	NA	NA	7	93	9	91	Chester (2000)
Ocean	15	85	5	95	17	83	3	97	2	98	5	95	Chester (2000)

NA = not available.

Krauskopf (1956) originally suggested that the concentration of Pb, as well as certain other trace metals, could be controlled by adsorption onto the ferric and manganese oxyhydroxides–clay mineral–organic matter. The extent of Pb adsorption onto hydrous Fe and Mn oxides is influenced by the physical characteristics of the adsorbent (specific surface, crystallinity, etc.) and the composition of the aqueous phase (pH, Eh, complexation, competing cations). In a recent study of Fe and Pb speciation, reactivity, and cycling in a lacustrine environment, Taillefert et al. (2000) determined that Pb is entrained during the formation of Fe-exocellular polymeric substances (EPS) that aggregate in a water column near the chemocline. It is not yet clear whether the metal is complexed to the EPS or adsorbed directly to the Fe oxide. However, extraction data from lake sediments suggest that the Pb–FeO_x phase is available to chemical attack (see below).

The average concentration of Pb in the lithosphere is about 14 $\mu g\, g^{-1}$ and the most abundant sources of the metal are the minerals galena (PbS), anglesite ($PbSO_4$), and cerussite ($PbCO_3$). The most important environmental sources for Pb are gasoline combustion (presently a minor source, but in the past 40 years a major contributor to Pb pollution), Cu–Zn–Pb smelting, battery factories, sewage sludge, coal combustion, and waste incineration.

11.3.2.1.2 Zinc

Zinc (atomic no. 30) is a bluish-white, relatively soft metal with a density of 7.133 $g\, cm^{-3}$. It has an atomic weight of 65.39, a melting point of 419.6 °C, and a boiling point of 907 °C. Zinc is divalent in all its compounds and is composed of five stable isotopes ($^{64}Zn = 49\%$) and a common radioisotope, ^{65}Zn, with a half-life of 245 days. It belongs to group IIb of the periodic table which classifies it as a heavy metal whose geochemical affinity is chalcophilic.

In freshwater, the uncomplexed Zn^{2+} ion dominates at an environmental pH below 8 whereas the uncharged $ZnCO_3^0$ ion is the main species at higher pH (Hem, 1972). Complexing of Zn with SO_4^{2-} becomes important at high sulfate concentrations or in acidic waters. Hydrolysis becomes significant at pH values greater than 7.5; hydroxy complexes of $ZnOH^-$ and $Zn(OH)_2^0$ do not exceed carbonate species at typical environmental concentrations of 15 $\mu g\, l^{-1}$ for world stream water (Reimann and de Caritat, 1998). More recent data of Gaillardet et al. (see **Chapter 7.7**) places the concentration of dissolved Zn in average world river water at 0.60 $\mu g\, l^{-1}$. Significant complexing with organic ligands may occur in stream and lake waters with highly soluble organic carbon concentrations. The concentration of Zn in ocean water is 0.39 $\mu g\, l^{-1}$ (Chester, 2000), which is close to its value in world river water.

There are several factors that determine the relative abundance of dissolved and particulate Zn in natural aquatic systems. These include media pH, biogeochemical degradation processes that produce dominant complexing ligands, cation exchange and adsorption processes that control the chemical potential of solid substrates, and the presence of occluded oxyhydroxide compounds (Adriano, 1986). At pH values above 7, aqueous complexed Zn begins to partition to particulate Zn as a result of sorption onto iron oxyhydroxide. The clay mineral montmorillonite is particularly efficient in removing Zn from solution by adsorption (Krauskopf, 1956; Farrah and Pickering, 1977).

The average Zn content of the lithosphere is, ~80 $\mu g\, g^{-1}$ and the most abundant sources of Zn are the ZnS minerals sphalerite and wurtzite and to a lesser extent smithsonite ($ZnCO_3$), willemite (Zn_2SiO_4), and zincite (ZnO) (Reimann and de Caritat, 1998). The smelting of nonferrous metals and the burning of fossil fuels and municipal wastes are the major Zn sources contributing to air pollution.

11.3.2.1.3 Cadmium

Cadmium has an atomic number of 48, an atomic weight of 112.40 consisting of eight stable isotopes ($^{112,114}Cd$ are most abundant), and a density of 8.65 $g\, cm^{-3}$ (Nriagu, 1980a). In several aspects Cd is similar to Zn (it is a neighbor of Zn in the periodic table); in fact it is almost always associated with Zn in mineral deposits and other earth materials. Cadmium is a soft, silvery white, ductile metal with a faint bluish tinge. It has a melting point of 321 °C and a boiling point of 765 °C. It belongs to group IIb of elements in the periodic table and in aqueous solution has the stable 2+ oxidation state. Cadmium is a rare element (67th element in order of abundance) with a concentration of ~0.1 $\mu g\, g^{-1}$ in the lithosphere and is strongly chalcophilic, like Zn.

In a natural, aerobic freshwater aquatic system with typical Cd–S–CO_2 concentrations (Hem, 1972), Cd^{2+} is the predominant species below pH 8, $CdCO_3^0$ is predominant from pH 8 to 10, and $Cd(OH)_2^0$ is dominant above pH 10. The solubility of Cd is minimum at pH 9.5 (Hem, 1972). The speciation

of Cd is generally considered to be dominated by dissolved forms except in cases where the concentration of suspended particulate matter is high such as 'muddy' rivers and reservoirs and near-bottom benthic boundary layers, and underlying bottom sediments in rivers and lakes (Li et al., 1984). The distribution coefficient between the particulate and the dissolved Cd is remarkably consistent for a wide range of riverine and lacustrine situations (Lum, 1987). The sorption of Cd on particulate matter and bottom sediments is considered to be a major factor affecting its concentration in natural waters (Gardiner, 1974). Pickering (1980) has quantitatively evaluated the role clay minerals, humic substances, and hydrous metal oxides in Cd adsorption and concludes that some fraction of the particle-bound Cd is irreversibly held by the solid substrate. The concentration of dissolved Cd in average world river water is 0.08 $\mu g\,l^{-1}$ (see **Chapter 7.7**). This concentration is identical to that of Cd in ocean water (0.079 $\mu g\,l^{-1}$; Chester, 2000).

11.3.2.1.4 Chromium

Chromium has an atomic number of 24, an atomic weight of 51.996 consisting of four stable isotopes ($^{52}Cr = 84\%$), and a density of 7.14 g cm^{-3} (Adriano, 1986). Crystalline Cr is steel-gray in color, lustrous, hard metal that has a melting point of 1900 °C and a boiling point of 2642 °C. It belongs to group VIb of the transition metals and in aqueous solution Cr exists primarily in the trivalent (+3) and hexavalent (+6) oxidation states. Chromium, as well as Zn, are the most abundant of the 'heavy metals' with a concentration of about 69 $\mu g\,g^{-1}$ in the lithosphere (Li, 2000).

In most natural waters at near neutral pH, Cr^{III} is the dominant form due to the very high redox potential for the couple Cr^{VI}/Cr^{III} (Rai et al., 1989). Chromium(III) forms strong complexes with hydroxides. Rai et al. (1987) report that the dominant hydroxo species are $CrOH^{2+}$ at pH values 4–6, $Cr(OH)_3^0$ at pH values from 6 to 11.5, and $Cr(OH)_4^-$ at pH values above 11.5. The OH^- ligand was the only significant complexer of Cr^{III} in natural aqueous solutions that contain environmental concentrations of carbonate, sulfate, nitrate, and phosphate ions. The only oxidant in natural aquatic systems that has the potential to oxidize Cr^{III} to Cr^{VI} is manganese dioxide. This compound is common on Earth's surface and thus one can expect to find some Cr^{VI} ions in natural waters. The predominant Cr^{VI} species at environmental pH is CrO_4^{2-} (Hem, 1985). The principal Cr^{III} solid compound that is known to control the solubility of Cr^{III} in nature is $Cr(OH)_3^0$. However, Sass and Rai (1987) have shown that $Cr/Fe(OH)_3$ has an even lower solubility. This compound is a solid solution and thus its solubility is dependent on the mole fraction of Cr; the lower the mole fraction, the lower the solubility (Sass and Rai, 1987). Most Cr^{VI} solids are expected to be relatively soluble under environmental conditions. In the absence of solubility-controlling solids, Cr^{VI} aqueous concentrations under neutral pH conditions will primarily be controlled by adsorption/desorption reactions (Rai et al., 1989). Under environmental conditions, iron oxides are the predominant adsorbents of chromate (Cr^{VI}) in acidic to neutral pH range and oxidizing environments. The Cr concentration in average world river water is 0.7 $\mu g\,l^{-1}$ (see **Chapter 7.7**) and that in ocean water is 0.21 $\mu g\,l^{-1}$ (Chester, 2000).

Chromium occurs in nature mainly in the mineral chromite; Cr also occurs in small quantities in many minerals in which it replaces Fe^{3+} and Al^{3+} (Faust and Aly, 1981). The metallurgy industry uses the highest quality chromite ore whilst the lower-grade ore is used for refractory bricks in melting furnaces. Major atmospheric emissions are from the chromium alloy and metal producing industries. Smaller emissions come from coal combustion and municipal incineration. In the aquatic environment, the major sources of Cr are electroplating and metal finishing industries. Hexavalent Cr^{VI} is a potent carcinogen and trivalent Cr^{III} is an essential trace element (Krishnamurthy and Wilkens, 1994).

11.3.2.1.5 Copper

Copper has an atomic number of 29, an atomic weight of 63.546, consists of two stable isotopes ($^{63}Cu = 69.2\%$; $^{65}Cu = 30.8\%$), and has a density of 8.94 g cm^{-3} (Webelements, 2002). Metallic Cucompounds (sulfides) are typically brassy yellow in color while the carbonates are a variety of green- and yellow-colored. The metal is somewhat malleable with a melting point of 1356 °C and a boiling point of 2868 °C. It belongs to group Ib of the transition metals and in aqueous solution Cu exists primarily in the divalent oxidation state although some univalent complexes and compounds of Cu do occur in nature (Leckie and Davis, 1979). Copper is a moderately abundant heavy metal with a concentration in the lithosphere of about 39 $\mu g\,g^{-1}$ (Li, 2000).

Chemical models for the speciation of Cu in freshwater (Millero, 1975) predict that free $Cu^{2+}(aq)$ is less than 1% of the total dissolved Cu and that $Cu(CO_3)_2^{2-}$ and $CuCO_3^0$ are equally important for the average river water. Leckie and Davis (1979) showed that the $CuCO_3^0$ complex is the most important one near the neutral pH. At pH values above 8, the dihydroxo–Copper(II) complex predominates. The chemical form of Cu is critical to the behavior of the element in geochemical and biological processes (Leckie and Davis, 1979). Cupric Cu forms strong complexes with many organic compounds.

In the sedimentary cycle, Cu is associated with clay mineral fractions, especially those rich in coatings containing organic carbon and manganese oxides. In oxidizing environments ($Cu–H_2O–O_2–S–CO_2$ system), Cu is likely to be more soluble under acidic than under alkaline conditions (Garrels and Christ, 1965). The mineral malachite is favored at pH values above 7. Under reducing conditions, Cu solubility is greatly reduced and the predominant stable phase is cuprous sulfide (Cu_2S) (Leckie and Nelson, 1975). In natural aquatic systems, some of the Cu is dissolved in freshwater streams and lakes as carbonate and organic complexes; a larger fraction is associated with the solid phases. Much of the particulate Cu is fixed in the crystalline matrix of the particles (Gibbs, 1973). Some of the riverine reactive particulate Cu may be desorbed as the freshwater mixes with seawater. The biological cycle of Cu is superimposed on the geochemical cycle. Copper is an essential element for the growth of most of the aquatic organisms but is toxic at levels as low as 10 $\mu g\,l^{-1}$ (Leckie and Davis, 1979). Copper has a greater affinity, than most of the other metals, for organic matter, organisms, and solid phases (Leckie and Davis, 1979) and the competition for Cu between the aqueous and the solid phases is very strong. Krauskopf (1956) noted that the concentration of copper in natural waters, 0.8–3.5 $\mu g\,l^{-1}$

(Boyle, 1979), is far below the solubility of known solid phases. Davis et al. (1978) found that the adsorption behavior of Cu in natural systems is strongly dependent on the type and concentration of inorganic and organic ligands. Recent data of Gaillardet et al. (see **Chapter 7.7**) places the concentration of dissolved Cu in average world river water at 1.5 $\mu g\,l^{-1}$ and that in ocean water at 0.25 $\mu g\,l^{-1}$ (Chester, 2000).

The most common Cu minerals, from which the element is refined into the metal, are Chalcocite (Cu_2S), Covellite (CuS), Chalcopyrite ($CuFeS_2$), Malachite and Azurite (carbonate compounds). It is not surprising that Cu is considered to have a chalcophillic geochemical affinity. In the past, the major source of Cu pollution was smelters that contributed vast quantities of Cu–S particulates to the atmosphere. Presently, the burning of fossil fuels and waste incineration are the major sources of Cu to the atmosphere and the application of sewage sludge, municipal composts, pig and poultry wastes are the primary sources of anthropogenic Cu contributed to the land surface (Alloway, 1995).

11.3.2.1.6 Nickel

Nickel has an atomic number of 28, an atomic weight of 58.71 consisting of five stable isotopes of which ^{58}Ni (67.9%) and ^{60}Ni (26.2%) are the most abundant, and a density of 8.9 $g\,cm^{-3}$ (National Science Foundation, 1975). Nickel is a silvery white, malleable metal with a melting point of 1455 °C and a boiling point of 2732 °C. It has high ductility, good thermal conductivity, moderate strength and hardness, and can be fabricated easily by the procedures which are common to steel (Nriagu, 1980b). Nickel belongs to group VIIIa and is classified as a transition metal (the end of the first transition series) whose prevalent valence states are 0 and 2+. However, the majority of nickel compounds are of the Ni^{II} species.

Morel et al. (1973) showed that the free aquo species (Ni^{2+}) dominates at neutral pH (up to pH 9) in most aerobic natural waters; however, complexes of naturally occurring ligands are formed to a minor degree ($OH^- > SO_4^{2-} > Cl^- > NH_3$). Under anaerobic conditions that often occur in the bottom sediments of lakes and estuaries, sulfide controls the solubility of Ni. Under aerobic conditions, the solubility of Ni is controlled by either the co-precipitate $NiFe_2O_4$ (Hem, 1977) or Ni $(OH)_{2(s)}$ (Richter and Theis, 1980). The latter authors performed laboratory adsorption experiments for Ni in the presence of silica, goethite, and amorphous manganese oxide and found that manganese oxide removed 100% of the Ni over the pH range 3–10. The iron oxide began to adsorb Ni at pH 5.5, the oxide's zero point of charge. Hsu (1978) found that Ni was associated with both amorphous iron and manganese oxides that coated silica sand grains.

In 1977, Turekian noted that the calculated theoretical concentrations of Ni and other tracemetals in seawater were in orders of magnitude higher than the measured values. Turekian (1977) hypothesized that the role of particulate matter was most important in sequestering reactive elements and transporting them from the continents to the ocean floor. For lakes, Allan (1975) demonstrated that atmospheric inputs were responsible for Ni concentrations in sediments from 65 lakes surrounding a nickel smelter. As Jenne (1968) and Turekian (1977) note, hydrous iron and manganese oxides have a large capacity for sorption or co-precipitation with trace metals such as Ni. These hydrous oxides exist as coatings on the particles, particularly clays, and can transport sequestered metals to great distances (Snodgrass, 1980). In the major rivers of the world, Ni transport is divided into the following phases (Snodgrass, 1980): 0.5% solution, 3.1% adsorbed, 47% as precipitated coating, 14.9% complexed by organic matter, and 34.4% crystalline material.

The concentration of Ni in the lithosphere is 55 $\mu g\,g^{-1}$ (Li, 2000) and the concentration of dissolved Ni in stream water is 2 $\mu g\,l^{-1}$ (Turekian, 1971). More recent data on the concentration of dissolved Ni in average world river water indicates the value to be 0.8 $\mu g\,l^{-1}$ (see **Chapter 7.7**) and the Ni concentration in ocean water to be 0.47 $\mu g\,l^{-1}$ (Chester, 2000). Natural emissions of Ni to the atmosphere are dominated by wind-blown dusts while anthropogenic sources that represent 65% of all emission sources are dominated by fossil-fuel combustion, waste incineration and nonferrous metal production (Nriagu, 1980b). Major uses of Ni include its metallurgical use as an alloy (stainless steel and corrosion-resistant alloys), plating and electroplating, as a major component of Ni–Cd batteries, and as a catalyst for hydrogenating vegetable oils (National Science Foundation, 1975).

11.3.2.2 Occurrence in Rocks, Soils, Sediments, Anthropogenic Materials

Table 4 presents the average concentration of six heavy metals (Pb, Zn, Cd, Cr, Cu, Ni) in a variety of earth materials, soils, sediments, and natural waters. For Pb it can be seen that the solid-phase concentration increases little along the transport gradient from the Earth's crust to world soils to lake sediments ($14 < 22 < 23\ \mu g\,g^{-1}$; Table 4). However, stream sediment and particularly riverine particulate matter is substantially enriched (50–68 $\mu g\,g^{-1}$) suggesting that anthropogenic inputs from the past use of leaded gasoline, the prevalent burning of fossil fuels and municipal waste, and land disposal of sewage sludge are mobilized from soils and become concentrated in transported particulate matter. The Pb content of soils in England and Wales (UK) is much higher (74 $\mu g\,g^{-1}$) than that (12 $\mu g\,g^{-1}$) found in remote soils of the USA (Alloway, 1995). This is due in part to the more densely populated regions of the UK that were sampled and the inclusion of metalliferous mining areas. Shallow marine sediments appear not to be enriched in Pb related to source materials (crustal rocks and world soils; Table 4) and deep-sea sediments appear to be the final repository of Pb that becomes concentrated in a variety of authigenic phases.

Zinc and Cd show a similar pattern with riverine particulate Zn (250 $\mu g\,g^{-1}$) greatly exceeding average Zn in terrestrial earth materials ($68 \pm 32\ \mu g\,g^{-1}$) and world soils ($66 \pm 17\ \mu g\,g^{-1}$), and particulate Cd (1.2 $\mu g\,g^{-1}$) greatly exceeding the terrestrial earth materials and soil concentrations (0.14 ± 0.08 and $0.23 \pm 0.15\ \mu g\,g^{-1}$). As for Pb, UK soils are significantly greater in Zn and Cd concentrations relative to USA soils, a fact that reflects the urban and metalliferous character of the UK soils (Alloway, 1995). Stream–lake–shallow marine sediments are all more concentrated in Zn ($113 \pm 18\ \mu g\,g^{-1}$) than crustal rocks and soils ($64 \pm 3\ \mu g\,g^{-1}$). As in the case of Pb, deep-sea clays are the ultimate repository for Zn also.

Chromium has the highest concentration of all the six heavy metals in the Earth's crust (Table 4), mainly due to a

Table 4 Heavy metals in the Earth's crustal materials, soils, freshwater sediments, and marine sediments

Material	*Pb*	*Zn*	*Cd*	*Cr*	*Cu*	*Ni*	*References*
Crust	14.8	65	0.10	126	25	56	Wedepohl (1995)
Granite	18, 17	40, 50	0.15, 0.13	20, 10	15, 20	8, 10	Adriano (1986); Drever (1988)
Basalt	8, 6	100, 105	0.2, 0.2	220, 170	90, 87	140, 130	"
Shale	23, 20	100, 95	1.4, 0.3	120, 90	50, 45	68, 68	"
Sandstone	10, 7	16, 16	<0.03,	35, 35	2, 2	2, 2	"
Limestone	9, 9	29, 20	0.05, 0.03	10, 11	4, 4	20, 20	"
Soils (general)	19	60	0.35	54	25	19	Adriano (1986)
Soils (World)	30	66	0.06	68	22	22	Kabata-Pendias (2000)
Soils, UK	74	97	0.8	41	23	25	Alloway (1995)
Soils, USA	12	57	0.27		30	24	"
Stream sediments	51 ± 28	132 ± 67	1.57 ± 1.27	67 ± 24	39 ± 13	44 ± 19	Various sources[a]
Lake sediment	22	97	0.6	48	34	40	**Table 2**
River particulates	68	250	1.2	100	100	90	"
Shallow marine sediment	23	111	0.2	79	43	44	Li (2000); Chester (2000)
Deep-sea clay	80	170	0.4	90	250	230	Li (2000)
Streams	1	30	0.01	1	7	2	Drever (1988)
Ocean	0.03	2	0.05	0.2	0.5	0.5	Drever (1988)

Units are $\mu g\ g^{-1}$ dry weight. Dissolved metal data for streams and ocean water are expressed in units $\mu g\ l^{-1}$.
[a]Various Sources: Dunnette (1992), Aston et al. (1974), Presley et al. (1980), Olade (1987), Mantei and Foster (1991), Zhang et al. (1994), Osintsev (1995), Chiffoleau et al. (1994), Borovec et al. (1993), Gocht et al. (2001).

very high concentration in basalt and shale. Average crustal rocks ($72 \pm 75\ \mu g\ g^{-1}$) are similar in Cr concentration to world soils ($73 \pm 19\ \mu g\ g^{-1}$) and the average Cr concentration in stream sediment–riverine particulates–lake sediment–shallow marine sediment ($74 \pm 22\ \mu g\ g^{-1}$). Only deep-sea clay is slightly enriched relative to all the other earth materials (**Table 4**). From these data it is apparent that natural Cr concentrations of various earth materials that constitute the weathering-transport continuum from continent to oceans have not been seriously altered by man's activities. As has been seen before, this is not the case for Pb, Zn, and Cd. These metals, along with Cu and Ni, are the backbone of the world's metallurgical industry and thus man's mining and smelting activities that have gone on for centuries have greatly altered the natural cycles.

The Cu concentration of crustal rocks ($32 \pm 34\ \mu g\ g^{-1}$) is approximately equivalent to that for average soils ($25 \pm 4\ \mu g\ g^{-1}$). However, as the earth material is weathered and transported to streams–lakes–shallow marine sediments there is a minimal enrichment in Cu concentration ($39 \approx 34 \approx 43\ \mu g\ g^{-1}$) (**Table 4**). And, as for Pb–Zn–Cd, riverine particulate matter is greatly enriched ($100\ \mu g\ g^{-1}$) relative to the other sedimentary materials. While the Pb–Zn–Cd concentrations of deep-sea clay are enriched 1.5 times that of the continental sedimentary materials, Cu is enriched approximately five times. The substantial enrichment of Cu in oceanic pelagic clay relative to terrestrial earth materials is due to the presence of ubiquitous quantities of ferromanganese oxides in surficial ocean sediments (Drever, 1988).

The Ni concentration of crustal rocks ($58 \pm 53\ \mu g\ g^{-1}$) is substantially greater than the average world soils ($23 \pm 3\ \mu g\ g^{-1}$), but essentially equal to continental sedimentary materials ($49 \pm 13\ \mu g\ g^{-1}$). Riverine particulate matter ($90\ \mu g\ g^{-1}$) is nearly twice the Ni concentration of these continental sedimentary materials and deep-sea clay is nearly three times ($230\ \mu g\ g^{-1}$) that concentration. As noted for Cu, the substantial Ni enrichment of deep-sea clays is due to the presence of ferromanganese micronodules in the oxidized surficial sediment column (Drever, 1988).

Table 5 gives the average concentration of six heavy metals in anthropogenic by-products; that is, materials refined from natural materials such as fly ash from coal and smelting of metal ores or by-products from man's use such as sewage sludge and animal waste. It is evident that smelting of the metal ores is a major contributor to the environmental pollution caused by atmospheric transport of heavy metals (**Table 5**). However, fly ash emissions from coal-fired power plants is probably a more important source of atmospheric heavy-metal pollution due to the fact that these power plants are the main sources of electricity for much of the world's population. In addition, sewage sludge is a major contributor of heavy-metal pollution in soils as land disposal of human waste becomes the only practical solution. It is not surprising that riverine particulates are so enriched in Pb, Zn, Cd, Cu, and Ni as soils polluted with atmospheric emissions from mining and smelting activities, and those altered by the addition of sewage sludge are swept into streams and rivers that eventually empty into the ocean.

11.3.2.3 Geochemical Phase Associations in Soils and Sediments

Not all metals are equally reactive, toxic, or available to biota. The free ion form of the metal is thought to be the most available and toxic (Luoma, 1983). With regards to reactivity, it is generally thought that different metal ions display differing affinities for surface binding sites across the substrates (Warren and Haack, 2001). The speciation or dissolved forms of a metal in solution is of primary importance in determining the partitioning of the metal between the solid and solution phases. Mineral surfaces, especially those of Fe oxyhydroxides, have been studied well by aquatic chemists. This is due to their

Table 5 Average concentration of six heavy metals in anthropogenic by-products

By-Product	*Pb*	*Zn*	*Cd*	*Cr*	*Cu*	*Ni*	*References*
Coal	15	53	0.4	27	16	17	Tillman (1994), Adriano (1986)
Fly ash	43	144	0.5	115	56	84	Hower et al. (1999), Adriano (1986)
Soils down-wind of smelters	28, 2200	61, 3000	25, 91		184	306	Adriano (1986), Alloway (1995)
Fertilizers	235	288, 371	32, 35	151, 60	18, 84	36, 20	”
Sewage sludge	1049, 820	3025, 2490	72, 18	1221, –	1085, –	319, –	”
Animal waste	45, 11	93, 130	0.36, 0.55	16, 30	20, 31	29, 19	Adriano (1986), Kabata-Pendias and Pendias (2001)

Units are $\mu g\ g^{-1}$ dry weight.

ubiquitous and abundant nature and their proven geochemical affinity (Honeyman and Santschi, 1988). Metals can be incorporated into solid minerals by a number of processes; nonspecific and specific adsorption, co-precipitation, and precipitation of discrete oxides and hydroxides (Warren and Haack, 2001). Furthermore, Fe and Mn oxyhydroxides form surface coatings on other types of mineral surfaces such as clays, carbonates, and grains of feldspar and quartz. The three most common environmental solid substrates are Fe-oxides, Mn-oxides, and natural organic matter (NOM) (Warren and Haack, 2001).

Sediments are an important storage compartment for metals that are released to the water column in rivers, lakes, and oceans. Because of their ability to sequester metals, sediments can reflect water quality and record the effects of anthropogenic emissions (Forstner, 1990). Particles as substrates of pollutants originate from two sources; (a) particulate materials transported from the watershed that are mostly related to soils and (b) endogenic particulate materials formed within the water column. Since adsorption of metal pollutants onto air- and waterborne particles is the primary factor in determining the transport, deposition, reactivity, and potential toxicity of these metals, analytical techniques should be related to either the chemistry of the particle surface or to the metal species that is highly enriched on the particle surface (Forstner, 1990). In the absence of highly-sophisticated solid-state techniques, chemical methods have been devised to characterize the reactivity of metal-rich phases adsorbed to solid particle surfaces. Single leaching and combined sequential extraction schemes have been developed to estimate the relative phase associations of sedimentary metals in various aquatic environments (Pickering, 1981). The most widely applied extraction scheme was developed by Tessier et al. (1979) in which the extracted components were defined as exchangeable, carbonates, easily-reducible Mn oxides, moderately-reducible amorphous Fe oxides, sulfides and organic matter, and lithogenic material.

Partition studies on river sediments were first reported by Gibbs (1973) for suspended loads of the Amazon and Yukon rivers. Nickel was the main heavy metal bound to hydroxide coatings while a lithogenic crystalline phase concentrated the Cr and Cu. Salomons and Forstner (1980), in an extraction study of river sediments from different regions of the world, found that less polluted or unpolluted river systems exhibit an increase in the relative amount of the metals' lithogenic fraction and that the excess of metal contaminants released to the aquatic environment by man's activities exist in relatively unstable chemical associations such as exchangeable and reducible. With the exception of Cd and Mn, the amount of heavy metals in exchangeable positions is generally low (Salomons and Forstner, 1984). In addition to this, Zn is often concentrated in the easily reducible phase (amorphous Fe/Mn oxyhydroxides), and Fe–Pb–Cu–Cr are concentrated in themoderately reducible phase (crystalline Fe/Mn oxyhydroxides) (Salomons and Forstner, 1984). As can be seen later, for reservoir and lake sediments, Pb is almost completely extracted by the mildly acidic hydroxylamine hydrochloride but Zn is only partially extracted by this chemical that defines the easily-reducible phase.

In a series of landmark papers by Tessier and coworkers, the role of hydrous Fe/Mn oxides in controlling the heavy-metal concentrations in natural aquatic systems has been defined by careful field and laboratory studies by comparing with theory (Tessier et al., 1985). They concluded that the adsorption of Cd, Cu, Ni, Pb, and Zn onto Fe-oxyhydroxides is an important mechanism in the lowering of heavy-metal concentrations in oxic pore waters of Canadian-Shield lakes. These heavy-metal concentrations were below the concentrations prescribed by equilibrium solubility models. In a more recent study, Tessier et al. (1989) concluded that Zn is sorbed onto Fe oxyhydroxides and that their field data fit reasonably well into a simple model of surface complexation. They also concluded that other substrates (Mn oxyhydroxides, organic matter, clays) can sorb Zn. Also, removal of Zn by phytoplankton has been shown to be an important mechanism for controlling the dissolved Zn concentrations in the eutrophic Lake Zurich (Sigg, 1987). Finally, Tessier et al. (1996) expanded their studies to include adsorbed organic matter. Their results strongly suggest that pH plays an important role in determining which types of particle surface binding sites predominate in the sorption of heavy metals in lakes. In circumneutral lakes metals are bound directly to hydroxyl groups of the Fe/Mn oxyhydroxides, and in acidic lakes metals are bound indirectly to these oxyhydroxides via adsorption of metals complexed by NOM.

Some words of caution should be included concerning these 'solid speciation' sediment extraction techniques. Kersten and Forstner (1987) noted that "useful information on solid speciation influencing the mobility of contaminants in biogeochemically reactive sediments by the chemical leaching approach requires proper and careful handling of the anoxic sediment samples." Martin et al. (1987) showed that the specificity and reproducibility of the extraction method greatly

depends on the chemical properties of the element and the chemical composition of the samples. They state that "these methods provide, at best, a gradient for the physicochemical association strength between trace elements and solid particles rather than their actual speciation." The problem of post-extraction readsorption of As, Cd, Ni, Pb, and Zn has been addressed by Belzile et al. (1989) who found that by using the 'Tessier method' (Tessier et al., 1979) on trace-element spiked natural sediments it is possible to recover the added trace elements within the limits of experimental error.

In a recent study of extraction of anthropogenic trace metals from sediments of US urban reservoirs, Conko and Callender (1999) showed that Pb had the highest anthropogenic content accounting for 80–90% of the total metal concentration. Three extractions were used: (1) easily-reducible 0.25 M Hydroxylamine HCL in 0.25 N HCl (Chao, 1984); (2) weak-acid digest (Hornberger et al., 1999); and (3) Pb-isotope digest of 1 N HNO_3 + 1.75 N HCl (Graney et al., 1995). Chao (1984) extraction, originally thought to extract only amorphous Mn oxyhydroxides, is now considered to be an acid-reducible extraction that solubilizes amorphous hydrous Fe and Mn oxides (Sutherland and Tack, 2000). Hornberger et al.'s (1999) weak-acid digest (0.6 N HCl) is thought to represent the bioavailable fraction of the metal (Hornberger et al., 2000). Graney et al.'s (1995) HNO_3 + HCl acid digest is the most aggressive of the three extracts and has been shown to represent, using Pb isotopes, the anthropogenic fraction of Pb in lacustrine sediments. A plot of extractable Pb and total Pb for a 1997 sediment core from the suburban Lake Anne watershed in Reston, Virginia (Callender and Van Metre, 1997) is presented in **Figure 1(a)**. It can be seen that between 85 and 95% of the total Pb is extracted by these chemicals. In general, the Chao extraction recovered 95% of the total Pb and since this technique is thought to specifically extract amorphous Fe and Mn oxyhydroxides, Conko and Callender (1999) postulated that most of the Pb is bound by these amorphous oxides. **Figure 1(b)** is a plot of various extractions and total Zn in the same Lake Anne core. Only 70% of the total Zn was extracted by any of the three techniques mentioned before; thus the remaining Zn must be associated with other sedimentary phases. Conko and Callender (1999) suggest Zn fixation by 2 : 1 clay minerals (i.e., montmorillonite), whereby sorbed Zn is fixed in the alumina octahedral layer, is an important phase (Pickering, 1981). An additional phase could be biotic structures that are postulated by Webb et al. (2000) as substrates where Zn occurs in intimate combination with Fe and P. While Lake Anne sediment is a typical siliclastic material, Lake Harding (located south of Atlanta, Georgia) sediment is reddish in color and consists of appreciably more iron and aluminum oxides. Much of the iron oxides are undoubtedly crystalline in character and may not be attacked by the mild extraction techniques listed above (especially the Chao extraction). **Figure 2** shows a plot of the extractable and total Pb in a sediment core from Lake Harding. Contrary to the Lake Anne Pb data where 95% is extractable, only 75% of the total Pb in Lake Harding is extractable. The Chao easily-reducible extraction yielded the lowest extraction efficiences. It is clear from these data that the type and nature of phase components that comprise natural aquatic sediments are most important for understanding the efficiency of any extraction scheme. Very little is known about the relationship between easily-extracted phases removed by sequential extraction (Tessier et al., 1979) and those liberated by single leaches. Sutherland (2002) compared the two approaches using soil and road deposited sediment in Honolulu, Hawaii. The results indicated that the dilute HCl leach was slightly more aggressive than the sequential procedure but that there was no significant difference between the Pb and Zn concentrations liberated by the two approaches. Further, the data also indicated that a

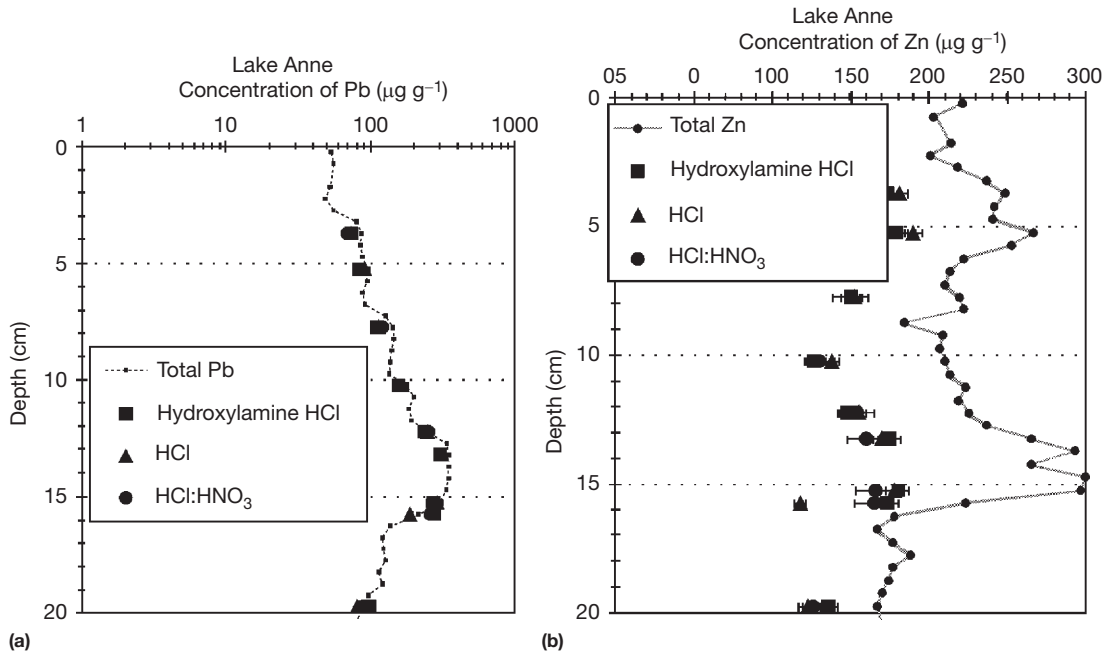

Figure 1 Temporal distribution of total and extractable lead (a) and zinc (b) in a sediment core from Lake Anne, Reston, Virginia, USA.

dilute HCl leach was a valuable, rapid, cost-effective analytical tool for contamination assessment. The Hawaii data also indicated that between 75% and 80% of the total Pb is very labile and anthropogenically enhanced (Sutherland, 2002; Sutherland and Tack, 2000). On the other hand, while labile Zn comprises 75% of the total, it is equally distributed between acid extractable and reducible (Sutherland et al., 2000). The extractable Pb data agrees well with the lacustrine Pb data presented in **Figure 1(a)**. The single HCl leach method on Hawaii sediments (Sutherland, 2002) extracts about 50% of the total Zn; a figure even lower than the 70% for lake sediments. Unfortunately, no information was available concerning the phase distribution of Zn in these sediments.

An important reason for testing 'selective' leach procedures on sediments that are subjected to anthropogenic influence is to determine whether such leaches can be used to measure the anthropogenic metal content of sedimentary materials. For Lake Anne sediment, Conko and Callender (1999) calculated the anthropogenic Pb and Zn content by subtracting the background metal concentrations from the total metal content. These were then compared to the 'anthropogenic' leach concentrations. For both Pb and Zn, there was essentially no difference between the two procedures. These techniques were applied to several other lake sediments with similar successes suggesting that a mild acid leach might be used to estimate the labile, anthropogenic metal content of a variety of sedimentary materials.

Terrestrial materials (river sediments, lake sediments, and urban particulate matter) appear to have between 50% and 70% exchangeable Pb and Zn while marine sediments contain very little exchangeable metal but appreciably more reducible and much more residual Pb and Zn (Kersten and Forstner, 1995). This may not be too surprising as exchangeable metals are released once freshwater mixes with salt water and redistribution in the marine environment results in some precipitated phases (carbonates, Fe/Mn oxyhydroxides) and the relative increase in the lithogenic fraction. In future, the solid-phase identification techniques should be used to classify the sediments that are to be subjected to 'selective' extraction techniques for the purpose of understanding the heavy metal phase associations.

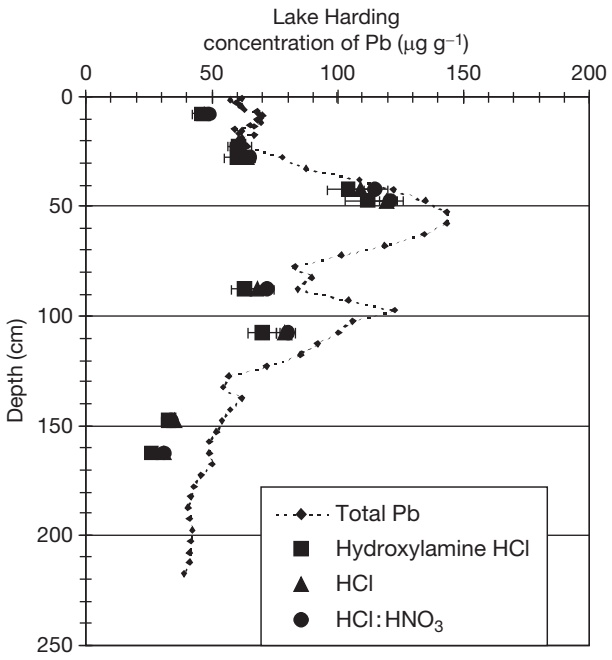

Figure 2 Temporal distribution of total and extractable lead in a sediment core from Lake Harding, Atlanta, Georgia, USA.

11.3.3 Atmospheric Emissions of Metals and Geochemical Cycles

Both natural and perturbed geochemical cycles include several subcycle elements, not the least of which is the emission of metals into the atmosphere. Atmospheric metals deposited on the land and ocean surface are a part of the runoff from land into the ocean and become incorporated in marine sediments. Thus, the two major pathways whereby heavy metals are injected into the natural geochemical cycles are atmospheric and fluvial. Considering the land surface, atmospheric emissions from stationary and mobile facilities and aqueous emissions from manufacturing and sewage disposal facilities are the primary sources of heavy metal contamination. As for the ocean, atmospheric deposition and continental runoff are the primary inputs. Duce et al. (1991) summarized the global inputs of metals to the ocean for the 1980s and these data are presented in **Table 6**. Riverine inputs are substantially greater than the atmospheric inputs, especially particulate riverine inputs that account for 95% of the total (Chester, 2000). For Pb and Zn, riverine inputs are 20 and 30 times greater than the corresponding atmospheric inputs. For Cd the factor is only 5, while for Cu and Ni the factors are 45 and 30, respectively. Global atmospheric inputs to land and ocean for the same time period are substantially greater (2–3 times, **Table 6**) than atmospheric deposition to the ocean. This is due to the presence of major pollution sources (mining, smelting, fossil-fuel combustion, waste incineration, manufacturing facilities) on the land masses. In fact, for Pb during the 1970s and 1980s, the use of leaded gasoline in vehicles resulted in the emission of four times the metal to the land surface compared to the ocean (**Table 6**).

From the above data it is obvious that atmospheric emissions on land are a major source of heavy-metal contamination to our natural environment. In the following sections the focus will be on these emissions due to the fact that there are numerous data available to construct emission estimates (Nriagu and

Table 6 Global deposition of metals to the ocean for the 1980s

Pb	*Zn*	*Cd*	*Cu*	*Ni*
Atmospheric				
90	137	3.1	34	25
Riverine				
1602	3906	15.3	1510	1411
World atmosphere				
342	177	8.9	63	86

All deposition values are thousand metric tons per year.
Source: Duce et al. (1991).

Pacyna, 1988) and that historical atmospheric emissions have been archived in continental ice accumulations (Greenland and Antarctica). The metal emission estimates of Nriagu and Pacyna (1988) are the most complete, and recent data are available for worldwide metal emissions.

11.3.3.1 Historical Heavy Metal Fluxes to the Atmosphere

Claire Patterson and his co-workers have pioneered the study of natural earth materials to uncover the 'secrets of the ages'. As early as 1963, Tatsumoto and Patterson (1963) related the high concentrations of Pb in surface seawater off Southern California to automotive aerosol fallout. In the United States it was found that Pb in gasoline was the largest single source of air pollution. Aerosols account for about one-third of the industrial Pb added to the oceans (Patterson et al., 1976). Murozumi et al. (1969) provided a very convincing argument that airborne Pb particulates can be transported over vast distances in their classic study of the Greenland ice sheet. Their data indicated that before 1750 the concentration of Pb in the atmosphere began to increase above 'natural' levels and that this was mainly due to the lead smelters, and that the sharp increase in the atmospheric Pb occurred around 1950 due to the burning of Pb alkyls in gasoline after 1940.

More recently, Claude Boutron and his co-workers in France have published high-quality data for Pb–Zn–Cd–Cu in Greenland snows (Boutron et al., 1991; Hong et al., 1994; Candelone et al., 1995). **Table 7** gives heavy metal deposition fluxes for the Summit Central Greenland Icesheet sampling locality. Lead increased dramatically between BP 7760 and AD 1773 (Industrial Revolution), and subsequently through 1850–1960 (Pb alkyl additives to automobile gasoline) (Nriagu, 1990a). Candelone et al. (1995) have successfully extended the uncontaminated metal record in ice from Central Greenland. Besides the above Pb record, for Zn, Cd, and Cu there is a clear increasing trend from 1773 to the 1970s (**Table 7**). However, between BP 7760 and AD 1773, there is essentially no change in metal flux. In fact, Zn decreased slightly; there is no change in Cd; and Cu increased slightly (**Table 7**). Over the past 200 years, Zn fluxes started to increase but it was not until 1900s that the increase became more rapid. On the other hand, for Cd and Cu, it was not until after the 1850s that their atmospheric concentrations and fluxes increased substantially (Candelone et al., 1995). The maximum remote atmospheric concentrations of Zn occurred around 1960 while those for Cd and Cu occurred around 1970 (Candelone et al., 1995). Finally, 1992 icesheet data indicate that the remote atmospheric Pb fluxes (**Table 7**) decreased by 6.5-fold in response to the banning of leaded gasoline throughout most of the world. Zinc and Cu decreased only 1.5 times while Cd decreased about 2.5 times (**Table 7**). These large increases in historical metal fluxes to the remote atmosphere are undoubtedly related to the major changes in the large scale anthropogenic emissions to the atmosphere in the northern hemisphere.

There is a wealth of data available on the world production of heavy metals during the past century or so (Nriagu, 1990b). Candelone et al. (1995) present historical Zn–Cd–Cu concentrations in snow/ice deposited at Summit, Central Greenland from 1773 to 1992. If one assumes that the 1773 concentrations are the result of natural atmospheric emissions, then the ratio of 1980s concentrations to 1773 concentrations are a measure of anthropogenic contamination of the remote atmosphere to that date. These ratios are 4, 7, and 3 for Zn, Cd, and Cu, respectively (figure 3 in Candelone et al., 1995). Compare this to the 1983 total emissions divided by the natural emissions (Nriagu, 1990b). These values are 3.9, 6.4, and 2.3 for Zn, Cd, and Cu, respectively. It appears that historical changes in Zn–Cd–Cu deposition in the Greenland icesheet are consistent with the estimates of metal emissions to the global atmosphere (Candelone et al., 1995). These emissions are primarily a result of smelting/refining, manufacturing processes, fossil-fuel combustion, and waste incineration (Nriagu,1990b).

Table 7 Heavy metal deposition fluxes at Summit, Central Greenland

Age	*Pb*	*Zn*	*Cd*	*Cu*
BP 7760	1.3	53	0.6	3.9
1773	18	37	0.6	5.0
1850	35	70	0.6	5.3
1960s–1970s	250	200	4.1	22
1992	39	120	1.8	17

All values are in picograms per cm^2 per year.
Source: Candelone et al. (1995).

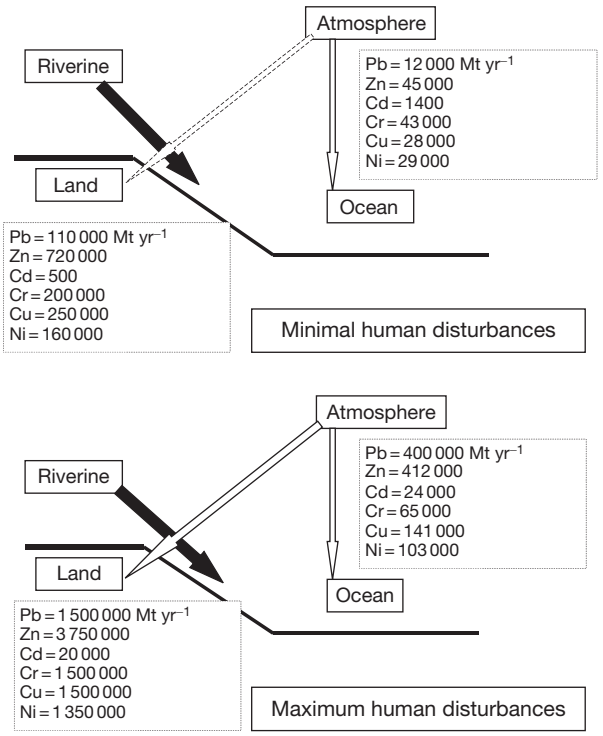

Figure 3 Schematic diagrams of perturbed heavy metal cycles representing prehistoric times of minimal human disturbances and modern times of maximum human disturbances. Data sources for minimum human disturbances: Nriagu (1990b), Bertine and Goldberg (1971). Data sources for maximum human disturbances: Martin and Whitfield (1981), Garrels et al. (1973), Lantzy and Mackenzie (1979), Nriagu and Pacyna (1988), Duce et al. (1991).

A similar analysis for Pb yields the following results: ice-sheet concentration ratio is about 15 and atmospheric emission ratio is about 20. While this is not too bad a comparison, it is not as good as for the other three metals (Zn–Cd–Cu). It is clear that most of the Pb increase in snow/ice samples from Greenland is due to the use of leaded gasoline after the 1950s (Murozumi et al., 1969).

Going back to the Holocene era (BP 7760 years) where dated ice cores give metal concentrations that reflect a time when man's impact on the global environment was minimal, Candelone et al. (1995) measured Zn–Cd–Cu concentrations that were comparable to values for ice dated at AD 1773. Even by AD 1900 the concentrations of Zn and Cu were only 1.3 and 1.5 times those recorded for the AD 1773 date (Candelone et al., 1995). Cadmium concentrations had increased more than four times during this period and Pb concentrations had increased nearly 10 times. In fact for Pb, the concentrations recorded in the icesheet have increased at least 30 times between BP 7760 and AD 1900. (Candelone et al., 1995). It is obvious that much Pb was emitted to the atmosphere long before the Industrial Revolution and that some Cd was emitted during the early stages of the Industrial Revolution. It is possible that Cd was a by-product of the Pb mining and smelting during the Greco-Roman civilization (2500–BP 1700 years).

11.3.3.2 Perturbed Heavy Metal Cycles

In this discussion of heavy metals, geochemical cycles are treated in a simple manner; emissions from land and oceans to the global atmosphere and subsequent deposition on the land and ocean surface, and runoff from the land to the ocean and eventual deposition in marine sediments. Only two components of this simple cycle will be discussed due to the availability of relatively accurate and complete data; deposition of metals from the atmosphere to the land and ocean surface, and continental runoff to the ocean.

Figure 3 presents these data for two simple scenarios: minimal human disturbances and maximum human disturbances. For the minimal human disturbances senario, it was assumed that deposition from the atmosphere was due to natural sources (Nriagu, 1990b) and that there was minimal anthropogenic impact on the Earth's surface. The continental runoff (riverine) data was taken from Bertine and Goldberg (1971) who calculated the amounts of metals entering into the world's oceans as a result of the weathering cycle. They accounted for both the dissolved and particulate phases by using the marine rates of sedimentation. It can be seen from **Figure 3** that for Pb–Zn–Cr–Cu–Ni, continental runoff was 5–10 times greater than the natural atmospheric inputs. For Cd, the atmospheric fluxes are greater than the continental runoff suggesting that continental rocks are depleted in Cd or that there are poor quality Cd data for these two sources. The latter explanation seems to be the most likely.

For the maximum human disturbances scenario, riverine inputs were calculated with the data of Martin and Whitfield (1981). As can be seen from **Table 2** in this chapter, Pb–Zn–Cd–Cu–Ni are strongly enriched (by man's activities) when compared to the average Earth's upper crust and soils and the Cr enrichment is found to be only somewhat enriched (**Table 2**). Atmospheric input data was computed as the average of global emissions data for the 1970s and 1980s (Garrels et al., 1973; Lantzy and Mackenzie, 1979; Nriagu and Pacyna, 1988; and Duce et al., 1991), and was assumed to be the time of maximum anthropogenic emissions to the atmosphere. For the maximum human disturbances scenario, riverine inputs are still larger than the atmospheric inputs except that Pb–Cr are only three times greater, Zn is six times greater, Cu is 10 times greater, Ni is 13 times greater, and Cd is about equal. These differences are undoubtedly due to the magnitude of different source functions.

A calculation of maximum/minimum ratio from the atmospheric input data in **Figure 3** yields the following results: Pb = 33, Zn = 9, Cd = 17, Cr = 1.5, Cu = 5, Ni = 4. We know that the burning of leaded gasoline is responsible for the large increase of Pb. Enormous metal production of Zn and Cd ores as well as refuse incineration are responsible for the increases of these metals. In addition, marine aerosols are an important source of Cd (Li, 1981). Obviously, Cu–Ni production from ores increased during this period but not nearly as much as for Zn–Cd. Also, combustion of fossil fuels contributed somewhat to the increase of Cu and Ni. The main source of Cr is steel and iron manufacturing which appears to not be as important an impact on the atmospheric environment as sources for the other metals. The pollution sources of Cr are minimal as reflected in the balance between riverine input and marine sediment output (Li, 1981).

A similar calculation for the riverine inputs (**Figure 3**) yields the following results: Pb = 14, Zn = 5, Cd = 40, Cr = 7.5, Cu = 6, Ni = 8. With the exception of Pb and Cd, the increases for Zn–Cr–Cu–Ni are similar. Smelting wastes and coal fly ash releases are the common sources of these four metals. Gasoline residues are an obvious source of the Pb increases and urban refuse incineration is a major source of the Cd increase (Nriagu and Pacyna, 1988).

11.3.3.3 Global Emissions of Heavy Metals

Table 8 presents the data on the global emissions of heavy metals to the atmospheric and terrestrial environments for the 1970s and 1980s. The atmospheric and riverine input (weathering mobilization) data are the same as that used for the minimum and maximum human disturbances to the geochemical cycling of the heavy metals presented in the previous section. Total industrial discharges of heavy metals are the calculated discharges into soils and water minus the emissions to the atmosphere (Nriagu, 1990b). Only a fraction of the heavy-metal production from mines is released into the atmosphere in the same year (Nriagu, 1990b). For instance for Pb, in the year 1983, about 30% of the metal produced from mining is used for metal production, other sources, and is wasted as industrial discharges (**Table 8**): Zn 27%, Cd 190%, Cr 16%, Cu 14%, and Ni 57%. It is not surprising that the price of base metals fluctuate so widely in that there appears to be a substantial excess of supply over demand (**Table 8**). This is not the case for Cd; the data presented in **Table 8** suggest that there may be a deficit in the supply of Cd. It appears unlikely but it may be that there is a sufficient demand for Cd that can just about balance the mine production. Another explanation is that the estimate of Cd from industrial discharges might be in error. Other discrepancies in Cd estimates have also been

Table 8 Global emissions of heavy metals to the atmosphere and terrestrial environment during 1970s and 1980s

Element	*Atmospheric input*[a]	*Weathering mobilization*[b]	*Total industrial discharges*[c]	*Production from mines*[d]	*World Metal production (Atmos.)*[e]	*Other sources (Atmos.)*[f]	*Emissions H_2O, soil (Atmos.)*[g]	*Global natural emissions*[h]
Pb	400 000	295 000	565 000	3 077 000	83 800	292 000	875 000	12 000
Zn	412 000	1 390 000	1 427 000	6 040 000	125 800	67 000	2 083 000	45 000
Cd	24 000	15 000	24 000	19 000	8500	3500	43 000	1400
Cr	65 000	1 180 000	1 010 000	6 800 000	28 500	25 000	1 397 000	43 000
Cu	141 000	635 000	1 048 000	8 114 000	35 400	15 500	1 428 000	28 000
Ni	103 000	540 000	356 000	778 000	15 900	71 000	614 000	29 000

Units are metric tons per year. Atmospheric Input (a) = World Metal Production (e) + Other Sources to the Atmosphere (f) + Natural Emissions to the Atmosphere (h).
Pb: 400 000 = 388 000; Zn: 412 000? 238 000; Cd: 24 000 ≅ 13 400; Cr: 65 000 ≅ 96 500; Cu: 141 000 ≅ 79 000; Ni: 103 000 ≅ 116 000.
[a]Source: Lantzy and Mackenzie (1979), Garrels et al. (1973), Nriagu and Pacyna (1988), Duce et al. (1991).
[b]Bertine and Goldberg (1971).
[c,d,h]Nriagu (1990b).
[e–g]Nriagu and Pacyna (1988).

noted and it is reasonable to think that since the concentrations of Cd are so low in natural earth materials, the analytical data may not be good.

In order to assess the internal consistency of the emissions, as shown in **Table 8**, a calculation was made whereby the mean atmospheric input was equated to the world metal production emitted to the atmosphere plus natural emissions and other sources to the atmosphere. With the exceptions of Cu and Zn, the quantities of emissions balance rather well. There is no obvious reason why Cu is out of balance by nearly a factor of 2 (atmospheric input > sources). For Zn, with an imbalance of 1.7 for atmospheric input > sources, there is an obvious problem with other sources in that the impact of rubber tire wear. This source term will be addressed in the next section. However, even with this term, the right side of the equation would increase to a maximum emissions figure of 300 000 t yr^{-1} (**Table 8**). It is possible that maximum Cu and Zn emissions to the atmosphere have been overestimated but there is no way to check this with the available data.

11.3.3.4 US Emissions of Heavy Metals

While there is a reasonable amount of data pertaining to global emissions of heavy metals during the last half of the twentieth century, there is a wealth of data available for emissions of heavy metals to the US atmosphere. Most of this has been calculated from USEPA and US Bureau of Mines materials production data combined with emission factors for a variety of source functions (Pacyna, 1986). In this section data plots will be presented to show the calculated emissions of several heavy metals to the US atmosphere over a decade of time. Some of the data, such as that for Pb, are from the published literature. On the other hand, much of the data for Zn has been calculated by the author and his colleagues and is presented for the first time.

11.3.3.4.1 Lead

With the scientific realization that Pb had contaminated the global atmosphere (Murozumi et al., 1969), scientists set out to identify the major sources of this contamination. The late Claire Patterson, formerly of the California Institute of Technology, was the leader in this field. In an earlier paper concerning Pb contamination and its effect on human beings, Patterson (1965) wrote "the industrial use of lead is so massive today that the amount of lead mined and introduced into our relatively small urban environments each year is more than 100 times greater than the amount of natural lead leached each year from soils by streams and added to the oceans over the entire earth". This conclusion was reached by Chow and Patterson (1962) in their landmark study of Pb isotopes in pelagic sediments. This information, coupled with the well-known health impacts of Pb (USEPA, 2000a,b), arose the interest of toxicologists worldwide and prompted detailed studies of the cycling of this element in the environment. Ingested Pb (food, water, soil, and dust) damages organs, affects the brain and nerves, the heart and blood, and particularly affects young children and adults (USEPA, 2000a,b). With the use of leaded gasoline that began in the 1930s (Nriagu, 1990a), the public outcry about the outbreak of severe lead poisoning, and the drastic increase in the US in automobile miles traveled, the US Congress passed an amendment to the Clean Air Act (Callender and Van Metre, 1997) banning the use of leaded gasoline. The USEPA (2000a,b), in their most recent air pollutant emission trends report, showed that since 1973 the quantity of Pb emitted to the environment (**Table 9**) has decreased drastically from about 200 000 t to about 500 t in 1998. As a comparison, European Pb emissions for 1979/1980 were released at a rate of 80 800 t yr^{-1} (Pacyna and Lindgren, 1997) while those for the US were 66 600 tons per year (USEPA, 2000a,b).

Figure 4 presents the important EPA emissions data on a five-year time scale from 1970 to 1995. In the 1970s and 1980s, it is clear that leaded gasoline consumption was the overwhelming emitter of Pb to the environment with metal processing a far second. Presently, the total amount of Pb emitted to the environment is a paltry 2500 t (USEPA, 2000a,b), with metal processing and waste disposal being the main emitters. While the US consumption of leaded gasoline has all but stopped, it is not the case for the rest of the world. As of 1993 when leaded gasoline consumption in North America (mostly Mexico) emitted 1400 t of Pb to the atmosphere, the rest of the world emitted 69 000 tons of Pb to the atmosphere (Thomas, 1995).

Table 9 Total US emissions of lead (Pb) to the atmosphere

Source category	*1970*	*1975*	*1980*	*1985*	*1990*	*1995*
Waste incineration	1995	1447	1097	790	729	552
Fossil fuel combustion	9269	9385	3899	469	454	446
Metals processing	21 971	9000	2745	1902	1968	1864
Gasoline consumption	164 800	123 657	58 688	17 208	1086	475

Units are metric tons.
Source: USEPA (1998, 2000a,b).

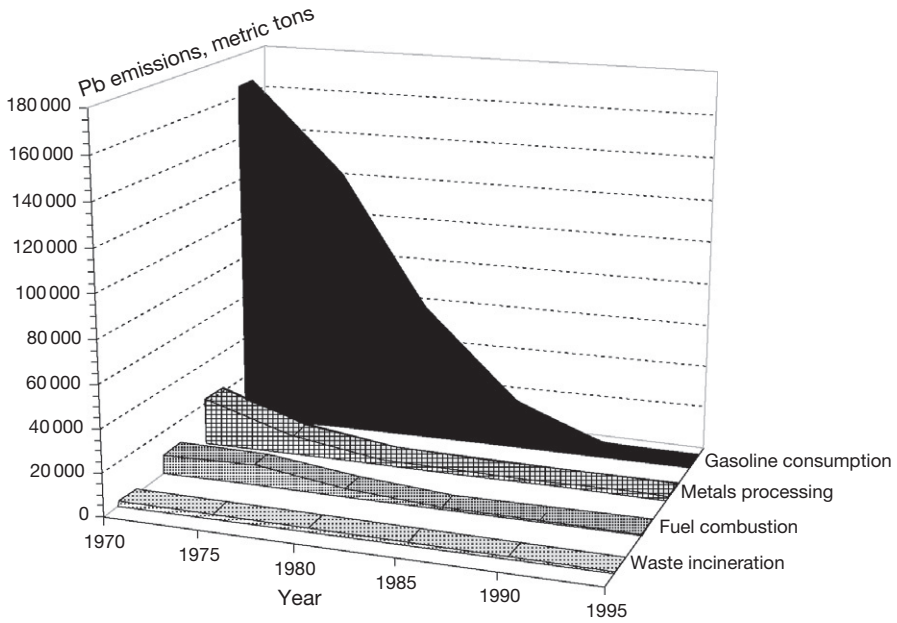

Figure 4 Three-dimensional plot of lead emissions to the US atmosphere for the period 1970–1995. Data from USEPA (2000a).

11.3.3.4.2 Zinc

The US atmospheric emissions data for Zn are somewhat sparse. Nriagu (1979) published data on the worldwide anthropogenic emission of Zn to the atmosphere during 1975 (**Table 10**). The author has taken this report as a model for the type of Zn emissions that appear to be important and has added several categories such as cement and fertilizer production and automobile rubber tire wear.

The reason why the emission data for Zn are sparse is that until recently it was thought that Zn was not harmful to the environment and that health risks were minimal compared to other heavy metals. Zinc is an essential micronutrient and plays a role in DNA polymerization (Sunda, 1991) and nervous system functions (Yasui et al., 1996). Zinc is generally less toxic than other heavy metals (Nriagu, 1980a); however, it is known to cause a variety of acute and toxic effects in aquatic biota. Several studies have established links between human activities and environmental Zn enrichment (Pacyna, 1996).

Figure 5 is a plot of second tier Zn emissions to the atmosphere for the period 1960–1995 in five-year time intervals. The only important Zn emission category not included in **Figure 5** is Zn mining. This is and has been the largest Zn emission category with 102 000 t in 1960 to 112 000 in 1970, declining to 48 000 in 1980, and stabilizing at about 32 000 t in the 1990s (Nriagu and Pacyna, 1988; www.minerals.usgs.gov). Obviously, emissions from Zn mining and smelting are the overwhelming sources. Total US Zn emissions for the 1980s amount to approximately 60 000 t yr^{-1} while European Zn emissions total 43 000 t yr^{-1} (Pacyna and Lindgren, 1997). Mining–smelting emissions overwhelm others that are important but it is difficult to plot these clearly on **Figure 5** if Zn mining is also included.

Of the five Zn emission categories plotted in **Figure 5**, waste incineration and rubber tire wear are the most important. Note that in general these emissions have increased during the last 40 years such that the second-tier emissions total approximately one-half of the Zn mining–smelting emissions.

11.3.3.4.3 Cadmium

Cadmium has received a wide variety of uses in American industries with the largest being electroplating and battery manufacture. Its emission from natural sources (erosion and volcanic activity) are negligible. The dominant sources of Cd emissions to the atmosphere are primary metals smelting (Cu and Pb), secondary metals production, fossil-fuel combustion, waste incineration, iron and steel production, and rubber tire wear. **Figure 6** is a plot of Cd emissions to the US atmosphere for five-year time periods from 1970 to 1990. Between 1970 and 1980, primary metals smelting was the primary source of

Table 10 Total US Emissions of zinc (Zn) to the atmosphere

Source category	*1960*	*1965*	*1970*	*1975*	*1980*	*1985*	*1990*	*1995*
Cement production[a]	617	716	729	667	735	754	752	846
Fertilizer production[b]	1000	1000	1054	1329	1632	1525	1390	1365
Copper mining[c]	1035	1163	1200	983	915	795	1185	1448
Iron and steel[d]	1628	2160	2236	1952	1682	1223	1342	1374
Fossil Fuel combustion[e]	1532	1719	2141	1878	1916	1984	1658	1298
Rubber tire wear [f]	3747	4901	5503	5044	5983	7258	8329	8847
Waste incineration[g]	6367	7280	5920	5006	3232	5659	7298	7941
Zinc mining[h]	101 500	126 280	111 440	55 580	47 600	36 540	36 820	32 480

Units are metric tons.

[a]Source: Nriagu and Pacyna (1988), http://minerals.usgs.gov/minerals/pubs/commodity/cement/stat/tbl1.txt.

[b]Source: Nriagu and Pacyna (1988), http://minerals.usgs.gov/minerals/pubs/commodity/phosphate_rock/stat/tbl1.txt.

[c]Source: Nriagu and Pacyna (1988), http://minerals.usgs.gov/ minerals/pubs/commodity/of01-006/copper.

[d]Source: Nriagu and Pacyna (1988), http://minerals.usgs.gov/minerals/pubs/commodity/of01-006/ironand steel.

[e]Source: Pacyna (1986), Statistical Abstracts of the United States (1998) (Coal and Oil production data).

[f]Source: Councell et al. (2004).

[g]Source: Pacyna (1986), USEPA (1998).

[h]Source: Nriagu and Pacyna (1988), http://minerals.usgs.gov/minerals/pubs/commodity/of01-006/zinc.

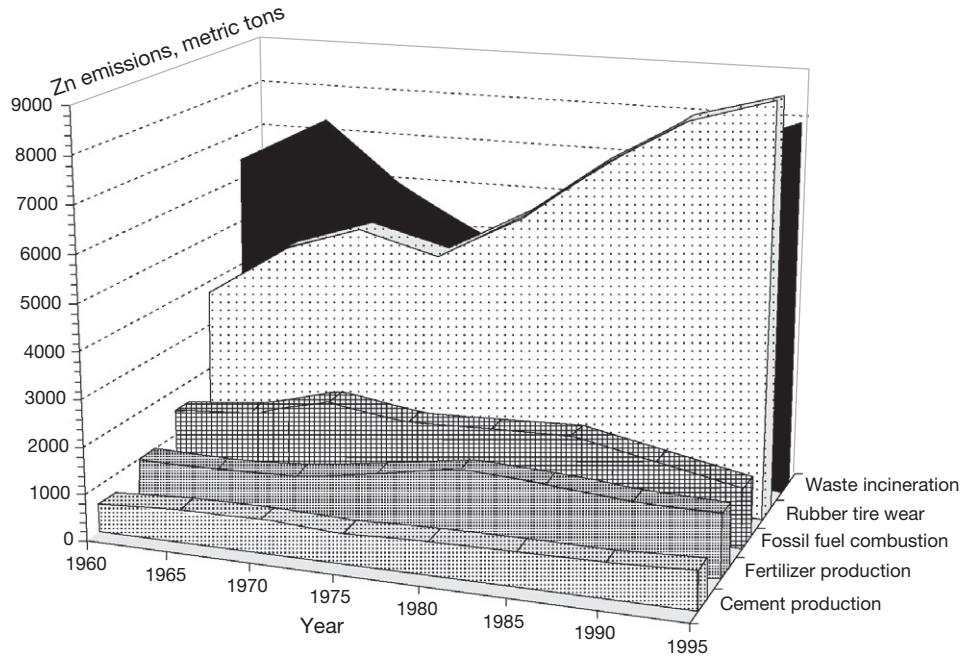

Figure 5 Three-dimensional plot of second tier zinc emissions to the US atmosphere for the period 1960–1995. Data from Councell et al. (2004), Nriagu and Pacyna (1988), minerals.usgs.gov/minerals/pubs/commodity/cement/stat/tbl1.txt, minerals.usgs.gov/minerals/pubs/commodity/phosphate_rock/stat/tbl1.txt, Pacyna (1986), USEPA (1998), Statistical Abstracts of the United States (1998), author's calculations.

Cd emissions to the atmosphere. Then fossil-fuel combustion became the primary emitter (60%) with Cu–Pb smelting accounting for much of the remainder (30%) (Wilber et al., 1992). These emissions were concentrated in the central part of the US (Wilber et al., 1992). By 1990, fossil fuel emissions decreased significantly, a fact that is probably related to the increased efficiency of stack emission controls; and secondary metal production became the major source of Cd to the US atmosphere (**Figure 6**). In the 1980s, Cd emissions to the US atmosphere amounted to 650 t yr^{-1} (**Table 11**). European emissions were nearly double this amount, i.e., 1150 t yr^{-1} (Pacyna and Lindgren, 1997).

11.3.4 Historical Metal Trends Reconstructed from Sediment Cores

11.3.4.1 Paleolimnological Approach

Many governmental agencies collect the data routinely for the assessment of the quality of rivers, streams, lakes, and coastal oceans. Water-quality monitoring involves temporal sampling of water resources that are affected by natural random events, seasonal phenomena, and anthropogenic forces. Testing water quality, monitoring data at regular intervals has become a common feature and an important exercise for water managers who are interested in checking whether the investment of large

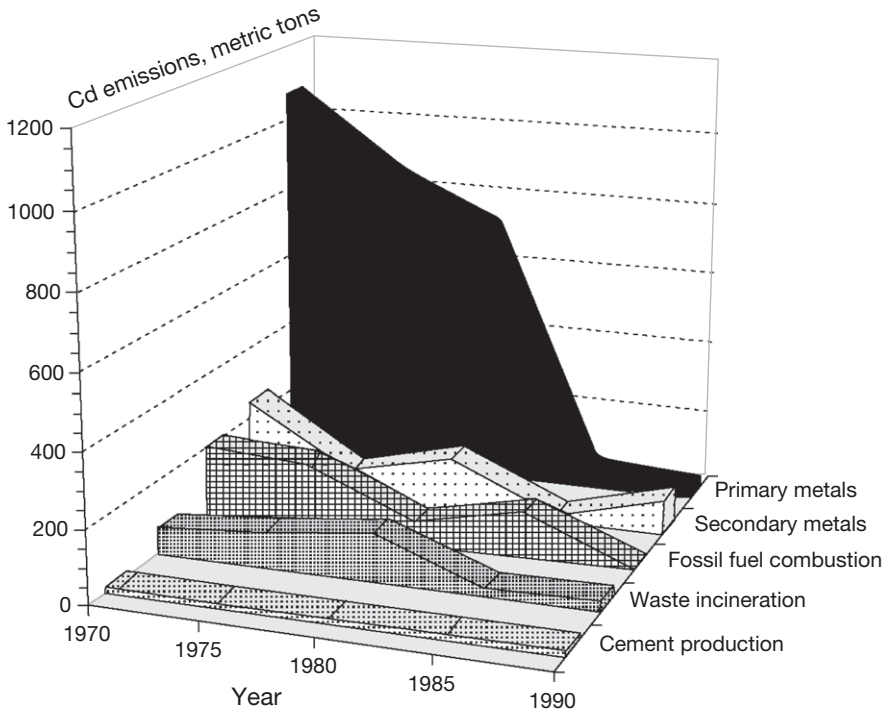

Figure 6 Three-dimensional plot of cadmium emissions to the US atmosphere for the period 1970–1990. (sources Davis and Associates, 1970; USEPA, 1975a,b, 1976, 1978; Wilber et al., 1992).

Table 11 Total U.S. emissions of cadmium (Cd) to the atmosphere

Source category	*1970*[a]	*1975*[b]	*1980*[c]	*1985*[d]	*1990*[e]
Rubber tire wear	6	6	5	5	5
Cement production	14	13	14	14	15
Waste incineration	72	97	131	21	28
Fossil fuel combustion	200	186	60	121	7
Secondary metals	245	75	143	15	96
Primary metals	1075	860	728	54	32

Units are metric tons.
[a]Source: Davis and Associates (1970).
[b]Source: USEPA (1975a,b, 1976).
[c]Source: USEPA (1978).
[d]Source: Wilber et al. (1992).
[e]Source: USEPA (2000b).

sums of money has improved the water quality of various water resources during the past 30 years. In addition, trends available by such monitoring can provide a warning of degradation of water quality.

Historical water quality databases suffer from many limitations such as lack of sufficient data, changing sampling and analytical methods, changing detection limits, missing values and values below the analytical reporting level. With regard to trace metal data, the problem is even more difficult in that many metals occur at environmental concentrations so low (parts per billion or less) that current (up until the early 1990s) routine analytical methodology was unable to detect ambient concentrations with adequate sensitivity and precision. Even the best statistical techniques, when applied to questionable data, can produce misleading results. For example, Pb in the Trinity River, south of Dallas, TX, USA. Abundant dissolved Pb data for the period 1977–1992 (Van Metre and Callender, 1996) indicate that there were no trends in Pb; in fact, the concentrations were scattered from 0 to 5 ppb. On the other hand, Pb in sediment cores from Lake Livingston, downstream from the Trinity River sampling station, showed a decline in Pb concentration from 1970 to 1993 (Van Metre and Callender, 1996). Thus, from the core data, one can conclude that there is a declining trend in Pb in the Trinity River.

For these very reasons, the US Congress supported the US Geological Survey's National Water Quality Assessment Program with its goals to describe the status and trends in water quality of our Nation's surface and groundwater, and to provide an understanding of the natural and human factors that affect the observed conditions and trends. The US public is eager to know whether the water quality of US rivers and lakes has benefited from the expenditure of billions of dollars since the passage of the Clean Air and Clean Water Acts in the 1970s.

An alternate approach to statistical analyses of historical water-quality data is to use metal distributions in dated sediment cores to assess the past trends in anthropogenic hydrophobic constituents that impact watersheds (paleolimnological approach). It is well known that marine and lacustrine sediments often record natural and anthropogenic events that occur in drainage basins, local and regional air masses, or are forced upon the aquatic system (Valette-Silver, 1993). A good example of the former is the increase in erosional inputs to lakes in response to anthropogenic activities in the drainage basin (Brush, 1984). Atmospheric pollution resulting from the cultural and industrial activities (Chow et al.,1973) is a compelling example of the latter. Thus, aquatic sediments are archives of

natural and anthropogenic change. This is especially true for hydrophobic constituents such as heavy metals.

Because of their large adsorption capacity, fine-grained sediments are a major repository for the contaminants and a record of the temporal changes in contamination. Thus, sediments can be used for historical reconstruction. To guarantee a reliable age dating, and, therefore, to be useful in the historical reconstruction, the core sediment must be undisturbed, fine-grained, and collected in an area with a relatively fast sedimentation rate. These conditions are often found in lakes where studies in the 1970s by Kemp et al. (1974) and Forstner (1976) used lake sediments to understand the pollution history of several Laurentian Great Lakes and some European lakes. However, there is a serious limitation in using sediment cores from many natural lakes in that the sedimentation rate is generally too slow in providing the proper time resolution to discern modern pollution trends. Lacustrine sediments usually accumulate at rates less than 1 cm yr^{-1} (Krishnaswami and Lal, 1978) and often at rates less than 0.3 cm yr^{-1} (Johnson, 1984). Thus, there may be sufficient time for early diagenesis, such as microbiologically-mediated reactions, to occur. On the other hand, in lacustrine environments where sediments accumulate at rates exceeding 1 and may exceed 5–10 cm yr^{-1} (Ritchie et al., 1973), such as in surface-water reservoirs, rapid sedimentation exerts a pronounced influence on sedimentary diagenesis.

A brief discussion of sedimentary diagenesis is warranted as post-depositional chemical, and physical stability is probably the most important factor in preserving heavy-metal signatures that may be recorded in aquatic sediments. For sediments to provide a historical record of pollution, the pollutant must have an affinity for the sedimentary particles. It is well known that most of the metals, and certainly the heavy metals discussed in this chapter, are hydrophobic in nature and allow partition to the solid phase. Once deposited in the sediment, the pollutants should not undergo chemical mobilization within the sediment column nor should the sediment column be disturbed by physical and biological processes.

Natural lacustrine and estuarine sediments whose accumulation rates are low, generally below 0.25 cm yr^{-1}, often do not satisfy the above requirements. The biophysical term bioturbation refers to surficial sediments mixed by the actions of deposit feeders, irrigation tube dwellers, and head-down feeders (Boudreau, 1999). In general, these bioturbation processes do not occur in reservoirs where sediment accumulation rates exceed 1 and often 5 cm yr^{-1} (Callender, 2000). At these rates, the sediment influx at the water–sediment interface is too great for benthic organisms to establish themselves.

On the other hand, geochemical mobility affects every sedimentary environment; varying in degree, from slowly accumulating natural lacustrine and estuarine sediments to rapidly accumulating reservoir sediments. The major authigenic solid substrates for adsorption and co-precipitation of heavy metals in aquatic sediments are the hydrous oxides of iron (Fe) and manganese (Mn) (Santschi et al., 1990). These primary metal oxides sorb/co-precipitate Pb–Cr–Cu (Fe oxyhydroxides) and Zn–Cd–Pb (Mn oxyhydroxides) (Santschi et al., 1990). Manganese oxides begin to dissolve in mildly oxidizing sediments while Fe oxides are reduced in anoxic sediments (Salomons and Forstner, 1984). In the mildly oxidizing zone, Mn^{2+} diffuses upward and precipitates as Mn oxide in the stronger oxidizing part of the sediment column. At greater sediment depths, Fe oxide reduction to Fe^{2+} begins and ferrous iron diffuses upward and precipitates as Fe oxide in the mildly oxidizing part of the sediment sequence (Salomons and Forstner, 1984).

An example from a slowly-accumulating (0.01–0.1 cm yr^{-1}) sediment profile in a freshwater lake in Scotland (Williams, 1992) should suffice to illustrate the formation of diagenetic metal profiles. Early diagenetic processes, such as those described before, have promoted extensive metal enrichment immediately beneath the water–sediment interface. The oxic conditions, near the water–sediment interface, that promote metal precipitation and enrichment (Mn, Fe, Pb, Zn, Cu, Ni) are entirely confined to strata of post-industrial age (Williams, 1992).

Callender (2000) extensively studied the geochemical effects of rapid sedimentation in aquatic systems and postulated that rapid sedimentation exerts a pronounced influence on early sedimentary diagenesis. The following are two case studies that illustrate this point. The Cheyenne River Embayment of Lake Oahe, one of the several impoundments on the upper Missouri River, accumulates sediment at an average rate of 9 cm yr^{-1} (Callender and Robbins, 1993). Three interstitial-water Fe profiles from the same site taken over a three-year period (August 1985, August 1986, June 1987), when superimposed on the same depth axis, show the effects of interannual variations in sediment inputs such that in 1986 a rapid input of oxidized material suppressed the dissolved Fe concentration to less than 0.1 mg l^{-1} to a depth of 8 cm. In 1985 when there was a drought and sediment inputs were reduced substantially, near-surface sediment became nearly anoxic and the interstitial Fe concentration rose to a very high 26 mg l^{-1} (Callender, 2000). In Pueblo Reservoir on the upper Arkansas River in central Colorado, cores of bottom sediments showed distinct reddish-brown layers that indicate rapid transport and sedimentation of Fe-rich colloids formed by the discharge of acid-mine waters from abandoned mines upstream (Callender, 2000). The amorphous sedimentary Fe profile from a sediment core near the river mouth shows two peaks at depths that correspond to the dates of heavy metal releases from the mines. Although the amorphous Fe oxyhydroxide concentrations are only 10% of the total Fe concentrations, they are adequate to adsorb Pb (Fergusson, 1990) and produce the anthropogenic Pb concentrations found in the core (Callender, 2000). Copper and Zn show similar distributions in this core whose sedimentation rate is 5 cm yr^{-1}.

In these examples as well as for most aquatic sediments, the principal diagenetic reactions that occur in these sediments are aerobic respiration and the reduction of Mn and Fe oxides. Under the slower sedimentation conditions in natural lakes and estuaries, there is sufficient time (years) for particulate organic matter to decompose and create a diagenetic environment where metal oxides may not be stable. When faster sedimentation prevails, such as in reservoirs, there is less time (months) for bacteria to perform their metabolic functions due to the fact that the organisms do not occupy a sediment layer for any length of time before a new sediment is added (Callender, 2000). Also, sedimentary organic matter in reservoir sediments is considerably more recalcitrant than that in natural lacustrine and estuarine sediments as reservoirs receive more terrestrial organic matter (Callender, 2000).

The author hopes that this discussion of sedimentary diagenesis, as it applies to heavy-metal signatures in natural

lacustrine and reservoir sediments, will help the reader interpret the results presented in the following sections on reconstructed metal trends from age-dated reservoir sediment cores.

The approach that Callender and Van Metre (1997) have taken is to select primarily reservoir lakes that integrate a generally sizeable drainage basin that is impacted by a unique landuse such as agriculture, mining, stack emissions, suburban 'sprawl', or urban development with some commercial and light industrial activity. Sediment cores are taken to sample the post-impoundment section as much as possible and to penetrate the pre-impoundment material. Core sampling is accomplished with a variety of coring tools (box cores, push cores, piston cores) in order to recover a relatively undisturbed sediment section. The recovered sediment is sampled on approximately an annual sediment thickness and samples are preserved (chilled, then frozen) for future analytical determinations. In the laboratory, sediment samples are weighed, frozen, freeze-dried, weighed again, and ground to a fine powder. Elemental concentrations are determined on concentrated acid digests (nitric and hydrofluoric in microwave pressure vessels) by inductively coupled plasma-atomic emission spectrometry (ICP/AES) or by graphite furnace atomic adsorption spectrometry (GF/AAS).

For reservoirs to be a good medium for detecting the trends in heavy metals, several conditions need to be satisfied. First, the site sampled should be continuously depositional over the life of the reservoir. This condition is most easily satisfied by sampling in the deeper, lacustrine region of the reservoir where sedimentation is slower but more uniform and the sediments predominantly consist of silty clay material. The second condition is that the sediments sampled should not be subject to significant physical and chemical diagenesis; that is, mobilization of chemical constituents after deposition. Callender (2000) has written an extensive paper indicating that rapid sedimentation promotes minimal diagenesis and preserves historical metal signatures. The third condition is that the chemical quality of reservoir bottom sediments should be related to the water quality of the influent river and that the influent water quality be representative of the drainage basin.

11.3.4.2 Age Dating

In general, reservoir sediments can be dated by several techniques. In one technique, the sediment surface is dated by the time of coring while in the other the date is derived from a visual inspection of the cored sediment column which often penetrates the pre-impoundment surface. The primary age dating tool for reservoir sediments is by counting the radioactive isotope ^{137}Cs which has a half-life period of 30 years (Robbins and Edgington, 1975; McCall et al., 1984). The ^{137}Cs activity of freeze-dried sediment samples is measured by counting the gamma activity in fixed geometry with a high-resolution, intrinsic germanium detector gamma-spectrometer (Callender and Robbins, 1993). Depending on the penetration depth of the core and the age of the reservoir, ^{137}Cs can provide one or two date markers and can be used to evaluate the relative amount of postdepositional mixing or sediment disturbance (Van Metre et al., 1997). The peak ^{137}Cs activity in the sediment core is assigned a date of 1964, consistent with the peak in atmospheric fallout levels of ^{137}Cs for 1963–1964. In reservoirs constructed prior to or around 1950, the first occurrence of ^{137}Cs, if it did not appear to have been effected by postdepositional sediment mixing, was assigned a date of 1953 which is consistent with the generally accepted date of 1952 for the first large-scale atmospheric testing of nuclear weapons by the US in Nevada (Beck et al., 1990). This is also the date of the first globally-detectable levels of ^{137}Cs in the atmosphere. In some cases dates for samples between the known date-depth markers were assigned using constant mass accumulation rates (MARs), and in other cases the MARs were varied.

In natural lacustrine and slowly-accumulating reservoir sediments, core dating with the isotope ^{210}Pb has been used extensively (Schell and Barner, 1986). Appleby and Oldfield (1983) found that the constant rate of ^{210}Pb supply model (CRS) provides a reasonably accurate sedimentation chronology. The basic assumption of the CRS model is that the rate of supply of excess ^{210}Pb to the lake is constant. This model, thus, assumes that the erosive processes in the catchment are steady and give rise to a constant rate of sediment accumulation (MAR) (Appleby and Oldfield, 1983). In practice, for reservoirs, this assumption is rarely met because, for example, an increase in the MAR caused by land disturbances, such as those associated with the urban development, transports additional surficial soils and sediments to the lake. This additional erosion increases the MAR and also increases the rate of supply of ^{210}Pb to the lake. In general, because excess ^{210}Pb is an atmospheric fallout radionuclide, the model works better in low sedimentation rate, atmospherically dominated lakes with undisturbed watersheds, than in high sedimentation rate, fluvially dominated urban lakes and reservoirs.

Another problem with age dating of reservoir sediment is the concept of sediment focusing. This concept was developed to correct for postdepositional resuspension and redistribution of sediment in parts of the lake (Hermanson, 1991). A common focus correction factor is derived from the inventory of ^{137}Cs in the sediment column compared to the estimated total ^{137}Cs fallout at the sampling site (Hermanson, 1991). The same concept was found to not work well for lakes and reservoirs where the catchment area far exceeds the lake area. Such is the case for most reservoirs (Van Metre et al., 2000). In these cases where the catchment area is 10–100 times the lake area, sediment focusing in the lake basin is overwhelmed by the concentration effect of atmospheric fallout over the catchment area being funneled into the lake or reservoir. The catchment area focus corrections are calculated the same way as lake basin focus corrections except that there may be some variation in the ^{137}Cs flux to large catchment areas and that there will almost always be a correction factor greater than 1. These focus corrections must be calculated in order to compare the contaminant fluxes between the sites within a lake basin and between lake basins.

11.3.4.3 Selected Reconstructed Metal Trends

11.3.4.3.1 Lead and leaded gasoline: consequence of the clean air act

Of the six heavy metals discussed in this chapter, Pb has been studied extensively with respect to the environmental effects. Clair Patterson, the father of environmental Pb studies, in one of his many major publications concerning the global Pb cycle (Patterson and Settle, 1987), noted that during pre-industrial times Pb in the troposphere originated from soil dusts and

volcanic gases. In modern times (1950–1980) the proportion of natural Pb in the atmosphere is overwhelmed by the industrial sources of smelter emissions and automobile exhausts. Lead air pollution levels measured near our Nation's roadways decreased 97% between 1976 and 1995 due to the consequence of the Clean Air Act that eliminated leaded gasoline which interfered with the performance of catalytic converters.

For remote locations on a more global scale, Boyle et al. (1994) showed that the stable Pb concentration in North Atlantic waters decreased at least three-fold from 1979 to 1988. Wu and Boyle (1997) confirmed and extended this time series to 1996 whereby the concentration of stable Pb apparently stabilized at 50 pmol kg^{-1} in surface waters near Bermuda. Shen and Boyle (1987) presented a 100-year record of Pb concentration in corals from Bermuda and the Florida Straits showing that Pb peaked in the 1970s and declined thereafter. Veron et al. (1987) found high Pb concentrations in northeast Atlantic surficial sediments and noted that the quantity of Pb stored in these sediments is of the same order of magnitude as the amount of pollutant Pb present in the water column.

On a more local level, man's activities in the urban/suburban environment have produced a strong imprint of Pb on the land surface. In the US, automobile and truck travel are the primary means of moving people and goods around the continent. With the introduction of leaded gasoline in the 1950s, the mean annual atmospheric concentration of Pb nearly tripled in value, especially near population centers (Eisenreich et al., 1986). A substantial proportion of these

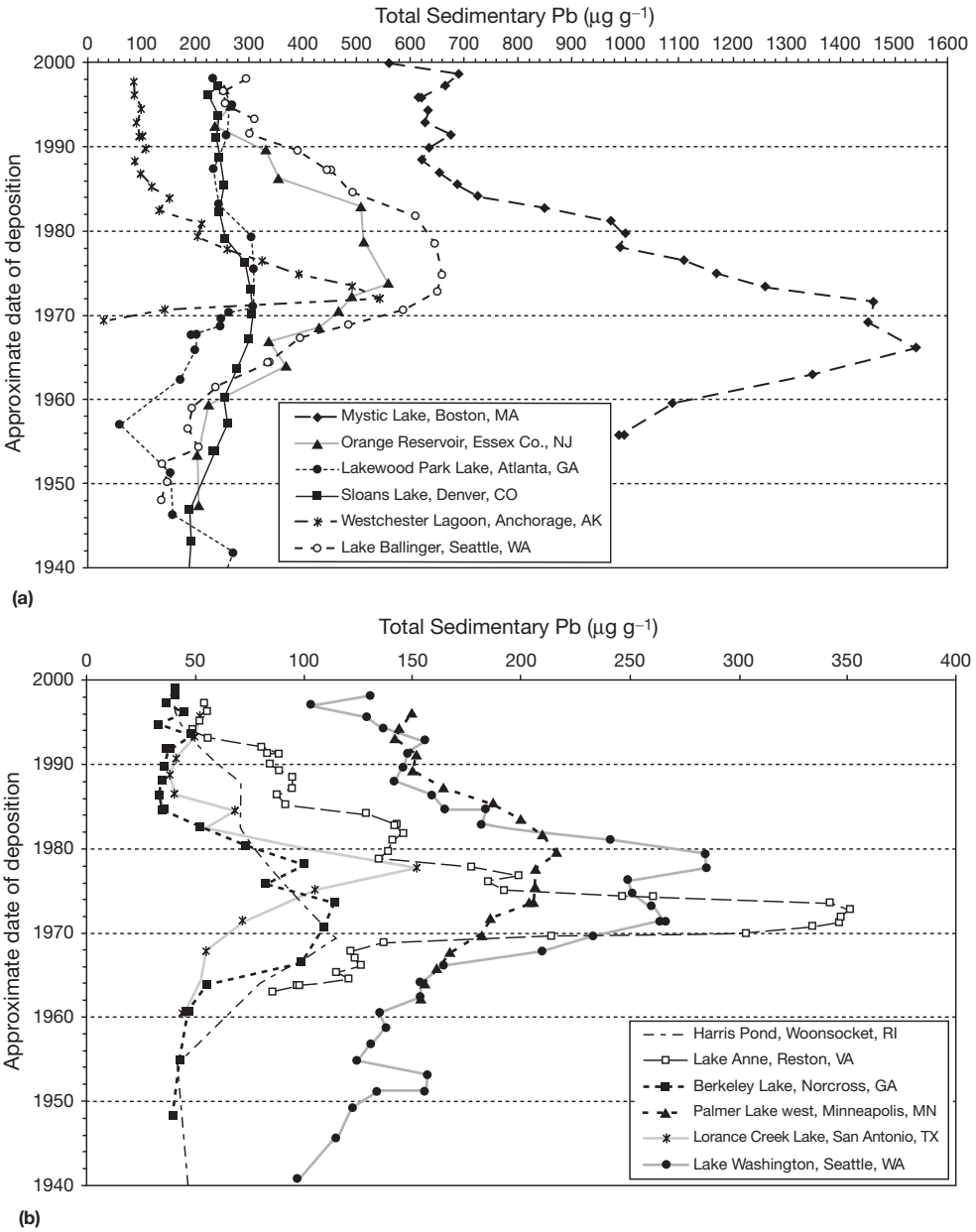

Figure 7 Temporal distribution of total sedimentary lead in sediment cores from (a) urban reservoirs, (b) suburban reservoirs and lakes, and (c) atmospheric reference site reservoirs.

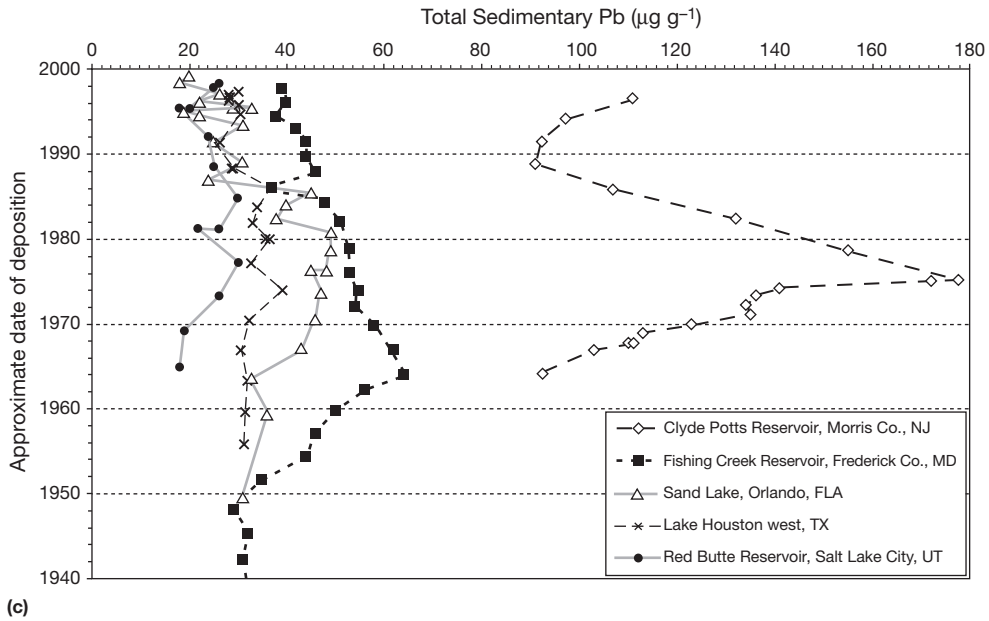

Figure 7 (continued).

atmospheric emissions of Pb have been deposited relatively close to the source. Figure 7(a)–(c) presents the age-dated sedimentary Pb profiles for reservoirs and lakes from urban–suburban–rural localities. One can see that the peak concentrations decrease from 700 to 300 to 100 μg g^{-1} as the distance from urban centers increase. All but two of the Pb peak concentrations date between 1970 and 1980, and are consistent with the decline in US atmospheric Pb concentrations following the ban of unleaded gasoline in 1972 (Callender and Van Metre, 1997). Sedimentary Pb data from many urban centers around the US (Boston, New York, New Jersey, Atlanta, Orlando, Minneapolis, Dallas, Austin, San Antonio, Denver, Salt Lake City, Las Vegas, Los Angeles, Seattle, and Anchorage) have been subjected to statistical trend analysis (B.J. Mahler, personal communication, 2002) and the results plotted in Figure 8. It is obvious that essentially all urban reservoirs and lake records show a very significant decline in Pb since 1975 and that this trend is most probably a result of the ban on leaded gasoline that was instituted in 1972.

11.3.4.3.2 Zinc from rubber tire wear

Contrary to the distribution of Pb in sediment cores whereby peak concentrations occurred during the 1970s, the concentration of sedimentary Zn often increases to the 1990s. It was observed in the atmospheric emissions of metals that waste incineration was one of the major contributors to the second tier of Zn emissions to the US atmosphere. Figure 9(a) presents age-dated sedimentary Zn data from a spectrum of urban/suburban sites around the US It is obvious that the general trend of sedimentary Zn is one of increasing concentrations from 1950s to 1990s. However, the general increasing trend for Zn is not as prevalent as that for Pb and at a few of the urban/suburban/reference sites noted for the Pb trend map there is no significant trend in sedimentary Zn concentration (B.J. Mahler, personal communication, 2002). Figure 5 shows that rubber tire wear is the most important and increasing contributor to the second tier of Zn emissions to the US atmosphere. Tire tread material has a Zn content of about 1% by weight. A significant quantity of tread material is lost to road surfaces by abrasion prior to tire replacement on a vehicle. In Figure 9(b) the anthropogenic Zn data for urban/suburban core sites is regressed against the mass sedimentation rate (MSR) for each core site. When MSR-normalized anthropogenic Zn is plotted against average annual daily traffic (AADT) data for the various metropolitan areas shown in Figure 9(a), a significant regression results (Figure 9(c)) suggesting that there is a causal relationship between anthropogenic Zn and vehicle traffic. Councell et al. (2004) produced data that estimates the magnitude of the Zn releases to the environment from rubber tire abrasion. Two approaches, wear rate (g km^{-1}) and tread geometry (abrasion to wear bars), were used to assess the magnitude of this nonpoint source of Zn in the US for the period 1936–1999. For 1999, the quantity of Zn released by tire wear in the US is estimated to be between 10 000 and 11 000 t.

Two specific case studies focused on the impact of vehicle tire wear to the Zn budget of watersheds in the Washington, DC metropolitan area. For Lake Anne, a suburban watershed located 40 km southwest of Washington, DC, the wet deposition atmospheric flux of Zn was 8 μg cm^{-2} yr^{-1} (Davis and Galloway, 1981) and the flux of Zn estimated from tire wear was 31 μg cm^{-2} yr^{-1} (Landa et al. 2002). The measured accumulation rate of Zn in age-dated sediment cores from Lake Anne is 41 μg cm^{-2} yr^{-1} (Landa et al., 2002) suggesting that tire-wear Zn inputs to suburban watersheds can be significantly greater than atmospheric inputs. In a rural/atmospheric reference site watershed, located ~90 km northwest of Washington, DC, the atmospheric Zn flux is 12 μg cm^{-2} yr^{-1} (Davis and Galloway, 1981) and that from tire wear is only 1 μg cm^{-2} yr^{-1} (Landa et al., 2002). There are only dirt roads leading to cabins in this protected watershed and it is obvious that vehicle tire wear is only a minor component of the Zn flux in this remote

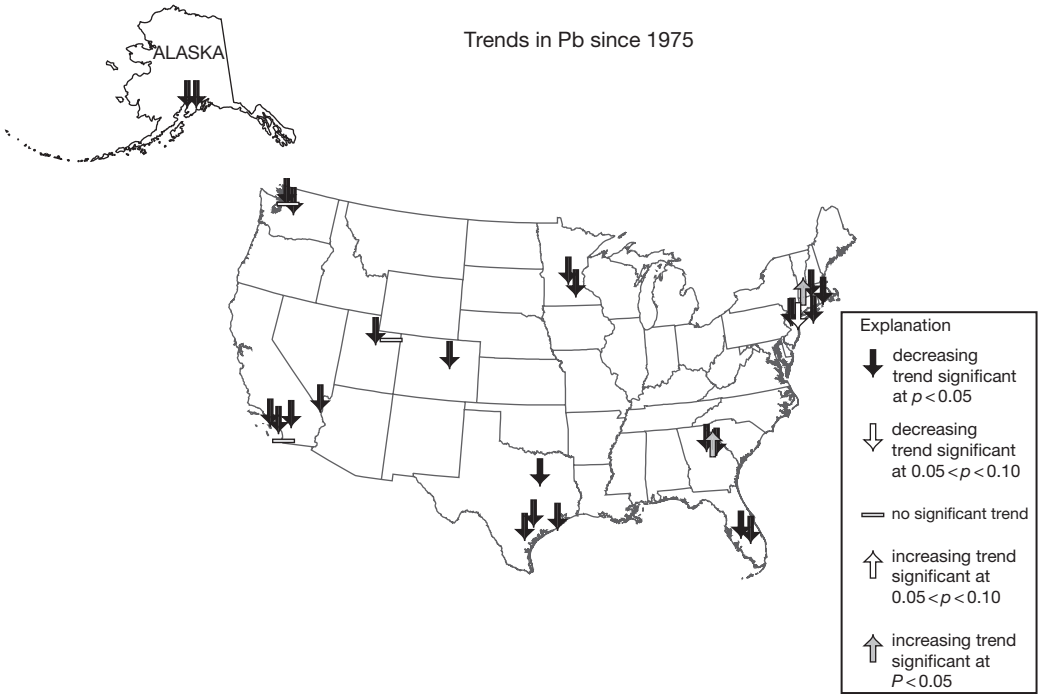

Figure 8 Map showing statistical trends in lead from sediment cores located throughout the US.

watershed. One conclusion drawn from these case studies and the substantial set of age-dated sediment core Zn profiles is that those watersheds that are impacted by vehicular traffic receive significant amounts of Zn via tire abrasion and that this Zn-enriched particulate matter is fluvially transported to lakes and reservoirs.

11.3.4.3.3 Metal processing and metal trends in sediment cores

While the relationship between Pb and Zn distributions in reservoir and lake sediment cores and environmental forcing functions (leaded gasoline use and vehicular traffic) are clear, the same is not true in the case of other metals such as Cd, Cr, Cu, and Ni. These metals do have one common, major source: nonferrous and ferrous metal production. Approximately 70% of the Cd and Cr anthropogenic emissions, 50% of the Cu, and 21% of the Ni anthropogenic emissions come from mining–smelting–metal processing. In an attempt to interpret metal trend maps for these four metals, historical US metal mining and production statistics have been shown in Figure 10. Copper is the only metal whose production increased during the past 25 years. Starting in 1985, the primary production of Cu has increased from about one million metric tons to a maximum of about two million metric tons in 1998 (Figure 10). Arizona has the largest Cu mining production followed by Utah, New Mexico, and Montana. Thus, all the major point sources of Cu exist in the western states. Figure 11 shows the statistical trends (since 1975) for Cu in sediment cores from 30 reservoir and lake sites around the US (B.J. Mahler, personal communication, 2002). Increasing or decreasing trends in the upper part of sediment cores were tested statistically for eight trace metals. Significant trends in sediments deposited since 1975 were tested using a Spearman's rank correlation (Helsel and Hirsch, 1992). Trends were determined to be significantly increasing or decreasing based on a p value of less than 0.05 (B.J. Mahler, personal communication, 2002). The Cu trend indicators in Figure 11 show that there are increasing trends significant at $p < 0{:}05$ at the core sites in Washington–California–Nevada and that there are no significant trends in Cu at core sites in the Midwest and Southwest. Such a pattern suggests that an increase in Cu mining in the Rocky Mountain States may cause airborne emissions that impact the western US but that these emissions are not transported east to the mid-continent. Along the Atlantic coast, from Georgia to Massachusetts, there are some sites that show an increasing trend in sedimentary Cu. It should be noted that many of the east coast sites are small ponds used for water supply and recreation and that some have been treated with $CuSO_4$ to control the algae. In addition, many of these sites are located in the east coast urban/suburban corridor and obviously receive a multitude of anthropogenic contaminants.

Limited space does not allow for the presentation of all metal trend maps such as those presented for Pb and Cu. Of the three remaining metals (Cd, Cr, Ni), the trends in Ni since 1975 is representative of the other metals as well. For the western half of the US, there are nine sites where there is a significant decreasing trend in Ni (Figure 12). This corresponds to the decrease in Ni smelter production for the 1970s and 1980s (Figure 10). There are a few increasing Ni trends along the east coast of the US, a pattern that may reflect the location of many nickel consumption facilities in Pennsylvania, West Virginia, and New Jersey. The trends in Cr since 1975 are very similar to those for Ni; for the western half of the US there are eight sites where there is a significant decreasing trend. Along the east coast of the US there is only one site in the Boston area that shows an increasing trend.

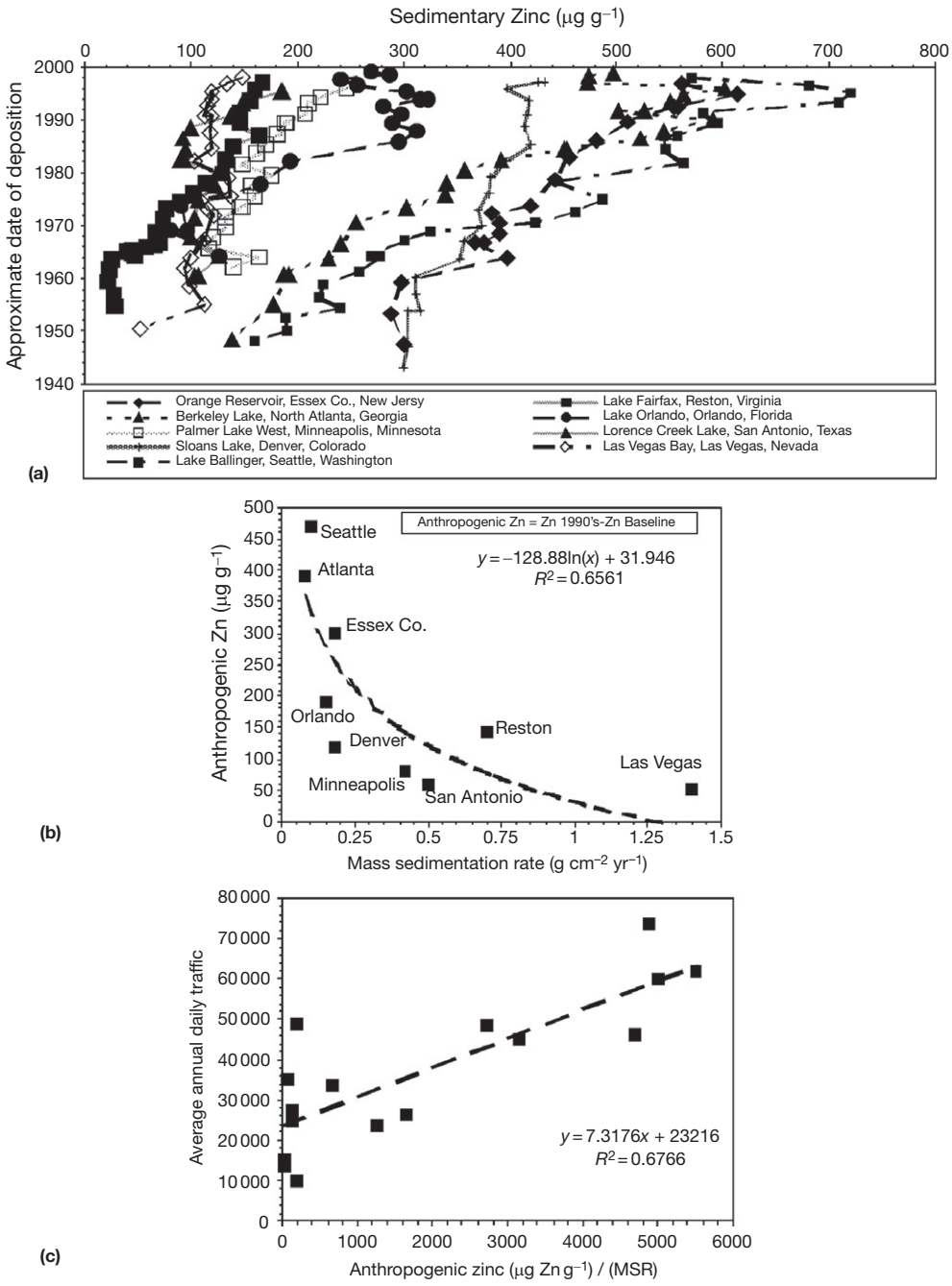

Figure 9 (a) Temporal distribution of total sedimentary zinc in US reservoir sediment cores, (b) regression of anthropogenic zinc versus MSR for US reservoir sediment cores, (c) MSR-normalized anthropogenic zinc versus average annual daily traffic for urban and suburban watersheds throughout the US.

Thus, the overall decreasing Cr trend for the US reflects the four-fold decrease in chromite (Cr ore) consumption by metallurgical and chemical firms in the US since 1970 (Figure 10). The trends in Cd since 1975 are not as strongly skewed toward decreasing trends as those for Ni and Cr. This is probably due to the fact that much of the Cd in the US is recovered by the processing of Zn ore and as one can see from Figure 10, Zn production has leveled out in the 1980s and 1990s. In fact, the preponderance of coring sites in the US (20 out of 30) show no significant trend in Cd.

11.3.4.3.4 Reduction in power plant emissions of heavy metals: clean air act amendments and the use of low sulfur coal

Only recently have electric utility power plant emissions been included on the US Environmental Protection Agency's (USEPA) Toxic Release Inventory which reported that electric utilities ranked highest for industrial toxic air emissions in 1998. These emissions were likely to be an important component of toxic air releases in the past, particularly prior to the passage of the Clean Air Act of 1970.

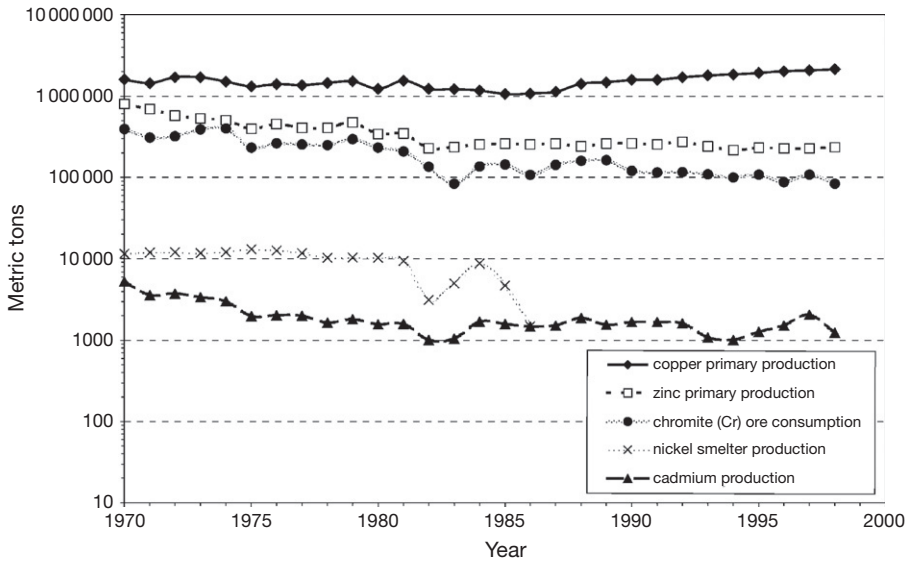

Figure 10 Historical production of nonferrous metals in the US Data from US Geological Survey, Mineral Resources Program.

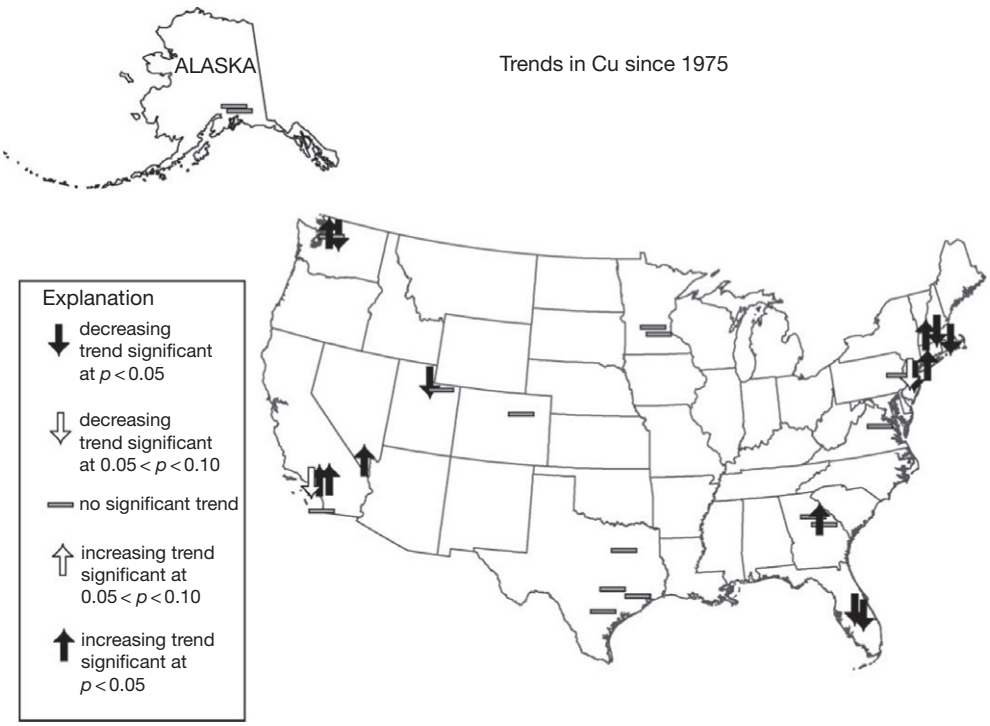

Figure 11 Map showing statistical trends in copper from sediment cores located throughout the US.

A sediment core from one reservoir (Mile Tree Run Reservoir) located in southwestern West Virginia was selected for the purpose of identifying particulate signatures of coal-fired power plant emissions from the nearby Ohio River Valley region. Arsenic (As) and some Pb and Zn releases to the environment may reflect coal-related geochemical processes. Stream sediments from the Appalachian Basin Region are particularly enriched in As compared to the sediments outside the Basin. While some As enrichment may come from the weathering of As-rich coal, this area of West Virginia is underlain primarily by sandstone which is low in trace-element composition. Thus, the elevated As contents are not likely to have an origin in the regional country rock but might have originated from numerous large coal-fired power plants situated along the Ohio River.

Figure 13(a) shows the temporal distribution of Ti-normalized As, Pb, and Zn in the sediment core from Mile Tree Run Reservoir. These Ti-normalized metal peaks date back to 1987, 1966, and 1946, respectively (Figure 13(a)). Figure 13(b) shows the temporal distribution of Ti-normalized sulfur (S),

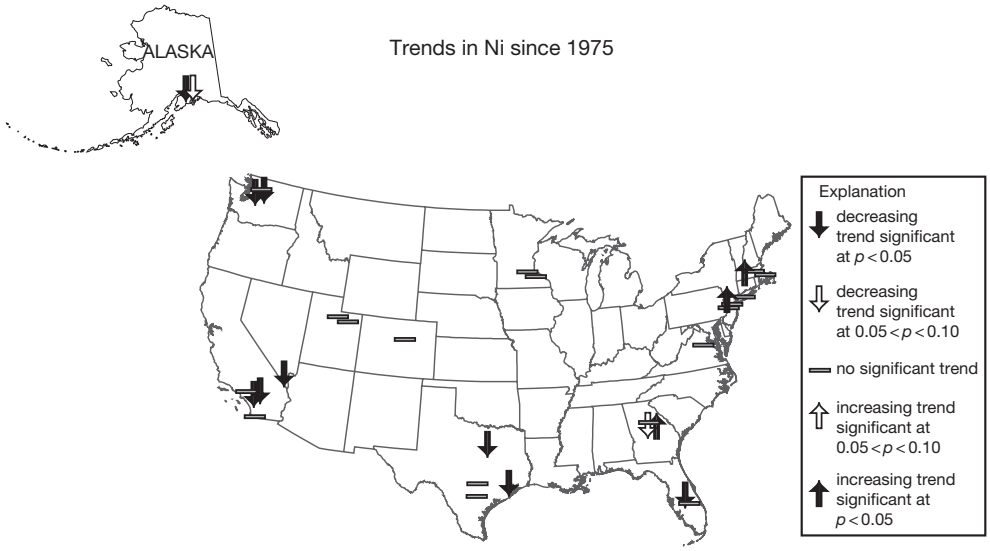

Figure 12 Map showing the statistical trends in nickel from sediment cores located throughout the US.

isothermal remnant magnetization (IRM) (a magnetite proxy), and Fe in the same core. Peaks in these constituents correspond to the aforementioned dates. These dates match the maximum values in combined coal production for the states of West Virginia, Pennsylvania, and Ohio (M.B. Goldhaber, personal communication, 2002). The temporal profile for the magnetic property IRM that is indicative of the mineral magnetite is shown in **Figure 13(b)** (M.B. Goldhaber, personalcommunication, 2002).

Figure 14(a) and **(b)** are scatter plots between Zn and coal production, and Zn and IRM (magnetite). Note the excellent correlations suggesting that Zn relates to atmospheric input (fly ash) from power plants. A glance at **Table 2** shows that Zn in fly ash is substantially enriched compared to average soils. One can also see this relationship for Mile Tree Run watershed soils in **Figure 13(a)**. Arsenic also has a very strong positive correlation with IRM in the Mile Tree Run Reservoir core. This element is known to be strongly associated with magnetite, an important fly ash mineral that is formed in the high temperature combustion of coal (Locke and Bertine, 1986). Such a geochemical association is not surprising in that it is thought that magnetite is formed from the pyrite in coal that is subjected to high temperature combustion. It is also well known that As is a minor element associated with pyrite.

The simultaneous decline after 1985 of the correlated Fe–As–Pb–Zn and magnetite peaks (**Figure 13(a)** and **(b)** suggests that the amount of power plant particulate emissions decreased since the 1977 amendment of the Clean Air Act that mandated reduced amounts of sulfur in the feed coal (Hower et al., 1999). It appears that this action resulted in lower metal and magnetite quantities in the fly ash combusted residue. Despite this decrease, soil samples from the Mile Tree Run Reservoir watershed are strongly enriched in As, Pb, and Zn when compared to average soils (**Table 2**) and local bedrock (Callender et al., 2001), indicating a regional power plant emissions impact on the geochemical landscape.

11.3.4.3.5 European lacustrine records of heavy metal pollution

Much of the recent literature pertaining to European studies of heavy metal pollution using sediment cores to track time trends focused on Pb. Petit et al. (1984) used the stable isotope geochemistry to identify Pb pollution sources and to evaluate the relative importance of anthropogenic sources to total Pb fluxes in a semi-rural region of western Europe. Thomas et al. (1984) showed that metal enrichment factors for Pb–Zn–Cd were significantly above unity, indicating a diffuse contribution through atmospheric transport from industrialized areas. A comparison with atmospheric fluxes showed good agreement for diffuse atmospheric supply of Pb, Zn, and Cd in the lake sediments (Thomas et al., 1984).

Much work has been done on Lake Constance situated on the borders of Germany, Austria, and Switzerland. The lake has undergone extensive cultural eutrophication due to the surrounding population, industrial activity, and the input of River Rhine. Muller et al. (1977) found that sedimentary Pb and Zn concentrations peaked around 1965. They also noted that there was a strong positive correlation between heavy-metal content and PAHs in the sediment core. Muller et al. (1977) suggested that coal burning was the source of this relationship. In a more recent study of Lake Constance sediments, Wessels et al. (1995) also noted high concentrations of Pb and Zn that began around 1960. However, they postulated that the origin of the Pb increase was emissions by regional industry and the origin of the Zn increase was a combination of urban runoff and coal burning.

Two groups, one in Switzerland and the other in Sweden, have used age-dated sediment cores from peat bogs and natural lake sediments to record the history of atmospheric Pb pollution dating back to several thousand years.

In Switzerland, Shotyk and co-workers (Shotyk et al., 1998) rebuilt the history of atmospheric Pb deposition over the last 12 000 years. They cored ombrotrophic peat bogs that are hydrologically isolated from the influence of local groundwaters and surfacewaters, and receive their inorganic solids

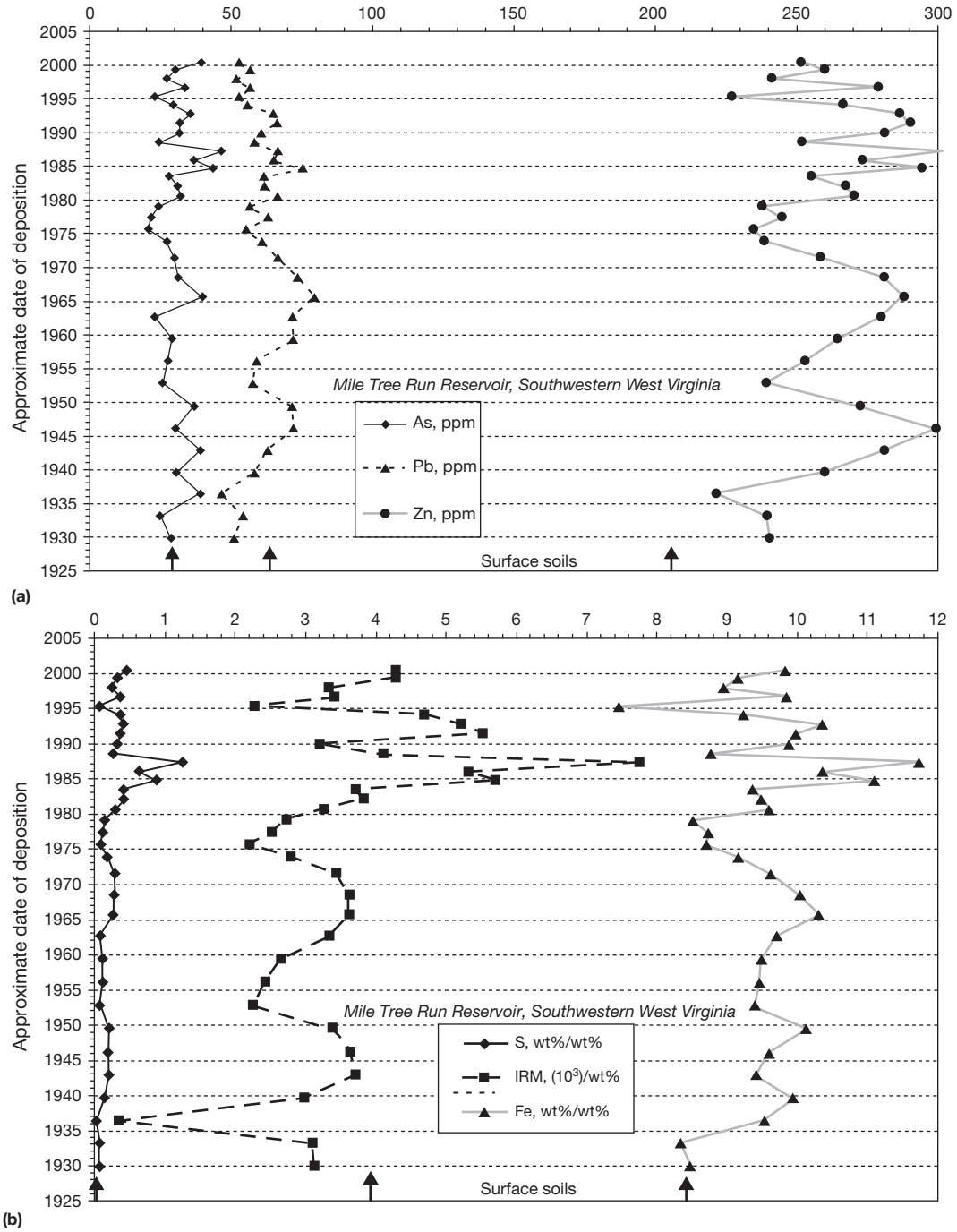

Figure 13 (a) Temporal distribution of Ti-normalized As–Pb–Zn (ppm/wt%) in a sediment core from Mile Tree Run Reservoir, Southwestern West Virginia, USA; (b) Temporal distribution of Ti-normalized S–IRM–Fe (wt%/wt%) in the Mile Tree Run Reservoir sediment core.

exclusively by atmospheric deposition. Whereas slowly-accumulating natural lake sediments appear to be affected by chemical diagenesis, studies have shown that peat bogs provide a reliable record of changes in atmospheric metal deposition (Roos-Barraclough and Shotyk, 2003). Their radiocarbon dated core profiles of stable Pb and $^{206}Pb/^{207}Pb$ isotopic ratios indicate that enhanced fluxes of Pb were caused by climatic changes between 10 500 and 8250 years before present (BP). Soil erosion, caused by forest clearing and agricultural tillage, increased Pb deposition subsequent to this time. Beginning 3000 yr BP, Pb pollution from mining and smelting was recorded by a significant increase in normalized Pb concentrations (Pb/Sc) and a decreasing $^{206}Pb/^{207}Pb$ ratio. Around BP 2100, Roman Pb mining became the most important source of atmospheric Pb pollution; and in AD 1830 the effects of the Industrial Revolution were recorded by a very large peak in Pb enrichment. The $^{206}Pb/^{207}Pb$ ratio declined significantly around AD 1940 indicating the use of leaded gasoline which was

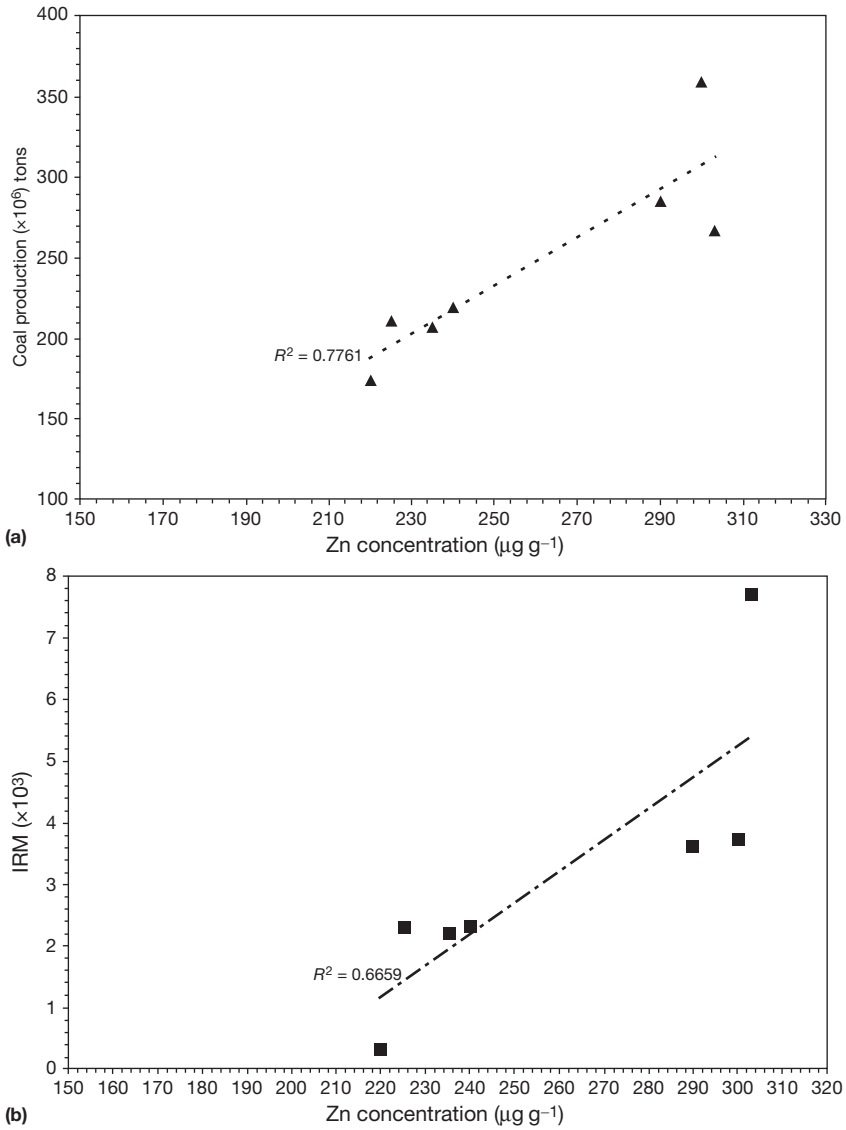

Figure 14 (a) Scatter plot of Appalachian Basin temporal coal production versus temporal concentration of Zn in a Mile Tree Run Reservoir sediment core, (b) Scatter plot of the temporal concentration of IRM (magnetite) versus the temporal concentration of Zn in the Mile Tree Run Reservoir sediment core.

subsequently discontinued in AD 1979 (Shotyk et al., 1998). In an earlier paper, Shotyk et al. (1996) noted that there were significant enrichments in As and Sb as well as for Pb dating back to Roman times (BP 2100). These enrichments in As and Sb were thought to be related to Pb mining and smelting.

In Sweden, Brannvall and his colleagues published several papers culminating in a summary paper (Brannvall et al., 2001) describing four thousand years of atmospheric Pb pollution in northern Europe. They cored 31 lakes throughout Sweden; some were age-dated with radiocarbon while others had varved sediments. Their stable Pb and $^{206}Pb/^{207}Pb$ isotope data indicate that the first influx of noncatchment atmospheric Pb occurred between 3500 and 3000 years ago. The large world production of Pb (80 000 t yr^{-1}) during Greek and Roman times 2000 years ago caused widespread atmospheric Pb pollution. There was a decline in the atmospheric Pb flux between AD 400 and 900. Brannvall et al. (2001) note that the Medieval period, rather than the Industrial Revolution, was the real beginning of the contemporary Pb pollution era. This era extended from AD 1000 to 1800. Lead peaked in the mid-twentieth century in Sweden (1950s–1970s) due to the use of leaded gasoline and fossil-fuel combustion. The recent decline in atmospheric Pb deposition since 1980 is very steep and significant. Johansson (1989) analyzed the heavy-metal content of some 54 lakes in central and northern Sweden, and noted that the Pb content of surface sediment was 50 times greater than the background concentration and that this Pb enrichment decreased substantially from south to north. Ek et al. (2001) studied the environmental effects of one thousand years of Cu production in Central Sweden. Metal analyses of the lake sediments showed that Cu pollution was restricted to a smaller area near the emission sources and that Pb, Zn, and Cd pollution was

widespread. Sedimentary metal enrichments began about AD 1000 and peaked in the seventeenth century when Central Sweden produced two-thirds of the world's Cu supply.

Sedimentary lacustrine records of heavy metal pollution in Lough Neagh (northern Ireland) and Lake Windermere (England) suggest that there have been two periods of metal disturbance since the AD 1600. Both lakes are situated within rural catchments. In Lough Neagh (Rippey et al., 1982), a change in the catchment erosion regime during the seventeenth century produced an increase in the sedimentary Cd–Cu–Pb concentrations. This change in erosion was a result of widespread and comprehensive forest clearance. A second and larger change occurred about AD 1880 when the concentrations of Cr, Cu, Zn, and Pb increased toward the sediment surface. Sediments from Lake Windermere also show a pronounced increase in Cu–Pb–Zn concentrations within the upper part of the sediment column (Hamilton-Taylor, 1979). Since the catchments are not proximal to the local anthropogenic sources such as mining, smelting, or wastewater inputs, it is possible that a substantial part of these metal enrichments are due to a more regional or even global atmospheric input that was generated by many anthropogenic processes related to the Industrial Revolution.

References

Adriano DC (1986) *Trace Elements in the Terrestrial Environment*. New York: Springer.

Alexander CR, Smith RG, Calder FD, Schropp SJ, and Windom HL (1993) The historical record of metal enrichment in two Florida estuaries. *Estuaries* 16: 627–637.

Allan RJ (1975) Natural versus unnatural heavy metal concentrations in lake sediments in Canada. *Proceedings International Conference on Heavy Metals in the Environment* 2: 785–808.

Alloway BJ (1995) *Heavy Metals in Soils*, 2nd edn. London, UK: Blackie Academic and Professional.

Anikiyev VV, Perepelitsa SA, and Shumilin Ye N (1993) Effects of man-made and natural sources on the heavy-metal patterns in bottom sediments in the Gulf of Peter the Great, Sea of Japan. *Geokhimiya* 9: 1328–1340.

Appleby PG and Oldfield F (1983) The assessment of ^{210}Pb data from sites with varying sediment accumulation rates. *Hydrobiologia* 103: 29–35.

Aston SR, Thornton I, Webb JS, Purves JB, and Milford BL (1974) Stream sediment composition: An aid to water quality assessment. *Water, Air, & Soil Pollution* 3: 321–325.

Beck HL, Helfer IK, Bouville A, and Deicer M (1990) Estimates of fallout in the continental US from Nevada weapons testing based on gummed-film monitoring data. *Health Physics* 59: 565–576.

Belzile N, Lecomte P, and Tessier A (1989) Testing readsorption of trace elements during partial chemical extractions of bottom sediments. *Environmental Science & Technology* 23: 1015–1020.

Bertine KK and Goldberg ED (1971) Fossil fuel combustion and the major sedimentary cycle. *Science* 173: 233–235.

Borovec Z, Tolar V, and Mraz L (1993) Distribution of some metals in sediments of the central part of the Labe (Elbe) River, Czech Republic. *Ambio* 22: 200–205.

Boudreau BP (1999) Metals and models: diagenetic modeling in freshwater lacustrine sediments. *Journal of Paleolimnology* 22: 227–251.

Boutron CF, Gorlach U, Candelone J-P, Bolshov MA, and Deimas RJ (1991) Decrease in anthropogenic lead, cadmium and zinc in Greenland snows since the late 1960s. *Nature* 353: 153–156.

Boyle EA (1979) Copper in natural waters. In: Nriagu JO (ed.) *Copper in the Environment, Part I: Ecological Cycling*, pp. 77–88. New York: Wiley.

Boyle EA, Sherrell RM, and Bacon MP (1994) Lead variability in the western North Atlantic Ocean and central Greenland ice: Implications for the search for decadal trends in anthropogenic emissions. *Geochimica et Cosmochimica Aeta* 58: 3227–3238.

Brannvall ML, Bindler R, Emteryd O, and Renberg I (2001) Four thousand years of atmospheric lead pollution in northern Europe: A summary from Swedish lake sediments. *Journal of Paleolimnology* 25: 421–435.

Brush GS (1984) Patterns of recent accumulation in Chesapeake Bay (Virginia-Maryland, USA) tributaries. *Chemical Geology* 44: 227–242.

Callender E (2000) Geochemical effects of rapid sedimentation in aquatic systems: Minimal diagenesis and the preservation of historical metal signatures. *Journal of Paleolimnology* 23: 243–260.

Callender E, Goldhaber MB, Reynolds RL, and Grosz A (2001) Geochemical signatures of power plant emissions as revealed in sediment cores from West Virginia reservoirs. *Annual Meeting of the Geological Society of America* (Abstracts).

Callender E and Robbins JA (1993) Transport and accumulation of radionuclides and stable elements in a Missouri River reservoir. *Water Resources Research* 29: 1787–1804.

Callender E and Van Metre PC (1997) Reservoir sediment cores show US lead declines. *Environmental Science & Technology* 31: 424A–428A.

Candelone J-P, Hong S, Pellone C, and Boutron CF (1995) Post-industrial revolution changes in large-scale atmospheric pollution of the northern hemisphere by heavy metals as documented in central Greenland snow and ice. *Journal of Geophysical Research* 100: 16 605–16 616.

Chao TT (1984) Use of partial dissolution techniques in geochemical exploration. *Journal of Geochemical Exploration* 20: 101–135.

Chester R (2000) *Marine Geochemistry*, 2nd edn. Oxford: Malden.

Chiffoleau J-F, Cossa D, Auger D, and Truquet I (1994) Trace metal distribution, partition and fluxes in the Seine estuary (France) in low discharge regime. *Marine Chemistry* 47: 145–158.

Chow T and Patterson CC (1962) The occurrence and significance of lead isotopes in pelagic sediments. *Geochimica et Cosmochimica Aeta* 26: 263–308.

Chow TJ, Bruland KW, Bertine KK, Soutar A, Koide M, and Goldberg ED (1973) Lead pollution: Records in southern California coastal sediments. *Science* 181: 551–552.

Coakley JP and Poulton DJ (1993) Source-related classification of St. Lawrence Estuary sediments based on spatial distribution of adsorbed contaminants. *Estuaries* 16: 873–886.

Conko KM and Callender E (1999) Extraction of anthropogenic trace metals from sediments of two US urban reservoirs. *Abstracts, 1999 Fall Meeting American Geophysical Union*.

Councell TB, Duckenfield KU, Landa ER, and Callender E (2004) Tire-wear particles as a source of zinc to the environment. *Environmental Science & Technology* 38: 4206–4214.

Davis WE and Associates (1970) *National Inventory of Sources and Emissions of Cadmium*. National Technical Information Service Report. PB 192250, Springfield, VA.

Davis AO and Galloway JN (1981) Atmospheric lead and zinc deposition in lakes in the eastern United States. In: Eisenreich SJ (ed.) *Atmospheric Pollutants in Natural Waters*, pp. 401–408. Ann Arbor: Ann Arbor Science.

Davis JA, James RO, and Leckie JO (1978) Surface ionization and complexation at the oxide/water interface:1. Computation of electrical double layer properties in simple electrolytes. *Journal of Colloid and Interface Science* 63: 480.

Dolske DA and Sievering H (1979) Trace element loading of southern Lake Michigan by dry deposition of atmospheric aerosol. *Water, Air, & Soil Pollution* 12: 485–502.

Dominik J, Mangini A, and Prosi F (1984) Sedimentation rate variations and anthropogenic metal fluxes into Lake Constance sediments. *Environmental Geology* 5: 151–157.

Drever JI (1988) *The Geochemistry of Natural Waters*, 2nd edn. New York: Prentice-Hall.

Duce RA, Liss PS, Merrill JT, et al. (1991) The atmospheric input of trace species to the world ocean. *Global Biogeochemical Cycles* 5: 193–259.

Dunnette DA (1992) Assessing global river quality, overview and data collection. In: Dunnette DA and O'Brien RJ (eds.) *The Science of Global Change: The Impact of Human Activities on the Environment, ACS Symposium 483*, pp. 240–286. American Chemical Society.

Eisenreich SJ (1980) Atmospheric input of trace elements to Lake Michigan. *Water, Air, & Soil Pollution* 13: 287–301.

Eisenreich SJ, Metzer NA, Urban NR, and Robbins JA (1986) Response of atmospheric lead to decreased use of lead in gasoline. *Environmental Science & Technology* 20: 171–174.

Ek AS, Lofgren S, Bergholm J, and Qvarfort U (2001) Environmental effects of one thousand years of copper production at Falun Central Sweden. *Ambio* 30: 96–103.

Farrah H and Pickering WF (1977) Influence of clay-solute interactions an aqueous heavy metal ion levels. *Water, Air, & Soil Pollution* 8: 189–197.

Faust SD and Aly OM (1981) *Chemistry of Natural Waters*. Ann Arbor: Ann Arbor Science.

Fergusson JE (1990) *The Heavy Elements: Chemistry, Environmental Impact, and Health Effects*, p. 614. Oxford: Pergamon.

Forstner U (1976) Lake sediments as indicators of heavy-metal pollution. *Naturwissenschaften* 63: 465–470.

Forstner U (1981) Recent heavy metal accumulation in limnic sediments. In: Wolf KH (ed.) *Handbook of Strata-Bound and Stratiform Ore Deposits*, pp. 179–269. Elsevier.

Forstner U (1990) Inorganic sediment chemistry and elemental speciation. In: Baudo R, Giesy JP, and Mantau H (eds.) *Sediments: Chemistry and Toxicity on In-Place Pollutants*, pp. 61–105. Lewis.

Gardiner J (1974) The chemistry of cadmium in natural water: II. The adsorption of cadmium on river muds and naturally occurring solids. *Water Research* 8: 157–164.
Garrels RJ and Christ CL (1965) *Solutions, Minerals and Equilibria*. New York: Harper and Row.
Garrels RM, Mackenzie FT, and Hunt C (1973) *Chemical Cycles and the Global Environment: Assessing Human Influences*. Los Altos: William Kaufmann.
Gibbs RJ (1973) Mechanisms of trace metal transport in rivers. *Science* 180: 71–73.
Gocht T, Moldenhauer K-M, and Puttmann W (2001) Historical record of polycyclic aromatic hydrocarbons (PAH) and heavy metals in floodplain sediments from the Rhine River (Hessisches Ried, Germany). *Applied Geochemistry* 16: 1707–1721.
Govindaraju K (1989) 1989 compilation of working values and sample description for 272 geostandards. *Geostandards Newsletter* 13: 1–113.
Graney JR, Halliday AN, Keeler GJ, Nriagu JO, Robbins JA, and Norton SA (1995) Isotopic record of lead pollution in lake sediments from the northeastern United States. *Geochimica et Cosmochimica Acta* 59: 1715–1728.
Hamilton-Taylor J (1979) Enrichments of zinc lead, and copper in recent sediments of Windermere, England. *Environmental Science & Technology* 13: 693–697.
Hanson PJ (1997) Response of hepatic trace element concentrations in fish exposed to elemental and organic contaminants. *Estuaries* 20: 659–676.
Heit M, Klusek C, and Baron J (1984) Evidence of deposition of anthropogenic pollutants in remote Rocky Mountain lakes. *Water, Air, & Soil Pollution* 22: 403–416.
Helsel DR and Hirsch RM (1992) *Statistical Methods in Water Resources, Studies in Environmental Science* 49: Amsterdam: Elsevier.
Hem JD (1972) Chemistry and occurrence of cadmium and zinc in surface water and ground water. *Water Resources Research* 8: 661–679.
Hem JD (1976) Geochemical controls on lead concentrations in stream water and sediments. *Geochimica et Cosmochimica Acta* 40: 599–609.
Hem JD (1977) Reactions of metal ions at surfaces of hydrous iron oxide. *Geochimica et Cosmochimica Acta* 41: 527–538.
Hem JD (1985) *Study and Interpretation of the Chemical Characteristics of Natural Water*. US Geological Survey: Survey Water-Supply Paper 2254, US Government Printing Office.
Hem JD and Durum WH (1973) Solubility and occurrence of lead in surface water. *Journal American Water Works Association* 65: 562–568.
Hermanson MH (1991) Chronology and sources of anthropogenic trace metals in sediments from small, shallow arctic lakes. *Environmental Science & Technology* 25: 2059–2064.
Honeyman BD and Santschi PH (1988) Metals in aquatic systems. *Environmental Science & Technology* 22: 862–871.
Hong S, Candelone J-P, Patterson CC, and Boutron CF (1994) Greenland ice evidence of hemispheric lead pollution two millennia ago by Greek and Roman civilizations. *Science* 265: 1841–1843.
Hornberger MI, Luoma SN, Van Geen A, Fuller CC, and Anima RJ (1999) Historical trends of metals in the sediments of San Francisco Bay, California. *Marine Chemistry* 64: 39–55.
Hornberger MI, Luoma SN, Cain DJ, et al. (2000) Linkage of bioaccumulation and biological effects to changes in pollutant loads in south San Francisco Bay. *Environmental Science & Technology* 34: 2401–2409.
Hower JC, Robl TL, and Thomas GA (1999) Changes in the quality of coal combustion by-products produced by Kentucky power plants, 1978 to 1997: Consequences of Clean Air Act directives. *Fuel* 78: 701–712.
Hsu CL (1978) *Heavy Metal Uptake by Soils Surrounding a Fly Ash Pond*. MS Thesis, University of Notre Dame.
Jenne EA (1968) Controls on Mn, Fe, Co, Ni, Cu and Zn concentrations in soils and water: The significant role of hydrous Mn and Fe oxides. In: *Trace Inorganics in Water*, *American Chemical Society Advances in Chemistry Series 73*, pp. 337–387.
Johansson K (1989) Metals in sediment of lakes in Northern Sweden. *Water, Air, & Soil Pollution* 47: 441–455.
Johnson TC (1984) Sedimentation in large lakes. *Annual Review of Earth and Planetary Sciences* 12: 179–204.
Kabata-Pendias A (2000) *Trace Elements in Soils and Plants*, 3rd edn. Boca Raton: CRC Press.
Kabata-Pendias A and Pendias H (1992) *Trace Elements in Soils and Plants*, 2nd edn. Boca Raton: CRC Press.
Kabata-Pendias A and Pendias H (2001) *Trace Elements in Soils and Plants*, 3rd edn. Boca Raton: CRC Press.
Kemp ALW, Anderson TW, Thomas RL, and Mudrochova A (1974) Sedimentation rates and recent sediment history of Lake Ontario, Erie, and Huron. *Journal of Sedimentary Petrology* 44: 207–218.
Kemp ALW and Thomas RL (1976) Impact of man's activities on the chemical composition in the sediments of Lakes Ontario, Erie, and Huron. *Water, Air, & Soil Pollution* 5: 469–490.
Kemp ALW, Williams JDH, Thomas RL, and Gregory ML (1978) Impact of man's activities on the chemical composition of the sediments of Lakes Superior and Huron. *Water, Air, & Soil Pollution* 10: 381–402.
Kersten M and Forstner U (1987) Effects of sample pretreatment on the reliability of solid speciation data of heavy metals-implications for the study of early diagenetic processes. *Marine Chemistry* 22: 299–312.
Kersten M and Forstner U (1995) Speciation of trace metals in sediments and combustion waste. In: Ure AM and Davidson CM (eds.) *Chemica Speciation in the Environment*, pp. 234–275. London: Blackie Academic and Professional.
Krauskopf KB (1956) Factors controlling the concentration of thirteen rare metals in sea-water. *Geochimica et Cosmochimica Acta* 9: 1–32.
Krishnamurthy S and Wilkens MM (1994) Environmental chemistry of chromium. *Northeastern Geology* 16: 14–17.
Krishnaswami S and Lal D (1978) Radionuclide limnochronol. In: Lerman A (ed.) *Lakes-Chemistry, Geology, Physics*, pp. 153–177. New York: Springer-Verlag.
Landa ER, Callender E, Councell TB, and Duckenfield KV (2002) Where the rubber meets the soil: Tire wear particles as a source of zinc to the environment. *Abstracts, Annual Meeting of the Soil Science Society of America*.
Lantzy RJ and Mackenzie FT (1979) Atmospheric trace metals: Global cycles and assessment of man's impact. *Geochimica et Cosmochimica Acta* 43: 511–525.
Leckie JO and Davis JA (1979) Aqueous environmental chemistry of copper. In: Nriagu JO (ed.) *Copper in the Environment*, pp. 90–121. New York: Wiley.
Leckie JO and Nelson MB (1975) Role of natural hetrerogeneous sulfide systems in controlling the concentration and distribution of heavy metals. *Paper presented at the Second International Symposium on Environmental Biogeochemistry,* Ontario, Canada.
Li Y-H (1981) Geochemical cycles of elements and human perturbation. *Geochimica et Cosmochimica Acta* 45: 2073–2084.
Li Y-H (2000) *A Compendium of Geochemistry*. Princeton: Princeton University Press.
Li Y-H, Burkhardt L, and Teraoka H (1984) Desorption and coagulation of trace elements during estuarine mixing. *Geochimica et Cosmochimica Acta* 48: 1879–1884.
Locke G and Bertine KK (1986) Magnetite in sediments as an indicator of coal combustion. *Applied Geochemistry* 1: 345–356.
Lum RR (1987) Cadmium in freshwaters: The Great Lakes and St. Lawrence River. In: Nriagu JO and Sprague JB (eds.) *Cadmium in the Aquatic Environment*, pp. 35–50. New York: Wiley.
Luoma SN (1983) Bioavailability of trace metals to aquatic organisms: A review. *Science of the Total Environment* 28: 1–23.
Mantei EJ and Foster MV (1991) Heavy metals in stream sediments: Effects of human activities. *Environmental Geology Water Science* 18: 95–104.
Martin J-M and Meybeck M (1979) Elemental mass balance of material carried by major world rivers. *Marine Chemistry* 7: 173–206.
Martin J-M, Nirel P, and Thomas AJ (1987) Sequential extraction techniques: Promises and problems. *Marine Chemistry* 22: 313–341.
Martin J-M and Whitfield M (1981) The significance of the river input of chemical elements to the ocean. In: Wong CS, Boyle E, Bruland KW, Burton JD, and Goldberg ED (eds.) *Trace Elements in Seawater*, pp. 265–296. New York: Plenum Press.
Martin J-M and Windom HL (1991) Present and future roles of ocean margins in regulating marine biogeochemical cycles of trace elements. In: Mantoura RFC, Martin J-M, and Wollast R (eds.) *Ocean Margin Process in Global Change*, pp. 45–67. New York: Wiley-Interscience.
McCall PL, Robbins JA, and Matisoff G (1984) ^{137}Cs and ^{210}Pb transport and geochronologies in urbanized reservoirs with raoidly increasing sedimentation rates. *Chemical Geology* 44: 36–65.
Mecray EL, King JW, Appleby PG, and Hunt AS (2001) Historical trace metal accumulation in the sediments of an urbanized region of the Lake Champlain watershed Burlington, Vermont. *Water, Air, & Soil Pollution* 125: 201–230.
Millero FJ (1975) The physical chemistry of estuaries. In: Church T (ed.) *Marine Chemistry in the Coastal Environment, ACS Symposium Series 18*, pp. 25–55. American Chemical Society.
Morel FMM, McDuff RE, and Morgan JJ (1973) Interactions and chemostasis in aquatic chemical systems: Role of pH, pE, solubility, and complexation. In: Singer PC (ed.) *Trace Metals and Metal-Organic Interactions in Natural Waters*, pp. 157–200. Ann Arbor: Ann Arbor Science.
Mudroch A, Sarazin L, and Lomas T (1988) Summary of surface and background concentrations of selected elements in the Great Lakes sediments. *Journal of Great Lakes Research* 14: 241–251.
Muller G, Grimmer G, and Bohnke H (1977) Sedimentary record of heavy metals and polycyclic aromatic hydrocarbons in Lake Constance. *Naturwissenschaften* 64: 427–431.

Murozumi M, Chow TJ, and Patterson CC (1969) Chemical concentrations of pollutant lead aerosols, terrestrial dusts and sea salts in Greenland and Antarctic snow strata. *Geochimica et Cosmochimica Acta* 33: 1247–1294.
National Science Foundation (1975) *Nickel*. Washington, DC: National Academy of Sciences.
Nightingale PD and Liss PS (2003) Gases in seawater. In: Holland HD and Turekian KK (eds.) *Treatise on Geochemistry*, vol. 6, pp. 49–81. Oxford: Elsevier.
Nriagu JO (1979) Global inventory of natural and anthropogenic emissions of trace metals to the atmosphere. *Nature* 279: 409–411.
Nriagu JO (1980a) Global cadmium cycle. In: Nriagu JO (ed.) *Cadmium in the Environment. Part I: Ecological Cycling,* pp. 1–12. New York: Wiley.
Nriagu JO (1980b) Global cycle and properties of nickel. In: Nriagu JO (ed.) *Nickel in the Environment*, pp. 1–26. New York: Wiley.
Nriagu JO (1988a) A silent epidemic of environmental metal poisoning*? Environmental Pollution* 50: 139–161.
Nriagu JO (1990a) The rise and fall of leaded gasoline. *Science of the Total Environment* 921: 13–18.
Nriagu JO (1990b) Global metal pollution. *Environment* 32: 7–33.
Nriagu JO and Pacyna JM (1988) Quantitative assessment of worldwide contamination of air, water, and soils by trace metals. *Nature* 33: 134–139.
Nriagu JO, Kemp ALW, Wong HKT, and Harper N (1979) Sedimentary record of heavy metal pollution in Lake Erie. *Geochimica et Cosmochimica Acta* 43: 247–258.
Olade MA (1987) Dispersion of cadmium, lead, and zinc in soils and sediments of a humid tropical ecosystem in Nigeria. In: Hutchinson TC and Meema KM (eds.) *Lead, Mercury, Cadmium and Arsenic in the Environment*, pp. 303–312. New York: Wiley, SCOPE 31.
Osintsev SP (1995) Heavy metals in the bottom sediments of the Katun' River and the Ob' upper reaches. *Water Resources* 22: 42–49.
Pacyna JM (1986) Atmospheric trace elements from natural and anthropogenic sources. In: Nriagu JO and Davidson CI (eds.) *Toxic Metals in the Atmosphere*, pp. 33–50. New York: Wiley.
Pacyna JM (1996) Monitoring and assessment of metal contaminants in the air. In: Chang LW (ed.) *Toxicology of Metals*, pp. 9–28. Boca Raton: CRC Press.
Pacyna JM and Lindgren ES (1997) Atmospheric transport and deposition of toxic compounds. In: Brune D, Chapman DV, Gwynne MD, and Pacyna JM (eds.) *The Global Environment*, pp. 386–407. New York: Wiley.
Patterson CC (1965) Contaminated and natural lead environments of man. *Archives of Environmental Health* 11: 344–360.
Patterson CC and Settle DM (1987) Review of data on eolian fluxes of industrial and natural lead to the lands and seas in remote regions on a global scale. *Marine Chemistry* 22: 137–162.
Patterson CC, Settle D, Schaule B, and Burnett M (1976) Transport of pollutant lead to the ocean and within ocean ecosystems. In: Windon HI and Duce RA (eds.) *Marine Pollution Transfer*, pp. 23–38. Heath.
Petit D, Mennessier JP, and Lamberts L (1984) Stable lead isotopes in pond sediments as a tracer of past and present atmospheric lead pollution in Belgium. *Atmospheric Environment* 18: 1189–1193.
Pickering WF (1980) Cadmium retention by clays and other soil or sediment components. In: Nriagu JO (ed.) *Cadium in the Environment. Part I: Ecological Cycling*, pp. 365–397. New York: Wiley.
Pickering WF (1981) Selective chemical extraction of soil components and bound metal species. *CRC Critical Reviews in Analytical Chemistry* 12: 233–266.
Presley BJ, Trefry JH, and Shokes RF (1980) Heavy metal inputs to Mississippi Delya sediments. *Water, Air, & Soil Pollution* 13: 481–494.
Rai D, Eary LE, and Zachara JM (1989) Environmental chemistry of chromium. *Science of the Total Environment* 86: 15–23.
Rai D, Sass BM, and Moore DA (1987) Chromium (III) hydrolysis constants and solubility of chromium (III) hydroxide. *Inorganic Chemistry* 26: 345–349.
Reimann C and de Caritat P (1998) *Chemical Elements in the Environment*. Berlin: Springer.
Richter RO and Theis TL (1980) Nickel speciation in a soil/ water system. In: Nriagu JO (ed.) *Nickel in the Environment*, pp. 189–202. New York: Wiley.
Rippey B, Murphy RJ, and Kyle SW (1982) Anthropogenically derived changes in the sedimentary flux of Mg Ni, Cu, Zn, Hg, Pb, and P in Lough Neagh, Northern Ireland. *Environmental Science & Technology* 16: 23–30.
Ritchie JC, McHenry JR, and Gill AC (1973) Dating recent reservoir sediments. *Limnology and Oceanography* 18: 254–263.
Robbins JA and Edgington DN (1975) Determination of recent sedimentation rates in Lake Michigan using Pb-210 and Cs-137. *Geochimica et Cosmochimica Acta* 39: 285–304.
Roos-Barraclough F and Shotyk W (2003) Millennial scale records of atmospheric mercury deposition obtained from ombrotrophic and minerotrophic peatlands in the Swiss Jura Mountains. *Environmental Science & Technology* 37: 235–244.
Rowell HC (1996) Paleolimnology of Onondaga Lake: the history of anthropogenic impacts on water quality. *Lake and Reservoir Management* 12: 35–45.
Salomons W (1983) Trace metal cycling in a polluted lake (Ijsselmeer, the Netherlands). *Delft Hydraulics Laboratory Report* S 357, 50 pp.
Salomons W and Forstner U (1980) Trace metal analysis on polluted sediments: II. Evaluation of environmental impact. *Environmental Technology Letters* 1: 506–517.
Salomons W and Forstner U (1984) *Metals in the Hydrocycle*. New York: Springer-Verlag.
Santschi P, Hohener P, Benout G, and Buchholtz-ten Brink M (1990) Chemical processes at the sediment-water interface. *Marine Chemistry* 30: 269–315.
Sass BM and Rai D (1987) Solubility of amorphous chromium (II)-iron (III) hydroxide solid solutions. *Inorganic Chemistry* 26: 2228–2232.
Schell WR and Barner RS (1986) Environmental isotope and anthropogenic tracers of recent lake sedimentation. In: Fontes JC and Fritz P (eds.) *Handbook of Environmental Isotope Geochemistry, The Terrestrial Environment*, pp. 169–206. Amsterdam: Elsevier.
Scudlark JR and Church TM (1997) Atmospheric deposition of trace elements to the mid-Atlantic bight. In: Baker JE (ed.) *Atmospheric Deposition of Contaminants to the Great Lakes and Coastal Waters*, pp. 195–208. SETAC Press.
Settle DM and Patterson CC (1980) Lead in albacore: Guide to lead pollution in Americans. *Science* 207: 1167–1176.
Shafer MM and Armstrong DE (1991) Trace element cycling in southern Lake Michigan: Role of water column particle components. In: Baker RA (ed.) *Organic Substances and Sediments in Water*, vol. 2. pp. 15–47. Chelsea: Lewis Publishers.
Shen GT and Boyle EA (1987) Lead in corals: Reconstruction of historical industrial fluxes to the surface ocean. *Earth and Planetary Science Letters* 82: 289–304.
Shotyk W, Cheburkin AK, Appleby PG, Frankhauser A, and Kramers JD (1996) Two thousand years of atmospheric arsenic, antimony, and lead deposition recorded in an ombrotrophic peat bog profile, Jura Mountains, Switzerland. *Earth and Planetary Science Letters* 145: E1–E7.
Shotyk W, Weiss D, Appleby PG, et al. (1998) History of atmospheric lead deposition since 12,370 ^{14}C yr BP from a peat bog, Jura Mountains, Switzerland. *Science* 281: 1635–1640.
Sigg L (1987) Surface chemical aspects of the distribution and fate of metal ions in lakes. In: Stumm W (ed.) *Aquatic Surface Chemistry*, pp. 319–349. New York: Wiley.
Snodgrass WJ (1980) Distribution and behavior of nickel in the aquatic environment. In: Nriagu JO (ed.) *Nickel in the Environment*, pp. 203–274. New York: Wiley.
Sunda WG (1991) Trace metal interactions with marine phytoplankton. *Biological Oceanography* 6: 411–442.
Sutherland RA (2002) Comparison between non-residual Al Co, Cu, Fe, Mn, Ni, Pb and Zn released by a three-step sequential extraction procedure and a dilute hydrochloric acid leach for soil and road deposited sediment. *Applied Geochemistry* 17: 353–365.
Sutherland RA and Tack FMG (2000) Metal phase associations in soils from an urban watershed, Honolulu, *Hawaii*. *Science of the Total Environment* 256: 103–113.
Sutherland RA, Tack FMG, Tolosa CA, and Verloo MG (2000) Operationally defined metal fractions in road deposited sediment Honolulu, Hawaii. *Journal of Environmental Quality* 29: 1431–1439.
Taillefert M, Lienemann C-P, Gaillard JF, and Perret D (2000) Speciation, reactivity, and cycling of Fe and Pb in a meromictic lake. *Geochimica et Cosmochimica Acta* 64: 169–183.
Tatsumoto MT and Patterson CC (1963) The concentration of common lead in some Atlantic and Mediterranean waters and in snow. *Nature* 199: 350–352.
Tessier A, Cambell PGC, and Bisson M (1979) Sequential extraction procedure for the speciation of particulate trace metals. *Analytical Chemistry* 51: 844–851.
Tessier A, Carignan R, Dubreuil B, and Rapin F (1989) Partitioning of zinc between water column and the oxic sediments in lakes. *Geochimica et Cosmochimica Acta* 53: 1511–1522.
Tessier A, Fortin D, Belzile N, DeVitre RR, and Leppard GG (1996) Metal sorption to diagenetic iron and manganese oxyhydroxides and associated organic matter: Narrowing the gap between field and laboratory measurements. *Geochimica et Cosmochimica Acta* 60: 387–404.
Tessier A, Rapin F, and Carignan R (1985) Trace metals in oxic lake sediments: Possible adsorption onto iron oxyhydroxides. *Geochimica et Cosmochimica Acta* 49: 183–194.
Thomas VM (1995) The elimination of lead in gasoline. *Annual Review of Energy and the Environment* 20: 301–324.
Thomas M, Petit D, and Lamberts L (1984) Pond sediments as historical record of heavy metals fallout. *Water, Air, & Soil Pollution* 23: 51–59.
Tillman DA (1994) *Trace Metals in Combustion Systems*. New York: Academic Press.

Turekian KK (1971) Rivers, tributaries, and estuaries. In: Hood DW (ed.) *Impingement of Man on the Oceans*, pp. 9–74. New York: Wiley.

Turekian KK (1977) The fate of metals in the oceans. *Geochimica et Cosmochimica Acta* 41: 1139–1144.

Turekian KK and Wedepohl KH (1961) Distribution of the elements in some major units of the Earth's crust. *Geological Society of America Bulletin* 72: 175–192.

United States Environmental Protection Agency (1975a) *Scientific and Technical Assessment Report on Cadmium*. EPA-600/6-6-75-003, US Government Printing Office.

United States Environmental Protection Agency (1975b) *Technical and Microanalysis of Cadmium and its Compounds*. EPA-560/3-75-005, US Government Printing Office.

United States Environmental Protection Agency (1976) *Cadmium: Control Strategy Analysis*. EPA-GCA-TR-75-36-G, US Government Printing Office.

United States Environmental Protection Agency (1978) *Sources of Atmospheric Cadmium*. EPA-68-02-2836, US Government Printing Office.

United States Environmental Protection Agency (1998) *Characterization of Municipal Solid Waste in the United States: 1997 Update*. EPA530-R-98-007.

United States Environmental Protection Agency (2000a) *National Air Pollutant Emission Trends, 1900–1998*. EPA-454/R-00-002, US Government Printing Office.

United States Environmental Protection Agency (2000b) *Deposition of Air Pollutants to the Great Waters*. EPA-453/R-00-005, US Government Printing Office.

United States Department of Commerce (1998) *Statistical Abstracts of the United States 1998*. US Government Printing Office.

Valette-Silver NJ (1993) The use of sediment cores to reconstruct historical trends in contamination of estuarine and coastal sediments. *Estuaries* 16: 577–588.

Van Metre PC and Callender E (1996) Identifying water-quality trends in the Trinity River Texas, USA, 1969–1992, using sediment cores from Lake Livingston. *Environmental Geology* 28: 190–200.

Van Metre PC, Callender E, and Fuller CC (1997) Historical trends in organochlorine compounds in river basins identified using sediment cores from reservoirs. *Environmental Science & Technology* 31: 2339–2344.

Van Metre PC, Mahler BJ, and Furlong ET (2000) Urban sprawl leaves its PAH signature. *Environmental Science & Technology* 34: 4064–4070.

Veron A, Lambert CE, Isley A, Linet P, and Grousset F (1987) Evidence of recent lead pollution in deep north-east Atlantic sediments. *Nature* 326: 278–281.

Wahlen M and Thompson RC (1980) Pollution records from sediments of three lakes in New York State. *Geochimica et Cosmochimica Acta* 44: 333–339.

Warren LA and Haack EA (2001) Biogeochemical controls on metal behavior in freshwater environments. *Earth-Science Reviews* 54: 261–320.

Webb SM, Leppard GG, and Gaillard J-F (2000) Zinc speciation in a contaminated aquatic environment: characterization of environmental particles by analytical electron microscopy. *Environmental Science & Technology* 34: 1926–1933.

WebElements. http://www.webelements.com/webelements/elements/text/Cu.html (accessed June 16, 2002).

Wedepohl KH (1968) Chemical fractionation in the sedimentary environment. In: Ahrens LH (ed.) *Origin and Distribution of the Elements*, pp. 999–1015. New York: Pergamon Press.

Wedepohl KH (1995) The composition of the continental crust. *Geochimica et Cosmochimica Acta* 59: 1217–1232.

Wessels M, Lenhard A, Giovanoli F, and Bollhofer A (1995) High resolution time series of lead and zinc in sediments of Lake Constance. *Aquatic Sciences* 57: 291–304.

Wilber GG, Smith L, and Malanchuk JL (1992) Emissions inventory of heavy metals and hydrophobic organics in the Great Lakes Basin. In: Schnoor JL (ed.) *Fate of Pesticides and Chemicals in the Environment*, pp. 27–50. New York: Wiley.

Williams TM (1992) Diagenetic metal profiles in recent sediments of a Scottish freshwater loch. *Environmental Geology and Water Sciences* 20: 117–123.

Wren CD, Maccrimmon HR, and Loescher BR (1983) Examination of bioaccumulation and biomagnification of metals in a Precambrian shield lake. *Water, Air, & Soil Pollution* 19: 277–291.

Wu J and Boyle EA (1997) Lead in the western North Atlantic Ocean: Completed response to leaded gasoline phaseout. *Geochimica et Cosmochimica Acta* 61: 3279–3283.

Yasui M, Strong MJ, Ota K, and Verity MA (1996) *Mineral and Metal Neurotoxicology*. Boca Raton: CRC Press.

Zhang J, Huang WW, and Wang JH (1994) Trace-metal chemistry of the Huanghe (Yellow River), China—Examination of the data from *in situ* measurements and laboratory approach. *Chemical Geology* 114: 83–94.

11.4 Geochemistry of Mercury in the Environment

WF Fitzgerald, University of Connecticut, Groton, CT, USA
CH Lamborg, Woods Hole Oceanographic Institution, Woods Hole, MA, USA

11.4.1 Introduction

Mercurial, the metaphor for volatile unpredictable behavior, aptly reflects the complexities of one of the most insidiously interesting and scientifically challenging biogeochemical cycles at Earth's surface. Elemental mercury is readily recognized as a silvery liquid at room temperature. Its gas phase is geochemically important as mercury and some of its compounds have relatively high vapor pressures. Mercury (Hg, from the Latin *hydrargyrum* or 'watery silver') is sulfur loving (i.e., chalcophilic) and extremely active biologically. It is mobilized tectonically, and significant deposits are found in mineralized regions characterized by subduction zones and deep-focus earthquakes (Schluter, 2000). Many of the major deposits are shown in **Figure 1** (Kesler, 1994).

The remarkable and useful qualities of mercury and its major mineralized form (cinnabar, HgS) have been well known for thousands of years. The Almadén mine in Spain, for example, the "richest known single source of cinnabar and quicksilver," has been active for more than 2500 years (Goldwater, 1972). Recently, using data from dated lake sediment cores, Cooke et al. (2009) reported that mercury mining began in the Peruvian Andes more than 3000 years ago (*c.* 1400 BC). Mercury products (e.g., thermostats, batteries, switches, fluorescent lighting) and applications (e.g., chlor-alkali production, dentistry, pharmaceuticals, catalysis) have been a practical part of modern life, while the wastes have been quite detrimental. Today, mercury emissions associated with fossil fuel burning, especially coal, and high-temperature combustion processes (e.g., municipal waste incineration; cement

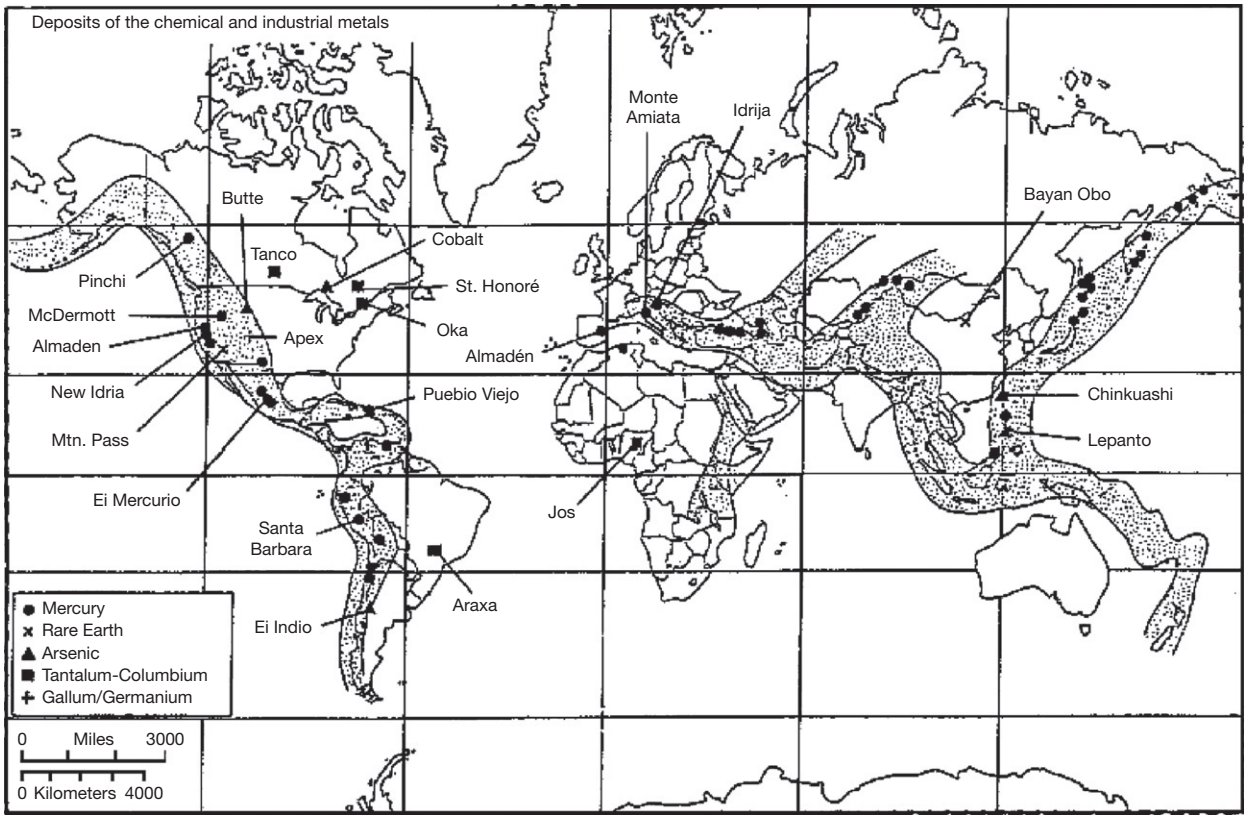

Figure 1 The global Hg belt. Reproduced with permission from Kesler SE (1994) *Mineral Resources, Economics and the Environment*. New York: MacMillan.

production) represent primary sources of pollutant mercury released to the environment on a global scale. As a result, mercury emissions since the mid-nineteenth century appear to have been in step with increases in emissions of CO_2 (Lamborg et al., 2002a). During the past decade, emissions, discharges, and nonpoint source inputs of mercury appear to have peaked and may be diminishing in many developed countries. Unfortunately, and on a global scale, declines are countered by increases in anthropogenic mercury releases from developing nations, particularly in Asia (Pacyna et al., 2010). For example, there appears to be a substantial enhancement of mercury emissions from small- and large-scale gold mining. Additionally, environmental gains through pollution controls, remediation, and regulations are tempered by the large reservoir of historic mercury, the pollution 'legacy,' residing in watersheds and sediments of many terrestrial, freshwater, and marine environments.

Although mercury has been used in 'spring tonics,' as a 'cure' for syphilis and a panacea for other afflictions, it is now recognized as a highly toxic trace metal that concentrates in aquatic food webs. According to Clarkson (1997), the principal human exposure to inorganic mercury species is from elemental mercury vapor, which is derived principally from industries such as gold and silver mining and chlor-alkali plants, and from dental amalgams. Deleterious health effects (e.g., 'Mad Hatter's disease') have been known since ancient times, and as Clarkson states, "severe exposure results in a triad of symptoms, erethism, tremor, and gingivitis." Today, however, the principal mercury-related human health concern is associated with exposure to the highly neurotoxic organomercury species, monomethylmercury (MMHg). This exposure is almost entirely due to consumption of fish and fish products (Fitzgerald and Clarkson, 1991; National Research Council, 2000). Inorganic mercury, whether natural or pollution derived, can be readily methylated in aquatic systems. Mercury methylation appears to be predominantly biotic, although some abiotic production is likely in natural waters (Benoit et al., 2003; Gårdfeldt et al., 2003). In situ methylation of 'reactive' or bioavailable mercury by sulfate-reducing bacteria (SRB) has been documented to result in the accumulation of MMHg in freshwater foodwebs and fish (e.g., Gilmour and Henry, 1991; Hall et al., 1998; Jensen and Jernelöv, 1969; Watras and Bloom, 1994; Watras et al., 1994; Westöö, 1966; Wiener et al., 1990a; Wood et al., 1968). Recent reports suggest that additional bacterial functional groups (i.e., iron-reducing bacteria; Fleming et al., 2006; Kerin et al., 2006) may have a role. These linkages are quite evident in the elevated MMHg in fish from reservoirs created by dam construction and subsequent flooding of landscapes (e.g., Bodaly et al., 1984; Cox et al., 1979; Tremblay et al., 1998). A similar process is thought to occur in the marine water column, possibly through the formation of dimethyl Hg (DMHg) followed by its decomposition to MMHg (Mason and Fitzgerald, 1993; Mason and Sullivan, 1999; Mason et al., 1998). Microbially mediated methylation continues to amplify the insidiousness of current and historic mercury pollution and health risks to wildlife and humans. Indeed, toxicologically, methylation of inorganic mercury is the most important transformation affecting the behavior and fate of mercury in aquatic systems.

Its accumulation in freshwater and marine fish can reach levels that could not only pose a threat to human health (Davidson et al., 2000; Granjean et al., 1997; Mahaffey et al., 2009; Mergler et al., 2007), but also reduce the reproductive success of piscivorous wildlife (e.g., Scheuhammer, 1991; special section of *Environmental Toxicology and Chemistry*, 1998, 17/2: 137–227, 12 papers, M. W. Meyer, editor) and the fish themselves (Hammerschmidt et al., 2002; Sandheinrich and Wiener, 2011; Wiener and Spry, 1996; Wiener et al., 1990b). Wiener et al. (2002) and Scheuhammer et al. (2007) present reviews of mercury toxicology in a number of different animal species.

MMHg poisoning is known as 'Minamata disease.' Between 1950 and 1975, major industrially related mass poisonings, severe debilitation, and many deaths occurred in Minamata and Niigata, Japan, and in Iraq. The Japanese poisonings resulted from consumption of locally caught fish and seafood that had been contaminated principally by MMHg discharged with wastewater from factories making acetaldehyde (Chisso Co. Ltd. and Showa Denko Co. Ltd.). The MMHg was synthesized abiotically as a by-product during the production of acetaldehyde (inorganic mercury was used as a catalyst). In the Iraqi tragedy, the source was contaminated bread, which had been made with flour unknowingly milled from wheat treated with MMHg as a fungicide (Bakir et al., 1973). There is an extensive scientific, medical, and general literature, as well as news accounts of these tragedies. The following works on the Japanese poisonings provide an overview and a useful starting point for a more in-depth examination: Smith and Smith (1975), Japan Public Health Association (2001), The Social Scientific Study Group on Minamata Disease (2001) and George (2001). There are other examples of sites severely contaminated by mercury and the interested reader is directed to the volume entitled *Mercury Contaminated Sites – Characterization, Risk Assessment and Remediation*, edited by Ebinghaus et al. (1998), which also contains descriptions of the Minamata situation.

In the mid-twentieth century, Goldschmidt (1954) cryptically summarized knowledge of the environmental cycling of mercury thus: "not much information is available concerning the geochemistry of mercury." Moreover, as he emphasized for that period, "most of the modern analytical data are due to A. Stock and co-workers," which were derived from their pre-World War II studies (e.g., Stock and Cucuel, 1934). In contrast, over the first decade of the twenty-first century, scores of environmentally related mercury publications appeared each year. There is an abundance of distributional data, an enhanced knowledge of the biogeochemical cycling of mercury and the impact of anthropogenic activities, a fuller appreciation of the utility, dangers, and complexities characterizing the mobilization, interactions, and fate of this biologically active element, and an awareness of the daunting challenges inherent in studying a metal that includes a gas phase as a major feature of its biogeochemistry at Earth's surface. The potential risks of human exposure to MMHg, especially prenatally, and the potential deleterious ecological consequences from localized to global-scale mercury pollution have given much impetus to mercury studies and regulatory activities internationally. As of the summer of 2011, there have been ten international conferences on 'Mercury as a Global Pollutant' since 1990. The city of Minamata, the venue for the sixth conference in 2001, provided conferees with poignant evidence of the tragic legacy of mercury contamination. The abstracts and publications from these broadly based meetings, which include basic biogeochemistry, environmental and pollution-related studies, ecological and human toxicology, and analytical developments, chronicle the rapid worldwide expansion of mercury research and knowledge.

This chapter focuses principally on the low-temperature environmental biogeochemistry of mercury. The current understanding of mercury cycling at Earth's surface (soils, sediments, natural waters, and the atmosphere) is presented. The coverage, as appropriate, includes anthropogenic interferences (i.e., mercury pollution) and biological mediation, which significantly affect the speciation, behavior, and fate of mercury in the environment. Complementary information on geochemical cycling of mercury in and among the various earthly reservoirs is presented in other chapters of the *Treatise on Geochemistry*.

11.4.1.1 The Global Mercury Cycle

Major features of the global mercury cycle have been illustrated using the relatively simple three-reservoir mass balance developed by Mason, Fitzgerald, and Morel in 1994 ('MFM'). Refinements are considered in **Section 11.4.7**. The MFM model provides estimates of natural and anthropogenic fluxes and an assessment of impact from human-related mercury emissions on the natural cycle for 1990 (**Figure 2(a)**). The preindustrial situation is shown in **Figure 2(b)**. It is evident that the atmosphere and oceans play important roles in the distribution and redistribution of mercury at Earth's surface. Indeed, atmospheric mercury deposition into the oceans greatly exceeds riverine inputs. The MFM model also suggests that the natural cycle of mercury has been severely perturbed. Human-related mercury emissions dominate the cycle such that most of the mercury in the atmosphere and surface oceans is anthropogenic. Moreover, the integrated estimate for total loadings from globally dispersed, anthropogenic mercury emissions between 1890 and 1990 is 1000 Mmol (200 kt). The MFM simulation predicts that ~95% of this mercury is sequestered in terrestrial systems, and the remainder in the oceans and atmosphere. The MFM estimate for the globally dispersed anthropogenic contribution is similar to the most recent estimate of 9.7 Mmol $year^{-1}$ recently reported (Pacyna and Pacyna, 2002; Pacyna et al., 2006, 2010; Streets et al., 2009).

Elemental mercury, a monatomic gas, is the dominant atmospheric form and has a long residence time in the troposphere (Fitzgerald et al., 1981; Lamborg et al., 2000, 2002a; Lindqvist et al., 1991; Slemr et al., 1981). Such longevity allows emissions of mercury to the atmosphere from natural and anthropogenic sources to be dispersed widely across Earth's surface. The redox couple of Hg^0 with the stable mercuric ion (Hg^0/Hg^{2+}; $E^\circ = 0.85$ V) is similar to that of the Fe(II)/Fe(III) couple, thereby providing the potential for dynamic oxidation and reduction cycling in the range of common environmental redox (i.e., pε) conditions. A unique and important example of this is the biologically and abiotically mediated reduction of Hg^{2+} resulting in widespread supersaturation of Hg^0 in freshwater and saltwater and its subsequent evasion

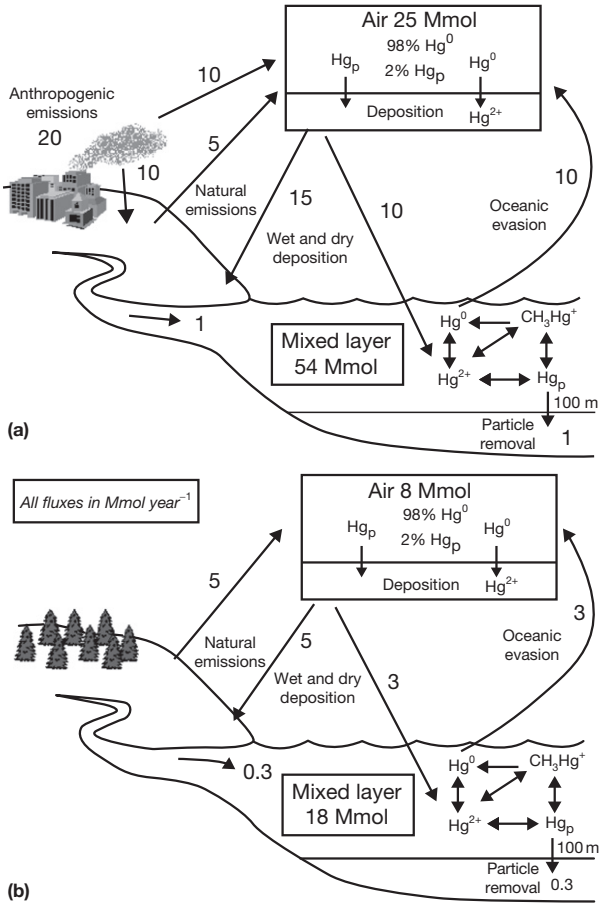

Figure 2 Fluxes of Hg on a global scale. (a) The current condition and (b) the preindustrial condition. All fluxes in Mmol of Hg year^{-1}. Note the balance of deposition to and evasion from the ocean, making soils the primary sink on decade/century timescales. One result of human activity has been a tripling of Hg in the atmosphere and surface ocean. Reproduced from Mason RP, Fitzgerald WF, and Morel FMM (1994) The biogeochemical cycling of elemental mercury – Anthropogenic influences. *Geochimica et Cosmochimica Acta* 58(15): 3191–3198.

(Amyot et al., 1997; Kim and Fitzgerald, 1986; Mason and Fitzgerald, 1993; Rolfhus, 1998). Field and laboratory observations in aqueous systems have documented the important influence of photochemical and bacterial reactions on the in situ reduction of Hg^{2+} (Amyot et al., 1997; Barkay et al., 2003; Mason and Fitzgerald, 1993; Rolfhus, 1998; Rolfhus and Fitzgerald, 2001), and therefore link Hg^0 production and evasion from the ocean to the complex biogeochemical cycles of carbon, nitrogen, phosphorus, and sulfur. Through evasion, the ocean prolongs the residence of mercury at Earth's surface and exacerbates the human perturbation of the global mercury cycle. The MFM analysis shows such oceanic emission of Hg^0 to be substantial (10 Mmol) and comparable to the atmospheric input of mercury to the oceans. As anticipated, cycling at the sea surface, distribution, production, oxidation, and other transformations for Hg^0 in the oceans are receiving increasing attention (e.g., Andersson et al., 2008a,b; Kotnik et al., 2007; Poulain et al., 2007; Selin, 2009; Soerensen et al., 2010a,b; Sommar et al., 2010; Strode et al., 2007).

Although the marine biogeochemical cycling of mercury is greatly simplified in the MFM simulation, the importance of the ocean as both a sink for atmospheric deposition and a substantial source of mercury to the atmosphere (Kim and Fitzgerald, 1986; Lindqvist et al., 1991; Mason et al., 1994; Nriagu, 1989) is consistent with models that use more realistic physical and biogeochemical oceanic dynamics (Hudson et al., 1995; Lamborg et al., 2002a; Mason et al., 2001; Selin et al., 2008).

The oceans actively and significantly participate in the transport and transformation of this toxic metal. Thus, there is an obvious need to increase the knowledge and understanding concerning the biogeochemical cycling of mercury and MMHg, and the impact of anthropogenically related inputs in the marine environment. A cursory examination of papers presented at the international mercury conferences is sufficient to show that there has been much interest in, and support for, studies examining linkages between the cycling of mercury in the atmosphere, anthropogenic emissions/discharges, deposition to terrestrial systems, and the bioaccumulation of MMHg in freshwaters (e.g., *Mercury in Temperate Lakes Program* – Watras et al., 1994; *METAALICUS Project*; Ebinghaus and Krüger, 1996; Petersen et al., 1995; USEPA Mercury Study Report to Congress, 1997; *The Nordic Network* – Lindqvist et al., 1991; Iverfeldt, 1991a). In contrast, mercury cycling in the oceans has received less attention. This is unfortunate as there is evidence, for example, that the mercury content in fish

has been increasing over the past several decades in the North Atlantic (e.g., Monteiro and Furness, 1997). Moreover, in 2001, the growing recognition of human exposure to MMHg from marine fish and fish products prompted the US Food and Drug Administration (USFDA) to place four pelagic marine fish (tilefish, king mackerel, swordfish, and shark) on their consumer advisory list (USFDA Consumer Advisory, 2001). The advisory emphasizes the need for women of childbearing age to limit their consumption of marine fish to 12 oz week^{-1} (0.34 kg week^{-1}).

A more stringent fish consumption advisory reference dose (Schober et al., 2003) was issued by the US Environmental Protection Agency (USEPA) in 2001. Women of childbearing age were cautioned to limit their MMHg intake to 0.1 μg kg^{-1} of body weight per day. It is illuminating to translate this recommendation into fish consumption. A summary of the MMHg content in some major marine fish and shellfish is presented in **Table 1**. Using fresh tuna with an average MMHg concentration of 0.32 μg g^{-1} wet weight (**Table 1**) as an example, the recommended weekly consumption for a 50–70 kg woman of childbearing age would be 35–49 μg or the equivalent of ~110–155 g (~4–5.5 oz, half a typical can) of fresh tuna. This is much smaller than the USFDA recommendation, which is equivalent to 0.5 μg kg^{-1} of body weight per day (however, a maximum of 12 oz of fish per week is recommended). The current provisional advisory from the Joint Food and Agricultural Organization/World Health Organization Expert Committee on Food Additives (JECFA, 2000) is 0.5 μg kg^{-1} of body weight per day. For further information regarding MMHg and fish consumption, the reader is referred to the useful and informative publication from the US National Academy of Sciences entitled 'Toxicological Effects of Methylmercury' (NAS, 2000). The examining committee from the National Research Council of the NAS reached the following consensus: "the value of EPA's current reference dose for MeHg, 0.1 μg kg^{-1} day^{-1} is scientifically justifiable for the protection of public health."

In summary, mercury entering the marine environment may continue to actively participate in aquatic chemistry, while much of the mercury deposited from the atmosphere to terrestrial systems is sequestered. Given the importance of the oceans as a whole in global mercury cycling, and international concerns and issues regarding human exposure to MMHg through marine fish and seafood consumption, the current situation is one of insufficient study and undersampling. While there have been a few open-ocean cruises to examine mercury biogeochemistry (e.g., Cossa et al., 1997, 2009; Dalziel, 1992; Dalziel and Yeats, 1985; Gill and Bruland, 1987; Gill and Fitzgerald, 1988; Horvat et al., 2003; Kim and Fitzgerald, 1986; Lamborg et al., 1999, 2008; Laurier et al., 2004; Leermakers et al., 2001; Mason and Fitzgerald, 1993; Mason and Sullivan, 1999; Mason et al., 1998; Sunderland et al., 2009), almost no longer term, seasonally oriented mid-ocean studies have been conducted. This state of data limitation is poised to change, however, with a number of oceanographic studies of Hg biogeochemistry currently under way as of this writing. Indeed, Hg is a prominent part of the recently initiated GEOTRACES Program, a major long-term multicountry international oceanic study of trace elements and isotopes in seawater. However, we emphasize that even in the more accessible nearshore zones, the biogeochemistry of mercury is understudied. In this regard, estuaries and adjacent coastal waters, as regions of high biological productivity, MMHg production, and fishery activity, are of special interest. They are major repositories for natural and pollutant mercury (see **Section 11.4.6**).

Table 1 Levels of total mercury (μg g^{-1} wet weight) in seafood (USFDA, 2001). Most (>95%) of the total mercury in edible fish tissue is MMHg.

Fish species	*Mean (range)*	n[a]
Tilefish	1.45 (0.65–3.73)	60
Swordfish	1.00 (0.10–3.22)	598
King Mackerel	0.73 (0.30–1.67)	213
Shark	0.96 (0.05–4.54)	324
Tuna (fresh or frozen)	0.32 (ND–1.30)	191
Tuna (canned)	0.17 (ND–0.75)	248
Atlantic cod	0.19 (ND–0.33)	11
Pollock	0.20 (ND–0.78)	107
Mahi mahi	0.19 (0.12–0.25)	15
American lobster	0.31 (0.05–1.31)	88

ND denotes that the mercury level was not detectable.
[a]Number of samples analyzed.
Sources: Grieb TM, Driscoll CT, Gloss SP, Schofield CL, Bowie GL, and Porcella DB (1990) Factors affecting mercury accumulation in fish in the upper Michigan Peninsula. *Environmental Toxicology and Chemistry* 9(7): 919–930; Bloom NS (1992) On the chemical form of mercury in edible fish and marine invertebrate tissue. *Canadian Journal of Fisheries and Aquatic Sciences* 49: 1010–1017; Hammerschmidt CR, Wiener JG, Frazier BE, and Rada RG (1999) Methylmercury content of eggs in yellow perch related to maternal exposure in four Wisconsin lakes. *Environmental Science & Technology* 33(7): 999–1003.

11.4.2 Fundamental Geochemistry

In this section, we consider aspects of the fundamental geochemistry and biogeochemistry of mercury used later in the chapter. These topics include: (1) solid Earth abundance and distribution, (2) isotopic composition and recent advances in mercury cosmochemistry, (3) the formation and distribution of minable mercury deposits, and (4) mercury in fossil fuels.

11.4.2.1 Solid Earth Abundance and Distribution

A summary of mercury data from the report of Turekian and Wedepohl (1961) is shown in **Table 2**. Due to the chalcophilic nature of its associations, mercury is found in higher abundances in intrusive magmatic rocks and locations of subaerial and submarine volcanism. Peak concentrations in these rocks may be as high as several percent in ore-grade minerals (e.g., 35% mercury in sphalerite; Ozerova, 1996). Also, as a result of this association, the distribution of highest mercury concentrations in rocks at the surface and near surface mirrors regions of current and past tectonic activity and has been described as the 'global mercury belt' (e.g., Gustin et al., 2000). As noted in greater detail in **Section 11.4.3**, mercury concentrations in soils weathered from this material can be very high as well (e.g., Steamboat Springs, NV, USA: 1.2–14.6 ppm; Gustin et al., 2000) and represent a potentially significant source of mercury to the atmosphere at a variety of spatial scales through

Table 2 Mercury content of selected rocks and sediments

Rock type	*Hg content (ppm)*
Ultrabasic igneous	0.0*X*[a]
Basaltic rocks	0.09
High- and low-Ca granites	0.08
Syenites	0.0*X*
Shales	0.4
Sandstones	0.03
Carbonates	0.04
Deep-sea carbonate sediment	0.0*X*
Deep-sea clays	0.*X*

[a]The *X* notation indicates order of magnitude estimate.
Source: Turekian KK and Wedepohl KH (1961) Distribution of the elements in some major units of the Earth's crust. *Geological Society of America Bulletin* 72: 175–192.

low-temperature volatilization. These rocks and their weathered products are rich in other metals as well, and emission of mercury from soils and rock has been used as a tool for large-scale ore and petroleum exploration as well as an indicator of tectonic activity (e.g., Klusman and Jaacks, 1987; McCarthy, 1968; Varekamp and Buseck, 1983). These general characterizations are significant then, as we later consider the cause for concentrations of mercury in soils removed from the mercury belt that are also elevated above the crustal abundances.

Also indicated in Turekian and Wedepohl's compilation is a relatively high concentration of mercury in sedimentary material rich in organic carbon, such as shales. Mercury associations with organic matter are considered in later sections (**Sections 11.4.5** and **11.4.8**). Here, we stress that such associations can lead not only to higher concentrations of mercury in these types of rock units but also in the transport of mercury away from sites of sediment accumulation as a result of petroleum movement (Fein and Williams-Jones, 1997; White, 1967). The mercury content of major rock types has not been systematically revisited since Turekian and Wedepohl's report, and there is evidence that some of their values may be overestimates. As an example, the recovery and analysis of glacial till in Glacier Bay National Park by Engstrom and Swain (1997) indicated much lower concentrations of mercury (<10 ppb). It is reasonable to assume, however, that the mercury concentration trends across rock types suggested by Turekian and Wedepohl and the geochemistry they suggest are valid.

11.4.2.2 Isotopic Distributions

Mercury has a relatively even distribution of its seven stable isotopes (196, 0.15%; 198, 10.0%; 199, 16.7%; 200, 23.2%; 201, 13.2%; 202, 29.8%; 204, 6.8%; Friedlander et al., 1981; Lauretta et al., 2001). This pattern presented cosmochemists with a formidable task when mercury isotopic distributions in meteorites were examined (e.g., Jovanovic and Reed, 1976; Thakur and Goel, 1989). Analytical difficulties apparently resulted in inaccurate determinations of the bulk abundance and isotopic composition of some meteorites, leading to the so-called 'mercury problem'; examined meteorites did not show the same bulk abundance and isotopic distribution as terrestrial material (Grevesse, 1970; Lauretta et al., 1999). Subsequent advances in mass spectrometry, and especially the development of multicollectors, have shown that the isotopic distributions of mercury in terrestrial and extraterrestrial material are very similar (e.g., Allende meteorite: 0.03–0.3 ppm; Lauretta et al., 2001).

With so many isotopes from which to choose, one might expect examination of mercury isotopic fractionation in natural media to be a profitable area of research as it has been, for example, with lead, light metals, nonmetals, and an increasing number of transition metals (e.g., Alleman et al., 2001; Anbar, 2004; Hoefs, 2004; Richter et al., 1992; Rouxel et al., 2004). Indeed, this area of research has yielded a number of surprising results, many since the first edition of the *Treatise on Geochemistry* was published (e.g., Bergquist and Blum, 2007; Biswas et al., 2008; Evans et al., 2001; Gehrke et al., 2009, 2011; Gratz et al., 2010; Hintelmann and Lu, 2003; Klaue et al., 2000; Kritee et al., 2007, 2008; Senn et al., 2010; Sherman et al., 2009, 2010; Smith et al., 2005, 2008). The wide range of stable isotopes is being used in deliberate addition experiments ranging from bench scale to whole watershed scale (e.g., Hintelmann and Evans, 1997; Hintelmann et al., 2002). These advances will be highlighted in **Section 11.4.8**.

The radioisotope ^{203}Hg has played an important role in laboratory investigations of mercury biogeochemistry (e.g., Costa and Liss, 1999; Gilmour and Riedel, 1995; Stordal and Gill, 1995). Continued production of ^{203}Hg-enriched material has been curtailed recently, and so, future mechanistic studies will feature the use of stable isotopes instead.

11.4.2.3 Minable Deposits

As mentioned, higher mercury concentrations in rock and soil are associated with the global mercury belt. However, the occurrence of minable deposits is not continuous along this belt. In addition to Almadén (Spain), the most productive mercury mines include Idrija (Slovenia), New Almaden (California, USA), and Huancavelica (Peru). Very high concentrations of mercury have been reported to be associated with oceanic hydrothermal sulfide chimneys and their weathered remains (e.g., Koski et al., 1994; Ozerova, 1996; Stoffers et al., 1999). In all of these cases, mercury occurs almost exclusively as cinnabar (red HgS), with smaller amounts of metacinnabar (black HgS) and elemental mercury (often as inclusion with HgS in minerals such as sphalerite and chalcopyrite). HgS is extremely insoluble ($\log K_{so}$ (cinnabar) = −36.8; Martell et al., 1998) under typical surface water conditions, and thus transport of mercury from these mineral rich environments at the Earth's surface generally involves sediment transport (e.g., Ganguli et al., 2000). The fate of cinnabar in anoxic sediments is addressed in **Section 11.4.5**. Transport of mercury to and from ore bodies invariably involves hydrothermal systems in the subsurface, with HgS solubility strongly controlled by fluid pH, temperature, and chloride, sulfide, and organic carbon contents (Varekamp and Buseck, 1984; White, 1967).

11.4.2.4 Occurrence of Mercury in Fossil Fuels

Even with the stated stability of cinnabar, mercury is mobile in the surface environment. This is indicated by the relatively high concentration of mercury in organic-rich deposits, such as

Table 3 Mercury content of fossil fuels

Sample type	*Total Hg (ng g^{-1})*
Coal	
China[a]	220
Std. Ref. Mat.[b]	77.4–433.2
Global estimate[c]	20–1000
Unrefined petroleum[d]	
Crude oil	<d.l. to >7000
Condensate	<d.l. to >12 000
Refined petroleum[d]	
Light distillates	1 ± 3
Utility fuel oil	1 ± 1
Asphalt	0.3 ± 0.3
Gasoline	0.2–3
Diesel	0.4–3
Kerosene	0.04
Heating oil	0.59
Naphtha	3–60
Petroleum coke	0–250

[a]Wang et al. (2000).
[b]Long and Kelly (2002).
[c]Pacyna and Pacyna (2002).
[d]Wilhelm (2001) and the references therein.

fossil fuels and shales. As we will explore later, mercury has high affinities for organic carbon as well as sulfide. Interest in fossil fuel recovery and burning as a source of mercury to the environment has led to a few published studies in this area; some of these data are summarized in Table 3. With notable exceptions, concentrations in coal appear higher than those in oil, suggesting preferential burial of mercury in terrestrial and coastal systems rather than in pelagic marine environments. Though mercury concentrations are not as high in various refined petroleum materials as in coal, the oil and gas recovery process often liberates large amounts of mercury leading to localized contamination of marine sediments (e.g., Grieb et al., 2001). The concentration of mercury is sufficiently high in some crude petroleum materials to also pose a corrosion hazard to the drilling and transportation apparatus and represents a significant engineering problem (e.g., Bloom, 2000; Wilhelm, 1999).

11.4.3 Sources of Mercury to the Environment

There have been few well-designed studies to constrain mercury emission estimates from natural sources and allow global extrapolations. Indeed, some work has been extraordinarily misleading. For example, in flawed studies based on the accumulation of mercury and other metals in glacial ice, Jaworowski et al. (1981) estimated the annual mercury flow into the atmosphere at 1000 Mmol with an anthropogenic contribution at 50 Mmol! Low- and high-temperature volatilization processes were offered by Jaworowski et al. as a potential explanation for the huge natural fluxes of mercury. Such inaccuracies, as well as the paucity of reliable investigations, begs the question "What is the appropriate flux range for global mercury emissions from sources such as volcanism, biomass burning, and low-temperature volatilization from natural waters and soils?" The MFM simulation (Mason et al., 1994) of the global mercury cycle estimates natural terrestrial emissions at 5 Mmol annually. Such emissions would include inputs from subaerial volcanism under erupting and non-erupting conditions, and the preindustrial mercury fluxes from mineralized regions, forest fires, biological activities, and natural waters. Today, volcanism and volatilization from mineralized regions may be the only purely natural sources of mercury, because, and as illustrated in Figure 2, anthropogenic mercury contamination is present throughout the atmosphere, biosphere, the terrestrial realm, and the hydrosphere. Thus, a portion of the emissions from these secondary reservoirs represents recycled pollutant mercury; this component has often been overlooked when the source strengths from 'natural sources' have been compared and assessed relative to modern anthropogenic mercury inputs.

11.4.3.1 Volcanic Mercury Emissions

The determination of global volcanic mercury fluxes from direct measurements is at best a hazardous, expensive, labor-intensive, and, perhaps, impossible task. Reasonably well-constrained global estimates, however, can be achieved through use of elemental ratios and a geochemical indexing approach. Sulfur provides an appropriate index, since it is a major component of volcanic emanations, and there is agreement on its global flux to the atmosphere. An example of this approach is the work of Patterson and Settle (1987), who combined Pb/S, Tl/S, and Bi/S ratios measured in volcanic gases collected under eruptive and quiescent (fumarolic) conditions with the global volcanic sulfur flux to "approximate global volcanic emissions of these three metals to the atmosphere." One of the present authors (WFF) measured mercury during the Patterson and Settle study. Results from this research were presented at two conferences (Fitzgerald, 1981, 1996), and Fitzgerald's estimate of 40 tons $year^{-1}$ appears in the paper by Patterson and Settle (1987). Given the potential importance of volcanic mercury inputs, and the limited number of investigations, a detailed description of the mercury study is included here.

Patterson, Settle, Buat-Menard (University of Bordeaux), Fitzgerald, and colleagues (see Acknowledgments) evaluated volcanic metal fluxes using an experimental design based on the hypothesis that metal volatilization would be dependent on temperature, sulfur and halogen composition of magma and mobilization by volcanic gases. Therefore, volcanoes and fumaroles were selected to provide a range of temperatures and S/Cl ratios. The characteristics of the volcanic gas samples are tabulated in Table 4. The four volcanoes examined were Kilauea (Hawaii, USA), Mt. Etna (Sicily, Italy), Vulcano (Aeolian Islands, Italy), and White Island (New Zealand).

Plumes were sampled for mercury using a simple gas train consisting of a preblanked (pyrolyzed) glass fiber prefilter stage for particulate phases, followed by two gold traps arranged in tandem to collect gaseous mercury (Bloom and Fitzgerald, 1988; Fitzgerald and Gill, 1979). The fumarolic collections were made with a gas sampling train designed by Clair Patterson and modified for mercury (Patterson and Settle, 1987; shown here in Figure 3). Any mercury associated with aerosols or the gas phase that escaped the two cold

Table 4 Volcano sampling locations and gas characteristics

Volcano	*Date*	*Type of gas*	*Temp. (°C)*	*S (wet gas) (mg S m^{-3})*	*S/Cl (weight)*	*Cl/F (weight)*	*Hg/S (weight)*	*Hg/Bi (weight)*
Kilauea Caldera	6/23/77	Fumarole	100	22 800	40	2	0.9	
Kilauea Pu'u O'o	5/12/84	Eruptive plume	1140	110	9		0.7	0.0019
Mt. Etna Bocca Nuova[a]	6/7/80	Eruptive plume	1100	4.3	0.7	8	11–14	
Mt. Etna SE Crater	6/8/80	Eruptive plume	1100	2.5	0.7	4	<13	
Vulcano Site A	6/11/80	Fumarole	280	5500	0.3	90	0.9	
White Island Site A	7/22/83	Fumarole	180	33 000	45	30	0.9	
White Island Site B	7/22/83	Fumarole	590	54 000			~0.44	0.024
White Island Site C	7/22/83	Fumarole[b]	650			180		0.0015

[a]Dedeurwaerder et al. (1982).
[b]Collected using plume filter device.
Source: Reproduced from Patterson CC and Settle DM (1987) Magnitude of lead flux to the atmosphere from volcanoes. *Geochimica et Cosmochimica Acta* 51(3): 675–681.

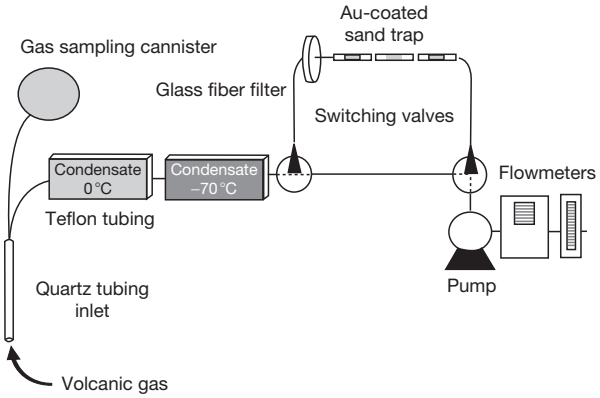

Figure 3 Hg sampling apparatus used to collect fumarole gas samples. Reproduced from Patterson CC and Settle DM (1987) Magnitude of lead flux to the atmosphere from volcanos. *Geochimica et Cosmochimica Acta* 51(3): 675–681.

traps was collected by a gas-sampling train analogous to the plume samplers. The gas was pumped through this system at ~1 l min^{-1}.

In general, and as illustrated for the 1977 study of 100 °C fumarole at Kilauea, essentially all of the mercury and the other metals are trapped in the 0 °C condensate (**Table 5**). Thus, fumarolic gas collectors for metal studies can be simplified. The observed Hg/S weight ratio in the Kilauea condensate was 0.9×10^{-6}. The Hg/S ratios from the other investigations are summarized in **Table 4**. Values range from 0.7×10^{-6} to 14×10^{-6} with a suggestion that Hg/S may increase as the S/Cl decreases. Dedeurwaerder et al. (1982) were part of the Mt. Etna study and their results for the Bocca Nuevo plume are included in the summary. Their plume sampling apparatus was based on the Fitzgerald technique and similar to that described above. The sulfur-flux weighted mean volcanic Hg/S from all locations is 5×10^{-6}.

Estimates of global volcanic sulfur emissions are summarized in **Table 6**. We have chosen a value of 9×10^{6} tons of sulfur per year as representative of the recent estimates. Therefore, by applying the determined Hg/S ratio, a global mercury flux from subaerial volcanism is estimated to be ~45 tons year^{-1}, or 0.23 Mmol annually. These average emissions are only 5–10% of the primary natural flux of 2.5–5 Mmol year^{-1} estimated by Mason et al. (1994) and Seigneur et al. (2001). Thus, and under long-term mean conditions, other types of terrestrial volatilization processes for mercury would dominate. Given this conclusion, it is important to place additional constraints on the validity of the 45 tons year^{-1} estimate for subaerial volcanic mercury emissions.

First, Varekamp and Buseck (1986) reported an average Hg/S weight ratio of 7.4×10^{-6} for emissions under non-erupting conditions from Mt. Hood, Mt. Shasta, and Mt. St. Helens in the United States, and from Mt. Etna. In 1981, these investigators reported a very high Hg/S weight ratio of 6000×10^{-6} for Mt. St. Helens under erupting conditions (Varekamp and Buseck, 1981). However, the mercury and sulfur measurements were not measured simultaneously and, according to Varekamp (personal communication), should not be used for a global-scale analysis of this kind. Thus, we suggest that a mean Hg/S ratio of 5×10^{-6} and the annual emission estimate of 45 tons is of the appropriate magnitude. Nriagu and Becker (2003), using the same Hg/S ratio and a more detailed volcanic SO_2 emissions inventory, derived much the same conclusion (~95 tons year^{-1}; 60% eruptive, 40% degassing).

Second, the scale of volcanic mercury fluxes can be approximated indirectly. For example, using the Hg/Bi ratios listed in **Table 4** as well as the Lambert et al. (1988) estimate for annual global bismuth emissions of 1500 tons, we obtain a range for

Table 5 Mercury and sulfur concentrations in volcanic gas at sulfur fumarole site, Kilauea caldera

Collection	*Hg concentration*	*Total Hg (ng)*	*Total S (g)*	*Hg/S ratio (weight)*
0 °C condensate	120 ng g^{-1}	59200	4.0	14.8×10^{-6}
270 °C condensate	10 ng g^{-1}	150	0.1	1.5×10^{-6}
Volcanic gas free of water	0.88 ng g^{-1}	230	60	3.9×10^{-9}
Total ambient air	10.2 ng m^{-3}	59600	64	9.3×10^{-7}

Table 6 Estimates of the global annual sulfur flux from volcanic activity

Method	*S flux (10^6 tons $year^{-1}$)*[a]	*References*
Rate of S loss per volcano	5.0	Stoiber and Jepsen (1973)
	3.8	Cadle (1975)
	4–5	Friend (1973)
S measurements from selected Volcanoes	9.4 Nonexplosive (4.5) Explosive (4.9)	Stoiber et al. (1987)
Literature review	9	Spiro et al. (1992)
Satellite survey of SO_2 emissions	6.5 Nonexplosive (4.5; Stoiber et al., 1987) Explosive (2.0)	Bluth et al. (1993)
Satellite and modeling	7.5–10.5	Halmer et al. (2002)

[a]Volcanic sulfur emissions and speciation are examined by Oppenheimer in **Chapter 4.4**.

the global volcanic mercury flux of 2–36 tons $year^{-1}$. Hinkley et al. (1999) suggests that the Lambert et al. values are a factor of 3 or 4 too high.

A comparable value of 18 tons annually is obtained using Olafsson's (1975) estimate of mercury emissions (7×10^5 g Hg/6×10^{14} g ejecta) for the volcanic eruption at Heimay, Iceland, and an estimate of 6 km^3 ($\sim 15 \times 10^{15}$ g) for annual, subaerial lava production (~20% of total annual lava production being subaerial; Crisp, 1984; Varekamp, personal communication).

Thus, annual global volcanic mercury emissions estimated or measured in several ways are <0.5 Mmol (100 tons), and our work yielded an average value of 0.23 Mmol (45 tons). This scaling serves two purposes: (1) it provides a framework for further, needed studies of mercury cycling associated with volcanism, and (2) it provides a reasonably well constrained estimate for global emissions for modeling and assessment of human perturbations of the natural mercury cycle. It is clear that average volcanic mercury inputs are small relative to estimates for modern anthropogenic mercury fluxes (~10 Mmol; Pacyna and Pacyna, 2002; Streets et al., 2009) to the global mercury cycle. Indeed, assuming steady state between emissions and deposition, the average yearly terrestrial deposition of mercury from volcanism should be ~0.09 μg m^{-2}. Since volcanic eruptions vary in time and space, large-scale eruptions might be apparent in natural archives such as lake sediments (**Chapter 11.3**), and ice cores. Carefully collected and dated lake sediments, however, do not reveal unusually high accumulations in strata coincident with large explosive aperiodic volcanic eruptions (e.g., Pinatubo in 1991, Krakatau in 1883, or Tambora in 1815). In contrast, and according to Schuster et al. (2002), volcanic mercury depositional signals may be evident in a study of the Fremont Glacier in Wyoming, USA. For example, their results suggest an average global mercury depositional peak increase of 16 μg m^{-2} $year^{-1}$ from the 1883 Krakatau eruption, which released ~21 km^3 of volcanic material (Rampino and Self, 1984). As the preeruption mercury deposition was ~2 μg m^{-2} $year^{-1}$, the Krakatau event is extraordinarily prominent at ~8× the background. In contrast, a mercury signal associated with the June 1991 Mount Pinatubo eruption in the Philippines, which released ~5 km^3 ash and pumice and $\sim 50 \times 10^{12}$ g SO_2 or 25×10^{12} g S (USGS Fact Sheet 113–97), is not evident in the Fremont Glacier ice core. If Mt. Pinatubo were assumed to be analogous to Krakatau according to the Fremont ice core, then the predicted mercury deposition would be ~4× less or ~4 μg m^{-2} $year^{-1}$. The anthropogenically enhanced background mercury deposition for 1991 in the ice core was considerably larger at ~11 μg m^{-2} $year^{-1}$. Thus, and given the large pollution-derived mercury deposition, the uncertainty inherent in reconstructed fluxes and the assumptions, the lack of a mercury signal from Mt. Pinatubo could reasonably be expected.

We suggest that the work of Schuster et al. (2002), while somewhat speculative and not well constrained, is provocative and stimulating. Moreover, there is reasonable coherence with the Hg/S for volcanic emissions shown in **Table 4**. For example, the Hg/S of 5×10^{-6} when combined with the 25×10^{12} g sulfur emission estimates for the Mt. Pinatubo eruption yields a mercury input of 125×10^6 g mercury or ~0.6 Mmol. This is just 6% of the 10 Mmol anthropogenic mercury emissions estimated by the MFM simulation for the global contribution in 1990. Therefore, the measured Hg/S ratio suggests the Mt. Pinatubo eruption would not be detectable as well. Similarly, the massive Krakatau eruption would have represented a ~2.4 Mmol input, enhancing global Hg deposition by 1 μg m^{-2} $year^{-1}$. It must be noted, however, that work from long peat cores has suggested that large aperiodic volcanic eruptions may have left detectable signals in that archiving medium as well (e.g., Martinez-Cortizas et al., 1999; Roos-Barraclough et al., 2002). The lack of identifiable volcanic signals in lacustrine sediments is likely due to the 'smoothing' effect that a several-year residence time of mercury within a lake and its watershed would exert on such short-duration signals.

In summary, it has been demonstrated that Hg/S ratios measured for a variety of volcanic plumes and fumaroles, when indexed to estimates of global sulfur emissions from volcanism, yield a mean volcanic mercury flux of 0.23 Mmol (45 tons), which is consistent with other estimates and observations. Accordingly, average yearly mercury emission from volcanoes is small relative to natural terrestrial fluxes to the atmosphere (2.5–5 Mmol) and modern pollution mercury entering the global cycle (10 Mmol). Over the 100 year time period used in the MFM simulation, anthropogenic mercury inputs to the global atmosphere were 1000 Mmol, while average mercury emissions from volcanoes would be 23 Mmol. Periodic large eruptions, such as Tambora, Krakatau, Mt. St.

Helens, and Mt. Pinatubo, would add significantly to this flux but for very short periods.

Our assessment for the importance of volcanic mercury emissions to the global inventory has been confirmed by recent investigations. Indeed, reported Hg/S mass ratios show reasonable agreement with our earlier studies (**Tables 4** and **5**). At White Island, for example, Wardell et al. (2008) found mean Hg/S values to range from 2.8×10^{-6} to 4.5×10^{-6} for replicate samples, while Bagnato et al. (2007) reported a mean Hg/S mass ratio of 17×10^{-6} for Mt. Etna. We note that Mt. Erebus, Antarctica, yielded an overall average reported to be 20×10^{-6} (Wardell et al., 2008; Hg was not detected in many samples). In 2009, Bagnato and coworkers investigating mercury emissions from La Soufriere Volcano, Guadeloupe Island (Lesser Antilles) found average Hg/S mass ratios of 0.4×10^{-6} and 3.2×10^{-6} for the plume and fumarolic gases, respectively. At Vulcano Island, Italy, the average Hg/S index for fumarolic gas was 0.7×10^{-6} and the plume measurements yielded an average of 0.2×10^{-6} (Zambardi et al., 2009). Witt et al., (2008a,b) reported Hg/S mass ratios for two fumarolic gas plumes at the Tatun Volcanic Field, Taiwan to be 2.4×10^{-6} and 5×10^{-6}. Witt et al. (2008a) made plume measurements for mercury and sulfur dioxide from the Masaya and Telica volcanoes, Nicaragua. These yielded the highest mean Hg/S mass ratio at 40×10^{-6} with a range between 0.2×10^{-6} and 70×10^{-6}. Nevertheless, and given the uncertainties, a mean volcanic Hg/S mass ratio of 5×10^{-6} remains appropriate. Finally, the net contribution of volcanic mercury fluxes to the global atmosphere may be smaller than our assessment due to the potential for rapid oxidation of mercury by co-emitting bromine as well as subsequent oxidation by ozone (von Glasow, 2010).

11.4.3.2 Mercury Input to the Oceans via Submarine Volcanism

To our knowledge, there are only two published reports of Hg concentrations in submarine hydrothermal fluids (Crespo-Medina et al., 2009; Lamborg et al., 2006). That work described hot fluids emerging from the Sea Cliff field (part of Gorda Ridge) as containing somewhat elevated total Hg concentrations (~10 pM) but that were comprised of nearly 100% MMHg. Lacking additional data, we can turn to the results of subaerial volcanism as a guide to the representativeness of the Sea Cliff data. First, we assume that the Hg/S of 5×10^{-6} established for subaerial volcanism (**Table 4**) can be applied to the hydrothermal inputs associated with submarine tectonic activity, and second, that oceanic lava production is ~5× as large as the amounts formed subaerially (e.g., Crisp, 1984). Accordingly, the submarine inputs would be ~1.3 Mmol annually. An upper estimate of 1.8 Mmol $year^{-1}$ was proposed by Fitzgerald et al. (1998), who used oceanic mercury profiles and an estimate for the rate of vertical mixing in the water column. The agreement for these estimates negates the extraordinarily large fluxes (20–40×) suggested by heat flow calculations (e.g., Rasmussen, 1994), and provides additional support for an average Hg/S ratio for volcanic emissions of $\sim 5 \times 10^{-6}$. An input of 1–2 Mmol $year^{-1}$ is significant and comparable to worldwide river input as estimated by Mason et al. (1994). It is probable, however, that only a small fraction of the tectonically associated marine mercury inputs mixes with bulk ocean water. It is likely that mercury will be removed from the hydrothermal fluids through co precipitation of metal sulfides and scavenging by precipitating hydrous oxides of manganese and iron as hydrothermal fluids mix with the oxygenated seawater near their entry points. The Sea Cliff results appear consistent with this view, as they are not highly elevated above seawater. Moreover, elevated levels of mercury are present in the hydrothermally derived metal-rich deposits found on the East Pacific Rise (Boström and Fisher, 1969) and the Gorda Ridge (Koski et al., 1994). Stoffers et al. (1999) observed some nascent elemental mercury around the sulfide chimneys of the White Island (New Zealand) complex, but given the scaling arguments above it would appear that submarine volcanism does not represent a significant source of mercury to the global ocean. The observation from the Sea Cliff study that much of the Hg in emerging fluid may be methylated is intriguing and requires further study, but could suggest that hydrothermal systems are significant sources of methylated Hg to the deep sea. As we note below (**Section 11.4.5.1.2**), deep sea concentrations of methylated Hg have not been observed to be elevated, suggesting the hydrothermal supply of these forms is demethylated relatively rapidly.

11.4.3.3 Low-Temperature Volatilization

As noted in the previous section, direct low-temperature weathering inputs from mineralized mercury deposits to aquatic environments occur primarily through sediment transport of cinnabar-containing material. Volatilization is an additional form of low-temperature weathering in which mercury is unparalleled by other metals. The volatility of elemental mercury is well documented, and to the extent that mercury-containing materials possess some fraction of their burden in the elemental form, weathering by volatilization will occur. Other mercury species are somewhat volatile as well (**Table 7**), but most are less so by orders of magnitude than elemental mercury. Volatilization of mercury from soils and rock to the atmosphere has only recently received significant attention. Unlike air–water gas exchange, air–soil/rock gas exchange has not been described in theoretical terms; thus, all that is known of mercury volatilization is from direct flux measurements and the results of soil manipulation experiments. Several others (e.g., Poissant and Casimir, 1998 and references therein) have noted from measured fluxes and their temperature dependence, the similarity of estimated and theoretical activation energies of vaporization (~60 and 85 kJ mol^{-1}, respectively).

Measurements using flux chambers and micrometeorological techniques are the most numerous (see special section of *Journal of Geophysical Research* 104(D17), 1999). As noted in **Section 11.4.2**, Klusman and colleagues (e.g., Klusman and Jaacks, 1987) attempted to develop a tracer approach based on measurements of $^{222}Rn/He/Hg$ to estimate the flux of mercury from soils indexed to the fluxes of the other gases. Their work, however, has not been extended beyond small-scale applications. Finally, isotope addition experiments, including those of Schluter (2000) using radioactive ^{203}Hg additions and those of Lindberg and colleagues using stable isotopes in the METAALICUS program (see **Section 11.4.8**), are proving very insightful.

The results from some volatilization measurements over a number of substrates are shown in **Table 8**, and vary widely. In

general terms, the various studies indicate that higher concentrations of mercury in the soil/rock substrates lead to higher evasional fluxes. Other factors are strongly influential as well. These include temperature, light, wind speed, and soil moisture (e.g., Gustin et al., 1999). It is clear that evasion of mercury from mineralized areas can be significant; however, the results from other substrates are currently limited by the large uncertainties and variability inherent in making such difficult measurements. Gustin and colleagues have made efforts to scale up their measurements, made primarily from Nevada, to the western United States and Mexico (10 Mg $year^{-1}$; Gustin et al., 2000). Thus, this important area of research is still developing and should be active in the future.

In his review of soil volatilization experiments, Schluter (2000) also highlighted the importance of the dissolved organic carbon (DOC) concentration in the soil fluids, with higher concentrations of fulvic acids, for instance, leading to an enhancement of mercury reduction and evasion by generating Hg(I) and then aiding the disproportionation reaction ($2Hg(I) = Hg(0) + Hg(II)$) through sequestration of Hg(II). The source of the reducing equivalents in soils appears to be species generated indirectly through photoreduction of some kind (e.g., organic carbon and Fe(II); Schluter, 2000). The flux from nonenriched soils, though, is substantially lower than that from the mineralized areas and may average around 0.2 μg m^{-2} $year^{-1}$ (Schluter, 2000).

Combining estimates for volcanic and low-temperature inputs of mercury from mineralized areas and nonenriched soils to the atmosphere allows an estimate of the total amount of natural terrestrial emissions to be made. The volcano work benefits from the existence of tracing species such as sulfur that make tractable the scaling of individual measurements to the global scale. In the case of low-temperature volatilization, however, no such index has yet been developed. Therefore, translating values such as those of Table 8 into global fluxes is difficult.

Using the data from Nevada (Gustin et al., 2000; 0.011 Mmol $year^{-1}$; 1.8×10^{11} m^2 area) an emission rate of ~10 μg m^{-2} $year^{-1}$ for the global mercury belt areas can be estimated. Further assuming that these enriched areas represent no more than ~15% of the continental area suggests a maximum contribution for volatilization from these areas of ~5.6 Mmol $year^{-1}$. The addition of the small volcanic contribution suggests that natural emissions of mercury to the atmosphere are <5.8 Mmol $year^{-1}$ and that subaerial and submarine emissions combined are <7.1 Mmol $year^{-1}$.

The volatilization estimates are crude extrapolations, as they are based on assumptions of soil concentration distributions and understanding of driving forces behind volatilization. They do suggest, however, that the emissions measured and estimated in some of the work cited are consistent in the first order with Mason et al. (1994) and that natural land-based sources of mercury to the atmosphere are consistent and likely to be ~5 Mmol $year^{-1}$. It has also been noted that a flux of 5 Mmol $year^{-1}$ for natural sources is consistent with the rate of atmospheric deposition in the preindustrial past indicated by analysis of lake sediments (e.g., Lamborg et al., 2002b). Finally, it must be noted that emissions from soils removed from natural enrichments likely contain a significant fraction of mercury initially mobilized by anthropogenic activities and subsequently deposited in soils (see Section 11.4.3.6).

Table 7 Henry's law constants for selected mercury species (at STP)

Equilibrium	*H (M atm^{-1})*
$Hg^0_{(g)} \leftrightarrow Hg^0_{(aq)}$	0.11
$Hg(OH)_{2(g)} \leftrightarrow Hg(OH)_{2(aq)}$	1.2×10^4
$HgCl_{2(g)} \leftrightarrow HgCl_{2(aq)}$	1.4×10^6
$(CH_3)_2Hg_{(g)} \leftrightarrow (CH_3)_2Hg_{(aq)}$	0.13
$CH_3HgCl_{(g)} \leftrightarrow CH_3HgCl_{(aq)}$	2.2×10^3

Sources: Sanemasa I (1975) Solubility of elemental mercury-vapor in water. *Bulletin of the Chemical Society of Japan* 48(6): 1795–1798; Iverfeldt A and Lindqvist O (1982) Distribution equilibrium of methyl mercury chloride between water and air. *Atmospheric Environment* 16(12): 2917–2925; Lindqvist O and Rodhe H (1985) Atmospheric mercury – A review. *Tellus* 27B: 136–159.

11.4.3.4 Anthropogenic Sources

The human-related sources of mercury to the environment are numerous and widespread. Most direct inputs of mercury from point sources to aquatic systems have largely been contained in most developed countries. Inputs of mercury to the environment via the atmosphere are of the greatest concern. These emissions, coupled with long-distance transport of elemental mercury, have resulted in elevated concentrations of mercury in fish from locations that are removed from anthropogenic sources (e.g., open ocean, and semiremote regions in the United States, Canada, Scandinavia; Wiener et al., 2002). A summary of the fluxes from major sources over the last few years is shown in Table 9. High-temperature processes, principally coal and cement production, and municipal waste burning dominate anthropogenic inputs of mercury to the atmosphere. As noted in Section 11.4.1, small- and large-scale gold mining may be a significant source of Hg to the atmosphere (Pacyna, et al., 2010). The emission of anthropogenic mercury is higher in the northern hemisphere, as a result of greater industrial activity and population density. Between 1990 and 1995 the emissions from developed economies in

Table 8 Some examples of measured fluxes over natural soils

Location	*Method*	*Soil conc. (ng g^{-1})*	*Evasional flux (ng m^{-2} h^{-1})*	*References*
Sweden	FC	NA	−2 to 2	Xiao et al. (1991)
Tennessee, USA	FC	61–469	−1.81 to 54.94	Carpi and Lindberg (1998)
Quebec, Canada	FC	NA	0.62–8.29	Poissant and Casimir (1998)
Nevada, USA	FC and MM	1200–214 600	50–600	Gustin et al. (1999)
Nova Scotia, Canada	FC	NA	−1.4 to 4.3	Boudala et al. (2000)

FC, flux chamber; MM, micrometeorology (Bowen ratio).

Table 9 Major classes of anthropogenic emissions of mercury to the atmosphere in 1995 and 2005

Source type[a]	*1995 flux (Mmol year^{-1})*	*2005 flux (Mmol year^{-1})*[b]
Stationary combustion	7.4	4.4
Non-ferrous metal production	0.8	0.7
Cement production	0.7	0.9
Waste disposal and product use	0.6	0.6
Pig iron and steel production	0.1	0.3
Gold production	n.c.	0.6
Mercury production (primary)	n.c.	<0.1
Caustic soda production	n.c.	0.2
Cremation	n.c.	0.1
Artisinal gold mining	n.c.	1.8
Total	9.6	9.7

n.c., not considered.

[a]Stationary combustion includes fossil fuel burning power plants, while waste disposal includes municipal waste combustion.

[b]Note the apparent large reduction in Hg emissions from stationary combustion and increases from gold production and mining.

Sources: Reproduced from Pacyna EG and Pacyna JM (2002) Global emission of mercury from anthropogenic sources in 1995. *Water, Air, and Soil Pollution* 137(1–4), 149–165; Pacyna EG, Pacyna JM, Sundseth K, et al. (2010) Global emission of mercury to the atmosphere from anthropogenic sources in 2005 and projections to 2020. *Atmospheric Environment* 44(20): 2487–2499.

North America and Europe have declined substantially. Unfortunately, they have almost been completely replaced by emissions from countries, especially in Asia, that have rapidly developing economies that are coal-driven. Accordingly, Asian sources of mercury currently constitute 56% of all anthropogenic emissions. Based on the Pacyna and Pacyna inventory and the natural source strength suggested by Mason et al. (1994), human activity contributes approximately two-thirds of the mercury emitted from land-based sources each year. Similarly, these estimates suggest that the emission and deposition fluxes of mercury are currently 3× what they were in the prehuman environment. Such estimates are now widely supported by the reconstruction of mercury deposition from remote lakes worldwide (more below; e.g., Fitzgerald et al., 1998). Reconstruction of deposition in the recent past (~30 years) is less certain. Many of the lake sediment archives examined thus far either accumulate too slowly or possess enough inherent variability that recent changes are difficult to definitively reconstruct. Furthermore, lake watersheds act to buffer rapid changes. As a result, there is evidence from a variety of archiving media for increases, decreases, and relatively little change in Hg deposition in the last few decades (e.g., Bindler et al., 2001; Fain et al., 2009a; Fitzgerald, 1995; Fitzgerald et al., 2005; Kraepiel et al., 2003; Roos-Barraclough et al., 2002; Shotyk et al., 2003). Some of these observations are quite clear, but perhaps regionally confined (e.g., Iverfeldt et al., 1995; Kamman and Engstrom, 2002).

Looking toward the future, recent reports (Pacyna et al., 2010; Streets et al., 2009) combined the emissions factors used to develop current anthropogenic Hg emissions and applied them to a few industrial development scenarios. Streets and colleagues estimated from these scenarios that by the year 2050, annual Hg emissions could vary from −0.4 to 96%, with the high end representative of a 'business as usual' scenario. This implies that the next 40 years could see an increase in the amount of Hg entering the global environment that is comparable to the previous 150.

11.4.3.5 Mining

Mining has been a long-standing and continuing source of environmental mercury contamination. Indeed, a partial analog to the alchemist's quest to transmute base metals into gold is contained in the *patio* process in which naturally occurring but trace amounts of gold and silver are amalgamated (concentrated) using large amounts of liquid mercury. The dense amalgam can be separated from the crushed, parent rock or from placer and alluvial deposits, often with much loss of mercury to air and aquatic systems. The gold or silver is recovered by heating the amalgam and vaporizing the mercury. This technology has been employed broadly and often crudely since its introduction by Bartolome de Medina in 1557 (Nriagu, 1979). Historically, uses of mercury in gold and silver mining were especially significant in the Americas from the mid-1500s to the turn of the twentieth century. This unhealthy and ecologically damaging practice continues today, and on a large scale, in many countries (e.g., China, Brazil, Philippines, Kenya, and Tanzania). In their review of current gold mining, Lacerda and Salomons (1998) found that environmental losses of mercury are large, 1–1.7 kg kg^{-1} gold recovered. Much of the pollutant mercury accumulates in the surrounding lands, watersheds, waterways, and mine tailings, and the associated environmental and human-health concerns are primarily local and regional. However, there are global worries as well, because a portion of the mercury is emitted to the atmosphere (Porcella et al., 1997).

Mercury losses occur not only with the processing and recovery of gold and silver, but in the mining and production of mercury. For example, the nineteenth century 'gold rush' in the western United States was fueled by mercury mining in California. Egleston (1887) reports that between 1850 and 1889, the mercury yield from California mines, especially from the New Almaden operation (85%), was 1 518 380 flasks (~34.5 kg per flask). This was comparable to the combined output of the two other major mines, the Almaden (Spain) and Idrija, Austria (now Slovenia), which produced 1 291 636 and 347 586 flasks, respectively, over the same time period. Moreover, and as Egleston emphasizes, "according to the best California authorities, the loss in the best constructed furnaces as near as can be approximated is not <15–20%, and in many of the works the losses will probably amount to double that." Mercury mining activities continue today in Spain though with a higher sensitivity to preventing mercury releases to the environment. Despite this, mercury mines remain significant sources of mercury to watersheds and coastal marine systems including inoperative sites such as Idrija and Clear Lake, CA, that supply mercury from abandoned tailings.

11.4.3.6 Biomass Burning, Soil and Oceanic Evasion – Mixed Sources

There are three prominent processes that release mercury of mixed natural and anthropogenic origin to the atmosphere. These three include biomass burning (deliberate and natural) and the evasion of mercury from soils and the ocean. The general factors controlling emission of mercury from soils

have been discussed in the section on low-temperature volatilization. The mercury released from soils that are not naturally enriched (unlike some of the mineralized substrates described) is mercury derived principally from atmospheric deposition and is released from the upper horizon pool (Schluter, 2000 and references therein). As the mercury that is deposited from the atmosphere is of mixed origin, so is the mercury emitted to the atmosphere from these soils. Therefore, though mercury may be released from completely natural and undisturbed soils as regulated by ambient biogeochemical processes, the current flux is not entirely natural. In the case of nonenriched soils, this is not very significant as these materials are net sinks of atmospheric mercury deposition (see **Section 11.4.6**). In the case of biomass burning and especially oceanic evasion, however, the fluxes to the atmosphere may be very important in the global mercury cycle. As with soils though, these processes mobilize both natural and anthropogenic mercury and represent sources of mixed origin. In this way, these media act to recycle mercury in the environment, extending the residence time of mercury at the Earth's surface.

Recent measurements of mercury in biomass burning plumes from research aircraft suggest that this process releases substantial amounts of mercury. Brunke et al. (2001) and Friedli et al. (2001) used CO and CO_2 as indexing species to establish fluxes of mercury of ~1–5 Mmol $year^{-1}$. A first-order estimate, based on the relative strengths of truly anthropogenic emissions and truly natural emissions, suggests that some two-thirds of the mercury released by biomass burning was initially released by human activities (i.e., 0.67–3.4 Mmol $year^{-1}$ anthropogenic; 0.33–1.6 Mmol $year^{-1}$ natural).

Oceanic evasion is a major component of the mercury cycle. As described in greater detail in **Section 11.4.5**, there are a number of processes that may lead to evasion of elemental mercury from the ocean. Mason et al. (1994) found that evasion from the ocean had tripled in magnitude in concert with the increase in anthropogenic activities. Therefore, as with biomass burning, nearly two-thirds of the mercury currently evading from the ocean is anthropogenic.

11.4.3.7 Watersheds and Legacy Mercury

Watersheds are sources of mercury to the aquatic environment. The movement of mercury through watersheds is intimately connected with that of organic matter, especially DOC (e.g., Dittman et al., 2010). However, as in the case of biomass burning and evasion, the mercury released from watersheds is of mixed origin. Because the residence time of mercury within watersheds is fairly long (see **Section 11.4.6**), the potential for the buildup of 'legacy' mercury exists. This feature is relevant when considering how rapidly a system might respond to decreased mercury loadings. Therefore, though decreases in mercury deposition to a watershed may occur, the watershed will contribute more mercury to its receiving waters than enters it each year. Legacy mercury, however, was released to the environment as a result of human activity and should be viewed as an anthropogenic source term.

In a few recent studies, watersheds were shown to be important sources of Hg to receiving waters above what might be viewed as 'typical.' In these studies, groundwater was identified as an important transporter of Hg and wastewater addition to the aquifers was implicated as a possible cause for the mobilization (Barringer and Szabo, 2006; Black et al., 2009; Bone et al., 2007). This is likely to be a very active area of research in the future.

11.4.4 Atmospheric Cycling and Chemistry of Mercury

Mercury is found in the atmosphere in both gas and particle phases. Greater than 95% of mercury exists as gas-phase elemental mercury (Bloom and Fitzgerald, 1988; Fitzgerald and Gill, 1979; Iverfeldt, 1991a). Concentrations of total gaseous mercury (TGM; including elemental, ionic and gaseous alkylated forms such as DMHg) in remote areas are typically in the range of 1–2 ng (as mercury) m^{-3}. Concentrations below 1 ng m^{-3} are to be found under certain conditions (more below) and higher values are often observed in urban/suburban locations. Some selected concentration and deposition data are shown in **Table 10**. Particle-phase atmospheric mercury appears to be largely Hg^{2+} and comprises a few percent of total atmospheric mercury in the troposphere (Fitzgerald et al., 1991; Iverfeldt, 1991a). There is only one published report of mercury in the stratosphere to our knowledge and no measurements in other regions of the upper atmosphere (Murphy et al., 1998). Not surprisingly, the authors found the concentration of particulate mercury increased above the tropopause as a result of enhanced oxidation of elemental mercury by ozone

Table 10 Atmospheric deposition concentration data

Location	*TGM (ng m^{-3})*	*Hg_T in precip. (ng l^{-1})*	*Deposition ($\mu g\ m^{-2}\ year^{-1}$)*	*Calculated lifetime (years)*[a]	*Reference(s)*
Florida, USA	1.4–3.1	13–23	15–28	0.3–0.7	Guentzel et al. (1995) and Gill et al. (1995)
Tennessee, USA	5.8 ± 3.6	3	30	1.2	Lindberg et al. (1992)
Michigan, USA	2.0	10	9 ± 3	1.4	Hoyer et al. (1995)
S. Atlantic Ocean	1.4	4	6	1.5	Lamborg et al. (1999)
Wisconsin, USA	1.6 ± 0.4	6	7	1.5	Lamborg et al. (1995)
Alert, Canada	1.2	~15	5	1.5	Schroeder et al. (1998) and Schroeder (personal communication)
Global average	1.6	NA	5.6	1.8	Lamborg et al. (2002a)
Eq. Pacific	1.3	3	4	2	Mason and Fitzgerald (1993)
Sweden	2.9 ± 0.7	10	13 ± 12	2 ± 1	Lindqvist et al. (1991)

[a]Lifetime with respect to wet deposition. Overall lifetime is equivalent to this value divided by the ratio of total deposition and wet deposition.

and the condensation of the less volatile Hg^{2+} onto ambient particles.

Recent years have seen a sharp rise in research regarding the production and fate of Hg^{2+} in the gas phase (the so-called 'reactive gaseous mercury' or RGM; Engle et al., 2005; Fain et al., 2009b; Fu et al., 2008; Landis et al., 2002; Sheu and Mason, 2001; Skov et al., 2006; Stratton and Lindberg, 1995; Swartzendruber et al., 2006). This is likely driven by the emergence of commercially available instruments designed to collect and measure this form of Hg, along with the whole atmospheric Hg species suite. The recognition that a significant fraction (a few percent) of atmospheric Hg is in a highly soluble and surface-reactive form has led to a major re-evaluation of the pathways of removal for this metal and a reassessment of loadings and fluxes in the environment. This is explored in greater detail below.

The vertical profile of mercury in the troposphere has been determined in a few cases (Banic et al., 2003; Landis and Stevens, 2001; Swartzendruber et al., 2008; Talbot et al., 2007). In most situations, it appears that there is little change in the total mercury mixing ratio with altitude, indicating thorough vertical mixing and an atmospheric residence time that is long enough to make this possible. Talbot et al. (2007) noted extremely low concentrations of Hg in the upper troposphere, apparently in situations when stratospheric injection had taken place and confirming the stratosphere measurements of Murphy et al. (1998). There have been some suggestions that elemental mercury decreases with altitude, while RGM increases, creating a gradient for atmospheric deposition on large scales of the more soluble and surface active Hg^{2+}. For example, Landis and Stevens (2001) have suggested that the vertical RGM gradient is on the order of 400 pg m^{-3} over the troposphere (6340 m, isobaric). This is a rather large gradient, representing ~25% of the total atmospheric mercury. Applying a vertical eddy diffusivity of 1 m^2 s^{-1} (Seinfeld, 1986) to this gradient provides an estimate of the potential rate of removal of RGM on a large scale of 2 μg m^{-2} $year^{-1}$ (or ~10–30% of the observed flux at most locations). It must be noted that these datasets are being developed only now and, therefore, the flux estimate made above is highly speculative.

The situation of horizontal profiling is better developed. **Figure 4** illustrates data from a number of sampling locations worldwide, showing a small but discernible interhemispheric gradient in TGM. Values for TGM in the northern hemisphere (NH; ~1.7 ng m^{-3}) are larger than in the south (~1.2 ng m^{-3}) as a result of the NH representing a greater proportion of land-based natural and anthropogenic emissions. Horizontal gradients on smaller scales (i.e., plumes) have also been observed including continental-scale, urban plumes, and single industries (Fitzgerald, 1995 and the references therein; Lamborg et al., 2002a).

Assuming little vertical variation in the mixing ratio of total mercury in the troposphere and using the available horizontal surface-based measurements, Mason et al. (1994) estimated the total atmospheric burden of mercury to be 25 Mmol (5 ktons; **Figure 2(a)**). Accordingly, the average tropospheric air column mercury burden is ~10 μg m^{-2}. If the emissions of mercury as outlined in **Section 11.4.3** equal 40 Mmol $year^{-1}$, then the average residence time of mercury in the atmosphere is ~0.6 year. Such a residence time is relatively long on

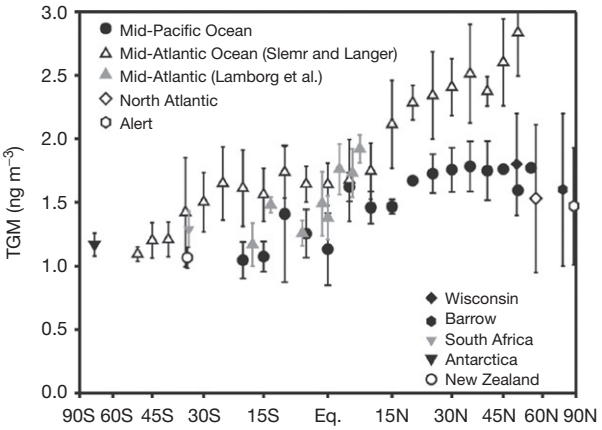

Figure 4 Total gaseous Hg in the atmosphere at several locations. Notice the discernible interhemispheric gradient, resulting from greater emissions of Hg to the atmosphere in the more industrialized northern hemisphere (data from Fitzgerald (1995) – Mid-Pacific (filled circles); Slemr and Langer (1992) – Mid-Atlantic (open triangles); Lamborg et al. (1999) – Mid-Atlantic (shaded triangles); Mason et al. (1998) – North Atlantic (open diamonds); Schroeder et al. (1998) – Alert, N.W.T. (open hexagons); Lamborg et al. (1995) – rural Wisconsin, USA (filled diamonds); Lindberg et al. (2002) – Point Barrow, Alaska, USA (filled hexagons); Ebinghaus et al. (2002) – Cape Town, RSA (shaded inverted triangles) and Antarctica (filled inverted triangles); Fitzgerald (1989) – Ninety Mile Beach, NZ (open circles); figure from Lamborg et al., 2002a).

atmospheric timescales (e.g., the mixing time for the hemispheres is ~1.3 years; Geller et al., 1997), and thus we should expect to find mercury reasonably well mixed vertically and intrahemispherically as we do. This global-scale value is within the range of similar estimates made from various specific locations (**Table 10**).

It was quickly realized that the mercury species to be found in greatest abundance in precipitation was ionic mercury (e.g., Fogg and Fitzgerald, 1979). Some typical values of total mercury in precipitation are shown in **Table 10**. Extensive databases of precipitation mercury concentrations are available from monitoring networks in the US, Canada, and Nordic countries (e.g., US Mercury Deposition Network: http://nadp.sws.uiuc.edu/mdn). The discrepancy between the dominant gas and precipitation phase species implied a process of oxidation of elemental mercury in the atmosphere and its subsequent scavenging as being a major component of the mercury cycle. Since the initial work, and partially in response to increased governmental interest in long-range atmospheric transport of pollutant mercury, there has been an extraordinary increase in research on the atmospheric chemistry of mercury. Many mechanisms for elemental mercury oxidation in the atmosphere have been proposed and a few have been studied in detail through laboratory experiments (e.g., Ariya and Ryzhkov, 2003; Donohoue et al., 2005, 2006; Hall et al., 1995; Lin and Pehkonen, 1999; Munthe, 1992; Pal and Ariya, 2004a,b; Raofie and Ariya, 2003, 2004; Sommar et al., 2001; Tokos et al., 1998). These include homogeneous gas-phase and heterogeneous-phase reactions occurring in cloud-water/precipitation and aerosols. The principal constraint on gas-phase oxidation is that the overall reaction rate must be similar to the residence time of mercury. However, the work done in

laboratory settings has indicated that the combined effect of oxidation by ozone, hydroxyl radical, and especially halogen radicals (Cl and Br) results in too short a lifetime of elemental Hg with respect to oxidation. This requires that oxidation be partially balanced by reduction in heterogeneous phase reactions, leading to complex cycling of mercury species within cloud-water or aerosols that includes influences by sorbent surfaces such as soot (Pleijel and Munthe, 1995). Some of the proposed mechanisms are shown in **Figure 5**. The ongoing challenge for those studying atmospheric mercury is to identify which of these mechanisms is actually influential in the atmosphere and under what conditions. The atmospheric chemistry embedded in the transport and deposition models of Selin et al. (2008) and Holmes et al. (2010), which included many of these reactions, estimated the atmospheric residence of mercury to be ~0.5 year. Their simulations highlighted the importance of aqueous-phase reduction reactions in controlling the atmospheric residence time of mercury. In more urbanized environments and close to sources, dry deposition of particulate mercury emitted from sources or forming shortly after emission is likely to be the dominant removal mechanism (e.g., Chiaradia and Cupelin, 2000; Keeler et al., 1995).

One of the more dramatic observations in mercury biogeochemistry in recent years is the so-called 'spring time depletion' of mercury in high latitudes. Schroeder et al. (1998) were the first to observe this phenomenon at Alert on the northern tip of Ellesmere Island (Canada). TGM at this location shows a fairly steady value of 1.5 ng m^{-3}, typical of stations representative of the global pool in the northern hemisphere. However, at the advent of polar sunrise and lasting for several weeks, the concentration begins to fluctuate between the baseline value and near zero, with the depletion episodes lasting hours to days. There is also a high correlation between depletion of mercury and ozone, thus forging a connection between mercury and the chemistry and physics of Arctic haze formation and breakdown (**Figure 6**; Barrie and Hoff, 1985; MacDonald et al., 2000). Further work by Bill Schroeder and his colleagues as well as others in the Arctic (e.g., Lindberg et al., 2002; Lu et al., 2001; Munthe and Berg, 2001 and references therein) and Antarctic (Ebinghaus et al., 2002) confirms this phenomenon as recurrent, seasonal, and occurring in both polar regions (though perhaps more dramatically in the Arctic). Working at mid-ocean, Mason et al. (2001) have observed a rapid oxidation of mercury near the air–sea interface resulting from reactions with sea-spray halogens, and which was supported by modeling (Hedgecock and Pirrone, 2001). As Lindberg et al. (2002) and others have observed, the reaction in the Arctic is also coincident with a buildup of reactive bromine compounds in the polar atmosphere, pointing to a possible mechanistic similarity between the Arctic and mid-ocean phenomena (e.g., Ariya and Ryzhkov, 2003; Balabanov et al., 2005; Donohoue et al., 2005, 2006; Goodsite et al., 2004; Mao et al., 2010; Raofie and Ariya, 2003). In both cases, the generation of significant concentrations of oxidized mercury in the gas phase may lead to significant dry depositional fluxes in addition to fluxes associated with precipitation. The assessment made by Schroeder et al. (1998) when describing the depletion events initially was that, perhaps, 0.5 Mmol of mercury was deposited into the Arctic as a result of this phenomenon (a boundary layer of 500 m over 2×10^5 km^2 containing 1.84 ng m^{-3} emptied of its mercury 5 times: 4.6 μg m^{-2} $year^{-1}$). This is significant but not an enormous unanticipated sink for mercury on a global scale. However, the flux could still be quite significant for delicate Arctic ecosystems and their human inhabitants. As recent modeling has indicated (Holmes et al., 2010), it appears that the halogen chemistry first implicated as important in the cycling of atmospheric Hg in the Arctic is likely responsible for a great deal of the oxidation and removal of Hg on a global scale, marking Schroeder's observations as one of the latest revolutions in our understanding of environmental Hg cycling.

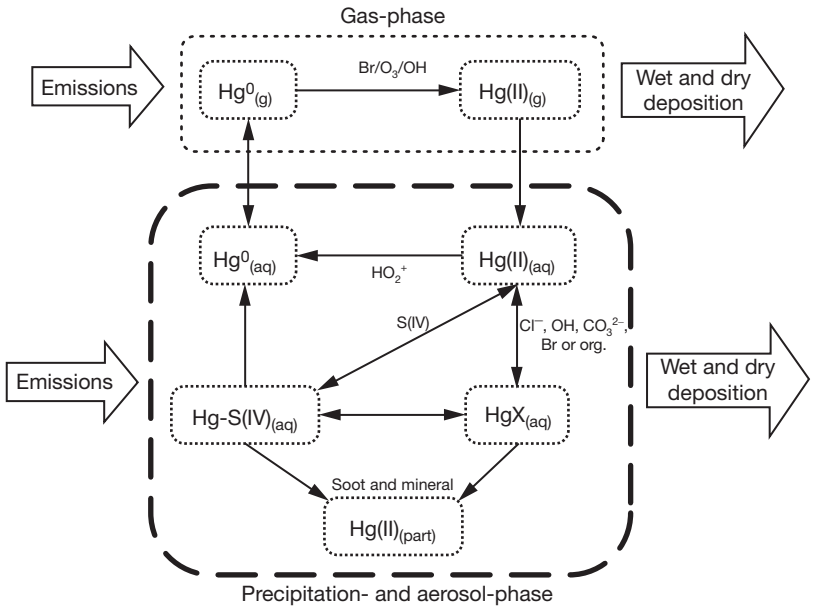

Figure 5 Summary of some of the important physical and chemical transformations of mercury in the atmosphere; figure style adapted from Shia et al. (1999); reactions from Shia et al. (1999) and Lin and Pehkonen (1999) and the references therein.

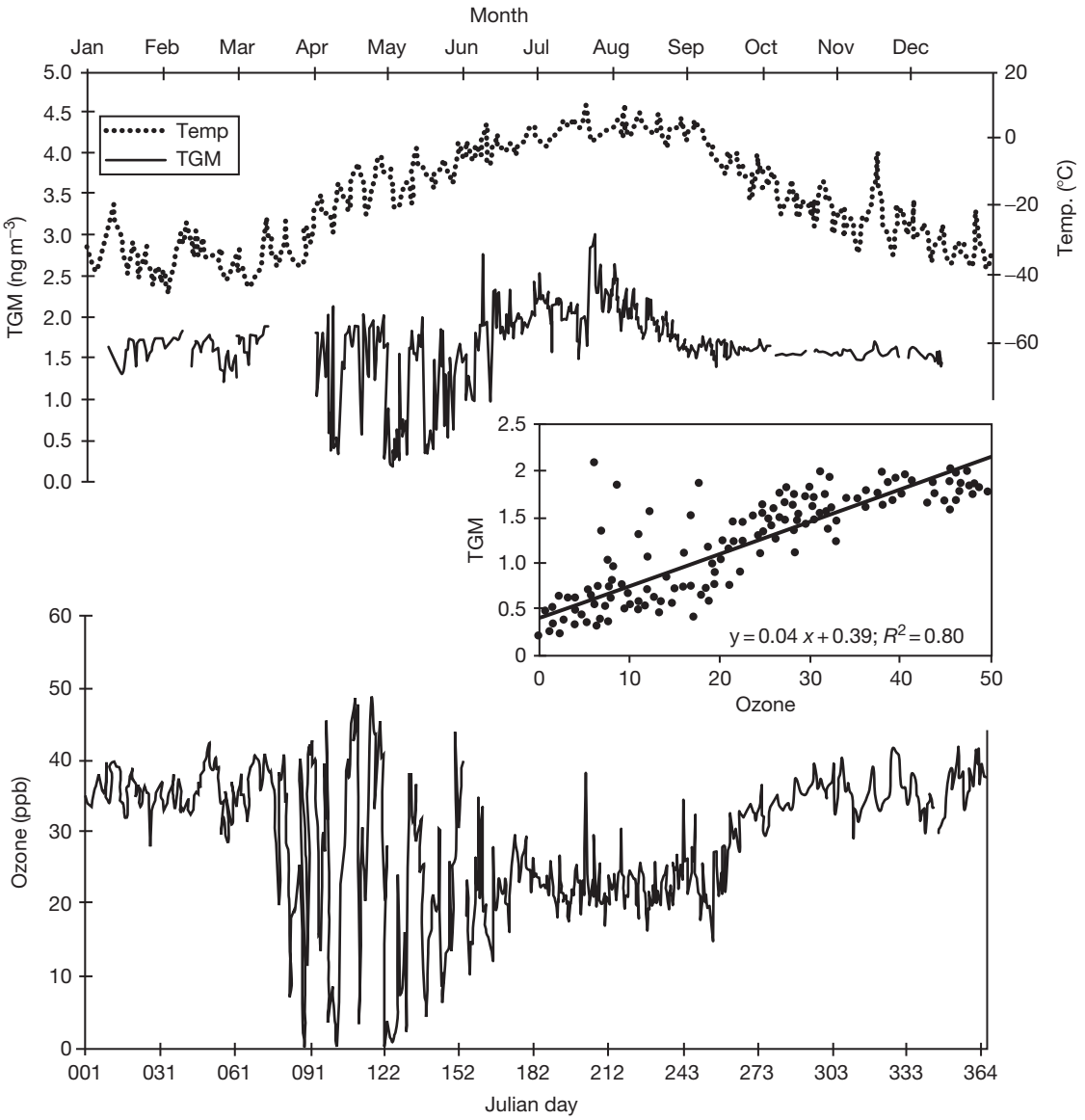

Figure 6 Depletion of Hg^0 in the atmosphere during Arctic spring as observed by Schroeder et al. (1998) at Alert. The traces, from top to bottom, are surface air temperature, total gaseous mercury, and ozone. The inset illustrates the correlation between mercury and ozone during the spring depletion period. Reproduced with permission from Schroeder WH, Anlauf KG, Barrie LA, et al. (1998) Arctic springtime depletion of mercury. *Nature* 394(6691): 331–332.

Research on pathways of mercury dry deposition in addition to particle phase and RGM suggests that plants (especially trees) may take up elemental mercury from the atmosphere into their leaves above a certain 'compensation point' concentration (Benesch et al., 2001; Hanson et al., 1995; Rea et al., 2002). Elemental mercury absorbed in this way could then be deposited to soils in the form of litterfall (e.g., Grigal et al., 2000; Johnson and Lindberg, 1995; Lee et al., 2000; St Louis et al., 2001). Forest foliage may also act as a particle interceptor, effectively increasing the dry deposition velocity of particles (throughfall; Iverfeldt, 1991b). Throughfall and litterfall studies suggest that the removal of mercury from the atmosphere in forests might be as much as 3× more than 'open-field' deposition.

Long-term monitoring datasets of mercury in the troposphere have now been developed at several locations. A compilation of results from sites in the northern hemisphere show little change in TGM concentrations over the last decade (Slemr et al., 2003). However, one group used the air stored in glacial firn to reconstruct the concentration of atmospheric Hg in the center of Greenland and found a peak in concentration in the 1970s, with recent decades showing a relatively steep decline (Fain et al., 2009a). Such research efforts are being performed in a social context of decreased mercury emissions from a number of countries (see **Section 11.4.3**). It is therefore difficult to predict the future direction of secular change of mercury in the atmosphere. However, as suggested, it may be that the reduced emissions from developed countries and relatively uncontrolled sources in Eastern Europe, for example, will be offset by increased emissions associated with developing economies such as China (e.g., Pacyna et al., 2010).

However, assuming for the moment that the atmosphere is near a steady state between emissions and deposition (Mason et al., 1994), the emissions estimates of **Section 11.4.3** can be used to gauge the magnitude of the depositional flux (40 Mmol year^{-1}). This flux is not uniform, with low latitudes receiving more mercury per unit area than high latitudes and continental regions more than oceanic areas. These general trends are the result of several factors. If wet deposition tends to be more important in the removal of mercury than dry processes, wetter regions such as the tropics can be expected to have higher overall fluxes of mercury. This trend is evident even on regional scales, as for instance, the flux of mercury to lakes on the wet side of New Zealand's South Island is much higher than on the dry side (Lamborg et al., 2002b). The difference between mid-continent and mid-ocean fluxes of mercury from the atmosphere appears to be one driven principally by transport from the continents, where sources to the atmosphere are strong, a process traced using ^{222}Rn (Lamborg et al., 1999).

11.4.5 Aquatic Biogeochemistry of Mercury

A brief overview of the marine biogeochemical cycle of mercury was presented in the introduction. Here, a broader picture of the reactions and species-specific interactions involving mercury in natural waters appears in **Figure 7**. This mechanistic scheme, taken from Fitzgerald and Mason (1997), is derived in part from the simulation of the biogeochemistry of mercury in temperate lakes (Hudson et al., 1994). Hudson et al. (1994) as part of the successful and scientifically influential Mercury in Temperate Lakes (MTL) Program conducted in northern Wisconsin, USA, developed a mercury cycling model (MCM). Comparable models have been developed for other freshwater environments such as the Florida Everglades (Beals et al., 2002) and Onondaga Lake, a highly mercury-contaminated and US EPA designated 'Superfund' site (Gbondo-Tugbawa and Driscoll, 1998). We anticipate, as information increases, analogous biogeochemical MCMs will be developed and applied for marine systems. Accordingly, we have chosen to illustrate major features of the aquatic cycling of mercury using the nearshore environment as a generalized working analog for aquatic systems.

Although organic and inorganic ligands and organisms differ in fresh and salty environments, much of the biogeochemical processing and movement of mercury are expected to be similar. Representative distribution and speciation data for mercury in natural waters are presented in **Table 11**. MMHg was first determined in freshwaters by Bloom (Bloom, 1989; Watras et al., 1994), and is now well documented (e.g., Mason and Sullivan, 1997; Verta and Matilainen, 1995). In 1990, Mason and Fitzgerald reported finding methylated mercury species, including DMHg, in the open-ocean waters of the

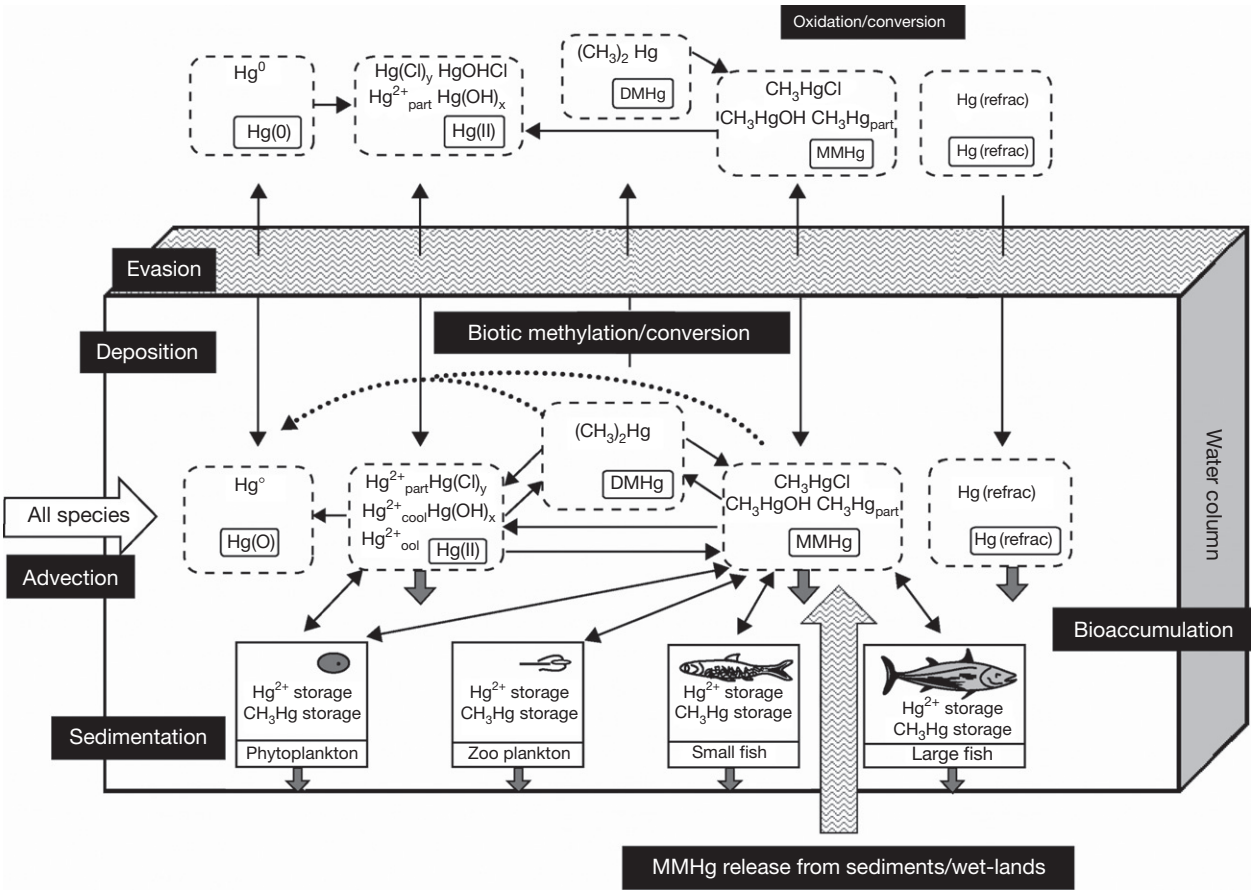

Figure 7 Generalized view of mercury biogeochemistry in the aquatic environment. Prominent processes are labeled (Hudson et al., 1994).

Table 11 Mercury species concentrations in a variety of natural waters. All data in pM, except where noted

Location	*Dissolved total Hg*	*Particulate total Hg*	*Dissolved reactive Hg*	*Dissolved MMHg*	*Particulate MMHg*	*Dissolved DMHg*	*Dissolved Hg^0*	*Reference(s)*
Freshwaters								
Lake Michigan, USA	1.6	0.58	NA	0.025–0.05	0.01–0.015	NA	0.140 ± 0.085	Mason and Sullivan (1997)
Lake Superior, USA/Canada	~0.5–5[a]	0.04–0.43[b]	0.08–0.57	0.008–0.064	0.00005–3.9[b]	NA	0.03–0.17	Rolfhus et al. (2003)
Lake Hoare, Antarctica[a]	2.7–6.8	NA	0.4–1.2	<0.4–1.2	NA	NA	NA	Vandal et al. (1998)
Everglades	5–10[a]	NA	0.15–0.5[a]	0.25–2.5[a]	NA	NA	0.025–0.225	Hurley et al. (1998)
Wisconsin Lakes, USA	3–6	1–2	NA	0.1–0.9	0.15–0.35	<0.003	0.035–0.355	Watras et al. (1994) and Fitzgerald et al. (1991)
Estuaries/coastal								
San Francisco Bay, USA	0.4–174	0.3–439	NA	0–1.6	0–1.92	NA	0.043–9.8	Conaway et al. (2003)
Long Island Sound, USA	1.6–13.1	<0.1–24.1	<0.1–7.6	0–3.3	<0.01–2.91	NA	0.037–0.89	Vandal et al. (2002) and Rolfhus and Fitzgerald (2001)
North Sea and Scheldt Estuary	0.5–14	0.1–6[b]	NA	0.05–1.37	0.0009–0.0435[b]	NA	0.06–0.8	Baeyens and Leermakers (1998) and Leermakers et al. (2001)
Siberian Estuaries	0.7–17	0.15–9.4	NA	NA	NA	NA	NA	Coquery et al. (1995)
Loire and Seine Estuaries	1–6	0.42–13.3[b]	<0.4–2.1	NA	<0.0015–0.0296[b]	NA	<0.05–0.454	Coquery et al. (1997)
Chesapeake Bay, USA[a]	~3–40	NA	NA	~0.05–0.8	NA	NA	~0.1	Mason and Lawrence (1999)
Pettaquamscutt R., USA	~1–25	~0–18	0.4–8[a]	<0.05–4	<0.05–6.88	NA	<0.025–0.4	Mason et al. (1993)
Brazilian Lagoons	18.5–55.2	18–230	0.18–0.43	NA	NA	NA	NA	Lacerda and Goncalves (2001)
Open ocean[c]								
Mediterranean Sea	0.8–6.4[a]	NA	<0.2–0.97[a]	<0.15[a]	NA	<0.13–0.29	<0.02–0.39	Cossa et al. (1997)
Black Sea	1.6–11.8	NA	NA	<0.025–1.04	NA	<0.002–0.041	0.21–1.16	Cossa and Coquery (2005) and Lamborg et al. (2008)
North Pacific	0.1–2	NA	NA	0.02–0.5[d]	NA	0.00–0.02	NA	Laurier et al. (2004), Hammerschmidt and Bowman (2012), and Sunderland et al. (2009)
Eq. Pacific Ocean[a]	NA	0.11–5.87	0.4–6.9	<0.05–0.58	NA	<0.005–0.67	0.015–0.69	Mason and Fitzgerald (1993)
North Atlantic	2.4 ± 1.6	0.035 ± 0.02	0.8 ± 0.44	1.04 ± 1.08[e]	NA	0.08 ± 0.07	0.48 ± 0.31	Mason et al. (1998)
South Atlantic	2.9 ± 1.7[a]	0.1 ± 0.05	1.7 ± 1.2[a]	<0.05–0.15	NA	<0.01–0.1	1.2 ± 0.8	Mason and Sullivan (1999)

[a]These samples were unfiltered. NA, not available.

[b]Units of nmol Hg g^{-1} of suspended material, dry weight.

[c]See **Section 11.4.5.1.2** for a summary of the latest unpublished data.

[d]Some of the values are from Sunderland et al., 2009, and are the sum of DMHg and MMHg.

[e]Likely includes anomalously high results.

equatorial Pacific Ocean (Mason and Fitzgerald, 1990, 1993). Their presence has been confirmed for the Atlantic Ocean, Mediterranean Sea, and estuaries (Cossa et al., 1994; Mason and Sullivan, 1999; Mason et al., 1998). Likewise, the production and supersaturation of Hg^0 is well documented in fresh and salt waters since the initial papers were published by Vandal et al. (1991) for lakes and Kim and Fitzgerald (1986) for the equatorial Pacific Ocean. As **Figure 7** shows, the cycling of Hg^0 and MMHg is intimately linked by their competing and critical roles in the aquatic biogeochemistry of mercury (substrate hypothesis). Notice that, in general, the speciation, transformation pathways, reactions and processes can be connected to reactive mercury. This reactant or 'substrate' should be viewed broadly to encompass labile inorganic and organically associated mercury species. Sources include atmospheric deposition/exchange, watersheds, riverine inputs, sewage and other human-related discharges.

Using **Table 11** as background and **Figure 7** as a guide, important features associated with mercury cycling in all natural waters, but especially seawater, are reemphasized and highlighted in the following summary:

1. The principal source of the toxic species, MMHg, in marine and many freshwater aquatic systems is in situ biologically mediated conversion of labile reactive mercury. As discussed, SRB have been implicated as the primary synthesizers (Compeau and Bartha, 1985; Gilmour and Henry, 1991; Winfrey and Rudd, 1990), though recent studies suggest that iron-reducing delta-Proteobacteria can methylate (Fleming et al., 2006; Kerin et al., 2006), and may even be the dominant methylators in low-sulfate environments (Hammerschmidt et al., 2006). The mechanisms of mercury methylation are still not understood, as is demonstrated by the presence of DMHg in some environments (i.e., water and sediments; Fitzgerald et al., 2011; Kirk and Louis, 2009) but whose role is not known. The bioamplification of MMHg in the aquatic food chain yields concentrations in fish that are often more than a million times greater than its levels in water. Many freshwater systems also receive significant inputs of MMHg from their watersheds, particularly wetlands (e.g., Hultberg et al., 1994; Hurley et al., 1995; St Louis et al., 1996). Salt marshes can also be prolific generators of MMHg, but do not appear to be larger sources than coastal sediments (Langer et al., 2001). They are, however, important nurseries for many aquatic organisms and could represent locations of significant MMHg accumulation in the early life stages of some fish species.
2. Hg^0 is an important species in air and water, and in situ direct reduction of labile reactive mercury by biotic (i.e., bacterial) and abiotic (i.e., photochemical) means is a principal pathway for its aqueous production (Amyot et al., 1994, 1997; Costa and Liss, 1999; Rolfhus, 1998); biological demethylation mechanisms (see **Figure 7**) yield small amounts of Hg^0 (Mason et al., 1993). The mechanisms of reduction are unclear and the focus of current study. The reverse reaction, oxidation of Hg^0, also occurs (e.g., Amyot et al., 1997; Lalonde et al., 2001). Thus, ambient Hg^0 concentrations can be expected to vary in space and time in response to changes in the forces that drive the reduction and oxidation reactions (e.g., bacterial activity, light, temperature, DOC, total mercury). Examples of diel and seasonal variations in Hg^0, consistent with this view, are becoming more common in the literature (e.g., Amyot et al., 2001; Andersson et al., 2008b; Balcom et al., 2004; Lindberg et al., 2000; O'Driscoll et al., 2003; Rolfhus and Fitzgerald, 2001; Soerensen et al., 2010a,b; Tseng et al., 2003; Tseng et al., 2004).
3. Reiterating, in situ Hg^0 production (natural waters are generally supersaturated) and emissions to the atmosphere are major processes; they exert a first-order (primary) control on the overall biogeochemistry and bioavailability of mercury in aqueous systems, and the water–air fluxes must be considered in global/regional atmospheric and aquatic biogeochemical models of the mercury cycle; the reduction reactions (leading to aqueous emissions of Hg^0) are recycling mercury derived from both natural and anthropogenic sources of mercury, and thereby, extending the lifetime of pollutant and natural mercury in active reservoirs.
4. The aqueous production of Hg^0 competes for reactant (i.e., labile reactive mercury) with the in situ biological synthesis of MMHg; thus, water bodies with a large production of Hg^0 will have less bioavailable mercury, smaller amounts of MMHg in biota and reduced mercury accumulation in the sediment (Fitzgerald et al., 1991; Rada et al., 1993; Wiener et al., 1990b).
5. Given the affinity of Hg^{2+} for sulfur (i.e., sulfhydryl groups) and its ability to form very stable organomercury chelates, organic complexation will exert an important control on the bioavailability of mercury.
6. Inorganic complexation with sulfur is a primary reaction in reducing environments. This reaction may occur in oxygenated waters where, for example, microenvironments develop such that oxygen is depleted and sulfate reduction takes place. This is one possible explanation for the presence of MMHg and DMHg in ocean surface waters. There is a triad of competing ligands for free mercury in most aqueous systems. Organic ligands compete with chloride in saltwater and with hydroxide in freshwater, while sulfur becomes especially competitive as oxygen levels decline, and SRB activity increases.

As a point of analytical and environmental interest, Hg^0 is more readily measured in natural waters than MMHg. Since the in situ production of MMHg and Hg^0 is proportional to the supply of reactive mercury, a comprehensive understanding of the aqueous Hg^0 cycle and its temporal and spatial patterns may provide a means to constrain and improve predictive models for the aquatic and atmospheric biogeochemistry of mercury and MMHg in natural waters. For a sense of the potential geochemical benefits from automated Hg^0 measurements, the reader is referred to some recent field studies of Hg^0 (e.g., Amyot et al., 2001; Andersson et al., 2011; Balcom et al., 2000; Lindberg et al., 2000).

11.4.5.1 Environmental Mercury Methylation

Given the importance of in situ synthesis of MMHg (and DMHg) through conversion of less toxic mercury species and its prominent role in the aquatic cycling of mercury (**Figure 7**), aqueous mercury methylation merits added consideration. As

outlined, bacterial mediation enhances the rates at which mercury, a 'soft acid,' can form alkylated species in aquatic environments. This extraordinary interaction and its potential consequences have provided the rationale for much environmentally related mercury research over the past three decades. Indeed, the biologically mediated synthesis of alkylated mercury species can readily account for most of the MMHg accumulating in biota, especially large fish, in most marine and freshwaters (Benoit et al., 2003; Fitzgerald and Watras, 1989; Hammerschmidt et al., 2004; Rolfhus and Fitzgerald, 1995; Watras et al., 1994; Wiener et al., 1990a).

11.4.5.1.1 Nearshore regions

The nearshore environment provides a useful biogeochemical framework for outlining current knowledge regarding mercury methylation in aqueous systems. Mechanistically, recent work in freshwaters and nearshore sediments has not only pointed to SRB as methylating agents, but transition regions between oxygenated and anoxic conditions (e.g., low oxygen/hypoxic) as the principal sites of MMHg production (e.g., Gilmour and Henry, 1991; Hammerschmidt and Fitzgerald, 2004; Hammerschmidt et al., 2004; Langer et al., 2001; Watras et al., 1994). While mercury methylation does occur in the water column and is especially important throughout most of the oceans (i.e., pelagic regions; e.g., Topping and Davies, 1981), the major sites for production are associated with particles and depositional environments such as lake and coastal/estuarine sediments, wetlands, and marshes (Gilmour et al., 1998; Hammerschmidt et al., 2006; Langer et al., 2001; Watras et al., 1994). Microbial production of MMHg in sediment is influenced by a number of environmental factors that affect either the activity of methylating organisms (i.e., SRB) or the availability of inorganic mercury for methylation. For example, recent studies of MMHg levels in bulk surface sediment (e.g., Benoit et al., 1998a; Gilmour et al., 1998; Hammerschmidt and Fitzgerald, 2004; Krabbenhoft et al., 1999; Mason and Lawrence, 1999; Sunderland et al., 2006) have shown dependencies on inorganic mercury, organic matter, and sulfide. In marine and estuarine sediments, where seawater provides ample sulfate, rates of sulfate reduction are influenced mostly by availability of organic matter and temperature (Skyring, 1987). King et al. (1999, 2000, 2001) have demonstrated that the rate of mercury methylation is closely related to that of sulfate reduction.

Intensive examination of the genomes of SRB and other methylating bacteria has recently revealed two genes (hgca and hgcb) which appear to be necessary for biological methylation in anaerobes (Parks et al., 2013). The presence/absence of these genes appears to explain why some bacterial species and strains are capable of methylating Hg, but others are not (Gilmour et al., 2011).

Estuarine/marine systems that are highly productive or receive autochthonous inputs of organic matter are prime locales for enhanced rates of mercury methylation and ecosystem exposure to MMHg. However, recent studies have illustrated that although significant mercury methylation occurs in such environs, production of MMHg is attenuated by accumulation of sulfide, the metabolic by-product of sulfate reduction (**Figure 8**; Gilmour and Henry, 1991). In estuarine and marine sediments, where activity of SRB is high and largely

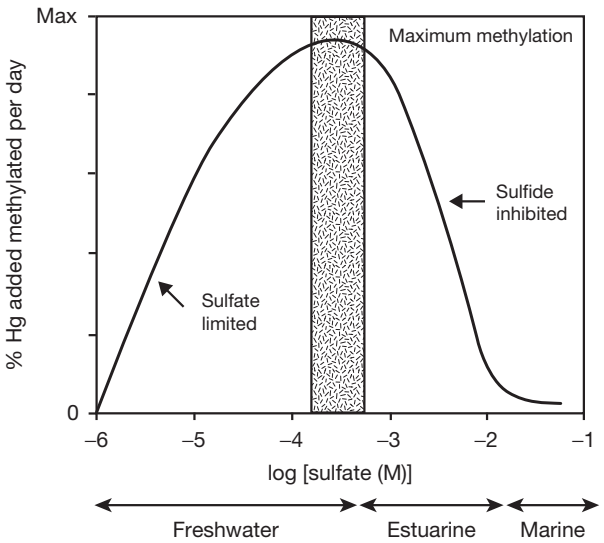

Figure 8 Sulfate/sulfide controls on mercury methylation in aquatic environments – the 'Gilmour curve.' At relatively low sulfate concentrations (most freshwaters), methylation of mercury is limited by the rate of sulfate reduction. At higher sulfate concentrations (saltwaters), sulfide buildup from relatively high rates of sulfate reduction results in decreased bioavailability of mercury. Reproduced from Langer CS, Fitzgerald WF, Visscher PT, and Vandal GM (2001) Biogeochemical cycling of methylmercury at Barn Island Salt Marsh, Stonington, CT, USA. *Wetlands Ecology and Management* 9: 295–310; Gilmour CC and Henry EA (1991) Mercury methylation in aquatic systems affected by acid deposition. *Environmental Pollution* 71(2–4): 131–169.

independent of sulfate, sulfide inhibition of mercury methylation is clearly demonstrated by the inverse relationship with sulfate. In contrast, mercury methylation in freshwater systems is directly related to sulfate, which limits SRB metabolism. Hence, maximum mercury methylation occurs in sediments where organic matter and sulfate are sufficiently high as to stimulate SRB metabolism, but not so high as to cause accumulation of sulfide that inhibits the availability of mercury for methylation (Gilmour and Henry, 1991, **Figure 8**, the 'Gilmour curve').

A mechanism by which sulfide affects methylation of mercury has been proposed by Benoit et al. (1999a,b, 2001a,b). Sulfide affects the chemistry of inorganic mercury in sediments by precipitating it as solid mercuric sulfide and forming dissolved mercury–sulfide complexes, including HgS^0, HgS_2^{2-}, and $HgHS_2^-$. HgS^0 is a major dissolved mercury–sulfide complex when sulfide is $<10^{-5}$ M and charged complexes, mainly as $HgHS_2^-$, are dominant at greater levels (**Figure 9**; Benoit et al., 1999a). The mechanism for uptake of inorganic mercury by methylating bacteria is not known, though the research of Benoit et al. points to diffusion of neutrally charged HgS^0 through the cellular membrane as the key factor. As a result, maximum rates of mercury methylation occur in sediments where SRB activity is significant but the accumulation of sulfide is minimized, thereby favoring speciation of dissolved Hg–S complexes as HgS^0.

Sulfide oxidation occurs both microbially and abiotically. In coastal sediments that are not subject to water column anoxia, burrowing animals mix the upper few centimeters of

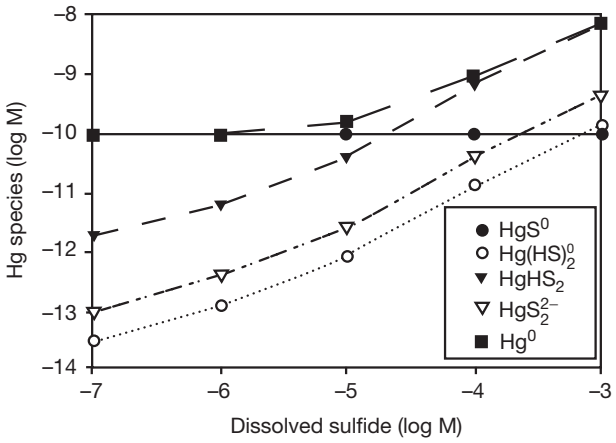

Figure 9 Dissolved mercury speciation in sediment pore waters as a function of sulfide concentration. Note that the most bioavailable form, HgS^0, is the dominant chemical form at log $S \lesssim (-4.7)$. Reproduced with permission from Benoit JM, Gilmour CC, Mason RP, and Heyes A (1999) Sulfide controls on mercury speciation and bioavailability to methylating bacteria in sediment pore waters. *Environmental Science & Technology* 33(6): 951–957.

sediment (i.e., bioturbation), homogenizing the sedimentary solid-phase and pore-water constituents (e.g., Gerino et al., 1998). In doing so, underlying anoxic (i.e., sulfidic) sediments are mixed with overlying oxic sediments, thereby minimizing accumulation of sulfide via dilution and abiotic and microbially mediated oxidation reactions. Sulfide-oxidizing bacteria (SOB) are chemolithotrophs that use sulfide as a source of energy and reducing power. Bioturbation also can stimulate SRB activity by translocating organic matter from surface sediments to depth (Gerino et al., 1998; Hines and Jones, 1985; Skyring, 1987). Hence, bioturbation of estuarine sediments likely stimulates mercury methylation by both enhancing SRB activity and minimizing accumulation of sulfide. Biologically mediated reworking of coastal/estuarine sediments, in general, keeps some portion of the historic (buried) inventory of anthropogenic mercury ('mercury pollution legacy') active (e.g., Benoit et al., 2009; Shull et al., 2009). Given that legacy mercury can be methylated and mobilized in the coastal zone (unlike in lakes), a significant delay is likely between reductions in modern loadings and expected declines in MMHg in the fish stock. This unfortunate expectation for marine systems must be emphasized when considering the expected and observable benefits from 'zero mercury use' environmental legislation and remediation efforts.

In sediments that are less bioturbated, SOB promote mercury methylation by minimizing accumulation of sulfide. These bacteria proliferate in redox transition zones overlying SRB. By consuming sulfide, SOB minimize its accumulation, promoting speciation of mercury–sulfide complexes as HgS^0 and facilitating uptake of inorganic mercury by proximal SRB. The well-defined relationships between redox transition zones, rates of mercury methylation, and MMHg distributions in salt marsh sediments are illustrated in **Figure 10** (Langer et al., 2001). These results are consistent with those predicted by the hypotheses of Benoit et al. (1999a,b). Clearly, the diverse chemistry and microbiology of the redox transition zone makes it an important location for MMHg synthesis in sediments. Thus, and as outlined, there is a triad of competing controlling reactions involving mercury loadings, organic matter, and sulfur that affect the bioavailability of mercury to methylating bacteria.

Demethylation in the water column and sediments is receiving increasing attention. Both abiotic (e.g., Sellers et al., 1996, 2001) and biotic (e.g., Barkay et al., 2003; Hintelmann et al., 2000; Kritee et al., 2009; Marvin-Dipasquale and Oremland, 1998; Marvin-Dipasquale et al., 2000; Pak and Bartha, 1998) processes are implicated. The result is that MMHg accumulation in aquatic systems represents a balance between methylation, bioaccumulation, and the demethylation processes. In sediments, MMHg decomposition is particularly important, and it is possible that some sediments represent net sinks, rather than net sources, for MMHg in the water column.

Most recently, Hammerschmidt, Fitzgerald, and coworkers (Fitzgerald et al., 2011) have been conducting comprehensive investigations of the biogeochemistry and speciation of Hg in sediments and waters on the continental margin of the northwest Atlantic Ocean (i.e., off New England). Among their findings are oceanographically consistent distributions for MMHg and DMHg in the waters of the shelf and slope. Results from three oceanographic cruises (2008–2010) suggest that total Hg in filtered seawater is relatively uniform throughout the study area. In contrast, dissolved MMHg increases typically with depth and DMHg is present in waters near the sediment–water interface on the shelf. Peaks of MMHg and DMHg in slope water are consistent with mobilization from sediment. These distributions suggest that both MMHg and, uniquely, DMHg are produced and mobilized from deposits on the continental margin. MMHg gradients on the shelf yield estimates for benthic MMHg fluxes that are similar to those determined in other coastal studies. Comparable distribution patterns were found by Kirk and Louis (2009) at stations in the Canadian Arctic Archipelago and Hudson Bay. Although, these new and exploratory results require confirmation, analogous sedimentary production and mobilization in other continental margins worldwide would represent an important source of methylated species to the marine environment.

11.4.5.1.2 Open-ocean mercury cycling

In contrast to the nearshore, mercury methylation in the water column is thought to be the primary source of MMHg in the open ocean, though lateral inputs from continental shelves are also potentially important sources (Hammerschmidt and Fitzgerald, 2006). As noted above and shown in **Table 11**, DMHg is found in seawater, but has not been commonly observed in freshwaters (Mason and Fitzgerald, 1993; Mason and Sullivan, 1999; Mason et al., 1993). Indeed, MMHg is the predominant alkylated species in temperate lakes, while DMHg and MMHg are both detectable constituents of the dissolved mercury pool in ocean water. The unique presence of DMHg in seawater prompted Mason and Fitzgerald (1993, 1996) to propose the following reaction sequence: where DMHg would be the principal product from the methylation of inorganic mercury with MMHg and Hg^0 derived from the decomposition reactions (see p. 24). The primary source of Hg^0 in aqueous systems, however, remains the in situ direct reduction of labile reactive mercury by biotic (i.e., bacterial)

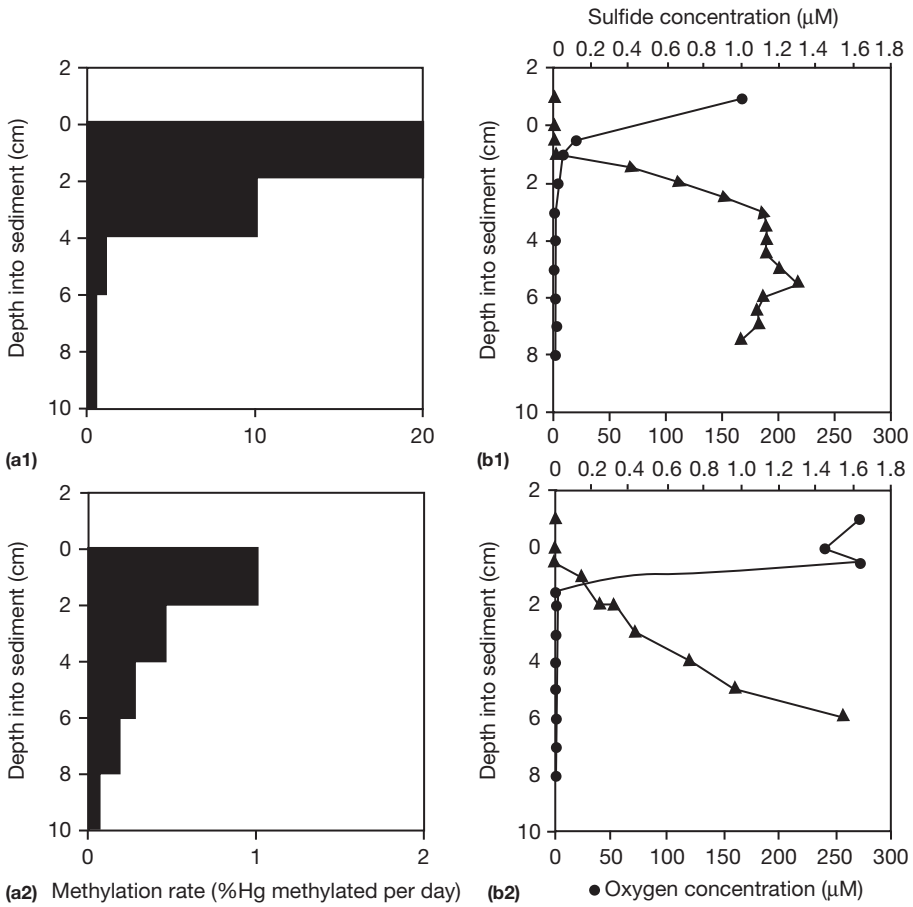

Figure 10 Vertical profiles of methylation rates (a1, a2) and sulfide/oxygen concentrations (b1, b2) in the sediments of sandy (1) and muddy (2) sites in a salt marsh (Barn Island, Connecticut, USA). Maximum methylation occurs in the top 2 cm of these sediments and is coincident with the redox transition zone. Note also that the rates are an order of magnitude faster in the sandy sediments. Reproduced with permission from Langer CS, Fitzgerald WF, Visscher PT, and Vandal GM (2001) Biogeochemical cycling of methylmercury at Barn Island Salt Marsh, Stonington, CT, USA. *Wetlands Ecology and Management* 9: 295–310.

and abiotic (i.e., photochemical) processes (Figure 7). Decomposition is the principal loss term for DMHg, while particulate scavenging and decomposition are important sinks for dissolved MMHg. This view of mercury cycling in the ocean is very speculative. DGM formation has been little studied, and the organisms responsible for methylation in the open ocean are not known (nor have the pathways been elucidated). New enriched isotope spiking and incubation experiments (e.g., Lehnerr et al., 2011; Monperrus et al., 2007) have suggested that the pathways for Hg species formation and destruction are multifold, and that there may be rapid interchange between all four of the principal Hg species in seawater.

11.4.5.1.3 Open-ocean mercury profiles

An appreciation of the challenges of ultra-trace metal investigations can be gained from a consideration of mercury speciation and distributional information for open ocean. A classic vertical distributional profile for mercury in the northeast Pacific Ocean is shown in Figure 11 (Gill and Bruland, 1987). As expected with a biogeochemically active element, mercury shows a nonconservative distribution, one that is

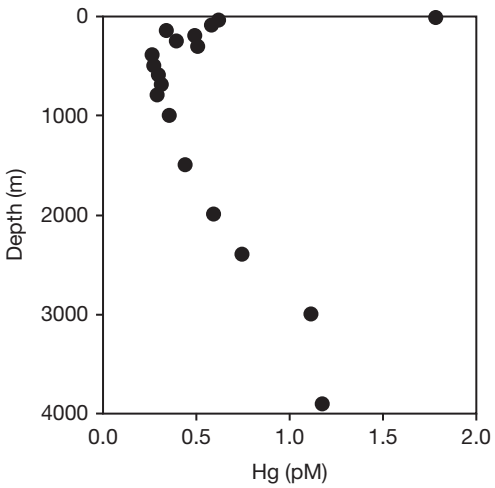

Figure 11 Vertical profile of total dissolved mercury in the northeast Pacific Ocean. Reproduced from Gill GA and Bruland KW (1987) Mercury in the northeast pacific. *Eos, Transactions American Geophysical Union* 68: 1763, from the Vertex VII cruise, station T7, August 6–10, 1987.

not governed by simple mixing of ocean waters. Total mercury concentrations range from 1.8 pM at the surface to 0.3 pM in the upper ocean minimum. The atmospheric mercury enrichment in the near-surface waters was captured due to recent rains and short-term stratification. The minimum is indicative of mercury removal via particulate scavenging processes that are biologically mediated. The gradual increase in mercury at depth may reflect regeneration processes. Today, given the analytical improvements since the Gill and Bruland report (e.g., Bowman and Hammerschmidt, 2011), a more comprehensive suite of mercury species can be determined, along more insightful biogeochemical reaction-based explanations for the distributional patterns in space and time. A summary of such extensive mercury measurements appears in Table 11.

An example of data comes from the Third IOC Baseline Trace Metal Cruise, which took place during May–June of 1996 in the equatorial and South Atlantic (Mason and Sullivan, 1999). We selected vertical profiles for mercury species for one station (#8 at 17° S, 25° W) from among six others examined as part of the Mason and Sullivan Program. These data are presented in Figure 12. DMHg, Hg^0 (total dissolved gaseous mercury – the small contribution of DMHg), and total mercury are plotted versus depth. In addition, and as a reference, the distributions of dissolved silicon and salinity are shown. First, the results confirm the presence of methylated mercury species, especially DMHg, and Hg^0 in oxygenated ocean waters. Here, however, and in contrast to the North Atlantic (Table 11), MMHg levels were at the detection level (0.05 pM). Mason et al. (1998) noted, given the uncertainty and the high detection limit (0.5 pM) in their study, that the values reported for MMHg in the North Atlantic may be too high. If these values were greater than for the South Atlantic, this trend would suggest that MMHg is either decomposing or scavenged more rapidly than it is formed. The prominence of Hg^0 (>50%) relative to the total mercury present (average of 2.4 ± 1.4 pM) is a most striking feature. Its abundant presence at depth is consistent with the hypothesis outlined above in which MMHg, which is produced as DMHg, decomposes. A portion of the MMHg is scavenged by particulate matter and Hg^0 is produced as the relatively stable product (under dark conditions) of the decomposition of the MMHg.

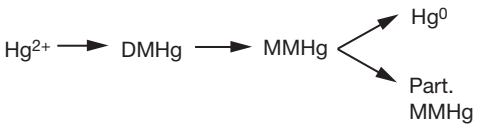

Most DMHg is produced in the near-surface waters, but, as illustrated in Figure 12, little is found in the euphotic zone because DMHg is readily decomposed photochemically. DMHg accumulates in the intermediate depths (see profile) above 1500 m. Below 1500 m, small but significant concentrations (0.02–0.03 pM) occur, but they are considerably smaller

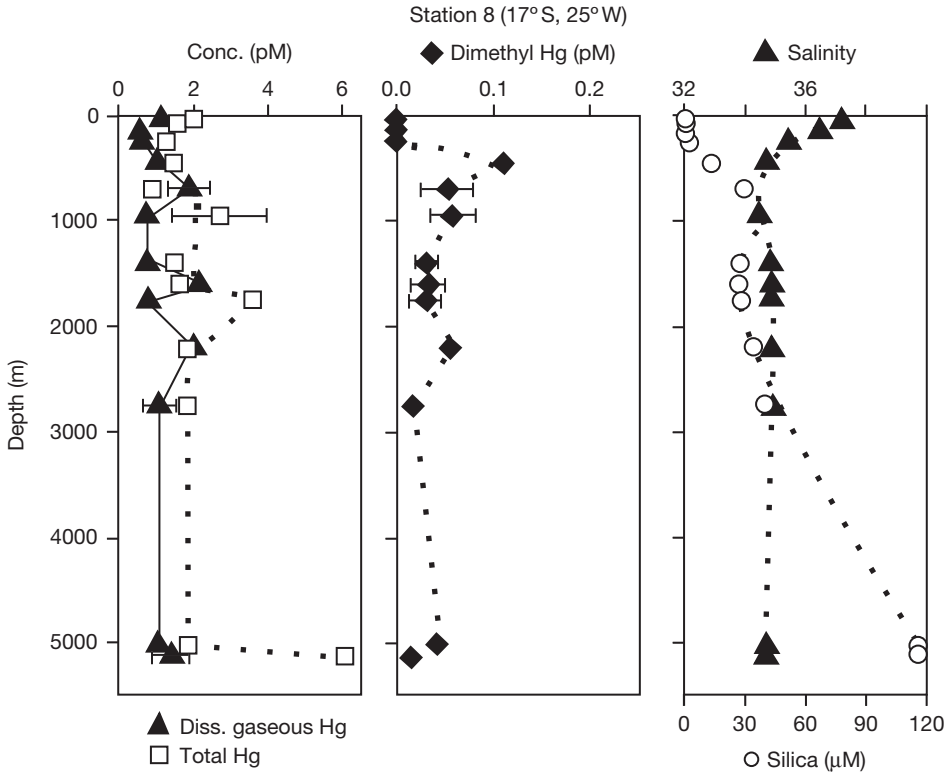

Figure 12 Vertical profiles of total dissolved mercury and mercury species in the South Atlantic, from station 8 of the IOC Baseline South Atlantic Cruise. MonomethylHg was below detection at all depths, while measurable dimethylHg was found within and below the thermocline. Dissolved gaseous mercury, dominated by Hg^0, represents the majority of mercury at many depths at this location. Reproduced with permission from Mason RP and Sullivan KA (1999) The distribution and speciation of mercury in the south and equatorial atlantic. *Deep Sea Research Part II: Topical Studies in Oceanography* 46(5): 937–956.

than values (0.16 ± 0.8 pM) in the source region of the North Atlantic Deep Water (NADW; Mason et al., 1998). While the DMHg decline in the modestly advecting NADW (southward travel time ~100 years to reach the study regions of South Atlantic and equatorial Atlantic) is significant, decomposition rate estimates for DMHg in advecting deep ocean waters imply that sufficient production must be occurring to yield measurable concentrations (Mason and Sullivan, 1999). This production is presumably fueled by the very small transport of carbon from the surface regions to below 1500 m.

In summary, mercury speciation studies in oceanic systems are revealing the complex interactions of this biologically active and reactive element. However, and as emphasized, the spatial and temporal coverage is sparse and many of the biogeochemical insights and hypotheses attempting to explain the behavior and fate of in-marine systems are speculative. Indeed, the challenging and complicated marine biogeochemistry of mercury beckons the curious and innovative. There is much to discover.

As evidence of this, we highlight two additional recent studies. The first is an analysis of total and methylated Hg on samples collected as part of the ongoing CLIVAR Repeat Hydrography Cruises (e.g., Measures et al., 2008; Sunderland et al., 2009). Sunderland and colleagues noted the substantial increase in methylated Hg associated with lower oxygen conditions in the permanent thermocline region of the water column. While this had been broadly observed before (Mason and Fitzgerald, 1990), they used estimates for apparent oxygen utilization and water mass age to demonstrate that the amount of methylated Hg correlated well with rates of organic carbon degradation (rather than just oxygen concentration), forging a link between primary productivity in the surface water with the methylation of Hg in waters below. This trend in elevated methylated Hg in thermocline waters is well described as a result of recent analytical advances (Bowman and Hammerschmidt, 2011) and will be featured in forthcoming publications that will aid the examination of both lateral sources and in situ production of methylated Hg (Cossa et al., 2009; Hammerschmidt and Bowman, 2012). In addition, the ongoing GEOTRACES program will dramatically enhance the number of available data on Hg concentrations and speciation in the ocean. Some intriguing findings from these studies include the observations that deep ocean water methylated Hg levels are both relatively low and do not increase near the sediment–water interface and that the deep Pacific and Atlantic oceans appear to have similar concentrations.

11.4.6 Removal of Mercury from the Surficial Cycle

The work summarized in **Section 11.4.3** notwithstanding, most studies indicate that soils and terrestrial sediments act as net sinks of mercury on timescales of centuries. Such a statement is supported by a review of the mercury content of soils from around the world and supporting data that allow determinations of mercury inventories in various soil horizons (**Table 12**). For comparison, we have estimated the 'excess mercury' inventories (xsHg) resulting from anthropogenic activities using the integrated human emission inventory over the last 100 years estimated by Mason et al. (1994; 947 Mmol total, 447 Mmol globally uniform, 500 Mmol near source). As the continental area of the globe is $\sim 1.5 \times 10^8$ km^2 and assuming uniform distribution and no soil loss, we expect to find from 0.6 mg m^{-2} in remote areas to 2.6 mg m^{-2} in 'non-remote' areas (taken to be one-third of the continental area). Most of the lake sediment data cited fit this range reasonably well. The soil data also display agreement depending on the assumed depth of penetration of the modern mercury signal. Matilainen et al. (2001) found that additions of radioactive ^{203}Hg were quantitatively retained in the organic humus layer of their test soils (O-horizon), and thus we might expect little vertical penetration of the modern signal. This leads to the conclusion that most of the mercury that has been deposited to soils in the last ~100 years is still present in active biogeochemical zones in these systems.

These estimates suggest that human-related contributions to soil loadings of mercury (the excess mercury) are a significant if not always dominant contributor to the total soil column mercury inventory. The natural weathering inputs of mercury to soils may be examined if we assume that the residence time of mercury within soils is similar to that of organic carbon, citing the strong associations between mercury and humic materials already mentioned. Estimates of organic carbon residence within soils are wide ranging and dependent on ecological setting, but may average ~100 years. This approach is supported by the observation that agricultural fields, which experience net losses of organic carbon as a result of human use, show lower mercury inventories than undisturbed soils (Grigal et al., 1994). As 100 years is the approximate timescale over which major human perturbation has taken place, we may subtract the estimated excess mercury loading from the total inventory to arrive at an estimate of the weathering input (**Table 12**). In most instances, the natural and excess loadings are comparable as was the ratio of natural to human-related emissions inventories during that period. Thus, it appears that on millennial timescales, soils are not net sinks for mercury, and release their burden to natural waters through runoff and erosion and to the atmosphere by volatilization and from fires.

Such bulk, integrative studies are supported by short-term studies of mercury loadings to watersheds and subsequent runoff in surface streams. A number of studies have indicated that 70–95% of the mercury deposited under these conditions is retained within the soils of the watersheds. Retention estimates made in this way could be biased low due to the slow release of 'legacy mercury' deposited over the previous decades that increases in magnitude as the total watershed inventory increases (e.g., Aastrup et al., 1991; Kamman and Engstrom, 2002; Krabbenhoft et al., 1995; Lamborg et al., 2002b; Lawson and Mason, 2001; Mierle, 1990; Scherbatskoy et al., 1998; Swain et al., 1992).

The flux of mercury from the continents to the ocean in river runoff has been estimated to be ~1–5 Mmol year^{-1} (Cossa et al., 1996; Mason et al., 1994). While some of this material is volatilized as outlined in **Section 11.4.5**, most is buried in coastal sediments (e.g., Fitzgerald et al., 2000). Deeper coastal sediments or remote, surface lacustrine sediments are of the order of 10–50 ng g^{-1} dry weight. Typical surface sediments, even from systems not receiving direct inputs from

Table 12 Concentrations of mercury in marine and terrestrial deposits and estimates of the anthropogenic mercury inventory (xsHg)

Location(s)	*Soil/sed. Hg conc. (ng g^{-1})*	*Soil/sed. Hg inventory (mg m^{-2})*	*References*
Soils			
Cedar Creek, MN, USA	140 ± 30	0.3 ± 0.2	Grigal et al. (1994)
Organic layer			
0–10 cm	36 ± 7	3.4 ± 0.5	
10–50 cm	11 ± 4	7 ± 4	
Fr. Guiana (rain forest)	122–318		Roulet and Lucotte (1995)
0–30 cm			
Sweden O Horizon	320 ± 10	~1.5	Alriksson (2001)
B Horizon	43 ± 3		
C Horizon	13 ± 1		
Nevada, USA	100–15 000		Gustin et al. (1999)
Lake sediments			
Northern Quebec, Canada	25–450		Lucotte et al. (1995)
N.S. and N.Z. lakes	10–300	0.32–0.95[a]	Lamborg et al. (2002b)
Ice cores			
Fremont glacier, USA	0.002–0.035	~1[a]	Schuster et al. (2002)
Model estimate			
Est. avg. anthrop. signal		0.6–2.6[a]	This work; Mason et al. (1994)
Coastal sediments			
Long Island Sound, USA	<30–600	~30–170[a]	Varekamp et al. (2000)
Northern Adriatic Sea	20–230	~13[a]	Fabbri et al. (2001)
Chesapeake Bay, USA	60–1000	NA	Mason and Lawrence (1999)
Gulf of Cadiz, Spain	~50–250	~75[a]	Cossa et al. (2001)
Gulf of Trieste, Adriatic Sea	100–23 300	~12 000[a]	Covelli et al. (2001)
Florida Bay, USA	~10–236	~1.6[a]	Kang et al. (2000)
San Francisco Bay, USA	20–700 (MMHg: 0–3.5)	NA	Conaway et al. (2003)
S. Baltic Sea	2–340	1.2[a]	Pempkowiak et al. (1998)
S. China Sea, Malaysia	20–127	NA	Kannan and Falandysz (1998)
Anadyr est., Bering Sea, Russia	77–2100	NA	Kannan and Falandysz (1998)
Mouth of St. Lawrence est., Canada	~50–100	~4.5[a]	Gobeil and Cossa (1993)
Greenland	~6–275	NA	Asmund and Nielsen (2000)
Santa Barbara Basin, USA	60–160	NA	Young et al. (1973)
Pelagic sediments			
Arctic Ocean	10–116	NA	Gobeil et al. (1999)
Kara Sea	75–2045	NA	Siegel et al. (2001)
W. Mediterranean	~80	NA	Cossa et al. (1997)
Laptev Sea	25–140	NA	Cossa et al. (1996)

[a]Includes just the anthropogenic, or excess Hg.

industrial activities, can be 10 × the background value. Extreme examples, such as the nearshore sediments of the Gulf of Trieste (NE Adriatic Sea), which receives the river discharge from the mercury mining and mineralized area of Idrija, are also to be found (**Table 12**). This enrichment of surface coastal sediments is not likely to be due to sediment diagenesis as the flux of mass and mercury to the sediment overwhelms upward diffusion (Gobeil and Cossa, 1993). Thus, the excess mercury associated with the enrichments may be used to gauge the impact of human activity on the coastal zone, as shown in **Table 12**. Many of the values estimated here are larger than that expected from release of mercury from watersheds following atmospheric deposition. This estimate was made by assuming ~25% of the continental deposition (250 Mmol) was delivered to 10% of the ocean area (3.6×10^7 km^2) giving 4 mg m^{-2}. This difference is the result of periods when significant nonatmospheric point- and area-source inputs to coastal systems and their watersheds were in effect. Such a condition exists currently, for example, in the case of relatively unrestricted gold mining in Amazonia, resulting in large documented accumulations of mercury in the river sediments and presumably in the coastal sediments of the western equatorial Atlantic (e.g., Lechler et al., 2000). The residence time of mercury in this pool is difficult to estimate given our relatively sparse data, but is likely to be similar to the residence time of the sedimentary material. For example, Herut et al. (1996) found that mercury contamination of the sediments of Haifa Bay, Israel, was disappearing in a manner consistent with sediment remobilization, and could have a half-life in excess of 100 years. These sediments then represent a significant sink for mercury on the global scale. This pool should also be viewed as an environmental and public health concern for the future because this material is concentrated in a relatively small area of the ocean and one that is biologically productive and commercially important (see **Section 11.4.5**).

Finally, open-ocean sediments receive a portion of the mercury deposited to the ocean. Here, the data are particularly sparse and only a handful of studies are available to guide

our discussion. Concentrations of mercury in these materials can be found in Table 12. Given the slow rate of accumulation and rapid recycling of material in the upper ocean, it is to be expected that little of this mercury is of anthropogenic origin, though one study claims to observe surface enrichments consistent with pollution inputs in a relatively nearshore and heavily impacted region (Siegel et al., 2001). Gobeil et al. (1999) found evidence for diagenetic remobilization of mercury along with Fe/Mn and Mercone et al. (1999) have proposed coupled Hg/Se diagenesis and mineral formation under the slow sediment accumulation conditions present in the open ocean. They argued that this remobilization could result in surface enrichments not associated with anthropogenic inputs. We estimate the total amount of mercury associated with marine sediments to be 6×10^7 Mmol (~10 ng of Hg per gram of sediments, 1% organic carbon content and 12×10^{15} tons organic carbon total; Lalli and Parsons, 1993). With inputs of mercury to open-ocean sediments on the order of 1 Mmol $year^{-1}$ (Mason et al., 1994), the sedimentary pool should be expected to represent the primary sink for mercury on million year timescales.

11.4.7 Models of the Global Cycle

Secular change in the global mercury cycle as a result of human activity is one of the major themes in this chapter and a focus of research currently. One of the most insightful research activities in pursuit of this theme has been the development of historical archives of mercury change. As of this writing, this development effort has focused on three archives: peat bogs, lake sediments, and ice cores. All are used to reconstruct historical changes in the flux of mercury from the atmosphere.

Peat cores are generally collected from bogs dominated by *Sphagnum* moss species and from systems that are ombrotrophic ('rain fed'). Under these conditions, it is assumed that the moss is only able to receive mercury from the atmosphere as these systems are isolated from groundwater and geologic inputs other than dust. Mercury delivered to the moss is incorporated in the living material at the surface and remains associated even as the moss continues to grow vertically. Therefore, collection and sectioning of a peat core, followed by dating and mercury analysis, should reveal any changes in the rate of incorporation of mercury into the moss. As discussed by Benoit et al. (1998b), the source of the mercury archived could include mercury associated with rain and dust as well as elemental mercury taken up from the gas phase by the moss. A number of studies have made successful use of the peat archive (e.g., Benoit et al., 1998b; Jensen and Jensen, 1991; Martinez-Cortizas et al., 1999; Norton et al., 1997). There are, however, other reports of variable element mobilities, including the dating isotope ^{210}Pb (e.g., Damman, 1978; Norton et al., 1997; Urban et al., 1990). In our work in Nova Scotia, we found evidence for mobility of lead but not mercury (Lamborg et al., 2002a). We therefore submit that peat archives, or sections of archives, that are dated with ^{210}Pb may yield inaccurate estimates of mercury deposition in the near past, while other dating techniques may result in reliable data. For example, in Nova Scotia, we dated surface peat using a co-occurring moss species *Polytrichum* that develops annual markings on the male gametophytes. The results of that analysis, when compared to lake sediments and rain measurements, indicated that dry deposition of dust or uptake of elemental mercury and/or RGM by the *Sphagnum* may contribute some of the mercury archived in peat, but that the contribution was likely small.

Sediments collected from remote lakes have been the most profitable of the archives studied to date. In most cases, lake sediments are free of diagenetic mobility that plagues the use of peat (e.g., Rydberg et al., 2008), allowing reliable dating and more precise reconstructions (see **Chapter 11.3**). The lake approach does have drawbacks, however, as suitable lakes (small watersheds, simple morphology, and little in/outflow) are often difficult to find in a location of interest. In the higher latitudes of the northern hemisphere, where extensive glaciation was in effect, small seepage lakes tend to be more common, and thus much of this reconstruction work has been performed in Scandinavia, Canada, and the northern United States (e.g. Bindler et al., 2001; Fitzgerald et al., 2005; Lockhart et al., 1998; Swain et al., 1992). Suitable lakes are being investigated currently in additional locations such as in the tropics, the temperate, subpolar southern hemisphere, and the Arctic (e.g., Kirk et al., 2011; Muir et al., 2009; Yang et al., 2010). Extension of lake sediment studies to these new regions should bolster the conclusions from the northern studies. The general picture emerging from the use of lake sediments (and peat) is one of a widespread, global-scale two to four times increase in the amount of mercury delivered from the atmosphere since the advent of the industrial revolution. As noted in **Section 11.4.3.4**, many of the lake systems studied thus far have had slow sediment accumulation rates and watersheds that act as low-pass filters, rendering accurate reconstructions of secular change in Hg deposition in the last few decades very difficult. However, the similarity in timing and scale of the increased mercury deposition across these varied systems leaves little doubt that the signal is real and the result of the substantial impact that human activity has had on the global mercury cycle. Application of this information to modeling efforts (see below) represents an important step forward in our understanding of how the mercury cycle operates.

Ice core archives are receiving increasing attention. In general, these archives are not as useful as sediments due to the relatively low rate of accumulation (usable ice cores are generally to be found in dry high latitudes and accumulate at slow rates). Furthermore, work by Marc Amyot and colleagues (Lalonde et al., 2002) has suggested that mercury deposited in snow is photoactive and may be lost from the media following reduction to elemental mercury. However, as described in **Section 11.4.3**, Schuster et al. (2002) analyzed ice core samples from the relatively rapidly accumulating (~70 cm $year^{-1}$) Fremont Glacier (Wyoming, USA) to reconstruct deposition over the last 270 years. As indicated in **Table 12**, their results are consistent with predictions made for the inventory of anthropogenic mercury made here based on the model of Mason et al. (1994). Therefore, mountain glaciers may represent an important archive for future development. We noted that this glacial core also apparently preserved signals associated with volcanic eruptions that have not been found in lake sediment archives, but that these signals are difficult to interpret as they appear not to be self-consistent. In a more conventional

location for ice core studies, Boutron et al. (1998) used snow blocks to estimate changes in mercury deposition to Greenland over the last 40 years. Their work illustrates other fundamental difficulties associated with studying Hg in ice cores (small sample sizes and exceptionally low levels, <1 pg g^{-1}). Going further back, Vandal et al. (1993) used core material from Dome C in Antarctica to reconstruct mercury accumulation at that location to before the last glacial maximum (*c.*34 ka BP). This unique study found evidence that increased deposition of mercury to Antarctica during that last glacial maximum was attributable to increased evasion from the ocean and suggests that mercury in ice cores may be a useful paleoproductivity proxy.

Seabird feathers may provide a proxy for oceanic mercury secular change (Monteiro and Furness, 1997). This dataset includes feathers retrieved from museum specimens of exclusively pelagic, piscivorous seabirds such as shearwaters and petrels. While there is scatter associated with the values, as should be expected from such a natural archive, an increase of $\sim 3\times$ between 1885 and 1994 can be seen in the mercury concentration of the feathers. Furness, Monteiro and coworkers have extended their work to include studies on the movement of mercury within living birds and the relationship between prey concentrations of mercury and those observed in the birds' feathers (Monteiro and Furness, 2001; Monteiro et al., 1998), which aid in the interpretation of the feather record. This approach has so far been applied to the NE Atlantic (Azores), and should be extended to other ocean regions.

A number of mathematical models have been developed to test the consistency of a variety of environmental mercury data sets as well as aid in generating testable hypotheses concerning those aspects of the global mercury cycle that are difficult to observe directly (Bergan and Rodhe, 2001; Bergan et al., 1999; Holmes et al., 2010; Hudson et al., 1995; Lamborg et al., 2002a; Lantzy and MacKenzie, 1979; Mason et al., 1994; Millward, 1982; Seigneur et al., 2003; Selin et al., 2008; Shia et al., 1999; Soerensen et al., 2010b; Strode et al., 2007; Sunderland et al., 2008). The earliest efforts were limited by the general lack of high-quality data available at the time. Mason et al. (1994) therefore can be said to be the first global mercury model capable of providing meaningful insight into the whole cycle. The findings of MFM, including their reconstruction of the cycle in its preindustrial and modern forms, have been illustrated (**Figure 2**) and discussed in **Section 11.4.1**. As demonstrated, the atmospheric deposition predictions from MFM can be compared to anthropogenic mercury inventories in soils and sediments and appear to accurately predict the flux of mercury from the atmosphere to these archives. Additional insights from MFM include an atmosphere/ocean system that is nearly balanced, indicating the influential role of oceanic evasion in redistributing and sustaining the lifetime of mercury at the Earth's surface. Furthermore, MFM found that anthropogenic activities should have tripled the current atmospheric deposition of mercury, resulting in a tripling of the amount of mercury entering terrestrial and marine ecosystems. As indicated by the lake sediment archives, this is what is found. Finally, the MFM model estimated that only 50% of the mercury emitted to the atmosphere as a result of human activities is able to participate in the global cycle, and that the remaining mercury is removed from the atmosphere close to the source. Thus, the MFM treatment describes the current condition of the mercury cycle as one significantly perturbed by human activity on local, regional, and global scales.

As with any modeling effort, MFM was partially supported by a number of assumptions based on, in some cases, scant information. Since MFM, several other modeling efforts have sought to address particular hypotheses concerning some of these assumptions. For example, Hudson et al. (1995) included additional reservoirs to their simulated ocean than were used in MFM in an effort to gauge the importance of ocean mixing in modulating mercury increases in the environment. They also introduced a more complex emissions source function indexed to CO_2 that released less mercury overall than in MFM, and did so in a nonlinear fashion. The conclusions from this work were quite similar to MFM but did indicate that ocean mixing should be considered an important process in the global-scale biogeochemistry of mercury. Perhaps most importantly, ocean mixing increases the size of the oceanic pool and as a result increases the predicted residence time of mercury in the ocean. An increased oceanic residence time could result in an increased overall rate of mercury methylation, particularly as much of this time would be spent in the lower oxygen/microbially active region of the permanent oceanic thermocline. Additional consideration of the oceanic biogeochemistry of mercury by Mason and Fitzgerald (1996) support this model view, particularly as an explanation for local imbalances in the air–sea exchange of mercury in certain regions such as the equatorial Pacific. Hudson et al. (1995) were also the first authors to directly compare their results to those provided by the lake sediments and noted, among other findings, that emissions from gold and silver mining prior to 1900, predicted to be significant, were not to be found in the archives.

Three other global models (Bergan and Rodhe, 2001; Bergan et al., 1999; Shia et al., 1999) focused on the atmospheric aspects of the global cycle and placed constraints on which of the several chemical mechanisms proposed for elemental mercury oxidation are likely to be important at this scale. Particularly noteworthy are the efforts by Bergan and colleagues, who exploited the data on interhemispheric concentrations of elemental mercury in the air. Exchange between the two hemispheres is relatively slow ($\sim$1.3 years) due to physical forcing, but yet the north/south gradient of elemental mercury is relatively weak (Fitzgerald, 1995; Lamborg et al., 1999; Slemr and Langer, 1992). As the emissions of mercury in the northern hemisphere are estimated to be larger than in the south, Bergan and colleagues used gradient and mixing time information to place constraints on the atmospheric lifetime of mercury. More recently, we extended this approach through inverse box modeling (Lamborg et al., 2002a), which used the gradient and lake sediment data explicitly to constrain both the atmospheric lifetime as well as aspects of the oceanic cycle including evasion, particle scavenging, and burial. This particular model (the global/regional interhemispheric mercury model, or GRIMM) suggested that evasion from the ocean is less than that estimated in MFM and that the ocean is a net sink.

Most recently, the latest laboratory information regarding elemental Hg oxidation (see **Section 11.4.4**) and the influence of RGM on dry deposition of Hg have been incorporated into high spatial resolution atmospheric general circulation models that also include soil and ocean chemistry

(Holmes et al., 2010; Selin et al., 2008; Smith-Downey et al., 2010; Strode et al., 2007). Laboratory results suggesting that the lifetime of elemental Hg in the atmosphere with respect to oxidation and deposition (~0.6 year) is much shorter than previously thought were successfully incorporated and were demonstrated to be consistent with atmospheric distributions on a global scale. To reconcile short atmospheric lifetimes of elemental mercury with interhemispheric distributions that look like a much longer lived gas, the new models emphasize the importance of ocean evasion in facilitating global atmospheric transport.

11.4.8 Developments in Studying Mercury in the Environment on a Variety of Scales

11.4.8.1 Acid Rain and Mercury Synergy in Lakes

As noted, sulfate reduction is thought to be the driving biogeochemical process behind mercury methylation in many ecosystems. In freshwaters that are relatively low in sulfate, recent increases in sulfate deposition associated with the acid rain phenomenon are hypothesized to result in increased rates of sulfate reduction and subsequently in mercury methylation (e.g., Gilmour and Henry, 1991; see **Chapter 11.10**, for details on acid rain geochemistry). Thus, not only are lakes receiving more total mercury than in the preindustrial past, they may be methylating a greater proportion of this load. Swain and Helwig (1989), for example, have noted that the concentration of mercury in Minnesota fish (usually dominated by MMHg), has increased by 10×, while deposition of mercury has increased by only 3×. Work by Branfireun et al. (1999, 2001) have recreated this phenomenon through sulfate additions to microcosms in the Experimental Lakes Area of Ontario, and there are ongoing efforts to expand this research to watershed/whole-lake scales (D. R. Engstrom, personal communication).

11.4.8.2 METAALICUS

METAALICUS is a project titled *Mercury Experiment To Assess Atmospheric Loading In Canada and the United States*. As described in this chapter, the atmosphere is the principal avenue for the mobilization of mercury in the environment and anthropogenic mercury emissions to the atmosphere, especially from coal combustion, have contaminated all the major reservoirs. We noted the strong interest and support for studies examining linkages between the cycling of mercury in the atmosphere, anthropogenic emissions, deposition to terrestrial systems, and the bioaccumulation of MMHg in freshwaters. We have suggested that there has been much emphasis on freshwater fish contamination at the expense of marine studies, given that the major exposure of humans to MMHg is through the consumption of marine fish and seafood products. Given our concerns as a caveat, we note that many scientists and 'stakeholders' think that an unequivocal connection between direct atmospheric mercury deposition and the levels of MMHg in fish in freshwater or marine systems has not been established. In other words, if mercury deposition is reduced, through, for example, controls on mercury emissions from coal-burning power plants, would MMHg concentrations in fish decline? The METAALICUS team of scientists from the United States and Canada have attempted to empirically address questions of linkages between mercury deposition and the bioaccumulation of MMHg in fish. They conducted a whole ecosystem experiment in which stable isotopes of mercury are added to a lake, its upland watershed and adjoining wetland, and mercury in fish as well as the food chain are examined.

Though the principal fieldwork has been concluded, the work is ongoing and, to date, several papers have been published (Amyot et al., 2004; Babiarz et al., 2003; Branfireun et al., 2005; Graydon et al., 2009; Harris et al., 2007; Hintelmann et al., 2002; Kelly et al., 2003; Lalonde et al., 2003; Southworth et al., 2007; St Louis et al., 2004). Several important findings have arisen from the project. First and foremost, the fish responded very quickly to Hg added directly to the lake. Though intuitively this was to be expected, such a direct connection between deposition and accumulation in fish had not been observed. Other important findings include the relative lack of influence from Hg added to the lake's watershed. Particularly surprising was the lack of appearance for Hg added to the lake's wetland, which is in direct hydraulic contact with the lake. These findings suggest that the ability of the watershed, both upland and wetland, to retain Hg has been underestimated. However, there has been a slow but measurable release of Hg from the upland, indicating that while slowed, the movement of Hg within the whole lake system has not been halted. Such findings will be enormously helpful for predicting the response of lakes in a future where Hg deposition has been lowered, but where legacy Hg still remains within watersheds. We wish to reemphasize that in productive nearshore regions of marine ecosystems, the legacy of pollution derived mercury in the surficial sediments is likely to predominate over 'new mercury' as a substrate for methylation. The intense bioturbation in coastal marine sediments can keep much historical mercury active, relative to the more quiescent sediments of lakes. Unfortunately, the mechanistic predictions for declines in fish mercury levels following controls on mercury emissions, derived from the successful METAALICUS program, may not be applicable to the marine environment.

The detailed mechanistic studies represented in METAALICUS, designed to illustrate the connections between atmospheric deposition and Hg accumulation in fish, have recently been supported in a broad-scale way (Hammerschmidt and Fitzgerald, 2005). This study noted a highly significant correlation between the methylHg content of mosquitoes (which are aquatic predators during their larval life stages) and local atmospheric Hg deposition.

11.4.8.3 Fractionation of Mercury Isotopes

With improvements in inductively coupled plasma-mass spectrometry, there has been a flurry of research regarding fractionation of the stable isotopes of mercury. This work was spurred by the initial demonstration that accurate and precise measurements of Hg isotopes could be made in natural media, starting with meteorites, rocks and ores (e.g., Evans et al., 2001; Gehrke et al., 2009; Hintelmann and Lu, 2003; Lauretta et al., 2001; Sherman et al., 2009; Smith et al., 2005). As analytical improvements are continuing and the amount of Hg needed to make the measurements has decreased, more media are now being examined and experiments conducted, both of which are

revealing surprising results. Chief among these is the observation of mass-independent isotope fractionation (MIF), which has been observed in only a few elements (Bergquist and Blum, 2007; Jackson et al., 2008). However, mass-dependent fractionation (MDF) has been documented as well, and we summarize a few of the findings for both kinds of behavior below.

As with many other isotope systems, one of the most attractive uses of isotopes is to identify sources of material in the environment, or apportion relative contributions when more than one source is possible. The isotopic composition of coal, one of the leading anthropogenic sources of Hg to the environment, has been measured in samples from around the world and reveals large ranges in both MDF and MIF (e.g., Biswas et al., 2008; Evans et al., 2001). By combining MDF and MIF signals, Biswas and colleagues were able to identify some sources of coal that had unique isotopic signatures, but there were no large-scale trends to be discerned (for example, United States vs. China). Isotope tracing did work well in confirming the sources of Hg in San Francisco Bay, however, as processing of ore in the region for use in gold mining produced isotopically light elemental Hg and relatively heavier mine wastes (Gehrke et al., 2011). The isotopic signal at the northern end of the Bay reflected the light material used in gold mining in the Sierra Nevada Mountains, while Hg found in the sediments of the south end of the Bay were much closer to that of the waste which was weathering in the New Idrija region. In general, however, source apportionment has not yet been as fruitful an application of Hg isotopic trends as initially hoped.

Identification of important biogeochemical processes does, however, appear to be an excellent application of Hg isotopic systematics. This is due in large part to the connection between the MIF phenomenon and photochemistry. The seminal study of Bergquist and Blum (2007) demonstrated that the MIF signal can be imprinted on aqueous Hg during either photochemical reduction of Hg(II) to Hg^0, or the photochemical degradation of MMHg to Hg(II). Furthermore, they identified a MIF signal in fish that bore the same properties as the photodemethylation process observed in the lab. While some have argued that MIF might be happening within foodwebs and therefore not reflect aqueous photochemistry (Das et al., 2009), the nominal explanation is that residual MMHg left behind following demethylation in natural waters is the source of Hg in fish. While this is somewhat unsurprising at first glance, the water–fish MIF connection was recently used to posit that coastal and pelagic fish receive their Hg from two different and separate pathways (Senn et al., 2010). As the photochemistry that generates MIF and MDF in natural waters leads to the production of at least some of the Hg^0 that evades to the atmosphere, one might anticipate that fractionation signals will be observed in the air and precipitation. Such signals have been documented (e.g., Carignan et al., 2009; Estrade et al., 2010; Gratz et al., 2010; Sherman et al., 2010), and might result from fractionation in the air or in some industrial emissions as well as in natural waters. Finally, *in vitro* bacterial fractionation of Hg during reduction and methylation has been documented (e.g., Kritee et al., 2008, 2009) and offers a tool for directly observing the balance between biological and abiological cycling of Hg in natural waters. However, methods for determining the ambient Hg isotope distribution in the aqueous phase are yet to be proven.

The field of Hg isotopes is still maturing. The number of instances and processes appearing to result in Hg fractionation are still being established. Unfortunately, it is uncertain if these measurements will ultimately be as useful as initially hoped. Regardless, this will be an area of intense research activity in the foreseeable future.

11.4.8.4 Tracing Atmospheric Mercury with ^{210}Pb and Br

As noted in **Section 11.4.4**, an ongoing effort among researchers studying the atmospheric chemistry of mercury is the determination of which reaction mechanisms are most influential in the field. Tracers are exceptionally powerful tools in this regard, as they greatly simplify the process of scaling up individual measurements to a wide range of scales. They are often integrative as well, so that discrete measurements of mercury and tracers in a particular medium at a particular time can be easily generalized to a whole year or area. Two tracers have recently shown some promise in understanding the large-scale behavior of mercury in the atmosphere and in complementary ways: ^{210}Pb and Br.

Lamborg et al. (1999, 2000) have demonstrated a strong correlation between Hg and ^{210}Pb in precipitation from samples collected in remote continental (Wisconsin) and mid-ocean (tropical South Atlantic) locations. The relationship from these collections was very similar and indicates that ^{210}Pb may be a useful tracer of mercury in precipitation. The geochemistry of ^{210}Pb is well described and this tracer has been useful for atmospheric studies of numerous kinds. The correlation between these two species implicates, by analogy, a homogeneous gas-phase oxidation of mercury that is first order as ^{210}Pb is generated from the homogeneous-phase first-order radioactive decay of ^{222}Rn. As the flux of ^{222}Rn to the atmosphere is known and constant, the current flux of mercury to and from the atmosphere can be estimated from Hg/^{210}Pb ratios, and the universality of the ratio used to examine regionality of mercury deposition (Lamborg et al., 2013) .

Two findings suggest that bromine may also be an important tracer and clue in the atmospheric chemistry of mercury. Lindberg et al. (2002) have noted that the advent of mercury depletion events in the Arctic is coincident with the buildup of reactive bromine compounds (such as BrO) in the polar atmosphere. Halogen compounds are potent oxidizers of mercury, stabilizing the Hg(II) created by forming halogen complexes. For example, BrCl is routinely used to oxidize solutions for mercury analysis in the laboratory. It has also been noted that such reactive compounds can be created in situ from sea salt in aerosols in the marine boundary layer (e.g., Disselkamp et al., 1999), supporting the hypothesis contained in Mason et al. (2001) of a rapid oxidation of elemental mercury over the ocean. Roos-Barraclough et al. (2002) presented findings from long peat cores that showed a strong correlation between higher deposition of mercury coincident with higher deposition of bromine over relatively long timescales (centuries). The cause of this correlation is still unknown and may have as much to do with sources of mercury to the atmosphere as well as the atmospheric chemistry of mercury.

11.4.8.5 Mercury and Organic Matter Interactions

Mercury, the quintessential soft metal, forms exceptionally strong associations with natural organic matter (e.g., Mantoura et al., 1978). This behavior has been recognized as influential in a number of aspects of mercury biogeochemistry. For example, lakes have often been shown to have higher mercury in higher DOC waters (e.g., Vaidya et al., 2000). This indicates that watersheds (the principal supply of DOC in lakes) can contribute significant amounts of mercury as well, and that the DOC mobilization from uplands mobilizes mercury and MMHg (Dittman et al., 2010). In addition, higher concentrations of DOC provide enhanced complexation capacity for mercury in the water column of lakes, enhancing mercury solubility and increasing mercury residence within the lake (e.g., Ravichandran et al., 1999). There are also competing effects of DOC on the reduction of mercury within natural waters. Recently, Amyot et al. (1997), Rolfhus (1998), Costa and Liss (1999) and O'Driscoll et al. (2006) have indicated that DOC may act to both enhance and inhibit mercury reduction (and therefore mercury evasion) in both freshwater and saltwater depending on the concentration of organic carbon in the water. The mechanisms for these intricate redox processes are not well known, but DOC is clearly an important master variable.

The magnitude of mercury–organic interactions (strength of the complexes and the abundance of the complexing agents) has been studied through partitioning experiments of various kinds. Mantoura et al. (1978), a frequently cited report, made use of a form of size exclusion chromatography to separate free mercury from organically complexed mercury. Other important work includes that of Hintelmann et al. (1997), who employed dialysis membranes to estimate MMHg partitioning between organic and inorganic complexes, and the work of Benoit et al. (2001c), who used calibrated octanol–water partitioning behavior of mercury species to study mercury-binding ligands in sediment pore waters from the Everglades. For other trace metals, electrochemical techniques have often been used, and one such study has been published for mercury (Wu et al., 1997). Watson et al. (1999) have suggested that the gold stripping electrodes used for this determination do not quantitatively release mercury, making this approach somewhat suspect. Lamborg et al. (2003), who developed a wet chemical analog to the electrochemical approach, found affinity results similar to those of Benoit et al. and the high end of Mantoura et al. from bulk water samples (most of the other studies have been performed on isolated DOC fractions), while Han (Han and Gill, 2005; Han et al., 2006) and Hsu-Kim (Hsu and Sedlak, 2003; Hsu-Kim and Sedlak, 2005) made use of competitive ligands to titrate even stronger, though less abundant, ligand classes. The general assumption has been that it is the reduced sulfur moieties (thiols) in the macromolecules of natural water DOC that are the sites for binding, and recent spectroscopic evidence supports this (Hesterberg et al., 2001; Xia et al., 1999). However, Lamborg et al. (2003) have found ligand concentrations, when normalized to DOC, which suggest mercury-binding functional group abundances on the order of parts per million. This is well below the abundance of reduced sulfur, which is generally found to be in the parts per thousand range. It therefore appears that the locations for mercury binding are rare in the DOC pool but still present in 10–1000 × excess of mercury.

In saltwater, organic matter complexation of mercury may not compete with the more abundant chloride ion (see **Section 11.4.5**). In estuaries, ligand exchange was observed by Rolfhus and Fitzgerald (2001) and Tseng et al. (2001). One result of the exchange of mercury from organic to inorganic complex forms is a general increase in the reactivity of mercury within estuaries. The change in complexation can result in dramatic changes in the reactivity of the mercury as a result (e.g., enhanced Hg^0 production, Rolfhus and Fitzgerald, 2001; enhanced Hg methylation by cysteine, Schaeffer and Morel, 2009).

11.4.9 Summary

In this chapter, we have summarized some of the gains made in understanding the environmental biogeochemistry of mercury since Goldschmidt's groundbreaking work. Much of this advancement has come since the early 1970s, and the growth in mercury research continues at breakneck pace. This is fortunate as there is a need for urgency, we believe, in these endeavors. While human activity has perturbed the mercury cycle by a smaller degree than, for example, lead, the implications for continued perturbation on human and ecological health are enormous.

The way forward will be a fascinating and challenging one. As we have summarized, this is because the biogeochemistry of mercury operates at a variety of time and space scales and in many environmental media. Due to the complexity of the processes and the minute quantities of material often encountered in the environment, future research will also require new hypotheses and new instrumentation. Similarly, and as with so many environmental research efforts, new collaborations among scientific disciplines will be required.

Acknowledgments

Foremost, we thank the editor, Barbara Sherwood-Lollar. Rob Mason and Gary Gill provided some graphs, Todd Hinkley and Johan Varekamp provided guidance for the volcano section. The volcano study was aided greatly by F. LeGuern, CNRS and P. Buat-Menard, University of Bordeaux, France; W. Giggenbach (deceased), DSIR, New Zealand; J. Spedding (deceased), University of Auckland, New Zealand; L.P. Greenland, USGS, C. C. Patterson (deceased) and D. Settle (retired). Chad Hammerschmidt assisted with the sections on methylation. Dan Engstrom, Don Porcella, Jim Wiener, and Kris Rolfhus graciously read drafts and provided many useful suggestions.

References

Aastrup M, Johnson J, Bringmark E, Bringmark L, and Iverfeldt A (1991) Occurrence and transport of mercury within a small catchment-area. *Water, Air, and Soil Pollution* 56: 155–167.

Alleman LY, Church TM, Veron AJ, Kim G, Hamelin B, and Flegal AR (2001) Isotopic evidence of contaminant lead in the South Atlantic troposphere and surface waters. *Deep Sea Research Part II: Topical Studies in Oceanography* 48(13): 2811–2827.

Alriksson A (2001) Regional variability of Cd, Hg, Pb and C concentrations in different horizons of Swedish forest soils. *Water, Air, and Soil Pollution: Focus* 1(3): 325–341.
Amyot M, Auclair JC, and Poissant L (2001) In situ high temporal resolution analysis of elemental mercury in natural waters. *Analytica Chimica Acta* 447(1–2): 153–159.
Amyot M, Gill GA, and Morel FMM (1997) Production and loss of dissolved gaseous mercury in coastal seawater. *Environmental Science & Technology* 31(12): 3606–3611.
Amyot M, Mierle G, Lean DRS, and McQueen DJ (1994) Sunlight-induced formation of dissolved gaseous mercury in lake waters. *Environmental Science & Technology* 28(13): 2366–2371.
Amyot M, Southworth G, Lindberg SE, et al. (2004) Formation and evasion of dissolved gaseous mercury in large enclosures amended with ($HgCl_2$)-Hg-200. *Atmospheric Environment* 38(26): 4279–4289.
Anbar AD (2004) Iron stable isotopes: Beyond biosignatures. *Earth and Planetary Science Letters* 217: 223–236.
Andersson ME, Gardfeldt K, Wangberg I, and Stromberg D (2008a) Determination of Henry's law constant for elemental mercury. *Chemosphere* 73: 587–592.
Andersson ME, Sommar J, Gardfeldt K, and Jutterstrom S (2011) Air-sea exchange of volatile mercury in the North Atlantic Ocean. *Marine Chemistry* 125: 1–7.
Andersson ME, Sommar J, Gardfeldt K, and Lindqvist O (2008b) Enhanced concentrations of dissolved gaseous mercury in the surface waters of the Arctic Ocean. *Marine Chemistry* 110(3–4): 190–194.
Ariya PA and Ryzhkov A (2003) Atmospheric transformation of elemental mercury upon reactions with halogens. *Journal de Physique IV* 107: 57–59.
Asmund G and Nielsen SP (2000) Mercury in dated Greenland marine sediments. *Science of the Total Environment* 245: 61–72.
Babiarz CL, Hurley JP, Krabbenhoft DP, et al. (2003) A hypolimnetic mass balance of mercury from a dimictic lake: Results from the METAALICUS project. *Journal de Physique IV* 107: 83–86.
Baeyens W and Leermakers M (1998) Elemental mercury concentrations and formation rates in the Scheldt Estuary and the North Sea. *Marine Chemistry* 60(3–4): 257–266.
Bagnato E, Aiuppa A, Parello F, et al. (2007) Degassing of gaseous (elemental and reactive) and particulate mercury from Mount Etna Volcano (southern Italy). *Atmospheric Environment* 41(35): 7377–7388.
Bakir F, Damluji SF, Aminzaki L, et al. (1973) Methylmercury poisoning in Iraq – Interuniversity report. *Science* 181(4096): 230–241.
Balabanov NB, Shepler BC, and Peterson KA (2005) Accurate global potential energy surface and reaction dynamics for the ground state of $HgBr_2$. *Journal of Physical Chemistry A* 109(39): 8765–8773.
Balcom PH, Fitzgerald WF, Lamborg CH, et al. (2000) Mercury cycling in and emissions from Long Island Sound. In: Nriagu J (ed.) *11th Annual International Conference on Heavy Metals in the Environment*, Contribution 1045. University of Michigan, School of Public Health, Ann Arbor, MI, 6–10 August.
Balcom PH, Fitzgerald WF, Vandal GM, et al. (2004) Mercury sources and cycling in the Connecticut River and Long Island Sound. *Marine Chemistry* 90(1–4): 53–74.
Banic CM, Beauchamp ST, Tordon RJ, et al. (2003) Vertical distribution of gaseous elemental mercury in Canada. *Journal of Geophysical Research* 108(D9): 4264.
Barkay T, Miller SM, and Summers AO (2003) Bacterial mercury resistance from atoms to ecosystems. *FEMS Microbiology Reviews* 27: 355–384.
Barrie LA and Hoff RM (1985) Five years of air chemistry observations in the Canadian Arctic. *Atmospheric Environment* 19(12): 1995–2010.
Barringer JL and Szabo Z (2006) Overview of investigations into mercury in ground water, soils, and septage, New Jersey coastal plain. *Water, Air, and Soil Pollution* 175(1–4): 193–221.
Beals DI, Harris RC, and Pollman C (2002) Predicting fish mercury concentrations in Everglades marshes: Handling uncertainty in the Everglades mercury cycling model (E-MCM) with a Monte Carlo approach. *Abstracts of Papers of the American Chemical Society* 223: 200-ENVR.
Benesch JA, Gustin MS, Schorran DE, Coleman J, Johnson DA, and Lindberg SE (2001) Determining the role of plants in the biogeochemical cycling of mercury on an ecosystem level. *6th International Conference on Mercury as a Global Pollutant*. Minamata, Japan, October 15–19.
Benoit JM, Fitzgerald WF, and Damman AWH (1998a) The biogeochemistry of an ombrotrophic bog: Evaluation of use as an archive of atmospheric mercury deposition. *Environmental Research* 78(2): 118–133.
Benoit JM, Gilmour CC, Mason RP, Riedel GS, and Riedel GF (1998b) Behavior of mercury in the Patuxent River estuary. *Biogeochemistry* 40(2–3): 249–265.
Benoit JM, Gilmour CC, Heyes A, Mason RP, and Miller CL (2003) Geochemical and biological controls over methylmercury production and degradation in aquatic ecosystems. *Biogeochemistry of Environmentally Important Trace Elements*. *ACS Symposium Series*, vol. 835, pp. 262–297. Washington, DC: American Chemical Society.
Benoit JM, Gilmour CC, and Mason RP (2001a) Aspects of bioavailability of mercury for methylation in pure cultures of *Desulfobulbus propionicus* (1pr3). *Applied and Environmental Microbiology* 67(1): 51–58.
Benoit JM, Gilmour CC, and Mason RP (2001b) The influence of sulfide on solid phase mercury bioavailability for methylation by pure cultures of *Desulfobulbus propionicus* (1pr3). *Environmental Science & Technology* 35(1): 127–132.
Benoit JM, Mason RP, Gilmour CC, and Aiken GR (2001c) Constants for mercury binding by dissolved organic matter isolates from the Florida Everglades. *Geochimica et Cosmochimica Acta* 65(24): 4445–4451.
Benoit JM, Gilmour CC, Mason RP, and Heyes A (1999a) Sulfide controls on mercury speciation and bioavailability to methylating bacteria in sediment pore waters. *Environmental Science & Technology* 33(6): 951–957.
Benoit JM, Mason RP, and Gilmour CC (1999b) Estimation of mercury–sulfide speciation in sediment pore waters using octanol–water partitioning and implications for availability to methylating bacteria. *Environmental Toxicology and Chemistry* 18(10): 2138–2141.
Benoit JM, Shull DH, Harvey RM, and Beal SA (2009) Effect of bioirrigation on sediment–water exchange of methylmercury in Boston Harbor, Massachusetts. *Environmental Science & Technology* 43(10): 3669–3674.
Bergan T, Gallardo L, and Rodhe H (1999) Mercury in the global troposphere: A three-dimensional model study. *Atmospheric Environment* 33(10): 1575–1585.
Bergan T and Rodhe H (2001) Oxidation of elemental mercury in the atmosphere; constraints imposed by global scale modelling. *Journal of Atmospheric Chemistry* 40(2): 191–212.
Bergquist BA and Blum JD (2007) Mass-dependent and -independent fractionation of Hg isotopes by photoreduction in aquatic systems. *Science* 318(5849): 417–420.
Bindler R, Renberg I, Appleby PG, Anderson NJ, and Rose NL (2001) Mercury accumulation rates and spatial patterns in lake sediments from West Greenland: A coast to ice margin transect. *Environmental Science & Technology* 35(9): 1736–1741.
Biswas A, Blum JD, Bergquist BA, Keeler GJ, and Xie ZQ (2008) Natural mercury isotope variation in coal deposits and organic soils. *Environmental Science & Technology* 42(22): 8303–8309.
Black FJ, Paytan A, Knee KL, et al. (2009) Submarine groundwater discharge of total mercury and monomethylmercury to central California coastal waters. *Environmental Science & Technology* 43(15): 5652–5659.
Bloom NS (1989) Determination of picogram levels of methylmercury by aqueous phase ethylation, followed by cryogenic gas chromatography with atomic fluorescence detection. *Canadian Journal of Fisheries and Aquatic Sciences* 46: 1131–1140.
Bloom NS (2000) Analysis and stability of mercury speciation in petroleum hydrocarbons. *Fresenius' Journal of Analytical Chemistry* 366(5): 438–443.
Bloom N and Fitzgerald WF (1988) Determination of volatile mercury species at the picogram level by low-temperature gas chromatography with cold-vapor atomic fluorescence detection. *Analytica Chimica Acta* 208: 151–161.
Bluth GJS, Schnetzler CC, Krueger AJ, and Walter LS (1993) The contribution of explosive volcanism to global atmospheric sulphur dioxide concentrations. *Nature* 366(6453): 327–329.
Bodaly RA, Hecky RE, and Fudge RJP (1984) Increases in fish mercury levels in lakes flooded by the Churchill River diversion, Northern Manitoba. *Canadian Journal of Fisheries and Aquatic Sciences* 41(4): 682–691.
Bone SE, Charette MA, Lamborg CH, and Gonneea ME (2007) Has submarine groundwater discharge been overlooked as a source of mercury to coastal waters? *Environmental Science & Technology* 41: 3090–3095.
Boström K and Fisher DE (1969) Distribution of mercury in East Pacific sediments. *Geochimica et Cosmochimica Acta* 33: 743–745.
Boudala FS, Folkins I, Beauchamp S, Tordon R, Neima J, and Johnson B (2000) Mercury flux measurements over air and water in Kejimkujik National Park, Nova Scotia. *Water, Air, and Soil Pollution* 122(1–2): 183–202.
Boutron CF, Vandal GM, Fitzgerald WF, and Ferrari CP (1998) A forty year record of mercury in central Greenland snow. *Geophysical Research Letters* 25(17): 3315–3318.
Bowman K and Hammerschmidt CR (2011) Extraction of monomethylmercury from seawater for low-femtomolar determination. *Limnology and Oceanography: Methods* 9: 121–128.
Branfireun BA, Bishop K, Roulet NT, Granberg G, and Nilsson M (2001) Mercury cycling in boreal ecosystems: The long-term effect of acid rain constituents on peatland pore water methylmercury concentrations. *Geophysical Research Letters* 28(7): 1227–1230.

Branfireun BA, Krabbenhoft DP, Hintelmann H, Hunt RJ, Hurley JP, and Rudd JWM (2005) Speciation and transport of newly deposited mercury in a boreal forest wetland: A stable mercury isotope approach. *Water Resources Research* 41(6); Art. No. W06016.

Branfireun BA, Roulet NT, Kelly CA, and Rudd JWM (1999) In situ sulphate stimulation of mercury methylation in a boreal peatland: Toward a link between acid rain and methylmercury contamination in remote environments. *Global Biogeochemical Cycles* 13(3): 743–750.

Brunke EG, Labuschagne C, and Slemr F (2001) Gaseous mercury emissions from a fire in the Cape Peninsula, South Africa, during January 2000. *Geophysical Research Letters* 28(8): 1483–1486.

Cadle RD (1975) Volcanic emissions of halides and sulfur compounds to troposphere and stratosphere. *Journal of Geophysical Research* 80(12): 1650–1652.

Carignan J, Estrade N, Sonke JE, and Donard OFX (2009) Odd isotope deficits in atmospheric Hg measured in lichens. *Environmental Science & Technology* 43(15): 5660–5664.

Carpi A and Lindberg SE (1998) Application of a Teflon™ dynamic flux chamber for quantifying soil mercury flux: Tests and results over background soil. *Atmospheric Environment* 32(5): 873–882.

Chiaradia M and Cupelin F (2000) Gas-to-particle conversion of mercury, arsenic and selenium through reactions with traffic-related compounds? Indications from lead isotopes. *Atmospheric Environment* 34(2): 327–332.

Clarkson TW (1997) The toxicology of mercury. *Critical Reviews in Clinical Laboratory Sciences* 34(4): 369–403.

Compeau GC and Bartha R (1985) Sulfate-reducing bacteria – Principal methylators of mercury in anoxic estuarine sediment. *Applied and Environmental Microbiology* 50: 498–502.

Conaway CH, Squire S, Mason RP, and Flegal AR (2003) Mercury speciation in the San Francisco Bay estuary. *Marine Chemistry* 80(2–3): 199–225.

Cooke CA, Balcom PH, Biester H, and Wolfe AP (2009) Over three millennia of mercury pollution in the Peruvian Andes. *Proceedings of the National Academy of Sciences of the United States of America* 106(22): 8830–8834.

Coquery M, Cossa D, and Martin JM (1995) The distribution of dissolved and particulate mercury in three Siberian estuaries and adjacent arctic coastal waters. *Water, Air, and Soil Pollution* 80(1–4): 653–664.

Coquery M, Cossa D, and Sanjuan J (1997) Speciation and sorption of mercury in two macro-tidal estuaries. *Marine Chemistry* 58: 213–227.

Cossa D, Averty B, and Pirrone N (2009) The origin of methylmercury in open Mediterranean waters. *Limnology and Oceanography* 54(3): 837–844.

Cossa D and Coquery M (2005) The Mediterranean mercury anomaly, a geochemical or a biological issue. In: Saliot A (ed.) *Handbook of Environmental Chemistry*, vol. 5K: *The Mediterranean Sea*, pp. 177–208. Berlin: Springer-Verlag.

Cossa D, Coquery M, Gobeil C, and Martin J-M (1996) Mercury fluxes at the ocean margins. In: Baeyens W, Ebinghaus R, and Vasiliev O (eds.) *Global and Regional Mercury Cycles: Sources, Fluxes and Mass Balances*. *NATO ASI Series 2*. *Environment*, vol. 21, pp. 229–248. Dordrecht, The Netherlands: Kluwer Academic Publishers.

Cossa D, Elbaz-Poulichet F, and Nieto JM (2001) Mercury in the Tinto–Odiel estuarine system (Gulf Of Cadiz, Spain): Sources and dispersion. *Aquatic Geochemistry* 7(1): 1–12.

Cossa D, Martin JM, Takayanagi K, and Sanjuan J (1997) The distribution and cycling of mercury species in the western Mediterranean. *Deep Sea Research Part II: Topical Studies in Oceanography* 44(3–4): 721–740.

Cossa D, Sanjuan J, and Noel J (1994) Mercury transport in waters of the Strait of Dover. *Marine Pollution Bulletin* 28(6): 385–388.

Costa M and Liss PS (1999) Photoreduction of mercury in sea water and its possible implications for Hg-0 air–sea fluxes. *Marine Chemistry* 68(1–2): 87–95.

Covelli S, Faganeli J, Horvat M, and Brambati A (2001) Mercury contamination of coastal sediments as the result of long-term cinnabar mining activity (Gulf of Trieste, northern Adriatic Sea). *Applied Geochemistry* 16(5): 541–558.

Cox JA, Carnahan J, Dinunzio J, McCoy J, and Meister J (1979) Source of mercury in fish in new impoundments. *Bulletin of Environmental Contamination and Toxicology* 23(6): 779–783.

Crespo-Medina M, Chatziefthimiou AD, Bloom NS, et al. (2009) Adaptation of chemosynthetic microorganisms to elevated mercury concentrations in deep-sea hydrothermal vents. *Limnology and Oceanography* 54(1): 41–49.

Crisp JA (1984) Rates of magma emplacement and volcanic output. *Journal of Volcanology and Geothermal Research* 20(3–4): 177–211.

Dalziel JA (1992) Reactive mercury on the Scotian Shelf and in the adjacent northwest Atlantic Ocean. *Marine Chemistry* 37(3–4): 171–178.

Dalziel JA and Yeats PA (1985) Reactive mercury in the central North Atlantic Ocean. *Marine Chemistry* 15(4): 357–361.

Damman AWH (1978) Distribution and movement of elements in ombrotrophic peat bogs. *Oikos* 30(3): 480–495.

Das R, Salters VJM, and Odom AL (2009) A case for in vivo mass-independent fractionation of mercury isotopes in fish. *Geochemistry, Geophysics, Geosystems* 10: Q11012.

Davidson PW, Palumbo D, Myers GJ, et al. (2000) Neurodevelopmental outcomes of Seychellois children from the pilot cohort at 108 months following prenatal exposure to methylmercury from a maternal fish diet. *Environmental Research* 84(1): 1–11.

Dedeurwaerder H, Decadt G, and Baeyens W (1982) Estimations of mercury fluxes emitted by Mount Etna Volcano. *Bulletin of Volcanology* 45(3): 191–196.

Disselkamp RS, Chapman EG, Barchet WR, Colson SD, and Howd CD (1999) BrCl production in NaBr/NaCl/HNO_3/O_3 solutions representative of sea-salt aerosols in the marine boundary layer. *Geophysical Research Letters* 26(14): 2183–2186.

Dittman JA, Shanley JB, Driscoll CT, et al. (2010) Mercury dynamics in relation to dissolved organic carbon concentration and quality during high flow events in three northeastern US streams. *Water Resources Research* 46: W07522.

Donohoue DL, Bauer D, Cossairt B, and Hynes AJ (2006) Temperature and pressure dependent rate coefficients for the reaction of Hg with Br and the reaction of Br with Br: A pulsed laser photolysis-pulsed laser induced fluorescence study. *Journal of Physical Chemistry A* 110(21): 6623–6632.

Donohoue DL, Bauer D, and Hynes AJ (2005) Temperature and pressure dependent rate coefficients for the reaction of Hg with Cl and the reaction of Cl with Cl: A pulsed laser photolysis-pulsed laser induced fluorescence study. *Journal of Physical Chemistry A* 109(34): 7732–7741.

Ebinghaus R, Kock HH, Temme C, et al. (2002) Antarctic springtime depletion of atmospheric mercury. *Environmental Science & Technology* 36(6): 1238–1244.

Ebinghaus R and Krüger O (1996) Emissions and local deposition estimates of anthropogenic mercury in north western and central Europe. In: Baeyens W, Ebinghaus R, and Vasiliev O (eds.) *Global and Regional Mercury Cycles: Sources, Fluxes and Mass Balances*, *NATO ASI Series 2*. *Environment*, vol. 21, pp. 135–159. Dordrecht, The Netherlands: Kluwer Academic Publishers.

Ebinghaus R, Turner RR, Lacerda LD, and Vasiliev BO (1998) *Mercury Contaminated Sites – Characterization, Risk Assessment and Remediation*. New York: Springer.

Egleston T (1887) *The Metallurgy of Silver, Gold, and Mercury in the United States*. New York: Wiley.

Engle MA, Gustin MS, Lindberg SE, Gertler AW, and Ariya PA (2005) The influence of ozone on atmospheric emissions of gaseous elemental mercury and reactive gaseous mercury from substrates. *Atmospheric Environment* 39(39): 7506–7517.

Engstrom DR and Swain EB (1997) Recent declines in atmospheric mercury deposition in the upper midwest. *Environmental Science & Technology* 31(4): 960–967.

Estrade N, Carignan J, and Donard OFX (2010) Isotope tracing of atmospheric mercury sources in an urban area of northeastern France. *Environmental Science & Technology* 44(16): 6062–6067.

Evans RD, Hintelmann H, and Dillon PJ (2001) Measurement of high precision isotope ratios for mercury from coals using transient signals. *Journal of Analytical Atomic Spectrometry* 16(9): 1064–1069.

Fabbri D, Gabbianelli G, Locatelli C, Lubrano D, Trombini C, and Vassura I (2001) Distribution of mercury and other heavy metals in core sediments of the northern Adriatic Sea. *Water, Air, and Soil Pollution* 129(1–4): 143–153.

Fain X, Ferrari CP, Dommergue A, et al. (2009a) Polar firn air reveals large-scale impact of anthropogenic mercury emissions during the 1970s. *Proceedings of the National Academy of Sciences of the United States of America* 106(38): 16114–16119.

Fain X, Obrist D, Hallar AG, McCubbin I, and Rahn T (2009b) High levels of reactive gaseous mercury observed at a high elevation research laboratory in the Rocky Mountains. *Atmospheric Chemistry and Physics* 9(20): 8049–8060.

Fein JB and Williams-Jones AE (1997) The role of mercury-organic interactions in the hydrothermal transport of mercury. *Economic Geology* 92(1): 20–28.

Fitzgerald WF (1981) Volcanic mercury emissions and the global mercury cycle. *Symposium on the Role of the Ocean in Atmospheric Chemistry. IAMAP 3rd Scientific Assembly*, Hamburg, Germany, 17–28 August.

Fitzgerald WF (1989) Atmospheric and oceanic cycling of mercury. In: Riley JP and Chester R (eds.) *Chemical Oceanography*, vol. 10, ch. 57, pp. 151–186. New York: Academic Press.

Fitzgerald WF (1995) Is mercury increasing in the atmosphere – The need for an atmospheric mercury network (AMNET). *Water, Air, and Soil Pollution* 80(1–4): 245–254.

Fitzgerald WF (1996) Mercury emissions from volcanoes. *4th International Conference on Mercury as a Global Pollutant*. Hamburg, Germany, 4–8 August 1996.

Fitzgerald WF and Clarkson TW (1991) Mercury and monomethylmercury: Present and future concerns. *Environmental Health Perspectives* 96: 159–166.

Fitzgerald WF, Engstrom DR, Lamborg CH, Tseng CM, Balcom PH, and Hammerschmidt CR (2005) Modern and historic atmospheric mercury fluxes in northern Alaska: Global sources and Arctic depletion. *Environmental Science & Technology* 39: 557–568.

Fitzgerald WF, Engstrom DR, Mason RP, and Nater EA (1998) The case for atmospheric mercury contamination in remote areas. *Environmental Science & Technology* 32(1): 1–7.

Fitzgerald WF and Gill GA (1979) Subnanogram determination of mercury by two-stage gold amalgamation applied to atmospheric analysis. *Analytical Chemistry* 51: 1714–1720.

Fitzgerald WF, Gill GA, and Hewitt AD (1981) Mercury: A trace atmospheric gas. *Presented at the Symposium on the Role of the Ocean in Atmospheric Chemistry, IAMAP 3rd Scientific Assembly*. Hamburg, Germany, 17–28 August.

Fitzgerald WF, Hammerschmidt CR, and Bowman KL (2011) Distribution and fluxes of monomethyl and dimethyl mercury on the continental margin of the northwest Atlantic Ocean. *American Society of Limnology and Oceanography Aquatic Sciences Meeting*, San Juan, PR, 13–18 February.

Fitzgerald WF and Mason RP (1997) Biogeochemical cycling of mercury in the marine environment. *Metal Ions in Biological Systems* 34: 53–111.

Fitzgerald W, Mason RP, and Vandal GM (1991) Atmospheric cycling and air–water exchange of mercury over mid-continental lacustrine regions. *Water, Air, and Soil Pollution* 56(1): 745–767.

Fitzgerald WF, Vandal GM, Rolfhus KR, Lamborg CH, and Langer CS (2000) Mercury emissions and cycling in the coastal zone. *Journal of Environmental Sciences* 12: 92–101.

Fitzgerald WF and Watras CJ (1989) Mercury in surficial waters of rural Wisconsin lakes. *Science of the Total Environment* 87/88: 223–232.

Fleming EJ, Mack EE, Green PG, and Nelson DC (2006) Mercury methylation from unexpected sources: Molybdate-inhibited freshwater sediments and an iron-reducing bacterium. *Applied and Environmental Microbiology* 72(1): 457–464.

Fogg TR and Fitzgerald WF (1979) Mercury in southern New England coastal rains. *Journal of Geophysical Research* 84(NC11): 6987–6989.

Friedlander G, Kennedy JW, Macias ES, and Miller JM (1981) *Nuclear and Radiochemistry*, 3rd edn. New York: Wiley.

Friedli HR, Radke LF, and Lu JY (2001) Mercury in smoke from biomass fires. *Geophysical Research Letters* 28(17): 3223–3226.

Friend JP (1973) The global sulfur cycle. In: Rasool SI (ed.) *Chemistry of the Lower Atmosphere*, pp. 177–201. New York: Plenum Press.

Fu XW, Feng XB, Zhu WZ, Zheng W, Wang SF, and Lu JY (2008) Total particulate and reactive gaseous mercury in ambient air on the eastern slope of the Mt. Gongga area, China. *Applied Geochemistry* 23(3): 408–418.

Ganguli PM, Mason RP, Abu-Saba KE, Anderson RS, and Flegal AR (2000) Mercury speciation in drainage from the New Idria mercury mine, California. *Environmental Science & Technology* 34(22): 4773–4779.

Gårdfeldt K, Munthe J, Stromberg D, and Lindqvist O (2003) A kinetic study on the abiotic methylation of divalent mercury in the aqueous phase. *Science of the Total Environment* 304(1–3): 127–136.

Gbondo-Tugbawa S and Driscoll CT (1998) Application of the regional mercury cycling model (RMCM) to predict the fate and remediation of mercury in Onondaga Lake, New York. *Water, Air, and Soil Pollution* 105(1–2): 417–426.

Gehrke GE, Blum JD, and Marvin-DiPasquale M (2011) Sources of mercury to San Francisco Bay surface sediment as revealed by mercury stable isotopes. *Geochimica et Cosmochimica Acta* 75(3): 691–705.

Gehrke GE, Blum JD, and Meyers PA (2009) The geochemical behavior and isotopic composition of Hg in a mid-Pleistocene western Mediterranean sapropel. *Geochimica et Cosmochimica Acta* 73(6): 1651–1665.

Geller LS, Elkins JW, Lobert JM, et al. (1997) Tropospheric SF_6: Observed latitudinal distribution and trends, derived emissions and interhemispheric exchange time. *Geophysical Research Letters* 24(6): 675–678.

George TS (2001) *Minamata: Pollution and the Struggle for Democracy in Postwar Japan, Harvard East Asian Monographs* vol. 194. Cambridge, MA: Harvard University Press.

Gerino M, Aller RC, Lee C, et al. (1998) Comparison of different tracers and methods used to quantify bioturbation during a spring bloom: 234-Thorium, luminophores and chlorophyll *a*. *Estuarine, Coastal and Shelf Science* 46(4): 531–547.

Gill GA and Bruland KW (1987) Mercury in the northeast Pacific. *Eos, Transactions American Geophysical Union* 68: 1763.

Gill GA and Fitzgerald WF (1988) Vertical mercury distributions in the oceans. *Geochimica et Cosmochimica Acta* 52: 1719–1728.

Gill GA, Guentzel JL, Landing WM, and Pollman CD (1995) Total gaseous mercury measurements in Florida – The FAMS project (1992–1994). *Water, Air, and Soil Pollution* 80(1–4): 235–244.

Gilmour CC, Elias DA, Kucken AM, et al. (2011) Sulfate-reducing bacterium *Desulfovibrio desulfuricans* ND132 as a model for understanding bacterial mercury methylation. *Applied and Environmental Microbiology* 77(12): 3938–3951.

Gilmour CC and Henry EA (1991) Mercury methylation in aquatic systems affected by acid deposition. *Environmental Pollution* 71(2–4): 131–169.

Gilmour CC and Riedel GS (1995) Measurement of Hg methylation in sediments using high specific-activity Hg-203 and ambient incubation. *Water, Air, and Soil Pollution* 80(1–4): 747–756.

Gilmour CC, Riedel GS, Ederington MC, et al. (1998) Methylmercury concentrations and production rates across a trophic gradient in the northern Everglades. *Biogeochemistry* 40(2–3): 327–345.

Gobeil C and Cossa D (1993) Mercury in sediments and sediment pore-water in the Laurentian Trough. *Canadian Journal of Fisheries and Aquatic Sciences* 50(8): 1794–1800.

Gobeil C, Macdonald RW, and Smith JN (1999) Mercury profiles in sediments of the Arctic Ocean basins. *Environmental Science & Technology* 33(23): 4194–4198.

Goldschmidt VM (1954) *Geochemistry*. London: Oxford University Press.

Goldwater LJ (1972) *A History of Quicksilver*. Baltimore: York Press.

Goodsite ME, Plane JMC, and Skov H (2004) A theoretical study of the oxidation of HgO to $HgBr_2$ in the troposphere. *Environmental Science & Technology* 38(6): 1772–1776.

Granjean P, Weihe P, White RF, et al. (1997) Cognitive deficit in 7-year-old children with prenatal exposure to methylmercury. *Neurotoxicology and Teratology* 19: 417–428.

Gratz LE, Keeler GJ, Blum JD, and Sherman LS (2010) Isotopic composition and fractionation of mercury in Great Lakes precipitation and ambient air. *Environmental Science & Technology* 44(20): 7764–7770.

Graydon JA, St Louis VL, Hintelmann H, et al. (2009) Investigation of uptake and retention of atmospheric Hg(II) by boreal forest plants using stable Hg isotopes. *Environmental Science & Technology* 43(13): 4960–4966.

Grevesse N (1970) Solar and meteoritic abundances of mercury. *Geochimica et Cosmochimica Acta* 34(10): 1129–1130.

Grieb TM, Petcharuttana Y, Roy S, Bloom N, and Brown K (2001) Mercury studies in the central Gulf of Thailand. In: *6th International Conference on Mercury as a Global Pollutant*. Minamata, Japan, October 15–19.

Grigal DF, Kolka RK, Fleck JA, and Nater EA (2000) Mercury budget of an upland-peatland watershed. *Biogeochemistry* 50(1): 95–109.

Grigal DF, Nater EA, and Homann PS (1994) Spatial distribution patterns of mercury in an east-central Minnesota landscape. In: Watras C and Huckabee J (eds.) *Mercury Pollution: Integration and Synthesis*, ch. III.2, pp. 305–312. Ann Arbor, MI: Lewis.

Guentzel JL, Landing WM, Gill GA, and Pollman CD (1995) Atmospheric deposition of mercury in Florida – The FAMS project (1992–1994). *Water, Air, and Soil Pollution* 80(1–4): 393–402.

Gustin MS, Lindberg SE, Austin K, Coolbaugh M, Vette A, and Zhang H (2000) Assessing the contribution of natural sources to regional atmospheric mercury budgets. *Science of the Total Environment* 259(1–3): 61–71.

Gustin MS, Lindberg S, Marsik F, et al. (1999) Nevada STORMS project: Measurement of mercury emissions from naturally enriched surfaces. *Journal of Geophysical Research* 104(D17): 21831–21844.

Hall BD, Rosenberg DM, and Wiens AP (1998) Methyl mercury in aquatic insects from an experimental reservoir. *Canadian Journal of Fisheries and Aquatic Sciences* 55(9): 2036–2047.

Hall B, Schager P, and Ljungstrom E (1995) An experimental study on the rate of reaction between mercury vapor and gaseous nitrogen dioxide. *Water, Air, and Soil Pollution* 81(1–2): 121–134.

Halmer MM, Schmincke HU, and Graf HF (2002) The annual volcanic gas input into the atmosphere, in particular into the stratosphere: A global data set for the past 100 years. *Journal of Volcanology and Geothermal Research* 115(3–4): 511–528.

Hammerschmidt CR and Bowman KL (2012) Vertical methylmercury distribution in the subtropical North Pacific. *Marine Chemistry* 132–133: 77–82.

Hammerschmidt CR and Fitzgerald WF (2004) Geochemical controls on the production and distribution of methylmercury in near-shore marine sediments. *Environmental Science & Technology* 38(5): 1487–1495.

Hammerschmidt CR and Fitzgerald WF (2005) Methylmercury in mosquitoes related to atmospheric mercury deposition and contamination. *Environmental Science & Technology* 39(9): 3034–3039.

Hammerschmidt CR and Fitzgerald WF (2006) Methylmercury cycling in sediments on the continental shelf of southern New England. *Geochimica et Cosmochimica Acta* 70(4): 918–930.

Hammerschmidt CR, Fitzgerald WF, Lamborg CH, Balcom PH, and Tseng CM (2006) Biogeochemical cycling of methylmercury in lakes and tundra watersheds of Arctic Alaska. *Environmental Science & Technology* 40(4): 1204–1211.

Hammerschmidt CR, Fitzgerald WF, Lamborg CH, Balcom PH, and Visscher PT (2004) Biogeochemistry of methylmercury in sediments of Long Island Sound. *Marine Chemistry* 90(1–4): 31–52.
Hammerschmidt CR, Sandheinrich MB, Wiener JG, and Rada RG (2002) Effects of dietary methylmercury on reproduction of fathead minnows. *Environmental Science & Technology* 36(5): 877–883.
Han S and Gill GA (2005) Determination of mercury complexation in coastal and estuarine waters using competitive ligand exchange method. *Environmental Science & Technology* 39: 6607–6615.
Han SH, Gill GA, Lehman RD, and Choe KY (2006) Complexation of mercury by dissolved organic matter in surface waters of Galveston Bay, Texas. *Marine Chemistry* 98(2–4): 156–166.
Hanson PJ, Lindberg SE, Tabberer TA, Owens JG, and Kim KH (1995) Foliar exchange of mercury vapor – Evidence for a compensation point. *Water, Air, and Soil Pollution* 80(1–4): 373–382.
Harris RC, Rudd JWM, Amyot M, et al. (2007) Whole-ecosystem study shows rapid fish-mercury response to changes in mercury deposition. *Proceedings of the National Academy of Sciences of the United States of America* 104(42): 16586–16591.
Hedgecock IM and Pirrone N (2001) Mercury and photochemistry in the marine boundary layer-modelling studies suggest the in situ production of reactive gas phase mercury. *Atmospheric Environment* 35(17): 3055–3062.
Herut B, Hornung H, Kress N, and Cohen Y (1996) Environmental relaxation in response to reduced contaminant input: The case of mercury pollution in Haifa Bay, Israel. *Marine Pollution Bulletin* 32(4): 366–373.
Hesterberg D, Chou JW, Hutchison KJ, and Sayers DE (2001) Bonding of Hg(II) to reduced organic sulfur in humic acid as affected by S–Hg ratio. *Environmental Science & Technology* 35(13): 2741–2745.
Hines ME and Jones GE (1985) Microbial biogeochemistry and bioturbation in the sediment of Great Bay, New Hampshire. *Estuarine, Coastal and Shelf Science* 20: 729–742.
Hinkley TK, Lamothe PJ, Wilson SA, Finnegan DL, and Gerlach TM (1999) Metal emissions from Kilauea, and a suggested revision of the estimated worldwide metal output by quiescent degassing of volcanoes. *Earth and Planetary Science Letters* 170(3): 315–325.
Hintelmann H and Evans RD (1997) Application of stable isotopes in environmental tracer studies – Measurement of monomethylmercury (CH_3Hg^+) by isotope dilution ICP-MS and detection of species transformation. *Fresenius' Journal of Analytical Chemistry* 358(3): 378–385.
Hintelmann H, Harris R, Heyes A, et al. (2002) Reactivity and mobility of new and old mercury deposition in a Boreal forest ecosystem during the first year of the METAALICUS study. *Environmental Science & Technology* 36(23): 5034–5040.
Hintelmann H, Keppel-Jones K, and Evans RD (2000) Constants of mercury methylation and demethylation rates in sediments and comparison of tracer and ambient mercury availability. *Environmental Toxicology and Chemistry* 19(9): 2204–2211.
Hintelmann H and Lu SY (2003) High precision isotope ratio measurements of mercury isotopes in cinnabar ores using multi-collector inductively coupled plasma mass spectrometry. *Analyst* 128(6): 635–639.
Hintelmann H, Welbourn PM, and Evans RD (1997) Measurement of complexation of methylmercury(II) compounds by freshwater humic substances using equilibrium dialysis. *Environmental Science & Technology* 31(2): 489–495.
Hoefs J (2004) *Stable Isotope Geochemistry*, 5th edn. Berlin: Springer-Verlag.
Holmes CD, Jacob DJ, Corbitt ES, et al. (2010) Global atmospheric model for mercury including oxidation by bromine atoms. *Atmospheric Chemistry and Physics* 10(24): 12037–12057.
Horvat M, Kotnik J, Logar M, Fajon V, Zvonaric T, and Pirrone N (2003) Speciation of mercury in surface and deep-sea waters in the Mediterranean Sea. *Atmospheric Environment* 37: S93–S108.
Hoyer M, Burke J, and Keeler G (1995) Atmospheric sources, transport and deposition of mercury in Michigan – 2 years of event precipitation. *Water, Air, and Soil Pollution* 80(1–4): 199–208.
Hsu H and Sedlak DL (2003) Strong Hg(II) complexation in municipal wastewater effluent and surface waters. *Environmental Science & Technology* 37(12): 2743–2749.
Hsu-Kim H and Sedlak DL (2005) Similarities between inorganic sulfide and the strong Hg(II)-complexing ligands in municipal wastewater effluent. *Environmental Science & Technology* 39(11): 4035–4041.
Hudson RJM, Gherini SA, Fitzgerald WF, and Porcella DB (1995) Anthropogenic influences on the global mercury cycle – A model-based analysis. *Water, Air, and Soil Pollution* 80(1–4): 265–272.
Hudson RJM, Gherini SA, Watras CJ, and Porcella DB (1994) Modeling the biogeochemical cycle of mercury in lakes: The mercury cycling model (MCM) and its application to the MTL study lakes. In: Watras C and Huckabee J (eds.) *Mercury Pollution: Integration and Synthesis*, ch. V.1, pp. 473–526. Ann Arbor, MI: Lewis.
Hultberg H, Iverfeldt A, and Lee YH (1994) Methylmercury input/output and accumulation in forested catchments and critical loads for lakes in southwestern Sweden. In: Watras C and Huckabee J (eds.) *Mercury Pollution: Integration and Synthesis*, ch. III.3, pp. 313–322. Ann Arbor, MI: Lewis.
Hurley JP, Benoit JM, Babiarz CL, et al. (1995) Influences of watershed characteristics on mercury levels in Wisconsin rivers. *Environmental Science & Technology* 29(7): 1867–1875.
Hurley JP, Krabbenhoft DP, Cleckner LB, Olson ML, Aiken GR, and Rawlik PS (1998) System controls on the aqueous distribution of mercury in the northern Florida Everglades. *Biogeochemistry* 40(2–3): 293–310.
Iverfeldt A (1991a) Occurrence and turnover of atmospheric mercury over the Nordic countries. *Water, Air, and Soil Pollution* 56: 251–265.
Iverfeldt A (1991b) Mercury in forest canopy throughfall water and its relation to atmospheric deposition. *Water, Air, and Soil Pollution* 56: 553–564.
Iverfeldt A, Munthe J, Brosset C, and Pacyna J (1995) Long-term changes in concentration and deposition of atmospheric mercury over Scandinavia. *Water, Air, and Soil Pollution* 80(1–4): 227–233.
Jackson TA, Whittle DM, Evans MS, and Muir DCG (2008) Evidence for mass-independent and mass-dependent fractionation of the stable isotopes of mercury by natural processes in aquatic ecosystems. *Applied Geochemistry* 23(3): 547–571.
Japan Public Health Association (2001) *Methylmercury Poisoning in Minamata and Niigata*. Japan: Japan Public Health Association.
Jaworowski Z, Bysiek M, and Kownacka L (1981) Flow of metals into the global atmosphere. *Geochimica et Cosmochimica Acta* 45(11): 2185–2199.
JECFA (2000) *Safety Evaluation of Certain Food Additives and Contaminants, WHO Food Additives Series 44: Methylmercury*. Geneva, Switzerland: World Health Organization.
Jensen A and Jensen A (1991) Historical deposition rates of mercury in Scandinavia estimated by dating and measurement of mercury in cores of peat bogs. *Water, Air, and Soil Pollution* 56(1): 769–777.
Jensen S and Jernelöv A (1969) Biological methylation of mercury in aquatic organisms. *Nature* 223: 753–754.
Johnson DW and Lindberg SE (1995) The biogeochemical cycling of Hg in forests – Alternative methods for quantifying total deposition and soil emission. *Water, Air, and Soil Pollution* 80(1–4): 1069–1077.
Jovanovic S and Reed GWJ (1976) Interrelations among isotopically anomalous mercury fractions from meteorites and possible cosmological inferences. *Science* 193: 888–891.
Kamman NC and Engstrom DR (2002) Historical and present fluxes of mercury to Vermont and New Hampshire lakes inferred from Pb-210 dated sediment cores. *Atmospheric Environment* 36(10): 1599–1609.
Kang WJ, Trefry JH, Nelsen TA, and Wanless HR (2000) Direct atmospheric inputs versus runoff fluxes of mercury to the lower Everglades and Florida Bay. *Environmental Science & Technology* 34(19): 4058–4063.
Kannan K and Falandysz J (1998) Speciation and concentrations of mercury in certain coastal marine sediments. *Water, Air, and Soil Pollution* 103(1–4): 129–136.
Keeler G, Glinsorn G, and Pirrone N (1995) Particulate mercury in the atmosphere – Its significance, transport, transformation and sources. *Water, Air, and Soil Pollution* 80(1–4): 159–168.
Kelly CA, Rudd JWM, and Holoka MH (2003) Effect of pH on mercury uptake by an aquatic bacterium: Implications for Hg cycling. *Environmental Science & Technology* 37(13): 2941–2946.
Kerin EJ, Gilmour CC, Roden E, Suzuki MT, Coates JD, and Mason RP (2006) Mercury methylation by dissimilatory iron-reducing bacteria. *Applied and Environmental Microbiology* 72(12): 7919–7921.
Kesler SE (1994) *Mineral Resources, Economics and the Environment*. New York: MacMillan.
Kim JP and Fitzgerald WF (1986) Sea-air partitioning of mercury over the equatorial Pacific Ocean. *Science* 231: 1131–1133.
King JK, Kostka JE, Frischer ME, and Saunders FM (2000) Sulfate-reducing bacteria methylate mercury at variable rates in pure culture and in marine sediments. *Applied and Environmental Microbiology* 66(6): 2430–2437.
King JK, Kostka JE, Frischer ME, Saunders FM, and Jahnke RA (2001) A quantitative relationship that demonstrates mercury methylation rates in marine sediments are based on the community composition and activity of sulfate-reducing bacteria. *Environmental Science & Technology* 35(12): 2491–2496.
King JK, Saunders FM, Lee RF, and Jahnke RA (1999) Coupling mercury methylation rates to sulfate reduction rates in marine sediments. *Environmental Toxicology and Chemistry* 18(7): 1362–1369.

Kirk JL and Louis VLS (2009) Multiyear total and methyl mercury exports from two major sub-Arctic rivers draining into Hudson Bay, Canada. *Environmental Science & Technology* 43(7): 2254–2261.

Kirk JL, Muir DCM, Antoniades D, et al. (2011) Climate change and mercury accumulation in Canadian high and subarctic lakes. *Environmental Science & Technology* 45(3): 964–970.

Klaue B, Kesler SE, and Blum JD (2000) Investigation of natural fractionation of stable mercury isotopes by inductively coupled plasma mass spectrometry. In: Nriagu J (ed.) *11th Annual International Conference on Heavy Metals in the Environment*, Contribution 1101. University of Michigan, School of Public Health, Ann Arbor, MI, 6–10 August.

Klusman RW and Jaacks JA (1987) Environmental influences upon mercury, radon and helium concentrations in soil gases at a site near Denver, Colorado. *Journal of Geochemical Exploration* 27(3): 259–280.

Koski RA, Benninger LM, Zierenberg RA, and Jonasson IR (1994) Composition and growth history of hydrothermal deposits in Escanaba Trough, Southern Gorda Ridge. In Morton JL, Zierenberg RA, and Reiss CA (eds.) *Geologic, Hydrothermal, and Biologic Studies at Escanaba Trough, Gorda Ridge, Offshore Northern California*, pp. 293–324. Reston, VA: US Geological Survey.

Kotnik J, Horvat M, Tessier E, et al. (2007) Mercury speciation in surface and deep waters of the Mediterranean Sea. *Marine Chemistry* 107(1): 13–30.

Krabbenhoft DP, Benoit JM, Babiarz CL, Hurley JP, and Andren AW (1995) Mercury cycling in the Allequash Creek watershed, northern Wisconsin. *Water, Air, and Soil Pollution* 80(1–4): 425–433.

Krabbenhoft DP, Wiener JG, Brumbaugh WG, Olson ML, DeWild JF, and Sabin TJ (1999) *A National Pilot Study of Mercury Contamination of Aquatic Ecosystems Along Multiple Gradients*. In: Morganwalp DW and Buxton HT (eds.) *US Geological Survey Toxic Substances Hydrology Program - Proceedings of the Technical Meeting, vol. 2, Contamination of Hydrologic Systems and Related Ecosystems, US Geological Survey Water-Resources Investigations Report 99-4018B*, pp. 147–160. Reston, VA: US Geological Survey.

Kraepiel AML, Keller K, Chin HB, Malcolm EG, and Morel FMM (2003) Sources and variations of mercury in tuna. *Environmental Science & Technology* 37(24): 5551–5558.

Kritee K, Barkay T, and Blum JD (2009) Mass dependent stable isotope fractionation of mercury during *mer* mediated microbial degradation of monomethylmercury. *Geochimica et Cosmochimica Acta* 73(5): 1285–1296.

Kritee K, Blum JD, and Barkay T (2008) Mercury stable isotope fractionation during reduction of Hg(II) by different microbial pathways. *Environmental Science & Technology* 42(24): 9171–9177.

Kritee K, Blum JD, Johnson MW, Bergquist BA, and Barkay T (2007) Mercury stable isotope fractionation during reduction of Hg(II) to Hg(0) by mercury resistant microorganisms. *Environmental Science & Technology* 41(6): 1889–1895.

Lacerda LD and Goncalves GO (2001) Mercury distribution and speciation in waters of the coastal lagoons of Rio de Janeiro, SE Brazil. *Marine Chemistry* 76(1–2): 47–58.

Lacerda LD and Salomons W (1998) *Mercury from Gold and Silver Mining: A Chemical Time Bomb?* Berlin: Springer-Verlag.

Lalli CM and Parsons TR (1993) *Biological Oceanography: An Introduction*. Oxford: Elsevier Butterworth-Heinemann.

Lalonde JD, Amyot M, Doyon MR, and Auclair JC (2003) Photo-induced Hg(II) reduction in snow from the remote and temperate Experimental Lakes Area (Ontario, Canada). *Journal of Geophysical Research* 108(D6): 4200.

Lalonde JD, Amyot M, Kraepiel AML, and Morel FMM (2001) Photooxidation of Hg(0) in artificial and natural waters. *Environmental Science & Technology* 35(7): 1367–1372.

Lalonde JD, Poulain AJ, and Amyot M (2002) The role of mercury redox reactions in snow on snow-to-air mercury transfer. *Environmental Science & Technology* 36(2): 174–178.

Lambert G, Cloarec MF, and Pennisi M (1988) Volcanic output of SO_2 and trace metals – A new approach. *Geochimica et Cosmochimica Acta* 52(1): 39–42.

Lamborg CH, Engstrom DR, Fitzgerald WF, and Balcom PH (2013) Apportioning global and non-global components of mercury deposition through ^{210}Pb indexing. *Science of the Total Environment* 448: 132–140.

Lamborg CH, Fitzgerald WF, Damman AWH, Benoit JM, Balcom PH, and Engstrom DR (2002a) Modern and historic atmospheric mercury fluxes in both hemispheres: Global and regional mercury cycling implications. *Global Biogeochemical Cycles* 16(4): 1104.

Lamborg CH, Fitzgerald WF, O'Donnell J, and Torgersen T (2002b) A non-steady-state compartmental model of global-scale mercury biogeochemistry with interhemispheric atmospheric gradients. *Geochimica et Cosmochimica Acta* 66(7): 1105–1118.

Lamborg CH, Fitzgerald WF, Graustein WC, and Turekian KK (2000) An examination of the atmospheric chemistry of mercury using Pb-210 and Be-7. *Journal of Atmospheric Chemistry* 36(3): 325–338.

Lamborg CH, Fitzgerald WF, Vandal GM, and Rolfhus KR (1995) Atmospheric mercury in northern Wisconsin – Sources and species. *Water, Air, and Soil Pollution* 80(1–4): 189–198.

Lamborg CH, Rolfhus KR, Fitzgerald WF, and Kim G (1999) The atmospheric cycling and air–sea exchange of mercury species in the south and equatorial Atlantic Ocean. *Deep Sea Research Part II: Topical Studies in Oceanography* 46(5): 957–977.

Lamborg CH, Tseng CM, Fitzgerald WF, Balcom PH, and Hammerschmidt CR (2003) Determination of the mercury complexation characteristics of dissolved organic matter in natural waters with "reducible Hg" titrations. *Environmental Science & Technology* 37(15): 3316–3322.

Lamborg CH, Von Damm KL, Fitzgerald WF, Hammerschmidt CR, and Zierenberg RA (2006) Mercury and monomethylmercury in fluids from Sea Cliff submarine hydrothermal field, Gorda Ridge. *Geophysical Research Letters* 33: L17606.

Lamborg CH, Yigiterhan O, Fitzgerald WF, Balcom PH, Hammerschmidt CR, and Murray JW (2008) Vertical distribution of mercury species at two sites in the western Black Sea. *Marine Chemistry* 111: 77–89.

Landis MS and Stevens RK (2001) Preliminary results from the USEPA mercury speciation network and aircraft measurement campaigns. *6th International Conference on Mercury as a Global Pollutant*. Minamata, Japan, October 15–19.

Landis MS, Stevens RK, Schaedlich F, and Prestbo EM (2002) Development and characterization of an annular denuder methodology for the measurement of divalent inorganic reactive gaseous mercury in ambient air. *Environmental Science & Technology* 36(13): 3000–3009.

Langer CS, Fitzgerald WF, Visscher PT, and Vandal GM (2001) Biogeochemical cycling of methylmercury at Barn Island Salt Marsh, Stonington, CT, USA. *Wetlands Ecology and Management* 9: 295–310.

Lantzy RJ and MacKenzie FT (1979) Atmospheric trace metals: Global cycles and assessment of man's impact. *Geochimica et Cosmochimica Acta* 43: 511–525.

Lauretta DS, Devouard B, and Buseck PR (1999) The cosmochemical behavior of mercury. *Earth and Planetary Science Letters* 171(1): 35–47.

Lauretta DS, Klaue B, Blum JD, and Buseck PR (2001) Mercury abundances and isotopic compositions in the Murchison (CM) and Allende (CV) carbonaceous chondrites. *Geochimica et Cosmochimica Acta* 65(16): 2807–2818.

Laurier FJG, Mason RP, Gill GA, and Whalin L (2004) Mercury distributions in the North Pacific Ocean – 20 years of observations. *Marine Chemistry* 90: 3–19.

Lawson NM and Mason RP (2001) Concentration of mercury, methylmercury, cadmium, lead, arsenic, and selenium in the rain and stream water of two contrasting watersheds in western Maryland. *Water Research* 35(17): 4039–4052.

Lechler PJ, Miller JR, Lacerda LD, et al. (2000) Elevated mercury concentrations in soils, sediments, water, and fish of the Madeira River Basin, Brazilian Amazon: A function of natural enrichments? *Science of the Total Environment* 260(1–3): 87–96.

Lee YH, Bishop KH, and Munthe J (2000) Do concepts about catchment cycling of methylmercury and mercury in boreal catchments stand the test of time? Six years of atmospheric inputs and runoff export at Svartberget, northern Sweden. *Science of the Total Environment* 260(1–3): 11–20.

Leermakers M, Galletti S, De Galan S, Brion N, and Baeyens W (2001) Mercury in the southern North Sea and Scheldt Estuary. *Marine Chemistry* 75(3): 229–248.

Lehnherr I, St Louis VL, Hintelmann H, and Kirk JL (2011) Methylation of inorganic mercury in polar marine waters. *Nature Geoscience* 4(5): 298–302.

Lin CJ and Pehkonen SO (1999) Aqueous phase reactions of mercury with free radicals and chlorine: Implications for atmospheric mercury chemistry. *Chemosphere* 38(6): 1253–1263.

Lindberg SE, Brooks S, Lin CJ, et al. (2002) Dynamic oxidation of gaseous mercury in the Arctic troposphere at polar sunrise. *Environmental Science & Technology* 36(6): 1245–1256.

Lindberg SE, Meyers TP, Taylor GE, Turner RR, and Schroeder WH (1992) Atmosphere–surface exchange of mercury in a forest – Results of modeling and gradient approaches. *Journal of Geophysical Research* 97(D2): 2519–2528.

Lindberg SE, Vette AF, Miles C, and Schaedlich F (2000) Mercury speciation in natural waters: Measurement of dissolved gaseous mercury with a field analyzer. *Biogeochemistry* 48(2): 237–259.

Lindqvist O, Johansson K, Aastrup M, et al. (1991) Mercury in the Swedish environment – Recent research on causes, consequences and corrective methods. *Water, Air, and Soil Pollution* 55(1–2): 1–261.

Lockhart WL, Wilkinson P, Billeck BN, et al. (1998) Fluxes of mercury to lake sediments in central and northern Canada inferred from dated sediment cores. *Biogeochemistry* 40(2–3): 163–173.

Long SE and Kelly WR (2002) Determination of mercury in coal by isotope dilution cold-vapor generation inductively coupled plasma mass spectrometry. *Analytical Chemistry* 74(7): 1477–1483.

Lu JY, Schroeder WH, Barrie LA, et al. (2001) Magnification of atmospheric mercury deposition to polar regions in springtime: The link to tropospheric ozone depletion chemistry. *Geophysical Research Letters* 28(17): 3219–3222.

Lucotte M, Mucci A, Hillairemarcel C, Pichet P, and Grondin A (1995) Anthropogenic mercury enrichment in remote lakes of northern Quebec (Canada). *Water, Air, and Soil Pollution* 80(1–4): 467–476.

MacDonald RW, Barrie LA, Bidleman TF, et al. (2000) Contaminants in the Canadian Arctic: 5 years of progress in understanding sources, occurrence and pathways. *Science of the Total Environment* 254(2–3): 93–234.

Mahaffey KR, Clickner RP, and Jeffries RA (2009) Adult women's blood mercury concentrations vary regionally in the United States: Association with patterns of fish consumption (NHANES 1999–2004). *Environmental Health Perspectives* 117(1): 47–53.

Mantoura RF, Dickson A, and Riley JP (1978) The complexation of metals with humic materials in natural waters. *Estuarine and Coastal Marine Science* 6: 387–408.

Mao H, Talbot RW, Sive BC, Kim SY, Blake DR, and Weinheimer AJ (2010) Arctic mercury depletion and its quantitative link with halogens. *Journal of Atmospheric Chemistry* 65: 145–170.

Martell AE, Smith RM, and Motekaitis RJ (1998) *NIST Critically Selected Stability Constants of Metal Complexes Data Base*. Gaithersburg, MD: US Department of Commerce.

Martinez-Cortizas A, Pontevedra-Pombal X, Garcia-Rodeja E, Novoa-Munoz JC, and Shotyk W (1999) Mercury in a Spanish peat bog: Archive of climate change and atmospheric metal deposition. *Science* 284(5416): 939–942.

Marvin-DiPasquale M, Agee J, McGowan C, et al. (2000) Methyl-mercury degradation pathways: A comparison among three mercury-impacted ecosystems. *Environmental Science & Technology* 34(23): 4908–4916.

Marvin-DiPasquale MC and Oremland RS (1998) Bacterial methylmercury degradation in Florida Everglades peat sediment. *Environmental Science & Technology* 32(17): 2556–2563.

Mason RP and Fitzgerald WF (1990) Alkylmercury species in the equatorial Pacific. *Nature* 347: 457–459.

Mason RP and Fitzgerald WF (1993) The distribution and biogeochemical cycling of mercury in the equatorial Pacific Ocean. *Deep Sea Research Part I: Oceanographic Research Papers* 40(9): 1897–1924.

Mason RP and Fitzgerald WF (1996) Sources, sinks and biogeochemical cycling of mercury in the ocean. In: Baeyens W, Ebinghaus R, and Vasiliev O (eds.) *Global and Regional Mercury Cycles: Sources, Fluxes and Mass Balances*. *NATO ASI Series 2*. *Environment*, vol. 21, pp. 249–272. Dordrecht, The Netherlands: Kluwer Academic Publishers.

Mason RP, Fitzgerald WF, Hurley J, Hanson AK, Donaghay PL, and Sieburth JM (1993) Mercury biogeochemical cycling in a stratified estuary. *Limnology and Oceanography* 38(6): 1227–1241.

Mason RP, Fitzgerald WF, and Morel FMM (1994) The biogeochemical cycling of elemental mercury – Anthropogenic influences. *Geochimica et Cosmochimica Acta* 58(15): 3191–3198.

Mason RP and Lawrence AL (1999) Concentration, distribution, and bioavailability of mercury and methylmercury in sediments of Baltimore Harbor and Chesapeake Bay, Maryland, USA. *Environmental Toxicology and Chemistry* 18(11): 2438–2447.

Mason RP, Lawson NM, and Sheu GR (2001) Mercury in the Atlantic Ocean: Factors controlling air–sea exchange of mercury and its distribution in the upper waters. *Deep Sea Research Part II: Topical Studies in Oceanography* 48(13): 2829–2853.

Mason RP, Rolfhus KR, and Fitzgerald WF (1998) Mercury in the North Atlantic. *Marine Chemistry* 61(1–2): 37–53.

Mason RP and Sullivan KA (1997) Mercury in Lake Michigan. *Environmental Science & Technology* 31(3): 942–947.

Mason RP and Sullivan KA (1999) The distribution and speciation of mercury in the South and equatorial Atlantic. *Deep Sea Research Part II: Topical Studies in Oceanography* 46(5): 937–956.

Matilainen T, Verta M, Korhonen H, Uusi-Rauva A, and Niemi M (2001) Behavior of mercury in soil profiles: Impact of increased precipitation, acidity, and fertilization on mercury methylation. *Water, Air, and Soil Pollution* 125(1–4): 105–119.

McCarthy JH (1968) Experiments with mercury in soil gas and air applied to mineral exploration. *Mineral Engineering* 20: 46.

Measures CI, Landing WM, Brown MT, and Buck CS (2008) High-resolution Al and Fe data from the Atlantic Ocean CLIVAR-CO_2 repeat hydrography A16N transect: Extensive linkages between atmospheric dust and upper ocean geochemistry. *Global Biogeochemical Cycles* 22(1): GB1005.

Mercone D, Thomson J, Croudace IW, and Troelstra SR (1999) A coupled natural immobilisation mechanism for mercury and selenium in deep-sea sediments. *Geochimica et Cosmochimica Acta* 63(10): 1481–1488.

Mergler D, Anderson HA, Chan HM, et al. (2007) Methylmercury exposure and health effects in humans: A worldwide concern. *Ambio* 36(1): 3–11.

Mierle G (1990) Aqueous inputs of mercury to Precambrian Shield lakes in Ontario. *Environmental Toxicology and Chemistry* 9(7): 843–851.

Millward GE (1982) Non-steady state simulations of the global mercury cycle. *Journal of Geophysical Research* 87(NC11): 8891–8897.

Monperrus M, Tessier E, Amouroux D, Leynaert A, Huonnic P, and Donard OFX (2007) Mercury methylation, demethylation and reduction rates in coastal and marine surface waters of the Mediterranean Sea. *Marine Chemistry* 107(1): 49–63.

Monteiro LR and Furness RW (1997) Accelerated increase in mercury contamination in North Atlantic mesopelagic food chains as indicated by time series of seabird feathers. *Environmental Toxicology and Chemistry* 16(12): 2489–2493.

Monteiro LR and Furness RW (2001) Kinetics, dose–response, and excretion of methylmercury in free-living adult Cory's shearwaters. *Environmental Science & Technology* 35(4): 739–746.

Monteiro LR, Granadeiro JP, and Furness RW (1998) Relationship between mercury levels and diet in Azores seabirds. *Marine Ecology Progress Series* 166: 259–265.

Muir DCG, Wang X, Yang F, et al. (2009) Spatial trends and historical deposition of mercury in eastern and northern Canada inferred from lake sediment cores. *Environmental Science & Technology* 43(13): 4802–4809.

Munthe J (1992) The aqueous oxidation of elemental mercury by ozone. *Atmospheric Environment A-General* 26(8): 1461–1468.

Munthe J and Berg T (2001) Reply to comment on "Atmospheric mercury species in the European Arctic: Measurement and modeling" by Berg et al. *Atmospheric Environment* 14: 2569–2582. *Atmospheric Environment* 35(31): 5379–5380.

Murphy DM, Thomson DS, and Mahoney TMJ (1998) In situ measurements of organics, meteoritic material, mercury, and other elements in aerosols at 5 to 19 kilometers. *Science* 282(5394): 1664–1669.

NAS (2000) *National Academy of Sciences Report: Toxicological Effects of Methylmercury*. Washington, DC: National Academy Press.

Norton SA, Evans GC, and Kahl JS (1997) Comparison of Hg and Pb fluxes to hummocks and hollows of ombrotrophic Big Heath Bog and to nearby Sargent Mt. Pond, Maine, USA. *Water, Air, and Soil Pollution* 100(3–4): 271–286.

NRC (2000) *National Research Council Report: Toxicological Effects of Methylmercury*. Washington, DC: National Academic Press.

Nriagu JO (1979) Production and uses of mercury. In: Nriagu JO (ed.) *The Biogeochemistry of Mercury in the Environment*. Amsterdam: Elsevier.

Nriagu JO (1989) A global assessment of natural sources of atmospheric trace metals. *Nature* 338(6210): 47–49.

Nriagu J and Becker C (2003) Volcanic emissions of mercury to the atmosphere: Global and regional inventories. *Science of the Total Environment* 304(1–3): 3–12.

O'Driscoll NJ, Siciliano SD, and Lean DRS (2003) Continuous analysis of dissolved gaseous mercury in freshwater lakes. *Science of the Total Environment* 304(1–3): 285–294.

O'Driscoll NJ, Siciliano SD, Lean DRS, and Amyot M (2006) Gross photoreduction kinetics of mercury in temperate freshwater lakes and rivers: Application to a general model of DGM dynamics. *Environmental Science & Technology* 40(3): 837–843.

Olafsson J (1975) Volcanic influence on sea water at Heimaey. *Nature* 255: 138–141.

Ozerova NA (1996) Mercury in geological systems. In: Baeyens W, Ebinghaus R, and Vasiliev O (eds.) *Global and Regional Mercury Cycles: Sources, Fluxes and Mass Balances*. *NATO ASI Series 2*. *Environment*, vol. 21, pp. 463–474. Dordrecht, The Netherlands: Kluwer Academic Publishers.

Pacyna EG and Pacyna JM (2002) Global emission of mercury from anthropogenic sources in 1995. *Water, Air, and Soil Pollution* 137(1–4): 149–165.

Pacyna EG, Pacyna JM, Steenhuisen F, and Wilson S (2006) Global anthropogenic mercury emission inventory for 2000. *Atmospheric Environment* 40: 4048–4063.

Pacyna EG, Pacyna JM, Sundseth K, et al. (2010) Global emission of mercury to the atmosphere from anthropogenic sources in 2005 and projections to 2020. *Atmospheric Environment* 44(20): 2487–2499.

Pak KR and Bartha R (1998) Mercury methylation and demethylation in anoxic lake sediments and by strictly anaerobic bacteria. *Applied and Environmental Microbiology* 64(3): 1013–1017.

Pal B and Ariya PA (2004a) Studies of ozone initiated reactions of gaseous mercury: Kinetics, product studies, and atmospheric implications. *Physical Chemistry Chemical Physics* 6(3): 572–579.

Pal B and Ariya PA (2004b) Gas-phase $HO^{\bullet}$-initiated reactions of elemental mercury: Kinetics, product studies, and atmospheric implications. *Environmental Science and Technology* 38(21): 5555–5566.

Parks JM, Johs A, Podar M, et al. (2013) The genetic basis for bacterial mercury methylation. *Science* 339: 1332–1335.

Patterson CC and Settle DM (1987) Magnitude of lead flux to the atmosphere from volcanos. *Geochimica et Cosmochimica Acta* 51(3): 675–681.
Pempkowiak J, Cossa D, Sikora A, and Sanjuan J (1998) Mercury in water and sediments of the southern Baltic Sea. *Science of the Total Environment* 213(1–3): 185–192.
Petersen G, Iverfeldt A, and Munthe J (1995) Atmospheric mercury species over central and northern Europe – Model calculations and comparison with observations from the Nordic air and precipitation network for 1987 and 1988. *Atmospheric Environment* 29(1): 47–67.
Pleijel K and Munthe J (1995) Modeling the atmospheric mercury cycle-chemistry in fog droplets. *Atmospheric Environment* 29(12): 1441–1457.
Poissant L and Casimir A (1998) Water–air and soil–air exchange rate of total gaseous mercury measured at background sites. *Atmospheric Environment* 32(5): 883–893.
Porcella DB, Ramel C, and Jernelov A (1997) Global mercury pollution and the role of gold mining: An overview. *Water, Air, and Soil Pollution* 97(3–4): 205–207.
Poulain AJ, Chadhain SMN, Ariya PA, et al. (2007) Potential for mercury reduction by microbes in the high Arctic. *Applied and Environmental Microbiology* 73: 2230–2238 (Erratum 73: 3769).
Rada RG, Powell DE, and Wiener JG (1993) Whole-lake burdens and spatial distribution of mercury in surficial sediments in Wisconsin seepage lakes. *Canadian Journal of Fisheries and Aquatic Sciences* 50(4): 865–873.
Rampino MR and Self S (1984) Sulfur-rich volcanic eruptions and stratospheric aerosols. *Nature* 310(5979): 677–679.
Raofie F and Ariya PA (2003) Kinetics and products study of the reaction of BrO radicals with gaseous mercury. *Journal de Physique IV* 107: 1119–1121.
Raofie F and Ariya PA (2004) Product study of the gas-phase BrO-initiated oxidation of Hg^0: Evidence for stable Hg^{1+} compounds. *Environmental Science & Technology* 38(16): 4319–4326.
Rasmussen PE (1994) Current methods of estimating atmospheric mercury fluxes in remote areas. *Environmental Science & Technology* 28(13): 2233–2241.
Ravichandran M, Aiken GR, Ryan JN, and Reddy MM (1999) Inhibition of precipitation and aggregation of metacinnabar (mercuric sulfide) by dissolved organic matter isolated from the Florida Everglades. *Environmental Science & Technology* 33(9): 1418–1423.
Rea AW, Lindberg SE, Scherbatskoy T, and Keeler GJ (2002) Mercury accumulation in foliage over time in two northern mixed-hardwood forests. *Water, Air, and Soil Pollution* 133(1–4): 49–67.
Richter FM, Rowley DB, and Depaolo DJ (1992) Sr isotope evolution of seawater – The role of tectonics. *Earth and Planetary Science Letters* 109(1–2): 11–23.
Rolfhus KR (1998) *The Production and Distribution of Elemental Hg in a Coastal Marine Environment*. PhD Thesis, University of Connecticut.
Rolfhus KR and Fitzgerald WF (1995) Linkages between atmospheric mercury deposition and the methylmercury content of marine fish. *Water, Air, and Soil Pollution* 80(1–4): 291–297.
Rolfhus KR and Fitzgerald WF (2001) The evasion and spatial/temporal distribution of mercury species in Long Island Sound, CT-NY. *Geochimica et Cosmochimica Acta* 65(3): 407–418.
Rolfhus KR, Sakamoto HE, Cleckner LB, et al. (2003) Distribution and fluxes of total and methylmercury in Lake Superior. *Environmental Science & Technology* 37(5): 865–872.
Roos-Barraclough F, Martinez-Cortizas A, Garcia-Rodeja E, and Shotyk W (2002) A 14,500 year record of the accumulation of atmospheric mercury in peat: Volcanic signals, anthropogenic influences and a correlation to bromine accumulation. *Earth and Planetary Science Letters* 202(2): 435–451.
Roulet M and Lucotte M (1995) Geochemistry of mercury in pristine and flooded ferralitic soils of a tropical rain forest in French Guiana, South America. *Water, Air, and Soil Pollution* 80(1–4): 1079–1088.
Rouxel O, Fouquet Y, and Ludden JN (2004) Subsurface processes at the Lucky Strike hydrothermal field, Mid-Atlantic Ridge: Evidence from sulfur, selenium, and iron isotopes. *Geochimica et Cosmochimica Acta* 68(10): 2295–2311.
Rydberg J, Galman V, Renberg I, Bindler R, Lambertsson L, and Martinez-Cortizas A (2008) Assessing the stability of mercury and methylmercury in a varved lake sediment deposit. *Environmental Science & Technology* 42(12): 4391–4396.
Sandheinrich MB and Wiener JG (2011) Methylmercury in freshwater fish: Recent advances in assessing toxicity of environmentally relevant exposures. In: Beyer N and Meador J (eds.) *Environmental Contaminants in Biota: Interpreting Tissue Concentrations*, pp. 169–190. Boca Raton, FL: Taylor and Francis.
Schaefer JK and Morel FMM (2009) High methylation rates of mercury bound to cysteine by *Geobacter sulfurreducens*. *Nature Geoscience* 2(2): 123–126.
Scherbatskoy T, Shanley JB, and Keeler GJ (1998) Factors controlling mercury transport in an upland forested catchment. *Water, Air, and Soil Pollution* 105(1–2): 427–438.
Scheuhammer AM (1991) Effects of acidification on the availability of toxic metals and calcium to wild birds and mammals. *Environmental Pollution* 71(2–4): 329–375.
Scheuhammer AM, Meyer MW, Sandheinrich MB, and Murray MW (2007) Effects of environmental methylmercury on the health of wild birds, mammals and fish. *Ambio* 36(1): 12–18.
Schluter K (2000) Review: Evaporation of mercury from soils. An integration and synthesis of current knowledge. *Environmental Geology* 39(3–4): 249–271.
Schober SE, Sinks TH, Jones RL, et al. (2003) Blood mercury levels in U.S. Children and women of childbearing age, 1999–2000. *Journal of the American Medical Association* 289: 1667–1674.
Schroeder WH, Anlauf KG, Barrie LA, et al. (1998) Arctic springtime depletion of mercury. *Nature* 394(6691): 331–332.
Schuster PF, Krabbenhoft DP, Naftz DL, et al. (2002) Atmospheric mercury deposition during the last 270 years: A glacial ice core record of natural and anthropogenic sources. *Environmental Science & Technology* 36(11): 2303–2310.
Seigneur C, Karamchandani P, Lohman K, Vijayaraghavan K, and Shia RL (2001) Multiscale modeling of the atmospheric fate and transport of mercury. *Journal of Geophysical Research* 106(D21): 27795–27809.
Seigneur C, Karamchandani P, Vijayaraghavan K, Lohman K, Shia RL, and Levin L (2003) On the effect of spatial resolution on atmospheric mercury modeling. *Science of the Total Environment* 304(1–3): 73–81.
Seinfeld JH (1986) *Atmospheric Chemistry and Physics of Air Pollution*. New York: Wiley-Interscience.
Selin NE (2009) Global biogeochemical cycling of mercury: A review. *Annual Review of Environment and Resources* 34: 43–63.
Selin NE, Jacob DJ, Yantosca RM, Strode S, Jaegle L, and Sunderland EM (2008) Global 3-D land–ocean–atmosphere model for mercury: Present-day versus preindustrial cycles and anthropogenic enrichment factors for deposition. *Global Biogeochemical Cycles* 22: GB2011.
Sellers P, Kelly CA, and Rudd JWM (2001) Fluxes of methylmercury to the water column of a drainage lake: The relative importance of internal and external sources. *Limnology and Oceanography* 46(3): 623–631.
Sellers P, Kelly CA, Rudd JWM, and MacHutchon AR (1996) Photodegradation of methylmercury in lakes. *Nature* 380: 694–697.
Senn DB, Chesney EJ, Blum JD, Bank MS, Maage A, and Shine JP (2010) Stable isotope (N, C, Hg) study of methylmercury sources and trophic transfer in the northern Gulf of Mexico. *Environmental Science & Technology* 44(5): 1630–1637.
Sherman LS, Blum JD, Johnson KP, Keeler GJ, Barres JA, and Douglas TA (2010) Mass-independent fractionation of mercury isotopes in Arctic snow driven by sunlight. *Nature Geoscience* 3(3): 173–177.
Sherman LS, Blum JD, Nordstrom DK, McCleskey RB, Barkay T, and Vetriani C (2009) Mercury isotopic composition of hydrothermal systems in the Yellowstone Plateau volcanic field and Guaymas Basin sea-floor rift. *Earth and Planetary Science Letters* 279(1–2): 86–96.
Sheu GR and Mason RP (2001) An examination of methods for the measurements of reactive gaseous mercury in the atmosphere. *Environmental Science and Technology* 35(6): 1209–1216.
Shia RL, Seigneur C, Pai P, Ko M, and Sze ND (1999) Global simulation of atmospheric mercury concentrations and deposition fluxes. *Journal of Geophysical Research* 104(D19): 23747–23760.
Shotyk W, Goodsite ME, Roos-Barraclough F, et al. (2003) Anthropogenic contributions to atmospheric Hg, Pb and As accumulation recorded by peat cores from southern Greenland and Denmark dated using the ^{14}C "bomb pulse curve" *Geochimica et Cosmochimica Acta* 67(21): 3991–4011.
Shull DH, Benoit JM, Wojcik C, and Senning JR (2009) Infaunal burrow ventilation and pore-water transport in muddy sediments. *Estuarine, Coastal and Shelf Science* 83(3): 277–286.
Siegel FR, Kravitz JH, and Galasso JJ (2001) Arsenic and mercury contamination in 31 cores taken in 1965, St. Anna Trough, Kara Sea, Arctic Ocean. *Environmental Geology* 40(4–5): 528–542.
Skov H, Brooks SB, Goodsite ME, et al. (2006) Fluxes of reactive gaseous mercury measured with a newly developed method using relaxed eddy accumulation. *Atmospheric Environment* 40(28): 5452–5463.
Skyring GW (1987) Sulfate reduction in coastal ecosystems. *Geomicrobiology Journal* 5(3–4): 295–374.
Slemr F, Brunke EG, Ebinghaus R, et al. (2003) Worldwide trend of atmospheric mercury since 1977. *Geophysical Research Letters* 30(10) Art. No. 1516.
Slemr F and Langer E (1992) Increase in global atmospheric concentrations of mercury inferred from measurements over the Atlantic Ocean. *Nature* 355(6359): 434–437.
Slemr F, Seiler W, and Schuster G (1981) Latitudinal distribution of mercury over the Atlantic Ocean. *Journal of Geophysical Research* 80: 1159.
Smith WE and Smith AM (1975) *Minamata*. New York: Holt, Rinehart and Winston.

Smith CN, Kesler SE, Blum JD, and Rytuba JJ (2008) Isotope geochemistry of mercury in source rocks, mineral deposits and spring deposits of the California Coast Ranges, USA. *Earth and Planetary Science Letters* 269(3–4): 398–406.

Smith CN, Kesler SE, Klaue B, and Blum JD (2005) Mercury isotope fractionation in fossil hydrothermal systems. *Geology* 33(10): 825–828.

Smith-Downey NV, Sunderland EM, and Jacob DJ (2010) Anthropogenic impacts on global storage and emissions of mercury from terrestrial soils: Insights from a new global model. *Journal of Geophysical Research* 115: G03008.

Social Scientific Study Group on Minamata Disease (2001) *In the Hope of Avoiding Repetition of a Tragedy of Minamata Disease (What We Have Learned from the Experience)*. Minamata, Japan: National Institute for Minamata Disease.

Soerensen AL, Skov H, Jacob DJ, Soerensen BT, and Johnson MS (2010a) Global concentrations of gaseous elemental mercury and reactive gaseous mercury in the marine boundary layer. *Environmental Science & Technology* 44(19): 7425–7430.

Soerensen AL, Sunderland EM, Holmes CD, et al. (2010b) An improved global model for air–sea exchange of mercury: High concentrations over the North Atlantic. *Environmental Science & Technology* 44(22): 8574–8580.

Sommar J, Andersson ME, and Jacobi HW (2010) Circumpolar measurements of speciated mercury, ozone and carbon monoxide in the boundary layer of the Arctic Ocean. *Atmospheric Chemistry and Physics* 10(11): 5031–5045.

Sommar J, Gardfeldt K, Stromberg D, and Feng XB (2001) A kinetic study of the gas-phase reaction between the hydroxyl radical and atomic mercury. *Atmospheric Environment* 35(17): 3049–3054.

Southworth G, Lindberg S, Hintelmann H, et al. (2007) Evasion of added isotopic mercury from a northern temperate lake. *Environmental Toxicology and Chemistry* 26(1): 53–60.

Spiro PA, Jacob DJ, and Logan JA (1992) Global inventory of sulfur emissions with $1° \times 1°$ resolution. *Journal of Geophysical Research* 97(D5): 6023–6036.

St Louis VL, Rudd JWM, Kelly CA, Beaty KG, Flett RJ, and Roulet NT (1996) Production and loss of methylmercury and loss of total mercury from boreal forest catchments containing different types of wetlands. *Environmental Science & Technology* 30(9): 2719–2729.

St Louis VL, Rudd JWM, Kelly CA, et al. (2001) Importance of the forest canopy to fluxes of methyl mercury and total mercury to boreal ecosystems. *Environmental Science & Technology* 35(15): 3089–3098.

St Louis VL, Rudd JWM, Kelly CA, et al. (2004) The rise and fall of mercury methylation in an experimental reservoir. *Environmental Science & Technology* 38(5): 1348–1358.

Stock A and Cucuel F (1934) The quantitative determination of microamounts of mercury. *Naturwissenchaften* 22: 390.

Stoffers P, Hannington M, Wright I, Herzig P, de Ronde C, and Party SS (1999) Elemental mercury at submarine hydrothermal vents in the Bay of Plenty, Taupo Volcanic Zone, New Zealand. *Geology* 27(10): 931–934.

Stoiber RE and Jepsen A (1973) Sulfur dioxide contributions to atmosphere by volcanos. *Science* 182(4112): 577–578.

Stoiber RE, Williams SN, and Huebert B (1987) Annual contribution of sulfur dioxide to the atmosphere by volcanos. *Journal of Volcanology and Geothermal Research* 33(1–3): 1–8.

Stordal MC and Gill GA (1995) Determination of mercury methylation rates using a 203-Hg radiotracer technique. *Water, Air, and Soil Pollution* 80(1–4): 725–734.

Stratton WJ and Lindberg SE (1995) Use of a refluxing mist chamber for measurement of gas-phase mercury(II) species in the atmosphere. *Water, Air, and Soil Pollution* 80(1–4): 1269–1278.

Streets DG, Zhang Q, and Wu Y (2009) Projections of global mercury emissions in 2050. *Environmental Science & Technology* 43(8): 2983–2988.

Strode SA, Jaegle L, Selin NE, et al. (2007) Air–sea exchange in the global mercury cycle. *Global Biogeochemical Cycles* 21(1): GB1017.

Sunderland EM, Cohen MD, Selin NE, and Chmura GL (2008) Reconciling models and measurements to assess trends in atmospheric mercury deposition. *Environmental Pollution* 156: 526–535.

Sunderland EM, Gobas FAPC, Branfireun BA, and Heyes A (2006) Environmental controls on the speciation and distribution of mercury in coastal sediments. *Marine Chemistry* 102(1–2): 111–123.

Sunderland EM, Krabbenhoft DP, Moreau JW, Strode SA, and Landing WM (2009) Mercury sources, distribution, and bioavailability in the North Pacific Ocean: Insights from data and models. *Global Biogeochemical Cycles* 23: GB2010.

Swain EB, Engstrom DR, Brigham ME, Henning TA, and Brezonik PL (1992) Increasing rates of atmospheric mercury deposition in midcontinental North America. *Science* 257: 784–787.

Swain EB and Helwig DD (1989) Mercury in fish from northeastern Minnesota lakes: Historical trends, environmental correlates, and potential sources. *Journal of the Minnesota Academy of Science* 55: 103–109.

Swartzendruber PC, Chand D, Jaffe DA, et al. (2008) Vertical distribution of mercury, CO, ozone, and aerosol scattering coefficient in the Pacific Northwest during the spring 2006 INTEX-B campaign. *Journal of Geophysical Research* 113(D10): D10305.

Swartzendruber PC, Jaffe DA, Prestbo EM, et al. (2006) Observations of reactive gaseous mercury in the free troposphere at the Mount Bachelor Observatory. *Journal of Geophysical Research* 111(D24): D24301.

Talbot R, Mao H, Scheuer E, Dibb J, and Avery M (2007) Total depletion of Hg^0 in the upper troposphere–lower stratosphere. *Geophysical Research Letters* 34(23): L23804.

Thakur AN and Goel PS (1989) Huge variations in the isotopic ratio Hg-196/Hg-202 in some acid-insoluble residues of Sikhote Alin and other iron-meteorites. *Earth and Planetary Science Letters* 96(1–2): 235–246.

Tokos JJS, Hall B, Calhoun JA, and Prestbo EM (1998) Homogeneous gas-phase reaction of Hg-0 with H_2O_2, O_3, CH_3I, and $(CH_3)_2S$: Implications for atmospheric Hg cycling. *Atmospheric Environment* 32(5): 823–827.

Topping G and Davies IM (1981) Methylmercury production in the marine water column. *Nature* 290: 243–244.

Tremblay A, Lucotte M, and Schetagne R (1998) Total mercury and methylmercury accumulation in zooplankton of hydroelectric reservoirs in northern Quebec (Canada). *Science of the Total Environment* 213(1–3): 307–315.

Tseng CM, Amouroux D, Abril G, Tessier E, Etcheber H, and Donard OFX (2001) Speciation of mercury in a fluid mud profile of a highly turbid macrotidal estuary (Gironde, France). *Environmental Science & Technology* 35(13): 2627–2633.

Tseng CM, Balcom PH, Lamborg CH, and Fitzgerald WF (2003) Dissolved elemental mercury investigations in Long Island Sound using on-line Au amalgamation-flow injection analysis. *Environmental Science & Technology* 37(6): 1183–1188.

Tseng CM, Lamborg C, Fitzgerald WF, and Engstrom DR (2004) Cycling of dissolved elemental mercury in Arctic Alaskan lakes. *Geochimica et Cosmochimica Acta* 68(6): 1173–1184.

Turekian KK and Wedepohl KH (1961) Distribution of the elements in some major units of the Earth's crust. *Geological Society of America Bulletin* 72: 175–192.

Urban NR, Eisenreich SJ, Grigal DF, and Schurr KT (1990) Mobility and diagenesis of Pb and Pb-210 in peat. *Geochimica et Cosmochimica Acta* 54(12): 3329–3346.

USEPA (1997) Mercury Study Report to Congress. *EPA-452/R-97-003*. Washington, DC: US Environmental Protection Agency.

USFDA (2001) *Mercury Levels in Seafood Species*. Washington, DC: US Food and Drug Administration, Center for Food Safety and Applied Nutrition, Office of Seafood.

Vaidya OC, Howell GD, and Leger DA (2000) Evaluation of the distribution of mercury in lakes in Nova Scotia and Newfoundland (Canada). *Water, Air, and Soil Pollution* 117(1–4): 353–369.

Vandal GM, Fitzgerald WF, Boutron CF, and Candelone JP (1993) Variations in mercury deposition to Antarctica over the past 34,000 years. *Nature* 362(6421): 621–623.

Vandal GM, Fitzgerald WF, Rolfhus KR, Lamborg CH, Langer CS, and Balcom PH (2002) Sources and cycling of mercury and methylmercury in Long Island Sound, *CWF-326-R, Final Report to the Connecticut Department of Environmental Protection*.

Vandal GM, Mason RP, McKnight D, and Fitzgerald W (1998) Mercury speciation and distribution in a polar desert lake (Lake Hoare, Antarctica) and two glacial meltwater streams. *Science of the Total Environment* 213(1–3): 229–237.

Vandal G, Mason R, and Fitzgerald W (1991) Cycling of volatile mercury in temperate lakes. *Water, Air, & Soil Pollution* 56(1): 791–803.

Varekamp JC, Buchholtz ten Brink MR, Mecray EL, and Kreulen B (2000) Mercury in Long Island Sound sediments. *Journal of Coastal Research* 16: 613–626.

Varekamp JC and Buseck PR (1981) Mercury emissions from Mount St Helens during September 1980. *Nature* 293(5833): 555–556.

Varekamp JC and Buseck PR (1983) Mercury anomalies in soils: A geochemical exploration method for geothermal areas. *Geothermics* 12(1): 29–47.

Varekamp JC and Buseck PR (1984) The speciation of mercury in hydrothermal systems, with applications to ore deposition. *Geochimica et Cosmochimica Acta* 48(1): 177–185.

Varekamp JC and Buseck PR (1986) Global mercury flux from volcanic and geothermal sources. *Applied Geochemistry* 1(1): 29–47.

Verta M and Matilainen T (1995) Methylmercury distribution and partitioning in stratified Finnish forest lakes. *Water, Air, and Soil Pollution* 80(1–4): 585–588.

von Glasow R (2010) Atmospheric chemistry in volcanic plumes. *Proceedings of the National Academy of Sciences of the United States of America* 107(15): 6594–6599.

Wang Q, Shen WG, and Ma ZW (2000) Estimation of mercury emission from coal combustion in China. *Environmental Science & Technology* 34(13): 2711–2713.

Wardell LJ, Kyle PR, and Counce D (2008) Volcanic emissions of metals and halogens from White Island and Erebus Volcano (Antarctica) determined with chemical traps. *Journal of Volcanology and Geothermal Research* 177(3–4): 734–742.

Watras CJ and Bloom NS (1994) The vertical distribution of mercury species in Wisconsin lakes: Accumulation in plankton layers. In: Watras CJ and Huckabee JW (eds.) *Mercury Pollution: Integration and Synthesis*, pp. 137–152. Ann Arbor, MI: Lewis.

Watras CJ, Bloom NS, Hudson RJM, et al. (1994) Sources and fates of mercury and methylmercury in Wisconsin lakes. In: Watras CJ and Huckabee JW (eds.) *Mercury Pollution: Integration and Synthesis*, ch. i.12, pp. 153–180. Ann Arbor, MI: Lewis.

Watson CM, Dwyer DJ, Andle JC, Bruce AE, and Bruce MRM (1999) Stripping analyses of mercury using gold electrodes: Irreversible adsorption of mercury. *Analytical Chemistry* 71(15): 3181–3186.

Westöö G (1966) Determination of methylmercury compounds in foodstuffs: I. Methylmercury compounds in fish, identification and determination. *Acta Chemica Scandinavica* 20(8): 2131–2137.

White DE (1967) Mercury and base-metal deposits with associated thermal and mineral waters. In: Barnes HL (ed.) *Geochemistry of Hydrothermal Ore Deposits,* ch. 13. New York: Holt, Rinehart and Winston.

Wiener JG, Fitzgerald WF, Watras CJ, and Rada RG (1990a) Partitioning and bioavailability of mercury in an experimentally acidified Wisconsin lake. *Environmental Toxicology and Chemistry* 9(7): 909–918.

Wiener JG, Martini RE, Sheffy TB, and Glass GE (1990b) Factors influencing mercury concentrations in walleyes in northern Wisconsin lakes. *Transactions of the American Fisheries Society* 119: 862–870.

Wiener JG, Krabbenhoft DP, Heinz GH, and Scheuhammer AM (2002) Ecotoxicology of mercury. In: Hoffman DJ and Rattner BA (eds.) *Handbook of Ecotoxicology*. Boca Raton, FL: Lewis.

Wiener JG and Spry DJ (1996) Toxicological significance of mercury in freshwater fish. In: Beyer WN, Heinz GH, and Redmon-Norwood AW (eds.) *Environmental Contamination of Wildlife*, pp. 297–339. Boca Raton, FL: Lewis.

Wilhelm SM (1999) Conceptual design of mercury removal systems for liquid hydrocarbons. *Hydrocarbon Processing* 78(4): 61.

Wilhelm SM (2001) Estimate of mercury emissions to the atmosphere from petroleum. *Environmental Science & Technology* 35(24): 4704–4710.

Winfrey MR and Rudd JWM (1990) Environmental factors affecting the formation of methylmercury in low pH lakes. *Environmental Toxicology and Chemistry* 9(7): 853–869.

Witt MLI, Fischer TP, Pyle DM, Yang TF, and Zellmer GF (2008a) Fumarole compositions and mercury emissions from the Tatun Volcanic Field, Taiwan: Results from multi-component gas analyzer, portable mercury spectrometer and direct sampling techniques. *Journal of Volcanology and Geothermal Research* 178(4): 636–643.

Witt MLI, Mather TA, Pyle DM, Aiuppa A, Bagnato E, and Tsanev VI (2008b) Mercury and halogen emissions from Masaya and Telica volcanoes, Nicaragua. *Journal of Geophysical Research* 113(B6): B06203.

Wood JM, Kennedy FS, and Rosen CG (1968) Synthesis of methyl-mercury compounds by extracts of a methanogenic bacterium. *Nature* 220: 173–174.

Wu Q, Apte SC, Batley GE, and Bowles KC (1997) Determination of the mercury complexation capacity of natural waters by anodic stripping voltammetry. *Analytica Chimica Acta* 350: 129–134.

Xia K, Skyllberg UL, Bleam WF, Bloom PR, Nater EA, and Helmke PA (1999) X-ray absorption spectroscopic evidence for the complexation of Hg(II) by reduced sulfur in soil humic substances. *Environmental Science & Technology* 33(2): 257–261.

Xiao ZF, Munthe J, Schroeder WH, and Lindqvist O (1991) Vertical fluxes of volatile mercury over forest soil and lake surfaces in Sweden. *Tellus B* 43(3): 267–279.

Yang HD, Engstrom DR, and Rose NL (2010) Recent changes in atmospheric mercury deposition recorded in the sediments of remote equatorial lakes in the Rwenzori Mountains, Uganda. *Environmental Science & Technology* 44(17): 6570–6575.

Young DR, Johnson JN, Soutar A, and Isaacs JD (1973) Mercury concentrations in dated varved marine sediments collected off Southern California. *Nature* 244: 273–275.

Zambardi T, Sonke JE, Toutain JP, Sortino F, and Shinohara H (2009) Mercury emissions and stable isotopic compositions at Vulcano Island (Italy). *Earth and Planetary Science Letters* 277(1–2): 236–243.

11.5 The Geochemistry of Acid Mine Drainage

DW Blowes and CJ Ptacek, University of Waterloo, Waterloo, ON, Canada
JL Jambor[†], University of British Columbia, Vancouver, BC, Canada
CG Weisener, University of Windsor, Windsor, ON, Canada
D Paktunc and WD Gould, Natural Resources Canada, Ottawa, ON, Canada
DB Johnson, Bangor University, Bangor, UK

This article is a revision of the previous edition article by D.W. Blowes, C.J. Ptacek, J.L. Jambor, and C.G. Weisener, volume 9, pp. 149–204, © 2003, Elsevier Ltd.

[†]Deceased

11.5.1 Introduction

11.5.1.1 Scale of the Problem

Mine wastes are the largest volume of materials handled in the world (ICOLD, 1996). The generation of acidic drainage and the release of water containing high concentrations of dissolved metals from these wastes are an environmental problem of international scale. Acidic drainage is caused by the oxidation of sulfide minerals exposed to atmospheric oxygen. Although acid drainage is commonly associated with the extraction and processing of sulfide-bearing metalliferous ore deposits and sulfide-rich coal, acidic drainage can occur wherever sulfide minerals are excavated and exposed to atmospheric oxygen. Engineering projects, including road construction, airport development, and foundation excavation, are examples of civil projects that have resulted in the generation of acidic drainage. On US Forest Service lands, there are between 20 000 and 50 000 mines releasing acidic drainage (USDA, 1993). Kleinmann et al. (1991) estimated that more than 6400 km of rivers and streams in the Eastern United States have been adversely affected by mine-drainage water. Between 8000 and 16 000 km of streams have been affected by metal mining in the Western United States. The annual worldwide production of mine wastes exceeded 4.5 billion tonnes in 1982 (ICOLD, 1996). In Canada alone, there are approximately 980 million tonnes of mine wastes, with the potential to cause acidic drainage (Government of Canada, 1991). The estimated costs for remediating mine wastes internationally total in the tens of billions of dollars (Feasby, 1993).

11.5.1.2 Overview of the Mining Process and Sources of Low-Quality Drainage

The recovery of metals from sulfide-rich ore bodies proceeds through a series of steps: from mining to crushing to mineral recovery (i.e., concentration), followed typically by smelting of the sulfide concentrates and thence to metal refining; although the nature of the ore body dictates the processes used to extract metals from ores, each of these steps generates a waste stream. The volumes of the waste streams can be large. For example, the production of 1 tonne of copper typically requires the excavation and processing of 100 tonnes of ores, not including the removal of overburden or rock to access the ore. Each of the steps of metal production can lead to the generation of low-quality water.

11.5.1.3 Sources of Low-Quality Drainage

11.5.1.3.1 Mine workings

Minerals are typically excavated by underground mining, strip mining, or open-pit mining. The selection of the mining technique is dictated by the physical structure, location, and grade or value of the ore body and by the characteristics of the

adjacent geological materials. Although open-pit mining and underground mining are the two most common mining techniques, placer mining and solution mining also have been used for mineral extraction. Placer mining involves excavation of river or stream sediments and separation of valuable minerals by gravity, by selective flotation, or by chemical extraction. Most solution mining is by heap leaching in which the extractant solution is trickled over broken ore on the surface or in underground workings; less common is injection into underground geological formations. The consequence of the excavation of open-pits and other mining-related disturbances is that sulfide minerals previously isolated from the atmosphere are exposed to oxygen. The oxidation of sulfide minerals ensues.

11.5.1.3.2 Open-pits

Open-pit mining is a surface mining technique employed to extract ores from large deposits that are relatively close to the surface. By design, open-pit mining can expose large surface areas of wall rock to atmospheric oxygen. If the wall rocks contain iron sulfide minerals, open-pits can be an important source of acidic drainage during and following mining as long as they remain exposed. Open-pits are typically several hundreds of meters deep and wide. For example, the Kennecott Copper Mine in Utah, United States, is 4 km wide and 1.2 km deep. Thus, large surfaces of rocks are exposed as potential sources of acidic drainage.

11.5.1.3.3 Waste rock

Open-pit and underground mining result in the excavation of large volumes of rock to gain access to ore bodies. After the ore body is accessed, ore for processing is separated from the host rock on the basis of economic cutoff values. Ore of higher metal grade is processed, and rock below the cutoff grade is put to waste. Frequently, ore is segregated into high-grade and low-grade ore stockpiles. Ore is the material that will yield a profit; thus, the metal contents of the discrimination between high-grade and low-grade ores will vary with the costs of mining activities and the value of the metals extracted. The waste rock from mining operations may be used in construction activities at the mine site. Excess waste rock is deposited in waste-rock piles whose composition differs greatly from mine to mine because of variations in ore-deposit and host-rock mineralogy and because of differences in the processing techniques and ore-grade cutoff values. Daily production of waste rock in Canada is estimated to be 1 000 000 tonnes (Government of Canada, 1991). Because of the large volume of rock excavated in open-pit operations, waste-rock piles may be tens of hectares in area and tens of meters in height (Ritchie, 1994).

11.5.1.3.4 Mill tailings

The ore extracted in most nonferrous, metalliferous mining operations is rich in base or precious metals, but the ore minerals are generally too dilute for direct processing using metallurgical techniques. Thus, most ores are processed through comminution steps that involve crushing and grinding to a fine-grain size and concentration steps such as gravity, magnetic, and flotation for beneficiation or upgrading of the ore minerals in the matrix. The grain size of the milled rock is dictated by the process used for mineral recovery. Typical grain sizes range from 25 μm to 1.0 mm. At many plants, differential flotation is used to separate the valuable sulfide minerals containing base or precious metals from others (e.g., pyrite [FeS_2] or pyrrhotite [$Fe_{0.875-1}S$]) that have no to little commercial value. A flotation concentrator may contain several circuits for the selective recovery of a variety of metal sulfides and the production of a series of metal-sulfide concentrates. The concentrate from the flotation step is retained for further metallurgical processing. Mill tailings are the residual material, including sulfide gangue minerals, that is discharged to tailings impoundments, typically as a slurry of water and finely ground rock. Mineral particles are removed from the slurry by gravity sedimentation, and the water is often recycled to the mill or discharged.

The ratio of tailings to concentrate can be very large, particularly at gold and precious-metal mines at which the concentrate may represent only a small fraction (e.g., ~1%) of the ore processed. The mining industry produces immense amounts of mine tailings. The mass of tailings produced daily in Canada is estimated to be 950 000 tonnes (Government of Canada, 1991). Tailings impoundments may be very large. For example, the Inco Ltd. Central Tailings Disposal Area covers an area of 25 km^2 with tailings up to 50 m in depth, and the ultimate capacity is more than 725 million tonnes (Puro et al., 1995).

Mill tailings are typically retained in impoundments. The retaining dams of many impoundments are constructed of coarse-grained tailings or of tailings combined with waste rock. These types of impoundments are designed to drain, thereby enhancing their structural integrity but resulting in the development of a thick zone of only partial saturation. The entry of gas-phase oxygen into the unsaturated tailings results in sulfide-mineral oxidation and in the release of low-quality drainage.

11.5.1.3.5 Wastes from extractive metallurgy operations

Metallurgical processing following milling (i.e., communition and concentrating) involves extractive metallurgy operations such as hydrometallurgy, pyrometallurgy, and electrometallurgy. Hydrometallurgy includes leaching operations performed in aqueous media using various chemicals and oxidizing agents (e.g., pressure leaching, pressure oxidation (POX), heap leaching, and bioleaching/oxidation). Resultant oxidation and leaching products are fine-grained residue formed during the process, which includes compounds such as elemental sulfur, various sulfate compounds, jarosite, goethite, and hematite.

Pyrometallurgy operations such as smelting and roasting involve processing of ores and other materials at high temperatures (i.e., often >1000 °C) and in the absence of aqueous media. Environmental issues related to pyrometallurgy involve gaseous and particulate emissions (e.g., SO_2, CO_2, CO, Hg, As-, Sb-, Se-, and Te-oxides). Significant amounts of SO_2 gas is produced from the oxidation of sulfide minerals during pyrometallurgical treatments. Although most of the SO_2 is captured and converted to sulfuric acid or elemental sulfur and/or reacted with lime to form gypsum, the quantities of roaster and smelting gases are significant. In addition, smelting operations produce wastes such as slags and sludge that are disposed in waste impoundments and sludge ponds. Electrometallurgy operations utilizing electrical energy for electrolysis include electrorefining and electrowinning unit operations. Wastes contain small quantities of fine-grained residue and slimes incorporating impurity elements originating from the anodes.

11.5.2 Mineralogy of Ore Deposits

11.5.2.1 Coal Deposits

Coal is a fossil fuel that represents the remains of flora that accumulated as peat in swamps and bogs during geological and prehistoric times. The accumulation occurred in submerged conditions, thereby preventing complete decay of the organic material to $CO_2 + H_2O$ during the early stage of maturation. Reflecting its origin, coal occurs in beds, maximum thicknesses approximate 90 m, and typical mining thicknesses are 1–4 m.

The uses of coal include electricity generation, steelmaking, and cement production. The carbon content of coal varies from about 70% to 95 wt% with most of the remainder consisting of O, H, N, and S. The O content generally ranges from about 2% to 20%, and the major change that occurs during coalification is a decrease in the O content and an increase in the carbon content. With this change, the physical properties and thermal yield per unit weight also change, and various classifications have been devised to reflect those properties. A common commercial subdivision is into 'brown coal' and 'hard coal,' which in turn is an indication of the degree of induration. Coals can also be grouped under four types with decreasing energy content: anthracite, bituminous, subbituminous, and lignite.

Proven coal reserves are estimated to be 826 billion tonnes (World Energy Council, 2009). The bituminous type forms about 52% of the world reserves followed by subbituminous type at 30% and lignite at 17%. The reserves are about equally distributed among Europe and Asia region (33%), Asia Pacific region (31.4%), and North America (29.8%) with the United States, Russia, China, and India having the biggest reserves. According to International Energy Agency (2010) figures, current world production is about 5990 Mt (million metric tonnes) of hard coal and 913 Mt of brown coal. Germany, at about 160 Mt, is the largest producer of brown coal, with Russia a distant second. China's production of 2971 Mt of hard coal is the world's highest, followed by the United States (919 Mt). India ranks third and produces 526 Mt. In recent years, the United States has undergone a pronounced shift to mining of Western coal, predominantly subbituminous, which has a lower average content of sulfur than coals from Appalachia. Wyoming alone now accounts for about a third of all US production. According to the statistics given by BP Statistical Review of World Energy (2010), the production and consumption of coal in the Asia Pacific region have more than doubled within the last decade (i.e., 1000–2200 Mt oil equivalent in 1999). This is in sharp contrast to the figures from North America, and Europe and Eurasia regions where the production and consumption figures have decreased slightly.

Environmental concerns have been focused on the gaseous (oxides of sulfur and nitrogen and greenhouse gases such as carbon dioxide and methane), particulate, and trace-element emissions (e.g., mercury, selenium, and arsenic), on the environmental quality of the ash and slag residues, and on acidic drainage that may ensue as a consequence of the exposure of mining-related wastes and mine openings to atmospheric weathering. Many of the environmentally least desirable aspects concerning the utilization of coal are related to the presence of mineral matter, especially Fe disulfides. The disulfides are a principal source for SO_2 emissions during combustion, and in mine wastes, the oxidation of FeS_2 is the principal cause of the development of acidic drainage.

Stach et al. (1982) list more than 40 minerals that have been identified as occurring in coal, and recent observations have expanded the total to more than a hundred. Finkelman (1980a,b) concluded that coals yielding >5 wt% ash have had the bulk of their minerals derived by detrital processes.

Table 1 summarizes and presents an interpretation of the occurrence of the principal nondetrital minerals in coal. The chief detrital minerals are quartz and clay minerals (including K–Al micas), and these minerals commonly form up to 90% of the mineral matter in coals. The bulk of the remainder typically consists of carbonates and pyrite. Renton (1982) observed that most discrete mineral grains observed in coal are about 20 μm in diameter, and few exceed 100 μm. Exceptions are concretions, nodules, and 'balls' that typically contain one or more of pyrite, marcasite [FeS_2], calcite [$CaCO_3$], and siderite [$FeCO_3$] and which may be many centimeters in diameter. As well, aggregates of pyrite and marcasite occur within coal and as fracture (cleat) mineralization. The most common cleat-filling minerals are calcite, pyrite, and kaolinite [$Al_2Si_2O5(OH)_4$] (Renton, 1982). Vassilev et al. (1996) observed that higher rank coals are enriched in elements associated with probable detrital minerals, whereas lower rank coals are enriched in elements associated with probable authigenic minerals and organic material. The magnitude of the concentrations of trace elements in coal is summarized in **Table 2**. Modern

Table 1 Some minerals observed in coal deposits[a]

Mineral group	*Inherent*	*Extraneous source*
Clay minerals	Kaolinite, illite–sericite[b], mixed-layer clays, smectite	Illite–sericite[b], chlorite
Carbonates	Calcite, siderite, dolomite–ankerite	Calcite, dolomite–ankerite
Sulfides	Pyrite, marcasite, sphalerite, galena, chalcopyrite, pyrrhotite, greigite	Pyrite, marcasite, sphalerite, galena, chalcopyrite
Oxides	Quartz, Fe oxyhydroxides, hematite	Quartz, goethite, lepidocrocite
Phosphates	Apatite, crandallite-group minerals, vivianite	Apatite
Others	Gypsum, halite	Sulfates, chlorides, nitrates

[a]Interpreted partly from data in Mackowsky (1968), Renton (1982), Stach et al. (1982), Harvey and Ruch (1986), Birk (1989), Ward (1989), Speight (1994), and Spears (1997). The extraneous source minerals typically form after consolidation has progressed to the state at which the coal can sustain fracturing, and the minerals occur as fracture fillings and in cavities. The minerals in each group are listed in approximate decreasing order of abundance.

[b]Sericite is a general term for fine-grained, mica-like minerals. Illite has been assigned a specific composition by the International Mineralogical Association (Rieder et al., 1998), but illite and sericite are used here only to designate mica-type minerals. The mineral ankerite has a formula Fe > Mg, but the name is commonly used for ferroan dolomite [$Ca(Mg,Fe)(CO_3)_2$].

Table 2 The magnitude of the trace-element contents (ppm) of coal and coal ash

	Coal		*Coal ash*	
Element	*Average*[a]	*Range*[b]	*Average*[c]	*Range*[d]
Antimony	3.0	0.05–10		200?
Arsenic	5.0	0.5–80	500	100–500?
Barium	500	20–1000		300–900
Beryllium	3	0.1–15	45	1–10
Bismuth	5.5		20	2–50
Boron	75	5–400	600	
Cadmium	1.3	0.1–3	5	5?
Chlorine	1000	50–2000		
Chromium	10	0.5–60		100–400
Cobalt	5	0.5–30	300	300
Copper	15	0.5–50		20–200
Fluorine		20–500		
Gallium	7	1–20	100	100?
Germanium	5	0.5–50	500	50–500
Lead	25	2–80	100	5–50?
Lithium	65	1–80		
Manganese	50	5–300		
Mercury	0.01	0.02–1		0.02–0.5?
Molybdenum	5	0.1–10	50	100–200
Nickel	15	0.5–50	700	50–800
Phosphorus	500	10–3000		
Scandium	5	1–10	60	
Selenium	3	0.2–1.4		60?
Silver	0.50		2	1–5
Strontium	500	15–500		80–170?
Thallium		<0.2–1		1?
Thorium		0.5–10		
Tin		1–10		16–200?
Titanium	500	10–2000		
Uranium	1.0	0.5–10	400	
Vanadium	25	2–100		100–1000
Zinc	50	5–300		100–1000?
Zirconium		5–200		100–500?

[a]From the US National Committee for Geochemistry, as cited in Valković (1983).
[b]Swaine (1990).
[c]Mason (1958).
[d]Krauskopf (1955).

technology utilizes coal washing, fluidized bed combustion, activated carbon injection, gasification of coal, flue gas desulfurization, and particulate control devices to improve energy extraction while limiting the gaseous and liquid emissions. The lower temperatures of those processes affect the fate of the individual trace elements that are emitted or are associated with the residues from the consumed coal (**Table 2**; Clarke, 1993).

11.5.2.2 Base-Metal Deposits

Base metal is a wide-ranging term that refers either to metals inferior in value to those of gold and silver or, alternatively, to metals that are more chemically active than gold, silver, and the platinum metals (AGI, 1957). Accordingly, a review of base-metal mineralogy would encompass much of the world's metal production and geology. Usage of the 'base metal' term in the mining and minerals industry is rather loose, but a common application is to the nonferrous metals excluding precious metals. These include copper, lead, zinc, nickel, and tin. Kesler (1994), however, grouped nickel with ferroalloy metals along with manganese, chromium, silicon, cobalt, molybdenum, vanadium, tungsten, niobium, and tellurium and copper, lead, zinc, and tin as base metals. Among the base metals, tin is by far the least significant in terms of volumes consumed and monetary value.

World mine production of copper in 2009 exceeded 15 Mt, about a third of which is from Chile. Other large producers are Peru and the United States, followed closely by China, Indonesia, and Australia. The most important ore mineral is chalcopyrite [$CuFeS_2$] and also significant are bornite [Cu_5FeS_4] and chalcocite [Cu_2S]. These three minerals make up about 90% of the primary copper production. The first two are the primary minerals, whereas chalcocite forms principally by their weathering and subsequent reprecipitation of the solubilized Cu as enriched 'blankets' of chalcocite ore beneath the oxidation zone.

Copper ore is predominantly derived from porphyry copper deposits, with lesser but significant contributions from massive sulfide, skarn, and other types of deposits. The host rocks for porphyry copper deposits are felsic granitoid intrusions, and in skarn deposits, the intrusions penetrate limestone and associated sedimentary-derived assemblages. The deposits are typically large (commonly hundreds of million tonnes) and of low grade (commonly <1% Cu), with successful exploitation dependent mainly on open-pit access and on daily large-tonnage extraction and processing.

Based on the 2009 figures, the world mine production of zinc is about 11 Mt, with almost all of it derived from sphalerite [(Zn,Fe)S], which is also the principal primary source of Cd and several other metals, such as Ge and In. China, Peru, and Australia are the largest producers, but several other countries including Canada, the United States, and India mine significant amounts. About half of the annual consumption is for the manufacture of galvanized products to resist corrosion, primarily in the automotive and construction industries.

Sources of sphalerite in mineral deposits are diverse. Large production is obtained chiefly from skarn (e.g., Antamina, Peru); from volcanogenic massive sulfide deposits (e.g., Kidd Creek and Brunswick No. 12, Canada) in which pyrite is the predominant mineral; from sedimentary-exhalative (SEDEX) deposits (e.g., Broken Hill and Mt. Isa, Australia) in which layers of Pb, Zn, and Fe sulfides occur in fine-grained clastic sedimentary rocks; and from Mississippi Valley-type deposits (e.g., Viburnum Trend, United States) in which sphalerite and galena [PbS] were deposited in large amounts in cavities, breccias, and as replacements of calcareous sedimentary rocks consisting predominantly of limestone.

Whereas sphalerite is the principal mineral source of Zn, galena is the main source of Pb. The annual world mining production of lead reached about 4 Mt in 2009, and the annual consumption is nearing 9 Mt, with the difference made up by recycling. The largest primary producers are China, Australia, and the United States, and the largest consumers are China and the United States. More than 75% of lead consumption is for the manufacture of lead–acid automotive batteries, which also are the principal source of recycled scrap. Unlike Zn, which is an essential biological trace element, Pb has no similar

function and is an important environmental hazard (Kesler, 1994). The processing of Pb and Zn concentrates is almost totally by conventional pyrometallurgical smelting, but the most abundant anthropogenic sources of Pb have been coal combustion and gasoline additives (Kesler, 1994).

Nickel production from primary sources includes Ni sulfide deposits located principally in Canada, Russia, Australia, and South Africa and laterite deposits in New Caledonia, Indonesia, Colombia, Brazil, Cuba, and the Dominican Republic. Russia is the top producer of Ni from the Norilsk–Talnakh Ni sulfide deposits that are considered to be the largest in the world. Canada, Indonesia, and Australia are the other important Ni producers. Stainless steel and alloys account for more than 80% of Ni consumption. Nickel sulfide deposits are associated with mafic and ultramafic complexes where pentlandite is the main mineral source of Ni. Pyrrhotite and chalcopyrite are the other abundant sulfide minerals. Laterite deposits are remnants of highly weathered mafic and ultramafic rocks. Nickel is hosted by silicate minerals and Fe(III) oxyhydroxides such as goethite.

11.5.2.3 Precious-Metal Deposits

The precious-metal group consists of gold, silver, and the platinum-group elements (PGEs). The world's leading producer of Au is China, followed by Australia, the United States, Russia, and South Africa forming nearly half of the total world production figure of 2572 Mt in 2009. Most mining of Au is done specifically for that metal rather than for a polymetallic assemblage, and most Au is produced from auriferous quartz veins also known as lode deposits. However, appreciable amounts (i.e., ~20%) of Au are recovered as a by-product from the processing of base-metal ores, especially Cu deposits. A characteristic feature of all types of deposits is that nearly all of the Au occurs as the native metal, commonly with Ag in solid solution. Another type of economically important Au deposits is known as the refractory Au where Au occurs in solid solution or as nanoparticulate form in arsenical pyrite and/or arsenopyrite. Gold is recovered from such ores by the destruction of the host sulfide through roasting, POX, or bacterial oxidation (BIOX) processes prior to cyanidation. Environmental concerns related to roasting are the high-As emissions and the disposal of the As_2O_3 that precipitates from the condensed gases. The use of pressurized autoclaves to oxidize the host sulfide minerals has increased to decrease As emissions. Another environmental concern has been the use of mercury to recover gold by amalgamation. This practice has been largely discontinued because the effects of mercury poisoning are well known, but a legacy of pollution remains in many areas, and amalgamation on a small scale is still practiced by artisan miners in countries such as Brazil, Guyana, and Indonesia.

Gold in recent years has found increased markets in electrical and electronic applications, but these account for <5% of the annual consumption. About 90% of the annual production is utilized for jewelry and arts purposes.

Peru, China, Mexico, and Chile are the largest producers of silver, whose main usage is in photography, plating, jewelry, and electronic and electrical applications. More than two-thirds of the world's production of silver in 2009 was obtained as a by-product from smelting of base-metal ores including those from copper–gold deposits. For example, the world's largest silver producer is the metamorphosed, stratabound Cannington deposit in Australia. The deposit is of the Broken Hill type and contains about 44 Mt grading 11.6% Pb, 4.4% Zn, and 538 g t^{-1} Ag (Walters and Bailey, 1998). The dominant sulfide assemblage is galena–sphalerite–pyrrhotite, and the high-Ag content is related mainly to the presence of argentiferous galena and freibergite [$(Ag,Cu,Fe)_{12}Sb_4S_{13}$].

Mexico, one of the leading silver producers by country, obtains about half of its output from mines in which silver is the principal ore metal. Many of the mines are epithermal fissure veins, and most host a polymetallic assemblage whose exploitation is economically dependent on the high-Ag values. Although acanthite [Ag_2S] and native silver predominate in some veins, in others, much of the Ag occurs in Ag sulfosalts and as Ag substitutions in tetrahedrite [$(Cu,Fe,Ag)_{12}Sb_4S_{13}$] and other minerals.

The platinum-group metals consist of ruthenium, rhodium, palladium, osmium, iridium, and platinum. Each of the metals occurs naturally in its native form, and in economically exploitable deposits, the elements occur overwhelmingly as individual platinum-group mineral (PGM) species. Mutual substitution of the various PGEs is common, but substitutions in other minerals, such as base-metal sulfides, typically occur to only a limited extent. A comprehensive review of PGM and PGE geochemistry is given in Cabri (2002).

The platinum-group metals are generally grouped with gold and silver as precious-metal commodities, but the platinum-group metals have little in common with the other precious metals in terms of their primary geological host-rock associations. The world's largest producer of platinum and rhodium is South Africa, with most of the metal obtained from mines that exploit thin (centimeters rather than meters), PGM-rich layers (averaging <10 g t^{-1} PGE) in the Bushveld Complex, a layered mafic intrusion that is also a principal source of chromium and vanadium. Platinum and palladium account for all but a very small percentage of the world's PGE production. Whereas the Bushveld Complex accounts for more than a quarter of the world's palladium production, more than double that amount is obtained as a by-product from Cu–Ni mines in layered intrusive complexes such as those at Sudbury, Canada, and Norilsk–Talnakh, Russia; the latter is the world's largest primary source of palladium. Braggite [(Pt,Pd)S], cooperite [PtS], sperrylite [$PtAs_2$], michenerite [PdBiTe], moncheite [$PdTe_2$], and Pt–Fe alloys are among the principal sources of PGE.

The principal consumption of PGE is as a catalyst, especially the use of platinum, or the more favored palladium because of its superior high-temperature performance, in catalytic converters in motor vehicles. Among the diverse other chief uses are electrical and electronic applications, jewelry, fabrication of laboratory equipment, and dental repairs.

11.5.2.4 Uranium Deposits

Canada, Australia, and Kazakhstan are the world's largest producers of uranium. Together, they form about 63% of the world's uranium production. All Canadian production is from rich deposits in the Athabasca Basin of Northern Saskatchewan; among those is the McArthur River mine, which

has the world's largest high-grade deposit, estimated at 152 000 t of U from ore grading, 15–18% U. These 'unconformity'-type Saskatchewan deposits, which are also the principal deposit type for Australian uranium production, contain mainly uraninite [UO_2] with associated coffinite [$U(SiO_4)_{1-x}(OH)_{4x}$] and brannerite [$(U,Ca,Y,Ce)(Ti,Fe)_2O_6$] (Plant et al., 1999). The chief uses of uranium are in nuclear power plants and weaponry.

11.5.2.5 Diamond Deposits

The world's annual production of natural diamonds, including both the gemstone and industrial types, is about 159 million carats (1 carat = 200 mg). Almost all is derived from kimberlite or its weathered remnants, but Australian production is from the Argyle mine at which the host rock is lamproite. Kimberlites are olivine- and volatile-rich potassic ultrabasic rocks of variable geological age that typically form near-vertical carrot-shaped 'pipes' intruded into Archean cratons. The volatile-rich component is predominantly CO_2 in the carbonate minerals calcite and dolomite, and the texture is characteristically inequigranular, with large grains (macrocrysts), usually of magnesian olivine [Mg_2SiO_4], in a fine-grained, olivine-rich matrix.

Russia, Botswana, Congo, Australia, and Canada, in decreasing order, account for more than 80% of the carats (both gemstone and industrial) produced in 2008. In terms of gemstone carats, Botswana, Russia, and Canada account for over 70% of the world production, whereas South Africa production is ranked sixth and with less than 0.5% of the world production, Australia is ranked eleventh.

11.5.2.6 Other Deposits

Table 3 summarizes the data on the principal sources and uses of numerous other metals. The listing is not intended to be comprehensive.

11.5.3 Sulfide Oxidation and the Generation of Oxidation Products

A principal environmental concern associated with mining results from the oxidation of sulfide minerals within the waste

Table 3 Principal 'mineral' sources and usage of various metals

	Principal 'mineral' sources	*Principal usage*
Aluminum	Gibbsite [$Al(OH)_3$], böhmite [$AlO(OH)$]	Transportation, packaging
Antimony	Stibnite [Sb_2S_3], by-product from Pb sulfides	Flame-retardant chemical, hardener for Pb in batteries
Arsenic	By-product as As_2O_3	Wood preservatives
Beryllium	Beryl [$Be_3Al_2Si_6O_{18}$] from pegmatite, bertrandite [$Be_4Si_2O_7(OH)_2$] from tuff	Be–Cu alloys (telecommunications)
Bismuth	By-product, mainly from galena	Pharmaceuticals, chemicals
Cadmium	By-product from sphalerite	Batteries
Chromium	Chromite [$FeCr_2O_4$] in mafic–ultramafic intrusions	Stainless steel
Cobalt	Laterites, Ni–Cu sulfide ores, linnaeite [$Co^{2+}Co_2{}^{3+}S_4$] from sedimentary-hosted Cu–Co deposits	Superalloys, alloys with steel
Gallium	By-product from sphalerite	GaAs in electronic devices
Germanium	By-product from sphalerite	Fiber-optic systems
Indium	By-product from sphalerite	Electronics, LCD screens
Iron	Hematite [Fe_2O_3], goethite [FeOOH], magnetite [$Fe^{2+}Fe_2{}^{3+}O_4$]	Iron and steel
Magnesium	Brines, seawater, magnesite [$MgCO_3$]	Al alloys, die casting
Manganese	Mn oxides, hydroxides	Alloys with steel
Mercury	Cinnabar [HgS]	Electrolysis, batteries
Molybdenum	Molybdenite [MoS_2] from porphyry Mo and Cu deposits	Alloys with iron, steel
Nickel	Laterite, pentlandite [$(Fe,Ni)_9S_8$] in mafic–ultramafic intrusions	Steel and nonferrous alloys
Niobium	Pyrochlore [$(Ca,Na)_2Nb_2O_6(OH,F)$] from carbonatites	Alloys with steel, superalloys
Rare earths	Bastnäsite-Ce [$(Ce,La)(CO_3)F$] from carbonatites	Chemical catalyst, automotive catalytic converters, glass polishing, ceramics
Rhenium	By-product from molybdenite	Pt–Rh catalysts, superalloys
Scandium	By-product	Al alloys, halide lighting additive
Selenium	By-product from Cu anode slimes	Glass, metallurgical additive, electronics
Silicon	Quartz [SiO_2]	Additive to steel
Strontium	Celestine [$SrSO_4$]	Television faceplate glass, ceramics
Tantalum	Tantalite–columbite [$(Fe,Mn,Mg)Ta_2O_6$-$(Fe,Mn,Mg)Nb_2O_6$] from pegmatites	Electronic components
Tellurium	By-product from refining Cu ores	Steel and copper additive
Thallium	By-product from Cu–Zn–Pb sulfide ores	Semiconductor materials, electronics
Thorium	Monazite [$(REE,Th)PO_4$] by-product from heavy-mineral sands	Refractory applications, catalyst
Tin	Cassiterite [SnO_2] in placers	Plating on cans and containers, solder
Titanium	Ilmenite [$FeTiO_3$] from heavy-mineral sands	TiO_2 pigment
Tungsten	Scheelite [$CaWO_4$] from skarns, ferberite [$Fe^{2+}WO_4$] from veins	Tungsten carbide
Vanadium	Magnetite [$Fe^{2+}(Fe^{3+},V^{3+})_2O_4$] in mafic–ultramafic intrusions	Steel additive
Yttrium	By-product from bastnäsite REE production	Phosphors
Zirconium	Zircon [$ZrSiO_4$] from heavy-mineral sands	Refractory facings and bricks

materials and mine workings and the transport and release of oxidation products. The principal sulfide minerals in mine wastes are pyrite and pyrrhotite, but others are susceptible to oxidation, releasing elements such as Al, As, Cd, Co, Cu, Hg, Ni, Pb, and Zn to the water flowing through the mine waste.

11.5.3.1 Sulfide-Mineral Oxidation

11.5.3.1.1 Pyrite oxidation

Pyrite is the most abundant sulfide mineral in Earth's crust. It is commonly associated with coal, base-metal, and gold deposits. It is also commonly found elsewhere in crustal rocks unrelated to mineral deposits. Pyrite oxidation and the factors affecting the kinetics of oxidation (O_2, Fe^{3+}, temperature, pH, E_h, and the presence or absence of microorganisms) have been the focus of extensive study because of their importance in both environmental remediation and mineral separation by flotation (Brown and Jurinak, 1989; Buckley and Woods, 1987; Evangelou and Zhang, 1995; Luther, 1987; McKibben and Barnes, 1986; Moses et al., 1987; Nordstrom, 1982; Sasaki et al., 1995; Wiersma and Rimstidt, 1984; Williamson and Rimstidt, 1994). The reviews of pyrite oxidation and the formation of acid mine drainage (AMD) are given by Lowson (1982), Evangelou (1995), Evangelou and Zhang (1995), Nordstrom and Southam (1997), Nordstrom and Alpers (1999a), Rimstidt and Vaughan (2003), and Rosso and Vaughan (2006).

The oxidation of pyrite can occur when the mineral surface is exposed to an oxidant and water either in oxygenated or anoxic systems, depending on the oxidant. The process is complex and can involve chemical, biological, and electrochemical reactions. The chemical oxidation of pyrite can follow a variety of pathways involving surface interactions with dissolved O_2, Fe^{3+}, and other mineral catalysts (e.g., MnO_2). The oxidation of pyrite by atmospheric oxygen produces one mole of Fe^{2+}, two moles of SO_4^{2-}, and two moles of H^+ for every mole of pyrite oxidized (Nordstrom, 1982):

$$FeS_2(s) + \frac{7}{2}O_2 + H_2O \rightarrow Fe^{2+} + 2SO_4^{2-} + 2H^+ \qquad [1]$$

The Fe(II) thus released may be oxidized to Fe(III):

$$Fe^{2+} + \frac{1}{4}O_2 + H^+ \rightarrow Fe^{3+} + \frac{1}{2}H_2O \qquad [2]$$

Fe(III) oxyhydroxides such as ferrihydrite (nominally $5Fe_2O_3{\cdot}9H_2O$) may precipitate:

$$Fe^{3+} + 3H_2O \rightarrow Fe(OH)_3 + 3H^+ \qquad [3]$$

where $Fe(OH)_3$ is a surrogate for ferrihydrite. Adding eqns [1]–[3] yields the overall reaction:

$$FeS_2(s) + \frac{15}{4}O_{2(aq)} + \frac{7}{2}H_2O_{(aq)} \rightarrow 2SO_4^{2-} + Fe(OH)_{3(s)} + 4H^+{}_{(aq)} \qquad [4]$$

This overall reaction results in the release of four moles of H^+ for each mole of pyrite oxidized.

11.5.3.1.1.1 Chemical oxidation by Fe^{3+} and O_2

Initially, pyrite oxidation involves the adsorption of O_2 and water to the partly protonated pyrite surface by bonding to Fe^{2+} (Fornasiero et al., 1994). Various sulfide species and Fe oxyhydroxide intermediate products can form on the pyrite surface, depending on the pH. According to Todd et al. (2003), in oxygenated aqueous solutions under acidic conditions (pH < 4), an Fe(III) hydroxysulfate is the main oxidation product. As the pH is increased, an Fe(III) oxyhydroxide appears beside an Fe(III) hydroxysulfate, and under alkaline conditions, goethite dominates the pyrite surfaces. Singer and Stumm (1970) suggested that, under acidic conditions, the major oxidant of pyrite is Fe^{3+}, whereas O_2 becomes the predominant oxidant at circumneutral pH because of the diminished solubility of Fe^{3+}. Pyrite oxidation by Fe^{3+} at circumneutral pH has also been observed (Brown and Jurinak, 1989; Evangelou and Zhang, 1995; Moses et al., 1987), but the reaction cannot be sustained without the presence of dissolved O_2 to perpetuate the oxidation to Fe^{3+}. When O_2 is the oxidant under near-neutral pH conditions, one O atom in the sulfate is derived from dissolved O_2, with the remainder derived from H_2O. Under acidic conditions, all four O atoms in sulfate are derived from H_2O (Reedy et al., 1991). Although both Fe^{3+} and oxygen can bind chemically to the surface, the more rapid oxidation rates for Fe^{3+} compared to those for O_2 are due to a more efficient electron transfer for Fe^{3+} (Luther, 1987). A molecular orbital model proposed by Luther (1987) is consistent with pyrite oxidation data obtained by McKibben and Barnes (1986), Moses et al. (1987), and Wiersma and Rimstidt (1984).

Rate data from the literature for the reaction of pyrite with dissolved O_2 were compiled by Williamson and Rimstidt (1994) to produce a rate law that is applicable for more than four orders of magnitude in O_2 concentration and over a pH range of 2–10:

$$R = 10^{-8.19(\pm0.04)} \frac{m_{DO}^{0.5(\pm0.04)}}{m_{H^+}^{0.11(\pm0.01)}} \qquad [5]$$

where R is the rate of pyrite dissolution in units of mol m^{-2} s^{-1}.

A series of batch and mixed flow reactor experiments were performed at pH <3 to determine the effect of SO_4^{2-}, Cl^-, ionic strength and dissolved O_2 on the rate of pyrite oxidation by Fe^{3+}. Of these, only dissolved O_2 had any appreciable effect on the rate of pyrite oxidation in the presence of Fe^{3+}. Williamson and Rimstidt (1994) combined their experimental results with kinetic data reported from the literature to formulate rate laws that are applicable over a range spanning six orders of magnitude in Fe^{3+} and Fe^{2+} concentrations and for a pH range of 0.5–3.0 when fixed concentrations of dissolved O_2 are present:

$$R = 10^{-6.07(\pm0.57)} \frac{m_{Fe^{3+}}^{0.93(\pm0.07)}}{m_{Fe^{2+}}^{0.40(\pm0.06)}} \qquad [6]$$

where R is the rate of pyrite dissolution in units of mol m^{-2} s^{-1}.

A wide variation in empirical rate laws has been developed to describe pyrite oxidation. The wideness of the range could be due to several factors, among which are the differences in sample preparation, different ratios of surface area to volume, types of pyrite (e.g., low T, high T, framboidal, and massive), and presence of impurities and substitutions in the pyrite or in the solution. The activation energies determined for pyrite oxidation range from 50 kJ mol^{-1} for pH 2–4 to 92 kJ mol^{-1} for pH 6–8, regardless of whether dissolved O_2 or Fe(III) is used as the oxidant (Nicholson, 1994; Wiersma and Rimstidt,

Table 4 Summary of proposed rate expressions for the dissolution of pyrite in solutions containing dissolved oxygen and ferric ion

Source	*Rate expression: dissolved oxygen*	*Rate expression: dissolved iron*
Garrels and Thompson (1960)		$r_{FeS_2} = \frac{k\left[Fe^{3+}\right]}{\sum[Fe]}$
Mathews and Robins (1972, 1974)	$r_{FeS_2} = k[O_2]^{0.81}$	$r_{FeS_2} = \frac{k\left[Fe^{3+}\right]}{\sum[Fe]\left[H^+\right]^{0.44}}$
Lowson (1982)		$r_{FeS_2} = \frac{k\left[Fe^{3+}\right]\left[Fe^{2-}\right]}{\sum[Fe]}$
McKibben and Barnes (1986)	$r_{FeS_2} = k[O_2]^{0.5}$	$r_{FeS_2} = \frac{k\left[Fe^{3+}\right]^{0.58}}{\left[H^+\right]^{0.5}}$
Williamson and Rimstidt (1994)	$r_{FeS_2} = k[O_2]^{0.5}\left[H^+\right]^{-0.11}$	$r_{FeS_2} = \frac{k\left[Fe^{3+}\right]^{0.3}}{\left[Fe^{2+}\right]^{0.47}\left[H^+\right]^{0.32}}$
Holmes and Crundwell (2000)	$r_{FeS_2} = k\left[H^+\right]^{-0.18}[O_2]^{0.5}$	$r_{FeS_2} = k\left[H^+\right]^{-0.5}\left(\frac{k_{Fe^{3+}}\left[Fe^{3+}\right]}{k_{Fe^{2+}}\left[Fe^{2+}\right]k_{FeS_2}\left[H^+\right]^{-0.5}}\right)^{0.5}$

Source: Holmes PR and Crundwell FK (2000) The kinetics of the oxidation of pyrite by ferric ions and dissolved oxygen: An electrochemical study. *Geochimica et Cosmochimica Acta* 64: 263–274.

1984). **Table 4** provides a summary of the proposed rate expressions for the dissolution of pyrite in solutions containing dissolved O_2 and Fe(III). The activation energies are observed to be higher for pH values in the range of 6–8 than in the range from 2 to 4. Casey and Sposito (1991) suggested that the proton adsorption/desorption reactions can contribute up to 50 kJ mol^{-1} to the experimental activation energy of dissolution reactions for silicate minerals. The hydrogen ion activity or pH, therefore, may play an important role in the observed activation energy for the oxidation of sulfide minerals. Regardless, the high activation energies observed indicate that the rate-limiting step in pyrite oxidation is related to electron transfer at the pyrite surface.

Holmes and Crundwell (2000) studied the kinetics of pyrite oxidation and reduction independently using electrochemical techniques. The kinetics of the half reactions are related to the overall dissolution reaction assuming no accumulation of charge on the surface. This assumption was used to derive expressions for the mixed potential and rate of dissolution, which agreed with those obtained by McKibben and Barnes (1986) and Williamson and Rimstidt (1994). The results showed that the electrochemical reaction steps occurring at the mineral–solution interface control the rate of dissolution. As summarized by Rimstidt and Vaughan (2003), the steps are (1) cathodic reaction transferring electrons from the pyrite surface to the aqueous oxidant species, (2) electron transport from the anodic to cathodic site, and (3) anodic reaction involving H_2O molecules interacting with S atoms to form a sulfoxy species. Reactivity of pyrite can be influenced by subtle changes in the composition of pyrite because of its semiconductor nature (Rimstidt and Vaughan, 2003). In other words, highly variable minor- and trace-element compositions of pyrite including Au, As, Sb, Co, and Ni (Abraitis et al., 2004) and the stoichiometric variability in terms of excess S or its deficiency would influence the electrical properties of pyrite and its reactivity.

Secondary Fe(III) oxyhydroxide coatings that develop at neutral pH values can reduce the rate of pyrite oxidation by limiting the transport of reactants to pyrite surfaces. According to Huminicki and Rimstidt (2009), Fe(III) oxyhydroxide coatings grow in two stages: the formation of Fe oxyhydroxide colloids and their attachment to pyrite surfaces followed by the interstitial precipitation of Fe oxyhydroxide material between the colloidal particles. Both stages play a role in limiting the transport of oxidant to pyrite surfaces.

11.5.3.1.2 Pyrrhotite oxidation

Pyrrhotite is a common Fe sulfide mineral. Although there have been numerous studies of the oxidation of pyrite, fewer studies have focused on pyrrhotite oxidation (Buckley and Woods, 1985; Janzen et al., 2000; Jones et al., 1992; Nicholson and Scharer, 1994; Pratt et al., 1994a,b; Thomas et al., 1998). The pyrrhotite structure is based on hexagonal close packing but is disordered (i.e., NiAs-type structure), giving rise to nonstoichiometric and stoichiometric compositions in which x in the formula $Fe_{1-x}S$ can vary from 0.125 (Fe_7S_8) to 0 (FeS). The Fe vacancies within the structure may be charge-compensated by Fe^{3+} (Vaughan and Craig, 1978) or an approximation thereof. Analyses of cleaved pyrrhotite surfaces under vacuum showed Fe(III)–S interactions on the pyrrhotite surface (Pratt et al., 1994a). The deficiency in Fe within the pyrrhotite structure can result in a symmetry that varies from monoclinic (Fe_7S_8) to hexagonal ($Fe_{11}S_{12}$), with the composition progressing to stoichiometric troilite (FeS). Orlova et al. (1988) examined the reaction rates for monoclinic and hexagonal pyrrhotite and concluded that the hexagonal form was the more reactive.

The deficiency of Fe in the pyrrhotite structure may affect the oxidation behavior. Nicholson and Scharer (1994) observed a dependency of activation energy on pH; the energy ranged from 52 to 58 kJ mol^{-1} at pH 2–4 and almost doubled to 100 kJ mol^{-1} at circumneutral pH (i.e., 6). These values are similar to activation energies noted for pyrite, suggesting a

chemical-controlled reaction. Orlova et al. (1988) observed a range of activation energies for both monoclinic and hexagonal varieties ranging from 50 to 46 kJ mol^{-1}, respectively. It was argued that the lower activation energy was a function of the hexagonal crystal structure. Janzen et al. (2000), however, did not observe consistent trends between activation energy and crystal structure.

11.5.3.1.2.1 Chemical oxidation by O_2 and Fe^{3+}

Pyrrhotite dissolution can proceed through oxidative or nonoxidative reactions. Oxidative dissolution can be at least 10^3 times slower than nonoxidative reactions (Thomas et al., 1998). Dissolved O_2 and Fe^{3+} can be important oxidants of pyrrhotite. When oxygen is the primary oxidant, the overall reaction may be written as

$$\mathrm{Fe_{1-x}S} + \left(2 - \frac{1}{2}x\right)\mathrm{O_2} + x\mathrm{H_2O} \Rightarrow (1-x)\mathrm{Fe^{2+}} + \mathrm{SO_4^{2-}} + 2x\mathrm{H^+} \quad [7]$$

The production of protons is linked to the mineral stoichiometry. Up to one-quarter mole of the protons produced are derived from the oxidation of one mole of the Fe-deficient form ($x = 0.125$), whereas no protons are produced from the stoichiometric form, which is troilite ($x = 0$). The release of protons can also result from the oxidation of the dissolved Fe, resulting from the precipitation of ferric hydroxide:

$$\mathrm{Fe^{2+}} + \frac{1}{4}\mathrm{O_2} + \frac{5}{2}\mathrm{H_2O} \Rightarrow \mathrm{Fe(OH)_{3(S)}} + 2\mathrm{H^+} \quad [8]$$

In other circumstances, the oxidation reactions may not proceed to completion. Partial oxidation may result in only a small proportion of the S being transformed to sulfate, with the remainder accumulating as reduced sulfur species (polysulfides and elemental sulfur) at the mineral surface (Janzen et al., 2000):

$$\mathrm{Fe_{1-x}S_{(S)}} + \left(\frac{1-x}{2}\right)\mathrm{O_2} + 2(1-x)\mathrm{H^+} \Rightarrow (1-x)\mathrm{Fe^{2+}} + \mathrm{S_x^{n<0}} + (1-x)\mathrm{H_2O} \quad [9]$$

The rates of oxidation of both pyrite and pyrrhotite at 25 °C and the standard atmospheric oxygen indicate that pyrrhotite can react 20–100 times faster than pyrite. During oxidation of a particle of pyrrhotite, Fe diffuses to the exposed surface, thereby creating a S-enriched inner zone that contains disulfide- and polysulfide-like species (Mycroft et al., 1995).

11.5.3.1.2.2 Nonoxidative mechanism

Nonoxidative dissolution of pyrrhotite occurs in acidic solutions when predominant S^{2-} surface species are exposed. The reaction occurs as

$$\mathrm{FeS} + 2\mathrm{H^+} \Rightarrow \mathrm{Fe^{2+}} + \mathrm{H_2S} \quad [10]$$

Jones et al. (1992) observed restructuring of sulfur-rich pyrrhotite surfaces in deoxygenated acid, resulting in the development of a surface dominated by a discontinuous layer of a tetragonal intermediate Fe_2S_3 structure. Janzen et al. (2000) showed a significant release of Fe^{2+} from pyrrhotite in acidic solutions in which oxygen was not present. Although Fe^{2+} concentrations increased linearly with time, sulfate values remained unchanged, with sulfur from pyrrhotite dissolution remaining in a reduced state (S^{2-}). Thomas et al. (1998, 2001) proposed a dissolution mechanism that allows two distinct pathways: (1) Fe leaves the surface, with no additional electrons released from the structure, and (2) after a critical accumulation of charge, the reduction of polysulfide to sulfide occurs, resulting in the release of negative charge from the surface in the form of HS^-. The significant feature of this process is the delay between the release of Fe^{2+} and HS^-.

11.5.3.1.3 Oxidation of other metal sulfides

11.5.3.1.3.1 Sphalerite

The oxidation of sphalerite is dependent on a number of factors, among which are the concentration of oxidants, such as dissolved O_2 or Fe(III) in the solution, the temperature, and the pH (Bobeck and Su, 1985; Crundwell, 1988; Olanipekun, 1999; Perez and Dutrizac, 1991; Rimstidt et al., 1994). For sphalerite, Vaughan and Craig (1978) reported a solubility product of $K_{sp} = 1 \times 10^{-20.6}$ at 25 °C in water. Other researchers have reported similar values (Daskalakis and Helz, 1993).

For sphalerite in dilute Fe(III) solutions, Rimstidt et al. (1994) obtained a dissolution rate of 7.0×10^{-8} mol m^{-2} s^{-1} with a corresponding activation energy of 27 kJ mol^{-1} over a range of 25–60 °C. The concentration of Fe(III) used was 10^{-3} M, which is similar to dissolved Fe concentrations ($2–9 \times 10^{-3}$ M) typically observed in acidic mine waters (Lin, 1997). The overall oxidation reaction for pure sphalerite, assuming that all sulfur is oxidized to sulfate, is

$$\mathrm{ZnS} + 4\mathrm{H_2O} \Rightarrow \mathrm{Zn^{2+}} + \mathrm{SO_4^{2-}} + 8\mathrm{H^+} \quad [11]$$

The x-ray photoelectron spectroscopy (XPS) examination of oxidized sphalerite showed the development of a surface layer of metal-deficient sulfide (Buckley et al., 1989) whose formation in acid solution is described by

$$\mathrm{ZnS} \Rightarrow \mathrm{Zn_{1-x}S} + x\mathrm{Zn^{2+}} + 2x\mathrm{e^-} \quad [12]$$

Weisener et al. (2003, 2004) observed increased rates of oxidation and increased acid consumption as a function of the amount of solid-solution Fe in sphalerite [(Zn,Fe)S]. Apparent activation energies of 21–28 kJ mol^{-1} obtained at 25–85 °C are similar to the values reported by Rimstidt et al. (1994). Weisener et al. (2003, 2004) suggested that the production of polysulfide species results in a lower diffusion gradient at the mineral surface, thus leading to lower reactivity with potential oxidants and to diffusion-limited release of Zn and Fe from the bulk mineral. Elemental sulfur was not observed to limit the reactivity of the mineral surface. The accumulation of polysulfides and S^0 on the sphalerite surface under oxygenated conditions can affect the acid-neutralization capacity because the polysulfides and S^0 consume acid when pH is <3. The resulting formation of a S-enriched surface slows the subsequent rate of dissolution of sphalerite in the absence of bacteria. Under these conditions, S^0 does not passivate the surface (Weisener, 2002). Moncur et al. (2009) showed that the stability of sphalerite in tailings impoundments is generally greater than that of pyrrhotite but less than that of pyrite.

11.5.3.1.3.2 Galena and chalcopyrite

Galena and chalcopyrite are commonly associated with acid-generating minerals, such as pyrite and pyrrhotite. Acid ferric sulfate solutions, generated through the oxidation of Fe sulfides, can enhance the oxidation of Pb- and Cu-bearing

sulfide minerals. The oxidation of galena has been studied by Buckley and Woods (1984a), Tossell and Vaughan (1987), Fornasiero et al. (1994), Kim et al. (1995), Prestidge et al. (1995), Basilio et al. (1996), Kartio et al. (1996, 1998), Chernyshova and Andreev (1997), Jennings et al. (2000), Nowak and Laajalehto (2000), Shapter et al. (2000), and others. The XPS studies showed that S^0 formed when galena was oxidized in a hydrogen peroxide solution and that metal-deficient surfaces resulted from oxidation by dilute acetic acid solutions (Buckley and Woods, 1984a). In natural oxygenated environments, galena will weather to anglesite, which is weakly soluble below pH 6 (Lin, 1997; Shapter et al., 2000):

$$PbS_{(s)} + 2O_{2(aq)} \Rightarrow Pb^{2+}_{(aq)} + {SO_4}^{2-}{}_{(aq)} \quad [13]$$

$$Pb^{2+}_{(aq)} + {SO_4}^{2-}{}_{(aq)} \Rightarrow PbSO_{4(s)} \quad [14]$$

Galena may also be oxidized by Fe(III) under acidic conditions (Rimstidt et al., 1994):

$$PbS + 8Fe^{3+} + 4H_2O \Rightarrow 8H^+ + {SO_4}^{2-} + Pb^{2+} + 8Fe^{2+} \quad [15]$$

The oxidation of galena in air may result in the formation of lead hydroxide and lead oxide (Buckley and Woods, 1984a; Evans and Raftery, 1982; Laajalehto et al., 1993). The oxidation in aqueous solutions may lead to the formation of lead oxides and lead sulfate surface products (Fornasiero et al., 1994; Kartio et al., 1996; Kim et al., 1995; Nowak and Laajalehto, 2000). In the absence of oxygen, both Pb and sulfide ions are released to the solution in the form of free Pb ions and hydrogen sulfide (Fornasiero et al., 1994). Jennings et al. (2000) showed that galena was not acid-generating when exposed to accelerated oxidation using hydrogen peroxide. This reaction resulted in the accumulation of anglesite on the mineral surface.

An XPS study by Buckley and Woods (1984b) showed that freshly fractured chalcopyrite surfaces exposed to air formed a ferric oxyhydroxide overlayer with a Fe-deficient region composed of CuS_2. Acid-treated surfaces of fractured chalcopyrite showed an increase in the thickness of the CuS_2 layer and the presence of elemental sulfur. Hackl et al. (1995) suggested that dissolution of chalcopyrite is passivated by a thin (<1 μm) Cu-rich surface layer, which forms as a result of solid-state changes. The passivating surface layer consists of Cu polysulfide, CuS_n, where $n \geq 2$. Hackl et al. (1995) described the dissolution kinetics as a mixed diffusion and chemical reaction whose rate is controlled by the rate at which the Cu polysulfide is leached. The oxidation of chalcopyrite in the presence of ferric ions under acidic conditions can be expressed as

$$CuFeS_2 + 4Fe^{3+} \Rightarrow 5Fe^{2+} + Cu^{2+} + 2S^0 \quad [16]$$

Hiroyoshi et al. (1997) monitored the oxygen consumption, sulfur formation, total Fe, and Fe(II) concentrations at different pH levels during the oxidation of chalcopyrite. On the basis of the reaction products formed, it was concluded that ferrous ions catalyzed the oxidation by dissolved oxygen in acidic media:

$$CuFeS_2 + 4H^+ + O_2 \Rightarrow Cu^{2+} + Fe^{2+} + 2S^0 + 2H_2O \quad [17]$$

This conclusion agrees with the observation and interpretations made from testing monomineralic chalcopyrite with peroxide solution; acid production was not observed. Chalcopyrite can be acid-consuming via the production of S^0 (Smart et al., 2000).

The dissolution of chalcopyrite also can be influenced strongly by galvanic effects. The presence of pyrite or molybdenite in association with chalcopyrite can cause accelerated rates of chalcopyrite dissolution (Dutrizac and MacDonald, 1973), whereas the presence of Fe-rich sphalerite and galena can slow the dissolution.

11.5.3.1.3.3 Mercury sulfides

Cinnabar [HgS], the principal ore of mercury, is the most thermodynamically stable form at low temperature (Barnett et al., 2001; Benoit et al., 1999). The presence of trace impurities, such as Zn, Se, and Fe, can impede the conversion of metacinnabar, which is the high-temperature form, to cinnabar. The trace impurities decrease the inversion temperature and thus retard the conversion (Barnett et al., 1997). Therefore, in some environments, the availability of impurities will favor the in situ formation of metacinnabar over cinnabar. The formation of HgS is favored under reducing conditions, in part, because of the high affinity of Hg compounds for S. Cinnabar is kinetically resistant to oxidation and can remain in the soil and tailings impoundments even under oxidizing conditions (Barnett et al., 1997). Although little has been published on its oxidation rates in soils, the observed persistence of HgS in soils at mine sites suggests that its weathering is slow under typical oxidative environments (Barnett et al., 1997; Gray et al., 2000).

11.5.3.1.4 Oxidation of arsenic sulfides

The oxidation of arsenopyrite [FeAsS] releases both S and As. Buckley and Walker (1988) studied the oxidation of arsenopyrite in alkaline and in acidic aqueous solutions. In air, the mineral reacted rapidly, and the oxidation of As to As(III) was more rapid than the oxidation of Fe on the same surface. Only a small amount of sulfur oxidation occurred. Under acidic conditions, the mineral formed S-rich surfaces.

Nesbitt et al. (1995) conducted a detailed study of the oxidation of arsenopyrite in oxygenated solutions. Arsenic and S were observed to exist in multiple oxidation states near the pristine surface. After reaction with air-saturated distilled water, Fe(III) oxyhydroxides formed the dominant Fe surface species, and As(V), As(III), and As(I) were as abundant as As(−I) surface species. An appreciable amount of sulfate was observed on the mineral surface. Arsenic was more readily oxidized than S, and similar rates of the oxidation of As(−I) and $Fe(II)^+$ surface species were observed. Nesbitt et al. (1995) concluded that continued diffusion of As to the surface under these conditions can produce large amounts of As^{3+} and As^{5+}, promoting rapid selective leaching of arsenites and arsenates. According to Walker et al. (2006), arsenite forms 60% of the total arsenic releases, while the remainder is made of arsenate and that the molar proportion of arsenic to sulfur is approximately 1:1, suggesting that the dissolution is congruent. Arsenopyrite oxidation involves the following reactions yielding ${H_2AsO_4}^{2-}$ and ${HAsO_4}^{-}$ ions in equal proportions (Walker et al., 2006):

$$4FeAsS + 11O_2 + 6H_2O \Rightarrow 4Fe^{2+} + 4H_3AsO_3 + 4{SO_4}^{2-} \quad [18]$$

$$2H_3AsO_3 + O_2 = 2{HAsO_4}^{2-} + 4H^+ \quad [19]$$

$$2H_3AsO_3 + O_2 = 2{H_2AsO_4}^{-} + 2H^+ \quad [20]$$

Further acidity is produced with the oxidation of dissolved Fe and its precipitation as a ferric hydroxide as described earlier

for pyrite. Overall, oxidation of one mole of arsenopyrite would result in the formation of 3.5 protons.

Rimstidt et al. (1994) measured the rate of reaction of arsenopyrite under conditions typical of AMD environments. Arsenopyrite was observed to be more reactive than pyrite, chalcopyrite, galena, and sphalerite. Oxidation of arsenopyrite led to the formation of scorodite on the surface. The activation energies for arsenopyrite oxidation varied from 18 kJ mol^{-1} at 0–25 °C to a slightly negative E_a of 6 kJ mol^{-1} at 25–60 °C. Rimstidt et al. (1994) attributed the negative activation energies to competition between the dominant reactions that occur at all temperatures and the less vigorous side reactions that contribute to rate-limiting behavior at higher temperatures. Oxidation of arsenopyrite in acidic media is faster than in air, in water, or in alkaline solutions (Corkhill and Vaughan, 2009).

Oxidation of arsenopyrite by dissolved oxygen at 25 °C and circumneutral pH (6–7) indicates that the rate of arsenopyrite oxidation is essentially independent of dissolved oxygen and that oxidative dissolution is congruent with respect to As and S (Walker et al., 2006). McKibben et al. (2008) determined the rate of arsenopyrite oxidation to be four orders of magnitude faster than that of Walker et al. (2006). The reason for this discrepancy is due to the use of As release rate by Walker et al. (2006) as opposed to the use of Fe release rate by McKibben et al. (2008) as representing the oxidative dissolution of arsenopyrite. McKibben et al. (2008) indicated the incongruency of arsenopyrite dissolution in acidic solutions. Incongruent dissolution also was evident from the surface characterization studies of Nesbitt et al. (1995) and Nesbitt and Muir (1998), indicating preferential enrichment of As in the oxidized surfaces of arsenopyrite. In other words, As and S releases from the surfaces of arsenopyrite were much slower than the release of Fe; therefore, the rates of As release from arsenopyrite would not represent the oxidative dissolution of arsenopyrite. Similar to pyrite, arsenopyrite oxidation is a three-step electrochemical process involving cathodic reaction, electron transport, and anodic reaction (Corkhill and Vaughan, 2009).

An investigation of the surface composition and the chemical state of three naturally weathered arsenopyrite samples exposed for periods ranging from 14 days to 25 years showed that the arsenopyrite surface has an effective passivating layer that protects the mineral from further oxidation (Nesbitt and Muir, 1998). The same samples were then reacted with mine-waste waters, which caused extensive leaching of the arsenopyrite surface below the oxidized overlayers. The acidic nature of the solution caused dissolution of the previously accumulated ferric arsenite and arsenate salts. In mine tailings, Paktunc et al. (2004) reported that arsenopyrite grains are often surrounded by secondary minerals, such as scorodite, arseniosiderite, and goethite and suggested that the relict arsenopyrite would be protected from further oxidative dissolution by the rims limiting the reaction to diffusion of reactants and products. Furthermore, As releases would be controlled by the solubility and stability of the secondary products. Similar occurrences of relict arsenopyrite enveloped by secondary products were reported by Salzsauler et al. (2005) and Moncur et al. (2009).

Pyrite can contain significant amounts of arsenic. Concentrations of up to 10 wt% (Fleet et al., 1993), 19 wt% (Reich et al., 2005), and 12 wt% (Paktunc et al., 2006) have been reported to occur in association with gold deposits. Micro x-ray absorption fine structure (XAFS) spectra collected from a range of arsenical pyrite grains having different morphologies and arsenic concentrations from 0.03 to 4.4 wt% are characterized by the dominant edge aligned with As^{1-} valence state similar to that of arsenopyrite and that of As substitutes for S in the structure (Paktunc, 2008). Based on XAFS results, it appears that As occurs in clusters within the pyrite structure (Paktunc, 2008; Savage et al., 2000), and such clustering of As atoms in the structure causes about 2.6% expansion of the unit cell, making pyrite more susceptible to oxidative dissolution (Savage et al., 2000). Arsenic substitutes for S in the pyrite structure forming As–S dianion groups and the presence of arsenic in pyrite would make it more reactive and accelerate its dissolution (Abraitis et al., 2004; Blanchard et al., 2007).

Oxidation of arsenic sulfides including orpiment and realgar produces arsenite as the dominant arsenic species and several intermediate sulfur species (Lengke and Tempel, 2003). Oxidation rates increase with pH, dissolved oxygen concentrations, and temperature. In comparison with pyrite, oxidation rates of orpiment and realgar are lower at pH 2.5–9, whereas those of amorphous arsenic sulfides are higher at neutral to alkaline pH (Lengke and Tempel, 2003). Under acidic conditions, arsenopyrite oxidizes four to five orders of magnitude faster than orpiment and realgar and three to four orders of magnitude faster than arsenical pyrite (McKibben et al., 2008).

11.5.3.2 Bacteria and Sulfide-Mineral Oxidation

11.5.3.2.1 Mechanisms of sulfide-mineral dissolution and the role of microorganisms

The mechanism(s) by which acidophilic microorganisms catalyze the dissolution of sulfide minerals has/have long been the subject of conjecture and debate. Much of the current consensus on this issue, described in the succeeding texts, comes from the insights provided by research groups headed by Wolfgang Sand and Helmut Tributsch over the past 10 years or so.

Sulfide minerals can be divided into those, such as sphalerite (ZnS) and chalcocite (Cu_2S), that are acid-soluble and those, such as pyrite (FeS_2) and tungstenite (WS_2), that are acid-insoluble. As their name suggests, the first of these are susceptible to acid dissolution by bacteria such as *Acidithiobacillus thiooxidans* that oxidize elemental sulfur and reduced inorganic sulfur compounds (RISCs) to sulfuric acid. In contrast, acid-insoluble sulfide minerals are stable in dilute solutions of sulfuric acid but are subject to oxidative dissolution. In acidic liquors, ferric iron is a more important oxidant of sulfide minerals than molecular oxygen, and therefore, bacteria, such as *Leptospirillum* spp., that oxidize ferrous iron to ferric assume the primary role in sulfide-mineral destruction. Even with acid-soluble sulfides, rates of mineral dissolution in acidic media are greatly accelerated when ferric iron is available **(Table 6)**.

Two different mechanisms (the 'thiosulfate' and 'polysulfide' mechanisms) have been proposed for the biologically accelerated dissolution of sulfide minerals in acidic environments (Schippers and Sand, 1999; **Figure 1**). Acid dissolution of susceptible sulfide minerals is initiated by the mineral being attacked by protons (hydronium ions), releasing the metal component and generating hydrogen sulfide (eqn [21]):

$$MS + 2H_3O^+ \rightarrow M^{2+} + H_2S + 2H_2O \qquad [21]$$

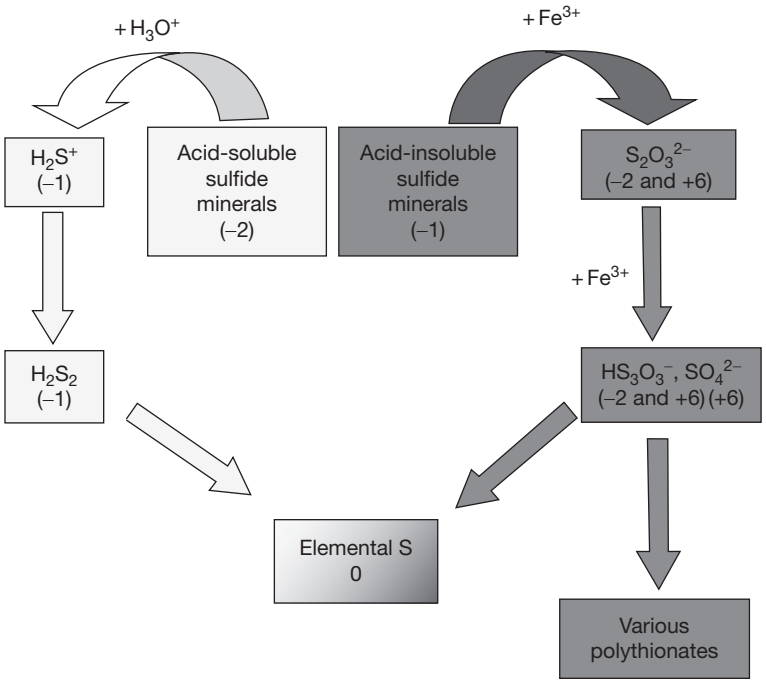

Figure 1 Oxidation pathways for acid-soluble and acid-insoluble sulfide minerals.

The hydrogen sulfide formed is oxidized, by acidophilic microorganisms, to sulfuric acid, allowing the process to continue (eqn [22]):

$$H_2S + 2O_2 + 2H_2O \rightarrow 2H_3O^+ + SO_4^{2-} \quad [22]$$

Acid-soluble sulfides may also be attacked by ferric iron (eqn [23]), in which case, the first free sulfur compound is thought to be an unstable sulfide cation (H_2S^+) that first dimerizes (to H_2S_2) and then oxidizes via various polysulfides (from which the mechanism derives its name) to elemental sulfur (eqn [24]), which is also oxidized by some acidophilic bacteria and archaea to sulfuric acid (eqn [25]), allowing the cycle of acid dissolution of the sulfide minerals to continue (eqn [21]):

$$MS_n + Fe^{3+} + H_3O^+ \rightarrow M^{2+} + 0.5H_2S_n + Fe^{2+} + H_2O \quad [23]$$

$$0.5H_2S_n + Fe^{3+} + H_2O \rightarrow 0.125S_8 + Fe^{2+} + H_3O^+ \quad [24]$$

$$0.125S_8 + 1.5O_2 + 3H_2O \rightarrow 2H_3O^+ + SO_4^{2-} \quad [25]$$

In acidic solutions, acid-insoluble minerals are oxidized by soluble ferric iron (eqn [26]), with a total of six successive one-electron transfer steps required to break the sulfur–metal bonds in minerals such as pyrite:

$$FeS_2 + 6Fe^{3+} + 9H_2O \rightarrow 7Fe^{2+} + S_2O_3^{2-} + 6H_3O^+ \quad [26]$$

Since the initial sulfur product released from the degrading mineral is thiosulfate, this form of oxidative sulfide-mineral dissolution has been described as the 'thiosulfate mechanism' (Rohwerder et al., 2003). Thiosulfate is unstable in acidic solutions (more so when ferric iron is present) and oxidizes via tetrathionate and other sulfur oxyanions, ultimately to sulfate (eqn [27]):

$$S_2O_3^{2-} + 2O_2 + 3H_2O \rightarrow 2H_3O^+ + 2SO_4^{2-} \quad [27]$$

Many acidophilic bacteria have been shown to attach to, and to form biofilms on, sulfide minerals (Rohwerder et al., 2003). The attachment may be (semi-)permanent and specific to certain sulfide minerals, though different species of acidophiles, and even strains within a species, have been shown to display significant differences in how rapidly and permanently they attach to mineral (pyrite, schwertmannite, and glass) surfaces (Ghauri et al., 2007). How acidophilic bacteria attach to sulfide-mineral surfaces is now quite well understood. In the case of *Acidithiobacillus ferrooxidans*, an acidophile that can oxidize both ferrous iron and reduced sulfur, ferric iron is complexed by two uronic acid residues in the bacterial glycocalyx, and the resulting net positive charge facilitates attachment to the negatively charged pyrite (Rohwerder et al., 2003). Once attached, further production of exopolymeric substances (EPS) by the bacteria enhances the development of biofilms on the mineral surfaces, within which conditions (pH, dissolved oxygen concentrations) may differ from the bulk solution phase and be more conducive for mineral dissolution. The biofilm formation and mineral attack by *Leptospirillum ferrooxidans*, an iron-oxidizing acidophile that is unable to oxidize reduced sulfur, appear to be different to that of *At. ferrooxidans*. When it is grown on pyrite, the EPS produced by *L. ferrooxidans* is dotted with small particles, which Tributsch and Rojas-Chapana (2007) identified as colloidal, microcrystalline pyrite. The oxidation of these microscopic grains appears to support the growth of biofilm communities of *L. ferrooxidans*. The pitting

caused by this process can develop into deep holes within sulfide minerals, a process described as 'electrochemical machining.' Colloidal sulfur was detected in the EPS of *At. ferrooxidans* attached to pyrite, and Tributsch and Rojas-Chanapa (2007) provided evidence for the role of thiol groups (e.g., in cysteine) being involved in the breakup of interfacial chemical complexes by *At. ferrooxidans*.

However, it has long been recognized that physical contact between bacteria and sulfide minerals is not a prerequisite for accelerated dissolution of the latter to occur. Historically, two scenarios were described to account for mineral dissolution catalyzed by either bacteria that were attached to sulfide minerals (the 'direct' mechanism) or planktonic-phase cells that generate the oxidant (ferric iron) in the solution, which subsequently diffuses and oxidizes the mineral (the 'indirect' mechanism). It is now recognized that ferric iron mediates oxidative dissolution of acid-insoluble sulfide minerals in both scenarios. Ferric iron is tightly associated with the glycocalyx of attached cells and is recycled with biofilms of iron-oxidizing acidophiles. The terms 'contact' and 'noncontact' leaching, proposed by Hallberg and Johnson (2001), are now used widely to describe that which is mediated by attached and free-swimming bacteria and archaea, respectively.

One consequence of mineral dissolution being possible by noncontact leaching is that, while the hydronium ions and ferric iron necessary for leaching may be generated in situ, they can also originate from an external location, which may be distant from the minerals themselves. For example, acidic ferric iron-rich solutions formed in the aerated surface zones of tailings lagoons can percolate to lower anoxic zones and cause oxidative dissolution of pyrite and other potentially reactive minerals, which are often considered to be secure when stored in oxygen-free environments. However, although oxidation of pyrite by ferric iron can occur in anoxic environments (eqn [28], which is valid for both aerobic and anoxic environments, as oxygen is not involved), regeneration of ferric iron is an oxygen-requiring reaction (eqn [28]):

$$Fe^{2+} + 0.25O_2 + H_3O^+ \rightarrow Fe^{3+} + 1.5H_2O \qquad [28]$$

Given the different roles of acidophilic bacteria and archaea in the dissolution of sulfide minerals, a division of different physiological groups based on their roles has been proposed (Johnson, 2010). The primary mineral degraders are those autotrophic, mixotrophic, and heterotrophic species that catalyze the oxidation of ferrous iron to ferric iron (**Section 11.5.3.2.2**), thereby generating the oxidant that initiates the breakdown of pyrite and most other metal sulfides. Secondary acidophiles are sulfur-oxidizing bacteria and archaea. The sulfuric acid that they generate maintains conditions that favor the activities of other acidophiles, and extreme acidity (pH <2.5) causes ferric iron to remain in the solution. Lastly, tertiary acidophiles are those obligate and facultative heterotrophic bacteria and archaea that degrade organic carbon, some of which inhibit the growth of some iron and sulfur oxidizers. Most acidic mineral-oxidizing environments, including biomining sites and those involved in the genesis of mine-impacted waters, are colonized by microbial consortia comprising different species of all three of these groups (Rawlings and Johnson, 2007). A schematic representation of the roles of primary, secondary, and tertiary acidophiles in the dissolution of pyrite is shown in **Figure 2**.

11.5.3.2.2 Biodiversity of iron- and sulfur-oxidizing acidophilic microorganisms

Mine-impacted waters can be colonized by a wide diversity of microorganisms. Eukaryotic life-forms observed in, and sometimes isolated from, mine-impacted waters include species of acidophilic and acid-tolerant microalgae, fungi and yeasts, protozoa, and some multicellular animals such as rotifers

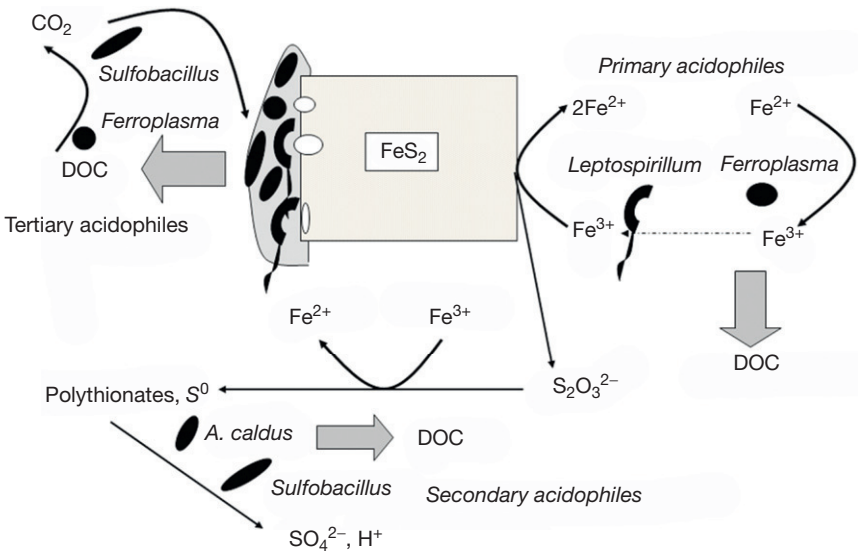

Figure 2 Microbial consortium involved in the oxidative dissolution of pyrite. Iron-oxidizing autotrophs constitute the primary mineral degraders, the secondary sulfuric acid-generating bacteria, the secondary-level subgroup, and the dissolved organic carbon (DOC)-degrading acidophiles, the tertiary-level subgroup. Reproduced with permission from Johnson DB (2010) The biogeochemistry of biomining. In: Barton L and Mandl M (eds.) *Geomicrobiology: Molecular and Environmental Perspective*, pp. 401–426. Dordrecht: Springer.

(Johnson, 2007). However, prokaryotic microorganisms (archaea and particularly bacteria) are found in greater numbers of individuals and of species than eukaryotes, and these have been the focus of a large body of applied and fundamental research.

Bacteria with contrasting physiological characteristics can thrive in mine-impacted waters. These species differ in their requirements for oxygen (obligate aerobes, and facultative and obligate anaerobes), methods of carbon assimilation (obligate and facultative autotrophs, and heterotrophs), and the nature of their electron donors (organic or inorganic). The common characteristic of all prokaryotes that are active in acidic mine waters is that they are metabolically active in low-pH environments, which are highly toxic to most other life-forms. Acidophiles can be divided into three groups, depending on their pH for optima for growth. Extreme acidophiles grow best at pH < 3, moderate acidophiles at pH 3–5, while acid-tolerant species have pH optima at above pH 5 but are able to grow at pH 3. Additional stress factors, such as elevated osmotic potentials and metal concentrations in mine-impacted waters, further restrict their indigenous biodiversities. Acidophiles also vary in their response to temperature. Thermophilic species include those that grow optimally at 40–60 °C (moderate thermophiles) or at 60–80 °C (extreme thermophiles), while thermotolerant acidophiles grow optimally at <40 °C but can also grow at >45 °C. Most acidophiles are mesophilic (growing between about 15 and 40 °C), while a subgroup of these that have been less studied (psychrotolerant species) can grow at <5 °C. Given the temperatures of the majority of mine-impacted waters, mesophilic and psychrotolerant species might be anticipated to be abundant in many of these environments, though there are notable exceptions, such as within the former Richmond Mine at Iron Mountain, California (Nordstrom et al., 2000).

The main protagonists involved in the formation of acidic mine waters, for reasons described in Section 11.5.3.2.1, are acidophilic bacteria and archaea that can catalyze the dissimilatory oxidation of ferrous iron or reduced forms of sulfur (Table 5). Other prokaryotes (and sometimes even the same species, under different environmental conditions) can, however, catalyze the dissimilatory reduction of ferric iron or elemental sulfur (or sulfur oxyanions) and thereby allow the cycling of these elements, which are among the most abundant of all in mine-impacted waters, at mine water/sediment interfaces (Johnson and Hallberg, 2009a,b; Johnson et al., 2012).

Acidophilic bacteria and archaea that oxidize iron. Some bacteria and archaea can catalyze the dissimilatory oxidation of ferrous iron but appear not to also oxidize reduced sulfur. The most widely studied of these are *Leptospirillum* spp., a species of the deep-branching *Nitrospira* phylum. These are obligately acidophilic and autotrophic bacteria that are well known for their key roles in biomining operations and in the formation of acid rock drainage. Three species of *Leptospirillum* have been validated, but the sole strain of one of these (*Leptospirillum thermoferrooxidans*) has been lost. *L. ferrooxidans* and *Leptospirillum ferriphilum* can coexist in mine-impacted waters, though the higher temperature for growth of most strains of the latter means that they are less commonly encountered in most mine waters. A third species, *Leptospirillum ferrodiazotrophum* awaits validation, though it appears to have many similar traits to *L. ferrooxidans*. *Leptospirillum* spp. generally grow more slowly than iron-oxidizing *Acidithiobacillus* spp., though their tolerance to ferric iron and affinity for ferrous iron tend to be significantly greater. In terms of mine water microbiology, these differences often result in *Acidithiobacillus* spp. being the numerically dominant iron oxidizers in freshly discharged, ferrous iron-rich waters, and *Leptospirillum* becoming increasingly significant downstream as ferrous iron concentrations fall and those of soluble ferric iron increase.

Two other iron-oxidizing species of bacteria that do not oxidize sulfur are known to be important in mine waters. One of these has been described recently (and also awaits

Table 5 Characteristics of iron- and sulfur-oxidizing prokaryotes that have been found in mine-impacted waters

	Oxidation of Fe^{2+}	*S*	*Carbon assimilation*[a]	*pH range (approx.)*	*T-response*	*Other traits*
Acidiferrobacter thiooxydans	+	+	A	1.2 to >3	T	Reduction of Fe^{3+}
Acidimicrobium ferrooxidans	+	–	A/H	1.3 to >3	T	Reduction of Fe^{3+}
Acidiphilium acidophilum	–	+	A/H	1.5 to 6.5	M	Reduction of Fe^{3+}
Acidithiobacillus caldus	–	+	A	1 to 4	T	
Acidithiobacillus ferrivorans	+	+	A	1.9 to >3	P	Reduction of Fe^{3+}
Acidithiobacillus ferrooxidans	+	+	A	1.3 to >3	M	Reduction of Fe^{3+}
Acidithiobacillus thiooxidans	–	+	A	0.5 to 5.5	M	Some strains are halotolerant
Ferrimicrobium acidiphilum	+	–	H	1.4 to >3	M	Reduction of Fe^{3+}
Ferroplasma spp.	+	–	H	0.8 to >2	T	Reduction of Fe^{3+}
Ferrovum myxofaciens	+	–	A	2 to >4	P	Copious production of exopolymeric substances
L. ferrooxidans	+	–	A	1.3 to >2	M	
L. ferriphilum	+	–	A	0.8 to >2	T	
Sulfobacillus spp.	+	+	A/H	1 to >3	T	Reduction of Fe^{3+}
Thiobacillus prosperus	+	+	A	1 to 4.5	M	Halophilic
Thiomonas spp.	–	+	A/H	3 to 8	M (T, one species)	Some species oxidize As(III)

[a]Carbon assimilation: A = autotroph, H = heterotroph; T-response: P = psychrotolerant, M = mesophilic, and T = thermotolerant or moderately thermophilic.

validation), though, paradoxically, it is the most readily observed in mine-impacted waters, due to its tendency to form macroscopic growths. *Ferrovum myxofaciens* is a *Betaproteobacterium* that shares several key characteristics with *Leptospirillum* spp. (**Table 5**), though it is far less acid-tolerant (the lower pH for its growth being ~2.0). Its most notable trait, however, is its propensity for generating copious amounts of EPS that enmesh the cells and cause them to grow in gelatinous biofilms or, more characteristically, in flowing mine-impacted waters, as 'acid streamers' (Kimura et al., 2011). Although streamer growths can be formed by other acidophiles (Johnson, 2009), those in lower-temperature (<30 °C) mine-impacted waters of pH 2–4 are often dominated by *Fv. myxofaciens*.

In contrast with both *Leptospirillum* spp. and *Fv. myxofaciens*, *Ferrimicrobium (Fm.) acidiphilum* (a Gram-positive *Actinobacterium*) is an obligate heterotroph, obtaining energy from the oxidation of ferrous iron, and carbon from an organic source (such as yeast extract) rather than carbon dioxide. However, a coculture of *Fm. acidiphilum* and the sulfur-oxidizing autotroph *At. thiooxidans* can degrade pyrite in the absence of an added organic carbon source by establishing a syntrophic relationship involving carbon transfer and access to reduced sulfur (polythionates, etc.). *Acidimicrobium ferrooxidans* is also a Gram-positive *Actinobacterium*, but in contrast to mesophilic *Ferrimicrobium*, this iron oxidizer is a moderate thermophile and therefore of more limited distribution in most mine-impacted waters. The thermotolerant iron-oxidizing archaeon, *Ferroplasma*, is also considered by most researchers to be obligately heterotrophic. Its occurrence in acidic mine waters has not yet been widely documented (except at Iron Mountain), though related euryarchaea have been detected in low-temperature mine waters (e.g., Kimura et al., 2011).

11.5.3.2.2.1 Acidophilic bacteria and archaea that oxidize sulfur

Some acidophilic bacteria and archaea can utilize the energy available from oxidizing various forms of reduced sulfur (oxidation states from −2 to +4) ultimately to sulfate (oxidation state +6) but do not oxidize iron (Dopson and Johnson, 2012). Elemental sulfur and polythionate RISCs are typical substrates for these prokaryotes. Some (mostly archaea) are thermophiles and are generally not found in mine waters. Prokaryotes that oxidize sulfur at lower temperatures (5–30 °C) are exclusively bacteria and include *At. thiooxidans*, which was the first acidophile to be described in 1919. *Acidithiobacillus caldus* shares many physiological traits with *At. thiooxidans*, with the notable exception that it is a moderate thermophile rather than a mesophile (**Table 5**).

Several species of *Thiomonas* have been described (e.g., Slyemi et al., 2011), though some of these have been combined into a single species on the basis of comparative 16S rRNA gene analysis (Battaglia-Brunet et al., 2011). *Thiomonas* spp. are moderate, rather than extreme, acidophiles and are generally not found in extremely acidic and metal-rich mine waters. They can grow autotrophically or as heterotrophs using organic carbon. All *Thiomonas* spp. can use the energy from oxidizing reduced sulfur to support their growth, though in closed environments (e.g., in laboratory shake-flask cultures), this oxidation reaction can cause problems as the consequent

Table 6 Comparison of sulfide-mineral oxidation rates from abiotic, microbial, and field measurements

Process	*Rates of oxidation pH < 2, 25 °C*			*Source*
	Abiotic	*Microbial*	*Field*	
Pyrite oxidation by [Fe^{2+}]	3×10^{-12} mol l^{-1} s^{-1}	3×10^{-7} mol l^{-1} s^{-1}	5×10^{-7} mol l^{-1} s^{-1}	Singer and Stumm (1968, 1970) and Nordstrom (1985)
Pyrite oxidation by [Fe^{3+}]	1×10^{-3} to 2×10^{-8} mol m^{-2} s^{-1} 2.7×10^{-7} mol m^{-2} s^{-1}			McKibben and Barnes (1986) and Rimstidt et al. (1994)
Pyrite oxidation by [DO]	0.3×10^{-9} to 3×10^{-9} mol m^{-2} s^{-1} 1.2×10^{-9} mol m^{-2} s^{-1} 0.5×10^{-9} mol m^{-2} s^{-1}	8×10^{-8} mol m^{-2} s^{-1}		McKibben and Barnes (1986), Olson (1991), Weisener (2002), and Nicholson (1994)
Pyrite nonoxidative dissolution	1.9×10^{-10} mol m^{-2} s^{-1}			Weisener (2002)
Oxidation of waste dump			0.03×10^{-8} mol m^{-2} s^{-1}	Ritchie (1994)
Oxidation in high relative humidity	~10^{-8} mol m^{-2} s^{-1}			Jerz and Rimstidt (2000)
Pyrrhotite oxidation by [DO]	1.3×10^{-8} mol m^{-2} s^{-1} 4×10^{-9} mol m^{-2} s^{-1}			Nicholson and Scharer (1994) and Janzen et al. (2000)
Pyrrhotite oxidation by [Fe^{3+}]	3.5×10^{-8} mol m^{-2} s^{-1}			Janzen et al. (2000)
Pyrrhotite nonoxidative dissolution	5×10^{-10} mol m^{-2} s^{-1} 6×10^{-7} mol m^{-2} s^{-1}			Janzen et al. (2000) and Thomas et al. (1998, 2000)
Sphalerite oxidation by [Fe^{3+}]	3×10^{-7} to 7×10^{-7} mol m^{-2} s^{-1}			Rimstidt et al. (1994)
Sphalerite oxidation by [DO]	1×10^{-8} to 3×10^{-8} mol m^{-2} s^{-1}			Weisener (2002)
Chalcopyrite oxidation by [Fe^{3+}]	9.6×10^{-9} mol m^{-2} s^{-1}			Rimstidt et al. (1994)
Galena oxidation by [Fe^{3+}]	1.6×10^{-6} mol m^{-2} s^{-1}			Rimstidt et al. (1994)

decrease in pH can be sufficient to cause their rapid mortality. Some species of *Thiomonas* (e.g., *Thiomonas intermedia* and *Thiomonas arsenitoxydans*) can also obtain energy from oxidizing arsenic (III) to arsenic (V) and therefore have potential for remediating As-contaminated mine waters (As(V) rapidly combines with schwertmannite and other ferric precipitates in mine waters, whereas As(III) is more bioavailable). Claims that some *Thiomonas* spp. can directly oxidize ferrous iron have been questioned, as pH perturbations in solid and liquid cultures of these bacteria can give rise to spontaneous chemical oxidation of iron.

Acidiphilium acidophilum is another classified acidophilic sulfur-oxidizing bacterium that is somewhat unusual in that, although it is capable of growing as a heterotroph (a trait that characterizes all other known species of *Acidiphilium)*, it can also grow autotrophically using reduced sulfur as an energy source, which is unique among species of this genus. It was originally considered to be a species of *Thiobacillus* (*Thiobacillus acidophilus*), though it was later reclassified as an *Acidiphilium* sp. on the basis of 16S rRNA gene sequencing. Interestingly, other species of *Acidiphilium* (which are widely distributed in mine waters) can also accelerate the oxidation of reduced sulfur though only when provided with organic carbon.

11.5.3.2.2.2 Acidophilic bacteria and archaea that oxidize both iron and sulfur

Some acidophilic bacteria that are commonly encountered in acidic mine waters are capable of accelerating the dissimilatory oxidation of both ferrous iron and reduced sulfur. Of these, the Gram-negative species *Acidithiobacillus* spp., *Acidiferrobacter thiooxydans*, and *Thiobacillus prosperus* are obligate autotrophs, while the Gram-positive species can use organic compounds as a carbon source and also fix carbon dioxide.

At. ferrooxidans is, by far, the most well studied of all acidophiles and was first isolated and characterized in the late 1940s. It is capable of growing autotrophically by oxidation of reduced sulfur or hydrogen, as well as ferrous iron, and can grow in anaerobic (using ferric iron as an electron acceptor, in place of oxygen) and aerobic environments. It is very frequently encountered in acidic mine waters, though its faster growth than many other iron oxidizers (such as *L. ferrooxidans*) means that it tends to dominate enrichment cultures of mine waters that contain ferrous iron, often leading to erroneous conclusions of its relative abundance and significance in these environments. It is now recognized that bacteria that have been classified as *At. ferrooxidans* comprise at least four phylotypes (species) on the basis of multigene sequence analysis (Amouric et al., 2011). One of these phylotypes had previously been recognized as the novel species, *At. ferrivorans*. This iron/sulfur oxidizer has many physiological traits in common with *At. ferrooxidans*, though an important difference is that it is a psychrotolerant bacterium (growing at 4 °C and above), and appears to be particularly well distributed in low-temperature mine waters. *At. ferrivorans* is also less acidophilic than *At. ferrooxidans*, and it grows poorly (if at all) on hydrogen. Amouric et al. (2011) also provided evidence of different biochemical pathways for iron oxidation in iron-oxidizing acidithiobacilli, including *At. ferrooxidans* and *At. ferrivorans*.

At least two other species of obligately autotrophic iron- and sulfur-oxidizing acidophilic bacteria are known, and although these are also *Proteobacteria*, they are only distantly related to *Acidithiobacillus* spp. *Af. thiooxidans* was initially named *Thiobacillus ferrooxidans* strain m-1, though fairly soon after its isolation (in the early 1980s), it was apparent that these bacteria were phylogenetically distant from other (bona fide) strains of *At. ferrooxidans* (Harrison, 1982). The original strain was isolated from coal spoil refuse in Missouri, United States, and there have been relatively few reports of its occurrence in other acidic waters (described in Hallberg et al. 2011b). *T. prosperus*, on the other hand, still awaits official classification over 20 years since first being isolated from the island of Vulcano (Italy), though closely related strains have been isolated more recently by Davis-Belmar et al. (2008). The key trait of *T. prosperus*-like acidophiles is their requirement for salt (sodium chloride), a compound that tends to inhibit the growth of more well-known iron oxidizers, including *At. ferrooxidans*, at relatively small concentrations. *T. prosperus*-like acidophiles have, to date, been isolated from acidic marine-impacted waters, though it might be anticipated that they could also thrive in saline mine waters. Interestingly, growth of both *Af. thiooxydans* and *T. prosperus* on ferrous iron has been reported to be stimulated by the inclusion of reduced sulfur, such as tetrathionate, in growth media.

A number of species of Gram-positive iron- and sulfur-oxidizing acidophilic bacteria have been described, the majority belonging to the spore-forming *Firmicutes* phylum. While most of these are thermotolerant or moderately thermophilic, and would not be anticipated to thrive in most mine waters, some unclassified species (possibly belonging to novel genera) have been detected in low-temperature mine waters (e.g., Kimura et al., 2011).

11.5.4 Acid-Neutralization Mechanisms at Mine Sites

The oxidation of sulfide minerals in mine waste-rock piles and tailings impoundments generates acidic waters containing high concentrations of SO_4, Fe(II), and other metals. The water affected by sulfide oxidation is displaced into underlying or adjacent geological materials, or it is discharged directly to the adjacent surface-water flow system. Geochemical reactions with the gangue minerals result in progressive increases in the pore-water pH and the attenuation of some dissolved metals. A sequence of geochemical reactions occurring in the mine wastes and in the underlying aquifers results in profound changes in the concentrations of dissolved constituents and in the mineralogy and physical properties of the mine waste and aquifer materials. Low-pH conditions promote the dissolution of many metal-bearing solids and the desorption of metals from solid surfaces. Increases in pH through acid-neutralization reactions can lead to pronounced declines in the concentrations of dissolved metals released from mine wastes.

11.5.4.1 Mechanisms of Acid Neutralization

The acid generated through sulfide oxidation reacts with the nonsulfide gangue minerals within the mine wastes. The most significant pH-buffering reactions in mine settings are the dissolution of carbonate minerals, aluminum hydroxide and ferric oxyhydroxide minerals, and aluminosilicate minerals.

11.5.4.1.1 Carbonate-mineral dissolution

The most abundant carbonate minerals in mine wastes are calcite [$CaCO_3$], dolomite [$CaMg(CO_3)_2$], ankerite [$Ca(Fe, Mg)(CO_3)_2$], siderite [$FeCO_3$], or mixtures thereof. The dissolution of calcite can be described as

$$CaCO_3 + H^+ \Leftrightarrow Ca^{2+} + HCO_3^- \quad [29]$$

or, at low pH, as

$$CaCO_3 + 2H^+ \leftrightarrow Ca^{2+} + CO_2 + H_2O \quad [30]$$

The dissolution of carbonate minerals has the potential to raise the pH of the pore water to near neutral. The dissolution of carbonate minerals releases Ca, Mg, Mn, Fe, and other cations that are as solid-solution substitutions or as impurities and increases the alkalinity of the water. At many sites, the mass of carbonate minerals contained in the mine wastes exceeds that of the sulfide minerals, and the rapid dissolution of carbonate minerals is sufficient to maintain neutral pH conditions through the mines or their waste piles. Neutral pH conditions have been observed in tailings impoundments derived from processing carbonate-bearing vein-type gold deposits (Blowes, 1990; McCreadie et al., 2000) and in open-pits derived from gold mining (Shevenell et al., 1999).

Many mines and mine wastes derived from massive sulfide ore deposits have a sulfide content in excess of the carbonate-neutralization capacity. At these sites, the available carbonate content is completely consumed, with the most soluble and most reactive carbonate minerals depleted first. Calcite is depleted initially, followed by dolomite–ankerite and siderite (Blowes and Ptacek, 1994). As the carbonate content of the waste dissolves, the pH is buffered to near neutral. The depletion of carbonate minerals through consumption by acid-neutralization reactions has been documented for a number of settings, including base-metal mine-tailings impoundments (Blowes and Jambor, 1990; Dubrovsky, 1986; Dubrovsky et al., 1984; Gunsinger et al., 2006a,b; Johnson et al., 2000; Moncur et al., 2005), aquifers impacted by drainage from mine wastes (Morin et al., 1988), and coal-mine spoils (Cravotta, 1994). In these studies, the greatest depletion occurs at the advancing acid front. An abrupt increase in solid-phase carbonate concentration is observed, suggesting that the dissolution of carbonate minerals is rapid. Measurements of the carbonate content of mine wastes, in front of and behind of the carbonate dissolution front, indicate that carbonate depletion occurs over a small distance along the path of groundwater flow and that carbonate minerals are absent behind the acid front (Dubrovsky et al., 1984; Johnson et al., 2000). Detailed laboratory column studies conducted by Jurjovec et al. (2002, 2003) confirmed that the depletion of carbonate minerals in response to an advancing acid front is rapid. Jurjovec et al. (2002, 2003) observed stable pH conditions, while alkalinity and cations were produced through carbonate dissolution, followed by a pronounced drop in pH after carbonate minerals were depleted (**Figure 3**).

The solubility products for the dissolution of calcite, dolomite–ankerite, and siderite vary, with calcite having the highest solubility product and siderite the lowest (**Table 7**). Field observations suggest that dissolution of the most soluble of these minerals will proceed first, followed by dissolution of the next most soluble mineral. As Fe sulfide minerals oxidize, Fe(II) can be released to anoxic pore waters and can react with the HCO_3^- produced through calcite dissolution, thereby forming siderite. Observations from field sites, coupled with geochemical modeling results, suggest that secondary siderite does form through this reaction (e.g., Blowes and Jambor, 1990; Ho et al., 1984; Moncur et al., 2005; Morin et al., 1988; Ptacek and Blowes, 1994). Al et al. (2000) identified secondary siderite on calcite surfaces, consistent with theoretical predictions. In laboratory studies conducted by Jurjovec et al. (2002, 2003), the dissolution of various carbonate minerals, including calcite, dolomite–ankerite, and siderite, could not be distinguished. Under the near-neutral pH conditions maintained by carbonate-mineral dissolution, the precipitation of crystalline and amorphous metal hydroxides is favored. Cations released through sulfide oxidation and the dissolution

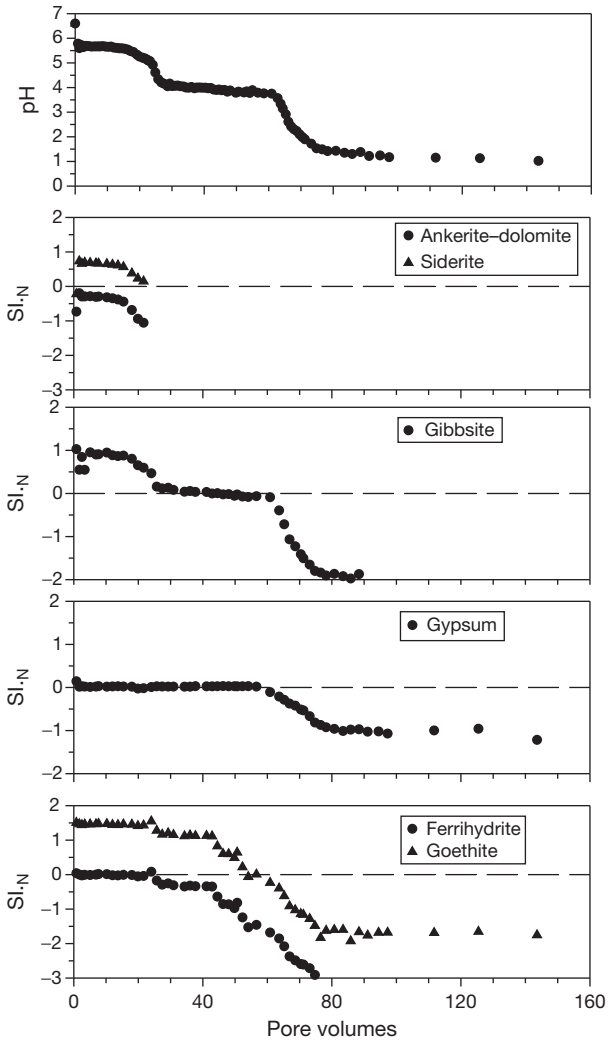

Figure 3 pH-buffering sequence observed in mine tailings: results of laboratory column experiment with 0.1 N H_2SO_4 input solution (reproduced from Jurjovec J, Ptacek CJ, and Blowes DW (2002) Acid neutralization mechanisms and metal release in mine tailings: A laboratory column experiment. *Geochimica et Cosmochimica Acta* 66: 1511–1523). $SI._N$ is the saturation index normalized per mole of reactant.

Table 7 Solubility products for selected phases that form at mine-drainage sites

Mineral	*Reaction*	*log k*
Oxides and hydroxides		
Goethite	$FeOOH_{(s)} + 3H^{+}_{(aq)} \leftrightarrow Fe^{3+}_{(aq)} + 2H_2O_{(l)}$	−1.0
Ferrihydrite	$Fe(OH)_{3(s)} + 3H^{+}_{(aq)} \leftrightarrow Fe^{3+}_{(aq)} + 3H_2O_{(l)}$	3.0–5.0
Gibbsite	$Al(OH)_{3(s)} + 3H^{+}_{(aq)} \leftrightarrow Al^{3+}_{(aq)} + 3H_2O_{(l)}$	7.94
Boehmite	$AlOOH_{(s)} + 3\,H^{+} \leftrightarrow Al^{3+}_{(aq)} + 2H_2O_{(l)}$	7.83
Sulfates		
Gypsum	$CaSO_4{\cdot}2H_2O_{(s)} \leftrightarrow Ca^{2+}_{(aq)} + SO_4{}^{2-}_{(aq)} + 2H_2O_{(l)}$	−4.58
Celestine	$SrSO_{4(s)} \leftrightarrow Sr^{2+}_{(aq)} + SO_4{}^{2-}_{(aq)}$	−6.62
Barite	$BaSO_4 \leftrightarrow Ba^{2+}_{(aq)} + SO_4{}^{2-}_{(aq)}$	−0.97
Carbonates		
Calcite	$CaCO_{3(s)} \leftrightarrow Ca^{2+}_{(aq)} + CO_3{}^{2-}_{(aq)}$	−8.48
Dolomite	$CaMg(CO_3)_{2(s)} \leftrightarrow Ca^{2+}_{(aq)} + Mg^{2+}_{(aq)} + 2CO_3{}^{2-}_{(aq)}$	−17.09

Source: Nordstrom DK and Munoz JL (1994) *Geochemical Thermodynamics*. Boston, MA: Blackwell Scientific.

of carbonate and aluminosilicate minerals can lead to the formation of secondary hydroxide phases that accumulate in the waste solids. These phases may subsequently dissolve as additional acid is produced through sulfide-mineral oxidation reactions. The dissolution of these secondary minerals contributes to acid neutralization.

11.5.4.1.2 Dissolution of hydroxide minerals

After the carbonate minerals are depleted, the pH falls until equilibrium with the most soluble secondary hydroxide mineral is attained. An abrupt increase in the concentration of dissolved Al has been observed to coincide with carbonate depletion at several mine-tailings impoundments. These observations suggest that the initial hydroxide mineral to dissolve is an aluminum hydroxide. Although a discrete Al-bearing phase has not been isolated, it is generally assumed to be amorphous Al hydroxide [$Al(OH)_3$] or gibbsite [crystalline $Al(OH)_3$]. Dissolution of this Al-bearing phase buffers the pH in the region of 4.0–4.5 (Blowes and Jambor, 1990; Dubrovsky, 1986; Gunsinger et al., 2006b; Johnson et al., 2000; Moncur et al., 2005). Although repeated attempts have been made, the presence of these Al-bearing phases has not been confirmed through mineralogical studies. After the secondary Al phases present in the tailings are depleted, the pH falls until equilibrium with an Fe oxyhydroxide mineral, typically ferrihydrite (nominally $9Fe_2O_8{\cdot}5H_2O$) or goethite (α-FeOOH), has been attained. Dissolution of ferric oxyhydroxide minerals typically maintains pH values in the range of 2.5–3.5.

11.5.4.1.3 Dissolution of silicate minerals

Gangue minerals associated with sulfide-rich tailings include various aluminosilicate minerals such as chlorite, smectite, biotite, muscovite, plagioclase, and amphibole and other silicate minerals such as olivine and pyroxene. Their contribution to acid-neutralization reactions has been examined in a number of field studies and through controlled laboratory experiments. During the period of carbonate- and hydroxide-mineral dissolution, aluminosilicate minerals may also dissolve, thus consuming H^+ and releasing H_4SiO_4, Al^{3+}, and other cations, including K, Ca, Mg, and Mn. Silicate dissolution is generally not rapid enough to buffer the pore water to a specific pH. Such reactions, however, do consume H^+ and contribute to the overall acid-neutralization potential of mine wastes. For instance, biotite has high neutralization capacity in that the dissolution of one mole of biotite (e.g., $KMg_{1.5}Fe_{1.5}Al\,Si_3O_{10}(OH)_2$) can consume between 7 and 10 H^+ depending upon the type of dissolution. In addition to H^+ consumption, Al and other metals released from aluminosilicate minerals may accumulate in secondary products such as amorphous $Al(OH)_3$ or gibbsite that act as secondary pH buffers. As with other phases contributing to acid neutralization, the mass and composition of silicates vary from site to site and within an individual site.

Detailed field studies conducted at the Heath Steele tailings impoundment, New Brunswick, Canada, illustrate the role of aluminosilicate-mineral dissolution in contributing to acid neutralization. The tailings contain in excess of 85 wt% sulfide minerals, where partial oxidation has led to the production of low-pH pore waters ($pH < 0.5$) and the extensive dissolution of aluminosilicate minerals. Blowes (1990) noted increased concentrations of Al and Si (up to 2500 and 200 mg l^{-1}, respectively) due to the dissolution of the aluminosilicate minerals. In the deeper tailings, a diverse silicate gangue was observed, including chlorite, muscovite, quartz, and an Fe-bearing amphibole. In the upper 30 cm of the tailings, a less diverse silicate gangue, extensively depleted in chlorite and amphibole, was observed. The order of depletion of the aluminosilicate minerals followed closely the order predicted on the basis of the zero point of charge of the aluminosilicate mineral.

Johnson et al. (2000) documented the depletion of aluminosilicates at the Nickel Rim mine-tailings impoundment. There solid-phase Al and biotite are depleted in the upper oxidized portion of the tailings, whereas biotite is abundant in the underlying unoxidized tailings. At the Sherridon tailings impoundment, Manitoba, Moncur et al. (2003, 2005) observed extensive depletion of biotite, chlorite, and possibly, smectite in the upper 1 m of the tailings. At this site, there is evidence of secondary replacement of other aluminosilicates, namely, plagioclase, cordierite, and amphibole. At Sherridon, the first appearance of biotite occurs at 72 cm, which coincides with the first appearance of secondary sulfides (marcasite). Chlorite and smectite first appear at a 90 cm depth, indicating the greater tendency for dissolution. In a controlled laboratory experiment using a 0.1 M H_2SO_4 solution, Jurjovec et al. (2002) observed extensive depletion of chlorite and minor depletion of biotite as a result of acid leaching of the tailings.

Dissolution rates of biotite and iron-rich chlorite at acidic pH (Nagy, 1995; Ritchie, 1994) are slow in comparison with calcite but several orders of magnitude faster than K-feldspars and albite (Lasaga et al., 1994; Stillings and Brantley, 1995). In addition, biotite and chlorite can be considered as slightly more reactive than muscovite. Dissolution rates of olivine at acidic pH (i.e., 3.98×10^{-11}–1.02×10^{-12} mol $cm^{-2}\,s^{-1}$) as reported by Wogelius and Walther (1991) and Sverjensky (1992) are comparable to the oxidative dissolution rates of pyrite. Other minerals with relatively fast dissolution rates under acidic conditions that are comparable with the oxidation rates of pyrite include Ca end-member of plagioclase (anorthite) and wollastonite. In addition, Fe-rich pyroxenes

and amphiboles may also be considered as having potentials to neutralize acidity. The presence of Fe^{2+} or other cations that may oxidize reduces the structural stability; therefore, the rates for ferromagnesian minerals may be higher depending upon their Mg to Fe ratios.

11.5.4.1.4 Development of pH-buffering sequences

The sequence of pH-buffering reactions observed within tailings impoundments results in a progressive increase in the pore-water pH along the groundwater flow path. These changes in pH occur as long zones of relatively uniform pH, which are dominated by a single pH-buffering reaction, separated by fronts or relatively sharp changes in pH as a buffering phase is depleted (**Figure 3**). Field data from the Nickel Rim tailings impoundment, as were presented by Johnson et al. (2000), illustrate a pH-buffering sequence. At the Nickel Rim site, the pH of the pore water at the base of the impoundment is near neutral, varying from 6.5 to 7.0. The geochemical calculations suggest that the pore water in this zone approaches or attains equilibrium with respect to calcite. Overlying the calcite-buffered zone, calcite is absent from the tailings, and the pH is buffered by the dissolution of siderite and possibly by the dissolution of dolomite. The complete depletion of carbonate minerals is accompanied by a sharp decline in pH from 5.8 to 4.5. Immediately above the depth of carbonate-mineral depletion, the pH is relatively uniform, varying from 4.0 to 4.5, the dissolved Al concentrations increase sharply, and the pore water approaches or attains equilibrium with respect to gibbsite. Near the surface of the impoundment, the pH decreases sharply from 4.0 to 3.5, then more gradually from 3.5 to approximately 2.5. Throughout this decrease in pH, the pore water is undersaturated with respect to ferrihydrite and approaches equilibrium with respect to goethite.

11.5.5 Geochemistry and Mineralogy of Secondary Minerals

In mineral processing and mine-waste settings, the secondary minerals are those that form during and after processing and after disposal of the wastes. Thus, the mined material may contain both the primary, fresh minerals and the oxidation products that were formed through geological processes (e.g., paleoweathering). In rare cases, a mineral deposit will consist wholly of oxidized material, but in the acid-drainage setting, all of these minerals are deemed to constitute the primary assemblage because they were formed prior to processing of ores and disposal as wastes. After final discharge or even during temporary storage of wastes and low-grade ores, crystallization of secondary minerals occurs in situ principally as a result of oxidation of the primary sulfide assemblage. However, upon removal from its disposal site, as occurs during a sampling program, a waste may form additional minerals as the material dries; such products, which are predominantly water-soluble salts that crystallize during evaporation of the pore water, are classified as 'tertiary' minerals (Jambor, 1994; Jambor and Blowes, 1998).

11.5.5.1 Soluble Sulfates: Iron Minerals

Iron sulfates form under low-pH conditions and are generally highly soluble. The most common secondary Fe sulfate minerals associated with oxidized mine wastes are of the type $Fe^{2+}SO_4{\cdot}nH_2O$, wherein n ranges from 7 to 1. The minerals of the most frequent occurrence and abundance are melanterite ($n=7$), rozenite ($n=4$), and szomolnokite ($n=1$); the pentahydrate (siderotil) and hexahydrate (ferrohexahydrite) have also been reported but are much less widespread and occur sparingly. The divalent salts seem to form in the earliest stages of sulfide-mineral oxidation, but they are observed more commonly as superficial evanescent coatings that appear during dry periods and are susceptible to solubilization during rainfall events. Melanterite has been reported from several localities as a precipitate from greenish pools of Fe-rich solutions that drained from pyritiferous deposits, and the mineral has also been noted to form a hardpan layer in pyrite-rich tailings at the Heath Steele Mines, New Brunswick, Canada (Blowes et al., 1992), in the main hardpan of the Sherridon tailings in Manitoba (Moncur et al., 2005, 2009), and in high-sulfide mine wastes at the Berikul mine site in Russia (Sidenko et al., 2005). The tetrahydrate, rozenite, more typically forms as a dehydration product of melanterite.

Although the soluble salts of ferric iron may crystallize on a microscale in the earliest stages of Fe sulfide oxidation, in field settings, the paragenesis indicates that the progression is from the early formation of the divalent salts of Fe to minerals containing both ferrous and ferric Fe and thence to the trivalent-Fe minerals (Jambor et al., 2000a,b). For minerals devoid of other cations, the most commonly occurring of the mixed-valence type is copiapite $[Fe^{2+}Fe_4{}^{3+}(SO_4)_6(OH)_2{\cdot}20H_2O]$, and less common is römerite $[Fe^{2+}Fe_2{}^{3+}(SO_4)_4{\cdot}14H_2O]$. Among the trivalent-Fe minerals, the most common are coquimbite $[Fe_2{}^{3+}(SO_4)_3{\cdot}9H_2O]$, ferricopiapite $[Fe_{2/3}{}^{3+}Fe_4{}^{3+}(SO_4)_6(OH)_2{\cdot}20H_2O]$, and rhomboclase $[(H_5O_2)^{1+}Fe^{3+}(SO_4)_2{\cdot}2H_2O]$. Also common is fibroferrite $[Fe^{3+}(SO_4)(OH){\cdot}5H_2O]$, which, however, is relatively insoluble except in acidic conditions.

A notable locality for acid drainage is Iron Mountain, California, where oxidation of pyritiferous massive sulfide deposits has resulted in the formation of many of the aforementioned soluble salts in the underground workings. The precipitation order of the salts at Iron Mountain follows the divalent to trivalent trend (Nordstrom and Alpers, 1999b). These secondary iron sulfates form and evolve during dry periods through dehydration, oxidation, and neutralization reactions, and they are dissolved during wet periods by releasing metals and acidity into local environments.

11.5.5.2 Soluble Sulfates: Other Elements

Other than the soluble sulfates of Fe, only those of Mg and Al are of moderately common occurrence in association with acid drainage. The Mg salts are chiefly of the type $MgSO_4{\cdot}nH_2O$, with epsomite $[MgSO_4{\cdot}7H_2O]$ and hexahydrite $[MgSO_4{\cdot}6H_2O]$ the predominant minerals. Occurrences of the pentahydrate (pentahydrite) and the tetrahydrate (starkeyite), which are known from a few localities, could be categorized as rare, and the monohydrate (kieserite), although identified as a weathering product of pyritiferous shales, has not yet been observed specifically in association with acid drainage.

Whereas the oxidation of pyrite provides the principal source for the Fe analogues of the simple Mg sulfates, the chief source of the latter is dolomite [$CaMg(CO_3)_2$]. Dissolution of dolomite attenuates the acidity generated by pyrite oxidation, thereby releasing Ca and Mg to form gypsum [$CaSO_4{\cdot}2H_2O$], simple Mg salts, and more complex ones such as magnesiocopiapite [$MgFe_4^{3+}(SO_4)_6(OH)_2{\cdot}20H_2O$]. Thus, both gypsum and Mg sulfates may form without the development of acid drainage if dolomite is sufficiently abundant to neutralize the acidity that is generated by oxidation of the associated sulfides.

The formation of soluble salts containing Al is paragenetically later than that of the simple Mg salts because Al is sourced from aluminosilicates, the dissolution of which is typically slow and requires low-pH conditions to accelerate the process. The most common soluble sulfates of Al are members of the halotrichite–pickeringite series [$Fe^{2+}Al_2(SO_4)_4{\cdot}22H_2O$–$MgAl_2(SO_4)_4{\cdot}22H_2O$] and of less widespread occurrence are aluminocopiapite [$Al_{2/3}Fe_4^{3+}(SO_4)_6(OH)_2{\cdot}20H_2O$] and alunogen [$Al_2(SO_4)_3{\cdot}17H_2O$].

Various soluble salts, such as kalinite [$KAl(SO_4)_2{\cdot}11H_2O$], blödite [$Na_2Mg(SO_4)_2{\cdot}4H_2O$], and bilinite [$Fe^{2+}Fe_2^{3+}(SO_4)_4{\cdot}22H_2O$], occur sparingly but may be locally prominent. The most common of the Cu salts is chalcanthite [$CuSO_4{\cdot}5H_2O$]. Both goslarite [$ZnSO_4{\cdot}7H_2O$] and gunningite [$ZnSO_4{\cdot}H_2O$] have been reported as secondary minerals in sphalerite-bearing wastes, but the salts occur sparingly.

11.5.5.3 Less Soluble Sulfate Minerals

Gypsum, which has a moderate solubility in water, is the most abundant secondary mineral in sulfide-rich tailings due to high-sulfate concentrations resulting from sulfide oxidation and high-Ca concentrations arising from lime and/or limestone use during metallurgical processing and tailings neutralization. Jarosite [$KFe_3(SO_4)_2(OH)_6$], which is relatively insoluble (**Table 7**), is the other abundant and widespread secondary mineral associated with acid drainage. Bassanite [$2CaSO_4{\cdot}H_2O$] has also been identified as a secondary mineral in tailings impoundments, but the quantities are minute and are insignificant relative to those of gypsum. Jarosite is, by definition, K-dominant, but as a mine-drainage precipitate, it invariably is oxonium-bearing, commonly with $K > H_3O > Na$. In the early stages of acid generation, the bulk of the K at most localities is derived by incongruent dissolution of trioctahedral micas. Various other members of the jarosite supergroup occur in acid-drainage settings; other members detected are natrojarosite [$NaFe_3(SO_4)_2(OH)_6$], hydronium jarosite [$(H_3O)Fe_3(SO_4)_2(OH)_6$], plumbojarosite [$PbFe_6(SO_4)_4(OH)_{12}$], alunite [$KAl_3(SO_4)_2(OH)_6$], and As-bearing species, but all are of rare occurrence relative to jarosite. Jarosite is also common in weathered zones of sulfide ore deposits and in acid sulfate soils. Furthermore, jarosite is an important compound in hydrometallurgy because its formation is widely utilized to control Fe, sulfate, alkalis, and impurity elements. Precipitation of jarosite occurs from acidic ($pH < 3$) solutions rich in Fe(III), SO_4, and alkalis such as K and Na at elevated temperatures (Dutrizac and Kaiman, 1976; Majzlan and Myneni, 2005). Dissolution of jarosite produces acidity.

Among the Al sulfate salts, jurbanite [$Al(SO_4)(OH){\cdot}5H_2O$] is commonly used in geochemical modeling, but the mineral itself is of extremely rare occurrence; the most common Al hydroxysulfates associated with acid drainage correspond to crystalline and amorphous felsöbányaite (basaluminite) [$Al_4(SO_4)(OH)_{10}{\cdot}4H_2O$] and hydrobasaluminite [$Al_4(SO_4)(OH)_{10}{\cdot}15H_2O$].

A poorly crystalline hydroxysulfate, schwertmannite (Bigham et al., 1990), having the ideal formula $Fe_8O_8(OH)_6SO_4{\cdot}nH_2O$, may be the most common direct precipitate of Fe from acidic effluents at pH 2–4 (Bigham and Nordstrom, 2000). The composition deviates from the ideal formula in terms of the proportions of Fe, OH, and SO_4. Although schwertmannite occurs in acidic waters and soils and commonly the initial precipitate from AMD, it is difficult to identify because of its poor crystallinity and the almost invariable presence of associated Fe oxyhydroxides and jarosite, but numerous occurrences have been reported in the literature. Schwertmannite typically occurs as 'hedgehog'-type rounded aggregates with filamentous or needlelike whiskers (Bigham and Nordstrom, 2000; Loan et al., 2004) or spheroidal aggregates (Peretyazhko et al., 2009; Regenspurg et al., 2004) that are typically less than a micrometer. Its structure is described by Bigham et al. (1990) as having some similarities to that of akaganeite [β-FeO(OH,Cl)] where double chains of FeO octahedra share corners to produce square tunnels extending parallel to the *c*-axis. Transmission electron microscopy (TEM) and nanodiffraction studies of Loan et al. (2004) did not find any evidence for an akaganeite-like structure. Instead, the TEM observations suggested that the schwertmannite whiskers possess structures similar to maghemite and highly disordered ferrihydrite. Recently, Fernandez-Martinez et al. (2010) proposed a structural model similar to the original akaganeite-like structure having two sulfate molecules per unit cell where one sulfate occurs as an inner-sphere and the other as an outer-sphere complex within the akaganeite tunnel structure. Schwertmannite is metastable, and it transforms to goethite (Bigham et al., 1996; Peretyazhko et al., 2009; Schwertmann and Carlson, 2005) and to jarosite at low pH (Majzlan and Myneni, 2005). Its transformation rate to goethite increases with an increase in pH (Regenspurg et al., 2004) and temperature (Schwertmann and Carlson, 2005), whereas it decreases with increases in the concentrations of sulfate and dissolved organic carbon (Knorr and Blodau, 2007). Detailed studies of the oxidation of pyrite and pyrrhotite indicate that schwertmannite is not an early formed mineral, and the occurrences suggest an origin in which the requisite Fe and SO_4 have undergone solubilization, transportation, and subsequent precipitation rather than maintaining an intimate association with precursor sulfides. Regenspurg et al. (2004) describe schwertmannite as the first mineral that forms from oxidation and hydrolysis of Fe(II)SO_4 solutions at pH 5–6.

The principal ore mineral of Pb is galena [PbS], and the predominant sulfates derived from it are anglesite [$PbSO_4$] and plumbojarosite. Partial substitution of Pb for the alkali-site cations also occurs in other members of the jarosite supergroup. An unusual sink for Cu and Al is the mineral hydrowoodwardite [$Cu_{1-x}Al_x(OH)_2(SO_4)_{x/2}(H_2O)_n$], recently discovered as a supergene product at several old mines in Saxony, Germany (Witzke, 1999). The same mineral was

almost simultaneously reported to occur as bluish coatings on weathered waste rocks and in stream sediments at two former mines in Northern Italy (Dinelli et al., 1998).

11.5.5.4 Metal Oxides and Hydroxides

The oxidation of Fe sulfides invariably leads to the formation of goethite [α-FeOOH] both in intimate association with the sulfides and in distal precipitates. Other oxyhydroxide minerals identified as secondary precipitates are crocite [γ-FeOOH] and akaganéite [β-FeO(OH,Cl)], but occurrences are generally insignificant relative to the abundance and distribution of goethite, which is thermodynamically the most stable iron oxyhydroxide at low temperatures. However, lepidocrocite has been observed to be important at some sites; for example, Roussel et al. (2000) determined the mineral to be the principal component of suspended particulate matter in drainage from an As-rich tailings impoundment in France, and Bowell and Bruce (1995) observed lepidocrocite to be a significant component of ochres that precipitated from low-pH (<5) waters at the Levant Mine in Cornwall, England. In general, Fe (III) oxyhydroxides are the other abundant secondary minerals forming from slightly acidic to neutral drainages in sulfidic mine tailings.

Ferrihydrite is a poorly crystalline mineral of widespread occurrence in soils and secondary alteration products of hydrothermal ore deposits, mining wastes, AMD settings, and iron-bearing sediments. In addition, it has a considerable importance in mineral processing and extractive metallurgy (Jambor and Dutrizac, 1998). Ferrihydrite is commonly referred to as 'amorphous $Fe(OH)_3$,' poorly crystalline iron oxyhydroxide, or colloidal ferric hydroxide. Its particle size is defined by Waychunas et al. (1996) as being in the 0.8–1.5 nm range and in the 2–6 nm range by Janney et al. (2000). There are several varieties of ferrihydrite identified by the number of broad peaks in the x-ray diffraction (XRD) patterns such as the two-line and six-line varieties. The two-line variety is less crystalline and smaller in size in comparison to the six-line variety (Drits et al., 1993; Manceau and Drits, 1993). Ferrihydrite is considered to be a mixture rather than a single compound (Drits et al., 1993; Marchand and Rancourt, 2009). Recently, Michel et al. (2007, 2010) proposed a new structural model for ferrihydrite based on synchrotron x-ray total scattering data. The structure is analogous to akdalaite ($Al_{10}O_{14}(OH)_2$) having 20% iron in tetrahedral coordination and possessing a low density of defects. Iron octahedra and tetrahedra share corners and edges, and unlike the conventional model (Drits et al., 1993), there are no face-sharing octahedra. The new model received critism due to its shortcomings in describing XRD, x-ray absorption spectroscopy, and Mössbauer data and not being in accordance with the fundamental crystal chemical principles (Hiemstra and van Riemsdijk, 2009; Manceau, 2009, 2010, 2011; Rancourt and Meunier, 2008).

Mixing of acidic waters with oxygenated freshwaters and neutralization of acidic mine effluents result in the formation of Fe(III) oxyhydroxides. These Fe(III) oxyhydroxide compounds and minerals begin as small clusters of Fe(O,OH, $OH_2)_6$ octahedra that evolve into larger polymeric units with time, eventually reaching colloidal sizes (Combes et al., 1989). Precipitation of ferrihydrite is favored when oxidation of Fe^{2+} and hydrolysis occur rapidly from supersaturated solutions. Due to their nanoparticle or colloidal sizes, Fe(III) oxyhydroxides have high surface areas; therefore, they can play important roles in terms of immobilizing heavy metals and toxic elements through sorption.

Ferrihydrite is metastable and transforms to hematite or goethite with aging (Combes et al., 1989; Waychunas et al., 2005) or to hematite through internal structural arrangements combined with dehydration (Schwertmann et al., 2004). The transformation from ferrihydrite to hematite occurs at neutral pH. In contrast, transformation of ferrihydrite to goethite requires dissolution and recrystallization because face-sharing FeO octahedra are not present in the goethite structure. Instead, the goethite structure consists of edge-sharing and corner-sharing FeO octahedra. Because of the energy barriers involving breakage of the Fe–O bonds linking octahedra through a face-sharing arrangement, ferrihydrite–goethite transformation requires disintegration of the structure through dissolution (Combes et al., 1990).

The presence of ferrihydrite in precipitates from mine-waste effluents is commonly reported, but unequivocal identifications of its presence in mine-waste solids, such as tailings, have been fewer. For the latter, because the crystallinity is poor and the mineral forms only a small proportion of the total waste solids, recourse is generally made to selective dissolution whereby the fraction that is more soluble in certain reagents is inferred to represent ferrihydrite rather than goethite, which is more dissolution-resistant. In addition, the likelihood of finding ferrihydrite in tailings is slim due to its metastability.

Although hematite [αFe_2O_3] is a common product of the oxidation of sulfide-bearing mineral deposits, only a few unequivocal occurrences are known in mine-drainage settings (e.g., Boulet and Larocque, 1996; Hochella et al., 1999). Various Fe oxides and oxyhydroxides, including hematite, maghemite [γ-Fe_2O_3], and ilmenite [$Fe^{2+}TiO_3$], have been observed as microcrystalline aggregates that have formed within acidophilic microorganisms in sediments affected by effluents from tailings at Elliot Lake, Ontario, Canada (Mann and Fyfe, 1989). Minerals of the spinel group, which includes magnetite [$Fe^{2+}Fe_2{}^{3+}O_4$], have been detected, but most associations are on a minute scale. However, the presence of extensive accumulations of magnetite derived by the anoxic reduction of transported Fe in mining-impacted lake-bottom sediments has been reported by Cummings et al. (2000).

Manganese oxides–oxyhydroxides which are known to be potent scavengers of trace metals in both aquatic and terrestrial environments (Villalobos et al., 2005) have been observed at a few acid-drainage localities. For example, Benvenuti et al. (2000) observed pyrolusite [MnO_2] and pyrochroite [$Mn(OH)_2$] in weathered jig tailings and waste rock at a site in Tuscany, Italy. At the Clark Fork River Superfund site, Hochella et al. (2005) reported the occurrence of a vernadite-like mineral (nominally $MnO_2{\cdot}nH_2O$) having high sorption capacity due to its exceptionally high surface area. It occurs as a mixture with ferrihydrite and carries significant amounts of heavy metals such as Pb, Cu, Zn, and As. Hochella et al. (1999) identified hydrohetaerolite [$Zn_2Mn_4{}^{3+}O_8{\cdot}H_2O$] among the secondary minerals in stream sediments at an acid-drainage

site in Montana, and nsutite [γ-MnO_2], birnessite [$Na_4Mn_{14}O_{27}{\cdot}9H_2O$], and minerals in the ranciéite–takanelite series [$(Ca,Mn^{2+})Mn_4{}^{4+}O_9{\cdot}3H_2O$–$(Mn^{2+},Ca)Mn_4{}^{4+}O_9{\cdot}H_2O$] were among the various Mn minerals detected in precipitates in the streambed of Pinal Creek, Arizona (Lind and Hem, 1993). At Pinal Creek, the acidic groundwater plume reacted with calcite-bearing alluvium, initially forming 'amorphous Fe oxide' as pH increased, and subsequently precipitating the Mn-bearing assemblage farther downstream, where the pH of the stream water was near neutral. Similar relationships were observed by Hudson-Edwards et al. (1996), who identified cesarolite [$PbH_2Mn_3O_8$], coronadite [$Pb(Mn^{4+},Mn^{2+})_8O_{16}$], woodruffite [$(Zn,Mn^{2+}Mn_3{}^{4+}O_7{\cdot}1\text{-}2H_2O$], and hydrohetaerolite in contaminated stream sediments of the Tyne River catchment, northeastern England, and noted the disappearance of these minerals in downstream areas in which the pH of the water was lower.

The presence of plumboferrite [$\sim PbFe_4O_7$] in the Tyne River sediments was reported by Hudson-Edwards et al. (1996), and the mineral has also been identified as a secondary product in tailings (Morin et al., 1999). Although Al hydroxides play a prominent role in geochemical modeling, few occurrences of such material have been described. Bove et al. (2000) reported the presence of an amorphous Al hydroxide precipitate in a stream channel that drains an acid sulfate hydrothermal system near Silverton, Colorado, and Bove et al. (2000) reported the occurrence of a poorly crystalline Al hydroxide in particulate matter that was filtered from seeps below an abandoned waste-rock dump in New Mexico; however, detailed characterizations were not published. Diaspore [AlOOH] has been reported to occur as a secondary mineral in a waste-rock dump in Tuscany, Italy (Benvenuti et al., 1997). In the study by Hochella et al. (1999), a nearly pure amorphous Si–Al oxyhydroxide (Si:Al = 2:1) rather than $Al(OH)_3$ was identified as the major sink for Al in the local drainage system.

The occurrence of secondary $SiO_2{\cdot}nH_2O$ has been observed in several tailings impoundments, predominantly as amorphous hydrated pseudomorphs after biotite. Cristobalite [SiO_2] has also been detected in the pseudomorphs. Partial replacement of various other minerals by amorphous silica has also been observed.

An extensive suite of supergene minerals, including chlorides, sulfates, and arsenates, occurs at Levant Mine, Cornwall, England, where ingress of seawater has influenced the variety of minerals in the suite. In stagnant pools of mine drainage at the mine, cuprite [Cu_2O] and native copper have precipitated within the ochres (Bowell and Bruce, 1995).

11.5.5.5 Carbonate Minerals

Like the precipitation of secondary $Al(OH)_3$, that of secondary siderite [$FeCO_3$] is widely employed in geochemical models. Secondary siderite and associated Fe oxyhydroxides were determined to have formed as coatings, up to 1000-nm thick, on ankerite–dolomite in the Kidd Creek tailings impoundment at Timmins, Ontario, Canada (Al et al., 2000). At Elliot Lake, Ontario, nodules of siderite, each <10 μm across, and calcite in aggregates, up to 400 μm across, occur as secondary minerals in a small tailings impoundment (Paktunc and Davé, 2002). The precipitation of the carbonate minerals at the Elliot Lake site was interpreted to result from high alkalinity related to the presence of decaying organic debris.

At the Matchless pyritiferous deposit in Namibia, huntite [$CaMg_3(CO_3)_4$] occurs within high-pH zones in an oxidized tailings impoundment (Dill et al., 2002). The high-pH zones are sandwiched between low-pH layers, with phyllosilicate-rich layers acting as aquitards that impede vertical movement and homogenization of the pore waters.

Wastes from Pb-rich mineral deposits typically form anglesite in sulfate-dominant environments, but in limestone-dominated host rocks and in gangue containing abundant carbonates, both cerussite [$PbCO_3$] and hydrocerussite [$Pb_3(CO_3)_2(OH)_2$] have been reported as secondary minerals in mining-related wastes. Several carbonate and hydroxycarbonate minerals of Cu and Zn were reported by Hudson-Edwards et al. (1996) as secondary products in stream sediments in the Tyne Basin, England.

11.5.5.6 Arsenic Oxides

Common arsenic oxide minerals include arsenates or As^{5+} species such as scorodite, arseniosiderite, and pharmacosiderite and aresnites or As^{3+} species such as claudetite (As_2O_3) and arsenolite (As_2O_3). Arsenates are common in mine wastes and mine-drainage settings, mainly because of the common and widespread occurrence of arsenopyrite and arsenian pyrite as gangue minerals. Once discarded in tailings or as constituents of waste rocks, arsenopyrite and arsenian pyrite oxidize to form secondary arsenates as discussed earlier and as indicated from the occurrence of scorodite around relict arsenopyrite particles (Moncur et al., 2005, 2009; Paktunc et al., 2004; Salzsauler et al., 2005). Arsenate minerals are also common in the oxidized (paleoweathered) portions of some gold deposits (Paktunc, unpublished data) and impacted soils (Ashley and Lottermoser, 1999). The common secondary arsenates in mine wastes include scorodite, amorphous ferric arsenate, arseniosiderite, yukonite, and pharmacosiderite (Filippi et al., 2007; Foster et al., 1998a; Morin and Calas, 2006; Paktunc et al., 2003, 2004, 2008; Walker et al., 2009). Among the secondary arsenates, scorodite is the most abundant variety due to its higher stability in the near-surface environments (Harvey et al., 2006; Paktunc and Bruggeman, 2010).

By far, the most important sink for arsenate is sorption to Fe oxyhydroxides. Examples include Fuller et al. (1993), Nriagu (1994), Kimball et al. (1995), Manceau (1995), Waychunas et al. (1996), Lutzenkirchen and Lovgren (1998), Manning et al. (1998), Raven et al. (1998), Webster et al. (1998), Foster et al. (1998b), Ding et al. (2000), Jain and Loeppert (2000), and Farquhar et al. (2002). Fe oxyhydroxides have the capacity to adsorb significant amounts of arsenate as bridging or bidentate–binuclear type complexes (Fuller et al., 1993; Paktunc et al., 2004, 2008; Waychunas et al., 1996). Sorption of As on clays is reported by Manning and Goldberg (1996), Foster et al. (1998a), Lin and Puls (2000), and Garcia-Sanchez et al. (2002) and on schwertmannite by Carlson et al. (2002).

Arsenopyrite and arsenian pyrite are the common carriers of gold in refractory gold deposits. In order to liberate the contained gold, these sulfide minerals are decomposed through accelerated oxidation at high temperature and/or pressure. Roasting, POX, and BIOX are the proven technologies in the

pretreatment of refractory gold ores. The POX of sulfide concentrate from refractory gold ores in autoclaves produces residue containing various arsenates including scorodite, sulfoarsenates, sulfates, and As-bearing hematite and jarosite. Arsenates and sulfoarsenates include compounds referred to as type 1 and type 2 (Swash and Monhemius, 1994) and phase 3 and phase 4 (Dutrizac and Jambor, 2003). Phase 3 has a highly variable composition ($Fe_{0.9-1.3}As_{0.3-0.6}S_{0.4-0.7}O_4(OH)_{0.3-3.3}$), and its As-rich end-member is similar to type 2 ($Fe_{1.2-1.3}As_{0.6-0.8}S_{0.2-0.4}O_4(OH)_{2.6-3.5}$) in terms of both the long- and short-range structures (Paktunc, 2009). Spherical Fe sulfarsenates from the Red Lake autoclave reported by McCreadie et al. (1998) is similar in composition to phase 3. Jarosite can accommodate limited arsenate in the structure through substitution of sulfate (Dutrizac and Jambor, 2000; Paktunc and Dutrizac, 2003; Savage et al., 2000).

During roasting pretreatment of the refractory gold ores, the host sulfide minerals are progressively transformed to pyrrhotite, magnetite, and hematite (Swash and Ellis, 1986) and to maghemite and hematite (Paktunc et al., 2006) as the sulfur is driven off as SO_2 from the sulfide minerals. Arsenic that occurs in -1 valence state in arsenian pyrite and arsenopyrite is volatilized as As_2O_3 and in some cases oxidized to As_2O_5 under the highly oxidizing conditions of the roaster. Depending upon the roasting conditions and the efficiency of the process, some of this As is trapped in maghemite and hematite, which report to the cyanidation circuit for gold extraction (Paktunc et al., 2006). These high-temperature Fe oxide oxidation products typically appear as porous and concentrically layered grains. McCreadie et al. (2000) reported that hematite and maghemite occurring as porous grains measuring 20–50 μm across are the As-rich phases in the residue from the Red Lake roaster. These grains have inclusions of a variety of gangue minerals and also have a high-As content, which varies widely between and within grains but is not correlated with the type of iron oxide. No discrete As phases were identified on the surfaces of the grains, and the As is not part of the crystal structure. The As was presumably incorporated during the roasting process. Arsenic is released due to bacterially mediated reduction of As-rich hematite and maghemite in the roaster tailings at the Campbell Mine (McCreadie et al., 2000). Foster et al. (1998a) reported that arsenic occurs in the roasted sulfide ore of the Spencerville mine in California as As^{5+} species in jarosite and as sorbed complexes on hematite and ferric oxyhydroxide grains. Micro x-ray absorption near edge structure studies indicated that arsenic occurs as both As^{3+} and As^{5+} species in maghemite and hematite (Paktunc, 2008). Walker et al. (2005) reported similar speciation data on the Fe oxide particles in the tailings of the Giant Gold Mine roaster. It appears that As^{3+} species are preferentially enriched in maghemite (Paktunc, 2008, 2009). Although modern roasters allow effective capture of As from off-gases as As_2O_3 (arsenolite) through condensation and collection in bags, complete removal of As from roaster circuits remains challenging, and there are major environmental issues with the disposal of pure As_2O_3 wastes stored in bags. For example, more than 100 000 tonnes of As_2O_3 are temporarily stored in the underground workings of the Giant Gold Mine at Yellowknife and permanent disposal is a major environmental concern.

Trivalent arsenic oxide species also occur as secondary oxidation products after arsenopyrite and arsenian pyrite in mine-drainage settings, although they are rare in comparison to the As^{5+} species. Reported occurrences of As^{3+} oxides in mine wastes and impacted soil/sediments include arsenolite (Ashley and Lottermoser, 1999), picropharmacolite [$Ca_4Mg(AsO_3OH)_2(AsO_4)_2{\cdot}11H_2O$] (Juillot et al., 1999), and tooeleite [$Fe_6(AsO_3)_4(SO_4)(OH)_4{\cdot}4H_2O$] (Morin et al., 2003).

11.5.5.7 Phosphates

Secondary phosphates occur rarely in acid-drainage settings. Pyromorphite [$Pb_5(PO_4)_3Cl$] has been identified in tailings (Morin et al., 1999) and in mining-related stream sediments (Hudson-Edwards et al., 1996). Brushite [$CaHPO_4{\cdot}2H_2O$] was reported by Dill et al. (2002) to be present in the oxidized tailings of the Matchless Mine, Namibia, but the absence of an adequate source of PO_4 in the primary mineral assemblage indicated that the anion was most likely derived from a flotation reagent.

11.5.5.8 Secondary Sulfides

The principal secondary sulfides that have been observed in oxidized mine wastes are marcasite [FeS_2] and covellite [CuS], which have distinctly different origins. The initial oxidation of pyrrhotite results in the solid-state diffusion of Fe toward grain boundaries at which the Fe is oxidized (Pratt and Nesbitt, 1997; Pratt et al., 1994a,b). Upon further Fe migration and the consequent enhanced S enrichment of the original pyrrhotite, replacement by marcasite is affected. Hence, pseudomorphism of the pyrrhotite by marcasite and other oxidation products, including native sulfur, is common if leaching rates are not rapid.

In contrast to the spatial restriction of marcasite to replacement of pyrrhotite, most covellite in mine wastes results from redeposition of solubilized Cu that is typically derived from primary chalcopyrite. Sorption of Cu on Fe oxyhydroxides is common, but redeposition as a sulfide occurs where reductive conditions are present. Such conditions seem to be available locally on a microscale in proximity to altering pyrrhotite, but on a broader scale, the formation of covellite is predominant at the interface between the oxidized and reduced zones of a waste body, thus emulating the supergene enrichment process that takes place in sulfide deposits, especially those of porphyry copper. In mine wastes, other Cu sulfides that resemble covellite in reflected light may also be present, but small grain size has impeded specific identification.

Occurrences of secondary pyrite with framboidal and massive morphologies were reported in the Elliot Lake uranium mine tailings (Paktunc and Davé, 2002). The geochemical conditions in the tailings that promote the formation of pyrite at depths of greater than 0.75 m are described as neutral to weakly alkaline and reducing assisted by microbial activity.

In permeable reactive barriers (PRBs) (described in **Section 11.5.5.9**), chalcopyrite, bornite [Cu_5FeS_4], greigite [$Fe^{2+}Fe_2{}^{3+}S_4$], and abundant framboidal pyrite have been observed as secondary precipitates within the reactive medium emplaced to treat waters laden with heavy metals and sulfate derived from oxidized tailings and sulfide concentrates

(Jambor et al., 2005). Organic carbon is added to the barrier mixture to promote sulfate reduction. The occurrence of mackinawite [Fe_9S_8] at one of the barriers was described by Herbert et al. (1998).

Nanometer-scale secondary sulfides associated with sulfide-reducing bacteria were reported by Fortin and Beveridge (1997) to have formed within the pyritiferous tailings at Kidd Creek, Timmins, Ontario. The sulfides were identified as mackinawite, amorphous FeS, and pyrite. A bacterially associated secondary Ag_2S phase, possibly acanthite, was observed by Davis (1997) in the Kidd Creek tailings.

11.5.5.9 Role of Microorganisms in the Formation and Dissolution of Secondary Minerals

Microorganisms have a major impact on the behavior and cycling of metals in the environment. Their role influences metal behavior through mediation of a variety of opposing mechanisms, including assimilation/adsorption and mineralization, precipitation and dissolution, oxidation and reduction, and methylation and dealkylation (Johnson, 2006). Sometimes, these processes are interrelated; for example, redox changes can result in the release of metal ions that are more or less soluble under prevailing environmental conditions, leading to their spontaneous precipitation or dissolution. Whereas the dissolution of pyrite and other sulfide minerals is central to the genesis of AMD, other microbially mediated processes can occur downstream at the point of discharge of water from a mine, leading to the formation of new (secondary) mineral phases, and these, in turn, may also be subjected to dissolution. While most of these processes involve redox transformations, other aspects of microbial metabolism (e.g., oxygenic photosynthesis by acidophilic and acid-tolerant microalgae, which results in increased alkalinity in mine waters) can also cause or contribute to the formation of secondary minerals.

At its point of discharge, AMD frequently contains little or no dissolved oxygen, and the dominant (or even exclusive) form of soluble iron present is Fe(II) (e.g., Rowe et al., 2007). Oxygenation of AMD streams by diffusion, mass transport, and oxygenic photosynthesis creates conditions favorable to the diverse species of bacteria and archaea that can obtain energy from the dissimilatory oxidation of ferrous iron. Ferrous iron oxidation is a proton-consuming reaction (eqn [31]), which causes, at least in the short term, the pH to increase

$$Fe^{2+} + 0.25O_2 + H^+ \rightarrow Fe^{3+} + 0.5H_2O \qquad [31]$$

However, ferric iron is far less soluble under most physiological conditions than is ferrous and reacts with hydroxyl ions (i.e., the reaction is pH-dependent) to form a variety of amorphous (e.g., ferric hydroxide, eqn [32]) and mineral phases:

$$Fe^{3+} + 3OH^- \rightarrow Fe(OH)_3 \qquad [32]$$

This reaction (referred to as iron 'hydrolysis') causes the pH to decrease, and because two protons are 'produced' for each iron atom, which oxidizes and hydrolyzes, the pH of AMD is often found to be lower downstream than at its point of discharge, as a result of these combined reactions.

In iron-rich mine waters, the dominant ferric iron mineral that forms is very much determined by the pH. In relatively high-pH waters, ferrihydrite is a frequently encountered secondary ferric iron mineral (eqn [33]):

$$10Fe^{3+} + 16H_2O \rightarrow Fe_{10}O_{14}(OH)_2 + 30H^+ \qquad [33]$$

However, at lower pH (~2.3–4), schwertmannite is often the dominant secondary ferric precipitate found in AMD (eqn [34]):

$$8Fe^{3+} + SO_4{}^{2-} + 14H_2O \rightarrow Fe_8O_8(OH)_6(SO_4) + 22H^+ \qquad [34]$$

Both of these are hydrous oxide minerals, but the formation of schwertmannite generates less acidity than does ferrihydrite (2.75 protons for each ferric ion precipitated, compared to 3) and also results in coprecipitation of sulfate, a useful attribute with regard to mine water remediation. However, schwertmannite is metastable with regard to goethite (Schwertmann and Cornell, 2000) and releases sulfate when it is transformed to the latter (eqn [35]):

$$Fe_8O_8(OH)_6(SO_4) + 2H_2O \rightarrow 8FeO{\cdot}OH + SO_4{}^{2-} + 2H^+ \qquad [35]$$

Ferrihydrite is also a metastable mineral and transforms to goethite and/or hematite (Schwertmann and Cornell, 2000).

Below pH ~2.3, the solubility of ferric iron is greatly increased and extremely acidic, iron-rich mine waters can assume colors ranging from light orange to burgundy red. However, a third type of secondary ferric minerals can precipitate under such extreme conditions. Jarosites are a group of basic hydrous sulfate ferric iron minerals. Jarosite also is a principle waste product formed during metallurgical mill processing, where it can be confined to large repositories (Al et al., 1994; Dutrizac, 1999; Dutrizac and Jambor, 2000; Welham et al., 2000). Structurally, jarosite is a member of the jarosite–alunite group of minerals with a general formula of $DG_3(TO_4)_2(OH,H_2O)_6$. The D sites can be occupied by monovalent (i.e., K, Na, Ag, Tl, and H_3O), divalent (i.e., Ca, Sr, Ba, and Pb), trivalent (Bi and rare earth element (REE)), and quadrivalent (Th and U) ions; G sites in this case can undergo solid-solution substitution with Al, Fe^{3+}, and T sites by S^{6+}, As^{5+}, or P^{5+} with lesser amounts of Cr and/or Si (Stoffregen et al., 2000). Jarosites are most commonly encountered in low-pH, high-ferric iron/sulfate-containing liquors that also contain significant concentrations of basic metal cations, such as process waters at biomining sites as well as mine-waste sites and mine waters (e.g., at Iron Mountain, California; Nordstrom et al., 2000). Due to its low solubility in water, jarosite will scavenge metals, allowing it to serve as an excellent medium for trace-metal attenuation. Jarosite thus is important with respect to the fate and transport of metals in AMD environments (Accornero et al., 2005; Lee et al., 2005).

Some microorganisms appear to have a role in forming secondary ferric iron minerals in AMD beyond that of generating ferric iron (which is primarily a microbiological process in acidic (pH ~4) waters). Filaments of ferrihydrite, deposited as trailing stalks attached to bacterial cells, are produced by one of the longest known of all bacteria, *Gallionella ferruginea*, a neutrophilic bacterium not commonly encountered in AMD. However, there is evidence that the EPS produced in abundance by the acidophilic iron oxidizer, *Fv. myxofaciens*, can serve as a site of nucleation for schwertmannite precipitates. *Ferrovum*-like bacteria have been identified as the dominant bacteria present in a pilot-scale system used for remediating

iron-rich groundwater in Germany, where the major precipitate formed is schwertmannite (Heinzel et al., 2009).

Metal sulfides can also form as secondary minerals in mine waters, though these are less frequently encountered than secondary ferric minerals. Many metals frequently found in elevated concentration in AMD from metal mines (e.g., copper and zinc) form highly insoluble sulfide phases that can precipitate (in the case of copper) even in extremely acidic mine waters. The prerequirement here is a source of sulfide (often denoted as S^{2-}, whereas H_2S is actually the dominant form below pH 6.8). Sulfide is produced as a waste product in several biological processes, the most important of which involve the dissimilatory reduction of sulfate, elemental sulfur, and polythionates by sulfate- and sulfur-reducing bacteria (Jameson et al., 2010). These bacteria are obligate or facultative anaerobes that only produce hydrogen sulfide in anoxic conditions, such as in sediments or within thick microbial biofilms and mats in mine streams, where sulfate, etc. (as opposed to oxygen), is used as a terminal electron acceptor. An electron donor (energy source) is also required, which can be organic (e.g., small molecular weight alcohols, such as ethanol) or inorganic (e.g., hydrogen) in nature. Since AMD streams are characterized by having very elevated concentrations of dissolved sulfate, there is great potential in these waters for bacterial sulfide formation. The availability of a suitable electron donor is usually the limiting factor for bacterial sulfidogenesis in AMD streams and sediments (mine waters are generally oligotrophic with regard to dissolved organic carbon), though colonization by acidophilic algae can lead to large inputs of organic carbon in mine waters, which in turn can support massive streamer/mat growths where sulfidogenic bacteria proliferate (e.g., Rowe et al., 2007).

Bacterial sulfate reduction is a proton-consuming reaction, whereas the formation of metal sulfides from the reaction between the dissolved metals and hydrogen sulfide generates protons. Whether the net reaction is pH-neutral or proton-consuming depends on the concentration of a metal(s) in the AMD that can form a sulfide phase under the prevailing pH conditions. Equations [36] and [37] show a hypothetical example for mine water sediment containing 1 mM of both Cu and Zn and 5 mM of Fe(II), where the electron donor is glycerol. At pH 2, only CuS forms (due to its much lower solubility product than those of ZnS and FeS), and the net reaction is alkali-generating (eqn [36]):

$$2C_3H_8O_3 + 3.5SO_4^{2-} + 5H^+ + Cu^{2+} + Zn^{2+} + 5Fe^{2+} \rightarrow 6CO_2 + 2.5H_2S + CuS + Zn^{2+} + 5Fe^{2+} + 8H_2O \quad [36]$$

Such a scenario has been described in AMD draining a copper mine in Spain (Cantareras) where only CuS was identified in the anaerobic microbial mat growth, even though the mine water also contained appreciable concentrations of Zn and Fe (Rowe et al., 2007). At pH 4, both Zn and Cu sulfides form, but not FeS (even though there still may be free sulfide available), as its solubility product is too large. The net reaction is now less proton-consuming (eqn [37]):

$$2C_3H_8O_3 + 3.5SO_4^{2-} + 3H^+ + Cu^{2+} + Zn^{2+} + 5Fe^{2+} \rightarrow 6CO_2 + 1.5H_2S + CuS + ZnS + 5Fe^{2+} + 8H_2O \quad [37]$$

The secondary minerals that form in AMD streams and sediments are themselves potentially subject to microbial dissolution. Secondary sulfides, such as the primary sulfides, are stable as long as conditions remain anoxic, but when sediments are disturbed by high-streamflow rates, etc., and exposed to oxygen, they are susceptible to the same processes of microbial oxidative dissolution as described in **Section 11.5.3.2.1** In contrast, secondary ferric iron minerals (jarosites, schwertmannite, and ferrihydrite) are subject to reductive dissolution in oxygen-depleted (or limiting) environments. Some species of bacteria and archaea are able to use ferric iron as an electron acceptor in anaerobic respiration (Lovley, 1993), and ferric iron reduction also can occur during fermentative metabolism. While dissimilatory ferric iron reduction has been most intensively studied with neutrophilic bacteria such as *Geobacter* spp., the ability to reduce iron appears to be particularly widespread among heterotrophic and autotrophic acidophiles (Coupland and Johnson, 2008; Johnson and Hallberg, 2009a,b). The reasons for this capacity are probably the elevated concentrations of iron that characterize AMD and related environments and also the greatly enhanced solubility of ferric iron at extremely low pH, making it more accessible as an electron acceptor.

Heterotrophic acidophilic bacteria, such as *Acidiphilium* spp. and *Ferrimicrobium acidiphilum*, use organic electron donors to fuel ferric iron reduction (Bridge and Johnson, 2000; Johnson et al., 2009), while autotrophic acidophiles, such as *Acidithiobacillus* spp., use reduced forms of sulfur and, occasionally, hydrogen (Hallberg et al., 2010; Ohmura et al., 2002). Mixotrophic acidophiles, such as *Sulfobacillus* spp. and *Am. ferrooxidans*, can use both organic and inorganic electron donors, and since these, such as *Acidithiobacillus* spp., are also iron oxidizers, they are capable of iron cycling when grown as pure cultures (Bridge and Johnson, 1998).

Bridge and Johnson (2000) compared rates of reductive dissolution of ferric iron minerals by *Acidiphilium* sp. SJH, using glycerol as an electron donor. They found that the iron mineral reduction rates followed the pattern amorphous $Fe(OH)_3$ > magnetite > goethite = natrojarosite > akageneite > (potassium) jarosite and that hematite was not reduced under the experimental conditions used. The rates of mineral dissolution were also faster at lower pH and that contact between the bacteria and the mineral phase was not necessary for reduction of the latter. They concluded that *Acidiphilium* sp. SJH caused the reductive dissolution of ferric iron minerals by an indirect mechanism in which bacterial reduction of soluble ferric iron caused a shift in equilibrium between the mineral phase and soluble ferric iron (which was affected by pH), thereby causing accelerated dissolution of the minerals. The optimum ferric iron reduction by *Acidiphilium* sp. SJH was observed under microaerobic rather than strictly anoxic conditions. Reductive dissolution of amorphous ferric hydroxide, goethite, and jarosite has also been reported for moderately thermophilic acidophiles (Bridge and Johnson, 1998), and recently, Hallberg et al. (2011a) have reported that reductive dissolution of goethite in a limonitic nickel laterite ore, using elemental sulfur as an electron donor, resulted in extraction of >80% of nickel, most of which was intimately associated with the goethite fraction.

In mine-impacted sediments, jarosite may decompose to form a variety of secondary mineral phases, for example, schwertmannite, iron oxides (usually goethite), and hydroxides

(Baron and Palmer, 1996; Gasharova et al., 2005; Smith et al., 2006; Welham et al., 2000). Depending on the geochemical conditions, these secondary minerals may also sequester metals such as Pb, Zn, Ni, Cr, As, and Ag either through adsorption or incorporation into their crystalline structure (Hudson-Edwards et al., 1999; Paktunc and Dutrizac, 2003; Sidenko and Sherriff, 2005).

Dissolution of jarosite (Bridge and Johnson, 2000) and schwertmannite (Coupland and Johnson, 2008; Gramp et al., 2009; Kusel et al., 1999) through the action of acidophilic iron and sulfate-reducing bacteria (SRB) under acidic conditions (pH <2.5) has been demonstrated. The bacteria, in this case, accelerate the dissolution of these ferric iron hydroxysulfate minerals by an indirect mechanism, such that the bacterial reduction of the dissolved Fe(III) results in a shift in equilibrium between solid Fe(III) phases, promoting dissolution of the mineral. As noted earlier, soluble ferric iron derived from acid dissolution of the ferric iron minerals appears to be the form of iron used by iron-reducing acidophiles. In contrast, concentrations of dissolved Fe(III) in equilibrium with the solid would be too low to support such an indirect mechanism at circumneutral pH. However, dissimilatory metal-reducing bacteria have been shown to thrive under circumneutral conditions, although most commonly through direct mechanisms utilizing metal sites (i.e., iron) as a terminal electron acceptor from the mineral itself (Crowe et al., 2007; Hansel et al., 2003; Nevin and Loveley, 2002; Weisener et al., 2011). In this respect, many questions remain regarding the long-term stability of metal-substituted iron hydroxysulfate minerals under prolonged reducing conditions and perhaps moderate pH settings associated with AMD settings either proximal or downstream.

Jones et al. (2006) investigated the microbial susceptibility of K jarosite. In this study, the dissolution character was controlled by a function of temperature and particle size and differences in experimental conditions (media, organisms, number of cells, etc.). These observations appear to be the case for other metal-substituted jarosite minerals. Jones et al. (2006) and Weisener et al. (2008) both show similar trends in sulfate release rates during reductive dissolution compared to ferrous iron for two different jarosite compounds containing different D-substituted elements (i.e., K vs. Ag). The effect of these trace metals relative to iron and sulfate is often not clear, especially when the range of redox-sensitive metals (i.e., As, Cr, Se, Pb, Tl, and Ag) that can occupy lattice positions in these hydroxy sulfate phases is considered. In the latter case, Ag was observed to form intracellularly within bacteria in part due to its very low solubility, coupled with the potential for metal-reducing bacteria (i.e., *Shewanella putrefaciens* and *Geobacter metallireducens*) to use Ag along with ferric iron as a terminal electron acceptor. Similar trends have been observed for Pb-substituted iron hydroxy sulfate minerals (Smeaton et al., 2009). However, in this case, Pb was observed to precipitate within the cytoplasmic membrane, in contrast to the cell wall, of the same bacterial species. Smeaton et al. (2009) note that, within such systems, key genetic differences related to how specific organisms regulate toxicity may be a deciding factor. These differences would certainly have a strong influence on potential pathways that would regulate metals in these AMD environments.

Other investigations have focused on the biogeochemical cycling of solid-phase Fe and S mineral phases often observed in these systems with the aim of understanding the oxidative and reductive pathways of hydroxysulfate end-members and their mineral counterparts (Gramp et al., 2009). The authors note that the reduction of Fe(III) hydroxysulfate occurs via solution-phase transformations, resulting in the dissolution and remobilization of minor trace metals occupying the D location. However, the precise initial mechanism associated with the biological reduction of sulfate is undetermined, but it is hypothesized that electron transfer in sulfate reducers to the surfaces of the mineral and the reduction of low concentrations of sulfate in the solution result in a shift in the equilibrium toward Fe(III) hydroxysulfate solubilization (Gramp et al., 2009).

In reduced aqueous environments, the presence of As in the solution can be a function of both biotic and abiotic mechanisms. The release of As to groundwater from anthropogenic sources is problematic in some areas proximal to mining operations (Williams, 2001) and can be strongly influenced by the microbial communities found within the mine wastes. The prevalent and notably most toxic As species in these systems are the inorganic forms: arsenate [As(V) as $HAsO_4^{2-}$ or $H_2AsO_4^-$] and arsenite [As(III) as H_3AsO_3 or $H_2AsO_3^-$], which act to disrupt cellular processes by posing as an analogue of phosphate or by binding to sulfhydryl groups, respectively (Oremland and Stolz, 2003). The geochemical controls on the fate of As in mine environments are complicated by a number of interacting biotic and abiotic processes, and thus the limits on its mobilization are often difficult to isolate (Smedley and Kinniburgh, 2002). In general, As provenance is most strongly associated with that of Fe. Iron oxides and oxyhydroxides provide sorption sites for As (Bowell, 1994) along with many clay minerals (Violante and Pigna, 2002). Extensive studies of As sorption have demonstrated that pH and redox conditions are the major factors affecting As sorption onto mineral phases (Burton et al., 2009; Casiot et al., 2005). However, factors such as surface area, mineralogy, and the presence of competing ions also may control As sorption (Lim et al., 2008). Following the onset of reducing conditions, adsorbed and coordinated arsenate can be remobilized during the microbial Fe(III) to Fe(II) transformations of Fe oxides (e.g., Cummings et al., 1999). Furthermore, As-bearing phases, such as scorodite [$FeAsO_4{\cdot}2H_2O$)], can be reduced by a variety of dissimilatory iron-reducing bacteria (Babechuk et al., 2009; Cummings et al., 1999; Newman et al., 1997; Papassiopi et al., 2003), leading to the release of Fe(II) and As(V). In some cases, dissimilatory release of As is thought to be a prerequisite for subsequent arsenate reduction (Cummings et al., 1999). The transformation of arsenic between pentavalent and trivalent states also can occur directly through microbial oxidation and reduction (Lee et al., 2010). Recent studies focusing on arsenic-rich mine tailings from the Ketza River mine, Canada, suggest that the stability of these mineral phases is dependent upon the increasing Fe/As ratio (Paktunc et al., 2003, 2004). Leaching tests performed by the authors have shown that the tailings material has significant As concentrations associated with Fe(III) oxyhydroxides. The adsorbed As associated with the Fe(III) oxyhydroxides was less soluble compared to other crystalline minerals such as arseniosiderite [$Ca_2Fe_3(AsO_4)_3O_2{\cdot}3H_2O$] (Paktunc et al., 2004).

The susceptibility of As-bearing Ca–Fe hydroxide minerals collected from tailings cores at the Ketza River mine (Yukon,

Canada) was investigated by Weisener et al. (2011). In this study, samples were collected from exposed and saturated tailings within the impoundment area. The principle concern was to establish the materials' behavior when exposed to reducing conditions in the presence of bacteria. The rates of Fe and As reduction using two strains of dissimilatory As- (*S. putrefaciens* ANA3) and Fe-reducing (*S. putrefaciens* 200R) bacteria were measured. Coatings containing Ca, Fe, and As in the tailings surfaces appeared to have an inhibitory effect on the bacteria slowing the rates of reduction for Fe and As. In part, this reduction in dissolution rate is likely due to surface area characteristics. However, when the carbonate coatings were removed through acid treatment and reinocculated with the bacteria strains, a significant increase in the rate of Fe and As reduction occurred. While, simultaneous reduction of both As(v) and Fe(iii) was observed in this study in both cases, As(iii) respiration rates showed a significant increase in the untreated material compared to Fe(ii) and was likely due to favorable thermodynamic conditions utilizing different electron receptor half reactions, for example, As(iii/v) reduction versus Fe(ii/iii).

11.5.6 AMD in Mines and Mine Wastes

11.5.6.1 Underground Workings

Access to deeply buried ore bodies is attained through underground mining. Workings are excavated to provide access to the ore body (**Figure 4**) and to mine the ore. These operations typically involve the removal of rock with no or little valuable metal content. Mining and economic limitations frequently result in large amounts of residual sulfide minerals being left adjacent to the excavated stopes. The extent of oxidation of these residual sulfides is primarily dependent on the surface area of exposed sulfide minerals and the duration of exposure to oxygen (Morin and Hutt, 1997). After a mine is decommissioned, the weathering products of these exposed sulfides may become a source of acidity, sulfate, and dissolved metals.

Many underground mines are allowed to flood shortly after mining ceases, thus limiting the extent of sulfide-mineral oxidation. In areas where the water table is deep or where adits have been excavated to drain the mine workings, extensive oxidation of the wall rock may persist for years or decades after mining ends. The extent of sulfide oxidation and the quality of the water derived from a mine site are dependent on the duration of exposure to atmospheric O_2, the local geological conditions, and the methods of mining used.

Nordstrom and Alpers (1999b) and Nordstrom et al. (2000) described the generation of extremely acidic water at the Iron Mountain Mine near Redding, California, where a series of tunnels had been excavated to allow access to deep portions of the ore body. The excavation of drainage tunnels from these sites had the effect of exposing large volumes of sulfide minerals, principally pyrite with lesser amounts of chalcopyrite and sphalerite, to oxidation. Large accumulations of secondary sulfate solids, such as römerite, rhomboclase, and Zn–Cu-bearing melanterite, have been observed as efflorescences on the mine walls and as stalagmites and stalactites (Nordstrom and Alpers, 1999b). Water dripping from the mine walls and in pools contained extremely high concentrations of dissolved solids (up to 760 000 mg l^{-1} SO_4, 86 mg l^{-1} Fe, and very high concentrations of other metals) and had a pH as low as −3.6 (Nordstrom et al., 2000; **Table 8**). During dry periods, secondary minerals form within the mine workings and the dissolved metals in pools become concentrated from evaporative effects. After rainfall events, flushing of the accumulated oxidation products results in effluents that have very high-metal concentrations. The concentrations of dissolved metals associated with the Iron Mountain site are much higher

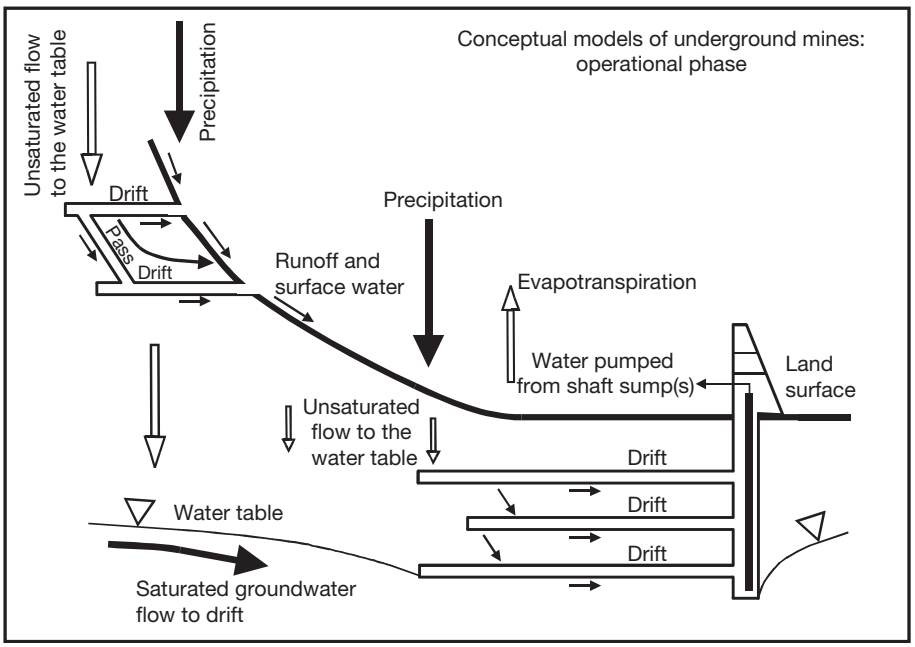

Figure 4 Schematic diagram showing underground mine workings. Modified from Morin KA and Hutt NM (1997) *Environmental Geochemistry of Minesite Drainage: Practical Theory and Case Studies*. Vancouver, BC: MDAG Publishing.

Table 8 Example of water chemistry observed in mine workings

	Königstein Mine[a] *Groundwater in fourth aquifer*	*Königstein Mine*[a] *Unsaturated unleached blocks*	*Königstein Mine*[a] *Unsaturated leached blocks*	*Königstein Mine*[a] *Flooded leached blocks*	*Richmond Mine Portal*[b]	*Carlton Mine Tunnel*[c]	*Roosevelt Mine Tunnel*[d]
pH (SU)	5.99	1.88	2.92	1.88	0.5–1.0	7.81	7.69
E_h (mV)	307	747	807	651	–	–	–
TDS (mg l^{-1})	1736	12 322	3827	13 296	–	–	–
SO_4 (mg l^{-1})	33	8220	2090	8800	20 000–108 000	1292	849
As (mg l^{-1})	–	–	–	–	34–59	–	–
Cd (mg l^{-1})	–	–	–	–	4–19	–	–
Cr_T (mg l^{-1})	<0.002	0.97	0.072	1.34	–	–	–
Cu (mg l^{-1})	–	–	–	–	120–650	–	–
Fe_T (mg l^{-1})	1.51	1171	15.32	1570	13 000–19 000	0.006	0.012
Pb (mg l^{-1})	0.013	2.1	0.010	1.43	–	–	–
Zn (mg l^{-1})	<0.01	132	24	164	700–2600	0.044	0.22
Ra (Bq kg^{-1})	104 ± 7	0.520 ± 0.047	0.0073 ± 0.0016	2.74 ± 0.24	–	–	–
Th (Bq kg^{-1})	n.a.	1333 ± 100	49 ± 6	1051 ± 95	–	–	–
U (mg l^{-1})	<0.02	12.3	18.1	50	–	–	–

[a]Königstein Mine, Germany (Biehler and Falck, 1999).
[b]Richmond Mine portal, California, United States (Nordstrom et al., 2000).
[c]Carlton Mine Tunnel, Colorado, United States (Eary et al., 2003).
[d]Roosevelt Mine Tunnel, Colorado, United States (Eary et al., 2003).

than those observed in drainage from other base metal and gold mines, such as the Carlton Mine and the Roosevelt Mine in Colorado (**Table 8**).

At the Wismut Königstein mine, near Dresden, Germany, acidic solutions were used in an in situ leaching procedure to extract uranium from a sandstone aquifer. During mining, zones of the mine were isolated, and acidic leaching solutions were percolated through blocks of aquifer material. The residual sulfuric acid was collected at the base of the block. The blocks were blasted to enhance permeability. In addition to the acid used in the leaching process, acidity was released by the oxidation of sulfide minerals contained in the sandstone (Biehler and Falck, 1999). The concentrations of dissolved constituents vary in the vicinity of the mine (**Table 8**). Low concentrations of sulfate and dissolved metals are observed in the groundwater. Higher concentrations are observed in the mined blocks, with the maximum concentrations observed in blocks that had been leached and flooded. Wismut plans to decommission the Königstein mine. The fate of dissolved metals and radionuclides in the flooding water is an important factor in the development of decommissioning plans (Bain et al., 2001).

The effects of Au mining on groundwater quality was assessed at the Cripple Creek Mining District, Cripple Creek, Colorado, using field measurements of water quality, mineralogical analyses, and geochemical modeling techniques (Eary et al., 2003). The underground workings were dewatered using a series of drainage adits. These adits have not been plugged, allowing the workings to continue to be exposed to atmospheric O_2. The Au ore occurs as disseminated native Au and is generally associated with pyrite. Oxidation reactions have produced low-pH conditions (pH <3), with elevated concentrations of SO_4 (>2000 mg l^{-1}), Fe (>200 mg l^{-1}), and other dissolved metals in the shallow groundwater. Deeper drainage waters are near neutral in pH (>7) and have low concentrations of dissolved metals. The upper host rocks were depleted in carbonate minerals, suggesting the increase in pH was a result of carbonate-mineral dissolution reactions. The removal of Fe was attributed to the formation of ferrihydrite, Mn to the formation of Mn oxyhydroxides and rhodochrosite, and Zn to the formation of Zn silicates and/or Zn substitutions in calcite. The predictions suggest that the neutralizing capacity of the rock will result in continued improvements in water quality for the foreseeable future (Eary et al., 2003).

11.5.6.2 Open-Pits

Open-pits are excavated to extract ore from near-surface ore bodies. Many open-pits are adjacent or connected to underground workings. Open-pit mining has increased substantially over the past two decades as improved metallurgical techniques, and the increased scale of mechanical operations has made it possible to extract metals from low-grade ores (Miller et al., 1996). These improvements have made large-scale open-pit mining of low-grade Cu and Au ores economically viable. Open-pits are excavated through a series of benches that provide access to the ore and maintain the stability of the pit walls. In areas where the water table is high, it may be necessary, during the mining operation, to dewater the pits and surrounding materials by using pumping or diversion techniques (**Figure 5**).

The excavation of the open-pit and dewatering expose portions of the ore body and country rock, which were previously buried or submerged, to atmospheric oxygen. The oxidation of sulfide minerals within the wall rock results in the release of acidity, sulfate, dissolved metals, and other trace elements (Davis and Ashenberg, 1989). The extent of sulfide oxidation is dependent on the surface area of the exposed sulfide minerals and the duration of mining. In upper portions of the pit, where benches may be pushed back only occasionally, sulfide

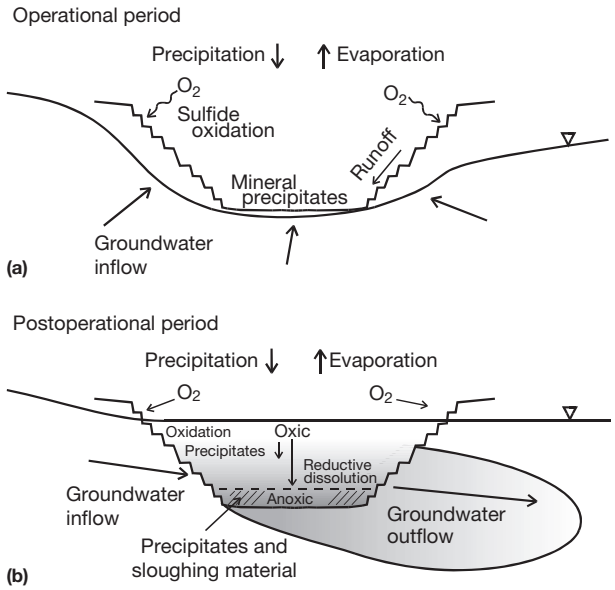

Figure 5 Schematic diagram of an open-pit mine during and after operation. Modified from Eary and Castendyk (1999).

minerals may oxidize for a prolonged period of time. The quantity of sulfide minerals exposed is dependent on their abundance and on the surface area of the pit walls. The pit-wall surface area is considerably greater than would be estimated from an ideal three-dimensional model because of irregularities in the pit walls, the presence of fractures and faults intersecting the pit walls, and the accumulation of rubble zones (Morin and Hutt, 1997). The reactive surface of a pit wall has been estimated to be 27–161 times larger than the ideal three-dimensional surface area (MEND, 1995). The total reactive rock-surface area for an open-pit can be large. For example, the reactive rock-surface area at the Island Copper Mine, near Port Hardy, British Columbia, Canada, was estimated to be 244 000 000 m^2, with a 161:1 ratio of reactive to modeled planar surfaces (MEND, 1995). Many pits are backfilled with sulfide-bearing waste rock, tailings, and other materials, some of which may have oxidized extensively prior to placement in the pit. The presence of these backfill materials may also contribute to the generation of low-quality effluent.

After mining is complete, pumping is terminated and the pits are allowed to flood. The principal components of water gain are precipitation, groundwater inflow, and surface-water inflow. The final elevation of the pit lake will depend on the local hydrological conditions and the geological properties of the surrounding rocks. The principal components of water loss are evaporation and groundwater and surface-water outflow. A water balance based on these principal components can be constructed to estimate the relative magnitude of each component and to assist in the prediction of pit-water quality (Eary and Castendyk, 2009). For the Spenceville Mine at Spenceville, California, Levy et al. (1997) estimated that the principal inflow components were surface runoff > precipitation ≥ groundwater inflow and the principal outflow components were direct evaporation > groundwater outflow as the pit reflooded. On this basis, it was concluded that 2 years had been required to reflood the pit. After the pit had filled, the outflow of surface water commenced and the magnitude of the groundwater and surface-water outflow components increased. In contrast, the Berkeley Pit at Butte, Montana, filled over a period of three decades and is anticipated to continue to fill for several more years (Gammons and Duaime, 2006), thus allowing prolonged exposure of sulfide minerals on the pit walls and the possible accumulation of secondary minerals. These secondary minerals may dissolve into precipitation runoff or into inflowing groundwater or during pit refilling. After the pit floods, further oxidation of sulfide minerals by atmospheric oxygen below the pit-lake surface will be limited because of the low solubility of O_2 in water. The sulfide minerals above the surface of the pit lake will continue to oxidize long after mining has ceased. In addition, oxidation of sulfide minerals with Fe(III) as an electron acceptor may continue within the flooded zone of the pit (Gammons and Duaime, 2006).

The chemistry of pit lakes depends on a number of factors, among which are the geology of the pit walls and surrounding geological materials, the duration of sulfide oxidation, and the local hydrologic conditions (**Table 9**; Miller et al., 1996; Shevenell et al., 1999). Some pit lakes have near-neutral pH and contain low concentrations of dissolved constituents. These lakes may be suitable for recreational use (Shevenell et al., 1999). Other lakes, however, are acidic and contain high concentrations of dissolved metals and may be hazardous to waterfowl (Miller et al., 1996; Morin and Hutt, 1997). Miller et al. (1996) and Shevenell et al. (1999) compared the water chemistry of several pit lakes in the Western United States. Pit lakes associated with sulfide ores and carbonate-deficient rocks generated acidic water containing high concentrations of dissolved metals, whereas pits excavated in country rock containing abundant carbonates were neutral in pH and contained low concentrations of dissolved metals. Some elements, including As, Se, and Hg, were present at high concentrations under the neutral pH conditions that are predominant in carbonate-rich terrains. Eary and Castendyk (2009) summarized the typical host-rock composition, acid–base characteristics, and the expected pit-lake water quality associated with major ore-deposit types.

The relative depth, which is the ratio of the maximum pit depth to the mean diameter of the pit lake expressed as percentage, typically is greater than for natural lakes. The large relative depth typical of pit lakes, combined with the high concentrations of dissolved solids in some pit-lake waters, results in a stable stratification; hence, seasonal turnover and metal cycling are limited. For example, Ramstedt et al. (2003) observed a halocline, redoxcline, and thermocline at different depths in the Udden pit lake, northern Sweden. The limited mixing that persists in some pit lakes can result in the development of a permanently anoxic zone at the base of a lake. Sanchez-España et al. (2008) examined 22 mine pit lakes of the Iberian Pyrite Belt in Spain and noted that many of the lakes exhibited a thermal and chemical stratification with a well-defined chemocline, separating an anoxic Fe(II)-rich monimolimnion from a well-mixed, oxygenated upper layer. The stratification isolates the anoxic zone from the atmosphere, limiting Fe(II) oxidation and providing an environment suitable for anaerobic bacteria, including Fe-reducing bacteria and SRB (Sanchez-España et al., 2008). In lakes derived from metal mining, concentrations of organic carbon may be low enough to limit the extent of Fe and sulfate reduction, whereas open-pits derived from coal mines may have sufficient organic

Table 9 Example of water chemistry observed in existing pit lakes

Constituent	*EPA drinking water standard*	*Berkeley Pit Butte, MT, 10/16/87*	*Robinson District*		*Yerington Pit Yerington, NV, 1991*	*Getchell Mine*			*Cortez Pit Cortez, NZ 1992–93*
			Liberty Pit 1993 (0.5 m)	*Kimbley Pit 1993 (0.5 m)*		*South Pit*[a] *4/28/82*	*Center Pit*[a] *4/28/92*	*North Pit*[a] *4/28/92*	
pH[b]	6.5–8.5 (s)	2.8	3.21	7.61	8.45	5.96	5.27	7.67	8.07
TDS[c]	100 (s)		6240	3580	631	2110	2140	2420	432
Cl	250 (s)	9	48.9	286	36	34.4	30.2	25.7	24.4
F	1.4–2.4		18.5	3.01	1.4	2.4	2.4	1.6	2.4
NO_3 as N	10		<.04	<0.02	0.67	0.01	0.01	0.01	0.207
SO_4	250 (s)	5740	3700	1800	270	1380	1410	1570	90.2
As	0.5	0.05	<0.005	<0.005	0.003	0.009	0.008	0.38	0.038
Ba	1		<0.002	<0.002	0.034				0.06
Cd	0.01	1.3	0.647	<0.005	<.001	<.005	<0.005	<0.005	
Cr	0.05		0.107	0.059	<0.005	<.02	<0.02	<0.02	
Cu	1 (s)	156	37.1	0.06	0.16	0.04	0.04	<0.005	
Fe	0.3 (s)	386	62.2	<0.05	0.01	0.8	2.1	0.16	0.134
Pb	0.05		<0.005	<0.005	<0.005	<.05	<0.05	<.05	0.0043
Mn	0.05 (s)	95	116	0.17	0.32	1.8	4.3	0.13	0.0017
Hg	0.002		<0.0002	<0.0002	<0.0005	<0.2	<0.2	<0.02	0.00046
Se	0.01		<0.005	<.005	0.13	<.002	<0.002	0.003	
Ag	0.05		0.022	0.021	<.01	<.005	<0.005	<0.005	
Zn	5 (s)	280	52.1	1.81	0.01	0.33	0.4	0.02	0.002
Ca		462	506	605	93	401	438	530	45.4
Mg		201	344	156	15	79.3	61.9	72.7	18.1
K		10	63	11.4	6.9	7.85	6.36	10.82	11.7
Na		72	53.6	95.3	76	56.3	40	38.1	68.6
Total alk.			0	189	24				

[a]Filtered samples; composites of samples from various depths.
[b]Amounts are in mg l^{-1}; pH is given in pH units.
[c]Total dissolved solids.
Source: Eary LE (1996) Geochemical and equilibrium trends in mine pit lakes. *Applied Geochemistry* 14: 963–987.

carbon to promote extensive sulfate reduction (Pfeiffer et al., 2002; Ramstedt et al., 2003). In the oxic portion of the water column, oxidation of ferrous iron and precipitation of ferric oxyhydroxide solids may occur. These solids can scavenge trace metals and can settle through the water column. The upper, oxic portion of a lake may therefore contain lower concentrations of dissolved constituents than the deeper waters. The distribution of dissolved constituents in the pit will affect the quality of water discharged from the pit into the adjacent groundwater system and surface-water outflow. For example, very high concentrations of dissolved Zn have been observed in groundwater adjacent to the Brunswick No. 6 open-pit at Bathurst, New Brunswick (Morin and Hutt, 1997). Eary (1999) provides a summary of secondary minerals that may form in open-pits. Recently, the Acid Drainage Technology Initiative, metal mining sector (ADTI-MMS) developed a comprehensive guidebook for assessing the characteristics, fate, and remediation of pit lakes that result from metal and coal mining (Eary and Castendyk, 2009).

11.5.6.3 Waste-Rock Piles

Waste rock, the large volume of rock excavated to access the ore and low-grade ore that cannot be processed economically, is commonly deposited in large piles that are typically 30–100 m high but range up to 500 m in height and several square kilometers in area (**Figure 6**). Waste-rock piles may be deposited in successive lifts or benches, or waste rock may be end dumped from the top of the pile, enhancing sorting and segregation according to particle size. The selection of a disposal technique will depend on the site conditions, economic considerations, and environmental policy.

Waste-rock materials vary in grain size from fine-grained sand and gravel-sized materials to large blocks up to several meters in diameter (Ritchie, 1994). The hydrology of waste-rock piles is an active area of research (Gelinas et al., 1992; MEND, 1994; Nichol et al., 2002; Ritchie, 1994). Measurements made on waste-rock piles and in laboratory columns suggest that the coarse nature of waste rock leads to a relatively large gas-filled porosity and high permeability. Ritchie (1994) summarized the characteristics of waste-rock piles (**Table 10**). This summary indicates that the travel time for vertical transport of water from the surface to the base of a 15 m high waste-rock pile is approximately 3 years. These calculations assume that water transport through the waste rock can be described in the same manner as water flow through an unsaturated soil. Recent studies of waste materials at a mine site in Northern Saskatchewan suggest that more than one flow regime may be present in waste-rock piles, with a portion of the water moving along rapid flow paths (Nichol et al., 2002). At many locations, waste-rock piles are constructed on permeable geological materials (Ritchie,

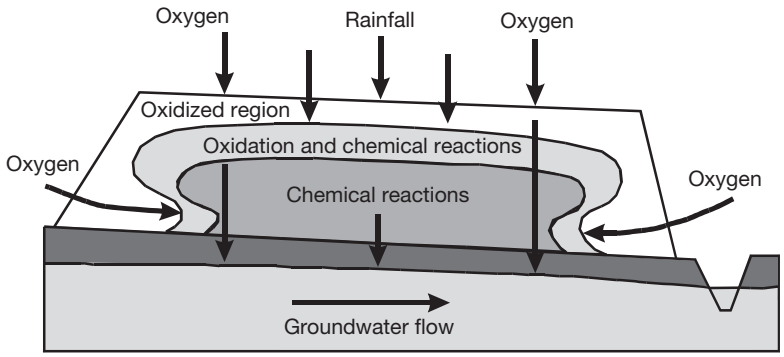

Figure 6 Schematic diagram of a waste-rock dump. Reproduced with permission from Ritchie AIM (1994) Sulfide oxidation mechanisms: Controls and rates of oxygen transport. In: Blowes DW and Jambor JL (eds.) *The Environmental Geochemistry of Sulfide Mine-Wastes*, vol. 22, pp. 201–246. Nepean, ON: Mineralogical Association of Canada.

Table 10 Physical properties of a typical dump of mine waste

Symbol	*Definition*	*Value*	*Units*
L	Dump height	15	m
A	Dump area	25	ha
ρ_r	Bulk density of dump material	1500	kg m^{-3}
ρ_{rs}	Sulfur density as pyrite	30 (2%)	kg m^{-3}
Q_w	Infiltration rate	0.5	m $year^{-1}$
ε_g	Porosity of the dumped material	0.4	
ε_w	Water-filled porosity at specified infiltration	0.1	
K_s	Saturated hydraulic conductivity of dump	10	m day^{-1}
D	Oxygen diffusion coefficient in the dump	5×10^{-6}	m^2 s^{-1}
C_o	Oxygen concentration in air	0.265	kg m^{-3}
ε	Mass of oxygen consumed per unit mass sulfur oxidized	1.75	
S^*	Mass of oxygen consumed per unit volume and unit time by the dump material	1×10^{-8}	kg m^{-1} s^{-1}
ρ_c	Carbonate density	0.6 (0.04%)	kg m^3

Source: Ritchie AIM (1994) Sulfide oxidation mechanisms: Controls and rates of oxygen transport. In: Blowes DW and Jambor JL (eds.) *The Environmental Geochemistry of Sulfide Mine-Wastes*, vol. 22, pp. 201–246. Mineralogical Association of Canada.

1994). At these locations, pore water affected by geochemical reactions within the waste-rock pile may be displaced into the underlying geological materials. Travel through the base of a waste-rock pile, 25 ha in area and undersaturated flow conditions, is anticipated to require 5 years or more (Ritchie, 1994). Under conditions that prevail in most waste-rock piles, the supply of oxygen limits the rate and extent of sulfide-mineral oxidation (Ritchie, 1994). Initially, the oxygen that is contained in a waste-rock pile upon deposition is consumed. This oxygen is gradually replenished by the oxygen from the surface of the pile via four gas-transport mechanisms: diffusion, advection, convection, and barometric pumping, with the last probably the least significant (**Figure 6**).

The rate of oxygen diffusion is proportional to the diffusivity of the waste-rock pile. Although the diffusivity of waste rock is high because of the low moisture content of the waste rock, diffusive transport of oxygen is sufficiently slow that this process limits the rate of sulfide oxidation. Advective transport of oxygen results from changes in gas pressure between the waste-rock pile and the atmosphere. Wind has the potential to drive oxygen deeper into the pile than would occur under diffusive transport mechanisms alone (Amos et al., 2009; Ritchie, 1994; **Figure 6**). The oxidation of pyrite is exothermic, and the progressive accumulation of heat can result in high temperatures in a waste-rock pile undergoing intense oxidation. Temperatures in excess of 60 °C have been measured in oxidizing waste-rock piles. These increased temperatures induce the convective transport of atmospheric oxygen into the pile (Ritchie, 1994, 2003; **Figure 7**).

Convective transport of oxygen results in the penetration of oxygen deep into the waste-rock pile, accelerating the rate of oxidation of sulfide minerals and reinforcing the development of the convection cell (Cathles, 1979, 1994). The accelerated rate of oxidation near the pile margins both increases the short-term release of contaminants and decreases the duration of sulfide oxidation at those sites. Measurements of temperature and gas-phase oxygen concentrations in a waste-rock pile at the Rum Jungle mine site in Australia illustrate the regimes of gas transport within the pile (Harries and Ritchie, 1985). On the surface of the pile, away from the pile margins, the temperature remains relatively uniform and the concentration of oxygen in the pore gas decreases from atmospheric levels (20.9%) to $<1\%$ within 10 m. Gas transport in this region of the pile is dominated by diffusion. At its western margin, temperatures of up to 50 °C were observed within the pile. High O_2 concentrations coincide with these high temperatures, indicating that convective transport of gas is drawing oxygen-rich air from the margin of the pile to approximately 150 m into the interior of the pile. The convective transport of O_2 in this region accelerates the rate of sulfide oxidation at the pile margin relative to the pile surface.

Although seemingly dramatic in its effects, the convective transport of atmospheric gases is of relatively limited importance because a zone of only about 100 m inward from the pile margins is affected. Based on model calculations, Ritchie (1994) estimated that approximately 150 years would be required to oxidize all of the pyrite in a typical waste-rock pile containing 2 wt% pyrite. The duration of oxidation is longer if

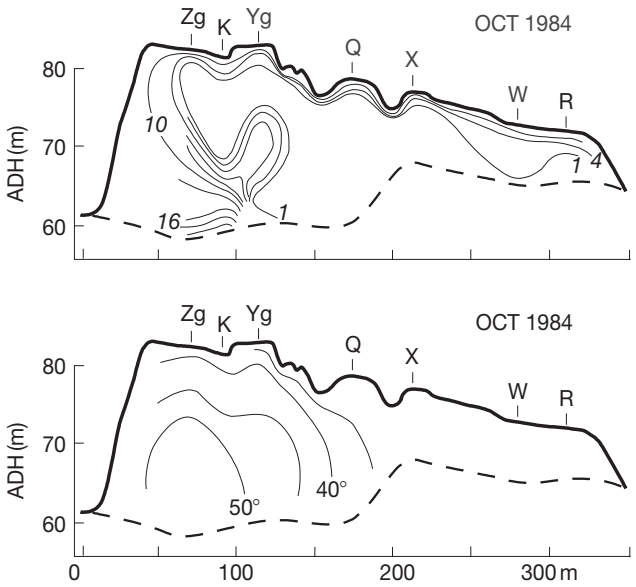

Figure 7 Measurements of temperature and oxygen concentration in the Rum Jungle Mine waste-rock pile. Reproduced from Harries JR and Ritchie AIM (1985) Pore gas composition in waste rock dumps undergoing pyritic oxidation. *Soil Science* 140: 143–152.

the pile has a greater sulfide content. The rapid oxidation of sulfide minerals in waste-rock piles can generate low-pH conditions and release very high concentrations of dissolved constituents to the pore water that flows through the waste-rock pile. Because of the difficulty associated with obtaining water samples from unsaturated waste rock, few measurements of water chemistry from within waste-rock piles are available. Measurements made within the unsaturated zone at the Mine Doyon waste-rock pile show low-pH waters containing very high concentrations of dissolved SO_4, Fe, and Al (**Table 11**; Gelinas et al., 1992, MEND, 1994).

The transport and release of dissolved constituents from the oxidation zone are controlled by the physical hydrogeologic processes that control water flow through the unsaturated pile. These processes include diffusion, flow through the porous matrix, and preferential flow through more permeable pathways. The interaction between these flow and transport processes is complex because of waste pile heterogeneity (Nichol et al., 2005), structure, and geometry (Lamontagne et al., 1999; Lefebvre et al., 2001). Transient flow conditions can result in spatial variations in flow patterns and flow intensities, which lead to spatial variability in flushing rates and, thus, variability in drainage solute and metal loadings (Nichol et al., 2005; Velbel, 1993).

11.5.6.4 Coal-Mine Spoils

One of the most serious environmental concerns associated with coal mining is the production of AMD. Coal mining exposes sulfur-bearing minerals to atmospheric oxygen and water. Pyrite is the principal source of acid production in coal spoils (Rose and Cravotta, 1998). Concerns associated with acidic coal-mine drainage include sedimentation of chemical

Table 11 Concentrations of dissolved constituents in samples collected in lysimeters installed into the Mine Doyon waste-rock pile

Sample	*92-1 L3A*	*92-1 L4A*	*92-1 L5A*	*92-2 L3A*	*92-2 L4A*	*92-2 L5A*
Depth (m)	1.67	2.42	4.05	1.67	2.54	4.07
pH (SU)	6.81	6.81	6.97	1.77	2.03	1.9
Cond. (μS)	1242	1625	2315	21185	17588	22532
E_h (mV)	249	250	226	514	484	432
Fe_T (mg l^{-1})	0	0	0	16614	2878	7888
SO_4 (mg l^{-1})	629	1550	0	63029	43210	40750
Al (mg l^{-1})	–	–	–	2324	2412	2634

MEND (1994) Monitoring and modeling of acid mine drainage from waste rock dumps. *Natural Resources Canada MEND Report* 1.14.2g.

precipitates, soil erosion, and loss of aquatic habitats in contact with waters with high-metal loads (Williams et al., 2002). A bimodal distribution of coal-mine drainage has been observed, with acidic (pH 3–5) and near-neutral (pH 5–7) pH values (Brady et al., 1997). **Figure 8** illustrates the range of pH values observed for both bituminous and anthracite coals of the Eastern United States. Acidic drainage associated with coal spoils develops where carbonate minerals, such as calcite and dolomite, or other calcareous strata that could neutralize acid production are insufficient to neutralize the acidity released by sulfide oxidation. Coal-mine effluents can range in composition from acidic to alkaline, depending on the host-rock geology. Effluents can have pH values as low as 2 and high concentrations of SO_4, Fe, Mn, and Al, along with common elements such as Ca, Na, K, and Mg. The latter constituents are commonly elevated due to aggressive acidic dissolution of carbonate, oxide, and aluminosilicate minerals along flow paths that are downgradient from the sources of oxidizing pyrite (Cravotta, 1994).

In cases where neutral or alkaline mine drainage predominates, problems may arise because of elevated concentrations of SO_4, Fe, Mn, and other solutes that are derived from sulfide oxidation or from reactions with carbonate or aluminosilicate minerals. Dissolved Fe and Al may precipitate as the pH increases, and these precipitates can act as substrates for adsorption and coprecipitation (Brake et al., 2001; Foos, 1997; Stumm and Sulzberger, 1992). The dissolution of siderite, which is commonly associated with coal spoils, followed by the precipitation of Fe(III) oxyhydroxides generates no net alkalinity (Rose and Cravotta, 1998).

High-sulfate concentrations are not dependent on pH conditions and can pose a significant problem in both acidic and alkaline conditions (Rose and Cravotta, 1998). The formation of hydrous sulfate minerals in coal spoils can be significant sources of 'stored acidity' (Alpers et al., 1994). This stored acidity can be released when the soluble secondary minerals are dissolved during periods of recharge or runoff and when Fe or Al components of the minerals undergo hydrolysis (Rose and Cravotta, 1998). An example of this effect is the dissolution of halotrichite and coquimbite, respectively:

Halotrichite

$$FeAl_2(SO_4)_4{\cdot}22H_2O + \frac{1}{4}O_2 \leftrightarrow Fe(OH)_3 + 2Al(OH)_3 + 4SO_4^{2-} + 8H^+ + 13{\cdot}5H_2O \quad [38]$$

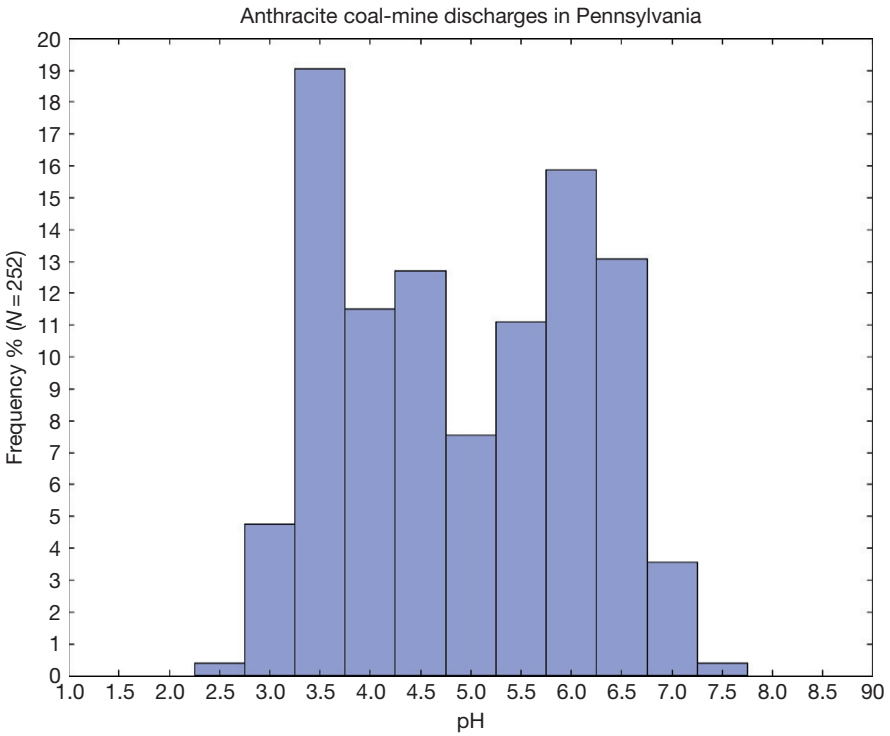

Figure 8 The bimodal distribution of pH in coal-mine drainage, where approximately half of the discharges from bituminous and anthracite coal mines are acidic with a pH less than 5 (http://pa.water.usgs.gov/projects/amd/index.html).

Coquimbite

$$Fe_2(SO_4)_3 \cdot 9H_2O \leftrightarrow 2Fe(OH)_3 + 3SO_4^{2-} + 6H^+ + 3H_2O \quad [39]$$

The storage and release of acidity by these mechanisms can cause considerable temporal variability in water quality and can cause acid drainage to continue even after pyrite oxidation has ceased.

11.5.6.5 Tailings Impoundments

Mine tailings are the finely ground residue from ore extraction. The grain size of the tailings depends on the nature of the ore and the milling process. Size measurements (Robertson, 1994) of tailings from four mines in Ontario, Canada, indicated the tailings materials to be predominantly silt and fine to medium sand with $<10\%$ clay content. Tailings are transported from the mill and are discharged into an impoundment as a slurry containing ~ 30 wt% solids. The method of deposition affects the distribution of tailings particles within the impoundment. Discharge commonly takes place at elevated perimeter dams; hence, there is potential for extensive hydraulic sorting, with coarser fractions settling near the discharge point and the finer fractions settling in distal portions of the impoundment (Robertson, 1994). At some sites, tailings are thickened to >60 wt% solids prior to deposition. Thickening the tailings allows a more rapid settling of the solids, which therefore reduces the potential for hydraulic sorting, resulting in a more uniform grain-sized distribution than is observed in conventional tailings areas (Al, 1996; Robinsky, 1978).

During tailings disposal, water is continuously added to the impoundment, and the water table remains near the impoundment surface. After tailings deposition ceases, precipitation becomes the dominant source of recharge to the impoundment. The water table falls to an equilibrium position controlled by the rate of precipitation, the rate of evapotranspiration, and the hydraulic properties of the tailings and the underlying materials (Blowes and Jambor, 1990; Dubrovsky et al., 1984).

The fine-grain size of mine tailings results in a high moisture-retaining potential for these materials, which is a situation distinctly different from that in waste-rock piles. Whereas waste-rock piles commonly have a large open and free-draining porosity, mine tailings drain slowly, maintaining a large residual moisture content under gravity drainage. Measured moisture contents of conventional tailings impoundments vary from 10% to 100% saturation (Blowes, 1990; Smyth, 1981). The residual moisture content of thickened tailings is greater than that observed for conventional tailings (Al and Blowes, 1996; Robinsky et al., 1991). The high residual moisture content of mine tailings results in a low gas-filled porosity and in rapid changes in hydraulic gradient in response to precipitation (Al and Blowes, 1996; Blowes and Gillham, 1988).

Precipitation that falls on the impoundment surface migrates downward and laterally through the tailings impoundment into underlying geological materials (**Figure 9**). Groundwater velocities in tailings impoundments are relatively low. Coggans et al. (1998) estimated that the groundwater vertical velocity ranged from 0.2 to 1.0 m a^{-1} at the Inco Ltd. Copper Cliff Central Tailings area in Sudbury, Ontario, whereas horizontal velocities were on the order of 10–15 m a^{-1}. At the Nickel Rim tailings impoundment, also

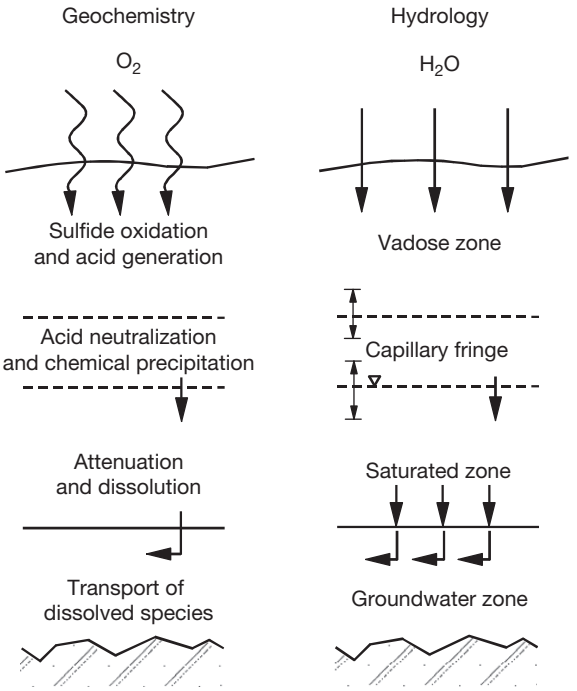

Figure 9 Schematic diagram showing the hydrology and geochemistry of a decommissioned min-tailings impoundment. Reproduced with permission from Blowes DW and Ptacek CJ (1994) Acid-neutralization mechanisms in inactive mine tailings. In: Blowes DW and Jambor JL (eds.) *The Environmental Geochemistry of Sulfide Mine-Wastes*, vol. 22, pp. 271–292. Nepean, ON: Mineralogical Association of Canada.

near Sudbury, Johnson et al. (2000) estimated groundwater vertical velocities ranged from 0.1 to 0.5 m a^{-1} and horizontal velocities ranged from 1 to 16 m a^{-1}.

The surface area of tailings impoundments varies from less than 10 ha to several square kilometers, and the thicknesses of the tailings deposits vary from a few meters to more than 50 m. The relatively low groundwater velocities and the large areal extent of tailings impoundments result in long time intervals between the time of groundwater infiltration and the time of groundwater discharge to an underlying aquifer or to the surface water environment (**Figure 10**). These long travel times result in the delay of measurable environmental degradation at the groundwater discharge point until long into the life of the impoundment. The severity of the negative environmental effects associated with tailings impoundments may not be evident until long after mine closure and decommissioning of the impoundments. The subsequent prevention and remediation of low-quality drainage waters are more difficult than during the active mining. The long travel distances and low groundwater velocities result not only in the potential for prolonged release of contaminants from the tailings impoundment but also in large long-term treatment costs. For example, Coggans (1992) combined estimates of the rate of sulfide oxidation with estimates of groundwater velocity at the Inco Copper Cliff Central Tailings area in Sudbury, Ontario, and predicted (1) that the peak release of sulfide-oxidation products will occur approximately 50 years after the impoundment is decommissioned and (2) that high concentrations of oxidation products will persist for approximately 400 years thereafter.

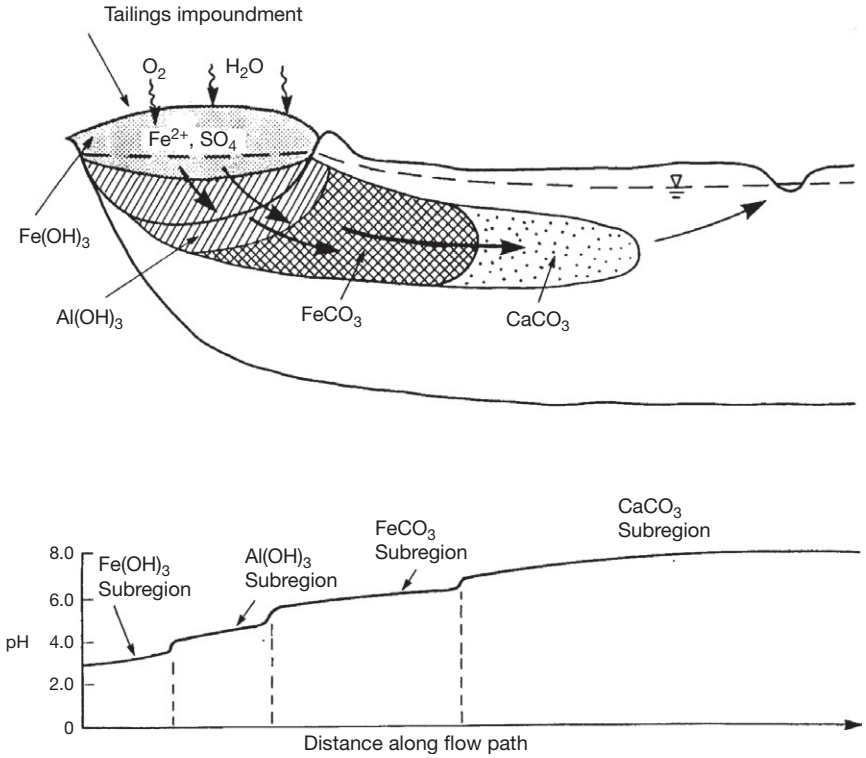

Figure 10 Schematic diagram of tailings impoundment and underlying aquifer, and pH-buffering regions. Reproduced with permission from Blowes DW and Ptacek CJ (1994) Acid-neutralization mechanisms in inactive mine tailings. In: Blowes DW and Jambor JL (eds.) *The Environmental Geochemistry of Sulfide Mine-Wastes*, vol. 22, pp. 271–292. Nepean, ON: Mineralogical Association of Canada.

In most tailings impoundments, gaseous diffusion is the most significant mechanism for oxygen transport. The rate of diffusion of oxygen gas is dependent on the concentration gradient and the diffusion coefficient of the tailings material. The diffusion coefficient of tailings is dependent on the air-filled porosity of the tailings; the coefficient increases as the air-filled porosity increases, and the coefficient decreases as the moisture content increases. Several empirical relationships have been developed to describe the dependence of the gas diffusion coefficient on the tailings moisture content (e.g., Reardon and Moddle, 1985). These relationships indicate a maximum diffusion coefficient at low moisture contents, with a gradual decline in diffusion coefficient as moisture content increases to about 70% saturation, followed by a more rapid decline as the moisture content increases further. The relationship between moisture content and diffusion coefficient results in rapid oxygen diffusion in the shallow portion of the vadose zone of a tailings impoundment, where the moisture content is low. The rapid diffusion of oxygen in this zone replenishes oxygen consumed by the oxidation of sulfide minerals. As the sulfide minerals in the shallow portion of the tailings are depleted, the rate of sulfide oxidation decreases due to the longer diffusion distance and the higher moisture content of the deeper tailings.

In many tailings impoundments, a variety of sulfide minerals is present. Jambor (1994) reported a general sequence of sulfide-mineral reactivity observed in several tailings impoundments, from the most readily attacked to the most resistant, to be pyrrhotite > galena–sphalerite > pyrite–arsenopyrite > chalcopyrite > magnetite. Blowes and Jambor (1990) observed systematic variations in sulfide-mineral alteration versus depth at the Waite Amulet tailings impoundment, Rouyn-Noranda, Quebec. On the basis of the observations, the degree of alteration was classified into a numerical scale as shown in **Table 12**. The sulfide alteration index indicates the relative degree of alteration of sulfides. Because pyrrhotite is the sulfide mineral most susceptible to alteration, the extent of its replacement forms the basis for the alteration index. When plotted versus depth on a vertical axis, the alteration index correlated well with geochemical parameters measured in adjacent drill holes and with gas-phase O_2 and CO_2 concentrations (**Figure 11**; Blowes and Jambor, 1990).

Table 12 Alteration-index criteria for sulfides in oxidized tailings

Index	*Alteration*
10	Almost complete oxidation of sulfides; traces of chalcopyrite ± pyrite
9	Only sparse pyrite and chalcopyrite; no pyrrhotite or sphalerite
8	Pyrite and chalcopyrite are common, but chalcopyrite proportion is higher than normal possibly because of pyrite dissolution; no pyrrhotite or sphalerite
7	Pyrite and chalcopyrite proportions are normal; pyrrhotite is absent, but sparse sphalerite is present
6	Pyrrhotite is absent but is sphalerite common
5	Pyrrhotite is represented by marcasite pseudomorphs
4	First appearance of pyrrhotite but only as remnant cores
3	Cores of pyrrhotite are abundant
2	Well-developed cores of pyrrhotite are with narrower alteration rims; replacement by marcasite is decreasing, while pseudomorphs are absent
1	Alteration restricted to narrow rims on pyrrhotite

The microbially mediated oxidation of sulfide minerals within mine-tailings impoundments generates acidic conditions and releases high concentrations of dissolved metals (**Table 12**). Mill tailings at the Heath Steele Mines in New Brunswick contain up to 85 wt% sulfide minerals (Blowes et al., 1991; Boorman and Watson, 1976). Pore-water pH values as low as 1.0 and concentrations of dissolved SO_4 up to 85 000 mg l^{-1} were observed in the shallow pore water of the tailings impoundment (**Figure 12**; Blowes et al., 1991). This water also contained up to 48 000 mg l^{-1} Fe, 3690 mg l^{-1} Zn, 70 mg l^{-1} Cu, and 10 mg l^{-1} Pb. The shallow pore waters at the Waite Amulet tailings impoundment in northwestern Quebec contain 21 000 mg l^{-1} SO_4, 9.5 mg l^{-1} Fe, 490 mg l^{-1} Zn, 140 mg l^{-1} Cu, and 80 mg l^{-1} Pb. The pH of this water varies from 2.5 to 3.5 (Blowes and Jambor, 1990). High concentrations of dissolved Zn (48 mg l^{-1}), Cu (30 mg l^{-1}), Ni (2.8 mg l^{-1}), and Co (1.5 mg l^{-1}) were observed in the shallow groundwater at the inactive Laver Cu mine in northern Sweden (Holmström et al., 1999). These low-pH conditions and high concentrations of dissolved metals occur within the shallowest portions of the tailings impoundment. As this water is displaced downward through the tailings or through adjacent aquifer materials, the pH gradually rises, and many metals are removed from the solution by precipitation, coprecipitation, or adsorption reactions. High concentrations of Fe(II) and SO_4, however, move down through the tailings and aquifer sediments relatively unattenuated (Dubrovsky et al., 1984; Johnson et al., 2000; Moncur et al., 2005). As this groundwater discharges from the tailings impoundment, Fe(II) oxidizes and precipitates as ferric (oxy)hydroxide and ferric hydroxysulfate minerals. These reactions release H^+, generating acidic conditions within surface waters. The transport of Fe(II) along the groundwater flow path, therefore, provides the vehicle for transporting acidity long distances from the oxidation zone to the surface-water flow system.

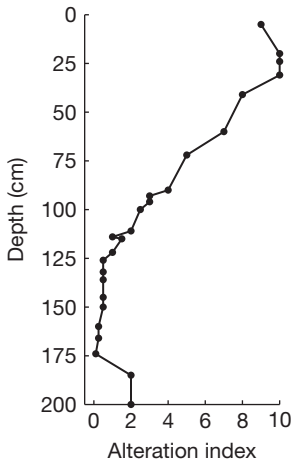

Figure 11 Sulfide alteration index (SAI) for oxidized tailings at the Sherridon mine, Manitoba. Reproduced from Moncur MC, Ptacek CJ, Blowes DW, and Jambor JL (2005) Release, transport and attenuation of metals from an old tailings impoundment. *Applied Geochemistry* 20: 639–659.

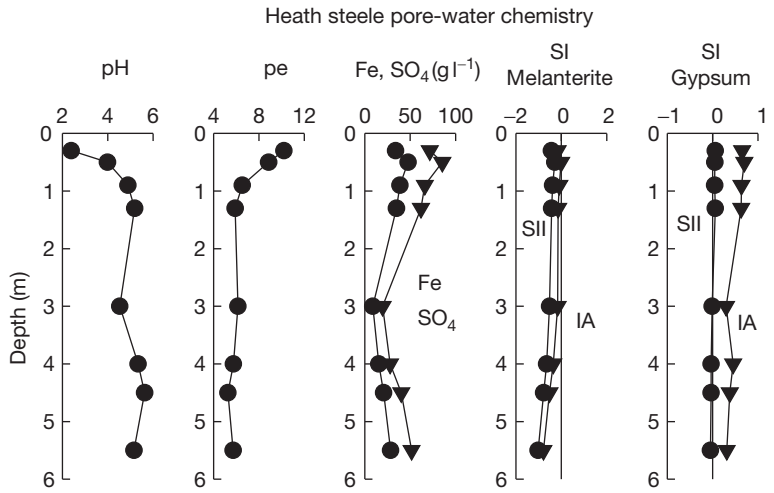

Figure 12 Pore-water chemistry and saturation indices versus depth at the tailings site of the Heath Steele Mines (reproduced from Blowes DW, Reardon EJ, Cherry JA, and Jambor JL (1991) The formation and potential importance of cemented layers in inactive sulfide mine tailings. *Geochimica et Cosmochimica Acta* 55: 965–978). IA represents saturation indices calculated using an ion-association model and SII represents saturation indices calculated using a specific ion-interaction model.

11.5.7 Bioaccumulation and Toxicity of Oxidation Products

Metals released from mines and mine sites, and in some cases from the natural weathering of ore deposits, can harm aquatic biota in adjacent water bodies (Borgmann et al., 2001). Metals are present in aqueous environments in a variety of species, some of which are bioavailable with various toxicities and potential for bioaccumulation. Transformations among these species depend on the physical and chemical characteristics of the water body. Metal toxicity can be acute or chronic. For example, Al can coordinate or precipitate to form species that result in sudden fish kills in waters near mine sites. Other metals, such as Hg, can bioaccumulate, leading to chronic toxicity (Domagalski, 2001). The extent of bioaccumulation and the toxicity of metals within natural environments are controlled by a number of factors, among which are the pH, oxidation–reduction potential, organic carbon content, concentrations and compositions of other dissolved species, and composition of the sediment (Warren and Haak, 2001).

11.5.7.1 Uptake and Bioaccumulation

Bioaccumulation and biomagnification are two terms commonly used for metal toxicity. Bioaccumulation refers to how pollutants (metals) enter a food chain and relates to the accumulation of contaminants, in biological tissues by aquatic organisms, from sources such as water, food, and particles of suspended sediment (Wang and Fisher, 1999). Bioaccumulation involves, relative to the ambient value, an increased concentration of a metal in a biological organism over time. Accumulation in living things can occur whenever metals are taken up and stored faster than they are metabolized or excreted (Markich et al., 2001). Understanding the dynamic processes of bioaccumulation can have important ramifications in protecting human beings and other organisms from the adverse effects of metal exposure, and hence, bioaccumulation is an important consideration in the regulation and treatment of metals associated with AMD.

Among the terms that are important in conjunction with bioaccumulation are uptake, bioavailability, bioconcentration, and biomagnification. Uptake describes the entrance of a chemical into an organism such as by breathing, swallowing, or absorbing it through the skin without regard to subsequent storage, metabolism, and excretion. Bioavailability refers to the availability of a compound to cross an organism's cellular membrane from the medium the organism inhabits at a given time (Semple et al., 2004). Bioconcentration is the specific bioaccumulation process by which the concentration of a chemical in an organism becomes higher than its concentration in the air or water around the organism. Although the process is the same for natural and anthropogenic chemicals, the term bioconcentration usually refers to chemicals foreign to the organism. For fish and other aquatic animals, bioconcentration after uptake through the gills or, in some circumstances, through the skin is usually the most important bioaccumulation process. Biomagnification refers to the tendency of pollutants to concentrate as they move from one trophic level to the next. The process occurs when a chemical or metal becomes increasingly concentrated as it moves up through a food chain, that is, the dietary linkages between single-celled plants and increasingly larger animal species. The natural bioaccumulation process is essential for the growth and nurturing of organisms (Heikens et al., 2001). Bioaccumulation of substances to harmful levels, however, may also occur.

Acid and alkaline mine waters commonly contain high concentrations of dissolved metals and metal-oxide particulates. The acidification of wetlands can elevate the concentrations of metals and increase the potential bioavailability in aquatic plants and freshwater biota (Albers and Camardese, 1993) and can influence the uptake of metals in both submerged and rooted plants (Sparkling and Lowe, 1998). Arsenic concentrations in freshwater macrophytes affected by effluents

from a Au mine were examined by Dushenko et al. (1995). Macrophytes concentrated As relative to sediment concentrations, with submerged species containing much higher levels of As than those in air-exposed plants. The differences observed were attributed to growth form and the ability of plants to exclude As with increasing sediment concentrations. Plants in the vicinity of high-As values showed clear indications of necrosis of leaf tips and reduced micronutrient levels of Cu, Mn, and Zn in root tissues.

A study of As contamination in wood mice proximal to abandoned mine sites has shown that the extent of accumulation depends on the level of habitat contamination (Erry et al., 2000). Rai et al. (2002) observed that seeds appreciably bioconcentrate toxic metals, in the order Pb > Cr > Cu > Cd. The concentrations of these metals correlated positively with metal concentrations in adjacent water and sediments, which had been impacted by domestic and industrial discharges.

11.5.7.2 Toxicity of Oxidation Products

Metals such as Fe, Cu, Cd, Cr, Pb, Hg, Se, and Ni can produce reactive oxygen species, resulting in lipid peroxidation, DNA damage, depletion of sulfhydryls, and Ca homeostasis (Stohs and Bagchi, 1995). The inherent toxicities produced by the oxidation of these metals generally involve symptoms of neurotoxicity and hepatotoxicity. Metal reactions can be influenced by oxidation–reduction reactions, which often occur in aqueous environments impacted by mine-waste effluents. Species that contain more than one oxidation state in natural waters are inherently more mobile, reactive, and will exhibit differences in toxicity (Ahmann et al., 1997; Brown et al., 1999a,b; Ledin and Pedersen, 1996; Lin, 1997; Nordstrom and Alpers, 1999a; Warren and Haak, 2001). Depending on the metal concentrations entering the environment, most oxidation products in excess of natural requirements can produce toxic responses to aquatic biota.

Iron is an essential element for metabolic systems, but in Fe-rich solutions, toxicity can develop in both fish and biota. Iron toxicity has occurred in aquatic plants exposed to Fe-rich groundwater (Lucassen et al., 2000). Iron species can also affect the gill performance in fish, causing acute toxicity and accumulation on the gills (Dalzell and MacFarlane, 1999). In mine-waste discharge, Fe(III) sulfate and oxyhydroxide precipitates can accumulate on the gill epithelium, resulting in clogging and damage, decreasing the available surface area, and increasing the diffusion distance for respiratory exchange (Dalzell and MacFarlane, 1999).

Arsenic in aquatic environments is usually more concentrated in sediments and pore water than in the overlying water column (Ahmann et al., 1997; Smedley and Kinniburgh, 2002; Williams, 2001). The most abundant forms of As are arsenate [As(V)] and arsenite [As(III)], but methylated forms can occur in mine-impacted environments (i.e., methylarsenic acid and dimethylarsenic acid) (Smedley and Kinniburgh, 2002). The principal pathway of As toxicity is through dietary exposure to sediment and suspended particulates by fish, followed by human consumption. Environmental exposure to As is a causal factor in human carcinogenous and other related health issues. Chronic exposure symptoms in humans include hyperkeratosis, hyperpigmentation, skin malignancies, and peripheral arteriosclerosis. Water provides the dominant pathway for As exposure in humans (Williams, 2001).

Mercury speciation is dependent on the available oxygen, pH, and dominant redox conditions, which often are site specific. Mercury can be present as either elemental Hg or mercuric phases (i.e., Hg^{2+}, HgS, and $HgCl_2$) associated with reduced anoxic environments. Under these conditions, Hg is considered to be relatively insoluble and is less toxic to biota. Under more oxidative conditions, such as those associated with roasting by-products (calcines) from separation procedures, Hg can form soluble sulfates and oxychlorides. Further reduction by SRB can cause the inadvertent methylation of the dissolved Hg (Rytuba, 2000). The methylation of Hg and adsorption of Hg and methylmercury onto Fe oxyhydroxides are important processes that control the fate and transport of Hg species in waters impacted by Hg-containing mine drainage. The primary mechanisms controlling the accumulation of methylmercury and inorganic Hg in aquatic food chains are not sufficiently understood, but it is speculated that bacteria in anoxic sedimentary environments associated with the reduction of SO_4^{2-} and S_2^{2-} are responsible (Domagalski, 2001; Rytuba, 2000). The formation of methymercury within sediments and suspended particulate matter has the potential to increase bioaccumulation across all trophic levels, resulting in biomagnification up the food web. Mercury concentrations in fish are ultimately determined by methylmercury accumulation at the bottom of the food chain, which is governed by water chemistry, primarily pH and chloride concentration (Mason et al., 1996).

Accumulation of methylmercury in fish is a consequence of the greater trophic transfer efficiency of methylmercury than of inorganic Hg. For example, methylmercury concentrations in phytoplankton accumulate in the cell cytoplasm, and assimilation by zooplankton is four times more efficient than occurs for inorganic Hg, which is bound in cellular membranes (Mason et al., 1996). The toxicity of methylmercury is high because of its increased stability and its affinity for lipid-based compounds and because its ionic properties lead to an increased ability to penetrate the membranes of living organisms. Because methylmercury is lipid-soluble, it can penetrate the blood–brain barrier. This penetration can affect the central nervous systems of most vertebrates by concentrating in the cerebellum and cerebral cortex, binding tightly to sulfhydryl groups. Developing fetuses are subject to risk exposure because methylmercury can cross the placental barrier (Domagalski, 2001; USEPA, 2000).

11.5.7.3 Assessment of Toxicity

11.5.7.3.1 Predictive models

Models are important tools for the prediction of metal toxicity in aquatic systems. The models relate metal toxicity to site-specific differences in the chemical composition of surface waters. For example, Di Toro et al. (2001) and Santore et al. (2001) summarized the biotic ligand model approach to account for compositional effects on the acute toxicity of metals to aquatic organisms. The model is based on the premise that mortality occurs when the metal biotic ligand complex reaches a critical concentration. The biotic ligand in fish is either known or suspected to be the Ca- or Na-channel proteins

within the gill surface that facilitate the ionic composition of the blood. The biotic ligand will therefore interact with metal cations in the solution. In natural systems, the amount of metal that binds to the gill surface is determined by the competition between the toxic metal and other metals such as Ca. The model is a generalization of free ion-activity model that relates toxicity to the concentration of the divalent metal ions in the solution. The difference in this model is the presence of competitive binding at the biotic ligand, which accounts for the protective effects of other cations, and the direct influences from pH. The model is applied using the Windermere humic aqueous model (WHAM) (Tipping, 1994) to describe metal complexation to organic matter, in conjunction with normal chemical speciation models such as MINTEQA2 (Allison et al., 1990).

11.5.7.3.2 Biologic sensors

Metal contaminants can be monitored using biologic sensors. These sensors can be divided into two groups: active and passive. Active monitoring utilizes well-defined species under controlled conditions, whereas passive monitoring refers to direct observation or chemical analysis of indigenous plant and wildlife. Widespread health concerns have led to the adoption and development of a variety of methods for rapid toxicity assessment. These methods include biosensor devices that incorporate biological whole cells on electrode substrates (e.g., cyanobacteria, microalgae, and fish cells) and substrate monitoring (e.g., bivalves, fish parasites, plants, and mosses).

Natural organisms can provide information pertaining to the chemical state within an environment not through their presence or absence but through their ability to concentrate heavy metals within tissues. For example, sentinel organisms, which include bivalves, have been used to monitor the concentrations of bioavailable metals and toxicity in aquatic ecosystems (Byrne and O'Halloran, 2001; Hall et al., 2002; Lau et al., 1998). Bivalves have been used to monitor heavy-metal pollutants from Au-mine operations in Sarawak, Malaysia (Lau et al., 1998).

Plants and algae species have also been used as biosensors to detect high concentrations of metals from contaminated aquatic ecosystems. Long-term evaluation of Zn and Cd concentrations using two species of brown algae was conducted in Sepetiba Bay, Rio de Janeiro, Brazil (Amado Filho et al., 1999).

11.5.7.3.3 Molecular tools

In the last 10 years, there has been rapid advance in the application of molecular based techniques within the geologic science with respect to their use in discerning microbial structure and effect in natural and anthropogenic systems. Although there are abundant applications of molecular techniques to delineate environmental processes, this section concentrates on the emerging use of these techniques to investigate the mechanisms associated with AMD. The biogeochemistry associated with sulfide-rich waste-rock storage and tailings is complex as certain variables including heat generation from sulfide oxidation; pH gradients, oxygen depletion, and nutrient matter can influence microbial colonization. Overall, the anaerobic biogeochemical processes at work in waste-rock piles are poorly understood (Schippers, 2003). Recent studies have shown that the microbial diversity observed in waste-rock storage sites typically consists of a variety of aerobic and anaerobic species such as autotrophic, heterotrophic, and/or lithotrophic bacteria. The latter have the ability to utilize inorganic compounds as an energy source. An extensive review of this genus has recently been compiled from a variety of mine sites around the globe (Schippers et al., 2010). It is the application of molecular based techniques that makes this possible. Some molecular methods used consist of variations of fluorescence in situ hybridization (FISH) and catalyzed reporter deposition-FISH (CARD-FISH), quantitative polymerase chain reaction (qPCR), denaturing gradient gel electrophoresis, and terminal restriction enzyme fragment length polymorphism. These molecular tools provide an opportunity to profile microbial ecophysiology and quantify individual bacteria groups (Edwards et al., 2003; Fike et al., 2008; Huang et al., 2007; Norland et al., 2009; Schippers, 2007). These tools also can be used to assess microbial community diversity and population. With all techniques there are inherent limitations and caution should be used when interpreting fingerprinting results. Some techniques will only profile more abundant ribotypes within a community but do not detect rare ribotypes.

Metagenomic sequencing of microbial communities in mine-impacted environments promises new perspectives of metabolic activities and pathways in these systems (Hutchens, 2009). Recent applications of these methods have begun to shed light on the complexity of mine-waste dumps. Based on DNA extraction and quantification (qPCR), it has been shown that 'bacteria' typically dominate over 'archaea' and 'Eukarya' with *Acidithiobacillus* spp. being the most abundant Fe(II) and sulfur oxidizers detected (Kock and Schippers, 2006, 2008). Furthermore, the authors report that *Leptospirillum*, an iron oxidizer, and *sulfobacillus* were detected either in low abundance or not at all. These observations can provide valuable insight into how researchers model the biogeochemistry of these systems. Recent work by Norland et al. (2009) has provided further key evidence to describe symbiotic relationships of microbial communities in AMD environments. Based on the application of FISH and high-resolution geochemical imaging using scanning transmission x-ray microscopy, they propose that a microbial cooperative is involved in sulfur cycling in these systems reminiscent of the structure observed for marine consortia. In this study, the authors note the formation of 'sulfur pod cooperative,' which mediate internal redox conditions that can differ from the bulk pore-water solutions. This study provides an interesting interpretation and holds promise for assessing future systems, which are controlling environmental gradients in these AMD sites.

11.5.8 Methods of Prediction

11.5.8.1 Laboratory Static Procedures

Static tests are intended to predict whether a sample, and the rock or soil that it represents, will be acid-producing after exposure to weathering. The distinguishing characteristic of a static test is that it is a one-time determination, whereas kinetic tests involve repeated cycles in which dosages of humidity or aqueous solutions are applied over a period of time. Thus, kinetic tests can provide information on weathering rates and the abundances of ions in the leachates, data not obtainable

from a static test. Nevertheless, static tests are widely used because they have the advantages of being rapid and simple to perform, and commensurate with those advantages is a relatively low cost per determination. Hence, static tests are commonly performed on large numbers of samples for an individual project and for potentially exploitable mineral and coal deposits, the results are commonly used to provide guidance as to which rocks may merit further study, such as by kinetic tests. At active mines, static tests may be used to monitor the potential of various wastes, such as overburden and barren or sulfide-bearing low-grade rocks that host the ores, to generate acidic drainage. The results may be used to govern how and where those wastes are disposed.

Numerous types of static tests have been developed, and some of the laboratory procedures and the variety of tests or their individual development have been described in various publications, such as those by MEND (1991), Lawrence and Wang (1997), Morin and Hutt (1997), White et al. (1999), and Jambor (2003). By far, the most widely adopted static test, both for metalliferous and coal deposits, is the acid–base account (ABA) of Sobek et al. (1978). As is implied by its name, ABA involves a determination of the acid-producing potential (AP) of a sample and a determination of the base that is potentially releasable; the latter is generally referred to as the neutralization potential (NP). The two chemically determined values therefore provide a net accounting of the expected behavior during weathering. A common form of expressing the result is to obtain the net NP (NNP) by simple subtraction of the two chemically determined values:

$$\mathrm{NNP} = \mathrm{NP} - \mathrm{AP} \qquad [40]$$

If NP > AP, the resulting value for NNP will be positive, thus indicating that the sample should have some acid-neutralizing capacity; the opposite, with AP > NP, is taken as an indication that the sample will be acid-generating.

The value for AP is obtained by measuring the sample's weight percentage of sulfur (or wt% $S_{sulfide}$ in some jurisdictions). It is assumed that the S is present as pyrite [FeS_2] and that the pyrite will weather in accordance with the reaction:

$$\mathrm{FeS_2} + \frac{15}{4}\mathrm{O_2} + \frac{7}{2}\mathrm{H_2O} \Rightarrow \mathrm{Fe(OH)_3} + 2\mathrm{SO_4}^{2-} + 4\mathrm{H}^{+} \qquad [41]$$

Hence, each mole of S produces $2H^+$, or stated alternatively, each mole of pyrite produces two moles of H^+. Most nonsulfide minerals will react with acid to some extent, and if the effect of the mineral dissolution is to decrease the acidity of the original solution, then the mineral contributes NP, the amount of which is relative to the acidity consumption effected by calcite in the reaction:

$$\mathrm{CaCO_3} + 2\mathrm{H}^{+} \Rightarrow \mathrm{Ca}^{2+} + \mathrm{CO_2} + \mathrm{H_2O} \qquad [42]$$

The $2H^+$ produced per mole of S in eqn [41] can be neutralized by 1 mol of $CaCO_3$, as in eqn [42]. Therefore, 1 mol of $CaCO_3$ is equivalent to 1 mol of S, and their approximate molecular weight values are 100 and 32, respectively; hence, $100 \div 32 = 3.125$, and 1 g of S is equivalent to 3.125 g of $CaCO_3$. If S is in kg t^{-1}, which is a unit commonly employed, the AP of a sample is its wt% S multiplied by 31.25 to obtain a value expressed in kg t^{-1} of $CaCO_3$ equivalence. The NP of calcite, because it is in g t^{-1}, is 1000. The NP of material is obtained by the addition of acid to a 2 g mass of a sample to determine how much of the acid it consumes (neutralizes). The step-by-step procedures and calculations are given by Sobek et al. (1978), MEND (1991), and Morin and Hutt (1997).

The relationship between the result from a static test and what may occur during weathering is strictly empirical. Many assumptions are involved in the derivation of the NP and AP values, and static tests are a surrogate for weathering, not an emulation of it. Nonetheless, those aspects aside, probably the chief arguments concerning interpretations of static-test results, have been focused on which value constitutes an environmentally 'safe' NNP, on which minerals will provide NP to prevent ARD rather than just mitigate it, and on which minerals contribute to static-test NP even though their effects on ARD are minimal except over longtime periods.

Part of the answer to the arguments has been the measurement of the NP values of specific minerals (Jambor et al., 2002) and the replacement, by some regulatory agencies, of the absolute value of NNP, adopting in its place the ratio of NP/AP for environmental assessments. Like other environmental parameters, the ratio deemed to be appropriate is different in various jurisdictions. Whether NNP values or NP/AP ratios are used, however, they are but one part of a more comprehensive, site-specific environmental evaluation that includes kinetic (dynamic) laboratory tests, commonly.

11.5.8.2 Mineralogical Prediction

Mineralogical factors such as the types, quantity and distribution of sulfide, carbonate and fast-dissolving silicate minerals, and their dissolution and oxidation rates are important in the prediction of AMD. Neutralization capacity and acid generation capacity of the samples can be determined from mineral quantities and the stoichiometry of neutralization and acid-generating reactions (Paktunc, 1999). This mineralogical approach provides an independent assessment of the static ABA test results, which are known to have limitations and uncertainties. Jambor et al. (2007) determined the NP potentials of a range of rocks by the Sobek method and compared the measured NP values with those calculated from the NP of individual minerals (Jambor et al., 2002) and mineral quantities. Although the measured values are always higher than those of the calculated NP values, there is a relationship controlled by the fast-dissolving silicate minerals such as Ca-rich plagioclase and olivine.

Knowledge of the oxidation and dissolution rates of the minerals present in the samples is important for assessing how fast the acidity is produced and whether or not the carbonate and silicate minerals present would dissolve fast enough to effectively neutralize the acidity. Kinetic considerations require that not only the types and quantity of the sulfide and carbonate minerals but also their distribution and availability within the sample need to be known.

The presence of more than one type or generation of pyrite possessing different morphological and chemical features in a deposit such as framboidal and massive types of pyrite and Au and As concentrations in pyrite (Paktunc et al., 2003) would require further considerations on the oxidative dissolution rates of pyrite with orders of magnitude differences.

Differences in the chemical composition of pyrite (Rimstidt and Vaughan, 2003) such as the stoichiometry and minor elements and the particle size would influence the oxidation rates and acid production rates.

The effectiveness of the neutralization capacity can be determined from assessing the particle size and mineral liberation properties. For instance, a study involving long-term column leaching experiments conducted for evaluating the oxidation and leaching characteristics of coarse pyritic uranium tailings with limestone amendments showed that the tailings amended with coarse-grained (6–7 mm) limestone produced acidic drainage after about 2 years of leaching despite the limestone amendment was stoichiometrically adequate for effective neutralization (Paktunc and Dave, 1999). On the contrary, the tailings amended with fine-grained (−44 μm) limestone where there was no acidic drainage during 7.5 years of leaching indicating the importance of availability or effectiveness of the neutralization capacity.

Another important mineralogical feature to consider is the degree of liberation of pyrite or pyrrhotite in the samples. This is especially important for waste rocks but equally applicable to tailings where the sulfide particle size is smaller than average tailings particles. ABA tests inherently assume that sulfide represented by the bulk S concentrations is available. This is acceptable in the case where the sulfide minerals are fully liberated. If sulfide mineral particles are not fully liberated, that means not all of their surfaces are exposed and available for reaction with water and oxygen. The effect of this feature was demonstrated by column leaching studies carried out on three waste-rock samples containing similar quantities of pyrite and calcite but with differing amounts of liberated, locked, and encapsulated pyrite (Paktunc and Davé, 2000). The tailings with essentially liberated pyrite particles produced acidic drainage after about 4 years of leaching, whereas the other two tailings where pyrite particles also occurred as encapsulated and locked particles did not produce acidic drainage during the entire leaching period of 7.5 years.

11.5.8.3 Laboratory Dynamic Procedures

Laboratory dynamic tests are conducted by exposing small volumes of rock to repeated weathering cycles. These tests are commonly referred to as kinetic tests and are intended to assess the potential for acid generation and metal leaching under flow conditions that are designed to emulate field conditions. The objectives of dynamic testing programs vary from confirming the hypothesis developed through static testing to estimating the rates of sulfide oxidation and metal release and to assessing the potential for secondary mineral formation and metal attenuation. Various testing procedures have been developed (DIAND, 1992), among which are well-standardized ones (ASTM, 2001). The test apparatus ranges from humidity cells, which contain approximately 1 kg of sample (ASTM, 2001) to columns containing up to 100 kg of sample (Bennett et al., 1999). The operational steps of the tests vary from procedure to procedure, and the steps may dictate the rate, duration, and volume of sample irrigation, the rate and duration of sample aeration, and the frequency of collection of supernatant samples.

The interpretation of dynamic test data depends on the objective and design of the testing procedure. Although some tests are designed to estimate individual parameters, such as the rate of sulfide-mineral oxidation (Bennett et al., 1999), other tests are intended to provide estimates of the rate of release of dissolved metals and the rate of depletion of sulfide minerals and acid-neutralizing carbonate minerals (ASTM, 2001; DIAND, 1992). It is important that the test design address the objectives. Tests that accelerate the rate of water washing of the sample may not accelerate the rate of sulfide oxidation if that reaction is dependent on the exposed surface area and the extent of bacterial catalysis but independent of the rate of irrigation. Furthermore, many of the products of sulfide oxidation are sparingly soluble at the neutral or moderately acidic pH values that may be observed in the early stages of the test program. Care must be taken to incorporate the masses of these phases into sulfide-oxidation or metal-leaching calculations.

11.5.8.4 Geochemical Models

11.5.8.4.1 Geochemical modeling approaches

A summary of the computer models available to describe inorganic geochemistry in static batch systems was prepared by Alpers and Nordstrom (1998). This summary indicates that a diverse series of models was developed in the 1970s and 1980s, and by the late 1990s, this diversity had decreased to a smaller number of well-supported models. **Figure 13** illustrates the current evolution of coupled chemical–hydrological-speciation modeling programs.

Geochemical speciation models and geochemical speciation mass-transfer models are used widely to describe water chemistry in mine-drainage environments. Most of these models are based on the ion-association theory (Garrels and Thompson, 1960) and use the extended Debye–Hückel model or derivative models, such as the Davies or WATEQ equation, for activity corrections (Nordstrom and Munoz, 1994). A variety of geochemical speciation mass-transfer models has been developed over the past decades (**Figure 13**; Allison et al., 1990; Alpers and Nordstrom, 1998; Ball and Nordstrom, 1987; Parkhurst, 1998; Parkhurst et al., 1985). These models have become highly sophisticated and are able to describe increasingly complex geochemical reactions. Activities derived from the speciation calculations are used to determine mineral saturation indices and predict the extent of mass transfer among aqueous, gaseous, and solid phases, over a range in temperature. Processes described by these models include geochemical speciation, acid–base equilibrium, redox equilibrium, precipitation/dissolution, and adsorption/desorption. The most recent versions of these models are able to incorporate descriptions of kinetically controlled reactions and descriptions of one-dimensional solute transport (e.g., Parkhurst, 1998).

Models based on the ion-pair approach are generally for application to dilute waters, such as those observed in relatively uncontaminated lakes or groundwater systems. Efforts to improve predictions of ion activities and mineral saturation indices for mine-drainage settings (e.g., Ball and Nordstrom, 1987; Nordstrom et al., 1990) have included the addition of extensions to the Debye–Hückel equation to cover a wider concentration range, the inclusion of a large number of

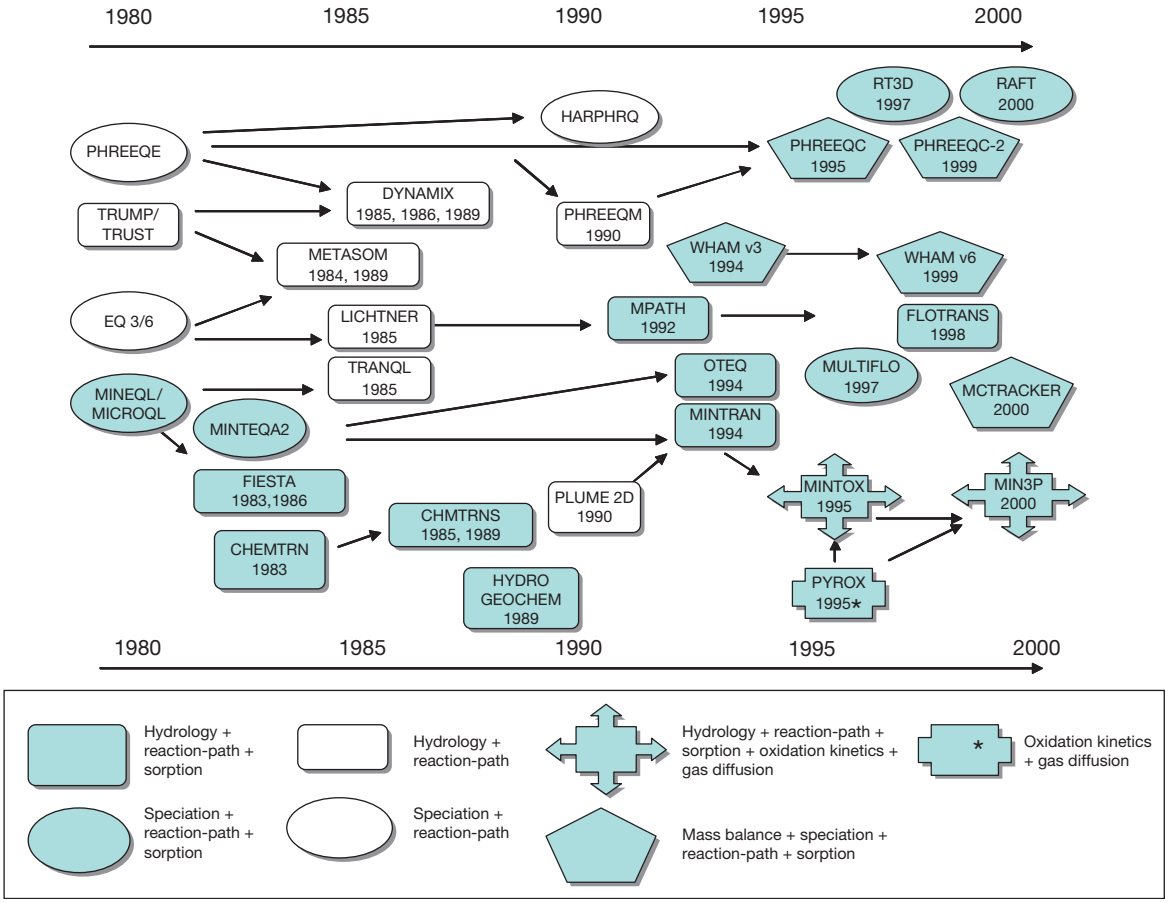

Figure 13 The evolution of coupled chemical–hydrological-speciation modeling programs. Modified from Alpers CN and Nordstrom DK (1998) Geochemical modeling of water–rock interactions in mining environments. In: Plumlee GS and Logsdon MJ (eds.) *The Environmental Geochemistry of Mineral Deposits. Reviews in Economic Geology*, vol. 6A, pp. 289–323. Littleton: Society of Economic Geologists.

ion-association constants and complexation constants specific to mine-drainage settings, and the addition of mineral-solubility constants for phases typically encountered in mine-drainage environments. As a result, the ion-association approach for predicting metal-speciation and mineral-stability fields is generally accurate for mine waters characterized by relatively high concentrations of dissolved solids (ionic strengths up to 1 m) and a relatively broad range in temperature (e.g., Ball and Nordstrom, 1987; Nordstrom et al., 1990).

11.5.8.4.2 Application of geochemical speciation mass-transfer models

Geochemical speciation and geochemical speciation mass-transfer models are used to assist in the interpretation of data collected in mines, deposits of mine wastes, and bodies of receiving water. These models can be used to infer the geochemical reactions that affect the concentrations of major ions and dissolved metals in mine waters and pore waters of mine wastes, to assess the stability of secondary minerals present in mine wastes, and to predict the concentrations of dissolved metals that can be anticipated in mine and mine-waste discharge. The application of these models can be constrained by other observations, particularly characterization of the primary and secondary mineralogy, by measurements of groundwater and surface-water flow directions and velocity, by water-balance calculations, and by measurements of environmental isotopes (e.g., ^{2}H, ^{3}H, ^{18}O, and ^{34}S). Geochemical speciation calculations have been used to assist in the interpretation of water chemistry associated with underground mine workings (Eary et al., 2003), open-pits (Davis and Ashenberg, 1989; Eary, 1999; Ramstedt et al., 2003; Tempel et al., 2000), tailings impoundments (Blowes and Jambor, 1990; Blowes et al., 1992; Gunsinger et al., 2006b; Johnson et al., 2000; Moncur et al., 2005), rivers (Runkel and Kimball, 2002; Runkel et al., 1996), and lakes (Moncur et al., 2006).

Waters associated with mine sites may contain high concentrations of dissolved solids as a result of intense sulfide-oxidation and evaporative processes. Specialized models are required for calculation of ion activities and mineral saturation indices for sites characterized by these high concentrations. The most widely accepted approach for prediction of ion activities and mineral solubilities in complex concentrated electrolyte mixtures is based on the Pitzer ion-interaction formalism (Pitzer, 1973) as summarized in Pitzer (1991). Models based on the Pitzer formalism have been developed for application to various geochemical systems, from acidic to basic, dilute to concentrated, and over a range in temperature, total pressure, and partial pressures of component gases (Clegg and Whitfield,

1991; Pitzer, 1991). The first applications of Pitzer-based models to geochemical systems involved calculations of ion-activity and mineral-solubility relations in waters containing seawater components (e.g., Clegg and Whitfield, 1991; Plummer et al., 1988; Weare, 1987). These efforts have been expanded to include development of ion-interaction-based models for a wide range of chemical compositions, including those derived from sulfide-oxidation processes (Baes et al., 1993; Ptacek and Blowes, 2000; Reardon and Beckie, 1987). Mine drainage containing high concentrations of dissolved metals, sulfate, and acid has been reported for sites in Canada (in excess of 300 000 mg l^{-1}; Blowes et al., 1991; Moncur et al., 2003, 2006) and in the United States (in excess of 900 000 mg l^{-1}; Nordstrom and Alpers, 1999b, Nordstrom et al., 2000).

Geochemical models based on the Pitzer approach have been applied to describe mineral-stability relationships in concentrated mine-drainage waters. At the Heath Steele site in New Brunswick, Canada, high concentrations in pore waters were observed in shallow tailings as a result of sulfide oxidation. Mineral saturation indices calculated using a Pitzer-based model for melanterite, gypsum, and siderite were close to 0.0 where these minerals were observed to occur, whereas saturation index values calculated using the conventional ion-pair model indicated supersaturated conditions (Blowes et al., 1991; Ptacek and Blowes, 1994). Tailings pore waters should have achieved equilibrium with respect to melanterite and gypsum, and possibly siderite, within the observed residence time in the tailings. At the Sherridon mine site in Sherridon, Manitoba, mineral saturation indices for melanterite, gypsum, and siderite also were close to 0.0 where these minerals were observed (Moncur et al., 2005). These results suggest that the Pitzer-based models have the potential to provide predictions of mineral-stability relationships that are consistent with observations at mine-drainage sites with concentrated pore waters.

11.5.8.5 Reactive-Transport Models

Reactive-transport models couple the equations that describe physical transport processes with equations that describe geochemical reactions. These models can be divided into three basic categories: (1) equilibrium models, (2) partial equilibrium models, and (3) kinetic models. The three are differentiated by the approach used to solve the equations for chemical reactions. Equilibrium-based models apply the local equilibrium assumption (LEA) in which all chemical reactions are assumed to proceed to completion or attain equilibrium within each time step. This assumption facilitates coupling between the physical transport step and the geochemical reaction step. In most models, the iteration between the transport step and the chemical step assures convergence between the two modules (Walter et al., 1994a,b). In some cases, however, the two steps proceed sequentially with no iteration between them. A comparison conducted by Walter et al. (1994a) suggests that the error arising from use of the sequential approach is modest. Partial equilibrium models identify a reaction, or a series of reactions, for which the equilibrium assumption is unrealistic. Kinetic expressions are then applied to describe these reactions. The remaining geochemical reactions are described using the LEA (Wunderly et al., 1996). Kinetic models provide the opportunity to consider the rates of all chemical reactions that occur. In several of these models, the chemical reactions are directly substituted into the transport equations and are solved simultaneously (Lichtner, 1993; Mayer et al., 2002; Steefel and Lasaga, 1994; Steefel and van Capellan, 1998). These models provide a comprehensive description of the geochemical system.

Reactive-transport models have been used to describe sulfide oxidation and transport of its products through mine wastes. Liu and Narasimhan (1989a,b) used a reactive-transport model to describe the transport of dissolved constituents at a uranium mine site. Sulfide oxidation and transport of oxidation products at the inactive Nordic uranium tailings impoundment were described using reactive-transport models (Walter et al., 1994; Wunderly et al., 1996). The transport of metal contaminants at Pinal Creek, Arizona, was modeled by Brown et al. (1998). Sulfide oxidation and transport of oxidation products through the Nickel Rim tailings impoundment, Sudbury, Ontario, were simulated by Bain et al. (2000) and by Mayer et al. (2002). The performance of a PRB at the Nickel Rim mine site was simulated using the reactive-transport model MIN3P (Mayer et al., 2006). These simulations that included the reaction mechanisms proposed by Benner et al. (2000), together with the flow system parameters and temperature conditions measured at the Nickel Rim site, provide good agreement with the field observations. MIN3P also was applied by Brookfield et al. (2006) to describe sulfide oxidation and subsequent reactive transport of oxidation products at the INCO Central Tailings Disposal Area, Copper Cliff, Canada. Acero et al. (2009) applied a coupled model that includes the Pitzer ion-association model and kinetically based geochemical reactions coupled to a dynamic flow and solute transport model to describe sulfide oxidation and reactive transport in laboratory column experiments. The performance of a PRB at the Nickel Rim mine site was simulated using the reactive-transport model MIN3P (Mayer et al., 2006). These simulations that included the reaction mechanisms proposed by Benner et al. (2000), together with the flow system parameters and temperature conditions measured at the Nickel Rim site, provide good agreement with the field observations.

11.5.9 Approaches for Remediation and Prevention

Extensive degradation of surface waters by the effluents from abandoned mines and mine wastes has the treatment of effluents imperative in many mining districts throughout the world. Because the degradation of surface-water resources is obvious, often, the remediation of surface waters is the first step in remediation. However, prevention of oxidation in mine wastes and treatment of contaminated groundwater have become areas of active research in mine rehabilitation efforts over the past two decades. An understanding of the geochemical and hydrological processes that result in the release and transport of the products of sulfide oxidation guides the development and implementation of remedial technologies at many mine sites. Among the various remedial strategies that have been developed for implementation at mine sites are the collection and treatment of contaminated surface water and groundwater, passive treatment of contaminated surface water using constructed wetlands, treatment of contaminated

groundwater using PRBs or other in situ remedial approaches, and emplacement of covers on tailings impoundments and waste-rock piles to prevent oxygen ingress or infiltration of precipitation. Mine-site remediation may focus on application of one of these strategies or, more commonly, the integration of a combination of these approaches. The selection of appropriate technologies depends on the physical conditions of the site, the mineralogy of the wastes, and the extent of existing sulfide oxidation.

11.5.9.1 Collection and Treatment

The most common approach to remediate sulfide-bearing mine wastes is collection of the effluent and treatment by pH neutralization and metal precipitation. At many mine sites, water is collected from ponds and ditches and is conveyed to a central treatment facility. The most common approach to water treatment is through pH neutralization using lime, with the subsequent precipitation of metals as a ferric hydroxide sludge. Over the past decade, substantial improvements have been made in treatment efficiency, particularly in the development of high-density sludge systems that both remove greater amounts of dissolved metals and produce lower volumes of waste sludges. The wastes derived from these treatment plants may be disposed of in dedicated facilities or may be codisposed with mill tailings. Little research has focused on the stability of treatment sludges within tailings impoundments. Zinck (1999) assessed the stability of sludges from wastewater treatment plants from several mine sites in Canada. Although the results suggested that these sludges are stable under the conditions that prevail in many mine-tailings impoundments, the stability of codisposal waste products from metal refineries seems to differ. For example, Al (1996) observed that jarosite residue, derived from the Kidd Creek metallurgical plant at Timmins, Ontario, was unstable in the tailings impoundment at that site. At the Campbell mine at Red Lake, Ontario, As-bearing hematite and maghemite residues derived from the roaster circuit in the Au refinery were mixed with flotation tailings and were codischarged to the tailings impoundment. The biologically mediated reductive dissolution of the roaster residue was determined to release As to the tailings pore water, which has been subsequently displaced into an underlying aquifer (McCreadie et al., 2000; Stichbury et al., 2000).

Alternative water-treatment technologies have recently been developed and applied for the treatment of mine-site effluents. Biologically mediated systems that reduce sulfate and promote the precipitation of insoluble metal sulfides have been developed for treatment of mine-waste streams. Reverse osmosis systems have been applied for treatment of mine-waste effluents or for polishing the effluent from facilities that use lime treatment.

11.5.9.2 Controls on Sulfide Oxidation

11.5.9.2.1 Physical barriers

Figure 14 shows a schematic diagram of a mine-waste impoundment. The generation of acidic drainage results from the exposure of sulfide minerals in the vadose zone of the tailings impoundment to atmospheric O_2. Oxygen penetrates the sulfide-bearing wastes by downward and inward movement. Limiting O_2 transport into mine wastes has the potential to limit the extent of sulfide oxidation and the rate of contaminant release. Various physical barriers have been applied or proposed to prevent oxygen ingress; the most commonly used barriers are covering the wastes with water, which limits oxygen transport because of its low-diffusion coefficient, emplacement of covers composed of soil materials designed to maintain high degrees of saturation and low gas-phase diffusivities, and emplacement of synthetic covers, which can be specified to maintain low rates of oxygen transport. In addition to covers that impede oxygen transport, covers composed of oxygen-consuming materials, such as wood wastes, have been applied to prevent oxidation of underlying sulfide minerals.

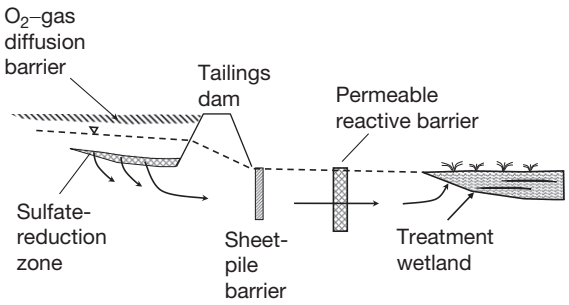

Figure 14 Schematic diagram of a mine-waste impoundment with a combined remediation approach, including a cover to prevent O_2 and water ingress, in situ mixing to geochemically stabilize waste, permeable reactive barrier in aquifer to treat subsurface drainage, and wetland for surface treatment of drainage.

To be most effective, physical barriers must be applied either at the time that mine-waste deposition ceases or shortly thereafter. The rate of sulfide oxidation is greatest immediately after mine-waste deposition ceases, whereupon the moisture content declines. Measurements of concentrations of dissolved constituents in inactive tailings impoundments and modeling of the rate of sulfide oxidation in these wastes indicate that extensive oxidation occurs during the first decade after tailings disposal is complete and that the rate of sulfide oxidation rapidly declines thereafter as the zone of active oxidation migrates deeper into the impoundment and the path for oxygen diffusion lengthens (Johnson et al., 2000; Mayer et al., 2002). These observations suggest that, for sites where mine-waste oxidation has progressed for more than a decade, the emphasis of remedial programs should shift from preventing sulfide oxidation to managing the fate of dissolved oxidation products.

11.5.9.2.1.1 Subaqueous disposal

The solubility of O_2 in water is low, approximately 8–13 mg l^{-1}, at normal surficial temperatures. Furthermore, the diffusion coefficient of O_2 in water (2×10^{-9} m^2 s^{-1}) is much lower than the diffusion coefficient of O_2 in air (1.78×10^{-5} m^2 s^{-1}). These characteristics have been exploited to limit the rate of sulfide-mineral oxidation by covering mine wastes with water. Subaqueous disposal can be achieved by depositing the wastes in natural water bodies, including lakes or marine systems, or in constructed impoundments designed to maintain the water cover. The extent of sulfide oxidation in tailings submerged in lakes in northern Manitoba was observed to be much less extensive than oxidation in adjacent subaerial tailings impoundments

(Pedersen et al., 1993). The development of reduced conditions in the sediments overlying the tailings resulted in the formation of authigenic sulfide minerals.

The environmental implications of dedicating a lake to mine-waste disposal can be significant. Mining companies proposing subaqueous disposal in natural water bodies face regulatory hurdles, and in some jurisdictions, disposal of mine wastes in natural water bodies is not permitted. In addition, mine sites may be remote from water bodies that have the size or depth to accommodate the mass of mine wastes generated through mineral exploitation. In these settings, construction of surface repositories with sufficient retention capacity to maintain water covers over wastes has been constructed (Davé and Vivyurka, 1994). To maintain structural stability of the repository, it is desirable to minimize the depth of the free water cover. Water covers of 1 m or less have been placed on inactive tailings impoundments (Vigneault et al., 2001; Yanful and Verma, 1999). Shallow water covers may be susceptible to resuspension of tailings by wind and wave action (Yanful and Verma, 1999). Furthermore, where sunlight penetrates the water cover, a periphyton layer may develop on the surface of the exposed tailings, producing oxygen at the tailings surface (Vigneault et al., 2001). As a result of these processes, complete prevention of sulfide oxidation may not be attained in repositories with shallow water covers (Vigneault et al., 2001; Yanful and Verma, 1999). For example, Martin et al. (2001) observed more extensive oxidation in shallow lake bed sediments than in similar sediments in deeper portions of a lake in Peru. Although, shallow water covers do not completely prevent sulfide oxidation, these covers do substantially lessen the rate of oxidation relative to rates observed under subaereal conditions. Vigneault et al. (2001) estimate that tailings submerged beneath a 0.3 m water cover oxidized at a rate approximately 2000 times less than the rate observed for in moist tailings exposed to oxygen in humidity cell experiments.

11.5.9.2.1.2 Dry covers

Retaining dams constructed at many mine-waste disposal facilities are composed of coarse-grained mill tailings or mill tailings combined with waste rock. Many of these structures were designed to retain tailings during deposition and to drain and consolidate after deposition is complete. Consolidation enhances the stability of the retaining dam and is a component of the impoundment design. Alternative cover designs may include layers that maintain high moisture contents under negative pressures. These dry covers maintain a near-saturated layer several meters above the water table. Dry covers typically are composed of layers of soil materials with variable grain-sized characteristics (Holmström et al., 2001; Nicholson et al., 1989). In their simplest form, these covers can be composed of a single layer of fine-grained material. In 1988, a fine-grained cover was applied to the surface of waste-rock piles at the Rum Jungle mine site in the Northern Territory, Australia (Harries and Ritchie, 1985, 1987). The performance of the Rum Jungle cover has been monitored regularly since installation (Harries and Ritchie, 1985, 1987; Timms and Bennett, 2000). Analysis and modeling of the field data indicate that the cover decreased the rate of oxidation of the underlying sulfide minerals by one-third to one-half of the initial rate and that recent data indicates that both the oxidation rate and the rate of infiltration have increased (Timms and Bennett, 2000).

More complex covers may be comprised of several layers, each with different soil characteristics. A cover installed at the Bersbo site in Sweden included layers of fine-grained clay and coarse-grained aggregate material and a protective layer of natural till (Lundgren, 2001).

Dry covers may also be installed with the objective of preventing the infiltration of precipitation into the underlying mine wastes. These covers are designed to retain moisture during wet seasons and promote evapotranspiration of this moisture during dry periods (Bews et al., 1997; Durham et al., 2000).

11.5.9.2.1.3 Synthetic covers

Covers composed of synthetic materials have been emplaced at mine-waste sites to prevent ingress of both oxygen and water. Synthetic materials used include polyethylene, concrete, and asphalt. A complex cover includes a sealing layer consisting of concrete stabilized with fly ash at the Bersbo site in Sweden in 1988. This cover includes a granular stabilization layer, the concrete sealing layer, and a 2-m-thick protective till cover. Instruments were installed through the barrier at the time of implementation, and monitoring since then has shown that, although the cover formed a suitable oxygen barrier, changes in barometric pressure cause migration of O_2 into the waste material (Lundgren, 2001).

To prevent the release of contaminants from an inactive Cu–Zn mine-tailings impoundment near Joutel, Québec, a geomembrane and a protective clay cover overlain by 0.5–1.5 m of till were placed on the impoundment surface (Lewis et al., 2000). The performance of this barrier is the subject of a long-term monitoring program.

11.5.9.2.1.4 Oxygen-consuming materials

Covers containing organic materials have been applied to the surface of mine wastes (Tassé et al., 1994). The principal objective of these covers is to prevent oxygen entry into the mine wastes by intercepting and consuming oxygen in the cover material. Wood wastes and other waste forms of organic carbon have been evaluated to assess their potential as cover materials. Reardon and Poscente (1984) evaluated the potential application of wood wastes as an oxygen-consuming barrier for sulfide-bearing mine tailings. The conclusion is that these materials may provide an effective oxygen barrier, but the life-span of the organic carbon cover would be insufficient for this approach to be viable. Tassé et al. (1994) described the performance of a wood-waste cover installed at a mine site in Québec. At this site, the cover provided an effective barrier to the ingress of O_2 into the underlying tailings.

Organic materials, such as wood waste or waste materials derived from pulp-and-paper operations, have the potential to leach organic acids, which subsequently move into the underlying tailings. For freshly deposited tailings, in which the oxidation of sulfide minerals has been minimal, the presence of these organic acids is not anticipated to have deleterious environmental effects. If an organic cover is emplaced over weathered sulfide-bearing mine tailings, however, accumulations of ferric iron-bearing secondary minerals may be reductively dissolved by the organic acids released from the cover materials. Extraction experiments conducted by Ribet et al. (1995)

indicated that most of the metals present in the shallow portions of the Nickel Rim tailings impoundment, Sudbury, Ontario, were in the oxidized form and would be susceptible to release by reductive dissolution.

11.5.9.2.2 Chemical treatments

A variety of methods has been developed to prevent sulfide-mineral oxidation at the particle scale. Chemical treatments have been proposed to encapsulate sulfide minerals in inert materials, thereby preventing oxidation at the sulfide-mineral surface. Huang and Evangelou (1994) proposed encapsulation with silicate coatings. Silicate binds with ferric iron on the sulfide-mineral surface, rendering the surface inert. Huang and Evangelou (1994) and Ueshima et al. (2004) proposed using phosphate to bind on sulfide surfaces in a similar manner. Laboratory experiments indicated that the rate of oxidation at the sulfide-mineral surface was much less in the presence of phosphate and silicate anions. Silicate coating of sulfide grains was also evaluated by Georgopoulou et al. (1995) and by Fytas and Bousquet (2002). Belzile et al. (1997) also observed that coating pyrite grains with either acetyl acetone or sodium silicate reduced the oxidation rate of pyrite grains. All of these studies indicated that coatings formed on the surfaces of sulfide minerals substantially decreased the rate of sulfide oxidation relative to that of pristine sulfide minerals. In addition to chemical treatments that incorporate the addition of anionic reagents, accelerated oxidation of sulfide particles by using strong oxidants, such as permanganate, has been proposed. The objective is to oxidize the surface of the sulfide grain, creating a protective armor layer.

11.5.9.2.3 Bactericides

The rate of abiotic pyrite oxidation declines as the pH decreases below 3.5. Under these conditions, bacterially mediated pyrite oxidation predominates. Numerous researchers have evaluated the use of bactericides, principally anionic surfactants, to prevent bacterial activity and limit the rate of sulfide oxidation. Bactericides can be applied either directly to mine-waste surfaces or as intimate mixtures with the mine wastes (Ericson and Ladwig, 1985). Preliminary results using this approach were encouraging (Dugan, 1987a,b; Sobek, 1987). Slow release of surfactants from rubber-based pellets is an approach that has been developed to extend the life-span of these surfactants in field applications. The toxicity of low-molecular-weight organic acids to microorganisms is well documented. At low-pH values, they have a neutral charge and are able to diffuse across the membrane and deprotonate in the cytoplasm killing the microorganism (Aston et al., 2009). However, organic acids would be too expensive for use in the field and would also degrade very rapidly. Thiocyanate has also been evaluated as an inhibitor of sulfide-mineral oxidation in waste rock (Olson et al., 2004), but thiocyanate is toxic and it would be difficult to obtain regulatory approval for its use. Stichbury et al. (1995) proposed the use of thiol-blocking agents to inhibit bacteria involved in the early stages of sulfide oxidation. In shake-flask cultures and in column experiments, Stichbury et al. (1995) observed reduced sulfide oxidation that persisted over a 1-year study. In a 2-year field study, the inhibitor mixture completely prevented the growth of *At. ferrooxidans* and lessened the growth of *At. thiooxidans* and *Thiobacillus thioparus* (Lortie et al., 1999). Lower concentrations of sulfate, iron, and dissolved metals were observed in the treated field plots than were observed in untreated control plots. The effectiveness of the inhibitors was observed to decline following the first year after application, and thus, they would not be suitable for long-term application. This observation suggests that inhibitors may be best applied in settings where prevention of sulfide oxidation is required for limited periods only. Examples are stockpiling of waste rock before it is placed in underground workings, stockpiles of mill tailings that will be subsequently used for mine backfill, or waste-rock and tailings piles during periods of temporary closure.

11.5.9.3 Passive Remediation Techniques

11.5.9.3.1 Types of passive systems

Passive treatment systems can be based on chemical or biological processes or a combination of both (Neculita et al., 2007). Systems for the treatment of mine drainage will often consist of several treatment cells in series based on different treatment processes (Johnson and Hallberg, 2005). Passive chemical systems include anoxic limestone drains (ALDs), limestone channels, and PRBs, and biological systems include constructed wetlands, bioreactors, and PRBs. PRBs will be discussed in another section of this article.

11.5.9.3.2 Anaerobic bioreactors

Anaerobic bioreactors (ABRs) consist of organic matter to provide substrates for microbial activity, sand and gravel for permeability, and limestone for alkalinity generation (Johnson and Hallberg, 2005; Kaksonen and Puhakka, 2007). They are generally operated in the upflow mode to develop anaerobic conditions more rapidly and to reduce compaction (Mattes et al., 2011). Although a number of processes are responsible for attenuating contaminant concentrations in ABRs, the key process is sulfate reduction. Sulfate reduction generates alkalinity and precipitates metals by the formation of metal sulfides. Because SRB only utilize simple organic compounds such as low-molecular-weight organic acids and alcohols as electron donors, they are dependent on other organisms to provide these substrates (Gould and Kapoor, 2003; Logan et al., 2005; Pruden et al., 2007). The major components of plant-derived organic matter are lignin, cellulose, and more reactive low-molecular-weight organic compounds. Lignin degrades much more slowly than the other materials but will contribute to the longevity of the ABR. The more reactive organic compounds will be consumed rapidly. Most of the electron donors for sulfate reduction will be provided by cellulose degradation. During degradation, cellulose is hydrolyzed to sugars, which are then fermented into alcohols and organic acids which can then be used by the SRB (Gould and Kapoor, 2003). In most ABR systems with the exception of pH extremes, carbon availability is the limiting factor. Microbiological studies of laboratory ABRs indicate that the key microorganisms are the anaerobic cellulose degraders and that cellulose hydrolysis is the rate-determining step (Logan et al., 2005; Pruden et al., 2007).

11.5.9.3.3 Constructed wetlands

Constructed wetlands have been used for water treatment since the early 1950s (Hedin and Nairn, 1992). The interest in using constructed wetlands for the remediation of mine drainage stems from their ability to filter particulate matter, thus reducing suspended solids, their ability to reduce biochemical oxygen demand and remove and store nutrients and heavy metals, and their natural buffering capacity (Greenway and Simpson, 1996; Hsu and Maynard, 1999; Machemer and Wildeman, 1992; Mayes et al., 2009; Perry and Kleinmann, 1991). However, wetland systems can lose their effectiveness if the influent pH is too low (Hsu and Maynard, 1999). The influent pH can be increased by treating the influent with an alkalinity-generating system such as anoxic limestone channel or an ALD prior to the wetland (Cravotta, 2010; Zipper and Skousen, 2010). If properly designed and maintained, constructed wetlands can result in the improvement of the quality of drainage water derived from mines (Walton-Day, 1999). The mechanisms that promote acid neutralization and metal retention include dissolution of primary carbonate minerals, formation and precipitation of metal hydroxides, microbially mediated sulfate reduction, formation of metals sulfides, complexation of metals by organic carbon, ion exchange, and direct uptake by plants (Bendell-Young and Pick, 1996). Batty et al. (2008) designed a wetland for the treatment of drainage from an abandoned coal mine with Fe and Mn concentrations of 45 and 2 mg l^{-1}, respectively. The system consisted of two oxidation ponds (total area 800 m^2) and three wetlands (total area 3000 m^2). The iron was removed in the first part of the system, but manganese was only removed in the latter stages of the system. Wetlands can be designed to function under aerobic or anaerobic conditions. Aerobic wetlands consist of *Typha* and other wetland vegetation planted in shallow relatively impermeable sediments comprised of soil, mine spoil, or clay. The vegetation in anaerobic wetlands is planted in deep (>30 cm) permeable sediments consisting of peat, soil, organically enriched compost, sawdust, etc., which are sequenced between crushed limestone or are mixed (http://www.wvu.edu/~agexten/landrec/passtr/passtrt.htm).

Anaerobic constructed wetlands promote bacterially mediated sulfate reduction. These reactions have the potential to remove metals, as well as high concentrations of sulfate, from mine drainage. A growing concern associated with the use of wetlands to attenuate metals is the potential for the wetland soils to become latent sinks of toxic metals (Gopal, 1999). Heal and Salt (1999) monitored a constructed-wetland system impacted by acidic metal-rich drainage from ironstone mine spoils. Mine waters (pH 2.7, 247 mg l^{-1} total Fe) passing through the wetland were monitored for 12 months. After installation, the acidity declined by 33%, and Fe, Mn, and Al concentrations declined by 20–40%. The performance of the constructed wetland showed favorable response to metal loads during the summer months, but the rates of metal removal decreased significantly in the winter months (Heal and Salt, 1999). Sobolewski (1996) monitored the performance of a constructed peat-based wetland for long-term treatment of mine drainage at the former Bell Copper Mine near Smithers, B.C., Canada. Copper concentrations were used to provide estimates of the long-term potential for removal of Cu from the mine-drainage site. Two Cu species were identified: Cu sulfides and Cu bound to organic material. Removal from mine effluent containing low concentrations of Cu at near-neutral pH was through sulfide formation. Removal from acidic drainage containing higher Cu concentrations was by complexation to organic matter. The effectiveness of the constructed-wetland system to remove metals under low-pH conditions and with high-metal concentrations was insufficient to be suitable for long-term remediation.

The definition of appropriate operating conditions is required to assure success of wetland treatment systems. Acidic drainage containing high concentrations of dissolved metals discharged from abandoned underground mines in Kentucky, United States, was intercepted by a wetland constructed in 1989 to reduce the concentration of metals (Barton and Karathanasis, 1998). The initial attempt to treat the drainage water using the wetland failed after 6 months because of insufficient utilization of the treatment area, inadequate alkalinity production, and high-metal loadings. A renovation added two ALDs and a series of anaerobic subsurface compartments to promote vertical flow through a successive alkalinity-producing system. The renovated system was monitored over 19 months and showed improved performance in metal removal. Iron concentrations decreased from 787 to 39 mg l^{-1}, the pH increased from 3.38 to 6.46, and the acidity decreased from 2244 to 199 mg l^{-1} (carbonate equivalent) (Barton and Karathanasis, 1998). The mass loading of metals was reduced by an average of 98% for Al, 95% for Fe, 55% for sulfate, and 49% for Mn.

Improving the efficiency of metal removal using wetlands has proved to be difficult. Successful wetland treatment systems are frequently overdesigned in order to handle variations in influent loading and also to prolong the effective lifetime of the wetland (Hedin, 2008). Detailed assessments of long-term performance of wetland systems with a focus on metal-retention mechanisms, eutrophication, and flushing rates and their effects on downgradient ecosystems are required if wetland treatment is to be applied in temperate regions.

11.5.9.3.4 Permeable reactive barriers

PRBs are used for treatment and prevention of mine-drainage waters within aquifers receiving discharge from mine wastes. These systems are constructed by excavating a portion of the aquifer downgradient from the waste disposal area and filling the excavation with a permeable mixture composed of reactive components (Blowes et al., 2000a,b). Among the mixtures designed for treating mine-drainage waters have been organic carbon in the form of composted municipal wastes, wood wastes, and by-products from pulp-and-paper manufacturing (Benner et al., 1999; Blowes et al., 1994), zerovalent iron (Blowes et al., 2000a; Morrison et al., 2002; Naftz et al., 2002), limestone, and phosphate-based adsorbent materials (Conca et al., 2002).

Reactive mixtures containing organic carbon are designed to support the bacterially mediated reduction of sulfate and the precipitation of metal sulfides (Blowes et al., 1994; Cocos et al., 2002; Waybrant et al., 1998, 2002). SRB oxidize organic carbon by using SO_4 as the electron acceptor, thereby generating H_2S and releasing dissolved inorganic carbon:

$$2(CH_2O)_x(NH_3)_y(H_3PO_4)_z + xSO_4^{2-} \Rightarrow 2xHCO_3^- + xH_2S + 2yNH_3 + 2zH_3PO_4 \quad [43]$$

where '$(CH_2O)_x(NH_3)_y(H_3PO_4)_z$' represents organic matter undergoing oxidation and x, y, and z are stoichiometric coefficients. The H_2S produced through sulfate reduction combines with metal cations to form metal sulfides:

$$Me^{2+} + S^{2-} \Rightarrow MeS \quad [44]$$

These metal sulfides are stable below the water table within the reactive barrier. Sulfate reduction also releases dissolved inorganic carbon, which neutralizes the pH and favors the precipitation of metal carbonate minerals, for example, $FeCO_3$ and $MnCO_3$ (Waybrant et al., 2002).

The first full-scale reactive barrier for treatment of mine drainage was installed at the Nickel Rim mine site, near Sudbury, Ontario in 1995 (Benner et al., 1997). The barrier contains a reactive mixture composed of 50 vol% organic carbon, 49 vol% pea gravel, and 1 vol% limestone. The organic carbon used was a composted waste of leaf mulch and wood chips derived from a municipal recycling program. Semiannual monitoring of the reactive barrier for 5 years after installation showed consistent removal of dissolved sulfate and dissolved metals and increases in pH and alkalinity (Benner et al., 1999). Enumeration of SRB within the barrier indicated that a large population of SRB had become established within a year following installation (Benner et al., 2000). Measurements of the sulfur isotopic ratio indicated enrichment of ^{34}S–SO_4 in the barrier effluent, which is consistent with the hypothesis that the sulfate removal was through bacterially mediated sulfate reduction. Measurements of the solid-phase sulfide content indicated accumulations of acid-volatile sulfides within the barrier material and lesser accumulations of total reducible sulfide (Herbert et al., 1998, 2000).

The aqueous geochemistry data obtained from the Nickel Rim site indicates that the rate of sulfate reduction is dependent on temperature, with sulfate reduction more rapid during the warm summer months than during the cooler winter months. The relationship between temperature and reaction rate could be explained using an Arrhenius-type relationship (Benner et al., 2002).

A pilot-scale reactive barrier for treating metals and sulfate was installed in 1997 at an industrial site in Vancouver, Canada (Ludwig et al., 2002; McGregor et al., 2002). Monitoring of the barrier between 1997 and 2001 showed that initial concentrations of up to 8570 $\mu g\,l^{-1}$ Cu were decreased to 17 $\mu g\,l^{-1}$ after passage through the barrier, Zn decreased from 2780 to $<140\,\mu g\,l^{-1}$, and Cd and Ni declined from 21 and 210 $\mu g\,l^{-1}$ to concentrations of <0.2 and $<6\,\mu g\,l^{-1}$, respectively (McGregor et al., 2002). The performance of the pilot-scale barrier led to the installation, in 2002, of a full-scale reactive barrier that is 400 m long and 17 m deep, with a maximum thickness of 5 m.

PRBs have also been installed at uranium mine-tailings impoundments to remove U and other metals. A reactive barrier containing three reactive components, as part of a side-by-side comparison, was installed at the Fry Canyon Mine site, Utah. The reactor systems included hydrous ferric oxide for the adsorption of U, zerovalent iron to induce U reduction and precipitation, and bone char that is rich in phosphate to induce the precipitation of U-bearing phosphates. Monitoring showed removal of U in all of these systems (Blowes et al., 2000a,b; Fuller et al., 2002; Naftz et al., 2002). A full-scale permeable barrier using zerovalent iron for reduction and precipitation of U was installed in 1999 in Monticello, Utah (Morrison et al., 2002). This barrier treats U, Mo, Se, and V.

PRBs have significant advantages over the conventional approaches for groundwater remediation. The barriers are passive systems whose effectiveness can persist for several years to decades. Moreover, the reactive material can be adjusted to target specific contaminants from a mine site, and the contaminants precipitated within the barrier are isolated from the surface-water environment and biota (Blowes et al., 2000a,b).

11.5.9.3.5 Other in situ techniques

The addition of organic carbon to mill tailings has the potential to enhance sulfate-reduction reactions and reprecipitation of metal sulfides within tailings impoundments (Blowes and Ptacek, 1992b). The addition of organic carbon below the equilibrium water table position will isolate the organic carbon from oxidation by atmospheric O_2. The addition of organic carbon to sulfide-rich tailings was evaluated in pilot test experiments conducted at the Kidd Creek Zn–Cu metallurgical site, Timmins, Ontario (Hulshof et al., 2003, 2006), and at the Greens Creek Z–Pb mine, near Anchorage, Alaska (Lindsay et al., 2009, 2011a, b,c). At the Kidd Creek metallurgical site, the addition of organic carbon was added to the sulfide-rich tailings in two test cells, one containing pulp waste from a pulp-and-paper mill and the second containing wood waste, principally tree branches and bark. The organic carbon was mixed thoroughly with the tailings and deposited in test cells, and the changes in water chemistry were monitored over a two-year period. In the test cell containing pulp waste, the organic carbon promoted the growth and activity of SRB, resulting in the precipitation of secondary sulfide minerals and declines in the concentrations of dissolved metals, principally Fe and Zn. The rate and extent of metal removal were greater in the test cell containing pulp waste than in the test cell containing wood waste (Hulshof et al., 2006).

The effectiveness of the addition of organic carbon in the form of peat, spent brewing grain, and municipal sewage sludge was evaluated at the Greens Creek Mine, Alaska, through the construction and monitoring of seven test cells (Lindsay et al., 2009, 2011a,b,c). The test cells were installed by excavating tailings materials, mixing with organic carbon, and placing the mixture within the excavation. A low permeability liner on the sides of the test cells was used to limit horizontal flow in the test cells. The base of the test cells remained open and connected to the underlying tailings impoundment. Monitoring over 4 years indicated that populations of IRB and SRB were established in all of the test cells within the first year of installation, but the largest and most active populations were observed in the test cells containing spent brewing grain (Lindsay et al., 2011b). The precipitation of metal sulfides resulted in substantial decreases in the concentrations of sulfate and dissolved metals, principally Zn. The declines in Zn concentrations were accompanied by an increase in dissolved As, which was attributed to microbially mediated reduction of iron oxyhydroxides and release of coprecipitated As, followed by a subsequent decrease in dissolved As. Mineralogical study of samples collected from the test cells indicated the accumulation of poorly crystalline Zn and Fe sulfides (Lindsay et al., 2011b,c).

11.5.10 Summary and Conclusions

The exposure of sulfide minerals contained in mine wastes to atmospheric oxygen results in the oxidation of these minerals. The oxidation reactions are accelerated by the catalytic effects of Fe hydrolysis and sulfide-oxidizing bacteria. The oxidation of sulfide minerals results in the depletion of minerals in the mine waste and the release of H^+, SO_4, Fe(II), and other metals to the water flowing through the wastes. The most abundant solid-phase products of the reactions are typically ferric oxyhydroxide or hydroxysulfate minerals. Other secondary metal sulfate, hydroxide, hydroxy sulfate, carbonate, arsenate, and phosphate precipitates form. These secondary phases limit the concentrations of dissolved metals released from mine wastes.

At many sites, the acid produced by sulfide oxidation is consumed by the pH-buffering reactions of the nonsulfide gangue minerals contained in the wastes. As these acid-neutralization reactions proceed, the pH of the pore water progressively increases, enhancing the potential for attenuation of dissolved metals by adsorption and precipitation reactions. The quality of aqueous effluents from tailings impoundments and waste-rock piles is dependent on the extent of the acid-producing sulfide-oxidation reactions versus the acid-consuming pH-buffering reactions. Regardless of the degree of acid neutralization, the effluent water from the waste material contains increased concentrations of dissolved constituents.

Oxidation products transported from the mine waste can enter streams, lakes, and oceans. A series of further reactions occur upon the discharge of this mine-drainage water, resulting in acidification and metal release. Complex geochemical models and reactive-transport models have been developed and are important tools in the prediction of the environmental impacts of mine wastes and in developing remedial alternatives. The remedial technologies developed and refined over the past two decades are being applied increasingly, thereby decreasing the magnitude of the negative effects of mining operations.

References

Abraitis PK, Pattrick RAD, and Vaughan DJ (2004) Variations in the compositional, textural and electrical properties of natural pyrite: A review. *International Journal of Mineral Processing* 74: 41–59.

Accornero M, Marini L, Ottonello G, and Zuccolini MV (2005) The fate of major constituents and chromium and other trace elements when acid waters from the derelict Libiola mine (Italy) are mixed with stream waters. *Applied Geochemistry* 20: 1368–1390.

Acero P, Ayora C, Carrera J, Saaltink MW, and Olivella S (2009) Multiphase flow and reactive transport model in vadose tailings. *Applied Geochemistry* 24: 1238–1250.

AGI (1957) *Glossary of Geology and Related Sciences*. Washington, DC: American Geological Institute.

Ahmann D, Krumholz LR, Lovley DR, and Morel FMM (1997) Microbial mobilization of arsenic from sediments of the Aberjona watershed. *Environmental Science and Technology* 31: 2923–2930.

Al TA (1996) *The Hydrology and Geochemistry of Thickened, Sulfide-Rich Tailings, Kidd Creek Mine, Timmins, Ontario*. PhD Thesis, University of Waterloo.

Al TA and Blowes DW (1996) Storm-water hydrograph separation of run off from a mine-tailings impoundment formed by thickened tailings discharge at Kidd Creek, Timmins, Ontario. *Journal of Hydrology* 180: 55–78.

Al TA, Blowes DW, Jambor JL, and Scott JD (1994) The geochemistry of mine-waste rock pore-water affected by the combined disposal of natrojarosite and base-metal sulfide tailings at Kidd Creek, Timmins, Ontario. *Canadian Geotechnical Journal* 31: 502–512.

Al TA, Martin CJ, and Blowes DW (2000) Carbonate-mineral/water interactions in sulfide-rich mine tailings. *Geochimica et Cosmochimica Acta* 64: 3933–3948.

Albers PH and Camardese MB (1993) Effects of acidification on metal accumulation by aquatic plants and invertebrates. 1. Constructed wetlands. *Environmental Toxicology and Chemistry* 12: 959–967.

Allison JD, Brown DS, and Novo-Gradac KJ (1990) *MINTEQA2/PRODEFA2, A Geochemical Assessment Model for Environmental Systems: Version 3.0 User's Manual*. Athens, GA: U.S. Environmental Protection Agency.

Alpers CN, Blowes DW, Nordstrom DK, and Jambor JL (1994) Secondary minerals and acid mine water chemistry. In: Blowes DW and Jambor JL (eds.) *The Environmental Geochemistry of Sulfide Mine-Wastes*, vol. 22, pp. 247–270. Nepean, ON: Mineralogical Association of Canada.

Alpers CN and Nordstrom DK (1998) Geochemical modeling of water–rock interactions in mining environments. In: Plumlee GS and Logsdon MJ (eds.) *The Environmental Geochemistry of Mineral Deposits*, *Reviews in Economic Geology*, vol. 6A, pp. 289–323. Littleton, CO: Society of Economic Geologists Inc.

Amado Filho GM, Andrade LR, Karez CS, Farina M, and Pfeiffer WC (1999) Brown algae species as biomonitors of Zn and Cd at Sepetiba Bay, Rio de Janeiro, Brazil. *Marine Environmental Research* 48: 213–224.

Amos RT, Blowes DW, Smith L, and Sego DC (2009) Measurement of wind-induced pressure gradients in a waste rock pile. *Vadose Zone Journal* 6: 953–962.

Amouric A, Brochier-Armanet C, Johnson DB, Bonnefoy V, and Hallberg KB (2011) Phylogenetic and genetic variation among Fe(II)-oxidizing acidithiobacilli supports the view that these comprise multiple species with different ferrous iron oxidation pathways. *Microbiology* 157: 111–122.

Ardau C, Blowes DW, and Ptacek CJ (2008) Comparison of laboratory testing protocols to field observations of the weathering of sulfide-bearing mine tailings. *Journal of Geochemical Exploration* 100: 182–191.

Armstrong DC (1995) Acid sulfate alteration in a magmatic hydrothermal environment, Barton Peninsula, King-George Island, Antarctica. *Mineralogical Magazine* 59(396): 429–441.

Ashley PM and Lottermoser BG (1999) Arsenic contamination at the Mole River mine, northern New South Wales. *Australian Journal of Earth Sciences* 46: 861–874.

ASTM (2001) Standard test method for accelerated weathering of solid materials using a modified humidity cell. Method D5744-96

Aston JE, Apel WA, Lee BD, and Peyton BM (2009) Toxicity of select organic acids to the slightly thermophilic acidophile *Acidithiobacillus caldus*. *Environmental Toxicology and Chemistry* 28: 279–286.

Babechuk M, Weisener CG, Fryer B, and Maunders C (2009) Microbial reductive dissolution of stable ferrous arsenate mineral phases: A case for arsenic mobility. *Applied Geochemistry* 24: 2332–2341.

Baes CF Jr., Reardon EJ, and Moyer BA (1993) Ion interaction model applied to the $CuSO_4$–H_2SO_4–H_2O system at 25 °C. *Journal of Physical Chemistry* 97: 12343–12348.

Bain JG, Blowes DW, Robertson WD, and Frind EO (2000) Modelling of sulfide oxidation with reactive transport at a mine drainage site. *Journal of Contaminant Hydrology* 41: 23–47.

Bain JG, Mayer KU, Blowes DW, et al. (2001) Modelling the closure-related geochemical evolution of groundwater at a former uranium mine. *Journal of Contaminant Hydrology* 52: 109–135.

Ball JW and Nordstrom DK (1987) WATEQ4F – A personal computer Fortran translation of the geochemical model WATEQ2 with revised data base. *US Geological Survey Open-File Report* 87–50.

Banfield JF and Welch SA (2000) Microbial controls on mineralogy of the environment. In: Vaughan DJ and Wogelius RA (eds.) *Environmental Mineralogy*, vol. 2, pp. 173–196. European Mineralogical Union.

Barnett MO, Harris LA, Turner RR, et al. (1997) Formation of mercuric sulfide in soil. *Environmental Science and Technology* 31: 3037–3043.

Barnett MO, Turner RR, and Singer PC (2001) Oxidative dissolution of metacinnabar (β-HgS) by dissolved oxygen. *Applied Geochemistry* 16: 1499–1512.

Baron D and Palmer CD (1996) Solubility of jarosite at 4–35 °C. *Geochimica et Cosmochimica Acta* 60(2): 185–195.

Barron JL and Lueking DR (1990) Growth and maintenance of *Thiobacillus ferrooxidans* cells. *Applied and Environmental Microbiology* 56: 2801–2806.

Barton CD and Karathanasis AD (1998) Renovation of a failed constructed wetland treating acid mine drainage. *Environmental Geology* 39: 39–50.

Basilio CI, Kartio IJ, and Yoon R-H (1996) Lead activation of sphalerite during galena flotation. *Mining Engineering* 9(8): 869–879.

Battaglia-Brunet F, El Achbouni H, Quemeneur M, Hallberg KB, Kelly DP, and Joulian C (2011) Proposal that the arsenite-oxidizing organisms, *Thiomonas cuprina* and '*Thiomonas arsenivorans*' be reclassified as strains of *Thiomonas delicata*. *International Journal of Systematic and Evolutionary Microbiology* 61: 2816–2821.

Batty L, Hooley D, and Younger P (2008) Iron and manganese removal in wetland treatment systems: Rates, processes and implications for management. *Science of the Total Environment* 394: 1–8.

Belzile N, Maki S, Chen Y-W, and Goldsack D (1997) Inhibition of pyrite oxidation by surface treatment. *Science of the Total Environment* 196: 177–186.

Bendell-Young L and Pick FR (1996) Base cation composition of pore water, peat and pool water of fifteen Ontario peatlands: Implications for peatland acidification. *Water, Air, and Soil Pollution* 96: 155–173.

Benner SG, Blowes DW, Gould WD, Herbert RB Jr., and Ptacek CJ (1999) Geochemistry of a permeable reactive barrier for metals and acid mine drainage. *Environmental Science and Technology* 33: 2793–2799.

Benner SG, Blowes DW, and Ptacek CJ (1997) A full-scale porous reactive wall for prevention of acid mine drainage. *Ground Water Monitoring and Remediation* 17: 99–107.

Benner SG, Blowes DW, Ptacek CJ, and Mayer KU (2002) Rates of sulfate removal and metal sulfide precipitation in a permeable reactive barrier. *Applied Geochemistry* 17: 301–320.

Benner SG, Gould WD, and Blowes DW (2000) Microbial populations associated with the generation and treatment of acid mine drainage. *Chemical Geology* 169: 435–448.

Bennet PC, Hiebert FK, and Rogers JR (2000) Microbial control of mineral-groundwater equilibria: Macroscale to microscale. *Hydrogeology Journal* 8: 47–62.

Bennett JW, Comarmond MJ, Clark NR, Carras JN, and Day S (1999) Intrinsic oxidation rates of coal reject measured in the laboratory. *Proceedings of Sudbury '99 Mining and the Environment* 1: 9–17.

Benoit JM, Gilmour CC, Mason RP, and Heyes A (1999) Sulfide controls on mercury speciation and bioavailability to methylating bacteria in sediment pore waters. *Environmental Science and Technology* 33: 951–957.

Benvenuti M, Mascaro I, Corsini F, Lattanzi P, Parrini P, and Tanelli G (1997) Mine waste dumps and heavy metal pollution in abandoned mining district of Boccheggiano (Southern Tuscany, Italy). *Environmental Geology* 30: 238–243.

Benvenuti M, Mascaro I, Corsini F, et al. (2000) Environmental mineralogy and geochemistry of waste dumps at the Pb(Zn)–Ag Bottino mine, Apuane Alps, Italy. *European Journal of Mineralogy* 12: 441–453.

Berger AC, Bethke CM, and Krumhansl JL (2000) A process model of natural attenuation in drainage from a historic mining district. *Applied Geochemistry* 15: 655–666.

Berthelot D, Leduc LG, and Ferroni GD (1993) Temperature studies of iron oxidizing autotrophs and acidophilic heterotrophs isolated from uranium mines. *Canadian Journal of Microbiology* 39: 384–388.

Bews BE, O'Kane MA, Wilson GW, Williams D, and Currey N (1997) The design of a low flux cover system, including lysimeters, for acid generating waste rock in semi-arid environments. *Proceedings of the Fourth International Conference on Acid Rock Drainage,* 2, pp. 747–762. MEND, Natural Resources Canada.

Biehler D and Falck WE (1999) Simulation of the effects of geochemical reactions on groundwater quality during planned flooding of the Königstein uranium mine, Saxony, Germany. *Hydrogeology Journal* 7: 284–293.

Bigham JM and Nordstrom DK (2000) Iron and aluminum hydroxysulfates from acid sulfate waters. In: Alpers CN, Jambor JL, and Nordstrom DK (eds.) *Sulfate Minerals – Crystallography, Geochemistry, and Environmental Significance*. *Reviews in Mineralogy and Geochemistry*, vol. 40, pp. 352–403. Mineralogical Society of America.

Bigham JM, Schwertmann U, Carlson L, and Murad E (1990) A poorly crystallized oxyhydroxysulfate of iron formed by bacterial oxidation of Fe(II) in acid mine waters. *Geochimica et Cosmochimica Acta* 54: 2743–2758.

Bigham JM, Schwertmann U, Traina SJ, Winland RL, and Wolf M (1996) Schwertmannite and the chemical modeling of iron in acid sulfate waters. *Geochimica et Cosmochimica Acta* 60: 2111–2121.

Birk D (1989) Quantitative coal mineralogy of the Sydney Coalfield, Nova Scotia, Canada, by scanning electron microscopy, computerized image analysis, and energy-dispersive X-ray spectrometry. *Canadian Journal of Earth Sciences* 27: 163–179.

Blanchard M, Alfredsson M, Brodholt J, Wright K, Richard C, and Catlow A (2007) Arsenic incorporation into FeS_2 pyrite and its influence on dissolution: A DFT study. *Geochimica et Cosmochimica Acta* 71: 624–630.

Blodau C and Peiffer S (2003) Thermodynamics and organic matter: Constraints on neutralization processes in sediments of highly acidic waters. *Applied Geochemistry* 18: 25–36.

Blowes DW (1990) *The Geochemistry, Hydrogeology and Mineralogy of Decommissioned Sulfide Tailings. A Comparative Study*. PhD Thesis, University of Waterloo.

Blowes DW and Gillham RW (1988) The generation and quality of streamflow on inactive uranium tailings near Elliot Lake, Ontario. *Journal of Hydrology* 97: 1–22.

Blowes DW and Jambor JL (1990) The pore-water geochemistry and the mineralogy of the vadose zone of sulfide tailings, Waite Amulet, Québec, Canada. *Applied Geochemistry* 5: 327–346.

Blowes DW, Jambor JL, Appleyard EC, Reardon EJ, and Cherry JA (1992) Temporal observations of the geochemistry and mineralogy of a sulfide-rich mine-tailings impoundment, Heath Steele mines, New Brunswick. *Exploration and Mining Geology* 1: 251–264.

Blowes DW, Lortie L, Gould WD, Jambor JL, and Hanton-Fong CJ (1995) Geochemical, mineralogical and microbiological characterization of a sulfide-bearing, carbonate-rich, gold mine tailings impoundment, Joutel, Québec. *Applied Geochemistry* 31: 687–705.

Blowes DW and Ptacek CJ (1992a) Geochemical remediation of groundwater by permeable reactive walls: Removal of chromate by reaction with iron-bearing solids. *Proceedings of Subsurface Restoration Conference, Third International Conference on Ground Water Quality Research, June 21–24, Dallas, TX* 214–216.

Blowes DW and Ptacek CJ (1992b) Treatment of mine tailings. US Patent 4990031, Canadian Patent 1327027, UK Patent GB 2219617 B.

Blowes DW and Ptacek CJ (1994) Acid-neutralization mechanisms in inactive mine tailings. In: Blowes DW and Jambor JL (eds.) *The Environmental Geochemistry of Sulfide Mine-Wastes*, vol. 22, pp. 271–292. Mineralogical Association of Canada.

Blowes DW, Ptacek CJ, Benner SG, McRae CWT, and Puls RW (2000a) Treatment of dissolved metals and nutrients using permeable reactive barriers. *Journal of Contaminant Hydrology* 45.

Blowes DW, Ptacek CJ, Benner SG, McRae CWT, and Puls RW (2000b) Treatment of dissolved metals and nutrients using permeable reactive barriers. *Journal of Contaminant Hydrology* 45: 120–135.

Blowes DW, Ptacek CJ, and Jambor JL (1994) Remediation and prevention of low-quality drainage from mine wastes. In: Blowes DW and Jambor JL (eds.) *The Environmental Geochemistry of Sulfide Mine-Wastes*, vol. 22, pp. 365–380. Mineralogical Association of Canada.

Blowes DW, Reardon EJ, Cherry JA, and Jambor JL (1991) The formation and potential importance of cemented layers in inactive sulfide mine tailings. *Geochimica et Cosmochimica Acta* 55: 965–978.

Bobeck GE and Su H (1985) The kinetics of dissolution of sphalerite in ferric chloride solution. *Metallurgical and Materials Transactions B* 16b: 413–424.

Boon M and Heijnen JJ (2001) Solid–liquid mass transfer limitation of ferrous iron in the chemical oxidation of FeS_2 at high redox potential. *Hydrometallurgy* 62: 57–66.

Boorman RS and Watson DM (1976) Chemical processes in abandoned sulfide tailings dumps and environmental implications for Northeastern New Brunswick. *CIM Bulletin* 69(772): 86–96.

Borgmann U, Norwood WP, Reynoldson TB, and Rosa F (2001) Identifying cause in sediment assessments: Bioavailability and sediment quality triad. *Canadian Journal of Fisheries and Aquatic Sciences* 58: 950–960.

Boulet MP and Larocque ACL (1996) A comparative mineralogical and geochemical study of sulfide mine tailings at two sites in New Mexico, USA. *Environmental Geology* 33: 130–142.

Bove DJ, Mast MA, Wright WG, Verplanck PL, Meeker GP, and Yager DB (2000) Geologic control on acidic and metal-rich waters in the southeast Red Mountains area, near Silverton, Colorado. *Proceedings from the Fifth International Conference on Acid Rock Drainage, 1*, pp. 523–533. Society for Mining, Metallurgy, and Exploration, Inc.

Bowell RJ (1994) Sorption of arsenic by iron oxides and oxyhydroxides in soils. *Applied Geochemistry* 9: 279–286.

Bowell RJ and Bruce I (1995) Geochemistry of iron ochres and mine waters from the Levant mine, Cornwall. *Applied Geochemistry* 10: 237–250.

BP (2010) BP Statistical Review of World Energy, June 2010, 44 p. www.bp.com/statisticalreview

Brady BC, Rose AW, and Cravotta CA III (1997) Bimodal distribution of pH coal-mine drainage (abs). Geological Society of America, GSA Abstracts with Programs, 29(1): 32.

Brake SS, Connors KA, and Romberger SB (2001) A river runs through it: Impact of acid mine drainage on the geochemistry of West Little Sugar Creek pre- and post-reclamation at the Green Valley coal mine, Indiana, USA. *Environmental Geology* 40: 1471–1481.

Breed AW and Hansford GS (1999) Effects of pH on ferrous-iron oxidation kinetics of *Leptospirillum ferrooxidans* in continuous culture. *Biochemical Engineering Journal* 3: 193–201.

Bridge TAM and Johnson DB (1998) Reduction of soluble iron and reductive dissolution of ferric iron-containing minerals by moderately thermophilic iron-oxidizing bacteria. *Applied and Environmental Microbiology* 64: 2181–2186.

Bridge TAM and Johnson DB (2000) Reductive dissolution of ferric iron minerals by *Acidiphilium* SJH. *Geomicrobiology Journal* 17: 193–206.

Brookfield AE, Blowes DW, and Mayer KU (2006) Integration of field measurements and reactive solute transport modelling to evaluate contaminant transport at a sulfide mine tailings impoundment. *Journal of Contaminant Hydrology* 88: 1–22.

Brown JG, Bassett RL, and Glynn PD (1998) Analysis and simulation of reactive transport of metal contaminants in ground water in Pinal Creek Basin, Arizona. In: teefel CI and van Cappellen P (eds.) *Special Issue – Reactive Transport Modeling of Natural Systems*, *Journal of Hydrology*, vol. 209, pp. 225–250.

Brown GE Jr., Henrich VE, Casey WH, Clark DL, et al. (1999a) Metal oxide surfaces and their interactions with aqueous solutions and microbial organisms. *Chemical Reviews* 99: 77–174.

Brown AD and Jurinak JJ (1989) Pyrite oxidation in aqueous mixtures. *Journal of Environmental Quality* 18: 545–550.

Brown DA, Sherriff BL, Sawicki JA, and Sparling R (1999b) Precipitation of iron minerals by a natural microbial consortium. *Geochimica et Cosmochimica Acta* 63: 2163–2169.

Buckley AN and Walker W (1988) The surface composition of arsenopyrite exposed to oxidizing environments. *Applied Surface Science* 35: 227–240.

Buckley AN and Woods RW (1984a) An X-ray photoelectron spectroscopic study of the oxidation of galena. *Applications of Surface Science* 17: 401–414.

Buckley AN and Woods RW (1984b) An X-ray photoelectron spectroscopic study of the oxidation of chalcopyrite. *Australian Journal of Chemistry* 37: 2403–2413.

Buckley AN and Woods RW (1985) X-ray photoelectron spectroscopy of oxidized pyrrhotite surfaces. *Applications of Surface Science* 22/23: 280–287.

Buckley AN and Woods RW (1987) The surface oxidation of pyrite. *Applied Surface Science* 27: 437–452.

Buckley AN, Wouterlood HJ, and Woods R (1989) The surface composition of natural sphalerites under oxidative leaching conditions. *Hydrometallurgy* 22: 39–56.

Burton ED, Bush RT, Johnston SG, et al. (2009) Sorption of arsenic(V) and arsenic(III) to schwertmannite. *Environmental Science and Technology* 43: 9202–9207.

Byrne PA and O'Halloran J (2001) The role of bivalve molluscs as tools in estuarine sediment toxicity testing: A review. *Hydrobiologia* 465: 209–217.

Cabri LJ (2002) *The Geology, Geochemistry, Mineralogy and Beneficiation of Platinum-Group Elements*. Montreal: Canadian Institute of Mining, Metallurgy and Petroleum.

Carlson L, Bigham JM, Schwertmann U, Kyek A, and Wagner F (2002) Scavenging of As from acid mine drainage by schwertmannite and ferrihydrite: A comparison with synthetic analogues. *Environmental Science and Technology* 26: 1712–1719.

Casey WH and Sposito G (1991) On the temperature dependence of mineral dissolution rates. *Geochimica et Cosmochimica Acta* 56: 3825–3830.

Casiot C, Lebrun S, Morin G, Bruneel O, Personné JC, and Elbaz-Poulichet F (2005) Sorption and redox processes controlling arsenic fate and transport in a stream impacted by acid mine drainage. *Science of the Total Environment* 347: 122–130.

Cathles LM (1979) Predictive capabilities of a finite difference model of copper leaching in low grade industrial sulfide waste dumps. *Mathematical Geology* 11: 175–191.

Cathles LM (1994) Attempts to model the industrial-scale leaching of copper-bearing mine waste. In: Alpers CN and Blowes DW (eds.) *Environmental Geochemistry of Sulfide Oxidation*, vol. 550, pp. 123–131. Washington, DC: American Chemical Society.

Chernyshova IV and Andreev SI (1997) Spectroscopic study of galena surface oxidation in aqueous solutions. *Applied Surface Science* 108: 225–236.

Clarke LB (1993) The fate of trace elements during combustion and gasification: An overview. *Fuel* 72: 731–736.

Clegg SL and Whitfield M (1991) Activity coefficients in natural waters. In: Pitzer KS (ed.) *Activity Coefficients in Electrolyte Solutions*, 2nd edn., pp. 279–434. Boca Raton, FL, USA: CRC Press.

Cocos IA, Zagury GJ, Clément B, and Samson R (2002) Multiple factor design for reactive mixture selection for use in reactive walls in mine drainage treatment. *Water Research* 32: 167–177.

Coggans CJ (1992) *Hydrogeology and Geochemistry of the Inco Ltd. Copper Cliff, Ontario, Mine Tailings Impoundments*. MSc Thesis, University of Waterloo.

Coggans CJ, Blowes DW, Robertson WD, and Jambor JL (1998) The hydrogeochemistry of a nickel-mine tailings impoundment, Copper Cliff, Ontario. *Reviews in Economic Geology* 6B: 447–465.

Combes JM, Manceau A, and Calas G (1990) Formation of ferric oxides from aqueous solutions: A polyhedral approach by X-ray absorption spectroscopy. II. Hematite formation from ferric gels. *Geochimica et Cosmochimica Acta* 54: 1083–1091.

Combes JM, Manceau A, Calas G, and Bottero JY (1989) Formation of ferric oxides from aqueous solutions: A polyhedral approach by X-ray absorption spectroscopy. I. Hydrolysis and formation of ferric gels. *Geochimica et Cosmochimica Acta* 53: 583–594.

Conca J, Strietelmeier E, Lu N, et al. (2002) Treatability study of reactive materials to remediate groundwater contaminated with radionuclides, metals, and nitrates in a four-component permeable reactive barrier. In: Naftz DL, Morrison SJ, Davis JA, and Fuller CC (eds.) *Handbook of Groundwater Remediation Using Permeable Reactive Barriers – Applications to Radionuclides, Trace Metals, and Nutrients*, pp. 221–252. Academic Press.

Corkhill CL and Vaughan DJ (2009) Arsenopyrite oxidation – A review. *Applied Geochemistry* 24: 2342–2361.

Coupland K and Johnson DB (2008) Evidence that the potential for dissimilatory ferric iron reduction is widespread among acidophilic heterotrophic bacteria, FEMS Microbiol. *Letters* 279: 30–35.

Cravotta CAIII (1994) Secondary iron sulfate minerals as sources of sulfate and acidity – The geochemical evolution of acidic ground water at a reclaimed surface coal mine in Pennsylvania. In: Alpers CN and Blowes DW (eds.) *Environmental Geochemistry of Sulfide Oxidation*, vol. 550, pp. 345–364. Washington, DC: American Chemical Society.

Cravotta CA III (2010) Abandoned mine drainage in the Swatara Creek Basin, Southern Anthracite Coalfield, Pennsylvania, USA: Performance of treatment systems. *Mine Water and the Environment* 29: 200–216.

Crowe SA, O'Neil AH, Kulezycki E, Weisener CG, Roberts JA, and Fowle DF (2007) Reductive release of trace metals from sediments: The importance of manganese. *Geomicrobiology Journal* 24: 157–165.

Crundwell FK (1988) Effect of iron impurity in zinc sulfide concentrates on the rate of dissolution. *AIChE Journal* 34: 1128–1134.

Cummings DE, Caccavo F Jr, Fendorf S, and Rosenzweig RF (1999) Arsenic mobilization by the dissimilatory Fe(III)-reducing bacterium Shewanella alga BrY. *Environmental Science and Technology* 33: 723–729.

Cummings DE, March AW, Bostick B, et al. (2000) Evidence for microbial Fe(III) reduction in anoxic, mining-impacted lake sediments (Lake Coeur d'Alene, Idaho). *Applied and Environmental Microbiology* 66: 154–162.

Dalzell DJB and Macfarlane NAA (1999) The toxicity of iron to brown trout and effects on the gills: A comparison of two grades of iron sulfate. *Journal of Fish Biology* 55: 301–315.

Daskalakis KD and Helz GR (1993) The solubility of sphalerite (ZnS) in sulfidic solutions at 25 °C and 1 atm pressure. *Geochimica et Cosmochimica Acta* 57: 4923–4931.

Davé NK and Vivyurka AJ (1994) Water cover on acid generating uranium tailings – Laboratory and field studies. *Proceedings of the International Land Reclamation and Mine Drainage Conference and the Third International Conference on the Abatement of Acidic Drainage, 1*, pp. 297–306. U.S. Bureau of Mines.

Davis BS (1997) Geomicrobiology of the oxic zone of sulfide mine tailings. In: McIntosh JM and Groat LA (eds.) *Biological–Mineralogical Interactions*, vol. 25, pp. 93–112. Nepean: Mineralogical Association of Canada.

Davis A and Ashenberg D (1989) The aqueous geochemistry of the Berkeley Pit, Butte, Montana, USA. *Applied Geochemistry* 4: 23–36.

Davis-Belmar CS, Nicolle JLC, and Norris PR (2008) Ferrous iron oxidation and leaching of copper ore with halotolerant bacteria in ore columns. *Hydrometallurgy* 94: 144–147.

Demas SY, Hall AM, Fanning DS, Rabenhorst MC, and Dzantor EK (2004) Acid sulfate soils in dredged materials from tidal Pocomoke Sound in Somerset County, MD, USA. *Australian Journal of Soil Research* 42(5–6): 537–545.

Di Toro DM, Allen HE, Bergman HL, Meyer JS, Paquin PR, and Santore RC (2001) Biotic ligand model of acute toxicity of metals. 1. Technical basis. *Environmental Toxicology and Chemistry* 20: 2383–2396.

DIAND (1992) *Guidelines for Acid Rock Prediction in the North*. Canada Department of Indian Affairs and Northern Development

Dill HG, Pöllmann H, Bosecker K, Hahn L, and Mwiya S (2002) Supergene mineralization in mining residues of the Matchless cupreous pyrite deposit (Namibia) – A clue to the origin of modern and fossil duricrusts in semiarid climates. *Journal of Geochemical Exploration* 75: 43–70.

Dinelli E, Morandi N, and Tateo F (1998) Fine-grained weathering products in waste disposal from two sulphide mines in the Northern Apennines, Italy. *Clay Minerals* 33: 423–433.

Ding M, DeJong BHWS, Roosendaal SJ, and Vredenberg A (2000) XPS studies on the electronic structure of bonding between solid and solutes: Adsorption of arsenate, chromate, phosphate, Pb^{2+}, and Zn^{2+} ions on amorphous black ferric oxyhydroxide. *Geochimica et Cosmochimica Acta* 64: 1209–1219.

Dold B and Fontbote L (2001) Element cycling and secondary mineralogy in porphyry copper tailings as a function of climate, primary mineralogy, and mineral processing. *Journal of Geochemical Exploration* 74(1–3): 3–55.

Domagalski J (2001) Mercury and methylmercury in water and sediment of the Sacramento River Basin, California. *Applied Geochemistry* 16: 1677–1691.

Dopson M and Johnson DB (2012) Biodiversity, metabolism and applications of acidophilic sulfur-metabolizing micro-organisms. *Environmental Microbiology* http://dx.doi.org/10.1111/j.1462-2920.2012.02749.x.

Drits VA, Sakharov BA, Salyn AL, and Manceau A (1993) Structural model for ferrihydrite. *Clay Minerals* 28: 185–208.

Dubrovsky NM (1986) *Geochemical Evolution of Inactive Pyritic Tailings in the Elliot Lake Uranium District*. PhD Thesis, University of Waterloo.

Dubrovsky NM, Morin KA, Cherry JA, and Smyth DJA (1984) Uranium tailings acidification and subsurface contaminant migration in a sand aquifer. *Water Pollution Research Journal of Canada* 19: 55–89.

Dugan PR (1987a) Prevention of formation of acid drainage from high-sulfur coal refuse by inhibition of iron- and sulfur-oxidizing microorganisms. I. Preliminary experiments in controlled shaken flasks. *Biotechnology and Bioengineering* 29: 41–48.

Dugan PR (1987b) Prevention of formation of acid drainage from high-sulfur coal refuse by inhibition of iron- and sulfur-oxidizing microorganisms. II. Inhibition in "Run of mine" refuse under simulated field conditions. *Biotechnology and Bioengineering* 29: 49–54.

Durham AJP, Wilson GW, and Currey N (2000) Field performance of two low infiltration cover systems in semi arid environment. *Proceedings from the Fifth International Conference on Acid Rock Drainage,* 2, pp. 1319–1326. Society for Mining, Metallurgy, and Exploration, Inc.

Dushenko WT, Bright DA, and Reimer KJ (1995) Arsenic bioaccumulation and toxicity in aquatic macrophytes exposed to gold-mine effluent: Relationships with environmental partitioning, metal uptake and nutrients. *Aquatic Botany* 50: 141–158.

Dutrizac JE (1999) The effectiveness of jarosite species for precipitating sodium jarosite. *Journal of the Minerals Metals & Materials Society* 51(12): 30–32.

Dutrizac JE and Jambor JL (2000) Jarosites and their application in hydrometallurgy. In: Alpers CN, Jambor JL, and Nordstrom DK (eds.) *Sulfate Minerals – Crystallography, Geochemistry, and Environmental Significance. Reviews in Mineralogy and Geochemistry*, vol. 40, pp. 406–452. Mineralogical Society of America.

Dutrizac JE and Jambor JL (2007) Characterization of the iron arsenate–sulphate compounds precipitated at elevated temperatures. *Hydrometallurgy* 86: 147–163.

Dutrizac JE and Kaiman S (1976) Synthesis and properties of jarosite-type compounds. *The Canadian Mineralogist* 14: 151–158.

Dutrizac JE and MacDonald RJC (1973) The effect of some impurities on the rate of chalcopyrite dissolution. *Canadian Metallurgical Quarterly* 12(4): 409–420.

Eary LE (1999) Geochemical and equilibrium trends in mine pit lakes. *Applied Geochemistry* 14: 963–987.

Eary LE and Castendyk DN (2009) The state of the art of pit lake research. In: Castendyk DN and Eary LE (eds.) Mine Pit Lakes: Characteristics, Predictive Modelling, and Sustainability, pp. 275–289. Littleton, CO: Society for Mining, Metallurgy and Exploration.

Eary LE, Runnells DD, and Esposito KJ (2003) Geochemical controls on ground water composition at the Cripple Creek Mining District, Cripple Creek, Colorado. *Applied Geochemistry* 18: 1–24.

Edwards KJ, Bond PL, Druschel GK, McGuire MM, Hamers RJ, and Banfield JF (2000) Geochemical and biological aspects of sulfide mineral dissolution: Lessons from Iron Mountain, California. *Chemical Geology* 169: 383–397.

Edwards KJ, Gihring TM, and Banfield JF (1999) Geomicrobiology of pyrite (FeS_2) dissolution: A case study at Iron Mountain, California. *Geomicrobiology Journal* 16: 155–179.

Edwards KJ, McCollom TM, Konishi H, and Buseck PR (2003) Seafloor bio-alteration of sulfide minerals: Results from in-situ incubation studies. *Geochimica et Cosmochimica Acta* 67: 2843–2856.

Edwards KJ, Schrenk MO, Hamers RJ, and Banfield JF (1998) Microbial oxidation of pyrite: Experiments using microorganisms from extreme acidic environment. *American Mineralogist* 83: 1444–1453.

Ericson PM and Ladwig J (1985) *Control of acid formation by the inhibition of bacteria and by coating pyrite surfaces*. Final Report to the West Virginia Department of Natural Resources, 68 pp.

Erry BV, Macnair MR, Meharg AA, and Shore RF (2000) Arsenic contamination in wood mice (*Apodemus sylvaticus*) and bank voles (*Clethrionomys glareolus*) on abandoned mine sites in southwest Britain. *Environmental Pollution* 110: 179–187.

Evangelou VP (1995) *Pyrite Oxidation and its Control: Solution Chemistry, Surface Chemistry, Acid Mine Drainage (AMD), Molecular Oxidation Mechanisms, Microbial Role, Kinetics, Control, Ameliorates and Limitations, Microencapsulation*. Boca Raton, FL: CRC Press.

Evangelou VP and Zhang YL (1995) A review: Pyrite oxidation mechanisms and acid mine drainage prevention. *Critical Reviews in Environmental Science and Technology* 25(2): 141–199.

Evans S and Raftery E (1982) Electron spectroscopic studies of galena and its oxidation by microwave-generated oxygen species and by air. *Chemical Society, Faraday Transactions* 1(78): 3545–3560.

Falkowski PG, Fenchel T, and Delong EF (2009) The microbial engines that drive Earths biogeochemical cycles. *Science* 320: 1034–1038.

Farquhar ML, Charnock JM, Livens FR, and Vaughan DJ (2002) Mechanisms of arsenic uptake from aqueous solution by interaction with goethite, lepidocrocite, mackinawite, and pyrite: An X-ray absorption spectroscopy study. *Environmental Science and Technology* 36: 1757–1762.

Feasby DG, Blanchette M, and Tremblay G (1991) The mine environment neutral drainage program. Second International Conference on the Abatement of Acidic Drainage, Tome 1, pp. 1–26. MEND Secretariat.

Feasby DG (1993) The mine environment neutral drainage (MEND) program. *Canadian Institute of Mining Bulletin* 86: 71.

Fernandez-Martinez A, Timon V, Roman-Ross G, Cuello GJ, Daniels JE, and Ayora C (2010) The structure of schwertmannite, a nanocrystalline iron oxyhydroxysulfate. *American Mineralogist* 95: 1312–1322.

Ferris FG (1993) Microbial biomineralization in natural environments. *Earth Science* 47: 233–250.

Fike DA, Gammon CL, Ziebis W, and Orphan VJ (2008) Micron-scale mapping of sulfur cycling across the oxycline of a cyanobacterial mat: A paired nanoSIMS and CARD-FISH approach. *ISME Journal* 2: 749–759.

Filippi M, Dousova B, and Machovic V (2007) Mineralogical speciation of arsenic in soils above the Mokrsko-west gold deposit, Czech Republic. *Geoderma* 139: 154–170.

Finkelman RB (1980a) Modes of occurrence of trace elements and minerals in coal: An analytical approach. In: Filby RH, Carpenter BS, and Ragaini RC (eds.) *Atomic and Nuclear Methods in Fossil Energy Research*, pp. 141–149. New York: Plenum.

Finkelman RB (1980b) *Modes of Occurrence of Trace Elements in Coal*. PhD Thesis, University of Maryland

Fleet ME, Chryssoulis SL, MacLean PJ, Davidson R, and Weisener CG (1993) Arsenian pyrite from gold deposits: Au and As distribution investigated by SIMS and EMP, and color staining and surface oxidation by XPS and LIMS. *The Canadian Mineralogist* 31: 1–17.

Flemming EJ, Mack EE, Green PG, and Nelson DC (2006) Mercury methylation from unexpected sources: Molybdate-inhibited freshwater sediments and an iron reducing bacterium. *Applied and Environmental Microbiology* 72: 457–464.

Florig HK (1997) China's air pollution risks. *Environmental Science and Technology* 31: 274A–279A.

Foos A (1997) Geochemical modelling of coal drainage, Summit County, Ohio. *Environmental Geology* 31: 205–210.

Fornasiero D, Li F, Ralston J, and Smart RSC (1994) Oxidation of galena surfaces. *Journal of Colloid and Interface Science* 164: 333–344.

Fortin D and Beveridge TJ (1997) Microbial sulfate reduction within sulfidic mine tailings: Formation of diagenetic Fe sulfides. *Geomicrobiology Journal* 14: 1–21.

Fortin D, Ferris FG, and Beveridge TJ (1997) Surface-mediated mineral development by bacteria. In: Banfield J and Nealson KH (eds.) *Reviews in Mineralogy*, pp. 161–180. Washington, DC: Mineralogical Society of America.

Foster AL, Brown GE Jr., Ingle TN, and Parks GA (1998a) Quantitative arsenic speciation in mine tailings using X-ray absorption spectroscopy. *American Mineralogist* 83: 553–568.

Foster AL, Brown GE Jr., and Parks GA (1998b) X-ray absorption fine-structure spectroscopy study of photocatalyzed, heterogeneous As(III) oxidation in kaolin and anatase. *Environmental Science and Technology* 32: 1444–1452.

Fowler TA (2001) On the kinetics and mechanism of the dissolution of pyrite in the presence of *Thiobacillus ferrooxidans*. *Hydrometallurgy* 59: 257–270.

Fuller CC, Davis JA, and Waychunas GA (1993) Surface chemistry of ferrihydrite: Part 2. Kinetics of arsenate adsorption and coprecipitation. *Geochimica et Cosmochimica Acta* 57: 2271–2282.

Fuller CC, Piana MJ, Bargar JR, Davis JA, and Kohler M (2002) Evaluation of apatite materials for use in permeable reactive barriers for the remediation of uranium-contaminated groundwater. In: Naftz DL, Morrison SJ, Davis JA, and Fuller CC (eds.) *Handbook of Groundwater Remediation Using Permeable Reactive Barriers – Applications to Radionuclides, Trace Metals, and Nutrients*, pp. 255–280. Academic Press.

Fytas K and Bousquet P (2002) Silicate micro-encapsulation of pyrite to prevent acid mine drainage. *CIM Bulletin* 95(1063): 96–99.

Gammons CH and Duaime TE (2006) Long term changes in limnology and geochemistry of the Berkeley pit lake, Butte, Montana. *Mine Water and the Environment* 25: 76–85.

Garcia-Sanchez A, Alvarez-Ayuso E, and Rodriguez-Martin F (2002) Sorption of As(V) by some oxyhydroxides and clay minerals. Application to its immobilization in two polluted mining soils. *Clay Minerals* 37: 187–194.

Garrels RM and Thompson ME (1960) Oxidation of pyrite by iron sulfate solutions. *The Australian Journal of Science* 258-A: 57–67.

Garrels RM and Thompson ME (1962) A chemical model for seawater at 25 °C and one atmosphere total pressure. *American Journal of Science* 260: 57–66.
Gasharova B, Gottlicher J, and Becker U (2005) Dissolution at the surface of jarosite: An in situ AFM study. *Chemical Geology* 215(1–4): 499–516.
Gelinas P, Lefebvre R, and Choquette M (1992) Monitoring of acid mine drainage in a waste rock dump. In: Singhal K, et al. (ed.) *Environmental Issues and Waste Management in Energy and Minerals Production*, pp. 747–756. Balkema.
Georgopoulou ZJ, Fytas K, Soto H, and Evangelou B (1995) Pyrrhotite coating to prevent oxidation. *Proceedings of Sudbury '95 Mining and the Environment* 1: 7–17.
Ghauri MA, Okibe N, and Johnson DB (2007) Attachment of acidophilic bacteria to solid surfaces: The significance of species and strain variations. *Hydrometallurgy* 85: 72–80.
Gopal B (1999) Natural and constructed wetlands for wastewater treatment: Potentials and problems. *Water Science and Technology* 40(3): 27–35.
Gould WD (1994) The nature and role of microorganisms in the tailings environment. In: Blowes DW and Jambor JL (eds.) *The Environmental Geochemistry of Sulfide Mine-Wastes*, vol. 22, pp. 163–184. Mineralogical Association of Canada.
Gould WD and Kapoor A (2003) The microbiology of acid mine drainage. In: Jambor JL, Blowes DW, and Ritchie AIM (eds.) *Environmental Aspects of Mine Wastes*, vol. 31, pp. 203–226. Mineralogical Association of Canada.
Government of Canada (1991) *State of Canada's Environment*. Ottawa: Ministry of Supply and Services.
Gramp JP, Wang H, Bigham JM, Jones FS, and Tuovinen OH (2009) Biosynthesis and reduction of Fe(III)-hydroxysulfates. *Geomicrobiology Journal* 26: 275–280.
Gray JE, Theodorakos PM, Bailey EA, and Turner RR (2000) Distribution, speciation and transport of mercury in stream sediment, stream-water, and fish collected near abandoned mercury mines in southwestern Alaska USA. *Science of the Total Environment* 260: 21–33.
Greenway M and Simpson JS (1996) Artificial wetlands for wastewater treatment, water reuse and wildlife in Queensland Australia. *Water Science and Technology* 33(10–11): 221–229.
Gunsinger MR, Ptacek CJ, Blowes DW, and Jambor JL (2006a) Evaluation of long-term sulfide oxidation processes within pyrrhotite-rich tailings, Lynn Lake, Manitoba. *Journal of Contaminant Hydrology* 83: 149–170.
Gunsinger MR, Ptacek CJ, Blowes DW, Jambor JL, and Moncur MC (2006b) Mechanisms controlling acid neutralization and metal mobility within a Ni-rich tailings impoundment. *Applied Geochemistry* 21: 1301–1321.
Hackl RP, Dreisinger DB, Peters E, and King JA (1995) Passivation of chalcopyrite during oxidative leaching in sulfate media. *Hydrometallurgy* 39: 25–48.
Hall LW Jr., Anderson RD, and Alden RW III (2002) A ten year summary of concurrent ambient water column and sediment toxicity tests in the Chesapeake Bay water shed: 1990–1999. *Environmental Monitoring and Assessment* 76: 311–352.
Hallberg KB, González-Toril E, and Johnson DB (2010) *Acidithiobacillus ferrivorans* sp. nov.; facultatively anaerobic, psychrotolerant, iron- and sulfur-oxidizing acidophiles isolated from metal mine-impacted environments. *Extremophiles* 14: 9–19.
Hallberg KB, Grail BM, du Plessis C, and Johnson DB (2011a) Reductive dissolution of ferric iron minerals: A new approach for bioprocessing nickel laterites. *Minerals Engineering* 24: 620–624.
Hallberg KB, Hedrich S, and Johnson DB (2011b) *Acidiferribacter thiooxydans*, gen. nov. sp. nov.; an acidophilic, thermo-tolerant, facultatively anaerobic iron- and sulfur-oxidizer of the family *Ectothiorhodospiraceae*. *Extremophiles* 15: 271–279.
Hallberg KB and Johnson DB (2001) Biodiversity of acidophilic prokaryotes. *Advances in Applied Microbiology* 49: 37–84.
Hansel C, Benner SG, Neiss J, Dohnalkova A, Kukkadapu RK, and Fendorf S (2003) Secondary mineralization pathways induced by dissimilatory iron reduction of ferrihydrite under advective flow. *Geochimica et Cosmochimica Acta* 67: 2977–2992.
Harries JR and Ritchie AIM (1985) Pore gas composition in waste rock dumps undergoing pyritic oxidation. *Soil Science* 140: 143–152.
Harries JR and Ritchie AIM (1987) The effect of rehabilitation on the rate of oxidation of pyrite in a mine waste rock dump. *Environmental Geochemistry and Health* 9: 27–36.
Harrison AP Jr. (1982) Genomic and physiological diversity amongst strains of *Thiobacillus ferrooxidans*, and genomic comparison with *Thiobacillus thiooxidans*. *Archives of Microbiology* 131: 68–76.
Harvey MC, Schreiber ME, Rimstidt JD, and Griffith MM (2006) Scorodite dissolution kinetics: Implications for arsenic release. *Environmental Science and Technology* 40: 6709–6714.
Harvey RD and Ruch RR (1986) Mineral matter in Illinois and other U. S. coals. In: Vorres KS (ed.) *Mineral Matter and Ash in Coals*, vol. 301, pp. 10–40. Washington, DC: American Chemical Society.
Heal KV and Salt CA (1999) Treatment of acidic metal-rich drainage from reclaimed ironstone mine spoil. *Water Science and Technology* 39(12): 141–148.
Hedin RS (2008) Iron removal by a passive system treating alkaline coal mine drainage. *Mine Water and the Environment* 27: 200–209.
Hedin RS and Nairn RW (1992) *Passive Treatment of Coal Mine Drainage*. pp. 2–43. Pittsburgh, PA, USA: U.S. Bureau of Mines.
Heikens A, Peijnenburg WJ, and Hendricks GM (2001) Bioaccumulation of heavy metals in terrestrial invertebrates. *Environmental Pollution* 113: 385–393.
Heinzel E, Janneck E, Glombitza F, Schlömann M, and Seifert J (2009) Population dynamics of iron-oxidizing communities in pilot plants for the treatment of acid mine waters. *Environmental Science and Technology* 43: 6138–6144.
Herbert RB Jr., Benner SG, and Blowes DW (2000) Solid phase iron–sulfur geochemistry of a reactive barrier for treatment of mine drainage. *Applied Geochemistry* 2000: 1331–1343.
Herbert RB Jr., Benner SG, Pratt AR, and Blowes DW (1998) Surface chemistry and morphology of poorly crystalline iron sulfides precipitated in media containing sulfate-reducing bacteria. *Chemical Geology* 144: 87–97.
Hiemstra T and van Riemsdijk WH (2009) A surface structural model for ferrihydrite I: Sites related to primary charge, molar mass, and mass density. *Geochimica et Cosmochimica Acta* 73: 4423–4436.
Hiroyoshi N, Hirota M, Hirajima T, and Tsunekawa M (1997) A case of ferrous sulfate addition enhancing chalcopyrite leaching. *Hydrometallurgy* 47: 37–45.
Ho GE, Murphy PJ, Platell N, and Wajon JE (1984) Iron removal from TiO_2 – Plant acidic wastewater. *Journal of Environmental Engineering* 110: 828–846.
Hochella MF, Kasama T, Putnis A, Putnis CV, and Moore JN (2005) Environmentally important, poorly crystalline Fe/Mn hydrous oxides: Ferrihydrite and a possibly new vernadite-like mineral from the Clark Fork River Superfund Complex. *American Mineralogist* 90: 718–724.
Hochella MF Jr., Moore JN, Golla U, and Putnis A (1999) A TEM study of samples from acid mine drainage systems: Metal–mineral association with implications for transport. *Geochimica et Cosmochimica Acta* 63: 3395–3406.
Holley EA, McQuillan AJ, Craw D, Kim JP, and Sander SG (2007) Mercury mobilization by oxidative dissolution of cinnabar (α-HgS) and metacinnabar (β-HgS). *Chemical Geology* 240: 313–325.
Holmes PR and Crundwell FK (2000) The kinetics of the oxidation of pyrite by ferric ions and dissolved oxygen: An electrochemical study. *Geochimica et Cosmochimica Acta* 64: 263–274.
Holmström H, Ljungberg J, Ekström M, and Öhlander B (1999) Secondary copper enrichment in tailings at the Laver mine, Northern Sweden. *Environmental Geology* 38: 327–342.
Holmström H, Salmon UJ, Carlsson E, Petrov P, and Öhlander B (2001) Geochemical investigations of sulfide-bearing tailings at Kristineberg, Northern Sweden, a few years after remediation. *Science of the Total Environment* 273: 111–133.
Hsu SC and Maynard JB (1999) The use of sulfur isotopes to monitor the effectiveness of constructed wetlands in controlling acid mine drainage. *Environmental Engineering and Policy* 1: 223–233.
Huang WE, Stoecker K, Griffiths R, et al. (2007) Raman-FISH: combining stable-isotope Raman spectroscopy and fluorescence in situ hybridization for the single cell analysis of identity and function. *Environmental Microbiology* 9(8): 1878–1889.
Huang X and Evangelou VP (1994) Suppression of pyrite oxidation rate by phosphate addition. In: Alpers CN and Blowes DW (eds.) *Environmental Geochemistry of Sulfide Oxidation*, vol. 550, pp. 562–573. Washington, DC: American Chemical Society.
Hudson-Edwards KA, Macklin MG, Curtis CD, and Vaughan DJ (1996) Processes of formation and distribution of Pb-, Zn-, Cd-, and Cu-bearing minerals in the Tyne Basin, northeast England: Implications for metal-contaminated river systems. *Environmental Science and Technology* 30: 72–80.
Hudson-Edwards KA, Schell C, and Macklin MG (1999) Mineralogy and geochemistry of alluvium contaminated by metal mining in the Rio Tinto area, Southwest Spain. *Applied Geochemistry* 14(8): 1015–1030.
Hulshof AHM, Blowes DW, and Gould WD (2006) Evaluation of in situ layers for treatment of acid mine drainage: A field comparison. *Water Research* 40: 1816–1826.
Hulshof A, Blowes DW, Ptacek CJ, and Gould WD (2003) Microbial and nutrient investigations into the use of in situ layers for treatment of tailings effluent. *Environmental Science and Technology* 37: 5027–5033.
Huminicki MC and Rimstidt JG (2009) Iron oxyhydroxide coating of pyrite for acid mine drainage control. *Applied Geochemistry* 24: 1626–1634.
Hutchens E (2009) Microbial selectivity on mineral surfaces: Possible implications for weathering processes. *Fungal Biology Reviews* 23: 115–121.
ICOLD (1996) *A Guide to Tailings Dams and Impoundments: Design, Construction, Use and Rehabilitation*. International Commission on Large Dams, Bulletin (United Nations Environment Programme) No. 106, 239 pp.
International Energy Agency (2010) *Coal Information 2010*, 530 p. Annual IEA Statistical Publications. ISBN: 978-92-64-08420-9.

Jain A and Loeppert RH (2000) Effect of competing anions on the adsorption of arsenate and arsenite by ferrihydrite. *Journal of Environmental Quality* 29: 1422–1430.

Jambor JL (1994) Mineralogy of sulfide-rich tailings and their alteration products. In: Blowes DW and Jambor JL (eds.) *The Environmental Geochemistry of Sulfide Mine-Wastes*, vol. 22, pp. 59–102. Mineralogical Association of Canada.

Jambor JL (2003) Mine-waste mineralogy and mineralogical perspectives of acid–base accounting. In: Jambor JL, Blowes DW, and Ritchie AIM (eds.) *Environmental Aspects of Mine Wastes*, vol. 31. Mineralogical Association of Canada.

Jambor JL and Blowes DW (1998) Theory and applications of mineralogy in environmental studies of sulfide-bearing mine wastes. In: Cabri LJ and Vaughan DJ (eds.) *Modern Approaches to Ore and Environmental Mineralogy*, vol. 27, pp. 367–401. Mineralogical Association of Canada.

Jambor JL, Blowes DW, and Ptacek CJ (2000a) Mineralogy of mine wastes and strategies for remediation. In: Vaughan DJ and Wogelius RA (eds.) *Environmental Mineralogy. European Mineralogical Union Notes in Mineralogy*, ch. 7, vol. 2, pp. 255–290. Hungary: Eötvös/Budapest University Press.

Jambor JL, Raudsepp M, and Mountjoy K (2005) Mineralogy of permeable reactive barriers for the attenuation of subsurface contaminants. *Canadian Mineralogist* 43: 2117–2140.

Jambor JL and Dutrizac JE (1998) Occurrence and constitution of natural and synthetic ferrihydrite, a widespread iron oxyhydroxide. *Chemical Reviews* 98: 2549–2586.

Jambor JL, Dutrizac JE, Groat LA, and Raudsepp M (2002) Static tests of neutralization potentials of silicate and aluminosilicate minerals. *Environmental Geology* 43: 1–17.

Jambor JL, Dutrizac JE, and Raudsepp M (2007) Measured and computed neutralization potentials from static tests of diverse rock types. *Environmental Geology* 52: 1019–1031.

Jambor JL, Nordstrom DK, and Alpers CN (2000b) Metal-sulfate salts from sulfide oxidation. In: Alpers CN, Jambor JL, and Nordstrom DK (eds.) *Sulfate Minerals – Crystallography, Geochemistry, and Environmental Significance. Reviews in Mineralogy and Geochemistry*, vol. 40, pp. 303–350. Mineralogical Society of America.

Jameson E, Rowe OF, Hallberg KB, and Johnson DB (2010) Sulfidogenesis and selective precipitation of metals at low pH mediated by *Acidithiobacillus* spp. and acidophilic sulfate reducing bacteria. *Hydrometallurgy* 104: 488–493.

Janney DE, Cowley JM, and Buseck PR (2000) Transmission electron microscopy of synthetic 2- and 6-line ferrihydrite. *Clays and Clay Minerals* 48: 111–119.

Janzen MP, Nicholson RV, and Scharer JM (2000) Pyrrhotite reaction kinetics: Reaction rates for oxidation by oxygen, ferric iron and nonoxidative dissolution. *Geochimica et Cosmochimica Acta* 64: 1511–1522.

Jennings SR, Dollhopf DJ, and Inskeep WP (2000) Acid production from sulfide minerals using hydrogen peroxide weathering. *Applied Geochemistry* 15: 247–255.

Jerz JK and Rimstidt JD (2000) A reactor to measure pyrite oxidation in air. *Proceedings from the Fifth International Conference on Acid Rock Drainage, 1*, pp. 55–60. Society for Mining, Metallurgy, and Exploration, Inc.

Johnson DB (2006) Biohydrometallurgy and the environment: Intimate and important associations. *Hydrometallurgy* 83: 153–166.

Johnson DB (2007) Physiology and ecology of acidophilic microorganisms. In: Gerday C and Glansdorff N (eds.) *Physiology and Biochemistry of Extremophiles*, pp. 257–270. Washington, DC: ASM press.

Johnson DB (2009) Extremophiles: Acid environments. In: Schaechter M (ed.) *Encyclopaedia of Microbiology*, pp. 107–126. Oxford: Elsevier. ISBN: 978-0-12-373944-5.

Johnson DB (2010) The biogeochemistry of biomining. In: Barton L and Mandl M (eds.) *Geomicrobiology: Molecular and Environmental Perspective*, pp. 401–426. Dordrecht, Germany: Springer.

Johnson DB, Bacelar-Nicolau P, Okibe N, Thomas A, and Hallberg KB (2009) Characteristics of *Ferrimicrobium acidiphilum* gen. nov., sp. nov., and *Ferrithrix thermotolerans* gen. nov., sp. nov.: Heterotrophic iron-oxidizing, extremely acidophilic Actinobacteria. *International Journal of Systematic and Evolutionary Microbiology* 59: 1082–1089.

Johnson RH, Blowes DW, Robertson WD, and Jambor JL (2000) The hydrogeochemistry of the Nickel Rim mine tailings impoundment, Sudbury, Ontario. *Journal of Contaminant Hydrology* 41: 49–80.

Johnson DB and Hallberg KB (2005) Acid mine drainage remediation options: A review. *Science of the Total Environment* 338: 3–14.

Johnson DB and Hallberg KB (2009a) Carbon, iron and sulfur metabolism in acidophilic micro-organisms. *Advances in Microbial Physiology* 54: 202–256.

Johnson DB and Hallberg KB (2009b) Carbon, iron and sulfur metabolism in acidophilic micro-organisms. *Advances in Microbial Physiology* 54: 202–256.

Johnson DB, Kanao T, and Hedrich S (2012) Redox transformations of iron at extremely low pH: Fundamental and applied aspects. *Frontiers in Microbiology* 3: http://dx.doi.org/10.3389/fmicb.2012.00096 Article 96.

Jones CF, LeCount S, Smart RSC, and White TJ (1992) Compositional and structural alteration of pyrrhotite surfaces in solution: XPS and XRD studies. *Applied Surface Science* 55: 65–85.

Jones EJP, Nadeau TL, Voytek MA, and Landa ER (2006) Role of microbial iron reduction in the dissolution of iron hydroxysulfate minerals. *Journal of Geophysical Research* 111: G01012.

Jones B and Renaut RW (2003) Hot spring and geyser sinters: The integrated product of precipitation, replacement, and deposition. *Canadian Journal of Earth Sciences* 40(11): 1549–1569.

Juillot F, Ildefonse P, Morin G, Calas G, de Kersabiec AM, and Benedetti M (1999) Remobilization of arsenic from buried wastes at an industrial site: Mineralogical and geochemical control. *Applied Geochemistry* 14: 1031–1048.

Jurjovec J, Ptacek CJ, and Blowes DW (2002) Acid neutralization mechanisms and metal release in mine tailings: A laboratory column experiment. *Geochimica et Cosmochimica Acta* 66: 1511–1523.

Jurjovec J, Ptacek CJ, Blowes DW, and Jambor JL (2003) The effect of natrojarosite addition to mine tailings. *Environmental Science and Technology* 37: 158–164.

Kaksonen AH and Puhakka JA (2007) Sulfate reduction based bioprocesses for the treatment of acid mine drainage and the recovery of metals. *Engineering in Life Sciences* 7: 541–564.

Kartio I, Laajalehto K, Kaurila T, and Suoninen E (1996) A study of galena (PbS) surfaces under controlled potential in pH 4.6 solution by synchrotron radiation excited photoelectron spectroscopy. *Applied Surface Science* 93: 167–177.

Kartio IJ, Laajalehto K, Suoninen E, Buckley AN, and Woods R (1998) The initial products of the anodic oxidation of galena in acidic solution and the influence of mineral stoichiometry. *Colloids and Surfaces A: Physicochemical and Engineering Aspects* 133: 303–311.

Kesler SE (1994) *Mineral Resources, Economics and the Environment*. USA: Macmillan.

Kim BS, Hayes RA, Prestidge CA, Ralston J, and Smart RSC (1995) Scanning tunneling microscopy studies of galena: The mechanisms of oxidation in aqueous solution. *Langmuir* 11: 2554–2562.

Kimball BA, Callender E, and Axtmann EV (1995) Effects of colloids on metal transport in a river receiving acid mine drainage, upper Arkansas River, Colorado, U.S.A. *Applied Geochemistry* 10: 285–306.

Kimura S, Bryan CG, Hallberg KB, and Johnson DB (2011) Biodiversity and geochemistry of an extremely acidic, low temperature subterranean environment sustained by chemolithotrophy. *Environmental Microbiology* http://dx.doi.org/10.1111/j.1462-2920.2011.02434.x.

Kleinmann RPL, Edenborn HM, and Hedin RS (1991) Biological treatment of mine water – An overview. In: Second International Conference on the Abatement of Acidic Drainage, Tome 1, pp. 27–42. MEND Secretariat.

Knorr KH and Blodau C (2007) Controls on schwertmannite transformation rates and products. *Applied Geochemistry* 22: 2006–2015.

Kock D and Schippers A (2006) Geomicrobiological investigation of two different mine waste tailings generating acid mine drainage. *Hydrometallurgy* 83: 167–175.

Kock D and Schippers A (2008) Quantitative microbial community analysis of three different sulfidic mine tailings dumps generating acid mine drainage. *Applied and Environmental Microbiology* 74: 5211–5219.

Krauskopf KB (1955) Sedimentary deposits of rare metals. In: Bateman AM (ed.) *Economic Geology Fiftieth Anniversary Volume*, pp. 411–463. Economic Geology Pub. Co.

Kusel K, Dorsch T, Acker G, and Stackebrandt E (1999) Microbial reduction of Fe(III) in Acidic sediments: Isolation of *acidiphilium cryptum* Jf-5 capable of coupling the reduction of Fe(III) to the oxidation of glucose. *Applied and Environmental Microbiology* 65: 3633–3640.

Laajalehto K, Smart RSC, Ralston J, and Suoninen E (1993) STM and XPS investigation of reaction of galena in air. *Applied Surface Science* 64: 29–39.

Lamontagne A, Lefebvre R, Poulin R, and Leroueil S (1999) Modelling of acid mine drainage physical processes in a waste rock pile with layered co-mingling. *Proceedings, 52nd Canadian Geotechnical conference,* Regina, Saskatchewan, 24–27 October, pp. 479–485.

Lasaga AC, Soler JM, Ganor J, Burch TE, and Nagy KL (1994) Chemical weathering rate laws and global geochemical cycles. *Geochimica et Cosmochimica Acta* 58: 2361–2386.

Lau S, Mohamed M, Tan Chi Yen A, and Su'ut S (1998) Accumulation of heavy metals in freshwater molluscs. *Science of the Total Environment* 214: 113–121.

Lawrence RW and Wang Y (1997) Determination of neutralization potential in the prediction of acid rock drainage. *Proceedings of the Fourth International Conference on Acid Rock Drainage* 1, pp. 451–464, MEND, Natural Resources Canada.

Leblanc M, Achard B, Othman DB, Luck JM, Bertrand-Sarfati J, and Personné JC (1996) Accumulation of arsenic from acid mine waters by ferruginous bacterial accretions (stromatolites). *Applied Geochemistry* 11: 541–554.

Ledin M and Pedersen K (1996) The environmental impact of mine wastes – Roles of microorganisms and their significance in treatment of mine wastes. *Earth-Science Reviews* 41: 67–108.
Lee P, Kang MJ, Choi SH, and Touray JC (2005) Sulfide oxidation and the natural attenuation of arsenic and trace metals in the waste rocks of the abandoned Seobo tungsten mine, Korea. *Applied Geochemistry* 20(9): 1687–1703.
Lee KY, Kim KW, and Kim SO (2010) Geochemical and microbial effects on the mobilization of arsenic in mine tailings soils. *Environmental Geochemistry and Health* 32: 31–44.
Lefebvre R, Hockley D, Smolensky J, and Gelinas P (2001) Multiphase transfer processes in waste rock piles producing acid mine drainage. 1. Conceptual model and system characterization. *Journal of Contaminant Hydrology* 52: 137–164.
Lengke MF and Tempel RN (2003) Natural realgar and amorphous AsS oxidation kinetics. *Geochimica et Cosmochimica Acta* 67: 859–871.
Lengke MF and Tempel RN (2005) Geochemical modeling of arsenic sulfide oxidation kinetics in a mining environment. *Geochimica et Cosmochimica Acta* 69: 341–356.
Levy DB, Custis KH, Casey WH, and Rock PA (1997) The aqueous geochemistry of the abandoned Spenceville Copper Pit, Nevada County, California. *Journal of Environmental Quality* 26: 233–243.
Lewis BA, Gallinger RD, and Wiber M (2000) Poirier site reclamation program. *Proceedings from the Fifth International Conference on Acid Rock Drainage, 2*, pp. 959–968. Society for Mining, Metallurgy, and Exploration, Inc.
Lichtner PC (1993) Scaling properties of time-space kinetic mass transport equations and the local equilibrium assumption. *American Journal of Science* 293: 257–296.
Lim MS, Yeo IW, Roh Y, Lee KK, and Jung MC (2008) Arsenic reduction and precipitation by *Shewanella* sp.: Batch and column tests. *Geosciences Journal* 30: 153–162.
Lin Z (1997) Mineralogical and chemical characterization of wastes from a sulfuric acid industry in Falun Sweden. *Environmental Geology* 30(3/4): 153–162.
Lin Z and Puls RW (2000) Adsorption, desorption, and oxidation of arsenic affected by clay minerals and aging process. *Environmental Geology* 39: 753–759.
Lind CJ and Hem JD (1993) Manganese minerals and associated fine particulates in the streambed of Pinal Creek, Arizona, U.S.A.: A mining-related acid drainage problem. *Applied Geochemistry* 8: 67–80.
Lindsay MBJ, Blowes DW, Condon PD, and Ptacek CJ (2009) Managing pore-water quality in mine tailings by inducing microbial sulfate reduction. *Environmental Science and Technology* 43: 7086–7091.
Lindsay MBJ, Blowes DW, Condon PD, and Ptacek CJ (2011a) Organic carbon amendments for passive in situ treatment of mine drainage: Field experiments. *Applied Geochemistry* 26: 1169–1183.
Lindsay MBJ, Blowes DW, Ptacek CJ, and Condon PD (2011b) Transport and attenuation of metal(loid)s in mine tailings amended with organic carbon: Column experiments. *Journal of Contaminant Hydrology* 125: 26–38.
Lindsay MBJ, Wakeman KD, Rowe OF, et al. (2011c) Microbiology and geochemistry of mine tailings amended with organic carbon for passive treatment of pore water. *Geomicrobiology Journal* 28: 229–241.
Linklater CM, Sinclair DJ, and Brown PL (2005) Coupled chemistry and transport modelling of sulphidic waste rock dumps at the Aitik mine site, Sweden. *Applied Geochemistry* 20: 275–293.
Liu CW and Narasimhan TN (1989a) Redox-controlled multiple-species reactive chemical treatment. 1. Model development. *Water Resources Research* 25: 868–882.
Liu CW and Narasimhan TN (1989b) Redox-controlled multiple-species reactive chemical treatment. 2. Verification and application. *Water Resources Research* 25: 883–910.
Loan M, Cowley JM, Hart R, and Parkinson GM (2004) Evidence on the structure of synthetic schwertmannite. *American Mineralogist* 89: 1735–1742.
Logan MV, Reardon KF, Figueroa LA, McLain JET, and Ahmann DM (2005) Microbial community activities during establishment, performance, and decline of bench-scale passive treatment systems for mine drainage. *Water Research* 39: 4537–4551.
Lortie L, Gould WD, Stichbury M, Blowes DW, and Thurel A (1999) Inhibitors for the prevention of acid mine drainage (AMD). *Proceedings of Sudbury'99 Mining and the Environment II Conference,* 13–17 September, Sudbury, ON 1191–1198.
Lovley DR (1993) Dissimilatory metal reduction. *Annual Review of Microbiology* 47: 263–290.
Lowson RT (1982) Aqueous oxidation of pyrite by molecular oxygen. *Chemical Reviews* 82: 461–497.
Lucassen EC, Smolders AJP, and Roelofs JGM (2000) Increased ground levels cause iron toxicity in *Glyceria fluitans* (L.). *Aquatic Botany* 66: 321–327.
Ludwig RD, McGregor RG, Blowes DW, Benner SG, and Mountjoy K (2002) A permeable reactive barrier for the treatment of dissolved metals. *Ground Water* 40: 59–66.
Lundgren T (2001) The dynamics of oxygen transport into soil covered mining waste deposits in Sweden. *Journal of Geochemical Exploration* 74: 163–173.
Luther IGW (1987) Pyrite oxidation and reduction: Molecular orbital theory considerations. *Geochimica et Cosmochimica Acta* 51: 3193–3199.
Lutzenkirchen J and Lovgren L (1998) Experimental study of arsenite adsorption to goethite. *Mineralogical Magazine* 62A: 927–928.
Machemer SD and Wildeman TR (1992) Adsorption compared with sulfide precipitation as metal removal processes from acid mine drainage in a constructed wetland. *Journal of Contaminant Hydrology* 9: 115–131.
Mackowsky M-T (1968) Mineral matter in coal. In: Murchison D and Westoll TS (eds.) *Coal and Coal-Bearing Strata*, pp. 309–321. Elsevier.
Majzlan J and Myneni SCB (2005) Speciation of iron and sulfate in acid waters: Aqueous clusters to mineral precipitates. *Environmental Science and Technology* 39: 188–194.
Manceau A (1995) The mechanism of anion adsorption on iron oxides: Evidence for the bonding of arsenate tetrahedra on free $Fe(O, OH)_6$ edges. *Geochimica et Cosmochimica Acta* 59: 3647–3653.
Manceau A (2009) Evaluation of the structural model for ferrihydrite derived from real-space modeling of high-energy X-ray diffraction data. *Clay Minerals* 44: 19–34.
Manceau A (2010) PDF analysis of ferrihydrite and the violation of Pauling's Principia. *Clay Minerals* 45: 225–228.
Manceau A (2011) Critical evaluation of the revised akdalaite-model for ferrihydrite. *American Mineralogist* 96: 521–533.
Manceau A and Drits VA (1993) Local structure of ferrihydrite and feroxyhite by EXAFS spectroscopy. *Clay Minerals* 28: 165–184.
Mann H and Fyfe WS (1989) Metal uptake and Fe-, Ti-oxide biomineralization by acidophilic microorganisms in mine-waste environments, Elliot Lake, Canada. *Canadian Journal of Earth Sciences* 26: 2731–2735.
Manning BA, Fendorf SE, and Goldberg S (1998) Surface structures and stability of arsenic(III) on goethite: Spectroscopic evidence for inner-sphere complexes. *Environmental Science and Technology* 32: 2383–2388.
Manning BA and Goldberg S (1996) Modeling arsenate competitive adsorption on kaolinite, montmorillonite and illite. *Clays and Clay Minerals* 44: 609–623.
Marchand P and Rancourt DG (2009) General model for the aqueous precipitation of rough surface nanocrystals and application to ferrihydrite genesis. *American Mineralogist* 94: 1428–1439.
Markich SJ, Brown PL, and Jeffree RA (2001) Divalent metal accumulation in freshwater bivalves: An inverse relationship with metal phosphate solubility. *Science of the Total Environment* 275: 27–41.
Martin AJ, McNee JJ, and Pedersen TF (2001) The reactivity of sediments impacted by metal-mining in Lago Junin, Peru. *Journal of Geochemical Exploration* 74: 175–187.
Mason B (1958) *Principles of Geochemistry*. New York: Wiley.
Mason RP, Reinfelder JR, and Morel FMM (1996) Uptake, toxicity, and trophic transfer of mercury in a coastal diatom. *Environmental Science and Technology* 30: 1835–1845.
Mathews CT and Robins RG (1972) The oxidation of ferrous disulfide by ferric sulfate. *Australian Chemical Engineering* 13: 21–25.
Mathews CT and Robins RG (1974) Aqueous oxidation of iron disulfide by molecular oxygen. *Australian Chemical Engineering* 15: 19–24.
Mattes A, Evans LJ, Gould WD, Duncan WFA, and Glasauer S (2011) The long term operation of a biologically based treatment system that removes As, S and Zn from industrial (smelter operation) landfill seepage. *Applied Geochemistry* 26: 1886–1896.
Mayer KU, Benner SG, and Blowes DW (2006) Process-based reactive transport modeling of a permeable reactive barrier for the treatment of mine drainage. *Journal of Contaminant Hydrology* 85: 195–211.
Mayer KU, Frind EO, and Blowes DW (2002) Multicomponent reactive transport modeling in variably saturated porous media using a generalized formulation for kinetically controlled reactions. *Water Resources Research* 38: 1174–1195.
Mayes WM, Batty LC, Younger PL, et al. (2009) Wetland treatment at extremes of pH: A review. *Science of the Total Environment* 407: 3944–3957.
McCreadie H, Blowes DW, Ptacek CJ, and Jambor JL (2000) The influence of reduction reactions and solids composition on pore-water arsenic concentrations. *Environmental Science and Technology* 34: 3159–3166.
McCreadie H, Jambor JL, Blowes DW, Ptacek C, and Hiller D (1998) Geochemical behaviour of autoclave-produced ferric arsenates and jarosite in a gold mine tailings impoundment. *Waste Characterization and Treatment*, pp. 61–78. Littleton, CO: Society for Mining, metallurgy and Exploration Inc.
McGregor R, Benner S, Ludwig R, Blowes D, and Ptacek C (2002) Sulfate reduction permeable reactive barriers to treat acidity, cadmium, copper, nickel, and zinc: Two case studies. In: Naftz DL, Morrison SJ, Davis JA, and Fuller CC (eds.) *Handbook of*

Groundwater Remediation Using Permeable Reactive Barriers – Applications to Radionuclides, Trace Metals, and Nutrients, pp. 495–522. Academic Press.
McKibben MA and Barnes HL (1986) Oxidation of pyrite in low temperature acidic solutions: Rate laws and surface textures. *Geochimica et Cosmochimica Acta* 50: 1509–1520.
McKibben MA, Tallant BA, and del Angel JK (2008) Kinetics of inorganic arsenopyrite oxidation in acidic aqueous solutions. *Applied Geochemistry* 23: 121–135.
MEND (1991) Acid rock drainage prediction manual. MEND Project 1.16.1b, *Report by Coastech Research*. MEND, Natural Resources Canada.
MEND (1994) Monitoring and modeling of acid mine drainage from waste rock dumps. *Natural Resources Canada MEND Report 1.14.2g*.
MEND (1995) *MINEWALL 2.0 Literature Review and Conceptual Models*. MEND Project 1.15.2b. Energy Mines and Resources Canada.
Michel FM, Barrónc V, Torrent J, et al. (2010) Ordered ferrimagnetic form of ferrihydrite reveals links among structure, composition, and magnetism. *Proceedings of the National Academy of Sciences of the United States of America* 107: 2787–2792.
Michel FM, Ehm L, Antao SM, et al. (2007) The structure of ferrihydrite, a nanocrystalline material. *Science* 316: 1726–1729.
Miller GC, Lyons WB, and Davis A (1996) Understanding the water quality of pit lakes. *Environmental Science and Technology* 30: 118–123A.
Moncur MC, Jambor JL, Ptacek CJ, and Blowes DW (2009) Mine drainage from the weathering of sulfide minerals and magnetite. *Applied Geochemistry* 24: 2362–2373.
Moncur MC, Ptacek CJ, Blowes DW, and Jambor JL (2003) Fate and transport of metals from an abandoned tailings impoundment after 70 years of sulfide oxidation. *Proceedings of Sudbury '03, Mining and the Environment III, Sudbury, ON*.
Moncur MC, Ptacek CJ, Blowes DW, and Jambor JL (2005) Release, transport and attenuation of metals from an old tailings impoundment. *Applied Geochemistry* 20: 639–659.
Moncur MC, Ptacek CJ, Blowes DW, and Jambor JL (2006) Spatial variations in water composition at a lake impacted by mine drainage. *Applied Geochemistry* 21: 1799–1817.
Morin G and Calas G (2006) Arsenic in soils, mine tailings, and former industrial sites. *Elements* 2: 97–101.
Morin KA, Cherry JA, Dave NK, Lim TP, and Vivyurka AJ (1988) Migration of acidic groundwater seepage from uranium-tailings impoundments, 1. Field study and conceptual hydrogeochemical model. *Journal of Contaminant Hydrology* 2: 271–303.
Morin KA and Hutt NM (1997) *Environmental Geochemistry of Minesite Drainage: Practical Theory and Case Studies*. Vancouver, BC: MDAG Publishing.
Morin G, Juillot F, Casiot C, et al. (2003) Bacterial formation of tooeleite and mixed Arsenic(III) or Arsenic(V) – Iron(III) gels in the Carnoulès acid mine drainage, France. A XANES, XRD, and SEM study. *Environmental Science and Technology* 37: 1705–1712.
Morin G, Ostergren JD, Juillot F, Ildefonse P, Calas G, and Brown GE Jr. (1999) XAFS determination of the chemical form of lead in smelter-contaminated soils and mine tailings: Importance of adsorption processes. *American Mineralogist* 84: 420–434.
Morrison SJ, Carpenter CE, Metzler DR, Bartlett TR, and Morris SA (2002) Design and performance of a permeable reactive barrier for containment of uranium, arsenic, selenium, vanadium, molybdenum, and nitrate at Monticello, Utah. In: Naftz DL, Morrison SJ, Davis JA, and Fuller CC (eds.) *Handbook of Groundwater Remediation Using Permeable Reactive Barriers – Applications to Radionuclides, Trace Metals, and Nutrients*, pp. 371–399. New York: Academic Press.
Moses CO, Nordstrom DK, Herman JS, and Mills AL (1987) Aqueous pyrite oxidation by dissolved oxygen and ferric iron. *Geochimica et Cosmochimica Acta* 51: 1561–1571.
Mycroft JR, Nesbitt HW, and Pratt AR (1995) X-ray photoelectron and Auger electron spectroscopy of air oxidized pyrrhotite: Distribution of oxidized species with depth. *Geochimica et Cosmochimica Acta* 59: 721–733.
Naftz DL, Fuller CC, Davis JA, et al. (2002) Field demonstration of three permeable reactive barriers to control uranium contamination in groundwater, Fry Canyon, Utah. In: Naftz DL, Morrison SJ, Davis JA, and Fuller CC (eds.) *Handbook of Groundwater Remediation Using Permeable Reactive Barriers – Applications to Radionuclides, Trace Metals, and Nutrients*, pp. 401–434. San Diego, CA: Academic Press.
Nagy KL (1995) Dissolution and precipitation kinetics of sheet silicates. In: White AF and Brantley SL (eds.) *Chemical Weathering Rates of Silicate Minerals*. *Reviews in Mineralogy*, vol. 31, pp. 173–225. Mineralogical Society of America.
Neculita C-M, Zagury GJ, and Bussiére B (2007) Passive treatment of acid mine drainage in bioreactors using sulfate-reducing bacteria: Critical review and research needs. *Journal of Environmental Quality* 36: 1–16.
Nesbitt HW and Muir IJ (1998) Oxidation states and speciation of secondary products on pyrite and arsenopyrite reacted with mine waste waters and air. *Mineralogy and Petrology* 62: 123–144.
Nesbitt HW, Muir IJ, and Pratt AR (1995) Oxidation of arsenopyrite by air and air-saturated, distilled water, and implications for mechanism of oxidation. *Geochimica et Cosmochimica Acta* 59: 1773–1786.
Nevin KP and Loveley DR (2002) Mechanism for accessing insoluble Fe(III) oxide during dissimilatory Fe(III) reduction by *geothrix fermentans*. *Applied and Environmental Microbiology* 68: 2294–2299.
Newman DK, Kennedy EK, Coates JD, et al. (1997) Dissimilatory arsenate and sulfate reduction in *Desulfotomaculum auripigmentum* sp. nov. *Archives of Microbiology* 168: 380–388.
Nichol C, Beckie R, and Smith L (2002) Characterization of unsaturated flow at different scales in waste rock. *Groundwater 2002 – Proceedings of the International Association of Hydrologists Conference*, Madrid, Spain: International Association of Hydraulic Engineering and Research.
Nichol C, Smith L, and Beckie R (2005) Field-scale experiments of unsaturated flow and solute transport in a heterogeneous porous medium. *Water Resources Research* 41: W05018.
Nicholson RV (1994) Iron-sulfide oxidation mechanisms: Laboratory studies. In: Blowes DW and Jambor JL (eds.) *The Environmental Geochemistry of Sulfide Mine-Wastes*, vol. 22, pp. 164–183. Nepean, Ontario: Mineralogical Association of Canada.
Nicholson RV, Gillham RW, Cherry JA, and Reardon EJ (1989) Reduction of acid generation in mine tailings through the use of moisture-retaining layers as oxygen barriers. *Canadian Geotechnical Journal* 26: 1–8.
Nicholson RV and Scharer JM (1994) Pyrrhotite oxidation kinetics. In: Alpers CN and Blowes DW (eds.) *Environmental Geochemistry of Sulfide Oxidation*, vol. 550, pp. 14–30. USA: American Chemical Society.
Nordstrom DK (1982) Aqueous pyrite oxidation and the consequent formation of secondary iron minerals. In: Hossner LR, Kittrick JA, and Fanning DF (eds.) *Acid Sulfate Weathering*. Madison, WI: Soil Science Society of American Press.
Nordstrom D K (1985) The rate of ferrous iron oxidation in a stream receiving acid mine effluent. In *Selected Papers in the Hydrogeological Sciences*, pp. 113–119. U.S. Geological Survey Water-Supply.
Nordstrom DK and Alpers CN (1999a) Geochemistry of acid mine waters. In: Plumlee GS and Logsdon MJ (eds.) *The Environmental Geochemistry of Mineral Deposits*, vol. 6A, pp. 133–157. Society of Economic Geologists, Inc.
Nordstrom DK and Alpers CN (1999b) Negative pH, efflorescent mineralogy, and consequences for environmental restoration at the Iron Mountain Superfund site, California. *Proceedings of the National Academy of Sciences of the United States of America* 96: 3455–3462.
Nordstrom DK, Alpers CN, Ptacek CJ, and Blowes DW (2000) Negative pH and extremely acidic mine waters from Iron Mountain, California. *Environmental Science and Technology* 34: 254–258.
Nordstrom DK and Munoz JL (1994) *Geochemical Thermodynamics*. Boston, MA: Blackwell Scientific.
Nordstrom DK, Plummer LN, Langmuir D, et al. (1990) Revised chemical equilibrium data for major water–mineral reactions and their limitations. In: Melchior DC and Bassett RL (eds.) *Chemical modeling of aqueous systems II*, *American Chemical Society Symposium Series*, vol. 416, pp. 398–413.
Nordstrom DK and Southam G (1997) Geomicrobiology of sulfide mineral oxidation. In: Banfield JF and Nealson KH (eds.) *Geomicrobiology: Interactions Between Microbes and Minerals*, vol. 35, pp. 361–385. Washington, DC: Mineralogical Society of America.
Norland KL, Southam G, Tylisza T, et al. (2009) Microbial architecture of environmental sulfur processes: A novel syntrophic sulfur-metabolizing consortia. *Environmental Science and Technology* 43: 8781–8786.
Nowak P and Laajalehto K (2000) Oxidation of galena surface – An XPS study of the formation of sulfoxy species. *Applied Surface Science* 157: 101–111.
Nriagu JO (ed.) (1994) *Arsenic in the Environment, Part I: Cycling and Characterization*. *Advances in Environmental Science and Technology*, vol. 26. New York: Wiley.
Ohmura N, Sasaki K, Matsumoto N, and Saiki H (2002) Anaerobic respiration using Fe^{3+}, S^0 and H_2 in the chemolithotrophic bacterium *Acidithiobacillus ferrooxidans*. *Journal of Bacteriology* 184: 2081–2087.
Olanipekun EO (1999) Kinetics of sphalerite leaching in acidic ferric chloride solutions. *Transactions of Indian Institute of Metallurgy* 52(2–3): 81–86.
Olson GJ (1991) Rate of pyrite bioleaching by *Thiobacillus ferrooxidans* – Results of an interlaboratory comparison. *Applied and Environmental Microbiology* 57: 642–644.
Olson G, Clark T, Mudder T, and Logsdon M (2004) Control and prevention of microbially-catalyzed acid rock drainage with thiocyanate. *SME Annual Meeting Preprints* 2004: 273–278.
Oremland RS and Stolz JF (2003) The ecology of arsenic. *Science* 300: 939–944.
Orlova TA, Stupnikov VM, and Krestan AL (1988) Mechanism of oxidative dissolution of sulfides. *Zhurnal Prikladnoĭ Khimii* 61: 2172–2177.

Paige CR, Snodgrass WJ, Nicholson RV, and Scharer JM (1997) An arsenate effect on ferrihydrite dissolution kinetics under acidic oxic conditions. *Water Research* 31: 2370–2382.

Paktunc D (1999) Mineralogical constraints on the determination of neutralization potential and prediction of acid mine drainage. *Environmental Geology* 39: 103–112.

Paktunc D (2008) Speciation of arsenic in pyrite by micro-X-ray absorption fine-structure spectroscopy (XAFS). *Proceedings of the Ninth International Congress for Applied Mineralogy (ICAM2008) 8–10 September 2008, Brisbane, Queensland, The Australasian Institute of Mining and Metallurgy, 8/2008,* 155–158.

Paktunc D (2009) Arsenic speciation in wastes resulting from pressure oxidation, roasting and smelting. In: Lentz DR, Thorne KG, and Beal K-L (eds.) *Proceedings of the 24th International Applied Geochemistry Symposium (IAGS); 1–4 June, 2009, vol. II*, Fredericton, Canada, 881–884.

Paktunc D and Bruggeman K (2010) Solubility of nanocrystalline scorodite and amorphous ferric arsenate: Implications for stabilization of arsenic in mine wastes. *Applied Geochemistry* 25: 674–683.

Paktunc D and Dave NK (1999) Acidic drainage characteristics and residual sample mineralogy of unsaturated and saturated coarse pyritic uranium tailings. In: Goldsack D, Belzile N, Yearwood P, and Hall G (eds.) *Proceedings, Sudbury'99 Mining and the Environment II, Sudbury 13–17, 1999, vol. 1,* pp. 221–230.

Paktunc D and Davé NK (2000) Mineralogy of pyritic waste rock leached by column experiments and prediction of acid mine drainage. In: Rammlmair D (ed.) *Applied Mineralogy*, pp. 621–623. Balkema.

Paktunc D and Davé NK (2002) Formation of secondary pyrite and carbonate minerals in the Lower Williams Lake tailings basin, Elliot Lake, Ontario, Canada. *American Mineralogist* 87: 593–602.

Paktunc D and Dutrizac J (2003) Characterization of arsenate-for-sulfate substitution in synthetic jarosite using X-ray diffraction and X-ray absorption spectroscopy. *The Canadian Mineralogist* 41: 905–919.

Paktunc D, Dutrizac J, and Gertsman V (2008) Synthesis and phase transformations involving scorodite, ferric arsenate and arsenical ferrihydrite: Implications for arsenic mobility. *Geochimica et Cosmochimica Acta* 72: 2649–2672.

Paktunc D, Foster A, Heald S, and Laflamme G (2004) Speciation and characterization of arsenic in gold ores and cyanidation tailings using X-ray absorption spectroscopy. *Geochimica et Cosmochimica Acta* 68: 969–983.

Paktunc D, Foster A, and Laflamme J (2003) Speciation and characterization of arsenic in Ketza River Mine tailings using X-ray absorption spectroscopy. *Environmental Science and Technology* 37: 2067–2074.

Paktunc D, Kingston D, Pratt A, and McMullen J (2006) Distribution of gold in pyrite and in products of its transformation resulting from roasting of refractory gold ore. *The Canadian Mineralogist* 44: 213–227.

Papassiopi N, Vaxevanidou K, and Paspaliaris I (2003) Investigating the use of iron reducing bacteria for the removal of arsenic from contaminated soils. *Water, Air, and Soil Pollution* 3: 81–90.

Parkhurst DL (1998) PHREEQC website (http://wwwbrr.cr.usgs.gov/projects/GWC_coupled/phreeqc/).

Parkhurst DL, Thorstenson DC, and Plummer LN (1985) PHREEQE – A computer program for geochemical calculations. *U.S. Geological Survey Water-Resources Investigations Report* 80-96

Pedersen TF, Mueller B, McNee JJ, and Pelletier CA (1993) The early diagenesis of submerged sulphide-rich mine tailings in Anderson Lake, Manitoba. *Canadian Journal of Earth Sciences* 30: 1099–1109.

Peretyazhko T, Zachara JM, Boily J-F, et al. (2009) Mineralogical transformations controlling acid mine drainage chemistry. *Chemical Geology* 262: 169–178.

Perez IP and Dutrizac JE (1991) The effect of iron content of sphalerite on its rate of dissolution in ferric sulphate and ferric chloride media. *Hydrometallurgy* 26: 211–232.

Perry A and Kleinmann RLP (1991) The use of constructed wetlands in the treatment of acid mine drainage. *Natural Resource Forum* 15(3): 178–184.

Pitzer KS (1973) Thermodynamics of electrolytes. I. Theoretical basis and general equations. *Journal of Physical Chemistry* 77: 2300–2308.

Pitzer KS (1991) Ion interaction approach: Theory and data correlation. In: Pitzer KS (ed.) *Activity Coefficients in Electrolyte Solutions*, pp. 75–153. Boca Raton, FL: CRC Press.

Plant JA, Simpson PR, Smith B, and Windley BF (1999) Uranium ore deposits – products of the radioactive earth. In: Burns PC and Finch R (eds.) *Uranium: Mineralogy, Geochemistry and the Environment. Reviews in Mineralogy*, vol. 38, pp. 255–319. Washington, DC: Mineralogical Society of America.

Plummer LN, Parkhurst DL, Fleming GW, and Dunkle SA (1988) A computer program incorporating Pitzer's equations for calculation of geochemical reactions in brines. *Geological Survey Water-Resources Investigations Report* 88-4153.

Pratt AR, Muir IJ, and Nesbitt HW (1994a) X-ray photoelectron and Auger electron spectroscopic studies of pyrrhotite and mechanisms of air oxidation. *Geochimica et Cosmochimica Acta* 58: 827–841.

Pratt AR and Nesbitt HW (1997) Pyrrhotite leaching in acid mixtures of HCl and H_2SO_4. *American Journal of Science* 297: 807–828.

Pratt AR, Nesbitt HW, and Muir IJ (1994b) Generation of acids from mine waste: Oxidative leaching of pyrrhotite in dilute H_2SO_4 solutions at pH 3.0. *Geochimica et Cosmochimica Acta* 58: 5147–5159.

Prestidge CA, Skinner WM, Ralston J, and Smart RSC (1995) The interaction of iron(III) species with galena surfaces. *Colloids and Surfaces* 105(2–3): 325–339.

Pruden A, Messner N, Pereyra L, Hanson RE, Hiibel SR, and Reardon KF (2007) The effect of inoculum on the performance of sulfate-reducing columns treating heavy metal contaminated water. *Water Research* 41: 904–914.

Ptacek CJ and Blowes DW (1994) Influence of siderite on the pore-water chemistry of inactive mine-tailings impoundments. In: Alpers CN and Blowes DW (eds.) *Environmental Geochemistry of Sulfide Oxidation*, vol. 550, pp. 172–189. Washington, DC: American Chemical Society.

Ptacek CJ and Blowes DW (2000) Prediction of sulfate mineral solubility in concentrated waters. Sulfate Minerals: Crystallography, Geochemistry, and Environmental Significance. In: Alpers CN, Jambor JL, and Nordstrom DK (eds.) *Reviews in Mineralogy and Geochemistry*, vol. 40, pp. 513–540, Mineralogical Society of America.

Puro M, Kipkie WB, Knapp RA, MacDonald TJ, and Stuparyk RA (1995) Inco's Copper Cliff tailings area. *Proceedings of Sudbury'95 Mining and the Environment* 1: 181–191.

Rai UN, Tripathi RD, Vajpajee P, Vidyanath J, and Ali MB (2002) Bioaccumulation of toxic metals (Cr, Cd, Pb, and Cu) by seeds of Euryale ferox Salisb. *Chemosphere* 46: 267–272.

Ramstedt M, Carlsson E, and Lövgren L (2003) Aqueous geochemistry in the Udden pit lake, Northern Sweden. *Applied Geochemistry* 18: 97–108.

Rancourt DG and Meunier JF (2008) Constraints on structural models of ferrihydrite as a nanocrystalline material. *American Mineralogist* 93: 1412–1417.

Raven KP, Jain A, and Loeppert RH (1998) Arsenite and arsenate adsorption on ferrihydrite: Kinetics, equilibrium, and adsorption envelopes. *Environmental Science and Technology* 32: 344–349.

Rawlings DE and Johnson DB (2007) The microbiology of biomining: Development and optimization of mineral-oxidizing microbial consortia. *Microbiology* 153: 315–324.

Reardon EJ and Beckie RD (1987) Modelling chemical equilibria of acid-mine drainage: The $FeSO_4$–H_2SO_4–H_2O system. *Geochimica et Cosmochimica Acta* 51: 2355–2368.

Reardon EJ and Moddle PM (1985) Gas diffusion coefficient measurements on uranium mill tailings: Implications to cover layer design. *Uranium* 2: 111–131.

Reardon EJ and Poscente PJ (1984) A study of gas compositions in sawmill waste deposits: Evaluation of the use of wood waste in close-out of pyritic tailings. *Reclamation and Revegetation Research* 3: 109–128.

Reedy BJ, Beattie JK, and Lowson RT (1991) A vibrational spectroscopic ^{18}O study of pyrite oxidation. *Geochimica et Cosmochimica Acta* 55: 1609–1614.

Regenspurg S, Brand A, and Peiffer S (2004) Formation and stability of schwertmannite in acidic mining lakes. *Geochimica et Cosmochimica Acta* 68: 1185–1197.

Reich M, Kesler SE, Utsu nomiya S, Palenik CS, Chryssoulis S, and Ewing RC (2005) Solubility of gold in arsenian pyrite. *Geochimica et Cosmochimica Acta* 69: 2781–2796.

Renton JJ (1982) Mineral matter in coal. In: Meyers RA (ed.) *Coal Structure*, pp. 283–326. New York: Academic Press.

Ribet I, Ptacek CJ, Blowes DW, and Jambor JL (1995) The potential for metal release by reductive dissolution of weathered mine tailings. *Journal of Contaminant Hydrology* 17: 239–273.

Rieder M, Cavazzini G, D'Yakonov YS, et al. (1998) Nomenclature of the micas. *The Canadian Mineralogist* 36: 905–912.

Rimstidt JD, Chermak JA, and Gagen PM (1994) Rates of reaction of galena, sphalerite, chalcopyrite and arsenopyrite. In: Alpers CN and Blowes DW (eds.) *Environmental Geochemistry of Sulfide Oxidation*, vol. 550, pp. 2–13. Washington, DC: American Chemical Society.

Rimstidt JD and Vaughan DJ (2003) Pyrite oxidation: A state of the art assessment of the reaction mechanism. *Geochimica et Cosmochimica Acta* 67: 873–880.

Ritchie AIM (1994) Sulfide oxidation mechanisms: Controls and rates of oxygen transport. In: Blowes DW and Jambor JL (eds.) *The Environmental Geochemistry of Sulfide Mine-Wastes*, vol. 22, pp. 201–246. Mineralogical Association of Canada.

Ritchie AIM (2003) Oxidation and gas transport in piles of sulfidic material. In: Jambor JL, Blowes DW, and Ritchie AIM (eds.) *Environmental Aspects of Mine Wastes. Short Course*, vol. 31, pp. 73–94. Ottawa, ON: Mineralogical Association of Canada.

Robertson WD (1994) The physical hydrogeology of mill-tailings impoundments. In: Blowes DW and Jambor JL (eds.) *The Environmental Geochemistry of Sulfide Mine-Wastes*, vol. 22, pp. 1–17. Mineralogical Association of Canada.

Robinsky E (1978) Tailings disposal by the thickened discharge method for improved economy and environmental control. In: *Tailings Disposal Today, Proceedings of the Second International Tailings Symposium*, vol. 2, pp. 75–92.

Robinsky E, Barbour SL, Wilson GW, Bordin D, and Fredlund DG (1991) Thickened sloped tailings disposal: An evaluation of seepage and abatement of acid drainage. *Second International Conference on the Abatement of Acidic Drainage, 1*, pp. 529–550. MEND Secretariat.

Rohwerder T, Gehrke T, Kinzler K, and Sand W (2003) Bioleaching review. Part A: Progress in bioleaching: Fundamentals and mechanisms of bacterial metal sulfide oxidation. *Applied Microbiology and Biotechnology* 63: 239–248.

Rose AW and Cravotta CA III (1998) Geochemistry of coal mine drainage. In: Brady BC, Smith MW, and Schueck J (eds.) *Coal Mine Drainage Prediction and Pollution in Pennsylvania*, pp. 1–22. Bureau of Mining and Reclamation.

Rosso KM and Vaughan DJ (2006) Reactivity of sulfide mineral surfaces. In: Vaughan DJ (ed.) *Sulfide Mineralogy and Geochemistry*, *Reviews in Mineralogy and Geochemistry*, vol. 61, pp. 557–608.

Roussel C, Bril H, and Fernandez A (2000) Arsenic speciation: Involvement in evaluation of environmental impact caused by mine wastes. *Journal of Environmental Quality* 29: 182–188.

Rowe OF, Sánchez-España J, Hallberg KB, and Johnson DB (2007) Microbial communities and geochemical dynamics in an extremely acidic, metal-rich stream at an abandoned sulfide mine (Huelva, Spain) underpinned by two functional primary production systems. *Environmental Microbiology* 9: 1761–1771.

Runkel RL, Bencala KE, and Broshears RE (1996) An equilibrium-based simulation model for reactive solute transport in small streams. In: *Geological Survey Water-Resources Investigations Report* 94-4014, pp. 775–780.

Runkel RL and Kimball BA (2002) Evaluating remedial alternatives for an acid mine drainage stream – Application of a reactive transport model. *Environmental Science and Technology* 36: 1093–1101.

Rytuba JJ (2000) Mercury mine drainage and processes that control its environmental impact. *Science of the Total Environment* 260: 57–71.

Salzsauler KA, Sidenko NV, and Sherriff BL (2005) Arsenic mobility in alteration products of sulfide-rich, arsenopyrite-bearing mine wastes, Snow Lake, Manitoba, Canada. *Applied Geochemistry* 20: 2303–2314.

Sánchez-España, Pamo EI, Pastor ES, Ercilla MD (2008) The acidic mine pit lakes of the Iberian Pyrite Belt: An approach to their physical limnology and hydrogeochemistry. *Applied Geochemistry*, 23: 1260–1287.

Sand W, Rohde K, Sobotke B, and Zenneck C (1992) Evaluation of *Leptospirillum ferrooxidans* for leaching. *Applied and Environmental Microbiology* 58: 85–92.

Santore RC, Di Toro DM, Paquin PR, Allen HE, and Meyer E (2001) Biotic ligand model of the acute toxicity of metals. 2. Application to acute copper toxicity in freshwater fish and Daphnia. *Environmental Toxicology and Chemistry* 20: 2397–2402.

Sasaki K, Tsunekawa M, Ohtsuka T, and Konno H (1995) Confirmation of a sulfur-rich layer on pyrite after oxidative dissolution by Fe(III) ions around pH 2. *Geochimica et Cosmochimica Acta* 59: 3155–3158.

Sasaki K, Tsunekawa M, Ohtsuka T, and Konno H (1998) The role of sulfur oxidizing bacteria *Thiobacillus thiooxidans* in pyrite weathering. *Colloids and Surfaces* 133: 269–278.

Savage KS, Tingle TM, O'Day PA, Waychunas GA, and Bird DK (2000) Arsenic speciation in pyrite and secondary weathering phases, Mother Lode gold district, Tuolumne County, California. *Applied Geochemistry* 15: 1219–1244.

Schippers A (2003) MiMi – Long-term anaerobic microbial processes in remediated mine tailings. The MISTRA-programme MiMi, Mitigation of the environmental impact from mining waste. MiMi Print, Luleå, Sweden, MiMi 2003:1

Schippers A, Kock D, Schwartz M, Bottcher ME, Vogel H, and Hagger M (2007) Geomicrobiological and geochemical investigation of a pyrrhotite-containing mine waste tailings dam near Selebi-Phikwe Botswana. *Journal of Geochemical Exploration* 92: 151–158.

Schippers A, Breuker A, Blazejak A, Bosecker K, Kock D, and Wright TL (2010) The biogeochemistry and microbiology of sulfidic mine waste and bioleaching dumps and heaps, and novel Fe(II)-oxidizing bacteria. *Hydrometallurgy* 104: 342–350.

Schippers A and Sand W (1999) Bacterial leaching of metal sulfides proceeds by two indirect mechanisms via thiosulfate or via polysulfides and sulfur. *Applied and Environmental Microbiology* 65: 319–321.

Schwertmann U and Carlson L (2005) The pH-dependent transformation of schwertmannite to goethite at 25 °C. *Clay Minerals* 40: 63–66.

Schwertmann U and Cornell RM (2000) *Iron Oxides in the Laboratory: Preparation and Characterization*, 2nd edn. Weinheim, Germany: Wiley-VCH.

Schwertmann U, Stanjek H, and Becher H-H (2004) Long-term in vitro transformation of 2-line ferrihydrite to goethite/hematite at 4, 10, 15 and 25 °C. *Clay Minerals* 39: 433–438.

Semple KT, Doick KJ, Jones KC, Burauel P, Craven A, and Harms H (2004) Defining bioavailability and bioaccessibility of contaminated soil and sediment is complicated. *Environmental Science and Technology* 38: 228A–231A.

Shamshuddin J, Muhrizal S, Fauziah I, and Van Ranst E (2004) A laboratory study of pyrite oxidation in acid sulfate soils. *Communications in Soil Science and Plant Analysis* 35(1–2): 117–129.

Shapter JG, Brooker MH, and Skinner WM (2000) Observation of oxidation of galena using Raman spectroscopy. *International Journal of Mineral Processing* 60: 199–211.

Shevenell L, Connors KA, and Henry CD (1999) Controls on pit lake water quality at sixteen open-pit mines in Nevada. *Applied Geochemistry* 14: 669–687.

Sidenko NV, Lazareva EV, Bortnikova SB, Kireev AD, and Sherriff BL (2005) Geochemical and mineralogical zoning of high-sulfide mine-waste at the Berikul mine-site, Kemerovo region, Russia. *The Canadian Mineralogist* 43: 1141–1156.

Sidenko NV and Sherriff BL (2005) The attenuation of Ni, Zn and Cu, by secondary Fe phases of different crystallinity from surface and ground water of two sulfide mine tailings in Manitoba, Canada. *Applied Geochemistry* 20(6): 1180–1194.

Singer PC and Stumm W (1968) Kinetics of the oxidation of ferrous iron. In: *2nd Symposium on Coal Mine Drainage Research*, pp. 12–34. National Coal Association/Bituminous Coal Research.

Singer PC and Stumm W (1970) Acid mine drainage-rate determining step. *Science* 167: 1121–1123.

Slyemi D, Moinier D, Brochier-Armanet C, Bonnefoy V, and Johnson DB (2011) Characteristics of a phylogenetically-ambiguous, arsenic-oxidizing *Thiomonas* sp. (strain 3As). *Archives of Microbiology* 193: 439–449.

Smart R St C, Jasieniak M, Prince KE, and Skinner WM (2000) SIMs studies of oxidation mechanisms and polysulfide formation in reacted sulfide surfaces. *Minerals Engineering* 13: 857–870.

Smeaton C, Fryer J, and Weisener CG (2009) Intracellular precipitation of Pb by Shewanella putrefaciens CN32 during the reductive dissolution of Pb-jarosite. *Environmental Science and Technology* 43: 8091–8096.

Smedley PL and Kinniburgh DG (2002) A review of the source, behaviour and distribution of arsenic in natural waters. *Applied Geochemistry* 17: 517–568.

Smith AML, Dubbin WE, Wright K, and Hudson-Edwards KA (2006) Dissolution of lead- and lead–arsenic-jarosites at pH 2 and 8 and 20 °C: Insights from batch experiments. *Chemical Geology* 229(4): 344–361.

Smyth DJA (1981) *Hydrogeological and Geochemical Studies Above the Water Table in an Inactive Uranium Tailings Impoundment near Elliot Lake, Ontario*. MSc Thesis, University of Waterloo.

Sobek AA (1987) The use of surfactants to prevent AMD in coal refuse and base metal tailings. *Proceedings of Acid Mine Drainage Workshop*, Halifax, Nova Scotia, March 1987, pp. 357–390. Ottawa, ON: Environment Canada.

Sobek AA, Schuller WA, Freeman JR, and Smith RM (1978) Field and laboratory methods applicable to overburdens and minesoils. EPA-600/2-78-954. U.S. Environmental Protection Agency.

Sobolewski A (1996) Metal species indicate the potential of constructed wetlands for long term treatment of metal mine drainage. *Ecological Engineering* 6: 259–271.

Southam G and Beveridge TJ (1992) Enumeration of *Thiobacilli* within pH-neutral and acidic mine tailings and their role in the development of secondary mineral soil. *Applied and Environmental Microbiology* 58: 1904–1912.

Southam G and Beveridge TJ (1994) The in vitro formation of placer gold by bacteria. *Geochimica et Cosmochimica Acta* 58: 4527–4530.

Sparkling DW and Lowe TP (1998) Metal concentrations in aquatic macrophytes as influenced by soil and acidification. *Water, Air, and Soil Pollution* 108: 203–221.

Spears DA (1997) Environmental impact of minerals in UK coals. In: Gayer R and Pešek J (eds.) *European Coal Geology and Technology*, *Geological Society London Special Publication*, vol. 125, 287–295.

Speight JG (1994) *The Chemistry and Technology of Coal*. New York: Marcel Dekker.

Stach E, Mackowsky M-T, Teichmüller M, Taylor GH, Chandra D, and Teichmüller R (1982) *Stach's Textbook of Coal Petrology*. Berlin: Gebrüder Borntraeger.

Steefel CI and Lasaga AC (1994) A coupled model for transport of multiple chemical species and kinetic precipitation/dissolution reactions with application to reactive flow in single phase hydrothermal systems. *American Journal of Science* 294: 529–592.

Steefel CI and van Capellan P (1998) Reactive transport modelling of natural systems. *Journal of Hydrology* 209: 1–7.

Stichbury M-LK, Bain JG, Blowes DW, and Gould WD (2000) Microbially-mediated reductive dissolution of arsenic bearing minerals in a gold mine tailings impoundment. *Proceedings of Fifth International Conference Acid Rock Drainage*, 1 97–103.

Stichbury M, Bechard G, Lortie L, and Gould WD (1995) Use of inhibitors to prevent acid mine drainage. *Proceedings of Sudbury'95Mining and the Environment*2: 613–622.

Stillings LL and Brantley SL (1995) Feldspar dissolution at 25 °C and pH 3: Reaction stoichiometry and the effect of cations. *Geochimica et Cosmochimica Acta* 59: 1483–1496.

Stoffregen RE, Alpers CN, and Jambor JL (2000) Alunite-jarosite crystallography, thermodynamics, and geochronology. In: Alpers CN, Jambor JL, and Nordstrom DK (eds.) *Sulfate Minerals – Crystallography, Geochemistry and Environmental Significance. Reviews in Mineralogy & Geochemistry*, vol. 40, pp. 453–479. Washington, DC: Mineralogical Society of America.

Stohs SJ and Bagchi D (1995) Oxidative mechanisms in the toxicity of metal ions. *Free Radical Biology & Medicine* 18: 321–336.

Stumm W and Sulzberger B (1992) The cycling of iron in natural environments: Considerations based on laboratory studies of heterogeneous redox processes. *Geochimica et Cosmochimica Acta* 56: 3233–3257.

Sverjensky DA (1992) Linear free energy relations for predicting dissolution rates of solids. *Nature* 358: 310–313.

Swaine DJ (1989) Environmental aspects of trace elements in coal. *Journal of Coal Quality* 8: 67–71.

Swaine DJ (1990) *Trace Elements in Coal*. London: Butterworths.

Swash PM and Ellis P (1986) The roasting of arsenical gold ores: A mineralogical perspective. *GOLD 100, Proceedings of International Conference on Gold*. South African Institute of Mining and Metallurgy, vol. 2, pp. 235–257.

Swash PM and Monhemius AJ (1994) Hydrothermal precipitation from aqueous solutions containing iron(III), arsenate and sulphate. In: *Hydrometallurgy '94*. Institute of Mining and Metallurgy and the Society of Chemical Industry, pp. 177–190. England: Chapman & Hall.

Tassé N, Germain MD, and Bergeron M (1994) Composition of interstitial gases in wood chips deposited on reactive tailings – Consequences for their use as an oxygen barrier. In: Alpers CN and Blowes DW (eds.) *Environmental Geochemistry of Sulfide Oxidation*, vol. 550, pp. 631–644. American Chemical Society.

Tempel RG, Shevenell LA, Lechler P, and Price J (2000) Geochemical modeling approach to predicting arsenic concentrations in a mine pit lake. *Applied Geochemistry* 15: 475–492.

Thomas JE, Jones CF, Skinner WM, and Smart RSC (1998) The role of surface sulfur species in the inhibition of pyrrhotite dissolution in acid conditions. *Geochimica et Cosmochimica Acta* 62: 1555–1565.

Thomas JE, Skinner WM, and Smart RSC (2001) A mechanism to explain sudden changes in rates and products for pyrrhotite dissolution in acid solution. *Geochimica et Cosmochimica Acta* 65: 1–12.

Timms GP and Bennett JW (2000) The effectiveness of covers at Rum Jungle after fifteen years. *Proceedings from the Fifth International Conference on Acid Rock Drainage, 2*, pp. 813–818. Society for Mining, Metallurgy, and Exploration, Inc.

Tipping E (1994) WHAM – A chemical equilibrium model and computer code for waters, sediments, and soils incorporating a discrete site/electrostatic model of ion-binding by humic substances. *Computational Geosciences* 20: 973–1023.

Todd EC, Sherman DM, and Purton JA (2003) Surface oxidation of pyrite under ambient atmospheric and aqueous (pH = 2 to 10) conditions: Electronic structure and mineralogy from X-ray absorption spectroscopy. *Geochimica et Cosmochimica Acta* 67: 881–893.

Tossell JA and Vaughan DJ (1987) Electronic structure and the chemical reactivity of the surface of galena. *The Canadian Mineralogist* 25(3): 381–392.

Tributsch H (2001) Direct versus indirect bioleaching. *Hydrometallurgy* 59: 177–185.

Tributsch H and Bennett JC (1981a) Semiconductor-electrochemical aspects of bacterial leaching: II Survey of rate controlling metal sulfide properties. *Journal of Chemical Technology and Biotechnology* 31: 627–635.

Tributsch H and Bennett JC (1981b) Semiconductor-electrochemical aspects of bacterial leaching:I Oxidation of Metal. *Journal of Chemical Technology and Biotechnology* 31: 565–577.

Tributsch H and Rojas-Chapana J (2007) Biological strategies for obtaining energy by degrading sulfide minerals. In: Rawlings DE and Johnson DB (eds.) *Biomining*, pp. 263–280. Heidelberg: Springer-Verlag.

Ueshima M, Fortin D, and Kalin M (2004) Development of iron-phosphate biofilms on pyritic mine waste rock surfaces previously treated with natural phosphate rock. *Geomicrobiology Journal* 21: 313–323.

USDA (1993) Acid drainage from mines on the National Forest: A management challenge. *U.S. Forest Service Publication*. 1505, pp. 1–12.

USEPA (2000) Bioaccumulation testing and interpretation for the purpose of sediment quality assessment. pp. 1–475.

Valković V (1983) *Trace Elements in Coal*, vol. 1. Boca Raton, FL: CRC Press.

Vassilev SV, Kitano K, and Vassileva CG (1996) Some relationships between coal rank and chemical and mineral composition. *Fuel* 75: 1537–1542.

Vaughan DJ and Craig JR (1978) *Mineral Chemistry of Metal Sulfides*. Cambridge: Cambridge University Press.

Velbel MA (1993) Constancy of silicate-mineral weathering-rate ratios between natural and experimental weathering: Implications for hydrologic control of differences in absolute rates. *Chemical Geology* 105: 89–99.

Vigneault B, Campbell PGC, Tessier A, and de Vitre R (2001) Geochemical changes in sulfidic mine tailings stored under a shallow water cover. *Water Research* 35: 1066–1076.

Villalobos M, Bargar J, and Sposito G (2005) Trace metal retention on biogenic manganese oxide nanoparticles. *Elements* 1: 223–226.

Violante A and Pigna M (2002) Competitive sorption of arsenate and phosphate on different clay minerals and soils. *Soil Science Society of America Journal* 68: 1788–1796.

Walker SR, Jamieson HE, Lanzirotti A, Andrade CF, and Hall GEM (2005) The speciation of arsenic in iron oxides in mine wastes from the giant gold mine, N.W.T.: Application of synchrotron micro-XRD and micro-xanes at the grain scale. *The Canadian Mineralogist* 43: 1205–1224.

Walker SR, Parsons MB, Jamieson HE, and Lanzirotti A (2009) Arsenic mineralogy of near-surface tailings and soils: Influences on arsenic mobility and bioaccessibility in the nova scotia gold mining districts. *The Canadian Mineralogist* 47: 533–556.

Walker FP, Schreiber ME, and Rimstidt JD (2006) Kinetics of arsenopyrite oxidative dissolution by oxygen. *Geochimica et Cosmochimica Acta* 70: 1668–1676.

Walter AL, Frind EO, Blowes DW, Ptacek CJ, and Molson JW (1994a) Modelling of multicomponent reactive transport in groundwater. 1. Model development and testing. *Water Resources Research* 30: 3137–3148.

Walter AL, Frind EO, Blowes DW, Ptacek CJ, and Molson JW (1994b) Modelling of multicomponent reactive transport in groundwater. 2. Metal mobility in aquifers impacted by acidic mine tailings discharge. *Water Resources Research* 30: 3149–3158.

Walters S and Bailey A (1998) Geology and mineralization of the Cannington Ag–Pb–Zn deposit: An example of Broken Hill-type mineralization in the Eastern succession, Mount Isa inlier, Australia. *Economic Geology* 93: 1307–1329.

Walton-Day K (1999) Geochemistry of the processes that attenuate acid mine drainage in wetlands. *Reviews in Economic Geology* 6A: 215–228.

Wang WX and Fisher NS (1999) Delineating metal accumulation pathways for marine invertebrates. *Science of the Total Environment* 237/238: 459–472.

Ward CR (1989) Minerals in bituminous coals of the Sydney basin (Australia) and the Illinois basin (U.S.A.). *International Journal of Coal Geology* 13: 455–479.

Warren LA and Haak EA (2001) Biogeochemical controls on metal behaviour in freshwater environments. *Earth-Science Reviews* 54: 261–320.

Waybrant KR, Blowes DW, and Ptacek CJ (1998) Prevention of acid mine drainage using in situ porous reactive walls: Selection of reactive mixtures. *Environmental Science and Technology* 32: 1972–1979.

Waybrant KR, Ptacek CJ, and Blowes DW (2002) Treatment of mine drainage using permeable reactive barriers: Column experiments. *Environmental Science and Technology* 36: 1349–1356.

Waychunas GA, Fuller CC, Rea BA, and Davis JA (1996) Wide angle X-ray scattering (WAXS) study of 'two-line' ferrihydrite structure: Effect of arsenate sorption and counterion variation and comparison with EXAFS results. *Geochimica et Cosmochimica Acta* 60: 1765–1781.

Waychunas GA, Trainor T, Eng P, et al. (2005) Surface complexation studied via combined grazing-incidence EXAFS and surface diffraction: Arsenate on hematite (0001) and (1012). *Analytical and Bioanalytical Chemistry* 383: 12–27.

Weare JH (1987) Models of mineral solubility in concentrated brines with application to field observations. In: Carmichael ISE and Eugster HP HP (eds.) *Thermodynamic Modeling of Geological Materials: Minerals, Fluids and Melts. Reviews in Mineralogy*, vol. 17, pp. 143–176. Mineralogical Society of America.

Webster JG, Swedlund PJ, and Webster KS (1998) Trace metal adsorption onto an acid drainage iron(III) oxy hydroxy sulfate. *Environmental Science and Technology* 23: 1361–1368.

Weisener CG (2002) *The Reactivity of Iron and Zinc Sulfide Mineral Surfaces: Adsorption and Dissolution Mechanisms*. PhD Thesis, University of South Australia.

Weisener CG, Babechuk M, Fryer J, and Maunders C (2008) Microbial biochemical alteration of silver jarosite in mine wastes: Implications for trace metal behavior in terrestrial systems. *Geomicrobiology Journal* 25: 1–10.

Weisener CG, Guthrie J, Smeaton C, Paktunc D, and Fryer J (2011) The effect of Ca-Fe-As coatings on microbial leaching of metals in arsenic bearing mine waste. *Journal of Geochemical Exploration* 110: 23–30.

Weisener CG, Smart RS, and Gerson A (2003) Spectroscopic characterisation of leached sphalerite surfaces as a function of temperature at pH 1. *Geochimica et Cosmochimica Acta* 67: 823–830.

Welham NJ, Malatt KA, and Vukcevic S (2000) The stability of iron phases presently used for disposal from metallurgical systems – A review. *Minerals Engineering* 13(8–9): 911–931.

White WW III, Lapakko KA, and Cox RL (1999) Static-test methods most commonly used to predict acid-mine drainage: Practical guidelines for use and interpretation. In: Plumlee GS and Logsdon MJ (eds.) *The Environmental Geochemistry of Mineral Deposits. Part A: Processes, Techniques, and Health Issues. Reviews in Economic Geology*, vol. 6A, pp. 325–338. Littleton: Society of Economic Geologists.

Wiersma CL and Rimstidt JD (1984) Rates of reaction of pyrite and marcasite with ferric iron at pH 2. *Geochimica et Cosmochimica Acta* 48: 85–92.

Williams M (2001) Arsenic in mine waters: An international study. *Environmental Geology* 40: 267–278.

Williams DJ, Bigham JM, Cravotta CA III, Traina SJ, Andersen JE, and Lyon JG (2002) Assessing mine drainage pH from color and spectral reflectance of chemical precipitates. *Applied Geochemistry* 17: 1273–1286.

Williamson MA and Rimstidt JD (1994) The kinetics and electrochemical rate-determining step of aqueous pyrite oxidation. *Geochimica et Cosmochimica Acta* 58: 5443–5454.

Witzke T (1999) Hydrowoodwardite, a new mineral of the hydrotalcite group from Königswalde near Annaberg, Saxony/Germany and other localities. *Neues Jahrbuch Mineral Monatsh* 75–86.

Wogelius RA and Walther JV (1991) Olivine dissolution at 25oC: Effects of pH, CO_2 and organic acids. *Geochimica et Cosmochimica Acta* 55: 943–954.

World Energy Council (2009) *Survey of Energy Resources Interim Update 2009, 96 p.* ISBN: 0 946121 34 6.

Wunderly MD, Blowes DW, Frind EO, and Ptacek CJ (1996) A multicomponent reactive transport model incorporating kinetically controlled pyrite oxidation. *Water Resources Research* 32: 3173–3187.

Yanful EK and Orlandea MP (2000) Controlling acid drainage in a pyritic mine waste rock. Part II: Geochemistry of drainage. *Water, Air, and Soil Pollution* 124(3–4): 259–284.

Yanful EK and Verma A (1999) Oxidation of flooded mine tailings due to resuspension. *Canadian Geotechnical Journal* 36: 826–845.

Yunmei Y, Yongxuan Z, Williams-Jones AE, Zhenmin G, and Dexian L (2004) A kinetic study of the oxidation of arsenopyrite in acidic solutions: Implications for the environment. *Applied Geochemistry* 19: 435–444.

Zinck JM (1999) Stability of lime treatment sludges. In: *Proceedings of 101st CIM Annual General Meeting,* Calgary, May 1999.

Zipper CE and Skousen JG (2010) Influent water quality affects performance of passive treatment systems for acid mine drainage. *Mine Water Environment* 29: 135–143.

11.6 Radioactivity, Geochemistry, and Health

MD Siegel and CR Bryan, Sandia National Laboratories, Albuquerque, NM, USA

Published by Elsevier Ltd.

Abbreviations

AR	Activity ratio
DDREF	Dose rate effectiveness factor
EAR	Excess absolute risk or rate
ERR	Excess relative risk
ISL	In situ leaching
ISR	In situ recovery
LET	Linear energy transfer
LNT	Linear no-threshold
LOAEL	Lowest observed adverse-effect level
MCL	Maximum contaminant level
MNA	Monitored natural attenuation
MRL	Minimum risk level
NA	Natural attenuation

NEM	Nonelectrostatic model
NOAEL	No-observed adverse-effect Level
NORM	Naturally occurring radioactive materials
PDI	Potential determining ion
RfD	Reference dose
SCM	Surface complexation model
SIT	Specific interaction theory
TENORM	Technologically enhanced naturally occurring radioactive material
TLM	Triple-layer model
UMT	Uranium mill tailings

Nomenclature

C_L	Concentration of contaminant in solution
C_S	Concentration of contaminant sorbed onto solid
D	Dose
D_0	Dose at time 0
H	Equivalent dose; $H = D \times w_r$
HE	Effective dose; $\mathrm{HE} = w_t \times (D \times w_r)$
K_d	Distribution of sorption coefficient
R_d	Sorption ratio (equivalent to K_d)
T_r	Radiologic half-life
T_b	Biological half-life
T_{eff}	Effective half-life; $T_{eff} = (T_r + T_b)/(T_r \times T_b)$
w_r	Radiation weighting factor
w_t	Tissue weighting factor
ρ	Bulk density of a porous medium
θ	Porosity

11.6.1 Introduction

11.6.1.1 Approach and Outline of Chapter

In the decade that has passed between the first edition of the Treatise on Geochemistry and the current second edition, a number of events have impacted the direction of research into the nature of radioactive contamination in the environment. The attack on the Twin Towers of the World Trade Center in September 2001 led to increased concerns over the risks posed by terrorists who might use nuclear bombs or 'dirty' bombs as weapons of mass destruction or 'mass distraction' for political purposes. New drinking-water regulations and exploitation of deep groundwater aquifers led to new interest in the occurrence of naturally occurring radioactive materials (NORM), including radium, in brackish waters. The occurrence of these radionuclides in waters associated with coalbed methane resources has led to concerns about the safe disposal of radioactive wastes associated with new fossil fuel sources. The growing consensus that nuclear power must play a significant role in energy policy in the twenty-first century has raised concerns about the risks associated with the front and back ends of the nuclear fuel cycle, and with the safety of reactor operations. Previous uranium mining efforts in the United States (US) and elsewhere have left a legacy of abandoned mining sites posing environmental hazards and worker health problems. Since 1987, the US repository program for spent nuclear fuel (SNF) has focused on a single proposed site, Yucca Mountain in Nevada, and the US Department of Energy (DOE) submitted a license application for the site to the Nuclear Regulatory Commission (NRC) in June 2008 (DOE, 2008). However, in early 2010, the DOE initiated legal steps to withdraw the license application, and at the time of this writing, the future of the program is in question and is being addressed through administrative, legal, and congressional forums. The decision to withdraw the license application has left the US without a clear plan for disposal of these wastes. Finally, the release of radioactive contamination associated with damage done to the Fukushima nuclear reactors in Japan in March 2011 by an earthquake and tsunami raised concerns about radionuclide transport and the resulting health effects in exposed populations.

This review addresses three major questions:

1. What are the major sources of radioactive contamination on the planet?
2. What controls radionuclide migration in the environment?
3. What are the likely impacts of exposure to radioactive contamination on human health?

This chapter is divided into two major sections. The first part of the chapter updates the basic geochemical and environmental data on radionuclide behavior obtained from research carried out from 2002 to 2011. Recent studies of radionuclide speciation, solubility, and sorption are reviewed, drawing upon the major US and European nuclear waste and remediation programs. The second half of the chapter focuses on three applications of this information: (1) NORM associated with drinking water resources or deep brackish waters, (2) radioactive contamination resulting from uranium mining, and (3) contamination associated with historical nuclear activities such as nuclear weapons production or nuclear waste disposal. Table 1 describes the groups of radionuclides discussed in this chapter and also shows their relative importance to each of these areas. For each application, data on natural occurrence, the major sources of contamination, important geochemical processes controlling distribution and transport of the key radionuclides, and environmental epidemiological studies describing the association between exposure and human health are reviewed. In addition, appendices providing more detailed information on health physics and toxicology, relevant to exposure to radioactive contamination, have been included.

11.6.1.2 Previous Reviews and Scope of the Chapter

This review emphasizes scientific work from the period 1990 to 2011, but it is recognized that any overview of the 'current' state of knowledge will likely be outdated before it is

Table 1 Radionuclide groups and relative importance for occurrence as discussed in this chapter

Radionuclide or radionuclide groups	*Drinking water*	*Mining*	*Waste management weapons production and nuclear accidents*
Radium and progeny	M	M	m
Thorium	N	m	M
Uranium	M	M	M
Transuranics	N	n	M
Fission products	N	n	M

M, major importance; m, minor importance; n, relatively not important.

published. Several major books have been written on the subject of radionuclide chemistry; notable ones include Seaborg and Katz (1954), Katz et al (1986), Ivanovich (1992), and Choppin et al. (1995). This chapter updates similar literature reviews that have been published in the last few decades, such as those by Allard (1983), Krauskopf (1986), Choppin and Stout (1989), Hobart (1990), Kim (1993), Silva and Nitsche (1995), Murphy and Shock (1999), Szabó et al. (2006), and Choppin (2007), and chapters in Barney et al. (1984), Langmuir (1997), Zhang and Brady (2002), and Morss et al. (2007). Recently, the US Environmental Protection Agency (EPA) published a 3-volume set of reports dealing with monitored natural attenuation (MNA) for metals and radionuclides (EPA, 2010). Volume 3 in the series (*Monitored Natural Attenuation of Inorganic Contaminants in Ground Water Volume 3 Assessment for Radionuclides Including Tritium, Radon, Strontium, Technetium, Uranium, Iodine, Radium, Thorium, Cesium, and Plutonium–Americium)* contains a fairly comprehensive review of radioactive decay chains, occurrence, speciation, solubility, and adsorption properties of the radionuclides.

This chapter focuses on the interactions of radionuclides with geomedia in near-surface low-temperature environments. Because of the importance of uranium mining to this topic, a brief overview of the mineralogy or economic geology of uranium deposits is included; the reader is referred to the series of review articles describing the mineralogy and paragenesis of uranium deposits and the environmental geochemistry of uranium and decay products published by the Mineralogical Society of America (Burns and Finch, 1999). The use of radium and uranium isotopes as environmental tracers is briefly described; however, an adequate treatment of the use of radionuclides in studies of the atmosphere, hydrosphere, or lithosphere is not provided here. Similarly, an exhaustive overview of the nuclear fuel cycle or weapons production is not discussed. The interested reader is advised to turn to other excellent general summaries of these topics and included references, for example, Eisenbud (1987). National symposia dealing with the disposal of nuclear waste and remediation of radioactive environmental contamination have been held annually by the Material Research Society (e.g., see Smith et al., 2010) and the American Nuclear Society (ANS) (see, e.g., ANS, 2011) for the last three decades. In this chapter, only limited information is provided about the role of microbes in the biogeochemistry of uranium and the actinides. Chapelle (1993) and Konhauser (2007) provide more comprehensive treatments of microbial growth, metabolism, and ecology for geoscience applications.

This chapter supplements and does not repeat the information presented in the corresponding chapter in the First Edition of the Treatise on Geochemistry Siegel and Bryan (2003). Much of the basic information describing methods in speciation, solubility and sorption experiments, and thermodynamic or reactive transport modeling is not repeated here. In addition, due to limitations in space, no update is given on recent work concerning colloid transport of radionuclides and only a cursory overview of studies of natural analogs for candidate nuclear waste disposal sites is provided. Finally, in Siegel and Bryan (2003), considerable attention is devoted on how geochemical studies were used in support of performance assessment calculations for the Waste Isolation Pilot Plant (WIPP) for transuranic (TRU) wastes and the proposed high-level waste (HLW) repository at Yucca Mountain. That information is not repeated here and is only briefly updated; comprehensive updates to those approaches can be found in the Yucca Mountain license application submitted to the NRC (DOE, 2008) and supporting documents (e.g., SNL, 2007a,b).

11.6.2 Radioactive Processes and Sources

11.6.2.1 Radioactive Processes

Only certain combinations of protons and neutrons result in stable atomic nuclei. **Figure 1** shows a section of the chart of the nuclides, on which nuclides are plotted as a function of their proton number (Z) and neutron number (N). The radioactive decay chain for ^{238}U is indicated; only ^{206}Pb has a stable combination of protons and neutrons. At low atomic numbers (below $Z=20$), isotopes with proton–neutron ratios of approximately 1 are stable, but a progressively higher proportion of neutrons is required to produce stability at higher atomic numbers. Unstable nuclei undergo radioactive decay – spontaneous transformations involving emission of particles and/or photons, resulting in changes in Z and N, and transformation of that atom into another element. Several types of radioactive decay may occur:

- β^- decay – a negatively charged beta particle (electron) and an antineutrino are emitted from the nucleus of the atom, and one of the neutrons is transformed into a proton. Z increases by 1 and N decreases by 1.
- β^+ decay – a positively charged beta particle (positron) and a neutrino are emitted from the nucleus, and a proton is transformed into a neutron. Z decreases by 1 and N increases by 1.
- Electron capture – an unstable nucleus may capture an extranuclear electron, commonly a K-shell electron, resulting in the transformation of a proton to a neutron. This results in the same change in Z and N as β^+ decay and commonly, nuclides with a deficiency of neutrons can decay by either mechanism.
- α decay – nuclei of high atomic number (heavier than cerium), and a few light nuclides, may decay by emission of an α particle, a ^{4}He nucleus consisting of two protons and two neutrons. Z and N both decrease by 2.

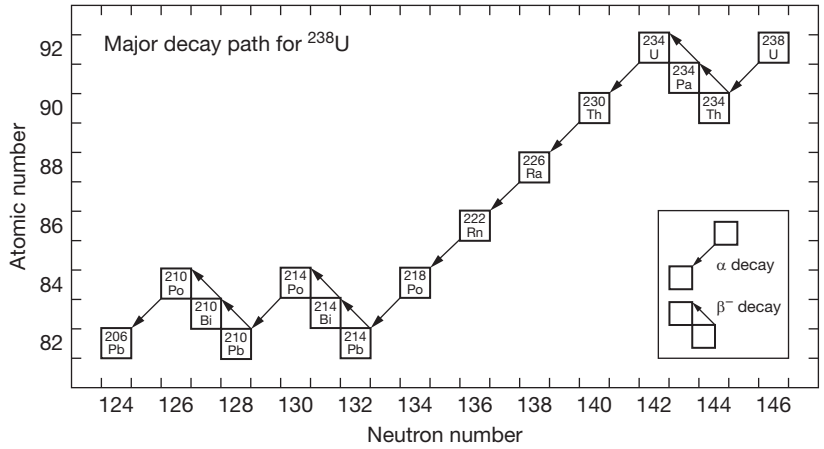

Figure 1 The major decay path for ^{238}U. A small fraction of decays will follow other possible decay paths – for example, decaying by β^- emission from ^{218}Po to ^{218}At, and then by α emission to ^{214}Bi – but ^{206}Pb is the stable end product in all cases.

Table 2 The major decay paths for several important actinides (isotope, half-life, and decay mode)

^{238}U decay series			*^{235}U decay series*			*^{232}Th decay series*			*^{237}Np decay series*		
^{238}U	4.47×10^9 years	α	^{235}U	7.04×10^8 years	α	^{232}Th	1.40×10^{10} years	α	^{237}Np	2.14×10^6 years	α
^{234Th}	24.1 days	β^-	^{231}Th	1.06 days	β^-	^{228}Ra	5.76 years	β^-	^{233}Pa	27.0 days	β^-
^{234}Pa	1.17 m	β^-	^{231}Pa	3.28×10^4 years	α	^{228}Ac	6.15 h	β^-	^{233}U	1.59×10^5 years	α
^{234}U	2.46×10^5 years	α	^{227}Ac	21.8 years	β^-	^{228}Th	1.91 years	α	^{229}Th	7.30×10^3 years	α
^{230Th}	7.54×10^4 years	α	^{227}Th	18.7 days	α	^{224}Ra	3.66 days	α	^{225}Ra	14.9 days	β^-
^{226}Ra	1.60×10^3 years	α	^{223}Ra	11.4 days	α	^{220}Rn	55.6 s	α	^{225}Ac	10.0 days	A
^{222}Rn	3.82 days	α	^{219}Rn	3.96 s	α	^{216}Po	0.145 s	α	^{221}Fr	4.8 m	A
^{218}Po	3.10 m	α	^{215}Po	1.78×10^{-3} s	α	^{212}Pb	10.6 h	β^-	^{217}At	3.2×10^{-2} s	A
^{214}Pb	27.0 m	β^-	^{211}Pb	36.1 m	β^-	^{212}Bi	1.01 h	β^-	^{213}Bi	45.6 m	β^-
^{214}Bi	19.9 m	β^-	^{211}Bi	2.14 m	α	^{212}Po	45 s	α	^{213}Po	3.8×10^{-6} s	A
^{214}Po	1.64×10^{-4} s	α	^{207}Tl	4.77 m	β^-	^{208}Pb	Stable		^{209}Pb	3.25 h	β^-
^{210}Pb	22.3 years	β^-	^{207}Pb	Stable					^{209}Bi	Stable	
^{210}Bi	5.01 days	β^-									
^{210}Po	138 days	α									
^{206}Pb	Stable										
^{239}Pu decay series			^{238}Pu decay series			^{241}Am decay series					
^{239}Pu	2.41×10^4 years	α	^{238}Pu	87.7 years	α	^{241}Am	432.7 years	α			
^{235}U	As above		^{234}U	As above		^{237}Np	As above				

Source: Baum et al. (2002).

In each case, the daughter nucleus is commonly left in an excited state and decays to the ground state by emission of gamma rays. If there is a significant delay between the two processes, the γ emission is considered a separate event. Decay by γ emission, resulting in no change in Z or N, is called an isomeric transition (e.g., decay of ^{99m}Tc to ^{99}Tc).

Many radioactive elements decay to produce unstable daughters. The radioactivity of many forms of radioactive contamination is primarily owing to daughter products with short half-lives. The longest such decay chains that occur naturally are those for ^{238}U, ^{235}U, and ^{232}Th, which decay through a series of intermediate daughters to ^{206}Pb, ^{207}Pb, and ^{208}Pb, respectively (see **Table 2**). The decay of ^{238}U to ^{206}Pb results in the production of eight alpha particles and six beta particles; that of ^{235}U to ^{207}Pb, seven alpha and four beta particles; and that of ^{232}Th to ^{208}Pb, six alpha and four beta particles. Thus, understanding the geochemistry of radioactive contamination requires consideration of the chemistries of both the abundant parents and of the transient daughters, which have much lower chemical concentrations. After several half-lives of the longest-lived intermediate daughter, a radioactive parent and its unstable daughters will reach secular equilibrium, and the contribution of each nuclide to the total radioactivity will be the same. Thus, a sample of ^{238}U will, after about a million years, have a total α activity that is about eight times that of the uranium alone.

Heavy nuclei can also decay by *fission*, by splitting into two parts. Although some nuclei can spontaneously fission, most require an input of energy. This is most commonly accomplished by absorption of neutrons, although alpha particles, gamma rays, and even x-rays may also induce fission. Fission is usually asymmetric – two unequal nuclei, or *fission products*, are produced, with atomic numbers ranging from 66 to 172.

Fission product yields vary with the energy of the neutrons inducing fission; under reactor conditions, fission is highly asymmetric, with production maxima at masses of ~95 and ~135. High-energy neutrons result in more symmetric fission with a less bimodal distribution of products.

Fission products generally contain an excess of neutrons and are radioactive, decaying by successive β^- emissions to stable nuclides. The high radioactivity of SNF and of the wastes generated by fuel reprocessing for nuclear weapons production is largely owing to fission products, and decreases rapidly over the first few tens of years. In addition to the daughter nuclei, neutrons are released during fission (2.5–3 neutrons per fission event for thermal neutrons), creating the potential for a fission chain reaction – the basis for nuclear power and nuclear weapons.

The basic unit of measure for radioactivity is the number of atomic decays per unit time. In the International System of Units (Système international d´unités, or SI) system, this unit is the Becquerel (Bq), defined as one decay per second. An older, widely used measure of activity is the Curie (Ci), equal to 3.7×10^{10} Bq. The units used to describe the dose, or energy absorbed by a material exposed to radiation, are dependent upon the type of radiation and the material. The dose absorbed by any material, by any radiation, is measured in rads (radiation-absorbed dose), where1 rad corresponds to 100 ergs per gram of absorbed energy. The SI equivalent is the Gray (Gy), which is equal to 100 rads. Historically, the unit describing biological damage is the rem (roentgen-equivalent man). The dose in rem is equal to the dose in rad multiplied by a quality factor, which varies with the type of radiation. The SI unit for equivalent dose is the Sievert (Sv), which is equivalent to 100 rem. Further details on the biological effects of radiation can be found in **Appendix A** of this chapter.

11.6.2.2 Overview of Radioactive Sources and Exposure

11.6.2.2.1 Natural sources of radioactivity

Radioactive materials have been present in the environment since the accretion of the earth. The decay of radionuclides provides an important source of heat that drives many of the large-scale earth processes. The most abundant naturally occurring radionuclides are ^{40}K, ^{232}Th, ^{238}U, and ^{235}U. Average crustal concentrations of uranium (mostly 238) and thorium (mostly 232) are 2.7 and 9.6 $\mu g\, g^{-1}$, respectively. Both elements are enriched in silicate-rich igneous rocks (4.4 and 16 $\mu g\, g^{-1}$, respectively, in granites) and are highly enriched in zircons (2000 and 2500 $\mu g\, g^{-1}$ respectively). In groundwater, average uranium concentrations range from <0.1 (reducing) to 100 $\mu g\, l^{-1}$ (oxidizing) (Langmuir, 1997). The average thorium concentration in groundwater is <1 $\mu g\, l^{-1}$ and is not affected by solution redox conditions.

The major decay paths for the naturally occurring isotopes of uranium and thorium are shown in **Table 2**. Other actinides of environmental importance include ^{237}Np, ^{238}Pu, ^{239}Pu, and ^{241}Am. These have decay series similar to and overlapping those of uranium and thorium. ^{237}Np ($t_{1/2} = 2.14 \times 10^6$ years, α) decays to ^{209}Bi through a chain of intermediates, emitting seven α and four β^- particles. ^{238}Pu ($t_{½} = 86$ years, α) decays into ^{234}U, an intermediate daughter on the ^{238}U decay series. ^{239}Pu ($t_{1/2} = 2.44 \times 10^4$ years, α) decays into ^{235}U. ^{241}Am ($t_{1/2} = 458$ years, α) decays into ^{237}Np. Small amounts of actinides (^{237}Np and ^{239}Pu) occur naturally owing to neutron capture reactions with ^{238}U.

Other naturally occurring radionuclides include actinium, technetium, and protactinium. Natural ^{99}Tc is a product of ^{238}U spontaneous fission (Curtis, 1999). The bulk of the natural global inventory of actinide radioactivity in the upper 100 m of the lithosphere (about 10^{22} Bq, or 2.7×10^{11} Ci) is owing to activity of uranium and thorium isotopes (Ewing, 1999; Santschi and Honeyman, 1989). This is about equal to the total activity of ^{40}K in the world ocean. **Table 2** in Siegel and Bryan (2003) provides additional examples of large-scale sources of natural and anthropogenic radioactivity in the environment throughout the world.

11.6.2.2.2 Nuclear waste

There are several classes of nuclear waste; each type is regulated by specific environmental regulations and each has a preferred disposal option.

Spent fuel (SF) consists of irradiated fuel elements removed from commercial reactors or special fuels from test reactors. It is highly radioactive and generates a lot of heat; therefore, remote handling and heavy shielding are required. It is considered a form of HLW because of the uranium, fission products, and transuranics that it contains. HLW includes highly radioactive liquid, calcined or vitrified wastes generated by reprocessing of SF. Until the project was terminated, both SF and HLW from commercial reactors were to be entombed in the geological repository at Yucca Mountain about 100 miles northwest of Las Vegas, Nevada. At the turn of the twentieth century, it was estimated that the inventory of nuclear reactor waste in the US would reach 1.3×10^{21} Bq by 2020 (Ewing, 1999). Initially, the bulk of the radioactivity is owing to short-lived radionuclides ^{137}Cs and ^{90}Sr. After 1000 years, the bulk of the radioactivity is owing to the decay of ^{241}Am, ^{243}Am, ^{239,240}Pu, and ^{237}Np. At longest time periods, a mixture of the isotopes ^{129}I, ^{210}Pb, and ^{226}Ra dominate the smaller amount of radioactivity that remains (Campbell et al., 1978). Disposal of HLW and SF in the US is regulated by 40 CFR Part 191 (EPA, 2001) and 10 CFR Part 60 (NRC, 1983). Current regulations focus on the time period up to 10 000 and 1 000 000 years after emplacement, when radioactivity is dominated by the decay of isotopes of americium, neptunium, and plutonium, and the long-lived fission products ^{129}I and ^{99}Tc.

Transuranic waste (TRU) is defined as waste contaminated with alpha-emitting radionuclides of atomic number greater than 92 and half-life greater than 20 years in concentrations greater than 100 nCi g^{-1} (3.7×10^3 Bq g^{-1}). TRU is primarily a product of the reprocessing of SF and the use of plutonium in the fabrication of nuclear weapons. In the US, the disposal of TRU at the WIPP in Southeastern New Mexico (NM) is regulated by 40 CFR Part 194 (EPA, 1996).

Uranium mill tailings (UMT) are large volumes of radioactive residues that result from the processing of uranium ore. In the US, the DOE has the responsibility for remediating mill-tailing surface sites and associated groundwater under the Uranium Mill Tailings Radiation Control Act (UMTRCA) of 1978 and its modification in 1988. *LLW* are radioactive wastes not classified as HLW, TRU, SF, or uranium mill tailings. They are generated by institutions and facilities using radioactive

materials and may include lab waste, towels, and lab coats contaminated during normal operations. Disposal of LLW is governed by agreements between states through state compacts at several facilities in the continental US Geochemical data; conceptual models and performance assessment methodologies relevant to LLW are summarized in Serne et al. (1990).

NORM includes radionuclides that are naturally present in the rocks and minerals of the earth's crust and cosmogenic radionuclides in the atmosphere and crust by cosmic rays. The principal 'primordial' radionuclides are isotopes of heavy elements belonging to the radioactive series headed by the three long-lived isotopes ^{238}U (uranium series), ^{235}U (actinium series), and ^{232}Th (thorium series). The principal radionuclide of concern in NORM is ^{226}Ra, a member of the uranium series.

Technologically Enhanced Naturally Occurring Radioactive Material (TENORM) is produced when NORM is concentrated or exposed to the environment by activities such as mineral extraction, purification, or waste treatment. Of significant importance are wastes produced by uranium and phosphate mining, coal ash generation, geothermal energy production, and municipal drinking water treatment. Radionuclide concentrations in TENORM are often orders of magnitude higher than in the parent NORM.

11.6.2.2.3 Sites of radioactive environmental contamination

In the US and other countries, radioactive contamination is of particular importance in the vicinity of nuclear weapons production sites, near proposed or existing nuclear waste disposal facilities, and in areas where uranium mining was carried out. In Europe and the Former Soviet Union (FSU), large areas have been contaminated by nuclear weapons production and uranium mining. The extent of contamination in the FSU is greater than in the US because of less strict regulations on the control of nuclear materials and mining. **Section 11.6.2.2** provides details about the nature of geochemical processes important for UMTs and in situ uranium mining. The US DOE estimates that nuclear weapons production activities have led to radioactive contamination of approximately 63 million cubic meters of soil and 1310 million cubic meters of groundwater in the US (DOE, 1997a,b). The contamination is located at 64 DOE environmental management sites in 25 states. The Hanford Reservation in Washington State provides a good example of the diverse sources of radioactive contamination associated with weapons production. At this site, nine plutonium production reactors were built in the 100 Area; HLWs are stored in buried tanks in the 200 Area where SF was processed; and nuclear fuel was fabricated in the 300 Area. A complex mixture of radioactive and hazardous wastes is either stored in aging underground tanks or has been discharged to seeps or trenches and to the vadose zone in surface impoundments. The total inventory at the Hanford Site is estimated to be 360–370 MCi (1.33×10^{19}–1.37×10^{19} Bq); between 0.22 and 6.5 MCi (8.1×10^{15}–2.4×10^{17} Bq) has been released to the ground (National Research Council, NRC, 2001). The status of efforts to remediate this contamination can be found in DOE (2006).

Naturally occurring uranium deposits have been an important source of information on the long-term behavior of actinides and fission products in the environment. Important sites of natural radioactivity (natural analogs) include the Pena Blanca deposit (Murphy, 1999; Pearcy et al., 1994), the Alligator River Region (Davis, 2001; Duerden et al., 1992; Payne et al., 1992), Cigar Lake (Curtis, 1999; Vilks et al., 1993), and the Oklo natural reactor (Brookins, 1990; Jensen and Ewing, 2001; Pourcelot and Gauthier-Lafaye, 1999). For a detailed summary of work in this area with applications to high-level nuclear waste disposal,the reader is referred to Simmons and Stuckless (2010).

11.6.2.2.4 Exposure to background and anthropogenic sources of radioactivity

Exposure to natural sources of radon (produced in the decay chain of crustal ^{238}U) averages 2 mSv year^{-1} while other natural sources account for 1 mSv year^{-1} (NRC, 1995). Total exposure to anthropogenic sources averages about 0.6 mSv year^{-1}, with medical x-ray tests accounting for about two thirds of the total. The average exposure related to the nuclear fuel cycle is estimated to be less than 0.01 mSv year^{-1} and is comparable to that associated with the release of naturally occurring radionuclides from the burning of coal in fossil-fuel plants (Ewing, 1999; McBride et al., 1978). At the other end of the range of exposures are those associated with nuclear blasts and reactor leaks. Details on exposures to the blast and fallout from nuclear detonations at Hiroshima and Nagasaki, the dose to workers involved in the cleanup of Chernobyl nuclear power plant after the 1986 accident, and the radiation dose on the shores of Lake Karachay near the Chelyabinsk-65 complex are discussed in more detail in **Section 11.6.4.3.4** and **Appendix A**.

11.6.3 Radionuclide Geochemistry: Principles and Methods

Analysis of the risk from radioactive contamination requires consideration of the release rates and rate of dispersion of the radioactive contamination through potential exposure pathways. Information about the specific activity and decay chain of the radioactive material, the physical and chemical nature of the host phase, and accessibility to environmental transport are all needed to convert the amounts of radioactivity of the source to estimates of the exposure to humans.

Prediction of the fate of radionuclides released from a contaminated area must consider a series of processes including (1) contact of the radioactive source with groundwater, and release of aqueous species and particulate matter, (2) transport of aqueous species and colloids through the saturated zone, the vadose zone, or the atmosphere, and (3) uptake of radionuclides by exposed populations or ecosystems. The chemistry of the radionuclides will control their transport properties by controlling their solubility, speciation, sorption, and transport by particulates. These are strong functions of the compositions of the groundwater and geomedia and the atomic structure of the radionuclides. Simplifications in predictions of radionuclide mobility are difficult to make; instead, site-specific measurements and thermodynamic calculations for the site-specific conditions are needed to make meaningful statements about radionuclide behavior. A wide variety of experimental techniques are used in radiochemical studies; a review of this subject is beyond the scope of this chapter. The interested reader should refer to the reviews and textbooks of actinide chemistry listed in **Sections 11.6.1.2** and **11.6.3.1**. Some

general points, which should be considered in evaluating available data relevant to environmental radioactive contamination, are described in Siegel and Bryan (2003) and are summarized briefly below.

11.6.3.1 Aqueous Speciation and Solubility

11.6.3.1.1 Experimental studies

Good summaries of accepted experimental techniques can be found in the references that are cited for individual radionuclides in the sections below. Nitsche (1991) provides a useful general summary of the principles and techniques of solubility studies. A large number of techniques have been used to characterize the speciation of radionuclides. These include potentiometric methods, optical absorbance, and vibrational spectroscopy. Silva and Nitsche (1995) summarize the use of conventional optical absorption and laser-based photothermal spectroscopy for detection and characterization of solution species and provide an extensive citation list. A recent review of the uses of Raman and infrared spectroscopy to distinguish various uranyl hydro complexes is given by Tsushima et al. (2007).

Extraction techniques to separate oxidation states and complexes are combined with radiometric measurements of various fractions. A series of papers by Choppin and coworkers referenced below provides good descriptions of these techniques; see, for example, Caceci and Choppin (1983) and Schramke et al. (1988). Cleveland and coworkers used a variety of extraction techniques to characterize the speciation of plutonium, neptunium, and americium in natural waters (Cleveland and Rees, 1981; Cleveland et al., 1983a,b; Rees et al., 1983).

A variety of methods have been used to characterize the solubility-limiting radionuclide solids and the nature of sorbed species at the solid/water interface in experimental studies. Electron microscopy and standard x-ray diffraction techniques can be used to identify some of the solids from precipitation experiments. X-ray absorption spectroscopy can be used to obtain structural information on solids and is particularly useful for investigating noncrystalline and polymeric actinide compounds that cannot be characterized by x-ray diffraction analysis (Silva and Nitsche, 1995). X-ray absorption near-edge spectroscopy can provide information about the oxidation state and the local structure of actinides in solution, in solids, or at the solution/solid interface. Many of the surface spectroscopic techniques have been reviewed by Bertsch and Hunter (2001) and Brown et al. (1999). Rai and coworkers have carried out a number of experimental studies of solubility and speciation of plutonium, neptunium, americium, and uranium that illustrate combinations of various solution and spectroscopic techniques (Felmy et al., 1989, 1990; Rai et al., 1980, 1997, 1998; Xia et al., 2001).

11.6.3.1.2 Aqueous speciation and solubility models

Several geochemical codes are commonly used for calculations of radionuclide speciation and solubilities. Reviews of the codes can be found in Serne et al. (1990), Mangold and Tsang (1991), Nuclear Energy Agency (NEA, 1996), and US EPA (1999a). Extensive databases of thermodynamic property values and kinetic rates are required for these codes and several such databases for the actinides have been developed over the last three decades. Of historical importance are the compilations and reviews of Lemire and Tremaine (1980), Phillips et al. (1988), and Fuger et al. (1990). Comprehensive and consistent databases have been based on compilations produced by the NEA for plutonium and neptunium (Lemire et al., 2001), americium (Silva et al., 1995), uranium (Grenthe et al., 1992), and technetium (Rard et al., 1999). These books contain suggested values for ΔG, ΔH, C_p, and log K_f for formation reactions of radionuclide species. More recent publications often use these compilations as reference and add additional parameter values or correct errors (Guillaumont et al., 2003; Van der Lee and Lomenach, 2004). Ideally, as new species are identified or suspect ones eliminated and as constants of previously recognized species are revised, the entire reaction network should be used to rederive all of the constants (Grenthe et al., 1992; Wagman et al., 1982). The NEA Thermochemical Data Base (TDB) Project (http://www.oecd-nea.org/databank/access.html) provides information about the latest self-consistent database maintained by this organization.

For most solubility and speciation studies, calculations of the activity coefficients of aqueous species are required. For waters with relatively low ionic strength (0.01–0.1 molal), simple corrections such as the Debye Huckel relationships are used (Langmuir, 1997, p. 127). This model accounts for the electrostatic, nonspecific, long-range interactions between water and the solutes. At higher ionic strengths, short-range interactions must be taken into account. The NEA has developed a database for ionic strengths up 3.0 molal based on the specific interaction theory (SIT) approach of Bronsted (1922), Scatchard (1936), and Guggenheim (1966). It has been used to obtain equilibrium constants and free energies for the NEA databases (Grenthe et al., 1992; Lemire et al., 2001; Rard et al., 1999; Silva et al., 1995). In some cases, the US DOE has used the more complex Pitzer for calculations of radionuclide speciation and solubility in its Nuclear Waste Management Programs. This model includes concentration-dependent interaction terms and is valid up to ionic strengths greater than 10 molal.

11.6.3.2 Sorption

11.6.3.2.1 Experimental studies

Several different approaches have been used to measure sorption of radionuclides by geomedia. These include (1) the laboratory batch method, (2) the laboratory flowthrough (column) method, and (3) the in situ field batch sorption method. Laboratory batch tests are the simplest experiments; they can be used to collect distribution coefficient (K_d) values or other partitioning coefficients to parameterize sorption and ion exchange models. (The term sorption is often used to describe a number of surface processes including adsorption, ion exchange, and coprecipitation that may be included in the calculation of a K_d. For this reason, some geochemists use the term sorption ratio (R_d) instead of distribution coefficient (K_d) to describe the results of batch sorption experiments. In this chapter, both terms are used in order to be consistent with the terminology used in the original source of information summarized.) The different sorption models are summarized in **Section 11.6.3.2.2**.

Descriptions of the *batch techniques* for radionuclide sorption and descriptions of calculations used to calculate

distribution coefficients can be found in ASTM (2010), Park et al. (1992), Siegel et al. (1995a), and US EPA (1999a).

In batch systems, the distribution or sorption coefficient (K_d or R_d) describes the partitioning of a contaminant between the solid and liquid phases. The K_d is commonly measured under equilibrium or at least steady-state conditions, unless the goal of the experiment is to examine the kinetics of sorption. It is defined as follows:

$$K_d(\text{ml g}^{-1}) = \frac{C_S}{C_L}, \quad [1]$$

where C_S is the concentration of the contaminant on the solid and C_L is the concentration in solution.

Measured batch K_d values can be used to calculate a retardation factor (R), which describes the ratio of the rate of groundwater movement to the rate of radionuclide movement:

$$R = 1 + \frac{K_d \rho}{\theta}, \quad [2]$$

where ρ is the bulk density of the porous medium and θ is the porosity. This equation can be rearranged, and contaminant retardation values measured from column breakthrough curves can be used to calculate K_ds.

Many published data from batch sorption measurements are subject to a number of limitations as described by Siegel and Erickson (1984, 1986), Serne and Muller (1987), and by US EPA (1999a). These include a solution:solid ratio that is much higher than that present in natural conditions, an inability to account for multiple sorbing species, an inability to measure different adsorption and desorption rates and affinities, and an inability to distinguish between adsorption and coprecipitation.

Batch methods are also used to collect data used to calculate equilibrium constants for surface complexation models (SCMs). Commonly for these models, sorption is measured as function of pH and the surface charge of the geomedia. The proton is the surface potential determining ion (PDI) of oxyhydroxides of iron and manganese and of the high-energy edge sites in aluminosilicates. Considerable data have been collected describing the influence of pH on sorption of radionuclides. Sorption edges are most commonly (and usefully) given for single oxidation states of the radionuclide. Comparisons of sorption edges for different radionuclides on the same substrate or for a single radionuclide on several substrates can be made by referring to their pH_{50} values (the pH at which 50% of the radionuclide is adsorbed). Radionuclides that form weaker surface complexes can only sorb appreciably when the concentration of competing protons is low (high pH) and therefore have high pH_{50} values. For example, Kohler et al. (1992) show that goethite strongly sorbs Np(V) from $NaClO_4$ solutions while quartz only weakly sorbs Np(V). The pH_{50} sorption values for Np(V) decrease in the order goethite < hematite < gibbsite < albite < quartz.

A variety of methods have been used to characterize the nature of sorbed species at the solid/water interface in experimental studies. Surface spectroscopy techniques such as extended x-ray absorption fine structure spectroscopy have been used to characterize uranyl and neptunyl complexes sorbed onto oxides/hydroxides and clays (Arai et al., 2007; Bargar et al., 1999, 2000; Chisholm-Brause et al., 1992, 1994; Combes et al., 1992; Dent et al., 1992; Duff et al., 2002). The information obtained from surface spectroscopy can help constrain the interpretation of the results for batch sorption tests by revealing the stoichiometry of the sorbed species.

Laboratory column tests are more difficult to perform but overcome some of the limitations of batch tests. Proper design, descriptions of experimental procedures and methods of data interpretation for column tests can be found in EPA (1999a), Relyea (1982), Van Genuchten, and Wierenga (1986), Triay et al. (1992, 1993, 1996c), Torstenfelt et al. (1985a,b), Siegel et al. (1995b), Sims et al. (1996), and Gabriel et al. (1998). In these experiments, the concentration of the radionuclide in the column effluent is monitored to obtain a breakthrough curve; the shape of the curve provides information about sorption equilibrium and kinetics and other properties of the crushed rock or intact rock column. In situ (field) batch sorption tests use measurements of the radionuclide contents of samples of rock cores and consanguineous pore water obtained at a field site. Applications of this technique are described in Jackson and Inch (1989), McKinley and Alexander (1993), Read et al. (1991), Ward et al. (1990), and Payne et al. (2001).

11.6.3.2.2 Sorption models

The available approaches to describing sorption have different levels of complexity and robustness, and include:

1. Linear sorption (K_d or R_d).
2. Nonlinear sorption (Freundlich and other isotherms).
3. Constant-charge (ion-exchange) model.
4. Constant-capacitance model.
5. Diffuse-layer model.
6. Double-layer model.
7. Triple-layer model (TLM).

The simplest model (linear sorption or K_d) is widely used in contaminant transport models, and K_d values are relatively easy to obtain using the batch methods described above. However, the radionuclide concentration, pH, major and minor element composition, rock mineralogy, particle size, and solid-surface-area/solution volume ratio must be specified for each K_d value. The TLM (Davis and Leckie, 1978a,b) is an example of an SCM. These models describe sorption within a framework similar to that used to describe associations between metals and ligands in solutions (Davis and Kent, 1990; Kent et al., 1988; Stumm, 1992). Reactions involving surface sites and solution species are postulated on the basis of experimental data and theoretical principles. Mass/charge balance and mass action laws are used to predict sorption as a function of solution chemistry. Different SCMs incorporate different assumptions about the nature of the solid–solution interface. These include the number of distinct surface planes where cations and anions can attach (double layer vs. triple layer) and the relations between surface charge, electrical capacitance, and activity coefficients of surface species. An additional model, the CD-MUSIC model (Hiemstra and Van Riemsdijk, 1999, 1996; Tournassat et al., 2004), is based on chemical bonding principles and the physical structure of the surface. A generalized (2-site) diffuse-layer model (Dzombak and Morel, 1990) has been used extensively to model laboratory studies of metals and radionuclides. Models of reactive transport of uranium in the environment using the 2-site model are

described by Davis and Curtis (2003) and Davis et al. (2004, 2006). Wang et al. (2001a,b) compiled a set of internally self-consistent sorption constants for Pu, Np, and other radionuclides using a single-site double-layer odel for goethite. Bradbury and Baeyens (2005) obtained surface complexation constants for Th(IV), Np(V), and U(VI) on strong sites in montmorillonite and for U(VI) on the weak sites using a 2-site protolysis NEM surface complexation and cation exchange model.

Several approaches have been used to represent variability of sorption under natural conditions. These include (1) sampling K_d values from a probability distribution function (pdf), (2) calculating a K_d using thermodynamic data, and (3) using SCMs in reactive transport codes. Because of the diversity of solutions, minerals, and radionuclides that will be present at the contaminated site and potential repository sites, a large body of empirical radionuclide sorption data has been generated. Databases of K_d values that can be used to estimate pdfs for various geologic media are summarized by Barney (1981a, b), Tien et al. (1985), DOE (1988), Bayley et al. (1990), McKinley and Scholtis (1992), and Triay et al. (1997). Attempts have been made to find statistical relations between experimental variables and the measured sorption ratios (R_ds). Several of these studies were summarized by Mucciardi and Orr (1977), Mucciardi (1978), and Serne and Muller (1987). Approaches to using thermodynamic sorption models to predict or guide the collection of K_d data are also summarized by the NEA (2001).

K_ds, whether sampled from probability distribution functions or calculated by regression equations or SCMs, can be used in many contaminant transport models. Alternate forms of the retardation factor equation that use a K_d (eqn [2]) and are appropriate for porous media, fracture porous media or discrete fractures have been used to calculate contaminant velocity and discharge (Erickson, 1983; Neretnieks and Rasmuson, 1984).

An important question regarding radionuclide migration is whether the sorption in whole rocks can be predicted from the properties of constituent minerals. Alternative sorption models include those based on weighted radionuclide K_d values for individual component minerals ('sorptive additivity') (Jacquier et al., 2001; Meyer et al., 1984), a 'competitive-additivity' approach based on surface complexation theory (Tripathi et al., 1993), and a component additivity approach (Davis et al., 1998) in which the wetted surface of complex mineral assemblage is assumed to be composed of a mixture of one or more reference minerals. These have been applied to radionuclides as described by McKinley et al. (1995), Waite et al. (2000), Prikryl et al. (2001), Arnold et al. (2001), Davis (2001), and Davis et al. (2002). In some cases, the sorption behavior of a mineral assemblage can be approximated by using only one of its components such as ferrihydrite or goethite (Barnett et al., 2002; Ward et al., 1994). The generalized composite approach is an alternative approach in which surface complexation constants are obtained by fitting experimental data for the natural mineral assemblage directly (Davis et al., 1998; Kob, 1988). A non-electrostatic (NEM) form of this approach fits the pH-dependence sorption of the radionuclide without representation of the electrostatic interaction terms found in other SCMs (see, e.g., Zavarin and Bruton, 2004a,b).

11.6.3.2.3 Reactive transport models

An alternative approach to describe radionuclide transport couples chemical speciation calculations to transport equations. Such models of *reactive transport* have been developed and demonstrated by a number of researchers including Parkhurst (1995), Lichtner et al. (1996), Bethke (1998), Yeh et al. (1995, 2011), and others reviewed in Steefel and Van Cappellen (1998), Lichtner et al. (1996), and Zhang et al. (2011). Uses of such models to simulate radionuclide transport of uranium in 1-D column experiments are illustrated by Sims et al. (1996) and Kohler et al. (1996). Simulations of two-dimensional (2-D) reactive transport of neptunium and uranium are illustrated by Yeh et al. (2002, 2011) and Criscenti et al. (2002), respectively. Considerable progress in this area has been made since the publication of the First Edition of the Treatise on Geochemistry. CORE^{2D} V4 (Samper et al., 2011) is the most recent version in a family of computer programs in the CORE series: a COde for modeling partly or fully saturated water flow, heat transport and multicomponent REactive solute transport. It can model abiotic reactions including acid–base, aqueous complexation, redox, mineral dissolution/precipitation, gas dissolution/exsolution, ion exchange, sorption reactions (linear K_d, Freundlich and Langmuir isotherms, and surface complexation using constant capacitance, diffuse-layer and TLMs), and microbial processes. The code has been used to model solute transport in aquifers including uranium transport in the Andújar aquifer (Spain) and for simulation of the long-term geochemical evolution of the near field of a high-level waste (HLW) repository in clay (Yang et al., 2008). HYDROGEOCHEM5 is the latest version of a family of reactive transport codes developed over the last two decades by several generations of graduate students and collaborators led by Prof. GT Yeh, currently at the University of Central Florida. The code is a comprehensive model of coupled fluid flow, thermal, and reactive chemical processes, and has been used to model transport of Np, U, and other radionuclides in laboratory- and field-scale applications (Yeh et al., 2011). The HYTEC code is generated by coupling the geochemical code CHESS (Van der Lee, 1998) with a choice of several transport codes. *CH*emical *E*quilibrium with *S*pecies and *S*urfaces (CHESS) can simulate a range of aqueous geochemical calculations including chemical equilibrium, kinetic reactions, colloidal transport, and transport through porous media, and was developed for the purpose of coupling with hydrodynamic models. A parallel version of the code is available. The HYTEC code has been applied in a number of studies relevant to radionuclide transport including comparison to analytical solutions, comparison to results from other numerical codes, and laboratory and field applications as reported in Van der Lee et al. (2002) and De Windt et al. (2003). Applications to radionuclide transport include benchmark calculations of UO_2 oxidative dissolution and uranium migration, interactions between cement and a clayey host-rock of an underground repository for intermediate-level radioactive waste (in support of performance assessment over a time scale of 100 000 years), and diffusion of an alkaline plume, mineralogical buffering, ion exchange, and clogging of the pore space at the cement/claystone interface controlling migration of a selected group of radionuclides (Cs, Ra, Tc, and U). Other coupled reactive transport codes used for simulations of transport of radionuclides in the environment include PFLOTRAN

(Hammond et al., 2011) and others described in Zhang et al. (2011). Routine use of these codes in performance assessment calculations is still limited by the substantial computing time requirements.

11.6.3.3 Colloids

11.6.3.3.1 Introduction

Colloidal suspensions are defined as suspensions of particles with a mean diameter less than 0.45 μm, or a size range from 1 nm to 1 μm. They represent potentially important transport vectors for highly insoluble or strongly sorbing radionuclides in the environment if they are not filtered out by the host rock. In fractured rock, local transport of radionuclides by colloids may be important. Previous reviews of the behavior of colloids in natural systems and their potential role in transporting contaminants include those of Moulin and Ouzounian (1992), Ryan and Elimelech (1996), Kretzschmar et al. (1999), Honeyman and Ranville (2002), Degueldre (1997), Degueldre et al. (2000), Siegel and Bryan (2003), and Novikov et al. (2006). Degueldre et al. (2000) and Honeyman and Ranville (2002) summarize techniques used to sample colloids from groundwater and to characterize particle concentration and size distributions.

Two types of colloids are recognized in the literature. Intrinsic colloids (also called 'true' colloids, type I colloids, precipitation colloids, or 'Eigencolloids') consist of radioelements with very low solubility limits. Intrinsic colloids may occur near the radionuclide source term, where aqueous concentrations are solubility limited, but it is unknown if they are produced or are stable in the far field, where concentrations are sorption limited and are commonly well below the solubility limits. Intrinsic colloids potentially could be produced by direct degradation of the nuclear waste or by remobilization of precipitated actinide compounds (Avogadro and de Marsily, 1984; Bates et al., 1992; Kim, 1994). An(IV) colloids have been shown to considerably increase the total radionuclide concentration in solution relative to dissolved concentrations (Altmaier et al., 2004).

Carrier colloids (also known as 'pseudocolloids,' type II colloids, or 'Fremdkolloides') consist of mineral or organic phases (in natural waters primarily organic complexes, silicates, and oxides) and microbial cells (biocolloids) to which radionuclides are sorbed. In nuclear waste repositories, carrier colloids will be produced by degradation of engineered barrier materials and waste components: Fe-based waste package materials can produce iron oxyhydroxide colloids, degradation of bentonite backfills can produce clay colloids, and alteration of HLW glass can produce a variety of silicate particulates. Both sparingly soluble and very soluble radionuclides can be associated with this type of colloid, and may be stabilized via surface reduction reactions (e.g., conversion of Np or Pu to sparingly soluble reduced-phase coprecipitates) or as stabilized epitaxial phases (Powell et al., 2011). Finally, radionuclides can be associated with microbial cells and be transported as biocolloids.

Naturally occurring colloids and radionuclide-colloid associations have been characterized at several natural analog sites for nuclear waste repositories. These include the Cigar Lake Uranium deposit in altered sandstone (Vilks et al., 1993); the altered schist at the Koongarra Uranium deposit (Payne et al., 1992); altered volcanic rock sites in Pocos de Caldas, Brazil (Miekeley et al., 1991); shallow freshwater aquifers above the salt-hosted Gorleben repository test site in Germany (Dearlove et al., 1991); the Grimsel test site in the Swiss Alps (Degueldre et al., 1989); the Whiteshell Research area in fractured granite in Canada (Vilks et al., 1991); the El Borrocal site in weathered fractured granite near Madrid, Spain (Gomez et al., 1992); and 24 springs and wells near or within the Nevada Test Site (Kingston and Whitbeck, 1991). Degueldre (1997) summarized the occurrence of colloids in groundwater from 17 different sites near a proposed Swiss repository site for low-level nuclear waste. Major international studies of the occurrence of natural colloids and their potential importance to the European nuclear waste disposal program were carried out by the MIRAGE 2 (Migration of Radionuclides in the Geosphere) project and the Complex Colloid Group of the Commission of European Communities; these are reviewed in Moulin and Ouzounian (1992). Although locally and globally there are wide variations in colloid concentration and size distribution, several general trends can be observed. Many of the observed particle concentrations fall within the range 0.01–5 mg l^{-1}; however, concentrations of >200 mg l^{-1} have been observed. There is an inverse correlation between particle concentration and particle size.

Sorption of radionuclides by colloids is affected by the same solution composition parameters discussed in the previous section on sorption processes. The important parameters include pH, redox conditions, the concentrations of competing cations such as Mg^{2+} and K^{+}, and the concentrations of organic ligands and carbonate. The high surface area of colloids leads to relatively high uptake of radionuclides compared to the rock matrix. This means that a substantial fraction of mobile radionuclides could be associated with carrier colloids in some systems. The association of radionuclides with naturally occurring colloids and studies of radionuclide uptake by colloids in laboratory systems give some indication of the potential importance of colloid-facilitated radionuclide transport in the environment as discussed by Lieser et al. (1990), Kim (1994), and Runde et al. (2002a), and reviewed by Siegel and Bryan (2003).

Penrose et al. (1990) and Nuttall et al. (1991) suggest that colloidal transport of strongly sorbing actinides such as plutonium and americium is potentially significant in the unsaturated zone and in shallow aquifers near Los Alamos, NM. Similarly, Kersting et al. (1999) provide evidence that measurable amounts of Pu and perhaps Co, Eu, and Cs produced by nuclear weapons tests (1956–92) at the Nevada Test site have been transported at least 1.3 km from the blast sites by colloids. More recently, association of plutonium with colloids at a distance 3 km from their probable source at Mayak Production Facility, Urals, Russia has been observed (Novikov et al., 2006). Between 70 and 90 mol% of the plutonium detected at that distance is likely Pu(IV) hydroxides or carbonates sorbed onto amorphous iron colloids and it is likely that uranyl species are sorbed onto the colloids. More information about radioactive contamination from the Mayak site is presented in **Section 11.6.4.3.4**.

11.6.3.3.2 Microbial and humic colloids

The transport of radionuclides and metals adsorbed to microbes has been considered by a number of researchers including McCarthy and Zachura (1989), Han and Lee

(1997), and Gillow et al. (2000). Because of their small size (<10 μm diameter), these colloids can be transported rapidly through fractured media and either filtered out or be transported through porous media. Microbes can sorb to geologic media, thereby retarding transport. Alternatively, under conditions of low nutrient concentrations, the microbes can reduce their size and adhesion capabilities and become more easily transported. Studies performed in support of WIPP compliance certification indicated that, under relevant redox conditions, microbially bound actinides contributed significantly to the concentration of mobile actinides in WIPP brines (Gillow et al., 2000; Strietelmeyer et al., 1999).

Evidence for strong sorption of actinides and fission products by humic substances, both in dilute and high ionic strength media, is provided by experimental studies and thermodynamic calculations. Humic substances have experimentally been shown to strongly complex the trivalent actinides (Artinger et al., 1998; Czerwinski et al., 1996; Morgenstern et al., 2000); Th(IV) (Nash and Choppin, 1980); U(VI) and probably U(IV) (Czerwinski et al., 1994; Zeh et al., 1997); and Np(V) (Kim and Sekine, 1991; Marquardt and Kim, 1998; Marquardt et al., 1996; Rao and Choppin, 1995) at mildly acidic to neutral pH. Under basic conditions, actinide–humic substance complexation is strongly a function of the carbonate concentration, because carbonate competes effectively with the humic acid as a ligand (Unsworth et al., 2002; Zeh et al., 1997). Little data are available for tetravalent actinides, but Tipping (1993) suggests, based on thermodynamic modeling, that these should be even more strongly complexed by humic substances than other oxidation states. Several studies have shown that actinide–humic acid complexes are thermodynamically stable in high ionic strength solutions (Czerwinski et al., 1996; Labonne-Wall et al., 1999; Marquardt et al., 1996). However, destabilization of humic colloids at high ionic strength (Buckau et al., 2000) and competition for humic acid sites by divalent metal cations (Marquardt et al., 1996; Tipping, 1993) may limit the importance of colloidal transport of actinides in brines.

In addition to possible transport of radionuclides by microbial colloids, microbe–actinide chemical interactions are important for the genesis of uranium ore bodies, dissolution of radioactive waste, and remediation of contaminated sites. Suzuki and Banfield (1999) discuss the similarities between the uranium–microbe interactions and transuranic–microbe interactions. Macaskie (1991) notes that it is possible to extrapolate the data for microbial uranium accumulation to other actinides. Hodge et al. (1973) observe that the biological behavior of uranium, thorium, and plutonium resemble that of ferric iron. Microbial reduction of Pu(VI), in some cases all the way to Pu(III), has been reported several times (Boukhalfa et al., 2007; Icopini et al., 2009; Livens et al., 2010; Panak and Nitsche, 2001; Renshaw et al., 2009). The case for neptunium is more complex; some microbes capable of reducing uranium and plutonium can reduce Np(V), but others cannot (Livens et al., 2010). Microbial processes may even be important under oxic conditions; Ohnuki et al. (2007) found that organic compounds released by *Bacillus subtilis*, a common soil bacterium, reduce P(VI) to Pu(V) in solution, but reduction to Pu(IV) does not occur; however, plutonium sorbed onto the microbe surface does reduce to Pu(IV). Microbes can also affect the speciation and transport of multivalent fission products. For example, Fe^{3+}-reducing bacteria and sulfate-reducing bacteria can reduce soluble pertechnetate to insoluble Tc(IV), as discussed by Lloyd et al. (1997).

11.6.3.3.3 Models for transport of radionuclides by colloids

Several numerical models have been developed to assess the potential magnitude of colloidal-facilitated transport of radionuclides compared to the transport of dissolved species (Avogadro and de Marsily, 1984; Cvetkovic et al., 2004; Nuttall et al., 1991; Smith and Degueldre, 1993; Van der Lee et al., 1992; Vilks et al., 1998); many are reviewed by Siegel and Bryan (2003). Contardi et al. (2001) used an SCM to examine the potential effect of colloidal transport on the effective retardation factors for Am, Th, U, Np, and Pu in waters from the proposed repository site at Yucca Mountain. They concluded that colloid-facilitated transport could lead to significantly higher doses to an exposed population. They found that colloidal transport reduced the effective retardation of strongly sorbed radionuclides such as Am and Th, whereas U, Np, and Pu(V) are less strongly sorbed by colloids and therefore were relatively unaffected by colloidal transport. Honeyman and Ranville (2002) developed a framework to determine the conditions under which colloid-facilitated contaminant transport will be important compared to the transport of solution species. They concluded that such conditions will be relatively rare in the environment. Vilks (1994) proposed that colloids do not have to be considered in the safety assessment for the Canadian repository in granite. He argued that the clay-based buffer to be used in the repository will filter out any colloids produced by degradation of the waste package. In addition, the concentration of naturally occurring colloids is too low to provide a substantial transport vector for radionuclides that escape to the far field of the repository. Experiments by Yamaguchi et al. (2007) offer some corroboration for Vilks' argument; they found that Pu transport through a compacted bentonite-sand mixture is retarded relative to Np, because the Pu is present dominantly as colloids, which are too big to travel through the tight clay pores.

11.6.4 Environmental Radioactivity and Health Effects Relevant to Drinking Water, the Nuclear Fuel Cycle, and Nuclear Weapons

This section provides a more detailed case-study approach to our description of radioactive contamination of the environment and impacts on human health. Radionuclides significant to environmental geochemistry comprise three overlapping groups: (1) common naturally occurring radioelements such as members of the uranium decay series (radium, thorium, and uranium), (2) thorium and the transuranics, and (3) fission products. As shown in **Table 1**, the environmental occurrence of the three groups overlaps. The first group is important to public health regulations of drinking water and for assessing the environmental impact of resource development. The latter two groups are important in association with nuclear waste and nuclear weapon production. Radium is primarily important to drinking water regulations and uranium mining. It is discussed first because its chemistry is relatively simple

compared to the other radionuclides. Uranium geochemistry is relevant to drinking water regulations, resource extraction, and nuclear waste, and its chemistry is similar to thorium and the transuranics (actinide series). General trends in the geochemistry of actinides are discussed first and then site-specific information about uranium mining and nuclear waste disposal is provided in Sections 11.6.4.2.2 and 11.6.4.2.3, respectively. The geochemistry of the fission products is described last; their behavior is important to nuclear waste disposal as well as in assessing the short-term impact of accidents at nuclear facilities. Because natural background concentrations of radionuclides are important in discussions of health regulations and cleanup goals, the sections on radium and uranium begin with discussions of natural occurrence and processes that control their distributions. The results of laboratory and modeling studies of geochemical behavior are discussed for all three groups; then relevant treatment, remediation, and risk assessment techniques are summarized. Finally, experimental and epidemiological studies of health effects are described.

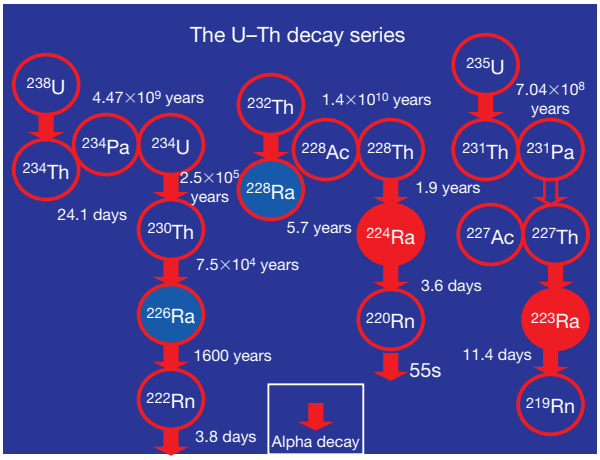

Figure 2 U–Th decay series showing parents and half-lives of ^{226}Ra, ^{228}Ra, ^{223}Ra, and ^{224}Ra (after A. Vengosh, 2007, pers. comm.).

11.6.4.1 Radium in Groundwater

Radium and its radioactive daughters present the most important ongoing radionuclide hazard to human health of all the groups described in Table 1. The 2003 USEPA Standard for radionuclides in drinking water (USEPA, 2013) is designed to prevent deaths due to cancer from radium ingestion and renal disease from uranium exposure. Previously, it had been estimated that residential drinking water exposure to radon, the decay product of radium, accounted for 5000 to over 20 000 deaths per year from lung cancer (EPA, 2003; Mills, 1991; Puskin and Nelson, 1989) and was considered the second most common cause of lung cancer after cigarette smoking. The occupational exposure of uranium miners to radon gas and its decay products in the 1960s to 1980s led to many deaths among workers, and continues to affect relationships between the Navajo Nation and the rest of the US and to impact development of uranium resources in the Southwestern US.

11.6.4.1.1 Geological occurrence

Radium isotopes are produced by radioactive decay of uranium and thorium parents (Figures 1 and 2). Granitic rocks rich in U and Th underlie local mountain-block cores in the western US from Colorado (CO) to Montana to California, and serve as the source of U and Th to sediments of the region. The valley-fill sediments derived from these granitic cores are further enriched in U through diagenetic reactions (Goldhaber et al., 1978). However, the abundance of radium in aquifers is not related solely to the abundance of the parents in the solids. As discussed below, Ra concentrations are also controlled by sorption, desorption, and ion exchange. Factors related to geology and climate that affect the acidity, redox potential, degree of mineralization, and composition of groundwaters, as well as their potential residence time, can affect sorption and thereby the occurrence pattern of Ra isotopes.

Radium in groundwater can be derived from multiple sources including (1) Ra ingrowth via decay of the dissolved Th parents in the solution; (2) dissolution from the aquifer minerals; (3) alpha-recoil from the parent nucleus in the aquifer rocks and on the clay and oxide surface coatings; (4) adsorption/desorption exchange with Ra adsorbed on the surface coating, clays, and oxides; and (5) coprecipitation with and/or dissolution of secondary minerals (e.g., barite). Direct ingrowth from thorium is generally negligible in fresh near-neutral water owing to the much lower solubility of thorium than radium, and dissolution is not favored in fresh water systems because it is too slow relative to the half-lives of short-lived radium isotopes. Radium isotopes are continuously released to groundwater contained in pore space of porous media or within fractures in bedrock by alpha-recoil mechanisms from mineral surfaces or surface coatings (Fleischer, 1980; Tricca et al., 2001), and this can be the primary source of radium in groundwater when other sources of radium to water are negligible (Krishnaswami et al., 1982).

In recent reports by the US Geological Society (USGS) (Focazio et al., 2001; Z. Szabó, 2010, USGS, pers. comm.), Ra concentrations and isotopic ratios analyzed in water samples collected from 1270 public and private (domestic) wells in 45 states covering eight geologic rock types in the principal aquifers in the US were analyzed. The samples were drawn from aquifers accounting for about 75% of the estimated withdrawals of groundwater for drinking water supply. Concentrations of combined Ra (^{226}Ra + ^{228}Ra) greater than 5 pCi l^{-1} (0.19 Bq l^{-1}) were found in five geologic rock types: glacial deposits, coastal plain sands, sandstones, carbonate rock, and crystalline rock. The maximum concentration of combined Ra was 20.4 pCi l^{-1} (0.75 Bq l^{-1}) in water from a quartzose sand aquifer in the North Atlantic Coastal Plain.

The review of the data shows that radium concentration is highest in waters with low pH and/or low dissolved-oxygen, especially in aquifers with poor sorptive capacity, even if Ra is not abundant in the aquifer solids. Two types of water have high radium contents: one group has low pH, and in places, high concentrations of nitrate or another acid anion, and high concentrations of divalent cations. The other group has low concentrations of dissolved oxygen (DO concentration <1 mg l^{-1}), high concentrations of iron or manganese, and in places, high concentrations of dissolved solids associated with some combination of high concentrations of calcium, barium, potassium, sulfate, and bicarbonate. Ra is poorly

soluble in the oxidizing and alkaline aquifer systems of the western US comprised of detrital sediments, lower tertiary/cretaceous sandstones, and quaternary alluvium.

11.6.4.1.2 Geochemical controls on Ra concentrations

Over the pH range of 3–10, the uncomplexed ion Ra^{2+} is expected to be the dominant aqueous species for dissolved radium (Baes and Mesmer, 1976; Langmuir and Riese, 1985). In sulfate-rich, acidic waters, $RaSO_4(aq)$ concentrations may be appreciable. In natural waters, radium concentrations are limited by coprecipitation, adsorption, dissolution, and radioactive processes. With the exception of sparingly soluble $RaCO_3$ and $RaSO_4$ (Langmuir and Melchior, 1985), most radium-bearing solids have high solubilities. Typically, groundwater concentrations of radium are too low for precipitation of pure $RaSO_4$, but radium can coprecipitate with barium as $(Ba,Ra)SO_4$, or with calcium in gypsum in groundwater containing moderate-to-high sulfate concentrations (Beddow et al., 2006; Kaplan et al., 2010; Langmuir and Melchior, 1985; Yoshida et al., 2009). In groundwater with high alkalinity, radium may coprecipitate with calcium during calcite precipitation (Yoshida et al., 2008).

Recent overviews of radium adsorption processes in subsurface systems have been provided in International Atomic Energy Agency (IAEA, 2006), US EPA (2010), and Kaplan et al. (2010). Radium uptake onto clay minerals is controlled by ion exchange based on apparent reversibility and selectivity of the adsorption process (Ames et al., 1983a,b; Centeno et al., 2004; Tachi et al., 2001). Amorphous Fe-hydroxides adsorb orders of magnitude more Ra than clay minerals and Ra is preferentially sorbed onto Mn-oxyhydroxides over Fe-oxyhydroxides (Ames et al., 1983a,b; Moore and Reid, 1973). Analyses of natural Fe-hydroxide samples have shown that the Fe-hydroxide contained substantially more ^{226}Ra than the surrounding rock matrix (Korner and Rose, 1977). The Ra is adsorbed quickly onto Fe-oxyhydroxide, in a matter of seconds to minutes (Krishnaswami et al., 1982). High concentrations of Ra in groundwater, therefore, are often associated with the reductive dissolution of Fe and Mn, which limits potential sorption to oxyhydroxides.

The pH of the groundwater affects Ra adsorption and mobility. As the pH decreases, the point of zero charge for Fe and Mn hydroxides (about pH 8 and 6, respectively), and less commonly for Al-hydroxides (about pH 5), is approached or reached. At low pH, divalent cations such as Ra are much less likely to be adsorbed because of the electrostatic repulsion from the positively charged surfaces. Other divalent cations including Ca, Mg, Sr, Fe, and Mn compete for adsorption sites, and sorbed cations block the sorption of Ra in solution. In general, at high levels of TDS (total dissolved solids), Ra can be very mobile because of this competition for sorption sites.

In acidic waters, the H^+ cation itself competes effectively with divalent cations such as Ca and Mg (Appelo, 1994), and by analogy, with Ra, for sorption sites. This effect has been invoked to explain increasing Ra concentrations related to nitrate pollution in poorly buffered (acidic) aquifers in the eastern US (Szabo et al., 2005; Szabo et al., 1997). Nitrification results in the release of substantial amounts of hydrogen ion and the acid-buffering capacity of waters (and soils) is so low that the hydrogen ions reach the water table without being neutralized and may decrease the pH. The concentration of Ra in the water increases because the hydrogen ion outcompetes divalent cations for adsorption sites (Appelo, 1994).

11.6.4.1.3 Isotopic ratios

11.6.4.1.3.1 $^{228}Ra/^{226}Ra$ ratios

The $^{228}Ra/^{226}Ra$ activity ratios (ARs) can indicate the source of radium as well as the geochemical processes that control its mobility. ^{238}U is the parent of ^{226}Ra and ^{232}Th is the parent of ^{228}Ra. The $^{228}Ra/^{226}Ra$ AR is often considered to be equal to the average Th/U AR in the aquifer rocks (Dickson, 1990); for igneous rocks, this would be in the range of 1–1.4, corresponding to a Th/U weight ratio of 3–4, the ratio of these elements in the earth's crust. However, other rock types commonly vary from this range – for instance, carbonates are preferentially enriched in uranium relative to thorium, whereas clastic rocks may be enriched in thorium relative to readily leached uranium, because Th is present in trace minerals resistant to chemical and physical weathering. Post-depositional enrichment or depletion of these elements in the aquifer rocks could result in variations in this ratio. Other processes can result in differences between the Ra isotopic composition of the rocks and the water. Dissolution of Ra-containing minerals would result in low ratios of the short-lived to long-lived Ra isotopes (e.g., low $^{228}Ra/^{226}Ra$ ARs) relative to the host aquifer rocks, given the slow dissolution rate and relatively faster decay of the short-lived Ra isotopes. In contrast, combination of the recoil process and decay of the dissolved radium isotopes and their rapid adsorption would increase the relative abundances of the short-lived Ra isotopes (i.e., higher $^{228}Ra/^{226}Ra$ ARs).

^{226}Ra is enriched relative to ^{228}Ra in waters from a variety of rock types, but especially in the carbonate-rock-type aquifer systems; this is likely owing to the enrichment of U (relative to Th) in carbonate minerals (Sturchio et al., 2001). Enrichment of ^{226}Ra relative to ^{228}Ra is also common in water samples from clastic sedimentary rocks where post-depositional enrichment of U relative to Th was likely. The high solubility of ^{238}U relative to ^{232}Th is the cause for its widespread distribution, redistribution, and enrichment relative to background levels in numerous sedimentary environments. Uranium forms soluble complexes with the carbonate and bicarbonate anions under oxygen-rich conditions (see **Section 11.6.4.2**), hence the high mobility. Uranium becomes chemically enriched relative to Th in sediment after reduction and precipitation along the interface between a reducing zone (commonly organic-C-rich) and an oxidizing zone, where U-rich reduction fronts (or 'roll' fronts) form (Goldhaber et al., 1978).

Enrichment of ^{232}Th relative to typical background concentrations in the sedimentary environment is seen in channel-lag deposits of dense materials such as zircon, sphene, allanite, and titanite (King et al., 1982). The low solubility of ^{232}Th (see **Section 11.6.4.2**) limits removal in percolating groundwater and the ^{228}Ra may be only slightly mobile. Thus, ^{228}Ra is most commonly present in higher concentrations than ^{226}Ra ($^{228}Ra/^{226}Ra$ values >1) in water from aquifers where the matrix is Th-rich unconsolidated coastal or alluvial sand and in waters from sandstone (with Th-rich resistate minerals) aquifers.

Vengosh et al. (2009) note that Ra activity in groundwater is controlled by a balance between the recoil process and

adsorption on clay minerals and oxides. In studies of aquifers in the Middle East, they argue that high radium abundances and high $^{228}Ra/^{226}Ra$ ratios in a sandstone aquifer with low salinity and high redox potential are due to low clay content and corresponding low sorption potential. This finding is particularly important in a region such as the Nubian Sandstone aquifer, which has been viewed as potential freshwater resources. If high radium contents are common in the clay-poor permeable sandstone aquifer, the water resource in the region is smaller than previously estimated.

11.6.4.1.3.2 $^{224}Ra/^{228}Ra$ ARs

Differences in ^{224}Ra occurrence and isotope ratios depend upon the geology of the principal aquifer and effects of water chemistry and recoil of ^{224}Ra. The AR of ^{224}Ra to ^{228}Ra is generally highest (median, 3.25) in the detrital sediments of the western US (lower tertiary/cretaceous sandstones and quaternary alluvium. Ra is poorly soluble in these oxidizing and alkaline aquifer systems, but the concentrations of ^{224}Ra are somewhat enhanced in solution relative to those of ^{228}Ra. This can be explained by alpha recoil of ^{224}Ra from the Th-rich (^{228}Ra-bearing) detrital sands in the western US. The process is analogous to 'recoil enrichment' for the isotope ^{234}U relative to the parent isotope ^{238}U (Osmond and Cowart, 1976). ^{224}Ra might be most enriched by the physical recoil mechanism relative to ^{228}Ra in waters where Ra is sparingly soluble (oxic and moderately-to-strongly alkaline waters, as in the western US), whereas relative ^{224}Ra enrichment is least where Ra is soluble. Concentrations of ^{224}Ra correlate positively with concentrations of sulfate and U in the sulfate-rich waters. This difference in occurrence and concentration trends between ^{224}Ra and ^{228}Ra in the mineralized and sulfate-rich waters of the western US is consistent with the proposed alpha-recoil mode of enhanced mobilization for ^{224}Ra in this region (Z. Szabó, 2010; USGS, pers. comm.).

The concentration of ^{224}Ra has regulatory and public health implications. ^{224}Ra and its decay products can contribute substantially to gross alpha-particle activity of water consumed by people (Focazio et al., 2001). The effectiveness of the use of gross alpha-particle activity both as a standard in itself (15 pCi l^{-1}; 0.56 Bq l^{-1}) and as a compliance-monitoring 'screen' for combined Ra has been shown to depend on the holding time between sample collection and analysis because of the presence of ^{224}Ra (Parsa, 1998; Szabo et al., 2005). In regions where ^{228}Ra is known to be present, the US EPA recommends that gross alpha-particle activity be determined within 48–72 h in order to account for the presence of the short-lived alpha-particle-emitting isotopes such as ^{224}Ra (EPA, 2000b).

11.6.4.1.4 Radium removal and generation of TENORM

Conventional water-treatment processes designed to remove suspended solids and dissolved chemical contaminants from drinking water supplies also remove radium (and other radionuclides). Lime-softening sludges from water supplies in Illinois and Wisconsin that have raw-water ^{226}Ra concentrations of 1–5 pCi l^{-1} (0.04–0.2 Bq l^{-1}) have ^{226}Ra concentrations of 6–30 pCi g^{-1} (0.2–1.1 kBq kg^{-1}). Several treatment processes are used to specifically remove radium from drinking water sources. These include coprecipitation with barium sulfate and selective sorbents such as ion-exchange resins, barium sulfate-coated alumina, and manganese dioxide-coated polymers. The sludges from these processes can have ^{226}Ra concentrations as high as 100 000 pCi g^{-1} (3700 kBq kg^{-1}), and brines from the regeneration of high-efficiency radium-removal resins might have such high radium concentrations that they require disposal in low-level-waste burial grounds (EPA, 2011a; NAS, 1999b). As mentioned previously, water softener brines discharged into septic systems in certain areas can lead to elevated radium concentrations (Szabo et al., 2010).

Such wastes are classified as TENORM. In addition to the generation of TENORM associated with drinking water resources, industrial sources of radium can be locally significant. Such sources include phosphate, metals and uranium mining areas, areas impacted by oil-fields, and facilities where nuclear materials have been manufactured or processed (NAS, 1999b). Most of the uranium, thorium, and decay products originally present in coal remain with the ash upon combustion. Composited fly ash plus bottom ash typically has a mean ^{226}Ra concentration of about 3.7 pCi g^{-1} (0.14 kBq kg^{-1}) (NAS, 1999b).

Uranium exists as impurities in phosphate rock ore used in the production of phosphoric acid and elemental phosphorus phosphates and is associated with the generation of TENORM containing radium. Concentrations of up to 200 ppm are obtained by substitution for calcium in the structure of the mineral fluorapatite ($Ca_5(PO_4)_3F$) (EPA, 2011a; NAS, 1999b). The phosphate ore is treated with sulfuric acid to yield phosphoric acid and a gypsum-rich waste (phosphogypsum or PG), which contains trace amounts of coprecipitated $^{226}RaSO_4$. Most of the uranium is concentrated in the phosphoric acid, whereas about 80% of the ^{226}Ra in the ore is concentrated in the PG with average ^{226}Ra activities of about 30 pCi g^{-1} (1.1 kBq kg^{-1}). About 5 tons of PG are produced for every ton of phosphoric acid. Small volumes of pipe scales that contain ^{226}Ra at up to 100 000 pCi g^{-1} (3700 kBq kg^{-1}) are also produced at wet-process plants.

Uranium production from surface-mining operations in the western US has generated large volumes of waste overburden with elevated concentrations of uranium and its decay products. In a typical mining operation in the 1980s, the ratio of the volume of overburden to ore was about 60:1 with an average ^{226}Ra concentration in uranium-mine overburden of about 25 pCi g^{-1} (0.9 kBq kg^{-1}) (NAS, 1999b). UMTs, which are the ore residues discharged to a waste pond after extraction of the uranium, contain most of the uranium-decay-product activity; these will be discussed in more detail in **Section 11.6.4.2.2**.

Metal mining and processing has generated by far the largest TENORM solid-waste volume. At the beginning of the twentieth century, the potential US inventory was estimated to have been about 50 billion tons with concentrations less than ten times background (NAS, 1999b). This was comprised of ores deposits whose mining and extraction might generate TENORM and included ores of rare-earth elements, molybdenum, gold, aluminum, lead-zinc, iron, tin, vanadium, copper, and other metals, placer deposits containing thorium and its decay products, bauxite and other ores that result from intense weathering. High sulfate concentrations in processing and disposal operations limit the mobility of radium; however, the presence of high concentrations of other anions associated

with metal-extraction processing, particularly chloride, will lead to increased radium mobility. For example, at a mine in Oregon, chlorination of zircon-bearing sands for extraction of zirconium, niobium, tantalum, and hafnium, led to process tailings with about 500 pCi g^{-1} (20 kBq kg^{-1}), presumably as soluble $RaCl_2$. Seepage water at this tailings disposal site contained up to 45 000 pCi l^{-1} (1700 Bq l^{-1}) (NAS, 1999b).

Oil and natural-gas reservoirs commonly contain large quantities of brines, which come to the surface during pumping operations. As they flow through pipes at the oil field, temperatures drop and a scale consisting of sulfates, carbonates, and silicates of calcium, strontium, and barium precipitates along the interior walls. About 100 tons of scale per oil well are produced in the US (EPA, 2011a). The brines can contain elevated concentrations of ^{226}Ra and ^{228}Ra. Coprecipitated radium results in a radioactive scale with typical activities of 100–10 000 pCi g^{-1} (4–400 kBq kg^{-1}); however, ^{226}Ra concentrations as high as 92 500–400 000 pCi g^{-1} (3700–15 000 kBq kg^{-1}) have been reported (Bou-Rabee et al., 2009; NAS, 1999b). Radium isotopes in barite can be used to determine the age and origin of such scales (Zielinski et al., 2001). Workers at oil-production platforms can be exposed to gamma rays, soil contamination can be present at pipe-reaming facilities, and radioactive sludges need to be handled as TENORM waste. Radon isotopes produced by decay of the radium are also a concern. The gamma ray dose rates from scales with 100 kBq kg^{-1} are 1000 times the background rate from terrestrial and cosmic ray sources; however, doses calculated from occupational exposure studies show that the effective doses will typically be below regulatory limits for workers and the general public (Bou-Rabee et al., 2009). Radium-containing TENORM can also be generated in geothermal-energy production: temperature changes lead to precipitation of solids from hot formation waters in piping, equipment, and retention ponds at the surface (EPA, 2011a). Recently, concerns have been raised over contamination of drinking water supplies and generation of TENORM by hydraulic fracturing operations during development of low-permeability natural gas reservoirs in the US. ^{226}Ra activities have ranged from over 2000–16 000 pCi l^{-1} (70–590 Bq l^{-1}) in production brines from gas fields in the Marcellus Shale in Pennsylvania and New York (NYSDOH, 2009). These brines must be treated as TENORM. Isotopic and geochemical analysis of shallow groundwater sources in the area have indicated contamination of drinking water sources by methane in areas near gas production wells, however, there was no evidence of contamination by radium from the deep brines associated with the natural gas (Osborn et al., 2011).

11.6.4.1.5 Health effects owing to radium exposure

A large population was exposed to relatively high radium radioactivities during the last century. Several thousand people were exposed to radium salts for therapeutic purposes in the first three decades of the twentieth century. Radium was accepted treatment for rheumatism and mental disorders. Radium was used in luminescent paint before World War I and many workers were exposed to radium doses ranging from tens to thousands of micrograms through internal and external routes while applying the paint to watch dials and military instruments. Radium-224 injection was used extensively in Europe for the treatment of tuberculosis and ankylosing spondylitis (a painful joint disease). These populations have provided extensive epidemiological data for studies over the last 70 years to understand the health effects of radium exposure (Harley, 2001; NAS, 1988a,b).

Radium is similar to calcium in its geochemical and metabolic behaviors and once ingested, radium is incorporated onto surfaces in the mineralized portion of bone. The primary health effect observed from the ingestion of ^{226,228}Ra is cancer of the bone (osteogenic sarcomas). The target cells for the cancers are in the marrow, about 10 μm from surfaces of the inner cavity of the bone. After exposure, the Ra diffuses into the interior of the bone and the target cells are no longer in the range of the alpha particles of ^{226}Ra. Radium-224 is also an alpha emitter with a half-life of 3.62 days; the short half-life means that the alpha dose is delivered entirely while the isotope is on the bone surface. Carcinomas of the paranasal sinuses and mastoid air cells also have been related to exposure to radium radioisotopes. Here the cells at risk are the epithelial cells of the mucosa lining the cavities (NAS, 1988a,b). Harley (2001) notes that no study has identified a statistically significant excess of leukemia after even massive doses of radium. This implies that the target cells for leukemia residing in bone marrow are outside the short range of the alpha particles (70 μm) produced by decay of radium isotopes (see **Figure 2**).

Total dose and risk are related to retention of radium by the body. The long half-life of ^{226}Ra (1600 years) allows distribution throughout the skeleton over life. A number of toxicokinetic models have been developed to describe radium retention and sarcoma risk as a function of radium intake and dose (Harley, 2001; NAS, 1988a,b). Radium retention has been modeled most commonly as a simple power law dependence on time (days) ($R = 0.54\ t^{-0.52}$). After 1 year of exposure about 2% of the radium is retained in the body; after 30 years, 0.5% still remains.

The annual risk of sarcoma is related to unit dose from ^{226}Ra and ^{228}Ra as:

$$I = \left[10^{-5} + \left(9.8 \times 10^{-6}\right)D^2\right] \exp\left[\left(-1.5 \times 10^{-2}\right)D\right],$$

where I = total bone sarcomas per person per year at risk, D = total mean skeletal dose in Gy from ^{226}Ra plus 1.5 times mean skeletal dose from ^{228}Ra (Harley, 2001; Rowland et al., 1978).

It has been suggested (Raabe et al., 1980) that there is a threshold dose and dose rate for bone sarcoma risk. If the dose rate or the total dose to the skeleton is lower than 0.004 Gy day^{-1} or 0.8 Gy, respectively, then bone cancer will not appear during the lifetime of the exposed person. This proposed threshold is relevant to discussions of the use of the linear no-threshold (LNT) model for risk assessment used to support environmental regulations (see **Appendix A**).

The radioactive progeny of radium isotopes include radon and several alpha- and beta-radiation emitters that have important health effects in specific populations. There have been multiple large follow-up studies of underground miners who were exposed to high concentrations of radon (^{222}Rn) and radon decay products. The carcinogens are actually the short-term decay products of ^{222}Rn (^{218}Po, ^{214}Po), which are deposited on the bronchial airways during inhalation and exhalation. Because of their short range, the alpha particles

transfer most of their energy to the thin layer of bronchial epithelium cells. These cells are known to be involved in the induction of cancer, and it is clear that even relatively short exposures to the high levels possible in mines lead to excess lung cancers. The results of the studies on miners have been used as a basis for estimation of the risks to the general public from exposures to radon in homes. There is considerable controversy over this topic. Although the health effects owing to the high radon exposures experienced by the miners have been well established, the risks at the lower exposure levels in residences are difficult to establish owing to uncertainties in the dose–response curve and the confounding effects of smoking and urbanization. The reader is referred to extensive documentation by the National Academy of Sciences (NAS, 1998) and the National Institutes of Health (NIH, 1994) for more information.

Regulations of acceptable exposure to radionuclides in the US are based on radionuclide slope factors (risk coefficients for total cancer morbidity), which are calculated for each radionuclide individually, based on its metabolic, chemical, and radioactive properties (EPA, 1999d, Federal Guidance Report No. 13). These attempts to take into account the age- and gender-dependence of radionuclide intake, metabolism, dosimetry, radiogenic risk, and competing causes of death in estimating the cancer risk from low-level exposures to radionuclides in the environment. When combined with site-specific media concentration data and appropriate exposure assumptions, slope factors can be used to estimate lifetime cancer risks to members of the general population owing to radionuclide exposures. Radionuclides in drinking water are regulated under the revised (as of 2000) Radionuclides Rule 66 FR 76708 (December 7, 2000) Vol. 65, No. 236 (USEPA, 2013). The 2000 revisions are designed to ensure that all customers of community water systems will receive water that meets the maximum contaminant levels (MCLs) for radionuclides in drinking water. The current standards are combined ^{226,228}Ra of 5 pCi l^{-1} (0.19 Bq l^{-1}); a gross alpha standard for all alphas of 15 pCi l^{-1} (0.56 Bq l^{-1}) (not including radon and uranium); a combined standard of 4 mrem $year^{-1}$ for beta emitters. The regulation also sets a drinking water MCL of 30 μg l^{-1} for uranium based on its nephrotoxicity rather than radioactivity, as discussed in a later section and in **Appendix B**. Other regulations relevant to radium in the environment are discussed in connection to uranium mining and milling in the next section.

11.6.4.2 Uranium and Other Actinides [An(III), An(IV), An(V), An(VI)]

In this section, the environmental chemistry of the actinides is considered in several different geochemical environments that are relevant to the 'front' and 'back' ends of the nuclear fuel cycle. Actinide transport in the oxic, near-surface environment is important with respect to in situ uranium mining and remediation of UMTs sites; it is also an important environment for transport at contaminated sites associated with nuclear weapons production (e.g., the US Hanford and Savannah River facilities, the Russian Mayak site, and others). The designated US repository site for SNF at Yucca Mountain, Nevada is in the vadose zone, and both percolating waters that would transport radionuclides to the water table, and the groundwater below the water table, are oxic. Other repository programs worldwide are evaluating potential sites for the permanent geologic storage of SNF and actinide-containing waste that are reducing. These sites include host rocks of crystalline rock (e.g., the Swedish, Finnish, and Canadian programs), clay (e.g., the French, Belgian, and Swiss programs), and salt [the German and US transuranic waste (TRU) programs]. Groundwaters from these lithologies range from dilute to saline in granites and clays, to highly saline in salt. Initially, a description of general trends in the geochemistry of the actinides is given. Subsequent sections describe site-specific behavior of uranium at uranium mining locations and impacts on human health and the behavior of actinides at potential nuclear waste disposal sites.

11.6.4.2.1 General trends in speciation, solubility, and sorption of the actinides

Actinides are hard acid cations (i.e., comparatively rigid electron clouds with low polarizability) and form ionic species as opposed to covalent bonds (Langmuir, 1997; Silva and Nitsche, 1995). Several general trends in their chemistry can be described (although there are exceptions). Owing to similarities in ionic size, coordination number, valence, and electron structure, the actinide elements of a given oxidation state have chemical properties that are either similar or vary systematically (Choppin, 1999; David, 1986; Vallet et al., 1999). For a given oxidation state, the relative stability of actinide complexes with hard base ligands can be divided into three groups in the order: CO_3^{2-}, $OH^- > F^-$, HPO_4^{2-}, $SO_4^{2-} > Cl^-$, NO_3^-. Within those ligand groups, stability constants generally decrease in the order $An^{4+} > An^{3+} \approx AnO_2^{2+} > AnO_2^+$ (Lieser and Mohlenweg, 1988; Silva et al., 1995). In addition, the same order describes the decreasing stability (increasing solubility) of actinide solids formed with a given ligand (Langmuir, 1997).

These trends have allowed the use of an oxidation state analogy modeling approach, in which data for the behavior of one actinide can be used as an analog for others in the same oxidation state. An oxidation state analogy was used for the WIPP to evaluate the solubility of some actinides and to develop a more complete set of modeling parameters for actinides included in the repository performance calculations. The results are assumed to be either similar to the actual case or can be shown to vary systematically (Fanghänel and Kim, 1998; Neck and Kim, 2001; Wall et al., 2002). The similarities in chemical behavior extend beyond the actinides to the lanthanides – Nd(III) is commonly used as a nonradioactive analog for the +III actinides. For instance, complexation and hydrolysis constants and Pitzer ion interaction parameters used in modeling Am(III) speciation and solubility for the WIPP were extracted from a suite of published experimental studies involving not only Am(III) but also Pu(III), Cm(III), and Nd(III) (DOE, 1996a).

11.6.4.2.1.1 Oxidation state

Differences among the potentials of the redox couples of the actinides account for much of the differences in their speciation and environmental transport. Detailed information about the redox potentials for these couples can be found in numerous references (Hobart, 1990; Runde et al., 2002a; Silva and

Nitsche, 1995). This information is not repeated here, but a few general points should be made. Important oxidation states for the actinides under environmental conditions are described in **Table 3**. Depending on the actinide, the potentials of the III/IV, IV/V, V/VI, and/or IV/VI redox couples can be important under near-surface environmental conditions. When the redox potentials between oxidation states are sufficiently different, then one or two redox states will predominate; this is the case for uranium, neptunium, and americium (Runde et al., 2002a). The behavior of uranium is controlled by the predominance of U(VI) species under oxidizing conditions and U(IV) under reducing conditions. In the intermediate Eh range and neutral pH possible under many settings, the solubility of neptunium is controlled primarily by the Eh of the aquifer and will vary between the levels set by $Np^{IV}(OH)_{4(s)}$ (10^{-8} M under reducing conditions) and $Np^{V}{}_2O_{5(s)}$ (10^{-5} M under oxidizing conditions). Redox potentials of Pu in the III, IV, V, and VI states are similar (around 1.0 V), therefore, plutonium can coexist in up to four oxidation states in some solutions (Langmuir, 1997; Runde et al., 2002a). However, Pu(V) and Pu(IV) are most commonly observed in environmental conditions (Choppin, 2007) and sorption of plutonium is strongly influenced by reduction of Pu(V) to Pu(IV) at the mineral–water interface. More discussions of these behaviors will be found in the individual sections for each actinide that follow.

11.6.4.2.1.2 Complexation and solubility

In dilute aqueous systems, the dominant actinide species at neutral to basic pH are hydroxy- and carbonato-complexes (Choppin, 2007). Similarly, solubility-limiting solid phases are commonly oxides, hydroxides, or carbonates. The same is generally true in high ionic strength brines, because common brine components – Na^+, Ca^{2+}, Mg^{2+}, Cl^-, $SO_4{}^{2-}$– do not complex as strongly with actinides. However, weak mono-, bis-, and tris-chloro complexes with hexavalent actinides (U(VI) and Pu(VI)), can contribute significantly to the solubility of these actinides in chloride-rich brines. Runde et al. (1999) measured shifts in the apparent solubility product constants for uranyl and plutonyl carbonate of nearly one log unit as chloride concentrations increased to 0.5 M. Carbonate complexes are important for radionuclides (Choppin, 2007); thorium, plutonium, neptunium, and uranium all have strong carbonate complexes under environmental conditions. Carbonate complexation also leads to decreased sorption by forming strong anionic complexes that will not sorb to negatively charged mineral surfaces. The potential importance of carbonate complexes with respect to increasing actinide solubility and decreasing sorption influenced a decision by the DOE to use MgO as the engineered barrier in the WIPP repository. MgO and its hydration products sequester CO_2 through formation of carbonates and hydroxycarbonates, as well as buffering the pH at neutral to moderately basic values, where actinide solubilities are at a minimum. In some potential repository settings, carbonate-poor and Ca-rich alkaline plumes may form owing to corrosion of cementitious waste forms. In these waters, tetravalent actinides form stable An–Ca–OH complexes (Altmaier et al., 2008; Fellhauer et al., 2010).

Dissolved organic carbon may be present as strong complexing ligands that increase the aqueous concentration limits of actinides (Olofsson and Allard, 1983). In environments with high organic matter from natural or anthropogenic sources, complexation of actinides with ligands such as EDTA and other organic ligands may decrease the extent of sorption onto rocks. Langmuir (1997) suggests that to a first approximation, complexation of An^{4+}, $AnO_2{}^+$, and $AnO_2{}^{2+}$ with humic and fulvic acids can be ignored because the actinides form such strong hydroxyl and carbonato-complexes in natural waters. In contrast, however, although An^{3+} species form OH^- and/or $CO_3{}^{2-}$ complexes, important actinide/humic–fulvic complexation does occur.

The low solubilities and high sorption affinity of thorium and americium severely limit their mobility under environmental conditions. However, because each exists in a single oxidation state – Th(IV) and Am(III) – under environmentally relevant conditions, they are relatively easy to study. In addition, their chemical behaviors provide valuable information about the thermodynamic properties of trivalent and tetravalent species of uranium, neptunium, and plutonium.

11.6.4.2.1.3 Actinide sorption

In general, actinide sorption will decrease in the presence of ligands that complex with the radionuclide (most commonly humic or fulvic acids, $CO_3{}^{2-}$, $SO_4{}^{2-}$, F^-) or cationic solutes that compete with the radionuclide for sorption sites (most commonly Ca^{2+}, Mg^{2+}). In general, sorption of the (IV) species of actinides (Np, Pu, U) is greater than the sorption of the (V) species.

Attempts to propose representative K_d values for actinides have met with controversy. For example, Silva and Nitsche (1995) suggested average K_d values for actinides in the order $An^{4+} > An^{3+} > AnO_2{}^{2+} > AnO_2{}^+$, as 500, 50, 5, and 1, respectively. This order corresponds to the order of the pH_{50} values of sorption edges for Th(IV), Am(III), Np(V), and Pu(V) in studies of sorption by γ-Al_2O_3 (Bidoglio et al., 1989); and of Pu(IV), U(VI), and Np(V) in studies of sorption by α-FeOOH (Turner, 1995). Calculated or measured element-specific K_ds for natural soils and geomedia for many environmental sites, however, are quite different from these values because sorption of radionuclides is very dependent on the radionuclide oxidation state, groundwater composition, and nature of rock surface, all of which may be variable and/or poorly characterized along the flow path. K_ds for site-specific conditions should be obtained from available databases (Barney, 1981a,b; Bayley et al., 1990; Cantrell et al., 2003; DOE, 1988; EPA, 1999a; McKinley and Scholtis, 1992; Tien et al., 1985; Triay et al., 1997; Vilks, 2009) instead of using broad 'generic' ranges whenever possible.

As discussed previously, plots of pH sorption edges are useful in summarizing the sorption of radionuclide by substrates that have amphoteric sites (i.e., SOH, SO^-,

Table 3 Important actinide oxidation states in the environment

Actinide element	*Oxidation states*			
Thorium		IV		
Uranium		IV		VI
Neptunium		IV	V	
Plutonium		IV	V	VI
Americium	III			
Curium	III			

SOH_2^+). The pH sorption edges of actinides are similar for different aluminosilicates (quartz, α-alumina, clinoptilolite, montmorillonite, and kaolinite). For example, Np(V) and U(VI) exhibit similar pH-dependent sorption edges that are independent of specific aluminosilicate identity (Bertetti et al., 1998; Pabalan et al., 1998). In the natural environment, and in the altered environment relevant to nuclear waste disposal, sorption onto carbonates, clays, and iron oxides/hydroxides is especially important. However, while sorption may result in actinide retardation and even immobilization, sorption onto colloidal grains can also result in enhanced transport (Honeyman and Ranville, 2002; Kersting et al., 1999; Novikov et al., 2006).

Stout and Carroll (1993), Carroll et al. (1992), Van Cappellen et al. (1993), Meece and Benninger (1993), Brady et al. (1999), and Reeder et al. (2001) summarize empirical data and theoretical models of actinide–carbonate mineral interactions. The surface PDI on carbonate minerals may be Ca^{2+} or Mg^{2+}. Increased solution concentration of Ca^{2+} will lead to decreased actinide sorption, which then leads to complex sorption behavior if the carbonate concentration and pH of the solution are varied. Carroll et al. (1992) studied the uptake of Nd(III), U(VI), and Th(VI) by pure calcite in dilute $NaHCO_3$ solutions using a combination of surface analysis techniques. They found that U (VI) uptake was limited to monolayer sorption and uranium–calcium solid solution was minimal even in solutions supersaturated with rutherfordine (UO_2CO_3). In contrast, they found that surface precipitation and carbonate solid solution was extensive for thorium and neodymium. Similarly, irreversible sorption and surface precipitation of americium onto carbonates were observed by Shanbhag and Morse (1982) and Higgo and Rees (1986).

Clay minerals are ubiquitous in the natural environment and are of added importance because many international programs are evaluating the potential placement of nuclear waste repositories in clay host rocks. Moreover, both clay and granite-based repository concepts implement a backfill of bentonite, a type of montmorillonite. For these reasons, many studies have evaluated actinide sorption onto clay minerals including montmorillonite (e.g., Bachmaf and Merkel, 2011; Bertetti et al., 1998; Chisholm-Brause et al., 1992, 1994; Kowal-Fouchard et al., 2004; Lujaniene et al., 2007; McKinley et al., 1995; Pabalan and Turner, 1997; Pabalan et al., 1998; Stumpf et al., 2004; Tsunashima et al., 1981; Turner et al., 1998); illite (Bradbury and Baeyens, 2009; Lujaniene et al., 2007, 2010), and kaolinite (Bachmaf and Merkel, 2011; Stumpf et al., 2004). Many studies have evaluated uranyl sorption onto smectites and have found that sorption occurs both by ion exchange and by surface complexation (Bradbury and Baeyens, 2005; Kowal-Fouchard et al., 2004; Turner et al., 1996). However, Sylwester et al. (2000) found that, in the presence of a competing ion, uranyl sorbed to smectite only by surface complexation at near-neutral pH, and (Bachmaf and Merkel, 2011) concluded that uranyl sorption could be explained by surface complexation alone. Similarly, Turner et al. (1998) found that Np(V) sorption onto montomorillonite involved only surface complexation. Uranyl-sorbed species are hydroxy complexes and sorption is inhibited by higher carbonate concentrations, as carbonato complexes become dominant (Hartmann et al., 2008; Pabalan and Turner, 1997). Illite and kaolinite also sorb uranyl strongly, and high sorption by kaolinite has been attributed to the abundance of aluminol sites (Bachmaf and Merkel, 2011). Other actinides also have high affinities for clays (e.g., Bradbury and Baeyens, 2009; Stumpf et al., 2004; Turner et al., 1998). Pu(IV) and Am (III) experiments with natural soils (Lujaniene et al., 2007, 2010) and U(VI) and Cm(III) experiments with claystones (Hartmann et al., 2008) showed that in both cases, the clay phases were the dominant sorbents, even in the presence of abundant iron hydroxides and carbonates.

Actinide sorption onto Fe-oxides/oxyhydroxides has been widely studied, both because Fe-minerals are common in natural settings and because many repository concepts for permanent disposal of radioactive waste have iron- or steel-engineered components (e.g., waste packages, emplacement rails or invert supports, emplacement ground support materials) that will corrode over time. For most sorbents, sorption onto iron oxides is initially rapid and is followed by continued slow uptake, generally for the duration of the experiment. Desorption is initially rapid and reversible, but with increasing contact time, an increasing fraction of the total becomes more strongly fixed. The strongly bound fraction may be 'irreversibly' sequestered, but more commonly, will desorb slowly over time.

Several mechanisms have been proposed for the development of the more strongly bound fraction, including

- Incorporation of metal ions into the Fe-oxide structure by isomorphic substitution. This mechanism has been suggested to occur during recrystallization of ferrihydrite to recrystallization to hematite and possibly goethite, but may also be effective during growth or coarsening (Ostwald ripening) of Fe-oxides. Many divalent metal ions are sequestered in this manner; among the actinides, this mechanism has been proposed for Am(III) (Schafer et al., 2003), U(VI) (Duff et al., 2002; Nico et al., 2009; Payne et al., 1994), and Th(IV) (McQueen et al., 2004). However, Gerth (1990) found that U(IV) did *not* enter the goethite structure during recrystallization. Watson (1996) was shown that entrapment of adsorbed contaminant ions by crystal growth permanently sequesters such ions from the environment, as solid-state diffusion of ions out of mineral structures is too slow at near-surface temperatures to allow for release.
- Overgrowth and encapsulation of sorbed or precipitated phases, during recrystallization of ferrihydrite as goethite or hematite. Th(IV) sequestration via overgrowth of surface precipitates of ThO_2 was reported by Gerth (1990).
- Formation of slowly dissolving metal hydroxide surface precipitates. This mechanism has been proposed for uranium mobilization by goethite (Bruno et al., 1995); and for immobilization of Pu(IV) (Duff, 2001).
- Slow diffusion of ions into and out of the crystal structure. Although suggested as a mechanism by Coughlin and Stone (1995), Watson (1996) showed that solid-state diffusion is far too slow a process at environmentally relevant temperatures for this process to be important.
- A time-dependent change in the metal–surface site stoichiometry, resulting in a more stable surface complex. Two different versions of this have been proposed:

- The development of a more strongly sorbed component could represent two-site sorption, with slow transformation from a weakly sorbing fast site to a high-affinity slow site. SCMs for iron oxyhydroxide advocate the presence of two sites, with a high-energy site comprising 2–5% of the total (e.g., Dzombak and Morel, 1990), although one model, the CD-MUSIC model (Hiemstra and VanRiemsdijk, 1996, 1999), relates site energies to the coordination of surface metal ions, resulting in higher numbers of high-energy sites. This process has been proposed to explain the development of a strongly sorbed Pu component on goethite (Painter et al., 2002; Wittman et al., 2005).
- For Pu, a special mechanism has been proposed: sorbed Pu(V) reduces to Pu(IV) on the goethite surface, which is both stabilized in the reduced oxidation state and more strongly sorbed. The proposed mechanism for this, on both goethite and hematite, is surface-mediated disproportionation of sorbed Pu(V) to Pu(VI) and Pu(IV) (Fjeld et al., 2003; Keeney-Kennicutt and Morse, 1985; Powell et al., 2005; Runde, 2002; Sanchez et al., 1985). This process has been widely used to explain why NpO_2^+ sorption to iron oxyhydroxides is much less than PuO_2^+ sorption.

11.6.4.2.2 Behavior of uranium in the environment and impacts on human health

This section describes the geochemical properties, geochemical processes that control the environmental occurrence of uranium, and the impacts of uranium mining on the environment and human health. The impacts of past uranium mining practices are briefly discussed and the principles of in situ recovery (ISR) are reviewed. This section also addresses the principle processes that must be considered in evaluating whether natural attenuation (NA) will be effective as a risk management strategy for remediated uranium mine sites. General trends in uranium geochemistry are described in the preceding section and behavior under conditions relevant to nuclear waste disposal are described in Section 11.6.4.2.3. More detailed information on the health effects related to exposure to uranium is found in Appendix B.

11.6.4.2.2.1 Radiochemical, geochemical, and biogeochemical properties of uranium

Natural uranium consists of 99.284% ^{238}U, 0.711% ^{235}U, and 0.005% ^{234}U by weight (49% ^{238}U, 2% ^{235}U, and 49% ^{234}U by radioactivity) and has a specific activity of 0.68 $\mu Ci\,g^{-1}$ (25 $kBq\,g^{-1}$) (ATSDR, 2011). Uranium isotope decay chains lead to a variety of radioactive daughter products that may be more dangerous to human health than the parents. Radium isotopes are a common contaminant of concern in drinking water systems and have been described in a previous section. Thorium is important to the understanding of radium radiochemistry, an important constituent of TENORM and UMTs as discussed below and also important in discussions of nuclear waste disposal (see Section 11.6.4.2.3). Here,the focus is on the properties of uranium that control transport and on its nephrotoxicity, the health effect most important for uranium. Because of the low specific activity of ^{238}U, it is not considered an important radiocarcinogen; only when enriched to significant levels of ^{235}U, (at 97.3%, the specific activity = 2.1 $\mu Ci\,g^{-1}$; 78 $kBq\,g^{-1}$) is the radioactive hazard significant. Depleted uranium, a by-product of the enrichment process has less specific activity (0.33 $\mu Ci\,g^{-1}$; 12 $kBq\,g^{-1}$) than natural uranium. The EPA has established a MCL of 0.03 $mg\,l^{-1}$ and set a MCL goal of no uranium in drinking water.

Uranium is highly mobile and soluble under near-surface oxidizing conditions and thus presents an exposure hazard to humans and ecosystems. Under most conditions, uranium geochemistry is dominated by redox conditions, pH, carbonate concentrations, and sorption. Under oxidizing near-surface conditions, U(VI) is the stable oxidation state. Figure 3 shows the aqueous speciation of U(VI) and the solubility of crystalline schoepite (β-$UO_2(OH)_2$) under atmospheric conditions ($pCO_2 = 10^{-3.5}$) over the pH range 4–9. The calculations

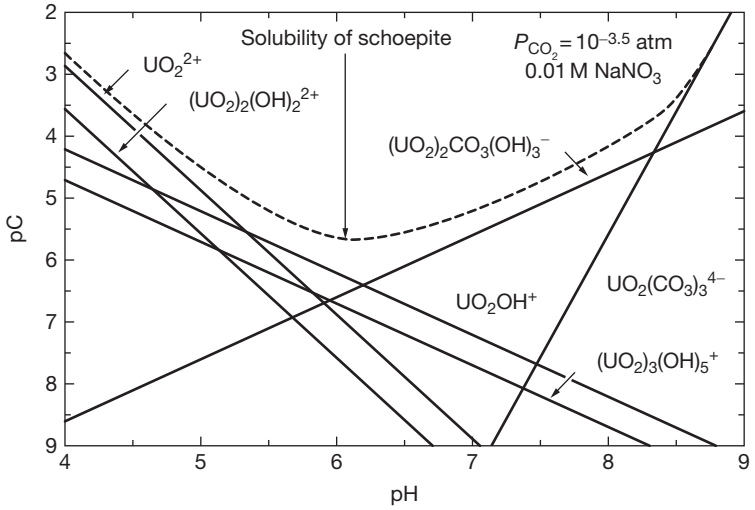

Figure 3 Aqueous speciation of uranium(VI) and the solubility of crystalline schoepite (β-$UO_2(OH)_2$) under atmospheric conditions ($pCO_2 = 10^{-3.5}$). Reproduced by permission of Nuclear Regulatory Commission modified from Davis (2001) *Surface Complexation Modeling of Uranium(VI) Adsorption on Natural Mineral Assemblages*, p. 12.

were carried out with the HYDRAQL code (Papelis et al., 1988) using a thermodynamic database described by Davis et al. (2001), which is based primarily on the compilation of Grenthe et al. (1992). The figure shows that over the pH range 6–8, the mixed hydroxy-carbonato binuclear complex $(UO_2)_2CO_3(OH)_3^-$ is predicted to predominate; that at lower pH, the uranyl ion (UO_2^{2+}) is most important; and that at higher pH, the polycarbonate $UO_2(CO_3)_3^{4-}$ has the highest concentration. In **Figure 3**, the total concentration of uranium is limited by the solubility of schoepite; therefore, it varies as a function of pH and can exceed 10^{-3} M.

The relative importance of the multinuclear uranyl complexes is different from those shown in **Figure 3** at different fixed total uranium concentrations. For example, if the total uranium concentration is limited to $<10^{-8}$ M (e.g., by slow leaching of uranium from a nuclear waste form), then the species $UO_2(OH)_{2(aq)}$ predominates at pH 6–7. At higher total uranium concentrations (e.g., 10^{-4} M), the multinuclear uranyl hydroxy complex $(UO_2)_3(OH)_5^+$ predominates at pH 5–6.5 (Davis et al., 2001). Accurate modeling of uranyl speciation in solution requires consideration of a large number of multinuclear uranyl hydroxyl complexes. Note that the solubility curve would be shifted slightly if thermodynamic data from the more recent compilation of thermodynamic data for uranyl species (Redkin and Wood, 2007) were used. The Redkin and Wood compilation includes additional multinuclear uranyl complexes and modifies Grenthe's equilibrium constants slightly.

When calcium (or other alkaline earth metals such as magnesium) are present at moderate concentrations in groundwater, Ca-carbonato complexes will dominate the aqueous speciation of U(VI) under typical pH conditions and moderate levels of alkalinity (>1 mmol l^{-1} as $CaCO_3$) (Amonette et al., 2010; Dong and Brooks, 2006, 2008; Prat et al., 2009). In alkaline waters, carbonate complexes will dominate; however, phosphate complexes may be important when phosphate concentrations are high (Bonhoure et al., 2007). In areas affected by uranium solution mining using sulfuric acid, $UO_2SO_{4(aq)}$ will be an important aqueous species. Bernhard et al. (1998) studied uranium speciation in water from uranium mining districts in Germany (Saxony) using laser spectroscopy, and found that $Ca_2UO_2(CO_3)_{3(aq)}$ was the dominant species in neutral pH carbonate- and Ca-rich mine waters; $UO_2(CO_3)_3^{4-}$ was the dominant aqueous species in basic (pH = 9.8), carbonate-rich, Ca-poor mine waters; and $UO_2SO_{4(aq)}$ dominated in acidic (pH = 2.6), sulfate-rich mine waters. Under reducing conditions, U(IV) species predominate and precipitates as a highly insoluble UO_2 phase. As discussed below, in uranium tailings disposal sites, oxidizing conditions are dominant, but confinement and microbial activity may lead to localized reducing conditions.

Uncertainties in the identity and solubility product of the solubility-limiting uranium solid in laboratory studies lead to considerable uncertainty in estimates of the solubility under natural conditions. Depending on whether amorphous $UO_2(OH)_2$ or crystalline schoepite (β-$UO_2(OH)_2$ is assumed to limit the solubility in solutions open to the atmosphere, the value of the minimum solubility and the pH at which it occurs change (Davis et al., 2001; Siegel and Bryan, 2003; Tripathi, 1983). Moreover, in oxic natural waters, other uranyl phases such as uranyl silicates may limit uranium solubility. In Yucca Mountain J-13 water, Langmuir (1997) calculated that $Ca(H_3O)_2(UO_2)_2(SiO_4)_2.3H_2O_{(cr)}$ would be the solubility-limiting phase, and would limit uranyl solubilities to 5.4×10^{-9} M. However, as measured uranyl solubilities in natural waters are generally much higher than this, uranyl silicate precipitation does not seem to control uranium solubilities in natural waters, possibly because of kinetic limitations.

Coprecipitation will also limit aqueous uranium concentrations. Studies by Reeder et al. (2001) and others (see also review by Landa, 2004) suggest that coprecipitation of U, Ra, and other contaminants in carbonate minerals commonly occurs. Uranyl has been coprecipitated by biogenic calcite and abiotically produced calcite and aragonite. Studies by Kelly et al. (2003) have shown that uranyl ion substitutes for a calcium and two adjacent carbonate ions in a stable lattice position in U-rich calcite.

Microbes can both react with and control the local geochemical environment of uranium (and other actinides) and affect their solubility and transport. Francis et al. (1991) report that oxidation is the predominant mechanism of dissolution of UO_2 from uranium ores. However, the dominant oxidant is not molecular oxygen but Fe(III) produced by oxidation of Fe(II) in pyrite in the ore by the bacteria *Thiobacillus ferroxidans*. The Fe(III) oxidizes the UO_2 to UO_2^{2+}. The rate of bacterial catalysis is a function of a number of environmental parameters including temperature, pH, TDS, f_{O2} and other factors important to microbial ecology. The oxidation rate of pyrite may be increased by 5–6 orders of magnitude owing to the catalytic activity of microbes such as *Thiobacillus ferroxidans* (Abdelouas et al., 1999).

Suzuki and Banfield (1999) and Abdelouas et al. (1999) provide well-documented overviews of the geomicrobiology of uranium with discussion of applications to environmental transport and remediation of sites contaminated with uranium and actinides. Suzuki and Banfield (1999) classify methods of microbial uranium accumulation as either *metabolism-dependent* or *metabolism-independent*. The former consists of precipitation or complexation with metabolically produced ligands, processes induced by active cellular pumping of metals, or enzyme-mediated changes in redox state. Examples include precipitation of uranyl phosphates owing to the activity of enzymes such as phosphatases, formation of chelating agents in response to metal stress, and precipitation of uraninite through enzymatic uranium reduction. *Metabolism-independent processes* involve physicochemical interactions between ionic actinide species and charged sites in microorganisms; these can occur with whole living cells or cell fragments. Uranium can be accumulated in the cells by passive transport mechanisms across the cell membrane or by biosorption, a term that includes nondirected processes such as adsorption, absorption, ion exchange, or precipitation. Suzuki and Banfield (1999) describe the effects of pH and concentrations of other cations and anions on uranium uptake by a variety of organisms. Uptake of uranium by microbes can be described using the techniques and formalisms used to analyze the sorption of metals by metal hydroxide surfaces such as the Freundlich, Langmuir, and surface-complexation sorption models (Fein et al., 1997; Fowle and Fein, 2000). A large number of species of bacteria, algae, lichen, and fungi have been shown to accumulate high levels of uranium through these processes.

Suzuki and Banfield provide examples of organisms whose uranium uptake capacities range from approximately 50 to 500 mg U per gram dry cell weight. Maximum uptake occurs from pH 4–5.

Microorganisms can develop resistance to the chemical and radioactive effects of actinides through genetic adaptation. In contaminated environments such as UMTs and mines, uranium accumulation levels exceed those observed in laboratory experiments with normal strains of bacteria. Suzuki and Banfield (1999) describe several mechanisms used by microbes to detoxify uranium. Microbial–uranium interactions have been studied for technological applications such as bioleaching, which is an important method for uranium extraction (Berthelot et al., 1997). As discussed in later section, in situ stabilization of uranium plumes by microbial reduction is an important method for remediation (Barton et al., 1996). Microbial ecology in high uranium environments has been studied in uranium mill tail wastes, and the effects of microbes on the stability of radioactive wastes buried in geological repositories is discussed by Francis (1994) and Pedersen (1996).

11.6.4.2.2.2 Environmental distribution of uranium

A number of programs of the USGS, US EPA, IAEA, and other agencies have provided surveys of uranium concentrations in air, soils, and water. The information summarized here is taken from these and other reviews as noted (ATSDR, 2011; EPA, 2007; NCRP, 1984; USGS, 2006). Uranium may be redistributed in the environment by anthropogenic contamination and natural processes such as groundwater and surface water transport and resuspension of soils containing uranium through wind and water erosion and volcanic eruptions. The primary industrial processes that cause contamination associated with the nuclear fuel cycle include the mining, milling, and processing of uranium ores or uranium end products; the production of phosphate fertilizers from uranium-bearing phosphate rocks; and the disposal of uranium mine tailings.

11.6.4.2.2.2.1 Overview: relationship between geochemical properties and distribution Uranium deposited from the air by wet or dry precipitation will be deposited on land or in surface waters. If land deposition occurs, the uranium can be reincorporated into soil, resuspended in the atmosphere (typically factors are around 10^{-6}), washed from the land into surface water, incorporated into groundwater, or deposited on or adsorbed onto plant roots. As discussed in more detail above, factors that control mobility of uranium in ground and surface water and soils include oxidation–reduction potential, pH, and adsorption characteristics of consanguineous solids. The formation of complexes with inorganic ligands (e.g., CO_3^{-2}, OH^-) or humic acid, and reduction of U(VI) to U(IV) are important (Allard et al., 1979; ATSDR, 2011; Siegel and Bryan, 2003). In most surface waters, sediments act as a sink for uranium and the uranium concentrations in sediments and suspended solids are several orders of magnitude higher than in surrounding water (Swanson, 1985). Uranium is likely to be in solution as an anionic carbonate complex in oxygenated water with high alkalinity; however, in acidic waters ($pH < 6$) containing low concentrations of inorganic ions and high concentrations of dissolved organic matter, the uranium may exist as a soluble organic complex (Ranville et al., 2007). When the neutral hydroxy complex of uranium predominates, sorption in acidic soils is maximized. At pH 6 and above and in the presence of high carbonate or hydroxide concentrations, sorption will be less owing to the predominance of anionic complexes such as $[UO_2(OH)_4]^{-2}$, especially in soils with low anion-exchange capacity, resulting in increased mobility.

The uptake or bioconcentration of uranium by plants or animals is the mechanism by which uranium in soil, air, and water enters into the food chain. Uranium may be deposited onto plants by direct deposition from air or water, by resuspension, or it can adhere to the outer membrane of the plant's root system. Adsorption through plant leaves or roots is very limited. The levels of uranium in aquatic organisms decline with each successive trophic level because of very low assimilation efficiencies (low bioconcentration or bioaccumulation factors) in higher trophic animals (ATSDR, 2011; Swanson, 1985).

11.6.4.2.2.2.2 Air Uranium is introduced into the atmosphere primarily by resuspension of soil, mining and milling activities, uranium processing facilities, and by burning coal. Background airborne uranium concentrations are typically quite low, in the attocurie m^{-3} (10^{-3} nBq m^{-3}) range, respectively (ATSDR, 2011). In geographic areas such as the western US that contain high levels of uranium in the rocks and soil, considerable amounts of natural uranium is introduced into the air by erosion and wind activity (USGS, 2010a). Uranium ore has concentrations of uranium up to 1000 times the average concentration normally found in soil (NCRP, 1984) and can be exposed as a result of open-pit, in situ leach, or underground mining operations. Airborne dust near uranium mining or milling operations has been shown to contain concentrations in the 1 pCi l^{-1} (0.037 Bq l^{-1}) range (ATSDR, 2011; Brugge et al., 2005; Lapham et al., 1989; NCRP, 1984). Airborne releases are associated with the actual mining, as well as ore crushing and grinding, high-temperature processes such as calcining or sintering, and from yellowcake drying and packaging at the mill. Ore stockpiles can also be a source of airborne emissions (NCRP, 1993). Wind erosion of tailings at uranium mining and milling activities will also result in the resuspension of uranium progeny (e.g., ^{226}Ra and ^{222}Rn) (Bigu et al., 1984; Hans et al., 1979; USGS, 2010a,b).

The dust may be a source of uranium for surface and groundwater pollution. Uranium in airborne dust has the same uranium concentration and isotopic ratios as the soil particles that produce it as long as the surface material from which it originated has not experienced significant weathering by moisture. Johnson et al. (2009) evaluated groundwater samples with elevated uranium near an open dump Tuba City, Arizona (AZ). On the basis of $^{234}U/^{238}U$ AR values, Johnson et al. argued that the uranium in the groundwater plume (AR values about 1.5) was not derived from an upstream UMTs site (AR values of about 1.0). Instead, they concluded that the elevated uranium by the dump was derived from cycling of uranium derived from weathering of reworked Chinle sediments in the soil zone.

The operation of coal-burning power plants using coal containing significant quantities of uranium can also release significant amounts of uranium into the environment. In 1984, it was estimated that a 550-MWe plant with a coal

input of 1.5 million tons per year with a uranium content of approximately 3 tons could release 0.06–0.2 Ci (2.2–7.4 GBq), or 90–300 kg of ^{238}U and ^{234}U per year (NCRP, 1984).

11.6.4.2.2.2.3 Rocks and soils The average uranium concentration in US soils and crust is about 3 μg g^{-1} (2 pCi g^{-1}; 0.074 Bq g^{-1}). Acidic rocks such as granites contain higher uranium concentrations (e.g., 4.8 μg g^{-1}), while basic rocks such as basalts contain lower concentrations (e.g., 0.6 μg g^{-1}) (Clark et al., 2006). Some parts of the US, particularly the western portion such as the Colorado Plateau, exhibit higher than average uranium levels owing to natural geologic conditions. In the US, major ore deposits are located in Colorado, Utah, Arizona, New Mexico, Wyoming, Nebraska, and Texas. Uranium ores contain between 0.05 and 0.2% uranium, up to 1000 times the levels normally found in soil (ATSDR, 2011).

The mineralogy of uranium-bearing minerals is very complex with more than 260 uranium-bearing minerals recognized. This topic is not reviewed here; the reader is referred to reviews such Burns and Finch (1999) and Clark et al. (2006). Uranium ores occur in a variety of geological settings including hydrothermal, magmatic, metasomatic, volcanic, sedimentary, and metamorphic deposits with distinctive mineral assemblages (Plant et al., 1999). Uranium minerals can result from primary or secondary deposition; commonly occurring minerals include uraninite (a uranium-oxide), coffinate (a uranium-silicate), pitchblende (a form of uraninite), and carnotite (a uranium-vanadate). Uranium phosphates, arsenates, vandates, and carbonates are common secondary minerals, and uranium sulfates, molybdates, tellurites, and selenites are less common.

Wastes from uranium milling contain only low levels of uranium; however, the levels of uranium progeny (e.g., radium) remain essentially unchanged from the ore. Uncontrolled erosion of these wastes from open tailings piles not protected from the weather occurred at a uranium mill site near Shiprock, NM, resulting in contamination of the surrounding area (Hans et al., 1979). Uranium releases also occur as a result of phosphate mining for production of phosphorous, which is used in phosphoric acid and phosphate fertilizers (NCRP, 1984). Phosphate rock from Florida, Texas, South Carolina and southeastern Idaho contains as much as 120 μg g^{-1} (80 pCi g^{-1}; 3.0 Bq g^{-1}) uranium, a concentration sufficiently high to be considered as a commercial source of uranium (NCRP, 1975). Uranium concentrations in phosphate rock in north and central Florida range from 6.8 to 124 μg g^{-1} (4.5–83.4 pCi g^{-1}; 0.17–3.1 Bq g^{-1}) (EPA, 1985). Uranium concentrations in soils can also be elevated owing to uranium enrichment associated with the nuclear fuel cycle and the production of nuclear weapons. For example, at the USDOE Feed Material Production Center at Fernald, Ohio (OH) site uranium concentrations were up to 10–50 times the background level of 2.2 pCi g^{-1} (0.08 Bq g^{-1}) (ATSDR, 2011; Stevenson and Hardy, 1993).

11.6.4.2.2.2.4 Water: background concentration levels The National Uranium Resource Evaluation (NURE) program and the US EPA compiled data obtained from over 90 000 water samples (ATSDR, 2011; NCRP, 1984; USGS, 2006). The data included about 35 000 surface water samples, averaging 1.1 pCi l^{-1} (0.041 Bq l^{-1}); 55 000 groundwater samples, averaging 3.2 pCi l^{-1} (0.12 Bq l^{-1}); and 28 000 samples from domestic water supplies, averaging 1.7 pCi l^{-1} (0.063 Bq l^{-1}). The population-weighted average concentration of uranium in US community drinking water was calculated to range from 0.3 to 2.0 pCi l^{-1} (0.011–0.074 Bq l^{-1}), or 0.4–3.0 μg l^{-1} (Ohanian, 1989). The population-weighted concentrations of uranium for individual states in the US ranged from 0.09 μg l^{-1} (New Jersey) to 7.99 μg l^{-1} (New Mexico) with a national average of 0.82 μg l^{-1} in drinking water supplies surveyed by the National Inorganics and Radionuclides Survey (NIRS) (Longtin, 1991). Another study showed that the average uranium concentrations in drinking water exceeded 2 pCi l^{-1} (0.074 Bq l^{-1}) in South Dakota, Nevada, New Mexico, California, Wyoming, Texas, Arizona, and Oklahoma (OK) (Cothern and Lappenbusch, 1983). The drinking water samples with the highest total uranium concentrations sampled in the RadNet program were obtained from Santa Fe, NM; Lincoln, Nebraska; Las Vegas, Nevada; and Los Angeles, California (listed in descending concentration of total uranium) (ATSDR, 2011). Uranium concentrations as high as 1160 μg l^{-1} were measured in drinking water from a home in northwestern Connecticut (ATSDR, 2011). As discussed below, surface waters contaminated by waste discharge and groundwaters from natural uranium-bearing aquifers exhibit uranium concentrations higher than the average local natural background levels.

11.6.4.2.2.2.5 Water concentrations at contaminated sites Uranium has been detected in surface water samples at 22 of 67 hazardous waste sites and in groundwater samples at 37 of 67 hazardous waste sites where uranium has been identified in some environmental component (ATSDR, 2011). Contamination of surface water and groundwater by effluents from uranium mining, milling, and production operations has been well documented (Eadie and Kaufmann, 1977; Swanson, 1985; Yang and Edwards, 1984) and is described in more detail in the next section. Examples of uranium values in groundwater and surface water include the Uravan site, where uranium levels ranged from 1500 to 16 000 pCi l^{-1}(56–590 Bq l^{-1}), and the tailings pond of the United Nuclear site, where uranium concentrations were as high as 3900 pCi l^{-1}(14 Bq l^{-1}). At the latter site, a break in the tailings pond dam in 1979 sent 93 million gallons of tailings liquid into the Rio Puerco (ATSDR, 2011).

Uranium is discharged to surface water and/or groundwater during open and underground mining operations. Groundwater must be removed if an open-pit or underground mine extends below the water table. The excess water typically contains high levels of uranium and is discharged into the ground or nearby bodies of water and may cause measurable increases in uranium levels in nearby surface waters. Waste waters from open-pit mines are typically 1–2 orders of magnitude greater in volume and radioactivity content than waters from shaft or underground mines. During operation, a typical open-pit mine could discharge a million gallons of water daily, giving combined uranium, radium, and radon releases of approximately 0.5 mCi day^{-1} (18.5 MBq) or nearly 200 mCi - year^{-1} (7.4 GBq) (ATSDR, 2011).

Discharge of dewatering effluents from underground uranium mines and runoff from uranium mine tailings piles contaminated surface waters and aquifers in New Mexico with elevated levels of gross alpha activity and uranium (NMHED, 1989). The concentration of uranium in mine discharge water in New Mexico was 31 500 μg l^{-1}, equivalent to 22 700 pCi l^{-1}

(840 Bq l^{-1}) assuming that the uranium content is natural uranium (EPA, 1985). Contamination of groundwater and surface water can also occur by water erosion of tailings piles (Goode and Wilder, 1987; Veska and Eaton, 1991; Waite et al., 1988). Since extraction of uranium ore during the milling process averages 90–95% recovery, the primary contaminants from uranium tailings disposal sites are uranium progeny (e.g., ^{226}Ra).

11.6.4.2.2.3 Uranium exposure and human health

11.6.4.2.2.3.1 Exposure pathways Food and drinking water are the primary sources of uranium exposure for the general public. Estimates of uranium intake from drinking water range from 0.6 to 1.0 pCi day^{-1} (0.02–0.04 Bq day^{-1}), or 0.9–1.5 μg day^{-1}, with a US-population-weighted average of 0.8 pCi l^{-1} (0.03 Bq l^{-1}) uranium (ATSDR, 2011). The daily intake of uranium from food sources is about the same. Uranium from soil is not taken up by plants, but rather is adsorbed onto the roots. Thus, the highest levels of uranium are found in root vegetables, primarily unwashed potatoes. Intake of uranium by inhalation is small, compared to food and drinking water, with estimated values ranging from 0.0007 to 0.007 pCi day^{-1} (3×10^{-5}–3×10^{-4} Bq day^{-1}), or 0.0010–0.010 μg day^{-1} (ATSDR, 2011).

People who work in or live near uranium mining, processing, and manufacturing facilities may be exposed to higher levels of uranium. The potential for exposure to uranium is highest in activities such as mining, milling, and handling uranium; processing uranium ore end products (uranium dioxide, uranium hexafluoride); producing nuclear energy and nuclear weapons; producing phosphate fertilizers from phosphate rocks that contain much higher-than-average levels of uranium; and improperly disposing of wastes. Populations living near uranium mills or mines or other areas with elevated uranium in soil may be exposed to higher levels of uranium from locally grown vegetables. Individuals living and working near fossil fuel plants may also have higher than average exposures (ATSDR, 2011; Miller, 1977; NAS, Biological Effects of Ionizing Radiation (BEIR) IV 1988a; NCRP, 1984; Tadmor, 1986).

Depleted uranium was used in the military conflicts in Iraq during 1991 and 2003, in Bosnia during 1994, and in Kosovo during 1999. The primary routes of exposure to depleted uranium include inhalation of aerosols formed during the high-energy collisions of depleted uranium munitions with vehicle armor, embedding of depleted uranium fragments in wounds to the body, and ingestion resulting from contact with depleted uranium residues on contaminated surfaces. Several studies have monitored the levels of uranium in the urine of individuals with reported exposure to the depleted uranium used during these conflicts. With the exception of individuals having depleted uranium-containing shrapnel embedded within their bodies, the levels of uranium measured in the urine of individuals reporting exposure were not different than levels in nonexposed individuals (ATSDR, 2011; Hooper et al., 1999; McDiarmid et al., 2001, 2004, 2009; Miller et al., 2008; Oeh et al., 2007a,b; Parkhurst and Guilmette, 2009; Toohey, 2003).

11.6.4.2.2.3.2 Environmental toxicology and epidemiology of uranium As discussed in detail in **Appendix B**, the chemical toxicity of uranium is more important than its radiological hazard. In body fluids, uranium is present as soluble U(VI) species, is rapidly absorbed from the gastrointestinal tract, and is rapidly eliminated from the body (60% within 24 h; Goyer and Clarkson, 2001). The uranyl carbonate complex in plasma is filtered out by the kidney glomerulus, the bicarbonate is reabsorbed by the proximule tubules, and the liberated uranyl ion is concentrated in the tubular cells. This produces systemic toxicity in the form of acute renal damage and renal failure. In addition, experimental animal studies and human epidemiology studies indicate that other uranium-related health effects of concern are developmental defects, reproductive outcomes, deoxyribonucleic acid (DNA) damage, and diminished bone growth. Many of the effects have been demonstrated most clearly in animals, but a growing body of human evidence has emerged from epidemiologic studies. More information from animal studies and details on the adsorption, distribution, and toxicity of uranium are provided in **Appendix B**.

Data from human epidemiological studies from environmental exposures support the health effects observed in animal studies at high doses. Pinney et al. (2003) found statistically significant elevations of urinary system diseases, including bladder and kidney disease, kidney stones, and chronic nephritis in community residents living in the area surrounding a US DOE uranium processing plant in Fernald, OH. During the period of operation from 1951 to 1958, an estimated 310 000 kg of airborne uranium was released, and 99 000 kg was released to surface water. Several ecological epidemiological studies examined possible associations between elevated levels of uranium in drinking water and indication of renal dysfunction (Kurttio et al., 2002; Limson-Zamora et al., 1998, 2009; Mao et al., 1995; Selden et al., 2009). In some, but not all of the studies, associations between biomarkers of degraded kidney function (e.g., urine levels of albumin, β2-microglobulin, glucose, and protein HC and elevated uranium levels in drinking water were observed. A lack of reliable dose–response data because of the wide range of exposure levels is considered a major weakness of these studies (ATSDR, 2011). As discussed in **Appendix B**, a chronic-duration oral minimum risk level (MRL) was not established because of the limitations in the human studies and lack of animal data examining the chronic toxicity of ingested uranium (ATSDR, 2011).

Several studies have examined the possibility that exposure to uranium can induce DNA repair deficiency in somatic cells as indicated by the frequency of chromosome aberrations. Au et al. (1995, 1998) examined blood samples from people living within 1.6 km of two U mining and milling sites and one U mining site in southern Texas ('exposed' population). These samples were compared with an 'unexposed' reference group located about 15 km predominantly upwind of the mining/milling areas. More chromosome aberrations were seen in the exposed individuals than in the reference population; however, the results were not statistically significant. In addition, gamma challenge assays suggested abnormal DNA repair capabilities in the blood cells of the exposed individuals.

A study of open-pit uranium miners (all nonsmokers) in Namibia (Brugge et al., 2005; Zaire et al., 1997) revealed a statistically significant increase in chromosomal aberrations in lymphocytes in the miner group. Prabhavathi et al. (2003) studied 160 nonsmoking workers employed in a nuclear fuel facility

where they were exposed to such uranyl compounds as uranium dioxide, uranium trioxide, uranyl fluoride, and uranyl nitrate. The results indicated a significant increase in the incidence of chromosomal aberrations, attributed to a cumulative effect of the chemical toxicity and radiotoxicity of uranyl compounds.

Studies of workers at uranium milling or nuclear facilities and residents living near uranium mining and milling facilities have not found significant increases in cancer mortality associated with uranium exposure when the effects of smoking and exposure to radon and its progeny are evaluated. Although increased mortality from lung cancer was noted in males living in Montrose County, CO (Boice et al., 2007b), and Grants, NM (Boice et al., 2010), occupational exposure to radon and smoking among underground uranium mine workers was considered to be the cause. Epidemiologic studies of workers at uranium mill and metal processing plants where there is little or no exposure to radon in excess of normal environmental levels showed no significant increase in overall deaths attributable to exposure to uranium (Archer et al., 1973; Boice et al., 2008; Polednak and Frome, 1981; Scott et al., 1972). Results of several other mortality assessments of populations living near uranium mining and milling operations have not demonstrated significant associations between mortality and exposure to uranium (ATSDR, 2011; Boice et al., 2003, 2007a).

11.6.4.2.2.4 Application: uranium contamination from mining

11.6.4.2.2.4.1 Overview of mining, processing, and disposal Open-pit mining, underground mining, and in situ leaching (ISL) (also known as ISR) have been used for mining uranium-containing ores. Waste from the first two techniques includes uranium mill tailings. About 41% of world uranium production comes from ISL and since 1994, most uranium in the US has been mined by this technique (ATSDR, 2011; WNA, 2011). The process of ISL essentially combines ore extraction and milling as discussed in detail in a subsequent section. Recent descriptions of other mining techniques and relevant ore deposits can be found in Merkel and Hasche-Berger (2008), Cuney and Kyser (2009), and Ulmer-Scholle (2011).

After mining, ores from open-pit or underground mines are crushed and leached in a uranium mill. Uranium production by mills and other sources in the United States from 1975 to 2009 ranged from 1100 (in 2003) to 21 852 (in 1981) short tons (ATSDR, 2011). The extraction of uranium from the ore by conventional or in situ methods generally involves leaching with sulfuric acid (H_2SO_4) or with carbonate (Na_2CO_3) if large amounts of carbonate are present.

The sulfuric acid leaching method can be represented by the following reaction:

$$UO_2 + 3H_2SO_4 + {}^1/_2O_2 \rightarrow \left[UO_2(SO_4)_3\right]^{4-} + H_2O + 4H^+.$$

Alkaline leaching with sodium carbonate proceeds by the following reactions:

$$UO_2 + {}^1/_2O_2 \rightarrow UO_3.$$

$$UO_3 + 3Na_2CO_3 + H_2O \rightarrow \left[UO_2(CO_3)_3\right]^{4-} + 4Na^+ + 2NaOH.$$

Uranyl ions are stripped from the extraction solvent and precipitated as yellowcake (predominantly U_3O_8), which is pressed, dried, banded, and shipped for refinement and enrichment. The waste from this process is called tailings and is discussed in detail in the next section.

Enriched uranium, which has a ^{235}U concentration >20% is produced by the conversion of yellowcake to uranium hexafluoride (UF_6) through a multistep chemical reaction beginning with dissolution in nitric acid, solvent extraction to remove impurities, precipitation with ammonium hydroxide, and fluorination. The final product, UF_6, is processed, producing enriched uranium and depleted uranium waste. Raffinate, a by-product of the yellowcake enrichment process is an acidic waste that contains trace amounts of toxic heavy metals as well as uranium, radium, and thorium and their decay products. As discussed below, this waste can leach into the groundwater from settling ponds or runoff to contaminate soils or groundwater when not disposed of properly.

11.6.4.2.2.4.2 Uranium mill tailings: introduction UMTs are the residual sand containing trace chemicals produced from the processing of uranium ore. About 75 000 tons of ore are required per year to produce the 150 tons of enriched uranium needed to fuel a 1000-mW electric nuclear power. Estimates of the total historical accumulation of uranium in licensed mill tailings piles in the US range from 200 to 240 million tons (Abdelouas, 2006; ATSDR, 2011; Landa, 2004; Murray, 1994). The worldwide mining of uranium has generated 9.38×10^8 cubic meters of tailings; the largest volume has been produced in Kazakhstan (2.09×10^8 cubic meters) (Abdelouas, 2006).

Historical disposal methods for processed uranium tailings have been discussed by Bearman (1979). In the late 1940s, mainly unconfined disposal systems were used. Untreated solid wastes were stored as open piles and, in some cases, were spread in urban areas where they were used as fill and as sand in concrete and brick mortar used to build structures, roads, walks, and driveways. Under the UMTRCA of 1978 (NRC, 2002), the US DOE designated 24 inactive tailings piles associated with nuclear weapons production for cleanup. These Title I sites contained a total of about 28 million tons of tailings and covered a total of approximately 1000 acres (ATSDR, 2011). Additional mill tailing sites licensed during or after 1978 by the USNRC or several states are regulated under the Title II program. By 2006, the US DOE had completed the surface remediation of all but one Title I site (Grand Junction, CO) and had transferred them to the long-term surveillance plan, which conducts annual inspections and groundwater monitoring at the disposal sites.

The US NRC licensed 16 Title II uranium recovery facilities under 10 CFR Part 40 regulations (USNRC, 2011). These included 12 conventional uranium mills and 4 ISL facilities. In 2010, one conventional uranium mill and four uranium in situ leach plants were in operation in the US (ATSDR, 2011). The remaining conventional uranium mill sites have completed, or are completing reclamation activities to provide long-term stabilization and closure of the tailings impoundments and the sites. The tailings from conventional milling consist of crushed rock in a processing fluid slurry and are placed in a tailings pile/cell, which is a constructed impoundment or a former uranium mine pit (the waste from ISL uranium extraction is produced in a processing plant, which separates the uranium from the mining solution; waste from this process is

disposed in a tailings pile at a mill site). The tailings pile construction must meet criteria in 10 CFR Part 40, **Appendix A**, including requirements for siting and design of the pile, cover performance and financial surety for decommissioning, reclamation, and long-term surveillance. The US NRC and US EPA groundwater standards for tailings sites and inactive sites are as follows: combined ^{226}Ra and ^{228}Ra: 0.185 Bq l^{-1}, gross alpha-particle activity: 0.555 Bq l^{-1}, combined ^{238}U and ^{234}U: 1.11 Bq l^{-1} (equivalent to 0.044 mg l^{-1} for equilibrium). Additional requirements apply to ^{226}Ra concentration at different depths in the soil, ^{222}Rn decay product concentration, and the level of gamma radiation. As discussed more fully in a later section, uranium mining by conventional underground and in situ extraction led to widespread contamination in Eastern Europe and the FSU. Discussion of recent cleanup of UMT in these areas is found in (Clarke and Parker, 2009).

The groundwater remediation phase of the UMTRA program mill tailings began in 1991. Although many of the tailings piles had been relocated to lined storage cells, the seepage of acidic metal-bearing solutions from the tailings into the ground had left a 'footprint' of contaminants that acted as a source for groundwater contaminant plumes. In 1997, the DOE proposed a three-pronged risk-based framework to remediation of the sites that included active, passive, and no-remediation strategies depending on site-specific conditions (DOE, 1996a,1997a,b). For example, at the Shiprock, NM site, DOE initiated an extraction system that removes contaminated water from the subsurface of the floodplain and terrace areas. Groundwater is extracted from 12 extraction wells and 2 interceptor drains and transported to a 111-acre solar evaporation pond located south of the disposal cell. The wells are strategically placed to extract groundwater from the contaminated plume. Pumping from the extraction wells may continue for as long as 20 years. At Tuba City, NM an active remediation system that consists of extraction wells was followed by treatment of the extracted water using ion exchange, degasification, and distillation. The treated water is cleaner than the site groundwater and injected into the aquifer. Descriptions of history and current status of management of the Title I and Title II sites can be found on the DOE office Legacy Management website (DOE, 2011).

In addition to the contamination of groundwater and surface water owing to seepage of fluids from unlined tailings, catastrophic or chronic failure of containment structures is a major cause of environmental impact. Chronic failures include dispersal of radioactive dust from dry tailings, erosion of tailings from outer surfaces of the containment structure, and effluent discharge. Hundreds of incidents involving active and inactive tailings dams have been reported; most of them were caused by slope instability, seepage, overtopping, and earthquakes (Strachan, 2002). A breached dam wall at a uranium tailings facility at Church Rock, NM, released 370 000 m^3 of radioactive water and 1000 tons of contaminated sediment, affecting some 110 km of the Rio Puerco (IAEA, 2004).

11.6.4.2.2.4.3 Geochemistry of mill tailings

11.6.4.2.2.4.3.1 Mineralogy of tailings Mill tailings contain crushed rock with fine-grained primary and secondary minerals. Primary minerals are phases that have resisted the leaching in the mill and remain relatively unchanged (silicate minerals such as quartz, feldspar, and clay, along with remaining sulfides). Secondary minerals (e.g., Fe-oxyhydroxides and Ca-sulfate) form by the precipitation of ore species and reagents added during processing and neutralization. The fine fraction of the tailings, including colloids, consists mainly of clay, sulfate salts [e.g., gypsum ($CaSO_4$:$2H_2O$), barite ($BaSO_4$)], and oxyhydroxides of Fe, Al, Mn, and Si. Radionuclides and metals can be associated with many of these mineral phases. Compositions of tailings from several sites reviewed by Abdelouas (2006) had compositional ranges (mg kg^{-1}) as follows: SO_4: 6760–110 552; Ca: 17 700–52 500; Al: 34 100–69 527; Fe: 27 000–7640; As: 48–5640; Pb: 72–749; V: 205–2 820; U: 126–350. Tailings typically contain all the ^{226}Ra initially present in the ore. Radioactive components include ^{226}Ra: 8.78–74 Bq g^{-1} and ^{230}Th: 3.93–32.3 Bq g^{-1}.

A number of processes lead to the formation of reactive Fe, Mn-oxyhydroxides, which scavenge dissolved and colloidal contaminants in UMT. These include (1) neutralization of tailings waste streams by the addition of process reagents such as MgO, CaO, or $CaCO_3$, (2) combination of acid- and alkaline-leach UMT (Landa, 1987) prior to discharge, (3) 'self-neutralization' in which residual acidity is consumed by reaction with tailings solids, such as clay minerals present in the ore (Fordham, 1993), and (4) processes in pre-oxidized, sulfidic, subaqueous UMT. In those tailings, surface disposal was followed by flooding and under water storage. During the initial, aerial period, dissolution of sulfides led to high ferrous iron concentrations in the pore waters. A layer of hydrous ferric oxide formed at the air–surface interface and at the water–surface interface upon flooding (Catalan et al., 2000; Martin et al., 2003).

As discussed previously, uranium (VI) can be strongly adsorbed by iron oxyhydroxides. ^{230}Th is also likely to be associated with iron oxyhydroxides. An Fe-oxide-rich 'red mud' contained about 58% of the ^{230}Th in the processed U ore from a H_2SO_4-leach U mill in Slovenia (Krizman et al., 1995). Radium in mill tailings is generally sorbed and coprecipitated with Fe–Mn oxyhydroxides, gypsum, and barite. Selective leaching trials have shown iron and manganese oxides to be important hosts of ^{226}Ra in acid-leach UMT (Somot et al., 1997). Coprecipitation with amorphous silica may play an important role in retention of ^{226}Ra and ^{230}Th (Landa, 2004). Jarosite [$KFe_3(SO_4)_2(OH)_6$] can also be an important host for ^{226}Ra and other environmental contaminants such as lead, mercury, copper, zinc, silver, chromium, arsenic, and selenium, which are incorporated into the jarosite structure by ionic substitution (Landa, 2004). Coprecipitation with carbonate and phosphate [e.g., autunite, $Ca(UO_2)_2(PO_4)_2$] may play a significant role in U stabilization in mill tailings disposal sites (Abdelouas et al., 1998, 2000; Ohnuki et al., 2004).

Diagenetic processes in aging UMT may influence the long-term behavior of uranium, radium, and other metals in these systems. Multiple, sequential reactions (sorption by iron oxyhydroxides, coprecipitation by barium sulfate) will immobilize radium. Amorphous iron oxyhydroxides may age to goethite, providing a more stable host for radium even under acidic condition owing to specific sorption below the zero point of charge.

11.6.4.2.2.4.3.2 Geochemistry of aqueous contamination from mill tailings Concentrations of uranium within tailings and in

runoff from mine tailing piles can be orders of magnitude higher than background values. Typical U concentrations in tailings pore waters range from less than 0.1 mg l^{-1} under reducing conditions to a few milligrams per liter under oxidizing conditions (Lottermoser and Ashley, 2005). The US EPA has measured uranium concentrations as high as 3.15 mg l^{-1} in mine-discharge water (Orloff et al., 2004).

Migration of contaminants from an unlined acid tailings repository and evaporation ponds into the local unconfined aquifer has been demonstrated by (Lottermoser and Ashley, 2005). U, ^{226}Ra, ^{210}Pb, As, Fe, and Mn are mobilized from the upper oxidized part of the tailings pile into surface water seepages. The spreading plume that originates from tailings dams can move at rates of several tens of meters per year (von der Heyden and New, 2004). In alkaline mill tailings, migration of U into groundwater is facilitated by the formation of stable uranyl carbonate complexes [$UO_2(CO_3)_2^{2-}$ and $UO_2(CO_3)_3^{4-}$] as shown by Abdelouas et al. (1998a) in groundwater near a tailings pile at an UMTRA site near Tuba City, AZ. In addition to U, the plume contained high concentrations of nitrate (~1 g l^{-1}) and sulfate (~2 g l^{-1}). A 12-m saturated zone was contaminated by the plume, which was moving at an average rate of 15 m $year^{-1}$.

Oxidation of sulfides, resulting in generation of acid pore waters, followed by seepage of acid waters, in particular from unlined mill tailings, are the main processes leading to the contamination of soils, surface water, and groundwater surrounding mill tailings. Oxidation may occur not only in the upper part of the tailings (Lottermoser and Ashley, 2005), but also in the bottom part due to infiltration of oxygen-rich groundwater. Desorption of uranium, radium, thorium, and hazardous elements occurs in low-pH waters, increasing their concentration. Low-pH waters may also dissolve large quantities of secondary phases, including Fe-oxyhydroxides and carbonates, containing radionuclides and heavy metals.

Under slightly acidic to alkaline conditions, thorium is highly insoluble (ThO_2, $Th(OH)_4$). However, the solubility of thorium increases in acidic aqueous solutions (pH < 4), therefore acidification of tailings waters may lead to the release of Th into the environment (Abdelouas, 2006). Ferric hydroxides formed as a result of neutralization of leachates from UMTs can have high concentrations of ^{230}Th (25.1 kBq kg^{-1}) compared to U ore (8.78 kBq kg^{-1}) and mill tailings (3.93 kBq kg^{-1}) (Krizman et al. 1995). In acidic tailings liquids, the ^{230}Th concentration may be very high (1.7×10^{-8} M), but it drops drastically at pH ≥ 4.6 (7.2×10^{-12}–2.4×10^{-13} M) (Lottermoser and Ashley, 2005). The processing history of the U ore may have a large impact on the bioavailability of ^{230}Th in UMT. Reif (1994) investigated the kinetics of ^{230}Th solubilization of the <38 μm sieve fraction of acid-leach (Rifle, CO) and alkaline-leach (Ambrosia Lake, NM) UMT in simulated lung fluid. The alkaline-leach UMT showed much greater release, yielding about 30% in 1 month versus about 2% for the acid-leach tailings. Because ^{230}Th may be responsible for the majority of the inhalation radiation dose associated with UMT, this difference may have public health implications (ATSDR, 2011).

11.6.4.2.2.4.3.3 Bacterial processes Bacteria activity in UMTs will affect the distribution and release of uranium and radium. Under reducing conditions, anaerobic bacteria in mill tailings sites reduce U(VI) to U(IV), resulting in the precipitation of highly insoluble uraninite, while at the same time, microbial iron reduction occurring in anaerobic zones of the red mud in the tailings can mobilize ^{230}Th. Sulfate-reducing bacteria have been identified in U heap leaching piles and UMT (Schippers et al., 1995). Dissolution of alkaline earth sulfate minerals such as barite ($BaSO_4$), may mobilize coprecipitated ^{226}Ra; this has been demonstrated in both laboratory studies (Landa et al., 1986) and observed at the Norman, OK, landfill research field site (Ulrich et al., 2003). Martin et al. (2003) describes the ^{226}Ra profile in a flooded (0.3–3 m water depth) mill tailings deposit cell. At shallow (<1.5 m) water depths, oxidizing conditions lead to low radium concentrations owing to coprecipitation with poorly crystallized barite. However, at greater depths (~2 m), reduction of sulfate by sulfate-reducing bacteria resulted in barite dissolution and release of radium. Other potential microbial reactions include sulfide oxidation, catalyzed by autotrophic bacteria such as *Acidithiobacillus ferrooxidans* and *Acidithiobacillus thiooxidans* (Abdelouas, 2006); dissolution of iron oxyhydroxides by the action of the Fe(III)-reducing bacteria can release radium; and microbial reduction and subsequent remobilization of U(VI), which was observed by Senko et al. (2002) at the Norman, OK field site. There, the intermediate products of denitrification (nitrite, nitrous oxide, and nitric oxide) were able to oxidize U(IV) and mobilize previously reduced U.

Sulfate-reducing and iron-reducing microorganisms may also lead to jarosite dissolution and the release of Ra and other contaminants. The relative amounts of sulfate stored in phases such as jurbanite ($AlOHSO_4 5H_2O$) and jarosite, as compared to sulfate sorbed onto HFO, will affect the seepage of the acidic UMT pond solution into the aquifer, and then the flushing of the affected zone by uncontaminated upgradient groundwater after the source of the contamination is removed (Zhu et al., 2001). Fortine and Beveridge (1997) note that sulfate reduction in sulfidic mine tailings is most likely limited by the supply of organic carbon. In UMT, organic carbon supplies may include solvents used in the milling circuit, carbonaceous ores such as lignites, wood chips used in covers, and sewage sludge and other organic amendments used during decommissioning activities to promote establishment of a vegetative cover and to limit oxygen penetration and pyrite oxidation (Landa, 2004).

11.6.4.2.2.4.3.4 Long-term behavior of mill tailings: soil analogs The mobility of radionuclides in soil horizons that develop over UMTs will depend on uptake and release by soil components (e.g., clay minerals, iron and manganese oxides, humic substances). Spodosols developed on hydrothermally altered Conway granite in the northeastern US (known for its high content of U and Th), provide a pedogenic natural analog. On the basis of selective extraction studies to assess the host phases of U and Th, Evans et al. (1997) concluded that Th appears to translocate from the A horizon to the B horizon. Iron oxides host phases for Th dissolve in the A horizon, and accumulate in new iron oxides precipitating in the B horizon. Organic matter and iron oxides are important hosts for U in these soils (Morton et al., 2001). Migration rates will be a complex function of both downward leaching and recycling to the surface by plant uptake of bioavailable fractions of the mobile radionuclides. Pedogenic processes (e.g., aggregation of fine particles, formation of secondary minerals, development of structural

planes and of root and earthworm channels that may act as preferential flow pathways) will modify the physical and hydraulic properties of engineered covers on UMT over time (Landa, 2004).

11.6.4.2.2.4.4 *ISR* of Uranium

11.6.4.2.2.4.4.1 General description ISR or ISL is a mining method in which specially formulated lixiviants are injected into uranium-containing porous rock formations. The solutions leach out the uranium from the rock and the resultant ore solutions are pumped to the surface for processing at surface facilities. During the processing, the uranium is extracted from the ore solution by ion exchange (IX), the IX resin is flushed with a brine to create a solution more concentrated with uranium, precipitated to form a sludge and then dried to produce yellow cake.

Rock formations that are amenable to in situ leach mining are typically porous, granular materials that contain high concentrations of uranium and are sandwiched between impermeable (usually clay-rich) rock strata. These conditions allow miners to inject the lixiviant into a designated vertical interval of the porous rock and control the direction that the ore solution travels as it moves to a withdrawal well. The injection wells in a single well 'pattern' are placed at the apices of a square, pentagon, or octagon with a single withdrawal well at the center. For narrow fronts, the well pattern of choice is often 'alternating single-line drive' – a single line of alternating well-types following the sinuosity of the ore front. Often these narrow fronts make up the majority of ore at a site.

Major ISL sites in the US occur in South Texas, Wyoming, Nebraska, and New Mexico. Descriptions of historic and current ISL sites are given by Montgomery (1987), Mudd (2001a), and Pelizza (2007, 2008). Deposit depths range from 33 to 760 m; ore zones are from several to tens of meters thick with porosities typically 20–30% and permeabilities of 0.09–1.43 m day^{-1}. Vanadium contents are variable in the low permeability deposits in Wyoming and Nebraska, molybdenum and humate contents can be high in the thick, high-permeability New Mexico deposits, and molybdenum contents are low in the thick, clean sand deposits of South Texas.

The following criteria are generally considered favorable to the success of ISL in an ore body (Montgomery, 1987; Underhill, 1992):

- Occurrence in porous and permeable rocks (usually a sand or sandstone).
- Confinement above and below by continuous impermeable strata such as clays or shales.
- Location below the water table.
- Artesian water pressure (15–75 m) relative to the overlying confining layer.
- Uranium mineralization in a readily leachable form, for example, coffinite or uraninite.
- Minimum grade and thickness sufficient for economic recovery of the contained uranium.
- Effective contact between the leach solution and uranium minerals.

The following are considered potential 'fatal flaws' for the suitability of a uranium deposit for ISL (Montgomery, 1987):

- Presence of humates or organics.
- Uranium mineralization in clays or silts.
- High molybdenum or vanadium concentrations.
- Thin, sinuous, and deep mineralization.
- Poor vertical solution confinement.
- Highly faulted formation.

11.6.4.2.2.4.4.2 Choice of leaching solution Because uranium is soluble under both acidic and alkaline conditions, it is possible to use either acidic or alkaline leaching. Sulfuric and nitric acid are commonly used in the former case; ammonia bicarbonate, sodium bicarbonate, or carbon dioxide have been used for alkaline leaching. Because uranium is soluble as U(VI) species, an oxidant must also be introduced to maintain oxidizing conditions; these include hydrogen peroxide, oxygen, or sodium chlorate ($NaClO_3$).

Historically, the choice of leaching chemistry has been dictated by (1) potential or desired uranium mineral dissolution rate; (2) potential chemical reactions between leaching solutions and gangue minerals and their effects on hydrologic properties of the aquifer such as a reduction in permeability, (3) requirements to restore groundwater quality to premining levels after the completion of ISL mining, and (4) cost of the chemicals (Mudd, 2001a). Some early ISL pilot operation in the US used ammonia bicarbonate leach solutions, however, reactions with clay minerals in the formations led to chemical and hydrologic problems. Ammonia adsorbed by the clays within the aquifer is undetectable by standard groundwater monitoring techniques. One estimate suggested that after mining, approximately 2 tons of ammonia remained adsorbed within an aquifer zone only 12×12 m in area (Mudd, 1998). Acid leaching was used in the USA in the late 1960s through to the early 1980s, and has been used extensively in Europe and the FSU. ISL projects in China, Mongolia, and Kazakhstan are also using or planning to use sulfuric acid ISL chemistry. In general, acid solutions will extract a higher proportion of uranium and at faster rates than alkaline solutions but acidic solutions will also mobilize high levels of toxic heavy metals (such as cadmium, selenium, vanadium, lead, and others). This has led to extensive groundwater contamination as discussed below. Lower levels of radium, however, are mobilized in sulfuric acid leach operations compared to alkaline leach operations because of the low solubility of radium sulfate.

Currently in the USA, all current or proposed ISL uranium production uses alkaline leaching chemistry with carbon dioxide or sodium carbonate and oxygen. Advantages of alkaline over acid leach solutions include (1) significantly lower levels of impurities, (2) higher efficiency of regenerating and recycling leaching solutions owing to less impurity problems, resulting in smaller waste stream flow rates, (3) relatively noncorrosive solutions with a lower probability for mechanical failure and spills, (4) lower precipitation of calcite and gypsum in the extraction process, and (5) the low cost of carbon dioxide and its negligible effect on aquifer permeability.

11.6.4.2.2.4.4.3 Processing After the pregnant lixiviant is extracted from the ore zone, it is pumped to the processing plant, where the uranium is extracted using standard metallurgical techniques such as solvent extraction or ion exchange. The ISL process leads to the formation of liquid and solid waste streams including bleed solutions, waste processing solutions, solid residues from the precipitation of minerals from the

highly concentrated solutions, solid waste from the processing plant (such as contaminated clothing and equipment), and other normal wastes from industrial facilities. The different wastewater streams are temporarily stored in a retention pond. The final disposal method can be either re-injection into the same aquifer, re-injection into a deeper aquifer that is unused and does not interact with other aquifers that are currently used, or evaporation of the water to leave a solid residue that can be disposed of in an engineered facility designed to minimize leakage of contaminants.

11.6.4.2.2.4.4.4 Site restoration Eventually, most of the uranium will be leached from the host rock volume within a well field and the concentration of uranium in the ore solution will drop to a low level. At this point, restoration of the well field to return the water quality of the aquifer to a 'safe' level begins. Both groundwater sweep and permeate injection are used in the groundwater restoration phase. In the former process, the depleted well field is pumped without reinjecting the withdrawn fluid; water from surrounding areas is drawn to the well field. The process water is treated to remove residual uranium and radium. In a later phase of restoration, process water is further cleansed by reverse osmosis and then re-injected to enhance groundwater restoration. In some cases, chemical remediation or bioremediation is attempted. Chemical remediation typically involves addition of a reducing chemical such as hydrogen sulfide or sodium sulfide Na_2S to cause the precipitation and immobilization of most contaminants. Bioremediation involves addition of nutrients such as acetate and molasses to promote the growth of indigenous bacteria, whose metabolic activities will lead to reducing conditions, as discussed previously. In the final restoration phase, pumping and re-injection of groundwater continues to obtain uniform conditions throughout the leaching zone. In theory, after a certain number of volumes of pore fluids are pumped through the depleted well field, the water remaining in the aquifer should no longer contain hazardous levels of contaminants.

Estimates of the restoration costs are dependent on estimates of the volume of pore water required to be flushed through the mined portions of the aquifer to return the groundwater to pre-mining or acceptable alternative water quality levels. Those estimates of fluid volume are based, in turn, on these restoration water quality criteria. Common ISR industry practice is to set the primary restoration to be a return to pre-mining baseline conditions. In the event that this is impossible, alternative restoration criteria can be established on a case-by case basis which will return water quality to MCLs specified in EPA's secondary and primary drinking water regulations or class of use criteria. As discussed later, the reliability of estimates of the required pore volumes and whether an ISL site can be returned to conditions that do not pose a threat to public health is a topic of considerable current controversy.

11.6.4.2.2.4.4.5 Environmental issues *Waste*: ISL mining may generate large volumes of wastewaters, which are often highly saline and contain toxic levels of heavy metals, process chemicals, and radionuclides. The bleed solution (the excess water pumped out over that injected) is often the most significant component. For ISL mines operated at 25 $l\,s^{-1}$ (a relatively small scale), the quantity of water pumped each day would be 2 160 000 l, which for a 2–5% bleed solution would form 43 200–108 000 $l\,day^{-1}$ to dispose of (or 15 768 000–39 420 000 $l\,year^{-1}$). Some ISL mines operate at flow rates of greater than 100 $l\,s^{-1}$, and thus the quantities of water involved are proportionally higher (Mudd, 1998).

Radiological hazards: The principle radioactive elements released during ISL uranium mining are uranium, thorium, radium, radon, and their decay products. Alkaline leaching mobilizes higher quantities of radium than acid leaching because of the low solubility of radium sulfate, whereas acid leaching mobilizes significant concentrations of thorium (Mudd, 1998). The main source of radiation exposure to workers in uranium mining operations is from radioactive radon gas, the decay products of radium and thorium. The radium and radon are transported in the mining and processing solutions to the surface and then pumped to retention ponds. Appreciable quantities of radon can be released and transported in the direction of prevailing winds significant distances away from the mine. The venting of uranium dust and residues that build up around the processing plant are also sources of environmental contamination.

Excursions: The most critical part of the ISL process is to control the movement of the chemical solutions within the aquifer. Any escape of these solutions outside the ore zone is considered an excursion, and can lead to contamination of surrounding groundwater systems. Potential causes of excursions can be released through old exploration holes that were not plugged adequately, plugging or blocking of the aquifer causing excess water pressure buildup and breaks in bores, and failures of injection/extraction pumps. Operation of the well-field patterns, that is, well flows relative to each other or 'well balance,' well pattern design, velocity and direction of natural groundwater movement, and so on, must be considered to minimize excursions. Well-field 'bleed,' in which water is withdrawn at a faster rate (about 1% higher) than it is injected, may be important. This creates a cone of depression that, in principle, should always cause water from surrounding areas to flow into the well pattern. The size and geometry of the cone of depression can be predicted to a certain extent with standard groundwater modeling theory and computer models; however, the predictions are only as reliable as the description of the rock layer geometry and porosity. Well-field bleed by itself will not preclude excursions; well-field operation can cause an excursion at 10% bleed, or have no excursions with 0% bleed. During the early phases of well-field development, simple models with rough estimates of geohydrologic properties obtained from exploration wells are used in the calculations. As the well field is developed and more information is obtained from the production wells, the predicted behavior of the cone of depression is refined.

Poor recovery and post-restoration releases: Poor recovery and post-restoration releases of contaminant from ISL sites can be related to several geochemical processes. These include precipitation of minerals containing trace metals and radionuclides, ion exchange with clays, and processes related to the presence of organic matter within the aquifer. In acid mining, clogging of the well with precipitates, such as jarosite (Landa, 2004; Mudd, 2001a) can inhibit flow. As mentioned previously, jarosite can contain significant amounts of contaminants (As, Pb, Hg, Cu, Zn, Cr, Se, Ra), which may be released to the environment during aquifer flushing with previously

uncontaminated groundwater (Mudd, 1998). During the post-mining period at an ISL site, when either active restoration measures or passive flushing by upgradient groundwater are underway, lower sulfate concentrations and higher pH, or the action of sulfate-reducing and iron-reducing microorganisms, may lead to jarosite dissolution and the release of Ra and other contaminants (Landa, 2004).

The presence of swelling clays such as montmorillonite undergoing ion exchange can lead to structural instability and a significant reduction in permeability of the aquifer material involved (Landa, 2004). At several early ISL sites in the USA, ion exchange of sodium or ammonium ions with clays caused severe problems with loss of permeability (Charbeneau, 1984; Mudd, 1998). This loss of permeability led to lower flow rates through the aquifer and higher pumping costs. In addition, any element that is adsorbed onto a clay can later be released upon a change in overall groundwater chemistry, hampering the restoration of groundwater quality. The presence of organic matter within aquifer can lead to enhanced solubilities of trace metals and radionuclides and potential release after the ISL operations are completed. In addition, the presence of organic matter or humates can also lead to the growth of microbial populations, aquifer plugging, and reduced permeability (Brierley and Brierley, 1982; Yates et al., 1983).

Several problems were encountered at acid leach ISL pilot and production sites developed in the US in the 1960s to 1980s. These can be summarized as (compiled from Charbeneau, 1984; Mudd, 2001a; Nigbor et al., 1982; Underhill, 1992):

- Precipitation of minerals, such as calcite ($CaCO_3$) and gypsum ($CaSO_4$), causing pipe blockages and solution control problems.
- Reprecipitation of uranium.
- Buildup of toxic heavy metals in solutions.
- Difficulty of restoring groundwater quality after ISL mining ceases for all environmentally sensitive elements.
- Clogging of the aquifer and well screens by bacterial growth.
- Inadequate engineering design of the processing plant and associated infrastructure, such as the evaporation pond.
- Leaking bore casings and well completion and construction.
- Clogging of the aquifer formation near production wells.
- Control of solution movement owing to the above problems.

The neutral to mildly basic pH established underground by modern ISR reagents is far less likely to produce the large-scale heavy metal mobilization caused by older acid-wash technologies. However, elements such as selenium, arsenic, vanadium, and molybdenum, which form oxy-anions and usually are found with the uranium in sandstone-type deposits, are still mobilized by acid-free ISR technologies (Erskine and Ardito, 2008; Schoeppner, 2008).

11.6.4.2.2.4.4.6 Case histories *Nine Mile Lake, Wyoming, USA*: Although the majority of ISL operations in the US use alkaline leaching solutions, several attempts to test acid leaching have been made (Mudd, 1998, 2001a; Staub et al., 1986). For example, pilot scale acid leaching operations were carried out at Nine Mile Lake in the Powder River Basin of Wyoming from 1976 to 1981 (Mudd, 2001a; Nigbor et al., 1982). This roll front uranium ore body has an average thickness of 3 m and lies within the Teapot Sandstone, which consists of upper and lower sands separated by 0.6–1.2 m of semipermeable shale and lignite. The dominant uranium mineral was uraninite (UO_2) with minor amounts of coffinite ($U(SiO_4)_{1-x}OH_{4x}$). The major clay mineral was kaolinite, with minor amounts of montmorillonite and the overall carbonate content was less than 0.1%. The Nine Mile Lake site was considered ideal for acid leach because of the low carbonate content of the ore body and the low cost of sulfuric acid. The test evaluated different methods of restoration and compared acid to alkaline leach effectiveness. Attempts to return the groundwater to pre-mining quality failed to restore U, V, Zn, Se, pH, and ^{226}Ra to pre-mining levels. Although the test showed that acid leach was effective, the test failed to demonstrate that acid leach was more cost-effective than the alkaline leach test owing to greater reagent consumption and the expense and difficulty of restoration. High levels of radioactive thorium were mobilized and the chemical state remained oxidizing and slightly acidic, leading to concerns over continued mobilization of many elements. For example, residual uranium content was the 5.65 times the pre-mining levels after restoration. There was no geochemical data or processes presented to demonstrate that this redox potential and acidity would be consumed as this groundwater flowed away from the ISL pattern through the aquifer (Mudd, 1998, 2001a; Staub et al., 1986).

Straz Deposit, Hamr District, Czech Republic: The Straz deposit in the Hamr District of the Czech Republic provides a good example of problems associated with full-scale acid ISL (Mudd, 2001b; Slezak, 1997). The Stráz site ceased producing uranium on April 1, 1996; the total uranium production by ISL was 13 968 tons (16 470 tons U_3O_8). Complex hydrogeological and biological conditions made application and success of ISL extremely difficult. The dissolution rates of uranium were slow, therefore large doses of chemicals were required (sulfuric acid at about 5% with nitric acid and nitrate as the main oxidants). Starting in 1968, more than 4 million tons of sulfuric acid, 300 000 tons of nitric acid, and 120 000 tons of ammonia were injected into the subsurface to mine uranium ore. The leaching solutions from the Stráz wellfields were not operated with a bleed system to maintain a cone of depression around the wellfields. More than 266 million cubic meters of groundwater (720 million cubic meters of aquifer material) in the North Bohemian Cretaceous Cenomanian and Turonian aquifers are contaminated with uranium, radium, and manganese and other solutes. Approximately 50% of the contaminated water is thought to be residual leaching solutions, with sulfate higher than 20 000 mg l^{-1} and salinities between 35 000 and 70 000 mg l^{-1}. Estimates of the contaminated area range from 6 km^2 to more than 24 km^2 and it threatens the watershed of the Plucnice River and the Dolánky water supply. Currently, restoration programs are aimed at determining the optimal strategy for long-term remediation and restoring groundwater quality. The technology being used for restoration involves pre-treatment, reverse osmosis, volume reduction by evaporation, crystallization, and processing of the concentrated saline solutions or brines. Additional ecologic problems have resulted from the ISL. The region, once covered

by pine forests, underwent significant deforestation for mining purposes and the forest is no longer sustainable.

Other sites: In Europe and the FSU, large areas have been contaminated by uranium mining. Aggressive acid leach techniques using large amounts of sulfuric and nitric acids were used in solution mining operations in the FSU. These operations created a legacy of widespread contamination comprised of large volumes of groundwater contaminated with acid and leached metals. Mudd (2001b) and IAEA (1992) summarize information about ISL practices in the FSU and Asia. The majority of the ISL projects used sulfuric acid, and the residual leaching solutions from ISL mines have migrated away from the mining zones. At the Haskovo site in Bulgaria, for example, surface waters in a valley downstream from the deposit have a sulfate concentration of 1400 $\mu g\, l^{-1}$ and a pH of 2.2. Private wells have high sulfate concentrations, indicating that the leaching solutions have impacted water supplies. At some sites, where there were surface spills owing to failure of distribution pipes, the uranium and radium content of soils is 10 and 2–3 times the background level, respectively.

Other ISL sites in the FSU include Konigstein and Ronneburg in Germany, Devadov in the Ukraine, Kazakhstan, and numerous deposits in Uzbekistan (IAEA, 1992). In Koenigstein, both underground and ISL mining in the stopes was carried out. The principal concerns for restoration of the site are centered around the flooding of the underground mine workings that occurs after the mine is closed down. There is significant potential for contamination of surrounding groundwater and surface water streams with uranium, radium, sulfate, iron, and heavy metals (Mudd, 2001b). Large-scale ISL mining using sulfuric acid began in Kazakhstan in 1978 and continues to expand at the present. Kazakhstan's uranium reserves are the second largest in the world (Australia has largest) and it is currently the world's largest producer of uranium.

11.6.4.2.2.4.4.7 Current controversies Interpretation of the success of historical attempts to restore sites mined using ISL techniques is one of the most controversial aspects of the uranium mining industry. Much of the controversy is owing to the disagreement over the level of restoration required to be protective of public health. As noted above, ISL industry practice is to set the primary restoration goal to be a return to pre-mining conditions. However, a return to pre-baseline conditions based on matching pre-mining concentrations of priority contaminants has rarely been accomplished. Instead, alternative restoration criteria based on pre-mining industrial class-of-use have been used by the mining industry. These criteria are defined by environmental regulations; groundwater in the production zones is not suitable for domestic use because of high concentrations of uranium, heavy metals, and other solutes; therefore, restoration to levels required for domestic use are not required.

Experiences at a number of US pilot sites is summarized by Mudd (1998, 2001a), Staub et al. (1986), and USNRC (2008). In many cases, failure to return the mining sites to pre-mining conditions has been documented, leading to opposition to proposed mining sites over the past 10 years (ENDAUM, 1997; Robinson et al., 1995). This failure has led some stakeholders to assert that current ISL practices are inherently unsafe and will eventually lead to contamination of nearby drinking water supplies (ENDAUM, 1997; Mudd, 1998, 2001a,b; Robinson et al., 1995). For example, the community in Crownpoint, NM is currently considering development of an alkaline leach ISL site. The Crownpoint Project is within the Navajo tribal community and considerable indigenous opposition over this proposed development remains.

11.6.4.2.2.4.4.8 NA for ISR sites A number of independent investigators and industry scientists have discussed the likelihood that adequate long-term restoration of ISR sites will occur by NA (Buma, 1979; Davis and Curtis, 2005; Davis et al., 2009; Pelizza, 2006). Pelizza (2006) argues that well fields are completed in a small fraction of the regional aquifers in Texas; therefore, the regional reducing capacity of the aquifer will prevail over any small pockets of residual oxidation that may persist after restoration of alkaline leach sites. At a recent workshop evaluating the uncertainties in the ability of NA to reduce uranium migration from ISR fields (Davis et al., 2009), three key areas of uncertainty were identified. The first category is uncertainty associated with basic characterization of the site. This includes factors such as historical mining activity, the current groundwater flow pattern and direction (and whether these have changed since the ore zone was formed), mineralogy, water chemistry, field parameters, mineral solubility, and solute speciation. The issue of characterizing baseline values from the entire aquifer exclusion zone versus the ore zone proper is particularly important. The second major source of uncertainty involves the geochemical mechanisms and potential efficacy of NA as a remedial alternative. Uncertainties include the reducing capacity of the system and the kinetics of reduction. In other words, upon cessation of mining, can the natural reduction capacity of the aquifer lead to reduction of contaminants on a reasonable time scale? The third category of uncertainty focuses on flow and transport and geochemical modeling at uranium ISR sites. Uncertainties include the appropriate use of scale (particularly with respect to heterogeneities), the source of thermodynamic data for geochemical modeling, and the distance, flow pathways, and travel times from ISR sites to private and/or municipal water supply wells.

A number of reactive transport simulations have attempted to evaluate the importance of different geochemical and operational factors to the potential success of restoration in returning the ore zone to pre-mining conditions. Success depends on site-specific geochemical and hydrological conditions, chemicals used for extracting uranium, and longevity of mining operations. Numerical simulations with the PHREEQC code by Davis and Curtis (2005) indicate that the long-term stability of the reducing geochemical conditions is dependent on post-restoration groundwater flow direction and the presence of sufficient concentration and mass of electron donors such as pyrite and uraninite. Their study has been used to support arguments that geochemical conditions in the mining zone are unlikely to be restored to pre-mining conditions.

Similar calculations using PHREEQC for the Smith Ranch Highland uranium deposit evaluated the behavior of uranium, arsenic, molybdenum, ^{226}Ra, selenium, vanadium, and other chemicals concentrated at these sites over a range of realistic site-specific geochemical and hydrologic conditions (Davis et al., 2009). In one set of simulations, only 10% of U(VI) species was calculated to adsorb onto hydrous ferric oxide present in the ore zone. This was because of significant U(VI) complexing with bicarbonate and carbonate in response to

carbon dioxide gas introduced during ISL uranium mining operations. Results of this simulation suggested that baseline conditions will not be achieved in 12.7 years after cessation of aquifer restoration. A number of other researchers have argued that the reducing capacity of rocks surrounding restored production zones should be effective in reducing contaminant levels. For example, site restoration data from the COGEMA Irigary mine and Crowe Butte Mine Unit 1 suggested to Demuth and Shramke (2006) that reducing conditions can be restored in post-restoration groundwater, in some cases without injection of reducing agents such as hydrogen sulfide. Additional reviews of restoration at mine sites have been provided by Pelizza (2008) indicating that although pre-mining baseline conditions for uranium, radium, and heavy metals were not re-established, those levels were too high for domestic use of water.

As discussed in more detail below, the US EPA (2007, 2010) and the ITRC (2010) have recently released guidance on implementation of a MNA framework for remediation of sites contaminated with radionuclides. Laboratory experiments, transport modeling, field data, and engineering cost analysis provide complementary information to be used in an assessment of the viability of an MNA approach. Information from kinetic sorption/desorption experiments, selective extraction experiments, reactive transport modeling, and historical cases analyses of plumes at several UMTRA sites (ITRC, 2010; Jove-Colon et al., 2001) and the Hanford 300 Area (ITRC, 2010) could potentially be used to establish a framework for evaluation of MNA for uranium and other metals from restored ISR sites.

11.6.4.2.2.4.5 Remediation of uranium-contaminated sites

A diverse set of approaches have been used or proposed for remediation of sites contaminated with uranium and its radioactive progeny. In many current remediation programs, simple excavation of contaminated soil and removal of contaminated groundwater by pumping are the preferred techniques. These techniques may be practical for removal of relatively small volumes of contaminated soils and water; however, after these source terms have been removed, large volumes of soil and water with low but potentially hazardous levels of contamination still remain. For radionuclides with low sorption, capture of contaminated water, and removal of radionuclides may be possible using permeable reactive barriers and bioremediation. Alternatively, radionuclides could be immobilized in place by injecting agents that lead to reductive precipitation or irreversible sorption. For strongly sorbing radionuclides, contaminant plumes will move very slowly and pose no potential hazards to current populations (Jove-Colon et al., 2001). However, regulations may require cleanup of sites to protect present and future populations under a variety of future-use scenarios. In these cases, it may be necessary to use soil-flushing techniques to mobilize the radionuclides and then to collect them. Alternatively, under an MNA approach, it might be demonstrated that contaminant plumes will not reach populations and that monitoring networks and contingency remedial plans are in place to protect populations if the plume moves more rapidly than predicted.

11.6.4.2.2.4.5.1 Permeable reactive barriers Permeable reactive barriers include reactive filter beds containing zero-valent iron (Fe^0), phosphate rock (apatite), silica sand, and organic materials (EPA, 1999c). The barriers can be installed by digging a trench in the flow path of a contaminated groundwater plume and backfilling with reactive material or injecting either a suspension of colloidal material or a solution containing a strong reductant (Abdelouas et al., 1999; Cantrell et al., 1995, 1997). The reactive filter material is used to reduce and precipitate the uranium from solution while allowing the treated water to flow through the reactive bed. In some installations, the drainfield can be designed to have removable cells should replacement and disposal of the reactive material be required. In others, a classic funnel and gate arrangement is used.

The use of Fe^0 to reduce and precipitate uranium out of solution has been shown to be effective by Gu et al. (1998) and Fiedor et al. (1998). The technique has been deployed in permeable reactive barriers at the Rocky Flats site in Colorado (Abdelouas et al., 1999), the Y-12 Plant near Oak Ridge National Laboratories (Watson et al., 1999), and other DOE sites. In this method, the Fe^0 reduces the U(VI) species to U(IV) aqueous species, which then precipitates as U(IV) solids (Fiedor et al., 1998; Gu et al., 1998). Reduction of U(VI) to U(IV) usually results in the precipitation of poorly crystalline U(IV) (e.g., uraninite, compositions ranging from UO_2 to $UO_{2.25}$) or mixed U(IV)/U(VI) solids (e.g., U_4O_9).

The solubility of uranium is strongly a function of its valence state, because U(IV) oxides and silicates have much lower solubilities than the corresponding uranyl phases, and because U(IV) does not form strong carbonate complexes. Hence, abiotic and biotic reduction of uranium are important processes in the concentration and fixation of U(VI), and potentially for remediation of uranium contaminant plumes in groundwater. Abiotic reduction of uranium generally involves reduced iron species as electron donors. Zero-valent iron effectively lowers uranium concentrations, and Fe^0 barriers are widely used for remediation of elevated uranium in groundwater, with about 120 barriers installed worldwide (Noubactep, 2010). Uranium removal by Fe^0 is widely attributed to reductive precipitation (Gu et al., 1998). However, it has also been argued that coprecipitation with iron corrosion products is the dominant mechanism (Noubactep, 2010). This view is supported by observations of U(IV) incorporation into green rust (Roh et al., 2000) and U(VI) incorporation into Fe(III) oxides during Fe(II)-catalyzed recrystallization of ferrihydrite (Nico et al., 2009; Stewart et al., 2009). Fe(II) minerals can also reduce uranium, including green rust (O'Loughlin et al., 2003) and pyrite. Finally, surface-catalyzed abiotic reduction of U(VI) by sorbed Fe(II) on clay surfaces may also be important in some systems (Chakraborty et al., 2010).

U(VI) readily precipitates in the presence of phosphate to form a number of sparingly soluble U-phosphate phases (e.g., saleeite, meta-autunite, and autunite) and also is removed by sorption and coprecipitation in apatite. Several studies have shown that hydroxyapatite is extremely effective at removing heavy metals, uranium, and other radionuclides from solution (Arey and Seaman, 1999; Gauglitz et al., 1992a,b). Apatite was shown to be effective at removing a number of metals including uranium at Fry Canyon, Utah (EPA, 2000a,b). Krumhansl et al. (2002) reviews the sorptive properties of a number of other materials for backfills around nuclear waste repositories and permeable reactive barriers. Injection of a reductant such as sodium dithionite creates a reducing zone that may be effective

in immobilizing uranium and other redox-active radionuclides. The technique is known as in situ redox manipulation. It has been shown to be moderately effective for chromium and is proposed for use at the Hanford site for remediation of a uranium groundwater plume (Fruchter et al., 1996).

11.6.4.2.2.4.5.2 Bioremediation A number of remediation techniques based on biological processes are in use. Examples include use of microbes to sequester uranium (as discussed previously) and phytoremediation of a number of metals. The former method involves reductive reactions by bacteria, particularly those of sulfate reduction (Lovely and Phillips, 1992) and direct reduction (Lovely and Phillips, 1992; Truex et al., 1997). Several techniques have been employed to generate high organic loading by growth of plant and algal biomass. Injection of nutrients into the subsurface and subsequent microbial bloom leads to low redox conditions favorable for reductive reactions, a significant decrease in the solubility and, consequently, removal of the metal onto the sediment.

Abdelouas et al. (1999) provide a good review of remediation techniques for UMTs and groundwater plumes. Biological processes used in bioremediation include biosorption, bioaccumulation, and bioreduction. Biosorption includes uptake of uranium by ion exchange or surface complexation by living microbes or the cell membranes of dead organisms. In bioaccumulation, the radionuclides are precipitated with enzymatic reactions (Abdelouas et al., 1999; Macaskie et al., 1996; and cited references). Bioreduction includes both direct reduction of radionuclides by organisms and indirect reduction. The latter involves creation of reducing conditions by the activity of sulfate and iron-reducing microbes and the subsequent reduction of the radionuclides by reductants such as H_2 and H_2S. Abdelouas et al. (1999) provide an excellent review of laboratory and field studies of microbes such as various *Desulfovibrio* species that have been shown to be effective in reducing hexavalent uranium by both of these processes.

A recent summary of microbial reduction of uranium (Wall and Krumholz, 2006) lists over 20 bacterial species shown to reduce U(VI) to U(IV). Microbes may utilize U(IV) directly as an electron acceptor, resulting in the formation of biogenic UO_2 nanocrystals (Lee et al., 2010). Energetically, O_2, Mn(IV), Fe(III), and NO_3^- are preferred relative to U(VI), which in turn is preferred relative to SO_4^{2-}, S^0, or CO_2 (Wall and Krumholz, 2006). However, the actual process responsible for uranium reduction may vary; reactions with other microbial byproducts have been, in many cases, shown to be more important than direct dissimilatory reduction of uranium. For example, sulfate-reducing bacteria can enzymatically reduce U(VI), but biogenic production by H_2S which then abiotically reduces U(VI), can be a more important pathway (Boonchayaanant et al., 2010). Also, in a system containing Fe(III) oxides, surface-catalyzed reduction by Fe(II) produced by dissimilatory iron reduction has been identified as the dominant pathway for uranium reduction (Behrends and Van Cappellen, 2005). Biogenic removal of uranium may not even require reduction; under anaerobic conditions, both U(VI) substitution into Fe(III) oxides during Fe(II)-catalyzed recrystallization of ferrihydrite (Nico et al., 2009) and U(VI) immobilization by sorption onto Fe(III) oxides formed by bio-oxidation of Fe(II) (Lack et al., 2002) have been reported. Finally, removal of U(VI) without reduction has also been accomplished via precipitation by biogenically produced phosphate (Beazley et al., 2007; Martinez et al., 2007).

Utilization of biogenic reduction of uranium as a remediation strategy faces several obstacles. Several processes may limit reduction of U(VI), including complexation with bicarbonate and organic ligands (Wall and Krumholz, 2006); formation of $Ca–UO_2–CO_3$ complexes at high Ca-concentrations (Neiss et al., 2007); and reaction with Fe(III)-containing clays, which can inhibit or delay U(VI) bioreduction, owing to surface-catalyzed reoxidation of U(IV) with concomitant reduction of Fe(III) to Fe(II) (Zhang et al., 2009). Remediation strategies based on U(VI) reduction strategies are also potentially vulnerable to reoxidation of the uranium. Biologically precipitated nanocrystals UO_2 are especially vulnerable to reoxidation (Singer et al., 2007), and can be oxidized by ferrihydrite, with concomitant production of uranyl and Fe(II) (Ginder-Vogel et al., 2010). Reoxidation could be limited by long-term injection of organic carbon; however, even under these conditions, uranium mobilization has been shown to increase with time, owing to enhanced microbial respiration and increasing carbonate/bicarbonate concentrations (Wan et al., 2008). Finally, Senko et al. (2002) showed that the biogenic intermediates of dissimilatory nitrate reduction, including nitrite, nitrous oxide, and nitric oxide, can reoxidize and mobilize U(IV), raising questions about the long-term effectiveness of bioremediation even if the system remains anaerobic.

Phytoremediation has been used to remove uranium and strontium from groundwaters and surface waters. Studies have been conducted on the uptake of heavy metals, uranium, and other radionuclides (Abdelouas et al., 1999; Cornish et al., 1995); both the uptake rates and the phytoconcentration of the radionuclides are high. The plants can be harvested and the volume of the residuals minimized by combusting the plant material.

11.6.4.2.2.4.5.3 Monitored natural attenuation As discussed previously, NA encompasses processes that lead to reduction of the mass, toxicity, mobility, or volume of contaminants without human intervention. The US EPA has recently published guidelines for the use of MNA for radionuclides and metals (EPA, 2007, 2010) at Superfund and other sites. For inorganic constituents, the most potentially important processes include dispersion and immobilization (precipitation, reduction, sorption, and coprecipitation).

The EPA approach has four steps or tiers:

Tier 1: Demonstration of dissolved plume stability via radioactive decay and/or active contaminant removal from groundwater.
Tier 2: Determination of the rate and mechanism of attenuation by immobilization.
Tier 3: Determination of the long-term capacity for attenuation and stability of immobilized contaminants.
Tier 4: Design of performance monitoring program, including defining triggers for assessing MNA failure, and establishing a contingency plan.

Additional guidance for implementing an MNA approach is provided by the Interstate Technology Regulatory Council (ITRC, 2010). The guidance document includes a number of case studies illustrating difficulties in past attempts to use MNA in a remediation plan. The studies include uranium

contamination at the US DOE Hanford 300 Area in Washington State, application of MNA as a remedy for the tritium plume under Site 300 at the Lawrence Livermore National Laboratory, and migration of a uranium contaminant groundwater plume the Monticello Mill Tailings site in Utah.

Studies of remediation options at UMTRA sites (ITRC, 2010) and the Hanford Site (Kelley et al., 2002) illustrate the complexity of adopting an MNA approach for uranium and strontium, respectively. Different approaches are required to establish the viability of MNA for these radioelements. One would expect that it would be easier to gain acceptance for an MNA approach for ^{90}Sr compared to $^{235/238}$U. This is because ^{90}Sr has a short half-life and uniformly strong sorption, whereas uranium isotopes have very long half-lives and complex sorption behavior. Strontium transport merely needs to be slowed enough by sorption to allow radioactive decay to remove the strontium, whereas demonstrating complete immobilization by a combination of precipitation, reduction, sorption, and coprecipitation is a key component of an MNA remedy for uranium. However, although extensive information was gathered at Hanford 100-N site in support of use of MNA for a ^{90}Sr plume that has reached the Columbia River (Kelley et al., 2002), use of MNA was rejected by the regulatory agencies and local citizen groups. Instead a combination of more active remediation technologies was selected for the final plan (DOE, 2010a,b). Although there has been little success to date in adopting MNA as the major component of remediation plans for sites contaminated with radionuclides, adoption of the EPA/ITRC framework for site-specific field, laboratory, and modeling studies may lead to future acceptance of the approach. This could lead to considerable cost-savings without endangering public health at certain sites.

11.6.4.2.3 Actinides and nuclear waste disposal

The general trends in speciation, sorption, and solubilities of actinides were previously described in **Section 11.6.4.2.1**. Here, the focus is on applications of these principles and data in studies in support of nuclear waste disposal. Throughout this section, the effects of redox condition and salinity on actinide solubility and speciation are discussed, and illustrated largely through reference to three extensively studied water compositions. These include (1) low ionic strength reducing waters from crystalline rocks at nuclear waste research sites in Sweden; (2) oxic water from the J-13 well at Yucca Mountain, Nevada; and (3) reference brines associated with the WIPP, an operating repository for TRU in the Permian salt beds of SE New Mexico.

The Swedish repository science program has investigated crystalline rock as a host rock for the disposal of radioactive waste and has measured the composition of granitic groundwaters (Andersson, 1990). Much of this was done at the Stripa site, an abandoned iron mine located in a granitic intrusion in south-central Sweden. At Stripa, shallow groundwaters are dilute, carbonate-rich, pH neutral, oxidizing waters of meteoric origin; naturally occurring uranium is present in concentrations of 10–90 $\mu g\,l^{-1}$. Once below this zone, the waters are slightly more saline (up to 1.3 $g\,l^{-1}$ TDSs), more basic (up to pH 10.1), and the Eh is lower – groundwater uranium concentrations are less than 1 p.p.b. (Andrews et al., 1989; Nordstrom et al., 1989). The trace amounts of sulfide and ferrous iron in the groundwater have little capacity for maintaining reducing conditions, and groundwater interactions with radioactive waste, waste containers, or repository backfill materials are likely to govern the redox conditions in a real repository (Nordstrom et al., 1989). A dilute, near-neutral, mildly reducing groundwater composition, representing a composite of analyses from several Swedish sites, is a suggested reference composition for deep granitic groundwaters (Andersson, 1990), and is referred to here as 'Stripa' or 'SKI-90' groundwater (SKI, 1991) see (**Table 4**).

The planned nuclear waste repository at Yucca Mountain, Nevada, is located in a thick sequence of tertiary volcanic tuffs. Although the status of the site is in question, studies related to the project represent a huge database of information on the solubility of radionuclides in dilute waters. The range of groundwater compositions sampled at Yucca Mountain is discussed by Perfect et al. (1995). Numerous geochemical studies have been carried out in high-Eh waters from the alluvium and tuffaceous rocks (e.g., UZ-TP-7) from the unsaturated zone, high-Eh waters from the saturated zone (e.g., J-13) within tuffaceous rocks, and in lower Eh-waters from a deeper Paleozoic carbonate aquifer (e.g., UE252p-1) (Tien et al., 1985; Triay et al., 1997). Water from the J-13 well has been used as a reference water (**Table 4**) in systematic studies of sorption, transport, and solubility (Nitsche et al., 1992). The composition of J-13 is controlled by a number of processes including dissolution of vitric and devitrified tuff, precipitation of secondary minerals, and ion exchange (Tien et al., 1985; Triay et al., 1997). The water is a very dilute, neutral pH, oxidizing Na-bicarbonate water (Ogard and Kerrisk, 1984).

The WIPP is an underground repository for the permanent disposal of defense-related TRU wastes (NAS, 1996). The facility is located in the US in southeastern New Mexico in the Salado Formation, a thick, bedded salt, at a depth of 655 m. The Castile Formation is an evaporite sequence below the Salado that may serve as a brine source if the repository is breached by human activities in the future. Brines from both formations are a mixture of Na^+, Mg^{2+},

Table 4 Compositions of low-ionic strength reference waters used in speciation and solubility calculations

Component	*Stripa (SKI-90)*[a] *(mM)*	*Yucca Mtn (J-13)*[b] *(mM)*
Na^+	1.39	1.96
K^+	0.0256	0.14
Ca^{2+}	0.5	0.29
Mg^{2+}	0.0823	0.07
Fe (total)	0.00179	–
SiO_2	0.0682	1.07
Cl^-	0.423	0.18
SO_4^{2-}	0.417	0.19
F^-	0.142	0.11
PO_4^{3-}	3.75×10^{-5}	–
HCO_3^-	2.0	2.81
pH	8.2	6.9
Eh (mV)	−0.3	0.34–0.7[c]

[a]SKI (1991) *SKI Project Summary*. SKB Technical Report 91–23, Stockholm, Sweden.
[b]Ogard AE and Kerrisk JF (1984) *Groundwater Chemistry Along The Flow Path Between a Proposed Repository Site and the Accessible Environment*. Los Alamos, NM: Los Alamos National Laboratory, LA-101188-MS.
[c]Range of Eh used in different works.

K^+, Ca^{2+}, Cl^-, and SO_4^{2-} and are saturated with respect to halite (NaCl) and anhydrite ($CaSO_4$) (DOE, 1996b). For the performance assessment calculations, the pH, pCO_2, and radionuclide solubilities and speciation were calculated assuming that the brines were in equilibrium with halite, anhydrite, brucite, and hydromagnesite ($Mg_5(CO_3)_4(OH)_2{\cdot}4H_2O$), minerals produced by hydration and carbonation of the MgO-engineered barrier. In addition, the TRU emplaced in the repository contains organic compounds, including acetate, citrate, EDTA, and oxalate, which were included in the solubility calculations (**Table 5**). The pC_{H+} of the modified brines was 9–10, and the Eh was assumed to be controlled by the metallic iron in the waste and waste packages. Compositions of the modified brines are provided in Brush et al. (2009). Speciation and solubility calculations in these brines were carried out using a Pitzer ion interaction model (DOE, 1996b) for the activity coefficients of the aqueous species (Pitzer, 1987, 2000). Pitzer parameters for the dominant nonradioactive species present in WIPP brines are summarized in Harvie and Weare (1980), Harvie et al. (1984), Felmy and Weare (1986), and Pitzer (1987, 2000). For the actinide species, the Pitzer parameters that were used are summarized in the WIPP Compliance Certification Application (CCA) (DOE, 1996a,b,c).

11.6.4.2.3.1 Speciation, solubility, and sorption of actinides in nuclear waste repository environments

11.6.4.2.3.1.1 Americium Silva et al. (1995) provide a detailed summary of experimental and theoretical studies of americium chemistry as well as a comprehensive, self-consistent database of reference thermodynamic property values. Solubility and speciation experiments with Am(III) indicate that the mixed hydroxycarbonate $AmOHCO_{3(cr)}$ is the solubility-limiting solid phase under most surface and subsurface conditions. At neutral pH, $AmOH^{2+}$, or $AmCO_3^+$ can be the dominant solution species depending on the carbonate concentration. Fanghänel and Kim (1998) evaluated the solubility of trivalent actinides in brines, using Cm(III) as a representative analog, and found that An(III) hydroxy and carbonato complexes are the most stable aqueous complexes. Multiple-ligand complexes with a high negative charge are more stable in brines than in dilute solutions, apparently because of the high cation concentrations. Chloride and sulfate complexes, although very weak, may be important aqueous species in some brines, especially at low pH.

Langmuir (1997) calculated a solubility of 5.6×10^{-8} M for J-13 water with the MINTEQA2 code (Allison et al., 1991) using the thermodynamic database of Turner et al. (1993) and a revised formation constant $\log K_{sp} = 7.2$ for $AmOHCO_{3(cr)}$ (compared to the NEA $\log K_{sp} = 8.605$ of Silva et al. (1995)). This is similar to the value of 1.2×10^{-9} M measured by Nitsche et al. (1993) in solubility experiments in J-13 water. Langmuir (1997) also calculated the solubility of americium for reducing water from crystalline rock (Sk-90 water) and obtained a value of $\leq 1.4 \times 10^{-7}$ M. This is similar to the range calculated by Bruno et al. (2000) using the EQ3NR (1992) code for slightly basic, reducing groundwaters in granite at Äspö and Gideå, Sweden.

In the WIPP speciation and solubility calculations, the solubility controlling solid phase for Am, and by analogy, for all +III actinides under WIPP conditions, was $Am(OH)_3$ (Brush et al., 2009). $AmEDTA^-$ was the dominant aqueous species ($Am(OH)^{2+}$ was the dominant inorganic species), and estimated americium solubilities in the reference Salado and Castile brines with the organic complexes were 1.66×10^{-6} and 1.51×10^{-6} M, respectively. When the organic compounds

Table 5 Compositions of brines used in WIPP speciation and solubility calculations

Component	*Salado brine (mM)*	*Salado brine w/organics (mM)*[a]	*Castile brine (mM)*	*Castile brine w/organics (mM)*[a]
Na^+	3530	4310	4870	5280
K^+	467	521	97	96.1
Ca^{2+}	14	9.8	12	11.2
Mg^{2+}	1020	584	19	13.6
Cl^-	5860	5400	4800	5230
SO_4^{2-}	177	210	170	176
Br^-	26.6	27.8	11	10.9
$B_4O_7^{2-}$	39.5	41.5	15.8	15.6
Total inorganic carbon		358		448
Total acetate	–	19.4	–	19.4
Total citrate	–	2.38	–	2.38
Total EDTA	–	0.0647	–	0.0647
Total oxalate	–	17.3	–	17.3
pH (Pitzer)[c]		8.69		8.98
pC_{H+}[b]		9.40		9.68
pCO_2, atm.		$10^{-5.5}$		$10^{-5.5}$
Ionic strength		7640		6770

DOE (1996a) *Programmatic Environmental Impact Statement For Ground Water Volume I (October 1996)*. Office of Legacy Management, U.S. Department of Energy; DOE (1996b) *Programmatic Environmental Impact Statement For Ground Water Volume II (October 1996)*. Office of Legacy Management, U.S. Department of Energy; Brush LH, Xiong L, and Long JL (2009) Results of the Calculations of Actinide Solubilities for the WIPP CRA-2009 PABC. Carlsbad, NM: Sandia National Laboratories, p. 47.

[a]In equilibrium with brucite and hydromagnesite.

[b]pC_{H+} = negative log of the molar concentration of H^+.

[c]The 'Pitzer' pH is the activity of the hydrogen ion calculated using the Pitzer ion activity model.

were excluded from the calculation, solubilities significantly lower (2.25×10^{-7} and 8.67×10^{-8} M, respectively).

Americium is strongly sorbed by tuffaceous rocks from Yucca Mountain in waters of low ionic strength (Triay et al., 1997). In a compilation by Tien et al. (1985), americium K_ds obtained with tuff in J-13 water ranged from 130 to 13 000 ml g^{-1}. Average values for devitrified, vitric, and zeolitized tuff were 2975, 1430, and 1513 ml g^{-1}, respectively. Turin et al. (2002) measured K_ds ranging from 410 to 510 ml g^{-1} using similar waters and tuffaceous rocks from Busted Butte on the Nevada Test Site. They also provide Freundlich isotherm parameters from the sorption measurements. A K_d range of 500–50 000 ml g^{-1} is reported for crystalline rocks by McKinley and Scholtis (1992); a value of 5000 ml g^{-1} is recommended for performance assessment.

Data are sparse for Am sorption in high ionic strength solutions. In experimental studies with near-surface sediments from the Gorleben site, Lieser et al. (1991) showed that americium sorption did not vary ($K_d \sim 1000$ ml g^{-1}) over a range of NaCl concentrations of 0–2 M, at a pH of 7.5. They concluded that americium sorption was not sensitive to ionic strength because at this pH, americium is nearly completely hydrolyzed. Thus, ion exchange reactions did not contribute to americium sorption, and competing ion concentrations had little effect on sorption K_ds. In situ studies of radionuclide transport through brackish bay sediments in Sweden (seawater solution compositions) measured K_ds of 1000–10 000 ml g^{-1} (Andersson et al., 1992).

11.6.4.2.3.1.2 Thorium Experimental and theoretical studies of thorium speciation, solubility, and sorption in low-ionic strength waters are described by Langmuir and Herman (1980), LaFlamme and Murray (1987), Östhols et al. (1994), Osthols (1995), and Quigley et al. (1996). Langmuir and Herman (1980) provide a critically evaluated thermodynamic database for natural waters at low temperature that is widely used. However, it does not contain information about important thorium carbonate complexes, and the stability of phosphate complexes may be overestimated (EPA, 1999b). In both low-ionic-strength groundwaters and in the WIPP brines, the solubility-limiting phase is $ThO_{2(am,\ hyd)}$ (also designated $Th(OH)_{4(am)}$). Thermodynamic calculations predict that the most stable phase is $ThO_{2(cr)}$; however, solubility experiments indicate that measured solubilities for $ThO_{2(cr)}$ are commonly much higher than predicted using thermodynamic data, and match those for the amorphous phase, possibly owing to the formation of an amorphous surface layer (Neck et al., 2003). In seawater, waters from Yucca Mountain, and reducing waters in crystalline rocks, the dominant aqueous species are $Th(OH)_{4(aq)}$ and mixed hydroxy–carbonate complexes. In alkaline lakes and other environments with high carbonate concentrations, thorium carbonate complexes are dominant (Altmaier et al., 2005; LaFlamme and Murray, 1987; Östhols et al., 1994). In organic-rich stream waters, swamps, soil horizons, and sediments, organic thorium complexes may predominate (Langmuir and Herman, 1980). Langmuir (1997) calculated similar thorium solubilities in J-13 water from Yucca Mountain ($\leq 6.0 \times 10^{-7}$) and in Stripa groundwater ($\leq 5.7 \times 10^{-7}$) using the thermodynamic database of Turner et al. (1993); however, these values are much higher than those calculated by Bruno et al. (2000) for waters from Äspö and Gideå using EQ3NR (about 2×10^{-10} M). They are also much higher than measured solubilities in ultrafiltered granitic water (~pH 9.0) from the Korean underground research facility (5.3×10^{-9}–7.3×10^{-9} M) (Kim et al., 2010). The authors of the latter study suggest that the measured values are well below the calculated solubility of $ThO_{2(am,\ hyd)}$ because of the formation of unidentified thorium colloids prior to saturation with that phase.

The solubility of $ThO_{2(am)}$ increases with increasing ionic strength; above pH 7 in 3.0 M NaCl solutions, the solubility is approximately three orders of magnitude higher than that measured in 0.1 M $NaClO_4$ solution (Felmy et al., 1991). Rai et al. (1997) describe solubility studies and a thermodynamic model for Th(IV) speciation and solubility in concentrated NaCl and $MgCl_2$ solutions. A Pitzer ion-interaction model was used to obtain a solubility product of $\log K_{sp} = -45.5$ for $ThO_{2(am)}$. In the speciation and solubility calculations for the WIPP performance assessment (**Table 5**), the important aqueous species were $Th(OH)_{4(aq)}$ (about 80% of the total) and $Th(OH)_3(CO_3)^-$ (about 20%); the corresponding estimated Th(IV) solubilities were 5.63×10^{-8} M in the Salado brine and 6.98×10^{-8} M in the Castile brine; the presence or absence of organics had no significant effect (Brush et al., 2009).

Thorium sorbs strongly to iron oxyhydroxides and humic matter (Hunter et al., 1988; Murphy, 1999; Nash and Choppin, 1980) and weakly to silica at neutral to basic pH (Osthols, 1995). Thorium sorption is sensitive to carbonate alkalinity because of the formation of negatively charged aqueous mixed hydroxy–carbonate complexes (LaFlamme and Murray, 1987); at alkalinities of 100 meq l^{-1}, thorium sorption by goethite decreases markedly. However, at the relatively low alkalinities measured at Yucca Mountain, this effect is not important for the proposed repository site (Triay et al., 1997). Measured thorium sorption ratios in J-13 water from Yucca Mountain for devitrified, vitric, and zeolitized tuff ranged from 140 to 23 800 ml g^{-1} (Thomas, 1987; Tien et al., 1985). Other compilations contain representative K_d values for thorium in crystalline rock that range from 100 to 5000 ml g^{-1} (McKinley and Scholtis, 1992) and from 20 to 300 000 ml g^{-1} for low-temperature geochemical environments (EPA, 1999b).

Thorium sorption at high ionic strength was examined using uranium series disequilibrium techniques by Laul (1992). Laul measured thorium retardation in saline groundwaters from the Palo Duro Basin, TX, and determined sorption K_ds of around 2100 ml g^{-1}. Because tetravalent actinides are strongly sorbed by mineral colloids and have a strong tendency to form intrinsic colloids, increases in ionic strength may have more effect on An(IV) transport through destabilization and flocculation of colloidal particles (Lieser and Hill, 1992), rather than through changes in the degree of sorption.

11.6.4.2.3.1.3 Neptunium Neptunium and plutonium are the radioelements of primary concern for the disposal of nuclear waste at the proposed repository at Yucca Mountain. This is owing to their long half-lives, radiotoxicity, and transport properties. Neptunium is considered to be the most highly mobile actinide because of its high solubility and low potential for sorption by geomedia. Its valence state (primarily Np(V) or Np(IV)) is the primary control of its environmental geochemistry. Oxide, hydroxide, and carbonate compounds are the most important solubility-limiting phases in natural waters.

In low-ionic strength, carbonate-free systems, $NpO_2(OH)$ and Np_2O_5 are stable Np(V) solids, while in brines, Np(V) alkaline carbonate solids are stable. Under reducing conditions, $Np(OH)_{4am}$ and NpO_2 are the stable Np(IV) solids. Under most near-surface environmental conditions, the dominant complexes of neptunium are those of the pentavalent neptunyl species (NpO_2^+). Np(IV) aqueous species may be important under reducing conditions possible at underground nuclear waste research facilities such as the WIPP and Stripa.

Kaszuba and Runde (1999) compiled thermodynamic data for neptunium relevant to Yucca Mountain. They updated the database of Lemire (1984) with recent experimental data and used the SIT to calculate ion activity coefficients. Their report has an extensive reference list and a list of interaction parameters. Kaszuba and Runde (1999) used the EQ3NR (Wolery, 1992) and the Geochemist's Workbench (Bethke, 1998) codes to calculate solubility and speciation in the J-13 and UE25p#1 well waters that span the expected geochemical conditions for the proposed HLW repository at Yucca Mountain. They predicted that $Np(OH)_{4(aq)}$ is the dominant aqueous complex in neutral solutions at Eh < 0 mV, while under oxidizing conditions, NpO_2^+ and $NpO_2CO_3^-$ are predominant at pH < 8 and pH 8–13, respectively.

Although the calculations of Kaszuba and Runde (1999) indicate that $NpO_{2(s)}$ is the thermodynamically stable solid for most Eh–pH conditions of environmental interest, that phase has never been observed to precipitate in solubility experiments in natural waters; instead $Np_2O_{5(s)}$ and amorphous $Np(OH)_{4(s)}$ precipitate. Figure 4 shows that if $Np_2O_{5(s)}$ controls the solubility under oxidizing conditions (Eh > 0.25 V), then the calculated solubility of neptunium decreases from $\sim 10^{-3.5}$ M at pH = 6, to 10^{-5} M at pH = 8. If amorphous $Np(OH)_{4(s)}$ controls the solubility under reducing conditions (Eh < −0.10 V), the solubility is approximately 10^{-8} M over the same pH range. In the intermediate Eh range and neutral pH conditions possible under many environmental settings, the solubility of neptunium is controlled primarily by the Eh of the aquifer and will vary between the levels set by the solubilities of $Np(OH)_{4(s)}$ and $Np_2O_{5(s)}$ (Figure 4). The inset in Figure 4 illustrates that at pH = 6.8, at Eh = −0.10 V, the concentration of neptunium in solution is approximately equal to that of the Np(IV) species and is controlled by the solubility of $Np(OH)_{4(s)}$. As the redox potential increases, Np(IV) in solution is oxidized to Np(V) and the aqueous concentration of neptunium increases. Phase transformation of $Np(OH)_{4(s)}$ to $Np_2O_{5(s)}$ occurs at about Eh = 0.25 V and then the solubility of the Np(V) oxide controls the aqueous neptunium concentration at higher Eh values.

The results of Kaszuba and Runde (1999) are broadly consistent with the calculations of Langmuir (1997). Langmuir calculated a slightly lower neptunium solubility for reducing conditions ($\leq 1.6 \times 10^{-9}$ M for Stripa water), but used formation constants that effectively eliminated the influence of $Np(OH)_5^-$. Langmuir (1997) used $NaNpO_2CO_3 3.5H_2O_{(cr)}$ as the solubility-limiting phase for Yucca Mountain J-13 water and calculated a solubility of 8.9×10^{-4} M, slightly higher than the range calculated by Kaszuba and Runde (1999) for $Np_2O_{5(s)}$. Although $NaNpO_2CO_3 3.5H_2O_{(cr)}$ and $Np_2O_{5(s)}$ have been observed experimentally in Np solubility experiments with J-13 water, they are metastable. Thermodynamic calculations predict that the less-soluble $NpO_{2(s)}$ will be the solubility-limiting phase even under oxic conditions, and Sassani et al. (2006) suggest that this phase could ultimately control Np transport at Yucca Mountain.

Aqueous neptunium species including bishydroxo and mixed hydroxy–carbonato species may be important, though not dominant, at higher pH and carbonate concentrations. Such conditions may exist at the Hanford Waste tanks, where $MNpO_2CO_3 \times nH_2O$ and $M_3NpO_2(CO_3)_2$ ($M = Na^+$, K^+) are predicted to be stable phases. The solubilities are 2–3 orders of magnitude higher than in waters in which Np_2O_5 is stable. Similarly, in the reducing granitic waters of the Korean underground research facility at high pH, Np(IV) hydroxy–carbonato complexes are calculated to be the dominant

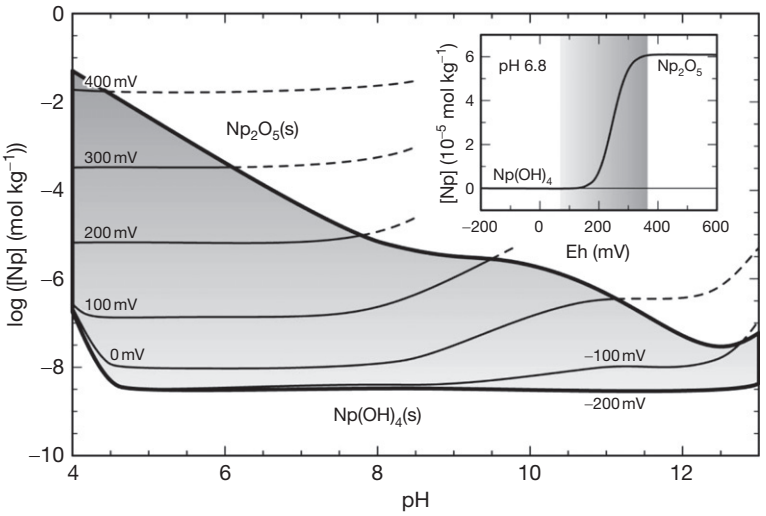

Figure 4 Calculated Np solubilities as a function of pH and Eh in J-13 groundwater variants (Table 4). $Np_2O_{5(s)}$ and $Np(OH)_{4(s)}$ were assumed to be the solubility-limiting phases. Inset shows regions of solubility control versus redox control (shaded area). Reprinted with permission from *Environmental Science & Technology* 1999, 33: 4433.

aqueous species (Kim et al., 2009). Under conditions expected in the near field of HLW geologic repositories in saline groundwater environments such as the salt domes and the bedded salts in Europe, Np(VI) species such as $NpO_2(CO_3)_3^{4-}$ might be important due to radiolysis. In the WIPP compliance calculations, the aqueous Np(V) concentrations were dominated by three species, each constituting more than 20% of the total: $NpO_2Ac_{(aq)}$, NpO_2^+, and $NpO_2(CO_3)^-$.

Neptunium is expected to be present in the WIPP in either the IV or V oxidation state. For the WIPP CCA speciation and solubility calculations, an upper bound for the solubility of Np (IV) was estimated from that of Th(IV), using the oxidation state analogy. As with U(IV), calculations suggest that this assumption is conservative (Wall et al., 2002). Modeling for the WIPP project suggested that Np(V) solubility in the reference Salado and Castile brines, with the organic components, is limited by $KNpO_2CO_3 \times 2H_2O_{(s)}$ and is 3.90×10^{-7} and 8.75×10^{-7} M, respectively (Brush et al., 2009). Many Np(V) species contributed to the total solubility, including $NpO_2Ac_{(aq)}$, NpO_2^+, and $NpO_2CO_3^-$ (each >25%), and NpO_2Ox^- (about 10%). Calculated solubilities were slightly lower in the organic-free systems (2.21×10^{-7} and 5.38×10^{-7} M, respectively). Experimental measurements of the solubility of Np(V) in laboratory solutions representing unaltered Salado brine yielded a value of 2.4×10^{-7} M, after allowing the brine systems to equilibrate for up to 2 years (Novak et al., 1996). The solubility-limiting phase was identified as $KNpO_2CO_3 \times nH_2O_{(s)}$, in agreement with the results of the WIPP performance-assessment modeling.

In general, sorption of Np(V) by aluminosilicates is expected to be low in waters at Yucca Mountain (Turner and Pabalan, 1999; Turner et al., 1998). K_ds for sorption of neptunium by zeolites and tuff particles were typically less than 10 ml g^{-1} in waters from that site (Runde et al., 2002b; Tien et al., 1985). The low neptunium sorption is owing to the relative dominance of the poorly sorbed hydrolyzed species $NpO_2(OH)_{(aq)}$ and the anionic $NpO_2CO_3^-$ species in solution. In contrast, the average K_ds for Np(V) uptake by colloidal hematite, montmorillonite and silica were 880, 150, and 550 ml g^{-1}, respectively, in Yucca Mountain J-13 water (Efurd et al., 1998), probably due to the high surface area of the particles. Similarly, McCubbin and Leonard (1997) reported neptunium K_ds of 1000–10 000 ml g^{-1} for particulates in seawater, but the oxidation state was uncertain. Like other tetravalent actinides, Np(IV) has a strong tendency to polymerize and form colloids and is strongly sorbed. Np(IV) migration is likely to occur as intrinsic colloids or sorbed species on pseudocolloids, and changes in ionic strength are likely to impact mobility mostly through destabilization of colloidal particles. Np(V) intrinsic colloids are not expected at neutral pH (Tanaka et al., 1992) and uptake by carrier colloids occurs by ion exchange and surface complexation. Competition for sorption sites between Np(V) species and other ions, especially Ca^{2+} and Mg^{2+}, could be significant (McCubbin and Leonard, 1997; Tanaka and Muraoka, 1999).

11.6.4.2.3.1.4 Plutonium Plutonium chemistry is complicated by the fact that it can exist in four oxidation states over an Eh range of −0.6 to 1.2 V and a pH range of 0–14. In the system Pu–O_2–H_2O, four triple points exist (Eh–pH where three oxidation states may coexist) and thus disproportionation reactions can occur in response to radiolysis or changes in Eh, pH, or the concentrations of other chemical species (Langmuir, 1997). The most important of these reactions are disproportionation of PuO_2^+ to PuO_2^{2+} and Pu^{4+} (Haschke, 2007) or disproportionation of plutonium facilitated by humic acid (Guillaumont and Adloff, 1992) and radiolysis (Nitsche et al., 1995).

Langmuir's Eh–pH calculations (1997) show that in systems containing only Pu, H_2O, and carbonate/bicarbonate (10^{-2} M), the stability field for the species Pu^{4+} is nearly nonexistent (limited to high Eh and very low pH) but the field for $Pu(OH)_{4(aq)}$ is extensive at pH > 5 and Eh < 0.5. Carbonato-complexes of Pu(VI) and Pu(V) are important at pH > 5 and higher Eh. Plutonium solubilities are generally low over most environmental conditions (< 10^{-8} M); Langmuir (1997) calculated solubilities of $\leq 6.6 \times 10^{-8}$ and $\leq 1.7 \times 10^{-9}$ M, respectively, in oxidizing Yucca Mountain J-13 water and reducing Stripa water; $Pu(OH)_{4(am)}$ was the solubility-limiting phase in both cases. The solubility fields for $PuO_{2(cr)}$ and $Pu(OH)_{4(am)}$ cover the Eh–pH field over pH > 5 at all Eh, and at lower pH values, cover substantial portions of the Eh–pH field where Eh > 0.5 V. In surface waters, both Pu(V) and Pu(IV) are commonly measured, but the Pu(IV) is dominantly colloidal material and most aqueous Pu is Pu(V) (Choppin, 2007). As discussed below, the system is different when other ligands, cations, and higher concentrations of carbonate are present.

Runde et al. (2002a) compiled an internally consistent database to calculate solubility and speciation of plutonium in more complex, low-ionic-strength waters. A specific interaction (SI) model (Grenthe et al., 1992) was used for ionic-strength corrections. The reader is referred to that work for details of the data sources and methods used for extrapolation and interpolation. Where reliable data for plutonium species were unavailable, thermodynamic constants were estimated from data for analogous americium, curium, uranium, and neptunium species. The most important solution species of plutonium are the aqueous ions, hydroxides, carbonates, and fluoride complexes. Important solids include oxides and hydroxides ($Pu(OH)_3$, PuO_2, $PuO_2 \times nH_2O$ [or $Pu(OH)_4$], PuO_2OH, $PuO_2(OH)_2$) and the carbonate PuO_2CO_3. The dominant solid phases and species are shown in an Eh–pH diagram for J-13 water variants in **Figure 5**. Note that in this system, the only triple point occurs at a pH of 2.4 where species in the IV, V, and VI oxidation states are calculated to be in equilibrium. In reference J-13 water (pH = 7, Eh = 0.43 V), $Pu(OH)_{4(aq)}$ dominates solution speciation, and $Pu(OH)_{4(s)}$ is the solubility-limiting phase. Under certain environments affected by interactions of groundwater and nuclear waste forms, Pu(V) or Pu(VI) could be produced by radiolysis or Pu(III) species could be produced by reduction.

Runde et al. (2002a) demonstrate that significant changes in plutonium solubility can occur due to the formation of Pu (V) and Pu(VI) species at pH > 6 or due to the formation of Pu (III) species at pH < 6. Using either $Pu(OH)_{4(s)}$ or the more crystalline $PuO_{2(s)}$ as the solubility controlling solids, Runde et al. (2002a) calculated plutonium solubilities over ranges of pH (3–10), Eh (0–0.6 V), and total carbonate concentration (0.1–2.8 mmol). For conditions typical of groundwater environments (pH range 6–9 and Eh range 0.05–0.45 V), Pu

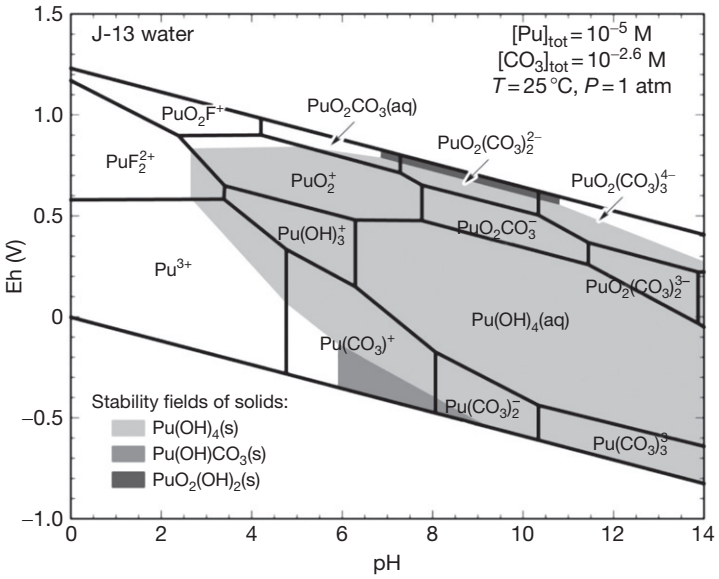

Figure 5 Eh–pH diagram showing dominant plutonium solid phases and species for J-13 water variants at 25 °C as calculated by Runde et al. (2002a). Solid lines indicate dominant solution species; shaded areas indicate solids supersaturated in 10^{-5} M Pu solutions. Precipitation of PuO_2 was suppressed in the calculations; see Runde et al. (2002a) for details. Reproduced by permission of Elsevier from *Applied Geochemistry*, 2002, 17: 844.

$(OH)_{4(aq)}$ is the dominant aqueous species. Under alkaline conditions, solubility increases with Eh due to the formation of Pu(V) and Pu(VI) solution species. At pH > 8 and Eh > 0.4 V, carbonate species are dominant. At pH values below 7, the solubility increases with decreasing Eh due to the stability of $Pu(OH)_3^+$. The calculated solubilities and speciation are sensitive to changes in both Eh and pH. For systems in which $Pu(OH)_{4(s)}$ is the stable solid, they ranged from $>10^{-2}$ M at pH = 4 and Eh = 0 V to 10^{-11} M at pH > 5 and Eh < 0.4 V. Calculated solubilities were about four orders of magnitude lower when $PuO_{2(s)}$ was the stable solid. Experimentally measured solubilities over this range of solution compositions are typically two orders of magnitude higher than calculated values (Runde et al., 2002a), possibly owing to the presence of Pu(IV) colloids (Capdevila and Vitorge, 1998; Efurd et al., 1998; Knopp et al., 1999), although the formation of a mixed valence state Pu solid, $PuO_{2+x(hyd)}$ may also be the cause (Jove-Colon and Finch, 2010; Neck et al., 2007). In experimental studies in J-13 water, at ambient temperature, plutonium solubility decreased from 5×10^{-8} M at pH = 6, to 9×10^{-9} M at pH = 9 (Efurd et al., 1998).

Because of the presence of Fe^0 and Fe(II), Pu(VI) is not expected to be stable under WIPP repository conditions. Pu (IV) is expected to be the dominant oxidation state, although Pu(III) was also considered to be a possibility in the WIPP CCA. In the WIPP performance assessment speciation and solubility calculations, Th(IV) was used as an analog for Pu (IV) (Brush et al., 2009; DOE, 1996a,b,c). Wall et al. (2002) evaluated the appropriateness of the analogy and found that this assumption was highly conservative and that predicted solubilities for Pu(IV) in Salado and Castile brines were 10–11 orders of magnitude lower than those for Th(IV). Similarly, Am(III) was used to estimate the solubility of Pu(III).

Studies of the sorption of plutonium are complicated by the high redox reactivity of Pu. Sorption of Pu(V) by pure aluminosilicates and oxyhydroxide phases is usually characterized by initial rapid uptake followed by slow irreversible sorption and may represent a reductive uptake mechanism catalyzed by the electrical double layer of the mineral surface (Runde et al., 2002a; Turner et al., 1998). In Yucca Mountain waters, the K_d ranges for Pu(V) uptake by hematite, montmorillonite, and silica colloids were 4.9×10^3–1.8×10^5, 5.8×10^3, and 8.1×10^3 ml g^{-1}, respectively. These are much higher than those observed for Np(V) in the same waters as described previously. High surface redox reactivity for plutonium and possible disproportionation of Pu(V) to Pu(VI) and Pu(IV) were observed in sorption studies using goethite by Keeney-Kennicutt and Morse (1985) and Sanchez et al. (1985). Desorption by plutonium was typically less from hematite than from aluminosilicates in studies with J-13 water described by Runde et al. (2002a).

11.6.4.2.3.1.5 Uranium General trends in uranium geochemistry relevant to oxic and near-surface conditions were discussed previously in **Section 11.6.4.2.2.** In water of low Eh, such as crystalline rock environments studied in the European nuclear waste programs, uranium solubility is controlled by saturation with UO_2 and coffinite ($USiO_4$) (Langmuir, 1997). Langmuir (1997) calculated uranium solubilities in the dilute, mildly reducing SKI-90 water with the MINTEQ2A code (Allison et al., 1991) and the thermodynamic database of Turner et al. (1993), with modifications for uranium described in Langmuir (1997). Using $UO_{2(am)}$ as the solubility-limiting phase, Langmuir calculated a solubility of $\leq 1.4 \times 10^{-8}$ M. This value, for the amorphous phase, should be considered the maximum soluble concentration that might be important for the short-term behavior of uranium. Over longer time periods, the solubilities are likely controlled by a more crystalline phase at levels that are several orders of magnitude lower than this. Langmuir (1997, pp. 501–502) also describes some of the controversy surrounding estimation of the solubility of UO_2. Estimates for the log K_{sp} of UO_2 range from −51.9 to −61.0, corresponding to soluble concentrations (as $U(OH)_{4(aq)}$)

ranging from 10^{-8} M (measured by Rai et al., 1990) to $10^{-17.1}$ M (computed by Grenthe et al., 1992). The reason for the wide range lies in the potential contamination of the experimental systems by O_2 and CO_2 and the varying crystallinity of the solid phase. Contamination and the presence of amorphous rather than crystalline UO_2 would lead to higher measured solubilities.

Reed et al. (1996) examined An(VI) stability in WIPP brines under anoxic conditions (1 atm H_2 gas) and found that U(VI) was stable as a carbonate complex in Castile brine at pH 8–10. Xia et al. (2001) also observed that U(VI) may be stable under some WIPP-relevant conditions, finding that while U(VI) was rapidly reduced to U(IV) by Fe^0 in water and 0.1 M NaCl, it was not reduced in the Castile brine, at pC_{H+} 8–13, over the course of a 55-day experiment. The possible occurrence of U(VI) was considered in WIPP performance-assessment calculations; by EPA mandate, a solubility of 10^{-3} M was assumed for An(VI) species. This may be considerably higher than actual U(VI) solubilities in WIPP brines. Lucchini et al. (2007) measured uranyl solubility in two WIPP brines, GWB and ERDA-6, under carbonate-free conditions (reaction with the MgO backfill will keep carbonate concentrations very low in WIPP brines), and at WIPP-relevant pC_{H+} values ($\geq$9), they obtained values of 10^{-5}–10^{-6} M for GWB, and $<10^{-6}$ M for ERDA-6.

A large number of studies of uranium sorption have been carried out in support of the nuclear waste disposal programs and the UMTs program (UMTRA) as described in **Sections 11.6.3.2** and **11.6.4.2.2**, respectively. Park et al. (1992) and Prasad et al. (1997) describe studies of sorption of uranyl ion by corrensite, the clay mineral lining many fractures in the fractured Culebra Dolomite member of the Rustler Formation above the WIPP in SE New Mexico. The studies were carried out in dilute and concentrated NaCl (0.1–3 M) solutions in the presence of Ca^{2+}, Mg^{2+}, carbonate, and citrate. Binding constants for the TLM were fit to the sorption edges. They found that the adsorption edges were typical of cation adsorption on mineral surfaces; the uranium was nearly completely bound to the surface at neutral and near-neutral pH values. Neither the background electrolyte (NaCl) nor Ca^{2+} or Mg^{2+} ions (at 0.05 M) influenced the adsorption, suggesting that uranyl binds at pH-dependent edge sites on the corrensite surface as an inner-sphere complex. Both carbonate and citrate reduced the adsorption of uranyl on corrensite in near-neutral solutions. Redden et al. (1998) carried out similar studies of uranium sorption by goethite, kaolinite, and gibbsite in the presence of citric acid. Davis (2001) and Jenne (1998) provide good summaries of studies of uranium sorption by synthetic and natural aluminosilicates and iron oxyhydroxides. Qualitative features of the sorption edges for these minerals are similar: U(VI) sorption at higher pH is typically low and likely is controlled by the predominance of the negatively charged uranyl–carbonate solution species. By analogy, sorption of U(VI) by aluminosilicates is predicted to be low in waters sampled at Yucca Mountain (Turner and Pabalan, 1999; Turner et al., 1998).

Luckscheiter and Kienzler (2001) examined uranyl sorption onto corroded HLW glass simulant in deionized water, 5.5 M NaCl, and 5.0 M $MgCl_2$, and found that sorption was greatly inhibited by the Mg-rich brine while the NaCl brine had little effect. Uranyl sorption at high ionic strength was also studied by Vodrias and Means (1993), who examined uranyl sorption onto crushed impure halite and limestone from the Palo Duro Basin, TX, in a synthetic Na–K–Mg–Ca–Cl brine ($I = 10.7$ M). They measured K_ds of 1.3 ml g^{-1} on the halite and 4–7 ml g^{-1} on the limestone. This is in contrast to a K_d of 2100 ml g^{-1} determined from uranium series disequilibrium measurements on formation brines from the same region (Laul, 1992). The isotopic ratios suggest that naturally occurring uranium was more strongly sorbed because it was present as U(IV).

11.6.4.2.3.1.6 Actinide sorption by uranium wastes In repository environments, the UO_2 fuel itself, or secondary U(IV) and U(VI) minerals that form by degradation of SNF and HLW forms, may play an important role in limiting actinide releases by sorption and coprecipitation. UO_2 strongly sorbs Np(V), which is partially reduced to Np(IV) on the mineral surface, and is strongly, perhaps irreversibly bound (Kazakovskaya et al., 2010). At low pH, Pu(IV) is reduced to trivalent Pu and is strongly retained on the UO_2 surface (Olsson et al., 2005). Th can be also sequestered by sorption/coprecipitation at low pH, a process that may be important in reducing repository settings if radiolytic dissolution of SNF is followed by distal reprecipitation of UO_2 (Rousseau et al., 2002). Secondary U (VI) oxides and hydroxides (Burns et al., 2004), and U(VI) silicate minerals such as uranophane and sodium boltwoodite (Douglas et al., 2005a,b), also sorb Np(V) and other actinides and sequester them by crystallographic substitution. This process may be important in limiting radionuclide releases from degrading SNF (Murphy and Grambow, 2008). Neptunium is also taken up by the uranium peroxide mineral metastudtite (Friese et al., 2004), but was shown to be sorbed rather than incorporated mineralogically, and was not permanently sequestered (Douglas et al., 2005b).

11.6.4.2.3.2 Geochemical models in risk assessment for nuclear waste

In performance assessment models, simple component process and sampling models are linked to provide a description of the release of radionuclides from idealized source terms, transport through engineered barriers and surrounding geomedia, and finally uptake by potentially exposed populations. The resulting doses are compared to environmental and health regulatory standards to determine the risk posed by the releases. A basic overview of the process of risk assessment is presented by Fjeld and Compton (1999). Probabilistic performance assessment methods have been developed to provide a basis for evaluation of the risk associated with the disposal of nuclear waste in geological repositories (Cranwell et al., 1987; Rechard, 1996, 2002; Wilson et al., 2002). Similar approaches are used for LLW disposal and uranium mill tailings. Development of risk assessment models by the European community is summarized in NEA (1991). The current status of risk assessment programs in several countries is reviewed in a session devoted to performance assessment at the 2001 Materials Research Society Symposium on the Scientific Basis for Nuclear Waste Management (McGrail and Cragnolino, 2002).

Abstraction of the properties of real systems into simple models is required for risk assessment. Heterogeneities in geochemical properties along potential flow paths, uncertainties in or lack of thermodynamic and kinetic parameter values, and the lack of understanding of geochemical processes all necessitate the use of a probabilistic approach to risk assessment.

System complexity and limitations in computer technology preclude precise representation of geochemical processes in risk assessment calculations. Uncertainties in properties of the engineered and natural barriers are incorporated into the risk assessment by using ranges and probability distributions for the parameter values (K_ds and maximum aqueous radionuclide concentrations) in Monte Carlo simulations, by regression equations to calculate sorption and solubility limits from sampled geochemical parameter ranges, and by the use of alternative conceptual models (see **Section 11.6.4.3.2.2**). Representation of the probabilistic aspects of geochemical processes in risk assessment is discussed in Siegel et al. (1983b, 1992), Chen et al. (2002), and Turner et al. (2002). Simplifications in solubility and sorption models used in performance assessment calculations for the WIPP (DOE, 1996a,b,c) and the proposed HLW repository at Yucca Mountain as reviewed in Siegel and Bryan (2003) and in **Section 11.6.3.2.2** of this chapter.

Performance assessment calculations of actinide speciation and solubility, and of the potential releases that could result if the repository is breached, were carried out as part of the CCA for the WIPP (DOE, 1996a,b,c). The calculations modeled actinide behavior in a generic Salado brine and a less magnesium-rich brine from the Castile Formation. Predicted repository conditions include (1) high ionic strength, requiring the use of a Pitzer ion interaction model for calculating activity coefficients; (2) the presence of magnesium oxide backfill, which will buffer pCO_2 and pH in the repository; (3) the presence of large amounts of iron and organics in the waste, establishing reducing conditions in the repository and constraining the actinides to their lower oxidation states, and (4) potentially significant quantities of the organic ligands acetate, citrate, oxalate, and EDTA will be present (DOE, 1996a,b,c). Discussion of the speciation, solubility, and sorption of the actinides under conditions relevant to the WIPP were included in previous sections. The use of an oxidation state analog for the actinides in WIPP performance assessment was reviewed in Siegel and Bryan (2003).

The geochemical setting of the proposed repository site for HLW at Yucca Mountain in Nevada was described previously. The results of performance assessment calculations for the proposed repository at Yucca Mountain suggest that the most significant contributors to risk are radionuclides that are highly soluble or poorly sorbing (^{99}Tc, ^{129}I, and ^{237}Np) in the oxidizing, Na-bicarbonate-rich waters at the site. In addition, other radionuclides such as ^{239}Pu, ^{241}Am, ^{238}U, and ^{230}Th may be important owing to colloidal transport or high dose-conversion factors. Sorption of a radionuclide may vary drastically over postulated flow paths and over time at Yucca Mountain. One approach to represent this variability in performance assessment calculations is to sample K_ds for transport equations from a probability distribution based on experimental measurements as discussed above (Siegel et al., 1983a; Wilson et al., 2002). Another approach is to calculate a range of K_ds from thermodynamic data for a range of groundwater compositions (Turner and Pabalan, 1999; Turner et al., 2002).

11.6.4.3 Fission Products

11.6.4.3.1 Introduction

Fission products of uranium and other actinides have been released to the environment during weapons production and testing, and by nuclear accidents. Because of their relatively short half-lives, they commonly account for a large fraction of the activity in radioactive wastes for the first several hundred years. Important fission products are shown in **Table 6**; all decay by emission of a beta particle. Many of these have very short half-lives and do not represent a long-term hazard in the environment, but they do constitute a significant fraction of the total released in a nuclear accident. Only radionuclides with half-lives of several years or longer represent a persistent environmental or disposal problem. Of primary interest are ^{90}Sr, ^{99}Tc, ^{129}I, and ^{137}Cs, and to a lesser degree, ^{79}Se and ^{93}Zr; all are β^- emitters.

While fission product mobility is mostly a function of the chemical properties of the element, the initial physical form of the contamination can also be important. For radioactive contaminants released as particulates – 'hot particles' – radionuclide transport is initially dominated by physical processes, namely, transport as aerosols (Wagenpfeil and Tschiersch, 2001) or as bedload/suspended load in river systems. As discussed in more detail later, at Chernobyl, the majority of fission products was released in fuel particles and condensed aerosols. Fission products were effectively sequestered – for example, little downward transport in soil profiles and little biological uptake – until dissolution of the fuel particles occurred and the fission products were released (Baryakhtar, 1995; Konoplev and Bulgakov, 1999; Konoplev et al., 1992; Petryaev et al., 1991). Thus, fuel particle dissolution kinetics controlled the release of fission products to the environment (Kashparov et al., 2004; Kashparov et al., 1999; Kruglov et al., 1994; Sokolik et al., 2001; Uchida et al., 1999).

11.6.4.3.2 Geochemistry of fission products

11.6.4.3.2.1 ^{90}Sr

Strontium occurs in only one valence state, (II). It does not form strong organic or inorganic complexes and is commonly present in solution as Sr^{2+}. The concentration is rarely solubility-limited in soil or groundwater systems because the solubility of common strontium phases is relatively high (EPA, 1999b; Lefevre et al., 1993). The concentration of strontium in solution is commonly controlled by sorption and ion exchange reactions with soil minerals. Parameters affecting strontium transport are cation exchange capacity (CEC), ionic strength, and pH (due to H^+ competition for amphoteric sites). Clay minerals – illite,

Table 6 Environmentally important fission products

Fission product	$t_{1/2}$, *years*
^{79}Se	6.5×10^5
^{90}Sr	28.1
^{93}Zr	1.5×10^6
^{99}Tc	2.12×10^5
^{103}Ru	0.11
^{106}Ru	0.56
^{110m}Ag	0.69
^{125}Sb	2.7
^{129}I	1.7×10^7
^{134}Cs	2.06
^{137}Cs	30.2
^{144}Ce	0.78

montmorillonite, kaolinite, and vermiculite – are responsible for most of the exchange capacity for strontium in soils (Goldsmith and Bolch, 1970; Sumrall and Middlebrooks, 1968). Zeolites (Ames and Rai, 1978) and Mn oxides/hydroxides also exchange or sorb strontium in soils. Because of the importance of ion exchange, strontium K_ds are strongly influenced by ionic strength of the solution, decreasing with increasing ionic strength (Mahoney and Langmuir, 1991; Nisbet et al., 1994); calcium and natural strontium are especially effective at competing with ^{90}Sr. Strontium in soils is largely exchangeably bound and does not become fixed with time (Serne and Gore, 1996). However, coprecipitation with calcium sulfate or carbonate and soil phosphates may also contribute to strontium retardation and fixation in soils (Ames and Rai, 1978).

11.6.4.3.2.2 ^{137}Cs

Cesium, like strontium, occurs in only one valence state, (I). Cesium is a very weak Lewis acid and has a low tendency to interact with organic and inorganic ligands (EPA, 1999b; Hughes and Poole, 1989); thus, Cs^+ is the dominant form in groundwater. Inorganic cesium compounds are highly soluble, and precipitation/coprecipitation reactions play little role in limiting cesium mobility in the environment. Retention in soils and groundwaters is controlled by sorption/desorption and ion exchange reactions. Cesium is sorbed by ion exchange into clay interlayer sites, and by surface complexation with hydroxy groups constituting broken bonds on edge sites, and the planer surfaces of oxide and silicate minerals. CEC is the dominant factor in controlling cesium mobility. Clay minerals such as illite, smectites, and vermiculite are especially important because they exhibit a high selectivity for cesium (Douglas, 1989; Smith and Comans, 1996). The selectivity is a function of the low hydration energy of cesium; once it is sorbed into clay interlayers, it loses its hydration shell and the interlayer collapses. Ions such as magnesium and calcium, are unable to shed their hydration shells and cannot compete for the interlayer sites. Potassium is able to enter the interlayer and competes strongly for exchange sites. Because it causes collapse of the interlayers, cesium does not readily desorb from vermiculite and smectite and may, in fact, be irreversibly sorbed (Douglas, 1989; Khan et al., 1994; Ohnuki and Kozai, 1994). Uptake by illitic clay minerals does not occur by ion exchange but rather by sorption onto frayed edge sites (Comans et al., 1989; Cremers et al., 1988; Smith et al., 1999), which are highly selective for cesium. Although illite has a higher selectivity for cesium, it has a much lower capacity than smectites because interlayer ion exchange does not occur.

Cesium mobility increases with ionic strength because of competition for exchange sites (Lieser and Peschke, 1982). Since cesium is rapidly and strongly sorbed by soil and sediment particles, it does not migrate downward rapidly through soil profiles, especially forest soils (Bergman, 1994; Panin et al., 2001; Rühm et al., 1996). Estimated downward migration rates for cesium released by the Chernobyl accident are on the order of 0.2–2 cm year^{-1} in soils in Bohemia (Hölgye and Malý, 2000), Russia (Sokolik et al., 2001), and Sweden (Isaksson et al., 2001; Rosén et al., 1999).

11.6.4.3.2.3 ^{99}Tc

Technetium occurs in several valence states, ranging from −1 to +7. In groundwater systems, the most stable oxidation states are (IV) and (VII) (Lieser and Peschke, 1982). Under oxidizing conditions, Tc(VII) is stable as pertechnetate, TcO_4^-. Pertechnetate compounds are highly soluble, and being anionic, pertechnetate is not sorbed onto common soil minerals and/or readily sequestered by ion exchange. Thus, under oxidizing conditions, technetium is highly mobile. Significant sorption of pertechnetate has been seen in organic-rich soils of low pH (Wildung et al., 1979), probably owing to the positive charge on the organic fraction and amorphous iron and aluminum oxides, and possibly coupled with reduction to Tc(IV).

Under reducing conditions, Tc(IV) is the dominant oxidation state because of biotic and abiotic reduction processes. Tc(IV) is commonly considered to be essentially immobile because it readily precipitates as low-solubility hydrous oxides and forms strong surface complexes on iron and aluminum oxides and clays. Tc(IV) behaves like other tetravalent heavy metals and occurs in solution as hydroxo and hydroxo–carbonato complexes. In carbonate-containing groundwaters, $TcO(OH)_{2(aq)}$ is dominant at neutral pH; at higher pH values, $Tc(OH)_3CO_3^-$ is more abundant (Eriksen et al., 1992). However, the solubility of Tc(IV) is low and is limited by precipitation of the hydrous oxide, $TcO_2 \times nH_2O$. The number of waters of hydration is traditionally given as $n = 2$ (Rard, 1983) but has more recently been measured as 1.63 ± 0.28 (Meyer et al., 1991). In systems containing H_2S or metal sulfides, the solubility-limiting phase for technetium may be Tc_2S_7 or TcS_2 (Rard, 1983).

Retention of pertechnetate in soil and groundwater systems usually involves reduction and precipitation as Tc (IV)-containing hydroxide or sulfide phases. Several mineral phases have been shown to fix pertechnetate through surface-mediated reduction/coprecipitation. These include magnetite (Byegård et al., 1992; Cui and Erikson, 1998; Haines et al., 1987) and a number of sulfides, including chalcocite, bournonite, pyrrhotite, tetrahedrite, and, to a lesser extent, pyrite and galena (Bock et al., 1989; Huie et al., 1988; Lieser and Bauscher, 1988; Strickert et al., 1980; Winkler et al., 1988). Sulfides are most effective at reducing technetium if they contain a multivalent metal ion in the lower oxidation state (Strickert et al., 1980). Technetium sorption by iron oxides is minimal under near-neutral, oxidizing conditions but is extensive under mildly reducing conditions, where Fe(III) remains stable. It is minimal on ferrous silicates (Vandergraaf et al., 1984). In addition, technetium may be fixed by bacterially mediated reduction and precipitation. Several types of Fe(III)- and sulfate-reducing bacteria have been shown to reduce technetium, either directly (enzymatically) or indirectly through reaction with microbially produced Fe(II), native sulfur, or sulfide (Lloyd and Macaskie, 1996; Lloyd et al., 2002; Lyalikova and Khizhnyak, 1996).

11.6.4.3.2.4 ^{129}I

Iodine can exist in the oxidation states −1, 0, +1, +5, and +7. However, the +1 state is not stable in aqueous solutions and disporportionates into −1 and +5. In surface and groundwaters at near-neutral pH, IO_3^- (iodate) is the dominant form in solution, while under acidic conditions, I_2 can form. Under anoxic conditions, iodine is present as I^- (iodide) (Allard et al., 1980; Liu and Van Gunten, 1988).

Iodide forms low-solubility compounds with copper, silver, lead, mercury, and bismuth, but all other metal iodides are quite soluble. As these metals are not common in natural environments, they have little effect on iodine mobility (Couture and Seitz, 1985). Retention by sorption and ion exchange appears to be minor (Lieser and Peschke, 1982). However, significant retention has been observed by the amorphous minerals imogolite and allophane (mixed Al/Si oxide/hydroxides, with SiO_2/Al_2O_3 ratios between 1 and 2). These minerals have high surface areas and positive surface charge at neutral pH and contribute significantly to the anion exchange capacity in soils (Gu and Schultz, 1991). At neutral pH, Al- and Fe-hydroxides are also positively charged and contribute to iodine retention, especially if iodine is present as iodate (Couture and Seitz, 1985). Sulfide minerals containing the metal ions that form insoluble metal iodides strongly sorb iodide, apparently through sorption and surface precipitation of the metal iodide. Iodate is also sorbed, possibly because it is reduced to iodide on the metal sulfide surfaces (Allard et al., 1980; Strickert et al., 1980). Lead, copper, silver, silver chloride, and lead oxides/hydroxides and carbonates can also fix iodine through surface precipitation (Allard et al., 1980; Bird and Lopata, 1980). None of these minerals are likely to be important in natural soils but may be useful in immobilizing iodine for environmental remediation.

Organic iodo compounds are not soluble and form readily through reaction with I_2 and, to a lesser extent, I^- (Couture and Seitz, 1985; Lieser and Peschke, 1982); retention of iodine in soils is mostly associated with the organic matter (Gu and Schultz, 1991; Kaplan et al., 2000; Muramatsu et al., 1990; Wildung et al., 1974; Yoshida et al., 1998). Several studies have suggested that fixation of iodine by organic soil compounds appears to be dependent upon microbiological activity, because sterilization by heating or radiation commonly results in much lower iodine retention (Bors et al., 1991; Koch et al., 1989; Muramatsu et al., 1990; Rädlinger and Heumann, 2000).

11.6.4.3.3 Application: the Chernobyl reactor accident

11.6.4.3.3.1 Introduction

On April 26, 1986, an explosion at the Chernobyl Nuclear Power Plant, and the subsequent fire in the graphite reactor core, released about 3% (6–8 metric tons) of the total fuel inventory of the reactor core. During the initial explosion, most radionuclide release occurred as fragments of unoxidized uranium dioxide fuel, which were deposited mostly in a plume extending 100 km to the west of the plant. The core fire lasted 10 days. Releases were once again dominated by fuel particles – however, because of the exposed core, these particles were partially or completely oxidized. For the first 4 days, high temperatures in the reactor resulted in the release of volatile radionuclides (Xe, Kr, I, Te, and Cs), much of which was deposited as condensed particles in plumes to the northwest, west, and northeast of the plant, extending as far as Scandinavia. Over the next 6 days, temperatures in the reactor decreased, and the release of volatile fission products decreased. The lower temperatures (600–1200°K) favored oxidation of the nuclear fuel, so fuel particles released during this phase were more heavily oxidized. Radionuclides released during this phase were deposited mostly in a southern plume, extending as far south as Greece.

11.6.4.3.3.2 Geochemical behavior

A major part of the radionuclides released at Chernobyl were deposited as 'hot particles,' either fuel particles with an average median diameter of 2–3 μm or condensed particles. Within the exclusion zone, extending 30 km from the plant, more than 90% of the radioactive contamination was in the form of fuel particles (Kashparov et al., 1999). This included about 80% of the ^{90}Sr and about 50–75% of the ^{137}Cs contamination. Particle size decreased with distance from the Chernobyl plant, and the proportion of condensed particles relative to the fuel particles increased. Other radionuclides released include the fission products ^{134}Cs, ^{144}Ce, ^{125}Sb, ^{106}Ru, ^{103}Ru, and ^{95}Zr, and the neutron activation products ^{110m}Ag and ^{54}Mn (Petropoulos et al., 2001). Because of the importance of fuel particles in terms of the total radionuclide release from Chernobyl, considerable attention has been given to fuel particle behavior in the environment. The transport properties of the radionuclides present in the fuel particles and the type of hazard that they represent changed as the particles weathered. Initially, particle (and radionuclide) transport was governed by physical processes. Particles were transported both as aerosols in the atmosphere and as suspended load in runoff and rivers. The primary hazards represented by the particles were inhalation and skin doses. Particle alpha activities were similar to that of the original nuclear fuel (2.5×10^8 Bq cm^{-3}) (Boulyga et al., 1999), while beta and gamma activities were somewhat lower due to loss of volatile fission products. The median fuel particle size released at Chernobyl (2–3 μm) falls within the respirable fraction of aerosols (defined as <7 μm), and such particles are easily re-suspended by anthropogenic or natural processes that disturb the soil. Fuel particles are not readily transported downward through the soil column, and soil sampling in the exclusion zone, carried out 10 years after the accident, showed that the particles were still concentrated in the upper 5 cm (Kashparov et al., 1999). Thirteen years after the accident, agricultural activities in the exclusion zone resulted in local airborne concentrations of hot particles of 50–200 particles per cubic meter (Boulyga et al., 1999).

Radionuclides sequestered in the fuel particles are not immediately available to the biosphere as the particles generally have a low solubility in water, simulated lung fluids, and HCl solutions (Chamberlain and Dunster, 1958; Oughton et al., 1993; Salbu et al., 1994). Release of biologically important radionuclides such as ^{90}Sr and ^{137}Cs into the biosphere requires weathering and dissolution of the fuel particles. Particle weathering rates vary with several source-related particle characteristics (particle size, oxidation state, and structure) and depend on environmental parameters such as soil pH and redox conditions. Field studies have shown that the fraction of exchangeable ^{90}Sr in soil increases as fuel particles dissolve (Baryakhtar, 1995; Kashparov et al., 1999; Konoplev and Bulgakov, 1999; Konoplev et al., 1992; Petryaev et al., 1991). Konoplev and Bulgakov (1999) used these observations to estimate the fraction of undissolved fuel particles present in soils in the Chernobyl 30-km exclusion zone. They found that the unoxidized fuel particles, deposited from the initial explosion in a plume to the west of Chernobyl, are more resistant to leaching and dissolution than the oxidized fuel particles released during the subsequent fire and deposited to the north, northeast, and south of the plant. Dissolution rates for the

unoxidized fuel particles were about one-third of those of oxidized particles, with 27–79% remaining undissolved in 1995, while only 2–30% of the oxidized fuel remained. Fuel particle dissolution rates also increased with increasing soil acidity and with decreasing particle size (Kashparov et al., 1999; Konoplev and Bulgakov, 1999).

These results are consistent with laboratory measurements of the effects of pH and oxidation state on the leachability of nuclear fuel particles (Kashparov et al., 2000). The increased leachability of the oxidized fuel particles may be due to (1) an increased solubility because of the change in oxidation state; (2) the higher surface area of the highly fractured oxidized particles; or (3) the diffusion of radionuclides (strontium, cesium) to grain boundaries and particle surfaces during the heating and oxidation process. Once released from the fuel particles, strontium and cesium are available to the biosphere and can be taken up by plants or can be transferred down the soil profile. At present, the relative rates of each process are not well enough constrained to predict future levels of ^{90}Sr and ^{137}Cs in vegetation in the exclusion zone (Kashparov et al., 1999).

In more distal areas, cesium and strontium concentrations in soils, lakes, and rivers were initially high from direct fallout but have progressively dropped as these elements move downward into the soil profile and are flushed or sedimented out of bodies of water. The estimated ecological half-life for ^{137}Cs in German forest soils is 2.8 ± 0.5 years for the l horizon and 7.7 ± 4.9 years for the Ah horizon (Rühm et al., 1996). ^{90}Sr concentrations in the Black Sea had dropped to pre-Chernobyl levels by 1994, and ^{137}Cs is predicted to reach pre-accident levels by 2025–30 (Kanivets et al., 1999). The main causes of the decreases are radioactive decay and loss through the Bosporus Strait. However, the relative proportion of ^{90}Sr entering the Black Sea as river input is increasing, as fuel particles in the major watersheds weather and release sequestered radionuclides. Smith et al. (1999) have shown that cesium removal from lakes and rivers is dominantly by lake outflow and by sedimentation. Cesium is strongly sorbed onto the frayed edge sites of illitic clay minerals, and cesium removal rates from lakes correlate with aqueous K^+ concentrations.

11.6.4.3.3.3 Environmental epidemiology

The explosion at the Chernobyl Power Station, released large quantities of radionuclides into the atmosphere. The accident caused 28 deaths of power plant employees and firemen due to radiation exposure within weeks. About 600 000 workers, termed 'liquidators' took part in major mitigation activities at the reactor and within the 30-km zone surrounding the reactor between 1986 and 1990. During 1986, 220 000 people were evacuated from areas surrounding the reactor, and after 1986, about 250 000 people were relocated from Belarus, the Russian Federation, and Ukraine. Dose distributions in countries near the reactor were heterogeneous and ranged from 0.2 to 64 mGy. Numerous epidemiologic studies have been carried out since the Chernobyl accident to investigate the potential late health consequences from the accident. These studies have focused largely on thyroid cancer in children. Other investigations have studied recovery operation workers and residents of contaminated areas. Additional studies of the occurrence of leukemia and solid tumors other than thyroid cancer among exposed individuals have also been carried out.

Many descriptive epidemiological studies suggest an increasing number of cases of thyroid cancer, particularly in the most heavily contaminated regions of Ukraine and Belarus, and Russia. There has been a significant increase of thyroid cancers among children in the areas contaminated by fallout from the Chernobyl explosion (Harley, 2001; UNSCEAR, 2000). The initial external exposures from Chernobyl were due to ^{131}I and short-lived isotopes. Subsequently, external exposures to ^{137}Cs and ^{134}Cs and internal exposures to radiocesium through consumption of contaminated foodstuffs were important. BEIR VII (NAS, 2006, pp. 216–223) lists 50 studies of the effects of fallout from the Chernobyl accident. Excess (thyroid) cancer incidence was observed only in those studies in which dose was determined by measuring contamination by specific radionuclides (e.g., ^{137}Cs). Over the period 1986–97, a steady increase in the number of thyroid cancers was observed in children under the age 14 at the time of the accident; by 1997, over 1600 thyroid cancers had been observed in children who were under the age of 17 at the time of the accident (Harley, 2001). However, the expected number of thyroid cancers is not well-constrained, and although there is little doubt that an excess of thyroid cancer has occurred in highly contaminated areas, there is still very little information regarding the quantitative relationship between radiation dose and cancer incidence. Most of the published findings are from ecologic studies that do not provide quantitative estimates of disease risk based on individual estimates of radiation dose. Only four analytical studies report dose response based on individual dose estimates. Quantitative estimates of risk from these studies are consistent with estimates from other radiation-exposed populations. There is evidence that two factors, a young age at exposure, and iodine deficiency, may be important modifiers of the risk of radiation-induced thyroid cancer. In contrast, no solid tumors other than thyroid cancer have been identified resulting from the accident.

The evidence from epidemiologic studies regarding the risk of leukemia comes from the studies of moderately or highly exposed Chernobyl recovery operation workers and the general population, who have been exposed at low-dose-rates (primarily from ^{137}Cs) for a number of years. The BEIR VII report concludes that the existing evidence does not show that rates of childhood or adult leukemia have increased as a result of radiation exposures from the Chernobyl accident. However, relatively small changes over time in the incidence of an uncommon disease such as childhood leukemia and in different geographic areas would be difficult to detect with ecologic studies. Similarly, the few studies of the general adult population have employed ecologic designs and are hard to interpret.

11.6.4.3.4 Application: contamination from weapons production at Chelyabinsk

11.6.4.3.4.1 Chelyabinsk complex

Large-scale contamination of the Urals in Russia is severe due to weapons production at the Chelyabinsk-65 complex near the city of Kyshtym. Cochran et al. (1993) provide an overview of the extent of the contamination at the site, drawing upon a number of Russian source documents. The main weapons production facility, the Mayak Chemical Combine, produced

over 5.5×10^{19} Bq of radioactive wastes from 1948 through 1992. Over 4.6×10^{18} Bq of long-lived radioactivity were discharged into open lake storage and other sites. During the period 1948–51, approximately 9.3×10^{16} Bq of medium level β activity liquid waste was discharged directly into the nearby Techa River; from March 1950 to November 1951, the discharge averaged 1.6×10^{14} Bq day^{-1}. During this period, about 124 000 people living downstream from the facility were exposed to elevated levels of radioactivity. In 1951, the medium level waste was discharged into nearby Lake Karachay. Through 1990, the lake had accumulated 4.4×10^{18} Bq of long-lived radionuclides (primarily ^{137}Cs [3.6×10^{18} Bq] and ^{90}Sr [7.4×10^{17} Bq]). By 1993, seepage of radionuclides from the lake had produced a radioactive groundwater plume that extended 2.5–3 miles from the lake. In 1993, the total volume of contaminated groundwater was estimated to be more than 4 million cubic meter, containing at least 1.8×10^{14} Bq of long-lived (>30-year half-life) fission products.

Several large-scale nuclear disasters have occurred at the Chelyabinsk-65 complex. Two of these events lead to the spread of radioactive contamination over large areas, exposure to large numbers of people and relocation of communities. In 1957, during the so-called 'Kyshtym Disaster,' an explosion of a HLW storage tank released 7.4×10^{17} Bq of radioactivity into the atmosphere (Medvedev, 1979; Trabalka et al., 1980). About 90% of the activity fell out in the immediate vicinity of the tank. Approximately 7.8×10^{16} Bq formed a kilometer-high radioactive cloud that contaminated an area greater than 23 000 km^2 to levels above 3.7×10^9 Bq km^{-2} of ^{90}Sr. This area was home to about 270 000 people; many of the inhabitants were evacuated after being exposed to radioactive contamination for several years.

A second disaster at the site occurred in 1967, after water in Lake Karachay evaporated during a hot summer that followed a dry winter. Dust from the lakeshore sediments was blown over a large area, contaminating 1800–2700 km^2 with a total of 2.2×10^{13} Bq of ^{137}Cs and ^{90}Sr. Approximately 41 000 people lived in the area contaminated at levels of 3.7×10^9 Bq km^{-2} of ^{90}Sr or higher. According to Botov (1992), releases of radioactive dust from the area continued through at least 1972. Since 1967, a number of measures have been taken to reduce the dispersion of radioactive contamination from Lake Karachay as described in Cochran et al. (1993) and NAS (2009) and sources documents cited therein.

11.6.4.3.4.2 Environmental epidemiology

A study of 28 100 individuals exposed along the Techa River, downstream from Chelyabinsk-65, revealed that a statistically significant increase in leukemia mortality arose between 5 and 20 years after the initial exposure (37 observed deaths vs. 14–23 expected deaths; see Cochran et al., 1993 and cited references and comments). BEIR VII describes several epidemiological studies of residents living near the Techa River in the vicinity of the Mayak plant. These include studies of cancer mortality in residents and their offspring, as well as pregnancy outcomes. There is some evidence of a statistically significant increase in total cancer mortality of the residents; however, there is no evidence of increase in their offspring (Kossenko, 1996). No evidence of a decrease in birth rate or fertility in the exposed population nor increased incidence of spontaneous abortions or stillbirths has been observed (Kossenko et al., 1994). There has been one study (Koshurnikova et al., 2002) of persons living in the town of Ozyorsk exposed to fallout from the nearby nuclear facility. This study reported an excess of thyroid cancer 3–4 times than expected relative to rates for the whole of Russia and a somewhat lower excess (1.5- to 2-fold higher) based on a comparison with Chelyabinsk Oblast rates; however, no estimates of radiation dose were included in this study.

11.6.5 Summary

This chapter provides descriptions of the most important examples of environmental radioactive contamination and their impacts on human health. The radionuclides comprise three overlapping groups in the environment: (1) common naturally occurring radioelements of the uranium decay series (radium, thorium, and uranium), (2) the actinides, and (3) the fission products of uranium and the transuranics. The first group is important to public health regulations of drinking water and for assessing the environmental impact of resource development. The latter two groups are important in association with the nuclear fuel cycle and nuclear weapons production. For each group, environmental occurrence and processes that control their distributions and environmental epidemiological studies of health effects are described. Cancer is the major effect of low radiation doses expected from exposure to radioactive contamination. Cancers most commonly observed in humans after exposure to ingested or inhaled radioactive contamination or to external ionizing radiation include those of the lungs, female breast, bone, thyroid, and skin.

Radium is primarily important to drinking water regulations, uranium mining, and production of TENORM. Concentrations of radium in groundwater are influenced by decay of the dissolved Th parents in the solution, dissolution from the aquifer and secondary minerals, alpha-recoil from the parent nucleus in the aquifer rocks and on the clay and oxide surface coatings, adsorption/desorption exchange with Ra adsorbed on the surface coating, clays, and oxides, and coprecipitation with secondary minerals. Two types of water have naturally high radium contents: one end member has low pH, and in places, high concentrations of acid anions and divalent cations. The other end member has low concentrations of dissolved oxygen (DO concentration <1 mg l^{-1}), high concentrations of iron or manganese, and high concentrations of dissolved solids. High concentrations of radium are associated with uranium deposits and uranium mill tailings. Radium is similar to calcium in its geochemical and metabolic behaviors and, once ingested, radium is incorporated onto surfaces in the mineralized portion of the bone. The primary health effect observed from the ingestion of ^{226,228}Ra is cancer of the bone (osteogenic sarcomas).

Uranium geochemistry is relevant to drinking water regulations, resource extraction, and nuclear waste; its chemistry is similar to thorium and the transuranics (actinide series). Owing to similarities in ionic size, coordination number, valence, and electron structure, the actinide elements of a given oxidation state have chemical properties that are either similar or vary systematically. For a given oxidation state, the

relative stability of actinide complexes with hard base ligands can be divided into three groups in the order: CO_3^{2-}, $OH^- > F^-$, HPO_4^{2-}, $SO_4^{2-} > Cl^-$, NO_3^-. Within those ligand groups, stability constants generally decrease in the order: $An^{4+} > An^{3+} \approx AnO_2^{2+} > AnO_2^+$.

In dilute aqueous systems, the dominant actinide species at neutral to basic pH are hydroxy- and carbonato-complexes. Similarly, solubility-limiting solid phases are commonly oxides, hydroxides, or carbonates. Sorption onto carbonates, clays, and iron oxides/hydroxides is especially important. In general, actinide sorption will decrease in the presence of ligands that complex with the radionuclide (most commonly humic or fulvic acids, CO_3^{2-}, SO_4^{2-}, F^-) or cationic solutes that compete with the radionuclide for sorption sites (most commonly Ca^{2+}, Mg^{2+}).

Open-pit mining, underground mining, and ISL (also known as ISR) have been used for mining uranium-containing ores. Wastes from the first two techniques include uranium mill tailings, composed of crushed rock with fine-grained primary and secondary minerals. Radionuclides and metals can be associated with many of these mineral phases and can be a source of groundwater contamination. WithISR or ISL mining techniques, lixiviants are injected into uranium-containing porous rock formations and the resultant ore solutions are pumped to the surface for processing at surface facilities. Because uranium is soluble under both acidic and alkaline conditions, it is possible to use either acidic or alkaline lixiviants. In general, acid solutions will extract a higher proportion of uranium and at faster rates than alkaline solutions but acidic solutions will also mobilize high levels of toxic heavy metals; this has led to extensive groundwater contamination. Currently in the USA, all current or proposed ISL uranium production uses alkaline leaching chemistry with carbon dioxide or sodium carbonate and oxygen.

Interpretation of historical evidence of past success or failures in restoring a site mined using ISL techniques is one of the most controversial aspects of the uranium mining industry. ISL industry practice is to set the primary restoration goal to match pre-mining conditions; however, a return to pre-baseline conditions has rarely been accomplished. Alternative restoration criteria based on pre-mining industrial class-of use have been used; restoration to levels required for domestic use have not been required because of high concentrations of uranium, heavy metals, and other solutes in the production zones. It is unclear whether adequate long-term restoration of ISR sites will occur by NA and if the regional reducing capacity of the aquifer will prevail over any small pockets of residual oxidation that may persist after restoration of alkaline leach sites. The key areas of uncertainty include site characterization (historical mining activity, current and future groundwater flow patterns, mineralogy, and water chemistry), and the likely efficacy of important geochemical mechanisms (reducing capacity and kinetics) of NA. The issue of characterizing baseline values from the entire aquifer exclusion zone versus the ore zone proper is particularly important in setting restoration goals.

The chemical toxicity of uranium is more important than its radiological hazard. Uranyl ion is concentrated in the tubular cells of the kidneys; this produces systemic toxicity in the form of acute renal damage and renal failure. Food and drinking water are the primary sources of uranium exposure for the general public and for populations who work in or live near uranium mining, processing, and manufacturing facilities. Several ecological epidemiological studies suggest possible associations between elevated levels of uranium in drinking water and indication of renal dysfunction. Studies of workers at uranium milling or nuclear facilities and residents living near uranium mining and milling facilities, however, have not found significant increases in cancer mortality associated with uranium exposure when the effects of smoking and exposure to radon and its progeny are evaluated.

The geochemistry of the fission products is important to nuclear waste disposal, weapons production as well as in assessing the short-term impact of accidents at nuclear facilities. Because of their relatively short half-lives, they commonly account for a large fraction of the activity in radioactive wastes for the first several hundred years. Of primary interest are ^{90}Sr, ^{99}Tc, ^{129}I, and ^{137}Cs, and to a lesser degree, ^{79}Se and ^{93}Zr; all are β^- emitters. While fission product mobility is mostly a function of the chemical properties of the element, the initial physical form of the contamination can also be important. For radioactive contaminants released as particulates – 'hot particles' – radionuclide transport is initially dominated by physical processes, namely, transport as aerosols or as bed-load/suspended load in river systems.

The explosion at the Chernobyl Power Station, released large quantities of fission product radionuclides into the atmosphere. Numerous epidemiologic studies have been carried out since the Chernobyl accident to investigate the potential late health consequences from the accident. Many descriptive epidemiological studies suggest an increasing number of cases of thyroid cancer, particularly in the most heavily contaminated regions of Ukraine and Belarus, and Russia. Large-scale contamination (primarily ^{137}Cs and ^{90}Sr) of the Urals in Russia is severe because of weapons production at the Chelyabinsk-65 complex near the city of Kyshtym. In addition to discharge of over 4.6×10^{18} Bq of radioactivity into open lake storage and the Techa River, several large-scale nuclear disasters have occurred. A study of 28 100 individuals exposed along the Techa River, downstream from Chelyabinsk-65, revealed that a statistically significant increase in leukemia mortality arose between 5 and 20 years after the initial exposure. There is some evidence of a statistically significant increase in total cancer mortality of the residents; however, there is no evidence of increase in their offspring.

Appendix A Radioactivity and Human Health

An understanding of the human health effects related to radioactivity and radioactive materials is essential for determining the significance of exposure to radioactive contamination and radioactivity in the environment. The subject is extremely complex, with a number of important controversies whose resolutions are beyond the scope of this chapter. Some general principles, however, are summarized below to guide the reader through the major issues important in assessing the risks associated with natural and anthropogenic environmental radioactivity. Several excellent reviews at a variety of levels of detail have been written and should be consulted by the reader

(ATSDR, 1990a,b,c, 1999; Cember, 1996; Harley, 2001; NAS, 1988b, 1998, 1999a, 2006; Shleien et al., 1998). Radiation exposures can lead to acute effects from very high doses and delayed effects from both single high exposure events and chronic low-level exposures. This section deals only with delayed effects because of their relevance to environmental exposures. Information about acute exposures can be found in Shleien et al. (1998), Harley (2001), and cited references. As explained later, however, many of the health effects models used a basis for environmental regulations that rely on extrapolation of the results of dose–response relationships at relatively high exposure levels to very low-level environmental exposures.

Basis for Health Effects from Radiation: Interactions between Ionizing Radiation and Human Tissue

Ionizing radiation loses energy when passing through matter by producing ion pairs. These can damage biological material directly or produce reactive species (free radicals) that can subsequently react with biomolecules. The *dose* is the mean energy imparted by ionizing radiation per mass. (The SI unit is the Gray (Gy), which is equal to 1 J kg^{-1}. The older unit is the rad, which equals 100 erg g^{-1}; 100 rad = 1 Gy). Ionizing radiation creates ion pairs in a substance such as air or tissue in relatively dense or sparse distribution depending upon the particle. Alpha particles with large mass produce relatively intense ionization tracks per unit distance relative to beta particles, and beta particles produce more dense ionization than gamma-rays. The ability to produce more or less ionization per unit path in a medium is described by the linear energy transfer (LET). Each track of low-LET radiation resulting from x-rays or gamma rays consists of a few ionizations across an average-sized cell nucleus. An electron set in motion by a gamma ray crossing an 8-μm-diameter nucleus gives an average of about 70 ionizations, equivalent to about 5 mGy (500 mrad) absorbed dose. A high-LET alpha particle produces many thousands of ionizations and gives a relatively high dose to the cell. For example, a 4-MeV alpha-particle track yields, on average, about 30 000 ionizations (3 Gy, 300 mrad) in an average-sized cell nucleus. Within the nucleus, even low-LET gamma radiation will give some microregions of relatively dense ionization over the dimensions of DNA structures owing to the low-energy electrons set in motion (UNSCEAR, 2000).

Ionization disrupts chemical bonding in cellular molecules such as DNA. Low-LET radiation generally leads to isolated events and these are readily repaired by cellular enzymes. The higher density of ionizations associated with high-LET radiation can lead to multiple disruptions of a DNA double helix and the damage may be irreparable. When a tissue is exposed to low doses of high-LET radiation, few cells will receive a relatively high dose but there will be greater probability of damage within that single DNA molecule compared to low-LET radiation, which leads to a more uniform distribution of dose. At doses of low LET radiation less than 1 mGy, a cell nucleus 8 mm in diameter will be traversed by multiple sparsely ionizing tracks.

The effect of the radiation damage depends on a combination of events on the cellular, tissue, and systemic levels. At acute doses of 0.1–5 Gy, damage to organisms can occur on the cellular level through single-strand and double-strand DNA breaks. These lead to mutations and/or cellular reproductive death after one or more divisions of the irradiated parent cell. The types of DNA damage have been classified according to their structure, and relative frequencies of different types of damage as a function of low-LET irradiation doses have been estimated. In order of increasing yield (number of defects per cell per Gray) the damages are double-strand breaks (40 defects per Gy^{-1}), DNA protein cross-link damages (150 defects Gy^{-1}), base damage (500 Gy^{-1}), and single-strand breaks (1000 Gy^{-1}). Loss or alteration of base sequence of DNA has genetic consequences (UNSCEAR, 2000). It is expected that the occurrence of more complex types of damage (i.e., double-strand breaks with adjacent damage) will increase with increasing LET and that this category of damage will be less repairable than the simpler forms of damage (Harley, 2001).

In addition to these direct forms of damage, ionizing radiation may ionize other molecules closely associated with DNA, which contain hydrogen or oxygen. Once ionized, these can form free radicals that can damage DNA (indirect effect). The indirect effect occurs over short distances within a cell and is limited by the reactivity of the radical, which determines how far it can diffuse. Exposure to high doses of radiation (>5 Gy) can lead to direct cell death before division due to interaction of free radicals with macromolecules such as lipids and proteins. The dose level at which significant damage occurs depends on the cell type. Cells that reproduce rapidly, such as those found in the bone marrow or the gastrointestinal tract, will be more sensitive to radiation than those that are longer lived, such as striated muscle or nerve cells. The effect of high radiation doses on organs depends on the various cell types in that system.

Cancer is the major effect of low radiation doses expected from exposure to radioactive contamination. Laboratory studies have shown that alpha, beta, and gamma radiation can produce cancer in virtually every tissue type and organ in animals studied (ATSDR, 2001). Cancers observed in humans after exposure to radioactive contamination or ionizing radiation include cancers of the lungs, female breast, bone, thyroid, and skin. Different kinds of cancers have different latency periods; leukemia can appear within 2 years after exposure, while cancers of the breast, lungs, stomach, and thyroid have latency periods greater than 20 years. Besides cancer, there is little evidence of other human health effects from low-level radiation exposure (Harley, 2001). A detailed understanding of the biochemical response to damage from ionizing radiation is a key element in the ongoing debate over the shape of the dose–response curve at very low doses considered to be safe for the general public in environmental regulations. This will be discussed in more detail in later sections.

Equivalent Dose and Biokinetics

Weighting parameters that take into account the radiation type, the biological half-life, and the tissue or organ at risk are used to convert the physically absorbed dose (in units of Gray or rad) to the biologically significant committed equivalent dose and effective dose, measured in units of Sv (or rem). An 'equivalent' dose, normalized for different types of radiation, is calculated using the values for LET of the various types of

radiation in water. As discussed above, the LET from alpha and beta particles is much greater than it is for gamma rays. A radiation weighting factor, w_r is defined as the ratio of the LET for gamma radiation to the radiation in question and the normalized (or weighted) dose H is called the equivalent dose: $H = D \times w_r$; where D is the dose in Grays (or rads) and H is the equivalent dose in Sieverts (or rems). Values of w_r are 5 for thermal neutrons, 20 for protons and alpha particles, and 1 for x-rays, gamma rays, beta particles, and electrons.

The effective dose H_E is a doubly weighted dose that is weighted for radiation type and tissue type: $H_E = w_t \times (D \times w_r)$. The unit is the Sievert or rem. The tissue weighting factor w_t is the ratio of the cancers to a particle organ from a partial body dose to the total cancers resulting from a whole body dose of the same dose. The sum of the weights for 12 specific organs plus a 'remainder' of other organs equals unity (see table 25-3, Harley, 2001). The dose rate is the dose per unit time and will decrease for short-lived ingested radionuclides as the radionuclide decays.

Toxicity and carcinogenicity of radioactive materials are derived from both chemical properties of the radioelements and the effects of ionizing radiation. If the kinetics of metabolism of a radionuclide is known, that is, its rate of intake, uptake, deposition, and excretion in a human, then the exposure to dose can be related. In general, substances in the body are removed through biological processes as well as by radioactive decay; therefore the effective half-life is shorter than the radiologic half-life. The relative importance of the radiological and chemical health effects are in part determined by the biological and radiological half-lives of the radionuclide and the mechanism of chemical toxicity of the radioelement. The longer a radionuclide is retained by the body or localized to a specific organ system, the greater the chance that the damage to DNA or proteins may not be repaired and a cancer may be initiated or promoted. The biological half-life of radioelement is determined in part by the chemical and physical form of the radioelement when it enters the body, the metabolic processes that it participates in, and the routes of elimination from the body. For example, ^{90}Sr and ^{226}Ra substitute for calcium and accumulate on the surfaces of bones. They have long biological half-lives (50 years) because they are recycled within the skeletal system. In young children, they are incorporated into growing bone where they can irradiate both the bone cells and bone marrow. High exposures can lead to bone cancer and cancers of the blood such as leukemia.

The total dose D can be directly related to health risk; it is expressed as

$$D = D_0 \times T_{eff} / \ln 2$$

where D_0 is the dose at time 0, T_{eff} is the effective half-life $= (T_r + T_b)/(T_r \times T_b)$, where T_r is the radiologic half-life and T_b is the biological half-life.

Dosimetry and Environmental Exposure

External and internal exposure pathways are important for human health effects. External exposure occurs from radiation sources outside the body such as soil particles on the ground surface, in surface water, and from particles dispersed in the air. It is most important for gamma radiation that has high penetrating potential; however, except for large doses, most of the radiation will pass through the body without causing significant damage. External exposure is less important for beta and alpha radiation, which are less penetrating and will deposit their energy primarily on the outer layer of the skin.

Internal exposures of alpha and beta particles are important for ingested and inhaled radionuclides. Dosimetry models are used to estimate the dose from internally deposited radioactive particles. The amount and mode of entry of radionuclides into the body, the movement and retention of radionuclides within various parts of the body, and the amount of energy absorbed by the tissues from radioactive decay are all factors in the computed dose (NAS, 1988a,b, 2006). The penetrating power of alpha radiation is low; therefore, most of the energy from alpha decay is absorbed in a relatively small volume in the gut or lungs surrounding an ingested or inhaled particle. The chance that damage to DNA or other cellular material will occur and the associated human health risk is higher for radioactive contamination composed of alpha emitters than for the other forms of radioactive contamination.

Ingestion of radioactive materials is most likely to occur from contaminated foodstuffs or water or eventual ingestion of inhaled compounds initially deposited in the lung. Ingestion of radioactive material may result in toxic effects as a result of either absorption of the radionuclide or irradiation of the gastrointestinal tract during passage through the tract, or a combination of both. The fraction of a radioactive material absorbed from the gastrointestinal tract is variable, depending on the specific element, the physical and chemical form of the material ingested, diet, as well as some other metabolic and physiological factors. The absorption of some elements is influenced by age, usually with higher absorption in the very young.

The inhalation route of exposure has long been recognized as being a major portal of entry for both nonradioactive and radioactive materials. The deposition of particles within the lung is largely dependent upon the size of the particles being inhaled. The retention of the particle in the lung depends on the location of deposition, in addition to the physical and chemical properties of the particles. Pulmonary clearance counteracts pulmonary retention. There are three distinct mechanisms of clearance that operate simultaneously. Ciliary clearance involves (escalator-like) movement of particles by rhythmic beating of hair-like cells on the surface of the upper respiratory tract. The second and third mechanisms (phagocytosis and absorption) act mainly in the deep respiratory tract. Phagocytosis is the engulfing of foreign bodies by alveolar macrophages and their subsequent removal by ciliary clearance or by entrance into the lymphatic system. Some inhaled soluble particles are absorbed into the blood and translocated to other organs and tissues.

Linear Nonthreshold Dose–Response Curve

There is considerable controversy over the shape of the dose–response curve at the chronic low-dose levels important for environmental contamination (see, e.g., Cohen, 1995; Tubiana and Aurengo, 2006; Tubiana et al., 2006). Proposed models include linear models, nonlinear (quadratic) models, and threshold models. Because risks at low dose must be

extrapolated from available data at high doses, the shape of the dose–response curve has important implications for the environmental regulations used to protect the general public. Detailed description of dosimetry models can be found in Cember (1996), BEIR IV (NAS, 1988a), Harley (2001), and BEIR VII (NAS, 2006).

The linear quadratic model is the most general model for description of the relation between low-dose exposure to ionizing radiation and the incidence of cancers. However, the BEIR VII committee endorsed the use of the LNT model for solid cancers and the linear-quadratic mode for leukemia. The committee viewed the LNT as a computationally convenient starting point; however, actual risk estimates modify this simplified model by using a dose and dose-rate effectiveness factor (DDREF). This factor has been developed to account for the fact that the lower the dose rate, the lower the health effect because the tissues can repair damage if the dose rate is low enough. A correction factor must thus be applied to avoid overconservatism in radiological regulations. The value of the DDREF has varied widely (from 2 to 10) over the last few years; BEIR VII suggests a DDREF of 2.5 (NAS, 2006).

BEIR VII concludes that the LNT should continue to be the basis for estimating health risks of exposure to ionizing radiation because no threshold has been identified and existing data are consistent with the LNT. The application of the LNT to cancer prediction and particularly to such predictions from collective dose estimates has been challenged recently by the Academie des Sciences and Academie Nationale de Medicine of France (Tubiana et al., 2006, 2008). This challenge is based on several grounds: (1) neither epidemiological studies nor experimental studies have shown evidence of carcinogenic effects at doses below 100 mSv and (2) the assumption that, *the likelihood that radiation-induced DNA damage will lead to cancer* is *independent of dose and dose-rate*, has not been verified by radiobiologic studies. In fact, recent data and modern theories of carcinogenesis suggest that the microenvironment of a cell will provide a number of processes that will mitigate the effects of the damage. These include DNA repair mechanisms as well as programmed death of damaged cells before they can replicate and pass on the mutation to descendants. These objections to the LNT are based on the examination of a number of studies, also reviewed in BEIR VII (Tubiana and Aurengo, 2006) as well as studies of Chernobyl survivors (Rozhdestvensky, 2004).

Epidemiological Studies of the Effects of Radiation

Many studies of the effects of radiation on human populations have been carried out. Five large epidemiological studies are reviewed by Harley (Harley, 2001). These include radium exposures by radium dial painters, atom bomb survivors, patients irradiated with x-rays for ankylosing spondylitis and ringworm (tinea capitis), and uranium miners exposed to radon. The first four studies examine health effects due to external exposures of high doses of ionizing radiation. The BEIR VII report includes summaries of over 130 epidemiological studies carried out between 1990 and 2006 (NAS, 2006). Numerous studies have considered the mortality and incidence of cancer among various occupationally exposed groups in the medical, manufacturing, nuclear, research, and aviation industries. Estimates of leukemia and cancer risks are derived from studies of the workers at the Mayak (Chelyabinsk) site in the FSU, the UK National Registry of Radiation Workers and the Three-Country Study (Canada–United Kingdom–United States) (NAS, 2006). Epidemiological studies of populations in the FSU exposed to fallout from the 1986 nuclear reactor explosion at Chernobyl and releases from the Chelyabinsk-65 complex demonstrate the health effects associated with exposure to radioactive iodine, strontium, and cesium as discussed in **Sections 11.6.4.3.3** and **11.6.4.3.4**.

The 'benchmark' studies establishing the long-term health effects of LET ionizing radiation are those analyzing survivors of the Hiroshima and Nagasaki atomic bombings in 1945. In addition, several studies have examined the risk for different cancers for populations living in the vicinity of nuclear power plants. Although the nuclear reactor studies are not used for the development of dosimetry models as have the other studies, they are of interest because they are considered relevant to the debate over the environmental hazards of nuclear power and its potential link to radioactive contamination in the environment. These two sets of epidemiological studies are described in more detail below.

Populations Living Near Nuclear Power Plants

Commercial nuclear power plants release small amounts of gaseous and liquid radiological effluents into the environment during normal operations. Environmental monitoring programs in the US and other countries routinely monitor potential radioactive air and water emissions from nuclear power plants. Of particular concern are potential releases of tritium, iodine-131 and iodine-129, carbon-14, radioactive particles, and noble gases. Effluent emissions from reactors and other components of the nuclear fuel cycle in the US are regulated by 10 CFR 50 and 40 CFR 190, respectively. According to the ANS, civilians living within 50 miles (80 km) of a nuclear power plant typically receive about 0.01 mrem (0.1 mSv) per year from the plant and more than 300 mrem anywhere in the US from natural sources. Additional doses are obtained from building materials, diet, medical procedures, and so on; the average dose from all sources is 620 mrem (ANS, 2011).

Over the last three decades, several epidemiological studies carried out to detect excess cancer deaths in populations living in the vicinity of nuclear power plants have yielded conflicting conclusions. An ecological study of risks of 16 types of cancer in populations living near nuclear facilities in the US was carried out by the National Cancer Institute (NCI, 1991). No excess cancer deaths were detected in the populations living in 107 countries containing/near 62 nuclear facilities. In BEIR VII (NAS, 2006), most of the studies of populations living around nuclear facilities are ecologic studies, which do not include individual estimates of radiation dose and therefore cannot provide an estimate of disease risk. The three case–control studies reviewed in BEIR VII found no increased risk of disease associated with radiation exposure.

More recently, a meta-analysis of 17 research papers (Baker et al. 2007) suggested evidence of elevated leukemia rates among children living near 136 nuclear facilities in the United Kingdom, Canada, France, US, Germany, Japan, and Spain. Elevated leukemia rates among children were also found by Kaatsch et al. (1998) in a study of residents living near 16

major nuclear power plants in Germany. However, both of these studies have been criticized on several methodological grounds and the results are not consistent with many other studies that have tended not to show increased cancer rates. Most recently, the British Committee on Medical Aspects of Radiation in the Environment (COMARE, 2011) reviewed data from the United Kingdom, France, Spain, Germany, Japan, and the US, and concluded that leukemia rates among children living near power plants in Britain were no higher than control populations. In addition, the report identified potential causes for calculated increased cancer rates in other studies that were due to weaknesses in their methodologies. There is still considerable interest in this topic however. In 2011, NAS began a multiyear study of the relationship between cancer incidences and proximity to nuclear power plants (NAS, 2011).

Survivors of Atomic Bomb Blasts at Hiroshima and Nagasaki

Ongoing analyses of epidemiological data describing the health of survivors of the Nagasaki and Hiroshima atomic bomb blasts have yielded important data (Douple et al., 2011; Little, 2009) about the effects of penetrating external radiations (gamma and neutron). For 63 years scientists in the Atomic Bomb Casualty Commission and its successor, the Radiation Effects Research Foundation have been assessing the long-term health effects in a population of approximately 200 000 survivors of the atomic bombings and in their children. A well-defined cohort has been studied longitudinally, individual radiation doses have been reconstructed, and excess relative risk (ERR) estimates for radiation-related health effects, including cancer and noncancer effects have been obtained. The results of the findings are summarized here; the original articles should be consulted for references to the supporting studies.

The studies include mortality and cancer incidence of a fixed sample of about 120 000 atomic-bomb survivors and control subjects (Life Span Study (LSS)), a cohort of *in utero*-exposed people and controls and another cohort of children of exposed and nonexposed parents who were conceived after the bombs. Because the direct atomic-bomb doses are from penetrating radiations arising from a large, localized source, it is possible to calculate doses systematically as a function of distance from the hypocenter, external shielding (buildings and terrain), and body self-shielding. Some survivors received nearly lethal large whole-body radiation doses (>2 Gy); however, the dose distribution is skewed toward the lower doses and the mean dose in the exposed LSS who received doses >0.005 Gy is about 0.2 Gy. Health effects studied included leukemia, solid cancers, chronic (noninfectious) diseases, and mutations and heritable DNA damage in offspring.

Over the course of the 63-year study of the LSS, excess leukemia deaths became the first major radiation-associated long-term health effect observed in the early 1950s, and were followed by solid-cancer deaths soon afterward. Noncancer disease deaths due to radiation became apparent in the mid-1960s. By 2002, there were 315 leukemia deaths in the LSS cohort and 98 (45%) of these are estimated to be excess deaths attributable to radiation exposure among the survivors exposed to >0.005 Gy. The proportion increases with increasing dose and reaches about 86% among those exposed to doses >1 Gy. The radiation-related risk is strongly modified by age and time after exposure; the higher excess deaths in the earlier years among those exposed at a young age is followed by a rapid decline with time. The shape of the curve for leukemias as a function of bone marrow dose is nonlinear, with an upward curvature in the range of 0–3 Gy and is different from the linear one seen for solid cancers.

The attributable fraction of all of the solid cancers among survivors exposed to >0.005 Gy (mean 0.21 Gy) was 11% and it increases with increasing dose to 48% among those who received at least 1 Gy. Unlike leukemia, the radiation-related risks for solid cancers typically show a gradual increase starting several years after the bombings. Health effects attributable to radiation exposure are described in terms of the excess absolute risk or rate (EAR) and the ERR. (The EAR is the rate of occurrence of disease between an exposed population and a comparable population with no exposure and is a measure of the absolute size of the effect. The ERR is the ratio of the EAR to the occurrence rate in the nonexposed comparison population; it is a measure of the strength of the effect of exposure and may have biological significance.) For solid cancers, the highest ERRs (>0.8, or >80% Gy^{-1}) are found for bladder, female breast, and lung cancers, and relatively high (0.5–0.8, or 50–80% Gy^{-1}) for cancers of the brain/central nervous system, ovary, thyroid, colon, and esophagus. The pattern of radiation-related risk for solid cancers as a group is approximately observed for most individual cancer sites. Other important results of this analysis include (1) both the ERR and EAR estimates for solid cancers are about 50% higher for women than for men, and (2) the ERR for people exposed to the bombs at a younger age is higher than those exposed at an older age (about twice as high after exposure at age 10 than at age 40). These data were used in BEIR VII (NAS, 2006). The analyses used the linearity of the dose–response curve for solid cancers and the quadratic response for leukemia to estimate that if a US population of 100 people were exposed to an acutely delivered dose of 0.1 Gy, there would be only about one person with cancer attributable to the radiation exposure, whereas 42 people would have been diagnosed as having cancer from other unknown sources.

Studies of 3300 individuals who were in their mother's womb at the time of exposure indicate that *in utero* exposure does not lead to greater adult cancer risk than childhood exposure does; however, an increase in mental retardation was observed. A study of 77 000 women was carried out to determine if radiation exposure would result in genetic effects in children of the survivors. No evidence of adverse pregnancy outcomes (congenital malformations, still births, and perinatal deaths within 1 week after birth) was observed and no effects of parental exposure have been observed in molecular genetic studies.

Regulating Radionuclide Releases to the Environment and Exposures to the Public

Federal regulations (e.g., 10 CFR Parts 20, 50, 61, 71), the Interagency Steering Committee on Radiation Standards, the NRC Committee in the BEIR Committee, and the National and International Commission on Radiological Protection (ICRP) and the National Council on Radiation Protection and

Measurements (NCRP) are the main sources of information estimating radiological health effects. The BEIR IV report (NAS, 1998) addressed the health risks of internally deposited alpha emitters (Rn, Po, Ra, Th, U, and Pu). Major emphasis is given to assessing the lung cancer risk associated with radon exposure. The BEIR V report addresses risk estimates for exposure to low-level ionizing radiation and much of its assessment is based on epidemiological data from the aforementioned exposed populations (e.g., survivors of the Hiroshima and Nagasaki atomic bombs, medical used of radiation, subjects who have had medical radiation treatments, etc.). In 2006, the NRC of the NAS published *Health Risks from Exposure to Low Levels of Ionizing Radiation BEIR VII Phase 2* (BEIR VII), which primarily addresses cancer and genetic risks from low doses of low-LET radiation based on additional clinical and epidemiological data.

Regulations of acceptable exposure to radionuclides in the US are based on estimates of the probability of radiogenic cancer mortality (fatal cancers) or morbidity (fatal plus nonfatal cancers) per unit activity of a given radionuclide inhaled or ingested, for internal exposure, or per unit time-integrated activity concentration in air or soil, for external exposure. Radionuclide slope factors (risk coefficients for total cancer morbidity) are calculated for each radionuclide individually, based on its metabolic, chemical, and radioactive properties (EPA, 1999d) (Federal Guidance Report No. 13). Risk coefficients derived in Federal Guidance Report No. 13, are used to calculate the slope factors and take into account the age- and gender-dependence of radionuclide intake, metabolism, dosimetry, radiogenic risk, and competing causes of death in estimating the cancer risk from low-level exposures to radionuclides in the environment. When combined with site-specific media concentration data and appropriate exposure assumptions, slope factors can be used to estimate lifetime cancer risks to members of the general population due to radionuclide exposures.

US Regulations

A large number of Federal regulations and recommendations establish 'permissible' radiation exposures to the general public and workers based on the above references. The USEPA issues legally binding Radiation Protection Guides (RPG). Other regulatory agencies such as the US NRC then issue regulations that are consistent with these RPGs. EPA regulations are published in Title 40, *Code of Federal Regulations* (e.g., 40CFR Parts 141, 190, 191, 192, 194, and 197). USNRC regulations are published in Title 10, *Code of Federal Regulations* (e.g., 10CFR Parts 20, 50, 61) (USNRC, 2011). Current US regulations limit whole body dose exposures (internal + external exposures) of radiological workers to 0.05 Sv $year^{-1}$ (5 rem $year^{-1}$). The EPA standards for nuclear waste repositories (40CFR191, 40CFR197) seek to limit exposures from all exposure pathways for the reasonably maximally exposed individual living 18 km from a nuclear waste repository to 0.15 mSv $year^{-1}$ (15 mrem $year^{-1}$) (Federal Register, February 22, 2001). EPA's regulations in 40 CFR 192 establish standards for protection of the public health, safety, and environment from radiological and nonradiological hazards associated with uranium ore processing, and disposal of resulting waste materials (USEPA, 2013). EPA also sets environmental standards for uranium extraction facilities under the Clean Air Act, Safe Drinking Water Act, and Clean Water Act. Radionuclides in drinking water are regulated under Radionuclides Rule 66 FR 76708 (December 7, 2000) Vol. 65, No. 236; under the National Primary Drinking Water Regulations (EPA, 2000c).

European Regulations

The World Health Organization (WHO) defines guidance levels for several radionuclides in drinking water (artificial and natural) below which no adverse radiological health effects are expected from the consumption of drinking water. These activities correspond to a committed effective dose below 0.1 mSv $year^{-1}$. For radon, the WHO guidelines recommend that controls should be implemented if the radon concentration of drinking water for public water supplies exceeds 100 Bq l^{-1}. The WHO recommends a guidance level of 15 μg l^{-1} natural uranium (corresponding to a ^{238}U activity concentration of 0.19 Bq l^{-1}) in the drinking water guidelines (WHO, 2004).

The European Drinking Water Directive 98/83/EC (European Commission, 1998) establishes standards for radioactivity in drinking water. A total indicative dose (the effective dose from radionuclides in drinking water except ^{3}H, ^{40}K, radon, and radon progenies) of 0.1 mSv $year^{-1}$ is allowed. Radon and the radon progenies are excluded from the European directive; however, the European Commission (2001) recommends that if ^{222}Rn activity concentrations are above 1000 Bq l^{-1}, treatment measures are justified. The dose contributions of ^{210}Po and ^{210}Pb may dominate the dose contributions of the radium isotopes (Gruber and Maringer, 2010). For the radon progenies, the Commission recommends that ^{210}Pb and ^{210}Po activities above 0.2 and 0.1 Bq l^{-1} respectively, are considered cause for concern (European Commission, 2001).

Appendix B Health Effects of Uranium

The health hazards associated with uranium are dependent on its radioactivity as well as upon its chemical and physical form, route of intake, and level of enrichment. The chemical form of uranium determines its solubility and, thus transportability in body fluids, as well as retention in the body and various organs. Uranium's chemical toxicity is the principal health concern, because soluble uranium compounds cause heavy metal damage to renal tissue. The radiological hazards of uranium may be a primary concern when inhaled, enriched, and insoluble uranium compounds are retained long term in the lungs and associated lymphatics. The health effects of uranium are associated with uranium itself as well as its radioactive progeny, primarily radium and its decay products. The chemical and radiological effects of uranium are discussed in this section; radium and its progeny were discussed previously in **Section 11.6.4.1.5**.

Absorption

Absorption of uranium from the lungs or digestive track is typically low and depends on solubility of the specific

compound. Generally, hexavalent uranium forms relatively soluble compounds and is adsorbed more readily than tetravalent uranium, which forms relatively insoluble compounds. Uranium can be absorbed through the skin; water-soluble uranium compounds are the most easily absorbed. Most of the uranium in the body leaves the body in the urine and feces.

Ingested uranium is less toxic than inhaled uranium, which may be partly due to the relatively low gastrointestinal absorption of uranium compounds. Estimates of the fraction of ingested uranium absorbed in the gastrointestinal tract in adults range from 0.1 to 6% depending on the solubility of the uranium compound (ATSDR, 2011; Weir, 2004). Typical absorption is 0.2% for insoluble compounds and 2% for soluble hexavalent compounds (ICRP, 1995, 1996). The results of animal studies suggest that very young animals can absorb greater quantities of uranium. The intestines of most young animals and human babies are more permeable than that of adults because infants must absorb immunity factors, such as antibodies, from the mother's milk (Brugge et al., 2005).

The deposition of inhalable uranium dust particles in the lungs depends on the particle size, and its absorption depends on its solubility in biological fluids (ICRP, 1996). Inhaled uranium compounds are adsorbed in the respiratory tract via transfer across cell membranes. Estimates of systemic absorption from inhaled uranium-containing dusts in occupational settings based on urinary excretion of uranium range from 0.76 to 5% (ATSDR, 2011).

Distribution

Absorbed uranium rapidly enters the bloodstream and complexes with citrate, bicarbonates, and protein in plasma. In body fluids, tetravalent uranium will oxidize to form uranyl ion (UO_2^{2+}). Dominant species are diffusible $UO_2HCO_3^+$ in equilibrium with a nondiffusible uranyl albumin complex. Under alkaline conditions, $UO_2HCO_3^+$is stable and is excreted. When the pH drops, the complex dissociates and binds to the cellular proteins in the tubular wall of the kidney (Weir, 2004). Approximately 67% of uranium in the blood is filtered in the kidneys and leaves the body in urine within 24 h; the remainder distributes to tissues, primarily the bone, liver, and kidney. In the animal and human skeletons, the uranyl ion replaces calcium in the hydroxyapatite complex of the solid bone (Landa, 2004; Weir, 2004). The retention half-times for uranium in bone is 11 days and 2–6 days in the kidney. Inhaled insoluble compounds deposited in the deep respiratory tract accumulate in the lungs and pulmonary lymph nodes. The human body burden of uranium is approximately 90 μg; with 66% of this total in the skeleton, 16% in the liver, 8% in the kidneys, and 10% in other tissues (ATSDR, 2011).

Toxicity

Results of experimental animal studies suggest that the more soluble uranium compounds (uranium hexafluoride, uranium tetrachloride, uranyl fluoride, uranyl nitrate) have the highest renal toxicity, followed by the less-soluble compounds (ammonium diuranate, sodium diuranate, uranium tetrafluoride) and the insoluble uranium compounds (uranium dioxide, uranium trioxide, uranium peroxide, triuranium octaoxide). Data from inhalation studies with animals suggest that soluble compounds are at least five times more toxic than insoluble compounds. The difference in toxicity is owing to the easier absorption of soluble compounds from the lung or gastrointestinal tract into the blood and distribution to other tissues (ATSDR, 2011; Tannenbaum et al., 1951). Regardless of the exposure duration or route, the animal data provide strong evidence that kidney damage is the principal toxic effect of uranium.

Uranium can damage the kidneys by any route of exposure as long as the uranium enters the blood. Several mechanisms for renal toxicity have been proposed. In the kidneys, uranium is released from the bicarbonate complex and complexes with phosphate ligands and proteins, which may damage the wall of the proximal tubule. Alternatively, uranium may inhibit both sodium transport-dependent and -independent ATP utilization and mitochondrial oxidative phosphorylation (Brady et al., 1989). In addition, cellular necrosis caused by high-LET alpha radiation emitted by uranium radioisotopes may contribute to the nephrotoxocity. Finally, increased susceptibility to osteoporosis could result as calcium leaking into the urine can cause a negative calcium balance (Zamora et al., 1998).

The Agency for Toxic Substances and Disease Registry (ATSDR, 2011) summarizes other noncancer health effects including respiratory, reproductive, developmental, and neurological effects associated with exposure to uranium by ingestion and inhalation; the information below is summarized from that source. Animal studies suggest that if inhaled, chronic exposure to insoluble uranium compounds can damage the respiratory tract. In studies of uranium miners exposed to airborne uranium dust, however, most of the reported noncancerous respiratory diseases were consistent with toxicity of inhalable dust particles other than uranium, such as silica. In general, adverse neurological effects have not been observed in studies of uranium workers, although tests to detect subtle neurological alterations were not conducted. Gulf War veterans exposed to depleted uranium sometimes showed poorer performance on neurological tests but the effects were not consistently observed.

Available data regarding reproductive and developmental effects of uranium in humans and animals are summarized by ATSDR (2011). No data describing human developmental effects from either inhalation or oral exposure were found. Animal studies suggest that oral uranium exposure at relatively high doses will affect reproductive and hormonal systems. Studies of inhalation exposure of uranium miners, millers, and processors indicated that male uranium miners had more first-born female children than expected, suggesting that uranium alpha radiation damaged the y-chromosomes of the miners. However, the associations were considered equivocal by the ATSDR; the workers were also exposed to ^{222}Rn, chlorine, hydrofluoric acid, lead sulfate, nickel, nitric acid and nitrogen oxides, silicon dioxide, and sulfuric acid (ATSDR, 2011).

Carcinogencity

Ingested and inhaled uranium are potentially carcinogenic because of the alpha radiation emitted by several of its isotopes. However, evidence linking human exposure to uranium and cancer has not been found. Although studies of uranium miners has shown a higher-than-expected rates of death from

lung cancer; the radiological effects of the progeny of uranium (radon and its decay products) and the miner's smoking habits are the likely causes. Uranium is assumed to be potentially carcinogenic by the National Institute for Occupational Safety and Health (NIOSH); however, based on animal studies, the mass equivalents for natural and depleted uranium for potential radiological effects are 3600 and 76 500 times higher, respectively, than the recommended short-term occupational exposure limits (ATSDR, 2011; NIOSH, 1997). Thus, as described below, the MRLs for chemical effects adequately protect against the possible radiotoxicity of natural and depleted uranium. Neither the International Agency for Research on Cancer, the USEPA, nor US Department of Human and Health Services have classified uranium as to its carcinogenicity (ATSDR, 2011; IRIS, 2011).

According to the NAS, bone sarcoma is the most likely cancer from oral exposure to uranium, in particular highly enriched uranium (NAS, 1988a). However, the NAS concluded that exposure to natural uranium may have no measurable effect. The BEIR IV report estimated a lifetime risk of excess bone sarcomas per million people of 1.5 if soluble uranium isotopes were ingested at a constant daily rate of 1 pCi day^{-1} (0.037 Bq day^{-1}). The number of bone sarcomas that occur naturally in a population of a million people is 750, thus the effect would likely be not measureable (see also Mays et al., 1985).

Environmental Health Regulations

Uranium-related health regulations are based on its chemical toxicity, primarily, nephrotoxicity, which varies according to solubility of the adsorbed uranium compound. Naturally occurring isotopic mixtures have low specific activities. The United Nations Scientific Committee on the Effects of Atomic Radiation (UNSCEAR) has considered that exposure limits for uranium in food and drinking water should be based on the chemical toxicity partly because radiological toxicity has not been observed in either humans or animals (UNSCEAR, 1993; Wrenn et al., 1985). However, few data linking chronic low-level exposures and health effects exist; this has implications for environmental regulations as discussed below.

Epidemiological and experimental animal studies are used to determine levels of exposure associated with subtle health effects in humans or animals (lowest observed adverse-effect level, LOAELs) or exposure levels below which no adverse effects (no-observed adverse-effect level, NOAELs) have been observed. Estimates of levels posing minimal risk to humans (MRLs) are based on the results of these experimental studies by reducing them by numerical safety factors that attempt to account for uncertainties associated with extrapolating the results from animal studies to humans, human variability, and other conservative assumptions. In some cases, other reference values for exposure limits such as Reference Doses (RfD) are derived from Benchmark Doses and associated confidence limits. For more details, see standard references on environmental health risk assessment such as ATSDR reports (ATSDR, 2011 and cited references), Klaassen (2001), and **Chapter 11.1**.

An MRL is defined as an estimate of daily human exposure to a substance that is likely to be without an appreciable risk of adverse effects (noncarcinogenic) over a specified duration of exposure. The MRLs are defined in terms of three exposure periods: acute (14 days or less), intermediate (15–364 days), and chronic (365 days or more). Separate MRLs have been derived for the effects from inhalation and oral exposure to uranium; however, several MRLs are not defined because reliable and sufficient data do not exist to identify the target organ(s) of effect or the most sensitive health effect(s) for a specific duration within a given route of exposure.

Available data provide evidence that the gastrointestinal tract, kidney, and developing organisms are target of uranium toxicity following acute oral exposure. Longer duration oral studies and inhalation studies identify the kidney as the most sensitive target of toxicity. However, no studies in laboratory animals examining the chronic toxicity of ingested uranium were identified by the ATSDR (2011). Therefore, owing to the additional uncertainty associated with limitations in the epidemiology studies examining both mortality (due to cancer) and morbidity (primarily nephrotoxicity), a chronic-duration oral MRL was not derived. Other agencies have derived other estimates of safe levels of uranium exposure. EPA derived an RfD of 0.003 mg kg^{-1} day^{-1} for uranium based on a LOAEL of 2.8 mg kg^{-1} day^{-1} for from animal studies and an uncertainty factor of 1000 (10 for the use of a LOAEL, 10 for intraspecies variability, and 10 for interspecies variability) (IRIS, 2011).

There has been considerable debate whether the current health standards set by the US EPA are sufficiently protective of human health (see, e.g., Brugge et al., 2005). Considering the safety factors for species and individual variation, the ingestion LOAEL corresponds to the daily consumption set by the WHO Drinking Water Standard at 0.002 mg l^{-1}; however, based on cost-benefit considerations, the MCL set by the US EPA in 2003 is 0.03 mg l^{-1}. The 2003 ruling for drinking water applies only to community water systems (CWS) and it was estimated that approximately 500 CWS would have to treat naturally occuring uranium. Further research is likely to be carried out, with particular attention on routes of exposure in communities near uranium sites, on the impact of uranium on indigenous populations, on the combined exposures of contaminant mixtures present at many uranium mining, milling and waste sites, on human developmental defects, and on health effects such as immune response at or below established exposure standards.

Acknowledgments

The authors thank Laura Connolly for her assistance in managing the large citation and references database for this chapter. Sandia National Laboratories is a multiprogram laboratory managed and operated by Sandia Corporation, a wholly owned subsidiary of Lockheed Martin Corporation, for the US Department of Energy's National Nuclear Security Administration under contract DE-AC04-94AL85000.

References

Abdelouas A (2006) Uranium mill tailings: Geochemistry, mineralogy and environmental impact. *Elements* 2(6): 335–341.

Abdelouas A, Lutze W, Gong W, et al. (2000) Biological reduction of uranium in groundwater and subsurface soil. *The Science of the Total Environment* 250(1–3): 21–35.

Abdelouas A, Lutze W, and Nuttall E (1998) Chemical reactions of uranium in ground water at a mill tailings site. *Journal of Contaminant Hydrology* 34(4): 343–361.

Abdelouas A, Lutze W, and Nuttall E (1999) In: Burns PC and Finch R (eds.) Uranium contamination in the subsurface; characterization and remediation. *Reviews in Mineralogy* 38(1): 433–473.

Allard B (1983) Actinide chemistry in geologic systems. *Kernia* 10(2): 97–102.

Allard B, Kipatsi H, Torstenfelt B, et al. (1979) Nuclide transport by groundwater in Swedish bedrock. In: McCarthy GJ (ed.) *Scientific Basis for Nuclear Waste Management*, vol. 1, pp. 403–410. New York: Plenum Press.

Allard B, Torstenfelt B, Andersson K, and Rydberg J (1980) Possible retention of iodine in the ground. *International Symposium on the Scientific Basis for Waste Management*, vol. 2, pp. 673–680. New York, NY: Plenum Press.

Allison JD, Brown DS, and Novo-Gradac KJ (1991) *MINTEQA2/PRODEFA2, A Geochemical Assessment Model for Environmental Systems*, 3.0. Athens, GA: U.S. Environmental Protection Agency.

Altmaier M, Neck V, and Fanghanel T (2004) Solubility and colloid formation of Th(IV) in concentrated NaCl and $MgCl_2$ solution. *Radiochimica Acta* 92(9–11): 537–543.

Altmaier M, Neck V, and Fanghanel T (2008) Solubility of Zr(IV), Th(IV) and Pu(IV) hydrous oxides in $CaCl_2$ solutions and the formation of ternary Ca–M(IV)–OH complexes. *Radiochimica Acta* 96(9–11): 541–550.

Altmaier M, Neck V, Muller R, and Fanghanel T (2005) Solubility of $ThO_2 \cdot xH_2O_{(am)}$ in carbonate solution and the formation of ternary Th(IV) hydroxide–carbonate complexes. *Radiochimica Acta* 93(2): 83–92.

Ames LL, McGarrah JE, and Walker BA (1983) Sorption of trace constituents from aqueous solutions onto secondary minerals. II. Radium. *Clays and Clay Minerals* 31(5): 335–342.

Ames LL, McGarrah JE, Walker BA, and Salter F (1983) Uranium and radium sorption on amorphous ferric oxyhydroxide. *Chemical Geology* 40: 135–148.

Ames L and Rai D (1978) *Radionuclide Interactions with Soil and Rock Media. Processes Influencing Radionuclide Mobility and Retention, Element Chemistry and Geochemistry, Conclusions and Evaluation. Radionuclide Interactions with Soil and Rock Media*, vol. I. Richland, WA: Pacific Northwest National Laboratory.

Amonette J, Wilkin RT, and Ford RG (2010) Uranium. In: Ford RG and Wilkin RT (eds.) *Monitored Natural Attenuation of Inorganic Contaminants in Ground Water Volume 3. Assessment for Radionuclides Including Tritium, Radon, Strontium, Technetium, Uranium, Iodine, Radium, Thorium, Cesium, and Plutonium-Americium*, vol. 3, pp. 53–68. Cincinnati, OH: National Risk Management Research Laboratory, Office of Research and Development, U.S. Environmental Protection Agency.

Andersson K (1990) *Natural Variability in Deep Groundwater Chemistry and Influence on Transport Properties of Trace Radionuclides. SK TR 90:17*. Swedish Nuclear Power Inspectorate.

Andersson K, Evans S, and Albinsson Y (1992) Diffusion of radionuclides in sediments – In situ studies. *Radiochimica Acta* 58(59): 321–327.

Andrews JN, Ford DJ, Hussain N, Trivedi D, and Youngman MJ (1989) Natural radioelement solution by circulating groundwaters in the Stripa granite. *Geochemica et Cosmochimica Acta* 53(8): 1791–1802.

ANS (2011) *Proceedings of the 13th International High-Level Radioactive Waste Management Conference*. American Nuclear Society (CD-ROM).

Appelo CAJ (1994) Cation and proton exchange, pH variations, and carbonate reactions in a freshening aquifer. *Water Resources Research* 30(10): 2793–2805.

Arai Y, Moran PB, Honeyman BD, and Davis JA (2007) In situ spectroscopic evidence for neptunium(V)-carbonate inner-sphere and outer-sphere ternary surface complexes on hematite surfaces. *Environmental Science & Technology* 33(14): 2481–2484.

Archer VE, Wagoner JK, and Lundin FE (1973) Cancer mortality among uranium mill workers. *Journal of Occupational Medicine* 15(1): 11–14.

Arey JS and Seaman JC (1999) Immobilization of uranium in contaminated sediments by hydroxyapatite addition. *Environmental Science & Technology* 33(2): 337–342.

Arnold T, Zorn T, Zanker H, Berhard G, and Nitsche H (2001) Sorption behavior of U(VI) on phyllite: Experiments and modeling. *Journal of Contaminant Hydrology* 47(2–4): 219–231.

Artinger R, Kienzler B, Schussler W, and Kim JI (1998) Effects of humic substances on the Am-241 migration in a sandy aquifer: Column experiments with Gorleben groundwater/sediment systems. *Journal of Contaminant Hydrology* 35(1–3): 261–275.

ASTM (2010) *Standard Test Method for Distribution Coefficients of Inorganic Species by the Batch Method*. West Conshohocken, PA: ASTM International. http://dx.doi.org/10.1520/C1733–10.

ATSDR (1990a) *Toxicological Profile for Thorium*. Atlanta, GA: Public Health Service. Agency for Toxic Substances and Disease Registry. U.S. Department of Health and Human Services.

ATSDR (1990b) *Toxicological Profile for Radium*. Atlanta, GA: Public Health Service. Agency for Toxic Substances and Disease Registry. U.S. Department of Health and Human Services.

ATSDR (1990c) *Toxicological Profile for Radon*. Atlanta, GA: Public Health Service. Agency for Toxic Substances and Disease Registry. U.S. Department of Health and Human Services.

ATSDR (1999) *Toxicological Profile for Uranium*. Atlanta, GA: Public Health Service. Agency for Toxic Substances and Disease Registry. U.S. Department of Health and Human Services.

ATSDR (ed.) (2001) *Appendix D. Overview of Basic Radiation Physics, Chemistry and Biology*. Atlanta, GA: Agency for Toxic Substances and Disease Registry, U.S. Department of Health and Human Services, Public Health Service.

ATSDR (2011) *Toxicological Profile for Uranium (Draft for Public Comment)*. Atlanta, GA: Agency for Toxic Substances and Disease Registry, U.S. Department of Health and Human Services, Public Health Service Pdf available at http://www.atsdr.cdc.gov/ToxProfiles/TP.asp?id=440&tid=77#bookmark16 (accessed on 26 July 2011).

Au WW, Lane RG, Legator MS, et al. (1995) Bio-marker monitoring of a population residing near uranium mining activities. *Environmental Health Perspectives* 103(5): 466–470.

Au WW, McConnell MA, Wilkinson GS, Ramanujam VMS, and Alcock N (1998) Population monitoring: Experience with residents exposed to uranium mining/milling waste. *Mutation Research* 405(2): 237–245.

Avogadro A and de Marsily G (1984) The role of colloids in nuclear waste disposal. In: McVay GL (ed.) *Scientific Basis for Nuclear Waste Management VII*, pp. 495–505. New York, NY: North-Holland.

Bachmaf S and Merkel BJ (2011) Sorption of uranium(VI) at the clay mineral-water interface. *Environmental Earth Sciences* 63: 925–934.

Baes CR Jr. and Mesmer RE (1976) *The Hydrolysis of Cations*. New York, NY: Wiley.

Baker PJ and Hoel DG (2007) Meta-analysis of standardized incidence and mortality rates of childhood leukemia in proximity to nuclear facilities. *European Journal of Cancer Care* 16(4): 355–362.

Bargar JR, Reitmeyer R, and Davis JA (1999) Spectroscopic confirmation of uranium (VI)-carbonato adsorption complexes on hematite. *Environmental Science & Technology* 33(14): 2481–2484.

Bargar JR, Reitmeyer R, Lenhart JJ, and Davis JA (2000) Characterization of U(VI)-carbonato ternary complexes on hematite: EXAFS and electrophoretic mobility measurements. *Geochimica et Cosmochimica Acta* 64(16): 2737–2749.

Barnett MO, Jardine PM, and Brooks SC (2002) U(VI) adsorption to heterogeneous subsurface media: Application of a surface complexation model. *Environmental Science & Technology* 36(5): 937–942.

Barney GS (1981a) *Radionuclide Reactions with Groundwater and Basalts from Columbia River Basalt Formations*, p. 47. Richland, WA: Atomics International Div., Rockwell Hanford Operations.

Barney GS (1981b) *Evaluation of Methods for Measurement of Radionuclide Distribution in Groundwater/Rock Systems*, p. 34. Richland, WA: Rockwell Hanford Operations RHO-BWI-LD-47.

Barney GS, Navratil JD, and Schulz WW (1984) Geochemical behavior of disposed radioactive waste. *American Chemical Society Symposium*, vol. 246. American Chemical Society.

Barton LL, Choudhury K, Thompson BM, Steenhoudt K, and Groffman AR (1996) Bacterial reduction of soluble uranium: The first step of in situ immobilization of uranium. *Radioactive Waste Management and Environmental Restoration* 20(2–3): 141–151.

Baryakhtar VG (1995) *Chernobyl Catastrophe*. Kiev, Russia: Export Publishing House.

Bates JK, Bradley JP, Teetsov A, Bradley CR, and Buchholtz M (1992) Colloid formation during waste form reaction: Implications for nuclear waste disposal. *Science* 256(5057): 649–651.

Baum EM, Knox HD, and Miller TR (2002) *Nuclides and Isotopes: Chart of the Nuclides*, 16th edn. Lockheed Martin: Knolls Atomic Power Laboratory.

Bayley SE, Siegel MD, Moore M, and Faith S (1990) *Sandia Sorption Data Management System Version 2 (SSDMS II) User's Manual*, p. 191. Albuquerque, NM: Sandia National Laboratories SAND-89-0371.

Bearman PJ (1979) A review of the environmental problems associated with the disposal of uranium tailings. *Environmental Geochemistry and Health* 1(2): 64–74.

Beazley MJ, Martinez RJ, Sobecky PA, Webb SM, and Taillefert M (2007) Uranium biomineralization as a result of bacterial phosphatase activity: Insights from bacterial isolates from a contaminated subsurface. *Environmental Science & Technology* 41(16): 5701–5707.

Beddow H, Black S, and Read D (2006) Naturally occurring radioactive material (NORM) from a former phosphoric acid processing plant. *Journal of Environmental Radioactivity* 86(3): 289–312.

Behrends T and Van Cappellen P (2005) Competition between enzymatic and abiotic reduction of uranium(VI) under iron reducing conditions. *Chemical Geology* 220(3–4): 315–327.

Bergman R (1994) The distribution of radioactive caesium in boreal forest ecosystems. Nordic radioecology – The transfer of radionuclides through Nordic ecosystems to man. *Studies in Environmental Science* 62: 335–379.

Bernhard G, Geipel G, Brendler V, and Nitsche H (1998) Uranium speciation in waters of different uranium mining areas. *Journal of Alloys and Compounds* 271–273: 201–205.

Bertetti FP, Pabalan RT, and Almendarez MG (eds.) (1998) *Studies of NeptuniumV Sorption on Quartz, Clinoptilolite, Montmorillonite, and Alumina*. San Diego, CA: Academic Press.

Berthelot D, Leuduc LG, and Ferroni GD (1997) Iron-oxidizing autotrophs and acidophilic heterotrophs from uranium mine environments. *Geomicrobiology Journal* 14(4): 317–324.

Bertsch PM and Hunter DB (2001) Applications of synchrotron-based X-ray microprobes. *Chemical Reviews* 101(6): 1809–1842.

Bethke CR (1998) *The Geochemist's Workbench Release*, 3.0 edn. Urbana-Champaign, IL: University of Illinois.

Bidoglio G, De Plano A, and Righetto L (1989) Interactions and transport of plutonium-humic acid particles in groundwater environments. In: Lutze W and Ewing RC (eds.) *Scientific Basis for Nuclear Waste Management XII, Materials Research Society Symposium Proceedings*, vol. 127, pp. 823–830. Pittsburgh, PA: Materials Research Society.

Bigu J, Grenier NK, Dave TP, et al. (1984) Study of radon gas concentration surface radon flux and other radiation variables from uranium mine tailings areas. *Uranium* 1: 257–277.

Bird GW and Lopata VJ (1980) Solution interaction of nuclear waste anions with selected geological materials. *International Symposium on the Scientific Basis for Waste Management II*, vol. 2, pp. 419–427. New York, NY: Plenum Press.

Bock WD, Bruhl H, Trapp T, and Winkler A (1989) Sorption properties of natural sulfides with respect to technetium. In: Lutze W and Ewing RC (eds.) *Scientific Basis for Nuclear Waste Management XII, Materials Research Society Symposium Proceedings*, vol. 127, pp. 973–977. Pittsburgh, PA: Materials Research Society.

Boice JD, Cohen SS, Mumma MT, et al. (2007) Mortality among residents of Uravan, Colorado who lived near a uranium mill, 1936–84. *Journal of Radiological Protection* 27(3): 299–319.

Boice JD, Cohen SS, Mumma MT, et al. (2008) A cohort study of uranium millers and miners of Grants, New Mexico, 1979–2005. *Journal of Radiological Protection* 28(3): 303–325.

Boice JD, Mumma MT, and Blot WJ (2007) Cancer and noncancer mortality in populations living near uranium and vanadium mining and milling operations in Montrose County, Colorado, 1950–2000. *Journal of Radiological Protection* 167(6): 711–726.

Boice JD, Mumma MT, and Blot WJ (2010) Cancer incidence and mortality in populations living near uranium milling and mining operations in Grants, New Mexico, 1950–2004. *Radiation Research* 175(5): 624–636.

Boice JD, Mumma M, Schweitzer S, et al. (2003) Cancer mortality in a Texas county with prior uranium mining and milling activities, 1950–2001. *Journal of Radiological Protection* 23(3): 247–262.

Bonhoure I, Meca S, Marti V, Pablo JD, and Cortina JL (2007) A new time-resolved laser-induced fluorescence spectrometry (TRLFS) data acquisition procedure applied to the uranyl-phosphate system. *Radiochimica Acta* 95(3): 165–172.

Boonchayaanant B, Gu BH, Wang W, Ortiz ME, and Criddle CS (2010) Can microbially-generated hydrogen sulfide account for the rates of U(VI) reduction by a sulfate-reducing bacterium? *Biodegradation* 21(1): 81–95.

Bors J, Martens H, and Kühn W (1991) Sorption studies of radioiodine on soils with special references to soil microbial biomass. *Radiochimica Acta* 52/53: 317–325.

Botov NG (1992) ALWP-67: A little-known big nuclear accident. *High Level Radioactive Waste Management*, vol. 2, pp. 2331–2338. American Nuclear Society.

Boukhalfa H, Icopini GA, Reilly SD, and Neu MP (2007) Plutonium(IV) reduction by the metal-reducing bacteria Geobacter metallireducens GS15 and Shewanella oneidensis MR1. *Applied and Environmental Microbiology* 73(18): 5897–5903.

Boulyga SF, Lomonosova EM, Zhuk JV, et al. (1999) Experimental study of radioactive aerosols in the vicinity of the Chernobyl nuclear power plant. *Radiation Measurements* 30(6): 703–707.

Bou-Rabee F, Al-Zamel AZ, Al-Fares RA, and Bem H (2009) Technologically enhanced naturally occurring radioactive materials in the oil industry (TENORM). A review. *Nukleonika* 54(1): 3–9.

Bradbury MH and Baeyens B (2005) Modelling the sorption of Mn(II), Co(II), Ni(II), Zn (II), Cd(II), Eu(III), Am(III), Sn(IV), Th(IV), Np(V) and U(VI) on montmorillonite: Linear free energy relationships and estimates of surface binding constants for some selected heavy metals and actinides. *Geochimica et Cosmochimica Acta* 69(4): 875–892. Erratum 869, 5391–5392.

Bradbury MH and Baeyens B (2009) Sorption modelling on illite. Part II: Actinide sorption and linear free energy relationships. *Geochimica et Cosmochimica Acta* 73(4): 1004–1013.

Brady HR, Kone CB, Brenner RM, et al. (1989) Early effects of uranyl nitrate on respiration and K transport in rabbit proximal tubule. *Kidney International* 36: 27–34.

Brady PV, Papenguth HW, and Kelly JW (1999) Metal sorption to dolomite surfaces. *Applied Geochemistry* 14(5): 569–579.

Brierley CL and Brierley JA (1982) Investigation of microbially induced permeability loss during in situ leaching. *Open File Report, OFR90-83*. U.S. Bureau of Mines, p. 69.

Bronsted JN (1922) Studies on solubility IV. The principals of the specific interactions of ions. *Journal of the American Chemical Society* 44(5): 877–898.

Brookins DG (1990) Radionuclide behaviour at the Oklo nuclear reactor, Gabon. *Waste Management* 10(4): 285–296.

Brown GE Jr., Henrich VE, Casey WH, et al. (1999) Metal oxide surfaces and their interactions with aqueous solutions and microbial organisms. *Chemical Reviews* 99(1): 77–174.

Brugge D, deLemos JL, and Oldmixon B (2005) Exposure pathways and health effects associated with chemical and radiological toxicity of natural uranium: A review. *Reviews on Environmental Health* 20(2): 177–193.

Bruno J, Cera E, Grive M, et al. (2000) Determination and uncertainties of radioelement solubility limits to be used by SKB in the SR 97' performance assessment exercise. *Radiochimica Acta* 88(9–11): 823–828.

Bruno J, Depablo J, Duro L, and Figuerola E (1995) Experimental-study and modeling of the U-VI-FE(OH) surface precipitation coprecipitation equilibria. *Geochimica et Cosmochimica Acta* 59(20): 4113–4123.

Brush LH, Xiong L, and Long JL (2009) *Results of the Calculations of Actinide Solubilities for the WIPP CRA-2009 PABC*, p. 47. Carlsbad, NM: Sandia National Laboratories.

Buckau G, Artinger R, Fritz P, et al. (2000) Origin and mobility of humic colloids in the Gorleben aquifer system. *Applied Geochemistry* 15(2): 171–179.

Buma G (1979) Geochemical arguments for natural stabilization following in-place leaching of uranium. In: Schlitt WJ and Shock DA (eds.) *In Situ Uranium Mining & Ground Water Restoration, Solution Mining Symposium, February 1979*, pp. 113–124. Society of Mining Engineers of AIME.

Burns PC, Deely KM, and Skanthakumar S (2004) Neptunium incorporation into uranyl compounds that form as alteration products of spent nuclear fuel: Implications for geologic repository performance. *Radiochimica Acta* 92(3): 151–159.

Burns PC and Finch R (eds.) (1999) *Uranium: Mineralogy, Geochemistry, and the Environment*. *Reviews in Mineralogy*, vol. 38. Washington, DC: Mineralogical Society of America.

Byegård J, Albinsson Y, Skarnemark G, and Skålberg M (1992) Field and laboratory studies of the reduction and sorption of technetium (VII). *Radiochimica Acta* 58(59): 239–244.

Caceci MS and Choppin GR (1983) The first hydrolysis constant of uranium (VI). *Radiochimica Acta* 33: 207–212.

Campbell JE, Dillon RT, Tierney MS, et al. (1978) *Risk methodology for geologic disposal of nuclear waste: Interim report*. NUREG/CR-0458; SAND78-0029, Albuquerque, NM: Sandia National Laboratories.

Cantrell KJ, Kaplan DI, and Gilmore TJ (1997) Injection of colloidal Fe^0 particles in sand with shear-thinning fluids. *Journal of Environmental Engineering* 123(8): 786–791.

Cantrell KJ, Kaplan DI, and Wietsma TW (1995) Zero-valent iron for the in situ remediation of selected metals in groundwater. *Journal of Hazardous Materials* 42(2): 201–212.

Cantrell KJ, Serne RJ, and Last GV (2003) *Hanford Contaminant Distribution Coefficient Database and Users Guide*, p. 83. Richland, WA: Pacific Northwest National Laboratory PNNL-13895 Rev.

Capdevila H and Vitorge P (1998) Solubility product of $Pu(OH)_4$(am). *Radiochimica Acta* 82: 11–16.

Carroll SA, Bruno J, Petit JC, and Dran JC (1992) Interactions of U(VI), Nd and Th(IV) at the calcite-solution interface. *Radiochimica Acta* 58/59: 245–252.

Catalan LJJ, Yanful EK, and St-Arnaud L (2000) Field assessment of metal and sulfate fluxes during flooding of pre-oxidized mine tailings. *Advances in Environmental Research* 4: 295–306.

Cember H (1996) *Introduction to Health Physics*. New York, NY: McGraw Hill.

Centeno LM, Faure G, Lee G, and Talnagi J (2004) Fractionation of chemical elements including the REEs and ^{226}Ra in stream contaminated with coal-mine effluent. *Applied Geochemistry* 19(7): 1085–1095.

Chakraborty S, Favre F, Banerjee D, et al. (2010) U(VI) sorption and reduction by Fe(II) sorbed on montmorillonite. *Environmental Science & Technology* 44(10): 3779–3785.
Chamberlain AC and Dunster J (1958) Deposition of radioactivity in north-west England from the accident at windscale. *Nature* 182(4636): 629–630.
Chapelle FH (1993) *Ground-Water Microbiology and Geochemistry*. New York, NY: Wiley.
Charbeneau RJ (1984) Groundwater restoration with in situ uranium leach mining. In: Bredehoeft JD, Geophysics Study Committee, and National Research Council (eds.) *Groundwater Contamination*, p. 12. Washington, DC: National Academy Press.
Chen Y, Loch AR, Wolery TJ, et al. (2002) Solubility evaluation for Yucca Mountain TSPA-SR. In: McGrail BP and Cragnolino GA (eds.) *Scientific Basis for Nuclear Waste Management XXV*. *Materials Research Society Symposium Proceedings*, vol. 713, pp. 775–782. Warrendale, PA: Materials Research Society.
Chisholm-Brause C, Conradson SD, Buscher CT, Eller PG, and Morris DE (1994) Speciation of uranyl sorbed at multiple binding sites on montmorillonite. *Geochimica et Cosmochimica Acta* 58(17): 3625–3631.
Chisholm-Brause C, Conradson SD, Eller PG, and Morris DE (1992) Changes in U(VI) speciation upon sorption onto montmorillonite from aqueous and organic solutions. *Scientific Basis for Nuclear Waste Management XV*. *Materials Research Symposium Proceedings*, vol. 257, pp. 315–322. Pittsburgh, PA: Materials Research Society.
Choppin GR (1999) Utility of oxidation state analogs in the study of plutonium behavior. *Radiochimica Acta* 85: 89–95.
Choppin GR (2007) Actinide speciation in the environment. *Journal of Radioanalytical and Nuclear Chemistry* 273(3): 695–703.
Choppin GR, Liljenzin JO, and Rydberg J (1995) *Radiochemistry and Nuclear Chemistry*. Oxford: Butterworth-Heinemann.
Choppin GR and Stout BE (1989) Actinide behavior in natural waters. *The Science of the Total Environment* 83(3): 203–216.
Clark DL, Neu MP, Runde W, et al. (2006) Uranium and uranium compounds. *Kirk–Othmer Encyclopedia of Chemical Technology*. New York: Wiley.
Clarke JH and Parker FL (2009) Uranium recovery and remediation of uranium mill tailings: Russian and U.S. experience. In: Schweitzer GE, Parker FL, and Robbins K (eds.) *Cleaning Up Sites Contaminated with Radioactive Materials: International Workshop*, National Academy of Sciences.
Cleveland JM and Rees TF (1981) Characterization of plutonium in Maxey Flats radioactive trench leachates. *Science* 212(4502): 1506–1509.
Cleveland JM, Rees TF, and Nash KL (1983a) Plutonium speciation in water from Mono Lake, California. *Science* 222(4630): 1323–1325.
Cleveland JM, Rees TF, and Nash KL (1983b) Plutonium speciation in selected basalt, granite, shale, and tuff groundwaters. *Nuclear Technology* 62: 298–310.
Cochran TB, Norris RS, and Suokko KL (1993) Radioactive contamination at Chelyabinsk-65, Russia. *Annual Review of Energy and the Environment* 18: 507–528.
Cohen BL (1995) Test of the Linear No-Threshold theory of radiation carcinogenesis in the low dose, low dose rate region. *Health Physics* 68: 157–174.
Comans RNJ, Middleburg JJ, Zonderhuis J, et al. (1989) Mobilization of radiocaesium in pore water in lake sediments. *Nature* 339(6223): 367–369.
COMARE (2011) Further consideration of the incidence of childhood leukemia around nuclear power plants in Great Britain. *Fourteenth Report; Committee on Medical Aspects of Radiation in the Environment*. ISBN: 978-0-85951-691-4.
Combes J, Chisholm-Brause D, Brown GE Jr., Parks GA, and Conradson SD (1992) EXAFS spectroscopic study of neptunium (V) sorption at the a-FeOOH/water interface. *Environmental Science & Technology* 26(376–383).
Contardi JS, Turner DR, and Ahn TM (2001) Modeling colloid transport for performance assessment. *Journal of Contaminant Hydrology* 47(2–4): 323–333.
Cornish JE, Goldberg WC, Levine RS, and Benemann JR (1995) Phytoremediation of soils contaminated with toxic elements and radionuclides. *Bioremediation of Inorganics* 3: 55–62.
Cothern CR and Lappenbusch WL (1983) Occurrence of uranium in drinking water in the U.S. *Health Physics* 45(1): 89–99.
Coughlin BR and Stone AT (1995) Nonreversible adsorption of divalent metal-ions (Mn-II, Co-II, Ni-II, Cu-II and Pb-II) onto goethite – Effects of acidification, FE-II addition, and picolinic-acid addition. *Environmental Science & Technology* 29(9): 2445–2455.
Couture RA and Seitz MG (1985) Sorption of anions and iodine by iron oxides and kaolinite. *Nuclear and Chemical Waste Management* 4(4): 301–306.
Cranwell RM, Campbell JE, Helton JC, et al. (1987) *Risk Methodology for Geologic Disposal of Radioactive Waste: Final Report*. Albuquerque, NM: Sandia National Laboratories SAND81-2573, NUREG/CR-2452.
Cremers A, Elsen A, De Preter P, and Maes A (1988) Quantitative analysis of radiocaesium retention in soils. *Nature* 335: 247–249.
Criscenti LJ, Cygan RT, Eliassi M, and Jove-Colon CF (2002) *Effects of Adsorption Constant Uncertainty on Contaminant Plume Migration*. U.S. Nuclear Regulatory Commission.
Cui D and Erikson T (1998) Reactive transport of Sr, Cs, and Tc through a column packed with fracture-filling material. *Radiochimica Acta* 82: 287–292.
Cuney M and Kyser K (2009) Recent and not-so-recent developments in uranium deposits and implications for exploration. *Mineralogical Association of Canada Short Course Series (24–25 May 2008)*, vol. 39. Quebec City, Quebec: Mineralogical Association of Canada MAC and the Society for Geology Applied to Mineral Deposits SGA.
Curtis D (1999) Nature's uncommon elements: Plutonium and technetium. *Geochimica et Cosmochimica Acta* 63(2): 275–285.
Cvetkovic V, Painter S, Turner D, Pickett D, and Bertetti P (2004) Parameter and model sensitivities for colloid-facilitated radionuclide transport on the field scale. *Water Resources Research* 40(6) Article #W06504.
Czerwinski K, Buckau G, Scherbaum F, and Kim JI (1994) Complexation of the uranylion with aquatic humic-acid. *Radiochimica Acta* 65(2): 111–119.
Czerwinski K, Kim JI, Rhee DS, and Buckau G (1996) Complexation of trivalent actinide ions (Am3+, Cm3+) with humic acid: The effect of ionic strength. *Radiochimica Acta* 72(4): 179–187.
David F (1986) Thermodynamic properties of lanthanide and actinide Ions in aqueous solution. *Journal of the Less Common Metals* 121: 27–42.
Davis JA (ed.) (2001) *Surface Complexation Modeling of Uranium(VI) Adsorption on Natural Mineral Assemblages*. Washington, DC: U.S. Nuclear Regulatory Commission NUREG/CR-6708.
Davis JA, Coston JA, Kent DB, and Fuller CC (1998) Application of the surface complexation concept to complex mineral assemblages. *Environmental Science & Technology* 32(19): 2820–2828.
Davis JA and Curtis GP (2003) *Application of Surface Complexation Modeling to Describe Uranium(VI) Adsorption and Retardation at the Uranium Mill Tailings Site at Naturita, Colorado*. Rockville, MD: U.S. Nuclear Regulatory Commission NUREG CR-6820.
Davis JA and Curtis GP (2005) *Consideration of Geochemical Issues in Groundwater Restoration at Uranium In-Situ Leach Mining Facilities*. Washington, DC: Office of Nuclear Regulatory Research, U.S. Nuclear Regulatory Commission NUREG/CR-6870.
Davis JA, Curtis GP, Wilkins MJ, et al. (2006) Processes affecting transport of uranium in a suboxic aquifer. *Physics and Chemistry of the Earth, Parts A/B/C* 31(10–14): 548–555.
Davis JA and Kent DB (1990) Surface complexation modelling in aqueous geochemistry. *Reviews in Mineralogy and Geochemistry* 23(1): 177–260.
Davis JA, Kohler M, and Payne TE (2001) Uranium(VI) aqueous speciation and equilibrium chemistry. *NUREG/CR-6708*. *Surface Complexation Modeling Uranium (Vi) Adsorption On Natural Mineral Assemblages*, pp. 11–18. Washington, DC: U.S. Nuclear Regulatory Commission.
Davis JA and Leckie JO (1978a) Surface ionization and complexation at the oxide/water interface. II. Surface properties of amorphous iron oxyhydroxide and adsorption on metal ions. *Journal of Colloid and Interface Science* 67(1): 90–107.
Davis JA and Leckie JO (1978b) Effect of adsorbed complexing ligands on trace metal uptake by hydrous oxides. *Environmental Science & Technology* 12(12): 1309–1315.
Davis PH, Longmire P, Siegel M, and Simmons A (2009) *Uncertainties in the Ability of Natural Attenuation to Reduce Uranium Migration from In Situ Uranium Recovery Fields*. Albuquerque, NM: Sandia National Laboratories. SAND2009-0622P, LA-UR-09-00503.
Davis JA, Meece DE, Kohler M, and Curtis GP (2004) Approaches to surface complexation modeling of uranium(VI) adsorption on aquifer sediments. *Geochimica et Cosmochimica Acta* 68(18): 3621–3641.
Davis JA, Payne TE, and Waite TD (2002) Simulation the pH and pCO_2 dependence of uranium(VI) adsorption by a weathered schist with surface complexation models. In: Zhang P and Brady P (eds.) *Geochemistry of Soil Radionuclides*, pp. 61–86. Madison, WI: Soil Science Society of America.
De Windt L, Burnol A, Montarnal P, and Van der Lee J (2003) Intercomparison of reactive transport models applied to UO_2 oxidative dissolution and uranium migration. *Journal of Contaminant Hydrology* 61(1–4): 303–312.
Dearlove JP, Longworth G, Ivanovich M, et al. (1991) A study of groundwater-colloids and their geochemical interactions with natural radionuclides in Gorleben aquifer systems. *Radiochimica Acta* 52: 83–89.
Degueldre C (1997) Groundwater colloid properties and their potential influence on radionuclide transport. *Scientific Basis for Nuclear Waste Management XX*.

Materials Research Society Symposium Proceedings, vol. 465, pp. 835–846. Warrendale, PA: Materials Research Society.
Degueldre C, Baeyens B, Goerlich W, et al. (1989) Colloids in water from a subsurface fracture in granitic rock, Grimsel test site. *Geochimica et Cosmochimica Acta* 53(3): 603–610.
Degueldre C, Triay IR, Kim JI, et al. (2000) Groundwater colloid properties: A global approach. *Applied Geochemistry* 15(7): 1043–1051.
Demuth H and Shramke J (2006) Fate and transport of Post-restoration Groundwater Constituents at In Situ Uranium Leach Facilities, Report Prepared for Uranium Resources, Inc. (May 2006). Littleton, CO: Petroteck Engineering Corporation; Loveland, CO: Enchemica LLC.
Dent AJ, Ramsay JDF, and Swanton SW (1992) An EXAFS study or uranyl ion in solution and sorbed onto silica and montmorillonite clay colloids. *Journal of Colloid and Interface Science* 150(1): 45–60.
Dickson BL (1990) Radium in ground water. *The Environmental Behavior of Radium*, vol. I, ch. 4-2, pp. 335–372. Vienna, Austria: International Atomic Energy Agency.
DOE (1988) *Site Characterization Plan, Yucca Mountain Site, Nevada Research and Development Area, Nevada*. Washington, DC: Office of Civilian Radioactive Waste Management, U.S. Department of Energy.
DOE (1996a) Title 40 – CFR Part 191 – Compliance certification application for the Waste Isolation Pilot Plant. *Federal Register* 1–21.
DOE (1996b) *Programmatic Environmental Impact Statement for Ground Water*, vol. I (October 1996). Office of Legacy Management, U.S. Department of Energy.
DOE (1996b) *Programmatic Environmental Impact Statement for Ground Water*, vol. II (October 1996). Office of Legacy Management, U.S. Department of Energy
DOE (1997a) *Record of Decision for Ground Water*. AMS: Office of Legacy Management, U.S. Department of Energy April 1997.
DOE (1997b) *Linking Legacies: Connecting the Cold War Nuclear Weapons Production Process to Their Environmental Consequences*, p. 231. Washington, DC: U.S. Department of Energy.
DOE (2006) *The Second CERCLA Five-Year Review Report for the Hanford Site*. Richland, WA: U.S. Department of Energy DOE/RL-2006-20.
DOE (2008) *Yucca Mountain Repository License Application*. Office of Civilian Radioactive Waste Management, U.S. Department of Energy DOE/RW-0573, Rev. 1.
DOE (2010a) *Proposed Plan for Amendment of the 100-NR-1/NR-2 Interim Action Record of Decision/June 2010*. Richland, WA: Richland Operations Office, U.S. Department of Energy DOE/RL-2009-54, REV. 0.
DOE (2010b) *Hanford Soil & Groundwater Remediation Project*. http://www.hanford.gov/?page=1105 (accessed on 25 July 2011)
DOE (2011) *Guidance and Reports* [Online]. Office of Legacy Management, U.S. Department of Energy. http://www.lm.doe.gov/pro_doc/guidance_reports.htm (accessed on 13 June 2011)
Dong W and Brooks SC (2006) Determination of the formation constants of ternary complexes of uranyl and carbonate with alkaline earth metals (Mg^{2+}, Ca^{2+}, Sr^{2+}, and Ba^{2+}) using anion exchange method. *Environmental Science & Technology* 40(15): 4689–4695.
Dong W and Brooks SC (2008) Formation of aqueous $MgUO_2(CO_3)_3^{2-}$ complex and uranium anion exchange mechanism onto an exchange resin. *Environmental Science & Technology* 42(6): 1979–1983.
Douglas LA (1989) Vermiculites. In: Dixon JB and Week SB (eds.) *Minerals in Soil Environments*, 2 edn. Madison, WI: Soil Science Society of America.
Douglas M, Clark SB, Friese JI, et al. (2005a) Neptunium(V) partitioning to uranium(VI) oxide and peroxide solids. *Environmental Science & Technology* 39(11): 4117–4124.
Douglas M, Clark SB, Friese JI, et al. (2005b) Microscale characterization of uranium (VI) silicate solids and associated neptunium(V). *Radiochimica Acta* 93(5): 265–272.
Douple EB, Mabuchi K, Cullings HM, et al. (2011) Long-term radiation-related health effects in a unique human population: Lessons learned from the atomic bomb survivors of Hiroshima and Nagasaki. *Disaster Medicine and Public Health Preparedness* 5(1): S122–S133.
Duerden P, Lever DA, Sverjensky DA, and Townley LR (1992) *Alligator River Analogue Project: Final Report*. Sandia National Laboratories.
Duff MC (2001) Speciation and transformations of sorbed Pu on geologic materials: wet chemical and spectroscopic observations. In: Kudo A (ed.) *Plutonium in the Environment: Proceedings of the Second International Symposium*, vol. 1, pp. 139–157. Netherlands: Elsevier.
Duff MC, Coughlin JU, and Hunter DB (2002) Uranium co-precipitation with iron oxide minerals. *Geochimica et Cosmochimica Acta* 66(20): 3533–3547.
Dzombak DA and Morel FMM (1990) *Surface Complexation Modeling, Hydrous Ferric Oxide*. New York, NY: Wiley.
Eadie GG and Kaufmann RF (1977) Radiological evaluation of the effects of uranium mining and milling operations on selected ground water supplies in the Grants Mineral Belt, New Mexico. *Health Physics* 32(4): 231–241.
Efurd DW, Runde W, Banar JC, et al. (1998) Neptunium and plutonium solubilities in a Yucca Mountain groundwater. *Environmental Science & Technology* 32(24): 3893–3900.
Eisenbud M (1987) *Environmental Radioactivity from Natural, Industrial, and Military Sources*. New York, NY: Academic Press.
ENDAUM (1997) Why Navajos resist new uranium mining. Eastern Navajo-Diné Against Uranium Mining. *The Workbook* 22(2): 52–62.
EPA (1985) *Drinking Water Criteria Document for Uranium*. Washington, DC: U.S. Environmental Protection Agency.
EPA (1996) Title 40 – CFR Part 194 – Criteria for the certification and re-certification of the Waste Isoloation Pilot Plant's compliance with the Title 40 – CFR Part 191 – Disposal regulations; final rule. *Federal Register* 61(28).
EPA (1999a) *The K_d Model Methods of Measurement and Application of Chemical Reaction Codes. Understanding Variation in Partition Coefficient, K_d, values*, vol. 1. Washington, DC: Office of Air and Radiation, U.S. Environmental Protection Agency.
EPA (1999b) *Review of Geochemistry and Available K_d Values for Cadmium, Cesium, Chromium, Lead, Plutonium, Radon, Strontium, Thorium, Tritium (^3H) and Uranium. Understanding Variation in Partition Coefficient, K_d, values*, vol. 2. Washington, DC: Office of Air and Radiation, U.S. Environmental Protection Agency.
EPA (1999c) *Field Applications of In Situ Remediation Technologies: Permeable Reactive Barriers*. Washington, DC: U.S. Environmental Protection Agency.
EPA (1999d) *Cancer Risk Coefficients for Environmental Exposure to Radionuclides*. Washington, DC: U.S. Environmental Protection Agency (PDF), EPA 402-R-99-001.
EPA (2000a) *National Primary Drinking Water Regulations; Radionuclides; Notice of Data Availability; Proposed Rule, 40 CFR Parts 141 and 142*, pp. 21576–21628. U.S. Environmental Protection Agency (EPA 815-2-00-003).
EPA (2000b) *Field Demonstration of Permeable Reactive Barriers to Remove Dissolved Uranium from Groundwater, Fry Canyon, Utah*. Washington, DC: U.S. Environmental Protection Agency.
EPA (2000c) CFR Parts 9, 141, and 142 (December 7, 2000). National primary drinking water regulations: Radionuclides: Final rule. *Federal Register* 65(236): 76708.
EPA (2001) Title 40 – CFR Part 197 – Public health and environmental radiation protection standards for Yucca Mountain, NV; final rule. *Federal Register* 66(114): 32074–32135.
EPA (2003) *Assessment of Risks from Radon in Homes*. Washington, DC: U.S. Environmental Protection Agency (EPA 402-R-03-003).
EPA (2007) *Monitored Natural Attenuation of Inorganic Contaminants in Groundwater*. vol. 1. Technical Basis for Assessment: Ada, OK: National Risk Management Research Laboratory, Groundwater and Ecosystems Restoration Division (EPA/600/R-07/139).
EPA (2010) *Monitored Natural Attenuation of Inorganic Contaminants in Groundwater. Assessment for Radionuclides Including Tritium, Radon, Strontium, Technetium, Uranium, Iodine, Radium, Thorium, Cesium, and Plutonium-Americium*, vol. 3. Cincinnati, OH: National Risk Management Research Laboratory, Office of Research and Development, U.S. Environmental Protection Agency.
EPA (2011a) Title 40 – CFR Part 192 – Health and environmental protection standards for uranium and thorium mill tailings and uranium In situ leaching processing facilities. *Federal Register*.
Erickson KL (1983) Approximations for adapting porous media radionuclide transport models to analysis of transport in jointed porous rocks. In: Brookins D (ed.) *Scientific Basis for Nuclear Waste Management*, vol. 6, pp. 473–480. Amsterdam: North-Holland.
Eriksen TE, Ndalamba P, Bruno J, and Caceci M (1992) The solubility of $TcO_2{\cdot}H_2O$ in neutral to alkaline solutions under constant pCO_2. *Radiochimica Acta* 58/59: 67–70.
Erskine DW and Ardito C (2008) Finding benchmarks at uranium mine sites. *Southwest Hydrology* 7(6): 24–25, 34.
European Commission (1998) Council Directive 98/83/EC of 3 November 1998 on the quality of water intended for human consumption. *Official Journal* 330: 32–54.
European Commission (2001) Commission recommendation of 20 December 2001 on the protection of the public against exposure to radon in drinking water supplies. 2001/982/Euratom, L344/85.
Evans CV, Morton LS, and Harbottle G (1997) Pedologic assessment of radionuclide distributions: Use of a radiopedogenic index. *Soil Science Society of American Journal* 61: 1440–1449.
Ewing RC (1999) Radioactivity and the 20th century. *Reviews in Mineralogy and Geochemistry* 38(1): 1–21.
Fanghänel T and Kim JI (1998) Spectroscopic evaluation of thermodynamics of trivalent actinides in brines. *Journal of Alloys and Compounds* 271–273: 728–737.

Fein JB, Daughney J, Yee N, and Davis TA (1997) A chemical equilibrium model for the sorpotion onto bacterial surfaces. *Geochimica et Cosmochimica Acta* 61(16): 3319–3328.

Fellhauer D, Neck V, Altmaier M, Lutzenkirchen J, and Fanghanel T (2010) Solubility of tetravalent actinides in alkaline $CaCl_2$ solutions and formation of $Ca_4[An(OH)_8]^{4+}$ complexes: A study of Np(IV) and Pu(IV) under reducing conditions and the systematic trend in the An(IV) series. *Radiochimica Acta* 98(9–11): 541–548.

Felmy AR, Dhanpat R, Schramke JA, and Ryan JL (1989) The solubility of plutonium hydroxide in dilute solution and in high-ionic-strength chloride brines. *Radiochimica Acta* 48: 29–35.

Felmy AR, Rai D, and Fulton RW (1990) The solubility of amohco$_3$(C) and the aqueous thermodynamics of the system Na^+–Am^{3+}–HCO_3^-–CO_3^{2-}–OH^-–H_2O. *Radiochimica Acta* 50(4): 193–204.

Felmy AR, Rai D, and Mason MJ (1991) The solubility of hydrous thorium(IV) oxide in chloride media: Development of an aqueous ion-interaction model. *Radiochimica Acta* 55(4): 177–185.

Felmy AR and Weare JH (1986) The prediction of borate mineral equilibria in natural waters: Application to Searles Lake, California. *Geochimica et Cosmochimica Acta* 50(12): 2771–2783.

Fiedor JN, Bostic WD, Jarabek RJ, and Farrell J (1998) Understanding the mechanism of uranium removal from groundwater by zero-valent iron using X-ray photoelectron spectroscopy. *Environmental Science & Technology* 32(10): 1466–1473.

Fjeld RA and Compton KL (1999) Risk assessment. In: Meyers RA and Dittrick DK (eds.) *Encyclopedia of Environmental Pollution and Cleanup*, vol. 2, pp. 1450–1473. New York, NY: Wiley.

Fjeld RA, Serkiz SM, McGinnis PL, Elci A, and Kaplan DI (2003) Evaluation of a conceptual model for the subsurface transport of plutonium involving surface mediated reduction of Pu(V) to Pu(IV). *Journal of Contaminant Hydrology* 67(1–4): 79–94.

Fleischer RL (1980) Isotopic disequilibrium of uranium: Alpha-recoil damage and preferential solution effects. *Science* 207: 979–981.

Focazio MJ, Szabo Z, Kraemer TF et al. (2001) Occurrence of selected radionuclides in ground water used for drinking water in the United States: A reconnaissance survey, 1998–99. *Water Resources Investigations Report 00-4273*. U. S. Geological Survey.

Fordham AW (1993) Porewater quality of uranium tailings during laboratory aging and its relation to the solid phase. *Australian Journal of Soil Research* 31: 365–390.

Fortin D and Beveridge TJ (1997) Microbial sulfate reduction within sulfidic mine tailings: Formation of diagenetic Fe sulfides. *Geomicrobiology Journal* 14: 1–21.

Fowle DA and Fein JB (2000) Experimental measurements of the reversibility of metal-bacteria adsorption reactions. *Chemical Geology* 168(1–2): 27–36.

Francis AJ (1994) Microbiological treatment of radioactive wastes. In: Schulz WW and Horwitz EP (eds.) *Chemical Pretreatment of Nuclear Waste for Disposal*, pp. 115–131. New York: Plenum Press.

Francis AJ, Dodge CJ, Gillow JB, and Cline JE (1991) Microbial transformations of uranium in wastes. *Radiochimica Acta* 52–53: 311–316.

Friese JI, Douglas M, Buck EC, Clark SB, and Hanson BD (2004) Neptunium(V) incorporation/sorption with uranium(VI) alteration products. In: Hanchar JM, StroesGascoyne S, and Browning L (eds.) *Scientific Basis for Nuclear Waste Management XXVIII*. *Materials Research Society Symposium Proceedings*, vol. 824, pp. 127–132. Warrendale, PA: Materials Research Society.

Fruchter JS, Amonette JE, Cole CR, et al. (1996) *In Situ Redox Manipulation field Injection Test Report – Hanford 100 H Area*. Richland, WA: Pacific Northwest National Laboratory.

Fuger J, Khodakovsky IL, Medvedev VA, and Navratil JD (1990) The Chemical Thermodynamics of Actinide Elements and Compounds. *The Actinide Aqueous Inorganic Complexes,* Part 12. Vienna: International Atomic Energy Agency.

Gabriel U, Gaudet JP, Spandini L, and Charlet L (1998) Reactive transport of uranyl in a goethite column: An experimental and modelling study. *Chemical Geology* 151(1–4): 107–128.

Gauglitz R, Holterdorf M, Franke W, and Marx G (1992a) Immobilization of heavy metals by hydroxylapatite. *Radiochimica Acta* 58(59): 253–257.

Gauglitz R, Holterdorf M, Franke W, and Marx G (1992b) Immobilization of actinides by hydroxylapatite. In: Sombret CG (ed.) *Scientific Basis for Nuclear Waste Management XV*. *Materials Research Society Symposium Proceedings*, vol. 257, pp. 567–573. Pittsburgh, PA: Materials Research Society.

Gerth J (1990) Unit-cell dimensions of pure and trace metal-associated goethites. *Geochimica et Cosmochimica Acta* 54(2): 363–371.

Gillow JB, Dunn M, Francis AJ, Lucero DA, and Papenguth HW (2000) The potential for subterranean microbes in facilitating actinide migration at the Grimsel Test Site and Waste Isolation Pilot Plant. *Radiochimica Acta* 88(9–11): 769–774.

Ginder-Vogel M, Stewart B, and Fendorf S (2010) Kinetic and mechanistic constraints on the oxidation of biogenic uraninite by ferrihydrite. *Environmental Science & Technology* 44(1): 163–169.

Goldhaber MB, Reynolds RL, and Rye RO (1978) Origin of a south Texas roll-type uranium deposit. II. Sulfide petrology and sulfur isotope studies. *Economic Geology* 73: 1690–1705.

Goldsmith WA and Bolch WE (1970) Clay slurry sorption of carrier-free radiocations. *Journal of the Sanitary Engineering Division of the American Society of Civil Engineers* 96(5): 1115–1127.

Gomez P, Turrero MJ, Moulin V, and Magonthier MC (1992) Characterization of natural colloids in groundwaters of El Berrocal, Spain. In: Kharaka YK and Maest AS (eds.) *Water–Rock Interaction*, pp. 797–800. Rotterdam: Balkema.

Goode DJ and Wilder RJ (1987) Ground-water contamination near a uranium tailings disposal site in Colorado. *Ground Water* 25(5): 545–554.

Goyer RA and Clarkson TW (2001) Toxic effects of metals. In: Klaassen CD (ed.) *Casarett and Doull's Toxicology: The Basic Science of Poisons*, 6th edn., pp. 811–867. New York: McGraw-Hill.

Grenthe I, Fuger J, Konings RJM, and Lemire RJ (1992) *Chemical Thermodynamics of Uranium*. Amsterdam: North-Holland.

Gruber V and Maringer FJ (2010) Public exposure by natural radionuclides in drinking water – Models for effective dose assessment and implications to guidelines. Third European IRPA Congress, June 14–18, 2010, Helsinki, Finland, Fontenay-aus-Roses, France: International Radiation Protection Association.

Gu B, Liang L, Dickey MJ, Yin X, and Dai S (1998) Reductive precipitation of uranium (VI) by zero-valent iron. *Environmental Science & Technology* 32(21): 3366–3373.

Gu B and Schultz RK (1991) Anion retention in soil: Possible application to reduce migration of buried technetium and iodine: A review. U.S. Nuclear Regulatory Commission, 32.

Guggenheim EA (1966) *Applications of Statistical Mechanics*. Oxford: Claredon Press.

Guillaumont R and Adloff JP (1992) Behavior of environmental pollution at very low concentration. *Radiochimica Acta* 58(59): 53–60.

Guillaumont R, Fanghanel T, and Fuger J, et al. (eds.) (2003) *Update on the Chemical Thermodynamics of Uranium, Neptunium, Plutonium, Americium and Technetium*. Amsterdam: Elsevier.

Haines RI, Owen DG, and Vandergraaf TT (1987) Technetium-iron oxide reactions under anaerobic conditions: A Fourier transform infrared, FTIR study. *Nuclear Journal of Canada* 1: 32–37.

Hammond GE, Lichtner PC, Lu C, and Mills RT (2011) PFLOTRAN: Reactive flow & transport code for use on laptops to leadership-class supercomputers. In: Zhang F, Yeh GT, and Parker J (eds.) *Groundwater Reactive Transport Models*. Oak Park, IL: Bentham Science.

Han BS and Lee KJ (1997) The effect of bacterial generation on the transport of radionuclides in porous media. *Annals of Nuclear Energy* 24(9): 721–734.

Hans J, Burris E, and Gorsuch T (1979) Radioactive waste management at the former Shiprock Uranium Mill Site New Mexico. *Health Physics* 37: 811.

Harley NH (2001) Toxic effects of radiation and radioactive materials. In: Klaassen CD (ed.) *Casarett and Doull's Toxicology*, 6th edn., pp. 917–944. New York, NY: McGraw-Hill.

Hartmann E, Geckeis H, Rabung T, Lutzenkirchen J, and Fanghanel T (2008) Sorption of radionuclides onto natural clay rocks. *Radiochimica Acta* 96: 699–707.

Harvie CE, Moller N, and Weare JH (1984) The prediction of mineral solubilities in natural waters: The Na–K–Mg–Ca–H–Cl–SO_4–OH–HCO_3–CO_3–CO_2–H_2O system to high ionic strengths at 25 °C. *Geochimica et Cosmochimica Acta* 48(4): 723–751.

Harvie CE and Weare JH (1980) The prediction of mineral solubilities in natural waters: The Na–K–Mg–Ca–Cl–SO4–H_2O system from zero to high concentration at 25 °C. *Geochimica et Cosmochimica Acta* 44(7): 981–997.

Haschke JM (2007) Disproportionation of Pu(IV): A reassessment of kinetic and equilibrium properties. *Journal of Nuclear Materials* 362(1): 60–74.

Hiemstra T and Van Riemsdijk WH (1999) Surface structural ion adsorption modeling of competitive binding of oxyanions by metal (hydr)oxides. *Journal of Colloid and Interface Science* 210(1): 182–193.

Hiemstra T and VanRiemsdijk WH (1996) A surface structural approach to ion adsorption: The charge distribution (CD) model. *Journal of Colloid and Interface Science* 179(2): 488–508.

Higgo JJW and Rees LVC (1986) Adsorption of actinides by marine sediments: Effect of the sediment/seawater ratio on the measured distribution ratio. *Environmental Science & Technology* 20: 483–490.

Hobart D (1990) Actinides in the environment. *Fifty years with Transuranium Elements, Robert A. Welch Foundations Conference on Chemical Research*, vol. 34, pp. 379–436.

Hodge HC, Stannard JN, and Hursh JB (1973) Uranium, plutonium, and transuranic elements. In: *Handbook of Experimental Pharmacology XXXVI*. New York: Springer.

Hölgye Z and Malý M (2000) Sources, vertical distribution, and migration rates of Pu-239, Pu-240, Pu-238, and Cs-137 in grassland soil in three localities of central Bohemia. *Journal of Environmental Radioactivity* 47(2): 135–147.

Honeyman BD and Ranville JF (2002) Colloid properties and their effects on radionuclide transport through soils and groundwater. In: Zhang P and Brady P (eds.) *Geochemistry of Soil Radionuclides*, pp. 131–164. Madison, WI: Soil Science Society of America.

Hooper FJ, Squibb KS, Siegel EL, et al. (1999) Elevated urine uranium excretion by soldiers with retained uranium shrapnel. *Health Physics* 77(5): 512–519.

Hughes MN and Poole RK (1989) *Metals and Micro-Organisms*. London: Chapman and Hall.

Huie Z, Zishu Z, and Lanying Z (1988) Sorption of radionuclides technetium and iodine on minerals. *Radiochimica Acta* 44/45: 143–145.

Hunter KA, Hawke DJ, and Choo LK (1988) Equilibrium adsorption of thorium by metal oxides in marine electrolytes. *Geochimica et Cosmochimica Acta* 52: 627–636.

IAEA (1992) Uranium In Situ Leaching. *Proceedings of a Technical Committee Meeting*. 5–8 October 1992. IAEA TECDOC-720, Vienna, Austria: International Atomic Energy Agency.

IAEA (2004a) Methods for assessing occupational radiation doses due to intakes of radionuclides. *Safety Reports Series, No. 37*. Vienna, Austria: International Atomic Energy Agency.

IAEA (2006) Applicability of monitored natural attenuation at radioactively contaminated sites. *Technical Reports Series No. 445*. International Atomic Energy Agency.

Icopini GA, Lack JG, Hersman LE, Neu MP, and Boukhalfa H (2009) Plutonium(V/VI) reduction by the metal-reducing bacteria *Geobacter metallireducens* GS-15 and *Shewanella oneidensis* MR-1. *Applied and Environmental Microbiology* 75(11): 3641–3647.

ICRP (1995) *Age-Dependent Doses to Members of the Public from Intake of Radionuclides: Part 3, Ingestion Dose Coefficients*. ICRP Publication 69. International Commission for Radiation Protection. Press, O. P

ICRP (1996) *Age-Dependent Doses to Members of the Public from Intake of Radionuclides: Part 4, Inhalation Dose Coefficients*. ICRP Publication 71. International Commission for Radiation Protection. Press, O. P

IRIS (2011) *Uranium, Natural and Uranium, Soluble Salts*. Washington, DC: U.S. Environmental Protection Agency System, I.R.I.

Isaksson M, Erlandsson B, and Mattsson S (2001) A 10-year study of the 137Cs distribution in soil and a comparison of Cs soil inventory with precipitation-determined deposition. *Journal of Environmental Radioactivity* 55(1): 47–59.

ITRC (2010) *A Decision Framework for Applying Monitored Natural Attenuation Processes to Metals and Radionuclides in Groundwater*. Washington, DC: Interstate Technology & Regulatory Council APMR-1.

Ivanovich M (1992) *The Phenomenon of Radioactivity*. Oxford: Oxford University Press.

Jackson RE and Inch KJ (1989) The In-situ absorption of Sr-90 in a sand aquifer at the Chalk River Nuclear Laboratories. *Journal of Contaminant Hydrology* 4: 27–50.

Jacquier P, Meier P, and Ly J (2001) Adsorption of radioelements on mixtures of minerals – Experimental study. *Applied Geochemistry* 16(1): 85–93.

Jenne EA (ed.) (1998) *Adsorption of Metals by Geomedia: Variables, Mechanisms, and Model Applications*. Richland, WA: Academic Press.

Jensen KA and Ewing RC (2001) The Okelobondo natural fission reactor, southeast Gabon: Geology, mineralogy, and retardation of nuclear-reaction products. *Geological Society of America Bulletin* 113(1): 32–62.

Johnson RH, Otton JK, and Horton RJ (2009) Results and interpretations of U.S. Geological Survey data collected in and around the Tuba City Open Dump, Arizona. *Open-File Report 2009–1154*. U.S. Geological Survey, p. 125.

Jove-Colon CF, Brady PV, Siegel MD, and Lindgren ER (2001) Historical case analysis of uranium plume attenuation. *Soil and Sediment Contamination* 10(1): 71–115.

Jove-Colon CF and Finch R (2010) Evaluation of Pu solubility using the mixed redox phase PuO_{2+x}: Modeling of existing experimental data. *Geochimica et Cosmochimica Acta* 74(12): A482.

Kaatsch P, Kaletsch U, Meinert R, and Michaelis J (1998) An extended study on childhood malignancies in the vicinity of German nuclear power plants. *Cancer Cause Control* 9: 529–533.

Kanivets VV, Voitsekhovitch OV, Simov VG, and Golubeva ZA (1999) The post-Chernobyl budget of ^{137}Cs and ^{90}Sr in the Black Sea. *Journal of Environmental Radioactivity* 43(2): 121–135.

Kaplan D, Ford R, and Wilkin R (2010) Radium. In: Ford RG and Wilkin RT (eds.) *Monitored Natural Attenuation of Inorganic Contaminants in Groundwater. Assessment for Radionuclides Including Tritium, Radon, Strontium, Technetium, Uranium, Iodine, Radium, Thorium, Cesium, and Plutonium-Americium*, vol. 3, pp. 79–90. Cincinnati, OH: National Risk Management Research Laboratory Office of Research and Development U.S. Environmental Protection Agency.

Kaplan DI, Serne RJ, Parker KE, and Kutnyakov IV (2000) Iodide sorption to subsurface sediments and illlitic minerals. *Environmental Science & Technology* 34: 399–405.

Kashparov VA, Ahamdach N, Zvarich SI, Yoschenko VI, Maloshtan IM, and Dewiere L (2004) Kinetics of dissolution of Chernobyl fuel particles in soil in natural conditions. *Journal of Environmental Radioactivity* 72: 335–353.

Kashparov VA, Oughton DH, Zvarich SI, Protsak VP, and Levchuk SE (1999) Kinetics of fuel particle weathering and ^{90}Sr mobility in the Chernobyl 30-km exclusion zone. *Health Physics* 76(3): 251–259.

Kashparov VA, Protsak VP, Ahamdach N, et al. (2000) Dissolution kinetics of particles of irradiated Chernobyl nuclear fuel: Influence of pH and oxidation state on the release of radionuclides in the contaminated soil of Chernobyl. *Journal of Nuclear Materials* 279(2–3): 225–233.

Kaszuba JP and Runde W (1999) The aqueous geochemistry of Np: Dynamic control of soluble concentrations with applications to nuclear waste disposal. *Environmental Science & Technology* 33(24): 4427–4433.

Katz JJ, Seaborg GT, and Morse LR (eds.) (1986) *The Chemistry of the Actinide Elements*. London: Chapman and Hall.

Kazakovskaya TV, Zakharova EV, and Haire MJ (2010) Sorption of Np by UO_2 under repository conditions. In: Rao L, Tobin JG, and Shuh DK (eds.) *Actinides 2009*, vol. 9. Bristol: Institute of Physics Publishing.

Keeney-Kennicutt WL and Morse JW (1985) The redox chemistry of $Pu(V)O_2^+$ interaction with common mineral surfaces in dilute solutions and seawater. *Geochimica et Cosmochimica Acta* 49(12): 2577–2588.

Kelley M, Maffit L, McClellan Y, Siegel MD, and Williams CV (2002) *Hanford 100-N Area Remediation Options Evaluation Summary Report*. Albuquerque, NM: Sandia National Laboratories.

Kelly SD, Newville MG, Cheng L, et al. (2003) Uranyl incorporation in natural calcite. *Environmental Science & Technology* 37: 1284–1287.

Kent DB, Tripathi VS, Ball NB, Leckie JO, and Siegel MD (1988) *Surface-Complexation Modeling of Radionuclide Adsorption in Subsurface Environments*. Washington, DC: US Nuclear Regulatory Commission.

Kersting AB, Efurd DW, Finnegan DL, et al. (1999) Migration of plutonium in ground water at the Nevada Test Site. *Nature* 397: 56–59.

Khan SA and Riaz-ur-Rehman and Kahn MA (1994) Sorption of cesium on bentonite. *Waste Management* 14(7): 629–642.

Kim JI (1993) The chemical behavior of transuranium elements and barrier functions in natural aquifer systems. In: Interrante CG and Pabalan RT (eds.) *Scientific Basis for Nuclear Waste Management XVI*. *Materials Research Society Symposium Proceedings*, vol. 294, pp. 3–21. Pittsburgh, PA: Materials Research Society.

Kim JI (1994) Actinide colloids in natural aquifer systems. *MRS Bulletin* 19(12): 47–53.

Kim SS, Baik MH, Choi JW, Shin HS, and Yun JI (2010) The dissolution of ThO_2(cr) in carbonate solutions and a granitic groundwater. *Journal of Radioanalytical and Nuclear Chemistry* 286(1): 91–97.

Kim SS, Baik MH, and Kang KC (2009) Solubility of neptunium oxide in the KURT (KAERI Underground Research Tunnel) groundwater. *Journal of Radioanalytical and Nuclear Chemistry* 280(3): 577–583.

Kim JI and Sekine T (1991) Complexation of neptunium(V) with humic-acid. *Radiochimica Acta* 55(4): 187–192.

King T, Michel J, and Moore WS (1982) Ground-water geochemistry of Ra-228, Ra-226, and Rn-222. *Geochimica et Cosmochimica Acta* 46: 1173–1182.

Kingston WL and Whitbeck M (1991) *Characterization of Colloids Found in Various Groundwater Environments in Central and Southern Nevada*. Las Vegas, NV: Desert Research Institute, University of Nevada System Water Resources Center Publication #45083.

Klaassen CD (2001) *Casarett and Doull's Toxicology*, 6th edn. New York, NY: McGraw-Hill.

Knopp R, Neck V, and Kim JI (1999) Solubility, hydrolysis, and colloid formation of plutonium(IV). *Radiochimica Acta* 86: 101–108.

Kob V (1988) Modeling of U(VI) sorption and speciation in a natural sediment-groundwater system. *Radiochimica Acta* 44/45: 403–406.

Koch JT, Rachar DB, and Kay BD (1989) Microbial participation in iodide removal from solution by organic soils. *Canadian Journal of Soil Science* 69: 127–135.

Kohler M, Curtis GP, Kent DB, and Davis JA (1996) Experimental investigation and modeling of uranium (VI) transport under variable chemical conditions. *Water Resources Research* 32(12): 3539–3551.

Kohler M, Weiland E, and Leckie JO (1992) Metal–ligand–surface interactions during sorption of uranyl and neptunyl on oxides and silicates. In: Kharaka YK and Maest AS (eds.) *7th International Symposium Water–Rock Interaction*, vol. 1, pp. 51–54. Rotterdam: A.A. Balkema.

Konhauser K (2007) *Introduction to Geomicrobiology*. Malden, MA: Blackwell Science.

Konoplev AV and Bulgakov AA (1999) Kinetics of the leaching of Sr-90 from fuel particles in soil in the near zone of the Chernobyl power plant. *Atomic Energy* 86(2): 136–141.

Konoplev AV, Bulgakov AA, Popov VE, and Bobovnikova TI (1992) Behaviour of long-lived radionuclides in a soil–water system. *Analyst* 117(6): 1041–1047.

Korner LA and Rose AW (1977) *Rn in Streams and Ground Waters of Pennsylvania as a Guide to Uranium Deposits*. Grand Junction, CO: U.S. Energy Research and Development Association Open-File Report GJBX 60(77).

Koshurnikova NA, Mushkacheva GS, Shilnikova NS, et al. (2002) Studies on the Ozyorsk population: Health effects. *Radiation and Environmental Biophysics* 41: 37–39.
Kossenko MM (1996) Cancer mortality among Techa River residents and their offspring. *Health Physics* 71: 77–82.
Kossenko MM, Izhevsky PV, Degteva MO, Akleev AV, and Vyushkova OV (1994) Pregnancy outcome and early health status of children born to the Techa River population. *Science of Total Environment* 142: 91–100.
Kowal-Fouchard A, Drot R, Simoni E, and Ehrhardt JJ (2004) Use of spectroscopic techniques for uranium (VI)/montmorillonite interaction modeling. *Environmental Science & Technology* 38: 1399–1407.
Krauskopf KB (1986) Aqueous geochemistry of radioactive waste disposal. *Applied Geochemistry* 1: 15–23.
Kretzschmar R, Borovec M, Grollimund D, and Elimelech M (1999) Mobile subsurfacecolloids and their role in contaminant transport. *Advances in Agronomy* 66: 121–194.
Krishnaswami S, Graustein WC, Turekian KK, and Dowd JF (1982) Radium, thorium, and radioactive isotopes in ground waters: Application to the in situ determination of adsorption-desorption rate constants and retardation factors. *Water Resources Research* 18: 1633–1645.
Krizman M, Byrne AR, and Benedik L (1995) Distribution of 230Th in milling wastes from the Zirovski vrh Uranium Mine (Slovenia), and its radioecological implications. *Journal of Environmental Radioactivity* 26: 223–235.
Kruglov SV, Vasil'eva NA, Kurinov AD, and Aleksakhin RM (1994) Leaching of radionuclides in Chernobyl fallout from soil by mineral acids. *Radiochemistry* 36(6): 598–602.
Krumhansl JL, Brady PV, and Zhang P (2002) Soil mineral backfills and radionuclide retention. In: Zhang P and Brady P (eds.) *Geochemistry of Soil Radionuclides*, pp. 191–210. Madison, WI: Soil Science Society of America.
Kurttio P, Auvinen A, Salonen L, et al. (2002) Renal effects of uranium in drinking water. *Environmental Health Perspectives* 110(4): 337–342.
Labonne-Wall N, Choppin GR, Lopez C, and Monsallier JM (1999) Interaction of uranyl with humic and fulvic acids at high ionic strength. In: Reed DT, Clark SB, and Rao L (eds.) *Actinide Speciation in High Ionic Strength Media*, pp. 199–211. New York, NY: Kluwer Academic/Plenum Publishers.
Lack JG, Chaudhuri SK, Kelly SD, et al. (2002) Immobilization of radionuclides and heavy metals through anaerobic bio-oxidation of Fe(II). *Applied and Environmental Microbiology* 68(6): 2704–2710.
LaFlamme BD and Murray JW (1987) Solid/solution interaction: The effect of carbonate alkalinity on adsorbed thorium. *Geochimica et Cosmochimica Acta* 51: 243–250.
Landa ER (1987) Radium-226 contents and Rn emanation coefficients of particle-size fractions of alkaline, acid and mixed U mill tailings. *Health Physics* 52: 303–310.
Landa ER (2004) Uranium mill tailings: Nuclear waste and natural laboratory for geochemical and radioecological investigations. *Journal of Environmental Radioactivity* 77(1): 1–27.
Landa ER, Miller CL, and Updegraff DM (1986) Leaching of 226Ra from uranium mill tailings by sulfate reducing bacteria. *Health Physics* 51(509–518).
Langmuir D (1997) *Aqueous Environmental Chemistry*. Upper Saddle River, NJ: Prentice Hall.
Langmuir D and Herman JS (1980) The mobility of thorium in natural waters at low temperatures. *Geochimica et Cosmochimica Acta* 44: 1753–1766.
Langmuir D and Melchior D (1985) The geochemistry of Ca, Sr, Ba, and Ra sulfates in some deep brines from the Palo Duro Basin, Texas. *Geochimica et Cosmochimica Acta* 49(11): 2423–2432.
Langmuir D and Riese AC (1985) The thermodynamic properties of radium. *Geochimica et Cosmochimica Acta* 49(7): 1593–1601.
Lapham SC, Millard JB, and Samet JM (1989) Health implications of radionuclide levels in cattle raised near U mining and milling facilities in Ambrosia Lake, New Mexico. *Health Physics* 36(3): 327–340.
Laul JC (1992) Natural radionuclides in groundwaters. *Journal of Radioanalytical and Nuclear Chemistry* 156(2): 235–242.
Lee SY, Baik MH, and Choi JW (2010) Biogenic formation and growth of uraninite (UO_2). *Environmental Science & Technology* 44(22): 8409–8414.
Lefevre F, Sardin M, and Schweich D (1993) Migration of Sr in clayey and calcareous sandy soil: Precipitation and ion exchange. *Journal of Contaminant Hydrology* 13(4): 215–229.
Lemire RJ (1984) *An Assessment of the Thermodynamic Behavior of Neptunium in Water and Model Groundwaters from 25 to 150 °C*. Pinawa, MB: Atomic Energy of Canada Limited.
Lemire RJ, Fuger J, Nitsche H, and Potter P (2001) *Chemical Thermodynamics of Neptunium and Plutonium*. Amsterdam: Elsevier.
Lemire RJ and Tremaine PR (1980) Uranium and plutonium equilibria in aqueous solutions to 200 °C. *Journal of Chemical Engineering Data* 25(4): 361–370.
Lichtner PC, Steefel CI, and Oelkers EH (1996) *Reactive transport in porous media*. *Reviews in Mineralogy* 34. Washington, DC: Mineralogical Society of America.
Lieser KH, Ament A, Hill RN, Singh U, and Thybusch B (1990) Colloids in groundwater and their influence on migration of trace elements and radionuclides. *Radiochimica Acta* 49: 83–100.
Lieser KH and Bauscher C (1988) Technetium in the hydrosphere and in the geosphere II. Influence of pH, of complexing agents, and of some minerals on the sorption of technetium. *Radiochimica Acta* 44(45): 125–128.
Lieser KH and Hill R (1992) Hydrolysis and colloid formation of thorium in water and consequences for its migration behavior: Comparison with uranium. *Radiochimica Acta* 56(1): 37–45.
Lieser KH, Hill R, Mühlenweg U, et al. (1991) Actinides in the environment. *Journal of Radioanalytical and Nuclear Chemistry* 147(1): 117–131.
Lieser KH and Mohlenweg U (1988) Neptunium in the hydrosphere and in the geosphere. *Radiochimica Acta* 43: 27–35.
Lieser KH and Peschke S (1982) The geochemistry of fission products (Cs, I, Tc, Sr, Zr, Sm). *Nuclear Energy Agency-Organisation for Economic Co-operation and Development (NEA-OECD)*, *Workshop on Geochemistry and Waste Disposal* 67–88.
Limson-Zamora M, Tracy BL, Zielinski JM, et al. (1998) Chronic ingestion of uranium in drinking water: A study of kidney bioeffects in humans. *The Journal of Toxicological Sciences* 43(1): 68–77.
Limson-Zamora M, Zielinski JM, Moodie GB, et al. (2009) Uranium in drinking water: Renal effects of long-term ingestion by an aboriginal community. *Archives of Environmental and Occupational Health* 64(4): 228–241.
Little MP (2009) Cancer and non-cancer effects in Japanese atomic bomb survivors. *Journal of Radiological Protection* 29(2A): A43–A59.
Liu Y and Van Gunten HR (1988) Migration chemistry and behavior of iodine relevant to geological disposal of radioactive wastes: A literature review with a compilation of sorption data. Paul Scherrer Institute Report No. 19.
Livens FR, Al-Bokari M, and Fomina M (2010) Microbial transformations of actinides in the environment. In: Rao L, Tobin JG, and Shuh DK (eds.) *Actinides 2009*, vol. 9, Bristol, UK: Institute of Physics Publishing Ltd.
Lloyd JR, Chenses J, Glasauer S, et al. (2002) Reduction of actinides and fission products by Fe(III)-reducing bacteria. *Geomicrobiology Journal* 19: 103–120.
Lloyd JR, Cole JA, and Macaskie LE (1997) Reduction of technetium from solution by escherichia coli. *Journal of Bacteriology* 179(6): 2014–2021.
Lloyd JR and Macaskie LE (1996) A novel phosphorimager-based technique for monitoring the microbial reduction of technetium. *Applied and Environmental Microbiology* 62(2): 578–582.
Longtin J (1991) Occurrences of radionuclides in drinking water, a national survey. Scientific background for the development of regulations for radionuclides in drinking water. In: Cothern CF and Rebers PA (eds.) *Radon, Radium and Uranium in Drinking Water*, pp. 97–140. Michigan: Lewis Publishers.
Lottermoser BG and Ashley PM (2005) Tailings dam seepage at the rehabilitated Mary Kathleen uranium mine, Australia. *Journal of Geochemical Exploration* 85: 119–137.
Lovely DR and Phillips EJP (1992) Reduction of uranium by Desulfovibrio desulfuricans. *Applied and Environmental Microbiology* 58(3): 850–856.
Lucchini JF, Borkowski M, Richmann MK, Ballard S, and Reed DT (2007) Solubility of Nd^{3+} and UO_2^{2+} in WIPP brine as oxidation-state invariant analogs for plutonium. *Journal of Alloys and Compounds* 444–445(Special Issue): 506–511.
Luckscheiter B and Kienzler B (2001) Determination of sorption isotherms for Eu, Th, U, and Am on the gel layer of corroded HLW glass. *Journal of Nuclear Materials* 298: 155–162.
Lujaniene G, Benes P, Stamberg K, et al. (2010) Effect of natural clay components on sorption of Cs, Pu and Am by the clay. *Journal of Radioanalytical and Nuclear Chemistry* 286(2): 353–359.
Lujaniene G, Motiejunas S, and Sapolaite J (2007) Sorption of Cs, Pu and Am on clay minerals. *Journal of Radioanalytical and Nuclear Chemistry* 274: 345–353.
Lyalikova NN and Khizhnyak TV (1996) Reduction of heptavalent technetium by acidophilic bacteria on the genus *Thiobacillus*. *Microbiology* 65(4): 468–473.
Macaskie LE (1991) The application of biotechnology to the treatment of wastes produced from the nuclear fuel cycle: Biodegradation and the bioaccumulation as a means of treating radionuclide-containing streams. *Critical Reviews in Biotechnology* 11(1): 41–112.
Macaskie LE, Lloyd JR, Thomas RAP, and Tolley MR (1996) The use of micro-organisms for the remediation of solutions contaminated with actinide elements, other radionuclides, and organic contaminants generated by nuclear fuel cycle activities. *Nuclear Technology* 35(4): 257–271.
Mahoney JJ and Langmuir D (1991) Adsorption of Sr on kaolinite, illite, and montmorillonite at high ionic strengths. *Radiochimica Acta* 54: 139–144.
Mangold DC and Tsang CF (1991) A summary of subsurface hydrological and hydrochemical models. *Reviews of Geophysics* 29(1): 51–79.

Mao Y, Desmeules M, Schaubel D, et al. (1995) Inorganic components of drinking water and microalbuminuria. *Environmental Research* 71(2): 135–140.
Marquardt C, Herrmann G, and Trautmann N (1996) Complexation of neptunium(V) with humic acids at very low metal concentrations. *Radiochimica Acta* 73(3): 119–125.
Marquardt C and Kim JI (1998) Complexation of Np(V) with fulvic acid. *Radiochimica Acta* 81(3): 143–148.
Martin AJ, Crusius J, McNee J, and Yanful EK (2003) The mobility of radium-226 and trace metals in pre-oxidized subaqueous uranium mill tailings. *Applied Geochemistry* 18(7): 1095–1110.
Martinez RJ, Beazley MJ, Taillefert M, et al. (2007) Aerobic uranium (VI) bioprecipitation by metal-resistant bacteria isolated from radionuclide- and metal-contaminated subsurface soils. *Environmental Microbiology* 9(12): 3122–3133.
Mays CW, Rowland RE, Stehaney AF, et al. (1985) Cancer risk from the lifetime intake of Ra and U isotopes. *Journal of Occupational Medicine* 48(5): 635–647.
McBride JP, Moore RE, Witherspoon JP, and Blanco RE (1978) Radiological impact of airborne effluents of coal and nuclear power plants. *Science* 202(4372): 1045–1050.
McCarthy JF and Zachura JM (1989) Surface transport of contaminants. *Environmental Science & Technology* 23: 496–502.
McCubbin D and Leonard KS (1997) Laboratory studies to investigate short-term oxidation and sorption behavior of neptunium in artificial and natural seawater solutions. *Marine Chemistry* 56: 107–121.
McDiarmid MA, Engelhardt SM, Dorsey CD, et al. (2009) Surveillance results of depleted uranium-exposed Gulf War I veterans: Sixteen years of follow-up. *Journal of Toxicology and Environmental Health Part A* 72(1): 14–29.
McDiarmid MA, Engelhardt SM, and Oliver M (2001) Urinary uranium concentrations in an enlarged Gulf War veteran cohort. *Health Physics* 80(3): 270–273.
McDiarmid MA, Engelhardt S, Oliver M, et al. (2004) Health effects of depleted uranium on exposed Gulf War veterans: A 10-year follow-up. *Journal of Toxicology and Environmental Health. Part A* 67(4): 277–296.
McGrail BP and Cragnolino GA (eds.) (2002) *Scientific Basis for Nuclear Waste Management XXV*. In: *Materials Research Society Symposium Proceedings*, vol. 713. Warrendale, PA: Materials Research Society.
McKinley IG and Alexander JL (1993) Assessment of radionuclide retardation: Uses and abuses of natural analogue studies. *Journal of Contaminant Hydrology* 13(1–4): 727–732.
McKinley IG and Scholtis A (1992) *A Comparison of Sorption Databases Used in Recent Performance Assessments. Radionuclide Sorption from the Safety Evaluation Perspective*. Paris: Nuclear Energy Agency-Organisation for Economic Co-operation and Development (NEA-OECD).
McKinley JP, Zachara JM, Smith SC, and Turner GD (1995) The influence of hydrolysis and multiple site-binding reactions on adsorption of U(VI) to montmorillonite. *Clays and Clay Minerals* 43(5): 586–598.
McQueen KG, Munro DC, Grey D, and Le Gleuher M (2004) Weathering-controlled fractionation of ore and pathfinder elements part II: The lag story unfolds. In: Roach IC (ed.) *Regolith*, pp. 241–246. Canberra: CRC LEME.
Medvedev ZA (1979) *Nuclear Disaster in Urals*. New York, NY: Norton.
Meece DE and Benninger LK (1993) The coprecipitation of Pu and other radionuclides with CaCO3. *Geochimica et Cosmochimica Acta* 57: 1447–1458.
Merkel BJ and Hasche-Berger A (eds.) (2008) *Uranium Mining and Hydrogeology*. Berlin: Springer.
Meyer RE, Arnold WD, Case FI, and O'Kelley GD (1991) Solubilities of Tc(IV) oxides. *Radiochimica Acta* 55: 11–18.
Meyer RE, Palmer DA, Arnold WD, and Case FI (1984) Adsorption of nuclides on hydrous oxides: Sorption isotherms on natural materials. In: Barney GS, Navratil JD, and Schultz WW (eds.) *Geochemical Behavior of Disposed Radioactive Waste*, vol. 246, ch. 5, pp 79–94.
Miekeley N, Coutinho de Jesus H, Porto da Siveira CL, and Degueldre C (1991) *Chemical and Physical Characterization of Suspended Particles and Colloids in Waters from the Osamu Utsumi and Morro de Ferro Analog Study Sites, Poco de Caldas, Brazil*. Stockholm, Sweden: SKB, SKB Technical Report 90-18.
Miller HT (1977) Radiation exposures associated with surface mining for uranium. *Health Physics* 32(6): 523–527.
Miller BG, Colvin AP, Hutchison PA, et al. (2008) A normative study of levels of uranium in the urine of British Forces personnel. *Occupational and Environmental Medicine* 65(6): 398–403.
Mills WA (1991) Analysis of the health risks from ingested radon. In: Cothern CF and Rebers PA (eds.) *Radon, Radium and Uranium in Drinking Water*, pp. 17–26. Michigan: Lewis Publishers.
Montgomery AH (1987) Adapting uranium in situ mining technology for new commercial operations: In situ leaching of uranium: Technical, environmental and economic aspects. In: *Proceedings of a Technical Committee Meeting* (November 3–6, 1987), Vienna, Austria: International Atomic Energy Agency IAEA TECDOC-492, p. 22.
Moore WS and Reid D (1973) Extraction of radium from natural waters using manganese impregnated acrylic fibers. *Deep Sea Research* 23: 647–651.
Morgenstern M, Lenze R, and Kim JI (2000) The formation of mixed-hydroxo complexes of Cm(III) and Am(III) with humic acid in the neutral pH range. *Radiochimica Acta* 88(1): 7–16.
Morss LR, Edelstein NM, and Fuger J (2007) *The Chemistry of the Actinide and Transactinide Elements*, 3rd edn. The Netherlands: Springer.
Morton LS, Evans CV, Harbottle G, and Estes GO (2001) Pedogenic fractionation and bioavailability of uranium and thorium in naturally radioactive spodosols. *Soil Science Society of America Journal* 65: 1197–1203.
Moulin V and Ouzounian G (1992) Role of colloids and humic substances in the transport of radio-elements through the geosphere. *Applied Geochemistry* 1: 179–186.
Mucciardi AN (1978) Statistical investigation of the mechanics controlling radionuclide sorption, Part II Task 4. *Second Contractor Information Meeting* II: pp. 333–425. Richland, WA: Battelle Northwest Laboratory.
Mucciardi AN and Orr EC (1977) Statistical investigation of the mechanics controlling radionuclide sorption. *Waste Isolation Safety Assessment Program, Task 4, Contractor Information Meeting*, pp. 151–188. Richland, WA: Battelle Northwest Laboratory.
Mudd GM (1998) An environmental critique of in situ leach uranium mining: The case against uranium solution mining, Summer 1997. Research Report: Melbourne.
Mudd GM (2001a) Critical review of acid in situ leach uranium mining: 1. USA and Australia. *Environmental Geology* 41(3–4): 390–403.
Mudd GM (2001b) Critical review of acid in situ leach uranium mining: 2. Soviet Block and Asia. *Environmental Geology* 41(3–4): 404–416.
Muramatsu Y, Uchida S, Sriyotha P, and Sriyotha K (1990) Some considerations on the sorption and desorption phenomena of iodide and iodate on soil. *Water, Air, and Soil Pollution* 49(1–2): 125–138.
Murphy WM (1999) Natural analogs and performance assessment for geologic disposal of nuclear waste. In: Smith RW and Shoesmith DW (eds.) *Scientific Basis for Nuclear Waste Management XXIII. Materials Research Society Symposium Proceedings*, vol. 608, pp. 533–544. Warrendale, PA: Materials Research Society.
Murphy WM and Grambow B (2008) Thermodynamic interpretation of neptunium coprecipitation in uranophane for application to the Yucca Mountain repository. *Radiochimica Acta* 96(9–11): 563–567.
Murphy WH and Shock EL (1999) Environmental aqueous geochemistry of actinides. *Reviews in Mineralogy* 38: 221–253.
Murray RL (1994) *Understanding Radioactive Waste*, 4th edn. Columbus, OH: Batelle Pacific Northwest Laboratories, Battelle Press.
NAS (1988a) *Health Risks of Radon and Other Internally Deposited Alpha Emitters. National Academy of Sciences Report BEIR IV*. Washington, DC: Committee on the Biological Effects of Ionizing Radiations National Research Council National Academy Press.
NAS (1988b) *The Effects of Exposure to Low Levels of Ionizing Radiation. National Academy of Sciences Report BEIR V*. Washington, DC: Committee on the Biological Effects of Ionizing Radiations, National Research Council. National Academy Press.
NAS (1996) *The Waste Isolation Pilot Plant: A Potential Solution for the Disposal of Transuranic Waste*. pp. 6, 79–80. Washington, DC: National Academy Press.
NAS (1998) *Health Effects of Exposure to Radon. National Academy of Sciences Report BEIR VI*. Washington, DC: National Academy Press.
NAS (1999a) *Health Effects of Exposure to Radon. National Academy of Sciences Report BEIR VI*. Washington, DC: National Academy Press.
NAS (1999b) *Evaluation of Guidelines for Exposures to Technologically Enhanced Naturally Occurring Radioactive Materials*. Washington, DC: Committee on Evaluation of EPA Guidelines for Exposure to Naturally Occurring Radioactive Materials, National Research Council; National Academy Press, National Academy of Sciences.
NAS (2006) *Health Effects of Exposure to Low Levels of Ionizing Radiation: Phase 2. National Academy of Sciences Report BEIR VII*. Washington, DC: Committee on the Biological Effects of Ionizing Radiations National Research Council National Academy Press.
NAS (2009) *Cleaning Up Sites Contaminated with Radioactive Materials: International Workshop Proceedings*. ISBN: 0-309-12762-9. http://www.nap.edu/catalog/12505.html (accessed on 10 July 2011). Committee on Cleaning Up of Radioactive Contamination: Russian Challenges and U.S. Experience, Office for Central Europe and Asia, Russian Academy of Sciences and National Research Council, pp. 234.
NAS (2011) *Analysis of Cancer Risks in Populations Near Nuclear Facilities: Phase 1*. National Academy of Sciences. http://dels.nas.edu/global/nrsb/CancerRisk.
Nash KL and Choppin GR (1980) Interaction of humic and fulvic acids with Th(IV). *Journal of Inorganic and Nuclear Chemistry* 42: 1045–1050.

National Research Council (2001) *Science and Technology for Environmental Cleanup at Hanford*. Washington, DC: National Academy Press.

NCI (1991) *No Excess Mortality Risk Found in Counties with Nuclear Facilities*. National Cancer Institute. http://www.cancer.gov/cancertopics/factsheet/Risk/nuclear-facilities.

NCRP (1975) *Natural Background Radiation in the United States*. Bethesda, MD: National Council on Radiation Protection and Measurements. NCRP Report No. 45, pp. 4–6.

NCRP (1984) *Exposures from the Uranium Series with Emphasis on Radon and Its Daughter*. Bethesda, MD: National Council on Radiation Protection and Measurements. NCRP Report No. 77.

NCRP (1993) *Limitation of Exposure to Ionizing Radiation*. Bethesda, MD: National Council on Radiation Protection and Measurements. NCRP Report No. 116.

NEA (1991) *Disposal of Radioactive Waste: Review of Safety Assessment Methods*. Paris: Nuclear Energy Agency 73.

NEA (1996) *Survey of Thermodynamic and Kinetic Data Bases [Online]*. Nuclear Science Committee, Nuclear Energy Agency Available: http://www.nea.fr/html/science/chemistry/tdbsurvey.html.

NEA (2001) Using thermodynamic sorption models for guiding radioelement distribution coefficient (K_d) investigations. A status report. *Radioactive Waste Management*, p. 194.

Neck V, Altmaier M, Muller R, et al. (2003) Solubility of crystalline thorium dioxide. *Radiochimica Acta* 91(5): 253–262.

Neck V, Altmaier M, Seibert A, et al. (2007) Solubility and redox reactions of Pu(IV) hydrous oxide: Evidence for the formation of $PuO_{2+x(s,hyd)}$. *Radiochimica Acta* 95(4): 193–207.

Neck V and Kim JL (2001) Solubility and hydrolysis of tetravalent actinides. *Radiochimica Acta* 89(1): 1–16.

Neiss J, Stewart BD, Nico PS, and Fendorf S (2007) Speciation-dependent microbial reduction of uranium within iron-coated sands. *Environmental Science & Technology* 41(21): 7343–7348.

Neretnieks I and Rasmuson A (1984) An approach to modeling radionuclide migration in a medium with strongly varying velocity and block sizes along the flow path. *Water Resources Research* 20(12): 1823–1836.

Nico PS, Stewart BD, and Fendorf S (2009) Incorporation of oxidized uranium into Fe (hydr)oxides during Fe(II) catalyzed remineralization. *Environmental Science & Technology* 43(19): 7391–7396.

Nigbor MT, Engelmann WH, and Tweeton DR (1982) Case history of a pilot-scale acidic in situ uranium leaching experiment. *Report of Investigations 8652*. U.S. Bureau of Mines, p. 81.

NIH (1994) *Radon and Lung Cancer Risk: A Joint Analysis of 11 Underground Miner Studies*. Bethesda, MD: National Institutes of Health, U.S. Department of Health and Human Services.

NIOSH (1997) *NIOSH Pocket Guide to Chemical Hazards*. Public Health Services. Centers for Disease Control and Prevention. National Institute for Occupational Safety and Health. U.S. Department of Health and Human Services.

Nisbet AF, Mocanu N, and Shaw S (1994) Laboratory investigation into the potential effectiveness of soil-based countermeasures for soils contaminated with radiocaesium and radiostrontium. *The Science of the Total Environment* 149(3): 145–154.

Nitsche H (1991) Solubility studies of transuranium elements for nuclear waste-disposal: Principles and overview. *Radiochimica Acta* 52–53: 3–8.

Nitsche H, Gatti RC, Standifer EM, et al. (1993) *Measured solubilities and speciations of Neptunium, Plutonium and Americium in a typical groundwater (J-13) from the Yucca Mountain region*. Los Alamos National Laboratory.

Nitsche H, Roberts K, Gatti RC, et al. (1992) *Plutonium Solubility and Speciation Studies in a Simulant of Air Intake Shaft Water from the Culebra Dolomite at the Waste Isolation Pilot Plant*. Albuquerque: Sandia National Laboratories.

Nitsche H, et al. (1995) *Solubility and Speciation Results from Over- and Undersaturation Experiments on Np, Pu, and Am in Water from Yucca Mountain Region Well UE-25p#1*. Los Alamos, NM: Los Alamos National Laboratories.

NMHED (1989) *Summary Report on the Church Rock Uranium Mill Tailings Spill: A Health and Environment Assessment*. Santa Fe, NM: New Mexico Health and Environment Department.

Nordstrom DK, Ball JW, Donahoe RJ, and Whittemore D (1989) Groundwater chemistry and water-rock interactions at Stripa. *Geochimica et Cosmochimica Acta* 53: 1727–1740.

Noubactep C (2010) The fundamental mechanism of aqueous contaminant removal by metallic iron. *Water South Africa* 36(5): 663–670.

Novak CF, Moore RC, and Bynum RV (1996) Prediction of dissolved actinide concentrations in concentrated electrolyte solutions: A conceptual model and model results for the Waste Isolation Pilot Plant (WIPP). *International Conference on Deep Geological Disposal of Radioactive Waste*, vol. 5, pp. 83–92. Albuquerque, NM: Sandia National Laboratories.

Novikov AP, Kalmykov SN, Utsunomiya S, et al. (2006) Colloid transport of plutonium in the far-field of the Mayak Production Association, Russia. *Science* 314: 638–641.

NRC (1983) Title 10 – CFR Part 60 – Disposal of high-level radioactive wastes in geologic repositories: Technical criteria: Final rule. *Federal Register* 48(120).

NRC (1995) *Technical Bases for Yucca Mountain Standards*, 205 pp. Washington, DC: National Research Council.

NRC (2002) *107th Congress 1st Session*. Washington, DC: U.S. Nuclear Regulatory Commission NUREG 0980 Vol. 1 No. 6.

Nuttall HE, Jain R, and Fertelli Y (1991) Radiocolloid transport in saturated and unsaturated fractures. In: *2nd Annual International Conference on High Level Radioactive Waste Management, Las Vegas, NV* pp. 189–196.

NYSDOH (2009) *Comments, July 21, 2009, Supplemental Generic Environmental Statement on the Oil and Gas Regulatory Program Well Permit Issuance for Horizontal Drilling and Hydraulic-Fracturing To Develop the Marcellus Shale and Other Low Permeability Gas Reservoirs*. Troy, NY: New York State Department of Health, Bureau of Environmental Radiation Protection New York State Dept of Health.

Oeh U, Li WB, Hollriegl V, et al. (2007) Daily uranium excretion in German peacekeeping personnel serving on the Balkans compared to ICRP model prediction. *Radiation Protection Dosimetry* 127(1–4): 329–332.

Oeh U, Priest ND, Roth P, et al. (2007) Measurements of daily urinary uranium excretion in German peacekeeping personnel and residents of the Kosovo region to assess potential intakes of depleted uranium (DU). *The Science of the Total Environment* 381(1–3): 77–87.

Ogard AE and Kerrisk JF (1984) *Groundwater Chemistry Along the Flow Path Between a Proposed Repository Site and the Accessible Environment*. Los Alamos, NM: Los Alamos National Laboratory LA-101188-MS.

Ohanian EV (1989) *National Primary Drinking Water Regulations for Radionuclides. Safe Drinking Water Act: Amendments, Regulations and Standards*, pp. 45–55.

Ohnuki T and Kozai N (1994) Sorption characteristics of radioactive cesium and strontium. *Radiochimica Acta* 66/67: 327–331.

Ohnuki T, Kozai N, Samadfam M, et al. (2004) The formation of autunite (Ca $(UO_2)_2(PO_4)_2{\cdot}nH_2O$) within the leached layer of dissolving apatite: Incorporation mechanism of uranium by apatite. *Chemical Geology* 211(1–2): 1–14.

Ohnuki T, Yoshida T, Ozaki T, et al. (2007) Chemical speciation and association of plutonium with bacteria, kaolinite clay, and their mixture. *Environmental Science & Technology* 41(9): 3134–3139.

Olofsson U and Allard B (Directors) (1983) *Complexes of Actinides with Naturally Occurring Organic Substances, Literature Survey Technical*. KBS Report. Stockholm, Sweden.

O'Loughlin EJ, Kelly SD, Cook RE, Csencsits R, and Kemner KM (2003) Reduction of uranium(VI) by mixed iron(II)/iron(III) hydroxide (green rust): Formation of UO_2 nanoparticles. *Environmental Science & Technology* 37(4): 721–727.

Olsson M, Glänneskog H, Jakobsson A-M, Nilsson H, and Albinsson Y (2005) Sorption of trivalent plutonium onto UO_2 and the effect of the solid phase on the Pu oxidation state. *Radiochimica Acta* 93: 341–346.

Orloff KG, Mistry K, Charp P, et al. (2004) Human exposure to uranium in groundwater. *Environmental Research* 94(3): 319–326.

Osborn S, Vengosh A, Warner NR, and Jackson RB (2011) Methane contamination of drinking water accompanying gas-well drilling and hydraulic fracturing. *Proceedings of the National Academy of Sciences* 108(20): 8172–8176.

Osmond JK and Cowart JB (1976) The theory and uses of natural uranium isotopic variations in hydrology. *Atomic Energy Review* 14(621–679).

Osthols E (1995) Thorium sorption on amorphous silica. *Geochimica et Cosmochimica Acta* 59(7): 1235–1249.

Östhols E, Bruno J, and Grenthe I (1994) On the influence of carbonate on mineral dissolution: III. The solubility of microcrystalline ThO_2 in CO_2–H_2O media. *Geochimica et Cosmochimica Acta* 58(2): 613–623.

Oughton DH, Salbu B, Brand TL, Day JP, and Aarkrog A (1993) Underdetermination of Strontium-90 in soils containing particles of irradiated uranium oxide fuel. *Analyst* 118(9): 1101–1105.

Pabalan RT and Turner DR (1997) Uranium(6+) sorption on montmorillonite: Experimental and surface complexation modeling study. *Aquatic Geochemistry* 2(3): 203–226.

Pabalan RT, Turner DR, Bertetti FP, and Prikryl JD (eds.) (1998) *Uranium(VI) Sorption onto Selected Mineral Surfaces: Key Geochemical Parameters*. San Diego, CA: Academic Press.

Painter S, Cvetkovic V, Pickett D, and Turner DR (2002) Significance of kinetics for sorption on inorganic colloids: Modeling and experiment interpretation issues. *Environmental Science & Technology* 36(24): 5369–5375.

Panak PJ and Nitsche H (2001) Interaction of aerobic soil bacteria with plutonium(VI). *Radiochimica Acta* 89(8): 499–504.

Panin AV, Walling DE, and Golosov VN (2001) The role of soil erosion and fluvial processes in the post-fallout redistribution of Chernobyl-derived caesium-137: A case study of the Lapki Catchment, central Russia. *Geomorphology* 40(3–4): 185–204.

Papelis C, Hayes KF, and Leckie JO (1988) *HYDRAQL: A Program for the Computation of Chemical Equilibrium Composition of Aqueous Batch Systems Including Surface-Complexation Modeling of Ion Absorption Solution Oxide/Solution Interface*. Stanford, CA: Environmental Engineering and Science, Dept. of Civil Engineering, Stanford University.

Park S-W, Leckie JO, and Siegel MD (1992) *Surface Complexation Modeling of Uranyl Adsorption on Corrensite from the Waste Isolation Pilot Plant Site*. Albuquerque, NM: Sandia National Laboratories.

Parkhurst DL (1995) *User's Guide to PHREEQC, a Computer Model for Speciation, Reaction-Path, Advective-Transport and Inverse Geochemical Calculations*. Reston, VA: U.S. Geological Survey (U.S. Geological Survey Water-Resources Investigations Report 95-4227).

Parkhurst MA and Guilmette RA (2009) Overview of the Capstone depleted uranium study of aerosols from impact with armored vehicles: Test setup and aerosol generation, characterization, and application in assessing dose and risk. *Health Physics* 96(3): 207–220.

Parsa B (1998) Contribution of short-lived radionuclides to alpha-particle radioactivity in drinking water and their impact on the Safe Drinking Water Act Regulations. *Radioactivity and Radiochemistry* 9: 41–50.

Payne TE, Davis JA, and Waite TD (1994) Uranium retention by weathered schists – The role of iron minerals. *Radiochimica Acta* 66(67): 297–303.

Payne TE, Edis R, and Seo T (1992) Radionuclide transport by groundwater colloids at the Koongarra Uranium Deposit. In: Sombret CG (ed.) *Scientific Basis for Nuclear Waste Management XV*. *Materials Research Society Symposium Proceedings*, vol. 257, pp. 481–488. Pittsburgh, PA: Materials Research Society.

Payne TE, Fenton BR, and Waite TD (2001) Comparison of "in-situ distribution coefficients" with experimental R_d values for uranium(VI) in the Koongarra Weathered Zone. In: Davis JA (ed.) *Surface Complexation Modeling Uranium(VI) Adsorption on Natural Mineral Assemblages*, pp. 133–142. Washington, DC: U.S. Nuclear Regulatory Commission.

Pearcy E, Prikryl JD, Murphy WM, and Leslie BW (1994) Alteration of uraninite from the Nopal I deposit, Pena Blanca District, Chihuahua, Mexico, compared to degradation of spent nuclear fuel in the proposed U.S. high-level nuclear waste repository at Yucca Mountain, Nevada. *Applied Geochemistry* 9: 713–732.

Pedersen K (1996) Investigations of subterranean bacteria in deep crystalline bedrock and their importance for the disposal of nuclear waste. *Canadian Journal of Microbiology* 42(4): 382–400.

Pelizza M (2006) Modern in situ uranium recovery technology assures no adverse impacts on adjacent aquifer uses. In: *Gulf Coast Association of Geologic Societies 2007, Annual Convention*, 21–23 October 2007.

Pelizza M (2007) Modern in situ uranium recovery technology assures no adverse impacts on adjacent aquifer uses. In: *Gulf Coast Association of Geologic Societies 2007, Annual Convention*, 21–23 October 2007.

Pelizza MS (2008) In situ recovery of uranium. *Southwest Hydrology* 7(6): 28–29 34.

Penrose WR, Polzer WL, Essington EH, Nelson DM, and Orlandini KA (1990) Mobility of plutonium and americium through a shallow aquifer in a semiarid region. *Environmental Science & Technology* 24: 228–234.

Perfect DL, Faunt CC, Steinkampf WC, and Turner AK (1995) *Hydrochemical Database for the Death Valley Region, Nevada and California*. Denver, CO: U.S. Geological Survey U.S. Geological Survey Open-File Report 94-305.

Petropoulos NP, Anagnostakis MJ, Hinis EP, and Simopoulos SE (2001) Geographical mapping and associated fractal analysis of the long-lived Chernobyl fallout radionuclides in Greece. *Journal of Environmental Radioactivity* 53(1): 59–66.

Petryaev EP, Ovsyannikova SV, Rubinchik S, Lubkina IJ, and Sokolik GA (1991) Condition of Chernobyl fallout radionuclides in the soils of Belorussia. Proceedings of AS of Byelorussian Soviet Socialist Republic (BSSR). *Physico-Energentical Sciences* 4: 48–55.

Phillips SL, Hale FV, Silvester LF, and Siegel MD (1988) *Thermodynamic Tables for Nuclear Waste Isolation*. *Aqueous Solutions Database*, vol 1. Albuquerque, NM: Sandia National Laboratories.

Pinney SM, Freyberg RW, Levine GE, et al. (2003) Health effects in community residents near a uranium plant at Fernald, Ohio, USA. *Inernational Journal of Occupational Medicine and Environmental Health* 16(2): 139–153.

Pitzer KS (1987) A thermodynamic model for aqueous solutions of liquid-like density. *Thermodynamic Modeling of Geological Materials: Minerals, Fluids, and Melts* 17(1): 97–142.

Pitzer KS (2000) *Activity Coefficients in Electrolyte Solutions*, 2nd edn. Boca Raton, FL: CRC Press.

Plant J, Simpson PR, Smith B, and Windley BF (1999) Uranium ore deposits: Products of the radioactive Earth. *Reviews in Mineralogy and Geochemistry* 38(1): 255–319.

Polednak AP and Frome EL (1981) Mortality among men employed between 1943 and 1947 at a uranium-processing plant. *Journal of Occupational Medicine* 23(3): 169–178.

Pourcelot L and Gauthier-Lafaye F (1999) Hydrothermal and supergene clays of the Oklo natural reactors: Conditions of radionuclide release, migration and retention. *Chemical Geology* 157(1–2): 155–174.

Powell BA, Dai Z, Zavarin M, Zhao P, and Kersting AB (2011) Stabilization of plutonium nano-colloids by epitaxial distortion on mineral surfaces. *Environmental Science & Technology* 45: 2698–2703.

Powell BA, Fjeld RA, Kaplan DI, Coates JT, and Serkiz SM (2005) $Pu(V)0_2^+$ adsorption and reduction by synthetic hematite and goethite. *Environmental Science & Technology* 39(7): 2107–2114.

Prabhavathi PA, Padmavathi P, and Reddy PP (2003) Chromosomal aberrations in the leucocytes of men occupationally exposed to uranyl compounds. *Bulletin of Environmental Contamination and Toxicology* 70(2): 322–327.

Prasad A, Redden G, and Leckie JO (1997) *Radionuclide Interactions at Mineral/Solution Interfaces in the WIPP Site Subsurface Environment*. Albuquerque, NM: Sandia National Laboratories.

Prat O, Vercouter T, Ansoborlo E, et al. (2009) Uranium speciation in drinking water from drilled wells in southern Finland and its potential links to health effects. *Environmental Science & Technology* 43(10): 3941–3946.

Prikryl JD, Jain A, Turner DR, and Pabalan RT (2001) $Uranium^{VI}$ sorption behavior on silicate mineral mixtures. *Journal of Contaminant Hydrology* 47(2–4): 241–253.

Puskin JS and Nelson CB (1989) Perspective on risks from residential radon exposure. *Journal of the Air Pollution Control Association* 39: 915–920.

Quigley MS, Honeyman BD, and Santschi PH (1996) Thorium sorption in the marine environment: Equilibrium partitioning at the hematite/water interface, sorption/desorption kinetics and particle tracing. *Aquatic Geochemistry* 1: 277–301.

Raabe OG, Book SA, and Parks NJ (1980) Bone cancer from radium: Canine dose response explains data for mice and humans. *Science* 208: 61–64.

Rädlinger G and Heumann KG (2000) Transformation of iodide in natural and wastewater systems by fixation on humic substances. *Environmental Science & Technology* 34(18): 3932–3936.

Rai D, Felmy AR, Hess HJ, and Moore DA (1998) A thermodynamic model of solubility of UO_2(am) in the aqueous K^+–Na^+–HCO_3^-–CO_3^{2-}–OH^-–H_20 system. *Radiochimica Acta* 82: 17–25.

Rai D, Felmy AR, and Ryan JL (1990) Uranium(VI) hydrolysis constants and solubility product of $UO_2{\cdot}xH_2O$(am). *Inorganic Chemistry* 29: 260–264.

Rai D, Felmy AR, Sterner SM, et al. (1997) The solubility of Th(IV) and U(IV) hydrous oxides in concentrated NaCl and $MgCl_2$ solutions. *Radiochimica Acta* 79(4): 239–247.

Rai D, Serne RJ, and Moore DA (1980) Solubility of plutonium compounds and their behavior in soils. *Soil Science Society of America Journal* 44(3): 490–495.

Ranville JF, Hendry MJ, Reszat TN, Xie Q, and Honeyman BD (2007) Quantifying uranium complexation by groundwater dissolved organic carbon using asymmetrical flow field-flow fractionation. *Journal of Contaminant Hydrology* 91: 233–246.

Rao L and Choppin GR (1995) Thermodynamic study of the complexation of neptunium(V) with humic acids. *Radiochimica Acta* 69(2): 87–95.

Rard JA (1983) *Critical Review of the Chemistry and Thermodynamics of Technetium and Some of its Inorganic Compounds and Aqueous Species*. Livermore, CA: Lawrence Livermore National Laboratory, University of California.

Rard JA, Rand MH, Anderegg G, and Wanner H (1999) *Chemical Thermodynamics of Technetium*. Amsterdam: North-Holland.

Read D, Hooker PJ, Ivanovich M, and Milodowski AE (1991) A natural analogue study of an abandoned uranium mine in Cornwall, England. *Radiochimica Acta* 52(53): 349–356.

Rechard RP (1996) *An Introduction to the Mechanics of Performance Assessment Using Examples of Calculations Done for the Waste Isolation Pilot Plant Between 1990 and 1992*, p. 286. Albuquerque NM: Sandia National Laboratories.

Rechard RP (2002) General approach used in the performance assessment for the Waste Isolation Pilot Plant. In: McGrail BP and Cragnolino GA (eds.) *Scientific Basis for Nuclear Waste Management XXV*. *Materials Research Society Symposium Proceedings*, vol. 713, pp. 213–228. Warrendale, PA: Materials Research Society.

Redden GD, Li J, and Leckie JO (1998) Adsorption of U(VI) and citric acid on goethite, gibbsite, and kaolinite. In: Jenne EA (ed.) *Adsorption of Metals by Geomedia*, pp. 291–315. San Diego, CA: Academic Press.

Redkin AF and Wood SA (2007) Uranium(VI) in aqueous solutions at 25°C and a pressure of 1 bar: Insight from experiments and calculations. *Geochemistry International* 45(11): 1111–1123.

Reed DT, Wygmans DG, and Richman MK (1996) *Actinide Stability/Solubility in Simulated WIPP Brines: Interim Report Under SNL WIPP Contract AP-2267*. Albuquerque, NM: Sandia National Laboratories.

Reeder RJ, Nugent M, Tait CD, et al. (2001) Coprecipitation of uranium(VI) with calcite: XAFS, micro-XAS, and luminescence characterization. *Geochimica et Cosmochimica Acta* 65(20): 3491–3503.

Rees TF, Cleveland JM, and Nash KL (1983) The effect of composition of selected groundwaters from the basin and range province on plutonium, neptunium, and americium speciation. *Nuclear Technology* 65(1): 131–137.

Reif RH (1994) Evaluation of in vitro dissolution rates of thorium in uranium mill tailings. *Health Physics* 67: 545–547.

Relyea JF (1982) Theoretical and experimental considerations for the use of the column method for determining retardation factors. *Radioactive Waste Management and the Nuclear Fuel Cycle* 3(3): 151–166.

Renshaw JC, Law N, Geissler A, Livens FR, and Lloyd JR (2009) Impact of the Fe(III)-reducing bacteria Geobacter sulfurreducens and Shewanella oneidensis on the speciation of plutonium. *Biogeochemistry* 94(2): 191–196.

Robinson P, Shuey C, and Morgan R (1995) *Uranium Mining in Navajo Ground Water: The risks outweigh the benefits*. 28 February 1995. Comments on the draft environmental impact statement to construct and operate the Crownpoint Uranium Solution Mining Project, New Mexico: Southwest Research and Information Center, p. 28. Plus appendices.

Roh Y, Lee SY, Elless MP, and Foss JE (2000) Incorporation of radioactive contaminants into pyroaurite-like phases by electrochemical synthesis. *Clays and Clay Minerals* 48(2): 266–271.

Rosén K, Öborn I, and Lönsjö H (1999) Migration of radiocaesium in Swedish soil profiles after the Chernobyl accident, 1987–1995. *Journal of Environmental Radioactivity* 46(1): 45–66.

Rousseau G, Fattahi M, Grambow B, Boucher F, and Ouvrard G (2002) Coprecipitation of thorium with UO_2. *Radiochimica Acta* 90(9–11): 523–527.

Rozhdestvensky LM (2004) Analysis of epidemiological data on radiocarcinogenic effects and approaches to determining the low-dose upper limit in terms of existence of biologically harmful effect threshold of ionizing radiation. In: Burlakova EB and Naidich VI (eds.) *The Effects of Low Dose Radiation: New Aspects of Radiobiological Research Prompted by the Chernobyl Nuclear Disaster*, pp. 290–325. Boston, MA: VSP.

Rowland RE, Stehney AF, and Lucas HF (1978) Dose-response relationships for female radium dial painters. *Radiation Research* 76: 368–383.

Rühm W, Kammerer L, Hiersche L, and Wirth E (1996) Migration of ^{137}Cs and ^{134}Cs in different forest soil layers. *Journal of Environmental Radioactivity* 33(1): 63–75.

Runde W (2002) Geochemical interactions of actinides in the environments. In: Zhang P and Brady P (eds.) *Geochemistry of Soil Radionuclides*, pp. 21–44. Madison, WI: Soil Science Society of America.

Runde W, Conradson SD, Efurd W, et al. (2002) Solubility and sorption of redox-sensitive radionuclides (Np, Pu) in J-13 water from Yucca Mountain site: Comparison between experiment and theory. *Applied Geochemistry* 17(6): 837–853.

Runde W, Neu MP, Condrdson SD, et al. (2002) Geochemical speciation of radionuclides in soil and solution. In: Zhang P and Brady P (eds.) *Geochemistry of Soil Radionuclides*, pp. 45–60. Madison, WI: Soil Science Society of America.

Runde W, Neu MP, and Reilly SD (eds.) (1999) *Actinyl(VI) Carbonates in Concentrated Sodium Chloride Solutions: Characterization, Solubility, and Stability*. New York, NY: Kluwer Academic/Plenum Press.

Ryan JN and Elimelech M (1996) Colloid mobilization and transport in groundwater. *Colloids and Surfaces A: Physicochemical and Engineering Aspects* 107: 1–56.

Salbu B, Krekling T, Oughton DH, et al. (1994) Hot particles in accidental releases from Chernobyl and windscale nuclear installations. *Analyst* 119(1): 125–130.

Samper J, Yang C, and Zheng L (eds.) (2011) *CORE^{2D} V4: A Code for Water Flow, Heat and Solute Transport, Geochemical Reactions, and Microbial Processes*. Bentham Science.

Sanchez AL, Murray JW, and Sibley TH (1985) The adsorption of plutonium IV and V on goethite. *Geochimica et Cosmochimica Acta* 49(11): 2297–2307.

Santschi PH and Honeyman BD (1989) Radionuclides in aquatic environments. *Radiation Physics and Chemistry* 34(2): 213–240.

Sassani DC, Van Luik A, and Summerson J (2006) Neptunium solubility in the near-field environment of a proposed Yucca Mountain Repository. In: Vaniseghem P (ed.) *Scientific Basis for Nuclear Waste Management XXIX*. *Materials Research Society Symposium Proceedings*, vol. 932, pp. 991–998. Warrendale, PA: Materials Research Society.

Scatchard G (1936) Concentrated solutions of strong electrolytes. *Chemical Reviews, American Chemical Society* 19(3): 309–327.

Schafer T, Artinger R, Dardenne K, et al. (2003) Colloid-borne Americium migration in gorleben groundwater: Significance of iron secondary phase transformation. *Environmental Science & Technology* 37(8): 1528–1534.

Schippers A, Hallmann R, Wentzien S, and Sand W (1995) Microbial diversity in uranium-mine waste heaps. *Applied and Environmental Microbiology* 61: 2930–2935.

Schoeppner J (2008) Remediation from uranium mining in New Mexico. *Southwest Hydrology* 7(6): 22–23.

Schramke JA, Dhanpat R, Fulton RW, and Choppin GR (1988) Determination of aqueous plutonium oxidation states by solvent extractions. *Journal of Radioanalytical and Nuclear Chemistry* 130(2): 333–346.

Scott LM, Bahler KW, De La Garza A, et al. (1972) Mortality experience of uranium and nonuranium workers. *Health Physics* 23: 555–557.

Seaborg GT and Katz JJ (1954) *The Actinide Elements*. New York: McGraw-Hill.

Selden AI, Lundholm C, Edlund B, et al. (2009) Nephrotoxicity of uranium in drinking water from private drilled wells. *Environmental Research* 109(4): 486–494.

Senko JM, Istok JD, Suflita JM, and Krumholz LR (2002) In-situ evidence for uranium immobilization and remobilization. *Environmental Science & Technology* 36(7): 1491–1496.

Serne RJ, Arthur RC, and Krupka KM (1990) *Review of Geochemical Processes and Codes for Assessment of Radionuclide Migration Potential at Commercial LLW Sites*. Richland, WA: Division of Low-Level Waste Management and Decommissioning Office of Nuclear Regulatory Commission.

Serne RJ and Gore VL (1996) *Strontium-90 Adsorption-Desorption Properties and Sediment Characterization at the 100 N-area*. Richland, WA: Pacific Northwest National Laboratory.

Serne RJ and Muller AB (1987) A perspective on adsorption of radionuclide on to geologic media. In: Brookins DG (ed.) *The Geological Disposal of High Level Radioactive Wastes*, pp. 407–443. Athens, Greece: Theophrastus.

Shanbhag PM and Morse JW (1982) Americium interaction with calcite and aragonite surfaces in seawater. *Geochimica et Cosmochimica Acta* 46: 241–246.

Shleien B, Slaback LA Jr., and Birky BK (1998) *Handbook of Health Physics and Radiological Health*. Baltimore, MD: Williams and Wilkins. ISBN: 0-683-18334-6.

Siegel MD and Bryan CR (2003) Environmental geochemistry of radioactive contamination. In: Holland HD and Turekain KK (eds.) *Environmental Geochemistry, Treatise on Geochemistry*, vol. 9, pp. 205–262. Oxford: Elsevier.

Siegel MD, Chu MS, and Pepping RE (1983a) Compliance assessments of hypothetical geological nuclear waste isolation systems with the draft EPA standard. In: Brookins DG (ed.) *Scientific Basis for Nuclear Waste Management VI*, pp. 497–506. Amsterdam: Elsevier.

Siegel MD, Chu MS, and Pepping RE (1983b) Compliance assessments of hypothetical geological nuclear waste isolation systems with the Draft EPA Standard. In: Brookins DG (ed.) *Scientific Basis for Nuclear Waste Management VI*. *Material Research Society Symposium, Proceedings*, vol. 15. Elsevier.

Siegel MD and Erickson KL (1984) Radionuclide releases from a hypothetical nuclear waste repository: Potential violations of the proposed EPA standard by radionuclides with multiple aqueous species. In: Post RG (ed.) *Waste Management '84*, vol. 1, pp. 541–546. University of Arizona.

Siegel MD and Erickson KL (1986) Geochemical sensitivity analysis for performance assessment of HLW repositories: Effects of speciation and matrix diffusion. In: *Symposium on Groundwater Flow and Transport Modeling for Performance Assessment of Deep Geologic Disposal of Radioactive Waste: A Critical Evaluation of the State of the Art*, pp. 467–490.

Siegel MD, Holland HD, and Feake C (1992) Geochemistry. In: Hunter RL and Mann CJ (eds.) *Techniques for Determining Probabilities of Geologic Events and Processes*. *Studies in Mathematical Geology*, vol. 4, pp. 185–206. New York, NY: Oxford University Press.

Siegel MD, Ward DB, Bryan CR, and Cheng WC (1995a) *Characterization of Materials for a Reactive Transport Model Validation Experiment*. Albuquerque, NM: Sandia National Laboratories.

Siegel MD, Ward DB, Bryan CR, and Cheng WC (1995b) *Batch and Column Studies of Adsorption of Li, Ni, and Br by a Reference Sand for Contaminant Transport Experiments*. Albuquerque, NM: Sandia National Laboratories.

Silva RJ, Bidoglio G, Rand MH, et al. (1995) *Chemical Thermodynamics of Americium*. New York: Elsevier.

Silva RJ and Nitsche H (1995) Actinide environmental chemistry. *Radiochimica Acta* 70(71): 377–396.

Simmons AM and Stuckless JS (2010) *Analogues to Features and Processes of a High-Level Radioactive Waste Repository Proposed for Yucca Mountain, Nevada*. Professional Paper 1779, p. 195. U.S. Geological Survey.

Sims R, Lawless RA, Alexander JL, Bennett DG, and Read D (1996) Uranium migration through intact sandstone: Effect of pollutant concentration and the reversibility of uptake. *Journal of Contaminant Hydrology* 21(1–4): 215–228.

Singer DM, Farges F, and Brown GE (2007) Biogenic UO_2 – Characterization and surface reactivity. In: Hedman B and Painetta P (eds.) *X-Ray Absorption Fine*

Structure-XAFS13, vol. 882, pp. 277–279. Melville, NY: American Institute of Physics.

SKI (1991) *SKI Project Summary*. SKB Technical Report 91–23. Stockholm, Sweden

Slezak J (1997) National experience on groundwater contamination associated with uranium mining and milling in the Czech Republic. In: *IAEA Advisory Group Meeting on Technical Options for Clean-up of Radioactively Contaminated Groundwater*.

Smith JT and Comans RNJ (1996) Modelling the diffusive transport and remobilisation of ^{137}Cs in sediments: The effects of sorption kinetics and reversibility. *Geochimica et Cosmochimica Acta* 60(6): 995–1004.

Smith JT, Comans RNJ, and Elder DG (1999) Radiocaesium removal from European lakes and reservoirs: Key processes determined from 16 Chernobyl-contaminated lakes. *Water Research* 33(18): 3762–3774.

Smith PA and Degueldre C (1993) Colloid-facilitated transport of radionuclides through fractured media. *Journal of Contaminant Hydrology* 13: 143–166.

Smith K, Kroeker S, Uberuaga B, and Wittle K (2010) *Scientific Basis for Nuclear Waste Management XXXIV. Materials Research Society Symposium Proceedings,* vol. 1265. San Francisco, CA: Cambridge University Press.

SNL (2007a) *Dissolved Concentration Limits of Elements with Radioactive Isotopes*. Las Vegas, NV: Sandia National Laboratories ANL-WIS-MD-000010 REV 06.

SNL (2007b) *EBS Radionuclide Transport Abstraction*. Las Vegas, NV: Sandia National Laboratories ANL-WIS-PA-000001 REV 03.

Sokolik GA, Ivanova TG, Leinova SL, Ovsiannikova SV, and Kimlenko IM (2001) Migration ability of radionuclides in soil-vegetative cover of Belarus after Chernobyl accident. *Environment International* 26(3): 183–187.

Somot S, Pagel M, and Thiry J (1997) Speciation of radium in uranium mill tailings from Ecarpiere (Vendee, France). *Comptes Rendus de l'Academie des Sciences* 325(2): 111–118.

Staub WP, Hinkle NE, Williams RE, et al. (1986) *An Analysis of Excursions at Selected In Situ Uranium Mines in Wyoming and Texas*. NUREG/CR-3967 and ORNL/TM-9956. U.S. Nuclear Regulatory Commission.

Steefel CI and Van Cappellen P (1998) Reactive transport modeling of natural systems. *Journal of Hydrology* 209(1–4).

Stevenson KA and Hardy EP (1993) Estimate of excess uranium in surface soil surrounding the feed materials production center using a requalified data base. *Health Physics* 65(3): 283–287.

Stewart BD, Nico PS, and Fendorf S (2009) Stability of uranium incorporated into Fe (hydr)oxides under fluctuating redox conditions. *Environmental Science & Technology* 43(13): 4922–4927.

Stout DL and Carroll SA (1993) *A Literature Review of Actinide–Carbonate Mineral Interactions*. Albuquerque, NM: Sandia National Laboratories.

Strachan C (2002) Review of tailings dam incident data, Tailings Management Guide. *Mining Environmental Management* 7–9.

Strickert R, Friedman AM, and Fried S (1980) The sorption of technetium and iodine radioisotopes by various minerals. *Nuclear Technology* 49: 253–266.

Strietelmeyer BA, Gillow JB, Dodge CJ, and Pansoy-Hjelvik ME (eds.) (1999) *Toxicity of Actinides to Bacterial Strains Isolated from the Waste Isolation Pilot Plant (WIPP) Environment*. New York, NY: Kluwer Academic/Plenum Press.

Stumm W (1992) *Chemistry of the Solid–Water Interface*. John Wiley & Sons.

Stumpf T, Hennig C, Bauer A, Denecke MA, and Fanghanel T (2004) An EXAFS and TRLFS study of the sorption of trivalent actinides onto smectite and kaolinite. *Radiochimica Acta* 82: 133–138.

Sturchio NC, Banner JL, Binz CM, Heraty LB, and Musgrove M (2001) Radium geochemistry of ground waters in Paleozoic carbonate aquifers, midcontinent U.S.A. *Applied Geochemistry* 16: 109–122.

Sumrall CL III and Middlebrooks EJ (1968) Removal of radioisotopes from water by slurrying with Yazoo and Zilpha clays. *Journal of American Water Works Association* 60(4): 485–494.

Suzuki Y and Banfield JF (1999) Geomicrobiology of uranium. *Reviews in Mineralogy* 38(1): 393–432.

Swanson SM (1985) Food chain transfer of U-series radionuclides in northern Saskatchewan aquatic system. *Health Physics* 49(5): 747–770.

Sylwester ER, Hudson EA, and Allen PG (2000) The structure of uranium (VI) sorption complexes on sioica, alumina, and montmorillonite. *Geochimica et Cosmochimica Acta* 64(14): 2431–2438.

Szabo Z, dePaul VT, Kraemer TF, and Parsa B (2005) Occurrence of radium-224 and comparison to that of radium-226 and radium-228 in water from the unconfined Kirkwood-Cohansey aquifer system, southern New Jersey. *Scientific Investigations Report 2004-5224*. U.S. Geological Survey.

Szabo Z, Jacobsen E, Kraemer TF, and Parsa B (2010) Environmental fate of Ra in cation exchange regeneration brine waste disposed to septic tanks, New Jersey Coastal Plain, U.S.A.: Migration to the water table. *Journal of Environmental Radioactivity* 101: 33–44.

Szabo Z, Rice DE, MacLeod CL, and Barringer TH (1997) Relation of distribution of radium, nitrate, and pesticides to agricultural land use and depth, Kirkwood-Cohansey aquifer system, New Jersey Coastal Plain, 1990–91. *Water Resources Investigations Report 96-4165A*. U.S. Geological Survey.

Szabó Z, Toriashi T, Vallet V, and Grenthe I (2006) Solution coordination chemistry of actinides: Thermodynamics, structure and reaction mechanisms. *Coordination Chemistry Reviews* 250(7–8): 784–815.

Tachi Y, Shibutani T, Sato H, and Yui M (2001) Experimental and modeling studies on sorption and diffusion of radium in bentonite. *Journal of Contaminant Hydrology* 47: 171–186.

Tadmor J (1986) Atmospheric release of volatilized species of radioelements from coal-fired plants. *Health Physics* 50(2): 270–273.

Tanaka T and Muraoka S (1999) Sorption characteristics of ^{237}Np, ^{238}Pu, ^{241}Am in sedimentary materials. *Journal of Radioanalytical and Nuclear Chemistry* 240(1): 177–182.

Tanaka S, Yamawaki M, Nagasaki S, and Moriyama H (1992) Geochemical behavior of neptunium. *Journal of Nuclear Science and Technology* 29(7): 706–718.

Tannenbaum A, Silverstone H, and Koziol J (1951) Tracer studies of the distribution and excretion of uranium in mice, rats, and dogs. In: Tannenbaum A (ed.) *Toxicology of Uranium Compounds*, pp. 128–181. New York, NY: McGraw-Hill.

Thomas K (1987) *Summary of Sorption Measurements Performed with Yucca Mountain, Nevada Tuff Samples and Water from Well J-13*. Los Alamos, NM: Los Alamos National Laboratory.

Tien P-L, Siegel MD, Updegraff CD, Wahi KK, and Guzowski RV (1985) *Repository Site Data Report for Unsaturated Tuff, Yucca Mountain, Nevada*, p. 400. Washington, DC: U.S. Nuclear Regulatory Commission.

Tipping E (1993) Modeling the binding of europium and the actinides by humic substances. *Radiochimica Acta* 62: 141–152.

Toohey RE (2003) Excretion of depleted uranium by Gulf War veterans. *Radiation Protection Dosimetry* 105(14): 171–174.

Torstenfelt B (1985a) Migration of the actinides thorium, protactinium, uranium, neptunium, plutonium, and americium in clay. *Radiochimica Acta* 39: 105–112.

Torstenfelt B (1985b) Migration of the fission products strontium, technetium, iodine and cesium in clay. *Radiochimica Acta* 39: 97–104.

Tournassat C, Ferrage E, Poinsignon C, and Charlet L (2004) The titration of clay minerals II. Structure-based model and implications for clay reactivity. *Journal of Colloid and Interface Science* 273(1): 234–246.

Trabalka JR, Eyman LD, and Auerbach SI (1980) Analysis of the 1957–1958 Soviet nuclear accident. *Science* 209(4454): 345–352.

Triay IR, Furlano AC, Weaver SC, et al. (1996) *Comparison of Neptunium Sorption Results Using Batch and Column Techniques*. Los Alamos, NM: Los Alamos National Laboratory.

Triay IR, Meijer A, Conca JL, et al. (1997) *Summary and Synthesis Report on Radionuclide Retardation for the Yucca Mountain Site Characterization Project*. Los Alamos, NM: Los Alamos National Laboratories LA-13262-MS.

Triay IR, Mitchell AJ, and Ott MA (1992) *Radionuclide Migration Laboratory Studies for Validation of Batch-Sorption Data*, pp. 99–109. Los Alamos, NM: Los Alamos National Laboratory.

Triay IR, Robinson BA, Mitchell AJ, Overly CM, and Lopez RM (1993) Transport of neptunium through Yucca Mountain tuffs. In: Interrante CG and Pabalan RT (eds.) *Scientific Basis for Nuclear Waste Management XVI. Materials Research Society Symposium Proceedings*, vol. 294, pp. 797–802. Pittsburgh, PA: Materials Research Society.

Tricca A, Wasserburg GJ, Porcelli D, and Baskaran M (2001) The transport of U- and Th-series nuclides in a sandy unconfined aquifer. *Geochimica et Cosmochimica Acta* 65(8): 1187–1210.

Tripathi V (1983) *Uranium(VI) Transport Modeling: Geochemical Data and Sub-Models*. PhD Thesis, Stanford University.

Tripathi VS, Siegel MD, and Kooner ZS (1993) Measurements of metal adsorption in oxide-clay mixtures: 'Competitive-additivity' among mixture components. In: Interrante CG and Pabalan RT (eds.) *Scientific Basis for Nuclear Waste Management XVI. Materials Research Society Symposium Proceedings*, vol. 294, pp. 791–796. Pittsburgh, PA: Materials Research Society.

Truex MJ, Peyton BM, Valentine NB, and Gorby YA (1997) Kinetics of U(VI) reduction by a dissimilatory Fe(III)-reducing bacterium under non-growth conditions. *Biotechnology and Bioengineering* 55(3): 490–496.

Tsunashima A, Brindley W, and Bastovanov M (1981) Adsorption of uranium from solutions by montmorillonite; compositions and properties of uranyl montmorillonites. *Clays and Clay Minerals* 29(1): 10–16.

Tsushima S, Rossberg A, Ikeda A, Muller K, and Scheinost AC (2007) Stoichiometry and structure of uranyl(VI) hydroxo dimer and trimer complexes in aqueous solution. *Inorganic Chemistry* 46: 10819–10826.

Tubiana M and Aurengo A (2006) Dose-effect relationships and estimation of the carcinogenic effects of low doses of ionising radiation: The Joint Report of the Academie des Sciences (Paris) and of the Academie Nationale de Medicine. *International Journal of Low Radiation* 2: 135–153.

Tubiana M, Aurengo A, Averbeck D, and Masse R (2006) The debate on the use of linear no threshold for assessing the effects of low doses. *Journal of Radiological Protection* 26: 317–324.

Tubiana M, Aurengo A, Averbeck D, and Masse R (2008) Low-dose risk assessment: the debate continues. *Radiation Research* 169: 246–247.

Turin HJ, Groffman AR, Wolfsberg LE, Roach JL, and Strietelmeier BA (2002) Tracer and radionuclide sorption to vitric tuffs of Busted Butte, Nevada. *Applied Geochemistry* 17(6): 825–836.

Turner DR (1995) *A Uniform Approach to Surface Complexation Modeling Of Radionuclide Sorption*. San Antonio, TX: Center for Nuclear Waste Regulatory Analyses.

Turner DR, Bertetti FP, and Pabalan RT (2002) Role of radionuclide sorption in high-level waste performance assessment: Approaches for the abstraction of detailed models. In: Zhang P and Brady P (eds.) *Geochemistry of Soil Radionuclides*, pp. 211–252. Madison, WI: Soil Science Society of America.

Turner DR, Griffin T, and Dietrich TB (1993) Radionuclide sorption modeling using the MINTEQA2 speciation code. In: Interrante CG and Pabalan RT (eds.) *Scientific Basis for Nuclear Waste Management XVI*. *Materials Research Society Symposium Proceedings*, vol. 294, pp. 783–789. Pittsburgh, PA: Materials Research Society.

Turner DR and Pabalan RT (1999) Abstraction of mechanistic sorption model results for performance assessment calculations at Yucca Mountain, Nevada. *Waste Management* 19(6): 375–388.

Turner DR, Pabalan RT, and Bertetti FP (1998) Neptunium(V) sorption on montmorillonite: An experimental and surface complexation modeling study. *Clays and Clay Minerals* 46: 256–269.

Turner GD, Sachara JM, McKinley JP, and Smith SC (1996) Surface-charge properties and UO_2^{2+} adsorption on a surface smectite. *Geochimica et Cosmochimica Acta* 60(18): 3399–3414.

Uchida S, Tagami K, Rühm W, and Wirth E (1999) Determination of ^{99}Tc deposited on the ground within the 30-km zone around the Chernobyl reactor and estimation of ^{99}Tc released into atmosphere by the accident. *Chemosphere* 39(15): 2757–2766.

Ulmer-Scholle DS (2011) *Uranium – How Is it Mined?* New Mexico Bureau of Geology and Mineral Resources.

Ulrich GA, Breit GN, Cozzarelli IM, and Suflita JM (2003) Sources of sulfate supporting anaerobic metabolism in a contaminated aquifer. *Environmental Science & Technology* 37: 1093–1099.

Underhill DH (1992) In-situ leach uranium mining in the United States of America: Past, present and future. In: *Uranium In Situ Leaching, Technical Committee Meeting*, 5–8 October 1992. IAEA TECDOC-720, 19–42.

UNSCEAR (1993) *Sources and Effects of Atomic Radiation*. New York, NY: United Nations Scientific Committtee on the Effects of Atomic Radiation, United Nations.

UNSCEAR (2000) *Sources and Effects of Ionizing Radiation*. *Report of the United Nations Scientific Committee on the Effects of Atomic Radiation*. New York: United Nations.

Unsworth ER, Jones P, and Hill SJ (2002) The effect of thermodynamic data on computer model predictions of uranium speciation in natural water systems. *Journal of Environmental Monitoring* 4: 528–532.

USEPA (2013) Radionuclides in Drinking Water Rule. http://water.epa.gov/lawsregs/rulesregs/sdwa/radionuclides/regulation.cfm (accessed April 7, 2013).

USGS (2006) *History of the National Uranium Resource Evaluation Hydrogeochemical and Stream Sediment Reconnaissance Program*. U.S. Geological Survey. http://pubs.usgs.gov/of/1997/ofr-970492/nurehist.htm (accessed on June 2011).

USGS (2010a) *Hydrological, Geological, and Biological Site Characterization of Breccia Pipe Uranium Deposits in Northern Arizona*. Reston, VA: U.S. Geological Survey Scientific Investigations Report 2010–5025.

USGS (2010b) *Geology, geochemistry, and Geophysics of the Fry Canyon Uranium/Copper Project Site, Southeastern Utah – Indications of Contaminant Migration*. Reston, VA: U.S. Geological Survey Scientific Investigations Report 2010–5075.

USNRC (2008) *Generic Environmental Impact Statement for In-Situ Leach Uranium Mining Facilities*, NUREG-1910, US Nuclear Regulatory Commission. http://www.nrc.gov/reading-rm/doc-collections/nuregs/staff/sr1910/ (accessed April 7, 2013).

USNRC (2011) Title 10 – CFR Part 40 – Domestic licensing of source material. http://www.nrc.gov/reading-rm/doc-collections/cfr/part040/ (accessed April 7, 2013).

Vallet V, Schimmelpfennig B, Maron L, et al. (1999) Reduction of uranyl by hydrogen: An Ab initio study. *Chemical Physics* 244(2–3): 185–193.

Van Cappellen P, Charlet L, Stumm W, and Wersin P (1993) A surface complexation model of the carbonate mineral-aqueous solution interface. *Geochimica et Cosmochimica Acta* 57: 3505–3518.

Van der Lee J (1998) *Thermodynamic and Mathematical Concepts of CHESS*. Fontainebleau, France: E´cole des Mines de Paris Technical Report LHMrRDr98r39, CIG.

Van der Lee J, De Windt L, Lagneau V, and Goblet P (2002) Presentation and application of the reactive transport code HYTEC. *Computational Methods in Water Resources* 1: 599–606.

Van der Lee J, Ledoux E, and de Marsily G (1992) Modeling of colloidal uranium transport in a fractured medium. *Journal of Hydrology* 139: 135–158.

Van der Lee J and Lomenach C (2004) Towards a common thermodynamic database for speciation models. *Radiochimica Acta* 92: 811–818.

Van Genuchten MT and Wierenga PJ (1986) Solute Dispersion Coefficients and Retardation Factors. In: *Methods of Soil Analysis, Part 1. Physical and Mineralogical Methods*, 2nd edn., pp. 1025–1054.

Vandergraaf TT, Tichnor KV, and George IM (1984) Reactions between technetium in solution and iron-containing minerals under oxic and anoxic conditions. In: Barney GS, Navratil JD, and Schultz WW (eds.) *Geochemical Behavior of Disposed Radioactive Waste*. Washington, DC: American Chemical Society.

Vengosh A, Hirschfeld D, Vinson D, et al. (2009) High naturally occurring radioactivity in fossil groundwater from the Middle East. *Environmental Science & Technology* 43: 1769–1775.

Veska E and Eaton RS (1991) Abandoned rayrock uranium mill tailings in the northwest territories: Environmental conditions and radiological impact. *Health Physics* 60(3): 399–409.

Vilks P (1994) *The Role of Colloids and Suspended Particles in Radionuclide Transport in the Canadian Concept for Nuclear Fuel Waste Disposal*. AECL-10280, COG-92-26. AECL Research.

Vilks P (2009) *Sorption in Highly Saline Solutions – State of the Science Review*. NWMO TR-2009-18, Atomic Energy of Canada Limited.

Vilks P, Caron F, and Haas M (1998) Potential for the formation and migration of colloidal material from a near-surface waste disposal site. *Applied Geochemistry* 13: 31–42.

Vilks P, Cramer JJ, Bachinski DB, Doern DC, and Miller HG (1993) Studies of colloids and suspended particles, Cigar Lake uranium deposit, Saskatchewan, Canada. *Applied Geochemistry* 8: 605–616.

Vilks P, Miller HG, and Doern DC (1991) Natural colloids and suspended particles in the Whiteshell Research area and their potential effect on radiocolloid formation. *Applied Geochemistry* 6(5): 565–574.

Vodrias EA and Means JL (1993) Sorption of uranium by brine-saturated halite, mudstone, and carbonate minerals. *Chemosphere* 26(10): 1753–1765.

von der Heyden CJ and New MG (2004) Groundwater pollution on the Zambian Copperbelt: Deciphering the source and the risk. *The Science of the Total Environment* 327(1–3): 17–30.

Wagenpfeil F and Tschiersch J (2001) Resuspension of coarse fuel hot particles in the Chernobyl area. *Journal of Environmental Radioactivity* 52(1): 5–16.

Wagman DD, Evans WH, Parker VB, Schumm RH, and Halow I (1982) The NBS tables of chemical thermodynamic properties. *Journal of Physical and Chemical Reference Data* 11(supplement 2): 2-1-2-34.

Waite TD, Davis JA, Fenton BR, and Payne TE (2000) Approaches to modelling uranium (VI) adsorption on natural mineral assemblages. *Radiochimica Acta* 88: 687–693.

Waite DT, Joshi SR, and Sommerstad H (1988) The effect of uranium mine tailings on radionuclide concentrations in Langley Bay, Saskatchewan Canada. *Archives of Environmental Contamination and Toxicology* 17(3): 373–380.

Wall NA, Giambalvo ER, Brush LH, and Wall DE (2002) The use of oxidation-state analogs for WIPP actinide chemistry. In: *223rd American Chemical Society National Meeting*, 7–11 April 2002. Unpublished presentation. Carlsbad, NM: Sandia National Laboratories.

Wall JD and Krumholz LR (2006) Uranium reduction. *Annual Review of Microbiology* 60: 149–166.

Wan JM, Tokunaga TK, Kim YM, et al. (2008) Effects of organic carbon supply rates on uranium mobility in a previously bioreduced contaminated sediment. *Environmental Science & Technology* 42(20): 7573–7579.

Wang P, Andrzej A, and Turner DR (2001a) Thermodynamic modeling of the adsorption of radionuclides on selected minerals. I: Cations. *Industrial Engineering Chemical Research* 40: 4428–4443.

Wang P, Andrzej A, and Turner DR (2001b) Thermodynamic modeling of the adsorption of radionuclides on selected minerals. II: Anions. *Industrial Engineering Chemical Research* 40: 4444–4455.

Ward DB, Brookins DG, Siegel MD, and Lambert SJ (1990) Natural-analog studies for partial validation of conceptual models of radionuclide retardation at the WIPP. In: Abrajano TA and Johnson LH (eds.) *Scientific Basis for Nuclear Waste Management XIV*. *Materials Research Society Symposium Proceedings*, vol. 212, pp. 703–710. Pittsburgh, PA: Materials Research Society.

Ward DB, Bryan C, and Siegel MD (1994) Detailed characterization and preliminary adsorption model for materials for an intermediate-scale reactive transport experiment. In: *1994 International Conference on High Level Radioactive Waste Management*, pp. 2048–2062. American Nuclear Society.

Watson EB (1996) Surface enrichment and trace-element uptake during crystal growth. *Geochimica et Cosmochimica Acta* 60(24): 5013–5020.

Watson D, Gu B, Phillips D, and Lee SY (1999) *Evaluation of Permeable Reactive Barriers for Removal of Uranium and Other Inorganics at the Department of ENERGY Y – 12 Plant, S-3 Disposal Ponds*. Oak Ridge, TN: Environmental Sciences Division, Oak Ridge National Laboratory.

Weir E (2004) Uranium in drinking water, naturally. *CMAJ* 170(6): 951–952.

WHO (2004) *Guidelines for Drinking Water Quality*, 3rd edn. Geneva: World Health Organization.

Wildung RE, McFadden KM, and Garland TR (1979) Technetium sources and behavior in the environment. *Journal of Environmental Quality* 8(2): 156–161.

Wildung RE, Routson RC, Serne RJ, and Garland TR (1974) *Pertechnetate, Iodide, and Methyl Iodide Retention by Surface Soils*, pp. 37–40. Richland, WA: Pacific Northwest National Laboratory.

Wilson ML, Swift PN, McNeish JA, and Sevougian SD (2002) Total-system performance assessment for the Yucca Mountain Site. In: McGrail BP and Cragnolino GA (eds.) *Scientific Basis for Nuclear Waste Management XXV*. *Materials Research Society Symposium Proceedings*, vol. 713, pp. 153–164. Warrendale, PA: Materials Research Society.

Winkler A, Bruhl H, Trapp C, and Bock WD (1988) Mobility of technetium in various rock and defined combinations of natural minerals. *Radiochimica Acta* 44(45): 183–186.

Wittman RS, Buck EC, and Hanson BD (2005) *Data Analysis of Plutonium Sorption on colloids in a Minimal Kinetics Model*. PNNL-15285: Pacific Northwest National Laboratory, p. 26.

WNA (2011) *World Uranium Mining*. http://www.world-nuclear.org/info/Nuclear-Fuel-Cycle/Mining-of-Uranium/World-Uranium-Mining-Production/ (accessed April 7, 2013).

Wolery TJ (1992) *EQ3/EQ6, A Software Package for Geochemical Modeling of Aqueous Systems, Package Overview and Installation Guide (Version 7.0)*. Lawrence Livermore National Laboratory.

Wrenn ME, Durbin PW, and Howard B (1985) Metabolism of ingested uranium and radium. *Health Physics* 48(5): 601–633.

Xia Y, Roa L, Rai D, and Felmy AR (2001) Determining the distribution of Pu, Np, and U oxidation states in dilute NaCl and synthetic brine solutions. *Journal of Radioanalytical and Nuclear Chemistry* 250(1): 27–37.

Yamaguchi T, Nakayama S, Nagao S, and Kizaki M (2007) Diffusive transport of neptunium and plutonium through compacted sand-bentonite mixtures under anaerobic conditions. *Radiochimica Acta* 95(2): 115–125.

Yang IC and Edwards KW (1984) Releases of radium and uranium into Ralston Creek and Reservoir Colorado, from uranium mining. In: Barney GS, Navratil JD, and Schulz W (eds.) *Geochemical Behavior of Disposed Radioactive Waste*. *ACSSymposium Series*, vol. 246, pp. 271–286. American Chemical Society.

Yang C, Samper J, and Montenegro L (2008) A coupled non-isothermal reactive transport model for long-term geochemical evolution of a HLW repository in clay. *Environmental Geology* 53: 1627–1638.

Yates MV, Brierley JA, Brierley CL, and Follin SE (1983) Effect of microorganisms on in situ uranium mining (October 1983). *Applied and Environmental Microbiology* 46(4): 779–784.

Yeh GT, Carpenter SL, Hopkins PL, and Siegel MD (1995) *Users' Manual for LEHGC: A Lagrangian-Eulerian Finite-Element Model of Hydrogeochemical Transport Through Saturated–Unsaturated Media*. Albuquerque, NM: Sandia National Laboratories.

Yeh GT, Li MH, and Siegel MD (2002) Fluid flow and reactive chemical transport in variably saturated subsurface media. In: Shen H, Cheng A, Wang K, Teng M, and Liu C (eds.) *Environmental Fluid Mechanics*, pp. 207–256. Reston, VA: American Society of Civil Engineers.

Yeh GT, Tripathi VJ, Gwo JP, et al. (2011) HYDROGEOCHEM: A coupled model of variably saturated flow, thermal transport and reactive biogeochemical transport. In: Zhang F, Yeh GT, and Parker JC (eds.) *E-Book on Mathematical Modeling of Reactive Transport in Groundwater*. Bentham Sciences Publishers.

Yoshida S, Muramatsu Y, and Uchida S (1998) Soil-solution distribution coefficients, K_ds of I^- and IO_3^- for 68 Japanese soils. *Radiochimica Acta* 82: 293–297.

Yoshida Y, Nakazawa T, Yoshikawa H, and Nakanishi T (2009) Partition coefficient of Ra in gypsum. *Journal of Radioanalytical and Nuclear Chemistry* 280: 541–545.

Yoshida Y, Yoshikawa H, and Nakanishi T (2008) Partition coefficients of Ra and Ba in calcite. *Geochemical Journal* 42: 295–304.

Zaire R, Notter M, Riedel W, and Theil E (1997) Unexpected rates of chromosomal instabilities and alterations of hormone levels in Namibian uranium miners. *Radiation Research* 147(5): 479–584.

Zamora ML, Tracy BL, Zielinski JM, Meyerhoff DP, and Moss MA (1998) Chronic ingestion of uranium in drinking water: A study of kidney bioeffects in humans. *Toxicological Sciences* 43: 68–77.

Zavarin M and Bruton CJ (2004a) *A Non-Electrostatic Surface Complexation Approach To Modeling Radionuclide Migration at the Nevada Test Site I. Iron Oxides and Calcite*. Livermore, CA: Lawrence Livermore National Laboratory UCRL-TR-208673.

Zavarin M and Bruton CJ (2004b) *A Non-Electrostatic Surface Complexation Approach to Modeling Radionuclide Migration at the Nevada Test Site II*. Livermore, CA: Lawrence Livermore National Laboratory *aluminosilicates* UCRL-TR-208672.

Zeh P, Czerwinski KR, and Kim JI (1997) Speciation of uranium in Gorleben groundwaters. *Radiochimica Acta* 76: 37–44.

Zhang P and Brady PV (eds.) (2002) Geochemistry of soil radionuclides. *SSSA Special Publication Number 59*, p. 252.

Zhang GX, Senko JM, Kelly SD, et al. (2009) Microbial reduction of iron(III)-rich nontronite and uranium(VI). *Geochimica et Cosmochimica Acta* 73(12): 3523–3538.

Zhang F, Yeh GT, and Parker JC (eds.) (2011) *E-Book on Mathematical Modeling of Reactive Transport in Groundwater*. Bentham Sciences Publishers.

Zhu C, Hu FQ, and Burden DS (2001) Multi-component reactive transport modeling of natural attenuation of an acid groundwater plume at a uranium mill tailings site. *Journal of Contaminant Hydrology* 52(1–4): 85–108.

Zielinski RA, Otton JK, and Budahn JR (2001) Use of radium isotopes to determine the age and origin of radioactive barite at oil-field production sites. *Environmental Pollution* 13: 299–309.

11.7 The Environmental and Medical Geochemistry of Potentially Hazardous Materials Produced by Disasters

GS Plumlee, SA Morman, GP Meeker, TM Hoefen, PL Hageman, and RE Wolf, US Geological Survey, Denver, CO, USA

Published by Elsevier Ltd.

11.7.1 Introduction

"A Toxic Gumbo-An environmental expert warns residents about the hazards of returning to New Orleans – now home to a dangerous brew of toxic chemicals and bacteria" – MSNBC.com coverage of Hurricane Katrina, September 2005

"Peru volcano spews deadly ash" – National Geographic News, April 2006

"U.S. Gulf oil spill poses public health threat" – The Nation's Health, American Public Health Association, August 2010

"Red Mud's Health Effects – Toxic Spills: Hungarian accident may have fewer long-term health effects than initially feared" – Chemical Engineering News

"Mississippi River floodwater could create long-term toxic impact" – PBS Newshour, May, 2011

"Cadmium spill threatens drinking water for millions" – Reuters, February, 2012

Natural and human-caused disasters (e.g., earthquakes, volcanic eruptions, wildfires, urban fires, landslides, hurricanes, tsunamis, floods, tornadoes, severe storms, windstorms, industrial spills, terrorist attacks, and armed conflicts) are well recognized for the substantial acute threats they pose to human health and safety and for their longer-lasting impacts from physical injuries and effects on chronic diseases and mental health (Hogan and Burstein, 2007; Landesman, 2006; Mason et al., 2010; Miller and Arquilla, 2008). As illustrated by the above news headlines, disasters can also result in substantial physical and chemical stresses on the environment, with resulting concerns for the health of the affected ecosystems and humans. Of particular concern are potentially hazardous materials (HM) (herein called 'disaster materials,' or DM) that can be released into the environment (Cook et al., 2008; Galea, 2007; Young et al., 2004). The descriptor 'potentially' is necessary because the actual adverse impacts of any given material will vary as a function of the amount(s) and form(s) in which it is released, the environment into which it is released, and other factors.

Once released into the environment, DM respond to and can be modified by many different physical, geochemical, and biogeochemical processes. These modifications can strongly influence the nature and magnitude of their potential environmental, ecological, and related human-health impacts. In many cases, the potential ecological, environmental, or health threats are diminished (e.g., contaminants are dispersed or diluted to nontoxic levels). However, in some cases, new materials, some of which are transient, can be produced that may enhance potential environmental and health threats.

Emergency responders have to focus on identifying rapidly the types and amounts of known specific HM produced by disasters and whether these materials are present in levels that pose a significant threat to the ecosystem or human health. As a result, the HM-focused sampling, characterization, and interpretation done as part of routine disaster responses may not fully define the range of materials produced by these extreme events, how these mixtures of materials behave in the environment, and how such mixtures and changes may influence impacts on affected ecosystems and humans.

Our research group at the US Geological Survey (USGS) has helped assess the environmental and health implications of materials produced by a variety of natural and anthropogenic disasters (e.g., Plumlee, 2009). A number of other researchers have studied some of the same disasters and other disasters for environmental or human health implications. Using ours and others' work, this chapter will summarize environmentally and toxicologically significant characteristics of a wide range of materials produced by a variety of disaster types, including volcanic gas or ash eruptions, landslides and debris flows, flooding (with a focus on Hurricane Katrina), a mud volcano eruption, wildfires at the wildland–urban interface, spills of metal mining or mineral-processing wastes, spills of coal slurry and coal fly ash (CFA), and building collapse (with a focus on the World Trade Center (WTC)). Several other important DM such as major oil spills (e.g., Aguilera et al., 2010; Thibodeaux et al., 2011), radioactive materials from nuclear accidents (e.g., Yoshida and Takahashi, 2012; **Chapter 11.6**), and releases of various industrial chemicals (ITE, 1997; NLM, 2012) have been covered elsewhere in the literature and are not discussed here. Plumlee et al. (2012) discuss some of these materials in the context of urban disasters.

This chapter illustrates the important roles that geochemists and other earth scientists can play in understanding DM and therefore in assisting in environmental disaster response and preparedness. These roles include, for example,

- characterizing in detail the physical, chemical, and microbial makeup of DM;
- identifying and discriminating potential multiple sources of the materials;
- monitoring, mapping, and modeling dispersal and evolution of the materials in the environment;
- understanding how the materials are modified by environmental processes;
- identifying key characteristics and processes that influence the materials' toxicity to exposed humans and ecosystems;
- informing decisions for material handling and disposal during cleanup;
- estimating shifts away from predisaster environmental baseline conditions; and
- using geochemical insights learned from past disasters to help estimate, prepare for, and increase societal resilience to environmental and related health impacts of future disasters.

Some examples presented in this chapter show how the examination of DM for potential environmental or health hazards can, in some cases, also provide useful insights into disaster origins and/or processes are also shown.

11.7.2 Potentially Hazardous Materials Produced by Disasters

Many types of natural and human-caused disasters have been shown to produce a range of hazardous solid, liquid, gaseous, aqueous, or biological materials that can, in sufficient amounts, pose threats to the environment, ecosystems, and humans (**Figure 1**, **Table 1**). Geogenic DM are materials produced from the earth by natural processes, for example, volcanic ash (VA) and gases, windblown dusts containing natural soil pathogens (such as the soil fungus *Coccidioides immitis* that causes valley fever), and smoke and ash released as combustion by-products by wildland wildfires. Geoanthropogenic DM are

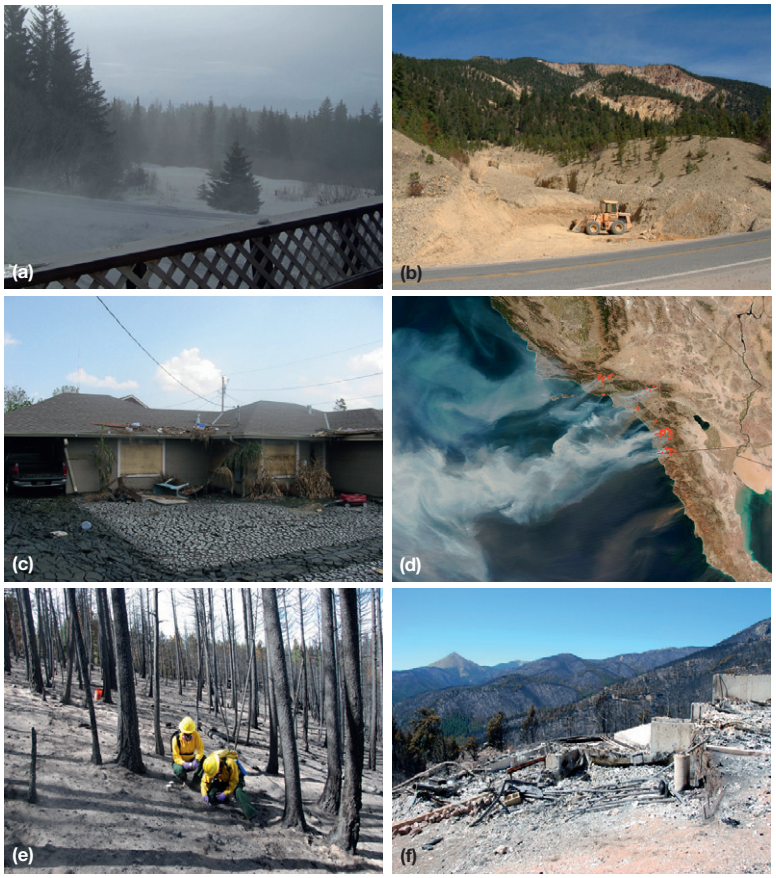

Figure 1 Photographic examples of materials produced by many different types of disasters or natural hazards. (a) Volcanic ash (VA) from the spring 2009 eruptions of Mount Redoubt, Alaska, United States, caused disruption of daily life in downwind Anchorage and other smaller towns such as Homer (shown in photograph) (photograph by Dennis Anderson). (b) Natural erosional scar areas with steep, denuded slopes (orange- to pink-colored cliffs in the background) form from acid-sulfate weathering of iron sulfide-rich hydrothermally altered rocks along the Red River, northern New Mexico. Debris flows from the scar areas triggered by thunderstorm runoff transport large volumes of weathered and unweathered material to downstream debris fans (middle ground of photo). The debris flows regularly cross a state highway (foreground) and have caused one fatal car accident (photograph by Geoff Plumlee). (c) Thick deposits of muddy flood sediments were left behind in an eastern New Orleans suburb following Hurricane Katrina in 2005 (photograph by John Lovelace, USGS). (d) This National Aeronautics and Space Administration (NASA) Moderate Resolution Imaging Spectroradiometer (MODIS) satellite image from 22 October 2007 shows dust plumes (brown) and smoke plumes (gray) from many wildfires (areas in red) at the wildland–urban interface in Southern California. Santa Ana winds fanned the fires and carried smoke and dust plumes into Los Angeles, San Diego, and other southern California cities, where millions of people were exposed to smoke, airfall ash, and dusts. (e) USGS scientists collect samples of white ash left behind after the Fourmile Canyon wildfire near Boulder, Colorado, United States (photograph by Gregg Swayze, USGS). (f) The Fourmile Canyon fire burned over 120 houses, from some of which ash and debris could be easily eroded into the local waterways by heavy rainfall runoff (photograph by Geoff Plumlee). (g) This June 2007 photograph by Handoko Wibowo shows the central vent (indicated by the steam cloud) and the surrounding mud erupted from the Lusi mud volcano in East Java, Indonesia. The factory and residence buildings flooded by the mud and the resulting land subsidence can be seen in the background. (h) In 1993, the failure of a siltation dam at the Marcopper open-pit copper mine, Marinduque Island, Philippines, during a typhoon released large volumes of sulfide mine wastes into the Mogpog River, northwest of the mine. As of 2003, mine wastes and acid-mine drainage still being released into the Mogpog from Marcopper were dominating the water and sediment loads in the small watershed, with the net result a river having little or no aquatic life. The river waters at the location in this photo were light blue due to the high levels of copper and were precipitating orange iron hydroxysulfates in the stream bed (photograph by Mark Logsdon). (i) The spring 1996 failure of a tailings impoundment at Marcopper released an estimated 1.5 million m^3 of pyritic tailings southward into the Makulapnit and Boac rivers. Tailings deposited in the riverbed had turned acid-generating due to sulfide oxidation, were well cemented by soluble salts formed by evaporation of acid waters in the tailings, and formed a prominent cliff that was incised by the river. By 2003, the tailings in this view were buried by and commingled with the unmineralized sediments deposited during typhoons (photograph by Geoff Plumlee). (j) This photograph, taken in early 2011, shows the inside of a house flooded in fall 2010 by the red mud spill from the bauxite-processing plant at Ajka, Hungary. The high-water mark of the flood is apparent on the walls, and deposits of the mud are visible on the floor. The high-water mark on the bathtub suggests it was picked up and floated by the flood (photograph by Todd Hoefen). (k) This photograph, taken in mid-September 2001, shows the view of Ground Zero at the World Trade Center (WTC) from a 31st-floor apartment. Note the extensive deposits of dust and debris on the roofs and the thick plume of smoke and dust emanating from Ground Zero (photograph by Mark Rushing). (l) The dust cloud from the WTC building collapses left behind extensive dust and debris deposits, even in multistory buildings where the windows were left open by the evacuating residents (photograph by Mark Rushing).

(Continued)

Figure 1 Continued

materials that were derived from the earth but have been influenced or modified by human activities or transformed by humans for use in society; these materials have also been termed 'naturally occurring, technologically enhanced materials,' or NOTEM. These include, for example, slurries from coal cleaning, coal fly ash, mine wastes or tailings, crude oil, soils or flood sediments contaminated by anthropogenic chemicals, and combustion by-products of wildfires at the wildland–urban interface. Anthropogenic DM include a spectrum of materials that are manufactured by humans, such as industrial or agricultural chemicals, petroleum products, and mineral-processing solutions. They also include waste products, such as sewage, debris, and smoke/ash by-products from the combustion of chemicals or buildings.

Many types of disasters can produce complex mixtures of multiple geogenic, geoanthropogenic, and/or anthropogenic materials. These mixtures can come either from a single complex source (such as a volcano or the collapse of the WTC towers) or from many different sources (such as multiple industrial facility types damaged by a flood or an earthquake).

For some disasters, mitigation or remediation treatments add more types of materials into the environment. For example, mitigation of oil spills in the surface water environment, such as the 2010 Deepwater Horizon oil spill, can involve the widespread application of chemical dispersants to or the purposeful combustion of spilled oil (Cooney, 2010; Oil Spill Commission, 2011). As another example, a variety of fire suppression chemicals are applied on vegetation near burning wildfires (Calfee and Little, 2003; Crouch et al., 2006; Kalabokidis, 2000). Although the efficacy and possible geochemical, environmental, ecological, and health consequences of such treatments have hopefully been extensively evaluated prior to their application, they nonetheless are often a source of considerable environmental and toxicological uncertainty and debate following disasters where they have been applied.

11.7.3 Medical Geochemistry – A Review and Update

In the previous editions of the *Treatise on Geochemistry*, Plumlee and Ziegler (2003, 2007) summarized the aspects of the emerging discipline 'medical' geochemistry, specifically the application of geochemical principles and methods to understand the interactions between body fluids and earth materials and how these interactions may influence toxicity. This discipline can also be appropriately termed 'toxicological geochemistry' (Plumlee et al., 2006a). The excellent papers in Sahai and Schoonen (2006) discuss other aspects of medical geochemistry and mineralogy, and those in Selinus et al. (2005) discuss the broader topic of medical geology. In the years since these publications, there have been many interesting advancements in medical and toxicological geochemistry, so a short review of key concepts and recent advancements is presented here, with a focus on DM.

Table 1 Examples of materials produced by different types of disasters

Disaster type	*Examples*	*Potentially hazardous materials*	*Key changes resulting from environmental processes*	*Characteristics of environmental or environmental health concern*
Volcanic gas venting to atmosphere	Kīlauea volcano, Hawaii (ongoing)	Acidic volcanic gases SO_2, HCl, HF, and CO_2	Major changes include dispersion, condensation onto water droplets, precipitation in solid salts, or sorption onto solid particulates	Gases are toxic in high levels. Condensates are acid irritants. Acid rain can leach lead from metal roofs. Fluoride from dry or wet deposition of HF can contaminate vegetation and water supplies
Volcanic degassing into lakes and atmosphere	Lake Nyos, Cameroon	CO_2 and possibly other gases	Lake bottom waters become charged with CO_2, which then can be released catastrophically when an event causes lake waters to overturn. Gases vented directly to atmosphere are dispersed or can condense in water droplets	CO_2 is an asphyxiant that settles into topographically low areas. Direct venting into atmosphere can kill vegetation
Volcanic ash (VA) eruptions	Mt. St. Helens, United States; Sakurajima, Japan; Soufrière Hills, Montserrat; Eyjafjallajokull, Iceland; Halema'uma'u summit crater, Kīlauea volcano, Hawaii; and many others	VA varies as a function of magma composition, eruption style, eruption duration, temperature, and other factors. VA can contain mineralogically complex mixtures with glass, many different silicates, oxides, and some sulfides. Acid gases can condense or sorb onto particulates and can have a fairly high proportion of inhalable or respirable particles, although particle clumping may decrease respirability	Proportion of respirable particles in ash cloud increases downwind due to the settling of coarser, denser phases. Proportions of adsorbed sulfate relative to fluoride, chloride can increase in ash cloud downwind. Ashfall into water bodies or rainfall interactions with ash can leach soluble acids, fluoride, and metals into water, creating potential problems in the waters but diminishing potential concerns with remaining ash. Rainfall runoff may also preferentially remove finer particles, which can be redeposited in sediments downstream	Potentially abundant respirable to inhalable particles. Broken glass shards and crystals can be abrasive. Respired crystalline silica, leachable iron or other metals, iron silicates, and iron sulfides may cause fibrotic response or oxidative stress in the lungs. Water-soluble or gastric-soluble fluoride can lead to fluorosis in humans or animals that drink ash-affected water or in animals that consume forage with adhered ash particles
Landslides, debris flows, or lahars	These can be sourced in geologically unstable rock lithologies, areas of steep topography, hydrothermally altered rocks, or deforested or wildfire-burned areas. Rapid-onset landslides and debris flows can be triggered by rainfall (Vargas, Venezuela, 1999) or earthquakes. Lahars are generally triggered by volcanic eruptions (Nevado del Ruiz, Columbia, 1985)	A wide range of materials can be present, depending upon bedrock lithology, soil type, soil composition, climate, trigger mechanism (i.e., earthquake vs. rainfall), and amounts and types of intermixed anthropogenic materials. Dusts containing contaminants or pathogens can be released during and after landslides. Runoff with potentially contaminated waters and sediments can be released during rainfall events	Landslides and debris flows can greatly enhance the amounts and surface areas of rocks available for weathering, erosion, and dust generation. As a result, landslides and debris flow deposits can be long-term sources of erodible, wind-borne, and water-transported pathogens and solid or leachable contaminants	Diverse possible contaminants or pathogens, such as asbestos, nickel, vanadium, and hexavalent chromium from ultramafic rocks; sulfides, metals, and soluble salts associated with weathered mineralized rocks; soil pathogens in dusts from earthquake-generated landslides; and entrained mineral/chemical toxicants and pathogens from damaged anthropogenic sources

(*Continued*)

Table 1 (Continued)

Disaster type	*Examples*	*Potentially hazardous materials*	*Key changes resulting from environmental processes*	*Characteristics of environmental or environmental health concern*
Flooding from extreme storms (high precipitation or wind-driven surges), tsunamis, or rapid snowmelt	Hurricanes Katrina (2005) and Floyd (1999)	Floodwaters and flood sediments can, depending upon their sources and upstream history, contain a wide range of natural and/or anthropogenic contaminants in solid or liquid form	Contaminants in floodwaters can be diluted and/or (depending upon their physical state, chemical makeup, and other characteristics) volatilized, photolytically degraded, biodegraded, taken up by plants or organisms, and sorbed onto solid sediment particles that can then settle out. Contaminants in flood sediments can also be diluted by uncontaminated sediments, volatilized, and photolytically degraded/transformed	Salt water contamination from coastal storm surges. Marsh-derived flood sediments may have acid-generating sulfides. Floodwaters can transport a wide range of water-, liquid-, or solid-based contaminants (salt water, asbestos, metals, metalloids, petroleum-related chemicals, polycyclic aromatic hydrocarbons, sewage components, pesticides, bacteria, viruses, etc.)
Wildfires at the wildland–urban interface and urban firestorms	Station fire, California (2009); multiple Southern California wildfires (2003–07); Oakland–Berkeley Hills fire (1991)	Smoke and related airborne particulate matter (PM), airfall ash, residual ash, and burned soils can contain a wide range of gaseous and solid, inorganic and organic toxicants. More heavily combusted ash can contain caustic alkali solids. There is generally a broader array of potential toxicants in combustion products from the built environment than from wildland fires. Dusts from burned areas can contain soil pathogens such as the soil fungus that causes valley fever	Fire gases, smoke, and related airborne PM are dispersed downwind from active fires. Solid material can settle out as airfall deposits. Residual ash and burned soils in burned wildland and urban areas can be resuspended by winds and human activities to produce high levels of airborne PM. Interactions of smoke and ash with rainfall or snowmelt can diminish caustic alkali content of residual ash. Some soil pathogens (i.e., the soil fungus that causes valley fever) can apparently survive in soils where the vegetation has been combusted by wildfires	Gases can be asphyxiants or irritants. Abundant respirable PM in smoke can cause a variety of respiratory and related problems. Alkali solids present in heavily combusted ash generate caustic alkalinity when they come into contact with surface waters or water-based body fluids. Metals such as lead, arsenic, hexavalent chromium, copper, and zinc are variably water-soluble and bioaccessible in the gastrointestinal fluids, respiratory tract fluids, perspiration, and eye fluids. Organic toxicants in smoke and ash can be taken up and have been linked to a variety of health problems. There have been increased cases of valley fever following wildfire in endemic areas, due to vegetation loss and enhanced dust generation
Mud volcano eruptions	Lusi mud volcano, East Java, Indonesia	Oil-related organic compounds in mud solids and waters. High fluoride, nitrate, and salinity in separated waters	Dried muds can become windblown. Organic compounds in surface muds will likely degrade by volatilization, biodegradation, and photolytic degradation	Possible contamination of water supplies by saline waters rich in fluoride, chloride, sulfate, etc. Nitrate may serve as a nutrient to promote algal blooms in the affected surface waters
Mine waste spills and mill tailings spills	Marcopper, Philippines (1993, 1996); Aznalcóllar, Spain (1998)	A wide range of potential mineral toxicants (e.g., asbestos, crystalline silica, and acid-generating and bioreactive iron sulfides),	Tailings with elevated levels of iron sulfides and low levels of carbonates can weather over time to produce acidic, metal-rich	Tailings spills have been shown to have immediate physical and chemical impacts on aquatic and terrestrial ecosystems. Acidic

		bioaccessible metal toxicants (e.g., Pb, As, Cd, Hg, and others), and processing chemicals (e.g., xanthates) can be present in tailings solids and liquids. The types and abundances of these are a function of the geology of the ore deposit being mined and processed and of the processing method used	drainage. Dusts can be generated from dried and weathered tailings deposits	and metal-rich runoff from weathered sulfide-rich tailings deposits during storm events can adversely affect aquatic ecosystems. Plants can take up metals from floodplain tailings deposits. Dusts containing iron sulfides and soluble iron sulfate salts may be bioreactive if inhaled. For a given elemental toxicant such as lead, some mineral forms (e.g., lead carbonate or lead oxide) are substantially more bioaccessible than others (e.g., lead sulfate or lead sulfide)
Spills of cyanide-bearing tailings and/or processing solutions	Baia Mare, Romania (2000)	Cyanide in spilled processing solutions is generally tied up primarily as moderately toxic weak-acid dissociable complexes with metals, such as copper or zinc. The abundances of the different complexes are a function of the deposit geology. Some toxic free cyanide may also be present. Much stronger cyanide complexes with iron or cobalt are also common but are less toxic unless exposed to sunlight. Cyanide solids, particularly those containing iron, are also common	Aqueous cyanide released into the environment can be diluted and can be degraded by: acidification through mixing with surface waters, with resulting volatilization of free cyanide; biodegradation; reaction with iron to form strong aqueous cyanide complexes or precipitate solid cyanide compounds; and photolytic degradation of strong cyanide complexes to form more toxic free or weak-acid dissociable cyanide. Breakdown of copper–cyanide or zinc–cyanide complexes may liberate enough of these metals to cause metal toxicity to aquatic organisms	Spills of cyanide processing solutions have had substantial immediate impacts on aquatic life in affected water bodies. However, it is unclear whether these impacts result from the physical effects of the tailings solids, toxicity of the cyanide, toxicity of metals released by environmental breakdown of metal–cyanide complexes, and/or toxicity resulting from application of reagents such as sodium hypochlorite intended to degrade the cyanide
Spill of mud by-products from bauxite processing	Ajka, Hungary, red mud spill (2010)	The Ajka plant did not recycle sodium hydroxide in its processing solutions, and so the mud had extreme levels of caustic alkalis in its water and mud components and when dried. The solid mud had somewhat elevated levels of As, V, Ni, Pb, Cr, Co, Mo, and Hg, and the water component had elevated levels of Al, As, B, Ga, Mo, and V	The muds were eventually diluted as the mudflow moved downstream. Some evaporative alkali salt crusts formed as the muds dried out and were available for redistribution as dusts. Foot or vehicle traffic were likely needed to disturb dried mud deposits sufficiently to generate substantial quantities of dusts. Rainfall on mud deposits likely helped consume the caustic alkalinity	Direct contact with the mud led to severe caustic alkali burns. Metals and metalloids in the mud deposits were somewhat water-soluble, bioavailable for uptake by plants, and bioaccessible. Caustic alkalis in dusts could cause caustic irritation of wet tissues. Toxicity testing indicated that the muds could generate mild inflammation of the respiratory tract
Coal slurry spills	Martin County, KY (2000)	Coal slurry has not been studied in detail but likely varies in potential toxicant content as a function of the geology and rank of the coal	Slurry and the waters separated from the slurry are likely diluted by progressive mixing with downstream surfacewater	Past slurry spills have had substantial adverse impacts on the affected aquatic ecosystems, such as fish kills. It is unclear whether these

(*Continued*)

Table 1 (Continued)

Disaster type	*Examples*	*Potentially hazardous materials*	*Key changes resulting from environmental processes*	*Characteristics of environmental or environmental health concern*
		being cleaned. The solids may have some level of inhalable to respirable particles and likely contain metals, iron sulfides, carbonates, crystalline silica, and organic components of the coal. The liquid component may have organic compounds leached from the coal (e.g., PAHs), chemicals used to wash coal, and elevated levels of sulfate, sodium, ammonium, iron, manganese, and other metals	inflows. Spilled slurry deposits with elevated levels of iron sulfides and low levels of carbonate minerals may turn acid-generating over time as the deposits weather. Dried slurry deposits may be the source of dusts. Rainfall onto slurry deposits may leach organic and inorganic components from the deposits	resulted from the physical impacts of the slurry solids, chemical impacts, or both. No studies are available that examine health impacts from human exposures to the slurry from these spills
Spills of wet-stored coal fly ash (CFA)	Kingston, TN (2008)	CFA, depending upon the coal, can contain some materials that produce acidic water leachates or more commonly materials that produce leachates with caustic alkalinity. CFA can also contain high levels of a variety of water-soluble and bioaccessible metal or metalloid toxicants, such as Pb, As, Tl, U, Hg, V, and Se. Wet-stored CFA likely has lower caustic alkalinity due to reactions with the water component. The water component may have elevated levels of metals or metalloids leached from the solids. Solids from the Kingston spill had elevated levels of metals and metalloids that were not highly water-soluble	Deposits from spilled wet-stored CFA will dry and become sources of dusts, particularly if disturbed by foot or vehicle traffic. Particle size distribution, mineralogy, and particle morphology of wet-stored CFA need further characterization. Rainfall on these deposits may continue to leach metals or metalloids from the solids, although likely at low levels	Physical impacts of spilled CFA solids from wet-stored impoundments can be substantial on aquatic ecosystems. Waters separated from wet-stored CFA sludge may also have a local impact on water quality and aquatic organisms due to alkalinity and toxicity of dissolved metals or metalloids. Dusts generated from dried CFA deposits may be a source of exposure to some metal and metalloid toxicants. Further work is needed on the bioaccessibility of metals and metalloids in wet-stored CFA solids
Building collapse	World Trade Center (WTC) collapse (2001)	Dust and debris from the WTC collapses were complex mixtures of pulverized materials used in building construction or found in buildings, including mineral toxicants (e.g., asbestos and crystalline silica), water-soluble minerals (wallboard gypsum), window glass, man-made glass fibers, acutely bioreactive materials (caustic calcium hydroxide from concrete particles), water-soluble metal or metalloid toxicants (Sb, Mo, and Cr(VI)), and metal or metalloid toxicants that are bioaccessible in gastric and/or lung fluids (Pb, Sb, Cu, Zn, etc.). Fires in the building prior to and following collapse produced smoke and soot with elevated levels of organic contaminants such as PAHs	Particle size distribution changed with distance way from the source as the heavier, coarser particles settle out preferentially. Rainfall reacted with and consumed some of the caustic alkalinity, leached soluble components from dust and debris into local waters, and enriched the residual materials in less water-soluble but potentially bioaccessible metals or metalloids such as lead	Health problems are now being recognized in people exposed to the dust cloud created by the WTC collapse; workers engaged in rescue, recovery, and cleanup at or near Ground Zero following the collapses; and local residents living near the WTC. These are attributed to various aspects of the dusts, such as the high levels of PM during the collapses, the caustic alkalinity of the dusts, and metals or metalloids in the dusts

See corresponding sections in the text for details and references cited.

11.7.3.1 Factors Influencing the Health Effects of Disaster Materials

Many factors can influence the health effects of DM and other earth materials on exposed humans and other organisms (Plumlee and Morman, 2011; Plumlee and Ziegler, 2007; Sullivan and Krieger, 2001). The initial factor is the exposure pathway, which includes the DM source, transport media (soil, dusts, sediments, air, water, foodstuffs, etc.), points of exposure, and exposure route. The exposure route is how humans take up DM or DM-contaminated materials and can be via inhalation, ingestion, or dermal/ocular contact. The dose, which is the intensity and duration of the exposure, is a key factor in the potential health effects.

The body has a range of physiological defenses against DM particles and other foreign matter. Inhaled particles can be trapped in the mucus lining the respiratory tract, cleared upward into the throat by ciliated cells, and then swallowed or expectorated. Alveolar macrophages are free-roaming cells that engulf foreign particles respired deep into the lungs; they either digest the particles or clear them into the lymph system or throat. Foreign matter trapped in the eyes can be dissolved or flushed by increased production of tears.

The phases present in DM ultimately play a key role in their potential health effects. For example, different natural or anthropogenic solid phases have different morphologies, chemical solubilities, and dissolution rates in the body's fluids, biological reactivities, and toxicant contents. These factors can all play a role in how the DM enter the body, interact with the body, and potentially cause toxicity.

The size of solid DM particles determines how readily they can be ingested and how deeply they can penetrate into the respiratory tract. Particles less than 250 μm are most readily ingested by hand-to-mouth transmission (EPA, 2008a). Those less than 100 μm may be inhaled into the upper respiratory tract, those less than 10 μm can penetrate into the bronchiolar portion of the lungs, and those less than 2.5–4 μm can be respired deep into the alveoli (McClellan, 2000). Mouth breathing as a result of exertion or nasal congestion, such as would likely occur during disasters that produce large amounts of atmospheric particulate matter (PM), allows coarser particles to penetrate deeper into the lungs (see figure 4 in Plumlee et al., 2006a; modified from ICRP, 1995).

The morphology of DM particles also influences how readily they are taken up and cleared by the body. Asbestos fibers less than ~0.5–1.0 μm wide and less than ~20 μm long can be respired deep into the alveoli, but those longer than ~5–10 μm are too long to be engulfed by the alveolar macrophages (Aust et al., 2011). These dimensions also apply to other 'respirable elongate mineral particles' (REMP; Aust et al., 2011) that do not necessarily meet the mineralogical or regulatory definitions of asbestos (Case et al., 2011; Gunter et al., 2007; NIOSH, 2003) but that are of potential concern from a toxicological perspective (Aust et al., 2011). Examples include the fibrous winchite and richterite amphibole at Libby, Montana, and fibrous erionite in Turkey, all of which have been clearly linked to high rates of asbestos-related disease (Carbone et al., 2011; Meeker et al., 2003; Sullivan, 2007). Large doses of nonelongate particles or smaller doses of some REMP can exceed the capacity of the lungs' various physical clearance mechanisms (Aust et al., 2011). Short REMP can also more easily become translocated to other parts of the body. The effective surface area of REMP has been shown to correlate with enhanced toxicity due to the increased surface area available for contact and interactions with cells (Aust et al., 2011).

Chemical reactions between DM and the body's fluids and tissues along the different exposure routes are key factors in their disposition and toxicity in the body (Plumlee and Ziegler, 2007; Plumlee et al., 2006a). The same mineral or solid phase can have greatly different solubilities and dissolution rates in the fluids of the eyes, fluids lining the respiratory tract (near-neutral pH, abundant mucoproteins, and surfactants), fluids in alveolar macrophage lysosomes (which are acidic and have abundant enzymes and oxidants), enzyme-rich saliva, acidic gastric fluids, and near-neutral-pH intestinal fluids (Plumlee and Ziegler, 2007). Biosoluble minerals dissolve quickly in the body, whereas biodurable minerals dissolve slowly and can persist in the lungs and tissues for years (Jurinski and Rimstidt, 2001). Halide, bromide, and some sulfate and carbonate compounds dissolve readily in both the respiratory tract and gastric fluids. Glasses, such as those in VA or man-made vitreous fibers found in building collapse dusts, can dissolve relatively quickly (over months to years) in the fluids of the respiratory tract. In contrast, crystalline silica and amphibole asbestos are highly biodurable in the lungs. Using published concentrations for dissolved electrolytes and silica in lung fluids, thermodynamic calculations show that the lung fluids are close to saturation with quartz (Plumlee and Ziegler, 2007). As a result, quartz grains do not have a thermodynamic driver to dissolve. In contrast, amphibole asbestos is highly undersaturated in the lung fluids, so its biodurability is kinetic (Plumlee and Ziegler, 2007; Taunton et al., 2010). Chrysotile asbestos is also undersaturated in the lung fluids but likely dissolves more rapidly than amphibole asbestos due to its scroll structure that unrolls as it dissolves, which, in turn, exposes more surface area for dissolution. This enhanced dissolution may be a factor in chrysotile's generally lower carcinogenicity than amphibole asbestos (Jurinski and Rimstidt, 2001).

The fate of inhaled gaseous DM in the respiratory tract is a function of the concentration of the gases in the inhaled air coupled with the solubility of the gases in the fluid lining the lungs. Water-soluble gases, such as sulfur dioxide, tend to be absorbed at higher levels in the respiratory tract than less soluble gases, such as nitrogen oxides (Newman, 2001).

The bioaccessibility of metal and metalloid toxicants measures how readily they are released into the body's fluids from solid, liquid, or aqueous DM and are available for uptake, whereas bioavailability measures how solubilized toxicants are actually absorbed by the body and transported to a site of toxic action (Hamel, 1998; Ruby et al., 1999). Mineralogy can play an important role in the bioaccessibility of various metal or metalloid toxicants; for example, lead carbonate and lead oxide minerals are much more bioaccessible in the gastric fluids than lead sulfides (Casteel et al., 2006). Not all bioaccessible toxicants are bioavailable, such as some metal toxicants that dissolve in stomach acids but reprecipitate or sorb onto other phases in the near-neutral intestinal fluids and are then excreted. For example, hexavalent chromium can be readily solubilized from various DM in the acidic gastric fluids and

in the near-neutral fluids of the lungs. It is readily reduced to Cr(III) in the acidic conditions of the stomach, through reactions with chloride and organic species, but reprecipitates as Cr (III) oxide/hydroxide phases in the higher-pH intestinal fluids and is excreted in the feces. Hexavalent chromium is much more persistent in the lung fluids, blood serum, and tissues, due to reduced kinetics of reduction reactions at pH 7.4 (Wolf et al., 2011). It is then readily absorbed and transported across cell membranes, similar to sulfate and phosphate species.

DM may be chemically bioreactive in the body. For example, water-soluble, acid-generating gases (e.g., sulfur dioxide or hydrogen chloride) or soluble acid-containing solids may cause acute, acid-related tissue irritation or damage. Efflorescent salts formed by evaporation of acid-rock drainage are an example of the latter (Plumlee and Morman, 2011). Wildfire ash (which is high in alkali and alkaline-earth hydroxides), and concrete particles produced by building collapse (which contain high levels of calcium hydroxide) can cause acute, alkali-related tissue irritation or damage and other health problems (Plumlee et al., 2005, 2007b; Rom et al., 2010).

DM particles can also be redox-bioreactive in the body. Reactions *in vivo* of dissolved oxygen or nitrogen with unresolved bonds on freshly broken mineral surfaces or with iron released from asbestos particles have been two of the most commonly cited examples of reactions that can cause acute or chronic generation of reactive oxygen species (ROS), reactive nitrogen species (RNS), and lipid peroxidation in the body. These then result in oxidative stress that can cause DNA damage, mutagenesis, toxicity, and cancer (Aust and Lund, 1990; Aust et al., 2002; Fubini and Areán, 1999; Horwell et al., 2007; Huang et al., 2011; Schoonen et al., 2006). Recent studies are implicating a number of additional phases and redox-variable elements, including pyrite and other iron sulfides in coal dusts, iron-rich VA, iron coatings on quartz grains, manganese(III) oxides, and hexavalent chromium in various materials (Franco et al., 2009; Harrington and Schoonen, 2012; Schoonen et al., 2006).

Biodurable DM can trigger chronic inflammation in the lungs as a result of the release of ROS/RNS from activated alveolar macrophages, lung epithelial cells, and mesothelial cells. These cells, which are activated by the presence of foreign particles, release a variety of chemical messengers, enzymes, and growth factors that promote tissue repair but can, over the long term, promote fibrosis and mutagenesis (Huang et al., 2011). The body's fibrotic response to mineral particles can vary according to mineralogy. For example, biodurable crystalline silica minerals, asbestos, and coal dusts are highly fibrogenic (they trigger fibrotic diseases of the lungs), whereas other biodurable minerals such as calcium phosphate are less so (De Capitani, 1989).

Research into the integrated toxicological effects (possibly synergistic or antagonistic) of complex toxicant mixtures, particularly for those found in DM, is relatively limited. The research that has been done indicates that multiple-toxicant exposures can either increase or decrease health impacts (ATSDR, 2004). For example, the combined exposure to both manganese and lead has been shown to enhance lead toxicity (Henn et al., 2012), as do exposures to lead and arsenic, and lead and methylmercury (ATSDR, 2004). Exposures to mixed dusts containing both REMP and other non-REMP types can result in different, sometimes greater, toxicity responses than with the REMP alone (Aust et al., 2011).

Individual-specific factors may promote or counteract toxic effects of exposure to DM. These include age, gender, genetics, habits (i.e., smoking), overall health, diet, and nutritional status. For example, children are more susceptible than adults to lead toxicity, and reduced nutritional status enhances absorption of lead from the intestines.

11.7.3.2 Interdisciplinary Methods Used to Study the Health Effects of Disaster Materials

Many health science methodologies are used to assess the potential health effects of exposures to DM and other earth materials (Sullivan and Krieger, 2001). The following discussion primarily cites as examples the many health science studies of emergency responders and others exposed to dusts and smoke following the attacks on and collapse of the WTC Towers on 11 September 2001. These studies show that medical issues resulting from exposures to DM may take many years to develop and so require long courses of study.

Medical care and monitoring of workers or populations that may have had exposures to DM are an important first step and continuing source of information in identifying and assessing potential health problems (e.g., Aldrich et al., 2010; Webber et al., 2011). Biological monitoring determines if DM toxicants are present in blood, urine, hair, or tissue samples and can thus provide further indications of exposures to and uptake of toxicants (e.g., Edelman et al., 2003). Induced sputum and bronchoalveolar lavage testing provides insights into the PM in the respiratory tract (Fireman et al., 2004; Rom et al., 2002). Epidemiological studies examine disease rates in rescue, response, or cleanup worker cohorts and in populations exposed environmentally to DM (e.g., Li et al., 2011; WTCHP, 2011; Zeig-Owens et al., 2011). Pathology studies examine tissue samples collected through biopsy or autopsy of individuals for evidence of diseases (Caplan-Shaw et al., 2011; Crowley et al., 2011; Izbicki et al., 2007; Meeker et al., 2010; Wu et al., 2010). *In vivo* uptake tests measure the uptake and absorption of toxicants from various materials by live animals (Casteel et al., 2006). Toxicity testing has been applied to a wide variety of earth materials and anthropogenic materials, including both *in vitro* (in the laboratory) tests using cell cultures (e.g., Franzi et al., 2011) and *in vivo* tests using live animals (e.g., Gavett et al., 2003; Wegesser et al., 2009). *In vitro* physiologically based extraction tests (PBETs) (also called *in vitro* bioavailability assessments, or IVBAs) are leach tests that model release of toxicants from materials into the simulated gastric, intestinal, lung, alveolar macrophage lysosomal, and other body fluids (Basta et al., 2007; Caboche et al., 2011; Drexler and Brattin, 2007; Gray et al., 2010; Hamel, 1998; Morman, 2012; Plumlee and Ziegler, 2007; Wolf et al., 2011).

Geochemists and other earth scientists, especially when working with collaborators in the health sciences, can make substantial contributions across this spectrum of health science investigations. Geochemists can provide the needed information on predisaster environmental baseline conditions. Earth scientists can provide health scientists with key predictive information about the minerals, other phases, and toxicants likely to be present in various DM based on lessons learned

from similar previous disasters (Plumlee et al., 2012). A wide variety of earth science methods can be applied to help characterize the nature of human exposures to DM, including (1) the toxicologically important size, shape, surface area, mineralogical, geochemical, and bioreactivity characteristics of DM samples, both as released from the source and as modified by environmental processes; (2) the content and oxidation state of elemental toxicants; (3) the isotopic composition of lead and some other elemental toxicants to help determine their sources; and (4) the likely biosolubility, bioaccessibility, and bioreactivity behavior in the body. Such characterization is essential to help understand the nature and potential sources of DM to which populations or individuals may have been exposed, the pathways by which exposures occurred, the characteristics of DM used as dosing materials for toxicity testing, and the DM sources of toxicants found to be elevated as a result of biomonitoring studies. Earth scientists can also help understand the exogenic versus endogenic origin of solid particles found in samples of sputum, in bronchoalveolar lavage fluids, or in tissues collected by biopsy or autopsy by interpreting mineralogy, mineral textures, and other pathology findings in a geochemical context (Caplan-Shaw et al., 2011; Meeker et al., 2010; Plumlee et al., 2006a; Wu et al., 2010).

11.7.4 Sampling, Analytical, and Remote Sensing Methods Applied to Disaster Materials

A wide range of analytical methods traditionally used for earth science investigations can be applied to understand key characteristics of DM that are important from an environmental or human health perspective, how these characteristics may change once in the environment, and how they may change in the human body. In this section, a brief overview is given of the sampling, analytical, and remote sensing methods that have been applied to DM. Many of the analytical methods mentioned in this section are discussed in more detail in *Treatise on Geochemistry* Volume 15, Analytical Geochemistry/Inorganic Instrument Analysis.

11.7.4.1 Spatially Extensive Sampling in Rapid Response and over the Long Term

Ideally, sampling of DM can be done to maximize understanding of spatial and temporal variability in the makeup of the materials. Sampling should be carried out as soon as possible after a disaster to collect fresh samples and to preserve possible ephemeral constituents. Even better, this sampling should be from spatially separated sites to assess for variable contributions from multiple sources or to assess chemical or physical changes that the materials undergo in the environment as they move away from a source. Repeated sampling of some sites over time following a disaster will help understand long-term changes in the materials in response to environmental processes, such as weathering, oxidation, wetting by rainfall, and others.

11.7.4.2 Safety during Sampling

The sampler must be protected from physical and other hazards in an inherently unsafe disaster environment to ensure safety. The sampler should be physically fit to withstand the rigors of sampling in such an environment. The sampler should also be protected from exposure to either likely or potential toxicants or pathogens contained in DM. Hence, appropriate training in disaster response safety, HM, and proper use of the personal protective equipment appropriate for a given event (e.g., toxicant-specific respirators and gloves vs. full TYVEX suits,) is essential for all personnel who may become involved with disaster response. Examples of training or certification USGS sampling crews have include the Occupational Safety and Health Environment (OSHA) 40-Hour Hazardous Waste Operations and Emergency Response Standard (HAZWOPER) training (http://www.osha.gov/html/faq-hazwoper.html) and the US Forest Service Red Card Certification for access to recently active wildfire areas (USFS, 2011). When seeking access to sample in areas affected by very recent disasters, familiarity with the roles, responsibilities, and interactions of the various federal, state, and local agencies and authorities involved with disaster response (e.g., Emergency Support Functions described by the Federal Emergency Management Agency (FEMA) at http://www.fema.gov/pdf/emergency/nrf/nrf-esf-intro.pdf) and with the Incident Command System used during disasters is also important.

11.7.4.3 Sampling Methods for Deposits of Solid Samples

Over the course of multiple disaster responses, a sampling scheme has been developed for solid deposits of DM (such as deposits of settled dust/debris, flood sediments, VA, and wildfire ash) and soils that underlie the deposits (Hoefen et al., 2009). Because deposits of many DM types can be quite heterogeneous, a key aspect of the sampling scheme is to try to collect (whenever time and logistics permit) a composite sample made up of multiple subsamples collected from evenly spaced increments, such as in a star pattern radiating from a centroid or along a transect. This method was based upon a method originally proposed by Smith et al. (2000) for sampling heterogeneous mine waste piles. A template that 'cookie cutters' the deposit material and underlying soils is used to ensure that the subsamples are each collected from the same surface area and allows total mass of material and various toxicants present in the material to be calculated per square surface area. If time or logistics preclude such detailed sampling, then a composite of multiple grab samples or even a single grab sample will have to suffice.

When underlying soils are collected, a standard depth of collection is typically the uppermost 5 cm (Smith et al., 2009). This is typically the portion of the soil column that is most easily disturbed and therefore the most likely source for exposures.

Different sample types are required for specific analytical methods (Hoefen et al., 2009). For example, samples for bulk inorganic analysis can be collected using plastic scoops (or in the case of indurated samples such as soils, stainless steel scoops) into high-density polyethylene (HDPE) widemouth bottles. Samples for analysis of organic contaminants are collected using a stainless steel spoon into baked brown glass jars and stored on ice. Samples for microbial analysis can be collected with sterile plastic scoops into new sterile centrifuge tubes.

The sampling methods described by Hoefen et al. (2009) were designed to collect samples that maximize understanding of geochemical processes and were not intended to meet

regulatory or litigation requirements. For samples that will be used for regulatory or litigation purposes, the analytical methods and analytes of interest should be determined before sampling and appropriate sample collection, preservation, and storage protocols are used to comply with chain-of-custody, analytical method, and holding time requirements. For studies that fall under the US Resource Conservation and Recovery Act regulations for wastes, appropriate test and sampling procedures can be found in EPA (2008c). The US Environmental Protection Agency (USEPA) Characterization and Monitoring Program also provides up-to-date research on a variety of topics related to sampling and analysis (http://www.epa.gov/esd/cmb/default.htm).

11.7.4.4 Sampling Methods for Airborne Particulate Matter and other Aerosols

Active air sampling for airborne PM and other aerosols (including water droplets and other aerosolized liquids) requires specialized pumps and sample collection devices (of which there are many different types) that need careful calibration, cleaning, and maintenance. The papers in Kulkarni et al. (2011) present a detailed discussion of these sampling methods. Typically, pumps pull air through filters, cascade impactors, or liquid impingers to trap the entrained PM (Kulkarni et al., 2011). High-volume air pumps with large surface area filters are designed to collect large amounts of material over extended periods of time. Personal air samplers are typically low-volume, collect on small surface area filters, and are designed to sample in as realistic a manner as possible the air being inhaled. Specialized samplers such as cascade impactors, cyclone separators, or button samplers can separate the PM by size to collect only respirable PM2.5 (<2.5 μm), inhalable PM10 (<10 μm), or in a series of size ranges. Specialized sampling equipment is also needed to collect samples for airborne microbes.

Stationary air samplers are those that are left at a single site for the period of sampling and provide useful indications about how PM may change over time. A number of studies have found that activity-based air sampling does a better job of measuring actual PM exposures to people than stationary monitors. In activity-based sampling, the persons doing the sampling wear personal air samplers while they participate in activities that would be done by potentially exposed people (e.g., a homeowner sweeping or cleaning up DM deposits).

A key aspect of PM sampling is to be aware that the sampling equipment, particularly low-volume samplers, can be easily overloaded during very dusty conditions. As a result, the sample collected may not be truly representative of the PM actually present over the course of the sampling period (e.g., see case study in NRC, 2010).

11.7.4.5 Field Analytical Methods for Solids

Handheld X-ray fluorescence (XRF) units have become popular for field analysis of elemental toxicants in soils or sediments, dust wipes or filters, and plastics (e.g., Dooyema et al., 2012; EPA, 2006; Hansen, 2012). The units can provide a very useful, rapid assessment in the field of potential elemental contaminants without time delays associated with the collection of samples, shipment to the analytical lab, and sample preparation for analysis. However, as with all analytical methodologies, the accuracy and precision of the results can depend strongly upon many different factors, including the element being analyzed, the analytical processing routine chosen (most units offer different analytical routines depending upon the likely contaminant concentrations), the concentrations of elements in field calibration standards compared to those in the target materials, the heterogeneity of the target materials, and the ambient conditions as the units are being used (EPA, 2006).

11.7.4.6 Sampling and Field Analysis Methods for Waters

Many different literature sources discuss appropriate water sampling techniques and field analytical methods that must be used to measure unstable parameters, such as temperature, pH, Eh, specific conductance, and dissolved oxygen, and field methods to measure other parameters, such as alkalinity, chloride, or fluoride, using kits or ion-specific electrodes in the field. The USGS National Field Manual for the Collection of Water-Quality Data (USGS, 2010) is an excellent and comprehensive source for field sampling and analysis protocols covering both inorganic and organic constituents. Ficklin and Mosier (1999) discuss sampling and field analysis of samples for inorganic constituents.

The key water sample types collected for inorganic analysis include (1) unfiltered acidified (with several drops of ultrapure nitric acid), for the total content of major and trace elements; (2) filtered (usually to <0.1 or 0.45 μm) acidified, for the analysis of dissolved trace elements; and (3) filtered unacidified, for the analysis of anions. Samples for aqueous inorganic mercury should be collected in 10% nitric acid-washed, triple-rinsed glass jars with a Teflon cap and preserved with 0.5 ml Ultrex HCl per 30 ml of sample, and once in the lab, BrCl is added (Hageman, 2007a).

The sampling methods designed specifically for the regulatory aspects of drinking water under the US Safe Drinking Water Act (SDWA) include the EPA Interactive Sampling Guide (http://water.epa.gov/type/drink/pws/smallsystems/samplingcd.cfm#two), the Sampling Guidance for Unknown Contaminants in Water, EPA-817-R-08-003 (http://www.epa.gov/watersecurity/pubs/guide_watersecurity_samplingforunknown.pdf), and the Response Protocol Toolbox for threats to drinking water systems, EPA 817-D-03-003, (http://www.epa.gov/watersecurity/pubs/guide_response_module3.pdf). Many states in the United States have their own sampling protocol guidance documents for sampling drinking water.

11.7.4.7 Processing and Preparation of Solid DM for Lab Analysis

Solid samples require processing prior to analysis (Hoefen et al., 2009). Contained waters in muds or wet sediments can be decanted, filtered, and analyzed. Wet samples must be air-dried at ambient temperature or freeze-dried prior to processing. Standard protocols for soil analysis (Smith et al., 2009) typically call for solids to be gently disaggregated and sieved to <2 mm. Splitting of samples is done using either cone and quartering or a Jones splitter. For many types of analysis, solid samples are ground using an automated agate mortar/pestle or micronizer, then homogenized prior to analysis.

11.7.4.8 Laboratory Methods for the Analysis of Disaster Materials

A wide range of analytical methods should be applied to DM in order to understand as much as possible about their sources, environmentally and toxicologically significant characteristics, and spatial and temporal changes. The following is a summary of most of the analytical methods that have been applied to DM samples. The details of the analytical methods are mostly described in Taggart (2002); otherwise, specific references are listed with the particular technique.

Bulk inorganic chemical composition of solids is typically measured on a sieved (<2 mm), ground split using inductively coupled plasma mass spectrometry (ICP-MS) for a 44-element suite. The USGS analyses use a four-acid (hydrochloric, hydrofluoric, nitric, and perchloric) digestion of the solid sample, which is typically considered a total digestion of most environmental materials. However, it is known that some acid-resistant mineral forms, such as chromite, cassiterite, and barite, as well as the rare earth elements, are not completely recovered using this method. In general, EPA (2008c) protocols (such as Method 3050B or 3051A) specify a less aggressive aqua regia digestion that typically yields, for a given sample, smaller total concentrations than the USGS four-acid digestion.

Major elements in solids (including chemical silica, which is not measured by ICP-MS) can be measured using laboratory wavelength dispersive XRF on a ground split that has been heated to 925 °C for 40 minutes to drive off volatile components, then fused with lithium tetraborate at 1120 °C. The amounts of volatile components (water, organic material, etc.) can be determined by weight loss during the initial heating of the sample.

Total carbon and total sulfur can be determined by combustion, carbonate carbon by coulometric titration, and organic carbon by the difference between total carbon and carbonate carbon.

Total inorganic mercury content of solids can be analyzed on a dried, ground split using continuous flow-cold vapor-atomic fluorescence spectrometry (CVAFS; Hageman, 2007a).

The inorganic cation and trace-element content of vegetation can be analyzed via ICP-MS or inductively coupled plasma atomic emission spectroscopy (ICP-AES) on an ashed, four-acid digested sample. A microwave-assisted digestion on a raw, dried material is also commonly used.

The identification of minerals and amounts of amorphous materials present in solids at levels above 1–2 wt% is accomplished using powder X-ray diffraction (XRD) analysis on a dried, ground sample.

Particle mineralogy, morphology, and chemical composition can be analyzed in dried, unground solid samples or air filters using scanning electron microscopy (SEM), electron probe microanalysis (EPMA), transmitted electron microscopy (TEM), or laser-ablation ICP-MS.

Particle size analysis is accomplished using a Malvern Mastersizer-S long bed laser analyzer. An unground, gently disaggregated, dried sample is introduced into an aqueous medium and pumped through the laser analyzer for grain size measurements.

Sulfur speciation (amounts of sulfur tied up in monosulfide, disulfide, elemental sulfur, and water- and acid-soluble sulfates) is analyzed using a sequential extraction scheme (Tuttle et al., 2003). Sulfur isotopic compositions of the various sulfur fractions can also be measured, as can the oxygen isotopic composition of sulfate species.

The concentrations of many organic chemicals in solids are measured by gas chromatography/mass spectroscopy (GC/MS) following an organic extraction using a microwave-assisted solvent extraction (Kvenvolden et al., 2002) and compound fractionation by adsorption chromatography (Kvenvolden et al., 1995).

A net acid production test (Fey et al., 2000) of a ground and micronized solid sample measures the maximum amount of acid that will ultimately be generated as a result of weathering and oxidation of sulfide minerals in mine wastes and other DM. A similar test for net alkali production could also be developed and applied to measure the amount of caustic alkalinity generated when DM containing caustic alkalis interact with rainwater.

Synchrotron-based XRF, XRD, and X-ray absorption spectroscopy (XAS) (Reeder et al., 2006) are increasingly applied to understand and map the mineralogy, phase composition, elemental associations, and oxidation states of elements such as chromium and arsenic in DM samples (e.g., Burke et al., 2012; Roy et al., 2007).

Some studies use sequential chemical extractions to glean information about the solid phases in which potential toxicants reside (e.g., Shi et al., 2010). These extractions submit the solid to a series of increasingly chemically aggressive leaches that are designed to extract elemental toxicants from various fractions or classes of solids, such as exchangeable, bound to carbonates, bound to iron or manganese oxides, bound to organic matter, and residual. However, these extractions are operationally defined based on the chemicals used and so provide the most accurate information when their results are interpreted using knowledge of the mineralogy and particle chemistry of the solids as determined by XRD, SEM, and other methods.

Various leach tests can be applied to DM to model how they will react with rainfall, seawater, or landfill leachate solutions. For example, we regularly use the USGS Field Leach Test (Hageman, 2007b) for rapid assessment of the potential reactivity and release of metals and anions into the environment from DM due to interactions with rainfall. This test involves a 5 min agitation of a DM sample with deionized water, typically in the proportions of 1 part solid to 20 parts water by weight. It has been compared extensively against the EPA Method 1312 Synthetic Precipitation Leaching Procedure (see discussion in Hageman, 2007b), which uses a much longer 18 h agitation time. When time is available to do both, valuable information can be gleaned about short-term versus long-term changes that can occur as rainfall reacts with DM. Similarly, EPA's Method 1311, the Toxicity Characteristic Leaching Procedure (TCLP) (EPA, 1992) and the simplified methods based upon the TCLP (Jeppson et al., 2006) can be used to model mobility of inorganic and organic contaminants from DM that are disposed of in landfills.

The bioaccessibility of various inorganic and organic toxicants from DM in a range of simulated body fluids is modeled by IVBAs, also called PBETs. We have carried out gastric and sequential gastric–intestinal IVBAs on a number of DM using gastric protocols based upon those of Drexler and Brattin

(2007) and intestinal protocols based on Basta et al. (2007). The Drexler and Brattin gastric IVBA has been validated (Casteel et al., 2006) for lead against juvenile swine uptake (a proxy for relative lead bioavailability in humans), and so the USEPA lists this test as a standard operational procedure for lead bioaccessibility. This gastric IVBA has not been validated against swine uptake for other toxicants but provides useful insights into their bioaccessibility.

Ansoborlo et al. (1999) and Stefaniak et al. (2006) provide excellent discussions of various simulated lung fluid (SLF) and macrophage lysosomal fluid IVBAs examining particle dissolution and uranium and beryllium bioaccessibility in the lung environment. We have modified and applied these types of IVBAs to DM and other earth materials using SLF, simulated alveolar macrophage lysosomal fluid, and serum-based fluid as the extracting fluids (Gray et al., 2010; Morman, 2012; Wolf et al., 2011); these model potential toxicant release from inhaled or respired particles. The gastric–intestinal leaches are performed on samples sieved to <250 μm, and the simulated lung and serum-based fluid leaches are done on samples sieved to <20 μm.

The chemical analysis of water samples, waters separated from wet DM, and leachate solutions can include (1) pH, specific conductance, alkalinity, and other parameters; (2) dissolved and total cations and metals by ICP-MS; (3) inorganic mercury by CVAFS; (4) dissolved organic carbon (DOC); (5) content of water-soluble organics by GC/MS; (6) stable hydrogen and oxygen isotopic composition; and (7) stable sulfur and oxygen isotopic composition of sulfate species.

Methods to determine the oxidation state (redox) speciation and temporal stability of variable-oxidation-state elements in waters, water leachates, and IVBA leachates are important to understand because of both the environmental and toxicological implications. For example, a method recently developed by Wolf et al. (2011) is now routinely used to simultaneously analyze for tri- and hexavalent chromium and tri- and pentavalent inorganic arsenic forms in waters, DM water leachates, and IVBA leachates. Iron redox speciation methods have been available for some time, but additional methods to rapidly determine oxidation state speciation of other potential elemental toxicants in solution, such as manganese, copper, molybdenum, and vanadium, are also needed.

A variety of methods have been developed to assess the toxicity of metals, mine wastes, contaminated sediments, and other materials on freshwater or marine aquatic organisms (e.g., Besser et al., 2009; Carr et al., 2003; Choate, 2012; Munns et al., 2002; Wildeman et al., 2007). These can readily be applied to assess impacts of DM on aquatic ecosystems.

Various techniques can be applied to understand the microbial makeup of water and solid samples. For example, multiplex polymerase chain reaction (PCR) analysis can be used to screen for the presence of microbe types (i.e., total *Bacillus* species) or specific pathogens, such as *Bacillus anthracis* (Griffin et al., 2009).

11.7.4.9 Remote Sensing Methods for Identification and Mapping of Disaster Materials

Remote sensing methods provide an important tool in the earth science toolbox for identifying types and compositions of DM, for mapping DM distribution in the environment, and for mapping damage to affected areas following a disaster. A variety of visible light (such as IKONOS), multispectral (such as Landsat 7 or MODIS), and hyperspectral (EO-Hyperion) satellite-based systems provide the best option for rapid detection and mapping of DM during and soon after disasters (e.g., Jennings et al., 2005; Klemas, 2010), especially when their orbit paths coincide temporally with the area affected by the disaster. However, these platforms are substantially (IKONOS and Landsat) to somewhat (EO-Hyperion) limited in the amount of compositional information that they can provide about the materials. Plane-based hyperspectral remote sensing platforms such as Airborne Visible and Infrared Imaging Spectrometer (AVIRIS), although challenging to deploy in a timely manner and limited in their lateral coverage away from their flight lines, can provide substantially more in the way of compositional and other types of information about DM (e.g., Clark et al., 2001, 2005, 2010; Kokaly et al., 2007, 2010; Swayze et al., 2005). The interpretation of hyperspectral remote sensing data benefits greatly from detailed mineralogical and chemical studies performed on samples collected in the field, most commonly in conjunction with ground calibration and verification for the AVIRIS at the time of the remote sensing flights. Reflectance spectroscopy measurements of DM in the field using a handheld reflectance spectrometer can provide initial interpretations of minerals and other phases present in DM, and laboratory reflectance spectroscopy measurements on collected samples provide more spectrally detailed information that can be linked to the results of laboratory mineralogical and chemical characterization of samples (e.g., Swayze et al., 2005).

11.7.5 Volcanic Eruptions and Volcanic Degassing

Volcanologists have been pioneers in the field of medical geology and have worked for decades with health experts to study the health impacts of VA and volcanic gases. Excellent summaries of the health characteristics and health impacts of VA, volcanic gases, and related materials are presented by Hillman et al. (2012), Horwell and Baxter (2006), Hansell et al. (2006), and Weinstein and Cook (2005). Ayris and Delmelle (2012) summarize the environmental effects of VA. Additional resources can be found in the websites of the International Volcanic Health Hazards Network (www.ivhhn.org) and USGS Volcano Hazards Program (http://volcanoes.usgs.gov/ash/index.html).

Various textbooks (e.g., Francis and Oppenheimer, 2003) and review articles (e.g., Witham et al., 2005) present a detailed discussion of the many complex factors that interact to control the composition of VA, gases, vog, and laze. These include the geologic setting of the volcano, magma composition (including water and other volatile content), temperature, depth of the source magma body, and eruption type (e.g., plinian, dome collapse, lava flow, and phreatomagmatic). The discussion here will focus on the characteristics that are most significant from an environmental or toxicological perspective.

11.7.5.1 Volcanic Gases, Vog, and Laze

Volcanic smog (known as vog) is a mixture of atmospheric gases, volcanic gases, and suspended liquid and solid particles.

It forms by the reaction of sulfur dioxide, hydrogen chloride, hydrogen fluoride, and other volcanic gases with atmospheric moisture, gases, dust, and sunlight (Sutton et al., 1997). Vog consists primarily of sulfuric acid and other sulfate compounds, but can also contain hydrochloric and hydrofluoric acids, and a variety of heavy metals, including selenium, mercury, and arsenic (Sutton et al., 1997). It is possible that vog may change in composition downwind from volcanic sources, becoming more enriched in sulfuric acid downwind relative to hydrochloric and hydrofluoric acids; this is related to the slower kinetics of gaseous sulfur dioxide conversion into sulfuric acid droplets compared to the rapid dissolution of hydrogen chloride and hydrogen fluoride into water aerosols (Delmelle, 2003).

Laze, a volcanic haze, forms when molten lava flows into the sea and vaporizes seawater (Sutton et al., 1997). It has many of the same characteristics as vog, with the exception that it probably contains higher levels of chloride and hydrochloric acid derived from seawater and may have lower concentrations of various heavy metals.

Delmelle (2003) summarized the environmental impacts resulting from dry deposition or wet deposition of volcanic gases on vegetation, surface water bodies, and soils. Direct toxicity effects of gases, such as SO_2, are generally only an issue where the gases are in highest concentration close to the vent from which the gases are emanating. Adverse health effects that have been noted as the result of vog produced by active Hawaiian volcanoes include irritation of the mucous membranes (eyes, nose, and throat), increased asthma, respiratory distress, increased susceptibility to respiratory ailments, headaches, watery eyes, and lack of energy (Sutton et al., 1997). These problems increased on the island of Hawaii during the eruption cycle of Kilauea volcano that began in 1986. These health effects are tied to the generation of acid in perspiration and fluids of the eyes and respiratory tract by condensation of SO_2 and other acid gases, uptake of acid-sulfate aerosol droplets, and dissolution of acid-bearing, sulfate- or chloride-rich salts from the vog particulates. Increased lead uptake by local residents has also been noted and results from the leaching of lead from metal roofing and flashing by rainfall that has been acidified by volcanic gases. Fluorosis can develop in livestock or wildlife that consume vegetation and entrained soils that have incorporated hydrogen fluoride deposited from vog.

11.7.5.2 Crater Lake Gas Eruption Disasters – Lake Nyos as an Example

Geochemistry played a key role in understanding the origins of the 1986 Lake Nyos gas disaster that killed 1700 people (Baxter et al., 1989; Evans et al., 1989). The primary cause was determined to be the eruption of large volumes of carbon dioxide-rich gases from the crater lake of a volcano, leading to the widespread asphyxiation of humans and animals living in low areas around and downstream from the volcano lake. Multiple studies agreed that the CO_2 was ultimately of volcanic origin. However, there was considerable debate about whether the eruption was phreatic in origin or resulted from limnic overturn and pressure release of lake waters that had, over many years, become CO_2-charged by volcanic degassing. The latter interpretation has generally garnered the most support based on a variety of geological and geochemical arguments. The burnlike lesions on a number of victims and survivors were originally interpreted as having resulted from the effects of other acid volcanic gases in the gas cloud (such as hydrogen fluoride, hydrogen chloride, hydrogen sulfide, and sulfur dioxide), but subsequent medical studies concluded that the lesions were more easily explained by loss of consciousness caused by exposure to carbon dioxide in air.

11.7.5.3 Volcanic Ash

VA erupted explosively from a volcano is generally composed of a mixture of pumice/glass shards (essentially quenched magma), fragments of older rocks from the volcano, and variable proportions of crystals or crystal fragments of various silicates and other less abundant mineral types. **Figure 1(a)** shows the dusty conditions in Homer, Alaska, created by ashfall from the 4 April 2009 eruption of Mt. Redoubt approximately 105 km away.

Acute respiratory health effects from exposures to VA have been noted, such as asthma, respiratory tract irritation, and possible related cardiopulmonary problems. These in part result from exposures to high levels of airborne or resuspended ash particles that can be inhaled deep into the bronchiolar or alveolar portions of the respiratory tract (<2.5 to 10 μm). As the ash cloud from a single eruption moves downwind, the coarser and heavier particles tend to settle out, and so the proportion of ash particles in the smallest size ranges typically increases substantially compared to those in coarser size ranges but decreases in total mass (**Figure 2**). Ash particle size distribution can also vary as a function of eruption type and dynamics, even in different eruptions from the same volcano. As noted by Horwell and Baxter (2006), ash particles have a strong tendency to clump, so it is likely that the proportion of ash particles that are actually respired can be much smaller than the amounts found via laser analysis of an aqueous ash suspension. Rainfall can change the particle size distribution of settled ash deposits, perhaps selectively removing the finer fraction through runoff (**Figure 2**).

The morphology of ash particles can also play a role in the irritation of the respiratory tract. For example, sharp edges on glass shards and broken crystals (**Figure 3**) may cause abrasion of the tissues lining the respiratory tract and eyes.

The potential toxicity of respirable crystalline silica in VA has been of concern from a respiratory health perspective for some time (Horwell and Baxter, 2006; Horwell et al., 2010). The number of detailed epidemiological or toxicological studies specific to VA is limited, and those that have been done to date on VA-exposed populations are not necessarily conclusive regarding the risk for development of silicosis, nonspecific pneumoconiosis, or other lung diseases (such as lung cancer or chronic obstructive pulmonary disease) that are more commonly linked to workplace exposures to high levels of relatively pure crystalline silica (Horwell and Baxter, 2006). Cristobalite, a variety of crystalline silica, is most abundant in ash from eruptions that result from the collapse of volcanic domes (Horwell and Baxter, 2006). The cristobalite forms initially by direct deposition from volcanic gases in the dome fractures. Cristobalite identification in VA via XRD requires a

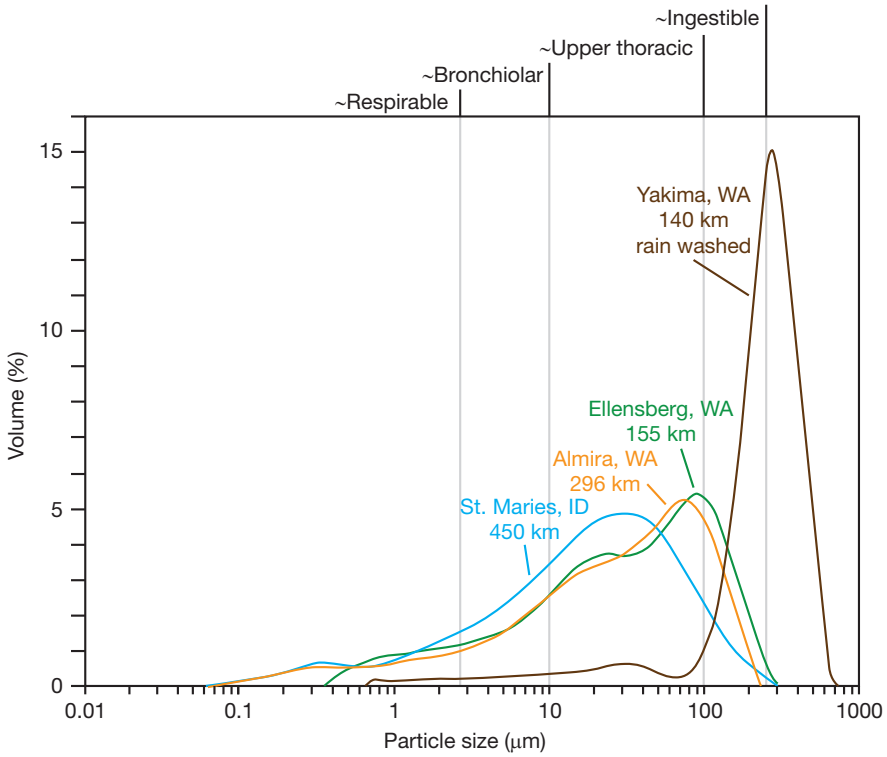

Figure 2 This plot shows the particle size distribution (as determined using Laser Malvern Mastersizer) of ash deposits from the 18 May 1980 Mt. St. Helens eruption, Washington State, United States, collected at progressively greater distances downwind from the volcano. Approximate upper size limits of physiological significance are also shown on the plot.

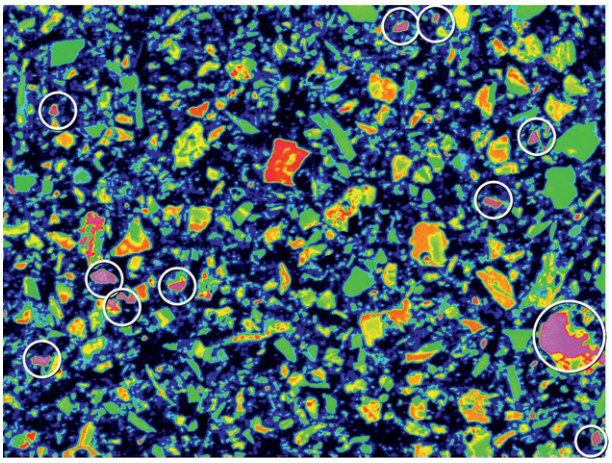

Figure 3 Modern scanning electron microscopy (SEM) image analysis software provides a means to relatively quickly assess the amounts of particular minerals in a DM sample. This SEM image is an element map of ash from the 2010 eruption of Mount Merapi volcano, Indonesia. The circles highlight phases where silica is the lone constituent (magenta) and show that many of the silica-only grains are greater than 15–25 μm in diameter and are attached to other mineral grains. The imaging software allows calculation of the areal percentage of silica-only phases present in the sample, in this case around 2% of the grains. The analysis was performed by Heather Lowers, USGS.

specialized pretreatment of the ash due to an XRD peak overlap with calcic plagioclase (Horwell et al., 2010). However, relatively new methods for element mapping and analysis using SEM can provide a relatively rapid indication of the proportion of pure silica phases along with key information on their occurrences and size distribution in settled ash samples (Figure 3). It is important to note that the potential toxicity of crystalline silica diminishes as it is diluted by other aluminosilicate minerals, and such a mitigating effect could clearly occur with VA, given the abundance of other silicate minerals and glass (Horwell and Baxter, 2006; Plumlee and Ziegler, 2007).

Fluorosis in livestock, wildlife, and more rarely in humans is also another important health concern at some geologically favorable volcanoes where the magmas or eruption processes lead to relatively fluorine-rich ash, such as the 2010 Eyjafjallajökull and other Iceland volcano eruptions; small 2008–09 Halema'uma'u crater eruptions, Kilauea volcano, Hawaii; 1995–96 Ruapehu eruptions, New Zealand; and 2007 Oldoinyo Lengai eruption, Tanzania. Fluoride, along with sulfate, chloride, acid, and some trace metals, can be tied up in relatively soluble salts in VA or is loosely sorbed onto VA particle surfaces (Witham et al., 2005). In most VA, these salts or sorbed species are a relatively small component of the total ash (compared to the large volume of glass and mineral particles) and result from interactions of ash particles with air and the gaseous components (including acidic gases) of the volcanic plume (Witham et al., 2005). In the case of most VA from fluoride-rich systems, the fluoride is relatively abundant and water-soluble – either the fluoride is leached into surface water supplies that are consumed or the bioaccessible fluoride is solubilized from ash that is consumed along with forage by grazing wildlife or livestock. For ash eruptions such as these, the presence of water-soluble fluoride is readily detected by water leach tests such as the USGS Field Leach Test

(Hageman, 2007b). In the case of Ruapehu, water leach tests did not indicate significant quantities of water-soluble fluoride, yet several thousand sheep died from fluorosis following the eruption. Cronin et al. (2003) concluded that the phreatomagmatic nature of some of the Ruapehu eruptions led to the formation of calcium and aluminum fluorides/phosphate phases in the ash, which are sparingly soluble in water but much more soluble in the digestive system of grazing animals. Morman and Plumlee (2010) and Caulkins et al. (2010) applied gastric IVBAs to examine whether such tests can better predict potential fluorosis hazards via an incidental VA ingestion.

The USGS Field Leach Test results on samples of ash that was deposited dry and not subsequently rained upon (Hageman, 2007b; Wang et al., 2010) suggest that short-term flushes of acid, anions, and some metals into rainwater or surface waters should be expected from most VA. Ash that has been rained upon or that is from phreatomagmatic eruptions involving significant water produces a substantially higher-pH leachate with high levels of major cations and lower levels of trace metals (Wang et al., 2010) due to the prior flushing of soluble components and the greater time for chemical reactions between the leachate solutions and the ash particles. These results suggest that the potential for release of acid and metals from ash is likely to diminish substantially over time as a result of interactions with rainfall.

In contrast to the silicate- and glass-dominated ash from most eruptions, ash from a series of relatively small eruptions in 2008–09 at the Halema'uma'u summit crater, Kīlauea volcano, Hawaii, contained a high proportion of calcium sulfates and complex phases containing iron, chloride, sulfate, aluminum, phosphate, and other elements, which formed as direct precipitates from magmatic gases on the fracture surfaces of wall rocks near the surface of the crater. The collapse of the wall rocks into the crater throat impeded gas flow, leading to overpressuring and eventual explosive release of the precipitate-rich material (Houghton et al., 2011). Due to the high proportion of these precipitates in the ejecta, water leachates from the Halema'uma'u ash samples are the most acidic and have the highest concentrations of soluble fluoride and various metal contents, which we have measured using the USGS Field Leach Test.

The VA from the Oldoinyo Lengai volcano in Tanzania is quite exotic due to the natrocarbonatitic, carbon dioxide-rich nature of the magmas (Mitchell and Dawson, 2007). The abundance of unusual carbonate phases produces the highest pH leachates of any VA that we have analyzed. Both water and gastric leachates have extremely high concentrations of fluoride and exotic elements (for VA leachates), such as molybdenum, arsenic, and vanadium. The fluorosis that would be predictable based on these results has been well known for years due to the fluorine-rich nature of the volcanic rocks in the region. However, the results also raise the possibility of toxicity from other elements that may be less well known. For example, soluble molybdenum levels in the tens of ppm suggest that molybdenosis in animals that graze in ash-affected areas or in areas of compositionally similar volcanic rocks may be a plausible concern.

Attention has only focused relatively recently on the potential health effects of ROS generation by metals released from respired VA. Horwell et al. (2003) found that ash from the Soufrière Hills volcano has high surface reactivity and generates high levels of ROS, which they attributed to the release of ferrous iron from the ash. More recently, Horwell et al. (2007) found that basaltic ash generates substantially more radical species in acellular lab experiments than more silicic ash, again postulated to result from iron release. Iron sulfides, which have been shown to generate high levels of ROS in lab experiments (Harrington and Schoonen, 2012), are present up to one or two percent by volume in silicic ash that we have studied from a number of volcanoes. It is unclear whether these sulfides are present in high enough levels to contribute substantially to ROS generation by, and therefore toxicity of, VA.

We have carried out IVBAs on ash from a number of different volcanoes and eruptions using lung fluid simulants and serum-based fluids as the extracting fluids. The results suggest that a variety of redox-variable elements, such as manganese, copper, cerium, and others, may be rather bioaccessible from respired ash particles, in many ash samples even more so than iron. Further work is needed to understand whether these elements could also contribute to ROS generation and potential toxicity of VA.

11.7.6 Landslides, Debris Flows, and Lahars

Landslides are relatively dry, slow- or fast-moving masses of rock, soil, and other materials. Debris flows are fast-moving masses of loose rock, soil, and other materials in which water-saturated sediments support and transport large boulders or other debris. Debris flows that form on volcanoes are termed lahars. Landslide deposits can be sources of debris flows due to the abundance of loose, easily erodible materials. Landslides and debris flows originate in areas of relatively steep topography and can be geogenic (e.g., volcanic, earthquake, geothermal, or rainfall triggers), geoanthropogenic (e.g., triggered by runoff in areas of deforestation or areas burned by human-caused wildfires), or anthropogenic (e.g., through failure of mine waste piles, CFA impoundments, or other containment structures) in origin. They can involve geogenic to anthropogenic materials. Landslides, debris flows, and lahars can cause large volumes of earth materials and entrained anthropogenic debris to be broken apart and exposed to weathering, erosion, redeposition, and dust generation.

Landslides, debris flows, and lahars are well recognized for the threats they pose to the physical safety of humans and other organisms in their paths (Petley et al., 2005) and for their physical impacts on the environment. For example, on 16 December 1999, extreme rainfall triggered debris flows that demolished urban areas in 24 drainages along a narrow strip of the Venezuelan coast in Vargas State, leading to the destruction of over 25 000 houses, damage to another 65 000 houses, and the estimated deaths of 15 000–30 000 people (García-Martínez and López, 2005).

There are some cases in the literature where exposures to landslide or debris flow materials have been of concern from a public health perspective and rarer cases where actual health problems have been documented from such exposures. Whether materials contained within landslides, debris flows, and lahars might pose environmental or health hazards is a function of the mineralogical, chemical, and pathogenic

makeup of the source materials coupled with the types and amounts of anthropogenic materials that are entrained.

11.7.6.1 Landslides and Debris Flows Sourced in Ultramafic Rocks

Ultramafic rocks, due to the abundance of materials with low shear strength such as serpentinite and asbestos, can commonly serve as source rocks for landslides and debris flows. The active Sumas Mountain/Swift Creek, Washington, United States, landslide is developed on a steep hill slope underlain by ultramafic rocks containing high levels of chrysotile asbestos (EPA, 2011a; Linneman et al., 2009). Rainfall runoff, sometimes in the form of debris flows, carries large volumes of chrysotile-containing material substantial distances downstream. The transported material is redeposited in stream sediments, natural levees, and floodplain sediment deposits, which can become wind-borne during dry periods and can be disturbed by human activities. In the past, dredging was used to keep the Swift Creek channel free of sediments and to reduce debris flow hazards. The dredged materials were used for road fill and home construction projects, which led to further distribution of the chrysotile-containing materials. Although the Washington State Department of Health found no evidence of elevated rates of asbestos-related disease in nearby residents, the EPA (2011a) did find that exposures to asbestos and some metals in the Swift Creek area were high enough to warrant implementation of measures to help reduce such exposures. In addition to chrysotile and amphibole asbestos (Van Gosen, 2009), the potential hazards that may be associated with landslides and debris flows from ultramafic rocks elsewhere are dusts or sediments that contain nickel, vanadium, or other metal/metalloid toxicants. Soluble hexavalent chromium released from the landslide rocks might also be a concern in some areas, resulting from the oxidation of trivalent chromium (which is relatively insoluble) by manganese in the surface environment (Wood et al., 2009).

11.7.6.2 Landslides and Debris Flows Sourced in Sulfide-Rich Rocks

Partially weathered, iron sulfide-bearing black shales or schists and hydrothermally altered/mineralized rocks can be sources of substantial landslides and debris flows. In the Great Smoky Mountains of Tennessee, landslides occur regularly in pyritic schists (Hammarstrom et al., 2005).

Along the Red River above Questa, New Mexico, United States, intense acid-sulfate weathering of pyritically altered andesites with accessory chalcopyrite (copper–iron sulfide), sphalerite (zinc sulfide), and galena (lead sulfide) has led to the formation of a series of spectacular erosional scar areas and associated debris fans (**Figure 1(b)**). The scar areas form by slumping and landsliding of the partially weathered rocks at their headwalls, and the runoff from summer thunderstorms erodes the landslide material and causes extreme debris flow events (Plumlee et al., 2009).

These landslides in sulfide-mineralized rocks expose fresh pyrite (and depending upon the geology, other sulfides) to weathering, which accelerates the formation of acidic drainage waters with high levels of metals, such as iron, aluminum, zinc, and copper see **Chapter 11.5**. Evaporation of the acid drainage during dry periods or in areas protected from rainfall leads to formation of sulfate-rich secondary salts. Dusts from the landslides and debris flows can be enriched in unweathered sulfides and secondary salts with bioaccessible acid, iron, and other metals, which may be bioreactive in the lungs (Plumlee and Morman, 2011). Dissolution of the soluble salts by rainfall events can also lead to pulses of acid and metals into surface waters, which can adversely affect downstream water quality and aquatic ecosystems (Hammarstrom et al., 2005; Plumlee et al., 2009). Results of the USGS Field Leach Test on debris from Questa scar areas illustrate the highly acid, metalliferous nature of the runoff that can occur, especially in comparison to leachate from debris in a nearby catchment underlain by rocks that are substantially less mineralized (**Figure 4**).

11.7.6.3 Volcanic Lahars

Volcano-sourced lahars are the largest, farthest traveled, and potentially most damaging of these phenomena. For example, the 1985 lahars from Nevado del Ruiz volcano in Columbia traveled up to 104 km downstream and killed 23 000 people (Pierson et al., 1990). The Nevado del Ruiz lahars were triggered by an eruption that interacted with the volcano's summit ice cap. As another example, the Osceola mudflow 5600 years BP removed a substantial portion of the upper Mt. Rainier volcano, including a substantial amount of hydrothermally altered rocks (John et al., 2008). The Osceola mudflow flowed to the north and west, eventually reaching Puget Sound. A number of towns have been developed in the Puyallup River valley on top of thick Osceola mudflow deposits. The Osceola mudflow contains a number of sulfide-rich clasts that can weather to produce small amounts of acid-rock drainage and soluble sulfate salts.

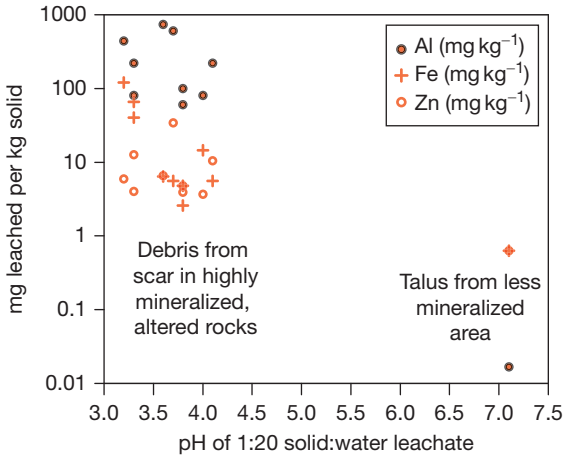

Figure 4 The USGS Field Leach Test illustrates that debris eroded from pyrite-mineralized, acid-sulfate-weathered scar areas along the Red River near Questa, New Mexico, produces highly acidic leachate waters with elevated levels of metals, such as iron, aluminum, and zinc. The plot was generated using the data from Smith et al. (2007).

11.7.6.4 Pathogens in Dusts from Earthquake-Generated Landslides

The outbreak of valley fever (coccidioidomycosis) following the 1994 Northridge, California, earthquake is cited as the best but an extremely rare example of an infectious disease outbreak associated with a geophysical disaster (Floret et al., 2006; Jibson, 2002). The outbreak resulted from exposures to dusts containing spores of the soil fungus *C. immitis*. The earthquake triggered landslides and resulting dust clouds in marine sedimentary rocks whose soil characteristics may have been ecologically favorable for the soil fungus to compete against other soil microbes, for example, high salinity and alkalinity, hot temperatures, coarser soil textures, soluble efflorescent salts, and potentially elevated borate salts that may act as antibiotics on bacteria that compete with the fungus (Fisher et al., 2007).

11.7.7 Hurricanes, Extreme Storms, and Floods – Katrina as an Example

11.7.7.1 An Overview of DM Produced by Hurricanes, Extreme Storms, and Floods

Hurricanes and extreme storms have the potential to cause substantial damage to the environment and human-built infrastructure from high winds, tornadoes, lightning strikes, and extreme precipitation with resulting runoff, erosion, and flooding (Young et al., 2004). Flooding can also result from other natural causes, such as rapid snowmelt, catastrophic failures of dams or levees triggered by either natural or human causes, and earthquake-generated tsunamis.

Storm-induced erosion can release into the environment a variety of metal/metalloid toxicants, mineral toxicants, and pathogens from rocks and soils in which they are naturally enriched, such as the examples discussed in the previous section on landslides and debris flows. Storm or flood damage to a wide variety of buildings, infrastructure, industrial facilities, and/or agricultural facilities could release many different types of debris, organic and inorganic contaminants, industrial wastes, sewage, and pathogens into the environment. Examples of such facilities include wastewater treatment plants (WWTPs), WWTPs that also process storm water runoff (termed combined sewage outflows, or CSOs), petroleum refineries, active or inactive metal mines, chemical manufacturing plants, warehouses storing HM, animal feeding operations, landfills, and others (Cozzani et al., 2010; Plumlee et al., 2011; Young et al., 2004). Storm runoff from agricultural lands, residential areas, and urban areas can release a variety of sediment-borne or waterborne anthropogenic contaminants (e.g., Hudak and Banks, 2006). Storm-related redistribution of contaminated sediments from riverbeds, lakebeds, or alluvial deposits has been noted to result in adverse environmental impacts on downstream ecosystems (e.g., Lecce et al., 2008). Surface water and shallow groundwater supplies used for human consumption, livestock consumption, or agricultural irrigation can become contaminated by a wide variety of contaminants or pathogens. Following storms, the contaminated sediments and debris that were redistributed by landslides or floodwaters dry out and can be redistributed as airborne PM by human disturbance and/or wind transport.

Adverse human health effects of storms and flooding include potential outbreaks of infectious disease from exposure to contaminated floodwaters (such as gastroenteritis, cholera, and *Escherichia coli* infections), consumption of contaminated drinking water, exposure to dusts from dried landslide or flood deposits containing soil pathogens (such as *C. immitis*), post-flood exposure to molds developed in water-soaked homes and buildings, vector-borne disease outbreaks (such as malaria and West Nile virus transmitted by mosquitos), and rodent-transmitted diseases (such as leptospirosis) and other infectious diseases (such as dengue fever). The greatest incidences of infectious diseases occur in developing countries where the public health infrastructure and treatment/mitigation capacity is more limited (Ahern et al., 2005; Barbeau et al., 2010; Cook et al., 2008; Noji, 2000; Young et al., 2004).

The potential for human health impacts linked to inorganic or organic toxicants released into the environment by storms has been widely speculated, but specific case studies documenting such links seem rare. Young et al. (2004) cite limited examples of short-term illnesses (such as respiratory problems) and potentially increased cancer rates following specific flood events but also note that much more work is needed to better understand potential linkages in this regard.

11.7.7.2 Hurricane Katrina Floodwaters, Flood Sediments, and Molds

Hurricane Katrina, which made landfall near New Orleans on 29 August 2005, and Hurricane Rita, which made landfall to the west of New Orleans several weeks later, triggered storm surges and multiple breaks in the levee system surrounding the city, leading to extensive flooding of the New Orleans area north and east of downtown. The American Society of Civil Engineers (ASCE, 2009) presented a detailed overview of the sequence of events that led to the flooding and its consequences. There were considerable concerns expressed in the media early in the flooding about the potential health threats posed by the 'toxic gumbo' of floodwaters, with possible chemical and microbial contamination coming from flooded WWTPs, oil refinery and other sources of oil spills, multiple Superfund sites, large numbers of older homes, and many other sources (Manuel, 2006). As the floodwaters were pumped from the city, they left behind extensive accumulations of flood sediments up to many centimeters thick on the streets, lawns, parking lots, and other flat surfaces, as well as in buildings (**Figure 1(c)**). During the flood dewatering and subsequent cleanup, there were concerns that these sediments might contain pathogens and chemical contaminants that could pose a health risk to emergency responders, cleanup workers, and local residents who came into contact with the wet sediments or inhaled dusts generated from dried sediments. A number of different governmental agencies and university research groups, including ours and other research groups at the USGS, carried out a range of studies on the Katrina floodwaters and flood sediments to examine potential characteristics of environmental or health significance.

Various groups analyzed floodwater samples collected in early September from Lake Pontchartrain and various New Orleans neighborhoods (Demcheck et al., 2007; Pardue et al., 2005; Presley et al., 2006). Collectively, they detected volatile

and semivolatile organic compounds, pesticides, and wastewater compounds but in relatively low concentrations. With the exception of arsenic, metals were within the ranges expected for storm water runoff but were below EPA maximum contaminant levels (MCLs) for drinking water. However, copper, nickel, and silver were sometimes measured in levels exceeding those protective of aquatic life in salt water. Fecal coliform bacteria (including *E. coli*) and *Aeromonas* (pathogenic bacteria not of sewage origin) were highly elevated in some floodwater samples but in ranges expected for storm water runoff. Fecal indicator bacteria in Lake Pontchartrain returned to prehurricane concentrations within 2 months of the flooding (Sinigalliano et al., 2007).

Large volumes of sediment-laden floodwaters were pumped out of the flooded areas in the weeks following Katrina, mostly into Lake Pontchartrain to the north but also to marshes to the east of New Orleans. Van Metre et al. (2006) examined the impacts on Lake Pontchartrain and found elevated concentrations of lead, zinc, polycyclic aromatic hydrocarbons (PAHs), and the legacy pesticide chlordane in the lake bottom sediments, but these were restricted to relatively limited areas along the shoreline near the entrance to one of the major canals (the 17th Street canal). They concluded that the impacts of the floodwater pumping on Lake Pontchartrain were spatially limited and most likely transient.

The flood sediments left behind after pumping of the floodwaters showed substantial spatial and temporal variability in their size makeup, with coarser sands deposited close to the ruptured levees soon after breeches and with finer clay to silt size fractions deposited throughout the area. Once dry, the silt- and clay-rich flood sediments formed hard, durable chunks that required considerable effort to break apart. As a result, these sediments would likely only release appreciable dust or loose particles if they were extensively disturbed (such as by being driven upon or otherwise mechanically pulverized). This situation is fortunate because our particle size analysis of disaggregated flood sediment samples indicates that a high proportion of the sediment is of the clay- to silt-size range that could be involuntarily ingested via hand-to-mouth contact (<250 μm) and that a smaller but still substantial proportion (1–16 volume %) of some sediment samples is in the respirable size range (less than 2–3 microns) (Plumlee et al., 2006b, 2007a).

Multiple studies found similar results regarding types, abundances, and distributions of metal and organic contaminants in flood sediments (Abel et al., 2010, and references therein; Plumlee et al., 2006b, 2007a; Rotkin-Ellman et al., 2010; Shi et al., 2010, and references therein). An important overall finding of our flood sediment study, based on SEM and XRD mineralogical characterization (Plumlee et al., 2006b, 2007a), was that the flood sediments were derived from multiple sources and that the spatial variations in sediment makeup and chemical composition across the New Orleans area resulted from variable contributions from these different sources (**Figures 5** and **6**). The flood sediments deposited in suburbs near marshes (Chalmette, Violet, and inland Slidell) primarily contained marine and brackish marsh mud with clays, abundant framboidal iron sulfide (as high as 5–10 wt %), and diatoms but overall relatively low levels of heavy metals and organic contaminants. The net acid production tests suggested that, should these flood sediments be left in contact with atmospheric oxygen, oxidation of the iron sulfides could eventually generate acid-sulfate waters containing elevated iron, aluminum, manganese, and copper released from the iron sulfide (**Figure 6**). The flood sediments near breached canals and Lake Pontchartrain (Lakeview, Ninth Ward, Rigolets, and lakefront Slidell) had abundant clay, diatoms, and sand but lesser iron sulfide (<1–5 wt%) and variable metal/organic contaminants, indicating contributions from brackish bottom sediments from Lake Pontchartrain north of New Orleans, levee materials, and materials eroded from beneath the levees near the breaches. Downtown New Orleans flood sediments contained clay and sand, no iron sulfides, abundant carbonates and urban materials (i.e., soda lime glass, glass fibers, concrete, and jewelry beads), and substantially higher concentrations of lead (as lead metal and lead oxides), arsenic, other metals, and semivolatile organic compounds (e.g., PAHs such as benzo(*a*)pyrene; termiticides such as chlordane, chlorpyrifos, permethrin, and fipronil; dieldrin; and phenol and carbazole) than flood sediments collected elsewhere. Many of these contaminants were in concentrations in excess of EPA residential soil screening levels (RSSLs). SEM analysis of the lead-rich sediment samples indicated that the lead particles were well within the ingestible size range. We concluded that these downtown sediment samples were primarily composed of floodwater-reworked local soils known from previous research (Mielke et al., 2004) to have very high levels of pre-Katrina metal and organic contamination. A later study comparing pre-Katrina soil samples to flood sediment samples (Rotkin-Ellman et al., 2010) concluded that the Katrina flooding resulted in the addition of new arsenic via flood sediments. Our study results and those of others identified contamination hot spots outside the downtown areas, which were likely from localized contaminant sources. The concentrations of various organic contaminants in flood sediment samples collected at the same locality near the Murphy Oil Refinery in Chalmette decreased between September and October 2005, indicating that degradation of the organic contaminants likely had occurred as a result of volatilization, biodegradation, and photodegradation (see results for benzo(*a*)pyrene in **Figure 5**; also see Plumlee et al., 2007a).

Ashley et al. (2008) sampled flood sediments from inside two homes in the Lakeview part of New Orleans north of downtown (an area where our study found only localized enrichments of lead, arsenic, and other heavy metals) and found substantially elevated levels of arsenic, cadmium, lead, vanadium, and semivolatile organic contaminants compared to outdoor samples measured by other studies (including ours). They concluded that the increased contaminant levels resulted from a winnowing effect that enriched the indoor samples with fine clay particles containing sorbed contaminants.

Our IVBA tests of the metal-rich downtown soils indicated that lead, arsenic, cadmium, zinc, and manganese were highly bioaccessible in the simulated gastric fluids (SGF), with more than 50% of the bulk metal concentration of each leached from the sample during the hour-long tests (**Figure 5**; Plumlee et al., 2006b, 2007a). These results and those of Abel et al. (2010) provided further indication (adding to conclusions already made by Mielke et al., 2004) that the pre-Katrina urban soils were an important exposure source for lead, that incidental ingestion was a viable exposure pathway for children living in the inner city prior to Katrina, and that

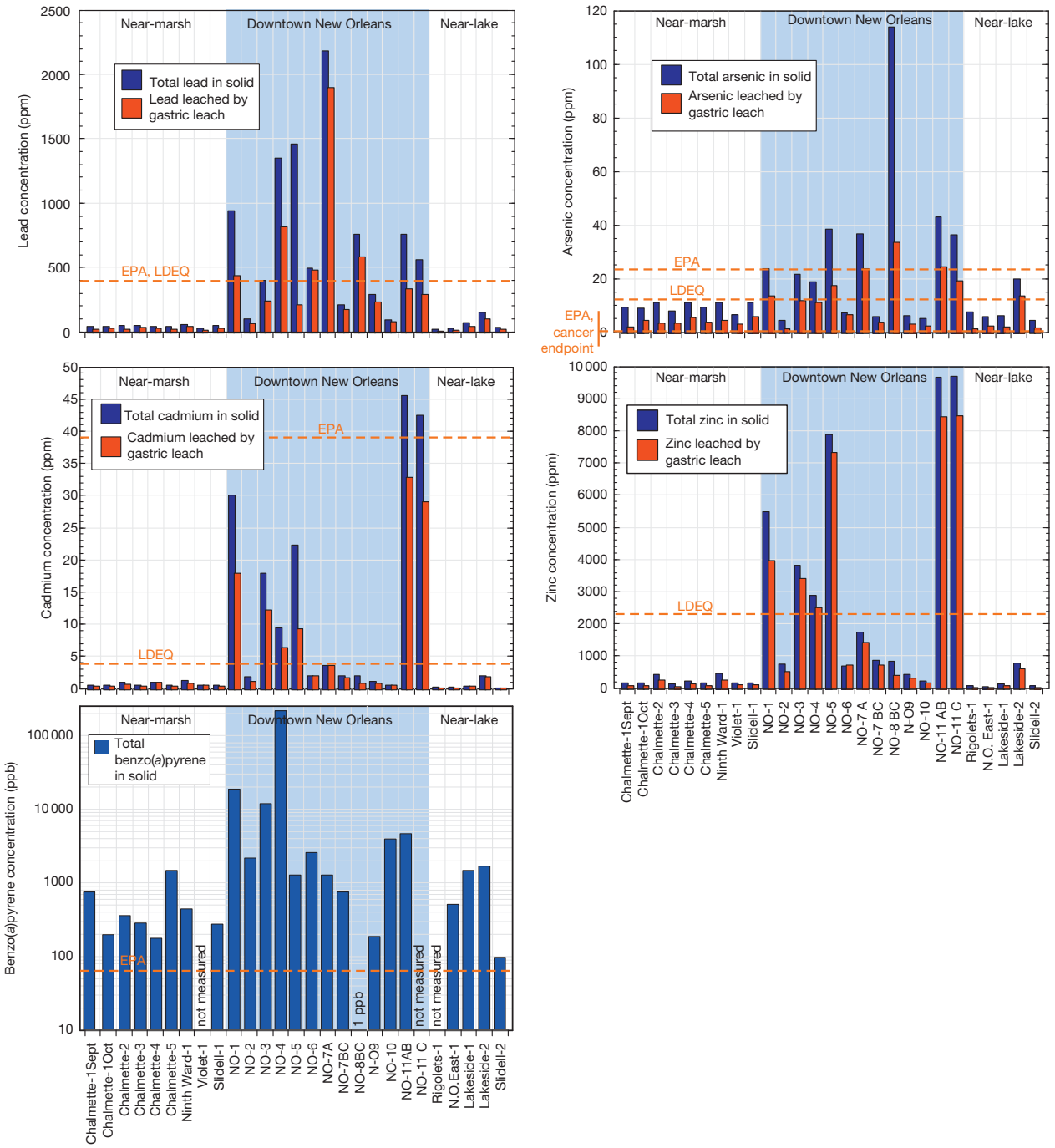

Figure 5 Hurricane Katrina flood sediments from downtown New Orleans were generally substantially enriched in many total metals, gastric-bioaccessible metals, and organic contaminants, such as the carcinogenic polycyclic aromatic hydrocarbon benzo(*a*)pyrene, compared to the flood sediment samples collected near Lake Pontchartrain and marshes. The US Environmental Protection Agency (USEPA) and Louisiana Department of Environmental Quality residential soil screening levels (RSSLs) are indicated by the dashed lines. Modified from figures in Plumlee GS, Foreman WT, Griffin DW, Lovelace JK, Meeker GP, and Demas CR (2007) Characterization of flood sediments from Hurricane Katrina and Rita and potential implications for human health and the environment. In: Farris GS, Smith GJ, Crane MP, Demas CR, Robbins LL, and Lavoie DL (eds.) *Science and the Storms: The USGS Response to the Hurricanes of 2005*, *US Geological Survey Circular 1306*, pp. 246–257. Washington, DC: US Government Printing Office.

post-Katrina soils and flood sediments in downtown New Orleans continue to pose a long-term exposure source for lead and other heavy metals.

The short-term environmental health impacts of exposure to Katrina floodwaters were mostly increased incidences of gastrointestinal illnesses, skin infections, and upper respiratory tract infections (ASCE, 2009), most likely related to microbial causes. Some cases of illness were induced by exposures to the natural bacterium *Vibrio vulnificus*, either through wounds or consumption of contaminated seafood. The latter is attributed

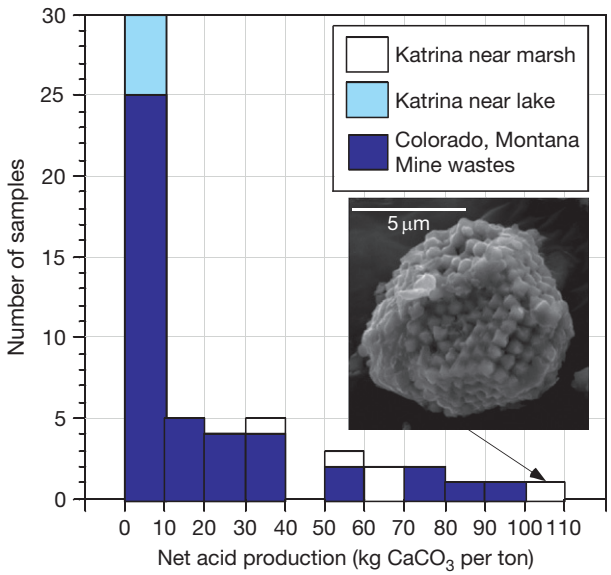

Figure 6 A test developed to predict net acid-generating potential in pyritic mine wastes revealed that the marsh-derived Katrina flood sediments had a very high acid-generating potential compared to the flood sediments collected near Lake Pontchartrain and the samples from many metal-rich mine wastes in Colorado and Montana. This resulted from the high levels of framboidal pyrite in the marsh-derived sediments (see SEM photomicrograph inset). Near-lake flood sediments had low levels of pyrite but also contained sufficient carbonates to neutralize most acid generated by iron sulfide oxidation. Downtown flood sediment samples had no pyrite and so were not acid-generating. Modified from figures in Plumlee GS, Foreman WT, Griffin DW, Lovelace JK, Meeker GP, and Demas CR (2007) Characterization of flood sediments from Hurricane Katrina and Rita and potential implications for human health and the environment. In: Farris GS, Smith GJ, Crane MP, Demas CR, Robbins LL, and Lavoie DL (eds.) *Science and the Storms: The USGS Response to the Hurricanes of 2005*, *US Geological Survey Circular 1306*, pp. 246–257. Washington, DC: US Government Printing Office.

as the cause of five fatalities (Manuel, 2006). Sinigalliano et al. (2007) found elevated levels of fecal indicator bacteria in sediments from flooded and unflooded areas following Katrina and in canal waters. They used these and other data to make the case that microbial pollution before, during, and following the hurricanes most likely resulted from the discharge of sewage-fouled waters within the city. They also expressed concerns reaffirmed by Dobbs (2007) that the city sediments could pose a longer-term source of microbial pollution to which residents could be exposed.

Griffin et al. (2009) performed PCR analysis on the splits of many of the same samples that we collected and analyzed (Plumlee et al., 2006b) and found indicators of *Bacillus anthracis* (the causative agent for the disease anthrax) in a strikingly high percentage of the samples (5 of 19 samples analyzed), especially when compared to the rates of *B. anthracis* indicated in soil samples collected on a north–south transect across the United States (5 of 104 samples). As part of a Gulf Coast soil sample transect, Griffin et al. (2009) analyzed new samples collected in 2007 from the same New Orleans sample locations and this time found no indications of *B. anthracis*. They concluded that the Katrina flooding enhanced *B. anthracis* growth (noting that flooding had also been linked to pre-Katrina anthrax outbreaks in Louisiana livestock) and that the bacteria may not survive in the uppermost soil levels during dry conditions following the flood event. Their results were obtained after the incubation period for the development of anthrax was exceeded. Fortunately, although the pathogen was clearly present in the short term after Katrina, there were no anthrax cases noted.

Barbeau et al. (2010) summarized studies of indoor and outdoor mold in New Orleans following Katrina. Very high levels of mold (particularly *Aspergillus*, *Penicillium*, and *Cladosporidium* fungi) were found in flooded homes, especially those that had been flooded to depths of greater than 3 ft. However, although residents and workers returning to clean up flooded homes were exposed to these very high levels of molds, there was not a corresponding increase in emergency room visits or hospitalization for health problems resulting from mold exposures. Barbeau et al. (2010) provided several possible explanations for this, such as that healthy people (who might be more likely to reoccupy or work in flooded homes) suffer fewer serious health effects from molds, that people with mild allergic symptoms (the most common effect of mold exposures) may not have sought respiratory care, or that persons reentering flooded homes had time-limited exposures to the molds.

The removal of the flood sediments and debris from flooded areas and hurricane-damaged or flooded buildings has been a long-term challenge since 2005. The results of the various characterization studies underscored the needs for appropriate health and safety protection of the people doing the work and the need for effective disposal of large quantities of contaminant- and pathogen-bearing materials. Our results finding that the flood sediments in eastern suburbs could be highly acid-generating due to abundant framboidal pyrite confirmed the cleanup managers' decisions to dispose of the muds and debris in landfills isolated from the atmosphere and rainfall. Otherwise, the acid drainage formed by sulfide oxidation (see **Chapter 11.5**) could have leached lead and other contaminants from the debris, thus presenting additional environmental hazards. This still may be an issue locally, as there have been media reports in the years since 2005 (e.g., USA Today, 3/26/2007) that illegal dumping of Katrina mud and debris in out-of-the way areas had become a problem.

11.7.8 Wildfires at the Wildland–Urban Interface

Wildland wildfires have always been a fundamental part of healthy natural ecosystems by helping to recycle nutrients, enhance soil productivity, reduce insect infestations, and initiate plant succession processes (Dombeck et al., 2004). Particularly in the United States, as humans have built communities in former wildland areas, wildfire suppression to protect these communities has substantially altered the natural ecological condition by allowing vegetation density to increase substantially and vegetation complexity to diminish greatly. As a result, wildfires have become more difficult to suppress, more devastating to the environment because they burn more intensely, and more likely to burn communities at the wildland–urban interface (**Figure 1(d)–(f)**).

Environmental impacts of wildland wildfires have been widely documented (Ice et al., 2004; Mendez, 2010; Moody

et al., 2008; Neary et al., 2008; Smith et al., 2011). Extensive physical impacts include increased runoff and erosion in burned areas, with increased transport of materials via damaging debris flows. Chemical impacts include, for example, loss of carbon and nutrients such as nitrogen from soils; increases in calcium, magnesium, sodium, potassium, sulfate, and chloride in soils; and increased availability of nitrogen, trace elements (iron, manganese, arsenic, chromium, and others), PAHs, other organic contaminants, and cyanide (a combustion by-product) in soils, sediments, and affected surface waters following fires. For example, elevated manganese is a commonly noted postfire problem in municipal water supplies drawn from surface waters in burned watersheds with conifer vegetation. Concerns with the potential environmental and ecological impacts of fire retardant chemicals (e.g., cyanide-bearing compounds used as corrosion inhibitors in the retardants) have also been discussed (Calfee and Little, 2003; Crouch et al., 2006; Kalabokidis, 2000).

The high toxicity of, and the resulting health effects from exposures to, smoke from fires in the built environment has been studied extensively (e.g., papers in Stec and Hull, 2010). There is a broader array of toxicants in the combustion products of fires in the built environment than in the combusted wildland vegetation. The impacts of wildfires on air quality and the resulting impacts of fire smoke on human health have also been studied extensively. Most health studies involve analysis of hospital admission data for populations affected by wildfires, toxicity testing of smoke, or health assessments and biomonitoring of firefighters. These studies have primarily focused on the adverse health effects from exposures to high levels of fine PM; irritant gases (hydrogen chloride, sulfur dioxide, hydrogen fluoride, nitrogen oxides, etc.); asphyxiant gases (carbon monoxide and hydrogen cyanide); organic chemicals such as formaldehyde, formalin, PAHs, or dioxins (some of which are considered carcinogens); other chemicals such as ozone; and combustion-produced free radicals (Bytnerowicz et al., 2009; Dennekamp and Abramson, 2011; Gaughan et al., 2008; Jalava et al., 2006; Künzli et al., 2006; Leonard et al., 2007; Lipsett et al., 2008; Neitzel et al., 2009; Shusterman et al., 1993; Viswanathan et al., 2006). All studies yield the conclusion that wildfire smoke exposures lead to a variety of acute health problems, such as eye and respiratory tract irritation, exacerbation of asthma, reduced lung function, bronchitis and other more serious respiratory tract problems, secondary cardiovascular effects, reduced immune system function, and biomarkers of increased oxidative stress in the body. These health issues are particularly problematic in sensitive populations such as those with preexisting asthma or other respiratory or cardiovascular diseases (Lipsett et al., 2008). Fewer studies have considered the potential contributions of exposures to ash or other inorganic constituents that can result from fires, such as caustic alkali solids, mineral toxicants, or metal toxicants (e.g., Harrison et al., 1995; LeBlond et al., 2008; Plumlee et al., 2007b).

The relatively short-term exposures of large populations to wildfire smoke (e.g., **Figure 1(d)**) may not pose a substantial risk for the development of long-term health problems, such as pneumoconiosis or cancer (Lipsett et al., 2008). However, all of the relatively small number of health studies of wildland firefighters conclude that much more research is needed to better understand the long-term health risks faced in this occupation (e.g., Gaughan et al., 2008; Neitzel et al., 2009). This is because wildland firefighting is increasingly a year-round rather than a seasonal occupation. Further, wildland firefighters typically do not wear the high level of respiratory protection (i.e., self-contained breathing apparatuses with full face masks) worn by urban firefighters, but wildland firefighters who fight fires at the wildland–urban interface are increasingly exposed to the potentially broader array of toxicants produced by burning buildings.

We are not aware of any detailed studies that have examined the health impacts from exposures to ash and debris encountered by people who clean up burned residences or by workers rehabilitating burned wildlands, although the potential for such risks has clearly been recognized and precautionary measures to avoid exposures are prescribed. For example, the state of California has issued advisories for safe ash cleanup, such as wearing long-sleeve shirts, gloves, eye protection, and respiratory protection (CADHHS, 2012).

11.7.8.1 Types of Ash Produced by Wildfires

Residual ash is left behind in a burned area following a wildfire. Ash particles and particles of underlying soils can easily be picked up by intense fire-caused updrafts and become entrained in the smoke plume from an active wildfire. Humans and animals can breathe in these suspended ash and soil particles, and the particles can eventually settle out downwind as airfall ash deposits.

Different types of ash are produced during a wildfire as a function of the burn severity, which, in turn, is a function of the maximum temperatures reached during combustion and the duration of the combustion at high temperatures. Black ash is composed of remnant vegetation material that has only been partially combusted. It is coarser grained and is composed primarily of charcoal and still has remnant plant structures that are visible in hand lens or by using SEM. In contrast, white ash results from a much more complete combustion and is composed of small calcium, magnesium, potassium, and sodium carbonates, oxides, hydroxides, sulfates, phosphates, and chlorides. White ash deposits are typically very fine-grained (**Figures 1(e)** and **7**), fluffy, and readily wind-borne. These ash particles are also small enough to be easily respired deep in to the lungs. Black ash deposits are not as readily wind-borne due to their coarser particle size.

Typically, a burned area can have patches of both residual black and white ash, in part reflecting variations in the amount of vegetation originally present. For example, grassy areas typically combust to form predominantly black ash. More heavily vegetated areas with closely spaced trees have greater fuel load, burn more intensely, and so can have much more abundant white ash.

The mineral phases, particle morphologies, and major-element chemical composition of ash from some vegetation types have been studied in detail (e.g., Canti, 2003; LeBlond et al., 2008).

11.7.8.2 Ash, Debris, and Burned Soil Characteristics of Potential Environmental or Health Concern

We have examined characteristics of potential environmental and health concern of residual ash and soil samples from

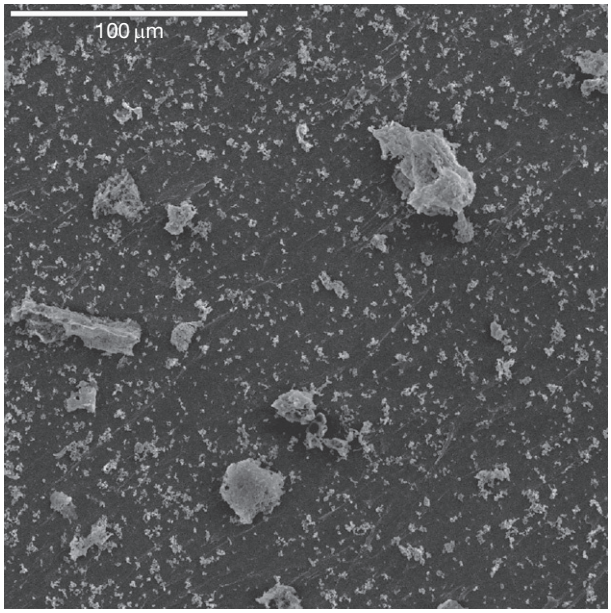

Figure 7 This scanning electron photomicrograph shows the characteristic particles of white ash left behind in a wildland area near San Diego, California, United States, burned by the 2007 Harris wildfire. A majority of the particles are inhalable to respirable in size and many are composed of caustic alkali phases, such as calcium, magnesium, or potassium hydroxide. The scale bar is 100 μm long. Image by Heather Lowers, USGS.

wildland, residential, and agricultural areas burned by a number of different wildfires at the wildland–urban interface in California and Colorado from 2007 to 2010. They have also characterized airfall ash samples collected in residential areas downwind from two of these fires in California (Hageman et al., 2008a,b; Hoefen et al., 2009; Plumlee et al., 2007b; Wolf et al., 2011). Most of the samples analyzed were collected within several days after combustion and so had not undergone any changes due to interactions with rainfall.

The results and those of other studies further confirm that ash and soil characteristics can vary considerably depending upon the source of the samples (e.g., wildlands, agricultural areas, or burned buildings), combustion intensity, vegetation type, and underlying bedrock geology.

SEM analysis shows that white ash particles are dominated by the alkali-metal and alkaline-earth oxides, carbonates, hydroxides, sulfates and phosphates mentioned previously. The white ash can be extremely fine-grained, with a predominance of particles in respirable to inhalable size ranges (**Figure 7**). Analysis of airfall ash shows that it is typically composed of a mix of larger black ash and smaller white ash particles (many in the respirable size range), with the amounts of larger black ash particles being greater in airfall ash deposits from wildfires driven by extreme horizontal winds. Airfall ash deposits can also have a mix of transported soil silicate minerals and particles likely derived from combusted buildings, such as metallic zinc. Ash and debris from burned buildings and residences can vary significantly in particle size, with abundant respirable particles up to large debris blocks. In addition to the minerals found in wildland black and white ash samples, ash from combusted residences or other buildings can have a variety of building-related materials or their combustion by-products, such as asbestos fibers, man-made vitreous fibers, wallboard gypsum, concrete, steel, and aluminum-, chromium-, lead-, zinc-, or copper-rich particles.

The ash and debris samples that we have analyzed from burned residences can often have elevated levels of copper, zinc, arsenic, cadmium, chromium, lead, chlordane (a legacy pesticide no longer used in construction), naphthalene, man-made glass fibers (fiberglass), and other chemicals or materials that would result from the burning of building materials (**Figure 8**; Plumlee et al., 2012). Lead and arsenic are commonly present in levels that exceed EPA residential SSLs (400 ppm lead and 22 ppm arsenic; EPA, 2011b). Some of the chromium present in the residential ash and debris is in the readily soluble, more toxic hexavalent form (Wolf et al., 2011); some may have been present before the fires as hexavalent chromium in building or household materials such as chrome–copper–arsenic (CCA)-treated wood, fabrics, or plastics; and some may have formed by the combustion of metallic or trivalent chromium (Panichev et al., 2008).

In comparison to the residential ash samples, our data show that wildland ash samples tend to have substantially lower levels of most potentially toxic heavy metals (**Figure 8**). The bulk chemical composition of the wildland ash changes with the increasing extent of combustion, with white ash being enriched in calcium, magnesium, potassium, and phosphate and depleted in most other elements compared to black ash. This may indicate that some potentially toxic elements (such as arsenic, lead, and others) are released from wildland vegetation into the smoke plume during combustion. Although more data are needed, there are indications in our dataset that different vegetation types behave differently with respect to the enrichment of metal toxicants in the ash versus their release into smoke during combustion. For example, one series of burned soil, black ash, and white ash samples collected in a burned oak forest in California showed enrichment of arsenic and mercury compared to ash samples from other vegetation types and enrichment of arsenic from the burned soil to black ash to white ash, rather than the depletion observed in this progression in all other vegetation types. Much more work is needed on organic contaminants (e.g., dioxins, furans, PAHs, and many different anthropogenic chemicals) in ash and burned soils – although our data is extremely limited due to the high cost of organic contaminant analysis, other studies have found elevated dioxins, furans, and PAHs in wildfire ash and smoke.

Our water leachate results using the USGS Field Leach Test (1 part ash to 20 parts deionized water, 5 min agitation) show a progression of increasing leachate pH and alkalinity from unburned soils to burned soils, black ash, white ash, airfall ash, and ash from burned residences (**Figure 9**). The white ash, airfall ash, and ash from burned residences could produce leachates with pH reaching nearly 13 at a 20:1 water/solid ratio. Over pH 10.5, the leachate is considered caustic. This increase in pH and alkalinity resulted from the increasing intensity of combustion that produced an increasing proportion of water-soluble oxides and hydroxides in the ash (Neary et al., 2008; Notario del Pino et al., 2008). Constituents that were highly enriched in the water leachates include calcium,

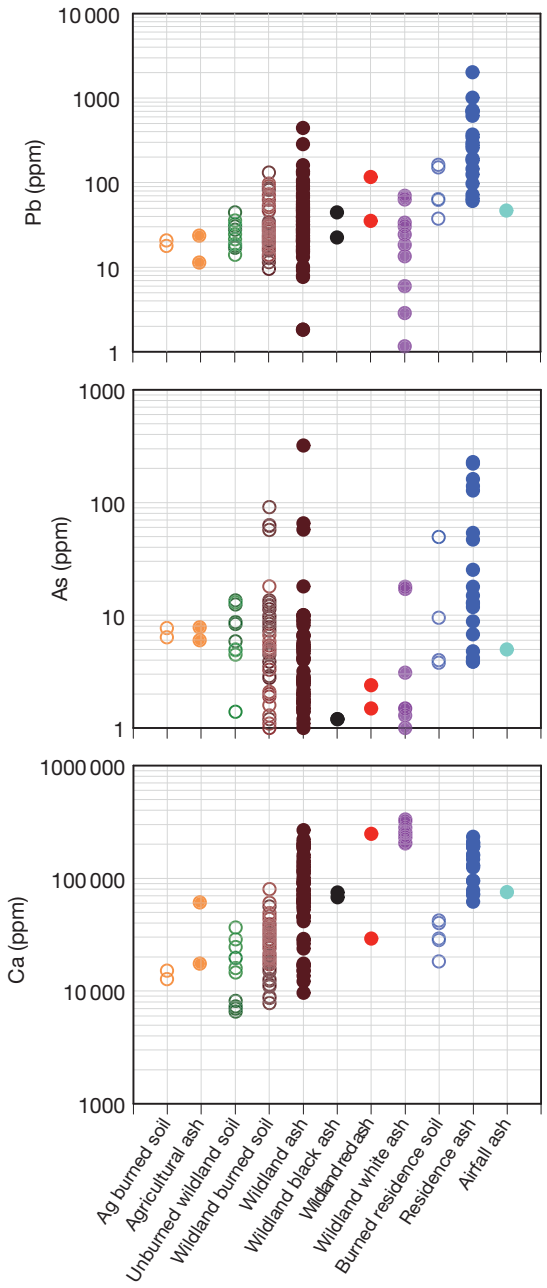

Figure 8 These plots show ranges in total lead, arsenic, and calcium concentrations for a variety of wildfire ash and burned soil types. Figures modified from Plumlee et al. (2008) to include additional data from 2009 California wildfires. Many ash samples from burned residences have higher concentrations of lead and arsenic than samples of wildland ash. In wildland ash samples, lead and arsenic generally decrease with increasing burn intensity (i.e., from black and black/white ash mixtures to white ash), possibly a result of volatilization during combustion. Increasing calcium concentrations with increasing burn intensity result from the formation of residual calcium hydroxides and oxides in the ash.

sodium, potassium, magnesium, chloride, and sulfate. Aluminum and silica were also extremely high in the water leachates but were likely present as colloids that were passed through the 0.45 μm filter used to filter the leachates prior to analysis. Nearly all potentially toxic metals were only leached in relatively minor amounts by water. Chromium, manganese, molybdenum, and occasionally arsenic were leached in somewhat greater amounts.

Our IVBAs of the ash samples using simulated gastric and lung fluids showed that a variety of metal or metalloid toxicants, particularly in the residential ash samples, are likely gastric-bioaccessible (including lead, zinc, copper, and arsenic) and/or lung fluid-bioaccessible (chromium, arsenic, and molybdenum). Speciation analysis indicates that the leachable chromium in both the water and lung fluid simulants is the more toxic hexavalent form (Wolf et al., 2011).

11.7.8.3 Potential Environmental and Health Concerns of Wildfire Ash

Our results and those of other studies can be used to help better understand and anticipate potential ecological and environmental health risks associated with wildfires. For example, the first rain to fall on a wildland-burned area may, depending upon the burn severity and storm characteristics, initially produce alkaline runoff that could potentially be detrimental to aquatic organisms. Any alkalinity impacts would likely diminish if rainfall is heavy and with increasing dilution over time and downstream. Colloidal silica and aluminum phases that are readily leachable from the ash may adversely affect aquatic organisms, as such particles have been shown to easily clog fish gills. Runoff from burned areas (particularly residential areas) may contain particulate and dissolved metal, metalloid, and organic toxicants that would be available for uptake by aquatic organisms.

Our results suggest that airfall ash deposited in small surface water bodies downwind from active fires may have a significant environmental impact on water quality due to the potentially smaller amounts of dilution that could occur than during the poststorm runoff. As one example of the potential chemical effects of airfall ash on water quality, a USGS colleague living several kilometers upwind of the massive 2009 Station fire near Los Angeles found that a relatively limited amount of airfall ash increased the pH of her 40 000 gallon salt water swimming pool by more than half a pH unit (L. Jones, oral comm., 2009). Our leachate tests of an airfall ash sample from the same fire produced a pH value near 13 at a 1:20 dilution (**Figure 9**). Metal, metalloid, or organic contaminants present in airborne ash from burning urban areas could similarly prove problematic to aquatic organisms and so may warrant further investigation. For example, we have found zinc particles in airfall ash samples from the May 2009 Jesusita fire near Santa Barbara, California.

The abundance of respirable, caustic alkali particles in more heavily combusted ash (**Figure 7**) and the high concentrations of metal toxicants in residential ash substantiate public health warnings that appropriate respiratory, eye, and skin protection should be worn by people exposed to heavy ash fallout or working in burned residences or wildland areas after fires. Some vegetation types, particularly grasses and reeds, can also produce fibrous crystalline silica phases that may be of potential respiratory health concern (e.g., LeBlond et al., 2008).

Some states or local jurisdictions in the United States require ash and debris from buildings burned by wildfires to be

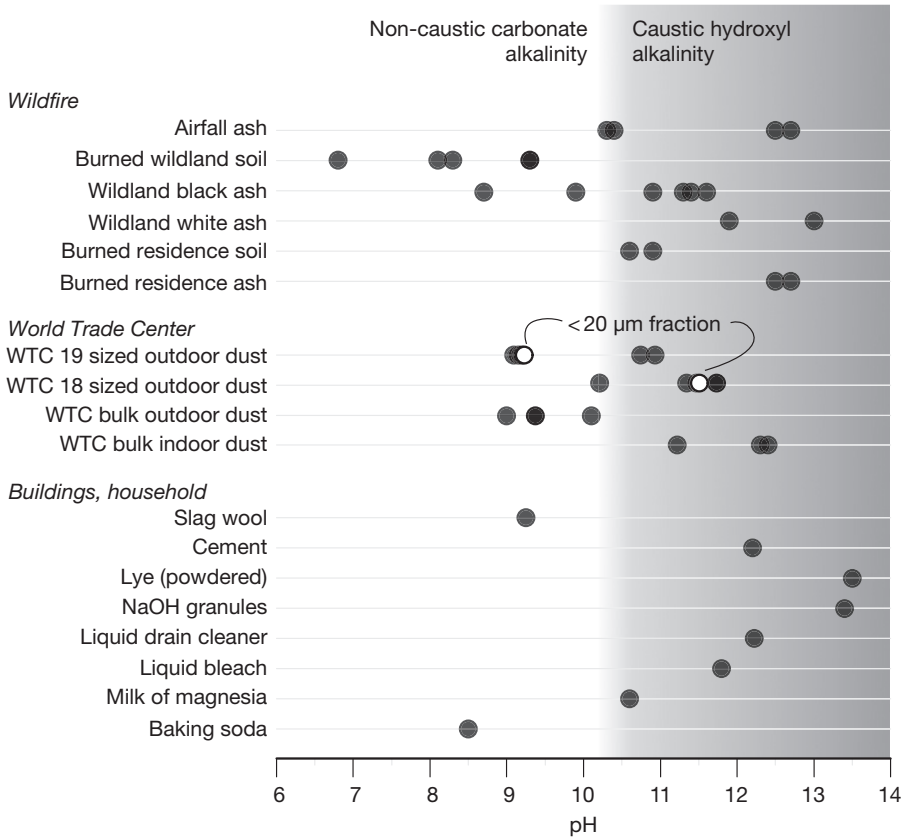

Figure 9 This plot compares pH results of the USGS Field Leach Test applied to residual ash, airfall ash and burned soils from wildfires, dusts from the WTC building collapses, and various building materials or household products. The test adds 1 part by weight of a material to 20 parts deionized water, the mixture is shaken gently for 5 minutes, and the resulting leachate is filtered to <0.45, then analyzed. Caustic hydroxyl alkalinity dominates over carbonate alkalinity at pH values above ~10.5. WTC and building material/household product data are from Plumlee et al. (2005). Wildfire data are in part from Plumlee et al. (2008) and are in part from our unpublished data from a wildfire manuscript in progress.

treated as HM and disposed of in high-level disposal facilities. The primary driving force behind this requirement is the concern regarding asbestos in the debris. This is so even though the amount of asbestos present likely diminishes with the decreasing age of the building, particularly those built after the late 1970s. However, the results show that a wide variety of organic and metal toxicants in addition to asbestos can also be present in sufficiently elevated levels to be of potential environmental or health concern when disposed of.

11.7.9 Mud and Waters from the Lusi Mud Eruption, East Java, Indonesia

On 29 May 2006, mud and gases began erupting from a vent 150 m away from a hydrocarbon exploration well near Sidoarjo, East Java, Indonesia (**Figure 1(g)**). The eruption, called the 'Lusi' (Lumpur 'mud' – Sidoarjo) (or, in Indonesia, 'Lapindo') mud volcano, has continued since, with rates reaching as high as 160 000 $m^3\,day^{-1}$ and continuing in excess of 100 000 $m^3\,day^{-1}$ into 2010. As of the fall of 2008, over 30 million m^3 of mud with temperatures ranging from 70 to 100 °C had erupted. However, as of mid-2011, web video images and news reports (Harsaputra, 2011) indicated that the eruption had slowed to around 10 000 $m^3\,day^{-1}$ and perhaps become more water-rich and that much of the mud accumulation is now dry at the surface. In spite of the recent decreases in flow, expectations are that the eruption will continue for many years (Davies et al., 2011).

The mud has been erupting primarily from a 60-m-wide central crater and has accumulated behind a system of levees and holding ponds (**Figure 1(g)**). The levees fail periodically. The mud has inundated an area in excess of 7 km^2. Although the mud accumulation behind the levees has created a topographic high that rises more than 20 m above the surrounding relatively flat ground, the eruption has also resulted in considerable subsidence of the original ground surface in the area around the main eruption vent (Abidin et al., 2008; Davies et al., 2011). Mud and decanted water are pumped into a nearby river, which then carries the mud to the ocean approximately 20 km to the east.

The mud inundation has caused over 35 000 persons to be displaced from more than a dozen villages in the area (McMichael, 2009). The inundation of numerous factories, farmland, and a major toll road (which has since been rerouted) has caused significant economic impacts on the region. In addition, a water-supply pipeline for the city of Surabaja to the north and a fiber-optic cable are in the area of subsidence and mud inundation. A gas pipeline near the eruption ruptured and exploded, reducing the supply of gas

available for local fertilizer production, which, in turn, led to local fertilizer shortages. According to the news reports cited by Abidin et al. (2008), 14 people have perished. Most, if not all, of these fatalities resulted from the gas pipeline explosion. In late February 2008, localized natural gas seeps or eruptions began to occur in residential and industrial areas outside the zone of major mud accumulation but within the area of subsidence (Davies et al., 2008). Several of these seeps and eruptions have combusted explosively when exposed to an ignition source, such as an electrical spark.

The mud eruption has been the focus of substantial scientific and media attention. Much of this attention has been on potential triggers of the eruption, whether it was caused by the exploration drilling, an earthquake, or a geothermal activity (Davies et al., 2010; Mazzini et al., 2012; Sawolo et al., 2009). Although relatively little scientific attention has focused on the potential environmental and health effects of the mud, a variety of media and environmental activist organization reports have expressed concerns regarding the potential adverse impacts of the mud on the affected river and marine environments and on the health of local residents exposed to the wet mud, waters that have contacted the mud, or dusts generated from dried mud deposits.

An environmental assessment carried out by a team from the United Nations Environment Program (UNEP) early in the eruption (UNEP/OCHA, 2006) measured low levels of potentially toxic heavy metals and organic contaminants in the mud that had erupted as of summer 2006. While the UNEP assessment provided very useful indications that the mud erupting in 2006 was not highly contaminated, the assessment did not examine the full range of characteristics of the mud that may be of potential concern from an environmental or public health perspective.

At the request of the US Department of State, the USGS has been providing technical assistance to the Indonesian Government on the geological and geochemical aspects of the mud eruption. Our group has analyzed the solid and separated the water components of two mud samples, collected in September 2007 and November 2008, and analyzed them for characteristics of possible environmental or human health concern (Plumlee et al., 2008). The mud samples contained a high proportion of ingestible (by hand–mouth transmission), inhalable, and respirable particles. The results confirmed the 2006 UNEP/Office for the Coordination of Humanitarian Affairs (OCHA) results that the levels of potentially toxic heavy metals or metalloids in the bulk mud were low. A complex mixture of organic compounds in the mud was likely derived from petroleum source rocks. The distribution and concentrations of some PAHs measured in the mud samples exceeded the EPA recommended interim sediment quality criteria. Although the mud samples contained several percent iron sulfides, net acid production tests indicated that enough carbonate material was also present to prevent the mud from becoming acid-generating due to weathering and sulfide oxidation in the near-surface environment. Hazama and Shizuma (2009) found that the activity concentrations of the naturally occurring radioactive materials in the mud were within acceptable limits.

Our data on the water separated from the muds showed that the water derived from settling mud deposits may have the potential to adversely affect the quality of surface- or groundwater sources for drinking water due to the high levels of fluoride, nitrate, iron, manganese, aluminum, sulfate, chloride, and total dissolved solids. The very high nitrate levels in the waters contained within the mud may present a source of nutrients that could enhance algal blooms and result in adverse impacts such as hypoxia in the affected freshwater and marine ecosystems.

In agreement with the previous studies, the water separated from the mud samples was compositionally and isotopically compatible with an origin as sedimentary formation water. The iron disulfide fraction of the mud sample was isotopically light and likely formed by bacterial sulfate reduction during diagenesis of clay-rich rocks from which the mud was derived. A smaller, isotopically heavy monosulfide fraction likely formed later by thermogenic reduction of formation-water sulfate to sulfide and reaction of the resulting sulfide with reactive iron in the mud.

Due in part to the small number of samples available for study, Plumlee et al. (2008) indicated that further linked earth science and public health studies were needed to more fully understand the potential environmental and health consequences of the erupting mud, waters, and gases and of the accumulating mud deposits and dusts generated from dried mud deposits. It is not clear to what extent these studies have been carried out.

11.7.10 Failures of Mill Tailings or Mineral-Processing Waste Impoundments

In the last several decades, a number of mill tailings or mineral-processing waste impoundments have failed, some of which have resulted in the catastrophic release of significant quantities of solid wastes, liquid wastes, and/or liquid processing solutions into the environment and some of which have caused human fatalities (Davies et al., 2000). Several have been studied from an environmental and health perspective and so provide useful insights into the issues of greatest environmental and health concern associated with such failures.

11.7.10.1 Mine Waste and Mill Tailings Impoundment Failures, Marinduque Island, Philippines

The Marcopper Mine, Marinduque Island, Philippines, was started in the late 1960s and had two open pits developed sequentially on two adjacent large-tonnage, low-grade porphyry copper ore bodies (Tapian and San Antonio). The ore bodies contained chalcopyrite and pyrite dispersed in quartz-filled fractures throughout the large volumes of hydrothermally altered igneous intrusive rock, the crystallization of which led to the formation of the ores.

In December 1993, extreme rainfall from a typhoon triggered the failure of a siltation dam at Marcopper that sent a debris flow of sulfidic mine wastes northwest from the mine into the Mogpog River (**Figure 1(h)**), eventually reaching the ocean (David, 2003; David and Plumlee, 2006; Oxfam, 2004; Plumlee et al., 2000, 2004). The mine wastes released from the impoundment had been eroded from large waste dumps around the San Antonio open pit. In March 1996, a plug in

the tunnel draining the Tapian open pit at Marcopper failed, releasing an estimated 1–3 million m^3 of mill tailings that had been stored in the open pit south and west into the Makulapnit and Boac river systems (**Figure 1(i)**), then into the ocean west of the island (David and Plumlee, 2006; Plumlee et al., 2000, 2004; UNEP, 1996).

A UNEP team dispatched to Marinduque in the weeks following the 1996 spill noted the catastrophic physical impacts of the tailings deposited in the downstream Makulapnit and Boac riverbeds and found the materials released in the tailings to be acutely toxic to aquatic test organisms (UNEP, 1996). They noted multiple sources of acid-rock drainage at the Marcopper mine site from the weathering of the pyrite-mineralized rocks. However, they concluded (based on a sodium nitrate leach) that the then fresh tailings deposited in the riverbeds posed little risk from a trace metal mobilization perspective and that the primary ecological risk was continued physical remobilization of the tailings. The UNEP team analyzed for but did not detect any processing-related chemicals (such as xanthate) in the waters remaining in the Tapian pit tailings impoundment. The tailings waters had near-neutral pH (6.9), which likely resulted from pH buffers added during the mill processing, and had high levels of copper (1.2 ppm).

The mining company did some remediation, such as replugging the drainage tunnel from the Tapian open pit, pushing tailings from the riverbed into the berms to prevent flooding of adjacent lowlands, contracting with local residents to fill sandbags with the tailings to make flood-control berms, and dredging a channel at the Boac river mouth to catch river-transported tailings before they entered the ocean. However, the bulk of the spilled tailings were left in or adjacent to the river due to the disagreements between the mining company and local residents as to how the tailings removed from the river should be disposed of. The company preferred submarine disposal in the ocean to the west of the island, an option opposed by the local residents due to environmental and perceived health impacts on the north shore of the island resulting from years of nearshore tailings disposal from Marcopper.

The USGS was asked to pull together an independent team to assess mining-related engineering, environmental, and health issues on Marinduque with funding from the Philippine Government (Wnuk, 2004). By the team's first visit in 2000, the Tapian pit was filling with pH 3–4 waters (**Figure 10**). Contrary to the findings of the UNEP assessment in 1996, tailings deposits that remained exposed above the Boac riverbed had become highly acid-generating due to the oxidation of pyrite in the hot monsoonal climate. Acid drainage formed during the monsoon season evaporated during the dry season, leaving behind a high component of soluble iron- and copper-rich sulfate salts in the tailings deposits. As a result, the USGS Field Leach Tests of these tailings produced acidic leachates with extremely high dissolved copper, iron, and aluminum (**Figure 10**; Plumlee et al., 2000). A leach test using seawater produced an even more acidic leachate with higher levels of dissolved metals, likely due to the enhanced metal complexing by seawater chloride (**Figure 10**). This suggested that disposal of the acid-generating tailings in the ocean could plausibly have additional implications for the marine environment that would not have been present when the tailings were fresh (Plumlee et al., 2000).

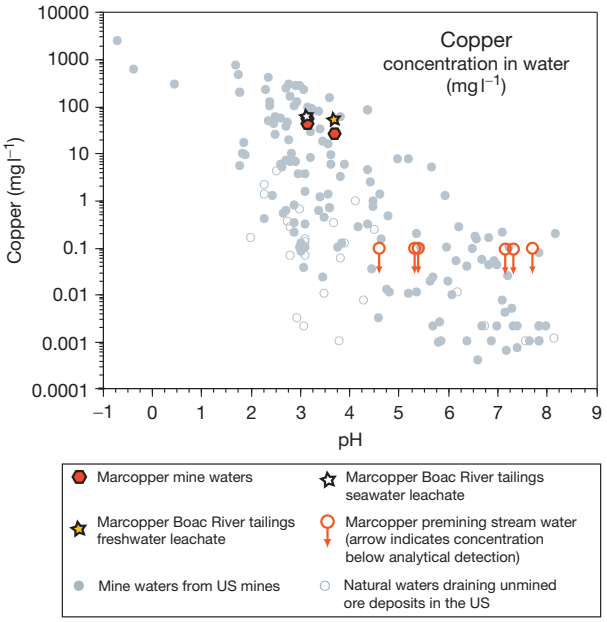

Figure 10 A tailings impoundment failure released an estimated 1.5–3 million m^3 of pyritic tailings from the Marcopper open-pit copper mine, Marinduque Island, Philippines, into the Boac River system. This plot shows pH and dissolved copper results from the USGS Field Leach Test using deionized water and seawater as the leachates on Boac River tailings collected in 2000. The data illustrate that the tailing had become acid-generating in the four years since the spill and that the runoff from the tailings during rain events would likely generate high levels of acids and metals dissolved from soluble acid-sulfate salts. For comparison, Marcopper mine water data and premining water quality data from the northern Marcopper mine site are shown.

The Boac River watershed is large, and the acid-rock drainage and acid-generating tailings from multiple sources at Marcopper are diluted by freshwaters and sediments derived from the unmineralized portions of the watershed. As a result, by the time of the USGS team's in 2003, the tailings remaining in the Makulapnit River had become largely buried or commingled with the unmineralized sediments transported into the river system during typhoons. Even though tailings deposits still remaining on the riverbanks were local sources for acid-rock drainage, the dilution and burial of the tailings in the riverbed were helping stimulate some recovery of the Boac River aquatic ecosystem (Plumlee et al., 2004). This recovery was unfortunately short-lived, as by 2003, the Tapian open pit had filled with acid-rock drainage that then started overflowing into the Makulapnit and Boac rivers, with accompanying impacts on the aquatic ecosystem (David and Plumlee, 2006).

Although the 1996 spill and its impacts on the Makulapnit River and Boac River watersheds received substantial media attention, people were made aware in 2000 of the 1993 debris flow and the devastating impacts of the sulfidic, acid-generating mine waste materials on the Mogpog River. Because the Mogpog River watershed is much smaller than the Boac River watershed and the mine site is the dominant source of both sediments (in the form of acid-generating mine wastes) and waters (in the form of copper-rich acid-rock drainage) for the Mogpog watershed, the river does not have the same 'self-mitigating' capacity that the Boac River has to help dilute the

solid and waterborne contaminants from Marcopper. The Mogpog has no prospect for recovery until massive mine waste piles are stabilized at the mine site and surface water management and erosion control are vastly improved.

The independent engineering assessment found that four siltation or water management dams at Marcopper were, as of 2003, at high risk of failure and that the impoundments behind two of them were filled with acid-generating mine wastes. Hence, there is a substantial risk for further catastrophic floods and/or debris flows of mineralized materials into both the Boac and Mogpog watersheds, particularly during the extreme rainfall and runoff produced by typhoons (Wnuk, 2004).

Local residents, public health authorities, and environmental NGOs repeatedly expressed very strong concerns regarding various adverse human health impacts from mining at Marcopper, including from long-term disposal of tailings from the 1970s until 1990 into the ocean north of the island, and from the 1993 and 1996 disasters. Of primary concern were the reported cases of lead and arsenic poisoning, which were attributed by the local residents and some public health authorities to exposures to Marcopper mine wastes. Our analyses showed that this linkage was difficult to verify, because these elements occurred in very low concentrations in the Marcopper tailings and wastes (Plumlee and Morman, 2011; Plumlee et al., 2004; Wnuk, 2004). The independent assessment team recommended that other potential exposure sources for possible cases of lead and arsenic poisoning be investigated (such as lead-bearing paint in schools and leaded gasoline combustion by-products) and that much more extensive study and monitoring be carried out to assess if the mining has had other potential adverse environmental and health impacts (Wnuk, 2004). For example, no contamination of shallow aquifers by acid drainage from the riverine tailings and wastes was found as of 2003 but could develop over time as waters migrate down from the tailings deposits into the subsurface. Potential health impacts from longer-term exposures to toxicants (such as manganese, aluminum, cadmium, and copper) in the mine wastes, tailings, dusts, and acid-rock drainage waters were also highlighted as being in need of further study as part of a broader population-based health assessment of those living or working in or near the mine and affected watersheds.

11.7.10.2 Mill Tailings Impoundment Failure, Aznalcóllar Mine, Spain

In 1998, the failure of a mill tailings impoundment at the silver–copper–lead–zinc Aznalcóllar Mine, Seville, Spain, released 4–5 million m^3 of acidic (pH ~3) waters and associated sulfidic tailings sludge into the Agrio River, which then flowed into the Guadiamar River, the Guadiamar river delta, and the wetlands of the Doñana Natural/National Parks (Grimalt et al., 1999). The mine was developed on a volcanogenic massive sulfide deposit hosted by marine volcanic and sedimentary rocks, with abundant arsenic-rich pyrite, chalcopyrite, sphalerite, galena, arsenopyrite (an iron–arsenic sulfide), and tetrahedrite (an antimony–copper sulfosalt with iron, zinc, arsenic, and silver).

The spill affected a large swath of agricultural lands along the rivers and wetlands in the parks. Extreme fish and shellfish kills resulting from the spill were documented, and some deaths of birds, amphibians, and small mammals were also noted but not ascertained with certainty to be spill-related. Some open groundwater wells were also contaminated by the sludge.

In contrast to Marinduque, a substantial remediation effort was undertaken in the months following the spill, much of which involved physical removal of the tailings deposits from the river floodplains. However, this activity also commonly removed the productive soils underlying the tailings deposits, leaving behind barren clays and sands (Grimalt et al., 1999).

Also in contrast to Marinduque, the Aznalcóllar spill has been the focus of many different studies examining the environmental, ecological, and health impacts, both soon after and over the years following the incident (Alastuey et al., 1999; Alzaga et al., 1999; Gil et al., 2006; Grimalt et al., 1999; Hudson-Edwards et al., 2005; Lacal et al., 2003; Vázquez et al., 2011, and other papers in the same journal volume).

Alastuey et al. (1999) found high levels of various metal toxicants in the tailings, including zinc (0.8%), lead (0.8%), arsenic (0.5%), copper (0.2%), antimony (0.05%), cobalt (62 ppm), thallium (50 ppm), cadmium, (25 ppm), silver (25 ppm), mercury (15 ppm) and selenium (10 ppm). They also found that concentrations of lead, silver, bismuth, and antimony increased with increasing distance downstream, which they attributed to the selective transport of very fine lead sulfide grains in the slurry. Evaporation of the acid tailings waters and initial sulfide oxidation led to the formation of water-soluble and bioaccessible acid-sulfate salts in the tailings deposits. Alzaga et al. (1999) found low levels of halogenated triphenylamines (which decreased with increasing distance downstream) and substituted carbazoles in the sludge deposits, which they concluded resulted from the mineral processing or from industrial wastes dumped into the tailings impoundment prior to release.

Similar to Marinduque, longer-term oxidation of pyrite and other sulfides in the floodplain tailings deposits, with the resulting generation of acid waters during wet periods and soluble acid-sulfate salts in dry periods, has enhanced the mobility of metals from the tailings, including iron, copper, zinc, arsenic, and cadmium (Hudson-Edwards et al., 2005). Although arsenic is readily water-solubilized, some is also associated with less bioaccessible iron oxides and jarosite. Lead was transformed into secondary lead sulfate as a result of the acidic, sulfate-rich waters (Lacal et al., 2003). Because lead sulfate and lead sulfide are not highly bioaccessible, it may be inferred that lead uptake via tailings ingestion by wildlife or humans likely was not an important exposure pathway (Plumlee and Morman, 2011).

The studies of waterfowl from the Doñana Natural/National Parks in the years following the spill (Taggart et al., 2006) found generally low levels of metals in bones and livers, suggesting that extensive cleanup efforts may have helped. A biomonitoring study of residents from the general area around the spill found elevated levels of arsenic and some other metals, compared to levels measured in populations elsewhere, but not in levels of potential health concern (Gil et al., 2006). Due to sulfide oxidation and rainfall-induced leaching over the long term, decreases in both total concentrations and ammonium sulfate-extractable concentrations of arsenic and other toxicants in the remaining sludge deposits have been observed (Vázquez et al., 2011).

11.7.10.3 Cyanide Processing Impoundment Failures – Baia Mare, Romania, as an Example

Cyanide-based processing is widely used by modern gold mining operations to extract gold from very low-grade ores because cyanide (applied in moderate concentrations as 'free' or uncomplexed sodium or potassium cyanide) forms a very strong aqueous complex with gold. Cyanide processing has commonly been raised as a potential concern from environmental or health perspectives because some cyanide forms can, in sufficiently high levels, be toxic to aquatic and terrestrial organisms (Donato et al., 2007; Eisler and Wiemeyer, 2004) and cyanide in its free form is notorious as a highly toxic human poison. Mineral beneficiation experts point out that environmental and health concerns are easily mitigated by appropriate engineering design and implementation of cyanide processing facilities (e.g., Young et al., 2001).

Johnson (in press) presents an excellent review of cyanide geochemistry. In addition to gold, other metals (cobalt, platinum, and iron) also form very strong nontoxic aqueous complexes with cyanide. Lead, silver, copper, zinc, manganese, and some other metals form moderately strong (termed weak-acid dissociable, or WAD) complexes with cyanide. WAD cyanide forms are toxic because they can break down readily into free cyanide. The metals that form strong or WAD cyanide complexes, if present in readily solubilized forms in the ores, can substantially reduce gold extraction efficiency and become enriched in the processing solutions. Sulfides in ores also react with cyanide to form relatively nontoxic aqueous thiocyanate, which also decreases extraction efficiency. Cyanide processing solutions are typically kept at pH values above 9.6 to preclude formation of hydrogen cyanide, which is easily volatilized, and so cyanide processing solutions can easily also leach from the ores and become enriched in oxyanion-forming toxicants such as arsenic that are geochemically mobile in alkaline waters. In addition to the volatilization of hydrogen cyanide triggered by a pH drop below 9.6 (such as through dilution by relatively acidic rain or surface waters), a variety of processes can transform or degrade cyanide in the environment (Johnson, in press). Ferricyanide ions can react with iron or other metals to precipitate insoluble ferricyanide compounds. Strong aqueous complexes with iron and cobalt, as well as some cyanide solids, can photodissociate to WAD cyanide in the presence of sunlight. Biodegradation by bacteria, particularly under oxygenated conditions, can also be important.

The collection, preservation, and analysis of samples for total cyanide and cyanide speciation are challenging (Johnson in press), both to collect samples rapidly enough to preserve transient cyanide species and to prevent changes in cyanide speciation and/or cyanide loss following collection. For example, keeping samples isolated from sunlight is key to prevent breakdown of cobalt or iron cyanide complexes. There are real-time detection systems developed for total cyanide (e.g., Timofeyenko et al., 2007), but we are not aware of any that are yet available to measure cyanide speciation in real time.

Cyanide-based gold extraction either involves milling or heap leach processing. Various milling methods use grinding to reduce particle size and increase surface area. Sulfide-rich gold ores require the additional milling step of roasting prior to cyanidation to oxidize sulfides that would lead to thiocyanate generation. Milling methods produce large volumes of water-rich tailings sludge that require disposal in tailings impoundments. Several cyanide tailings impoundments have failed over the years, leading to the release of fine-grained solids and cyanide-rich processing solutions into the environment. In contrast to milling-based cyanide extraction methods, heap leaching involves the sprinkling of cyanide solutions directly on large piles of crushed, sulfide-poor ore on impermeable pads. Although heap leach impoundments can fail, they may not have the high volumes of water and fine-grained materials that can lead to substantial downstream transport of solid and liquid wastes. However, plumbing breaks and leaks that develop in the impermeable pads have, for example, led to the release of cyanide processing solutions from heap leach pads into the environment or groundwater.

On 30 January 2000, rainfall onto or rapid melting of a snow-laden cyanide tailings impoundment at Baia Mare, Romania, led to the failure of the impoundment and the release of an estimated 100 000 m^3 of processing wastes containing as much as 100 tons of cyanide (in concentrations as high as 400 mg l^{-1} total cyanide and 120 mg l^{-1} free cyanide) into the Sasar River (Cunningham, 2005; DeVries, 2001; UNEP/OCHA, 2000). The facility had been reprocessing old tailings from a previous gold mining operation. The ores in the Baia Mare area are volcanic- and sediment-hosted Au–Cu–Ag–Pb–Zn–As epithermal vein ores with abundant pyrite, chalcopyrite, sphalerite, and galena and lesser amounts of marcasite and pyrrhotite (both iron sulfides), arsenopyrite, and various sulfosalts (sulfides with copper, arsenic, antimony, and bismuth).

The mining company reportedly added sodium hypochlorite to the spill effluent as it left the impoundment breach to try (unsuccessfully) to destroy the cyanide in the effluent. The waste plume from the failure was detected via transiently elevated concentrations of cyanide, copper, iron, manganese, and zinc in river waters as it flowed successively from the Sasar River into the Lapus, Somes, Tisza, and Danube rivers and eventually (several weeks later) into the Black Sea approximately 2000 km downstream. Governmental agencies from several of the affected countries (Romania, Hungary, Yugoslavia, and Bulgaria) did downstream sampling during the spill and reported total cyanide concentrations as high as 33 mg l^{-1} and copper concentrations as high as 18 mg l^{-1} in the Tisza River by February 1 as the spill plume crossed into Hungary (UNEP/OCHA, 2000). The levels in the plume decreased to 0.1 mg l^{-1} total cyanide and 0.05 mg l^{-1} copper by the time it reached cities well downstream on the Danube by February 24 (UNEP/OCHA, 2000). Even well downstream, the levels of cyanide, copper, iron and manganese exceeded various European country surface water quality standards.

The spill severely affected the aquatic ecosystem at all levels (Cordos et al., 2003). Hungary and Yugoslavia agencies reported extensive fish kills in the Tisza River, but no fish kills were reported on the Danube. Fish populations were observed to be recovering after the spill (perhaps due to fish reentering the affected reaches from unaffected areas above the spill) but with a smaller number of species; mollusk species were also severely affected (Cordos et al., 2003). Freshwater phyto- and zooplankton communities in the rivers were decimated during the passage of the plume but started recovering soon after the plume had passed (UNEP/OCHA, 2000).

The impacts on drinking water taken from the river were reportedly limited to villages close to the spill, which were provided with alternative water sources at some point after the spill had occurred. Shallow water wells near the mine site showed elevated levels of heavy metals but not cyanide. Most downstream cities utilized groundwater wells that showed no signs of contamination or were able to stop intake from the river as the plume passed.

As with Aznacóllar, a number of studies were carried out in the years following the spill on its impacts on sediment, soil, and water quality. Multiple studies (e.g., Bird et al., 2008; Cordos et al., 2003; UNEP/OCHA, 2000) found extremely high levels of copper, lead, mercury, cadmium, and zinc in sediments close to the mining site. All concluded that, although the tailings solids and waters had contaminated the riverbed and adjacent floodplain, the area had high levels of heavy metal contamination prior to the spill from mining, milling, and smelting. This heavy metal pollution in and of itself poses a significant long-term threat to animal and human health.

A variety of aspects of the Baia Mare spill remain poorly understood based on the available information. For example, although sodium hypochlorite was applied in undescribed quantities to the material as it emanated from the site, it is unclear how effective this treatment was in removing cyanide from the waters (substantial amounts of cyanide survived to be measured in downstream samples). Also unclear is whether the sodium hypochlorite was applied in sufficiently high levels that it itself had a detrimental impact on the aquatic ecosystem downstream. It is unclear from the available reports whether samples were collected in a manner that would preserve them from postsampling changes in cyanide content or speciation. Although it can be inferred based on the copper-rich nature of the effluent that a substantial quantity of the cyanide in the effluent was complexed with copper, data are lacking on the aqueous and solid cyanide speciation in the effluent and plume as it moved downstream. Such data would have substantially helped in understanding the geochemical evolution of cyanide in the system and how changes in cyanide speciation may have influenced potential toxicity effects on aquatic organisms. Further, concentrations of other important toxicants, such as arsenic, antimony, cadmium, and mercury, were not measured in the effluent or the waters at the time of the spill, so it is not known how these may have contributed to environmental impacts.

11.7.10.4 Red Mud Spill from Bauxite Processing, Hungary

In October 2010, an impoundment storing bauxite-processing residue at Ajka, Hungary, failed, resulting in the release of 0.9 to 1 million m^3 of caustic alkaline red mud into Torna Creek and River Marcal (Burke et al., 2012; Czövek et al., 2012; Gelencsér et al., 2011; Jordan et al., 2011; Mayes et al., 2011; Renforth et al., 2012; Ruyters et al., 2011). The mudflow inundated agricultural areas and several villages in lowlands downstream and eventually reached the Danube River. The mudflow killed 10 people and injured as many as 150 others and damaged or destroyed many houses, bridges, and other structures. Fish kills were also observed for several tens of kilometers downstream. Close to the impoundment, high-water marks on buildings and trees indicate that the flood surge exceeded 1.5–2 m and likely contaminated some open water wells. However, the sludge that was left behind typically was only 1–2 cm thick, indicating that the mud that escaped from the impoundment was relatively water-rich (**Figure 1(j)**).

Remediation efforts included removal of the mud from residential areas and some agricultural fields (with redisposal at the impoundment site), plowing of mud deposits into the soils of other agricultural fields, and treatment of the mud with gypsum and acetic acid. Following the spill, the company shifted from wet storage to dry storage of the processing by-products (Jordan et al., 2011), reducing the potential for a mud release in the future but increasing the potential for dust generation from the storage areas if appropriate dust control measures are not implemented.

The mud was composed predominantly of the aqueous and solid by-products of the Bayer process for transforming bauxite (in this case, karst bauxite) into aluminum oxide. However, the dam enclosing the mud storage impoundment that failed was constructed of CFA and so the mud also contained material eroded from the dam. The mineral phases identified (Gelencsér et al., 2011; Jordan et al., 2011) include a mixture of (1) remnant bauxite minerals (e.g., the aluminum hydroxide minerals gibbsite and boehmite, $AlOH_3$); (2) mud phases such as hematite (iron oxide) and cancrinite ($Na_6CaAl_6Si_6(CO_3)O_{24} \cdot 2H_2O$); (3) minerals of possible processing or fly ash origin such as 'hydrogarnet' ($Ca_3AlFe(SiO_4)(OH)_8$), calcite (calcium carbonate), and perovskite (calcium–titanium oxide); (4) possible soil minerals such as feldspars; and (5) processing- or remediation-related gypsum (calcium sulfate).

The Bayer process digests bauxite ores using sodium hydroxide. As a result, the water component of the mud had an extremely caustic pH of greater than 13. Some number of the injuries (and possibly fatalities) resulted from caustic alkali burns to people who came into contact with the mud.

Early remediation efforts involved the addition of gypsum and acetic acid to attempt to neutralize the caustic alkalinity. The addition of calcium sulfate, which is commonly practiced at bauxite residue disposal sites, causes caustic hydroxyl ions to react with the calcium released from the gypsum and atmospheric carbon dioxide, with the resulting formation of calcium carbonate (Renforth et al., 2012). It is likely that the amount of caustic alkalinity in mud deposits that were exposed to rainfall diminished with time as the hydroxide ions reacted with carbonic acid in rainfall.

Photographs in the literature indicate that the mud deposits left behind following the spill dried to a very hard, mud-cracked material that likely was not prone to dust generation unless pulverized by foot or vehicle traffic. Photographs and descriptions indicate that some fluffy efflorescent salts also developed on dried mud deposits. These may have been soluble caustic sodium hydroxides and gypsum that, in contrast to the red mud material, could easily become wind-borne.

Several studies found elevated levels of some elements in the water and solid components of the mud. Waters remaining in the impoundment following the spill had elevated levels of dissolved (<0.45 μm) aluminum (659 ppm), arsenic (3.6 ppm), boron (0.9 ppm), gallium (2.3 ppm), molybdenum (4 ppm), and vanadium (5.7 ppm) (Mayes et al., 2011). The solid component of the mud was found to contain elevated levels (tens to hundreds of ppm) of arsenic, vanadium,

nickel, lead, chromium, cobalt, molybdenum, and mercury (Burke et al., 2012; Gelencsér et al., 2011; Jordan et al., 2011). Chromium was predominantly in the less toxic trivalent form bound up in iron oxides, arsenic was in various arsenate forms, and vanadium was present in pentavalent form associated with calcium aluminosilicate phases (Burke et al., 2012).

Several studies applied sequential extraction, water leach, or other chemical extraction tests on samples of the muds (Burke et al., 2012; Jordan et al., 2011; Ruyters et al., 2011). One investigated the uptake of metals and metalloids from the mud by spring barley (Ruyters et al., 2011). These studies indicated that the various potentially toxic metals and metalloids in the mud were only rather sparingly mobilized. In plants, the most substantial impact on yield reduction and enhanced uptake of some metals resulted from the addition of soluble sodium hydroxide to the soils from the mud (Ruyters et al., 2011). The natural neutralization of caustic alkalinity from any remaining exposed mud deposits will over time change the mobility of various elements enriched in the muds. Various studies concluded that removal of mud deposits remaining in the environment is still warranted to minimize mobilization of all metals and metalloids (e.g., Burke et al., 2012).

A substantial public health concern following the spill was potential exposures to dusts generated from dried red mud deposits, with possible health effects caused by the caustic alkalinity and elevated levels of some metals. Gelencsér et al. (2011) analyzed samples of dust that they had resuspended from mud deposits using a leaf blower and concluded that respirable-sized particles, alkalinity, and metal or metalloid toxicants were not at levels of substantial concern. Similarly, Czovek et al. (2012) carried out inhalation toxicity testing on rats using ground mud samples and found only evidence of mild inflammation. They concluded that short-term exposures of healthy individuals to high concentrations of dusts from dried red mud deposits would not pose a greater hazard than exposures to urban dusts at comparable concentrations. Further work is needed, however, to assess potential health implications from exposures to dusts released from the revamped practice of dry storage of processing wastes following the spill.

Our group is currently working with the Hungarian Geological Survey to fill in some knowledge gaps on the mud deposits. For example, they are examining bioaccessibility characteristics of the muds and dusts that could be generated from the muds using the simulated gastrointestinal and lung fluids. They are also examining spectral reflectance characteristics of the mud to interpret hyperspectral remote sensing data that can then be used to help map the distribution of remaining mud deposits.

11.7.10.5 General Insights Regarding Environmental and Health Impacts of Mineral-Processing Impoundment Failures

The case studies presented in this section provide several important lessons regarding response to and preparedness for failures of mine waste, mill tailings, and mineral-processing storage impoundments. With the exception of cyanide, relatively little information has been collected on the environmental behavior of manufactured chemicals present in mineral-processing solutions that have been released as a result of impoundment failures. For example, chemicals such as xanthates used in mineral flotation have not been noted in postspill studies; however, it is unclear whether this absence is because they have not been looked for, are present in sufficiently low levels in the original discharge that they are rapidly diluted in the environment, or are rapidly degraded in the environment. Recently, Rostad et al. (2011) found no xanthates but did find high levels of DOC and xanthate degradation products and a surfactant in surface water samples from a lead–zinc mine–mill in Missouri. These results indicate that further studies of these compounds following tailing spills are warranted.

In the case of failures that release large volumes of cyanide-bearing solutions into the environment, rapid mobilization of field teams is needed to collect and analyze appropriately preserved samples of the solutions as they are released and subsequently modified in the environment. This level of effort is needed to more fully understand how various degradation processes influence the speciation and potential aquatic toxicity of released cyanide.

In the case of solids released by catastrophic impoundment failures, the geologic characteristics of the deposits being mined and processed provide important predictive insights (e.g., Plumlee, 1999; Plumlee and Morman, 2011) into the nature of the solids being released, such as (1) the abundance of various acid-generating sulfides or potential mineral toxicants such as asbestos or crystalline silica; (2) the types and abundances of potential metal or metalloid toxicants (e.g., arsenic, lead, and mercury); and (3) the mineral hosts for the toxicants (e.g., bioaccessible lead carbonate vs. nonbioaccessible lead sulfide or lead sulfate – see examples in Plumlee and Morman, 2011). Particularly, if an impoundment failure releases large volumes of sulfide-bearing tailings into the environment, measurement of the net acid production potential of the material released will help understand if the material may become acid-generating over time.

11.7.11 Failures of Coal Slurry or Coal Fly Ash Impoundments

Coal is the collective term that refers to organic-rich sedimentary rock materials formed by the fossilization of plant matter (see Chapter 9.8). Coal can have different ranks, depending on the temperature and pressure to which the organic matter has been subjected following deposition. Anthracite has the highest rank and the highest carbon content (95%). Progressively lower ranks of coal have progressively lower carbon content. Coal can also have variable amounts of accessory materials interspersed with the organic components, including a variety of clays, carbonate minerals, crystalline silica or other silicate minerals, and iron sulfides, such as pyrite and marcasite. In addition, coals can contain very high levels of a variety of potentially toxic metals and metalloids, such as mercury, cadmium, thallium, and arsenic. Many of these are present as trace elements within the sulfides, but they can also occur as trace constituents of the organic coal components.

Many coals are washed with a mixture of water and various proprietary chemicals at the mine site prior to transport. The goal is to remove as much of the noncombustible component (including sulfides and silicate minerals) as possible. The resulting slurry is either pumped to surface impoundments

for storage or is reinjected underground into old mine workings (Ducatman et al., 2010).

During coal combustion, the elements present in the original organic and mineral components of coal are redistributed as a result of the high temperatures into new gaseous and solid phases. Coarse bottom ash and (in cyclone boilers that combust at hotter temperatures) boiler slag are the materials that collect at the bottom of the coal combustion boilers and must be removed and stored as wastes. CFA is a highly complex particulate material, typically present in inhalable- to respirable-sized particles, produced by the combustion of ground coal and entrained in the hot flue gases. Modern coal-fired power plants remove CFA from their exhaust emissions using electrostatic precipitators, scrubbers, or filter bags and must then either repurpose (e.g., as a component of cements) or dispose of as waste the trapped CFA particles. Bottom ash, slag, and CFA that are not used for various engineering purposes are either stored in dry impoundments or piped as slurries into wet impoundments (also called ponds).

11.7.11.1 Coal Slurry Impoundment Failures

A number of coal slurry impoundment failures have been noted over the last two decades, either from failure of the dams holding back surface impoundments or when underground storage areas are breached. The dams are often composed of loose rubble from mining activity, reinforced with soil (Quaranta et al., 2004). For example, in October 2000 in Martin County, Kentucky, a surface coal slurry impoundment ruptured at its base and released its stored slurry into the underground mine workings. The slurry eventually reached the surface through two mine portals, and over 1.1 million m^3 of slurry was discharged into the local waterways. Thick deposits of residual, metal-rich sludge were left in the streambeds. The plume led to fish kills along 93 km of the Sandy River and its tributaries and caused disruption to the local water supplies in downstream cities with water intakes from the river. Extensive cleanup and removal of the riverine sludge deposits were carried out in the next 6 months, but substantial material remained in the streams and continued to affect fishery resources following the cleanup (Frey et al., 2001; McSpirit et al., 2007). Hower et al. (2000) describe a 1996 coal slurry spill and its resulting environmental impacts in Virginia, and other spills in the eastern United States have been noted in media reports. In 1972, the failure of a rubble dam released over 490 000 m^3 of coal slurry into Buffalo Creek (Logan County, West Virginia) killing 125 people, injuring over 1000 other people, and leaving 4000 people homeless (Vendetti, 2001).

There is relatively little information available in the literature about the composition (and, hence, the resulting environmental and health implications) of coal slurry. Slurry composition is likely a complex function of the geology, mineralogy, trace-element content, rank of the coal being processed, and proprietary chemicals used in the cleaning water (Ducatman et al., 2010; Orem et al., 2009; W. Orem, oral comm., 2011). Studies of groundwater quality near slurry impoundments may provide some insights into the composition of the coal slurry waters. These studies note elevated levels of sulfate, sodium, ammonium, iron, manganese, arsenic, chromium, zinc, and cadmium. However, due to the elevated levels of many of these constituents in the rocks that host the coal, a clear link back to the coal slurry is difficult to establish (Wigginton et al., 2008).

The slurry solids are enriched in the fine fraction of the ground coal, so it will have some abundance of inhalable to respirable particles. In addition to the organic coal components, the solids are enriched in quartz, clays, and other silicate components of the coals. Carbonates may be variably present based on the carbonate content of the coals and host rocks. For sulfur-rich coals, it is likely that the solids contain abundant sulfides and are enriched in the heavy metals or metalloids such as lead, arsenic, and other elements that reside in the sulfides. Organic contaminants are likely to include anthropogenic chemicals used in the washing water (including fuel oil components, kerosene, and polyacrylamide flocculant) and coal-derived chemicals in the coal solids and in waters leached from the coals such as PAHs (W. Orem, oral comm., 2011).

While some proportion of the fish kills caused by these releases could be attributed to the immediate physical effects of the slurry solids, the role of the chemical impacts is unclear. Potential long-term changes in the sludge residues left in the environment are not addressed in the available literature. It is possible that the slurry from coals with abundant sulfides and minimal carbonates could become acid-generating as the sulfides oxidize.

11.7.11.2 Coal Fly Ash Impoundment Failures

Fresh CFA is mineralogically and chemically complex and is a function of the rank, chemical composition, and mineralogy of the original coal coupled with the combustion conditions. It is composed of diagnostic spherical particles that can contain a variety of phases such as aluminosilicate glasses, quartz, mullite (an aluminum silicate), perovskite (calcium titanium oxide), iron oxides, lime (calcium oxide), periclase (magnesium oxide), phosphates, clays, anhydrite, and other sulfates. Sulfur dioxide and a wide variety of trace elements can be sorbed on the particle surfaces. CFA can concentrate uranium and thorium from the original coal and so can contain greater concentrations of radioactive elements or associated radioactivity than granites, basalts, or common shales. However, the concentrations of radioactive elements in CFA are less than those in some other common rock types, and so the radiation dose an average person in the United States receives from CFA is minor compared to the doses from other sources, such as medical X-rays (USGS, 1997).

Depending on the proportions of carbonates to iron sulfides in the coal prior to combustion, CFA can generate somewhat acidic (low carbonate/sulfide coal) to highly alkaline (high carbonate/sulfide coal) water leachates (USGS, 2002a) (**Figure 11**). The pH of some ash leachates can also be initially acidic due to the dissolution of acid-sulfate phases from particle surfaces, then turn alkaline as the waters react with minerals, such as lime (CaO) and periclase (MgO) (USGS, 2002a). The types and concentrations of metals and metalloids released from CFA into water leach solutions depend on their initial concentration in the coal and on the alkalinity or acidity of the CFA leachate. In general, metals such as cadmium, copper, manganese, iron, nickel, lead, and zinc are released in greatest quantities from acidic CFA leachates, whereas

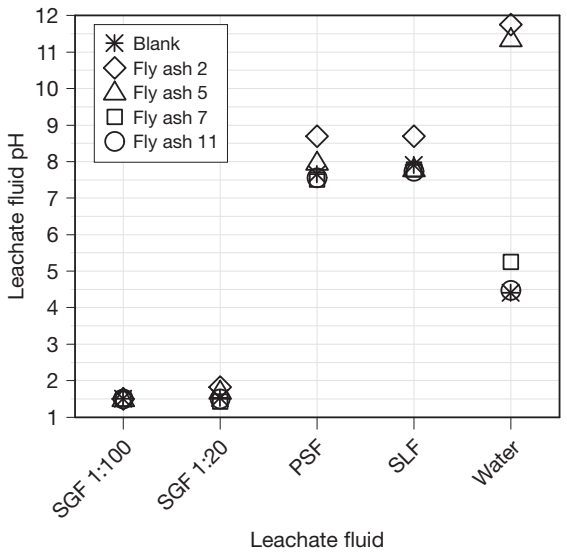

Figure 11 This plot shows the pH of simulated gastric fluids (SGF), serum-based fluids, simulated lung fluids (SLF), and water before (blank) and after leaching of four coal fly ash (CFA) samples. Two of the fly ash samples generate substantial amounts of caustic alkalinity, whereas the other two do not. Abbreviations are as follows: SGF 1:100 – samples leached with SGF at 1 part solid to 100 parts SGF by weight; SGF 1:20 – samples leached with SGF at 1 part solid to 20 parts SGF by weight; polysulfone (PSF) – samples leached with serum-based fluid at 1 part solid to 20 parts fluid by weight; SLF – samples leached with lung fluid simulant at 1 part solid to 20 parts fluid by weight; and water – 1 part solid to 20 parts deionized water by weight. SGF leaches were agitated at 37 °C for 1 hour; all other leaches were agitated at 37 °C for 24 hours. Recipes for the SGF are given by Morman (2012) and the PSF and SLF extraction fluids by Wolf et al. (2011). G. Plumlee, S. Morman, R. Finkelman unpublished data.

elements that form oxyanionic species such as arsenic, boron, molybdenum, selenium, antimony, and vanadium are released in greatest quantities from alkaline CFA leachates. Uranium in CFA is associated with the less reactive glassy phases and thorium is associated with insoluble phosphate phases, and so these radioactive elements tend not to be readily leachable into waters (USGS, 1997).

A variety of *in vitro* and *in vivo* toxicological studies have examined the potential health effects of CFA. Some studies have concluded that iron release from CFA can generate free radicals and therefore can trigger DNA damage and toxicity (Aust et al., 2002). Various *in vitro* assays summarized by Aust et al. (2002) showed that CFA samples generate ROS, interpreted to be due to the participation of iron from the CFA. Hence, the deleterious effects from inhalation exposure to CFA may be linked to its content of leachable iron, its alkali content, and the amounts of soluble salts that can dissolve to generate acid and thereby enhance iron release. The studies that examined CFA toxicity using *in vivo* and *in vitro* testing found a variety of effects such as inflammation, altered immunological mechanisms, and toxic impacts on cells (see, e.g., papers cited in Ruhl et al., 2009).

Twining et al. (2005) analyzed samples of CFA sieved to <10 μm from an Indiana power plant and found that a number of elements can be quite bioaccessible in SLF (zinc > nickel > copper > lead) and SGF (zinc, copper, vanadium > lead, nickel, strontium, uranium > thorium, aluminum, chromium). However, when the results were translated into potential daily exposure amounts and compared to implied threshold limits, the metals were indicated to be less problematic from a health hazard perspective than the CFA particulates themselves. The concentrations and potential bioaccessibility of other elements were not presented by the Twining study, but our analyses of CFA from the United States and other countries (**Figure 12**) indicate that metals or metalloids, such as manganese, arsenic, selenium, thallium, and uranium, can be present in somewhat to rather elevated concentrations, depending upon the source coal for the CFA. Bioaccessibility tests using SLF and SGF (our data) indicate that molybdenum, arsenic, zinc, chromium, thallium, uranium, and selenium tend to be relatively bioaccessible in CFA samples (**Figure 12**). Because a portion of uranium and thorium are associated with more biodurable CFA phases, it is possible that these may actually persist in the lung environment for some time if the particles are not cleared, potentially enhancing the chances of radiation-triggered toxicity.

Wet storage of CFA can substantially alter the chemical, mineralogical, chemical reactivity, and toxicant leachability/bioaccessibility characteristics of the original CFA (Singh and Kolay, 2002). Acid- or alkali-forming phases on particle surfaces are neutralized, and some proportion of the readily leachable elements can be taken into solution, then in some cases reprecipitated as other phases. Zeolites are a common phase formed when CFA reacts with water (Singh and Kolay, 2002).

In December 2008, the containment structure for a wet CFA impoundment at Kingston, Tennessee, failed, releasing more than 4.1 million m^3 of wet-stored CFA sludge directly into the Emory River, a tributary of the Clinch and Tennessee rivers. Ruhl et al. (2009, 2010) have carried out a multiyear study of the CFA spill and its impacts on the river environment. They reported elevated concentrations in the spill solids compared to background soils of a number of potentially toxic elements in the CFA deposits, most notably arsenic (avg. of 75 ppm), nickel (avg. 23 ppm), vanadium (avg. 77 ppm), manganese (avg. 102 ppm), mercury (150 ppb), and other elements such as chromium, cobalt, copper, zinc, and lead. They also found what they considered to be very high levels of radium (4.6–8.1 pC g^{-1} unit), levels that are at the upper end of values typically found in CFA. Elevated levels of arsenic and selenium were found in water samples only from a surface pond with restricted flow and in pore waters from river sediments collected downstream from the spill. The highest aqueous arsenic concentrations were associated with somewhat anoxic conditions in the pore waters, resulting in an abundance of As^{3+}. The concentrations of potentially toxic elements were low in free-flowing river waters due to the effects of dilution.

Ruhl et al. (2010) also carried out leach tests of the Kingston CFA using deionized water, local river water, and solutions having a range of pH values. They found that the particular elements that were released varied predictably as a function of pH, with oxyanion-forming elements being leached at high pH and other metals leached at lower pH. They also noted the lack of alkalinity generated by the Kingston CFA samples when leached with local river water or deionized water. The authors of this chapter interpret that this is likely due in part to the fact

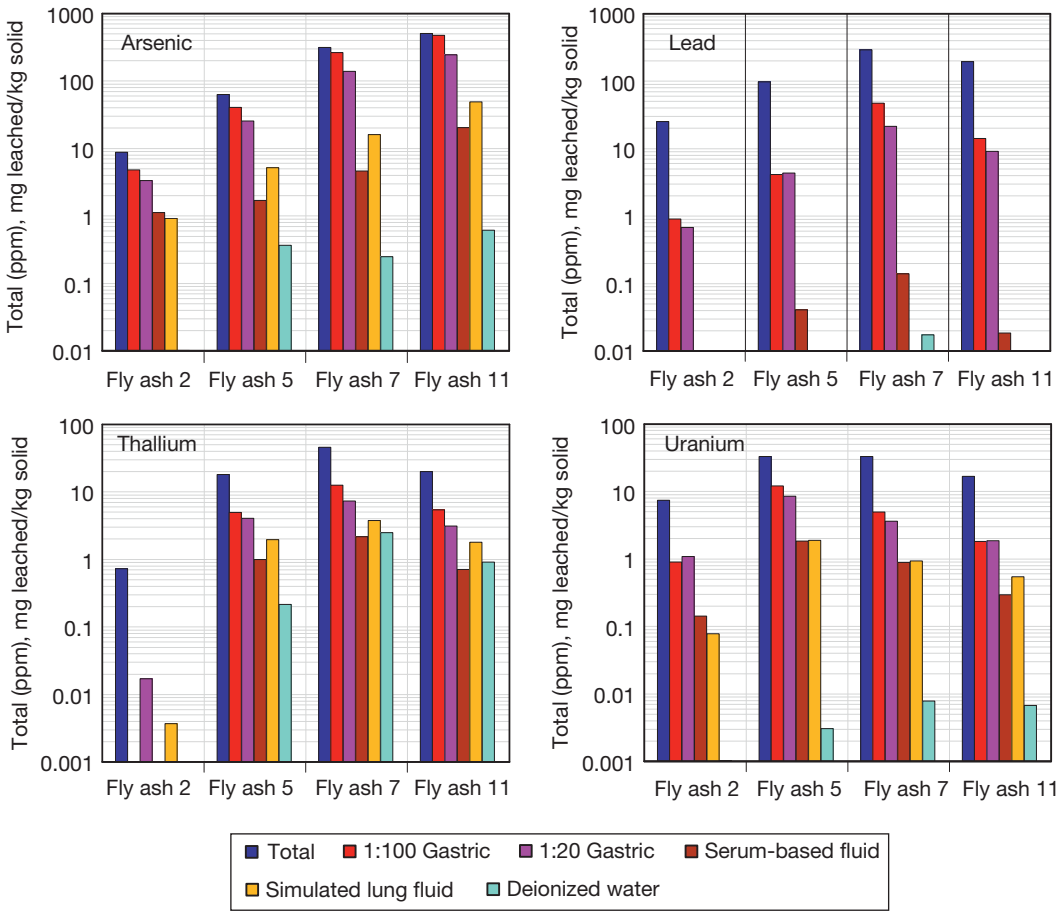

Figure 12 Total and leachable concentrations of arsenic, lead, thallium, and uranium of the four CFA samples whose leachate pH values were shown in **Figure 11**. The ash samples can vary substantially in their toxicant content and toxicant bioaccessibility. All four potential toxicants are indicated to be quite gastric-bioaccessible in these samples, and all but lead are indicated to be somewhat bioaccessible in the lung environment. Thallium concentrations in several of the fly ash leachates are the highest that we have measured in any water or simulated biofluid leaches of a wide variety of earth and environmental materials. G. Plumlee, S. Morman, R. Finkelman unpublished data.

that the Kingston CFA was stored wet, and so any caustic solids, such as lime and periclase, may have been neutralized in the impoundment prior to the spill. However, the Ruhl et al. (2009) pH 6–7 leachates were produced at very low CFA/water ratios, from 1:250 to 1:1000, and so the effects of caustic alkali materials present at low to moderate levels in the ash would have not been manifested in the leachates due to dilution. Leachate tests at substantially higher CFA/water ratios (e.g., 1:20) and SEM and XRD studies of the spill ash would be helpful to understand if these alkalinity-generating minerals were present.

Ruhl et al. (2009) also raised the possibility of potential health impacts resulting from exposures to dusts resuspended from the spilled and dried surficial deposits of Kingston CFA, citing concerns about the high levels of trace metals and radium in the CFA. A mineralogical study of the dried ash deposits would be helpful to understand the particle size distribution and the phases present. The IVBA tests using simulated gastrointestinal and lung fluids would also provide insights into the bioaccessibility/biodurability behavior of the CFA particles and their contained toxicants via inadvertent ingestion and inhalation pathways.

11.7.12 Building Collapse – The World Trade Center as an Example

Buildings can collapse catastrophically as a result of earthquakes, fires, armed conflicts, and terrorist attacks. The uncontrolled collapse of large buildings typically is associated with the generation of large dust clouds that spread out and leave deposits of settled dust throughout the adjacent urban areas and the formation of large volumes of debris at the building sites that are in need of disposal. Planned demolition of buildings also results in dust clouds and debris, but the buildings' contents and, as much as possible, the potentially HM present in the buildings are usually removed prior to demolition.

Although a unique case in terms of the size of the buildings affected, the tragic attacks on and collapse of the WTC towers in New York City (NYC) on 11 September 2001 provide a highly documented example of both the materials that can be generated and the resulting environmental health concerns. The WTC building collapses generated massive dust clouds that enveloped much of lower Manhattan. The dust clouds left behind deposits of dust, debris, and paper up to many inches thick, both outdoors and indoors in buildings where windows were open at the

time of the collapse or (in the case of buildings close to Ground Zero) where windows or walls were blown open by the force of the collapses, or whose air conditioning intake filtration systems were breached (**Figure 1(k)** and **1(l)**). Fires smoldered in the depths of the debris pile for several months following 9/11.

Concerns immediately developed regarding the potential health risks associated with various types of exposures (Landrigan et al., 2004; Lorber et al., 2007; WTCHP, 2011). Populations downwind were exposed to smoke with abundant PM, organic compounds, and acids from fires started by the jet impacts into the two towers. Large numbers of people in lower Manhattan suffered intense acute exposures to dusts generated by the collapses. Air quality monitoring data were not available during and immediately after the collapses, and so the exposures during this period must be inferred based largely on studies of the settled dust deposits. Over the following months, rescue and recovery workers at Ground Zero were exposed occupationally at higher levels to dusts generated by the cleanup, smoke from fires that smoldered within the debris at Ground Zero for some weeks after the attacks, and diesel combustion by-products produced during debris removal. Persons living and/or working in lower Manhattan were also exposed environmentally to the same sorts of materials (Lorber et al., 2007). Persons cleaning up dusts in building interiors were exposed to resuspended dusts during cleanup.

A variety of health and toxicological effects have been documented or postulated to date (Aldrich et al., 2010; Caplan-Shaw et al., 2011; Edelman et al., 2003; Fireman et al., 2004; Gavett et al., 2003; Landrigan et al., 2004; Li et al., 2011; Meeker et al., 2010; Perera et al., 2005; Prezant et al., 2002; Rom et al., 2002; Scanlon, 2002; Stephenson, 2002; Webber et al., 2011; WTCHP, 2011; Zeig-Owens et al., 2011). The short- to intermediate-term impacts resulting from exposures to the dusts and smoke include:

- intense burning of the eyes, mouth, and upper respiratory tract, nasal congestion, and gagging reflux of incidentally swallowed dust;
- sinusitis and laryngitis;
- development of the persistent 'WTC cough';
- other respiratory effects, such as shortness of breath, chronic chemically induced bronchitis, new-onset asthma, and exacerbation of existing asthma;
- elevated levels of metals (titanium, zinc, mercury, gold, tin, and nickel), degraded glass fibers, silicate minerals, calcium phosphate and silicate minerals, chrysotile asbestos, and glass shards in the induced sputum and/or bronchoalveolar lavage fluids of firefighters;
- chemical pneumonitis (rare, three cases);
- acute eosinophilic pneumonia (rare);
- corrosive damage to and irritation of respiratory tract;
- gastroesophageal reflux disease, resulting from corrosive damage to the gastrointestinal tract;
- elevated levels of lead, antimony, and cadmium in the urine of firefighters.

Based on toxicity testing of rats aspirated with various size-fractionated, deionized-water extracted WTC settled dust samples, Gavett et al. (2003) concluded that high-level acute exposures to WTC dusts $<2.5\ \mu m$ in size could cause pulmonary inflammation and airway hyperresponsiveness in people.

With the passage of more than a decade since the attacks and building collapses, a number of recent studies have been assessing the health of exposed populations. A variety of longer-term impacts are being recognized:

- Increased cases of asthma, obstructive airway disease, and bronchial hyperreactivity have been well documented.
- Large declines in lung function in NYC firefighters were noted in the first year after 2001, with little recovery in the following 6 years. Such a long-term lack of recovery following an exposure is unusual in firefighters exposed to smoke and fire.
- Moderate excess in rates of multiple cancer types have been seen in NYC firefighters.
- Increased cases of sarcoidosis (development of abnormal clusters of chronic inflammatory cells, or granulomas, in the lungs or other tissues) have been associated with work at Ground Zero.
- Upper and lower respiratory symptoms, interstitial fibrosis, small airway abnormalities, and abundant mineral particles in lung tissues have been noted in residential, pediatric, and local working populations exposed to WTC dust, gas, and fumes.
- Increased rates of interstitial lung disease have been documented in WTC responders.
- Developmental effects (such as small for gestational age) have been seen in newborns whose mothers were near Ground Zero on or shortly after 11 September 2001.
- Recent studies have found quartz, platy aluminosilicates, calcium phosphates, calcium carbonates, calcium sulfates, small glass shards, some chrysotile asbestos, talc, and feldspars, and carbon nanotubes in the lung and lung lymph node tissue samples taken from WTC responders or workers who developed lung disease.

These studies collectively indicate that the populations at greatest risk for adverse health impacts include (1) those who were exposed to extremely high levels of ambient PM at the times of and in the first few hours after the collapses, (2) rescue/recovery personnel who worked for extended periods of time at Ground Zero, (3) workers removing debris from Ground Zero, (4) pregnant women who were at or near Ground Zero during or shortly after the collapse (Perera et al., 2005), and (5) people who lived or worked near Ground Zero in the months following 9/11 (Landrigan et al., 2004). Risks in the general population living away from Ground Zero are not thought to be high for short- or long-term adverse health effects from environmental inhalation exposures to the dusts and smoke (Lorber et al., 2007). We are not aware of any studies that examined potential inadvertent ingestion exposures to WTC dusts, such as via ingestion of dusts cleared from the respiratory tract. Incidental ingestion of settled dusts by hand-to-mouth transmission could also occur in workers who ate without washing their hands or, hopefully less likely, in toddlers living in apartments that were not adequately cleaned.

A number of studies have characterized the materials and chemical composition of settled dust deposits and airborne dust, smoke, and other aerosols generated by the WTC collapse (Clark et al., 2005; Lowers and Meeker, 2005; Lowers et al., 2009; Meeker et al., 2005; Pleil et al., 2004; Plumlee et al., 2005; Swayze et al., 2005; and other papers in Chatfield and

Kominsky, 2001; Clark et al., 2001; Lioy et al., 2002; Marley and Gaffney, 2005; McGee et al., 2003; Millette et al., 2002; Offenberg et al., 2003, 2004; USGS, 2002b; Yiin et al., 2004). These studies varied greatly in the numbers of samples studied, when and where the samples were collected, the types of samples collected, the processing applied to the samples prior to analysis (e.g., size fractionation by sieving and/or aerodynamic separation), and the analytical methods applied.

The following discussion is taken largely from results of our USGS studies of 36 settled dust samples collected from around lower Manhattan a week after 9/11 (Clark et al., 2001, 2005, Meeker et al., 2005; Plumlee et al., 2005; Swayze et al., 2005). The results of other studies are also cited where they provide information not obtained by the USGS studies.

The USGS results found that, although the same general types of materials were present in all the samples studied, there were complex variations in materials makeup, particle size, and bulk chemical composition, both from sample to sample across lower Manhattan and within a given sample down to the micrometer scale (Clark et al., 2001; Meeker et al., 2005; Plumlee et al., 2005). These complex variations likely resulted from the combination of many different factors, such as the dynamics of the building collapses, the complex airflow patterns along the downtown street grid, the northwest-to-southeast prevailing wind direction on 11 September 2001, and the major rainstorm on 14 September 2001 that affected exposed outdoor dusts.

In general, the dusts produced by the collapse and the resulting settled dust deposits were mixtures of a wide variety of pulverized materials used in building construction and found within office buildings (**Figure 13**). These included glass fibers (mineral wool or slag wool used in ceiling tiles and insulation), gypsum (from wallboard), concrete components (portlandite, larnite, and other diagnostic phases), window glass shards, paper, rock-forming minerals such as quartz and feldspars (from aggregate in concrete, dimension stone, and other sources), iron-rich particles (from steel beams, welding, and other sources), zinc-rich particles (presumably from metal ductwork), lead-rich particles (solder and lead oxide from paints), bismuth-rich particles (from ceiling fire sprinkler heads), and others. The studies that examined fewer numbers of size-fractionated samples (e.g., McGee et al., 2003) tended not to identify as many different phases as those that examined greater numbers of bulk samples (Clark et al., 2001; Lowers and Meeker, 2005; Meeker et al., 2005).

Chrysotile asbestos was found in most settled dust samples at levels generally around 1–3 volume % and was also found in material coating a steel beam in the debris at Ground Zero at levels as high as 20 volume %. Low levels of amphibole asbestos fibers were identified only in one settled dust sample collected north of the WTC complex (Chatfield and Kominsky, 2001). Lioy et al. (2002) studied three outdoor settled dust samples that they size-fractionated after collection and found little to no asbestos in the <2.5 μm fraction. Wu et al. (2010) found fibers that they interpreted to be carbon nanotubes in both samples of the dusts and biopsied tissue samples and to be from combustion of organic compounds.

Lioy et al. (2002) found that the dominant particle size of their outdoor settled dust samples was in the 2.5 μm to tens of micrometer range, with $>50\%$ greater than 53 μm, and so concluded that only a small proportion of the particles would therefore reach the alveolar portion of the lungs. In contrast, Yiin et al. (2004) analyzed 16 samples collected inside two buildings near Ground Zero and found that more than 50% were <53 μm, indicating that the indoor dusts had greater proportions of inhalable and perhaps respirable particles. Particle clumping of fine particles onto the surfaces of coarser particles was observed in SEM images of many of the dust samples (Meeker et al., 2005), and so such clumping may have further diminished the proportion of particles reaching the alveoli. However, it is possible that inhaled particles coarser than 2.5 μm may have also penetrated deeper into the respiratory tract as a result of oral breathing, especially given the extremely dusty conditions at the time of the collapse and in the hours immediately following the collapse.

The hyperspectral remote sensing data collected over lower Manhattan following 9/11 (Clark et al., 2001, 2005) revealed clear zoning in the settled dust deposits around Ground Zero.

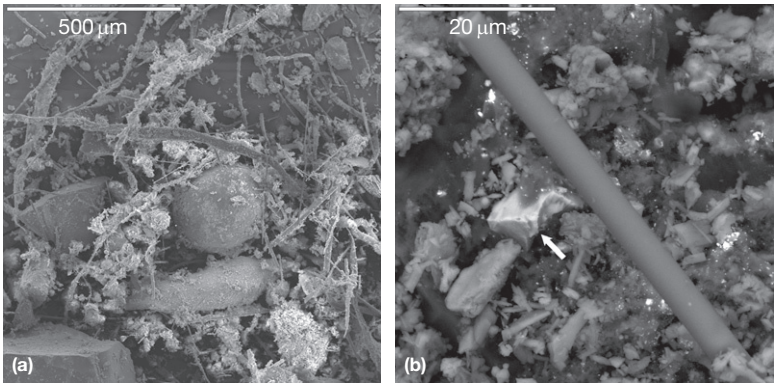

Figure 13 SEM photomicrographs of two indoor settled dust samples from the WTC illustrate the complex nature of the dusts. (a) This image is dominated by slag wool fibers and a slag wool sphere, with particles of concrete, window glass shards, gypsum from wallboards, and other materials. Note the small particles clumped onto the larger slag wool fibers. The scale bar is 500 μm. (b) Backscatter electron image of a WTC dust sample showing a slag wool fiber, zinc particle (lighter gray, noted by arrow), small lathlike crystals of gypsum, dark gray organic fibers, many small lead-rich particles (bright white), and other materials. The scale bar is 20 μm. SEM images acquired by G. Meeker.

This zoning was interpreted to be due to the differential settling of particles of different size and composition. The zoning pattern was elongated toward the southeast along the prevailing wind direction on 9/11.

The concentrations of major elements (oxygen, silicon, calcium, sulfur, magnesium, aluminum, iron, and carbon) in indoor dusts and outdoor dusts that had not been rained upon integrate the contributions of glass fibers, concrete, gypsum wallboard, metals, paper, and other materials within the office buildings (**Figure 14**) (Clark et al., 2001; Plumlee et al., 2005). Trace-element compositions (**Figure 14**) enriched in a variety of metals (zinc, barium, lead, copper, chromium, molybdenum, antimony, titanium, and bismuth) recorded contributions from paints, lighting, electrical wires, pipes, computer equipment, electronics, sprinkler heads, and other diverse materials. Many of these metals were substantially enriched in the settled dust samples compared to the soils of the eastern United States (Plumlee et al., 2005), and lead, antimony, and arsenic exceeded EPA residential soil standards in a substantial proportion of the samples. The size-fractionated samples collected prior to the rainstorm showed substantial decreases in silica and increases in sulfate with decreasing particle size, which were attributed by McGee et al. (2003) to the decreasing content of synthetic vitreous fibers and the increasing content of sulfate contributed from readily pulverized wallboard gypsum. The USGS data on sieved samples found no consistent trends in trace-element composition with decreasing particle size (Plumlee et al., 2005).

The rainstorm on 14 September strongly affected the mineralogy and chemical composition of a number of the outdoor samples. Compared to indoor samples, these outdoor samples that had been rained upon prior to collection showed increases in relatively insoluble components, such as silica, iron, lead, barium, titanium, and phosphorus, and decreases in water-soluble components, such as sulfate, calcium, and magnesium (**Figure 14**) (Plumlee et al., 2005).

Several studies performed water leach tests on bulk settled dust samples and size-fractionated samples, all using different solid/water ratios and times of agitation. Our tests on bulk and sieved settled dust samples, using 1:20 solid/water and 5 min reaction time, showed that the dusts were quite chemically reactive, generating leach solutions with very high pH (**Figure 9**) and alkalinities due to the rapid partial dissolution of calcium hydroxide from concrete particles. Indoor dust samples and two outdoor dust samples produced substantially higher pH levels (11.8–12.4) and caustic alkalinities ($\sim$600 mg l^{-1} $CaCO_3$) than most outdoor dust samples (pH 8.2–10.4; alkalinity $\sim$30 mg l^{-1} $CaCO_3$), another indication that most of the USGS suite of outdoor dust samples had reacted with rainfall or other water prior to collection. Some metals or metalloids in

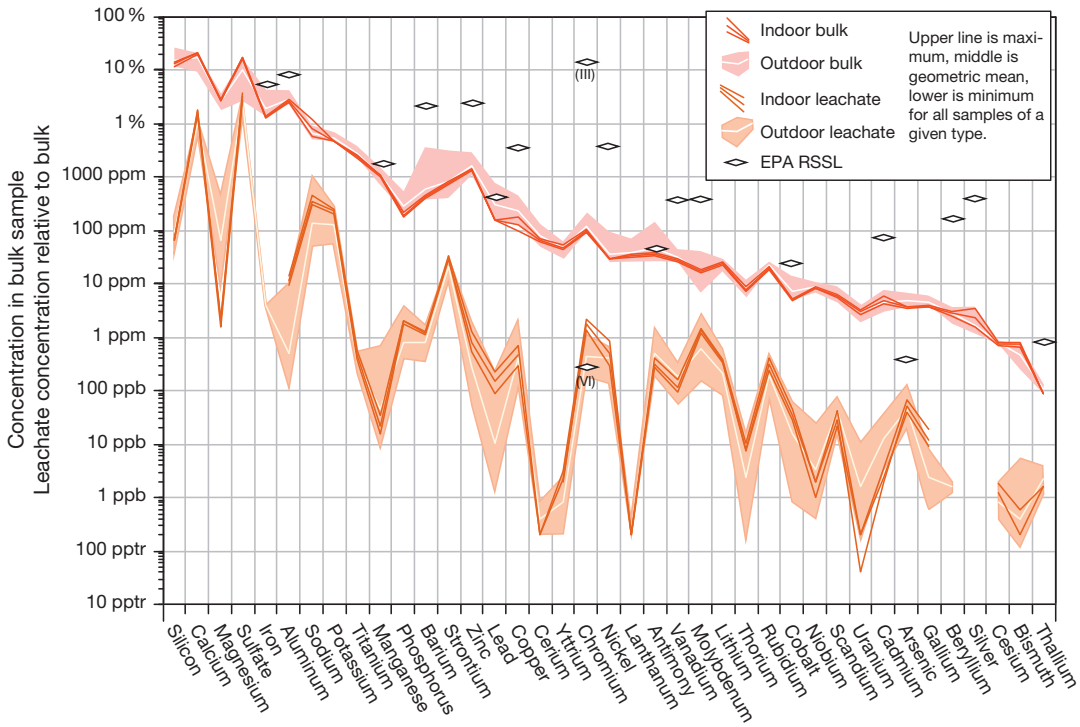

Figure 14 Plot showing ranges and geometric means of bulk and water-leachable element concentrations in a number of outdoor and two indoor settled dust samples from the WTC collapses. The leachate concentrations have been recalculated to mass leached per mass of solid. The diamonds show USEPA (EPA, 2011b) RSSLs that are available for some elements. Note that for water-soluble elements, high leachate concentrations in the indoor dusts generally correspond with low bulk concentrations in the outdoor dusts, illustrating the flushing of soluble dust components as a result of the rainfall event that occurred on 14 September 2001 before the samples were collected. Figure modified from Plumlee GS, Hageman PL, Lamothe PJ, et al. (2005) Inorganic chemical composition and chemical reactivity of settled dust generated by the World Trade Center building collapse. In: Gaffney JS and Marley NA (eds.) *Urban Aerosols and Their Impacts: Lessons Learned from the World Trade Center Tragedy. ACS Symposium Series*, vol. 919, pp 238–276. New York: Oxford University Press.

the dusts (chromium, antimony, molybdenum, barium, copper, zinc, cobalt, and nickel) are readily leached by deionized water (Figure 14). Many of these form oxyanion species or carbonate complexes that are most mobile at the alkaline pHs generated by the leachates.

There has been considerable attention to the caustic nature of the dusts, primarily for contributions to gastroesophageal reflux disease and irritation or damage to the eyes and respiratory tract. In contrast to the very high pH values measured by the USGS on indoor bulk samples, McGee et al. (2003) found lower pH values (8.9–10) in their leachates of the <2.5 μm size fraction of samples collected prior to the rainstorm. These values have since been cited (e.g., Lorber et al., 2007) to indicate that the respirable fraction of the dusts did not contain caustic particles. However, McGee et al. (2003) used a much more dilute solid/water ratio of 1:500 than the USGS ratio of 1:20, a factor that may have helped dilute caustic alkalinity measured in the smaller dust particles. We have since run 5 min water leach tests on several indoor and outdoor bulk samples at a solid/water ratio of 1:500, which generally produced pH values as much as one pH unit lower than leach tests performed on the same samples at 1:20 solid/water ratio. They also ran 1:20 solid/water leach tests on two sieve-sized outdoor dust samples, one of which yielded a pH of 11.3 in the <20 μm fraction compared to 12 in the bulk sample (Plumlee et al., 2005). Both these results suggest that the inhalable to respirable size fractions of the dusts did contain some caustic calcium hydroxide, although possibly not at the same levels as those found in coarser size fractions.

In vitro bioaccessibility assessments on settled dust samples using SLF as the extracting fluids (Plumlee et al., 2005) provided further insights into the potential chemical behavior of the dusts *in vivo*. The SLF produced leachates with smaller increases (~2 pH units) than those produced by the deionized-water leachates (>5 pH units). This resulted from the substantial pH-buffering capacity of the SLF components, but these smaller pH shifts were nonetheless an impressive indication of the caustic alkalinity present in the dusts. The concentration of phosphate in the SLF leachate dropped substantially from that in the SLF blank, likely due to reactions with calcium released from the concrete and gypsum particles and the resulting precipitation of insoluble calcium phosphate minerals. Metalloids such as antimony and chromium were relatively bioaccessible in the SLF (Figure 15). Metals such as copper and zinc were more soluble in SLF than in water due to chelation by chloride, citrate, and glycine. Lead was not substantially dissolved from the dusts by either water or SLF, possibly because the lead occurred in relatively insoluble phases in the dusts and/or formed insoluble phosphate precipitates. Chemical speciation calculations of the leachate fluids produced by the SLF indicate that the extraction fluids were highly supersaturated with a wide variety of silicates, including chrysotile and amphiboles. This indicated that the biodurability of these fibrous minerals *in vivo* could have been substantially enhanced by other dust components. We also ran gastric IVBAs on dust samples and found that a substantial portion of lead and some other metal or metalloid toxicants (e.g., antimony, manganese, aluminum, nickel, copper, zinc, and others) were likely gastric-bioaccessible in the dusts (Figure 15).

Lioy et al. (2002) found a wide variety of organic chemicals in bulk settled dust samples (not separated by size), including PAHs, polychlorobiphenyls (PCBs), dioxins, furans, and many others. Several of the PAHs were present in levels above EPA RSSLs. PCBs and dioxins were present but in low levels. Pleil et al. (2004) analyzed archived air filters collected around lower Manhattan following 9/11 and also found elevated levels

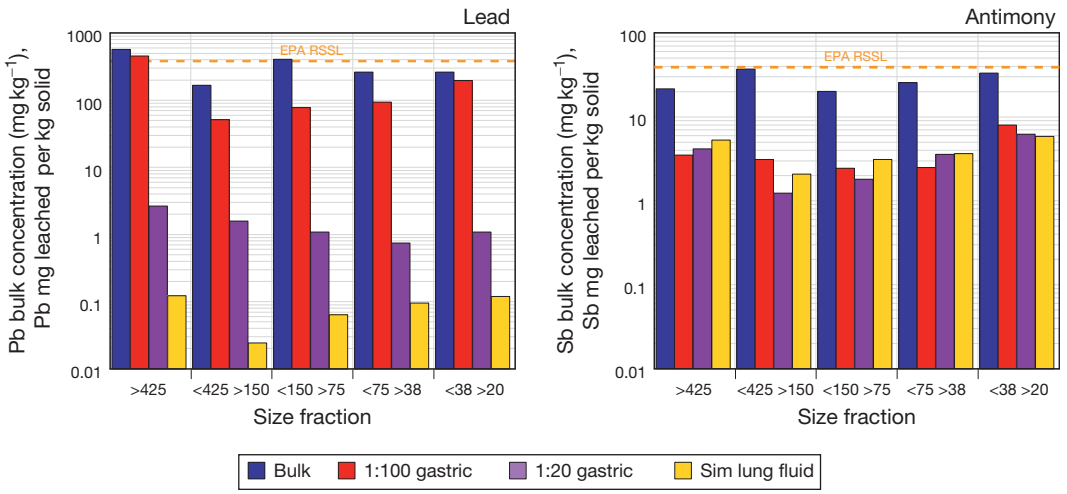

Figure 15 Plots showing total and fluid-leachable (by simulated gastric and lung fluids) concentrations of lead and antimony in various sieved size fractions (in μm) of WTC outdoor settled dust sample WTC18 (Plumlee et al., 2005 and our unpublished data). As shown in **Figure 8**, this sample generated caustic water leachate pH values and so had been relatively sheltered from the rainfall event on 14 September that affected many other outdoor WTC dust samples. The >425 μm fraction was ground prior to leaching to reduce the nugget effect of large pebble-sized chunks, whereas the smaller size range samples were not ground. Note that the bulk concentrations of lead and antimony do not vary consistently as a function of size fraction but that the 1:100 solid/liquid gastric extraction and SLF concentrations do increase with decreasing particle size range. The drop in leachable lead between the 1:100 and 1:20 gastric extractions resulted from the substantially higher pH reached by the 1:20 extraction and the coprecipitation of lead with phases that precipitated as a result of this pH increase. Note that antimony extraction is nearly as effective or more effective in the lung fluids than in the gastric fluids due to the enhanced mobility of antimony at the higher pH values of the SLF.

of PAHs. The high PAHs in the settled dusts were interpreted to be combustion by-products from the fires that burned in the WTC towers prior to the collapse. The PAHs found in the air filters were interpreted to be combustion products from the fires that burned in the debris at Ground Zero for several months following 9/11, diesel exhaust generated during cleanup, and PAHs from normal urban vehicular traffic. Exposures to these PAHs have been interpreted as a potential cause of reduced fetal growth in pregnant women exposed to the WTC dust event (Perera et al., 2005).

There are differences in the types of minerals or inorganic phases reported from studies of induced sputum and bronchoalveolar lavage fluids collected relatively soon after 9/11 (Fireman et al., 2004; Rom et al., 2002) versus those found later in pathology samples of lung tissues from WTC first responders or workers who developed lung disease (Caplan-Shaw et al., 2011; Meeker et al., 2010; Wu et al., 2010). In the former, there seem to be more components identifiable as from the WTC dusts (e.g., glass fibers and glass shards), whereas in the latter (with the exception of carbon nanotubes and chrysotile asbestos), the solid phases are not diagnostic of those found in the dusts. It is unclear if these differences reflect differences in the nature of the samples or long-term changes that result from processes in the lungs such as WTC dust particle clearance/dissolution or replacement of WTC dust particles by particles more stable in the lung environment.

In summary, the dusts generated by the WTC collapse were a complex and heterogeneous mixture of bioreactive, bioaccessible, and biodurable particles. The dust plume evolved as it traveled away from Ground Zero, with coarser particles deposited closer to Ground Zero. The settled dusts were dominated by slag wool (a man-made glass fiber used in ceiling tiles and insulation), gypsum (from wallboard), concrete particles, window glass shards, paper, and rock fragments (from aggregate used in concrete). One toxicologically significant characteristic of the dusts was the abundance of calcium hydroxide particles from the pulverized concrete, which generated caustic alkalinity when the dusts came into contact with water in the environment or water-based body fluids. Many other potential environmental or human toxicants were present, including crystalline silica (from concrete aggregate and dimension stone), lead (solder and lead oxide from paints), antimony (used as a fire retardant), zinc (ductwork, solders, and other uses), hexavalent chromium (insulation, combusted fabrics, and chrome plating), bismuth (ceiling fire sprinklers), chrysotile asbestos (1–3 volume %, from insulation), and PAHs (combustion products from fires and other sources). Several studies concluded that the settled dusts did not have a substantial fraction of respirable particles, although the extent to which the settled dusts on roads and sidewalks may have been further pulverized and resuspended by vehicle or foot traffic was not assessed by any study. The settled dusts underwent substantial changes once in the environment, primarily in response to a rainstorm that occurred on 14 September. The rainstorm helped neutralize caustic alkalinity in dust deposits that were not sheltered but also may have helped concentrate relatively water-insoluble but gastric-soluble toxicants such as lead. Over the long term, reactions with atmospheric moisture and carbon dioxide may have helped consume caustic alkalinity from sheltered or indoor dusts, particularly in the extremely small particle sizes. Chemical reactions between the body's fluids and the dust constituents may have triggered particle dissolution, precipitation of secondary phases in the respiratory tract such as calcium and lead phosphates, solubilization of some bioaccessible toxicants such as antimony and hexavalent chromium, and other changes in mineralogy. Incidental ingestion of dusts by hand-to-mouth contact or of dust particles cleared from the respiratory tract may be a previously unnoted exposure pathway for gastric-bioaccessible toxicants such as lead.

11.7.13 Disaster Preparedness

As can be seen from this chapter's coverage of the lengthy list of disasters that have had their environmental and health impacts studied in some detail, there is a growing database of knowledge from past environmental disaster responses that can be used to help anticipate impacts of similar future disasters. Environmental and medical geochemistry contributions can be made from the perspective of both long-term disaster preparedness and in the short term as particular disasters are looming and happening.

A key example is the development of disaster scenarios. These scenarios have, in the last decade, become a highly successful tool developed by the natural hazards community to engage emergency planners, businesses, universities, government agencies, and others in preparing for major natural disasters. The scenarios develop scientifically based models for particular disaster events and then gather expert input from a wide range of disciplines to help anticipate plausible physical, economic, societal, and other impacts of the disasters. Two excellent examples include the 2008 Great Southern California ShakeOut scenario, which modeled the impacts of a 7.8 magnitude earthquake on the southern San Andreas Fault (Porter et al., 2011a), and the 2009–11 ARkStorm (short for Atmospheric River, 1000-year storm) scenario, which modeled the impacts of a major, weeks-long winter storm hitting nearly all of California (Porter et al., 2011b). We have found that these disaster scenarios provide an excellent opportunity for environmental and medical geochemistry to contribute key insights into the potential environmental and health effects of the modeled disasters.

In the ARkStorm scenario, experts designed a scientifically plausible meteorological event to approximate the series of extreme storms that pummeled California for more than 40 days during the winter of 1861–62. Based upon the results of the meteorological model, a wide variety of other experts examined plausible physical, economic, and other impacts of such a series of storms on modern-day California. The ARkStorm would likely produce extreme precipitation across many parts of California, at levels that would likely exceed those experienced approximately once every 500 to 1000 years (**Figure 16**). Extensive flooding would likely overwhelm the state's flood-protection system (typically designed to withstand 100- to 200-year runoff events) and lead to the flooding of much of the Central Valley and portions of Orange County, Los Angeles County, San Diego, San Francisco Bay area, and other coastal communities. Storm-related flooding, high winds, runoff, erosion, and many landslides triggered by the

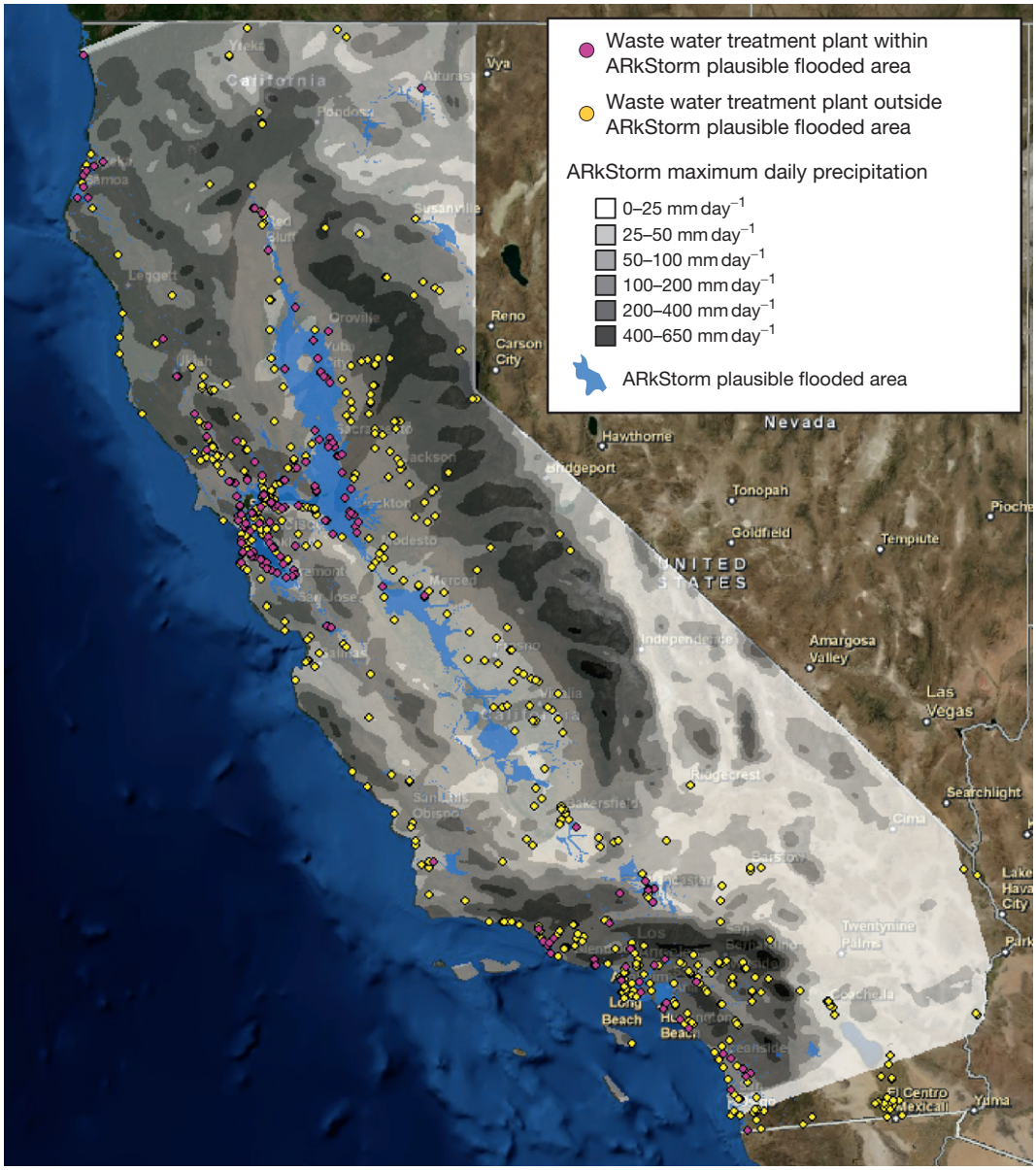

Figure 16 This figure (see Plumlee et al., 2011) shows the distribution of wastewater treatment plants (WWTPs) in California, superimposed on the plausible maximum daily precipitation amounts (gray scale) and flooded areas (light blue) predicted for the ARkStorm extreme winter storm scenario (Porter et al., 2011b). The ARkStorm scenario modeled the impacts of an extreme winter storm hitting modern-day California for 40+ days based on a similar storm that occurred from December 1861 to January 1862. The locations of the WWTPs were taken from the EPA Facilities Registry System database, a national database of sites or facilities that are the focus of some sort of environmental monitoring or regulatory oversight (http://www.epa.gov/enviro/html/frs_demo/geospatial_data/geo_data_state_single.html). Geographic information system (GIS) analyses such as these can be used to provide an indication of where contaminants specific to various types of facilities could be released into the environment. The plausible contaminants released from flooded or overloaded WWTPs include raw sewage; pathogenic bacteria, protozoans, and viruses; and a wide variety of pharmaceuticals, personal care products, and household and industrial chemicals.

storm would lead to extensive damage to homes, buildings, highways, and other infrastructure. Repair to water, power, and sewer lifelines would likely take months. Including business interruptions, the total costs of the storm likely would exceed $725 billion (Porter et al., 2011b).

Building upon the excellent framework developed to model ARkStorm precipitation, flooding, landslides, and other plausible physical impacts, Plumlee et al. (2011) developed a qualitative approach by which plausible environmental and related health impacts of the ARkStorm storm could be anticipated. The environmental health impacts of various past extreme storms were first used to identify plausible impacts that could be associated with the disaster scenario. Substantial insights were then gleaned using a Geographic Information Systems (GIS) approach to link ARkStorm effects maps with the data extracted from diverse database sources containing geologic, hazards, and environmental information (**Figure 16**). This type of analysis helped constrain where potential sources of

HM (and their likely types of contaminants or pathogens) would fall within areas of predicted ARkStorm-related precipitation, flooding, and winds. Our analysis indicated that many potential sources of mineral, chemical, and pathogen contaminants could be disturbed or damaged as a result of extreme precipitation, runoff, erosion, landslides, and flooding. These include natural sources such as rock units that host asbestos, heavy metals, or soil pathogens and many different types of anthropogenic sources such as urban areas, WWTPs, animal feeding operations, petroleum refineries, abandoned mine sites, industrial facilities, and others. Storm-related damages to the natural and built environments would therefore have the potential to cause considerable but complex and spatially/temporally variable environmental damage and contamination. These, in turn, would have the potential to cause substantial adverse impacts on aquatic and terrestrial ecosystems and some adverse impacts on human health. Although only a first step, this qualitative approach will help enhance planning for, mitigation of, and resilience to environmental health consequences of future disasters. This qualitative approach also requires careful communication to stakeholders that does not sensationalize or overstate potential problems but rather conveys the plausible impacts and outlines the next steps to improve understanding of potential risks and their mitigation.

11.7.14 Summary

In this chapter, we have presented data and interpretations from a large number of studies that have examined the environmental and health characteristics of HM produced by a variety of disasters. There are a number of useful insights that can be gleaned from these studies. For example, water leach tests of DM such as WTC dusts and CFA done by different groups using different solid/water ratios illustrate the difficulty in directly comparing results of studies carried out by different groups using different analytical methodologies.

There are many examples of recent disasters where the DM have mostly been cleaned up quite quickly, within weeks to months. However, there are also examples where cleanup takes years or is not carried out at all. Even in cases where the DM are largely cleaned up quickly, this chapter illustrates that there is nonetheless a strong need to evaluate the potential for long-term changes in DM that can significantly alter their environmental or health implications. Such long-term changes could occur, for example, in isolated places where the DM have escaped removal, if the DM are disposed of in areas open to the environment, or in areas where cleanup has not occurred. The primary examples are diverse DM containing iron sulfides that can become acid-generating when exposed in the environment.

Perhaps most importantly, the studies show that DM can be highly complex mixtures of materials with a range in their environmental behavior and characteristics that influence bioreactivity, biosolubility/biodurability, and potential toxicity. Depending upon the disaster, these materials can be produced from a single source or multiple sources. In response to environmental processes, the materials can change in their physical, mineralogical, and chemical makeup (and, hence, in their exposure pathways and toxicity to exposed humans and organisms) both spatially away from their source(s) and over time following a disaster. Hence, rapid deployment for initial sampling of DM at multiple locations around a disaster site, acquisition and analysis of remote sensing data that can be used to help extend analyses of individual samples to broader areas, and repeated sampling at the same localities over periods of time following disasters are all needed.

The complexity and spatial/temporal variability of the materials demonstrate that many different analytical methods, applied by earth scientists working in cooperation with health scientists, are needed to fully characterize the environmental and medical geochemical characteristics of DM and their potential exposure pathways to the affected ecosystems and humans. Traditional HM approaches of analyzing total concentrations of particular toxicants and whether or not these exceed known action levels, although absolutely necessary, are not sufficient to fully understand the range of potential environmental and related health threats.

Further, the potential health effects of these complex materials likely cannot be adequately assessed based solely on the toxicity of their individual components. The integrated effects of the whole material must be considered, along with the potentially complex chemical interactions between the individual components of the DM and the body's fluids.

Finally, the knowledge gleaned from studies of materials produced by past disasters can be used to help anticipate the potential environmental and health threats posed by DM produced by similar future disasters, thereby enhancing disaster preparedness and resilience. Disaster scenario development provides an excellent opportunity for the integration of environmental and medical geochemistry information on DM and anticipating plausible environmental and related health impacts of future disasters.

Acknowledgments

A number of scientists at the US Geological Survey (USGS) provided samples or analytical results used in a number of the figures or text discussions, including Monique Adams, Michael Anthony, Bob Finkelman, Bill Foreman, Harland Goldstein, Todd Hinkley, Lopaka Lee, and Tom Pierson. The authors are very grateful for insights provided by many additional collaborators within and outside the USGS, including specialists in public health, geologic hazards, and disaster response and preparedness. Reviews of all or parts of the manuscript by Jim Crock, Bill Orem, and Barbara Sherwood Lollar are greatly appreciated and led to significant improvements in content and readability.

Any use of trade, firm, or product names is for descriptive purposes only and does not imply endorsement by the US Government.

References

Abel MT, Cobb GP, Presley SM, et al. (2010) Lead distributions and risks in New Orleans following Hurricanes Katrina and Rita. *Environmental Toxicology and Chemistry* 29: 1429–1437.

Abidin HZ, Davies RJ, Kusuma MA, Andreas H, and Deguchi T (2008) Subsidence and uplift of Sidoarjo (East Java) due to the eruption of the Lusi mud volcano (2006–present). *Environmental Geology* 57: 833–844.

Aguilera F, Méndez J, Pásaro E, and Laffon B (2010) Review on the effects of exposure to spilled oils on human health. *Journal of Applied Toxicology* 30: 291–301.

Ahern M, Kovats RS, Wilkinson P, Few R, and Matthies F (2005) Global health impacts of floods: Epidemiologic evidence. *Epidemiologic Reviews* 27: 36–46.

Alastuey A, García-Sánchez A, López F, and Querol X (1999) Evolution of pyrite mud weathering and mobility of heavy metals in the Guadiamar valley after the Aznalcóllar spill, south-west Spain. *Science of the Total Environment* 242: 41–55.

Aldrich TK, Gustave J, Hall CB, et al. (2010) Lung function in rescue workers at the World Trade Center after 7 years. *The New England Journal of Medicine* 362: 1263–1272.

Alzaga R, Mesas A, Ortiz L, and Bayona JM (1999) Characterization of organic compounds in soil and water affected by pyrite tailing spillage. *Science of the Total Environment* 242: 167–178.

Ansoborlo E, Hengé-Napoli MH, Chazel V, GIbert R, and Guilmette RA (1999) Review and critical analysis of available in vitro dissolution tests. *Health Physics* 77: 638–645.

ASCE (2009) The New Orleans hurricane protection system: What went wrong and why. *Report by the American Society of Civil Engineers*, *Hurricane Katrina External Review Panel*. Reston, VA: American Society of Civil Engineers.

Ashley NA, Valsaraj KT, and Thibodeaux LJ (2008) Elevated in-home sediment contaminant concentrations – The consequence of a particle settling–winnowing process from Hurricane Katrina floodwaters. *Chemosphere* 70: 833–840.

ATSDR (2004) *Guidance Manual for the Assessment of Joint Toxic Action of Chemical Mixtures*. Atlanta, GA: US Department of Health and Human Services, Public Health Service.

Aust AE, Ball JC, Hu AA, et al. (2002) Particle characteristics responsible for effects on human lung epithelial cells. *Health Effects Institute Research Report Number* 110. Boston: HEI Publications.

Aust AE, Cook PM, and Dodson RF (2011) Morphological and chemical mechanisms of elongated mineral particle toxicities. *Journal of Toxicology and Environmental Health. Part B, Critical Reviews* 14: 40–75.

Aust AE and Lund LG (1990) The role of iron in asbestos-catalyzed damage to lipids and DNA. In: Reddy CC, Hamilton GA, and Madyasttha KM (eds.) *Biological Oxidation Systems*, vol. 2, pp. 597–605. San Diego, CA: Academic Press.

Ayris PM and Delmelle P (2012) The immediate environmental effects of tephra emission. *Bulletin of Volcanology* 74: 1905–1936.

Barbeau DN, Grimsley LF, White LE, El-Dahr JM, and Lichtveld M (2010) Mold exposure and health effects following hurricanes Katrina and Rita. *Annual Review of Public Health* 31: 165–178.

Basta NT, Foster JN, Dayton EA, Rodriguez RR, and Casteel SW (2007) The effect of dosing vehicle on arsenic bioaccessibility in smelter-contaminated soils. *Journal of Environmental Science and Health, Part A* 42: 1275–1281.

Baxter P, Kapila M, and Mfonfu D (1989) Lake Nyos disaster, Cameroon, 1986: The medical effects of large scale emission of carbon dioxide? *British Medical Journal* 298: 1437–1441.

Besser JM, Brumbaugh WG, Allert AL, Poulton BC, Schmitt CJ, and Ingersoll CG (2009) Ecological impacts of lead mining on Ozark streams: Toxicity of sediment and pore water. *Ecotoxicology and Environmental Safety* 72: 516–526.

Bird G, Brewer PA, Macklin MG, et al. (2008) River system recovery following the Novaţ-Roşu tailings dam failure, Maramureş County, Romania. *Applied Geochemistry* 23: 3498–3518.

Burke IT, Mayes WM, Peacock CL, Brown AP, Jarvis AP, and Gruiz K (2012) Speciation of arsenic, chromium, and vanadium in red mud samples from the Ajka spill site, Hungary. *Environmental Science & Technology* 46: 3085–3092.

Bytnerowicz A, Arbaugh MJ, Riebau AR, and Andersen C (2009) *Wildland Fires and Air Pollution*. *Developments in Environmental Science*, vol. 8. Amsterdam: Elsevier B.V.

Caboche J, Perdrix E, Malet B, and Alleman LY (2011) Development of an *in vitro* method to estimate lung bioaccessibility of metals from atmospheric particles. *Journal of Environmental Monitoring* 13: 621–630.

CADHHS (2012) Safe cleanup of fire ash. California Deaprtment of Health and Human Services, 8 p., http://www.calepa.ca.gov/Disaster/Documents/FireAsh.pdf.

Calfee RD and Little EE (2003) Effects of a fire-retardent chemical to fathead minnows in experimental streams. *Environmental Science and Pollution Research* 10: 296–300.

Canti MG (2003) Aspects of the chemical and microscopic characteristics of plant ashes found in archaeological soils. *CATENA* 54: 339–361.

Caplan-Shaw CE, Yee H, Rogers L, et al. (2011) Lung pathologic findings in a local residential and working community exposed to World Trade Center dust, gas, and fumes. *Journal of Occupational and Environmental Medicine* 53: 981–991.

Carbone M, Baris I, Bertino P, et al. (2011) Erionite exposure in North Dakota and Turkish villages with mesothelioma. *Proceedings of the National Academy of Sciences of the United States of America* 108(33): 13618–13623.

Carr RS, Nipper M, and Plumlee GS (2003) Survey of marine contamination from mining-related activities on Marinduque Island, Philippines: Porewater toxicity and chemistry. *Aquatic Ecosystem Health & Management* 6: 369–379.

Case BW, Abraham JL, Meeker G, Pooley FD, and Pinkerton KE (2011) Applying definitions of "asbestos" to environmental and "low-dose" exposure levels and health effects, particularly malignant mesothelioma. *Journal of Toxicology and Environmental Health. Part B, Critical Reviews* 14: 3–39.

Casteel SW, Weis CP, Henningsen GM, and Brattin WJ (2006) Estimation of relative bioavailability of lead in soil and soil-like materials using young swine. *Environmental Health Perspectives*. 114: 1162–1171.

Caulkins J, Delmelle P, Wickham M, and Faulks R (2010) Tracking multiple pathways of human exposure to volcanic fluoride. Cities on Volcanoes 6, Tenerife, Abstracts Volume, 175–176. http://www.citiesonvolcanoes6.com/.

Chatfield EJ and Kominsky JR (2001) Summary report: Characterization of particulate found in apartments after destruction of the World Trade Center.

Choate LM (2012) Procedure for determination of metal toxicity using MetPLATE™. In: Driscoll R, Hageman PL, Benzel WM et al. (eds.) *Assessment of the Geoavailability of Trace Elements from Minerals in Mine Wastes: Analytical Techniques and Assessment of Selected Copper Minerals*. *US Geological Survey Scientific Investigations Report 2011-5211*, pp. 44–50. Reston, VA: US Geological Survey.

Clark RN, Green RO, Swayze GA, et al. (2001) Environmental studies of the World Trade Center area after the September 11, 2001 attack. *US Geological Survey Open-File Report 01-0429*. http://pubs.usgs.gov/of/2001/ofr-01-0429.

Clark RN, Swayze GA, Hoefen TM, et al. (2005) Environmental mapping of the World Trade Center area with imaging spectroscopy after the September 11, 2001 attack. In: Gaffney JS and Marley NA (eds.) *Urban Aerosols and Their Impacts: Lessons Learned from the World Trade Center Tragedy*. *ACS Series*, vol. 919, pp. 66–83. New York: Oxford University Press.

Clark RN, Swayze GA, Leifer I, et al. (2010) A method for quantitative mapping of thick oil spills using imaging spectroscopy. *US Geological Survey Open-File Report 2010-1167*. Reston, VA: US Geological Survey.

Cook A, Watson J, van Buynder P, Robertson A, and Weinstein P (2008) 10th anniversary review: Natural disasters and their long-term impacts on the health of communities. *Journal of Environmental Monitoring* 10: 167–175.

Cooney C (2010) Burning Question—Gulf spill: EPA reports that surface slick burns produced very low levels of cancer-causing dioxins. *Chemical & Engineering News* 88: 7.

Cordos E, Rautlu R, Roman C, et al. (2003) Characterization of the rivers system in the mining and industrial area of Baia Mare, Romania. *European Journal of Mineral Processing and Environmental Protection* 3: 324–335.

Cozzani V, Campedel M, Renni E, and Krausman E (2010) Industrial accidents triggered by flood events: Analysis of past accidents. *Journal of Hazardous Materials* 175: 501–509.

Cronin SJ, Neall VE, Lecointre JA, Hedley MJ, and Loganathan P (2003) Environmental hazards of fluoride in volcanic ash: A case study from Ruapehu volcano, New Zealand. *Journal of Volcanology and Geothermal Research* 121: 271–291.

Crouch RL, Timmenga HJ, Barber TR, and Fuchsman PC (2006) Post-fire surface water quality: Comparison of fire retardant versus wildfire-related effects. *Chemosphere* 62: 874–889.

Crowley LE, Herbert R, Moline JM, et al. (2011) "Sarcoid like" granulomatous pulmonary disease in World Trade Center disaster responders. *American Journal of Industrial Medicine* 54: 175–184.

Cunningham SA (2005) Incident, accident, catastrophe: Cyanide on the Danube. *Disaster* 29: 99–128.

Czövek D, Novák Z, Somlai C, et al. (2012) Respiratory consequences of red sludge dust inhalation in rats. *Toxicology Letters* 209: 113–120.

David CP (2003) Establishing the impact of acid mine drainage through metal bioaccumulation and taxa richness of benthic insects in a tropical Asian stream (The Philippines). *Environmental Toxicology and Chemistry* 22: 2952–2959.

David CP and Plumlee GS (2006) Comparison of dissolved copper concentration trends in two rivers receiving ARD from an inactive copper mine (Marinduque Island, Philippines). In: Barnhisel RI (ed.) *Proceedings, 7th International Conference on Acid Rock Drainage (ICARD)*, March 26–30, 2006, St. Louis, MO, pp. 426–438. Lexington, KY: American Society of Mining and Reclamation (ASMR).

Davies E, Heriwati R, Richardson A (2008) Indonesians in Java village scared by seeping gas. Reuters, March 5, 2008, http://www.reuters.com/article/scienceNews/idUSJAK29258220080305.

Davies MP, Martin T, and Lighthall P (2000) Mine tailings dams: When things go wrong. *Proceedings of Tailings Dams 2000, Association of State Dam Safety Officials, US Committee on Large Dams,* Las Vegas, Nevada, pp. 261–273. http://www.infomine.com/publications/docs/Davies2002d.pdf.

Davies R, Manga M, Tingay M, Lusianga S, and Swarbrick R (2010) Discussion – Sawolo et al. (2009) the Lusi mud volcano controversy: Was it caused by drilling? *Marine and Petroleum Geology* 27: 1651–1657.

Davies RJ, Mathias SA, Swarbrick RE, and Tingay MJ (2011) Probabilistic longevity estimate for the Lusi mud volcano, East Java. *Journal of the Geological Society* 168: 517–523.

De Capitani EM (1989) Prevalence of pneumoconiosis in workers exposed to phosphate rocks. *Revista de Saúde Pública* 23: 98–106.

Delmelle P (2003) Environmental impacts of tropospheric volcanic gas plumes. In: Oppenheimer C, Pyle DM, and Barclay J (eds.) *Volcanic Degassing, Geological Society Special Publication 213*, pp. 381–399. London: Geological Society of London.

Demcheck DK, Stoeckel DM, Bushon RN, Blehert DS, and Hippe DJ (2007) Bacteriological water quality in and around Lake Pontchartrain following hurricanes Katrina and Rita. In: Farris GS, Smith GJ, Crane MP, Demas CR, Robbins LL, and Lavoie DL (eds.) *Science and the Storms: The USGS Response to the Hurricanes of 2005*, *US Geological Survey Circular 1306*, pp. 239–244. Washington, DC: US Government Printing Office.

Dennekamp M and Abramson MJ (2011) The effects of bushfire smoke on respiratory health. *Respirology* 16: 198–209.

DeVries FW (2001) Brief overview of the Baia Mare dam breach. In: Young CA, Twidwell LG, and Anderson CG (eds.) *Cyanide: Social, Industrial, and Economic Aspects*, pp. 11–14. Warrendale, PA: TMS.

Dobbs FC (2007) Aprés le déluge: Microbial landscape of New Orleans after the hurricanes. *Proceedings of the National Academy of Sciences of the United States of America* 104: 9103–9104.

Dombeck MP, Williams JE, and Wood CA (2004) Wildfire policy and public lands: Integrating scientific understanding with social concerns across landscapes. *Conservation Biology* 18: 883–889.

Donato DB, Nichols O, Possingham H, Moore M, Ricci PF, and Noller BD (2007) A critical review of the effects of gold cyanide-bearing tailings solutions on wildlife. *Environment International* 33: 974–984.

Dooyema C, Neri A, Lo Y, et al. (2012) Outbreak of fatal childhood lead poisoning related to artisanal gold mining in northwestern Nigeria, 2010. *Environmental Health Perspectives* 120: 601–607.

Drexler JW and Brattin WJ (2007) An *in vitro* procedure for estimation of lead relative bioavailability, with validation. *Human and Ecological Risk Assessment* 13: 383–401.

Ducatman A, Ziemkiewicz P, Quaranta J, Vandivort T, Mack B, and VanAken B (2010) Coal slurry waste underground injection assessment. *Final Report: Phase II. West Virginia Department of Health and Human Resources*.

Edelman P, Osterloh J, Pirkle J, et al. (2003) Biomonitoring of chemical exposure among New York City firefighters responding to the World Trade Center fire and collapse. *Environmental Health Perspectives* 111: 1906–1911.

Eisler R and Wiemeyer SN (2004) Cyanide hazards to plants and animals from gold mining and related water issues. *Reviews of Environmental Contamination and Toxicology* 183: 21–54.

EPA (1992) Method 1311 Toxicity characteristic leaching procedure. *US Environmental Protection Agency 1311-1*. http://www.epa.gov/wastes/hazard/testmethods/sw846/pdfs/1311.pdf.

EPA (2006) XRF technologies for measuring trace elements in soil and sediment: Niton XLi 700 Series XRF Analyzer. *US Environmental Protection Agency Innovative Technology Verification Report*, EPA/540/R-06/003. Washington, DC: US Environmental Protection Agency.

EPA (2008a) Child-specific exposure factors handbook (final report). *US Environmental Protection Agency Report EPA/600/R-06/096F*. Washington, DC: US Environmental Protection Agency.

EPA (2008b) Standard operating procedure for an *in vitro* bioaccessibility assay for lead in soil. *US Environmental Protection Agency Report EPA 9200.1-86*. Washington, DC: US Environmental Protection Agency.

EPA (2008c) Test methods for evaluating solid waste, physical/chemical methods. *US Environmental Protection Agency Publication SW-846*. Washington, DC: US Environmental Protection Agency.

EPA (2011a) *Sumas Mountain Asbestos*. US Environmental Protection Agency web site, updated 5/2011, http://yosemite.epa.gov/r10/cleanup.nsf/sites/swiftcreek.

EPA (2011b) *US Environmental Protection Agency Regional Screening Levels for Chemical Contaminants*. http://www.epa.gov/region9/superfund/prg/.

Evans WC, Kling GW, Tuttle ML, Tanyileke G, and White LD (1989) Gas buildup in Lake Nyos, Cameroon: The recharge process and its consequences. *Applied Geochemistry* 8: 207–221.

Fey DL, Desborough GA, and Church SE (2000) Comparisons of two leach procedures applied to metal-mining related wastes in Colorado and Montana and a relative ranking method for mine wastes. *Proceedings of the Fifth International Conference on Acid Rock Drainage*, Denver, Colorado, 21–24 May, vol. II, pp. 1477–1487. Littleton, CO: Society for Mining, Metallurgy, and Exploration.

Ficklin WH and Mosier E (1999) Field methods for sampling and analysis of environmental samples for unstable and selected stable constituents. In: Plumlee GS and Logsdon MJ (eds.) *The Environmental Geochemistry of Mineral Deposits. Part A: Processes, Techniques and Health Issues, Reviews in Economic Geology* 6A, pp. 71–116. Littleton, CO: Society of Economic Geologists, Inc.

Fireman EM, Lerman Y, Ganor E, et al. (2004) Induced sputum assessment in New York City firefighters exposed to World Trade Center dust. *Environmental Health Perspectives* 112: 1564–1569.

Fisher FS, Bultman MW, Johnson SM, Pappagianis D, and Zaborsky E (2007) *Coccidioides* niches and habitat parameters in the southwestern United States – A matter of scale. *Annals of the New York Academy of Sciences* 1111: 47–72.

Floret N, Viel J-F, Mauny F, Hoen B, and Piarroux R (2006) Negligible risk for epidemics after geophysical disasters. *Emerging Infectious Diseases* 12: 543–548.

Francis P and Oppenheimer C (2003) *Volcanoes*, 2nd edn. Oxford: Oxford University Press.

Franco R, Sánchez-Olea R, Reyes-Reyes EM, and Panayiotidis ML (2009) Environmental toxicity, oxidative stress and apoptosis: Ménage à trois. *Mutation Research – Genetic Toxicology and Environmental Mutagenesis* 674: 3–22.

Franzi LM, Bratt JM, Williams KM, and Last JA (2011) Why is particulate matter produced by wildfires toxic to lung macrophages? *Toxicology and Applied Pharmacology* 257: 182–188.

Frey KJ, Michaelson DP, and Davis WL (2001) Impacts of the Martin County coal slurry spill on fishery resources in eastern Kentucky streams: A case study. *Proceedings of the Annual Conference of the Southeastern Association of Fish and Wildlife Agencies* 55: 95–104.

Fubini B and Areán CO (1999) Chemical aspects of the toxicity of inhaled mineral dusts. *Chemical Society Reviews* 28: 373–381.

Galea S (2007) The long-term health consequences of disasters and mass traumas. *Canadian Medical Association Journal* 176: 1293–1294.

García-Martínez R and López JL (2005) Debris flows of December 1999 in Venezuela. In: Jakob M and Hungr O (eds.) *Debris-Flow Hazards and Related Phenomena*, pp. 519–538. Berlin: Springer.

Gaughan DM, Cox-Ganser JM, Enright PL, et al. (2008) Acute upper and lower respiratory effects in wildland firefighters. *Journal of Occupational and Environmental Medicine* 50: 1019–1028.

Gavett SH, Haykal-Coates N, Highfill JW, et al. (2003) World Trade Center fine particulate matter causes respiratory tract hyperresponsiveness in mice. *Environmental Health Perspectives* 111: 981–991.

Gelencsér A, Kováts N, Turóczi B, et al. (2011) The red mud accident in Ajka (Hungary): Characterization and potential health effects of fugitive dust. *Environmental Science & Technology* 45: 1608–1615.

Gil F, Capitán-Vallvey LF, De Santiago E, et al. (2006) Heavy metal concentrations in the general population of Andalusia, South of Spain: A comparison with the population within the area of influence of Aznalcóllar mine spill (SW Spain). *Science of the Total Environment* 372: 49–57.

Gray JE, Plumlee GS, Morman SA, et al. (2010) In vitro studies evaluating leaching of mercury from mine waste calcine using simulated human body fluids. *Environmental Science & Technology* 44: 4782–4788.

Griffin DW, Petrosky T, Morman SA, and Luna V (2009) A survey of the occurrence of *Bacillus anthracis* in North American soils over two long-range transects and within post-Katrina New Orleans. *Applied Geochemistry* 24: 1464–1471.

Grimalt JO, Ferrer M, and Macpherson E (1999) The mine tailing accident at Aznalcollar. *Science of the Total Environment* 242: 3–11.

Gunter ME, Belluso E, and Mottana A (2007) Amphiboles: Environmental and health concerns. *Reviews in Mineralogy and Geochemistry* 67: 453–516.

Hageman PL (2007a) Determination of mercury in aqueous and geologic materials by continuous flow-cold vapor-atomic fluorescence spectrometry (CVAFS). *US Geological Survey Techniques and Methods Report 5-D2*. Reston, VA: US Geological Survey.

Hageman PL (2007b) U.S. Geological Survey field leach test for assessing water reactivity and leaching potential of mine wastes, soils, and other geologic and environmental materials. *US Geological Survey Techniques and Methods Report 5-D3*. Reston, VA: US Geological Survey.

Hageman PL, Plumlee GS, Martin DA, et al. (2008a) Leachate geochemical results for ash samples from the June 2007 Angora wildfire near Lake Tahoe in Northern California, 2008. *US Geological Survey Open-File Report 2008-1170*. Reston, VA: US Geological Survey.

Hageman PL, Plumlee GS, Martin DA, et al. (2008b) Leachate geochemical results for ash and burned soil samples from the October 2007 Southern California wildfires.

US Geological Survey Open-File Report 2008-1139. Reston, VA: US Geological Survey.

Hamel SLC (1998) *The Estimation of Bioaccessibility of Heavy Metals in Soils Using Artificial Biofluids*. PhD Thesis, Rutgers University and University of Medicine and Dentistry of New Jersey.

Hammarstrom JM, Seal RR II, Meier AL, and Kornfeld JM (2005) Secondary sulfate minerals associated with acid drainage in the eastern US: Recycling of metals and acidity in surficial environments. *Chemical Geology* 215: 407–431.

Hansell AL, Horwell CJ, and Oppenheimer C (2006) The health hazards of volcanoes and geothermal areas. *Occupational and Environmental Medicine* 63: 149–156.

Hansen K (2012) Gold, lead, and death in Nigeria. *Earth Magazine* 57: 28–35.

Harrington A and Schoonen MAA (2012) Pyrite-driven reactive oxygen species formation in simulated lung fluid: Implications for coal workers' pneumoconiosis. *Environmental Geochemistry and Health* 34: 527–538.

Harrison R, Materna BL, and Rothman N (1995) Respiratory health hazards and lung function in wildland firefighters. *Occupational Medicine* 10: 857–870.

Harsaputra I (2011) Porong turnpike safe to use during exodus. Jakarta Post, 08/13/2011, http://www.thejakartapost.com/news/2011/08/13/porong-turnpike-safe-use-during-exodus.html.

Hazama R and Shizuma K (2009) Environmental assessment of natural radioactivity in soil samples from the LUSI mud volcano, Indonesia. *Environment Asia* 2(2): 45–49.

Henn BC, Bellinger DC, and Wright RO (2012) Associations of early childhood manganese and lead coexposure with neurodevelopment. *Environmental Health Perspectives* 120: 126–131.

Hillman SE, Horwell CJ, Densmore A, et al. (2012) Sakurajima volcano: A physico-chemical study of the health consequences of long-term exposure to volcanic ash. *Bulletin of Volcanology* 74: 913–930.

Hoefen TM, Kokaly RF, Martin DA, et al. (2009) Sample collection of ash and burned soils from the October 2007 Southern California Wildfires. *US Geological Survey Open-File Report 2009-1038*. Reston, VA: US Geological Survey.

Hogan DE and Burstein JL (eds.) (2007) *Disaster Medicine*, 2nd edn. Philadelphia, PA: Lippincott Williams and Wilkins.

Horwell CJ and Baxter PJ (2006) The respiratory health hazards of volcanic ash: A review for volcanic risk mitigation. *Bulletin of Volcanology* 69: 1–24.

Horwell CJ, Fenoglio I, and Fubini B (2007) Iron-induced hydroxyl radical generation from basaltic volcanic ash. *Earth and Planetary Science Letters* 261: 662–669.

Horwell CJ, Le Blond JS, Michnowicz SAK, and Cressey G (2010) Cristobalite in a rhyolitic lava dome: Evolution of ash hazard. *Bulletin of Volcanology* 72: 249–253.

Horwell CJ, Sparks RSJ, Brewer TS, Llewellin EW, and Williamson BJ (2003) The characterisation of respirable volcanic ash from the Soufrière Hills volcano, Montserrat, with implications for human health hazards. *Bulletin of Volcanology* 65: 346–362.

Houghton BF, Swanson DA, Carey RJ, Rausch J, and Sutton AJ (2011) Pigeonholing pyroclasts: Insights from the 19 March 2008 explosive eruption of Kīlauea volcano. *Geology* 39: 263–266.

Hower JC, Schram WH, and Thomas GA (2000) Forensic petrology and geochemistry: Tracking the source of a coal slurry spill, Lee County, Virginia. *International Journal of Coal Geology* 44: 101–108.

Huang SX, Jaurand MC, Kamp DW, Whysner J, and Hei TK (2011) Role of mutagenicity in asbestos fiber-induced carcinogenicity and other diseases. *Journal of Toxicology and Environmental Health. Part B, Critical Reviews* 14: 179–245.

Hudak PF and Banks KF (2006) Compositions of first flush and composite storm water runoff in small urban and rural watersheds, north-central Texas. *Urban Water Journal* 3: 43–49.

Hudson-Edwards KA, Jamieson HE, Charnock JM, and Macklin MG (2005) Arsenic speciation in waters and sediment of ephemeral floodplain pools, Ríos Agrio–Guadiamar, Aznalcóllar, Spain. *Chemical Geology* 219: 175–192.

Ice GG, Neary DG, and Adams PW (2004) Effects of wildfire on soils and watershed processes. *Journal of Forestry* 102: 16–20.

ICRP (1995) *Human Respiratory Tract Model for Radiological Protection*. ICRP Publication 66. New York: Elsevier.

ITE (1997) Environmental follow-up of industrial accidents. *Report by The Institute of Terrestrial Ecology for the UK Department of the Environment, Transport, and the Regions*. London: The Stationery Office.

Izbicki G, Chavko R, Banauch GI, et al. (2007) World Trade Center "sarcoid-like" granulomatous pulmonary disease in New York City Fire Department rescue workers. *CHEST* 131: 1414–1423.

Jalava PI, Salonen RO, Hälinen AI, et al. (2006) In vitro inflammatory and cytotoxic effects of size-segregated particulate samples collected during long-range transport of wildfire smoke to Helsinki. *Toxicology and Applied Pharmacology* 215: 341–353.

Jennings DB, Williams DJ, and Garofalo D (2005) Mapping the spatial extent of ground dust and debris from the collapse of the World Trade Center buildings. *US Environmental Protection Agency Report EPA/600/R-03/018*. Reston, VA: US Environmental Protection Agency.

Jeppson J, Ranville JF, and Wildeman TR (2006) TCLP investigations: The development of a rapid screening field test. *2006 Billings Land Reclamation Symposium*, http://www.asmr.us/Publications/Conference%20Proceedings/2006%20Billings/0282-Jeppson-CO-abs.pdf.

Jibson RW (2002) A public health issue related to collateral seismic hazards: The valley fever outbreak triggered by the 1994 Northridge, California earthquake. *Surveys in Geophysics* 23: 511–528.

John DA, Sisson TW, Breit GN, Rye RO, and Vallance JW (2008) Characteristics, extent and origin of hydrothermal alteration at Mount Rainier Volcano, Cascades Arc, USA: Implications for debris-flow hazards and mineral deposits. *Journal of Volcanology and Geothermal Research* 175: 289–314.

Johnson CA (in press) The fate of cyanide in leach wastes at gold mines: An environmental perspective. *Reviews in Economic Geology*.

Jordan G, Fügedi U, Bartha A, et al. (2011) The red mud catastrophe in Kolontár, Hungary: Applying geology. *European Geologist* 32: 9–13.

Jurinski JB and Rimstidt JD (2001) Biodurability of talc. *American Mineralogist* 86: 392–399.

Kalabokidis KD (2000) Effects of wildfire suppression chemicals on people and the environment – A review. *Global NEST: The International Journal* 2: 129–137.

Kelly C (2005) Guidelines for rapid environmental impact assessment in disasters. Benefield Hazard Research Centre, University College London and Care International.

Klemas V (2010) Tracking oil slicks and predicting their trajectories using remote sensors and models: Case studies of the Sea Princess and Deepwater Horizon oil spills. *Journal of Coastal Research* 26: 789–797.

Kokaly RF, Hoefen TM, Livo KE, et al. (2010) A rapid method for creating qualitative images indicative of thick oil emulsion on the ocean's surface from imaging spectrometer data: *US Geological Survey Open-File Report 2010-1107*. Denver, CO: US Geological Survey.

Kokaly RF, Rockwell BW, Haire SL, and King TVV (2007) Characterization of post-fire surface cover, soils, and burn severity at the CerroGrande Fire, New Mexico, using hyperspectral and multispectral remote sensing. *Remote Sensing of Environment* 106: 305–325.

Kulkarni P, Baron P, and Willeke K (eds.) (2011) *Aerosol Measurement: Principles, Techniques, and Applications*, 3rd edn. New York: Wiley.

Künzli N, Avol E, Wu J, et al. (2006) Health effects of the 2003 Southern California wildfires on children. *American Journal of Respiratory and Critical Care Medicine* 174: 1221–1228.

Kvenvolden KA, Hostettler FD, Carlson PR, Rapp JB, Threlkeld CN, and Warden A (1995) Ubiquitous tar balls with a California-source signature on the shorelines of Prince William Sound, Alaska. *Environmental Science & Technology* 10: 2684–2694.

Kvenvolden KA, Hostettler FD, Rosenbauer RJ, Lorenson TL, Castle WT, and Sugarman S (2002) Hydrocarbons in recent sediment of the Monterey Bay National Marine Sanctuary. *Marine Geology* 181: 101–113.

Lacal J, Pilar de Silva M, García R, Teresa SM, Procopio JR, and Hernández L (2003) Study of fractionation and potential mobility of metal in sludge from pyrite mining and affected river sediments: Changes in mobility over time and use of artificial ageing as a tool in environmental impact assessment. *Environmental Pollution* 124: 291–305.

Landesman LY (2006) *Public Health Management of Disasters: The Pocket Guide*. Washington, DC: American Public Health Association.

Landrigan PJ, Lioy PJ, Thurston G, et al. (2004) Health and environmental consequences of the world trade center disaster. *Environmental Health Perspectives* 112: 731–739.

LeBlond JS, Williamson B, Horwell CJ, Monro AK, Kirk CA, and Oppenheimer C (2008) Production of potentially hazardous respirable silica airborne particulate from the burning of sugarcane. *Atmospheric Environment* 42: 5558–5568.

Lecce S, Pavlowsky R, and Schlomer G (2008) Mercury contamination of active channel sediment and floodplain deposits from historic gold mining at Gold Hill, North Carolina, USA. *Environmental Geology* 55: 113–121.

Leonard SS, Castranova V, Chena BT, et al. (2007) Particle size-dependent radical generation from wildland fire smoke. *Toxicology* 236: 103–113.

Li J, Brackbill RM, Stellman SD, et al. (2011) Gastroesophageal reflux symptoms and comorbid asthma and posttraumatic stress disorder following the 9/11 terrorist attacks on World Trade Center in New York City. *American Journal of Gastroenterology* 106: 1933–1941.

Linneman SR, Pittman P, and Bayer T (2009) The source of asbestiform chrysotile at Swift Creek, WA—Geology, mineralogy and sediment transport. *Geological Society of America Abstracts with Programs* 41: 704.

Lioy P, Weisel CP, Millette JR, et al. (2002) Characterization of the dust/smoke aerosol that settled east of the World Trade Center (WTC) in lower Manhattan after the

collapse of the WTC 11 September 2001. *Environmental Health Perspectives* 110: 703–714.

Lipsett M, Materna B, Stone S, Therriault S, Blaisdell R, Cook J (2008) Wildfire smoke, a guide for public officials. California Office of Environmental Health Hazard Assessment. http://www.oehha.ca.gov/air/risk_assess/wildfire.html.

Logue JN (1996) Disaster, the environment, and public health: Improving our response. *American Journal of Public Health* 86: 1207–1210.

Lorber M, Gibb H, Grant L, Pinto J, Pleil J, and Cleverly D (2007) Assessment of inhalation exposures and potential health risks to the general population that resulted from the collapse of the World Trade Center towers. *Risk Analysis* 27: 1203–1221.

Lowers HA and Meeker GP (2005) Particle atlas of World Trade Center dust. *US Geology Survey Open-File Report 2005-1165*. http://pubs.usgs.gov/of/2005/1165/.

Lowers HA, Meeker GP, Lioy PJ, and Lippmann M (2009) Summary of the development of a signature for detection of residual dust from collapse of the World Trade Center buildings. *Journal of Exposure Science and Environmental Epidemiology* 19: 325–335.

Manuel J (2006) In Katrina's wake. *Environmental Health Perspectives* 114: A33–A39.

Marley NA and Gaffney JS (eds.) (2005) *Urban Aerosols and Their Impacts: Lessons Learned from the World Trade Center Tragedy. ACS Symposium Series*, vol. 919. New York: Oxford University Press.

Mason V, Andrews H, and Upton D (2010) The psychological impact of exposure to floods. *Psychology, Health & Medicine* 15: 61–73.

Mayes WM, Jarvis AP, Burke IT, et al. (2011) Dispersal and attenuation of trace contaminants downstream of the Ajka bauxite residue (red mud) depository failure, Hungary. *Environmental Science & Technology* 45: 5147–5155.

Mazzini A, Etiope G, and Svensen H (2012) A new hydrothermal scenario for the Lusi eruption, Indonesia. Insights from gas geochemistry. *Earth and Planetary Science Letters* 317–318: 305–318.

McClellan R (2000) Particle interactions with the respiratory tract. In: Gehr P and Heyder J (eds.) *Particle–Lung Interactions*, pp. 3–66. New York: Dekker.

McGee JK, Chen LC, Cohen MD, et al. (2003) Chemical analysis of World Trade Center fine particulate matter for use in toxicologic assessment. *Environmental Health Perspectives* 111: 972–980.

McMichael H (2009) The Lapindo mudflow disaster: Environmental, infrastructure, and economic impact. *Bulletin of Indonesian Economic Studies* 45: 73–83.

McSpirit S, Scott S, Gill D, Hardesty S, and Sims D (2007) Risk perceptions after a coal waste impoundment failure: A survey assessment. *Southern Rural Sociology* 22: 88–110.

Meeker GP, Bern AM, Brownfield IK, et al. (2003) The composition and morphology of amphibole from the Rainy Creek Complex, near Libby, Montana. *American Mineralogist* 88: 1955–1969.

Meeker G, Plumlee G, Baldwin M, and Prezant D (2010) Mineralogical analysis and geochemical characterization of exogenic and endogenic particles in thoracic tissue. *Geological Society of America Abstracts with Programs* 42(5): 354.

Meeker GP, Sutley SJ, Brownfield IK, et al. (2005) Materials characterization of dusts generated by the collapse of the World Trade Center. In: Gaffney JS and Marley NA (eds.) *Urban Aerosols and Their Impacts: Lessons Learned from the World Trade Center Tragedy. ACS Symposium Series*, vol. 919, pp. 84–102. New York: Oxford University Press.

Mendez GO (2010) Water-quality data from storm runoff after the 2007 fires, San Diego County, California. *US Geological Survey Open-File Report 2010-1234*. http://pubs.usgs.gov/of/2010/1234/pdf/ofr20101234.pdf.

Mielke HW, Wang G, Gonzales CR, Powell ET, Le B, and Quach VN (2004) PAHs and metals in the soils of inner-city and suburban New Orleans, Louisiana, USA. *Environmental Toxicology and Pharmacology* 18: 243–247.

Miller AC and Arquilla B (2008) Chronic diseases and natural hazards: Impacts of disasters on diabetic, renal, and cardiac patients. *Prehospital and Disaster Medicine* 23: 185–194.

Millette JR, Boltin R, Few P, and Turner W Jr. (2002) Microscopical studies of World Trade Center disaster dust particles. *Microscope* 50: 29–35.

Mitchell RH and Dawson JB (2007) The 24th September 2007 ash eruption of the carbonatite volcano Oldoinyo Lengai, Tanzania: Mineralogy of the ash and implications for formation of a new hybrid magma type. *Mineralogical Magazine* 71: 482–483.

Moody JA, Martin DA, and Cannon SH (2008) Post-wildfire erosion response in two geologic terrains in the western USA. *Geomorphology* 95: 103–118.

Morman SA (2012) In vitro bioaccessibility extractions. In: Driscoll R, Hageman PL, Benzel WM et al. (eds.) *Assessment of the Geoavailability of Trace Elements from Minerals in Mine Wastes: Analytical Techniques and Assessment of Selected Copper Minerals*, *US Geological Survey Scientific Investigations Report 2011-5211*, pp. 34–43. Reston, VA: US Geological Survey.

Morman SA and Plumlee G (2010) In vitro physiologically based extraction tests of volcanic ash from diverse volcanoes (abs.). Cities on Volcanoes 6, Tenerife, Abstracts Volume, p. 173. http://www.citiesonvolcanoes6.com/.

Munns WR, Berry WJ, and Dewitt TH (2002) Toxicity testing, risk assessment, and options for dredged material management. *Marine Pollution Bulletin* 44: 294–302.

Neary DG, Ryan KC, and DeBano LF (eds.) (2008) Wildland fire in ecosystems: Effects of fire on soils and water. *USDA General Technical Report RMRS-GTR-42*, vol. 4. Ogden, UT: US Department of Agriculture, Forest Service, Rocky Mountain Research Station.

Neitzel R, Naeher LP, Paulsen M, Dunn K, Stock A, and Simpson CD (2009) Biological monitoring of smoke exposure among wildland firefighters: A pilot study comparing urinary methoxyphenols with personal exposures to carbon monoxide, particular matter, and levoglucosan. *Journal of Exposure Science and Environmental Epidemiology* 19: 349–358.

Newman LS (2001) Clinical pulmonary toxicology. In: Sullivan JB Jr. and Krieger G (eds.) *Clinical Environmental Health and Exposures*, 2nd edn., pp. 206–223. Philadelphia, PA: Lippincott Williams and Wilkins.

NIOSH (2003) Method 7400. Asbestos and other fibers by PCM. Issue 2 (8/15/94). In: *NIOSH Manual of Analytical Methods*, 4th edn. NIOSH Publication No. 2003-154. Cincinnati, OH: National Institute for Occupational Safety and Health.

NLM (2012) Hazardous Substances Data Bank. US National Library of Medicine. http://toxnet.nlm.nih.gov/cgi-bin/sis/htmlgen?HSDB, accessed May 2012.

Noji EK (2000) The public health consequences of disasters. *Prehospital and Disaster Medicine* 15: 147–157.

Notario del Pino J, Dorta Almenar I, Rodríguez Rodríguez A, et al. (2008) Analysis of the 1:5 soil:water extract in burnt soils to evaluate fire severity. *CATENA* 74: 246–255.

NRC (2010) *Review of the Department of Defense Enhanced Particulate Matter Surveillance Program Report*. Washington, DC: The National Academies Press.

NWCG (2011) National Interagency Incident Management System, Wildland Fire Qualification System Guide. *National Wildfire Coordinating Group Report No. PMS 310-1*. http://www.nwcg.gov/pms/docs/pms310-1.pdf.

Offenberg JH, Eisenreich SJ, Chen LC, et al. (2003) Persistent organic pollutants in the dusts that settled across lower Manhattan after September 11, 2001. *Environmental Science & Technology* 37: 502–508.

Offenberg JH, Eisenreich SJ, Gigliotti CL, et al. (2004) Persistent organic pollutants in dusts that settled indoors in lower Manhattan after September 11, 2001. *Journal of Exposure Analysis and Environmental Epidemiology* 14: 164–172.

Oil Spill Commission (2011) *The Use of Surface and Subsea Dispersants during the BP Deepwater Horizon Oil Spill*. Washington DC: National Commission on the BP Deepwater Horizon Oil Spill and Offshore Drilling.

Orem W, Tatu C, Pavlovic N, et al. (2009) Health effects of energy resources. *US Geology Survey Fact Sheet 2009-3096*.

Oxfam (2004) *Water Quality in the Mogpog River, Marinduque Island, Republic of the Philippines*. A & SR Tingay Pty Ltd.

Panichev N, Mabasa W, Ngobeni P, Mandiwana K, and Panicheva S (2008) The oxidation of Cr(III) to Cr(VI) in the environment by atmospheric oxygen during the bush fires. *Journal of Hazardous Materials* 153: 937–941.

Pardue JH, Moe WM, McInnis D, et al. (2005) Chemical and microbiological parameters in New Orleans floodwater following Hurricane Katrina. *Environmental Science & Technology* 39: 8591–8599.

Perera FP, Tang D, Rauh V, et al. (2005) Relationships among polycyclic aromatic hydrocarbon-DNA adducts, proximity to the World Trade Center, and effects on fetal growth. *Environmental Health Perspectives* 113: 1062–1067.

Petley DN, Dunning SA, and Rosser NJ (2005) The analysis of global landslide risk through the creation of a database of worldwide landslide fatalities. In: Hungr O, Fell R, Couture R, and Eberhardt E (eds.) *Landslide Risk Management*, pp. 367–374. London: Taylor and Francis.

Pierson TG, Janda RJ, Thouret J-C, and Borrero CA (1990) Perturbation and melting of snow and ice by the 13 November 1985 eruption of Nevado del Ruiz, Colombia, and consequent mobilization, flow and deposition of lahars. *Journal of Volcanology and Geothermal Research* 41: 17–66.

Pleil JP, Vette AF, Johnson BA, and Rappaport SM (2004) Air levels of carcinogenic polycyclic aromatic hydrocarbons after the World Trade Center disaster. *Proceedings of the National Academy of Sciences of the United States of America* 101: 11685–11688.

Plumlee GS (1999) The environmental geology of mineral deposits. In: Plumlee GS and Logsdon MJ (eds.) *The Environmental Geochemistry of Mineral Deposits. Part A: Processes, Techniques and Health Issues. Reviews in Economic Geology*, vol. 6A, pp. 71–116. Littleton, CO: Society of Economic Geologists, Inc.

Plumlee GS (2009) Report from Ground Zero: How geoscientists aid in the aftermath of environmental disasters. *Earth Magazine* 54: 38–47.

Plumlee G, Alpers C, and Morman S (2011) Environmental and health issues. In: Porter K, Wein A, Alpers C, et al. (eds.) *Overview of the ARkStorm Scenario*. *US Geological Survey Open-File Report 2010-1312*, pp. 148–150. Denver, CO: US Geological Survey.

Plumlee GS, Casadevall TJ, Wibowo HT, et al. (2008) Preliminary analytical results for a mud sample collected from the LUSI mud volcano, Sidoarjo, East Java, Indonesia. *US Geological Survey Open-File Report 2008-1019*. Denver, CO: US Geological Survey.

Plumlee GS, Foreman WT, Griffin DW, Lovelace JK, Meeker GP, and Demas CR (2007a) Characterization of flood sediments from Hurricane Katrina and Rita and potential implications for human health and the environment. In: Farris GS, Smith GJ, Crane MP, Demas CR, Robbins LL, and Lavoie DL (eds.) *Science and the Storms: The USGS Response to the Hurricanes of 2005*, *US Geological Survey Circular 1306*, pp. 246–257. Washington, DC: US Government Printing Office.

Plumlee GS, Hageman PL, Lamothe PJ, et al. (2005) Inorganic chemical composition and chemical reactivity of settled dust generated by the World Trade Center building collapse. In: Gaffney JS and Marley NA (eds.) *Urban Aerosols and Their Impacts: Lessons Learned from the World Trade Center Tragedy*. *ACS Symposium Series*, vol. 919, pp. 238–276. New York: Oxford University Press.

Plumlee GS, Logsdon MJ, Boyle TP, David CP, and Carr RS (2004) Environmental assessment. In: Wnuk C (ed.) *Engineering, Health, and Environmental Issues Related to Mining on Marinduque Island, Philippines; Final Report of the Independent US Assessment Team,* Section 5. Washington, DC: The FUTURES Group International.

Plumlee GS, Ludington S, Vincent KR, Verplanck P, Caine JS, and Livo KE (2009) Questa baseline and pre-mining ground-water quality investigation, 7. A pictorial record of chemical weathering, erosional processes, and potential debris-flow hazards in scar areas developed on hydrothermally altered rocks. *US Geological Survey Open-File Report 2006-1207*. Reston, VA: US Geological Survey.

Plumlee GS, Martin DA, Hoefen T, et al. (2007b) Preliminary analytical results for ash and burned soils from the October 2007 Southern California Wildfires. *US Geological Survey Open-File Report 2007-1407*. Reston, VA: US Geological Survey. http://pubs.usgs.gov/of/2007/1407.

Plumlee GS, Meeker GP, Lovelace JK, et al. (2006b) USGS environmental characterization of flood sediments left in the New Orleans area after Hurricanes Katrina and Rita, 2005—Progress Report. *US Geological Survey Open-File Report 2006-1023*. Reston, VA: US Geological Survey. http://pubs.usgs.gov/of/2006/1023.

Plumlee GS and Morman SA (2011) Mine wastes and human health. *Elements Magazine* 7: 399–404.

Plumlee GS, Morman SA, and Cook A (2012) Environmental and medical geochemistry in urban disaster response and preparedness. *Elements Magazine* 8(6): 5.

Plumlee GS, Morman SA, and Ziegler TA (2006a) The toxicological geochemistry of earth materials: An overview of processes and the interdisciplinary methods used to understand them. In: Sahai N and Schoonen MAA (eds.) *Medical Mineralogy and Geochemistry*. *Reviews in Mineralogy and Geochemistry*, vol. 64, pp. 5–58. Mineralogical Society of America and Geochemical Society.

Plumlee GS, Morton RA, Boyle TP, Medlin JH, and Centeno JA (2000) An overview of mining-related environmental and human health issues, Marinduque Island, Philippines: Observations from a Joint U.S. Geological Survey – Armed Forces Institute of Pathology Reconnaissance field evaluation, May 12–19, 2000. *US Geological Survey Open-File Report 00-397*. Available on-line at http://pubs.usgs.gov/of/2000/ofr-00-0397/.

Plumlee GS and Ziegler T (2003) The medical geochemistry of dusts, soils, and other earth materials. In: Lollar BS (ed.) *Treatise on Geochemistry, Vol. 9: Environmental Geochemistry*, ch. 7, pp. 263–310. Oxford: Elsevier-Pergamon.

Plumlee GS and Ziegler T (2007) The medical geochemistry of dusts, soils, and other earth materials. In: Lollar BS (ed.) *Treatise on Geochemistry, Vol. 9: Environmental Geochemistry,* online edition, ch. 7, pp. 1–61. Oxford: Elsevier. http://www.sciencedirect.com/science/referenceworks/9780080437514.

Porter K, Jones L, Cox D, et al. (2011a) The ShakeOut scenario: A hypothetical Mw7.8 earthquake on the southern San Andreas Fault. *Earthquake Spectra* 27: 239–261.

Porter K, Wein A, Alpers C, et al. (2011b) Overview of the ARkStorm scenario. *US Geological Survey Open-File Report 2010-1312*. http://pubs.usgs.gov/of/2010/1312/.

Presley SM, Rainwater TR, Austin GP, et al. (2006) Assessment of pathogens and toxicants in New Orleans, LA following Hurricane Katrina. *Environmental Science & Technology* 40: 468–474.

Prezant DJ, Weiden M, Banauch GI, et al. (2002) Cough and bronchial responsiveness in firefighters at the World Trade Center site. *The New England Journal of Medicine* 347: 806–815.

Quaranta JD, Gutta B, Stout B, McAteer D, and Ziemkiewcz P (2004) Improving the safety of coal slurry impoundments in West Virginia. *Tailings and Mine Waste '04, Proceedings of the Eleventh Tailings and Mine Waste Conference*, Vail, Colorado, USA, pp. 279–283. Leiden, The Netherlands: A.A. Balkema Publishers.

Reeder RJ, Schoonen MAA, and Lanzirotti A (2006) Metal speciation and its role in bioaccessibility and bioavailability. In: Sahai N and Schoonen MAA (eds.) *Medical Mineralogy and Geochemistry*. *Reviews in Mineralogy and Geochemistry*, vol. 59, pp. 59–113. Mineralogical Society of America and Geochemical Society.

Renforth P, Mayes WM, Jarvis AP, Burke IT, Manning DA, and Gruiz K (2012) Contaminant mobility and carbon sequestration downstream of the Ajka (Hungary) red mud spill: The effects of gypsum dosing. *Science of the Total Environment* 421–422: 253–259.

Rom WN, Reibman J, Rogers L, et al. (2010) Emerging exposures and respiratory health: World Trade Center dust. *Proceedings of the American Thoracic Society* 7: 142–145.

Rom WN, Weiden M, Garcia R, et al. (2002) Acute eosinophilic pneumonia in a New York City firefighter exposed to World Trade Center dust. *American Journal of Respiratory and Critical Care Medicine* 166: 797–800.

Rostad CE, Schmitt CJ, Schumacher JG, and Leiker TJ (2011) An exploratory investigation of polar organic compounds in waters from a lead-zinc mine and mill complex. *Water, Air, & Soil Pollution* 217: 431–443.

Rotkin-Ellman M, Solomon G, Gonzales CR, Agwaramgbo L, and Mielke HW (2010) Arsenic contamination in New Orleans soil: Temporal changes associated with flooding. *Environmental Research* 110: 19–25.

Roy A, Bianchetti C, Tittsworth R, and Pardue J (2007) Speciation of heavy metals in Katrina sediments from New Orleans, Louisiana. *AIP Conference Proceedings* 882: 268–270.

Ruby MV, Schoof R, Brattin W, et al. (1999) Advances in evaluating the oral bioavailability of inorganics in soil for use in human health risk assessment. *Environmental Science & Technology* 33: 3697–3705.

Ruhl L, Vengosh A, Dwyer GS, Hsu-Kim H, and Deonarine A (2010) Environmental impacts of the coal ash spill in Kingston, Tennessee: An 18-month survey. *Environmental Science & Technology* 44: 9272–9278.

Ruhl L, Vengosh A, Dwyer GS, et al. (2009) Survey of the potential environmental and health impacts in the immediate aftermath of the coal ash spill in Kingston, Tennessee. *Environmental Science & Technology* 43: 6326–6333.

Ruyters S, Mertens J, Vassilieva E, Dehandschutter B, Poffijn A, and Smolders E (2011) The red mud accident in Ajka (Hungary): Plant toxicity and trace metal bioavailability in red mud contaminated soil. *Environmental Science & Technology* 45: 1616–1622.

Sahai N and Schoonen MAA (eds.) (2006) *Medical Mineralogy and Geochemistry*. *Reviews in Mineralogy and Geochemistry*, vol. 64. Mineralogical Society of America and Geochemical Society.

Sawolo N, Sutriono E, Istadi BP, and Darmoyo AB (2009) The LUSI mud volcano triggering controversy: Was it caused by drilling? *Marine and Petroleum Geology* 26: 1766–1784.

Scanlon PD (2002) World Trade Center cough—A lingering legacy and a cautionary tale. *The New England Journal of Medicine* 347: 840–842.

Schoonen MAA, Cohn CA, Roemer E, Laffers R, Simon S, and O'Riordan T (2006) Mineral-induced formation of reactive oxygen species. In: Sahai N and Schoonen MAA (eds.) *Medical Mineralogy and Geochemistry*. *Reviews in Mineralogy and Geochemistry* 64: pp. 179–221. Mineralogical Society of America and Geochemical Society.

Selinus O, Alloway B, and Centeno J, et al. (eds.) (2005) *Essentials of Medical Geology*. San Diego, CA: Elsevier Academic Press.

Shi H, Witt E III, Shu S, Su T, Wang J, and Adams C (2010) Toxic trace element assessment for soils/sediments deposited during hurricanes Katrina and Rita from southern Louisiana, USA: A sequential extraction analysis. *Environmental Toxicology and Chemistry* 29: 1419–1428.

Shusterman D, Kaplan JZ, and Canabarro C (1993) Immediate health effects of an urban wildfire. *The Western Journal of Medicine* 158: 133–138.

Singh DN and Kolay PK (2002) Simulation of ash–water interaction and its influence on ash characteristics. *Progress in Energy and Combustion Science* 28: 267–299.

Sinigalliano CD, Gidley ML, Shibata T, et al. (2007) Impacts of Hurricanes Katrina and Rita on the microbial landscape of the New Orleans area. *Proceedings of the National Academy of Sciences of the United States of America* 104: 9029–9034.

Smith KS, Hageman PL, Briggs PH, et al. (2007) Questa baseline and pre-mining ground-water quality investigation. 19. Leaching characteristics of composited materials from mine waste-rock piles and naturally altered areas near Questa, New Mexico. *US Geological Survey Scientific Investigations Report 2006-5165*. Reston, VA: US Geological Survey.

Smith KS, Ramsey CA, and Hageman PL (2000) Sampling strategy for rapid screening of mine-waste dumps on abandoned mine lands. In: *Proceedings of the Fifth*

International Conference on Acid Rock Drainage, Denver, Colorado, 21-24 May, vol. II, pp. 1453–1461. Littleton, CO: Society for Mining, Metallurgy and Exploration.
Smith HG, Sheridan GJ, Lane PNJ, Nyman P, and Haydon S (2011) Wildfire effects on water quality in forest catchments: A review with implications for water supply. *Journal of Hydrology* 396: 170–192.
Smith DB, Woodruff LG, O'Leary RM, et al. (2009) Pilot studies for the North American Soil Geochemical Landscapes Project – Site selection, sampling protocols, analytical methods, and quality control protocols. *Applied Geochemistry* 24: 1357–1368.
Sorey ML, Farrar CD, Gerlach TM, et al. (2000) Invisible CO_2 gas killing trees at Mammoth Mountain, California. *US Geological Survey Fact Sheet 172-96*. http://pubs.usgs.gov/dds/dds-81/Intro/facts-sheet/fs172-96.pdf.
Stec A and Hull R (2010) *Fire Toxicity*. Oxford: Woodhead Publishing.
Stefaniak AB, Day GA, Hoover MD, Breysse PN, and Scripsick RC (2006) Differences in dissolution behavior in a phagolysosomal simulant fluid for single-constituent and multi-constituent materials associated with beryllium sensitization. *Toxicology In Vitro* 20: 82–95.
Stephenson J (2002) Researchers probe health consequences following the World Trade Center attack. *Journal of the American Medical Association* 288: 1219–1221.
Sullivan PA (2007) Vermiculite, respiratory disease, and asbestos exposure in Libby, Montana: Update of a cohort mortality study. *Environmental Health Perspectives* 115: 579–585.
Sullivan JB Jr. and Krieger G (eds.) (2001) *Clinical Environmental Health and Exposures*, 2nd edn. Philadelphia, PA: Lippincott Williams and Wilkins 1323pp.
Sutton J, Elias T, Hendley JW II, Stauffer PH. Volcanic Air Pollution—A Hazard in Hawaii. *US Geological Survey Fact Sheet 169-97*. http://pubs.usgs.gov/fs/fs169-97/.
Swayze GA, Hoefen TM, Sutley SJ, et al. (2005) Spectroscopic and x-ray diffraction analyses of asbestos in the World Trade Center dust. In: Gaffney JS and Marley NA (eds.) *Urban Aerosols and Their Impacts: Lessons Learned from the World Trade Center Tragedy. ACS Symposium Series*, vol. 919, pp. 40–65. New York: Oxford University Press.
Taggart JE (2002) Analytical methods for chemical analysis of geologic and other materials. *US Geological Survey Open-File Report 02-223*. http://pubs.usgs.gov/of/2002/ofr-02-0223/.
Taggart MA, Figuerola J, Green AJ, et al. (2006) After the Aznalcóllar mine spill: Arsenic, zinc, selenium, lead and copper levels in the livers and bones of five waterfowl species. *Environmental Research* 100: 349–361.
Taunton AE, Gunter ME, Druschel GK, and Wood SA (2010) Geochemistry in the lung: Reaction-path modeling and experimental examination of rock-forming minerals under physiologic conditions. *American Mineralogist* 95: 1624–1635.
Thibodeaux LJ, Valsaraj KT, John VT, Papadopoulos KD, Pratt LR, and Pesika NS (2011) Marine oil fate: Knowledge gaps, basic research, and development needs; a perspective based on the Deepwater Horizon Spill. *Environmental Engineering Science* 28: 87–93.
Timofeyenko YG, Rosentreter JJ, and Mayo S (2007) Piezoelectric quartz crystal microbalance sensor for trace aqueous cyanide ion detection. *Analytical Chemistry* 79: 251–255.
Tuttle MLW, Briggs PH, and Berry CJ (2003) A method to separate phases of sulphur in mine-waste piles and natural alteration zones, and to use sulphur isotopic compositions to investigate release of metals and acidity into the environment. *Proceedings of the Sixth International Conference on Acid Rock Drainage (ICARD 6)*, Cairns, North Queensland, Australia, 14–17 July 2003, pp. 1141–1145.
Twining J, McGlinn P, Loi E, Smith K, and Gieré R (2005) Risk ranking of metals from fly ash dissolved in simulated lung and gut fluids. *Environmental Science & Technology* 39: 7749–7756.
UNEP (1996) Final report of the United Nations expert assessment mission to Marinduque Island, Philippines. United Nations Environment Programme, Water Branch.
UNEP/OCHA (2000) *Cyanide Spill at Baia Mare Romania*. United Nations Environment Programme/Office for the Co-ordination of Humanitarian Affairs.
UNEP/OCHA (2006) Environmental Assessment — Hot Mud Flow East Java, Indonesia. *United Nations Disaster Assessment and Coordination Mission Final Technical Report*, Joint United Nations Environment Program/Office for the Coordination of Humanitarian Affairs Environment Unit, http://ochanet.unocha.org/p/Documents/Indonesia_Hot_Mud_Flow_East_Java_final_report.pdf.
USFS (2011) *Wildland Fire Qualification System Guide*. US Forest Service National Interagency Incident Management System, PMS-310-1.
USGS (1997) Radioactive elements in coal and fly ash: Abundance, forms, and environmental significance. *US Geological Survey Fact Sheet FS-163-97*. http://pubs.usgs.gov/fs/1997/fs163-97/FS-163-97.pdf.
USGS (2002a) Characterization and modes of occurrence of elements in feed coal and fly ash—an integrated approach. *US Geological Survey Fact Sheet FS-038-02*. http://pubs.usgs.gov/fs/fs-0038-02/.
USGS (2002b) USGS environmental studies of the World Trade Center area, New York City, after September 11, 2001. *US Geological Survey Fact Sheet FS-050-02*.
USGS (2010) National field manual for the collection of water-quality data. *US Geological Survey Techniques of Water-Resources Investigations*, book 9, chs. A1-A9. http://water.usgs.gov/owq/FieldManual/.
Van Gosen BS (2009) The geologic relationships of industrial mineral deposits and asbestos in the western United States. *Preprints of the 2009 SME Annual Meeting*, 22-25 February 2009, Denver, Colorado, Preprint 09-061. Littleton, CO: Society for Mining, Metallurgy, and Exploration.
Van Metre PC, Horowitz AJ, Mahler BJ, et al. (2006) Effects of Hurricanes Katrina and Rita on the chemistry of bottom sediments in Lake Pontchartrain, Louisiana, USA. *Environmental Science & Technology* 40: 6894–6902.
Vázquez S, Hevia A, Moreno E, Esteban E, Peñalosa JM, and Carpena RO (2011) Natural attenuation of residual heavy metal contamination in soils affected by the Aznalcóllar mine spill, SW Spain. *Journal of Environmental Management* 92: 2069–2075.
Vendetti J. (2001) Storing coal slurry. *Geotimes*, Dec., 1pp. http://www.geotimes.org/dec01/NNcoal.html.
Viswanathan S, Eria L, Diunugala N, Johnson J, and McClean C (2006) An analysis of effects of San Diego wildfire on ambient air quality. *Journal of the Air & Waste Management Association* 56: 56–67.
Wang B, Michaelson G, Ping C, Plumlee G, and Hageman P (2010) Characterization of pyroclastic deposits and pre-eruptive soils following the 2008 eruption of Kasatochi Island Volcano, Alaska. *Arctic, Antarctic, and Alpine Research* 42: 276–284.
Webber MP, Glaser MS, Weakley J, et al. (2011) Physician-diagnosed respiratory conditions and mental health symptoms seven to nine years following the World Trade Center disaster. *American Journal of Industrial Medicine* 4: 661–671.
Wegesser TC, Pinkerton KE, and Last JA (2009) California wildfires of 2008: Coarse and fine particulate matter toxicity. *Environmental Health Perspectives* 117: 893–897.
Weinstein P and Cook A (2005) Volcanic emissions and health. In: Selinus O, Alloway B, and Centeno J, et al. (eds.) *Essentials of Medical Geology*, pp. 87–114. San Diego, CA: Elsevier Academic Press.
Wigginton A, Mitchell J, Evansc G, and McSpirit S (2008) Assessing the impacts of coal waste on residential wells in the Appalachian region of the Big Sandy watershed, Kentucky and West Virginia: An exploratory investigation. *The Journal of the Kentucky Academy of Science* 69: 152–163.
Wildeman TR, Smith KS, and Ranville JF (2007) A simple scheme to determine potential aquatic metal toxicity from mining wastes. *Environmental Forensics* 8: 119–128.
Witham CS, Oppenheimer C, and Horwell CJ (2005) Volcanic ash leachates: A review and recommendations for sampling methods. *Journal of Volcanology and Geothermal Research* 141: 299–326.
Wnuk C (ed.) (2004) *Engineering, Health, and Environmental Issues Related to Mining on Marinduque Island, Philippines. Final Report of the Independent US Assessment Team*. Washington, DC: The FUTURES Group International.
Wolf RE, Morman SA, Hageman PL, Hoefen TM, and Plumlee GS (2011) Simultaneous speciation of arsenic, selenium, and chromium: Species stability, sample preservation, and analysis of ash and soil leachates. *Analytical and Bioanalytical Chemistry* 401: 2733–2745.
Wood WW, Clark D, Imes JL, and Counceil TB (2009) Eolian transport of geogenic hexavalent chromium to ground water. *Ground Water* 48: 19–29.
WTCHP (2011) *First Periodic Review of Scientific and Medical Evidence Related to Cancer for the World Trade Center Health Program*. World Trade Center Health Program, US Centers for Disease Control and Prevention.
Wu M, Gordon RE, Herbert R, et al. (2010) Case report: Lung disease in World Trade Center responders exposed to dust and smoke: Carbon nanotubes found in the lungs of World Trade Center patients and dust samples. *Environmental Health Perspectives* 118: 499–504.
Yiin LM, Millette JR, Vette A, et al. (2004) Comparisons of the dust/smoke particulate that settled inside the surrounding buildings and outside on the streets of southern New York City after the collapse of the World Trade Center, September 11, 2001. *Journal of the Air & Waste Management Association* 54: 515–528.
Yoshida N and Takahashi Y (2012) Land-surface contamination by radionuclides from the Fukushima Daiichi nuclear power plant. *Elements Magazine* 8: 201–206.
Young S, Balluz L, and Malilay J (2004) Natural and technologic hazardous material releases during and after natural disasters: A review. *Science of the Total Environment* 322: 3–20.
Young CA, Twidwell LG, and Anderson CG (eds.) (2001) *Cyanide: Social, Industrial, and Economic Impacts*. Warrendale, PA: TMS.
Zeig-Owens R, Webber P, Hall CB, et al. (2011) Early assessment of cancer outcomes in New York City firefighters after the 9/11 attacks: An observational cohort study. *Lancet* 378: 898–905.

11.8 Eutrophication of Freshwater Systems

NA Serediak and EE Prepas, Lakehead University, Thunder Bay, ON, Canada
GJ Putz, University of Saskatchewan, Saskatoon, SK, Canada

This article is a revision of the previous edition article by EE Prepas and T Charette, volume 9, pp. 311–331, © 2003, Elsevier Ltd.

Glossary

Absorption Incorporation of dissolved material inside another substance or structure (e.g., water droplet or cell).
Adsorption Adhesion of atoms, ions, or molecules (e.g., gas, liquid, dissolved solid, biomolecule) to a surface.
Allotrope Different molecular forms of the same chemical element (e.g., graphite and diamond are allotropes of carbon).
Anaerobic A condition indicating the absence of oxygen as an electron acceptor; also termed anoxic.
Anthropogenic An environmental effect or condition resulting from human activities.
Apatite A group of calcium phosphate minerals most commonly bound to a hydroxyl (OH^-) or halide ion (often F^- or Cl^-) and the main source of phosphorus required by photosynthetic organisms.
Chlorophyll *a* Abbreviated chl*a*; from the Greek roots meaning 'green' (chloro) and 'leaf' (phyllo); an inner-sphere chelate found as a photosynthetic pigment in many primary producers and often measured as an indicator of phytoplankton biomass; though not all phytoplankton use chl*a* as the main electron donor in photosynthesis, it is the one most commonly encountered.
Hydrology The study of water and its forms, cycling, movement, distribution, and quantity.
Hydrophilic The condition of a molecule or substance being attracted to and tending to be dissolved by water.

Photosynthesis A redox reaction which converts carbon dioxide (CO_2) and water (H_2O) into carbohydrates (general formula CH_2O) and oxygen (O_2) following excitation by ultraviolet light.

Primary productivity Biomass production primarily as a result of photosynthesis, usually measured as a mass per unit area or per volume of water.

11.8.1 Introduction

Since the advent of modern ecology in the twentieth century, increasing attention has been paid to surface water ecosystems, especially lakes as downstream indicators of cumulative upstream point and diffuse-source impacts. One result of collective nutrient inputs is eutrophication, which can be severe enough to be evident at coarse visual levels as the 'greening' of lakes and streams (Edmondson, 1991; Schindler, 1974). Eutrophication has been varyingly defined as an increase in the production of organic matter (Nixon, 1995), enrichment with inorganic plant nutrients (Lawrence et al., 1998), or, more specifically, phosphorus and nitrogen overenrichment leading to excessive plant, algal, and cyanobacterial growth and anoxic events (Carpenter, 2005). Although eutrophication occurs naturally in some systems, its current frequency and intensity in freshwater is cause for immediate concern.

While freshwater is considered a renewable resource, its global allocation is restricted by proportional availability (Figure 1). Demands for clean sources are increasing while accessibility, quality, and supplies of freshwater are limited; escalated occurrences of eutrophication are applying additional pressure on a strained resource. Nutrient flow on a global scale has more than doubled for nitrogen and more than tripled for phosphorus (see Sections 11.8.2.1 and 11.8.2.2) relative to preindustrial estimates (Cassara, 2008). This is concurrent with increases in harmful algal blooms and associated detrimental effects on aquatic food webs, commercial fisheries, public health, recreation, and tourism (Hoagland et al., 2002). To appreciate eutrophication as a serious environmental hazard, it is worthwhile to examine the mechanisms and causes for its occurrence in freshwater.

11.8.1.1 Importance and Structure of Water

Water is the most common substance known to occur naturally in all three physical states: gas, liquid, and solid. Water molecules are composed of two hydrogen atoms bonded to one oxygen atom in a three-dimensional triangular (tetrahedral) configuration (Figure 2). The smaller, positively charged hydrogen ions are repelled both by each other and by the larger, negatively charged oxygen ion. This spatial arrangement yields a polarized molecule with an overall charge gradient ranging from one slightly negative to one slightly positive region (a dipole, as there are only two oppositely charged regions). Polar compounds like water are subject to additional intermolecular

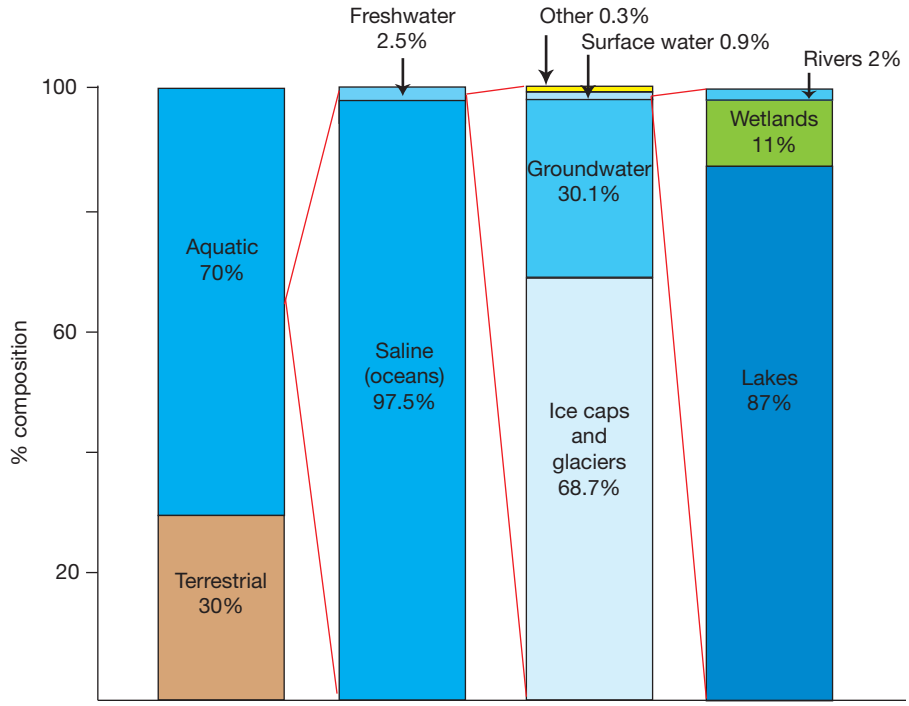

Figure 1 Global water resources as percentages of available water fractions. The 'other' category refers to water locked in biological structures, soil moisture, permafrost, etc. Adapted from values in Babkin VI and Klige RK (2003) The hydrosphere. In: Shiklomanov IA and Rodda JC (eds.) *World Water Resources at the Beginning of the Twenty-First Century*. New York: Cambridge University Press.

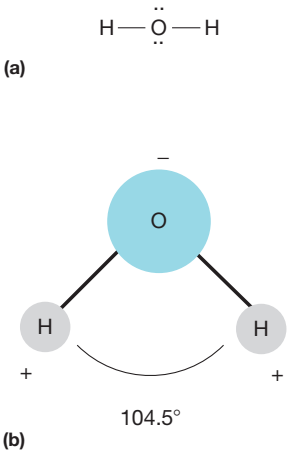

Figure 2 The two electron pairs in the Lewis diagram (a) force the hydrogen atoms into a characteristic configuration (b), creating a charge difference across the water molecule.

connections in fluid and solid states, such as hydrogen bonding and van der Waals forces. The combination of these forces and the molecular structure of water result in the unique properties of water to expand during freezing and to reach maximum density at about 4 °C. It is also amphoteric, meaning it can act as either a proton donor (acid) or acceptor (base), and is often referred to as a universal solvent for its ability to dissolve numerous substances. The fundamental characteristics of water make it an essential component of geochemical weathering.

11.8.1.2 Movement over and through Land

Beginning with precipitation (e.g., rain, snow, sleet, hail), water is deposited on the landscape and becomes a component of the weathering process (Figure 3). Unless it is experiencing a force greater than that of gravity, water migrates from relatively high elevations to relatively low points on the landscape, transporting and dissolving substances in its path. There are a number of things that will naturally affect the movement of water along established hydrologic pathways. These include

- freezing and thawing of water and soils
- spatial and temporal precipitation patterns
- watershed slope
- area and type of wetlands
- soil depth to bedrock or other impermeable surface
- soil type
- vegetation community composition, senescence, or combustion
- flow modifications (e.g., beaver activity, hydroelectric dams, urbanization, wetland conversion, withdrawals for agricultural, municipal, and industrial uses)

All of these attributes combine to shape the quantity and quality of water entering aquatic ecosystems from the surrounding land. As water proceeds over and through the landscape, its movement is one of the primary means of nutrient relocation from terrestrial sources to aquatic systems. Collection corridors for flowing water are termed lotic systems, and refer to rivers and streams that may be permanent or ephemeral (temporary). Although water is rarely static, points of accumulation do occur on the landscape (e.g., lakes, ponds, wetlands) and are termed lentic systems.

11.8.1.3 Implications for Overloading the System

Nutrients begin as minerals located in rock, soil, organic matter, or as airborne particles. Through the processes of mechanical and chemical weathering, decomposition (physical, chemical, and biological), mineralization and atmospheric deposition, nutrients are transformed into more biologically available, water-soluble components. The unique assembly of water and its passage over and through the landscape transports chemically accessible nutrients to aquatic organisms, which benefit directly. When nutrient delivery is increased through anthropogenic effects, inputs to surface water systems result in disproportionate amounts of easily incorporated chemicals relative to what would occur naturally. The function and structure of aquatic systems, which developed in concert with the terrestrial environment, are disrupted by the resulting nutrient imbalance.

11.8.2 Nutrient Cycles in Aquatic Ecosystems

In general, a nutrient is any substance required for growth and development that an organism cannot produce itself. However, the discussion of nutrients relative to aquatic systems usually relates to phosphorus and nitrogen, as their abundance can create the most problems in surface waters. The division between macro- and micronutrient categories is often a matter of perspective: silica is not an important constituent for many mid-summer phytoplankton (photosynthetic algae and cyanobacteria), but is vital for diatoms that tend to dominate algal communities in early spring. For many organisms, compounds required for growth and maintenance are obtained externally and environmental availability limits growth of both individuals and populations. However, organisms such as cyanobacteria are able to meet at least part of their nutrient needs through chemical conversions that take place internally, often under specific external conditions. Eutrophication works to the advantage of these species in particular, and often to the detriment of other organisms in the aquatic community.

What makes nutrient availability so pivotal rests on the theory of the limiting factor, or the Law of the Minimum. Usually attributed to Justus von Liebig, a gifted chemist, researcher, and teacher, who popularized the term, it was originally proposed by Karl Sprengel, a German botanist working in the field of agriculture (van der Ploeg et al., 1999). Sprengel noted that it was not availability of all nutrients that affected plant growth, but the amount of the least available nutrient relative to need that determined crop yield (Jungk, 2009). Traditional considerations placed nitrogen, followed by phosphorus, as limiting primary production in terrestrial, estuarine, and marine systems, while the reverse order was applied to freshwater systems. Phosphorus is still often considered the primary nutrient on which management should focus in

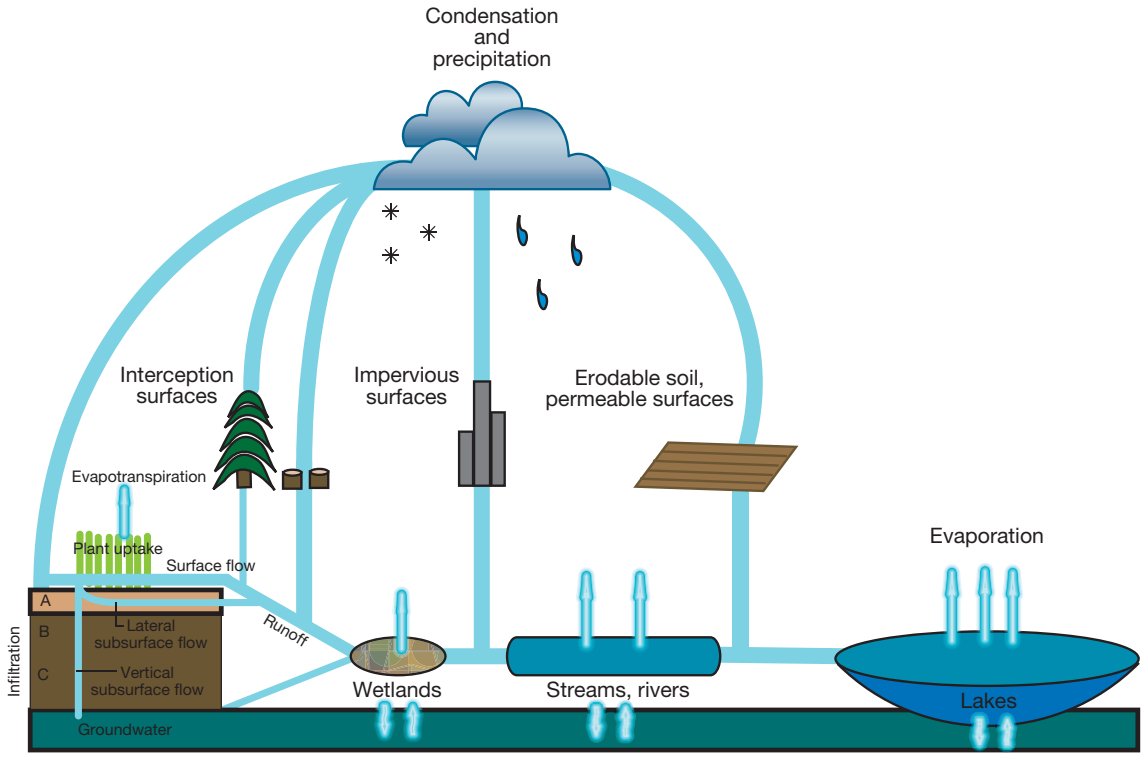

Figure 3 Generalized movement of water at the landscape scale. Climate influences precipitation volumes, and not all precipitation reaches aquatic systems as runoff. Conversion of precipitation to runoff is affected by factors that can increase (e.g., impervious surfaces, forest canopy removal, wetland conversion) or decrease (e.g., migration to deep groundwater through permeable soils, plant uptake, temporary storage, evaporation, evapotranspiration) water movement across the landscape. These same factors can affect nutrient concentrations within the runoff.

limiting the eutrophication of freshwater environments (Schindler et al., 2008), although nitrogen has been seen as limiting in lakes when levels of phosphorus were very high (Downing and McCauley, 1992). Additional analyses also suggest that both nitrogen and phosphorus are often equivalently limiting, and coincident enrichment creates a positive and synergistic response regardless of system location (Elser et al., 2007; Lewis and Wurtsbaugh, 2008). When limiting nutrients are supplied in excess, increased growth occurs relative to unenriched areas and the taxonomic diversity of communities that grow in response can change.

11.8.2.1 Phosphorus

The name phosphorus is derived from Greek and roughly means 'bearer of light,' although in Latin it translates as Lucifer and has been called the devil's element (Emsley, 2000). The discovery of phosphorus is credited to Hennig Brandt who in 1669 isolated a compound from his own urine in his search for the philosopher's stone (the mythical substance capable of turning base metals into gold). The material with the greenish glow gave its name to the wrongly assigned process by which it was thought to emit light: phosphorescence (reemission of light after surface excitation) instead of the correct chemiluminescence (glowing as a result of a cold chemical reaction). Phosphorus is a critical element in all known forms of life. Although toxic when ingested in certain forms and biologically unavailable in others, phosphorus bound as phosphate (PO_4-P) is water soluble and a necessary and vital component of many biological structures (e.g., nucleic acids, proteins, ATP, cell membranes) and processes (e.g., phosphorylation and photosynthesis).

Phosphorus is never found naturally as a free element owing to its extreme reactivity. It can exist in several allotropes (chemical forms), the most common of which are white and red phosphorus. Although white phosphorus was used industrially for many years, its instability under ambient conditions (i.e., when exposed to air), toxic vapors, and debilitating human health effects from chronic exposure led to its replacement by the far more stable red phosphorus under the Berne Convention of 1906 (Emsley, 2000). With no significant atmospheric component in the phosphorus cycle (**Figure 4**; see also **Chapter 10.13**), all sources originate from phosphate rock, which occurs as an apatite of either sedimentary or igneous origins (**Table 1**). The natural phosphorus cycle is quite slow owing to the inherently low solubility of many phosphorus-containing compounds. However, phosphorus is a strong adsorber and adheres tenaciously to the charged surfaces of many soil particles, particularly fine-grained clays and silts. Transmission of adsorbed phosphorus to aquatic ecosystems is enhanced by watershed activities that alter forest vegetation species composition and cover, disturb or expose soil, and increase overland or shallow subsurface flow, which enhances erosion (Sims et al., 1998). Once transported to aquatic systems, phosphorus undergoes chemical processes that result in increased amounts of more biologically available forms relative to other

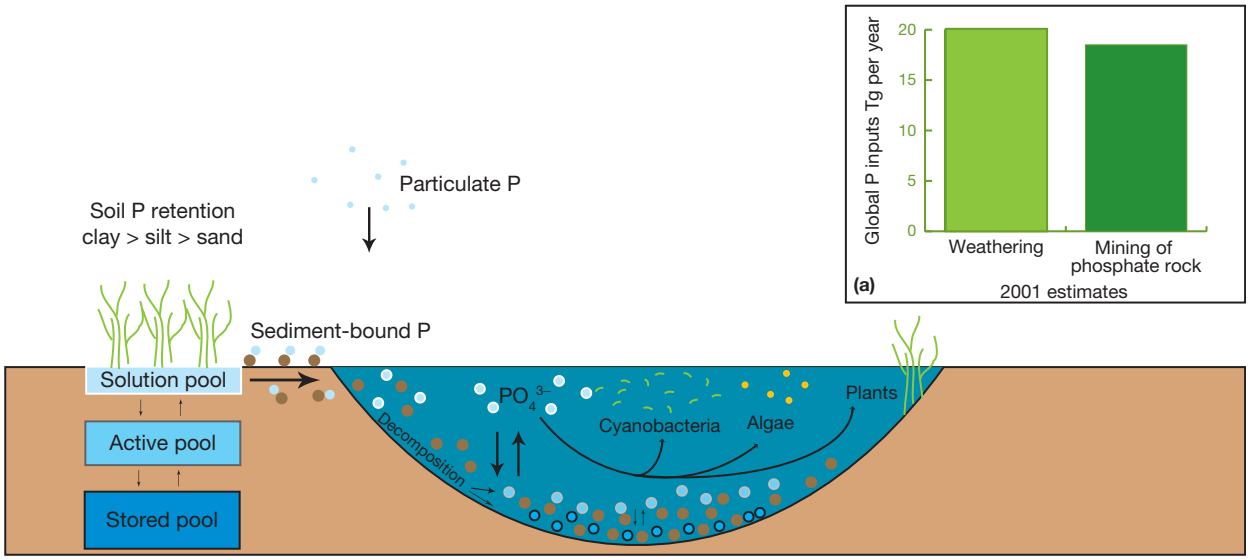

Figure 4 A simplified phosphorus cycle for a lake catchment. Much of the phosphorus that reaches surface water systems is transported and adsorbed to particles in the soil solution pool. Similar storage fractions exist in lake sediments, where phosphorus concentrations in the water column are affected by pH and oxygen-dependent sediment–water interactions. The inset graph shows phosphorus inputs to the global phosphorus cycle at the maximum range of estimated global P inputs from natural sources compared to anthropogenic inputs. Humans have roughly doubled the amount of phosphorus in circulation, even when compared to the higher end of natural input estimates. Adapted from values in Bennet EM, Carpenter SR, and Caraco NF (2001) Human impacts on erodable phosphorus and eutrophication: A global perspective. *Bioscience* 51: 227–234.

fractions present (Table 2). Anthropogenic activity can supercharge this cycle by delivering increased amounts of P directly to aquatic systems, thereby circumventing natural weathering processes. This occurs through movement of soluble, accessible P (e.g., chemical fertilizer, sewage, mining fines), the delivery of which can be exacerbated by watershed activities that increase transport rates.

11.8.2.2 Nitrogen

Unlike phosphorus, nitrogen occurs most commonly as an extremely stable atmospheric gas, dinitrogen (N_2). Dinitrogen gas comprises approximately 78% of our breathable atmosphere and is remarkably unreactive due to the strength of the triple bond. It was first identified as a separable and noncombusting component of air in 1772 by Scottish physician Daniel Rutherford, who called it noxious or fixed air. Although it can be difficult to create other compounds from elemental nitrogen, converting nitrogen-containing molecules back to N_2 gas is comparatively easy and often results in large, sometimes uncontrollable, energy releases. Nitrogen also occurs naturally in the form of solid minerals of ammonium salts, and as potassium nitrate, otherwise called saltpeter and known to alchemists since at least the Middle Ages. Purified nitrogen compounds, especially nitrate (NO_3-N), have two primary uses: as effective fertilizers, and as a main constituent of gunpowder and other incendiary devices (Leigh, 2004). Bat feces, or guano, is also an excellent and inexpensive source of crude nitrates. Like phosphorus, nitrogen is an essential nutrient and a key component of many crucial biological structures (e.g., amino and nucleic acids, neurotransmitters).

Since the primary form of nitrogen is as a stable atmospheric gas, natural systems must rely on processes that can break the triple bond since neither plants nor animals can directly access molecular N_2. Lightening strikes and volcanic activity produce localized amounts of bioavailable nitrogen that are dispersed with precipitation, a process known as atmospheric fixation. However, the naturally occurring main source of chemically accessible nitrogen is through direct bacterial fixation, the anaerobic process of converting N_2 gas directly to bioavailable forms. Once the triple bond is broken, nitrogen compensates for its nonreactive elemental state by a high propensity to combine with a seemingly endless number of ions and functional groups, only a small number of which are routinely analyzed (Table 3). The nitrogen cycle is a complex chemical tangle relative to that of phosphorus because of the strong atmospheric component (Figure 5). In addition to being vital nutrients, nitrogenous components are also important terminal electron acceptors for certain anaerobic forms of respiration. The chief constituents of the nitrogen cycle are bacteria and their ability to produce reactive forms of nitrogen, including ammonium, NH_4-N, and the far more watersoluble nitrate, NO_3-N (Figure 6). It is the propensity for nitrogen to occur as a stable, biologically inaccessible gas that traditionally made it a limiting nutrient, especially with coincidentally sufficient phosphorus sources.

From the years 1890 to 1990, anthropogenic inputs of reactive nitrogen to the global cycle increased almost nine times relative to preindustrial levels; primary sources include production of nitrogen-fixing crops (e.g., legumes, rice), extraction and combustion of fossil fuels, and the use of synthetic fertilizers (Galloway et al., 2003). In 1903 and1909, respectively, the Birkeland–Eyde and Haber–Bosch processes industrialized nitrogen fixation, with the latter globally established in the 1950s as the primary method (Figure 7; Smil, 2001). What cyanobacteria and other nitrogen-fixing bacteria had

Table 1 Phosphate (PO_4) mineral composition and the four primary apatite functional groups (R), of which fluorapatite is by far the most common. The crystal structure of all apatites is based on a double repeating unit, represented by the chemical formula being divisible by two (see also **Chapter 13.12**)

Common name	*Chemical formula*
Primary structure	$Ca_{10}(PO_4)_6(R)_2$
Fluorapatite	–F
Hydroxyapatite	–OH
Chlorapatite	–Cl
Bromapatite	–Br

Sources: Zumdahl SS (1993) *Chemistry*. Boston, MA: Houghton Mifflin; Wetzel RG (2001) *Limnology, Lake and River Ecosystems*, 3rd edn. San Diego, CA: Academic Press.

Table 2 Common analytical fractions of phosphorus. Organic and inorganic forms may co-occur in each fraction, and filtration is meant to separate soluble and insoluble contributions to the measure of total phosphorus. Concentrations in freshwater generally follow a gradient of [TP] > [TDP] > [SRP]. Phosphorus concentrations in surface water samples are often measured in $\mu g\ l^{-1}$ (parts per billion) of phosphate or $mol\ l^{-1}$ of phosphorus

Analytical fraction	*Abbreviation*	*Fraction and analytical separation*
Total phosphorus	TP	All phosphorus dissolved or suspended in the water sample; analyzed from unfiltered water following digestion
Total dissolved phosphorus Total soluble phosphorus	TDP TSP	Phosphorus analyzed from water after filtration through a 0.45 μm membrane filter and following digestion; the method is standardized to represent dissolved phosphorus, although fine particulates may be present in the filtrate
Soluble reactive phosphorus	SRP	Dissolved, biologically available phosphorus remaining in water filtered through a 45 μm membrane filter and analyzed within 12–24 h of sample collection
Particulate phosphorus	Part-P	All suspended and colloidal undissolved phosphorus, often determined by difference (TP − TDP)

Source: Eaton AE, Clesceri LS, Rice EW, and Greenberg AE (eds.) (2005) *Standard Methods for the Examination of Water and Wastewater*, centennial edition. American Public Health Association, American Water Works Association and Water Environment Federation joint publication.

Table 3 Common analytical fractions of nitrogen, based primarily on separation of organic and inorganic forms in dissolved and undissolved fractions. Surface water concentrations are often measured in $\mu g\ l^{-1}$ (parts per billion) of the compound or $mol\ l^{-1}$ nitrogen

Analytical fraction	*Abbreviation*	*Fraction and analytical separation*
Total nitrogen	TN	All nitrogen present within an unfiltered sample of water
Total Kjedahl nitrogen	TKN	All organic forms of nitrogen, both dissolved and undissolved, plus ammonia present in an unfiltered sample of water
Ammonia-N Ammonium-N	NH_3-N NH_4-N	A fraction of dissolved inorganic nitrogen often referred to as simply 'ammonia' although most methods measure NH_3-N + NH_4-N, the relative concentrations of which in surface waters are pH and temperature dependent; traditionally determined from an unfiltered sample, although many analytical instruments now require filtration
Nitrate	NO_3-N	A fraction of dissolved inorganic nitrogen and the conjugate base of nitric acid; analyzed from water filtered through a 0.45 μm membrane filter
Nitrite	NO_2-N	A fraction of dissolved inorganic nitrogen and the conjugate base of nitrous acid; analyzed from water filtered through a 0.45 μm membrane filter
Nitrate + Nitrite	NO_x	In practice, nitrate and nitrite are often measured together from surface water samples, since nitrite concentrations in the presence of oxygen are very small; analyzed from water filtered through a 0.45 μm membrane filter
Dissolved inorganic nitrogen	DIN	(NH_3-N + NH_4-N) + NO_x
Dissolved organic nitrogen	DON	TN − DIN

Source: Eaton AE, Clesceri LS, Rice EW, and Greenberg AE (Eds.) (2005) *Standard Methods for the Examination of Water and Wastewater*, centennial edition. American Public Health Association, American Water Works Association and Water Environment Federation joint publication.

been doing for billions of years prior, humans chemically engineered, and atmospheric nitrogen was converted into a commercially available product. Coincident with the synthesis of chemical fertilizers was the increase in use of fossil fuels and associated reactive nitrogen contributions. High rates of atmospheric nitrogen deposition have been implicated in causing conditions of nitrogen saturation (Aber et al., 1989), where chronic nitrogen inputs to forested ecosystems alter nitrogen cycling. Continuous nitrogen loading increases both nitrate losses in runoff and nitrogenous gas losses to the atmosphere, and decreases the ecosystem's ability to retain nitrogen, one side effect of which is increased nutrient input to receiving waters (see **Chapter 10.12**). Although food production created excess reactive nitrogen on purpose, the energy industry created it by accident (Galloway et al., 2003). In just over 100 years, the nitrogen cycle was short-circuited and supercharged with remarkable human efficiency.

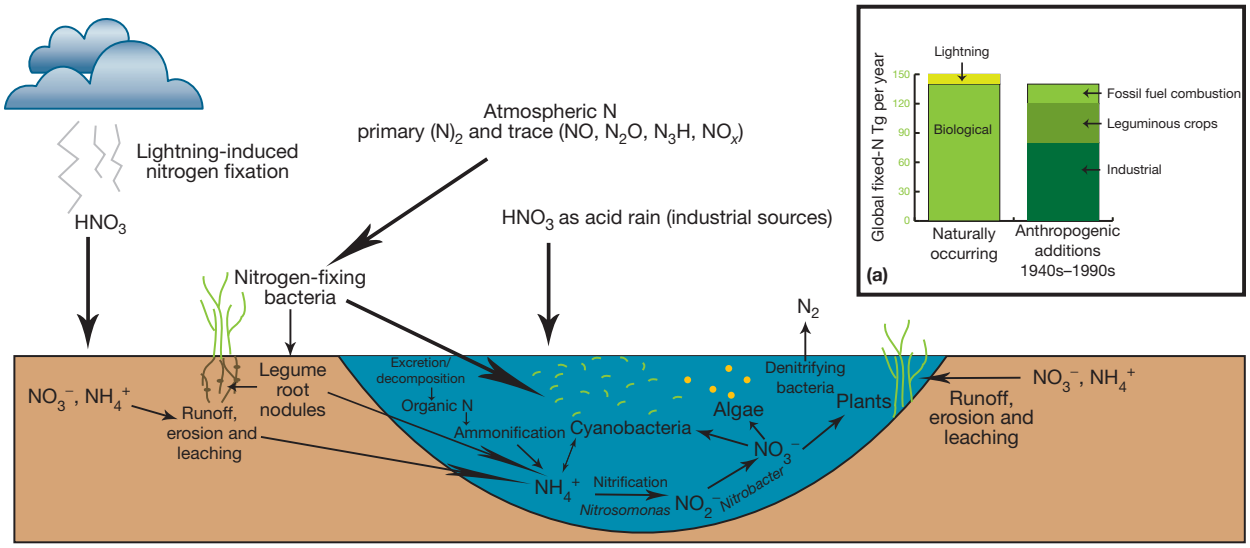

Figure 5 A simplified nitrogen cycle. Nitrogen reaches aquatic systems dissolved (NO_3-N) in water and adsorbed (NH_4-N) to particles moving in overland or shallow subsurface flow, or by direct fixation (of N_2) and deposition (of HNO_3). Although equilibrium occurs between ammonia (NH_3-N) and ammonium (NH_4-N) species, the latter is the dominant form present in most soil and freshwater systems and is the one represented here. Nitrogen cycling is driven by the activity of bacteria and fungi and is far more complex than is depicted here. The inset graph shows nitrogen at maximum ranges from natural sources compared to anthropogenic inputs. As with phosphorus, humans have roughly doubled the amount of nitrogen in circulation even when compared to the higher end of natural input estimates. Adapted from values in Vitousek PM, Aber JD, Howarth RW, et al. (1997) Human alteration of the global nitrogen cycle: Sources and consequences. *Ecological Applications* 7: 737–750.

11.8.3 Aquatic Ecosystem Structure

11.8.3.1 Nutrient Input Patterns

For aquatic systems, nutrient concentrations are measured from samples collected to address two primary input patterns:

- Point-source impacts from localized inputs (e.g., sewage outfalls), where paired samples are usually collected upstream and downstream of the pollution source.
- Nonpoint or diffuse impacts from unconfined sources (e.g., surficial runoff from disturbed soils, atmospheric deposition), where samples are collected all along the channel (time and funds permitting), or frequently at the most downstream point of the area of interest to represent cumulative watershed effect.

Nonpoint nutrient inputs are by far the more difficult of the two processes to measure and control, since transport is unconstrained by location and dependent upon geomorphology, level of watershed disturbance and surface and subsurface hydrology. Preventing or limiting eutrophication in aquatic systems has focused heavily on function and properties of the riparian zone, the area immediately adjacent to the channel bank or margin. Riparian zones are transitional areas that mark the interface between aquatic and terrestrial ecosystems, characterized by saturated soils and hydrophilic vegetation. They are often left as intact buffers to mitigate eutrophication impacts from overland and shallow subsurface nitrogen and phosphorus inputs into both lentic and lotic systems. Riparian zone effectiveness in reducing nutrient loading is highly variable between locations, and even within lengths along the same system. Removal of nitrogen from runoff prior to stream input is best achieved by riparian buffers of at least 50 m as subsurface removal appears to be a more effective mediator of excess nitrogen, and both herbaceous and forest–herbaceous riparian buffers are more effective at nitrogen conversion processes when wider (Mayer et al., 2006). Riparian buffers that retain persistent nitrogen inputs from agricultural sources may themselves become sources of forms of atmospheric nitrogen such as nitrous oxide (N_2O), an important greenhouse gas. This potentially trades prevention of aquatic nitrogen enrichment for an environmental impact of a different sort (Hefting et al., 2002).

11.8.3.2 Lotic Systems

Rivers, streams, brooks, and any other moving surface water constitute lotic systems. The classic assumption of flowing waters is that they do not experience the extreme, deleterious effects of eutrophication as do lakes, since any added nutrients or anoxia-inducing organic carbon loads are constantly aerated and moved downstream. Most flowing surface water is heterotrophic (Dodds, 2006; Hynes, 1975), meaning carbon is obtained from the surrounding landscape, or sources outside the stream channel (allochthonous), instead of within the water body itself (autochthonous). Hynes (1975) stated "the fertility of the valley rules that of the stream," meaning that it is the surrounding watershed, or all land draining into the stream, that defines its chemical character. The River Continuum Concept (Minshall et al., 1985; Vannote et al., 1980) stressed that lotic systems integrate physical gradients as they move through the landscape, linking processes upstream with those downstream. There are few effects in lotic systems that do not translate themselves somewhere else down the channel.

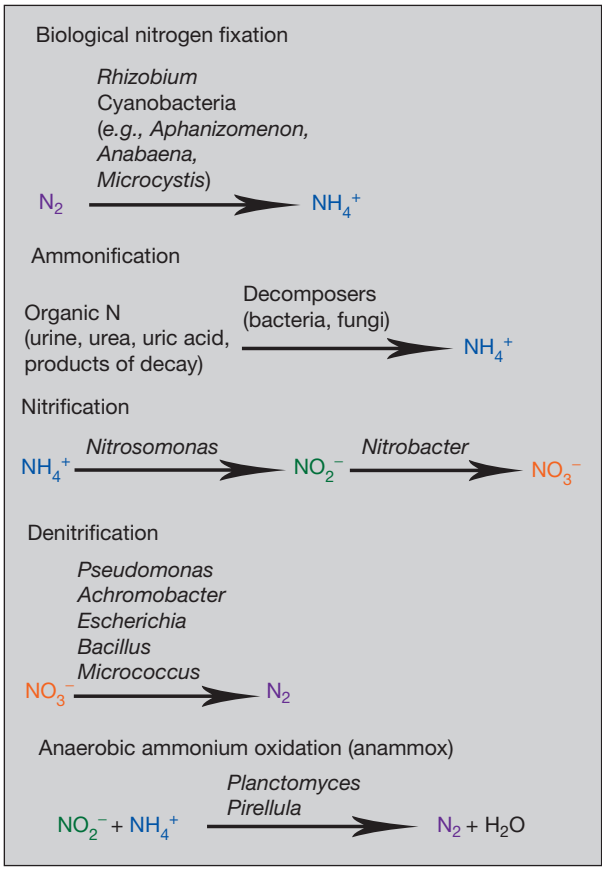

Figure 6 Nitrogen chemistry is often a consequence of bacterial and fungal activity. While some processes are strictly aerobic, such as oxidation reactions that produce NO_3^-, others (e.g., denitrification, anammox) are results of facultative anaerobes, which can function with or without the presence of oxygen. Adapted from equations in Wetzel RG (2001) *Limnology, Lake and River Ecosystems*, 3rd edn. San Diego, CA: Academic Press.

Trophic status (Table 4), or the measure of primary productivity relative to total phosphorus (TP) levels, has long been determined for lakes (Carlson, 1977), but the process has only recently been studied in lotic systems. Primary productivity is the amount of photosynthetic biomass obtained at a given time from a known volume of water, the most common equivalent measure of which is chlorophyll *a* (or chl*a* in $\mu g\,l^{-1}$). For flowing waters, trophic level has been proposed as a ratio of heterotrophic to autotrophic state. Respectively, these two states are determined by metabolic activity at night (oxygen demand for aerobic respiration) and gross primary production (accumulation of photosynthate mass) during daylight hours (Dodds, 2006). Regional stream trophic states provide a baseline for comparison between determined reference systems and lotic systems potentially affected by increased nutrient loading.

11.8.3.2.1 Determining order

Lotic systems constitute a network of surface water channels on the landscape that humans, with a propensity for classification, have divided into ranked orders. Channels are hierarchically categorized based on their Horton–Strahler number, a reflection of branching complexity (Figure 8). The index ranges from first order, for a small, headwater system with no tributaries, up to twelfth order at the mouth of the Amazon River. Approximately 80% of global lotic systems are first or second order (Waugh, 2002). Stream order is important when determining the effects of eutrophication on flowing water, since order is a reflection of both position in the landscape and size. For example, headwater streams are often small and respond rapidly to landscape perturbations (e.g., intense storms, flooding, fire, tree removal) relative to large, higher order systems, which reflect more collective effects.

11.8.3.2.2 Runoff, discharge, and loading rates

Relating a nutrient concentration to the landscape requires determination of watershed area, runoff, and discharge. A watershed consists of all land area surrounding a water body of interest where surface and shallow subsurface flow

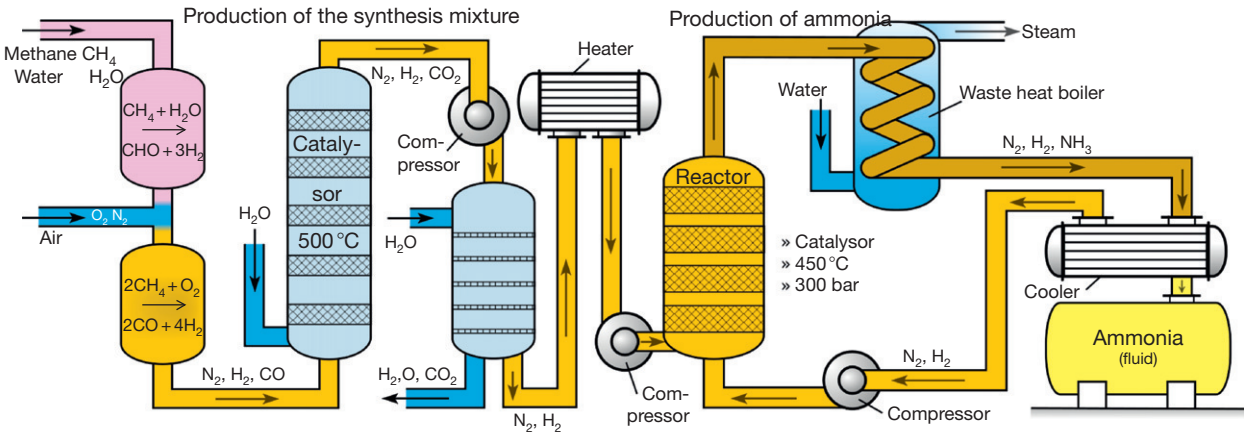

Figure 7 The anthropogenic alternative to biological fixation is the Haber–Bosch process of industrial fixation. The process is named after Fritz Haber, who developed the chemistry, and Carl Bosch, who scaled the method for industrial production. Both men later won Nobel Prizes for their efforts, and presumably credited the invaluable assistance of Robert Le Rossignol, who developed and built the requisite high-pressure system. Reproduced from Wright FE (2010) Flow diagram for the production of ammonia. Permission for use granted under the GNU Free Documentation License, version 1.2 or later.

Table 4 Trophic status of inland waters based on concentrations of epilimnetic total phosphorus (TP) and maximum chlorophyll *a* (chl*a*) and transparency as measured by Secchi disk depth. Trophic index (TI) is calculated using the three previous measurements as correlates. Note that as phosphorus and chlorophyll concentrations increase, transparency of the water decreases

Trophic status	*TP ($\mu g\ l^{-1}$) (Vollenweider, 1970)*	*Maximum chla ($\mu g\ l^{-1}$) (Mitchell and Prepas, 1990)*	*Secchi depth (m) (Carlson, 1977)*	*TI (Carlson, 1977)*
Oligotrophic	<5	<8	>8–4	<30–40
Oligomesotrophic	5–10	occasionally >8	–	–
Mesotrophic	10–30	8–25	4–2	40–50
Eutrophic	30–100	26–75	2–0.5	50–70
Hypereutrophic	>100	>75	0.5–<0.25	70–100+

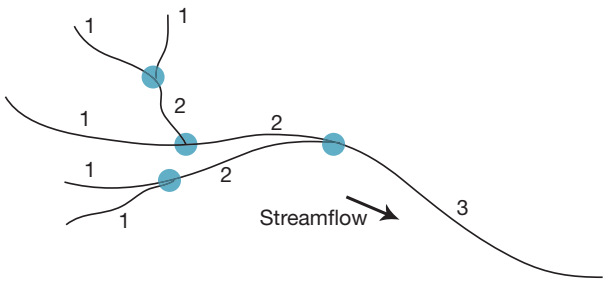

Figure 8 Stream order determination using the Horton–Strahler method. Streams are numbered based on branching hierarchy. Stream order only rises for downstream reaches after the confluence of identically ordered upstream systems. Reaches downstream of differently ordered stream confluences default to the stream with the highest order. Adapted from Brooks KN, Ffolliott PF, Gregersen HM, and DeBano LF (2003) *Hydrology and the Management of Watersheds*, 3rd edn. Ames, IA: Blackwell Publishing, Iowa State Press.

converge to a single point (Figure 9). Runoff is the precipitation within the watershed that reaches the channel as a contribution to flow, minus amounts lost to interception (e.g., soil wetting), evaporation (i.e., from soil, open water, leaf surfaces), transpiration (as a by-product of plant respiration), and landscape sinks (i.e., localized points of accumulation with slow or nonexistent outflow, and deep seepage to underground storage). Discharge is a measure of the rate of water volume flowing past a set location at a known point in time. Channel width, depth, and velocity are measured at regular intervals across a linear stretch of water (i.e., not at a bend in the river) to calculate discharge. Both discharge and runoff are used in conjunction to estimate loading rates. In general, areal loading rates are a product of nutrient concentrations and volume of discharge over a specified length of time divided by watershed area. Loading rates can change in response to season (e.g., decrease in nutrient release during periods of rapid plant growth, freezing in temperate systems), natural events (e.g., flooding, fire), or anthropogenic effects (e.g., agriculture, wetland conversion).

11.8.3.3 Wetlands

Regardless of the variation in form, wetlands are all defined by permanently or seasonally saturated hydric soils overlying a water table at or near ground level, characteristic hydrophilic plant cover, and often high biological diversity (Table 5). Wetlands provide a crossing point between terrestrial and aquatic systems, naturally different from each yet essential to both (Mitsch and Gosselink, 2007). The importance of wetlands in aquatic systems is being increasingly recognized as disproportionate to their areal presence on the landscape, which is especially true in lower latitudes (Krecek and Haig, 2006). Although globally protected in policy by the Ramsar Convention of 1971, wetlands, and particularly headwater wetlands, have come under steady pressure in the face of continued urban development, agricultural expansion, and forest harvesting practices. Wetlands provide regions in aquatic networks that function as:

- landscape filters via chemical deposition and binding
- areas that reduce surface water flow force
- collection basins for flood moderation in periods of high flow
- groundwater recharge zones

Additionally, wetland sediments can provide important adsorption sites for transported phosphorus, and increased surface area, oxic/anoxic zones, and bacterial availability for enhanced nitrogen cycling. Wetlands themselves are also important sources of colored dissolved organic carbon (CDOC), the presence of which can provide some short-term protection from the effects of increased nutrients (see Section 11.8.4.4.1). Although wetlands act as natural filters for adsorbed chemicals, particularly phosphorus, binding sites within the sediments can become exhausted with excess inputs. Rises in water levels (i.e., with storm events or snowmelt) can result in wetland discharge events that release nutrients to connected downstream systems. Wetlands can act as sinks during drier periods, or as sources of nutrients and other chemical constituents during times of increased water movement and landscape connectivity.

11.8.3.4 Lentic Systems

Lakes differ from wetland ecosystems in that they are more permanent water bodies, which may or may not be separated from direct contact with the water table, and which have, or seasonally develop, identifiable stratifications based on depth, light penetration, temperature, horizontal limits of plant growth, and trophic status (Figure 10; Table 4). Concentrations of dissolved oxygen (DO) and salts can also be factors in stratification of the water column. The intersection of adequate light availability, temperature, and nutrient levels are the main

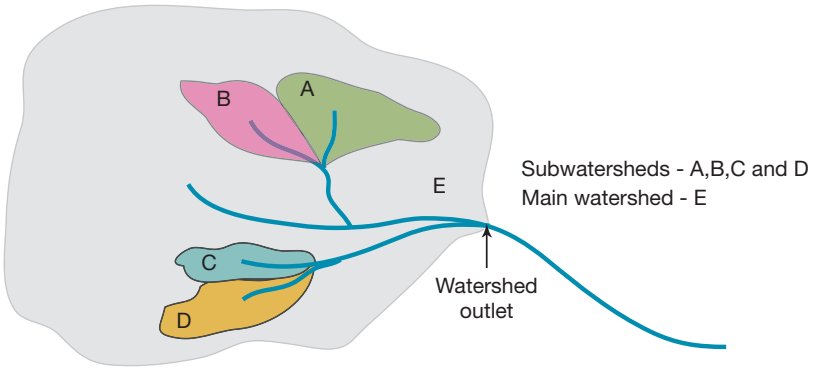

Figure 9 Watershed delineations are relative to position, since watersheds by definition converge to a single point. Small watersheds become part of larger watersheds as the point of reference moves downstream. The watersheds of downstream aquatic systems can quickly become very large as they incorporate the watersheds of all smaller systems flowing into them. Reproduced from Brooks KN, Ffolliott PF, Gregersen HM, and DeBano LF (2003) *Hydrology and the Management of Watersheds*, 3rd edn. Ames, IA: Blackwell Publishing, Iowa State Press.

factors that interact to create optimal conditions for green growth in lakes. When the control of nutrient limitation is removed, photosynthetic production can escalate dramatically.

When dissolved or adsorbed nutrients reach a lake their transport paths often diverge. Sediment-bound fractions will either settle quickly, sink slowly, or remain suspended as colloidal fractions, depending on sediment size and density. Dissolved fractions are subject to vertical and horizontal circulation patterns characteristic of the lake system, and more immediately available for uptake and use. As with wetlands, lakes can be both sinks and sources of accessible nutrients.

11.8.3.4.1 Temperature and mixing

Because of its inherent physical properties, water stratifies in response to temperature gradients within the water column. Cooler, denser water settles at the bottom, forming the hypolimnion, while a warmer, less dense layer remains at the surface, comprising the epilimnion; in between these two layers is a narrow region where the water temperature drops rapidly when measured from top to bottom (the metalimnion, or thermocline). Lakes will destratify and the water column will undergo mixing (turnover) with seasonal or wind effects that circulate the water (Figure 11). If turnover occurs once per year, the lake is said to be monomictic, and two turnovers per year classify a lentic system as dimictic. Lakes that only weakly stratify in warm conditions, such as shallow water systems, can undergo repeated mixing events and are said to be polymictic. Lakes that have multiple basins of varying depths which experience mixing in only parts of the lake (i.e., shallower regions) are meromictic. In tropical and subtropical regions, meromictic conditions prevail in very deep lakes which can remain persistently stratified in unfailingly warm temperatures, thermally isolating the colder hypolimnion.

In general, a metalimnion does not form in water that has cooled to the point of ice formation. In lakes which form ice during winter, gradual water density and temperature gradients will exist under ice relative to depth, with cooler, denser water located at the lake bottom. Temperatures at the surface can rise even while it is under ice cover, especially if low snow conditions permit increased light penetration and winter phytoplankton blooms. By late winter, lakes may exhibit chemical stratification in DO profiles near bottom sediments (Babin and Prepas, 1985). This is especially true in lakes with a high surface area to volume ratio and only weakly developed or shallow hypolimnetic zones in open water months. By late winter, DO concentrations in deep water may be at or near zero as oxygen is consumed by chemical processes at the sediment–water interface and by organisms that routinely overwinter in benthic regions. The resulting anoxic conditions and changes in hydrogen ion activity (pH) over the bottom sediments create a reducing environment conducive to liberating metal-bound and soil-adsorbed P fractions (Figure 12). The increased soluble P is circulated to surface waters in the spring after ice cover recedes and the seasonal rise in air temperatures results in lake water turnover. Shallow, polymictic systems are more susceptible to internal nutrient cycling regardless of location, due to their vertical compression and propensity for sediment and chemical resuspension.

11.8.3.4.2 Light, turbidity, and primary productivity

The majority of primary productivity in lakes is photosynthetic growth, which by definition requires sunlight. Concentrations of chl*a* ($\mu g\, l^{-1}$) are used to represent primary productivity, although it should be noted that not all photosynthetic pigments are restricted to being chlorophylls. Since chl*a* is measured from a known volume of filtered water, this can include any green growth suspended in the water column in addition to phytoplankton, such as small pieces of macrophytes (rooted aquatic vegetation) or zooplankton (microscopic animals) that have eaten green matter.

Primary productivity can be limited by conditions that constrain the depth of the euphotic zone, such as high turbidity. Turbidity is a measure of water column transparency which quantifies suspended material. The simplest method of measure is one which has changed little since its invention in 1865 by Father Pietro Angelo Secchi. Taking a Secchi depth involves lowering a 20 cm disk with alternating white and black quadrants over the shady side of a boat, ideally between 9 a.m. and 3 p.m. The midpoint between the depth at which the disk first disappears on the way toward the lake bottom and reappears on the way up is the Secchi depth. Multiplying this value by

Table 5 The five major wetland classes and associated characteristics

Wetland class	*pH range*	*Location*	*Hydrology*	*Dominant vegetation*
Bog	3–5	Arctic and subarctic regions, in areas of little to no relief	Receives only ombrotrophic (mineral poor) precipitation as water inputs; no runoff, little or no connection to groundwater	>40 cm peat accumulation; primarily *Sphagnum* moss, some willow (*Salix*), tamarack (*Larix*) and black spruce (*Picea mariana*)
Fen	5–8	Arctic and subarctic regions, in depression basins	Connected to groundwater, slow internal drainage; precipitation and moderate runoff as additional inputs	>40 cm peat accumulation; sedges (*Carex*, *Cyperus*), wildflowers, cedar (*Thuja*), tamarack and shrubs; little to no *Sphagnum* moss
Swamp	~7.2	Temperate to tropical regions, associated with streams, rivers, or lakes	Groundwater a primary input; may or may not be seasonally or annually flooded; may experience repeated flood 'pulses'	Trees and shrubs, predominantly dense coniferous or deciduous forests; not always immediately recognized as a wetland, especially during dry periods
Marsh	7–8	May be freshwater (primarily inland) or saltwater (primarily coastal)	Water inputs as groundwater, precipitation and runoff; can be important groundwater recharge areas	Reeds, rushes (*Typha*, *Phragmites*), grasses, sedges; also broad leafed and floated aquatic plants
Shallow open wetland	Similar to lakes and dependent on soils, bedrock and mode of origin	Transitional form between lake and marsh; many locations	Characterized by >75% open water; water column continually unstratified; water inputs from groundwater, precipitation, runoff and other water bodies	Depth <2 m; distinguished from lakes by at or near continuous submergent vegetation, such as milfoils (*Millefolium*); also duckweed (*Lemna*); emergent vegetation restricted to perimeters

Source: National Wetlands Working Group (1997) In: Warner BG and Rubec CDA (eds.) *The Canadian Wetland Classification System*, 2nd edn. Waterloo, ON: Wetlands Research Centre, University of Waterloo.

two gives, roughly, the depth of the lower limit of the euphotic zone (**Figure 10**; Lind, 1985). Turbidity can also be measured using a light meter, or with a collected water sample and a nephelometer. Each method relies on the same mechanism, which measures turbidity as equivalent to the amount of light reflected off the particles suspended in the water. Despite variation in results between users, Secchi depth is almost always collected as a contributing measurement to determining trophic index, since it is easy to take and the equipment rarely malfunctions even in the hands of the most inexperienced operator.

Turbidity is a major factor affecting primary productivity in that it affects light penetration into the water column. High turbidity can be caused by suspended sediments and inorganic particles, or by an active bloom itself. In this manner, certain species of phytoplankton that are unable to regulate their buoyancy and move to sunlight at the lake surface are self-limited in large blooms which decrease light penetration and reduce euphotic zone depth. However, shallow lakes can exhibit alternate stable states over a wide range of nutrient concentrations, of either macrophyte-dominated transparent conditions or phytoplankton-dominated turbid conditions. Turbidity measurements used to determine trophic status would not always accurately reflect primary productivity or related nutrient concentrations in bistable shallow water systems (Scheffer et al., 1993).

Seasonally in temperate regions and year round in polar regions, light penetration into the water column is also attenuated both by ice and snow cover, with primary productivity in temperate lakes usually at annual lows during winter months. Subtropical and tropical systems have no such limitations, and primary productivity in these regions is most often a function of nutrient availability, turbidity, and wind mixing.

11.8.3.4.3 Nutrient ratios and phytoplankton dynamics

The relative concentrations of requisite elements to each other have been used as an index of bloom dominance in lentic systems since Redfield (1934) determined the ratio of C:N:P for marine phytoplankton was 106:16:1, now suggested as an average stoichiometric ratio instead of an optimum (Klausmeier et al., 2004). In freshwater systems, ratios of epilimnetic nitrogen to phosphorus are often used to predict phytoplankton species dominance. Ratios of N:P that are approximately 16 are considered optimal for phytoplankton production in general. Ratios of N:P > 20 are defined as phosphorus limited and favoring green algae, and N:P < 10 are considered nitrogen limited, favoring cyanobacteria (Bulgakov and Levich, 1999). The composition of nutrient sources has also been suggested as playing a strong role in lake total nitrogen (TN) to TP ratios, where trophic status corresponded with TN:TP ratios. High TN:TP ratios (i.e., low TP concentrations) are found in oligotrophic lakes, where natural systems release much less phosphorus than nitrogen in runoff, and moderate TN:TP values corresponded to mesotrophic lakes with runoff from a larger variety of more fertile sources. Extremely low TN:TP values (i.e., very high TP concentrations) have been related to eutrophic systems whose ratios approximated that of sewage (Downing and McCauley, 1992). Although all blooms are seen as degradations in water quality, cyanobacteria have the potential to release potent

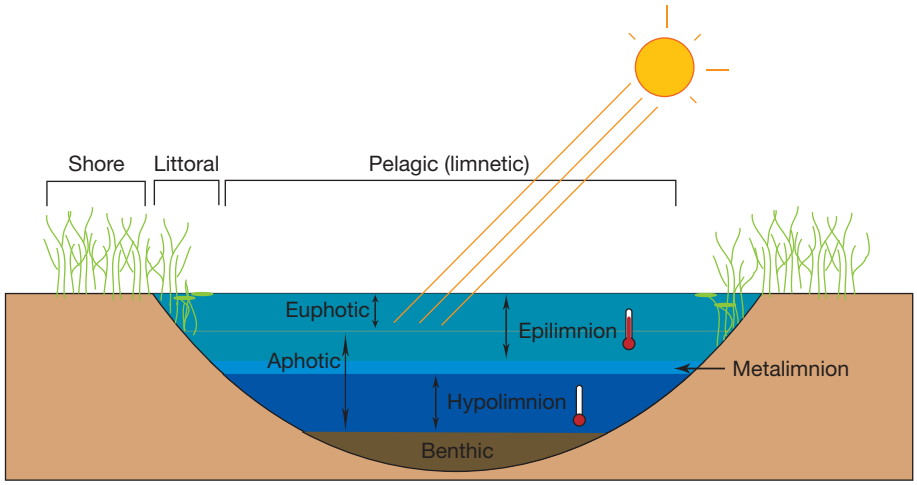

Figure 10 Lakes zones are delineated based on physical location (e.g., littoral, pelagic, benthic), light availability (e.g., euphotic, aphotic) and temperature (e.g., epilimnion, hypolimnion). Although lower limits of the euphotic and epilimnetic zones may sometimes occur at the same depth, this is not always the case.

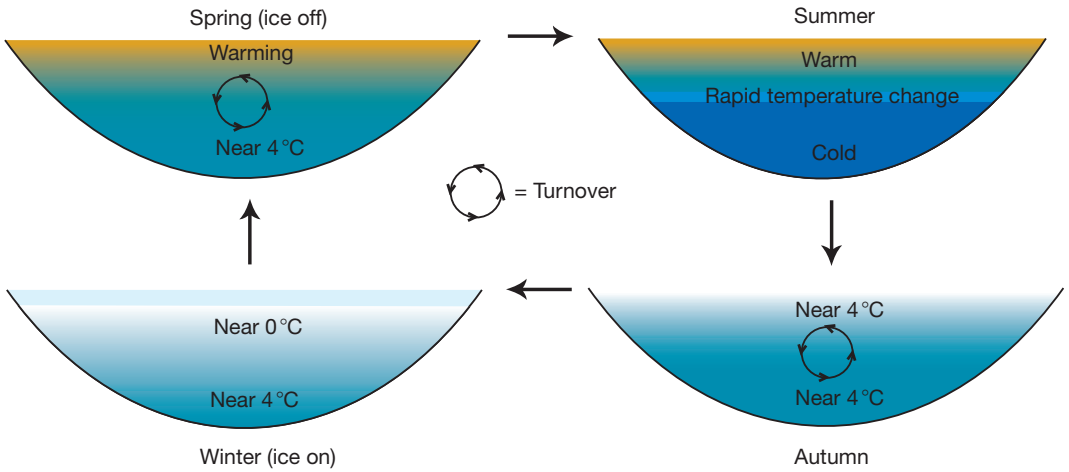

Figure 11 In temperate regions, lakes undergo seasonal stratification and mixing events. Shallow temperate lakes can mix and restratify repeatedly over summer months, while the hypolimnion in deeper lakes remains isolated until turnover events. The hypolimnion in very deep temperate lakes may not mix completely. Also, temperate and arctic lakes may stratify in winter months if algal blooms raise temperatures under the ice cover. At lower latitudes, deeper lakes trend toward depicted summer conditions year round, with shallow lakes subject to destratification from moderate cooling and wind events. The hypolimnion in very deep subtropical and tropical lakes may only rarely mix. Adapted from Mitchell P and Prepas E (eds.) (1990) *Atlas of Alberta Lakes*. Edmonton, AB: The University of Alberta Press.

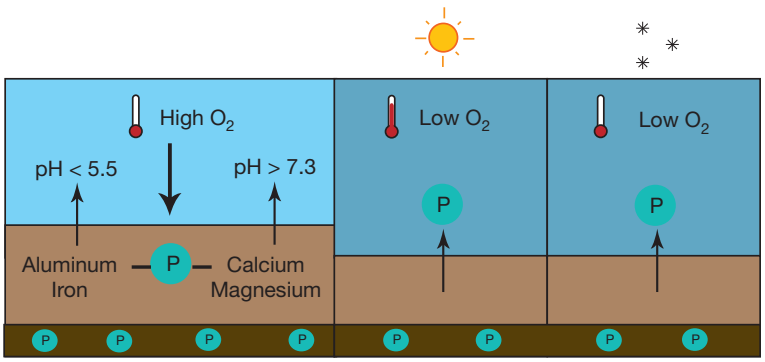

Figure 12 Phosphorus release from bottom sediments is affected by oxygen concentration and pH. Phosphorus will preferentially bind to many metals and form precipitates, but will return to the solution pool under reducing conditions, or if pH reaches acidic or alkaline levels. Low oxygen levels can occur in warm water, which is unable to maintain high dissolved oxygen concentration, but can also occur in cold water where oxygen has been depleted by consumption. Migration of phosphorus to the stored pool occurs with increased sedimentation and isolation from the water column. (see also **Chapter 13.2**)

toxins upon the death and decay of the active bloom and are held in even lower favor than algal blooms. Eutrophication is often followed by shifts in phytoplankton assemblages toward cyanobacteria, which are well suited to exploiting phosphorus-rich environments and outcompeting algal species (Steinberg and Hartmann, 1988).

11.8.4 Eutrophication

11.8.4.1 Ecological Succession versus Eutrophication

When an increase in nutrients occurs from either point sources or diffuse entry and increases primary productivity, quantified as chl*a* in $\mu g\ l^{-1}$, and causes a shift in trophic status, an aquatic system is said to be experiencing eutrophication. The distinction is important. Seasonal or otherwise intermittent nutrient increases may incur discrete bloom events, but a shift in trophic status requires nutrient inputs at a higher, sustained level. A resulting change in ecological functioning is indicative of true eutrophication.

With ecological succession, changes in trophic status are usually measured on longer timescales, that is, in the order of hundreds or thousands of years, although catastrophic events such as landslides or forest fires can accelerate this progression (see **Section 11.8.4.2**). Traditional succession theory classifies most surface water forms as intermittent features on the landscape. Younger systems begin as oligotrophic (nutrient-poor) water bodies that gradually experience sedimentation over time; the accumulated sediments fill the water body, physically changing shape, depth, and volume, and also altering it chemically through solution–dissolution processes at the sediment–water interface (Sawyer, 1966). This implies that existing aquatic systems are positioned as points on a temporal gradient that will naturally converge to eutrophication. Accelerating successional processes causes problems that can prove extremely difficult to reverse. Response to external conditions has been proposed as system dependent, relating loss of resilience to rate of ecosystem perturbation. Systems with low inherent capacity to change may experience dramatic shifts in structure and function relative to systems with greater elasticity to either stochastic or persistent events (Scheffer et al., 2001). Even relatively constant aquatic systems can experience catastrophic change in the face of introduced and unrelenting pressures.

11.8.4.2 Natural Eutrophication

Natural eutrophication has been separated from ecological succession to differentiate their relative time scales. While succession occurs over long periods, eutrophication as a result of either rapid increases in nutrient inflow rates or in-system concentration of nutrients does occur naturally in the form of:

- landslides
- mass wasting events (e.g., sediment deposition from flooding, beaver dam breaks)
- seasonal drought
- precipitation events following fire

The classification of drought-induced natural eutrophication becomes complicated beyond seasonal limits, when long-term trends of human-caused climate effects are considered and exceed estimated thresholds of what can be called natural.

11.8.4.3 Cultural Eutrophication

Hasler (1947) defined the term cultural eutrophication as an increase in the rate and intensity of harmful algal blooms occurring as a direct result of human-caused nutrient loading. Eutrophication from human-caused effects is often related to postindustrial era impacts. However in North America recent paleolimnological work suggests even prehistoric humans altered the trophic status of a lake through runoff from nearby permanent settlements and agricultural activities (Ekdahl et al., 2004). Cultural eutrophication has accompanied major milestones in human advancement, including:

- modernized agricultural practices (e.g., fertilizer use, manure inputs, pesticides bound to organophosphate adjuvants)
- population growth
- industrial activity (e.g., synthetic fertilizer production, fossil fuel extraction and combustion, forest clearcutting, agricultural practices)
- introduction of the flush toilet and centralized sewage treatment
- use of phosphate-containing cleaning agents (e.g., detergents, degreasers)
- urbanization and associated increases in impermeable surfaces (e.g., concrete, asphalt, rooftops)
- remote resource access and associated road construction
- wetland conversion and failure to protect sensitive areas

Anthropogenic pursuits have altered biogeochemical pathways for nitrogen and phosphorus in a dramatic fashion. That human activities are supplying an excess of biologically available nutrients to aquatic systems is clear; how we will mitigate cumulative effects from disparate sources is less so.

11.8.4.4 Conditions that Affect Eutrophication

There are naturally occurring situations that can limit or exacerbate the effects of eutrophication, with some being more seasonal and less persistent than others. Mechanisms include light limitation, precipitation, and extremes in water chemistry that either limit phytoplankton growth in the presence of nutrients, or affect internal nutrient cycling from the water column to the sediment layer.

11.8.4.4.1 Dissolved organic carbon

Carbon is the chemical foundation of all known life and in elemental form exists as stable, tetravalent allotropes of single carbon atoms combined with four hydrogen atoms. Although required for growth and development, carbon is not usually considered a limiting resource since it is readily available in both terrestrial and aquatic systems, and has a significant atmospheric component in its cycle. DOC is receiving increased research attention for its ability to absorb ultraviolet (UV) radiation, specifically photosynthetically active radiation (PAR). Since PAR is a requisite for photosynthesis in rooted aquatic plants (macrophytes), phytoplankton (microscopic plants and single-celled organisms) and cyanobacteria, a decrease in the depth to which light can penetrate water bodies can potentially limit primary production. However, not all DOC is created in the same manner nor in the same locations,

and the source can affect the structure. Forms of DOC originate as the products of decay or waste matter and can be divided into either colored DOC or uncolored DOC. The latter includes soluble fats, proteins, and carbohydrates that have no appreciable light absorbing capabilities and are often from autochthonous sources. Occurrence of CDOC is primarily a result of plant constituents (e.g., cellulose, lignins, tannins) that decompose and create complexes of humin, and humic and fulvic acids, often from allochthonous sources such as wetlands (**Table 6**; Wetzel, 2001; Williamson et al., 1999). Light attenuation due to CDOC exhibits seasonal variation in surface water, and effects are primarily restricted to the spring season in temperate regions. Solar radiation eventually decomposes colored complexes into simpler forms of uncolored DOC through photodecay or photobleaching (Molot and Dillon, 1997; Osborn et al., 2001), which then no longer inhibits light penetration into the water column see also **Chapters 7.8** and **12.6**).

11.8.4.4.2 Salinity

A saline freshwater lake may sound like a contradiction in terms, but in arid and semiarid regions, hydrologic processes that concentrate freshwater can occur resulting in extremely high total dissolved solid (TDS) concentrations (**Table 7**). Saline lakes occur in landlocked systems where net water losses (evaporation, transpiration) have exceeded net water inputs (precipitation, runoff, groundwater) for long enough that TDS concentrations exceed 500 mg l^{-1} (Mitchell and Prepas, 1990). Saline lakes exhibit unique flora and fauna and often low biodiversity, reflecting adaptations not present in most freshwater species for surviving high solute environments. There are instances of saline lakes receiving high nutrient inputs, given their co-occurrence with agricultural operations in grassland and prairie environments, or with indigenous animal populations in desert and polar environments. Despite high levels of total P (0.15–24 mg l^{-1}), some saline lakes fail to exhibit classic symptoms of eutrophication and instead show low primary productivity from limiting levels of iron (Evans and Prepas, 1997), although naturally eutrophic conditions have been observed in Antarctic lakes surrounded by a large penguin rookery (Bell and Laybourn-Parry, 1999). The hypersaline Great Salt Lake, Utah, exhibited increased chl*a* levels following experimental nutrient enrichment only when salinity levels were low enough for cyanobacteria to exist in the lake ($\leq$70 mg l^{-1} for this system) (Marcarelli et al., 2006). Overall, salinity levels in aquatic systems need to be very high for nutrient inputs not to increase chl*a* production, and high salinity in itself does not appear to reduce dissolved nitrogen and P concentrations.

Table 6 Dissolved organic carbon (DOC) and constituents of uncolored and colored (CDOC) fractions, with fractionation solubilities for CDOC

DOC fraction	*Constituents*	*Solubility*
Uncolored DOC	Decayed plant debris, polysaccharides, lignins, proteins	–
CDOC	Humin	Insoluble in acids and alkalis
	Humic acid	Insoluble in acid Soluble in alkalis
	Fulvic acid	Soluble in acids and alkalis

Source: Sparks DL (2003) *Environmental Soil Chemistry*, 2nd edn. San Diego, CA: Academic Press.

Table 7 Salinity levels and corresponding total dissolved solid (TDS) concentrations

Classification	*TDS (mg l^{-1})*
Freshwater	<500[a]
Slightly saline	500–1000[a]
Moderately saline	1000–5000[a]
Saline	>5000[a]
Ocean water	~35 000[b]

[a]Mitchell P and Prepas EE (1990) *Atlas of Alberta Lakes*. Edmonton, AB: University of Alberta Press.
[b]Office of Naval Research (http://www.onr.nav.mil/).

11.8.4.4.3 Fire

Effects of fire on aquatic nutrient enrichment relate to the size (area burned) and intensity (vertical heat transfer) of the fire itself. Nitrogenous compounds volatilize fairly easily (200 °C) and are often lost to the atmosphere in proportion to combusted organic matter. Phosphorous compounds have higher heats of volatilization (>500 °C) and are more likely to be transported as particulates in ash during the fire, or in the first rainy season postfire during wind erosion and runoff events (Boerner, 1982; Debano and Conrad, 1978). Water quality in five streams in Iowa, USA, degraded following fire. Although NO_3-N concentrations were higher in burned streams compared to reference streams, the negative effects on water quality were mostly related to increases in fine sediment transport and particulate organic matter. Stream periphyton (algae and bacteria growing on submerged aquatic surfaces) decreased following fire, possibly as a result of increase turbidity and light limitation (Minshall et al., 2001). Boreal subarctic headwater peatland lakes subject to fire experienced increases in P and inorganic nitrogen fractions, but no associated increase in chl*a*. This was also related to light limitation as a result of concurrent increases in DOC concentrations (McEachern et al., 2000). Ranalli (2004) summarized that measureable water quality effects following fire were likely if:

- receiving waters were oligotrophic or mesotrophic
- the residence time of the water body was short relative to the length of time nutrient concentrations remain elevated in runoff
- the watershed had steep slopes
- soil cation exchange capacity was low or nonexistent

11.8.4.4.4 Drought

Drought is a regular component of ecosystems in many regions, and considerations of its impacts have largely considered biotic survival during low flow periods. Overland transport of dissolved and adsorbed nutrients is limited or nonexistent in drought conditions, and water inputs are

restricted to those available from groundwater or direct precipitation. Drought accompanied by elevated temperatures may reduce water levels through evaporation. In a simulated summer drought, denitrification increased with drought severity and ammonium concentrations were severely decreased (Dowrick et al., 1998). Such a scenario would favor cyanobacterial dominance in phytoplankton communities as phosphorus, with no significant atmospheric component in its cycle, would increase in relative concentration in tandem with N depletion and further decrease the N:P ratio.

11.8.5 Two Case Studies in Eutrophication

The rate and magnitude of recovery from eutrophication can be highly variable. Response to nitrogen and phosphorus input control measures range from rapid return to preimpact conditions, to chronic effects of nutrient overenrichment. Hysteresis, or the lagging of the response following the impact, means eutrophication effects will persist in certain systems long after control measures have been put in place. This may require more consistent defense of management methods in the face of what appears to be maximum effort but minimal results. The following case studies provide examples of different nutrient input sources, aquatic system responses, and mitigation efforts undertaken in reaction to instances of cultural eutrophication (Table 8).

11.8.5.1 A Point-Source-Impacted Deep Water Lake

Lake Washington remains a classic case of point-source pollution and recovery, and a story that reflects both the commitment of individuals and the inherent characteristics of the lake itself (Figure 13). Lake Washington is situated in a heavily populated metropolitan area including the city of Seattle and neighboring smaller cities in the state of Washington, USA. The Cedar and Sammamish rivers are the primary inlets (90% of inflow), with only a few secondary inlets contributing an additional 10% of inflow. The original outlet was the Black River, which emptied into Puget Sound on the Pacific Ocean. However, the Black River was by-passed with the opening of the Lake Washington Ship Canal in 1917, which dropped the lake level approximately 3 m, permanently separated the two water bodies and dried out the river (Crowley, 1999). Currently, the sole outlet remains the Lake Washington Ship Canal, which also discharges into Puget Sound.

Beginning in the mid-1800s, Lake Washington began receiving sewage inputs from surrounding communities, including the then fledgling city of Seattle. In 1922, there were 30 sewage outfalls from Seattle draining into the lake, despite it being the city's source of drinking water, and despite a typhoid outbreak in 1907. Sewage from the west side of the lake was diverted to Puget Sound after completion of infrastructure in 1936 (Edmondson, 1991). In 1933, prior to full completion of the sewer diversion, the lake had been characterized as being in good condition, with low nutrient concentrations and high annual deep water DO concentrations (Scheffer and Robinson, 1939).

Despite the efforts at sewage diversion in 1936, from the 1940s to the 1950s, 11 additional secondary sewage treatment plants were in operation and discharging to Lake Washington. By 1963, the lake was significantly polluted and experiencing large and frequent summer algal blooms with accompanying decreased water clarity and increased chl*a* concentrations. Death and subsequent decay of the blooms released noxious odors and decreased deep water DO concentrations, severely hampering sport fishing and other recreational activities. By the 1960s, the trophic status of Lake Washington had degraded from mesotrophic to eutrophic (Edmondson, 1991). Concerted action from the community to improve the water quality in the lake was aided tremendously by the research and support of the late W.T. Edmondson, and in 1958, a public vote resulted in sewerage upgrades that diverted sewage flow away from the lake for a second time. Construction commenced in 1963 and after completion in 1968 the water quality rapidly improved. By 1975, the water once again had returned to mesotrophic conditions, with high mid-summer transparency, low nutrient levels (17 $\mu g\ l^{-1}$ P) and low phytoplankton abundance (Edmondson, 1977).

Lake Washington's remediation has much to do with its physical characteristics (Table 8). The lake is long and thin, with limited amounts of shallow areas, and only two defined inflows of water with low P concentrations. The reasonably small residence time (2.4 years) means water in the lake is replaced by inflow in fewer than 3 years. The lake is fairly deep, and sediment-bound nutrients that reach the bottom are unlikely to be repeatedly resuspended into the water column; P losses to sediments have been estimated at 49% of

Table 8 Comparison of physical parameters between Lake Washington, USA and Taihu Lake, China. The range for residence times and flushing coefficients for Taihu Lake reflect the numerous bays and variable water movement and storage patterns across this lake. Note that flushing coefficients are the inverse of residence time

Water body	*Current trophic status*	*Watershed area (km^2)*	*Surface area (km^2)*	*Maximum depth (m)*	*Mean depth (m)*	*Volume (m^3)*	*Residence time (year)*	*Flushing coefficient ($year^{-1}$)*
[a]Lake Washington, USA	Mesotrophic	1270	88	65	33	3.0	[c]2.4	[d]0.4
[b]Taihu Lake, China	Hypereutrophic	36500	2428	2.6	1.9	4.3	[e]0.3–12.8	[e]0.08–3.1

[a]Edmondson WT (1991) *The Uses of Ecology: Lake Washington and Beyond*. Washington, DC: University of Washington Press.
[b]Xu H, Yang LZ, Zhao GM, Jiao JG, Yin SX, and Liu ZP (2009) Anthropogenic impact on surface water quality in Taihu Lake region, China. *Pedosphere* 19: 765–778.
[c]International Lake Environment Committee-World Lake Database http://wldb.ilec.or.jp/ (accessed January 2011).
[d]Major Lakes Monitoring-King County Water and Land Resources Division http://green.kingcounty.gov/ (accessed April 2011).
[e]Hu L, Hu W, Zhai S, and Wu H (2010) Effects on water quality following water transfer in Lake Taihu, China. *Ecological Engineering* 36: 471–481.

Figure 13 Siegmund W (2006) Lake Washington, Interstate 90, Lacey V. Murrow Memorial Bridge, Seattle, Washington, USA. Permission for use granted under the GNU Free Documentation License, version 1.2 or later. The view from this vantage point shows the heavy settlement around Lake Washington's shoreline.

Figure 14 Unnamed source (2007) Taihu Lake. Released to the public domain 5 June 2007. This image, taken on 6 May 2006, shows an unnamed bay of Taihu Lake with light green water characteristic of an eutrophication event. In May of the following year, a massive cyanobacterial bloom prevented at least 2 million people from accessing their main source of freshwater. Information from Kahn J. 13 October 2007. Part 3: In China, a lake's champion imperils himself. The New York Times, Asia Pacific.

annual inputs (Edmondson, 1991). As Edmondson recognized, Lake Washington was an excellent candidate for rapid recovery once the identifiable problem of point-source sewage input was rectified. It should be noted, however, that the lake's improvement came at the expense of Puget Sound as the alternate receiving body for continued sewage discharge, which translates more into relocation than remediation.

11.8.5.2 A Nonpoint-Source-Impacted Shallow Water Lake

Shallow water lakes are recognized as dynamic, polymictic systems driven by sediment–water interactions that make them susceptible to long-term chronic eutrophication effects (Scheffer, 2004). Taihu Lake is one such example (**Figure 14**). Located approximately 100 km west of Shanghai, and positioned in the lower regions of the Yangtze River delta in one of the fastest developing areas of the country, Taihu is the third largest freshwater lake in China. The lake is situated in an area of low relief and its watershed receives loading from agriculture, industry and a human population at one of the highest densities in the world at nearly 1000 people per square kilometer (Chang, 1987). For these reasons, sediment loading and anthropogenic effects are major concerns for lakes in the region. The lake is a key drinking water source for many of the inhabitants of the surrounding areas and home to important fisheries for eel, crab, and carp.

Although the ratio of watershed area to surface area is similar between Lake Washington and Taihu Lake (14.4 and 15.0, respectively), depth and flow patterns are considerably different between the two lakes (**Table 8**). The range of flushing rates for Taihu Lake reflects its complex bathymetric characteristics. The lake receives inputs from an estimated 172 surface inflows, some of which can reverse flow in drier months. Water retention times are variable between major bays, with shorter residence times in the south and east portions of the lake relative to those in the north, particularly Meiliang Bay (Qin et al., 2007). Taihu Lake's large surface area is also susceptible to wave formation and wind mixing, which readily resuspend bottom sediments. In the 1980s, Taihu Lake began experiencing noticeable cyanobacterial blooms along its north end. In 2001, the presence of cyanotoxins was confirmed from samples collected in one of the lake's bays (Shen et al., 2003). In 2006, the lake experienced an enormous bloom dominated by cyanobacteria, which covered two-thirds of the lake surface and left millions of residents without drinking water.

Given Taihu Lake's large surface area, shallow depth, and soft littoral sediments, system recovery has been significantly affected by hysteresis. Superficial lake sediments are subject to wind mixing, which induces frequent resuspension of internal nutrients (Qin et al., 2004). Mechanisms responsible for macrophyte dominance in a clear water stable state (Scheffer et al., 1993) are being explored as remediation possibilities (Qin et al., 2003), while effective nutrient management plans continue in their development. Bulk water transfer to several heavily eutrophied bays has met with only limited success. Reductions in total P concentrations were noted, but only weak declines in total N and chl*a* concentrations were evident (Hu et al., 2010). It is highly likely that multiple, concurrent treatments will be required for successful remediation. The size, complex geometry, variable water retention times and numerous inputs into Taihu Lake render it an unlikely candidate for matching the rapid rehabilitation of Lake Washington.

11.8.6 Future Opportunities

The key to effective eutrophication control is balance, and recognizing when anthropogenic impacts require an equivalent effort in control and remediation. Although eutrophication can and does occur naturally, human-caused instances are increasing in number and intensity as remediation methods lag behind intensified inputs. There are many prospects for eutrophication control in systems where nutrient limitations and internal cycling processes have been removed or disrupted by human activities.

11.8.6.1 Management

Since all forms of P originate as mined or weathered minerals, sources are finite, and predictions have been made for the occurrence of peak phosphorus, the point at which resource depletion is matched by production capacity. After this point, resource availability decreases, resource quality declines, and finished product price increases dramatically, reflecting the growing difficulties in extraction and production. The Hubbert linearization curve (Hubbert, 1974) predicted the case of peak oil in the 1970s; applying the same principles for phosphorus has resulted in predictions for peak phosphorus ranging from 1989 (Dréy and Anderson, 2007) to roughly 2030 (Cordell et al., 2009). When the peak will occur is secondary to the certainty that it will occur. Alternatives may be found for oil, but elemental phosphorus is irreplaceable. However, phosphorus can be reclaimed and research opportunities require focus on increased efficiency of use, in situ retention and greater recapture and reuse, all of which can also reduce the effects of eutrophication. Efforts include:

- manure capture and urban mining (use of human sewage) for both direct fertilization and purified fertilizer production;
- human population control to reduce agricultural pressure;
- improvements in sanitation, including low water-use systems ranging from in-house to large municipal applications;
- use of green water (soil water) versus blue water (surface and groundwater) for global resource and food production; this relates more to tailoring renewable products to local growing conditions than to the amount of water required to grow the crop, and limits the risk of eutrophication from anthropogenic drought.

Alleviating eutrophication effects in situ has involved the use of established methods, such as hypolimnetic withdrawal (Nürnberg, 1987), hypolimnetic oxygenation (Prepas and Burke, 1997), or phosphorus precipitation following addition of calcium carbonate and lime (Prepas et al., 1990), all of which reduce nutrient concentrations from the dissolved pool. The pivotal example of Experimental Lake 227 (Schindler, 1974) led to the restriction of phosphate use in many detergents, an important watershed-level control measure. However, in Canada, as an example, measures to address additional sources such as automatic dishwasher detergents have only been put in place as recently as 2010 (Government of Canada, 2009), industrial sources of phosphate have not been well addressed, and agricultural and municipal runoffs remain important contributors (**Table 9**). These sorts of persistent, nonpoint nutrient inputs require additional characterization and preventive options relative to the more easily addressed point-source impacts. Future research and special consideration will also be required for sensitive areas such as shallow lakes, wetlands, and headwater systems. As natural nutrient conversion factories and early warning indicators of cumulative effects, these systems will need to function at full force for both detection and mitigation of eutrophication.

Table 9 Approximate phosphorus contributions from major sources to Canadian surface waters

Source	*Phosphorus load*	
Municipal waste, sewers and septic systems	14.3%	53% human waste 11% household cleaners and detergents 36% commercial and industrial sources
Industry	2.9%	
Agriculture	82.1%	
Aquaculture	0.7%	

Source: Adapted from values in Chambers PA, Guy M, Roberts ES, et al. (2001) *Nutrients and Their Impacts on the Canadian Environment*. Hull, QC: Agriculture and Agri-Food Canada, Environment Canada, Fisheries and Oceans Canada, Health Canada and Natural Resources Canada.

11.8.6.2 Monitoring

Long-term datasets can improve predictability by providing a solid base of accumulated information against which to test ecological modeling scenarios. Accumulated monitoring data also allow for the identification of trends and risk factors, where planning knowledge could minimize costly reclamations. Changes in trophic status represent a regime shift. These shifts may be preceded by an increase in variability discernable from levels inherent in ecological systems. Simulations suggest that higher standard deviations in summer epilimnetic P concentrations could precede a shift to eutrophic conditions by about a decade (Carpenter and Brock, 2006). Long-term monitoring data can provide validation for these types of predictive models that have the potential to sound the alarm before the effect is noticed.

Remote sensing is increasing in ecological applications as resource extraction moves farther from urban centers, and personnel, time, and funding for direct ecosystem sampling may be untenable. Identifying and monitoring sensitive and responsive critical areas, such as wetlands and headwater streams, will help in targeting prevention and mitigation efforts. Critical zones can be used as indicators of excess nutrient transport prior to downstream cumulative effects. As well, much remains unknown about phytoplankton community shifts in response to eutrophication. Ongoing analyses of phytoplankton community structure in Lake Washington and its response to nutrient inputs and subsequent control would not be possible without long-term ecological monitoring.

11.8.7 Conclusions

Improvement in trophic status is possible, although the case studies suggest some systems will exhibit prolonged response to eutrophication and require continued and determined management efforts. The detrimental effects of eutrophication are large and will continue to grow unless the influx of excess nutrients can be reduced, retained or redirected away from vulnerable surface waters. As Bill Bryson (2005) writes regarding species extinctions, humans are ". . . so remarkably careless about looking after things." Unfortunately, the same can be said for our attention to the functioning of many aquatic systems. In pursuit of food, shelter and water, we have maximized the first two at the expense of the last one, overfertilizing and choking valuable freshwater resources in the process. Management, monitoring, and sustained efforts will be required to reverse the trend.

References

Aber JD, Nadelhoffer KJ, Steudler P, and Melillo JM (1989) Nitrogen saturation in northern forest ecosystems. *BioScience* 39: 378–386.

Babin J and Prepas EE (1985) Modelling winter oxygen depletion rates in ice-covered temperate zone lakes in Canada. *Canadian Journal of Fisheries and Aquatic Sciences* 42: 239–249.

Bell EM and Laybourn-Parry J (1999) The plankton community of a young, eutrophic, Antarctic saline lake. *Polar Biology* 22: 248–253.

Boerner REJ (1982) Fire and nutrient cycling in temperate ecosystems. *BioScience* 32: 187–192.

Bryson B (2005) *A Short History of Nearly Everything*. Toronto: Anchor Canada.

Bulgakov NG and Levich AP (1999) The nitrogen:phosphorus ratio as a factor regulating phytoplankton community structure: Nutrient ratios. *Archiv für Hydrobiologie* 146: 3–22.

Carlson RE (1977) A trophic state index for lakes. *Limnology and Oceanography* 22: 361–369.

Carpenter SR (2005) Eutrophication of aquatic ecosystems: Bistability and soil phosphorus. *Proceedings of the National Academy of Sciences of the United States of America* 102: 10002–10005.

Carpenter SR and Brock WA (2006) Rising variance: A leading indicator of ecological transition. *Ecology Letters* 9: 311–318.

Cassara A (2008) *Measuring Eutrophication on a Global Scale*. World Resources Institute, EarthTrends. http://earthtrends.wri.org/updates/node/278 (accessed October 2010).

Chang WYB (1987) Large lakes of China. *Journal of Great Lakes Research* 13: 235–249.

Cordell D, Drangert J-O, and White S (2009) The story of phosphorus: Global food security and food for thought. *Global Environmental Change* 19: 292–305.

Crowley W (1999) Lake Washington Ship Canal. Essay 1444. Historylink.org. http://www.historylink.org/ (accessed November 2010).

Debano LF and Conrad CE (1978) The effect of fire on nutrients in a chaparral ecosystem. *Ecology* 59: 489–497.

Dodds WK (2006) Eutrophication and trophic state in rivers and streams. *Limnology and Oceanography* 51: 671–680.

Downing JA and McCauley E (1992) The nitrogen:phosphorus relationship in lakes. *Limnology and Oceanography* 37: 936–945.

Dowrick DJ, Hughes S, Freeman C, Lock MA, Reynolds B, and Hudson JA (1998) Nitrous oxide emissions from a gully mire in mid-Wales, UK, under simulated summer drought. *Biogeochemistry* 44: 151–162.

Drév P and Anderson B (2007) Peak phosphorus. Energy Bulletin. http://www.greb.ca/GREB/Publications_files/Peakphosphorus.pdf (accessed January 2011).

Edmondson WT (1977) Trophic equilibrium of Lake Washington. *US Environmental Protection Agency Report 600/3-77/087*. Washington, DC: US Environmental Protection Agency.

Edmondson WT (1991) *The Uses of Ecology: Lake Washington and Beyond*, Washington, DC: University of Washington Press.

Ekdahl EJ, Teranes JL, Guilderson TP, et al. (2004) Prehistorical record of cultural eutrophication from Crawford Lake, Canada. *Geology* 32: 745–748.

Elser JJ, Bracken MES, Cleland E, et al. (2007) Global analysis of nitrogen and phosphorus limitation of primary producers in freshwater, marine and terrestrial ecosystems. *Ecology Letters* 10: 1135–1142.

Emsley J (2000) *The 13th Element: The Sordid Tale of Murder, Fire, and Phosphorus*. New York: Wiley.

Evans JC and Prepas EE (1997) Relative importance of iron and molybdenum in restricting phytoplankton biomass in high phosphorus saline lakes. *Limnology and Oceanography* 42: 461–472.

Galloway JN, Aber JD, Erisman JW, et al. (2003) The nitrogen cascade. *Biogeochemistry* 53: 341–356.

Government of Canada (2009) Regulations amending the phosphorus concentration regulations. *Canada Gazette* 143. http://www.canadagazette.gc.ca/ (accessed February 2011).

Hasler AD (1947) Eutrophication of lakes by domestic drainage. *Ecology* 28: 383–395.

Hefting MM, Bobbink R, and de Caluwe H (2002) Nitrous oxide emission and denitrification in chronically nitrate-loaded riparian buffer zones. *Journal of Environmental Quality* 32: 1194–1203.

Hoagland P, Anderson DM, Kaoru Y, and White AW (2002) The economic effects of harmful algal blooms in the United States: Estimates, assessment issues, and information needs. *Estuaries* 25: 819–837.

Hu L, Hu W, Zhai S, and Wu H (2010) Effects on water quality following water transfer in Lake Taihu, China. *Ecological Engineering* 36: 471–481.

Hubbert MK (1974) US Energy Resources: A Review as of 1972. A background paper prepared at the request of Henry M. Jackson, Chairman, Committee on Interior and Insular Affairs, United States Senate, pursuant to Senate Resolution 45, *A National Fuels and Energy Policy Study: Serial No. 93-40 (92-75), Part 1*, Washington, DC: US Government Printing Office.

Hynes HBN (1975) The stream and its valley. *Verhandlungen des Internationalen Verein Limnologie* 19: 1–15.

Jungk A (2009) Carl Sprengel – The founder of agricultural chemistry: A re-appraisal commemorating the 150th anniversary of his death. *Journal of Plant Nutrition and Soil Science* 172: 633–636.

Klausmeier CA, Litchman E, Daufresne T, and Levin SA (2004) Optimal nitrogen-to-phosphorus stoichiometry of phytoplankton. *Nature* 429: 171–174.

Krecek J and Haig M (2006) Headwater wetlands. In: Krecek J and Haig M (eds.) *Environmental Role of Wetlands in Headwaters*, pp. 1–6. The Netherlands: Springer.

Lawrence E, Jackson ARW, and Jackson JM (1998) Eutrophication. *Longman Dictionary of Environmental Science*, pp. 144–145. London: Addison Wesley Longman.

Leigh GJ (2004) *The Word's Greatest Fix: A History of Nitrogen and Agriculture*. Oxford/New York: Oxford University Press.

Lewis WM and Wurtsbaugh WA (2008) Control of lacustrine phytoplankton by nutrients: Erosion of the phosphorus paradigm. *International Review of Hydrobiology* 93: 446–465.

Lind OT (1985) *Handbook of Common Methods in Limnology*, 2nd edn., Dubuque, IA: Kendall Hunt Publishing Co.

Marcarelli AM, Wurtsbaugh WA, and Griset O (2006) Salinity controls phytoplankton response to nutrient enrichment in the Great Salt Lake, Utah, USA. *Canadian Journal of Fisheries and Aquatic Sciences* 63: 2236–2248.

Mayer PM, Reynolds SK, McCutchen MD, and Canfield TJ (2006) Meta-analysis of nitrogen removal in riparian buffers. *Journal of Environmental Quality* 36: 1172–1180.

McEachern P, Prepas EE, Gibson JJ, and Dinsmore WP (2000) Forest fire induced impacts on phosphorus, nitrogen and chlorophyll a concentrations in boreal subarctic lakes of northern Alberta. *Canadian Journal of Fisheries and Aquatic Sciences* 57: 73–81.

Minshall GW, Brock JT, Andrews DA, and Robinson CT (2001) Water quality, substratum and biotic responses of five central Idaho (USA) streams during the first year following the Mortar Creek Fire. *International Journal of Wildland Fire* 10: 185–199.

Minshall GW, Cummins KW, Peterson RC, et al. (1985) Developments in stream ecosystem theory. *Canadian Journal of Fisheries and Aquatic Sciences* 42: 1045–1055.

Mitchell P and Prepas EE (1990) *Atlas of Alberta Lakes*. Edmonton, AB: University of Alberta Press.

Mitsch WJ and Gosselink JG (2007) *Wetlands*, 4th edn., New York: Wiley.

Molot LA and Dillon PJ (1997) Photolytic regulation of dissolved organic carbon in northern lakes. *Global Biogeochemical Cycles* 11: 357–365.

Nixon SW (1995) Coastal marine eutrophication: A definition, social causes, and future concerns. *Ophelia* 41: 199–219.

Nürnberg GK (1987) Hypolimnetic withdrawal as lake restoration technique. *Journal of Environmental Engineering* 113: 1006–1017.

Osborn CL, Morris DP, Thorn KA, and Moeller RE (2001) Chemical and optical changes in freshwater dissolved organic matter exposed to solar radiation. *Biogeochemistry* 54: 251–278.

Prepas EE and Burke JM (1997) Effects of hypolimnetic oxygenation on water quality in Amisk Lake, Alberta, a deep eutrophic lake with high internal phosphorus loading rates. *Canadian Journal of Fisheries and Aquatic Sciences* 54: 2111–2120.

Prepas EE, Murphy TP, Crosby JM, et al. (1990) Reduction of phosphorus and chlorophyll *a* concentrations following $CaCO_3$ and $Ca(OH)_2$ additions to hypereutrophic Figure Eight Lake, Alberta. *Environmental Science & Technology* 24: 1252–1258.

Qin B, Hu W, Gao G, Luo L, and Zhang J (2004) Dynamics of sediment resuspension and the conceptual schema of nutrient release in the large shallow Lake Taihu, China. *Chinese Science Bulletin* 49: 54–64.

Qin B, Song Y, and Gao G (2003) The role of pheriphytes in the shift between macrophyte and phytoplankton dominated systems in a shallow, eutrophic lake (Lake Taihu, China). *Science in China Series C, Life Sciences* 49: 597–602.

Qin B, Xu P, Wu Q, Luo L, and Zhang Y (2007) Environmental issues of Lake Taihu, China. *Hydrobiologia* 581: 3–14.

Ranalli AJ (2004) A summary of the scientific literature on the effects of fire on the concentration of nutrients in surface waters. *US Geological Survey Open-File Report 2004-1296*. Denver, CO: US Geological Survey.

Redfield AC (1934) On the proportions of organic derivations in sea water and their relation to the composition of plankton. In: Daniel RJ (ed.) *James Johnstone Memorial Volume*, pp. 177–192. Liverpool: University Press of Liverpool.

Sawyer CN (1966) Basic concepts of eutrophication. *Journal of the Water Pollution Control Federation* 38: 737–744.

Scheffer M (2004) *Ecology of Shallow Lakes*. Norwell, MA: Kluwer Academic Publishers.

Scheffer M, Carpenter S, Foley JA, Folke C, and Walker B (2001) Catastrophic shifts in ecosystems. *Nature* 413: 591–596.

Scheffer M, Hosper SH, Meijer M-L, Moss B, and Jeppesen E (1993) Alternative equilibria in shallow lakes. *Trends in Ecology and Evolution* 8: 275–279.

Scheffer VB and Robinson RJ (1939) A limnological study of Lake Washington. *Ecological Monographs* 9: 95–143.

Schindler DW (1974) Eutrophication and recovery in experimental lakes: Implications for lake management. *Science* 184: 897–899.

Schindler DW, Hecky RE, Findlay DL, et al. (2008) Eutrophication of lakes cannot be controlled by reducing nitrogen input: Results of a 37-year whole-ecosystem experiment. *Proceedings of the National Academy of Sciences of the United States of America* 105: 11254–11258.

Shen PP, Shi Q, Hua ZC, et al. (2003) Analysis of microcystins in cyanobacteria blooms and surface water samples from Meiliang Bay, Taihu Lake, China. *Environment International* 29: 641–647.

Sims JT, Simard RR, and Joern BC (1998) Phosphorus loss in agricultural drainage: Historical perspective and current research. *Journal of Environmental Quality* 27: 277–293.

Smil V (2001) *Enriching the Earth: Fritz Haber, Carl Bosch and the Transformation of World Food Production*. Cambridge, MA: MIT Press.

Steinberg CEW and Hartmann HM (1988) Planktonic bloom-forming cyanobacteria and the eutrophication of lakes and rivers. *Freshwater Biology* 20: 279–287.

van der Ploeg RR, Böhm W, and Kirkham MB (1999) On the origin of the theory of mineral nutrition of plants and the Law of the Minimum. *Soil Science Society of America Journal* 63: 1055–1106.

Vannote RL, Minshall GW, Cummins KW, Sedell JR, and Cushing CE (1980) The river continuum concept. *Canadian Journal of Fisheries and Aquatic Sciences* 37: 130–137.

Vitousek PM, Aber JD, Howarth RW, et al. (1997) Human alteration of the global nitrogen cycle: Sources and consequences. *Ecological Applications* 7: 737–750.

Vollenweider R (1970) *Scientific Fundamentals of the Eutrophication of Lakes and Flowing Water, with Particular Reference to Nitrogen and Phosphorus as Factors Responsible in Eutrophication*. Paris, France: OECD.

Waugh D (2002) *Geography: An Integrated Approach*, 3rd edn., Cheltenham, UK: Nelson Thornes.

Wetzel RG (2001) *Limnology, Lake and River Ecosystems*, 3rd edn. San Diego, CA: Academic Press.

Williamson CE, Morris DP, Pace ML, and Olson OG (1999) Dissolved organic carbon and nutrients as regulators of lake ecosystems: Resurrection of a more integrated paradigm. *Limnology and Oceanography* 44: 795–803.

11.9 Salinization and Saline Environments

A Vengosh, Duke University, Durham, NC, USA

Glossary

Additive agricultural chemicals chemicals added to irrigation water (e.g., nitrogen fertilizers, gypsum, dolomite, boron compounds).

Afforestation an establishment of a forest or plantation in an area where there were no trees.

Arsenate the oxic form (species) of arsenic in water; occurs in oxidizing water.

Arsenite the reduced form (species) of arsenic in water; occurs in reduced water.

Artificial recharge man-made recharge of aquifers through artificial basins or reverse pumping wells that replenish the aquifer as a compensation for overexploitation.

Base-exchange reactions chemical reactions that involve exchange of dissolved and adsorbed cations (e.g., Ca^{2+}, Mg^{2+}, Na^{+}) from adsorption sites on clay minerals and/or oxides.

Boron species boron in aquatic solutions occurs as uncharged boric acid ($B(OH)_3^0$) and borate ion ($B(OH)_4^-$) forms.

Boron isotopes the stable isotope ratio of boron, $^{11}B/^{10}B$, is defined in delta notation: $\delta^{11}B = \{[^{11}B/^{10}B]_{sample}/[^{11}B/^{10}B]_{STD} - 1\} \times 1000$, where STD is a standard.

Ca–chloride water composition the definition of water with a high proportion of calcium over the sum of sulfate and bicarbonate; $Ca/(SO_4 + HCO_3) > 1$ in equivalent units.

Chlorine radioactive isotope ratio the activity of the radioactive ^{36}Cl isotope is normalized to the total chloride content, $^{36}Cl/Cl$.

Conservative mixing mixing of two or more water bodies that involves nonreactive mixing of dissolved salts in the water; the concentrations of the dissolved water reflect the relative mixing proportions of the water bodies.

Criterion continuous concentration an estimate of the highest concentration of a material in surface freshwater to which an aquatic community can be exposed indefinitely without resulting in an unacceptable effect.

Cross-formational flow flow of groundwater from one aquifer, typically confined, to an overlying aquifer.

Denitrification reduction of nitrate molecule (NO_3^-) under reduced conditions to nitrogen gas.

Disinfection byproducts formation of hazardous byproducts during chlorine disinfection of drinking water, typically with high organic matter; generation of trihalomethanes (THMs), and specifically brominated trihalomethanes (e.g., bromodichloromethane; BDCM) during the disinfection process.

Dissociation of boric acid to borate ion an increase in the pH will convert boric acid to the borate ion species. The

dissociation constant is defined at the pH at which the fraction of boric acid is equal to that of borate ion.

Dissolved inorganic carbon the sum of dissolved inorganic carbon (DIC) species in a solution that is composed of carbon dioxide, carbonic acid, bicarbonate anion, and carbonate anion. The relative proportions of these species vary with pH.

Dolomitization a chemical reaction of Mg-rich water with calcium carbonate (e.g., limestone) rocks that involves Mg^{2+} and Ca^{2+} exchange, resulting in Ca-rich residual solution.

Efflorescent salt crusts salts that are generated in soil or shallow unsaturated zones that were formed by evaporation of saline soil solution that have reached the saturation level of different soluble minerals (e.g., gypsum, halite).

Electrical conductivity a field measure of the salinity of water, known also as specific conductance, that measures a solution's ability to conduct an electric current. The SI unit is siemens per centimeter (S cm^{-1}). A reciprocal quantity is electrical resistivity.

Endorheic rivers rivers that flow to inland basins and never reach the ocean.

Ethylene dibromide (EDB) type of soil fumigant enriched in bromide.

Evapotranspiration the combined evaporation and plant transpiration from soil surface; evaporation involves transport of water to the air from the soil solution, surface water, while transpiration accounts for water transport through a plant. The combined effect results in water loss and accumulation of salt residue.

Exchangeable adsorption sites one of the adsorption reaction processes involves exchange of cations (e.g., Ca^{2+}, Mg^{2+}, Na^{+}) from adsorption sites on clay minerals and/or oxides and water. The capacity of exchangeable adsorption sites varies among the mineral types and will determine the magnitude of the exchange reaction process.

Fossil water known also as nonrenewable groundwater, includes water that was recharged to an aquifer during historical/geological time and is not originated from the modern hydrological cycle. Fossil water is typically identified by radioactive age-dating isotopes (e.g., ^{14}C, tritium) and stable oxygen and hydrogen isotopes that are different from those of modern precipitation.

Freshening fresh groundwater flow and displacement of saline groundwater.

Imported water water that is used from external sources outside a region or an aquifer; typically, water is imported from areas of high abundance to areas where natural water resources are not sufficient to accommodate water demands.

Incongruent silicate mineral reactions a weathering chemical reaction that involves reaction of silicate minerals (e.g., aluminosilicates) in rocks and soils with carbon dioxide that generates clay minerals (e.g., kaolinite) and residual water enriched in bicarbonate. While in *congruent* dissolution the mineral is completely dissolved into solution, *incongruent* dissolution involves formation of a new mineral from the ions that were dissolved from mineral weathering.

Inner-sphere complex a chemical bond that is typically covalent between oxyanions and the electron-donating oxygen ion on a mineral surface without the presence of water molecules.

Ionic strength a measure of the salinity of a solution that is expressed as the square root of the sum of the individual ion concentrations (in molality unit; mol kg^{-1} $\{H_2O\}$) multiplied by the charge number of that ion. Generally, multivalent ions contribute strongly to the ionic strength of a solution relative to monovalent ions.

Isotopic fractionation preferential and/or selective incorporation of specific isotopes into different phases (dissolved, solid, vapor) that results in enrichment and/or depletion of the isotopes and changing of their ratios in the reaction products.

Meteoric water line the linear correlation between δ^2 H and $\delta^{18}O$ values in precipitation that reflects the local temperature and relative humidity; typically, the linear correlation has a slope $\sim$8 and an intercept value that increases with aridity (lower relative humidity), known as deuterium excess.

Mineral saturation the concentration level of ions from which different minerals will begin to precipitate into a solid state.

Mobilization leaching of ions and trace elements from a solid phase (e.g., mineral surface) to the dissolved phase in water.

Nitrogen isotopes the 'delta' notation, defined as $\delta^{15}N_{NO_3} = [(^{15}N/^{14}N)_{sample}/(^{15}N/^{14}N)_{AIR} - 1] \times 10^3$.

Osteosarcoma bone cancer associated with long-term exposure to radioactive nuclides that are bioaccumulated in bone tissue.

Outer-sphere complex a chemical bond that is typically an ion pair in which oxyanions and surface functional groups on a mineral surface are separated by one or more water molecules.

Overexploitation of an aquifer water pumping rates of an aquifer beyond the natural replenishment rates.

Oxyanions speciation of trace elements such as arsenic, selenium, and boron into anionic forms.

Sodium adsorption ratio (SAR) the relative activity of sodium ions in exchange reactions with soil.

Selenate, Se(VI) the oxidized form of selenium in oxidizing water.

Selenite, Se(IV) the reduced form of selenium in reducing water.

Sinkholes a natural depression or hole in land surface caused by subsurface dissolution of rocks.

Sodic subsoil a dense clay soil zone with high capacity for sodium adsorption, which reduces the hydraulic conductivity of the soil.

Softener backwash saline water saline effluents that are generated during the regeneration process of softener in which a brine is flushed through the ion-exchange column to remove calcium to provide available exchangeable sites for calcium removal process of softeners.

Stable oxygen and hydrogen isotopes in water $\delta^{18}O_{H_2O}$ $(=[(^{18}O/^{16}O)_{sample}/(^{18}O/^{16}O)_{STD} - 1] \times 10^3)$ and $\delta^2H_{H_2O}$

($=[(^{2}H/^{1}H)sample/(^{2}H/^{1}H)_{STD} - 1] \times 10^{3}$), where STD is standard mean ocean water (SMOW).

Strontium isotopes the ratio of radiogenic ^{87}Sr to stable ^{86}Sr isotopes, $^{87}Sr/^{86}Sr$.

Sulfur isotope in sulfate $\delta^{34}S_{SO_4}$ ($=[(^{34}S/^{36}S)_{sample}/(^{34}S/^{36}S)_{STD} - 1] \times 10^{3}$).

Total dissolved solids a measure of water salinity; the sum of dissolved salts in water.

Total organic carbon (TOC) The concentration of carbon bound in organic compounds in water; can be used as a measure of water quality.

Uranium decay chains a group of radioactive nuclides that are generated from the parent ^{238}U, ^{235}U, and ^{232}Th isotopes through cascades of radiogenic and radioactive nuclides of different half-lives, ending with the stable lead isotopes.

11.9.1 Introduction

One of the most conspicuous phenomena of water-quality degradation, particularly in arid and semiarid zones, is salinization of water resources. Rates of salinization vary widely: in some cases, it is a long-term phenomenon associated with geologic processes; in others, it is induced by human activities and thus very recent. The net result is that during the last century, many aquifers and river basins worldwide have become unsuitable for human consumption owing to high levels of salinity. Future exploitation of groundwater in the Middle East, for example, and in many other water-scarce regions in the world depends to a large extent on the degree and rate of salinization (Ranjan et al., 2006; Sowers et al., 2011; Vengosh and Rosenthal, 1994; Vengosh et al., 2001). Likewise, each year, large areas of soil become salinized and unusable for agriculture production (Dregne, 2002; Rengasamy, 2006).

Salinization is a global environmental phenomenon that affects diverse aspects of our lives: changing the chemical composition of natural water resources; degrading the quality of water supplied to domestic and agriculture sectors; affecting ecological systems by loss of biodiversity and taxonomic replacement by halotolerant species; contributing to loss of fertile soil; resulting in collapse of agricultural and fishery industries; changing local climatic conditions; and creating severe health problems (Dregne, 2002; Jackson et al., 2001; Postel, 1999; Rengasamy, 2006; Shiklomanov, 1997; Williams, 2001a,b; Williams et al., 2002). The damage due to salinity in the Colorado River Basin alone, for example, has been estimated to be between $500 and $750 million per year and could exceed $1 billion per year if the salinity in the Imperial Dam increased from 700 to 900 mg l^{-1} (US Department of the Interior, 2003). In Australia, accelerating soil salinization has become a profound environmental and economic disaster (Gordon et al., 2003; Rengasamy, 2006; Scanlon et al., 2005; Timms, 2005; Williams et al., 2002); Western Australia is "losing an area equal to one football oval an hour" due to spreading salinity (Murphy, 1999). In the early 2000s, the annual cost of dryland salinization in Australia was estimated at AU$700 million for lost land and AU$130 million for lost production (Williams et al., 2002). In short, salinization processes have become pervasive.

Salinity in water is usually defined as the sum of the dissolved constituents (total dissolved solids – TDS, in milligrams per liter) and occasionally also by one of the dissolved salt ions, typically the chloride content, although chloride comprises only a fraction of the total dissolved salts in water. The chloride to total dissolved solids (Cl/TDS) ratio varies from 0.1 in nonmarine saline waters to ~0.5 in marine saline waters. Water salinity is also defined by electrical conductivity (in microsiemens per centimeter), which is typically measured in the field during sampling. The typical instrument calibration by KCl solution may result, however, in different absolute 'salinity' values for different chemical compositions. In soil studies, the electrical conductivity and the ratio of $Na/\sqrt{(Ca+Mg)}$ (sodium adsorption ratio – SAR, in equivalent units) are often used as indirect measures of soil salinity.

In addition to chloride, high levels of other dissolved constituents may limit the use of water for domestic, agriculture, or industrial applications. In parts of China, eastern Africa, and India, for example, high fluoride content is associated with brackish to saline groundwater and causes severe dental and skeletal fluorosis (Ayenew et al., 2008; D'Alessandro et al., 2008; Misra and Mishra, 2007; Rango et al., 2009, 2010a,b,c; Shiklomanov, 1997). Hence, the 'salinity' problem is only the 'tip of the iceberg,' as high levels of sodium and chloride can be associated with high concentrations of other inorganic contaminants such as sulfate, boron, fluoride, and bioaccumulated elements such as selenium and arsenic (see **Chapter 11.2**). The salinization process may also enhance the mobilization of toxic trace elements in soils due to competition of ions for adsorption sitesand formation of metal–chloride complexes (Backstrom et al., 2003, 2004) and oxyanion complexes (Amrhein et al., 1998; Goldberg et al., 2008). Thus, the chemical evolution of the major dissolved constituents in a solution will determine the reactivity of trace elements with the host aquifer/streambed solids, and consequently their concentrations in water resources. For example, high concentrations of bicarbonate in groundwater can significantly enhance arsenic desorption from hydrous ferric oxide that could result in high As concentrations in HCO_3^--rich groundwater (Appelo et al., 2002; Czerniczyniec et al., 2007; Di Natale et al., 2008; Yu et al., 2006).

Salinity can also affect the radioactivity level of groundwater. Most naturally occurring radionuclides are highly retained to the aquifer matrix and are not soluble in associated groundwater. Radium is an exception since the ratio between adsorbed and dissolved radium depends on the salinity among other factors, and thus the concentration (activity) of dissolved radium typically increases with salinity (Herczeg et al., 1988; Krishnaswami et al., 1991; Miller and Sutcliffe, 1985; Moise et al., 2000; Sturchio et al., 2001; Tomita et al., 2010; Vinson, 2011; Vinson et al., 2009).

The World Health Organization (WHO) recommends that the chloride concentration of the water supply for human consumption should not exceed 250 mg l^{-1}. Yet, many countries have adopted higher national drinking water standards for

salinity, which can also vary for different regions within a country. For example, the US Environmental Protection Agency (EPA) has secondary (nonenforceable) standards of 250 mg l^{-1} for chloride and 500 mg l^{-1} for TDS (US Environmental Protection Agency, 2011b), yet each state in the United States has different enforceable standards (e.g., Florida – TDS of 500 mg l^{-1}, Utah – TDS of 2000 mg l^{-1}, California – TDS of 1000 mg l^{-1}). In Israel, the enforceable drinking water standard for chloride is much higher, at 600 mg l^{-1}.

Agriculture applications also depend upon the salinity level of irrigation water. Many crops, such as citrus, avocado, and mango, are sensitive to salt concentrations in irrigation water (Grieve and Poss, 2000; Kudo et al., 2010; Rengasamy, 2010; Scott et al., 2000; Wang et al., 2003). In addition, long-term irrigation with sodium-rich water results in a significant reduction of the hydraulic conductivity and hence the fertility of the irrigated soil. Similarly, various industrial sector applications require water of low salinity. The high-tech industry, for example, requires large amounts of water with low levels of dissolved salts. Hence, the salinity level of groundwater is one of the limiting factors that determine the suitability of water for various applications.

The salinity problem is a global phenomenon but it is more severe in water-scarce areas, such as arid and semiarid zones (**Figure 1**). Increasing demands for water have created tremendous pressures on water resources that have resulted in the lowering of ground and surface water levels and consequently increasing salinization. In the Middle East, for example, salinity is the main factor that limits water utilization, and future prospects for water use in Israel, the West Bank, the Gaza Strip, and Jordan are complicated by increasing salinization (Salameh, 1996; Vengosh and Rosenthal, 1994). The salinity problem thus has numerous grave economic, social, and political consequences (Sowers et al., 2011), particularly in cross-boundary basins that are shared by different communities (e.g., the Salinas Valley in California; Vengosh et al., 2002), friendly states (e.g., the Colorado River along the Mexico–US border; Stanton et al., 2001), and hostile states such as the Euphrates and Tigris rivers (Beaumont, 1996; Odemis et al., 2010), the Jordan River (Farber et al., 2004, 2005, 2007; Vengosh et al., 2001), the Gaza Strip (Ai-Yaqubi et al., 2007; Vengosh et al., 2005; Weinthal et al., 2005), the Aral Basin (Weinthal, 2002), and the Nile River (Elewa and El Nahry, 2009; Ohlsson, 1995).

Salinization of water resources also affects agricultural management. The composition of irrigation water will determine the salinity and fertility of the soil, and with time, the quality of the underlying water resource. The use of treated wastewater or other marginal waters (e.g., brackish water) with high contents of chloride, sodium, and boron is suitable only for salt-tolerant crops and requires special amending treatment of the soil. In addition, high boron in irrigation water and consequently in soil is also of concern in agriculture (Grieve and Poss, 2000; Koc, 2007), as boron is an essential micronutrient for plants but becomes toxic at high levels (typically >0.75 mg l^{-1} in irrigation water).

Finally, salinization processes are directly linked to global factors such as population growth and climate change. Increasing population leads to greater demands for food, which further increases the rate of freshwater withdrawal beyond the rate of natural replenishment (**Figure 2**), triggering salinization of aquifers. Furthermore, climate change models predict a reduction in precipitation in many arid and semiarid regions (**Figure 1**). A decrease in river discharge and aquifer replenishment coupled with an increase in temperature, and thus evaporation rates, would further worsen and accelerate salinization rates in the already salinized water resources of these regions.

This chapter provides an overview of global salinization phenomena and investigates the different mechanisms and geochemical processes that are associated with salinization. The overview includes salinization of rivers, lakes, and groundwater from different parts of the world. Special emphasis is given to the distinction between natural processes and anthropogenic forcing that generates salinity, such as wastewater

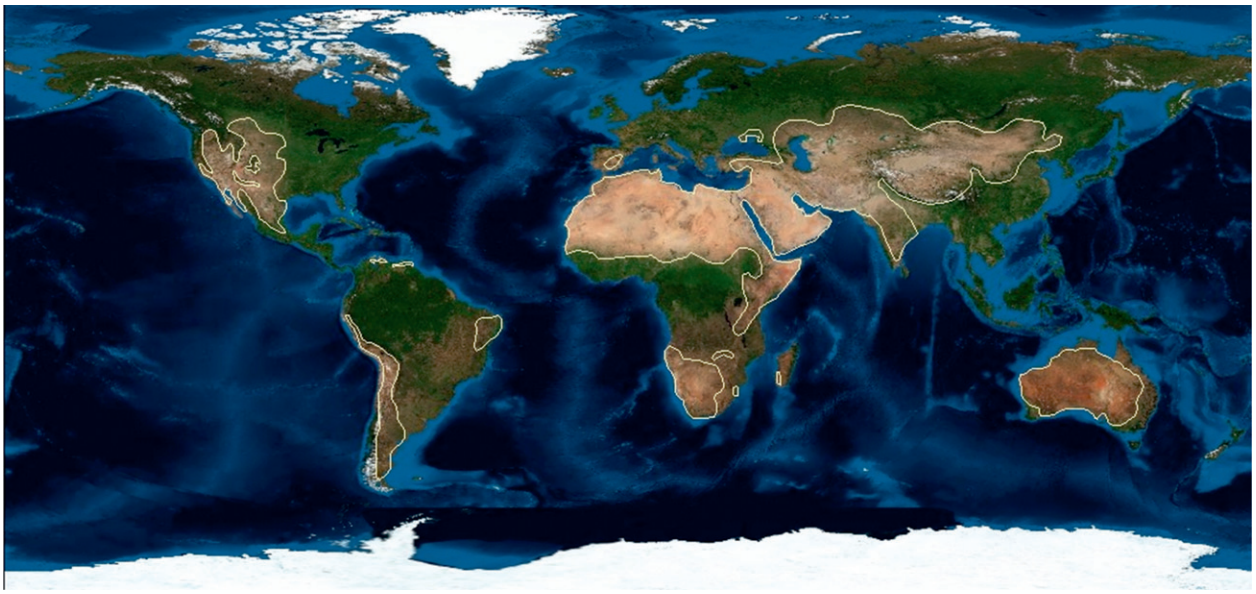

Figure 1 Map of arid and semiarid regions of the world.

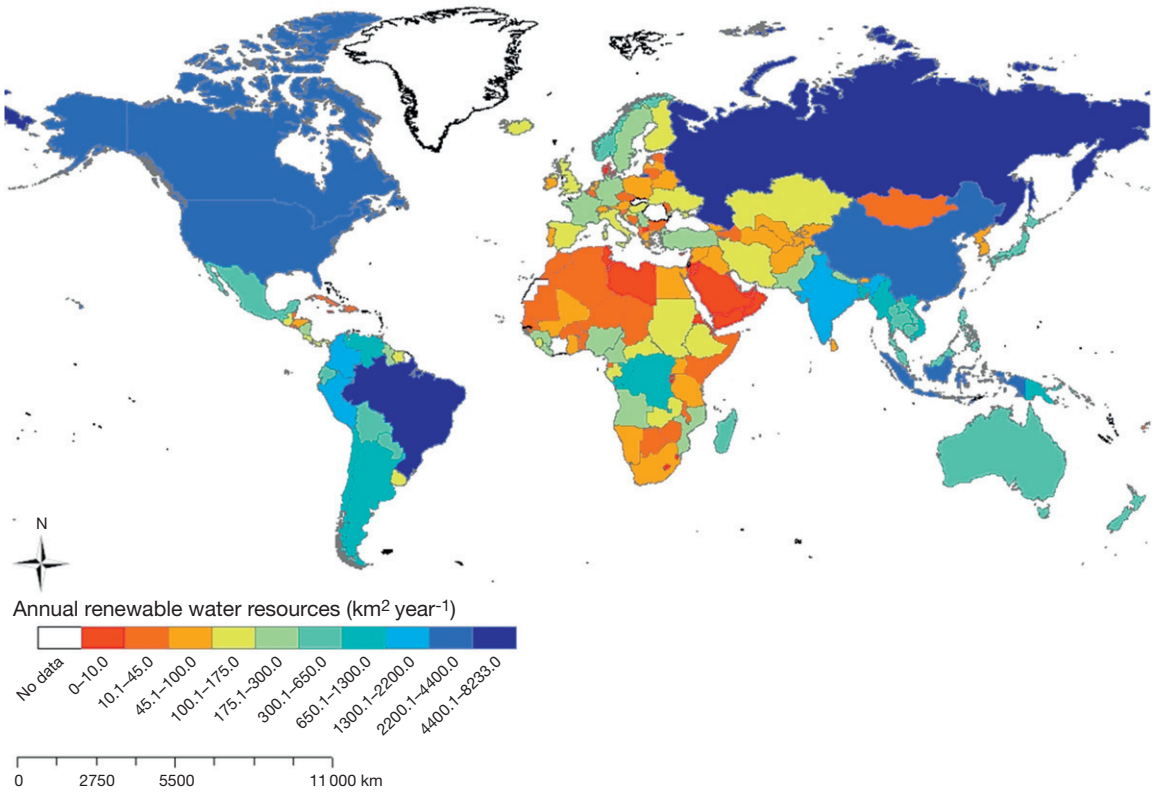

Figure 2 Global distribution of annual renewable water resources (billion cubic meters per year). Data from AQUASTAT database; Information System on Water and Agriculture, Food and Agriculture Organization, United Nation, http://www.fao.org/nr/water/aquastat/dbase/index.stm.

contamination and agricultural runoff. As such, two anthropogenic salinization cycles are introduced – the agricultural and domestic cycles. The role of the unsaturated zone in shaping the chemical composition of dryland salinization is also discussed. An overview of the effects of salinity on the occurrence of health-related contaminants such as fluoride, oxyanions (arsenic, selenium, boron), radionuclides, trihalomethanes, and fish-kill algae is presented. Some useful geochemical and isotopic fingerprinting tracers are introduced for elucidating the salinity sources. Finally, the chemical and isotopic compositions of man-made 'new water' that is produced from desalination are analyzed with implications for predicting the chemical and isotopic compositions of future water resources in the Anthropocene Era.

11.9.2 River Salinization

More than one-half of the world's major rivers (Figure 3) are being seriously depleted and polluted, which causes degradation of the surrounding ecosystems and threatens the health and livelihood of people who depend upon these rivers for drinking water and irrigation (Meybeck, 2003). Rivers are being depleted and contaminated because the global demand for water is rising sharply. The problem will be further exacerbated by the need to supply food and drinking and irrigation water for an additional estimated 2 billion people by 2025 (Serageldin, 2000). The World Commission on Water for the twenty-first century has developed a list of 'stressed rivers,' which includes the Yellow River in China, the Amu Darya and Syr Darya in Central Asia, the Colorado River in the western United States, the Nile River in Egypt, the Volga River in Russia, the Ganges River in India, and the Jordan River in the Middle East (Figure 3) (Serageldin, 2000).

Salinization of surface water can occur through either natural or anthropogenic processes or a combination of the two. In the natural setting, particularly in a dryland environment, salts are deposited and stored in the unsaturated zone and are eventually transported to shallow groundwater that discharges into adjacent rivers. Some rivers flow through arid regions although their source lies in wetter parts of upper basins (Colorado, Rio Grande, Orange, Nile, Euphrates, Tigris, Jordan, Indus, Murray; Figure 3). About 50% of arid land is located in 'endorheic' regions in which there is no flow to the ocean. In these regions, rivers flow into lakes such as the Caspian, Aral, Chad, Great Salt, Eyre, Dead Sea, and Titicaca, all without outlets.

Salinization of rivers also occurs due to human intervention, such as diversion of upstream natural flow or dam construction, and consequently significant reduction of natural flow discharge. The Amu Darya and Syr Darya in Central Asia, for example, were almost desiccated due to the diversion of water for cotton irrigation in the former Soviet Union (Weinthal, 2002). While historical annual flow in these two rivers is estimated at 122 billion cubic meters per year, by the mid-1980s, the Amu Darya and Syr Darya no longer flowed to the Aral Sea (Micklin, 1988, 1992).

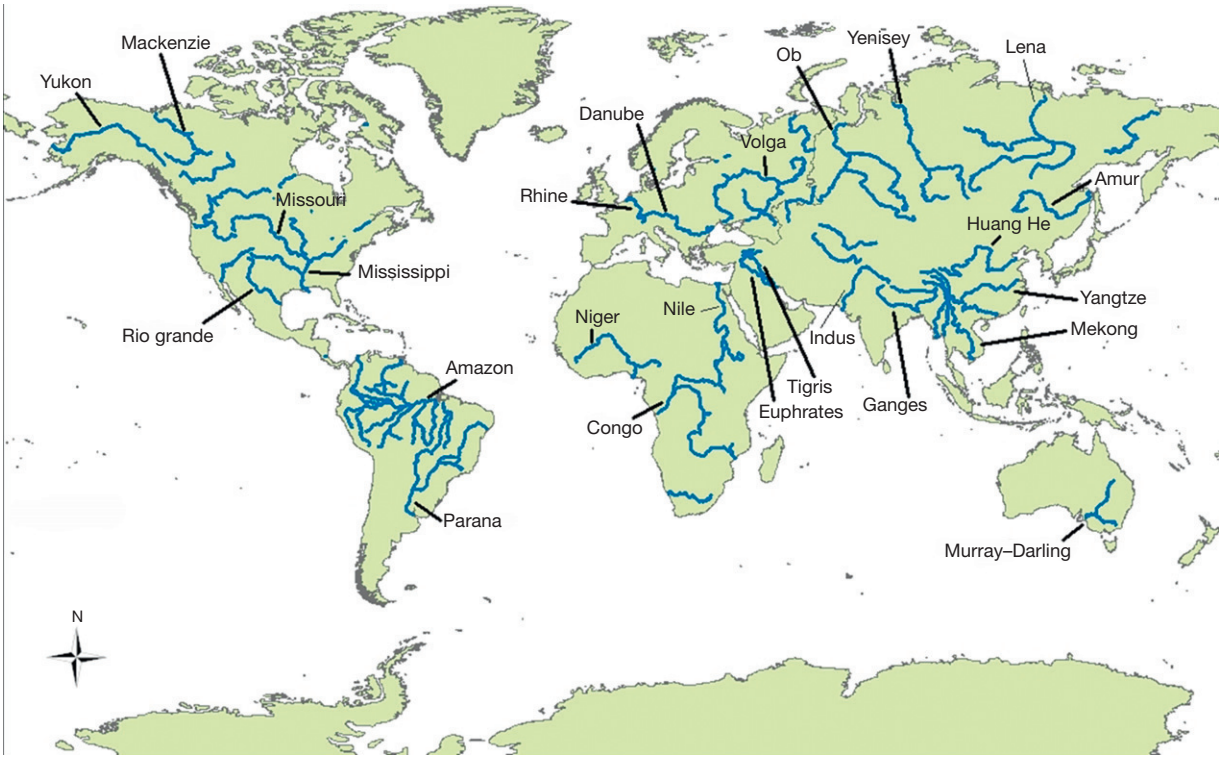

Figure 3 Map of major rivers of the world.

A.F. Pillsbury, in his classic 1981 paper, described how recycling of salts via irrigation and agricultural return flow controls the salinity of the downstream river in arid zones (Pillsbury, 1981). Once the natural salt balance is disturbed and salts begin to accumulate, either in the unsaturated zone or in drainage waters, the salinity in the downstream discharge water will increase. The salinity of the Colorado River is derived from a century of activity that includes upstream diversion of freshwater, massive irrigation, evapotranspiration and salt accumulation in the soil, and return of saline drainage flow back to the river (Pillsbury, 1981). Natural brines from Paradox Valley, for example, discharge to the Dolores River in Colorado, which is a tributary of the Colorado River. This brine discharge, with TDS of 250 000 mg l^{-1}, annually contributes about 2×10^8 kg of dissolved salts to the Colorado River system (Kharaka et al., 1997).

The Colorado River Basin encompasses about 630 000 km^2 in seven states in western United States and northern Mexico (**Figure 4**). The river serves 33 million people and provides the basis for the regional economy in agriculture, livestock grazing, mining, forestry, manufacturing, oil and gas production, hydropower production, recreation, and tourism. During 1906–1998, the unregulated flow rate of the Colorado River varied widely from 6.1 to 30.2 billion cubic meters per year, with an average annual natural flow of approximately 18.6 billion cubic meters per year at Lee's Ferry, about 15 km south of the Utah–Arizona border (Colorado River Board of California, 2011). The 1992 Colorado River Compact allocated 9.2 billion cubic meters per year for each of the Upper and Lower Basin states, with the right of the Lower Basin to increase its use by 1.2 billion cubic meters per year. The construction of reservoirs along the river (**Figure 4**) increases useable capacity of the Colorado river to about 74 billion cubic meters per year, from which Lake Powell (behind Glen Canyon Dam) and Lake Mead (behind Hoover Dam) have a combined capacity of approximately 62.8 billion cubic meters per year (Colorado River Board of California, 2011).

One of the major issues of concern for adequate management is the relatively high salinity of the Colorado River, with an estimated 9 million tons of salts passing the Hoover Dam annually (Colorado River Basin Salinity Control Forum, 2008). The salinity of the river increases as it flows downstream (**Figure 5**), but no systematic increase with time has been observed as salinity has fluctuated and overall decreased during the last four decades (**Figure 6**). These annual salinity variations have been shown to correlate inversely with the river flow (Butler and von Guerard, 1996). It has been estimated that about half of the salinity load in the Colorado River Basin is derived from natural saline discharge, 37% directly from irrigation, and the remaining 16% from reservoir-storage effects and municipal and industrial practices (US Bureau of Reclamation, 2003). The elevated salinity level of the Colorado River causes economic damage estimated at $600 million per year, mainly to the agriculture sector in which irrigation with saline water reduces crop yields and adds labor costs for irrigation management and drainage requirements. Urban utilization of the saline Colorado River adds further additional costs due to more frequent replacement of plumbing and water-using appliances, use of water softeners, and the purchase of bottled water (Colorado River Board of California, 2011).

Figure 4 Map of the Upper and Lower basins of the Colorado River.

Similarly, the rise of salinity in the Nile delta in Egypt has been attributed to a disturbance of the natural salt balance after the construction of the Aswan dam (Lake Nassar) and the reduction of natural outflow of water from the Nile River to the Mediterranean Sea. About 50 billion cubic meters per year of the Nile water is used for irrigation. The recycling of drainage water has increased the salinity of the northern part of the Nile close to the outlets to the Mediterranean Sea (Elewa and El Nahry, 2009; Kotb et al., 2000).

Reduction of the natural river flow and increasing discharge of saline drainage water are also the primary sources of increasing salinity in the Euphrates and Tigris rivers in Iraq (Fattah and Baki, 1980; Odemis et al., 2010; Robson et al., 1984). In addition, the water quality has deteriorated due to sewage pollution (Al-Muhandis, 1977; Mutlak et al., 1980). Upstream, in Turkey, the government has embarked since the mid-1960s on a large-scale program for the development of southeastern Turkey (Beaumont, 1996). The Southeastern Anatolia Project (GAP) with the Ataturk Dam is one of the largest water projects in the world, annually diverting for irrigation more than 13 billion cubic meters from the Euphrates and Tigris rivers. Consequently, the annual flow of the downstream Euphrates River has been reduced by 30–50%, out of an annual natural discharge of ~30 billion cubic meters per year (Beaumont, 1996). Massive irrigation in downstream Syria and Iraq has resulted in the formation of saline agricultural return flows that together with local shallow groundwater are discharged to the downstream sections of the river. As a result, the salinity of the Euphrates River, close to its confluence into the Persian Gulf, has risen to 3000 mg l^{-1} (Fattah and Baki, 1980; Robson et al., 1984).

In the dryland river environment, river salinization is also exacerbated by land clearing of deep-rooted natural vegetation, which accelerates recharge rates and causes groundwater tables to rise and dissolve salts in the unsaturated zone. In the Murray–Darling Basin in South Australia, soluble aerosols derived from the ocean are deposited in the drainage basin, concentrated by evapotranspiration, and discharged to the

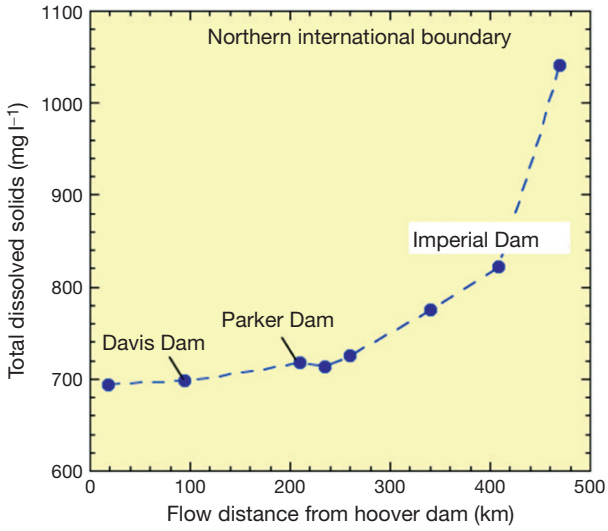

Figure 5 Variations in the salinity (mg l^{-1}) of the Colorado River with flow distance along the southern Colorado Basin as measured in October 2003. Distance along river (in km) is initiated from Hoover Dam (see locations in **Figure 4**). Data from unpublished results, Duke University.

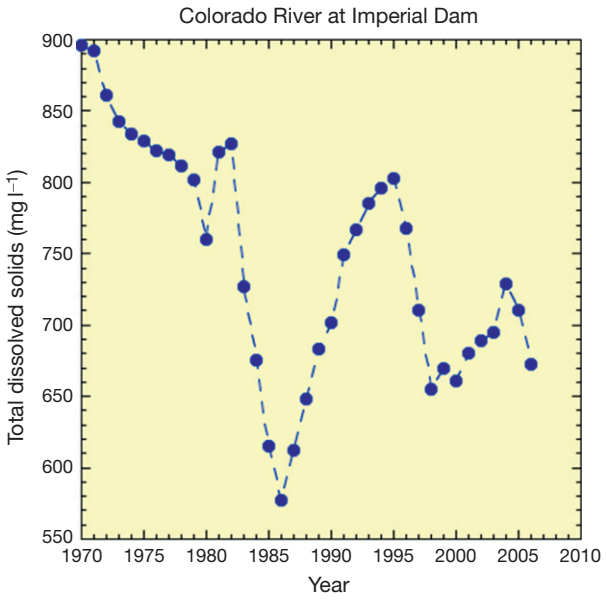

Figure 6 Time series of the salinity variations (mg l^{-1}) of the Colorado River at Imperial Dam since 1970. Data from Colorado River Basin Salinity Control Forum (2008).

Murray River (Herczeg et al., 1993; White et al., 2009). Large-scale cleaning of natural vegetation and its replacement by annual crops and pastures have increased the amount of water leaking through the unsaturated zone. Excess irrigation has also increased groundwater levels (Williams et al., 2002 and references therein). The rise of saline groundwater and mobilization of salts stored in the unsaturated zone have formed saline seepages that discharge to streams and the soil surface, which affects runoff salinity. Consequently, in the Murray River (**Table 1**) water salinity has gradually increased during the last 50 years such that Na^+ and Cl^- and overall major ion compositions are now similar to that of seawater (Herczeg et al., 1993). In the Sandspruit River, a tributary of the Berg River in the semiarid Western Cape Province of South Africa, salinization of the river (TDS range from 4500 to 9000 mg l^{-1}) was also attributed to accumulation and leaching of salts from the soil. Elemental mass-balance calculations suggest that the salts are derived from both recycling of meteoric aerosols and soil leaching (Flügel, 1995).

The Lower Jordan River along the border between Israel and Jordan (**Figure 7**) represents a different type of river salinization in the dryland environment. A tenfold reduction of surface water flow in the Jordan River (50–200 million cubic meters per year during the last 50 years relative to ~1400 million cubic meters per year in historic times) and intensification of shallow groundwater discharge resulted in salinization of the Jordan River (Farber et al., 2004, 2005; Holtzman et al., 2005; Shavit et al., 2002). During August 2001, the salinity of the southern end of the Jordan River, just before its confluence into the Dead Sea, reached 11 g l^{-1}, a quarter of the Mediterranean seawater salinity (**Figure 8**). Based on ion ratios (Na/Cl, Br/Cl) and strontium, boron, oxygen, and oxygen isotope variations, the rise of salinity in the southern section of the Jordan River (**Table 1**; **Figure 8**) was attributed to the discharge of saline groundwater (Farber et al., 2004, 2005; Vengosh et al., 2001). It was suggested that the shallow saline groundwater originated from both leaching of local saline marl sediments and upflow of underlying hypersaline brines (Farber et al., 2007).

Likewise, the salinity of the Rio Grande River increases to about 2000 mg l^{-1} along 1200 km flow distance. The parallel decrease of the Br/Cl ratio of the salinized river implies discharge of saline groundwater that interacted with halite deposits (Eastoe et al., 2010; Moore et al., 2008b; Phillips et al., 2003). Additional geochemical tools such as boron, strontium, and sulfur isotopes were used to suggest that the salinization of the Rio Grande River along the border of the United States and Mexico is derived from upwelling basin saline groundwater rather than anthropogenic (e.g., wastewater) sources (Moore et al., 2008b). The impact of evaporite dissolution was demonstrated also in the Ebro River Basin in Spain as long-term monitoring of the salinity (large variations, TDS up to 1000 mg l^{-1}) has shown that the TDS is mostly controlled by variations of SO_4^{2-}, Na^+, and Ca^{2+} ions, reflecting preferential dissolution of gypsum and carbonate minerals as part of surficial chemical weathering (Negrel et al., 2007).

Salinization of rivers can also occur in temperate climate zones due to direct anthropogenic contamination. For example, the Rhine River has suffered from discharge of potash mine drainage brines since the opening of potash mines more than 100 years ago. Chloride levels and salt fluxes have increased by a factor of 15–20. The rise of the annual chloride load at the Rhine River mouth (recorded since 1880) reflects an increase from a natural load of less than 5 kg s^{-1} to more than 300 kg s^{-1} in the 1960s (Meybeck and Helmer, 1989). Another example is the Arno River in northern Tuscany, Italy. Pollution by wastewater resulted in a downstream increase in Na^+, Cl^-, and SO_4^{2-} ions with a distinctive sulfur isotopic composition (Cortecci et al., 2002, 2007).

To summarize, there are five major sources of soluble salts in river basins: (1) meteoric salts, (2) salts derived from water–rock interaction (e.g., dissolution of evaporitic rocks), (3) salts

Table 1 Chemical composition of saline water from various sources

Site	*Source*	*TDS*	*Ca*	*Mg*	*Na*	*K*	*Cl*	*SO_4*	*HCO_3*	*NO_3*	*Br*	*B (ppb)*	*Na/Cl*	*SO_4/Cl*	*Br/Cl*	*B/Cl ($\times 10^{-3}$)*
Seawater (Red Sea)		41 390	418	1442	12 396	516	23 290	3077	161	–	75.6	5.3	0.86	0.05	1.5	0.8
Freshwater rivers																
Amazon River	Berner and Berner (2012)	39	5.2	1	1.5	0.8	1.1	1.7	20	–	–	6	2.1	0.6	–	18.2
Orinoco River	Berner and Berner (2012)	35	3.3	1	1.5	0.7	2.9	3.4	11	–	–	2	0.8	0.4	–	27.1
Mississippi (1905)	Berner and Berner (2012)	216	34	8.9	11	2.8	10.3	25.5	116	–	–	–	1.7	0.9	–	–
Mackenzie	Berner and Berner (2012)	211	33	10.4	7	1.1	8.9	36.1	111	–	–	12	1.2	1.5	–	4.4
Danube	Berner and Berner (2012)	307	49	9	9	1	19.5	24	190	–	–	–	0.7	0.5	–	–
Congo	Berner and Berner (2012)	34	2.4	1.4	2	1.4	1.4	1.2	13.4	–	–	3	2.2	0.3	–	7.2
Zambeze	Berner and Berner (2012)	58	9.7	2.2	4	1.2	1	3	25	–	–	–	6.7	1.1	–	–
Saline rivers																
Murray River, South Australia	Herczeg et al. (1993)	448	21	17	101	6	171	38	94	–	0.4	–	0.91	0.08	1.1	–
Jordan River (south end)	Vengosh et al. (2001)	1109	545	705	2300	170	5370	1650	254	20	81	2800	0.66	0.11	6.7	1.7
Tigris River (Baghdad, 1977)	Mutlak et al. (1980)	521	64	21.7	47.7	–	82.6	66.5	238	10	–	200	0.89	0.3	–	8.7
Saline lakes																
Salton Sea (1989)	Schroeder and Rivera (1993)	40 700	950	1300	11 000	220	17 000	10 000	185	–	13	12 000	1	0.22	0.3	2.3
Aral Sea (1991)	Linnikov and Podbereznyi (1996)	59 120	1020	3600	14 600	640	22 650	16 180	430	–	–	–	0.99	0.26	–	–
Caspian Sea	Peeters et al. (2000)	12 385	340	700	3016	88	5233	3008	–	–	–	–	0.89	0.2	–	–
Dead Sea Rift Valley	Starinsky (1974)	337 800	17 600	42 120	41 300	7600	224 200	280	200	–	4500	54 690	0.28	0.005	10	0.8
Seawater intrusion																

(*Continued*)

Table 1 (Continued)

Site	*Source*	*TDS*	*Ca*	*Mg*	*Na*	*K*	*Cl*	*SO_4*	*HCO_3*	*NO_3*	*Br*	*B (ppb)*	*Na/Cl*	*SO_4/Cl*	*Br/Cl*	*B/Cl ($\times10^{-3}$)*
Coastal aquifer, Israel	Vengosh et al. (1994)		980	245	2830	22	6304	470	206	–	21.3	950	0.69	0.03	1.5	5
Salinas Valley, California	Vengosh et al. (2002)		410	126	450	12	1670	212	62	–	5.4	245	0.42	0.05	1.5	4.8
Saline plumes and upcoming of brines																
Coastal aquifer, Israel (Beer Toviyya)	Vengosh et al. (1999a,b)	2560	176	97	545	3.9	1125	143	370	98	3.5	508	0.75	0.05	1.4	1.5
Ogallala aquifer, Texas	Mehta et al. (2000a,b)	67530	1460	388	23850	32	36120	5610	41	–	6.2	–	1	0.06	0.07	–
Dammam aquifer, Kuwait	Al-Ruwaih (1995)	4062	470	138	635	15.2	1241	1189	77	8	–	1500	0.77	0.35	–	3.9
Jordan Valley, Jericho, Cenomanian aquifer	Marie and Vengosh (2001)	8270	490	580	1700	110	4950	105	275	62	83	–	0.52	0.02	7.4	–
Pleistocene aquifer	Marie and Vengosh (2001)	3100	156	208	590	84	1372	295	363	29	10	–	0.66	0.16	3.3	–
Groundwater associated with freezing process																
Sweden	Bein and Arad (1992)	18200	3690	31	2850	12	11100	522	7	–	79	–	0.39	0.02	3.1	–
Finland	Bein and Arad (1992)	14400	3900	13	1500	7	8900	1	21	–	77	–	0.25	<0.01	3.8	–
Agricultural drainage																
San Joaquin Valley, California	Mitchell et al. (2000)	4580	192	242	952	–	499	2650	–	44	–	5940	2.9	1.9	–	3.9
Mendota, San Joaquin Valley, California	Kharaka et al. (1996)	14280	438	285	3720	3.1	1210	8350	250	25	3.4	–	4.7	2.5	1.2	–
Imperial Valley, California	Schroeder and Rivera (1993)	6715	310	330	1420	19	1200	3000	383	53	–	–	1.9	0.9		
Imperial Valley, California	Schroeder and Rivera (1993)	8250	560	320	1700	24	2600	2700	342	5	2.3	1700	1	0.4	0.4	2
Wastewaters																
Dan Reclamation Project, Israel (1993)	Vengosh and Keren (1996)	1300	80	30	264	34.2	361	112.5	420	–	0.4	500	1.1	0.11	0.5	6
Orleans, Cape Cod, Massachusetts	DeSimone et al. (1997)	1700	440	0.3	100	30	950	19	134	30	–	200	0.16	0.007	–	0.7

The ion concentrations are reported in mg l^{-1} (unless otherwise stated) whereas the ionic ratios are molar.

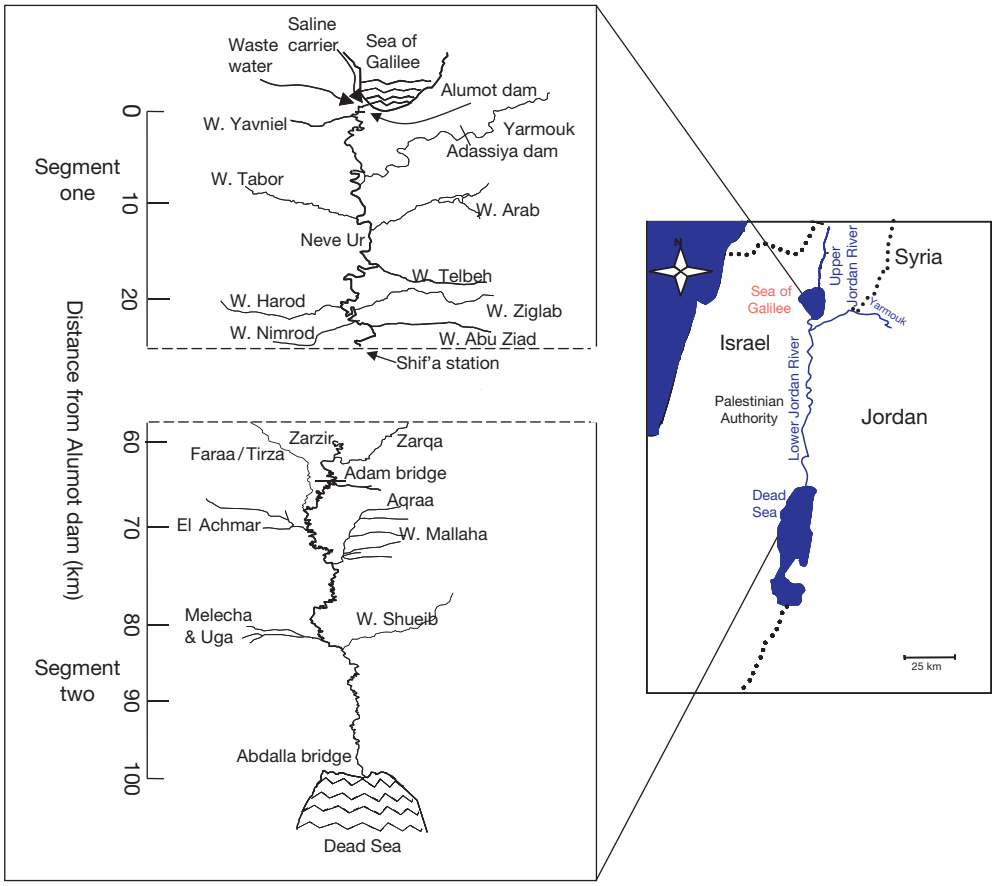

Figure 7 Map of the Jordan River between the Sea of Galilee (Lake Tiberias) and the Dead Sea along the border of Israel and Jordan.

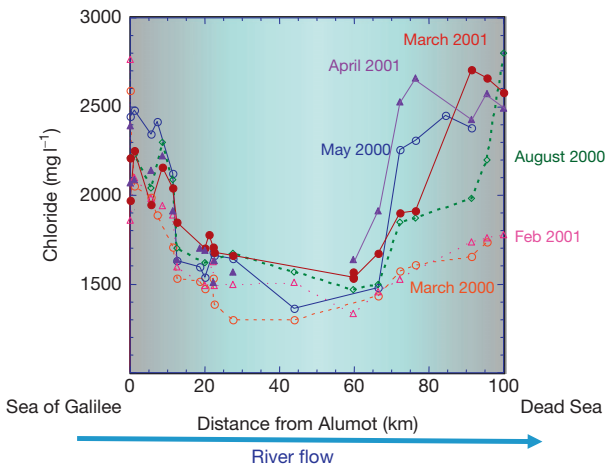

Figure 8 Variation of chloride content of the Jordan River with flow distance. Distance (km) refers to the beginning of the Jordan River flow (Alumot dam) downstream from the Sea of Galilee. Data from Farber et al. (2004).

derived from remnants of formation water entrapped in the basin, (4) geothermal waters, and (5) anthropogenic salts (e.g., wastewater effluent; Farber et al., 2004; Moore et al., 2008b; Vengosh et al., 2001; Williams, 2001a). Meteoric salts are concentrated via in-stream net evaporation and evapotranspiration along the river flow. In addition, meteoric salts can be recycled through irrigation in the watershed and development of saline agricultural drainage water that flows to the river.

Overall, rivers are one of the most sensitive hydrological systems to global and climatic changes. In addition to the reduction in precipitation and increased aridity that are projected for arid and semiarid regions as a result of global warming, population growth and increasing pressure on shallow aquifer systems combined with river contamination will cause a significant increase in river salinity. One example of these processes is the ongoing changes in the water quality of the Ganges River Basin, which supports approximately 500 million people, about 40% of the total population in India (Misra, 2011). The growing population and urbanization in the Ganges Basin has led to increased utilization of shallow groundwater, lowering the water table, and a reduction in surface and subsurface discharge to the Ganges River. At the same time, enormous solid waste production and disposal has filled small natural channels and changed flow patterns; this, coupled with accelerated disposal of domestic wastewater, has led to severe degradation of water quality. Compounding these ongoing changes, climate change models predict that a temperature rise may reduce precipitation by up to 16%, which could reduce the groundwater recharge by 50% (Misra, 2011). Thus, in spite of the enormous discharge of surface water in the

Ganges Basin (annual surface water potential of 525 billion cubic meters; Misra, 2011), even the mighty Ganges River is not immune to significant salinization.

11.9.3 Lake Salinization

Naturally occurring salt lakes typically reflect a hydrological equilibrium that has been developed over geological time (see Chapter 7.12). The wide range of the chemical compositions of natural salt lakes represents their different sources; salts that are derived from the evolution of freshwater inflows (e.g., the Great Salt Lake, Utah; Jones et al., 2009; Spencer et al., 1985), hydrothermal fluids (Qaidam Basin, China; Vengosh et al., 1995), remnants of evaporated seawater (Dead Sea, Israel; Katz and Starinsky, 2009; Starinsky, 1974; Stein et al., 1997; Torfstein et al., 2005; Waldmann et al., 2007), and long-term accumulation of marine aerosols (Lake Eyre, Australia; Chivas et al., 1991; Vengosh et al., 1991a).

The term *lake salinization* as used in this chapter, however, applies to direct anthropogenic activity and the ongoing transformation of freshwater lakes into salt lakes. In principle, the diversion of freshwater from one basin to another, or the diversion of natural lake inflows, are the principal processes that could result in lake salinization. The consequences may be devastating; for example, the diversion of almost all of the water from the Amu Darya and Syr Darya in central Asia to grow cotton and other crops (Weinthal, 2002) led to major desiccation of the Aral Sea (Micklin, 1988, 1992). From discharge rates of about 55 billion cubic meters per year during the 1960s, the river inflow to the Aral Sea decreased to 22 billion cubic meters per year in the 1970s, a range of 6–15 billion cubic meters per year during the 1980s and 1990s, and 2–10 billion cubic meters per year between 2000 and 2010 (Micklin, 2010). Water levels dropped by 30 m (55 m above sea level in 1950 to 25 m in 2010) and the water volume reduced from 1089 km^3 in 1960 (whole lake) to two separate small basins (the Western Basin with a volume of 56 km^3 and the Eastern Basin with a volume of 0.64 km^3) in 2009 (Micklin, 2010). The salinity rose exponentially from 10 g l^{-1} in the 1960s to over 100 g l^{-1} in the Western Basin and over 200 g l^{-1} in the Eastern Basin in 2008 (Figure 9; Zavialov et al., 2009). The rise of the salinity has led to the destruction of the once-thriving fisheries industry and has produced severe health problems in the region associated with resuspension of contaminated sediments from the desiccated lake to the atmosphere (Micklin, 1988, 1992, 2010).

Lake Chad in the Sahel region in Africa has shrunk by 75% in the last three decades because of both periodic droughts and massive diversions of water for irrigation. The rich fisheries that used to support the local population have collapsed entirely (Abramovitz, 1996; Roche, 1975). The salinity of the alkaline (pH 9.8) Mono Lake (90 g l^{-1}), situated in an arid basin in eastern California, has increased nearly twofold over the past 50–60 years as a consequence of watershed runoff diversions to the city of Los Angeles (Blum et al., 1998). Draining saline agricultural return flow from the Imperial Valley in southern California during the twentieth century into the lake of the Salton Sea resulted in salt accumulation and the creation of a salt lake with a salinity that rose from almost zero to 46 g l^{-1} in 2005 (Figure 10; Amrhein et al., 2001; Cohen, 2009; Cohen and Hyun, 2006; Hely et al., 1966; Schroeder and Rivera, 1993; Schroeder et al., 1991, 2002; Wardlaw and Valentine, 2005).

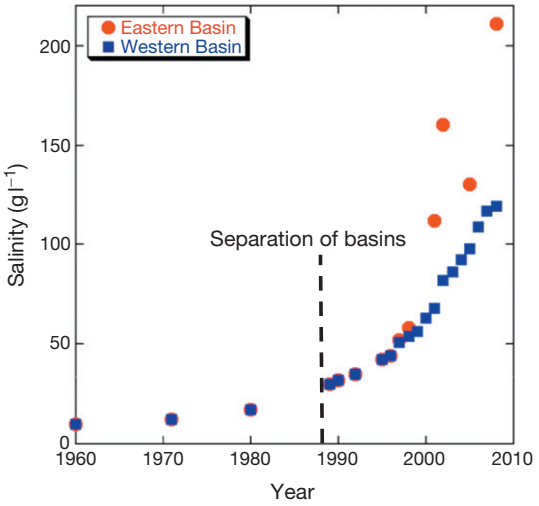

Figure 9 Time series of the salinity variations (mg l^{-1}) of the Aral Sea since 1960. Note that the desiccation of the lake generated in the late 1980s two separated lakes, the Eastern and Western basins. Data integrated from Linnikov and Podbereznyi (1996), Micklin (2010), and Zavialov et al. (2009).

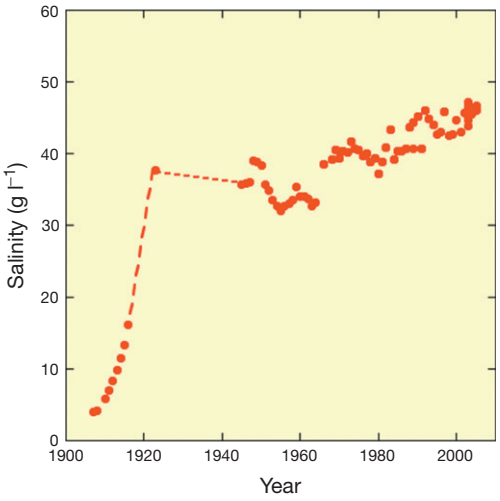

Figure 10 Historical salinization of the Salton Sea (California, USA) during the twentieth century. Data integrated from Amrhein et al. (2001), Cohen (2009), Cohen and Hyun (2006), Schroeder and Rivera (1993), and Schroeder et al. (1991).

The desiccation of the Dead Sea due to a significant reduction of freshwater discharge from the Jordan River (Farber et al., 2004; Holtzman et al., 2005; Shavit et al., 2002) and other tributaries, combined with potash salt production by Israel and Jordan, has resulted in a dramatic reduction of the water level (Figure 11), at a rate of about 1 m per year (Oren et al., 2010; Salameh and Wl-Naser, 1999; Yechieli et al., 1998). Since the early 1980s, the Dead Sea desiccation has been associated with increasing rates of formation of sinkholes along the lakeshores that have resulted in increasing damage to infrastructure (Closson and Abou Karaki, 2009; Closson et al., 2010; Ezersky et al., 2009; Shalev et al., 2006; Yechieli et al., 2006). A detailed

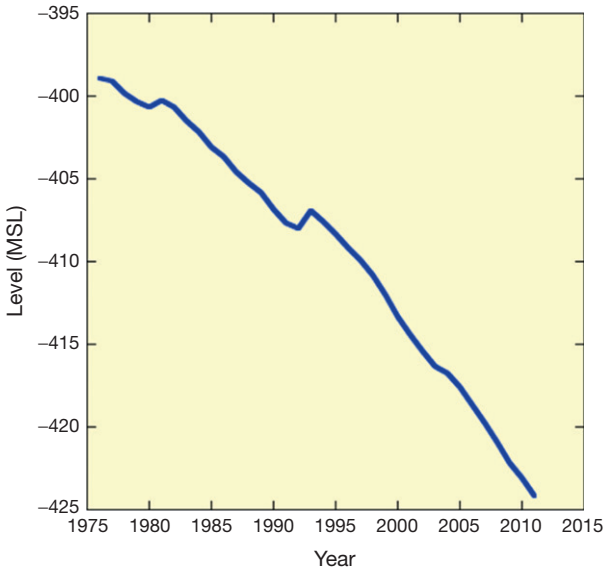

Figure 11 Historical variations of the Dead Sea (Israel) water level since 1975. Note the continued drop in lake level at a rate of about a meter per year. Data were kindly provided by Dr Irena Pankratov, Israel Water Authority.

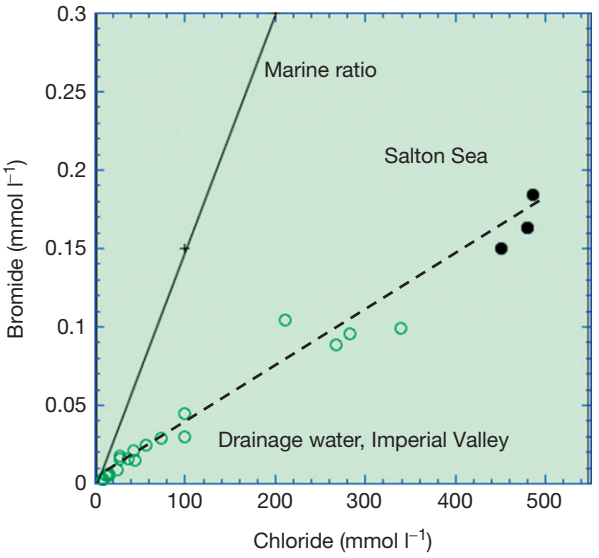

Figure 12 Bromide versus chloride concentrations (in mmol l^{-1}) of agricultural drainage waters in Imperial Valley (open circles) and Salton Sea (closed circles) in southern California, USA. Note the identical Br/Cl ratios measured in both the agricultural drainage waters and the saline lake, implying that the lake originated from the agricultural drainage inflows. The Br/Cl ratios are lower than the marine ratio, indicating that salinity originated from dissolution of halite mineral. Data were integrated from Amrhein et al. (2001), Schroeder et al. (1991), and Schroeder and Rivera (1993).

investigation revealed that more than a thousand sinkholes have developed along the western coast of the Dead Sea since the early 1980s, with the rate of formation accelerating (up to 150–200 sinkholes per year) with time. The sinkholes occur along a narrow strip 60 km long and <1 km wide and spread parallel to the general direction of the fault system associated with the Dead Sea Transform (Shalev et al., 2006; Yechieli et al., 2006). The desiccation of the Dead Sea caused the retreat of the saline water–freshwater–groundwater interface and the advance of freshwater into salt deposits along the Dead Sea shore, leading to salt dissolution and formation of the sinkholes. Data from groundwater associated with sinkholes show Na/Cl ratios (0.5–0.6) that are higher than that of typical Dead Sea brine (0.25), which confirm that halite dissolution is the major factor in generating sinkholes (Yechieli et al., 2006).

In general, the salinity and water chemistry of a lake is determined by (1) the imbalance between evaporation and water inflows, typically due to the diversion of freshwater discharge, climate change, and a reduction in precipitation that could induce water deficit and rise in salinity (Tweed et al., 2009); (2) the salinity and chemical composition of the inflow waters; and (3) precipitation of minerals within the lake once the concentrations of dissolved salts reach the saturation levels of these minerals (see **Chapter 7.12**). The effect of inflow water is demonstrated by the low (marine ratio of $<1.5\times10^{-3}$) Br/Cl ratios of the Salton Sea, which preserve the composition of the drainage and agriculture inflows from the Imperial Valley, originated from the Colorado River with low Br/Cl ratios (**Figure 12**).

Lake salinization can also occur by subsurface discharge of saline groundwater. The balance between the freshwater (typically surface water) and the saline subsurface inflows will determine the salinity of the lake. The Sea of Galilee (Lake Kinneret) in Israel is an example of subsurface discharge of saline groundwater to a freshwater lake. The chemical composition of the lake mimics the chemical composition of the saline groundwater, as shown by the relatively high Br/Cl ratio (Bergelson et al., 1999; Kolodny et al., 1999; Nishri et al., 1999) and ^{226}Ra activity (Raanan et al., 2009) of the Sea of Galilee. Variations of the lake levels and salinity during the last 60 years (**Figure 13**) reflect the balance between the surface freshwater inflows, groundwater discharge, evaporation, pumping to Israel National Water Carrier, and diversion of the surface saline inflows from the lake (Kolodny et al., 1999; Nishri et al., 1999). The large fluctuations and low lake levels during the last decade reflect the reduction of precipitation and consecutive drought that have affected this and other water resources in the Middle East during this time (Sowers et al., 2011).

During the early stages of lake salinization, the chemical composition of the saline lake water mimics the composition of the freshwater inflow. This was demonstrated in the case of the Aral Sea (**Table 1**) where the chemical composition of the brackish lake water during its early stages of salinization (salinity of 14 g l^{-1} in 1971) was identical to that of evaporated lake water during 1991 (salinity of 56 g l^{-1}; **Figure 14**) (Linnikov and Podbereznyi, 1996). Yet, as the Aral Sea continued to desiccate and the salinity continued to increase (**Figure 9**), the calcium and bicarbonate contents of the brines sampled from the East (TDS = 121.6 g l^{-1}) and West (97.7 g l^{-1}) basins during 2005–2006 were lower (**Figure 14**, data from Linnikov and Podbereznyi, 1996; Zavialov et al., 2009), indicating secondary precipitation of carbonate and perhaps gypsum in the shrinking lake. The Na/Cl ratio of the evolved saline lake was identical to the ratios measured during early stages of evolution (**Figure 14**), indicating that the lake

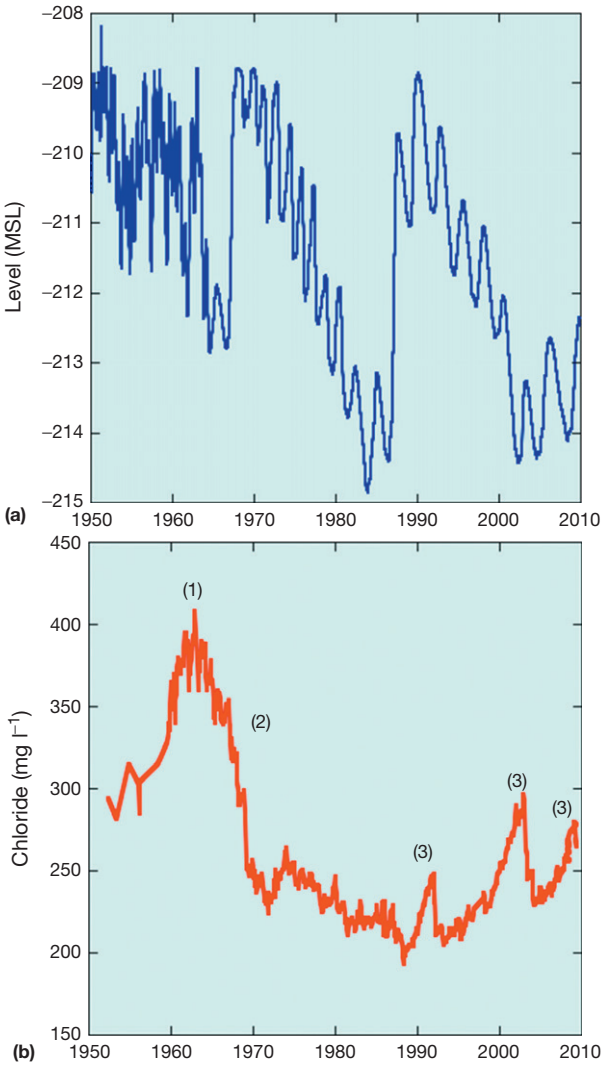

Figure 13 (a) Historical variations of the Sea of Galilee (Israel) water level since 1950. Note the sharp variations in the lake level particularly during the last 20 years. Data were kindly provided by Dr Irena Pankratov, Israel Water Authority; (b) Salinity variations of the Sea of Galilee (Israel) since 1950. Note the large variations in salinity that reflect (1) phase of a closed basin in which evaporation increased the lake salinity; (2) initiating pumping of the lake water to Israel National Water Carrier and diversion of the surface saline springs that flow to the lake; and (3) major drought episodes associated with a significant drop in the lake level. Data were kindly provided by Dr Irena Pankratov, Israel Water Authority.

water did not reach the halite saturation stage. Likewise, the rise of salinity of the Salton Sea (**Figure 10**) resulted in calcite and gypsum precipitation in the lake bottom sediments and temporal variations in the concentrations of Ca^{2+}, HCO_3^-, and SO_4^{2-} relative to Cl^-, in water from the Salton Sea (Schroeder et al., 2002). Similarly, brines from Australian ephemeral salt lakes have high Br/Cl ratios due to precipitation of halite crust, while brines from ephemeral salt lakes that lack halite crusts have Br/Cl ratios identical to inflow surface water and groundwater (Cartwright et al., 2009).

Saturation of the saline water and precipitation of minerals (Hardie and Eugster, 1970) have two important negative feedbacks that limit salt accumulation in salt lakes. In this respect, the saturation level of calcite, gypsum, and halite in brines will determine the salinity and composition of the residual brines. In the Salton Sea, the lake water had a total salinity of 46 g l^{-1}, and was oversaturated with respect to calcite, which controls the Ca^{2+} and HCO_3^- levels of the lake. Combined biologic activity, sulfate reduction processes, and base-exchange reactions (Na^+ removal) added additional dissolved Ca^{2+}, which enhanced calcite precipitation (Amrhein et al., 2001). At higher salinity levels, such as the Dead Sea (**Table 1**; Katz and Starinsky, 2009) with a salinity of 340 g l^{-1}, the low water activity and thus the low vapor pressure of the hypersaline brines impose low evaporation rates. Yechieli et al. (1998) predicted that despite a significant reduction in freshwater inflows to the Dead Sea, the Dead Sea will not totally desiccate but will reach a new equilibrium given the low water activity. The geometry of the lake basin and the size of the surface area are also important factors that control the amount of evaporation water (Yechieli et al., 1998). In sum, while the rate of salinization is rapid during the early stages of salinization, it decreases at later stages due to salt precipitation and low water activity of the brines. While the absolute salinity continues to increase, the *rate* of salinization is expected to decrease.

Global warming and reduction of precipitation in semiarid and arid climatic zones are expected to intensify the salinization of many salt lakes. In the Salton Sea in California, it has been predicted that salinity will rise from 46 g l^{-1} (**Figure 10**) to about 300 g l^{-1} by the end of the twenty-first century, with a rapid increase to about 200 g l^{-1} within the next 20–30 years (Cohen, 2009; Cohen and Hyun, 2006). The Australian salt lakes demonstrate perhaps the best example of further salinization of salt lakes due to climatic change. The salt lakes in Australia (Timms, 2005) were formed by long-term deposition of meteoric salts with seawater-like composition (Chivas et al., 1991; Vengosh et al., 1991a). Yet, a study of the Corangamite area in southeast Australia has revealed that a severe multiyear drought (11 years of below-average rainfall between 1997 and 2008) resulted in a 60% reduction in lake areas, an 80% decrease in volume, and a significant rise in salinity; conductivity rose from less than 50 mS cm^{-1} prior to 1997 to 200 mS cm^{-1} in 2006 in Lake Corangamite (Tweed et al., 2009). It is predicted that by 2025 most natural salt lakes will show adverse changes; many permanent salt lakes will decrease in size and increase in salinity, and many nonnatural saline lakes will be formed. In certain regions, such as in southern Australia, many seasonally filled salt lakes are likely to become drier for longer periods (Williams, 2002). Restoration plans for handling the ongoing salinity crisis of salt lakes such as the Salton Sea (Cohen, 2009; Cohen and Hyun, 2006) and the Aral Sea (Micklin, 2010) will have to deal with the challenges of further aridification that are associated with global warming and the inevitable intensification of salt lake salinization.

11.9.4 Groundwater Salinization

11.9.4.1 Seawater Intrusion and Saltwater Displacement in Coastal Aquifers

Saltwater intrusion is one of the most widespread and important processes that degrade water quality to levels exceeding

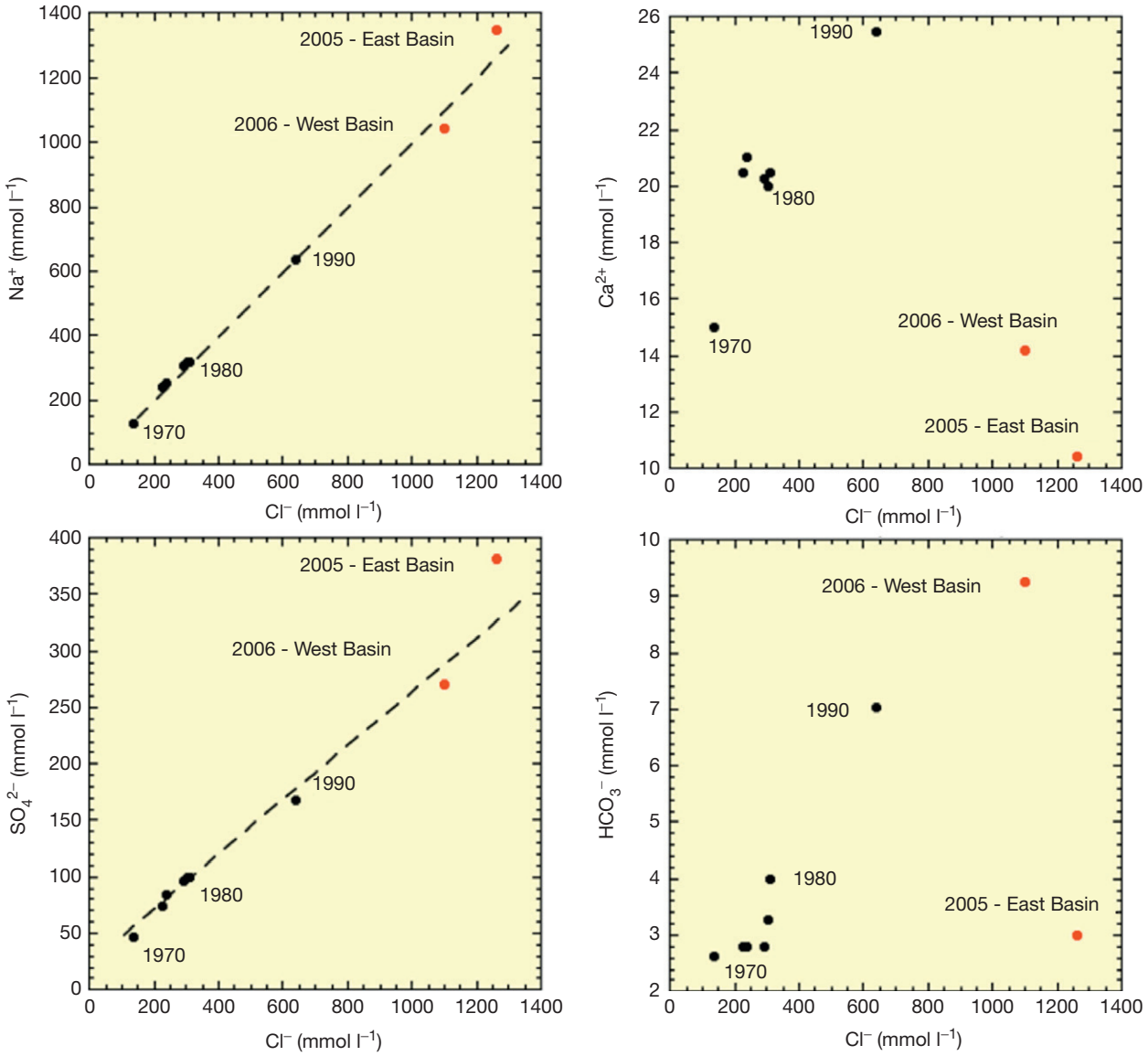

Figure 14 Concentrations of sodium, calcium, sulfate, and bicarbonate versus chloride contents (mmol l^{-1}) of the Aral Sea during different stages of lake desiccation and salinization, marked by the year of sampling. Note that the rise in salinity that was recorded in the lake since 1970 (see **Figure 9**) was associated with an apparent conservative increase of sodium and sulfate, while calcium and bicarbonate contents in the lately evolved lake were depleted relative to the expected conservative evaporation represented by chloride contents. These depletions suggest precipitation of secondary minerals such as calcium carbonate. Data were integrated from Linnikov and Podbereznyi (1996) and Zavialov et al. (2009).

acceptable drinking and irrigation water standards, and endanger future water exploitation in coastal aquifers. This problem is intensified due to population growth, and the fact that about 70% of the world's population occupies the coastal plain zones (Jones et al., 1999; Meybeck, 2003). Human activities (e.g., urbanization, agricultural development, tourism) in coastal areas increase the rate of groundwater salinization (Jones et al., 1999). In the United Sates, saltwater intrusion into coastal aquifers has been identified in the eastern Atlantic (Andreasen and Fleck, 1997; Lin et al., 2009; Meisler et al., 1985; Stringfield and LeGrand, 1969; Wicks and Herman, 1996; Wicks et al., 1995), and the southern (Langman and Ellis, 2010) and western Pacific (Izbicki, 1991, 1996; Todd, 1989; Vengosh et al., 2002) coasts. In Europe, seawater intrusion has been documented within many of the coastal aquifers, particularly along the Mediterranean Sea and its eastern part in the archipelagos in the Aegean Sea (Alcalá and Custodio, 2008; Custodio, 2010; de Montety et al., 2008). Along the eastern Mediterranean, seawater intrusion has been reported to significantly intrude the coastal aquifer of Israel (Russak and Sivan, 2010; Sivan et al., 2005; Vengosh et al., 2005; Yechieli and Sivan, 2011; Yechieli et al., 2009).

Seawater intrusion may occur in areas of high precipitation, such as the Jeju volcanic island in South Korea, where the annual average rainfall is about 1870 mm and the estimated groundwater recharge is 1.4×10^9 m^3 $year^{-1}$. Although the groundwater withdrawal in the volcanic island is only 5% of the estimated replenishment, Br/Cl and $\delta^{18}O$ data indicate that

seawater has intruded 2.5 km inland due to the high conductivity and heterogeneity of the basaltic aquifers (Kim et al., 2003; Koh et al., 2009; Park et al., 2005). The Jeju island salinization case demonstrates that the predicted rise of sea level could lead to seawater intrusion in similar volcanic islands in the Pacific and further salinization of their groundwater.

In many coastal aquifers around the world, modern seawater intrusion typically occurs due to extensive freshwater withdrawals. Average ocean water has a TDS of 35 g l^{-1} while internal seas may have higher (e.g., Mediterranean Sea, Red Sea; TDS ~40 g l^{-1}) or lower salinities. Nevertheless, seawater has a uniform chemistry due to the long residence time of its major constituents, with the following features: predominance of Cl^- and Na^+ with a molar ratio of 0.86, an excess of Cl^- over the alkali ions (Na + K), and Mg^{2+} greatly in excess over Ca^{2+} (Mg/Ca = 4.5–5.2; **Table 1**). Seawater also has uniform Br/Cl (1.5×10^{-3}), $\delta^{18}O_{H_2O}$ (0–1‰), $\delta^{34}S_{SO_4}$ (21‰), $\delta^{11}B$ (39‰), and $^{87}Sr/^{86}Sr$ (0.7092) values. In contrast, fresh groundwaters are characterized by highly variable chemical compositions, although the typical fresh groundwater is dominated by Ca–Mg–HCO_3 ions. In most cases, Ca^{2+} predominates over Mg^{2+} content. The variations of conservative constituents in a mixed groundwater (Cl^-, $\delta^{18}O_{H_2O}$, $\delta^2H_{H_2O}$ Br/Cl) reflect the relative mixing proportions of fresh groundwater and seawater. For stable oxygen and hydrogen isotopes, the slope of a mixing curve between seawater ($\delta^{18}O_{H_2O} \sim \delta^2H_{H_2O} \sim 0$‰) and freshwater in the coordination of $\delta^2H_{H_2O}$ versus $\delta^{18}O_{H_2O}$ will always be lower than the Meteoric Water Line (i.e., <8) (Gat, 1974).

Yet, the most striking phenomenon that characterizes seawater intrusion into coastal aquifers is the difference between the chemical composition of the saline water associated with saltwater intrusion and the theoretical mixture between seawater and groundwater (Jones et al., 1999). In many cases, the saline water has a Ca–chloride composition (i.e., the ratio of $Ca/(SO_4 + HCO_3) > 1$) with low ratios of Na^+, SO_4^{2-}, K^+, and boron to chloride relative to modern ocean water (**Table 1**).

This geochemical modification during seawater intrusion has been attributed to base-exchange reactions with the aquifer rocks (Appelo, 1994; Appelo and Geirnart, 1991; Appelo and Postma, 2005; Appelo and Willemsen, 1987; Jones et al., 1999; Sayles and Mangelsdorf, 1977). Typically cation exchangers in aquifers are clay minerals, organic matter, oxyhydroxides, and fine-grained rock materials, which have mostly Ca^{2+} adsorbed on their surfaces due to the predominance of Ca^{2+} in freshwater. When seawater intrudes into a coastal aquifer saturated with Ca-rich groundwater, Na^+ replaces part of the Ca^{2+} on the solid surface. As a result, Na^+ is retained by the solid phase while Ca^{2+} is released to the water. Consequently, the solute composition changes from an Mg–chloride into a Ca–chloride, the Na/Cl ratio decreases, and the (Ca + Mg)/Cl ratio increases (Appelo, 1994; Appelo and Geirnart, 1991; Appelo and Postma, 2005; Appelo and Willemsen, 1987; Custodio, 1987a, 1997; Jones et al., 1999). Under such conditions, the relative enrichments in calcium and magnesium as normalized to chloride concentrations should be balanced by the relative depletion of sodium (i.e., $\Delta Ca + Mg = -\Delta Na$; where Δ is the difference between a conservative mixing value and actual concentration in salinized groundwater; Vengosh et al., 2002). Together with Ca^{2+}, exchangeable Sr^{2+} is released to the dissolved phase (Johnson and DePaolo, 1994). The $^{87}Sr/^{86}Sr$ ratio of adsorbed strontium can therefore affect the Sr isotopic composition of the saline groundwater. In the Salinas Valley of central California, the $^{87}Sr/^{86}Sr$ ratio of salinized coastal groundwater increases with Ca^{2+} content (**Figure 15**), indicating the contribution of a high $^{87}Sr/^{86}Sr$ ratio source from the clays. Due to the accumulation of ^{87}Rb in potassium-rich clay minerals, it has been proposed that base-exchange reactions are associated with radiogenic $^{87}Sr/^{86}Sr$ input to saline water (Vengosh et al., 2002), while in dolomitization processes, Sr from old marine carbonate is characterized by a lower $^{87}Sr/^{86}Sr$ composition (e.g., the Dead Sea brines; Stein et al., 1997).

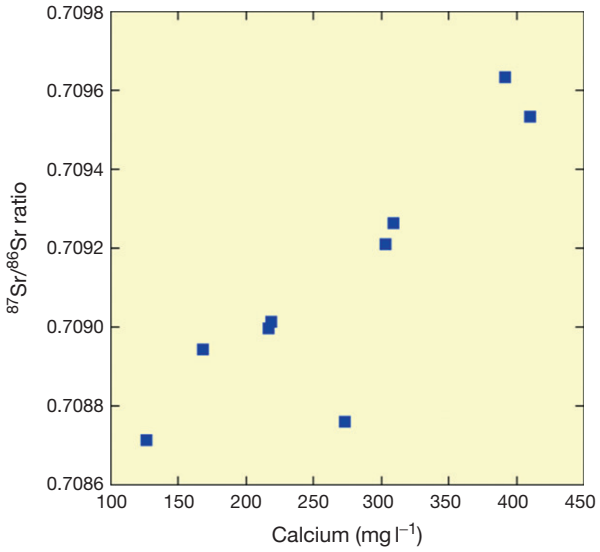

Figure 15 $^{87}Sr/^{86}Sr$ ratio versus calcium content of saline groundwater associated with seawater intrusion into the coastal aquifer of Salinas Valley, California, USA. The increase of $^{87}Sr/^{86}Sr$ with calcium concentration suggests that base-exchange reactions occur at an early stage of seawater intrusion and that strontium in exchange sites that is mobilized to the salinized water has a high $^{87}Sr/^{86}Sr$ ratio. Data from Vengosh et al. (2002).

In addition to base-exchange reactions, boron and potassium are typically adsorbed during seawater intrusion (Jones et al., 1999). The adsorption of boron is accompanied by an isotopic fractionation in which the light isotope, ^{10}B, is preferentially retained into the adsorbed phase, resulting in an enrichment of ^{11}B in the residual salinized groundwater. Consequently, saline groundwater associated with seawater intrusion is characterized by low B/Cl ratios ($< 8 \times 10^{-4}$) and high $\delta^{11}B$ values (>39‰) relative to those of seawater (**Figure 16**; Vengosh, 1998; Vengosh et al., 1994, 1999a,b). The intrusion of seawater into coastal aquifers is also associated with redox conditions along the saltwater–freshwater interface. Consequently, fractionation of sulfur isotopes during sulfate reduction processes results in high $\delta^{34}S_{SO_4}$ values in the residual sulfate, and thus saline groundwater associated with seawater intrusion is characterized by low SO_4/Cl ratios (<0.05) and high $\delta^{34}S_{SO_4}$ values (>20‰; Krouse and Mayer, 2000).

Climate change and fluctuations of sea levels during the Quaternary resulted in numerous cycles of seawater

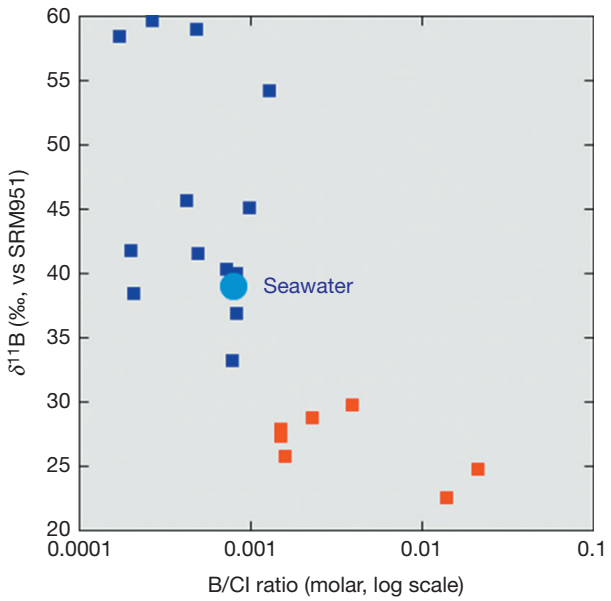

Figure 16 $\delta^{11}B$ values versus boron to chloride ratios (molar unit) in saline groundwater from the Mediterranean coastal aquifer associated with saltwater intrusion (Vengosh et al., 1994) and the North Carolina coastal aquifer associated with refreshing processes and reverse base-exchange reactions (Vinson et al., 2011). The comparison shows that seawater intrusion is associated with boron retention and ^{11}B enrichment while seawater displacement mobilizes boron from the aquifer rocks with lower $\delta^{11}B$ values.

encroachment but also fresh groundwater flow cycles into coastal aquifer saturated with saline groundwater and seaward displacement of intruded seawater. Fresh groundwater flow and displacement of saline groundwater (*freshening*) cause an opposite, defined as 'reverse,' base-exchange reaction. Ca^{2+} and Mg^{2+}, which are abundant in fresh groundwater, replace Na^{+} on the exchange sites of clay minerals with concomitant release of Na^{+} to the water. The flushing of the saline groundwater therefore generates Na–HCO_3-type saline groundwater with Na/Cl ratio >1 and low concentrations of Ca^{2+} and Mg^{2+} (Appelo, 1994; Appelo and Geirnart, 1991; Appelo and Postma 2005; Appelo and Willemsen, 1987; Chapelle and Knobel, 1983; Jones et al., 1999). The conspicuous difference in the chemical composition between saline groundwater originating from seawater intrusion and seawater displacement is critical in evaluating the sources and mechanisms of groundwater salinization in coastal aquifers (Russak and Sivan, 2010; Yechieli et al., 2009). The variations of Ca^{2+}, Sr^{2+}, Mg^{2+}, and K^{+} and ratios to chloride can be used to distinguish saline water originating from freshening processes (Russak and Sivan, 2010).

Another mechanism for the formation of Na–HCO_3 saline groundwater in coastal aquifers is oxidation of organic carbon that generates dissolved inorganic carbon (DIC), coupled with base-exchange reactions. Much study has been conducted in the Black Creek aquifer of South Carolina where the DIC concentration in groundwater near the Atlantic coast was 10 fold higher than that in groundwater from recharge areas (Chapelle and Knobel, 1983; Chapelle and McMahon, 1991; Knobel et al., 1998; McMahon and Chapelle, 1991). Thus, the bicarbonate content in the saline groundwater cannot be attributed only to fresh groundwater contribution but rather additional DIC must be generated within confined aquifers in order to account for the high HCO_3 concentrations in the saline groundwater. Generation of CO_2 from microbial respiration could produce carbonate mineral dissolution and thus Ca^{2+} mobilization, which would be exchanged by Na^{+}, resulting in the observed Na–HCO_3 composition (Vinson, 2011).

Saline Na–HCO_3 water is often associated with high boron contents and B/Cl ratios (i.e., greater than seawater) as demonstrated in southern Mediterranean coastal aquifers (Vengosh et al., 2005), the Saloum delta aquifer of Senegal (Faye et al., 2005), sandstone and shale aquifers in Michigan (Ravenscroft and McArthur, 2004), the delta aquifer of the Bengal Basin in southern Bangladesh (Halim et al., 2010; Ravenscroft and McArthur, 2004), and the coastal aquifer of North Carolina (Vinson et al., 2011). The relative enrichment of boron relative to the expected conservative mixing between seawater and freshwater suggests that boron is mobilized from the adsorption sites. One possible explanation for the relative boron enrichment is that the equilibrium between adsorbed and dissolved boron is reequilibrated during freshening processes resulting in desorption of boron. The strong correlation between Na/Cl and B/Cl ratios that characterize many of the saline Na–HCO_3-type groundwaters suggests that the arrival of low-saline, calcium-rich, and boron-poor water to the saline-saturated aquifer triggers the reverse-base-exchange reactions and boron mobilization to the water.

Since boron adsorption is associated with isotopic fractionation in which $^{10}B(OH)_4^-$ is retained onto adsorbed sites in clay minerals, the $\delta^{11}B$ value of adsorbed boron is typically lower than that of seawater. Spivack et al. (1987) showed that desorbed boron from marine sediments has a $\delta^{11}B$ value of about +15‰. During desorption of boron, all of the boron is mobilized without any isotopic discrimination (Spivack et al., 1987). Therefore, the $\delta^{11}B$ of a solution that originated from boron desorption is expected to be lower than that of seawater. This is demonstrated in Na–HCO_3 saline groundwater in the coastal aquifer of North Carolina that has both high B/Cl ratios and low $\delta^{11}B$ values relative to seawater (Vinson et al., 2011; **Figure 16**).

The ability to distinguish direct seawater intrusion from mixing of saline groundwater originating from displacement of seawater and freshening could be important for predicting salinization processes. Direct seawater intrusion would result in accelerated salinization rates, while mixing with saline groundwater that originated from diluted seawater could induce much lower salinization rates. This was demonstrated in the coastal aquifer of North Carolina (**Figure 16**) where the chemical and boron isotopic compositions of the saline groundwater indicate that it originated from diluted, apparently fossil seawater, which was consistent with a slow (2.5-fold in 20 years) rate of salinization (Vinson et al., 2011). Likewise, some areas of the Saloum delta aquifer of Senegal show evidence of seawater intrusion (low Na/Cl and B/Cl ratios) while others show evidence of freshening (high Na/Cl and B/Cl ratios; Faye et al., 2005).

Intrusion of modern seawater is not the only salinization process occurring in coastal aquifers, as salinization can also result from mixing with fossil seawater. Fossil seawater

represents past invasions of seawater into coastal aquifers accompanying rises in sea levels. Direct measurements and estimated residence times of seawater in coastal aquifers have been reported by using ^{14}C and tritium age-dating techniques in Germany (Hahn, 1991), India (Sukhija, 1996), coastal aquifers along the Gulf of Guinea in Togo (Akouvi et al., 2008), Japan (Yamanaka and Kumagai, 2006), the coastal plain of Suriname (Groen et al., 2000), and the Mediterranean coastal aquifer of Israel (Sivan et al., 2005; Yechieli and Sivan, 2011; Yechieli et al., 2000, 2009). It was shown, for example, that modern seawater intruded the upper and unconfined subaquifers of the coastal aquifer in Israel, whereas saline groundwater that occupies the underlying and confined subaquifers has an apparent age range of 10 000–15 000 years (Yechieli and Sivan, 2011).

11.9.4.2 Mixing with External Saline Waters in Noncoastal Areas

Many studies of regional aquifer systems have shown a general sequence of major ion evolution from low-saline Ca–Mg–HCO_3 water type to saline Na–SO_4–Cl groundwater along a hydraulic gradient (Hendry and Schwartz, 1988; Herczeg and Edmunds, 2000; Herczeg et al., 1991, 2001; Mazor, 1997). In addition to the increasing salinity, the ratio of Na^+ and Cl^- ions relative to the other dissolved salts (i.e., Na + Cl/TDS) increases with flow, as demonstrated in the saline groundwater from the Murray aquifer in South Australia (Herczeg et al., 2001) and the Cretaceous sandstone aquifer of the Milk River Formation, Alberta, western Canada (Hendry and Schwartz, 1988; Herczeg and Edmunds, 2000). The gradual increase of salinity and the chemical modification toward predominance of chloride and sodium ions is a result of several possible processes: (1) advection and diffusion of saline fluids entrapped in impermeable zones in the aquifer and/or outside the aquifer that are connected to an active permeable zone in the aquifer; and (2) dissolution of soluble salts such as gypsum and halite minerals within the aquifer. For example, several models have been postulated to explain the increase of salinity along flow paths in the Cretaceous sandstone aquifer of Milk River Formation. Hendry and Schwartz (1988) hypothesized that the salinity increase is due to diffusion of solute from the underlying aquitard. The entrapment of saline fluids in geological units of low hydraulic conductivity that are connected to active aquifers may result in diffusion of solutes and a gradual increase in the salinity of the aquifer (Herczeg and Edmunds, 2000).

Likewise, salinization of many aquifers is induced by flow of saline groundwater from adjacent or underlying aquifers (e.g., Bouchaou et al., 2009; Hsissou et al., 1999; Kloppmann et al., 2001; Magaritz et al., 1984; Maslia and Prowell, 1990; Sánchez-Martos and Pulido-Bosch, 1999; Sánchez-Martos et al., 2002; Vengosh and Benzvi, 1994; Vengosh et al., 1999a,b, 2002, 2005). For example, in the Upper Floridian aquifer in Georgia, USA, faults breach the nearly impermeable units of the underlying confined aquifer and allow upward leaking of saline groundwater (Maslia and Prowell, 1990). Similarly, extensive saline plumes in the Ogallala aquifer in the Southern High Plains, Texas, USA, are attributed to cross-formational flow from underlying evaporite units (Mehta et al., 2000a,b). The aquifer permeability will determine the flow paths of the underlying, typically pressurized, saline groundwater. This was demonstrated in deep reclaimed lake areas (polders) in the western Netherlands where saline groundwater from an underlying aquifer flows through paleochannel areas in the aquifer (de Louw et al., 2010). In the shallow (up to 150 m) Devonian formations of the Michigan Basin of southwestern Ontario, saline groundwater with geochemical characteristics similar to deep brines (e.g., high $\delta^2H_{H_2O}$, $\delta^{18}O_{H_2O}$, Br/Cl and low N/Cl and SO_4/Cl ratios) indicate that the high-salinity fluids migrated into discrete areas of the Devonian and Pleistocene formations. The cross-formational fluid flow from depth probably occurred along discrete fractures that were formed during or following deglaciation (Weaver et al., 1995). Finally, evidence for the migration of the Middle Devonian Marcellus brines to shallow aquifers in the Appalachian basin (northeastern Pennsylvania) was shown by saline groundwater with distinctive Br/Cl, $^{87}Sr/^{86}Sr$, and Ba/Sr fingerprints (Warner et al. 2012).

Saline plumes formed by uprising of saline groundwater are also a major source of salinity in the Mediterranean coastal aquifer of Israel (**Table 1**; **Figure 17**) (Vengosh et al., 1994, 1999b). Likewise, groundwater in the Gaza Strip is salinized by lateral flow of saline groundwater from the eastern part of the aquifer. The flow rate and thus the rate of salinization have been accelerated due to overexploitation and reduction of groundwater levels within the Gaza Strip to levels exceeding drinking water standards (Vengosh et al., 2005). This salinization phenomenon is one of the fundamental water-quality problems in the Gaza Strip where the salinity level of groundwater exceeds international drinking water standards. Diversion of the external saline flow via pumping and desalinization has been proposed to mitigate the highly salinized aquifer that is the only source of drinking and irrigation water for the rapidly growing population in the Gaza Strip (Weinthal et al., 2005).

Several models have been suggested to explain the origin of saline groundwater in nonmarine settings. These include brines originated from residual evaporated seawater entrapped as formation water, saline water originated from seawater freezing, and saline water generated by evaporite dissolution. Residual evaporated seawaters that were modified by water–rock interactions such as dolomitization are typically characterized by a Ca–chloride composition ($Ca/(SO_4 + HCO_3) > 1$) with an Na/Cl ratio below seawater ratio value (**Figure 18**), Br/Cl ≥ seawater ratio (1.5×10^{-3}), relative depletion of sulfate ($SO_4/Cl < 0.05$), $\delta^{34}S_{SO_4} \geq 20‰$, and $\delta^{11}B \geq 39‰$ (Carpenter et al., 1974; McCaffrey et al., 1987; Raab and Spiro, 1991; Starinsky, 1974; Stein et al., 1997; Vengosh et al., 1992; Wilson and Long, 1993). Upon hydrological contact and mixing of brines with fresh groundwater, the chemical composition of the hypersaline brine dominates the composition of the mixture owing to the extreme difference in salinity between the brines and the freshwater. Consequently, dilution or flushing of entrapped brines by low-saline groundwater has only a minor effect on the chemical and isotopic compositions of saline groundwater derived from brine intrusion.

In the Dead Sea Rift Valley, deep pressurized brines that are the residue of evaporated seawater (greater than 10-fold evaporation; Starinsky, 1974) are in hydrological contact with overlying fresh groundwater (Farber et al., 2007; Marie and Vengosh, 2001). Once the natural hydrological balance is disturbed due to exploitation of the overlying fresh groundwater,

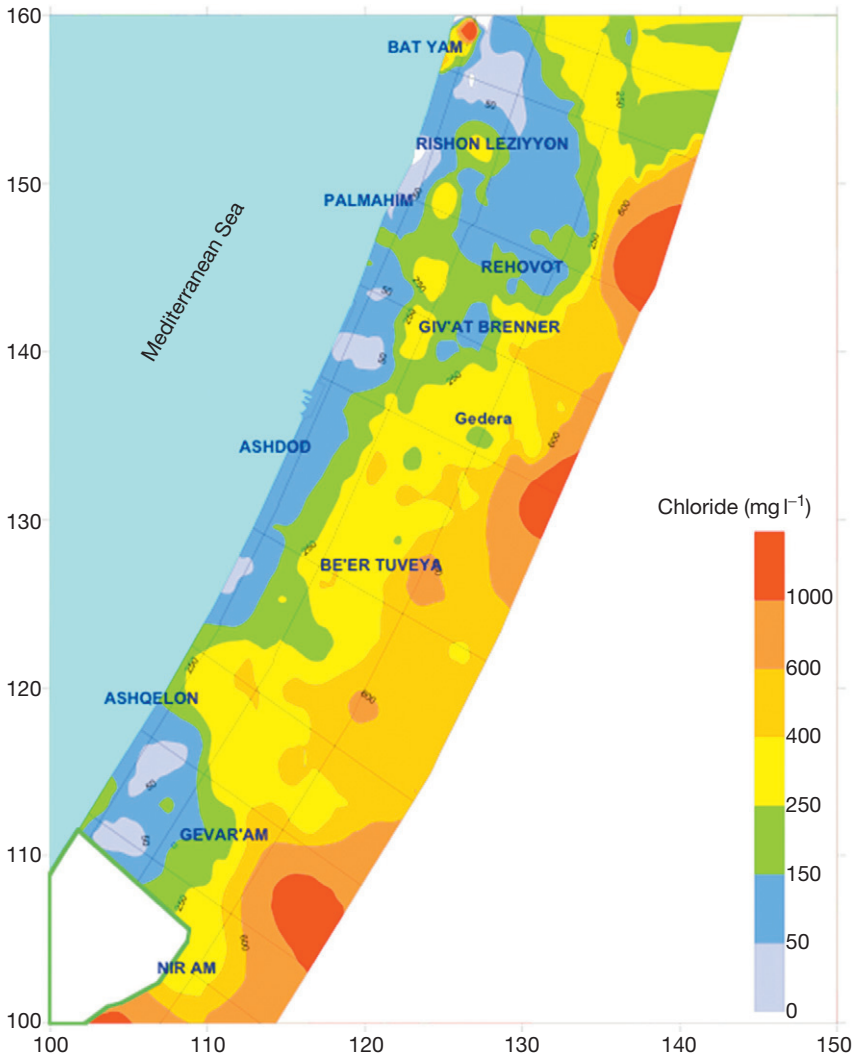

Figure 17 Chloride (in mg l^{-1}) distribution in groundwater from the central and southern part of the Mediterranean coastal aquifer of Israel. Note the saline plumes in the central and eastern parts of the aquifer.

the salinization process starts or accelerates. In the Jericho area in the southern Jordan Valley, rapid rates of salinization due to the upconing of underlying brines are found in wells located near the major Rift faults (Farber et al., 2004, 2005, 2007; Marie and Vengosh, 2001). Due to the high salinity of the apparent original brines (>100 g l^{-1}), mixture with only a small fraction of brine leads to devastating salinization phenomena in overlying freshwater resources.

An additional source of salinity in polar areas is residual brines derived from the freezing of seawater (Bottomley et al., 1999; Herut et al., 1990; Marion et al., 1999; Nelson and Thompson, 1954; Richardson, 1976; Stotler et al., 2009; Wang et al., 2000). Bein and Arad (1992) suggested that deep saline groundwater from Sweden and Finland, which is characterized by low Na/Cl and high Br/Cl ratios, is the remnant of frozen seawater formed during the last glaciations, followed by dilution with meteoric water (Bein and Arad, 1992).

Dissolution of evaporite minerals in sedimentary basins is also a common feature of salinization. This type of salinization process has been reported for groundwater in the Ogallala Formation in the Southern High Plains, Texas, USA (Mehta et al., 2000a,b), the Dammam aquifer in Kuwait (Al-Ruwaih, 1995), the Nubian Sandstone aquifer in the Sinai and Negev deserts (Rosenthal et al., 1998; Vengosh et al., 2007), the Great Artesian Basin in Australia (Herczeg et al., 1991; Love et al., 2000), and the Hammamet–Nabeul shallow aquifer in northeastern Tunisia (Moussa et al., 2011). In the case of halite dissolution, the saline water is dominated by Na^+ and Cl^- ions, Na/Cl ratio ~1, and Br/Cl < seawater ratio (e.g., the Ogallala Formation; **Table 1**; Mehta et al., 2000a,b). Salinization can also be derived from dissolution of marine Ca–sulfate (e.g., gypsum) as evidenced in Pinawa, Canada (Nesbitt and Cramer, 1993), the Salinas Valley in California (Vengosh et al., 2002), and the Nubian Sandstone aquifer in the Negev, Israel (Vengosh et al., 2007). Typically, gypsum dissolution would produce saline water with Ca/SO_4 ratio ~1. However, the dissolution of gypsum can also be associated with Ca^{2+} uptake onto the exchange substrate, displacing Na^+ to the solution. The residual water would be enriched in Na–SO_4 (Nesbitt and Cramer, 1993). Dissolution of gypsum would affect the sulfur isotopic composition of the salinized water. The $\delta^{34}S_{SO_4}$ values of marine sulfate varied over geological time, with a maximum

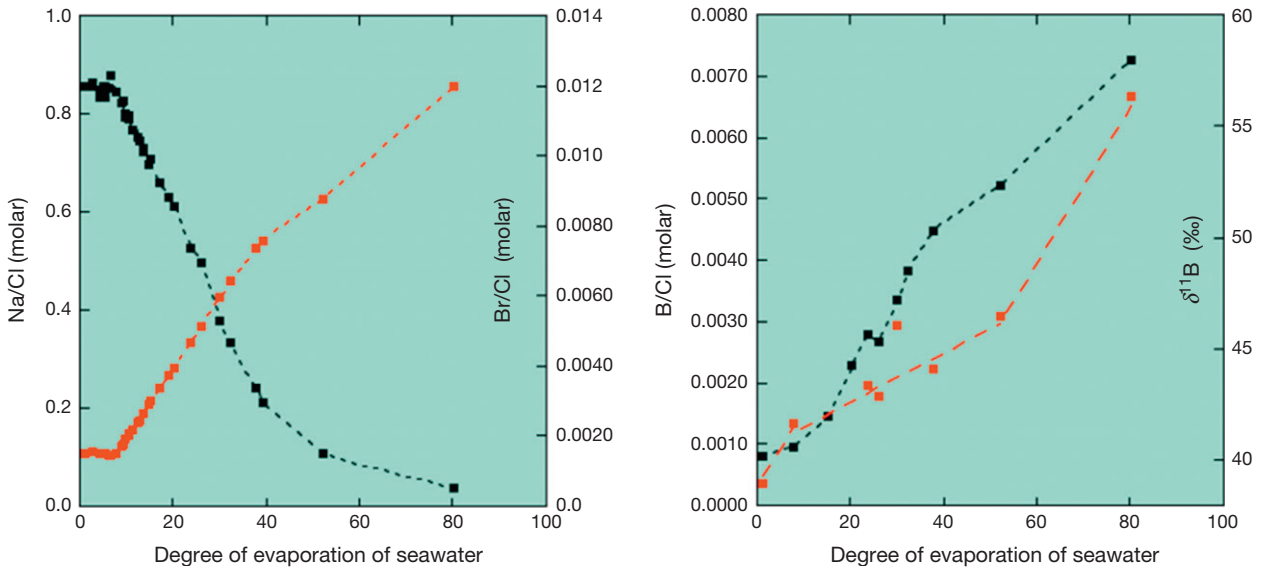

Figure 18 Variation of Na/Cl, Br/Cl, B/Cl, and δ^{11}B values during evaporation of seawater. Degree of evaporation is defined as the ratio of Br^- content in the solution at different stages of evaporation to the initial Br^- concentration in seawater. Data were integrated from McCaffrey et al. (1987), Raab and Spiro (1991), and Vengosh et al. (1992).

near +35‰ in the Cambrian and less than +10‰ in the Permian. In contrast, oxidation of sedimentary sulfides, which are significantly depleted in ^{34}S relative to oceanic sulfate, will result in low $\delta^{34}S_{SO_4}$ values with typical ranges of −30‰ to +5‰ (Krouse and Mayer, 2000). Likewise, the $^{87}Sr/^{86}Sr$ ratio of marine sulfate minerals will mimic the Sr isotopic composition of co-genetic seawater, and thus salinization resulting from gypsum dissolution will carry the isotopic imprint of the $^{87}Sr/^{86}Sr$ of ocean water at the time of the mineral deposition. This was demonstrated in the Nubian Sandstone aquifer of the Negev, Israel, where sulfate-rich groundwater flows from the underlying Jurassic aquifer to the overlying Nubian Sandstone aquifer. The chemical and isotopic compositions of the Jurassic groundwater ($\delta^{34}S_{SO_4}$ ~+14‰; $^{87}Sr/^{86}Sr$ ~0.707 64) was interpreted as reflecting dissolution of Late Triassic marine gypsum deposits as these isotopic signatures are consistent with the $\delta^{34}S_{SO_4}$ and $^{87}Sr/^{86}Sr$ values of the Jurassic seawater (Vengosh et al., 2007). Finally, the Sr isotope compositions of sulfate-rich saline waters from the High Atlas (Warner et al. , 2010) and Anti-Atlas (Ettayfi et al., 2012) mountains in Morocco are consistent with the Lower Cretaceous and Early Cambrian secular seawater Sr isotope ratios, respectively, reflecting interaction of groundwater with carbonate and sulfate aquifer rocks.

11.9.4.3 Salinization of Shallow Groundwater in River Basins

In many river basins in arid and semiarid zones, groundwater substitutes for surface water as the major water resource for domestic and agricultural applications. In arid regions, such as the Jordan Valley (Farber et al., 2007), the Lower Mesopotamian Plain of the Euphrates River, Iraq (Barica, 1972), the Hueco Bolson Basin of Texas and Chihuahua of the US–Mexico border (Eastoe et al., 2008, 2010), the alluvial aquifer system in arid Alice Springs in central Australia (Vanderzalm et al., 2011), the arid region of Namibia (Shanyengana et al., 2004), and the sub-Saharan Draa and Ziz basins in southern Morocco (Warner et al., 2010), the local populations are entirely dependent on agriculture and are concentrated near the river channels and/or associated oases. One of the factors affecting agricultural productivity is the salinity of the irrigation water; salinity is thus a key limiting factor in sustainable agricultural development and the overall livelihood of the local populations in these regions.

In some of the arid basins, surface water is imported from areas of higher precipitation and is stored in dammed reservoirs before being discharged for downstream irrigation. As discussed earlier in the chapter, salinization of surface water resulting from evaporation (either in the reservoirs or during irrigation), leads to saline agriculture return flows that are recharged into local aquifers. In addition, salinization of the shallow groundwater may result from dissolution of salts in the unsaturated zone and/or by lateral flow of adjacent saline groundwater, particularly due to reverse hydrological gradients in the inner parts of the alluvial aquifers evolved from differential pumping in the basin valley (**Figure 19**). In an attempt to delineate the sources and mechanisms of groundwater salinization in a managed arid watershed, one can define three types of geochemical tracers (R_1, R_2, R_3) that are capable of delineating the three principal saline sources (**Figure 20**):

(1) R_1 type – Tracers are used to identify *evaporation* (process 1 in **Figure 20**) and *mixing* with external groundwater (process 3), but do not identify salt dissolution. These tracers include water isotopes ($\delta^{18}O$, $\delta^{2}H$) and ion concentrations.
(2) R_2 type – Tracers are used to identify *dissolution of salts* (process 2 in **Figure 20**) and *mixing* with external groundwater (process 3), but not evaporation (process 1). These tracers include several ion ratios, particularly the ratios of conservative elements such as Br/Cl and B/Cl.
(3) R_3 type – Tracers that are sensitive to *mixing* with external groundwater (process 3), but not to evaporation and salt

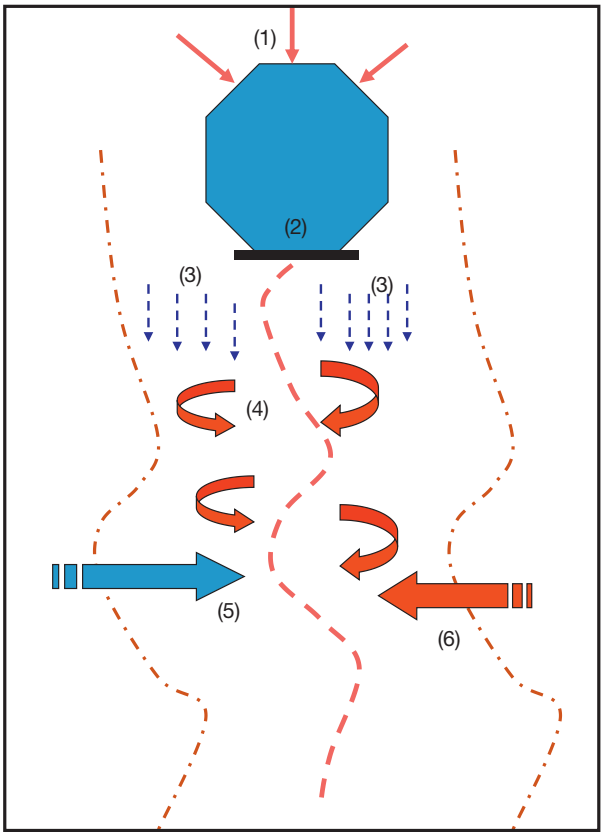

Figure 19 Schematic illustration of possible salinization mechanisms of surface water and shallow groundwater in alluvial aquifers where imported water is stored in dammed reservoirs and used for irrigation. The possible salinization includes (1) inflow of fresh and saline water to dammed reservoir; (2) evaporation from the reservoir; (3) evaporation during irrigation of the imported water; (4) dissolution of salts from the unsaturated zone during irrigation; (5) lateral flow of low-saline water to the alluvial aquifers; and (6) lateral flow of saline water to the alluvial aquifers.

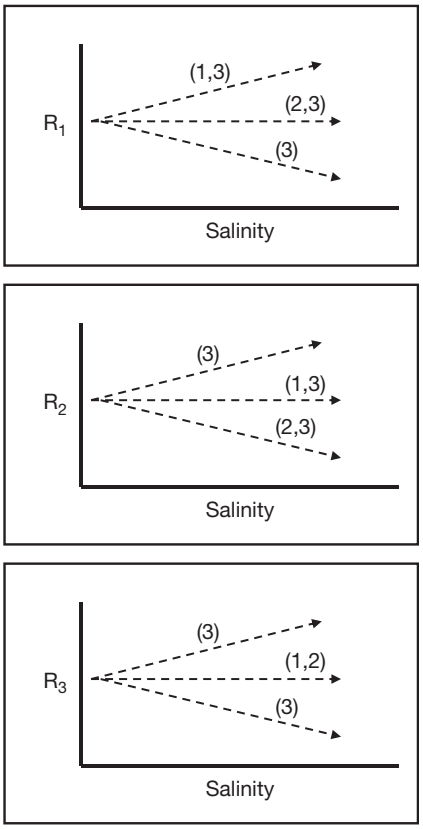

Figure 20 Schematic illustration of possible variations of three types of geochemical tracers (R_1, R_2, R_3) that are capable of delineating the three principal saline mechanisms of shallow groundwater in alluvial aquifers; see text for detailed explanation.

dissolution (processes 1 and 2). These tracers include the isotopic compositions of dissolved constituents in the water such as strontium ($^{87}Sr/^{86}Sr$), sulfur ($\delta^{34}S_{SO_4}$), and boron ($\delta^{11}B$) isotopes.

In the sub-Saharan Draa Basin of southern Morocco, winter snowmelt from the Atlas Mountains is captured in a reservoir, stored, and discharged downstream for irrigation in six oases. Shallow groundwater from the oases shows a large salinity range, with TDS up to 12 000 mg l^{-1}. The Br/Cl and B/Cl ratios of the shallow groundwater decrease with increasing salinity, which suggests that the major mechanism of salinization of the shallow groundwater in the Draa Basin is dissolution of salts stored in the unsaturated zone and salinization of the underlying shallow groundwater (Warner et al., 2010; 2013).

11.9.4.4 Salinization of Nonrenewable Groundwater

The impact of salinization is more conspicuous in an aquifer where the freshwater is not renewable (i.e., fossil; see Chapter 7.14). Numerous studies have shown that groundwater resources across the Sahara and the Sahel regions in northern Africa and in the arid zones of the Middle East are fossil and reflect paleorecharge during periods of higher rainfall in the late Pleistocene (Cook and Herczeg, 2000; Edmunds and Droubi, 1998; Edmunds and Gaye, 1994; Edmunds et al., 1999, 2002; Gaye and Edmunds, 1996; Phillips, 1994; Vengosh et al., 2007). Typically, fresh paleowaters overlie saline dense water bodies. With geological time, a fragile hydraulic equilibrium is generated between the two water bodies. Well construction and groundwater extraction can affect this delicate hydrological equilibrium. Exploitation of paleowaters, without modern replenishment, may lead to rapid salinization of groundwater resources. In the Middle East and northern Africa, salinization of fossil groundwater has had devastating effects since in some cases they are the only sources of potable water (Bouchaou et al., 2008, 2009; Salameh, 1996; Sowers et al., 2011; Vengosh and Rosenthal, 1994; Vengosh et al., 2007). In the Damman carbonate aquifer in Bahrain, for example, overexploitation has resulted in a drop of the piezometric surface by 4 m and an increase in the salinity by over 3 g l^{-1}, owing to a combination of leakage from a deeper aquifer, marine intrusion, sabkha water migration, and agricultural drainage. More than half of the area of the Damman aquifer has become saline as a result of overexploitation (Edmunds and Droubi, 1998). In southern Israel, the extraction of brackish paleowater from the Lower Cretaceous Nubian Sandstone aquifer in areas along the Rift Dead Sea Valley has resulted in mixing with Ca–chloride brine and the salinization of the associated groundwater (Yechieli et al., 1992). Another example is the Sakakah Aquifer in the northeastern part of Saudi Arabia where

mixing relationships between fossil fresh and saline (TDS up to 3000 mg l^{-1}) groundwater have degraded water quality (Al-Bassam, 1998).

In the Souss-Massa Basin in southwest Morocco, stable isotopes, tritium, and ^{14}C data for local groundwater indicate two types of groundwater: (1) fresh and young groundwater originating from recharge from the High Atlas Mountains, particularly in the eastern part of the basin; and (2) more saline and old (several thousands of years) groundwater in the western part of the basin, where most groundwater exploitation has taken place. The exploitation of fossil rather than the renewable groundwater in the aquifer has led to high salinization rates in the western part of the aquifer (Bouchaou et al., 2008).

11.9.5 Salinization of Dryland Environment

Salinity of water and soil in the dryland environment is a natural phenomenon resulting from a long-term accumulation of salts on the ground and lack of their adequate flushing in the unsaturated zone. Salt accumulation and formation of efflorescent crusts have been documented in the upper unsaturated zone (Cartwright et al., 2004, 2006, 2007b; Gee and Hillel, 1988; Jackson et al., 2009; Leaney et al., 2003; Nativ et al., 1997; Ng et al., 2009; Scanlon et al., 2009a,b; Stonestrom et al., 2009) and fracture surfaces (Kamai et al., 2009; Weisbrod et al., 2000) in many arid areas. The accumulation of soluble salts in soil occurs when evaporation exceeds precipitation and salts are not leached but remain in the upper soil layers in low-lying areas. Natural soil salinization, referred to as 'primary salinization,' occurs in arid and semiarid climatic zones. 'Secondary salinization' is the term used to describe soil salinized as a consequence of direct human activities (Dehaan and Taylor, 2002; Fitzpatrick et al., 2000; Shimojimaa et al., 1996). Excessive salinity in soil results in toxicity for crops, reduction in soil fertility, reduction of availability of water to plants by reducing the osmotic potential of the soil solution, and a significant change in the hydraulic properties of soil (Bresler et al., 1982; Frenkel et al., 1978; Hillel, 1980).

Most of the salts that have accumulated in the unsaturated zone in arid environments of the southwestern United States and in the Murray Basin, Australia, originated from long-term atmospheric deposition of chloride and sulfate salts (Scanlon et al., 2009a,b). The salt accumulation has been attributed to surface evaporation (Allison and Barnes, 1985; Allison et al., 1990), wetting and drying cycles (Chambers et al., 1996; Drever and Smith, 1978; Keren and Gast, 1981), soil capillarity, and capillarity transport of water and salts from bulk rock matrix toward the fracture surface (Weisbrod et al., 2000).

In the western United States, recharge typically occurs within surrounding highlands, and groundwater flows toward the basin centers. Along the flow path, the salinity of the groundwater increases by several orders of magnitude by both salt dissolution and evaporation (Richter and Kreitler, 1986, 1993). The chemistry of the residual saline groundwater is primarily controlled by the initial freshwater composition and the subsequent saturation of typical minerals (calcite, gypsum, spiolite, halite; Eugster and Jones, 1979; Hardie and Eugster, 1970). It has been demonstrated, for example, that evaporation and mineral precipitation control the salinity of groundwater that flows to Deep Spring Lake (Jones, 1965), Death Valley (Hunt et al., 1996), and the Sierra Nevada Basin (Garrels and MacKenzie, 1967).

While the source of the salts is natural, the process of *salinization* in the dryland environment refers to human intervention. The most widespread phenomenon of dryland salinization is the response to changes in land use, such as land clearing and replacing natural vegetation with annual crops and pastures. The natural vegetation in arid and semiarid zones uses any available water, and thus the amount of water that percolates below the root zone is minimal, estimated at between 1 and 5 mm $year^{-1}$ in the case of South Australia (Allison and Barnes, 1985). Over thousands of years, salts have accumulated in the unsaturated zone and their mobilization and leaching to the underlying saturated zone was constrained by the slow recharge flux. Large-scale replacement of the natural vegetation with annual crops and pastures with short roots significantly increased the amount of water percolating below the root zone, increasing the recharge rate and consequently the rate that salts leached into the underlying groundwater (Scanlon et al., 2009a; Williams, 2002). Thus, the salts that historically were stored in the root zone began to flush through the unsaturated to the saturated zone, causing salinization of the underlying groundwater. Leaney et al. (2003) predicted that salt flux from the unsaturated zone in the Murray–Darling Basin of southeastern Australia (with soil salinity up to 15 000 mg l^{-1}) will increase the salinity of the shallow groundwater (~1000 mg l^{-1}) by a factor of 2–6. Indeed, a systematic survey of salts in borehole samples collected beneath natural ecosystems, nonirrigated ('rain-fed') croplands, and irrigated croplands in the southwestern United States and in the Murray–Darling Basin in Australia showed increased mobilization of chloride and sulfate following land use changes (Scanlon et al., 2009a). Similar cases of soil and shallow groundwater salinization induced by land use changes were reported in Argentina (Lavado and Taboada, 1987), India (Choudhari and Sharma, 1984), and South Africa (Flügel, 1995).

Another type of anthropogenic-induced salinization in dryland environments is *afforestation*. Since deep tree roots can efficiently draw water from the underlying shallow groundwater, afforestation of grasslands may reverse the downward flux of groundwater from the soil to the saturated zone. As a result, transpiration of water by deep roots may leave its salt load in the unsaturated zone. Consequently, afforestation reduces natural groundwater recharge and causes salinization of the soil and shallow groundwater (Jackson et al., 2009; Jobbagy and Jackson, 2004; Nosetto et al., 2009). Evidence of soil and groundwater salinization due to tree establishment on grasslands has been shown in the northern Caspian region (Sapanov, 2000), Australia (Heuperman, 1999), and the Argentine Pampas (Berthrong et al., 2009; Jobbagy and Jackson, 2004; Nosetto et al., 2009). A systematic chemical survey of the upper 30 cm of soil in 153 plantation sites worldwide showed that afforestation is associated with a significant decrease in nutrient cations (Ca^{2+}, Mg^{2+}, K^{+}) and increase in sodium due to selective uptake of the cations by the plants (Berthrong et al., 2009; Jobbagy and Jackson, 2004).

One of the most dramatic large-scale salinization phenomena occurs in Australia (Allison and Barnes, 1985; Allison et al., 1990; Cartwright et al., 2004, 2006, 2007b; Fitzpatrick et al., 2000; Herczeg et al., 1993, 2001; Leaney et al., 2003; Peck and Hatton, 2003; Scanlon et al., 2009a;

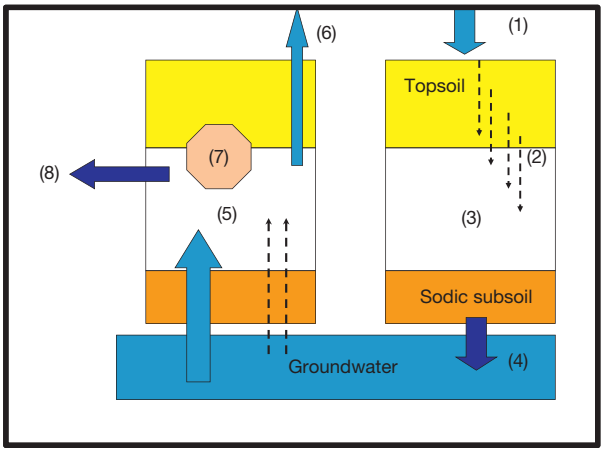

Figure 21 The dryland salinization cycle (the Australian model): (1) salt accumulation and precipitation of minerals; (2) selective dissolution and transport of soluble salts in the vadoze zone; (3) storage of salts influenced by soil permeability; (4) leaching and salinization of groundwater; (5) rise of saline groundwater; (6) capillarity evaporation of rising groundwater; (7) soil salinization; and (8) lateral solute transport and salinization of streams and rivers. Modified from Fitzpatrick RW, Merry R, Cox J (2000) What are saline soils and what happens when they are drained? *Journal of Australian Association of Natural Resource Management* 6: 26–30.

Williams et al., 2002). The Australian case is used here to describe the chemical evolution of solutes in the dryland environment. The dryland salinization cycle (**Figure 21**) is a complex process that begins with salt accumulation on the surface and soil, precipitation and dissolution of nonsoluble (carbonate) and soluble (gypsum and halite) minerals, and incongruent silicate mineral reactions (Eugster and Jones, 1979; Hardie and Eugster, 1970). The salts that accumulate in the soil are flushed into the vadose zone. Two factors control the rate of flushing: mineral solubility and soil physical properties such as permeability. The different solubility of different minerals leads to chemical separation of minerals within the unsaturated zone; the higher the solubility of the mineral, the longer will the ions derived from its dissolution travel in the unsaturated zone. This process is also known as wetting and drying and involves complete precipitation of dissolved salts during dry conditions and subsequent dissolution of soluble salts during wet periods (Drever and Smith, 1978). This results in an uneven distribution of ions along the unsaturated zone: Ca^{2+}, Mg^{2+}, and HCO_3^- tend to accumulate at relatively shallow depths, SO_4^{2-} at intermediate depths, and Na^+ and Cl^- are highly mobilized to greater depths of the unsaturated zone. The Na/Ca ratio fractionates along the travel of solute in the vadose zone; Ca^{2+} is removed by precipitation of carbonate minerals whereas Na^+ remains in solution, or even increases due to dissolution of halite. In addition, the mobilization of Na^+ triggers base-exchange reactions; Na^+ is adsorbed on clay and oxides, but the Ca^{2+} that is released from the adsorbed sites is taken up by precipitation of soil carbonate.

The overall chemical composition of the solutes that are generated in the dryland environment depends on the initial fluid and soil compositions. In Australia, the solutes are derived from marine aerosols and deposited on the soil (Herczeg et al., 2001; Scanlon et al., 2009a). ^{14}C ages of soil solutions reveal that most of the recharge occurred during wet climatic periods more than 20 000 years ago (Leaney et al., 2003). Likewise, decreases in ^{3}H and ^{14}C activities with groundwater depth from the Shepparton Formation in the southeast Murray Basin and northern Victoria, Australia, suggest dominantly preland clearing vertical recharge (Cartwright et al., 2006, 2007b). Consequently, with thousands of years of salt accumulation and numerous wet and dry cycles through the unsaturated zone, the saline groundwater in the dryland environment has become 'marine-like' with a predominance of Na^+ and Cl^- ions and Na/Cl and Br/Cl ratios identical to those of seawater (Herczeg et al., 1993, 2001; Mazor and George, 1992). In addition, the Australian salts lakes, which represent groundwater discharge zones, are characterized by marine chemical and isotopic (sulfur and boron) compositions modified by internal lake processes (Chivas et al., 1991; Vengosh et al., 1991a).

In addition to atmospheric deposition, water–rock interactions, triggered by generation of acids from CO_2 accumulation and oxidation of organic matter in the soil, can modify the original chemistry of the meteoric deposition. The 'nonmarine' signature of the saline groundwater and salt lakes in the western United States reflects the role of water–rock interactions in shaping the chemical composition of both initial and evolved groundwater in the arid zone in this region (Eugster and Jones, 1979; Hardie and Eugster, 1970). Numerous drying and wetting cycles may also result in precipitation of halite minerals in the saturated zone that change the chemistry of the recharge solutions. Variations in Br/Cl ratios in water from the Honeysuckle Creek area in the southeast Murray–Darling Basin in Australia indicate that the transformed salts are derived from a combination of *both* halite dissolution and a residual evaporated solution (Cartwright et al., 2004).

The second factor that controls salinization of dry land environments is the physical characteristics (e.g., permeability) of the soil. In the arid zone of Australia, rainfall was not always sufficient to leach the salts, and the clay layers in deep sodic subsoil prevents downward movement of water and salts, leading to a saline zone (Fitzpatrick et al., 2000). Differential residence time and salinity due to aquifer permeability was documented in groundwater from the Shepparton Formation in the southeast Murray Basin. Recharge in highly permeable paleovalleys produced relatively lower saline groundwater (TDS ~3000 mg l^{-1}) with a 'bomb pulse' ^{36}Cl signature, suggesting relatively young recharge. In contrast, recharge in areas of low permeability generated much higher salinity (TDS up to 60 000 mg l^{-1}) with low Br/Cl and low ^{36}Cl activities. The correlation between Br/Cl and $R^{36}Cl$ values suggests old halite dissolution and slow transport through the impermeable unsaturated zone (Cartwright et al., 2006).

In addition to the natural accumulation of salts in soil due to the decrease of soil permeability (also called 'subsoil transient salinity'; Fitzpatrick et al., 2000), anthropogenic salinization due to the rise of saline groundwater has also been described in South Australia (Allison and Barnes, 1985; Allison et al., 1990; Cox et al., 2002; Herczeg et al., 1993). The selective leaching process in the unsaturated zone generates two types of saline groundwater (1) Na–Cl groundwater; and (2) sulfate-rich water. The rising of Na–Cl groundwater creates halite-dominant soils, where chloride is the dominant anion. The rising of sulfate-enriched groundwater creates three types of

soils: (1) gypsic soil – under aerobic conditions and saturation of calcium sulfate; (2) sulfidic soil – under anaerobic conditions and sufficient organic carbon, bacteria uses the oxygen associated with sulfate and produces pyrite; (3) sulfunic soil – exposure of pyrite to oxygen in the air causes oxidation of pyrite and formation of sulfuric acid, which consequently reduces the soil pH and enhances leaching of basic cations, anions, and trace elements into the soil solution (Cox et al., 2002; Fitzpatrick et al., 2000).

The differentiation of soil permeability due to clay content, sodium uptake by clays, and mineral precipitation also prevents salts from flushing downward through the unsaturated zone, and causes lateral flow of saline soil solutions and shallow groundwater toward low-lying areas. The final stage of the dryland cycle is salinization of adjacent streams and rivers that occupy low-lying areas. The chemical composition of the salinized river in the dryland environment reflects the net results of salt recycling between soil, subsoil, groundwater, secondary soil, soil solution, and surface water (**Figure 21**).

11.9.6 Anthropogenic Salinization

11.9.6.1 Urban Environment and Wastewater Salinization

The salinity of domestic wastewater is a function of the combined salinity of the source water supplied to a municipality and the salts added directly by humans (**Figure 22**). The 'man-made' salts include detergents, washing powders, and salts generated in daily household operations such as salts used for dishwashers and for refreshing ion-exchange columns typically used in softeners. In Israel, for example, the average net human contribution of chloride, sodium, and boron to domestic wastewater were 125, 120, and 0.6 mg, respectively, for 1 l of wastewater in the early 1990s (Hoffman, 1993; Vengosh et al., 1994). Common treatment for sewage purification will reduce the turbidity, the concentrations of organic constituents, and the nutrient loads but will not remove the dissolved inorganic salts unless sewage is treated through tertiary treatment such as desalination (see Section 11.9.9). Consequently, in many arid and semiarid countries, treated sewage is commonly saline. In Israel, the chloride content of domestic sewage effluent from the Dan metropolitan area was between 300 and 400 mg l^{-1} during the early 1990s (Harussi et al., 2001; Vengosh et al., 1994).

Wastewater has become a valuable resource in many water-deficient countries and reusing treated wastewater for agriculture has substituted for natural water sources in some places in Europe (Bixio et al., 2006, 2008), the United States (Crook and Surampalli, 2005), and many Mediterranean (Maton et al., 2010) and Middle East countries. In Israel, treated sewage effluents have been increasingly used for agriculture (Friedler, 2001); from a total of 530×10^6 m^3 of sewage produced in 2010, 355×10^6 m^3 (about 75%) was treated and used for irrigation (Israel Water Authority, 2011). Likewise, Jordan has been increasingly using wastewater for the agricultural sector (Al-Khashman, 2009; Carr et al., 2011; Hadadin et al., 2010). Yet, the salinity and the presence of other inorganic constituents in wastewater pose a significant risk for soil and consequently for aquifer salinization following decades of irrigation (Banin and Fish, 1995; Beltrán, 1999; Fernandez-Cirelli et al., 2009; Klay et al., 2010; Tarchouna et al., 2010). Soil and groundwater salinization due to long-term application of treated wastewater have been reported, for example, in Israel (Gavrieli et al., 2001; Kass et al., 2005; Rebhun, 2004; Ronen et al., 1987; Vengosh and Keren, 1996), Cape Cod, Massachusetts, USA (DeSimone et al., 1997), Texas, USA (Duan et al., 2011), Tunisia (Klay et al., 2010), southern France (Tarchouna et al., 2010), Portugal (Stigter et al., 1998), and Senegal (Re et al., 2011). It is therefore crucial to reduce the salinity of wastewater if this resource is to become a sustainable alternative water source for agriculture. Possible solutions for salt reduction were outlined by Weber et al. (1996) and include

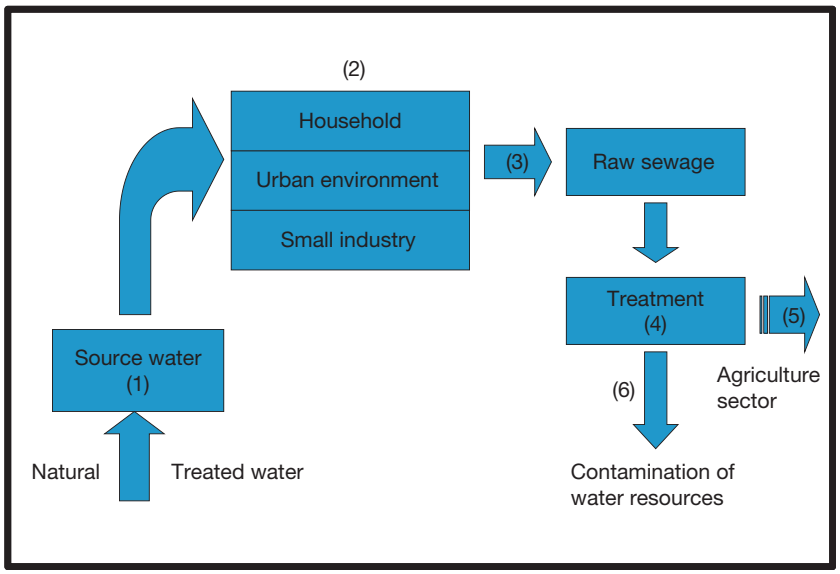

Figure 22 The domestic wastewater salinization cycle: (1) supply water to a municipality; (2) salts added within the urban environment; (3) sewage generation; (4) sewage treatment; (5) reuse of treated sewage for irrigation; (6) contamination of water resources.

separation of saline effluents from major treated sewage streams that are diverted from the sewage treatment plants; substitution of sodium by potassium salts in ion-exchangers; construction of centralized systems for the supply of soft water in industrial areas that would eliminate the need for softeners and thus reduce the impact of softener backwash saline water; precipitation of Ca^{2+} and Mg^{2+} in the effluents from ion-exchangers and recycling of the NaCI solution; a reduction of the discharge of salts by the meat-processing (koshering) process; and establishing new membrane technology for salt removal in treated wastewater effluents (Weber et al., 1996).

Boron is commonly high in domestic wastewater due to the use of synthetic Na–borate additives derived from natural Na–borate minerals that are used as bleaching agents (Nishikoori et al., 2011; Raymond and Butterwick, 1992; Vengosh et al., 1994; Waggott, 1969). Given that high concentrations of boron in irrigation water (>1 mg l^{-1} for most crops) could be toxic for many plants (Bastias et al., 2010; Davis et al., 2002; Karabal et al., 2003; Kaya et al., 2009; Lehto et al., 2010; Papadakis et al., 2004; Reid, 2010; Scialli et al., 2010; Smith et al., 2010; Sotiropoulos et al., 1999; Thompson et al., 1976), some countries have set regulations for reducing boron additives in detergents and washing powders. This has been implemented in Israel; in 1999, the Israeli Ministry of Environment established a new regulation to reduce the boron content in detergents from 8.4 g kg^{-1} (old standard) to 0.5 g kg^{-1} (2008 standard; Weber and Juanicó, 2004). The result was a reduction in the boron concentration in sewage from the Dan Region Sewage Reclamation Project near Tel Aviv (the Shafdan) from about 0.9 mg l^{-1} before the regulation during the early 1990s (Vengosh et al., 1994) to about 0.2 mg l^{-1} in 2006 (Kloppmann et al., 2009).

The typical chemical composition of saline domestic sewage is presented in **Table 1**. The use of household NaCl salt and Na-rich and B-rich detergents results in typical ionic ratios of Na/Cl > 1, a low Br/Cl ratio (i.e., Br/Cl < seawater ratio due to halite dissolution; Vengosh and Pankratov, 1998), and a high B/Cl ratio (greater than seawater ratio of 8×10^{-4}; Kloppmann et al., 2008a; Leenhouts et al., 1998; Vengosh et al., 1994, 1999a; Widory et al., 2004). Since Na–borate additives are derived from natural borate deposits (mainly from the western United States, Turkey, and China), the boron isotopic composition of wastewater is similar to the mineral borate isotopic ratios, with a typical $\delta^{11}B$ range of 0–10‰ (Eisenhut et al., 1995; Vengosh et al., 1994). This isotopic composition is different from those of other salinity sources (e.g., seawater intrusion with $\delta^{11}B > 39‰$; **Figure 23**) and thus several studies have utilized this method for tracing wastewater contamination in water resources (Bassett et al., 1995; Eisenhut et al., 1995; Hogan and Blum, 2003; Kloppmann et al., 2008a; Leenhouts et al., 1998; Vengosh et al., 1994, 1999a; Widory et al., 2004). The anthropogenic sulfate in wastewater also has a distinctive isotopic ratio (Houhou et al., 2010; Torssander et al., 2006). This tracer was used to detect pollution of the Arno River in northern Tuscany with a distinctive sulfur isotopic ratio ($\delta^{34}S_{SO_4} = 6–8‰$; Cortecci et al., 2007), urban groundwater contamination in Metro Manila, Philippines (Hosono et al., 2010), shallow groundwater of the Taipei urban area (Hosono et al., 2011), and groundwater from Shuicheng Basin, southwestern China (Li et al., 2010).

One of the major sources of salts that affect the salinity of domestic wastewater is the discharge of softener backwash effluent. In suburban and rural areas, where the local groundwater supply is hard (high Ca^{2+} and Mg^{2+} concentrations), softener backwash may be an important salinity source for the local watershed and groundwater. In the Greater Phoenix Metropolitan Area, Arizona, a population of 12 million people annually generated 45 500 tons of salts to wastewater from water softeners, which constitutes ~39% of the city's salt contribution (Daugherty et al., 2010). Kelly et al. (2008) estimated that an average of 125 kg $year^{-1}$ of salts are used for softening per house in rural communities in southeastern New York. Similarly, residential development in the Detroit metropolitan

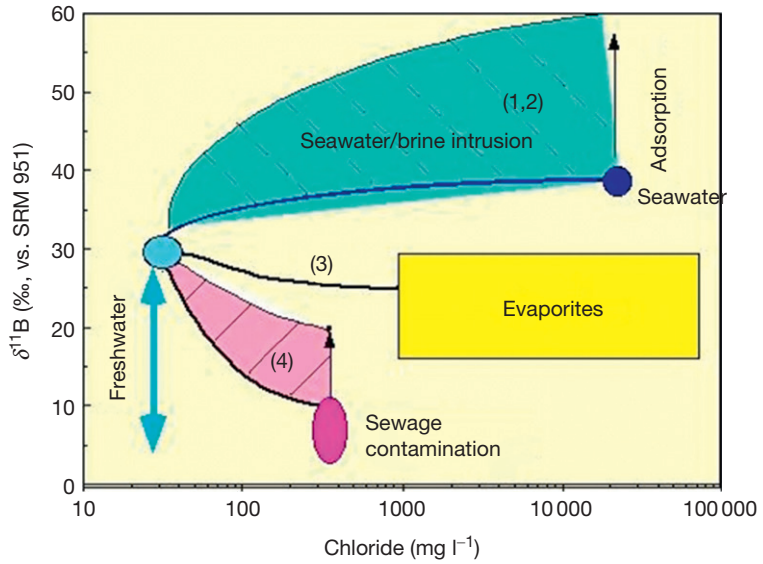

Figure 23 Schematic illustration of the expected boron isotope variations upon salinization by (1) seawater intrusion; (2) dissolution of marine evaporites; and (3) contamination from sewage effluents. Note the enrichment in ^{11}B that is associated with boron adsorption process. Data from Vengosh et al. (1994).

area resulted in increasing salinity in local streams (Thomas, 2000). During regeneration (refreshing) of softeners, an NaCl solution is passed through a resin and releases, by ion-exchange reactions, the adsorbed Ca^{2+} and Mg^{2+} ions that are retained from the supply water in order to increase the reactivity of the softener for the next load of Ca- and Mg-rich supply water. The chloride and sodium contents in backwash brine can reach to 10 000 and 6000 mg l^{-1}, respectively (Gross and Bounds, 2007). While sodium may be retained during the regeneration process due to the release Ca^{2+} and Mg^{2+} ions, excess utilization of NaCl solution for regeneration masks this differential uptake of sodium, resulting in Na/Cl ratios close to unity in backwash effluents. In addition to the large potential salinization of softener backwash effluents, introducing these brines into septic tanks, which are common in many private homes in rural areas in the United Sates, inhibits anaerobic digestion and thus reduces the efficiency of biological remediation such as nitrifying microorganisms. Consequently, nitrogen removal in septic tanks could be inhibited in systems receiving water softener backwash brine (Gross and Bounds, 2007).

11.9.6.2 Deicing and Salinization

Another significant source of anthropogenic salinization is the use of road deicing salts. Salt has been used for road deicing for several decades, particularly in the eastern and northeastern states of the United States and Canada. The use of road salt has improved fuel efficiency and reduced accidents, yet at the same time has caused salinization of associated watersheds and groundwater. The use of rock salt for road deicing in the United States has dramatically increased in the last 75 years (Jackson and Jobbagy, 2005; Richter and Kreitler, 1993). Contamination of water resources can occur from leaking of brine generated in storage piles of salt (Wilmoth, 1972) and from the dissolution of salts applied onto the roads (Howard and Beck, 1993; Williams et al., 2000). Deicing salts were found to be the major salinity source of the North Branch of the Chicago River through direct runoff flow and wastewater effluent discharge in the large metropolitan area of Chicago (Jackson et al., 2008). In cases where salt is applied as a powder, salt particles may become airborne and be transported considerable distances downwind (Jones and Hutchon, 1983; Richter and Kreitler, 1993). Kaushal et al. (2005) showed that widespread increases in suburban and urban development in the northeastern United States are associated with a continuous increase in chloride concentrations in local streams: from less than 10 mg l^{-1} during the late 1960s to 100 mg l^{-1} during the late 1990s. During winter, some streams in Maryland, New York, and New Hampshire have exceedingly high chloride concentrations (>4600 mg l^{-1}), up to 100 times greater than unimpacted forest streams during summer (Kaushal et al., 2005). Kelly et al. (2008) showed that between 1986 and 2005 chloride and sodium concentrations in a rural stream in southeastern New York increased by rates of 1.5 and 0.9 mg l^{-1} per year, respectively. The average chloride concentration increased from ~15 mg l^{-1} in 1986 to about 50 mg l^{-1} in 2005 (Kelly et al., 2008). If the chloride rise is extrapolated into the next century, it seems that many rural streams in the northeast of the United States will have baseline chloride contents exceeding the drinking water threshold of 250 mg l^{-1} (Jackson and Jobbagy, 2005). Hence, increases in roadways and deicer use are causing salinization of freshwaters, degrading habitat for aquatic organisms, and impacting large supplies of drinking water for humans throughout the region. Likewise, a survey of 23 springs in the Greater Toronto Area of southern Ontario in Canada recorded high chloride levels (up to 1200 mg l^{-1}), resulting from the winter application of road deicing salts (Williams et al., 2000).

The most common road deicing practice is to apply pure sodium chloride to main urban roads and highways. Calcium chloride salt is also used but not as frequently since it is more expensive and known to make road surfaces more slippery when wet (Richter and Kreitler, 1993). Hence, the predominant geochemical signal of road deicing is Na–Cl composition with a Na/Cl ratio close to unity (**Table 1**; Howard and Beck, 1993). In contrast, the use of calcium chloride salt would result in saline water with a Ca–chloride composition and $Na/Cl \ll 1$.

11.9.6.3 Agricultural Drainage and the Unsaturated Zone

The salinity of agriculture return flow is controlled by (1) the composition of the parent irrigation water; (2) the composition and source of additive commercial chemicals (e.g., nitrogen fertilizers, gypsum, dolomite, boron compounds), pesticides, and herbicides; and (3) the nature of the soil through which the irrigation water flows (Beltrán, 1999; Böhlke, 2002; Böhlke and Horan, 2000; Causape et al., 2004a,b; Corwin et al., 2007; Garcia-Garizabal and Causape, 2010; Gates et al., 2002; Johnson et al., 1999; Milnes and Renard, 2004; Suarez, 1989; Tanji and Valoppi, 1989; Tedeschi et al., 2001; Westcot, 1988). In the western United States, for example, saline drainage waters from the Imperial Valley in southern California are characterized by high sodium ($Na/Cl > 1$), sulfate, and boron and typically low Br/Cl ratios (**Table 1**; data from Schroeder and Rivera, 1993). The conspicuously low Br/Cl ($(3–4) \times 10^{-4}$) in the drainage water is one order of magnitude lower than seawater (1.5×10^{-3}) or atmospheric ($>1.5 \times 10^{-3}$) ratios (**Figure 12**; Davis et al., 1998). While this composition could be related to the chemistry of the Colorado River, which is the major water source for irrigation in this area, the high concentration of selenium in the drainage water is attributed to mobilization from oxidized alkaline soils derived predominantly from natural seleniferous marine sediments (Hern and Feltz, 1998; Grieve et al., 2001; Rhoades et al., 1989; Schroeder and Rivera, 1993; see **Chapter 11.2**). As a result, agricultural practices have caused significant changes in groundwater geochemistry due to mobilization of natural contaminants and intensification of water–rock interactions that further enhance water mineralization (Böhlke and Irwin, 1992).

The salinity of agricultural return flow also depends on the balance between the amount of salt entering the soil and the amount of salt that is removed (Westcot, 1988). A change from natural vegetation to agricultural crops and the application of irrigation water may add salts to the system. The amount of salt is further increased, as evaporation and transpiration exceed recharge. Approximately 60% of the supplied irrigation water will be transpired through growing crops but the majority of salts remain in the residual solution. Consequently,

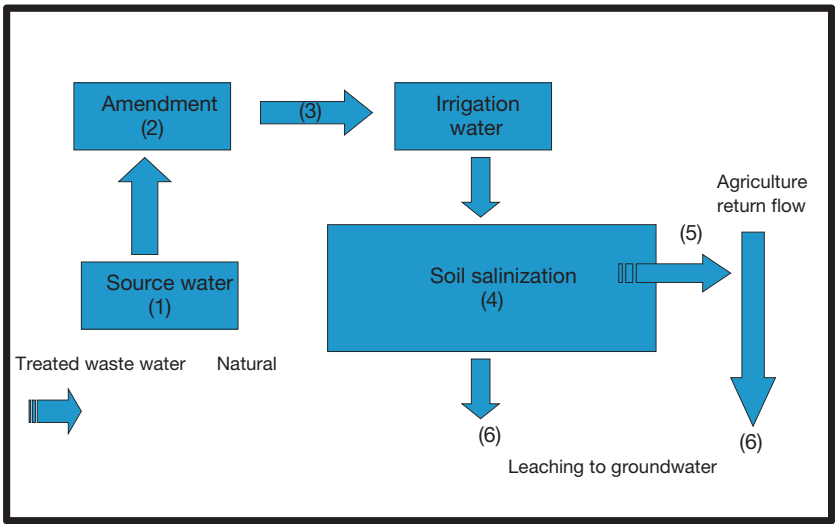

Figure 24 The agriculture salinization cycle: (1) supply water for irrigation; (2) salts added with fertilizers and amendment treatment; (3) generation of irrigation water; (4) soil salinization; (5) formation of agricultural return flow; (6) possible contamination of water resources.

adequate drainage is one of the key factors that control soil salinization; nevertheless, the nonreactivity of some of the soluble salts (i.e., conservative ions) makes them a long-term hazard.

The salinity of agricultural return flow is also a function of the salinity of the soil. In arid and semiarid areas, the natural salinity of the soil is high and thus flushing with irrigation water enhances salt dissolution in the soil. In some cases, the occurrence of contaminants in the protolith lead to high concentrations in agricultural effluents. A survey of the quality of drainage water in the western United States shows that the drainage waters are typically saline with elevated concentrations of sodium, selenium, boron, arsenic, and mercury (Hern and Feltz, 1998). In San Joaquin Valley, Salinas Valley, and Imperial Valley in California, drainage waters are highly saline and contaminate the associated ground- and surface waters (Amrhein et al., 2001; Glenn et al., 1999; Kharaka et al., 1996; Rhoades et al., 1989; Schroeder and Rivera, 1993). For example, the agricultural drainage salt generation during irrigation of crops in San Joaquin Valley in California annually exceeds 600 000 tons, which accumulates at a rapid rate, causing serious concern for the environment and the local agricultural industry (Jung and Sun, 2001). The soil reactivity is also enhanced by the composition of the irrigation water and added fertilizers. As high salinity is typically associated with high sodium content, exchangeable sodium replaces exchangeable calcium. As a result, the soil becomes impermeable. The 'sodium hazard' is expressed as the 'sodium adsorption ratio,' which represents the relative activity of sodium ions in exchange reactions with soil. Typically, irrigation waters with SAR values higher than 10 are considered to be sodium hazards (e.g., San Joaquin Valley; Mitchell et al., 2000). In cases of high SAR soil, gypsum or calcium carbonate can be applied to reverse the sodium exchange and improve soil physical properties (Agassi et al., 2003; Keren, 1991; Keren and Ben-Hur, 2003; Keren and Klein, 1995; Keren and Singer, 1988; Li and Keren, 2008, 2009; Nadler et al., 1996; Tarchitzky et al., 1999).

The chemical composition of agricultural drainage (Figure 24) is influenced by the quality of the water source that is used for irrigation. In many water-scarce areas, the only available water for irrigation is treated domestic sewage. Hence, the end product of urban wastewater (Figure 22) can be the initial water for agriculture (Figure 24). Other types of marginal waters (e.g., brackish waters) may also affect the salinity of agricultural return flows.

The second factor that determines the chemistry of the agriculture cycle is fertilizers and other types of additives that are directly added to the irrigation water. Nitrate is the predominant ion contributed by fertilizers (McMahon et al., 2008). Böhlke (2002) showed that artificial fertilizer is the largest nonpoint source of nitrogen in rural areas, consistent with the global increase in the use of nitrogen fertilizer since the middle of the twentieth century. Nitrate derived from fertilizers is characterized by relatively low $\delta^{15}N_{NO_3}$ values (−4‰ to +3‰; Kendall and Aravena, 2000, and references therein). ($\delta^{15}N_{NO_3} = [(^{15}N/^{14}N)_{sample}/(^{15}N/^{14}N)_{AIR} - 1] \times 10^3$. AIR refers to N_2 in air (Coplen et al., 2002).) Other major forms of nitrogen applied to crops are urea, ($CO(NH_2)_2$), ammonia (NH_3), ammonium nitrate (NH_4NO_3), and animal manure (Böhlke, 2002; Kendall and Aravena, 2000).

In addition to nitrogen application, other types of ammandates are added to the irrigation water. These include dolomite to provide calcium and magnesium for plant growth and to neutralize acid soils (Böhlke, 2002), and gypsum, which is used in soil with irrigation water having high SAR values in order to neutralize the exchangeable Na^+ in the soil (e.g., Salinas Valley, California; Vengosh et al., 2002). In addition, application of KCl salts as fertilizers results in chloride contamination, and use of Na–borate or Ca–borate fertilizers in boron-depleted soil contributes boron (Komor, 1997). The use of soil fumigants like ethylene dibromide (EDB) (Böhlke, 2002; Doty et al., 2003; Redeker et al., 2000) can lead to degradation and release of bromide to groundwater, as evidenced by conspicuously high Br/Cl ratios in shallow groundwater underlying strawberry cultivation in the Salinas Valley (Vengosh et al., 2002).

Another source of salinity that is associated with agricultural activity is animal waste, including cattle (Gooddy et al., 2002; Hao and Chang, 2003; Harter et al., 2002; Hudak, 1999, 2000a,b, 2003; Hudak and Blanchard, 1997) and swine manure (Krapac et al., 2002). It has been demonstrated that the salinity of soil and underlying groundwater increases significantly following long-term manure applications (Hao and Chang, 2003; Hudak, 1999, 2000a,b, 2003; Hudak and Blanchard, 1997; Krapac et al., 2002). Manure often has high concentrations of chloride (1700 mg l^{-1} in swine manure), sodium (840 mg l^{-1}), potassium (3960 mg l^{-1}), and ammonium with $\delta^{15}N_{NO_3}$ values > 9‰ (Krapac et al., 2002). Animal waste is also characterized by high Br/Cl ratios; cattle, horse, and goat wastes with Br/Cl ranging from 2.6×10^{-3} to 127×10^{-3} (Hudak, 2003) were shown to affect groundwater in Spain and Portugal (Alcalá and Custodio, 2008). In general, saline groundwater with high nitrate (with high $\delta^{15}N_{NO_3}$) combined with high Br/Cl and K/Cl ratios suggests contamination from animal wastes.

The third stage in the agriculture cycle (**Figure 24**) is transport and reactivity with the unsaturated zone. The unsaturated zone acts as a buffer and modifies the original chemical composition of the irrigation water (or any other recharge water). Microbial oxidation of ammonium releases protons (H^+) that generate acidity along with nitrate production in soils (Böhlke, 2002) that may induce dissolution of calcium carbonate minerals (Curtin et al., 1998; De Boer and Kowalchuk, 2001; Furrer et al., 1990; Murkved et al., 2007; Rudebeck and Persson, 1998; Vance and David, 1991). Consequently, nitrate-rich waters in carbonate aquifers are associated with high calcium derived from dissolution of the aquifer matrix. For example, in the mid-Atlantic coastal plain in the United States, groundwater recharged beneath fertilized fields has a unique Ca–Mg–NO_3 composition with positive correlations between nitrate and other inorganic constituents such as Mg^{2+}, Ca^{2+}, Sr^{2+}, Ba^{2+}, K^+, and Cl^- (Hamilton and Helsel, 1995; Hamilton et al., 1993). In the Gaza Strip, which is part of the Mediterranean coastal aquifer, dissolution of the Pleistocene carbonate aquifer matrix is reflected in high $^{87}Sr/^{86}Sr$ ratios in nitrate-rich groundwater, relative to groundwaters with lower nitrate concentrations that are associated with lower $^{87}Sr/^{86}Sr$ ratios (Vengosh et al., 2005).

Using irrigation water that is enriched in sodium with high SAR values triggers ion-exchange reactions (Agassi et al., 2003; Keren, 1991; Keren and Ben-Hur, 2003; Keren and Klein, 1995; Keren and Singer, 1988; Li and Keren, 2008, 2009; Nadler et al., 1996; Stigter et al., 1998; Tarchitzky et al., 1999). The capacity of ion exchange on clay minerals is limited, however, and depends on various lithological (e.g., clay content) and environmental (e.g., pH, solute composition) factors. Nonetheless, the uptake of Na^+ and release of Ca^{2+} (and Mg^{2+}) is a major geochemical modifier that is associated with transport of irrigation water in the unsaturated zone. The Na/Cl ratio is a good indicator of the efficiency of the base-exchange reactions; low Na/Cl ratios (i.e., below the original value of the irrigation water) reflect continuation of exchange reactions whereas the increase of the Na/Cl ratio toward the original Na/Cl value of the irrigation water suggests exhaustion of the exchangeable sites and reduction in the clay capacity for exchange reactions (Vengosh and Keren, 1996). Kass et al. (2005) showed that irrigation with Ca-rich water causes an opposite reaction where Na^+ is released and the residual groundwater has an Na/Cl that is higher than that of the irrigation water. Similarly, the ability of clay minerals to adsorb reactive elements (e.g., boron, potassium) is limited, and after long-term recharge or irrigation, the capacity of adsorption decreases (DeSimone et al., 1997; Stigter et al., 1998; Vengosh and Keren, 1996). In most cases, the potassium level in groundwater is low and the K/Cl ratios in groundwater associated with agricultural recharge are typically low due to adsorption of potassium onto clay minerals (Böhlke, 2002).

The amount of organic load associated with anthropogenic contamination and redox conditions also controls the reactivity of the unsaturated zone and consequently the salinity of associated water. In aerobic conditions, the degradation of organic matter will enhance acidity and result in accumulation of HCO_3^- and Ca^{2+} due to dissolution of the carbonate matrix of the host aquifer. In addition, the contents of sulfate and nitrate are expected to vary conservatively under oxic conditions in the unsaturated zone. Thus, high sulfate and nitrate contents, which are common in many irrigation waters, would also be preserved in underlying groundwater. In contrast, in anaerobic conditions, sulfate and nitrate reduction will enhance calcium carbonate precipitation, and hence sulfate (by sulfate reduction), nitrate (denitrification), and calcium (precipitation) will be removed during flux to the unsaturated zone (Böhlke, 2002; Böhlke and Horan, 2000; Gooddy et al., 2002). Under anaerobic conditions, the original chemical signature of the agricultural return flow would therefore be modified and the residual underlying groundwater would become relatively depleted in sulfate and nitrate concentrations, with high $\delta^{34}S_{SO_4}$ and $\delta^{15}N_{NO_3}$ values relative to the irrigation water.

11.9.7 Salinity and the Occurrence of Health-Related Contaminants

Salinization of water resources is often associated with an increase in the concentrations of *associated* contaminants, including inorganic constituents (e.g., fluoride, arsenic, boron, and radium), organic compounds such as toxic disinfection byproducts, and biological contaminants such as toxic saltwater algae. The occurrence of these contaminants in water resources has important implications for possible bioaccumulation in plants and the food chain, toxicity of the water, and direct effects on human health.

As shown in this section, numerous studies have shown that the concentrations of trace elements in water resources are typically correlated with the overall water salinity. In surface water, this positive correlation is directly linked to evaporation and the apparent conservative behavior of trace elements in the water. In groundwater, this correlation may be derived from surface evaporation of recharged water during the replenishment process, water–rock interactions that mobilize both major and trace elements, or the net salinity impacts on the solubility and/or reactivity of inorganic trace metals, resulting in progressively higher contents of trace elements with increasing salinity.

11.9.7.1 Fluoride and Salinity

Many water resources in China, eastern Africa, and India are characterized by high fluoride contents that are associated with elevated salinity and cause widespread dental and skeletal fluorosis (Ayenew et al., 2008; D'Alessandro et al., 2008; Misra and Mishra, 2007; Mor et al., 2009; Rango et al., 2009, 2010a,b,c; Shiklomanov, 1997; Viero et al., 2009). An example of fluoride contamination in lakes and groundwater is the Central Rift Valley of Ethiopia (Rango et al., 2009, 2010a,b,c, 2013), where fluoride concentrations linearly increase with salinity in both groundwater and alkaline (pH 10) lakes (**Figure 25**). While the linear relationships in groundwater reflect mobilization of fluoride together with major elements such as Na^+ and HCO_3^- (**Figure 25**) due to weathering of amorphous glass in the young basalts of the Rift Valley (Rango et al., 2010b), in alkaline lakes these correlations are due to surface evaporation and the associated concentration of ions. The salinization of groundwater and lakes in the Ethiopian Rift Valley has therefore direct implications for the levels of health-related contaminants such as fluoride. Since the local rural population in the East African Rift Valley consumes groundwater primarily as drinking water, the high fluoride levels in groundwater result in a high frequency of fluorosis (Rango et al., 2009, 2010a,b,c, 2012). In addition to fluoride, the extensive weathering of the basaltic rocks leads to mobilization of other health-related trace element contaminants to the groundwater such as arsenic, boron, and vanadium (Rango et al., 2010a).

11.9.7.2 Oxyanions and Salinity

The relationship between salinity and oxyanions, particularly arsenic, selenium, and boron, depends on two key factors: (1) the speciation of the oxyanions as a function of environmental conditions such as pH, redox state, temperature, pressure, and salinity; and (2) the type of bond that the oxyanion species makes with surface functional groups in oxides and clay minerals; an oxyanion may form *an inner-sphere complex* (i.e., a chemical bond that is typically covalent between the oxyanion and the electron-donating oxygen ion without the presence of water molecules) or *an outer-sphere complex* (i.e., an ion pair in which the oxyanion and the surface functional groups are separated by one or more water molecules; McBride, 1977; Sposito, 1984; Stumm and Morgan, 1995). While ionic strength has no effect on the degree of adsorption through inner-sphere complex formation, high salinity will reduce the adsorption of outer-sphere-forming ions because adsorption is suppressed by the competition of other anions (McBride, 1977). The affinity of oxyanion species to form surface complexes (inner- or outer-sphere complexes) depends on the valence of the adsorbed species. Increasing salinity will therefore reduce the adsorption capacity of some oxyanions species and increase their concentrations in the residual saline water.

11.9.7.2.1 Arsenic

The extent to which arsenic mobilization is affected by salinity depends on its valence state. As shown in **Chapter 11.2** at near-neutral pH, oxidized As(V) (arsenate) occurs as anionic $H_2AsO_4^-$ or $HAsO_4^{2-}$, subject to pH-sensitive adsorption onto metal oxides. Under reducing conditions, arsenic aquatic species are composed of arsenite (As(III)) in which the uncharged $H_3AsO_3^0$ is dissociated to $H_2AsO_3^-$ ($pK_a = 9.3$). Consequently, at $pH < 9$ the uncharged $H_3AsO_3^0$ is less effectively adsorbed than the anionic As(V) form. Given the differential reactivity of arsenic species, the relationship of arsenic with salinity depends primarily on the redox conditions. Previous studies have shown that under oxic conditions, arsenate ($H_2AsO_4^-$ and $HAsO_4^{2-}$ are the predominant species at neutral pH) adsorption onto Fe and Al amorphous oxides is

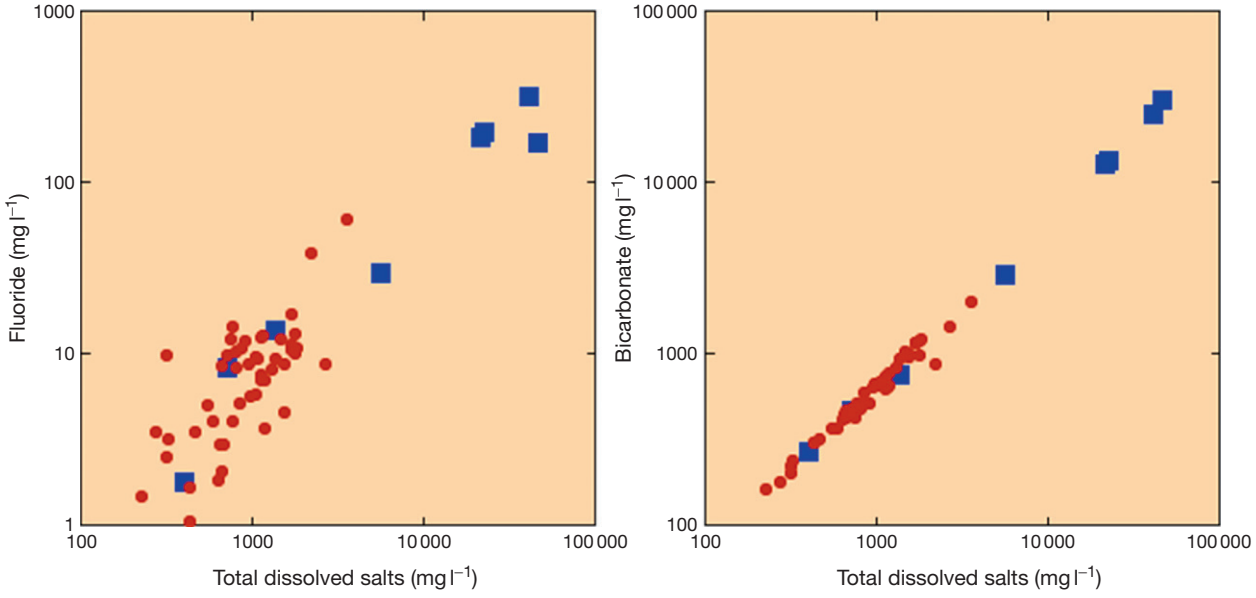

Figure 25 Fluoride and bicarbonate concentrations versus TDS (mg l^{-1}) in groundwater (red circles) and lakes (blue squares) from the Central Rift Valley in Ethiopia. While groundwater mineralization induces fluoride mobilization, evaporation processes further increase fluoride contents in alkaline (pH 10) lakes. Data from unpublished results, Duke University.

through an inner-sphere complex, which is not associated with the ionic strength of the solution (Goldberg and Johnston, 2001; Liu et al., 2008). In contrast, under reduced conditions, arsenite adsorption on amorphous Al oxides reaches an adsorption maximum at around pH 8 but decreases with increasing ionic strength (i.e., outer-sphere complex mechanism; Goldberg and Johnston, 2001). Thus, salinization under reduced conditions and neutral pH results in high As contents in the salinized water.

In addition to the possible *direct* effect of ionic strength on As adsorption, salinization of surface water could *indirectly* affect As distribution. One possible scenario is salinity-induced stratification of lake water that would generate reducing conditions in the bottom water, produce arsenite species, and, consequently, decrease the reactivity of the overall arsenic with oxides in sediments. For example, As contents were found to be linearly correlated with chloride contents in evaporation ponds from the San Joaquin Valley of California, in conjunction with the increase of the arsenite fraction of the total arsenic and organic arsenic. This trend was associated with increasing reducing conditions (high dissolved organic matter, low dissolved oxygen, and elevated sulfide concentrations) in the evaporation ponds (Gao et al., 2007). Although some removal of As to sediments in the pond was monitored (Gao et al., 2007), the reduced noncharged arsenic species was less reactive, resulting in the apparent conservative behavior of arsenic in the ponds. Likewise, saltwater intrusion into coastal and delta aquifers typically generates anoxic conditions, which will favor formation of uncharged arsenite species and will decrease arsenic removal. This was demonstrated in the reduced and high-salinity groundwater from the Red River Delta in Vietnam (Jessen et al., 2008). Another example of the high correlation between As and salinity under reduced conditions is oil field brines, as petroleum reservoir waters from sedimentary basins in southeastern Mexico show maximum As concentrations of 2000 $\mu g\,l^{-1}$ and a linear correlation with chloride content (Birkle et al., 2010).

Changes in salinity could also affect the environmental conditions that control the resilience of anaerobic bacteria, which grow by dissimilatory reduction of As(V) to As(III) (Blum et al., 1998). As demonstrated in the hypersaline alkaline Mono and Searles lakes in California, lake salinity can control the rate of microbial activity, such as arsenate reduction and arsenite oxidation, as well as the microbial population that triggers different biogeochemical reactions (e.g., denitrification and arsenate reduction; Blum et al., 1998; Kulp et al., 2007).

In oxic groundwater, where arsenate (As(V)) is the dominant species, salinity should not, in principle, affect As mobilization. Nonetheless, correlations between As and salinity have been observed in oxic groundwater from the Southern High Plains aquifer in Texas (Scanlon et al., 2009b) and the Sali River alluvial basin in northwest Argentina (Nicolli et al., 2010). While in Texas this correlation has been attributed to mixing of low saline groundwater with As-rich saline groundwater from the underlying Triassic Dockum aquifer (Scanlon et al., 2009b), in the shallow oxic aquifer in Argentina, the correlation results from evaporation combined with the high pH and Na—HCO_3 composition of the water that apparently reduces As adsorption (Nicolli et al., 2010). Likewise, in oxic groundwater from the Rift Valley of Ethiopia in which sodium and bicarbonate are the major components of the dissolved constituents (**Figure 25**), a positive correlation is observed between As and TDS, suggesting that As is derived from weathering of the volcanic glass (Rango et al., 2010b).

11.9.7.2.2 Selenium

Selenium is both a micronutrient essential for animal nutrition and a potentially toxic trace element for ecological systems. The US EPA has set a limiting factor of 5 $\mu g\,l^{-1}$ for *criterion continuous concentration*, which is an estimate of the highest concentration of a material in surface freshwater to which an aquatic community can be exposed indefinitely without resulting in an unacceptable effect (US Environmental Protection Agency, 2011a). As shown in **Chapter 11.2**, the dominant inorganic Se species are selenite, Se(IV), and selenate, Se(VI). While selenate is thermodynamically stable under oxidizing conditions, the transformation rates of Se(IV) to Se(VI) are sufficiently slow that both species can coexist in water in oxic environments (Masscheleyn et al., 1990). The reduced form, selenite, is strongly adsorbed by oxides while selenate adsorbs weakly and is readily leached to water (Dzombak and Morel, 1990). While the strong adsorption of selenite (SeO_3^{2-} species) is through inner-sphere surface complexes, the weak adsorption of selenate is through outer-sphere complexes and therefore is salinity-dependent (Hayes et al., 1988). This was demonstrated in experimental column studies, which showed that selenate is more mobile than other conservative anions such as sulfate and chloride (Goldhamer et al., 1986).

High correlations between selenium and salinity were reported in shallow groundwater from the San Joaquin Valley in California (Deverel and Fujii, 1987; Deverel and Gallanthine, 2007; Presser and Swain, 1990; Schoups et al., 2005; Tanji and Valoppi, 1989), brines of the Salton Sea in California (Schroeder et al., 2002), saline seeps associated with cultivated drylands of the Great Plains region of North America (Miller et al., 1981), and stream discharge to the Ashley Creek, part of the Upper Colorado River Basin in Utah (Naftz et al., 2008).

11.9.7.2.3 Boron

Boron is an essential element for plant growth but can be toxic at higher levels in irrigation water or soil solutions (Bastias et al., 2010; Davis et al., 2002; Karabal et al., 2003; Kaya et al., 2009; Lehto et al., 2010; Papadakis et al., 2004; Reid, 2010; Scialli et al., 2010; Smith et al., 2010; Sotiropoulos et al., 1999; Thompson et al., 1976). Numerous studies have shown that boron concentrations in water are highly correlated with salinity. Yet, boron can be reactive with clay minerals and oxides. Boron in aquatic solutions occurs as uncharged boric acid ($B(OH)_3^0$) and borate ion ($B(OH)_4^-$) species. The distribution of boron species in solution is controlled by pH and the dissociation of boric acid to borate ion depends on the temperature, pressure, and salinity (**Figure 26**; Dickson, 1990a; Millero, 1995). Empirical data calculated from Millero (1995) and Dickson (1990a) show that an increase in the salinity of water reduces the pK_B (K_B is the dissociation constant of boric acid; **Figure 26**). **Figure 27** illustrates the changes in the boron species distribution from freshwater salinity ($pK_B = 9.2$) to seawater salinity ($pK_B = 8.6$ at 25 °C). The higher pK_B values under low salinity conditions implies a higher

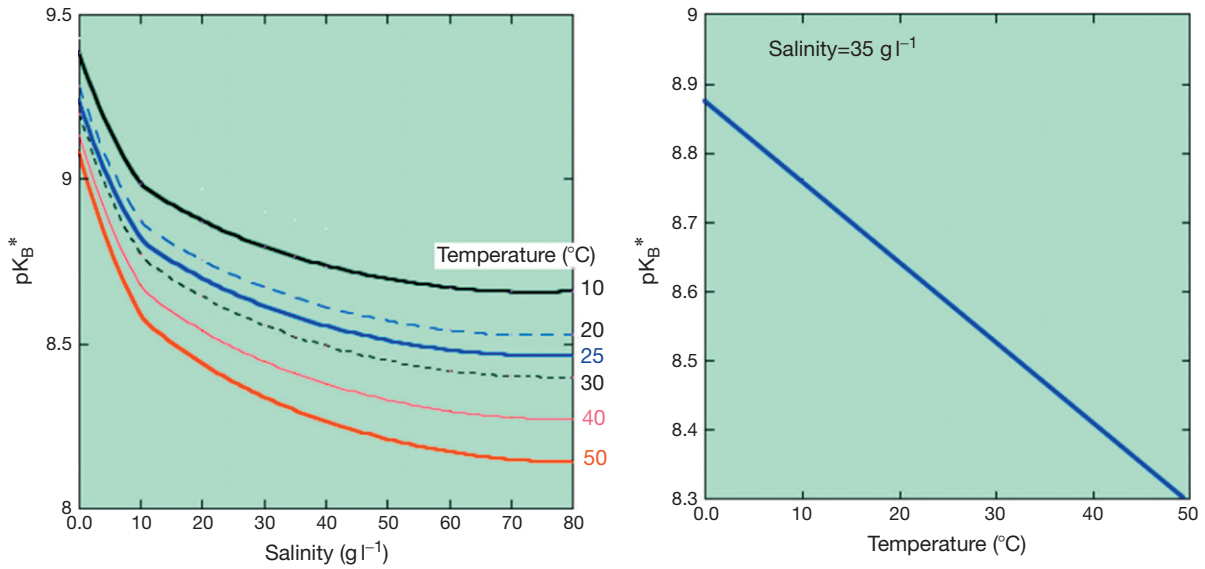

Figure 26 Modeling of the variations of the boric acid dissociation constant (expressed as pK_B^* values) as a function of salinity and temperature. Note that the pK_B^* value decreases with salinity and temperature. Empirical data were calculated from Millero (1995) and Dickson (1990a).

proportion of the borate ion in solution at pH below 9, and thus salinization will lead to a lower fraction of boric acid for a given pH (**Figure 26**).

Numerous experimental studies have shown that the adsorption of boron on oxides and clay minerals increases with pH at a maximum range of 8–9. The increase of adsorption with pH has led to the suggestion that the magnitude of borate ion ($B(OH)_4^-$) adsorption onto oxides and clay minerals is higher than that of the uncharged boric acid (Keren and Gast, 1981; Keren and Oconnor, 1982; Keren and Sparks, 1994; Keren et al., 1981; Mezuman and Keren, 1981). In contrast, Su and Suarez (1995) argued that uncharged boric acid is also adsorbed onto positively charged surfaces at low pH, and that the maximum adsorption of boric acid to form trigonally coordinated surface species occurs at a pH closer to the pK_B value of boric acid. Under higher pH conditions, the concentrations of hydroxyl ions increase and compete with borate ions for adsorption sites (Su and Suarez, 1995).

Experimental studies have also shown that boron adsorption onto oxides and clay minerals increases with ionic strength (Goldberg et al., 1993; Keren and Sparks, 1994; McBride, 1977). The effect of ionic strength suggests a mechanism involving an adsorption through an outer-sphere complex (McBride, 1977), which is salinity-dependent. However, it was found that this salinity effect is not universal and an inner-sphere adsorption mechanism applies for goethite, gibbsite, and kaolinite minerals while an outer-sphere adsorption (i.e., salinity-dependent) mechanism occurs for adsorption onto montmorillonite and bulk soils (Goldberg et al., 1993).

As shown in **Figure 27**, a rise in salinity will increase the fraction of borate ion in solution in the pH range of 7.5–9. Thus, a higher fraction of borate ion, which seems to be more effectively adsorbed, could result in overall higher boron retention with salinity. Since boron adsorption is associated with isotopic fractionation in which ^{11}B tends to incorporate preferentially into the trigonal species while ^{10}B is selectively fractionated into the tetrahedral form, selective removal of ^{10}B

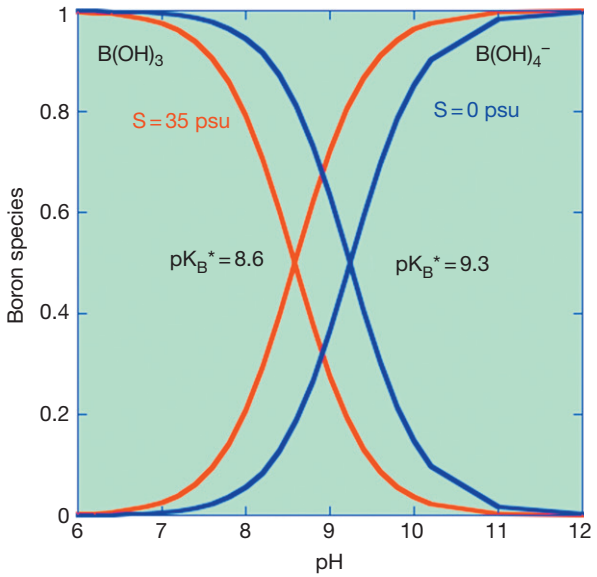

Figure 27 Modeling of the distribution of boron species boric acid and borate as a function of pH under low salinity conditions ($pK_B^* = 9.2$ at 25 °C) and seawater salinity ($pK_B^* = 8.6$ at 25 °C). Note that an increase in the salinity increases the fraction of borate ion for a given pH and increases the overall reactivity of boron with oxides and clay minerals. Data were calculated from Millero (1995) and Dickson (1990a).

$(OH)_4^-$ to the solid phase results in enriched $^{11}B/^{10}B$ ratios in the residual solution (Palmer et al., 1987; Spivack et al., 1987; Vengosh and Spivack, 2000). Consequently, despite the increase of boron concentration with salinity, in many cases, the salinization phenomena are accompanied by an increase in boron adsorption with lower boron to chloride ratios and higher $\delta^{11}B$ values relative to the expected theoretical mixing relationships between saline and freshwater end members. This was demonstrated in studies of seawater intrusion and

salinization by wastewater (Vengosh et al., 1994), salinization of groundwater in the Salinas Valley in California (Vengosh et al., 2002), and in the Mediterranean coastal aquifer of Israel (Vengosh et al., 1999b).

11.9.7.3 Naturally Occurring Radionuclides and Salinity

Groundwater may contain naturally occurring radionuclides produced during the decay of ^{238}U, ^{235}U, and ^{232}Th (see **Chapter 11.6**). Uranium (U) is a source of kidney toxicity as well as alpha radiation (US Environmental Protection Agency, 2000). High concentrations (activities) of naturally occurring radium (Ra), a decay product of ^{238}U and ^{232}Th, in drinking water increase the risks of developing osteosarcoma (bone cancer) and other health problems (Cohn et al., 2003; US Environmental Protection Agency, 2000). High levels of Ra in groundwater have been reported in reduced (Cecil et al., 1987; Vinson et al., 2009), acidic (Cecil et al., 1987; Dickson and Herczeg, 1992; Herczeg et al., 1988; Szabo and Zapecza, 1987; Vinson et al., 2009), and thermal waters (Kitto et al., 2005; Sturchio et al., 1993), as well as in low-saline fossil groundwater such as the Nubian Sandstone (Disi) aquifer in Jordan (Vengosh et al., 2009). Yet, the most common phenomenon is the high correlation between radium abundance and salinity (Carvalho et al., 2005; Hammond et al, 1988; Kraemer and Reid, 1984; Krishnaswami et al., 1991; Moatar et al., 2010; Moise et al., 2000; Otero et al., 2011; Raanan et al., 2009; Sturchio et al., 2001; Tomita et al., 2010 ; Vinson, 2011). Most of these studies have shown that the radium adsorption coefficient is decreased with increasing salinity, probably due to competition with other dissolved cations for adsorption sites (Dickson, 1990b; Krishnaswami et al., 1991; Sturchio et al., 2001; Webster et al., 1995).

A field-based experiment of $MgCl_2$ brine injection into fractured metamorphic and granitic rocks from the Hubbard Brook Experimental Forest in New Hampshire, USA, resulted in a large release of ^{226}Ra (from near zero to 1200 dpm l^{-1}) from ion-exchange sites on the fracture surfaces. This brine injection experiment demonstrated that when transient cation solutions are introduced to an aquifer system as part of salt water flow in an aquifer (e.g., seawater or brine intrusion, road salts applications, migration of leachates from landfills), significant Ra mobilization can occur from the aquifer rocks to groundwater (Wood et al., 2004).

In addition to salinity, the chemical composition of saline water also controls the retardation of Ra and the relationship with salinity (Tomita et al., 2010; Vinson, 2011). For example, sulfate-rich saline water is associated with Ra co-precipitation with secondary barite minerals, whereas reduced conditions trigger Ra mobilization from adsorbed sites due to reductive dissolution of Fe and Mn oxides in which radium is highly retained (Vinson, 2011). The control of both salinity and the redox state on Ra activity has been shown in several studies (e.g., Cecil et al., 1987; Sturchio et al., 2001; Vinson et al., 2009) and is illustrated in the case of the saline groundwater from the Cretaceous carbonate aquifer (Judea Group) in the Negev, Israel (unpublished data), that shows a linear correlation of ^{226}Ra with salinity and a reverse correlation with dissolved oxygen (**Figure 28**).

11.9.7.4 Trihalomethanes and Salinity

Chlorine disinfection is widely employed in municipal water systems. Elevated chloride and bromide contents in supply waters can lead to the formation of toxic disinfection byproducts, such as trihalomethanes (THMs), and specifically brominated THMs (e.g., bromodichloromethane – BDCM), during the chlorine disinfection process. The extent to which chlorine disinfection results in the formation of these

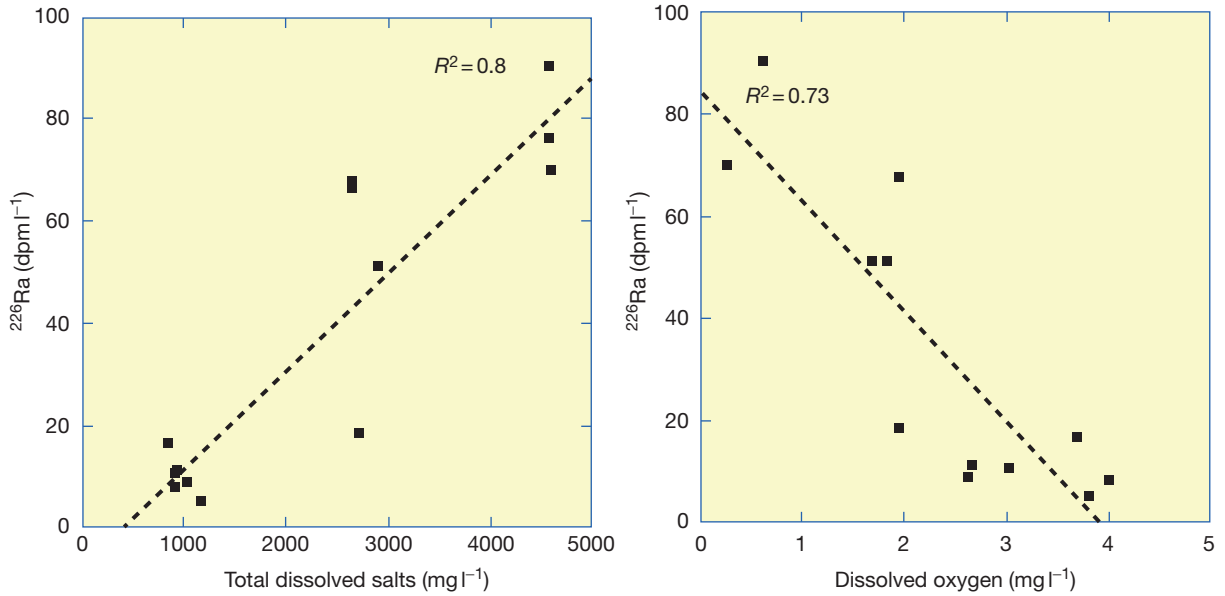

Figure 28 ^{226}Ra activity (decay per minute) versus total dissolved salts (mg l^{-1}) and dissolved oxygen (mg l^{-1}) in groundwater from the Lower Cretaceous carbonate aquifer (Judea Group) in the Negev, Israel. Note that the increase of ^{226}Ra activity with salinity is parallel to the inverse relationship with dissolved oxygen. Data from unpublished results, Duke University.

byproducts depends on the content and type of organic matter present, the quantity of chlorine used, pH, temperature, and reaction time (Chowdhury et al., 2010b). Epidemiological and toxicological studies have reported that brominated THMs such as BDCM are more carcinogenic than their chlorinated analogs (Krasner et al., 2002; Miltner et al., 2008; Nobukawa and Sanukida, 2000; Pressman et al., 2010; Richardson, 2008, 2009; Richardson and Ternes, 2005; Richardson et al., 2002, 2003, 2007). The US EPA set MCL values of 80 μg l^{-1} for total THMs and BDCM and 10 μg l^{-1} for bromate in drinking water, and has initiated the Stage 2 Disinfectants and Disinfection Byproducts Rule (Stage 2 Disinfectants and Disinfection Byproducts rule; US Environmental Protection Agency, 2012). In Canada, the regulatory limit is 16 μg l^{-1} for BDCM (Health Canada, 2007).

Several studies have shown that the bromide content and Br/Cl of treated water play an important role in the generation of brominated THMs (Chowdhury et al., 2010a,b; Heller-Grossman et al., 2001; Richardson et al., 2003; Uyak and Toroz, 2007; Xue et al., 2008). Experimental increases in the bromide ion concentration of treated water resulted in increasing rates of total THM formation, with higher BDCM and dibromochloromethane (DBCM) compounds and lower chloroform formation. A threefold increase of bromide content (from 40 to 120 μg l^{-1}) caused an increase in total THMs of ~30% and about a threefold increase in BDCM content (Chowdhury et al., 2010b).

The Sea of Galilee (Lake Kinneret) in Israel is an interesting natural case study with respect to these byproducts as the lake water is the major drinking water source for Israel (through the National Water Carrier) and the salt budget of the lake is controlled by the discharge of saline groundwater with high Br/Cl ratios, such as the Tiberias Hot Spring with chloride contents of 19 000 mg l^{-1} and Br/Cl ~0.005 (Kolodny et al., 1999; Nishri et al., 1999; Stiller et al., 2009). The salinity of the lake has fluctuated during the last decades due to variations in precipitation and water inflows coupled with human activities (e.g., pumping rates; **Figure 13(b)**). Studies in the early 2000s monitored chloride content of ~280 mg l^{-1}, total organic carbon (TOC) concentrations ranging between 4 and 6 mg l^{-1}, and high bromide ion concentrations (1.9 mg l^{-1}; Br/Cl ~ 3×10^{-3}). The combination of hydrophilic organic matter and high bromide contents resulted in high concentrations of THMs in Lake Kinneret water (summer = 606 μg l^{-1}), in which 96% of total THMs is in the form of brominated THMs, mostly as bromoform and dibromoacetic acid (Heller-Grossman et al., 2001; Richardson et al., 2003). Thus, high bromide levels in the source water can cause a significant shift in speciation to bromine-containing byproducts (Richardson et al., 2003).

Since the Br content and Br/Cl ratio of potable water play a significant role in the formation of brominated THMs, the origin and type of the saline waters that is involved in salinization of freshwater resources could also affect the occurrence and distribution of brominated THMs in chlorinated water. For example, salinization with a brine with a chloride content of ~100 000 mg l^{-1} into a freshwater reservoir at a dilution factor of ~350 would keep the chloride content below the WHO recommendation for drinking water of 250 mg l^{-1} (**Figure 29**). However, the Br/Cl ratio of the original brine would control the expected bromide contents in the salinized water. Three types of brines with identical chloride content of ~100 000 mg l^{-1} are considered: (1) an Appalachian brine from the eastern United States with Br/Cl = 4×10^{-3} (Osborn and McIntosh, 2010; Warner et al., 2012); (2) fivefold evaporated seawater below halite saturation with marine Br/Cl = 1.5×10^{-3}; and (3) brine originated from halite dissolution with low Br/Cl = 0.1×10^{-4}. Mixing simulations of these three brine types show significant bromide variations; at the drinking water threshold of chloride = 250 mg l^{-1}, dilution with the Appalachian brine, evaporated seawater, and halite dissolution yields bromide contents of 2.5, 0.9, and 0.05 mg l^{-1}, respectively (**Figure 29**). Consequently, dilution of brine with a high Br/Cl ratio would be sufficient to generate potable water based on the chloride standard, but with high bromide contents that could trigger generation of highly toxic brominated THMs during chlorination of the salinized potable water. The nature and mechanism by which the saline waters originated (e.g., evaporation of seawater beyond halite saturation, dissolution of halite, domestic wastewater) will control the Br/Cl ratios of the brine and consequently the bromide content of the salinized water. The bromide factor therefore increases the health risks associated with the formation of toxic brominated THMs.

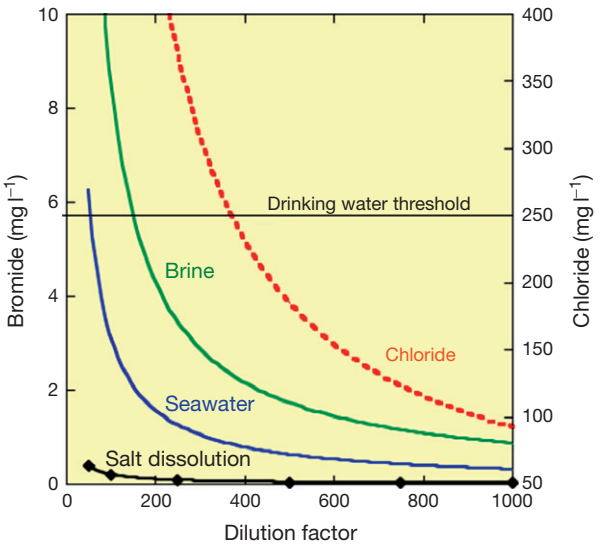

Figure 29 Modeling the dilution of a brine with chloride content of ~100 000 mg l^{-1} upon three different brine sources: (1) evaporated seawater such as the Appalachian brine from the eastern United States with Br/Cl = 4×10^{-3} (Osborn and McIntosh, 2010; Warner et al., 2012); (2) fivefold evaporated seawater below halite saturation with marine Br/Cl = 1.5×10^{-3}; and (3) brine originated from halite dissolution with low Br/Cl = 0.1×10^{-4}. Mixing simulations show that dilution of the brine to the drinking water threshold of chloride = 250 mg l^{-1} would result in differential bromide contents in the diluted water, based on the original Br/Cl ratios of the parent brines.

11.9.7.5 Salinity and Toxic Algae Bloom

Salinization of surface water could trigger harmful algae blooms toxic to fish. One of the most frequent causes of fish kills is the bloom of *Prymnesium parvum*. The *P. parvum* is a haptophyte alga, which is distributed worldwide. This alga is tolerant of large variations in temperature and salinity, and is capable of forming large fish-killing blooms (Baker et al., 2007, 2009;

Sager et al., 2008; Southard et al., 2010). This saltwater alga produces a potent toxin that is capable of killing fish, mussels, and salamanders (Sager et al., 2008). Studies of *P. parvum* blooms in lakes along the Brazos River in Texas, USA, have shown that large fish-killing blooms occurred when the freshwater inflows were low and the salinity was high (Roelke et al., 2011). In addition to the Brazos Basin in Texas, major fish kills, directly associated with *P. parvum* blooms, occurred in the Colorado, Red, and Rio Grande basins in the United States between 1981 and 2008, with an estimate of 34 million fish kills and an estimated economic loss of almost $13 million (Southard et al., 2010). The maximum growth of *P. parvum* occurs under specific environmental conditions such as temperature, salinity, and light. While *P. parvum* has been found in water with a range of salinity (TDS from 1000 to 100 000 mg l^{-1}), it was found that the maximal cell concentrations occurred at 26 °C and TDS of about 20 000 mg l^{-1}, about 60% of seawater salinity (Baker et al., 2007). Furthermore, the chemical composition of the saline water, particularly the abundance of cations, and the pH control the production of the toxins; under high pH conditions, toxins form, while at pH < 7, they are minimized and fish kills will not occur (Sager et al., 2008).

One of the recent significant fish kills that occurred directly from blooming of *P. parvum* and high salinity was the massive fish, salamander, and mussel kill on Dunkard Creek in September 2009. The Dunkard Creek watershed lies along the border of West Virginia and Pennsylvania, USA (Reynolds, 2009). The saline water discharged to the Dunkard Creek had TDS of about 23 000 mg l^{-1}, and was composed of Na–Cl–SO_4 ions with low concentrations of Ca^{2+} and Mg^{2+} (data from Reynolds, 2009). This composition is not consistent with the expected chemistry of produced water associated with oil and gas wells (e.g., high Ca^{2+}), or with water associated with coalbed methane production (high HCO_3^-, low SO_4^{2-}). The combined high chloride (6120 mg l^{-1}) and sulfate (10 800 mg l^{-1}) contents suggest an artificial blend probably from multiple sources. Yet, the impact of the discharged saline water on the blooming of *P. parvum* and associated fish kill in Dunkard Creek indicates that discharge of saline effluents can have devastating effects on ecological systems (Reynolds, 2009).

11.9.8 Elucidating the Sources of Salinity

Elucidating salinity sources in water resources is crucial for water management, model prediction, and remediation. Yet, the variety of salinization sources and processes makes this a difficult task. Ground- and surface water salinization can result from point sources (e.g., leakage or discharge of domestic wastewater) or nonpoint sources (e.g., agriculture return flows, irrigation with sewage effluent). Salinization can result from geologic processes such as natural saline-water flow from adjacent or underlying aquifers (Alcalá and Custodio, 2008; Bouchaou et al., 2008; Faye et al., 2005; Herczeg et al., 2001; Hsissou et al., 1999; Kloppmann et al., 2001; Maslia and Prowell, 1990; Mehta et al., 2000a,b; Sami, 1992; Sánchez-Martos and Pulido-Bosch, 1999; Sánchez-Martos et al., 2002; Shanyengana et al., 2004; Vengosh and Benzvi, 1994; Vengosh et al., 1999b, 2002, 2005; Warner et al., 2012). Alternatively, salinization can be induced by direct anthropogenic contamination or combined effects such as seawater intrusion. The multiple salinity sources therefore present a real challenge to water agencies and regulatory bodies.

The key to tracing salinity sources is the assumption that the chemical composition of the original saline source is preserved during the salinization process (i.e., conservative nature of the dissolved constituents). Due to the large differences in the solute content between saline waters and freshwaters, the chemical composition of the contaminated water mimics the composition of the saline source. However, the original composition of the saline source can be modified via water–rock interactions. For example, the composition of seawater is significantly modified by base-exchange reactions as it intrudes into coastal aquifers. Consequently, diagnostic tracers must be conservative. Nonetheless, nonconservative tracers are also useful in delineating salinization sources as long as the possible modification processes are understood.

Often, the chemical composition of salinized water does not point to a single source or salinization mechanism, given overlaps and similarities in the chemical compositions of different saline sources. For example, the Na/Cl ratio can be a good tracer to distinguish marine (e.g., seawater intrusion with Na/Cl < 0.86) from nonmarine or anthropogenic sources (Na/Cl ≥ 1). However, the reactivity of Na^+ in the unsaturated zone can reduce the Na/Cl ratio even in a nonmarine setting (e.g., DeSimone et al., 1997; Kass et al., 2005; Stigter et al., 1998; Vengosh and Keren, 1996). It is therefore essential to use *assemblages* of diagnostic chemical and isotopic tracers for accurate delineation of the salinity sources. Mazor (1997) and Herczeg and Edmunds (2000) reviewed most of the common geochemical tools that can be used to identify the different salinity sources of solutes. In general, dissolved constituents in salinized water can potentially be derived from (1) mixing between meteoric water and saline water such as seawater, connate brines, and hydrothermal waters trapped within or outside the aquifer; (2) dissolution of evaporites; (3) mineralization due to weathering of the aquifer minerals; (4) accumulation and leaching of salts in the unsaturated zone derived from long-term deposition of atmospheric fallout; or (5) anthropogenic contamination derived from sewage (domestic or industrial) effluents, deicing, agricultural return flows, oil- and gas-produced waters, and effluents from coal mining and coal ash leaching. Each of these sources has a unique and distinctive chemical and isotopic composition. While using individual tracers can provide useful information on these saline sources, *integration of multiple geochemical and isotopic tracers* can help resolve multiple salinity sources and provides a more robust and reliable evaluation of salinization processes (Alcalá and Custodio, 2008; Banner and Hanson, 1990; Böhlke, 2002; Boschetti et al., 2011; Bouchaou et al., 2008, 2009; Farber et al., 2004; Gattacceca et al., 2009; Hosono et al., 2010, 2011; Jørgensen and Banoeng-Yakubo, 2001; Kim et al., 2003; Langman and Ellis, 2010; Lu et al., 2008; Lucas et al., 2010; Millot and Negrel, 2007; Millot et al., 2007, 2010, 2011; Moller et al., 2008; Moore et al., 2008b; Otero et al., 2011; Sánchez-Martos and Pulido-Bosch, 1999; Sánchez-Martos et al., 2002; Sultan et al., 2008; Vengosh et al., 2002, 2005, 2007; Widory et al., 2004, 2005).

A summary of the geochemical and isotopic characteristics of some of these sources is given in **Table 2**. This section explores the use of assemblages of geochemical tracers, with

Table 2 Typical chemical and isotopic characteristics of major saline sources

Source	*TDS ($g\,l^{-1}$)*	*Na/Cl (molar ratio)*	*SO_4/Cl (molar ratio)*	*Br/Cl ($\times10^{-3}$, molar ratio)*	*B/Cl ($\times10^{-3}$, molar ratio)*	*$\delta^{11}B$ (‰)*	*$\delta^{34}S$ (‰)*	*$^{36}Cl/Cl$ ($\times10^{-15}$)*
Seawater	35	0.86	0.05	1.5	0.8	39	21	<5
Relics of evaporated seawater (brines)	>35	<0.86	<0.05	>1.5	<0.8	>39	>21	<5–100
Evaporite dissolution	>1	1	≫0.05	<1.5	<0.8	20–30	<21	<5
Hydrothermal water	0.2 to >1	>1	≫0.05	<1.5	>5	0±5	≪21	<5
Domestic wastewater	~1	>1	>0.05	<1.5	5	0–10	6–10	50–>100
Agricultural return flow	0.5–5	>1	≫0.05	<1.5	>0.8	20–30		50–>100

particular emphasis on the systematics of conservative (Br/Cl) and nonconservative (e.g., Na/Cl) elements, stable isotopes ($\delta^{18}O_{H_2O}$ and $\delta^{2}H_{H_2O}$), radioactive tracers (^{36}Cl and ^{129}I), and isotopes of dissolved constituents in the water ($\delta^{11}B$, $^{87}Sr/^{86}Sr$, $\delta^{34}S_{SO_4}$, and $\delta^{18}O_{SO_4}$).

The most common tracers that have been extensively used for delineating salinity sources are halogen ratios, due to the basic assumption that halogens behave conservatively in aquifer systems. In particular, the bromide to chloride ratio has been used extensively to delineate salinization processes (Alcalá and Custodio, 2008; Andreasen and Fleck, 1997; Cartwright et al., 2004, 2006, 2007a, 2009; Davis et al., 1998; Dror et al., 1999; Edmunds, 1996; Edmunds et al., 2003; Farber et al., 2004, 2007; Fontes and Matray, 1993; Freeman, 2007; Herczeg and Edmunds, 2000; Hsissou et al., 1999; Hudak and Blanchard, 1997; Katz et al., 2011; Kolodny et al., 1999; Leybourne and Goodfellow, 2007; Mandilaras et al., 2008; Matray et al., 1994; Mazor, 1997; Panno et al., 2006; Vengosh and Pankratov, 1998; Warner et al., 2012). **Figure 30** illustrates the possible variations of Br/Cl and B/Cl ratios for different salinity sources. While several salinity sources have distinctive low Br/Cl ratios (e.g., wastewater, deicing, evaporite dissolution) relative to other sources with high Br/Cl ratios (brines evolved from evaporated seawater, animal waste, coal ash), possible overlaps may occur. Furthermore, bromide may not always behave as a conservative tracer, as laboratory-controlled adsorption experiments have shown some bromide retention at pH < 7 that can lead to modification of Br/Cl ratios during water transport in clay-rich systems (Goldberg and Kabengi, 2010).

The second layer in the evaluation of a salinity source is using different cations to chloride ratios such as Na/Cl and Ca/Cl ratios. For example, seawater intrusion into coastal aquifers is associated with an inverse correlation between Na/Cl and Ca/Cl due to base-exchange reactions, resulting in low Na/Cl and high Ca/Cl ratios relative to seawater values (Appelo, 1994; Appelo and Geirnart, 1991; Appelo and Postma, 2005; Appelo and Willemsen, 1987; Custodio, 1987a,b, 1997; Jones et al., 1999). In contrast, wastewater and nonmarine salinity sources typically have Na/Cl > 1. This distinction may be biased, however, since the original Na/Cl ratio can be modified by water–rock interaction and base-exchange reactions that would reduce the Na/Cl ratio of saline water in nonmarine settings; hence, additional tracers are required.

Other common conservative tracers for salinization studies are the stable isotopes of the water molecule, oxygen ($\delta^{18}O_{H_2O}$)

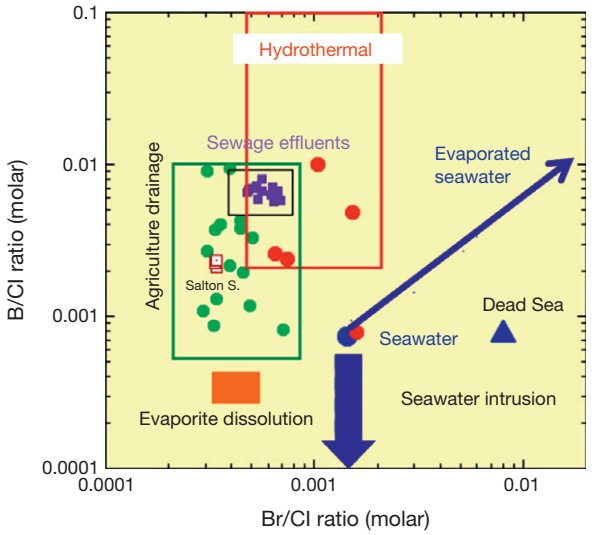

Figure 30 Elucidation of saline sources by using the variation of B/Cl versus Br/Cl ratios. Note the expected geochemical distinction between seawater, evaporated seawater, brines (e.g., Dead Sea), hydrothermal fluids, sewage effluents, agricultural drainage (e.g., Salton Sea), and evaporite dissolution.

and hydrogen ($\delta^{2}H_{H_2O}$) isotopes (see **Chapter 7.10**). The use of stable isotopes of oxygen and hydrogen for tracing salinity sources in surface water may be complicated by evaporation effects that will result in enrichment of $^{18}O_{H_2O}$ and $^{2}H_{H_2O}$ combined with low $\delta^{18}O_{H_2O}$ /$\delta^{2}H_{H_2O}$ ratios relative to the original composition of the saline water. However, natural or artificial recharge of saline surface water into an aquifer can be identified by distinctive enriched $^{18}O_{H_2O}$ and $^{2}H_{H_2O}$ compositions. This distinction was used to trace the distribution of saline-treated wastewater and imported water from the Sea of Galilee that are artificially recharged into the Mediterranean coastal aquifer of Israel. Both wastewater and imported water are characterized by high $\delta^{18}O_{H_2O}$ and $\delta^{2}H_{H_2O}$ values that are different from those of the regional groundwater and thus the stable isotope variations can be used to monitor the mixing of the external water in the aquifer (Vengosh et al., 1999b).

While dilution of saline water would create small changes in the solute ratios (e.g., Br/Cl) due to the relatively high concentration of the solutes in the saline source relative to freshwater, the original $\delta^{18}O_{H_2O}$ and $\delta^{2}H_{H_2O}$ values of saline

sources would be completely modified by mixing (dilution) with meteoric water (e.g., Banner et al., 1989; Bergelson et al., 1999; Hanor, 1994; Warner et al., 2012). Nevertheless, stable isotopes of oxygen and hydrogen in water can be used to evaluate mixing relationships in the case of seawater intrusion (Jones et al., 1999; Yechieli et al., 2000) or reflect agricultural return flows (Davisson and Criss, 1993; Kass et al., 2005). It is also possible to use the stable isotopes for detecting the origin of salinity derived from mixing with diluted saline water (e.g., residues of evaporated seawater, formation waters) that were diluted by freshwater with low $\delta^{18}O_{H_2O}$ and $\delta^{2}H_{H_2O}$ values, as opposed to salinization from direct seawater intrusion with higher $\delta^{18}O_{H_2O}$ and $\delta^{2}H_{H_2O}$ values. For example, Herczeg et al. (2001) showed that groundwaters in the Murray–Darling Basin have low $\delta^{18}O_{H_2O}$ and $\delta^{2}H_{H_2O}$ values relative to possible mixing between meteoric water and seawater, thus suggesting that the salinity of the groundwater in the basin is derived from atmospheric fallout with stable isotope meteoric composition and not from seawater intrusion. Similarly, Bergelson et al. (1999) showed that saline springs that emerge from the Sea of Galilee in the Jordan Rift Valley have low $\delta^{18}O_{H_2O}$ and $\delta^{2}H_{H_2O}$ values to account for direct evaporated brine and must therefore reflect multiple dilution stages of the original hypersaline brines. Finally, anthropogenic saline sources, such as domestic wastewaters that are treated or stored in open reservoirs, are often enriched in ^{18}O and ^{2}H, which can be used to trace their presence in contaminated groundwater (Vengosh et al., 1999b).

Radioactive isotopes of ^{36}Cl and ^{129}I that behave conservatively in the hydrological system are also important tools for studying salinization processes (see **Chapter 7.14**). Since 1952, atmospheric thermonuclear testing has significantly changed the ^{36}Cl budget in the atmosphere. The atmospheric ^{36}Cl fallout was several magnitudes higher than prenuclear flux, particularly between 1952 and 1970. Hence, the nuclear ^{36}Cl-pulse is an important hydrological tracer that is preserved in the hydrological system and its signal is modified only by dispersion and natural decay of ^{36}Cl (half-life ~301 000 years; Phillips, 2000). Modern meteoric chloride is characterized by a high $^{36}Cl/Cl$ ratio that is preserved during evaporative concentration and recycling of salts via precipitation–dissolution (Phillips, 2000). In contrast, other saline sources such as road salts and oilfield brines have significantly lower $^{36}Cl/Cl$ ratios. The distinction between meteoric and groundwater chloride (**Figure 31**) was used by several studies to estimate the relative proportion of meteoric and subsurface chlorine sources in the Jordan Valley and the Dead Sea (Magaritz et al., 1990; Yechieli et al., 1996), the closed basins in Antarctica (Lyons et al., 1998), and Lake Magadi of the East African Rift (Phillips, 2000).

Similarly, ^{129}I is a naturally occurring, cosmogenic and fissiogenic isotope ($T_{1/2} = 15.7$ My; Fabryka-Martin, 2000; Fabryka-Martin et al., 1991). Like ^{3}H, ^{14}C, and ^{36}Cl, ^{129}I was produced in bomb tests, but in greater abundance above the natural level. While some of the other anthropogenic radionuclides have returned to near prebomb levels, ^{129}I in the surface environment continues to be elevated due to subsequent emissions from nuclear fuel reprocessing facilities, and is transported via the atmosphere on a hemispheric scale. Modern meteoric waters are expected to have a large $^{129}I/^{127}I$ ratio ($>1000 \times 10^{-12}$) relative to that in old groundwater ($<10^{-12}$; Moran et al., 1999, 2002). By combining the isotopic ratios

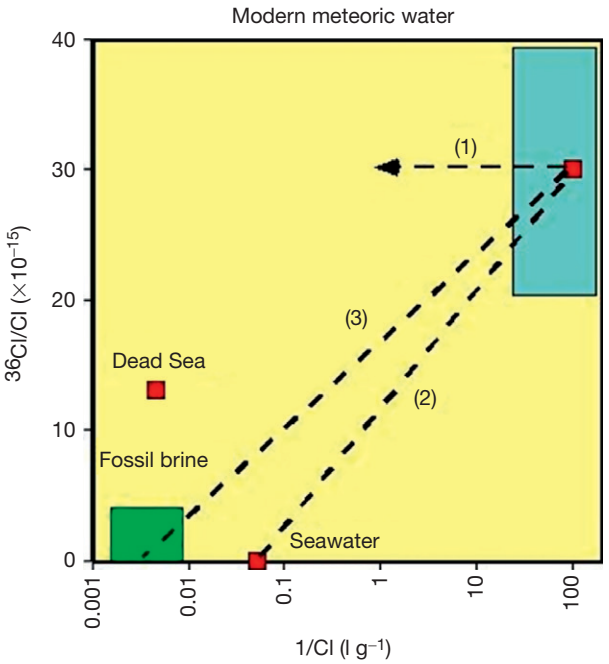

Figure 31 Schematic illustration of the expected $^{36}Cl/Cl$ variation versus the reciprocal of chloride (l g^{-1}) upon salinization by: (1) surface evaporation; (2) seawater intrusion; and (3) mixing with brines and/or dissolution of evaporites. Data were integrated from Magaritz et al. (1990), Yechieli et al. (1996), and Phillips (2000). The relatively high $^{36}Cl/Cl$ ratio in the Dead Sea suggests mixing with young meteoric chloride (Yechieli et al., 1996).

($^{36}Cl/Cl$, $^{129}I/I$) Ekwurzel et al. (2001) discriminated between different saline sources in the Souss-Massa Basin in Morocco, and particularly between modern saline recharge and older saline groundwater (**Figure 32**).

Using conservative tracers such as Br/Cl, $\delta^{18}O_{H_2O}$, and $^{36}Cl/Cl$ ratios, it is possible to discriminate river salinization processes (**Figure 33**). Recycling and evaporation of meteoric salts by in-stream river salinization would result in increasing $\delta^{18}O_{H_2O}$ and $\delta^{2}H_{H_2O}$ values with flow distance, but the Br/Cl and $^{36}Cl/Cl$ ratios in the river would not be expected to change with increasing salinity (**Figure 33**). River salinization via discharge of agricultural return flow would likely increase the $\delta^{18}O_{H_2O}$ values and may change the Br/Cl ratio, but the $^{36}Cl/Cl$ would not be changed (i.e., short-term recycling of modern meteoric chlorine with a high $^{36}Cl/Cl$ ratio). However, in dryland environments the long-term storage of chlorine in the subsurface can be expected to buffer the original $^{36}Cl/Cl$ ratio. Dissolution of halite deposits and formation of saline groundwater can be expected to form saline groundwater with a low Br/Cl ratio (e.g., Rio Grande Basin; Phillips et al., 2003; Mills et al., 2002) and a low $^{36}Cl/Cl$ would ratio. In contrast, an increase of the Br/Cl ratio with salinity reflects discharge of saline groundwater that originated from mixing with relics of evaporated seawater that are entrapped in the basin (e.g., Jordan River; Farber et al., 2004, 2005, 2007). In such a scenario, the $^{36}Cl/Cl$ ratio is also expected to be low (**Figure 33**).

While conservative tracers can provide some indication of the solute sources, reactive tracers are as valuable, as they can

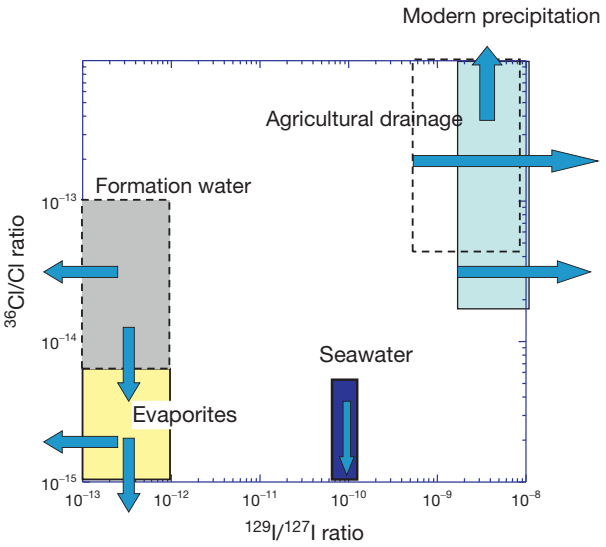

Figure 32 Elucidation of saline sources by using the variation of ^{36}Cl/Cl and ^{129}I/^{127}I ratios. Note the isotopic distinction between modern meteoric water and agricultural return relative to formation water, evaporite dissolution, and seawater. Arrows represent possible extended ranges. Data from Ekwurzel et al. (2001) and Moran et al. (2002).

provide essential information on both the original solutes and possible modifications upon interactions with the host sediments/rocks of the investigated aquifer. One example is the boron isotope ratio, which can be used as an indicator of both the solute sources and interaction with oxides and clay minerals in the aquifer rocks. The δ^{11}B values vary significantly from low values in nonmarine brines (e.g., Qaidam Basin, Tibet; δ^{11}B = 0 to +10‰; Vengosh et al., 1995) and anthropogenic sources such as coal (δ^{11}B as low as −70‰; Williams and Hervig, 2004) and coal ash leachates (δ^{11}B = −15‰; Ruhl et al., 2010), to high ratios in evaporated seawater (δ^{11}B = 55‰; Vengosh et al., 1992) and in the Dead Sea (δ^{11}B = 57‰; Vengosh et al., 1991b). Yet, boron tends to be adsorbed onto clay minerals and oxides, particularly under high salinity conditions (see Section 11.9.7.2). During the adsorption process, the light isotopes, in the form of B $(OH)_4^-$, incorporate preferentially into adsorbed sites whereas the residual dissolved boron in the form $B(OH)_3$ is enriched in ^{11}B. The magnitude of the boron isotope fractionation between the boron species has been debated; earlier studies have utilized the theoretical fractionation factor of 19‰ (α_{B3-B4} = 1.0193) proposed by Kakihana et al. (1977) while later theoretical (Byrne et al., 2006; Liu and Tossell, 2005) and experimental (Klochko et al., 2006) studies have suggested a larger fractionation of 27.2‰ (α_{B3-B4} = 1.0272). Adsorption experiments conducted by Palmer et al. (1987) also suggested a larger isotope fractionation of about 30‰ between adsorbed and dissolved boron. In contrast, boron mobilization from rocks is not associated with isotopic fractionation and the mobilization of boron from a typically lower δ^{11}B composition of rocks reduces the δ^{11}B values of the water.

Taking into account the possible isotopic modification upon water–rock interactions, boron isotopes can be used to trace salinization processes and to delineate multiple salinity sources (**Figure 34**; Vengosh and Spivack, 2000). Increasing numbers of studies (Barth, 1998; Farber et al., 2004; Forcada and Evangelista, 2008; Katz et al., 2009; Kloppmann et al., 2009; Kruge et al., 2010; Leenhouts et al., 1998; Naftz et al., 2008; Rabiet et al., 2005; Ruhl et al., 2010; Vengosh and Spivack, 2000; Vengosh et al., 1994, 2002, 2005; Widory et al., 2004, 2005) have utilized these variations to detect the origin of saline groundwater, such as seawater intrusion into coastal aquifers with high δ^{11}B values and low B/Cl ratios, as opposed to anthropogenic contamination with significantly lower δ^{11}B values and high B/Cl ratios, such as wastewater and leachates from coal and coal ash. **Figure 34** illustrates the B/Cl and boron isotope variations of some of the major salinity sources and shows the conspicuous differences between marine sources (e.g., seawater intrusion, evaporated seawater, connate brines, oil and gas brines) with high δ^{11}B values relative to wastewater, geothermal water, and contamination derived from leaching of coal and coal ash. During water transport and reactivity with oxides and clay minerals in the aquifer, the original isotopic fingerprints of the different end members will *always* be modified toward higher δ^{11}B values and lower B/Cl ratios due to the isotopic fractionation associated with boron retention. These modifications can mask the original isotopic fingerprints of the salinity sources but in many cases the *range* of the δ^{11}B values of the salinized groundwater will still be useful to distinguish different salinity sources. For example, in spite of isotopic fractionation associated with seawater intrusion and wastewater contamination, the δ^{11}B ranges of groundwater salinized from these two sources would be distinguishable (Vengosh et al., 1994).

The strontium isotope ratio is another sensitive tracer to delineate the origin of saline water, the type of rock source, and the impact of weathering processes (see **Chapter 7.11**). Due to the absence of isotopic fractionation, the isotopic composition of strontium mobilized from rocks during weathering is identical to that of the rock and thus strontium isotope geochemistry is a powerful tool for delineating solutes and salinization sources. Numerous studies have utilized strontium isotopes to detect the flow paths of groundwater in different aquifers (Banner and Hanson, 1990; Banner et al., 1989; Bullen et al., 1996, 1997; Katz and Bullen, 1996; Smith et al., 2009; Starinsky et al., 1980, 1983a,b; White et al., 1999), the composition of exchangeable strontium in clay minerals (Armstrong et al., 1998; Johnson and DePaolo, 1994; Vengosh et al., 2002), salinization from upflow of the Middle Devonian Marcellus brines in northeastern Appalachian basin (Warner et al., 2012), salinization from produced water from coal bed methane production (Brinck and Frost, 2007; Campbell et al., 2008), the origin of dissolved strontium in rivers (Farber et al., 2004; Moore et al., 2008b; Singh et al., 1998), mineralization of schist rocks with radiogenic Sr isotope ratios along the margin of the Lakhssas Plateau in the Anti-Atlas Mountains of southwestern Morocco (Ettayfi et al., 2012), and the interaction between groundwater, lake water, and aquifer minerals (Katz and Bullen, 1996; Lyons et al., 1995).

In carbonate or calcareous sand aquifers, the strontium isotopic composition of saline groundwater should mimic that of the host aquifer rocks. In cases where they are dissimilar, the groundwater must have interacted with external rock sources and thus must have flown in a different aquifer. For example, saline groundwater from central Missouri, USA, has high ^{87}Sr/^{86}Sr ratios that are considerably more radiogenic than the host Mississippian carbonates. The high ^{87}Sr/^{86}Sr

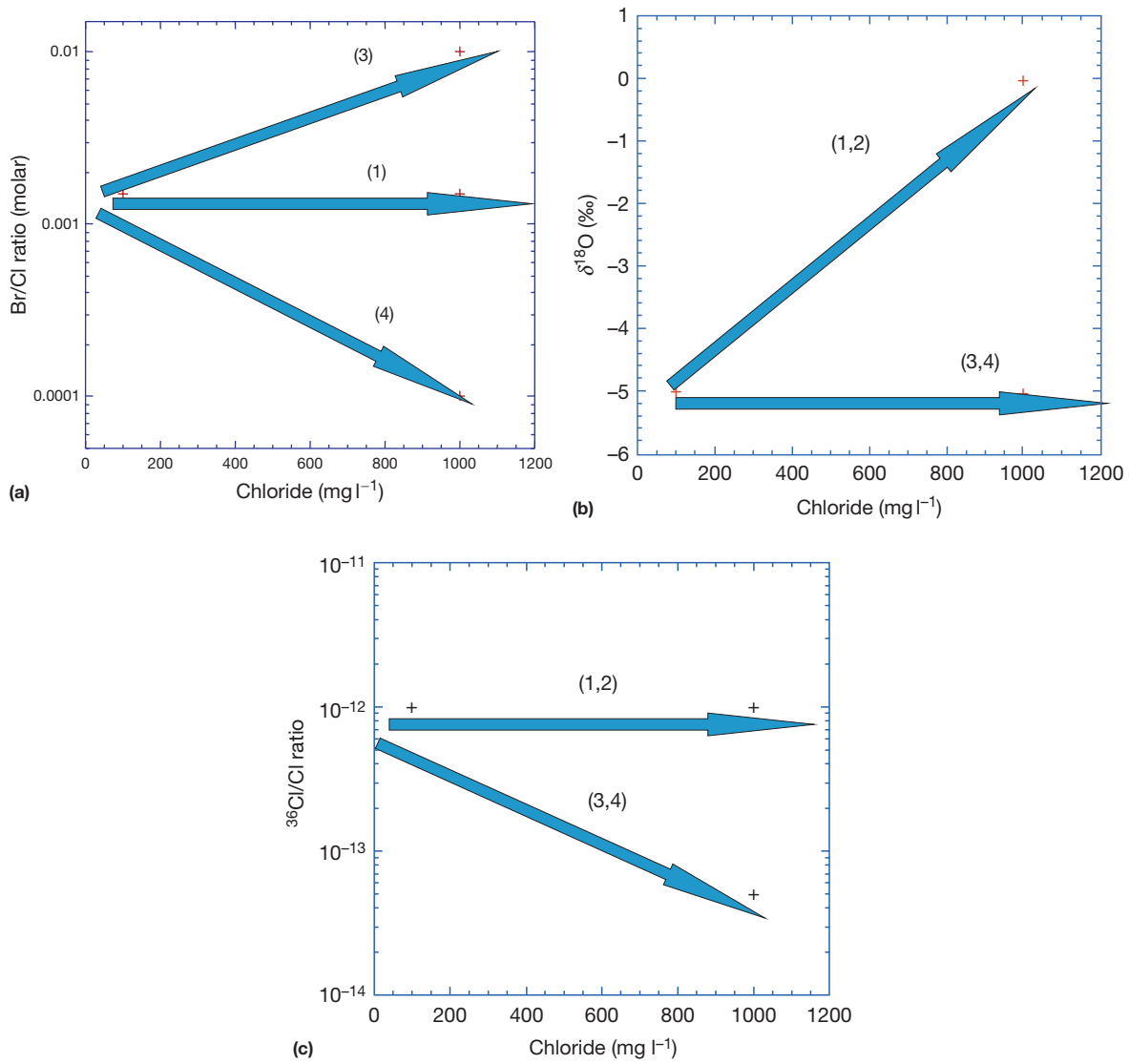

Figure 33 Schematic illustration of possible Br/Cl (a), $\delta^{18}O_{H_2O}$ (b), and $^{36}Cl/Cl$ (c) variations upon different river salinization scenarios: (1) surface evaporation of the river water; (2) recycling of salts via formation of agricultural return flow and discharge to the river; (3) discharge of external groundwater to the river with brine or old formation water components (i.e., high Br/Cl); and (4) discharge of external groundwater salinized by dissolution of evaporite deposits.

ratios suggested deep subsurface migration and water–rock interaction with Paleozoic and Precambrian strata (Banner et al., 1989). Similarly, the $^{87}Sr/^{86}Sr$ ratios of saline groundwater from the Mediterranean coastal aquifer of Israel are considerably lower than the $^{87}Sr/^{86}Sr$ ratios of the Pleistocene carbonate aquifer matrix, indicating an external source for the formation of the saline groundwater (Vengosh et al., 1999b). The flow of external saline water with a different $^{87}Sr/^{86}Sr$ ratio is therefore an important tool to delineate salinization processes. Several studies have used this approach, such as the cases of the Nubian Sandstone aquifer in the Negev, Israel (Vengosh et al., 2007), the Jordan River (Farber et al., 2004), the coastal aquifer of North Carolina (Vinson, 2011; Woods et al., 2000), the Oconee River Basin in the Piedmont region of northeastern Georgia (Rose and Fullagar, 2005), the RAK aquifer in southern Saudi Arabia (Sultan et al., 2008), the Lower Rio Grande in the New Mexico–Texas border region, USA (Moore et al., 2008b), the saline water in the Anti-Atlas Mountains of southwestern Morocco (Ettayfi et al., 2012), and the Souss-Massa Basin in Morocco (Bouchaou et al., 2008).

Strontium isotopes can also be used to trace salinization by agricultural return flow. Böhlke and Horan (2000) showed that some fertilizers and hence agricultural recharge have high radiogenic $^{87}Sr/^{86}Sr$ ratios, significantly different from those of natural strontium acquired by water–rock interactions in the aquifer. Although denitrification and carbonate dissolution may alter the strontium isotopic ratio in redox conditions, the association of distinctive $^{87}Sr/^{86}Sr$ ratios and nitrate concentrations suggests that the Sr composition is controlled by the input of fertilizers in groundwater (Böhlke and Horan, 2000).

The sulfur ($\delta^{34}S_{SO_4}$) and oxygen in sulfate ($\delta^{18}O_{SO_4}$) isotope variations in salinized groundwater can provide additional

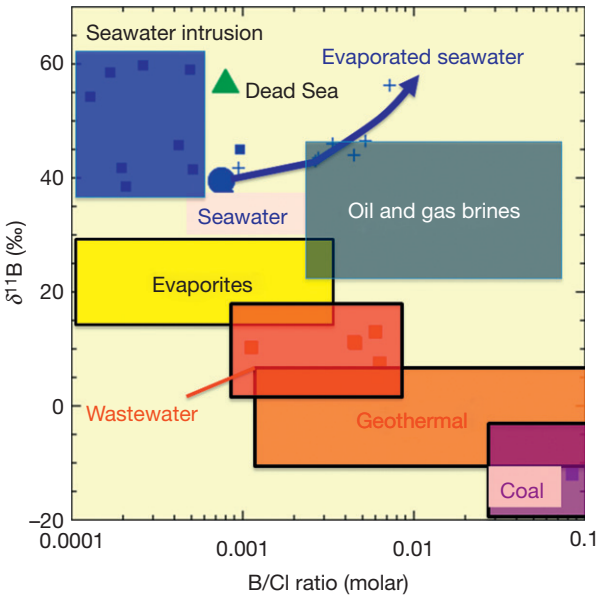

Figure 34 Elucidation of saline sources by using the variation of $\delta^{11}B$ versus B/Cl ratios. Note the expected geochemical distinction between seawater, evaporated seawater, brines (e.g., Dead Sea), and saltwater intrusion with typically high $\delta^{11}B$ values relative to hydrothermal fluids, sewage effluents, evaporite dissolution, and contamination from coal and coal ash leachates with significantly higher B/Cl ratios and lower $\delta^{11}B$ values.

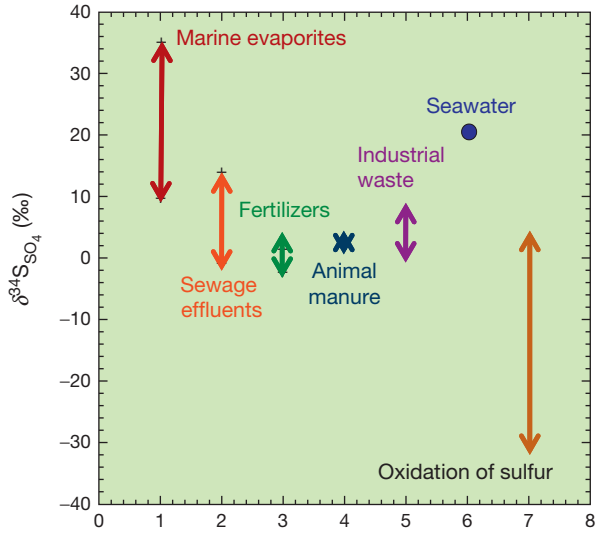

Figure 35 Variations of sulfur isotope ratio in sulfate ($\delta^{34}S_{SO_4}$) in different possible saline sources. Note the large range of $\delta^{34}S_{SO_4}$ values in marine evaporites that reflect the secular variations of $\delta^{34}S_{SO_4}$ in seawater with time and the high $\delta^{34}S_{SO_4}$ value of seawater relative to nonmarine and anthropogenic sources. Sulfate reduction processes are expected to increase the $\delta^{34}S_{SO_4}$ values in the residual sulfate.

information on the salinity sources. Seawater has distinctive isotopic characteristics ($\delta^{34}S_{SO_4}=+21‰$; $\delta^{18}O_{SO_4}=+9.5‰$) relative to nonmarine salinity sources, typically with lower $\delta^{34}S_{SO_4}$ and $\delta^{18}O_{SO_4}$ values (Figure 35). High sulfate in noncoastal groundwater could be derived from oxidation of reduced inorganic sulfur components with low $\delta^{34}S_{SO_4}$ and $\delta^{18}O_{SO_4}$ values (−30‰ to +5‰; −10‰ to +5‰, respectively), or from dissolution of sulfate deposits. The isotopic ratios of marine gypsum vary with geological age and range from +10‰ to +35‰ and +9‰ to +20‰ for $\delta^{34}S_{SO_4}$ and $\delta^{18}O_{SO_4}$, respectively. Sulfate reduction causes isotopic fractionation in which the heavy isotopes, ^{34}S and ^{18}O, become enriched in the residual sulfate-depleted water. Consequently, seawater intrusion and hypersaline brines are characterized by low SO_4/Cl ratios and high $\delta^{34}S_{SO_4}$ and $\delta^{18}O_{SO_4}$ values due to sulfate reduction processes (Kim et al., 2003; Krouse and Mayer, 2000; Moore et al., 2008b; Oulhote et al., 2011; Raab and Spiro, 1991; Sanz et al., 2007; Yamanaka and Kumagai, 2006). Examples for salinization of groundwater from dissolution of evaporite sulfate deposits include the Nubian Sandstone aquifer of the Negev, Israel (Vengosh et al., 2007) and the Hueco Bolson aquifer, located within the Trans-Pecos Texas region and the primary water resource for El Paso, Texas, USA, and Juarez, Mexico (Druhan et al., 2008).

Anthropogenic sources such as domestic wastewater ($\delta^{34}S_{SO_4}$ of −0.5‰ to 14.3‰; Houhou et al., 2010; Torssander et al., 2006), fertilizers (−2.1‰ to +1.6‰; Szynkiewicz et al., 2011), animal manure (+2.7‰; Szynkiewicz et al., 2011), and industrial waste (+1–8‰; Cortecci et al., 2002) have high sulfate (high SO_4/Cl ratios) with low $\delta^{34}S_{SO_4}$ characteristics (Figure 35). The $\delta^{34}S_{SO_4}$ data (range of −1.6‰ to +0.9‰) from the Rio Grande River in New Mexico and western Texas, USA, showed that the high sulfate content in the river was derived from local fertilizers and not from the associated Paleozoic evaporite rocks that are characterized by higher $\delta^{34}S_{SO_4}$ values (Szynkiewicz et al., 2011). Overall, while different saline sources can have distinctive sulfur isotopic fingerprints (Figure 35), under anaerobic conditions sulfate reduction can mask the original isotopic signature, and the $\delta^{34}S_{SO_4}$ and $\delta^{18}O_{SO_4}$ values of the salinized groundwater will *always* be higher than the expected mixing relationships between the freshwater and the saline sources.

11.9.9 Remediation and the Chemical Composition of Desalination

As the world experiences explosive population growth, increasing demands for food and energy are associated with depletion of worldwide water resources and degradation of water quality. About 70% of the world's freshwater is utilized, particularly for irrigated agriculture. In order to meet global food demands, agricultural production will have to increase by twofold or threefold during the coming decades and the exploitation of freshwater resources will further increase (Gleick, 1994, 1998; Hanasaki et al., 2008a,b ; Hern and Feltz, 1998; Kim et al., 2009 ; Oki and Kanae, 2006; Vorosmarty et al., 2000). The expected increase in the human population during this century (8–12 billion by the year 2050; Roush, 1994) will increase demands for freshwater and cultivation of marginal land. Furthermore, projections for future renewable water resources in arid and semiarid areas such as the Middle East and northern Africa are alarming; climate change coupled with projected increasing water demand are likely to amplify the already profound water shortage in these regions Sowers et al., 2011. The Intergovernmental Panel on Climate Change (IPCC) (Christensen et al., 2007) and other independent studies predict

a significant reduction in precipitation in the Middle East and northern Africa by the next century (Alpert et al., 2008; Arnell, 1999; Conway and Hulme, 1996; Evans, 2008; Milly et al., 2005; Sánchez et al., 2004; Suppan et al., 2008). The combination of reduced recharge, enhanced evaporation, and pumping beyond replenishment capacity will likely cause severe and adverse environmental impacts, and in particular increasing salinization of water resources.

In principle, two technical solutions can be adopted by water agencies facing long-term salinization of water resources – dilution and desalination. Dilution is the cheapest solution for pollution, which depends on the availability of freshwater resources. In many depleted or salinized aquifers, artificial recharge or irrigation of imported water occurs from areas of relatively high water abundance: for example, the northern–southern water transport in California, USA; the flow of snowmelt and rivers from the Atlas Mountains to the sub-Sahara Draa and Ziz basins in Morocco for irrigation of oases; and the transport of water from the Sea of Galilee in Israel through the National Water Carrier for artificial recharge in the Mediterranean coastal aquifer. This import and use of external water sources compensates, at least temporarily, for overexploitation and salinization of aquifers. Artificial recharge of external water will modify the oxygen and deuterium isotopic compositions of the natural groundwater. In some cases, where the recharge water is derived from upstream and higher elevation, the recharge will result in lower $\delta^{18}O_{H_2O}$ and $\delta^{2}H_{H_2O}$ values. This was demonstrated by the recharge of the Colorado River aqueduct water into the Pacific coastal aquifer of Orange County, California (Davisson et al., 1999; Williams, 1997). In contrast, in cases where the recharge water is derived from open-surface reservoirs with evaporation (e.g., recharge of Salinas River, California; Vengosh et al., 2002), lakes (e.g., recharge of imported water from the Sea of Galilee into the Mediterranean coastal aquifer, Israel; Vengosh et al., 1999b), and wastewater treated in open basins (Vengosh et al., 1999b), the $\delta^{18}O_{H_2O}$ and $\delta^{2}H_{H_2O}$ values are expected to be significantly higher than those of the natural groundwater. Given the water shortage, interbasin transfers are, however, a less feasible solution for most water-scarce regions.

Desalination, in contrast, could be the ultimate solution for providing potable water to water-scarce countries. The water crisis in the Middle East, for example, could be resolved primarily by large-scale desalination of seawater and brackish water (Glueckstern, 1992). In 1998, 12 500 desalination units around the world produced about 23 million cubic meters per day (Glueckstern and Priel, 1998). A decade later (2009), 14 451 desalination plants globally produced almost 60 million cubic meters per day of desalted water (International Desalination and Water Reuse, 2011), and under-construction and planned desalination plants are expected to generate an additional 11 and 25 million cubic meters per day of desalted water in the near future, respectively (data from desaldata.com updated to November 2010; Windler, 2011). Until 2000, the capacity of new installed desalination plants fluctuated between 1 and 2 million cubic meters per year, but since 2000, the capacity of newly installed desalination plants has increased rapidly to 6–7 million cubic meters per year (International Desalination and Water Reuse, 2011). One of the critical factors that led to the accelerated rates of desalination is the significant improvement in reverse osmosis (RO) membrane technology, replacing older technologies such as thermal desalination. By 2009, about half of the global desalted water was produced using RO desalination technology and newer desalination facilities are entirely based on membrane technology (Greenlee et al., 2009). Nonetheless, Saudi Arabia, which is currently the world leader in desalination with approximately 26% of global production capacity, almost entirely uses thermal desalination. The United States on the other hand, which is ranked second and produces 17% of the world's desalted water, uses predominantly (~70%) RO desalination technology (Greenlee et al., 2009). The world's largest RO desalination plant was installed in Israel in 2005 with a production capacity of 330 000 $m^3 day^{-1}$ (Dreizin, 2006; Kronenberg, 2004; Lokiec and Kronenberg, 2003; Sauvet-Goichon, 2007). Israel is expected to expand its desalination capacity so that it becomes the primary source for the domestic sector; it has already developed new desalination capacity of 345 million cubic meters per year and is planning to double this to 660 million cubic meters per year by 2013 (data from desaldata.com updated to November 2010; Windler, 2011).

Consequently, the chemical composition of future water resources in the twenty-first century is likely to reflect these human interventions – the creation of 'new water' from desalination. The rapid worldwide increase in desalination production generates new types of water that are added to the natural hydrological cycle through leakage, irrigation, and recycling by wastewater irrigation. The Anthropocene Era is therefore characterized by generating new 'man-made water.' Man-made water has different chemical and isotopic characteristics from natural waters. Given that RO is the leading desalination technology, the review of the geochemistry of desalted water is focused here on the effect of RO desalination.

The chemistry of RO desalted water depends on (1) the source water that is used for desalination, which can range from seawater to brackish to saline groundwater with a large spectrum of chemical compositions (Greenlee et al., 2009); (2) the ion selectivity through the membranes, which depends on ion mass, size, charge, and reactivity (Kloppmann et al., 2008b; Mukherjee and Sengupta, 2003); and (3) posttreatment processes that shape the chemistry of the produced water (Birnhack et al., 2011). While the composition of seawater is uniform, desalination of brackish to saline groundwater could generate desalted water with different chemical and isotopic compositions relative to natural waters. The most conspicuous difference is the stable isotope composition of desalted water; desalination generates low-saline water with $\delta^{18}O_{H_2O}$ and $\delta^{2}H_{H_2O}$ values that are identical to those of the saline water source. Thus, desalination of seawater generates freshwater with $\delta^{18}O_{H_2O}$ and $\delta^{2}H_{H_2O}$ of seawater, which are significantly different from the depleted $^{18}O_{H_2O}$ and $^{2}H_{H_2O}$ composition of meteoric water. For example, the stable isotope signatures of RO desalted freshwater from the Ashkelon desalination plant in Israel ($\delta^{18}O_{H_2O} \sim +2‰$; $\delta^{2}H_{H_2O} \sim +12‰$; **Figure 36**) and the Sabkha C desalination plant in Eilat, Israel ($\delta^{18}O_{H_2O} \sim 0‰$; $\delta^{2}H_{H_2O} \sim +2‰$), are clearly different from the stable isotope compositions of fresh meteoric water (Kloppmann et al.,

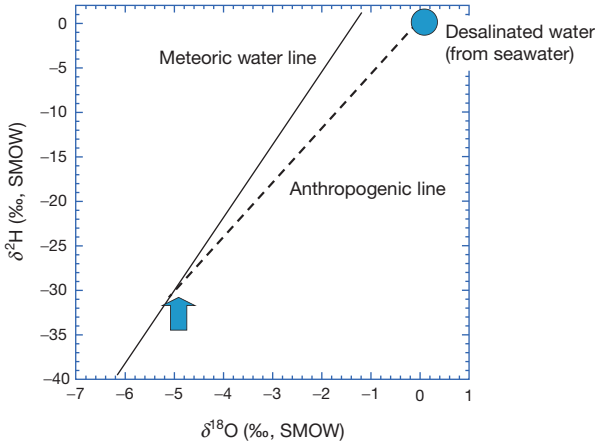

Figure 36 $\delta^2H_{H_2O}$ versus $\delta^{18}O_{H_2O}$ values of reverse osmosis (RO) desalted seawater and the Global Meteoric Water Line (Craig, 1961). The Anthropogenic Line lies on a possible mixing relationship between natural waters along the meteoric water line (arrow) and the desalted seawater. Future formation of a large volume of desalted seawater is expected to cause infiltration (e.g., leakage, reuse) of man-made freshwater with high $\delta^2H_{H_2O}$ and $\delta^{18}O_{H_2O}$ values relative to natural meteoric waters with lower $\delta^2H_{H_2O}$ and $\delta^{18}O_{H_2O}$ values.

2008b). Consequently, recharge of freshwater originating from desalination either by leakage in the urban environment or wastewater irrigation would have $\delta^{18}O_{H_2O}$ and $\delta^2H_{H_2O}$ values that lie along a mixing line between the natural and seawater values (**Figure 36**). The slope of the *Anthropogenic Line* depends on the $\delta^{18}O_{H_2O}$ and $\delta^2H_{H_2O}$ values of the meteoric water in the local area and will always be lower than those of natural meteoric lines with a slope <8 (**Figure 36**).

The second factor that controls the chemistry of RO desalted water is the preferential permeability of ions through the RO membrane. Ion transport through the membrane depends on ion mass, size, charge, and reactivity (Mukherjee and Sengupta, 2003). The rejection by the RO membrane is higher for heavier molecules; thus, the molar Na/Cl ratio is modified from 0.86 in seawater to 0.94 in desalted water (**Table 1**; data from Kloppmann et al., 2008b). The preferential selection by the RO membrane of double-charged ions (Ca^{2+}, Mg^{2+}, SO_4^{2-}) over single-charged ions (Cl^-, Na^+) also modifies the original chemical composition and ionic ratios of the desalted water. Thus, desalted seawater is modified into an Na–Cl freshwater type (Cl + Na/TDI ~ 0.93, in equivalent units) and the Ca/Cl, Mg/Cl, SO_4/Cl, and Ca/Na ratios of RO desalted water are significantly lower (by fivefold) relative to those in the original seawater (**Table 1**). Similarly, nanofiltration membranes, with a negatively charged hydrophobic rejection layer, tend to selectively reject multivalent ions but have low rejection efficiency for monovalent ions (Kharaka et al., 1996, 1997).

Perhaps one of the most conspicuous ion selections that are associated with RO desalination is the selective transport of noncharged species such as boric acid ($B(OH)_3^0$) and arsenic acid ($H_3AsO_3^0$) relative to the rejection of charged species. Pretreatment processes typically reduce the pH of the saline water source in order to reduce scaling, and consequently boron exists mostly in the form of uncharged boric acid (see **Figure 27** for the dependence of boron species on pH). For processed seawater (pH < 6.5) and saline groundwater from North Carolina (pH 7.8), it was calculated (based on salinity, pH, and pressure) that boric acid forms 99% (Kloppmann et al., 2008b) and 93% (Vinson, 2011) of the total boron, respectively. The noncharged nature of boric acid generates differential permeability of boron species through the RO membranes in which boric acid is not rejected as effectively as other, charged, ions. As a result, boron is enriched in desalted water with conspicuously high B/Cl ratios (Cengeloglu et al., 2008; Geffen et al., 2006; Georghiou and Pashafidis, 2007; Hyung and Kim, 2006; Kloppmann et al., 2008b; Mane et al., 2009; Ozturk et al., 2008; Parks and Edwards, 2005; Prats et al., 2000; Sagiv and Semiat, 2004; Tu et al., 2011; Vinson et al., 2011). The B/Cl of desalted water can reach 0.4 (Kloppmann et al., 2008b) relative to 8×10^{-4} in seawater, a 500-fold enrichment.

Given that boron isotope fractionation depends on the species distribution in which the heavy boron isotope ^{11}B tends to be enriched in boric acid, RO desalination can also induce isotopic fractionation. Under low pH desalination, where boric acid is the dominant species of boron, no isotope fractionation is expected, and thus the boron isotope composition of the desalted water will be identical to that of the saline source. This was demonstrated for both seawater (Kloppmann et al., 2008b) and brackish groundwater (Vinson et al., 2011) during RO desalination. In contrast, under high-pH desalination, where ^{11}B-depleted borate ion is rejected by the RO membrane, selective transport of boric acid species through the membrane will induce isotopic fractionation, which will result in ^{11}B-enriched desalted water (Kloppmann et al., 2008b). The Ashkelon RO desalination plant (Dreizin, 2006; Kronenberg, 2004; Lokiec and Kronenberg, 2003; Sauvet-Goichon, 2007) includes four cascade desalination stages, operating both at high- and low-pH conditions (Gorenflo et al., 2007), which reduce boron concentrations of the desalted water below 0.4 mg l^{-1}. At pH 9.5, where borate ion composes 95% of the dissolved boron, the desalted water is highly enriched in ^{11}B ($\delta^{11}B = 58‰$) relative to seawater (39‰; Kloppmann et al., 2008b).

In addition to boron, the absorption of noncharged arsenic by the RO membrane also depends on the prevalence of charged As species in the saline water source. Arsenic speciation in water depends on oxidation state and pH. Under reducing conditions, arsenic occurs as arsenite (As(III)) in which the uncharged $H_3AsO_3^0$ is the dominant species at pH below 9. Under oxic conditions, arsenate (As(V)) species are stable, particularly the monovalent species $H_2AsO_4^-$ (pH < 6.5) and the divalent species $HAsO_4^{2-}$ (pH > 6.5). Consequently, RO rejection for the charged As(V) in oxygenated water is more effective (George et al., 2006; Geucke et al., 2009; Moore et al., 2008a, Oreskovich and Watson, 2003; Walker et al., 2008). Desalination of reduced brackish to saline groundwater in which arsenic occurs as the reduced species arsenite (As(III)) therefore requires an additional treatment system to remove arsenic, as demonstrated in desalination of groundwater from the coastal aquifer of North Carolina (Vinson et al., 2011).

The third process that shapes the composition of desalted water is posttreatment of desalted water. Permeates after RO desalination contain low dissolved constituents and thus low buffering capacity that make the water very soft with low Ca^{2+} and Mg^{2+} contents (Birnhack et al., 2011; Delion et al., 2004;

Lahav and Birnhack, 2007). Such soft supply water could trigger corrosion of pipes (Sarin et al., 2004), a concern for older homes with lead-solder piping. In addition, several studies have shown an inverse relationship between magnesium content in drinking water and the pathogenesis of cardiovascular diseases (Mason, 2011). Furthermore, some studies have identified adverse effects on soils irrigated with desalted water (Lahav and Birnhack, 2007; Yermiyahu et al., 2007). Consequently, the Israeli Ministry of Health mandates specific water-quality characteristics for desalinated water before distribution in the drinking water system that include alkalinity as $CaCO_3$ >80 mg l^{-1}, Ca^{2+} between 80 and 120 mg l^{-1}, and pH < 8.5 (Birnhack et al., 2011).

In order to increase the alkalinity, posttreatment of RO desalted water could include (1) direct introduction of chemicals (e.g., hydrated lime – $Ca(OH)_2$, calcium salts); (2) blending with seawater or brackish groundwater; and (3) reaction with a calcite or dolomite rock matrix that will result in dissolution of Ca^{2+}, Mg^{2+} (for dolomite), and HCO_3^- into the desalted water. In order to accelerate the carbonate dissolution, either CO_2 or H_2SO_4 are added, followed by pH adjustment using NaOH base (Birnhack et al., 2011). These posttreatment techniques will change the composition of the desalted product. For example, in the Ashkelon desalination plant in Israel, addition of H_2SO_4 results in high Ca^{2+} and SO_4^{2-} contents relative to the RO permeate water, whereas calcite dissolution by carbon dioxide, as in the Larnaca desalination plant in Cyprus, resulted in moderate Ca^{2+} enrichment without any change in the conspicuously low SO_4/Cl ratio that characterizes the RO chemical fractionation (Kloppmann et al., 2008b). Nevertheless, the distinctive $\delta^{18}O_{H_2O}$, $\delta^2H_{H_2O}$, B/Cl, and $\delta^{11}B$ signatures associated with RO desalination are not affected by posttreatment processes and can be distinguished from natural water sources (Kloppmann et al., 2008b).

In addition to desalination of seawater and brackish groundwater, wastewater is another potential source that can be reused upon desalination. Since the dissolved inorganic constituents of sewage effluents are not removed during first and secondary sewage treatment procedures (Vengosh and Keren, 1996; Vengosh et al., 1994), high levels of salinity in treated water is one of the major limiting factors for using treated wastewater for irrigation (Rebhun, 2004). Desalination of treated wastewater could therefore provide an additional adequate water source upon removal of salts, organic matter, and pharmaceuticals (Deegan et al., 2011; Glueckstern and Priel, 1997; Glueckstern et al., 2008; Harussi et al., 2001; Ozaki and Li, 2002; Priel et al., 2006, 2009; Rebhun, 2004). Similar to RO desalination of seawater, the unique chemical and isotopic characteristics of wastewater are retained and even reinforced during desalination. This includes the stable isotope composition ($\delta^{18}O_{H_2O}$ and $\delta^2H_{H_2O}$) of treated wastewater that is typically enriched relative to groundwater (Vengosh et al., 1999a) and boron enrichment with a distinctive $\delta^{11}B$ range of 0–10‰ (Kloppmann et al., 2008a; Vengosh and Spivack, 2000; Vengosh et al., 1994, 1999a,b). For example, low-pH desalination of wastewater from Flanders, Belgium, showed desalted wastewater with high $\delta^{18}O_{H_2O}$ and $\delta^2H_{H_2O}$ values and high boron with high B/Cl ratios and low $\delta^{11}B$ values of ~0‰ (Kloppmann et al., 2008a).

Finally, the formation of new water from desalination also generates saline effluents that could become an undesirable salinization source. Seawater RO desalination plant recovery is typically limited to 40–65% of the volume of the inlet saline water and consequently the TDS levels of brines from seawater RO plants are usually in the range of 65 000–85 000 mg l^{-1}. The actual brine salinity will therefore be determined by the ratio of the permeate flow rate to feed flow rate (Voutchkov, 2011). For example, the RO desalination plant in Larnaka, Cyprus, generates brines with TDS of 74 200 mg l^{-1} relative to Mediterranean seawater with TDS of 41 125 mg l^{-1}, a concentration factor of 1.8 (data from Kloppmann et al., 2008b). In contrast, desalination of lower-salinity brackish groundwater or wastewater will allow larger fractional recoveries of 75–90% of the inlet water, which will result in larger concentration factors of 4–10 (Voutchkov, 2011). For example, the TDS of brines generated from desalination of brackish groundwater in Nitzna (Negev), Israel, was ~40 000 mg l^{-1}, relative to 4630 mg l^{-1} in the inlet water, a concentration factor of 8.6 (data from Kloppmann et al., 2008b). In addition to salts, brines from RO desalination may contain acids, bases, phosphates, and organic polymers due to the use of scale inhibitors (Voutchkov, 2011). Most of the coastal RO desalination plants dispose of their brines through ocean outfall (e.g., Ashkelon, Israel; Larnaka, Cyprus). RO brines are also disposed to the ocean via discharge canals from power plants in which the cooling water is blended with the RO brines, thus reducing the salinity of the discharged water (Voutchkov, 2011). Yet, in non-coastal areas, disposal of RO brines could become a limiting factor due to the large potential salinization effects of the brines. In areas where the brackish groundwater has high levels of radioactivity, such as the Nubian Sandstone aquifers of the Middle East (Vengosh et al., 2009), RO desalination would reject the charged radium nuclides but the residual brines would become enriched in radium (Rosenberg and Ganor, 2009).

The chemical and isotopic compositions of RO brines reflect the geochemical fractionation that occurs during RO desalination (Kloppmann et al., 2008b), particularly for constituents that are rejected or selected by the RO membrane. While the ratios of the major elements and isotopic compositions of stable oxygen and hydrogen in RO brines mimic the compositions of the inlet saline waters, dissolved constituents that are selectively transferred to RO permeates become depleted in the residual brines. For example, the B/Cl ratio of RO brines would drop to lower than the original saline water sources. This was demonstrated in brine compositions from the Eilat (Israel) desalination plant where brines in different sections of the desalination plant had lower B/Cl ratios relative to the saline inlet water (e.g., B/Cl = 6×10^{-4} in Sabkha C brine relative to inlet seawater with B/Cl ratio = 8×10^{-4}). The isotopic composition of boron in low-pH RO desalination brine will not be modified and will mimic the isotopic composition of the saline inlet water (Kloppmann et al., 2008b). Consequently, brines originated from RO desalination of seawater are expected to have low B/Cl ratios (<8×10^{-4}) and marine isotope ratio ($\delta^{11}B$ = ~39‰), which differ from the composition of saltwater intrusion due to elemental boron depletion and ^{11}B enrichment (<8×10^{-4}; $\delta^{11}B$ > 39‰; **Figure 34**) associated with boron adsorption during seawater intrusion (Vengosh et al., 1994).

Acknowledgments

The author dedicates this chapter to his mentors, professors Yehushua Kolodny and Avraham Starinsky from the Hebrew University of Jerusalem, Israel, who introduced him to the world of geochemistry, and to his graduate students over the years (Yohanan Artzi, Osnat Velder, Efrat Farber, Sharona Henig, Dana Roded , Nitzan Pery, Hadas Raanan, David Vinson, Laura Ruhl, Nathaniel Warner, Brittany Merola, Jennie Harkness) for continuing to challenge him. He is also grateful to Emily M. Klein from Duke University for a thorough and inspiring review.

References

Abramovitz JN (1996) Imperiled waters, impoverished future: The decline of freshwater ecosystems. *Worldwatch Paper 128*. Washington, DC: Worldwatch Institute.

Agassi M, Tarchitzky J, Keren R, Chen Y, Goldstein D, and Fizik E (2003) Effects of prolonged irrigation with treated municipal effluent on runoff rate. *Journal of Environmental Quality* 32: 1053–1057.

Ai-Yaqubi A, Aliewi A, and Mimi Z (2007) Bridging the domestic water demand gap in Gaza Strip-Palestine. *Water International* 32: 219–229.

Akouvi A, Dray M, Violette S, de Marsily G, and Zuppi GM (2008) The sedimentary coastal basin of Togo: Example of a multilayered aquifer still influenced by a palaeo-seawater intrusion. *Hydrogeology Journal* 16: 419–436.

Al-Bassam AM (1998) Determination of hydrochemical processes and classification of hydrochemical facies for the Sakakah Aquifer, northeastern Saudi Arabia. *Journal of African Earth Sciences* 27: 27–38.

Al-Khashman O (2009) Chemical evaluation of Ma'an sewage effluents and its reuse in irrigation purposes. *Water Resources Management* 23: 1041–1053.

Al-Muhandis MH (1977) Pollution of river water in Iraq. *International Association of Hydrological Sciences* 123: 467–470.

Al-Ruwaih FM (1995) Chemistry of groundwater in the Dammam Aquifer, Kuwait. *Hydrogeology Journal* 3: 42–55.

Alcalá FJ and Custodio E (2008) Using the Cl/Br ratio as a tracer to identify the origin of salinity in aquifers in Spain and Portugal. *Journal of Hydrology* 359: 189–207.

Allison GB and Barnes CJ (1985) Estimation of evaporation from the normally "dry" Lake Frome in South Australia. *Journal of Hydrology* 78: 229–242.

Allison GB, Cook PG, Barnett SR, Walker GR, Jolly ID, and Hughes MW (1990) Land clearance and river salinization in the western Murray Basin, Australia. *Journal of Hydrology* 119: 1–20.

Alpert P, Krichak SO, Shafir H, Haim D, and Osetinsky I (2008) Climatic trends to extremes employing regional modeling and statistical interpretation over the Eastern Mediterranean. *Global and Planetary Change* 63: 163–170.

Amrhein C, Crowley D, Holdren GC, et al. (2001) Effects of salt precipitation on historical and projected salinities of the Salton Sea. Summary comments from workshop at the University of California, Riverside, January 30–31 2001.

Amrhein C, Duff MC, Casey WH, and Westcot DW (1998) Emerging problems with uranium, vanadium, molybdenum, chromium, and boron. In: Dudley LM and Guitjens JC (eds.) *Agroecosystems and the Environment: Sources, Control, and Remediation of Potentially Toxic, Trace Element Oxyanions*. Washington, DC: American Association for the Advancement of Science.

Andreasen DC and Fleck WB (1997) Use of bromide:chloride ratios to differentiate potential sources of chloride in a shallow, unconfined aquifer affected by brackish-water intrusion. *Hydrogeology Journal* 5: 17–26.

Appelo CAJ (1994) Cation and proton exchange, pH variations, and carbonate reactions in a freshening aquifer. *Water Resources Research* 30: 2793–2805.

Appelo CAJ and Geirnart W (1991) Processes accompanying the intrusion of salt water. *Hydrogeology of Salt Water Intrusion–A Selection of SWIM Papers* II: 291–304.

Appelo CAJ and Postma D (2005) *Geochemistry, Groundwater and Pollution*. Amsterdam: A.A. Balkema.

Appelo CAJ, Van der Weiden MJJ, Tournassat C, and Charlet L (2002) Surface complexation of ferrous iron and carbonate on ferrihydrite and the mobilization of arsenic. *Environmental Science & Technology* 36: 3096–3103.

Appelo CAJ and Willemsen A (1987) Geochemical calculations and observations on salt water intrusions. I. A combined geochemical/mixing cell model. *Journal of Hydrology* 94: 313–330.

Armstrong SC, Sturchio NC, and Hendry MJ (1998) Strontium isotopic evidence on the chemical evolution of pore waters in the Milk River Aquifer, Alberta, Canada. *Applied Geochemistry* 13: 463–475.

Arnell NW (1999) Climate change and global water resources. *Global Environmental Change* 9: 31–49.

Ayenew T, Demlie M, and Wohnlich S (2008) Hydrogeological framework and occurrence of groundwater in the Ethiopian aquifers. *Journal of African Earth Sciences* 52: 97–113.

Backstrom M, Karlsson S, Backman L, Folkeson L, and Lind B (2004) Mobilisation of heavy metals by deicing salts in a roadside environment. *Water Research* 38: 720–732.

Backstrom M, Nilsson U, Hakansson K, Allard B, and Karlsson S (2003) Speciation of heavy metals in road runoff and roadside total deposition. *Water, Air, & Soil Pollution* 147: 343–366.

Baker JW, Grover JP, Brooks BW, et al. (2007) Growth and toxicity of *Prymnesium parvum* (Haptophyta) as a function of salinity, light, and temperature. *Journal of Phycology* 43: 219–227.

Baker JW, Grover JP, Ramachandrannair R, et al. (2009) Growth at the edge of the niche: An experimental study of the harmful alga *Prymnesium parvum*. *Limnology and Oceanography* 54: 1679–1687.

Banin A and Fish A (1995) Secondary desertification due to salinization of intensively irrigated lands: The Israeli experience. *Environmental Monitoring and Assessment* 37: 17–37.

Banner JL and Hanson GN (1990) Calculation of simultaneous isotopic and trace element variations during water–rock interaction with applications to carbonate diagenesis. *Geochimica et Cosmochimica Acta* 54: 3123–3137.

Banner JL, Wasserburg GJ, Dobson PF, Carpenter AB, and Moore CH (1989) Isotopic and trace element constraints on the origin and evolution of saline groundwaters from central Missouri. *Geochimica et Cosmochimica Acta* 53: 383–398.

Barica J (1972) Salinization of groundwater in arid zones. *Water Research* 6: 925–933.

Barth S (1998) Application of boron isotopes for tracing sources of anthropogenic contamination in groundwater. *Water Research* 32: 685–690.

Bassett RL, Buszka PM, Davidson GR, and Chongdiaz D (1995) Identification of groundwater solute sources using boron isotopic composition. *Environmental Science & Technology* 29: 2915–2922.

Bastias E, Alcaraz-Lupez C, Bonilla I, Martinez-Ballesta MC, Bolaoos L, and Carvajal M (2010) Interactions between salinity and boron toxicity in tomato plants involve apoplastic calcium. *Journal of Plant Physiology* 167: 54–60.

Beaumont P (1996) Agricultural and environmental changes in the upper Euphrates catchment of Turkey and Syria and their political and economic implications. *Applied Geography* 16: 137–157.

Bein A and Arad A (1992) Formation of saline groundwaters in the Baltic region through freezing of seawater during glacial periods. *Journal of Hydrology* 140: 75–87.

Beltrán JM (1999) Irrigation with saline water: Benefits and environmental impact. *Agricultural Water Management* 40: 183–194.

Bergelson G, Nativ R, and Bein A (1999) Salinization and dilution history of ground water discharging into the Sea of Galilee, the Dead Sea Transform, Israel. *Applied Geochemistry* 14: 91–118.

Berner EK and Berner RA (2012) *Global Environment: Water, Air and Geochemical Cycles*, 2nd edn. Princeton, NJ: Princeton University Press.

Berner EK and Berner RA (1987) *The Global Water Cycle: Geochemistry and Environment*. Englewood Cliffs, NJ: Prentice-Hall.

Berthrong ST, Jobbagy EG, and Jackson RB (2009) A global meta-analysis of soil exchangeable cations, pH, carbon, and nitrogen with afforestation. *Ecological Applications* 19: 2228–2241.

Birkle P, Bundschuh J, and Sracek O (2010) Mechanisms of arsenic enrichment in geothermal and petroleum reservoirs fluids in Mexico. *Water Research* 44: 5605–5617.

Birnhack L, Voutchkov N, and Lahav O (2011) Fundamental chemistry and engineering aspects of post-treatment processes for desalinated water – A review. *Desalination* 273: 6–22.

Bixio D, Thoeye C, De Koning J, Joksimovic D, Savic D, Wintgens T, and Melin T (2006) Wastewater reuse in Europe. *Desalination* 187: 89–101.

Bixio D, Thoeye C, Wintgens T, et al. (2008) Water reclamation and reuse: Implementation and management issues. *Desalination* 218: 13–23.

Blum JS, Bindi AB, Buzzelli J, Stolz JF, and Oremland RS (1998) *Bacillus arsenicoselenatis*, sp nov, and *Bacillus selenitireducens*, sp nov: two haloalkaliphiles from Mono Lake, California that respire oxyanions of selenium and arsenic. *Archives of Microbiology* 171: 19–30.

Böhlke JK (2002) Groundwater recharge and agricultural contamination. *Hydrogeology Journal* 10: 153–179.

Böhlke JK and Horan M (2000) Strontium isotope geochemistry of groundwaters and streams affected by agriculture, Locust Grove, MD. *Applied Geochemistry* 15: 599–609.

Böhlke JK and Irwin JJ (1992) Brine history indicated by argon, krypton, chlorine, bromine, and iodine analyses of fluid inclusions from the Mississippi Valley type lead-fluorite-barite deposits at Hansonburg, New Mexico. *Earth and Planetary Science Letters* 110: 51–66.

Boschetti T, Toscani L, Shouakar-Stash O, et al. (2011) Salt waters of the northern Apennine Foredeep Basin (Italy): Origin and evolution. *Aquatic Geochemistry* 17: 71–108.

Bottomley DJ, Katz A, Chan LH, et al. (1999) The origin and evolution of Canadian Shield brines: Evaporation or freezing of seawater? New lithium isotope and geochemical evidence from the Slave craton. *Chemical Geology* 155: 295–320.

Bouchaou L, Michelot JL, Qurtobi M, et al. (2009) Origin and residence time of groundwater in the Tadla basin (Morocco) using multiple isotopic and geochemical tools. *Journal of Hydrology* 379: 323–338.

Bouchaou L, Michelot JL, Vengosh A, et al. (2008) Application of multiple isotopic and geochemical tracers for investigation of recharge, salinization, and residence time of water in the Souss-Massa aquifer, Southwest of Morocco. *Journal of Hydrology* 352: 267–287.

Bresler E, McNeal BL, and Carter DL (1982) *Saline and Sodic Soils: Principles, Dynamics, Modeling. Advanced Series in Agricultural Sciences*, vol. 10. Berlin: Springer.

Brinck EL and Frost CD (2007) Detecting infiltration and impacts of introduced water using strontium isotopes. *Ground Water* 45: 554–568.

Bullen T, White A, Blum A, Harden J, and Schulz M (1997) Chemical weathering of a soil chronosequence on granitoid alluvium: II – Mineralogic and isotopic constraints on the behavior of strontium. *Geochimica et Cosmochimica Acta* 61: 291–306.

Bullen TD, Krabbenhoft DP, and Kendall C (1996) Kinetic and mineralogic controls on the evolution of groundwater chemistry and $^{87}Sr/^{86}Sr$ in a sandy silicate aquifer, northern Wisconsin, USA. *Geochimica et Cosmochimica Acta* 60: 1807–1821.

Butler DL and von Guerard P (1996) Salinity in the Colorado River in the Grand Valley, Western Colorado, 1994–95. US Geological Survey Fact Sheet FS–215-96.

Byrne RH, Yao W, Klochko K, Tossell JA, and Kaufman AJ (2006) Experimental evaluation of the isotopic exchange equilibrium $^{10}B(OH)_3 + ^{11}B(OH)_4^- = ^{11}B(OH)_3 + ^{10}B(OH)_4^-$ in aqueous solution. *Deep Sea Research Part I: Oceanographic Research Papers* 53: 684–688.

Campbell CE, Pearson BN, and Frost CD (2008) Strontium isotopes as indicators of aquifer communication in an area of coal bed natural gas production, Powder River Basin, Wyoming and Montana. *Rocky Mountain Geology* 43: 149–175.

Carpenter AB, Trout ML, and Pickett EE (1974) Preliminary report on the origin and chemical evolution of lead- and zinc-rich oil field brines in Central Mississippi. *Economic Geology* 69: 1191–1206.

Carr G, Potter RB, and Nortcliff S (2011) Water reuse for irrigation in Jordan: Perceptions of water quality among farmers. *Agricultural Water Management* 98: 847–854.

Cartwright I, Hall S, Tweed S, and Leblanc M (2009) Geochemical and isotopic constraints on the interaction between saline lakes and groundwater in southeast Australia. *Hydrogeology Journal* 17: 1991–2004.

Cartwright I, Hannam K, and Weaver TR (2007a) Constraining flow paths of saline groundwater at basin margins using hydrochemistry and environmental isotopes: Lake Cooper, Murray Basin, Australia. *Australian Journal of Earth Sciences* 54: 1103–1122.

Cartwright I, Weaver TR, and Fifield LK (2006) Cl/Br ratios and environmental isotopes as indicators of recharge variability and groundwater flow: An example from the southeast Murray Basin, Australia. *Chemical Geology* 231: 38–56.

Cartwright I, Weaver TR, Fulton S, Nichol C, Reid M, and Cheng X (2004) Hydrogeochemical and isotopic constraints on the origins of dryland salinity, Murray Basin, Victoria, Australia. *Applied Geochemistry* 19: 1233–1254.

Cartwright I, Weaver TR, Stone D, and Reid M (2007b) Constraining modern and historical recharge from bore hydrographs, ^{3}H, ^{14}C and chloride concentrations: Applications to dual-porosity aquifers in dryland salinity areas, Murray Basin, Australia. *Journal of Hydrology* 332: 69–92.

Carvalho IG, Cidu R, Fanfani L, Pitsch H, Beaucaire C, and Zuddas P (2005) Environmental impact of uranium mining and ore processing in the Lagoa Real District, Bahia, Brazil. *Environmental Science & Technology* 39: 8646–8652.

Causape J, Quilez D, and Aragüés R (2004a) Assessment of irrigation and environmental quality at the hydrological basin level: II. Salt and nitrate loads in irrigation return flows. *Agricultural Water Management* 70: 211–228.

Causape J, Quilez D, and Aragüés R (2004b) Salt and nitrate concentrations in the surface waters of the CR-V irrigation district (Bardenas I, Spain): Diagnosis and prescriptions for reducing off-site contamination. *Journal of Hydrology* 295: 87–100.

Cecil LD, Smith RC, Reilly MA, and Rose AW (1987) Radium-228 and radium-226 in the ground water of the Chickies Formation, Southeastern Pennsylvania. In: Graves G (ed.) *Radon, Radium, and other Radioactivity in Ground Water*, pp. 437–447. London: Lewis.

Cengeloglu Y, Arslan G, Tor A, Kocak I, and Dursun N (2008) Removal of boron from water by using reverse osmosis. *Separation and Purification Technology* 64: 141–146.

Chambers LA, Bartley JG, and Herczeg AL (1996) Hydrogeochemical evidence for surface water recharge to a shallow regional aquifer in northern Victoria, Australia. *Journal of Hydrology* 181: 63–83.

Chapelle FH and Knobel LL (1983) Aqueous geochemistry and the exchangeable cation composition of glauconite in the Aquia Aquifer, Maryland. *Ground Water* 21: 343–352.

Chapelle FH and McMahon PB (1991) Geochemistry of dissolved inorganic carbon in a Coastal Plain aquifer: 1 – Sulfate from confining beds as an oxidant in microbial CO_2 production. *Journal of Hydrology* 127: 85–108.

Chivas AR, Andrew AS, Lyons WB, Bird MI, and Donnelly TH (1991) Isotopic constraints on the origin of salts in Australian playas: 1 – Sulphur. *Palaeogeography, Palaeoclimatology, Palaeoecology* 84: 309–332.

Choudhari JS and Sharma KD (1984) Stream salinity in the Indian arid zone. *Journal of Hydrology* 71: 149–163.

Chowdhury S, Champagne P, and McLellan PJ (2010a) Factorial analysis of trihalomethanes formation in drinking water. *Water Environment Research* 82: 556–566.

Chowdhury S, Champagne P, and McLellan PJ (2010b) Investigating effects of bromide ions on trihalomethanes and developing model for predicting bromodichloromethane in drinking water. *Water Research* 44: 2349–2359.

Christensen JH, Hewitson B, and Busuioc A, et al. (eds.) (2007) *Regional Climate Projections*. Cambridge: Cambridge University Press.

Closson D and Abou Karaki N (2009) Human-induced geological hazards along the Dead Sea coast. *Environmental Geology* 58: 371–380.

Closson D, Abou Karaki N, and Hallot F (2010) Landslides along the Jordanian Dead Sea coast triggered by the lake level lowering. *Environmental Earth Sciences* 59: 1417–1430.

Cohen MJ (2009) Past and future of the Salton Sea. In: Gleick PH (ed.) *The World's Water 2008–2009*, pp. 127–138. Covelo, CA: Island Press.

Cohen MJ and Hyun KH (2006) *Hazard: The Future of the Salton Sea with No Restoration Project*. Oakland, CA: Pacific Institute.

Cohn P, Skinner R, Burger S, Fagliano J, and Klotz J (2003) *Radium in Drinking Water and the Incidence of Osteosarcoma*. Division of Epidemiology, New Jersey Department of Health and Senior Services, Environmental and Occupational Health.

Colorado River Basin Salinity Control Forum (2008) 2008 Review: Water Quality Standards for Salinity Colorado River System. http://www.crb.ca.gov/reports.html (accessed June 2011).

Colorado River Board of California (2011) California's Colorado River Water Use Plan. State of California http://www.crb.ca.gov/reports.html (accessed April 2011).

Conway D and Hulme M (1996) The impacts of climate variability and climate change in the Nile Basin on future water resources in Egypt. *Water Resources Development* 12: 277–296.

Cook P and Herczeg A (2000) *Environmental Tracers in Subsurface Hydrology*. Boston, MA: Kluwer.

Coplen TB, Hopple JA, Bohlke JK, et al. (2002) Compilation of minimum and maximum ratios of selected elements in naturally occurring terrestrial materials and reagents. *US Geological Survey Water-Resources Investigations Report 01-4222*. Denver, CO: US Geological Survey.

Cortecci G, Dinelli E, Bencini A, Adorni-Braccesi A, and La Ruffa G (2002) Natural and anthropogenic SO_4 sources in the Arno river catchment, northern Tuscany, Italy: A chemical and isotopic reconnaissance. *Applied Geochemistry* 17: 79–92.

Cortecci G, Dinelli E, and Boschetti T (2007) The River Arno catchment, northern Tuscany: chemistry of waters and sediments from the River Elsa and River Era sub-basins, and sulphur and oxygen isotopes of aqueous sulphate. *Hydrological Processes* 21: 1–20.

Corwin DL, Rhoades JD, and Simunek J (2007) Leaching requirement for soil salinity control: Steady-state versus transient models. *Agricultural Water Management* 90: 165–180.

Cox JW, Chittleborough DJ, Brown HJ, Pitman AM, and Varcoe JCR (2002) Seasonal changes in hydrochemistry along a toposequence of texture-contrast soils. *Australian Journal of Soil Research* 40: 581–604.

Craig H (1961) Isotopic variations in meteoric waters. *Science* 133: 1702–1703.

Crook J and Surampalli RY (2005) Water reuse criteria in the United States. In: Cubillo F (ed.) *Efficient Use and Management of Urban Water Supply*. London: IWA Publishing.

Curtin D, Campbell CA, and Jalil A (1998) Effects of acidity on mineralization: pH-dependence of organic matter mineralization in weakly acidic soils. *Soil Biology and Biochemistry* 30: 57–64.

Custodio E (1987a) Effect of human activities on salt-freshwater relationships in coastal aquifers. In: Custodio E and Bruggeman GA (eds.) *Groundwater Problems in Coastal Areas*. *Studies and Reports in Hydrology* 45. Paris: UNESCO.

Custodio E (1987b) Salt-fresh water interrelationship under natural conditions. In: Custodio E and Bruggeman GA (eds.) *Groundwater Problems in Coastal Areas*. *Studies and Reports in Hydrology* 45. Paris: UNESCO.

Custodio E (1997) Seawater intrusion in coastal aquifers: Guidelines for study, monitoring and control. *FAO Water Reports 11*. Rome: Food and Agriculture Organization of the United Nations.

Custodio E (2010) Coastal aquifers of Europe: An overview. *Hydrogeology Journal* 18: 269–280.

Czerniczyniec M, Farias S, Magallanes J, and Cicerone D (2007) Arsenic(V) adsorption onto biogenic hydroxyapatite: Solution composition effects. *Water, Air, & Soil Pollution* 180: 75–82.

D'Alessandro W, Bellomo S, Parello F, Brusca L, and Longo M (2008) Survey on fluoride, bromide and chloride contents in public drinking water supplies in Sicily (Italy). *Environmental Monitoring and Assessment* 145: 303–313.

Daugherty EN, Ontiveros-Valencia AV, Rice JS, Wiest MJ, and Halden RU (2010) Impact of point-of-use water softening on sustainable water reclamation: Case study of the Greater Phoenix Area. In: Halden RH (ed.) *Contaminants of Emerging Concern in the Environment: Ecological and Human Health Considerations*. *ACS Symposium Series*, vol. 1048, pp. 497–518. Washington, DC: American Chemical Society.

Davis SM, Drake KD, and Maier KJ (2002) Toxicity of boron to the duckweed, *Spirodella polyrrhiza*. *Chemosphere* 48: 615–620.

Davis SN, Whittemore DO, and Fabryka-Martin J (1998) Uses of chloride/bromide ratios in studies of potable water. *Ground Water* 36: 338–350.

Davisson ML and Criss RE (1993) Stable isotope imaging of a dynamic groundwater system in the southwestern Sacramento Valley, California, USA. *Journal of Hydrology* 144: 213–246.

Davisson ML, Hudson GB, Esser BK, and Ekwurzel B (1999) Tracing and age-dating recycled wastewater recharged for potable reuse in a seawater injection barrier, southern California. *Isotope Techniques in Water Resource Development and Management*. *Proceedings of an International Symposium,* Vienna, Austria, 10–14 May. IAEA-SM-361/36. Vienna, Austria: International Atomic Energy Agency.

De Boer W and Kowalchuk GA (2001) Nitrification in acid soils: micro-organisms and mechanisms. *Soil Biology & Biochemistry* 33: 853–866.

de Louw PGB, Essink G, Stuyfzand PJ, and van der Zee S (2010) Upward groundwater flow in boils as the dominant mechanism of salinization in deep polders, The Netherlands. *Journal of Hydrology* 394: 494–506.

de Montety V, Radakovitch O, Vallet-Coulomb C, Blavoux B, Hermitte D, and Valles V (2008) Origin of groundwater salinity and hydrogeochemical processes in a confined coastal aquifer: Case of the Rhone delta (Southern France). *Applied Geochemistry* 23: 2337–2349.

Deegan AM, Shaik B, Nolan K, Urell K, Oelgemoller M, Tobin J, and Morrissey A (2011) Treatment options for wastewater effluents from pharmaceutical companies. *International Journal of Environmental Science and Technology* 8: 649–666.

Dehaan RL and Taylor GR (2002) Field-derived spectra of salinized soils and vegetation as indicators of irrigation-induced soil salinization. *Remote Sensing of Environment* 80: 406–417.

Delion N, Mauguin G, and Corsin P (2004) Importance and impact of post treatments on design and operation of SWRO plants. *Desalination* 165: 323–334.

DeSimone LA, Howes BL, and Barlow PM (1997) Mass-balance analysis of reactive transport and cation exchange in a plume of wastewater-contaminated groundwater. *Journal of Hydrology* 203: 228–249.

Deverel SJ and Gallanthine SK (2007) Relation of salinity and selenium in shallow groundwater to hydrologic and geochemical processes, Western San Joaquin Valley, California. *Journal of Hydrology* 335: 223–224.

Deverel SJ and Fujii R (1987) Processes affecting the distribution of selenium in shallow groundwater of agricultural areas, Western San Joaquin Valley, California. *US Geological Survey Open-File Report 87–220*. Menlo Park, CA: US Geological Survey.

Di Natale F, Erto A, Lancia A, and Musmarra D (2008) Experimental and modelling analysis of As(V) ions adsorption on granular activated carbon. *Water Research* 42: 2007–2016.

Dickson AG (1990a) Thermodynamics of the dissociation of boron-acid in synthetic seawater from 273.15 to 318.15 K. *Deep Sea Research Part I: Oceanographic Research Papers* 37: 755–766.

Dickson BL (1990b) Radium in groundwater. In: *The Environmental Behaviour of Radium*, IAEA Technical Reports Series 310, pp. 355–372. Vienna: International Atomic Energy Agency.

Dickson BL and Herczeg AL (1992) Naturally-occurring radionuclides in acid—Saline groundwaters around Lake Tyrrell, Victoria, Australia. *Chemical Geology* 96: 95–114.

Doty SL, Shang TQ, Wilson AM, et al. (2003) Metabolism of the soil and groundwater contaminants, ethylene dibromide and trichloroethylene, by the tropical leguminous tree, *Leuceana leucocephala*. *Water Research* 37: 441–449.

Dregne HE (2002) Land degradation in the drylands. *Arid Land Research and Management* 16: 99–132.

Dreizin Y (2006) Ashkelon seawater desalination project – Off-taker's self costs, supplied water costs, total costs and benefits. *Desalination* 190: 104–116.

Drever JI and Smith CL (1978) Cyclic wetting and drying of the soil zone as an influence on the chemistry of ground water in arid terrains. *American Journal of Science* 278: 1448–1454.

Dror G, Ronen D, Stiller M, and Nishri A (1999) Cl/Br ratios of Lake Kinneret, pore water and associated springs. *Journal of Hydrology* 225: 130–139.

Druhan JL, Hogan JF, Eastoe CJ, Hibbs BJ, and Hutchison WR (2008) Hydrogeologic controls on groundwater recharge and salinization: A geochemical analysis of the northern Hueco Bolson aquifer, Texas, USA. *Hydrogeology Journal* 16: 281–296.

Duan RB, Fedler CB, and Sheppard CD (2011) Field study of salt balance of a land application system. *Water, Air, & Soil Pollution* 215: 43–54.

Dzombak DA and Morel FMM (1990) *Surface Complexation Modeling: Hydrous Ferric Oxide*. New York: John Wiley.

Eastoe CJ, Hibbs BJ, Granados Olivas A, Hogan J, Hawley J, and Hutchison WR (2008) Isotopes in the Hueco Bolson Aquifer, Texas (USA) and Chihuahua (Mexico): Local and general implications for recharge sources in alluvial basins. *Hydrogeology Journal* 16: 737–747.

Eastoe CJ, Hutchison WR, Hibbs BJ, Hawley J, and Hogan JF (2010) Interaction of a river with an alluvial basin aquifer: Stable isotopes, salinity and water budgets. *Journal of Hydrology* 395: 67–78.

Edmunds WM (1996) Bromine geochemistry of British groundwaters. *Mineralogical Magazine* 60: 275–284.

Edmunds WM and Droubi A (1998) Groundwater salinity and environmental change. *Isotope Techniques in the Study of Past and Current Environmental Changes in the Hydrosphere and Atmosphere*. *Proceedings of an International Symposium*, Vienna, Austria, pp. 503–518. Vienna, Austria: International Atomic Energy Agency.

Edmunds WM, Fellman E, and Goni IB (1999) Lakes, groundwater and paleohydrology in the Sahel of NE Nigeria: Evidence from hydrogeochemistry. *Journal of Geological Society* 156: 345–355.

Edmunds WM, Fellman E, Goni I, and Prudhomme C (2002) Spatial and temporal distribution of groundwater recharge in northern Nigeria. *Hydrogeology Journal* 10: 205–215.

Edmunds WM and Gaye CB (1994) Estimating the spatial variability of groundwater recharge in the Sahel using chloride. *Journal of Hydrology* 156: 47–59.

Edmunds WM, Guendouz AH, Mamou A, Moulla A, Shand P, and Zouari K (2003) Groundwater evolution in the Continental Intercalaire aquifer of southern Algeria and Tunisia: Trace element and isotopic indicators. *Applied Geochemistry* 18: 805–822.

Eisenhut S, Heumann KG, and Vengosh A (1995) Determination of boron isotopic variations in aquatic systems with negative thermal ionization mass spectrometry as a tracer for anthropogenic influences. *Fresenius' Journal of Analytical Chemistry* 354: 903–909.

Ekwurzel B, Moran JE, Hudson GB, et al. (2001) An isotopic investigation of salinity and water sources in the Souss-Massa Basin (Morocco). *First International Conference on Saltwater Intrusion and Coastal Aquifers (SWICA)-Monitoring, Modeling and Management*. Essaouira, Morocco 23–25 April.

Elewa HH and El Nahry AH (2009) Hydro-environmental status and soil management of the River Nile Delta, Egypt. *Environmental Geology* 57: 759–774.

Ettayfi N, Bouchaou L, Michelot JL, et al. (2012) Geochemical and isotopic (oxygen, hydrogen, carbon, strontium) constraints for the origin, salinity, and residence time of groundwater from a carbonate aquifer in the Western Anti-Atlas Mountains, Morocco. *Journal of Hydrology* 438: 97–111.

Eugster HP and Jones BF (1979) Behavior of major solutes during closed-basin brine evolution. *American Journal of Science* 279: 609–631.

Evans JP (2008) 21st century climate change in the Middle East. *Climatic Change* 92: 417–432.

Ezersky M, Legchenko A, Camerlynck C, and Al-Zoubi A (2009) Identification of sinkhole development mechanism based on a combined geophysical study in Nahal Hever South area (Dead Sea coast of Israel). *Environmental Geology* 58: 1123–1141.

Fabryka-Martin J (2000) Iodine-129 as a groundwater tracer. In: Cook P and Herczeg AL (eds.) *Environmental Tracers in Subsurface Hydrology*. pp. 504–510. Boston, MA: Kluwer Academic.

Fabryka-Martin J, Whittemore DO, Davis SN, Kubik PW, and Sharma P (1991) Geochemistry of halogens in the Milk River aquifer, Alberta, Canada. *Applied Geochemistry* 6: 447–464.

Farber E, Vengosh A, Gavrieli I, et al. (2004) The origin and mechanisms of salinization of the Lower Jordan River. *Geochimica et Cosmochimica Acta* 68: 1989–2006.

Farber E, Vengosh A, Gavrieli I, et al. (2005) Management scenarios for the Jordan River salinity crisis. *Applied Geochemistry* 20: 2138–2153.

Farber E, Vengosh A, Gavrieli I, et al. (2007) The geochemistry of groundwater resources in the Jordan Valley: The impact of the Rift Valley brines. *Applied Geochemistry* 22: 494–514.

Fattah QN and Baki SJA (1980) Effects of drainage systems on water quality of major Iraqi rivers. *International Association of Hydrological Sciences* 130: 265–270.

Faye S, Maloszewski P, Stichler W, Trimborn P, Faye SC, and Gaye CB (2005) Groundwater salinization in the Saloum (Senegal) delta aquifer: Minor elements and isotopic indicators. *Science of the Total Environment* 343: 243–259.

Fernandez-Cirelli A, Arumi JL, Rivera D, and Boochs PW (2009) Environmental effects of irrigation in arid and semi-arid regions. *Chilean Journal of Agricultural Research* 69: 27–40.

Fitzpatrick RW, Merry R, and Cox J (2000) What are saline soils and what happens when they are drained? *Journal of the Australian Association of Natural Resource Management* 6: 26–30.

Flügel W-A (1995) River salination due to dryland agriculture in the Western Cape Province, Republic of South Africa. *Environment International* 21: 679–686.

Fontes JC and Matray JM (1993) Geochemistry and origin of formation brines from the Paris Basin, France. 1. Brines associated with triassic salts. *Chemical Geology* 109: 149–175.

Forcada EG and Evangelista IM (2008) Contributions of boron isotopes to understanding the hydrogeochemistry of the coastal detritic aquifer of Castellon Plain, Spain. *Hydrogeology Journal* 16: 547–557.

Freeman JT (2007) The use of bromide and chloride mass ratios to differentiate salt-dissolution and formation brines in shallow groundwaters of the Western Canadian Sedimentary Basin. *Hydrogeology Journal* 15: 1377–1385.

Frenkel H, Goertzen JO, and Rhoades JD (1978) Effects of clay type and content, exchangeable sodium percentage, and electrolyte concentration on clay dispersion and soil hydraulic conductivity. *Soil Science Society of America Journal* 42: 32–39.

Friedler E (2001) Water reuse – An integral part of water resources management: Israel as a case study. *Water Policy* 3: 29–39.

Furrer G, Sollins P, and Westall JC (1990) The study of soil chemistry through quasi-steady-state models: II. Acidity of soil solution. *Geochimica et Cosmochimica Acta* 54: 2363–2374.

Gao S, Ryu J, Tanji KK, and Herbel MJ (2007) Arsenic speciation and accumulation in evapoconcentrating waters of agricultural evaporation basins. *Chemosphere* 67: 862–871.

Garcia-Garizabal I and Causape J (2010) Influence of irrigation water management on the quantity and quality of irrigation return flows. *Journal of Hydrology* 385: 36–43.

Garrels RM and MacKenzie FT (1967) Origin of the chemical composition of some springs and lakes. In: Gould RF (ed.) *Equilibrium Concepts in Natural Water Systems. ACS Advances in Chemistry*, vol. 67, pp. 222–242. Washington, DC: American Chemical Society.

Gat JR (1974) Local variability of the isotope composition of groundwater. In: *Isotope Techniques in Groundwater Hydrology, 1974. Proceedings of a Symposium Organized by the International Atomic Energy Agency*. Vienna, Austria, 11–15 March, vol. 2, pp. 51–60. Vienna: IAEA.

Gates TK, Burkhalter JP, Labadie JW, Valliant JC, and Broner I (2002) Monitoring and modeling flow and salt transport in a salinity-threatened irrigated valley. *Journal of Irrigation and Drainage Engineering* 128: 87–99.

Gattacceca JC, Vallet-Coulomb C, Mayer A, et al. (2009) Isotopic and geochemical characterization of salinization in the shallow aquifers of a reclaimed subsiding zone: The southern Venice Lagoon coastland. *Journal of Hydrology* 378: 46–61.

Gavrieli I, Yechieli Y, Kass A, Vengosh A, and Starinsky A (2001) The impact of freshwater and wastewater irrigation on the chemistry of shallow groundwater: A case study from the Israeli Coastal Aquifer. *Geological Survey of Israel, Report GSI/35/01*. Jerusalem, Israel: Geological Survey of Israel.

Gaye CB and Edmunds WM (1996) Groundwater recharge estimation using chloride, stable isotopes and tritium profiles in the sands of northwestern Senegal. *Environmental Geology* 27: 246–251.

Gee GW and Hillel D (1988) Groundwater recharge in arid regions: Review and critique of estimation methods. *Hydrological Processes* 2: 255–266.

Geffen N, Semiat R, Eisen MS, Balazs Y, Katz I, and Dosoretz CG (2006) Boron removal from water by complexation to polyol compounds. *Journal of Membrane Science* 286: 45–51.

George CM, Smith AH, Kalman DA, and Steinmaus CM (2006) Reverse osmosis filter use and high arsenic levels in private well water. *Archives of Environmental & Occupational Health* 61: 171–175.

Georghiou G and Pashafidis L (2007) Boron in groundwaters of Nicosia (Cyprus) and its treatment by reverse osmosis. *Desalination* 215: 104–110.

Geucke T, Deowan SA, Hoinkis J, and Patzold C (2009) Performance of a small-scale RO desalinator for arsenic removal. *Desalination* 239: 198–206.

Gleick PH (1994) Water and energy. *Annual Review of Energy and the Environment* 19: 267–299.

Gleick PH (1998) Water in crisis: Paths to sustainable water use. *Ecological Applications* 8: 571–579.

Glenn EP, Cohen MJ, Morrison JI, Valdés-Casillas C, and Fitzsimmons K (1999) Science and policy dilemmas in the management of agricultural waste waters: The case of the Salton Sea, CA, USA. *Environmental Science & Policy* 2: 413–423.

Glueckstern P (1992) Desalination – Present and future. *Water and Irrigation Review* 12: 4–11.

Glueckstern P and Priel M (1997) Optimized brackish water desalination plants with minimum impact on the environment. *Desalination* 108: 19–26.

Glueckstern P and Priel M (1998) Advanced concept of large seawater desalination systems for Israel. *Desalination* 119: 33–45.

Glueckstern P, Priel M, Gelman E, and Perlov N (2008) Wastewater desalination in Israel. *Desalination* 222: 151–164.

Goldberg S, Forster HS, and Heick EL (1993) Boron adsorption mechanisms on oxides, clay-minerals, and soils inferred from ionic-strength effects. *Soil Science Society of America Journal* 57: 704–708.

Goldberg S, Hyun S, and Lee LS (2008) Chemical modeling of arsenic(III, V) and selenium(IV, VI) adsorption by soils surrounding ash disposal facilities. *Vadose Zone Journal* 7: 1185–1192.

Goldberg S and Johnston CT (2001) Mechanisms of arsenic adsorption on amorphous oxides evaluated using macroscopic measurements, vibrational spectroscopy, and surface complexation modeling. *Journal of Colloid and Interface Science* 234: 204–216.

Goldberg S and Kabengi NJ (2010) Bromide adsorption by reference minerals and soils. *Vadose Zone Journal* 9: 780–786.

Goldhamer DA, Grismer M, Nielsen DR, and Biggar JW (1986) Transport of selenium in San Joaquin soils: Influence of soil and water physical and chemical properties. University of California 1985–1986, Technical Progress Report.

Gooddy DC, Clay JW, and Bottrell SH (2002) Redox-driven changes in porewater chemistry in the unsaturated zone of the chalk aquifer beneath unlined cattle slurry lagoons. *Applied Geochemistry* 17: 903–921.

Gordon L, Dunlop M, and Foran B (2003) Land cover change and water vapour flows: Learning from Australia. *Philosophical Transactions of the Royal Society Series B* 358: 1973–1984.

Gorenflo A, Brusilovsky M, Faigon M, and Liberman B (2007) High pH operation in seawater reverse osmosis permeate: First results from the world's largest SWRO plant in Ashkelon. *Desalination* 203: 82–90.

Greenlee LF, Lawler DF, Freeman BD, Marrot B, and Moulin P (2009) Reverse osmosis desalination: Water sources, technology, and today's challenges. *Water Research* 43: 2317–2348.

Grieve CM and Poss JA (2000) Wheat response to interactive effects of boron and salinity. *Journal of Plant Nutrition* 23: 1217–1226.

Grieve CM, Poss JA, Suarez DL, and Dierig DA (2001) Lesquerella growth and selenium uptake affected by saline irrigation water composition. *Industrial Crops and Products* 13: 57–65.

Groen J, Velstra J, and Meesters AGCA (2000) Salinization processes in paleowaters in coastal sediments of Suriname: Evidence from δ^{37}Cl analysis and diffusion modelling. *Journal of Hydrology* 234: 1–20.

Gross M and Bounds T (2007) Water softener backwash brine stresses household septic tanks and treatment systems. *Small Flows Magazine* 8: 8–10.

Hadadin N, Qaqish M, Akawwi E, and Bdour A (2010) Water shortage in Jordan – Sustainable solutions. *Desalination* 250: 197–202.

Hahn J (1991) Aspects of groundwater salinization in the Wittmund (East Friesland) coastal area. *Hydrogeology of Salt Water Intrusion – A Selection of SWIM Papers* II: 251–269.

Halim MA, Majumder RK, Nessa SA, et al. (2010) Evaluation of processes controlling the geochemical constituents in deep groundwater in Bangladesh: Spatial variability on arsenic and boron enrichment. *Journal of Hazardous Materials* 180: 50–62.

Hamilton PA, Denver JM, Phillips PJ, and Shedlock RJ (1993) Water quality assessment of the Delmarva Peninsula, Delaware, Maryland, and Virginia: Effects of agricultural activities on the distribution of nitrate and other inorganic constituents in the surficial aquifers. *US Geological Survey Open-File Report 93–40*. Menlo Park, CA: US Geological Survey.

Hamilton PA and Helsel DR (1995) Effects of agriculture on ground-water quality in five regions of the United States. *Ground Water* 33: 217–226.

Hammond DE, Zukin JG, and Ku TL (1988) The kinetics of radioisotope exchange between brine and rock in geothermal system. *Journal of Geophysical Research* 93: 13175–13186.
Hanasaki N, Kanae S, Oki T, et al. (2008a) An integrated model for the assessment of global water resources Part 1: Model description and input meteorological forcing. *Hydrology and Earth System Sciences* 12: 1007–1025.
Hanasaki N, Kanae S, Oki T, et al. (2008b) An integrated model for the assessment of global water resources Part 2: Applications and assessments. *Hydrology and Earth System Sciences* 12: 1027–1037.
Hanor JS (1994) Origin of saline fluids in sedimentary basins. In: Parnell J (ed.) *Geofluids: Origin, Migration and Evolution of Fluids in Sedimentary Basins, Geological Society Special Publication 78*, pp. 151–174. London: Geological Society of London.
Hao X and Chang C (2003) Does long-term heavy cattle manure application increase salinity of a clay loam soil in semi-arid southern Alberta? *Agriculture Ecosystems and Environment* 94: 89–103.
Hardie LA and Eugster HP (1970) The evolution of closed-basin brines. *Mineralogical Society of America, Special Publications* 3: 273–290.
Harter T, Davis H, Mathews MC, and Meyer RD (2002) Shallow groundwater quality on dairy farms with irrigated forage crops. *Journal of Contaminant Hydrology* 55: 287–315.
Harussi Y, Rom D, Galil N, and Semiat R (2001) Evaluation of membrane processes to reduce the salinity of reclaimed wastewater. *Desalination* 137: 71–89.
Hayes KF, Papelis C, and Leckie JO (1988) Modeling ionic strength effects on anion adsorption next term at hydrous oxide/solution interfaces. *Journal of Colloid and Interface Science* 125: 717–726.
Health Canada (2007) *Canadian Drinking Water Guidelines*. Online Available at http://www.hc-sc.gc.ca/ewh-semt/water-eau/drink-potab/guide/index-eng.php (accessed April 2011).
Heller-Grossman L, Manka J, Limoni-Relis B, and Rebhun M (2001) THM, haloacetic acids and other organic DBPs formation in disinfection of bromide rich Sea of Galilee (Lake Kinneret) water. *Water Science & Technology: Water Supply* 1: 259–266.
Hely AG, Hughes GH, and Irelan B (1966) *Hydrologic Regimen of Salton Sea, California*. *Geological Survey Professional Paper 486-C*. Washington, DC: US Government Printing Office.
Hendry MJ and Schwartz FW (1988) An alternative view on the origin of chemical and isotopic patterns in groundwater from the Milk River Aquifer, Canada. *Water Resources Research* 24: 1747–1763.
Herczeg AL, Dogramaci SS, and Leaney FWJ (2001) Origin of dissolved salts in a large, semi-arid groundwater system: Murray Basin, Australia. *Marine and Freshwater Research* 52: 41–52.
Herczeg AL and Edmunds WM (2000) Inorganic ions as tracers. In: Cook P and Herczeg AL (eds.) *Environmental Tracers in Subsurface Hydrology*. pp. 31–77. Boston, MA: Kluwer Academic.
Herczeg AL, Simpson HJ, Anderson RF, Trier RM, Mathieu GG, and Deck BL (1988) Uranium and radium mobility in groundwaters and brines within the Delaware Basin, Southeastern New Mexico, U.S.A.. *Chemical Geology* 72: 181–196.
Herczeg AL, Simpson HJ, and Mazor E (1993) Transport of soluble salts in a large semiarid basin: River Murray, Australia. *Journal of Hydrology* 144: 59–84.
Herczeg AL, Torgersen T, Chivas AR, and Habermehl MA (1991) Geochemistry of ground waters from the Great Artesian Basin, Australia. *Journal of Hydrology* 126: 225–245.
Hern J and Feltz HR (1998) Effects of irrigation on the environment of selected areas of the western United States and implications to world population growth and food production. *Journal of Environmental Management* 52: 353–360.
Herut B, Starinsky A, Katz A, and Bein A (1990) The role of seawater freezing in the formation of subsurface brines. *Geochimica et Cosmochimica Acta* 54: 13–21.
Heuperman A (1999) Hydraulic gradient reversal by trees in shallow water table areas and repercussions for the sustainability of tree-growing systems. *Agricultural Water Management* 39: 153–167.
Hillel D (1980) *Fundamentals of Soil Physics*. New York: Academic Press.
Hoffman D (1993) Use of potassium and nanofiltration plants for reducing the salinity of urban wastewater. Adam Technical and Economic Services, Water Department, Agricultural Ministry of Israel.
Hogan JF and Blum JD (2003) Boron and lithium isotopes as groundwater tracers: A study at the Fresh Kills Landfill, Staten Island, New York, USA. *Applied Geochemistry* 18: 615–627.
Holtzman R, Shavit U, Segal-Rozenhaimer M, et al. (2005) Quantifying ground water inputs along the Lower Jordan River. *Journal of Environmental Quality* 34: 897–906.
Hosono T, Siringan F, Yamanaka T, et al. (2010) Application of multi-isotope ratios to study the source and quality of urban groundwater in Metro Manila, Philippines. *Applied Geochemistry* 25: 900–909.
Hosono T, Wang C-H, Umezawa Y, et al. (2011) Multiple isotope (H, O, N, S and Sr) approach elucidates complex pollution causes in the shallow groundwaters of the Taipei urban area. *Journal of Hydrology* 397: 23–36.
Houhou J, Lartiges BS, France-Lanord C, Guilmette C, Poix S, and Mustin C (2010) Isotopic tracing of clear water sources in an urban sewer: A combined water and dissolved sulfate stable isotope approach. *Water Research* 44: 256–266.
Howard KWF and Beck PJ (1993) Hydrogeochemical implications of groundwater contamination by road de-icing chemicals. *Journal of Contaminant Hydrology* 12: 245–268.
Hsissou Y, Mudry J, Mania J, Bouchaou L, and Chauve P (1999) Utilisation du rapport Br/Cl pour déterminer l'origine de la salinité des eaux souterraines: Exemple de la plaine du Souss (Maroc). *Comptes Rendus de l'Académie des Sciences – Series IIA – Earth and Planetary Sciences* 328: 381–386.
Hudak PF (1999) Chloride and nitrate distributions in the Hickory aquifer, Central Texas, USA. *Environment International* 25: 393–401.
Hudak PF (2000a) Regional trends in nitrate content of Texas groundwater. *Journal of Hydrology* 228: 37–47.
Hudak PF (2000b) Sulfate and chloride concentrations in Texas aquifers. *Environment International* 26: 55–61.
Hudak PF (2003) Chloride/bromide ratios in leachate derived from farm-animal waste. *Environmental Pollution* 121: 23–25.
Hudak PF and Blanchard S (1997) Land use and groundwater quality in the Trinity Group outcrop of North-Central Texas, USA. *Environment International* 23: 507–517.
Hunt CB, Robinson TW, Bowles WA, and Washburn AL (1996) *Hydrologic Basin, Death Valley, California*. *Geological Survey Professional Paper 494-B*. Washington, DC: US Government Printing Office.
Hyung H and Kim J-H (2006) A mechanistic study on boron rejection by sea water reverse osmosis membranes. *Journal of Membrane Science* 286: 269–278.
International Desalination & Water Reuse (2011) The International Desalination and Water Reuse Quarterly industry website. Online Available at http://www.desalination.biz/index.asp?channel=0 (accessed June 2011).
Israel Water Authority (2011) Israel Water Authority web site. Online Available at http://www.water.gov.il/hebrew/Pages/home.aspx (accessed May 2011).
Izbicki JA (1991) Chloride sources in a California coastal aquifer. In: *Ground Water in the Pacific Rim Countries*, *Proceedings of the Symposium Sponsored by the Irrigation and Drainage Division of the American Society of Civil Engineers,* Honolulu, Hawaii, July 23–25, 1991.
Izbicki JA (1996) Seawater intrusion in a coastal California aquifer. US Geological Survey Fact Sheet FS-125-96.
Jackson PR, Garcia CM, Oberg KA, Johnson KK, and Garcia MH (2008) Density currents in the Chicago River: Characterization, effects on water quality, and potential sources. *Science of the Total Environment* 401: 130–143.
Jackson RB, Carpenter SR, Dahm CN, et al. (2001) Water in a changing world. *Ecological Applications* 11: 1027–1045.
Jackson RB and Jobbagy EG (2005) From icy roads to salty streams. *Proceedings of the National Academy of Sciences of the United States of America* 102: 14487–14488.
Jackson RB, Jobbagy EG, and Nosetto MD (2009) Ecohydrology in a human-dominated landscape. *Ecohydrology* 2: 383–389.
Jessen S, Larsen F, Postma D, et al. (2008) Palaeo-hydrogeological control on groundwater As levels in Red River delta, Vietnam. *Applied Geochemistry* 23: 3116–3126.
Jobbagy EG and Jackson RB (2004) Groundwater use and salinization with grassland afforestation. *Global Change Biology* 10: 1299–1312.
Johnson JS, Baker LA, and Fox P (1999) Geochemical transformations during artificial groundwater recharge: Soil–water interactions of inorganic constituents. *Water Research* 33: 196–206.
Johnson TM and DePaolo DJ (1994) Interpretation of isotopic data in groundwater–rock systems: Model development and application to Sr isotope data from Yucca Mountain. *Water Resources Research* 30: 1571–1587.
Jones BF (1965) Geochemical evolution of closed basin water in the western Great Basin. In: Rau JL (ed.) *Second Symposium on Salt*. Northern Ohio Geological Society.
Jones BF, Naftz DL, Spencer RJ, and Oviatt CG (2009) Geochemical Evolution of Great Salt Lake, Utah, USA. *Aquatic Geochemistry* 15: 95–121.
Jones BF, Vengosh A, Rosenthal E, and Yechieli Y (1999) Geochemical investigations. In: Bear J, Cheng AHD, Soreq S, Ouazar D, and Herrera I (eds.) *Seawater Intrusion in Coastal Aquifers – Concepts, Methods and Practices*, ch. 3, pp. 51–72. Dordrecht, The Netherlands: Kluwer Academic.
Jones PH and Hutchon H (1983) Road salt in the environment. In: Schreiber BC and Harner HL (eds.) *6th International Symposium on Salt*. Alexandria, VA: Salt Institute.
Jørgensen NO and Banoeng-Yakubo BK (2001) Environmental isotopes (^{18}O, ^{2}H, and $^{87}Sr/^{86}Sr$) as a tool in groundwater investigations in the Keta Basin, Ghana. *Hydrogeology Journal* 9: 190–201.

Jung J and Sun G (2001) Recovery of sodium sulfate from farm drainage salt for use in reactive dyeing of cotton. *Environmental Science & Technology* 35: 3391–3395.

Kakihana H, Kotaka M, Satoh S, Nomura M, and Okamoto M (1977) Fundamental studies on the ion-exchange of boron isotopes. *Bulletin of the Chemical Society of Japan* 50: 158–163.

Kamai T, Weisbrod N, and Dragila MI (2009) Impact of ambient temperature on evaporation from surface-exposed fractures. *Water Resources Research* 45: W02417.

Karabal E, Yücel M, and Öktem HA (2003) Antioxidant responses of tolerant and sensitive barley cultivars to boron toxicity. *Plant Science* 164: 925–933.

Kass A, Gavrieli I, Yechieli Y, Vengosh A, and Starinsky A (2005) The impact of freshwater and wastewater irrigation on the chemistry of shallow groundwater: A case study from the Israeli Coastal Aquifer. *Journal of Hydrology* 300: 314–331.

Katz A and Starinsky A (2009) Geochemical history of the Dead Sea. *Aquatic Geochemistry* 15: 159–194.

Katz BG and Bullen TD (1996) The combined use of $^{87}Sr/^{86}Sr$ and carbon and water isotopes to study the hydrochemical interaction between groundwater and lakewater in mantled karst. *Geochimica et Cosmochimica Acta* 60: 5075–5087.

Katz BG, Eberts SM, and Kauffman LJ (2011) Using Cl/Br ratios and other indicators to assess potential impacts on groundwater quality from septic systems: A review and examples from principal aquifers in the United States. *Journal of Hydrology* 397: 151–166.

Katz BG, Griffin DW, and Davis JH (2009) Groundwater quality impacts from the land application of treated municipal wastewater in a large karstic spring basin: Chemical and microbiological indicators. *Science of the Total Environment* 407: 2872–2886.

Kaushal SS, Groffman PM, and Likens GE (2005) Increased salinization of fresh water in the northeastern U.S. *Proceedings of the National Academy of Sciences of the United States of America* 102: 13517–13520.

Kaya C, Tuna AL, Dikilitas M, Ashraf M, Koskeroglu S, and Guneri M (2009) Supplementary phosphorus can alleviate boron toxicity in tomato. *Scientia Horticulturae* 121: 284–288.

Kelly VR, Lovett GM, Weathers KC, et al. (2008) Long-term sodium chloride retention in a rural watershed: Legacy effects of road salt on streamater concentration. *Environmental Science & Technology* 42: 410–415.

Kendall C and Aravena R (2000) Nitrate isotopes in groundwater systems. In: Cook P and Herczeg AL (eds.) *Environmental Tracers in Subsurface Hydrology*. pp. 261–297. Boston, MA: Kluwer Academic.

Keren R (1991) Adsorbed sodium fraction effect on rheology of montmorillonite–kaolinite suspensions. *Soil Science Society of America Journal* 55: 376–379.

Keren R and Ben-Hur M (2003) Interaction effects of clay swelling and dispersion and $CaCO_3$ content on saturated hydraulic conductivity. *Australian Journal of Soil Research* 41: 979–989.

Keren R and Gast RG (1981) Effects of wetting and drying and of exchangeable cations, on boron adsorption and release by montmorillonite. *Soil Science Society of America Journal* 45: 478–482.

Keren R, Gast RG, and Baryosef B (1981) pH-dependent boron adsorption by Na-montmorillonite. *Soil Science Society of America Journal* 45: 45–48.

Keren R and Klein E (1995) Sodium/calcium montmorillonite suspension and light scattering. *Soil Science Society of America Journal* 59: 1032–1035.

Keren R and O'Connor GA (1982) Effect of exchangeable ion and ionic strength on boron adsorption by montmorillonite and illite. *Clays and Clay Minerals* 30: 341–346.

Keren R and Singer MJ (1988) Effect of low electrolyte concentration on hydraulic conductivity of sodium/calcium–montmorillonite–sand system. *Soil Science Society of America Journal* 52: 368–373.

Keren R and Sparks DL (1994) Effect of pH and ionic-strength on boron adsorption by pyrophyllite. *Soil Science Society of America Journal* 58: 1095–1100.

Kharaka YK, Ambats G, Presser TS, and Davis RA (1996) Removal of selenium from contaminated agricultural drainage water by nanofiltration membranes. *Applied Geochemistry* 11: 797–802.

Kharaka YK, Ambats G, Thordsen JJ, and Davis RA (1997) Deep well injection of brine from Paradox Valley, Colorado: Potential major precipitation problems remediated by nanofiltration. *Water Resources Research* 33: 1013–1020.

Kim H, Yeh PJF, Oki T, and Kanae S (2009) Role of rivers in the seasonal variations of terrestrial water storage over global basins. *Geophysical Research Letters* 36: L17402. http://dx.doi.org/10.1029/2009gl039006.

Kim Y, Lee K-S, Koh D-C, et al. (2003) Hydrogeochemical and isotopic evidence of groundwater salinization in a coastal aquifer: A case study in Jeju volcanic island, Korea. *Journal of Hydrology* 270: 282–294.

Kitto ME, Parekh PP, Torres MA, and Schneider D (2005) Radionuclide and chemical concentrations in mineral waters at Saratoga Springs, New York. *Journal of Environmental Radioactivity* 80: 327–339.

Klay S, Charef A, Ayed L, Houman B, and Rezgui F (2010) Effect of irrigation with treated wastewater on geochemical properties (saltiness, C, N and heavy metals) of isohumic soils (Zaouit Sousse perimeter, Oriental Tunisia). *Desalination* 253: 180–187.

Klochko K, Kaufman AJ, Yao W, Byrne RH, and Tossell JA (2006) Experimental measurement of boron isotope fractionation in seawater. *Earth and Planetary Science Letters* 248: 261–270.

Kloppmann W, Chikurel H, Picot G, et al. (2009) B and Li isotopes as intrinsic tracers for injection tests in aquifer storage and recovery systems. *Applied Geochemistry* 24: 1214–1223.

Kloppmann W, Négrel P, Casanova J, Klinge H, Schelkes K, and Guerrot C (2001) Halite dissolution derived brines in the vicinity of a Permian salt dome (N German Basin). Evidence from boron, strontium, oxygen, and hydrogen isotopes. *Geochimica et Cosmochimica Acta* 65: 4087–4101.

Kloppmann W, Van Houtte E, Picot G, et al. (2008a) Monitoring reverse osmosis treated wastewater recharge into a coastal aquifer by environmental isotopes (B, Li, O, H). *Environmental Science & Technology* 42: 8759–8765.

Kloppmann W, Vengosh A, Guerrot C, Millot R, and Pankratov I (2008b) Isotope and ion selectivity in reverse osmosis desalination: Geochemical tracers for man-made freshwater. *Environmental Science & Technology* 42: 4723–4731.

Knobel LL, Chapelle FH, and Meisler H (1998) *Geochemistry of the Northern Atlantic Coastal Plain Aquifer System. US Geological Survey Professional Paper 1404-L*. Washington, DC: US Government Printing Office.

Koc C (2007) Effects on environment and agriculture of geothermal wastewater and Boron pollution in great Menderes basin. *Environmental Monitoring and Assessment* 125: 377–388.

Koh DC, Chae GT, Yoon YY, Kang BR, Koh GW, and Park KH (2009) Baseline geochemical characteristics of groundwater in the mountainous area of Jeju Island, South Korea: Implications for degree of mineralization and nitrate contamination. *Journal of Hydrology* 376: 81–93.

Kolodny Y, Katz A, Starinsky A, Moise T, and Simon E (1999) Chemical tracing of salinity sources in Lake Kinneret (Sea of Galilee), Israel. *Limnology and Oceanography* 44: 1035–1044.

Komor SC (1997) Boron contents and isotopic compositions of hog manure, selected fertilizers, and water in Minnestoa. *Journal of Environmental Quality* 26: 1212–1222.

Kotb THS, Watanabe T, Ogino Y, and Tanji KK (2000) Soil salinization in the Nile Delta and related policy issues in Egypt. *Agricultural Water Management*. 43: 239–261.

Kraemer TF and Reid DF (1984) The occurrence and behavior of radium in saline formation water of the US Gulf coast region. *Chemical Geology* 46: 153–174.

Krapac IG, Dey WS, Roy WR, Smyth CA, Storment E, Sargent SL, and Steele JD (2002) Impacts of swine manure pits on groundwater quality. *Environmental Pollution* 120: 475–492.

Krasner S, Chinn R, Pastor S, Sclimenti M, Weinberg H, Onstad G, and Richardson S (2002) The occurrence of disinfection by-products of health concern in drinking water. *Epidemiology* 13: 160.

Krishnaswami S, Bhushan R, and Baskaran M (1991) Radium isotopes and ^{222}Rn in shallow brines, Kharaghoda (India). *Chemical Geology* 87: 125–136.

Kronenberg G (2004) The largest SWRO plant in the world – Ashkelon 100 million m^3/y BOT project. *Desalination* 166: 457–463.

Krouse HR and Mayer B (2000) Sulphur and oxygen isotopes in sulphate. In: Cook P and Herczeg AL (eds.) *Environmental Tracers in Subsurface Hydrology*, pp. 195–231.Boston: Kluwer Academic.

Kruge MA, Permanyer A, Serra J, and Yu D (2010) Geochemical investigation of an offshore sewage sludge deposit, Barcelona, Catalonia, Spain. *Journal of Analytical and Applied Pyrolysis* 89: 204–217.

Kudo N, Sugino T, Oka M, and Fujiyama H (2010) Sodium tolerance of plants in relation to ionic balance and the absorption ability of microelements. *Soil Science and Plant Nutrition* 56: 225–233.

Kulp TR, Han S, Saltikov CW, Lanoil BD, Zargar K, and Oremland RS (2007) Effects of imposed salinity gradients on dissimilatory arsenate reduction, sulfate reduction, and other microbial processes in sediments from two California soda lakes. *Applied and Environmental Microbiology* 73: 5130–5137.

Lahav O and Birnhack L (2007) Quality criteria for desalinated water following posttreatment. *Desalination* 207: 286–303.

Langman JB and Ellis AS (2010) A multi-isotope (δD, $\delta^{18}O$, $^{87}Sr/^{86}Sr$, and $\delta^{11}B$) approach for identifying saltwater intrusion and resolving groundwater evolution along the Western Caprock Escarpment of the Southern High Plains, New Mexico. *Applied Geochemistry* 25: 159–174.

Lavado RS and Taboada MA (1987) Soil salinization as an effect of grazing in a native grassland soil in the Flooding Pampa of Argentina. *Soil Use and Management* 3: 143–148.

Leaney FW, Herczeg AL, and Walker GR (2003) Salinization of a fresh palaeo-ground water resource by enhanced recharge. *Ground Water* 41: 84–92.
Leenhouts JM, Basset RL, and Iii TM (1998) Utilization of intrinsic boron isotopes as co-migrating tracers for identifying potential nitrate contamination sources. *Ground Water* 36: 240–250.
Lehto T, Ruuhola T, and Dell B (2010) Boron in forest trees and forest ecosystems. *Forest Ecology and Management* 260: 2053–2069.
Leybourne MI and Goodfellow WD (2007) Br/Cl ratios and O, H, C, and B isotopic constraints on the origin of saline waters from eastern Canada. *Geochimica et Cosmochimica Acta* 71: 2209–2223.
Li F and Keren R (2008) Native $CaCO_3$ mineral dissolution and its contribution to sodic calcareous soil reclamation under laboratory conditions. *Arid Land Research and Management* 22: 1–15.
Li FH and Keren R (2009) Calcareous sodic soil reclamation as affected by corn stalk application and incubation: A laboratory study. *Pedosphere* 19: 465–475.
Li XD, Liu CQ, Harue M, Li SL, and Liu XL (2010) The use of environmental isotopic (C, Sr, S) and hydrochemical tracers to characterize anthropogenic effects on karst groundwater quality: A case study of the Shuicheng Basin, SW China. *Applied Geochemistry* 25: 1924–1936.
Lin J, Snodsmith JB, Zheng CM, and Wu JF (2009) A modeling study of seawater intrusion in Alabama Gulf Coast, USA. *Environmental Geology* 57: 119–130.
Linnikov OD and Podbereznyi VL (1996) Prevention of sulfate scale formation in desalination of Aral Sea water. *Desalination* 105: 143–150.
Liu GJ, Zhang XR, McWilliams L, Talley JW, and Neal CR (2008) Influence of ionic strength, electrolyte type, and NOM on As(V) adsorption onto TiO_2. *Journal of Environmental Science and Health Part A: Toxic/Hazardous Substances & Environmental Engineering* 43: 430–436.
Liu Y and Tossell JA (2005) Ab initio molecular orbital calculations for boron isotope fractionations on boric acids and borates. *Geochimica et Cosmochimica Acta* 69: 3995–4006.
Lokiec F and Kronenberg G (2003) South Israel 100 million m^3/y seawater desalination facility: Build, operate and transfer (BOT) project. *Desalination* 156: 29–37.
Love AJ, Herczeg AL, Sampson L, Cresswell RG, and Fifield LK (2000) Sources of chloride and implications for ^{36}Cl dating of old groundwater, Southwestern Great Artesian Basin, Australia. *Water Resources Research* 36: 1561–1574.
Lu HY, Peng TR, and Liou TS (2008) Identification of the origin of salinization in groundwater using multivariate statistical analysis and geochemical modeling: A case study of Kaohsiung, Southwest Taiwan. *Environmental Geology* 55: 339–352.
Lucas Y, Schmitt AD, Chabaux F, et al. (2010) Geochemical tracing and hydrogeochemical modelling of water–rock interactions during salinization of alluvial groundwater (Upper Rhine Valley, France). *Applied Geochemistry* 25: 1644–1663.
Lyons WB, Tyler SW, Gaudette HE, and Long DT (1995) The use of strontium isotopes in determining groundwater mixing and brine fingering in a playa spring zone, Lake Tyrrell, Australia. *Journal of Hydrology* 167: 225–239.
Lyons WB, Welch KA, and Sharma P (1998) Chlorine-36 in the waters of the McMurdo Dry Valley lakes, southern Victoria Land, Antarctica: Revisited. *Geochimica et Cosmochimica Acta* 62: 185–191.
Magaritz M, Kaufman A, Paul M, Boaretto E, and Hollos G (1990) A new method to determine regional evapotranspiration. *Water Resources Research* 26: 1759–1762.
Magaritz M, Nadler A, Kafri U, and Arad A (1984) Hydrogeochemistry of continental brackish waters in the southern Coastal Plain, Israel. *Chemical Geology* 42: 159–176.
Mandilaras D, Lambrakis N, and Stamatis G (2008) The role of bromide and iodide ions in the salinization mapping of the aquifer of Glafkos River basin (northwest Achaia, Greece). *Hydrological Processes* 22: 611–622.
Mane PP, Park P-K, Hyung H, Brown JC, and Kim J-H (2009) Modeling boron rejection in pilot- and full-scale reverse osmosis desalination processes. *Journal of Membrane Science* 338: 119–127.
Marie A and Vengosh A (2001) Sources of salinity in ground water from Jericho Area, Jordan Valley. *Ground Water* 39: 240–248.
Marion GM, Farren RE, and Komrowski AJ (1999) Alternative pathways for seawater freezing. *Cold Regions Science and Technology* 29: 259–266.
Maslia ML and Prowell DC (1990) Effect of faults on fluid flow and chloride contamination in a carbonate aquifer system. *Journal of Hydrology* 115: 1–49.
Mason P (2011) Magnesium, drinking water, and health. Online Available at http://www.mgwater.com/index.shtml (accessed June 2011).
Masscheleyn PH, Delaune RD, and Patrick WH (1990) Transformations of selenium as affected by sediment oxidation reduction potential and pH. *Environmental Science & Technology* 24: 91–96.
Maton L, Psarras G, Kasapakis G, et al. (2010) Assessing the net benefits of using wastewater treated with a membrane bioreactor for irrigating vegetables in Crete. *Agricultural Water Management* 98: 458–464.
Matray JM, Lambert M, and Fontes JC (1994) Stable isotope conservation and origin of saline waters from the Middle Jurassic aquifer of the Paris Basin, France. *Applied Geochemistry* 9: 297–309.
Mazor E (1997) *Chemical and Isotopic Groundwater Hydrology, the Applied Approach*. New York: Dekker.
Mazor E and George R (1992) Marine airborne salts applied to trace evapotranspiration, local recharge and lateral groundwater flow in Western Australia. *Journal of Hydrology* 139: 63–77.
McBride MA (1977) A critique of diffuse double layer models applied to colloid and surface chemistry. *Clays and Clay Minerals* 45: 598–608.
McCaffrey MA, Lazar B, and Holland HD (1987) The evaporation path of seawater and the coprecipitation of Brand K with halite. *Journal of Sedimentary Petrology* 57: 928–937.
McMahon PB, Bohlke JK, Kauffman LJ, et al. (2008) Source and transport controls on the movement of nitrate to public supply wells in selected principal aquifers of the United States. *Water Resources Research* 44: W04401. http://dx.doi.org/10.1029/2007wr006252.
McMahon PB and Chapelle FH (1991) Geochemistry of dissolved inorganic carbon in a Coastal Plain aquifer. 2. Modeling carbon sources, sinks, and $\delta^{13}C$ evolution. *Journal of Hydrology* 127: 109–135.
Mehta S, Fryar AE, and Banner JL (2000a) Controls on the regional-scale salinization of the Ogallala aquifer, Southern High Plains, Texas, USA. *Applied Geochemistry* 15: 849–864.
Mehta S, Fryar AE, Brady RM, and Morin RH (2000b) Modeling regional salinization of the Ogallala aquifer, Southern High Plains, TX, USA. *Journal of Hydrology* 238: 44–64.
Meisler H, Leahy PP, and Knobel LL (1985) *Effect of Eustatic Sea-Level Changes on Saltwater-Freshwater in the Northern Atlantic Coastal Plain*. *US Geological Survey Water-Supply Paper 2255*. Washington, DC: US Government Printing Office.
Meybeck M (2003) Global analysis of river systems: From Earth system controls to Anthropocene syndromes. *Philosophical Transactions of the Royal Society Series B* 358: 1935–1955.
Meybeck M and Helmer R (1989) The quality of rivers: From pristine stage to global pollution. *Global and Planetary Change* 1: 283–309.
Mezuman U and Keren R (1981) Boron adsorption by soils using a phenomenological adsorption equation. *Soil Science Society of America Journal* 45: 722–726.
Micklin PP (1988) Desiccation of the Aral Sea: A water management disaster in the Soviet Union. *Science* 241: 1170–1176.
Micklin PP (1992) The Aral crisis: Introduction to the special issue. *Post-Soviet Geography* 33: 269–282.
Micklin P (2010) The past, present, and future Aral Sea. *Lakes and Reservoirs: Research and Management* 15: 193–213.
Miller MR, Brown PL, Donovan JJ, Bergatino RN, Sonderegger JL, and Schmidt FA (1981) Saline seep development and control in the North American Great Plains – Hydrogeological aspects. *Agricultural Water Management* 4: 115–141.
Miller RL and Sutcliffe H (1985) Occurrence of natural radium-226 radioactivity in ground water of Sarasota County, Florida. *US Geological Survey Water-Resources Investigations Report 84-8237*. Denver, Co: US Geological Survey.
Millero FJ (1995) Thermodynamics of the carbon dioxide system in the oceans. *Geochimica et Cosmochimica Acta* 59: 661–677.
Millot R, Guerrot C, Innocent C, Negrel P, and Sanjuan B (2011) Chemical, multi-isotopic (Li–B–Sr–U–H–O) and thermal characterization of Triassic formation waters from the Paris Basin. *Chemical Geology* 283: 226–241.
Millot R and Negrel P (2007) Multi-isotopic tracing (δ^7Li, $\delta^{11}B$, $^{87}Sr/^{86}Sr$) and chemical geothermometry: Evidence from hydro-geothermal systems in France. *Chemical Geology* 244: 664–678.
Millot R, Negrel P, and Petelet-Giraud E (2007) Multi-isotopic (Li, B, Sr, Nd) approach for geothermal reservoir characterization in the Limagne Basin (Massif Central, France). *Applied Geochemistry* 22: 2307–2325.
Millot R, Petelet-Giraud E, Guerrot C, and Negrel P (2010) Multi-isotopic composition (δ^7Li–$\delta^{11}B$–δD–$\delta^{18}O$) of rainwaters in France: Origin and spatio-temporal characterization. *Applied Geochemistry* 25: 1510–1524.
Mills SK, Phillips FM, Hogan J, and Hendrix JMH (2002) Deep thoughts: What is the influence of deep groundwater discharge on salinization of the Rio Grande? *American Geological Society Annual Meeting*. Denver, October 2002.
Milly PCD, Dunne KA, and Vecchia AV (2005) Global pattern of trends in stream flow and water availability in a changing climate. *Nature* 438: 347–350.
Milnes E and Renard P (2004) The problem of salt recycling and seawater intrusion in coastal irrigated plains: An example from the Kiti aquifer (Southern Cyprus). *Journal of Hydrology* 288: 327–343.

Miltner RJ, Speth TF, Richardson SD, Krasner SW, Weinberg HS, and Simmons JE (2008) Integrated disinfection by-products mixtures research: Disinfection of drinking waters by chlorination and ozonation/postchlorination treatment scenarios. *Journal of Toxicology and Environmental Health, Part A* 71: 1133–1148.

Misra AK (2011) Impact of urbanization on the hydrology of Ganga Basin (India). *Water Resources Management* 25: 705–719.

Misra AK and Mishra A (2007) Study of quaternary aquifers in Ganga Plain, India: Focus on groundwater salinity, fluoride and fluorosis. *Journal of Hazardous Materials* 144: 438–448.

Mitchell JP, Shennan C, and Singer MJ (2000) Impacts of gypsum and winter cover crops on soil physical properties and crop productivity when irrigated with saline water. *Agricultural Water Management*. 45: 55–71.

Moatar F, Shadizadeh SR, Karbassi AR, Ardalani E, Derakhshi RA, and Asadi M (2010) Determination of naturally occurring radioactive materials (NORM) in formation water during oil exploration. *Journal of Radioanalytical and Nuclear Chemistry* 283: 3–7.

Moise T, Starinsky A, Katz A, and Kolodny Y (2000) Ra isotopes and Rn in brines and ground waters of the Jordan-Dead Sea Rift Valley: Enrichment, retardation, and mixing. *Geochimica et Cosmochimica Acta* 64: 2371–2388.

Moller P, Weise SM, Tesmer M, et al. (2008) Salinization of groundwater in the North German Basin: Results from conjoint investigation of major, trace element and multi-isotope distribution. *International Journal of Earth Sciences* 97: 1057–1073.

Moore KW, Huck PM, and Siverns S (2008a) Arsenic removal using oxidative media and nanofiltration. *Journal of the American Water Works Association* 100: 74–83.

Moore SJ, Bassett RL, Liu B, Wolf CP, and Doremus D (2008b) Geochemical tracers to evaluate hydrogeologic controls on river salinization. *Ground Water* 46: 489–501.

Mor S, Singh S, Yadav P, et al. (2009) Appraisal of salinity and fluoride in a semi-arid region of India using statistical and multivariate techniques. *Environmental Geochemistry and Health* 31: 643–655.

Moran JE, Oktay SD, and Santschi PH (2002) Sources of iodine and iodine 129 in rivers. *Water Resources Research* 38: 1149.

Moran JE, Oktay S, Santschi PH, and Schink DR (1999) Atmospheric dispersal of ^{129}iodine from nuclear fuel reprocessing facilities. *Environmental Science & Technology* 33: 2536–2542.

Moussa AB, Zouari K, and Marc V (2011) Hydrochemical and isotope evidence of groundwater salinization processes on the coastal plain of Hammamet-Nabeul, north-eastern Tunisia. *Physics and Chemistry of the Earth Parts A/B/C* 36: 167–178.

Mukherjee P and Sengupta AK (2003) Ion exchange selectivity as a surrogate indicator of relative permeability of ions in reverse osmosis processes. *Environmental Science & Technology* 37: 1432–1440.

Murkved PT, Dörsch P, and Bakken LR (2007) The N_2O product ratio of nitrification and its dependence on long-term changes in soil pH. *Soil Biology and Biochemistry* 39: 2048–2057.

Murphy J (1999) *Salinity – Our Silent Disaster*. Australian Broadcasting Corporation.

Mutlak S, Salih B, and Tawfiq S (1980) Quality of Tigris River passing through Baghdad for irrigation. *Water, Air, & Soil Pollution* 13: 9–16.

Nadler A, Levy GJ, Keren R, and Eisenberg H (1996) Sodic calcareous soil reclamation as affected by water chemical composition and flow rate. *Soil Science Society of America Journal* 60: 252–257.

Naftz DL, Bullen TD, Stolp BJ, and Wilkowske CD (2008) Utilizing geochemical, hydrologic, and boron isotopic data to assess the success of a salinity and selenium remediation project, Upper Colorado River Basin, Utah. *Science of the Total Environment* 392: 1–11.

Nativ R, Adar E, Dahan O, and Nissim I (1997) Water salinization in arid regions–observations from the Negev desert, Israel. *Journal of Hydrology* 196: 271–296.

Negrel P, Roy S, Petelet-Giraud E, Millot R, and Brenot A (2007) Long-term fluxes of dissolved and suspended matter in the Ebro River Basin (Spain). *Journal of Hydrology* 342: 249–260.

Nelson KH and Thompson TG (1954) Deposition of salts from seawater by frigid concentration. *Journal of Marine Research* 13: 166–182.

Nesbitt HW and Cramer JJ (1993) Genesis and evolution of HCO_3-rich and SO_4-rich groundwaters of Quaternary sediments, Pinawa, Canada. *Geochimica et Cosmochimica Acta* 57: 4933–4946.

Ng GHC, McLaughlin D, Entekhabi D, and Scanlon B (2009) Using data assimilation to identify diffuse recharge mechanisms from chemical and physical data in the unsaturated zone. *Water Resources Research* 45: W09409. http://dx.doi:10.1029/2009wr007831.

Nicolli HB, Bundschuh J, Garcia JW, Falcon CM, and Jean JS (2010) Sources and controls for the mobility of arsenic in oxidizing groundwaters from loess-type sediments in arid/semi-arid dry climates – Evidence from the Chaco-Pampean plain (Argentina). *Water Research* 44: 5589–5604.

Nishikoori H, Murakami M, Sakai H, Oguma K, Takada H, and Takizawa S (2011) Estimation of contribution from non-point sources to perfluorinated surfactants in a river by using boron as a wastewater tracer. *Chemosphere* 84: 1125–1132.

Nishri A, Stiller M, Rimmer A, Geifman Y, and Krom M (1999) Lake Kinneret (The Sea of Galilee): The effects of diversion of external salinity sources and the probable chemical composition of the internal salinity sources. *Chemical Geology* 158: 37–52.

Nobukawa T and Sanukida S (2000) The genotoxity of by-products by chlorination and ozonation of the river water in the presence of bromide ions. *Water Science & Technology* 42: 259–264.

Nosetto MD, Jobbagy EG, Jackson RB, and Sznaider GA (2009) Reciprocal influence of crops and shallow ground water in sandy landscapes of the Inland Pampas. *Field Crops Research* 113: 138–148.

Odemis B, Sangun MK, and Evrendilek F (2010) Quantifying long-term changes in water quality and quantity of Euphrates and Tigris rivers, Turkey. *Environmental Monitoring and Assessment* 170: 475–490.

Ohlsson L (1995) *Hydropolitics*. London: Zed Books.

Oki T and Kanae S (2006) Global hydrological cycles and world water resources. *Science* 313: 1068–1072.

Oren A, Plotnikov IS, Sokolov S, and Aladin NV (2010) The Aral Sea and the Dead Sea: Disparate lakes with similar histories. *Lakes and Reservoirs: Research and Management* 15: 223–236.

Oreskovich RW and Watson IC (2003) Dealing with arsenic (III) in brackish water RO permeate. In: *International Desalination Association Proceedings*, 1–12 BAH03.

Osborn SG and McIntosh JC (2010) Chemical and isotopic tracers of the contribution of microbial gas in Devonian organic-rich shales and reservoir sandstones, northern Appalachian Basin. *Applied Geochemistry* 25: 456–471.

Otero N, Soler A, Corp RM, Mas-Pla J, Garcia-Solsona E, and Masque P (2011) Origin and evolution of groundwater collected by a desalination plant (Tordera, Spain): A multi-isotopic approach. *Journal of Hydrology* 397: 37–46.

Oulhote Y, Le Bot B, Deguen S, and Glorennec P (2011) Using and interpreting isotope data for source identification. *Trends in Analytical Chemistry* 30: 302–312.

Ozaki H and Li HF (2002) Rejection of organic compounds by ultra-low pressure reverse osmosis membrane. *Water Research* 36: 123–130.

Ozturk N, Kavak D, and Kose TE (2008) Boron removal from aqueous solution by reverse osmosis. *Desalination* 223: 1–9.

Palmer MR, Spivack AJ, and Edmond JM (1987) Temperature and pH controls over isotopic fractionation during adsorption of boron on marine clay. *Geochimica et Cosmochimica Acta* 51: 2319–2323.

Panno SV, Hackley KC, Hwang HH, et al. (2006) Source identification of sodium and chloride in natural waters: Preliminary results. *Ground Water* 44: 176–187.

Papadakis IE, Dimassi KN, Bosabalidis AM, Therios IN, Patakas A, and Giannakoula A (2004) Boron toxicity in 'Clementine' mandarin plants grafted on two rootstocks. *Plant Science* 166: 539–547.

Park SC, Yun ST, Chae GT, Yoo IS, Shin KS, Heo CH, and Lee SK (2005) Regional hydrochemical study on salinization of coastal aquifers, western coastal area of South Korea. *Journal of Hydrology* 313: 182–194.

Parks JL and Edwards M (2005) Boron in the environment: *Critical Reviews in Environmental Science and Technology* 35: 81–114.

Peck AJ and Hatton T (2003) Salinity and the discharge of salts from catchments in Australia. *Journal of Hydrology* 272: 191–202.

Peeters F, Kipfer R, Achermann D, et al. (2000) Analysis of deep-water exchange in the Caspian Sea based on environmental tracers. *Deep Sea Research Part I: Oceanographic Research Papers* 47: 621–654.

Phillips FM (1994) Environmental tracers for water movement in desert soils of the American Southwest. *Soil Science Society of America Journal* 58: 15–24.

Phillips FM (2000) Chlorine-36. In: Cook P and Herczeg A (eds.) *Environmental Tracers in Subsurface Hydrology*, pp. 299–348. Boston, MA: Kluwer Academic.

Phillips FM, Mills S, Hendrickx MH, and Hogan J (2003) Environmental tracers applied to quantifying causes of salinity in arid-region rivers: Results from the Rio Grande Basin, southwestern USA. In: Alsharhan AS and Wood WW (eds.) *Water Resources Perspectives: Evaluation, Management and Policy*, pp. 327–334. Amsterdam: Elsevier.

Pillsbury AF (1981) The salinity of rivers. *Scientific American* 245: 54–65.

Postel SL (1999) *Pillar of Sand: Can the Irrigation Miracle Last?* New York: Worldwatch Institute.

Prats D, Chillon-Arias MF, and Rodriguez-Pastor M (2000) Analysis of the influence of pH and pressure on the elimination of boron in reverse osmosis. *Desalination* 128: 269–273.

Presser TS and Swain WC (1990) Geochemical evidence for Se mobilization by the weathering of pyritic shale, San Joaquin Valley, California, U.S.A.. *Applied Geochemistry* 5: 703–717.

Pressman JG, Richardson SD, Speth TF, et al. (2010) Concentration, chlorination, and chemical analysis of drinking water for disinfection byproduct mixtures health

effects research: US EPA's four lab study. *Environmental Science & Technology* 44: 7184–7192.
Priel M, Gelman E, Glueckstern P, Balkwill A, David I, and Arviv R (2009) Optimization of wastewater desalination. *Desalination and Water Treatment* 7: 71–77.
Priel M, Glueckstern P, and Perlov N (2006) Seawater vs. different raw-water sources desalination. *Desalination* 199: 317–318.
Raab M and Spiro B (1991) Sulfur isotopic variations during seawater evaporation with fractional crystallization. *Chemical Geology* 86: 323–333.
Raanan H, Vengosh A, Paytan A, Nishri A, and Kabala Z (2009) Quantifying saline groundwater flow into a freshwater lake using the Ra isotope quartet: A case study from the Sea of Galilee (Lake Kinneret), Israel. *Limnology and Oceanography* 54: 119–131.
Rabiet M, Brissaud F, Seidel J-L, Pistre S, and Elbaz-Poulichet F (2005) Deciphering the presence of wastewater in a medium-sized Mediterranean catchment using a multitracer approach. *Applied Geochemistry* 20: 1587–1596.
Rango T, Kravchenko J, Atlaw B, McCornick PG, Jeuland M, Merola M, and Vengosh A (2012) Groundwater quality and its health impact: an assessment of dental fluorosis in rural inhabitants of the Main Ethiopian Rift. *Environment International* 43: 37–47.
Rango T, Bianchini G, Beccaluva L, Ayenew T, and Colombani N (2009) Hydrogeochemical study in the Main Ethiopian Rift: New insights to the source and enrichment mechanism of fluoride. *Environmental Geology* 58: 109–118.
Rango T, Bianchini G, Beccaluva L, and Tassinari R (2010a) Geochemistry and water quality assessment of central Main Ethiopian Rift natural waters with emphasis on source and occurrence of fluoride and arsenic. *Journal of African Earth Sciences* 57: 479–491.
Rango T, Colombani N, Mastrocicco M, Bianchini G, and Beccaluva L (2010b) Column elution experiments on volcanic ash: Geochemical implications for the main Ethiopian rift waters. *Water, Air, & Soil Pollution* 208: 221–233.
Rango T, Kravchenko J, Atlaw B, et al. (2012) Groundwater quality and its health impact: An assessment of dental fluorosis in rural inhabitants of the Main Ethiopian Rift. *Environment International* 43: 37–47.
Rango T, Petrini R, Stenni B, Bianchini G, Slejko F, Beccaluva L, and Ayenew T (2010c) The dynamics of central Main Ethiopian Rift waters: Evidence from δD, $\delta^{18}O$ and $^{87}Sr/^{86}Sr$ ratios. *Applied Geochemistry* 25: 1860–1871.
Ranjan SP, Kazama S, and Sawamoto M (2006) Effects of climate change on coastal fresh groundwater resources. *Global Environmental Change* 16: 388–399.
Ravenscroft P and McArthur JM (2004) Mechanism of regional enrichment of groundwater by boron: The examples of Bangladesh and Michigan, USA. *Applied Geochemistry* 19: 1413–1430.
Raymond K and Butterwick L (1992) Perborate. In: Qude NTD (ed.) *Detergents*, pp. 288–318. New York: Springer.
Re V, Faye SC, Faye A, et al. (2011) Water quality decline in coastal aquifers under anthropic pressure: The case of a suburban area of Dakar (Senegal). *Environmental Monitoring and Assessment* 172: 605–622.
Rebhun M (2004) Desalination of reclaimed wastewater to prevent salinization of soils and groundwater. *Desalination* 160: 143–149.
Redeker KR, Wang NY, Low JC, McMillan A, Tyler SC, and Cicerone RJ (2000) Emissions of methyl halides and methane from rice paddies. *Science* 290: 966–969.
Reid R (2010) Can we really increase yields by making crop plants tolerant to boron toxicity? *Plant Science* 178: 9–11.
Rengasamy P (2006) World salinization with emphasis on Australia. *Journal of Experimental Botany* 57: 1017–1023.
Rengasamy P (2010) Osmotic and ionic effects of various electrolytes on the growth of wheat. *Australian Journal of Soil Research* 48: 120–124.
Reynolds L (2009) *Update on Dunkard Creek*. US Environmental Protection Agency: USEPA Region 3 Environmental Analysis and Innovation Division Office of Monitoring and Assessment Freshwater Biology Team.
Rhoades JD, Bingham FT, and Letey J (1989) Use of saline drainage water for irrigation: Imperial Valley study. *Agricultural Water Management* 16: 25–36.
Richardson C (1976) Phase relationships in sea ice as a function of temperature. *Journal of Glaciology* 17: 507–519.
Richardson SD (2008) Environmental mass spectrometry: Emerging contaminants and current issues. *Analytical Chemistry* 80: 4373–4402.
Richardson SD (2009) Water analysis: Emerging contaminants and current issues. *Analytical Chemistry* 81: 4645–4677.
Richardson SD, Plewa MJ, Wagner ED, Schoeny R, and DeMarini DM (2007) Occurrence, genotoxicity, and carcinogenicity of regulated and emerging disinfection by-products in drinking water: A review and roadmap for research. *Mutation Research – Reviews* 636: 178–242.
Richardson SD, Simmons JE, and Rice G (2002) Disinfection byproducts: The next generation. *Environmental Science & Technology* 36: 198A–205A.
Richardson SD and Ternes TA (2005) Water analysis: Emerging contaminants and current issues. *Analytical Chemistry* 77: 3807–3838.
Richardson SD, Thruston AD, Rav-Acha C, et al. (2003) Tribromopyrrole, brominated acids, and other disinfection byproducts produced by disinfection of drinking water rich in bromide. *Environmental Science & Technology* 37: 3782–3793.
Richter BC and Kreitler CW (1986) Geochemistry of salt water beneath the Rolling Plains, North-Central Texas. *Ground Water* 24: 735–742.
Richter BC and Kreitler CW (1993) *Geochemical Techniques for Identifying Sources of Ground-Water Salinization*. Boca Raton, FL: C. K. Smokely/CRC Press.
Robson JF, Stoner RF, and Perry JH (1984) Disposal of drainage water from irrigated alluvial plains. *Water Science & Technology* 16: 41–55.
Roche MA (1975) Geochemistry and natural ionic and isotopic tracing – two complementary ways to study the natural salinity regime of the hydrological system of Lake Chad. *Journal of Hydrology* 26: 153–171.
Roelke DL, Grover JP, Brooks BW, et al. (2011) A decade of fish-killing *Prymnesium parvum* blooms in Texas: Roles of inflow and salinity. *Journal of Plankton Research* 33: 243–253.
Ronen D, Magaritz M, Almon E, and Amiel AJ (1987) Anthropogenic anoxification ("eutrophication") of the water table region of a deep phreatic aquifer. *Water Resources Research* 23: 1554–1560.
Rose S and Fullagar PD (2005) Strontium isotope systematics of base flow in Piedmont Province watersheds, Georgia (USA). *Applied Geochemistry* 20: 1571–1586.
Rosenberg YO and Ganor J (2009) Radium co-precipitation in evaporitic systems. *Geochimica et Cosmochimica Acta* 73: A1119.
Rosenthal E, Jones BF, and Weinberger G (1998) The chemical evolution of Kurnob Group paleowater in the Sinai-Negev province – A mass-balance approach. *Applied Geochemistry* 13: 553–569.
Roush W (1994) Population: The view from Cairo. *Science* 265: 1164–1167.
Rudebeck A and Persson T (1998) Nitrification in organic and mineral soil layers in coniferous forests in response to acidity. *Environmental Pollution* 102: 377–383.
Ruhl LS, Vengosh A, and Dywer GS (2010) Isotopic and geochemical tracers for evaluating the environmental impact of the Tennessee Valley Authority coal ash spill in Kingston, TN. *Geochimica et Cosmochimica Acta* 74: A889.
Russak A and Sivan O (2010) Hydrogeochemical tool to identify salinization or freshening of coastal aquifers determined from combined field work, experiments, and modeling. *Environmental Science & Technology* 44: 4096–4102.
Sager DR, Barkoh A, Buzan DL, et al. (2008) Toxic *Prymnesium parvum*: A potential threat to U.S. reservoirs. *American Fisheries Society Symposium* 62: 261–273.
Sagiv A and Semiat R (2004) Analysis of parameters affecting boron permeation through reverse osmosis membranes. *Journal of Membrane Science* 243: 79–87.
Salameh E (1996) *Water Quality Degradation in Jordan*. *The Higher Council of Science and Technology*. Jordan: Royal Society for the Conservation of Nature.
Salameh E and Wl-Naser H (1999) Does the actual drop in Dead Sea level reflect the development of water sources within its drainage basin? *Acta Hydrochimica et Hydrobiologica* 27: 5–11.
Sami K (1992) Recharge mechanisms and geochemical processes in a semi-arid sedimentary basin, Eastern Cape, South Africa. *Journal of Hydrology* 139: 27–48.
Sánchez E, Gallardoa C, Gaertner MA, Arribas A, and Castro M (2004) Future climate extreme events in the Mediterranean simulated by a regional climate model: A first approach. *Global and Planetary Change* 44: 163–180.
Sánchez-Martos F and Pulido-Bosch A (1999) Boron and the origin of salinization in an aquifer in southeast Spain. *Comptes Rendus de l'Académie des Sciences – Series IIA – Earth and Planetary Sciences* 328: 751–757.
Sánchez-Martos F, Pulido-Bosch A, Molina-Sánchez L, and Vallejos-Izquierdo A (2002) Identification of the origin of salinization in groundwater using minor ions (Lower Andarax, Southeast Spain). *Science of the Total Environment* 297: 43–58.
Sánz E, Ayora C, and Soler A (2007) Tracing salinity sources of S'Almadrava karstic brackish spring (Mallorca, Spain) with sulfur and oxygen isotopes. In: Bullen TD and Wang Y (eds.) *Proceedings of the 12th International Symposium on Water–Rock Interaction*, Kunming, China, 31 July–5 August 2007, *Water–Rock Interaction*, vols. 1 and 2. London: Taylor and Francis.
Sapanov MK (2000) Water uptake by trees on different soils in the Northern Caspian region. *Eurasian Soil Science* 33: 1157–1165.
Sarin P, Snoeyink VL, Lytle DA, and Kriven WM (2004) Iron corrosion scales: Model for scale growth, iron release, and colored water formation. *Journal of Environmental Engineering – ASCE* 130: 364–373.
Sauvant MP and Pepin D (2000) Geographic variation of the mortality from cardiovascular disease and drinking water in a French small area (Puy de Dome). *Environmental Research* 84: 219–227.
Sauvant MP and Pepin D (2002) Drinking water and cardiovascular disease. *Food and Chemical Toxicology* 40: 1311–1325.

Sauvet-Goichon B (2007) Ashkelon desalination plant – A successful challenge. *Desalination* 203: 75–81.

Sayles FL and Mangelsdorf PC Jr. (1977) The equilibration of clay minerals with sea water: Exchange reactions. *Geochimica et Cosmochimica Acta* 41: 951–960.

Scanlon BR, Nicot JP, Reedy RC, Kurtzman D, Mukherjee A, and Nordstrom DK (2009b) Elevated naturally occurring arsenic in a semiarid oxidizing system, Southern High Plains aquifer, Texas, USA. *Applied Geochemistry* 24: 2061–2071.

Scanlon BR, Reedy RC, Stonestrom DA, Prudic DE, and Dennehy KF (2005) Impact of land use and land cover change on groundwater recharge and quality in the southwestern US. *Global Change Biology* 11: 1577–1593.

Scanlon BR, Stonestrom DA, Reedy RC, Leaney FW, Gates J, and Cresswell RG (2009a) Inventories and mobilization of unsaturated zone sulfate, fluoride, and chloride related to land use change in semiarid regions, southwestern United States and Australia. *Water Resources Research* 45: W00A18. http://dx.doi:10.1029/2008wr006963.

Schoups G, Hopmans JW, Young CA, et al. (2005) Sustainability of irrigated agriculture in the San Joaquin Valley, California. *Proceedings of the National Academy of Sciences of the United States of America* 102: 15352–15356.

Schroeder RA, Orem WH, and Kharaka YK (2002) Chemical evolution of the Salton Sea, California: Nutrient and selenium dynamics. *Hydrobiologia* 473: 23–45.

Schroeder RA and Rivera M (1993) Physical, chemical and biological data for detailed study of irrigation drainage in the Salton Sea area, California. *US Geological Survey Open-File report 93-83*. Menlo Park, CA: US Geological Survey.

Schroeder RA, Setmire JG, and Densmore JN (1991) Use of stable isotopes, tritium, soluble salts, and redox-sensitive elements to distinguish ground water from irrigation water in the Salton Sea basin. In: Ritter WF (ed.) *Irrigation and Drainage*, pp. 524–530, 1991 National Conference, July 22–26, 1991, Honolulu, Hawaii: American Society of Civil Engineers.

Scialli AR, Bonde JP, Brüske-Hohlfeld I, Culver BD, Li Y, and Sullivan FM (2010) An overview of male reproductive studies of boron with an emphasis on studies of highly exposed Chinese workers. *Reproductive Toxicology* 29: 10–24.

Scott BJ, Ridley AM, and Conyers MK (2000) Management of soil acidity in long-term pastures of south-eastern Australia: A review. *Australian Journal of Experimental Agriculture* 40: 1173–1198.

Serageldin I (2000) World's Rivers in Crisis: Some are Dying; Others Could Die. Online Available at http://www.worldwatercouncil.org/Vision/6902B03438178538C125683A004BE974.htm (accessed June 2011).

Shalev E, Lyakhovsky V, and Yechieli Y (2006) Salt dissolution and sinkhole formation along the Dead Sea shore. *Journal of Geophysical Research* 111: B03102. http://dx.doi:10.1029/2005jb004038.

Shanyengana ES, Seely MK, and Sanderson RD (2004) Major-ion chemistry and ground-water salinization in ephemeral floodplains in some arid regions of Namibia. *Journal of Arid Environments* 57: 211–223.

Shavit U, Holtzman R, Segal M, et al. (2002) Water sources and quality along the Lower Jordan River, regional study. In: Rubin H, Nachtnebel P, Shamir U, and Furst J (eds.) *Water Resources Quality, 4th International Austrian-Israeli Technion Symposium, 23-25 April, 2001,* Vienna, Austria. pp. 127–148.

Shiklomanov IA (1997) *Comprehensive Assessment of the Freshwater Resources of the World*. Stockholm: United Nation Commission for Sustainable Development, World Meteorological Organization and Stockholm Environment Institute.

Shimojimaa E, Yoshioka R, and Tamagawa I (1996) Salinization owing to evaporation from bare-soil surfaces and its influences on the evaporation. *Journal of Hydrology* 178: 109–136.

Singh SK, Trivedi JR, Pande K, Ramesh R, and Krishnaswami S (1998) Chemical and strontium, oxygen, and carbon isotopic compositions of carbonates from the Lesser Himalaya: Implications to the strontium isotope composition of the source waters of the Ganga, Ghaghara, and the Indus rivers. *Geochimica et Cosmochimica Acta* 62: 743–755.

Sivan O, Yechieli Y, Herut B, and Lazar B (2005) Geochemical evolution and timescale of seawater intrusion into the coastal aquifer of Israel. *Geochimica et Cosmochimica Acta* 69: 579–592.

Smith JP, Bullen TD, Brabander DJ, and Olsen CR (2009) Strontium isotope record of seasonal scale variations in sediment sources and accumulation in low-energy, subtidal areas of the lower Hudson River estuary. *Chemical Geology* 264: 375–384.

Smith TE, Grattan SR, Grieve CM, Poss JA, and Suarez DL (2010) Salinity's influence on boron toxicity in broccoli: I. Impacts on yield, biomass distribution, and water use. *Agricultural Water Management* 97: 777–782.

Sotiropoulos TE, Therios IN, and Dimassi KN (1999) Calcium application as a means to improve tolerance of kiwifruit (*Actinidia deliciosa* L.) to boron toxicity. *Scientia Horticulturae* 81: 443–449.

Southard GM, Fries LT, and Barkoh A (2010) *Prymnesium parvum*: The Texas experience. *Journal of the American Water Resources Association* 46: 14–23.

Sowers J, Vengosh A, and Weinthal E (2011) Climate change, water resources, and the politics of adaptation in the Middle East and North Africa. *Climatic Change* 104: 599–627.

Spencer RJ, Eugster HP, Jones BF, and Rettig SL (1985) Geochemistry of Great Salt Lake, Utah. 1. Hydrochemistry since 1850. *Geochimica et Cosmochimica Acta* 49: 727–737.

Spivack AJ, Palmer MR, and Edmond JM (1987) The sedimentary cycle of boron isotopes. *Geochimica et Cosmochimica Acta* 51: 1939–1949.

Sposito GA (1984) *The Surface Chemistry of Soils*. New York: Oxford University Press.

Stanton J, Kent Olson D, Brock JH, and Gordon RS (2001) The environmental and economic feasibility of alternative crops in arid areas: Considering mesquite in Baja California, Mexico. *Journal of Arid Environments* 48: 9–22.

Starinsky A (1974) *Relationship Between Calcium-Chloride Brines and Sedimentary Rocks in Israel*. PhD Thesis, The Hebrew University.

Starinsky A, Bielski M, Ecker A, and Steinitz G (1983a) Tracing the origin of salts in groundwater by Sr isotopic composition (the Crystalline Complex of the southern Sinai, Egypt). *Chemical Geology* 41: 257–267.

Starinsky A, Bielski M, Lazar B, Steinitz G, and Raab M (1983b) Strontium isotope evidence on the history of oilfield brines, Mediterranean Coastal Plain, Israel. *Geochimica et Cosmochimica Acta* 47: 687–695.

Starinsky A, Bielski M, Lazar B, Wakshal E, and Steinitz G (1980) Marine $^{87}Sr/^{86}Sr$ ratios from the Jurassic to Pleistocene: Evidence from groundwaters in Israel. *Earth and Planetary Science Letters* 47: 75–80.

Stein M, Starinsky A, Katz A, Goldstein SL, Machlus M, and Schramm A (1997) Strontium isotopic, chemical, and sedimentological evidence for the evolution of Lake Lisan and the Dead Sea. *Geochimica et Cosmochimica Acta* 61: 3975–3992.

Stigter TY, van Ooijen SPJ, Post VEA, Appelo CAJ, and Carvalho Dill AMM (1998) A hydrogeological and hydrochemical explanation of the groundwater composition under irrigated land in a Mediterranean environment, Algarve, Portugal. *Journal of Hydrology* 208: 262–279.

Stiller M, Rosenbaum JM, and Nishri A (2009) The origin of brines underlying Lake Kinneret. *Chemical Geology* 262: 293–309.

Stonestrom DA, Scanlon BR, and Zhang L (2009) Introduction to special section on Impacts of Land Use Change on Water Resources. *Water Resources Research* 45: W00A00. http://dx.doi:10.1029/2009WR007937.

Stotler RL, Frape SK, Ruskeeniemi T, Ahonen L, Onstott TC, and Hobbs MY (2009) Hydrogeochemistry of groundwaters in and below the base of thick permafrost at Lupin, Nunavut, Canada. *Journal of Hydrology* 373: 80–95.

Stringfield VT and LeGrand HE (1969) Relation of sea water to fresh water in carbonate rocks in coastal areas, with special reference to Florida, U.S.A., and Cephalonia (Kephallinia), Greece. *Journal of Hydrology* 9: 387–404.

Stumm W and Morgan JJ (1995) *Aquatic Chemistry: Chemical Equilibria and Rates in Natural Waters*. New York: John Wiley & Sons.

Sturchio NC, Banner JL, Binz CM, Heraty LB, and Musgrove M (2001) Radium geochemistry of ground waters in Paleozoic carbonate aquifers, midcontinent, USA. *Applied Geochemistry* 16: 109–122.

Sturchio NC, Bohlke JK, and Markun FJ (1993) Radium isotope geochemistry of thermal waters, Yellowstone National Park, Wyoming, USA. *Geochimica et Cosmochimica Acta* 57: 1203–1214.

Su CM and Suarez DL (1995) Coordination of adsorbed boron – A FTIR spectroscopic study. *Environmental Science & Technology* 29: 302–311.

Suarez DL (1989) Impact of agricultural practices on groundwater salinity. *Agriculture Ecosystems and Environment* 26: 215–227.

Sukhija BS (1996) Differential of paleomarine and modern seawater intruded salinities in coastal groundwaters (of Karaikal and Tanjavur, India) based on inorganic chemistry, organic biomarker fingerprints and radiocarbon dating. *Journal of Hydrology* 174: 173–201.

Sultan M, Sturchio N, Sefry SA, Milewski A, Becker R, Nasr I, and Sagintayev Z (2008) Geochemical, isotopic, and remote sensing constraints on the origin and evolution of the Rub Al Khali aquifer system, Arabian Peninsula. *Journal of Hydrology* 356: 70–83.

Suppan P, Kunstmann H, Heckel A, and Rimmer A (eds.) (2008) *Impact of Climate Change on Water Availability in the Near East*. Berlin: Springer.

Szabo Z and Zapecza OS (1987) Relation between radionuclide activities and chemical constituents in groundwater of Newark Basin, New Jersey. In: Graves G (ed.) *Radon, Radium, and other Radioactivity in Ground Water*. London: Lewis.

Szynkiewicz A, Witcher JC, Modelska M, Borrok DM, and Pratt LM (2011) Anthropogenic sulfate loads in the Rio Grande, New Mexico (USA). *Chemical Geology* 283: 194–209.

Tanji K and Valoppi L (1989) Groundwater contamination by trace elements. *Agriculture Ecosystems and Environment* 26: 229–274.

Tarchitzky J, Golobati Y, Keren R, and Chen Y (1999) Wastewater effects on montmorillonite suspensions and hydraulic properties of sandy soils. *Soil Science Society of America Journal* 63: 554–560.

Tarchouna LG, Merdy P, Raynaud M, Pfeifer HR, and Lucas Y (2010) Effects of long-term irrigation with treated wastewater. Part I: Evolution of soil physico-chemical properties. *Applied Geochemistry* 25: 1703–1710.
Tedeschi A, Beltrun A, and Arages R (2001) Irrigation management and hydrosalinity balance in a semi-arid area of the middle Ebro river basin (Spain). *Agricultural Water Management* 49: 31–50.
Thomas MA (2000) The effect of residential development on ground-water quality near Detroit, Michigan. *Journal of the American Water Resources Association* 36: 1023–1038.
Thompson JAJ, Davis JC, and Drew RE (1976) Toxicity, uptake and survey studies of boron in the marine environment. *Water Research* 10: 869–875.
Timms BV (2005) Salt lakes in Australia: Present problems and prognosis for the future. *Hydrobiologia* 552: 1–15.
Todd DK (1989) *Sources of Saline Intrusion in the 400-foot Aquifer, Castroville Area, California*. Salinas, CA: Monterey County Flood Control and Water Conservation District.
Tomita J, Satake H, Fukuyama T, Sasaki K, Sakaguchi A, and Yamamoto M (2010) Radium geochemistry in Na-Cl type groundwater in Niigata Prefecture, Japan. *Journal of Environmental Radioactivity* 101: 201–210.
Torfstein A, Gavrieli I, and Stein M (2005) The sources and evolution of sulfur in the hypersaline Lake Lisan (paleo-Dead Sea). *Earth and Planetary Science Letters* 236: 61–77.
Torssander P, Morth CM, and Kumpulainen R (2006) Chemistry and sulfur isotope investigation of industrial wastewater contamination into groundwater aquifers, Pitea County, N. Sweden. *Journal of Geochemical Exploration* 88: 64–67.
Tu KL, Nghiem LD, and Chivas AR (2011) Coupling effects of feed solution pH and ionic strength on the rejection of boron by NF/RO membranes. *Chemical Engineering Journal* 168: 700–706.
Tweed S, Leblanc M, and Cartwright I (2009) Groundwater-surface water interaction and the impact of a multi-year drought on lakes conditions in South-East Australia. *Journal of Hydrology* 379: 41–53.
US Bureau of Reclamation (2003) Quality of Water: Colorado River Basin. *Progress Report No. 21*, Washington, DC: US Department of the Interior.
US Department of the Interior (2003) Colorado River Basin Salinity Control Program. Online Available at http://www.usbr.gov/uc/progact/salinity/ (accessed June 2011).
US Environmental Protection Agency (EPA) (2000) *National Primary Drinking Water Regulations; Radionuclides; Final Rule*. US Environmental Protection Agency.
US Environmental Protection Agency (EPA) (2011a) National Recommended Water Quality Criteria: Criterion Continuous Concentration. Online Available at http://www.epa.gov/waterscience/criteria/wqctable/index.html (accessed June 2011).
US Environmental Protection Agency (EPA) (2011b) Drinking Water Contaminants. Online Available at http://water.epa.gov/drink/contaminants/index.cfm (accessed June 2011).
US Environmental Protection Agency (EPA) (2012) Stage 2 Disinfectants and Disinfection Byproducts Rule. Online Availble at http://water.epa.gov/lawsregs/rulesregs/sdwa/stage2/regulations.cfm (accessed July 2012).
Uyak V and Toroz I (2007) Investigation of bromide ion effects on disinfection by-products formation and speciation in an Istanbul water supply. *Journal of Hazardous Materials* 149: 445–451.
Vance GF and David MB (1991) Chemical characteristics and acidity of soluble organic substances from a northern hardwood forest floor, central Maine, USA. *Geochimica et Cosmochimica Acta* 55: 3611–3625.
Vanderzalm JL, Jeuken BM, Wischusen JDH, et al. (2011) Recharge sources and hydrogeochemical evolution of groundwater in alluvial basins in arid central Australia. *Journal of Hydrology* 397: 71–82.
Vengosh A (1998) The isotopic composition of anthropogenic boron and its potential impact on the environment. *Biological Trace Element Research* 66: 145–151.
Vengosh A, Barth S, Heumann KG, and Eisenhut S (1999a) Boron isotopic composition of freshwater lakes from central Europe and possible contamination sources. *Acta Hydrochimica et Hydrobiologica* 27: 416–421.
Vengosh A and Benzvi A (1994) Formation of salt plume in the coastal plain aquifer of Israel – The Beer Toviyya region. *Journal of Hydrology* 160: 21–52.
Vengosh A, Chivas AR, McCulloch MT, Starinsky A, and Kolodny Y (1991a) Boron isotope geochemistry of Australian salt lakes. *Geochimica et Cosmochimica Acta* 55: 2591–2606.
Vengosh A, Chivas AR, Starinsky A, Kolodny Y, Baozhen Z, and Pengxi Z (1995) Chemical and boron isotope compositions of non-marine brines from the Qaidam Basin, Qinghai, China. *Chemical Geology* 120: 135–154.
Vengosh A, Farber E, Shavit U, Holtzman R, Segal M, Gavrieli I, and Bullen TM (2001) Exploring the sources of salinity in the Middle East: a hydrologic, geochemical and isotopic study of the Jordan River. In: Cidu R (ed.) *10th International Symposium on Water-Rock Interaction, WRI-10, 2001b Sardinia, Italy*, pp. 71–79. Amsterdam: A.A. Balkema.
Vengosh A, Gill J, Davisson ML, and Hudson GB (2002) A multi-isotope (B, Sr, O, H, and C) and age dating (^{3}H–^{3}He and ^{14}C) study of groundwater from Salinas Valley, California: Hydrochemistry, dynamics, and contamination processes. *Water Resources Research* 38: 1008. http://dx.doi:10.1029/2001WR000517.
Vengosh A, Hening S, Ganor J, et al. (2007) New isotopic evidence for the origin of groundwater from the Nubian Sandstone Aquifer in the Negev, Israel. *Applied Geochemistry* 22: 1052–1073.
Vengosh A, Heumann KG, Juraske S, and Kasher R (1994) Boron isotope application for tracing sources of contamination in groundwater. *Environmental Science & Technology* 28: 1968–1974.
Vengosh A, Hirschfeld D, Vinson D, et al. (2009) High naturally occurring radioactivity in fossil groundwater from the Middle East. *Environmental Science & Technology* 43: 1769–1775.
Vengosh A and Keren R (1996) Chemical modifications of groundwater contaminated by recharge of treated sewage effluent. *Journal of Contaminant Hydrology* 23: 347–360.
Vengosh A, Kloppmann W, Marei A, et al. (2005) Sources of salinity and boron in the Gaza strip: Natural contaminant flow in the southern Mediterranean coastal aquifer. *Water Resources Research* 41: W01013. http://dx.doi:10.1029/2004WR003344.
Vengosh A and Pankratov I (1998) Chloride/bromide and chloride/fluoride ratios of domestic sewage effluents and associated contaminated groundwater. *Ground Water* 36: 815–824.
Vengosh A and Rosenthal E (1994) Saline groundwater in Israel: Its bearing on the water crisis in the country. *Journal of Hydrology* 156: 389–430.
Vengosh A and Spivack AJ (2000) Boron in Ground Water. In: Cook P and Herczeg A (eds.) *Environmental Tracers in Subsurface Hydrology*, pp. 479–485. Boston, MA: Kluwer.
Vengosh A, Spivack AJ, Artzi Y, and Ayalon A (1999b) Geochemical and boron, strontium, and oxygen isotopic constraints on the origin of the salinity in groundwater from the Mediterranean coast of Israel. *Water Resources Research* 35: 1877–1894.
Vengosh A, Starinsky A, Kolodny Y, and Chivas AR (1991b) Boron isotope geochemistry as a tracer for the evolution of brines and associated hot springs from the Dead Sea, Israel. *Geochimica et Cosmochimica Acta* 55: 1689–1695.
Vengosh A, Starinsky A, Kolodny Y, Chivas AR, and Raab M (1992) Boron isotope variations during fractional evaporation of sea water: New constraints on the marine vs. nonmarine debate. *Geology* 20: 799–802.
Viero AP, Roisenberg C, Roisenberg A, and Vigo A (2009) The origin of fluoride in the granitic aquifer of Porto Alegre, Southern Brazil. *Environmental Geology* 56: 1707–1719.
Vinson DS (2011) *Radium Isotope Geochemistry in Groundwater Systems: The Role of Environmental Factors*. PhD Thesis, Duke University.
Vinson DS, Schwartz HG, Dwyer GS, and Vengosh A (2011) Evaluating salinity sources of groundwater and implications for sustainable reverse osmosis desalination in coastal North Carolina, USA. *Hydrogeology Journal* 19: 981–994.
Vinson DS, Vengosh A, Hirschfeld D, and Dwyer GS (2009) Relationships between radium and radon occurrence and hydrochemistry in fresh groundwater from fractured crystalline rocks, North Carolina (USA). *Chemical Geology* 260: 159–171.
Vorosmarty CJ, Green P, Salisbury J, and Lammers RB (2000) Global water resources: Vulnerability from climate change and population growth. *Science* 289: 284–288.
Voutchkov N (2011) Overview of seawater concentrate disposal alternatives. *Desalination* 273: 205–219.
Waggott A (1969) An investigation of the potential problem of increasing boron concentrations in rivers and water courses. *Water Research* 3: 749–765.
Waldmann N, Starinsky A, and Stein M (2007) Primary carbonates and Ca-chloride brines as monitors of a paleo-hydrological regime in the Dead Sea basin. *Quaternary Science Reviews* 26: 2219–2228.
Walker M, Seiler RL, and Meinert M (2008) Effectiveness of household reverse-osmosis systems in a Western US region with high arsenic in groundwater. *Science of the Total Environment* 389: 245–252.
Wang WX, Vinocur B, and Altman A (2003) Plant responses to drought, salinity and extreme temperatures: Towards genetic engineering for stress tolerance. *Planta* 218: 1–14.
Wang Y, Chen X, Meng G, Wang S, and Wang Z (2000) On changing trends of δD during seawater freezing and evaporation. *Cold Regions Science and Technology* 31: 27–31.
Wardlaw GD and Valentine DL (2005) Evidence for salt diffusion from sediments contributing to increasing salinity in the Salton Sea, California. *Hydrobiologia* 533: 77–85.

Warner NR, Lgourna Z, Bouchaou L, et al. (2013) Integration of geochemical and isotopic tracers for elucidating water sources and salinization of shallow aquifers in the sub-Saharan Drâa Basin, Morocco. *Applied Geochemistry* (in press; http://www.sciencedirect.com/science/article/pii/S088329271300070X).

Warner NR, Jackson RB, Darrah TH, et al. (2012) Geochemical evidence for possible natural migration of Marcellus Formation brine to shallow aquifers in Pennsylvania. *Proceedings of the National Academy of Sciences of the United States of America* 109: 11961–11966.

Warner N, Lgourna Z, Boutaleb S, et al. (2010) A geochemical approach for the evaluation of water availability and salinity in closed basins: The Draa Basin, Morocco. *American Geophysical Union, Fall Meeting*, San Francisco, December 2010.

Weaver TR, Frape SK, and Cherry JA (1995) Recent cross-formational fluid-flow and mixing in the shallow Michigan Basin. *Geological Society of America Bulletin* 107: 697–707.

Weber B, Avnimelech Y, and Juanico M (1996) Salt enrichment of municipal sewage: New prevention approaches in Israel. *Environmental Management* 20: 487–495.

Weber B and Juanicó M (2004) Salt reduction in municipal sewage allocated for reuse: The outcome of a new policy in Israel. *Water Science & Technology* 50: 17–22.

Webster IT, Hancock GJ, and Murray AS (1995) Modeling the effect of salinity on radium adsorption from sediments. *Geochimica et Cosmochimica Acta* 59: 2469–2476.

Weinthal ES (2002) *State Making and Environmental Cooperation: Linking Domestic and International Politics in Central Asia*. Cambridge, MA: MIT Press.

Weinthal E, Vengosh A, Marei A, Gutierrez A, and Kloppmann W (2005) The water crisis in the Gaza strip: Prospects for resolution. *Ground Water* 43: 653–660.

Weisbrod N, Nativh R, Adar KM, and Ronend D (2000) Salt accumulation and flushing in unsaturated fractures in an arid environment. *Ground Water* 38: 452–461.

Westcot DW (1988) Reuse and disposal of higher salinity subsurface drainage water – A review. *Agricultural Water Management* 14: 483–511.

White AF, Bullen TD, Vivit DV, Schulz MS, and Clow DW (1999) The role of disseminated calcite in the chemical weathering of granitoid rocks. *Geochimica et Cosmochimica Acta* 63: 1939–1953.

White I, Macdonald BCT, Somerville PD, and Wasson R (2009) Evaluation of salt sources and loads in the upland areas of the Murray-Darling Basin, Australia. *Hydrological Processes* 23: 2485–2495.

Wicks CM and Herman JS (1996) Regional hydrogeochemistry of a modern coastal mixing zone. *Water Resources Research* 32: 401–407.

Wicks CM, Herman JS, Randazzo AF, and Jee JL (1995) Water–rock interactions in a modern coastal mixing zone. *Geological Society of America Bulletin* 107: 1023–1032.

Widory D, Kloppmann W, Chery L, Bonnin J, Rochdi H, and Guinamant J-L (2004) Nitrate in groundwater: an isotopic multi-tracer approach. *Journal of Contaminant Hydrology* 72: 165–188.

Widory D, Petelet-Giraud E, Negrel P, and Ladouche B (2005) Tracking the sources of nitrate in groundwater using coupled nitrogen and boron isotopes: A synthesis. *Environmental Science & Technology* 39: 539–548.

Williams AE (1997) Stable isotope tracers: Natural and anthropogenic recharge, Orange County, California. *Journal of Hydrology* 201: 230–248.

Williams DD, Williams NE, and Cao Y (2000) Road salt contamination of groundwater in a major metropolitan area and development of a biological index to monitor its impact. *Water Research* 34: 127–138.

Williams J, Walker GR, and Hatton TJ (2002) Dryland salinization: A challenge for land and water management in the Australian landscape. In: Haygarth PM and Jarvis SC (eds.) *Agriculture, Hydrology, and Water Quality*. Wallingford, UK: CAB International.

Williams LB and Hervig RL (2004) Boron isotope composition of coals: A potential tracer of organic contaminated fluids. *Applied Geochemistry* 19: 1625–1636.

Williams WD (2001a) Anthropogenic salinisation of inland waters. *Hydrobiologia* 466: 329–337.

Williams WD (2001b) Salinization: Unplumbed salt in a parched landscape. *Water Science & Technology* 43: 85–91.

Williams WD (2002) Environmental threats to salt lakes and the likely status of inland saline ecosystems in 2025. *Environmental Conservation* 29: 154–167.

Wilmoth BM (1972) Salty ground water and meteoric flushing of contaminated aquifers in West Virginia. *Ground Water* 10: 99–106.

Wilson TP and Long DT (1993) Geochemistry and isotope chemistry of Ca–Na–Cl brines in Silurian strata, Michigan Basin, U.S.A. *Applied Geochemistry* 8: 507–524.

Wood WW, Kraemer TF, and Shapiro A (2004) Radon (^{222}Rn) in ground water of fractured rocks: A diffusion/ion exchange model. *Ground Water* 42: 552–567.

Woods TL, Fullagar PD, Spruill RK, and Sutton LC (2000) Strontium isotopes and major elements as tracers of ground water evolution: Example from the Upper Castle Hayne Aquifer of North Carolina. *Ground Water* 38: 762–771.

Xue S, Zhao QL, Wei LL, and Jia T (2008) Effect of bromide ion on isolated fractions of dissolved organic matter in secondary effluent during chlorination. *Journal of Hazardous Materials* 157: 25–33.

Yamanaka M and Kumagai Y (2006) Sulfur isotope constraint on the provenance of salinity in a confined aquifer system of the southwestern Nobi Plain, central Japan. *Journal of Hydrology* 325: 35–55.

Yechieli Y, Abelson M, Bein A, Crouvi O, and Shtivelman V (2006) Sinkhole "swarms" along the Dead Sea coast: Reflection of disturbance of lake and adjacent groundwater systems. *Geological Society of America Bulletin* 118: 1075–1087.

Yechieli Y, Gavrieli I, Berkowitz B, and Ronen D (1998) Will the Dead Sea die? *Geology* 26: 755–758.

Yechieli Y, Kafri U, and Sivan O (2009) The inter-relationship between coastal sub-aquifers and the Mediterranean Sea, deduced from radioactive isotopes analysis. *Hydrogeology Journal* 17: 265–274.

Yechieli Y, Ronen D, and Kaufman A (1996) The source and age of groundwater brines in the Dead Sea area, as deduced from ^{36}Cl and ^{14}C. *Geochimica et Cosmochimica Acta* 60: 1909–1916.

Yechieli Y and Sivan O (2011) The distribution of saline groundwater and its relation to the hydraulic conditions of aquifers and aquitards: Examples from Israel. *Hydrogeology Journal* 19: 71–81.

Yechieli Y, Sivan O, Herut B, Vengosh A, Ronen D, and Lazar B (2000) ^{14}C and tritium dating of seawater intruding into the Israeli coastal aquifer. *Radiocarbon* 43: 773–781.

Yechieli Y, Starinsky A, and Rosenthal E (1992) Evolution of brackish groundwater in a typical arid region – Northwern Arava Rift-Valley, Southern Israel. *Applied Geochemistry* 7: 361–374.

Yermiyahu U, Tal A, Ben-Gal A, Bar-Tal A, Tarchitzky J, and Lahav O (2007) Environmental science – Rethinking desalinated water quality and agriculture. *Science* 318: 920–921.

Yu XY, Amrhein C, Zhang YQ, and Matsumoto MR (2006) Factors influencing arsenite removal by zero-valent iron. *Journal of Environmental Engineering - ASCE* 132: 1459–1469.

Zavialov PO, Ni AA, Kudyshkin TV, Ishniyazov DP, Tomashevskaya IG, and Mukhamedzhanova D (2009) Ongoing changes of ionic composition and dissolved gases in the Aral Sea. *Aquatic Geochemistry* 15: 263–275.

11.10 Acid Rain – Acidification and Recovery

SA Norton, University of Maine, Orono, ME, USA
J Kopáček, Institute of Hydrobiology, Ceske Budejovice, Czech Republic
IJ Fernandez, University of Maine, Orono, ME, USA

This article is a revision of the previous edition article by S.A. Norton, J. Veselý, volume 9, pp. 367–406, © 2003, Elsevier Ltd.

11.10.1 Introduction

Air pollution by acids has been known as a problem for centuries (Brimblecombe, 1992; Camuffo, 1992; Ducros, 1845; Smith, 1872). Nevertheless, only in the mid-1900s did it become clear that it was a problem for more than just industrially developed areas and that precipitation quality could affect aquatic resources (Gorham, 1955). The last three decades of the twentieth century saw tremendous progress in the documentation of the chemistry of the atmosphere, precipitation, and the systems impacted by atmospheric deposition. Acidification in ecosystems results in chemical changes to soil, soil solutions, and surface and groundwater, which progressively increase from episodic through seasonal to chronic stages. The most fundamental changes during chronic acidification are an increase in exchangeable H^+ (hydrogen ion) or Al^{3+} (aluminum) in soils, an increase in H^+ activity (≅concentration) and Al^{3+} in water in contact with that soil, and a decrease in alkalinity (ALK) in waters draining from the watershed. As terrestrial systems and runoff acidify, terrestrial and aquatic biota change.

Acidic surface waters occur in many parts of the world as a consequence of natural processes and also from atmospheric deposition of strong acids (e.g., Canada, Jeffries et al., 1986; the United Kingdom, Evans and Monteith, 2001; Sweden, Swedish Environmental Protection Board, 1986; Finland, Forsius et al., 1990; Norway, Henriksen et al., 1988a; and the United States, Brakke et al., 1988). The concern over acidification in the temperate regions of the northern hemisphere has been driven by the potential for acceleration of natural acidification by pollution of the atmosphere with acidic or acidifying compounds. Atmospheric pollution (**Figure 1**) has resulted in an increased flux of acid to and through ecosystems. Depending on the ability of an ecosystem to neutralize the increased flux of acidity, acidification can increase imperceptibly or accelerate at rates that endanger ecosystem services and function.

Concerns about acid (or acidic) rain in its modern sense were publicized by Svante Odén (a Swedish soil scientist) in

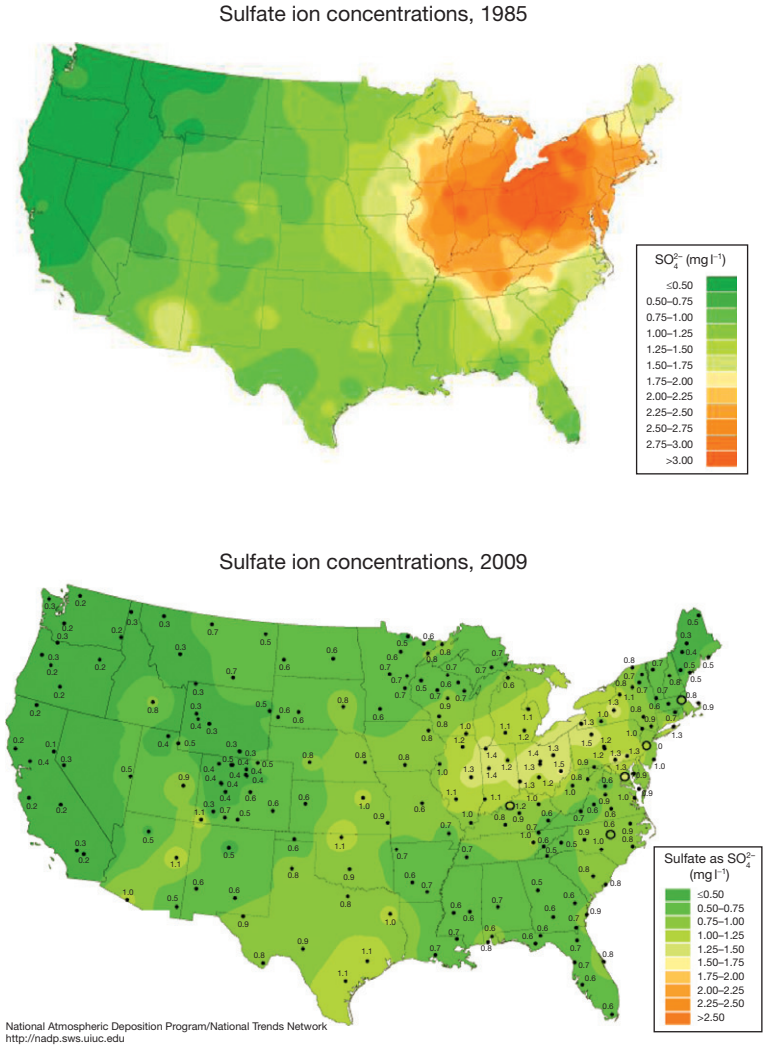

(a)

Figure 1 (Continued)

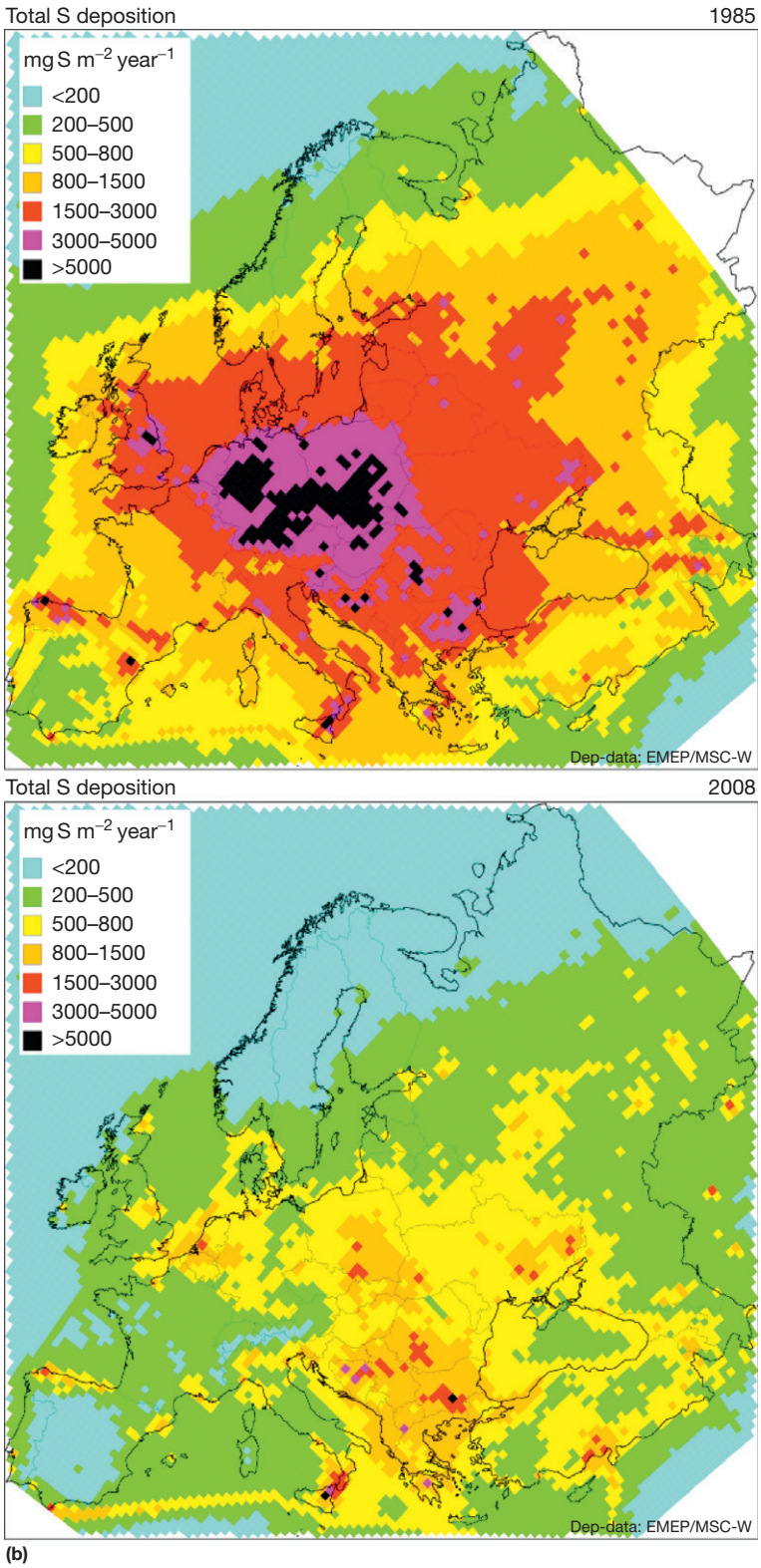

(b)

Figure 1 (a) Concentration of SO_4 in the United States for 1985 and 2009 (National Atmospheric Deposition Program) and (b) deposition of SO_4 in Europe for 1985 and 2008 (European Monitoring and Evaluation Programme (EMEP) with help from M. B. Posch).

1968 (Cowling, 1982). Odén argued, initially in the Swedish press, that long-term increases in the atmospheric deposition of acid could lower the pH of surface waters, cause a decline in fish stocks, deplete soils of nutrients, and accelerate damage to materials. By the 1970s, acidification of surface waters was reported to occur in many countries in Europe as well as North America. The late twentieth century effort to understand the impacts of acid rain was driven primarily by reports of damaged or threatened freshwater fisheries and secondarily by damaged forests. Perhaps the earliest linkage between acidic surface water and damage to fish was made by Dahl (1921) in southern Norway. There, spring runoff was sufficiently acidic to kill trout. It was not until the 1970s that a strong link was hypothesized between depressed pH, mobilization of Al^{3+} from soil, and fish status (Schofield and Trojnar, 1980). The relationship between acidification of soils and forest health started with hypotheses in the 1960s and has slowly developed. Acid rain enhances the availability of some nutrients (e.g., nitrogen (N)), and may either enhance (short term) or diminish (long term) the availability of others (e.g., calcium (Ca), magnesium (Mg), potassium (K), and phosphorus (P)). Damage to anthropogenic structures (e.g., buildings, statues), human health, and visibility also raises concern. The history of these early developments was summarized by Cowling (1982). Since the 1970s, sulfur (S) and N emissions to the atmosphere have been reduced 50–85 and 0–30%, respectively, in North America and Europe. The emission reductions have occurred as a consequence of knowledge gained, implemented policies, and economic factors. While recovery of water quality is underway in some areas, problems of acidification persist, and they are now complicated by effects of climate change (Schindler, 1997).

11.10.2 What Is Acidification?

Acidity of waters is typically expressed by the pH ($=-\log[H^+]$) as an intensity factor and by acid-neutralizing capacity (ANC), or ALK, as a capacity factor. The latter is commonly expressed in microequivalents (i.e., micromoles of charge) per liter ($\mu eq\ l^{-1}$). *Acidic* water has a pH below 7.0. Acidic water is commonly defined as having a pH below that of (distilled) water in equilibrium with atmospheric carbon dioxide (CO_2), 5.65. Whichever definition is adopted, the process of water *acidification* involves a decrease in pH and ANC, with accompanying secondary chemical changes.

Early definitions of ALK took the following form (in equivalents):

$$\text{Carbonate alkalinity} = (HCO_3^- + CO_3^{2-} + OH^-) - (H^+) \quad [1]$$

This carbonate ALK was determined by titration with acid to a known pH end point. As the understanding of water chemistry grew, it became clear that other ions played a role in ALK and a more comprehensive definition of ALK was advanced:

$$\begin{aligned}\text{Alkalinity} = {} & (HCO_3^- + CO_3^{2-} + OH^- + A^{x-} \\ & + \text{other weak acid anions}) \\ & -(H^+ + [M^{3+}(OH^-)_n]^{3-n})\end{aligned} \quad [2]$$

where A^{x-} = organic anions from dissociation of dissolved organic acids and $(M^{3+}(OH^-)_n)^{3-n}$ represents variously charged (hydroxylated) species of metals, particularly Al^{3+} and $Fe^{3+\text{ or }2+}$, in solution. The ANC of a solution can be defined as charge balance ANC (Hemond, 1990; Reuss and Johnson, 1986). In equivalents,

$$\sum(+) = \sum(-) \quad [3]$$

$$\begin{aligned}&(Ca^{2+} + Mg^{2+} + Na^+ + K^+ + [M^{3+}(OH^-)_n]^{3-n} \\ &\quad + NH_4^+ + H^+) = (OH^- + F^- + Cl^- + NO_3^- + SO_4^{2-} \\ &\quad + CO_3^{2-} + HCO_3^- + A^{x-} + \text{other weak acid anions})\end{aligned} \quad [4]$$

Rearranging we get,

$$\begin{aligned}&(Ca^{2+} + Mg^{2+} + Na^+ + K^+ + NH_4^+) \\ &\quad - (SO_4^{2-} + NO_3^- + Cl^- + F^-) = (OH^- + CO_4^{2-} \\ &\quad + HCO_3^- + A^{x-} + \text{other weak acid anions}) \\ &\quad - (H^+ + [M^{3+}(OH^-)_n]^{3-n})\end{aligned} \quad [5]$$

The right-hand side of eqn [5] is the expanded definition of ALK. Therefore,

$$\begin{aligned}&\sum(\text{Strong base cations}) - \sum(\text{Strong acid anions}) \\ &\quad = \text{alkalinity} = \text{acid neutralizing capacity} \\ &\quad = \sum(\text{Weak acid anions}) - \sum(\text{Weak acid cations})\end{aligned} \quad [6]$$

or

$$\text{ANC} = \text{ALK} = (\text{SBC}) - (\text{SAA}) = (\text{WAA}) - (\text{WAC}) \quad [7]$$

Thus, in equivalents,

$$\begin{aligned}\text{ANC} = {} & (HCO_3^- + CO_3^{2-} + OH^- + A^{x-}) \\ & - (H^+ + [M^{3+}(OH)_n]^{3-n})\end{aligned} \quad [8a]$$

or

$$\begin{aligned}\text{ANC} = {} & (Ca^{2+} + Mg^{2+} + Na^+ + K^+ + NH_4^+) \\ & - (SO_4^{2-} + NO_3^- + Cl^- + F^-)\end{aligned} \quad [8b]$$

Two ecosystem-level premises follow:

1. All elemental inorganic and biotic cycles are linked and work together toward an equilibrium; if we independently change some part of this system (e.g., H^+), all cycles shift toward a new equilibrium of the whole system.
2. Ion charge balance must prevail.

ANC is a summative term that indicates the state of acidification of the water. A declining ANC, for whatever reason, connotes ongoing acidification. According to eqn [8b], all processes adding strong acid anions (SAA) to the system without adding an equivalent amount of strong base cations (SBC) (e.g., acid rain, nitrification, mineral sulfide oxidation, S-org or S^{2-} oxidation), or removal of SBC without an equivalent amount of SAA (e.g., biomass growth, SBC depletion from soils by exchange for Al^{3+} and H^+), lead to acidification (lower ANC) of the system. In contrast, processes removing SAA without equivalent removal of SBC (denitrification, NO_3 assimilation, SO_4 reduction), or adding SBC without equivalent addition of SAA (weathering, dust deposition, liming), increase ANC.

The ANC or ALK (eqn [8a]) of solutions is commonly measured by Gran titration. In this process, some A^{x-} and $(M^{3+}(OH^-)_n)^{3-n}$ are titrated, contributing to the ANC. In this chapter, we equate ALK with the term ANC. Concentrations on the right side of eqn [2] vary with soil partial pressure of CO_2 (pCO_2), but maintain electroneutrality in combination with other dissolved species. The ANC defined by eqn [8b] is commonly calculated as the residual of individual analyses of water for SBC and SAA. The sum of errors in individual analyses, particularly if concentrations are high, can lead to substantial errors in the calculated ANC. Alternatively, in waters with high concentrations of sea salt or dissolved organic carbon (DOC), the ANC can be calculated from the right side of eqn [2] as (carbonate ALK + the estimated contribution of DOC to anions) − (estimated concentration of ionic M) (Evans et al., 2001a; Köhler et al., 1999). Each mg of DOC l^{-1} adds 3–6 μeq l^{-1} to carbonate ALK. The discrepancy between ANC and carbonate ALK, due to DOC and/or M species for low-ANC waters, may exceed 50 μeq l^{-1}.

In this chapter, we focus on acidification processes affecting surface waters that drain soils and bedrock for which chemical weathering is slow. Bedrock lithologies and soils that contain free carbonate minerals (e.g., calcite, $CaCO_3$) and/or abundant ferromagnesian silicate minerals (e.g., pyroxene, $(Ca,Mg)SiO_3$) release base cations at much higher rates (Sverdrup, 1990; White and Brantley, 1995), rapidly consuming H^+ in the process, and thus they are much less susceptible to acidification, requiring considerably more time or stronger acid to deplete base cations from the soil and bedrock.

11.10.3 Long-Term Acidification

11.10.3.1 Has Long-Term Acidification Occurred?

Prior to 1960, freshwater pH was infrequently measured and colorimetric methods for pH measurements were commonly inaccurate (Haines et al., 1983), particularly in waters with low ionic strength. Thus, reconstruction of pH for lakes and streams from the literature for even the mid-1950s is problematic. However, dated lake sediment cores have been analyzed for fossil diatom and chrysophyte assemblages. Statistical interpretation of the fossil assemblages enables inferences about longer term trends in past lake environmental conditions, especially pH (Battarbee et al., 1990; Charles and Smol, 1988; Dixit et al., 1992), and also DOC, ALK, and dissolved Al (Davis, 1987). Decreases in atmospheric deposition of acidic compounds since 1990 have coincided with increases in measured lake water ANC and pH, as well as pH inferred from fossil remains. The latter changes have been observed directly, which affirms that the reconstructions of earlier natural acidification were valid.

Reconstruction of the pH history of several northern hemisphere lakes using fossil assemblages showed that the lakes were alkaline shortly after deglaciation but had acidified markedly by the early Holocene (the last 10 000 years of earth history) (Norton et al., 2011; Pražáková et al., 2006; Renberg, 1990; Ryan and Kahler, 1987; Whitehead et al., 1986).

Neutral to alkaline pH in soil and surface water shortly after deglaciation was caused by weathering of an abundance of finely divided 'rock flour' and highly soluble minerals such as calcite (Engstrom et al., 2000) and apatite ($Ca_5(PO_4)_3(OH,F,Cl)$) (Boyle, 2007; Kopáček et al., 2007; Norton et al., 2011) to produce positive ANC in watersheds. In Sweden, for example, the initial decrease in diatom-inferred pH from as high as 8 to as low as 6 after deglaciation was followed by a long-term decrease from ~6 to 5, caused by the development of vegetation and soils, terrestrial production of DOC, and release of organic acids to some lakes (Renberg, 1990). The inferences about organic acids are borne out by speciation studies of Al in sediment cores (Kopáček et al., 2007; Norton et al., 2011). These natural soil-forming processes acidified soil and surface water over thousands of years in glaciated terrain before the onset of modern acidic precipitation ('acid rain') (Figure 2). Through time, weathering rates slowed as small particles were weathered rapidly, soluble minerals were dissolved and depleted in upper soil horizons, and incongruent weathering reactions became diffusion controlled on larger grains. As a result of declining weathering rate, natural acid inputs were

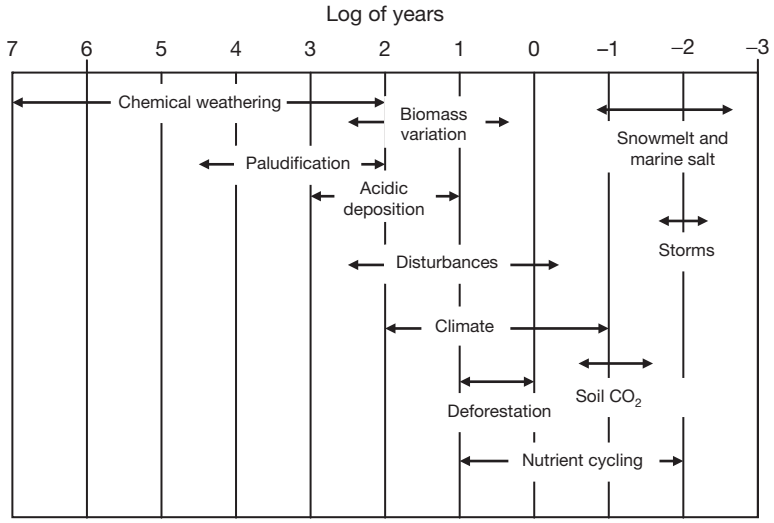

Figure 2 Timescale of processes leading to surface water acidification.

incompletely neutralized, and the pH of solutions draining from the upper soil layers to surface waters declined. Coupled biological and chemical evidence for long-term acidification is rare. Engstrom et al. (2000) studied a chronosequence (substituting space for time at one locality) of postglaciation lakes in Alaska, USA, and demonstrated declining pH and ALK with exposure time, with initial lake pHs near 8 and declining pH over several hundred to several thousand years to as low as 5. Similar conclusions were reached for a 16 600 year postglacial record for Sargent Mountain Pond, Maine, USA (Norton et al., 2011) and a somewhat shorter record from Plešné Lake, Czech Republic (Kopáček et al., 2009).

For most streams and lakes in glaciated terrain, the pH was rarely <5 until the post-1800 period. Exceptions include lakes rich in organic acidity (high DOC). Diatom-inferred pH values for soft water lakes in the Sierra Nevada Mountains (California, USA) and the European Alps showed fluctuations that were attributed to climate change during the nineteenth century (Psenner and Schmidt, 1992; Whiting et al., 1989). Cold periods were associated with lower pH values. During warm periods, the pH was higher due to increased evaporation, longer water retention times, stronger lake stratification, and enhanced assimilation of inorganic S and N. These temperature-driven fluctuations of pH were disrupted by the onset of significant acidic deposition shortly before 1900. In acid-sensitive systems, anthropogenic acidification has been much faster than natural acidification, and the pH and ANC has decreased below the natural prehistoric minima for many lakes, as inferred from diatom and chrysophyte species.

11.10.3.2 What Controls Long-Term Acidification?

Prior to acid rain, the principal sources of acid input to watersheds were from elevated CO_2 in soils (carbonic acid acidity) and DOC from the metabolism of organic matter (eqns [9a] and [9b]).

$$CO_2 + H_2O = H^+ + HCO_3^- \quad [9a]$$

$$H_n(A) = xH^+ + H_{n-x}A^{(x-)} \quad [9b]$$

Organic acidity is produced primarily in the organic-rich layer of forested ecosystems (the 'forest floor') or fens and bogs. The pH of soil solutions in organic-rich forest soils may be lower than 4 because of the dissociation of organic acids, caused largely by dissociation of carboxylic groups (−COOH). The concentration of (A^{x-}) can be estimated from chemical analyses of the major base cations, acid anions, and ALK as an 'anion deficit,' measured by titration with acid, or calculated from DOC concentrations in conjunction with models for organic acidity (Driscoll et al., 1994; Hruška et al., 2001; Köhler et al., 1999; Oliver et al., 1983). Complexation of Al and Fe by organic ligands enhances the mobilization of these metals, but at the same time reduces the toxicity of dissolved Al. Much of the DOC acidity is lost to aerobic respiration as soil solutions descend through the unsaturated mineral soil, producing substantial amounts of CO_2. Carbonic acid acidity is produced throughout the soil column but typically reaches a maximum below the forest floor. Aerobic respiration can increase the soil CO_2 pressure (pCO_2) to as much as two orders of magnitude higher than the atmospheric value to produce pHs as low as 4.5.

Natural acidity is also contributed from emissions of acidic or acidifying compounds from volcanoes (Camuffo, 1992; Pyle et al., 1996), including compounds of S, N, chloride (Cl), and NH_3 (ammonia), from the ocean (e.g., methylsulfonate) (Charlson et al., 1987), and from wetlands (e.g., H_2S) (Gorham et al., 1987). Ecosystem conditions that have sulfide weathering or mineralization rates sufficient to supply H_2SO_4 in significant amounts over an extended period of time are rare. Where this occurs, it is most commonly caused by land disturbance associated with construction (e.g., Hindar and Lydersen, 1994), mining or quarrying activities (i.e., acid mine drainage), recent volcanism (Wood et al., 2006), or recent deglaciation (Engstrom and Wright, 1984). Certain changes in the hydrology of soils can mobilize substantial quantities of acidic compounds. For example, runoff from marine sediments in Finland, eustatically uplifted since deglaciation, has high concentrations of SO_4 from the oxidation of sulfide minerals (principally pyrite, FeS_2) contained within these postglacial marine sediments (Forsius et al., 1990). Runoff from recently drained peatlands can contain high concentrations of SO_4 derived from oxidation of sulfide minerals and organically bound S, as well as elevated DOC. Studies of the chemistry of wetlands (Bayley et al., 1988; Gorham et al., 1985) show empirically and experimentally that SO_4 from atmospheric sources or added as a treatment is removed from bog water by some combination of precipitation as sulfide minerals, transformation into reduced organic S, or reduction to H_2S with emission to the atmosphere. Reduced organic S can be reoxidized during lower groundwater levels and then leached from the system as the water table rises (Dillon et al., 1997). DOC from wetlands can contribute substantial acidity to the runoff, particularly if water tables vary.

Neutralization of soil solution acidity from any source (commonly incorrectly termed 'acid buffering,' which refers only to the resistance to change) is typically caused by the leaching of Ca from bedrock and soil. Magnesium is most commonly the second most important cation released during weathering. Rarely, there are watersheds with unusual silicate bedrock (e.g., serpentinite (serpentine, $Mg_3Si_2O_5(OH)_4$)), or unmetamorphosed ultramafic rocks (e.g., dunite (olivine, Mg_2SiO_4)) that produce Mg-HCO_3 surface waters (Krám et al., 1997) where Mg exceeds Ca in runoff. Acidification is greatest in regions where bedrock and soils are more chemically resistant to weathering, where soils and glacial deposits are thin, rainfall is greater, temperature is higher, and production of organic acids is higher. For example, much of Fennoscandinavia, Scotland, Wales, the Adirondack Mountains of New York, USA, and the Muskoka Region of Ontario and eastern Nova Scotia, Canada, have recently acidified lake districts as a consequence of atmospheric inputs of SO_4 and NO_3, in combination with granitic or quartzite/shale bedrock and relatively high concentrations of naturally occurring DOC. Surface waters draining mafic, ultramafic, or calcareous bedrock are relatively unaffected by acidification because of the high base cation weathering rates. Surface waters draining noncalcareous sandstone, granite, and schist are more likely to be impacted by acid rain (Kuylenstierna and Chadwick, 1989). The highly soluble minerals calcite and apatite are commonly

present in small amounts in many rock types. In postglacial time, these two minerals likely controlled pH and Ca in runoff for up to several thousand years before weathering rates became dominated by slower weathering silicates such as amphibole, biotite, and feldspars (Ca, Na, K, Al silicates) (Boyle, 2007).

Although weathering plays an important role in the neutralization of acid, rates at which base cations are released in natural systems from weathering are not well known. Weathering rates vary with bedrock and soil composition, concentration of organic ligands, temperature, soil moisture and pH, precipitation amounts and pH, redox (reduction/oxidation) conditions, and vegetation (see, e.g., Klaminder et al., 2011; Sverdrup, 1990; White and Brantley, 1995). Chemical weathering rates of aluminosilicate minerals increase at lower pH in laboratory experiments.

Field-based experiments have yielded a better understanding of the rate at which base cations can be supplied to offset the input of strong mineral acids (Bain and Langan, 1995; Swoboda-Colberg and Drever, 1993). For many elements, chemical budgets for watersheds have been constructed by the simplistic relationship:

$$\text{Weathering rate} = \text{stream solute output} - \text{atmospheric solute input} \quad [10]$$

Equation [10] ignores numerous quantitatively important processes including changes in biomass (living and dead), changes in exchangeable soil pools for cations and anions, contributions from dry deposition, and gaseous losses to the atmosphere (e.g., for S and N). A more comprehensive equation for a watershed element mass balance might be:

$$\begin{aligned}\text{Weathering rate} = {} & [\text{stream output} + \text{gaseous efflux}] \\ & - [\text{atmospheric input (wet)} + \text{atmospheric input (dry)}] \\ & \pm \Delta\text{biomass storage} \pm \Delta\text{secondary soil pools} \\ & (\text{e.g., exchangeable, adsorbed})\end{aligned} \quad [11]$$

Commonly, the weathering rate is calculated by adding and subtracting many fluxes, each of which is difficult to assess (Pačes, 1983; Velbel, 1985; White and Blum, 1995). No long-term calibrated watershed studies measure all these variables well and therefore the weathering rates determined from them are only approximate. For example, Bormann and Likens (1979) calculated that Ca weathering from 1963 to 1974 was approximately 11.5 kg ha^{-1} year^{-1} at Hubbard Brook Experimental Forest (HBEF), New Hampshire, USA, assuming that all the excess Ca was from weathering of primary minerals. At HBEF, surface waters have very low ALK and have likely been acidified, and they are susceptible to episodic acidification. On the basis of a more complete analysis, Bailey et al. (2003) were not able to resolve the primary weathering from depletion of exchangeable base cations from the soil. At an ecologically and geologically similar site at Bear Brook Watershed in Maine (BBWM), USA, Ca weathering rates were calculated on a similar basis. Assuming steady state for many of the unknown variables, the estimated rates ranged from 11 to 15 kg ha^{-1} year^{-1} for 1988–1992 and 1.5 kg ha^{-1} year^{-1} for 1988–2000 in the reference watershed, respectively (Norton et al., 1999; Watmough et al., 2005).

Numerous studies suggest that proportions of Ca derived from the watershed compared to the Ca derived from atmospheric inputs can be inferred by using Sr (strontium) isotope data. The Sr isotope ratios ($^{87}Sr/^{86}Sr$) for the bedrock, atmospheric input, and output are combined in a linear mixing model to infer the ultimate sources of Ca (bedrock/soil complex vs. atmosphere). The explicit assumption of this technique is that Ca and Sr behave similarly during all biogeochemical processes. This assumption has been challenged (Bullen et al., 2002).

Several studies have suggested that acid deposition accelerates weathering (e.g., Miller et al., 1993). However, Norton et al. (1999) concluded on the basis of runoff chemistry at BBWM that chemical weathering was not affected during a 20 year experimental acidification of an entire watershed (Navrátil et al., 2010). There, Swoboda-Colberg and Drever (1993) acidified in situ soil columns, after removal of the forest floor (organic horizon). They stripped exchangeable cation pools from the mineral soil with strong acid leaching until a steady-state rate of leaching of cations occurred. This steady-state loss was attributed to primary chemical weathering. The values (kg ha^{-1} year^{-1}) were 200–400 times higher than those based on the whole watershed (eqn [11], simplified). Dahlgren et al. (1990) used reconstructed soils from the same watershed and determined that experimental acidification of the columns with H_2SO_4 was accompanied by increased leaching of base cations from the exchangeable pools and dissolution of Al from a solid phase. Silica release was not enhanced by their acidic treatments. Generally, silica is relatively unchanged in nearly all field-scale acidification experiments with the major exception of the wollastonite ($CaSiO_3$) treatment at HBEF (Cho et al., 2010), suggesting no substantial change in congruent weathering rates. In summary, most field experiments and watershed studies suggest that *variations* in short-term base cation release to runoff are dominated by ion exchange equilibria or ecosystem perturbations (e.g., ice storms, wind damage, fire), not changes in weathering rates. As exchangeable base cation supplies become depleted and pH declines, mobilization of ionic Al becomes increasingly important.

Laboratory experimental rates of weathering (typically expressed as mol m^{-2} s^{-1}) are generally 2–3 orders of magnitude higher than field rates. These differences are partly an artifact of differing experimental methods, non-steady-state processes (Holdren and Adams, 1982), differences in hydrological conditions between the field and laboratory, disturbance effects, and effective mineral surface area in contact with reacting water. The chemical weathering in soil can be inhibited or virtually stopped in dry periods (Zilberbrand, 1999). Alternatively, as acidic soil solutions dry, the increasing concentrations of solutes causes pH to decline and ionic strength to increase, which should increase weathering rates in a restricted volume of soil solution. Clearly, extrapolating experimental weathering rates determined in the laboratory to the field and regionalization of the results are problematic. The balance between primary weathering sources of base cations and desorption of base cations in contributing to runoff concentrations is difficult to determine. Thus, the resilience of soils to acidification is still poorly understood. Unfortunately, accurate weathering data are important to realistically calibrate

some dynamic and static models of soil and water acidification (e.g., PROFILE, Sverdrup and De Vries, 1994; Sverdrup and Warfvinge, 1993).

Several types of evidence from soils have been used to estimate long-term weathering rates. The historical approach uses the reduction in base cation concentrations (Johansson and Tarvainen, 1997) or labile minerals (e.g., biotite and hornblende; Frogner, 1990) in the soil profile with respect to chemically unaltered C-horizon soil as an index of weathering. If the age of the soil is known (e.g., post-Wisconsinan in North America, Weichselian in northern Europe), this method provides long-term average weathering rates that are generally greater than present day rates (Klaminder et al., 2011). Weathering rate decreases with increasing soil age (Engstrom et al., 2000) and may follow a power-law equation (Taylor and Blum, 1995). Modern weathering rates could be <10% of the rate immediately after deglaciation.

The base cation status of surface water is also controlled partly by hydrology. Steeper topography generally has thinner soils, shortening contact time between soil solutions and mineral soil, thereby decreasing the rate of chemical weathering and ALK production. Seepage lakes, containing neither surface inlets nor outlets, can recharge or receive discharge from the local groundwater system. In the former case, the lake water chemistry can be similar to atmospheric deposition, modified by evaporation and in-lake processes. As groundwater flow paths change so that more water flows through a seepage lake, the ANC of the lake typically increases as a consequence of the entering ground water having been in contact with mineral soil. For all lakes, residence time of water is important in determining evaporative changes in water composition (Webster and Brezonik, 1995) and the extent to which the in-lake processes alter the acid–base status of the water inputs (see **Section 11.10.5.6**).

11.10.4 Short-Term and Episodic Acidification

Short-term (days to weeks) and episodic (hours to days) acidification events (**Figure 2**) are caused by a variety of mechanisms including pulsed inputs of water (high discharge from snowmelt or rain) causing preferential dilution of base cations, release of oxidized S and N from organic or inorganic pools (Dillon et al., 1997), atmospheric input of marine aerosols (the salt effect; Wright et al., 1988), and increased leaching of DOC (Hruška et al., 2001). These mechanisms are controlled by weather and climate change. Many aspects of episodic acidification have been thoroughly reviewed by Wigington et al. (1990).

Watersheds have five major lines of defense against short-term and episodic acidification: (1) cation desorption, (2) anion adsorption, (3) Al dissolution, (4) protonation of weak acid anions, and (5) dehydroxylation of metal species.

1. Chemical weathering of silicate minerals in soils is a relatively slow source of base cations, but the total long-term neutralization capacity of soils is typically large. In contrast, ion exchange reactions (cation and anion exchange) in soil are relatively rapid, and tend to buffer H^+, SO_4^{2-}, base cation, and ANC concentrations. The sum of the exchange sites for cations (expressed in moles of charge per kg soil) is termed the cation exchange capacity (CEC). The percentage of the cation exchange sites occupied by the base cations Ca, Mg, Na, and K is traditionally termed the base saturation (BS). The rest of the cation exchange sites are occupied primarily by Al and H. In concept, if desorption of base cations exceeds the weathering rate release of those base cations, BS of soil decreases, site occupancy by Al and H increases, and soil acidification occurs; subsequently, more of the charge balance in runoff is maintained by the export of H^+ and Al^{3+}. The soil- and surface-water thus become more susceptible to short-term and episodic acidification (Wigington et al., 1996) that can last for hours to months.
2. In soils rich in Fe and Al secondary phases, excess SO_4 from the atmosphere can be reversibly adsorbed or desorbed, thereby retarding acidification or recovery from acidification, respectively (David et al., 1991a,b; Navrátil et al., 2009). Well-drained forest soils, such as in southern Europe or the central and southern United States, that were not glaciated during the Wisconsinan, are commonly rich in sesquihydroxides (Al and Fe hydroxides) that cause high SO_4 adsorption capacity (e.g., Cosby et al., 1986). However, even young postglacial soils have an enhanced ability to adsorb SO_4 (Kahl et al., 1999).

   Substantial decreases of atmospheric input of S in Europe and North America in the last two decades (**Figure 1**) have caused a general decline in surface water SO_4 (Evans et al., 2001b; Stoddard et al., 1998). Many soils have switched from being a sink to a source of S (Driscoll et al., 1998; Prechtel et al., 2001). Fluxes of SO_4 in runoff from watersheds with thin (e.g., alpine) soil and low SO_4 adsorption capacity have decreased rapidly (Kopáček et al., 2001a) in comparison to watersheds with deeply weathered and thick soils (Alewell, 2001). Stable isotope ($\delta^{34}S$) studies and budget calculations suggest that the pool of organic S in forest floor and biological S turnover are important contributors to SO_4 export. Organic cycling of deposited atmospherically derived S plays an equally important role in polluted coniferous forests in the Czech Republic (and probably elsewhere; Houle and Carignan, 1995) where over 80% of the total S content in soils is organically bound (Novák et al., 2003). Sulfur isotope studies indicated that up to 80% of sulfate in stream water in polluted areas of the Czech Republic was organically cycled (Novák et al., 2000).
3. As the pH of soil water decreases below 5.5–5.0 and soil cation exchange sites become depleted of base cations, desorption of exchangeable Al and dissolution of solid Al secondary phases become important because Al hydrolysis increasingly dominates acid neutralization processes. For example,

$$Al(OH)_3 + 3H^+ = Al^{3+} + 3H_2O \qquad [12]$$

   Commonly, studies of changing water quality do not differentiate whether increased dissolved Al is from desorption of Al from soils, or from dissolution of a solid Al phase. Both processes have been demonstrated at some sites. In very acidic forest soils, dissolution of Fe can also contribute to acid neutralization (Borg, 1986; Matschullat et al., 1992; Norton et al., 2004; Ulrich, 1983). Dissolution of Mn solid secondary phases could be rarely important and occurs

probably only during early acidification stages when Mn is rapidly mobilized (Puhe and Ulrich, 2001).

4. Weak acid anions are loosely defined as anions from acids whose dissociation constants are in the range of pHs exhibited by surface waters (~4–11). Two important acid groups are included. In the system CO_2–H_2O, there is an equilibrium among the various C-bearing species as a consequence of CO_2 dissolving in water

$$H_2O + CO_2 = H_2CO_3 \qquad K = 10^{-1.5} \quad pK = 1.5 \qquad [13]$$

$$H_2CO_3 = H^+ + HCO_3^- \qquad K = 10^{-6.5} \quad pK = 6.5 \qquad [14]$$

$$HCO_3^- = H^+ + CO_3^{2-} \qquad K = 10^{-10.3} \quad pK = 10.3 \qquad [15]$$

For eqn [14], H_2CO_3 and HCO_3^- are present in equal concentrations at pH = 6.5. Any process not involving dissolving or evasion of CO_2 that tends to lower the pH will result in production of H_2CO_3 at the expense of HCO_3^-, a process called protonation. Carbonate ALK (eqn [1]) is reduced.

Dissolved organic acid typically consists of a mixture of organic acids whose p*K*s (the negative log of the equilibrium constant) may range from very small values (strong organic acids) to as high as the bicarbonate–carbonic acid p*K* (eqn [14]) (weak organic acids). Any weak organic anions are also subject to protonation (Hruška et al., 2003; Oliver et al., 1983), supplying additional acid neutralization capacity to the soil water and surface water (eqn [2]).

5. Some dissolved metals, for example, Al, Fe, and Mn, are speciated with differing amounts of hydroxyl, for example, Al^{3+}, $Al(OH)^{2+}$, $Al(OH)_2^+$, $Al(OH)_3$, and $Al(OH)_4^-$. The relative abundance of each species is a function of pH, similar to organic acids and the CO_2-bearing species. Thus, a process that tends to acidify the water can be partly neutralized by consumption of H^+, which can be represented as, for example,

$$Al(OH)^{2+} + H^+ = Al^{3+} + H_2O \qquad [16]$$

11.10.5 Drivers of Short-Term and Episodic Acidification

Susceptibility to episodic acidification is increased because of longer term acidification, driven by excess loading of SO_4 and NO_3, higher ambient DOC, and aggrading biomass, all of which chronically lower base cations, pH, and ANC.

11.10.5.1 High Discharge from Snowmelt and Rain

During snowmelt, acidic pollutants are preferentially eluted. Consequently, acidic pulses are released and may enter streams and lakes, particularly early in the snowmelt process, and these solutions may have little contact with soils (Jeffries, 1990; Johannessen and Henriksen, 1978). Base cation concentrations become diluted concurrently with elevated concentrations of SAA. The associated pH and ALK depressions can have severe biological impacts on fish and other biota, particularly during their sensitive early life stages. This meltwater may be close to 0 °C and thus typically does not mix downward in lakes with warmer, more dense lake water if the lake is covered with ice. The result is a shallow layer of relatively low pH water directly beneath the ice. Acidic episodes kill fish long before the system is chronically acidic; recovery from acidic episodes is a key to biotic recovery. In circumneutral streams and lakes, dilution of Ca is an important factor for fish mortality (Tranter et al., 1994).

11.10.5.2 Pulsed Release of SO_4 and NO_3 from Soils

Episodic release of SO_4 and/or NO_3 from soils, unaccompanied by equivalent base cations, may depress pH and ANC, on a timescale of individual high discharge events, or seasonally. Episodically elevated concentrations of SO_4 in runoff may be caused by prolonged drought, lowering of the groundwater table, subsequent oxidation of S stored in organic matter, and then leaching during higher discharge (Dillon et al., 1997). Seasonal release of stored S is most strong from watersheds with a high areal percentage of wetlands (Kerr et al., 2011). Increases in DOC may accompany the elevated SO_4, enhancing the depression of pH. Normal fluctuations of hydrology are typically unaccompanied by substantial variation in stream SO_4 because of anion exchange equilibria in mineral soils and stream sediment. The flux of NO_3 is dominated more by biological processes, being strongly diminished in many streams during the vegetation growing season versus the dormant season. Consequently, many watersheds have a strong seasonal cyclicity for release of NO_3 (Navrátil et al., 2010; Stoddard, 1994). Superimposed on this seasonality is a short-term release of NO_3 caused by flushing of mineralized N (as NO_3) from shallow soils during periods of higher flow. It is common for NO_3 to vary more in runoff (on both a percentage and absolute basis) than SO_4 (Navrátil et al., 2010), apparently because most soils have a low NO_3 exchange capacity.

The elevated SAA fluxes from acidic soils during events are usually associated with elevated terrestrial export of H^+ and ionic Al forms, which are potentially toxic for water biota (e.g., Gensemer and Playle, 1999). Inorganic Al and DOC interactions and the proportion of ionic and organically bound (nontoxic) Al forms cause variability in fish mortality, as does duration of exposure in an acidic episode (Baldigo and Murdoch, 1997). Changing flow paths during hydrological events (i.e., proportion of snowmelt or rainwater and soil water in the total water input to lakes) are of overwhelming importance in controlling the chemical character of episodes in streams (Davies et al., 1992). For example, acid-sensitive fish species were absent in streams of the northeastern United States that had median pH < 5.0–5.2 and inorganic Al > 100–200 μg l^{-1} during high flow (Baker et al., 1996).

11.10.5.3 Marine Aerosols

Deposition of marine salt aerosol causes episodic acidification of runoff near the coast by alteration of cation exchange equilibria within strongly acidic soil. During the 'sea-salt effect,' marine aerosol Na and Mg displace primarily H, Al, and Ca from soil exchange sites. The Na/Cl and Mg/Cl equivalent

ratios in runoff can decline below ocean water values, 0.86 and 0.2, respectively, as Na and Mg cations are adsorbed by the soil. The pH of runoff can decline as much as 2 pH units during these sea-salt episodes. The ANC of runoff is reduced while BS and soil pH are increased very slightly. Wiklander (1975) was one of the first to suggest acidification of leachate by the sea-salt effect. The process has been demonstrated experimentally at the laboratory scale (Skartveit, 1981) and at the watershed scale (Wright et al., 1988). Individual high salt inputs can be reflected in surface water chemistry for months to a few years (Evans et al., 2001c; Godsey et al., 2010; Kirchner et al., 2000; Norton and Kahl, 2000). The maximum effect from sea-salt input occurs in thin acidic soils that have low BS and low CEC. Most soils have relatively low Cl exchange capacity. Thus, Cl behaves conservatively. The sites most responsive to sea-salt inputs are those at an intermediate distance from the coast where occasional major sea-salt inputs can generate large proportional changes in Cl and other marine ions (Harriman et al., 1995). Major regional events with pH depressions sufficient to kill fish have been documented by Hindar et al. (1994). These events can occur in areas even where acidification from strong acids is absent. Salt-driven acidification episodes can be relatively common in acidic bogs although it has not been well documented. Pugh et al. (1996) demonstrated a salt acidification effect in an ombrotrophic/poor fen site. The salt originated from road runoff, but the chemical changes in runoff were otherwise analogous.

11.10.5.4 Organic Acidity

The most acidic stream flows in polluted regions commonly have disproportionately higher concentrations of H^+, NO_3^-, SO_4^{2-} and inorganic Al. In unpolluted regions, as in northern Sweden (Hruška et al., 2001) or in North Shore rivers, Quebec, Canada (Campbell et al., 1992), episodic acidification can be primarily caused by dilution of base cations and increase in organic anions during high discharge. In northern Quebec, for example, 'inorganic anion deficits' increased from around 35 to 70–100 μeq l^{-1}, representing up to 20 mg DOC l^{-1} during high flow at snowmelt, causing pH to decline from near 7 to about 5 (Campbell et al., 1992). The episodic pH depression associated with DOC operates independently of anthropogenic acidity and likely is responsible for substantial episodic acidification. Fortunately, as DOC and H^+ increase, much of the potentially toxic metals that are mobilized (especially Al) becomes bound (complexed) with the DOC and is thus biologically much less reactive. Since about 1980, depending on location, atmospheric deposition of SO_4 has declined as has runoff SO_4. Concurrently, DOC concentration has increased at most localities, especially in watersheds with significant percentage of wetland (Monteith et al., 2007). The correlation between declining SO_4 and increasing DOC suggests a mechanistic linkage. Decreasing ionic strength and increasing soil water pH have been suggested to cause increasing solubility of DOC. Some of the increase in DOC concentration can be attributable to climatic warming, causing increased mineralization of organic matter. Altered hydrology, such as earlier snowmelt, can also enhance DOC export from watersheds. Elevated atmospheric deposition of N can also stimulate mineralization of organic matter. Acidity from increased DOC partially offsets decreased SO_4, inhibiting recovery from acid rain (Arvola et al., 2010). An additional effect of increasing DOC is the increased mobilization of Al and Fe (and other metals) from soils, and subsequent impact on phosphorus (P) cycling (see Section 11.10.6.2).

11.10.5.5 Dilution

It is common during periods of snowmelt or high rainfall to have most runoff passing through shallow soils or even overland. As a consequence, soil cation exchange processes can be largely by-passed. This causes dilution of base cations in the runoff; however, SO_4 in runoff is less diluted than elements originating in the watershed because some SO_4 exists in the snow or rain that makes up the runoff. Consequently, SAA decrease less than SBC, causing acidification. Such acidification can also occur seasonally as a result of NO_3 mobilization (Laudon and Norton, 2010).

11.10.5.6 In-Lake Processes Affecting pH and ANC

In circumneutral lakes, the water ANC and pH are primarily affected by CO_2 assimilation (eqn [17]; left to right = production of organic matter) and dissimilation of organic matter (reversed eqn [17]; CO_2 production):

$$CO_2 + H_2O = CH_2O + O_2 \qquad [17]$$

Changes in concentrations of dissolved CO_2 affect concentrations of HCO_3^- and H^+ (eqns [13] and [14]), and lake water pH. The pH maxima occur in the epilimnion near midday due to the highest photosynthetic activity and the largest depletion of CO_2 concentrations. Dissimilation of settling organic matter increases CO_2 concentrations and decreases pH in deeper waters. Consequently, pH is usually higher in the epilimnion than in the hypolimnion of circumneutral lakes. An inverse pH–depth relationship (lower pH values in the surface layer than above the bottom) is typical for strongly acidified lakes, with a depleted carbonate buffering system. The reasons for this difference are low pH and negligible carbonate system buffering in acidic waters. Changes in H^+ concentrations associated with the CO_2 assimilation and dissimilation are relatively small in acidic waters due to low dissociation of H_2CO_3 at pH < 5 (eqn [14]). In contrast, the effects of other in-lake processes generating or consuming H^+ (such as ionic exchange across the sediment–water interface, biotic reduction of SO_4 and NO_3, photochemical and bacterial oxidation of organic acids, hydrolysis of $(M^{3+}(OH^{1-})_n)^{3-n}$, and dissociation or protonation of organic acids) on water pH are more pronounced (and straightforward) in acidic than in circumneutral lakes because the associated H^+ fluxes are not buffered by the carbonate buffering system.

Laboratory and in situ experiments have demonstrated that stream and lake sediments in contact with the water column are effective ion exchangers for base cations (e.g., Cook et al., 1986; Oliver and Kelso, 1983), anions (Navrátil et al., 2010; Norton et al., 2000), and Al (Henriksen et al., 1988b; Tipping and Hopwood, 1988). Because of the reversible cation-exchange processes, pH depression can be buffered during episodic acidification, as is recovery of ANC during de-acidification (see Section 11.10.8). Exchange of H^+ for base cations in sediment is commonly reported as a significant ANC

source during the early stage of stream and lake water acidification (e.g., Psenner, 1988; Schiff and Anderson, 1986).

Sulfate and NO_3 are used as electron acceptors during microbial dissimilation of organic matter in anoxic conditions that are typical for sediments but also may occur in the hypolimnion of a productive lake. The biochemical reductions of SO_4 and NO_3 are important H^+ consuming (ANC generating) processes:

$$2CH_2O + SO_4^{2-} + 2H^+ = H_2S + 2CO_2 + 2H_2O \quad [18]$$

$$5CH_2O + 4NO_3^- + 4H^+ = 2N_2 + 7H_2O + 5CO_2 \quad [19]$$

The rate of SO_4 and NO_3 reduction in sediments is normally governed by diffusion. Total amount of the reduced SO_4 and NO_3 thus increases with SO_4 and NO_3 concentrations in lake water and water residence time (Kelly et al., 1987). As acidification progresses and terrestrial exports of SO_4 and NO_3 to the lake increase, the contribution of SO_4 and NO_3 biochemical reduction to the total in-lake ANC generation increases, and typically becomes the dominant process (Cook et al., 1986; Rudd et al., 1986; Schindler, 1986). However, net storage of SO_4 (as reduced S) in sediment is typically a small percentage of excess SO_4 in lake water (Norton et al., 1988). Besides denitrification (eqn [19]), NO_3 is assimilated during photosynthesis by phytoplankton, consuming 1 mol of H^+ per 1 mol of NO_3 consumed (eqn [20]). This process is an important ANC source in productive lakes with either naturally high (e.g., Plešné Lake; Kopáček et al., 2004) or artificially elevated (e.g., Davison et al., 1995) P concentrations.

$$NO_3^- + R - OH + H^+ = R - NH_2 + 2O_2 \quad [20]$$

DOC is not conservative in water. It can be metabolized, condensed, photooxidized, or precipitated during acidification. Sunlight can effectively reduce concentrations of allochthonous recalcitrant organic matter, decrease its average molecular weight, and produce numerous biologically available compounds, like acetic, formic, citric, malonic, and oxalic acids (Bertilsson and Tranvik, 2000; Kieber et al., 1989; Steinberg and Kühnel, 1987). Both the total photochemical oxidation of organic acid anions to inorganic carbon (mono- and dioxide) and the microbial uptake of the produced low molecular weight organic acids influence in-lake concentrations of A^{x-} and H^+. This in-lake removal of allochthonous DOC was a significant internal ANC-producing process in the acidified Adirondack, New York, USA, and Bohemian Forest, Czech Republic, lakes (Driscoll and Postek, 1996; Kopáček et al., 2003). DOC's proportion in the total in-lake ANC production has probably increased during the recovery phase, as terrestrial export of SO_4 decreased and that of DOC increased (Monteith et al., 2007). The photochemical cleavage of higher molecular weight DOC decreases water color and increases transparency. The altered light regime in water (including UV permeability) has then further consequences on chemistry, biota, and the thermal structure of lakes (Schindler et al., 1996).

11.10.6 Effects of Acidification

11.10.6.1 Release of Al and other Elements

Acidification of surface waters to a pH of ~5 or below causes sharp increases in concentrations of dissolved Al (Driscoll and Postek, 1996; Lawrence et al., 1987; Schecher and Driscoll, 1987) and trace metals (e.g., Be, Veselý et al., 2002a; Cd, Alfaro-De la Torre and Tessier, 2002; Mn, Borg, 1986 (but see Navrátil et al., 2007 for a different perspective); and Zn, Veselý and Majer, 1996; Veselý et al., 1985; **Figure 3**). Increased concentrations of dissolved inorganic Al during soil and water acidification are the primary cause of fish mortality in acidic waters (Baker et al., 1996). The controls on Al concentration as pH declines include ion exchange, dissolution of solid-phase Al (typically referred to as 'gibbsite' = $Al(OH)_3$) with variable solubility constants (Mulder and Stein, 1994), and equilibrium with solid Al–organic complexes (Cronan et al., 1986). Concurrently, the Al aqueous speciation changes toward more of the uncomplexed free ion. Free Al^{3+} and H^+ outcompete trace metal cations on soil exchange sites, the concentrations of OH^- and HCO_3^- ligands are negligible, and the relative importance of organocomplexes may decline as pH declines. Potentially toxic substances such as Al^{3+} become more biologically available. At BBWM, increases of Al in a low pH and low DOC stream, caused by experimental acidification of a watershed, were entirely inorganic Al and apparently related to solubility of an unidentified Al phase (Postek et al., 1996). Mechanisms regulating the release of Al from amorphous inorganic and organic compounds in soil are uncertain (LaZerte and Findeis, 1995; Mulder and Stein, 1994). Laboratory experiments suggested a combination of kinetically limited Al release from primary and secondary minerals and organic compounds together with the complexation of Al with DOC (Berggren and Mulder, 1995). During acid episodes, Al can increase to more than 1 mg l^{-1} and such a concentration can be chronically maintained in waters of heavy polluted regions (Veselý et al., 1998b). The dissolution of Al is further enhanced by formation of soluble complexes, especially with fluoride and sulfate (Schecher and Driscoll, 1987). Mixing of these acidic Al-rich waters with higher pH waters commonly causes Al precipitation, also a problem for fish (Reinhardt et al., 2004; Rosseland et al., 1992; Teien et al., 2006; Weatherley et al., 1991). Rare earth elements (REE) and beryllium (Be) behave similarly to Al in streams. They are mobilized by DOC and by declining pH during acidic episodes (REE data from BBWM, Norton, unpublished; Tang and Johannesson, 2003; Veselý et al., 2002b; Wood et al., 2006).

Many pollutants other than S and N occur in modern atmospheric deposition. The history of deposition of these pollutants has been determined by chemical and isotopic analyses of ice cores (e.g., Boutron et al., 1995), lake sediment cores (e.g., Renberg et al., 2000), peat cores (e.g., Shotyk et al., 1996), soils (Bindler et al., 1999), vegetation (Steinnes, 1995), and direct measurements (e.g., NADP–NTN, 2009). Most metals have enhanced mobility as a consequence of acidification. Mercury (Hg) and lead (Pb) are relatively conservative in watersheds, in large part because of fixation by particulate organic matter or sorption to sesquihydroxide secondary phases. Atmospheric deposition of Pb increased in eastern and central North America and northern Europe by as much as 50 times preindustrial values, peaking in the 1970s. It has declined since then to generally <5% of peak values (**Figure 4**). Biological impact of atmospherically deposited Pb, except in grossly polluted regions, has not been demonstrated to be significant. The deposition of Hg is strongly influenced by dry

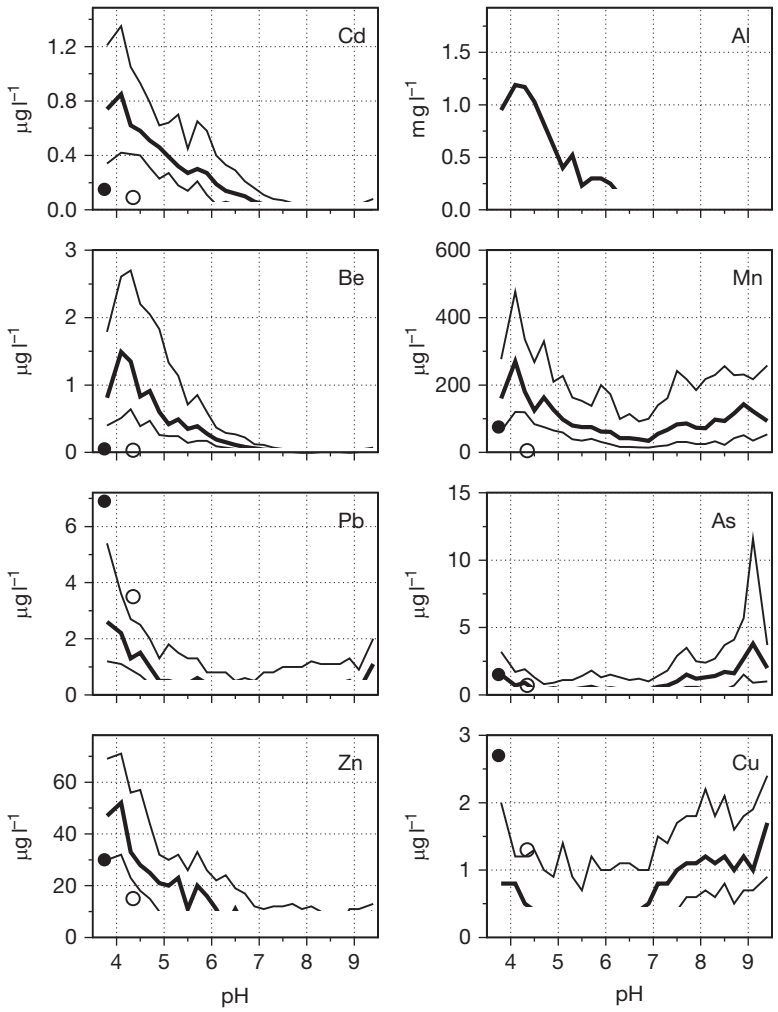

Figure 3 Relationship among median, upper, and lower quartiles of Al, As, Be, Cd, Cu, Mn, Pb, and Zn, and pH in Czech Republic brooks in the late 1980s. Values were calculated after sorting the water samples ($n = 12\,988$) into groups with 0.2 pH unit ranges. Volume-weighted average concentrations in bulk precipitation (○) and throughfall (●) in 1991 samples from the Bohemian Forest are shown (modified from Veselý J and Majer V (1996) The effect of pH and atmospheric deposition on concentrations of trace elements in acidified freshwaters: A statistical approach. *Water, Air, and Soil Pollution* 88: 227–246; Veselý J and Majer V (1998) Hydrogeochemical mapping of Czech freshwaters. *Bulletin of the Czech Geological Survey* 73: 183–192). The decline of Be, Cd, Mn, and Zn at very low pH is likely caused by acidification-related depletion of exchangeable trace metals from the watershed soils.

deposition of Hg to plant surfaces. Thus, Hg deposition was low when Caribou Bog (Orono, Maine, USA) (Figure 4) was a lake, high during the fen stage as the lake filled in, and then low during the ombrotrophic stage, until the present era of pollution. Similarly, at Sargent Mountain Pond (Maine, USA), Hg deposition increased dramatically slightly before the Younger Dryas and afterward, as a consequence of the development of forest vegetation. Modern deposition of Hg at both sites reached unprecedented values as a consequence of anthropogenic emissions. Mercury has increased in atmospheric deposition by more than 100% since the mid-1800s, peaking in the 1970s and declining since then (Figure 4).

Mercury becomes methylated under reducing conditions, enters the aquatic food chain through phytoplankton, is magnified as much as 10^6 -fold in the food chain, and reaches maximum concentrations in piscovorous fish. The increase of SO_4 in the environment from acid rain could have stimulated methylation of Hg because of enhanced biotic reduction of SO_4 in wetlands, groundwater, and lakes, thus increasing methyl-Hg in fish and the humans who consume the fish (Morel et al., 1998). The trend for the deposition of Cd from the atmosphere is generally parallel to that of Hg for eastern Canada and the United States (Alfaro-De la Torre and Tessier, 2002; Norton et al., 2007). Additional information on trace elements and Hg is included in Chapters 11.3 and 11.4, respectively, of this volume.

11.10.6.2 Nutrient Availability

The initial response to acid rain is an increase in the mobilization and export of base cations and, commonly, SO_4 and NO_3 from the watershed. In general, soil acidification and associated leaching of Mg, Ca, and K, and elevated Al mobilization are usually associated with less favorable nutritional status, whereas N deposition tends to increase the fertility of naturally

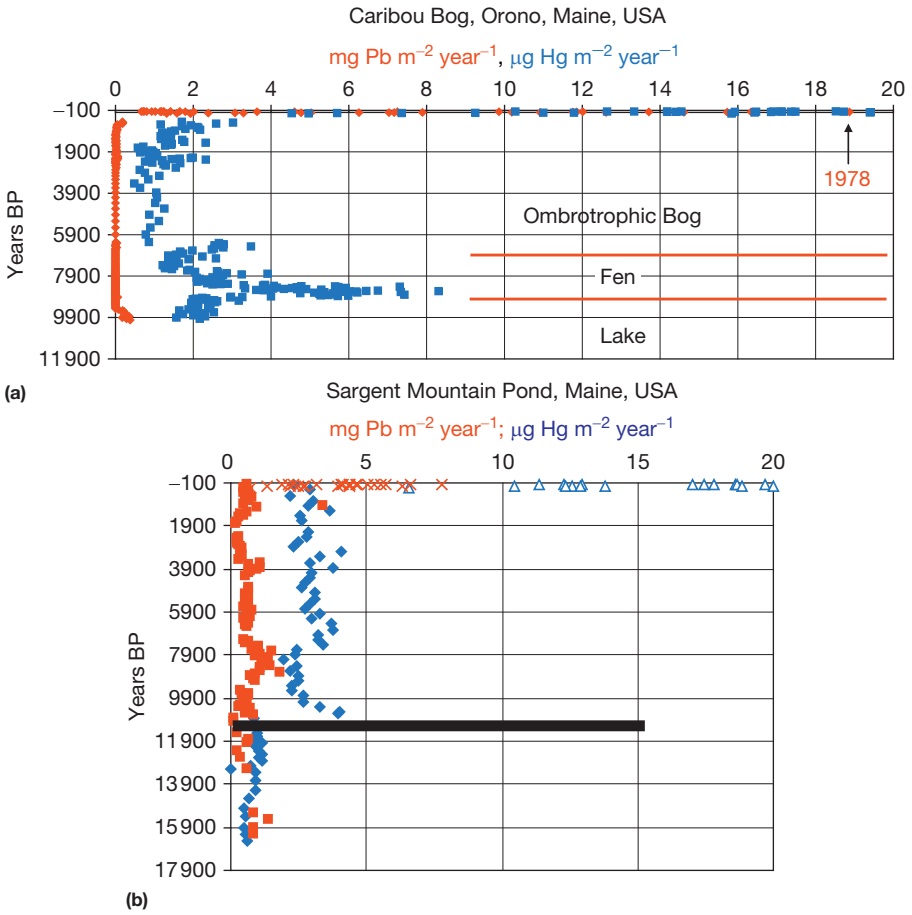

Figure 4 (a) Accumulation rate of Hg and Pb in Holocene time at Caribou Bog, Maine (modified from Roos-Barraclough F, Givelet N, Shotyk W, and Norton SA (2006) Use of Br and Se in peat to reconstruct the natural and anthropogenic fluxes of atmospheric Hg: A ten-thousand year record from Caribou Bog, Maine, USA. *Environmental Science & Technology* 40: 3188–3194). Note the differing influence of vegetation on the flux of Hg and Pb in preindustrial time and the unprecedented high accumulation rates in the last 100 years. (b) Accumulation rate of Hg and Pb in early postglacial to ca. AD 2004 sediment of Sargent Mountain Pond, Maine, USA (Norton, unpublished). The bold dashed horizontal line is the approximate time of the Younger Dryas, after which the landscape was fully forested. The recent sediment data (open symbols) are spliced to data from a long core.

N-limited terrestrial ecosystems (Puhe and Ulrich, 2001). The elevated N deposition thus may correspond to a period of fertilization of plants in forests and in N-limited surface waters. However, prolonged increased leaching of exchangeable base cations and subsequent decline in exchangeable pools of base cations in soils (Fernandez et al., 2003; Kirchner, 1992; Likens et al., 1996) can have a long-term impact on terrestrial ecosystem health. As the molar ratio (Ca + Mg + K)/Al in soil solution declines during acidification, nutrient uptake by roots can be impaired. Limited Ca or Mg uptake, associated with elevated Al concentrations and low pH in the rooting zone, slows growth and decreases the stress tolerance of trees (Cronan and Grigal, 1995), and adversely affects tree physiology (Šantrůčková et al., 2007). Declining Ca in runoff, which may occur during acidification or recovery, has been implicated in reduced fecundity and survival of Ca-rich *Daphnia* species (Jeziorski et al., 2008). Similar effects might be expected in other organisms that require higher Ca in water.

Although P is not commonly the subject of acid rain geochemistry research, ecosystem alterations due to acidification inevitably alter P dynamics in watersheds. Reinhardt et al. (2004) demonstrated that the export of P in runoff from the experimentally acidified catchment at BBWM had increased nearly by a factor of 10, along with Al. SanClements et al. (2010) reported that an important source of this P and Al was in the B horizon of these forested Spodosols, a locus of secondary Al and Fe accumulation and thus, significant P adsorption capacity. They suggested that mobilization of Al by the experimental acidification also resulted in P mobilization, and that this effect was evident at both BBWM and a similar experimental watershed acidification study at the Fernow Watershed in West Virginia, USA. Evidence also existed to suggest that for the period of time of accelerated P mobilization, which could be transient, P was more available to biota, with biocycling of this P resulting in redistributions within the ecosystem.

Minimally polluted forest ecosystems export mostly organically bound N and NH_4, instead of inorganic oxidized N (NO_3) (e.g., Hedin et al., 1995; Perakis and Hedin, 2002). Increased atmospheric deposition of N can initially have a

positive growth effect on N-limited ecosystems. Turnover of mineralized N in the forest floor is generally an order of magnitude higher than atmospheric input of inorganic N, which creates only a small addition to a large N soil pool. Nitrogen demands by biota must be satisfied first, and a certain amount of N can be immobilized in forest organic matter, before N saturation and chronic NO_3 leaching occur (Aber et al., 1989, 1998; Stoddard et al., 2001). Ecosystems vary widely in their capacity to retain N inputs. Excess N is exported mostly as NO_3, increasing the concentration of SAA in water, contributing to acidification. Nitrate leakage is greatest from high-elevation, steep sites, and from mature forests with high soil N stores and low soil C/N ratio (Fenn et al., 1998), and lowest from watersheds containing extensive wetlands. Concentrations and seasonality of NO_3 in stream water are used as indices of N saturation (Stoddard, 1994). Mosello et al. (2000) and Kopáček et al. (2001a) indicated that retention of N in watersheds decreased with time under acidification stress. In contrast, slightly elevated terrestrial N retention may be connected to reduction of acidic deposition during the recovery phase (Lorz et al., 2002; Veselý et al., 1998a, 2002a). Increased concentration of NO_3 in streams increases P demand and the risk of P limitation in stream microbial communities, as demonstrated at BBWM (Simon et al., 2010). This P limitation can be exacerbated by the mobilization of Al from soils and subsequent precipitation of $Al(OH)_3$ in streams, increasing the capacity for adsorption of dissolved P. Davison et al. (1995) used whole-lake treatment with P to overcome acidification by excess NO_3.

Export of NO_3 in surface waters is linked to soil microbial activity and the soil C/N ratio (Yoh, 2001). Empirical data showed that a C/N ratio of the forest floor <25 and throughfall deposition above 9–10 kg N ha^{-1} $year^{-1}$ were thresholds for leaching NO_3 in Europe (Dise and Wright, 1995; Gundersen et al., 1998), with similar findings reported for North America (Aber et al., 2003). In the European data, the slope of the relationship between N input and NO_3 leached was twice for sites where $C/N < 25$. Higher rates of NO_3 leaching also occurred at sites with $pH < 4.5$ and high N input (MacDonald et al., 2002). However, N leakage was about half that of deposition at high-elevation alpine sites in the Rocky Mountains of Colorado, USA (Williams et al., 1996). The export of NO_3 from N-saturated forests also reflects the soil's potential for nitrification and land-use history. Goodale and Aber (2001) reported that although net N mineralization did not vary by land-use history, nitrification rates doubled at old-growth sites compared to younger hardwood forests disturbed by fire and harvesting about a century ago. Enhanced nitrification at old-growth sites could have resulted from excess N accumulation relative to C accumulation in soils. Carbon mineralization rates and C/N ratios were comparable in spruce forest soils for two neighboring watersheds in the Bohemian Forest, Czech Republic, while potential net N mineralization and nitrification differed by 50–70%; higher potentials were associated with higher leaching of NO_3 (Kopáček et al., 2002a). In Europe, as SO_4 deposition and runoff SO_4 has declined, NO_3 has become the major anion in some surface waters. Nitrate thus dominates the acidification status of these systems, as well as being the most important driver of episodic acidification and Al mobility (Kopáček et al., 2009).

The productivity of temperate freshwaterlakes and streams is generally limited by the availability of phosphorus, although light limitation can be of primary importance in already P-poor lakes (Karlsson et al., 2009). Phosphorus occurs in many rocks, primarily in the mineral apatite, which has a relatively high weathering rate. Consequently, older soil profiles are depleted in apatite. Monazite ($(REE)PO_4$) is common in many rocks but the mineral is very insoluble. Much P is concentrated in organic-rich soils and is strongly recycled or sequestered by adsorption in Al- and Fe-rich illuvial soil layers (SanClements et al., 2009). Lakes predisposed to acidification thus have low concentrations of base cations and P. Acidification of catchments can result in a slightly increased export of dissolved P from soils (Roy et al., 1999). Roy et al. (1999) and Reinhardt et al. (2004) found that two contiguous acidifying streams contained high concentrations of particulate acid-soluble Al and Fe hydroxides and acid-soluble particulate P during acidic episodes. Particulate P was 10–50 times higher than dissolved P and highest in the lower pH stream. Ionic Al species hydrolyze downstream or in lakes at higher pH, as polymeric Al species are formed with large specific surfaces and with strong affinity for PO_4^{3-}. The P in acidified streams and lakes (typically with a pH in the 5.5–6.5 range) can be scavenged by these Al- or Fe-rich particles. If the Al hydroxide is deposited as sediment, the flux of P into sediment can be irreversible (Kopáček et al., 2001b), even during periods of hypolimnetic anoxia when pH typically increases, Fe hydroxide dissolves, and adsorbed P would normally be released to the water column (Amirbahman et al., 2003; Einsele, 1936). Thus, stream acidification can lead to downstream oligotrophication as suggested by Dickson (1978).

As DOC has increased during the decline of SO_4 in runoff, the mobilization of Al to lakes should have increased because Al–DOC complexes, regardless of pH trend. Kopáček et al. (2000, 2005) have demonstrated that precipitation of $Al(OH)_3$ in the water column of Plešné Lake, Czech Republic, removes P from the lake P-cycle, thereby lowering biologically available P. The source of the Al is partly from inorganic mobilization because of acidification and dominantly from complexation with soil DOC, followed by Al liberation due to photooxidation of the complex in the lake water column. If Al partially controls bioavailability of P, then there is likely a linkage between P and Hg in fish. Higher dissolved P in a lake enhances the food chain, thereby diluting the Hg concentration in algae and the subsequent food chain, including fish. Conversely, if P is lowered in the water column, productivity is reduced and Hg concentration will be higher in the food chain, particularly fish. This concept of biodilution (Chen and Folt, 2005) is not fully understood but is a pressing problem.

11.10.7 Effects of a Changing Physical Climate on Acidification

Global and regional climate models predict spatially variable changes in temperature and precipitation. Consequently, temperature, the timing of runoff maxima, and seasonality can all be expected to change. These changes will alter concentrations and fluxes of solutes and particulates, altering the acid–base status of runoff. Year-to-year changes need to be distinguished

from biologically driven seasonal cycles that control a number of components in runoff to varying degrees, including NO_3, SO_4, DOC, K, and Mg (see, e.g., Likens et al., 1994; Navrátil et al., 2010). These changes are difficult to distinguish from climate change effects occurring over decades to centuries because of the complexity of potential ecosystems responses. Increases in precipitation may not result in increasing discharge if accompanied by higher temperature (Clair and Ehrman, 1996). As major atmospheric circulation patterns change, the input of marine aerosols can also be substantially altered (Evans et al., 2001c). Empirical evidence has emerged that temperature variability can partially control important abiotic reactions involving Al (Lydersen et al., 1990; Veselý et al., 2003).

Wright et al. (2006, 2010) evaluated the relative sensitivity of several possible climate-induced effects on the recovery of soil and surface water from acidification. The results show that several of the factors are of only minor importance (increase in pCO_2 in soil air and runoff), several are important at only a few sites (sea salts at near-coastal sites), and several are important at nearly all sites (increased concentrations of organic acids in soil solution and runoff). In addition, changes in forest growth and decomposition of soil organic matter are important at forested sites and sites at risk of nitrogen saturation. Increased temperature and adequate moisture would produce at least a transient increase in the mineralization of organic matter, producing an increased release of DOC and nutrients.

11.10.7.1 NO_3

Current mean annual concentrations of NO_3 in stream water generally correlate with the magnitude of N atmospheric deposition and the N saturation status of the terrestrial ecosystem (Aber et al., 1989, 2003; Stoddard et al., 2001; Wright et al., 2001). Nitrate concentrations of many watersheds are commonly highest during the spring snowmelt period and lowest during summer base flow. This pattern implies that nitrification occurs during winter months, with NO_3 accumulating in the soil until flushed by snowmelt, as well as NO_3 stored in the snowpack. However, peak spring and winter NO_3 concentrations vary markedly from year to year. Cyclic interannual variations in these peak NO_3 concentrations have been ascribed to (1) summer drought due to oxidation of organic N in dried out soils (Harriman et al., 2001; Reynolds et al., 1992; Ulrich, 1983); (2) cold dry winters (Mitchell et al., 1996), and also warmer soils during mild winters (Kaste et al., 2008); and (3) variable mean annual temperature (Murdoch et al., 1998). Synchronous variation in NO_3 concentrations among lakes and a strong negative correlation with the winter North Atlantic Oscillation (NAO) Index and mean winter temperature occurred in the United Kingdom. Low NAO winters increased NO_3 in the UK monitored waters (Monteith et al., 2000).

Snow is an insulator against freezing of forest soils (Kaste et al., 2008). Physical disruption during soil freezing can increase fine root mortality and reduce plant N uptake, thereby allowing soil NO_3 levels to increase even with no increase in net mineralization or nitrification (Groffman et al., 2001). The annual mean soil temperature is correlated with mineralization and can shift the C/N ratio of forest floor as much as 0.5 per 1 °C (Yoh, 2001). Thus, climate could become an increasingly important factor governing soil C/N and regulating the NO_3 production due to a metabolic balance between C as a source of energy and N as the commonly most limiting nutrient. Soils with higher C/N ratios typically have lower nitrification and decomposition rates, and almost always demonstrate lower NO_3 leaching losses.

Warming by 3–5 °C increased rates of mineralization of soil organic matter and NO_3 flux in runoff in the climate change experiment (CLIMEX) in Norway (Wright, 1998). The ecosystem switched from being a net sink to a net source of inorganic N, probably due to acceleration of decomposition of soil organic matter induced by higher temperature. In contrast, artificially warmed soils in a coniferous forest in Maine, USA, had lower rates of N cycling, and forest floor N concentration was a better predictor of potential net N mineralization than was total C or the C/N ratio (Fernandez et al., 2000), the results of which were more a function of local factors such as soil moisture availability. A meta-analysis of experimental soil warming studies from around the world showed a strong positive relationship between increased warming and net N mineralization (Rustad et al., 2001), although treatment duration among the 32 research sites was only in the range of 2–9 years, and longer term responses remain unstudied. Generally, the C/N ratio alone is a poor predictor of N leaching or retention.

11.10.7.2 SO_4

In oligotrophic boreal lakes of Ontario, Canada, a drought in the 1980s decreased the water table and lake levels, exposing watershed soils and littoral sediments that contain reduced S. During the drought, the length of the ice-free season, duration of stratification, depth of the photic zone, and light extinction increased while precipitation and then nutrient inputs to the lakes decreased. Sulfur was reoxidized and mobilized to the lakes during subsequent wet periods (Dillon et al., 1997; Jeffries et al., 1995). Drought occurred in Ontario in years following strong El Niño/ENSO events (Dillon et al., 1997), another major circulation feature in addition to the NAO (Jones et al., 2001). When the ENSO Index was strongly negative, the frequency of drought in the following summer was high. If long-term changes in global or regional climate alter the frequency or magnitude of El Niño/ENSO-related droughts (Dai and Wigley, 2000) the recovery of acidified lakes will be longer and more complex.

11.10.7.3 CO_2

Carbon dioxide was the first atmospheric gas shown to be increasing because of human activities and it is often implicated in global warming. Small seasonal variation in atmospheric CO_2 concentrations reflect the net respiration/photosynthesis of the northern hemisphere and possible forcing by El Niño (Bacastow, 1976). The recent increase in atmospheric CO_2 of about 0.5% $year^{-1}$, documented with direct measurement since 1958 and indirectly by ice core analyses (IPCC, 2007; Schneider, 1989), is largely from the burning of fossil fuels, deforestation, and other alterations of land use. This atmospheric CO_2 increase has little direct impact on freshwater acidification but could be indirectly linked through climate change caused by greenhouse gas effects from the increased atmospheric CO_2. Wright (1998) experimentally

increased ambient air CO_2 by 100% in a miniwatershed in Risdalsheia, southern Norway. This increase, in combination with warming of soil by 3–5 °C, produced an increased concentration of NO_3 in runoff. A more insidious development as a consequence of increased atmospheric CO_2 is acidification of the oceans' surface waters (Caldeira and Wickett, 2003; Sabine et al., 2004). The increase of atmospheric CO_2 by about 50% over the last 100 years has resulted in a probable titration of the bicarbonate–carbonate pH buffer system, with a lowering of pH by about 0.1 unit. The full consequences of this acidification are not known. An important consequence will be that carbonate-depositing organisms will have to expend more energy during calcite precipitation. Earth has experienced much higher atmospheric CO_2 (and related higher temperature) but the rate of change now is likely greater than at any time in Earth's history. The warming associated with additional greenhouse gases will likely accelerate some biochemical processes (mineralization of organic matter to produce DOC and CO_2) and provide negative feedback to others (such as the solubility of CO_2 in freshwater).

The increase of atmospheric CO_2 could have imperceptibly decreased the pH of precipitation, but the partial pressure of CO_2 (pCO_2) in soils is far more important to the acid–base status of surface water. Variation in forest soil pCO_2 is influenced by temperature and moisture in soils as well as release of excess soil CO_2 to the atmosphere. Warmer conditions increase microbial and root respiration in the soil thereby increasing soil pCO_2 above the long-term average value and producing short-term increases in runoff ANC, and vice versa. Norton et al. (2001) found that intraseasonal variation in pCO_2 caused by variable snow pack thickness could induce variation in ANC in runoff of 10–15 $\mu eq\,l^{-1}$. Such variability can exceed increases in ANC caused by a 15–20 $\mu eq\,l^{-1}$ decline of SO_4 in runoff. Decline in soil pCO_2, despite increased temperature and possibly increased soil respiration, could result from lower soil moisture content and greater efflux of soil CO_2. Strong seasonality of soil pCO_2, while normal, likely induces variation of 10–20 $\mu eq\,l^{-1}$in ALK. Variations of water pH would depend on the soil pH.

11.10.7.4 Organic Acids

DOC consists of a complicated mixture of organic acids with differing p*K* values (the pH at which half of the organic acid is protonated). DOC species with low p*K*s contain 'strong' acid anions, analogous to SO_4 and NO_3. Their contribution to the acidification status can overwhelm that of SO_4 and NO_3 in DOC-rich surface waters. Variable export of DOC from forests is controlled by organic production and decomposition, sorption by soil, and flushing, all connected to local climate (Kalbitz et al., 2000). For example, DOC discharged from subwatersheds in the Rhode River watershed, Maryland, USA, varied eightfold (Correll et al., 2001). Temperature effects on DOC concentrations were weak and fluxes were not correlated with temperature in a Norway spruce forest in Germany (Michalzik and Matzner, 1999). Drought in western Ontario, Canada caused a decline in DOC export from watersheds, or more removal from lake water columns because of the longer water residence times (Schindler et al., 1996). In a whole watershed acidification, Gjessing (1992) studied the response of Lake Skjervatjern, western Norway, to additions of NH_4NO_3 and H_2SO_4, and cycles of drought. DOC concentrations decreased in the lake as a result of drought-related decreased input of DOC from the watershed, and in-lake processes that consumed DOC. It is not fully clear why DOC concentrations have generally increased over the last two decades in European and North American soft waters (Bouchard, 1997; Evans and Monteith, 2001), but this increase seems to be most likely related to increasing pH and decreasing ionic strength of soil water due to reduced anthropogenic SO_4 and Cl deposition (Monteith et al., 2007). In addition, Anesio and Granéli (2003) showed that DOC is more photoreactive in acidified waters. Thus, with recovery underway as a consequence of reduced SO_4 deposition, photoreactivity may be decreasing, resulting in an increase in DOC. Wright et al. (2010) reported that artificially increased salt loading at Gårdsjøn watershed, Sweden, caused a decline in DOC export, supporting the ionic strength hypothesis. Evans et al. (2008a) examined results from 12 European and North American field N addition experiments and found variable response in DOC export related to the chemical form of N addition. They suggested that changes in acidity, such as ANC forcing, might be the more important factors governing DOC export although cause and effect remained undefined. If the quality of the DOC remains constant while the concentration increases, recovery of ANC in a regime of decreasing atmospheric pollution (S and N) will be retarded because of added organic anion acidity. Altered toxicity to fish will depend on whether the increased DOC is saturated with Al.

11.10.7.5 Evaporation/Hydrology

In many upper Midwest lakes of the United States, the widespread decrease in lake SO_4 observed farther east was prevented during a 4 year drought that caused evaporative concentration of the already acidic seepage lakes (Webster and Brezonik, 1995). Lower than normal precipitation reduced seepage lake water levels and groundwater elevations. A decrease and eventual cessation of groundwater inflow, caused by the drought, led to losses of ANC, Ca, and Mg in lakes. Groundwater-dominated (seepage) lakes of Wisconsin, USA, responded to drought, with no relationship between concentrations of solutes in the lake and precipitation (Webster et al., 2000). Landscape position, defined by the spatial position of a lake within a hydrologic flow system, accounted for differences in chemical response to drought (Webster et al., 1996). In the lakes of surface water-dominated Ontario, Canada, chemical response of conservative solutes such as Ca or Cl in low-ANC lakes was negatively related to precipitation amount. In regions with low precipitation and/or high evapotranspiration, such as Finland and central Czech Republic, increased precipitation would cause a decrease of SAA in surface water, and a decline in base cation leaching, which could be more than is caused by dilution because of cation resorption by soils.

11.10.7.6 Marine Aerosols

The sea-salt effect, which has until recently been considered only as an episodic process, may also operate over decadal periods in relation to the NAO Index. The NAO is derived

from the atmospheric pressure difference between the Azore Islands and Iceland. The NAO strongly affects winter temperature and precipitation in regions bordering the North Atlantic (Hurrell, 1995; Jones et al., 2001). High winter NAO Index values are associated with wet and warm, frontally dominated winter weather in northwestern Europe. Such periods are coincident with more marine salt input, increasing Cl (Evans et al., 2001c). Most importantly, the episodic input of the base cations Na^+ and Mg^{2+} may cause desorption of H^+ and Al^{3+}, with potentially significant impact on biota (e.g., Hindar et al., 1994).

11.10.7.7 Biological Feedbacks

Climate variability and atmospheric deposition alter vegetation and microbial activity. Elevated concentrations of atmospheric CO_2 can increase, at least for some period of time, forest growth and nutrient uptake, as does increased N deposition. Warming lengthens the growing season, increases primary production (uptake) and decomposition, thereby accelerating cycling of nutrients. Forested ecosystems can respond to climate warming by increasing inorganic N leaching caused by enhanced mineralization (Mol-Dijkstra and Kros, 2001; Wright, 1998). Changes in vegetative community structure through stand development or human disturbance can produce significant changes in dry deposition of acidic compounds through canopy interception, evapotranspiration, hydrology, and base cation sequestration in biomass. Simulations by the nutrient cycling model (NuCM) at six US sites suggested that increasing temperature caused N release from the forest floor. At N-saturated sites, N leaching increased. At the N-limited sites, increased growth (uptake) occurred (Johnson et al., 2000), limiting any increases in N loss. These examples illustrate the complexity of ecosystem response to multiple stressors, and the challenge of incorporating biological mechanisms into models of acidification and recovery.

11.10.8 Acidification Trajectories through Recent Time

Long-term natural acidification trajectories are reflected in freshwater responses to base cation depletion in soils that occurs as a result of pedogenesis in humid environments coupled with an increasing production of DOC. Variations in the acidification trajectory can be induced by variations in the original mineralogy of the soil, hydrology, temperature, biomass accumulation, and the concentrations of weak acids (carbonic and organic). With the onset of accelerated acidification induced from atmospheric deposition of strong acid, the export of base cations (mainly Ca) should increase, either because of their desorption from the soil complex or because of an increase of mineral weathering. Although variations in mineral weathering as a consequence of acidification were studied intensively in the 1980s (see, e.g., Schnoor, 1990; Swoboda-Colberg and Drever, 1993), experimental studies at both the laboratory and watershed scale (e.g., Dahlgren et al., 1990; Fernandez et al., 2003) indicate that increased export of base cations is largely attributable to desorption on decadal timescales or less.

Within a yearly cycle for watersheds that are nearly steady state with respect to acid–base status, Ca and other base cations in runoff commonly vary inversely with discharge (e.g., Feller and Kimmins, 1979). This relationship is caused primarily by dilution of runoff with precipitation (Laudon and Norton, 2010). Although base cation concentrations vary considerably, their ratios commonly remain relatively constant (**Figure 5**), indicating that short-term variability is controlled by ion exchange equilibria among Al, H, Ca, Mg, K, and Na, with Na and K playing only a minor role. Thus, samples with lower concentration (**Figure 5**) are from high-flow events. If acid loading is substantially increased to a system (cf. West Bear, **Figure 5**), the exchangeable base cation soil pool resists acidification by desorbing base cations (and adsorbing H^+) and the soils adsorb SO_4. The trajectory of changes in the Ca concentration in runoff during acidification related to anthropogenic acidity should follow the path shown in **Figure 6(a)**. A reduction in acid loading reverses these processes. This conceptual model divides the history of anthropogenic acidification and recovery into seven stages:

Stage 1 corresponds to a 'steady state' where base cation concentrations in runoff are relatively constant, averaged over periods longer than an annual cycle. The rate of export of base cations is equal to the rate of chemical weathering of minerals containing these elements. BS of soils is also relatively constant. The end of Stage 1 represents the onset of a step increase in acid loading to an elevated constant value. *Stage 2* corresponds to the period of increasing export of base cations as a consequence of the increased acid loading. Concurrently, the ANC of the stream and BS of the soils decrease. As acidification progresses and soil exchangeable base cations become depleted, base cation concentrations in solution peak, and then decline. *Stage 3* is a period of decreasing stream base cation and ANC concentrations, with increasing H^+ and Al in runoff, and decreasing BS in the soils. *Stage 4* is a new steady state where runoff chemistry approximates Stage 1 steady-state values, and

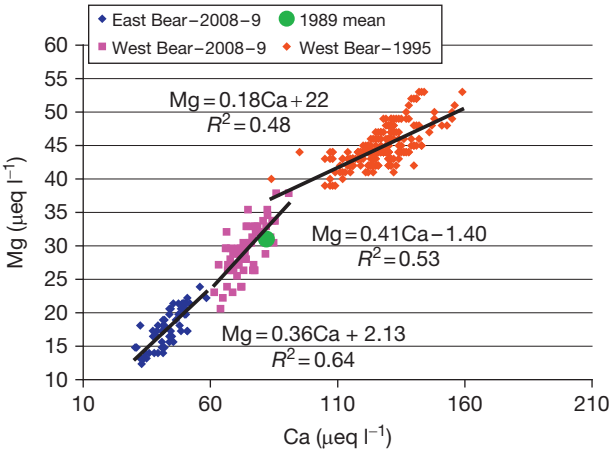

Figure 5 Weekly concentrations of Ca and Mg in East and West Bear brooks, watersheds, Maine, USA, for 2008–2009, and for 1995 for West Bear Brook (Norton, unpublished) showing strong ion exchange control on the Mg/Ca ratios. The green point is the mean value for 1989 for both watersheds (see **Figure 7**). Note (1) decrease of Ca and Mg in West Bear from 1995 to 2008–2009, (2) preferential depletion of Mg, and (3) decrease of Ca and Mg in East Bear.

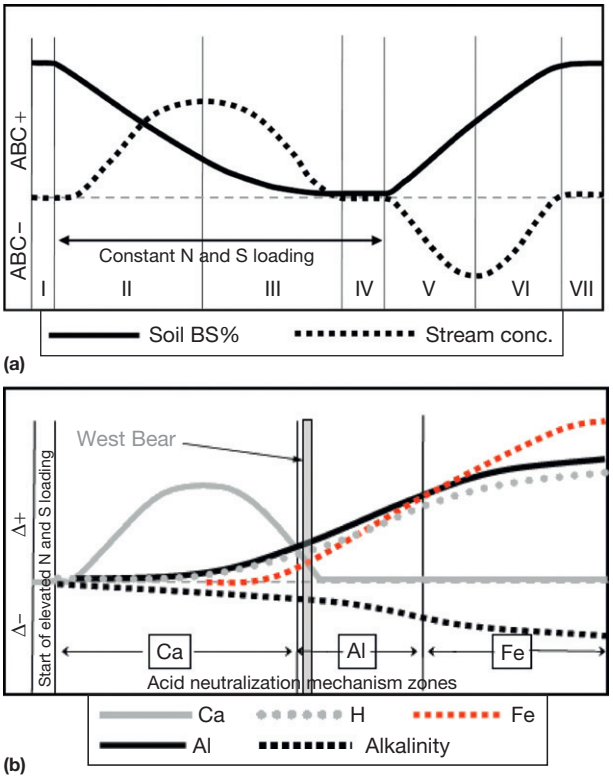

Figure 6 (a) Changes in base cations in stream runoff as a consequence of acidification and deacidification. Modified from Fernandez IJ, Rustad LE, Norton SA, Kahl JS, and Cosby BJ (2003) Experimental acidification causes soil base cation depletion in a New England forested watershed. *Soil Science Society of America Journal* 67: 1909–1919. (b) Evolution of dominant neutralization mechanisms by Ca, Al, and Fe during acidification. Modified from Fernandez IJ, Rustad LE, Norton SA, Kahl JS, and Cosby BJ (2003) Experimental acidification causes soil base cation depletion in a New England forested watershed. *Soil Science Society of America Journal* 67: 1909–1919.

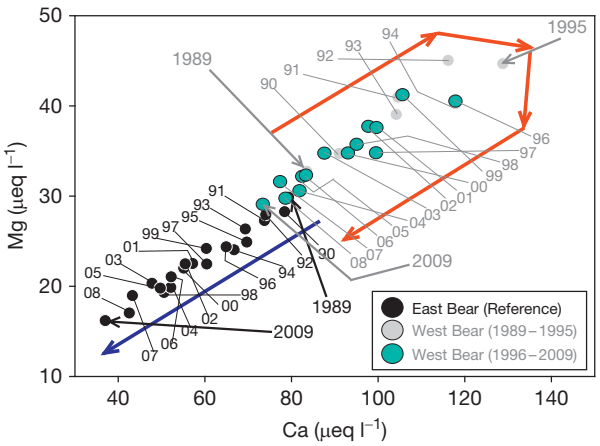

Figure 7 Volume-weighted annual mean concentrations of Ca and Mg for East and West Bear watersheds, Maine, USA, from 1989 to 2009 (Fernandez and Norton, unpublished).

the rate of export equals the weathering rate. However, BS of the soil is now lower and episodic acidification is easily induced. *Stage 5* starts when the excess acid loading from the atmosphere stops. With continued weathering, part of the supply of base cations is adsorbed onto the impoverished soil exchange complex, lowering the runoff cation concentrations to values below preacidification values. The concentration of base cations decreases to a minimum value and then in *Stage 6* it increases, as the BS and stream concentrations approach their preacidification steady-state values. *Stage 7* is the recovered steady state, equivalent to Stage 1.

This scenario suggests that anthropogenic acidification, unlike natural acidification, is largely reversible and the depleted BS of soils may be restored, provided weathering and atmospheric inputs of base cations are higher than their rate of leaching. The oversimplified acidification trajectory is linked with a timescale that is highly site specific and the details of the processes will depend on many factors. Nonetheless, there is strong evidence for such a scenario, including laboratory studies of soils (Dahlgren et al., 1990), ecosystem-level experiments (Fernandez and Norton, 2010), and empirical data (Jenkins et al., 2001). Regrettably, there are not sufficiently long time series to document all stages of this process but studies of watersheds not in steady state can be placed within this evolutionary scheme. In watersheds with low exchangeable base cation reservoirs, anthropogenic acidification can deplete base cations rather quickly. In these watersheds, Al (Neal et al., 1997; Veselý et al., 1998b) or Fe (e.g., Borg, 1986) are typically the dominant cations exported. The conceptual models of Figure 6 are captured in the paired watershed experiment at BBWM, where one watershed (West Bear) was treated with $(NH_4)_2SO_4$ to accelerate acidification. Acidification of the West Bear watershed has been accelerated from Stage 1 through Stages 2 and 3 in a decade (Fernandez and Norton, 2010), responding at first with increasingly greater leaching of Ca and Mg (Figure 7) for 7 years (equivalent to Stage 2), followed by declining leaching of Ca and Mg as soil BS declined (Stage 3). As base cations became depleted, Al replaced base cations as the principal neutralizer of incoming acid, and Fe started to mobilize as the more easily mobilized forms of soil Al became depleted (Figure 6(b)). Meanwhile, slower acidification of the untreated watershed (East Bear) resulted in a continuous decline over 22 years of observation during declining atmospheric deposition of SO_4. Either East Bear has entered Stage 5 (recovery) or is still in the late stages of Stage 3.

11.10.9 Longitudinal Acidification

In general, soil water pH increases with depth below the forest floor in well-drained forest soils because of decreasing soil organic matter sources of DOC, metabolism of acidic DOC, and increasingly weatherable minerals with depth. Consequently, pH in headwater streams generally increases downstream (Driscoll et al., 1988) because (1) soils and flow paths are typically shallow at higher elevation, (2) higher elevations more commonly support coniferous forests whereas deciduous vegetation is typically more common at lower elevation, (3) larger watersheds typically have more heterogeneous geology, with the possibility of higher ANC-producing bedrock/soil,

(4) lower elevation terrain is typically underlain by bedrock with higher ANC-producing chemistry, and (5) mountainous areas typically receive larger quantities of pollutants relative to lowlands due to orographic precipitation effects and interception of cloud droplets with high concentrations of pollutants (Grennfelt and Hultberg, 1986; Lovett, 1992). Thus, there is a general pattern that watersheds are more acid sensitive at upper elevations and acidify from the top down (Hauhs, 1989; Matschullat et al., 1992; Norton, 1989).

Base cations removed from the upper part of a watershed are generally lost from the system, mostly remaining in solution. Some of the base cations are temporarily stored in stream sediment or in wetlands. The concentration of base cations typically increases downstream. Mobilized ionic Al (dominantly) (Roy et al., 1999), Fe, and Mn (Borg, 1986) move downstream where they can be precipitated in higher pH regions of streams (Veselý et al., 1985) or lakes (Kopáček et al., 2001b), scavenging trace metals and P. These Al- and Fe-rich precipitates represent translocated ANC. The acid neutralizing capacity, represented by exchangeable base cations and Al- and Fe-rich precipitates, must be stripped by progressive acidification before an entire stream can become chronically acidic.

Flat topography and a cool, moist climate provide favorable conditions for organic matter accumulation. Bogs and fens along the surface water flow path may substantially alter water chemistry, commonly adding DOC, and removing NO_3 and SO_4. All other chemical factors being equal, humic waters (those rich in DOC) are more acidic. These waters, commonly naturally acidic, are more common at low elevation on flat terrain with relatively low precipitation, such as in Finland (Kortelainen and Mannio, 1990). Streams that are recharged primarily by springs have relatively stable chemistry (Lange et al., 1995) and low DOC.

11.10.10 Some Areas with Recently or Potentially Acidified Soft Waters

11.10.10.1 Eastern Canada

Much of eastern Canada is underlain by slowly weathering rocks with few carbonate minerals. This area includes large parts of Ontario, Quebec, Newfoundland, New Brunswick, Labrador, and Nova Scotia. The regional climate ranges from relatively dry, cool, and continental in western Ontario, the site of the classic Experimental Lakes Area (ELA) (see, e.g., Schindler et al., 1990), to relatively wet cool maritime (see Jeffries, 1997, for an overview). Sudbury, Ontario, once the site of the world's largest point source of SO_2 emissions, has been the focus of chemical and biological studies, first describing the trajectory of acidification and then recovery (Gunn, 1995), after the point source emissions were dramatically reduced. This west-to-east transect also corresponds to a strong gradient of atmospheric deposition of SO_4 and NO_3, with the highest pollution in eastern Ontario and western Quebec. Consequently, the various lake districts have distinctly different water qualities. The Ontario and Quebec lakes are dominated by relatively low DOC drainage lakes whose modified acid–base chemistry has been dominated by SO_4 input. Nova Scotian lakes and streams, on the other hand, are predisposed to impact from atmospheric deposition because of their relatively low Ca and high DOC. The time series of lake chemistries are long, high quality, and commonly of high spatial and temporal resolution so that both the processes of acidification and recovery can be studied, as well as the effects of climate and marine aerosol gradients.

11.10.10.2 Eastern United States

The Adirondack Mountain Region of New York was the first area in the United States to be identified as under stress from acidic deposition. It is close to the region of highest S and N deposition for the United States (**Figure 1**), receives between 1 and 1.5 m of precipitation, and is underlain by large areas of Ca-poor bedrock and thin soils developed from till. In 1985, the US Environmental Protection Agency conducted a statistically designed national survey to characterize terrane at risk from anthropogenic acidification (Brakke et al., 1988). They identified additional areas outside New York that were receiving significant acid rain and had bedrock and soils that placed them at risk of acidification. Since then, there have been few comprehensive federally sponsored surveys of lake or stream chemistry. Fewer sites have been studied more intensively (e.g., Stoddard et al., 1998). In the last half of the 1990s, SO_4 in deposition declined, but recovery of ANC in acidified systems has been slow to nonexistent (Kahl et al., 2004). At some localities, base cations are decreasing faster than SAA (NO_3 and SO_4) in surface water (Warby et al., 2005, 2009), implying that either acidification from SAA is still continuing or other contemporary processes are occurring (Yanai et al., 1999).

South of the glaciated region in the eastern United States there are few natural lakes, but many streams draining old thin soils developed on Ca-poor bedrock exist. Webb et al. (1989) surveyed 344 trout streams draining the Blue Ridge Mountains in Virginia and found many low-ALK streams with low Ca and Mg. Sulfate concentrations, while the highest of all ions, were maintained at less than one third of values in equilibrium with atmospheric deposition because of soil sulfate retention. The soils, dominantly Ultisols, strongly adsorbed SO_4 and had not yet equilibrated with the elevated concentrations in deposition, thus delaying acidification. The desorption of SO_4 also delays recovery as atmospheric deposition of SO_4 declines.

Some of the longest time series of environmental measurements of soils and soil solutions, precipitation quality, and nutrient cycling for the United States come from the Walker Branch Watershed, Tennessee and from the Coweeta Watershed, North Carolina. As for HBEF, much research there was originally designed to evaluate the impact of forest practices on soil fertility. A common characteristic of the older soils is the relatively low concentration of Ca and Mg because of long-term natural acidification. The accumulation of abundant sesquihydroxide secondary phases in the soils results in adsorption of excess SO_4 from the atmosphere, even as base cations are being depleted by acidic deposition (Johnson et al., 1982, 1988).

11.10.10.3 British Isles

The United Kingdom Acid Waters Monitoring Network (UKAWMN) was established in 1988 to assess the effect of emission reduction on selected acid-sensitive sites in the

United Kingdom (Evans and Monteith, 2001). Widespread declines in nonmarine SO_4 concentration did not occur between 1988 and the mid-1990s. Sulfate concentrations have declined substantially since the mid-1990s (Ferrier et al., 2001; Harriman et al., 2001). The most strikingly consistent observation from UKAWMN is the gradual regional increase in DOC, which has slowed recovery. The increase in organic acidity has been of a similar magnitude to the decrease in mineral acidity (Evans and Monteith, 2001). There has also been a general reduction in winter storms connected with the sea-salt effect from the early 1990s with a reduction in Cl and a slight reduction in acidity. Over the past 50 years, patterns of storminess over the United Kingdom, connected with marine salt input, have oscillated on an approximately 10 year cycle (Evans et al., 2001c). Long-term studies at several research sites have enabled detection and understanding of acidification-related processes in addition to acidification from air pollution (e.g., Plynlimon Wales; Neal, 1997).

Aherne et al. (2002) reported, from a stratified pseudorandom survey of 200 lakes in the Republic of Ireland, that variations in lake chemistry were strongly influenced by marine aerosol deposition. The acidity for lakes with pH <6 was dominated by organic acidity, followed by SO_4 (primarily in the east) and NO_3.

11.10.10.4 Scandinavia

Acidification of freshwaters has been and remains a major environmental problem for the three Nordic countries (Finland, Norway, and Sweden) where freshwaters have low ionic strength and low concentrations of nutrients. This is mainly due to low bedrock weathering rates and thin soils (Henriksen et al., 1998; Skjelkvåle et al., 2001b). From western Norway to eastern Finland, there is a gradient from high (~3 m) to low (~0.5 m) precipitation and from mountainous areas with thin and patchy soils to forested areas with relatively thick, commonly organic, soils. Clearwater lakes and streams with low base cation concentrations and low ANC dominate in western Norway and brown, high DOC lakes and streams with higher concentrations of solutes dominate in Finland (Mannio, 2001; Skjelkvåle et al., 2001a). For the northern half of Sweden, changes in water chemistry can be largely attributed to variation in climate (Fölster and Wilander, 2002). Surveys of 485 lakes in Norway conducted in 1986 and again in 1995 reveal widespread chemical recovery from acidification (Henriksen et al., 1998). At first, most of the decrease in nonmarine SO_4 was compensated by a decrease in base cations such that ANC remained unchanged (Stage 4 of the acidification trajectory; see **Section 11.10.8**). But as SO_4 continued to decrease, the concentrations of nonmarine Ca and Mg stabilized and ANC increased (Skjelkvåle et al., 1998). The cessation of further increases of NO_3 in the 1990s suggested that N saturation was a long-term process in Nordic countries. Concentrations of DOC or TOC (total organic carbon) have increased significantly in numerous Scandinavian lakes during the last two decades (Monteith et al., 2007).

11.10.10.5 Continental Europe

Geology, weathering rates, and soil composition in much of continental Europe provide better acid neutralizing ability than in most of Scandinavia. Most of central Europe was not glaciated during the Pleistocene. Consequently, soils are richer in secondary Al and Fe phases, enabling them to adsorb more of the excess SO_4 from atmospheric deposition. Highly variable bedrock type and thicker soils cause spatial heterogeneity of susceptibility to acidification and chemical recovery of surface water. Acidification of higher elevation watersheds, with less accumulation of weathering products, was rapid and recovery quicker in sensitive areas of central Europe (Evans et al., 2001b; Veselý et al., 2002a), accelerated by large decreases in atmospheric deposition of not only SO_4 but also both reduced and oxidized nitrogen compounds. Streams draining watersheds on deeply weathered preglacial soils have no or only a slight decrease in SO_4 concentrations and no chemical recovery, even with a substantial decline of acidic deposition (Alewell, 2001; Alewell et al., 2001). Variable soils coupled with regional variation in deposition produced isolated, severely acidified regions at higher elevations of the Czech Republic (Veselý and Majer, 1996, 1998), Slovakia, and Poland (Kopáček et al., 2002b). These sites have undergone regional decline in NO_3 concentrations (up to 60%) since the mid-1980s (Veselý et al., 2002a). However, in northwestern Italy, NO_3 concentrations increased by about 25% from the 1970s to the 1990s (Mosello et al., 2000). Sites in the central and southern parts of the Netherlands have large NH_3/NH_4 deposition with high potential for nitrification and acidification (De Vries et al., 1995), although deposition has declined since about 2000.

While impacts of acidification on fish status are the main concern in Scandinavia and North America, damage to planted coniferous forests at high-elevation sites in central Europe was critical. For example, about 100 000 ha of *Picea abies* died in the Czech Republic in the 1970s and 1980s, and more than 50% of the forest suffered 'irreversible' damage (Moldan and Schnoor, 1992). Remarkably, emissions of S and inorganic N were reduced nearly 92 and 60%, respectively, between 1985 and 2008, and the forests are slowly returning to a healthy status (Šantrůčková et al., 2007).

11.10.10.6 South America

Much of South America is relatively free of significant air pollution. Nitrate concentrations in remote Chilean and Argentinian streams are low. Dissolved organic nitrogen is responsible for most of the high N losses, 0.2–3.5 kg N ha^{-1} $year^{-1}$, from these forests (Perakis and Hedin, 2002). In Amazonia there is strong internal recycling of N with little export from undisturbed watersheds. The rain is slightly acidic (pH 5.2) with inputs of 3.7–8.7 kg SO_4-S ha^{-1} $year^{-1}$ and about 0.8 kg NO_3-N ha^{-1} $year^{-1}$ (Forti et al., 2001). Abundant DOC depresses the pH of some larger tributary streams of the Amazon (Williams, 1968). The MAGIC acidification model (Modeling the Acidification of Groundwater In Catchments, Cosby et al., 1985) has been used to assess the effects of conversion of a tropical Amazonian rain forest watershed to pasture on water quality (Neal et al., 1992). The modeling demonstrated the sensitivity of tropical rainforest runoff to deforestation, even without climate changes (Forsius et al., 1995).

11.10.10.7 Eastern Asia

In contrast to North America and Europe, emissions of SO_2, NO_x, NH_3, and metals are rising markedly in many developing countries. In East Asia (Japan, Korea, China, Mongolia, and Taiwan), emissions of SO_2, NO_x, and NH_3 are projected to increase by about 46, 95, and 100%, respectively, by 2030 (Klimont et al., 2001). By 2020, Asian emissions of SO_2, NO_x, and NH_3 may equal or exceed the combined emissions of Europe and North America (Galloway, 1995). By 2010, emissions of CO_2 by China exceeded those of the United States. Annual mean concentrations of SO_2 in air as high as 1300 ppb have occurred in industrial areas of Thailand (Wangwongwatava, 2001). Fujian and Guizhou provinces in south China received significantly acidic rain. Although total S deposition in China is relatively high (Larssen et al., 1998), alkaline dust and NH_3 emissions neutralize much of the SO_4 acidity of precipitation. Regional long-term data for surface waters susceptible to acidification are sparse (Fu et al., 2007) but growing. Osterberg et al. (2008) showed, through analysis of ice cores from coastal southwestern Alaska (Mount Logan), that trace metal deposition was low and relatively constant until about 1980, when deposition of Pb, As, and Bi started increasing dramatically. This is coincident with the emergence of China as an important user of coal as it rapidly industrialized. At the same time, deposition of these metals in eastern North America and Europe has been rapidly declining.

Total deposition of S compounds over Japan was more than twice the human emissions because of volcanic activity. The emission of SO_2 from Japan is <5% of the total emissions in East Asia. As for China, there are few regional long-term datasets to determine environmental impact from S and N emissions.

11.10.11 Experimental Acidification and Deacidification of Low-ANC Systems

Numerous experiments have been conducted to understand the chemical linkages between atmospheric deposition of acidic compounds and acidification of soils, streams, and lakes. Experiments have included additions of acid, exclusion of acids, and the application of limestone ($CaCO_3$) or other acid-neutralizing compounds to add ANC directly to surface water or soils. Many of the studies are discussed in Dise and Wright (1992), Rasmussen et al. (1993), Jenkins et al. (1995), and Van Breemen and Wright (2004). We highlight a few studies here.

11.10.11.1 Experimental Acidification of Lakes

Lake 223 in the ELA in northwestern Ontario, Canada, and Little Rock Lake (LRL) in northern Wisconsin, USA, were progressively acidified by in-lake addition of H_2SO_4 from their original pH values of 6.1–6.8 to 4.7–5.1 (Schindler et al., 1990). Both lakes generated an important part of their ANC internally by microbial reduction of SO_4, and to a lesser extent by reduction of NO_3. ANC production increased in LRL as approximately 50% of the H_2SO_4 added was neutralized by microbial reduction in sediments. Acidification disrupted N cycling. Nitrification was inhibited in Lake 223, whereas in LRL, N fixation was greatly decreased at lower pH.

Lake 302S in the ELA was experimentally acidified from an original pH of 6.0–6.7 to pH 4.5. The DOC drastically declined from 7.2 to 1.4–1.6 mg l^{-1}, comparable to clear arctic and alpine lakes (Schindler et al., 1996). The increased clarity allowed greater penetration of solar radiation, including UV. The thermal structure of the water column was altered, impacting circulation and nutrient regeneration. Results from both Lake 223 and lakes near Sudbury, Canada, suggest a recovery of lacustrine communities when acidification stress is reversed. Fish reproduction resumed at pHs similar to those at which reproduction ceased when the lake was being acidified.

Dystrophic (humic-rich) Lake Skjervatjern and its watershed, western Norway, were acidified with a combination of H_2SO_4 and NH_4NO_3 as part of the humic experiment (HUMEX) (Gjessing, 1992). The research studied the role of humic substances during acidification of surface waters, and the impacts of acidic deposition on chemical and biological properties of humic water (Kortelainen et al., 1992). The watershed and lake were physically divided with a curtain for the treatment. The DOC of Lake Skjervatjern was partly controlled by variable water retention time in the lake basin. DOC decreased with increasing retention time. DOC and water color decreased during acidification, followed by an increase likely caused by fertilization of the watershed with N. Periods with high precipitation and discharge coincided with increased concentration and quality of DOC (Gjessing et al., 1998).

These few experiments illustrate clearly that acidification of surface waters causes a decline in DOC, and fairly quickly, either through altered processes in the watershed or in the lake. The reverse of this change was to be anticipated during the recovery from decreased atmospheric loading of SO_4, and has been documented in many lakes in the northern hemisphere (Monteith et al., 2007). The changes in base cation dynamics are slower to respond, being buffered by soil, and thus slower to recover.

11.10.11.2 Experimental Acidification of Wetlands

Bayley et al. (1988) added H_2SO_4 to a bog in western Ontario, Canada, to evaluate the chemical and biological response of wetlands to atmospheric inputs of SO_4. Sulfate was substantially retained in true bogs, or reduced to H_2S and reemitted to the atmosphere. The fate of SO_4 is unclear because of very strong intraannual variation in concentration due to oscillating oxidation and reduction processes within bogs. The fate of NO_3 in true bogs seems quite unequivocal in that bogs always have lower concentrations than are present in precipitation. The N budget (net storage or reemission to the atmosphere) of bogs has not been well studied. Both S and N can be stored in reduced form as organic matter, released to the atmosphere as gaseous compounds, leached to surface water as organically bound S and N, or as the oxidized anion. It seems unlikely that true bogs (with pHs near 4) can be significantly acidified by any reasonable loading of acid from the atmosphere because of the organic acid buffering (Gorham et al., 1987).

11.10.11.3 Experimental Acidification of Terrestrial Ecosystems

At HBEF, New Hampshire, USA, Likens et al. (1977) pioneered the paired watershed approach to biogeochemical experiments,

which included many related to the impact of acidification. For over 35 years, they have examined long- and short-term data for precipitation chemistry, stream chemistry, cation supply from various sources, variable forestry practices, and performed smaller scale experiments with moisture, soil CO_2, salt additions, and Ca amendments to the forest floor. The long-term high-resolution data derived from HBEF have provided important insights into the variability of our chemical climate and have demonstrated the necessity of long-term data to sort out important long-term process from short-term variability (Cho et al., 2010; Driscoll et al., 1989).

BBWM, USA, is a paired watershed (~10 ha each) study with one forested watershed treated with $(NH_4)_2SO_4$ and the other serving as a reference (Fernandez and Norton, 2010; Norton and Fernandez, 1999). The major changes in stream chemistry for the 1989–2009 manipulation period include decreased pH and ALK, and increased export of base cations, SO_4, NO_3, Al, P, Fe, and Mn. DOC and silica remained essentially constant, suggesting that acidification from ~5.2 to 4.6 was largely controlled by increased nitrification of ammonium plus resident organic N, increased SO_4 flux, desorption of base cations, and dissolution of secondary Al, Fe, and Mn phases from the soil. Fernandez et al. (2003) showed that the excess base cation export in runoff was matched by the loss of exchangeable base cations from soil in the experimentally acidified watershed over the first decade of treatments, in agreement with MAGIC model predictions. Runoff SO_4 has declined in the treated watershed at BBWM as a consequence of increased SO_4 adsorption in the acidifying soils. This process was also observed at HBEF (Nodvin et al., 1986) as a consequence of transient increased nitrification (and soil water acidification) due to tree harvesting. The effect of lower pH on SO_4 adsorption has also been reproduced in laboratory experiments (Navrátil et al., 2009).

Watersheds in the Fernow Experimental Forest, West Virginia, USA, have also been artificially acidified with $(NH_4)_2SO_4$ since 1989 (Adams et al., 2006; Edwards et al., 2002; Fernandez et al., 2010). They reported some parallel results on the trajectory of response to experimental acidification such as the increased export of Ca and especially Mg (Al was not measured), but they had substantial SO_4 retention in the older, unglaciated soils.

Risdalsheia, southern Norway (Wright et al., 1993) is in a region substantially impacted by acidification during the twentieth century. It has been the site for many paired watershed chemical manipulations. At Risdalsheia, a miniwatershed, including the canopy, was covered by a transparent roof to exclude ambient acid precipitation. 'Clean' reconstituted rain with natural concentrations of sea salts was applied underneath the roof. Loadings of SO_4, NO_3, and NH_4 were experimentally reduced by about 80%; the remaining 20% occurred as dry deposition of gases and particles. Later, the same miniwatershed was subjected to 3–5 °C warming and elevated CO_2 (to 560 ppmv). The flux of N in runoff increased by about 5–12 mmol m^{-2} $year^{-1}$ (Wright, 1998), probably due to increased mineralization and nitrification rates in the soils because of higher temperature. The pH did not increase substantially because of high concentrations of DOC that buffered pH. Long-term simulations by the SMART2 (Simulation Model for Acidification's Regional Trends) model (Mol-Dijkstra and Kros, 2001) predicted a long-term increase of N in runoff.

Wright also conducted a series of experiments at Sogndal, western Norway, a pollution-free site with more than one meter of rain. Using the paired watershed design, H_2SO_4 and a combination of H_2SO_4 and HNO_3 were added to the terrestrial part of several watersheds over a long period of time. The acidification trajectory involved increased export of base cations and Al, and decreased ANC and pH (Frogner, 1990). Episodic acidification due to atmospheric deposition of marine aerosols was also demonstrated experimentally at Sogndal. Diluted sea water (~600 mg Cl l^{-1}) was added to a miniwatershed, simulating a salty rain event. The runoff response included depressed pH and ALK, and increased export of Al, Ca, and Mg desorbed from the soil (Wright et al., 1988).

Gårdsjøn, Sweden, has been home to the famous roof experiment (Andersson and Olsson, 1985; Hultberg and Skeffington, 1998). The watershed complex included terrestrial and aquatic experiments, with acid additions, terrestrial liming, acid exclusion experiments, ^{15}N additions, and salt additions. Located in southwestern Sweden, the terrestrial and aquatic system had been acidified by anthropogenic acidity from the atmosphere. In a somewhat analogous experiment to that at Risdalsheia, a roof was installed below the canopy of a small watershed to catch all throughfall. The precipitation plus chemicals leached from the canopy were reconstituted to contain only the normal marine salts and then distributed below the roof. This essentially was a step function reduction in acid rain, to assess how ecosystems recover. A subwatershed was part of a European network of manipulations where excess N (as NH_4 or NO_3), labeled with ^{15}N, was added to systems (see Wright and Rasmussen, 1998; Wright and von Breeman, 1995). This tracer enabled scientists to track the ecosystem processing, sequestration, and release of N. The NITREX (NITRogen saturation EXperiments) (Dise and Wright, 1992) project involved chemical manipulations with N and N isotopes in Norway, Sweden, Wales, Switzerland, The Netherlands, and Denmark (Moldan and Wright, 2011; Wright and Rasmussen, 1998).

11.10.11.4 Experimental Acidification of Streams

Chemical acidification experiments in streams have the advantage of having a chemical and biological reference (upstream of any chemical additions), easy sampling, and repeatability. Understanding the role of sediments during episodic acidification also yields information about the behavior of soils, from which much of the sediment is derived. A classic experiment for stream acidification was conducted by Hall et al. (1980) at HBEF. They demonstrated the ability of stream sediments to yield base cations and Al, thus resisting the depression of pH by addition of HCl. While much of this acid neutralizing ability was exhausted, stream sediment clearly played a role in ameliorating episodic acidification and recovery. Similar experiments have been conducted in the United Kingdom (Tipping and Hopwood, 1988), Norway (Henriksen et al., 1988b), and Maine, USA (Goss and Norton, 2008; Norton et al., 1992, 2000).

In summary, the studies indicate that stream sediments (inorganic and organic) are a pool of reversibly exchangeable

base cations, Al (probably precipitated plus exchangeable), P, and other trace metals including Be, Cd, Fe, and Mn. Stream sediment also has SO_4 adsorption capacity, which contributes to the delay and diminution of episodic acidification, and delays recovery. The effectiveness of the sediment exchange processes is proportional to grain size and organic matter content. Stream water has the ability to buffer excursions of pH if there is sufficient DOC and HCO_3^- weak acid acidity, as demonstrated by Hruška et al. (1999).

11.10.12 Remediation of Acidity

11.10.12.1 Ca Additions

Treatment with limestone ($CaCO_3$), or something chemically similar that yields ALK during rapid dissolution, has been used as a general antidote for acidification of terrestrial and aquatic systems, first on an experimental basis and then as a long-term management strategy under field conditions. There is no general agreement on the usefulness of liming as a countermeasure to anthropogenic acidification. Nonetheless, all countries with significant acidification problems have studied this method of remediation. Many studies are reviewed in Porcella et al. (1989). Liming generates ANC but not in a way consistent with the natural system and generally not at the same place as natural processes. Thus, while pH may be restored to preacidification values in soil or surface waters, the system chemistry may not resemble preacidification conditions and biota may not recover along the trajectory they followed during acidification.

For example, Dillon et al. (1979) followed the response of several lakes in the vicinity of Sudbury, Ontario, Canada. Wright (1985) conducted a three lake study at the Hovvatn site in southern Norway. There, two lake basins were limed in 1981 by several methods, including dispersal on ice and along the shore. A contiguous lake with similar initial chemistry served as a reference lake. A major finding was the rapid loss of ALK generated by the dissolution of $CaCO_3$, due to flushing of the lake with acidic water from the watershed. Similar findings appear in most studies, although detailed response is complicated by differing hydrology of individual lakes. It is clear that direct addition of the $CaCO_3$ to a lake has to be done on a more or less continuing basis to avoid large excursions in pH or a return to acidic conditions. The cost related to aerial applications of lime is enormous, commonly on the order of $200 (United States – 2005 equivalents) per ton. Nonetheless, some nations have adopted liming as a strategy to protect or restore surface water pH. For example, Sweden started expending substantial funds in a program that limes hundreds of lakes per year, on a rotating basis (Henrikson and Brodin, 1992). This program has continued to 2010. Since 1990, about half of the Swedish subsidy for liming has been used in northern Sweden where natural organic acids can be more important than acid deposition in determining the acidity of surface waters (Bishop, 1997; Laudon et al., 2001). Thus, liming programs need to distinguish naturally acidic surface waters from those that have been acidified by excess SO_4 and NO_3 (Bishop et al., 2008).

Other experiments have included liming low pH, high Al, high DOC streams during episodic acidification, as in the West River Sheet Harbor, Nova Scotia. The net effect was to raise pH, ANC, and Ca but the accompanying precipitation of Al presented a serious stress for at least anadromous fish (Rosseland et al., 1992; Teien et al., 2006). Liming directly on the land (e.g., at Gårdsjøn, Sweden; Hultberg and Skeffington, 1998) was also partially effective in restoring exchangeable Ca reservoirs in soil, but a considerable dose is necessary to improve ANC in draining waters. Reacidification of limed lakes can result in elevated trace metal concentrations as sediments desorb metals and adsorption of metals in the water column declines.

Acidified lakes near or above tree line commonly have acidophilic vegetation in the watershed that can be severely damaged by direct application of lime, for example, at Tjønnstrond, Norway (Traaen et al., 1997), even though water quality (lower Al, higher ANC, pH, and Ca) was restored for a decade, fish habitat became more hospitable, and exchangeable Ca was partially restored in the catchment soils. Additionally, organic matter may be lost from soil as mineralization increases due to higher pH.

At HBEF, wollastonite ($CaSiO_3$), a relatively soluble silicate mineral, was applied to an entire watershed (W-1, Peters et al., 2004). The response was for runoff to have elevated Ca, pH, Si, and ANC, and decreased inorganic Al, as the soils increased exchangeable Ca concentrations (Cho et al., 2010). Soil pH increased and exchangeable Al declined. As with application of $CaCO_3$ to watersheds, the effects persisted and can be expected to persist for even longer than lime applications because of the slower dissolution rate of the wollastonite.

11.10.12.2 Nutrient Additions to Eliminate Excess NO_3

Forests have a large capacity to retain N and to increase growth even after years of large anthropogenic input of N (Prescott et al., 1995). Similarly, adding P can increase N uptake by trees and significantly reduce NO_3 concentrations in soil solution (Stevens et al., 1993). Adding P as an N management strategy would presumably lead to reduced export of NO_3 in surface water. Concurrently, it would lead to increased uptake of Ca and Mg, thereby potentially increasing acidification. Adding P to lakes (Davison et al., 1995) and streams (Hessen et al., 1997; Simon et al., 2010) has been shown to reduce NO_3 concentrations, increase ANC, and increase the pH of the water (eqn [20]). Modest P addition ($<15\ \mu g\ P\ l^{-1}$, still avoiding eutrophication) instead of liming, thus may increase lake water pH and reduce NO_3 in a cost-effective way. However, in lakes where Al is precipitating (see **Section 11.10.5.2**), the addition of P can have a transitory effect because the P is irreversibly scavenged from the water column. Increased leaching of NO_3 from watersheds could be producing P limitation in streams and lakes.

11.10.12.3 Land Use

11.10.12.3.1 Deforestation

Understanding rates and processes of immobilization and leaching of N from soil organic matter under different levels of N deposition is crucial for assessment of future acidification.

The tight internal N cycle is broken as summer soil temperature, moisture, stream discharge, and storm-peak discharge increase, and when the vegetation is disturbed by harvesting, forest decline, fire, wind-throw, insect defoliation, and canopy damage by ice storms. Harvesting effects on stream chemistry have been studied extensively in North America, notably at Hubbard Brook (Bormann and Likens, 1979; Lawrence et al., 1987) and the Catskill Mountains (McHale et al., 2007), and in Wales (Reynolds et al., 1995). Deforestation in Wales resulted in a 5–7 year long NO_3 pulse in stream water related to increased mineralization and nitrification in the soil, and to more inorganic N available for leaching due to decreased biological uptake. The elevated NO_3 export from deforested areas is accompanied by elevated losses of base cations from soils and high leaching of ionic Al (Huber et al., 2004; McHale et al., 2007). Forest disturbances caused by harvesting, wind, or fire over the past several centuries have long-term impacts on forests' vulnerability to N saturation and their future capacity to store C and N (Goodale and Aber, 2001). Temporarily enhanced production of NO_3 and H^+ increases adsorption of SO_4 to soil (Gbondo-Tugbawa et al., 2002; Navrátil et al., 2009), and H^+ can exchange for Al and Ca in the soil (Henriksen and Kirkhusmo, 2000). The removal of biomass by harvesting is a removal of base cations, contributing to longer term base cation decreases in streams, thereby increasing the susceptibility of the stream to other acidifying stresses. Decreasing the canopy (by harvesting, defoliation, ice storm damage, or change in species) causes a decrease in the flux of pollutants to the forest floor because of decreased dry deposition (Hultberg and Grennfelt, 1992).

11.10.12.3.2 Afforestation

Aggrading forests contribute to surface water acidification in a number of ways: (1) Water discharge decreases because of enhanced evapotranspiration, causing evaporative concentration of pollutants, (2) hydrological pathways become modified (Waters and Jenkins, 1992), (3) coniferous afforestation commonly results in increasing DOC, (4) dry deposition of acidifying pollutants to a forest canopy increases as the canopy develops and effective leaf area index increases, and (5) inputs of pollutants in fog and rime ice (e.g., Ferrier et al., 1994) are also increased with the development of a canopy. Total deposition of S and other pollutants in throughfall in forests is typically several times higher than in bulk deposition outside the forest (Beier et al., 1993; Hansen et al., 1994; Rustad et al., 1994), with the exception of nutrients like N that can be biologically immobilized in the forest canopy. Episodic acidification caused by marine aerosols probably is enhanced in degree and frequency in forested areas, particularly in polluted areas (Jenkins et al., 1990).

The Plynlimon, Wales, studies of effects of conifer afforestation and deforestation have been carried out since shortly after World War II (Neal, 1997). There, forest plots with varied ages and their surface water discharge and chemistry have been studied for decades to help define the role of forests in acidification processes. Base cations and NH_4 were sequestered in biomass (Nilsson et al., 1982) with a concurrent release of H^+. The increase of storage of N and base cations in biomass decreases as the forest matures and consequently the acidifying effect of an aggrading forest decreases as standing biomass and dead biomass reach steady state. The time to steady state is species specific (Emmett et al., 1993).

11.10.13 Chemical Modeling of Acidification of Soft Water Systems

11.10.13.1 Steady-State Models

The response of the chemistry of soil, soil solutions, and surface waters to acid deposition has been simulated using steady state and dynamic models since the early 1980s. Models were developed to: (1) interpret the past, (2) guide future research, (3) support policy decisions (Forsius et al., 1997; Henriksen and Posch, 2001), and (4) aid in the explanation of observed ecosystem behavior (Gbondo-Tugbawa et al., 2002). Initial steady-state models used empirical data, in either space or time, to understand and predict regional lake chemistry (e.g., using lake populations; Henriksen, 1980) and stream chemical behavior (e.g., Christophersen and Neal, 1990). Kirchner (1992) developed a watershed-based static model for assessment of acidification vulnerability, based on runoff chemistry. Empirical models remain as powerful tools even as dynamic models have grown in complexity, parallel to computer development.

'Critical loads' are a quantitative estimate of the exposure to one or more pollutants below which significant harmful effects on specified sensitive components of the environment do not occur, according to present knowledge (Nilsson and Greenfelt, 1988). The exceedances of critical loads for impacts on soils and surface waters have been the basis for negotiations of emission reductions in Europe. The concept and usefulness of critical loads has spread to Canada and, recently, to the United States. The steady-state model for critical loads implies that only the final results of a certain deposition level are considered. Time to reach the final state is not considered. Critical loads of acidity for surface waters assume that the input of acids to a watershed will not exceed the weathering rate, less a stated amount of ANC ($0–50\ \mu eq\ l^{-1}$) in the long term. Early studies of critical loads focused more on S. As S in atmospheric deposition declined, N became a focus. The steady-state water chemistry (SSWC) model (Henriksen et al., 1995) considered only the extant N leaching level. The First-order Acidity Balance (FAB) model (Henriksen and Posch, 2001) for lakes assumed the N immobilization rate to be equal to the long-term annual amount of N that is used for alteration of the C/N ratio in the soil, plus N lost to denitrification and retained within the lake. This is the worst case of NO_3 leaching to surface waters. The FAB model, for example, predicts that more of the Norwegian lakes (46% in comparison to 37% by the SSWC model) could experience exceedances of the critical loads for acidifying deposition in the future (Kaste et al., 2002). Emission reductions negotiated in Gothenburg, Sweden, in 1999 were expected to reduce the area of exceedance of critical load for acidity from 93 million ha in Europe in 1990 to 15 million in 2010 (UN-ECE, 1999). Empirical and modeling studies indicate that recovery is underway (Aherne et al., 2008; Evans et al., 2008a,b).

Critical loads for pollutant metals (especially Cd, Hg, and Pb) are being considered in Europe (Skjelkvåle and Ulstein, 2002), even as the deposition of these three metals are sharply declining.

11.10.13.2 Dynamic Models

The static models for critical loads for S and N neglect the time component of acidification. Static models exclude long-term processes that can be nonstationary, including acid neutralization by soil adsorption of SO_4, altered biochemistry of N compounds, desorption of cations, and increasing DOC, all in a constant physical climate. These processes can delay acidification and recovery. The numerical models ILWAS (Integrated Lake Water Acidification Study) (Gherini et al., 1985), MAGIC (Cosby et al., 1985, 2001), SMART (De Vries et al., 1989), SAFE (Soil Acidification in Forest Ecosystems) (Warfvinge et al., 1993), PnET-BGC/CHESS (Krám et al., 1999), AHM (Alpine Hydrochemical Model) (Meixner et al., 2000), PROFILE (Sverdrup and Warfvinge, 1993), and NuCM (Johnson et al., 2000) are based on mathematical formulations of hydrological and biogeochemical processes in soil and waters. The models have been used for both forecasts and hindcasts of water quality in watersheds using data on topography, meteorology, soil chemistry, weathering rates, and acidic deposition. The reliability of model prediction increases with the length of observed data used for calibration. These dynamic models, although varying in detail, are based on similar principles: charge balance of ions in the soil solution and mass balances of the elements considered. Thus they describe the changes of the element pools over time.

The MAGIC and SMART models have been developed and improved for regional scale application. These models have a high degree of process aggregation to minimize data requirements for application at large scales or at multiple sites. The opposite is true for models having relatively complex process formulations, which are developed for application on a site scale, for example, ILWAS. ILWAS is perhaps the most mechanistic and synthetic model, providing detailed description of watershed acidification.

MAGIC is likely the most widely applied model for soil and surface water acidification and recovery studies. It is a process-oriented model, lumping key soil processes at the watershed scale over monthly or yearly time steps (Cosby et al., 1985). MAGIC has a soil–soil solution equilibrium section in which the chemical composition of soil solution is governed by SO_4 adsorption, CO_2 equilibria, cation exchange, and leaching of Al. The mass balance section assumes the flux of major ions is governed by atmospheric inputs, chemical weathering inputs, net uptake in biomass, and loss to runoff. MAGIC version 7 incorporated the major controls on N fluxes through time (Cosby et al., 2001). Nitrogen leaching to surface waters is modeled as a function of total inorganic N deposition, plant uptake of N, soil uptake or immobilization of N, and nitrification of reduced N. The MAGIC 7 model assumes that the net retention or release of incoming inorganic N in the soil is determined by the C/N ratio of soil organic matter.

Modeling by MAGIC is fairly successful in predicting S and cation dynamics (**Figure 8**) in freshwater, although stable S isotope research indicates that biological S turnover (not modeled) is an important process (Alewell, 2001; Gbondo-Tugbawa et al., 2002; Novák et al., 2000). Similarly, N cycle modeling is still evolving and further studies are needed to verify N immobilization processes used under varying N and S deposition scenarios. The size, kinetics, and uptake capacity of soil are critical factors determining response to increased N loading, and are influenced by land-use history (Goodale and Aber, 2001; Magill et al., 1997).

The SMART model (De Vries et al., 1989) estimates long-term chemical changes in soil and soil water in response to changes in atmospheric deposition. The model structure is based on the mobile anion concept, incorporating the charge balance principle. SMART2 adds forest growth and biocycling processes, which enable modeling soil N availability and forest growth (Mol-Dijkstra and Kros, 2001). In SMART2, total nutrient uptake is described as a demand function, which consists of maintenance uptake in leaves and net growth uptake in stems. Immobilization of N is dependent on the soil C/N ratio.

The assumption employed in models is that equilibrium chemistry is applicable in all relevant situations. This implies that the reaction of soil pH and other parameters to a change in input is virtually instantaneous and processes such as diffusion are neglected. Long-term, large-scale acidification models are difficult to calibrate and validate because of the paucity of sufficient long-term (>50 years) observations.

11.10.14 Chemical Recovery from Anthropogenic Acidification

The many spatial and temporal lake and stream surveys conducted in many countries, plus experiments, have demonstrated the linkages between emissions of acidic compounds to the atmosphere and terrestrial and aquatic acidification. Mandated and implemented reductions in air pollution in North America and Europe have occurred since the 1970s. The long-term experiment of ecosystem acidification from air pollution is seeing a reduction of the dose in North America and Europe, but not eastern Asia.

Long-term acidification related to soil depletion of soluble ALK-producing minerals is irreversible without soil scarification or substantial soil amendments that, as for liming lakes, must be an ongoing process. Shorter term acidification due to atmospheric deposition is largely reversible if the flux of mobile acidic anions (primarily SO_4 and NO_3) can be reduced to the point where chemical weathering and atmospheric inputs can provide sufficient base cations to allow soils to recharge their BS (Stages 5 and 6; **Figure 6(a)**). Recovery from acidification caused by acidic deposition has been demonstrated in whole ecosystem experiments (e.g., in Sweden by Hultberg and Skeffington, 1998, and in Norway by Wright et al., 1993) and probably occurred in some acid-sensitive central European lakes impacted by local smelting in preindustrial times. More generally, partial recovery of ANC has occurred in many areas impacted by acid rain (Evans and Monteith, 2001; Evans et al., 2001b; Wright et al., 2005). The general pattern of recovery involves a reduction of SO_4 (and in some localities, NO_3) in surface water that exceeds reductions in base cations associated with recovery of soil BS and reduced atmospheric inputs of base cations associated with emission control of particulates (e.g., Hedin et al., 1994). ANC increases because of a decline of SO_4 relative to base cations in runoff. Repeated surveys in the United Kingdom, Scandinavia, the Czech Republic and elsewhere indicate recovery since 1990 in many, but not all, individual lakes and streams (Jenkins et al., 2001; **Figure 9**). In the

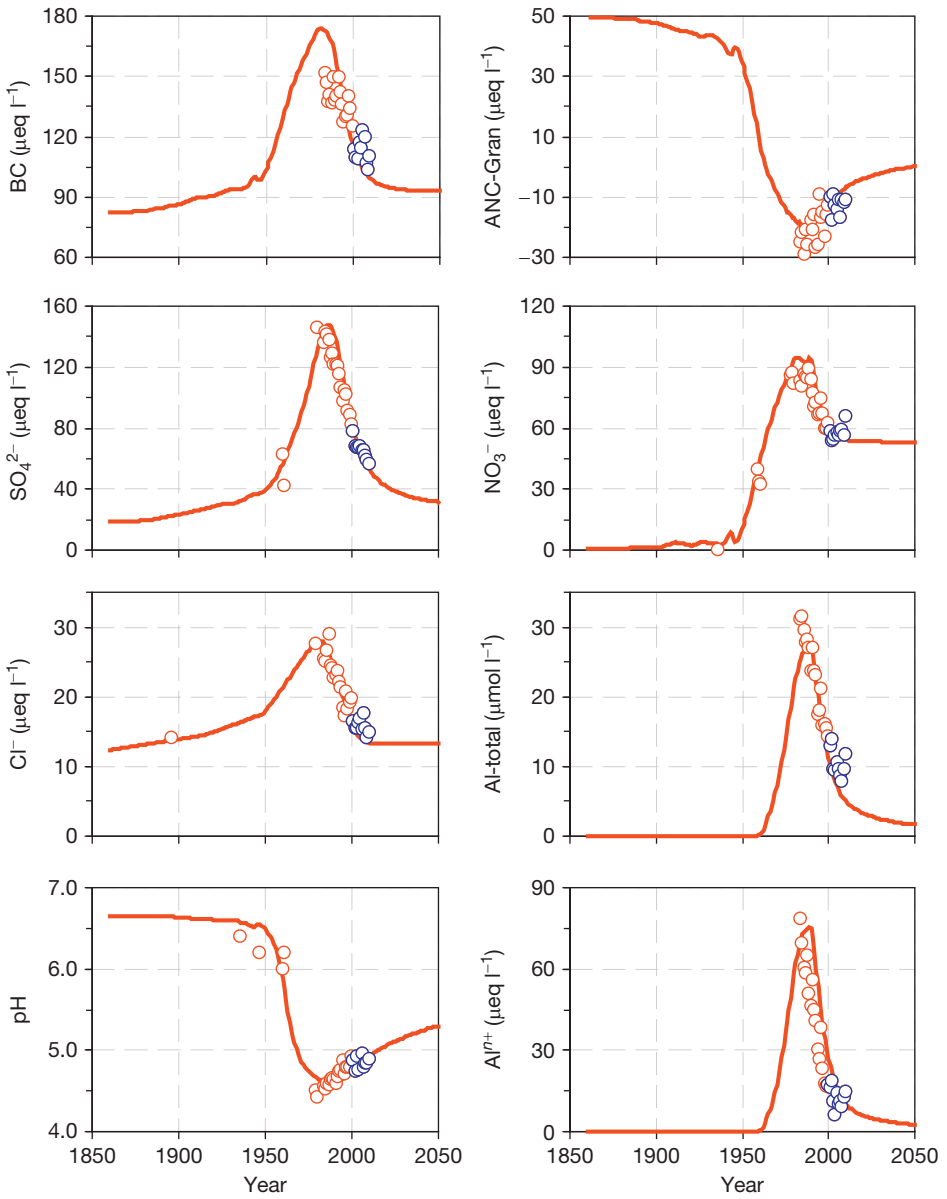

Figure 8 Measured (open circles) and modeled (lines) trends in water chemistry of Černé Lake, Bohemian Forest, Czech Republic. The model (MAGIC 7; Cosby et al., 2001) was calibrated on long-term data prior to year 2001 (red circles). The best agreement was obtained with a 300% higher SO_4 adsorption capacity than determined experimentally, and slightly decreasing N retention during the acidic deposition peak (Majer et al., 2003). The forecast is based on the projected decrease in S and N emission/deposition rate in central Europe according to the Gothenburg Protocol (UN-ECE, 1999). Blue circles represent data measured in 2001–2010, and which are in reasonable agreement with those predicted by the model.

northeastern United States, recovery of ANC has accompanied reduction of atmospheric SO_4 while atmospheric NO_3 has remained relatively constant (Kahl et al., 2004; Stoddard et al., 1998, 1999, 2001). Considerable recovery in sensitive areas of central Europe includes not only reduction in SO_4, but also Al, NO_3, and Cl concentrations (Veselý et al., 2002a). The chemical path of lake recovery can follow a hysteresis loop (Kopáček et al., 2002b), also suggested by the artificial acidification and recovery of stream sediments (**Figure 10(a)** and **10(b)**). A simple linear recovery of pH, ANC, and elevated Al from reduced SO_4 and NO_3 atmospheric deposition is unlikely, due to concurrent variations in climate, including variations in temperature, precipitation, marine aerosol input (**Section 11.10.7**), and DOC production. For example, an increase in temperature (~1.3 °C) over 17 years accelerated the decrease of inorganic Al during recovery by about 13% in strongly acidified lakes in the Czech Republic; temperature increase was the second most important cause of Al reduction after the SAA decrease (Veselý et al., 2003; **Figure 11**).

The increased export of P from acidifying watersheds appears to covary with decreasing pH and increasing export of Al. Initially, as soils acidify, retention of P (as PO_4^{3-}) would increase as the adsorption capacity of the soil increases (Navrátil et al., 2009). However, with continued decline in

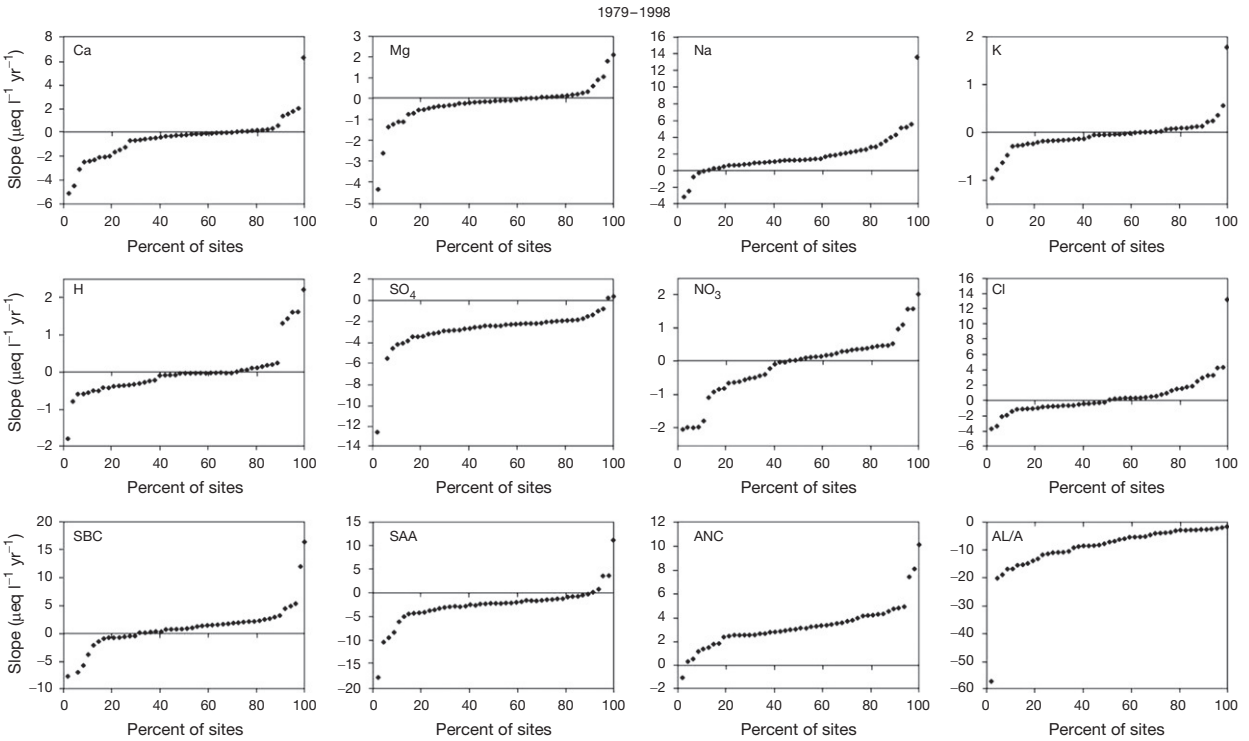

Figure 9 Recovery of regional alkalinity between 1979 and 1998 in a suite of lakes in Scotland, United Kingdom. Reprinted from Ferrier RC, Helliwell RC, Cosby BJ, Jenkins A, and Wright RF (2001) Recovery from acidification of lochs in Galloway, south-west Scotland, UK: 1979–1998. *Hydrology and Earth System Sciences* 5: 421–431, with permission.

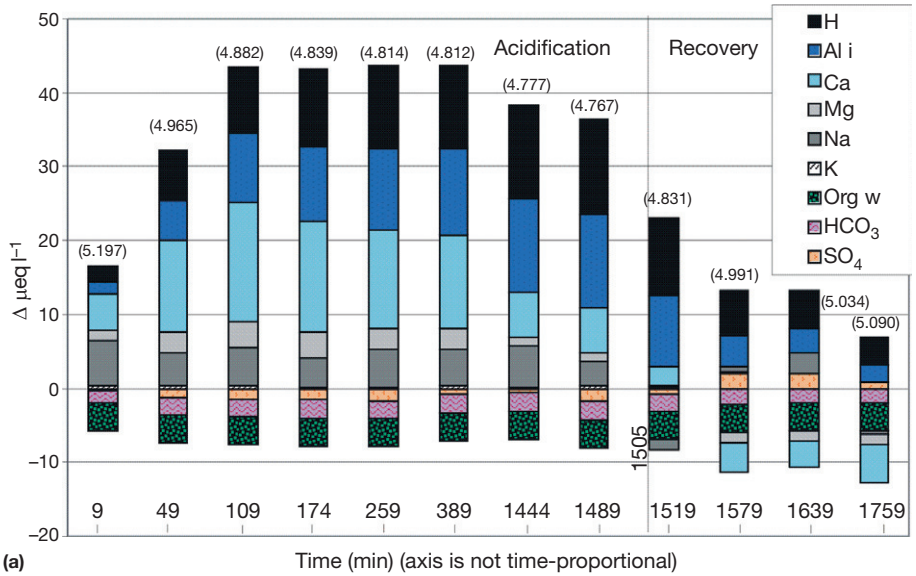

Figure 10 (Continued)

pH, leaching of P from soils can result from desorption of Al-binding sites within the soil, or even dissolution of secondary $Al(OH)_3$. In either case, the loss is largely irreversible because of earlier depletion of the primary source of P, apatite ($Ca_5(PO_4)_3$), from mineral soil.

The importance of these secondary effects on acid–base status, metal concentration, and toxicity is still being studied. As part of the RECOVER2010 project (Ferrier et al., 2003a), the current state of acidification was simulated by MAGIC7 and projected for many European and eastern Canadian watersheds (see special issue of *Hydrology and Earth System Sciences*; Ferrier et al., 2003b). Sufficient time has not elapsed since declining acid inputs to assess the accuracy of the model predictions (Majer et al., 2003), yet the general decline of SO_4, and

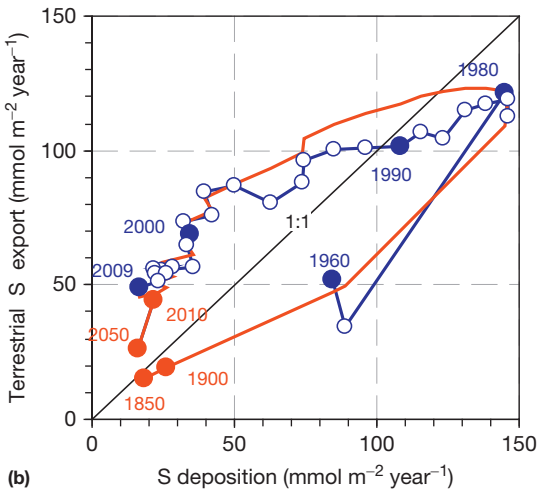

Figure 10 (a) Experimental episodic acidification and recovery of the low ANC East Bear Brook, Maine, USA, showing solute dynamics (reprinted with permission from Goss and Norton, 2008). Acid (HCl) was added to the brook from time = 0 to 1505 min; samples were taken at 16 m below the acid addition at the indicated times. Note reversibility during acidification and recovery as SO_4 first adsorbs and then desorbs, while Ca and Mg desorb and then adsorb. (b) Input and output fluxes of S in the watershed of Černé Lake (Bohemian Forest, Czech Republic). The blue points are observed lake water SO_4 concentrations, and red points and lines are simulated by MAGIC (Majer et al., 2003). Terrestrial fluxes were calculated from concentration data using average annual runoff (1365 mm), and annual in-lake SO_4 removal of 22% (based on a mass budget study in 2000; unpublished data). The relationship exhibits a significant hysteresis in terrestrial SO_4 leaching compared to the input–output equilibrium (1:1 line), with significant SO_4 retention in the watershed from 1850 to 1990, and leaching substantially higher than atmospheric input since 1990. A new steady state will not probably establish by 2050.

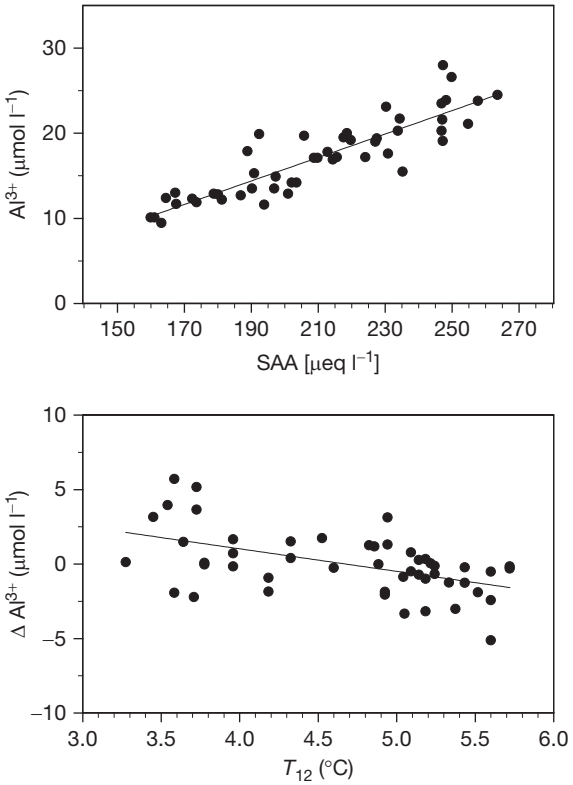

Figure 11 (a) The linear relationship between Al^{3+} and the sum of strong acid anions (SAA) for Cerné Lake, Czech Republic, 1984–2001. (b) The relationship between the residuals of the Al^{3+}–SAA relationship (a) and the mean temperature for the 12 months preceding the sample (T_{12}) from Cerné Lake, Czech Republic, 1984–2001. Modified from Veselý J, Majer V, Kopáček J, and Norton SA (2003) Climate warming accelerates decreased aluminum concentrations in lakes recovering from acidification. *Limnology and Oceanography* 48: 2346–2354.

generally increasing pH and ANC are clear (Figure 8). The major uncertainties with the model predictions are linked with the poorly understood biochemistry of N. This collection of studies was followed by a special issue of *Hydrology and Earth System Sciences* (Dillon and Wright, 2008) where both individual ecosystems and collections of lakes were modeled empirically and with MAGIC7 to predict recovery from acidification in a changing physical climate.

In general, systems that had been acidified most, recovered ANC more quickly. However, many aquatic systems in North America and Europe show little or no recovery, or even continue to acidify as base cations decline faster than the reduction in SO_4 plus NO_3 (Warby et al., 2005, 2009; Figure 9). The causes of continued acidification during reduced air pollution are likely a complex interaction of many secondary processes including changes in climate-driven hydrology and temperature (Forsius et al., 2010), biomass uptake, net respiration in soils, N processing, regeneration of soil BS, and long-term fluxes of marine aerosols. These secondary effects can mask the recovery of systems from reduced S input for some time. With increasing N saturation in many systems, episodic acidification could become more frequent for systems already damaged by a history of base cation depletion (Kopáček et al., 2009; Figure 12).

Acknowledgments

We are very appreciative of many thoughtful interactions with colleagues, too numerous to identify, in Europe, North America, and Asia concerning acid rain and its impacts. They have been generous with ideas and presented us opportunities to understand the breadth and depth of research related to anthropogenic acidification. Anthropogenic acidification was perhaps the most important and heavily researched environmental problem in large areas of the northern hemisphere from 1975 to 2005. The attention paid to the terrestrial and aquatic resources at risk has provided the world with an understanding of how they function that is critical to preparing us for assessing the effect of climate change on these same resources. It will also inform emerging nations, such as China and India, of the potential for environmental damage.

The body of research on ecosystem acidification has been built substantially by hundreds of scientists in several dozen countries. Several billion dollars (US equivalent) have been spent achieving significant understanding about where our systems were prior to acid rain, their present status, and their probable future with various scenarios of atmospheric pollution and abatement, and climate change. More than 100 books

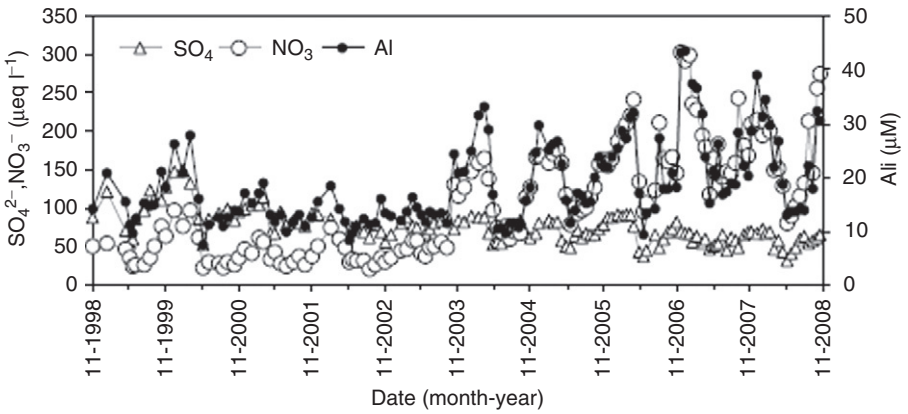

Figure 12 Increasing role of NO_3 in episodic and chronic acidification and Al mobility at Plesné Lake, Czech Republic. Reprinted from Kopáček J, Hejzlar J, Kaňa J, Norton SA, Porcal P, and Turek J (2009) Trends in aluminium export from a glaciated mountain area to surface waters: Effects of soil development, atmospheric acidification, and nitrogen-saturation. *Journal of Inorganic Biochemistry* 103: 1439–1448, with permission.

and thousands of articles have been published on the topic over the last 35 years. The literature we cite identifies many individuals and organizations responsible for this progress. Not everybody could be recognized, of course. One amazing characteristic of the research effort has been the international cooperation that evolved as a consequence of the people involved and the realization that atmospheric pollution knows no political borders. Its consequences could be understood and remediation implemented only with international political cooperation, driven by excellent science. That cooperation is one of the important secondary results of the effort. We thank the people who, early on, had the vision to identify the ability of human activity to degrade our chemical climate through atmospheric pollution and who stimulated so many people to look, experiment, and understand. These people include, but are not limited to, Svante Odén in Sweden, David Schindler and Peter Dillon in Canada, Ellis Cowling and Gene Likens in the United States, Arne Henriksen and Richard Wright in Norway, and Bernard Ulrich in former West Germany. They were pioneers and still are.

The first version of this chapter was cowritten with the late Josef Veselý of the Czech Geological Survey. His interests and skills ranged from the atomic level to catchments; his timescale of interest ranged from minutes to millennia. His mastery of biogeochemistry was an inspiration to many scientists. We dedicate this revision to him.

References

Aber JD, Goodale CL, Ollinger SV, et al. (2003) Is nitrogen deposition altering the nitrogen status of northeastern forests? *Bioscience* 53: 375–389.

Aber J, McDowell W, Nadelhoffer K, et al. (1998) Nitrogen saturation in temperate forests ecosystems. *Bioscience* 48: 921–934.

Aber JD, Nadelhoffer KJ, Steudler P, and Mellillo JM (1989) Nitrogen saturation in northern forest ecosystems. *Bioscience* 39: 378–386.

Adams MB, DeWalle DR, and Hom JL (eds.) (2006) *The Fernow Watershed Acidification Study*. Dordrecht, The Netherlands: Springer.

Aherne J, Futter MN, and Dillon PJ (2008) The impacts of future climate change and sulphur emission reductions on acidification recovery at Plastic Lake, Ontario. *Hydrology and Earth System Sciences* 12: 383–392.

Aherne J, Kelly-Quinn M, and Farrell EP (2002) A survey of lakes in the Republic of Ireland: Hydrochemical characteristics and acid sensitivity. *Ambio* 31: 452–459.

Alewell C (2001) Predicting reversibility of acidification: The European sulfur story. *Water, Air, and Soil Pollution* 130: 1271–1276.

Alewell C, Armbruster M, Bittersohl J, et al. (2001) Are there signs of acidification reversal in freshwaters of the low mountain ranges in Germany? *Hydrology and Earth System Sciences* 5: 367–378.

Alfaro-De la Torre MC and Tessier A (2002) Cadmium deposition and mobility in the sediments of an acidic oligotrophic lake. *Geochimica et Cosmochimica Acta* 66: 3549–3562.

Amirbahman A, Pearce AR, Bouchard RJ, Norton SA, and Kahl JS (2003) Relationship between hypolimnetic phosphorous and iron release from eleven lakes in Maine, USA. *Biogeochemistry* 65: 369–386.

Andersson F and Olsson B (eds.) (1985) *Lake Gårdsjön – An Acid Forest Lake and Its Catchment*, *Ecological Bulletins* , vol. 37. Stockholm: Swedish Natural Science Research Council.

Anesio AM and Granéli W (2003) Increased photoreactivity of DOC by acidification: Implications for the carbon cycle in humic lakes. *Limnology and Oceanography* 48: 735–744.

Arvola L, Rask M, Ruuhijärvi J, et al. (2010) Long-term patterns in pH and colour in small acidic boreal lakes of varying hydrological and landscape settings. *Biogeochemistry* 101: 269–279.

Bacastow RB (1976) Modulation of atmospheric carbon dioxide by the southern oscillation. *Nature* 261: 116–118.

Bailey SW, Buso DC, and Likens GE (2003) Implications of sodium mass balance for interpreting the calcium cycle of a northern hardwood ecosystem. *Ecology* 84: 471–484.

Bain DC and Langan SJ (1995) Weathering rates in catchments calculated by different methods and their relationship to acidic inputs. *Water, Air, and Soil Pollution* 85: 1051–1056.

Baker JP, VanSickle J, Gagen CJ, et al. (1996) Episodic acidification of small streams in the northeastern United States: Effects on fish populations. *Ecological Applications* 6: 422–437.

Baldigo BP and Murdoch PS (1997) Effect of stream acidification and inorganic aluminum on mortality of brook trout (*Salvelinus fontinalis*) in the Catskill Mountains, New York. *Canadian Journal of Fisheries and Aquatic Sciences* 54: 603–615.

Battarbee RW, Mason J, Renberg I, and Talling JF (1990) *Palaeolimnology and Lake Acidification*. London: The Royal Society.

Bayley SE, Parker B, Vitt D, and Rosenburg D (1988) Experimental acidification of a freshwater wetland. Wildlife Toxicology Fund, Final Report.

Beier C, Hansen K, and Gundersen P (1993) Spatial variability of throughfall fluxes in a spruce forest. *Environmental Pollution* 81: 257–267.

Berggren D and Mulder J (1995) The role of organic matter in controlling aluminum solubility in acid mineral soils. *Geochimica et Cosmochimica Acta* 59: 4167–4180.

Bertilsson S and Tranvik LJ (2000) Photochemical transformation of dissolved organic matter in lakes. *Limnology and Oceanography* 45: 753–762.

Bindler R, Brännvall M-L, and Renberg I (1999) Natural lead concentrations in pristine boreal forest soils and past pollution trends: A reference for critical load models. *Environmental Science & Technology* 33: 3362–3367.

Bishop KH (1997) Liming of acid surface waters in northern Sweden: Questions of geographical variation and the precautionary principle. *Transactions of the Institute of British Geographers* 22: 49–60.

Bishop K, Rapp L, Köhler S, and Korsman T (2008) Testing the steady-state water chemistry model predictions of pre-industrial lake pH with paleolimnological data from Northern Sweden. *Science of the Total Environment* 407: 723–729.

Borg H (1986) Metal speciation in acidified mountain streams in central Sweden. *Water, Air, and Soil Pollution* 30: 1007–1014.

Bormann FH and Likens GE (1979) *Pattern and Process in a Forested Ecosystem*. New York: Springer-Verlag.

Bouchard A (1997) Recent lake acidification and recovery trends in southern Quebec, Canada. *Water, Air, and Soil Pollution* 94: 225–245.

Boutron CF, Candelone J-P, and Hong S (1995) Greenland snow and ice cores: Unique archives of large-scale pollution of the troposphere of the Northern Hemisphere by lead and other heavy metals. *Science of the Total Environment* 160/161: 233–241.

Boyle JF (2007) Loss of apatite caused irreversible early Holocene lake acidification. *The Holocene* 17: 539–544.

Brakke DF, Landers DH, and Eilers JM (1988) Chemical and physical characteristics of lakes in the northeastern United States. *Environmental Science & Technology* 22: 155–163.

Brimblecombe P (1992) History of atmospheric acidity. In: Radojevic M and Harrison RM (eds.) *Atmospheric Acidity*, pp. 267–304. London: Elsevier Applied Science.

Bullen T, Wiegand B, Chadwick O, Vitousek P, Bailey S, and Creed I (2002) New approaches to understanding calcium budgets in watersheds: Sr isotopes meet Ca isotopes. In: *BIOGEOMON 2002, the 4th International Symposium on Ecosystem Behaviour*, Reading, UK, 17-21 August 2002.

Caldeira K and Wickett ME (2003) Anthropogenic carbon and ocean pH. *Nature* 425: 365.

Campbell PGC, Hansen HJ, Dubreuil B, and Nelson WO (1992) Geochemistry of Quebec North Shore salmon rivers during snowmelt: Organic acid pulse and aluminum mobilization. *Canadian Journal of Fisheries and Aquatic Sciences* 49: 1938–1952.

Camuffo D (1992) Acid rain and the deterioration of monuments: How old is the problem? *Atmospheric Environment* 26B: 241–247.

Charles DF and Smol JP (1988) New methods for using diatoms and chrysophytes to infer past pH of low alkalinity lakes. *Limnology and Oceanography* 33: 1451–1462.

Charlson RJ, Lovelock JE, Andreae MO, and Warren SG (1987) Oceanic phytoplankton, atmospheric sulfur, cloud albedo and climate. *Nature* 326: 655–661.

Chen CY and Folt CL (2005) High plankton densities reduce mercury biomagnification. *Environmental Science & Technology* 39(1): 115–121.

Cho Y, Driscoll CT, Johnson CE, and Siccama TG (2010) Chemical changes in soil and soil solution after calcium silicate addition to a northern hardwood forest. *Biogeochemistry* 100: 3–20. http://dx.doi.org/10.1007/s10533-009-9397-6.

Christophersen N and Neal C (1990) Linking hydrochemical, geochemical and soil chemical processes on the catchment scale: An interplay between modeling and field work. *Water Resources Research* 26: 3077–3086.

Clair TA and Ehrman JM (1996) Variations in discharge and dissolved organic carbon and nitrogen export from terrestrial basins with changes in climate: A neural network approach. *Limnology and Oceanography* 41: 921–927.

Cook RB, Kelly CA, Schindler DW, and Turner MA (1986) Mechanisms of hydrogen ion neutralization in an experimentally acidified lake. *Limnology and Oceanography* 31: 134–148.

Correll DL, Jordan TE, and Weller DE (2001) Effects of precipitation, air temperature, and land use on organic carbon discharges from Rhode river watersheds. *Water, Air, and Soil Pollution* 128: 139–159.

Cosby BJ, Ferrier RC, Jenkins A, and Wright RF (2001) Modeling the effects of acid deposition: Refinements, adjustments and inclusion of nitrogen dynamics in the MAGIC model. *Hydrology and Earth System Sciences* 5: 499–517.

Cosby BJ, Hornberger GM, Galloway JN, and Wright RF (1985) Modeling the effects of acid deposition: Assessment of a lumped-parameter model of soil water and stream water chemistry. *Water Resources Research* 21: 51–63.

Cosby BJ, Hornberger GM, Wright RF, and Galloway JN (1986) Modeling the effects of acid deposition: Controls of long-term sulfate dynamics by soil sulfate adsorption. *Water Resources Research* 22: 1283–1302.

Cowling EB (1982) Acid precipitation in historical perspective. *Environmental Science & Technology* 16: 110A–123A.

Cronan CS and Grigal DF (1995) Use of calcium/aluminum ratios as indicators of stress in forest ecosystems. *Journal of Environmental Quality* 24: 209–226.

Cronan CS, Walker WJ, and Bloom PR (1986) Predicting aqueous aluminium concentrations in natural waters. *Nature* 324: 140–143.

Dahl K (1921) Research on the die-off of brown trout in mountain lakes in southwestern Norway (in Norwegian). *Norsk Jæger-og Fiskeforenings Tidsskrift* 49: 249–267.

Dahlgren RA, McAvoy DC, and Driscoll CT (1990) Acidification and recovery of a spodosol Bs horizon from acidic deposition. *Environmental Science & Technology* 24: 531–537.

Dai AG and Wigley TML (2000) Global patterns of ENSO-induced precipitation. *Geophysical Research Letters* 27: 1283–1286.

David MB, Fasth WJ, and Vance GF (1991) Forest soil response to acid and salt additions of sulfate: I. Sulfur constituents and net retention. *Soil Science* 151: 136–145.

David MB, Vance GF, and Fasth WJ (1991) Forest soil response to acid and salt additions of sulfate: II. Aluminum and base cations. *Soil Science* 151: 208–219.

Davies TD, Tranter M, Wigington PJ, and Eshleman KN (1992) Acidic episodes in surface waters in Europe. *Journal of Hydrology* 132: 25–69.

Davis RB (1987) Paleolimnological diatom studies of acidification of lakes by acid rain: An application of quaternary science. *Quaternary Science Reviews* 6: 147–163.

Davison W, George DG, and Edwards NJA (1995) Controlled reversal of lake acidification by treatment with phosphate fertilizer. *Nature* 377: 504–507.

De Vries W, Leeters EEJM, and Hendriks CMA (1995) Effects of acid deposition on Dutch forest ecosystems. *Water, Air, and Soil Pollution* 85: 1063–1068.

De Vries W, Posch M, and Kämäri J (1989) Simulation of the long-term soil response to acid deposition in various buffer ranges. *Water, Air, and Soil Pollution* 48: 349–390.

Dickson W (1978) Some effects of the acidification of Swedish lakes. *Verhandlung International Verein Limnology* 20: 851–856.

Dillon PJ, Molot LA, and Futter M (1997) The effect of El Niño-related drought on the recovery of acidified lakes. *Environmental Monitoring and Assessment* 46: 105–111.

Dillon PJ and Wright RF (eds.) *Special Issue. Role of Climate Change in Recovery of Acidified Surface Water (EUROLIMPACS). Hydrology and Earth System Sciences* 12: 333–522.

Dillon PJ, Yan ND, Scheider WA, and Conroy N (1979) Acidic lakes in Ontario, Canada: Characterization, extent and responses to base and nutrient additions. *Archives of Hydrobiological Beih Ergebn Limnological* 13: 317–336.

Dise NB and Wright RF (1992) The NITREX project (Nitrogen saturation experiments). *Directorate-General for Science, Research and Development Environment Research Programme, Ecosystems Report No. #2*. Brussels: Commission of the European Communities.

Dise NB and Wright RF (1995) Nitrogen leaching from European forests in relation to nitrogen deposition. *Forest Ecology and Management* 71: 153–162.

Dixit SS, Smol JP, Kingston JC, and Charles DF (1992) Diatoms: Powerful indicators of environmental change. *Environmental Science & Technology* 26: 23–33.

Driscoll CT, Lehtinen MD, and Sullivan TJ (1994) Modeling the acid–base chemistry of organic solutes in Adirondack, New York, lakes. *Water Resources Research* 30: 297–306.

Driscoll CT, Likens GE, and Church MR (1998) Recovery of surface waters in the northeastern US from decreases in atmospheric deposition of sulfur. *Water, Air, and Soil Pollution* 105: 319–329.

Driscoll CT, Likens GE, Hedin LO, Eaton JS, and Bormann FH (1989) Changes in the chemistry of surface waters: 25-Year results at the Hubbard Brook Experimental Forest. *Environmental Science & Technology* 23: 137–143.

Driscoll CT and Postek KM (1996) The chemistry of aluminum in surface waters. In: Sposito G (ed.) *The Environmental Chemistry of Aluminum*, pp. 363–418. Boca Raton, FL: CRC Press.

Driscoll CT, Yatsko CP, and Unangst FJ (1988) Longitudinal and temporal trends in the water chemistry of the North Branch of the Moose River. *Biogeochemistry* 3: 37–61.

Ducros M (1845) Observation d' une pluie acide. *Journal de Pharmacie et de Chimie* 3: 273–277.

Edwards PJ, Wood F, and Kochenderfer JN (2002) Baseflow and peakflow chemical responses to experimental applications of ammonium sulfate to a forested watershed in north-central West Virginia, USA. *Hydrological Processes* 16: 2287–2310.

Einsele W (1936) Über die Beziehungen des Eisenkreislaufs zum Phosphatkreislauf im eutrophen See. *Archives of Hydrobiology* 29: 664–686.

Emmett BA, Reynolds B, Stevens PA, et al. (1993) Nitrate leaching from afforested Welsh catchment – Interactions between stand age and nitrogen deposition. *Ambio* 22: 386–394.

Engstrom DR, Fritz SC, Almendinger JE, and Juggins S (2000) Chemical and biological trends during lake evolution in recently deglaciated terrain. *Nature* 408: 161–166.

Engstrom DR and Wright HE Jr. (1984) Chemical stratigraphy of lake sediments as a record of environmental change. In: Haworth EY and Lund JWG (eds.) *Lake Sediments and Environmental History*, pp. 11–67. Minneapolis, MN: University of Minnesota Press.

Evans CD, Cullen JM, Alewell C, et al. (2001b) Recovery from acidification in European surface waters. *Hydrology and Earth System Sciences* 5: 283–297.

Evans CD, Goodale C, Simon L, et al. (2008a) Does elevated nitrogen deposition or ecosystem recovery from acidification drive increased dissolved organic carbon loss from upland soil? A review of evidence from field nitrogen addition experiments. *Biogeochemistry* 91: 13–35.

Evans CD, Harriman R, Monteith DT, and Jenkins A (2001a) Assessing the suitability of acid neutralising capacity as a measure of long-term trends in acid waters based on two parallel datasets. *Water, Air, and Soil Pollution* 130: 1541–1546.

Evans CD and Monteith DT (2001c) Chemical trends at lakes and streams in the UK Acid Waters Monitoring Network, 1988–2000: Evidence for recent recovery at a national scale. *Hydrology and Earth System Sciences* 5: 351–366.

Evans CD, Monteith DT, and Harriman R (2001c) Long-term variability in the deposition of marine ions at west coast sites in the UK Acid Waters Monitoring Network: Impacts on surface water chemistry and significance for trend determination. *Science of the Total Environment* 265: 115–129.

Evans CD, Reynolds R, Hinton B, et al. (2008b) Effects of decreasing acid deposition and climate change on acid extremes in an upland stream. *Hydrology and Earth System Sciences* 12: 337–351.

Feller MC and Kimmins JP (1979) Chemical characteristics of small streams near Haney in southwestern British Columbia. *Water Resources Research* 15: 247–258.

Fenn ME, Poth MA, Aber JD, et al. (1998) Nitrogen excess in North American ecosystems: Predisposing factors, ecosystem responses, and management strategies. *Ecological Applications* 8: 706–733.

Fernandez IJ, Adams MB, SanClements MD, and Norton SA (2010) Comparing decadal responses of whole-watershed manipulations at the Bear Brook and Fernow experiments. *Environmental Monitoring and Assessment* 171: 149–162.

Fernandez IJ and Norton SA (2010) The Bear Brook Watershed in Maine – The second decade – Preface. *Environmental Monitoring and Assessment* 171: 1–2.

Fernandez IJ, Rustad LE, Norton SA, Kahl JS, and Cosby BJ (2003) Experimental acidification causes soil base cation depletion in a New England forested watershed. *Soil Science Society of America Journal* 67: 1909–1919.

Fernandez IJ, Simmons JA, and Briggs RD (2000) Indices of forest floor nitrogen status along a climate gradient in Maine, USA. *Forest Ecology and Management* 134: 77–187.

Ferrier RC, Helliwell RC, Cosby BJ, Jenkins A, and Wright RF (2001) Recovery from acidification of lochs in Galloway, south-west Scotland, UK: 1979–1998. *Hydrology and Earth System Sciences* 5: 421–431.

Ferrier RC, Jenkins A, and Elston DA (1994) The composition of rime ice as an indicator of the quality of winter deposition. *Environmental Pollution* 87: 259–266.

Ferrier RC, Wright RF, Jenkins A, and Barth H (2003a) Predicting recovery of acidified freshwaters in Europe and Canada: An introduction. *Hydrology and Earth System Sciences* 7: 431–435.

Ferrier RC, Wright RF, and Jenkins A, Barth H (eds.) (2003b) *Special Issue: Predicting Recovery of Acidified Freshwaters in Europe and Canada. Hydrology and Earth System Sciences* 7: 429–617.

Fölster J and Wilander A (2002) Recovery from acidification in Swedish forest streams. *Environmental Pollution* 117: 379–389.

Forsius M, Alveteg M, Jenkins A, et al. (1997) MAGIC, SAFE, and SMART model applications at integrated monitoring sites: Effects of emission reduction scenarios. *Water, Air, and Soil Pollution* 105: 21–30.

Forsius M, Kämäri J, Kortelainen P, Mannio J, Verta M, and Kinnunen K (1990) Statistical lake survey in Finland: Regional estimates of lake acidification. In: Kauppi P, Antitila P, and Kenttämies K (eds.) *Acidification in Finland*, pp. 759–780. Berlin: Springer-Verlag.

Forsius MC, Neal C, and Jenkins A (1995) Modeling perspective of the deforestation impact in stream water quality of small preserved forested areas in the Amazonian rainforest. *Water, Air, and Soil Pollution* 79: 325–337.

Forsius M, Saloranta T, Arvola L, et al. (2010) Physical and chemical consequences of artificially deepened thermocline in a small humic lake – A paired whole-lake climate change experiment. *Hydrology and Earth System Sciences* 14: 2629–2642.

Forti MC, Carvalho A, Melfi AJ, and Montes CR (2001) Deposition patterns of SO_4, NO_3 and H^+ in the Brazilian territory. *Water, Air, and Soil Pollution* 130: 1121–1126.

Frogner T (1990) The effect of acid deposition on cation fluxes in artificially acidified catchments in western Norway. *Geochimica et Cosmochimica Acta* 54: 769–780.

Fu B, Zhuang X, Jian G, Shi J, and Lu Y (2007) Environmental problems and challenges in China. *Environmental Science & Technology* 41: 7597–7602.

Galloway JN (1995) Acid deposition: Perspectives in time and space. *Water, Air, and Soil Pollution* 85: 15–24.

Galloway JN, Norton SA, and Church MR (1983) Freshwater acidification from atmospheric deposition of sulfuric acid: A conceptual model. *Environmental Science & Technology* 17: 541–545.

Gbondo-Tugbawa SS, Driscoll CT, Mitchell MJ, Aber JD, and Likens GE (2002) A model to simulate the response of a northern hardwood forest ecosystem to change in S deposition. *Ecological Applications* 12: 8–23.

Gensemer RW and Playle RC (1999) The bioavailability and toxicity of aluminum in aquatic environments. *Critical Reviews in Environmental Science & Technology* 29: 315–450.

Gherini SA, Mok L, Hudson RJM, Davis GF, Chen CW, and Goldstein RA (1985) The ILWAS model, formulation and application. *Water, Air, and Soil Pollution* 26: 425–459.

Gjessing ET (1992) The HUMEX Project: Experimental acidification of a catchment and its humic lake. *Environment International* 18: 535–543.

Gjessing ET, Riise G, and Lydersen E (1998) Acid rain and natural organic matter (NOM). *Acta Hydrochimica et Hydrobiologica* 26: 131–136.

Godsey SE, Kirchner JW, Palucis M, et al. (2010) Generality of fractal 1/f scaling in catchment tracer time series, and its implications for catchment travel time distribution. *Hydrological Processes* 24: 1660–1671.

Goodale CL and Aber JD (2001) The long-term effects of land-use history on nitrogen cycling in northern hardwood forests. *Ecological Applications* 11: 253–267.

Gorham E (1955) On the acidity and salinity of rain. *Geochimica et Cosmochimica Acta* 7: 231–239.

Gorham E, Eisenriech SJ, Ford J, and Santelman MV (1985) The chemistry of bog waters. In: Stumm W (ed.) *Chemical Processes in Lakes*, pp. 339–362. New York: Wiley.

Gorham E, Janssens JA, Wheeler GA, and Glaser PH (1987) The natural and anthropogenic acidification of peatlands. In: Hutchinson TC and Memma KM (eds.) *Effects of Atmospheric Pollutants on Forests, Wetlands, and Agricultural Ecosystems*, pp. 493–512. Berlin: Springer-Verlag.

Goss HV and Norton SA (2008) Contrasting chemical response to artificial acidification of three acid-sensitive streams in Maine, USA. *Science of the Total Environment* 404: 245–252.

Grennfelt P and Hultberg H (1986) Effects of nitrogen deposition on the acidification of terrestrial and aquatic ecosystems. *Water, Air, and Soil Pollution* 30: 945–963.

Groffman PM, Driscoll CT, Fahey TJ, Hardy JP, Fitzhugh RD, and Tierney GL (2001) Effects of mild winter freezing on soil nitrogen and carbon dynamics in a northern hardwood forest. *Biogeochemistry* 56: 191–213.

Gundersen P, Callesen I, and De Vries W (1998) Nitrate leaching in forest ecosystems is related to forest floor C/N ratio. *Environmental Pollution* 102: 403–407.

Gunn JM (ed.) (1995) *Restoration and Recovery of an Industrial Region*. New York: Springer-Verlag.

Haines TA, Akielaszek JJ, Norton SA, and Davis RB (1983) Errors in pH measurement with colorimetric indicators in low alkalinity waters. *Hydrobiologia* 107: 57–61.

Hall R, Likens GE, Fiance SB, and Hendrey GR (1980) Experimental acidification of a stream in the Hubbard Brook Experimental Forest, New Hampshire. *Ecology* 61: 976–989.

Hansen K, Draaijers GPJ, Ivens WPMF, Gundersen P, and Leeuwen NFM (1994) Concentration variations in rain and throughfall collected sequentially during individual rain events. *Atmospheric Environment* 28: 3195–3205.

Harriman R, Anderson H, and Miller JD (1995) The role of sea-salts in enhancing and mitigating surface water acidity. *Water, Air, and Soil Pollution* 85: 553–558.

Harriman R, Watt AW, Christie AEG, et al. (2001) Interpretation of trends in acidic deposition and surface water chemistry in Scotland during the past three decades. *Hydrology and Earth System Sciences* 5: 407–420.

Hauhs M (1989) Lange Bramke: An ecosystem study of a forested catchment. In: Adriano DC and Havas M (eds.) *Acid Precipitation. Case Studies*, vol. 1, pp. 275–304. New York: Springer-Verlag.

Hedin LO, Armesto JJ, and Johnson AH (1995) Patterns of nutrient loss from unpolluted, old-growth temperate forests: Evaluation of biogeochemical theory. *Ecology* 76: 493–509.

Hedin LO, Granat L, Likens GE, et al. (1994) Steep declines in atmospheric base cations in regions of Europe and North America. *Nature* 367: 351–354.

Hemond HF (1990) Acid neutralizing capacity, alkalinity, and acid–base status of natural waters containing organic acids. *Environmental Science & Technology* 24: 1486–1489.

Henriksen A (1980) Acidification of freshwaters – A large scale titration. In: Drablos D and Tollans A (eds.) Ecological Impact of Acid Precipitation, pp. 68–74. Oslo: SNSF Project.
Henriksen A and Kirkhusmo LA (2000) Effects of clear-cutting of forest on the chemistry of a shallow groundwater aquifer in southern Norway. *Hydrology and Earth System Sciences* 4: 323–331.
Henriksen A, Lien L, Traaen TS, Sevalrud IS, and Brakke DF (1988) Lake acidification in Norway – Present and predicted chemical status. *Ambio* 17: 259–266.
Henriksen A and Posch M (2001) Steady-state models for calculating critical loads of acidity for surface waters. *Water, Air, and Soil Pollution: Focus* 1: 375–398.
Henriksen A, Posch M, Hultberg H, and Lien L (1995) Critical loads of acidity for surface waters – Can the ANC_{limit} be considered variable? *Water, Air, and Soil Pollution* 85: 2419–2424.
Henriksen A, Skjelkvåle BL, Mannio J, et al. (1998) Northern European Lake Survey – 1995. Finland, Norway, Sweden, Denmark, Russian Kola, Russian Karelia, Scotland and Wales. *Ambio* 27: 80–91.
Henriksen A, Wathne BM, Røgeberg EJS, Norton SA, and Brakke DF (1988) The role of stream substrates in aluminum mobility and acid neutralization. *Water Research* 22: 1069–1073.
Henrikson L and Brodin YW (eds.) (1992) *Liming of Acidified Surface Waters: A Swedish Synthesis*, Berlin: Springer-Verlag.
Hessen DO, Henriksen A, and Smelhus AM (1997) Seasonal fluctuations and diurnal oscillations in nitrate of a heathland brook. *Water Research* 31: 1813–1817.
Hindar A, Henriksen A, Torseth K, and Semb A (1994) Acid water and fish death. *Nature* 372: 327–328.
Hindar A and Lydersen E (1994) Extreme acidification of a lake in southern Norway caused by weathering of sulfide-containing bedrock. *Water, Air, and Soil Pollution* 77: 17–25.
Holdren GR and Adams JE (1982) Parabolic dissolution kinetics of silicate minerals: An artifact of nonequilibrium precipitation processes? *Geology* 10: 186–190.
Houle D and Carignan R (1995) Role of SO_4 adsorption and desorption in the long-term S-budget of a coniferous catchment on the Canadian shield. *Biogeochemistry* 28: 161–182.
Hruška J, Köhler S, and Bishop K (1999) Buffering processes in a boreal dissolved organic carbon-rich stream during experimental acidification. *Environmental Pollution* 106: 55–65.
Hruška, J, Kohler S, Laudon H, and Bishop K (2003) Is a universal model of organic acidity possible: Comparison of the acid/base properties of dissolved organic carbon in the boreal and temperate zones. *Environmental Science & Technology* 37: 1726–1730.
Hruška J, Laudon H, Johnson CE, Köhler S, and Bishop K (2001) Acid/base character of organic acids in boreal streams during snowmelt. *Water Resources Research* 37: 1013–1026.
Huber C, Baumgarten M, Göttlein A, and Rotter V (2004) Nitrogen turnover and nitrate leaching after bark beetle attack in mountainous spruce stands of the Bavarian Forest national park. *Water, Air, and Soil Pollution: Focus* 4: 391–414.
Hultberg H and Grennfelt P (1992) Sulfur and seasalt deposition as reflected by throughfall and runoff chemistry in forested catchments. *Environmental Pollution* 75: 215–222.
Hultberg H and Skeffington R (1998) *Experimental Reversal of Acid Rain Effects: The Gårdsjön Roof Project*. New York: Wiley.
Hurrell JW (1995) Decadal trend in the North Atlantic Oscillation: Regional temperatures and precipitation. *Science* 269: 676–679.
IPCC (2007) *Intergovernmental Panel on Climate Change, Fourth Assessment Report: Climate Change 2007 (AR4)*. Geneva: IPPC.
Jeffries DS (1990) Buffering of pH by sediments in streams and lakes. In: Norton SA, Lindberg SE, and Page AL (eds.) *Soils, Aquatic Processes, and Lake Acidification*. *Advances in Environmental Science, Acidic Precipitation*, vol. 4, pp. 107–132. New York: Springer-Verlag.
Jeffries DS (1997) *1997 Canadian Acid Rain Assessment, Vol. 3: Aquatic Effects*. Burlington, Canada: Ministry of the Environment.
Jeffries DS, Clair TA, Dillon PJ, Papineau M, and Stainton MP (1995) Trends in surface water acidification at ecological monitoring sites in southeastern Canada. *Water, Air, and Soil Pollution* 85: 577–582.
Jeffries DS, Wales DL, Kelso JRM, and Linthurst RA (1986) Regional chemical characteristics of lakes in North America. Part 1: Eastern Canada. *Water, Air, and Soil Pollution* 31: 551–569.
Jenkins A, Cosby BJ, Ferrier RC, Walker TAB, and Miller JD (1990) Modelling stream acidification in afforested catchments – An assessment of the relative effects of acid deposition and afforestation. *Journal of Hydrology* 120: 163–181.
Jenkins A, Ferrier RC, and Kirby C (eds.) (1995) Ecosystem manipulation experiments: Scientific approaches, experimental design and relevant results. *Ecosystems Research Report* 20. Brussels: Commission of the European Communities.
Jenkins A, Ferrier RC, and Wright RF (eds.) (2001) Assessment of recovery of European surface waters from acidification 1970–2000. *Hydrologyand Earth System Sciences* 5: 274–282.
Jeziorski A, Yan ND, Paterson AM, et al. (2008) The widespread threat of calcium decline in fresh waters. *Science* 322: 1374–1377.
Johannessen M and Henriksen A (1978) Chemistry of snowmelt water: Changes in concentration during melting. *Water Resources Research* 14: 615–619.
Johansson M and Tarvainen T (1997) Estimation of weathering rates for critical load calculations in Finland. *Environmental Geology* 29: 158–164.
Johnson DW, Henderson GS, Huff DD, et al. (1982) Cycling of organic and inorganic sulfur in a chestnut oak forest. *Oecologia* 54: 141–148.
Johnson DW, Henderson GS, and Todd DE (1988) Changes in nutrient distribution in forests and soils of Walker Branch watershed, Tennessee, over an eleven-year period. *Biogeochemistry* 5: 275–293.
Johnson DW, Susfalk RB, Gholz HL, and Hanson PJ (2000) Simulated effects of temperature and precipitation change in several forest ecosystems. *Journal of Hydrology* 235: 183–204.
Jones PD, Osborn T, and Briffa KR (2001) The evolution of climate over the last millennium. *Science* 292: 662–667.
Kahl J, Norton S, Fernandez I, et al. (1999) Nitrogen and sulfur input–output budgets in the experimental and reference watersheds, Bear Brook Watershed in Maine (BBWM). *Environmental Monitoring and Assessment* 55: 113–131.
Kahl JS, Stoddard JL, Haueber R, et al. (2004) Have U.S. surface waters responded to the Clean Air Act Amendments. *Environmental Science & Technology* 38: 485A–490A.
Kalbitz K, Solinger J-H, Park B, Michalzik B, and Matzner E (2000) Control on the dynamics of dissolved organic matter: A review. *Soil Science* 165: 277–304.
Karlsson J, Byström P, Ask J, Persson L, and Jansson M (2009) Light limitation of nutrient-poor lake ecosystems. *Science* 460: 506–509.
Kaste Ø, Austnes K, Vestgarden LS, and Wright RF (2008) Manipulation of snow in small headwater catchments at Storgama, Norway: Effects on leaching of inorganic nitrogen. *Ambio* 37: 29–37.
Kaste Ø, Henriksen A, and Posch M (2002) Present and potential nitrogen outputs from Norwegian soft water lakes – An assessment made by applying steady-state first-order acidity balance (FAB) model. *Hydrology and Earth System Sciences* 6: 101–112.
Kelly CA, Rudd JWM, Hesslein RH, et al. (1987) Prediction of biological acid neutralization in acid-sensitive lakes. *Biogeochemistry* 3: 129–140.
Kerr JG, Eimers MC, Creed IF, et al. (2011) The effect of seasonal drying on sulphate dynamics in streams across southeastern Canada and the northeastern USA. *Biogeochemistry*. http://dx.doi.org/10.1007/s10533-011-9664-1.
Kieber DJ, McDaniel J, and Mopper K (1989) Photochemical source of biological substances in sea water. Implications for carbon cycling. *Nature* 341: 637–639.
Kirchner JW (1992) Heterogeneous geochemistry of catchment acidification. *Geochimica et Cosmochimica Acta* 56: 2311–2327.
Kirchner JW, Feng X, and Neal C (2000) Fractal stream chemistry and its implications for contaminant transport in catchments. *Nature* 403: 524–527.
Klaminder J, Lucas RW, Futter MN, et al. (2011) Silicate mineral weathering rate estimates: Are they precise enough to be useful when predicting the recovery of nutrient pools after harvesting? *Forest Ecology and Management* 261: 1–9.
Klimont Z, Cofala J, Schopp W, et al. (2001) Projections of SO_2, NO_x, NH_3 and VOC emissions in East Asia. *Water, Air, and Soil Pollution* 130: 193–198.
Köhler SJ, Hruška J, and Bishop K (1999) Influence of organic acids site density on pH modelling of Swedish lakes. *Canadian Journal of Fisheries and Aquatic Sciences* 56: 1461–1470.
Kopáček J, Borovec J, Hejzlar J, Ulrich K-U, Norton SA, and Amirbahman A (2005) Aluminum control of phosphorus sorption by lake sediments. *Environmental Science & Technology* 39: 8784–8789.
Kopáček J, Brzáková M, Hejzlar J, Nedoma J, Porcal P, and Vrba J (2004) Nutrient cycling in a strongly acidified mesotrophic lake. *Limnology and Oceanography* 49: 1202–1213.
Kopáček J, Hejzlar J, Borovec J, Porcal P, and Kotorová I (2000) Phosphorus inactivation by aluminum in the water column and sediments: A process lowering in-lake phosphorus availability in an acidified watershed-lake ecosystem. *Limnology and Oceanography* 45: 212–225.
Kopáček J, Hejzlar J, Kaňa J, Norton SA, Porcal P, and Turek J (2009) Trends in aluminium export from a glaciated mountain area to surface waters: Effects of soil development, atmospheric acidification, and nitrogen-saturation. *Journal of Inorganic Biochemistry* 103: 1439–1448.

Kopáček J, Hejzlar J, Kaňa J, Porcal P, and Klementová Š (2003) Photochemical, chemical, and biological transformations of dissolved organic carbon and its impact on alkalinity production in acidified lakes. *Limnology and Oceanography* 48: 106–117.

Kopáček J, Kaňa J, Šantrůčková H, et al. (2002a) Physical, chemical, and biochemical characteristics of soils in watersheds of the Bohemian Forest Lakes: II. Čertovo and Černé Lake. *Silva Gabreta* 8: 67–93.

Kopáček J, Marešová M, Hejzlar J, and Norton SA (2007) Natural inactivation of phosphorus by aluminum in pre-industrial lake sediments. *Limnology and Oceanography* 52: 1147–1155.

Kopáček J, Stuchlík E, Veselý J, et al. (2002b) Hysteresis in reversal of central European mountain lakes from atmospheric acidification. *Water, Air, and Soil Pollution: Focus* 2: 91–114.

Kopáček J, Ulrich K, Hejzlar J, Borovec J, and Stuchlík E (2001b) Natural inactivation of phosphorus by aluminum in atmospherically acidified water bodies. *Water Research* 35: 3783–3790.

Kopáček J, Veselý J, and Stuchlík E (2001a) Sulphur and nitrogen fluxes and budgets in the Bohemian Forest and Tatra Mountains during the Industrial Revolution (1850–2000). *Hydrology and Earth System Sciences* 5: 391–405.

Kortelainen P, David MB, Roila T, and Makinen I (1992) Acid–base characteristics of organic-carbon in the HUMEX Lake Skjervatjern. *Environment International* 18: 621–629.

Kortelainen P and Mannio J (1990) Organic acidity in Finnish lakes. In: Kauppi P, Anttilla P, and Kenttämies K (eds.) *Acidification in Finland*, pp. 849–864. Berlin: Springer-Verlag.

Krám P, Hruška J, Wenner BS, Driscoll CT, and Johnson CE (1997) The biogeochemistry of base cations in two forest catchments with contrasting lithology in the Czech Republic. *Biogeochemistry* 37: 173–202.

Krám P, Santore RC, Driscoll CT, Aber JD, and Hruška J (1999) Application of the forest–soil–water model (PnET-BGC/CHESS) to the Lysina catchment, Czech Republic. *Ecological Modelling* 120: 9–30.

Kuylenstierna JCI and Chadwick MJ (1989) The relative sensitivity of ecosystems in Europe to the indirect effects of acidic depositions. In: Kämäri J, Brakke DF, Jenkins A, and Wright RF (eds.) *Regional Acidification Models*, pp. 3–22. Berlin: Springer-Verlag.

Lange H, Hauhs M, and Schmidt S (1995) Long-term sulfate dynamics at Lange Bramke (Harz) used for testing two acidification models. *Water, Air, and Soil Pollution* 79: 339–351.

Larssen T, Xiong JL, Vogt RD, Seip HM, Liao BH, and Yhao DW (1998) Studies of soils, soil water and stream water at a small catchment near Guiyang, China. *Water, Air, and Soil Pollution* 101: 137–162.

Laudon H and Norton SA (2010) Causes, drivers, and evolution of episodic acidification at the Bear Brook Watershed in Maine, USA. *Environmental Monitoring and Assessment* 171: 59–69.

Laudon H, Westling O, Löfgren S, and Bishop K (2001) Modeling pre-industrial ANC and pH during spring flood in northern Sweden. *Biogeochemistry* 54: 171–195.

Lawrence GB, Fuller RD, and Driscoll CT (1987) Release of aluminum following whole-tree harvesting at the Hubbard Brook Experimental Forest, New Hampshire, USA. *Journal of Environmental Quality* 16: 383–390.

LaZerte BD and Findeis J (1995) The relative importance of oxalate and pyrophosphate extractable aluminum to the acidic leaching of aluminum in podzol B horizons from the Precambrium Shield, Ontario, Canada. *Canadian Journal of Soil Science* 75: 43–54.

Likens GE, Bormann FH, Pierce RS, Eaton JS, and Johnson NM (1977) *Biogeochemistry of a Forested Ecosystem*. New York: Springer-Verlag.

Likens GE, Driscoll CT, and Buso DC (1996) Long-term effects of acid rain: Response and recovery of a forest ecosystem. *Science* 272: 244–246.

Likens GE, Driscoll CT, Buso DC, et al. (1994) The biogeochemistry of potassium at Hubbard Brook. *Biogeochemistry* 25: 61–125.

Lorz C, Armbruster M, and Feger KH (2002) Temporal development of water chemistry in three forested watersheds in Germany as influenced by contrasting deposition regimes – Results from long-term monitoring and model applications. In: *BIOGEOMON 2002, the 4th International Symposium on Ecosystem Behaviour,* Reading, UK, 17–21 August 2002, p. 141. Reading. UK: University of Reading.

Lovett GM (1992) Atmospheric deposition and canopy interactions of nitrogen. In: Johnson DW and Lindberg SE (eds.) *Atmospheric Deposition and Forest Nutrient Cycling*. *Ecological Studies*, vol. 91, pp. 152–166. New York: Springer-Verlag.

Lydersen E, Salbu B, Polèo ABS, and Muniz IP (1990) The influence of temperature on aqueous aluminum chemistry. *Water, Air, and Soil Pollution* 51: 203–215.

MacDonald JA, Dise NB, Matzer E, Armbruster M, Gundersen P, and Forsius M (2002) Nitrogen input together with ecosystem nitrogen enrichment predict nitrate leaching from European forests. *Global Change Biology* 8: 1028–1033.

Magill AH, Aber JD, Hendricks JJ, Bowden RD, Melillo JM, and Steudler PA (1997) Biogeochemical response of forest ecosystems to simulated chronic nitrogen deposition. *Ecological Applications* 7: 402–415.

Majer V, Cosby BJ, Kopáček J, and Veselý J (2003) Modelling reversibility of Central European mountain lakes from acidification: Part I – The Bohemian forest. *Hydrology and Earth System Sciences* 7: 494–509.

Mannio J (2001) *Responses of Headwater Lakes to Air Pollution Changes in Finland*. *Monographs of the Boreal Environment Research* 18. Helsinki: Finnish Environment Institute.

Matschullat J, Andreae H, Lessman D, Malessa V, and Siewers U (1992) Catchment acidification – From the top down. *Environmental Pollution* 77: 143–150.

McHale MR, Burns DA, Lawrence GB, and Murdoch PS (2007) Factors controlling soil water and stream water aluminum concentrations after a clearcut in a forested watershed with calcium-poor soils. *Biogeochemistry* 84: 311–331.

Meixner T, Bales RC, Williams MW, Campbell DH, and Baron JS (2000) Stream chemistry modeling of two watersheds in the Front Range, Colorado. *Water Resources Research* 36: 77–87.

Michalzik B and Matzner E (1999) Dynamics of dissolved organic nitrogen and carbon in a Central European Norway spruce ecosystems. *European Journal of Soil Science* 50: 579–590.

Miller EK, Blum JD, and Friedland AJ (1993) Determination of soil exchangeable-cation loss and weathering rates using Sr isotopes. *Nature* 362: 438–441.

Mitchell MJ, Driscoll CT, Kahl JS, Likens GE, Murdoch PS, and Pardo LH (1996) Climatic control of nitrate loss from forested watersheds in northeast United States. *Environmental Science & Technology* 30: 2609–2612.

Moldan B and Schnoor JL (1992) Czechoslovakia – Examining a critically ill environment. *Environmental Science & Technology* 26: 14–21.

Moldan F and Wright RF (2011) Nitrogen leaching and acidification during 19 years of NH_4NO_3 additions to a coniferous-forested catchment at Gårdsjön, Sweden (NITREX). *Environmental Pollution* 159: 431–440.

Mol-Dijkstra JP and Kros H (2001) Modelling effects of acid deposition and climate change on soil and run-off chemistry at Risdalsheia, Norway. *Hydrology and Earth System Sciences* 5: 499–517.

Monteith DT, Evans CD, and Reynolds B (2000) Are temporal variations in the nitrate content of UK upland freshwaters linked to the North Atlantic Oscillation? *Hydrological Processes* 14: 1745–1749.

Monteith DT, Stoddard JL, Evans CD, et al. (2007) Dissolved organic carbon trends resulting from changes in atmospheric deposition chemistry. *Nature* 450: 537–540.

Morel FMM, Kraepiel AML, and Amyot M (1998) The chemical cycle and bioaccumulation of mercury. *Annual Review of Ecology and Systematics* 29: 543–566.

Mosello R, Marchetto A, Brizzio MC, Rogora M, and Tartari GA (2000) Results from the Italian participation in the international co-operative programme on assessment and monitoring of acidification of rivers and lakes (ICP Waters). *Journal of Limnology* 59: 47–54.

Mulder J and Stein A (1994) The solubility of aluminum in acidic forest soils: Long-term changes due to acid deposition. *Geochimica et Cosmochimica Acta* 58: 85–94.

Murdoch PS, Burns DA, and Lawrence GB (1998) Relation of climate change to the acidification of surface waters by nitrogen deposition. *Environmental Science & Technology* 32: 1642–1647.

National Atmospheric Deposition Program (NRSP-3)/National Trends Network (2009) NADP Program Office, Illinois State Water Survey, 2204 Griffith Dr., Champaign, IL 61820

Navrátil T, Norton SA, Fernandez IJ, and Nelson SJ (2010) Twenty-year inter-annual trends and seasonal variations in precipitation and stream water chemistry at the Bear Brook Watershed in Maine, USA. *Environmental Monitoring and Assessment* 171: 23–46.

Navrátil T, Rohovec J, Amirbahman A, Norton SA, and Fernandez IJ (2009) Controls of natural amorphous aluminum hydroxide on sulfate and phosphate anions in sediment-solution systems. *Water, Air, and Soil Pollution* 201: 87–98.

Navrátil T, Shanley JB, Skřivan P, Krám P, Mihaljevič M, and Drahota P (2007) Manganese biogeochemistry in a central Czech Republic catchment. *Water, Air, and Soil Pollution* 186: 149–165.

Neal C (1997) A view of water quality from the Plynlimon catchments. *Hydrology and Earth System Sciences* 1: 743–753.

Neal C, Fisher R, Smith CJ, et al. (1992) The effects of tree harvesting on stream-water quality at an acidic and acid-sensitive spruce forested area: Plynlimon, mid-Wales. *Journal of Hydrology* 135: 305–319.

Neal C, Wilkinson J, Neal M, et al. (1997) The hydrochemistry of the headwaters of the River Severn, Plynlimon. *Hydrology and Earth System Sciences* 1: 583–617.

Nilsson J and Grennfelt P (1988) Critical loads for sulphur and nitrogen. Report from a Workshop Held at Skokloster, Sweden, 19-24 March 1988.

Nilsson SI, Miller HG, and Miller JD (1982) Forest growth as a possible cause of soil and water acidification: An examination of the concepts. *Oikos* 39: 40–49.

Nodvin SC, Driscoll CT, and Likens GE (1986) The effect of pH on sulfate adsorption by a forest soil. *Soil Science* 142: 69–75.

Norton SA (1989) Watershed acidification – A chromatographic process. In: Kamari J, Brakke DF, Jenkins A, Norton SA, and Wright RF (eds.) *Regional Acidification Models*, pp. 89–101. Berlin: Springer-Verlag.

Norton SA, Brownlee JC, and Kahl JS (1992) Artificial acidification of a non-acidic and an acidic headwater stream in Maine, USA. *Environmental Pollution* 77: 123–128.

Norton SA, Cosby BJ, Fernandez IJ, Kahl JS, and Church MR (2001) Long-term and seasonal variations in CO_2: Linkages to catchment alkalinity generation. *Hydrology and Earth System Sciences* 5: 83–91.

Norton SA and Fernandez IJ (eds.) (1999) *The Bear Brook Watershed in Maine: A Paired Watershed Experiment – The First Decade (1987–1997)*. The Netherlands: Kluwer Academic Publishers.

Norton SA, Fernandez IJ, Kahl JS, and Reinhardt RL (2004) Acidification trends and the evolution of neutralization mechanisms through time at the Bear Brook Watershed in Maine (BBWM), USA. *Water, Air, and Soil Pollution: Focus* 4: 289–310.

Norton SA and Kahl JS (2000) Impacts of marine aerosols on surface water chemistry at Bear Brook Watershed, Maine. *Verhandlung International Verein Limnology* 27: 1280–1284.

Norton S, Kahl J, Fernandez I, et al. (1999) The Bear Brook Watershed, Maine (BBWM), USA. *Environmental Monitoring and Assessment* 55: 7–51.

Norton SA, Mitchell MJ, Kahl JS, and Brewer GF (1988) In-lake alkalinity generation by SO_4 reduction: A paleolimnological assessment. *Water, Air, and Soil Pollution* 39: 33–45.

Norton SA, Perry RH, Saros J, et al. (2011) The controls on phosphorus availability in a boreal lake ecosystem since deglaciation. *Journal of Paleolimnology* 46: 107–122.

Norton SA, Wagai R, Navrátil T, Kaste JM, and Rissberger FA (2000) Response of a first-order stream in Maine to short-term in-stream acidification. *Hydrology and Earth System Sciences* 4: 383–391.

Norton SA, Wilson T, Handley M, and Osterberg EC (2007) Atmospheric deposition of cadmium in the northeastern USA. *Applied Geochemistry* 22: 1217–1222.

Novák M, Buzek F, Harrison AF, Přechová E, Jačková I, and Fottová D (2003) Similarity between C, N and S stable isotope profiles in European spruce forest soils: Implications for the use of $\delta^{34}S$ as a tracer. *Applied Geochemistry* 18: 765–779.

Novák M, Kirchner JW, Groscheová H, et al. (2000) Sulphur isotope dynamics in two Central European watersheds affected by high atmospheric deposition of SO_x. *Geochimica et Cosmochimica Acta* 64: 367–383.

Oliver BG and Kelso JRM (1983) A role for sediments in retarding the acidification of headwater lakes. *Water, Air, and Soil Pollution* 20: 379–389.

Oliver BG, Thurman EM, and Malcolm RL (1983) The contribution of humic substances to the acidity of colored natural waters. *Geochimica et Cosmochimica Acta* 47: 2031–2035.

Osterberg E, Mayewski P, Kreutz K, et al. (2008) Ice core record of rising lead pollution in the North Pacific atmosphere. *Geophysical Research Letters* 35: L05810.

Pačes T (1983) Rate constants of dissolution derived from the measurements of mass balance in hydrochemical catchments. *Geochimica et Cosmochimica Acta* 47: 1855–1863.

Perakis SS and Hedin LO (2002) Nitrogen loss from unpolluted South American forests mainly via dissolved organic compounds. *Nature* 415: 416–419.

Peters SC, Blum JD, Driscoll CT, and Likens GE (2004) Dissolution of wollastonite during the experimental manipulation of Hubbard Brook Watershed 1. *Biogeochemistry* 67(3): 309–329.

Porcella DB, Schofield CL, DePinto JV, et al. (1989) Mitigation of acidic conditions in lakes and streams. In: Norton SA, Lindberg SE, and Page AL (eds.) *Acidic Precipitation. Soils, Aquatic Processes, and Lake Acidification*, vol. 4, pp. 159–186. New York: Springer-Verlag.

Postek KM, Driscoll CT, Kahl JS, and Norton SA (1996) Changes in the concentrations and speciation of aluminum in response to an experimental addition of ammonium sulfate to the Bear Brook Watershed, Maine, USA. *Water, Air, and Soil Pollution* 85: 1733–1738.

Pražáková M, Veselý J, Fott J, Majer V, and Kopáček J (2006) The long-term succession of cladoceran fauna and palaeoclimate forcing: A 14,600-year record from Plešné Lake, the Bohemian Forest. *Biologia, Bratislava* 61(supplement 20): S387–S399.

Prechtel A, Alewell C, Armbruster M, et al. (2001) Response of sulphur dynamics in European catchments to decreasing sulphate deposition. *Hydrology and Earth System Sciences* 5: 311–325.

Prescott CE, Kishchuk BE, and Weetman GF (1995) Long term effects of repeated N fertilization and straw application in a jack pine forest. 3. Nitrogen availability in the forest floor. *Canadian Journal of Forest Research* 25: 1991–1996.

Psenner R (1998) Alkalinity generation in a soft-water lake: Watershed and in-lake processes. *Limnology and Oceanography* 33: 1463–1475.

Psenner R and Schmidt R (1992) Climate driven pH control of remote alpine lakes and effects of acid deposition. *Nature* 356: 781–783.

Pugh AL, Norton SA, Schauffler M, et al. (1996) Interactions between peat and salt-contaminated runoff in Alton Bog, Maine, USA. *Journal of Hydrology* 182: 83–104.

Puhe J and Ulrich B (2001) *Global Climate Change and Human Impacts on Forest Ecosystems*. Berlin: Springer-Verlag.

Pyle DM, Battie PD, and Bluth GJS (1996) Sulphur emissions to the stratosphere from explosive volcanic eruptions. *Bulletin of Volcanology* 57: 663–671.

Rasmussen L, Brydges T, and Mathy P (1993) Experimental manipulations of biota and biogeochemical cycling in ecosystems: Approach, methodologies, findings. Ecosystem Research Report *No. #4*. Brussels: Commission of the European Communities.

Reinhardt RL, Norton SA, Handley M, and Amirbahman A (2004) Mobilization of and linkages among P, Al, and Fe during high discharge episodic acidification at the Bear Brook Watershed in Maine, USA. *Water, Air, and Soil Pollution: Focus* 4: 311–323.

Renberg I (1990) A 12,600 year perspective of the acidification of Lilla Öresjön, southwest Sweden. *Philosophical Transactions of the Royal Society Series B* 237: 357–361.

Renberg I, Brännvall M-L, Bindler R, and Emteryd O (2000) Atmospheric lead pollution history during four millennia (2000 BC to 2000 AD) in Sweden. *Ambio* 29: 150–156.

Reuss JO and Johnson DW (1986) *Acid Deposition and Acidification of Soils and Waters*. *Ecological Studies*, vol. 59. New York: Springer-Verlag.

Reynolds B, Emmett BA, and Woods C (1992) Variations in streamwater nitrate concentrations and nitrogen budgets over 10 years in a headwater catchment in mid-Wales. *Journal of Hydrology* 136: 155–175.

Reynolds B, Stevens PA, Hughes S, Parkinson JA, and Weatherley NS (1995) Stream chemistry impacts of conifer harvesting in Welsh catchments. *Water, Air, and Soil Pollution* 79: 147–170.

Roos-Barraclough F, Givelet N, Shotyk W, and Norton SA (2006) Use of Br and Se in peat to reconstruct the natural and anthropogenic fluxes of atmospheric Hg: A ten-thousand year record from Caribou Bog, Maine, USA. *Environmental Science & Technology* 40: 3188–3194.

Rosseland BO, Blakar IA, Bulger A, et al. (1992) The mixing zone between limed and acidic river waters: Complex aluminium chemistry and extreme toxicity for salmonids. *Environmental Pollution* 78: 3–8.

Roy SJ, Norton SA, and Kahl JS (1999) Phosphorous dynamics at Bear Brooks, Maine, USA. *Environmental Monitoring and Assessment* 55: 133–147.

Rudd JWM, Kelly CA, St. Louis V, Hesslein RH, Furutani A, and Holoka MH (1986) Microbial consumption of nitric and sulfuric acids in acidified north temperate lakes. *Limnology and Oceanography* 31: 1267–1280.

Rustad LE, Kahl JS, Norton SA, and Fernandez IJ (1994) Multi-year estimates of dry deposition at the Bear Brook Watershed in Eastern Maine, USA. *Journal of Hydrology* 162: 319–336.

Rustad LE, Marion GM, Norby RJ, et al. (2001) A meta-analysis of the response of soil respiration, net nitrogen mineralization, and aboveground plant growth to experimental ecosystem warming. *Oecologia* 126: 543–562.

Ryan DF and Kahler DM (1987) Geochemical and mineralogical indications of pH in lakes and soils in central New Hampshire in the early Holocene. *Limnology and Oceanography* 32: 751–757.

Sabine CL, Feely RA, Gruber N, et al. (2004) The oceanic sink for anthropogenic CO_2. *Science* 305: 367–371.

SanClements MD, Fernandez IJ, and Norton SA (2009) Soil and sediment phosphorus fractions in a forested watershed at Acadia National Park, ME, USA. *Forest Ecology and Management* 258: 2318–2325.

SanClements MD, Fernandez IJ, and Norton SA (2010) Controls on phosphorus fractions in acidic soils of humid temperate forests. *Soil Science Society of America Journal* 74: 2175–2186.

Šantrůčková H, Šantrůček J, Šetlík J, Svoboda M, and Kopáček J (2007) Carbon isotopes in tree rings of Norway spruce exposed to atmospheric pollution. *Environmental Science & Technology* 41: 5778–5782.

Schecher WD and Driscoll CT (1987) An evaluation of uncertainty associated with the aluminum equilibrium calculations. *Water Resources Research* 23: 525–534.
Schiff SL and Anderson RF (1986) Alkalinity production in epilimnetic sediments: Acidic and non-acidic lakes. *Water, Air, and Soil Pollution* 31: 941–948.
Schindler DW (1986) The significance of in-lake production of alkalinity. *Water, Air, and Soil Pollution* 239: 149–157.
Schindler DW (1997) Widespread effects of climatic warming on freshwater ecosystems in North America. *Hydrological Processes* 11: 1043–1067.
Schindler DW, Curtis PJ, Parker BR, and Stainton MP (1996) Consequences of climate warming and lake acidification for UV-B penetration in North American boreal lakes. *Nature* 379: 705–708.
Schindler DW, Frost TM, Mills KH, et al. (1990) Comparisons between experimentally- and atmospherically-acidified lakes during stress and recovery. *Proceedings of the Royal Society of Edinburgh Section B: Biological Sciences* 97: 193–226.
Schneider S (1989) The changing climate. *Scientific America* 261: 274.
Schnoor JL (1990) Kinetics of chemical weathering: A comparison of laboratory and field weathering rates. In: Stumm W (ed.) *Aquatic Chemical Kinetics*, pp. 475–504. New York: Wiley Interscience.
Schofield CL and Trojnar JR (1980) *Polluted Rain*. New York: Plenum Press.
Shotyk W, Cheburkin AK, Appleby PG, Fankhauser A, and Kramers JD (1996) Two thousand years of atmospheric arsenic, antimony, and lead deposition recorded in an ombrotrophic peat bog profile, Jura Mountains, Switzerland. *Earth and Planetary Science Letters* 145: E1–E7.
Simon K, Chadwick MA, Huryn AD, and Valett HM (2010) Stream ecosystem response to chronic deposition of nitrogen and acid at the Bear Brook Watershed, Maine. *Environmental Monitoring and Assessment* 171: 83–92.
Skartveit A (1981) Relationships between precipitation chemistry, hydrology, and runoff acidity. *Nordic Hydrology* 12: 55–60.
Skjelkvåle BL, Mannio J, Wilander A, and Andersen T (2001b) Recovery from acidification of lakes in Finland, Norway and Sweden 1990–1999. *Hydrology and Earth System Sciences* 5: 327–337.
Skjelkvåle BL, Stoddard JL, and Anderson T (2001a) Trends in surface water acidification in Europe and North America. *Water, Air, and Soil Pollution* 130: 787–792.
Skjelkvåle BL and Ulstein M (2002) *Proceedings from the Workshop on Heavy Metals (Pb, Cd, and Hg) in Surface Waters: Monitoring and Biological Impact*. Norwegian Institute for Water Research, Report, pp. 21–22.
Skjelkvåle BL, Wright RF, and Henriksen A (1998) Norwegian lakes show widespread recovery from acidification: Results of national surveys of lakewater chemistry 1986–1997. *Hydrology and Earth System Sciences* 2: 555–562.
Smith RA (1872) *Air and Rain: The Beginnings of Chemical Climatology*. London: Longmans Green & Co.
Steinberg C and Kühnel W (1987) Influence of cation acids on dissolved humic substances under acidified conditions. *Water Research* 21: 95–98.
Steinnes E (1995) A critical evaluation of the use of naturally growing moss to monitor the deposition of atmospheric metals. *Science of the Total Environment* 160/161: 243–249.
Stevens PA, Harrison AF, Jones HE, Williams TG, and Hughes S (1993) Nitrate leaching from a Sitka spruce plantation and the effect of fertilisation with phosphorus and potassium. *Forest Ecology and Management* 58: 233–247.
Stoddard JL (1994) Long-term changes in watershed retention of nitrogen. Its causes and aquatic consequences. In: Baker LA (ed.) *Environmental Chemistry of Lakes and Reservoirs. ACS Advances in Chemistry No. 237,* pp. 223–284. Washington: American Chemical Society.
Stoddard JL, Driscoll CT, Kahl JS, and Kellogg JH (1998) A regional analysis of lake acidification trends for the northeastern U.S., 1982–1994. *Environmental Monitoring and Assessment* 51: 399–413.
Stoddard JL, Jeffries DS, Lükewille A, et al. (1999) Regional trends in aquatic recovery from acidification in North America and Europe. *Nature* 401: 575–578.
Stoddard JL, Traaen TS, and Skjelkvåle BL (2001) Assessment of nitrogen leaching ICP-Waters sites (Europe and North America). *Water, Air, and Soil Pollution* 130: 781–786.
Sverdrup H (1990) *The Kinetics of Base Cation Release Due to Chemical Weathering*. Lund, Sweden: Lund University Press.
Sverdrup H and De Vries W (1994) Calculating critical loads for acidity with the simple mass balance method. *Water, Air, and Soil Pollution* 72: 143–162.
Sverdrup H and Warfvinge P (1993) Calculating field weathering rates using a mechanistic geochemical model PROFILE. *Applied Geochemistry* 8: 273–283.
Swedish Environmental Protection Board (1986) *Acid and Acidified Waters*. Solna Sweden: Swedish Environmental Protection Board.
Swoboda-Colberg NG and Drever JI (1993) Mineral dissolution rates in plot scale field and laboratory experiments. *Chemical Geology* 105: 51–69.
Tang J and Johannesson KH (2003) Speciation of rare earth elements in natural terrestrial waters: Assessing the role of dissolved organic matter from the modeling approach. *Geochimica et Cosmochimica Acta* 67: 2321–2339.
Taylor A and Blum JD (1995) Relation between soil age and silicate weathering rates determined from the chemical evolution of a glacial chronosequence. *Geology* 23: 979–982.
Teien H-C, Krogland F, Salbu B, and Rosseland BO (2006) Gill reactivity of aluminium-species following liming. *Science of the Total Environment* 358: 206–220.
Tipping E and Hopwood J (1988) Estimating streamwater concentrations of aluminum released from streambeds during 'acid episodes'. *Environmental Technology Letters* 9: 703–712.
Traaen TS, Frogner T, Hindar A, Kleiven E, Lande A, and Wright RF (1997) Whole-catchment liming at Tjonnstrond, Norway: An 11-year record. *Water, Air, and Soil Pollution* 94: 163–180.
Tranter M, Davies TD, Wigington PJ, and Eshleman KN (1994) Episodic acidification of fresh-water systems in Canada – Physical and geochemical processes. *Water, Air, and Soil Pollution* 72: 19–39.
Ulrich B (1983) Soil acidity and its relation to acid deposition. In: Ulrich B and Pankrath J (eds.) *Effects of Accumulation of Air Pollutants in Forest Ecosystems*, pp. 127–146. Dordrecht, The Netherlands: D. Reidel Publishing Co.
UN-ECE (1999) *The 1999 Gothenburg Protocol to Abate Acidification, Eutrophication and Ground-Level Ozone*. http://www.unece.org/env/lrtap.
Van Breemen N and Wright RF (2004) History and prospect of catchment biogeochemistry: A European perspective based on acid rain. *Ecology* 85: 2363–2368.
Velbel MA (1985) Geochemical mass balance and weathering rates in forested watersheds of the Southern Blue Ridge. *American Journal of Science* 285: 904–930.
Veselý J, Hruška J, and Norton SA (1998b) Trends in water chemistry of acidified Bohemian lakes from 1984 to 1995: II. Trace elements and aluminum. *Water, Air, and Soil Pollution* 108: 425–443.
Veselý J, Hruška J, Norton SA, and Johnson CE (1998a) Trends in the chemistry of acidified Bohemian lakes from 1984 to 1995: I. Major solutes. *Water, Air, and Soil Pollution* 108: 107–127.
Veselý J and Majer V (1996) The effect of pH and atmospheric deposition on concentrations of trace elements in acidified freshwaters: A statistical approach. *Water, Air, and Soil Pollution* 88: 227–246.
Veselý J and Majer V (1998) Hydrogeochemical mapping of Czech freshwaters. *Bulletin of the Czech Geological Survey* 73: 183–192.
Veselý J, Majer V, Kopáček J, and Norton SA (2003) Climate warming accelerates decreased aluminum concentrations in lakes recovering from acidification. *Limnology and Oceanography* 48: 2346–2354.
Veselý J, Majer V, and Norton SA (2002a) Heterogeneous response of central European streams to decreased acidic atmospheric deposition. *Environmental Pollution* 120: 275–281.
Veselý J, Norton SA, Skřivan P, et al. (2002b) Environmental chemistry of beryllium. In: Grew ES (ed.) *Beryllium – Mineralogy, Petrology and Geochemistry. Reviews in Mineralogy and Geochemistry*, vol. 50, pp. 291–317. Washington, DC: Mineralogical Society of America.
Veselý J, Šulcek Z, and Majer V (1985) Acid–base changes in streams and their effect on the contents of some heavy metals in stream sediment. *Bulletin of the Czech Geological Survey* 60: 9–23.
Wangwongwatava S (2001) Step-by-step approach to establish acid deposition monitoring network in East Asia (EANET): Thailand's experiences. *Water, Air, and Soil Pollution* 130: 151–162.
Warby RAF, Johnson CE, and Driscoll CT (2005) Chemical recovery of surface waters across the northeastern United States from reduced inputs of acidic deposition: 1984–2001. *Environmental Science & Technology* 39: 6548–6554.
Warby RAF, Johnson CE, and Driscoll CT (2009) Continuing acidification of organic soils across the northeastern U.S.: 1984–2001. *Soil Science Society of America Journal* 73(1): 274–284.
Warfvinge P, Falkengren-Grerup U, and Sverdrup H (1993) Modelling long-term base cation supply in acidified forest stands. *Environmental Pollution* 80: 1–14.
Waters D and Jenkins A (1992) Impacts of afforestation on water quality trends in two catchments in mid-Wales. *Environmental Pollution* 77: 167–172.
Watmough SA, Aherne J, Alewell C, et al. (2005) Sulphate, nitrogen and base cation budgets at 21 forested catchments in Canada, the United States and Europe. *Environmental Monitoring and Assessment* 109: 1–36.
Weatherley NS, Rutt GP, Thomas SP, and Ormerod SJ (1991) Liming acid stream: Aluminium toxicity to fish in mixing zones. *Water, Air, and Soil Pollution* 55: 345–353.

Webb JR, Cosby BJ, Galloway JN, and Hornberger GM (1989) Acidification of native brook trout streams in Virginia. *Water Resources Research* 25: 1367–1377.

Webster KE and Brezonik PL (1995) Climate confounds detection of chemical trends to acid deposition in upper Midwest lakes in the USA. *Water, Air, and Soil Pollution* 85: 1575–1580.

Webster KE, Kratz TK, Bowser CJ, Magnuson JJ, and Rose WJ (1996) The influence of landscape position on lake chemical responses to drought in northern Wisconsin. *Limnology and Oceanography* 41: 977–984.

Webster KE, Soranno PA, Baines SB, et al. (2000) Structuring features of lake districts: Landscape controls on lake chemical responses to drought. *Freshwater Biology* 43: 499–515.

White AF and Blum AE (1995) Effects of climate on chemical weathering in watersheds. *Geochimica et Cosmochimica Acta* 59: 1729–1747.

White AF and Brantley SL (1995) *Chemical Weathering Rates of Silicate Minerals*. *Reviews in Mineralogy*, vol. 31. Washington, DC: Mineralogical Society of America.

Whitehead DR, Charles DF, Jackson ST, Reed SE, and Sheehan MC (1986) Late glacial and Holocene acidity changes in Adirondack (N.Y.) lakes. In: Smol JP, Battarbee RW, Davis RB, and Meriläinen J (eds.) *Diatoms and Lake Acidity*, pp. 251–274. Dordrecht, The Netherlands: Junk.

Whiting MC, Whitehead DR, Holmes RW, and Norton SA (1989) Paleolimnological reconstruction of recent acidity changes in four Sierra Nevada lakes. *Journal of Paleolimnology* 2: 284–304.

Wigington PJ, Davies TD, Tranter M, and Eshleman KN (1990) Episodic acidification of surface waters due to acidic deposition. *US National Acid Precipitation Assessment Program, State of Science and Technology Report 12*. Washington, DC: National Acid Precipitation Assessment Program.

Wigington PJ, DeWalle DR, Murdoch PS, et al. (1996) Episodic acidification of small streams in the northeastern United States: Ionic controls of episodes. *Ecological Applications* 6: 389–407.

Wiklander L (1975) The role of neutral salts in the ion exchange between acid precipitation and soil. *Geoderma* 14: 93–105.

Williams PM (1968) Organic and inorganic constituents of the Amazon River. *Nature* 216: 937–938.

Williams MW, Baron JS, Caine N, Sommerfeld R, and Sanford R (1996) Nitrogen saturation in the Rocky Mountains. *Environmental Science & Technology* 30: 640–646.

Wood SA, Gammons CH, and Parker SR (2006) The behavior of rare earth elements in naturally and anthropogenically acidified waters. *Journal of Alloys and Compounds* 418: 161–165.

Wright RF (1985) Chemistry of Lake Hovvatn, Norway, following liming and reacidification. *Canadian Journal of Fisheries and Aquatic Sciences* 42: 1103–1113.

Wright RF (1998) Effect of increased carbon dioxide and temperature on runoff chemistry at a forested catchment in southern Norway. *Ecosystems* 1(2): 216–225.

Wright RF, Aherne J, Bishop K, et al. (2006) Modelling the effect of climate change on recovery of acidified freshwaters: Relative sensitivity of individual processes in the MAGIC model. *Science of the Total Environment* 365: 154–166.

Wright RF, Aherne J, Bishop K, et al. (2010) Interaction of climate change and acid deposition. In: Kernan M, Battarbee R, and Moss B (eds.) *Climate Change Impacts on Freshwater Ecosystems*, pp. 152–179 Oxford: Blackwell Publishing Ltd.

Wright RF, Alewell C, Cullen JM, et al. (2001) Trends in nitrogen deposition and leaching in acid-sensitive streams in Europe. *Hydrology and Earth System Sciences* 5: 299–310.

Wright RF, Larssen T, Camarero L, et al. (2005) Recovery of acidified European surface waters. *Environmental Science & Technology* 39: 64A–72A.

Wright RF, Lotse E, and Semb A (1993) RAIN Project: Results after 8 years of experimentally reduced acid deposition to a whole catchment. *Canadian Journal of Fisheries and Aquatic Sciences* 50: 258–268.

Wright RF, Norton SA, Brakke DF, and Frogner T (1988) Acidification of stream water by whole-catchment experimental addition of dilute seawater. *Nature* 334: 422–424.

Wright RF and Rasmussen L (1998) Introduction to the NITREX and EXMAN projects. *Forest Ecology and Management* 101: 1–7.

Wright RF and van Breemen N (eds.) (1995) The NITREX project: An introduction. *Forest Ecology and Management* 71: 1–5.

Yanai RD, Siccama TG, Arthur MA, Federer CA, and Friedland AJ (1999) Accumulation and depletion of base cations in forest floors in the northeastern US. *Ecology* 80: 2774–2787.

Yoh M (2001) Soil C/N ratio as affected by climate: An ecological factor of forest NO_3 leaching. *Water, Air, and Soil Pollution* 130: 661–666.

Zilberbrand M (1999) On equilibrium constants for aqueous geochemical reactions in water unsaturated soils and sediments. *Aquatic Geochemistry* 5: 195–206.

11.11 Tropospheric Ozone and Photochemical Smog

S Sillman, University of Michigan, Ann Arbor, MI, USA

Abbreviations

PAN	Peroxyacetyl nitrate ($CH_3CO_3NO_2$)
PM_{10}	Summed mass per unit volume of aerosols with individual particle size below 10 μm
$PM_{2.5}$	Summed mass per unit volume of aerosols with individual particle size below 2.5 μm
RH	A hydrocarbon in photochemical reactions
RO_2	An organic radical consisting of a hydrocarbon chain (R) terminating in O_2
ROOH	An organic peroxide, consisting of a hydrocarbon chain (R) terminating in OOH
TSP	Total suspended particulates
VOC	Volatile organic compounds

Symbols

$h\nu$	Representation of a photon in photolytic reactions, where ν represents frequency and h represents Planck's constant
NO_x	Nitrogen oxides, equal to the sum of nitric oxide (NO) and nitrogen dioxide (NO_2)
NO_y	Total reactive nitrogen, equal to the sum of all nitrogen-containing species (weighted by the number of nitrogen atoms), excluding ammonia (NH_3) or ammonium (NH_4)
NO_z	Summed reaction products of NO_x, equal to $NO_y - NO_x$
O_x	Odd oxygen, here used to represent the sum of ozone, atomic oxygen, and nitrogen dioxide

11.11.1 Introduction

The question of air quality in polluted regions represents one of the issues of geochemistry with direct ties to human well-being. Human health and well-being, along with the well-being of plants, animals, and agricultural crops, is dependent on the quality of the air we breathe. Since the start of the industrial era, air quality has become a matter of major importance, especially in large cities or urbanized regions with heavy automobile traffic and industrial activity.

Concern over air quality was found as far back as the 1600s. Originally, polluted air in cities resulted from the burning of wood or coal, largely as a source of heat. The Industrial Revolution in England saw a great expansion in the use of coal, both for industrial uses and for heating in rapidly growing cities. London suffered from devastating pollution events during the late 1800s and early 1900s, with thousands of excess deaths attributed to air pollution (Brimblecombe, 1987). Smaller events occurred at locations in continental Europe and the United States with heavy coal use. These events were caused by directly emitted pollutants (primary pollutants), including sulfur dioxide (SO_2), carbon monoxide (CO), and particulates. They were especially acute in cities with northerly locations during fall and winter when sunlight is at a minimum. These original pollution events gave rise to the term 'smog' (a combination of smoke and fog), which aptly described these early air pollution events. Events of this type have become much less severe since the 1950s in western Europe and the United States as natural gas replaced coal as the primary source of home heating, as industrial smokestacks were designed to emit at higher altitudes (where dispersion is more rapid), and as industries were required to install pollution control equipment.

Beginning in the 1950s, a new type of pollution, photochemical smog became a major concern. Photochemical smog consists of ozone (O_3) and other closely related species ('secondary pollutants') that are produced photochemically from directly emitted species, in a process that is driven by sunlight and is accelerated by warm temperatures. This smog is largely the result of gasoline-powered engines (especially automobiles), although coal-fired industry can also generate photochemical smog. The process of photochemical smog formation was first identified by Haagen-Smit and Fox (1954) in association with Los Angeles, a city whose geography makes it uniquely susceptible to this type of smog formation. Sulfate aerosols and organic particulates are often produced concurrently with ozone, giving rise to a characteristic milky-white haze associated with this type of air pollution.

Today, ozone and particulates are recognized as the air pollutants that are most likely to adversely affect human health. In the United States, most major metropolitan areas have had periodic air pollution events with ozone in excess of government health standards. Violations of local health standards also occur in major cities in Canada and in much of Europe. Other cities around the world (especially Mexico City) also experience very high ozone levels. In addition to urban-scale events, elevated ozone occurs in region-wide events in the eastern United States and in western Europe, with excess ozone extending over areas of 1000 km or more. In recent years, region-wide events have also occurred over the Mediterranean, in northern China (possibly extending to Korea and Japan), and possibly also in the Middle East (e.g., Guttikunda et al., 2005; Lelieveld et al., 2002; Li et al., 2001; Mauzerall et al., 2000). Ozone plumes with similar extent are found in the tropics (especially in central Africa) at times of high biomass burning (e.g., Chatfield et al., 1998; Jenkins et al., 1997). In some cases, ozone associated with biomass burning has been identified at distances up to 10 000 km from sources (Schultz et al., 1999).

Ozone also has significant impact on the global troposphere, and ozone chemistry is a major component of global tropospheric chemistry. Global background ozone concentrations are much lower than urban or regional concentrations during pollution events, but there is evidence that the global background has risen as a result of human activities (e.g., Volz and Kley, 1988; Wang and Jacob, 1998). A rise in global background ozone can make local pollution events everywhere more acute and can also cause ecological damage in remote locations that are otherwise unaffected by urban pollution. Ozone at the global scale is also related to greenhouse warming, and the various particulates include some that contribute to warming (soot or black carbon) and others that cause cooling (sulfates). The complex relation between ozone, particulates, and climate is only now being unraveled.

This chapter provides an overview of photochemical smog at the urban and regional scale, focused primarily on ozone and including a summary of information about particulates. It includes the following topics: dynamics and extent of pollution events, health and ecological impacts, relation between ozone and precursor emissions, including hydrocarbons and nitrogen oxides (NO_x); sources, composition, and fundamental properties of particulates; chemistry of ozone and related species; methods of interpretation based on ambient measurements; and the connection between air pollution events and the chemistry of the global troposphere. Because there are many similarities between the photochemistry of ozone during pollution events and the chemistry of the troposphere in general, this chapter will include some information about global tropospheric chemistry and the links between urban-scale and global-scale events. Additional treatment of the global troposphere is found in Volume 5 of *Treatise on Geochemistry*. The chemistry of ozone formation discussed here is also related to topics discussed in greater detail elsewhere in this volume: acid rain and acidification (**Chapter 11.10**) and hydrocarbons (**Chapters 11.12** and **11.13**).

11.11.2 General Description of Photochemical Smog

11.11.2.1 Primary and Secondary Pollutants

The term 'primary pollutants' refers to species whose main source in the atmosphere is direct emissions or introduction from outside (e.g., from soils). These species are contrasted with secondary pollutants, whose main source is photochemical production within the atmosphere.

The distinction between primary and secondary pollutants is conceptually useful because primary and secondary species usually show distinctly different patterns of diurnal and

seasonal variations in polluted regions of the atmosphere. The ambient concentrations of primary species are controlled largely by proximity to emission sources and rates of dispersion. The highest concentrations of these species tend to occur at nighttime or early morning and in winter in northerly locations because atmospheric dispersion rates are slowest at these times. By contrast, high concentrations of secondary species such as ozone are often associated with atmospheric conditions that favor photochemical production. The highest concentrations of ozone usually occur during the afternoons and in summer (in midlatitudes) or during the dry season (in the tropics). The highest concentrations of ozone and other secondary species also occur at locations significantly downwind of emission sources, rather than in immediate proximity to precursor emissions. These diurnal and seasonal cycles are discussed in detail in Section 11.11.4.

11.11.2.2 Ozone

Ozone occurs naturally in the troposphere, largely as a result of downward mixing from the stratosphere. This downward mixing includes both direct transport of ozone and transport of NO_x, which leads to photochemical formation of ozone in the troposphere. Ozone mixing ratios in the stratosphere (from approximately 20–60 km above ground level) are as high as 15 000 parts per billion (ppb). This is higher than ozone concentrations at ground level, even in the most polluted regions, by a factor of 100. Approximately 95% of the Earth's ozone is located in the stratosphere. Ozone in the troposphere is much lower and generally decreases from the top of the troposphere to ground level. The ozone that is transported downward from the stratosphere is removed through photochemical processes in the troposphere (which include both production and removal of ozone, but with removal rates exceeding production rates). Ozone is also removed through dry deposition at the Earth's surface. Removal of ozone in the troposphere happens on a timescale of approximately 3 months. In the absence of human activities, ozone concentrations would vary from 200 ppb in the upper troposphere to 10–20 ppb at ground level.

11.11.2.2.1 Urban ozone

Ozone is formed in polluted urban areas from photochemical reactions involving two classes of precursors: hydrocarbons (or, more generally, volatile organic compounds or VOC) and nitrogen oxides (NO_x, consisting of nitric oxide (NO) and nitrogen dioxide (NO_2)). During a typical urban air pollution event, peak O_3 reaches a value of 120–180 ppb.

The first city to record ozone levels high enough to be of public concern was Los Angeles. Beginning in the 1950s, Los Angeles routinely recorded peak ozone in excess of 125 ppb, a value that was later established as the health standard in the United States. During the 1970s and 1980s, ozone in excess of the health standard occurred as often as 180 days $year^{-1}$ in the Los Angeles metropolitan area. In the 1990s, Mexico City also began to experience ozone levels comparable to Los Angeles with ozone in excess of 125 ppb on approximately 180 days $year^{-1}$ (e.g., see Sosa et al., 2000). Events with ozone in excess of 200 ppb are quite rare and generally occur only in cities with the most severe ozone problems. Ozone as high as 490 ppb has been recorded in Los Angeles (NRC, 1991) and in Mexico City. Stringent control measures have succeeded in lowering the frequency and severity of air quality violations in Los Angeles (beginning in the 1990s) and in Mexico City (after 2000), but Los Angeles still records violations on approximately 25 days $year^{-1}$. In both cities, the initial reduction in ozone was achieved largely through controls on autoemissions.

Most other major cities in the United States and in Europe also record events with ozone in excess of 125 ppb, but these occur only a few times per year. Severe air pollution events occur less frequently in these cities because the meteorological conditions that favor rapid formation of ozone (high sunlight, warm temperatures, and low rates of dispersion) occur less frequently. Significant excess ozone is formed only when temperatures are above 20 °C, and severe events are usually associated with temperatures of 30 °C or higher. The major cities of the northeastern United States and northern Europe have ozone above 80 ppb on approximately 30–60 days $year^{-1}$. At other times, a combination of cool temperatures and/or clouds would prevent ozone formation, regardless of the level of precursor emissions. In humid tropical regions, ozone excursions are limited by the frequent occurrence of convective clouds and rain, which has the effect of dispersing urban pollutants as well as suppressing ozone formation due to lack of sunlight. Thus, days with high ozone are generally limited to summer (in the middle and high latitudes) and dry seasons (in the tropics).

The most severe pollution events occur when a combination of light winds and suppressed vertical mixing prevent the dispersion of pollutants from an urban center. The process of ozone formation typically requires several hours and occurs only at times of bright sunlight and warm temperatures. For this reason, peak ozone values typically are found downwind of major cities rather than in the urban center. During severe events with light winds, high ozone concentrations are more likely to occur closer to the city center.

11.11.2.2.2 Regional pollution events and long-distance transport

Peak ozone in urban plumes is found most commonly 50–100 km downwind of the city center. Once formed, ozone in urban plumes has an effective lifetime of approximately 3 days. For this reason, urban plumes with high ozone can travel for great distances. Transport of ozone can be even longer in the middle and upper troposphere, where the lifetime of ozone extends to 3 months.

Although peak ozone most commonly occurs 50–100 km downwind from urban centers, plumes with high ozone have frequently been observed at distances of 300 km or more from their source regions. Ozone in excess of 150 ppb has frequently been observed on Cape Cod (Massachusetts), attributed to emissions in the New York metropolitan area 400 km away. Similar excess ozone has been observed along the shores of Lake Michigan apparently due to emissions in the Chicago area that have traveled 300 km across the lake. Ozone as high as 200 ppb has been observed in Acadia National Park, Maine, attributed to transport from Boston (300 km away) and New York (700 km away) (see Figure 1). The plume from the

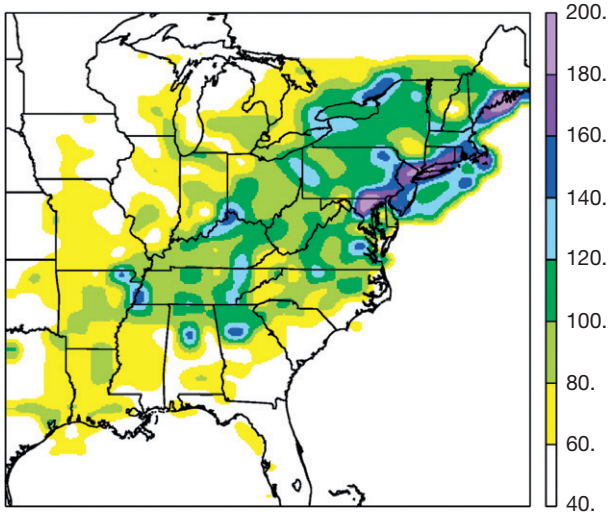

Figure 1 Peak ozone concentrations in the eastern United States during a severe air pollution event (15 June 1988) based on surface observations at 350 EPA monitoring sites. The shadings represent values of 40–60 ppb (lightest shading) to 180–200 ppb (darkest shading) with 20 ppb intervals in between. First printed in Sillman (1993).

New York–Boston corridor has also been observed by aircraft over the North Atlantic Ocean at a distance of several hundred kilometers from the source region (Daum et al., 1996). In Europe, plumes from cities in Spain have been predicted to transport over the Mediterranean Sea, also at distances several hundred kilometers from the source region (Millan et al., 1997).

Well-defined plumes with excess ozone are also associated with large coal-fired power plants in the United States. The largest power plants can have rates of NO_x emissions that are comparable to the summed emission rate from a city as large as Washington DC. Because these power plants have relatively low emissions of CO or volatile organics, the rate of ozone formation is slower, and peak ozone occurs further downwind (100–200 km). Ozone as high as 140 ppb has been observed in plumes from individual power plants (Gillani and Pleim, 1996; Miller et al., 1978; Ryerson et al., 1998, 2001; White et al., 1983). These plumes have been observed by aircraft for distances up to 12 h downwind from the plume sources. It is more difficult to observe plumes at greater downwind distances because well-defined plumes are usually dispersed following overnight transport (Clarke and Ching, 1983).

In addition to transport in well-defined plumes, ozone in excess of 80 ppb is found to extend over broad regions (500×500 km or larger) during region-wide events. These events are associated with stagnant high-pressure systems that bring several consecutive days of high temperatures, sunlight, and suppressed atmospheric mixing to a polluted area. Region-wide events of this type have been frequently observed in the eastern United States and less frequently in western Europe. Elevated ozone during these events affects rural areas as well as urban and suburban locations. These events are caused by the combined effect of emissions from large and small cities, industries, and power plants rather than emissions from a single urban center, and can include ozone that has formed and accumulated over a period of several days. Emissions from cities within the affected region create plumes with additional excess ozone added to (and subsequently contributing to) the regional background. Region-wide pollution from multiple sources may be responsible for extensive high ozone (above 80 ppb) observed in the Mediterranean and in eastern China and possibly extending across the Sea of Japan to Korea and Japan (Guttikunda et al., 2005; Lelieveld et al., 2002; Mauzerall et al., 2000).

An event of this sort is illustrated in **Figure 1**. During this event, ozone in excess of 90 ppb was observed at every surface monitoring site (including both urban and rural sites) over an area extending from Ohio to Virginia and Maine, approximately 1000×1000 km. Higher ozone (150–200 ppb) was found throughout the cities of the northeast corridor (Washington, Philadelphia, New York, and Boston). The plume of high ozone in the northeast corridor extended to Maine. Locally high ozone was also found near several other cities.

There has been considerable speculation that the rapid worldwide growth of cities and industries will cause the scale of these region-wide events to increase and to eventually involve intercontinental transport. Ozone concentrations of 80 ppb have been observed at Sable Island, Nova Scotia, transported from source regions 2000 km distant in the United States (e.g., Parrish et al., 1993). Layers of elevated ozone aloft over the South Atlantic Ocean and over the western Pacific have both been attributed to biomass burning in Africa (Chatfield et al., 1998; Jenkins et al., 1997; Schultz et al., 1999). Model calculations have estimated that emissions from East Asia can cause a significant increase in background ozone levels in the western United States (Cooper et al., 2010; Horowitz and Jacob, 1999; Lelieveld and Dentener, 2000). Measurements have identified possible transport from North America in air over Europe (Stohl and Trickl, 1999). Long-range transport of sulfate aerosols is also possible (Barth and Church, 1999).

While such long-range transport of ozone is possible, it might be viewed as part of the global tropospheric balance.

Signals for transport of ozone from East Asia to North America and from North America to Europe have been detected in measurements and predicted in models (Cooper et al., 2010; Fiore et al., 2009). The contribution of intercontinental transport (including both direct transport of O_3 and transport of precursors) is typically 4–7 ppb (Fiore et al., 2002b, 2009) and roughly 20% of the size of the contribution from local/regional emissions. However, due to the huge spatial extent of this transport (effectively encompassing the entire northern hemisphere), the cumulative damage to human health and agriculture from even a small increase in ozone can be large. Global impacts on the continental scale include transport on timescales of several months (based on the lifetime of ozone and some precursors in the free troposphere) and are associated with dispersion throughout the northern hemisphere (merging with general tropospheric chemistry) as well as with specific transport events.

11.11.2.2.3 Ozone and the global troposphere

Surface ozone concentrations in the remote northern hemisphere range from 20 to 40 ppb with a seasonal maximum in May. Background ozone in the southern hemisphere is

significantly lower (20–25 ppb). These background ozone concentrations are both affected by global-scale photochemistry, which includes both production and destruction of ozone. It is believed that emissions resulting from human activities have increased the global background ozone, especially in the northern hemisphere (e.g., see Cooper et al., 2010; Fiore et al., 2009; Lelieveld and Dentener, 2000; Wang and Jacob, 1998; and Volume 4 of this series).

Although the transport of ozone plumes from source regions provides dramatic evidence of the global impact of human activities, the chemical content of the global troposphere is more likely to be affected by photochemistry during average conditions rather than by episodic transport events. The rates of photochemical production and destruction of ozone in the free troposphere (defined as the region extending from the top of the planetary boundary layer, approximately 2–3 km above the ground, to the top of the troposphere) are much larger in terms of total molecules produced than the rate of production in polluted source regions. Production rates in polluted regions are much higher on a per volume basis, but the volume of the free troposphere is large enough so that photochemical production there greatly exceeds the amount of ozone molecules produced in source regions.

NO_x, the critical precursor for ozone formation, typically has daytime concentrations of 5–20 ppb in urban areas, 0.5–1 ppb in polluted rural areas during region-wide events, and 10–100 parts per trillion (ppt) in the remote troposphere. A NO_x concentration of 1 ppb is associated with ozone formation at rates of 2–5 ppb per hour, which is fast enough to allow ozone concentrations to increase to 90 ppb when air stagnates in a polluted region for 2 days or more. Ozone production rates as high as 100 ppb per hour have been observed in urban locations (e.g., in the Texas Air Quality Study in Houston, Kleinman et al., 2002). Production rates are much slower in the free troposphere, and loss usually exceeds production. However, NO_x concentrations of 100 ppt, which are much too small to allow the formation of episodic high ozone, would still allow ozone to remain at a steady-state concentration of approximately 80 ppb. The current level of background ozone in the lower troposphere (20–40 ppb) is closely related to the photochemical steady state, achieved over several months, based on concentrations of NO_x and organics in the remote troposphere.

There is an obvious close relation between smog events in polluted regions and conditions in the global troposphere because the global troposphere is strongly impacted by pollutants that are emitted primarily in cities or polluted regions. However, the relation between polluted regions and the global troposphere can often be counterintuitive. In general, the rate of ozone formation per NO_x ('ozone production efficiency,' discussed in more detail below) is higher when NO_x concentrations are lowest. Consequently, the global impact of emissions is actually higher when there is rapid dispersion of pollutants from a polluted region. The exported pollutants produce more total ozone (though with lower peak concentration) when they undergo photochemical processing in downwind rural areas or in the remote troposphere rather than in a polluted region during a stagnation event. Ozone precursors lead to ozone formation in the remote troposphere even when local conditions (e.g., clouds and low temperatures) prevent the formation of ozone in the polluted source region.

11.11.2.2.4 Ozone precursors: NO_x, CO, and volatile organics

Ozone in urban areas is produced from two major classes of precursors: NO_x, consisting of NO and NO_2, and VOC. The ozone formation process is also closely associated with the hydroxyl radical (OH, see below for a complete description). The process of ozone formation is initiated by the reaction of organics (usually primary hydrocarbons) with OH. The subsequent reaction sequence involves NO_x and results simultaneously in the production of ozone, oxidation of organics to CO_2, and oxidation of NO_x to nitric acid (HNO_3). In urban areas, the ozone formation process is also accompanied by the conversion of NO_x to organic nitrates such as peroxyacetyl nitrate ($CH_3CO_3NO_2$, often abbreviated as PAN), which has the effect of transporting NO_x to the remote troposphere.

In addition to their impact on ozone, NO_x and VOC are associated with various other pollutants which impact human health and activities. NO_2 causes impairment of lung functions and generally has the same level of toxicity as ozone, although ambient concentrations are usually much lower. NO_2 is produced in the atmosphere by chemical conversion from directly emitted NO, although some NO_2 is also emitted directly into the atmosphere. NO_2 is usually grouped together with NO as NO_x because conversion from NO to NO_2 is rapid (with timescales of 5 min or less), and because the ambient mixing ratios of NO_2 show a pattern of behavior that resembles primary rather than secondary pollutants. HNO_3 contributes to acid rain and contributes to the formation of particulates (see **Section 11.11.2.3**). Both primary and secondary VOC include species that are directly toxic (see **Chapters 11.12** and **11.13**), and secondary organics produced from directly emitted VOC are major components of particulates. CO is also a toxic gas, although ambient concentrations are rarely high enough to raise health concerns.

In the remote troposphere, the ozone formation process is initiated primarily by the oxidation of CO and methane (CH_4) rather than volatile organics. CO and CH_4 are both long-lived species (2 month lifetime for CO, 9–14 years for CH_4) and are widely distributed in the remote troposphere. They have less direct impact on urban photochemistry because most of the CO emitted in urban areas is exported to the remote troposphere. However, the effect of CH_4 in particular has been identified as a major influence on ambient ozone because increases in CH_4 lead to increases in ozone worldwide and thus contribute indirectly to urban and regional pollution events (Fiore et al., 2002a; West et al., 2006).

Shorter lived volatile organics (with lifetimes ranging from 1 h to 3 days) are more important in terms of urban photochemistry because they undergo reactions rapidly enough to contribute to ozone formation during local air pollution events. Alkenes, aromatics, and oxygenated organic species such as formaldehyde (HCHO) are especially important in terms of urban photochemistry because they initiate reaction sequences that generate additional OH radicals (which catalyze further ozone production) in addition to producing ozone directly. This is discussed further in **Chapter 11.12** of this volume.

The relative impact of NO_x and VOC on ozone formation during pollution events represents a major source of uncertainty. The chemistry of ozone formation is highly nonlinear, so that the exact relation between ozone and precursor emissions depends on the photochemical state of the system. Under some conditions, ozone is found to increase with increasing NO_x emissions and to remain virtually unaffected by changes in VOC. For other conditions, ozone increases rapidly with increased emission of VOC and decreases with increasing NO_x. This split into NO_x-sensitive and NO_x-saturated (or VOC-sensitive) photochemical regimes is a central feature of ozone chemistry and a major source of uncertainty in terms of pollution control policy.

An analogous split between NO_x-sensitive and NO_x-saturated chemistry occurs in the remote troposphere, but the implications are somewhat different. Increased CO, CH_4, and VOC always contribute to increased ozone in the remote troposphere, even under NO_x-sensitive conditions (Jaegle et al., 1998, 2001), whereas ozone in polluted regions with NO_x-sensitive chemistry is largely insensitive to CO and VOC.

NO_x emissions in polluted regions originate from two major sources: gasoline- and diesel-powered vehicles (primarily automobiles) and coal-fired power plants. Volatile organics are also generated largely by gasoline- and diesel-powered vehicles and by a variety of miscellaneous sources, all involving petroleum fuel or petroleum products. Coal-fired industry does not generate significant amounts of organics.

Although the question of NO_x versus VOC sensitivity and the related policy issue of NO_x versus VOC controls is complex and uncertain, there are a few concepts and trends that are useful for gaining a good general understanding. NO_x-sensitive conditions occur when there is excess VOC and a high ratio of VOC to NO_x, while VOC-sensitive conditions occur when there is excess NO_x and low VOC/NO_x. The ratio of summed VOC to NO_x, weighted by the reactivity rate of each individual VOC, provides a good indicator for NO_x- versus VOC-sensitive chemistry.

Among freshly emitted pollutants, the initial rate of ozone formation is often controlled by the amount and chemical composition of VOC. For this reason, ozone formation in urban centers is often (but not always) controlled by VOC. As air moves downwind, ozone formation is increasingly controlled by NO_x rather than VOC (Milford et al., 1989). Ozone in far downwind and rural locations is often (but not always) controlled by upwind NO_x emissions (Roselle and Schere, 1995). Rural areas also tend to have NO_x-sensitive conditions due to the impact of biogenic VOC (see next section). However, this description represents a general trend only and is not universally valid. NO_x-sensitive conditions can occur even in large urban centers, and VOC-sensitive conditions can occur even in aged plumes. For a more complete discussion, see NARSTO (2000) and Sillman (1999).

11.11.2.2.5 Impact of biogenics

In addition to anthropogenic sources, there are significant biogenic sources of organics. Isoprene (C_5H_8) is emitted by a variety of deciduous trees (especially oaks), and these emissions have a significant impact on ozone formation. Terpenes (e.g., α-pinene and $C_{10}H_{10}$) are emitted primarily by conifers and are precursors of particulates (see **Section 11.11.2.3**). Emission of biogenic VOC often equals or exceeds the rate of emission of anthropogenic VOC at the regional scale, and even within urban areas, biogenic VOC can account for a significant percentage of total VOC reactivity. Biogenic VOC are especially important because they have a relatively short lifetime (1 h or less) and consequently contribute to local ozone formation during pollution events.

The major significance of biogenic VOC with regard to ozone lies in their implications for the effectiveness of control strategies and their impact on ozone–NO_x–VOC chemistry. The presence of biogenic VOC in polluted regions effectively increases the ratio of VOC to NO_x, especially when ratios are weighted by the rate of reactivity. Consequently, regions with biogenic VOC are more likely to have ozone formation that is sensitive to NO_x rather than VOC (Chameides et al., 1988; Pierce et al., 1998; Simpson, 1995).

Biogenic emissions also influence chemistry in the free troposphere. On a global scale, the emission of biogenic VOC greatly exceeds anthropogenic emissions. The global impact of biogenics is somewhat limited due to their short atmospheric lifetime, so that high concentrations are limited to source regions. By contrast, the longer lived CO and CH_4 are ubiquitous in the troposphere.

Biogenic sources of NO_x are generally too small to contribute significantly to pollution events. Biogenic emissions represent approximately 5% of the total NO_x emissions in the United States (compared to 50% of the total VOC) (Williams et al., 1992). Biogenic NO_x emissions can be important in intensively farmed regions, where soil emission of NO_x is enhanced by heavy use of fertilizer.

11.11.2.3 Particulates

Particulates, or aerosols, have wide-ranging impacts on both human activities and environmental quality. (Technically, the term 'aerosol' refers to a mixture of solid and liquid particles suspended in a gaseous medium, whereas the term 'suspended particulates' refers to the suspended particles themselves. In practice, the terms 'aerosols' and 'particulates' are often used interchangeably.) First, aerosols have been identified as one of the major health hazards, affecting the respiratory system, associated with air pollution (along with ozone). Second, because degradation of visibility in polluted air is due almost entirely to aerosols (Seinfeld and Pandis, 1998), particulates are the most noticeable aspect of air pollution. Third, removal of acidic aerosols from the atmosphere, through deposition on soils and water surfaces or through rainout, can cause ecological damage. Acid rain (**Chapter 11.10**) is the best-known example of this type of damage. Fourth, sulfate aerosols affect the global climate directly (by enhancing atmospheric reflectivity) and indirectly (by affecting the growth and reflectivity of clouds). This is believed to have a significant cooling effect on the atmosphere, although there is large uncertainty for assessing the impact of human activities on climate (Forster et al., 2007). Other aerosols (e.g., black carbon) rapidly absorb solar radiation and can possibly increase global warming (Chung and Seinfeld, 2002; Jacobson, 2002; Ramanathan and Carmichael, 2008).

Aerosols are associated with major uncertainties in climate predictions and in estimations of the impact of human activities on climate. These uncertainties are largely due to indirect effects on climate. Aerosols affect climate through direct effect

on incoming and outgoing solar radiation, which can be calculated with relatively little uncertainty. However, aerosols also affect the optical properties of clouds (first indirect effect) and cloud lifetimes, extent, and precipitation rates (second indirect effect). These effects account for much of the uncertainty in current predictions for future climate (Forster et al., 2007). A major current concern is that policies to reduce concentrations of atmospheric sulfate would lead to increased global warming, especially if emissions of black carbon (which tend to exacerbate warming trends) increase.

As was the case with ozone, aerosols also occur naturally in the atmosphere. Aerosols play an important role in the atmosphere's hydrologic cycle. Formation of cloud droplets occurs on hygroscopic aerosols, and nucleation of ice also needs a particle to initiate ice formation. Precipitation, which is enhanced by the presence of large aerosols or ice, strongly depends on these ice and cloud condensation nuclei. Most (though not all) of the damaging effects are due to anthropogenic rather than naturally occurring aerosols.

Aerosols are composed of a large variety of species, from both natural and anthropogenic materials. Naturally occurring aerosols include sea salt, mineral dust, pollens and spores, organic aerosols derived from biogenic VOC, and sulfate aerosols derived from reduced sulfur gases. Anthropogenic aerosols consist of soot (also known as black carbon), sulfate derived from SO_2 emitted from coal burning, organics derived from anthropogenic VOC, and fly ash. Biomass burning (either naturally occurring or anthropogenic) also creates aerosols. Aerosols include both primary species and species produced by photochemical reactions.

Aerosols are generally divided into two groups, fine particles (with size below 2.5 μm) and larger coarse particles, because of their distinct impacts on human activities and environmental quality.

The fine and coarse particles differ from each other in terms of their origin, chemical composition, and their atmospheric effects. Coarse particles are usually the result of mechanical wear on preexisting solid substances: mineral dust (i.e., soil particles), sea salt, solid organic matter from plants, flakes from automobile tires and from buildings, etc. By contrast, fine particles are largely the result of chemistry – either combustion chemistry in fires, smokestacks and internal combustion engines or photochemistry in the atmosphere, cloud droplets, and water aerosols. Chemical and photochemical production followed by condensation (in combustion processes) or nucleation (in the atmosphere) result in the formation of solid particles of very small size (0.005–0.1 μm), a size range that is referred to as the nuclei mode. After formation, these particles lead to formation of larger particle sizes (0.1–1 μm) through the process of coagulation or through deposition of chemically formed particulate material on existing nuclei. These accumulation mode particles are the major cause of health and visibility effects associated with particulates. The process of coagulation does not lead to significant amounts of particles with size greater than 2.5 μm, so that the fine particles (nuclei and accumulation mode) have distinctly different sources than the coarse particles.

Observed distributions of particle sizes (Figure 2) often show two separate peaks in particle mass, at 0.1–1 μm and at 3–20 μm, reflecting the different origin of coarse and fine particles.

Apart from their origin, there are other important differences between coarse and fine particulates. Fine particulates are usually acidic in nature and rapidly dissolve in water (and in some cases, are formed through aqueous chemistry in cloud droplets or water aerosols). Coarse particulates are usually nonacidic and hydrophobic. Coarse particulates are removed from the atmosphere through gravitational settling, on timescales of 1 day or less depending on the size of the individual particles. Fine particulates are too small to be removed by gravitational settling. They are removed either by rainout (wet deposition) or by direct deposition to ground surfaces (dry deposition). The dry deposition rate for fine particulates is typically 0.1 cm s^{-1} (Seinfeld and Pandis, 1998) and allows these particulates to remain in an atmospheric boundary layer of typical depth for 10 days or more. Removal by wet deposition is often more rapid (2–5 days, Rasch et al., 2000), although this depends on local climatology. The slow removal rate allows the concentration of fine particulates to build up during multiday pollution events. Fine particulates are often transported for distances of 300 km or more in the atmosphere, more readily than coarse particulates (although coarse mineral dust from desert regions can be transported on continental scales, e.g., Prospero, 1999). Fine particulates have a much larger impact on atmospheric visibility than coarse particulates. Most importantly, adverse health impacts are associated primarily with fine particulates (see **Section 11.11.2.4**).

The major sources of fine particles in the ambient atmosphere are: sulfates, which are produced photochemically from SO_2; organics, which are produced chemically from both anthropogenic and biogenic VOC; black carbon (soot), which is emitted directly from anthropogenic industry and transportation; and nitrates, which are formed from NO_x. Sulfates and organic compounds are typically the largest components of fine particulates in urban and industrialized regions. Sulfate aerosols have been historically the largest aerosol component, especially in regions with coal-fired industry. They are currently the dominant aerosol in the eastern and midwestern United States, although their concentrations may be significantly reduced in the future by planned reductions of sulfur emissions. Nitrates form aerosols in combination with ammonia (NH_3), usually from agricultural sources. The resulting ammonium nitrate aerosol (NH_4NO_3) is often a significant component of particulates in locations that include both intensive agriculture and urban NO_x sources in close proximity (e.g., Los Angeles and Milan). Organic particulates from biomass burning (largely in the tropics) also contribute significantly to the total amount of particulates at the global scale. Trace metals (iron, lead, zinc, mercury, etc.) are also present in small quantities as aerosol components. These contribute little to the total particulate mass but are often of concern because they may be individually toxic (see **Chapter 11.3**).

Particulate concentrations in the atmosphere are frequently expressed in terms of total suspended particulates (TSP, as mass per unit volume) or as the summed mass of particulates with individual size below a given diameter (typically, $PM_{2.5}$ for particulates smaller than 2.5 μm or PM_{10} for particulates smaller than 10 μm). In urban centers in the United States and Europe, typical particulate concentrations are 15–30 μg m^{-3} for $PM_{2.5}$, 30–50 μg m^{-3} for PM_{10}, and 50–100 μg m^{-3} for TSP, with peak concentrations approximately three times

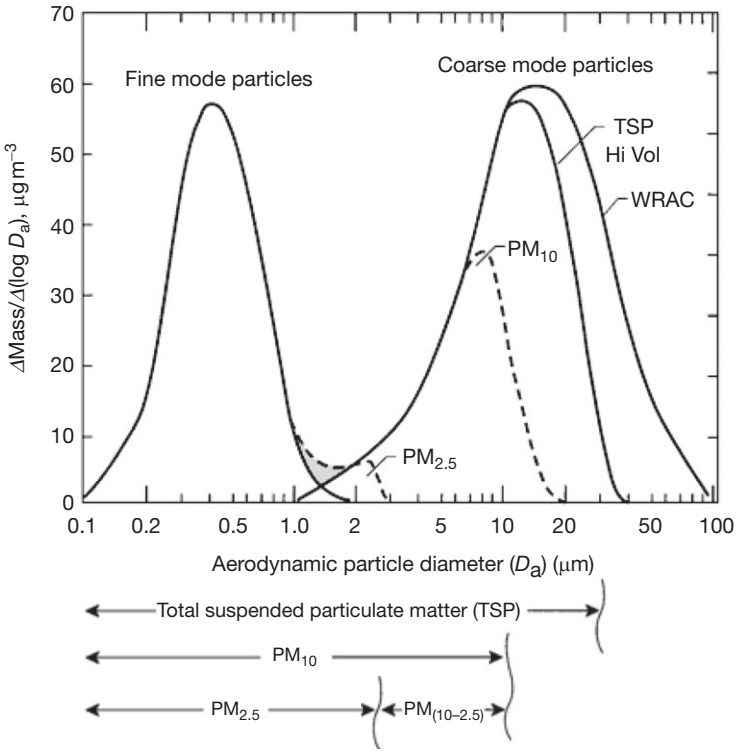

Figure 2 Representative example of a mass distribution of ambient particulate matter as a function of particle diameter. Mass distribution per particle size interval is shown as ΔMASS/Δ(logD_a) (in μg m^{-3}) plotted against particle size (D_a) in μm. The figure also shows the range of aerosol sizes included in various methods of aerosol measurement: wide range aerosol classifiers (WRAC), total suspended particulate (TSP) samplers, PM_{10}, and $PM_{2.5}$ samplers. Reproduced from Lippman M and Schlesinger RB (2000) Toxicological bases for the setting of health-related air pollution standards. *Annual Review Public Health* 21: 309–333.

higher (e.g., Baltensberger et al., 2002; Blanchard et al., 2002; Jacobson, 1997; Seinfeld and Pandis, 1998). Rural and remote PM_{10} concentrations are typically below 10 μg m^{-3}. Several rapidly growing megacities in industrializing regions (Delhi, Bombay, Cairo, Mexico City, and Bangkok) have TSP in excess of 400 μg m^{-3} (Mage et al., 1996). Particulate concentrations as high as 5000 μg m^{-3} (TSP) have been observed during historically severe episodes, for example, in the Ruhr valley, Germany, in 1966, and in London in1952 (Anderson, 1999; Brimblecombe, 1987). Particulate concentrations (as TSP, PM_{10}, and $PM_{2.5}$) are most frequently measured, but often, the chemical composition of particulates is equally important, in terms of atmospheric analysis and environmental impacts.

The distribution of aerosols (shown in **Figure 2** per unit mass) can also be expressed in terms of the total number of particles, which places greater emphasis on the smaller particles and provides information about the nuclei mode and the process of accumulation. Aerosol concentrations are sometimes expressed in terms of aerosol surface area, which is closely related to visibility impacts.

The role of chemistry in producing sulfate particulates is especially noteworthy. Sulfates are emitted directly from coal-fired industries, but most atmospheric sulfates are produced photochemically from SO_2 (also emitted from coal-fired industries). Sulfates are produced in two ways: by gas-phase oxidation (a process which is often linked to ozone formation), and by aqueous-phase reactions. The aqueous reactions can proceed on timescales of a few minutes or less in cloud droplets, so that atmospheric sulfur is rapidly converted to sulfates in the presence of clouds. This cloud-formed sulfate is often removed from the atmosphere by rain (see **Chapter 11.10**) or dispersed vertically by dynamics associated with clouds. Sulfates can also be produced in hygroscopic or wetted aerosolswhich are present in the atmosphere at times of high relative humidity, and in fog. Dangerously high levels of sulfates were generated during the classic London fogs of the early 1900s, which combined stagnant meteorology, fog, and high sulfur concentrations (Brimblecombe, 1987).

Ozone air pollution events generally have lower concentrations of sulfates than the winter fog events because the dynamics that lead to ozone production usually has much more rapid vertical dilution than the fog events. However, ozone events can lead to significant enhancement of sulfates, especially at the regional scale. The same photochemical processes that lead to ozone formation also cause rapid photochemical conversion of SO_2 to sulfates. Conversion of SO_2 to sulfates during air pollution events occurs at a timescale of 1–2 days. This allows for significant accumulation of sulfates during regional air pollution events.

11.11.2.4 Environmental and Health Impacts

The impact of ozone, acid aerosols, and other related pollutants on human health has been the subject of intense scrutiny

(Dockery et al., 1993; Hoening, 2000; Holgate et al., 1999; Lippman, 2000; Lippman and Schlesinger, 2000; Wilson and Spengler, 1996). There is evidence that current ambient levels of both ozone and acid aerosols have significant health impacts. In addition, ozone has been linked with both damage to agricultural crops (Mauzerall and Wang, 2001) and forests (US Congress, 1989). Particulates are responsible for most of the visibility degradation associated with air pollution (Seinfeld and Pandis, 1998).

The most direct and striking evidence for health effects from air pollution is found in particulates. A series of studies in the United States have shown that mortality rates correlate with exposure to particulates (Dockery et al., 1993; Lippman and Schlesinger, 2000). These studies found that high exposure to particulates were correlated with increased mortality from respiratory or cardiopulmonary diseases, but not with increased death rates from other causes. The increase in mortality rates was significant (10–26%), and the associated premature deaths were believed to represent a 2–3 year shortening of life spans. The associated range of particulate concentrations was 30–80 $\mu g\, m^{-3}$ for TSP and 10–30 $\mu g\, m^{-3}$ for fine particulates ($PM_{2.5}$), approximately half of which consisted of sulfates. The studies were able to statistically rule out alternate causes of increased mortality, including incidence of smoking, presence of air-borne allergens, temperature, humidity, or the presence of other air pollutants. Increased mortality was specifically associated with fine particulates rather than coarse particulates and was linked with both sulfate and nonsulfate fine particulates. There have also been numerous episodic events in United States and in Europe (including the well-known London fogs) in which elevated particulates, SO_2, and other primary pollutants, have been correlated with excess deaths and admissions to hospitals (Anderson, 1999; Brimblecombe, 1987). Although particulates have been correlated with excess mortality, the physiological cause of damage from particulates is less clear. It is also uncertain whether the impact of particulates is to their chemical composition or only to the particulate size.

Ambient ozone has not been clearly linked to excess mortality possibly because it is difficult to statistically separate ambient ozone from other possible causative factors. Ambient ozone is strongly correlated to temperature (see **Section 11.11.4**), so that excess deaths associated with ozone are hard to separate from deaths associated with heat. However, ambient levels of ozone have been linked to impairment of respiratory functions both in laboratory studies and in studies of individuals under ambient conditions. A 10–20% reduction in forced expiratory volume was found to result from exposure to ozone mixing ratios of 80–100 ppb for 6 h or for exposure to 180–200 ppb for 2 h. Studies with laboratory animals suggest that this type of impairment can lead to permanent lung damage. Studies have also identified increased inflammation of the lungs, coughing, and other asthmatic symptoms following exposure to ambient ozone as low as 80 ppb (Brauer and Brook, 1997). Autopsies on auto accident victims in Los Angeles also showed evidence of long-term lung damage. See Lippman and Schlesinger (2000) and Lippman (2000) for a complete summary. More recent studies have suggested that health effects occur for ozone as low as 60 ppb, and that effects are worse for periods of persistent high ozone (Bell et al., 2004).

Based on the above evidence, the United States Environmental Protection Agency (EPA) proposed in 1997 to strengthen and change the format of National Ambient Air Quality Standards for both particulates and ozone. The previous standards (dating from 1979) were a 1 h maximum mixing ratio of 125 ppb for O_3 and an annual average concentration of 75 $\mu g\, m^{-3}$ (PM_{10}) for particulates. The proposed new standard for O_3 would be an 8 h average mixing ratio of 85 ppb. The change to a standard based on 8 h averages rather than single-hour peak concentrations was based on the studies described above that showed damage resulting from prolonged exposure. The proposed health standard for particulates would be based on $PM_{2.5}$ rather than PM_{10}, because $PM_{2.5}$ reflects the concentration of fine particulates more closely than PM_{10} (Wilson and Suh, 1997; see **Figure 2**) and would be 15 $\mu g\, m^{-3}$ for annual average concentrations and 50 $\mu g\, m^{-3}$ for 24 h average peak concentrations. Implementation of the new standards was delayed by court challenges and the change of administration in the United States in 2000, but was implemented in 2004. In 2008, EPA lowered the health standard for O_3 to 75 ppb (8 h average).

Acute health effects have also been identified as a result of exposure to NO_2 and CO, but these effects were found only for exposure to NO_2 above 250 ppb and CO above 10 000 ppb, amounts that were 10 times higher than ambient concentrations (Bascomb et al., 1996; Holgate et al., 1999). These species are primarily of concern as possible indoor air pollutants because ambient mixing ratios are often significantly higher indoors (Jones, 1999).

Visibility degradation associated with air pollution is almost entirely due to fine particulates, although coarse particulates and a few gaseous species (e.g., NO_2) may also contribute (Seinfeld and Pandis, 1998). Visibility degradation associated with fine particulates occurs through the process of Mie scattering, which is most efficient for particulate sizes close to the wavelength of visible light (0.4–0.7 μm).

Damage to agricultural crops from air pollution is primarily associated with ozone, while ecological damage is associated with both ozone and deposition of acid particulates (**Chapter 11.10**). Ozone enters plants through the plant stomata and can interfere with various cell functions. Many plants respond to elevated ozone by closing the stomata, which limits internal damage but slows growth rates. Negative impacts include reduced rate of plant photosynthesis, increased senescence, and reduced rates of reproduction. These impacts can result from ozone as low as 60–80 ppb, a level frequently surpassed in rural and agricultural areas subject to regional air pollution events. Reductions in crop yields have been found for ozone as low as 40 ppb, especially for soybeans which are especially vulnerable to ozone damage (Mauzerall and Wang, 2001; Wang and Mauzerall, 2004). It has been estimated that crop damage from ozone in the United States causes monetary losses of $1–2 billion per year (US Congress, 1989). Similar monetary losses have been estimated for China, and forecasts suggest that a 20% reduction of crop yields due to ozone could occur in China by 2020 (Aunon et al., 2000). Global losses are estimated at $11–18 billion, including a 4–15% reduction in the wheat crop. For a review of agricultural impacts, see Mauzerall and Wang (2001) and Wang and Mauzerall (2004).

Ozone and particulates both have a range of possible impacts on climate. Ozone itself is a greenhouse gas, and the

anthropogenic increase in O_3 between 1900 and 2000 is estimated to have caused an increase in temperature of 0.2 °C in the nontropical northern hemisphere (Shindell et al., 2006). The amount of warming attributed to O_3 is roughly 20% as much as is contributed by CO_2, and consequences are perhaps less dangerous because O_3 does not persist and accumulate in the atmosphere as does CO_2. The effect of the major ozone precursors, NO_x and VOC, are more complicated because these species also influence atmospheric reactivity in general. It has been estimated that NO_x emissions have a small net cooling effect on the atmosphere, despite their contribution to ozone formation, due to their role in increasing the atmospheric OH radical and decreasing atmospheric CH_4 (Wild et al., 2001). CH_4 itself is both a direct greenhouse gas and an ozone precursor.

The two main particulates, sulfates and black carbon, have large but opposite effects on climate. Anthropogenic sulfates are believed to have a significant cooling impact (also approximately 20% compared to the current impact of increased CO_2), while black carbon is expected to have a large warming impact. This has led to concerns that control measures that focus on sulfates and omit black carbon may exacerbate climate change. Evaluation of aerosol impacts is complicated because they affect cloud radiative properties, cloud extent and lifetime, snow albedo, and melting rates, all of which influence climate (indirect effects) in addition to their direct effect on radiation (Forster et al., 2007; Ramanathan and Carmichael, 2008).

11.11.2.5 Long-Term Trends in Ozone and Particulates

Attempts to identify changes in air pollutant concentrations over time have been the subject of great interest, both as a basis for evaluating the effectiveness of existing controls and as a way of identifying the sources of possible problems for the future. Evaluating trends for ozone is difficult because day-to-day and seasonal variations in ozone depend largely on meteorology. This is especially true in the northern United States and western Europe, where annual changes in ozone depend on the frequency of occurrence of hot, dry conditions that promote ozone formation. In addition, ozone concentrations are of interest in terms of extreme events rather than climatic averages. Trends in the occurrence of these extreme events are difficult to evaluate in a way that is statistically robust. Trends in primary pollutants are easier to evaluate because these pollutant concentrations are less dependent on meteorology.

For many years, it appeared that efforts to lower the frequency and severity of air pollution events in the United States had little or no effect. Fiore et al. (1998) evaluated 10 year trends in ozone in the United States by statistically filtering out changes in meteorology. They found a statistically significant downward trend in southern California and in New York, but not elsewhere. The downward trend was somewhat more pronounced when trends were evaluated based on more extreme events. Estimates for changes in NO_x in the United States during the 1990s suggest either a modest (10–15%) reduction (Fenger, 1999) or no reduction (Bowen and Valiela, 2001; Butler et al., 2001). Significant downward trends were found for SO_2 (Fenger 1999). Kuebler et al. (2001) reported a significant decrease in precursor emissions in Switzerland but little change in O_3, possibly due to transport from elsewhere in Europe or to an increase in global background O_3. A significant decrease in ozone was found only in Los Angeles, where the number of days with ozone exceeding the original United States air quality standard (125 ppb) decreased from 180 days · year^{-1} in the 1970s and 1980s to 25–45 days year^{-1}.

By contrast, a significant reduction in O_3 during pollution events appeared throughout the United States during the early 2000s. The reduction in O_3 can be seen most clearly in plots for diurnal peak O_3 versus temperature. These plots show that O_3 in polluted regions increases with temperature, which increases the speed of photochemical production from local sources. Observations showed that the rate of increase of O_3 with temperature decreased by approximately 30% during the 2000s, suggesting a similar 30% decrease in ozone photochemical production. Similarly, exceedences of the original United States air quality standard (125 ppb peak hourly value) occurred much less frequently in the 2000s than previously. The improvement in air quality was attributed largely to reductions in NO_x emissions from coal-fired power plants (Bloomer et al., 2009; Frost et al., 2006), which were proposed by the US EPA in 1999 and implemented in 2005. The US standard for air quality was also made more strict in the 2000s, changing from 125 ppb (hourly) to an 8 h average of 85 ppb (2002) and then to an 8 h average of 75 ppb (2009), as recognition of the adverse health impacts became more widespread. Currently, there are still widespread exceedences of the air quality standard even though there have been significant improvements in air quality.

As mentioned above, there have been sharp reductions in both sulfate particulates and soot since the 1950s, largely due to the conversion from coal to natural gas as the primary source of home heating (Fenger, 1999).

Concentrations of both ozone and particulates have increased over the past 20 years in many parts of the developing world, including cities in Asia and Latin America (e.g., Guttikunda et al., 2005; Lelieveld et al., 2002; Mage et al., 1996; Mauzerall et al., 2000). It is possible that continued growth will lead to increases in global background concentrations in the future (e.g., Lelieveld and Dentener, 2000,). Some observations suggested that ozone concentrations over the Pacific Ocean increased during the early 2000s as a result of the growth of industrial activity in East Asia (Parrish et al., 2004). As mentioned above, emissions from Europe and the United States are also known to affect the chemistry of the troposphere on a global scale and lead to increased O_3 throughout the northern hemisphere.

11.11.3 Photochemistry of Ozone and Particulates

11.11.3.1 Ozone

The central concepts of ozone photochemistry are as follows: the split into NO_x-sensitive and NO_x-saturated photochemical production regimes, the role of the OH radical, and the concept of ozone production efficiency per NO_x.

11.11.3.1.1 Ozone formation

The ozone formation process is almost always initiated by a reaction involving a primary hydrocarbon (abbreviated here as RH), other organic or CO with the OH radical. The reaction

with OH removes a hydrogen atom from the hydrocarbon chain, which then acquires O_2 from the atmosphere to form a radical with the form RO_2. (For example, methane (CH_4) reacts with OH to form the RO_2 radical CH_3O_2, propane (C_3H_8) reacts to form $C_3H_7O_2$, etc.) The equivalent reaction for CO forms HO_2, a radical with many chemical similarities to the various RO_2 radicals.

$$RH + OH \xrightarrow{[O_2]} RO_2 + H_2O \quad [1]$$

$$CO + OH \xrightarrow{[O_2]} HO_2 + CO_2 \quad [2]$$

This is followed by reactions of RO_2 and HO_2 with NO, resulting in the conversion from NO to NO_2:

$$RO_2 + NO \xrightarrow{[O_2]} R'CHO + HO_2 + NO_2 \quad [3]$$

$$HO_2 + NO \rightarrow OH + NO_2 \quad [4]$$

Here, R′CHO represents intermediate organic species, typically including aldehydes and ketones. Photolysis of NO_2 results in the formation of atomic oxygen (O), which reacts with atmospheric O_2 to form ozone:

$$NO_2 + h\nu \rightarrow NO + O \quad [5]$$

The conversion of NO to NO_2 is the characteristic step that leads to ozone formation, and the rate of conversion of NO to NO_2 is often used to represent the ozone formation rate. The process does not remove either OH or NO from the atmosphere, so that the OH and NO may initiate additional ozone-forming reactions.

For $NO_x > 0.5$ ppb (typical of urban and polluted rural sites in the eastern United States and Europe), reactions [3] and [4] represent the dominant reaction pathways for HO_2 and RO_2 radicals. In this case, the rate of ozone formation is controlled largely by the rate of the initial reaction with hydrocarbons or CO (reactions [1] and [2]). Analogous reaction sequences lead to the formation of various other gas-phase components of photochemical smog (e.g., formaldehyde, HCHO, and PAN) and to the formation of organic aerosols.

11.11.3.1.2 Odd hydrogen radicals

The rate of ozone production is critically dependent on the availability of odd hydrogen radicals (defined by Kleinman (1986) as the sum of OH, HO_2, and RO_2) and in particular by the OH radical. The OH radical is important because reaction sequences that lead to either the production or removal of many tropospheric pollutants are also initiated by reactions involving OH. In particular, the ozone production sequence is initiated by the reaction of OH with CO (reaction [1]) and hydrocarbons (reaction [2]). The split into NO_x-sensitive and VOC-sensitive regimes, discussed below, is also closely associated with sources and sinks of radicals.

Odd hydrogen radicals are produced by photolysis of ozone, formaldehyde, and other intermediate organics:

$$O_3 + h\nu \xrightarrow{[H_2O]} 2OH + O_2 \quad [6]$$

$$HCHO + h\nu \xrightarrow{2O_2} 2HO_2 + CO \quad [7]$$

They are removed by reactions that produce peroxides and HNO_3:

$$HO_2 + HO_2 \rightarrow H_2O_2 + O_2 \quad [8]$$

$$RO_2 + HO_2 \rightarrow ROOH + O_2 \quad [9]$$

$$OH + NO_2 \rightarrow HNO_3 \quad [10]$$

Formation of PAN is also a significant sink for odd hydrogen. Removal of OH occurs on timescales of 1 s or less, and removal of odd hydrogen radicals as a group usually occurs on timescales of 5 min or less.

The supply of radicals is dependent on photolytic reactions, so that most significant gas-phase chemistry only occurs during the daytime. The supply of radicals is also linked to the availability of water vapor (H_2O) through reaction [6]. Both the photochemical production and loss of pollutants are slower in winter, due to lack of sunlight and lower H_2O. Photochemical loss rates are also slower in the upper troposphere, where temperatures are lower and mixing ratios of H_2O are much smaller.

The role of NO_x as a sink for odd hydrogen radicals (primarily through reaction [10]) is especially noteworthy. When ambient NO_x mixing ratios are large, reaction [10] drives the radical mixing ratios to very low levels, with the result that photochemical production and loss rates are much slower. Under such NO_x-saturated conditions, rates of production of ozone and other secondary species and rates of photochemical removal of pollutants are significantly slowed.

11.11.3.1.3 O_3, NO, and NO_2

Rapid interconversion among the species O_3, NO, and NO_2 occurs through the reactions

$$NO + O_3 \rightarrow NO_2 + O_2 \quad [11]$$

and

$$NO_2 + h\nu \rightarrow NO + O \quad [5]$$

followed by the reaction of atomic oxygen with O_2 to form O_3. Taken together, reactions [1] and [2] produce no net change in ozone. Each of these reactions occurs rapidly, on a timescale of 200 s or less. Typically, the two major components of NO_x (NO and NO_2) adjust to establish a near steady state between reactions [1] and [2]. However, these reactions can lead to a significant decrease in ozone concentrations in the vicinity of large NO_x sources. More than 90% of NO_x emissions consist of NO rather than NO_2, so that the process of approaching a steady state among reactions [5] and [11] (which usually has NO_2 mixing ratios equal to or greater than those of NO) involves conversion of O_3 to NO_2. This process (sometimes referred to as NO_x titration) is important mainly in plumes extending from large point sources. NO_x mixing ratios in these plumes can be 100 ppb or higher, and O_3 is often depressed to very low levels. These plumes typically lead to a net increase in ozone, but only following dispersion and travel downwind (e.g., Gillani and Pleim, 1996; Ryerson et al., 1998, 2001). The process of NO_x titration also can lead to very low O_3 in urban centers at night, when the reverse reaction [5] is zero. Ambient O_3 is usually low at night (<30 ppb) due to removal through deposition in the shallow nocturnal boundary layer. Nighttime NO_x emissions followed by reaction [11] often drive these concentrations to 1 ppb or lower.

The process of NO_x titration has little impact on O_3 during conditions that favor photochemical production because production rates (via reactions [1]–[5]) greatly exceed losses associated with NO_x titration.

Analyses of ozone chemistry often use the concept of odd oxygen, $O_x = O_3 + O + NO_2$ (Logan et al., 1981), as a way to separate the process of NO_x titration from the processes of ozone formation and removal that occur on longer timescales. Odd oxygen is unaffected by reactions [5] and [11] and remains constant in situations dominated by NO_x titration, such as the early states of a power plant plume. Production of odd oxygen occurs only through NO_x–VOC–CO chemistry, and loss of odd oxygen occurs through conversion of NO_2 to PAN and HNO_3 or through slower ozone loss reactions (e.g., reaction [6]), rather than through the more rapid back-and-forth reactions [1] and [2]. The chemical lifetime of odd oxygen relative to these losses is typically 2–3 days in the lower troposphere. (The lifetime of odd oxygen in the middle and upper troposphere is much longer (1 month or more) because the rate of removal via reaction [6] ($O_3 + h\nu \rightarrow 2OH$) depends on the availability of H_2O. Typically, H_2O mixing ratios in the middle and upper troposphere are lower than at ground level by a factor of 10 or more.) This lifetime is often more useful for describing atmospheric processes associated with ozone than the chemical lifetime of ozone relative to reaction [11].

The ambient ratio NO_2/NO is controlled by a combination of the interconversion reactions [11] and [5] and the ozone-producing reactions [3] and [4]. Because the ozone-producing reactions involve conversion of NO to NO_2 and affect the ratio NO_2/NO, measured values of this ratio can be used (especially in the remote troposphere) to identify the process of ozone formation. When the ratio NO_2/NO is higher than it would be if determined solely by reactions [5] and [11], it provides evidence for ozone formation (e.g., Ridley et al., 1992). Reactions [3]–[5] and [11] can be combined to derive the summed concentration of HO_2 and RO_2 radicals from measured O_3, NO, NO_2, and solar radiation (e.g., Duderstadt et al., 1998, see also Trainer et al. (2000) for complete citations).

11.11.3.1.4 O_3– NO_x–VOC sensitivity and OH

The split into NO_x-sensitive and NO_x-saturated regimes is often illustrated by an isopleth plot, which shows O_3 as a function of its two main precursors, NO_x and VOC. As shown in **Figure 3**, the rate of ozone production is a nonlinear function of the NO_x and VOC concentrations. When VOC/NO_x ratios are high, the rate of ozone production increases with increasing NO_x. Eventually, the ozone production rate reaches a local maximum and subsequently decreases as NO_x concentrations are increased further. This local maximum (the 'ridge line') defines the split into NO_x-sensitive and NO_x-saturated regimes. At high VOC/NO_x ratios, the rate of ozone production increases with increasing NO_x and is largely insensitive to VOC. At low VOC/NO_x ratios (above the 'ridge line' in **Figure 3**), the rate of ozone production increases with increasing VOC and decreases with increasing NO_x. This split into NO_x-sensitive and NO_x-saturated regimes has immediate implications for the design of effective control policies for ozone. Ozone in a NO_x-sensitive region can be reduced only by reducing NO_x. Ozone in a VOC-sensitive region can be reduced either by reducing VOC or by reducing NO_x to extremely low levels.

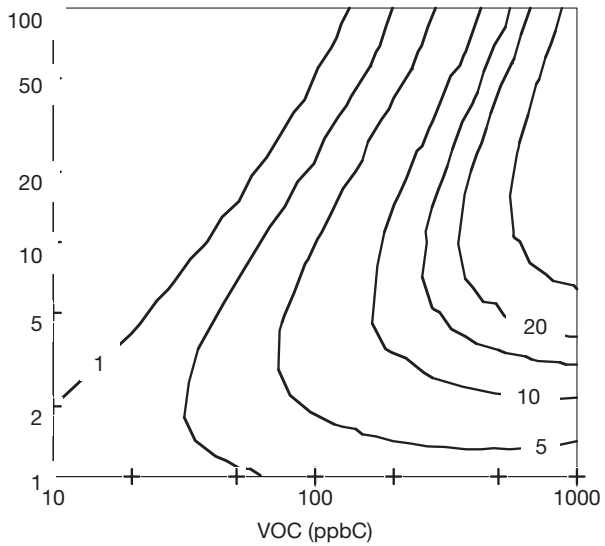

Figure 3 Isopleths giving net rate of ozone production (ppb per hour, daytime average, and solid line) as a function of VOC (ppbC) and NO_x (ppb). Reproduced from Sillman S (1999) The relation between ozone, NO_x and hydrocarbons in urban and polluted rural environments. *Atmospheric Environment* 33(12): 1821–1845.

Isopleth plots such as **Figure 3** are commonly used to show ozone concentrations as a function of NO_x and VOC emission rates. Representations of ozone concentrations versus emission rates are always critically dependent on assumptions about rates of vertical mixing and the time allowed for photochemical production of ozone. The format shown here, relating ozone production rates to NO_x and VOC, is also sensitive to various assumptions (O_3 and water vapor concentrations, solar radiation, and the specific composition of VOC) but shows less variation than O_3 concentrations.

The split into NO_x-sensitive and NO_x-saturated regimes is closely related to the cycle of odd hydrogen radicals, which controls the rate of photochemical production of ozone. The NO_x-saturated regime occurs when the formation of HNO_3 via reaction [10] represents the dominant sink for odd hydrogen, while the NO_x-sensitive regime occurs when the peroxide-forming reactions [8] and [9] represent the dominant sinks (Kleinman, 1991; Sillman et al., 1990). When HNO_3 dominates, then the ambient level of OH decreases with increasing NO_x and is largely unaffected (or increases slightly) with increasing VOC. The rate of ozone formation is determined by the rate of the reaction of hydrocarbons and CO with OH (reactions [1] and [2]) and consequently increases with increasing VOC and decreases with increasing NO_x. This is the VOC-sensitive regime. When peroxides represent the dominant sink for odd hydrogen, then the sum $HO_2 + RO_2$ is relatively insensitive to changes in NO_x or VOC. The rate of ozone formation, approximately equal to the rate of reactions [5] and [6], increases with increasing NO_x and is largely unaffected by VOC. This is the NO_x-sensitive regime. These patterns can be seen in **Figures 4** and **5**, which show OH and $HO_2 + RO_2$ as a function of NO_x and VOC for conditions corresponding to the isopleths in **Figure 3**. The 'ridge line' in **Figure 3** that separates NO_x-sensitive and VOC-sensitive chemistry corresponds to

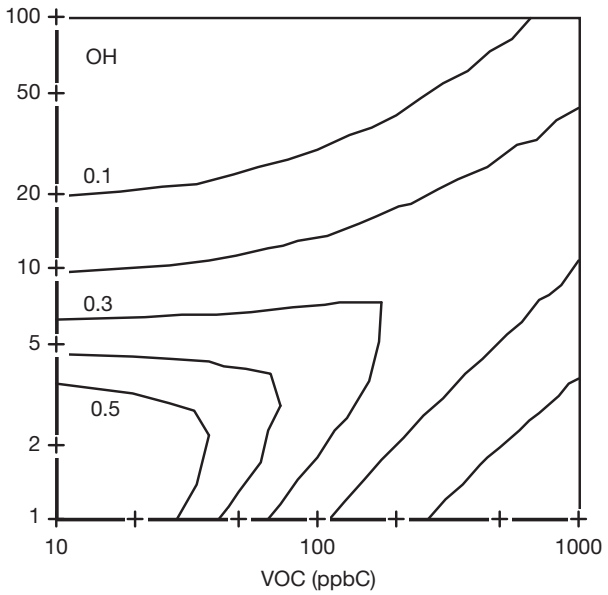

Figure 4 Isopleths showing the concentration of OH (ppt) as a function of VOC (ppbC) and NO_x (ppb) for mean summer daytime meteorology and clear skies, based on 0-d calculations shown in Milford et al. (1994) and in **Figure 3**. The isopleths represent 0.1, 0.2, 0.3, 0.4, and 0.5 ppt.

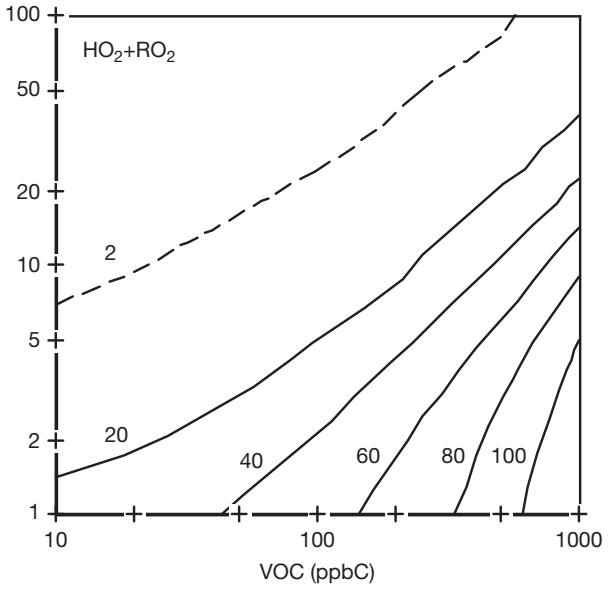

Figure 5 Isopleths showing the concentration of HO_2+RO_2 (ppt) as a function of VOC (ppbC) and NO_x (ppb) for mean summer daytime meteorology and clear skies, based on 0-d calculations shown in Milford et al. (1994) and in **Figure 3**. The isopleths represent 2 ppt (dashed line) and 20, 40, 60, 80, and 100 ppt (solid lines).

high OH, while HO_2+RO_2 is highest in the region corresponding to NO_x-sensitive chemistry. OH is lowest for conditions with either very high NO_x (due to removal of OH through formation of HNO_3, reaction [10]) or very low NO_x (due to the slow rate of conversion from HO_2 to OH through reaction [4]).

This somewhat mechanistic description can be summarized in broadly conceptual terms as follows: when the source of odd hydrogen radicals (equal to reactions [6] and [7]) exceeds the source of NO_x (related to reaction [10]), then chemistry follows a NO_x-sensitive pattern. When the source of NO_x approaches or exceeds the source of radicals, then chemistry shows a NO_x-saturated pattern and O_3, OH, and the rate of photochemistry in general decrease with further increases in NO_x (Kleinman, 1991, 1994).

The split into NO_x-sensitive and NO_x-saturated regimes affects formation rates of many other secondary species, including gas-phase species and particulates. There are significant variations for individual species: organics such as PAN and organic particulates show greater sensitivity to VOC, while nitrate formation shows greater sensitivity to NO_x and almost never decreases with increasing NO_x. However, many of the features of the ozone–NO_x–VOC sensitivity shown in **Figure 3** also appear for these other species.

11.11.3.1.5 Ozone formation in the remote troposphere

In the remote troposphere, an analogous process of ozone formation occurs. The reaction sequence leading to ozone formation is initiated primarily by CO and CH_4 rather than by the volatile organics. The reactions [2] and [4] above ($CO+OH \rightarrow HO_2$, $HO_2+NO \rightarrow NO_2$, etc.) in particular lead to ozone formation throughout the troposphere. Rates of ozone formation are much lower than in polluted regions, but total production greatly exceeds production in polluted regions. The distinguishing factor of remote chemistry is that there is a competing reaction sequence that results in the removal of O_3. Removal of O_3 occurs through the reaction

$$HO_2 + O_3 \rightarrow OH + 2O_2 \qquad [12]$$

This reaction competes with the ozone formation reaction [4] in the remote troposphere when NO_x is low (<50 ppt) and can lead to a steady-state concentration of ozone in the remote troposphere determined by the NO_x concentration. The addition of CH_4 and other organics to the remote troposphere increases O_3 because the resulting RO_2 radicals contribute to ozone formation (via reaction [3]) but do not contribute to the removal of O_3.

Jaegle et al. (1998, 2001) have described an analogous split between NO_x-sensitive and NO_x-saturated photochemical regimes in the remote troposphere. However, most analyses show that ozone in the remote troposphere would increase in response to increases in either NO_x, CO, CH_4, or various VOC. Ozone at the global scale is also affected by complex coupling between these species and OH (e.g., Wild and Prather, 2000) and shows very different sensitivity to precursors than in polluted regions.

11.11.3.1.6 Ozone production efficiency

The concept of ozone production efficiency per NO_x was developed by Liu et al. (1987), Lin et al. (1988), and Trainer et al. (1993) as a method for evaluating ozone production, especially in the global troposphere. Ozone production efficiency represents the ratio of net production of ozone to removal of NO_x ($=P(O_3+NO_2)/L(NO_x)$). Liu et al. (1987) and Lin et al. (1988) found that production efficiencies are highest at low NO_x concentrations, even when VOC is assumed to increase with increasing NO_x. Lin et al. also found that production

efficiencies increase with VOC. In theory, ozone production efficiencies are given by the ratio between reactions [1]+[2] and [10], that is, by the ratio of the sum of reactivity-weighted VOC and CO to NO_x, although they are also influenced by the rate of formation of organic nitrates. An updated analysis (**Figure 6**) showed the same pattern but with lower values than initially reported by Liu et al. (1987) and Lin et al. (1988). Ozone production efficiencies in polluted regions are likely to be even lower than shown in **Figure 6** because these calculations typically do not include removal of ozone (even though removal of NO_x is directly linked to removal of ozone through the reaction sequence [11] followed by reaction [10]), and also do not count net formation of PAN or nighttime formation of HNO_3 in the sum of NO_x losses. Various studies (e.g., Nunnermacker et al., 1995; Ryerson et al., 1998, 2001; Sillman et al., 1998; Trainer et al., 2000) estimated an ozone production efficiency of three to five during pollution events.

11.11.3.2 Chemistry of Aerosols

Formation of aerosols in the gas phase is often initiated by the reaction of precursors with the OH radical, and is therefore sensitive to many of the same factors (sunlight, NO_x, and VOC) that affect ozone formation. This is especially true for secondary organic aerosols. Formation of organic aerosols is often initiated by the reactions between VOC and OH (equivalent to reaction [1]) followed by reaction with NO (equivalent to reaction [2]) to produce secondary organics. These secondary organics often also react with OH, leading to additional reaction sequences analogous to reactions [1] and [2].

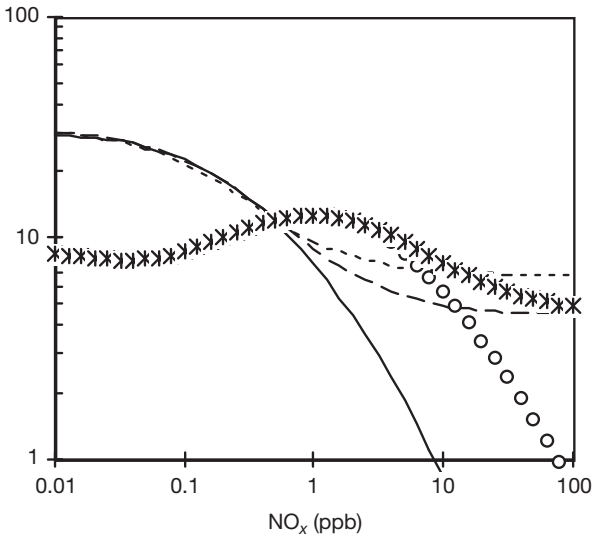

Figure 6 Ozone production efficiency, expressed as the rate of production of odd oxygen (O_3+NO_2) divided by the loss of NO_x, from steady-state calculations. The calculations assume: (1) CO and CH_4 only (solid line), (2) anthropogenic VOC with VOC/NO_x=10 (dashed line), (3) anthropogenic VOC with VOC/NO_x=20 (short dashed line), (4) CH, CH_4, and 1 ppb isoprene (circles), and (5) anthropogenic VOC/NO_x=10 and 1 ppb isoprene (asterisks). Reproduced from Sillman S (1999) The relation between ozone, NO_x and hydrocarbons in urban and polluted rural environments. Atmospheric Environment 33(12): 1821–1845, based on similar unpublished analyses by Greg Frost (NOAA Aeronomy lab).

Secondary organics are also formed from reactions between VOC and O_3. These processes are closely linked with the ozone formation process and have the same complex dependence on OH, NO_x, and VOC as ozone does. They differ from the ozone formation process in that the secondary organics are associated only with specific organic precursors, whereas virtually all reactive organics can initiate reaction sequences that lead to ozone formation.

Formation of organic aerosols from photochemically produced VOC occurs when the mixing ratios of individual VOC exceeds the saturation mixing ratio (usually expressed in terms of vapor pressure). Organic aerosols can also be formed by condensation and formation of a solution with preexisting particles, a process that can occur at vapor pressures below the saturation mixing ratio. Generally, only organics with seven or more carbon atoms lead to the formation of particulates, and yields tend to be higher for species with higher carbon number. The most common secondary organics are alkyl dicarboxylic acids with the form $HOOC(CH_2)_nCOOH$, for $n=1$–8. There has been much recent speculation about the sources of organic aerosols in the atmosphere, which include both direct emissions and secondary formation, from both anthropogenic and biogenic sources (e.g., Donahue et al., 2009; Dzepina et al., 2009; Fu et al., 2009; Heald et al., 2008).

Production of sulfate and nitrate aerosols is also initiated by gas-phase reactions involving OH. Nitrate aerosols are produced from NO_x through reaction [10] followed by the combination of HNO_3 with atmospheric NH_3 to produce ammonium nitrate aerosol (NH_4NO_3). Production of nitrates can also occur at night through a reaction on aerosol surfaces:

$$NO_2 + NO_3 \rightarrow N_2O_5 \qquad [13]$$

$$N_2O_5 + H_2O \xrightarrow{\text{aerosol}} 2HNO_3 \qquad [14]$$

where NO_3 is produced by the nighttime gas-phase reaction of NO_2 with O_3. The resulting HNO_3 again forms an aerosol by combining with NH_3. This reaction sequence is significant only at night because during the daytime NO_3 rapidly photolyzes. The nighttime reaction produces significant amounts of HNO_3 and has a significant impact on both urban smog chemistry and global tropospheric chemistry (Dentener and Crutzen, 1993), although the reaction of NO_2 with OH [11] is the largest source of HNO_3 in the atmosphere. The rate of nitrate formation shows a complex dependence on NO_x and VOC, in a manner similar to O_3 (Meng et al., 1997).

The amount of nitrate aerosol is controlled partly by the production of HNO_3 (via reactions [11]–[13]) and partly by the availability of NH_3 to form ammonium nitrate. Ammonium nitrate aerosol forms in equilibrium with gas-phase NH_3 and HNO_3:

$$NH_3(g) + HNO_3(g) \leftrightarrow NH_4NO_3(s) \qquad [15]$$

The availability of NH_3 in the atmosphere is affected by the amount other acid aerosols, such as sulfates, which also form compounds with NH_3. As a result, formation of nitrate aerosol can show complex dependence on emission rates of NH_3 and SO_2 as well as on NO_x and VOC (Pandis, 2003).

Production of sulfates occurs through the gas-phase reaction of SO_2 with OH. Sulfates are also produced in the aqueous

phase, in both cloud droplets and liquid water aerosols. The aqueous reaction sequences that lead to formation of sulfates are initiated by the reaction of dissolved SO_2 (in the forms of H_2SO_3, HSO_3^-, or SO_3^{2-}) with one of three species: aqueous hydrogen peroxide (H_2O_2), O_3, or OH. Trace metals can also catalyze the formation of sulfates. Aqueous hydrogen peroxide and O_3 are both formed by dissolution of gas-phase species, and their abundance is determined by gas-phase photochemistry (reaction [9] for production of hydrogen peroxide). The rate of sulfate formation during episodes may be limited by the availability of these oxidants, especially during winter in the midlatitudes. The seasonal cycle of SO_2 is affected by seasonally varying emission rates, abundance of clouds, and meteorological dispersion, in addition to the availability of oxidants (e.g., Rasch et al., 2000).

Once formed, sulfates readily combine with atmospheric NH_3 to form ammonium sulfate ($(NH_4)_2SO_4$) or ammonium bisulfate (NH_4HSO_4). Formation of these species can be a significant sink of atmospheric NH_3. As mentioned above, the interaction between sulfates, nitrates, and NH_3 is a cause of nonlinearity in aerosol source–receptor relationships.

Trace metals also undergo complex chemical transformations in the aqueous phase, including reactions that form sulfates. These metals enter the aqueous phase through dissolved particulates. Trace metals are especially important for the chemical transformation of mercury. These reactions are the source of considerable uncertainty at present, due in part to large variation in trace metal composition of particulates.

11.11.3.3 Ozone–Aerosol Interactions

Heterogeneous reactions on aerosol surfaces can affect gas-phase photochemistry, including both urban smog chemistry and the chemistry of the global troposphere (e.g., Jacob, 2000). Several types of possible interactions have been identified. Photolysis rates can be significantly lower during pollution events with high particulate concentrations, and the reduced photolysis rates can slow the rate of formation of ozone and other secondary reaction products (Dickerson et al., 1997). Significant conversion of NO_x to HNO_3 occurs in nighttime reactions on aerosol surfaces (Dentener and Crutzen, 1993). This reaction can affect the formation of both ozone (by removing NO_x) and aerosol nitrate during pollution events. It also can represent a significant sink for NO_x in the global troposphere. Heterogeneous conversion of NO_2 to HONO, leading to formation of OH radicals, may also impact ozone formation rates in large cities.

Formation of ammonium nitrate aerosol also affects the global troposphere by transporting NO_x from polluted regions to remote locations (Horowitz et al., 1998). Gas-phase organic nitrates such as PAN, formed in polluted regions and exported to the remote troposphere, are often a significant source of NO_x in remote locations. Because ammonium nitrate is relatively long-lived (with a lifetime of days to weeks, similar to other fine particulates), it can also transport NO_x to the remote troposphere.

As discussed above, the formation of ozone and aerosols in polluted regions is frequently coupled because they involve many of the same precursors and have closely related precursor sensitivity (Meng et al., 1997).

11.11.4 Meteorological Aspects of Photochemical Smog

Meteorology affects the development of photochemical smog in two ways: through dynamics (especially vertical mixing) and through temperature.

11.11.4.1 Dynamics

Dynamics has a direct effect on smog formation because it affects the rate of dilution of emitted pollutants and dispersion out of the polluted region. During stagnant conditions, polluted air is exported from an urban area very slowly and may remain within a polluted region (or recirculate through the region) for several days. The most important aspect of dynamics is vertical mixing.

Vertical mixing over land follows a diurnal cycle that is strongly influenced by sunlight. At nighttime, the land surface cools, producing a stable atmospheric structure near the surface (with cooler air below) that suppresses vertical mixing. Under these conditions, vertical mixing near the surface is driven solely by friction between the surface and the synoptic wind and is opposed by the thermally stable vertical structure. During the night and early morning, pollutants emitted near the surface are often mixed only to a height of 100 m. Elevated emissions from smokestacks (which often rise to an altitude of 500–1000 m due to the heat content of the emitted species) remain in a narrow atmospheric layer aloft and are not mixed to the surface. During the daytime, solar radiation warms the surface, and this heat causes convective mixing of the atmosphere. On sunny afternoons, this convective mixing typically reaches a height of 2000 m. This mixing has the effect of diluting primary emissions, but it also causes elevated plumes from smokestacks to mix down to the surface. It also causes pollutants that were formed in the convective mixed layer on the previous day to mix down to the surface.

The region of the atmosphere that is in direct contact with the surface (on a timescale of 1 h or less) is commonly referred to as the boundary layer or mixed layer. Technically, the boundary layer refers to the region of the atmosphere that is dynamically influenced by the surface (through friction or convection driven by surface heating). Less formally, the boundary layer is used to represent the layer of high pollutant concentrations in source regions. The top of the boundary layer in urban areas is characterized by a sudden decrease in pollutant concentrations and usually by changes in other atmospheric features (water vapor content, thermal structure, and wind speeds).

Concentrations of primary pollutants show a diurnal cycle that is a direct result of the pattern of vertical mixing in the atmosphere. Concentrations of NO_x, CO and SO_2, and elemental carbon particulates are typically higher at night than at midday, even though emission rates are approximately three times higher during the day. Peak concentrations of primary pollutants usually occur during early and midmorning when emission rates are high and rates of vertical mixing are still relatively low. Pollutant concentrations decrease during the day as convective mixing increases and reach the diurnal minimum from noon to 6 p.m. (see **Figure 7**).

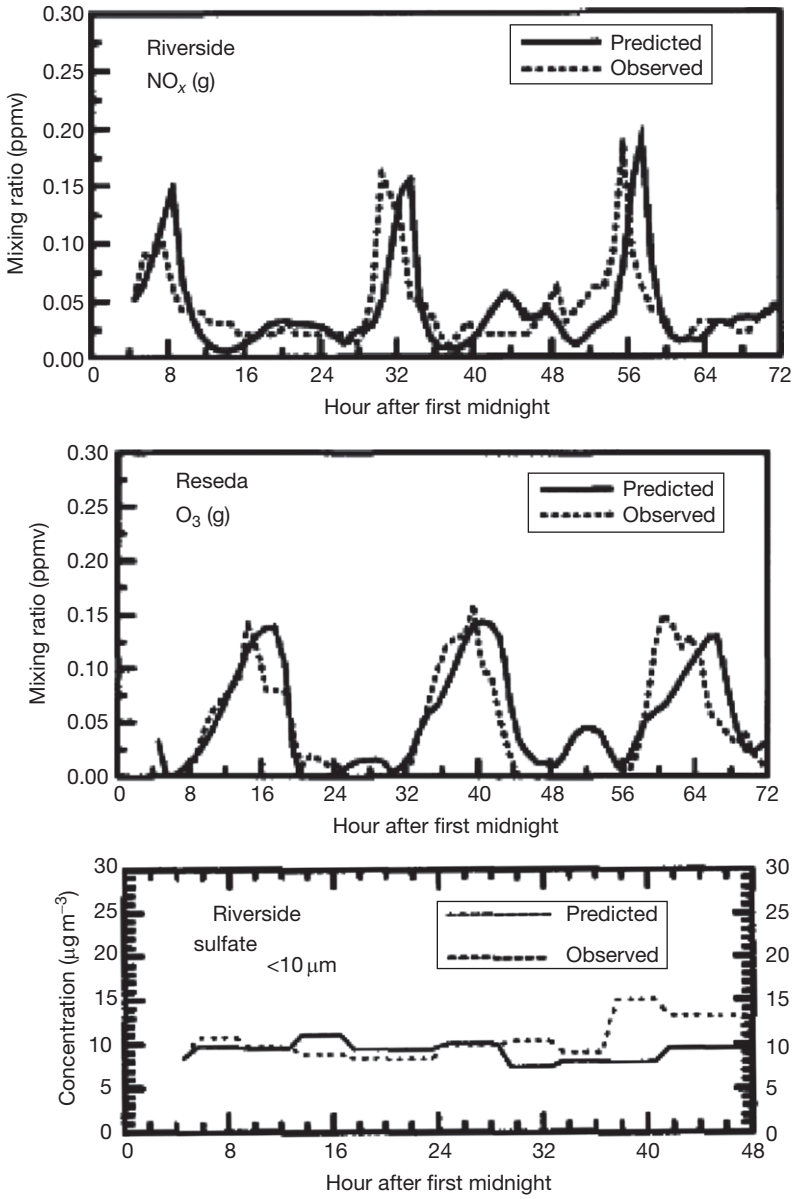

Figure 7 Time series for NO_x and O_3 (in parts per million, ppm) and sulfate (PM_{10}, μg m^{-3}) versus hour at Riverside, CA, 26–28 August 1988. Dashed lines represent measurements, and solid lines represent model predictions. Reproduced from Jacobson MZ, Lu R, Turco RP, and Toon OP (1996) Development and application of a new air pollution modeling system – Part I. Gas-phase simulations. *Atmospheric Environment* 30: 1939–1963; Jacobson MZ (1997) Development and application of a new air pollution modeling system – Part III. Aerosolphase simulations. *Atmospheric Environment* 31: 587–608.

Ozone and other secondary pollutants show a very different diurnal pattern. Because ozone is only produced photochemically during the day, it typically reaches a diurnal maximum during the afternoon. Ozone is removed near the surface at night, both through surface deposition and through nighttime reactions with primary pollutants, and consequently reaches its minimum at night. Nighttime ozone concentrations are typically lower in urban centers than in the surrounding rural area because primary pollutants react to remove ozone in the nighttime surface layer. During large-scale pollution episodes, ozone may decrease to very low values at ground level at night, but high ozone concentrations remain in a layer (typically 200–2000 m above the surface). Ozone concentrations increase rapidly during the morning as convective mixing begins, and ozone from above the ground is mixed down to the surface. Subsequently, ozone concentrations continue to increase as photochemistry results in additional ozone formation. A similar diurnal pattern is shown by HNO_3, PAN, and many other secondary pollutants. Other secondary species such as sulfate particulates and many secondary hydrocarbons are not removed from the atmosphere at night. These species show much smaller diurnal variations than either O_3 or the primary species (see Figure 7).

Due to the contrasting diurnal patterns of primary and secondary pollutants, ozone and other secondary pollutants

appear to anticorrelate with their precursor species (NO_x and VOC) if measured concentrations are plotted for a full diurnal cycle. Peak ozone occurs during and after the time of maximum sunlight, which is also the time of maximum vertical dilution. Concentrations of primary pollutants reach their diurnal minimum at this time.

Severe pollution episodes that involve primary pollutants are associated with meteorology that suppresses vertical mixing during the daytime. This is most common in winter in northerly locations (when solar radiation is minimal) and is often accompanied by fog near the surface. These conditions do not produce high levels of ozone and other secondary pollutants because low temperatures and lack of sunlight prevents ozone formation. The warm temperatures and high sunlight that lead to rapid ozone formation also tend to cause a relatively deep convective mixed layer. Severe ozone events are often associated with persistent high-pressure systems and subsidence inversions, which limit vertical dispersion and prevent the formation of clouds (which would vent the polluted boundary layer). However, the height of the daytime mixed layer is usually 1500–2000 m even during these events.

The city of Los Angeles is uniquely vulnerable to ozone because dynamics in Los Angeles can cause air to be trapped in a relatively shallow layer even at times of warm temperatures and high solar radiation. This occurs when relatively cool marine air is trapped in the Los Angeles basin under much warmer air from the inland desert. Convective mixing heights during these events are often just 500 m.

11.11.4.2 Ozone and Temperature

As stated above, ozone in polluted regions shows a strong dependence on temperature. This dependence on temperature is important as a basis for understanding variations in ozone concentrations from year to year or between cities. As shown in Figure 8, elevated ozone is always associated with temperatures in excess of 20 °C and often with temperatures above 30 °C. In the eastern United States and Europe, year-to-year variations in ozone concentrations are often the result of variations in temperature and cloud cover, rather than in changes in emission of pollutants.

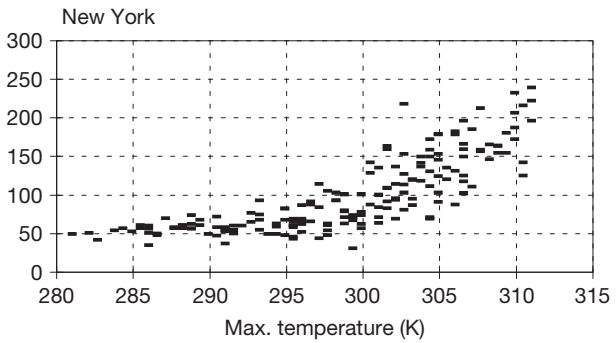

Figure 8 Diurnal peak O_3 (ppb) versus maximum surface temperature observed in the New York–New Jersey–Connecticut metropolitan area for 1 April through 30 September 1988. Reproduced from Sillman S and Samson PJ (1995) The impact of temperature on oxidant formation in urban, polluted rural and remote environments. *Journal of Geophysical Research* 100: 11497–11508. With permission from John Wiley & Sons.

The reason for the dependence on temperature is due largely to the chemistry of ozone formation. Cardellino and Chameides (1990) and Sillman and Samson (1995) found that the temperature dependence was associated with the temperature-dependent decomposition rate of PAN. PAN becomes longer lived at lower temperatures, and formation of PAN results in the removal of NO_x, hydrocarbons, and odd hydrogen radicals (described below), all of which suppress ozone formation. PAN, also a component of photochemical smog, tends to reach maximum values at intermediate temperatures (5–10 °C). Jacob et al. (1993) proposed that ozone correlates with temperature partly because the meteorological conditions that favor ozone formation (high solar radiation and light winds) tend to be associated with warm temperatures. In addition, the emission rate of biogenic hydrocarbons (a major ozone precursor, discussed above) increases sharply with increasing temperature.

The dependence of ozone on temperature is an example of a phenomenon that only affects ozone in polluted regions and does not have a similar impact on the global troposphere. Warm temperatures and stagnant conditions lead to ozone formation in polluted regions, which is subsequently exported to the free troposphere. In the absence of these conditions, ozone precursors are exported to the free troposphere, and they eventually lead to ozone formation at a slightly higher rate (Sillman and Samson, 1995). PAN formed in polluted regions eventually decomposes in the free troposphere producing NO_x and leading to ozone formation.

As was described above, changes in ozone due to reductions in pollutant emissions can only be identified from statistics over a multiyear period, long enough to identify a statistically robust signal beyond year-to-year variations in meteorological conditions (R) (e.g., Fiore et al., 1998). A signal for change in response to emissions can also be obtained from the correlation between ozone and temperature. As described above, the rate of increase of O_3 with temperature has declined by approximately 30% for the time period 2003–2007 compared to 1987–2002 for all regions of the United States (Bloomer et al., 2009), reflecting lower precursor emissions (primarily NO_x) and lower formation rates during pollution events.

11.11.5 New Directions: Evaluation Based on Ambient Measurements

Some of the most important results have involved the use of high-quality field measurements as a basis for deriving information about photochemical smog.

Since the original analysis of smog formation by Haagen-Smit and Fox (1954), analysis of photochemical smog has relied mainly on two methods: calculations with photochemical models to identify the chemical relation between ozone and its precursors; and experiments involving smog chambers that duplicate the smog formation process in a laboratory setting. Since 1954, the model calculations have expanded from zero-dimensional models (representing only photochemical transformations) to three-dimensional chemical transport models with sophisticated treatment of emissions and horizontal and vertical transports. The photochemical transformations associated with urban smog involve thousands of individual species

(mostly VOC), which cannot be conveniently included in model calculations. Instead, models use condensed photochemical mechanisms that approximate the chemistry of the thousands of individual VOC by a smaller number of either lumped species (which represent the composite of several individual species) or surrogate species (which use the chemistry of selected individual species to represent a group of related species). Condensed mechanisms are also necessary because the reaction rates and products have not been measured for all individual VOC species and are often inferred by analogy with species for which experimental data are available. The accuracy of condensed mechanisms is tested by comparing results of these mechanisms to smog chamber experiments (e.g., Dodge, 2000; Stockwell et al., 1997; Zaveri and Peters, 1999).

Models for photochemical smog formation are still subject to various uncertainties. Estimates for emission rates represent the largest uncertainty. In 1995, it was discovered that biogenic VOC emissions in the United States had been underestimated by a factor of four (Geron et al., 1994). This discovery led to a major change in model predictions for the impact of NO_x and VOC on ozone formation in the eastern United States (Pierce et al., 1998, see also Chameides et al., 1988) and led to greater emphasis on control of NO_x emission sources. Results from the Texas Air Quality Study in 2000 also suggest that emissions of anthropogenic VOC from industrial sources are much larger than represented in emission inventories (Daum et al., 2004). The accuracy of emission inventories effectively limits our ability to understand the process of smog formation.

Representation of meteorology during smog events has been greatly improved by the development of mesoscale meteorological models with sophisticated assimilation of ambient data (Seaman, 2000). Uncertainties related to dynamics are likely to remain because the smog events are usually associated with light and variable wind speeds. These stagnant conditions strain the ability to accurately estimate rates of dispersion of air pollutants through either measurements or dynamical models.

The accuracy of photochemical mechanisms is an additional source of uncertainty. Known uncertainties in photochemical reaction rates and stoichiometries cause an uncertainty of 20% in calculated ozone formation rates (Gao et al., 1996).

Perhaps, the biggest challenge is the need to evaluate model predictions and assumptions based on ambient measurements. Initially, research results and regulations involving photochemical smog were based largely on model simulations, which were evaluated based only on their ability to reproduce the observed ozone concentration during specific smog events (NARSTO, 2000; NRC, 1991). This evaluation is problematic because model calculations can yield reasonably correct ozone in comparison with measurements even when individual assumptions (e.g., about emission rates) are incorrect. In particular, comparison with ambient ozone provides no basis for evaluating the accuracy of model predictions for the response of ozone to changes in emission rates of NO_x and VOC. It frequently happens that different model scenarios for the same event would give opposite predictions for the impact of NO_x versus VOC controls, without showing a difference in predicted ozone concentrations (Reynolds et al., 1996; Sillman et al., 1995).

Over the past 15 years, there has been a major expansion in the range of ambient measurements of species related to smog formation, especially in polluted rural environments. These measurements have included primary NO_x and VOC, a range of long-lived secondary reaction products and direct measurement of the OH and HO_2 radicals that control the photochemistry of smog formation. These measurements should permit a more extensive evaluation of the current understanding of the smog formation process and either validate or correct current assumptions. Critical issues that can be addressed by existing field measurements include the following: the accuracy of emission inventories, accuracy of predictions for the impact of NO_x versus VOC on ozone formation, rates of ozone formation per NO_x, and the general accuracy of ozone chemistry.

One approach based on ambient measurements is the correlation between ozone and the sum of total reactive nitrogen (NO_y, defined as the sum of NO_x, HNO_3, aqueous NO_3^-, organic nitrates, etc., but not including NH_3) and the correlation between ozone and the sum of NO_x reaction products (NO_z, defined as NO_y–NO_x). Trainer et al. (1993) used these correlations to estimate the ozone production efficiency per NO_x. The ozone production efficiency is related to the observed slope between ozone and NO_z, although the actual ozone production efficiency is lower than the observed slope due to the more rapid removal of NO_z (Chin et al., 1994; Sillman et al., 1998). The correlation between O_3 and NO_z, along with other similar correlations involving ozone, reactive nitrogen, and hydrogen peroxide, is also related to the split between NO_x-sensitive and NO_x-saturated photochemistry. Ozone production efficiency per NO_x in models is consistently higher for NO_x-sensitive conditions than for NO_x-saturated conditions, so that ratios such as O_3/NO_z are expected to be higher for NO_x-sensitive locations relative to NO_x-saturated locations (Sillman, 1995; Sillman and He, 2002).

Measured correlations between O_3, NO_y, and NO_z (**Figure 9**) illustrate the distinctly different chemistry and meteorology for different types of environments: polluted rural sites in the eastern United States, the moderately polluted cities of Nashville (United States) and Paris, and the extreme case of Los Angeles. Nashville, Paris, and the polluted rural sites all have features that are typical of the majority of polluted events and locations. All are continental sites and (in contrast to Los Angeles) do not have unusual mesoscale meteorology. Elevated ozone occurs during events characterized by warm temperatures and sunshine and is formed in a well-mixed daytime convective layer extending to 1500–2000 m or higher. Chemistry is active, and by the afternoon, most of the directly emitted NO_x has been converted to PAN, HNO_3, and other reaction products. The sum NO_y is dominated by these reaction products rather than by primary NO_x. The ozone mixing ratio increases with increasing NO_y, and the O_3–NO_y slope is surprisingly similar at all three locations. By contrast, Los Angeles has much higher mixing ratios of NO_y, NO_x, and other primary pollutants. The density of emissions in Los Angeles is not significantly higher than in Paris or other large cities, but in Los Angeles, the daytime convective mixed layer is frequently capped by an inversion and extends only to 500 m or lower. The high NO_x suppresses photochemical activity, and most reactive nitrogen remains in the form of NO_x. In contrast to the other sites, O_3 and NO_y are poorly correlated. Measurements also show that O_3 in Los Angeles is strongly correlated with the sum of NO_x reaction products (NO_z) because the same photochemical processes that lead to formation of O_3

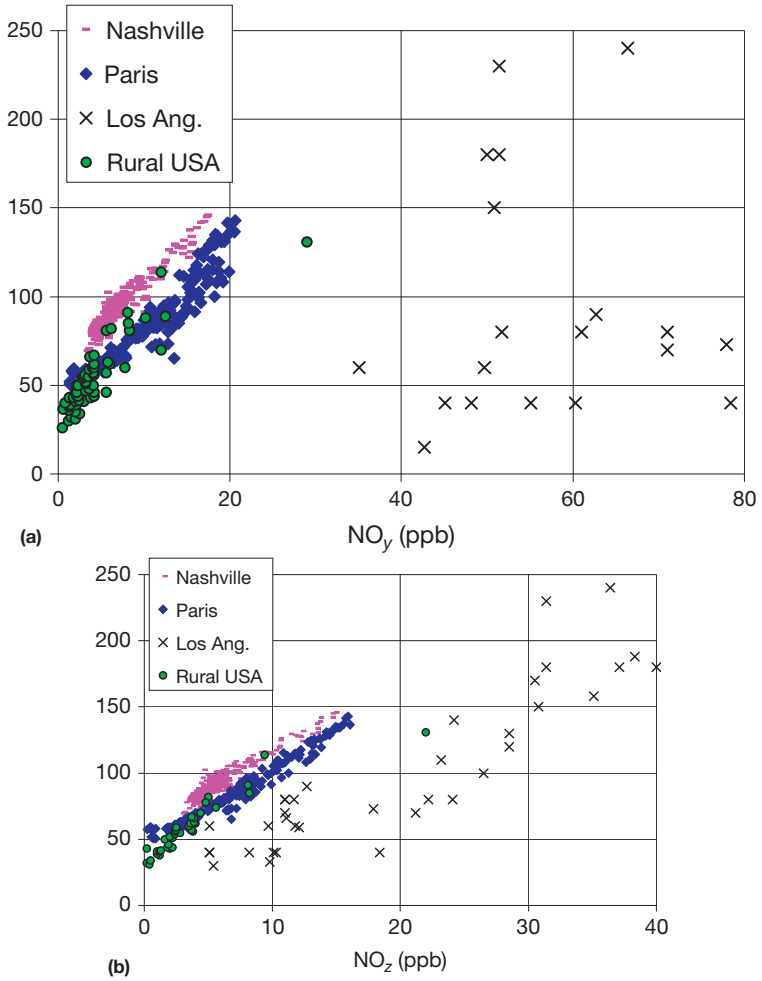

Figure 9 Measured correlations between (a) O_3 and NO_y, and (b) O_3 and (NO_y–NO_x) (also known as NO_z), all in ppb. Measurements are shown from field campaigns in Nashville (pink dashes), Paris (blue diamonds), Los Angeles (X's), and from four rural sites in the eastern United States (green circles). From measurements reported by Sillman et al. (2003) and Trainer et al. (1993).

also lead to the conversion of NO_x to reaction products. However, the O_3–NO_z slope is significantly lower for Los Angeles than for the other sites. The low O_3–NO_z slope is evidence that photochemistry in Los Angeles differs significantly from photochemistry elsewhere (probably reflecting strongly NO_x-saturated conditions in Los Angeles).

Similar measured correlations have identified distinctly different photochemical conditions (probably reflecting strongly NO_x-saturated conditions) in plumes from power plants (e.g., Gillani and Pleim, 1996; Ryerson et al., 1998, 2001) and at rural sites in the United States during autumn (Hirsch et al., 1996; Jacob et al., 1995).

Correlations among related primary species are useful as a basis for evaluating emission inventories (McKeen et al., 1996; Parrish et al., 1998; Trainer et al., 2000). Because the emission sources of individual VOC and NO_x are often collocated (even when the specific sources differ), these species show a strong correlation in the ambient atmosphere (see **Figure 10**). Isoprene is an obvious exception because its source is biogenic and not collocated with anthropogenic sources.

Several methods have been developed for inferring O_3–NO_x–VOC sensitivity from measured NO_x and VOC. Early efforts used the ratio of ambient VOC to NO_x during the morning in an urban center to infer conditions at downwind locations in the afternoon, but this approach had many problems: it failed to account for biogenic emissions, did not recognize the different impacts of fast-reacting and slow-reacting organics, and did not address the regional-scale nature of pollution events. Due to the complexities of transport, it is difficult to relate ambient ozone or ozone sensitivity to VOC or NO_x directly. However, it is possible to relate the instantaneous rate of production of O_3 to ambient VOC and NO_x. Kleinman et al. (2005) have developed simple expressions for determining the sensitivity of instantaneous production of ozone to VOC and NO_x as a function of ambient NO_x, sunlight, and reactivity-weighted VOC.

Based on existing model capabilities and field measurements, it should be possible to evaluate and modify current models for ozone photochemistry with the following goals: (1) show individual VOC mixing ratios and VOC reactivity (defined as the sum of individual primary VOC weighted by their respective rate constants with OH) that is consistent with ambient measurements and with inferences from measured VOC–VOC and VOC–NO_y correlations; (2) show reasonable

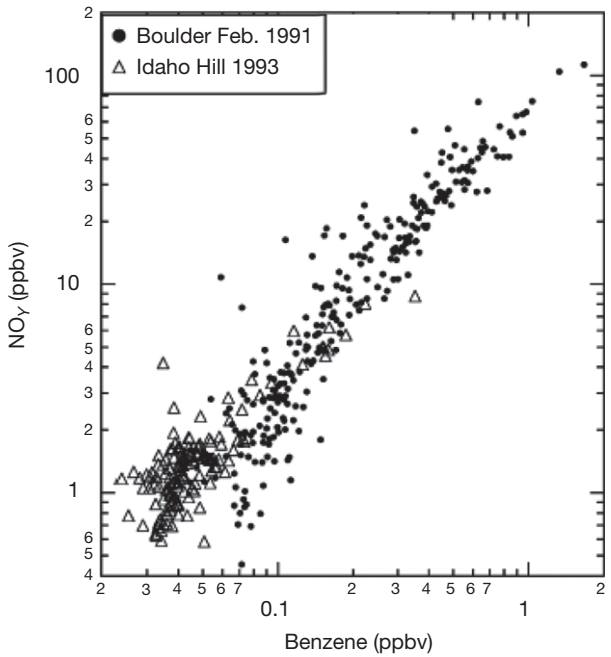

Figure 10 Measured correlations between benzene and NO_y during winter at an urban site (Boulder, CO) and at a rural site (Idaho Hill, CO). Reproduced from Trainer M, Parrish DD, Goldan PD, Roberts J, and Fehsenfeld FC (2000) Review of observation-based analysis of the regional factors influencing ozone formation. *Atmospheric Environment* 34: 2045–2062. Based on measurements reported by Goldan et al. (1995, 1997).

agreement with measured isoprene and HCHO, if available; and (3) show reasonable agreement with measured correlation between ozone and reactive nitrogen species and/or sums. The first two goals would have the effect of evaluating the accuracy of emission inventories while the third goal would evaluate the accuracy of photochemical production rates. Model applications that met these criteria would be very likely to predict the relation between ozone and precursor emissions correctly. Conversely, major errors in photochemistry or in emission inventories would be quickly apparent in this type of analysis. Analyses of these species should also facilitate the identification of long-term trends in both ozone and its precursors.

The relation between ambient levels and precursor emissions is somewhat easier to identify for particulates than for ozone because the chemical composition of individual particulates provides evidence for their origin: sulfate particulates are associated to SO_2 emissions; organic particulates with specific VOC, and so on. A variety of statistical methods have been used to identify source types for particulates based on chemical composition, especially in terms of trace metal components (e.g., Henry, 1992; Seinfeld and Pandis, 1998). This type of analysis requires sophisticated measurement of the chemical composition of individual particulates, rather than the more common measurement of summed concentrations. Statistical methods have also been used to gain information about ozone and ozone precursors (e.g., Buhr et al., 1995; Stehr et al., 2000).

The source and composition of organic aerosols are still a major area of uncertainty. The composition of organic particulates consists of hundreds of individual compounds, and much of their chemical content has not been identified. The relative amounts of primary versus secondary organics contained in these aerosols, and the relative contribution of anthropogenic versus biogenic emissions and of different anthropogenic emission sources are all uncertain. In addition, the formation of secondary organics, sulfate and nitrate aerosols are all affected by nonlinear photochemical processes, which lead to uncertainty concerning source–receptor relationships. It is possible, for example, that reduction of sulfur emissions can free up NH_3 and lead to higher concentrations of nitrate aerosols, thus counteracting the benefits of reduced sulfates (Ansari and Pandis, 1998).

The most challenging research area pertaining to photochemical smog is the attempt to measure or infer concentrations of primary radical species (OH, HO_2, and/or HO_2+RO_2) and compare these measurements with calculations based on current photochemical mechanisms. Measured or inferred radical species also would allow the instantaneous rate of ozone production to be calculated and compared to expected values. Summed HO_2+RO_2 can be inferred indirectly through measurements of NO, NO_2, O_3, and the photolysis rate of NO_2 as described above (Cantrell et al., 1993; see Trainer et al., 2000 for complete references). The most recent analyses have combined measured OH and/or HO_2 with NO and NO_2 as a test for consistency (Shirley et al., 2006; Thornton et al., 2002). Results of these attempts have been somewhat ambiguous. Measured OH can be compared with expected values by performing a constrained steady-state calculation in which OH is calculated based on measured concentrations of long-lived species. This is possible only if a complete set of measured VOC is available, since OH concentrations depend on the removal rate through OH–VOC reactions. Many evaluations have found discrepancies between measured and model OH by up to a factor of two (Carslaw et al., 1999; Eisele et al., 1996; Frost et al., 1999; George et al., 1999; McKeen et al., 1997; Poppe et al., 1994; Tan et al., 2001; Volz-Thomas and Kolahgar, 2000). In some cases where measured OH was lower than model values, it appeared likely that OH was removed by additional unmeasured VOC (McKeen et al., 1997). However, the accuracy of OH and HO_x in models has not been adequately demonstrated. Thornton et al. (2002) also reported apparent inconsistencies between measured radical concentrations and broader ozone photochemistry.

Acknowledgments

I want to thank Mary Barth and Spyros Pandis for their thorough review of this document and many helpful suggestions, especially with regard to aerosols.
Support for this work was provided by the National Science Foundation under grants #ATM-9713567 and #ATM-0207841 and by the EPA STAR grant program (grant # RD833377010). Although support was by NSF and EPA, it does not necessarily reflect the views of those agencies and no official endorsement should be inferred.

References

Anderson HR (1999) Health effects of air pollution episodes. In: Holgate ST, Samet JM, Koren HS, and Maynard RL (eds.) *Air Pollution and Health*, pp. 460–482. London/San Diego: Academic Press.

Ansari AS and Pandis SN (1998) Response of inorganic PM to precursor concentrations. *Environmental Science & Technology* 32: 2706–2714.
Atkinson R (2000) Atmospheric chemistry of VOCs and NO_x. *Atmospheric Environment* 34: 2063–2102.
Aunon K, Bernston TK, and Seip HM (2000) Surface ozone in China and its possible impact on crop yields. *AMBIO* 29: 294–301.
Avnery S, Mauzerall DL, Liu J, and Horowitz LW (2011) Global crop yield reductions due to surface ozone exposure: 1. Year 2000 crop production losses and economic damage. *Atmospheric Environment* 45: 2284–2296.
Baltensberger U, Streit N, Weingartner E, et al. (2002) Urban and rural aerosol characterization of summer smog events during the PIPAPO field campaign in Milan, Italy. *Journal of Geophysical Research* 107(D22): 8193.
Barth MC and Church AT (1999) Regional and global distributions and lifetimes of sulfate aerosols from Mexico City and southeast China. *Journal of Geophysical Research* 104: 30231–30239.
Bascomb R, Bromberg PA, Costa DL, et al. (1996) Health effects of outdoor air pollution. *American Journal of Respiratory and Critical Care Medicine* 153: 477–498.
Bell ML, McDermott A, Zeger SL, Samet JM, and Dominici F (2004) Ozone and short-term mortality in 95 US urban communities, 1987–2000. *Journal of the American Medical Association* 292(19): 2372–2378.
Blanchard CL (2000) Ozone process insights from field experiments – Part III: Extent of reaction and ozone formation. *Atmospheric Environment* 34: 2035–2043.
Blanchard P, Brook JR, and Brazal P (2002) Chemical characterization of the organic fraction of atmospheric aerosol at two sites in Ontario, Canada. *Journal of Geophysical Research* 107(D21): 8348.
Bloomer BJ, Stehr JW, Piety CA, Salawitch RJ, and Dickerson RR (2009) Observed relationships of ozone air pollution with temperature and emissions. *Geophysical Research Letters* 36: L09803.
Bowen JL and Valiela I (2001) Historical changes to atmospheric nitrogen deposition to Cape Cod, Massachusetts, USA. *Atmospheric Environment* 35: 1039–1051.
Brauer M and Brook JR (1997) Ozone personal exposures and health effects for selected groups residing in the Fraser Valley. *Atmospheric Environment* 31: 2113–2121.
Brimblecombe P (1987) *The Big Smoke: A History of Air Pollution in London Since Medieval Times*. London: Methuen.
Buhr M, Parrish D, Elliot J, et al. (1995) Evaluation of ozone precursor source types using principal component analysis of ambient air measurements in rural Alabama. *Journal of Geophysical Research* 100: 22853–22860.
Butler TJ, Likens GE, and Stunder BJB (2001) Regional-scale impacts of phase I of the Clean Air Act Amendments in the USA: The relation between emissions and concentrations, both wet and dry. *Atmospheric Environment* 35(6): 1015–1028.
Cantrell CA, Shetter RE, Calvert JG, et al. (1993) Peroxy radicals as measured in ROSE and estimated from photostationary state deviations. *Journal of Geophysical Research* 98: 18355–18366.
Cardellino CA and Chameides WL (1990) Natural hydrocarbons, urbanization, and urban ozone. *Journal of Geophysical Research* 95: 13971–13979.
Carslaw N, Creasey DL, Heard DE, et al. (1999) Modeling OH, HO_2 and RO_2 radicals in the marine boundary layer: 1. Model construction and comparison with field measurements. *Journal of Geophysical Research* 104: 30241–30256.
Chameides WL, Lindsay RW, Richardson J, and Kiang CS (1988) The role of biogenic hydrocarbons in urban photochemical smog: Atlanta as a case study. *Science* 241: 1473–1474.
Chatfield RB, Vastano JA, Li L, Sachse GW, and Conners VS (1998) The Great African plume from biomass burning: Generalizations from a three-dimensional study of TRACE A carbon monoxide. *Journal of Geophysical Research* 103: 28059–28078.
Chin M, Jacob DJ, Munger JW, Parrish DD, and Doddridge BG (1994) Relationship of ozone and carbon monoxide over North America. *Journal of Geophysical Research* 99(14): 565–573.
Chung SH and Seinfeld JH (2002) Global distribution and climate forcing of carbonaceous aerosols. *Journal of Geophysical Research* 107(D19): 4407.
Clarke JF and Ching JKS (1983) Aircraft observations of regional transport of ozone in the northeastern United States. *Atmospheric Environment* 17: 1703–1712.
Cooper OR, Parrish DD, Stohl A, et al. (2010) Increasing springtime ozone mixing ratios in the free troposphere over western North America. *Nature* 463: 344–348.
Daum PH, Kleinman LI, Newman L, et al. (1996) Chemical and physical properties of anthropogenic pollutants transported over the North Atlantic during NARE. *Journal of Geophysical Research* 101: 29029–29042.
Daum PH, Kleinman LI, Springston SR, et al. (2004) Origin and properties of plumes of high ozone observed during the Texas 2000 Air Quality Study (TexAQS 2000). *Journal of Geophysical Research* 109: D17306.
Demerjian KL (2000) A review of national monitoring networks in North America. *Atmospheric Environment* 34: 1861–1884.
Dentener FJ and Crutzen PJ (1993) Reaction of N_2O_5 on tropospheric aerosols: Impact on the global distribution of NO_x, O_3, and OH. *Journal of Geophysical Research* 98: 7149–7162.
Dickerson RR, Kondragunta S, Stenchicov G, Civeraolo KL, Doddridge BG, and Holben BN (1997) The impact of aerosols on solar ultraviolet radiation and photochemical smog. *Science* 278: 827–830.
Dockery DW, Pope CA, Xu X, et al. (1993) An association between air pollution and mortality in six U.S. cities. *New England Journal of Medicine* 329: 1753–1759.
Dodge MC (2000) Chemical oxidant mechanisms for air quality modeling: Critical review. *Atmospheric Environment* 34: 2103–2130.
Donahue NM, Robinson AL, and Pandis SN (2009) Atmospheric organic particulate matter: From smoke to secondary organic aerosol. *Atmospheric Environment* 43: 94–106.
Duderstadt KA, Carroll MA, Sillman S, et al. (1998) Photochemical production and loss rates at Sable Island, Nova Scotia during the North Atlantic Regional Experiment 1993 summer intensive. *Journal of Geophysical Research* 103: 13531–13555.
Dzepina K, Volkamer RM, Madronich S, et al. (2009) Evaluation of recently-proposed secondary organic aerosol models for a case study in Mexico City. *Atmospheric Chemistry and Physics* 9: 5681–5709.
Eisele FL, Tanner DJ, Cantrell CA, and Calvert JG (1996) Measurements and steady state calculations of OH concentrations at Mauna Loa Observatory. *Journal of Geophysical Research* 101: 14665–14679.
Fenger J (1999) Urban air quality. *Atmospheric Environment* 33: 4877–4900.
Fiore AM, Jacob DJ, Bey I, et al. (2002a) Background ozone over the United States in summer: Origin, trend, and contribution to pollution episodes. *Journal of Geophysical Research* 107(D15): 4275.
Fiore AM, Jacob DJ, Field BD, Streets DG, Fernandes SD, and Jang C (2002b) Linking ozone pollution and climate change: The case for controlling methane. *Geophysical Research Letters* 29(19): 1919.
Fiore AM, Jacob DJ, Logan JA, and Yin JH (1998) Long-term trends in ground level ozone over the contiguous United States, 1980–1995. *Journal of Geophysical Research* 103: 1471–1480.
Fiore AM, Dentener FJ, Wild O, et al. (2009) Multimodel estimates of intercontinental source-receptor relationships for ozone pollution. *Journal of Geophysical Research* 114: D04301.
Forster P, Ramaswamy V, Artaxo P, et al. (2007) Changes in atmospheric constituents and in radiative forcing. In: Solomon S, Qin D, and Manning M, et al. (eds.) *Climate Change 2007: The Physical Science Basis. Contribution of Working Group I to the Fourth Assessment Report of the Intergovernmental Panel on Climate Change*. Cambridge/New York: Cambridge University Press.
Frost GJ, Trainer M, Mauldin RL III, et al. (1999) Photochemical modeling of OH levels during the First Aerosol Characterization Experiment (ACE 1). *Journal of Geophysical Research* 104: 16041–16052.
Frost GJ, McKeen SA, Trainer M, et al. (2006) Effects of changing power plant NO_x emissions on ozone in the eastern United States: Proof of concept. *Journal of Geophysical Research* 111: D12306.
Fu TM, Jacob DJ, and Heald CL (2009) Aqueous-phase reactive uptake of dicarbonyls as a source of organic aerosol over eastern North America. *Atmospheric Environment* 43: 1814–1822.
Gao D, Stockwell WR, and Milford JB (1996) Global uncertainty analysis of a regional-scale gas phase chemical mechanism. *Journal of Geophysical Research* 101: 9071–9078.
George LA, Hard TM, and O'Brian RJ (1999) Measurement of free radicals OH and HO_2 in Los Angeles smog. *Journal of Geophysical Research* 104: 11643–11655.
Geron CD, Guenther AB, and Pierce TE (1994) An improved model for estimating emissions of volatile organic compounds from forests in the eastern United States. *Journal of Geophysical Research* 99: 12773–12791.
Gillani NV and Pleim JE (1996) Sub-grid-scale features of anthropogenic emissions of NO_x and VOC in the context of regional Eulerian models. *Atmospheric Environment* 30: 2043–2059.
Goldan PD, Kuster WC, and Fehsenfeld FC (1997) Non-methane hydrocarbon measurements during the tropospheric OH photochemistry experiment. *Journal of Geophysical Research* 102: 6315–6324.
Goldan PD, Trainer M, Kuster WC, et al. (1995) Measurements of hydrocarbons, oxygenated hydrocarbons, carbon monoxide and nitrogen oxides in an urban basin in Colorado: Implications for emissions inventories. *Journal of Geophysical Research* 100: 22771–22785.
Guenther A, Geron C, Pierce T, Lamb B, Harley P, and Fall R (2000) Natural emissions of non-ethane volatile organic compounds, carbon monoxide, and oxides of nitrogen from North America. *Atmospheric Environment* 34: 2205–2230.
Guttikunda SK, Tang Y, Carmichael GR, et al. (2005) Impacts of Asian megacity emissions on regional air quality during spring 2001. *Journal of Geophysical Research* 110: D20301.

Haagen-Smit AJ and Fox MM (1954) Photochemical ozone formation with hydrocarbons and automobile exhaust. *Journal of the Air Pollution Control Association* 4: 105–109.

Heald CL, Henze DK, Horowitz LW, et al. (2008) Predicted change in global secondary organic aerosol concentrations in response to future climate, emissions, and land use change. *Journal of Geophysical Research* 113: D05211.

Henry RC (1992) Dealing with near collinearity in chemical mass balance receptor models. *Atmospheric Environment* 26A(5): 933–938.

Henry RC, Lewis CW, Hopke PK, and Williamson HW (1984) Review of receptor modeling fundamentals. *Atmospheric Environment* 18: 1507–1515.

Hirsch AI, Munger JW, Jacob DJ, Horowitz LW, and Goldstein AH (1996) Seasonal variation of the ozone production efficiency per unit NO_x at Harvard Forest, Massachusetts. *Journal of Geophysical Research* 101: 12659–12666.

Hoening JQ (2000) *Health Effects of Ambient Air Pollution: How Safe Is the Air We Breathe?* Norwell/Dordrecht: Kluwer Academic Publishers.

Holgate ST, Samet JM, Koren HS, and Maynard RL (eds.) (1999) *Air Pollution and Health*. London/San Diego: Academic Press.

Horowitz LW and Jacob DJ (1999) Global impact of fossil fuel combustion on atmospheric NO_x. *Journal of Geophysical Research* 104: 23823–23840.

Horowitz LW, Liang J, Gardner GM, and Jacob DJ (1998) Export of reactive nitrogen from North America during summertime: Sensitivity to hydrocarbon chemistry. *Journal of Geophysical Research* 103: 13451–13476.

IPCC (2001) Climate change 2001: The scientific basis. In: Houghton JT, Ding Y, and Griggs DJ, et al. (eds.) *Contribution of Working Group I to the Third Assessment Report of the Intergovernmental Panel on Climate Change*. p. 881. Cambridge/ New York: Cambridge University Press.

Jacob DJ (2000) Heterogeneous chemistry and tropospheric ozone. *Atmospheric Environment* 34: 2131–2159.

Jacob DJ, Heikes BG, Dickerson RR, Artz RS, and Keene WC (1995) Evidence for a seasonal transition from NO_x- to hydrocarbon-limited ozone production at Shenandoah National Park, Virginia. *Journal of Geophysical Research* 100: 9315–9324.

Jacob DJ, Logan JA, Gardner GM, et al. (1993) Factors regulating ozone over the United States and its export to the global atmosphere. *Journal of Geophysical Research* 98: 14817–14827.

Jacobson MZ (1997) Development and application of a new air pollution modeling system – Part III. Aerosol-phase simulations. *Atmospheric Environment* 31: 587–608.

Jacobson MZ (2002) Control of fossil-fuel particulate black carbon and organic matter, possibly the most effective method of slowing global warming. *Journal of Geophysical Research* 107(D19): 4410.

Jacobson MZ, Lu R, Turco RP, and Toon OP (1996) Development and application of a new air pollution modeling system – Part I. Gas-phase simulations. *Atmospheric Environment* 30: 1939–1963.

Jaegle L, Jacob DJ, Brune WH, and Wennberg PO (2001) Chemistry of HO_x radicals in the upper troposphere. *Atmospheric Environment* 35: 469–490.

Jaegle L, Jacob DJ, Brune WH, et al. (1998) Sources of HO_x and production of ozone in the upper troposphere over the United States. *Geophysical Research Letters* 25: 1705–1708.

Jenkins GS, Mohr K, Morris VR, and Arino O (1997) The role of convective processes over the Zaire-Congo Basin to the southern hemispheric ozone maximum. *Journal of Geophysical Research* 102: 18963–18980.

Jones AP (1999) Indoor air quality and health. *Atmospheric Environment* 33: 4535–4564.

Kanakidou M, Singh HB, Valentin KM, and Crutzen PJ (1991) A two-dimensional study of ethane and propane oxidation in the troposphere. *Journal of Geophysical Research* 96: 15395–15414.

Kleinman LI (1986) Photochemical formation of peroxides in the boundary layer. *Journal of Geophysical Research* 91: 10889–10904.

Kleinman LI (1991) Seasonal dependence of boundary layer peroxide concentration: The low and high NO_x regimes. *Journal of Geophysical Research* 96: 20721–20734.

Kleinman LI (1994) Low and high-NO_x tropospheric photochemistry. *Journal of Geophysical Research* 99: 16831–16838.

Kleinman LI (2000) Ozone process insights from field experiments – Part II: Observation-based analysis for ozone production. *Atmospheric Environment* 34: 2023–2034.

Kleinman LI, Daum PH, Imre D, et al. (2002) Ozone production rate and hydrocarbon reactivity in five urban areas: A cause of high ozone concentration in Houston. *Geophysical Research Letters* 29(10): 1467.

Kleinman LI, Daum PH, Lee Y-N, et al. (2005) A comparative study of ozone production in five U.S. metropolitan areas. *Journal of Geophysical Research* 110: D02301.

Kuebler J, van den Bergh H, and Russell AG (2001) Long-term trends of primary and secondary pollutant concentrations in Switzerland and their response to emission controls and economic changes. *Atmospheric Environment* 35: 1351–1363.

Lelieveld J, Berresheim H, Borrmann S, et al. (2002) Global air pollution crossroads over the Mediterranean. *Science* 298: 794–799.

Lelieveld J and Dentener FJ (2000) What controls tropospheric ozone? *Journal of Geophysical Research* 105: 3531–3552.

Li QB, Jacob DJ, Logan JA, et al. (2001) A tropospheric ozone maximum over the Middle East. *Geophysical Research Letters* 28: 3235–3238.

Lin X, Trainer M, and Liu SC (1988) On the nonlinearity of tropospheric ozone. *Journal of Geophysical Research* 93: 15879–15888.

Lippman M (ed.) (2000) *Environmental Toxicants: Human Exposures and Their Health Effects*. New York: Wiley-Interscience.

Lippman M and Schlesinger RB (2000) Toxicological bases for the setting of health-related air pollution standards. *Annual Review of Public Health* 21: 309–333.

Liu SC, Trainer M, Fehsenfeld FC, et al. (1987) Ozone production in the rural troposphere and the implications for regional and global ozone distributions. *Journal of Geophysical Research* 92: 4191–4207.

Logan JA, Prather MJ, Wofsy SC, and McElroy MB (1981) Tropospheric chemistry: A global perspective. *Journal of Geophysical Research* 86: 7210–7254.

Mage D, Ozolins G, Peterson P, et al. (1996) Urban air pollution in the megacities of the world. *Atmospheric Environment* 30: 681–686.

Mauzerall DL, Narita D, Akimoto H, et al. (2000) Seasonal characteristics of tropospheric ozone production and mixing ratios over east Asia: A global three-dimensional chemical transport model analysis. *Journal of Geophysical Research* 105: 17895–17910.

Mauzerall DL and Wang X (2001) Protecting agricultural crops from the effects of tropospheric ozone exposure: Reconciling science and standard setting in the United States, Europe, and Asia. *Annual Review of Energy and the Environment* 2001(26): 237–268.

McKeen SA, Liu SC, Hsie E-Y, et al. (1996) Hydrocarbon ratios during PEM-WEST A: A model perspective. *Journal of Geophysical Research* 101: 2087–2109.

McKeen SA, Mount G, Eisele F, et al. (1997) Photochemical modeling of hydroxyl and its relationship to other species during the tropospheric OH photochemistry experiment. *Journal of Geophysical Research* 102: 6467–6493.

McMurry PH (2000) A review of atmospheric aerosol measurements. *Atmospheric Environment* 34: 1959–2000.

Meng Z, Dabdub D, and Seinfeld JH (1997) Chemical coupling between atmospheric ozone and particulate matter. *Science* 277: 116–119.

Milford J, Gao D, Sillman S, Blossey P, and Russell AG (1994) Total reactive nitrogen (NO_y) as an indicator for the sensitivity of ozone to NO_x and hydrocarbons. *Journal of Geophysical Research* 99: 3533–3542.

Milford J, Russell AG, and McRae GJ (1989) A new approach to photochemical pollution control: Implications of spatial patterns in pollutant responses to reductions in nitrogen oxides and reactive organic gas emissions. *Environmental Science & Technology* 23: 1290–1301.

Millan MM, Salvador R, Mantilla E, and Kallos G (1997) Photooxidant dynamics in the Mediterranean basin during summer: Results from European research projects. *Journal of Geophysical Research* 102: 8811–8823.

Miller DF, Alkezweeny AJ, Hales JM, and Lee RN (1978) Ozone formation related to power plant emissions. *Science* 202: 1186–1188.

NARSTO (2000) *An Assessment of Tropospheric Ozone Pollution: A North American Perspective*. The NARSTO Synthesis Team. Available at http://camraq.owt.com/Narsto.

NARSTO (2003) *NARSTO Particulate Matter Science for Policy Makers: A NARSTO Assessment*. Parts 1 and 2, EPRI 1007735. Available at http://www.cgenv.com/ Narsto.

National Research Council (NRC) (1991) *Rethinking the Ozone Problem in Urban and Regional Air Pollution*. NRC Committee on Tropospheric Ozone Formation and Measurement. Washington, DC: National Academy Press.

Nunnermacker LJ, Imre D, Daum PH, et al. (1995) Characterization of the Nashville urban plume on July 3 and July 18, 1995. *Journal of Geophysical Research* 103: 28129–28148.

Parrish DD and Fehsenfeld FC (2000) Methods for gas-phase measurements of ozone, ozone precursors and aerosol precursors. *Atmospheric Environment* 34: 1921–1957.

Parrish DD, Holloway JS, Trainer M, Murphy PC, Forbes GL, and Fehsenfeld FC (1993) Export of North American ozone pollution to the North Atlantic Ocean. *Science* 259: 1436–1439.

Parrish DD, Trainer M, Young V, et al. (1998) Internal consistency tests for evaluation of measurements of anthropogenic hydrocarbons in the troposphere. *Journal of Geophysical Research* 103: 22339–22359.

Parrish DD, Dunlea EJ, Atlas EL, et al. (2004) Changes in the photochemical environment of the temperate North Pacific troposphere in response to increased Asian emissions. *Journal of Geophysical Research* 109: D23S18.

Pierce T, Geron C, Bender L, Dennis R, Tonnesen G, and Guenther A (1998) Influence of increased isoprene emissions on regional ozone modeling. *Journal of Geophysical Research* 103: 25611–25630.

Placet M, Mann CO, Gilbert RO, and Niefer MJ (2000) Emissions of ozone precursors from stationary sources: A critical review. *Atmospheric Environment* 34: 2183–2204.

Poppe D, Zimmermann J, Bauer R, et al. (1994) Comparison of measured OH concentrations with model calculations. *Journal of Geophysical Research* 99: 16633–16642.

Prospero JM (1999) Long-term measurements of the transport of African mineral dust to the southeastern United States: Implications for regional air quality. *Journal of Geophysical Research* 104: 15917–15927.

Ramanathan V and Carmichael G (2008) Global and regional climate changes due to black carbon. *Nature Geoscience* 1: 221–227.

Rasch PJ, Barth MC, Kiehl JT, Schwartz SE, and Benkovitz CM (2000) A description of the global sulfur cycle and its controlling processes in the National Center for Atmospheric Research Community Climate Model, Version 3. *Journal of Geophysical Research* 105: 1367–1385.

Reynolds S, Michaels H, Roth P, et al. (1996) Alternative base cases in photochemical modeling: Their construction, role, and value. *Atmospheric Environment* 30(12): 1977–1988.

Ridley BA, Madronich S, Chatfield RB, et al. (1992) Measurements and model simulations of the photostationary state during the Mauna Loa Observatory Photochemistry Experiment: Implications for radical concentrations and ozone production and loss rates. *Journal of Geophysical Research* 97: 10375–10388.

Roselle SJ and Schere KL (1995) Modeled response of photochemical oxidants to systematic reductions in anthropogenic volatile organic compound and NO_x emissions. *Journal of Geophysical Research* 100: 22929–22941.

Russell A and Dennis R (2000) NARSTO critical review of photochemical models and modeling. *Atmospheric Environment* 34: 2283–2324.

Ryerson TB, Buhr MP, Frost GJ, et al. (1998) Emissions lifetimes and ozone formation in power plant plumes. *Journal of Geophysical Research* 103: 22569–22584.

Ryerson TB, Trainer M, Holloway JS, et al. (2001) Observations of ozone formation in power plant plumes and implications for ozone control strategies. *Science* 292: 719–723.

Sawyer RF, Harley RA, Cadle SH, Norbeck JM, Slott R, and Bravo HA (2000) Mobile sources critical review: 1998 NARSTO assessment. *Atmospheric Environment* 34: 2161–2182.

Schultz MG, Jacob DJ, Wang Y, et al. (1999) On the origin of tropospheric ozone and NO_x over the tropical South Pacific. *Journal of Geophysical Research* 104: 5829–5843.

Seaman NL (2000) Meteorological modeling for air quality assessments. *Atmospheric Environment* 34: 2231–2260.

Seinfeld JH and Pandis SN (1998) *Atmospheric Chemistry and Physics: From Air Pollution to Climate Change*. New York: Wiley.

Shindell D, Faluvegi G, Lacis A, Hansen J, Ruedy R, and Aguilar E (2006) Role of tropospheric ozone increases in 20th-century climate change. *Journal of Geophysical Research* 111: D08302.

Shirley TR, Brune WH, Ren X, et al. (2006) Atmospheric oxidation in the Mexico City Metropolitan Area (MCMA) during April 2003. *Atmospheric Chemistry and Physics* 6: 2753–2765.

Sillman S (1993) Tropospheric ozone: The debate over control strategies. *Annual Review of Energy and Environment* 18: 31–56.

Sillman S (1995) The use of NO_y, H_2O_2 and HNO_3 as indicators for O_3-NO_x-ROG sensitivity in urban locations. *Journal of Geophysical Research* 100: 14175–14188.

Sillman S (1999) The relation between ozone, NO_x and hydrocarbons in urban and polluted rural environments. *Atmospheric Environment* 33(12): 1821–1845.

Sillman S, Al-Wali K, Marsik FJ, et al. (1995) Photochemistry of ozone formation in Atlanta, GA: Models and measurements. *Atmospheric Environment* 29: 3055–3066.

Sillman S and He D (2002) Some theoretical results concerning O_3-NO_x-VOC chemistry and NO_x-VOC indicators. *Journal of Geophysical Research* 107: D224659.

Sillman S, He D, Pippin M, et al. (1998) Model correlations for ozone, reactive nitrogen and peroxides for Nashville in comparison with measurements: Implications for VOC-NO_x sensitivity. *Journal of Geophysical Research* 103: 22629–22644.

Sillman S, Logan JA, and Wofsy SC (1990) The sensitivity of ozone to nitrogen oxides and hydrocarbons in regional ozone episodes. *Journal of Geophysical Research* 95: 1837–1851.

Sillman S and Samson PJ (1995) The impact of temperature on oxidant formation in urban, polluted rural and remote environments. *Journal of Geophysical Research* 100: 11497–11508.

Sillman S, Vautard R, Menut L, and Kley D (2003) O_3-NO_x-VOC sensitivity and NO_x-VOC indicators in Paris: Results from models and Atmospheric Pollution Over the Paris Area ESQUIF measurements. *Journal of Geophysical Research*.

Simpson D (1995) Biogenic emissions in Europe. 2: Implications for ozone control strategies. *Journal of Geophysical Research* 100: 22891–22906.

Sosa G, West J, San Martini F, Molina LT, and Molina MJ (2000) Air quality modeling and data analysis for ozone and particulates in Mexico City. *MIT Integrated Program on Urban, Regional and Global Air Pollution Report No. 15*. Available from http://eaps.mit.edu/megacities/index.html

Stehr JW, Dickerson RR, Hallock-Waters KA, Doddridge BG, and Kirk D (2000) Observations of NO_y, CO and SO_2 and the origin of reactive nitrogen in the eastern U.S. *Journal of Geophysical Research* 105: 3553–3563.

Stockwell WR, Kirchner F, and Kuhn M (1997) A new mechanism for regional atmospheric chemistry modeling. *Journal of Geophysical Research* 102: 25847–25879.

Stohl A and Trickl T (1999) A textbook example of long-range transport: Simultaneous observation of ozone maxima from stratospheric and North American origin in the free troposphere over Europe. *Journal of Geophysical Research* 104: 30445–30462.

Tan D, Faloona I, Brune WH, et al. (2001) HO_x budgets in a deciduous forest: Results from the PROPHET summer 1998 campaign. *Journal of Geophysical Research* 106: 24407–24428.

Thornton JA, Wooldridge PJ, Cohen RC, et al. (2002) Ozone production rates as a function of NO_x abundances and HO_x production rates in the Nashville urban plume. *Journal of Geophysical Research* 107(D12): 4146.

Trainer M, Parrish DD, Buhr MP, et al. (1993) Correlation of ozone with NO_y in photochemically aged air. *Journal of Geophysical Research* 98: 2917–2926.

Trainer M, Parrish DD, Goldan PD, Roberts J, and Fehsenfeld FC (2000) Review of observation-based analysis of the regional factors influencing ozone formation. *Atmospheric Environment* 34: 2045–2062.

US Congress (1989) *Catching Our Breath: Next Steps for Reducing Urban Ozone*. Office of Technology Assessment OTA-O-412. Washington, DC: US Government Printing Office.

Volz A and Kley D (1988) Evaluation of the Montsouris series of ozone measurements made in the nineteenth century. *Nature* 332: 240–242.

Volz-Thomas A and Kolahgar B (2000) On the budget of hydroxyl radicals at Schauinsland during the Schauinsland Ozone Precursor Experiment (SLOPE96). *Journal of Geophysical Research* 105: 1611–1622.

Wang Y and Jacob DJ (1998) Anthropogenic forcing on ozone, and OH since preindustrial times. *Journal of Geophysical Research* 103: 31123–31135.

Wang X and Mauzerall DL (2004) Characterizing distributions of surface ozone and its impact on grain production in China, Japan and South Korea: 1990 and 2020. *Atmospheric Environment* 38: 4383–4402.

West JJ, Fiore AF, Horowitz LW, and Mauzerall DL (2006) Global health benefits of mitigating ozone pollution with methane emission controls. *Proceedings of the National Academy of Sciences of the United States of America* 103(11): 3988–3993.

White WH, Patterson DE, and Wilson WE Jr. (1983) Urban exports to the nonurban troposphere: Results from project MISTT. *Journal of Geophysical Research* 88: 10745–10752.

Wild O and Prather MJ (2000) Excitation of the primary tropospheric chemical mode in a global three dimensional model. *Journal of Geophysical Research* 105: 24647–24660.

Wild O, Prather MJ, and Akimoto H (2001) Indirect long-term global radiative cooling from NO_x emissions. *Geophysical Research Letters* 28: 1719–1722.

Williams EJ, Guenther A, and Fehsenfeld FC (1992) An inventory of nitric oxide emissions from soils in the United States. *Journal of Geophysical Research* 97: 7511–7519.

Wilson R and Spengler JD (eds.) (1996) *Particles in Our Air: Concentrations and Health Effects*. Cambridge, MA: Harvard School of Public Health, Harvard University Press.

Wilson WE and Suh HH (1997) Fine particles and coarse particles: Concentration relationships relevant to epidemiologic studies. *Journal of the Air and Waste Management Association* 47: 1238–1249.

Zaveri RA and Peters LK (1999) A new lumped structure photochemical mechanism for large-scale applications. *Journal of Geophysical Research* 104: 30387–30415.

11.12 Volatile Hydrocarbons and Fuel Oxygenates

IM Cozzarelli, U.S. Geological Survey, Reston, VA, USA
JR Mckelvie, Currently at Nuclear Waste Management Organization, Toronto, ON, Canada
AL Baehr, U.S. Geological Survey, W. Trenton, NJ, USA

This article is a revision of the previous edition article by I.M. Cozzarelli, A.L. Baehr, volume 9, pp. 433–474, © 2003, Elsevier Ltd.

11.12.1 Introduction

11.12.1.1 Scope of the Problem

Petroleum hydrocarbons (hydrocarbons that result from petroleum products such as oil, gasoline, or diesel fuel) are among the most commonly occurring and widely distributed contaminants in the environment. Volatile hydrocarbons are the lighter fraction of petroleum hydrocarbons and, together with fuel oxygenates, are most often released from crude oil and liquid petroleum products produced from crude oil. The demand for crude oil stems from the world's ever-growing energy need. From 1970 to 2007, world primary energy production more than doubled, with fossil fuels (crude oil, natural gas, and coal) accounting for approximately 86% of all energy produced globally in 2007 (**Figure 1**; Energy Information Administration, 2010a). World crude oil production was 73 million barrels (bbl) day^{-1} (1.16×10^{10} l day^{-1}) in 2007 (Energy Information Administration, 2010a). With a global consumption of 86 million bbl day^{-1} (1.37×10^{10} l day^{-1}) in 2007 (Energy Information Administration, 2010a), the world's dependence on oil as an energy source is clearly a leading contributor to global warming and worsening air and water quality.

Petroleum products are present in Earth's subsurface as solids, liquids, or gases. This chapter presents a summary of the environmental problems and issues related to the use of liquid petroleum, or oil. The focus is on the sources of volatile hydrocarbons and fuel oxygenates and the geochemical behavior of these compounds when they are released into the environment. Methyl *tert*-butyl ether (MTBE) use in gasoline as an octane booster began in the 1970s to replace lead additives. It became the most widely used fuel oxygenate in the United States, and in 1999, the US Environmental Protection Agency (USEPA) included it in its Contaminant Candidate List because of its widespread occurrence in groundwater. In 2000 they initiated efforts to eliminate or limit the use of MTBE as a fuel additive (US Environmental Protection Agency, 2000) and since 2007, MTBE has not been used in the United States and ethanol has emerged as its primary replacement. Although oxygenates include compounds other than MTBE and ethanol (EtOH),

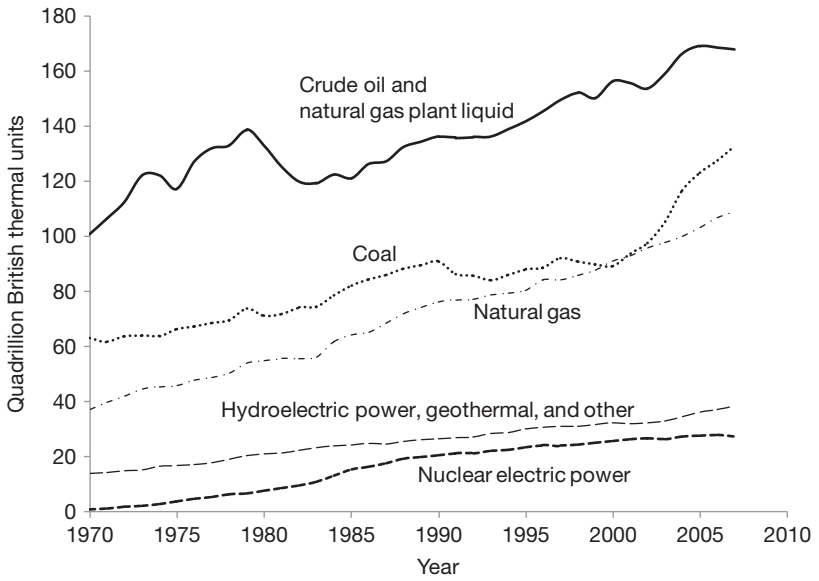

Figure 1 World primary energy production by source from 1970 to 2007. Modified from Energy Information Administration (2010a) *Annual Energy Review 2009*. DOE/EIA-0384(2009). Washington, DC: US Energy Information Administration.

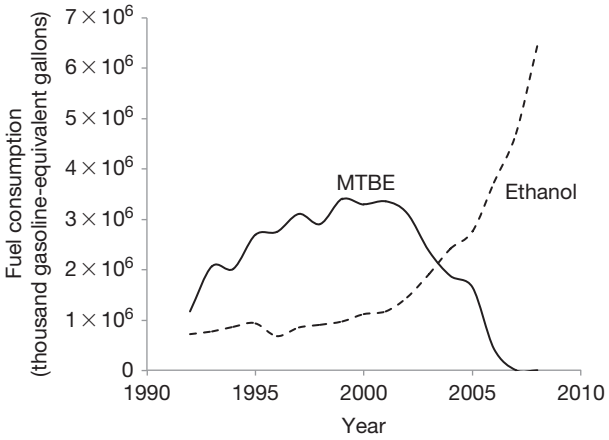

Figure 2 MTBE and ethanol consumption in reformulated gasoline in the United States. Modified from Energy Information Administration (2010a) *Annual Energy Review 2009*. DOE/EIA-0384(2009). Washington, DC: US Energy Information Administration.

most of the information presented here focuses on these oxygenates because of their historical and emerging widespread use in gasoline (**Figure 2**). The environmental impact of higher molecular weight hydrocarbons that also originate from petroleum products is described in **Chapter 11.13**.

Crude oil occurs within the Earth and is a complex mixture of natural compounds composed largely of hydrocarbons containing only hydrogen and carbon atoms. The minor elements of sulfur, nitrogen, and oxygen constitute less than 3% of most petroleum (Hunt, 1996). Releases to the environment occur during the production, transport, processing, storage, use, and disposal of these hydrocarbons. The petroleum industry classifies oil naturally occurring in a liquid phase as either conventional oil or nonconventional oil. Conventional oil can be explored and produced by conventional primary and secondary recovery techniques, whereas nonconventional oil, such as heavy oils, tar sands, and synthetic oils, is more difficult to extract from the host rock and requires specialized methods (Tissot and Welte, 1984). The history of liquid petroleum usage dates back centuries. Marco Polo described its use as a fuel for lamps in 1291 (Testa and Winegardner, 2000). In the mid-nineteenth century, Native Americans used crude oil skimmed from creeks and rivers as a medicinal ointment (Energy Information Administration, 1999). Commercial production in the United States began in 1859 with kerosene production for use in lamps. At the turn of the century, the emphasis shifted to gasoline with the invention of the automobile, and in the 1930s and 1940s, a substantial market for heating oil developed.

In 2007, 86% of the world's energy came from fossil fuels, with oil consumption alone supplying ~33% of that energy (Energy Information Administration, 2010a). Oil, with its high BTU (British thermal unit) density and ease of transport, is the most valuable fuel in the world today, and the world demand for crude oil is ever increasing. The *International Energy Outlook 2010* reference case predicts world marketed energy consumption to grow by 49% from 2007 to 2035, with liquid fossil fuels continuing to provide a large percentage to the energy mix (Energy Information Administration, 2010b). As demand increases and known oil reserves (**Table 1**) are depleted, more emphasis will be placed on new discoveries and improved recovery technologies. Sources such as tar sands and oil shales are likely to become more important, bringing environmental problems inherent to the production, transport, and processing of these resources to new sectors of the environment.

Reserves of crude oil, the raw material used to make petroleum products, are not evenly distributed around the world (**Table 1**). Statistics regarding the production levels of the major oil-producing nations in the world are published by

the US Department of Energy's (DOE) Energy Information Administration (EIA) (Energy Information Administration, 2010a). Nations in the Organization of Petroleum Exporting Countries (OPEC) produce about 43% of the world's total of nearly 73 million bbl day^{-1} (bpd) (1.16×10^{10} l day^{-1}). In 2007, the top three oil producers were Russia at 9.4 million bpd (1.50×10^{9} l day^{-1}), Saudia Arabia at 8.7 million bpd (1.39×10^{9} l day^{-1}), and the United States at 5.1 million bpd (8.04×10^{8} l day^{-1}). Oil and gas are being produced in virtually all geographic areas intersecting a wide range of ecological habitats including tropical rain forests, Middle Eastern deserts, Arctic regions, and deep offshore marine environments.

The petroleum industry has two main components: exploration/recovery and refinement/delivery. Crude oil is delivered to refineries and refined products are delivered to consumers through a large transportation network that includes tankers, barges, pipelines, and railroads. This transportation network links suppliers and producers across the world. Above-ground tanks, below-ground tanks and caverns, and offshore facilities store petroleum at various stages in this distribution system. The largest underground storage facilities in the United States are part of the US Strategic Petroleum Reserve maintained by the US Government for times of supply shortage (Energy Information Administration, 1999). The global and complex nature of this industry means that every environmental compartment (air, land, water, biota) and all nations are affected by petroleum spills and waste products.

Table 1 Proved oil reserves (January, 2009)

Region	*Crude oil reserves (billion barrels)*
North America	207.7
Central & South America	122.7
Europe	13.7
Eurasia	98.9
Middle East	746.0
Africa	117.1
Asia & Oceania	34.0
Total	1340.0

Source: Energy Information Administration (2010a)

Petroleum products can be released into the environment at all stages of petroleum use, from exploration, production, transportation, storage, use, and disposal (**Figure 3**). Concentrated releases of compounds are known as point sources. An example of a point source petroleum release during production is the Deepwater Horizon blowout of 2010 in the Gulf of Mexico, which is estimated to have leaked 7.0×10^{5} m^3 of oil (7.0×10^{8} l) (Crone and Tolstoy, 2010). Another well-known case of petroleum contamination is the huge oil spill in the Santa Barbara Channel in 1969 due to the blowout of a Union Oil Co. of California development well that leaked more than 50 000 bbl (7.9×10^{6} l) of oil into the channel. The *Exxon Valdez* tanker spill, which released 258 000 bbl (4.1×10^{7} l), is an example of a major point source release associated with transportation; the spilled oil spread 750 km from the original spill site and impacted 1750 km of shoreline (Bence et al., 1996; Wolfe et al., 1994). Highly publicized contamination of coastal waters by petroleum spills, such as the Santa Barbara spill, is credited with being the catalyst that thrust the modern environmental movement to the forefront of American conscience and politics in the early 1970s (Williams, 1991). In addition to these large offshore spills, widespread smaller releases to the environment, such as gasoline leaking from underground storage tanks (USTs) and pipelines, introduce hydrocarbon and fuel oxygenate compounds into the air, water, and solids of the subsurface.

The more volatile components of oil partition preferentially into the atmosphere and hydrosphere, and, to a lesser extent, the geosphere (e.g., sorption onto sediments) and biosphere (i.e., bioaccumulation), whereas the higher molecular weight fraction of oil is less soluble and less volatile and impacts

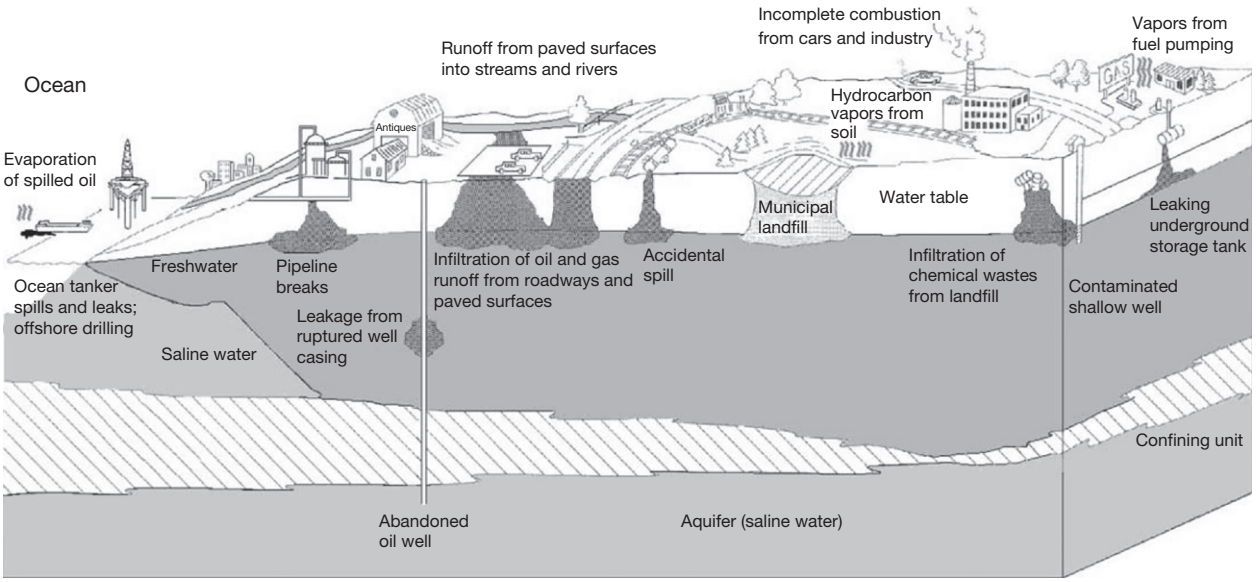

Figure 3 Modes of contamination by petroleum products during production, transport, use, and disposal. Reproduced from Fetter CW (1993) *Contaminant Hydrology*. New York: Macmillan Publishing Company.

the biosphere and geosphere more directly, as described by Abrajano et al. (Chapter 11.13). Usage causes compounds from petroleum products to separate and enter the environment. For example, incomplete fuel combustion in an automobile engine or a home-heating furnace results in the release of compounds to the atmosphere where they can be widely dispersed. Compounds in the exhaust gas of a motor boat partition in river or lake water, allowing for mixing and transport in the water body. These examples are illustrative of chronic low level and widespread release of compounds referred to as nonpoint sources.

Nonpoint sources can cause compounds to be dispersed throughout the hydrosphere, which can complicate efforts to evaluate the effect of point source spills. Current sampling and analytical techniques allow for the detection of volatile organic compounds (VOCs) at low concentrations – on the order of 0.1 $\mu g\,l^{-1}$ and less. As a result, VOCs have been detected frequently in ambient shallow groundwater in urban areas across the United States in studies conducted as part of the US Geological Survey (USGS) National Water-Quality Assessment (NAWQA) program (Moran et al., 2005; Rowe et al., 2007; Squillace et al., 1996, 1999). The importance of VOCs at low concentrations in ambient water is unclear. If these low concentrations are the result of plumes emanating from point sources, then concentrations could possibly increase with time. If the source were diffuse (nonpoint), as in the case of atmospheric sources, then changes in VOC concentrations in groundwater over time would be constrained by atmospheric concentrations.

Widely distributed and frequent point source spills can be considered nonpoint sources when the scale of concern is large in space or time. For example, the USEPA estimates that 200 million gallons of used oil is improperly disposed of each year (http://www.epa.gov/osw/conserve/materials/usedoil/oil.htm#facts). This large quantity of improperly disposed motor oil could be a regional source of benzene, toluene, ethylbenzene, and xylenes (BTEX) and MTBE as used motor oil contains BTEX on the order of 500–2000 $mg\,l^{-1}$ (Baker et al., 2002; Chen et al., 1994) and MTBE on the order of 100 $mg\,l^{-1}$. In a survey of 946 domestic wells designed to assess ambient groundwater quality in Maine, MTBE was detected in 15.8% percent of the wells, mostly at concentrations of less than 0.1 $\mu g\,l^{-1}$ (State of Maine Bureau of Health, 1998). Small and widely distributed spills of fuel-related products not necessarily associated with leaking storage tanks were identified as likely sources.

11.12.1.2 Petroleum Chemical Composition

Petroleum in its natural form is of limited use. Therefore, further processing, or refining, is needed to create the wide array of petroleum products in use today (Energy Information Administration, 1999). The refining process results in products from the original crude oil with different hydrocarbon compositions. In industrialized societies, the most notable products are motor gasoline and distillate fuels such as home-heating fuel (Figure 4). The United States leads the world in the generation of refined petroleum products, with gasoline accounting for just under half of the entire product.

A refinery converts crude oil into useful products by multistep processes that may include distillation, extraction, catalytic or thermal cracking, and finally hydrotreating to remove unwanted compounds. The chemical components of the crude oil are separated by their different physical and chemical properties, thus creating products that have different compositions. The kinds of refined products generated from crude oil and their boiling point range are illustrated in Figure 5 (National Research Council, 1985). For example, gasoline is one of the lightest fractions and contains the lighter hydrocarbons (C_4–C_8 range, where n in C_n refers to the number of carbon atoms in the hydrocarbon chain), whereas bunker fuel (fuel for ships that may be a mixture of two or more of the distillate cuts shown in Figure 5 or a residual oil from a distillation run; National Research Council, 1985) has a higher boiling point and mostly contains the heavier components ($>C_{14}$). Thus, the release of these refined products into the environment affects environmental compartments such as soils, the atmosphere, or freshwater bodies in different ways.

11.12.1.2.1 Crude oil

Crude oil within the Earth is of biological origin, formed when the remains of once-living organisms were buried and subjected to heat and pressure over millions of years. The composition of the petroleum formed in a given geologic deposit depends chiefly on the nature of the original organic material and the basin's thermal history (Tissot and Welte, 1984). Petroleum hydrocarbons are a complex mixture of over 1000 compounds with different physical and chemical properties. The fate of these compounds in the environment is dependent on their chemical structure.

The main groups of compounds in crude oils are saturated hydrocarbons (such as normal and branched alkanes and cycloalkanes that contain no double bonds), aromatic hydrocarbons, resins and asphaltenes (higher molecular weight polycyclic compounds containing nitrogen, sulfur, and oxygen (NSO)), and organometallic compounds (Tissot and Welte, 1984). Unsaturated hydrocarbons (nonaromatic hydrocarbons containing one or more double or triple bonds), such as olefins, are essentially absent. Most producible crude oils contain, on average, from 30 to 35% each of n- and isoalkanes, cycloalkanes, and aromatics (Table 2), although there can be a large variation in the actual composition for individual crudes. The most abundant hydrocarbons in crude oil are in the light fraction ($\leq C_{15}$). For example, in most crude oils, the abundance of n-alkanes decreases beyond n-decane. In the aromatic fraction, benzene, toluene, and other low molecular weight alkylbenzenes are abundant (Tissot and Welte, 1984). Because of the process by which oil is made, no two oils have exactly the same history, and, therefore, no two crude oils have the same chemical composition.

Among the classes of compounds in crude oil, the alkanes, cycloalkanes, and aromatic fractions contain compounds that are volatile, and they are described in more detail in this chapter. The NSO compounds, resins and asphaltenes, and organometallic compounds are nonvolatile and, in general, are less mobile in the environment. Discussion of these compounds is beyond the scope of this chapter. Examples of some of the volatile hydrocarbons present in crude oil

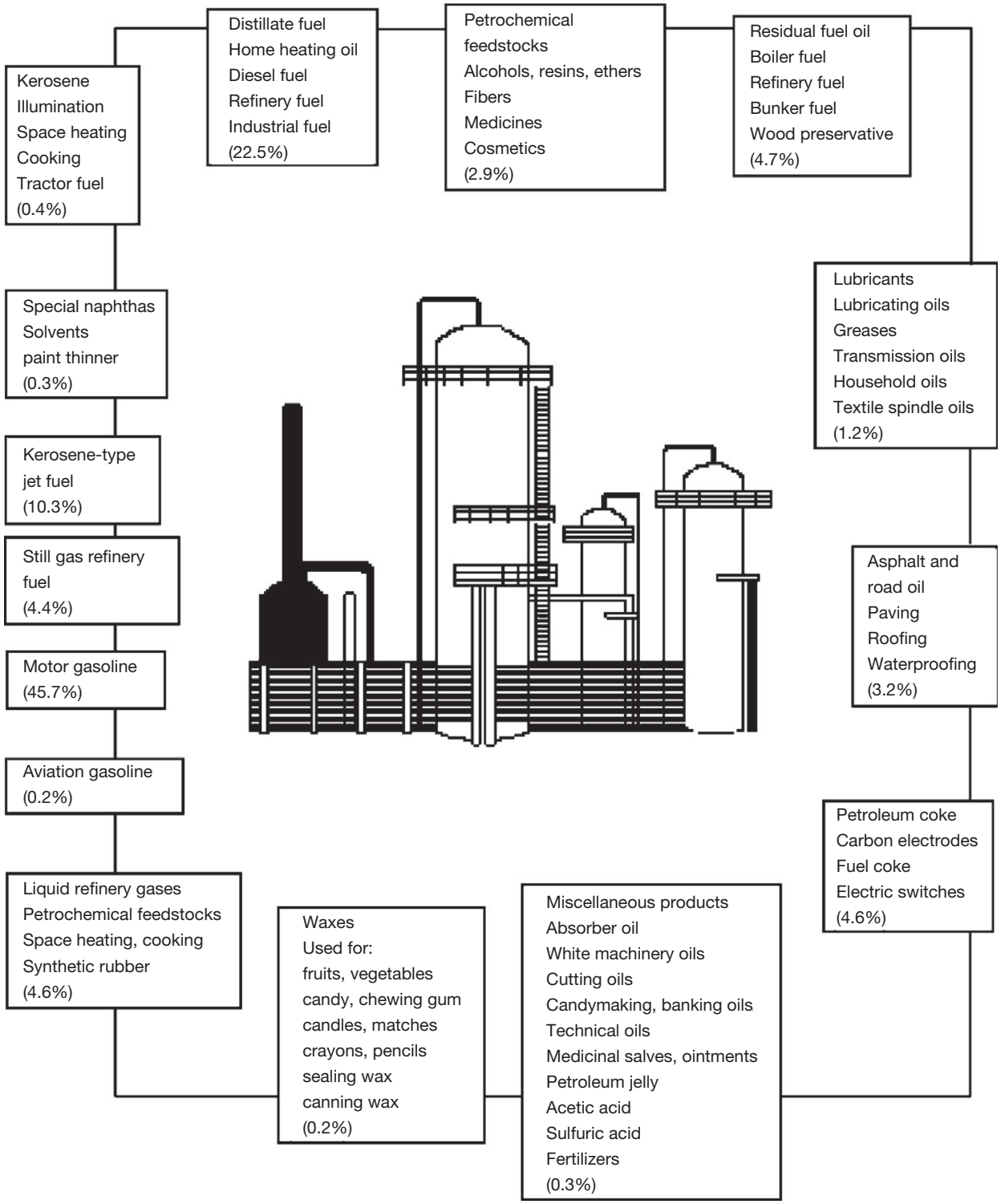

Figure 4 Petroleum products and uses. Reproduced from Energy Information Administration (1999). *Petroleum: An Energy Profile 1999*. DOE/EIA-0545(99), pp. 1–79. Washington, DC: Department of Energy.

for the major compound classes are shown in **Figure 6**. Benzene, toluene, xylenes, ethylbenzene, isopropylbenzene, naphthalene, and methyl- and dimethylnaphthalenes are among the most important volatile aromatic hydrocarbons because they are widely used and, once released into the environment, their mobility and toxicity make them a significant environmental threat (Merian and Zander, 1982). The occurrence of these compounds in the environment is almost exclusively anthropogenic, with the exception of natural hydrocarbon seeps.

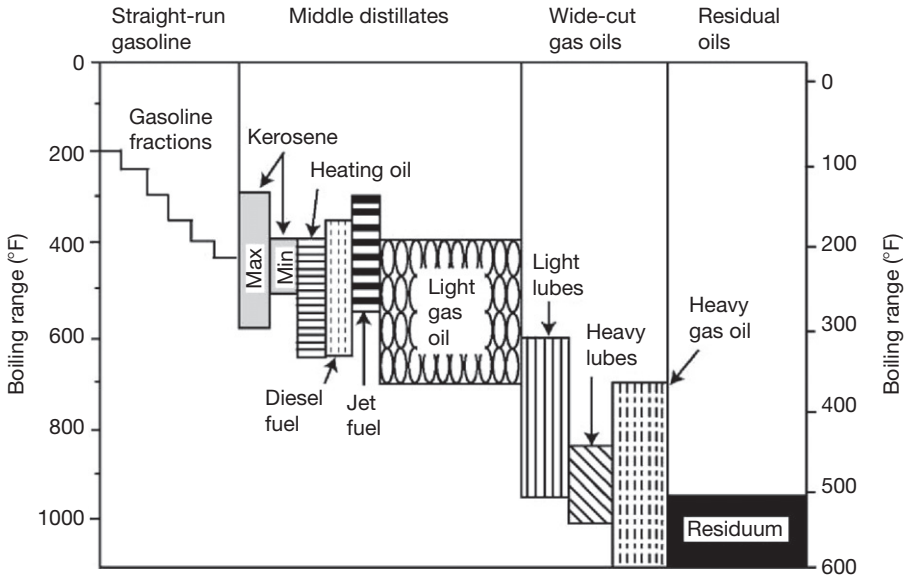

Figure 5 Common products obtained from crude oil distillation and cracking, and their boiling point range. Reproduced from National Research Council (1985). *Oil in the Sea: Inputs, Fates, and Effects*. Washington, DC: National Academy Press.

Table 2 Average composition of hydrocarbons in normal producible crude oils (% by weight of hydrocarbon)

Compound group	*Percentage*
n- + isoalkanes	33.3
Cycloalkanes	31.9
Aromatics	34.5
Saturated:aromatics	2.8
Alkanes:saturates	0.49

Source: Modified from Tissot BP and Welte DH (1984) *Petroleum Formation and Occurrence*. Berlin: Springer Verlag.
Total of 517 samples.

11.12.1.2.2 Fuels

Fuel products account for almost 90% of all the petroleum used in the United States. The leading fuel produced in the world is gasoline (Energy Information Administration, 1999). Because of its widespread use and the fact that it is composed of that fraction of crude oil with lower boiling points, gasoline is the single largest source of volatile hydrocarbons to the environment (**Table 3**). Motor gasoline comes in various blends with properties that affect engine performance. All motor gasolines are made of the relatively volatile components of crude oil.

Other fuels include distillate fuel oil (diesel fuel and heating oil), jet fuel, residual fuel oil, kerosene, aviation gasoline, and petroleum coke (**Figure 4**). In the petroleum refining process, heat distillation is used first to separate different hydrocarbon components. The lighter products are liquefied petroleum gases and gasoline, whereas the heavier products include heavy gas oils. Liquefied petroleum gases include ethane, ethylene, propane, propylene, *n*-butane, butylenes, and isobutane. Jet fuels are kerosene-based fuels that fall into the lighter distillate range of refinery output (**Figure 5**).

11.12.1.2.3 Fuel oxygenates

In the United States, passage of the 1990 Clean Air Act Amendments (CAAA) led to the development of Federal programs that required that oxygen-containing compounds be blended in gasoline to reduce carbon monoxide emissions. Examples of compounds used as oxygenates are MTBE, EtOH, ethyl *tert*-butyl ether (ETBE), *tert*-amyl methyl ether (TAME), and diisopropyl ether (DIPE) (Zogorski et al., 1997).

MTBE (chemical formula $C_5H_{12}O$) was the most common gasoline oxygenate before 2004 (**Figure 2**). MTBE use began in the 1970s as an octane booster to replace lead additives (Hogue, 2000), and, at that time, it was used in concentrations of 2–7% by volume in gasoline (Gullick and LeChevallier, 2000). As mandated by CAAA, gasoline used in metropolitan areas where carbon monoxide standards are not attained must contain not less than 2.7% oxygen by weight. By volume, this requirement corresponds to 14.8 and 7.3% for MTBE and EtOH, respectively. Gasoline oxygenated to this extent contains approximately 110 g of MTBE l^{-1}. As a result of its adoption as the primary oxygenate to satisfy the needs of the CAAA, MTBE increased in rank of use among organic chemicals produced from 39th in 1970 to 4th in 1998 (Thompson et al., 2000). The predominant use of MTBE as an oxygenate was because it was inexpensive to produce and had favorable blending characteristics with gasoline (Gullick and LeChevallier, 2000).

The USEPA established a drinking water health advisory of 20–40 μg l^{-1} MTBE in December 1997 (US Environmental Protection Agency, 1987).

In a sampling study of 1208 domestic wells in the United States, MTBE was the most frequently detected fuel oxygenate and the eighth most commonly detected VOC (Rowe et al., 2007). Perhaps the most publicized case of MTBE contamination of groundwater is the one involving public water supply wells in Santa Monica, California. In August 1995, the city of Santa Monica discovered MTBE in wells used for drinking water supply through routine analytical testing of well water.

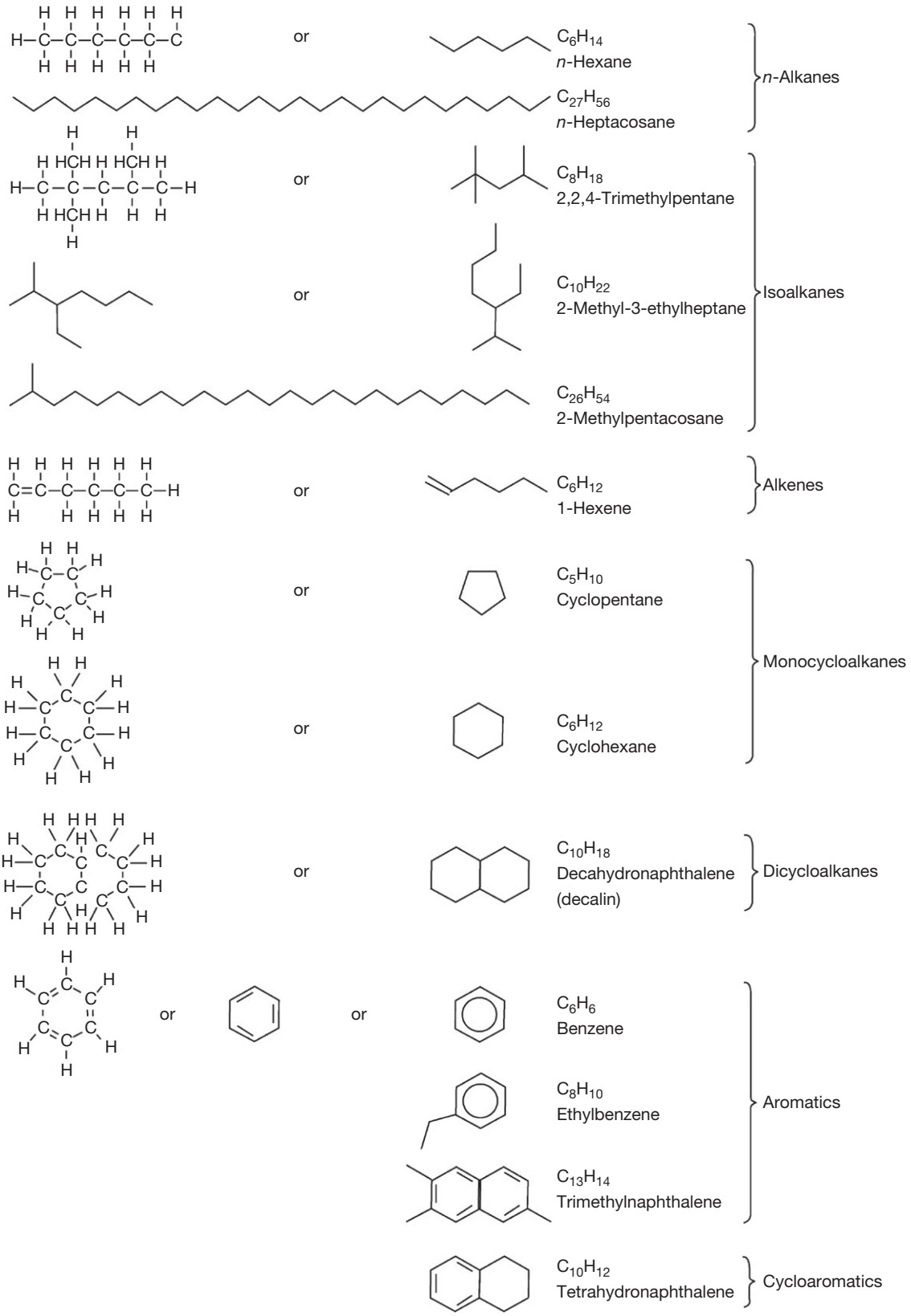

Figure 6 A sample of volatile hydrocarbons present in crude oil for the major compound classes, *n*-alkanes, isoalkanes, *n*-alkenes, cycloalkanes, aromatics, and cycloaromatics. Modified from Tissot BP and Welte DH (1984) *Petroleum Formation and Occurrence*. Berlin: Springer Verlag.

Table 3 Estimated composition of VOC emissions from gasoline evaporation at ambient air temperature

	Percentage
Alkanes	
Propane	1.0
n-Butane	17.0
Isobutane	7.0
n-Pentane	8.0
Isopentane	28.0
Hexane	20.0
Other alkanes $>C_6$	5.0
Alkenes	
Butene	3.0
Pentene	5.0
Other alkenes $>C_5$	3.0
Aromatic hydrocarbons	
Benzene	1.0
Toluene	1.5
Xylene	0.5

Source: Friedrich R and Obermeier A (1999) Anthropogenic emissions of volatile organic compounds. In: Hewitt CN (ed.) *Reactive Hydrocarbons in the Atmosphere*, pp. 1–39. San Diego, CA: Academic Press.

In 1996, levels of MTBE at the city's Charnock Wellfield rose to more than 600 $\mu g\,l^{-1}$ and, by 13 June 1996, all the five supply wells at the city's Charnock Wellfield were shut down because of persistent and increasing concentrations of MTBE contamination (US Environmental Protection Agency, 2000). The USEPA included MTBE on the Contaminant Candidate List in 1999 and, in 2000, initiated efforts to eliminate or limit the use of MTBE as a fuel additive (US Environmental Protection Agency, 2000). Since 2007, MTBE has not been used in the United States and ethanol has emerged as the primary replacement for MTBE in reformulated gasoline (**Figure 2**).

Due to the widespread occurrence of MTBE in groundwater, policymakers have recognized the need to consider the impact of fuel oxygenates on the environment (Powers et al., 2001). An assessment of the health and environmental impacts of the use of ethanol as a fuel oxygenate was conducted for the State of California by Lawrence Livermore National Laboratories and the University of California (California Environmental Policy Council, 1999). Ethanol can be released during production, storage, blending, distribution, and use (Rice et al., 1999). Due to the hygroscopic properties of ethanol-blended gasoline, ethanol and gasoline are received separately at gasoline distribution terminals and then are mixed as they are pumped into the tanker truck for delivery (McDowell et al., 2003; Rice et al., 1999). This can result in large spills of denatured ethanol that can lead to significantly higher ethanol concentrations in the subsurface than an ethanol-blended gasoline spill would cause (McDowell et al., 2003). For example, the 1999 ethanol release of 72 m^3 (19 000 gallon) at Pacific Northwest Terminal resulted in ethanol concentrations as high as 18 000 $mg\,l^{-1}$, which has been the subject of several studies (Beller et al., 2001; Buscheck et al., 2001; McDowell et al., 2003). Several laboratory, field, and modeling experiments assessing the fate of ethanol and, importantly, its impact on BTEX compounds, have occurred in the last decade (e.g., Chen et al., 2008b; Da Silva and Alvarez, 2002; Deeb et al., 2002; Lahvis, 2003b; Lovanh et al., 2002; Mackay et al., 2006) and are discussed further in **Section 11.12.4.2.3**.

11.12.1.2.4 Solvents, lubricants, and petrochemical feedstocks

The nonfuel use of petroleum is small compared with its fuel use. Nonfuel uses include solvents such as those used in paints, lacquers and printing inks, lubricating oils and greases, waxes used in candy making, packaging, and candles, petroleum jelly, asphalt, petroleum coke, and petrochemical feedstocks. Lubricating oils are complex mixtures containing linear and branched paraffins, cyclic alkanes, and aromatic hydrocarbons ($>C_{15}$ with boiling points between 300 and 600 °C) (Vazquez-Duhalt, 1989). As with all petroleum products, the exact nature of the chemical composition varies with the starting crude-oil composition and the refinery process. In general, lubricating oils are 73–80% aliphatic hydrocarbons, 11–15% monoaromatic hydrocarbons, and 4–8% polyaromatic and polar compounds. Motor oil can accumulate additional compounds, such as MTBE and BTEX, as it circulates through the engine (Chen et al., 1994).

Petrochemical feedstocks are used for the manufacture of chemicals, synthetic rubber, and a variety of plastics, and form the basis of synthetic fibers and drugs. Petrochemical feedstocks include solvents such as ethylene, propylene, butylenes, benzene, toluene, and xylenes. Large amounts of solvents are used in the chemical industry as reaction media, as a base for paints and thinners, and as propellants for sprays. The VOCs emitted as a result of solvent use are composed of a larger variety of species than those released from the use of fossil fuels (Friedrich and Obermeier, 1999). Depending on the product, the emissions of hydrocarbons during solvent use vary appreciably. The highest emissions of pure hydrocarbons come from adhesives, which release vapors containing typically about 20% by weight of pure toluene. With the exception of solvents, most products in this category largely contain the nonvolatile fraction of petroleum and therefore do not represent significant sources of volatile hydrocarbons to the environment.

11.12.1.3 Ecological Concerns and Human Exposure Pathways

The human exposure routes from hydrocarbons in the environment include inhalation, ingestion, and dermal absorption. The pathways of exposure can include direct contact with the hydrocarbon phase itself, inhalation of hydrocarbon vapors in indoor or outdoor air, and ingestion of contaminated food or water (**Figure 7**). Among children, ingestion of contaminated soils also is a potential concern (Calabrese et al., 1991). Ingestion of unintentional hydrocarbon contamination of food is rare and direct contact with hydrocarbons typically is limited to workers in the petroleum industry. Therefore, it does not appear to be a major risk for the general population (Daugherty, 1991).

Exposure to indoor hydrocarbon vapors can occur as a consequence of changes of land use from commercial or industrial to residential. Residual hydrocarbons in soils or groundwater may result in a chronic vapor exposure pathway. Analysis

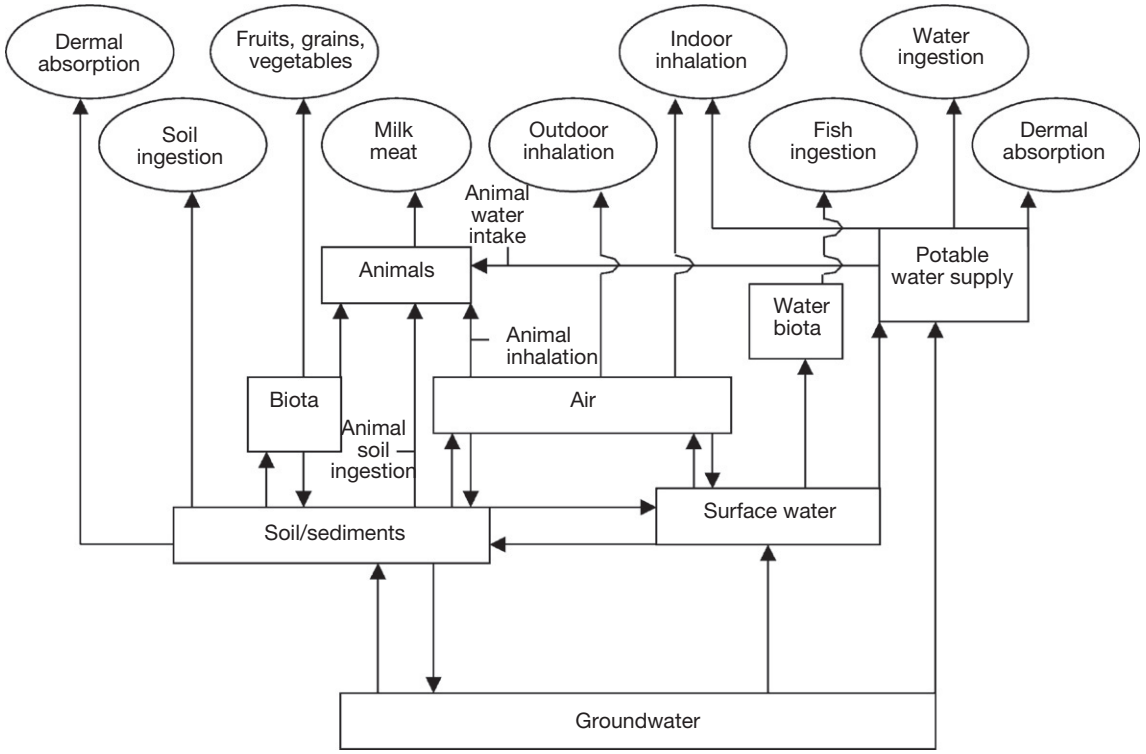

Figure 7 Modes of exposure to hydrocarbon contaminants. Reproduced from Kostecki PT and Calabrese EJ (1991) *Hydrocarbon Contaminated Soils and Groundwater: Analysis, Fate, Environmental and Public Health Effects, Remediation*. Chelsea, MI: Lewis Publishers.

of risk associated with exposure to hydrocarbons is typically undertaken in a multistep approach known as risk assessment. A thorough discussion of the use of risk assessment at contaminated sites is provided in **Chapter 11.1**. Assessing risks posed by hydrocarbon spills or wastes is complex and involves estimates of chemical concentrations at each potential exposure point, identification of the potential populations that may be exposed, and assessment of exposure pathways, intake rates, and the toxicity of the chemicals of concern.

Determining a safe level of exposure to petroleum hydrocarbons is a difficult process because petroleum is a complex mixture of thousands of compounds with varying degrees of toxicity to human health and the environment (Miller et al., 2000). No toxicity data are available for the vast majority of these compounds. Evaluation of the potential impact of petroleum released into the environment is complicated further by the fact that the composition of the released hydrocarbons changes over time because of natural degradation processes. One approach to assess the potential health effects of hydrocarbon exposure is to first use the entire complex mixture in a battery of short- and long-term toxicological tests to determine the combined toxicity of the complex mixture. Unfortunately, these data are not available for most petroleum products. Toxicity data on whole mixtures of petroleum products are only available for gasoline, jet fuel, and mineral oil. No whole mixture toxicity data are available for crude petroleum or drilling fluids or cuttings (Miller et al., 2000). A major shortcoming with the whole mixture approach is that once in the environment, the parent product separates into fractions based on differences in individual environmental transport characteristics (Miller et al., 2000). Because of these differences in transport characteristics, the mixture to which a receptor is exposed will vary in space and time. Thus, toxicity data on the original product will not necessarily reflect the toxicity of the product once it is released into the environment.

Specific toxicity data are available for only about 95 individual hydrocarbons of the over 1000 components of petroleum, and only 25 have sufficient toxicological data to develop exposure criteria (Miller et al., 2000). One approach to estimating exposure effects for a complex petroleum mixture is to base the estimates on the 25 compounds for which toxicity data exist. Individual toxicity data are largely available for the more toxic compounds and, thus, this approach may be overly conservative for more complex mixtures of petroleum, although the importance of simultaneous exposure to the multiple components of petroleum is largely unknown. Toxicological studies generally divide petroleum into fractions based on structure (such as aromatic or aliphatic) and molecular weight. Compounds greater than C_{38} are not considered bioavailable by dermal or oral routes (Miller et al., 2000). Indicator compounds are used to represent the toxicity of each fraction and different cleanup criteria are developed for each petroleum fraction. Most evaluations of the health effects of contamination consider single-point sources and there is little understanding of the effect of multiple points of exposure over time. Assessment of cumulative exposure risks is especially important for nonpoint sources of contamination that may result in longer term exposure.

Of most concern among the volatile fuel hydrocarbons from a human health perspective is benzene, a known

carcinogen. Alkenes and alkylbenzenes are considered more toxic than alkanes (Oestermark and Petersson, 1993). All alkenes are potentially genotoxic because of metabolic formation of epoxides (Oestermark and Petersson, 1993). Of particular concern are ethene and 1,3-butadiene. Although alkanes are generally considered less toxic than alkenes or alkylbenzenes, hexane is a known neurotoxin (Perbellini et al., 1980). Calabrese and Kenyon (1991) report on the toxicological assessment of numerous volatile hydrocarbons including benzene, toluene, ethylbenzene, xylenes, and *n*-hexane.

11.12.2 The Petroleum Industry

11.12.2.1 Petroleum Exploration, Production, and Processing

During petroleum exploration and production operations, hydrocarbons can be released to the environment by spillage of the crude oil itself or by the release or disposal of waste generated during the exploration and production process. The main categories in the petroleum refining process include separation (e.g., distillation), conversion (e.g., thermal cracking, alkylation), treatment (e.g., hydrosulfurization), and blending (Friedrich and Obermeier, 1999). Many of these processes release volatile hydrocarbons directly to the atmosphere with additional releases to the atmosphere and geosphere occurring because of leaks from equipment and spills.

The techniques needed to remove or extract crude oil from the Earth vary depending on the type of rock the oil is found in (such as sandstone or limestone) and its porosity and permeability. Oil is typically removed from the subsurface by onshore and offshore wells drilled into petroleum-bearing formations. The petroleum underground is usually under great pressure and will, therefore, flow into the lower pressure environment created by the open well. With high enough pressure, the oil will flow up through the well. Many wells, however, especially those that have been in production a long time (tens of years), require artificial lift methods, or pumping, because pressure within the reservoir is insufficient to lift the oil to the surface. When oil no longer flows sufficiently using these methods, secondary and tertiary, or enhanced recovery, methods are used. These methods may use water, gases, or other chemicals to flush the oil out of the rock, or use heat to thin the oil and increase its flow rate. These methods produce not only crude oil but also water or other chemical wastes that contain hydrocarbons.

In terms of volume and toxicity, drilling fluids and drill cuttings are among the most significant waste streams from exploration and development activities in the oil and gas industry (US Environmental Protection Agency, 1987). The composition of drilling fluids is complex and varies depending upon the specific down-hole conditions such as the geology of the formation. A major part of the undiscovered oil and natural gas resources outside the Middle East lie in offshore areas (US Geological Survey, 2000). In 1999, over 150 countries had some type of drilling or production operations offshore (Jones et al., 2000). Cuttings, the geological core materials brought to the surface by the drilling fluids, primarily are formation rock along with drilling fluids that adhere to their surface. Cuttings are typically disposed of by either discharge to the sea, hauled to shore for disposal, or injection back into the formation (Jones et al., 2000). The volume of cuttings generated can be 4–5 times more than the borehole volume because of excessive caving of formations into the borehole.

Produced water is the aqueous phase separated from recovered hydrocarbons produced during oil well production, and injection water used to maintain pressure in the reservoir. Over the life of an oil field, the volumes and composition of produced water vary greatly. Produced water discharges are continuous and represent the largest volume waste stream in production operations (Stephenson, 1992). The quantity discharged at any particular treatment facility depends on the number of wells handled by that facility. The discharge rates range from less than 500 bbl day^{-1} (7.9×10^4 l day^{-1}; most of the platforms in the Gulf of Mexico) to over 600 000 bbl day^{-1} (9.5×10^7 l day^{-1}; three production-processing platforms in the South Java Sea).

Drilling fluids can be water-based fluids (WBFs), oil-based fluids (OBFs), and synthetic-based fluids (SBFs). An OBF has diesel, mineral oil, or some other oil as its continuous fluid phase. Although wells drilled with OBF technology produce less waste volumes than those drilled with WBFs, they contain priority pollutants and have far greater toxicity. In many cases offshore, this waste is barged to shore for land disposal or recycled because of restrictions on offshore discharge. Despite their unique and valuable properties, the use of OBF is declining because of the added cost of barging waste fluids to shore and the development of more attractive alternatives such as SBFs (Jones et al., 2000).

Drilling and production discharges to the marine environment present different environmental concerns than those in onshore areas. Discharge of OBF cuttings poses the most severe environmental impact on the seafloor of the three fluid types. On the seafloor, OBF cuttings can increase oil in the sediments and decrease biological abundance and diversity of immobile bottom-dwelling organisms (Hartley and Watson, 1993). The overall effect of an OBF cuttings discharge is, in part, determined by the concentration of the oil remaining on the cuttings and its toxicity. In zones severely affected by OBF cuttings discharge, the rate of recovery depends upon the energy level of the environment and the seafloor ecology. At many North Sea drilling sites, cuttings are found in large piles 100–150 ft (30–46 m) high and 200 ft (61 m) across on the seafloor (Jones et al., 2000). Studies on the impact of oil wet cutting discharges in the oceans have been conducted for several decades. Benthic studies around offshore platforms using oil-based drilling muds have shown that the greatest disturbances are near the platform. Davies et al. (1984, 1989) found that within 500 m of the platform, hydrocarbon levels reached 10^1–10^5 times the background levels. Addy et al. (1984) discovered that the effects of drilling discharges were most severe with diesel-based muds followed by mineral oils, and the lowest effects were with water-based muds. Hydrocarbon inputs into the world's oceans have been the subject of various National Research Council (NRC) reports focusing on the sources, fate, and effects of these hydrocarbons (National Research Council, 1985, 2003).

The above discussion focuses on petroleum releases associated with the wastes typical of offshore operations. Larger releases of crude oil can occur due to accidents. A high profile, newsworthy, offshore petroleum release is the 2010 Deepwater

Horizon blowout in the Gulf of Mexico, which is thought to be the largest accidental marine oil spill in the history of the petroleum industry. Following an accident on board the Deepwater Horizon rig on 20 April 2010, an estimated 7.0×10^5 m^3 of oil (Crone and Tolstoy, 2010) was released before the flow was capped on 15 July 2010, resulting in the presence of a continuous plume of petroleum hydrocarbons more than 35 km in length at approximately 1100 m depth for several months (Camilli et al., 2010). The disaster has already resulted in several studies assessing the fate of the dispersed oil, in particular the response of native microorganisms to the hydrocarbons (Camilli et al., 2010; Hazen et al., 2010; Valentine et al., 2010).

A substantial number of investigations of the surface water and groundwater impacts of onshore produced-water releases have been conducted in the United States since the 1960s. Much of the focus has centered on the effect of the high concentrations of salts in oil field brines on soil fertility and erosion, vegetation health, and groundwater quality. It is estimated that there are nearly 683 square miles (1769 km^2) of brine-impacted soil in the state of Texas alone (McFarland et al., 1987). Evaluating the effect of nearly 3.5 million oil and gas wells drilled in the conterminous United States since the early 1800s is complicated in that there is no systematic collection of information at the state or national scale describing past produced-water releases either with regard to location or volumes of water released. Evaluation of aquifer or watershed susceptibility to this source is being investigated by the USGS using geographic information system (GIS) techniques (Otton and Mercier, 2000). The USGS (Breit et al., 2000) reviewed data from 77 650 archived records of water samples, and developed a database with internal consistency that may be useful for assessing the general patterns related to the chemical compositions of formation waters from different geologic settings (http://energy.cr.usgs.gov/prov/prodwat/). This database provides useful information on inorganic chemical species present in the oil field brines, but no such effort has yet been undertaken to compile a comprehensive database of the dissolved hydrocarbon concentrations in these waters, so the potential cumulative effect of this source on the environment is largely unknown. In addition, the USGS is conducting the Osage–Skiatook Petroleum Environmental Research Project to study the transport, fate, natural attenuation, and impacts produced by water contaminants at two study sites in Oklahoma (http://energy.cr.usgs.gov/health_environment/produced_waters/osage_more.html). A better understanding of the extent and fate of produced-water releases is necessary to ensure that appropriate remediation strategies are developed.

Other sources of pollution during oil exploration and production are evaporative losses of hydrocarbons, estimated at 45–68 million ton year^{-1} (Merian and Zander, 1982) and the catastrophic release of crude oil because of accidents such as well-site explosions. Evaporative losses during production of crude oil largely result in the release of *n*-alkanes up to C_8 (octane) into the atmosphere (Friedrich and Obermeier, 1999). During petroleum processing, the major sources of VOC emissions to the atmosphere are vacuum distillation (0.05 kg of VOC emissions m^{-3} of refinery feed), catalytic cracking (0.25–0.6 kg of VOC m^{-3} of feed), coking (0.04 kg of VOC m^{-3} of feed), chemical sweetening, and asphalt blowing (27 kg of VOC per ton of asphalt).

11.12.2.2 Petroleum Transportation and Storage

Transportation of crude oil and petroleum products occurs predominantly by tanker, pipeline, railway tank cars, and tank trucks, whereas storage occurs largely in surface or underground tanks and in underground caverns. The distribution and storage of crude oil and refined products result in releases of significant amounts of hydrocarbons to the atmosphere, surface waters, soils, and groundwater. Groundwater contamination by crude oil, and other petroleum-based liquids, is a particularly widespread problem. An estimated average of 83 crude oil spills occurred per year during 1994–1996 in the United States, each spilling about 50 000 bbl (7.9×10^6 l) of crude oil (Delin et al., 1998). The USEPA estimates that there are approximately 607 000 active USTs (at approximately 221 000 sites), which are regulated by the UST technical regulations (as of March, 2010, http://www.epa.gov/oust/pubs/ustfacts.pdf). As of September, 2010, the USEPA confirmed gasoline release from 494 997 USTs, of which 93 123 still require cleanup (http://www.epa.gov/oust/pubs/ustfacts.pdf). Leaking underground storage tanks (LUSTs) pose a significant threat to groundwater quality in the United States (http://www.epa.gov/oust/aboutust.htm) and have resulted in a significant impact on environmental health and safety.

Atmospheric emissions of volatile hydrocarbons from this sector of the petroleum industry have been summarized by Friedrich and Obermeier (1999). Gasoline, because it contains components with a high volatility, is the most important source of VOCs to the atmosphere during petroleum handling and storage. VOCs released into the atmosphere can undergo photochemical reactions with nitrous oxides in the atmosphere, producing ground-level ozone, or photochemical smog, as described in more detail in **Chapter 11.11**. The estimated composition of VOC emissions because of evaporation of gasoline is given in **Table 3**.

Seaports handle large amounts of petroleum products and have facilities on site to store these products. At the Port of Los Angeles alone, for example, there are approximately 500 above-ground storage tanks with a capacity to hold 500 million gallons (1.9×10^9 l) of product (Rice, 1991). Although the lasting effects of oil spills on the open seas may be less than the effect of the many subsurface leaks and spills of petroleum products or the atmospheric pollution caused by the use of petroleum products, oil spills on the open seas create a major public policy impact because they spread rapidly and provide powerful visual images. According to Williams (1991) and Wolfe et al. (1994), after being relatively quiet in the 1980s, the American environmental movement was revitalized by the massive and well-publicized oil spill from the *Exxon Valdez* oil tanker. The publicized images of environmental devastation had a galvanizing effect on the causes of environmental organizations.

Pipelines usually are used to transport crude oil from the exploration and discovery site to the refinery location, as well as to transport petroleum products to end users. Crude oil travels through pipelines under pressure at speeds up to 6 miles per hour. Pipeline breaches can result in explosive releases of crude oil or petroleum products. One of the better studied onland hydrocarbon spills occurred near Bemidji, Minnesota, in 1979, when the land surface and shallow subsurface were

contaminated following a crude oil pipeline burst that spilled approximately 1.7×10^6 l (about 10 700 bbl) of crude oil onto a glacial outwash deposit (Baedecker et al., 1993; Delin et al., 1998; Eganhouse et al., 1993; Essaid et al., 2011). Crude oil sprayed on the land surface covering an area estimated at 7500 m^2 (Delin et al., 1998) and percolated through the unsaturated zone to the water table near the rupture site. Some of the sprayed oil also flowed over the surface toward a small wetland. Groundwater contamination by aromatic hydrocarbons resulted from this spill, as well as contamination of the sediments and unsaturated zone soil gas.

Among the approximately 600 000 USTs that are subject to Federal regulation, releases have been confirmed at 494 997 of the sites (http://www.epa.gov/oust/pubs/ustfacts.pdf). It has been estimated that about 95% of USTs store petroleum fuels (Lund, 1995) and that gasoline usage represents approximately 80% of the volume of motor fuel consumption (Zogorski et al., 1997). The UST problem, therefore, is largely one of gasoline released to the subsurface. MTBE is much more water-soluble (50 000 mg l^{-1}) than the BTEX compounds (ranging in solubility from 1780 for benzene to 152 mg l^{-1} for ethylbenzene) and was present in oxygenated gasoline in larger amounts than the BTEX compounds. Therefore, when oxygenated gasoline containing MTBE spilled, MTBE was the principal compound in groundwater on a mass basis, which, coupled with its high solubility and low biodegradability (relative to volatile hydrocarbons), led to it posing the greatest threat for groundwater contamination from leaking USTs (Shih et al., 2004). As the use of ethanol as a fuel oxygenate increases, it is possible that BTEX compounds will become the greatest problem from UST leaks in the future (Chen et al., 2008b). Ethanol itself is not anticipated to reach high concentrations as it is rapidly consumed by native bacterial populations found in the environment (Dakhel et al., 2003; Suflita and Mormile, 1993; Zhang et al., 2006). The impact of petroleum and MTBE releases in the subsurface on groundwater quality and restoration of contaminated aquifers have been the subject of numerous books and reviews (e.g., Alvarez and Illman, 2006; Farhadian et al., 2008; Rosell et al., 2006; Shih et al., 2004; Vandecasteele, 2008).

11.12.2.3 Petroleum Usage

Worldwide petroleum consumption rose from about 21 million bpd (3.4×10^9 l day^{-1}) in 1960 to about 86 million bpd (1.4×10^{10} l day^{-1}) in 2008. The United States is the largest consumer and accounts for approximately 23% of this consumption, consuming 19.5 million bpd (3.1×10^9 l day^{-1}) in 2008 (Energy Information Administration, 2010a). The equivalent of approximately 8.5 million bpd (1.4×10^9 l day^{-1}) is consumed as gasoline in the United States by the transportation sector annually, which resulted in a peak usage of approximately 13 million gallons day^{-1} (4.9×10^7 l day^{-1}) of MTBE in 1999 (Energy Information Administration, 2000).

Petroleum usage has impacted water and air quality. Urban runoff as a source of petroleum to the marine environment has been well documented (Eganhouse and Kaplan, 1981; Latimer et al., 1990). It is estimated that anthropogenic hydrocarbon emissions to the atmosphere total 103 Tg of carbon $year^{-1}$, of which 21% is associated with transportation activities (Kansal, 2009). In urban atmospheres, the composition of volatile aromatic hydrocarbons has been found by numerous investigators to be similar to that of gasoline, indicating gasoline as a source (Merian and Zander, 1982). A study of 39 US cities reported that median concentrations of BTEX in air were 12.6 ppb benzene, 33.8 ppb toluene, 5.9 ppb ethylbenzene, 18.1 ppb *m*- and *p*-xylene, and 7.2 ppb *o*-xylene (Seila et al., 1989). Worldwide, the estimated contribution to the atmosphere from evaporation of motor fuels alone is roughly 100 000 ton benzene, 50 000 ton toluene, and 15 000 ton higher aromatics per year (Merian and Zander, 1982). Incomplete combustion of fossil fuels also can lead to the emission of hydrocarbons and other gases into the atmosphere. Emissions from internal combustion engines include significant amounts of alkanes such as methane, butane, and isobutane; alkenes such as ethene, propene, and isobutene; and aromatics such as benzene, toluene, xylenes, and ethylbenzene (Friedrich and Obermeier, 1999). In the transportation sector, two-stroke engines, such as in mopeds, release the highest amounts of VOCs to the atmosphere, whereas gasoline engines equipped with three-way catalysts have the lowest emissions of VOCs.

Moran et al. (2005) reviewed the occurrence and distribution of MTBE and gasoline hydrocarbons in samples of groundwater collected by the USGS's NAWQA program and found that the probability of detecting MTBE was only weakly related to the density of leaking USTs. This suggests that more research is needed to understand the sources and transport of MTBE to groundwater (Moran et al., 2005; State of Maine Bureau of Health, 1998). Scavenging and deposition of atmospheric VOCs (Goldstein and Galbally, 2007) can also be a nonpoint source of contamination to groundwater resources (Pankow et al., 1997). For example, during peak MTBE usage, concentrations of MTBE in the atmosphere above urban areas were sufficiently high to cause its detection in groundwater at concentrations of 0.1 μg l^{-1} or less (Baehr et al., 1999). In their study of Southern New Jersey groundwater quality, USGS researchers (Baehr et al., 1999; Stackelberg et al., 1997) compared atmospheric concentration data of MTBE and other VOCs over a 2 year period. Among the VOCs most frequently detected in groundwater (trichloromethane (chloroform), MTBE, 1,1,1-trichloroethane (TCA), and tetrachloroethane (PCE)), atmospheric concentrations of MTBE alone were sufficiently high to cause detection in water samples. It was concluded that the presence of VOCs (other than MTBE) resulted from nonatmospheric sources, whereas the atmospheric source of MTBE potentially could cause detection at the 0.1 μg l^{-1} concentration, provided MTBE was not degraded in the unsaturated zone (Baehr et al., 2001). Atmospheric concentrations of MTBE are being monitored and will decrease with its elimination from gasoline (CEPA Air Resources Board, 1999). Coincidentally, atmospheric emissions of ethanol are expected to increase as it is added to reformulated gasoline. The substitution of ethanol for MTBE is not expected to have a significant impact on air quality and VOC emission estimates (CEPA Air Resources Board, 1999).

Table 4 Pathways relevant to the phase transfer of compounds from petroleum product sources to environmental compartments by partition processes

Transfer from	*Examples*	*Transfer to*	*Process*
Free product	Gasoline, jet fuel, diesel fuel, crude oil, heating oil, motor oil, lubricants	Water	Solubilization
		Air	Volatilization
		Solid phases	Sorption
Water	Ocean, estuary, river, lake, precipitation, unsaturated-zone moisture, groundwater	Air	Volatilization
		Solid phases	Sorption
Air	Atmosphere, unsaturated-zone gas	Water	Dissolution
		Solid phases	Sorption
Solid phases	Atmospheric particles, soil organic matter, suspended sediment, aquifer solids, biota	Water	Desorption
		Air	Volatilization

11.12.2.4 Disposal of Petroleum Wastes

Fuels and heating oils are intended to be consumed during usage with little or no waste produced aside from gases released into the atmosphere. One exception is used motor oil that is disposed of in landfills or down storm drains and can be a source of groundwater contamination. Bjerg et al. (Chapter 11.16) evaluate the landfill as a source of volatile hydrocarbons to groundwater and present the concentrations typically found in leachate-impacted aquifers. Used motor oil (as discussed in Section 11.12.1.1), which contains BTEX and MTBE from interaction with gasoline during use, also presents a major environmental problem from improper disposal, partly because it is so widely used and handled. Almost 60% of the motor oil used in the United States is utilized by vehicle owners changing their own oil and the USEPA estimates that over 200 million gallons of used oil are improperly disposed of each year in the United States (http://www.epa.gov/wastes/conserve/materials/usedoil/oil.htm#facts).

11.12.3 Environmental Transport Processes

The presence of petroleum compounds through the environment is initiated by product usage and the partitioning of compounds from the initial product to multiple phases in the environment. Exposure pathways are then established because the compounds are transported within the bulk fluid phases of the atmosphere and hydrosphere or as solid phases in the case of suspended sediment or biota. Phase partitioning of petroleum and fuel oxygenates and the physical transport processes that affect them are discussed in Sections 11.12.3.1 and 11.12.3.2, respectively.

11.12.3.1 Phase Partitioning

The phases relevant to the transfer of compounds from petroleum product sources and the processes by which these transfers occur are listed in Table 4. The product phase usually is an organic liquid; however, compressed gases and waste slurries are examples of gaseous and aqueous phase sources, respectively. When the product is released, the primary factor governing the rate of mass transfer of product constituents to the environment is the concentration of the constituents at phase interfaces. Models of chemical equilibrium are used to estimate these concentrations. For example, if the product is liquid and immiscible in water, then the equilibrium concentrations at the product and aqueous phase interface (product–aqueous phase equilibrium), by the process of solubilization (Table 4), is expressed as:

$$C_k = \gamma_k \chi_k C_{\text{sol}} \qquad [1]$$

where C_k is the aqueous phase concentration of the kth constituent, C_{sol} is the solubility of the constituent (g cm^{-3}), γ_k is the activity coefficient, and χ_k is the mole fraction of the compound in the product (organic liquid) phase. The index k identifies the constituent in a product consisting of N compounds ($k = 1, 2, 3, \ldots, N$). If the product consists of a nearly pure compound (e.g., reagent grade benzene), then $\gamma_k \chi_k \rightarrow 1$. Eqn [1] is used to determine equilibrium between free product (the nonaqueous phase petroleum) and dilute aqueous phases in terms of pure compound properties (solubility) adjusted for the composition of the product (mole fraction). The activity coefficient reflects the effect of phase composition on the equilibrium relation (nonideal behavior). If $\gamma_k \approx 1$, then eqn [1] reduces to Raoult's law, which states idealized behavior in both phases. Raoult's law provides a working approximation for predicting the level of water contamination. Solubilities and other properties for select compounds are listed in Table 5. The list provides a comparison between the different classes of compounds. More comprehensive lists of properties are provided in the cited references. The Chemical Abstracts Service (CAS) number reported is useful when using online databases (e.g., Syracuse Research Corporation, Web site: http://srcinc.com/what-we-do/environment.aspx). The temperature dependence of solubility is generally neglected at Earth's surface and near-surface temperatures.

The cosolvent effect is the term commonly used to identify nonideal behavior involving aqueous/immiscible phase equilibrium. The effect can result in higher aqueous concentrations ($\gamma_k > 1$) than those predicted by Raoult's law. For traditional fuels and other petroleum products discussed here, the cosolvent effect is negligible because the total concentration in the aqueous phase is on the order of 100 mg l^{-1} (about 0.01%

Table 5 Solubilities and other properties of select petroleum hydrocarbons and fuel oxygenates

	Formula	*CAS number*	*Molecular weight, w_k (g mol^{-1})*	*Specific volume, v_k at 25 °C (cm^3 g^{-1})*	*Solubility, C_{sol} at 25 °C (mg l^{-1})*	*Vapor pressure p at 25 °C (atm)*	*Henry H_k at 25 °C*	*Octanol/water log_{10} K_{OW}*
Aromatic hydrocarbons (Mackay et al., 1992a,b, 1993)								
Benzene	C_6H_6	71-43-2	78.1	1.14	1780	0.125	0.225	2.13
Methylbenzene (toluene)	C_7H_8	108-88-3	92.1	1.15	515	0.038	0.274	2.69
1,4-Dimethylbenzene (*p*-xylene)	C_8H_{10}	106-42-3	106.2	1.16	185	0.012	0.271	3.18
1,2-Dimethylbenzene (*o*-xylene)	C_8H_{10}	95-47-6	106.2	1.14	175	0.012	0.286	3.15
1,3-Dimethylbenzene (*m*-xylene)	C_8H_{10}	108-38-3	106.2	1.13	159	0.011	0.296	3.20
Ethylbenzene	C_8H_{10}	100-41-4	106.2	1.15	152	0.013	0.358	3.13
Isopropylbenzene	C_9H_{12}	98-82-8	120.2	1.16	61	0.006	0.485	3.63
1,2,4-Trimethylbenzene	C_9H_{12}	95-63-6	120.2	1.14	57	0.003	0.230	3.60
n-Propylbenzene	C_9H_{12}	103-65-1	120.2	1.16	52	0.004	0.420	3.69
n-Butylbenzene	$C_{10}H_{14}$	104-51-8	134.2	1.16	15	0.001	0.494	4.26
Alkanes								
n-Butane	C_4H_{10}	106-97-8	58.1	1.73	61.4	2.398	92.8	–
n-Pentane	C_5H_{12}	109-66-0	72.2	1.6	38.5	0.675	51.7	3.45
n-Hexane	C_6H_{14}	110-54-3	86.3	1.52	9.5	0.199	74.0	4.11
n-Heptane	C_7H_{16}	142-82-5	100.2	1.46	3	0.060	82.3	5.00
n-Octane	C_8H_{18}	111-65-9	114.2	1.42	0.7	0.018	118.5	5.15
Alkenes								
1-Butene	C_4H_8	106-98-9	56.1	1.68	222	0.293	3.0	–
1-Pentene	C_5H_{10}	109-67-1	70.1	1.56	148	0.839	16.2	2.2
1-Hexene	C_6H_{12}	592-41-6	84.2	1.49	50	0.245	16.8	3.39
2-Heptene	C_7H_{14}	592-77-8	98.2	1.43	15	0.064	17.0	–
1-Octene	C_8H_{16}	111-66-0	112.2	1.4	2.7	0.023	38.9	4.57
Cycloalkanes								
Cyclopentane	C_5H_{10}	287-92-3	70.1	1.34	156	0.418	7.7	–
Cyclohexane	C_6H_{12}	110-82-7	84.2	1.29	55	0.125	7.8	2.86
Methylcyclohexane	C_7H_{14}	108-87-2	98.2	1.3	14	0.061	17.5	–
Propylcyclopentane	C_8H_{16}	2040-96-2	112.2	1.3	2	0.016	37.1	–
Ethers (oxygenate additives) (Zogorski et al., 1997)								
Methyl *tert*-butyl ether (MTBE)	$C_5H_{12}O$	1634-04-4	88.2	1.34	50 000	0.329	0.024	1.20
Ethyl *tert*-butyl ether (ETBE)	$C_6H_{14}O$	637-92-3	102.2	1.37	26 000	0.200	0.032	1.74

(*Continued*)

Table 5 (Continued)

	Formula	*CAS number*	*Molecular weight*, w_k *(g mol^{-1})*	*Specific volume*, v_k *at 25 °C (cm^3 g^{-1})*	*Solubility*, C_{sol} *at 25 °C (mg l^{-1})*	*Vapor pressure* p *at 25 °C (atm)*	*Henry* H_k *at 25 °C*	*Octanol/water* log_{10} K_{OW}
tert-Amyl methyl ether (TAME)	$C_6H_{14}O$	994-05-8	102.2	1.3	20 000	0.090	0.019	–
Diisopropyl ether (DIPE)	$C_6H_{14}O$	108-20-3	102.2	1.35	9000	0.197	0.092	1.52
Ethanol (Deeb et al., 2003; Lahvis 2003b)	C_2H_6O	64-17-5	46.07	0.787	miscible	0.078	0.00024	−0.31

The Henry coefficient is obtained from the solubility and vapor pressure data from this table as follows: $H_k = (w_k p/RT)/C_{sol}$. Other values are provided in **Table 6**

hydrocarbons). This mixture is dilute enough so that the hydrocarbon solutes do not appreciably interact. Activity coefficients can be calculated using the Universal Functional Activity Coefficient (UNIFAC) method (Fredenslund et al., 1975). The high concentrations of fuel oxygenates like MTBE and ethanol in groundwater at spill sites have raised the question as to whether or not they could increase aqueous concentrations of the BTEX group via the cosolvent effect (Chen et al., 2008a; Powers et al., 2001; Zogorski et al., 1997). It has been shown that the cosolvency effect arises only when the cosolvent is present in water at 1% (10 000 mg l^{-1}) or higher (Pinal et al., 1990, 1991). These concentrations are much higher than typically would be encountered in the environment. For example, gasoline that contains 15% MTBE by volume, when equilibrated with water, results in no more than 7500 mg l^{-1} (approximately 0.75%) of MTBE in water (Barker et al., 1991). No cosolvency effect for BTEX was noted for gasolines containing any of the following compounds and volume percentages: 15% MTBE, 10% EtOH, 10% TAME, and 10% isopropyl alcohol by volume (Barker et al., 1991; Poulsen et al., 1992). In experiments with MeOH, no cosolvency effect was noted until the MeOH concentrations in water exceeded 8% by volume, at which point aqueous BTEX concentrations increased in proportion to increasing methanol content of the aqueous phase (Barker et al., 1991; Poulsen et al., 1992).

When ethanol is used in a gasoline as an oxygenate, its volume tends to be ≤10% (McDowell et al., 2003). Gasoline with ethanol added at 10% or less is referred to as gasohol (McDowell et al., 2003). While this concentration will not result in cosolvency effects, questions have been raised about the effects that higher ethanol concentrations, such as the 85% ethanol in E85 fuel, may have on BTEX compounds. Chen et al. (2008a) suggest that ethanol concentrations high enough to increase the solubility of BTEX are likely to occur only at the interface between nonaqueous-phase liquid (NAPL) and groundwater, but note that the cosolvent effect of E85 could be significant. In addition, denatured ethanol can be spilled during blending of gasoline and ethanol (McDowell et al., 2003; Rice et al., 1999) and can come into contact with existing BTEX contamination (McDowell et al., 2003). Studies at the Pacific Northwest Terminal, where 72 m^3 of ethanol was released into an existing hydrocarbon plume, indicate that ethanol reduced the surface and interfacial tension and resulted in a significant change in the size, shape, and saturation of the existing gasoline pool (McDowell et al., 2003).

Crude oil and its derived products are mixtures of many types of compounds. Although knowledge of the exact composition of a product is needed to make equilibrium calculations, this information generally is unavailable because product quality is based on engineering specifications like octane number and not on a specific composition. Furthermore, many compounds of interest are present in products in small quantities: therefore, estimates for χ_k can be off by multiples, resulting in inaccurate equilibrium concentration prediction. Approximations to χ_k, however, can be made given some knowledge of product composition for the purpose of estimating the magnitude of equilibrium concentrations. The mole fraction is defined in terms of concentration in the product phase as:

$$\chi_k = \frac{I_k/w_k}{\sum_{j=1}^{N}(I_j/w_j)} \quad \text{definition of mole fraction} \qquad [2]$$

where χ_k is the mole fraction, I_k is the concentration of the compound in the product phase (in g cm^{-3}, for example, grams of benzene per cubic centimeter of crude oil), and w_k is the molecular weight (g mol^{-1}). The volumetric fraction is defined as:

$$\chi_k^v = \frac{I_k/v_k}{\sum_{j=1}^{N} I_j/v_j} \quad \text{definition of volumetric fraction} \qquad [3]$$

where v_k (**Table 5**) is the specific volume of a compound (cm^3 g^{-1}) in the mixture that can be approximated by the reciprocal of the compound's density. The mass fraction is defined as:

$$\chi_k^m = \frac{I_k}{\sum_{j=1}^{N} I_j} = \frac{I_k}{\rho} \quad \text{definition of mass fraction} \qquad [4]$$

where $\rho = \sum_{j=1}^{N} I_j$ is the density of the product.

To meet requirements that wintertime fuel contain 2.7% oxygen by weight, MTBE was added to gasoline so that the final product consisted of 14.7% MTBE by volume ($\chi_k^v = 0.147$). MTBE and the other compounds in gasoline have similar specific volumes; therefore, $\chi_k^v \approx \chi_k^m$. Finally, the molecular weight of MTBE is on the order of the average molecular weight of gasoline compounds; therefore, $\chi_k \approx \chi_k^m \approx \chi_k^v$. A constituent

Table 6 Composition of a gasoline oxygenated with MTBE and associated equilibrium concentrations in water

Compound	*Formula*	*Molecular weight* w_k *(g mol^{-1})*	*Volumetric fraction,* χ_k^v	*Mass fraction,* χ_k^m	*Mole fraction,* χ_k	*Solubility,* C_{sol} *(mg l^{-1}) (from Table 5)*	*Concentration* $C_k = \chi_k C_{sol}$ *(mg l^{-1})*
MTBE	$C_5H_{12}O$	88.1	0.15	0.1544	0.1589	50 000	7945
Aromatics							
Benzene	C_6H_6	78.1	0.0136	0.0165	0.0192	1780	34.2
Toluene	C_7H_8	92.1	0.0699	0.0834	0.0822	515	42.3
Xylenes	C_8H_{10}	106.2	0.0912	0.0963	0.0823	175	14.4
C_9	C_9H_{12}	120.2	0.063	0.0751	0.0567	57	3.2
C_{10}	$C_{10}H_{14}$	134.2	0.0306	0.0364	0.0246	15	0.4
C_{11}	$C_{11}H_{16}$	148.2	0.0134	0.016	0.0098	10.5	0.1
C_{12}	$C_{12}H_{18}$	162.3	0.0007	0.0008	0.0005	5	0
Subtotal		–	0.28	0.32	0.28	–	94.6
Alkanes							
C_4	C_4H_{10}	58.1	0.053	0.0442	0.069	61.4	4.2
C_5	C_5H_{12}	72.2	0.137	0.1184	0.1488	40	6
C_6	C_6H_{14}	86.2	0.114	0.1045	0.11	9.5	1
C_7	C_7H_{16}	100.2	0.0687	0.0646	0.0585	3	0.2
C_8	C_8H_{18}	114.2	0.0617	0.0597	0.0474	0.5	0
Subtotal		–	0.43	0.39	0.43	–	11.4
Alkenes							
C_4	C_4H_8	56.1	0.0011	0.0009	0.0015	222	0.3
C_5	C_5H_{10}	70.1	0.0333	0.0295	0.0382	148	5.7
C_6	C_6H_{12}	84.2	0.029	0.0269	0.029	50	1.5
C_7	C_7H_{14}	98.2	0.0135	0.0132	0.0122	15	0.2
C_8	C_8H_{16}	112.2	0.0017	0.0017	0.0014	2.7	0
Subtotal		–	0.08	0.07	0.08	–	7.7
Cycloalkanes							
C_5	C_5H_{10}	70.1	0.002	0.002	0.0027	160	0.4
C_6	C_6H_{12}	84.2	0.0109	0.0117	0.0127	55	0.7
C_7	C_7H_{14}	98.2	0.0137	0.0146	0.0135	14	0.2
C_8	C_8H_{16}	112.2	0.0092	0.01	0.0081	2	0
Subtotal		–	0.04	0.04	0.04	–	1.3

breakdown for a gasoline oxygenated with MTBE (Lahvis, 2003a) is given in Table 6. The compositional breakdown shows the similarity between the definitions of volume, mass, and mole fraction. The gasoline, on a mass basis, consists of about 15.5% MTBE, 32% aromatics, and 39% alkanes; however, MTBE is the primary contaminant in the aqueous phase on a mass basis (7945 mg l^{-1}) followed by the aromatic constituents (94.6 mg l^{-1}). Although alkanes constitute the majority of mass in the gasoline, their contribution to water contamination (11.4 mg l^{-1}) is relatively minor compared to other gasoline compounds. The contribution of alkenes and cycloalkanes (7.7 and 1.3 mg l^{-1}, respectively) to water contamination is also relatively minor. If MTBE were not blended into the gasoline, then the total hydrocarbon solubility would be approximately 15% greater: $1.15(94.6+11.4+7.7+1.3)=132.3$ mg l^{-1}.

Equilibrium between product and gaseous phases (product–gaseous phase equilibrium) is expressed in an analogous way to the product and aqueous phase equilibrium as:

$$G_k = \gamma_k \chi_k G_{vap} \quad \text{product-gaseous phase equilibrium} \qquad [5]$$

where G_k is the concentration of the compound in the gaseous phase (g l^{-1}), G_{vap} is the concentration in the gaseous phase in equilibrium with the pure compound, and, as for the aqueous–product phase equilibrium, γ_k and χ_k are the activity coefficient and mole fraction in the product phase, respectively. Again, this is a form of Raoult's law, and generally it is assumed that $\gamma_k = 1$ (ideal behavior for equilibrium involving gaseous phase). Gaseous phase data often are reported in terms of partial pressure. The ideal gas law is used to convert to concentration units as:

$$G_{vap} = \frac{\omega_k}{RT} p \quad \text{Ideal Gas Law} \qquad [6]$$

where p is the partial pressure of the pure compound in atmospheres, T is temperature in degrees Kelvin, and R is the gas constant, $R = 82.05783$ cm^3 atm mol^{-1} K^{-1}. Values for p at 25 °C are provided in Table 5.

The temperature dependence of p is modeled by the Clausius–Clapeyron equation as:

$$\frac{1}{p}\frac{dp}{dT} = \frac{\Delta H}{RT^2} \quad \text{Clausius–Clapeyron equation} \qquad [7]$$

where ΔH is the latent heat of vaporization or change in enthalpy associated with the phase change (cm^3 atm mol^{-1}). Integration of eqn [7] yields:

$$\ln(p/p_0) = A - B/T \quad \text{vapor pressure as function of temperature} \qquad [8]$$

where $A = \Delta H/RT_0$, $B = \Delta H/R$, and p_0 is the value for p at temperature T_0. If ΔH is given in units of calorie mol^{-1} and

Table 7 Vapor pressure of petroleum compounds as a function of temperature

Compound	ΔH^a *(cal mol^{-1})*	p*(T) in atm*			
		5 °C	*15 °C*	*25 °C*[b]	*35 °C*
Aromatic hydrocarbons					
Benzene	8079.8	0.047	0.078	0.125	0.195
Methylbenzene (toluene)	9078.1	0.012	0.022	0.038	0.062
1,4-Dimethylbenzene (*p*-xylene)	10126.6	0.003	0.006	0.012	0.020
1,2-Dimethylbenzene (*o*-xylene)	10372.6	0.003	0.006	0.012	0.020
1,3-Dimethylbenzene (*m*-xylene)	10186.3	0.003	0.006	0.011	0.019
Ethylbenzene	10088.4	0.004	0.007	0.013	0.022
Isopropylbenzene	10778.6	0.002	0.003	0.006	0.011
1,2,4-Trimethylbenzene	11447.3	0.001	0.001	0.003	0.005
n-Propylbenzene	11038.9	0.001	0.002	0.004	0.008
n-Butylbenzene	12266.5	0.000	0.001	0.001	0.003
Alkanes					
n-Butane	5020.3	1.304	1.787	2.398	3.158
n-Pentane	6312.4	0.314	0.466	0.675	0.954
n-Hexane	7537.6	0.080	0.128	0.199	0.301
n-Heptane	8734.2	0.021	0.036	0.060	0.097
n-Octane	9909.2	0.005	0.010	0.018	0.031
Alkenes					
1-Butene	4829.2	0.163	0.221	0.293	0.382
1-Pentene	6083.1	0.401	0.587	0.839	1.171
1-Hexene	7310.7	0.101	0.159	0.245	0.365
2-Heptene	8672.1	0.022	0.038	0.064	0.102
1-Octene	9634.6	0.007	0.013	0.023	0.039
Cycloalkanes					
Cyclopentane	6811.6	0.183	0.281	0.418	0.608
Cyclohexane	7883.9	0.048	0.079	0.125	0.193
Methyl-cyclohexane	8445.2	0.022	0.037	0.061	0.097
Propyl-cyclopentane	9811.3	0.005	0.009	0.016	0.028
Ethers (oxygenate additives)					
Methyl *tert*-butyl ether (MTBE)	7122.0	0.139	0.217	0.329	0.486
Ethanol	10131.9	0.023	0.043	0.078	0.135

$\ln(p/p_0) = A - B/(T + 273.15)$, where $A = [(0.5035)\Delta H]/(T_0 + 273.15)$ and $B = (0.5035)\Delta H$.

[a]Values from Lide (2002) and Mayer and Svoboda (1985)

[b]Values for $T_0 = 25$ °C from **Table 5**

temperature in °C, then $A = (0.5035)\Delta H/(T_0 + 273.15)$ and $B = (0.5035)\Delta H$ because 1 calorie mol^{-1} = 41.32 cm^3 atm mol^{-1}. This equation results from the following: 1 atm = 101 325 Pa, 1 Pa = 1 kg m^{-1} s^{-2}, 1 J = 1 kg m^2 s^{-2}, 1 calorie = 4.187 J, and $R = 82.05783$ cm^3 atm mol^{-1} K^{-1}. The calculation of the temperature dependence of vapor pressure for select compounds is presented in **Table 7**. For example, the concentration of benzene in air at a filling station would be approximately four times higher on a warm day (35 °C) compared to a cold day (5 °C).

Equilibrium between aqueous and gaseous phases is modeled according to Henry's law as:

$$G_k = H_k C_k \quad \text{Henry's Law} \qquad [9]$$

where H_k is the Henry's law coefficient (dimensionless) for the compound. Because both the aqueous and gaseous phases are assumed to be dilute with respect to the organic compounds, there is no activity coefficient or nonideal behavior associated with this interface. The temperature dependence of H_k is calculated in the same way as vapor pressure, referred to as the van't Hoff equation:

$$\frac{d\ln(H_k)}{dT} = \frac{\Delta H_{Henry}}{RT^2} \quad \text{Henry's coefficient as function of temperature} \qquad [10]$$

where ΔH_{Henry} is the change in enthalpy associated with the aqueous/gaseous phase transfer (in cm^3 atm mol^{-1}). Integration of eqn [10] yields:

$$\ln(H_k/H_{k0}) = A - B/T \qquad [11]$$

where $A = \Delta H_{Henry}/RT_0$, $B = \Delta H_{Henry}/R$, and H_{k0} is the value for H_k at temperature T_0. If ΔH_{Henry} is given in units of calorie mol^{-1} and temperature in °C, then $A = (0.5035)\Delta H_{Henry}/(T_0 + 273.15)$ and $B = (0.5035)\Delta H_{Henry}$. The temperature dependence for MTBE and select aromatics is given in **Table 8**. The parameter values were selected from references cited in the review by Rathbun (1998). Henry's law coefficients at 25 °C for other compounds are provided in **Table 5**.

The temperature dependence of H_k for MTBE can result in appreciable changes in MTBE concentration in precipitation. For example, given the same gaseous concentrations in the atmosphere, the concentration of MTBE at equilibrium in

Table 8 Henry's coefficient of MTBE, ethanol and monoaromatic hydrocarbons as a function of temperature

Compound	ΔH_{Henry} *(cal mol^{-1})*	ΔH_{k0} *at* $T_0 = 25\,^{\circ}C$ *dimensionless*	H_k			
			$T = 0\,^{\circ}C$	$T = 10\,^{\circ}C$	$T = 20\,^{\circ}C$	$T = 30\,^{\circ}C$
MTBE (Robbins et al., 1993)	15334.6	0.026	0.002	0.007	0.017	0.04
Ethanol (Snider and Dawson, 1985)	13108.2	2.15×10^{-4}	2.84×10^{-5}	6.66×10^{-5}	1.47×10^{-4}	3.10×10^{-4}
Aromatics (Dewulf et al., 1995)						
Benzene	7720	0.195	0.059	0.098	0.156	0.242
Toluene	8574	0.227	0.06	0.105	0.177	0.288
1,4-Dimethylbenzene (*p*-xylene)	9755.7	0.244	0.054	0.102	0.184	0.32
1,2-Dimethylbenzene (*o*-xylene)	9676.3	0.173	0.039	0.073	0.131	0.226
1,3-Dimethylbenzene (*m*-xylene)	8570	0.247	0.066	0.115	0.193	0.314
Ethylbenzene	10113.2	0.274	0.057	0.111	0.205	0.363

$\ln(H_k/H_{k0}) = A - B/T$, where $A = [(0.5035)\Delta H_{Henry}]/(T_0 + 273.15)$ and $B = (0.5035)\Delta H_{Henry}$.

rain at 10 °C compared to that at 30 °C is approximately six times greater. Therefore, MTBE detection would be expected to be higher in precipitation and runoff during cooler months (Baehr et al., 1999). Similar to MTBE, ethanol will partition strongly into the aqueous phase. Ethanol is miscible in water and has a low Henry's constant (H_k) of 0.00024 (Lahvis, 2003b).

Sorption involves mass transfer of VOCs to a solid phase such as particulates in the atmosphere, bed sediments of a stream or lake, or the solid matrix of subsurface porous media. Solid surfaces attract water electrostatically except for cases involving extremely dry sediment, in which case an aqueous phase surrounding the solid surfaces is involved in the process. Sorption, therefore, has been defined as any accumulation of a dissolved organic compound by solid particles (Voice and Weber, 1983). Sorption of VOCs is conceptually different than partitioning into the bulk fluid phases of the environment because the composition of the solid must be taken into consideration to obtain an equilibrium relation. The natural organic content of sediment is fundamental to sorption because VOCs are hydrophobic. Sediments in lake beds rich in natural organic matter, such as humin or humic acid, would hold more VOCs than a sand largely devoid of natural organic matter.

Sorption of VOCs involves the processes of adsorption and partitioning. Partitioning is the incorporation of the VOC into the natural organic matter associated with the solid and is analogous to the dissolution of an organic compound into an organic solvent. Adsorption is the formation of a chemical or physical bond between the VOC and the mineral surface of a solid particle (Rathbun, 1998). The equilibrium relation between aqueous and solid phase concentrations then is expressed as

$$S = [f_{oc}K_{oc} + (1 - f_{oc})K_m]C \qquad [12]$$

where S is the mass of the VOC sorbed per unit mass of solid (g kg^{-1}), C is the concentration in the aqueous phase (g l^{-1}), f_{oc} is the weight fraction of organic carbon in the solid (dimensionless), K_{oc} is the normalized sorption coefficient because of organic matter partitioning (l kg^{-1} of organic carbon), and K_m is the sorption coefficient because of mineral adsorption (l kg^{-1} of mineral sediment). Karickhoff (1984) presented guidelines for estimating the relative contribution of adsorption and partitioning. For small ($<C_{10}$) nonpolar organics, which describes essentially all of the compounds listed in **Table 5** (except for ether oxygenates), adsorption is important compared to partitioning only if $f_{oc} < 0.02$. The threshold for ethers such as MTBE, which are in the category of neutral organics with polar functional groups, is $f_{oc} < 0.04$. Rathbun (1998) provides a review of K_{oc} values for aromatic hydrocarbons and various sediments.

The octanol–water partition coefficient K_{ow} for an organic compound is the ratio of the compound concentration in octanol saturated with water to that in water saturated with octanol. This property of the VOC can be used to estimate K_{oc} as it is directly related to the tendency of a compound to partition in natural organic matter from aqueous solution (Karickhoff, 1981). The octanol–water partition coefficient also provides a measure of the propensity of a compound to bioaccumulate (Rathbun, 1998) in fatty tissue of aquatic biota. Values of K_{ow} are provided in **Table 5**.

Eqn [12] is referred to as a linear isotherm. Linearity assumes that sorption sites on the solid surfaces are unlimited; therefore, the model only may be applicable for lower concentrations. An alternative formulation is

$$S = K_f C^{1/n} \qquad [13]$$

where K_f and n are constants of the Freundlich-type isotherm (Voice and Weber, 1983). Values for n usually range from 0.7 to 1.1 (Lyman et al., 1990).

A good example of how physical properties affect the partitioning of hydrocarbons released into the environment can be gleaned from the results obtained at the Bemidji, Minnesota, crude oil spill research site. Although the alkane fraction of the hydrocarbons largely remained in the oil phase following the spill, the lighter, more volatile, aliphatic fractions were found in the unsaturated zone ($<C_5$, Chaplin et al., 2002). The aromatic hydrocarbons from C_6 to C_{10}, which are soluble in water and have lower Henry's Law constants, were transported downgradient in groundwater, further than other organic

compounds (Baedecker and Eganhouse, 1991; Eganhouse et al., 1993). The major hydrocarbon types found downgradient from the oil were volatile aromatic hydrocarbons in groundwater and nonvolatile alkanes in sediment. Over a time period of decades, the *n*-alkanes in the oil and sediment were gradually depleted (Bekins et al., 2005). The higher molecular weight hydrocarbons, predominantly normal alkanes in the C_{11}–C_{33} range and the isoprenoid hydrocarbons, pristane and phytane, have low water solubilities and occurred in groundwater only near the oil source. In a study conducted in 1995, 16 years after the spill, Furlong et al. (1997) found that the *n*-alkanes were largely absent from the groundwater at the Bemidji site, even close to the oil, whereas polycyclic aromatic hydrocarbons (PAHs) persisted in the water downgradient from the oil. A review in Wisconsin of closed leaking underground storage tank sites that rely on natural attenuation to remove contaminant mass, showed that at eight out of ten sites monitored, naphthalene was observed at more downgradient monitoring wells than was benzene (Evanson et al., 2009), presumably due to its long-term persistence in the source phase. Additional information about the fate of low-solubility PAHs in the environment is provided by Abrajano et al. (**Chapter 11.13**).

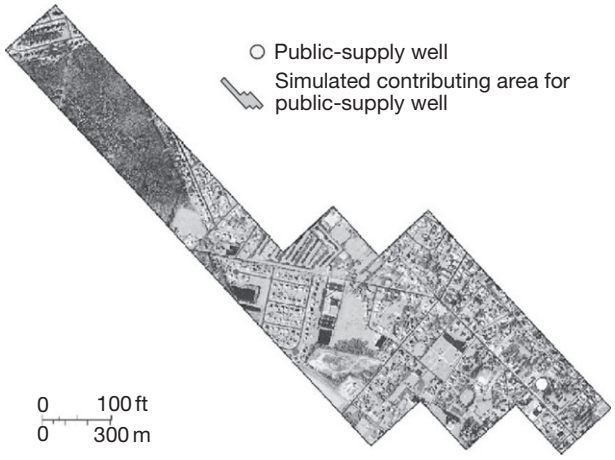

Figure 8 Simulated contributing area to a shallow and moderate-depth monitoring and public-supply well. Reproduced from Kauffman LJ, Baehr AL, Ayers MA, and Stackelberg PE (2001) Effects of land use and travel time on the distribution of nitrate in the Kirkwood-Cohansey Aquifer system in southern New Jersey. *US Geological Survey Water-Resources Investigation Report 01-4117*. Denver, CO: US Geological Survey.

11.12.3.2 Physical Transport

While phase partitioning describes how molecular constituents of petroleum products interact at interfaces, such as between a liquid petroleum and aqueous phase, once transferred to an environmental compartment, the compounds can undergo physical mixing processes, and chemical and biologically mediated transformations. The phase transfers described earlier can be viewed as the beginning of the overall process of transport through the atmosphere, hydrosphere, geosphere, or biosphere. Methods of predicting transport are discipline-specific, and dependent on the scale of investigation, and the part of the environment (e.g., atmosphere, ocean, streams, groundwater) that is most affected. Mathematical models of transport quantify the movement, dilution, and chemical and biochemical attenuation of contaminants through the relevant environmental compartments. The bases of transport models rely on conservation principles (conservation of mass, momentum, and energy) that are represented as a series of equations such as those described in Domenico and Schwartz (1998).

Although a detailed discussion of physical transport processes is beyond the scope of this chapter, it is important to note that quantification of the bulk movement of air in the atmosphere or water in the hydrosphere can provide a qualitative interpretation of chemical transport. A simplistic example is that stagnant air masses induce conditions favorable for smog formation because chemicals can increase in concentration over an urban area. Therefore, basic weather predictions can be used to anticipate air quality. In general, models of fluid movement define the flow field in which contaminants can be transported via advection. For example, delineation of the area over which water recharging a surficial aquifer eventually will travel to the public supply well (well contributing area, **Figure 8**) was achieved with a groundwater flow model simulation. In aggregate, land use and associated contamination within the contributing area caused low-level detection of MTBE and other compounds in samples taken from the well. The accumulation of point sources within the contributing area can be interpreted as an urban nonpoint source. Estimated travel times of groundwater from point of recharge to the well can be calculated from a groundwater flow model simulation and are useful in determining the effect of land use throughout the contributing area (Kauffman et al., 2001).

Accumulation of point sources from land use of petroleum products also can affect surface waters. For example, urban riverine inputs of volatile hydrocarbons to the marine environment have been studied in the coastal waters of Spain by Gomez-Belinchon et al. (1991). Volatile petroleum hydrocarbon inputs from two rivers were found to account for a mass flux of 47 and 96 ton $year^{-1}$ of alkylbenzenes and 38 and 66 ton $year^{-1}$ of *n*-alkanes each. Although this was a significant mass flux, the concentrations of alkylbenzenes and *n*-alkanes in this coastal area originating from marine traffic actually outnumbered the contribution from the rivers.

11.12.4 Transformation Processes

Chemical and biological transformation processes, in addition to the physical transport processes, control the ultimate fate of hydrocarbons released into the environment. The transformation reactions differ depending on the environmental compartment within which the hydrocarbons reside and vary with chemical structure. When hydrocarbons are released to the atmosphere or surface waters, photochemical oxidation, an abiotic process, can occur. In soils and ground- and surface waters that are biologically mediated, degradation of hydrocarbons is the most important transformation process. In the absence of light, chemical degradation reactions at earth-surface temperature and pressure are relatively unimportant compared to biologically mediated degradation reactions.

11.12.4.1 Abiotic Transformation

Approximately 25% of the average oil spill on the open ocean evaporates and, in the gaseous state, hydrocarbons are readily photooxidized (National Research Council, 1985). The dissolved fraction of petroleum also is subject to photooxidation. Mill et al. (1980) documented the photooxidation of isopropylbenzene in the presence of humic substances. A review of the photochemical oxidation of petroleum in water reported that oxidation of alkanes and alkylbenzenes, such as *sec*-butylbenzene and *tert*-butylbenzene, has been observed in photooxidation studies and the products produced have included acids, carbonyl compounds, alcohols, peroxides, and ethers (Payne and Phillips, 1985). Photooxidation in the atmosphere of volatile aromatic hydrocarbons (benzene, toluene, and xylenes) has been studied in the presence of catalysts, such as nitrous oxide and carbon monoxide, as reviewed by Merian and Zander (1982). The products formed from these reactions include nitro-substituted phenols and aldehydes. A review of gas-phase reactions in the troposphere for alkanes, alkenes, alkynes, oxygenates, and aromatic hydrocarbons is presented by Atkinson (1990).

The largest sink for alkanes in the atmosphere is reaction with OH and NO_3 radicals. The formation of photochemical smog is described in detail in **Chapter 11.11**. Monoaromatic hydrocarbons react only slowly with O_3 and NO_3 radicals in the troposphere. The only important atmospheric processes for monoaromatic hydrocarbons, and naphthalene and dinaphthalenes are reactions with OH radicals (Atkinson, 1990). The products of these reactions include aldehydes, cresols, and, in the presence of NO, benzylnitrates. Methane can be an important contributor to ozone formation, especially in the remote troposphere, as described in **Chapter 11.11**.

Photooxidation has been reported at crude oil spills. It results in depletion of *n*-alkanes below nC_{15} and alkylaromatics such as C_1- and C_2-substituted naphthalenes relative to unoxidized oil (Payne and Phillips, 1985). In terms of a material balance, photooxidation has been found to be a minor process (National Research Council, 1985) but it does result in changes in the residual oil composition and can affect the subsequent behavior of an oil spill on the open ocean (Payne and Phillips, 1985). Autooxidation reactions of hydrocarbons in the absence of light have not been well studied.

11.12.4.2 Biotic Transformation

While chemical oxidation processes may occur largely in the atmosphere, and on land surface or open waters where sunlight is a catalyst, biologically mediated processes dominate in soils and groundwater. The more water-soluble components of crude oil and petroleum products discussed in **Section 11.12.1.2** of this chapter, benzene and the lower molecular weight alkylbenzenes, are the hydrocarbons most frequently reported in groundwater downgradient from spills and leaks. These hydrocarbons are biologically reactive and their fate in the subsurface is controlled by microbiological as well as physical and chemical processes.

It has been known for nearly a century that certain microorganisms are able to degrade petroleum hydrocarbons and use them as a sole source of carbon and energy for growth. The early studies of bacterial degradation of hydrocarbons are summarized by Gibson and Subramanian (1984), while reviews of the microbial metabolism of hydrocarbons were presented by Davis (1967), Atlas (1984), Chapelle (1993), Rosenberg and Ron (1996), and Heider et al. (1998). There are four types of microbial metabolism that release energy: photometabolism; fermentation; aerobic respiration; and anaerobic respiration (Reineke, 2001). Fermentation does not require oxygen or other electron acceptors such as NO_3^-, or $Fe(III)_s$, and depends on the capability of microorganisms to use part of the organic molecule as an electron acceptor. The respiration of organic material, on the other hand, does require an electron acceptor and proceeds as a series of coupled oxidation and reduction steps. In almost all shallow subsurface environments, petroleum hydrocarbons can serve as electron donors in microbial metabolism (Wiedemeier et al., 1999). The oxidation of hydrocarbons results in the release of electrons that are transferred to oxygen, or, in the case of anoxic environments, alternate electron acceptors such as sulfate. Respiration reactions release more energy for cell growth than fermentation reactions, and as such, respiration reactions have been studied much more extensively. Aerobic and anaerobic respiration reactions are described in more detail in the following sections for aromatic and aliphatic hydrocarbons as well as for fuel oxygenates.

There are several factors that have been shown to affect the biodegradability of petroleum hydrocarbons, including hydrocarbon structure (i.e., aliphatic or aromatic), degree of branching and saturation, and chain length (Baker and Herson, 1994). In comparison to hydrocarbons, less is known about the biodegradability of MTBE and other fuel oxygenates. Early studies suggested that MTBE was difficult to biodegrade (Yeh and Novak, 1994, 1995) because of the resistance to microbial attack of the tertiary carbons (Suflita and Mormile, 1993) or the presence of the very stable and chemically unreactive ether linkage (Salanitro et al., 1994). It has been argued that these early studies documenting apparent MTBE recalcitrance were correct at the time as MTBE had only recently been introduced into the subsurface and microbial communities had not developed the enzymes or appropriate microbial populations necessary to degrade MTBE (Mackay and Einarson, 2006). However, in recent years, biodegradation of MTBE has been documented in numerous laboratory microcosm studies under both aerobic and anaerobic conditions (see reviews by Babé et al., 2007; Fayolle et al., 2001; Schmidt et al., 2004) and at contaminated field sites (Kolhatkar et al., 2002; Kuder et al., 2005; Schirmer et al., 1999; Zwank et al., 2005).

With the shift from MTBE to ethanol in oxygenated gasoline, laboratory and field studies have been conducted to anticipate the impacts that ethanol releases will have on groundwater quality. In addition to the direct effects of ethanol on the petroleum it is released with, concerns have been raised over the potential for ethanol to come into contact with preexisting contamination (Mackay et al., 2007). It is possible that high-concentration ethanol releases onto a preexisting hydrocarbon NAPL may exacerbate groundwater impacts, by dissolving and mobilizing BTEX compounds (Stafford et al., 2009). In addition, laboratory studies indicate that the presence of ethanol decreases the biodegradation rate of BTEX (Lovanh

et al., 2002), likely due to competition for electron acceptors (Chen et al., 2008b). Studies evaluating the impact of ethanol on groundwater quality are further discussed in **Section 11.12.4.2.3**.

11.12.4.2.1 Aerobic processes

Oxygen is the preferred electron acceptor by microorganisms because of the high-energy yield of these processes. Aerobic degradation of hydrocarbons can occur when indigenous populations of bacteria capable of aerobic degradation of hydrocarbons are supplied with molecular oxygen and nutrients required for cell growth. The aerobic pathway of hydrocarbon degradation has been studied extensively in petroleum-contaminated soils. The capability to degrade hydrocarbons in aerobic environments is present in a wide variety of bacteria and fungi that contain the genetic capability of incorporating molecular oxygen into the hydrocarbon structure (Gibson and Subramanian, 1984; Rosenberg and Ron, 1996), thus creating the widespread potential for hydrocarbon oxidation wherever oxygen and nutrients are available. In fact, studies involving complex mixtures of hydrocarbons, such as gasoline, have demonstrated that microorganisms can degrade most of the hydrocarbons present in gasoline (Jamison et al., 1975).

The biodegradation of aromatic hydrocarbons under aerobic conditions was reviewed by Gibson and Subramanian (1984), Smith (1994), Rosenberg and Ron (1996), and Bosma et al. (2001). Both prokaryotic and eukaryotic microorganisms have the enzymatic potential to oxidize aromatic hydrocarbons (Rosenberg and Ron, 1996). Bacteria and fungi degrade aromatic hydrocarbons in different ways, however. Bacteria are able to utilize the compounds as a sole source of carbon and energy whereas fungi appear to cometabolize aromatic hydrocarbons to hydroxylated products (Reineke, 2001). The first step in fungal metabolism is the formation of an epoxide (Reineke, 2001), whereas bacteria initiate the oxidation of unsubstituted aromatic compounds by incorporating both atoms of molecular oxygen into the aromatic ring to form a *cis*-dihydrodiol, as reviewed by Gibson and Subramanian (1984). Further oxidation of the *cis*-dihydrodiol leads to catechol formation (**Figure 9**). The aromatic ring is then cleaved by the *ortho*- or *meta*-cleavage pathways, ultimately producing low molecular weight compounds such as pyruvate and acetaldehyde, which can be further oxidized via the Krebs cycle (e.g., Baker and Herson, 1994). In the case of toluene, for example, the presence of an alkyl substituent group on the benzene ring presents microorganisms with an additional site of attack, and oxidation of this side chain results in the formation of benzylalcohols, benzaldehydes, and alkylbenzoic acids (**Figure 9**).

The oxidation of straight chain alkanes proceeds, in general, by oxidation of the terminal methyl group (**Figure 10**) to form intermediates including the corresponding alcohols, aldehydes, or carboxylic acids (Bouwer and Zehnder, 1993). In the presence of oxygen, a class of enzymes called oxygenases mediates this reaction. Fatty acids derived from alkanes are then oxidized further to acetate and propionate by β-oxidation (Rosenberg and Ron, 1996). Unsaturated hydrocarbons, such as alkenes and alkynes, are degraded by similar mechanisms (Bouwer and Zehnder, 1993). The most degradable *n*-alkanes are the C_{10}–C_{18} compounds while longer chain alkanes are less biodegradable because their lower aqueous solubilities limit uptake by microorganisms (Bosma et al., 2001). Although *n*-alkanes are the predominant hydrocarbons by volume in many petroleum products, such as crude oils, those with chain lengths $> C_{15}$ also are typically less mobile in subsurface and aquatic environments, again because of their relatively low solubilities (Eganhouse et al., 1993).

Aerobic degradation reactions require available moisture, nitrogen, and phosphorus in addition to molecular oxygen (Rosenberg and Ron, 1996). In oil spills in aquatic environments, where oxygen and moisture are plentiful, the limitation to biodegradation, therefore, tends to be nutrient availability. A review of the basic requirements for aerobic biodegradation

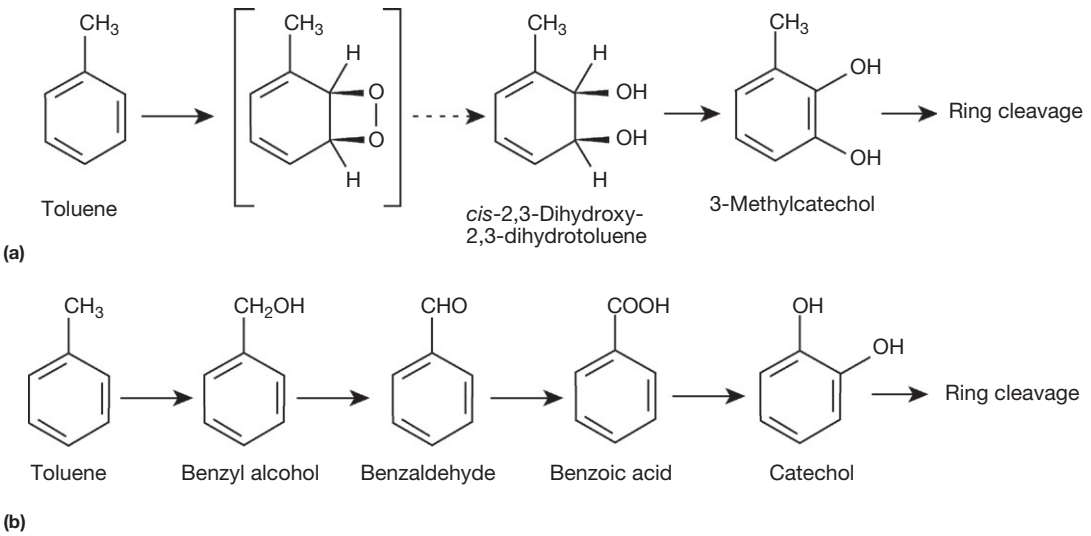

Figure 9 Aerobic toluene degradation pathway by (a) aromatic ring attack by dioxygenation and (b) side chain attack by stepwise oxidation. Modified from Smith MR (1990) The biodegradation of aromatic hydrocarbons by bacteria. *Biodegradation* 1: 191–206.

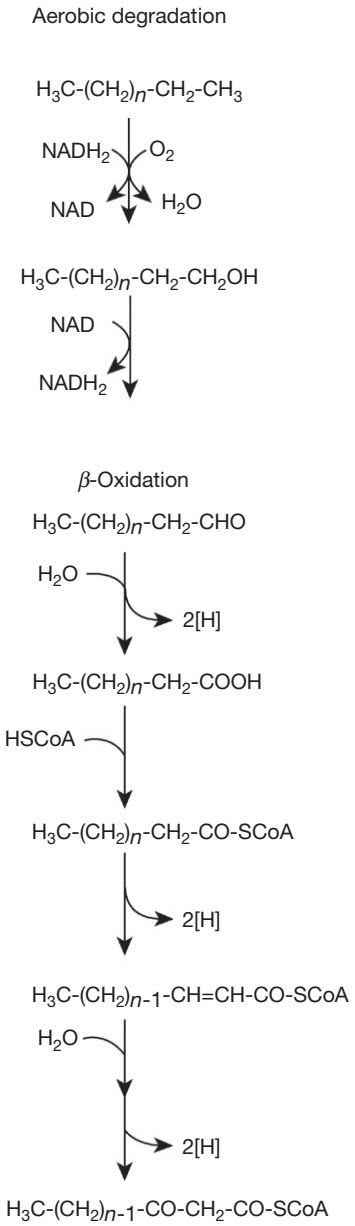

Figure 10 Alkane degradation under aerobic conditions, showing incorporation of oxygen from molecular oxygen into the aliphatic compound, producing a fatty acid. Fatty acids are oxidized further by β-oxidation. [H] indicates reducing equivalents that are either required or formed in the reaction step. Modified from Bouwer EJ and Zehnder A (1993) Bioremediation of organic compounds-putting microbial metabolism to work. *Bioremediation* 11: 360–367.

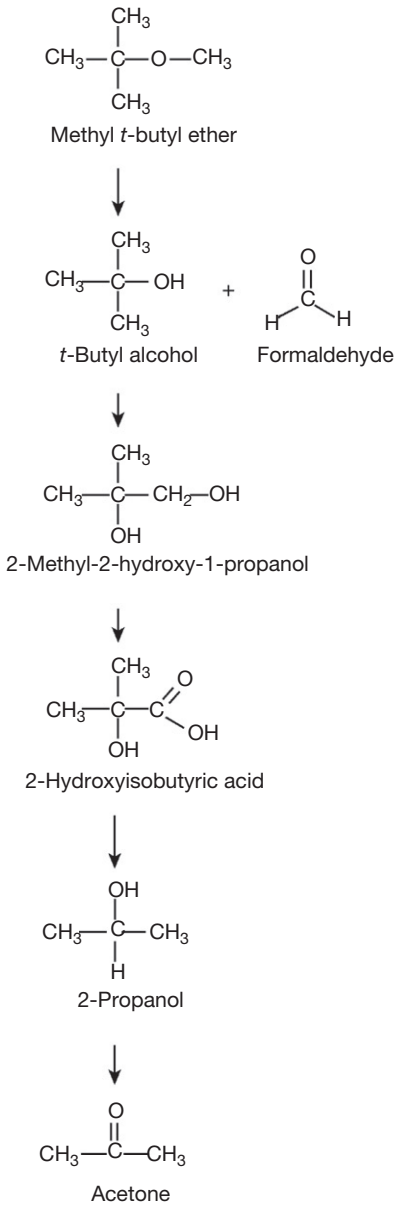

Figure 11 A demonstrated pathway for MTBE biodegradation under aerobic conditions. Modified from Deeb RA, Scow KM, and Alvarez-Cohen L (2000) Aerobic MTBE biodegradation: An examination of past studies, current challenges and future research directions. *Biodegradation* 11: 171-186.

and the quantification of this process at sites contaminated with hydrocarbons is presented by Rifai (1997).

The degradation processes and rates of transformation of fuel oxygenates, such as MTBE, and potential metabolites of degradation are less understood. Although early studies indicated that MTBE was resistant to microbial attack, more recent laboratory studies have shown that MTBE can biodegrade under oxygen-rich conditions (Babé et al., 2007; Deeb et al., 2000; Fayolle et al., 2001; Schmidt et al., 2004). Mixed and pure bacterial cultures have been used in the study of MTBE biodegradation under carefully controlled conditions. One of the first studies of a bacterial culture capable of MTBE biodegradation was of a microbial consortium enriched from activated sludge (Salanitro et al., 1994). In this study, MTBE was utilized as a primary growth substrate with the production of *tert*-butyl alcohol (TBA) as a transient intermediate, although growth rates were slow. At MTBE concentrations above 5 mg l^{-1}, removal rates decreased. Studies with related cultures showed that MTBE was biodegraded at concentrations as high as 80 mg l^{-1} in laboratory microcosm experiments in

which these cultures were added to soils and groundwater (Salanitro et al., 1999).

The pathway of MTBE aerobic degradation involves cleavage of the ether bond of MTBE yielding TBA and formaldehyde as shown in **Figure 11** (Deeb et al., 2000). This first involves the initial attack by a monooxygenase enzyme (Fayolle et al., 2001; Smith et al., 2003b) and the formation of the hemiacetal intermediate *tert*-butoxymethanol through the addition of singlet oxygen to the methyl group. This intermediate is then either oxidized by an alcohol dehydrogenase enzyme to *tert*-butyl formate (TBF) and then rapidly hydrolyzed to TBA by esterase (Hardison et al., 1997; Smith et al., 2003b), or it undergoes direct dismutation to form TBA directly (Smith et al., 2003a; Steffan et al., 1997). To date, none of the monooxygenases enabling growth on MTBE have been isolated or genetically sequenced (Lopes Ferreira et al., 2006). The proposed *tert*-butoxymethanol intermediate formed by the oxidation of the methyl group has not been measured. The evidence supporting the initial oxidation of the methyl group is therefore primarily based upon the presence of TBF during aerobic biodegradation of MTBE by some microorganisms or the ability of microorganisms to grow on TBF as a substrate. Recent studies suggest that not all aerobic MTBE-degrading strains may produce TBA by these initial reactions; some may, instead, directly cleave the ether bond (Bastida et al., 2010; McKelvie et al., 2009; Rosell et al., 2007). As such, additional isotopic, enzymatic, and microbial investigations are necessary to elucidate the mechanism by which individual strains biodegrade MTBE.

Although research on the biodegradation of MTBE under natural conditions is limited, the potential for significant in situ aerobic transformation of MTBE in surface water was demonstrated by Bradley et al. (2001), who identified MTBE-degrading capabilities in microorganisms indigenous to stream and lake bed sediments at 11 different sites. MTBE biodegradation under aerobic conditions in aquifers contaminated with petroleum products has been demonstrated at the Canadian Forces Base (CFB) Borden (Schirmer and Barker, 1998; Schirmer et al., 1999), although at slow rates, much slower than typically observed for BTEX compounds. Field experiments involving diffusive addition of oxygen into an aquifer with an existing MTBE plume (Vandenberg Air Force Base (VAFB), California) demonstrated that native aerobic MTBE-degrading microorganisms were stimulated to degrade MTBE (Wilson et al., 2002).

11.12.4.2.2 Anaerobic processes

Anoxic conditions frequently develop in subsurface environments affected by high concentrations of dissolved hydrocarbons because of rapid aerobic biodegradation rates and the limited supply of oxygen. In the absence of oxygen, the oxidized forms of other inorganic species, and some organic species, such as humic substances, are used by microorganisms as electron acceptors. Because of the prevalence of petroleum product leaks and spills in oxygen-restricted subsurface environments, these reactions are the most often studied hydrocarbon degradation reactions. Anaerobic degradation reactions are described in more detail in **Chapter 11.16** for another common contaminant, landfill leachate that likewise occurs in oxygen-restricted environments (Christensen et al., 2000). In many studies, the nonconservative behavior of dissolved aromatic hydrocarbons from anoxic groundwater has been attributed to anaerobic degradation reactions (e.g., Barker and Wilson, 1997; Barker et al., 1986; Cozzarelli et al., 1990, 1999; Eganhouse et al., 1996; Reinhard et al., 1984; Schwarzenbach et al., 1983; Wilson et al., 1990).

The most commonly available electron acceptors in subsurface environments include both solid and dissolved phase

Table 9 Theoretical stoichiometry and energetics of mineralization of aromatic and aliphatic hydrocarbons under a range of redox conditions

Chemical equation	*Change in free energy* ΔG^0
Denitrification	
$C_6H_5(CH_3) + 7.2\,NO_3^- + 0.2\,H^+ \rightarrow 7\,HCO_3^- + 3.6\,N_2 + 0.6\,H_2O$	-493.6 kJ mol^{-1} NO_3^-
$C_6H_{14} + 7.6\,NO_3^- + 1.6\,H^+ \rightarrow 6\,HCO_3^- + 3.8\,N_2 + 4.8\,H_2O$	-492.8 kJ mol^{-1} NO_3^-
$C_8H_{18} + 10\,NO_3^- + 2\,H^+ \rightarrow 8\,HCO_3^- + 5\,N_2 + 6\,H_2O$	-493.1 kJ mol^{-1} NO_3^-
Nitrate ammonification (example of toluene)	
$C_6H_5(CH_3) + 4.5\,NO_3^- + 2\,H^+ + 7.5\,H_2O \rightarrow 7\,HCO_3^- + 4.5\,NH_4^+$	-493.1 kJ mol^{-1} NO_3^-
Iron(III) reduction (selected examples)	
$C_6H_5(CH_3) + 36\,Fe(OH)_3 + 29\,HCO_3^- + 29\,H^+ \rightarrow 36\,FeCO_3 + 87\,H_2O$	-39.1 kJ mol^{-1} Fe
$C_6H_5(CH_3) + 36\,\alpha\text{-}FeO(OH) + 29\,HCO_3^- + 29\,H^+ \rightarrow 36\,FeCO_3 + 51\,H_2O$	-12.3 kJ mol^{-1} Fe
Sulfate reduction	
$C_6H_5(CH_3) + 4.5\,SO_4^{2-} + 2\,H^+ + 3\,H_2O \rightarrow 7\,HCO_3^- + 4.5\,H_2S$	-45.6 kJ mol^{-1} SO_4^{2-}
$C_6H_{14} + 4.75\,SO_4^{2-} + 3.5\,H^+ \rightarrow 6\,HCO_3^- + 4.75\,H_2S + H_2O$	-44.2 kJ mol^{-1} SO_4^{2-}
$C_8H_{18} + 6.25\,SO_4^{2-} + 4.5\,H^+ \rightarrow 8\,HCO_3^- + 6.25\,H_2S + H_2O$	-44.6 kJ mol^{-1} SO_4^{2-}
Methanogenesis (selected example)	
$C_6H_5(CH_3) + 7.5\,H_2O \rightarrow 2.5\,HCO_3^- + 4.5\,CH_4 + 2.5\,H^+$	-28.5 kJ mol^{-1} CH_4

Source: Modified from Spormann AM and Widdel F (2000) Metabolism of alkylbenzenes, alkanes, and other hydrocarbons in anaerobic bacteria. *Biodegradation* 11: 85–105.

Notes on compounds: Free energy formation (ΔG_f^0, in kJ mol^{-1}) of hydrocarbons used in the presented equations: $C_6H_5(CH_3)$, toluene (lq): +114.2; C_6H_{14}, hexane (lq): −3.8; C_8H_{18}, octane (lq): +6.41

Free energy formation (ΔG_f^0, in kJ mol^{-1}) of iron oxides used in the presented equations: $Fe(OH)_3$, ferric hydroxide (amorphous), −699; α-FeO(OH), goethite (crystalline): −488.6

For adequate comparison of the free energetics of the indicated reactions, $\Delta G^{0'}$ values have to be related to the same number of electrons transferred. Hence, the values for denitrification and iron(III) reduction must be multiplied by 1.6 and 8, respectively, resulting in free energy changes per 8 mol electrons (i.e., per 1.6 mol NO_3^- and 8 mol Fe, respectively).

species. Bjerg et al. (Chapter 11.16, Table 4) review these processes in landfill-impacted aquifers and provide quantitative values for the oxidative capacity of two aquifers. As shown in Table 9, the reactions involving mineralization of aromatic and aliphatic hydrocarbons under a range of redox conditions are exergonic, and, therefore, considered useful to microorganisms. The biggest factor in determining the energy produced for the reaction is the type of available electron acceptor, not the type of hydrocarbon (i.e., aliphatic vs. aromatic). Reactions proceed based largely on the free-energy yield, which is greatest for the denitrification pathway and least for the methanogenic pathway (Stumm and Morgan, 1996). In aquifers, as geochemical conditions change, a sequence of reactions occurs, reflecting the ecological succession of progressively less efficient modes of metabolism. The energy yields for common oxidation–reduction reactions were reviewed by Wiedemeier et al. (1999) and Spormann and Widdel (2000).

Thus, natural attenuation studies of hydrocarbons often focus on the availability of electron acceptors (e.g., Barker and Wilson, 1997; Cozzarelli et al., 1995; Gieg et al., 1999; McGuire et al., 2002; Skubal et al., 2001). Numerous studies have focused on the availability of electron acceptors in both the sediment (e.g., Baedecker et al., 1993; Bekins et al., 2001a; Chapelle et al., 2002; Cozzarelli et al., 2001a; Heron and Christensen, 1994, 1995) and the aqueous phase (e.g., Ball and Reinhard, 1996; Cozzarelli et al., 1999) as a key control of the fate of hydrocarbons in subsurface environments. In most sediment, $Fe(III)_s$, as iron oxides, is abundant and readily reduced by microorganisms. Although less abundant, manganese oxides ($Mn(IV)_s$) are easily reducible by microorganisms. Anaerobic bacteria have been isolated that can use other metals also as electron acceptors, such as the oxyanions of arsenate or selenate (Stolz and Oremland, 1999) and uranium (Abdelouas et al., 2000; Francis et al., 1994; Lovley and Anderson, 2000; Lovley and Phillips, 1992; Lovley et al., 1991; Tebo and Obraztsova, 1998). Anaerobic microbial oxidation of toluene coupled to humus respiration was demonstrated by the use of enriched anaerobic sediments from the Amsterdam petroleum harbor and the Rhine River (Cervantes et al., 2001); the humic acids were utilized as terminal electron acceptors. In most aquifers, nitrate and sulfate are supplied during groundwater recharge by precipitation. In coastal areas, mixing with seawater and contamination of groundwater with fertilizers can significantly increase the concentrations of these constituents. A number of studies have demonstrated a heterogeneous distribution of hydraulic conductivity within a given sedimentary deposit (e.g., Barber et al., 1992; Bekins et al., 2001a; Cozzarelli et al., 1999; Davis et al., 1993; Hess et al., 1992; Robin et al., 1991) that may control the introduction of these electron acceptors to the contaminated zone. In situ microorganisms are poised to take advantage of these changes in electron acceptor availability, and the dominant microbial degradation reactions shift as a result of these changes. These shifting reactions result in the development of redox zones, as determined by geochemical and microbial signatures that are variable in space and time. These concepts are illustrated in Chapter 11.16, Figure 3, and are not reproduced here.

Among the hydrocarbons, the volatile aromatic hydrocarbons, exemplified by the BTEX compounds, have been the most studied in terms of their anaerobic biodegradation potential. This is because of their toxicity, and much greater water solubility and anaerobic degradability relative to the aliphatic, alicyclic, and polycyclic hydrocarbons. Many approaches have been used to study the fate of hydrocarbons under anoxic conditions including field studies, microcosm experiments using sediments and water from contaminated sites, and mixed-culture and pure-culture laboratory studies. The first evidence of anaerobic degradation of monoaromatic hydrocarbons in the environment was observed in methanogenic microcosm experiments with petroleum-contaminated sediments by Ward et al. (1980). Shortly thereafter, Schwarzenbach et al. (1983) and Reinhard et al. (1984) reported the selective removal of alkylbenzenes in anoxic zones of contaminated groundwater, providing evidence for the anaerobic degradation of these compounds by aquifer microorganisms. There were numerous studies in the 1980s focusing on anaerobic degradation of aromatic hydrocarbons, including studies by Vogel and Grbić-Galić (1986), who used an anaerobic methanogenic consortium derived from sewage sludge to verify that oxidation of these substrates occurred in the absence of molecular oxygen. In addition, Wilson et al. (1986) reported the degradation of benzene and alkylbenzenes in methanogenic microcosms derived from a landfill leachate-contaminated aquifer. Both of these laboratory studies, involving mixed cultures of bacteria, highlighted the importance of microorganisms in the degradation of alkylbenzenes under methanogenic conditions. At the same time, evidence that these processes might be important in determining the fate of alkylbenzene in the environment was reported by Eganhouse et al. (1987), who documented the apparent in situ microbial degradation of selected alkylbenzenes in the iron-reducing and methanogenic zones of an aquifer contaminated with crude oil near Bemidji, Minnesota.

Many subsequent laboratory biodegradation studies, conducted using soils or sediment from contaminated sites, have confirmed the transformation of benzene and alkylbenzenes under nitrate-reducing (Hutchins et al., 1991; Kuhn et al., 1988; Major et al., 1988; Zeyer et al., 1986), iron-reducing (Baedecker et al., 1993; Lovley et al., 1989), and sulfate-reducing (Beller et al., 1992a; Edwards et al., 1992; Haag et al., 1991) conditions. Pure-culture studies of nitrate-reducing (e.g., Dolfing et al., 1990; Evans et al., 1991), iron-reducing (e.g., Lovley and Lonergan, 1990), and sulfate-reducing (e.g., Beller et al., 1996; Rabus et al., 1993) bacteria have provided insight into the biochemical mechanisms involved in the anaerobic degradation of alkylbenzenes, and have identified specific microorganisms that can use these compounds as sole carbon sources. Spormann and Widdel (2000) provide a summary of the pure-culture studies of alkylbenzene metabolism.

While anaerobic alkylbenzene degradation had been well documented by the early 1990s, conclusive evidence for the anaerobic degradation of benzene remained controversial until the mid-1990s (Krumholz et al., 1996), and only more recently has it been well documented (Kazumi et al., 1997; Lovley, 2000). Microbial degradation of benzene has been noted in slurries constructed with sediments from various geographical locations, ranging in composition from aquifer sands to fine-grained estuarine muds, under methanogenic, sulfate-reducing,

and iron-reducing conditions (Kazumi et al., 1997), demonstrating the likely widespread occurrence of this process in the environment. Anaerobic degradation of benzene under nitrate-reducing conditions has been demonstrated in both enrichment cultures (Burland and Edwards, 1999) and pure cultures (Coates et al., 2001). The shortage of, and the difficulty associated with maintaining, benzene-degrading pure cultures has limited the understanding of benzene anaerobic biodegradation pathways. As summarized by Mancini et al. (2008), proposed benzene reaction mechanisms include, but are not limited to, hydroxylation of benzene to phenol by a hydroxyl free radical, hydroxylation of benzene to phenol by one electron transfer, and methylation of benzene to toluene. Benzoate and phenol frequently have been detected as intermediates of anaerobic benzene degradation in methanogenic, sulfate-reducing, and iron-reducing enrichment cultures, while phenol and toluene have been detected as intermediates during nitrate-reducing conditions (Botton and Parsons, 2007; Caldwell and Suflita, 2000; Chakraborty and Coates, 2005; Grbić-Galić and Vogel, 1987; Kunapuli et al., 2007; Ulrich et al., 2005).

The microbial metabolism of aromatic hydrocarbons has been reviewed extensively in the last decade (Cao et al., 2009; Chakraborty and Coates, 2004; Farhadian et al., 2008; Foght, 2008; Phelps and Young, 2001; Spormann and Widdel, 2000) and examination of these reviews reveals that our understanding of the biodegradation pathways is constantly changing. Although a detailed discussion of the specific metabolic pathways is beyond the scope of this chapter, it is important to briefly discuss the types of transformations and intermediate products that result. The metabolic intermediates of anaerobic microbial oxidation of petroleum hydrocarbons include aromatic, aliphatic, and alicyclic organic acids, phenols, and aldehydes (e.g., Beller et al., 1992b; Cozzarelli et al., 1990, 1994; Grbić-Galić and Vogel, 1987; Heider et al., 1998; Kuhn et al., 1988; Wilkes et al., 2000). Benzoic acid has been reported in laboratory studies of anaerobic toluene and benzene degradation by both mixed cultures (e.g., Grbić-Galić and Vogel, 1987) and pure cultures (for a review of these studies, see Beller, 2000). *m*-Toluic acid has been identified as an intermediate by pure cultures of *m*-xylene-degrading denitrifying bacteria (Seyfried et al., 1994), while cometabolism of *o*- and *p*-xylenes by toluene-degrading cultures has been found to result in the accumulation of *o*- and *p*-toluic acids (e.g., Beller et al., 1996; Rabus and Widdel, 1995).

Although a pathway involving the oxidation of the methyl substituent group of alkylbenzenes has been proposed in studies of the anaerobic degradation of toluene under nitrate-reducing (Kuhn et al., 1988), iron-reducing (Lovley and Lonergan, 1990), sulfate-reducing (Haag et al., 1991), and methanogenic (Grbić-Galić and Vogel, 1987) conditions, the mechanism of biochemical activation of alkylbenzenes has been elusive. Toluene and xylene oxidation by fumarate addition has been documented and this mechanism results in the production of a new group of organic acid intermediates, benzylsuccinic acids, first identified by Evans et al. (1992) and Beller et al. (1992b). These investigators reported the accumulation of benzylsuccinic acid and benzylfumaric acid (later shown to be *E*-phenylitaconate; Beller, 2000) in pure cultures of toluene-degrading nitrate reducers and in enrichment cultures of toluene- and *o*-xylene-degrading sulfate reducers, respectively. This pathway produces benzylsuccinates or methylbenzylsuccinates (Beller and Spormann, 1997a, b; Biegert et al., 1996; Evans et al., 1992) by a novel mechanism in which the methyl group of the parent hydrocarbon is added to the double bond of fumarate to form benzylsuccinic acid (**Figure 12**). Benzylsuccinic acid appears to be the first intermediate produced during anaerobic toluene metabolism by pure cultures of nitrate-, iron-, and sulfate-reducing bacteria and in mixed cultures of methanogens (these studies are reviewed by Beller, 2000, 2002) with subsequent formation of benzoic acid. The enzyme responsible for catalyzing this step of the reaction is benzylsuccinate synthase (BSS) and the identification of bacteria harboring genes for BSS provides a new tool for quantifying hydrocarbon-degrading bacteria in environmental samples (Beller et al., 2002). Additional evidence indicates that this same mechanism may extend to other alkylbenzenes. Wilkes et al. (2000) reported the selective removal of alkylbenzenes from crude oil by sulfate-reducing enrichment culture with the production of methylbenzylsuccinates and alkylbenzoic acids. In laboratory incubations under sulfate-reducing and methanogenic conditions, sediment-associated microorganisms from a gas condensate-contaminated aquifer anaerobically biodegraded toluene, ethylbenzene, xylene, and toluic acid isomers to their corresponding benzylsuccinic acid derivatives with stoichiometric amounts of sulfate consumed or methane produced (Elshahed et al., 2001). The benzylsuccinates were biodegraded further to toluates, phthalates, and benzoate. Some of the metabolites were also detected in groundwater samples from an aquifer where alkylbenzene concentrations had decreased over time, suggesting that anaerobic microbial metabolism of these contaminants also occurred in situ.

Although oxidized aromatic compounds clearly are important metabolites in the anaerobic degradation of aromatic hydrocarbons, the conditions under which these intermediates accumulate in the environment are poorly understood. Although benzylsuccinic acid has been documented as a metabolic intermediate of toluene degradation under diverse electron-accepting conditions, the extracellular yield of this metabolite under methanogenic conditions can be low (Beller and Edwards, 2000) and it is sometimes not detected in subsurface environments where toluene is actively degrading under anaerobic conditions (Beller, 2002). Other investigators have found that the degradation of aromatic hydrocarbons, such as toluene, can occur in enrichment cultures without the accumulation of any extracellular intermediates under both denitrifying and iron-reducing conditions (Baedecker et al., 1993; Kuhn et al., 1988; Lovley and Lonergan, 1990; Lovley et al., 1989), whereas transient formation of intermediates of toluene degradation, including *p*-cresol, *o*-cresol, and benzoic acid, occurred under methanogenic conditions (Grbić-Galić and Vogel, 1987). In the in situ environment, as well as in laboratory experiments containing mixed microbial communities, the intermediates themselves are subject to degradation. In subsurface environments contaminated with petroleum products, the availability of electron acceptors has been shown to be an important control on the apparent

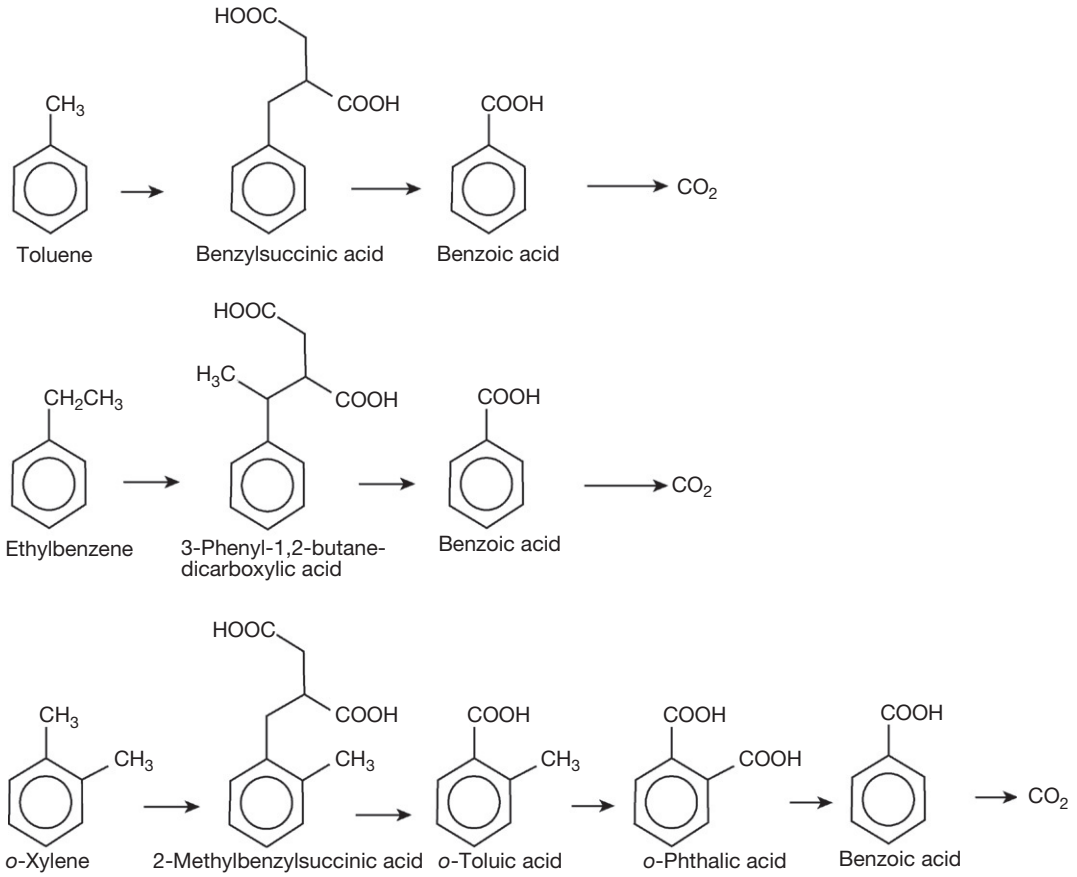

Figure 12 Proposed pathways of anaerobic degradation of toluene, ethylbenzene, and *o*-xylene by the fumarate addition pathway. Modified from Elshahed MS, Gieg LM, McInerney MJ, and Suflita JM (2001) Signature metabolites attesting to the *in situ* attenuation of alkylbenzenes in anaerobic environments. *Environmental Science & Technology* 35(4): 682–689.

rates of microbial degradation of aromatic compounds in situ and the accumulation of metabolic intermediates, such as trimethylbenzoates (Cozzarelli et al., 1994). Identification of the metabolites of biodegradation can thus be used as indicators of the degradation of hydrocarbons in petroleum-contaminated environments (see **Section 11.12.5.3**).

Because of its abundance in anoxic aquatic environments and its importance as a greenhouse gas, methane transformation by anaerobic oxidation has been the subject of numerous studies. The processes involved in, and the rates associated with, anaerobic methane oxidation in the environment have been the subject of several reviews (Caldwell et al., 2008; Knittel and Boetius, 2009; Spormann and Widdel, 2000). In marine systems, sulfate reduction has been shown to be an important part of the methane oxidation process (Boetius et al., 2000; Orphan et al., 2002). More recently, direct, anaerobic oxidation of methane coupled to denitrification has been demonstrated in microbial consortia isolated from anoxic freshwater sediments (Ettwig et al., 2010; Raghoebarsing et al., 2006). Landfills, however, and not hydrocarbon contaminations per se, are the main source of anthropogenic methane emissions in the United States and, therefore, methane degradation processes are not discussed further in this chapter (see **Chapter 11.16** for a discussion of methane generation from landfills).

Among the low molecular weight *n*-alkanes, hexane and octane have been the most frequently studied by microbiologists in their attempt to elucidate the metabolic pathways of aliphatic hydrocarbon biodegradation. Evidence for the utilization of *n*-alkanes by anaerobic bacteria was first indicated in the 1940s by Novelli and ZoBell (1944) and Rosenfeld (1947). Depletion of long-chain *n*-alkanes (C_{15}–C_{34}) from diesel fuel and crude oil under sulfate-reducing conditions has been reported by Coates et al. (1997) and Caldwell et al. (1998). Degradation of *n*-alkanes has also been reported for *n*-hexadecane (Bregnard et al., 1996; Rabus et al., 2001) and *n*-hexane under nitrate-reducing conditions (Bregnard et al., 1996; Rabus et al., 2001) and for *n*-hexadecane under methanogenic conditions (Anderson and Lovley, 2000). Microbial anaerobic degradation of alkanes has been the subject of several reviews (Grossi et al., 2008; Rojo, 2009; Spormann and Widdel, 2000; Wentzel et al., 2007). Several nitrate-reducing and sulfate-reducing bacterial strains capable of degrading *n*-alkanes have been isolated as summarized by Spormann and Widdel (2000) and Grossi et al. (2008). Despite this, knowledge on the processes involved with anaerobic degradation of *n*-alkanes, in particular the long chains, is still limited and warrants further study (Grossi et al., 2008; Wentzel et al., 2007). The two known mechanisms of anaerobic *n*-alkane degradation are fumarate addition (Rabus et al., 2001) and carboxylation (So and Young, 1999).

Both pathways can occur simultaneously and have been also observed as initial reactions during anaerobic degradation of some aromatic hydrocarbons (Grossi et al., 2008). Anaerobic bacterial alkane degradation is a slow process and it is common for individual strains to degrade only a narrow range of *n*-alkanes (Wentzel et al., 2007 and references therein).

The anaerobic degradation of alicyclic hydrocarbons has been documented by Rios-Hernandez et al. (2003), who investigated the metabolism of ethylcyclopentane (ECP) by sulfate-reducing enrichment cultures obtained from a gas condensate-contaminated aquifer. During biodegradation of ECP, intermediates produced included ethylcyclopentylsuccinic acids, ethylcylcopentylpropionic acid, ethylcyclopentylcarboxylic acid, and ethylsuccinic acid. Based on the identification of these intermediates, Rios-Hernandez et al. (2003) proposed that alicyclic hydrocarbons such as ECP can be activated anaerobically under sulfate-reducing conditions by addition to the double bond of fumarate to form the first intermediates, the benzylsuccinate derivatives. This result suggests that the anaerobic metabolites of alicyclic hydrocarbons could be used as indicators of their anaerobic degradation in situ, an approach that has been used in the study of alkanes and aromatic hydrocarbon degradation (Rios-Hernandez et al., 2003).

Although a few recent studies indicate that anaerobic degradation of MTBE can occur (e.g., Kolhatkar et al., 2002; Kuder et al., 2005; Zwank et al., 2005), other studies have demonstrated MTBE to be relatively recalcitrant in anaerobic aquifers (e.g., Bradley et al., 1999; Suflita and Mormile, 1993). In part due to the lack of pure cultures, little is known about the microbial metabolism of this compound under anoxic conditions. One of the first indications of anaerobic MTBE transformation came when Yeh and Novak (1994) found that MTBE could be degraded in microcosms constructed of clay soils and incubated under methanogenic conditions. Mormile et al. (1994) studied aquifer material collected from the Ohio River that had been impacted by oil storage and barge-loading facilities. MTBE degradation was associated with the appearance of TBA. In a subsequent study with aquifer material that had been contaminated with gasoline, Landmeyer et al. (1998) documented slow but measurable rates of MTBE biodegradation, although only about 3% of the added MTBE was degraded. Follow-up studies by Finneran and Lovley (2001) demonstrated that MTBE degradation rates increased after an adaptation period when Fe(III) and humic substances were added to sediments from this same site. In addition, Finneran and Lovley (2001) demonstrated the complete degradation of MTBE with the simultaneous production of CH_4 in bottom sediment from the Potomac River. Bacteria in the aquatic sediments also degraded TBA under anaerobic conditions. An EPA study (Wilson et al., 2000) provides perhaps the best evidence that degradation of MTBE occurs in the subsurface under methanogenic conditions. In this investigation, removal of MTBE in microcosms constructed with sediment from the former Fuel Farm Site at the US Coast Guard Support Center in Elizabeth City, North Carolina, occurred in both the presence and absence of BTEX.

O'Reilly et al. (2001) first proposed that anaerobic biodegradation of MTBE may proceed via an enzyme-catalyzed hydrolysis reaction consistent with an S_N1 or S_N2 nucleophilic substitution mechanism. Since that time, several studies have provided evidence supporting anaerobic biodegradation of MTBE via an S_N2 nucleophilic substitution reaction mechanism, involving direct breakage of the ether bond to form TBA (Kuder et al., 2005; Zwank et al., 2005). Biodegradation of the MTBE metabolite TBA has been demonstrated in microcosm studies under oxic, nitrate-reducing, sulfate-reducing, manganese-reducing (Bradley et al., 2002), and iron-reducing (Finneran and Lovley, 2001) conditions but not methanogenic conditions (Schmidt et al., 2004). The biodegradation pathway of TBA under anaerobic conditions has yet to be elucidated. Continued assessment of the fate of TBA at contaminated field sites is important as there is still little evidence supporting TBA in situ biodegradation under anaerobic conditions and it is unclear if TBA is more than just a dead-end product in methanogenic aquifers (Schmidt et al., 2004).

11.12.4.2.3 Fuel hydrocarbon and oxygenate mixtures

Researchers have shown considerable interest in the effects of MTBE, and more recently, of ethanol on other organic compounds, such as those in gasoline. As a result of the historical widespread use of MTBE in gasoline, BTEX and MTBE are often found as cocontaminants in the subsurface. Aerobic biodegradation studies have generally suggested that BTEX biodegradation rates are not inhibited by the presence of MTBE (Deeb et al., 2001), but rather that MTBE degradation tends to be inhibited by the presence of more readily biodegradable compounds (Deeb et al., 2000, 2001). For example, laboratory studies by Deeb and Alvarez-Cohen (2000) demonstrated no effect on aerobic BTEX biodegradation rates in a toluene-enriched mixed culture from a gasoline-contaminated aquifer that contained 2–100 mg l^{-1} MTBE. In contrast, several laboratory studies have demonstrated that the addition of BTEX compounds significantly decreases MTBE biodegradation rates (Deeb et al., 2001; Raynal and Pruden, 2008). In studies by Schirmer et al. (1999), MTBE aerobic biodegradation only occurred in the absence of BTEX in laboratory columns containing aquifer material from four different field sites. While most aerobic studies, including those discussed earlier, have demonstrated that BTEX impedes MTBE biodegradation, there are exceptions. For example, McMahon (1995) found that MTBE decreased toluene degradation rates by 10% and benzene degradation by up to five times compared to controls containing no MTBE, suggesting that in some cases MTBE can impede BTEX biodegradation. Overall, the above-mentioned studies highlight the need to consider substrate interaction effects when evaluating the metabolic capabilities of microorganisms. There has been comparatively much less study of MTBE and BTEX substrate interactions during anaerobic biodegradation compared to aerobic biodegradation. However, the persistence of MTBE relative to BTEX at anaerobic contaminated field sites suggests that the presence of MTBE does not hinder BTEX biodegradation, but rather that MTBE will be degraded only when more readily degradable substrates have been depleted.

Ethanol can be degraded by both aerobic and anaerobic processes (Powers et al., 2001). A field study by Zhang et al. (2006) released ethanol into a sand and gravel aquifer and monitored its fate. Ethanol was readily degraded with a

first-order biodegradation rate constant of 0.32 day^{-1}, which completely depleted the 6 mg l^{-1} of dissolved oxygen in the groundwater. Ethanol degradation processes were attributed as follows: 0.2% via deoxygenation, 8.3% via denitrification, 4.5% via sulfate reduction, and 77% via fermentation, methanogenesis, and cell growth (Zhang et al., 2006). Suflita and Mormile (1993) also demonstrated that ethanol was the most readily anaerobically biodegradable compound in a laboratory study of 21 fuel oxygenates with a biodegradation rate of 17.9 ± 0.6 ppm C day^{-1}. While the biodegradation of ethanol by microorganisms is well documented, the effect of the presence of ethanol together with hydrocarbons in the environment is less well studied. When ethanol is released with gasoline, the ethanol itself is rapidly degraded (Dakhel et al., 2003; Lahvis, 2003b; Mackay et al., 2006). At the concentrations of ethanol expected near the source of gasohol-contaminated sites, the preferential consumption of electron acceptors for ethanol degradation would likely contribute to longer BTEX plumes and a greater risk of exposure (Chen et al., 2008b; Da Silva and Alvarez, 2002). Church et al. (2000) demonstrated the effects of ethanol on benzene plume lengths. They concluded that in cases with low dissolved oxygen concentrations (2 mg l^{-1}), benzene plume lengths increased over 100% when ethanol was added compared to the benzene plume length simulated with gasoline only (containing no fuel oxygenates).

While numerous studies have demonstrated the potential for plume lengthening due to the coexistence of ethanol with BTEX, few studies have been done in anaerobic systems. Microcosm studies by Corseuil et al. (1998) showed that rapid degradation of ethanol under aerobic conditions can quickly produce anoxic conditions, which can lead to the persistence of benzene, which is the most recalcitrant of the BTEX compounds. Interestingly, toluene biodegradation was either enhanced or impeded depending on the anaerobic electron acceptor condition that prevailed, suggesting that in some cases, ethanol may have promoted the growth of toluene-degrading microorganisms. Similarly, microcosm studies by Ruiz-Aguilar et al. (2002) demonstrated that ethanol was often degraded before BTEX compounds and had a variable effect on BTEX degradation depending on the electron-accepting conditions and aquifer material source.

More recently, Mackay et al. (2006) conducted a controlled ethanol release field study at VAFB to assess the impact of ethanol on MTBE and BTEX anaerobic biodegradation (Beller et al., 2008; Feris et al., 2008; Mackay et al., 2006, 2007; McKelvie et al., 2007a). Two continuous side-by-side field releases were conducted within a preexisting MTBE plume to form two lanes. The first involved the continuous injection of site groundwater amended with benzene, toluene, and *o*-xylene (BToX) ('No ethanol lane'), while the other involved the continuous injection of site groundwater amended with BToX and ethanol ('With ethanol lane'). Initially, the BToX plumes in both lanes were the same length, but after an initial acclimation period, the plume in the 'No ethanol lane' retracted significantly, whereas the plume in the 'With ethanol lane' did not retract as quickly or as far. The preferential consumption of sulfate by ethanol was suggested to have led to the slower rates of BTEX biodegradation. Follow-up studies using quantitative polymerase chain reaction (qPCR) demonstrated that the presence of ethanol altered microbial community structure and function, which in turn lowered the aquifer redox state and led to a reduction in biodegradation rates of BToX (Feris et al., 2008). Hence, overall, the results suggest that ethanol may reduce biodegradation rates of aromatic fuel components in the subsurface (Beller et al., 2008; Feris et al., 2008, Mackay et al., 2006).

Interestingly, the same effect was not seen for the existing MTBE contamination. Substantial MTBE biodegradation did not occur in the 'No ethanol lane' but rather in the 'With ethanol lane' (Mackay et al., 2007; McKelvie et al., 2007a). This suggests that the ethanol release somehow stimulated MTBE biotransformation to TBA by creating a strongly acetogenic/methanogenic zone and/or providing the required nutrients and electron donors to establish an active microbial community (Mackay et al., 2007). During the ethanol release experiment, concentrations of TBA increased to a maximum of 1200 μg l^{-1} in the 'With ethanol lane' due to biodegradation of MTBE. Results suggest that the TBA produced did not undergo substantial, if any, biodegradation during the study timeframe (Mackay et al., 2007; McKelvie et al., 2007a). The physiological mechanism behind the stimulation of MTBE biodegradation by ethanol at VAFB has not yet been elucidated. Wilson et al. (2005a) outlined three possible biochemical processes under which MTBE may be biodegrading in the subsurface: (1) chemolithotrophic methanogenesis (biodegradation by methanogens); (2) MTBE carboxylation (biodegradation by acetogenic bacteria); and (3) MTBE direct hydrogenation (MTBE as an alternate electron acceptor). All these processes require molecular hydrogen (Wilson et al., 2005a). Ethanol itself was degraded very rapidly in the subsurface at VAFB and resulted in the production of acetate, butyrate, and propionate (Mackay et al., 2006). In addition, ethanol fermentation likely also occurred, resulting in the production of molecular hydrogen, which may have stimulated MTBE biodegradation. The apparent persistence of TBA shown in the VAFB study also highlights the need for additional studies of TBA in contaminated aquifers to determine whether TBA is a dead-end product in anaerobic groundwater systems, particularly under methanogenic conditions, as has been suggested (Bradley et al., 2002; Schmidt et al., 2004). Further study into the effects of ethanol on BTEX and MTBE biodegradation is warranted as the use of ethanol-based fuels continues to rise. In particular, the effect of microbial community and terminal electron acceptor processes on substrate interaction effects requires further assessment for accurate prediction of the fate of gasoline constituent mixtures.

11.12.5 Environmental Restoration

11.12.5.1 Natural Attenuation Processes

Natural attenuation relies on subsurface processes such as dilution, dispersion, sorption, volatilization, and biodegradation to effectively reduce contaminant toxicity, mobility, or volume to levels that are below drinking water guidelines (Wiedemeier et al., 1995). Natural attenuation of petroleum hydrocarbons in the environment has been the focus of many studies over the past decade and has become widely applied as a remedial option (National Research Council (US) Committee on Intrinsic Remediation, 2000). Recognition of the broad

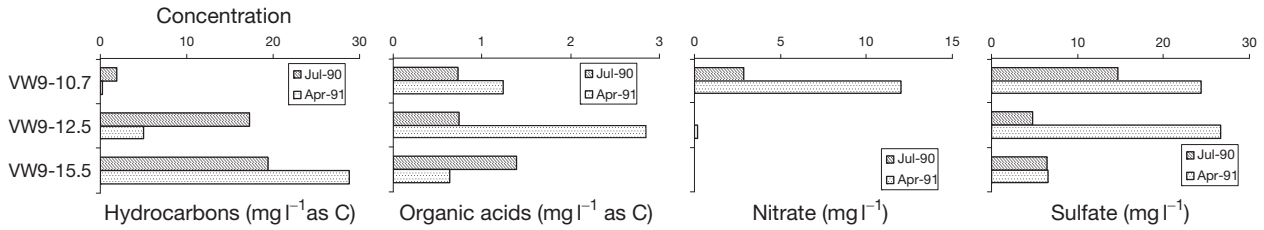

Figure 13 Concentration profiles for groundwater at the Galloway Township gasoline study site in July 1990 and April 1991 (modified from Cozzarelli IM, Herman JS, Baedecker MJ, and Fischer JM (1999) Geochemical heterogeneity of a gasoline-contaminated aquifer. *Journal of Contaminant Hydrology* 40(3): 261–284). The two shallow samples are within the sandy sediments (3.26 and 3.81 m below land surface, bls) and one deeper sample (at 4.72 m bls) is within the low-permeability clay-rich layer.

scope of the problem of groundwater contamination and the high cost of monitoring engineered groundwater clean-up systems has contributed to the skyrocketing interest in monitored natural attenuation as a remediation strategy (Bekins et al., 2001b). The conditions under which natural attenuation is likely to be an effective means of aquifer restoration were discussed by Barker and Wilson (1997) for BTEX compounds and by Chapelle (1999) for petroleum hydrocarbons. The theory, mechanisms, and applications of natural attenuation for fuels, including numerous case studies, were presented by Wiedemeier et al. (1999) and, therefore, do not require reiteration here. However, limits on the applicability of natural attenuation and some of the problems faced when attempting to document natural attenuation warrant discussion.

Heterogeneities in physical and chemical properties of aquifer sediments can constrain the possibilities for hydrologic transport and biogeochemical reactions and complicate the study of the fate of petroleum contaminants in situ. The potential difficulties in monitoring contaminant migration in heterogeneous systems were first illustrated by Patrick and Barker (1985) in a natural-gradient tracer test involving addition of dissolved benzene, toluene, and xylenes in groundwater. In the unconfined shallow glaciofluvial sand aquifer, the vertical scale of heterogeneity was on the order of 0.01 m, and hydraulic conductivity contrasts of up to an order of magnitude were demonstrated among sediment layers. Resulting retardation of hydrocarbons along individual layers and concentration-depth profiles at individual locations appeared erratic. In a study of a coastal plain aquifer, the rates of biodegradation of toluene and benzene were observed to vary as a function of sediment type due to different levels of microbial activity (Aelion, 1996). Natural attenuation of petroleum hydrocarbon in a heterogeneous aquifer in Denmark showed that strong seasonal variations in the flow field affected the availability of electron acceptors and the shape and extent of the hydrocarbon plume (Mossing et al., 2001).

Because of the complexities of the subsurface environment, documenting the natural attenuation of hydrocarbons requires multiple lines of evidence (National Research Council (US) Committee on Intrinsic Remediation, 2000; Wiedemeier et al., 1995) and a multiscale approach. It has been demonstrated that closely spaced sampling is required to identify microbiological processes in contaminated aquifers (Bekins et al., 1999; Smith et al., 1991). In fact, detailed studies of microbial processes may require a microscale approach to account for the microbe–mineral interactions that have been documented by Bennett et al. (2000). Coupling the study of microbiological and hydrogeologic processes is a particular challenge because the scales used in these investigations usually are quite different. This difference has resulted in limited knowledge of the interaction between hydrological and microbiological features of subsurface environments (Haack and Bekins, 2000).

Scientists conducting research as part of the USGS Toxic Substances Hydrology Program (for more information, see http://toxics.usgs.gov) have been characterizing chemical heterogeneity in an effort to better understand the natural attenuation of hydrocarbons in surficial aquifers. In one example of this approach, the scale of biogeochemical reactions was investigated in a physically and chemically heterogeneous surficial coastal plain aquifer contaminated by a gasoline spill (Cozzarelli et al., 1995, 1999). Hydrocarbons were degraded by microbially mediated reactions that varied over short vertical distances (tens of centimeters) and time (months) (**Figure 13**). Anaerobic processes, iron reduction and sulfate reduction, dominated within a low-permeability clay unit present between 4 and 4.5 m bls (below land surface), whereas in the more permeable sandy layers (less than 4 m bls), nitrate reduction and aerobic degradation occurred. Mixing with oxygenated recharge water resulted in increased degradation of hydrocarbons near the water table (at 3.26 m bls, **Figure 13**), whereas mixing with less contaminated groundwater limited the spread of hydrocarbons at the base of the plume. Assessment of aquifer heterogeneities and groundwater contamination was possible because of sampling at the submeter scale, a finer resolution than is attempted in many remedial investigations of contaminated aquifers. The information obtained in this type of study is essential to the development of models capable of simulating the fate of hydrocarbons at the scale of a contaminated site.

Steep gradients in the concentrations of organic and inorganic carbon, and the reactants and products associated with hydrocarbon degradation have also been observed by investigators at a site contaminated with crude oil at Bemidji, Minnesota (Bekins et al., 2001a; Cozzarelli et al., 2001b). The decade-long study of the hydrocarbon plume documented that the extent of contaminant migration and compound-specific behavior has changed as redox reactions, most notably iron reduction, have evolved over time. Previous work at the Bemidji site documented the loss of benzene and alkylbenzenes in groundwater downgradient from the crude oil source (Baedecker et al., 1993; Cozzarelli et al., 1990; Eganhouse et al., 1993, 1996) and established that microorganisms

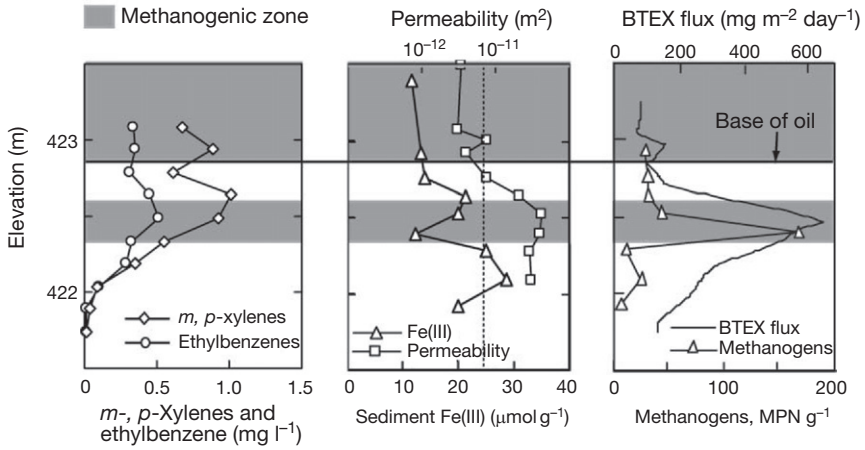

Figure 14 Microbial and chemical profiles from the crude oil-contaminated aquifer near Bemidji, Minnesota (reproduced from Bekins BA, Cozzarelli IM, Warren E, and Godsy EM (2002) Microbial ecology of a crude oil contaminated aquifer. *Proceedings of Groundwater Quality 2001 Conference. Third International Conference on Groundwater Quality*, Sheffield, UK, 18–21 June 2001. IAHS Publication No. 275, pp. 57–63.). Methanogenic zones are shaded gray.

degrade these compounds in the anoxic aquifer (Baedecker et al., 1993; Cozzarelli et al., 1994; Lovley et al., 1989). Zones of maximum hydrocarbon contamination at this site were found within the anoxic plume and were on the order of only 1–2 m in thickness (Bekins et al., 2001a; Cozzarelli et al., 2001a). Within the narrow anoxic zones, anaerobic degradation reactions resulted in significant loss of hydrocarbons as groundwater moved downgradient. Over time, on the order of years, concentration changes at a small scale, determined from analysis of pore-water samples drained from aquifer cores, indicated that the hydrocarbon plume was growing slowly as sediment iron oxides were depleted. Depletion of the unstable Fe(III) oxides near the subsurface crude oil source caused the zone of maximum concentrations of BTEX to spread within the anoxic plume (Cozzarelli et al., 2001a). Microbial data from the same profiles through the anaerobic portion of the contaminated aquifer (**Figure 14**) clearly show areas where the microbial populations have progressed from iron-reducers to methanogens (Bekins et al., 2001a). In monitoring the remediation of hydrocarbon-contaminated groundwater by natural attenuation, these investigators found that subtle concentration changes in observation well data from the anoxic zone were diagnostic of depletion of the intrinsic electron-accepting capacity of the aquifer and may allow early prediction of growth of a hydrocarbon plume.

The presence of cold-adapted, hydrocarbon-degrading microorganisms has been documented in Antarctic (Aislabie et al., 2000) and Arctic (Braddock and McCarthy, 1996; Eriksson et al., 2001; Lindstrom et al., 1999; Mohn and Stewart, 2000) soils, suggesting that there is potential for biodegradation to play a role in the remediation of the considerable petroleum hydrocarbon contamination that exists in these environments (Blanchette et al., 2004; Margesin and Schinner, 1999; Tumeo and Giunn, 1997). However, bioremediation in cold temperature environments may be hindered by low degradation rates (Eriksson et al., 2001) and can be difficult to identify and quantify often because of subtle changes in contaminant concentrations and electron acceptor concentration (Richmond et al., 2001). Microcosm studies can be very lengthy and can often take hundreds of days and may not definitively indicate that the process is actually occurring in situ. For example, despite demonstration of petroleum biodegradation potentials for Arctic samples in the laboratory approaching those seen in temperate regions, several groups have suggested that these potentials are unlikely to be achieved in situ where biodegradation is limited by the short annual thaw season (Braddock and McCarthy, 1996; Eriksson et al., 2001). In a study of a petroleum-contaminated subarctic aquifer beneath an oil refinery in Alaska, McKelvie et al. (2005) were able to demonstrate not only the biodegradation of toluene and xylene but also the likely persistence of benzene, highlighting the need to consider biodegradation on a compound-specific basis. Ulrich et al. (2010) reviewed 46 field studies of BTEX attenuation from sites with groundwater typically less than 15 °C and showed that biodegradation rates of individual BTEX compounds decrease by approximately 50% for a 10 °C decrease in temperature. Given that oil exploration and production in polar regions are likely to increase in the future, a better understanding of natural attenuation processes in these environments is important. The potential for bioremediation of petroleum hydrocarbons in groundwater under cold climate conditions is further reviewed by Stempvoort and Biggar (2008).

The natural attenuation potential of many compounds is not yet well understood (National Research Council (US) Committee on Intrinsic Remediation, 2000). Although natural attenuation of the aromatic hydrocarbon components of gasoline has been well established, less is known about the efficacy of natural attenuation of MTBE. Studies at the Borden aquifer (Ontario, Canada) indicated that MTBE had a retardation factor of approximately 1 and, as such, traveled at the average velocity of the groundwater (Hubbard et al., 1994). This is because, unlike BTEX compounds, sorption and volatilization are not major attenuation processes for MTBE (Hubbard et al., 1994; Shaffer and Uchrin, 1997; Squillace et al., 1996). Due to its high aqueous solubility (Squillace et al., 1996), once dissolved into groundwater, MTBE can easily migrate through the vadose zone (Dernbach, 2000), and large

MTBE plumes extending for kilometers have been documented at some contaminated sites (Johnson et al., 2000). A study by Wilson et al. (2000), conducted at the former Fuel Farm Site at the US Coast Guard Support Center at Elizabeth City, North Carolina, demonstrated MTBE removal in a methanogenic aquifer in which BTEX compounds undergo extensive anaerobic oxidation. The apparent attenuation of MTBE in the anoxic plume (average first-order attenuation rate of MTBE in the groundwater was calculated at 2.7 $year^{-1}$; Wilson et al., 2000) was consistent with the biodegradation rates measured in laboratory experiments.

11.12.5.2 Engineered or Enhanced Remediation

Engineered remediation of hydrocarbon-contaminated environments focuses on the destruction, dilution, or physical removal of the hydrocarbons to reduce their concentrations to levels that are environmentally acceptable. There are in situ technologies, involving treatment of the contaminants in place, as well as ex situ technologies, which involve physical removal of the contaminated material to another location. The environmental compartment within which the hydrocarbons reside largely dictates the remediation approach. Sometimes the approach involves the complete or partial transfer of the contaminant from one environmental compartment to another, thereby transferring the risk. For example, in the treatment of contaminated soil, one approach is aeration, which increases the inhalation exposure risk of workers and nearby residents (National Research Council, 1993). Remedial technologies currently used in the restoration of petroleum-contaminated aquifers were reviewed by Testa and Winegardner (2000). The restoration of contaminated aquifers requires that several objectives be accomplished, including both contaminant plume and source containment, and plume and source removal. Different technological approaches are often used to address each of these objectives and may include combinations of physical, chemical, and biological processes.

In beach sediments or in the terrestrial environment, where physical removal of the contaminant is difficult and expensive and ex situ cleanup technologies have appreciable limitations (National Research Council, 1993), a common cleanup approach is enhanced bioremediation. Enhanced bioremediation is an intensive area of research and numerous books have been written on this topic (Baker and Herson, 1994; Crawford and Crawford, 1996; Riser-Roberts, 1992). Enhanced bioremediation focuses on aiding the destruction of contaminants by microorganisms by providing electron acceptors, donors, nutrients, or microorganisms to the environmental system. The presence of hydrocarbons in the environment usually brings about a selective enrichment of indigenous hydrocarbon-degrading microorganisms in situ and, thus, seeding a contaminated site with microorganisms usually is not necessary (Rosenberg and Ron, 1996). Addition of nutrients or electron acceptors, however, is a common approach, and has been effective in increasing biodegradation of hydrocarbons following surface water petroleum spills. As discussed in **Section 11.12.4.2.1**, in aquatic environments, microbial requirements for oxygen and moisture are not limiting, but available nutrients, such as nitrogen and phosphorus, usually are limiting (Rosenberg and Ron, 1996). For example, commercial nitrogen- and phosphorus-containing fertilizers that have an affinity for hydrocarbons have been used to treat oil-contaminated shorelines.

Following the *Exxon Valdez* oil tanker spill, about 100 miles (161 km) of shoreline were treated with fertilizers in the largest marine bioremediation project ever undertaken. Despite numerous studies of the remediation project, no conclusive evidence for the long-term impact of fertilizer treatment on the removal of oil from the beaches was obtained (Rosenberg and Ron, 1996). More success has been achieved using time-release fertilizers to treat oil-contaminated sand. Rosenberg et al. (1992) demonstrated significant biodegradation of hydrocarbons at Zvulon Beach in Israel that was heavily contaminated with heavy crude oil, after addition of controlled-release, polymeric, hydrophobic fertilizer (because bacteria that can hydrolyze this fertilizer are rare, bacteria were added in this case).

The physicochemical characteristics of MTBE, including relatively high aqueous solubility and low Henry's constant, are such that removal by traditional treatment technologies, such as pump-and-treat, is difficult. For example, a common bioremediation approach in the unsaturated subsurface is known as 'bioventing,' which involves the forced air movement of oxygen through the petroleum-contaminated soil (Hinchee, 1995). The presence of MTBE in addition to petroleum hydrocarbon compounds complicates the use of these techniques because the volatility and aerobic biodegradation potential of MTBE and BTEX, for example, are different and the effects of their co-occurrence are largely unknown. The presence of MTBE in many cases of petroleum product releases to the environment has, therefore, appreciably changed the restoration options. Because of the slow rate of anaerobic degradation of MTBE, enhancement of aerobic degradation by enhanced oxygenation of an aquifer has been the focus of in situ bioremediation approaches (Salanitro et al., 2000; Wilson et al., 2002).

11.12.5.3 Innovative Tools to Assess Remediation

New analytical tools and approaches are being used to document the biodegradation of contaminants in situ as summarized in recent reviews by Bombach et al. (2010b) and Kuder and Philp (2008). These include the use of compound-specific stable isotope ratios (e.g., Dempster et al., 1997; Wilkes et al., 2000), identification of metabolism products (e.g., Beller, 2000), comprehensive two-dimensional gas chromatography (e.g., Gaines et al., 1999), and molecular techniques to identify microbial diversity and function (e.g., Kleikemper et al., 2002). Because disappearance of parent compounds is not always attributable to destructive attenuation mechanisms, the presence of oxidized metabolites of hydrocarbons is sometimes used as conclusive evidence of in situ microbial transformation. Beller (2000) reviews the use of metabolic indicators for detecting anaerobic degradation of alkylbenzenes; examples of these metabolites are shown in **Figure 15**. The metabolites of alkylbenzenes most frequently reported in aquifers contaminated with petroleum products are benzoic and alkylbenzoic acids. These compounds were first identified in a petroleum-contaminated aquifer by Cozzarelli et al. (1990), who found methyl-, dimethyl-, and trimethylbenzoic acids in anoxic groundwater downgradient from a crude oil spill in Bemidji,

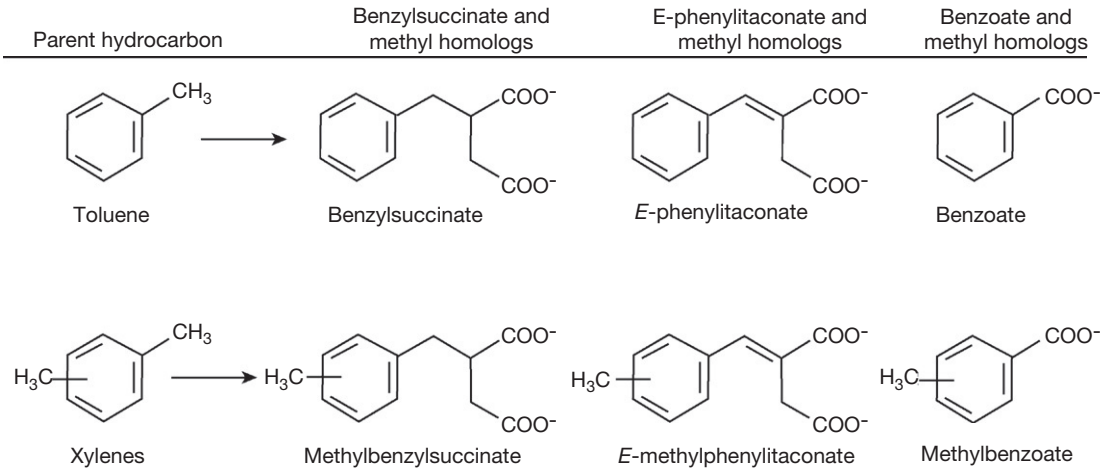

Figure 15 Potential indicators of in situ metabolism of toluene and xylene under anaerobic conditions. Modified from Beller HR (2000) Metabolic indicators for detecting *in situ* anaerobic alkylbenzene degradation. *Biodegradation* 11(2–3): 125–139.

Minnesota, where microbial degradation of alkylbenzenes was occurring. Among others who have observed these compounds in association with hydrocarbon contamination are Fang and Barcelona (1999), who identified dimethyl- and trimethylbenzoic acids in an anoxic aquifer contaminated with JP-4 jet fuel at Wurtsmith Air Force Base, Oscoda, Michigan.

Beller et al. (1995) first proposed the use of benzylsuccinic acid and its methylated analogs as useful indicators of anaerobic toluene and xylene degradation in a controlled-release experiment at Seal Beach (California). During the 2 month injection experiment, toluene, *o*-xylene, and *m*-xylene were depleted in the groundwater and the benzylsuccinate and *E*-phenylitaconate homologs corresponding to each of these hydrocarbons appeared in the groundwater. Concentration trends provided conclusive evidence that these metabolites were produced during anaerobic metabolism of the precursor hydrocarbons. Similar alkylbenzene transformation products were detected in a fuel-contaminated aquifer in Fallon (Nevada) (Beller, 2000). In a highly reduced gas condensate-contaminated aquifer, Elshahed et al. (2001) found benzylsuccinic acid analogs of ethylbenzene, *o*-, *m*-, and *p*-xylene metabolism in sulfate-reducing zones of the aquifer. Anaerobic metabolism of alkanes in situ also has been indicated by the presence of alkylsuccinates in six aquifers contaminated with petroleum products (Gieg and Suflita, 2002). The widespread occurrence of these metabolites at sites with both low and high hydrocarbon concentrations suggests that anaerobic degradation reactions are common in subsurface environments and that detection of metabolites may be a useful indicator of this process. Parisi et al. (2009) measured contaminant metabolite profiles in groundwater from a former refinery site to evaluate in situ microbial hydrocarbon metabolism. They compared a contaminant-free background aquifer to areas of the same aquifer impacted by hydrocarbon spills. A variety of metabolites indicative of hydrocarbon degradation were found in locations of the hydrocarbon contamination but not in the background well. The identified metabolites were indicative of degradation of several alkylbenzenes, naphthalenes, PAHs, alkanes, and potentially alicyclic hydrocarbons. Importantly, there was good agreement between field metabolic profiling and laboratory incubations with regard to which compounds were actively degrading and which were recalcitrant.

Numerous studies over the past two decades have established that hydrocarbon-degrading microorganisms are ubiquitous in soils, aquatic sediments, and aquifers. However, one aspect of documenting natural attenuation of hydrocarbons is demonstrating that the microbial populations necessary to carry out the specific transformations, outlined in **Section 11.12.4.2**, are active. This activity presents a practical constraint for many studies of natural attenuation because of the difficulty in accurately defining microbial activity in environmental samples (Bekins et al., 2002). Culture-based and molecular analyses of microbial populations in subsurface contaminant plumes have revealed important adaptation of microbial populations to plume environmental conditions (Haack and Bekins, 2000). The results of studies at the Bemidji crude oil site demonstrate that the subsurface geochemical and hydrological conditions affect subsurface microbial community structure appreciably (Bekins et al., 2001a, 2002).

Microbial population dynamics in petroleum-contaminated environments are sometimes characterized based on the analysis of lipids, such as phospholipid ester-linked fatty acids (PLFAs). These techniques can provide information on a variety of microbial characteristics and on overall community composition (Green and Scow, 2000). For example, Fang and Barcelona (1998) examined microbial biomass and community structure in a glaciofluvial aquifer located at Wurtsmith Air Force Base, Michigan, which had been contaminated with JP-4 fuel hydrocarbons released after the crash of a tanker aircraft. The fatty acids identified in the aquifer sediment ranged from C_{12} to C_{20}, including saturated, monounsaturated, branched, and cyclopropyl fatty acids, while the polyunsaturated fatty acids were virtually absent. The results of the PLFA analysis indicated considerable microbial heterogeneity of bacteria in the subsurface. The hydrocarbon-contaminated anaerobic zones had higher microbial biomass and metabolically more diverse microbial communities than those in aerobic zones. More recently, stable isotope probing has been used to track the incorporation of ^{13}C from labeled BTEX, MTBE, and TBA into PLFA, DNA, and RNA to evaluate biodegradation

potential and to identify and isolate petroleum hydrocarbon-biodegrading microorganisms (Bombach et al., 2010a; Busch-Harris et al., 2008; Herrmann et al., 2010; Kasai et al., 2006; Kunapuli et al., 2007).

Nucleic acid approaches, which involve the extraction of microbial DNA and RNA from environmental samples, have been applied to the study of natural attenuation of petroleum products in the last decade. With these techniques, the specific genes that are responsible for hydrocarbon-degrading capabilities in bacteria can be measured. These tools are especially useful for studying microbial diversity at impacted sites (Madsen, 2000). Various applications of these techniques in petroleum-contaminated environments are reviewed by Haack and Bekins (2000). For example, Stapleton and Sayler (1999) monitored changes in the molecular microbial ecology at the Natural Attenuation Test Site at Columbus Air Force Base, Mississippi by identifying hydrocarbon-degrading genes in situ. Exposure of indigenous microorganisms to BTEX and naphthalene was evaluated using an array of gene probes targeting common genotypes associated with the aerobic biodegradation of these compounds. Each of the targeted genotypes showed appreciable responses to hydrocarbon exposure and, combined with increased aerobic degradation potentials of the added hydrocarbons, provided conclusive evidence that an aerobic contaminant-degrading community successfully developed within the plume. The Natural Attenuation Study at Columbus AFB represents a successful application of molecular techniques in linking adaptations of indigenous microorganisms to hydrocarbon exposure. Currently, however, the number of known genes responsible for hydrocarbon degradation is small and broader application of this technology may enable the identification of the nucleic acid sequences of additional degradative genes (Haack and Bekins, 2000).

Carbon and hydrogen compound-specific isotope analysis (CSIA) has emerged as a useful tool for assessing the contribution of biodegradation versus nondegradative processes to natural attenuation in contaminated aquifers (Ahad et al., 2000; Harrington et al., 1999; Hunkeler et al., 2001a; Kelley et al., 1997; Mancini et al., 2002, 2003; Stehmeier et al., 1999). Chemical bonds formed by the light isotopes (e.g., ^{1}H–^{12}C) are generally weaker than bonds containing heavier isotopes (e.g., ^{1}H–^{13}C or ^{2}H–^{12}C). During petroleum hydrocarbon biodegradation, molecules containing light isotopes will therefore react at a slightly faster rate than those containing heavier isotopes, resulting in the progressive isotopic enrichment of the heavier isotope in the remaining compound. While biodegradation of BTEX and MTBE can involve substantial isotopic fractionation, particularly under anaerobic conditions, nondegradative attenuation processes such as dissolution, vaporization, and sorption result in carbon isotopic fractionation that is typically less than the analytical uncertainty of CSIA (Dempster et al., 1997; Harrington et al., 1999; Huang et al., 1999; Schuth et al., 2003; Slater et al., 1999, 2001). Similarly, nondegradative attenuation processes result in hydrogen isotopic fractionation typically less than the analytical uncertainty of CSIA (Schuth et al., 2003; Ward et al., 2000), except when more than 95% of the compound is sorbed (Schuth et al., 2003) or volatilized (Wang and Huang, 2003); however, such extreme removal processes are expected only during remediation efforts using absorbent materials or air sparging. While applications of stable isotope analysis to assess the fate of environmental contaminants is discussed in more detail elsewhere (e.g., Elsner et al., 2005; Hunkeler et al., 2008), discussion of its relevance to petroleum hydrocarbons and MTBE is summarized here.

CSIA has been used to verify the occurrence of in situ biodegradation of aromatic hydrocarbons (e.g., Griebler et al., 2004; Mancini et al., 2002; Richnow et al., 2003; Steinbach et al., 2004) and MTBE (e.g., Kolhatkar et al., 2002; Kuder et al., 2005; Zwank et al., 2005) at contaminated field sites. While early studies mainly focused on identifying the occurrence of in situ biodegradation through isotopic enrichment in ^{13}C or ^{2}H in downgradient wells relative to the source zone, more recently CSIA has been used to provide estimates of biodegradation rates in the subsurface (Fischer et al., 2006; McKelvie et al., 2007a; Morrill et al., 2005). In a multitracer test, a mixture of ring-deuterated and fully deuterated toluene and bromide (as a conservative tracer) were injected into the subsurface (Fischer et al., 2006). As the mass of toluene and bromide injected were known, the biodegradation rates were calculated by comparing the mass and isotopic composition of toluene released to the mass and isotopic composition of toluene crossing two control planes. There was good agreement between toluene biodegradation rates calculated using isotopic values and biodegradation rates calculated using changes in toluene concentration relative to bromide across the control planes (Fischer et al., 2006). Similarly, McKelvie et al. (2007a) found that MTBE first-order biodegradation rates calculated using measured isotopic values at VAFB were in good agreement with the rate constants calculated using contaminant mass discharge (Mackay et al., 2006). The good agreement found in MTBE biodegradation rates using carbon isotopic values and mass discharge methods suggests that CSIA can provide reliable biodegradation rate estimates if well density at a site is not sufficient to permit a mass discharge-based approach. The USEPA recently issued two manuals outlining how stable isotopic fractionation can be used to calculate the extent of biodegradation and biodegradation rates of organic contaminants, including MTBE and BTEX, in groundwater (Hunkeler et al., 2008; Wilson et al., 2005b), attesting to the growing acceptance of this technique as a biodegradation monitoring strategy.

In addition, CSIA can be used to identify biodegradation pathways (Elsner et al., 2005 and references therein). Laboratory studies measuring isotopic fractionation of MTBE (Gray et al., 2002; Hunkeler et al., 2001b; Kolhatkar et al., 2002; Kuder et al., 2005; McKelvie et al., 2009; Rosell et al., 2007; Zwank et al., 2005) and BTEX (Hunkeler et al., 2001a; Mancini et al., 2003, 2006, 2008; Meckenstock et al., 1999; Morasch et al., 2001, 2002, 2004) have provided insights into the initial enzymatic reactions involved in MTBE biodegradation. New techniques that yield site-specific isotopic values have the potential to yield additional insights into the fate of petroleum hydrocarbons and MTBE (Gauchotte et al., 2009; McKelvie et al., 2010). Such measurements have the potential to yield information about the origin of compounds (natural versus synthetically produced), their metabolic degradation pathways, and their parent compounds. For example, the use of quantitative site-specific ^{2}H nuclear magnetic resonance spectroscopy directly quantified the $^{2}H/^{1}H$ isotopic ratios of

the methoxy and tertiary butyl groups of MTBE and demonstrated that their isotopic ratios were reflective of their production from methanol and isobutene, respectively (McKelvie et al., 2010).

An increasing trend in the literature is the incorporation of a combination of several microbial and molecular-based methods to give a complete picture of biodegradation potential and occurrence at contaminated field sites (Abe et al., 2009; Beller et al., 2008; McKelvie et al., 2005, 2007b; Parisi et al., 2009; Weiss and Cozzarelli, 2008). Carbon and hydrogen isotopic fractionation during biodegradation of both BTEX and MTBE has been shown to follow an exponential relationship (Rayleigh model), and where the fractionation factor is small, significant biodegradation must occur before the observed isotopic fractionation is greater than the analytical uncertainty. Therefore, stable isotopic analysis alone may not be able to detect early onset of biodegradation and other lines of evidence are also important. For example, it is beneficial to use both CSIA and analysis of the unique metabolic intermediates when assessing bioremediation as a remedial option at contaminated sites, as analysis of metabolites may provide the earliest evidence of biodegradation, while stable carbon and hydrogen isotopes may continue to provide support for biodegradation in less contaminated wells where metabolites may be below detection limits (Beller et al., 2008; McKelvie et al., 2005). In addition, while microbial methods such as polymerase chain reaction (PCR) may indicate the presence of a petroleum-biodegrading microorganism, it is not unequivocal evidence that the process is occurring in situ and other molecular techniques such as CSIA and measurement of metabolic intermediates can be implemented to estimate the extent of petroleum biodegradation.

11.12.6 Challenges

The use of petroleum products is integral to the functioning of industrialized societies. Increased worldwide energy consumption results as economies expand to meet the instinctive need to improve living standards. Increased energy demand translates directly to increased use and release of petroleum products because use of alternative energy sources (e.g., nuclear, wind, hydroelectric, and solar power) remains a secondary strategy. Our global reliance on oil has resulted in the expansion of drilling and production activities to offshore marine environments and to polar regions. The release of petroleum compounds to the environment results in human and ecological exposure. Knowledge of the fate of the compounds throughout the environment, their distribution in the hydrosphere, biosphere, and geoshpere at a scale relevant to human consumption, and the toxicological consequences associated with chronic exposure to mixtures of petroleum and other compounds (e.g., pesticides) has not advanced to the point where environmental costs associated with product usage can be measured.

Much research has focused on the transport of BTEX contaminants in groundwater that results from releases from USTs. An evolving consensus within the research community is that natural attenuation from microbial breakdown and volatilization limits the movement of BTEX in ground and surface waters. This consensus has been supported by results of the USGS in its assessment of ambient shallow groundwater throughout urban areas, as BTEX compounds are not detected frequently. Although it has been established that detailed field investigations are essential for a thorough evaluation of natural attenuation, allowing the documentation of the biogeochemical processes responsible for contaminant destruction (Bekins et al., 2001b; National Research Council (US) Committee on Intrinsic Remediation, 2000), few of these studies have been undertaken. New tools are needed to allow the study of the fate of petroleum hydrocarbons and fuel oxygenates in diverse environments. Long-term detailed monitoring programs are essential to develop conceptual models of natural attenuation and studies need to allow the recognition that our understanding of microbial transformation pathways is constantly changing.

Field investigations of spatial and temporal variability of biogeochemical processes and resulting changes in groundwater and aquifer composition provide insights into how naturally occurring microorganisms degrade hydrocarbons in contaminated aquifers such as those underlying the Galloway and Bemidji sites. It is clear that understanding the environmental conditions that favor biodegradation depends on our ability to measure these processes at an appropriate scale. This knowledge forms the basis for applying either intrinsic or engineered in situ bioremediation as a groundwater cleanup strategy. Yet, long-term studies of the natural degradation of contaminants in the field are rare and studies of the impact of changes in important factors, such as the source term, are lacking. In addition, the fate of hydrocarbons in geologically heterogeneous systems is largely unknown and determining the appropriate spatial scale at which to sample in heterogeneous systems presents a major challenge to geochemists and microbiologists and will differ from site to site. New analytical tools will aid in the verification and quantification of contaminant fate processes in the environment. However, there is a need for an integrated approach to assess the contribution of biodegradation to natural attenuation that draws on multiple lines of evidence including stable isotope fractionation, analysis of metabolic intermediates and direct microbial evidence. Furthermore, understanding the environmental conditions that favor and limit intrinsic bioremediation will depend largely on the ability to characterize and quantify chemical and microbiological heterogeneity at a scale appropriate to the reactions being measured. This is particularly important in ecosystems such as the polar regions, where petroleum degradation processes are slow and hence difficult to quantify using decreases in contaminant concentrations alone.

MTBE usage in gasoline increased dramatically in the 1990s in response to programs in the United States (CAAA) and Europe to improve air quality. This resulted in the widespread occurrence of MTBE in the environment. MTBE degrades more slowly and is less volatile than BTEX. As a result, MTBE has been observed by many investigators to migrate farther in aquifers than BTEX at gasoline spill sites. Further, MTBE and its daughter product TBA are frequently detected in ambient groundwater. Additional studies are necessary to elucidate the mechanisms of MTBE and TBA transport and transformation to fully be able to predict their long-term fate in the

environment. The implication of the detection of MTBE at low concentrations in ambient groundwater is unclear. If the low concentrations of VOCs and MTBE found in regional water-quality studies (multistate) are the result of evolving plumes emanating from USTs, then concentrations could possibly increase with time. If the source were the atmosphere, changes in VOC concentrations in groundwater over time would be constrained by atmospheric concentrations and would therefore be expected to decrease with the elimination of MTBE from gasoline.

While MTBE usage has resulted in improved air quality in urban areas, it has challenged the UST spill natural attenuation paradigm because of its widespread occurrence. The classic environmental problem of improving atmosphere quality in exchange for degradation of the hydrosphere, or vice versa, has been demonstrated. The potential impact on water quality of other fuel oxygenates remains largely untested. The environmental implications associated with a shift from MTBE to ethanol as an oxygenate in fuels requires further study, as the release of ethanol to the environment is likely to dramatically rise in the future and its potential impact on BTEX and MTBE is not fully understood. Biodegradation by indigenous microorganisms is now recognized as the major attenuation mechanism for BTEX compounds in both oxic and anoxic groundwater environments. Ethanol is readily biodegraded in the environment compared to MTBE. However, the introduction of ethanol into the environment may rapidly decrease nutrients and electron acceptors needed for BTEX biodegradation, thereby inadvertently elongating petroleum plumes and increasing the likelihood of encountering groundwater receptors (Da Silva and Alvarez, 2002; Mackay et al., 2006). Improved understanding of BTEX and ethanol biodegradation and natural attenuation in the subsurface is necessary to fully predict the consequences of an increased reliance on ethanol-oxygenated gasoline and on high ethanol-content fuels such as E85. As the frequency of ethanol releases to the environment has the potential to dramatically increase, it is important that scientists and regulators are well prepared to deal with the implications.

Acknowledgments

The authors thank Jeanne Jaeschke and Robin Krest of the USGS and Melissa Whitfield Åslund (University of Toronto) for assistance with the reference database, tables, and figures. This manuscript was improved thanks to the thoughtful review comments of Hedeff I. Essaid of the USGS. The first edition benefited from comments from Robert Eganhouse (USGS), Barbara Bekins (USGS), Harry Beller (Lawrence Livermore National Laboratory), and an anonymous reviewer. This work was supported by the USGS National Research Program and Toxic Substances Hydrology Program.

References

Abdelouas A, Lutze W, Nuttall EH, Strietelmeier BA, and Travis BJ (2000) Biological reduction of uranium in groundwater and subsurface soil. *Science of the Total Environment* 250(1): 21–37.

Abe Y, Aravena R, Zopfi J, Parker B, and Hunkeler D (2009) Evaluating the fate of chlorinated ethenes in streambed sediments by combining stable isotope, geochemical and microbial methods. *Journal of Contaminant Hydrology* 107(1–2): 10–21.

Addy JM, Hartley JP, and Tibbetts PJC (1984) Ecological effects of low toxicity oil based mud drilling in the Beatrice oilfield. *Marine Pollution Bulletin* 15(12): 429–436.

Aelion CM (1996) Impact of aquifer sediment grain size on petroleum hydrocarbon distribution and biodegradation. *Journal of Contaminant Hydrology* 22(1–2): 21–109.

Ahad JME, Lollar BS, Edwards EA, Slater GF, and Sleep BE (2000) Carbon isotope fractionation during anaerobic biodegradation of toluene: Implications for intrinsic bioremediation. *Environmental Science & Technology* 34(5): 892–896.

Aislabie J, Foght J, and Saul D (2000) Aromatic hydrocarbon-degrading bacteria from soil near Scott Base, Antarctica. *Polar Biology* 23: 183–188.

Alvarez PJJ and Illman WA (2006) *Bioremediation and Natural Attenuation: Process Fundamentals and Mathematical Models*. Chichester, UK: John Wiley & Sons.

Anderson RT and Lovley DR (2000) Hexadecane decay by methanogenesis. *Nature* 404: 722–723.

Atkinson R (1990) Gas-phase tropospheric chemistry of organic compounds: A review. *Atmospheric Environment* 24A(1): 1–41.

Atlas RM (1984) *Petroleum Microbiology*. New York: Macmillan Publishing.

Babé A, Labbé D, Monot F, Greer CW, and Fayolle-Guichard F (2007) Biodegradability of oxygenates by microflora from MTBE-contaminated sites: New molecular tools. *The Handbook of Environmental Chemistry*, vol. 5Y, pp. 75–98.

Baedecker MJ, Cozzarelli IM, Eganhouse RP, Siegel DI, and Bennett PC (1993) Crude oil in a shallow sand and gravel aquifer-III. Biogeochemical reactions and mass balance modeling in anoxic groundwater. *Applied Geochemistry* 8: 569–586.

Baedecker MJ and Eganhouse RP (1991) Partitioning and transport of hydrocarbons from crude oil in a sand and gravel aquifer. *201st National Meeting of the American Chemical Society*, American Chemical Society, Division of Environmental Chemistry, Atlanta, Georgia, April 14–19, 1991, vol. 31, no. 1, pp. 463–466.

Baehr AL, Charles EG, and Baker RJ (2001) Methyl *tert*-butyl ether degradation in the unsaturated zone and the relation between MTBE in the atmosphere and shallow groundwater. *Water Resources Research* 37(2): 223.

Baehr AL, Stackelberg PE, and Baker RJ (1999) Evaluation of the atmosphere as a source of volatile organic compounds in shallow ground water. *Water Resources Research* 35(1): 127–136.

Baker RJ, Best EW, and Baehr AL (2002) Used motor oil as a source of MTBE, TAME, and BTEX to ground water. *Ground Water Monitoring & Remediation* 22(4): 46–51.

Baker KH and Herson DS (1994) *Bioremediation*. New York: McGraw-Hill.

Ball HA and Reinhard M (1996) Monoaromatic hydrocarbon transformation under anaerobic conditions at Seal Beach, California: Laboratory studies. *Environmental Toxicology and Chemistry* 15(2): 114–122.

Barber LB II, Thurman EM, and Runnells DD (1992) Geochemical heterogeneity in a sand and gravel aquifer: Effect of sediment mineralogy and particle size on the sorption of chlorobenzenes. *Journal of Contaminant Hydrology* 9: 35–54.

Barker JF, Gillham RW, Lemon L, Mayfield CI, Poulsen M, and Sudicky EA (1991) *Chemical Fate and Impact of Oxygenates in Ground Water: Solubility of BTEX from Gasoline-Oxygenate Compounds, American Petroleum Institute Publication 4531*. Washington, DC: American Petroleum Institute.

Barker JF, Tessmann JS, Plotz PE, and Reinhard M (1986) The organic geochemistry of a sanitary landfill leachate plume. *Journal of Contaminant Hydrology* 1: 171–189.

Barker JF and Wilson JT (1997) Natural biological attenuation of aromatic hydrocarbons under anaerobic conditions. In: Ward CH, Cherry JA, and Scalf MR (eds.) *Subsurface Restoration*, pp. 289–300. Chelsea, MI: Ann Arbor Press.

Bastida F, Rosell M, Franchini AG, et al. (2010) Elucidating MTBE degradation in a mixed consortium using a multidisciplinary approach. *FEMS Microbiology Ecology* 73: 370–384.

Bekins BA, Baehr AL, Cozzarelli IM, et al. (1999) Capabilities and challenges of natural attenuation in the subsurface: Lessons from the U.S. Geological Survey Toxics Substances Hydrology Program. *U.S. Geological Survey Toxic Substances Hydrology Program: Proceedings of the Technical Meeting, Charleston, South Carolina, March 8–12, 1999, US Geological Survey Water-Resources Investigations Report 99-4018C*, pp. 37–56. Denver, CO: US Geological Survey.

Bekins BA, Cozzarelli IM, Godsy EM, Warren E, Essaid HI, and Tuccillo ME (2001a) Progression of natural attenuation processes at a crude-oil spill site: II. Controls on spatial distribution of microbial populations. *Journal of Contaminant Hydrology* 53: 387–406.

Bekins BA, Cozzarelli IM, Warren E, and Godsy EM (2002) Microbial ecology of a crudeoil contaminated aquifer. *Proceedings of Groundwater Quality 2001. Third*

International Conference on Groundwater Quality, Sheffield, UK, 18–21 June 2001. IAHS Publication No, pp. 275: 57–63.

Bekins BA, Hostettler FD, Herkelrath WN, Delin GN, Warren E, and Essaid HI (2005) Progression of methanogenic degradation of crude oil in the subsurface. *Environmental Geosciences* 12: 139–152.

Bekins BA, Rittmann BE, and MacDonald JA (2001b) Natural attenuation strategy for goundwater cleanup focuses on demonstrating cause and effect. *Eos, Transactions of the American Geophysical Union* 82(5): 53, 57–58.

Beller HR (2000) Metabolic indicators for detecting *in situ* anaerobic alkylbenzene degradation. *Biodegradation* 11(2–3): 125–139.

Beller HR (2002) Analysis of benzylsuccinates in groundwater by liquid chromatography/tandem mass spectrometry and its use for monitoring *in situ* BTEX biodegradation. *Environmental Science & Technology* 36(12): 2724–2728.

Beller HR, Ding W-H, and Reinhard M (1995) Byproducts of anaerobic alkylbenzene metabolism useful as indicators of *in situ* bioremediation. *Environmental Science & Technology* 29(11): 2864–2870.

Beller H and Edwards E (2000) Anaerobic toluene activation by benzylsuccinate synthase in a highly enriched methanogenic culture. *Applied and Environmental Microbiology* 66(12): 5503–5505.

Beller HR, Grbić-Galić D, and Reinhard M (1992a) Microbial degradation of toluene under sulfate-reducing conditions and the influence of iron on the process. *Applied and Environmental Microbiology* 58(3): 786–793.

Beller HR, Kane SR, and Legler TC (2001) Chapter 4: Effect of ethanol on hydrocarbon-degrading bacteria in the saturated zone: Microbial ecology studies. In: Rice DW and Depue RT (eds.) *Subsurface Fate and Transport of Gasoline Containing Ethanol*, Report to the California State Water Resources Control Board, UCRL-AR-145380.

Beller HR, Kane SR, Legler TC, and Alvarez PJJ (2002) A real-time polymerase chain reaction method for monitoring anaerobic, hydrocarbon-degrading bacteria based on a catabolic gene. *Environmental Science & Technology* 36(18): 3977–3984.

Beller H, Kane SR, Legler TC, et al. (2008) Comparative assessments of benzene, toluene and xylene natural attenuation by quantitative polymerase chain reaction analysis of a catabolic gene, signature metabolites, and compound-specific isotope analysis. *Environmental Science & Technology* 42(16): 6065–6072.

Beller HR, Reinhard M, and Grbić-Galić D (1992b) Metabolic by-products of anaerobic toluene degradation by sulfate-reducing enrichment cultures. *Applied and Environmental Microbiology* 58(9): 3192–3195.

Beller HR and Spormann AM (1997a) Anaerobic activation of toluene and *o*-xylene by addition to fumarate in denitrifying strain T. *Journal of Bacteriology* 170(3): 670–676.

Beller HR and Spormann AM (1997b) Benzylsuccinate formation as a means of anaerobic toluene activation by sulfate-reducing strain PRTOL1. *Applied and Environmental Microbiology* 63(9): 3729–3731.

Beller HR, Spormann AM, Sharma PK, Cole JR, and Reinhard M (1996) Isolation and characterization of a novel toluene-degrading, sulfate-reducing bacterium. *Applied and Environmental Microbiology* 62(4): 1188–1196.

Bence AE, Kvenvolden KA, and Kennicutt MC (1996) Organic geochemistry applied to environmental assessments of Prince William Sound, Alaska, after the *Exxon Valdez* oil spill—a review. *Organic Geochemistry* 24(1): 7–42.

Bennett PC, Hiebert FK, and Rogers JR (2000) Microbial control of mineral-groundwater equilibria: Macroscale to microscale. *Hydrogeology Journal* 8(1): 47–62.

Biegert T, Fuchs G, and Heider J (1996) Evidence that anaerobic oxidation of toluene in the denitrifying bacterium *Thauera aromatica* is initiated by formation of benzylsuccinate from toluene and fumarate. *European Journal of Biochemistry* 238(3): 661–668.

Blanchette RA, Held BW, Jurgens JA, Aislabie J, Duncan S, and Farrell RL (2004) Environmental pollutants from the Scott and Shackleton expeditions during the 'Heroic Age' of Antarctic exploration. *Polar Record* 40: 143–151.

Boetius A, Ravenschlag K, Schubert CJ, et al. (2000) A marine microbial consortium apparently mediating anaerobic oxidation of methane. *Nature* 407: 623–626.

Bombach P, Chatzinotas A, New TR, Kästner M, Lueders T, and Vogt C (2010a) Enrichment and characterization of a sulfate-reducing toluene-degrading microbial consortium by combining *in situ* microcosms and stable isotope probing techniques. *FEMS Microbiology Ecology* 71: 237–246.

Bombach P, Richnow HH, Kästner M, and Fischer A (2010b) Current approaches for the assessment of *in situ* biodegradation. *Applied Microbiology and Biotechnology* 86(3): 839–852.

Bosma TNP, Harms H, and Zehnder AJB (2001) Biodegradation of xenobiotics in environment and technosphere. In: Beek B (ed.) *The Handbook of Environmental Chemistry, vol. 2, part K, Biodegradation and Persistence*, pp. 163–202. Berlin: Springer-Verlag.

Botton S and Parsons JR (2007) Degradation of BTX by dissimilatory iron-reducing cultures. *Biodegradation* 18: 371–381.

Bouwer EJ and Zehnder A (1993) Bioremediation of organic compounds – putting microbial metabolism to work. *Bioremediation* 11: 360–367.

Braddock JF and McCarthy KA (1996) Hydrologic and microbiological factors affecting persistence and migration of petroleum hydrocarbons spilled in a continuous-permafrost region. *Environmental Science & Technology* 30: 2626–2633.

Bradley PM, Landmeyer JE, and Chapelle FH (1999) Aerobic mineralization of MTBE and *tert*-butyl alcohol by stream-bed sediment microorganisms. *Environmental Science & Technology* 33(11): 1877–1879.

Bradley PM, Landmeyer JE, and Chapelle FH (2001) Widespread potential for microbial MTBE degradation in surface-water sediments. *Environmental Science & Technology* 35(4): 658–662.

Bradley PM, Landmeyer JE, and Chapelle FH (2002) TBA biodegradation in surface-water sediments under aerobic and anaerobic conditions. *Environmental Science & Technology* 36: 4087–4090.

Bregnard TP-A, Hohener P, Haner A, and Zeyer J (1996) Degradation of weathered diesel fuel by microorganisms from a contaminated aquifer in aerobic and anaerobic microcosms. *Environmental Toxicology and Chemistry* 15(3): 299–307.

Breit GN, Kharaka Y, and Rice CA (2000) Database of the composition of water produced with oil and gas. *7th International Petroleum Environmental Conference,* pp. 903–942.

Burland S and Edwards EA (1999) Anaerobic benzene biodegradation linked to nitrate reduction. *Applied and Environmental Microbiology* 65(2): 529–533.

Buscheck TE, O'Reilly K, Koschal G, and O'Regan G (2001) Ethanol in groundwater at the pacific northwest terminal. *Proceedings of the Sixth International Symposium on In-Situ and On-Site Bioremediation,* San Diego, California, 4–7 June 2001. Columbus, OH: Battelle Press.

Busch-Harris J, Sublette K, Roberts KP, et al. (2008) Bio-traps coupled with molecular biological methods and stable isotope probing demonstrate the *in situ* biodegradation potential of MTBE and TBA in gasoline-contaminated aquifers. *Groundwater Monitoring & Remediation* 28(4): 47–62.

Calabrese EJ and Kenyon EM (1991) *Air Toxics and Risk Assessment*. Chelsea, MI: Lewis.

Calabrese EJ, Stanek ES, and Gilbert CE (1991) A preliminary decision framework for deriving soil ingestion rates. In: Kostecki PT and Calabrese EJ (eds.) *Hydrocarbon Contaminated Soils and Groundwater: Analysis, Fate, Environmental and Public Health Effects, Remediation*, pp. 301–311. Chelsea, MI: Lewis Publishers.

Caldwell ME, Garrett RM, Prince RC, and Suflita JM (1998) Anaerobic degradation of long-chain n-alkanes under sulfate-reducing conditions. *Environmental Science & Technology* 32: 2191–2195.

Caldwell ME and Suflita JM (2000) Detection of phenol and benzoate as intermediates of anaerobic benzene biodegradation under different terminal electron-accepting conditions. *Environmental Science & Technology* 34: 1216–1220.

California Environmental Policy Council (1999) *Health and Environmental Assessment of the Use of Ethanol as a Fuel Oxygenate. State of California. UCRL-AR-135949*.

Caldwell SL, Laidler JR, Brewer EA, Eberly JO, Sandborgh SC, and Colwell FS (2008) Anaerobic oxidation of methane: Mechanisms, bioenergetics, and the ecology of associated microorganisms. *Environmental Science & Technology* 42(18): 6791–6799.

Camilli R, Reddy CM, Yoerger DR, et al. (2010) Tracking hydrocarbon plume transport and biodegradation at Deepwater Horizon. *Science* 330(6001): 201–204.

Cao B, Nagarajan K, and Loh K-C (2009) Biodegradation of aromatic compounds: Current status and opportunities for biomolecular approaches. *Applied Microbiology and Biotechnology* 85(2): 207–228.

CEPA Air Resources Board (1999) Air quality impacts of the use of ethanol in California reformulated gasoline. *Health and Environmental Assessment of the Use of Ethanol as a Fuel Oxygenate, Vol III*. Prepared by the California Environmental Protection Agency Air Resources Board, State of California, UCRL-AR-135949.

Cervantes F, Dijksma W, Duong-Dac T, Ivanova A, Lettinga G, and Field JA (2001) Anaerobic mineralization of toluene by enriched sediments with quinones and humus as terminal electron acceptors. *Applied and Environmental Microbiology* 67(10): 4471–4478.

Chakraborty R and Coates JD (2004) Anaerobic degradation of monoaromatic hydrocarbons. *Applied Microbiology and Biotechnology* 64(4): 437–446.

Chakraborty R and Coates JD (2005) Hydroxylation and carboxylation, two crucial steps of anaerobic benzene degradation by *Dechloromonas* strain RCB. *Applied and Environmental Microbiology* 71: 5427–5432.

Chapelle FH (1993) *Groundwater Microbiology and Geochemistry*. New York: Wiley.

Chapelle FH (1999) Bioremediation of petroleum hydrocarbon-contaminated ground water: The perspectives of history and hydrology. *Ground Water* 37(1): 122–132.

Chapelle FH, Bradley PM, Lovely DR, O'Neill K, and Landmeyer JE (2002) Rapid evolution of redox processes in a petroleum hydrocarbon-contaminated aquifer. *Ground Water* 40(4): 353–360.

Chaplin BP, Delin GN, Baker RJ, and Lahvis MA (2002) Long-term evolution of biodegradation and volatilization rates in a crude oil-contaminated aquifer. *Bioremediation Journal* 6: 237–255.

Chen YD, Barker JF, and Gui L (2008a) A strategy for aromatic hydrocarbon bioremediation under anaerobic conditions and the impacts of ethanol: A microcosm study. *Journal of Contaminant Hydrology* 96: 17–31.

Chen CS, Lai YW, and Tien C-J (2008b) Partitioning of aromatic and oxygenated constituents into water from regular and ethanol-blended gasolines. *Environmental Pollution* 156: 988–996.

Chen CS-H, Delfino JJ, and Rao PSC (1994) Partitioning of organic and inorganic components from motor oil into water. *Chemosphere* 28(7): 1385–1400.

Christensen TH, Bjerg PL, Banwart SA, Jakobsen R, Heron G, and Albrechtsen H-J (2000) Characterization of redox conditions in groundwater contaminant plumes. *Journal of Contaminant Hydrology* 45: 165–241.

Church CD, Trartnyek PG, Pankow J, et al. (2000) Effects of environmental conditions on MTBE degradation in model column aquifers. *Proceedings of the Technical Meeting of USGS Toxic Substances Hydrology Program,* Charleston, South Carolina 8–12 March 1999, pp. 93–101.

Coates JD, Chakraborty R, Lack JG, et al. (2001) Anaerobic benzene oxidation coupled to nitrate reduction in pure culture by two strains of *Dechloromonas*. *Nature* 411(6841): 1039–1043.

Coates JD, Woodward J, Allen J, Philp P, and Lovley DR (1997) Anaerobic degradation of polycyclic aromatic hydrocarbons and alkanes in petroleum contaminated marine harbor sediments. *Applied and Environmental Microbiology* 63(9): 3589–3593.

Corseuil HX, Hunt CS, dos Santos RCF, and Alvarez PJJ (1998) The influence of the gasoline oxygenate ethanol on aerobic and anaerobic BTX biodegradation. *Water Research* 32(7): 2065–2072.

Cozzarelli IM, Baedecker MJ, Eganhouse RP, and Goerlitz DF (1994) The geochemical evolution of low-molecular-weight organic acids derived from the degradation of petroleum contaminants in groundwater. *Geochimica et Cosmochimica Acta* 58(2): 863–877.

Cozzarelli IM, Bekins BA, Baedecker MJ, Aiken GR, Eganhouse RP, and Tuccillo ME (2001a) Progression of natural attenuation processes at a crude-oil spill site: I. Geochemical evolution of the plume. *Journal of Contaminant Hydrology* 53: 369–385.

Cozzarelli IM, Eganhouse RP, and Baedecker MJ (1990) Transformation of monoaromatic hydrocarbons to organic acids in anoxic groundwater environment. *Environmental Geology and Water Sciences* 16(2): 135–141.

Cozzarelli IM, Eganhouse RP, Godsy EM, Warren E, and Bekins BA (2001b) Measurement of biodegradation of hydrocarbons *in situ* under different redox conditions. *20th International Meeting on Organic Geochemistry,* Nancy, France, 10–14 September 2001, p. 2.

Cozzarelli IM, Herman JS, and Baedecker MJ (1995) Fate of microbial metabolites of hydrocarbons in a coastal plain aquifer: The role of electron acceptors. *Environmental Science & Technology* 29(2): 458–469.

Cozzarelli IM, Herman JS, Baedecker MJ, and Fischer JM (1999) Geochemical heterogeneity of a gasoline-contaminated aquifer. *Journal of Contaminant Hydrology* 40(3): 261–284.

Crawford RL and Crawford DL (1996) *Bioremediation Principles and Applications*. Cambridge: University Press.

Crone TJ and Tolstoy M (2010) Magnitude of the 2010 Gulf of Mexico oil leak. *Science* 330(6004): 634.

Dakhel N, Pasteris G, Werner D, and Höhener P (2003) Small-volume releases of gasoline in the vadose zone: Impact of the additives MTBE and ethanol on groundwater quality. *Environmental Science & Technology* 37(10): 2127–2133.

Da Silva MLB and Alvarez PJJ (2002) Effects of ethanol versus MTBE on benzene, toluene, ethylbenzene, and xylene natural attenuation in aquifer columns. *Journal of Environmental Engineering* 128(9): 862–867.

Daugherty S (1991) Regulatory approaches to hydrocarbon contamination from underground storage tanks. In: Kostecki PT and Calabrese EJ (eds.) *Hydrocarbon Contaminated Soils and Groundwater: Analysis, Fate, Environmental and Public Health Effects, Remediation*, pp. 24–63. Chelsea, MI: Lewis Publishers.

Davies JM, Addy JM, Blackman RAA, et al. (1984) Environmental effects of the use of oil-based drilling muds in the North Sea. *Marine Pollution Bulletin* 15(10): 363–370.

Davies JM, Bedborough DR, Blackman RAA, et al. (1989) The environmental effect of oil-based mud drilling in the North Sea. In: Engelhardt FR, Ray JP, and Gillam AH (eds.) *Drilling Wastes: Proceedings of the 1988 Conference on Drilling Wastes*, pp. 59–90. London/New York: Elsevier Applied Science.

Davis JB (1967) *Petroleum Microbiology*. New York: Elsevier.

Davis JM, Lohmann RC, Phillips FM, Wilson JL, and Love DW (1993) Architecture of the Sierra Ladrones Formation, central New Mexico: Depositional controls on the permeability correlation structure. *Geological Society of America Bulletin* 105: 998–1007.

Deeb RA and Alvarez-Cohen L (2000) Aerobic biotransformation of gasoline aromatics in multicomponent mixtures. *Bioremediation Journal* 4(2): 171–179.

Deeb RA, Chu K-H, Shih T, et al. (2003) MTBE and other oxygenates: Environmental sources, analysis, occurrence, and treatment. *Environmental Engineering Science* 20: 443–447.

Deeb RA, Hu H-K, Hanson JR, Scow KM, and Alvarez-Cohen L (2001) Substrate interactions in BTEX and MTBE mixtures by an MTBE-degrading isolate. *Environmental Science & Technology* 35(2): 312–317.

Deeb RA, Scow KM, and Alvarez-Cohen L (2000) Aerobic MTBE biodegradation: An examination of past studies, current challenges and future research directions. *Biodegradation* 11: 171–186.

Deeb RA, Sharp JO, Stocking A, et al. (2002) Impact of ethanol on benzene plume lengths: Microbial and modeling studies. *Journal of Environmental Engineering* 128(9): 868–875.

Delin GN, Essaid HI, Cozzarelli IM, Lahvis MH, and Bekins BA (1998) *Ground Water Contamination by Crude Oil Near Bemidji, Minnesota*, USGS Fact Sheet 084-98. Denver, CO:. US Geological Survey.

Dempster HS, Lollar BS, and Feenstra S (1997) Tracing organic contaminants in groundwater: A new methodology using compound-specific isotopic analysis. *Environmental Science & Technology* 31(11): 3193–3197.

Dernbach LS (2000) The complicated challenge of MTBE cleanups. *Environmental Science & Technology* 34: 516A–521A.

Dewulf J, Drijvers D, and Van Langenhove H (1995) Measurement of Henry's Law constant as a function of temperature and salinity for the low temperature range. *Atmospheric Environment* 29(3): 323–331.

Dolfing J, Zeyer J, Binder-Eicher P, and Schwarzenbach RP (1990) Isolation and characterization of a bacterium that mineralizes toluene in the absence of molecular oxygen. *Archives of Microbiology* 154: 336–341.

Domenico PA and Schwartz FW (1998) *Physical and Chemical Hydrogeology*, 2nd ed. New York: Wiley.

Edwards EA, Wills LE, Reinhard M, and Grbić-Galić D (1992) Anaerobic degradation of toluene and xylene by aquifer microorganisms under sulfate-reducing conditions. *Applied and Environmental Microbiology* 58(3): 794–800.

Eganhouse RP, Baedecker MJ, Cozzarelli IM, Aiken GR, Thorn KA, and Dorsey TF (1993) Crude oil in a shallow sand and gravel aquifer-II. Organic geochemistry. *Applied Geochemistry* 8: 551–567.

Eganhouse RP, Dorsey TF, and Phinney CS (1987) Transport and fate of monoaromatic hydrocarbons in the subsurface, Bemidji, Minnesota, research site. In: Franks BJ (ed.) *U.S. Geological Survey Program on Toxic Waste-Ground-Water Contamination: Proceedings of the Third Technical Meeting, Pensacola, Florida, March 23–27, 1987, USGS Open-File Report 87-109*, p. C-29. Denver, CO: US Geological Survey.

Eganhouse RP, Dorsey TF, Phinney CS, and Westcott AM (1996) Processes affecting the fate of monoaromatic hydrocarbons in an aquifer contaminated by crude oil. *Environmental Science & Technology* 30(11): 3304–3312.

Eganhouse RP and Kaplan IR (1981) Extractable organic matter in urban stormwater runoff. 1. Transport dynamics and mass emission rates. *Environmental Science & Technology* 15(3): 300–315.

Elshahed MS, Gieg LM, McInerney MJ, and Suflita JM (2001) Signature metabolites attesting to the *in situ* attenuation of alkylbenzenes in anaerobic environments. *Environmental Science & Technology* 35(4): 682–689.

Elsner M, Zwank L, Hunkeler D, and Schwarzenbach RP (2005) A new concept linking observable stable isotope fractionation to transformation pathways of organic pollutants. *Environmental Science & Technology* 39(18): 6896–6916.

Energy Information Administration (1999) *Petroleum: An Energy Profile 1999,* DOE/E1A-0545(99), pp. 1–79. Washington, DC: Department of Energy.

Energy Information Administration (2000) *Alternatives to Traditional Transportation Fuels 1999*. Washington, DC: US Energy Information Administration.

Energy Information Administration (2010a) *Annual Energy Review 2009*. DOE/EIA-0384 (2009). Washington, DC: US Energy Information Administration.

Energy Information Administration (2010b) *International Energy Outlook 2010*. DOE/EIA-0484(2010). Washington, DC: US Energy Information Administration.

Eriksson M, Ka J-O, and Mohn WW (2001) Effects of low temperature and freeze-thaw cycles on hydrocarbon biodegradation in arctic tundra soil. *Applied and Environmental Microbiology* 67: 5107–5112.

Essaid HI, Bekins BA, Herkelrath WN, and Delin GN (2011) Crude oil at the Bemidji site: 25 years of monitoring, modeling and understanding. *Ground Water* 49: 706–726.

Ettwig KF, Butler MK, Le Paslier D, et al. (2010) Nitrite-driven anaerobic methane oxidation by oxygenic bacteria. *Nature* 464: 543–548.

Evans PJ, Ling W, Goldschmidt B, Ritter ER, and Young LY (1992) Metabolites formed during anaerobic transformation of toluene and *o*-xylene and their proposed relationship to the initial steps of toluene mineralization. *Applied and Environmental Microbiology* 58(2): 496–501.

Evans PJ, Mang DT, and Young LY (1991) Degradation of toluene and *m*-xylene and transformation of *o*-xylene by denitrifying enrichment cultures. *Applied and Environmental Microbiology* 57(2): 450–454.

Evanson T, Pelayo A, and Bahr J (2009) Wisconsin closure protocol study. A retrospective study of LUST site closures between 1999 and 2000, April 2009. PUB-RR-805, Wisconsin Department of Natural Resources.

Fang J and Barcelona MJ (1998) Biogeochemical evidence for microbial community change in a jet fuel hydrocarbons-contaminated aquifer. *Organic Geochemistry* 29(4): 899–907.

Fang J and Barcelona MJ (1999) Evolution of aromatic hydrocarbon and metabolic intermediate plumes in a shallow sand aquifer contaminated with jet fuel. In: Stanley A (ed.) *Petroleum Hydrocarbons and Organic Chemicals in Ground Water: Prevention, Detection, and Remediation Conference*, pp. 51–56. Westerville, OH: National Ground Water Association.

Farhadian M, Vachelard C, Duchez C, and Larroche C (2008) *In situ* bioremediation of monoaromatic pollutants in groundwater: A review. *Bioresource Technology* 99(13): 5296–5308.

Fayolle F, Vandecasteele J-P, and Monot F (2001) Microbial degradation and fate in the environment of methyl *tert*-butyl ether and related fuel oxygenates. *Applied Microbiology and Biotechnology* 56: 339–349.

Feris K, Mackay D, De Sieyes N, et al. (2008) Effect of ethanol on microbial community structure and function during natural attenuation of benzene, toluene, and *o*-xylene in a sulfate-reducing aquifer. *Environmental Science & Technology* 42(7): 2289–2294.

Fetter CW (1993) *Contaminant Hydrology*. New York: Macmillan Publishing Company.

Finneran KT and Lovley DR (2001) Anaerobic degradation of methyl *tert*-butyl ether (MTBE) and *tert*-butyl alcohol (TBA). *Environmental Science & Technology* 35(9): 1785–1790.

Fischer A, Bauer J, Meckenstock RU, et al. (2006) A multitracer test proving the reliability of Rayleigh equation-based approach for assessing biodegradation in a BTEX contaminated aquifer. *Environmental Science & Technology* 40(13): 4245–4252.

Foght J (2008) Anaerobic biodegradation of aromatic hydrocarbons: Pathways and prospects. *Journal of Molecular Microbiology and Biotechnology* 15: 93–120.

Francis AJ, Dodge CJ, Lu F, Halada GP, and Clayton CR (1994) XPS and XANES studies of uranium reduction by *Clostridium* sp. *Environmental Science & Technology* 28: 636–639.

Fredenslund A, Jones R, and Prausnitz JM (1975) Group-contribution estimation of activity coefficients in nonideal liquid mixtures'. *Journal of the American Institute of Chemical Engineers* 21(6): 1086–1099.

Friedrich R and Obermeier A (1999) Anthropogenic emissions of volatile organic compounds. In: Hewitt CN (ed.) *Reactive Hydrocarbons in the Atmosphere*, pp. 1–39. San Diego, CA: Academic Press.

Furlong ET, Koleis JC, and Aiken GR (1997) Transport and degradation of semivolatile hydrocarbons in a petroleum-contaminated aquifer, Bemidji, Minnesota. In: Eganhouse RP (ed.) *Molecular Markers in Environmental Geochemistry, ACS Symposium Series* vol. 671, pp. 398–412. Washington, DC: American Chemical Society.

Gaines RB, Frysinger GS, Hendrick-Smith MS, and Stuart JD (1999) Oil spill source identification by comprehensive two-dimensional gas chromatography. *Environmental Science & Technology* 33(12): 2106–2112.

Gauchotte C, O'Sullivan G, Davis S, and Kalin RM (2009) Development of an advanced on-line position-specific stable carbon isotope system and application to methyl *tert*-butyl ether. *Rapid Communications in Mass Spectrometry* 23: 3183–3319.

Gibson DT and Subramanian V (1984) Microbial degradation of aromatic hydrocarbons. In: Gibson DT (ed.) *Microbial Degradation of Organic Compounds*, vol. 13, pp. 181–252. New York: Marcel Dekker Inc.

Gieg LM, Kolhatkar RV, McInerney MJ, et al. (1999) Intrinsic bioremediation of petroleum hydrocarbons in a gas condensate-contaminated aquifer. *Environmental Science & Technology* 33(15): 2550–2560.

Gieg LM and Suflita JM (2002) Detection of anaerobic metabolites of saturated and aromatic hydrocarbons in petroleum-contaminated aquifers. *Environmental Science & Technology* 36(17): 3755–3762.

Goldstein AH and Galbally IE (2007) Known and unexplored organic constituents in the Earth's atmosphere. *Environmental Science & Technology* 41(5): 1514–1521.

Gomez-Belinchon JI, Grimalt JO, and Albaiges J (1991) Volatile organic compounds in two polluted rivers in Barcelona (Catalonia, Spain). *Water Research* 25(5): 577–589.

Gray J, Couloume-Lacrampe G, Gandhi D, et al. (2002) Carbon and hydrogen isotopic fractionation during biodegradation of methyl *tert*-butyl ether. *Environmental Science & Technology* 36(9): 1931–1938.

Grbić-Galić D and Vogel TM (1987) Transformation of toluene and benzene by mixed methanogenic cultures. *Applied and Environmental Microbiology* 53(2): 254–260.

Green CT and Scow KM (2000) Analysis of phospholipid fatty acids (PLFA) to characterize microbial communities in aquifers. *Hydrogeology Journal* 8(1): 126–141.

Griebler C, Safinowski M, Vieth A, Richnow HH, and Meckenstock RU (2004) Combined application of stable carbon isotope analysis and specific metabolites determination for assessing *in situ* degradation of aromatic hydrocarbons in a tar oil-contaminated aquifer. *Environmental Science & Technology* 38: 617–631.

Grossi V, Cravo-Laureau C, Guyoneaud R, Ranchou-Peyruse A, and Hirschler-Réa A (2008) Metabolism of *n*-alkanes and *n*-alkenes by anaerobic bacteria: A summary. *Organic Geochemistry* 39(8): 1197–1203.

Gullick RW and LeChevallier MW (2000) Occurrence of MTBE in drinking water sources. *Journal of American Water Works Association* 92: 100–113.

Haack SK and Bekins BA (2000) Microbial populations in contaminant plumes. *Hydrogeology Journal* 8(1): 63–76.

Haag F, Reinhard M, and McCarty PL (1991) Degradation of toluene and *p*-xylene in anaerobic microcosms: Evidence for sulfate as a terminal electron acceptor. *Environmental Toxicology and Chemistry* 10: 1379–1389.

Hardison LK, Curry SS, Ciuffetti LM, and Hyman MR (1997) Metabolism of diethyl ether and cometabolism of methyl *tert*-butyl ether by a filamentous fungus, a *Graphium* sp. *Applied and Environmental Microbiology* 63: 3059–3067.

Harrington RR, Poulson SR, Drever JI, Colberg PJS, and Kelly EF (1999) Carbon isotope systematics of monoaromatic hydrocarbons: Vaporization and adsorption experiments. *Organic Geochemistry* 30(8A): 765–775.

Hartley JP and Watson TN (1993) Investigation of a North Sea oil platform drill cuttings pile. *Proceedings 25th Annual SPE et al. Offshore Technology Conference*, Houston, TX, 3–6 May 1993, pp. 749–756.

Hazen TC, Dubinsky EA, DeSantis TZ, et al. (2010) Deep-sea oil plume enriches indigenous oil-degrading bacteria. *Science* 330(6001): 204–208.

Heider J, Spormann AM, Beller HR, and Widdel F (1998) Anaerobic bacterial metabolism of hydrocarbons. *FEMS Microbiology Reviews* 22: 459–473.

Heron G and Christensen TH (1994) The role of aquifer sediment in controlling redox conditions in polluted groundwater. In: Dracos TH and Stauffer F (eds.) *Transport and Reactive Processes in Aquifers: Proceedings of the IAHR/AIHR Symposium on Transport and Reactive Processes in Aquifers*, Zurich, Switzerland, 11–15 April 1994, pp. 73–78. Rotterdam, The Netherlands: A. A. Balkema Publishers.

Heron G and Christensen TH (1995) Impact of sediment-bound iron on redox buffering in a landfill leachate polluted aquifer (Vejen, Denmark). *Environmental Science & Technology* 29: 187–192.

Herrmann S, Kleinsteuber S, Chatzinotas A, et al. (2010) Functional characterization of an anaerobic benzene-degrading enrichment culture by DNA stable isotope probing. *Environmental Microbiology* 12: 401–411.

Hess KM, Herkelrath WN, and Essaid HI (1992) Determination of subsurface fluid contents at a crude-oil spill site. *Journal of Contaminant Hydrology* 10: 75–96.

Hinchee RE, Kittel JA, and Reisinger HJ (1995) *Applied Bioremediation of Petroleum Hydrocarbons, Vol. 3. Third International In Situ and On-Site Bioremediation Symposium*. Columbus, OH: Battelle Press.

Hogue C (2000) Getting the MTBE out. *Chemical & Engineering News* 78(13): 6.

Huang L, Sturchio NC, Abrajano T Jr., Heraty LJ, and Holt BD (1999) Carbon and chlorine isotope fractionation of chlorinated aliphatic hydrocarbons by evaporation. *Organic Geochemistry* 30(8): 777–785.

Hubbard CE, Barker JF, O'Hannesin SF, Vandegriendt M, and Gillham RW (1994) *Transport and Fate of Dissolved Methanol, Methyl-tertiary Butyl-Ether, and Monoaromatic Hydrocarbons in a Shallow Sand Aquifer*. Washington, DC: American Petroleum Institute.

Hunkeler D, Anderson N, Aravena R, Bernasconi SM, and Butler BJ (2001a) Hydrogen and carbon isotope fractionation during aerobic biodegradation of benzene. *Environmental Science & Technology* 35(17): 3462–3467.

Hunkeler D, Butler BJ, Aravena R, and Barker JF (2001b) Monitoring biodegradation of methyl *tert*-butyl ether (MTBE) using compound-specific carbon isotope analysis. *Environmental Science & Technology* 35(4): 676–681.

Hunkeler D, Meckenstock RU, Sherwood Lollar B, Schmidt TC, and Wilson JT (2008) A guide for assessing biodegradation and source identification of organic ground water contaminants using Compound Specific Isotope Analysis (CSIA). *US Environmental Protection Agency, Report No. EPA 600/R-08/148*. Washington, DC: US Environmental Protection Agency.

Hunt JM (1996) *Petroleum Geochemistry and Geology*. New York: W. H. Freeman & Company.
Hutchins SR, Sewell GW, Kovacs DA, and Smith GA (1991) Biodegradation of aromatic hydrocarbons by aquifer microorganisms under denitrifying conditions. *Environmental Science & Technology* 25(1): 68–76.
Jamison VW, Raymond RL, and Hudson JOJ (1975) Biodegradation of high-octane gasoline in groundwater. *Developments in Industrial Microbiology* 16: 305–312.
Johnson R, Pankow J, Bender D, Price C, and Zogorski J (2000) MTBE: To what extent will past releases contaminate community water supply wells. *Environmental Science & Technology* 34(9): 210a–217a.
Jones FV, Leuterman AJJ, and Still I (2000) Discharge practices and standards for offshore operations around the world. *7th International Petroleum Environmental Conference*, Albuquerque, NM, November 2000, pp. 903–942. National Energy Technology Laboratory.
Kansal A (2009) Sources and reactivity of NMHCs and VOCs in the atmosphere: A review. *Journal of Hazardous Materials* 166: 17–26.
Karickhoff SW (1981) Semi-empirical estimation of sorption of hydrophobic pollutants on natural sediments. *Chemosphere* 10(8).
Karickhoff SW (1984) Organic pollutant sorption in aquatic systems. *Journal of Hydraulic Engineering* 110(6): 707–735.
Kasai Y, Takahata Y, Manefield M, and Watanabe K (2006) RNA-based stable isotope probing and isolation of anaerobic benzene-degrading bacteria from gasoline-contaminated groundwater. *Applied and Environmental Microbiology* 72: 3586–3592.
Kauffman LJ, Baehr AL, Ayers MA, and Stackelberg PE (2001) Effects of land use and travel time on the distribution of nitrate in the Kirkwood-Cohansey Aquifer system in southern New Jersey. *US Geological Survey Water-Resources Investigation Report 01-4117*. Denver, CO: US Geological Survey.
Kazumi J, Caldwell ME, Suflita JM, Lovley DR, and Young LY (1997) Anaerobic degradation of benzene in diverse anoxic environments. *Environmental Science & Technology* 31(3): 813–818.
Kelley CA, Hammer BT, and Coffin RB (1997) Concentrations and stable isotope values of BTEX in gasoline-contaminated groundwater. *Environmental Science & Technology* 31(9): 2469–2472.
Kleikemper J, Schroth MH, Sigler WV, Schmucki M, Bernasconi SM, and Zeyer J (2002) Activity and diversity of sulfate-reducing bacteria in a petroleum hydrocarbon-contaminated aquifer. *Applied and Environmental Microbiology* 68(4): 1516–1523.
Knittel K and Boetius A (2009) Anaerobic oxidation of methane: Progress with an unknown process. *Annual Review of Microbiology* 63: 311–334.
Kolhatkar R, Kuder T, Philp P, Allen J, and Wilson JT (2002) Use of compound-specific stable carbon isotope analyses to demonstrate anaerobic biodegradation of MTBE in groundwater at a gasoline release site. *Environmental Science & Technology* 36(23): 5139–5146.
Kostecki PT and Calabrese EJ (1991) *Hydrocarbon Contaminated Soils and Groundwater: Analysis, Fate, Environmental and Public Health Effects, Remediation*. Chelsea, MI: Lewis Publishers.
Krumholz LR, Caldwell ME, and Suflita JM (1996) Biodegradation of 'BTEX' hydrocarbons under anaerobic conditions. In: Crawford R and Crawford D (eds.) *Bioremediation: Principles and Applications*, pp. 61–69. Cambridge: Cambridge University Press.
Kuder T and Philp P (2008) Modern geochemical and molecular tools for monitoring in-situ biodegradation of MTBE and TBA. *Reviews in Environmental Science and Biotechnology* 7(1): 79–91.
Kuder T, Wilson JT, Kaiser P, Kolhatkar RV, Philp P, and Allen J (2005) Enrichment of stable carbon and hydrogen isotopes during anaerobic biodegradation of MTBE: Microcosm and field evidence. *Environmental Science & Technology* 39: 213–220.
Kuhn EP, Zeyer J, Eicher P, and Schwarzenbach RP (1988) Anaerobic degradation of alkylated benzenes in denitrifying laboratory aquifer columns. *Applied and Environmental Microbiology* 54(2): 490–496.
Kunapuli U, Lueders T, and Meckenstock RU (2007) The use of stable isotope probing to identify key iron-reducing microorganisms involved in anaerobic benzene degradation. *The ISME Journal* 1: 643–653.
Lahvis MA (2003b) Evaluation of small-volume releases of ethanol-blended gasoline at UST sites. *API Soil and Groundwater Research Bulletin* 19: 1–7.
Landmeyer JE, Chapelle FH, Bradley PM, Pankow JF, Church CD, and Tratnyek PG (1998) Fate of MTBE relative to benzene in a gasoline-contaminated aquifer (1993-98). *Ground Water Monitoring & Remediation* 18(4): 93–102.
Latimer JS, Hoffman EJ, Hoffman G, Fasching JL, and Quinn JG (1990) Sources of petroleum hydrocarbons in urban runoff. *Water, Air, and Soil Pollution* 52: 1–21.
Lide DR (2002) *CRC Handbook of Chemistry and Physics*. Boca Raton, FL: CRC Press, Inc.
Lindstrom JE, Barry RP, and Braddock JF (1999) Long-term effects on microbial communities after a subarctic oil spill. *Soil Biology and Biochemistry* 31: 1677–1689.
Lopes Ferreira N, Malandain C, and Fayolle-Guichard F (2006) Enzymes and genes involved in the aerobic biodegradation of methyl *tert*-butyl ether (MTBE). *Applied Microbiology and Biotechnology* 72: 252–262.
Lovanh N, Hunt CS, and Alvarez PJJ (2002) Effect of ethanol on BTEX biodegradation kinetics: Aerobic continuous culture experiments. *Water Research* 36(15): 3739–3746.
Lovley DR (2000) Anaerobic benzene degradation. *Biodegradation* 11(2–3): 107–116.
Lovley DR and Anderson RT (2000) Influence of dissimilatory metal reduction on fate of organic and metal contaminants in the subsurface. *Hydrogeology Journal* 8(1): 77–88.
Lovley DR, Baedecker MJ, Lonergan DJ, Cozzarelli IM, Phillips EJP, and Siegel DI (1989) Oxidation of aromatic contaminants coupled to microbial iron reduction. *Nature* 339: 297–299.
Lovley DR and Lonergan DJ (1990) Anaerobic oxidation of toluene, phenol, and *p*-cresol by the dissimilatory iron-reducing organism, GS-15. *Applied and Environmental Microbiology* 56(6): 1858–1864.
Lovley DR and Phillips EJ (1992) Reduction of uranium by *Desulfovibrio desulfuricans*. *Applied and Environmental Microbiology* 58(3): 850–856.
Lovley DR, Phillips EJP, Gorby YA, and Landa ER (1991) Microbial reduction of uranium. *Nature* 350: 413–416.
Lund L (1995) Changes in UST and LUST: The federal perspective. *Tank Talk* 10 (2 and 3): 7.
Lyman WJ, Reehl WJ, and Rosenblatt DH (1990) *Handbook of Chemical Property Estimation Methods: Environmental Behavior of Organic Compounds*. Washington, DC: American Chemical Society.
Mackay DM, De Sieyes NR, Einarson M, et al. (2006) Impact of ethanol on the natural attenuation of benzene, toluene, and *o*-xylene in a normally sulfate-reducing aquifer. *Environmental Science & Technology* 40(19): 6123–6130.
Mackay DM, De Sieyes NR, Einarson M, et al. (2007) Impact of ethanol on the natural attenuation of MTBE in a normally sulfate-reducing aquifer. *Environmental Science & Technology* 41(6): 2015–2021.
Mackay DM and Einarson MD (2006) Bioattenuation of MTBE—an evolving picture. In: *5th International Conference on Remediation of Chlorinated and Recalcitrant Compounds 2006*, Monterey, CA, 220-25 May. Columbus, OH: Battelle Press.
Mackay D, Shiu WY, and Ma KC (1992a) *Illustrated Handbook of Physical-Chemical Properties and Environmental Fate for Organic Chemicals Vol I: Monoaromatic Hydrocarbons, Chlorobenzenes, and PCBs*. Chelsea, MI: Lewis Publishers.
Mackay D, Shiu WY, and Ma KC (1992b) *Illustrated Handbook of Physical-Chemical Properties and Environmental Fate for Organic Chemicals Vol II: Polynuclear Aromatic Hydrocarbons, Polychlorinated Dioxins, and Dibenzofurans*. Chelsea, MI: Lewis Publishers.
Mackay D, Shiu WY, and Ma KC (1993) *Illustrated Handbook of Physical-Chemical Properties and Environmental Fate for Organic Chemicals Vol III: Volatile Organic Chemicals*. Chelsea, MI: Lewis Publishers.
Madsen EL (2000) Nucleic-acid characterization of the identity and activity of subsurface microorganisms. *Hydrogeology Journal* 8(1): 112–125.
Major DW, Mayfield CI, and Barker JF (1988) Biotransformation of benzene by denitrification in aquifer sand. *Ground Water* 26(1): 8–14.
Mancini SA, Couloume GL, Jonker H, et al. (2002) Hydrogen isotopic enrichment: An indicator of biodegradation at a petroleum hydrocarbon contaminated field site. *Environmental Science & Technology* 36(11): 2464–2470.
Mancini SA, Devine CE, Elsner M, et al. (2008) Isotopic evidence suggests different initial reaction mechanisms for anaerobic benzene biodegradation. *Environmental Science & Technology* 42: 8290–8296.
Mancini SA, Hirschorn SK, Elsner M, et al. (2006) Aerobic biodegradation of toluene: Effects of iron limitation on stable isotopic fractionation. *Environmental Science & Technology* 40(24): 7675–7681.
Mancini SA, Ulrich AC, Couloume GL, Sleep B, Edwards EA, and Lollar BS (2003) Carbon and hydrogen isotopic fractionation during anaerobic biodegradation of benzene. *Applied and Environmental Microbiology* 69(1): 191–198.
Margesin R and Schinner F (1999) Review: Biological decontamination of oil spills in cold environments. *Journal of Chemical Technology and Biotechnology* 74: 381–389.
McDowell CJ, Buscheck T, and Powers SE (2003) Behavior of gasoline pools following a denatured ethanol spill. *Ground Water* 41(6): 746–757.
McFarland ML, Ueckert DN, and Hartmann S (1987) Revegetation of oil well reserve pits in west Texas. *Journal of Range Management* 40(2): 122.
McGuire JT, Long DT, Klug MJ, Haack SK, and Hyndman DW (2002) Evaluating behavior of oxygen, nitrate, and sulfate during recharge and quantifying reduction

rates in a contaminated aquifer. *Environmental Science & Technology* 36(12): 2693–2700.
McKelvie JR, Elsner M, Simpson AJ, Sherwood Lollar B, and Simpson MJ (2010) Quantitative site-specific ^{2}H NMR investigation of MTBE: Potential for assessing contaminant sources and fate. *Environmental Science & Technology* 44(3): 1062–1068.
McKelvie JR, Hirschorn SK, Lacrampe-Couloume G, et al. (2007a) Evaluation of TCE and MTBE *in situ* biodegradation: Integrating stable isotope, metabolic intermediate and microbial lines of evidence. *Ground Water Monitoring & Remediation* 27(4): 62–78.
McKelvie JR, Mackay D, deSieyes M, Lacrampe-Couloume G, and Sherwood Lollar B (2007b) Quantifying MTBE biodegradation in the Vandenberg Air Force Base ethanol release study using stable carbon isotopes. *Journal of Contaminant Hydrology* 94: 157–165.
McKelvie JR, Hyman M, Elsner M, et al. (2009) Isotopic fractionation of MTBE suggests different initial reaction mechanisms during aerobic biodegradation. *Environmental Science & Technology* 43: 2793–2799.
McKelvie JR, Lindstrom JE, Beller HR, Richmond SA, and Sherwood Lollar B (2005) Analysis of anaerobic BTX biodegradation in a subarctic aquifer using isotopes and benzylscuccinates. *Journal of Contaminant Hydrology* 81(1–4): 167–186.
McMahon PB (1995) Effect of fuel oxidants on the degradation of gasoline components in aquifer sediments. *3rd International Symposium on In Situ and On-Site Bioreclamation,* San Diego, CA, April 1995.
Meckenstock RU, Morasch B, Warthmann R, et al. (1999) $^{13}C/^{12}C$ isotope fractionation of aromatic hydrocarbons during microbial degradation. *Environmental Microbiology* 1(5): 409–414.
Merian E and Zander M (1982) Volatile aromatics. In: Hutzinger O, Bock KJ, and Daum KA, et al. (eds.) *The Handbook of Environmental Chemistry: Anthropogenic Compounds*, vol. 3, Part B, pp. 117–161. Berlin: Springer-Verlag.
Mill T, Hendry DG, and Richardson H (1980) Free radical oxidants in natural waters. *Science* 207: 886–887.
Miller D, Rivera RG, Travis CC, Solis R, and Calva L (2000) An approach to soil restoration of hydrocarbon contamination using a carbon fractionation approach. *7th International Petroleum Environmental Conference*, Albuquerque, NM, November 2000, pp. 1264–1286. National Energy Technology Laboratory.
Mohn WW and Stewart GR (2000) Limiting factors for hydrocarbon biodegradation at low temperature in arctic soils. *Soil Biology and Biochemistry* 32: 1161–1172.
Moran MJ, Zogorski JS, and Squillace PJ (2005) MTBE and gasoline hydrocarbons in ground water of the United States. *Ground Water* 43(4): 615–627.
Morasch B, Richnow HH, Schink B, and Meckenstock RU (2001) Stable hydrogen and carbon isotope fractionation during microbial toluene degradation: Mechanistic and environmental aspects. *Applied and Environmental Microbiology* 67(10): 4842–4849.
Morasch B, Richnow HH, Schink B, Vieth A, and Meckenstock RU (2002) Carbon and hydrogen stable isotope fractionation during aerobic bacterial degradation of aromatic hydrocarbons. *Applied and Environmental Microbiology* 68(10): 5191–5194.
Morasch B, Richnow HH, Vieth A, Schink B, and Meckenstock RU (2004) Stable isotope fractionation caused by glycyl radical enzymes during bacterial degradation of aromatic compounds. *Applied and Environmental Microbiology* 70(5): 2935–2940.
Mormile MR, Liu S, and Suflita JM (1994) Anaerobic biodegradation of gasoline oxygenates: Extrapolation of information to multiple sites and redox conditions. *Environmental Science & Technology* 28(9): 1727–1732.
Morrill P, Lacrampe-Couloume G, Slater GF, et al. (2005) Quantifying chlorinated ethene degradation during reductive dechlorination at Kelly AFB using stable carbon isotopes. *Journal of Contaminant Hydrology* 76: 279–293.
Mossing C, Larsen LC, Hansen HCL, Seifert D, and Bjerg PL (2001) Monitored Natural Attenuation (MNA) of petroleum hydrocarbons in a heterogenous aquifer affected by transient flow. *Proceedings of the Sixth International In Situ and On-Site Bioremediation Symposium*, San Diego, California, 4–7 June 2001, vol. 2, pp. 11–18. Columbus, OH: Battelle Press.
National Research Council (1985) *Oil in the Sea: Inputs, Fates, and Effects*. Washington, DC: The National Academies Press.
National Research Council (1993) *In Situ Bioremediation When Does it Work?* Washington, DC: The National Academies Press.
National Research Council (2003) *Oil in the Sea: Inputs, Fates, and Effects*. Washington, DC: The National Academies Press.
National Research Council (US) Committee on Intrinsic Remediation (2000) *Natural Attenuation for Groundwater Remediation*. Washington, DC: The National Academies Press.
Novelli GD and ZoBell CE (1944) Assimilation of petroleum hydrocarbons by sulfate-reducing bacteria. *Journal of Bacteriology* 47: 447–448.
Oestermark U and Petersson G (1993) Volatile hydrocarbons in exhaust from alkylate-based petrol. *Chemosphere* 27(9): 1719–1728.
O'Reilly KT, Moir ME, Taylor CD, Smith CA, and Hyman MR (2001) Hydrolysis of *tert*-butyl methyl ether (MTBE) in dilute aqueous acid. *Environmental Science & Technology* 35: 3954–3961.
Orphan VJ, House CH, Hinrichs K-H, McKeegan KD, and deLong EF (2002) Multiple archaeal groups mediate methane oxidation in anoxic cold seep sediments. *Proceedings of the National Academy of Sciences of the United States of America* 99: 7663–7668.
Otton JK and Mercier TJ (2000) National watershed and aquifer susceptibility-evaluation of the impact of oil and gas production operation. *7th International Petroleum Environmental Conference*, Albuquerque, NM, November 2000, pp. 961–978. National Energy Technology Laboratory.
Pankow JF, Thomson NR, Johnson RL, Baehr AL, and Zogorski JS (1997) The urban atmosphere as a non-point source for the transport of MTBE and other volatile organic compounds (VOCs) to shallow groundwater. *Environmental Science & Technology* 31(10): 2821–2828.
Parisi VA, Brubaker GR, Zenker MJ, et al. (2009) Field metabolomics and laboratory assessments of anaerobic intrinsic bioremediation of hydrocarbons at a petroleum-contaminated site. *Microbial Biotechnology* 2(2): 202–212.
Patrick GC and Barker JF (1985) A natural-gradient tracer study of dissolved benzene, toluene and xylenes in ground water. *Proceedings of the Second Canadian/ American Conference on Hydrogeology*, pp. 141–147. National Water Well Association.
Payne JR and Phillips CR (1985) Photochemistry of petroleum in water. *Environmental Science & Technology* 19(7): 569–579.
Perbellini L, Brugnone F, and Pavan I (1980) Identification of the metabolites on *n*-hexane, cyclohexane, and their isomers in men's urine. *Toxicology and Applied Pharmacology* 53: 220–229.
Phelps CD and Young LY (2001) Biodegradation of BTEX under anaerobic conditions: A review. *Advances in Agronomy* 70: 329–357.
Pinal RP, Lee LS, and Rao SC (1991) Prediction of the solubility of hydrophobic compounds in nonideal solvents. *Chemosphere* 22(9–10): 939–951.
Pinal RP, Rao SC, Lee LS, and Cline PV (1990) Cosolvency of partially miscible organic solvents on the solubility of hydrophobic organic chemicals. *Environmental Science & Technology* 24(5): 639–647.
Poulsen M, Lemon L, and Barker JF (1992) Dissolution of monoaromatic hydrocarbons into groundwater from gasoline-oxygenate mixtures. *Environmental Science & Technology* 26(12): 2483–2489.
Powers SE, Hunt CS, Heermann SE, Corseuil HX, Rice D, and Alvarez PJJ (2001) The transport and fate of ethanol and BTEX in groundwater contaminated by gasohol. *Critical Reviews in Environmental Science and Technology* 31(1): 79–123.
Rabus R, Nordhaus R, Ludwig W, and Widdel F (1993) Complete oxidation of toluene under strictly anoxic conditions by a new sulfate-reducing bacterium. *Applied and Environmental Microbiology* 59(5): 1444–1451.
Rabus R and Widdel F (1995) Anaerobic degradation of ethylbenzene and aromatic hydrocarbons by new denitrifying bacteria. *Archives of Microbiology* 163: 96–103.
Rabus R, Wilkes H, Behrends A, et al. (2001) Anaerobic initial reaction of n-alkanes in a denitrifying bacterium: Evidence for (1-methylpentyl)succinate as initial product and for involvement of an organic radical in n-hexane metabolism. *Journal of Bacteriology* 183(5): 1707–1715.
Raghoebarsing AA, Pol A, van de Pas-Schoonen KT, et al. (2006) A microbial consortium couples anaerobic methane oxidation to denitrification. *Nature* 440: 918–921.
Rathbun RE (1998) *Transport, Behavior, and Fate of Volatile Organic Compounds in Streams. US Geological Survey Professional Paper* 1589. Washington, DC: US Government Printing Office.
Raynal M and Pruden A (2008) Aerobic MTBE biodegradation in the presence of BTEX by two consortia under batch and semi-batch conditions. *Biodegradation* 19(2): 269–282.
Reineke W (2001) Aerobic and anaerobic biodegradation pontentials of microorganisms. In: Beek B (ed.) *The Handbook of Environmental Chemistry Vol. 2 Part K-Biodegradation and Persistence*, pp. 1–161. Berlin: Springer-Verlag.
Reinhard M, Goodman NL, and Barker JF (1984) Occurrence and distribution of organic chemicals in two landfill leachate plumes. *Environmental Science & Technology* 18(12): 953–961.
Rice DW (1991) Unique problems of hydrocarbon contamination for ports. In: Kostecki PT and Calabrese EJ (eds.) *Hydrocarbon Contaminated Soils and Groundwater: Analysis, Fate, Environmental and Public Health Effects, Remediation*, pp. 71–75. Chelsea, MI: Lewis Publishers.
Rice DW, Powers SE, and Alvarez PJJ (1999) Potential scenarios for ethanol-containing gasoline released into surface and subsurface waters. *Health and Environmental Assessment of the Use of Ethanol as a Fuel Oxygenate*, vol. IV, ch. 1. State of California, UCRL-AR-135949.

Richmond SA, Lindstrom JE, and Braddock JF (2001) Assessment of natural attenuation of chlorinated aliphatics and BTEX in subarctic groundwater. *Environmental Science & Technology* 35: 4038–4045.

Richnow HH, Annweiler E, Michaelis W, and Meckenstock RU (2003) Microbial *in situ* degradation of aromatic hydrocarbons in a contaminated aquifer monitored by carbon isotope fractionation. *Journal of Contaminant Hydrology* 65: 101–120.

Rifai HS (1997) Natural aerobic biological attenuation. In: Ward CH, Cherry JA, and Scalf MR (eds.) *Subsurface Restoration*. Chelsea, MI: Ann Arbor Press, Inc.

Rios-Hernandez LA, Gieg LM, and Suflita JM (2003) Biodegradation of an alicyclic hydrocarbon by a sulfate-reducing enrichment from a gas condensate-contaminated aquifer. *Applied and Environmental Microbiology* 69(1): 434–443.

Riser-Roberts E (1992) *Bioremediation of Petroleum Contaminated Sites*. Boca Raton, FL: CRC Press.

Robbins GA, Wang S, and Stuart JD (1993) Using the static headspace method to determine Henry's Law constants. *Analytical Chemistry* 65(21): 3113–3118.

Robin MJL, Sudicky EA, Gillham RW, and Kachanoski RG (1991) Spatial variability of strontium distribution coefficients and their correlation with hydraulic conductivity in the Canadian Forces Base Bordon Aquifer. *Water Resources Research* 27(10): 2619–2632.

Rojo F (2009) Degradation of alkanes by bacteria. *Environmental Microbiology* 11(10): 2477–2490.

Rosell M, Barceló D, Rohwerder T, Breuer U, Gehre M, and Richnow HH (2007) Variations in $^{13}C/^{12}C$ and D/H enrichment factors of aerobic bacterial fuel oxygenate degradation. *Environmental Science & Technology* 41: 2036–2043.

Rosell M, Lacorte S, and Barceló D (2006) Analysis, occurrence and fate of MTBE in the aquatic environment over the past decade. *TrAC Trends in Analytical Chemistry* 25(10): 1016–1029.

Rosenberg E, Legmann R, Kushmaro A, Taube R, Adler E, and Ron EZ (1992) Petroleum bioremediation: A multiphase problem. *Biodegradation* 3: 337–350.

Rosenberg E and Ron EZ (1996) Bioremediation of petroleum contamination. In: Crawford RL and Crawford DL (eds.) *Bioremediation: Principles and Applications*. New York: Cambridge University Press.

Rosenfeld WD (1947) Anaerobic oxidation of hydrocarbons by sulfate-reducing bacteria. *Journal of Bacteriology* 54: 664–665.

Rowe BL, Toccalino PL, Moran MJ, Zogorski JS, and Price CV (2007) Occurrence and potential human-health relevance of volatile organic compounds in drinking water from domestic wells in the United States. *Environmental Health Perspectives* 115(11): 1539–1546.

Ruiz-Aguilar GML, Fernandez-Sanchez JM, Kane SR, Kim K, and Alvarez PJJ (2002) Effect of ethanol and methyl *tert*-butyl ether on monoaromatic hydrocarbon biodegradation: Response variability for different aquifer materials under various electron-accepting conditions. *Environmental Toxicology and Chemistry* 21(12): 2631–2639.

Salanitro JP, Diaz LA, Williams MP, and Wisniewski HL (1994) Isolation of a bacterial culture that degrades methyl *t*-butyl ether. *Applied and Environmental Microbiology* 60(7): 2593–2596.

Salanitro JP, Johnson PC, Spinnler GE, Maner PM, Wisniewski HL, and Bruce C (2000) Field-scale demonstration of enhanced MTBE bioremediation through aquifer bioaugmentation and oxygenation. *Environmental Science & Technology* 34(19): 4152–4162.

Salanitro JP, Spinnler GE, Neaville CC, Maner PM, Stearns SM, and Johnson PC (1999) Demonstration of the enhanced MTBE bioremediation (EMB) *in situ* process. *Proceedings from the Fifth International In Situ and On-Site Bioremediation Symposium*, *In Situ Bioremediation of Petroleum Hydrocarbon and Other Organic Compounds*, vol. 3, pp. 37–46. Columbus, OH: Battelle Press.

Schirmer M and Barker JF (1998) A study of long-term MTBE attenuation in the Borden Aquifer, Ontario, Canada. *Ground Water Monitoring & Remediation* 18(2): 113–122.

Schirmer M, Butler BJ, Barker JF, Church CD, and Schirmer K (1999) Evaluation of biodegradation and dispersion as natural attenuation processes of MTBE and benzene at the Borden field site. *Physics and Chemistry of The Earth Part B-Hydrology Oceans and Atmosphere* 24(6): 557–560.

Schmidt TC, Schirmer M, Weiss H, and Haderlein SB (2004) Microbial degradation of methyl *tert*-butyl ether and *tert*-butyl alcohol in the subsurface. *Journal of Contaminant Hydrology* 70: 173–203.

Schuth C, Taubald H, Bolano N, and Maciejczyk K (2003) Carbon and hydrogen isotope effects during sorption of organic contaminants on carbonaceous materials. *Journal of Contaminant Hydrology* 64: 269–281.

Schwarzenbach RP, Giger W, Hoehn E, and Schneider JK (1983) Behavior of organic compounds during infiltration of river water to groundwater. Field studies. *Environmental Science & Technology* 17(8): 472–479.

Seila RL, Lonnema WA, and Meeks SA (1989) Determination of C2–C12 ambient air hydrocarbons in 39 U.S. cities from 1984 through 1986. *US EPA Report EPA/600/53–89/1058*. Washington, DC: US Environmental Protection Agency.

Seyfried B, Glod G, Schocher RJ, Tschech A, and Zeyer J (1994) Initial reactions in the anaerobic oxidation of toluene and *m*-xylene by denitrifying bacteria. *Applied and Environmental Microbiology* 60(11): 4047–4052.

Shaffer KL and Uchrin CG (1997) Uptake of methyl tertiary butyl ether (MTBE) by groundwater solids. *Bulletin of Environmental Contamination and Toxicology* 59(5): 744–749.

Shih T, Rong Y, Harmon T, and Suffet M (2004) Evaluation of the impact of fuel hydrocarbons and oxygenates on groundwater resources. *Environmental Science & Technology* 38: 42–48.

Skubal KL, Barcelona MJ, and Adriaens P (2001) An assessment of natural biotransformation of petroleum hydrocarbons and chlorinated solvents at an aquifer plume transect. *Journal of Contaminant Hydrology* 49(1–2): 151–169.

Slater GF, Dempster HS, Sherwood Lollar B, and Ahad J (1999) Headspace analysis: A new application for isotopic characterization of dissolved organic contaminants. *Environmental Science & Technology* 33(1): 190–194.

Slater GF, Sherwood Lollar B, Sleep BE, and Edwards EA (2001) Variability in carbon isotopic fractionation during biodegradation of chlorinated ethenes: Implications for field applications. *Environmental Science & Technology* 35(5): 901–990.

Smith MR (1990) The biodegradation of aromatic hydrocarbons by bacteria. *Biodegradation* 1: 191–206.

Smith MR (1994) The physiology of aromatic hydrocarbon degrading bacteria. In: Ratledge C (ed.) *Biochemistry of Microbial Degradation*, pp. 347–378. Dordrecht, Netherlands: Kluwer Academic Publishers.

Smith RL, Harvey RW, and LeBlanc DR (1991) Importance of closely spaced vertical sampling in delineating chemical and microbiological gradients in groundwater studies. *Journal of Contaminant Hydrology* 7: 285–300.

Smith CA, O'Reilly KT, and Hyman MR (2003a) Characterization of the intial reactions during the cometabolic oxidation of methyl-*tert* butyl ether by propane-grown *Mycobacterium vaccae* JOB5. *Applied and Environmental Microbiology* 69: 796–804.

Smith CA, O'Reilly KT, and Hyman MR (2003b) Cometabolism of methyl tertiary butyl ether and gaseous *n*-alkanes by *Pseudomonas mendocina* KR-1 grown on C_5 to C_8 *n*-alkanes. *Applied and Environmental Microbiology* 69: 7385–7394.

So CM and Young LY (1999) Initial reaction in anaerobic alkane degradation by a sulfate reducer, strain AK-01. *Applied and Environmental Microbiology* 65(12): 5532–5540.

Spormann AM and Widdel F (2000) Metabolism of alkylbenzenes, alkanes, and other hydrocarbons in anaerobic bacteria. *Biodegradation* 11: 85–105.

Squillace PJ, Moran MJ, Lapham WW, Price CV, Clawges RM, and Zogorski JS (1999) Volatile organic compounds in untreated ambient groundwater of the United States, 1985–1995. *Environmental Science & Technology* 33(23): 4176–4187.

Squillace PJ, Zogorski JS, Wilber WG, and Price CV (1996) Preliminary assessment of the occurrence and possible sources of MTBE in groundwater in the United States, 1993–1994. *Environmental Science & Technology* 30(5): 1721–1730.

Stackelberg PE, Hopple JA, and Kauffman LJ (1997) Occurrence of nitrate, pesticides, and volatile organic compounds in the Kirkwood-Cohansey aquifer system, southern New Jersey. *US Geological Survey Water-Resources Investigation Report 97-4241*. Denver, CO: US Geological Survey.

Stafford BP, Cápiro NL, Alvarez PJJ, and Rixey WG (2009) Pore water characteristics following a release of neat ethanol onto pre-existing NAPL. *Groundwater Monitoring & Remediation* 29(3): 93–104.

Stapleton R and Sayler G (1999) Changes in subsurfacing catabolic gene frequencies during natural attenuation of petroleum hydrocarbons. *Environmental Science & Technology* 34(10): 1991–1999.

State of Maine Bureau of Health (1998) The presence of MTBE and other gasoline compounds in Maine's drinking water—a preliminary report. Bureau of Health, Department of Human Services, Bureau of Waste Management and Remediation, Department of Environmental Protection, Maine Geological Survey, Department of Conservation.

Steffan RJ, McClay K, Vainverg S, Condee CW, and Zhang D (1997) Biodegradation of gasoline oxygenates methyl *tert*-butyl ether, ethyl *tert*-butyl ether, and *tert*-amyl methyl ether by propane-oxidizing bacteria. *Applied and Environmental Microbiology* 63: 4216–4222.

Stehmeier LG, Francis MM, Jack TR, Diegorb E, Winsorb L, and Abrajano TAJ (1999) Field and in vitro evidence for in-situ bioremediation using compound-specific $^{13}C/^{12}C$ ratio monitoring. *Organic Geochemistry* 30: 821–833.

Steinbach A, Seifert R, Annweiler E, and Michaelis W (2004) Hydrogen and carbon isotope fractionation during anaerobic biodegradation of aromatic hydrocarbons - A field study. *Environmental Science & Technology* 38(2): 609–616.

Stempvoort DV and Biggar K (2008) Potential for bioremediation of petroleum hydrocarbons in groundwater under cold climate conditions: A review. *Cold Regions Science and Technology* 53: 16–41.

Stephenson MT (1992) A survey of produced water studies. In: Ray JP and Englehardt FR (eds.) *Produced Water: Technological/Environmental Issues and Solutions*, pp. 1–11. New York: Plenum Press.

Stolz JF and Oremland RS (1999) Bacterial respiration of arsenic and selenium. *FEMS Microbiology Reviews* 23(5): 615–627.

Stumm W and Morgan JJ (1996) *Aquatic Chemistry, Chemical Equilibria and Rates in Natural Waters*, 3rd edn. New York: John Wiley and Sons, Inc.

Suflita JM and Mormile MR (1993) Anaerobic biodegradation of known and potential gasoline oxygenates in the terrestrial subsurface. *Environmental Science & Technology* 27(5): 976–978.

Tebo BM and Obraztsova AY (1998) Sulfate-reducing bacterium grows with Cr(VI), U(VI), Mn(IV), and Fe(III) as electron acceptors. *FEMS Microbiology Letters* 162: 193–198.

Testa SM and Winegardner DL (2000) *Restoration of Contaminated Aquifer: Petroleum Hydrocarbons and Organic Compounds*. Boca Raton, FL: Lewis Publishers.

Thompson GW, Jollett MR, Cadena F, and Weisman C (2000) Removal of MTBE using organozeolites. *7th International Petroleum Environmental Conference*, Albuquerque, NM, November 2000, pp. 813–844. National Energy Technology Laboratory.

Tissot BP and Welte DH (1984) *Petroleum Formation and Occurrence*. Berlin: Springer Verlag.

Tumeo MA and Giunn DA (1997) Evaluation of bioremediation in cold regions. *Journal of Cold Regions Engineering* 11: 221–231.

Ulrich AC, Beller HR, and Edwards EA (2005) Metabolites detected during biodegradation of C-13(6)-benzene in nitrate-reducing and methanogenic enrichment cultures. *Environmental Science & Technoogy* 39: 6681–6691.

Ulrich AC, Tappenden K, Armstrong J, and Biggar KW (2010) Effect of cold temperature on the rate of natural attenuation of benzene, toluene, ethylbenzene and the three isomers of xylene (BTEX). *Canadian Geotechnical Journal* 47: 516–527.

US Environmental Protection Agency (1987) Report to Congress: Management of wastes from the exploration, development, and production of crude oil, natural gas, and geothermal energy. *US EPA Report EPA/530-SW-88-003*. Washington, DC: US Environmental Protectiona Agency.

US Environmental Protection Agency (2000) Methyl tertiary butyl ether (MTBE); advance notice of intent to initiate rulemaking under the Toxic Substances Control Act to eliminate or limit the use of MTBE as a fuel additive in gasoline; advance notice of proposed rulemaking. *Federal Register* 65(58): 16094–16109.

US Geological Survey (2000) *USGS World Petroleum Assessment 2000. New Estimates of Undiscovered Oil and Natural Gas, Including Reserve Growth, Outside the United Sates*. Denver, CO: US Geological Survey.

Valentine DL, Kessler JD, Redmond MC, et al. (2010) Propane respiration jump-starts microbial response to a deep oil spill. *Science* 330(6001): 208–211.

Vandecasteele J-P (2008) *Petroleum Microbiology: Concepts, Environmental Implications*, Industrial Applications. Paris: Editions Technip/IFP Publications.

Vazquez-Duhalt R (1989) Environmental impact of used motor oil. *Science of the Total Environment* 79: 1–23.

Vogel TM and Grbić-Galić D (1986) Incorporation of oxygen from water into toluene and benzene during anaerobic fermentative transformation. *Applied and Environmental Microbiology* 52(1): 200–202.

Voice TC and Weber WJ (1983) Sorption of hydrophobic compounds by sediments, soils, and suspended solids—I. Theory and background. *Water Research* 17(10): 1433–1441.

Wang Y and Huang Y (2003) Hydrogen isotopic fractionation of petroleum hydrocarbons during vaporization: Implications for assessing artificial and natural remediation of petroleum contamination. *Organic Geochemistry* 18: 1641–1651.

Ward JAM, Ahad JME, Lacrampe-Couloume G, Slater GF, Edwards EA, and Sherwood Lollar B (2000) Hydrogen isotope fractionation during methanogenic degradation of toluene: Potential for direct verification of bioremediation. *Environmental Science & Technology* 34: 4577–4581.

Ward DM, Atlas RM, Boehm PD, and Calder JA (1980) Microbial biodegradation and chemical evolution of oil from the Amoco spill. *Ambio* 9: 277–283.

Weiss JV and Cozzarelli IM (2008) Biodegradation in contaminated aquifers: Incorporating microbial/molecular methods. *Ground Water* 46(2): 305–322.

Wentzel A, Ellingsen TE, Kotlar H-K, Zotchev SB, and Throne-Holst M (2007) Bacterial metabolism of long-chain *n*-alkanes. *Applied Microbiology and Biotechnology* 76(6): 1209–1221.

Wiedemeier TH, Rifai H, Newell C, and Wilson JT (1999) *Natural Attenuation of Fuels and Chlorinated Solvents in the Subsurface*. New York: Wiley.

Wiedemeier TH, Wilson JT, Kampbell DH, Miller RN, and Hansen JE (1995) *Technical Protocol for Implementing Intrinsic Remediation with Long-Term Monitoring for Natural Attenuation of Fuel Contamination Dissolved in Groundwater*. US Air Force Center for Environmental Excellence.

Wilkes H, Boreham C, Harms G, Zengler K, and Rabus R (2000) Anaerobic degradation and carbon isotopic fractionation of alkylbenzenes in crude oil by sulphate-reducing bacteria. *Organic Geochemistry* 31(1): 101–115.

Williams B (1991) *U.S. Petroleum Strategies in the Decade of the Environment*. Tulsa, OK: Pennwell Publishing Company.

Wilson BH, Smith GB, and Rees JF (1986) Biotransformations of selected alkylbenzenes and halogenated aliphatic hydrocarbons in methanogenic aquifer material: A microcosm study. *Environmental Science & Technology* 20(10): 997–1002.

Wilson BH, Wilson JT, Kampbell DH, Bledsoe BE, and Armstrong JM (1990) Biotransformation of monoaromatic and chlorinated hydrocarbons at an aviation gasoline spill site. *Geomicrobiology Journal* 8: 225–240.

Wilson JT, Adair C, Kaiser P, and Kolhatkar R (2005a) Anaerobic biodegradation of MTBE at a gasoline spill site. *Ground Water Monitoring & Remediation* 25(3): 103–115.

Wilson JT, Kaiser PM, and Adair C (2005b) Monitored natural attenuation of MTBE as a risk management option at leaking underground storage tank sites. *US EPA Report EPA/600/R-04-179*. Cincinnati, OH: US Environmental Protection Agency.

Wilson JT, Cho JS, Wilson BH, and Vardy JA (2000) Natural attenuation of MTBE in the subsurface under methanogenic conditions. *US EPA Report EPA/600/R-00/006*. Cincinnati, OH: US Environmental Protection Agency.

Wilson RD, Mackay DM, and Scow KM (2002) *In situ* MTBE biodegradation supported by diffusive oxygen release. *Environmental Science & Technology* 36: 190–199.

Wolfe DA, Galt JA, Short J, et al. (1994) The fate of the oil spilled from the Exxon Valdez. *Environmental Science & Technology* 28(13): 561–567.

Yeh CK and Novak JT (1994) Anaerobic biodegradation of gasoline oxygenates in soils. *Water Environment Research* 66(5): 744–752.

Yeh CK and Novak JT (1995) The effect of hydrogen peroxide on the degradation of methyl and ethyl *tert-butyl* ether in soils. *Water Environmental Research* 67: 828–834.

Zeyer J, Kuhn EP, and Schwarzenbach RP (1986) Rapid microbial mineralization of toluene and 1,3-dimethylbenzene in the absence of molecular oxygen. *Applied and Environmental Microbiology* 52(4): 944–947.

Zhang Y, Khan IA, Chen X-H, and Spalding RF (2006) Transport and degradation of ethanol in groundwater. *Journal of Contaminant Hydrology* 82(3–4): 183–194.

Zogorski JS, Morduchowitz A, Baehr AL, et al. (1997) *Interagency Assessment of Oxygenated Fuels, Ch. 2: Fuel Oxygenates and Water Quality*. National Science and Technology Council, pp. 2-1–2-80. Washington, DC: Office of Science and Technology Policy, The Executive Office of the President.

Zwank L, Berg M, Elsner M, Schmidt TC, Schwarzenbach RP, and Haderlein SB (2005) New evaluation scheme for two-dimensional isotope analysis to decipher biodegradation processes: Application to groundwater contamination by MTBE. *Environmental Science & Technology* 39(4): 1018–1029.

11.13 High Molecular Weight Petrogenic and Pyrogenic Hydrocarbons in Aquatic Environments

TA Abrajano Jr. and B Yan, Rensselaer Polytechnic Institute, Troy, NY, USA
V O'Malley, Enterprise Ireland, Glasnevin, Republic of Ireland

This article is reproduced from the previous edition, volume 9, pp. 475–509, © 2003 Elsevier Ltd.

11.13.1 Introduction

Geochemistry is ultimately the study of sources, movement, and fate of chemicals in the geosphere at various spatial and temporal scales. Environmental organic geochemistry focuses such studies on organic compounds of toxicological and ecological concern (e.g., Schwarzenbach et al., 1993, 1998; Eganhouse, 1997). This field emphasizes not only those compounds with potential toxicological properties, but also the geological systems accessible to the biological receptors of those hazards. Hence, the examples presented in this chapter focus on hydrocarbons with known health and ecological concern in accessible shallow, primarily aquatic, environments.

Modern society depends on oil for energy and a variety of other daily needs, with present mineral oil consumption throughout the 1990s exceeding 3×10^9 t year^{-1} (NRC, 2002). In the USA, e.g., ~40% of energy consumed and 97% of transportation fuels are derived from oil. In the process of extraction, refinement, transport, use, and waste production, a small but environmentally significant fraction of raw oil materials, processed products, and waste are released inadvertently or purposefully into the environment. Because their presence and concentration in the shallow environments are often the result of human activities, these organic materials are generally referred to as 'environmental contaminants.' Although such reference connotes some form of toxicological or ecological hazard, specific health or ecological effects of many organic 'environmental contaminants' remain to be demonstrated. Some are, in fact, likely innocuous at the levels that they are found in many systems, and simply adds to the milieu of biogenic organic compounds that naturally cycle through the shallow environment. Indeed, virtually all compounds in crude oil and processed petroleum products have been introduced naturally to the shallow environments as oil and gas seepage for millions of years (NRC, 2002). Even high molecular weight (HMW) polyaromatic compounds were introduced to shallow environments through forest fires and natural coking of crude oil (Ballentine et al., 1996; O'Malley et al., 1997). The full development of natural microbial enzymatic systems that can utilize HMW hydrocarbons as carbon or energy source attests to the antiquity of hydrocarbon dispersal processes in the environment. The environmental concern is, therefore, primarily due to the rate and spatial scale by which petroleum products are released in modern times, particularly with respect to the environmental sensitivity of some ecosystems to these releases (Schwarzenbach et al., 1993; Eganhouse, 1997; NRC, 2002).

Crude oil is produced by diagenetic and thermal maturation of terrestrial and marine plant and animal materials in source rocks and petroleum reservoirs. Most of the petroleum in use today is produced by thermal and bacterial decomposition of phytoplankton material that once lived near the surface of the world's ocean, lake, and river waters (Tissot and Welte, 1984). Terrestrially derived organic matter can be regionally

significant, and is the second major contributor to the worldwide oil inventory (Tissot and Welte, 1984; Peters and Moldowan, 1993; Engel and Macko, 1993). The existing theories hold that the organic matter present in crude oil consists of unconverted original biopolymers and new compounds polymerized by reactions promoted by time and increasing temperature in deep geologic formations. The resulting oil can migrate from source to reservoir rocks where the new geochemical conditions may again lead to further transformation of the petrogenic compounds. Any subsequent changes in reservoir conditions brought about by uplift, interaction with aqueous fluids, or even direct human intervention (e.g., drilling, water washing) likewise could alter the geochemical makeup of the petrogenic compounds. Much of our understanding of environmental sources and fate of hydrocarbon compounds in shallow environments indeed borrowed from the extensive geochemical and analytical framework that was meticulously built by petroleum geochemists over the years (e.g., Tissot and Welte, 1984; Peters et al., 1992; Peters and Moldowan, 1993; Engel and Macko, 1993; Moldowan et al., 1995; Wang et al., 1999; Faksness et al., 2002).

Hydrocarbon compounds present in petroleum or pyrolysis by-products can be classified based on their composition, molecular weight, organic structure, or some combination of these criteria. For example, a report of the Committee on Intrinsic Remediation of the US NRC classified organic contaminants into HMW hydrocarbons, low molecular weight (LMW) hydrocarbons, oxygenated hydrocarbons, halogenated aliphatics, halogenated aromatics, and nitroaromatics (NRC, 2000). Hydrocarbons are compounds comprised exclusively of carbon and hydrogen and they are by far the dominant components of crude oil, processed petroleum hydrocarbons (gasoline, diesel, kerosene, fuel oil, and lubricating oil), coal tar, creosote, dyestuff, and pyrolysis waste products. These hydrocarbons often occur as mixtures of a diverse group of compounds whose behavior in near-surface environments is governed by their chemical structure and composition, the geochemical conditions and media of their release, and biological factors, primarily microbial metabolism, controlling their transformation and degradation.

Hydrocarbons comprise from 50% to 99% of compounds present in refined and unrefined oil, and compounds containing other elements such as oxygen, nitrogen, and sulfur are present in relatively smaller proportions. Hydrocarbon compounds have carbons joined together as single C—C bonds (i.e., alkanes), double or triple C=C bonds (i.e., alkenes or olefins), or via an aromatic ring system with resonating electronic structure (i.e., aromatics). Alkanes, also called paraffins, are the dominant component of crude oil, with the carbon chain forming either straight (*n*-alkanes), branched (isoalkanes), or cyclic (naphthenes) arrangement of up to 60 carbons (**Figure 1**). Aromatic compounds are the second major component of crude oil, with asphalthenes, consisting of stacks of highly polymerized aromatic structures(average of 16 rings), completing the list of major oil hydrocarbon components. Also shown in **Figure 1** are several important classes of compounds that are extensively used in 'fingerprinting' crude oil or petroleum sources: sterols derived from steroid, hopanol derived from bacteriohopanetetrols, and pristane and phytane derived from phytol (from chlorophyll) during diagenesis.

Polycyclic aromatic hydrocarbons (PAHs) that are made up of two or more fused benzene rings are minor components of crude oil (**Figures 1** and **2**), but they are by far the most important HMW compounds in terms of chronic environmental impact. Indeed, total PAH loading is used as the surrogate for the overall estimation of petroleum toxicity effects in environmental assessments (e.g., Meador et al., 1995; NRC, 2002). PAHs are characterized by two or more fused benzene rings (**Figure 2**), and many have toxic properties including an association with mutagenesis and carcinogenesis (e.g., Cerniglia, 1991; Neilson, 1998). The World Health Organization (WHO) and the US Environmental Protection Agency (US EPA) have recommended 16 parental (unsubstituted rings) PAHs as priority pollutants (**Figure 2**). Although petroleum sourced PAHs are major contributors in many surface and subsurface aquatic environments, another major contributor of PAHs to the environment is pyrolysis of fuel and other biomass. The latter are referred to as pyrogenic PAHs to distinguish them from the petrogenic PAHs derived directly from uncombusted petroleum, coal, and their by-products. Natural sources such as forest fires could be important in less inhabited and remote watersheds, but anthropogenic combustion of fossil fuel (e.g., petroleum, coal) and wood is the dominant source of pyrogenic PAHs (Neff, 1979; Bjorseth and Ramdahl, 1983; Ballentine et al., 1996; O'Malley et al., 1997).

11.13.2 Scope of Review

A number of previous reviews and textbooks on organic contaminant behavior in geochemical environments have already considered the general physical, chemical, and biological behavior of organic contaminants on the basis of their structure and composition. This review will focus on the geochemical behavior of a group of organic compounds referred to as HMW hydrocarbons, but will emphasize a class of compounds known as PAHs. Focus on PAHs is justified by their known toxicity and carcinogecity, hence the environmental concern already noted above. Monocyclic aromatic hydrocarbons comprise the LMW end of the aromatic hydrocarbon spectrum, which are discussed in more detail with other hydrocarbon fuels in **Chapter 11.12** of this volume.

Other chapters in this volume examine the LMW hydrocarbons and oxygenated hydrocarbons (see **Chapter 11.12**), halogenated compounds (see **Chapter 11.14**), and pesticides (see **Chapter 11.15**). Other general reviews and textbooks that summarize the sources and geochemical fate and transport of hydrocarbons in a variety of geological media are also available (e.g., Moore and Ramamoorthy, 1984; Schwarzenbach et al., 1993, 1998; Eganhouse, 1997; Volkman et al., 1997; NRC, 2000, 2002; Neilson, 1998; Abdul-Kassim and Simoneit, 2001; Beek, 2001). The following discussions focus on shallow aquatic environments, especially sediments, given the highly hydrophobic (mix poorly with water) and lipophilic (mix well with oil/fat) nature of most HMW hydrocarbon compounds. Nevertheless, the readers should recognize that in spite of our focus on a specific group of hydrocarbon compounds, the behavior of these compounds in aquatic systems will have broad similarity with the behavior of many other hydrophobic and lipophilic compounds discussed in other chapters in this volume. Indeed, most of these compounds are studied

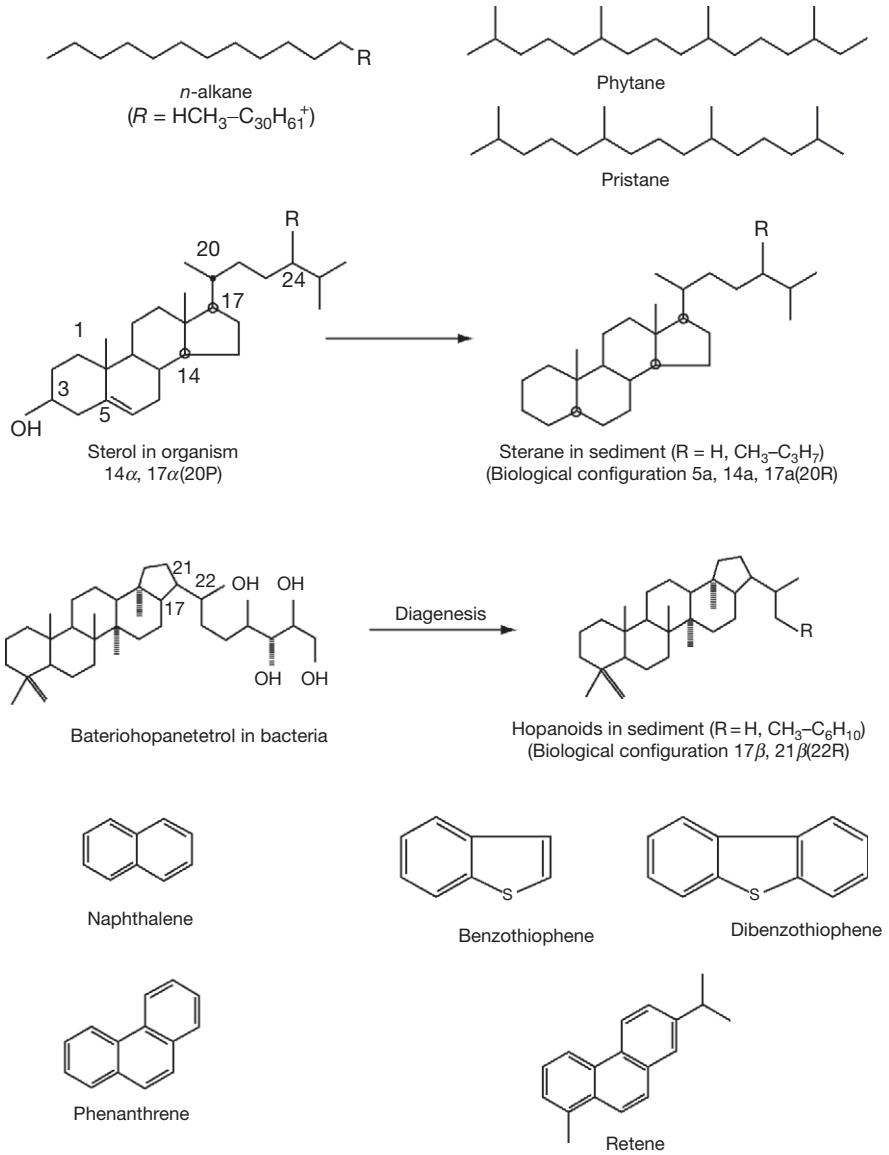

Figure 1 Examples of types of hydrocarbons found in crude oil and mentioned in the text.

simultaneously in shallow aquatic environments, sharing not only common geochemical behavior but also analytical procedures for extraction, isolation, and characterization (e.g., Peters and Moldowan, 1993; Eganhouse, 1997; Abdul-Kassim and Simoneit, 2001).

11.13.3 Sources

11.13.3.1 Petrogenic Hydrocarbons

Worldwide use of petroleum outpaced coal utilization by the 1960s, and accidental oil discharge and release of waste products CO_2, soot (black carbon), and PAHs also increased concomitantly. The more recent report of the NRC (2002) shows that oil production crept up from 7 Mt day^{-1} in the 1970s to 11 Mt day^{-1} by the end of 2000. The total discharge of petroleum into the world's ocean was estimated to be between 0.5 Mt and 8.4 Mt of petroleum hydrocarbons annually (NRC, 2002), which roughly constitutes 0.1% of the annual oil consumption rate. Of this total, 47% are derived from natural seeps, 38% from consumption of petroleum (e.g., land-based runoff, operational discharges, and atmospheric deposition), 12% from petroleum transport, and 3% from petroleum extraction. Used crankcase oils or engine lubricating oils are an important specific source of PAHs in urban environments. The world production of crankcase oil is estimated to be ~40 Mt year^{-1} and 4.4% of that is estimated to eventually reach aquatic environments (NRC, 1985).

Transportation-related release, in order of decreasing annual input, includes accidental releases during tank vessel spill, intentional ballast discharge, pipeline spills, and coastal facility spills. Spectacular oil releases recorded by massive oil spills from grounded tankers tend to capture the public attention, although chronic releases from operational discharges and land releases are quantitatively more important (NRC, 2002). Tank vessel spills account for less than 8% of worldwide

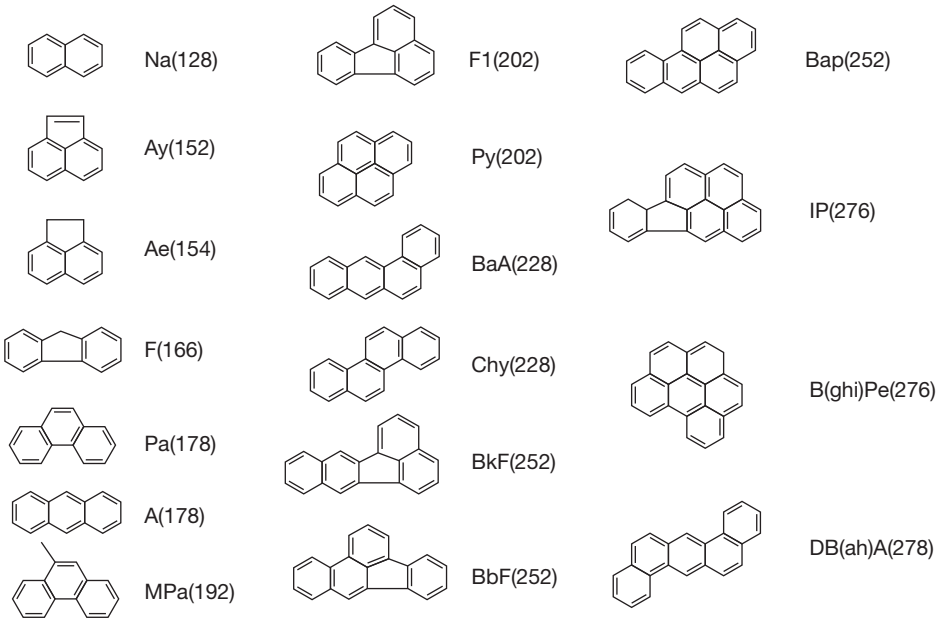

Figure 2 Structures of polycyclic aromatic hydrocarbons. Symbols used in this figure and text: Na (naphthalene), Ay (acetonaphthylene), Ae (acenaphthene), Fl (fluorene), Pa (phenanthrene), A (anthracene), MPa (methyl phenanthrene), F (fluoranthene), Py (pyrene), BaA (benz(a)anthracene), Chy (chrysene), BkF (benzo(k)fluoranthene), BbF (benzo(b)fluoranthene), BaP (benzo(a)pyrene), IP (indenopyrene), B(ghi)Pe (benzo(ghi)perylene), and Db(ah)A (dibenzo(ah)enthracene).

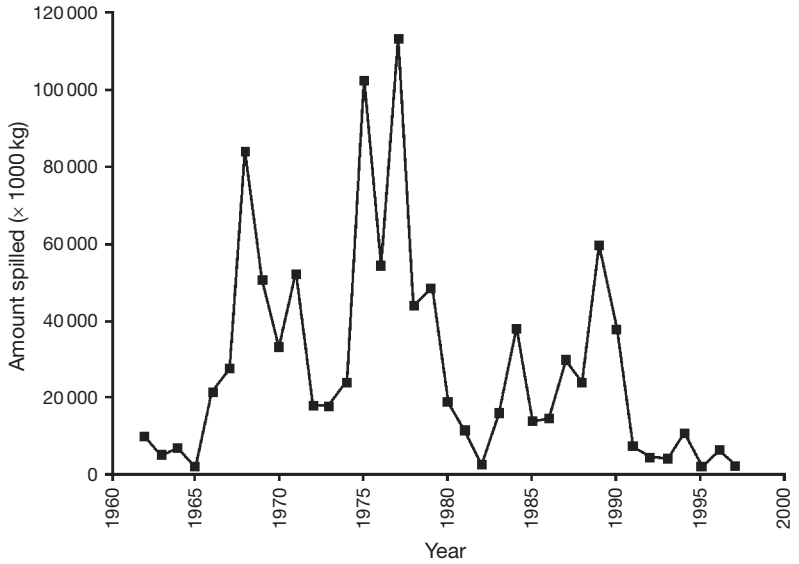

Figure 3 Oil spill trend in North American waters during the 1990s compared to the previous decades (data source NRC, 2002).

petroleum releases in the 1990s (NRC, 2002). For example, oil slick formed from ballast discharges in the Arabian Sea was estimated to exceed 5.4×10^4 m^3 for 1978 (Oostdam, 1980). For comparison, the volume released by the 2002 Prestige oil spill off the Northwest coast of Spain is 1.3×10^4 m^3. Other major oil spills with larger releases include the Torrey Canyon (1.17×10^5 m^3), Amoco Cadiz (2.13×10^5 m^3), Ixtoc blowout (5.3×10^5 m^3), Exxon Valdez (5.8×10^4 m^3), and 1991 Gulf War ($>10^6$ m^3). Studies by Kvenvolden et al. (1993a, 1993b, 1995) also showed the substantially greater input of long-term chronic releases of California oil in the Prince Williams Sound sediments compared to oil released from the Exxon Valdez. A report by the NRC (2002) points to the dramatic decline in oil spilled in North American waters during the 1990s compared to the previous decades (**Figure 3**), with vessel spills accounting for only 2% of total petroleum release to US waters. The 1980s recorded the largest number (391) and volume (2.55×10^5 m^3) of oil spilled to North American waters.

Land releases into groundwater aquifers, lakes, and rivers are dominated by urban runoff and municipal/industrial

discharges, but the actual amounts are difficult to quantify (NRC, 2002). Petroleum discharges from underground storage tanks are by far the dominant source of hydrocarbons in groundwater (see **Chapter 11.12**). However, surface releases from bulk supply depot, truck stops, industrial refueling facilities, and oil storage terminals could also be locally significant sources. It is noteworthy that substantial releases of hydrocarbons may also emanate from natural deposits of oil, heavy oil, shale oil,and bitumen. For example, the Athabasca River in northern Canada shows concentration levels of oil and grease of 850 $\mu g\, l^{-1}$ and $>3000\ \mu g\, l^{-1}$, respectively, from natural bitumen deposits (Moore and Ramamoorthy, 1984). Likewise, Yunker et al. (1993) and Yunker (1995) showed dominant input of natural hydrocarbons in the Mackenzie River. Indeed, natural seeps account for over 60% of petroleum releases to North American waters (NRC, 2002).

Petroleum hydrocarbon sources to North American and worldwide waters were summarized in a report by NRC (2002). In many cases of large petroleum spills, the specific source of petroleum spill is evident, and no geochemical fingerprinting is required to establish the source. Nevertheless, the inventory of petroleum compounds and biomarkers that are eventually sequestered in bottom sediments need not reflect sole derivation from a single source, even in cases of massive oil spills in the area (e.g., Kvenvolden et al., 1995; Wang et al., 1999). Where a mass balance of petroleum sources is required to properly design remediation or identify a point source, molecular methods for distinguishing sources of hydrocarbons have come to the fore.

Several geochemical methods for allocating sources of petrogenic hydrocarbons that are released to aquatic systems have been successfully applied (e.g., O'Malley et al., 1994; Whittaker et al., 1995; Abdoul-Kassim and Simoneit, 1995; Kvenvolden et al., 1995; Wang and Fingas, 1995; Dowling et al., 1995; Bieger et al., 1996; Kaplan et al., 1997; Eganhouse, 1997; Volkman et al., 1997; Mansuy et al, 1997; Hammer et al., 1998; Wang et al., 1999; McRae et al., 1999, 2000; Mazeas and Budzinski, 2001; Hellou et al., 2002; Faksness et al., 2002; NRC, 2002; Lima et al., 2003). The fingerprints used are either molecular or isotopic, and are variably affected by weathering processes. They include overall molecular distribution of hydrocarbons (e.g., range of carbon numbers and odd-even predominance), source specific biomarkers (e.g., terpanes and steranes), so-called 'diagnostic molecular ratios,' and stable isotope compositions. The level of specificity by which a source can be pinpointed is dependent on the fingerprint used to tag the specific source and the multiplicity of hydrocarbon sources involved. Faksness et al. (2002) presented a flow chart for oil spill identification using a tiered molecular discrimination scheme based on the overall hydrocarbon distribution, source-specific markers, and diagnostic ratios (**Figure 4**) target compounds have been used for source identification of spilled oil including: (1) saturated hydrocarbons + pristane and phytane; (2) volatile alkylated aromatics including benzene, toluene, ethyl benzene, and xylene (BTEX); (3) alkylated and nonalkylated PAHs and heterocyclics; and (4) terpanes and steranes (Volkman et al., 1997; Wang et al., 1999). For example, Wang and Fingas (1995) and Douglas et al. (1996) suggested that alkylated dibenzothiophenes are sufficiently resilient to a wide range of weathering reactions to be useful fingerprints for sources of crude oil. Kvenvolden et al. (1995) used the abundances of sterane and hopane biomarkers to differentiate specific crude oil sources in Prince William Sound, Alaska. The use of resilient biomarker signatures has matured to the point that they are widely used for specific litigation cases for assigning liability for oil releases (e.g., Kaplan et al., 1997; Wang et al., 1999).

The molecular distribution of PAHs in petroleum and crankcase oils is quite distinct from pyrogenic sources that will be discussed in the following section (**Figure 5**). This contrast provides an excellent basis for source apportionment of HMW hydrocarbons in the environment. Petrogenic PAHs consist primarily of two- and three-ring parental and methylated compounds with lower concentrations of HMW PAHs (**Figure 5**) (Bjorseth and Ramdahl, 1983; Pruell and Quinn, 1988; Vazquez-Duhalt, 1989; Latimer et al., 1990; O'Malley, 1994). PAH formation during oil generation is attributed both to the aromatization of multi-ring biological compounds (e.g., sterols) and to the fusion of smaller hydrocarbon fragments into new aromatic structures (e.g., Radke, 1987; Neilson and Hynning, 1998; Simoneit, 1998). Steroids are probably the most well understood in terms of biological origin and geological fate, and a simplification of the proposed pathways of sterol diagenesis and catagenesis is summarized in **Figure 6** (after Mackenzie, 1984). Crude oils usually formed at temperatures below 150 °C have a predominance of alkylated (i.e., possessing alkyl side chains) over parental PAHs. O'Malley (1994) characterized hundreds of variably used crankcase oils, and of these samples, 25.5% comprised of four- and five-ring parental compounds, and virgin crankcase oil samples were found to contain no resolvable PAHs (cf. Pruell and Quinn, 1988; Latimer et al., 1990). Since virgin crankcase oils are devoid of measurable PAHs, the most probable source of PAHs in used crankcase oil are the thermal alteration reactions (i.e., aromatization) of oil components such as terpenoids in the car engine (Pruell and Quinn, 1988; Latimer et al., 1990). As with true diagenetic PAHs (**Figure 6**), the distribution of PAHs in used crankcase oils apparently depends on several factors including temperature of reaction, engine design, and general operating conditions of the engine. Since the engine operating temperatures are generally high, the likely products resulting from these reactions include three-, four-, and five-ring unsubstituted compounds such as Pa, Fl, Py, BaA, Chy, BeP, and BaP (see **Figure 2** caption for abbreviations). Pruell and Quinn (1988) also suggested that LMW compounds (one- and two-ring) might be accumulated in crankcase oils from admixed gasoline. The relative stability of pyrogenic PAHs to weathering makes them attractive markers for discrimination of oil sources (**Figure 5**) (Pancirov and Brown, 1975; O'Malley, 1994; Wang et al., 1999). However, Volkman et al. (1997) advocate caution in the use of aromatic compounds because of the relatively small variations between different oils and the differential aqueous solubility of these compounds (see below). Some HMW PAHs may be present in crude oil, albeit, at very low concentrations. Finally, crude oils are also rich in heterocyclic species particularly thiophenes (e.g., dibenzothiophenes). Significant molecular variations of these compounds have been reported for individual crude oil samples, and these are mainly attributed to oil origin and maturity (Neff, 1979). Other important potential sources of petrogenic PAHs identified in sedimentary environments are asphalt and tire and brake wear (Wakeham et al., 1980a;

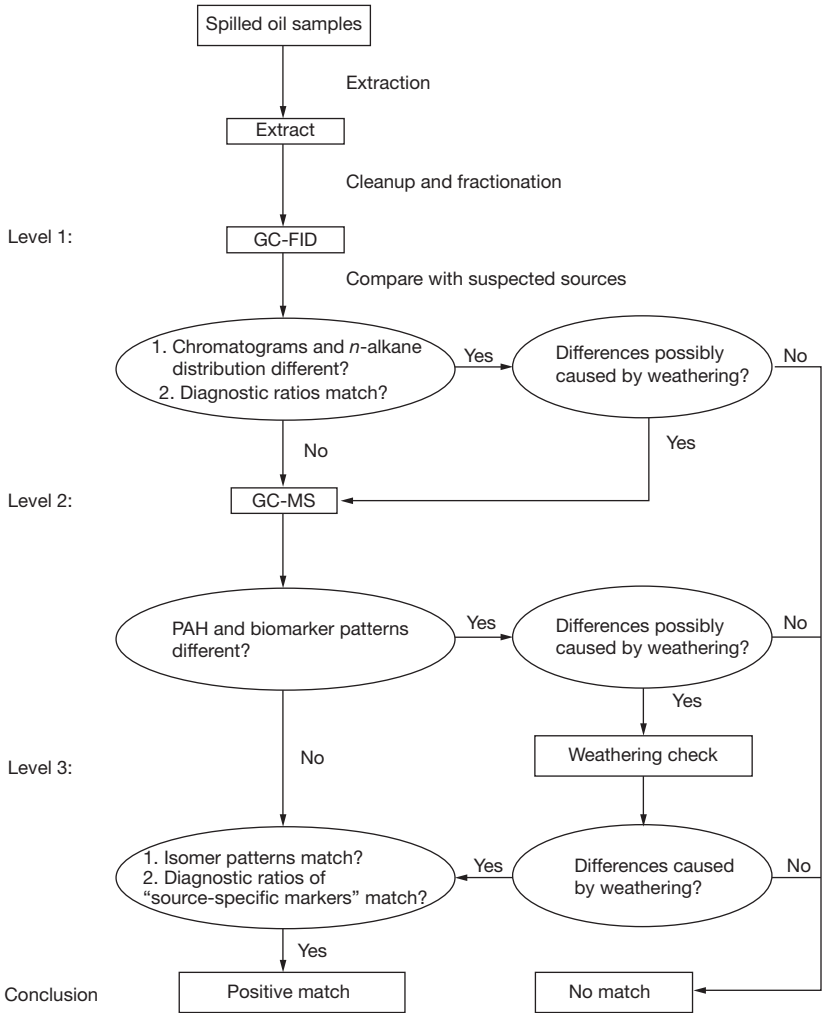

Figure 4 Tiered oil spill source identification scheme using molecular chemistry. The increasing level of source specificity required (down the diagram) is provided by global distributions of *n*-alkanes (level 1), PAH and biomarker distribution patterns (level 2), and isomeric and other diagnostic marker ratios (level 3), respectively (reproduced by permission of Nordtest from *Revision of the Nordtest Methodology for Oil Spill Identification*, **2002**, 110).

Broman et al., 1988; Takada et al., 1990; Latimer et al., 1990; Reddy and Quinn, 1997).

Although previous workers have suggested bacterial synthesis as a possible source of biogenic PAHs in modern sediments, Hase and Hites (1976) have shown that bacteria more likely only bioaccumulate them from the growth medium. Anaerobic aromatization of tetracyclic triterpenes appeared to have been demonstrated by Lohmann et al. (1990) by incubating radiolabeled β-amyrin,but the quantitative importance of these synthesis pathways remains unresolved (e.g., Neilson and Hynning, 1998). The early diagenesis of sedimentary organic matter is certain to lead to the formation of a number of PAHs from alicyclic precursors (e.g., Neilson and Hynning, 1998; Simoneit, 1998). Examples of reactions are the diagenetic production of phenanthrene and chrysene derivatives from aromatization of pentacyclic triterpenoids originating from terrestrial plants, early diagenesis of abietic acids to produce retene (**Figure 7**), and in situ generation of perylene from perylene quinones (Youngblood and Blumer, 1975; Laflamme and Hites, 1978; Wakeham et al., 1980b; Venkatesan, 1988; Lipiatou and Saliot, 1991; Neilson and Hynning, 1998; Simoneit, 1998; Wang et al., 1999). Perylene and retene are the two most prominent PAHs found in recently deposited sediments (Lipiatou and Saliot, 1991). The origin of perylene has been linked to terrestrial precursors (4,9-dihydroxyperylene-3,10-quinone, the possible candidate), marine precursors, and anthropogenic inputs (Blumer et al., 1977; Laflamme and Hites, 1978; Prahl and Carpenter, 1979; Venkatesan, 1988; Lipiatou and Saliot, 1991). The diagenetic pathway for retene is well constrained (**Figure 7**), but it can also be produced from wood combustion (Wakeham et al., 1980b; Lipiatou and Saliot, 1991; Neilson and Hynning, 1998).

11.13.3.2 Pyrogenic Sources of HMW Hydrocarbons

The burial maturation of sedimentary organic matter leading to oil and coal formation and possible biosynthesis are only two of three possible pathways for generating HMW hydrocarbons. Pyrolysis or incomplete combustion at high

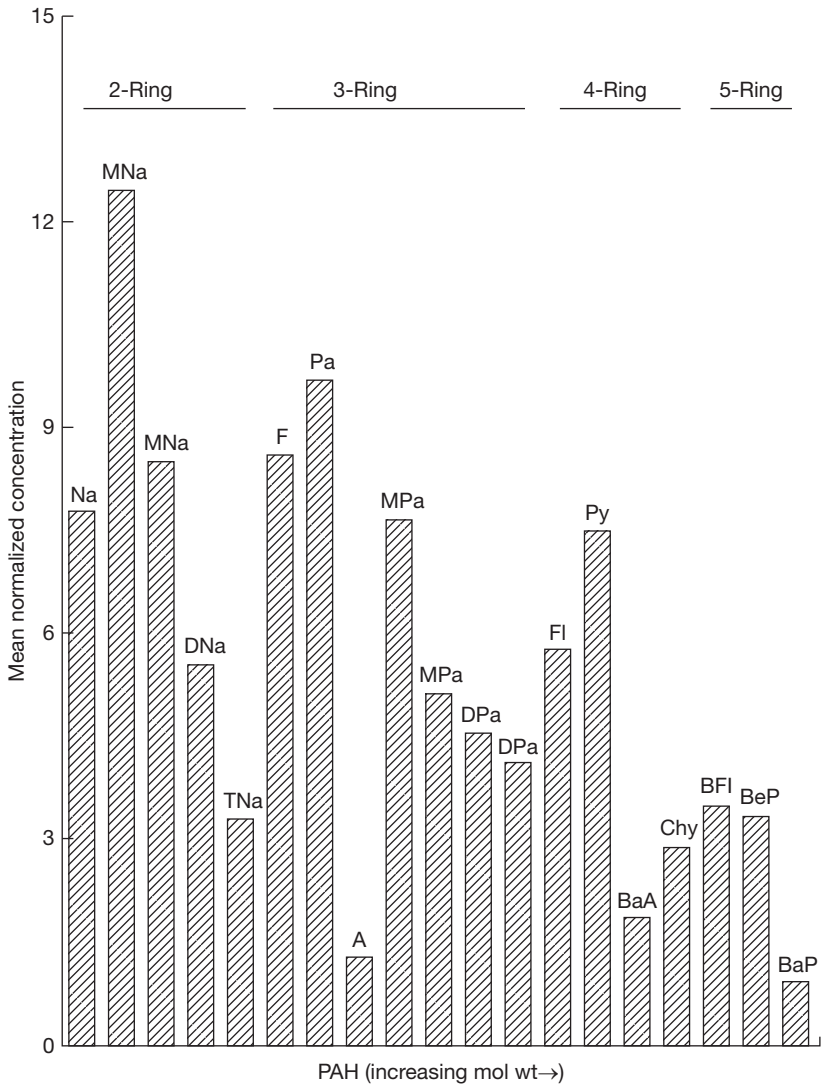

Figure 5 PAHs distribution in petrogenic sources. Compound symbols as in **Figure 2** with the modifier 'M' (methylated), 'D' (dimethylated), and 'T' (trimethylated) added for alkylated PAH.

temperatures also generates a wide variety of LMW and HMW hydrocarbons depending on the starting materials, environmental condition of pyrolysis, and kinetic factors (e.g., gas circulation). Whereas lower molecular compounds generated by pyrolysis have generated significant interest (e.g., butadiene, formaldehyde), the condensed structures from naphthalene to 'black carbon' or soot has been the focus of interest amongst the HMW hydrocarbons.

Indeed, pyrolysis of petroleum and fossil fuel comprise quantitatively the most important source of PAHs in modern sediments (Youngblood and Blumer, 1975; Laflamme and Hites, 1978; Neff, 1979; Wakeham et al., 1980a,b; Sporstol et al., 1983; Bjorseth and Ramdahl, 1983; Kennicutt II et al., 1991; Lipiatou and Saliot, 1991; Canton and Grimalt, 1992; Brown and Maher, 1992; Steinhauer and Boehm, 1992; Yunker et al., 1993, 1995; O'Malley et al., 1996; Lima et al., 2003). For example, sedimentary PAH distribution shows some common molecular features including the dominance of four- and five-ring PAHs (Fl, Py, BaA, Chy, BeP, and BaP), Pa/A ratio between 2 and 6, high Pa/MPa ratio and Fl/Py ratio close to unity. As noted above, the common characteristics related to direct petrogenic-related sources are a series of two- and three-ring parental and alkylated compounds (Na, MNa, Pa, and MPa), low Pa/MPa and Fl/Py ratios, and an unresolved complex mixture (UCM) (Kennicutt II et al., 1991; Volkman et al., 1992; Wang et al., 1999). Although these sedimentary hydrocarbons may bear the imprint of petrogenic sources, the overall molecular attributes are signatures of high-temperature pyrolysis of fossil fuels and natural sources (e.g., forest fires) (Youngblood and Blumer, 1975; Laflamme and Hites, 1978; Lake et al, 1979; Killops and Howell, 1988; Ballentine et al., 1996). Individual markers such as perylene and retene, which are thought to be formed by the diagenetic alteration of biogenic compounds, are also typical of recently deposited sediments (Wakeham et al., 1980a; Venkatesan, 1988; Lipiatou and Saliot, 1991; Yunker et al., 1993, 1995),

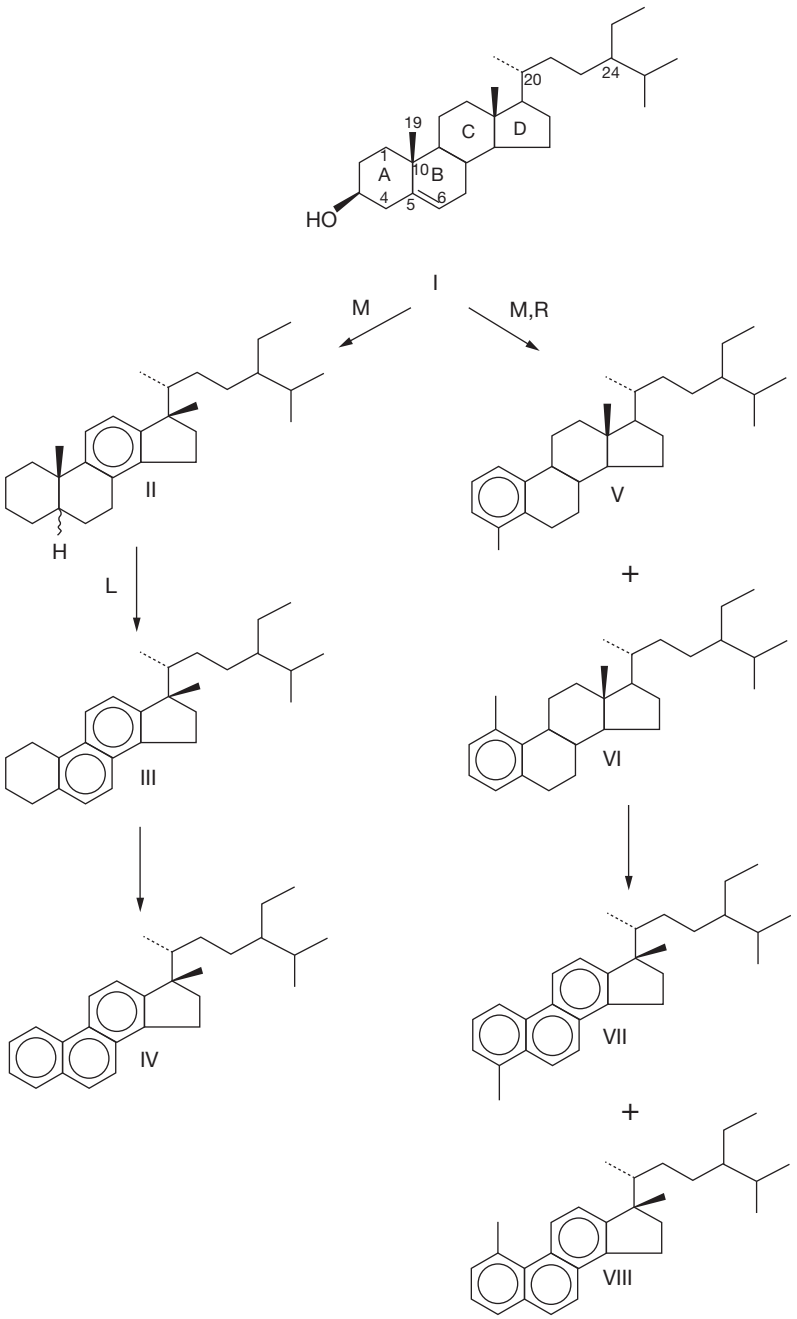

Figure 6 Diagenetic conversion of sterol (I) to various aromatic hydrocarbons during diagenesis. Abbreviation 'M' implies that the reaction involved multiple steps, 'R' represents aromatization of the A ring, and 'L' represents the aromatization of the B ring. Compounds II, V, and VI are intermediates for the formation of triaromatic steroids (after Mackenzie, 1984).

although combustion sources of perylene are also known (e.g., Wang et al., 1999).

The mechanisms by which pyrolytic production of PAHs occur are complex, and have been widely studied since the 1950s (Badger et al., 1958; Howsam and Jones, 1998). Pyrolytic production of PAHs is generally believed to occur through a free radical pathway, wherein radicals of various molecular weights can combine to yield a series of different hydrocarbon products. Therefore, the formation of PAHs is thought to occur in two distinct reaction steps: pyrolysis and pyrosynthesis (Lee et al.,1981). In pyrolysis, organic compounds are partially cracked to smaller unstable molecules at high temperatures. This is followed by pyrosynthesis or fusion of fragments into larger and relatively more stable aromatic structures. Badger et al. (1958) was the first to propose this stepwise synthesis using BaP from free radical recombination reactions (**Figure 8**). Compounds identified in subsequent studies suggest that the C_2 species react to form C_4, C_6, and C_8 species, and confirm the mechanisms proposed by Badger et al. (1958) (Howsam and Jones, 1998; **Figure 8**). Despite the large

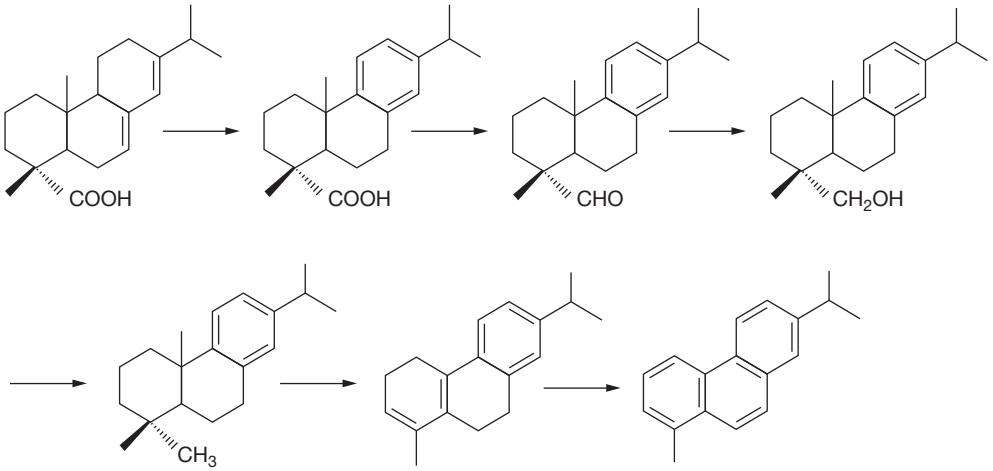

Figure 7 Diagenetic pathway for formation of retene from abietic acid (after Wakeham et al., 1980a).

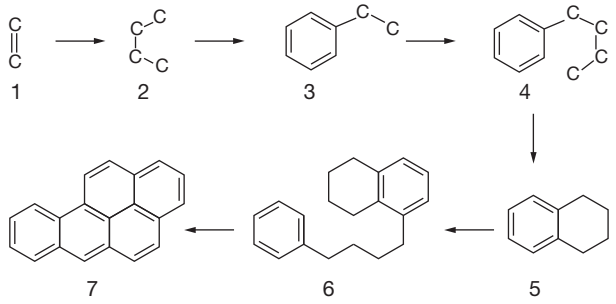

Figure 8 Stepwise pyrosynthesis of benzo(a)pyrene through radical recombination involving acetylene (1), a four carbon unit such as vinylacetylene or 1,3-butadiene, and styrene or ethylbenzene (3) (reproduced by permission of Royal Society of Chemistry from *Journal of the Chemistry Society*, **1958**, *1958*, 2449–2461).

quantities of different PAHs formed during primary reactions, only a limited number enter the environment. This is because initially formed PAHs themselves can be destroyed during combustion as a result of secondary reactions that lead to the formation of either higher condensed structures or oxidized carbon (Howsam and Jones, 1998). For example, the pyrolysis of naphthalene can yield a range ofHMW species such as perylene and benzofluoranthenes, possibly as a result of cyclodehydrogenation of the binaphthyls (Howsam and Jones, 1998). This may be particularly important for compounds that are deposited on the walls of open fireplaces along with soot particulates close to the hot zone of the flame.

PAHs isolated from important pyrogenic sources vary widely in composition, and they are quite distinct from the PAH distribution of petrogenic PAHs (**Figure 9**) (Alsberg et al., 1985; Westerholm et al., 1988; Broman et al., 1988; Freeman and Cattell, 1990; Takada et al., 1990; Rogge et al, 1993; O'Malley, 1994; Howsam and Jones, 1998). For example, individual fireplace soot samples, from hard- and softwood-burning open fireplaces, were consistently dominated by three-, four-, and five-ring parental PAHs with generally lower concentrations of methylated compounds (**Figure 9**) (cf. Freeman and Cattell, 1990; Howsam and Jones, 1998). Vehicular emission and soot samples are also generally characterized by the presence of pyrolysis-derived three-, four-, and five-ring parental PAHs (Wakeham et al., 1980a; Stenbcrg, 1983; Alsberg et al., 1985; Westerholm et al., 1988; Broman et al., 1988; Takada et al., 1990). The range and concentration of PAHs that accumulate in car mufflers are dependent on car age, engine operating conditions, catalytic converter efficiency, and general driving conditions (Pedersen et al., 1980; Stenberg, 1983; Rogge et al., 1993). Rogge et al. (1993) also reported greater PAH emissions occurred from noncatalytic automobiles compared to vehicles with catalytic systems. Perylene, a pentacyclic hydrocarbon, reported to be predominantly of diagenic origin (Laflamme and Hites, 1978; Prahl and Carpenter, 1979; Wakeham et al., 1980b; Simoneit, 1998; Wang et al., 1999) was also identified in some of the investigated car soots samples, although in very low concentrations (Blumer et al., 1977). Lipiatou and Saliot (1992) reported that perylene may also be derived from coal pyrolysis. In contrast to the pyrogenic sources, **Figure 9** also shows the enhanced concentration of two-ring compounds, especially a whole series of methylated phenanthrenes and naphthalenes in petrogenic sources.

11.13.4 Pathways

HMW hydrocarbons can enter surface aquatic systems directly by spillage, accidental release, and natural oil seeps, or indirectly through sewers, urban, and highway runoff. Once hydrocarbons enter aquatic environments, they become rapidly associated with particulate matter, and are deposited in bottom sediments of surface waters or sorbed onto aquifer materials in groundwater systems (Radding et al., 1976; Schwarzenbach et al., 1993; Luthy et al., 1997) (**Figure 10**). In surface-water systems, physical factors, such as turbulence, stability and composition of colloidal particles, deep-water currents, surface waves, and upwelling influence the length of time they remain suspended in the water column. The rate at which hydrocarbons are incorporated into bottom sediments is controlled by sedimentation rate, bioturbation, and bottom sediment–water column exchanges. In groundwater systems, the transport of hydrocarbons depends on whether or not they comprise a separate nonaqueous phase liquid (NAPL), groundwater flow velocities,

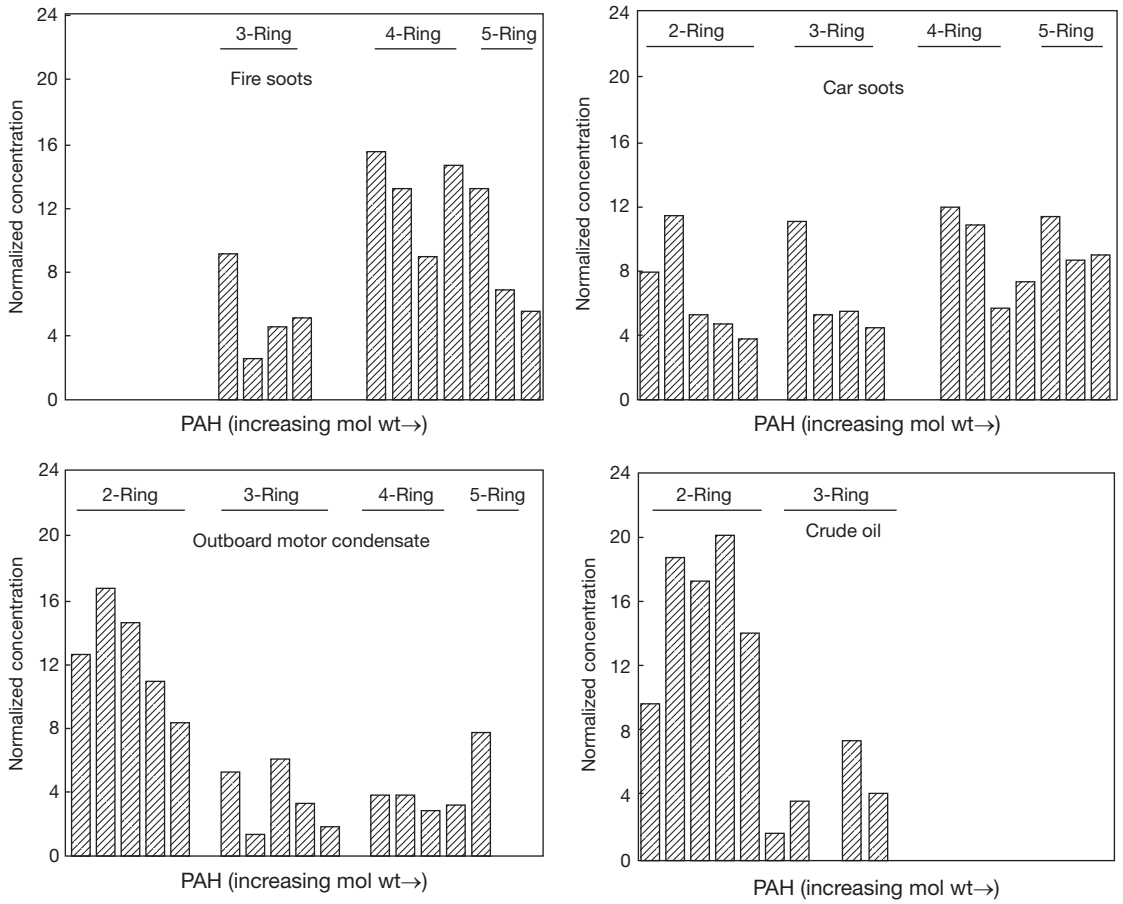

Figure 9 Molecular distribution/signatures of fire soot, car soot, outboard motor concentrate, and crude-oil PAH sources (after O'Malley, 1994).

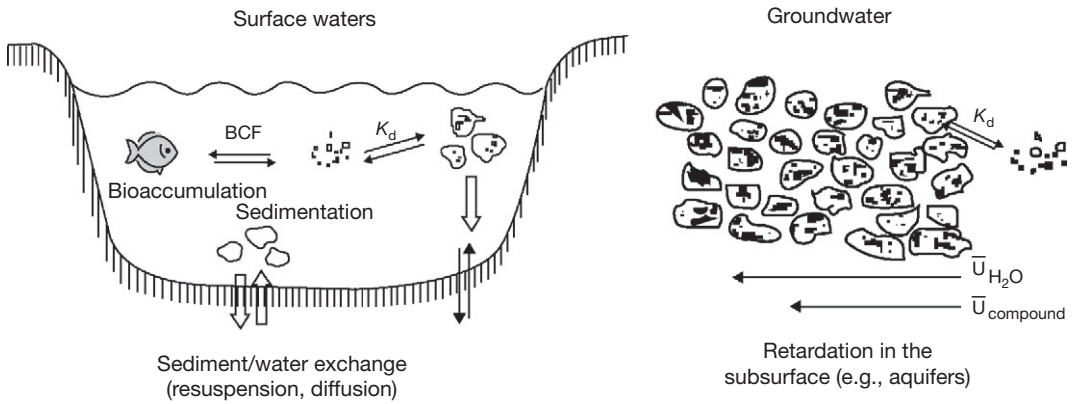

Figure 10 Solid–water exchange processes in groundwater and surface-water environments illustrating sorption to particulates (K_d) and biological concentration factor (BCF). Retardation in groundwater aquifer signified by the difference between water and compound velocities (U) (after Schwarzenbach et al., 1998).

and geochemical partitioning that are discussed below. HMW hydrocarbons likewise enter groundwater environments directly or indirectly from domestic and industrial effluents and urban runoff, and direct spillage of petroleum and petroleum products (e.g., ballast discharge, underground storage tanks).

An important alternate pathway of hydrocarbons to aquatic systems, however, is deposition of airborne particulates including anthropogenic (e.g., soot particles) and natural biogenic (e.g., monoterpenes, difunctional carboxylic acids) aerosols (Simoneit, 1984, 1986; Strachan and Eisenreich, 1988; Baker and Eisenreich, 1990; Eisenreich and Strachan, 1992; Currie et al., 1999). Indeed, the importance of 'organic aerosols' from anthropogenic and natural sources is now extensively recognized (e.g., Simoneit, 1984, 1986; Ellison et al.,

1999). A major part of the extractable and elutable organic matter in urban aerosols consists of an UCM, mainly the branched and cyclic hydrocarbons that originate from car exhaust (e.g., Simoneit, 1984; Rogge et al., 1993). The resolved organic compounds in aerosol extracts consist of *n*-alkanes and fatty acids and PAHs. Whereas health, environmental, and climatic concerns have targeted the reaction products and intermediates formed from tropospheric reactions of labile hydrocarbons and carboxylic acids in these aerosols, the focus of toxicological concern has been on the PAHs.

In the case of PAHs, it is generally recognized that virtually all emissions to the atmosphere are indeed associated with airborne aerosols (Suess, 1976; Simoneit, 1986; McVeety and Hites, 1988; Strachan and Eisenreich, 1988; Baek et al., 1991; Eisenreich and Strachan, 1992; Currie et al., 1999; Offenberg and Baker, 1999). For example, Eisenreich and Strachan (1992) and Strachan and Eisenreich (1988) showed that upwards of 50% of the PAH inventory of the Great Lakes is deposited via atmospheric fallout. PAHs are initially generated in the gas phase, and then as the vapor cools; they are adsorbed onto soot particulates (Howsam and Jones, 1998). The highest concentrations of HMW PAHs in airborne particulates occur in the $<5\,\mu m$ particle size range (Pierce and Katz, 1975; Offenberg and Baker, 1999). PAH distribution between the gas and particulate phase is generally influenced by the following factors: vapor pressure as a function of ambient temperature, availability of fine particulate material, and the affinity of individual PAHs for the particulate organic matrix (Goldberg, 1985; Baek et al., 1991; Schwarzenbach et al., 1993). Atmospheric concentrations of PAHs are normally high in winter and low during the summer months (Pierce and Katz, 1975; Gordon, 1976; Howsam and Jones, 1998), an observation attributed to increased rates of photochemical activity during the summer and increased consumption of fossil fuels during the winter period.

Residence times of particulate PAHs in the atmosphere and their dispersal by wind are determined predominantly by particle size, atmospheric physics, and meteorological conditions (Howsam and Jones, 1998; Offenberg and Baker, 1999). The main processes governing the deposition of airborne PAHs include wet and dry deposition and, to a smaller extent, vapor phase deposition onto surfaces. Particles between 5 μm and 10 μm are generally removed rapidly by sedimentation and by wet and dry deposition (Baek et al., 1991). However, PAHs associated with fine particulates (<1–$3\,\mu m$) can remain suspended in the atmosphere for a sufficiently long time to allow dispersal over hundreds or thousands of kilometers (McVeety and Hites, 1988; Baek et al., 1991).

PAHs in domestic sewage are predominantly a mixture of aerially deposited compounds produced from domestic fuel combustion and industrial and vehicle emissions, combined with PAHs from road surfaces that have been flushed into sewage. Road surface PAHs are derived primarily from crankcase oil, asphalt, and tire and brake wear (Wakeham et al., 1980a; Broman et al., 1988; Takada et al., 1990; Rogge et al., 1993; Reddy and Quinn, 1997). Some PAHs are removed from sewage during primary treatment (sedimentation). Not all urban runoff enters the sewer system, and some sewer designs allow runoff to be independently discharged to aquatic systems without primary treatment. The quantity of runoff from an urban environment is generally governed by the fraction of paved area within a catchment and the annual precipitation. During periods of continued rainfall, road surfaces are continually washed and the contributions of PAHs to watersheds are generally low. However, significant episodic contributions to aquatic systems can occur after prolonged dry periods or during spring snow melt (Hoffman et al., 1984; Smirnova et al., 1998). The distribution and quantity of PAHs in industrial effluents depends on the nature of the operation and on the degree of treatment prior to discharge. In some urban areas, industrial effluents are combined with domestic effluents prior to treatment, or they are independently treated before being discharged to sewer systems. Once particle-associated hydrocarbons are deposited in sediments or sorbed onto aquifer material, the subsequent fate is determined by the physics of sediment and water transport, and the biogeochemical reactions described below.

11.13.5 Fate

Shallow geochemical environments consist of solid, aqueous, and air reservoirs and their interfaces. Hydrocarbon compounds partition into these various reservoirs in a manner determined by the structure and physical properties of the compounds and the media, and the mechanism of hydrocarbon release. The structure and physical properties of the compounds and media understandably impact their sorption, solubility, volatility, and decomposition behavior (e.g., Schwarzenbach et al., 1993). In addition, hydrocarbon partitioning in real systems is holistically a disequilibrium process; hence, the distribution of hydrocarbons depends as much on the pathway taken as on the final physical state of the system (e.g., Schwarzenbach et al., 1993; Luthy et al., 1997). Shallow aquatic systems may tend towards some equilibrium distribution (**Figure 10**), but this is seldom, if ever, truly attained.

Processes affecting hydrocarbon distribution and fate in multiphase aquatic systems can be characterized either as inter-media exchange or as transformational reactions (Mackay, 1998). The latter pertains to processes that involve molecular transformation of the compound, whereas the former is concerned with the movement of the molecularly intact compound from one medium to another. For the purpose of this review, we focus on the three most important exchange processes dictating the geochemical fate of hydrocarbons in aquatic environments: sorption, volatilization, and water dissolution. Sorption characterizes exchange between water and particulate phases (sediments or aquifer media), volatility characterizes exchange between air and water or air and solid, and dissolution pertains to the ability of contaminants to be present as true solutes in the aqueous media. A process of potential importance in some oil spills, emulsification, is not covered here but the readers are referred to a recent document published by NRC (2002), and references cited therein. Similarly, discussion of molecular reaction will focus on the two dominant transformation processes of hydrocarbons in geologic media: photolytic and biological transformation. Photolysis pertains to light-assisted chemical reactions that can affect compounds in the atmosphere and in the photic zone of water columns. Biological transformation is often accomplished by

microorganisms, and could take place in aerobic or anaerobic environments. Purely chemical transformations, including hydrolysis, redox, and elimination reactions, are not examined here, because they are unlikely to be the dominant reaction pathways in shallow aquatic systems (NRC, 2002). For example, the theoretical pK_a values of hydrocarbons are exceedingly high; hence, they tend not to participate in acid–base reactions. Redox reactions involving alkenes can take place at surface geochemical conditions, but this compound group is not present in major amounts in petroleum hydrocarbon spills or pyrogenic products.

Hydrocarbons are hydrophobic and lipophilic compounds. As free liquid, gas, or solid phases, they are quite immiscible in water primarily because of their low polarity. In a competition between aqueous solution, air and solids, HMW hydrocarbons tend to partition heavily into the solid phases, and hence they are also sometimes referred to as 'particle-associated compounds.' This is true in both the atmospheric reservoir, where they associate with atmospheric particulates, and surface and groundwater systems, where they exhibit affinity for suspended particles and aquifer solids. In the case of nonhalogenated NAPL, the separate liquid phase is generally lighter than the aqueous phase, and hence they tend to physically 'float' on the aqueous surface. Such is the case for oil spills either in surface water (e.g., ocean, streams, and lake) or in groundwater (e.g., underground storage tanks).

The hydrophobicity can be expressed by the dimensionless octanol/water partition coefficient (K_{ow}):

$$K_{OW} = C_{i,O}/C_{i,W}$$

where $C_{i,O}$ is the concentration of i in octanol and $C_{i,W}$ is the concentration of i in water. Many of the thermodynamic properties describing the partitioning of hydrocarbons in air, water, biota, or solid have been successfully, albeit empirically, related to K_{OW}. The value of K_{OW} among petroleum hydrocarbons, especially PAHs, tends to be very high (10^3 to $>10^6$), and this preference for the organic phase, either as a free phase or in organic particulates, is a major control on the fate and distribution of hydrocarbons in aquatic systems. The lipophilic affinity of PAHs is also a major contributor to enrichment of these compounds in organisms and organic-rich sediments.

11.13.5.1 Sorption

Solid–water exchange of hydrocarbons is a primary control on their aqueous concentration in groundwater and surface aquatic environments (**Figures 10** and **11**). The specific partitioning of hydrocarbons between solid and aqueous phase could be described by the distribution coefficient (K_d):

$$K_d = C_{i,\,solid}/C_{i,W}$$

where $C_{i,solid}$ is the concentration of i in the solid (mol kg^{-1}) and $C_{i,W}$ is the concentration of i in water (mol l^{-1}). For hydrophobic compounds, K_d tends to be constant only within a limited concentration range, and the more general Freundlich isotherm is commonly used:

$$C_{i,\,solid} = K_d C_{i,w}^n$$

where n is a parameter relating to the nonlinearity of the sorption process (e.g., Schwarzenbach et al., 1993; Luthy et al., 1997). Hydrocarbons tend to partition preferentially to organic matter; hence, the K_d is often written to take explicit account of this preference:

$$K_d = C_{i,OM} f_{OC}/C_{i,W}^{\,n} = K_{i,OC} f_{OC}$$

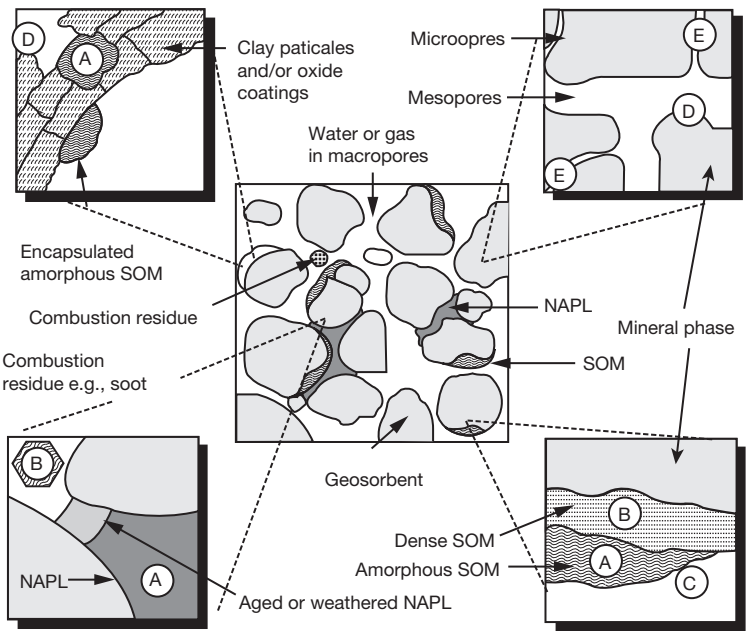

Figure 11 Heterogenous solid compartments in soils and sediments. NAPL signifies nonaqueous phase liquid and SOM represents soil organic matter. **A** – absorption into amorphous organic matter or NAPL, **B** – absorption into soot or black carbon, **C** – adsorption onto water-wet organic surfaces, **D** – adsorption to non-porous mineral surfaces, and **E** – adsorption into microvoids or microporous minerals (reproduced by permission of American Chemical Society from *Environmental Science & Technology* **1997,** 31, 3341–3347).

where $K_{i,OC}$ is the distribution coefficient between organic matter and aqueous phase and f_{OC} is the fraction of organic carbon (~0.5 fraction of organic matter, f_{OM}) in the solid substrate. Note that the above formulation assumes insignificant sorption on mineral matter, which is generally true for 'threshold' $f_{OC} > 0.0005$ (Schwarzenbach et al., 1993). Typical soils have a f_{OC} range of 0.005–0.05, whereas coarse aquifers have a f_{OC} range of 0–0.025.

'Linear free energy relationships' are quite frequently used for estimating K_d or $K_{i,OC}$. This linear correlation comes in the form

$$\log K_{i,OC} = a \log K_{OW} - b$$

where a and b are linear fitting parameters, and K_{OW} is the aforementioned octanol/water partition coefficient (e.g., Chiou et al., 1979, 1998; Karickhoff, 1981; Schwarzenbach et al., 1993). For example, $K_{i,OC}$ of PAHs could be estimated from their K_{OW} by assuming that $K_{i,OC} = 0.41 K_{OW}$ (Karickhoff's, 1981).

Hydrocarbon sorption on sediments or atmospheric particulates can involve either absorption or adsorption, which connotes surface attachment or subsurface dissolution, respectively. No distinction between these two processes is made here, except to note that sorption in geochemical systems often involves both (Kleineidam et al., 2002). Laboratory experiments have shown that HMW petroleum hydrocarbons rapidly associate with sediment surfaces, with sorption uptake of up to 99% in 48 h at hydrocarbon concentrations of 1–5 mg l^{-1} (e.g., Knap and Williams, 1982). The rate and extent of sorption depends on the competitive affinity of the compounds between the aqueous or gaseous solution and the solid surface. The latter, in turn, depends on the nature of the crystallographic or amorphous substrate, especially the presence, type, and amount of organic matter in the solid and colloidal phase (e.g., Witjayaratne and Means, 1984; Luthy et al., 1997; Ramaswami and Luthy, 1997; Gustafsson and Gschwend, 1997; Villholth, 1999; MacKay and Gschwend, 2001). The extent of preference for the solid surface is often described in terms of the sorption coefficient, K_d, as defined above.

The use of single distribution coefficient for organic matter would imply a constancy of sorption behavior on all organic substrates, and that the nature of organic matter substrate is not critical for sorption assessment. The impact of the heterogeneous nature of organic matter substrates on geosorption has been explored, and it has become evident that the wide variety of organic matter properties requires accounting of substrate specific K_{OM} values (e.g., Luthy et al., 1997; Kleineidam et al., 1999, 2002; Chiou et al., 1998; Bucheli and Gustafsson, 2000; Karapanagioti et al., 2000) (**Figure 11**). For example, Karapanagioti et al. (2000) and Kleineidam et al. (1999) demonstrated the distinct Freundlich K_d (and $K_{i'OC}$) for phenanthrene sorption on different organic substrates as well as mineral matter substrates (**Figure 12**) (Karickhoff et al., 1979). Bulk $K_{i'OC}$ characteristics of naphthalene, phenanthrene, and pyrene were examined by Chiou et al. (1998), and they concluded that significant differences exist in $K_{i'OC}$ of pristine terrestrial soil organic matter and sediment organic matter, and that sorption is enhanced in sediments with organic contaminants present. Furthermore, there is now increasing recognition of the explicit role of black carbon (soot)

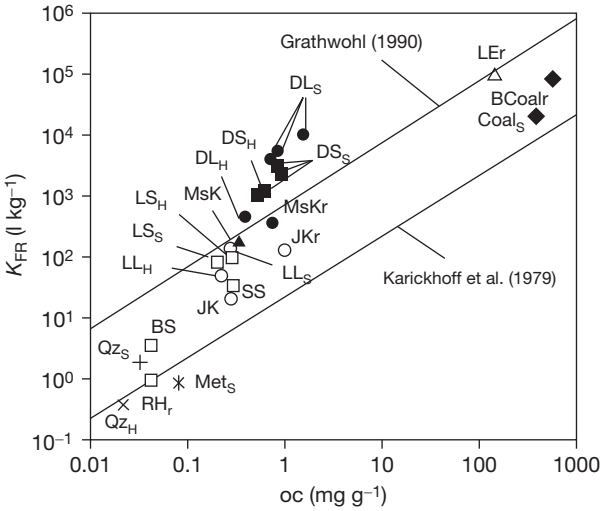

Figure 12 Phenanthrene sorption coefficients on different organic substrates. K_{FR} is the Freundlich coefficient and oc is organic carbon content. Remaining symbols are per table 2 of Kleineidam et al. (1999): D/L – dark/light, L – limestone, S – sandstone, Met – igneous and metamorphic rocks, Qz – quartz, and BS – bituminous shale (reproduced by permission of American Chemical Society from *Environmental Science & Technology.*, **1999,** 33, 1637–1644).

sorption particularly in regards to explaining much higher field measured K_d values compared to previously suggested 'overall' K_d values (e.g., Chiou et al., 1979; Karickhoff et al., 1979; Karickhoff, 1981; Gustafsson and Gschwend, 1997; Accardi-Dey and Gschwend, 2003). It appears that the cohesive compatibility between PAHs and aromatic components of the organic substrate is a major factor in enhancement of sorption (e.g., Gustafsson and Gschwend, 1997; Chiou et al., 1998; Bucheli and Gustafsson, 2000; MacKay and Gschwend, 2001; Accardi-Dey and Gschwend, 2003). Accardi-Dey and Gschwend (2003) proposed treating organic sorption as a composite of organic carbon absorption and black carbon adsorption:

$$K_d = K_{i,OC} f_{OC} + f_{BC} K_{BC} C_{i,W}^{n-1}$$

where f_{BC} is the fraction of black carbon in the sample, K_{BC} is the black carbon distribution coefficient, and n is the Freundlich exponent as before. Note also that f_{OC} is now the fraction of organic carbon that excludes the black carbon component. Whereas this approach apparently explained discrepancies in modeled and field-calculated K_d and the nonlinear K_d observed in the laboratory, it remains to be seen if non-BC organic carbon can indeed be represented by a single K_d (i.e., $= K_{i,OC}$) in the general case.

11.13.5.2 Volatilization

When petroleum products enter surface-water systems, the lighter aliphatic and aromatic hydrocarbons spread out along the surface of the water and evaporate. The volatilization half-life of naphthalene, e.g., is 0.5–3.2 h (Mackay et al., 1992). The naphthalene that does not evaporate sorbs to the particulate matter as noted above or is transformed into water in oil emulsion. In general, evaporation is the primary mechanism

of loss of volatile and semivolatile components of spilled oil (e.g., Fingas, 1995; Volkman et al., 1997; NRC, 2002). After a few days of oil spill at sea, ~75 % of light crude, 40% of medium crude, and 10 % of heavy crude oil will be lost by evaporation (NRC, 2002). The specific evaporation rates are influenced by a number of factors including meteorological factors, stratification of the water column, flow and mixing of water, and sequestration by mineral and natural organic sorbent matter.

The partitioning between air and water is characterized by the Henry's law constant (K_H):

$$K_H = P_{i,\,AIR,}/C_{i,\,W}$$

where $P_{i,AIR,}$ is the partial pressure of i in and $C_{i,w}$ is the molarity of i in the aqueous phase. K_H is often estimated from $P_{0,}/C_{i,sat,}$ where P_0 is the vapor pressure of the compound and $C_{i,sat}$ is the solubility (see below). High K_H implies higher volatility, and results from a combination of high vapor pressure and low aqueous solubility. The vapor pressure of hydrocarbon compounds, along with their affinity for the sorption surfaces, dictates the partitioning between the atmosphere and atmospheric particulate phases. Hence, P_0 is a primary control on the atmospheric fate and transport of hydrocarbons. For example, a hydrocarbon that is tightly bound to the particulate phase is less likely to be altered during transportation and deposition (Baek et al., 1991). The subsequent fate of hydrocarbons deposited in surface waters is further influenced volatilization behavior because of possible surface losses to the atmosphere (Strachan and Eisenreich, 1988; Baker and Eisenreich, 1990; Eisenreich and Strachan, 1992; Lun et al., 1998; Gustafson and Dickhut, 1997).

The dependence of vapor pressure on temperature follows from a simplified solution to the Clapeyron equation (Schwarzenbach et al., 1993):

$$\ln\ P_0 = -B/T + A$$

where $B = \Delta H_{vap}/R$ and $A = \Delta S_{vap}/R$. ΔH_{vap} and ΔS_{vap} are, respectively, the molar enthalpy and molar entropy of vaporization and R is the gas constant (8.314 Pa m^3 mol^{-1} K^{-1}). ΔH_{vap} is principally the energy required to break van der Waals and hydrogen bonds in going from the condensed phase to vapor. ΔS_{vap} is a compound-specific constant, which has been shown to correlate with compound boiling point (Schwarzenbach et al., 1993). Increase in temperature results in more condensed phase hydrocarbons moving into the vapor phase, while a temperature decrease results in more vapor phase hydrocarbons appearing in the condensed phase (e.g., Lane, 1989; Baker and Eisenreich, 1990; Mackay, 1998). Thus, particulate hydrocarbon deposition is likely greater during colder periods, but the effect is highest on the lower molecular weight compounds (e.g., naphthalene) with significant vapor pressure. Likewise, the relative behavior of hydrocarbons between water surface and air is dictated by their relative vapor pressures such that a net flux of PAHs into the atmosphere can take place in warm summer months and the reverse taking place during the colder months (e.g., Baker and Eisenreich, 1990; Gustafson and Dickhut, 1997). Mackay (1998) and Mackay and Callcott (1998) provided more detailed analysis of this partitioning behavior using the so-called 'fugacity approach.' To mass balance PAH partitioning between the atmosphere and water, they used the dimensionless parameter K_{AW}, the air–water partition coefficient, as $K_{AW} = K_H/RT$ (cf. Baker and Eisenreich, 1990; Schwarzenbach et al., 1993). Along with solid–water partitioning discussed above and solubility values discussed below, they showed mass balance partitioning models for PAHs in a model 'seven-phase geomedia' (Mackay and Callcott, 1998). For a detailed discussion of the 'fugacity approach,' the reader is referred to Mackay (1998).

As noted above, volatilization losses from the aqueous phase to the atmosphere are also influenced by the aqueous solubility of the compound (i.e., $P_0/C_{i,}$sat). Higher solubility results in lower K_H for compounds of identical vapor pressures. Although the impact of solubility on volatilization loss is critical for LMW hydrocarbons, the effect of solubility on the behavior of HMW compounds has broader significance for understanding their transport and fate (see below).

11.13.5.3 Water Dissolution and Solubility

HMW hydrocarbons have a wide range of solubility, reported as S or $C^{sat}_{i,W}$ (i.e., aqueous concentration at saturation), but these solubilities are generally very low (e.g., Readman et al., 1982; Means and Wijayaratne, 1982; Whitehouse, 1984; Mackay and Callcott, 1998). For example, water solubility of PAHs tends to decrease with increasing molecular weight from 4×10^{-4} M for naphthalene to 2×10^{-8} M for benzo(a)pyrene (Schwarzenbach et al., 1993). Linear fused PAHs (e.g., naphthalene and anthracene) also tend to be less soluble than angular or pericondensed structures (e.g., phenanthrene and pyrene). Furthermore, alkyl substitution decreases water solubility of the parental PAHs. In spite of their low solubility, dissolution is one of the most important media exchange processes leading to the primary destruction pathway of hydrocarbons in aquatic systems – biodegradation. Metabolic utilization of hydrocarbons requires that they be transported as dissolved components into the cells, a process often assisted by extracellular enzymes released by the microorganisms after a quorum has been reached (Ramaswami and Luthy, 1997; Neilson and Allard, 1998). The presence of dissolved humic acids in solution also enhances solubility (Chiou et al., 1979, 1983; Fukushima et al., 1997; Chiou and Kyle, 1998). Solubility enhancement may also be achieved using surfactants, a method employed in many previous PAH and oil cleanup efforts.

Temperature affects aqueous solubility in a manner dictated by the enthalpy of solution (ΔH^0_s) according to (Schwarzenbach et al., 1993)

$$\ln C^{sat}_{i,\,w} = -\Delta H^0_s/RT + \Delta S^0_s/R$$

The temperature effects on solubility for liquid and solid hydrocarbons vary greatly because of the large melting enthalpy component to ΔH^0_s for solids (for which all PAHs are at room temperature). In general, PAH solubility increases with temperature, prompting present interest in thermophilic degradation of HMW PAHs. Hydrocarbons, including PAHs, also exhibit 'salting-out' effects in saline solutions. This effect is exemplified by the so-called Setschenow formulation (Schwarzenbachs et al., 1993): $\log C^{sat}_{i,\,salt} = \log C^{sat}_{i,\,W} - K_s S$ where $C^{sat}_{i,\,salt}$ is the saturation concentration or solubility in the saline

solution, $C_{i,W}^{sat}$ is the saturation concentration in pure water defined previously, K_s is the Setschenow constant, and S is the total molar salt concentration. For example, the Setschenow constant for pyrene at 25 °C is 0.31–0.32 (Schwarzenbach et al., 1993) so that at the salinity of seawater, $C_{i,W}^{sat}$, is 54% greater than $C_{i,salt}^{sat}$. This salting-out effect could be large enough to manifest in the localization of PAH contamination in estuarine environments (e.g., Whitehouse, 1984).

HMW hydrocarbons and especially PAHs with no polar substituents are very hydrophobic, which along with their lipophilic characteristics and low vapor pressure explain why they are not efficiently transported in aqueous form.

11.13.5.4 Photochemical Reactions

Photochemical reactions involving electromagnetic radiation in the UV-visible light range can induce structural changes in organic compounds. Direct photochemical reactions occur when the energy of electronic transition in the compounds corresponds to that of the incident radiation, with the compound acting as the light-absorbing molecule (i.e., chromophore). Hence, the structure of hydrocarbons determines the extent by which they are prone to photodecomposition, but photolytic half-lives are also significantly dependent on compound concentration and substrate properties (e.g., Behymer and Hites, 1985, 1988; Paalme et al., 1990; Reyes et al., 2000; NRC, 2002). In general, aromatic and unsaturated hydrocarbons are more prone to UV absorption and decomposition, with increasing numbers of conjugated bonds resulting in lower energy required for electronic transition. Photodissociation is not likely an important weathering mechanism for HMW straight-chain hydrocarbons, because these compounds do not absorb light efficiently (e.g., Payne and Phillips, 1985). Nevertheless, these hydrocarbons may be transformed through the process of indirect photodissociation wherein another molecule (e.g., humic and fulvic acids) or substrate (mineral or organic) acts as the chromopore (NRC, 2002). Aromatic structures are prone to direct photochemical reaction in a manner that depends on molecular weight and degree of alkylation.

Laboratory experiments have shown that PAHs are photoreactive under atmospheric conditions (Zafiriou, 1977; Behymer and Hites, 1988; Schwarzenbach et al., 1993; Reyes et al., 2000) and in the photic zone of the water column (Zepp and Schlotzhauer, 1979; Payne and Phillips, 1985; Paalme et al., 1990). The existence of PAH oxidation products in atmospheric particulate matter indicates that PAHs react with oxygen or ozone in the atmosphere (Schwarzenbach et al., 1993; Howsam and Jones, 1998), but the reaction with hydroxyl (OH) radicals during daylight conditions is considered to be the major reaction sink of these compounds in the atmosphere. There is great variation in the reported half-lives of various PAHs due to photolysis, largely because of the differences in the nature of the substrate on which the PAHs are adsorbed and the degree to which they are bound (Behymer and Hites, 1985; Paalme et al., 1990; Schwarzenbach et al., 1993). Carbon content and the color of substrates are important factors in controlling PAH reactivity (Behymer and Hites, 1988; Reyes et al., 2000), and the suppression of photochemical degradation of PAHs adsorbed on soot and fly-ash has been attributed to particle size and substrate color. Darker substrates absorb more light and thereby protect PAHs from photolytic degradation reactions (Behymer and Hites, 1988).

Photo-oxidation by singlet oxygen appears to be the dominant chemical degradation process of PAHs in aquatic systems (Lee et al., 1978; Hinga, 1984; Payne and Phillips, 1985). The degree to which PAHs are oxidized in an aqueous system depends on the PAH type and structure, water column characteristics (such as oxygen availability), temperature and depth of light penetration, and residence time in the photic zone (Payne and Phillips, 1985; Paalme et al., 1990; Schwarzenbach et al., 1993). Paalme et al. (1990) have shown that the rate of photochemical degradation of different PAHs in aqueous solutions can differ by a factor of >140 depending on their chemical structure, with perylene, benzo(b)fluoranthene, and coronene showing the greatest stability. Alkyl PAHs are more sensitive to photo-oxidation reactions than parental PAHs, probably due to benzyl hydrogen activation (e.g., Radding et al., 1976). Payne and Phillips (1985) reported that benz(a)anthracene and benzo(a)pyrene are photolytically degraded 2.7 times faster in summer than in winter. Once deposited in sediments, photoxidation reactions are generally significantly reduced due to anoxia and limited light penetration. PAH residence times in sediments depend on the extent of physical, chemical, and biological reactions occurring at the sediment–water interface, as well as the intensity of bottom currents (Hinga, 1984).

11.13.5.5 Biodegradation

Biodegradation is perhaps the most important reaction mechanism for the degradation of hydrocarbons in aquatic environments. Aliphatic compounds in crude oil and petroleum products are readily degraded, with a prominent initial microbial preference for straight chain compounds (e.g., Atlas and Bartha, 1992; Prince, 1993; Volkman et al., 1997; Wang et al., 1999; Heider et al., 1999; Bosma et al., 2001; NRC, 2002). The aerobic pathway shows conversion of alkane chains to fatty acids, fatty alcohols and aldehyde, and carboxylic acids that are then channeled into the central metabolism for subsequent β-oxidation (**Figure 13**; cf. see **Chapter 11.15**). Anaerobic degradation proceeds with nitrate, Fe^{3+}, or sulfate as the terminal electron acceptor, with no intermediate alcohols in the alkane degradation (**Figure 13**). The degradation pathway involves an O_2-independent oxidation to fatty acids, followed by β-oxidation. Sulfate reducers apparently show specificity towards utilization of short chain alkanes (C_6–C_{13}) (Bosma et al., 2001). Laboratory experiments on complex oil-blends further showed composition changes accompanying biodegradation. For example, Wang et al. (1998) examined the compositional evolution of Alberta Sweet Mixed Blend oil upon exposure to defined microbial inoculum, with total petroleum hydrocarbons (9–41%), and specifically the total saturates (5–47%) and *n*-alkanes (>90%), showing varying degrees of degradation. They further showed that susceptibility to *n*-alkane degradation is an inverse function of chain length, the branched alkanes are less susceptible than straight-chain *n*-alkanes, and that the most resilient saturate components are the isoprenoids, pristane and phytane. Even amongst isoprenoids, however, there is still a notable inverse dependence between chain length and degradation susceptibility. The relative susceptibility of w-alkanes to biodegradation compared to the

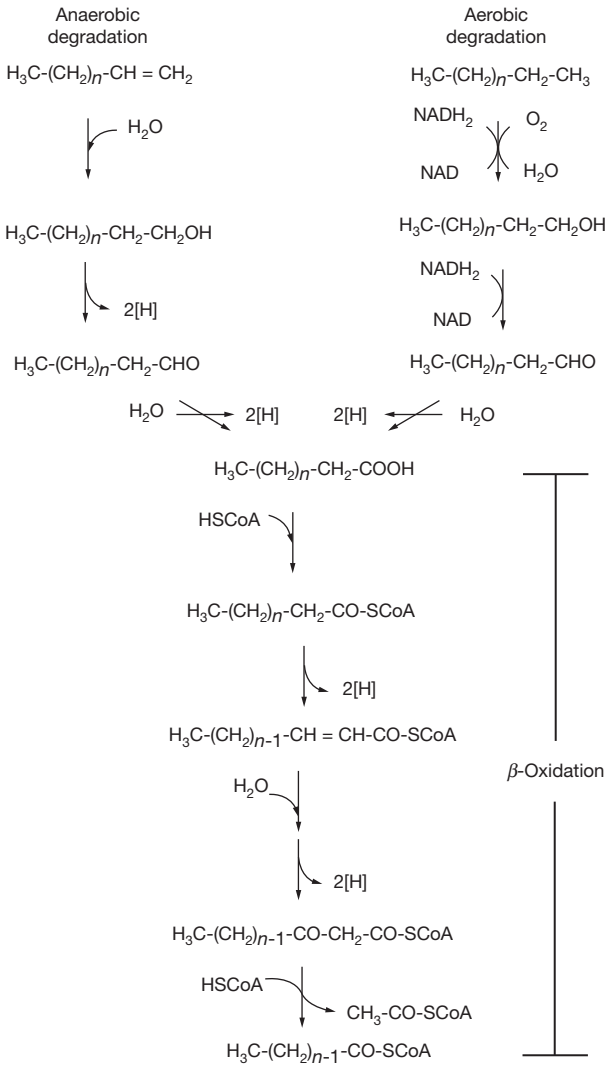

Figure 13 Generalized aerobic and anaerobic biodegradation pathways for *n*-alkanes (reproduced by permission of Springer from *The Handbook of Environmental Chemistry*, **2001**, pp. 163–202).

isoprenoids is the basis for using C_{17}/pristane and *n*-C_{18}/phytane ratios for distinguishing biodegradation from volatilization effects because the latter discriminates primarily on the basis of molecular weight. Additionally, Prince (1993) noted the relative resilience of polar compounds compared to corresponding hydrocarbons. Interesting deviations from this generalized biodegradation pattern were nevertheless noted by others, including the observation that some Exxon Valdez spill site microbial communities preferentially degraded naphthalene over hexadecane at the earliest stages of biodegradation (e.g., Sugai et al., 1997).

Numerous cases of crude oil and refined petroleum spill into surface environments have provided natural laboratories for examination of the biodegradation of petrogenic compounds in a variety of environmental conditions (e.g., Kaplan et al., 1997; Prince, 1993; Wang et al., 1998; NRC, 2002). The observations on compositional patterns of biodegradation noted above are generally replicated in these natural spills. For example, a long-term evaluation of compositional variation of Arabian light crude in a peaty mangrove environment was conducted by Munoz et al. (1997), who showed the same pattern of initial preferential loss of *n*-alkanes followed by isoprenoids, and ultimately the biomarkers in the order steranes, hopanes, bicyclic terpanes, tri- and tetracyclic terpanes, diasteranes, and the aromatic biomarkers. However, an interesting report on the biodegradation patterns in the crude-oil spill site in Bemidji, Minnesota, showed an apparent reversal in the biodegradation preference of *n*-alkanes, wherein HMW homologues show faster degradation rates (Hostetler and Kvenvolden, 2002). The overall resilience of terpane and sterane compounds to biodegradation has been well recognized; hence, biomarker ratios are widely used as indicators of oil spill sources even in highly weathered oils (e.g., Volkman et al., 1997).

Aromatic hydrocarbons in the atmosphere and open waters may undergo volatilization and photodecomposition, but microbial degradation is the dominant sink below the photic zone (Gibson and Subramanian, 1984). As with aliphatic hydrocarbons, biodegradation of aromatic compounds involves the introduction of oxygen into the molecule forming catechol (cf. **Chapter 11.12**). Microbial degradation has also been recognized as the most prominent mechanism for removing PAHs from contaminated environments (Neilson, 1998; NRC, 2000, 2002). Microbial adaptations may result from chronic exposure to elevated concentrations as shown by the higher biodegradation rates in PAH-contaminated sediments than in pristine environments (Neilson, 1998; NRC, 2000). Nevertheless, it is also known that preferential degradation of PAHs will not occur in contaminated environments where there are more accessible forms of carbon (NRC, 2000). A summary of the turnover times for naphthalene, phenanthrene, and BaP in water and sediment is shown in **Table 1**. In general, PAH biodegradation rates are a factor of 2–5 slower than degradation of monoaromatic hydrocarbons (cf. **Chapter 11.12**), and of a similar magnitude as HMW *n*-alkanes (C_{15}–C_{36}) under similar aerobic conditions. The ability of microorganisms to degrade fused aromatic rings is determined by their combined enzymatic capability which can be affected by several environmental factors (McElroy et al., 1985; Cerniglia, 1991; Neilson and Allard, 1998; Bosma et al., 2001). The most rapid biodegradation of PAHs occurs at the water–sediment interface (Cerniglia, 1991). Prokaryotic microorganisms primarily metabolize PAHs by an initial dioxygenase attack to yield *cis*-dihydrodiols and finally catechol (e.g., **Figure 14**). Biodegradation and utilization of lower molecular weight PAHs by a diverse group of bacteria, fungi, and algae has been demonstrated (**Table 2**; Neilson and Allard, 1998; Bosma et al., 2001). For example, many different strains of microorganisms have the ability to degrade napththalene including *Pseudomonas*, *Flavobacterium*, *Alcaligenes*, *Arthrobacter*, *Micrococcus*, and *Bacillus*.

The degradation pathways of higher molecular weight PAHs – such as pyrene, benzo(e)pyrene, and benzo(a)pyrene – are less well understood (Neilson and Allard, 1998). Because these compounds are more resistant to microbial degradation processes, they tend to persist longer in contaminated environments (Van Brummelen et al., 1998; Neilson and Allard, 1998; Bosma et al., 2001). However, the degradation of fluoranthene, pyrene, benz(a)anthracene, benzo(a)pyrene, benzo (b)fluorene, chrysene, and benzo(b)fluoranthene has been reported in laboratory conditions (Barnsley, 1975; Mueller

Table 1 Turnover times for naphthalene, phenanthrene, and benzo(a)pyrene in water and sediment.

PAH and environment	*Temp. (°C)*	*Times (d)*
Naphthalene		
Estuarine water	13	500
Estuarine water	24	30–79
Estuarine water	10	1–30
Seawater	24	330
Seawater	12	15–800
Estuarine sediment	25	21
Estuarine sediment		287
Estuarine sediment	22	34
Estuarine sediment	30	15–20
Estuarine sediment	2–22	13–20
Stream sediment	12	>42
Stream sediment	12	0.3
Reservoir sediment	22	62
Reservoir sediment	22	45
Phenanthrene		
Estuarine sediment	25	56
Estuarine sediment	2–22	8–20
Reservoir sediment	22	252
Reservoir sediment	22	112
Sludge-treated soil	20	282
Benzo(a)pyrene		
Estuarine water	10	2–9000
Estuarine sediment	22	>2800
Estuarine sediment	2–22	54–82
Stream sediment	12	>20 800
Stream sediment	12	>1250
Reservoir sediment	22	>4200
Sludge-treated soil	20	>2900

Source: O'Malley (1994).

et al., 1988, 1990; Schneider et al., 1996; Ye et al., 1996; Neilson and Allard, 1998). Elevated temperatures increase the rate of biotransformation reactions *in vitro*. For example, laboratory studies have shown a 50% loss of phenanthrene after 180 days at 8 °C in water compared to 75% loss in 28 days at 25 °C (Sherrill and Sayler, 1981; Lee et al., 1981). It is widely believed that PAHs with three or more condensed rings tend not to act as sole substrates for microbial growth, but may be the subject of co-metabolic transformations. For example, co-metabolic reactions of pyrene, 1,2-benzanthracene, 3,4-benzopyrene, and phenanthrene can be stimulated in the presence of either naphthalene or phenanthrene (Neilson and Allard, 1998). Nevertheless, the degradation of PAHs even by co-metabolic reactions is expected to be very slow in natural ecosystems (e.g., Neilson and Allard, 1998).

Biodegradation effects on aromatic hydrocarbons is a subject of much interest both from the standpoint of characterizing oil spill evolution and engineered bioremediation (Wang et al., 1998; Neilson and Allard, 1998). Wang et al. (1998) noted that the susceptibility to biodegradation increases with decreasing molecular weight and degree of alkylation. For example, the most easily degradable PAHs examined are the alkyl homologues of naphthalene, followed by the

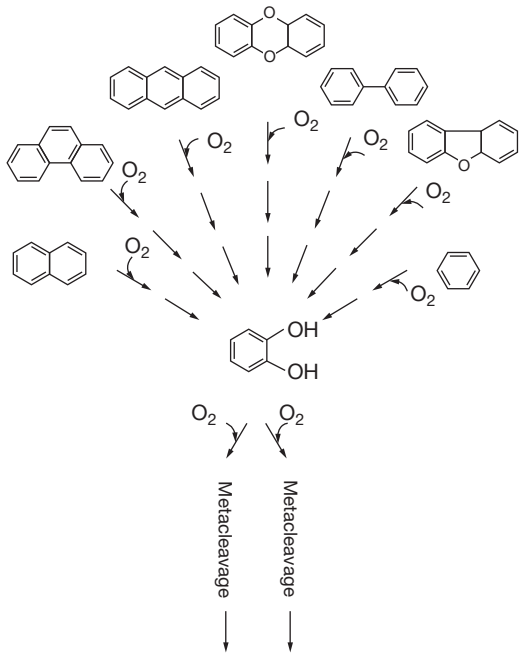

Figure 14 Generalized aerobic biodegradation pathways for aromatic hydrocarbons (after Bosma et al., 2001).

alkyl homologues of dibenzothiophene, fluorene, phenanthrene, and chrysene. Also noteworthy is the observation that microbial degradation is isomer specific, leading to the suggestion that isomer distribution of methyl dibenzothiophenes are excellent indicators of degree of biodegradation (Wang et al., 1998). Finally, in spite of the focus of biodegradation studies on aerobic degradation, recent work has demonstrated the capacity of sulfate-reducing bacteria in degrading HMW PAH (e.g., BaP) (Rothermich et al., 2002).

11.13.6 Carbon Isotope Geochemistry

The present review of hydrocarbon sources, pathways, and fate in aquatic environments highlights the current state of understanding of HMW hydrocarbon geochemistry, but it also provides a useful starting point for exploring additional approaches to unraveling the sources and fate of hydrocarbons in aquatic environments. It is clear that the degree and type of hydrocarbons ultimately sequestered in particulates, sediments, or aquifer materials depend not only on the nature and magnitude of various source contributions, but also on the susceptibility of the hydrocarbons to various physical, chemical, and microbial degradation reactions. As we have already shown, the latter alters the overall molecular signatures of the original hydrocarbon sources, complicating efforts to apportion sources of hydrocarbons in environmental samples. Nevertheless, resilient molecular signatures that either largely preserve the original source signatures or alter in a predictable way have been employed successfully to examine oil sources as already discussed (Wang et al., 1999). Additionally, carbon-isotopic composition can be used to help clarify source or 'weathering reactions' that altered the hydrocarbons of interest. In what follows, we will examine the emerging application of

Table 2 Biodegradation and utilization of lower molecular weight PAHs by a diverse group of bacteria, fungi, and algae.

Organism	*Substrate*
Pseudomonas sp.	Naphthalene
	Phenanthrene
	Anthracene
	Fluoranthene
	Pyrene
Flavobacteria sp.	Phenanthrene
	Anthracene
Alcaligenes sp.	Phenanthrene
Aeromonas sp.	Naphthalene
	Phenanthrene
Beijerenckia sp.	Phenanthrene
	Anthracene
	Benz(a)anthracene
	Benzo(a)pyrene
Bacillus sp.	Naphthalene
Cunninghamella sp.	Naphthalene
	Phenanthrene
	Benzo(a)pyrene
Micrococcus sp.	Phenanthrene
Mycobacterium sp.	Phenanthrene
	Phenanthrene
	Fluorene
	Fluoranthene
	Pyrene

Source: O'Malley, 1994.

carbon-isotopic measurements in unravelling the sources and fate of PAHs in shallow aquatic systems. Similar approaches to studying aliphatic compounds have been employed in a number of hydrocarbon apportionment studies (e.g., O'Malley, 1994; Mansuy et al., 1997; Dowling et al., 1995), and the approach has indeed been a principal method used for oil–oil and oil source rock correlation for decades (e.g., Sofer, 1984; Schoell, 1984; Peters et al., 1986; Faksness et al., 2002). The key to using carbon isotopes for understanding the geochemistry of HMW hydrocarbons in shallow aquatic systems is to distinguish two reasons why the abundance of stable isotopes in these compounds might vary: (1) differences in carbon sources and (2) isotope discrimination introduced after or during formation. In what follows, we will first describe and compare the carbon-isotope systematics in the pyrogenic and petrogenic PAH sources. Then we will examine possible changes in the carbon-isotope compositions in these compounds as a result of one or more weathering reactions. Finally, we will use the PAH inventory of an estuarine environment in eastern Canada as an example of how the molecular characteristics discussed earlier in this chapter can be blended with compound-specific carbon-isotope signatures to distinguish PAH sources and pathways.

11.13.6.1 Carbon Isotope Variations in PAH Sources

11.13.6.1.1 Pyrogenesis

The isotopic signature imparted on individual PAHs during formation is determined by both the isotopic composition of the precursor compounds and the formation conditions. Since these two factors can vary widely during pyrolysis or diagenesis, the potential exists for PAHs produced from different sources and from a variety of processes to have equally variable isotopic signatures. Isotopic characterization of bulk organic and aromatic fractions has been performed for many years (e.g., Sofer, 1984; Schoell, 1984), but the advent of compound-specific isotopic characterization methods for individual organic compounds has immensely increased the database for assessing the range of PAH isotopic compositions.

The specific mechanisms controlling the isotopic signatures of individual pyrogenic PAHs are only partly understood (O'Malley, 1994; Currie et al., 1999). It is expected that the pyrolysis of isotopically distinct precursor materials would result in PAHs with different isotopic signatures. Due to the nature of PAH formation pathways discussed earlier in this chapter, the $\delta^{13}C$ of pyrolysis-derived compounds may be dictated by a series of primary and secondary reactions that precursor and intermediate compounds undergo prior to the formation of the final PAHs. The isotopic effects associated with ring cleavage reactions of intermediate precursors (LMW compounds) may result in ^{13}C enriched higher molecular weight species formed by the fusion of these reduced species. Variations in the $\delta^{13}C$ of the higher molecular weight condensed compounds may, therefore, depend on the $\delta^{13}C$ of the precursor and intermediate species. In the absence of pyrosynthetic recombination reactions, produced PAHs will have isotopic compositions that are largely dictated by those of the original precursor compounds. Alkylation or dealkylation reactions at specific sites of a parent molecule will alter the isotopic composition of that compound only to the extent that the alkyl branch is isotopically different from the substrate PAHs.

O'Malley (1994) performed the first characterization of compound-specific carbon-isotope characterization of primary and secondary PAH sources. Irrespective of the range observed in the $\delta^{13}C$ of the wood-burning soot PAHs, the overall trend in the mean $\delta^{13}C$ values indicates that lower molecular weight compounds (three-ring) are isotopically more depleted than four-ring PAHs, whereas five-ring compounds have $\delta^{13}C$ values similar to the three-ring species (**Figure 15**). Since PAHs are the products of incomplete combustion, the range of isotopic values generated during pyrolysis is related to the isotopic signature of their initial precursors and the fractionations that are associated with primary and secondary reactions noted above. The trend observed in the $\delta^{13}C$ of the three-, four-, and five-ring PAHs in thispyrolysis process indicates the following possibilities: (1) the individual compounds were derived from isotopically distinct precursors in the original pyrolysis source that underwent pyrolysis and pyrosynthesis possibly at different temperature ranges; (2) the overall isotopic variation was primarily dictated by the formation and carbon branching pathways that occurred during pyrosynthesis; or (3) some combination of (1) and (2).

Benner et al. (1987) analyzed the $\delta^{13}C$ of various wood components and reported that cellulose, hemicellulose, and an uncharacterized fraction (solvent extractable) were, respectively, 1.3‰, 0.3‰, and 1.0‰ more enriched in ^{13}C than the total wood tissue, whereas lignins were 2.6‰ more depleted than the whole plant. Wood combustion in open wood fireplaces could resemble a stepped combustion process where hemicellulose normally degrades first, followed by cellulose and then the lignins. If the carbon isotopic compositions of

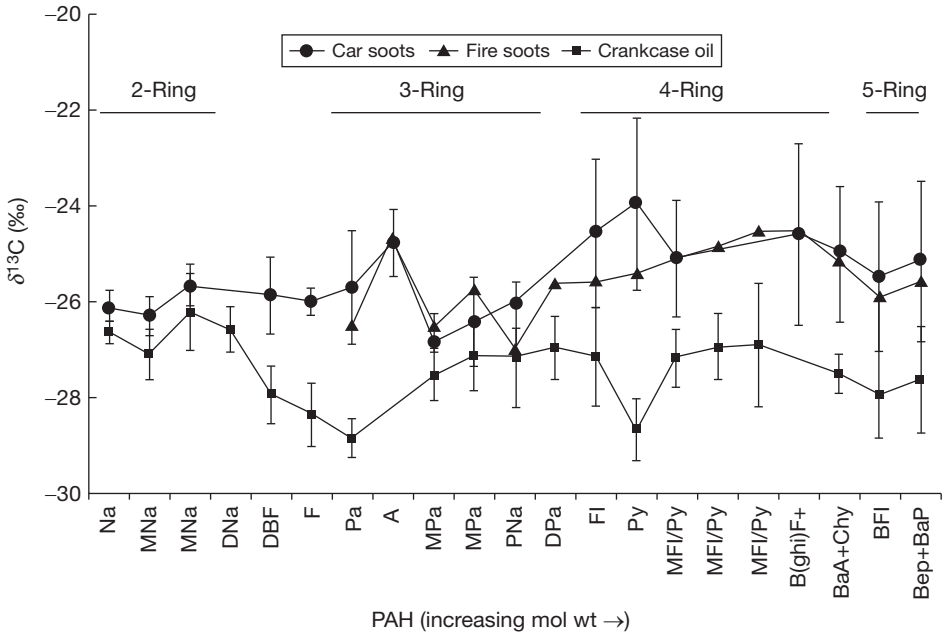

Figure 15 $\delta^{13}C$ of PAHs from car soot (automobile emission; 10 samples), fire soot (wood burning; 11 samples), and crankcase oil (12 samples). Error bars are 2σ variation within each source type (after O'Malley, 1994).

hemicellulose, cellulose, and lignin are sole factors in determining the overall isotopic signature of the wood-burning soot, then the $\delta 5^{13}C$-depleted PAHs may be primarily derived from lignin, while the more enriched compounds may originate from the heavier cellulose or uncharacterized fractions. The uncharacterized fraction of wood also contains certain compounds that are good PAH precursors (e.g., terpenes, fatty acids, and other aromatic compounds including acids, aldehydes, and alcohols).

As an alternative, the trend in the isotopic signature of wood-burning soot PAHs may be controlled by secondary condensation and cyclodehydrogenation reactions during pyrolysis to produce more condensed HMW compounds. Therefore, during the pyrolysis process, LMW compounds, generally formed at lower temperatures, may be actual precursors to the higher molecular weight species that are formed subsequently. Holt and Abrajano (1991) concluded from kerogen partial combustion studies that ^{13}C-depleted carbon is preferentially oxidized during partial combustion leaving a ^{13}C-enriched residue (cf. Currie et al., 1999). Therefore, the PAH-forming radicals produced at lower temperatures are expected to be depleted in ^{13}C compared to radicals formed at higher temperatures. Despite the difference in the combustion/ pyrolysis processes, materials, and conditions, the $\delta^{13}C$ of the parental PAHs isolated from car soots follow a similar trend to the wood-burning soot PAHs (**Figure 15**). This similarity argues for the prevailing role of pyrolytic secondary reactions in imparting the resulting PAH $\delta^{13}C$ values. Unlike open wood burning, the combustion process in the gasoline engine may be described as spontaneous or shock combustion (Howsam and Jones, 1998), whereby gasoline is initially vaporized and mixed with air prior to combustion in the combustion chamber. The PAHs produced during this process are reported to be primarily dependent on the fuel:air ratio and the initial aromaticity of the fuel (Begeman and Burgan, 1970; Jensen and Hites, 1983).

The complex controls on the carbon isotopic composition of produced PAHs during wood burning is also apparent in PAH produced by coal pyrolysis (McRae et al., 1999, 2000; Reddy et al., 2002). PAHs that have been isotopically characterized by McRae et al. (1999) showed progressive ^{12}C enrichment in successively higher temperatures offormation (−24‰ to −31‰). One analysis of a coal tar standard reference material (SRM) by Reddy et al. (2002) yielded compound specific $\delta^{13}C$ values in the ^{13}C-enriched end of this range (−24.3‰ to −24.9‰). MacRae et al. (1999) reasoned that the isotopic changes observed at increasing temperature reflect the competition between original PAHs in the coal (mostly two and three rings), and those produced by high-temperature condensation and aromatization. Interestingly, the polycondensed higher molecular weight PAHs showed enrichment in ^{12}C, perhaps indicating the incorporation of the early ^{12}C-enriched fragments produced by during pyrolysis (cf. Holt and Abrajano, 1991). Creosote produced from coal tar likewise exhibits a wide range of $\delta^{13}C$ composition (e.g., Hammer et al., 1998), mimicking the observation made by McRae et al. (1999).

11.13.6.1.2 Pedogenesis

Carbon isotopic compositions of PAHs in petroleum and petroleum source rocks are among the earliest targets of compound-specific carbon isotopic analysis. Freeman (1991) analyzed individual aromatic compounds in the Eocene Messel Shale and demonstrated the general tendency of aromatic compounds to be consistently enriched in ^{13}C compared to the aliphatic fraction. This pattern is consistent with diagenetic effects associated with aromatization of geolipids (Sofer, 1984; Simoneit, 1998). As already noted, several examples of diagenetically produced PAHs (e.g., substituted Pa, Chy, retene, and

perylene) result from the aromatization of precursors such as pentacyclic triterpenoids (Wakeham et al., 1980b; Mackenzie, 1984; Peters and Moldowan, 1993; Neilson and Hynning, 1998; Simoneit, 1998). The aromatization of natural compounds to produce PAHs is not expected to result in significant isotopic alterations, a contention supported by the successful use of compound-specific carbon-isotope signatures to trace precursor–product relationships in diagenetic systems (e.g., Hayes et al., 1989; Freeman, 1991). It is notable, however, that the range of $\delta^{13}C$ values to be expected from potential precursors (e.g., triterpenoids) remains to be fully defined. O'Malley (1994) reported depletion in ^{13}C (up to 2‰) methylated naphthalene homologues compared to their corresponding parental compound. The $\delta^{13}C$-depleted isotopic values observed in these petrogenic-associated PAHs may be dictated by the similarly depleted nature of the precursor compounds. Published $\delta^{13}C$ values of petrogenic-associated PAHs are limited, and it is more than likely that further analysis will reveal more variations that would reflect the isotopic composition of precursor compounds and the nature and degree of diagenetic reactions.

In contrast to the wood fireplace and car soot signatures, the $\delta^{13}C$ of the PAHs isolated from crankcase oil were generally depleted in ^{12}C (Figure 15). Also, the range of $\delta^{13}C$ values measured was only marginally enriched compared to the range of bulk isotopic values (-29.6‰ and -26.8‰) reported for virgin crankcase oil. Unlike fuel pyrolysis, where a significant portion of the precursor source materials is initially fragmented into smaller radicals prior to PAH formation, the PAHs in used crankcase oil are largely derived from a series of thermally induced aromatization reactions of natural precursors that exist in the oil. Crankcase oils derived from petroleum consist primarily of naphthenes with minor *n*-alkane content ($<C_{25}$) and traces of steranes and triterpanes (Simoneit, 1998). Of the parental compounds isolated from the crankcase oils, Pa and Py were generally more depleted in ^{13}C than Fl, BaA/Chy, BFl, and BeP/BaP (Figure 15). The difference in the isotopic values of these two groups of parental compounds suggests that they may be derived from different precursors in the oil. The similarity in the isotopic values of Pa and Py indicates that they may be derived from precursor materials, which have a common origin or a common synthesis pathway that is distinct from those followed by other HMW PAHs. The assignment of aromatic structures to their biological precursors in crude oils has proved difficult (Radke, 1987). However, it is now well established that the saturated or partially unsaturated six-membered rings in steroids and poly cyclic terpenoids undergo a process of stepwise aromatization (MacKenzie, 1984; Simoneit, 1998).

Our measurements of crude and processed oil products other than crankcase oil are shown in Figure 16, but these measurements are largely restricted to naphthalene and methylated naphthalene (unpublished data). The PAHs isolated from the bulk outboard motor condensate are isotopically very similar to the mean isotopic values of the PAHs in used crankcase oil, except that the outboard motor condensates were generally more enriched in ^{13}C (Figure 16). This similarity to crankcase oils was also observed in their PAH molecular signatures. The apparent enrichment in ^{13}C of naphthalene and its methylated derivatives in the outboard motor samples may be due to the partial combustion of gasoline that is

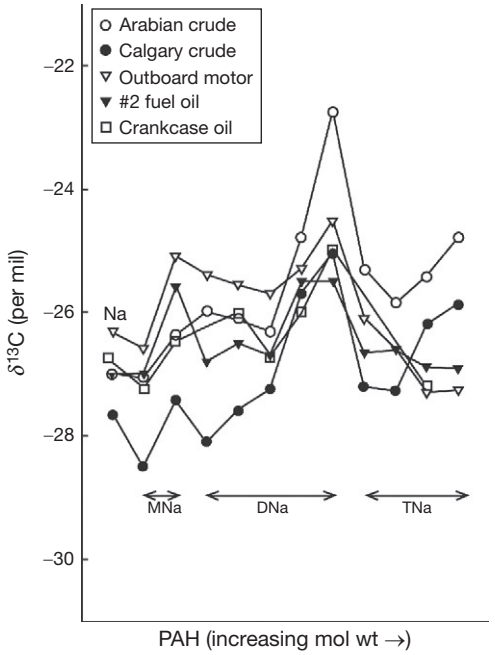

Figure 16 $\delta^{13}C$ of crude oil, outboard motors, and fuel oil. Also shown is the crankcase oil $\delta^{13}C$ signature.

characteristic of two-stroke outboard motor engines. The $\delta^{13}C$ of the PAHs isolated from the crude petroleum samples have similar trends (compound-to-compound variations), except that the Calgary crude PAHs are generally lighter (−32.2‰ to −25.1‰) than the Arabian sample (−30.0‰ to −22.7‰; Figure 16). This variation in isotopic values is possibly related to the origin or maturity of these samples. Differences in the $\delta^{13}C$ values of the isomeric compounds suggest that these compounds may originate from different precursor products or by different formation pathways. Naphthalene and methylated naphthalenes in #2 fuel oil had isotopic values within the range observed for the crude oils and other petroleum products investigated ($\delta^{13}C$). Mazeas and Budzinski (2001) also reported compound-specific $\delta^{13}C$ measurement of an oil sample, and their values fell in the range of −24‰ to −29‰. However, their measurements of PAHs from a crude oil SRM showed more enriched $\delta^{13}C$ values (−22‰ to −26‰). The latter values are the most ^{12}C-enriched values we have seen in petroleum-related compounds to date.

11.13.6.2 Weathering and Isotopic Composition

Once PAHs are emitted to the environment, the extent of alteration of the isotopic signature during transformation reactions depends on the nature of the carbon branching pathways involved in the reaction. Isotopic fractionation as a result of kinetic mass-dependent reactions (e.g., volatilization or diffusion) is unlikely to be significant, because the reduced mass differences between the light and heavy carbon in these HMW compounds are small. Substitution reactions, resulting in the maintenance of ring aromaticity, are also not likely to significantly alter the isotopic signature of the substrate molecule, although it is possible that the extent of substitution could result in kinetic isotope effects (KIEs). Experiments conducted

to examine possible KIEs on biotic and abiotic transformation (e.g., volatilization, sorption, photodegradation, and microbial degradation) have shown the overall resilience of the compound-specific carbon-isotope signatures inherited from PAH sources (O'Malley, 1994; O'Malley et al., 1994; Stehmeir et al., 1999; Mazeas et al., 2002). The HMW of these compounds apparently preempts significant carbon-isotopic discrimination during abiotic transformation processes (e.g., volatilization and photodegradation). For example, no fractionation from photolytic degradation was observed on the $\delta^{13}C$ of standard PAHs experimentally exposed to natural sunlight. The $\delta^{13}C$ of F, Pa, Fl, Py, and BbF during the various exposure periods were particularly stable despite up to a 40% reduction in the initial concentration of pyrene (**Figure 17**). The absence of significant KIE in the systems studied here may be related to the relatively HMW of the compounds and low reduced mass differences involved.

Microbial degradation experiments likewise showed negligible shifts in the $\delta^{13}C$ values of Na and Fl even after >90% biodegradation (**Figure 18**) (O'Malley et al., 1994). Bacteria degrade PAHs by enzymatic attack which can be influenced by a number of environmental factors (Cerniglia, 1991). Alteration of the original isotopic values of Na and Fl may have been expected, since most PAH degradation pathways involve ring cleavage (loss of carbon) (Mueller et al., 1990; Cerniglia, 1991). For bacterial degradation to occur, the PAHs are normally incorporated into the bacterial cells where enzymes are produced (van Brummelen et al., 1998; Neilson and Allard, 1998). The pathways by which PAHs enter bacterial cells may dictate whether isotopic alterations will occur as a result of microbial degradation. This pathway is not well understood, but it is postulated that bacteria either ingests PAHs that are associated with organic matter, or because of their lipophilic properties, PAHs may diffuse in solution across the cell wall membrane. Hayes et al. (1989) suggested that organisms do not isotopically discriminate between heavy and light carbon when ingesting organic material from homogenous mixtures. In this case, the isotopic ratio of the unconsumed residue will not be different from the starting material. Even if cell wall diffusion was the predominant pathway, isotopic fractionation will again be limited by the small relative mass difference between ^{12}C and ^{13}C containing PAHs. It is for this reason that most isotopic fractionations in biological systems can be traced back to the initial C_1 (i.e., CO_2 and CH_4) fixation steps. Since no enrichments were observed in the biodegradation residue of naphthalene and fluoranthene, no observable mass discrimination can be attributed to biodegradation for these compounds. If the controlling steps for the biodegradation of higher molecular weight PAHs are similar, isotopic alterations resulting from microbial degradation would likely be insignificant in many natural PAH occurrences. It is notable that recent experiments on naphthalene and toluene show that some carbon-isotopic discrimination can occur under certain conditions (Meckenstock et al., 1999; Diegor et al., 2000; Ahad et al., 2000; Morasch et al., 2001; Stehmeir et al., 1999). Yanik et al. (2003) also showed some carbon-isotope fractionation, interpreted as biodegradation isotope effect, in field weathered petroleum PAHs. If the presence of isotopic discrimination during biodegradation is shown for some systems, it is likely contingent on the specific pathways utilized during microbial metabolism. This may be a fruitful area of further inquiry.

11.13.6.3 Isotopic Source Apportionment of PAHs in St. John's Harbor: An Example

The earliest example of using compound specific carbon-isotope compositions for apportioning PAH sources in aquatic systems is the study of St. John's Harbor, Newfoundland by O'Malley et al. (1994, 1996). This is an ideal setting for utilizing carbon isotopes because the molecular evidence is

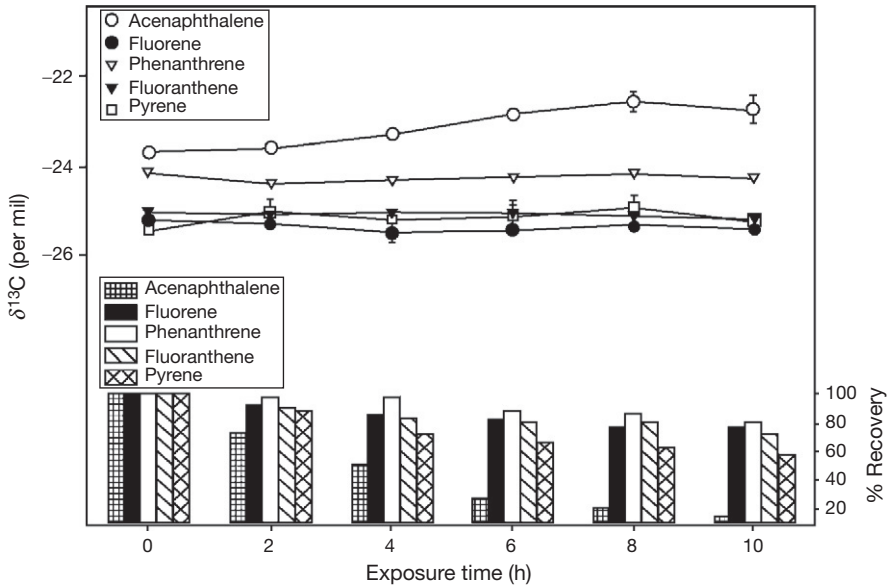

Figure 17 Carbon-isotope effects of PAH photolysis. Top line diagram shows negligible shifts in $\delta^{13}C$ for F, Pa, Fl, and P. Only Ae shows a shift in $\delta^{13}C$ (0.5‰) beyond differences in replicate experiments (1σ = error bar or size of data point). Lower histogram shows percentage of PAHs that were not photodegraded.

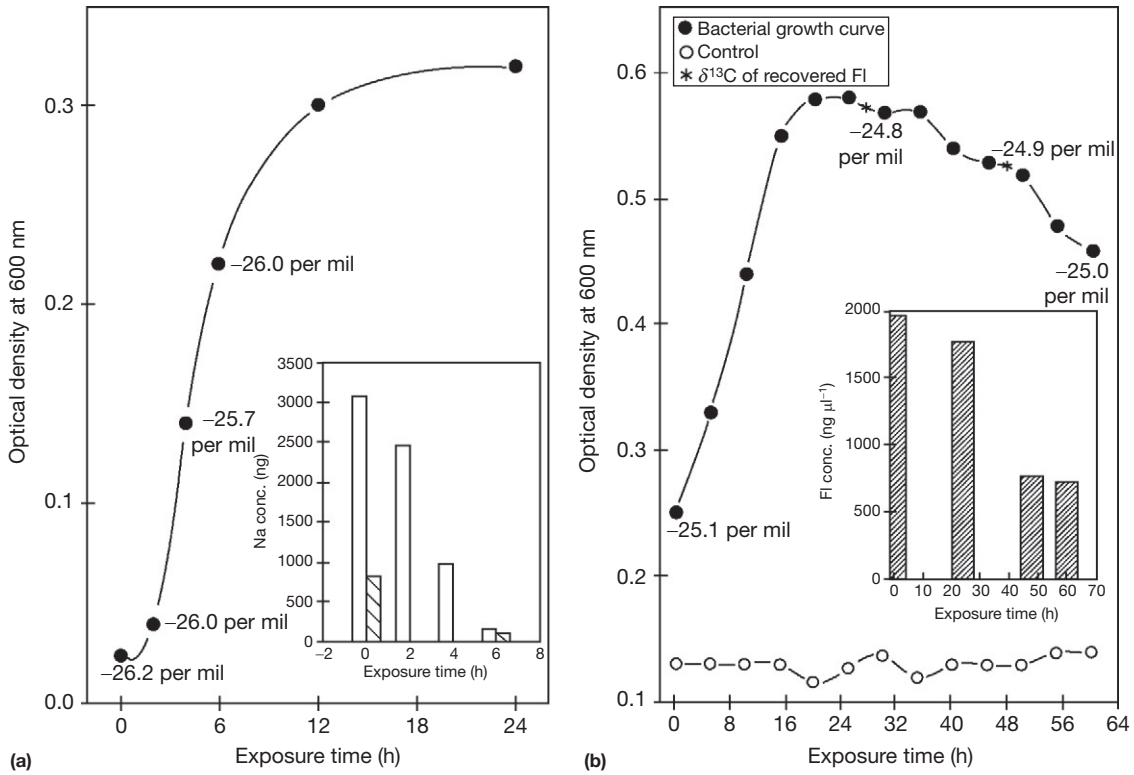

Figure 18 Carbon-isotope effects of PAH biodegradation: (a) biodegradation of Na with *Pseudomonas putida*, Biotype B ATCC 17484 and (b) biodegradation of Fl with *Pseudomonas paucimobilis*, strain EPA 505. Inset shows decline in PAH concentration over the same time period.

equivocal. The surface sediments in St. John's Harbor were characterized by high but variable concentrations of three-, four-, and five-ring parental PAHs suggestive of pyrogenic sources, the presence of methylated PAHs and a UCM indicative of petrogenic inputs, and occasional presence of retene and perylene, implicating diagenetic input. The relatively low Pa/A ratio (1.9) in the surface sediment, which is indicative of significant pyrolysis contributions, is similar to those calculated in previous studies (Killops and Howell, 1988; Brown and Maher, 1992). The Fl/Py ratio (1.2), indicative of pyrolysis, is comparable to the Fl/Py ratios reported for sediments from other similar systems (e.g., Penobscot Bay, Boston Harbor, Severn Estuary, Bedford Harbor, and Halifax Harbor) (Killops and Howell, 1988; Pruell and Quinn, 1988; Gearing et al., 1981; Hellou et al., 2002). Similarly, the BaA/Chy ratio (0.80) also indicates that BaA and Chy are of pyrogenic origin. However, unlike Fl and Py, the generally higher BaA/Chy ratio suggests that the primary source of these particular compounds may be related to car emissions. The BaP/BeP and the Pa/MPa ratios of the sediment cannot be clearly reconciled with any of the primary source signatures. This could indicate that these ratios have limited value for source apportionment because of the reactivity of BaP and methylated Pa in the environment (e.g., Canton and Grimalt, 1992).

The reactivity of MPa and BaP seems to have resulted in the alteration of their source compositional ratios during transportation/deposition, and thus may not be a reliable source indicator. In addition to the compositional attributes of the parental PAHs, the presence of methylated compounds and a UCM in the surface sediments indicates possible petrogenic inputs of PAHs to the Harbor. The UCM is generally indicative of petroleum and petroleum products, and is a widely used indicator of petrogenic contamination in sediments (Prahl and Carpenter, 1979; Volkman et al., 1992, 1997; Simoneit, 1998). It is commonly assumed that a UCM consists primarily of an accumulation of multibranched structures that are formed as a result of biodegradation reactions of petroleum (Volkman et al., 1992). Since no clear indication of petroleum-derived inputs can be discerned from the compositional ratios of the prominent PAHs in the sediments, it is apparent that the isomeric ratios of the prominent petrogenic PAHs are masked by pyrogenic-derived components.

There is no characteristic trend in the $\delta^{13}C$ between the LMW and HMW PAHs in the surface sediments of St. John's Harbor. However, the isotopically enriched A and the trend between Pa and MPa are indicative of pyrogenic PAH sources, whereas the marginally depleted Py compared to Fl suggests inputs of petrogenic sources. The isotopic signatures of the PAHs from all the surface samples are broadly similar, and can be quantitatively related to the prominent primary sources (**Figure 19**). Significant enrichments of Pa, MPa, and A relative to the four- and five-ring compounds are consistently observed in all the individually analyzed samples. This may be attributed to the input of road sweep material via the sewer system. The consistency in the $\delta^{13}C$ of Pa (–25.9‰ to –25.2‰) in the surface sediments suggests that it is possibly derived from an isotopically enriched source of pyrogenic origin. Evidence of some petrogenic input is, nevertheless, indicated by the relatively ^{13}C- depleted pyrene, a trend that was consistently observed in most of the samples investigated. The results of mass

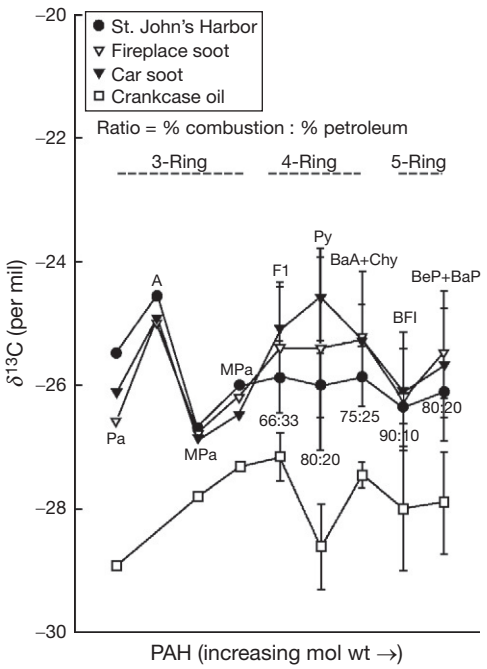

Figure 19 δ^{13}C of St. John' s Harbor sediments compared to the three primary PAH sources in the Harbor. Error bars show 2σ variability in the source δ^{13}C. Ratios shown (e.g., 80 : 20) are the approximate balance of crankcase oil and fireplace soot (assuming two-component mixing) in the Harbor sediments.

balance mixing calculation are diagrammatically shown in Figure 20. The δ^{13}C of the four- and five-ring PAHs isolated from the various sediments generally form positive mixing arrays between the wood-burning and car soot and crankcase oil end-members, quantitatively substantiating molecular data that mixtures of these prominent primary sources could explain the range of δ^{13}C values observed in these particular sediments. The validity of these mixing arrays is further supported by unchanging relative positions of the individual sites (e.g., E, F, and J; Figure 20) in the mixing array (accounting for experimental error) regardless of the projection used. In general, as indicated by the dominance of the three-, four-, and five-ring parental PAHs in the molecular signatures, PAHs of pyrolysis origin seem to be dominant contributors to the Harbor sediments. This is shown by the bulk of the data points, which are concentrated close to the two pyrolysis/combustion end-members (Figure 20). From the position of the mean values on the mixing curves, the average pyrolysis input is estimated to be ~70% while the remaining 30% of the PAHs seem to be derived from crankcase oil contributions. Sites H and J are particularly enriched in pyrolysis-derived PAHs, while the maximum input of crankcase oil (≈50%) consistently occurred at site E indicating the heterogeneous nature of these sediments which was not evident from the molecular signatures. The percentage input of crankcase oil is similar to the range (20–33%) estimated from Figure 19.

The relative importance of the two primary pyrolysis sources (wood-burning soot versus car soot) as PAH contributors to the sediments is also evident in these mixing curves. With the exception of sites A, H, K, and L, which plot closer to the wood-burning soot/crankcase oil mixing array, all the remaining sites tend to be concentrated close to the car soot/crankcase oil mixing curve (Figure 20). This indicates that a significant portion of the pyrolysis-derived PAHs in the Harbor is of car emission origin. Despite the lack of distinct evidence in the molecular signature data to suggest the importance of car soot emissions in the pyrolysis signatures, inputs of car soot PAHs to the sediments are indicated by the low Pa/A and elevated BaA/Chy compositional ratios. The dominance of car soot PAHs compared to wood-burning soots suggests that a significant part of wood-burning emissions is being transported away from the sampling area due to wind dispersion, and that car soot inputs mainly occur as a result of road runoff. The presence of retene, identified in most of the surface sediments samples, is mainly related to early diagenesis rather than from wood-burning sources, despite having a similar δ^{13}C value to these sources. This is supported by the apparent absence of retene in the open-road and sewage sample molecular signatures, which are identified to be the predominant pathways for PAH input to the Harbor. There was also a notable absence of retene in the atmospheric air samples collected in the St. John's area. The input of petroleum or petroleum products to the sediments is not surprising since most of the individual samples are characterized by the presence of a prominent UCM.

The prominence of car soot and crankcase oil PAHs in sediments supports the suggestion that road runoff and runoff via the sewer system, and not atmospheric deposition, is the main pathway for PAH input to the Harbor sediments. This is also reflected by the similarity in the isotopic values of the PAHs in the sewage and sediment samples (Figure 21). Input of road sweep materials to the sediments was also supported by the presence of asphalt-like particulates similar to those observed in the open-road sweeps. Due to the absence of major industries in the St. John's area, sewage is dominated by domestic sources. Sewage PAH content is, therefore, predominantly derived from aerially deposited pyrolysis products, car emissions, crankcase oil by direct spillage and engine loss (NRC, 2002), and road sweep products such as weathered asphalt, tire, and brake wear. The occurrence of early diagenesis in these sediments is supported by the presence of perylene in the deeper samples which is suggested to be derived from diagenetic alteration reactions based on the Py/Pery ratio. Reliable isotopic measurements could not be performed on perylene due to coelution with unidentified HMW biological compounds.

In conclusion, using both the molecular signatures and the δ^{13}C of the PAHs isolated from St. John's Harbor, sources of pyrogenic and petrogenic PAHs along with diagenetic sources are positively identified. From a combination of the molecular abundance data and the δ^{13}C of the individual PAHs, car emissions are identified as important contributors of pyrolysis-derived compounds, whereas an average of 30% was derived from crankcase oil contributions. Direct road runoff, runoff via the storm sewers, and snow dumping are identified to be the most likely pathways for PAH input to the Harbor using both the molecular signature and carbon-isotope data. In this particular site, the combined use of molecular and carbon isotopic data elucidated the prominent sources of PAHs in the sediments. However, the use of isotopic data has the added

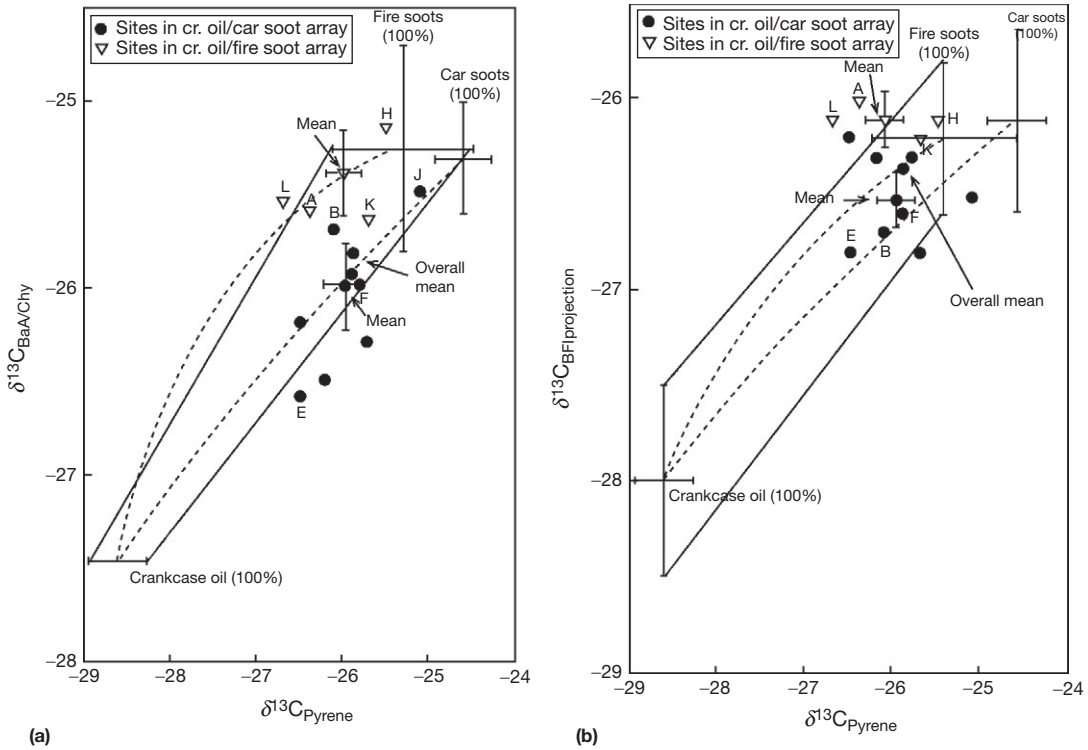

Figure 20 Carbon-isotopic mixing diagram for St. John's Harbor sediments using identified PAH source end-members: (a) $\delta^{13}C_{Pyrene}$ versus $\delta^{13}C_{BaA+Chy}$ and (b) $\delta^{13}C_{Pyrene}$ versus $\delta^{13}C_{BF1}$ projection. Data points are subdivided into retene-(▽) and non-retene-containing samples (●).

advantage that some quantification of sources can be undertaken with more confidence (O'Malley et al., 1996). It should be noted that these mixing equations used only the more stable higher molecular weight four- and five-ring compounds to avoid uncertainties related to possible weathering fractionations that could affect lower molecular weight compounds.

11.13.7 Synthesis

The unwanted release of petrogenic and pyrogenic hydrocarbon contaminants in the environment represents a major global challenge for pollution prevention, monitoring, and cleanup of aquatic systems. Understanding the geochemical behavior of these compounds in aqueous environments is a prerequisite to identifying point and nonpoint sources, understanding their release history or predicting their transport and fate in the environment. This review examined the physical and chemical properties of HMW hydrocarbons and environmental conditions and processes that are relevant to understanding of their geochemical behavior, with an explicit focus on polycyclic (or polynuclear) aromatic hydrocarbons (PAHs). PAHs represent the components of greatest biological concern amongst pyrogenic and petrogenic hydrocarbon contaminants. The molecular diversity of PAHs is also useful for holistically characterizing crude oil and petrogenic sources and their weathering history in aquatic systems. The majority of PAHs resident in surface aquatic systems, including lake, river, and ocean sediments, and groundwater aquifers are derived from pyrolysis of petroleum, petroleum products, wood, and other biomass materials. Finally, HMW hydrocarbons share the hydrophobic and lipophilic behavior of PAH; hence, all the discussions of the geochemical behavior of PAHs are indeed relevant to HMW hydrocarbons in general.

The molecular distribution and compound specific carbon-isotopic composition of hydrocarbons can be used to qualify and quantify their sources and pathways in the environment. Molecular source apportionment borrows from molecular methods that were developed and applied extensively for fundamental oil biomarker studies, oil–oil and oil source rock correlation analysis. Additionally, petroleum refinement produces well-defined mass and volatility ranges that are used as indicators of specific petroleum product sources in the environment. Compound-specific carbon-isotopic measurement is a more recent addition to the arsenal of methods for hydrocarbon source apportionment. Carbon isotopic discrimination of *n*-alkanes, biomarkers, and PAHs has shown that the technique is highly complementary to molecular apportionment methods.

HMW hydrocarbons are largely hydrophobic and lipophilic; hence, they become rapidly associated with solid phases in aquatic environments. This solid partitioning is particularly pronounced in organic-matter-rich sediments, with the result that the bulk solid–water partition coefficient is generally a linear function of the fraction of organic carbon or organic matter present in the sediments. Under favorable conditions, organic-rich sediments preserve potential records of the sources and flux of hydrocarbons in a given depositional system. The bulk molecular compositions of hydrocarbons are altered in aquatic environments as a result of selective dissolution, volatilization, sorption, photolysis, and biodegradation.

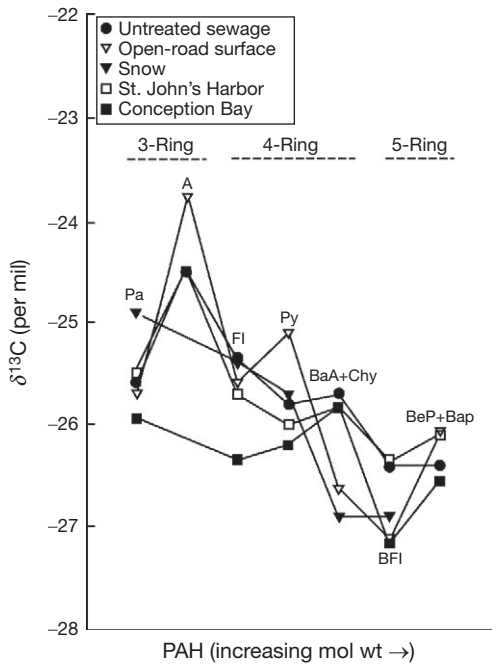

Figure 21 Comparison of PAH $\delta^{13}C$ from the St. John's Harbor sediment, road surface sweep, road-side snow pile, and sewer effluent. Also shown for comparison is the average (18 samples) PAH $\delta^{13}C$ of sediments from a separate harbor outside of the St. John's Harbor watershed (Conception Bay).

This review has summarized our understanding of the effect of these 'weathering reactions' on molecular and isotopic composition. Understanding hydrocarbon weathering is important for understanding sources of past deposition, and they may also provide insights on the timing of hydrocarbon release. Carbon isotope compositions of HMW hydrocarbons are not significantly altered by most known weathering and diagenetic reactions, enabling the use of isotopic signatures as source indicators of highly weathered hydrocarbons.

Several additional areas of research will likely yield major additional advances in understanding of petrogenic and pyrogenic hydrocarbon geochemistry. For example, developments in compound-specific isotope analysis of D/H ratios in individual hydrocarbon compounds will provide additional constraints on the origin, mixing, and transformation of hydrocarbons in shallow aquatic systems. Bacterial degradation experiments similar to those presented in this review have been completed, and no D/H fractionations in naphthalene and fluoranthene were observed (Abrajano, unpublished). This contrasts with large, but bacterial species-dependent, D/H fractionation already observed for toluene (e.g., Ward et al., 2000; Morasch et al., 2001). The dependence of D/H fractionation on the degrading microorganisms and the environment of degradation for mono- and PAHs are clearly fertile areas of further investigation. Similarly, the characterization of D/H signatures of PAH sources is a topic of ongoing interest. Compound-specific measurement of δD of fire soot (12 samples) reveals a wide range from –40‰ to –225‰, which overlaps with the observed range (–50‰ to –175‰) for crankcase oil (18 samples) (Abrajano, unpublished). Whereas source discrimination of the type shown for carbon isotopes does not appear promising for hydrogen, the factors governing the acquisition of D/H signatures of PAHs will likely yield unique insight into their pathways and transformation in the environment (e.g., Morasch et al, 2001).

Likewise, the continued development of compound-specific radiocarbon dating techniques ushers an exciting dimension to the study of PAHs and other hydrocarbons in modern sediments (e.g., Eglinton et al., 1997; Eglinton and Pearson, 2001; Pearson et al., 2001; Reddy et al., 2002). In particular, compound-specific radiocarbon determination offers a clear distinction to be made between 'new carbon' (e.g., wood burning) and 'old carbon' (petroleum and petroleum combustion).

Finally, there is now increasing recognition of a critical need for detailed characterization of the mechanisms of solid phase association of hydrocarbons in sediments or aquifer solid phase. The likelihood that the sorption/desorption behavior, bioavailability, and overall cycling of hydrocarbons depend critically on the nature of solid phase association provides a strong impetus for future work.

Acknowledgments

Financial support for our continuing studies of hydrocarbon sources and pathways in surface and groundwater systems from the US National Science Foundation (Hydrologic Sciences, EAR-0073912) is gratefully acknowledged. The RPI Isotope Hydrology and Biogeochemistry Facility was also partially supported by the US National Science Foundation (BES-9871241). The St. John's Harbor study was initiated through generous support from the Natural Science and Engineering Research Council and the Department of Fisheries and Oceans (Canada).

References

Abdul-Kassim TAT and Simoneit BRT (1995) Petroleum hydrocarbon fingerprinting and sediment transport assessed by molecular biomarker and multivariate statistical analysis in the eastern harbour of Alexandria, Egypt. *Marine Pollution Bulletin* 30: 63–73.

Abdul-Kassim TAT and Simoneit BRT (2001) Pollutant-solid phase interactions: Mechanism, chemistry and modeling. In: *The Handbook of Environmental Chemistry*, vol. 5, part E, 314pp. Berlin: Springer.

Accardi-Dey AM and Gschwend P (2003) Reinterpreting literature sorption data considering both absorption into organic carbon and adsorption onto black carbon. *Environmental Science & Technology* 37: 99–106.

Ahad JME, Lollar BS, Edwards EA, Slater GF, and Sleep BE (2000) Carbon isotope fractionation during anaerobic biodegradation of toluene: Implications for intrinsic bioremediation. *Environmental Science & Technology* 34: 892–896.

Alsberg T, Stenbcrg U, Westerholm R, et al. (1985) Chemical and biological characterization of organic material from gasoline exhaust particles. *Environmental Science & Technology* 19: 43–49.

Atlas RM and Bartha R (1992) Hydrocarbon biodegradation and oil spill bioremediation. *Advances in Microbial Ecology* 12: 287–338.

Badger GM, Buttery RG, Kimber RW, Lewis GE, Moritz AG, and Napier IM (1958) The formation of aromatic hydrocarbons at high temperatures: Part 1. Introduction. *Journal of the Chemical Society* 1958: 2449–2461.

Baek SO, Field RA, Goldstone ME, Kirk PW, Lester JN, and Perry R (1991) A review of atmospheric polycyclic aromatic hydrocarbons: Sources, fate and behaviour. *Water, Air, & Soil Pollution* 60: 279–300.

Baker JE and Eisenreich SJ (1990) Concentrations and fluxes of polycyclic aromatic hydrocarbons and polychlorinated biphenyls across the air–water interface of Lake Superior. *Environmental Science & Technology* 24: 342–352.

Ballentine DC, Macko SA, Turekian VC, Gilhooly WP, and Martincigh B (1996) Tracing combustion-derived atmospheric pollutants using compound-specific carbon isotope analysis. *Organic Geochemistry* 25: 97–108.

Barnsley EA (1975) The bacterial degradation of fluoranthene and benzo(a)pyrene. *Canadian Journal of Microbiology* 21: 1004–1008.

Beek B (2001) *The Handbook of Environmental Chemistry. Parl K: Biodegradation and Persistence*, vol. 2. Berlin: Springer.

Begeman CR and Burgan JC (1970) *Polynuclear hydrocarbon emission from automotive engines*. Detroit, MI: Society of Automotive Engineers. SAE Paper 700469.

Behymer TD and Hites RA (1985) Photolysis of polycyclic aromatic hydrocarbons adsorbed on simulated atmospheric particulates. *Environmental Science & Technology* 19: 1004–1006.

Behymer TD and Hites RA (1988) Photolysis of polycyclic aromatic hydrocarbons adsorbed on fly ash. *Environmental Science & Technology* 22: 1311–1319.

Benner R, Fogel ML, Sprague EK, and Hodson RE (1987) Depletion of ^{13}C in lignin and its implications for stable carbon isotope studies. *Nature* 329: 708–710.

Bieger T, Hellou J, and Abrajano TA (1996) Petroleum biomarkers as tracers of lubricating oil contamination. *Marine Pollution Bulletin* 32: 270–274.

Bjorseth A and Ramdahl T (1983) Sources and emissions of PAHs. *Handbook of Polycyclic Aromatic Hydrocarbons Emission Sources and Recent Progress in Analytical Chemistry*, 432pp. Dekker.

Blumer M, Blumer W, and Reich T (1977) Polycyclic aromatic hydrocarbons in soils of a mountain valley: Correlation with highway traffic and cancer incidence. *Environmental Science & Technology* 11(12): 1082–1084.

Bosma TNP, Harms H, and Zehnder JB (2001) Biodegradation of xenobiotics in the environment and technosphere. In: Beek B (ed.) *The Handbook of Environmental Chemistry, Park K: Biodegradation and Persistence*, vol. 63. p. 202, Berlin: Springer.

Broman D, Coimsjo A, Naf C, and Zebuhr Y (1988) A multisediment trap study on the temporal and spatial variability of polycyclic aromatic hydrocarbons and lead in an anthropogenic influenced archipelago. *Environmental Science & Technology* 22 (10): 1219–1228.

Brown G and Maher W (1992) The occurrence, distribution and sources of polycyclic aromatic hydrocarbons in the sediments of the Georges River estuary, Australia. *Organic Geochemistry* 18(5): 657–658.

Bucheli TD and Gustafsson O (2000) Quantification of the soot-water distribution coefficient of PAHs provides mechanistic basis for enhanced sorption observations. *Environmental Science & Technology* 34: 5144–5151.

Canton L and Grimalt JO (1992) Gas chromatographic-mass spectrometric characterization of polycyclic aromatic hydrocarbon mixtures in polluted coastal sediments. *Journal of Chromatography* 607: 279–286.

Cerniglia CE (1991) Biodegradation of organic contaminants in sediments: Overview and examples with polycyclic aromatic hydrocarbons. In: Baker RA (ed.) *Organic Substances and Sediments in Water*, vol. 3, pp. 267–281. Chelsea, MI: Lewis Publishers.

Chiou CT and Kyle DE (1998) Deviations from sorption linearity on soils of polar and nonpolar organic compounds at low relative concentrations. *Environmental Science & Technology* 32: 338–343.

Chiou CT, Peters LJ, and Freed VH (1979) Physical concept of soil-water equilibria for nonionic organic compounds. *Science* 206: 831–832.

Chiou CT, Porter PE, and Schmeddling DW (1983) Partition equilibria of nonionic organic compounds between soil organic matter and water. *Environmental Science & Technology* 17: 227–231.

Chiou CT, McGroddy SE, and Kile DE (1998) Partition charateristics of polycyclic aromatic hydrocarbons on soils and sediments. *Environmental Science & Technology* 32: 264–269.

Currie LA, Klouda GA, Benner BA, Garrity K, and Eglinton TI (1999) Isotopic and molecular marker validation, including direct molecular 'dating' (GC/AMS). *Atmospheric Environment* 33: 2789–2806.

Diegor E, Abrajano T, Patel T, Stehmeir L, Gow J, and Winsor L (2000) Biodegradation of aromatic hydrocarbons: Microbial and isotopic studies. Goldschmidt Conference (Cambridge Publications). *Journal of Conference Abstracts* 5: 350.

Douglas GS, Bence EA, Prince RC, McMillen SJ, and Butler EL (1996) Environmental stability of selected petroleum hydrocarbon source and weathering ratios. *Environmental Science & Technology* 30: 2332–2339.

Dowling LM, Boreham CJ, Hope JM, Marry AM, and Summons RE (1995) Carbon isotopic composition of ocean transported bitumens from the coastline of Australia. *Organic Geochemistry* 23: 729–737.

Eganhouse RP (ed.) (1997) *Molecular Markers in Environmental Geochemistry. ACS Symposium Series*, 426p. Washington, DC: American Chemical Society.

Eglinton TI and Pearson A (2001) Ocean Process tracers: Single compound radiocarbon measurements. In: *Encyclopedia of Ocean Sciences*. London: Academic Press.

Eglinton TI, Benitez-Nelson BC, Pearson A, McNichol AP, Bauer JE, and Druffel ERM (1997) Variability in radiocarbon ages of individual organic compounds from marine sediments. *Science* 277: 796–799.

Eisenreich SJ and Strachan WMJ (1992) Estimating atmospheric deposition of toxic substances to the Great Lakes—an update. *A Workshop Held at Canadian Centre for Inland Waters, Burlington, Ontario, Jan. 31-Feb. 2, (1992),* 29pp.

Ellison GB, Tuck AF, and Vaida V (1999) Atmospheric processing of organic aerosols. *Journal of Geophysical Research* 104: 11633–11641.

Engel MH and Macko SA (1993) Organic Geochemistry. In: *Principles and Applications,* 861p, New York: Plenum.

Faksness LG, Weiss HM, and Daling PS (2002) *Revision of the Nordtest Methodology for Oil Spill Identification,* 110p. Sintef Applied Chemistry Report STF66 A02028, N-7465 Trondheim, Norway.

Fingas MF (1995) A literature review of the physics and predictive modeling of oil spill evaporation. *Journal of Hazardous Materials* 42: 157–175.

Freeman KH (1991) *The Carbon Isotopic Composition of Individual Compounds from Ancient and Modern Depositional Environments*, pp. 42–92. PhD Thesis, Indiana University.

Freeman DJ and Cattell FC (1990) Wood burning as a source of polycylic aromatic hydrocarbons. *Environmental Science & Technology* 24: 1581–1585.

Fukushima M, Oba K, Tanaka S, Kayasu K, Nakamura H, and Hasebe K (1997) Elution of pyrene from activated carbon into an aqueous system containing humic acid. *Environmental Science & Technology* 31: 2218–2222.

Gearing PJ, Gearing JN, Pruell RJ, Wade TL, and Quinn JG (1980) Partitioning of no. 2 fuel oil in controlled estuarine ecosystems, sediments and suspended particulate matter. *Environmental Science & Technology* 14: 1129.

Gibson DT and Subramanian V (1984) Microbial degradation of aromatic hydrocarbons. In: Gibson DT (ed.) *Microbial Degradation of Organic Compounds*, pp. 181–252. New York: Dekker.

Goldberg ED (1985) *Black Carbon in the Environment: Properties and Distribution,* 198p, New York: Wiley.

Gordon RJ (1976) Distribution of airborne polycyclic aromatic hydrocarbons throughout Los Angeles. *Environmental Science & Technology* 10: 370–373.

Gustafsson O and Gscwend PM (1997) Soot as a strong partition medium for polycyclic aromatic hydrocarbons in aquatic systems. In: Eganhouse RP (ed.) *1997, Molecular Markers in Environmental Geochemistry, ACS Symposium Series*, pp. 365–381. Washington, DC: American Chemical Society.

Gustafson KE and Dickhut RM (1997) Gaseous exchange of polycyclic aromatic hydrocarbons across the air-water interface of southern Chesapeake Bay. *Environmental Science & Technology* 31: 1623–1629.

Hammer BT, Kelley CA, Coffin RB, Cifuentes LA, and Mueller JG (1998) $\delta^{13}C$ values of polycyclic aromatic hydrocarbons collected from two creosote-contaminated sutes. *Chemical Geology* 152: 43–58.

Hase A and Hites RA (1976) On the origins of polycyclic aromatic hydrocarbons in recent sediments: Biosynthesis by anaerobic bacteria. *Geochimica et Cosmochimica Acta* 40: 1141–1143.

Hayes JM, Freeman KH, Popp BN, and Hoham CH (1989) Compound-specific isotopic analysis: A novel tool for reconstruction of ancient biogeochemical processes. *Advances in Organic Geochemistry* 16(4–6): 1115–1128.

Heider J, Spormann AM, Beller HR, and Widdel F (1999) Anaerobic bacterial metabolism of hydrocarbons. *FEMS Microbiology Reviews* 22: 459–473.

Hellou J, Steller S, Leonard J, and Albaiges J (2002) Alkanes, terpanes, and aromatic hydrocarbons in surficial sediments of Halifax Harbor. *Polycyclic Aromatic Compounds* 22: 631–641.

Hinga KR (1984) *The Fate of Polycyclic Aromatic Hydrocarbons in Enclosed Marine Ecosystems*. PhD Thesis, University of Rhode Island.

Hoffman EJ, Mills GL, Latimer JS, and Quinn JG (1984) Urban runoff as a source of polycyclic hydrocarbons to coastal environments. *Environmental Science & Technology* 18: 580.

Holt B and Abrajano TA (1991) Chemical and isotopic alteration of organic matter during stepped combustion. *Analytical Chemistry* 63: 2973–2978.

Hostetler F and Kvenvolden K (2002) Forensic implications of spilled oil biodegradation in anaerobic environments. *Geological Society of America Abstracts with Programs*. Denver, Colorado, October, 2002

Howsam M and Jones KC (1998) Sources of PAHs in the environment. In: Neilson AH (ed.) *PAHs and Related Compounds, The Handbook of Environmental Chemistry*, vol. 3, part I, pp. 138–174. Berlin: Springer.

Jensen TE and Hites RA (1983) Aromatic diesel emissions as function of engine conditions. *Analytical Chemistry* 55: 594–599.

Kaplan IR, Galperin Y, Lu ST, and Lee RP (1997) Forensic environmental geochemistry: Differentiation of fuel types, their sources and release time. *Organic Geochemistry* 27: 289–317.

Karapanagioti H, Kleineidam S, Sabatini D, Grathwohl P, and Ligouis B (2000) Impacts of heterogeneous organic matter on phenanthrene sorption: Equilibrium and kinetic studies with aquifer material. *Environmental Science & Technology* 34: 406–414.

Karickhoff SW (1981) Semi-empirical estimation of sorption of hydrophobic pollutants on natural sediments and soils. *Chemosphere* 10: 833–846.

Karickhoff SW, Brown DS, and Scott TA (1979) Sorption of hydrophobic pollutants on natural sediments. *Water Research* 13: 241–248.
Kennicutt MC II, Brooks JM, and McDonald TJ (1991) Origins of hydrocarbons in Bering Sea sediments: I. Aliphatic hydrocarbons and fluorescence. *Organic Geochemistry* 17(1): 75–83.
Killops SD and Howell VJ (1988) Sources and distribution of hydrocarbons in Bridgewater Bay (Severn Estuary, UK) intertidal surface sediments. *Estuarive Coastal and Shelf Science* 27: 237–261.
Kleineidam S, Rugner H, Ligouis B, and Grathwol P (1999) Organic matter facie and equilibrium sorption of phenanthrene. *Environmental Science & Technology* 33: 1637–1644.
Kleineidam S, Schuth CH, and Grathwol P (2002) Solubility-normalized combined adsorption-partitioning sorption isotherms for organic pollutants. *Environmental Science & Technology* 36: 4689–4697.
Knap AH and Williams PJL (1982) Experimental studies to determine the fate of petroleum hydrocarbons in refinery effluent on an estuarine system. *Environmental Science & Technology* 16: 1–4.
Kvenvolden KA, Hostettler FD, Rapp JB, and Carlson PR (1993a) Hydrocarbons in oil residue on beaches of islands of Prince William Sound, Alaska. *Marine Pollution Bulletin* 26: 24–29.
Kvenvolden KA, Carlson PR, Threlkeld CN, and Warden A (1993b) Possible connection between two Alaskan catastrophies occurring 25 yr apart (1964 and 1989). *Geology* 21: 813–816.
Kvenvolden KA, Hostettler FD, Carlson PR, Rapp JB, Threlkeld C, and Warden A (1995) Ubiquitous tar balls with a California source signature on the shorelines of Prince William Sound, Alaska. *Environmental Science & Technology* 29(10): 2684–2694.
Laflamme RE and Hites RA (1978) The global distribution of polycyclic aromatic hydrocarbons in recent sediments. *Geochimica et Cosmochimica* 42: 289–303.
Lake JL, Norwood C, Dimock D, and Bowen R (1979) Origins of polycyclic aromatic hydrocarbons in estuarine sediments. *Geochimica et Cosmochimica Acta* 43: 1847–1854.
Lane DA (1989) The fate of polycyclic aromatic compounds in the atmosphere during sampling. In: Vo-Dinh (ed.) *Chemical Analysis of Polycyclic Aromatic Compounds, Chemical Analysis Series*, vol. 101, pp. 30–58. Wiley-Interscience.
Latimer JS, Hoffman EJ, Hoffman G, Fasching JL, and Quinn JG (1990) Sources of petroleum hydrocarbons in urban runoff. *Water, Air, & Soil Pollution* 52: 1–21.
Lee ML, Novotny MV, and Bartle KD (1981) *Analytical Chemistry of Polycyclic Aromatic Compounds*. New York: Academic Press.
Lee RF, Gardner WS, Anderson JW, Blaylock JW, and Barwell CJ (1978) Fate of polycyclic aromatic hydrocarbons in controlled ecosystems enclosures. *Environmental Science & Technology* 12: 832–838.
Lima AC, Eglinton TI, and Reddy CM (2003) High resolution record of pyrogenic polycyclic aromatic hydrocarbon deposition during the 20th Century. *Environmental Science & Technology* 37: 53–61.
Lipiatou E and Saliot A (1991) Fluxes and transport of anthropogenic and natural polycyclic aromatic hydrocarbons in the western Mediterranean sea. *Marine Chemistry* 32: 51–71.
Lohmann F, Trendel JM, Hetru C, and Albrecht P (1990) C-29 trtiated amyrin: Chemical synthesis aiming at the study of aromatization processes in sediments. *Journal of Labelled Compounds and Radiopharmaceuticals* 28: 377–386.
Lun R, Lee K, De Marco L, Nalewajko C, and Mackay D (1998) A model of the fate of polycyclic aromatic hydrocarbons in the saguenay ford. *Environmental Toxicology and Chemistry* 17: 333–341.
Luthy RG, Aiken GR, Brusseau ML, et al. (1997) Sequestration of hydrophobic organic contaminants by geosorbents. *Environmental Science & Technology* 31: 3341–3347.
MacKay AA and Gschwend P (2001) Enhanced concentration of PAHs in a coal tar site. *Environmental Science & Technology* 31(35): 1320–1328.
Mackay D (1998) Multimedia mass balance models of chemical distribution and fate. In: Schuurmann G and Markert B (eds.) *Ecotoxicology*, ch. 8, pp. 237–257. NY and Spektrum, Berlin: Wiley.
Mackay D and Callcott D (1998) Partitioning and physical chemical properties of PAHs. PAHs and Related Compounds. In: Neilson AH (ed.) *The Handbook of Environmental Chemistry, Volume 3*, Part I, pp. 325–346. Berlin, Heidelberg: Springer.
Mackay D, Shiu WY, and Ma KC (1992) *Illustrated Handbook of Physical-Chemical Properties and Environmental Fate for Organic Chemicals, volume II, 1992*. Boca Raton: Lewis.
MacKenzie AS (1984) Application of biological markers in petroleum geochemistry. In: Brooks J and Welte DH (eds.) *Advances in Petroleum Geochemistry*, vol. 1, pp. 115–214. London: Academic Press.
Mansuy L, Philp RP, and Allen J (1997) Source identification of oil spills based on the isotopic composition of individual components in weathered oil samples. *Environmental Science & Technology* 31: 3417–3425.
Mazeas L and Budzinski H (2001) Polycyclic aromatic hydrocarbon $^{13}C/^{12}C$ ratio measurement in petroleum and marine sediments: Application to standard reference material and a sediment suspected of contamination from Erika oil spill. *Journal of Chromatography* A 923: 165–176.
Mazeas L, Budzinski H, and Raymond N (2002) Absence of stable carbon isotope fractionation of saturated and polycyclic aromatic hydrocarbons during aerobic bacterial degradation. *Organic Geochemistry* 33: 1259–1272.
McElroy AE, Farrington JW, and Teal JM (1985) Bioavailability of polycyclic aromatic hydrocarbons in the aquatic environment. In: Varanasi U (ed.) *Metabolism of Polycyclic Aromatic Hydrocarbons in the Aquatic Environment*, pp. 1–39. Boca Raton: CRC Press.
McRae C, Sun CG, Snape CE, Fallick A, and Taylor D (1999) $\delta^{13}C$ values of coal-derived PAHs from different processes and their application to source apportionment. *Organic Geochemistry* 30: 881–889.
McRae C, Snape CE, Sun CG, Fabbri D, Tartari D, Trombini C, and Fallick A (2000) Use of compound specific stable isotope analysis to source anthropogenic natural gas-derived polycyclic aromatic hydrocarbons in lagoon sediments. *Environmental Science & Technology* 34: 4684–4686.
McVeety BD and Hites RA (1988) Atmospheric deposition of polycyclic aromatic hydrocarbons to water surfaces: A mass balance approach. *Atmospheric Environment* 22(3): 511–536.
Meador J, Stein J, Reichert W, and Varanasi U (1995) Bioaccumulation of polycyclic aromatic hydrocarbons by marine organisms. *Reviews of Environmental Contamination and Toxicology* 143: 80–164.
Means JC and Wijayaratne R (1982) Role of natural colloids in the transport of hydrophobic pollutants. *Science* 215: 968.
Meckenstock RU, Morasch B, Wartmann R, et al. (1999) $^{13}C/^{12}C$ isotope fractionation of aromatic hydrocarbons during microbial degradation. *Environmental Microbiology* 1: 409–414.
Moldowan JM, Dahl JE, McCaffrey MA, Smith WJ, and Fetzer JC (1995) Application of biological marker technology to bioremediation of refinery by-products. *Energy & Fuels* 9(1): 155–162.
Moore JW and Ramamoorthy S (1984) *Organic Chemicals in Natural Waters Applied Monitoring and Impact Assessment*, 289pp. NY: Springer.
Morasch B, Schink B, Richnow H, and Meckenstock RU (2001) Hydrogen and carbon isotope fractionation upon bacterial toluene degradation: Mechanistic and environmental aspects. *Applied and Environmental Microbiology* 67: 4842–4849.
Mueller JG, Chapman PJ, and Pritchard PH (1988) Action of a fluoranthene-utilizing bacterial community on polycyclic aromatic hydrocarbons components of Creosote. *Applied and Environmental Microbiology* 55(12): 3085–3090.
Mueller JG, Chapman PJ, Blattmann BO, and Pritchard PH (1990) Isolation and characterization of a flouranthene utilizing strain of *Pseudomonas paucimobilis*. *Applied and Environmental Microbiology* 56(4): 1079–1086.
Munoz D, Guiliano M, Doumenq P, Jacquot F, Scherrer P, and Mille G (1997) Long term evolution of petroleum biomarkers in mangrove soil (Guadaloupe). *Marine Pollution Bulletin* 34: 868–874.
Neff JM (1979) *Polycyclic Aromatic Hydrocarbons in the Aquatic Environment. Sources, Fates and Biological Effects*. London: Applied Science Publishers.
Neilson AH (1998) *PAHs and Related Compounds Biology*, 386p. NY: Springer.
Neilson AH and Allard AS (1998) Microbial metabolism of PAHs and heteroarenes. In: Neilson AH (ed.) *The Handbook of Environmental Chemistry*, vol. 3, part I. pp. 2–80. Berlin, Heidelberg: Springer.
Neilson A and Hynning P (1998) PAHs: Products of chemical and biochemical transformation of alicyclic precursors. In: Neilson AH (ed.) *The Handbook of Environmental Chemistry*, vol. 3, part 1, pp. 224–273. Berlin, Heidelberg: Springer.
NRC (1985) Oil in the Sea: Inputs, Fates, and Effects. Committee on Oil in the Sea: Inputs, Fates, and Effects, National Research Council, 601p.
NRC (2000) Natural Attenuation for Groundwater Remediation, Committee on Intrinsic Remediation, Water Science and Technology Board, Board on Radioactive Waste Management, National Research Council, 292pp.
US National Research Council (NRC) (2002) Oil in the Sea III: Inputs, Fates, and Effects. Committee on Oil in the Sea: Inputs, Fates, and Effects, National Research Council, 446p.
Offenberg JH and Baker JE (1999) Aerosol size distributions of polycyclic aromatic hydrocarbons in urban and over-water atmospheres. *Environmental Science & Technology* 33: 3324–3331.
O'Malley VP (1994) *Compound-Specific Carbon Isotope Geochemistry of Polycyclic Aromatic Hydrocarbons in Eastern Newfoundland Estuaries*. PhD Thesis, Memorial University of Newfoundland.
O'Malley VP, Burke RA, and Schlotzhauer WS (1997) Using GC-MS/Combustion/IRMS to determine the $^{13}C/^{12}C$ ratios of individual hydrocarbons produced from the combustion of biomass materials—application to biomass burning. *Organic Geochemistry* 27: 567–581.

O'Malley V, Abrajano TA, and Hellou J (1994) Determination of $^{13}C/^{12}C$ Ratios of individual PAHs from environmental samples: Can PAHs sources be source apportioned? *Organic Geochemstry* 21: 809–822.

O'Malley V, Abrajano TA, and Hellou J (1996) Isotopic apportionment of individual polycyclic aromatic hydrocarbon sources in St. Johns Harbour. *Environmental Science & Technology* 30: 634–638.

Oostdam BL (1980) Oil pollution in the Persian Gulf and approaches 1978. *Marine Pollution Bulletin* 11: 138–144.

Paalme L, Irha N, Urbas E, Tsyban A, and Kirso U (1990) Model studies of photochemical oxidation of carcinogenic polyaromatic hydrocarbons. *Marine Chemistry* 30: 105–111.

Pancirov RJ and Brown RA (1975) Analytical methods for PAHs in crude oils, heating oils and marine tissues. *Conference Proceedings on Prevention and Control of Oil Pollution*. Washington, DC, API. 103–113.

Payne JR and Phillips CR (1985) Photochemistry of petroleum in water. *Environmental Science & Technology* 19: 569.

Pearson A, McNichol AP, Benitez-Nelson BC, Hayes JM, and Eglinton TI (2001) Origins of lipid biomarkers in santa monica basin surface sediment: A case study using compound-specific Δ14C analysis. *Geochimica et Cosmochimica Acta* 65: 3123–3137.

Pedersen PS, Ingwersen J, Nielsen T, and Larsen E (1980) Effects of fuel, lubricant, and engine operating parameters on the emission of polycyclic aromatic hydrocarbons. *Environmental Science & Technology* 14(1): 71–79.

Peters KE and Moldowan JM (1993) *The Biomarker Guide, Interpreting Molecular Fossils in Petroleum and Ancient Sediments*. Englewood Cliffs, NJ: Prentice-Hall.

Peters KE, Moldowan JM, Schoell M, and Hempkins WB (1986) Petroleum isotopic and biomarker composition related to source rock organic matter and depositional environment. *Organic Geochemistry* 10: 17–27.

Peters KE, Scheuerman GL, Lee CY, Moldowan JM, Reynolds RN, and Pena MM (1992) Effects of refinery processes on biological markers. *Energy & Fuels* 6: 560–577.

Pierce RC and Katz M (1975) Dependency of polynuclear aromatic hydrocarbon content on size distribution of atmospheric aerosols. *Environmental Science & Technology* 9: 347–353.

Prahl FG and Carpenter R (1979) The role of zooplankton fecal pellets in the sedimentation of polycyclic aromatic hydrocarbons in Dabob Bay, Washington. *Geochimica et Cosmochimica Acta* 43: 1959–1972.

Prince RC (1993) Petroleum oil spill bioremediation in marine environments. *Critical Reviews in Microbiology* 19: 217–239.

Pruell JR and Quinn JG (1988) Accumulation of polycyclic aromatic hydrocarbons in crankcase oil. *Environmental Pollution* 49: 89–97.

Radding SB, Mill T, Gould CW, et al. (1976) The environmental fate of selected polynuclear aromatic hydrocarbons. US Environmental Protection Agency EPA560/5-75-009.

Radke M (1987) Organic Geochemistry of aromatic hydrocarbons. In: Brooks J and Welte DH (eds.) *Advances in Petroleum Geochemistry*, vol. 2, pp. 141–207. New York: Academic Press.

Ramaswami A and Luthy RG (1997) Mass transfer and bioavailability of PAHs compounds in coal tar NAPL-slurry systems: 1. Model development. *Environmental Science & Technology* 31: 2260–2267.

Readman JW, Mantoura RFC, Rhead MM, and Brown L (1982) Aquatic distribution and heterotrophic degradation of polycyclic aromatic hydrocarbons (PAHs) in the Tamer estuary. *Estuarine, Coastal and Shelf Science* 14: 369–389.

Reddy C and Quinn JG (1997) Environmental chemistry of benzothiazoles derived from rubber. *Environmental Science & Technology* 31: 2847–2853.

Reddy C, Reddy CM, Pearson A, et al. (2002) Radiocarbon as a tool to apportion the sources of polycyclic aromatic hydrocarbons and black carbon in environmental samples. *Environmental Science & Technology* 36: 1774–1787.

Reyes CS, Medina M, Crespo-Hernandez C, et al. (2000) Photochemistry of pyrene on unactivated and activated silica surfaces. *Environmental Science & Technology* 34: 415–421.

Rogge WF, Hildemann LM, Mazurek MA, Cass GR, and Simoneit BR (1993) *Environmental Science & Technology* 27: 1892–1904.

Rothermich MM, Hayes LA, and Lovley D (2002) Anaerobic, sulfate-dependent degradation of polycyclic aromatic hydrocarbons in petroleum-contaminated harbor sediment. *Environmental Science & Technology* 36: 4811–4817.

Schneider J, Grosser R, Jayasimhulu K, Xue W, and Warshawsky D (1996) Degradation of pyrene, benz(a)anthracene, and benz(a)pyrene by *Mycobacterium* sp. strain RGHII-135, isolated from a former coal gasification site. *Applied and Environmental Microbiology* 157: 7–12.

Schoell M (1984) Stable isotopes in petroleum research. In: Brooks J and Welte DH (eds.) *Advances in Petroleum Geochemistry*, vol. 1, pp. 215–245. London: Academic Press.

Schwarzenbach RP, Gschwend PM, and Imboden DM (1993) *Environmental Organic Chemistry*, 681p, NY: Wiley.

Schwarzenbach RP, Haderlein SB, Muller SR, and Ulrich MM (1998) Assessing the dynamic behavior of organic contaminants in natural waters. In: Macalady DL (ed.) *Perspectives in Environmental Chemistry*, pp. 138–166. NY: Oxford University Press.

Sherrill TW and Sayler GS (1981) Phenanthrene biodegradation in freshwater environments. *Applied and Environmental Microbiology* 39: 172–178.

Simoneit BRT (1984) Organic matter of the troposphere: III. Characterization and sources of petroleum and pyrogenic residues in aerosols over the western United States. *Atmospheric Environment* 18: 51–67.

Simoneit BRT (1986) Characterization of organic constituents in aerosols in relation to their origin and transport: A review. *International Journal of Environmental Analytical Chemistry* 23: 207–237.

Simoneit BRT (1998) Biomarker PAHs in the environment. In: Neilson AH (ed.) *PAHs and Related Compounds Chemistry*, pp. 175–215. NY: Springer.

Smirnova A, Abrajano T, Smirnov A, and Stark A (1998) Distribution and sources of polycyclic aromatic hydrocarbons in the sediments of lake Erie. *Organic Geochemistry* 29: 1813–1828.

Sofer Z (1984) Stable carbon isotope compositions of crude oils: Application to source depositional environments and petroleum alteration. *American Association of Petroleum Geologists Bulletin* 68(1): 31–48.

Sporstol S, Gjos N, Lichtenthaler RG, et al. (1983) Source identification of aromatic hydrocarbons in sediments using GC-MS. *Environmental Science & Technology* 17(5): 282–286.

Stehmeir LG, Francis M McD., Jack TR, Diegor E, Winsor L, and Abrajano TA (1999) Field and *in vitro* evidence for *in-situ* bioremediation using compound-specific $^{13}C/^{12}C$ ratio monitoring. *Organic Geochemistry* 30: 821–834.

Steinhauer MS and Boehm PD (1992) The composition and distribution of saturated and aromatic hydrocarbons in nearshore sediments, river sediments, and coastal peat in the Alaskan beaufort sea: Implications for detecting anthropogenic hydrocarbon inputs. *Marine Environmental Research* 33: 223–253.

Stenberg UR (1983) PAHs Emissions from automobiles. *In: Handbook of Polycyclic Aromatic Hydrocarbons. Emission Sources and Recent Progress in Analytical Chemistry*, vol 2, pp. 87–111. New York: Marcel Dekker.

Strachan WMJ and Eisenreich SJ (1988) Mass balancing of toxic chemicals in the Great Lakes: The role of atmospheric deposition. Windsor, Ontario: International Joint Commission.

Suess MJ (1976) The environmental load and cycle of polycyclic aromatic hydrocarbons. *Science of the Total Environment* 6: 239–250.

Sugai SF, Lindstrom JE, and Braddock JF (1997) Environmental influences on the microbial degradation of Exxon Valdez oil spill on the shorelines of Prince William Sound, Alaska. *Environmental Science & Technology* 31: 1564–1572.

Takada H, Onda T, and Ogura N (1990) Determination of polycyclic aromatic hydrocarbons in urban street dusts and their source materials by capillary gas chromatography. *Environmental Science & Technology* 24(8): 1179–1186.

Tissot BP and Welte DH (1984) *Petroleum Formation and Occurrence*, 2nd edn., 699p, Berlin: Springer.

Van Brummelen TC, van Hattum B, Crommentuijn T, and Kalf DE (1998) Bioavailability and ecotoxicology of PAHs. In: Neilson AH (ed.) *PAHs and Related Compounds Chemistry*, pp. 175–215. NY: Springer.

Vazquez-Duhalt R (1989) Environmental impact of used motor oil. *Science of the Total Environment* 79: 1–23.

Venkatesan MI (1988) Occurrence and possible sources of perylene in marine sediments-a review. *Marine Chemistry* 25: 1–27.

Villholth KG (1999) Colloid characterization and colloidal phase partitioning of polycyclic aromatic hydrocarbons in two creosote-contaminated aquifers in Denmark. *Environmental Science & Technology* 33: 691–699.

Volkman JK, Holdsworth DG, Neill GP, and Bavor HJ (1992) Identification of natural, anthropogenic and petroleum hydrocarbons in aquatic sediments. *Science of the Total Environment* 112: 203–219.

Volkman JK, Revill AT, and Murray AP (1997) Applications of biomarkers for identifying sources of natural and pollutant hydrocarbons in aquatic environments. In: Eganhouse RP (ed.) *Molecular Markers in Environmental Geochemistry ACS Symposium Series*, pp. 110–132. Washington, DC: American Chemical Society.

Wakeham SG, Schaffner C, and Giger W (1980a) Polycyclic aromatic hydrocarbons in recent lake sediments: II. Compounds derived from biogenic precursors during early diagenesis. *Geochimica et Cosmochimica Acta* 44: 415–429.

Wakeham SG, Schaffner C, and Giger W (1980b) Polycyclic aromatic hydrocarbons in recent lake sediments: I. Compounds having anthropogenic origins. *Geochimica et Cosmochimica Acta*. 44: 403–413.

Wang Z and Fingas M (1995) Use of methyldibenzothiophenes as markers for differentiation and source identification of crude and weathered oils. *Environmental Science & Technology* 29: 2842–2849.

Wang Z, Fingas M, Blenkinsopp S, et al. (1998) Comparison of oil composition changes due to biodegradation and physical weathering in different oils. *Journal of Chromatography* A809: 89–107.

Wang Z, Fingas M, and Page DS (1999) Oil spill identification. *Journal of Chromatography* A843: 369–411.

Ward JAM, Ahad JME, Lacrampe-Couloume G, Slater GF, Edwards EA, and Lollar BS (2000) Hydrogen isotope fractionation during methanogenic degradation of toluene: Potential for direct verification of bioremediation. *Environmental Science & Technology* 34: 4577–4581.

Westerholm R, Stenbcrg U, and Alsberg T (1988) Some aspect of the distribution of polycyclic aromatic hydrocarbons (PAHs) between particles and gas phase from diluted gasoline exhausts generated with the use of a dilution tunnel, and its validity for measurement in air. *Atmospheric Environment* 22(5): 1005–1010.

Whitehouse BG (1984) The effects of temperature and salinity on the aqueous solubility of polynuclear aromatic hydrocarbons. *Marine Chemistry* 14.

Whittaker M, Pollard SJT, and Fallick TE (1995) Characterisation of refractory wastes at heavy oil-contaminated sites: A review of conventional and novel analytical methods. *Environmental Technology* 16: 1009–1033.

Wijayaratne RD and Means JC (1984) Adsorption of polycyclic aromatic hydrocarbons by natural estuarine colloids. *Marine Environmental Research* 11: 77–89.

Yanik P, O'Donnell TH, Macko SA, Qian Y, and Kennicutt MC (2003) The isotopic compositions of selected crude oil PAHs during biodegradation. *Organic Geochemistry* 34: 291–304.

Ye D, Siddiqui MA, Maccubbin AE, Kumar S, and Sikka HC (1996) Degradation of polynuclear aromatic hydrocarbons by *Sphingomonas paucimbilis*. *Environmental Science & Technology* 30: 136–142.

Youngblood WW and Blumer M (1975) Polycyclic aromatic hydrocarbons in the environment: Homologous series in soils and recent marine sediments. *Geochimica et Cosmochimica Acta* 39: 1303–1314.

Yunker MB, MacDonald RW, Cretney WJ, Fowler BR, and McLaughlin FA (1993) Alkane, terpene, and polycyclic aromatic hydrocarbon geochemistry of the mackenzie river and mackenzie shelf: Riverine contributions to beaufort sea coastal sediment. *Geochimica et Cosmochimica Acta*. 57: 3041–3061.

Yunker MB, MacDonald RW, Veltkamp DJ, and Cretney WJ (1995) Terrestrial and marine biomarkers in a seasonally ice-covered arctic estuary-integration of multivariate and biomarkers approaches. *Marine Chemistry* 49: 1–50.

Zafiriou OC (1977) Marine organic photochemistry previewed. *Marine Chemistry* 5: 497–522.

Zepp RG and Schlotzhauer PF (1979) Photoreactivity of selected aromatic hydrocarbons in water. In: Jones PW and Leber P (eds.) *Polynuclear Aromatic Hydrocarbons*, pp. 141–158. Ann Arbor, MI: Ann Arbor Science Publishers.

11.14 Biogeochemistry of Halogenated Hydrocarbons

P Adriaens and C Gruden, The University of Michigan, Ann Arbor, MI, USA
ML McCormick, Hamilton College, Clinton, NY, USA

This article is reproduced from the previous edition, volume 9, pp. 511–539, © 2003 Elsevier Ltd.

11.14.1 Introduction

Halogenated hydrocarbons originate from both natural and industrial sources. Whereas direct anthropogenic emissions to the atmosphere and biosphere are often easy to assess, particularly when they are tied to major industrial activities, the attribution of emissions to other human activities (e.g., biomass burning), diffuse sources (e.g., atmospheric discharge, run off), and natural production (e.g., soils, fungi, algae, microorganisms) are difficult to quantify. The widespread occurrence of both alkyl and aryl halides in groundwater, surface water, soils, and various trophic food chains, even those not affected by known point sources, suggests a substantial biogeochemical cycling of these compounds (Wania and Mackay, 1996; Adriaens et al., 1999; Gruden et al., 2003). The transport and reactive fate mechanisms controlling their reactivity are compounded by the differences in sources of alkyl-, aryl-, and complex organic halides, and the largely unknown impact of biogenic processes, such as enzymatically mediated halogenation of organic matter, fungal production of halogenated hydrocarbons, and microbial or abiotic transformation reactions (e.g., Asplund and Grimvall, 1991; Gribble, 1996; Watling and Harper, 1998; Oberg, 2002). The largest source may be the natural halogenation processes in the terrestrial environment, as the quantities detected often exceed the amount that can be explained by human activities in the surrounding areas (Oberg, 1998). Since biogeochemical processes result in the distribution of a wide range of halogenated hydrocarbon profiles, altered chemical structures, and isomer distributions in natural systems, source apportionment (or environmental forensics) can often only be resolved using multivariate statistical methods (e.g., Goovaerts, 1998; Barabas et al., 2003; Murphy and Morrison, 2002).

This chapter will describe the widespread occurrence of halogenated hydrocarbons, interpret their distribution and biogeochemical cycling in light of natural and anthropogenic sources, biotic and abiotic reactivity, and prevailing cycling mechanisms. Specific emphasis will be placed on the potential role of biotic and abiotic transformation reactions in soil, water, and sediment environments resulting in environmental sequestration and phase transfer.

11.14.2 Global Transport and Distribution of Halogenated Organic Compounds

The biogeochemistry of halogenated pollutants has to be reviewed within the context of transport and phase partitioning, and the impact of these processes on their distribution and

reactivity in various environmental compartments. Whereas the authors recognize that these atmospheric processes dominate the global biogeochemistry of halogenated hydrocarbons, there are substantial differences in the types of biogeochemical controls that impact biogenic, anthropogenic, and complex halogenated organic matter at local (contaminant hot spots), regional (e.g., Great Lakes), and global (e.g., temperate and polar latitudes) scales. Since this chapter aims to discuss persistent organic pollutants (POPs), biogenic pollutants (e.g., the halomethanes), and anthropogenic non-POPs (e.g., chloroethenes, chlorofluoro-hydrocarbons), an operational separation between POPs and non-POPs based on their distribution mechanisms and physical–chemical properties which render them as belonging to either class is useful to provide context for the remainder of this chapter.

11.14.2.1 Persistent Organic Pollutants

POPs are generally considered as long-lived organic compounds that become concentrated as they move through the food chain, exhibiting toxic effects on animal reproduction, development, and immunological function. These compounds are dominated by chlorinated hydrocarbons, including many pesticides: DDT, hexachlorobenzene (HCB), chlordane, heptachlor, toxaphene, aldrin, dieldrin, endrin, mirex, polychlorinated biphenyls (PCBs), and chlorinated dibenzo-*p*-dioxins and furans (PCDD/F) (Bidleman, 1999). The chemistry of these compounds is very complex and spans orders of magnitude variability in their solubility, vapor pressure, and partitioning behavior as a function of chlorine content and substitution pattern. For example, there are 210 congeners of PCBs, 135 congeners of furans, and 75 congeners of dioxins. In addition, many compounds are chiral in nature (e.g., the hexachlorocyclohexane-HCH group), a property which also confers differential reactivity on the molecule. Based on observations dating back to mid-1960s, it has become apparent that POPs have the capability of being transported over thousands of kilometers (e.g., Sladen et al., 1966; Peterle, 1969), during which these compounds have the opportunity to fractionate, react, and bioaccumulate in global food chains.

Several global maps have been generated that document the distribution of these compounds based on the analysis of tree bark samples (Simonich and Hites, 1995), pine needles and lichens (Ockenden et al., 1998a), rural soils and isolated water bodies (Baker and Hites, 2000a,b), and butter samples (Kalantzi et al., 2001). Aside from global latitudinal fractionation (e.g., Ockenden et al., 1998b), analysis for organochlorine insecticides and PCBs over the Great Lakes indicate the existence of local and regional volatilization pathways, rather than long-range transport (e.g., McConnell et al., 1998). These regional and global distribution phenomena and their implications have been recognized in a number of multilateral venues (Montreal, Stockholm, UN, etc.), and the need for identifying and classifying chemicals for their propensity to long-range transport, and characterization of POP distribution mechanisms is an urgent topic of research.

11.14.2.1.1 Global distribution mechanisms

Even though substantial experimentation and monitoring of POPs in the atmosphere, the world's soils, vegetation, and oceans indicate a widespread (mainly latitudinal) distribution, the present knowledge on the global dynamics of POPs is incomplete. The processes controlling their distribution can only be assessed by integration of models with the available datasets (Dachs et al., 2002), or by constructing hypothetical environments to explore how a given chemical is likely to partition, react, and be transported (MacKay and Wania, 1995). The advantage of the latter approach is that chemical behavior is the only variable under consideration, and problems associated with environmental characterization and limiting chemical analyses are avoided. The former allows for a validation of this approach with multivariate data sets. Based on these approaches, two main mechanisms controlling air–water fluxes and enrichment of contaminants in polar regions and food webs have been advanced: temperature-controlled global fractionation and condensation, and oceanic controlled phytoplankton uptake with particle sinking.

For a quarter of a century, the concept of global distillation has been developed to describe the tendency of certain contaminants to evaporate from temperate and tropical regions and condense in cold climates (Goldberg, 1975). More recently, a 'grasshopper effect' analogy was used to describe the tendency of POPs to undergo cycles of deposition and re-emission during transport (Wania and MacKay, 1996). Accordingly, properties such as vapor pressure and partition coefficient will impact this tendency for any given POP compound, resulting in distinctive condensation temperatures and degree of fractionation with latitude. These cycles are thought to be strongly influenced by diurnal and seasonal variability of environmental conditions, such as temperature, due to its influence on air–surface and air–water partitioning. Indeed, the influence of air–water exchange has been shown to dominate depositional processes in many aquatic systems for a wide range of POPs such as PCBs and HCHs (Totten et al., 2001; Wania and MacKay, 1996). Large-scale surveys of organochlorine pesticides and PCBs in ocean air and water show features which support these effects (Iwata et al., 1993), and many aryl halides in atmospheric air masses show strong temperature-dependent diurnal cycling (e.g., Lee et al., 2000), providing support for rapid air–surface exchange of semi-volatile organic compounds. On a regional scale, significant temperature-dependent air–water exchange of toxaphene (polychlorinated bornanes and bornenes) in the Great Lakes has been demonstrated, whereby the colder temperatures and lower sedimentation rates in Lake Superior are responsible for its higher aqueous concentrations (Swackhamer et al., 1999).

Large differences in exchange fluxes were calculated depending on mechanistic assumptions. Consider the following two limiting cases: (1) all of the POPs in water are truly dissolved and available to participate in gas exchange, and (2) all of the POPs are bound to particles or colloidal material and unable to revolatilize. When the fugacity in surface water was taken into account, net deposition occurred only in colder regions; in the case of (1), air-to-sea deposition occurred in all ocean regions (Iwata et al., 1993). Further, the controlling influence of temperature in determining the transport and sinks of POPs via cold condensation, global distillation, and latitudinal fractionation has been supported by climatic models (Wania and MacKay, 1996). Experimental observations have validated this model for terrestrial and limnic systems, but are scarce in the marine environment (e.g., Grimalt

et al., 2001; Meijer et al., 2002), indicating that other mechanisms may play a role in the global distribution of POPs.

Vertical scavenging of POPs in oceans following sorption to particulate organic matter, and subsequent removal from participation in dynamic air–water exchange as the result of particulate sinking to deep waters and sediments has been demonstrated, resulting in vertical profiles in the water column (e.g., Dachs et al., 1999a,b). Hence, deposition fluxes of POPs in the water column may at least in part be considered to represent a significant control for revolatilization as they are impacted by sinking particles and biogeochemical processes such as phytoplankton uptake (Dachs et al., 2002). Support for the role of phytoplankton was derived from findings that air–water exchange and phytoplankton uptake behave as coupled processes in aquatic environments (Dachs et al., 1999a,b). These mutual interferences in atmospherically driven aquatic systems result from (1) the impact of the magnitude of air–water exchange on phytoplankton trophic status (biomass and growth rate), and (2) the impact of air–water exchange on POPs concentrations in phytoplankton (Dachs et al., 2000). These combined processes result in lower PCB concentrations in zooplankton at increased biomass concentrations, due to a dilution effect (particle dilution). Similar effects are expected for phytoplankton. Further, higher growth rates lead to lower PCB concentrations in the phytoplankton due to dilution by the new organic matter introduced in the ecosystem (growth dilution) (Dachs et al., 2000). Since biomass productivity at low latitudes is limited, it would be expected that POPs uptake and settling processes would not be very important at these latitudes. Indeed, Dachs et al. (2002) demonstrated, using a combination of field measurements of atmospheric PCBs, PCDDs, and PCDFs, and remote sensing data of ocean temperature, wind speed and chlorophyll, that deposition in mid-high latitudes is driven by sinking marine particulate matter, rather than by cold condensation. However, the relative contribution of this process is highly dependent on the physical chemical properties of the POPs under consideration.

11.14.2.1.2 Contaminant classification

Hence, it appears that, independent of the distribution mechanism, physical–chemical properties govern the impact of the various mechanisms on the POPs, resulting in differential latitudinal fractionation (Bidleman, 1999; Wania and MacKay, 1996). To capture partitioning behavior, Wania and MacKay (1996) proposed a classification of POPs as a function of octanol–air partition coefficient (K_{OA}), vapor pressure of the subcooled liquid (PL), and condensation temperature (T_c). As shown in Table 1, four categories of global transport behavior are proposed, ranging from low to high mobility, for a range of POPs.

It has been argued that the K_{OA} values can be used as a unifying property for describing volatilization of POPs from soils and sorption to aerosols. The limited experimentally obtained values typically are supplemented by estimates from octanol–water and air–water partition coefficients. The value of condensation temperature lies in its ability to estimate sorption of atmospheric contaminants to aerosols (Bidleman, 1988). At T_c, the chemical is equally partitioned between the gas phase and aerosols. Since POPs exist in the atmosphere both as gases (vapor phase), and in condensed form adsorbed to aerosol particles, the characteristic temperature of condensation provides a measure of depositional preference (Wania and MacKay, 1996). Hence, based on the integration of this information, it is argued that PCBs, PCDDs, and most organochlorine pesticides will preferentially accumulate in mid-latitude to polar regions. Since these regions also exhibit the highest phytoplankton biomass (Dachs et al., 2002) as a source for POPs uptake and particle sinking, they may represent a sink for POPs.

11.14.2.2 Biogenic Pollutants and Anthropogenic Non-POPs

In accordance with the rationale presented earlier, biogenic organohalides such as the halomethanes, and anthropogenic sources such as the chlorofluorocarbons (CFC), methylchloroform, and carbon tetrachloride are highly mobile and are atmospherically dispersed without significant depositional impacts (Table 1), as they tend to exhibit log K_{OA} values of less than 6.5 (Wania, 2003). Their global environmental impacts are predominantly derived from their long residence times which allow for substantial migration into the stratosphere. Here, solar UV photolysis results in dechlorination and ozone depletion reactions. This is particularly the case for the chlorofluorocarbons (Sherwood Rowland, 1991). Despite their global distribution, some deposition as a result of atmospheric gas exchange with natural waters has resulted in the presence of CFCs in young groundwaters (recharged within the last

Table 1 Global transport behavior of POPs.

Classification	*Low mobility*	*Relatively low mobility*	*Relatively high mobility*	*High mobility*
Global Transport Behavior	Rapid deposition and retention close to source	Preferential deposition and accumulation in mid-latitudes	Preferential deposition and accumulation in polar latitudes	Worldwide atmospheric dispersion, no deposition
Chlorobenzenes			5–6 chlorines	0–4 chlorines
PCBs	8–9 chlorines	4–8 chlorines	1–4 chlorines	
PCDD/Fs	4–8 chlorines	2–4 chlorines	0–1 chlorine	
Organochlorine pesticides	mirex	Polychlorinated camphenes, DDTs, chlordanes	HCB, HCHs dieldrin	
log K_{OA}	10	8	6	
log P_L	−4	−2	0	
T_c (°C)	+30	−10	−50	

After Wania and MacKay (1996).

50 years), resulting in diurnal, weekly and seasonal patterns (Ho et al., 1998), which has allowed for groundwater dating provided information on the local or regional emissions is available. Similarly, evidence has been presented suggesting that anaerobic sediments and soils may represent a sink for CFCs, as a result of microbial uptake (Lovley and Woodward, 1992). Similarly, the distribution of biogenic halomethanes in the atmosphere as the result of emissions from tropical forests and marine biological activity exhibits environmental impact derived from atmospheric oxidation reactions, and wet deposition of the resulting acid intermediates. The air–water exchange for the halomethane compounds is thought to be limited, and the net fluxes are in the direction of (re-)volatilization. The presence of other alkyl halides of anthropogenic origin such as the chloroethenes and tetrachloromethane in groundwaters and surface waters are usually considered to be the result of local discharges (e.g., Lendvay et al., 1998a,b), rather than from atmospheric sources as described for the CFCs.

The impact of deposition on global distribution has been noted for the CFC replacements hydrochlorofluorocarbons (HCFCs), the chlorinated solvents tetrachloroethene (PCE), and trichloroethene (TCE), as these compounds undergo gas phase oxidation and photochemical degradation, resulting in the formation of carbonyl halides (e.g., CCI_2O) and haloacetyl halides (e.g., bromo-, chloro-, and fluoroacetates). As these compounds are polar and water soluble, they are transported via aerosols, rain, and fog, which impacts their tropospheric lifetime and depositional fluxes (Rompp et al., 2001; de Bruyn et al., 1995). It is not clear whether and to what extent there is evidence of latitudinal fractionation of these compounds.

11.14.3 Sources and Environmental Fluxes

Halogenated hydrocarbons in the atmosphere and biosphere are derived from a large number of natural and anthropogenic sources. The ultimate environmental sinks for most halogenated compounds, whether they are released to the atmosphere or directly discharged in waterways, are the Earth's soils, sediments, and waterways (**Figure 1**). Little is known about the relative contributions of point sources and nonpoint sources of contamination. The global distribution and fluxes of aryl (e.g., polychlorinated biphenyls, dibenzo-*p*-dioxins and dibenzofurans, and halogenated pesticides) and alkyl (e.g., C_1–C_4 chlorinated, fluorinated, iodinated, and brominated alkanes) halides are better established. Through a comparative assessment of areas affected by urbanization and relatively pristine areas such as remote lakes, anthropogenic sources (e.g., industrial effluents) may be distinguished from natural halogenated hydrocarbon production mechanisms and pathways. Since the 1990s, it has become clear that most halogens, particularly chlorine, bromine, and iodine, participate in a complex biogeochemical cycle. Whereas environmental phase partitioning and transport are expected to dominate the environmental behavior of halogenated hydrocarbons, their reactivity in soils and sediments impact the natural and anthropogenic sources and global mass balances of these chemicals. The focus of this chapter will be on quantifying the impacts of reactivity on environmental behavior, while recognizing the multiplicity of controls on their biogeochemistry.

11.14.3.1 Adsorbable Organic Halogens

Frequently, halogenated hydrocarbons in environmental matrices are quantified, in bulk, by a standard analytical procedure for adsorbable organic halogens (AOX). Originally conceived to monitor the formation of chlorinated organic compounds in drinking water, the data derived from environmental characterization have been interpreted as an indicator of anthropogenic activity (Kuhn et al., 1977). For example, in Germany, AOX concentrations of 5 $\mu g\,l^{-1}$ were used to discriminate between negligible and moderate influence of industrial activity (Hoffman, 1986). Later studies indicated that the apparent relationship between AOX and industrial activity was affected by another environmental variable, the amount of organic matter present (Asplund et al., 1989). In a subsequent review on the natural occurrence of halogenated hydrocarbons in 135 lakes in southern Sweden (Asplund and Grimvall, 1991), AOX concentrations of 11–185 $\mu g\,Cl\,l^{-1}$ were observed, with correlations to both color (pigmentation, Pt) and total

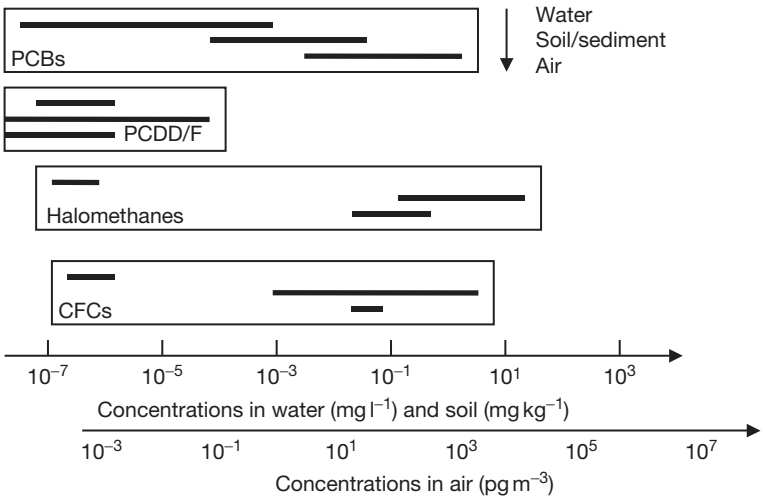

Figure 1 Distribution of selected aliphatic and aromatic organohalides in various environmental compartments.

organic carbon (TOC) (Figure 2). The ratio of halogenated hydrocarbons to organic carbon for soil samples was very stable (0.2–2.8 mg Cl per g C). In surface water samples of diverse origin, the ratio was higher (0.8–14.5 mg Cl per g C) and exhibited more variation. Mass balances for AOX, based on long-range atmospheric deposition of industrial compounds predicted an average concentration of only 15 μg Cl l^{-1} in bulk precipitation, indicating that natural production may be a substantial source of halogenated hydrocarbons. This hypothesis was further supported by the observation that AOX concentrations in runoff were, on average, 10-fold higher than in precipitation.

Indeed, in recent years evidence has emerged for the existence of a natural chlorine cycle (Figure 3) involving production and mineralization of halogenated hydrocarbons at the air–soil interface affecting deposition, volatilization, and leaching processes (Oberg, 2002). This is not surprising considering that chlorine, one of the most abundant elements, represents the sixth most common constituent of soil organic matter (0.01–0.5% DW) and is deposited globally through the action of sea spray (range: <1 kg ha^{-1} inland to 100 kg ha^{-1} in coastal areas). Hence, up to tons of AOX can be found per km^2 in some environments (Oberg, 1998). Despite published reviews on the subject (e.g., Gribble, 1996; Oberg, 2002), discussion on the chlorine cycle is not yet fully integrated in the biogeochemistry literature on the microbial ecology of biodegradation and biotransformation (Adriaens et al., 1999). The number of naturally produced chlorinated compounds is on the order of 1500, and covers alkenes, alkanes, terpenes, steroids, fatty acids, and glycopeptides, including compounds previously assumed to emanate exclusively from anthropogenic activity (Adriaens et al., 1999; Oberg, 2002). Most of these compounds have been shown to undergo microbial and abiotic transformation reactions resulting in the liberation of the halogen ions in the environment (Section 11.14.5). As opposed to mineralization, halogenated hydrocarbons are formed in many micro- and macro-ecosystems via the following processes: intra- and extracellular defense mechanisms (e.g., Neidleman and Geigert, 1986), biosynthesis (Harper et al., 1990), and production of reactive (e.g., HOCl) catalysts to oxidize organic substrates (Oberg et al., 1997; Johansson et al., 2000). From a biotransformation perspective, the halogenated (chlorinated) substrates have been shown to serve as a source of carbon and/or energy generation to (mostly) bacteria (Adriaens and Hickey, 1994; Adriaens and Vogel, 1995; Adriaens et al., 1999; Adriaens and Barkovskii, 2002). The structural similarity between anthropogenic and natural compounds may explain why some microorganisms have evolved the capability to respire or otherwise degrade selected halogenated hydrocarbons (van der Meer et al., 1992; Holliger and Schraa, 1994; Copley, 1998).

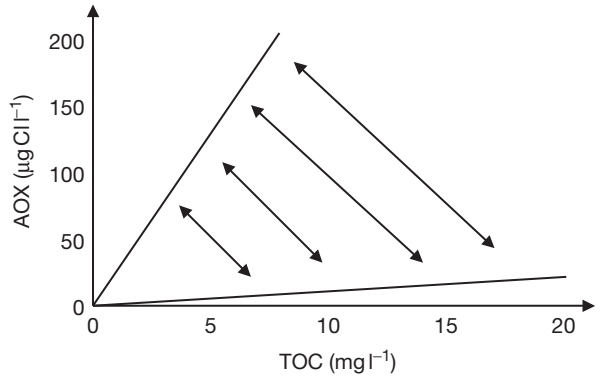

Figure 2 Concentration ranges (in delineated area) of AOX as a function of color and TOC in Swedish lakes and rivers (after Asplund and Grimvall, 1991).

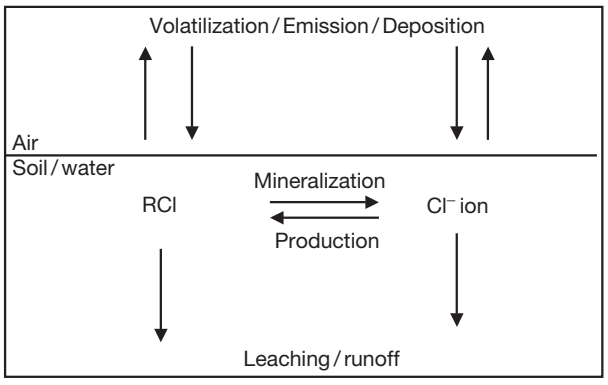

Figure 3 A conceptual model of the chlorine cycle in soils, with dominant processes indicated (after Oberg, 2002).

These observations point towards the shortcomings of using AOX as the sole source and mass balance indicator for halogenated hydrocarbons, and this operational designation would only be useful when known point sources of contamination (e.g., pulp mills and chemical manufacturing) or natural production (e.g., forest soils) are present. Sufficient chemical resolution of the composition of AOX will be required to further dissect the source attribution of selected aliphatic and aromatic compounds (Dahlman et al., 1993, 1994; Johansson et al., 1994; Laniewski et al., 1995).

11.14.3.2 Alkyl Halides

The natural and anthropogenic production of alkyl halides has recently been studied (Laturnus et al., 1995, 2002; Watling and Harper, 1998; Carpenter et al., 1999; Giese et al., 1999). This group of compounds is composed of methanes (CFC, tetrachloro-, trichloro-, chloro-, bromo- and iodo-, diiodo-, and chloroiodo-), propanes (1- and 2-iodo-, 1-iodo-2-methyl-), butanes (1- and 2-iodo), acetates (trifluoro-), and ethenes (tetrachloro-, trichloro-). Whereas naturally produced alkyl halides tend to be substituted with one or two halogens, those of industrial origin are generally poly-substituted (Key et al., 1997). Chloromethane and bromomethane are the most abundant halogenated hydrocarbons in the atmosphere (Butler, 2000; Harper et al., 2001), with the former catalyzing an estimated 17% of ozone destruction. Only CFC11 ($CFCl_3$) and CFC12 (CF_2Cl_2) exhibit greater ozone-depleting effects (Harper, 2000). In contrast to the CFCs, chloro- and bromomethane are mainly of nonindustrial origin. For example, as of early 2000s, 50% of the global annual input (4×10^{12} t) of chloromethane cannot be accounted for (Butler, 2000). Important sources that have been previously omitted from

mass balance calculations include halogenated hydrocarbons resulting from natural oxidation processes during degradation of organic matter, biomass burning, oceanic emissions, wood rotting fungi, and release by higher plant species (Keppler et al., 2000; Harper, 2000; Watling and Harper, 1998; Rhew et al., 2000; Laturnus et al., 2002). Even though a significant contributor of halomethanes was believed to be of marine origin, the ocean is, for the most part, undersaturated in bromomethane and insufficiently supersaturated in methyl chloride to explain more than a small percentage of the total atmospheric flux (**Figure 1**; Butler, 2000).

Evidence has indicated that terrestrial–coastal ecosystems, and abiotic formation mechanisms under acidic, iron-reducing conditions may help explain the flux deficit (Rhew et al., 2000; Yokouchi et al., 2000; Keppler et al., 2000; Dimmer et al., 2001). For example, the median biotic fluxes of halomethanes ($CHCl_3$, CH_3Br, CH_3Cl, CH_3I) from peat land ecosystems were estimated to be on the order of $(0.9–4.5) \times 10^9$ g year^{-1}, with the highest values incurred for chloroform and the lowest for bromomethane (Dimmer et al., 2001). Marine algae and vegetation in coastal marshes have been identified as potential sources of bromo- and chloromethane (Rhew et al., 2000), as well as of volatile iodinated C_1–C_4 hydrocarbon production (Giese et al., 1999). Fluxes from coastal marshes may account for up to 10% of atmospheric halomethanes, and those of microalgae ranging from 0.005% to 3%. Wood-rotting fungi (particularly *Phellinius* and *Inonotus* Basidiomycetes) have long been recognized as significant sources of chloromethane emissions, resulting from biosynthesis pathways (Watling and Harper, 1998). Estimations of the global fungal contributions are dependent on assumptions for the amount of woody tissue decomposed, chloride content of wood, and the global abundance of chloromethane-releasing species, and are on the order of 1.6×10^5 t year^{-1} with 75% emanating from tropical forest. Those same characteristics and enzyme systems which allow Basidiomycetes to decompose complex organic matter also allow these fungi to degrade complex halogenated hydrocarbons such as polychlorinated biphenyls (PCBs) and chlorophenols to low molecular weight compounds which are released in the environment and often incorporated in soil organic matter (de Jong and Field, 1997). However, the relative trends of formation as compared to degradation have not been assessed, and thus the impact of environmental transformation processes to halogenated hydrocarbon flux reduction is not known.

Lastly, a relatively recently identified source is the abiotic formation of halocarbons in acidic soils amended with the halide ion in the presence of elevated concentrations of iron (III). Considering the importance of insoluble iron(III) oxide and oxyhydroxides in the sedimentary environment, elevated salinities in soils, and the availability of organic carbon, the potential of this mechanism to release halomethanes is substantial (Keppler et al., 2000). Interestingly, this reaction is independent of microbial activity and sunlight. One important means to help discriminate between the contributions of the various biotic and abiotic sources to haloalkane production may be the application of carbon isotope ratios (Harper et al., 2001). Isotopic fractionation values have now become available for biogenic sources, allowing investigators to discriminate between fungal and plant contributions to chloromethane production.

11.14.3.3 Aryl Halides

Substantial insights have been gleaned into the sources and biogeochemistry of target aryl halides (mostly POPs), such as fluorinated organics (Key et al., 1997), polychlorinated dibenzo-*p*-dioxins (PCDD) and furans (Baker and Hites, 2000a,b; Cole et al., 1999; Gruden et al., 2003; Gaus et al., 2002; Lohmann et al., 2000), polychlorinated biphenyls (Ockenden et al., 1998a,b; Breivik et al., 2002a,b), toxaphene (Swackhamer et al., 1999; James et al., 2001), and organochlorine pesticides (McConnel et al., 1998; Lee et al., 2000). Based on a comprehensive inventory of the types and sources of chemical contamination in the environment, Swoboda-Colberg (1995) identified the petrochemical and pesticide industry as the main sources of aryl halides. Particularly, the herbicide and wood treatment industry have used (1) simple aromatic compounds (e.g., chlorobenzenes, chlorophenols) and their derivatives (e.g., chlorophenoxyacetates), (2) cyclodienes (e.g., heptachlor, dieldrin, heptasulfan), and (3) organonitrogen pesticides (e.g., alachlor, linuron). The natural production of aryl halides discharged into the environment by plants, microorganisms, marine organisms and other processes is rapidly being recognized as a fully integrated component of the biosphere (Gribble, 1996). This fraction is comprised of chlorinated pyrroles and indoles, as well as phenols, phenolic ethers, benzenes, hydroquinone, and orcinol methyl ethers (**Figure 4(a)**). Combustion and biotic formation processes have been identified as sources for the natural (non-anthropogenic) production of aryl halides, such as PCDD/F (Bumb et al., 1980) and other aromatically bound halogens (Dahlman et al., 1993; Gribble, 1996). Particularly Basidiomycetes have a widespread capacity for halogenated hydrocarbon biosynthesis and degradation (de Jong and Field, 1997). Many aryl halides have biotic origin, provided the right precursor molecule is present. For example, aerobic wastewater treatment processes and extracellular soil enzymes such as peroxidases and laccases have been demonstrated to produce PCDD and PCDF from chlorophenol precursors (Svenson et al., 1989). Anaerobic processes result in natural dechlorination processes and the formation of lesser chlorinated, and thus more soluble and volatile, compounds (Häggblom, 1992; Adriaens et al., 1999; Gruden et al., 2003). Even including these processes, it has been suggested that environmental levels exceed known natural and anthropogenic sources by a significant margin, resulting in the conundrum that measurements of depositional fluxes exceed known emissions.

In a review, Baker and Hites (2000a) conducted an extensive mass balance investigation on PCDD/F, and estimated that annual emissions are on the order of 3000 kg year^{-1} with depositional fluxes totaling $(0.3–1) \times 10^4$ kg year^{-1}. Most of the mass balance discrepancy was found to be due to the octachlorinated dioxin congener (OCDD), which is dominant in most terrestrial environments. Based on time trends of dioxin profiles in Siskiwit Lake (Lake Superior) sediment cores, it was argued that photochemical synthesis of OCDD from pentachlorophenol (PCP) in atmospheric condensed water may be a more substantial source of OCDD than combustion (Baker and Hites, 2000b). With sediments identified as the ultimate sinks for aryl halides, there is substantial interest in ongoing attenuation processes relevant to these systems. Gevao et al. (1997), using PCB analysis in a dated sediment core

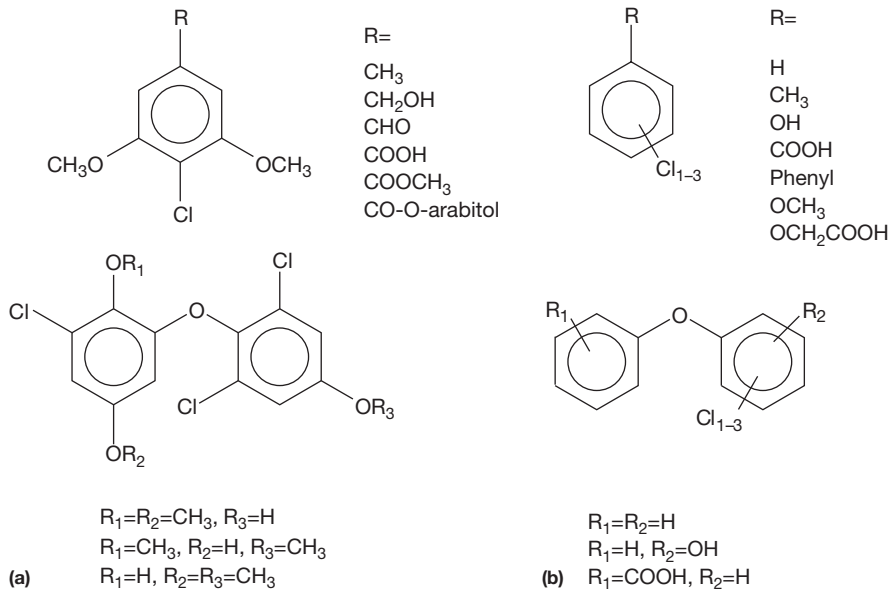

Figure 4 Selected structural features of aromatic organohalides produced by Basisiomycetes in soils (a), and degraded by microorganisms (b).

(Estwaithe Water, UK), demonstrated a predominance of lesser-chlorinated congeners in more recent sediments. This trend may indicate a postdepositional mobility of PCBs favoring the diffusive transport of the more soluble and volatile congeners of the overall pool of PCBs in these sediments.

Further evidence for re-emission of the PCB sediment burden via the water column to the atmosphere was obtained by Jeremiasson et al. (1994) in a mass balance study in Lake Superior. A similar mechanism may be operative in the Hudson–Raritan estuary, where dioxin profiles at the air–water interface were dominated by dichlorinated PCDD (diCDD) (Lohmann et al., 2000). Fugacity calculations indicated the water column as the source, however, dioxin profiles in the sediment column were only analyzed for tetra- to octaCDD. It is unclear whether the diCDD constitute original source material or are the result of environmental transformation (dechlorination) processes (Gruden et al., 2003). Gaus et al. (2002) provided supporting evidence for the potential contribution of natural dechlorination reactions to the alteration of dioxin profiles in sediments. Based on analysis of a global range of sediments, the authors observed the existence of a 'sediment pattern' rich in 1,4-chlorines which increased with time (depth), indicating that the chlorines in 2, 3,7, and 8 positions may have been selectively removed. The nomenclature is shown below:

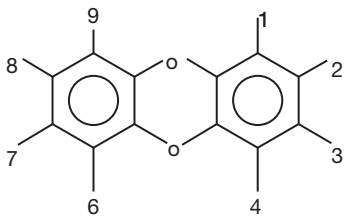

Nomenclature for PCDDs

To demonstrate the relevance of dioxin formation processes in sediments, Barabas et al. (2003) applied environmental forensics tools (polytopic vector analysis) to deconvolute sediment (Passaic River, NJ) dioxin patterns in a number of source and reactivity constituents. In addition to the validation of a half dozen source patterns, the authors were able to extract a dechlorination pattern which was depleted in heptaCDD and enhanced in 2,3,7,8-tetraCDD. This pattern was responsible for up to 7% (mean: 3%) of the total sample variance in a 12-mile stretch of the river, and the loading of the profile generally increased with depth, indicating a correlation between time and pattern occurrence. Further analysis of structured (undisturbed) sediment cores indicated that the dechlorination contribution to the presence of TCDD was ~90–100% in samples with low total dioxin loadings. Considering the similarity in structural features between biogenic aryl halides and aryl halides that have been biologically degraded, these versatile microbial degradation processes likely contribute significantly to the chlorine cycle (**Figure 4(b)**).

11.14.4 Chemical Controls on Reactivity

The existence of a chlorine cycle and the scattered evidence of biogeochemical cycles for halogenated hydrocarbons involve a wide range of environmentally relevant reaction mechanisms and pathways leading to their widespread distribution and matrix-dependent profiles. The extent to which biotic and abiotic reactions influence the chlorine (halogen) cycle depends on complex interactions between the intrinsic molecular properties of these compounds and characteristics of the environment.

11.14.4.1 Phase Partitioning

The elemental composition, structure, and substituents found in natural and anthropogenic halogenated hydrocarbons influence the physical–chemical properties of these compounds, and thus their distribution between the various environmental phases as well as their intrinsic molecular reactivity. Vapor

pressure, aqueous solubility, octanol–water partition coefficient, and octanol–air partition coefficient are the predominant properties that dictate the partitioning of the compounds between the various environmental phases (e.g., Cole et al., 1999; Harner et al., 2000). Fugacity calculations are the primary means for interpreting, correlating, and predicting the multimedia concentrations of halogenated hydrocarbons (MacKay, 1991). Since the three 'solubilities' (air, water, octanol) generally demonstrate a linear but inverse correlation to LeBas molar volume, it would follow that bulkier molecules are less soluble in all three matrices. For example, the aqueous solubilities of halogenated C_1 and C_2 alkanes and alkenes are 2–8 times higher than those of the most soluble (lesser chlorinated) PCBs; the solubility range of PCB congeners themselves spans five orders of magnitude between mono- and octaCDD (Schwarzenbach et al., 1993). The presence of polar functional groups such as hydroxyl, carboxyl, or methyl substituents tends to increase the solubility. Conversely, the less water-soluble compounds have the tendency to partition into solvent, lipid, or organic phases.

These properties and principles govern the transfer of organic chemicals between different environmental compartments. Of particular interest to halogenated hydrocarbon reactivity discussed in this treatise is the air–water interface (emissions, water column outgassing), and the solid–water interface (sorptive processes, sequestration, mineral-mediated reactions). For example, the role of air–water diffusive exchange in large aquatic systems may provide a source or sink for volatile compounds such as the halomethanes (Butler, 2000), PCBs (Achman et al., 1993; McConnell et al., 1998; Zhang et al., 1999), toxaphene (Swackhamer et al., 1999), organochlorine insecticides (McConnell et al., 1998), and PCDD/F (Lohmann et al, 2000). The solid–water interface is perhaps the most dominant phase transfer affecting reactivity in the terrestrial environment, as halogenated hydrocarbons undergo a wide range of matrix interactions, including nondestructive processes such as sorption and sequestration (Luthy et al., 1997), and destructive processes such as microbial, organic- and mineral-mediated transformations (Adriaens et al., 1999; Adriaens and Barkovskii, 2002). Sorption and sequestration processes are strongly influenced by the structural features (backbone and functional groups), and the characteristics of the naturally occurring humic substances (e.g., Dahlman et al., 1993). It is widely believed that these sequestration processes limit the availability of halogenated hydrocarbons to biotic and abiotic reactions or catalysts. These complex biogeochemical interactions will be discussed in more detail in **Section 11.14.5**.

11.14.4.2 Reaction Energetics

The propensity of halogenated hydrocarbons to react in the various relevant environmental compartments is often explained in terms of the energetic properties associated with their chemical structure (Dolfing and Harrison, 1992; Lynam et al., 1998; Tratnyek and Macalady, 2000). These properties include, but are not limited to, redox potential ($E^{0\prime}$, mV), Gibbs free energy of formation ($\Delta G^{0\prime}$, kJ/reaction), carbon-halogen bond strength, and ionization potential. **Figure 5(a)** illustrates that the redox potential of most halogenated hydrocarbons corresponds to the range where microbial iron- and nitrate-reduction prevail. Hence, these compounds are likely susceptible to biological reduction (resulting in dechlorination/dehalogenation) as they reside in a range where the addition of electrons is energetically favorable.

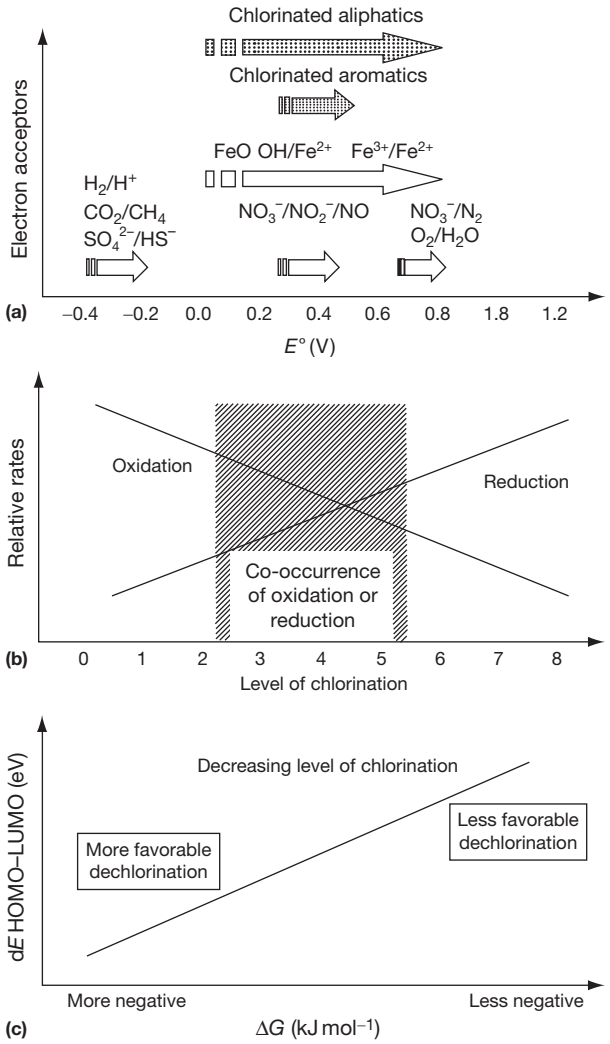

Figure 5 Thermodynamic parameters associated with organohalide reactivity: (a) electon accepting species versus redox potential; (b) relative importance of oxidation versus dechlorination rates as a function of number of chlorines [1-8]; and (c) trend between energy difference of the HOMO and LUMO electron layers and Gibbs free energy of reaction.

By similar reasoning, we can further conclude that oxidation reactions will be most favorable for the lesser-halogenated isomers. This concept is illustrated in **Figure 5(b)** where relative rates of oxidation and reduction are plotted as a function of level of chlorination. In practice, the literature has revealed that there may be a (chemical-dependent) zone where oxidation and reduction reactions are equally likely. This zone captures aryl halides with four to six chlorines, and alkyl halides with one to three chlorines per molecule. **Figure 5(c)** shows a trend between the Gibbs free energy for reductive dechlorination and the HOMO–LUMO gap (HOMO = highest occupied molecular orbital, LUMO = lowest unoccupied molecular orbital). It has been argued that the size of the gap is directly correlated to compound reactivity, as it reflects the energy barrier associated with electron transfer. Hence, higher

chlorinated (halogenated) compounds would, according to this plot, be chemically more reactive than lesser-halogenated isomers. It should be noted that there has been very limited biochemical validation of this concept, though correlations are apparent during reductive dechlorination and OH radical oxidation. Other molecular descriptors of chemical reactivity of halogenated hydrocarbons, such as electronic, steric, and hydrophobic parameters, have widely been used to predict reaction kinetics as a function of substituent effects, and to probe reaction mechanisms (Peijnenburg et al., 1992; Lynam et al., 1998; Zhao et al., 2001; Lindner et al., 2003).

11.14.5 Microbial Biogeochemistry and Bioavailability

Microbiota, reactive surfaces, and natural organic matter, represent the main causative agents affecting halogenated hydrocarbon transformation and mineralization reactions in the terrestrial environment. This is accomplished by a complex web of interactions between the ecophysiology (structure and function) of microbial communities and the inorganic geochemical characteristics (dissolved and solid phases), which is mainly controlled by the energetics of the prevailing oxidation and reduction reactions involved in the carbon cycle (Adriaens et al., 1999; Adriaens and Barkovskii, 2002). The extent to which these reactions affect the fate of halogenated hydrocarbons is determined by the governing matrix interactions.

11.14.5.1 Ecological Considerations

A fundamental issue in the biogeochemistry of natural environmental systems is the means by which organic carbon transport, geochemical processes and microbial activity combine to produce spatial and temporal variations in redox zonation. The development of redox zones is based on the availability of labile (i.e., biodegradable) organic carbon which can be oxidized, and solid or soluble inorganic compounds which can be used as electron acceptors (reduced) by microbial activities (Chapelle et al., 1996; Christensen et al., 2000). The succession of terminal electron accepting processes (TEAPs) proceeds in order of decreasing redox potential and free-energy yield, and is generally in the order of: oxygen reduction, nitrate reduction, manganese reduction, iron reduction, sulfate reduction, and methanogenesis. For more in-depth discussion on this topic, please refer to Bjerg et al. (**Chapter 11.16**). Since the reduction potential of a given redox couple depends on both the abundance and speciation (free, complexed, solid) of the electron donors and acceptors, the prevailing TEAPs in anaerobic environments are often dictated by the available mineral forms of iron and sulfur (Heron and Christensen, 1995; Postma and Jacobson, 1996; Jacobson et al., 1998). The extent of reduction of these species is then controlled by the availability of labile organic matter. Since the development of redox zones is a nonequilibrium process it has been argued that fermentation reactions, which provide soluble labile organic compounds (acetate, hydrogen), are the rate limiting processes in establishing the prevailing TEAP (Postma and Jacobson, 1996).

Generally, in the presence of labile organics or contamination, the TEAP sequence results in increasingly oxidized conditions at distance from the source of organic. Whereas the redox clines (distances for redox gradients) are on the order of millimeters within soil aggregates and vertical sediment cores (Henrichs and Reeburgh, 1987; Fenchel et al., 1998), they can range from meters to tens of meters in groundwater systems (Chapelle, 1993; Christensen et al., 2000). Largely controlled by solute transport in the matrix under consideration (refer to **Section 11.14.5.2**), the occurrence and extent of each TEAP is dependent on the concentrations of both the electron donor and electron acceptor, the presence and activities of microbial populations, and the temporal changes in site hydrology (Christensen et al., 1997; Hunter et al., 1999). Hence, to interpret TEAP conditions in natural systems, the relative depletion of electron acceptors (or oxidation capacity, OXC) or accumulation of reduced respiration products (total reduction capacity, TRC) is usually complemented with redox and dissolved hydrogen gas measurements, and verified with microbial community analysis (Chapelle et al., 1996; Ludvigsen et al., 1997; Lendvay et al., 1998a,b; Skubal et al., 2001; McGuire et al., 2000). TEAP conditions and redox zonation affect the chemical form, mobility, and persistence of many anthropogenic contaminants and natural halogenated hydrocarbons alike, due to the direct or indirect activities (e.g., the accumulation of reactive iron oxides or sulfides) of the prevailing microbial communities (e.g., Adriaens et al., 1999; McCormick et al., 2002a). The various catabolic contributions of microbiota to environmental transformation processes and pathways will be discussed in **Section 11.14.6**.

Limited quantitative information is available on the fluxes and reactivity of organic matter in soils and subsurface environments (**Figure 6**). With concentrations of low molecular weight (labile) organic matter (whether dissolved or solid-associated) in uncontaminated aquifers on the order of ng l^{-1} to μg l^{-1}, the rates of biogeochemical transformations in these oligotrophic environments tend to be orders of magnitude lower than those found in surface soils or lake and marine sediments (e.g., Capone and Kiene, 1988; Murphy and Schramke, 1998; Hunter et al., 1999). Estimates for carbon oxidation rates in pristine groundwater systems have been measured and calculated based on geochemical modeling to be $\sim 10^{-3}$–10^{-8} mmol CH_2Ol^{-1} day^{-1} (Murphy and Schramke, 1998), and approximately one to two orders of magnitude higher in contaminated environments (Ludvigsen et al., 1998). These rates are not constant, but are dependent on the fluxes of dissolved organic carbon (DOC) and geochemical species (e.g., Skubal et al., 2001).

In sediments, the rates of redox zone development in sediment depth profiles are strongly correlated with sedimentation rates (Henrichs and Reeburgh, 1987). Indeed, spatial and temporal variations in microbial processes have been observed in terrestrial, estuarine, and coastal aquatic sediments: aerobic and denitrifying activity is confined to the top few centimeters of sediments, sulfate-reduction has been observed over 50–60 cm of sediment thickness, which is underlain by a zone of methanogenic activity (Skyring, 1987; Carlton and Klug, 1990). Thus, sulfate-reduction is expected to be the dominant process responsible for organic matter oxidation to carbon dioxide in estuarine and coastal sediments, unless high sedimentation ratios prevail and methanogenic conditions develop in the deeper layers (Skyring, 1987). Sulfate-reducing processes significantly affect porewater and sediment chemistry, including a decrease in pH with a concurrent rise in alkalinity and sulfides, carbonate precipitation, ammonia production, and reduction of iron(III) hydroxide minerals by

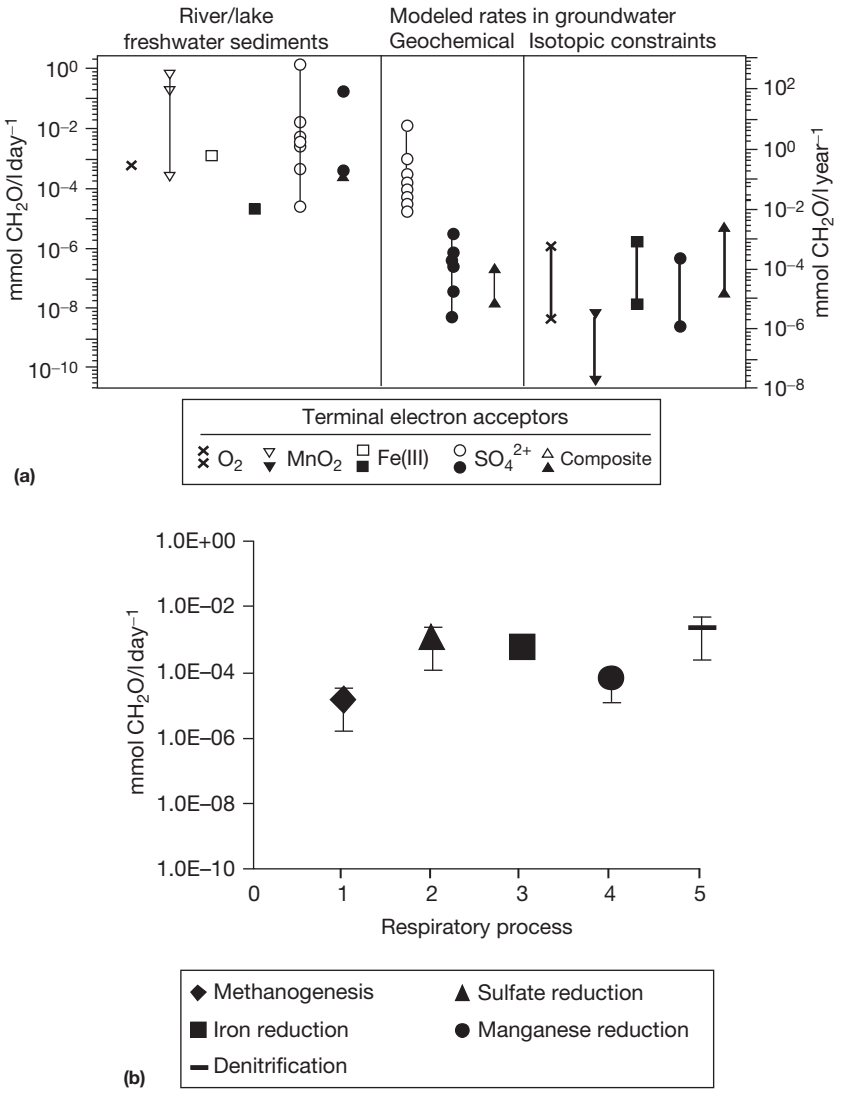

Figure 6 Distribution of reported organic matter turnover under the various TEAPs in pristine surface water sediments and groundwater aquifers (a) and landfill-leachate contaminated groundwater (b). The respiration rates in pristine groundwater ((a) middle and right panels) were modeled using total electron acceptor species concentration (geochemical) and carbon isotope fractionation (isotopic constraints) (after Murphy and Schramke, 1998 and Ludvigsen et al., 1998).

sulfides. Estimated carbon oxidation fluxes from sediments of varying geochemistry range from 3 to 458 mmol C m^{-2} day^{-1} (Capone and Kiene, 1988). The predominant global contributions to anaerobic carbon metabolism occur in shallow sediments (7.5–1300 g C m^{-2} $year^{-1}$ and estuaries and bays (2–150 g C m^{-2} $year^{-1}$). Of the various electron acceptors, sulfate ((370–1300) $\times$ 10^{12} g C $year^{-1}$ is the predominant contributor to global carbon production as compared to oxygen ((150–1900) $\times$ 10^{12} g C $year^{-1}$ nitrate ((20–84) $\times$ 10^{12} g C $year^{-1}$, and methane ((30–52) $\times$ 10^{12} g C $year^{-1}$) (Henrichs and Reeburgh, 1987).

In topsoils, the development of redox zones is directly related to the soil volumetric water content ($cm^3$of water per cm^3), as this determines the composition and activity of soil biota (Fenchel et al., 1998). Water potential is affected by both solute and matrix characteristics, which subsequently affect the ecophysiology of microorganisms. The soil biota which are of interest to this chapter include bacteria, and low-water potential-tolerant fungi. The impact of water and oxygen limitations on the terrestrial nitrogen cycle have been well documented and affect the relative rates of ammonification, respiration, nitrification, and denitrification (Tiedje, 1988). The carbon equivalent oxidation fluxes due to denitrification globally amount to (13–233) $\times$ 10^{12} g C $year^{-1}$ (including wetlands). Taking into account all soil respiration processes on the order of 6 $\times$ 10^{16} g C $year^{-1}$ are liberated into the atmosphere (Schlesinger, 1991). Hence, the flux of oxidation equivalents in topsoils and sediments govern the geochemical cycling of the subsurface and, by governing relevant biogenic production and biomineralization activity, has potentially the greatest impact on the chlorine cycle.

11.14.5.2 Matrix Interactions

The physical–chemical properties of halogenated hydrocarbons in general, and of aryl halides (mainly POPs) in

particular, include relatively low vapor pressures (aryl halides), high octanol–water partition coefficients, very high octanol–air partition coefficients, and generally low solubility. These features, in combination with the complex chemical characteristics of natural soil and sediment organic matter, affect the availability of these compounds to biochemical or abiotic reactions (Luthy et al., 1997). Additionally, due to the multitude of reactive phenolic and carboxylic functional groups in sediment organic matter and many aryl halides (or their transformation products), ample opportunity exists for cross-linking and other sequestration reactions (Luthy et al., 1997; Adriaens et al., 1999; Adriaens and Barkovskii, 2002) which remove these contaminants effectively out of the biogeochemical cycle controlled by transport and phase partitioning processes.

The incorporation of parent halogenated hydrocarbons or their transformation products in soil organic matter has been indicated by the formation of operationally defined 'polar material' and polymeric humic substances by addition or condensation reactions (Scheunert et al., 1992; Adriaens and Barkovskii, 2002). Particularly under aerobic conditions, phenolic dimers or polymers, humic addition products, and condensation products have been observed (Andreux et al., 1993). Apparently a significant fraction of anthropogenic halogenated hydrocarbon molecules (and their transformation products) can ultimately be incorporated in natural soil constituents. A factor which complicates the evaluation of soil-bound residues is that all organic matter recovered from natural sites, including that which is not contaminated, is chlorinated to some extent due to the incorporation of inorganic salts in low and high molecular weight humic-like substances (e.g., Oberg, 1998). Numerous attempts have been made to identify the types of structures in organic matter found in the environment (e.g., unpolluted waters, marine sediments, and coniferous forest soils) that are chlorinated. Using an oxidative degradation technique, several mono- and dichlorinated aromatic structures, exhibiting hydroxy-, methoxy-, and ethoxy-substituents have been detected (e.g., Dahlman et al., 1993); however, the chlorine bound to such structures corresponded to a small fraction of the total organic chlorine (AOX). Considering that the natural AOX can often exceed the anthropogenic AOX in concentration, the absolute determination of matrix-bound material as the result of microbial degradation reactions as compared to microbial formation reactions may be difficult to estimate.

Transport in porous matrices also affects the availability of halogenated hydrocarbons to microbial or abiotic reactions. In soils or sediments where advective fluid flow is minimal, transport is governed by diffusion, whereas in groundwater systems both advective and diffusive transport processes are operative. Field measurements for sorbed halogenated hydrocarbons in sediments indicate that transport of even the most soluble components is on the order of decade-long time frames for centimeters distance (e.g., Gevao et al., 1997; Zhang et al., 1999). Halogenated hydrocarbons in topsoils (and water bodies), which are exposed to significant diurnal or seasonal temperature changes, undergo advection-driven (heat) air–surface exchange processes in timeframes on the order of hours to days (e.g., Lee et al., 2000). Similarly, in low organic sandy/silty groundwater aquifers, advective transport, in combination with substantial longitudinal dispersion and sorption mechanisms, controls the movement of halogenated hydrocarbons on the order of centimeter per day (Wiedemeier et al., 1999).

11.14.6 Environmental Reactivity

Halogenated compounds have been distributed in the ambient environment in one form or another for millions of years. Even compounds such as dioxins appear to have been formed in million-year old ball clays (Ferrario and Byrne, 2000) by as of yet unknown mechanisms, and are by-products during natural incineration processes such as forest fires. In addition, plants, algae, and microorganisms produce and release these compounds for various physiological and ecological reasons, indicating that some latent activity for biosynthesis and biodegradation may have evolutionary roots. Thus, it is not surprising that our knowledge of microbial degradation pathways for stable environmental contaminants keeps expanding, as new enrichment techniques aimed at harnessing and exploring the microbial ecological potential are developed (Palleroni, 1995; Fathepure and Tiedje, 1999).

Aside from microbial mediation, halogenated hydrocarbons and inorganic halide ions may be transformed in the environment by a variety of abiotic species including reduced or oxidized organic matter, reactive surfaces, and other soluble species (Adriaens et al., 1996; Fu et al., 1999; Butler and Hayes, 2000; McCormick et al., 2002a). By definition, abiotic reaction implies that no direct microbial mediation is required. Thus, these reactions are not necessarily limited to the terrestrial environment (e.g., photolysis, hydroxide radical-mediated oxidation). Indirectly, anaerobic microbial populations such as iron-, manganese-, and sulfate-reducers are responsible for the formation of reactive biogenic minerals and surfaces (Fredrickson and Gorby, 1996; Rugge et al., 1998; Thamdrup, 2000; McCormick et al., 2002a). Considered collectively, the abundance of photoreactive particles in atmospheric aerosols (Andreae and Crutzen, 1997), as well as the reducing power of the estimated (1500–2000) $\times$ 10^{12} g organic carbon stored in soil layers (Post et al., 1982), indicate that terrestrial and atmospheric abiotic reactivity has the potential to exceed biotic transformation in the global biogeochemical chlorine (halogen) cycle. While limited mass balances have been developed on the global distribution and fluxes of halogenated hydrocarbon formation, estimates of degradation fluxes in the global environment have not been developed, and the information available is at best limited to local contamination burdens. To limit the extent of the review, only those processes that have applicability to natural terrestrial environmental systems will be described.

11.14.6.1 Microbial Reactivity

The microbiology of halogenated hydrocarbon transformation has been discussed in a number of treatises over the years (Vogel et al., 1987; Häggblom, 1992; Mohn and Tiedje, 1992; Adriaens and Hickey, 1994; Adriaens and Vogel, 1995; Adriaens et al., 1999; Adriaens and Barkovskii, 2002). Since the present chapter includes alkyl and aryl halides, this section will review the most salient features of the enzymes and degradation processes relevant to these compounds, under aerobic and anaerobic conditions. Among all microbiota that may participate in the halogen cycle, fungi will be featured separately, as they have been found to substantially contribute to halogenated hydrocarbon formation, as well as biodegradation (de Jong and Field, 1997).

The evolution of regulators and catabolic genes has resulted in an extraordinary metabolic versatility of microorganisms to transform or mineralize halogenated hydrocarbons, either via growth (energy-coupled) or nongrowth (cometabolic; nonenergetic) processes (**Table 2**). Whereas the latter are often operationally defined based on specific laboratory conditions, increasing evidence suggests that many aryl and alkyl halides are involved as fortuitous inducers controlling pathway-specific regulation, even though they do not serve as substrates for catabolic enzymes (Fathepure and Tiedje, 1999; Copley, 1998). This gratuitous induction may then result in a partial transformation of the halogenated substrate, often resulting in enzyme inhibition (van Hylckema-Vlieg et al., 2000). The cometabolic nature of dehalogenation has, however, undergone a substantial revision during the 1990s, due to the discovery of a novel microbial respiration process, dehalorespiration. This process allows many anaerobic microorganisms to generate energy through the promotion of a proton-motive force resulting from the dechlorination step (Holliger and Schraa, 1994; Fathepure and Tiedje, 1999). Hence, for these organisms to thrive in contaminated environmental systems, halogenated compounds (e.g., chloroethenes, chlorobenzoates, chlorophenols, PCDD) need to be present as the electron acceptors, and simple organic acids (e.g., acetate, formate, ...) as the electron donors. The presence of dehalorespiring microorganisms has been demonstrated globally, in halogenated hydrocarbon-impacted environments. Considering the redox potentials of aryl and alkyl halides (**Figure 5(a)**), these processes are energetically very favorable as they are at par with iron and nitrate reduction. Indeed, environmental transformation of halogenated hydrocarbons has been observed across the entire spectrum of respiratory TEAP zones (Adriaens et al., 1999).

Table 2 Examples of halogenated and nonhalogenated compounds degraded via microbial growth and cometabolic processes

Process	*Halogenated*	*Nonhalogenated*
Mineralization		
Aerobic	Mono-, dichlorobenzenes/ benzoates/phenols; 2,4-D; 2,4,5-T; chlorinated aliphatic acids	BTEX, saturated/ unsaturated hydrocarbons, naphthalene, creosote compounds
Anaerobic	Chlorobenzoates/ phenols, dichloromethane	BTEX, aliphatic acids
Co-metabolism		
Aerobic	Di-pentachlorobenzenes/ benzoates/ phenols/ biphenyls; mono-dichlorodioxins/furans; chloroethenes;	PAH; long chain/ branched hydrocarbons
Anaerobic	Di-hexachlorobenzenes, di-decachloro biphenyls; di-octachlorodioxins; PCE, trichloromethane; DDT; Lindane	PAH, aliphatics

Abbreviations: 2,4,-D: 2,4-dichlorophenoxyacetic acid; 2,4,5-T: trichlorophenoxyacetic acid; BTEX: benzene, toluene, ethylbenzene, xylenes; PAH: polycyclic aromatic hydrocarbons.

Acclimation of microorganisms to halogenated hydrocarbons in the environment has resulted in a wide range of aerobic and anaerobic mechanisms to initiate aryl halide degradation, including oxidative, hydrolytic, and reductive dehalogenation, via novel recruitment and adaptation of proteins (Copley, 1998; van der Meer et al., 1992). Whereas the oxidative and reductive processes occur predominantly under strictly aerobic and anaerobic conditions, respectively, hydrolytic processes prevail in aerobic and micro-aerophilic conditions. Some studies have indicated, e.g., the importance and ubiquity of haloalkane dehalogenase, dichloromethane dehalogenase, tetrachlorohydroquinone dehalogenase, and perchloroethylene and trichloroethylene reductive dehalogenases (reviewed in Copley, 1998). It appears that complete or partial halogen removal is the predominant first step during microbial transformation of many important halogenated pollutants, resulting in the accumulation of hydroxylated and/or lesser halogenated intermediates (**Table 3**). Hydroxylated aromatics are considered 'activated' as the functional group destabilizes the aromatic II-electrons. In contrast, hydroxyalkanes are precursors for microbial dehydrogenase and hydroxylase activity. The compounds are then rendered more susceptible to other chemical transformations, such as ring cleavage and the formation of carboxylated acids, resulting in the production of catabolic intermediates to enter the tricarboxylic acid (TCA) or derivative cycles. The extensive removal of halogens through reductive dehalogenation under anaerobic conditions allows either for aerobic processes to commence, or for hydrogenase- and hydratase-type of anaerobic ring reduction and hydrolysis to produce catabolic intermediates (Adriaens and Hickey, 1994; Adriaens et al., 1999).

Table 3 Enzyme classes capable of transforming and dehalogenating organohalides under aerobic and anaerobic conditions

Enzyme class	*Substrates*	*Reaction*
Monooxygenases (e.g., methane, peroxidases...)	Alkanes (C_1-C_{18}) Alkenes (C_2) Aromatics (phenol, toluene,....)	$RX + O_2 \rightarrow ROH + H_2O + X^-$ $ArX + O_2 \rightarrow ArOH + H_2O + X^-$
Dioxygenases	Alkenes (C_2) Aromatics (benzene, naphthalene,....)	$RX = RX + O2 \rightarrow$ unstable oxirane+ halogenated by-products $ArX + O_2 \rightarrow Ar(OH)_2$
Ring-cleavage dioxygenases	(Halogenated) 1,2-dihydroxy-aromatics	$Ar(OH)_2 + O_2 \rightarrow$ (halogenated) *ortho*- or *meta*-ring fission products
Dehalogenases (haloalkane, DCM, PCE/TCE reductive, aromatic hydrolytic)	Aliphatic acids, Aromatic acids	$RX + H_2O \rightarrow ROH + HX$ (aerobic) $RX + H_2 \rightarrow RH + HX$ (anaerobic) $ArX + H_2O \rightarrow ArOH + HX$ (aerobic) $ArX + H_2 \rightarrow RH + HX$ (anaerobic)

Abbreviations: DCM: dichloromethane; PCE: perchloroethene; TCE: trichloroethene.

Observations of these reactions in the natural environment indicate that they take place on the order of years per chlorine removed for aryl halides in sediments (Brown et al., 1987; Adriaens et al., 1999; Fu et al., 2001; Gaus et al., 2002), and months to years for alkyl halides or pesticides in groundwater (Potter and Carpenter, 1995; Wiedemeier et al., 1999; Skubal et al., 2001). Accurate calculations account for the metabolic rates measured in sediments or soils (Henrichs and Reeburgh, 1987; Schlesinger, 1991; Murphy and Schramke, 1998). For example, Fu et al. (2001) estimated the rate of cometabolic dioxin dechlorination in estuarine Passaic River sediments at 3–8 pg of diCDD per gram sediment per year, based on sediment respiration rates, and the ratios of dioxin dechlorination as compared to methane production, which represented the dominant TEAP under which these reactions occurred.

Whereas all previously described degradation reactions are catalyzed by archea and bacteria or by unspecified populations under various TEAPs, Basidiomycetes or wood-rotting fungi appear to be responsible for both biotic halogenated hydrocarbon production (e.g., **Figure 4**), and their transformation or mineralization (de Jong and Field, 1997). The source of organic chlorine in soil, and its subsequent volatilization has been ascribed to haloperoxidases, a group of enzymes that catalyzes the halogenation of humic substances in the presence of hydrogen peroxide and halide ions (Neidleman and Geigert, 1986). Chloroperoxidases oxidize chloride, bromide, and iodide and have been extracted from the fungus *Caldariomyces fumago*, in soil extracts and in spruce forest soils (Laturnus et al., 1995; Asplund and Grimvall, 1991; Asplund et al., 1993). The enzyme activity is pH-dependent (2.5–4.0), and its specific activity decreases with depth. The main reactive chlorine formed is HOCl, which then reacts with any other organic substrate for biodegradation purposes, while forming organic chlorine as a by-product (Johansson et al., 2000). Aside from this haloperoxidase-like activity in (mainly) forest soils, halogenated hydrocarbons (>80 identified to date), and halomethanes are produced by 68 genera from 20 different Basidio-mycete families (de Jong and Field, 1997; Watling and Harper, 1998). The aryl halides include anisyl (methoxylated chlorobenzyl) compounds (15–75 mg kg^{-1} wood or litter), monomeric and polymeric hydroquinone methyl ethers (74–2400 mg kg^{-1}), orcinol (dimethoxy) methyl ethers, anthraquinones, and a wide range of other compounds (de Jong and Field, 1997). Many of these compounds are produced for physiological functions such as antibiotic activity and lignin degradation. The haloalkanes are dominated by chloro- and bromomethane, as indicated earlier.

Besides halogenated hydrocarbon production, the Basidiomycetes are also capable of aryl halide mineralization, and hence part of the *de novo* biosynthesized halogenated hydrocarbons may be fully mineralized. The remainder becomes incorporated into humus (de Jong and Field, 1997), and may produce PCDD/F as a by-product (de Jong et al., 1994). The white-rot fungi, which are capable of degrading hemicellulose, lignin, and cellulose through an extracellular, oxidative enzyme system, also have the capability to biotransform a wide range of chlorinated pollutants via a nonspecific free-radical mechanism (e.g., Bumpus et al., 1985; Barr and Aust, 1994). These pollutants include aliphatic halogenated hydrocarbons such as chloroform, trichloroethylene, and tetrachloromethane (**Table 3**). Aromatic halogenated hydrocarbons degraded by white rot fungi include chlorolignins (bleach kraft mill effluents), pentachlorophenol, PCDD/F, PCBs, and pesticides such as DDT (1,1,1-trichloro-2,2-bis (4-chlorophenyl)ethane) and atrazine with mineralization wrates ~10–70% (reviewed in de Jong and Field, 1997). The balance between production and mineralization of the more complex aromatic by-products is unclear, but all evidence points towards a net accumulation (Oberg, 2002). For example, Watling and Harper (1998) describe the accumulation of chloroanisyl compounds at 15–75 mg kg^{-1} in wood or litter colonized by fungi in forest environments, and the presence of chlorinated hydroquinone metabolites at levels ranging from 74 mg kg^{-1} to 2400 mg kg^{-1} in fungal tissue.

11.14.6.2 Surface-Mediated Reactivity

Since the 1990s, there has been a trend toward using zero-valent metals to dehalogenate groundwater contaminants via surface-mediated reactions (e.g., Gillham and O'Hannesin, 1994; Matheson and Tratnyek, 1994). Since these reactive metals are not indigenous to natural environments, this section will consider the analogous manner in which biogenic ferrous and sulfidic minerals may contribute to the chlorine cycle. Iron is the fourth most abundant element in the Earth's crust, accounting for 3.6% by mass (on average) of Earth's surface rocks (Martin and Meybeck, 1979). In contrast, sulfur is the fourteenth most abundant element in the Earth's crust with the content of surface rocks varying from 0.027% to 0.240% by mass (Bowen, 1979). This abundance in many natural environments (soils, groundwater, surface water) sustains substantial dissimilative iron reduction and sulfate reduction in the presence of labile organic matter. It is then not surprising that these respiratory processes, and their associated microbial communities (DIRB: dissimilatory iron reducing bacteria; SRB: sulfate reducing bacteria) are dominant in marine, estuarine, and many groundwater environments. More importantly with respect to the present chapter, DIRB and SRB activity results in the accumulation of a variety of reactive iron-oxides, -hydroxides, and -sulfides as their respiratory end-products (Fredrickson et al., 1998; Lovley, 1991; Rickard, 1969; Rickard et al., 1995; Vaughan and Lennie, 1991; Zachara et al., 2002).

The variety of common oxidation states encountered for iron (II, III) and sulfur(−II, 0, II, IV, VI) results in complex and varied speciation for these elements in natural environments. Limiting the scope to only those oxidation states and species that commonly support anaerobic respiration, narrows the discussion to primarily the oxides of iron(III) and sulfur(II, IV, VI). Oxides of Fe(III) are primarily found as insoluble oxide or hydroxide particle coatings and aggregates (Thamdrup, 2000), and can comprise several mass percent of freshwater or marine sediments (Coey et al., 1974; Raiswell and Canfield, 1998; Thamdrup, 2000). The ferrous iron, Fe(II), that is produced as a consequence of iron respiration may accumulate in solution, adsorb to the surfaces of surrounding minerals or become incorporated into new biogenic minerals through a variety of chemical or microbially mediated pathways (schematically represented in **Figure 7**). In contrast to the oxides of Fe(III), the oxides of sulfur form soluble oxyanions that may be found in a variety of mixed oxidation-state polynuclear complexes (Erlich, 1996). Those

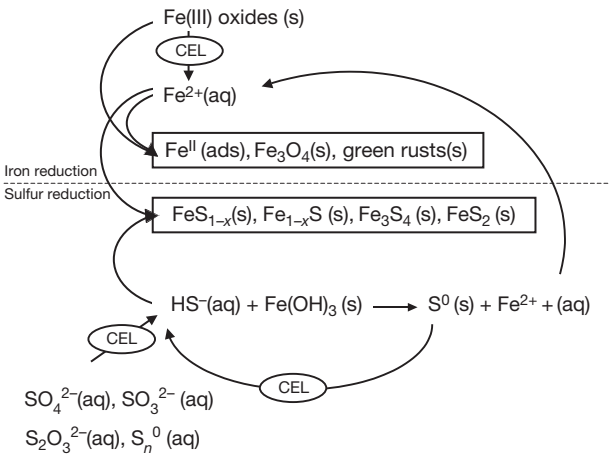

Figure 7 Formation of mineral and sorbed Fe(II) species under iron-reducing conditions. (source McCormick et al., 2002b)

most commonly known to support anaerobic respiration include sulfate (SO_4^{2-}), sulfite (SO_3^{2-}), and thiosulfate ($S_2O_3^{2-}$). However, elemental sulfur can also serve as a terminal electron acceptor for some species of eubacteria and archea (Schauder and Kroeger, 1993). The ultimate and most common product of sulfur respiration is sulfide, S(−II). In the presence of iron, biogenic S(−II) can precipitate as numerous insoluble sulfides, including pyrite (FeS_2), mackinawite (FeS_{1-x}), pyrrhotite ($Fe_{1-x}S$), and greigite (Fe_3S_4) (Rickard, 1969; Rickard et al., 1995). As indicated by **Figure 7**, collectively DIRB and SRB can significantly alter the chemical and mineralogical speciation in their environment.

Despite the importance of biogeochemical iron- and sulfur-cycling (Rickard et al., 1995; Schlesinger, 1991; Lovley, 1997; Erlich, 1996), the ability of biogenic ferrous and sulfidic minerals to mediate organohalide transformations has received limited attention. The thermodynamic feasibility of these reactions to occur under iron-reducing conditions is illustrated in **Figure 8**, which incorporates some of the dominant redox couples (mineral and biological) relevant to this TEAP. The range of substrates presently known to undergo dechlorination in the presence of reduced iron oxides and iron sulfides includes, among others: tetrachloromethane, hexachloroethane, tetra- and trichloroethylene, bromoform, chloropicrine, hexachlorobenzene, and possibly PCBs (Kriegman-King and Reinhard, 1992; Svenson et al., 1989; Butler and Hayes, 2000; Cervini-Silva et al., 2000). Since most of these studies were confined to abiotic laboratory systems, it is difficult to assess the relative impact of surface-mediated reactions on organohalide fluxes in the natural environment. However, some insights may be gleaned from a recent study by McCormick et al. (2002a), who compared the reaction kinetics of tetrachloromethane transformation in the presence of the dissimilative iron-reducer *Geobacter metallireducens* and biogenic magnetite generated by this same strain. Due to the abundance of reduced mineral surfaces, the abiotic contribution to CCl_4 transformation was found to be at least two orders of magnitude greater than the cell mediated (co-metabolic) reaction (McCormick et al., 2002a). Considering that the reported dechlorination rates observed with iron sulfides are orders of magnitude faster than those with reduced iron oxides (Butler and Hayes, 2000), it is likely that the contribution of these solids will exceed the microbial rates as well.

11.14.6.3 Organic-Matter-Mediated Reactivity

Soil and sediment organic matter affect environmental transformation reactions through direct participation in reduction (e.g., dechlorination) and oxidation (halogenation) reactions (e.g., Svenson et al., 1989; Barkovskii and Adriaens, 1998; Fu et al., 1999; Keppler et al., 2000), or by serving as an electron acceptor for microbial respiration (Lovley et al., 1996). The latter reaction has been coupled to the microbial capability to oxidize vinyl chloride and *cis*-dichloroethene (Bradley et al., 1998). With quinonic and phenolic groups constituting from 13% to 56% (molar concentration) of all oxygen functional groups in natural organic matter (Schlesinger, 1991), environmental transformation reactions mediated by natural organic matter may potentially contribute significantly to the fate of halogenated hydrocarbons (Oberg, 1998, 2002).

Couples such as hydroquinone/quinone have been hypothesized to dominate the redox properties of humic and fulvic acids, and to act either as electron transfer mediators or as the direct donors of electrons for dechlorination reactions (Schwarzenbach et al., 1990; Dunnivant et al., 1992). For example, it has been shown in sediment–water systems that the rates of alkyl halide reduction increase with organic matter content (Peijnenburg et al., 1992). Further support for this hypothesis was obtained by Svenson et al. (1989), who reported a first-order dependence between rates of hexachloroethane reduction and hydroxyl concentrations. Aside from alkyl halides, structural features of organic matter have been shown to catalyze (Fu et al., 1999) or accelerate (Barkovskii and Adriaens, 1998) the dechlorination of dioxins (**Figure 9**).

A correlation between reaction rates, molecular structure of the humic or fulvic acid, and content of reactive sites is more difficult to demonstrate. It has been hypothesized that the hydroquinone or quinone is the main reactive site for electron transfer during dechlorination reactions. Phenolic acidity, as based on the inflection point during titration of organic matter, is indicative of the hydroquinone content within humic materials. Published information indicates that the quinone content of humic acids is generally higher than for fulvic acid (Stevenson, 1994).

In their study on the reductive dehalogenation of hexachloroethane, carbon tetrachloride, and bromoform, Svenson et al. (1989) found that the addition of humic acid or organic matter from aquifer material to aqueous solutions containing bulk electron donors increased the reduction rate by up to 10-fold. Although they did not determine the phenolic acidity, Peijnenburg et al. (1992) established a positive correlation between the reductive rate constants of a range of aryl halides and the organic carbon content of sediment systems. According to the rationale outlined earlier, a humic material with high hydroquinone/quinone content should facilitate a more effective electron transfer to electron acceptor molecules. Just as organic matter-mediated formation has been argued to contribute substantially to the global production of halomethanes, the involvement of humics in environmental

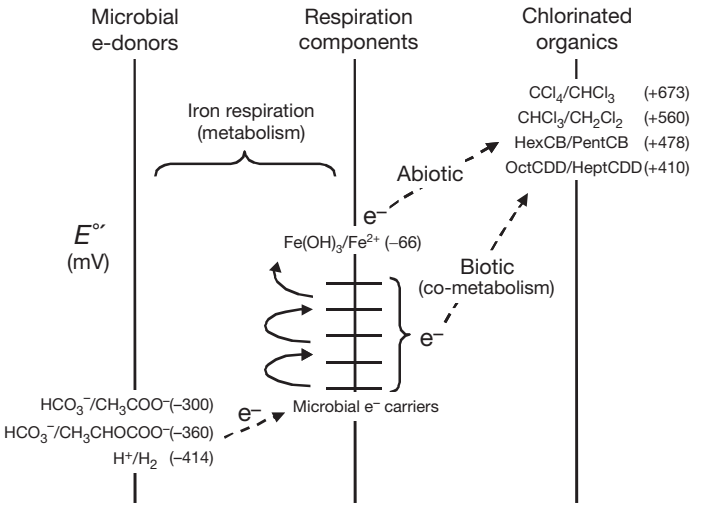

Figure 8 Comparison of microbial, mineral, and chloromethane redox pairs under iron-reducing conditions (after McCormick et al., 2002a).

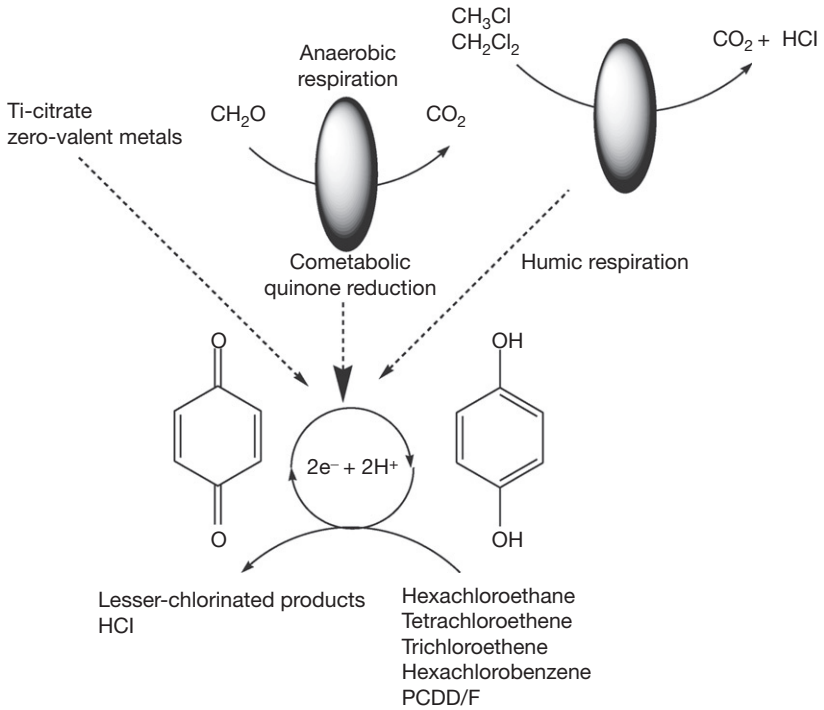

Figure 9 Model representation of organic-mediated dehalogenation reactions in the presence (oval) and absence of microorganisms.

dehalogenation reactions of trace halogenated hydrocarbons may be more substantial than currently assumed. Support for this hypothesis may be derived from observations that dioxin dechlorination patterns in sediment systems (Albrecht et al., 1999) indicate the influence of a humic-dechlorination signature in model systems (Fu et al., 1999). The predominant congener endpoints observed in the model systems of Fu et al. (1999) were also observed at the air–water interface in the estuary from which the sediments were obtained (Lohmann et al., 2000), pointing towards the possible occurrence of a dioxin cycling mechanism influenced by organic catalysis.

11.14.6.4 Predictive Models: Structure–Reactivity Relationships

Structure–activity relationships (SARs) between chemical reactivity and molecular descriptors (**Figure 10**) for both alkyl and aryl halides are valuable tools to explore mechanistic determinants influencing activity, and to predict rate constants for environmental transformation within classes of compounds (Wolfe et al., 1980; Moore et al., 1990; Hermens et al., 1995). An abundance of these statistically significant correlations based on appropriate predictor variables is available, yet very few of these yield useful quantitative structure–activity

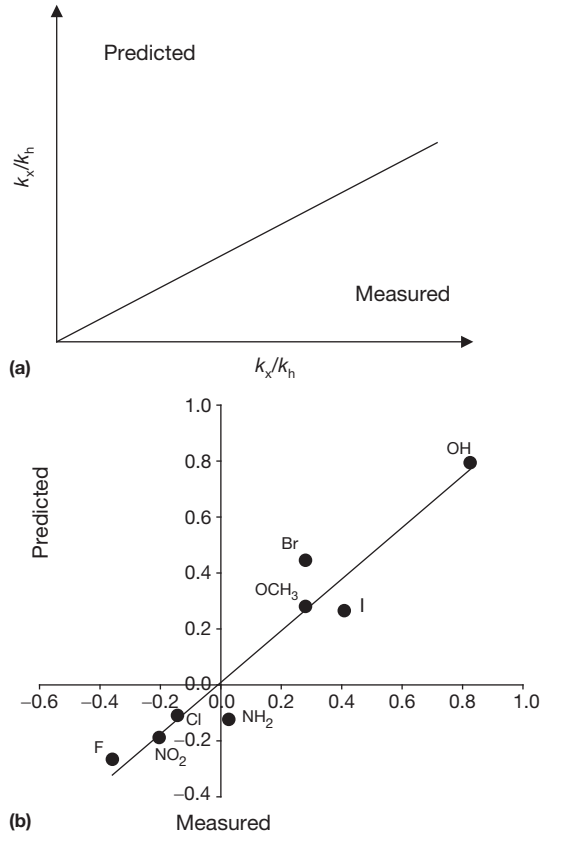

$k_x/k_h = 3.36 - 7.58(2.68)\ ^{12}C + 0.59(0.25)\ E_S - 0.56(0.23)\ \log K_{ow};\ R^2 = 0.92$

Figure 10 Theoretical (a) and practical (b) representation of QSARs. Panel b describes a QSAR for the methanotrophic oxidation (activity of methane mono-oxygenase) of *ortho*(C_{12})-substituted biphenyls. The structural backbone was biphenyl, and the substituents considered included all halogens, methyl-, methoxy-, hydroxyl-, nitro-, and amino-moieties (Lindner et al., 2003). The molecular descriptors used in (b) are ^{12}C (charge on the *ortho*-carbon), E_s (Taft's steric parameter), and log K_{ow}.

relationship expressions (QSARs). One of the limitations is the scarcity of relationships between readily available molecular descriptors and important microbial transformation reactions. Another relates to the lack of understanding of the contaminant–matrix interactions that govern the degradation process. Perhaps not surprisingly, the most robust SARs and QSARs have been generated for strictly abiotic transformation processes such as hydrolysis, direct photolysis, and oxidation. More recently, correlations have been generated describing fortuitous degradation processes (e.g., reductive dechlorination) or for enzymes exhibiting broad substrate specificities (e.g., soluble methane monooxygenase) (Roberts et al., 1993; Cozza and Woods, 1992; Rorije et al., 1995; Lynam et al., 1998; Lindner et al., 2003).

Most QSARs are based on the Hansch method, where biological response is expressed as a linear function of hydrophobic, electronic, and steric properties (refer to equation below and Figure 10; k_x = rate constant for substituted compound; k_h = rate constant for unsubstituted compound):

$$\frac{k_x}{k_h} = aX + bY + cZ + dX' + eY' + fZ' + gE + \text{error}$$

Descriptors: Electronic, Polar, Structural | Quantum-chemical | Environmental

Ab initio and semi-empirical molecular orbital calculations have been used to obtain molecular descriptors such as electron density distributions of the highest occupied II orbital, carbon–chlorine bond charges, heats of formation and ionization potentials, or HOMO–LUMO gaps (Okey and Stensel, 1996; Lynam et al., 1998; Zhao et al., 2001). One or more of these parameters have been found to be strongly correlated to the observed dechlorination pathways of dioxins and substituted benzenes (Cozza and Woods, 1992; Lynam et al., 1998), to the preferred methane monooxygenase oxidation pathways of *ortho*-substituted biphenyls (Lindner et al., 2003), or dioxygenase-mediated oxidation of dioxins and furans (Damborsky et al., 1998). For example, **Figure 10** shows a SAR between the measured and predicted oxygen uptake rates exhibited by a methanotrophic bacterium, *Methylosinus trichosporium* OB3b, against *ortho*(designated as C_{12})-substituted biphenyls. This particular SAR includes electronic (carbon charge), structural (compound width), and polarity (octanol–water partitioning coefficient) descriptors; no environmental or quantum-chemical descriptors were considered (Lindner et al., 2003).

Robust QSARs were developed to predict the reductive transformation constants of 45 halogenated monoaromatic hydrocarbons and 13 halogenated aliphatic hydrocarbons in anoxic sediments using either Hansch-type descriptors (the carbon–halogen bond strength, the summation of the Hammett sigma constants and inductive constants for the additional substituents, and the steric factors for these substituents) (Peijnenburg et al., 1992) or quantum-chemical descriptors (Rorije et al., 1995; Zhao et al., 2001). Whereas the electronic properties of the substituents exhibited a positive effect (increased the reaction rate), steric and bond strength factors decreased the predicted reaction rate. When the sediment organic matter content was included in the prediction, the electronic properties and quantum-chemical descriptors became less influential in predicting reaction rates. This indicates that the predicted reaction rate in more complex environmental samples is controlled by mass transfer limitations.

11.14.7 Implications for Environmental Cycling of Halogenated Hydrocarbons

The goal of this chapter was to assess the influence of environmental phase partitioning and transport on the biogeochemical cycling and terrestrial reactivity of halogenated hydrocarbons. Whereas the global environmental behavior with respect to POPs and non-POPs distribution can be described within regional or latitudinal contexts, the impact of terrestrial environmental transformations on contaminant biogeochemistry is of major importance at contaminant 'hot spots.' The biogeochemistry of volatile and semi-volatile halogenated hydrocarbons is very diverse and scale-dependent,

and differs in terms of major environmental reservoirs, transport pathways and transformation reactions. Particularly pertaining to the latter, the environmental degradation or mineralization fluxes and their contribution to the global halogenated hydrocarbon biogeochemical cycles are difficult to quantify, because of: (1) the local nature of the available databases of reactive surfaces, reactive organic matter, and microbial reactivity; (2) the differences in source characteristics of volatile, semi-volatile, and complex halogenated organic compounds; and (3) the slow natural reaction rates (especially degradation) relative to the overall environmental cycling of these contaminants.

Despite these limitations, the literature on the natural attenuation of anthropogenic substrates in terrestrial environments has provided some insights into environmental transformations affecting halogenated substrates under a wide range of environmental conditions, and may allow some extrapolations to regional or global impact (e.g., Wiedemeier et al., 1999; Lendvay et al., 1998a,b; Skubal et al., 2001). First, microbially mediated natural attenuation processes are abundant in contaminated environments, and affect the fate of hydrocarbons (e.g., Christensen et al., 1997; Bekins et al., 2001; Cozzarelli et al., 2001), chlorinated solvents (e.g., Lendvay et al., 1998a,b; Skubal et al., 2001), chlorinated pesticides (e.g., Potter and Carpenter, 1995; Zipper et al., 1998), and PCDD/F (Lohmann et al., 2000; Fu et al., 2001; Gaus et al., 2002) or PCBs (Brown et al., 1987; Flanagan and May, 1993) in a wide range of natural environments (soils, surface water sediments, groundwater). Second, there has been a bias towards the impact of biological processes on contaminant fate, and hence, the potential influence of abiotic reaction pathways is rarely considered. Finally, there is a dearth of quantitative contaminant mass balance estimates and fluxes associated with natural contaminated groundwater, sediment or soils, and those that are available are very local in scale.

In an attempt to assess the quantitative contribution of reactive processes to the overall cycling of anthropogenic source contamination, two examples will be considered: (1) vinyl chloride oxidation at groundwater–surface water interface (GSI) St. Joseph, Michigan (e.g., Lendvay et al., 1998a,b), and (2) dioxin dechlorination in estuarine sediment cores collected from the Passaic River, New Jersey (Albrecht et al., 1999; Fu et al., 2001). Case study 1 is relevant to the Great Lakes region, as 28% of the Michigan shoreline is affected by anthropogenic pollutants, with 600 sites contaminated by chlorinated solvents. The total estimated fluxes of all chlorinated solvents into Lakes Michigan and Huron, based on two sites recently investigated which were$\sim$10–30 kg year^{-1} (Lendvay et al., 1998a,b, 2002), would total (6–18) $\times$ 10^3 kg annually. Anaerobic dechlorination processes upgradient from the shoreline form lesser-chlorinated ethenes such as vinyl chloride and ethene, only 1–8% of which are then aerobically degraded at the GSI. Considering that this site and the Lake Michigan shoreline in general represent a 'high energy' GSI (in terms of seiche activity and reoxygenation of the aquifer) and may represent a 'best-case scenario' for natural attenuation at GSIs, the total contribution of microbial processes to minimizing alkyl halide fluxes to the Great Lakes is minimal, since >90% of the dissolved dechlorinated contaminant burden is discharged to the Lakes. Considering the elevated solubility of (lesser chlorinated) solvents (Schwarzenbach et al., 1993) limited transfer to the air–water boundary layer should be expected. However, the global fluxes of vinyl chloride and perhaps dichloroethenes discharged to surface water bodies as the result of anaerobic dechlorination processes in contaminant hot spots may be substantial. As indicated earlier, chloroethenes and particularly their atmospheric degradation products (carbonyl halides and acetyl halides) are subject to atmospheric transport and deposition and their source areas may be terrestrial or estuarine in origin.

The situation is somewhat different for POPs, such as chlorodioxins. Some estimates have indicated that up to 7% of the dioxin profile variance of the Passaic River sediments may be due to natural dechlorination (Barabas et al., 2003). Laboratory studies have indicated that mainly mono- and dichlorinated congeners can be expected to accumulate, at dechlorination rates on the order of one chlorine removed every seven years (Fu et al., 2001). One scenario suggests the lesser-chlorinated compounds would selectively diffuse up from buried sediments to the shallow layers (Gevao et al., 1997), where they then dissolve or are transported via particulate material (since lesser-chlorinated dioxins are sparingly soluble) and accumulate at the air–water interface (Lohmann et al., 2000). Estimated rates for diCDD production are in the picogram per gram sediment per year range, which could result in a global biotic production of tens of kilograms per year of diCDD alone, considering the volume of dioxin-contaminated sediments worldwide ($\sim$100 Mt; 3–15 Mt in the US). Similar rates, but higher concentrations can be expected for PCBs as the volume and concentrations of PCB-contaminated sediments are higher (Gevao et al., 1997; Breivik et al., 2002a,b). Average sediment and soil PCB concentrations are two to three orders of magnitude higher than PCDD, while the total impacted soil/sediment volume is probably similar to that of PCDD.

Overall, a meaningful synthesis of the processes influencing the distribution and cycling of aliphatic and aryl halides (**Figure 11**) within the context of biogeochemical controls requires a thorough understanding of the sources, reservoirs, transport pathways, transformation reactions, and scale dependence of each. Semi-volatile POPs, which include aromatic and alicyclic compounds, are mainly anthropogenic in nature. They exhibit a tendency to fractionate latitudinally, and undergo rapid air–water exchange processes resulting in frequent regional and latitudinal deposition and revolatilization. Based on mass flux estimates, the net flux is in the direction of deposition, which may eliminate a substantial fraction of the total POP load from the cycling process due to carbon sinking, soil or sediment biotransformation processes, POP sequestration in natural organic matter, and uptake by vegetation. Point releases of POPs in waterways sediments limit their cycling to the local or regional scale, through sequestration in sediment organic matter, re-release due to sediment disturbance, biogenic gas ebullition and upward diffusion of the more soluble compounds, ultimately impacting the air–water interface in estuaries. Preliminary results indicate that these processes impacting point sources may result in a net local or regional efflux to the atmosphere. Non-POP alkyl halides, which represent signature compounds derived from both biogenic and anthropogenic sources, are globally characterized by a net volatilization flux to the atmosphere and troposphere.

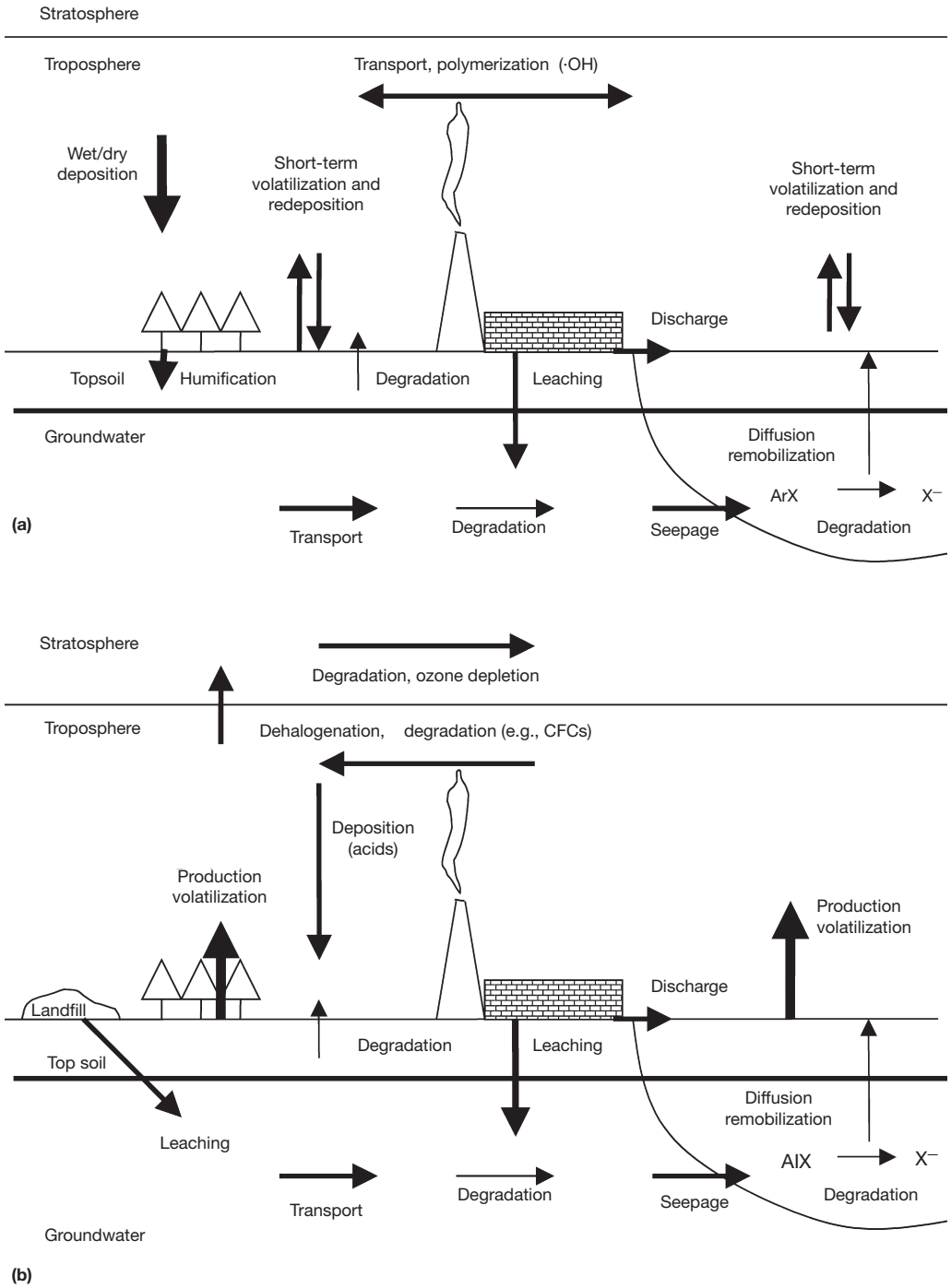

Figure 11 Schematic representation of biogeochemical cycling of aryl (a) and alkyl (b) organohalides in environmental systems (the thickness of the arrows indicate the relative importance of each process or pathway; note that the net flux of alkyl halides is towards volatilization, that of aryl halides towards deposition).

Deposition fluxes are thought to be less significant for the neutral parent compounds, but substantial for the atmospheric (ionic) degradation products. Considering the fairly rapid atmospheric reactions in clouds, the deposition fluxes are regional in nature, and no latitudinal fractionation has been observed. The multitude of point source releases of these compounds have resulted in locally impacted groundwaters and surface waters, where natural degradation reactions substantially contribute to their fate and transport, but are unlikely to impact the global biogeochemistry. Hence, Figure 11 is characterized by a difference in the relative importance of the fate pathways, sources, and sinks between POPs and non-POP halogenated hydrocarbons. Overall, the impact of biogenic production pathways, and degradation reactions on the scale of biogeochemical cycling is not clear at this time. Moreover, the impact of terrestrial environmental contaminant

formation, transformation, and sequestration reactions on explaining the global halocarbon deficit remains an open question.

11.14.8 Knowledge Gaps and Fertile Areas for Future Research

This chapter discussed the biogeochemistry of halogenated hydrocarbons in the environment with emphasis on environmental flux and reactivity, to develop a better understanding of the chlorine (halogen) cycle. A secondary goal was to integrate information on biotic and abiotic organochlorine production with their degradation processes in light of chemical and environmental controls on reactivity.

As has been indicated by many experts in the area of global cycling of POPs, analytical methods, and environmental characterization present a challenge to closing the mass balance of the chlorine cycle. AOX and aryl halides, as well as their transformation products tend to be associated with soil, sediment, and planktonic organic matter, either due to sorption or covalent bonding, which complicates the development of accurate mass balances and flux calculations, and quantitative analysis of natural transformation processes. As of early 2000s, several approaches are being explored to enable interpretation of the environmental fate of halogenated hydrocarbons. On a global and regional scale, the evaluative environments often used for modeling partitioning and transport behavior are being validated using increasingly comprehensive datasets on contaminants and environmental controlling variables such as wind speed, sediment resuspension, and remote sensing data on plankton blooms. Despite the availability of data and integrated models, the mechanistic understanding of global transport processes is highly dependent on adequate system description and characterization, which adds substantial spatial and temporal uncertainty to the interpretation of the data.

To address the issue of contaminant specificity relative to environmental reactivity and global transport, QSARs are becoming increasingly robust and will advance the modeling approaches to a new level (Grammatica et al., 2002). A fundamental assumption for this approach is that a change in compound structure results in a similar change in its behavior in the system. The parameters influencing reactivity should be chosen carefully, and relationships should be obtained using unbiased statistical analysis. Next-generation QSARs are currently being developed which include information on the genetic and physiological diversity of microorganisms within a given ecosystem. Another approach is based on contaminant fingerprint recognition in the environment, as a function of known sources and probable abiotic or biotic transformation processes. These fingerprints include congener, isomer, and enantiomer profiles, as well as isotopic fractionation. Evidence is emerging that these fingerprints may be able to discriminate between biotic and abiotic reactivity affecting halogenated hydrocarbons, as well as distinguish various source and sink contributions.

As testified by the multitude of reviews over the years, the fate of halogenated organic compounds as affected by microbial activity is extremely difficult to summarize, both with respect to pathways of transformation and reaction kinetics. This is due both to the great diversity in chemical structures (multiple and variable substituents) and the range of acclimation mechanisms and enzyme specificities. This review demonstrates that transition of mechanistic observations in the laboratory to fate prediction in environmental matrices is complicated by multiple attenuation processes and an overall lack of mass balance (due to either irreversible sequestration mechanisms or incomplete analysis for transformation products). Considering that these poorly understood issues have not even been resolved for PCBs and halomethanes, arguably the best-studied subsets of aromatic and aliphatic compounds; the state of the art with respect to their role and place in the chlorine (halogen) cycle has to be considered maturing at best.

Despite these limitations, great strides have been made during the 1990s with respect to understanding halogenated hydrocarbon biogeochemistry in terrestrial environments. Consider, e.g., the progress made in elucidating the genetic basis for microbial adaptation to structurally similar chemicals, and the requirements for transcriptional activation of key-metabolic enzymes in aryl and alkyl halide pathways. The breakthrough discovery that halorespiration and halogenation of natural organic matter may be more widespread than was previously assumed, opens up a vast array of new possibilities to understand the reactive component affecting the biogeochemistry of organohalides. Developments in molecular ecological characterization have afforded substantial advances in this area. For example, we can now monitor population shifts within complex communities as the result of aryl and alkyl halide induced stresses. Complementary to microbial research, the thermodynamic considerations of which transformations are likely to occur have aided in directing fate mechanism studies. First-principle (*ab initio*) model predictions have been shown to describe radical-catalyzed oxidations and reductions, and field observations have proven to be particularly useful to 'calibrate' fundamental research investigations on environmental fate predictions. Finally, the quantitative extrapolation of global POP uptake and the impact of sinking carbon has advanced a complementary mechanism for contaminant cycling to the temperature-controlled global fractionation deposition and revolatilization processes.

Ultimately, research in the halogen cycles and the interface between natural and anthropogenic fluxes is directed towards risk quantification and reduction, through research questions such as: "Do environmental transformation reactions reduce the exposure risk from organohalides?," "What is the role for organohalide transformation processes in controlling biogeochemical cycling?," "Do environmental sequestration and carbon sinking permanently remove POPs and other halogenated hydrocarbons from the global biogeochemical cycle?," or "What characteristics differentiate a POP from other environmental contaminants, and help explain their global distribution?" As of early 2000s, the incomplete information presents an enormous challenge to the regulatory community, as it is unclear how the available data should be incorporated into risk-based decision models. Hence, the field of biogeochemical contaminant cycling would significantly benefit from the weighted integration of phase partitioning, transport, and reactivity processes, by informing uncertainty-based geostatistical approaches across spatial (local impact on regional and global processes) and temperal (diurnal temperature controls on long-term reactivity) scales of interrogation.

Acknowledgments

The authors thank the Office of Naval Research, the National Science Foundation, the US Environmental Protection Agency (STAR Fellowship to MLM), the National Oceanic and Atmospheric Administration, and the Michigan Department for Environmental Quality for financial support. Since this document has not been submitted for review to either agency, no endorsement should be inferred. The lead author expresses his gratitude to all his students, postdocs, and technicians who have contributed to research providing insights in this important area during the last decade.

References

Achman DR, Hornbuckle KC, and Eiseneich SE (1993) Volatilization of polychlorinated biphenyls from Green Bay, Lake Michigan. *Environmental Science & Technology* 27: 75–87.

Adriaens P and Barkovskii AL (2002) Fate and microbial degradation of organohalides. In: Britton G (ed.) *Encyclopedia of Environmental Microbiology*, pp. 1238–1252. New York, NY: Wiley.

Adriaens P and Hickey WJ (1994) Physiology of biodegradative microorganisms. In: Stoner DL (ed.) *Biotechnology for the Treatment of Hazardous Waste*, pp. 45–71. Chelsea, MI: Lewis Publishers.

Adriaens P and Vogel TM (1995) Treatment processes for chlorinated organics. In: Young LY and Cerniglia C (eds.) *Microbiological Transformation and Degradation of Toxic Organic Chemicals*, pp. 427–476. New York, NY: Wiley.

Adriaens P, Chang PL, and Barkovskii AL (1996) Dechlorination of chlorinated PCDD/F by organic and inorganic electron transfer molecules in reduced environments. *Chemosphere* 32: 433–441.

Adriaens P, Barkovskii AL, and Albrecht ID (1999) Fate of chlorinated aromatic compounds in soils and sediments. In: Adriano DC, Bollag J-M, Frankenberger WT, and Sims R (eds.) *Bioremediation of Contaminated Soils, Soil Science Society of America/American Society of Agronomy Monograph*, pp. 175–212. Madison, WI: Soil Science Society of America Press.

Albrecht ID, Barkovskii AL, and Adriaens P (1999) Production and dechlorination of 2,3,7,8-tetrachloro-dibenzo-*p*-dioxin (TCDD) in historically-contaminated estuarine sediments. *Environmental Science & Technology* 33: 737–744.

Andreae MO and Crutzen PJ (1997) Atmospheric aerosols: Biogeochemical sources and role in atmospheric chemistry. *Science* 276: 1052–1058.

Andreux F, Scheunert I, Adrian P, and Schiavon M (1993) The binding of pesticide residues to natural organic matter, their movement and their bioavailability. In: Mansour M (ed.) *Fate and Prediction of Environmental Chemicals in Soils, Plants, and Aquatic Systems*, pp. 133–149. Boca Raton, FL: Lewis Publishers.

Asplund G and Grimvall A (1991) Organohalogens in nature. *Environmental Science & Technology* 25: 1346–1350.

Asplund G, Grimvall A, and Petterson C (1989) Naturally produced organic halogens (AOX) in humic substances from soil and water. *Science of the Total Environment* 81/82: 239–248.

Asplund G, Christiansen JV, and Grimvall A (1993) A chloroperoxidase-like catalyst in soil: Detection and characterization of some properties. *Soil Biology & Biochemistry* 25: 41–46.

Baker JI and Hites RA (2000a) Is combustion the major source of polychlorinated dibenzo-*p*-dioxins and dibenzo-furans? A mass balance investigation. *Environmental Science & Technology* 34: 2879–2886.

Baker JI and Hites RA (2000b) Siskiwit Lake revisited: Time trends of polychlorinated dibenzo-*p*-dioxin and dibenzofuran deposition at Isle Royale, Michigan. *Environmental Science & Technology* 34: 2887–2891.

Barabas N, Goovaerts P, and Adriaens P (2003) Modified polytopic vector analysis to identify and quantify a dioxin dechlorination signature in sediments: 2. Application to the Passaic River superfund site. *Environmental Science & Technology* (accepted).

Barkovskii AL and Adriaens P (1998) Affect of model humic constituents on microbial reductive dechlorination of polychlorinated dibenzo-*p*-dioxins. *Environmental Toxicology and Chemistry* 17: 1013–1021.

Barr DP and Aust SD (1994) Mechanisms white rot fungi use to degrade pollutants. *Environmental Science & Technology* 28: A78–A87.

Bekins BA, Cozzarelli IM, Godsy EM, Warren E, Essaid HI, and Tuccillo ME (2001) Progression of natural attenuation processes at a crude oil spill site: 2. Control on spatial distribution of microbial populations. *Journal of Contaminant Hydrology* 53: 387–406.

Bidleman TF (1988) Atmospheric processes. *Environmental Science & Technology* 22: 361–367.

Bidleman TF (1999) Atmospheric transport and air–surface exchange of pesticides. *Water, Air, & Soil Pollution* 115(11): 5–166.

Bowen HJM (1979) *Environmental Chemistry of the Elements*. London: Academic Press.

Bradley PM, Chapelle FH, and Lovley DR (1998) Humic acids as electron acceptors for anaerobic microbial oxidation of vinyl chloride and dichloroethene. *Applied and Environmental Microbiology* 64: 3102–3105.

Breivik K, Sweetman A, Pacyna JM, and Jones KC (2002a) Towards a global historical emission inventory for selected PCB congeners—a mass balance approach: 1. Global production and consumption. *Science of the Total Environment* 290: 181–198.

Breivik K, Sweetman A, Pacyna JM, and Jones KC (2002b) Towards a global historical emission inventory for selected PCB congeners—a mass balance approach: 2 Emissions. *Science of the Total Environment* 290: 199–224.

Brown JF Jr., Bedard DL, Brennan MJ, Carnahan JC, Feng H, and Wagner RE (1987) Polychlorinated biphenyl dechlorination in aquatic sediments. *Science* 236: 709–712.

Bumb RR, Crummett WB, and Cutie SS, et al. (1980) Trace chemistries of fire: A source of chlorinated dioxins. *Science* 210: 385–386.

Bumpus JA, Tien M, Wright D, and Aust SD (1985) Oxidation of persistent environmental pollutants by a white rot fungus. *Science* 228: 1434–1436.

Butler EC and Hayes KF (2000) Kinetics of the transformation of halogenated aliphatic compounds by iron sulfide. *Environmental Science & Technology* 34: 422–429.

Butler JH (2000) Better budgets for methyl halides? *Nature* 403: 260–261.

Capone DG and Kiene RP (1988) Comparison of microbial dynamics in marine and freshwater sediments: Contrasts in anaerobic carbon catabolism. *Limnology and Oceanography* 33: 725–749.

Carlton RG and Klug MJ (1990) Spatial and temporal variations in microbial processes in aquatic sediments: Implications for the nutrient status of lakes. In: Baudo R, Giesy J, and Muntau H (eds.) *Sediments: Chemistry and Toxicity of In-Place Pollutants*, pp. 107–127. Ann Arbor, MI: Lewis Publishers.

Carpenter LJ, Sturges WT, and Penkett SA, et al. (1999) Short-lived alkyl iodides and bromides at Mace Head, Ireland: Links to biogenic sources and halogen oxide production. *Journal of Geophysical Research* 104: 1679–1689.

Cervini-Silva J, Wu J, Larson RA, and Stucki JW (2000) Transformation of chloropicrin in the presence of iron-bearing minerals. *Environmental Science & Technology* 34: 915–917.

Chapelle FH (1993) *Groundwater Microbiology and Geochemistry*. New York: Wiley-Liss.

Chapelle FH, Haack SK, Adriaens P, Henry MA, and Bradley PM (1996) Comparison of Eh and H_2 measurements for delineating redox processes in a contaminated aquifer. *Environmental Science & Technology* 30: 3565–3569.

Christensen TH, Kjeldsen P, and Albrechtsen HJ, et al. (1997) Attenuation off landfill leachate pollutants in aquifers. *Crit. Rev. Environmental Science & Technology* 24: 119–202.

Christensen TH, Bjerg PL, Banwart SA, Jacobson R, Heron G, and Albrechtsen H-J (2000) Characterization of redox conditions in groundwater contaminant plumes. *Journal of Contaminant Hydrology* 45: 165–241.

Coey JM, Schindler DW, and Weber F (1974) Iron compounds in lake sediments. *Canadian Journal of Earth Sciences* 11: 1489–1493.

Cole JG, MacKay D, Jones KC, and Alcock RE (1999) Interpreting, correlating, and predicting the multimedia concentrations of PCCDD/Fs in the United Kingdom. *Environmental Science & Technology* 33: 399–405.

Copley SD (1998) Microbial dehalogenases: Enzymes recruited to convert xenobiotic substrates. *Current Opinion in Chemical Biology* 2: 613–617.

Cozza CL and Woods SL (1992) Reductive dehclorination pathways for substituted benzenes: A correlation with electronic properties. *Biodegradation* 2: 265–278.

Cozzarelli IM, Bekins BA, Baedecker MJ, Aiken GR, Eganhouse RP, and Tuccillo ME (2001) Progression of natural attenuation processes at a crude oil spill site: I. Geochemical evolution of the plume. *Journal of Contaminant Hydrology* 53: 369–385.

Dachs J, Eisenreich SJ, Baker JE, Ko FX, and Jeremiason J (1999a) Coupling of phytoplankton uptake and air–water exchange of persistent organic pollutants. *Environmental Science & Technology* 33: 3653–3660.

Dachs J, Bayona JM, Ittekkot V, and Albaiges J (1999b) Monsoon-driven vertical fluxes of organic pollutants in the Western Arabian Sea. *Environmental Science & Technology* 33: 3949–3956.

Dachs J, Eisenreich SJ, and Hoff RM (2000) Influence of eutrophication on air–water exchange, vertical fluxes and phytoplankton concentrations of persistent organic pollutants. *Environmental Science & Technology* 34: 1095–1102.

Dachs J, Lohmann R, Ockenden WA, Mejanelle L, Eisenrich SJ, and Jones KC (2002) Oceanic biogeochemical controls on global dynamics of persistent organic pollutants. *Environmental Science & Technology* 36: 4229–4237.

Dahlman O, Morck R, and Ljungquist P, et al. (1993) Chlorinated structural elements in high molecular weight organic matter from unpolluted waters and bleached kraft effluents. *Environmental Science & Technology* 27: 1616–1620.

Dahlman O, Reimann A, Ljungquist P, Boren H, and Grimvall A, et al. (1994) Characterization of chlorinated aromatic structures in high molecular weight BMKE materials and in fulvic acids from industrially unpolluted waters. *Water Science & Technology* 29: 81–91.

Damborsky J, Lynam M, and Kuty M (1998) Structure-biodegradability relationships for chlorinated dibenzo-*p*-dioxins and dibenzofurans. In: Wittich R (ed.) *Biodegradation of Dioxins and Furans*, pp. 165–228. Landes, TX.

deJong E and Field JA (1997) Sulfur tuft and turkey tail: Biosynthesis and biodegradation of organohalogens by Basidiomycetes. *Annual Review of Microbiology* 51: 375–414.

deJong E, Field JA, Spinnler HE, Wijnberg JBPA, and de Bont JAM (1994) Significant biogenesis of chlorinated aromatics by fungi in natural environments. *Applied and Environmental Microbiology* 60: 264–270.

deBruyn WJ, Shorter JA, Davidovits P, Worsnop DR, Zahniser MS, and Kolb CE (1995) Uptake of haloacetyl and carbonyl halides by water surfaces. *Environmental Science & Technology* 29: 1179–1185.

Dimmer CH, Simmonds PG, Nickless G, and Bassford MR (2001) Biogenic fluxes of halomethanes from Irish peatland ecosystems. *Atmospheric Environment* 35: 321–330.

Dolfing J and Harrison BK (1992) The Gibbs free energy of halogenated aromatic compounds and their potential role as electron acceptors in anaerobic environments. *Environmental Science & Technology* 26: 2213–2218.

Dunnivant FM, Schwarzenbach RP, and Macalady DL (1992) Reduction of substituted nitrobenzenes in aqueous solutions containing natural organic matter. *Environmental Science & Technology* 26: 2133–2141.

Erlich HL (1996) *Geomicrobiology*. New York, NY: Dekker.

Fathepure BZ and Tiedje JM (1999) Anaerobic bioremediation: Microbiology, principles, and applications. In: Adriano DC, Bollag J-M, Frankenberger WT Jr., and Sims RC (eds.) *Bioremediation of Contaminated Soils*, *Soil Science Society of America/American Society of Agronomy Monograph*, pp. 339–386. Madison, WI: Soil Science Society of America Press.

Fenchel T, King GM, and Blackburn TH (1998) *Bacterial Biogeochemistry: The Ecophysiology of Mineral Cycling*. New York: Academic Press.

Ferrario J and Byrne C (2000) The concentration and distribution of 2,3,7,8-dibenzo-*p*-dioxins/-furans in chickens. *Chemosphere* 40: 221–224.

Flanagan WP and May RJ (1993) Metabolite detection as evidence for naturally occurring aerobic PCB biodegradation in Hudson River sediments. *Environmental Science & Technology* 27: 2207–2212.

Fredrickson JK and Gorby YA (1996) Environmental processes mediated by iron-reducing bacteria. *Current Opinion in Biotechnology* 7: 287–294.

Fredrickson JK, Zachara JM, Kennedy DW, et al. (1998) Biogenic iron mineralization accompanying the dissimilatory reduction of hydrous ferric oxide by a groundwater bacterium. *Geochimica et Cosmochimica Acta* 62: 3239–3257.

Fu Q, Barkovskii AL, and Adriaens P (1999) Reductive transformation of dioxins: An assessment of the contribution of dissolved organic matter to dechlorination reactions. *Environmental Science & Technology* 33: 3837–3842.

Fu QS, Barkovskii AL, and Adriaens P (2001) Dioxin cycling in aquatic sediments: The Passaic River estuary. *Chemosphere* 43: 643–648.

Gaus C, Brunskill GJ, Connell DW, et al. (2002) Transformation processes, pathways, and possible sources of distinctive polychlorinated dibeno-*p*-dioxin signatures in sink environments. *Environmental Science & Technology* 36: 3542–3549.

Gevao B, Hamilton-Taylor J, Murdoch C, Jones KC, Kelly M, and Tabner BJ (1997) Depositional time trends and remobilization of PCBs in lake sediments. *Environmental Science & Technology* 31: 3274–3280.

Giese B, Laturnus F, Adams FC, and Wiencke C (1999) Release of volatile iodinated C1–C4 hydrocarbons by marine microalgae from various climate zones. *Environmental Science & Technology* 33: 2432–2439.

Gillham RW and O'Hannesin SF (1994) Enhanced degradation of halogenated aliphatics by zero-valent iron. *Ground Water* 32(6): 958–967.

Goldberg ED (1975) Synthetic organohalides in the sea. *Proceedings of the Royal Society Series B* 189: 277–289.

Goovaerts P (1998) Geostatistical tools for characterizing the spatial variability of microbiological and physico-chemical soil properties. *Biology and Fertility of Soils* 27: 315–334.

Grammatica P, Pozzi S, Consonni V, and DiGuardo A (2002) Classification of environmental pollutants for global mobility potential. *SAR and QSAR in Environmental Research* 13: 205–217.

Gribble GW (1996) Naturally occurring organohalogen compounds—a comprehensive survey. *Progress in the Chemistry of Organic Natural Products* 68: 1–423.

Grimalt JO, Fernandez P, Berdie L, et al. (2001) Selective trapping of organochlorine compounds in mountain lakes of temperate areas. *Environmental Science & Technology* 35: 2690–2697.

Gruden C, Fu QS, Barkovskii AL, Albrecht ID, Lynam MM, and Adriaens P (2003) Dechlorination of dioxins in sediments: Catalysts, mechanisms, and implications for remedial strategies and dioxin cycling. In: Häggblom MM and Bossert ID (eds.) *Dehalogenation: Microbial Processes and Environmental Applications*, pp. 347–372. Wiley.

Häggblom MM (1992) Microbial breakdown of halogenated aromatic pesticides and related compounds. *FEMS Microbiology Reviews* 103: 29–72.

Harner T, Green NJL, and Jones KC (2000) Measurements of octanol-air partition coefficients for PCDD/Fs: A tool in assessing air-soil equilibrium status. *Environmental Science & Technology* 34: 3109–3114.

Harper DB (2000) The global chloromethane cycle: Biosynthesis, biodegradation and metabolic role. *Natural Product Reports* 17: 337–348.

Harper DB, Buswell JA, Kennedy JT, and Hamilton JTG (1990) Chloromethane, methyl donor in veratryl alcohol biosynthesis in Phanerochaete chrysosporium and other lignin-degrading fungi. *Applied and Environmental Microbiology* 56: 3450–3457.

Harper DB, Kalin RM, Hamilton JTG, and Lamb C (2001) Carbon isotope ratios for chloromethane of biological origin: Potential tool in determining biological emissions. *Environmental Science & Technology* 35: 3616–3619.

Henrichs SM and Reeburgh WS (1987) Anaerobic mineralization of marine sediment organic matter: Rates and the role of anaerobic processes in the ocean carbon economy. *Geomicrobiology Journal* 5: 191–237.

Hermens J, Balaz S, Damborsky J, et al. (1995) Assessment of QSARs for predicting fate and effects of chemicals in the environment: An international European project. *SAR and QSAR in Environmental Research* 3: 223–236.

Heron G and Christensen TH (1995) Affect of sediment-bound iron on redox buffering in a landfill leachate polluted aquifer (Vejen, Denmark). *Environmental Science & Technology* 29: 187–192.

Ho DT, Schlosser P, Smethie WM Jr., and Simpson HJ (1998) Variability in atmospheric chlorofluorocarbons ($CC1_3F$ and $CC1_2F_2$) near a large urban area: Implications for groundwater dating. *Environmental Science & Technology* 32: 2377–2382.

Hoffman H-J (1986) Untersuchung der AOX-gehalte von Bayerischen fluessen. *Muenchener Beitraege zur Abwasser Fischerei und Flussbiologie* 40: 445–459.

Holliger C and Schraa G (1994) Physiological meaning and potential for application of reductive dechlorination by anaerobic bacteria. *FEMS Microbiology Reviews* 15: 297–305.

Hunter KS, Wang Y, and Van Cappellen P (1999) Kinetic modeling of microbially-driven redox chemistry of subsurface environments: Coupling transport, microbial metabolism and geochemistry. *Journal of Hydrology* 209: 53–80.

Iwata H, Tanabe S, Sokal N, and Tatsukawa R (1993) Distribution of persistent organochlorines in the oceanic air and surface seawater and the role of ocean on their global transport and fate. *Environmental Science & Technology* 27: 1080–1098.

Jacobson R, Albrechtsen H-J, Rasmussen M, Bay H, Bjerg PL, and Christensen TH (1998) H_2 concentrations in a landfill leachate plume (Grindsted, Denmark): In site energetics of terminal electron acceptor processes. *Environmental Science & Technology* 32: 2142–2148.

James RR, McDonald JG, Symonik DM, Swackhamer DL, and Hites RA (2001) Volatilization of toxaphene from Lakes Michigan and Superior. *Environmental Science & Technology* 35: 3653–3660.

Jeremiasson JD, Hornbuckle KC, and Eisenreich SJ (1994) PCBs in Lake Superior, 1978-1992: Decreases in water concentrations reflect loss by volatilisation. *Environmental Science & Technology* 28: 903–914.

Johansson C, Pavasars I, Boren H, and Grimvall A (1994) A degradation procedure for determination of halogenated structural elements in organic matter from marine sediments. *Environment International* 20: 103–111.

Johansson E, Kranz-Rulcker C, Zhang BX, and Oberg G (2000) Chlorination and biodegradation of lignin. *Soil Biology & Biochemistry* 32: 102–132.

Kalantzi OI, Alcock RE, Johnson PA, et al. (2001) The global distribution of PCBs and organochlorine pesticides in butter. *Environmental Science & Technology* 35: 1013–1018.

Keppler F, Eiden R, Niedan V, Pracht J, and Scholer HF (2000) Halocarbons produced by natural oxidation processes during degradation of organic matter. *Nature* 403: 298–301.

Key BD, Howell RD, and Criddle CS (1997) Fluorinated organics in the biosphere. *Environmental Science & Technology* 31: 2445–2454.

Kriegman-King MR and Reinhard M (1992) Transformation of carbon tetrachloride in the presence of sulfide, biotite, and vermiculite. *Environmental Science & Technology* 26: 2198–2206.

Kuhn W, Fuchs F, and Sontheimer H (1977) Untersuchungen zur Bestimmung des organisch gebundenen Chlors mit Hilfe eines neuartigen Anreicherungsverfahrens. *Zeitschrift für Wasser und Abwasser Forschung* 6: 192–194.

Laniewski K, Boren H, Grimvall A, Jonsson S, and von Sydow L (1995) Chemical characterization of adsorbable organic halogens (AOX) in precipitation. In: Grimvall A and de Leer EWB (eds.) *Naturally Produced Organohalogens*, pp. 113–130. Dordrecht, The Netherlands: Kluwer.

Laturnus F, Mehrtens G, and Gron C (1995) Haloperoxidase-like activity in spruce forest soil —A source of volatile halogenated organic compounds. *Chemosphere* 31: 3709–3719.

Laturnus F, Haselmann KF, Borch T, and Gron C (2002) Terrestrial natural sources of trichloromethane (chloroform, CHC13)—An overview. *Biogeochemistry* 60: 121–139.

Lee RGM, Burnett V, Harner T, and Jones KC (2000) Short-term temperature dependent air-surface exchange and atmospheric concentrations of polychlorinated napthalenes and organochlorine pesticides. *Environmental Science & Technology* 34: 393–398.

Lendvay JM, Dean SM, and Adriaens P (1998a) Temporal and spatial trends in biogeochemical conditions at a ground-water-surface water interface: Implications for natural bioattenuation. *Environmental Science & Technology* 32: 3472–3478.

Lendvay JM, Sauck WA, McCormick ML, et al. (1998b) Geophysical characterization, redox zonation, and contaminant distribution at a groundwater-surface water interface. *Water Resources Research* 34: 3545–3559.

Lendvay JM, Barcelona MJ, Daniels G, et al. (2002) Bioreactive barriers: Bioaugmentation and biostimulation for chlorinated solvent remediation. *Environmental Science & Technology* 37: 1422–1431.

Lindner AS, Whitfield C, Chen N, Semrau JD, and Adriaens P (2003) Quantitative structure-biodegradation relationships for *ortho*-substituted biphenyl compounds oxidized by *Methylosinus trichosporium* OB3b. *Environmental Toxicology and Chemistry* 22: 2251–2257.

Lohmann R, Nelson E, Eisenreich SJ, and Jones KC (2000) Evidence for dynamic air–water exchange of PCDD/Fs: A study in the Raritan Bay/Hudson River estuary. *Environmental Science & Technology* 34: 3086–3093.

Lovley DR (1991) Dissimilatory Fe(III) and Mn(IV) reduction. *Microbiological Reviews* 55: 259–287.

Lovley DR (1997) Microbial Fe(III) reduction in subsurface environments. *FEMS Microbiology Reviews* 20: 305–313.

Lovley DR and Woodward JC (1992) Consumption of freons CFC-11 and CFC-12 by anaerobic sediments and soils. *Environmental Science & Technology* 26: 925–929.

Lovley DR, Coates JD, Blunt-Harris EL, Phillips EJP, and Woodward JC (1996) Humic substances as electron acceptors for microbial respiration. *Nature* 382: 445–448.

Ludvigsen L, Albrechtsen H-J, Holst H, and Christensen TH (1997) Correlating phospholipid fatty acids (PLFA) in a landfill leachate polluted aquifer with biogeochemical factors by multivariate statistical methods. *FEMS Microbiology Reviews* 20: 447–460.

Ludvigsen L, Albrechtsen HJ, Heron G, Bjerg PL, and Christensen TH (1998) Anaerobic microbial redox processes in a landfill leachate contaminated aquifer (Grindsted, Denmark). *Journal of Contaminant Hydrology* 33: 273–291.

Luthy RG, Aiken GR, Brusseau ML, et al. (1997) Sequestration of hydrophobic organic contaminants by geosorbents. *Environmental Science & Technology* 31: 3341–3347.

Lynam M, Damborsky J, Kuty M, and Adriaens P (1998) Molecular orbital calculations to probe mechanism of reductive dechlorination of polychlorinated dioxins. *Environmental Toxicology and Chemistry* 17: 998–1005.

MacKay D (1991) *Multimedia Environmental Models: The Fugacity Approach*. Boca Raton, FL: CRC Press/Lewis Publishers.

MacKay D and Wania F (1995) Transport of contaminants to the Arctic: Partitioning, processes and models. *Science of the Total Environment* 160/161: 25–38.

Martin JM and Meybeck M (1979) Elemental mass-balance of material carried by major world rivers. *Marine Chemistry* 7: 173–206.

Matheson LJ and Tratnyek PG (1994) Reductive dehalogenation of chlorinated methanes by iron metal. *Environmental Science & Technology* 28: 2045–2053.

McConnell LL, Bidleman TF, Cotham WE, and Walla MD (1998) Air concentrations of organochlorine insecticides and polychlorinated biphenyls over Green Bay, WI, and the four lower Great Lakes. *Environmental Pollution* 101: 391–399.

McCormick ML (1999) *Reductive Dechlorination of Chlorinated Solvents under Iron Reducing Conditions*. PhD Thesis, The University of Michigan.

McCormick ML, Bouwer EJ, and Adriaens P (2002a) Carbon tetrachloride transformation in a defined iron-reducing culture: Relative kinetics of biotic and abiotic reactions. *Environmental Science & Technology* 36: 403–410.

McCormick ML, Jung PT, Koster van Groos PG, Hayes KF, and Adriaens P (2002b) Assessing biotic and abiotic contributions to chlorinated solvent transformation in iron-reducing and sulfidogenic environments. In: Thornton SF and Oswald SE (eds.) *Groundwater Quality: Natural and Enhanced Restoration of Groundwater Pollution*, pp. 119–125. Oxfordshire, UK: International Association of Hydrological Sciences.

McGuire JT, Smith EW, Long DT, et al. (2000) Temporal variations in parameters reflecting terminal electron accepting processes in an aquifer contaminated with waste fuel and chlorinated solvents. *Chemical Geology* 169: 471–485.

Meijer SN, Steinnes E, Ockenden WA, and Jones KC (2002) Influence of environmental variables on the spatial distribution of PCBs in Norwegian and UK soils: Implications for global cycling. *Environmental Science & Technology* 36: 2146–2153.

Mohn WW and Tiedje JM (1992) Microbial reductive dehalogenation. *Microbiological Reviews* 56: 482–507.

Moore SA, Pope JD, Barnett JT Jr., and Suarez LA (1990) Structure-activity relationships and estimation techniques for biodegradation of xenobiotics. Athens, GA: US Environmental Protection Agency. EPA 600/S3-89/ 080, Research and Development Report.

Murphy EM and Schramke JA (1998) Estimation of microbial respiration rates in groundwater by geochemical modeling constrained with stable isotopes. *Geochimica et Cosmochimica* 62(21/22): 3395–3406.

Murphy L and Morrison RD (2002) *Introduction to Environmental Forensics, p. 560*. San Diego: Academic Press.

Neidleman SL and Geigert J (1986) *Biohalogenation: Principles, Basic Roles and Applications*. Chichester: Ellis Horwood.

Oberg G (1998) Chloride and organic chlorine in soil. *Acta Hydrochimica et Hydrobiologica* 26: 137–144.

Oberg G (2002) The natural chlorine cycle—fitting the scattered pieces. *Applied Microbiology and Biotechnology* 58: 565–581.

Oberg G, Brunberg H, and Hjelm O (1997) Production of organically-bound halogens during degradation of birch wood by common white rot fungi. *Soil Biology & Biochemistry* 29: 191–197.

Ockenden WA, Steinnes E, Parker C, and Jones KC (1998a) Observations on persistent organic pollutants in plants: Implications for their use as passive air samplers and for POP cycling. *Environmental Science & Technology* 32: 2721–2726.

Ockenden WA, Sweetman AJ, Prest HF, Steinnes E, and Jones KC (1998b) Toward an understanding of the global atmospheric distribution of persistent organic pollutants: The use of semi-permeable membrane devices as time-integrated passive samplers. *Environmental Science & Technology* 32: 2703–2795.

Okey RW and Stensel HD (1996) A QSBR development procedure for aromatic xenobiotic degradation by unacclimated bacteria. *Water Environment Research* 65: 772–780.

Palleroni NJ (1995) Microbial versatility. In: Young LY and Cerniglia CE (eds.) *Microbial Transformation and Degradation of Toxic Organic Chemicals*, pp. 3–27. New York, NY: Wiley.

Peijnenburg WJGM, t'sHart MJ, den Hollander HA, van de Meent D, Verboom HH, and Wolfe NL (1992) QSARs for predicting reductive transformation rate constants of halogenated aromatic hydrocarbons in anoxic sediment systems. *Environmental Toxicology and Chemistry* 11: 310–314.

Peterle TJ (1969) DDT in Antarctic snow. *Nature* 224: 620–623.

Post WM, Emmanuel WR, Zinke PJ, and Stangenberger AL (1982) Soil carbon pools and world life zones. *Nature* 298: 156–159.

Postma D and Jacobson R (1996) Redox zonation: Equilibrium constraints on the Fe(III)/SO_4-reduction interface. *Geochimica et Cosmochimica Acta* 60: 3169–3175.

Potter TL and Carpenter TL (1995) Occurrence of Alachlor environmental degradation products in groundwater. *Environmental Science & Technology* 29: 1557–1564.

Raiswell R and Canfield DE (1998) Sources of iron for pyrite formation in marine sediments. *American Journal of Science* 298: 219–245.

Rhew RC, Miller BR, and Weiss RF (2000) Natural methyl bromide and methyl chloride emissions from coastal salt marshes. *Nature* 403: 292–295.

Rickard D, Martin AA, and Luther GW III (1995) Chemistry of iron sulfides in sedimentary environments. In: *Geochemical Transformations of Sedimentary Sulfur. ACS Symposium Series*, pp. 168–193. Washington, DC: American Chemical Society.

Rickard DT (1969) The microbiological formation of iron sulphides. *Stockholm Contributions in Geology* 20: 49–66.

Roberts AL, Jeffers PM, Wolfe NL, and Gschwend PM (1993) Structure-reactivity relationships in dehydrohalogenation reactions of polychlorinated and polybrominated alkanes. *Critical Reviews in Environmental Science & Technology* 23: 1–39.

Rompp A, Klemm O, Fricke W, and Frank H (2001) Haloacetates in fog and rain. *Environmental Science & Technology* 35: 1294–1298.

Rorije E, Langenberg JH, Richter J, and Peijnenburg WJGM (1995) Modeling reductive dehalogenation with quantum chemically derived descriptors. *SAR and QSAR in Environmental Research* 4: 237–252.

Rugge K, Hofstetter TB, Haderlein SB, et al. (1998) Characterization of predominant reductants in an anaerobic leachate-contaminated aquifer by nitroaromatic probe compounds. *Environmental Science & Technology* 32: 23–31.

Schauder R and Kroeger A (1993) Bacterial sulfur respiration. *Archives of Microbiology* 159: 491–497.

Scheunert I, Mansour M, and Andreux F (1992) Binding of organic pollutants to soil organic matter. *International Journal of Environmental Analytical Chemistry* 46: 189–222.

Schlesinger WH (1991) *Biogeochemistry: An Analysis of Global Change*. San Diego, CA: Academic Press.

Schwarzenbach PR, Stierly R, Lanz K, and Zeyer J (1990) Quinone and iron porphyrin mediated reduction of nitroaromatic compounds in homogenous aqueous solutions. *Environmental Science & Technology* 24: 1566–1574.

Schwarzenbach RP, Gschwendt PM, and Imboden DM (1993) *Environmental Organic Chemistry*. New York, NY: Wiley.

Sherwood Rowland F (1991) Stratospheric ozone in the 21st century: The chlorofluorocarbon problem. *Environmental Science & Technology* 25: 622–628.

Simonich SL and Hites RA (1995) Global distribution of persistent organochlorine compounds. *Nature* 269: 1851–1854.

Skubal KL, Barcelona MJ, and Adriaens P (2001) A field and laboratory assessment of natural bioattenuation in an aquifer contaminated by mixed organic waste. *Journal of Contaminant Hydrology* 49: 151–171.

Skyring GW (1987) Sulfate reduction in coastal ecosystems. *Geomicrobiology Journal* 5: 295–374.

Sladen WJL, Menzie CM, and Reichel WL (1966) DDT residues in Adelie penguins and a crabeater seal from Antarctica. *Nature* 210: 670–673.

Svenson A, Kjeller LO, and Rappe C (1989) Enzyme mediated formation of 2,3,7,8-tetrasubstituted chlorinated dibenzodioxins and dibenzofurans. *Environmental Science & Technology* 23: 900–1202.

Stevenson FJ (1994) *Humus Chemistry: Genesis, Composition, Reactions*. New York, NY: Wiley.

Swackhamer DL, Schottler S, and Pearson RF (1999) Air-water exchange and mass balance of toxaphene in the Great Lakes. *Environmental Science & Technology* 33: 3864–3872.

Swoboda-Colberg NG (1995) Chemical contamination of the environment: Sources, types, and fate of synthetic organic chemicals. In: Young LY and Cerniglia CE (eds.) *Microbial Transformation and Degradation of Toxic Organic Chemicals*, pp. 27–77. New York, NY: Wiley.

Thamdrup B (2000) Bacterial manganese and iron reduction in aquatic sediments. *Advances in Microbial Ecology* 16: 41–84.

Tiedje JM (1988) Ecology of denitrification and dissimilatory nitrate reduction to ammonium. In: Zehnder AJB (ed.) *Biology of Anaerobic Microorganisms*, pp. 179–244. New York, NY: Wiley.

Totten LA, Brunciak PA, Gigliotti CL, et al. (2001) Dynamic air–water exchange of polychlorinated biphenyls in the New York–New Jersey Harbor estuary. *Environmental Science & Technology* 35: 3834–3840.

Tratnyek PG and Macalady DL (2000) Oxidation–reduction reactions in the aquatic environment. In: Boethling RS and Mackay D (eds.) *Handbook of Property Estimation Methods for Chemicals*, pp. 383–415. Boca Raton, FL: Lewis Publishers.

van der Meer JR, de Vos WM, Harayama S, and Zehnder AJB (1992) Molecular mechanisms of genetic adaptation to xenobiotic chemicals. *Microbiological Reviews* 56: 677–694.

van Hylckema-Vlieg JET, Poelarends GJ, Mars AE, and Jansen DB (2000) Detoxification of reactive intermediates during microbial metabolism of halogenated compounds. *Current Opinion in Microbiology* 3: 257–262.

Vaughan DJ and Lennie AR (1991) The iron sulphide minerals: Their chemistry and role in nature. *Scientific Progress Edinburgh* 75: 371–388.

Vogel TM, Criddle CS, and McCarty PL (1987) Transformations of halogenated aliphatic compounds. *Environmental Science & Technology* 21: 722–736.

Wania F (2003) Assessing the potential of persistent organic chemicals for long-range transport and accumulation in polar regions. *Environmental Science & Technology* 37: 1344–1351.

Wania F and MacKay D (1996) Tracking the distribution of persistent organic pollutants. *Environmental Science & Technology* 30: 390A–396A.

Watling R and Harper DB (1998) Chloromethane production by wood-rotting fungi and an estimate of the global flux to the atmosphere. *Mycological Research* 102: 769–787.

Wiedemeier TH, Rifai HS, Newell CN, and Wilson JT (1999) *Natural Attenuation of Fuels and Chlorinated Solvents in the Subsurface*. New York, NY: Wiley.

Wolfe NL, Paris DF, Steen WC, and Baughman GL (1980) Correlation of microbial degradation rates with chemical structure. *Environmental Science & Technology* 14: 1143–1144.

Yokouchi Y, Noijiri Y, Barrie LA, et al. (2000) A strong source of methyl chloride to the atmosphere from tropical coastal land. *Nature* 403: 295–298.

Zachara JM, Kukkadapu RK, Fredrickson JK, Gorby YA, and Smith SC (2002) Biomineralization of poorly crystalline Fe(III) oxides by dissimilatory metal reducing bacteria (DMRB). *Geomicrobiology Journal* 19: 179–207.

Zhang H, Eisenreich SJ, Franz T, Baker JE, and Offenberg JH (1999) Evidence for increased gaseous PCB fluxes to Lake Michigan from Chicago. *Environmental Science & Technology* 33: 2129–2137.

Zhao H, Chen J, Quan X, Yang F, and Peijnenburg WJGM (2001) Quantitative structure-property relationship study on reductive dehalogenation of selected halogenated aliphatic hydrocarbons in sediment slurries. *Chemosphere* 44: 1557–1563.

Zipper C, Suter MJ-F, Haderlein SB, Gruhl M, and Kohler H-PE (1998) Changes in the enantiomeric ratio of (R) to (S) mecoprop indicate *in situ* biodegradation of this chiral herbicide in a polluted aquifer. *Environmental Science & Technology* 32: 2070–2076.

11.15 The Geochemistry of Pesticides

JE Barbash, United States Geological Survey, Tacoma, WA, USA

Published by Elsevier Ltd.

Nomenclature

a.i.	Active ingredient
f_{oc}	Mass fraction of organic carbon in soil (m/m)
k	Rate constant for the rate-limiting step of a chemical reaction (units depend on reaction order)
$1/n$	Freundlich exponent (dimensionless)
pK_a	The negative log of the equilibrium constant for the interconversion between a Brønsted acid and its conjugate base (dimensionless)
A	Arrhenius preexponential factor (same units as k)
C_{aq}	Concentration of solute dissolved in water (m/v)
C_{oc}	Amount of solute sorbed to soil organic carbon (m/m)
C_{α}	Carbon atom representing the site of a particular reaction on a molecule (the 'alpha carbon')
C_{β}	Carbon atom (the 'beta carbon') immediately adjacent to C_{α}
E_a	Activation energy (energy mol^{-1})
H	Henry's law constant (various forms)
K_f	Freundlich partition coefficient (v/m)
K_{oc}	Soil organic carbon–water partition coefficient (v/m)
K_{ow}	Octanol–water partition coefficient (dimensionless)
K_p	Soil–water partition coefficient (v/m)
K_{SA}	Soil–air partition coefficient (form depends upon units for H)
R	Universal gas constant (form depends on units for E_a)
S_N2	Bimolecular nucleophilic substitution reaction
T_{max}	Temperature above which substrate decomposition or enzyme inactivation occurs
T_{min}	Temperature below which biological functions are inhibited
T_{opt}	Temperature of maximum biotransformation rate
μ_{max}	Maximum rate of biotransformation (m/v/t)

 http://dx.doi.org/10.1016/B978-0-08-095975-7.00915-3

11.15.1 Introduction

The mid-1970s marked a major turning point in human history, for it was during this period that the ability of Earth's ecosystems to absorb most of the biological impacts of human activities appears to have been exceeded by the magnitude of those impacts. This conclusion is based partly upon estimates of the rate of carbon dioxide emission during the combustion of fossil fuels, relative to the rate of its uptake by terrestrial ecosystems (Loh, 2002). A very different threshold, however, had already been crossed several decades earlier with the birth of the modern chemical industry, which produced novel substances for which no such natural assimilative capacity existed. Among these new chemical compounds, none has posed a greater challenge to the planet's ecosystems than synthetic pesticides, compounds that have been intentionally released into the environment in vast quantities – several hundred million pounds of active ingredient (a.i.) per year in the United States alone (Kiely et al., 2004) – for many decades. To gauge the extent to which we are currently able to assess the ecological implications of this new development in Earth's history, this chapter presents an overview of current understanding regarding the sources, transport, fate and biological effects of pesticides, their transformation products, and selected adjuvants in the hydrologic system. (Adjuvants are the so-called 'inert ingredients' included in commercial pesticide formulations to enhance the effectiveness of the a.i.)

11.15.1.1 Previous Reviews of Pesticide Geochemistry

Pesticides have been in widespread use since the Second World War, and their environmental effects have been causing concern for at least four decades (Carson, 1962). As a result, numerous reviews summarizing the results from field and laboratory studies of their distribution, transport, fate, and biological effects in the hydrologic system have been published The principal features of many of these reviews have been summarized elsewhere for the atmosphere (Majewski and Capel, 1995), vadose zone and groundwater (Barbash and Resek, 1996), surface waters (Larson et al., 1997), stream sediments, and aquatic biota (Nowell et al., 1999). Other compilations of existing information on these topics have focused either on particular pesticide classes (e.g., Erickson and Lee, 1989; Gunasekara, 2005; Laskowski, 2002; Pehkonen and Zhang, 2002; Stamper and Tuovinen, 1998; Weber, 1990), or on individual pesticides (e.g., Huber and Otto, 1994; Moye and Miles, 1988). Information on the biological effects of pesticides on both target and nontarget organisms has been extensively reviewed (e.g., Howell et al., 1996; Kamrin, 1997; Kegley et al., 1999; Matsumura, 1985; Murphy, 1986; Smith, 1987; Solomon et al., 2000; Stinson and Bromley, 1991). Valuable overviews of environmental organic chemistry are also available (e.g., Capel, 1993; Schwarzenbach et al., 1993).

11.15.1.2 Scope of This Review

This chapter focuses on the sources, transport, fate and biological effects of synthetic organic pesticides, their transformation products and volatile pesticide adjuvants – collectively referred to herein as *pesticide compounds* – in the hydrologic system. Although there are thousands of substances that are currently registered for use as pesticide adjuvants in the United States (US Environmental Protection Agency, 2010), discussion of these chemicals is limited to those that are volatile organic compounds (VOCs) because they are the adjuvant group whose geochemical behavior has been most thoroughly documented. (VOCs are commonly used as solvents in commercial pesticide formulations; e.g., Wang et al., 1995.) Most of the pesticide compounds examined in this chapter are registered for use in the United States. Similarly, discussion of the use of these compounds focuses primarily on their applications within the United States. For space considerations, pesticides that are wholly inorganic (e.g., chlorine, sulfur, chromated copper arsenate, copper oxychloride), or contain metals (e.g., tributyltin) or metalloids (e.g., arsenicals) are not discussed in detail. Topics for which comprehensive, up-to-date reviews have already been published receive less attention than those for which fewer reviews are available. Consequently, greater emphasis is placed on the factors that influence the rates and mechanisms of transformation of pesticide compounds than on the biological effects of these substances, their patterns of use and occurrence, or their partitioning among environmental media.

11.15.1.3 Biological Effects of Pesticide Compounds

All pesticides are designed to kill, or otherwise control, specific animals or plants, so a great deal is known about the acute biological effects of these chemicals on their target organisms. Insecticides (including most fumigants) act as either physical poisons, protoplasmic poisons, stomach poisons, metabolic inhibitors, neurotoxins, or hormone mimics (Matsumura, 1985). Herbicides control or kill plants through a variety of mechanisms, including the inhibition of biological processes such as photosynthesis, mitosis, cell division, enzyme function, root growth, or leaf formation; interference with the synthesis of pigments, proteins, or DNA; destruction of cell membranes; or the promotion of uncontrolled growth (William et al., 1995). Fungicides act as metabolic inhibitors (Matheron, 2001). Most rodenticides are either anticoagulants, stomach poisons, or neurotoxins (Meister, 2000). Because most pesticides are poisons, considerable knowledge has also developed regarding the acute effects of these compounds on humans (e.g., Murphy, 1986).

Far more elusive, however, are the myriad sublethal effects on nontarget organisms (including humans) of chronic exposure to pesticide compounds. Of considerable concern in this regard is endocrine disruption, a phenomenon whose effects were first discovered five decades ago, but whose widespread impacts across a broad range of organisms and ecosystems have become known only since the 1990s (Colborn et al., 1993, 1996; Sumpter and Johnson, 2005), and may be inheritable (Anway et al., 2005). Other effects of chronic pesticide exposure in wildlife – some of which may themselves be related to endocrine disruption – include impaired homing abilities (Scholz et al., 2000) and reduced egg production in fish (Tillitt et al., 2010), hearing impairment in mammals (Song et al., 2005), eggshell thinning in birds, reduced immune function, liver and kidney damage, teratogenicity, neurotoxicity, delayed metamorphosis, smaller body size, reduced

activity, and reduced tolerance to cold or predatory stress (Colborn et al., 1993; Murphy, 1986; Osano et al., 2002; Relyea, 2005a; Smith, 1987; Teplitsky et al., 2005). Exposure to pesticides may also be a factor contributing to honeybee colony collapse disorder (Hendrikx et al., 2009). Ecological effects of pesticide exposure include decreased biodiversity and productivity (Relyea, 2005b), reduced rates of leaf litter decomposition (Schäfer et al., 2007), shifts in predator-to-prey ratios (Relyea et al., 2005; Rohr and Crumrine, 2005), reduced abundance of pesticide-sensitive species, and concomitant increases in the abundance of less sensitive species (Liess and Von Der Ohe, 2005). Recent evidence also suggests that many of the malformations and population declines that have been observed in amphibians over the past several decades may have been facilitated by exposure to pesticides at concentrations commonly encountered in the hydrologic system (e.g., Hayes, 2004; Hayes et al., 2002, 2006; Relyea, 2005c; Sparling et al., 2001). Documented or suspected effects in humans include cancer (Alavanja et al., 2004; Hardell and Eriksson, 1999; Patlak, 1996; President's Cancer Panel, 2010; Sanborn et al., 2004; Schreinemachers, 2000), immune system suppression (Repetto and Baliga, 1996), impaired neurological development (Colborn, 2006; Eskenazi et al., 2006; Grandjean et al., 2006), learning disorders (Guillette et al., 1998), attention deficit/hyperactivity disorder (Bouchard et al., 2010; Winrow et al., 2003), Gulf War syndrome (Winrow et al., 2003), Parkinson's disease (Brown et al., 2006), Alzheimer's disease and other forms of dementia (Hayden et al., 2010), fetal death (Bell et al., 2001), earlier onset of puberty (Guillette et al., 2006; Wang et al., 2005), birth defects (Garry et al., 2002; Winchester et al., 2009), and shifts in sex ratios (Garry et al., 2002).

Recent biomonitoring studies have provided information on the concentrations of pesticide compounds in the human body, their relations to diet, and their rates of elimination. As part of their third national assessment of exposures to a variety of anthropogenic chemicals and metals in the environment, the Centers for Disease Control and Prevention (2005) reported detections of 29 pesticide compounds in the blood or urine of the US population. For infants and children, most exposures to pesticides appear to come from their diet (Lu et al., 2005; National Research Council, 1993). Significantly lower concentrations of organophosphorus pesticide (OP) metabolites, for example, have been measured in the urine of children consuming organic fruits, vegetables, and juices (i.e., those produced without the use of synthetic pesticides), relative to those fed the same food items produced conventionally (Curl et al., 2003). Other work has shown that a dietary shift from conventionally grown foods to organic foods results in a statistically significant, rapid decrease (within 1–2 days) in urinary metabolite concentrations for two OP insecticides in children (malathion and chlorpyrifos), with a similarly rapid return to previous levels upon restoration of a conventional diet (Lu et al., 2005).

When, as is often the case, individual pesticides are present in the hydrologic system in combination with other pesticides (e.g., Gilliom et al., 2006; Kolpin et al., 2000; Larson et al., 1999; Squillace et al., 2002), the combined toxicity of the different chemicals may be either antagonistic, additive, or synergistic relative to the effects and toxicities of the individual pesticides alone, depending upon the compounds, organisms, and conditions (e.g., Anderson and Lydy, 2002; Belden and Lydy, 2000; Carder and Hoagland, 1998; Hayes et al., 2006; Howe et al., 1998; Pape-Lindstrom and Lydy, 1997; Relyea, 2009; Thompson, 1996). In addition, pesticide adjuvants may be responsible for substantial increases in the toxicity of commercial formulations relative to that of the a.i. alone (e.g., Benachour et al., 2007; Bolognesi et al., 1997; Howe et al., 2005; Lin and Garry, 2000; Oakes and Pollak, 1999; Relyea, 2005c; Renner, 2005). While most pesticide transformation products are less toxic than their parent compounds, in some instances, the reverse has been observed (Sinclair and Boxall, 2003). Despite these considerations, however, most of the water-quality criteria that have been established for the protection of aquatic life or human health in relation to individual pesticides do not account for the potential synergistic effects of other pesticides, adjuvants, or transformation products that may also be present. One exception to this is the decision by the US Environmental Protection Agency (2003) to include three of the chlorinated products of atrazine transformation (deethylatrazine (DEA), deisopropylatrazine, and diaminochlorotriazine) together with the parent compound in their assessments of the human and environmental health risks associated with atrazine use. In addition, the European Union's Drinking Water Directive specifies a maximum allowable concentration of 0.10 $\mu g\ l^{-1}$ for any single pesticide compound of concern in water (including parent compounds "and their relevant metabolites, degradation and reaction products"), and a maximum allowable total concentration of 0.50 $\mu g\ l^{-1}$ for all pesticide compounds that are detected (European Commission, 1998, pp. 15–16).

11.15.1.4 Variations in Pesticide Use over Time and Space

In 1964, an estimated 617 million pounds (280 x 10^6 kg) of pesticide a.i. were sold for either agricultural or nonagricultural use in the United States (**Figure 1**). This amount reached a maximum of 1.14 billion pounds (517 x 10^6 kg) a.i. in 1979 and decreased to 906 million pounds (411 x 10^6 kg) a.i. by 1987 (Kiely et al., 2004). However, despite ongoing efforts to reduce pesticide use through the introduction of integrated pest management practices and genetically engineered crops (e.g., US General Accounting Office, 2001), **Figure 1** indicates that the total mass of pesticides applied in the United States in 2001 (888 million pounds (403 x 10^6 kg) a.i.) was 98% of the amount applied in 1987. Worldwide use in 2001 totaled 5 billion pounds (2268 x 10^6 kg) of a.i. (Kiely et al., 2004). Relatively detailed estimates of agricultural pesticide use in 1992, 1997, and 2002 are available for individual counties across the United States (Thelin and Gianessi, 2000; US Geological Survey, 2010). Estimates of pesticide use in nonagricultural settings, however, are available only on a national scale, despite the fact that such use represented 24% of the total mass of a.i. sold in the United States in 2001 (Kiely et al., 2004). Summaries of the agricultural use of specific pesticides in individual countries around the world are available from the Database on Pesticides Consumption, maintained by the United Nations Food and Agriculture Organization (2003).

11.15.1.5 Environmental Distributions in Relation to Use

Figure 2 illustrates the variety of routes by which pesticides are dispersed within the hydrologic system after they are released, either intentionally through application or unintentionally

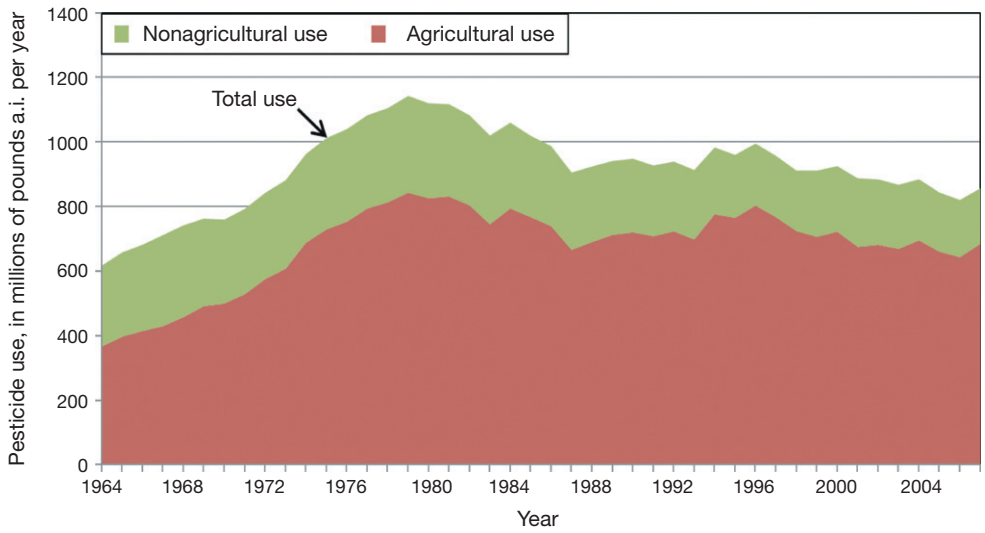

Figure 1 Estimated amounts of pesticide use in the United States for agricultural and nonagricultural purposes from 1964 to 2007. Data obtained from Grube A, Donaldson D, Kiely T, and Wu L (2011) Pesticides industry sales and usage – 2006 and 2007 market estimates. *USEPA 733-R-04-001*. Washington, DC: US Environmental Protection Agency (accessed at http://www.epa.gov/opp00001/pestsales/07pestsales/market_estimates06-07.pdf on 3 September 2011).

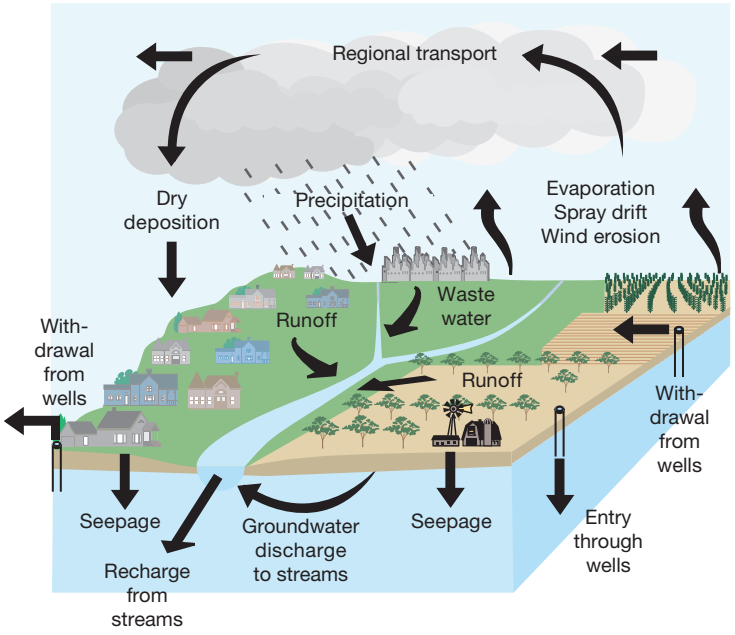

Figure 2 Pesticide movement in the hydrologic system. Reproduced from Barbash JE and Resek EA (1996) *Pesticides in Ground Water – Distribution, Trends, and Governing Factors*. Boca Raton, FL: CRC Press.

through spills or other accidents. As might be expected, spatial patterns of pesticide detection in air (Majewski et al., 1998), surface waters (Capel et al., 2001), groundwaters (Barbash et al., 1999), bed sediments, and aquatic biota (Wong et al., 2001) have generally been found to correspond with their patterns of application.

One of the best measures of our ability to predict the spatial distributions of any anthropogenic contaminant in the hydrologic system, however, is the degree to which its total mass can be accounted for after its release into the environment. Mass-balance studies of applied pesticides since the mid-1970s have had only limited success in this regard, even under highly controlled conditions. Of the initial amounts applied during numerous investigations – nearly all of which were conducted in agricultural settings – the proportions of applied a.i. detected in the hydrologic system have typically been 3% or less in surface waters (Capel et al., 2001; Clark and Goolsby, 2000; Wauchope, 1978), 5% or less in vadose zone waters or tile

drainage (Flury, 1996), and 5% or less in groundwater (Barbash and Resek, 1996). Estimates of the proportion of applied pesticides that move offsite in spray drift range from 1 to 75% (with considerable variation among different compounds, depending upon their volatility), while the amounts lost to the atmosphere through volatilization from the soil following application have been estimated at between 0.2 and 90%. Offsite losses through both spray drift and volatilization from soil depend upon a variety of factors such as pesticide properties, application method, formulation, and weather conditions (Asman et al., 2003; Majewski and Capel, 1995; Unsworth et al., 1999). High proportions – and often the majority – of the applied mass of pesticide a.i. have been measured in association with plant tissues and surface soils within the first few hours to days after application, but the percentages of applied mass detected in these media typically drop below 30% within a few months (Barbash and Resek, 1996). Much of the pesticide mass that has remained unaccounted for during these studies – but did not move offsite in the air, groundwater, or surface waters – may have formed covalent bonds with plant tissues or soil organic matter to form *bound residues* (e.g., Harris, 1967; Nicollier and Donzel, 1994; Xu et al., 2003) or undergone transformation to CO_2 or products for which chemical analyses are rarely conducted (Barbash and Resek, 1996). The fate of applied adjuvants – which usually constitute the majority of the mass of commercial pesticide formulations (Tominack, 2000) – is almost entirely unknown.

11.15.1.6 Overview of Persistence in the Hydrologic System

Given their broad diversity of chemical structures, it is not surprising that pesticide compounds exhibit a wide range of persistence in the hydrologic system. Such variability may be observed among different compounds within a given environmental medium (i.e., the atmosphere, water, soil, aquatic sediment, or biological tissues) or for the same compound in different environmental media. Since there are many thousands of compounds that are, or have been, used as pesticides, space considerations preclude a characterization of the environmental reactivity of all of them in this chapter. However, **Table 1** provides a brief overview of the persistence of several common herbicides, insecticides, fumigants, and fungicides (representing some of the principal chemical classes of each) in the atmosphere, surface water, soil, and aqueous sediments.

Table 1 Persistence of some commonly used pesticides in the atmosphere, surface water, soil, and aquatic sediments

Use class	*Chemical class*	*Example(s)*	*Suggested half-life class in*			
			Atm.	*Surface water*	*Soil*	*Aquatic sediment*
Herbicides	Acetanilides	Metolachlor	4	6	6	7
	Amino acid derivatives	Glyphosate	4	6	6	7
	Chlorophenoxy acids	2,4-D	2	3	5	6
		2,4,5-T	3	5	5	6
	Dinitroanilines	Isopropalin	2	5	6	7
		Trifluralin	4	6	6	7
	Triazines	Atrazine	1	8	6	6
		Simazine	3	5	6	7
	Ureas	Diuron	2	5	6	7
		Linuron	2	5	6	7
Insecticides	Carbamates	Aldicarb	1	5	6	8
		Carbaryl	3	4	5	6
		Carbofuran	1	4	5	6
	Organochlorines	Chlordane	3	8	8	9
		p,*p*′-DDT	4	7	8	9
		Lindane	4	8	8	9
	Organophosphates	Chlorpyrifos	2	4	4	6
		Diazinon	5	6	6	7
		Malathion	2	3	3	5
Fumigants	Organochlorines	Chloropicrin	4	3	3	4
Fungicides	Imides	Captan	2	2	5	5
	Organochlorines	Chlorothalonil	4	4	5	6
Half-life class definitions						
Class	Mean half-life	Range (h)				
1	5 h	<10				
2	~1 d	10–30				
3	~2 d	30–100				
4	~1 week	100–300				
5	~3 weeks	300–1000				
6	~2 months	1000–3000				
7	~8 months	3000–10 000				
8	~2 yr	10000–30 000				
9	~6 yr	>30 000				

Source: Mackay et al. (1997).

These data were taken from Mackay et al. (1997), who drew on an extensive body of published data to determine a 'half-life class' for 42 pesticide compounds in each of these four environmental media. As can be seen from the discussion in this chapter, the persistence of a given compound in a specific environmental setting is influenced by many different physical, chemical, and biological factors. Each estimate of the 'half-life class' in **Table 1** thus represents a generalized mean value selected from what was often a wide range available from previous studies. (The reader is referred to Mackay et al. (1997) for a summary of the methods by which these data were generated.) The data in **Table 1** indicate that the persistence of pesticide compounds generally increases among the four environmental media in the following order: atmosphere < surface waters < soils < aquatic sediments. According to Mackay et al. (1997), this pattern is a reflection of several circumstances, including the following: (1) chemical reaction rates in water are generally slower than those in air; (2) pesticides in aquatic sediments and soils are exposed to less sunlight than those in the atmosphere or surface waters, and are therefore less subject to photochemical reactions; and (3) pesticides sorbed to aquatic sediments and soils are often less accessible for biotransformation than those in the aqueous phase. The data in **Table 1** also suggest that pesticide compounds within the same chemical class may show similar patterns of persistence in a given environmental setting. However, variations in structure among compounds within the same chemical class may also result in substantial variations in reactivity in the same medium (cf. diazinon vs. malathion). To date, the most comprehensive attempt to account quantitatively for the myriad of environmental factors that control pesticide persistence in situ has been the work of Fenner et al. (2007), who examined 27 different predictor variables as candidates for inclusion in a multivariate regression to predict the rate of atrazine disappearance in aerobic soil. Developed using data obtained from published laboratory studies, the resulting equation explained 67% of the variation in the rates of atrazine disappearance in soil as a nonlinear function of temperature, pH, the weight percentages of sand and organic carbon in the soil, depth below ground surface, and the depth interval of assessment.

11.15.2 Partitioning among Environmental Matrices

The large-scale movement of persistent pesticide compounds within the hydrologic system is controlled primarily by their rates of advection in water and air masses, as well as by the movement of biota in which they might bioaccumulate. However, the partitioning of these compounds among different environmental media occurs in response to differences in their chemical potential, or *fugacity*, among these media (Mackay, 1979). Given the broad diversity of chemical structures that pesticide compounds encompass, it is not surprising that their affinities for different environmental media also span a wide range. For example, if they are sufficiently persistent, hydrophobic compounds such as DDT (1,1,1-trichloro-2,2-bis (4-chlorophenyl)ethane), dieldrin, chlordane, and other organochlorine insecticides (OCs) will, over time, preferentially accumulate in organic soils, lipid-rich biological tissues, and other media with high levels of organic carbon. Similarly, the extent to which pesticide compounds are taken up in the roots of plants generally increases in relation to the affinity of the compounds for lipids (Briggs et al., 1982). By contrast, more volatile compounds, such as chlorofluorocarbons (several of which are, or have been, used as adjuvants; Marquardt et al., 1998; US Environmental Protection Agency, 2010) and fumigants, will tend to reside primarily in soil gases and the atmosphere until they degrade. (The effects of transformation on the partitioning of pesticide compounds will be discussed in a later section.)

Mackay et al. (1997) provide detailed examples of fugacity calculations to illustrate how variations in the physical and chemical properties of pesticides affect their partitioning among environmental media. **Figure 3** displays the results from some of these calculations for three of the pesticides listed in **Table 1**. Consistent with the expectations described above, these computations predict that following their release into the hydrologic system, the relatively water-soluble herbicide atrazine will come to reside mostly in the aqueous phase, the more hydrophobic insecticide chlorpyrifos will tend to concentrate in soil, and the volatile fumigant chloropicrin will be present primarily in the vapor phase. Results from such calculations for a given compound help to focus attention on the media where it is likely to be present in the highest concentrations, and thus where a detailed understanding of its persistence and biological effects may be most critical.

11.15.2.1 Partitioning between Soils, Sediments, and Natural Waters

The movement of pesticide compounds between the solid and aqueous phases exerts considerable influence over the transport, persistence, and bioavailability of these compounds in natural waters. (The *bioavailability* of a compound is the extent to which it is accessible for uptake by living organisms. The term *natural waters* is used herein to refer to water occurring anywhere within the hydrologic system – including precipitation, surface waters, vadose zone water, and groundwater – regardless of whether or not it has been affected by human activities.) The principal phases among which this partitioning takes place are the aqueous solution itself, natural organic matter (NOM), mineral surfaces, and biological tissues. Because water in the vadose and saturated zones is in such intimate contact with natural solids, such partitioning is presumed to exert a more substantial influence over the movement and persistence of pesticide compounds below the land surface than in surface waters or the atmosphere.

Sorptive interactions with NOM are particularly important for neutral pesticide compounds, including those that are *Brønsted acids* (i.e., chemical species that can donate a hydrogen atom to another species, known as a *Brønsted base*; Stumm and Morgan, 1981). This is especially true in soils with mass fractions of organic carbon (f_{oc}) of 0.001 or more (Schwarzenbach and Westall, 1981). This threshold, however, is likely to vary inversely with the octanol–water partition coefficient (K_{ow}) among different compounds (McCarty et al., 1981). The discovery that soil–water partition coefficients (K_p) for neutral organic compounds often vary among different soils in direct relation to f_{oc} led to the development of the organic carbon–water partition coefficient, or K_{oc} ($K_{oc} = K_p/f_{oc}$; Hamaker and Thompson, 1972). The association of these compounds with

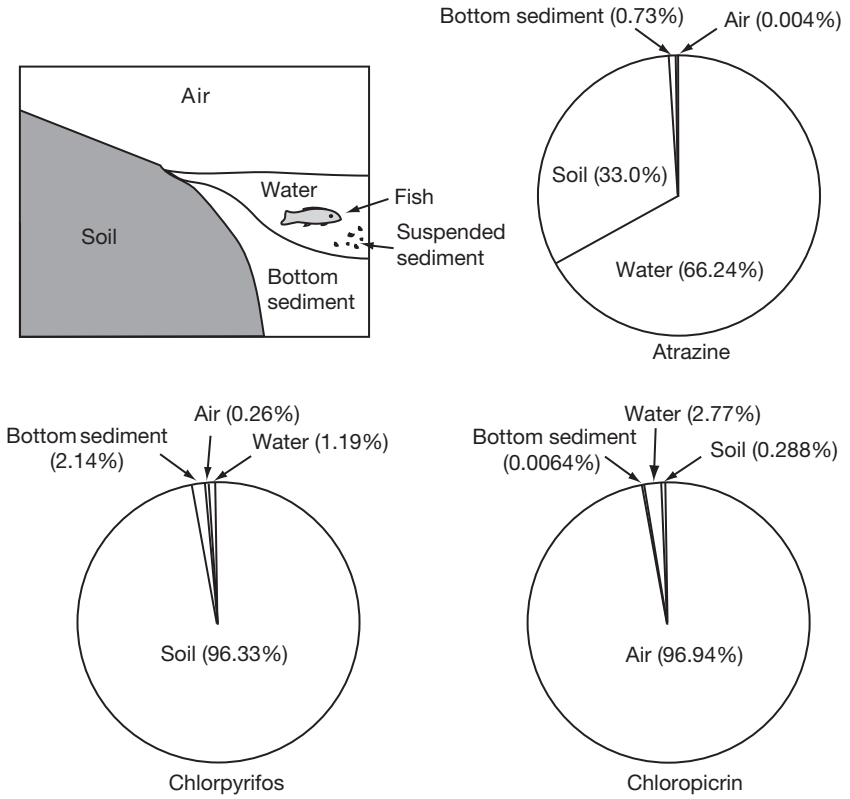

Figure 3 Distributions of atrazine, chlorpyrifos, and chloropicrin among air, surface water, soils, and aqueous sediments, based on fugacity calculations. Percentages sum to less than 100% because partitioning into fish and suspended sediment was not accounted for. Reproduced from Mackay D, Shiu W-Y, and Ma K-C (1997) *Illustrated Handbook of Physical–Chemical Properties and Environmental Fate for Organic Chemicals*, *Vol. V: Pesticide Chemicals*. New York: Lewis Publishers.

NOM is commonly viewed as being analogous to their dissolution in an organic solvent, especially since K_{oc} values are known to be inversely related to water solubility, directly related to K_{ow} and largely independent of competitive effects among solutes (Chiou, 1998, 2002). Considerable progress has been made over the past two decades in predicting K_{oc} from molecular structure (e.g., Reddy and Locke, 1994; Schüürmann et al., 2006).

Despite their normalization to f_{oc}, K_{oc} values for individual pesticide compounds still vary among different soils and sediments, though to a much lesser extent than K_p values (Curtis et al., 1986). These variations in K_{oc}, which typically span a factor of 10 or less for individual pesticide compounds (e.g., Mackay et al., 1997), are presumed to arise from variations in the sorption properties of the biogenic materials of which NOM is comprised (Shin et al., 1970), changes in the chemical properties of NOM caused by weathering (Chiou, 1998, 2002) or, for ionic compounds or Brønsted acids, variations in solution properties such as pH and salinity (Schwarzenbach et al., 1993).

The exchange of pesticide compounds between aqueous solution and the sorbed phase in soils is not instantaneous. Indeed, the more hydrophobic the compound, the longer the time required to reach sorption equilibrium. This phenomenon has been attributed to the effect of hydrophobicity on the rate at which an organic molecule diffuses through the polymeric structure of NOM within soil particles or aggregates (Brusseau and Rao, 1989; Curtis et al., 1986). Support for this explanation is provided by the fact that the amount of time required for pesticides to reach sorption equilibrium has been observed to be longer for soils containing higher amounts of NOM (e.g., Moreau and Mouvet, 1997).

A K_p value (and its corresponding K_{oc}) is most commonly determined for a given solute in a specific soil–water system by computing the slope of a *sorption isotherm* (i.e., a graph of sorbed concentration vs. dissolved concentration at equilibrium over a range of solute loadings). The widespread use of K_{oc} values assumes that the sorption isotherm is linear, that is, that the quantitative relation between the amount of solute sorbed to the soil organic carbon (C_{oc}) and the dissolved concentration (C_{aq}) is of the following form (Hamaker and Thompson, 1972):

$$C_{oc} = K_{oc} C_{aq}$$

However, the sorption of a number of pesticide compounds to some soils has been found to be more accurately described by the nonlinear Freundlich isotherm (e.g., Hamaker and Thompson, 1972; Widmer and Spalding, 1996), that is,

$$C_{oc} = K_f C_{aq}^{1/n}$$

Published values of Freundlich parameters (K_f and $1/n$) are relatively sparse, but are currently available for at least 60 pesticide compounds (Barbash, unpublished compilation).

Sorption to mineral surfaces (as opposed to NOM) is generally viewed as more of a displacement than a dissolution phenomenon. Because mineral surfaces tend to be more polar than NOM, sorption to the former is more substantial for polar and ionic compounds than for those that are more hydrophobic (Chiou, 1998, 2002; Curtis et al., 1986). Furthermore, since most NOM and mineral surfaces exhibit either a neutral or negative charge, sorption to soils and sediments is considerably stronger for pesticide compounds that are positively charged in solution – such as paraquat or diquat – than for neutral species, and weaker still for anions. As a consequence, measured K_p values in soils exhibit little dependence upon pH for pesticide compounds that are not Brønsted acids or bases (Haderlein and Schwarzenbach, 1993; Macalady and Wolfe, 1985). However, for those that are Brønsted acids or bases, K_p values increase dramatically as the pH is reduced below the pK_a value(s) for the compound (Broholm et al., 2001; Haderlein and Schwarzenbach, 1993). (The pK_a of a Brønsted acid/base pair is the negative logarithm of the equilibrium constant for their interconversion through the gain or loss of a proton. As such, the pK_a also represents the pH value below which the concentration of the acid exceeds that of the base, and above which the base dominates.) Schellenberg et al. (1984) introduced equations that may be used to quantify the effects of pH variations on K_p for Brønsted acids and bases.

Increases in temperature lead to a decrease in K_p values for most pesticide compounds (e.g., Katz, 1993), but some display the reverse trend (Chiou, 1998; Haderlein and Schwarzenbach, 1993; Hamaker and Thompson, 1972; Padilla et al., 1988). In most environmental settings, however, the effect of temperature on sorption is expected to be relatively minor – and, indeed, is nearly always neglected. Precipitation from solution may be significant for some pesticides, as is the case for glyphosate, which has been shown to form relatively insoluble metal complexes with Fe^{III}, Cu^{II}, Ca^{II}, and Mg^{II} at circumneutral pH (Subramaniam and Hoggard, 1988). (Roman numerals are used as superscripts in this chapter to denote chemical species that may be present either as dissolved ions or as part of the solid phase.)

While much of the preceding discussion has focused on the effect of water–solid partitioning on the movement of pesticide compounds below the land surface, such partitioning – along with diffusion, advection, and other physical, chemical, and biological processes (**Figure 4**) – may also influence the transport of these chemicals in surface waters. (Nowell et al. (1999) provide a detailed summary of current knowledge regarding

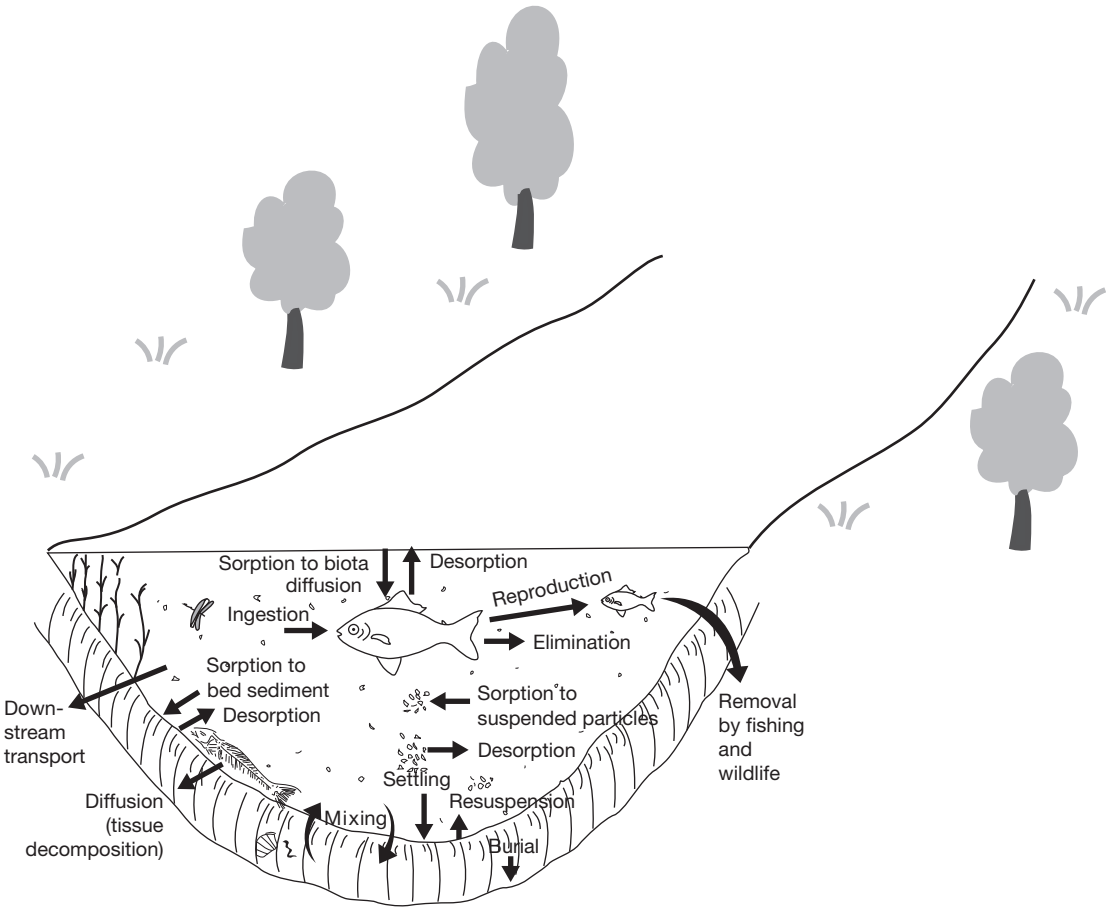

Figure 4 Pesticide movement to, from, and within sediment and aquatic biota in surface waters. Modified from Nowell LH, Capel PD, and Dileanis PD (1999) *Pesticides in Stream Sediment and Aquatic Biota – Distribution, Trends and Governing Factors*. Boca Raton, FL: CRC Press, with permission from CRC Press.

the influence of these processes on the transport of pesticide compounds in streams.) Compounds exhibiting a pronounced affinity for natural sediments – either because of hydrophobicity, low water solubility, or other chemical characteristics – are transported primarily with suspended sediments in surface waters, rather than in the aqueous phase (Wauchope, 1978). The deposition of sediments to which persistent pesticide compounds are sorbed leads to substantial increases in the residence time of these compounds in aquatic ecosystems. For this reason, detailed analyses of sediment cores obtained from lakes and reservoirs around the country have proved to be useful for observing long-term trends in the concentrations of OCs in aquatic environments over several decades (Van Metre and Mahler, 2005; Van Metre et al., 1998).

In addition to sorption and precipitation, the diffusive exchange of pesticide compounds between *mobile* and *immobile waters* also influences the rates at which these solutes move through the hydrologic system – or, more specifically, through the vadose and saturated zones. (The term *mobile water* refers to subsurface water that moves by comparatively rapid, advective flow along preferred flow paths within soils and other geologic media. By contrast, *immobile water* resides within the interior pores of soil particles and aggregates, and therefore migrates much more slowly, if at all.) This exchange is associated with the macroscopic phenomenon known as *preferential transport*, and can affect solute transport in ways that are similar to the effects of sorption, including the tailing of solute breakthrough curves, long-term uptake and release of solutes over time, and much of what is often erroneously attributed to the formation of bound residues (Barbash and Resek, 1996). The diffusion of pesticide compounds from mobile waters into zones of immobile water is also believed to exert substantial effects on bioavailability, since pesticide molecules may diffuse into the interior pore spaces of soil particles or aggregates and become inaccessible to organisms that might otherwise be able to degrade them (Zhang et al., 1998).

11.15.2.2 Partitioning between Aquatic Biota and Natural Waters

The movement and persistence of pesticide compounds in the hydrologic system are also affected by partitioning and transformation in the tissues of aquatic biota. Pesticide compounds accumulate in aquatic biota as a result of either passive partitioning from the water column or the ingestion of sediment or other organisms already containing the chemicals. The distribution of pesticides and other organic compounds between water and biological tissues has been most commonly described using a bioconcentration factor (BCF). (Compilations of BCF values for pesticides include those assembled by Kenaga (1980) and Mackay et al. (1997).) Since both the biota and sediments in aquatic ecosystems are in nearly constant contact with the water itself, the concentrations of pesticide compounds in aquatic sediments have been used as indicators of the anticipated levels of these substances in aquatic biota. This approach, most commonly implemented through the use of a biota–sediment accumulation factor (BSAF), has been shown to produce remarkably consistent results for a wide range of aquatic environments and organisms across the United States (Wong et al., 2001). Partitioning-based approaches for predicting pesticide concentrations in biota, however, do not account for the metabolism of these compounds *in vivo*. Nowell et al. (1999) provide a detailed examination of the history, theoretical basis, assumptions, and limitations of the BSAF model, as well as a comprehensive summary of existing data on the occurrence of pesticide compounds in aquatic fauna and flora across the United States.

11.15.2.3 Partitioning between Earth's Surface and the Atmosphere

Several types of observations suggest that atmospheric transport is principally responsible for the fact that pesticide residues are now likely to be detected in every terrestrial and marine ecosystem on the surface of our planet (e.g., Iwata et al., 1993; Majewski and Capel, 1995). First, as noted earlier, a large proportion of applied pesticide compounds may be transported in the air away from the original application sites as a result of either spray drift, wind erosion of soil, or volatilization from the plant, soil, and water surfaces to which the chemicals were applied (Majewski and Capel, 1995). (Large-scale movement of migrating biota may also represent an important – and, in some instances, the most important – mechanism for the global dispersal of pesticide compounds; Blais et al., 2005; Ewald et al., 1998.) Second, while terrestrial and aquatic ecosystems are spatially discontinuous, the atmosphere is a single, comparatively well-mixed medium that is in direct contact with the entire surface of the Earth. Finally, the atmosphere exhibits mixing times that, by comparison with the transformation rates of most of the compounds of interest (e.g., **Table 1**), are comparatively rapid – on the order of weeks to months for mixing within each of the northern and southern hemispheres, and 1–2 years for exchange between the hemispheres (Majewski and Capel, 1995). However, an understanding of the processes and factors that control the dissemination of pesticide compounds across the globe depends upon a knowledge not only of large-scale spatial patterns of pesticide use (e.g., US Geological Survey, 2010) and atmospheric transport (Bidleman, 1999; Majewski and Capel, 1995; Unsworth et al., 1999), but also of the mechanisms and rates of partitioning of these compounds between air and the materials at the Earth's surface.

11.15.2.3.1 Movement between air and natural waters

The parameter used most often to quantify partitioning between air and water, the Henry's law constant (H), takes several forms but is frequently calculated as the ratio between the vapor pressure and the aqueous solubility of the subcooled liquid. Suntio et al. (1988) listed the assumptions upon which the use of H to describe this partitioning is based, described methods for converting between the different forms in which H is expressed, and assembled a compilation of H values for 96 pesticides. The rate of transfer of a pesticide compound between air and water is a function of the contrast between its fugacities in the two phases (Bidleman, 1999). This exchange rate is also controlled by the rates of diffusion of the compound through the thin, adjacent films of air and water that comprise the interface between the two phases, as well as by wind speed, current velocity, turbulence, and the other factors that influence the thickness of these films (Thomas, 1990a).

While it is obvious that pesticide compounds will migrate away from their application sites immediately following their release, the directions of large-scale movement of persistent compounds over longer timescales may be more difficult to anticipate. Fugacity calculations and *enantiomer ratios*, however, have proved to be valuable tools for revealing the large-scale patterns of atmospheric transport of persistent pesticides. (Enantiomers are pairs of compounds that have the same chemical composition, but spatial arrangements of atoms that differ in such a way that the two molecules are mirror images of one another.) The first of these two methods involves estimating the fugacities of a given pesticide compound in pairs of environmental media that are in intimate physical contact (e.g., air/water or water/soil) in order to predict its future movement. If the fugacities of the compound in the two media are not equal, their ratio provides an indication of the likely direction of future exchange of the compound between the media of interest.

Enantiomer-based methods exploit the fact that some pesticide compounds are applied in known ratios of enantiomers, most commonly as *racemic* mixtures, that is, 1:1 ratios (Buser et al., 2000; Monkiedje et al., 2003). Although most abiotic transformation and partitioning processes are not affected by the structural differences between enantiomers (Bidleman, 1999), the biotransformation of some pesticide compounds has been found to be an *enantioselective* process, that is, one that exhibits a preference for one enantiomer over the other (e.g., Harner et al., 1999; Monkiedje et al., 2003). Consequently, for a pesticide compound that is applied as a racemic mixture but may undergo enantioselective biotransformation in the environment, an indication of whether or not the compound has undergone biotransformation since it was applied – and thus a rough indication of its residence time in the hydrologic system – may be discerned through the measurement of enantiomer concentration ratios (Bidleman, 1999) or, preferably, enantiomer fractions (Harner et al., 2000).

The use of both fugacity calculations and enantiomer ratios in the Great Lakes, for example, has revealed alternating, seasonal cycles of net deposition and net volatilization of OCs to and from the lake surfaces. However, these methods have also indicated that the concentrations of OCs in the lakes are in approximate long-term equilibrium with the overlying air. Thus, significant reductions in the levels of OCs in the lakes are unlikely to occur until their concentrations in the atmosphere decline. Similar observations have been made in other parts of the world, including Lake Baikal and Chesapeake Bay. Other investigations have indicated that global-scale patterns of deposition for some OCs may be more strongly controlled by temperature than by spatial patterns of application, with net volatilization occurring in more temperate regions and net deposition to soil and other solid surfaces – including snow and ice – in polar regions (Bidleman, 1999). This pattern of movement, sometimes referred to as *global distillation*, may help explain why such high levels of OCs are commonly detected in polar ecosystems (e.g., Hermanson et al., 2005; Nowell et al., 1999; Wania, 2003).

11.15.2.3.2 Movement between air, soil, and plant surfaces

The volatilization of a pesticide compound from soil is controlled by three general processes (Thomas, 1990b): (1) upward advection in the soil from capillary action caused by water evaporating at the surface (the *wick effect*); (2) partitioning between the solid, liquid, and gas phases within the soil; and (3) transport away from the soil surface into the atmosphere. If a compound is less volatile than water, the wick effect may cause it to concentrate at the soil surface, resulting in its precipitation from solution, an increase in its volatilization rate, and/or a suppression of the water evaporation rate. Thomas (1990b) summarizes a variety of methods that have been devised for estimating the rates of pesticide volatilization from soil following either surface- or depth-incorporated applications. Woodrow et al. (1997) found the rates of pesticide volatilization from recently treated soil, water bodies, and 'noninteractive' surfaces (including freshly treated plants, glass, and plastic) to be highly correlated with simple combinations of the vapor pressure, water solubility, K_{oc}, and application rates of the compounds of interest.

Pesticides in the vapor phase show considerable affinity for dry mineral surfaces, especially those of clays. However, since mineral surfaces generally exhibit a greater affinity for water than for neutral organic compounds, the vapor-phase sorption of pesticides to dry, low-f_{oc} materials diminishes markedly with increasing relative humidity (RH) as the pesticide molecules are displaced from the mineral surfaces by the adsorbed water (Chiou, 1998, 2002). One important consequence of this phenomenon is that the wetting of dry soils to which a pesticide has previously been applied (and thus sorbed) may lead to a sudden increase in the concentration of the compound in the overlying air (e.g., Majewski et al., 1993). At or above the RH required to cover all of the mineral surfaces with adsorbed water (a water content that some studies suggest is commonly at or below the wilting point), the sorption of pesticide vapor becomes controlled by interactions with the soil organic matter – rather than by competition with water – and the amount of pesticide taken up by the soil depends upon the soil f_{oc}. Organic matter has a much lower affinity for water than that exhibited by mineral surfaces. As a result, in organic rich soils, f_{oc} exerts considerably more influence over pesticide uptake than does RH, even under dry conditions (Chiou, 1998, 2002). Soil–air partition coefficients (K_{SA}) have typically been computed as the ratio between soil/water and air/water partition coefficients for the compounds of interest (e.g., $K_{SA}=K_p/H$), although methods for the direct measurement of K_{SA} have also been devised (Hippelein and McLachlan, 1998; Meijer et al., 2003).

Consistent with the observations for soil/air partitioning, plant/air partition coefficients for pesticides have been found to be correlated with K_{ow}/H (Bacci et al., 1990). (K_{ow} is commonly used as a measure of partitioning between biological tissues and water.) A direct correlation observed by Woodrow et al. (1997) between vapor pressure and the rates of volatilization from the surfaces of recently treated plants suggests that chemical interactions with plant surfaces exert only a minor influence on pesticide volatilization from plants during the first few hours following application. For persistent OCs that were banned in previous decades but are still widely detected in the environment, enantiomer ratios and other methods have been employed to distinguish between inputs from 'old' sources – that is, the ongoing atmospheric exchange of these compounds with soils, plants, and surface waters many years

after their application – and fresh inputs of the compounds in countries where their use continues, either legally or illegally (Bidleman, 1999).

11.15.3 Transformations

All transformations of pesticide compounds in the hydrologic system are initiated by either *photochemical* or *thermal* processes, depending upon whether or not the reactions are driven by solar energy. Following its introduction into the environment, the persistence of a pesticide molecule is determined by its chemical structure, as well as by the physical, chemical, and biological characteristics of the medium in which it is located. If it is exposed to sunlight of sufficient intensity within the appropriate wavelength range, the molecule may either be promoted to a higher energy state and react via *direct photolysis*, or it may undergo *indirect photolysis* by reacting with another species that has itself been promoted (either directly or indirectly) to a higher energy level by sunlight.

At the same time, however, the pesticide molecule may also be susceptible to thermal reactions. At a given temperature, the distribution of kinetic energy among all molecules of a particular chemical species exhibits a specific statistical form known as the *Boltzmann distribution*. For any given reaction, only those molecules possessing a kinetic energy exceeding a specific threshold, the *activation energy*, are likely to undergo that transformation (Atkins, 1982). Thermal reactions are those that occur as a result of collisions between molecules exceeding this energy barrier, either with or without biochemical assistance. Thus, if a pesticide molecule does not react by photolysis (either directly or indirectly), its persistence will be determined by the distribution of kinetic energy among the other chemical species with which it may undergo thermal reactions within the medium of interest.

Because pesticide compounds exhibit such a broad range of chemical structures, the variety of pathways by which they are transformed in the hydrologic system is also extensive, but all may be classified according to the manner in which the overall oxidation state of the molecule is altered, if at all. *Neutral* reactions leave the oxidation state of the original, or *parent* compound unchanged, while *electron-transfer* reactions (also referred to as *oxidation–reduction* or *redox* reactions) involve either an increase (*oxidation*) or a decrease (*reduction*) in oxidation state. Both neutral and electron-transfer mechanisms have been identified for thermal and photochemical transformations of pesticides. Most of the known transformation pathways involve reactions with other chemical species, but some are unimolecular processes – most commonly those that occur through direct photolysis. In many cases, pesticides may react via combinations of different types of reactions occurring simultaneously, sequentially or both (e.g., **Figure 5**). Several previous reviews have provided comprehensive summaries of the pathways that have been observed for the transformation of pesticide compounds in natural systems by either photochemical (e.g., Atkinson et al., 1999; Harris, 1990b; Mill and Mabey, 1985) or thermal mechanisms (e.g., Alexander, 1981; Barbash and Resek, 1996; Bollag, 1982; Castro, 1977; Coats, 1991; Gao et al., 2010; Kearney and Kaufman, 1972; Kuhn and Suflita, 1989; Roberts and Hutson, 1999; Roberts et al., 1998; Scow, 1990; Vogel et al., 1987). **Figure 6** illustrates several of the myriad reactions by which an individual pesticide may be transformed in the environment, using the example of metolachlor.

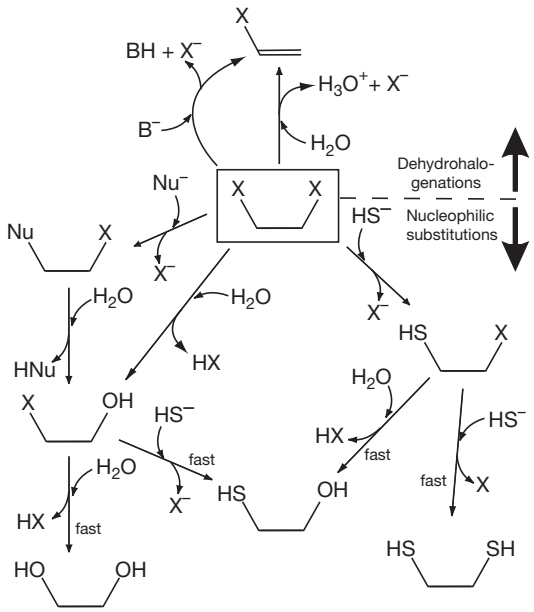

Figure 5 Chemical reactions leading to the dehalogenation of a 1,2-dihaloethane (X = Br for 1,2-dibromoethane (EDB), X = Cl for 1,2-dichloroethane) in an aqueous solution containing the bisulfide anion (HS^-) and one or more additional nucleophiles (Nu^-) that react with the compound via nucleophilic substitution (e.g., nitrate, hydroxide, or a buffer conjugate base), or bases (B^-) that react via dehydrohalogenation (e.g., hydroxide or a buffer conjugate base). Reproduced from Barbash JE (1993) *Abiotic Reactions of Halogenated Ethanes and Ethylenes with Sulfide, Nitrate and pH-Buffer Anions in Aqueous Solution*. PhD Thesis, Stanford University.

Pesticide compounds may be transformed with or without the assistance of living organisms, depending upon compound structure and the biogeochemical environment. Distinguishing between biological and abiotic mechanisms of transformation, however, is not always straightforward. For several pesticide compounds, both abiotic and microbially mediated transformations may occur simultaneously or sequentially (e.g., **Figure 6**; Bondarenko et al., 2004; Gan et al., 1999; Graetz et al., 1970; Lightfoot et al., 1987; Oremland et al., 1994; Skipper et al., 1967; Vogel and McCarty, 1987). Some transformations may occur either with or without biological assistance (e.g., Jafvert and Wolfe, 1987; Loch et al., 2002; Mandelbaum et al., 1993; Wolfe et al., 1986). Other reactions appear to be primarily, if not exclusively abiotic (Bondarenko et al., 2004; Haag and Mill, 1988a; Konrad et al., 1967). Under the conditions of most natural waters, the *mineralization* of pesticides containing carbon–carbon bonds – that is, their complete conversion to simple products such as CO_2, H_2O, and halide ions – does not take place abiotically (Alexander, 1981), although the abiotic conversion of CCl_4 to a variety of single-carbon products in the presence of dissolved sulfide and clay surfaces has been documented (Kriegman-King and Reinhard, 1992). The cleavage of aromatic rings also does not

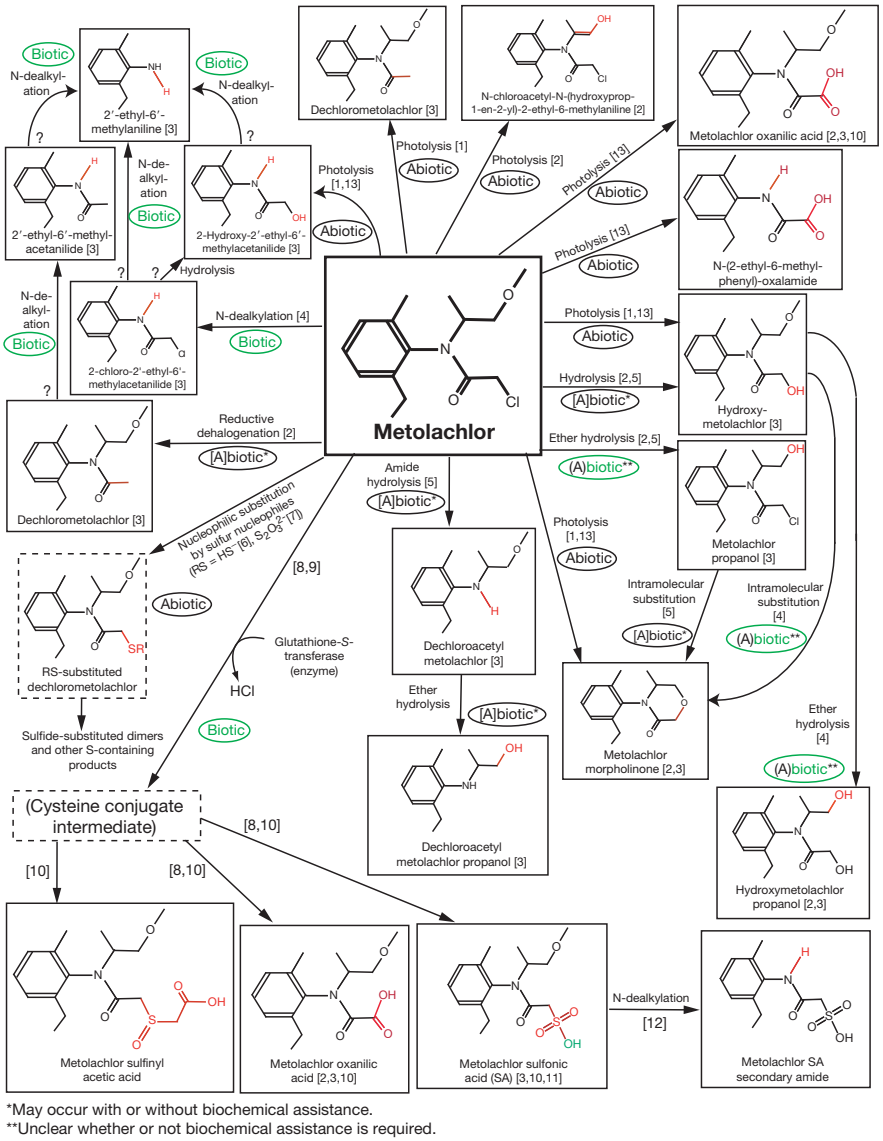

Figure 6 Some of the principal transformations of metolachlor in the environment. For each product, the part of the molecule undergoing transformation is shown in red. Numbers in brackets refer to the original sources of information for each reaction (adjacent to arrows) or compound detections in environmental media (inside boxes). Reaction mechanisms shown without reference numbers were inferred from the observed change in structure; those shown with a question mark ('?') indicate proposed, rather than reported, transformation pathways. Compounds shown without reference numbers adjacent to their names were reported by laboratory studies, but may not have been detected in the environment to date. Note that dechlorometolachlor and metolachlor oxanilic acid (like 2-hydroxy-2′ethyl-6′methylacetanilide, hydroxymetolachlor, and metolachlor morpholinone) have been found to be produced by both photochemical and thermal (nonphotochemical) reactions. References cited: [1] Kochany and Maguire (1994), [2] Chesters et al. (1989), [3] Hladik et al. (2005), [4] Liu et al. (1991), [5] Carlson (2003), [6] Stamper et al. (1997), [7] Gan et al. (2002), [8] Field and Thurman (1996), [9] Scarponi et al. (1991), [10] Graham et al. (1999), [11] Aga et al. (1996), [12] Lee and Strahan (2003), [13] Day and Hodge (1996).

appear to occur readily through abiotic means in natural waters. With the exception of direct photolysis, however, one or more organisms have been found to be capable of facilitating all of the major types of pesticide transformation reactions listed above (e.g., Alexander, 1981; Barbash and Resek, 1996; Castro, 1977; Coats, 1991; Kearney and Kaufman, 1972; Kuhn and Suflita, 1989; Scow, 1990; Zepp and Wolfe, 1987).

As noted earlier, transformation reactions of pesticide compounds are typically faster in air than in water (Mackay et al., 1997). However, general trends among the rates of different reactions per se are elusive, since chemical structure and the physical, chemical, and biological characteristics of the reaction medium may be as important in determining reaction rate as the nature of the reaction in question. The following discussion describes the circumstances under which pesticide compounds undergo each major type of reaction, and examines the various ways in which the rates of these transformations are controlled by chemical structure and the biogeochemical environment.

11.15.3.1 Photochemical Transformations

Pesticide compounds that may undergo direct photolysis in the hydrologic system are those for which the wavelengths

required for bond breakage fall within the range of the solar spectrum (e.g., Zepp et al., 1975). Because of this constraint, relatively few pesticide compounds undergo direct photolysis; those that have been observed to do so include several chlorophenoxy acids (and their esters), nitroaromatics, triazines, OPs, OCs, carbamates, polychlorophenols, ureas, and fumigants (e.g., Chu and Jafvert, 1994; Crosby and Leitis, 1973; Dilling et al., 1984; Harris, 1990b; Lam et al., 2003; Mansour and Feicht, 1994; Mill and Mabey, 1985; Zepp et al., 1984), as well as fipronil (Walse et al., 2004) and metolachlor (Kochany and Maguire, 1994). Most phototransformations of pesticide compounds occur through indirect photolysis, as a result of reaction with another species, known as a *sensitizer*, or a sensitizer-produced *oxidant*. The most common sensitizers for the phototransformation of pesticide compounds in natural waters include nitrate (Haag and Hoigné, 1985) and the humic and fulvic acids derived from NOM (e.g., Mansour and Feicht, 1994). Sensitizer-produced oxidants include hydrogen peroxide, singlet oxygen, hydroxyl, peroxy, and nitrate radicals, and photoexcited triplet diradicals (Cooper and Zika, 1983; Mackay et al., 1997; Mill and Mabey, 1985). The photoproduction of hydrogen peroxide has also been shown to be catalyzed by algae (Zepp, 1988). In contrast with its tendency to increase the rates of indirect photolysis by acting as a sensitizer, NOM may also *inhibit* the rates of direct photolysis (Kochany and Maguire, 1994) through light attenuation and, in some cases, the quenching of reactive intermediates (Mill and Mabey, 1985; Walse et al., 2004).

For some pesticide compounds, such as dinitroaniline herbicides (Weber, 1990), phototransformation occurs primarily in the vapor phase, rather than in the dissolved or sorbed phases. Perhaps the most environmentally significant pesticide phototransformation in the atmosphere, however, is the photolysis of the fumigant methyl bromide, since the bromine radicals created by this reaction are 50 times more efficient than chlorine radicals in destroying stratospheric ozone (Jeffers and Wolfe, 1996). Detailed summaries of the rates and pathways of phototransformation of pesticides and other organic compounds in natural systems, and discussions of the physical and chemical factors that influence these reactions, have been presented elsewhere (e.g., Atkinson et al., 1999; Harris, 1990b; Mill and Mabey, 1985; Zepp et al., 1984).

11.15.3.2 Neutral Reactions

The neutral reactions responsible for transforming pesticide compounds in the hydrologic system – listed in roughly decreasing order of the number of compounds known to be affected – include nucleophilic substitution, dehydrohalogenation, rearrangement, and addition. **Figure 7** displays some examples of these reactions for pesticides. Nucleophilic substitution involves the replacement of a substituent on the molecule (the *leaving group*) by an attacking species (the *nucleophile*). (A leaving group is any part of a molecule that is removed during a chemical reaction; March, 1985.) Electrophilic substitution reactions are also well known in organic chemistry (March, 1985). However, since nucleophiles are substantially more abundant than electrophiles in most natural waters, reactions with electrophiles are of relatively minor importance in the hydrologic system, and confined primarily to photolytic and biologically mediated transformations (Schwarzenbach et al., 1993).

Not surprisingly, the nucleophilic substitution reactions that have been studied most extensively for pesticide compounds in natural waters (e.g., Mabey and Mill, 1978; Washington, 1995) are those involving the three solutes that are present in all aqueous systems, that is, H_2O, its conjugate base (OH^-), and its conjugate acid (H_3O^+). These reactions are referred to as *neutral*, *base-catalyzed*, and *acid-catalyzed hydrolysis*, respectively. The first two of these reactions involve the direct displacement of the leaving group by the nucleophile (H_2O or OH^-), while in the third case, protonation near the *alpha* carbon (C_α, i.e., the one from which the leaving group is displaced) decreases the electron density on C_α, rendering it more susceptible to nucleophilic attack by H_2O (March, 1985). Some plants employ catalysts to hydrolyze pesticides in their tissues as a detoxification mechanism (Beynon et al., 1972). Extracellular biochemicals that may catalyze the hydrolysis of pesticide compounds include protease, esterase, and phosphatase enzymes (Huang and Stone, 2000). Other microbial enzymes that facilitate pesticide hydrolysis have been summarized by Bollag (1982). As discussed later, metals may also catalyze hydrolysis reactions.

Among the other nucleophiles whose reactions with pesticide compounds may be significant in the hydrologic system, perhaps the most important are reduced sulfur anions (Barbash and Reinhard, 1989a), particularly bisulfide, polysulfides (e.g., Barbash and Reinhard, 1989b; Lippa and Roberts, 2002; Loch et al., 2002; Miah and Jans, 2001; Roberts et al., 1992; Stamper et al., 1997), and thiosulfate (e.g., Ehrenberg et al., 1974; Wang et al., 2000). Reactions with these nucleophiles are often an indirect mechanism of biotransformation, as these and other reduced sulfur anions are derived primarily from biological activity. However, living organisms also actively employ a variety of nucleophilic enzymes to detoxify halogenated compounds by displacing halide. In addition to the enzyme-catalyzed hydrolyses mentioned earlier, another environmentally important example of these reactions is the displacement of chloride from chloroacetanilide herbicides by glutathione and glutathione-*S*-transferase (e.g., **Figure 6**) to form the corresponding sulfonic and oxanilic acids (Field and Thurman, 1996). (The initial step in this example is an illustration of a *synthetic reaction*, or *conjugation* in which a part of the original molecule is replaced with a substantially larger moiety(Bollag, 1982; Coats, 1991)). Work by Loch et al. (2002), however, suggests that the sulfonic acid products might also be generated through abiotic reactions of chloroacetanilide herbicides with reduced sulfur species.

Other nucleophiles of potential importance include pH buffer anions (**Figure 5**) since, as noted later, buffers are commonly used to stabilize pH during laboratory studies of pesticide transformations. Although it is only a weak nucleophile, the nitrate anion has also been found (Barbash, 1993; Barbash and Reinhard, 1992b) to displace bromide from the fumigant 1,2-dibromoethane (ethylene dibromide, or EDB) in aqueous solution (**Figure 5**), an observation worth noting because nitrate is probably the most widespread groundwater contaminant in the world.

Another neutral mechanism by which some pesticide compounds may be transformed is dehydrohalogenation, which involves the removal of a proton and a halide ion (HX) from a pair of adjacent carbon atoms (e.g., **Figures 5** and **7**). Under

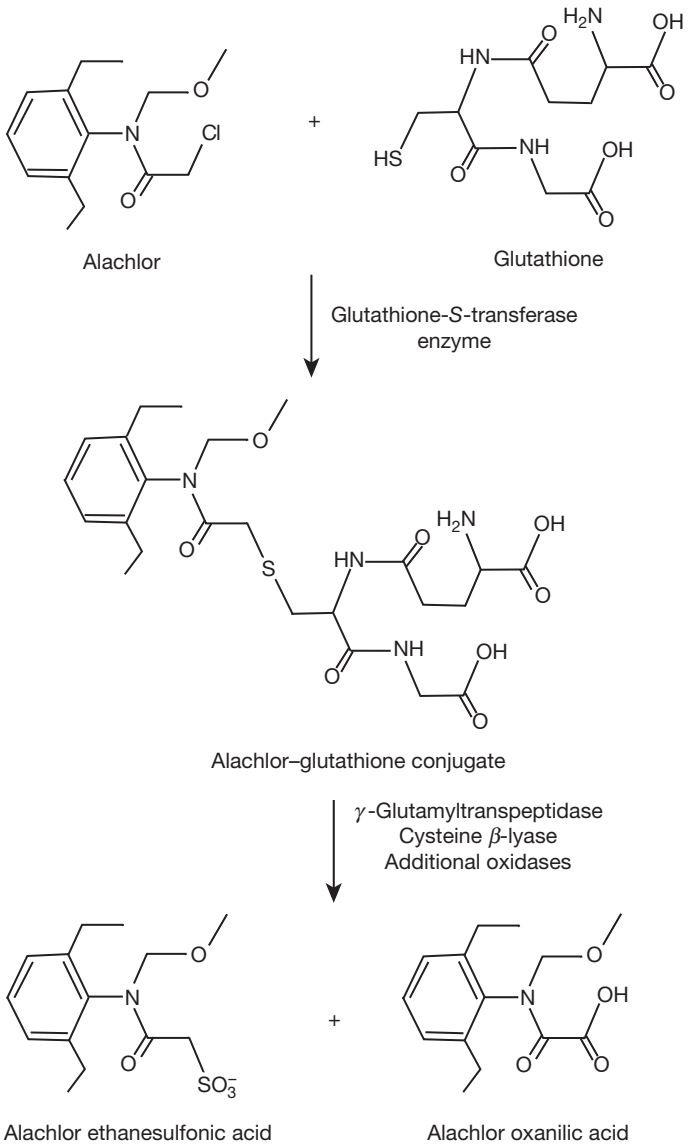

Figure 7 Some examples of neutral reactions of pesticide compounds: nucleophilic substitution (e.g., hydrolysis, Roberts and Stoydin, 1976); dehydrohalogenation (Kuhn and Suflita, 1989); intramolecular reactions (e.g., rearrangement, Newland et al., 1969); and addition (e.g., hydration, Sirons et al., 1973).

the comparatively mild conditions of most natural waters, only singly bonded carbons are likely to undergo this reaction, leading to the formation of the corresponding alkene. Pesticide compounds that have been observed to undergo dehydrohalogenation under environmentally relevant conditions include a number of fumigants, insecticides, and volatile adjuvants (Barbash and Reinhard, 1992a,b; Burlinson et al., 1982; Cline and Delfino, 1989; Deeley et al., 1991; Haag and Mill, 1988a; Jeffers et al., 1989; Kuhn and Suflita, 1989; Ngabe et al., 1993; Vogel and McCarty, 1987; Vogel and Reinhard, 1986).

Two other neutral mechanisms of pesticide transformation are intramolecular reactions and additions (Figure 7). Intramolecular reactions of pesticide compounds may leave the overall chemical composition of the parent unchanged (*rearrangements* – Newland et al., 1969; Russell et al., 1968), slightly altered (Coats, 1991), or substantially modified (Wang and Arnold, 2003; Wei et al., 2000). Addition reactions involve the coupling of a compound containing a double or triple bond with another molecule; examples involving pesticide compounds include the hydration of cyanazine to form cyanazine amide (Sirons et al., 1973), the hydration of acrolein to form 3-hydroxypropanal (Bowmer and Higgins, 1976), and the hypothesized addition of H_2S to polychloroethenes to form the corresponding polychloroethanethiols (Barbash, 1993; Barbash and Reinhard, 1992a).

11.15.3.3 Electron-Transfer Reactions

Thermodynamic considerations dictate that the likelihood with which a pesticide compound in a particular geochemical setting will undergo oxidation or reduction is governed in large part by the tendency of the other chemical species present to

accept or donate electrons, respectively (McCarty, 1972). In addition to the more transient oxidants mentioned earlier in relation to photochemical reactions, those that are most commonly present in natural waters – listed in roughly decreasing order of their tendency to accept electrons – include O_2, NO_3^-, Mn^{IV}, Fe^{III}, SO_4^{2-}, and CO_2. Conversely, the most common reductants in natural waters include CH_4 and other forms of reduced organic carbon, S^{II}, Fe^{II}, Mn^{II}, NH_4^+, and H_2O (Christensen et al., 2000). Extensive discussion of the chemistry of these and other naturally occurring oxidants and reductants in the hydrologic system has been provided elsewhere in this volume (see **Chapters 11.12** and **11.16**).

Many redox transformations of pesticide compounds that may take place in the hydrologic system have been observed to occur abiotically (e.g., Baxter, 1990; Carlson et al., 2002; Castro and Kray, 1966; Curtis and Reinhard, 1994; Jafvert and Wolfe, 1987; Klecka and Gonsior, 1984; Kray and Castro, 1964; Kriegman-King and Reinhard, 1992; Mochida et al., 1977; Strathmann and Stone, 2001; Tratnyek and Macalady, 1989; Wade and Castro, 1973; Wang and Arnold, 2003). Among the most common are reactions with both organic and inorganic forms of reduced iron, as well as reactions with reduced forms of nonferrous metals, such as Cr^{II}, Cu^{I}, Cu^{II}, and Sn^{II}. Reactions with these other metals may be important in natural waters affected by the use of copper-based fungicides or algicides for agriculture, aquaculture, wood preservation, or aquatic weed control; by the discharge of mine drainage or tanning wastes; or by the use of paints containing organotin fungicides on boats.

While many redox transformations of pesticide compounds can occur abiotically, virtually all such reactions in natural systems are facilitated, either directly or indirectly, by biological processes (Wolfe and Macalady, 1992). Some pesticide compounds may be taken up by living organisms and directly oxidized or reduced through the involvement of a variety of redox-active biomolecules (Bollag, 1982). Enzymes that have been found to be responsible for the biological oxidation of pesticide compounds include methane monooxygenase (Little et al., 1988) and mixed-function oxidases (Ahmed et al., 1980); those involved in reduction reactions consist primarily of transition metal complexes centered on iron, cobalt, or nickel (e.g., Chiu and Reinhard, 1995; Gantzer and Wackett, 1991). In addition to their ability to oxidize or reduce pesticide compounds directly, living organisms also exert indirect control over these reactions by regulating the predominant terminal electron-accepting processes (TEAPs) in natural waters (Lovley et al., 1994).

Although a large number of studies have been conducted to examine the persistence of pesticide compounds under the geochemical conditions encountered in soils and natural waters (Barbash and Resek, 1996), relatively few have reported these observations in terms of the dominant TEAPs under which these transformations are likely to occur. **Figure 8** summarizes the results from some of the studies from which such information may be extracted. In the figure, the location of each compound indicates the condition(s) under which it has been found to be relatively stable in natural waters. Most of the examples shown involve reductive dehalogenation, reflecting the fact that, as noted by Wolfe and Macalady (1992), most investigations of redox reactions involving pesticides have focused on this type of transformation. For each reaction shown, the shorter the arrow, the more precisely the results from the cited studies could be used to determine the boundary separating the regions of redox stability for parent and product(s). Thus, for example, the specific TEAP under which bromacil undergoes reductive debromination appears to have been more precisely determined than that under which trichloromethane (chloroform) undergoes dechlorination. (Data from other studies not used for the construction of **Figure 8**, however, may have helped to define these boundaries more precisely.) The figure also shows that the same type of reaction may require different TEAPs in order for the transformation of different compounds to take place. For example, while the dechlorination of tetrachloromethane to trichloromethane can occur under denitrifying conditions, the dechlorination of 2,4,5-T to 2,4-D and 2,5-D requires sulfate-reducing conditions. **Figure 8** also shows that transformations of the same parent compound may yield different products under the influence of different TEAPs (tetrachloromethane, dicamba).

Evidence for the importance of redox conditions in controlling the occurrence of redox-active pesticide compounds in ground water was provided by a series of statistically significant correlations ($p \leq 0.05$) observed between the concentrations of dissolved oxygen (DO) and those of several VOCs in shallow ground water beneath urban areas across the United States. Squillace et al. (2004) found that the concentrations of VOCs in which the carbon is relatively oxidized – that is, chloroform, bromodichloromethane (two compounds produced from the use of chlorine for water disinfection; e.g., Ivahnenko and Barbash, 2004), and 1,1,1-trichloroethane (an adjuvant) – exhibited significant positive relations with DO concentrations. By contrast, toluene (also an adjuvant) – in which the carbon is more reduced – showed an *inverse* relation with DO concentrations. Of particular relevance to **Figure 8** were the observations by Squillace et al. (2004) that the concentrations of 1,1-dichloroethane were positively correlated with those of 1,1,1-trichloroethane but *inversely* correlated with those of DO – suggesting that the presence of 1,1-dichloroethane may have been largely attributable to the reductive dechlorination of 1,1,1-trichloroethane under anoxic conditions.

For neutral reactions, the nature of the attacking species can often be inferred from the composition and structure of the reaction products. By contrast, the specific oxidants or reductants with which pesticide compounds undergo electron-transfer reactions in the hydrologic system are usually unclear (Wolfe and Macalady, 1992). This uncertainty arises both from the variety of different species that can serve as electron donors or acceptors in natural systems (many of which were listed earlier), and from the potential involvement of electron-transfer agents that may act as intermediaries in these reactions (**Figure 9**). The most common electron-transfer agents (or *electron carriers*) in natural waters appear to be redox-active moieties associated with NOM, since the rates of reduction of pesticides have been found to vary directly with the NOM content of soils (Glass, 1972) and sediments (Wolfe and Macalady, 1992). The specific components of NOM that are responsible for promoting the reduction of pesticide compounds in natural systems are elusive, but laboratory studies have demonstrated that these reactions may be facilitated by

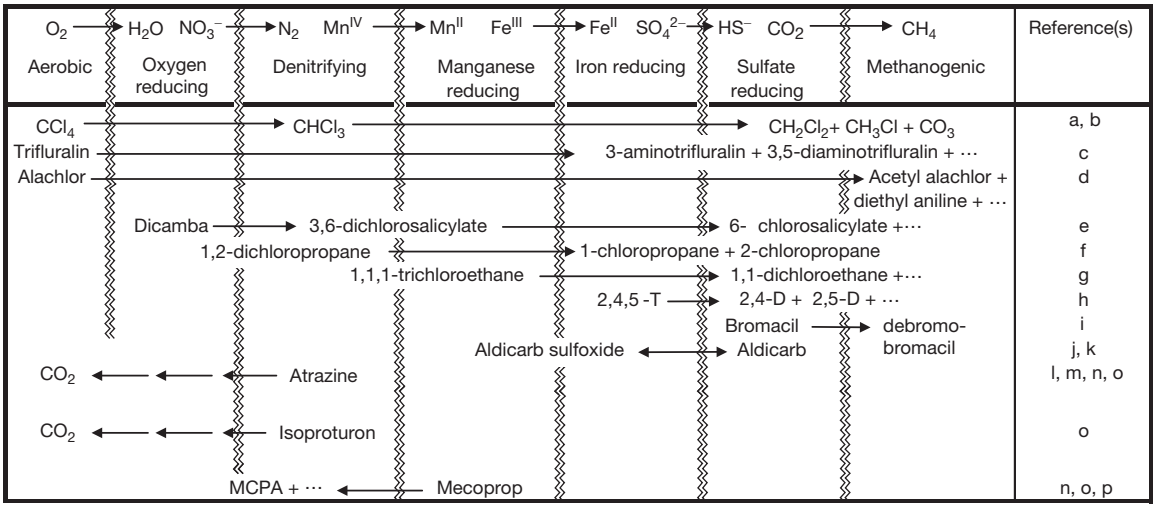

Figure 8 Some examples of electron-transfer reactions of pesticide compounds in relation to dominant terminal electron-accepting processes (TEAPs) in natural waters. TEAP sequence based on Christensen et al. (2000). Manganese, iron, sulfur, or carbon may be present in either the dissolved or solid phase. Location of each compound indicates the condition(s) under which it has been found to be relatively stable in natural waters. Incomplete lists of transformation products denoted by ellipsis (. . .); compounds shown are those inferred to have been derived directly from the parent compound. One-way arrows denote essentially irreversible reactions, two-way arrow denotes a reversible reaction, and multiple arrows in sequence denote multistep reactions. References cited: a: Egli et al. (1988), b: Picardal et al. (1995), c: Wang and Arnold (2003), d: Novak et al. (1997), e: Milligan and Häggblom (1999), f: Tesoriero et al. (2001), g: Klecka et al. (1990), h: Gibson and Suflita (1986), i: Adrian and Suflita (1990), j: Miles and Delfino (1985), k: Lightfoot et al. (1987), l: Nair and Schnoor (1992), m: Papiernik and Spalding (1998), n: Rügge et al. (1999), o: Larsen et al. (2000), p: Agertved et al. (1992).

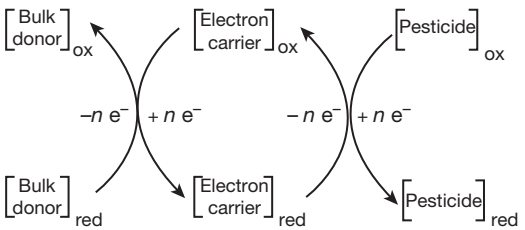

Figure 9 Hypothesized mechanism for the reductive transformation of a pesticide compound through the transfer of electrons from a bulk electron donor (e.g., FeS, Kenneke and Weber, 2003) to a pesticide molecule (e.g., methyl parathion, Tratnyek and Macalady, 1989) by an electron carrier (e.g., hydroquinone, Schwarzenbach et al., 1990). Reproduced from Schwarzenbach RP, Stierli R, Lanz K, and Zeyer J (1990) Quinone and iron porphyrin mediated reduction of nitroaromatic compounds in homogeneous aqueous solution. *Environmental Science & Technology* 24(10): 1566–1574, with permission from American Chemical Society.

several different redox-active moieties likely to be present in NOM (Chiu and Reinhard, 1995; Curtis and Reinhard, 1994; Gantzer and Wackett, 1991; Garrison et al., 2000; Klecka and Gonsior, 1984; Schwarzenbach et al., 1990; Tratnyek and Macalady, 1989; Wang and Arnold, 2003). These moieties are commonly thought to serve primarily as electron carriers in such reactions by cycling back and forth between electron acceptance from a 'bulk' electron donor (e.g., solid-phase iron sulfides; Kenneke and Weber, 2003) and electron donation to the pesticide compound (**Figure 9**). However, Glass (1972) proposed an alternate system in which iron serves as the electron carrier, and NOM as the bulk electron donor.

11.15.3.4 Governing Factors

The rates and mechanisms of transformation of a pesticide compound in the hydrologic system are determined by the concentration and structure of the compound of interest (*substrate*), as well as the physical, chemical, and biological circumstances under which each reaction takes place – including the concentrations and structures of other chemical species with which the substrate may react. As might be expected, these factors often show complex patterns of interdependence, such as the simultaneous influence of temperature and soil moisture on reaction rates, or the fact that pH can exert both direct and indirect effects on pesticide persistence. These influences, as well as their interactions, are discussed below.

11.15.3.4.1 Reactant concentrations

Except for intramolecular reactions and direct photolysis, most transformations of pesticide compounds in the hydrologic system are *bimolecular*, that is, their rate-limiting step involves a reaction between the substrate and another chemical species. In natural waters, these other species – which may be of biological or abiotic origin, or may be associated with the surfaces of natural materials – consist primarily of Brønsted acids and bases, nucleophiles, oxidants, reductants, and catalysts. Although there are some exceptions (e.g., Hemmamda et al., 1994; Huang and Stone, 2000), the rates of abiotic bimolecular transformation of pesticide compounds in *homogeneous* aqueous solution (i.e., in the absence of a solid phase) have been found to be first order with respect to the aqueous concentrations of both the substrate and the other reactant – and thus second-order overall – for a wide range of reactions (e.g., Burlinson et al., 1982; Curtis and Reinhard, 1994; Deeley et al., 1991; Haag and Mill, 1988b; Jafvert and Wolfe, 1987;

Klecka and Gonsior, 1984; Mill and Mabey, 1985; Roberts et al., 1992; Schwarzenbach et al., 1990; Strathmann and Stone, 2001; Tratnyek and Macalady, 1989; Walraevens et al., 1974; Wan et al., 1994; Wang and Arnold, 2003; Wei et al., 2000). The widespread use of transformation half-lives for quantifying the persistence of pesticide compounds in the hydrologic system (e.g., Mackay et al., 1997), however, is based on the assumption of *pseudo-first-order kinetics* with respect to the substrate, that is, that the concentrations of the other reactants are sufficiently high to remain effectively constant during the transformation of the substrate (Moore and Pearson, 1981). For heterogeneous reactions – which may involve the participation of soil, mineral, or biological surfaces – reaction rates may exhibit a different quantitative relation to the concentrations of the substrate (Zepp and Wolfe, 1987) or the other reactants (Kriegman-King and Reinhard, 1994).

Because the rates of biotransformation are influenced by a variety of factors related to the size, growth, and substrate utilization rate of the microbial populations involved, they often exhibit a more complex dependence upon substrate concentration than do the rates of abiotic transformation in homogeneous solution (D'Adamo et al., 1984). Under many circumstances, however, these more complex relations often simplify to being pseudo first order with respect to substrate concentration, particularly when the latter is substantially lower than that required to support half the maximum rate of growth of the organisms of interest. At concentrations well above this level, transformation rates may be independent of substrate concentration (Paris et al., 1981).

11.15.3.4.2 Structure and properties of the pesticide substrate

The development of synthetic pesticides has always depended upon an understanding of the effects of chemical structure on the toxicity to the target organism(s). (These effects are discussed in a later section.) However, as the deleterious effects of pesticide compounds on nontarget organisms became more widely known (e.g., Carson, 1962), it also became increasingly important to learn how the structures of these chemicals control their persistence in the hydrologic system. Indeed, the properties responsible for biological activity are often those that most affect environmental persistence as well (e.g., Liu et al., 2005; Scarponi et al., 1991; Smolen and Stone, 1997). In addition to their direct effects on reactivity (discussed below), variations in chemical structure will also influence persistence indirectly if they shift the partitioning among different phases in which reaction rates are substantially different. Because the ways in which the structure of a pesticide compound controls its reactivity depend, in turn, upon reaction mechanism, these effects will be examined separately for each of the major types of reactions.

(1) *Neutral reactions*. As noted previously, more studies have been conducted on neutral reactions (especially hydrolysis and dehydrohalogenation) than on other types of reaction involving pesticide compounds in aqueous solution. Thus, it is not surprising that these reactions have also yielded some of the most extensive understanding of the effects of structure on the reactivity of pesticide compounds in the hydrologic system. Investigations of this topic for hydrolysis and dehydrohalogenation have also provided some of the most statistically significant quantitative structure–reactivity relations (QSRRs) observed for pesticide compounds (e.g., Roberts et al., 1993; Schwarzenbach et al., 1993; Wolfe et al., 1978).

Several QSRR studies suggest that among the structural features with the greatest influence over hydrolysis rates are those that affect the pK_a of the leaving group. For example, the initial step in OP hydrolysis, which usually occurs at one of the three phosphate ester linkages, involves the displacement of the leaving group with the lowest pK_a (Smolen and Stone, 1997). As a result, for each of five organothiophosphate ester insecticides investigated by Smolen and Stone (1997), the initial product of hydrolysis was always a phenolate anion (**Figure 10**). This also explains why dimethyl ester OPs, such as methyl parathion and methyl azinphos, hydrolyze more rapidly than their diethyl ester counterparts (Lartiges and Garrigues, 1995). Similarly, for each of four groups of carbamates (*N*-methyl, *N*-phenyl, *N*,*N*-dimethyl, and *N*-methyl-*N*-phenyl), the second-order reaction rate constants for base-promoted hydrolysis have been found to be inversely correlated with the pK_a values of the displaced leaving groups (Wolfe et al., 1978). Several of the correlation equations devised for predicting pesticide hydrolysis rates from pK_a values have been compiled by Harris (1990a).

Many other structural effects on the rates of nucleophilic substitution reactions of pesticide compounds have been noted. For example, carbamates with two substituents (other than hydrogen) bound to nitrogen undergo base-promoted hydrolysis more slowly than those with only one (Wolfe et al., 1978), perhaps as a result of *steric hindrance* (i.e., the enhanced restriction of access to the reaction site by the presence of larger substituents near C_α). Steric hindrance is also believed to be responsible for some of the effects of structure on the rates of acid- and base-catalyzed hydrolysis of chloroacetamide herbicides – particularly the size of the ether or alkyl substituent bound to the amide nitrogen (Carlson, 2003; Carlson and Roberts, 2002). Data presented by Scarponi et al. (1991) suggest that similar factors may affect the rates of nucleophilic substitution reactions between chloroacetamides and glutathione. In a comprehensive analysis of the effects of structure on the rates and pathways of biotransformation of 30 amide-containing synthetic compounds (including several pesticides and pharmaceuticals), Helbling et al. (2010) identified steric hindrance as the principal factor responsible for the observation that all of the primary and secondary amides reacted by enzyme-catalyzed hydrolysis rather than N-dealkylation, while the opposite was true for the tertiary amides. Zepp et al. (1975) found that the rates of hydrolysis of 2,4-D esters (2,4-$C_6H_3Cl_2$—O—CH_2COOR) are higher if R contains an ether linkage near the ester carboxyl group than if R is a hydrocarbon moiety.

The bimolecular nucleophilic (S_N2) displacement of halide from haloalkane adjuvants and fumigants is slowed by the presence of alkyl groups or additional halogen atoms bound to the carbon at (C_α), or immediately adjacent to (C_β), the site of attack. Although bromide is a better leaving group than chloride (i.e., it is displaced more rapidly than chloride), trends in the relative rates of displacement of different

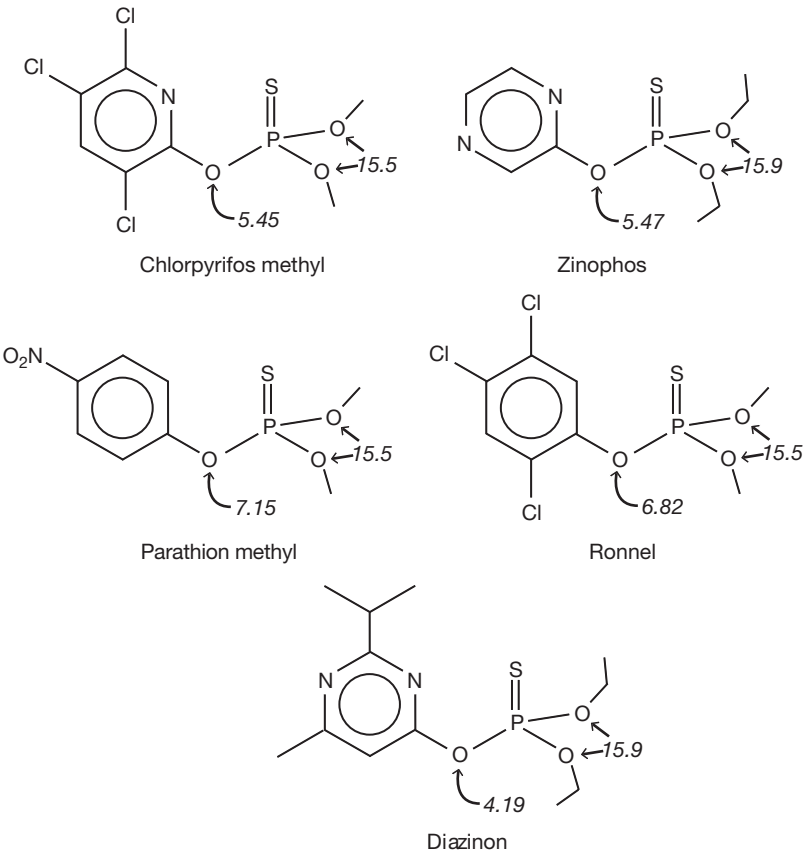

Figure 10 pK_a values for different leaving groups for a series of organothiophosphate insecticides. Leaving group with the lowest pK_a value in each compound is the one first displaced by hydrolysis. Reproduced from Smolen JM and Stone AT (1997) Divalent metal ion-catalyzed hydrolysis of phosphorothionate ester pesticides and their corresponding oxonates. *Environmental Science & Technology* 31(6): 1664–1673, with permission from American Chemical Society.

halogens may also depend upon the nature of the attacking species, as well as other substituents bound to C_α and C_β. These and other effects of structure on the rates of S_N2 displacement of halide from halogenated pesticide compounds have been examined extensively (e.g., Barbash, 1993; Barbash and Reinhard, 1989a; Roberts et al., 1993; Schwarzenbach et al., 1993; Stamper et al., 1997).

Since bimolecular dehydrohalogenation reactions are initiated by the abstraction of a hydrogen atom (from C_α) by a Brønsted base, they are promoted by structural factors that increase the ease with which this hydrogen atom can be removed from the molecule, such as the presence of halogens or other *electron-withdrawing* substituents bound to C_α. (These are moieties that withdraw electron density from the rest of the molecule, the effect being less pronounced with increasing distance from the substituent.) Because this transformation also involves the departure of halide from the adjacent carbon (C_β), rates of reaction are higher for the loss of HBr than for the loss of HCl (e.g., Barbash, 1993; Barbash and Reinhard, 1992a; Burlinson et al., 1982). Roberts et al. (1993) provided a comprehensive discussion of these and other effects of structure on the rates of dehydrohalogenation reactions.

(2) *Electron-transfer reactions*. Although many types of redox reactions involving pesticide compounds have been investigated (Barbash and Resek, 1996), most of what has been learned about the effects of substrate structure and properties on the rates of these reactions in the hydrologic system has come from studies of reductive dehalogenation (e.g., Peijnenburg et al., 1992b) and nitro group reduction (e.g., Schwarzenbach et al., 1993; Wang and Arnold, 2003). Other factors remaining constant, the rates of reductive dehalogenation increase with decreasing strength of the carbon–halogen bond being broken. As a result, the rates of these reactions generally (1) increase with increasing numbers of halogens on the molecule (e.g., Gantzer and Wackett, 1991; Jafvert and Wolfe, 1987), especially at C_α (Butler and Hayes, 2000; Klecka and Gonsior, 1984; Mochida et al., 1977); (2) decrease among halogens in the order I > Br > Cl (e.g., Jafvert and Wolfe, 1987; Kochi and Powers, 1970; Schwarzenbach et al., 1993; Wade and Castro, 1973); (3) are higher for the removal of halogen from *polyhaloalkanes* (polyhalogenated hydrocarbons lacking multiple carbon–carbon bonds) than from the corresponding *polyhaloalkenes* (polyhalogenated, nonaromatic hydrocarbons with one or more carbon–carbon double bonds) (Butler and Hayes, 2000; Gantzer and Wackett, 1991); and (4) are positively correlated with one-electron reduction potentials (e.g., Butler and

Hayes, 2000; Curtis and Reinhard, 1994; Gantzer and Wackett, 1991). A positive correlation of reaction rates with reduction potentials has also been reported for the reduction of nitroaromatic compounds (e.g., Schwarzenbach et al., 1990; Wang and Arnold, 2003). Systematic relations between the rates of reductive dechlorination of polyhaloethanes and electron densities on carbon have also been observed (Salmon et al., 1981).

Rates of reduction may also be influenced by the manner in which different substituents affect the distribution of electrons in the substrate molecule (*electronic* effects), or hinder access to reaction sites (steric effects). Because the initial, rate-limiting step in most of these reactions involves the addition of an electron to the substrate to form a carbon radical, reaction rates are generally increased by electron-withdrawing groups (e.g., halogens, acetyl, nitro), and decreased by *electron-donating* groups, that is, substituents such as alkyl groups that donate electron density to the rest of the molecule (e.g., Peijnenburg et al., 1992b; Wang and Arnold, 2003). The opposite pattern is expected for rates of oxidation (e.g., Dragun and Helling, 1985). For reactions involving aromatic compounds, electronic effects are substantially more pronounced for substituents located in positions that are either *ortho* or *para* to the substituent being replaced or altered (i.e., either one or three carbons away on the hexagonal aromatic ring) than for those in the *meta* position (i.e., located two carbons away). By contrast, steric effects are most important for substituents in the *ortho* position (Peijnenburg et al., 1992b; Schwarzenbach et al., 1993). These electronic and steric effects on the rates of electron-transfer reactions of pesticide compounds are in agreement with general reactivity theory (March, 1985).

(3) *Photochemical reactions*. As noted earlier, phototransformations in the hydrologic system occur only for those substrates that either absorb a sufficient amount of light energy within the solar spectrum, or react with photoexcited sensitizers or other photoproduced oxidants. In general, structures that promote light absorption include extensively conjugated hydrocarbon systems (i.e., those possessing alternating double and single bonds), substituents containing unsaturated heteroatoms (e.g., nitro, azo, or carbonyl) and, for substituted aromatics, halo, phenyl, and alkoxyl groups (Harris, 1990b; Mill and Mabey, 1985). As with reductive dehalogenation, the rates at which halogenated aromatics undergo photolysis are correlated with the strength of the carbon–halogen bond being broken, as well as with the tendency of other substituents to withdraw electrons or cause steric hindrance (Peijnenburg et al., 1992a). Photolysis rates have also been found (Katagi, 1992) to be correlated with changes in electron density caused by photoinduced excitation (i.e., the promotion of one or more electrons to higher energy states following the absorption of light energy). A comprehensive summary of the effects of chemical structure on photoreactivity for a broad range of pesticides was provided by Mill and Mabey (1985).

(4) *Biotransformations*. Some of the structural features that are associated with lower rates of biotransformation include increased branching and decreased length of hydrocarbon chains, decreased degree of unsaturation, larger numbers of rings in polynuclear aromatic hydrocarbons, the presence of methyl, nitro, amino, or halogen substituents on aromatic rings and, under oxic conditions, increasing numbers of halogens on the molecule (Scow, 1990). As might be expected, many of the ways in which variations in the structure of pesticide compounds affect their rates and mechanisms of biotransformation result from fundamental constraints of structure over chemical reactivity. For example, biotransformation rates among a variety of different pesticides have been found to be linearly correlated with their respective rates of base-catalyzed hydrolysis (Wolfe et al., 1980). Other effects of chemical structure on biodegradability are related more to biological factors than to purely chemical ones. Examples include features that increase the toxicity of the molecule (e.g., additional halogens) or affect the ease with which the appropriate enzyme(s) can access the reaction site (Bollag, 1982). One illustration of the latter effect is the observation, noted earlier, that biochemical reactions are often enantioselective, leading to variations in biotransformation rates among different *isomers* of the same pesticide compound (e.g., Falconer et al., 1995; Liu et al., 2005; Monkiedje et al., 2003; Peijnenburg et al., 1992b; Sakata et al., 1986; Wong et al., 2002). (Isomers are compounds that have the same chemical composition, but slightly different spatial arrangements of atoms. Enantiomers, for example, are isomers that, as noted earlier, are mirror images of one another.) The structural specificity of some biotransformation reactions is also demonstrated by the fact that unequal mixtures of isomers are sometimes produced from the transformation of a single compound (e.g., Parsons et al., 1984).

11.15.3.4.3 Structure and properties of other reactants

The rates and mechanisms of most pesticide transformations in the hydrologic system are, as noted earlier, influenced by the nature of the chemical species reacting with the pesticide compound during the rate-limiting step. These other species participate in the reactions either as Brønsted acids or bases, Lewis acids or bases (electrophiles or nucleophiles, respectively), oxidants, reductants, or catalysts. They may be present in the aqueous, solid, or gaseous phases, and may be of either abiotic or biological origin. In some cases, individual chemical species may react by different mechanisms simultaneously with the same pesticide compound. For example, Kriegman-King and Reinhard (1992) observed that in aqueous solution, hydrogen sulfide can react with tetrachloromethane as both a nucleophile (to form carbon disulfide and carbon dioxide) and a reductant (to form trichloromethane, dichloromethane, carbon monoxide, and other products).

Some reactants may play different roles in their interactions with pesticide compounds, depending on the geochemical conditions. Metals and their complexes, for example, may react with pesticide compounds as hydrolysis catalysts (e.g., Huang and Stone, 2000; Mortland and Raman, 1967; Schowanek and Verstraete, 1991; Smolen and Stone, 1997; Wan et al., 1994), direct reductants (e.g., Castro and Kray, 1963, 1966; Mochida et al., 1977; Strathmann and Stone, 2001, 2002a,b), or bulk electron donors through electron-transfer agents such as hydroquinones (e.g., Curtis and

Reinhard, 1994; Tratnyek and Macalady, 1989; Wang and Arnold, 2003). Most of what little information is available on how different metals and their complexes vary in their ability to promote transformations of pesticide compounds, however, focuses on their roles as direct reductants or hydrolysis catalysts (see references cited above); reduced iron appears to be the only metal that has been examined as a potential bulk electron donor in natural systems (Glass, 1972; Wang and Arnold, 2003).

A valuable framework for understanding the effects of chemical structure on reactivity is provided by the hard and soft acids and bases (HSAB) model, which classifies Lewis acids and bases as either 'hard' or 'soft.' Hard acids (e.g., H_3O^+, Na^+, Fe^{3+}) and bases (e.g., OH^-, CO_3^{2-}, Cl^-) are relatively small, exhibit low polarizability (and generally high electronegativity), and are more likely to form ionic bonds than covalent ones. Soft acids (e.g., Cd^{2+}, Hg^{2+}, Br_2) and bases (e.g., HS^-, $S_2O_3^{2-}$, I^-, CN^-) have the opposite characteristics (Fleming, 1976). Stated simply, the HSAB model posits that hard acids react most readily with hard bases, while soft acids react most readily with soft bases (Pearson, 1972). Thus, the soft base HS^- reacts with the fumigant 1,2-dichloroethane (**Figure 11**) almost exclusively through nucleophilic substitution at the (soft) carbon bonded to halogen (Barbash and Reinhard, 1989b), while the harder OH^- attacks the same compound primarily at one of the (hard) hydrogens, leading to dehydrochlorination (Walraevens et al., 1974). Similarly, for nucleophilic substitution reactions involving the thionate OPs (see **Figure 10** for compound structures), reaction occurs primarily at one of the (soft) carbon atoms bonded to oxygen in the ester linkages when the attacking species is HS^- (Miah and Jans, 2001), but at the (hard) phosphorus atom when the attacking species is OH^- (Smolen and Stone, 1997). Replacement of (soft) sulfur in thionate OPs with (hard) oxygen in the corresponding oxonate OPs further reduces the electron density on phosphorus, leading to higher rates of hydrolysis (Smolen and Stone, 1997).

Although the HSAB model has been criticized for being insufficiently quantitative (e.g., March, 1985), its predictions have been shown to be consistent with results from frontier molecular orbital calculations for a wide variety of reactions (Fleming, 1976; Klopman, 1968). Such calculations have, in turn, been shown to be useful for elucidating the effects of pesticide structure on reactivity (e.g., Katagi, 1992; Lippa and Roberts, 2002).

In addition to the nature of the *donor atom* (e.g., sulfur in bisulfide vs. oxygen in hydroxide), other features that govern the hardness of a nucleophile – and thus the rates and mechanisms of its reaction with pesticide compounds – include the oxidation state of the donor atom and the hardness, size, and structure of the remainder of the molecule. These patterns have been shown to be evident in reactivity trends observed, for example, among a variety of buffer anions and naturally occurring nucleophiles in their reactions with several haloaliphatic pesticide compounds (Barbash, 1993; Barbash and Reinhard, 1989a; Roberts et al., 1992).

While most applications of the HSAB model have focused on neutral reactions, the model also applies to electron-transfer reactions. The abilities of different transition elements (or other reductants) to reduce a given pesticide compound are generally presumed to increase with their softness – that is, with their ability to donate electrons, a characteristic that is commonly quantified using one-electron reduction potentials (e.g., Schwarzenbach et al., 1993). Reactivity trends reported among different reduced metal cations (e.g., Mochida et al., 1977; Strathmann and Stone, 2001), however, do not precisely track the order of their reduction potentials (Dean, 1985). The

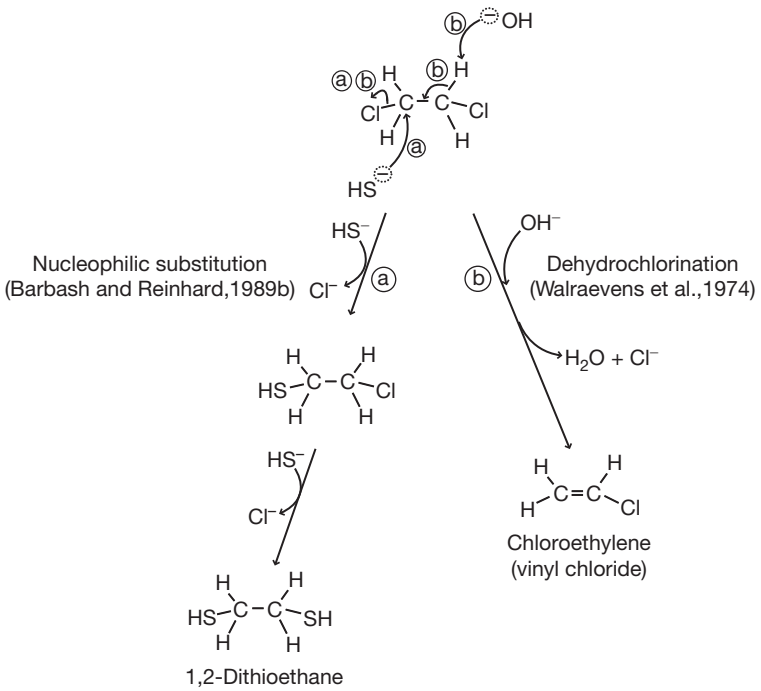

Figure 11 Principal reactions of the fumigant 1,2-dichloroethane with (a) bisulfide (Barbash and Reinhard, 1989b) and (b) hydroxide (Walraevens et al., 1974) in aqueous solution.

relative propensities of different metals to reduce pesticide compounds are therefore influenced by other factors. Related work suggests that such factors include pH and the nature of the coordinating ligand (Mochida et al., 1977; Strathmann and Stone, 2001, 2002a,b).

Comparisons among different metals with regard to their ability to catalyze the hydrolysis of pesticide compounds appear to be limited (e.g., Huang and Stone, 2000; Mortland and Raman, 1967; Smolen and Stone, 1997). Dramatic decreases in reactivity that have been observed upon precipitation at higher pH suggest, however, that metals catalyze hydrolysis much more effectively as ions in solution than as solid-phase (hydr)oxide surfaces (Huang and Stone, 2000).

Ligands have long been known to exert substantial effects upon the solubility, adsorption, and reactivity of transition elements in the hydrologic system. (Indeed, biochemical evolution has taken great advantage of the latter phenomenon, as shown by the critical roles played by metalloenzymes in many metabolic activities.) Several studies have demonstrated the effects of ligand structure on the rates of reductive transformation of pesticide compounds by transition metals, either as dissolved species (e.g., Gantzer and Wackett, 1991; Kochi and Powers, 1970; Mochida et al., 1977; Singleton and Kochi, 1967; Strathmann and Stone, 2001, 2002a,b) or as part of the solid phase (e.g., Torrents and Stone, 1991). One of the studies of greatest relevance to understanding the effect of ligands on the reactivity of pesticide compounds under natural conditions involved an examination by Klecka and Gonsior (1984) of the reductive dehalogenation of polychloroalkanes by ferrous iron in solution. This work indicated that the rates of these reactions are either wholly dependent upon (chloroform, 1,1,1-trichloroethane), or greatly accelerated by (tetrachloromethane) the coordination of the iron with a porphyrin ring (hematin), relative to the rate when iron is coordinated only to water (Fe^{2+}). Huang and Stone (2000) found that the three transition metal cations known to catalyze the hydrolysis of the carbamate insecticide dimetilan (Cu^{II}, Ni^{II}, and Zn^{II}) exhibit strong affinities for nitrogen- and oxygen-donor ligands. Pb^{II}, which did not catalyze this reaction, showed only a weak affinity for these ligands. As might have been expected, different ligands were found to cause varying degrees of catalytic activity for a given metal.

11.15.3.4.4 Physical factors

(1) *Temperature*. Because both the kinetic energy of molecules and the frequencies of their collisions increase with temperature, so do the rates of thermal reactions, including those that are biologically mediated. By contrast, the rate of photochemical conversion of a molecule from its ground state to an excited state is not dependent upon temperature. Overall rates of photochemical reaction may, however, exhibit either a positive or a negative dependence on temperature as the net result of competition among activation, quenching, and reaction steps (Mill and Mabey, 1985). Nevertheless, the detection in Arctic regions of pesticides that exhibit gas-phase lifetimes of only a few days in the more temperate climates where they were likely to have been applied (Bidleman, 1999) demonstrates the importance of accounting for temperature variations, as well as the rapidity of long-range atmospheric transport (mentioned earlier), in predicting the persistence of these compounds in the atmosphere.

The dependence of thermal reaction rates on temperature is most commonly found to be in accordance with the Arrhenius equation, that is,

$$\ln(k) = \ln(A) - \frac{E_a}{RT}$$

where k is the rate constant for the rate-limiting step of the reaction of interest, A is the Arrhenius preexponential factor, E_a is the activation energy, R is the universal gas constant, and T is the temperature of reaction (K). As is evident from the form of this equation, the quantities E_a/R and $\ln(A)$ may be estimated from the slope and intercept, respectively, of an Arrhenius plot, that is, a linear regression of $\ln(k)$ versus $1/T$ (e.g., **Figure 12**). Arrhenius plots exhibiting a significant departure from linearity are usually interpreted to imply the simultaneous operation of more than one transformation mechanism, with different mechanisms dominating over different temperature ranges. Pesticides for which this phenomenon has been observed include malathion (Wolfe et al., 1977), 1,2-dibromo-3-chloropropane (DBCP) (Deeley et al., 1991), triasulfuron, and primisulfuron (Dinelli et al., 1998).

The Arrhenius relation will not be observed above the temperature at which the decomposition or, as may occur for enzymes, inactivation of one or more of the reactants occurs (T_{max}). Indeed, adherence to this relation at temperatures well above T_{max} for most microorganisms has been used as evidence for an abiotic, rather than a biologically mediated mechanism of transformation (Wolfe and Macalady, 1992). For biotransformations, the Arrhenius equation also fails to describe the temperature dependence of reaction rates below the temperature at which biological functions are inhibited (T_{min}), and above the temperature of maximum transformation rate (T_{opt}). An empirical equation introduced by O'Neill (1968) may be used to estimate the rates of biotransformation as a function of ambient temperature, T_{min}, T_{opt}, T_{max} (in this case, the lethal temperature), E_a, and the maximum

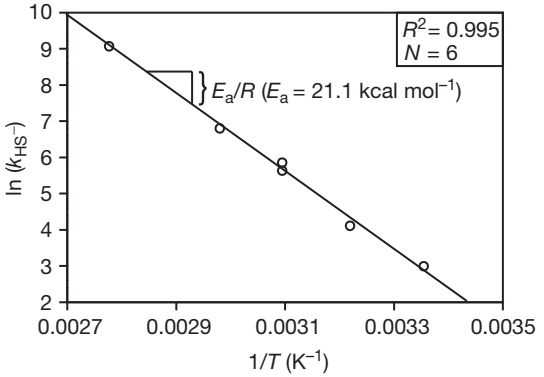

Figure 12 Arrhenius plot for the second-order rate constant (k_{HS-}) for the nucleophilic displacement of bromide from 1,2-dibromoethane (EDB) by bisulfide ion (HS^-). Reproduced from Barbash JE (1993) *Abiotic Reactions of Halogenated Ethanes and Ethylenes with Sulfide, Nitrate and pH-Buffer Anions in Aqueous Solution*. PhD Thesis, Stanford University.

biotransformation rate (μ_{max}). Because of the complexity of biochemical systems and the myriad different structures encompassed by pesticide compounds, T_{min}, T_{opt}, T_{max}, E_a, and μ_{max} are all likely to vary among different compounds, microbial species, and geochemical settings (e.g., Gan et al., 1999, 2000). However, Vink et al. (1994) demonstrated the successful application of the O'Neill function to describe the temperature dependence of biotransformation for 1,3-dichloropropene and 2,4-D in soils (**Figure 13**).

Although the dependence of reaction rates on temperature has been well known for over a century (Moore and Pearson, 1981), the temperatures at which transformation half-lives are measured are often not reported, either by the original publications or, more commonly, in data compilations (e.g., Nash, 1988; Pehkonen and Zhang, 2002; US Department of Agriculture-Agricultural Research Service, 1995). (A notable exception to this pattern is the University of Hertfordshire's Pesticide Properties Database, which provides the temperature of measurement for transformation rates – as well as for several other physical and chemical parameters – for over 700 pesticides and 350 pesticide transformation products; Lewis et al., 2007.) Similarly, as noted by Barbash and Resek (1996), the effects of temperature variations on transformation rates are rarely incorporated into simulations of pesticide fate in the hydrologic system. Several studies, however, have demonstrated the importance of adjusting transformation rates for seasonal and depth-related variations in temperature when predicting pesticide persistence (Beulke et al., 2000; Padilla et al., 1988; Watson, 1977; Wu and Nofziger, 1999). As is evident from the Arrhenius equation, the adjustment of pesticide transformation rates for variations in temperature requires the availability of data on E_a for the compound and setting of interest. Compilations of E_a values appear to be rare in the literature, but a few summaries are available for the transformations of a variety of herbicides (Nash, 1988; Smith and Aubin, 1993), adjuvants, and fumigants (Barbash, 1993), as well as for the activity of soil enzymes known to effect pesticide transformations (Wu and Nofziger, 1999). E_a values – or data from which they may be computed – are currently available for at least 105 pesticide compounds in the published literature (Barbash, unpublished compilation).

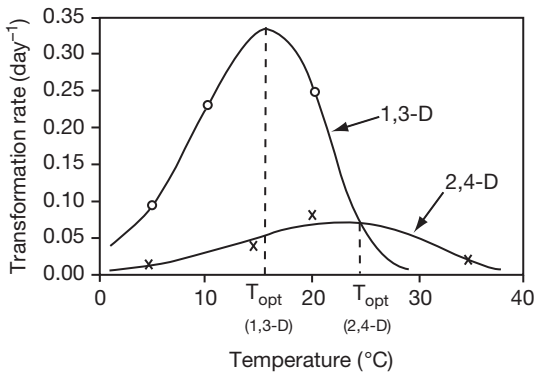

Figure 13 Variations in the rates of biotransformation of 1,3-dichloropropene (1,3-D,circles) and 2,4-D (crosses) with temperature in soils, fitted to the O'Neill function. Reproduced from Vink JPM, Nörtershäuser P, Richter O, Diekkrüger B, and Groen KP (1994) Modelling the microbial breakdown of pesticides in soil using a parameter estimation technique. *Pesticide Science* 40: 285–292, with permission from John Wiley & Sons Ltd on behalf of the SCI.

(2) *Soil moisture content*. Rates of pesticide transformation in soils have usually been found to increase with moisture content up to the *field capacity* of the soil (e.g., Anderson and Dulka, 1985; Burnside and Lavy, 1966; Cink and Coats, 1993; Roeth et al., 1969; Walker, 1974, 1987). (Field capacity is the amount of water remaining in a soil after the rate of gravity drainage becomes negligible.) This dependence has been described through the use of an empirical equation, introduced by Walker (1974), that expresses transformation half-life as an inverse exponential function of soil moisture content (up to field capacity). The Walker equation has been used to quantify the effects of soil moisture on the rates of transformation of atrazine (Rocha and Walker, 1995), propyzamide, napropamide (Walker, 1974), and at least 25 other pesticide compounds (Gottesbüren, 1991). Similarly, Parker and Doxtader (1983) found that the rate of transformation of 2,4-D in a sandy loam increased with decreasing soil moisture tension, but observed an exponential relation between the two variables that was different from that implied by the Walker equation.

The dependence of pesticide transformation rates on soil moisture is commonly assumed to reflect the influence of water content on biotransformation. For example, Parker and Doxtader (1983) attributed the moisture dependence of 2,4-D transformation rates to two different effects of reduced soil moisture on biological processes, that is, (1) reduced activity of microbial populations and (2) higher pesticide concentrations, which have been shown by other investigators (e.g., Cink and Coats, 1993) to inhibit microbial degradation. For soil moisture contents above field capacity, however, this relation might not be observed, especially for aerobic transformations that may be inhibited in saturated soils following the consumption of DO. Abiotic factors may also be involved, since a direct relation between pesticide transformation rates and soil moisture has also been observed in sterile soils (Anderson and Dulka, 1985). Furthermore, some nonbiological processes may exhibit the opposite effect; both the Lewis and Brønsted acidity of mineral surfaces – and thus their tendency to promote the oxidation or acid-catalyzed reactions of pesticide compounds, respectively – are enhanced with decreasing soil moisture (Voudrias and Reinhard, 1986).

(3) *Interactions among temperature, moisture and soil texture*. The effects of variations in temperature and moisture content on the rates of pesticide transformation in soil show a complex interdependence, the nature of which may vary among different compounds for the same soil, as well as among different soils for the same compound (Baer and Calvet, 1999; Nash, 1988; Walker, 1974). Equations used for describing the simultaneous effects of temperature and soil moisture on pesticide transformation rates have been reported by Parker and Doxtader (1983) and Dinelli et al. (1998). In a comprehensive review of 178 studies that compared observed pesticide concentrations in soils

with those predicted using a pesticide persistence model, Beulke et al. (2000) demonstrated the importance of accounting for spatial and temporal variations in temperature and moisture in estimating the rates of pesticide transformation. Interactions between abiotic and biological factors are likely to be responsible for the observation that the nature of the relation between soil moisture and the rates of pesticide transformation may, in turn, depend upon soil texture (e.g., Gan et al., 1999; Rocha and Walker, 1995). Rocha and Walker (1995) also observed that the effect of temperature on atrazine transformation could be a function of soil texture, as well. However, while the nonlinear regression model of Fenner et al. (2007) for atrazine (mentioned earlier) included temperature, pH, sand content, organic carbon content, and two depth-related parameters as explanatory variables, volumetric water content was not retained as a predictor variable in the final equation.

(4) *Solar energy input*. For pesticide compounds that undergo phototransformation in natural waters, the rate of reaction is controlled by a number of factors that affect the amount of light energy reaching the reactant(s) of interest. These include the *irradiance*, or the rate of energy input from the Sun (which, in turn, is controlled in part by latitude, season, and time of day) at the wavelengths of maximum light absorption for each reactant, as well as turbidity, color, and depth within the water body of interest. While the presence of suspended solids is generally presumed to reduce photolysis rates in surface water through light attenuation, in some instances the presence of suspended sediments has been observed to *increase* the rates of these reactions. This phenomenon has been attributed to forward scattering of the incident light by the suspended particles, which can result in an increase in the light path length (Mill and Mabey, 1985; Miller and Zepp, 1979). The effects of various physical and chemical factors on the rates of photochemical transformation of pesticide compounds have been summarized by Mill and Mabey (1985) and Harris (1990b). Zepp et al. (1975) presented graphical illustrations of how the rate of 2,4-D butoxyethyl ester photolysis varies with time of day (in Athens, GA; **Figure 14**), season, and latitude in the northern hemisphere (**Figure 15**). Zepp and Cline (1977) provided similar diagrams for the direct photolysis of carbaryl and trifluralin in water.

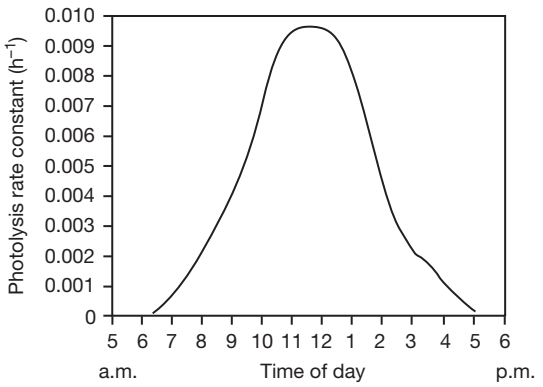

Figure 14 Dependence of the rate constant for the photolysis of 2,4-D butoxyethyl ester (in water at 28 °C) on the time of day in the southern United States. Reproduced from Zepp RG, Wolfe NL, Gordon JA, and Baughman GL (1975) Dynamics of 2,4-D esters in surface waters – Hydrolysis, photolysis, and vaporization. *Environmental Science & Technology* 9(13): 1144–1149, with permission from American Chemical Society.

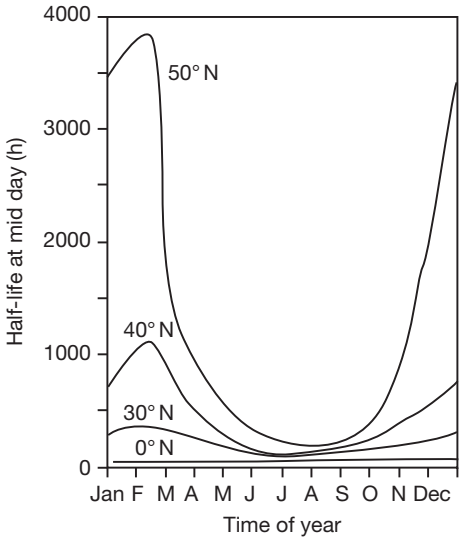

Figure 15 Dependence of the half-life for the photolysis of 2,4-D butoxyethyl ester (in water at 28 °C) on season and northern latitude. Reproduced from Zepp RG, Wolfe NL, Gordon JA, and Baughman GL (1975) Dynamics of 2,4-D esters in surface waters – Hydrolysis, photolysis, and vaporization. *Environmental Science & Technology* 9(13): 1144–1149, with permission from American Chemical Society.

11.15.3.4.5 Geochemical environment

As is the case for its physical properties, the geochemical characteristics of the reaction medium can also influence the rates and mechanisms of pesticide compound transformation in the hydrologic system, as well as the health and activity of the organisms capable of transforming these compounds. Such characteristics include redox conditions (discussed earlier), pH, ionic strength, the structure and concentrations of any surface-active substances (SAS), solvents or ligands that may be present, and the chemical properties of any interfaces with which the reactants may come in contact.

(1) *pH*. Changes in pH can affect the rates of pesticide compound transformation in both direct and indirect ways. Direct effects arise from the fact that shifts in pH reflect changes in the concentrations of two potentially important reactants that are present in all aqueous solutions, that is, H_3O^+ and OH^-. However, pH changes may also exert substantial indirect effects on pesticide transformations, through their influence on biological activity (e.g., Mallat and Barceló, 1998), the surface properties of reactive natural solids such as manganese oxides (Baldwin et al., 2001) and clays (Voudrias and Reinhard, 1986), and the concentrations of other reactants. For pesticide compounds that are Brønsted acids or bases, such as the sulfonylurea herbicides (Smith and Aubin, 1993), variations in

pH may influence transformation rates in solution if the reactivities of the conjugate acid and base are substantially different from one another.

Even if the aqueous concentration of a pesticide compound is independent of pH, however (as is the case for most parent compounds), its transformation rate may still vary with changes in pH if the attacking species is a Brønsted acid or base. In such instances, the pH dependence of the reaction rate will parallel that of the attacking species concentration. For pesticide compounds, this effect has been reported for nucleophilic substitution reactions involving H_3O^+, OH^- (e.g., Mabey and Mill, 1978), and HS^- (Haag and Mill, 1988b; Lippa and Roberts, 2002; Roberts et al., 1992), for reduction (Strathmann and Stone, 2002a,b; Wang and Arnold, 2003) or hydrolytic catalysis by divalent metal cations (Huang and Stone, 2000), and for reduction by model compounds employed to mimic the electron-transfer capabilities of hydroquinone moieties found in NOM (Curtis and Reinhard, 1994; Tratnyek and Macalady, 1989). Indeed, the latter observation may explain why the reduction of methyl parathion in anoxic sediments was reported by Wolfe et al. (1986) to occur more rapidly under alkaline conditions ($8 < pH < 10$) than under acidic conditions ($2 < pH < 6$). The relative rates among competing photochemical transformations for individual pesticide compounds may also shift with pH. Crosby and Leitis (1973), for example, observed pH-related shifts in the yields of different products from the aqueous photolysis of trifluralin, both in the presence and the absence of soil (**Figure 16**).

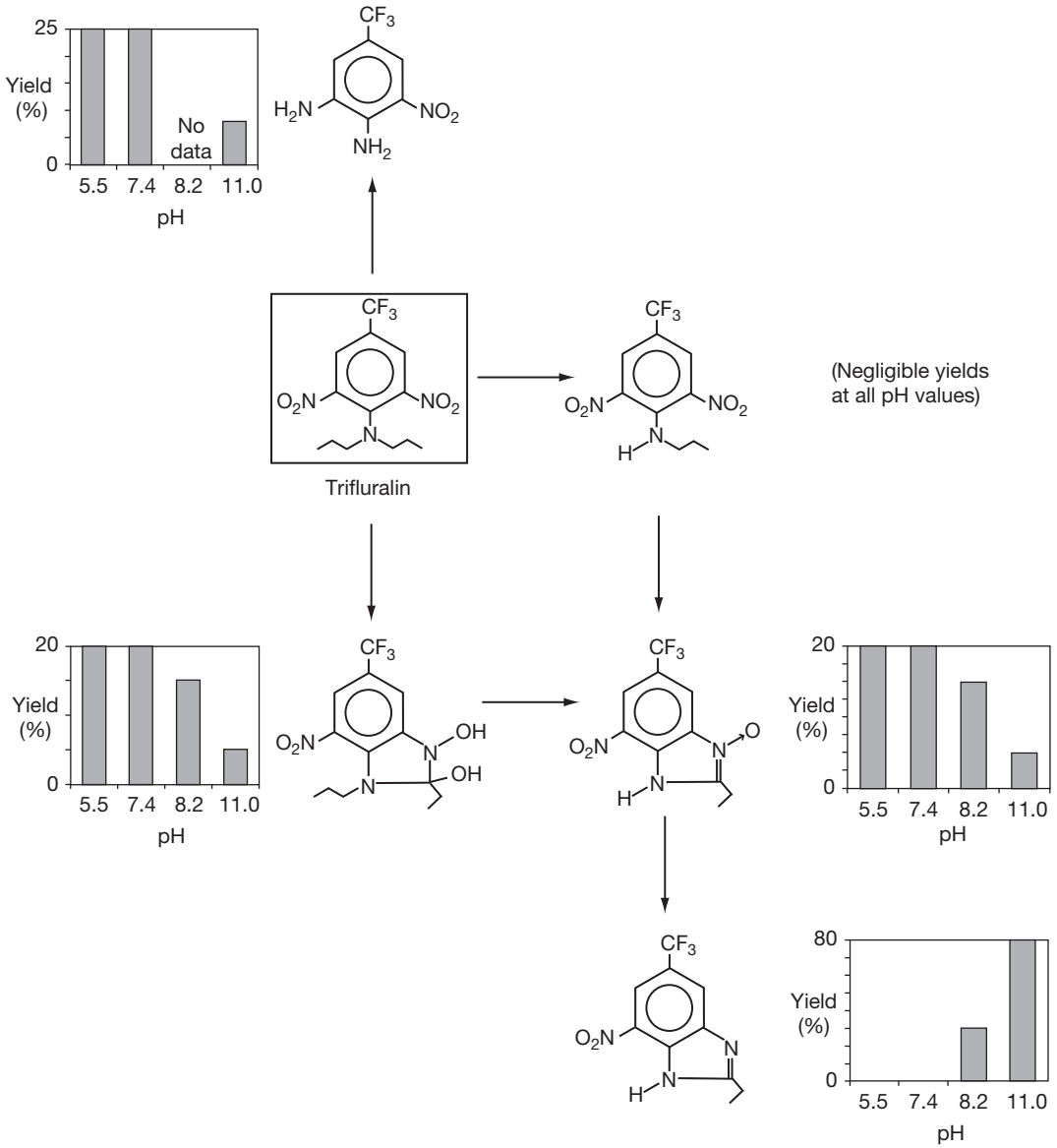

Figure 16 Effects of pH on the yields of different products during the photolysis of trifluralin in summer sunlight (Davis, CA) in water, either with or without soil present. For purposes of display, vertical axis for each product is normalized to the maximum yield for that compound, rather than to 100%. Yields among products at each pH value sum to less than 100% because data for minor products are not shown. Produced using data from Crosby DG and Leitis E (1973) The photodecomposition of trifluralin in water. *Bulletin of Environmental Contamination and Toxicology* 10: 237–241.

The overall rate at which a pesticide compound undergoes hydrolysis in water represents the sum of the rates of the acid-catalyzed, neutral and base-catalyzed processes (Mabey and Mill, 1978). For those pesticide compounds that react only with H_2O, the rate of hydrolysis is independent of pH (e.g., Hong et al., 2001; McCall, 1987). Some pesticide compounds, however, react with more than one of the three species of interest (H_3O^+, H_2O, and/or OH^-), resulting in a pattern of pH dependence that may display an abrupt shift above or below a particular threshold pH value (Mabey and Mill, 1978; Schwarzenbach et al., 1993). Few compilations of these threshold parameters appear to be available for pesticide compounds (Mabey and Mill, 1978; Mabey et al., 1983; Roberts et al., 1993; Schwarzenbach et al., 1993), but individual values may sometimes be inferred from published data (e.g., Bank and Tyrrell, 1984; Burlinson et al., 1982; Cline and Delfino, 1989; Jeffers et al., 1989; Lee et al., 1990; Lightfoot et al., 1987; Ngabe et al., 1993; Weintraub et al., 1986; Zepp et al., 1975). Other results suggest that these threshold parameter values may vary with temperature (Lightfoot et al., 1987).

The dependence of transformation rate on pH is not always consistent among pesticides within the same chemical class. For example, while the hydrolysis reactions of most OP (Konrad and Chesters, 1969; Konrad et al., 1969; Mabey and Mill, 1978) and carbamate insecticides (Wolfe et al., 1978) are primarily base-catalyzed, both diazinon (Konrad et al., 1967) and carbosulfan (Wei et al., 2000) are also subject to the acid-catalyzed reaction. Summaries of the pH dependence of hydrolysis rates for a variety of pesticides have been provided by Mabey and Mill (1978), Bollag (1982), Schwarzenbach et al. (1993), and Barbash and Resek (1996).

Several authors have combined the Arrhenius equation with kinetic equations reflecting the pH dependence of reaction rates in order to quantify the simultaneous dependence of pesticide transformation rates on temperature and pH (e.g., Dinelli et al., 1997; Lightfoot et al., 1987; Liqiang et al., 1994). Other work has demonstrated the extent to which E_a values for pesticide hydrolysis vary, if at all, with pH (Dinelli et al., 1997, 1998; Lee et al., 1990; Smith and Aubin, 1993).

Most of what is known about the effects of pH on the rates of pesticide transformation in aqueous solution has been learned from laboratory studies employing buffers to stabilize pH. However, since they are Brønsted acids and bases, pH buffers may also accelerate these reactions – or cause shifts in the relative rates of different transformation mechanisms – compared to what occurs in unbuffered solution (Barbash and Reinhard, 1989a, 1992b; Burlinson et al., 1982; Deeley et al., 1991; Li and Felbeck, 1972; Smolen and Stone, 1997). Such effects, though, are not observed for all pesticide compounds (Hemmamda et al., 1994; Hong et al., 2001; Kochany and Maguire, 1994; Smolen and Stone, 1997). Indeed, the absence of buffer effects has been used as evidence for unimolecular reaction mechanisms (Bank and Tyrrell, 1984). The varying tendencies of different buffers to accelerate hydrolysis and dehydrohalogenation are consistent with reactivity trends predicted by the HSAB model (Barbash, 1993) and, for hydrolysis, may be predicted quantitatively using a method introduced by Perdue and Wolfe (1983). Relatively few laboratory studies have accounted for buffer effects (e.g., Barbash and Reinhard, 1989a, 1992b; Burlinson et al., 1982; Li and Felbeck, 1972; Miles and Delfino, 1985; Smolen and Stone, 1997), but failing to make such corrections may lead to overestimates in the rates at which these reactions are likely to occur in natural waters.

(2) *Ionic strength*. Ionic strength is known to influence some chemical reactions, with both the magnitude of the effect and its direction (i.e., acceleration vs. inhibition) depending upon the nature of the reaction in question. The effects of ionic strength on pesticide transformations are of particular interest in saline environments such as coastal waters where pesticides are applied for aquaculture, or estuaries into which significant loads of pesticides are discharged by rivers that drain extensive agricultural (Clark and Goolsby, 2000; Hainly and Kahn, 1996; Hladik et al., 2005; Larson et al., 1995; Lippa and Roberts, 2002; Pereira et al., 1990) and nonagricultural areas (Bondarenko et al., 2004). Transition-state theory predicts that the effects of ionic strength on reaction rates will be smallest for neutral reactants, and become more pronounced with increasing ionic charge on the reactants (Lasaga, 1981). This is consistent with observations regarding the effects of ionic strength on the rates of hydrolysis of pesticide compounds over the range of salinities encountered in most natural waters. As predicted by transition-state theory, these effects have been found to be minor over the pH range (if any) within which a given pesticide compound is subject only (or primarily) to reaction with H_2O (Barbash and Reinhard, 1992b; Bondarenko et al., 2004; Liqiang et al., 1994), but substantial both at higher pH for those compounds that are subject to base catalysis (Bondarenko et al., 2004; Miles and Delfino, 1985) and at lower pH for those subject to acid catalysis (Wei et al., 2000). Also consistent with transition-state theory is the observation by Miles and Delfino (1985) that the effect of salt concentration on the rate of aldicarb sulfone hydrolysis is more pronounced (on a molar basis) for the divalent Ca^{2+} than for the monovalent Na^+. The effects of ionic strength on photochemical reactions do not appear to be extensively documented (e.g., Mill and Mabey, 1985), but Walse et al. (2004) observed a significant increase in the rate of photolysis of the insecticide fipronil upon the addition of 3% NaCl, suggesting that the rate of this reaction is likely to be higher in marine waters (which typically have salinities of approximately 3.5%) than in freshwater environments. Ionic strength may also affect pesticide persistence through its influence on the activity of the organisms responsible for biotransformations (Bondarenko et al., 2004).

(3) *Concentrations and structure of SAS*. SAS that may be present in the hydrologic system – either dissolved in the aqueous phase or as part of the soil – may influence the rates and mechanisms of pesticide transformation. These compounds include fatty acids, polysaccharides, humic substances, and other forms of NOM (Thurman, 1985), as well as the surface-active agents (or *surfactants*) commonly used in detergents or as adjuvants in commercial pesticide formulations. All SAS share the common property of *amphiphilicity*, that is, the ability to associate

simultaneously with both polar and nonpolar chemical species in aqueous solution. This property arises from the dual nature of their chemical structure, one portion of the molecule being relatively hydrophilic (and often ionic) and another portion being more hydrophobic. In aqueous solution, these compounds exhibit a tendency to self-associate into assemblages known as *submicellar aggregates* at low concentrations, and *micelles* (**Figure 17**) above a chemical-specific level (the *critical micelle concentration*). Micelles consist of an inner core formed by the more hydrophobic portions of the SAS molecules, surrounded by an outer layer consisting of their more hydrophilic portions (Fendler and Fendler, 1975).

When SAS are present in solution, pesticide compounds partition between the bulk aqueous solution and the (sub) micellar phase (**Figure 17**). This partitioning may affect the overall rates and products of transformation of these compounds if their rates of reaction in the (sub)micellar phase are significantly different from those in the aqueous phase (Barbash, 1987; Barbash and Resek, 1996; Macalady and Wolfe, 1987). In some cases, relatively minor variations in SAS structure can have substantial impacts on pesticide transformation rates (Kamiya et al., 1994). Even if reaction rates are not substantially different in the (sub)micellar phase, however, the presence of SAS may modify reaction rates in solution for sparingly soluble pesticide compounds by simply increasing their dissolved concentrations, as may occur in the presence of polar solvents (e.g., Barbash and Reinhard, 1989a; Schwarzenbach et al., 1993; Wei et al., 2000). Rates of biotransformation may be either increased or decreased by partitioning into a (sub)micellar phase, depending upon the effect of the particular SAS on bioavailability, and the nature of the microorganisms involved (Guha and Jaffé, 1996).

The influences of NOM – either in aqueous solution or in the soil phase – on the rates of transformation of pesticide compounds in water are consistent with general principles regarding the effects of SAS on chemical reactions. Because the polar regions of most NOM are either neutral or possess a negative charge, previous research suggests that the presence of NOM in natural waters is likely to accelerate the reactions of pesticide compounds with cations, have a negligible effect on their rates of reaction with neutral species, and inhibit their rates of attack by anions – and that these effects will increase with increasing NOM concentration (Barbash, 1987; Macalady and Wolfe, 1987). These trends are precisely what has been observed for the transformations of pesticide compounds by acid-catalyzed (Khan, 1978; Li and Felbeck, 1972), neutral (Macalady and Wolfe, 1985), and base-catalyzed hydrolysis (Macalady and Wolfe, 1985; Noblet et al., 1996; Perdue and Wolfe, 1982) in the presence of either dissolved or solid-phase NOM. The anticipated effects of SAS on the rates of other reactions that may transform pesticide compounds in natural waters (i.e., substitution reactions with other nucleophiles, dehydrohalogenation, reductive dehalogenation, and free-radical transformations) were reviewed by Barbash (1987).

(4) *Interfacial effects*. The rates and mechanisms of pesticide compound transformation (both biotic and abiotic) at interfaces in the hydrologic system (air/water, water/solid, and solid/air) are often markedly different from those in

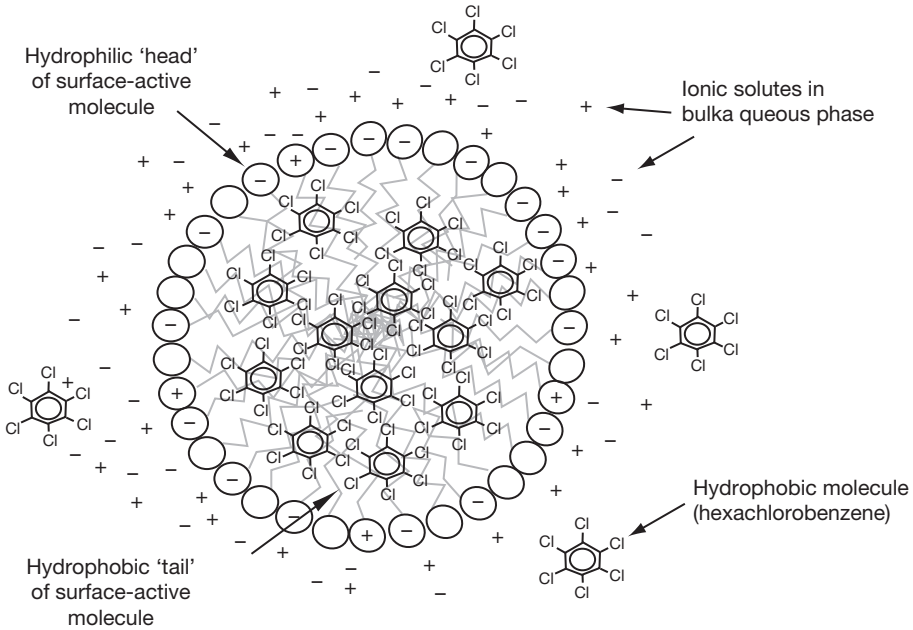

Figure 17 Cross-sectional view of the self-association of surface-active molecules into an idealized micelle. Hydrophobic portion of each surface-active molecule shown as a jagged line; hydrophilic portion shown as a circle. Hydrophobic pesticide molecules, represented by the fungicide hexachlorobenzene, will tend to accumulate within the hydrophobic core of the micelle at a higher concentration than in the bulk aqueous phase. Ionic species (e.g., hydroxide ion) will show the opposite distribution. Adapted from Fendler JH and Fendler EJ (1975) *Catalysis in Micellar and Macromolecular Systems*. San Francisco, CA: Academic Press.

the adjacent bulk phases (e.g., Barbash and Resek, 1996). The influence of the air/water interface on these reactions is likely to be most important within the surface microlayer of surface waters, where the more hydrophobic pesticide compounds are likely to concentrate (Zepp et al., 1975) – as alcohols, hydrocarbons, carotenoid pigments, chlorophylls, fatty acids, fatty acid esters, and other naturally derived SAS are known to do (Parsons and Takahashi, 1973). The gas/solid interface is likely to exert the greatest influence on reactivity at the surfaces of dry soils and plants, or in the atmosphere, where surface-catalyzed reactions of volatile halogenated compounds, including the fumigant methyl bromide, can deplete atmospheric ozone. Among the three principal types of interfaces in the hydrologic system, however, the solid/liquid interface appears to have received the most attention regarding this topic, and is therefore the main focus of the following discussion.

The presence of natural solids can significantly modify the rates of transformation in aqueous systems – relative to the rates observed in homogeneous solution – for many pesticide compounds, but may have little effect on others (Barbash and Resek, 1996). Factors that can influence the rates and mechanisms of transformation of pesticide compounds at the water/solid interface include the structure of the compound of interest (e.g., Baldwin et al., 2001; Torrents and Stone, 1991), the composition and surface structure of the mineral phase (e.g., Carlson et al., 2002; Kriegman-King and Reinhard, 1992; Wei et al., 2001), the solid-phase organic carbon content (e.g., Wolfe and Macalady, 1992), and the characteristics, health, and size of the resident microbial community.

Most of the ways in which natural water/solid interfaces influence the rates of transformation of pesticide compounds, however, are consistent with the various effects of related chemical species on these reactions in homogeneous solution, discussed in preceding sections. Russell et al. (1968), for example, observed that the hydrolysis of atrazine at low pH was greatly accelerated in suspensions of montmorillonite clay, relative to the rate of reaction in homogeneous solution at the same pH. The authors attributed this effect to the acid catalysis of the reaction by the clay surface, which exhibited a pH that was considerably lower (by as much as 3–4 pH units) than that of the bulk solution. As noted previously, the sorption of pesticide compounds to soil organic matter has been observed to influence the rates of their hydrolysis in the same manner as might be expected from the association of these compounds with SAS in solution, leading to an acceleration of the acid-catalyzed process (Li and Felbeck, 1972), a negligible effect on the neutral process, and an inhibition of the base-catalyzed process (Macalady and Wolfe, 1985).

In addition, several naturally occurring metal oxides exhibit semiconducting properties that may catalyze the photochemical production of hydroxyl and hydroperoxyl radicals in aqueous solution – species which, as noted earlier, can react with pesticide compounds (Zepp and Wolfe, 1987). Chemical structures located at the surfaces of natural solids may also participate in pesticide transformation reactions as Brønsted bases, oxidants (e.g., Voudrias and Reinhard, 1986), reductants (e.g., Wolfe et al., 1986), hydrolysis catalysts (Wei et al., 2001), complexing agents (e.g., Torrents and Stone, 1991), or sources of protons for hydrogen bonding (e.g., Armstrong and Chesters, 1968).

Rates of pesticide transformation may be either directly or inversely related to the amount of NOM in the solid phase, depending upon the reaction in question. The common observation of higher transformation rates in more organic-rich soils may result from either enhanced microbial activity in the presence of more abundant NOM (e.g., Veeh et al., 1996) or, for the case of reductive transformations in sterile soils, higher concentrations of biogenic reductants associated with the NOM (Wolfe and Macalady, 1992). By contrast, the inverse relations that have been reported between NOM and pesticide transformation rates are believed to be caused by substantial decreases in the rates of some reactions in the sorbed phase, relative to the dissolved phase (e.g., Graetz et al., 1970; Lartiges and Garrigues, 1995; Ogram et al., 1985; Walse et al., 2002; Zepp and Wolfe, 1987). Indeed, with regard to biotransformations, it is generally assumed that sorption reduces the bioavailability of pesticide compounds (e.g., Zhang et al., 1998). Phototransformations have also been found to occur either faster or more slowly in the sorbed phase, depending upon substrate structure and the nature of the solid phase (Mill and Mabey, 1985).

11.15.3.5 Effects of Transformations on Environmental Transport and Fate

As might be expected, the transformation of a pesticide can generate products with partitioning characteristics that are substantially different from those of the parent compound. For example, the hydrolysis of 1,3-dichloropropene (**Figure 7**) and EDB (Syracuse Research Corporation, 1988; US Department of Agriculture-Agricultural Research Service, 1995; Weintraub et al., 1986), as well as the hydration of acrolein (Bowmer and Higgins, 1976), all generate reaction products that are much less volatile – and more water soluble – than their parent compounds. Similarly, the herbicide DCPA (2,3,5,6-tetrachloro-1,4-benzenedicarboxylic acid), a relatively hydrophobic dimethyl ester, undergoes transformation in soil to yield progressively more mobile products as it hydrolyzes first to a 'half-acid' ester intermediate, and thence to the diacid, tetrachloroterephthalic acid (Ando, 1992; US Department of Agriculture-Agricultural Research Service, 1995; US Environmental Protection Agency, 1992). Indeed, one of the principal strategies employed by living organisms for detoxifying xenobiotic compounds is to convert them – typically through either oxidation or hydrolysis – to products that are more water soluble, and thus more readily excreted (Coats, 1991).

Neutral reactions do not always lead to an increase in the mobility of pesticide compounds in the hydrologic system, however. For example, for each of several chloroacetamide herbicides, the nucleophilic displacement of chloride by bisulfide has been observed to generate a product that in each case is less water soluble than the parent compound, with the solubilities of the products decreasing in the same order as those of their parent compounds (Stamper et al., 1997). Atrazine hydrolyzes to form hydroxyatrazine, which is less water soluble than its parent compound (Bayless, 2001; Erickson and Lee, 1989), and exhibits a nearly 20-fold greater affinity for soil organic matter (based on K_{oc}) than atrazine (Moreau and Mouvet,

1997). An early explanation for the latter phenomenon (Armstrong et al., 1967) suggested that because the replacement of the chlorine atom on atrazine with a hydroxyl group raises the pK_a of the substituted amino groups on the molecule, this also increases its tendency to form hydrogen bonds with soil surfaces.

The oxidation of pesticide compounds usually generates products with aqueous mobilities that are either similar to or greater than that of the parent compound. The oxidation of aldicarb, for example, produces aldicarb sulfoxide and aldicarb sulfone, both of which have lower K_{oc} values than aldicarb (Moye and Miles, 1988). Similarly, because most phototransformations involve either the hydrolysis or oxidation of the parent compound, they yield products that are generally more polar (Mill and Mabey, 1985), and thus more water soluble than the parent compound. Reduction reactions, by contrast, may result in products that are less water soluble than their parent compound. Examples include the reduction of aldicarb sulfoxide to aldicarb (Lightfoot et al., 1987; Miles and Delfino, 1985) and the reduction of phorate sulfoxide to phorate (Coats, 1991). The reactivity of transformation products may be either higher or lower than that of their parent compounds. However, those in the former category (i.e., reactive intermediates) are, of course, much less likely to be detected in the hydrologic system than more stable products.

11.15.3.6 Occurrence of Pesticide Transformation Products in the Hydrologic System

Observations regarding the concentrations of pesticide transformation products in the hydrologic system, and their variations in space in time, are of considerable value for understanding the fate of pesticides in the environment. Among other applications, such information can be useful for (1) increasing the proportion of applied parent compound that can be accounted for in water, soils, biota, and other environmental media; (2) enhancing our understanding of the physical, hydrologic, chemical, and biological processes that control the transport and fate of pesticide compounds in the hydrologic system; and (3) testing the accuracy of predictions regarding the types and concentrations of pesticides and their transformation products that are encountered in the environment (Barbash and Kolpin, 2010). Although published information on the occurrence of pesticide transformation products in environmental media has been reported since the mid-1970s (Barbash and Resek, 1996), such data were relatively sparse – relative to those for parent compounds – until the mid-1990s. Since that time, interest in transformation products has increased substantially. As a result, data on occurrence in various environmental media are now available for over 140 pesticide transformation products, derived from at least 84 parent compounds (Barbash and Kolpin, 2010; Barbash and Resek, 1996). Examples of most of the reactions that these results may now be used to investigate in situ are shown in **Figure 18** (for neutral reactions) and **Figure 19** (for electron-transfer and photolytic reactions).

Information on the occurrence of pesticide transformation products and their parent compounds in the environment has been employed in several ways to improve our understanding of the processes controlling the transport and fate of pesticides after they are applied to the land. For example, Burow et al. (1999) used data on the occurrence of DBCP and two of its transformation products to examine the relative importance of physical and chemical processes in controlling the fate of the fumigant in groundwater. Tesoriero et al. (2001) employed a combination of field and laboratory studies to demonstrate the importance of redox conditions in controlling the fate of another fumigant, 1,2-dichloropropane, in groundwater (**Figure 19**). Data on the occurrence of atrazine and DEA (also abbreviated as 'CIAT' by some authors; e.g., Erickson and Lee, 1989) in surface and groundwaters across the United States have provided persuasive evidence that the 'DEA fraction' (i.e., the molar proportion of atrazine-derived compounds that is present in a given environmental medium as DEA) increases with increasing residence time in the vadose zone (Barbash and Kolpin, 2010). This observation is consistent with the fact that microorganisms are essentially ubiquitous within the subsurface (e.g., Ghiorse, 1997; Issa and Wood, 1999), and that in the absence of light, the formation of DEA from atrazine requires microbial assistance. Upon examining data on the occurrence of atrazine and DEA in the subsurface beneath four field sites across the United States, Tesoriero et al. (2007) observed that the concentrations of DEA in groundwater are higher – relative to those of its parent compound – in areas with thicker vadose zones than in locations where the water table is more shallow. Such a finding is what might be anticipated for an oxidation reaction that, in the absence of light, is microbially mediated (**Figure 19**). Tesoriero et al. (2007) also found the DEA fraction in groundwater to be independent of groundwater residence time at all four sites. This conclusion is in agreement with previous research indicating that the rates of pesticide biotransformation typically decrease with increasing depth below the land surface, presumably because both the sizes of microbial populations and the concentrations of organic matter in the soil exhibit the same pattern (Barbash and Resek, 1996).

Measured concentrations of pesticides and their transformation products in environmental media have also been employed to test the predictions from computer simulations of the transport and fate of the parent compounds in the hydrologic system. Examples include investigations of the transport and fate of DBCP in groundwater (Burow et al., 1999), as well as atrazine, metolachlor, and glyphosate in the vadose zone (Barbash and Voss, 2007; Bayless, 2001; Bayless et al., 2008; Webb et al., 2008).

11.15.4 The Future

Future progress in understanding the geochemistry and biological effects of pesticide compounds will be fundamentally dependent upon the availability of more detailed information on the temporal and spatial patterns of application and occurrence of these compounds, especially in nonagricultural settings. However, while the spatial and temporal distributions of their sources differ considerably from those of other contaminants, most of the uncertainties that beset our current knowledge of the geochemistry and biological effects of pesticide compounds are essentially identical to those that pertain to industrial solvents, petroleum hydrocarbons, fire-fighting

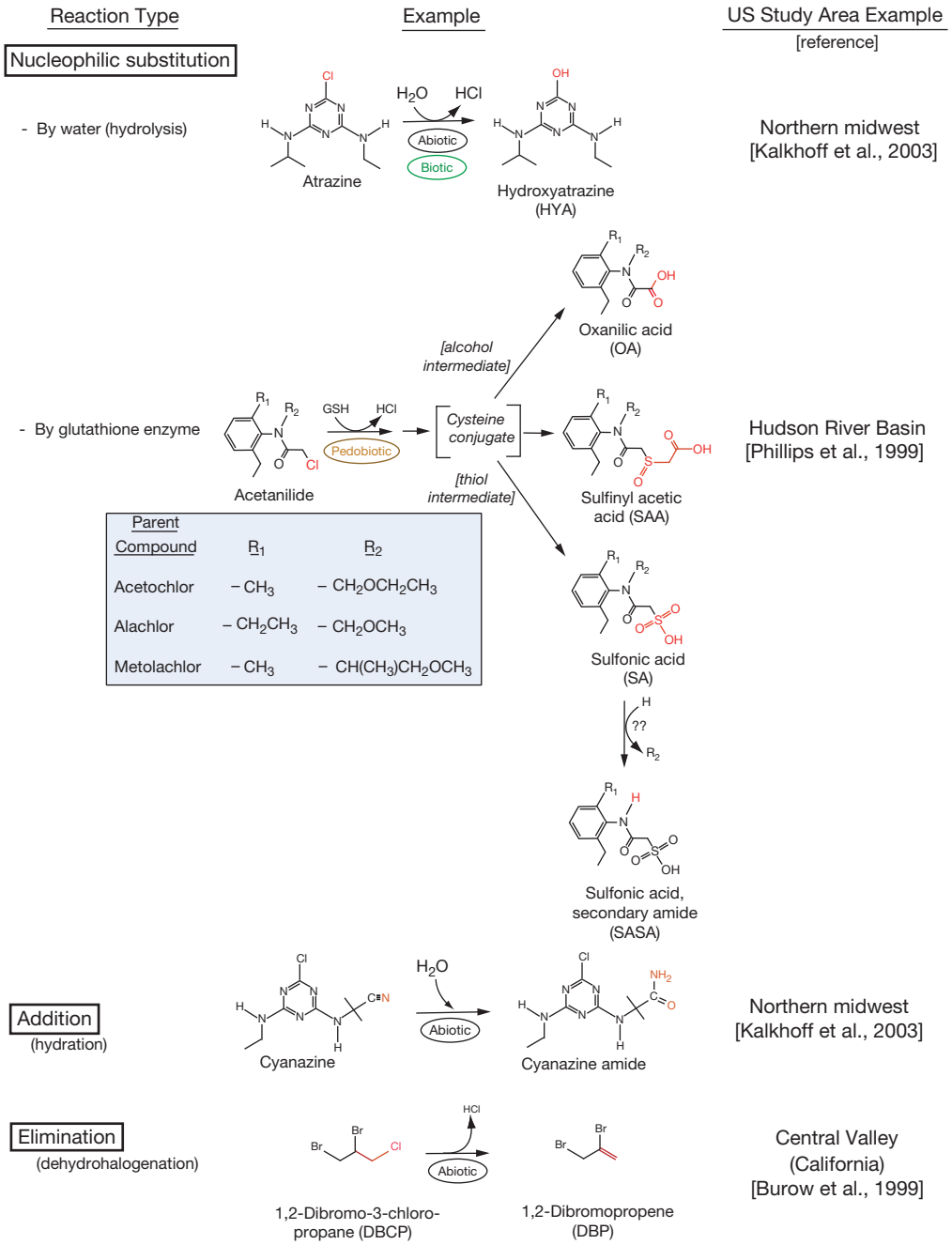

Figure 18 Examples of neutral reactions for which data on the occurrence of the products, as well as the pesticide parent compounds, have been reported in environmental media. The term 'pedobiotic' refers to processes occurring in the soil that are biologically mediated, primarily by microorganisms.

chemicals, personal care products, pharmaceuticals, mining wastes, and the other chemical effluvia of modern life. As with these and other anthropogenic contaminants, predictions regarding the transport, effects, and fate of pesticide compounds in natural waters must take more explicit account of a variety of complex phenomena that have received comparatively limited attention in such assessments to date. These include spray drift, large-scale atmospheric transport, preferential transport in the vadose and saturated zones, nonlinear sorption, time-dependent uptake by soils, endocrine disruption, toxicological interactions among pesticides and other contaminants present in mixtures, the effects of temperature and moisture content on transformation rates, and the transport, fate and biological effects of transformation products and adjuvants. Until significant progress is achieved in understanding these phenomena and accounting for the magnitude, timing, and spatial distributions of pesticide and adjuvant use and occurrence, the full implications of the ongoing release of these compounds into the Earth's ecosystems will remain unknown.

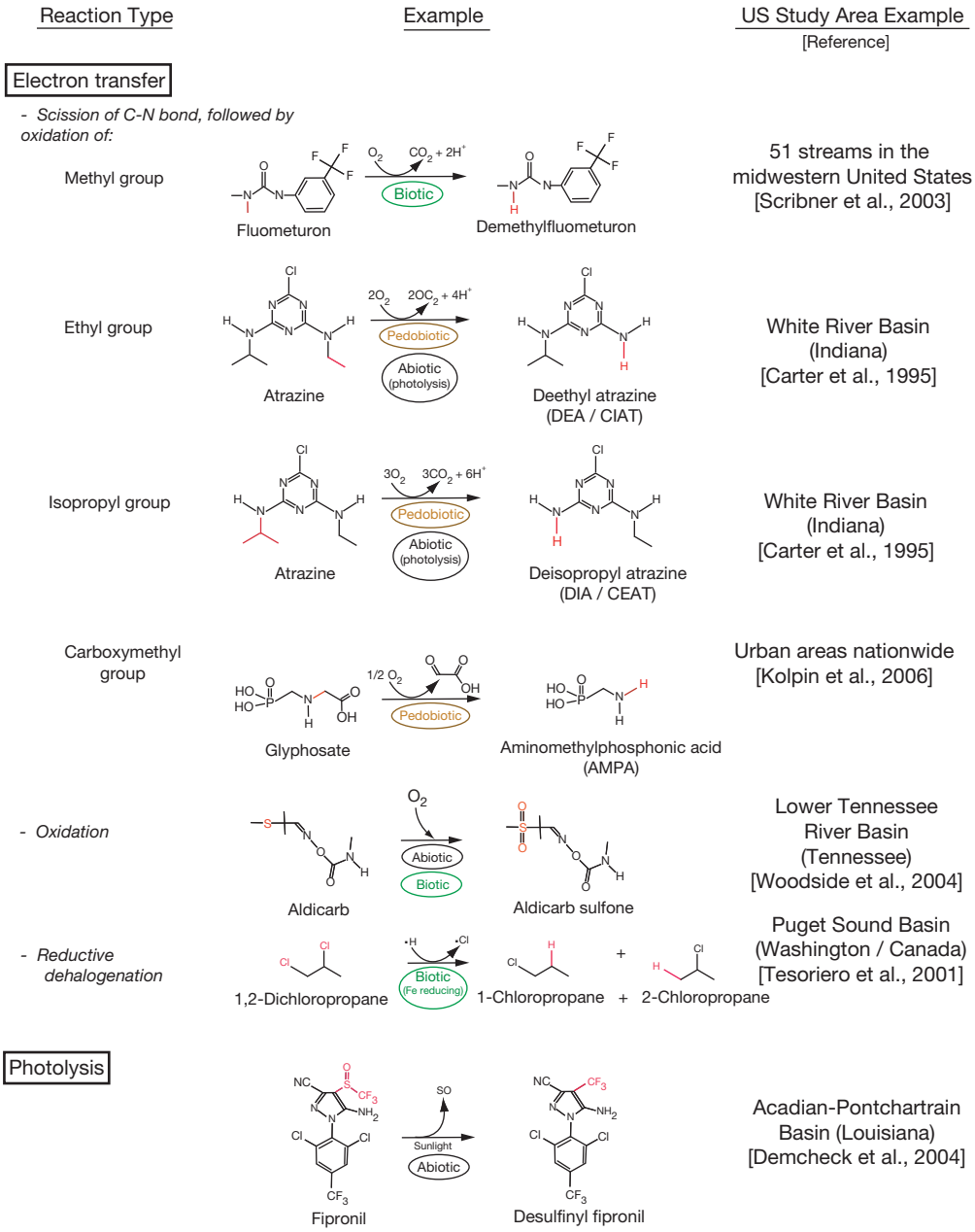

Figure 19 Examples of electron-transfer and photolytic reactions for which data on the occurrence of the products, as well as the pesticide parent compounds, have been reported in environmental media. The term 'pedobiotic' refers to processes occurring in the soil that are biologically mediated, primarily by microorganisms.

Acknowledgments

Although this chapter officially lists only one author, the assistance of several valued colleagues was indispensable to its production. The author would therefore like to thank both the editor for this volume, Professor Barbara Sherwood-Lollar, and the series editor, Mabel Peterson, for their incredible patience in awaiting the completion of the original version. In addition, the author owes an enormous debt of gratitude to two USGS colleagues, Drs. Paul Capel and Mark Sandstrom, for having provided extremely thorough, insightful, and helpful reviews of the original manuscript, as well as to these scientists and Dr. Jim Tesoriero for their careful reviews of the current version. The author also thanks the staff at the USGS library in Menlo Park, CA, for having provided copies of so many papers in such a timely manner, and many other colleagues – including Yvonne Roque and Drs. Lynn Roberts, Lisa Nowell, Bill Ball, Markus Flury, Peter Jeffers, Werner Haag, Farla Kaufman, and Chensheng Lu – for providing valuable assistance.

References

Adrian NR and Suflita JM (1990) Reductive dehalogenation of a nitrogen heterocyclic herbicide in anoxic aquifer slurries. *Applied and Environmental Microbiology* 56(1): 292–294.

Aga DS, Thurman EM, Yockel ME, Zimmerman LR, and Williams TD (1996) Identification of a new sulfonic acid metabolite of metolachlor in soil. *Environmental Science & Technology* 30(2): 592–597.

Agertved J, Rügge K, and Barker JF (1992) Transformation of the herbicides MCPP and atrazine under natural aquifer conditions. *Ground Water* 30(4): 500–506.

Ahmed AE, Kubic VL, Stevens JL, and Anders MW (1980) Halogenated methanes: Metabolism and toxicity. *Federation Proceedings* 39(13): 3150–3155.

Alavanja MCR, Dosemeci M, Samanic C, et al. (2004) Pesticides and lung cancer risk in the agricultural health study cohort. *American Journal of Epidemiology* 160(9): 876–885.

Alexander M (1981) Biodegradation of chemicals of environmental concern. *Science* 211(4478): 132–138.

Anderson JJ and Dulka JJ (1985) Environmental fate of sulfometuron methyl in aerobic soils. *Journal of Agricultural and Food Chemistry* 33(4): 596–602.

Anderson TD and Lydy MJ (2002) Increased toxicity to invertebrates associated with a mixture of atrazine and organophosphate insecticides. *Environmental Toxicology and Chemistry* 21(7): 1507–1514.

Ando CM (1992) Survey for chlorthal-dimethyl residues in well water of seven California counties. EH-92-01. Sacramento, CA: State of California Environmental Protection Agency.

Anway MD, Cupp AS, Uzumcu J, and Skinner MK (2005) Epigenetic transgenerational actions of endocrine disruptors and male fertility. *Science* 308(5727): 1466–1469.

Armstrong DE and Chesters G (1968) Adsorption catalyzed chemical hydrolysis of atrazine. *Environmental Science & Technology* 2(9): 683–689.

Armstrong DE, Chesters G, and Harris RF (1967) Atrazine hydrolysis in soil. *Soil Science Society of America Proceedings* 31: 61–66.

Asman W, Jørgensen A, and Jensen PK (2003) Dry deposition and spray drift of pesticides to nearby water bodies. Pesticides Research No. 66. Danish Environmental Protection Agency. (accessed at http://www2.mst.dk/udgiv/publications/2003/87-7972-945-2/pdf/87-7972-946-0.pdf on 20 December 2010).

Atkins PW (1982) *Physical Chemistry*, 2nd edn., San Francisco, CA: W.H. Freeman.

Atkinson R, Guicherit R, Hites RA, Palm W, Seiber JN, and de Voogt P (1999) Transformations of pesticides in the atmosphere: A state of the art *[sic]*. *Water, Air, and Soil Pollution* 115: 219–243.

Bacci E, Calamari D, Gaggi C, and Vighi M (1990) Bioconcentration of organic chemical vapors in plant leaves: Experimental measurements and correlation. *Environmental Science & Technology* 24(6): 885–889.

Baer U and Calvet R (1999) Fate of soil applied herbicides: Experimental data and prediction of dissipation kinetics. *Journal of Environmental Quality* 28: 1765–1777.

Baldwin DS, Beattie JK, Coleman LM, and Jones DR (2001) Hydrolysis of an organophosphate ester by manganese dioxide. *Environmental Science & Technology* 35(4): 713–716.

Bank S and Tyrrell RJ (1984) Kinetics and mechanism of alkaline and acidic hydrolysis of aldicarb. *Journal of Agricultural and Food Chemistry* 32(6): 1223–1232.

Barbash JE (1987) The effect of surface-active compounds on chemical reactions of environmental interest in natural waters. *Preprints of Extended Abstracts presented at the ACS National Meeting, American Chemical Society, Division of Environmental Chemistry* 27(2): 58–61.

Barbash JE (1993) *Abiotic Reactions of Halogenated Ethanes and Ethylenes with Sulfide, Nitrate and pH-Buffer Anions in Aqueous Solution*. PhD Thesis Stanford University.

Barbash JE and Kolpin DW (2010) The use of data on transformation product occurrence to infer the sources, transport and fate of organic contaminants in the hydrologic system. Invited presentation delivered at *TransCon2010 – Environmental Transformation of Organic Compounds*, Ascona, Switzerland (13 September 2010).

Barbash JE and Reinhard M (1989a) Reactivity of sulfur nucleophiles toward halogenated organic compounds in natural waters. In: Saltzman ES and Cooper WJ (eds.) *Biogenic Sulfur in the Environment*. *ACS Symposium Series*, vol. 393, pp. 101–138. Washington, DC: American Chemical Society.

Barbash JE and Reinhard M (1989b) Abiotic dehalogenation of 1,2-dichloroethane and 1,2-dibromoethane in aqueous solution containing hydrogen sulfide. *Environmental Science & Technology* 23(11): 1349–1358.

Barbash JE and Reinhard M (1992a) Abiotic reactions of halogenated ethanes and ethylenes in buffered aqueous solutions containing hydrogen sulfide. *Preprints of Extended Abstracts presented at the ACS National Meeting, American Chemical Society, Division of Environmental Chemistry* 32(1): 670–673.

Barbash JE and Reinhard M (1992b) The influence of pH buffers and nitrate concentration on the rate and pathways of abiotic transformation of 1,2-dibromoethane (EDB) in aqueous solution. *Preprints of Extended Abstracts presented at the ACS National Meeting, American Chemical Society, Division of Environmental Chemistry* 32(1): 674–677.

Barbash JE and Resek EA (1996) *Pesticides in Ground Water – Distribution, Trends, and Governing Factors*, Boca Raton, FL: CRC Press.

Barbash JE and Voss FD (2007) Use of a geographic information system with process-based simulation modeling to predict atrazine concentrations in shallow ground water across the United States: Simulation approach and testing against nationwide observations. *233rd American Chemical Society National Meeting*, Chicago, IL, 27 March 2007. Agrochemicals Division, Paper #123 (abstract available online at http://oasys2.confex.com/acs/233nm/techprogram/P1057615.HTM).

Barbash JE, Thelin GP, Kolpin DW, and Gilliom RJ (1999) Distribution of major herbicides in ground water of the United States. *US Geological Survey, Water-Resources Investigations Report 98-4245* (http://water.wr.usgs.gov/pnsp/rep/wrir984245/).

Baxter RM (1990) Reductive dechlorination of certain chlorinated organic compounds by reduced hematin compared with their behaviour in the environment. *Chemosphere* 21(4–5): 451–458.

Bayless ER (2001) Atrazine retention and degradation in the vadose zone at a till plain site in central Indiana. *Ground Water* 39(2): 169–180.

Bayless ER, Capel PD, Barbash JE, Webb RMT, Connell Hancock TL, and Lampe DC (2008) Simulated fate and transport of metolachlor in the unsaturated zone, Maryland, USA. *Journal of Environmental Quality* 37: 1064–1072.

Belden JB and Lydy MJ (2000) Impact of atrazine on organophosphate insecticide toxicity. *Environmental Toxicology and Chemistry* 19(9): 2266–2274.

Bell EM, Hertz-Picciotto I, and Beaumont JJ (2001) A case-control study of pesticides and fetal death due to congenital anomalies. *Epidemiology* 12: 148–156.

Benachour N, Sipahutar H, Moslemi S, Gasnier C, Travert C, and Séralini GE (2007) Time- and dose-dependent effects of roundup on human embryonic and placental cells. *Archives of Environmental Contamination and Toxicology* 53: 126–133.

Betarbet R, Sherer TB, MacKenzie G, Garcia-Osuna M, Panov AV, and Greenamyre JT (2000) Chronic systemic pesticide exposure reproduces features of Parkinson's disease. *Nature Neuroscience* 3(12): 1301–1306.

Beulke S, Dubus IG, Brown CD, and Gottesbüren B (2000) Simulation of pesticide persistence in the field on the basis of laboratory data – A review. *Journal of Environmental Quality* 29: 1371–1379.

Beynon KI, Stoydin G, and Wright AN (1972) A comparison of the breakdown of the triazine herbicides cyanazine, atrazine and simazine in soils and in maize. *Pesticide Biochemistry and Physiology* 2: 153–161.

Bidleman TF (1999) Atmospheric transport and air-surface exchange of pesticides. *Water, Air, and Soil Pollution* 115: 115–166.

Blais JM, Kimpe LE, McMahon D, et al. (2005) Arctic seabirds transport marine-derived contaminants. *Science* 309(5733): 445.

Bollag J-M (1982) Microbial metabolism of pesticides. In: Rosazza JP (ed.) *Microbial Transformations of Bioactive Compounds*, vol. 2, pp. 126–168. Boca Raton, FL: CRC Press.

Bolognesi C, Bonatti S, Degan P, et al. (1997) Genotoxic activity of glyphosate and its technical formulation Roundup. *Journal of Agricultural and Food Chemistry* 45: 1957–1962.

Bondarenko S, Gan J, Haver DL, and Kabashima JN (2004) Persistence of selected organophosphate and carbamate insecticides in waters from a coastal watershed. *Environmental Toxicology and Chemistry* 23(11): 2649–2654.

Bouchard MF, Bellinger DC, Wright RO, and Weisskopf MG (2010) Attention-deficit/hyperactivity disorder and urinary metabolites of organophosphate pesticides. *Pediatrics* 125(6): e1270–e1277.

Bowmer KH and Higgins ML (1976) Some aspects of the persistence and fate of acrolein herbicide in water. *Archives of Environmental Contamination and Toxicology* 5: 87–96.

Briggs GG, Bromilow RH, and Evans AA (1982) Relationships between lipophilicity and root uptake and translocation of non-ionised chemicals by barley. *Pesticide Science* 13: 495–504.

Broholm MM, Tuxen N, Rügge K, and Bjerg PL (2001) Sorption and degradation of the herbicide 2-methyl-4,6-dinitrophenol under aerobic conditions in a sandy aquifer in Vejen, Denmark. *Environmental Science & Technology* 35(24): 4789–4797.

Brown TP, Rumsby PC, Capleton AC, Rushton L, and Levy LS (2006) Pesticides and Parkinson's disease – Is there a link? *Environmental Health Perspectives* 114(2): 156–164.

Brusseau ML and Rao PSC (1989) The influence of sorbate-organic matter interactions on sorption nonequilibrium. *Chemosphere* 18(9/10): 1691–1706.

Burlinson NE, Lee LA, and Rosenblatt DH (1982) Kinetics and products of hydrolysis of 1,2-dibromo-3-chloropropane. *Environmental Science & Technology* 16(9): 627–632.

Burnside OC and Lavy TL (1966) Dissipation of dicamba. *Weeds* 14(3): 211–214.

Burow KR, Panshin SY, Dubrovsky NM, van Brocklin D, and Fogg GE (1999) Evaluation of processes affecting 1,2-dibromo-3-chloropropane (DBCP) concentrations in ground water in the eastern San Joaquin Valley, California: Analysis of chemical data and ground-water flow and transport simulations, *US Geological Survey Water-Resources Investigations Report 99-4059*. Menlo Park, CA: US Geological Survey.

Buser H-R, Poiger T, and Müller MD (2000) Changed enantiomer composition of metolachlor in surface water following the introduction of the enantiomerically enriched product to the market. *Environmental Science & Technology* 34(13): 2690–2696.

Butler EC and Hayes KF (2000) Kinetics of the transformation of halogenated aliphatic compounds by iron sulfide. *Environmental Science & Technology* 34(3): 422–429.

Capel PD (1993) Organic chemical concepts. In: Alley WM (ed.) *Regional Ground-Water Quality*, pp. 155–179. New York: Van Nostrand Reinhold.

Capel PD, Larson SJ, and Winterstein TA (2001) The behaviour of 39 pesticides in surface waters as a function of scale. *Hydrological Processes* 15: 1251–1269.

Carder JP and Hoagland KD (1998) Combined effects of alachlor and atrazine in benthic algal communities in artificial streams. *Environmental Contamination and Toxicology* 17(7): 1415–1420.

Carlson DL (2003) *Environmental Transformations of Chloroacetamide Herbicides: Hydrolysis and Reaction with Iron Pyrite*. PhD Thesis, Johns Hopkins University.

Carlson DL and Roberts AL (2002) Acid- and base-catalyzed hydrolysis of chloroacetamide herbicides. *Preprints of Extended Abstracts presented at the 224th ACS National Meeting, American Chemical Society, Division of Environmental Chemistry* 42(2): 317–320.

Carlson DL, McGuire MM, Fairbrother DH, and Roberts AL (2002) Dechlorination of the herbicide alachlor on pyrite (100) surfaces. *Preprints of Extended Abstracts presented at the 224th ACS National Meeting, American Chemical Society, Division of Environmental Chemistry* 42(2): 327–331.

Carson RL (1962) *Silent Spring*. Boston, MA: Houghton-Mifflin.

Carter DS, Lydy MJ, and Crawford CG (1995) Water-quality assessment of the White River Basin, Indiana: Analysis of available information on pesticides, 1972–92. *US Geological Survey Water-Resources Investigations Report 94-4024*. Menlo Park, CA: US Geological Survey.

Castro CE (1977) Biodehalogenation. *Environmental Health Perspectives* 21: 279–283.

Castro CE and Kray WC Jr. (1963) The cleavage of bonds by low valent transition metal ions: The homogeneous reduction of alkyl halides by chromous sulfate. *Journal of the American Chemical Society* 85: 2768–2773.

Castro CE and Kray WC Jr. (1966) Carbenoid intermediates from polyhalomethanes and chromium(II) the homogeneous reduction of geminal halides by chromous sulfate. *Journal of the American Chemical Society* 88: 4447–4455.

Centers for Disease Control and Prevention (2005) Third national report on human exposure to environmental chemicals. *Centers for Disease Control and Prevention, National Center for Environmental Health Publication Number 05-0570*. Atlanta, GA: Centers for Disease Control and Prevention. (available on-line at http://www.cdc.gov/exposurereport/).

Chesters G, Simsiman G, Levy J, Alhajjar B, Fathulla R, and Harkin J (1989) Environmental fate of alachlor and metolachlor. *Reviews of Environmental Contamination and Toxicology* 110: 1–74.

Chiou CT (1998) Soil sorption of organic pollutants and pesticides. In: Meyers RA (ed.) *Encyclopedia of Environmental Analysis and Remediation*, pp. 4517–4554. New York: Wiley.

Chiou CT (2002) *Partition and Adsorption of Organic Contaminants in Environmental Systems*, Hoboken, NJ: Wiley-Interscience.

Chiu P-C and Reinhard M (1995) Metallocoenzyme-mediated reductive transformation of carbon tetrachloride in titanium(III) citrate aqueous solution. *Environmental Science & Technology* 29(3): 595–603.

Christensen TH, Bjerg PL, Banwart SA, Jakobsen R, Heron G, and Albrechtsen H-J (2000) Characterization of redox conditions in groundwater contaminant plumes. *Journal of Contaminant Hydrology* 45: 165–241.

Chu W and Jafvert CT (1994) Photodechlorination of polychlorobenzene congeners in surfactant micelle solutions. *Environmental Science & Technology* 28(13): 2415–2422.

Cink JH and Coats JR (1993) Effect of concentration, temperature, and soil moisture on the degradation of chlorpyrifos in an urban Iowa soil. In: Racke KD and Leslie AR (eds.) *Pesticides in Urban Environments: Fate and Significance*. *ACS Symposium Series*, vol. 522, pp. 62–69. Washington, DC: American Chemical Society.

Clark GM and Goolsby DA (2000) Occurrence and load of selected herbicides and metabolites in the lower Mississippi river. *Science of the Total Environment* 248(2–3): 101–113.

Cline PV and Delfino JJ (1989) Transformation kinetics of 1,1,1-trichloroethane to the stable product 1,1-dichloroethene. In: Larson RA (ed.) *Biohazards of Drinking Water Treatment*, pp. 47–56. New York: Lewis Publishers.

Coats JR (1991) Pesticide degradation mechanisms and environmental activation. In: Somasundaram L and Coats JR (eds.) *Pesticide Transformation Products: Fate and Significance in the Environment*. *ACS Symposium Series*, vol. 459, pp. 10–31. Washington, DC: American Chemical Society.

Colborn T (2006) A case for revisiting the safety of pesticides: A closer look at neurodevelopment. *Environmental Health Perspectives* 114(1): 10–17.

Colborn T, Dumanoski D, and Myers JP (1996) *Our Stolen Future*, New York: Penguin.

Colborn T, vom Saal S, and Soto AM (1993) Developmental effects of endocrine-disrupting chemicals in wildlife and humans. *Environmental Health Perspectives* 101(5): 378–384.

Cooper WJ and Zika RG (1983) Photochemical formation of hydrogen peroxide in surface and ground waters exposed to sunlight. *Science* 220: 711–712.

Crosby DG and Leitis E (1973) The photodecomposition of trifluralin in water. *Bulletin of Environmental Contamination and Toxicology* 10: 237–241.

Curl CL, Fenske RA, and Elgethun K (2003) Organophosphorus pesticide exposure of urban and suburban preschool children with organic and conventional diets. *Environmental Health Perspectives* 111(3): 377–382.

Curtis GP and Reinhard M (1994) Reductive dehalogenation of hexachloroethane, carbon tetrachloride, and bromoform by anthrahydroquinone disulfonate and humic acid. *Environmental Science & Technology* 28(13): 2393–2401.

Curtis GP, Reinhard M, and Roberts PV (1986) Sorption of hydrophobic organic compounds by sediments. In: Davis JA and Hayes KF (eds.) *Geochemical Processes at Mineral Surfaces*. *ACS Symposium Series*, vol. 323, pp. 191–216. Washington, DC: American Chemical Society.

D'Adamo PD, Rozich AF, and Gaudy AF Jr. (1984) Analysis of growth data with inhibitory carbon sources. *Biotechnology and Bioengineering* 25: 397–402.

Day KE and Hodge V (1996) The toxicity of the herbicide metolachlor, some transformation products and a commercial safener to an alga (*Selenastrum capricornutum*), a cyanophyte (*Anabaena cylindrica*) and a macrophyte (*Lemma gibba*). *Water Quality Research Journal of Canada* 31(1): 197–214.

Dean JA (1985) *Lange's Handbook of Chemistry*, 13th edn. San Francisco, CA: McGraw-Hill.

Deeley GM, Reinhard M, and Stearns SM (1991) Transformation and sorption of 1,2-dibromo-3-chloropropane in subsurface samples collected at Fresno, California. *Journal of Environmental Quality* 20(3): 547–556.

Demcheck DK, Tollett RW, Mize SV, et al. (2004) Water quality in the Acadian-Ponchartrain drainages, Louisiana and Mississippi, 1999–2001. *US Geological Survey Circular 1232*. Denver, CO: US Geological Survey.

De Souza ML, Seffernick J, Martinez B, Sadowsky MJ, and Wackett LP (1998) The atrazine catabolism genes *atzABC* are widespread and highly conserved. *Journal of Bacteriology* 180: 1951–1954.

Dilling WL, Lickly LC, Lickly TD, Murphy PG, and McKellar RL (1984) Organic photochemistry: 19. Quantum yields for O, O-diethyl-O-(3,5,6-trichloro-2-pyridinyl) phosphorothioate (chlorpyrifos) and 3,5,6-trichloro-2-pyridinol in dilute aqueous solutions and their environmental phototransformation rates. *Environmental Science & Technology* 18(7): 540–543.

Dinelli G, Di Martino E, and Vicari A (1998) Influence of soil moisture and temperature on degradation of three sulfonylurea herbicides in soil. *Agrochimica* 42(1–2): 50–58.

Dinelli G, Vicari A, Bonetti A, and Catizone P (1997) Hydrolytic dissipation of four sulfonylurea herbicides. *Journal of Agricultural and Food Chemistry* 45(5): 1940–1945.

Dragun J and Helling CS (1985) Physicochemical and structural relationships of organic chemicals undergoing soil- and clay-catalyzed free-radical oxidation. *Soil Science* 139(2): 100–111.

Egli C, Tschan T, Scholtz R, Cook AM, and Leisinger T (1988) Transformation of tetrachloromethane to dichloromethane and carbon dioxide by *Acetobacterium woodii*. *Applied and Environemental Microbiology* 54(11): 2819–2824.

Ehrenberg L, Osterman-Golkar S, Singh D, and Lundqvist U (1974) On the reaction kinetics and mutagenic activity of methylating and β-halogenoethylating gasoline additives. *Radiation Botany* 14: 185–194.

Erickson LE and Lee KH (1989) Degradation of atrazine and related s-triazines. *Critical Reviews in Environmental Control* 19(1): 1–14.

Eskenazi B, Marks AR, Bradman A, et al. (2006) In utero exposure to dichlorodiphenyltrichloroethane (DDT) and dichlorodiphenyldichloroethylene (DDE) and neurodevelopment among young Mexican American children. *Pediatrics* 118(1): 233–241.

European Commission (1998) Council Directive 98/83/EC of 3 November 1998 on the quality of water intended for human consumption. Official Journal of the European Communities L330/32 (5/12/1998). (available online at http://eur-lex.europa.eu/LexUriServ/LexUriServ.do?uri= OJ:L:1998:330:0032:0054:EN:PDF).

Ewald G, Larsson P, Linge H, Okla L, and Szarzi N (1998) Biotransport of organic pollutants to an inland Alaska lake by migrating sockeye salmon (*Oncorhynchus nerka*). *Arctic* 51(1): 40–47.

Falconer RL, Bidleman TF, Gregor DJ, Semkin R, and Teixeira C (1995) Enantioselective breakdown of α-hexachlorocyclohexane in a small Arctic lake and its watershed. *Environmental Science & Technology* 29(5): 1297–1302.

Fendler JH and Fendler EJ (1975) *Catalysis in Micellar and Macromolecular Systems*. San Francisco, CA: Academic Press.

Fenner K, Lanz VA, Scheringer M, and Borsuk ME (2007) Relating atrazine degradation rate in soil to environmental conditions: Implications for global fate modeling. *Environmental Science & Technology* 41(8): 2840–2846.

Field JA and Thurman EM (1996) Glutathione conjugation and contaminant transformation. *Environmental Science & Technology* 30(5): 1413–1417.

Fleming I (1976) *Frontier Orbitals and Organic Chemical Reactions*. New York: Wiley.

Flury M (1996) Experimental evidence of transport of pesticides through field soils – A review. *Journal of Environmental Quality* 25: 25–45.

Gan J, Papiernik SK, Yates SR, and Jury WA (1999) Temperature and moisture effects on fumigant degradation in soil. *Journal of Environmental Quality* 28(5): 1436–1441.

Gan J, Qang Q, Yates SR, Koskinen WC, and Jury WA (2002) Dechlorination of chloroacetanilide herbicides by thiosulfate salts. *Proceedings of the National Academy of Sciences of the United States of America* 99(8): 5189–5194.

Gan J, Yates SR, Knuteson JA, and Becker JO (2000) Transformation of 1,3-dichloropropene in soil by thiosulfate fertilizers. *Journal of Environmental Quality* 29: 1476–1481.

Gantzer CJ and Wackett LP (1991) Reductive dechlorination catalyzed by bacterial transition-metal coenzymes. *Environmental Science & Technology* 25(4): 715–722.

Gao J, Ellis LBM, and Wackett LP (2010) The University of Minnesota biocatalysis/biodegradation database: Improving public access. *Nucleic Acids Research* 38: D488–D491 (Database accessible online at http://umbbd.msi.umn.edu/).

Garrison AW, Nzengung VA, Avants JK, et al. (2000) Phytodegradation of *p, p′*-DDT and the enantiomers of *o, p′*-DDT. *Environmental Science & Technology* 34(9): 1663–1670.

Garry VF, Harkins ME, Erickson LL, Long-Simpson LK, Holland SE, and Burroughs BL (2002) Birth defects, season of conception, and sex of children born to pesticide applicators living in the Red River Valley of Minnesota, USA. *Environmental Health Perspectives* 110(3): 441–449.

Ghiorse WC (1997) Subterranean life. *Science* 275: 789–790.

Gibson SA and Suflita JM (1986) Extrapolation of biodegradation results to groundwater aquifers: Reductive dehalogenation of aromatic compounds. *Applied and Environmental Microbiology* 52(4): 681–688.

Gilliom RJ, Barbash JE, Crawford CG, et al. (2006) Pesticides in the nation's streams and ground water, 1992–2001. US Geological Survey Circular 1291. Denver, CO: US Geological Survey.

Glass BL (1972) Relation between the degradation of DDT and the iron redox system in soils. *Journal of Agricultural and Food Chemistry* 20(2): 324–327.

Gottesbüren B (1991) *Concept, Development and Validation of the Knowledge-Based Herbicide Advisory System HERBASYS*. PhD Thesis, University of Hanover.

Graetz DA, Chesters G, Daniel TC, Newland LW, and Lee GB (1970) Parathion degradation in lake sediments. *Journal of the Water Pollution Control Federation* 42(2): R76–R94.

Graham WH, Graham DW, DeNoyelles F Jr., Smith VH, Larive CK, and Thurman EM (1999) Metolachlor and alachlor breakdown product formation patterns in aquatic field mesocosms. *Environmental Science & Technology* 33(24): 4471–4476.

Grandjean P, Harari R, Barr DB, and Debes F (2006) Pesticide exposure and stunting as independent predictors of neurobehavioral deficits in Ecuadorian school children. *Pediatrics* 117(3): e546–e556.

Guha S and Jaffé PR (1996) Biodegradation kinetics of phenanthrene partitioned into the micellar phase of nonionic surfactants. *Environmental Science & Technology* 30(2): 605–611.

Guillette EA, Conard C, Lares F, Aguilar MA, McLachlan J, and Guillette LJ Jr. (2006) Altered breast development in young girls from an agricultural environment. *Environmental Health Perspectives* 114(3): 471–475.

Guillette EA, Meza MM, Aquilar MG, Soto AD, and Garcia IE (1998) An anthropological approach to the evaluation of preschool children exposed to pesticides in Mexico. *Environmental Health Perspectives* 106(6): 347–353.

Gunasekara AS (2005) Environmental fate of pyrethrins. Sacramento, CA: California Department of Pesticide Regulation, Environmental Monitoring Branch. (available online at http://www.cdpr.ca.gov/docs/empm/pubs/fatememo/pyrethrin_efate2.pdf).

Haag WR and Hoigné J (1985) Photo-sensitized oxidation in natural water via OH• radicals. *Chemosphere* 14: 1659–1671.

Haag WR and Mill T (1988a) Effect of a subsurface sediment on hydrolysis of haloalkanes and epoxides. *Environmental Science & Technology* 22(6): 658–663.

Haag WR and Mill T (1988b) Some reactions of naturally occurring nucleophiles with haloalkanes in water. *Environmental Toxicology and Chemistry* 7: 917–924.

Haderlein SB and Schwarzenbach RP (1993) Adsorption of substituted nitrobenzenes and nitrophenols to mineral surfaces. *Environmental Science & Technology* 27(2): 316–326.

Hainly RA and Kahn JM (1996) Factors affecting herbicide yields in the Chesapeake Bay watershed, June 1994. *Journal of the American Water Resources Association* 32(5): 965–984.

Hamaker JW and Thompson JM (1972) Adsorption. In: Goring CAI and Hamaker JW (eds.) *Organic Chemicals in the Soil Environment*, vol. 1, pp. 49–143. New York: Dekker.

Hardell L and Eriksson M (1999) A case-control study of non-Hodgkin lymphoma and exposure to pesticides. *Cancer* 85: 1353–1360.

Harner T, Kylin H, Bidleman TF, and Strachan WM (1999) Removal of α- and γ-hexachlorocyclohexane and enantiomers of α-hexachlorocyclohexane in the eastern Arctic Ocean. *Environmental Science & Technology* 33(8): 1157–1164.

Harner T, Wiberg K, and Norstrom R (2000) Enantiomer fractions are preferred to enantiomer ratios for describing chiral signatures in environmental analyses. *Environmental Science & Technology* 34(1): 218–220.

Harris CI (1967) Fate of 2-chloro-s-triazine herbicides in soil. *Journal of Agricultural and Food Chemistry* 15(1): 157–162.

Harris JC (1990a) Rate of hydrolysis. In: Lyman WJ, Reehl WF, and Rosenblatt DH (eds.) *Handbook of Chemical Property Estimation Methods*, pp. 7(1)–7(48). Washington, DC: American Chemical Society.

Harris JC (1990b) Rate of aqueous photolysis. In: Lyman WJ, Reehl WF, and Rosenblatt DH (eds.) *Handbook of Chemical Property Estimation Methods*, pp. 8(1)–8(43). Washington, DC: American Chemical Society.

Hayden KM, Norton MC, Darcey D, et al. (2010) Occupational exposure to pesticides increases the risk of incident AD (Alzheimer disease): The Cache County study. *Neurology* 74(19): 1524–1530.

Hayes TB (2004) There is no denying this: Defusing the confusion about atrazine. *BioScience* 54(12): 1138–1149.

Hayes TB, Case P, Chui S, et al. (2006) Pesticide mixtures, endocrine disruption, and amphibian declines: Are we underestimating the impact? *Environmental Health Perspectives* 114 (supplement 1): 40–50.

Hayes TB, Collins A, Lee M, et al. (2002) Hermaphroditic, demasculinized frogs after exposure to the herbicide atrazine at low ecologically relevant doses. *Proceedings of the National Academy of Sciences of the United States of America* 99(8): 5476–5480.

Helbling DE, Hollender J, Kohler H-PE, and Fenner K (2010) Structure-based interpretation of biotransformation pathways of amide-containing compounds in sludge-seeded bioreactors. *Environmental Science & Technology* 44(17): 6628–6635.

Hemmamda S, Calmon M, and Calmon JP (1994) Kinetics and hydrolysis mechanism of chlorsulfuron and metsulfuron-methyl. *Pesticide Science* 40: 71–76.

Hendrikx P, Chauzat M-P, Debin M, et al. (2009) Bee mortality and bee surveillance in Europe. Scientific report submitted to the European Food Safety Authority (CFP/EFSA/AMU/2008/02). (available online at http://www.efsa.europa.eu/it/scdocs/doc/27e.pdf).

Hermanson MH, Isaksson E, Teixeira C, et al. (2005) Current-use and legacy pesticide history in the Austfonna Ice Cap, Svalbard, Norway. *Environmental Science & Technology* 39(21): 8163–8169.

Hippelein M and McLachlan MS (1998) Soil-air partitioning of semivolatile organic compounds: 1. Method development and influence of physical–chemical properties. *Environmental Science & Technology* 32(2): 310–316.

Hladik ML, Hsiao JJ, and Roberts AL (2005) Are neutral chloracetamide herbicide degradates of potential environmental concern? Analysis and occurrence in the upper Chesapeake Bay. *Environmental Science & Technology* 39(17): 6561–6574.

Hong F, Win KY, and Pehkonen SO (2001) Hydrolysis of terbufos using simulated environmental conditions: Rates, mechanisms, and product analysis. *Journal of Agricultural and Food Chemistry* 49(12): 5866–5873.

Howe CM, Berrill M, Pauli BD, Helbing CC, Werry K, and Veldhoen N (2005) Toxicity of glyphosate-based pesticides to four North American frog species. *Environmental Contamination and Toxicology* 23(8): 1928–1938.

Howe GE, Gillis R, and Mowbray RC (1998) Effect of chemical synergy and larval stage on the toxicity of atrazine and alachlor to amphibian larvae. *Environmental Contamination and Toxicology* 17(3): 519–525.

Howell DL, Miller KV, Bush PB, and Taylor JW (1996) Herbicides and wildlife habitat (1954–1996): An annotated bibliography on the effects of herbicides on wildlife habitat and their uses in habitat management. *US Department of Agriculture Forest Service, Technical Publication R8-TP 13*.

Huang C-H and Stone AT (2000) Synergistic catalysis of dimetilan hydrolysis by metal ions and organic ligands. *Environmental Science & Technology* 34(19): 4117–4122.

Huber R and Otto S (1994) Environmental behavior of bentazon herbicide. *Reviews of Environmental Contamination and Toxicology* 137: 111–134.

Issa S and Wood M (1999) Degradation of atrazine and isoproturon in the unsaturated zone: A study from southern England. *Pesticide Science* 55: 539–545.

Ivahnenko T and Barbash JE (2004) Chloroform in the hydrologic system – Sources, transport, fate, occurrence, and effects on human health and aquatic organisms. *US Geological Survey Scientific Investigations Report 2004-5137*. Denver, CO: US Geological Survey.

Iwata H, Tanabe S, Sakal N, and Tatsukawa R (1993) Distribution of persistent organochlorines in the oceanic air and surface seawater and the role of ocean [*sic*] on their global transport and fate. *Environmental Science & Technology* 27(6): 1080–1098.

Jafvert CT and Wolfe NL (1987) Degradation of selected halogenated ethanes in anoxic sediment-water systems. *Environmental Toxicology and Chemistry* 6: 827–837.

Jeffers PM, Ward LM, Woytowitch LM, and Wolfe NL (1989) Homogeneous hydrolysis rate constants for selected chlorinated methanes, ethanes, ethenes, and propanes. *Environmental Science & Technology* 23(8): 965–969.

Jeffers PM and Wolfe NL (1996) On the degradation of methyl bromide in sea water. *Geophysical Research Letters* 23(14): 1773–1776.

Kalkhoff SJ, Lee KE, Porter SD, Terrio PJ, and Thurman EM (2003) Herbicides and herbicide degradation products in Upper Midwest agricultural streams during August base-flow conditions. *Journal of Environmental Quality* 32: 1025–1035.

Kamiya M, Nakamura K, and Sasaki C (1994) Inclusion effects of cyclodextrins on photodegradation rates of parathion and paraoxon in aquatic medium [*sic*]. *Chemosphere* 28(11): 1961–1966.

Kamrin MA (1997) *Pesticide Profiles: Toxicity, Environmental Impact, and Fate*. Boca Raton, FL: CRC Press.

Katagi T (1992) Quantum chemical estimation of environmental and metabolic fates of pesticides. *Journal of Pesticide Science* 17(3): S221–S230 (in Japanese).

Katz BG (1993) Biogeochemical and hydrological processes controlling the transport and fate of 1,2-dibromoethane (EDB) in soil and ground water, central Florida. *US Geological Survey Water-Supply Paper 2402*. Tallahassee, FL: US Geological Survey.

Kearney PC and Kaufman DD (1972) Microbial degradation of some chlorinated pesticides. In: *Degradation of Synthetic Organic Molecules in the Biosphere: Natural, Pesticidal, and Various Other Man-Made Compounds*, pp. 166–189. Washington, DC: National Academy of Sciences.

Kegley S, Neumeister L, and Martin T (1999) *Disrupting the Balance: Ecological Impacts of Pesticides in California*. San Francisco, CA: Pesticide Action Network North America Regional Center.

Kenaga EE (1980) Predicted bioconcentration factors and soil sorption coefficients of pesticides and other chemicals. *Ecotoxicology and Environmental Safety* 4: 26–38.

Kenneke JF and Weber EJ (2003) Reductive dehalogenation of halomethanes in iron- and sulfate-reducing sediments: 1. Reactivity pattern analysis. *Environmental Science & Technology* 37(4): 713–720.

Khan SU (1978) Kinetics of hydrolysis of atrazine in aqueous fulvic acid solution. *Pesticide Science* 9: 39–43.

Kiely T, Donaldson D, and Grube A (2004) Pesticides industry sales and usage – 2000 and 2001 market estimates. 733-R-04-001. Washington, DC: US Environmental Protection Agency. (accessed at http://www.epa.gov/opp00001/pestsales/01pestsales/market_estimates2001.pdf on 20 December 2010).

Klecka GM and Gonsior SJ (1984) Reductive dechlorination of chlorinated methanes and ethanes by reduced iron(II) porphyrins. *Chemosphere* 13(3): 391–402.

Klecka GM, Gonsior SJ, and Markham DA (1990) Biological transformations of 1,1,1-trichloroethane in subsurface soils and ground water. *Environmental Toxicology and Chemistry* 9: 1437–1451.

Klopman G (1968) Chemical reactivity and the concept of charge- and frontier-controlled reactions. *Journal of the American Chemical Society* 90(2): 223–234.

Kochany J and Maguire RJ (1994) Sunlight photodegradation of metolachlor in water. *Journal of Agricultural and Food Chemistry* 42: 406–412.

Kochi JK and Powers JW (1970) The mechanism of reduction of alkyl halides by chromium (II) complexes: Alkylchromium species as intermediates. *Journal of the American Chemical Society* 92(1): 137–146.

Kolpin DW, Barbash JE, and Gilliom RJ (2000) Pesticides in ground water of the US, 1992–1996. *Ground Water* 38(6): 858–863.

Kolpin DW, Thurman EM, Lee EA, Meyer MT, Furlong ET, and Glassmeyer ST (2006) Urban contributions of glyphosate and its degradate AMPA to streams in the United States. *Science of the Total Environment* 354: 191–197.

Konrad JG, Armstrong DE, and Chesters G (1967) Soil degradation of diazinon, a phosphorothioate insecticide. *Agronomy Journal* 59: 591–594.

Konrad JG and Chesters G (1969) Degradation in soils of ciodrin, an organophosphate insecticide. *Journal of Agricultural and Food Chemistry* 17(2): 226–230.

Konrad JG, Chesters G, and Armstrong DE (1969) Soil degradation of malathion, a phosphorothioate insecticide. *Soil Science Society of America Proceedings* 33: 259–262.

Kray WC Jr. and Castro CE (1964) The cleavage of bonds by low-valent transition metal ions: The homogeneous dehalogenation of vicinal dihalides by chromous sulfate. *Journal of the American Chemical Society* 86: 4603–4608.

Kriegman-King M and Reinhard M (1992) Transformation of carbon tetrachloride in the presence of sulfide, biotite and vermiculite. *Environmental Science & Technology* 26(11): 2198–2206.

Kriegman-King M and Reinhard M (1994) Transformation of carbon tetrachloride by pyrite in aqueous solution. *Environmental Science & Technology* 28(4): 692–700.

Kuhn EP and Suflita JM (1989) Dehalogenation of pesticides by anaerobic microorganisms in soils and groundwater – A review. In: Sawhney BL and Brown KW (eds.) *Reactions and Movement of Organic Chemicals in Soils, Soil Science Society of America Special Publication No. 22*, pp. 111–180. Madison, WI: Soil Science Society of America.

Lam MW, Tantuco K, and Mabury SA (2003) PhotoFate: A new approach in accounting for the contribution of indirect photolysis of pesticides and pharmaceuticals in surface waters. *Environmental Science & Technology* 37(5): 899–907.

Larsen L, Sørensen SR, and Aamand J (2000) Mecoprop, isoproturon, and atrazine in and above a sandy aquifer: Vertical distribution of mineralization potential. *Environmental Science & Technology* 34(12): 2426–2430.

Larson SJ, Capel PD, Goolsby DA, Zaugg SD, and Sandstrom MW (1995) Relations between pesticide use and riverine flux in the Mississippi River Basin. *Chemosphere* 31(5): 3305–3321.

Larson SJ, Capel PD, and Majewski MS (1997) *Pesticides in Surface Waters – Distribution, Trends and Governing Factors*. Boca Raton, FL: CRC Press.

Larson SJ, Gilliom RJ, and Capel PD (1999) Pesticides in streams of the US-initial results from the National Water-Quality Assessment Program. *US Geological Survey Water-Resources Investigations Report 98-4222*. *Denver*, CO: US Geological Survey.

Lartiges SB and Garrigues PP (1995) Degradation kinetics of organophosphorus and organonitrogen pesticides in different waters under various environmental conditions. *Environmental Science & Technology* 29(5): 1246–1254.

Lasaga AC (1981) Transition state theory. In: Lasaga AC and Kirkpatrick RJ (eds.) *Kinetics of Geochemical Processes*. *Reviews in Mineralogy*, vol. 8, pp. 135–169. Washington, DC: Mineralogical Society of America.

Laskowski DA (2002) Physical and chemical properties of pyrethroids. *Reviews of Environmental Contamination and Toxicology* 174: 49–170.

Lee PW, Fukoto JM, Hernandez H, and Stearns SM (1990) Fate of monocrotophos in the environment. *Journal of Agricultural and Food Chemistry* 38(2): 567–573.

Lee EA and Strahan AP (2003) Methods of analysis by the U.S. Geological Survey Organic Geochemistry Research Group – Determination of acetamide herbicides and their degradation products in water using online solid-phase extraction and liquid chromatography/mass spectrometry. *US Geological Survey Open-File Report 03-173*. Menlo Park, CA: US Geological Survey.

Lewis KA, Green A, and Tzilivakis J (2007) Development of an improved pesticide properties database for risk assessment applications. Presented at the *Fifth Annual Conference of the European Federation of Information Technology in Agriculture*, Glasgow, Scotland, July 2007. (available online at http://sitem.herts.ac.uk/aeru/footprint/en/docs/Lewis_et_al.pdf).

Li G-C and Felbeck GT Jr. (1972) Atrazine hydrolysis as catalyzed by humic acids. *Soil Science* 114(3): 201–209.

Liess M and Von Der Ohe P (2005) Analyzing effects of pesticides on invertebrate communities in streams. *Environmental Toxicology and Chemistry* 24(4): 954–965.

Lightfoot EN, Thorne PS, Jones RL, Hansen JL, and Romine RR (1987) Laboratory studies on mechanisms for the degradation of aldicarb, aldicarb sulfoxide and aldicarb sulfone. *Environmental Toxicology and Chemistry* 6: 377–394.

Lin N and Garry VF (2000) In vitro studies of cellular and molecular developmental toxicity of adjuvants, herbicides and fungicides commonly used in Red River Valley, Minnesota. *Journal of Toxicology and Environmental Health* 60: 423–439.

Lippa KA and Roberts AL (2002) Nucleophilic aromatic substitution reactions of chloroazines with bisulfide (HS^-) and polysulfides (S_n^{2-}). *Environmental Science & Technology* 36(9): 2008–2018.

Liqiang J, Shukui H, Liansheng W, Chao L, and Deben D (1994) The influential factors of hydrolysis of organic pollutants in environment [*sic*]. *Chemosphere* 28(10): 1749–1756.

Little CD, Palumbo AV, Herbes SE, Lidstrom ME, Tyndall RL, and Gilmer PJ (1988) Trichloroethylene biodegradation by a methane-oxidizing bacterium. *Applied and Environmental Microbiology* 54: 951–956.

Liu S-Y, Freyer AJ, and Bollag J-M (1991) Microbial dechlorination of the herbicide metolachlor. *Journal of Agricultural and Food Chemistry* 39(3): 631–636.
Liu W, Gan J, Schlenk D, and Jury WA (2005) Enantioselectivity in environmental safety of current chiral insecticides. *Proceedings of the National Academy of Sciences of the United States of America* 102(3): 701–706.
Loch AR, Lippa KA, Carlson DL, Chin YP, Traina SJ, and Roberts AL (2002) Nucleophilic aliphatic substitution reactions of propachlor, alachlor, and metolachlor with bisulfide (HS^-) and polysulfides (S_n^{2-}). *Environmental Science & Technology* 36(19): 4065–4073.
Loh J (2002) *Living Planet Report 2002*. Gland, Switzerland: WWF-World Wide Fund For Nature. (available on the World Wide Web at http://panda.org/news_facts/publications/general/livingplanet/lpr02.cfm)
Lovley DR, Chapelle FH, and Woodward JC (1994) Use of dissolved hydrogen (H_2) concentrations to determine distribution of microbially catalyzed redox reactions in anoxic groundwater. *Environmental Science & Technology* 28(7): 1205–1210.
Lu C, Toepel K, Irish R, Fenske RA, Barr DB, and Bravo R (2005) Organic diets significantly lower children's dietary exposure to organophosphorus pesticides. *Environmental Health Perspectives* 114(2): 260–263.
Mabey WR, Barich V, and Mill T (1983) Hydrolysis of polychlorinated alkanes. American Chemical Society. *Preprints of Extended Abstracts presented at the ACS National Meeting, American Chemical Society, Division of Environmental Chemistry* 23(2): 359–361.
Mabey WR and Mill T (1978) Critical review of hydrolysis of organic compounds in water under environmental conditions. *Journal of Physical and Chemical Reference Data* 7(2): 383–425.
Macalady DL and Wolfe NL (1985) Effects of sediment sorption and abiotic hydrolyses: 1. Organophosphorothioate esters. *Journal of Agricultural and Food Chemistry* 33(2): 167–173.
Macalady DL and Wolfe NL (1987) Influences of aquatic humic substances on the abiotic hydrolysis of organic contaminants: A critical review. *Preprints of Extended Abstracts presented at the ACS National Meeting, American Chemical Society, Division of Environmental Chemistry* 27(1): 12–15.
Mackay D (1979) Finding fugacity feasible. *Environmental Science & Technology* 13(10): 1218–1223.
Mackay D, Shiu W-Y, and Ma K-C (1997) *Illustrated Handbook of Physical–Chemical Properties and Environmental Fate for Organic Chemicals, Vol V: Pesticide Chemicals*. New York: Lewis.
Majewski MS and Capel PD (1995) *Pesticides in the Atmosphere – Distribution, Trends and Governing Factors*. Boca Raton, FL: CRC Press.
Majewski MS, Desjardins R, Rochette P, Pattey E, Seiber J, and Glotfelty D (1993) Field comparison of an eddy accumulation and an aerodynamic-gradient system for measuring pesticide volatilization fluxes. *Environmental Science & Technology* 27(1): 121–128.
Majewski MS, Foreman WT, Goolsby DA, and Nakagaki N (1998) Airborne pesticide residues along the Mississippi River. *Environmental Science & Technology* 32(23): 3689–3698.
Mallat E and Barceló D (1998) Analysis and degradation study of glyphosate and of aminomethylphosphonic acid in natural waters by means of polymeric and ion-exchange solid-phase extraction columns followed by ion chromatography–post-column derivatization with fluorescence detection. *Journal of Chromatography A* 823: 129–136.
Mandelbaum RT, Wackett LP, and Allan DL (1993) Rapid hydrolysis of atrazine to hydroxyatrazine by soil bacteria. *Environmental Science & Technology* 27(9): 1943–1946.
Mansour M and Feicht EA (1994) Transformation of chemical contaminants by biotic and abiotic processes in water and soil. *Chemosphere* 28(2): 323–332.
March J (1985) *Advanced Organic Chemistry: Reactions, Mechanisms and Structure*, 3rd edn. New York: Wiley.
Marquardt S, Cox C, and Knight H (1998) *Toxic Secrets: 'Inert' Ingredients in Pesticides 1987–1997*. Eugene, OR: Northwest Coalition for Alternatives to Pesticides Available online at http://www.pesticide.org/inertsreport.pdf.
Matheron M (2001) Modes of action for plant disease management chemistries. Presented at the *11th Annual Desert Vegetable Crop Workshop,* Yuma, AZ, 6 December 2001 (accessed online at http://ag.arizona.edu/crops/diseases/papers/dischemistry.html on 9/22/02).
Matsumura F (1985) *Toxicology of Insecticides*, 2nd edn. New York: Plenum Press.
McCall PJ (1987) Hydrolysis of 1,3-dichloropropene in dilute aqueous solution. *Pesticide Science* 19: 235–242.
McCarty PL (1972) Energetics of organic matter degradation. In: Mitchell R (ed.) *Water Pollution Microbiology*, pp. 91–118. New York: Wiley-Interscience.
McCarty PL, Reinhard M, and Rittmann BE (1981) Trace organics in groundwater. *Environmental Science & Technology* 15(1): 40–51.
Meijer SN, Shoeib M, Jantunen LMM, Jones KC, and Harner T (2003) Air-soil exchange of organochlorine pesticides in agricultural soils: 1. Field measurements using a novel in situ sampling device. *Environmental Science & Technology* 37(7): 1292–1299.
Meister T (2000) *Farm Chemicals Handbook*, vol. 86. Willoughby, OH: Meister Publishing Company.
Miah HM and Jans U (2001) Reactions of phosphorothionate triesters with reduced sulfur species. Abstract presented at the *22nd Annual Meeting of the Society for Environmental Toxicology and Chemistry*, Baltimore, MD, November 2001
Miles CJ and Delfino JJ (1985) Fate of aldicarb, aldicarb sulfoxide, and aldicarb sulfone in Floridan groundwater. *Journal of Agricultural and Food Chemistry* 33(3): 455–460.
Mill T and Mabey WR (1985) Photochemical transformations. In: Neely WB and Blau G (eds.) *Environmental Exposure from Chemicals*, vol. I, pp. 175–216. Boca Raton, FL: CRC Press.
Miller GC and Zepp RG (1979) Effects of suspended sediments on photolysis rates of dissolved pollutants. *Water Research* 13: 453–459.
Milligan PW and Häggblom MM (1999) Biodegradation and biotransformation of dicamba under different reducing conditions. *Environmental Science & Technology* 33(8): 1224–1229.
Mochida I, Noguchi H, Fujitsu H, Seiyama T, and Takeshita K (1977) Reactivity and selectivity in the reductive elimination of halogen from haloalkanes by chromous, cuprous, and stannous ions. *Canadian Journal of Chemistry* 55: 2420–2425.
Monkiedje A, Spiteller M, and Bester K (2003) Degradation of racemic and enantiopure metalaxyl in tropical and temperate soils. *Environmental Science & Technology* 37(4): 707–712.
Moore JW and Pearson RG (1981) *Kinetics and Mechanism*, 3rd edn. New York: Wiley.
Moreau C and Mouvet C (1997) Sorption and desorption of atrazine, deethylatrazine, and hydroxyatrazine by soil and aquifer solids. *Journal of Environmental Quality* 26: 416–424.
Mortland MM and Raman KV (1967) Catalytic hydrolysis of some organic phosphate pesticides by copper(II). *Journal of Agricultural and Food Chemistry* 15(1): 163.
Moye HA and Miles CJ (1988) Aldicarb contamination of groundwater. *Reviews of Environmental Contamination and Toxicology* 105: 99–145.
Murphy SD (1986) Toxic effects of pesticides. In: Klaassen CD, Amdur MO, and Doull J (eds.) *Casarett and Doull's Toxicology: The Basic Science of Poisons*, pp. 519–581. New York: Macmillan.
Nair DR and Schnoor JL (1992) Effect of two electron acceptors on atrazine mineralization rates in soil. *Environmental Science & Technology* 26(11): 2298–2300.
Nash RG (1988) Dissipation from soil. In: Grover R (ed.) *Environmental Chemistry of Herbicides*, vol. 1, pp. 132–169. Boca Raton, FL: CRC Press.
National Research Council (1993) *Pesticides in the Diets of Infants and Children*. Washington, DC: National Academy Press (available online at http://books.nap.edu/catalog/2126.html).
Newland LW, Chesters G, and Lee GB (1969) Degradation of γ-BHC in simulated lake impoundments as affected by aeration. *Journal of the Water Pollution Control Federation* 41(5): R174–R188.
Ngabe B, Bidleman TF, and Falconer RL (1993) Base hydrolysis of α- and γ-hexachlorocyclohexanes. *Environmental Science & Technology* 27(9): 1930–1933.
Nicollier G and Donzel B (1994) Release of bound ^{14}C-residues from plants and soil using microwave extraction. Poster presented at the *8th International Congress of Pesticide Chemistry*, 4–9 July 1994. Washington, DC: American Chemical Society.
Noblet JA, Smith LA, and Suffet IH (1996) Influence of natural dissolved organic matter, temperature, and mixing on the abiotic hydrolysis of triazine and organophosphate pesticides. *Journal of Agricultural and Food Chemistry* 44(11): 3685–3693.
Novak PJ, Christ SJ, and Parkin GF (1997) Kinetics of alachlor transformation and identification of metabolites under anaerobic conditions. *Water Research* 31(12): 3107–3115.
Nowell LH, Capel PD, and Dileanis PD (1999) *Pesticides in Stream Sediment and Aquatic Biota – Distribution, Trends and Governing Factors*. Boca Raton, FL: CRC Press.
O'Neill RV (1968) Population energetics of the millipede, *Narceus americanus* (beauvois). *Ecology* 49(5): 803–809.
Oakes DJ and Pollak JK (1999) Effects of a herbicide formulation, Tordon 75D(R), and its individual components on the oxidative functions of mitochondria. *Toxicology* 136: 41–52.
Ogram AV, Jessup RE, Ou LT, and Rao PSC (1985) Effects of sorption on biological degradation rates of (2,4-dichlorophenoxy)acetic acid in soils. *Applied and Environmental Microbiology* 49(3): 582–587.

Oremland RS, Miller LG, and Strohnaier FE (1994) Degradation of methyl bromide in anaerobic sediments. *Environmental Science & Technology* 28(3): 514–520.

Osano O, Admiraal W, and Otieno D (2002) Developmental disorders in embryos of the frog *Xenopus laevis* induced by chloroacetanilide herbicides and their degradation products. *Environmental Toxicology and Chemistry* 21(2): 375–379.

Padilla F, LaFrance P, Robert C, and Villeneuve J (1988) Modeling the transport and the fate of pesticides in the unsaturated zone considering temperature effects. *Ecological Modelling* 44: 73–88.

Pape-Lindstrom PA and Lydy MJ (1997) Synergistic toxicity of atrazine and organophosphate insecticides contravenes the response addition mixture model. *Environmental Toxicology and Chemistry* 16(11): 2415–2420.

Papiernik SK and Spalding RF (1998) Atrazine, deethylatrazine, and deisopropylatrazine persistence measured in groundwater in situ under low-oxygen conditions. *Journal of Agricultural and Food Chemistry* 46(2): 749–754.

Paris DF, Steen WC, Baughman GL, and Barnett JT Jr. (1981) Second-order model to predict microbial degradation of organic compounds in natural waters. *Applied and Environmental Microbiology* 41(3): 603–609.

Parker LW and Doxtader KG (1983) Kinetics of the microbial degradation of 2,4-D in soil: Effects of temperature and moisture. *Journal of Environmental Quality* 12(4): 553–558.

Parsons TR and Takahashi M (1973) *Biological Oceanographic Processes*. New York: Pergamon.

Parsons F, Wood PR, and DeMarco J (1984) Transformations of tetrachloroethene and trichloroethene in microcosms and groundwater. *Journal of the American Water Works Association* 76: 56–59.

Patlak M (1996) Estrogens may link pesticides, breast cancer. *Environmental Science & Technology* 30(5): 210A–211A.

Pearson RG (1972) The influence of the reagent on organic reactivity. In: Chapman NB and Shorter J (eds.) *Advances in Linear Free Energy Relationships*, pp. 281–319. New York: Plenum.

Pehkonen SO and Zhang Q (2002) The degradation of organophosphorus pesticides in natural waters: A critical review. *Critical Reviews in Environmental Science & Technology* 32(1): 17–72.

Peijnenburg WJGM, de Beer KGM, den Haan MWA, Hollander HA, Stegeman MHL, and Verboom H (1992a) Development of a structure-reactivity relationship for the photohydrolysis of substituted aromatic halides. *Environmental Science & Technology* 26(11): 2116–2121.

Peijnenburg WJGM, den Hart MJ, van de Hollander HA, Meent D, Verboom HH, and Wolfe NL (1992b) QSARs for predicting reductive transformation rate constants of halogenated aromatic hydrocarbons in anoxic sediment systems. *Environmental Toxicology and Chemistry* 11: 301–314.

Perdue EJ and Wolfe NL (1982) Modification of pollutant hydrolysis kinetics in the presence of humic substances. *Environmental Science & Technology* 16(12): 847–852.

Perdue EM and Wolfe NL (1983) Prediction of buffer catalysis in field and laboratory studies of pollutant hydrolysis reactions. *Environmental Science & Technology* 17(11): 635–642.

Pereira WE, Rostad CE, and Leiker TJ (1990) Distribution of agrochemicals in the lower Mississippi River and its tributaries. *Science of the Total Environment* 97/98: 41–53.

Phillips PJ, Wall GR, Thurman EM, Eckhardt DQ, and vanHoesen J (1999) Metolachlor and its metabolites in tile drain and stream runoff in the Canajoharie Creek watershed. *Environmental Science & Technology* 33(20): 3531–3537.

Picardal F, Arnold RG, and Huey BB (1995) Effects of electron donor and acceptor conditions on reductive dehalogenation of tetrachloromethane by *Shewanella putrefaciens* 200. *Applied and Environmental Microbiology* 61(1): 8–12.

President's Cancer Panel (2010) Reducing environmental cancer risk – What we can do now. Washington, DC: National Cancer Institute (downloaded from http://deainfo.nci.nih.gov/advisory/pcp/pcp08-09rpt/PCP_Report_08-09_508.pdf on 8/5/10).

Reddy KN and Locke MA (1994) Prediction of soil sorption (K_{oc}) of herbicides using semiempirical molecular properties. *Weed Science* 42: 453–461.

Relyea RA (2005a) The lethal impacts of Roundup and predatory stress on six species of North American tadpoles. *Archives of Environmental Contamination and Toxicology* 48: 351–357.

Relyea RA (2005b) The impact of insecticides and herbicides on the biodiversity and productivity of aquatic communities. *Ecological Applications* 15(2): 618–627.

Relyea RA (2005c) The lethal impact of Roundup on aquatic and terrestrial amphibians. *Ecological Applications* 15(4): 1118–1124.

Relyea RA (2009) A cocktail of contaminants: How mixtures of pesticides at low concentrations affect aquatic communities. *Oecologia* 159(2): 363–376.

Relyea RA, Schoeppner NM, and Hoverman JT (2005) Pesticides and amphibians: The importance of community context. *Ecological Applications* 15(4): 1125–1134.

Renner R (2005) Are pesticide 'inerts' an unrecognized environmental danger? *Environmental Science & Technology* 39(20): 417A–418A.

Repetto R and Baliga S (1996) *Pesticides and the Immune System: The Public Health Risks*. Washington, DC: World Resources Institute.

Roberts AL, Jeffers PM, Wolfe NL, and Gschwend PM (1993) Structure-reactivity relationships in dehydrohalogenation reactions of polychlorinated and polybrominated alkanes. *Critical Reviews in Environmental Science & Technology* 23(1): 1–39.

Roberts TR and Hutson DH (1999) *Metabolic Pathways of Agrochemicals, Part II: Insecticides and Fungicides*. Cambridge, UK: Royal Society of Chemistry.

Roberts TR, Hutson DH, Lee PW, et al. (1998) *Metabolic Pathways of Agrochemicals, Part 1: Herbicides and Plant Growth Regulators*. Cambridge, UK: Royal Society of Chemistry.

Roberts AL, Sanborn PN, and Gschwend PM (1992) Nucleophilic substitution reactions of dihalomethanes with hydrogen sulfide species. *Environmental Science & Technology* 26(11): 2263–2274.

Roberts TR and Stoydin G (1976) The degradation of (*Z*)- and (*E*)-1,3-dichloropropenes and 1,2-dichloropropane in soil. *Pesticide Science* 7: 325–335.

Rocha F and Walker A (1995) Simulation of the persistence of atrazine in soil at different sites in Portugal. *Weed Research* 35(3): 179–186.

Roeth FW, Lavy TL, and Burnside OC (1969) Atrazine degradation in two soil profiles. *Weed Science* 17: 202–205.

Rohr JR and Crumrine PW (2005) Effects of an herbicide and an insecticide on pond community structure and processes. *Ecological Applications* 15(4): 1135–1147.

Rügge K, Bjerg PL, Mosbaek H, and Christensen TH (1999) Fate of MCPP and atrazine in an anaerobic landfill leachate plume (Grindsted, Denmark). *Water Research* 33(10): 2455–2458.

Russell JD, Cruz M, White JL, et al. (1968) Mode of chemical degradation of s-triazines by montmorillonite. *Science* 160: 1340–1342.

Sakata S, Mikami N, Matsuda T, and Miyamoto J (1986) Degradation and leaching behavior of the pyrethroid insecticide cypermethrin in soils. *Journal of Pesticide Science* 11(1): 71–79.

Salmon AG, Jones RB, and Mackrodt WC (1981) Microsomal dechlorination of chloroethanes: Structure-reactivity relationships. *Xenobiotica* 11(11): 723–734.

Sanborn M, Cole D, Kerr K, Vakil C, Sanin LH, and Bassil K (2004) *Pesticides Literature Review: Systematic Review of Pesticide Human Health Effects*. Toronto, ON: The Ontario College of Family Physicians (downloaded from the web at http://www.ocfp.on.ca/English/OCFP/Communications/Publications/default.asp?s=1#EnvironmentHealth on 26 April 2004).

Scarponi L, Perucci P, and Martinetti L (1991) Conjugation of 2-chloroacetanilide herbicides with glutathione: Role of molecular structures and of glutathione *S*-transferase enzymes. *Journal of Agricultural and Food Chemistry* 39(11): 2010–2013.

Schäfer RB, Caquet T, Siimes K, Mueller R, Lagadic L, and Liess M (2007) Effects of pesticides on community structure and ecosystem functions in agricultural streams of three biogeographical regions in Europe. *Science of the Total Environment* 382: 272–285.

Schellenberg K, Leuenberger C, and Schwarzenbach RP (1984) Sorption of chlorinated phenols by natural sediments and aquifer materials. *Environmental Science & Technology* 18(9): 652–657.

Scholz NL, Truelove NK, French BL, et al. (2000) Diazinon disrupts antipredator and homing behaviors in chinook salmon (*Oncorhynchus tsawytscha*). *Canadian Journal of Fisheries and Aquatic Sciences* 57: 1911–1918.

Schowanek D and Verstraete W (1991) Hydrolysis and free radial [*sic*] mediated degradation of phosphonates. *Journal of Environmental Quality* 20(4): 769–776.

Schreinemachers DM (2000) Cancer mortality in four northern wheat-producing States. *Environmental Health Perspectives* 108(9): 873–881.

Schüürmann G, Ebert R-U, and Kühne R (2006) Prediction of the sorption of organic compounds into organic matter from molecular structure. *Environmental Science & Technology* 40(22): 7005–7011.

Schwarzenbach RP, Gschwend PM, and Imboden DM (1993) *Environmental Organic Chemistry*. New York: Wiley.

Schwarzenbach RP, Stierli R, Lanz K, and Zeyer J (1990) Quinone and iron porphyrin mediated reduction of nitroaromatic compounds in homogeneous aqueous solution. *Environmental Science & Technology* 24(10): 1566–1574.

Schwarzenbach RP and Westall J (1981) Transport of nonpolar organic compounds from surface water to groundwater: Laboratory sorption studies. *Environmental Science & Technology* 15(11): 1360–1367.

Scow KM (1990) Rate of biodegradation. In: Lyman WJ, Reehl WF, and Rosenblatt DH (eds.) *Handbook of Chemical Property Estimation Methods*, pp. 9(1)–9(85). Washington, DC: American Chemical Society.

Scribner EA, Battaglin WA, Dietze JE, and Thurman EM (2003) Reconnaissance data for glyphosate, other selected herbicides, their degradation products, and antibiotics in 51 streams in nine Midwestern States, 2002. *US Geological Survey Open-File Report 03-217*. Denver, CO: US Geological Survey.

Seffernick JL, Shapir N, Schoeb M, Johnson G, Sadowsky MJ, and Wackett LP (2002) Enzymatic degradation of chlorodiamino-*s*-triazine. *Applied and Environmental Microbiology* 68(9): 4672–4675.

Shin Y-O, Chodan JJ, and Wolcott AR (1970) Adsorption of DDT by soils, soil fractions, and biological materials. *Journal of Agricultural and Food Chemistry* 18(6): 1129–1133.

Sinclair CJ and Boxall ABA (2003) Assessing the ecotoxicity of pesticide transformation products. *Environmental Science & Technology* 37(20): 4617–4625.

Singleton DM and Kochi JK (1967) The mechanism of reductive elimination of vic-dihalides by chromium(II). *Journal of the American Chemical Society* 89(25): 6547–6555.

Sirons GJ, Frank R, and Sawyer T (1973) Residues of atrazine, cyanazine, and their phytotoxic metabolites in a clay loam soil. *Journal of Agricultural and Food Chemistry* 21(6): 1016–1020.

Skipper HD, Gilmour CM, and Furtick WR (1967) Microbial versus chemical degradation of atrazine in soils. *Soil Science Society of America Proceedings* 31(5): 653–656.

Smith GJ (1987) *Pesticide Use and Toxicology in Relation to Wildlife: Organophosphorus and Carbamate Compounds*, *US Fish and Wildlife Service Resource Publication 170*. Washington, DC: US Fish and Wildlife Service.

Smith AE and Aubin AJ (1993) Degradation of [14-C]amidosulfuron in aqueous buffers and in an acidic soil. *Journal of Agricultural and Food Chemistry* 41(12): 2400–2403.

Smolen JM and Stone AT (1997) Divalent metal ion-catalyzed hydrolysis of phosphorothionate ester pesticides and their corresponding oxonates. *Environmental Science & Technology* 31(6): 1664–1673.

Solomon G, Ogunseitan OA, and Kirsch J (2000) *Pesticides and Human Health: A Resource for Health Care Professionals*. Physicians for Social Responsibility and Californians for Pesticide Reform. (available online at http://www.psrla.org/documents/pesticides_and_human_health.pdf).

Song L, Seeger A, and Santos-Sacchi J (2005) On membrane motor activity and chloride flux in the outer hair cell: Lessons learned from the environmental toxin tributyltin. *Biophysical Journal* 88: 2350–2362.

Sparling DW, Fellers GM, and McConnell LL (2001) Pesticides and amphibian population declines in California, USA. *Environmental Toxicology and Chemistry* 20(7): 1591–1595.

Squillace PJ, Moran MJ, and Price CV (2004) VOCs in shallow groundwater in new residential/commercial areas of the United States. *Environmental Science & Technology* 38(20): 5327–5338.

Squillace PJ, Scott JC, Moran MJ, Nolan BT, and Kolpin DW (2002) VOCs, pesticides, nitrate, and their mixtures in groundwater used for drinking water in the United States. *Environmental Science & Technology* 36(9): 1923–1930.

Stamper DM, Traina SJ, and Tuovinen OH (1997) Anaerobic transformation of alachlor, propachlor, and metolachlor with sulfide. *Journal of Environmental Quality* 26: 488–494.

Stamper DM and Tuovinen OH (1998) Biodegradation of the acetanilide herbicides alachlor, metolachlor, and propachlor. *Critical Reviews in Microbiology* 24(1): 1–22.

Stinson ER and Bromley PT (1991) *Pesticides and Wildlife: A Guide to Reducing Impacts on Animals and Their Habitat*. Blaksburg, VA: Virginia Cooperative Extension Communications.

Strathmann TJ and Stone AT (2001) Reduction of the carbamate pesticides oxamyl and methomyl by dissolved Fe^{II} and Cu^{I}. *Environmental Science & Technology* 35(12): 2461–2469.

Strathmann TJ and Stone AT (2002a) Reduction of the pesticides oxamyl and methomyl by Fe^{II}: Effect of pH and inorganic ligands. *Environmental Science & Technology* 36(4): 653–661.

Strathmann TJ and Stone AT (2002b) Reduction of oxamyl and related pesticides by Fe^{II}: Influence of organic ligands and natural organic matter. *Environmental Science & Technology* 36(23): 5172–5183.

Stumm W and Morgan JJ (1981) *Aquatic Chemistry: An Introduction Emphasizing Chemical Equilibria in Natural Waters*, 2nd edn. New York: Wiley.

Subramaniam V and Hoggard PE (1988) Metal complexes of glyphosate. *Journal of Agricultural and Food Chemistry* 36(6): 1326–1329.

Sumpter JP and Johnson AC (2005) Lessons from endocrine disruption and their application to other issues concerning trace organics in the aquatic environment. *Environmental Science & Technology* 39(12): 4321–4332.

Suntio LR, Shiu WY, Mackay D, Seiber JN, and Glotfelty D (1988) Critical review of Henry's Law constants for pesticides. *Reviews of Environmental Contamination and Toxicology* 103: 1–59.

Syracuse Research Corporation (1988) *Environmental Fate Database*. Available at http://esc.syrres.com/scripts/CHFcgi.exe (accessed on 4/11/03).

Teplitsky C, Piha H, Laurila A, and Merilä J (2005) Common pesticide increases costs of antipredator defenses in *Rana temporaria* tadpoles. *Environmental Science & Technology* 39(16): 6079–6085.

Tesoriero AJ, Löffler FE, and Liebscher H (2001) Fate and origin of 1,2-dichloropropane in an unconfined shallow aquifer. *Environmental Science & Technology* 35(3): 455–461.

Tesoriero AJ, Saad DA, Burow KR, Frick EA, Puckett LJ, and Barbash JE (2007) Linking ground-water age and chemistry data along flow paths: Implications for trends and transformations of nitrate and pesticides. *Journal of Contaminant Hydrology* 94: 139–155.

Thelin GP and Gianessi LP (2000) Method for estimating pesticide use for county areas of the conterminous United States. *US Geological Survey Open-File Report 00-250*. Denver, CO: US Geological Survey.

Thomas RG (1990a) Volatilization from water. In: Lyman WJ, Reehl WF, and Rosenblatt DH (eds.) *Handbook of Chemical Property Estimation Methods*, pp. 15(1)–15(34). Washington, DC: American Chemical Society.

Thomas RG (1990b) Volatilization from soil. In: Lyman WJ, Reehl WF, and Rosenblatt DH (eds.) *Handbook of Chemical Property Estimation Methods*, pp. 16(1)–16(50). Washington, DC: American Chemical Society.

Thompson HM (1996) Interactions between pesticides: A review of reported effects and their implications for wildlife risk assessment. *Ecotoxicology* 5: 59–81.

Thurman EM (1985) *Organic Geochemistry of Natural Waters*. Boston, MA: Martinus Nijhoff/Dr. W. Junk.

Tillitt DE, Papoulias DM, Whyte JJ, and Richter CA (2010) Atrazine reduces reproduction in fathead minnow (*Pimephales promelas*). *Aquatic Toxicology* 99(2): 149–159.

Tominack RL (2000) Herbicide formulations. *Clinical Toxicology* 38(2): 129–135.

Torrents A and Stone AT (1991) Hydrolysis of phenyl picolinate at the mineral/water interface. *Environmental Science & Technology* 25(1): 143–149.

Tratnyek PG and Macalady DL (1989) Abiotic reduction of nitro aromatic pesticides in anaerobic laboratory systems. *Journal of Agricultural and Food Chemistry* 37(1): 248–254.

United Nations Food and Agriculture Organization (2003) *Database on Pesticides Consumption*. United Nations Food and Agriculture Organization, Statistics Division. Available at http://www.fao.org/waicent/FAOINFO/economic/pesticid.htm (accessed 4/14/03).

Unsworth JB, Wauchope RD, Klein AW, et al. (1999) Significance of the long range transport of pesticides in the atmosphere. *Pure and Applied Chemistry* 71(7): 1359–1383.

US Department of Agriculture-Agricultural Research Service (1995) *Pesticide Properties Database*. Available on-line at http://www.arsusda.govrsml/ppdb2.html (last, update May, 1995).

US Environmental Protection Agency (2010) Inert ingredients permitted in pesticide products (accessed 13 November 2010, on the World-Wide Web at URL http://www.epa.gov/opprd001/inerts/).

US Environmental Protection Agency (1992) Another look: National survey of pesticides in drinking water wells, phase 2 report. *EPA Report EPA 579/09-91-020*. Washington, DC: US Environmental Protection Agency.

US Environmental Protection Agency (2003) Interim reregistration elegibility decision for atrazine. Case No. 0062. US Environmental Protection Agency (accessed 1/5/11 at http://www.epa.gov/oppsrrd1/REDs/atrazine_ired.pdf).

US General Accounting Office (2001) Agricultural pesticides: Management improvements needed to further promote integrated pest management. *US General Accounting Office Report GAO-01-815*. Washington, DC: US General Accounting Office.

US Geological Survey (2010) USGS Pesticide National Synthesis Project – Annual use maps (accessed at http://water.usgs.gov/nawqa/pnsp/usage/maps/ on 21 December 2010).

Van Metre PC and Mahler BJ (2005) Trends in hydrophobic organic contaminants in urban and reference lake sediments across the United States, 1970–2001. *Environmental Science & Technology* 39(15): 5567–5574.

Van Metre PC, Wilson JT, Callender E, and Fuller CC (1998) Similar rates of decrease of persistent, hydrophobic and particle-reactive contaminants in riverine systems. *Environmental Science & Technology* 32(21): 3312–3317.

Veeh RH, Inskeep WP, and Camper AK (1996) Soil depth and temperature effects on microbial degradation of 2,4-D. *Journal of Environmental Quality* 25: 5–12.

Vink JPM, Nörtershäuser P, Richter O, Diekkrüger B, and Groen KP (1994) Modelling the microbial breakdown of pesticides in soil using a parameter estimation technique. *Pesticide Science* 40: 285–292.

Vogel TM, Criddle CS, and McCarty PL (1987) Transformations of halogenated aliphatic compounds. *Environmental Science & Technology* 21(8): 722–736.

Vogel TM and McCarty PL (1987) Abiotic and biotic transformations of 1,1,1-trichloroethane under methanogenic conditions. *Environmental Science & Technology* 21(12): 1208–1213.

Vogel TM and Reinhard M (1986) Reaction products and rates of disappearance of simple bromoalkanes, 1,2-dibromopropane, and 1,2-dibromoethane in water. *Environmental Science & Technology* 20(10): 992–997.

Voudrias EA and Reinhard M (1986) Abiotic organic reactions at mineral surfaces. In: Davis JA and Hayes KF (eds.) *Geochemical Processes at Mineral Surfaces. ACS Symposium Series*, vol. 323, pp. 462–486. Washington, DC: American Chemical Society.

Wade RS and Castro CE (1973) Oxidation of iron(II) porphyrins by alkyl halides. *Journal of the American Chemical Society* 95(1): 226–230.

Walker A (1974) A simulation model for prediction of herbicide persistence. *Journal of Environmental Quality* 3(4): 396–401.

Walker A (1987) Herbicide persistence in soil. *Reviews of Weed Science* 3: 1–17.

Walraevens R, Trouillet P, and Devos A (1974) Basic elimination of HCl from chlorinated ethanes. *International Journal of Chemical Kinetics* VI: 777–786.

Walse SS, Morgan SL, Kong L, and Ferry JL (2004) Role of dissolved organic matter, nitrate, and bicarbonate in the photolysis of aqueous fipronil. *Environmental Science & Technology* 38(14): 3908–3915.

Walse SS, Shimizu KD, and Ferry JL (2002) Surface-catalyzed transformations of aqueous endosulfan. *Environmental Science & Technology* 36(22): 4846–4853.

Wan HB, Wong MK, and Mok CY (1994) Mercury(II) ion-promoted hydrolysis of some organophosphorus pesticides. *Pesticide Science* 42: 93–99.

Wang S and Arnold WA (2003) Abiotic reduction of dinitroaniline herbicides. *Water Research* 37: 4191–4201.

Wang Q, Gan J, Papiernik SK, and Yates SR (2000) Transformation and detoxification of halogenated fumigants by ammonium thiosulfate. *Environmental Science & Technology* 34(17): 3717–3721.

Wang W, Liszewski M, Buchmiller R, and Cherryholmes K (1995) Occurrence of active and inactive herbicide ingredients at selected sites in Iowa. *Water, Air, and Soil Pollution* 83: 21–35.

Wang RY, Needham LL, and Barr DB (2005) Effects of environmental agents on the attainment of puberty: Considerations when assessing exposure to environmental chemicals in the National Children's Study. *Environmental Health Perspectives* 113(8): 1100–1107.

Wania F (2003) Assessing the potential of persistent organic chemicals for long-range transport and accumulation in polar regions. *Environmental Science & Technology* 37(7): 1344–1351.

Washington JW (1995) Hydrolysis rates of dissolved volatile organic compounds: Principles, temperature effects, and literature review. *Ground Water* 33(3): 415–424.

Watson JR (1977) Seasonal variation in the biodegradation of 2,4-D in river water. *Water Research* 11: 153–157.

Wauchope RD (1978) The pesticide content of surface water draining from agricultural fields – A review. *Journal of Environmental Quality* 7(4): 459–472.

Webb RMT, Wieczorek MZ, Nolan BT, et al. (2008) Variations in pesticide leaching related to land use, pesticide properties, and unsaturated zone thickness. *Journal of Environmental Quality* 37: 1145–1157.

Weber JB (1990) Behavior of dinitroaniline herbicides in soils. *Weed Technology* 4: 394–406.

Wei J, Furrer G, Kaufmann S, and Schulin R (2001) Influence of clay minerals on the hydrolysis of carbamate pesticides. *Environmental Science & Technology* 35(11): 2226–2232.

Wei J, Furrer G, and Schulin R (2000) Kinetics of carbosulfan degradation in the aqueous phase in the presence of a cosolvent. *Journal of Environmental Quality* 29: 1481–1487.

Weintraub RA, Jex GW, and Moye HA (1986) Chemical and microbial degradation of 1,2-dibromoethane (EDB) in Florida ground water, soil, and sludge. In: Garner WY, Honeycutt RC, and Nigg HN (eds.) *Evaluation of Pesticides in Ground Water. ACS Symposium Series*, vol. 315, pp. 294–310. Washington, DC: American Chemical Society.

Widmer SK and Spalding RF (1996) Assessment of herbicide transport and persistence in groundwater: A review. In: Meyer MT and Thurman EM (eds.) *Herbicide Metabolites in Surface Water and Groundwater. ACS Symposium Series*, vol. 630, pp. 271–287. Washington, DC: American Chemical Society.

William RD, Burrill LC, Ball D, et al. (1995) *Pacific Northwest Weed Control Handbook 1995*. Corvallis, OR: Oregon State University Extension Service.

Winchester PD, Huskins J, and Ying J (2009) Agrichemicals in surface water and birth defects in the United States. *Acta Pediatrica* 98: 664–669.

Winrow CJ, Hemming ML, Allen DM, Quistad GB, Casida JE, and Barlow C (2003) Loss of neuropathy target esterase in mice links organophosphate exposure to hyperactivity. *Nature Genetics* 33: 477–485.

Wolfe NL, Kitchens BE, Macalady DL, and Grundl TJ (1986) Physical and chemical factors that influence the anaerobic degradation of methyl parathion in sediment systems. *Environmental Toxicology and Chemistry* 5: 1019–1026.

Wolfe NL and Macalady DL (1992) New perspectives in aquatic redox chemistry: Abiotic transformations of pollutants in groundwater and sediments. *Journal of Contaminant Hydrology* 9(1–2): 17–34.

Wolfe NL, Paris DF, Steen WC, and Baughman GL (1980) Correlation of microbial degradation rates with chemical structure. *Environmental Science & Technology* 14(9): 1143–1144.

Wolfe NL, Zepp RG, Gordon JA, Baughman GL, and Cline DM (1977) Kinetics of chemical degradation of malathion in water. *Environmental Science & Technology* 11(1): 88–93.

Wolfe NL, Zepp RG, and Paris DF (1978) Use of structure-reactivity relationships to estimate hydrolytic persistence of carbamate pesticides. *Water Research* 12: 561–563.

Wong CS, Capel PD, and Nowell LH (2001) National-scale, field-based evaluation of the biota-sediment accumulation factor model. *Environmental Science & Technology* 35(9): 1709–1715.

Wong CS, Lau F, Clark M, Mabury SA, and Muir DCG (2002) Rainbow trout (*Oncorhynchus mykiss*) can eliminate chiral organochlorine compounds enantioselectively. *Environmental Science & Technology* 36(6): 1257–1262.

Woodrow JE, Seiber JN, and Baker LW (1997) Correlation techniques for estimating pesticide volatilization flux and downwind concentrations. *Environmental Science & Technology* 31(2): 523–529.

Woodside MD, Hoos AB, Kingsbury JA, et al. (2004) *Water Quality in the Lower Tennessee River Basin, Tennessee, Alabama, Kentucky, Mississippi, and Georgia. US Geological Survey Circular 1233*. Denver, CO: US Geological Survey. (available online at http://water.usgs.gov/pubs/circ/2004/1233/).

Wu J and Nofziger DL (1999) Incorporating temperature effects on pesticide degradation into a management model. *Journal of Environmental Quality* 28: 92–100.

Xu JM, Gan J, Papiernik SK, Becker JO, and Yates SR (2003) Incorporation of fumigants into soil organic matter. *Environmental Science & Technology* 37(7): 1288–1291.

Zepp RG (1988) Sunlight-induced oxidation and reduction of organic xenobiotics in water. *EPA Report EPA/600/D-88/033*. Athens, GA: US Environmental Protection Agency Office of Research and Development.

Zepp RG and Cline DM (1977) Rates of direct photolysis in aquatic environment *[sic]*. *Environmental Science & Technology* 11(11): 359–366.

Zepp RG, Schlotzhauer PF, Simmons MS, Miller GC, Baughman GL, and Wolfe NL (1984) Dynamics of pollutant photoreactions in the hydrosphere. *Fresenius' Journal of Analytical Chemistry* 319: 119–125.

Zepp RG and Wolfe NL (1987) Abiotic transformation of organic chemicals at the particle–water interface. In: Stumm W (ed.) *Aquatic Surface Chemistry: Chemical Processes at the Particle–Water Interface*, pp. 423–455. New York: Wiley.

Zepp RG, Wolfe NL, Gordon JA, and Baughman GL (1975) Dynamics of 2,4-D esters in surface waters – Hydrolysis, photolysis, and vaporization. *Environmental Science & Technology* 9(13): 1144–1149.

Zhang W, Bouwer EJ, and Ball WP (1998) Bioavailability of hydrophobic organic contaminants: Effects and implications of sorption-related mass transfer on bioremediation. *Ground Water Monitoring and Remediation* 18(1): 126–138.

11.16 The Biogeochemistry of Contaminant Groundwater Plumes Arising from Waste Disposal Facilities

PL Bjerg, H-J Albrechtsen, P Kjeldsen, and TH Christensen, Technical University of Denmark, Lyngby, Denmark
IM Cozzarelli, U.S. Geological Survey, Reston, VA, USA

11.16.1 Introduction

Landfills of solid waste are abundant sources of groundwater pollution. The potential for generating strongly contaminated leachate from landfilled waste is very substantial; even for small landfills, the timescale can be measured in decades or centuries. This indicates that waste dumps with no measures to control leachate entrance into the groundwater still may constitute a source of groundwater contamination long time after dumping has ceased. In addition to these dumps, engineered landfills with liners and leachate collection systems may *also* constitute a source of groundwater contamination due to inadequate design, construction, and maintenance resulting in leakage of leachate.

Landfills may pose several environmental problems (explosion hazards, vegetation damage, dust and air emissions, etc.), but groundwater pollution by leachate is considered to be the most important one and the focus of this chapter. Landfills may differ significantly depending on the waste they receive, for example, mineral waste landfills for combustion ashes, hazardous waste landfills, and specific industrial landfills serving a single industry or municipal waste landfills receiving a mixture of municipal waste, construction and demolition waste, waste of small industries, and minor quantities of hazardous waste. The latter type of landfill (termed *old landfills* in this chapter) is very common all over the world. The municipal landfill is characterized by a high content of organic waste affecting the biogeochemical processes in the landfill body and the generation of strongly anaerobic leachate with a high content of dissolved organic carbon, salts, and ammonium, as well as specific organic compounds and metals released from the waste.

This chapter describes the biogeochemistry of a landfill leachate plume as it emerges from the bottom of a landfill and migrates in an aquifer. The landfill hydrology, source composition, and spreading of contaminants are described in the introductory sections. The focus in this chapter is on investigating the biogeochemical processes associated with the natural attenuation of organic contaminants in a leachate plume. Studies have shown that microbial processes and geochemical conditions change over time and distance in contaminant plumes, resulting in different rates of degradation (biotic and abiotic). The availability of electron acceptors, such as iron oxides or dissolved sulfate, is an important factor for evaluating the efficacy and sustainability of natural attenuation as a remedy for leachate plumes. Understanding of the complex environments developing in a leachate plume is important in assessing the risk to the groundwater resources and in developing cost-effective remediation strategies.

11.16.2 Source and Leachate Composition

Landfills as pollution sources have three key characteristics:

1. Landfills are large often heterogeneous sources both in volume and area.
2. Landfills host a mixture of inorganic and organic pollutants.
3. Landfills have an expected pollution potential lasting for decades and centuries.

The area of landfills typically ranges from a few ha up to more than 50 ha (Christensen et al., 2001), and the amount of waste can be enormous (100 000–5 000 000 m^3).

The presence of a mixture of contaminants in the landfill body affects the overall behavior of the pollution plume, and the interaction between various contaminants and also the natural setting is crucial for the understanding of the biogeochemistry of landfill leachate plumes. In comparison with other groundwater pollution sources, the complexity of the source means that many different compounds (inorganic and organic) and processes (geochemical and microbial) will be interacting in a landfill leachate plume.

Landfill leachate is generated by excess rainwater percolating through the landfilled waste layers. Combined physical, chemical, and microbial processes in the waste transfer pollutants from the waste material to the percolating water. Focusing on the common type of landfill receiving a mixture of municipal, commercial, and mixed industrial waste, but excluding significant amounts of concentrated specific chemical waste, landfill leachate may be characterized as a water-based solution of four groups of pollutants (Christensen et al., 1994):

- Dissolved organic matter, expressed as chemical oxygen demand (COD) or total organic carbon (TOC), including methane, volatile fatty acids (in particular in the acid phase of the waste stabilization, Christensen and Kjeldsen, 1989), and more refractory compounds, for example, fulvic-like and humic-like compounds.
- Inorganic macrocomponents: calcium (Ca^{2+}), magnesium (Mg^{2+}), sodium (Na^{+}), potassium (K^{+}), ammonium ($NH_4{}^{+}Z$), iron (Fe^{2+}), manganese (Mn^{2+}), chloride (Cl^{-}), sulfate ($SO_4{}^{2+}$), and hydrogen carbonate ($HCO_3{}^{-}$).
- Heavy metals: cadmium (Cd^{2+}), chromium (Cr^{3+}), copper (Cu^{2+}), lead (Pb^{2+}), nickel (Ni^{2+}), and zinc (Zn^{2+}).
- Xenobiotic organic compounds (XOCs) originating from household or industrial chemicals and present in relatively low concentrations in the leachate (usually less than 1 mg l^{-1} of individual compounds). These compounds include, among others, a variety of aromatic hydrocarbons, phenols, chlorinated aliphatic hydrocarbons, and pesticides.

Other compounds may be found in leachate from landfills, for example, borate, sulfide, arsenate, selenate, barium, lithium, mercury, and cobalt. In general, however, these compounds are not measured very often, and when measured, they are usually found in very low concentrations and are considered only of secondary importance.

Leachate composition varies significantly among landfills depending on waste composition, waste age, and landfilling technology. The waste can be divided into three main groups:

- Household waste
- Demolition waste
- Chemical and hazardous waste

In nonengineered landfills, the different types of waste are randomly distributed at the site. Historical records are often nonexistent, and investigations are often based on interviews, aerial photos (over time), and excavations. Experiences from Danish sites have shown that combining these methods is an efficient way to develop a good description of the composition of the landfilled waste (Kjeldsen, 1993; Kjeldsen et al., 1998a,b; Thomsen et al., 2012).

Investigations on leachate composition have often been based on only one or a few leachate samples from each landfill. In the context of groundwater pollution, the spatial distribution of the leachate quality must be appreciated, which requires a large number of sampling points (Kjeldsen et al., 1998a). For instance, significant spatial variability in leachate concentrations was observed in wells at the 10 ha large Grindsted Landfill (DK) (Kjeldsen et al., 1998a). Very low concentrations of almost all parameters (including XOCs) were found in areas covering about 60–70% of the landfill. A *hot spot*, occupying about 10% of the landfill area was found with concentrations 20–1000 times higher than in the low concentration area. Especially for large landfills, information on spatial variability in leachate concentrations is very important as basis for locating the main sources of the groundwater pollution plume and for the selection of cost-effective remedial actions.

Table 1 presents ranges of general leachate parameters compiled from data reported in the literature. The table is based mainly on data originating from newer landfills (leachate less than 25 years old). Data from older uncontrolled landfills may exhibit lower values than the minimum values given in the table (Assmuth and Strandberg, 1993; Kjeldsen and Christophersen, 2001). In general, landfill leachates may contain very high concentrations of dissolved organic matter and inorganic macrocomponents. The concentrations of these components may typically be up to a factor 10–500 higher than groundwater concentrations in pristine aquifers; however, a significant variability is recognized.

Leachate also contains a broad range of xenobiotic compounds (**Table 2**). Since the composition of chemical waste is highly variable, the compounds identified and their concentration ranges are difficult to summarize in general terms. An important subgroup is the volatile organic compounds (VOCs), which are organic compounds that tend to vaporize at room temperature and pressure. Typically, VOCs are an important component of the compounds in gasoline, lubricants, and solvents. Some VOCs are highly toxic or carcinogenic. Aromatic hydrocarbons and chlorinated aliphatic compounds are the most frequently found compounds in landfill leachate; however, they are also the most common compounds included in analytical programs. Phenols, pharmaceuticals, and pesticides, as well as other ionic or polar compounds (e.g., phthalates and aromatic sulfonates) have been identified as well (e.g., Barnes et al., 2004; Paxeus, 2000; Schwarzbauer et al., 2002).

Several parameters change dramatically as the organic waste in the landfill degrades. During the initial fermentation (acid phase), the leachate may show low pH values and high concentrations of many compounds, in particular high

Table 1 Composition of landfill leachate

Parameter	*Range*
pH (no unit)	4.5–9
Spec. cond. ($\mu S\ cm^{-1}$)	2500–35 000
Total solids	2000–60 000
Organic matter	
TOC	30–29 000
Biological oxygen demand (BOD_5)	20–57 000
COD	140–152 000
BOD_5/COD (ratio)	0.02–0.80
Organic nitrogen	14–2500
Inorganic macrocomponents	
Total phosphorus	0.1–23
Chloride	150–4500
Sulfate	8–7750
Hydrogencarbonate	610–7320
Sodium	70–7700
Potassium	50–3700
Ammonium-N	50–2200
Calcium	10–7200
Magnesium	30–15 000
Iron	3–5500
Manganese	0.03–1400
Heavy metals	
Arsenic	0.01–1
Cadmium	0.0001–0.4
Chromium	0.02–1.5
Cobalt	0.005–1.5
Copper	0.005–10
Lead	0.001–5
Mercury	0.00005–0.16
Nickel	0.015–13
Zinc	0.03–1000

Values in $mg\ l^{-1}$ unless otherwise stated.

Source: Kjeldsen P, Barlaz MA, Rooker AP, Baun A, Ledin A, and Christensen TH (2002) Present and long term composition of MSW landfill leachate – A review. *Critical Reviews in Environmental Science and Technology* 32: 297–336.

Table 2 The most frequently observed XOCs in landfill leachates

Compound	*Range ($\mu g\ l^{-1}$)*
Aromatic hydrocarbons	
Benzene	0.2–1630
Toluene	1–12 300
Xylenes	0.8–3500
Ethylbenzene	0.2–2300
Trimethylbenzenes	0.3–250
Naphthalene	0.1–260
Halogenated hydrocarbons	
Chlorobenzene	0.1–110
1,2-Dichlorobenzene	0.1–32
1,4-Dichlorobenzene	0.1–16
1,1-Dichloroethane	0.6–46
1,2-Dichloroethane	<6
1,1,1-Trichloroethane	0.1–3810
Trichloroethylene	0.05–750
Tetrachloroethylene	0.01–250
Dichloromethane	1.0–827
Trichloromethane	1.0–70
Phenols	
Phenol	0.6–1200
Cresols	1–2100
Pesticides	
Mecoprop[a]	0.38–150
Phthalates	
Diethylphthalate	10–660
Di-(2-ethylhexyl)phthalate	0.6–240
Di-*n*-butylphthalate	0.1–70
Butylbenzyl phthalate	0.2–8
Phosphonates	
Tri-*n*-butylphosphate	1.2–360
Miscellaneous	
Acetone	6–4400
Camphor[b]	20–260
Fenchone	7–80
Tetrahydrofuran	9–430

Only pollutants that have been observed in more than three independent investigations are included.

[a]2-(2-methyl-4-chlorophenoxy) propionic acid (MCPP).

[b]1,7,7-trimethylbicyclo(-bicyclo[2.2.1]-heptane-2-one.

Source: Kjeldsen P, Barlaz MA, Rooker AP, Baun A, Ledin A, and Christensen TH (2002) Present and long term composition of MSW landfill leachate – A review. *Critical Reviews in Environmental Science and Technology* 32: 297–336.

concentrations of easily degradable organic compounds, such as volatile fatty acids. Later, when the fermentation products are converted effectively to methane and carbon dioxide (methane phase), pH increases and the degradability of the organic carbon in the leachate decreases. A detailed discussion of the phases, which a landfill will experience, is given in Kjeldsen et al. (2002).

The data given in **Tables 1** and **2** are based on leachate sampled from landfills younger than 25 years. The values are difficult to extrapolate beyond the first 25 years of a landfill's life. Belevi and Baccini (1992) estimated by the use of leaching tests on municipal solid waste that leachate from landfills for centuries would contain significant concentrations of several compounds. The leachate will, in particular, contain nitrogen and organic carbon content in significant concentrations for several centuries, as discussed in detail by Kjeldsen et al. (2002).

In summary, leachate contains a variety of compounds (dissolved organic matter, inorganic compounds, heavy metals, and XOCs) due to the mixed composition of the waste disposed of in landfills. The spatial variability of the leachate quality is significant, and this may affect the leaching pattern from the landfill and the plumes formed. A landfill should be seen as a complex source, which is expected to last for decades or even centuries.

11.16.3 Spreading of Pollutants in Groundwater

All compounds in leachate entering an aquifer will be subjected to advection and dispersion (dilution) as the leachate mixes with the groundwater (Freeze and Cherry, 1979). For nonreactive components, of which chloride is the dominant component, dilution is the only attenuation mechanism. Dilution is the interaction of the leachate flow in the aquifer with the flow of groundwater. Leachate migration should be seen in terms of a three-dimensional plume developing in a three-dimensional geologic structure, where gradients, permeabilities, and physical

boundaries (geologic strata, infiltration, rivers, abstraction wells, etc.) determine the position and migration velocity of the plume. Dilution is governed by macroscopic dispersion and molecular diffusion but can also be affected by local vertical gradients, leachate density, and to some extent, viscosity.

Dispersion is the mathematical term in the solute transport equation (see Freeze and Cherry, 1979) accounting for dilution or mixing according to concentration gradients. The dispersivity has a longitudinal component (in the flow direction), a vertical component, and a horizontal, transverse component. The longitudinal dispersivity is important only for the concentrations in the front of leachate plumes. Of greater interest is the magnitude of the transverse dispersivities, which govern the transverse spreading of the plume. Data from field experiments (review by Adams and Gelhar, 1992; Gelhar et al., 1992; Jensen et al., 1993; Petersen, 2000) showed small transverse dispersivities (from millimeter to few centimeter) indicating limited transversal spreading of pollution plumes. Unfortunately, field data showing detailed horizontal delineation of landfill leachate plumes have not been presented since the early investigations from Borden Landfill (**Figure 1**). Vertical dispersivities are expected to be extremely small (Gelhar et al., 1992; Jensen et al., 1993), which means very limited vertical mixing due to dispersion alone. This has been confirmed in a number of landfill studies (see **Figure 2**, examples in Barker et al., 1986; Bjerg et al., 1995; Lønborg et al., 2006; Lyngkilde and Christensen, 1992b; Nicholson et al., 1983; Prommer et al., 2006), where the studies at Sjoelund Landfill (DK) in particular reveals steep vertical concentration gradients of chloride and other compounds (Bjerg et al., 2011).

The flow of leachate may, as mentioned, physically differ from the flow of groundwater at least with respect to the following three aspects:

Local water table gradients below and around the landfill will most likely differ from the general gradients because the landfill will usually have a different hydrology/hydrogeology compared to the surrounding area. Local water table mounds have been observed at the Borden Landfill (CAN) (MacFarlane et al., 1983), the Vejen Landfill (DK) (Kjeldsen, 1993), the Noordwijk Landfill (NL) (van Duijvenbooden and Kooper, 1981), and the Grindsted Landfill (DK) (Kjeldsen et al., 1998b). The reasons for water mounds in general are not fully understood (see later discussion in **Section 11.16.7.1**). The effects of local mounding are (1) enhanced lateral spreading of the leachate plume and (2) downward-directed hydraulic gradients in the groundwater zone beneath the landfill. The latter can cause an unexpected spreading pattern despite homogeneous aquifer conditions and limited density difference between leachate and the ambient groundwater. The enhanced lateral spreading of the plume may increase the volume of contaminated groundwater and spatial extent but provides increased dilution of contaminants.

The viscosity of the leachate may differ from the viscosity of the groundwater. A higher viscosity would theoretically lead to lower flow velocities, which could influence the dilution of the leachate plume; however, actual field evidence is scarce (Christensen et al., 2001).

The density of the leachate is a function of the temperature and the concentration of dissolved solids. Leachate with a total dissolved solid concentration of 20 000 mg l^{-1} is not uncommon (see **Table 1**), corresponding to a density that is over 1% higher than the groundwater density. Density differences may significantly affect the vertical positioning of the plume just below the landfill. Field observation on the downward movement of the plume is often difficult to separate from the effect of local water table mounds (Christensen et al., 2001). A better understanding of the effects of higher leachate densities in field situations is needed, because density effects could be the major cause of vertical leachate spreading in aquifers as *normal* vertical dispersion usually is very small, as discussed earlier.

In summary, transport and spreading of dissolved landfill leachate pollutants in aquifers will be governed by advection/dispersion. The local hydrogeology at the site in terms of water table mounds and seasonal variation in flow field may enhance the spreading horizontally and vertically. Also, density effects due to high concentrations of inorganic compounds may increase vertical transport, but the actual understanding of density transport in leachate plumes is poor. Density transport is likely to be of most importance close to the landfill but of less importance as dilution of the plume increases.

11.16.4 Biogeochemistry of Landfill Leachate Plumes

11.16.4.1 Redox Environments and Redox Buffering

The entry of strongly reduced landfill leachate into a pristine, often oxidized, aquifer, leads to the creation of very complex redox environments. Important processes include organic matter biodegradation, biotic and abiotic redox processes, dissolution/precipitation of minerals, complexation, ion exchange, and sorption. The resulting redox environments strongly influence both the inorganic and organic biogeochemistry of the aquifer and create the chemical framework for understanding the attenuation processes in the plume.

Characterization of redox environments in pollution plumes has been reviewed by Christensen et al. (2000b). A range of different approaches have been used in addressing redox conditions in pollution plumes:

- Redox potential
- Redox-sensitive compounds in groundwater samples
- Hydrogen concentrations in groundwater
- Concentrations of volatile fatty acids
- Sediment characteristics
- Microbial tools

However, it should be noted that the approaches are not standard and the value of each approach is a matter of discussion (Christensen et al., 2000b). In addition, the redox conditions in contaminant plumes are not only spatially variable but also temporally variable (McGuire et al., 2000).

In the following, the authors present the redox environments observed in landfill leachate plumes, based on the simplified presentation of redox conditions, as given in **Figure 3**. Later in this chapter, it is shown for two case stories (**Sections 11.16.5** and **11.16.6**) that the actual redox conditions may be somewhat more complex. In an aquifer with a continuous leachate release, a methanogenic zone evolves close to the landfill. Within this zone and downgradient from it, sulfate reduction may take place. Iron reduction takes place further downgradient where the conditions are less reducing. Zones of

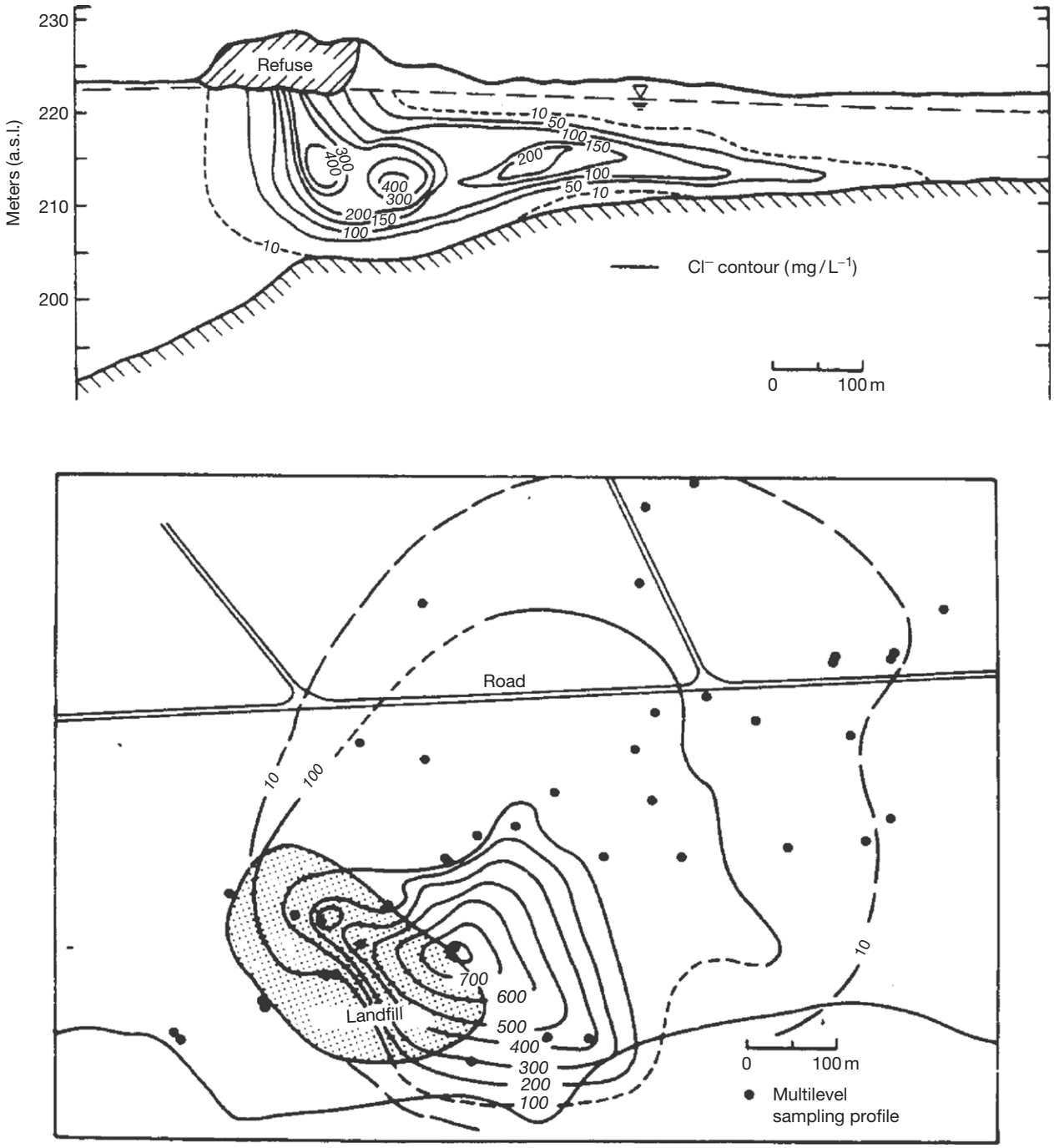

Figure 1 Horizontal and vertical transect contours of Cl^- (mg l^{-1}) in the Borden Landfill (CAN). Reproduced from MacFarlane DS, Cherry JA, Gillham RW, and Sudicky EA (1983) Migration of contaminants in groundwater at a landfill: A case study. 1. Groundwater flow and plume delineation. *Journal of Hydrology* 63: 1–29, with permission.

manganese and nitrate reduction have been observed, sometimes overlapping the iron-reducing zone. Finally, aerobic conditions may exist in the outskirts of the reduced plume if the pristine aquifer is oxidized and contains significant amounts of dissolved oxygen (>1 mg l^{-1}).

As illustrated in Figure 3, the content of reduced species (organic matter and ammonium) in groundwater along the flow line decreases. The redox potential increases with distance. Close to the landfill, dissolved electron acceptors, such as oxygen, nitrate, and sulfate, are depleted or lowered in concentration. Sulfide may be present due to sulfate-reducing processes. At some distances, the content of reduced dissolved species, such as sulfide, ferrous iron, and manganese, peaks as a result of redox processes. Also, the composition of the solid minerals changes with distance, as discussed in the succeeding text. Overall, the pollutants leaving the landfill will, unless removed from

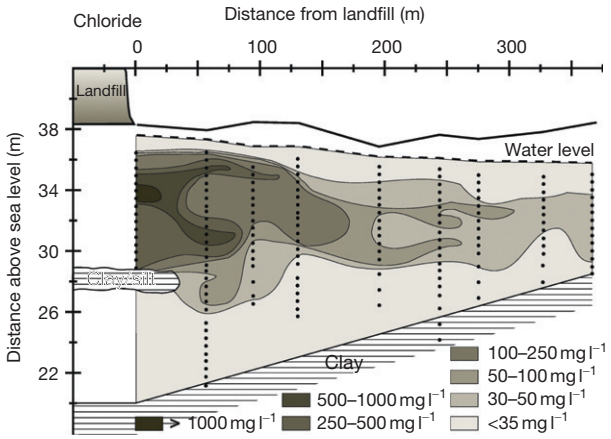

Figure 2 Vertical transect contours of Cl^- (mg l^{-1}) in the Vejen Landfill (DK). Reproduced from Lyngkilde J and Christensen TH (1992) Redox zones of a landfill leachate pollution plume (Vejen, Denmark). *Journal of Contaminant Hydrology* 10: 273–289, with permission.

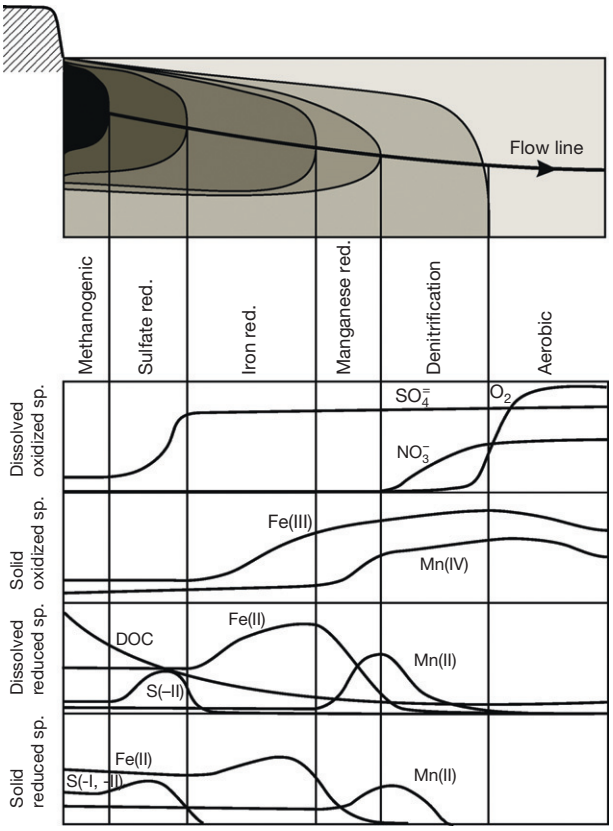

Figure 3 Schematic redox zonation in an originally aerobic aquifer downgradient from a landfill and the distribution of redox-sensitive species along a streamline in the plume. The axes are not to scale. Reproduced from Christensen TH, Kjeldsen P, Bjerg PL, et al. (2001) Biogeochemistry of landfill leachate plumes. *Applied Geochemistry* 16: 659–718, with permission.

the water, migrate through a series of redox zones and, over time, migrate into more oxidizing environments.

Leachate from landfills typically is strongly reduced, rich in organic matter and ammonium, and may be seen as infiltrating water with a great capacity for donating electrons (reduction capacity, RDC) during redox reactions. The produced electrons must be accepted by dissolved or solid-aquifer electron acceptors. The capacity of the aquifer to accept electrons is denoted by the oxidation capacity (OXC, Heron et al., 1994a; Scott and Morgan, 1990).

The set of reactions that creates the complex redox environments of landfill leachate plumes consists of combinations of two half reactions: one oxidation half reaction and one reduction half reaction. **Table 3** presents the most prominent overall redox reactions, along with their calculated Gibbs free energy change at standard conditions ($\Delta G_0(W)$). The lower (the more negative) the $\Delta G_0(W)$, the more energy is gained and the more willingly the reaction will proceed. Considering the processes of organic matter oxidation, it is evident that when all electron acceptors are present, oxygen will be used first, followed by nitrate, manganese, iron, and sulfate. Finally, methanogenesis and fermentation reactions dominate, when the most favorable electron acceptors are depleted.

Organic matter dominates the RDC for typical leachates (Christensen et al., 2001). Ammonium and methane may also contribute significantly, showing that the fate of these inorganic compounds in the aquifer may also affect the formation of redox environments. The aquifer OXC may be dominated by iron oxides, when calculated for an aquifer volume, including aquifer material and groundwater (**Table 4**). This is caused by the limited aqueous solubility of oxygen and the relatively low nitrate and sulfate contents in aquifers. The actual importance of the dissolved electron acceptors can, however, not be evaluated solely from an aquifer volume. In a flow system, the mixing of electron acceptors at the fringes of the plume will be a critical issue too. Mixing at the fringes will be governed by the transverse dispersivities (transversal and vertical). Seasonal recharge may play a role as well, as discussed by McGuire et al. (2000) for a mixed contaminant plume.

The relative importance of fringe and core processes will also depend on the degradability of the electron donor. In a phenol plume, Thornton et al. (2001) showed that the consumption of aqueous oxidants greatly exceeded the mineral oxidants. This was partly because very high phenol concentrations limited degradation inside the plume and partly because the iron reduction potential was small in the sandstone aquifer. This is not expected to be the case in a landfill leachate plume in sandy aquifers as the major electron donor (organic matter) is degradable by iron reduction and there probably will be a large iron RDC. Also, solid manganese oxides contribute to the OXC, as they can be reduced into dissolved manganese. However, when long-term aquifer changes are in question, iron reduction is likely to dominate, since iron concentrations typically are 20–50 times higher than manganese concentrations in aerobic glaciofluvial sediments (Heron, 1994).

Not all iron oxides are available for reduction. Some iron minerals are solid crystals or even the entire iron grains, which makes them resistant to microbial reduction (Heron et al., 1994b; Lovley, 1991; Postma, 1993). Other iron oxides or hydroxides are amorphous and readily reducible. Over time, even some crystalline minerals, such as goethite and hematite, may be reduced in the complex environment in leachate (Heron and Christensen, 1995). This indicates that the importance of iron as a redox buffer controlling the size of plumes is

Table 3 Most prominent redox reactions in landfill leachate plumes

Reaction	*Process*	*ΔG_0(W) (kcal mol^{-1})*
Methanogenic/fermentative organic matter mineralization	$2CH_2O \rightarrow CH_3COOH \rightarrow CH_4 + CO_2$	−22
Sulfate reduction/OMO	$2CH_2O + SO_4^{2-} + H^+ \rightarrow 2CO_2 + HS^- + 2H_2O$	−25
Iron reduction/OMO	$CH_2O + 4Fe(OH)_3 + 8H^+ \rightarrow CO_2 + 4Fe^{2+} + 11H_2O$	−28
Manganese reduction/OMO	$CH_2O + 2MnO_2 + 4H^+ \rightarrow CO_2 + 2Mn^{2+} + 3H_2O$	−81
Denitrification/OMO	$5CH_2O + 4NO_3^- + 4H^+ \rightarrow CO_2 + 2N_2 + 7H_2O$	−114
Aerobic respiration/OMO	$CH_2O + O_2 \rightarrow CO_2 + H_2O$	−120
CO_2 reduction	$HCO_3^- + H^+ + 4H_2 \rightarrow CH_4 + 3H_2O$	−55
Ammonium oxidation	$NH_3^+ + 2O_2 \rightarrow NO_3^- + 2H^+ + H_2O$	−72
Methane oxidation	$CH_4 + 2O_2 \rightarrow HCO_3^- + H^+ + H_2O$	−196

Dissolved organic matter is represented by the model compound CH_2O.
OMO is short for the reaction organic matter oxidation.
Source: Christensen TH, Kjeldsen P, Bjerg PL, et al. (2001) Biogeochemistry of landfill leachate plumes. *Applied Geochemistry* 16: 659–718.

Table 4 Oxidation capacity (OXC, milli equivalent per liter of aquifer) calculated for oxidized species in two aerobic aquifers

Species	*Reduction half reaction*	*Vejen (DK)*		*Sand Ridge (Illinois, United States)*	
		Content	*OXC (meq l^{-1})*	*Content*	*OXC (meq l^{-1})*
O_2	$O_2 + 4H^+ + 4e^- \rightarrow 2H_2O$	10 mg l^{-1}	0.44	9 mg l^{-1}	0.39
NO_3^-	$NO_3^- + 6H^+ + 5e^- \rightarrow 1/2N_2 + 3H_2O$	15 mg l^{-1}	1.9	0.95 mg l^{-1}	0.12
Mn(IV) (sediment)	$MnO_2 + 4H^+ + 2e^- \rightarrow Mn^{2+} + 2H_2O$	0.1 mg g^{-1}	6	0.39 mg g^{-1}	23
Fe(III) (sediment)	$FeOOH + 3H^+ + e^- \rightarrow Fe^{2+} + 3H_2O$	2 mg g^{-1}	60	6.8 mg g^{-1}	200
SO_4^{2-}	$SO_4^{2-} + 9H^+ + 8e^- \rightarrow HS^- + 4H_2O$	40 mg l^{-1}	1.2	36 mg l^{-1}	1.1

The calculations are based on the shown contents of oxidized species, the proposed reduction half reactions, and assumed physical parameters: porosities of 0.35 and bulk densities of 1.6 kg l^{-1}. The potential contributions from CO_2 and natural organic matter were not evaluated.
Source: Christensen TH, Kjeldsen P, Bjerg PL, et al. (2001) Biogeochemistry of landfill leachate plumes. *Applied Geochemistry* 16: 659–718.

not given just by the amount of iron oxides present. The composition and microbial availability of iron for reduction are key parameters. Methods for the actual quantification of the microbial iron RDC are, however, not developed. Reactive fractions have been addressed by mild chemical extractions (hydrochloric acid or ascorbic acid), but this is only an operationally defined quantity of easily dissolved, oxidized minerals. The actual pool of microbial available iron RDC may be better determined by the use of microbial assays.

The reduction of iron oxides and precipitation of the reduced metals as carbonates or sulfides changes the composition of the solids along a flow line (**Figure 3**). Overall, the mineral-bound iron oxides are reduced into dissolved ferrous iron, which partly precipitate and partly migrate downgradient into the more oxidized zones. When meeting oxygen, and maybe also manganese oxides, ferrous iron is oxidized and precipitates as amorphous iron hydroxides. The newly precipitated hydroxides form a very reactive and accessible electron acceptor. The migrating part of the reduced iron thus contributes to a regeneration of OXC further away from the landfill. This may be essential in controlling the size of the reduced zones, especially if the plume expands. The substantial buffering by iron oxides, thus, is related to the consumption of OXC and the buildup of reduced species in the strongly reduced part of the plume. Overall, iron acts to minimize the size of the plume by the redox buffering reactions, thus greatly retarding the migration of the reduced leachate and associated problematic compounds (Heron, 1994).

11.16.4.2 Microbial Activity and Redox Processes

Inside a landfill leachate plume, the environment is characterized by the presence of reduced species and the high concentrations of dissolved organic matter. This environment is partly due to the composition of the leachate from the landfill and partly due to microbial processes in the plume. Since this environment is very different from the uncontaminated, oligotrophic, often aerobic aquifers surrounding the plume, the composition of the microbial population of the plume is dramatically different from the indigenous microbial population in the uncontaminated aquifer.

Microbial populations in landfill leachate-contaminated aquifers are dominated by bacteria (eubacteria and archaea), as shown by the analysis of the PLFAs (phospholipid fatty acids) (Ludvigsen et al., 1999). The total number of bacteria reported for landfill leachate plumes is in the range of 4×10^4–1.5×10^9 cells per gram dry weight (dw), and the number of colony forming units, living cells, is in the range of 60–1×10^7 CFU per gram dw (Christensen et al., 2001). However, the large variation caused by different methods and the fact that different types of aquifers were studied mask any difference in the number of bacteria inside and outside the plume. The total number of bacteria in the aquifer downgradient from the Grindsted Landfill (DK) was fairly constant with the distance from the landfill, and the ATP content (an estimate of living cells) showed no significant trend (Ludvigsen et al., 1999). In contrast, considering the number of living bacteria estimated by PLFA

concentration, it was higher close to the landfill than further away from the landfill. From the measurements of ATP and PLFA, the viable biomass ranged from 10^4 to 10^6 viable cells per gram dw (Ludvigsen et al., 1999), clearly demonstrating the presence of a significant viable population.

The microbial community structure in the water phase in the landfill leachate plume is clearly different from the community structure outside the plume as shown in the Banisveld aquifer in the Netherlands (Röling et al., 2001) by 16S ribosomal DNA-based denaturing gradient gel electrophoresis (DGGE). Members of the β subclass of the class Proteobacteria dominated upstream the landfill, but this group was not encountered beneath the landfill where gram-positive bacteria dominated. Further downstream where the effect of the contamination decreased, the community structure partly shifted back, since the contribution of the gram-positive bacteria decreased and the β proteobacteria reappeared. However, the contribution of δ proteobacteria also increased strongly, and the β proteobacteria found here (*Acidovorax* and *Rhodoferax*) differed considerably from those found upstream (*Gallionella* and *Azoarcus*), so the community structure remained affected by the contamination. Surprisingly, this relationship was not evident in sediment samples, where the major part of the microbial population is associated, either because leachate has had little impact on the microorganisms associated with the 10 000–100 000-year-old sediments (Röling et al., 2001) or because the microorganisms in the water phase in the plume mainly were derived from the landfill.

The ability of microbial populations to use different organic substrates under anaerobic conditions was investigated by Röling et al. (2000). The contaminated samples were able to use a higher number of substrate than the samples from upstream and downstream. This pattern was observed in water samples and in sediment samples, but the populations in sediment samples were able to use up to three times more substrates than populations in water samples (Röling et al., 2000).

Microbial redox processes. Different metabolic types of bacteria (denitrifiers, manganese reducers, iron reducers, sulfate reducers, and methanogens) occur at landfill sites. Some of these metabolic types (sulfate reducers and methanogens) can be separated into different physiological groups, which use different carbon substrates as observed in the Norman Landfill (United States) leachate-contaminated aquifer (Beeman and Suflita, 1987, 1990, Harris et al., 1999). The microbial population changed in composition throughout the plume at the Grindsted Landfill (DK). Methanogens and sulfate reducers were abundant close to the landfill, but their numbers decreased in the more distant parts of the plume (Ludvigsen et al., 1999). The iron, manganese, and nitrate reducers constituted a surprisingly high fraction of the total cell numbers and varied little with distance. The ubiquitous presence of these groups of redox-specific populations provided the aquifer with a substantial potential for the different redox processes. Therefore, the dominance of one occurring redox process merely reflects the environment and the available electron acceptors than the composition of the microbial population.

The potential for microbially mediated redox processes has been documented in different landfill leachate plumes (Acton and Barker, 1992; Albrechtsen and Christensen, 1994; Cozzarelli et al., 2000; Ludvigsen et al., 1998; Nielsen et al., 1995a). Performance of bioassays with unamended groundwater and sediment samples verified the presence of the following metabolic activities in the Grindsted Landfill (DK) plume: denitrification, iron reduction, manganese reduction, sulfate reduction, and methane production (Ludvigsen et al., 1998), and similarly, iron reduction, sulfate reduction, and methane production were observed at the Norman Landfill (Cozzarelli et al., 2000). Examples of bioassays in different locations from the leachate plume at Grindsted Landfill are shown in **Figure 4**. The rates for the different processes can be estimated from such incubations, but representative rates cannot be selected. This is due to the fact that only few data exist for landfill sites (Ludvigsen et al., 1998) and that very large variations exist, as also pointed out by McGuire et al. (2002), who compared rates from different environments. Several different microbially mediated redox processes occur concomitantly in such microbial assays (Cozzarelli et al., 2000; Ludvigsen et al., 1998), and microbially mediated redox processes thus do not exclude each other. This is somewhat conflicting with a simple thermodynamic model based on Gibbs free energy (**Table 3**). However, in each sample, one electron-accepting process accounted for more than 70% of the equivalent carbon conversion when the measured rates of the electron-accepting processes were used to calculate the carbon conversion of organic matter to carbon dioxide (assuming oxidation level zero of the carbon in the organic matter) (Ludvigsen et al., 1998). This suggests that the concept of redox zones makes sense in terms of dominating redox levels but that other redox processes also may be taking place simultaneously (to be further discussed in **Section 11.16.7.2**). This may have further implications for the potential of a redox zone to degrade trace amounts of organic chemicals (Albrechtsen et al., 1999; Rügge et al., 1999b).

The microbially mediated redox processes mentioned earlier will thus utilize electron acceptors and produce reduced species. This will generate more reduced environments as long as there are electron donors available. The microbial population thus strongly affects its environment in the core of the plume. At the boundaries of the plume, complex microbial communities may exist, and steep redox gradients will be created when dissolved electron acceptors are consumed (Bjerg et al., 2011; Tuxen et al., 2006). In addition, reoxidation of sulfides or ferro species by oxygen diffusing into the plume may increase the concentration of sulfate and ferric iron, which can stimulate sulfate and iron reduction in these zones as observed at Norman Landfill (Cozzarelli et al., 2000).

In summary, significant numbers of bacteria, detected with several different approaches, are present in landfill leachate plumes. Methanogens, sulfate reducers, iron reducers, manganese reducers, and denitrifiers are believed to be widespread in leachate plumes. Microbial activity seems to occur throughout leachate plumes, although the actual activity (as measured by ATP, PLFA, and redox processes) is low compared to activity in topsoil. Several redox processes can take place in the same samples adding additional diversity to the concept of redox zones illustrated in **Figure 3**.

11.16.5 Overview of Processes Controlling Fate of Landfill Leachate Compounds

The four major compound classes in landfill leachate are dissolved organic carbon, inorganic compound, heavy metals,

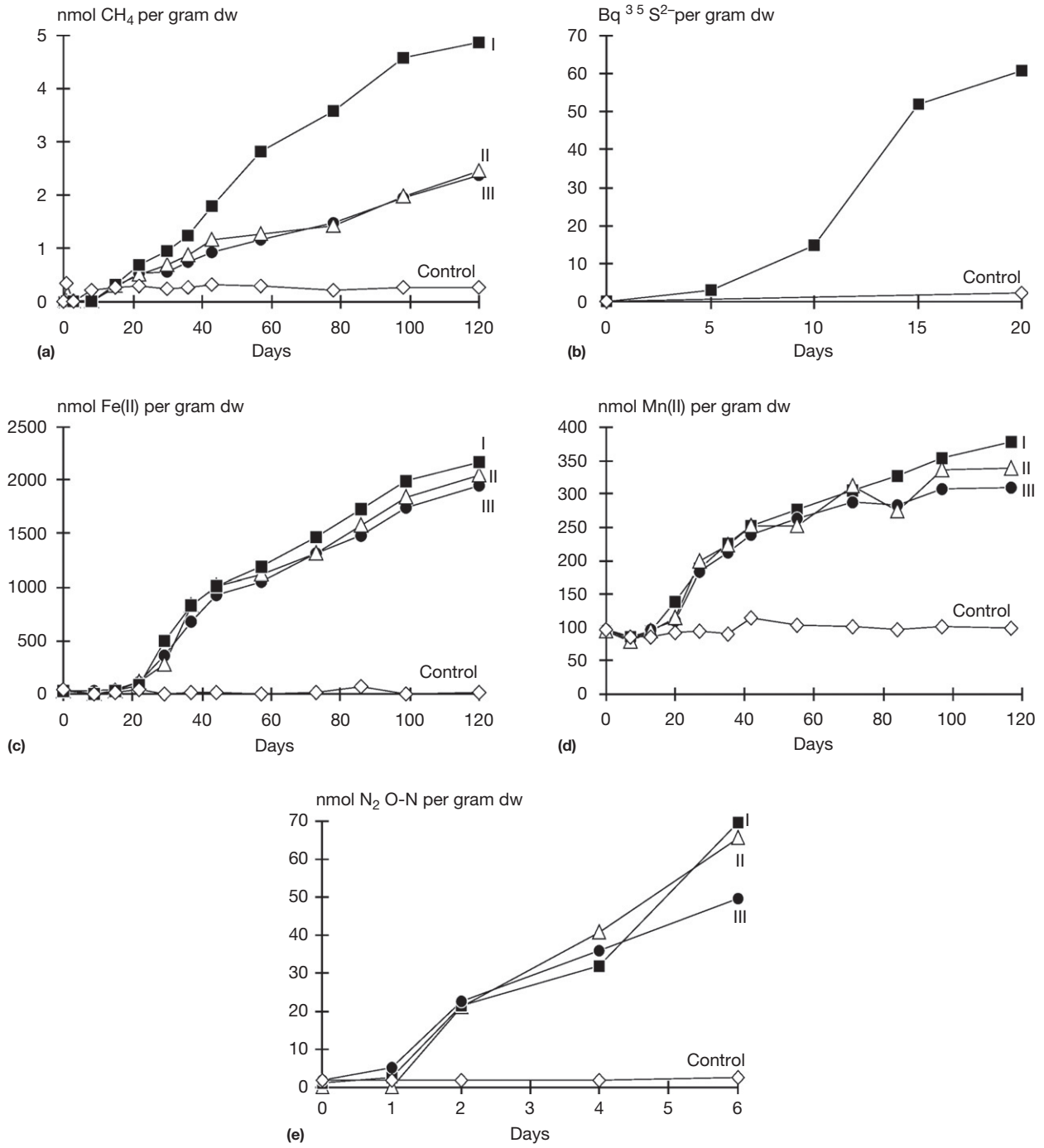

Figure 4 Unamended bioassays showing evidence of each redox reaction from the Grindsted Landfill (DK). The bioassays are performed with sample material from different locations in the plume representing different redox conditions. Reproduced from Ludvigsen L, Albrechtsen H-J, Heron G, Bjerg PL, and Christensen TH (1998) Anaerobic microbial redox processes in a landfill leachate contaminated aquifer (Grindsted, Denmark). *Journal of Contaminant Hydrology* 33: 273–291, with permission.

and XOCs. Typical levels in leachate are reported in Tables 1 and 2. In this section, the fate of these compounds in landfill leachate plumes is summarized. The emphasis is on XOCs, but in order to provide an overview, all compound classes are included. A detailed discussion of the fate of individual compounds in a landfill leachate plumes can be found in Christensen et al. (1994, 2001). A comprehensive investigation of the distribution and geochemistry of inorganic macrocomponents at the Borden Landfill (CAN) is presented by Nicholson et al. (1983).

11.16.5.1 Dissolved Organic Matter, Inorganic Macrocomponents, and Heavy Metals

11.16.5.1.1 Dissolved organic carbon

Volatile fatty acids constituting a substantial fraction of the dissolved organic carbon in acid-phase leachate are easily degraded according to reported laboratory studies. The dissolved organic matter dominating the methanogenic leachate does not sorb to any substantial degree onto aquifer material and seems fairly recalcitrant with respect to microbial degradation as seen in laboratory experiments (Kjeldsen, 1986). However, with respect to degradation of recalcitrant organic matter, laboratory experiments with short retention times, unstable redox conditions, and limited time for microbial adaptation may fail to simulate the conditions in a leachate-polluted aquifer. Observations of actual leachate plumes are usually too limited to provide insight into the fate of the dissolved organic matter. One exception is the report by Lyngkilde and Christensen (1992a) that demonstrated substantial degradation of dissolved organic matter in the anaerobic part of the leachate plume at Vejen Landfill (DK). The observations by DeWalle and Chian (1981) and Rügge et al. (1995) may support this, indicating that dissolved organic matter in methanogenic leachate is degradable to a large extent. Brun et al. (2002) quantified degradation of organic carbon in the Vejen Landfill leachate plume. They found half lives of 100 days in the anaerobic parts of the plume and 1–2 days in the aerobic zone. The anaerobic degradation rate compares to Sykes et al. (1982), who estimated an anaerobic half life at the Borden Landfill (CAN) of 400 days.

11.16.5.1.2 Inorganic macrocomponents

Anions in leachate plumes are mainly important due to their ability to form complexes and take part in dissolution/precipitation processes and their role as electron acceptors. The formation of complexes may increase the mobility of cations and heavy metals. In addition, many reactions are influenced by pH, which to a large extent is governed by the carbonic acid components, in particular HCO_3^-. The sulfur compounds, involved in the sulfate reduction process, are of certain interest, but the prevalence of sulfate reduction in leachate plumes is not very well understood (Murray et al., 1981). Nitrate and maybe sulfate as well may be depleted in the core of the plume, but they will certainly be significant players at plume boundaries.

The attenuation of cations is, besides by dilution, primarily governed by cation exchange processes (Nicholson et al., 1983). Calcium and magnesium are also influenced by complexation and dissolution/precipitation processes. The attenuation of ammonium and potassium due to cation exchange processes is significant, while sodium only has a low ability to take part in cation exchange processes. Calcium and, in some cases, also magnesium, typically dominating the cation exchange complex, could be expelled and move at the front of the leachate plume (Kehew et al., 1984).

Ammonium seems, at least based on the detailed investigation of the Grindsted Landfill (DK) leachate plume, to be significantly attenuated in the anaerobic part of the plume. The ammonium plume is of limited extent followed by zones of increased concentrations of nitrate and dinitrogen oxide, but the attenuation mechanisms are not understood. This issue deserves further research as ammonium may be seen as one of the critical compounds in a landfill leachate plume (Christensen et al., 2000a; see also detailed studies at the Norman Landfill in **Section 11.16.6**).

Dissolved iron and manganese in the leachate will be subjected to precipitation as sulfides or carbonates, ion exchange, oxidation, and dilution (Nicholson et al., 1983). These processes tend to lower the aqueous concentrations of iron and manganese along the flow lines, but reduction of sediment-associated iron and manganese oxides may increase their concentrations further out in the plume (Albrechtsen and Christensen, 1994), often exceeding the saturation indexes with respect to carbonates (Jensen et al., 2002). Organic complexation of iron and manganese seems only of modest importance. Further downgradient the landfill at higher redox potentials, iron and manganese may again precipitate as oxides.

11.16.5.1.3 Heavy metals

The behavior of heavy metals in a landfill leachate plume is simultaneously controlled by sorption, precipitation, and complexation, and proper evaluations of metal attenuation must account for this complex system. Generally, heavy metals do not constitute a groundwater pollution problem at landfills (Arneth et al., 1989) because landfill leachates usually contain only modest heavy metal concentrations and the metals are subjected to strong attenuation by sorption and precipitation in the landfill body (Kjeldsen et al., 2002). Sulfide-producing conditions result in extremely low solubilities of heavy metals (Bisdom et al., 1983). The presence of colloidal and organically complexed metals does enhance solubilities and mobilities (Christensen et al., 1996), but apparently not to the extent that the metals exhibit any appreciable migration in leachate plumes.

11.16.5.2 Xenobiotic Organic Compounds

Sorption: In aquifers characterized by low organic carbon content, most of the XOCs found in leachate plumes are only weakly attenuated by sorption. This applies to the aromatic hydrocarbons, chlorinated hydrocarbons, and the polar compounds. Very few detailed sorption studies involving landfill leachate have been reported (Kjeldsen et al., 1990; Larsen et al., 1992). Preliminary evidence suggests that the presence of leachate, in particular, in terms of dissolved organic carbon, does not affect the sorption of XOCs significantly, and as such, the traditional methods for estimating retardation in aquifers are valid.

The chlorinated aliphatic hydrocarbons are frequently identified in landfill leachate. Adriaens et al. (**Chapter 11.14**) reviewed their presence and fate in the environment. The chlorinated aliphatic hydrocarbons generally degrade by reductive dechlorination under anaerobic conditions (Vogel et al., 1987, where the chlorinated compounds can act as electron acceptors (halorespiration, Holliger et al., 1999)). This also means that the reductive dechlorination process requires an electron donor, such as naturally occurring carbon, petroleum hydrocarbons, or organic carbon, in landfill leachate. The greater availability of naturally occurring carbon likely contributes to the extremely rapid reductive dechlorination of chlorinated ethanes and ethenes that was observed in wetland sediments compared to sand

aquifers (Lorah and Olsen, 1999a,b; Lorah et al., 2003). Degradation under aerobic conditions of higher chlorinated aliphatic compounds, such as tetrachloroethylene (PCE) and trichloroethylene (TCE) has not been demonstrated, but degradation products, such as dichloroethylene (DCE) isomers (primarily *cis*-1,2-DCE), can be oxidized to carbon dioxide. The possibility that mono- and dichlorinated CAHs might degrade via anaerobic oxidation under methanogenic Fe(III)-reducing or Mn(IV)-reducing conditions was suggested by Bradley and others (Bradley, 2000); however, later experiments could not reproduce the results (Bradley et al., 2008). Recently, Gossett (2010) demonstrated that direct aerobic oxidation of vinylchloride (VC) can be sustained at dissolved oxygen concentrations below 20 $\mu g\,l^{-1}$ and concluded that some prior observations of VC disappearance under assumed anaerobic conditions may have been the result of aerobic oxidation at very low oxygen levels. The fate of chlorinated ethanes is much more complex than the fate of chlorinated ethenes, as reviewed by Scheutz et al. (2011). In microcosm and enrichment experiments with wetland sediments, Jones et al. (2002) found that addition of Fe(III) as either amorphous FeOOH or Fe(III) NTA slowed dechlorination of chlorinated ethanes and inhibited degradation of *cis*-DCE, *trans*-DCE, and VC. Degradation of the chlorinated ethanes and ethenes was most rapid under methanogenic conditions (Jones et al., 2002; Lorah et al., 2003).

Information obtained from different plumes, in general, is in accordance with observations from landfill leachate plumes, where the expectation is that PCE and TCE will be reductively dechlorinated. This is supported by the observations of lower chlorinated compounds, DCE and VC, in leachate plumes or degradation experiments. The transformation of chlorinated ethenes has been observed under various redox conditions ranging from methanogenic- to nitrate-reducing conditions (Bradley, 2000; Johnston et al., 1996; Nielsen et al., 1995a; Rügge et al., 1999b). Tetrachloromethane will rapidly degrade in landfill plumes by sediment-associated iron and organic carbon (Pecher et al., 1997; Rügge et al., 1999b). The transformation of 1,1,1-TCA in anaerobic environments is rapid and seems to be affected by both abiotic and biotic degradation processes (Bjerg et al., 1999; Nielsen et al., 1995b). Studies of full-scale landfill plumes have shown a significant degradation of TCE (Chapelle and Bradley, 1998) and 1,1-DCA (Ravi et al., 1998). However, in the case of 1,1-DCA, complete dechlorination to ethane was not shown. In summary, the current information suggests that landfill plumes host redox environments, microorganisms, and/or geochemical processes that effectively can attenuate chlorinated aliphatic hydrocarbons.

The aromatic hydrocarbons generally degrade readily under aerobic conditions, but also anaerobic degradation by pure bacterial cultures has been recognized (**Chapter 11.12**; Heider et al., 1999). The vast amount of data from natural attenuation studies of petroleum hydrocarbon plumes generally supports anaerobic degradation, especially for BTEX (benzene, toluene, ethylbenzene, and xylenes), under field conditions. The first-order degradation rates observed under unspecified anaerobic conditions (Lønborg et al., 2006; Suarez and Rifai, 1999) are typically 1 or 2 orders of magnitude lower than rates reported for aerobic conditions (Nielsen et al., 1996).

Detailed observations in landfill leachate plumes have indicated degradation of mainly toluene, xylenes, and C3–C5-benzenes (Barker et al., 1986; Eganhouse et al., 2001; Lyngkilde and Christensen, 1992b; Rügge et al., 1995). These studies use tracers or compound ratios to rule out dilution and sorption; however, direct proof of degradation is not provided. Isotopic ratios have been applied as a strong tool for identification of degradation. The Vejen Landfill site (DK) was revisited after 10 years (Baun et al., 2003; Richnow et al., 2003), and by the use of isotopic ratios ($^{13}C/^{12}C$) for aromatic hydrocarbons, evidence of degradation was provided for ethylbenzene and *m*-/*p*-xylene. Also, a specific degradation product, benzyl succinic acid (see review by Beller, 2000), was observed, documenting degradation of toluene in the plume (Ledin et al., 2005). It is noticeable that positive results regarding degradation of benzene are few. Baun et al. (2003) concluded that benzene was persistent in the anaerobic part of the Vejen Landfill plume (DK). Ravi et al. (1998) proved that benzene degradation took place in the very long plume at West KL Landfill (United States).

The degradability of toluene and xylenes observed in plumes has been supported by experimental evidence from field and laboratory experiments (Acton and Barker, 1992; Bjerg et al., 1999; Johnston et al., 1996; Nielsen et al., 1995a; Rügge et al., 1999b), while recalcitrance of benzene has been shown in experiments by the same authors. This adds to the belief that benzene is less readily degradable than most of the other BTEXs under strongly anaerobic conditions in landfill leachate plumes.

The phenolic compounds generally degrade readily under aerobic conditions. Information for anaerobic conditions is mixed, and no distinct pattern is evident. Studies indicate persistence of phenol, *o*-cresol, 2,4-dichlorophenol, and 2,6-dichlorophenol under iron-reducing and nitrate-reducing conditions (Nielsen et al., 1995a). Grbic-Galic (1990) reviewed the methanogenic transformation of phenolic and aromatic compounds in aquifers in more general terms and reported the transformation of several phenols.

The pesticides are another important group of pollutants (see **Chapter 11.15**). Many different herbicides have been identified in landfill leachate; however, only very little is known about pesticide degradation potentials in leachate plumes. Mecoprop is frequently observed in leachate (**Table 2**), and at the Vejen Landfill (DK), mecoprop was observed in the plume 130 m downgradient of the landfill at a concentration of 95 $\mu g\,l^{-1}$ (Lyngkilde and Christensen, 1992b). Baun et al. (2003) showed in a revisit at the site that MCPP was recalcitrant in the anaerobic part of the plume up to 135 m from the landfill. Rügge et al. (1999a) found in an injection experiment in the Grindsted Landfill (DK) plume that atrazine and mecoprop were recalcitrant under strongly anaerobic conditions. Anaerobic dechlorination of phenoxy acids including impurities and putative metabolites have been proposed (Reitzel et al., 2004). Rügge et al. (1995) identified in landfill leachate-affected groundwater different phenoxy acids resembling known herbicides, though, without the chlorine atoms attached. Milosevic et al. (2012, 2013) identified phenoxy acids in very high concentrations at Risby Landfill (Denmark) and suggested anaerobic degradation by use of a combined isotope and enantiomer analysis in a complex clayey till setting. Tuxen et al. (2003) proposed that a significant part of the phenoxy acids at the Sjoelund Landfill (DK) disappeared

due to degradation in the interface between the anaerobic leachate plume and the surrounding aerobic aquifer. Field scale studies and reactive solute transport modeling showed profileration of specific phenoxy acid degrading bacteria and metabolic activity in the fringe zone of the plume (Prommer et al., 2006; Tuxen et al., 2006). This is consistent with the expected aerobic degradation of phenoxy acids (Broholm et al., 2001). A conceptual model for the degradation of phenoxy acid pesticides and other aerobic degradable compounds was suggested by Bjerg et al. (2011). In conclusion, studies on pesticide degradation in different anaerobic environments are few, and due to their general recalcitrance in groundwater environments (Albrechtsen et al., 2001), they may turn out to be critical compounds in landfill leachate plumes.

Recently, information on XOC degradation in different landfill plume redox environments has been expanded. As more results become available, more XOCs are found to be degradable in the intermediate redox zones dominated by sulfate, iron, and nitrate reduction. Transformation of chlorinated aliphatics seems to occur not only under methanogenic conditions but also in less reducing zones. Aromatic hydrocarbons degrade readily in aerobic environments, but only slowly in reducing environments. Benzene may, in particular, be recalcitrant under strongly reducing conditions. As the understanding of how to perform degradation studies has improved significantly during the 1990s, more detailed information on complex degradation patterns and compound interactions have been revealed. Also, the use of isotopic ratios and identification of specific degradation products have improved the ability to prove degradation under field conditions. Overall, several compounds have been shown to disappear in plumes, but direct evidence of microbial degradation has only been established for some of these XOCs. Finally, the frequent findings of pesticides and recently more polar compounds also call for more focus on such compounds.

11.16.6 Norman Landfill (United States)

The Norman Landfill Research Site is a closed municipal solid waste landfill, formerly operated by the city of Norman, OK. The site is a research location for the Toxic Substances Hydrology Program of the US Geological Survey (USGS) (http://toxics.usgs.gov/). Scientists from the USGS, the University of Oklahoma, the US EPA, and numerous universities have installed wells and instruments to investigate the chemical, biological, and hydrologic processes in groundwater, wetland sediments, and surface water. The focus of the Norman investigations was on understanding the biogeochemical processes associated with the degradation of organic and inorganic contaminants in the leachate plume as it moves downgradient in the shallow aquifer and intersects a wetland. At Norman Landfill, interdisciplinary approaches combining geochemical, isotopic, and microbiological techniques at multiple spatial and temporal scales have been used to identify the important biogeochemical processes occurring in the aquifer (e.g., Báez-Cazull et al., 2007; Cozzarelli et al., 2000; Cozzarelli et al., 2011; Harris et al., 2006; Lorah et al., 2009; Scholl et al., 2006; Tuttle et al., 2009; Ulrich et al., 2003).

11.16.6.1 Source, Geology, and Hydrogeology

The field site is located in the alluvium of the Canadian River. The landfill received solid waste between 1922 and 1985. The waste initially was dumped into trenches that were about 3 m deep and that contained water to a depth of 1.5–2.5 m because of the shallow water table; the waste was subsequently covered with 15 cm of sand. No restrictions were placed on the type of material dumped at the landfill. In 1985, the landfill was closed, and the mounds, which had reached a maximum height greater than 12 m, were covered with local clay and silty-sand material. The Canadian River alluvium is 10–12 m thick and is predominantly sand and silty sand, with interbedded mud and gravel. The water table in the Canadian River alluvium fluctuates in response to rainfall and seasonal evapotranspiration and is usually less than 2 m below land surface near the landfill (Scholl et al., 2004). A shallow stream with areas ponded by beaver dams (referred to here as a slough), which is about 0.75 m deep, lies roughly parallel to the landfill and about 100 m to the southwest (**Figure 5**). Groundwater flows from the landfill toward the slough and Canadian River.

The hydraulic conductivity of subsurface materials near the landfill, which was measured by the use of slug tests, ranged from 7.3×10^{-2} to 24 m day^{-1} (Scholl et al., 1999). A discontinuous low hydraulic-conductivity interval that consisted of silt and clay was detected about 3–4 m below the water table along the transect where most data have been collected (**Figure 5**). A high hydraulic-conductivity layer containing coarse sand and gravel is located near the base of the alluvium at depth of about 10–12 m. Low-permeability shale and siltstone in the Hennessey Group of Permian age act as a lower boundary to vertical groundwater flow beneath the alluvium. The red color of the alluvium is attributed to very fine-grained (<0.1 μm) disseminated hematite that originated with the detrital sediments from the abundant red beds in the drainage basin. Sand layers contain quartz, illite–smectite, feldspars, and minor calcite and dolomite; mud layer mineralogy is similar but with greater amounts of clays that include illite–smectite, smectite, kaolinite, and chlorite (Breit et al., 2005). Authigenic phases in the aquifer include FeS, pyrite (FeS_2), barite ($BaSO_4$), and very fine (<0.1 μm) Fe(III) oxides. Mirabilite ($Na_2SO_4 \cdot 10H_2O$) and gypsum ($CaSO_4 \cdot 2H_2O$) occur in trace amounts as ephemeral accumulations on the land surface (Tuttle et al., 2009).

11.16.6.2 Landfill Leachate Plume

11.16.6.2.1 Biogeochemistry of the plume

Leachate recharging the underlying aquifer contained dissolved constituents derived from dissolution and degradation of buried waste material resulting in high NVDOC, HCO_3^-, NH_4^+, B, Cl^-, Fe^{2+}, and CH_4 concentrations; high $\delta^2 H_{H_2O}$ values; and low SO_4^{2-}, Ar, and N_2 concentrations in the aquifer (Cozzarelli et al., 2011). **Figure 6(a)** and **6(b)** illustrates a time series (1999 and 2006) of plume-scale concentrations of important inorganic and organic constituents in groundwater along the vertical longitudinal profile from MLS35 to MLS80 (**Figure 5**). Arsenic, barium, cadmium, chromium, cobalt, nickel, and strontium also had substantially higher concentrations in wells downgradient from the landfill

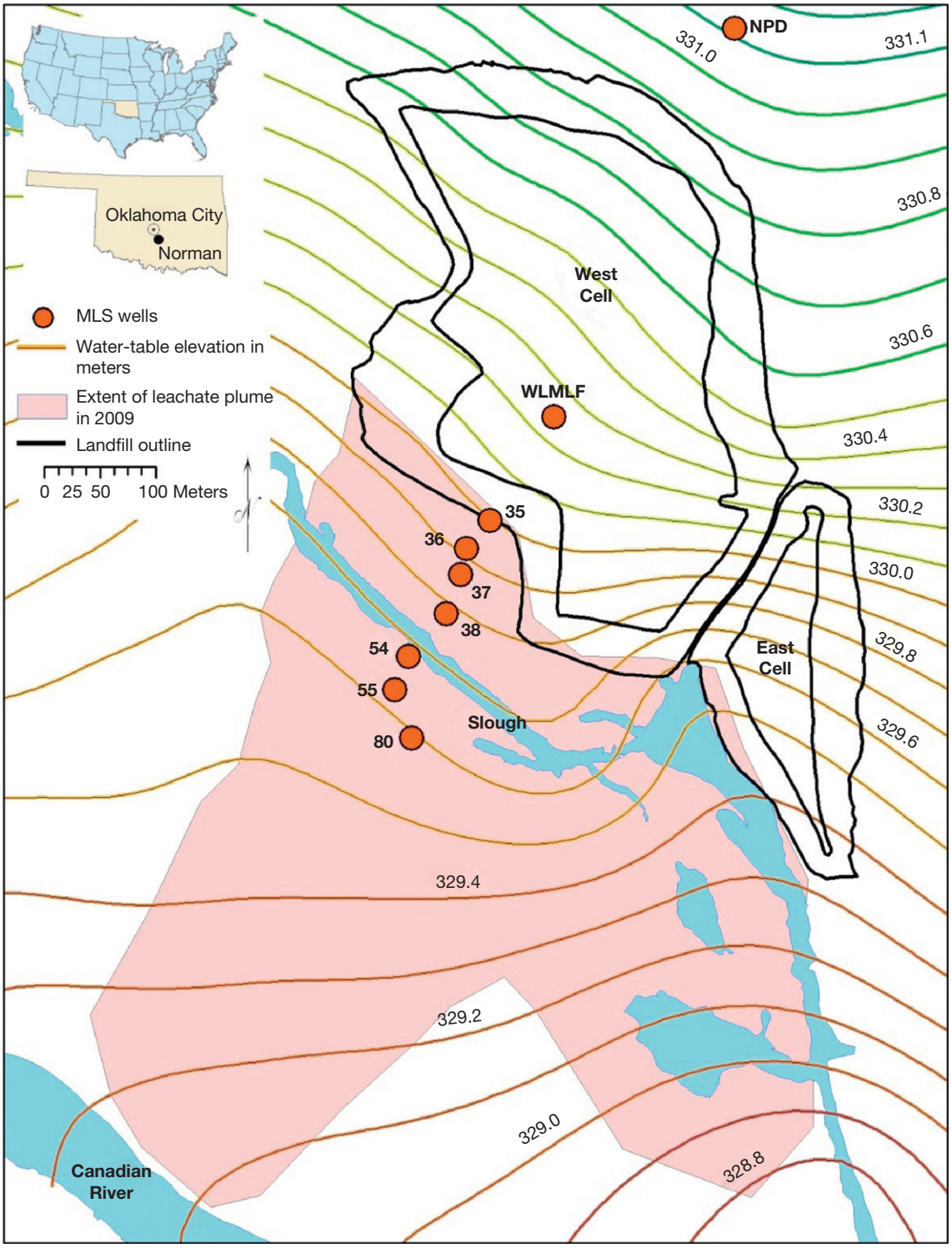

Figure 5 Map showing the Norman Landfill (United States) site. MLS35 through MLS80 represents the wells used to construct the transect, in the direction of groundwater flow, shown in **Figure 6**. WLMLF is the well in the landfill. NPD is the background well. The approximate extent of the plume was determined from specific conductance measurments in 2009.

than in background wells. Dynamic hydrologic conditions at the Norman Landfill have created a leachate plume that interacts with a shallow wetland and also migrates underneath the wetland toward the Canadian River. Spatial and temporal variability in the rates of processes in the shallow aquifer affects the plume-scale migration of leachate constituents. **Figure 7** illustrates a generalized conceptual model of transport and reaction zones in the landfill leachate-affected aquifer.

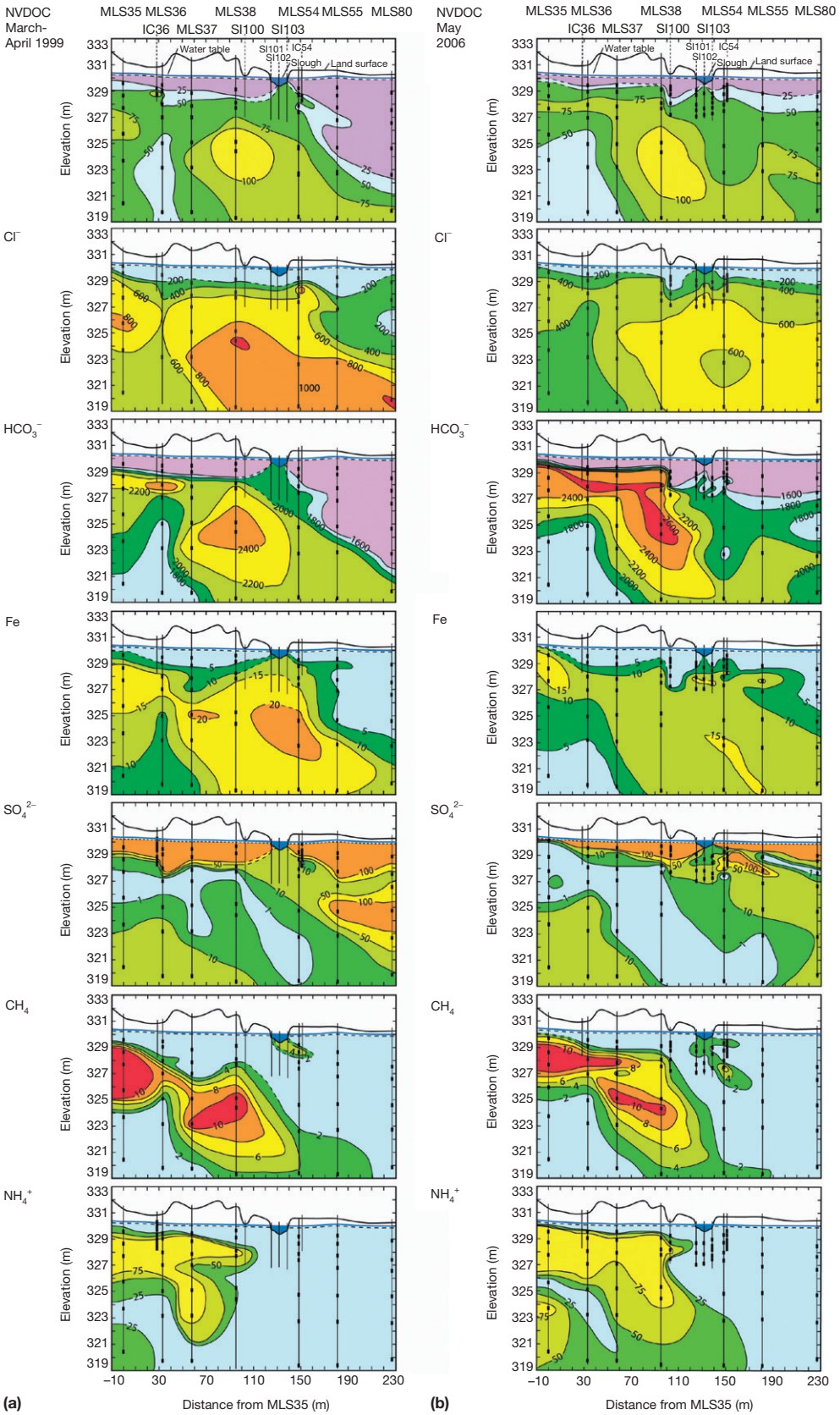

Figure 6 Concentrations of dissolved NVDOC (mg l^{-1} as C), chloride (mg l^{-1} as Cl^{-}), alkalinity (mg l^{-1} as HCO_3^{-}), iron (mg l^{-1} as Fe^{2+}), sulfate (mg l^{-1} as SO_4^{2-}), methane (mg l^{-1} as CH_4), and ammonium (NH_4^{+}, in mg l^{-1} as N) in March–April 1999 and May 2006. The location of the wells on transect MLS35-80 is shown in **Figure 5**.

Chloride and nonvolatile dissolved organic carbon (NVDOC) profiles along the well MLS35-80 transect in 1999 and 2006 confirm that the plume extends through the entire thickness of the alluvium between the landfill and the slough and has migrated beneath the slough (**Figure 6(a)** and **6(b)**). Groundwater at the edge of the landfill has high concentrations of NVDOC (maximum 113 mg l^{-1}) compared to groundwater collected upgradient and northeast of the landfill, where the median concentration was 3.3 mg l^{-1} (Cozzarelli et al., 2011). The high NVDOC concentrations result from the dissolution and partial degradation of organic waste in the landfill. The NVDOC, which reached a concentration of 300 mg l^{-1} in the landfill well (WLMLF), is a highly heterogeneous mixture of nonvolatile organic components and fragments from proteins, lignin, cellulose, hemicellulose, polysaccharides, lipids, and waxes that have undergone extensive biological and chemical reactions (Leenheer et al., 2003; Nanny and Ratasuk, 2002).

Temporal variability of constituents at the plume scale shows persistence in the NVDOC concentrations in the center of the plume, with a similar pattern to the Cl^- concentrations, indicating little differentiation between NVDOC and a conservative component (**Figure 6(a)** and **6(b)**). The biodegradability of NVDOC has been studied using a bioassay technique by Weiss et al. (2005) and with in situ experiments by Harris et al. (2006). These experiments indicated that the overall reactivity of the organic carbon in this system is poor and is consistent with the persistently high NVDOC concentrations observed in the plume. However, some degradation of organic compounds to inorganic compounds is evident by the increase in alkalinity (up to 7 times the background concentrations) of groundwater downgradient from the landfill resulting in an alkalinity plume similar in shape to the NVDOC plume (**Figure 6(a)** and **6(b)**). Background water pH values ranged from 6.9 to 7.2, whereas values throughout the high-chloride plume along transect MLS35–80 (**Figure 5**) ranged from 6.7 to 7.3.

Degradation processes in the leachate-contaminated aquifer have resulted in the depletion of oxidized chemical species (such as O_2 and SO_4^{2-}) and the accumulation of reduced products (such as Fe^{2+}) in groundwater (**Figure 6(a)** and **6(b)**). Groundwater within the plume between the landfill and the slough is largely anoxic (<0.2 mg l^{-1} dissolved oxygen), and therefore, the reactions that dominate within the plume are anaerobic. Aerobic respiration is of limited importance in most of the contaminated aquifer, except near the water table where mixing with oxygenated recharge water occurs (Scholl et al., 2006; Tuttle et al., 2009; see **Chapter 11.12**).

Ammonium was the dominant N species in the landfill leachate plume; concentrations in the center of the plume had a median value around 151 mg l^{-1} (concentrations expressed as mg l^{-1} of N), compared with approximately 1–2 mg l^{-1} in upgradient groundwater (see **Chapter 11.12**). The NH_4^+ plume formed downgradient from the landfill most likely results from the transport of NH_4^+ produced during the fermentation of organic matter within the refuse mounds. At the boundaries of the plume, the concentration of NH_4^+ decreases sharply. The front of the NH_4^+-rich region, as defined by the 75 mg l^{-1} contour (**Figure 6(a)** and **6(b)**), moved downgradient 35 m in the 7 years between 1999 and 2006 (average of 5 m $year^{-1}$), substantially slower than the estimated median groundwater flow velocity (15 m $year^{-1}$) and apparent flushing rate of high Cl^- (Cozzarelli et al., 2011). This pattern of slow front migration is consistent with a sustained leachate NH_4^+ supply that was attenuated by sorption and/or biodegradation/oxidation within the leachate plume. The concentrations and isotopic composition of ammonium indicate retention onto sediment by ion exchange and oxidation at the upper plume boundary are the major controls on the transport of ammonia in this system (Cozzarelli et al., 2011; Lorah et al., 2009). Periodically, nitrate concentrations greater than 70 mg l^{-1} (as N) were measured during monthly sampling of water table

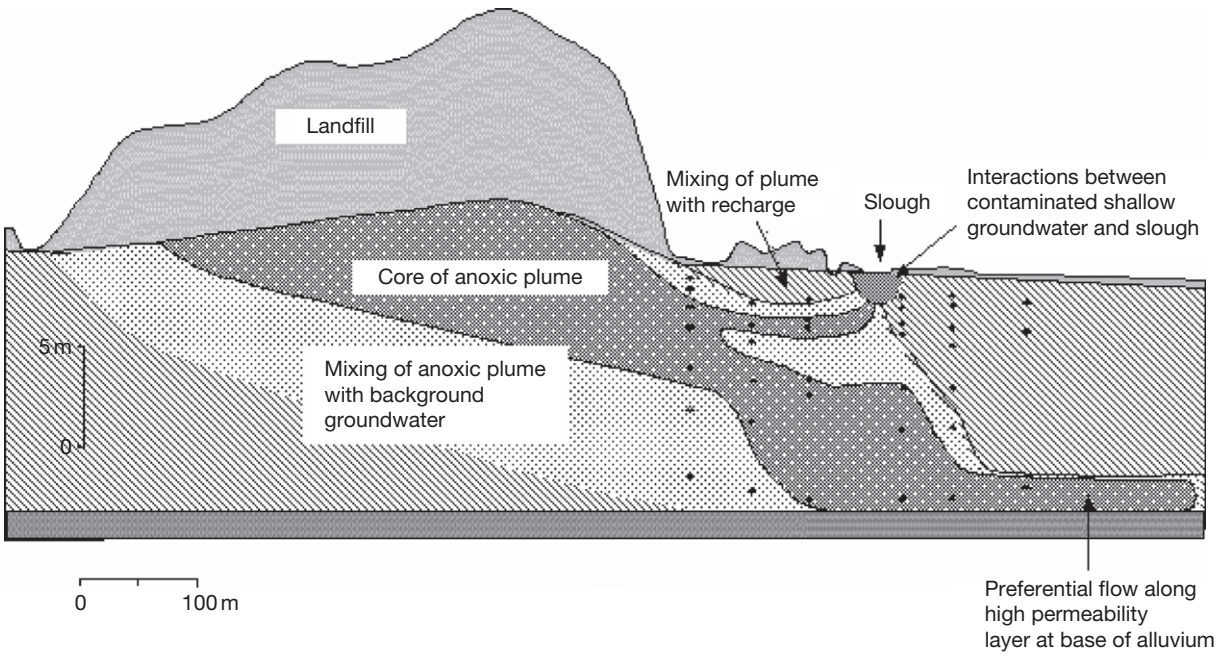

Figure 7 Conceptual model of redox (transport and reaction) zone at the Norman Landfill (United States).

wells that intersected the plume/recharge water mixing zone (Figure 7). Active redox cycling, including NH_4^+ oxidation and NO_3^- production and reduction, occur in this zone of transient hydrologic conditions.

High concentrations of Fe^{2+} in the groundwater (>23 mg l^{-1} Figure 6(a) and 6(b)) are consistent with microbial dissolution of sediment-bound Fe(III) oxides that are responsible for the pervasive red-brown color of the aquifer sediment. High concentrations of dissolved Fe^{2+} persisted along the length of the plume throughout the study period, consistent with transport under reducing conditions. Readily reactive iron oxides were depleted from the sediments within the saturated zone (Breit et al., 2005; 2008), indicating the source of the Fe^{2+} in the plume may largely be from dissolution and reduction of Fe(III) oxides farther upgradient or from dissolution of Fe in the landfill waste (Cozzarelli et al., 2000, 2011). Dissolved Fe^{2+} concentrations are irregular, spatially and temporally (Figure 6(a) and 6(b)), and although the shape of the Fe plume largely corresponds to the high NVDOC plume, high Fe^{2+} concentrations do not correspond directly to concentrations of CH_4 and HCO_3^- or the depletion of SO_4^{2-}. The variation may reflect the precipitation of secondary mineral phases or the heterogeneous availability of reactive-iron phases along variable flow paths. Báez-Cazull et al. (2007) found shallow groundwater beneath the slough was greatly oversaturated with respect to siderite, and Tuttle et al. (2009) describe the abundance of FeS and pyrite in the alluvium. With increased exposure to the plume over time, the remaining Fe(III) oxides are expected to become less accessible such that solution transport will eventually exceed the rate of Fe(III) oxide reduction and dissolved Fe^{2+} concentrations in the plume (Figure 6(a) and 6(b)) will decline.

The dominant dissolved S species in the leachate plume and background groundwater is SO_4^{2-} (Cozzarelli et al., 2011; Tuttle et al., 2009). Dissolved sulfide (H_2S) concentrations were generally <0.05 mg l^{-1}, consistent with the presence of dissolved Fe^{2+} and solid FeS and FeS_2 within the sediment. Sulfate reduction in the plume has resulted in the depletion of SO_4^{2-} from the center of the plume (Figure 6(a) and 6(b)), where sulfate concentrations were <1 mg l^{-1}. Near the lower boundary of the plume, SO_4^{2-} ranges from 10 to 60 mg l^{-1}, consistent with the mixing of background groundwater with SO_4^{2-}-depleted plume water. The plume-scale distribution of SO_4^{2-} concentrations shows that between 1999 and 2006, the extent of the SO_4^{2-} depletion zone had increased substantially. Numerous investigators have used the Norman Landfill as a model system to study the progress of SO_4^{2-} reduction in an anaerobic aquifer (Harris et al., 2006; Kneeshaw et al., 2007; Scholl et al., 2006; Tuttle et al., 2009; Ulrich et al., 2003). Quantitative analyses of the different SO_4^{2-} sources in the aquifer along with S isotopic analyses indicate SO_4^{2-} plays a major role in supporting biodegradation processes. Bacterial SO_4^{2-} reduction lowered SO_4^{2-} concentrations resulting in residual dissolved SO_4^{2-} having $\delta^{34}S$ values much greater than the recognized sulfate sources (Tuttle et al., 2009). The variable sources and sinks for sulfur in this aquifer reflect the effect of the leachate superimposed on natural sulfur cycling within the alluvium. Although dissolved sulfide concentrations in the plume were low, analysis of the sediment cores indicated that iron sulfides have accumulated in the aquifer. The highest concentrations of iron sulfides in the upper portion of the plume, measured by Ulrich et al. (2003), were detected just beneath the water table where increased sulfate reduction rates were measured (Figure 8). Tuttle et al. (2009)

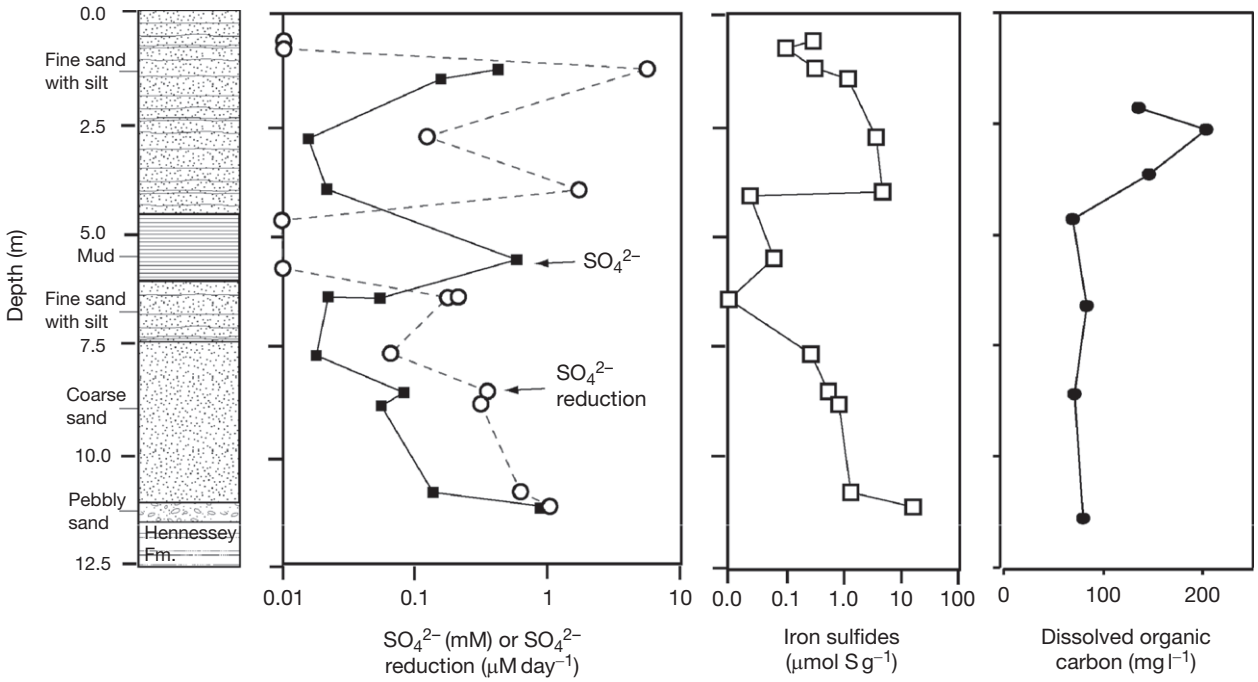

Figure 8 Depth profile (meters below land surface) of the stratigraphy, sulfate reduction rates, sulfate concentration, iron sulfide content of sediment, and dissolved organic carbon in groundwater obtained from an area adjacent to well 40. Reproduced from Ulrich GA, Breit GN, Cozzarelli IM, and Suflita JM (2003) Sources of sulfate supporting anaerobic metabolism in a contaminated aquifer. *Environmental Science and Technology* 37: 1093–1099.

and Scholl et al. (2006) proposed active S cycling in this zone; the oxidation of iron sulfides explained the relatively low $\delta^{34}S_{SO_4}$ values of sulfate measured in wells screened at this unsaturated/saturated zone interface where atmospheric oxygen was available to react with FeS phases.

Concentrations of CH_4 are highest in the center of the anoxic plume. The highest CH_4 concentrations occurred slightly beneath the top of the sulfate-depleted zone (**Figure 6(a)** and **6**(b)). The distribution of CH_4 concentrations did not change appreciably over 7 years, indicating that attenuation mechanisms balanced the production and transport of CH_4. The δD values for groundwater downgradient from the landfill indicate that the groundwater is enriched in deuterium (Cozzarelli et al., 2000; see **Chapter 11.12**). Hackley et al. (1996) reported 30–60‰ deuterium enrichment in leachate from three landfills in Illinois and speculated that most of the enrichment was a result of methanogenesis, with some enrichment resulting from isotopic exchange with hydrogen sulfide. The greatest enrichment in deuterium at the Norman Landfill was measured in the center of the plume where δD of H_2O values ranged from −10.6 to −3.4‰ in 1999, compared to background values of −45.8 to −27.9‰. The samples that contained the greatest enrichment in deuterium also had enriched ^{13}C of total dissolved inorganic carbon (TDIC) values. The $\delta^{13}C$ of TDIC values in the most contaminated groundwater downgradient from the landfill was as heavy as 11.9‰, which indicated significant enrichment in ^{13}C compared to typical $\delta^{13}C$ values for shallow groundwater from the Central Oklahoma aquifer, which ranged from −17.8‰ to −12.5‰ (Parkhurst et al., 1993). This large shift in isotopes to enriched values in the groundwater most likely results from biogenic CH_4 production. The high concentrations of CH_4 combined with the heavy δD of H_2O values at the edge of the landfill and analysis of landfill gases (see **Chapter 11.12**) indicate that methanogenesis largely occurs within and underneath the landfill and that the products of this process are transported in groundwater. Methane in the Norman Landfill leachate plume was attenuated by anaerobic oxidation within the center of the plume and aerobic oxidation near the water table (Grossman et al., 2002, see **Chapter 11.12**). Grossman et al. (2002) estimated that 27% of the plume CH_4 was oxidized in the anoxic core of the plume with an average oxidation rate of 56 μM $year^{-1}$.

11.16.6.2.2 Availability of electron acceptors

The fate of NVDOC was investigated in the plume in order to understand the natural attenuation potential of this system. As illustrated previously, the NVDOC concentrations showed little change with distance in the core of the plume, indicating that NVDOC was not efficiently degraded in this zone. The most rapid reactions in this system occurred at the upper boundary of the plume where electron acceptors are available (**Figure 7**). Direct rate measurements made in the laboratory combined with field observations and experiments suggest that sulfate reduction is the most important microbial reaction that affects aquifer geochemistry downgradient from the Norman Landfill. The core of the plume is strictly anaerobic and supports sulfate reduction and perhaps small amounts of iron reduction and methanogenesis, whereas the boundaries of the plume appear to support iron reduction and sulfate reduction, to a greater extent, due to the increased availability of reactive electron acceptors at these boundaries. Background groundwater in this system was reducing except near the water table, where oxygenated recharge mixes with anoxic groundwater and the plume during recharge events (**Figure 7**; Cozzarelli et al., 2011). The nonuniform availability of electron acceptors and the mixing of the contaminant plume with water at the plume boundaries have a significant effect on biogeochemical processes.

Soluble and solid-phase geochemical investigations coupled with laboratory rate experiments were used to evaluate the factors that control the availability of electron acceptors in this system (Cozzarelli et al., 2000; Scholl et al., 2006; Tuttle et al., 2009; Ulrich et al., 2003). The sources of electron acceptors vary significantly over relatively small spatial scales (on the order of meters). Several sources of sulfate that support sulfate-reducing activity in the leachate-affected aquifer have been identified. Each of these sources supplies sulfate to a different region of the aquifer to varying degrees. First, the oxidation of iron sulfides to sulfate and/or dissolution of sulfate during recharge events are important in shallow regions near the water table where high rates of sulfate reduction have been measured. In situ evidence for aerobic iron sulfide oxidation is found at the water table, where despite relatively high rates of sulfate reduction, the concentration of iron sulfide is comparatively low (**Figure 8**; Ulrich et al., 2003). Further, sulfate concentrations are highest near the water table and decrease rapidly with depth. Experiments conducted with sediment collected from the study site have shown that hydrogen sulfide precipitates rapidly in the sediments as immobile iron sulfide minerals. Such minerals were not easily oxidized to sulfate under anaerobic conditions in the presence of a variety of potential electron acceptors (Ulrich et al., 2003); however, when aerobic conditions prevail, as expected to seasonally occur at the water table, the iron sulfides readily oxidize and sulfate concentrations increased. The observation that iron sulfide oxidation near the water table contributes to the supply of SO_4^{2-} is analogous to findings from an uncontaminated aquifer in the Yegua formation of East Central Texas (Ulrich et al., 1998).

The abundance of solid forms of Fe and S in the sediment within the upper 2.8 m of aquifer was quantified to further assess whether water table fluctuations affected the availability of solid-phase electron acceptors at this plume boundary (Breit et al., 2008). Oxidation of FeS minerals during dry periods and decomposition of particulate organic material containing ester sulfates increased both the available Fe(III) iron and sulfate pools at this interface (Tuttle et al., 2009). More rapid Fe reduction is expected in the shallow alluvium where fine-grained and poorly crystalline Fe(III) oxides are regenerated in response to water-level fluctuations. At this mixing interface, the seasonal lowering of the water table can expose labile Fe(II)-containing phases to reoxidation, thereby renewing the supply of Fe(III) as an electron acceptor when the water table rises again. Iron reduction in sediment samples collected near the water table progressed at a rate of 6.5 nmol Fe per gram sediment per day (Cozzarelli et al., 2000).

Sulfate reduction within the core of the plume (at intermediate aquifer depths) is limited by the availability of sulfate, which is supplied by the slow process of barite ($BaSO_4$) dissolution. Under conditions of low dissolved sulfate (<1 mg l^{-1}), as is the case in the center of the anoxic leachate plume, barite is undersaturated and dissolves releasing both barium and sulfate to the solution. Barite grains within the core of the

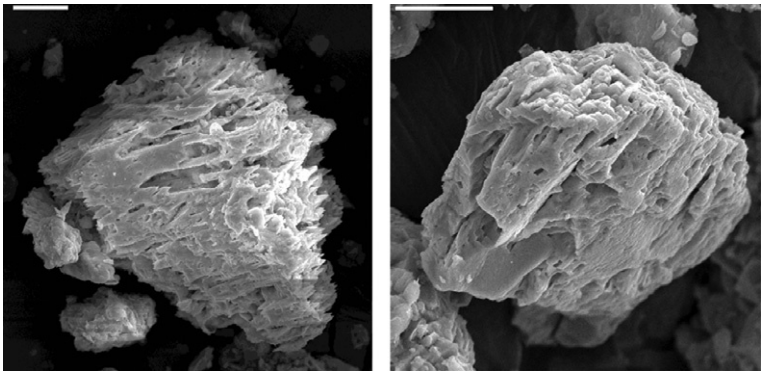

Figure 9 SEM micrographs contrasting textures of detrital barite grains. Grain on the left with dissolution textures was collected from sediment exposed to leachate; nearby porewater contains <10 mg l^{-1} sulfate. Grain on the right was collected from sediment unexposed to leachate and containing 100 mg l^{-1} sulfate. Bar scale is 10 μm. Reproduced from Ulrich GA, Breit GN, Cozzarelli IM, and Suflita JM (2003) Sources of sulfate supporting anaerobic metabolism in a contaminated aquifer. *Environmental Science and Technology* 37: 1093–1099.

plume show dissolution features (Figure 9). Rapid dissolution of barite is unlikely given its low solubility; however, the amount of barite present in the sediment is sufficient to impact the sulfate budget of the aquifer (Ulrich et al., 2003). In addition to the slow dissolution of barite, the isolation of Fe(III) oxides largely within clay particles further limits rates of oxidation–reduction reactions in the core of the anoxic plume. Complete reduction of Fe(III) oxides in these sediments is possible as indicated by the sparse intervals of gray alluvium (including mud clasts) recovered in sediment core near accumulations of entrained plant fragments, which likely favored reductive dissolution of Fe(III) oxides during the thousands of years of burial (Cozzarelli et al., 2011). The results of this analysis suggest that reductive dissolution of detrital Fe(III) oxides in reducing environments within the alluvium continues both within the leachate and in the generally anoxic background groundwater, but at a slow rate.

Another source of dissolved sulfate in the aquifer is through advective flux occurring above the confining layer at the bottom of the aquifer and at the upgradient mixing zone between the anoxic plume and background water. Hydraulic conductivity is relatively high (Scholl and Christenson, 1998) in this depth interval where coarse-grained sands and gravel are the predominant sediment types. The lower chloride concentration and lower specific conductance of groundwater in deeper portions of the aquifer relative to the leachate plume are consistent with mixing of leachate and uncontaminated groundwater. Dissolved sulfate in this interval approaches background concentrations and is important in maintaining rates of sulfate reduction near the base of the aquifer (Figure 8). Investigations of plume biogeochemistry (Cozzarelli et al., 2000) indicate that the influx of electron acceptors by mixing with recharge or upgradient groundwater is limited to the boundaries of the plume. Thus, although anaerobic oxidation was supported by electron acceptors from background groundwater in mixing zones, aquifer solids were more important as sources of electron acceptors in the core of the plume.

11.16.6.2.3 Fate of XOCs

Organic compounds identified in Norman Landfill leachate in 2000 included numerous organic wastewater contaminants (OWCs), including detergents, insect repellents, plasticizers, fire retardants, polycyclic aromatic hydrocarbons, and fecal indicators (Barnes et al., 2004; Cozzarelli et al., 2011). Although the concentrations of OWCs generally decreased downgradient from the landfill, a similar composition and distribution were detected in 2009 (Cozzarelli et al., 2011). Several OWCs detected in the core of the plume during both the 2000 and 2009 sampling events included bisphenol A (a plasticizer), *p*-cresol (a disinfectant), DEET (an insect repellent), and tri(2-chloroethyl) phosphate (a fire retardant). Persistence of these compounds 95 m downgradient from the edge of the landfill and over a 9-year period indicates that natural attenuation was relatively slow for these contaminants and that the landfill was a continuing source of OWCs.

Volatile organic compounds (VOCs) in the Norman Landfill leachate plume were measured in 1995, in 1996 (Eganhouse et al., 2001), and in 2009 (Cozzarelli et al., 2011). Some of the same compounds identified by Eganhouse et al. (2001) were still detectable in the leachate 14 years later, including those identified as good molecular markers of the leachate because of their apparent persistence within the core of the anoxic leachate plume – cholorobenzene, 1,4-dichlorobenzene, and isopropylbenzene. Naphthalene had the highest concentration of the VOCs detected (99.6 μg l^{-1} in WLMLF), and benzene was the only VOC with a concentration that exceeded the USEPA drinking-water standard (>20 μg l^{-1} in WLMLF). Low VOC concentrations in the leachate plume at Norman Landfill are similar to those of other *old* municipal landfills that were not used for the disposal of large quantities of industrial chemicals (Eganhouse et al., 2001).

Various in situ approaches have been used to assess the biodegradation potential and fate of priority pollutants and other emerging contaminants in the Norman Landfill leachate plume. Investigation of the distribution of volatile organic carbon compounds (VOCs) has provided evidence of natural attenuation of several priority pollutants (Eganhouse et al., 2001). Although VOCs make up <1% of the mass of organic carbon in the Norman Landfill leachate plume, they are useful indicators to show that biodegradation is occurring in the leachate plume. Eganhouse et al. (2001) compared concentrations of two different isomers of benzene, isopropylbenzene and *n*-propylbenzene, in landfill leachate. Isomers of benzene have the same number and type of atoms but the molecules

have slightly different structures. These different isomers of benzene have similar physical properties, so it should be affected by volatilization, dilution, and sorption in a similar manner. The concentration of *n*-propylbenzene decreases much faster as leachate flows away from the landfill than do the concentrations of isopropylbenzene. This decrease in concentration of *n*-propylbenzene is caused by biodegradation, indicating that biological degradation is decreasing the concentrations of some contaminants at Norman Landfill. These techniques can be applied at sites with contaminants other than landfill leachate.

In situ field experiments of microbial processes in zones with different chemical and physical properties have been conducted at Norman Landfill using push–pull test technology and small-scale tracer tests (Harris et al., 2007; Scholl et al., 2001; Senko et al., 2002). Push–pull tests are single-well injection–withdrawal tests (Istok et al., 1997). During the injection phase of the test, a solution consisting of groundwater amended with tracers, electron donors, or electron acceptors is injected or *pushed* into the aquifer. During the extraction phase, the test solution is pumped (*pulled*) from the same location and concentrations of tracer, reactants, and possible reaction products are measured as a function of time in order to construct breakthrough curves and to compute mass balances for each solute. Reaction rate coefficients are computed from the mass of reactant consumed and/or product formed. These tests can be conducted anywhere in the aquifer, making it possible to investigate processes and rates in different geologic textures and geochemical environments.

At Norman Landfill, investigators are using these field injection techniques to investigate how biodegradation rates vary with aquifer permeability (Scholl et al., 2001). Push–pull tracer tests were conducted to measure in situ biodegradation rates of simple organic acids in the leachate plume. Replicate wells were placed in three layers: medium sand, silt/clay lenses in sand, and poorly sorted gravel. In situ biodegradation rates of two simple organic acids, formate and lactate, were compared in three different permeability zones within the anoxic leachate plume at the site. These organic acids were used as microbial process probes since they degrade at different rates depending on the dominant microbial processes. The results show that there are differences in biodegradation in areas of different permeability. These may be related to differences in microbial community structure, sediment chemistry, and water flow regime.

The conceptual model of biogeochemical zones developed for the Norman Landfill study (**Figure 7**) provides a framework for understanding the transport of organic contaminants and provides insight into the natural attenuation of leachate compounds in the aquifer. This type of approach to assessing the active microbial processes and the availability of electron acceptors can be applied at other sites contaminated with leachate. Once the biogeochemical framework of a system is established, detailed experiments on the rates of processes and fate and transport of compounds of concern can be undertaken. In evaluating the effectiveness of natural attenuation, plume-scale chemical and isotopic patterns can elucidate long-term interactions between leachate and aquifer water and sediments, whereas monthly monitoring data allow the identification of transient processes along plume boundaries.

11.16.7 Grindsted Landfill Site (DK)

The Grindsted Landfill site in Denmark has been subjected to a number of investigations since 1992. The site has been investigated using a multidisciplinary approach by a large group of researchers with different background (environmental engineering, environmental chemistry, ecotoxicology, geology, and microbiology) from the Technical University of Denmark. The work has for certain topics been accomplished in cooperation with researchers from other universities and research institutions all over the world.

11.16.7.1 Source, Geology, and Hydrogeology

The site is located in the western part of Denmark on top of the original land surface (**Figure 10**). Disposal of waste took place between 1930 and 1977, and approximately 300 000 tonnes of waste have been deposited, mainly between 1960 and 1970 (Kjeldsen et al., 1998a). The waste consists of municipal solid waste (20%); bulky waste, garden waste, and street sweepings (5%); industrial waste (20%); sewage treatment sludge (30%); and demolition waste (25%). The spatial variability of the leachate quality was investigated by sampling (31 wells) below the landfill in the uppermost groundwater (a small unsaturated zone exists beneath the landfill). The results revealed a significant spatial variability in the leachate composition, and based on this, the landfill could be divided into four main areas (**Figure 11**). The average concentrations in the strong leachate were typically 20–40 times higher than in the weak leachate with respect to concentrations of ammonium, chloride, and NVOC. The strong leachate was located in the northern part of the landfill and originated from dumping of industrial waste. The large heterogeneities in the leachate quality may generate multiple plumes with different properties and call for differentiated remedial actions mainly directed toward the industrial hot spot area.

Geology: The Grindsted Landfill is located on a glacial outwash plain. The upper 10–12 m of the unconfined aquifer consists of an upper Quaternary sandy layer and a lower Tertiary sandy layer, locally separated by discontinuous silt and clay layers (Heron et al., 1998). Investigations of the hydraulic conductivity and hydraulic gradients resulted in pore flow velocities of approximately 50 and 10 m $year^{-1}$ for the Quaternary and Tertiary sandy layers, respectively. A clay layer of approximately 1 m thickness located 12 m below ground surface extends over a large area of the landfill. Below this layer is a more regional micaceous sandy layer of approximately 65 m thickness. This layer is vertically limited by another low-permeable clay layer approximately 80 m below ground surface.

The overall groundwater flow direction is northwesterly, but the isopotential contours are semicircular, indicating a diverging flow. Locally, inside and close to the landfill, the flow field shows significant seasonal variation (**Figure 12**). The reasons for this mounding have not been fully understood, but Kjeldsen et al. (1998b) suggest three possibilities: (1) higher infiltration in this part of the landfill; (2) lower hydraulic conductivity in the aquifer underlying this part of the landfill possibly due to differences in geology, bacterial growth, precipitates, or gaseous bubbles of methane and carbon

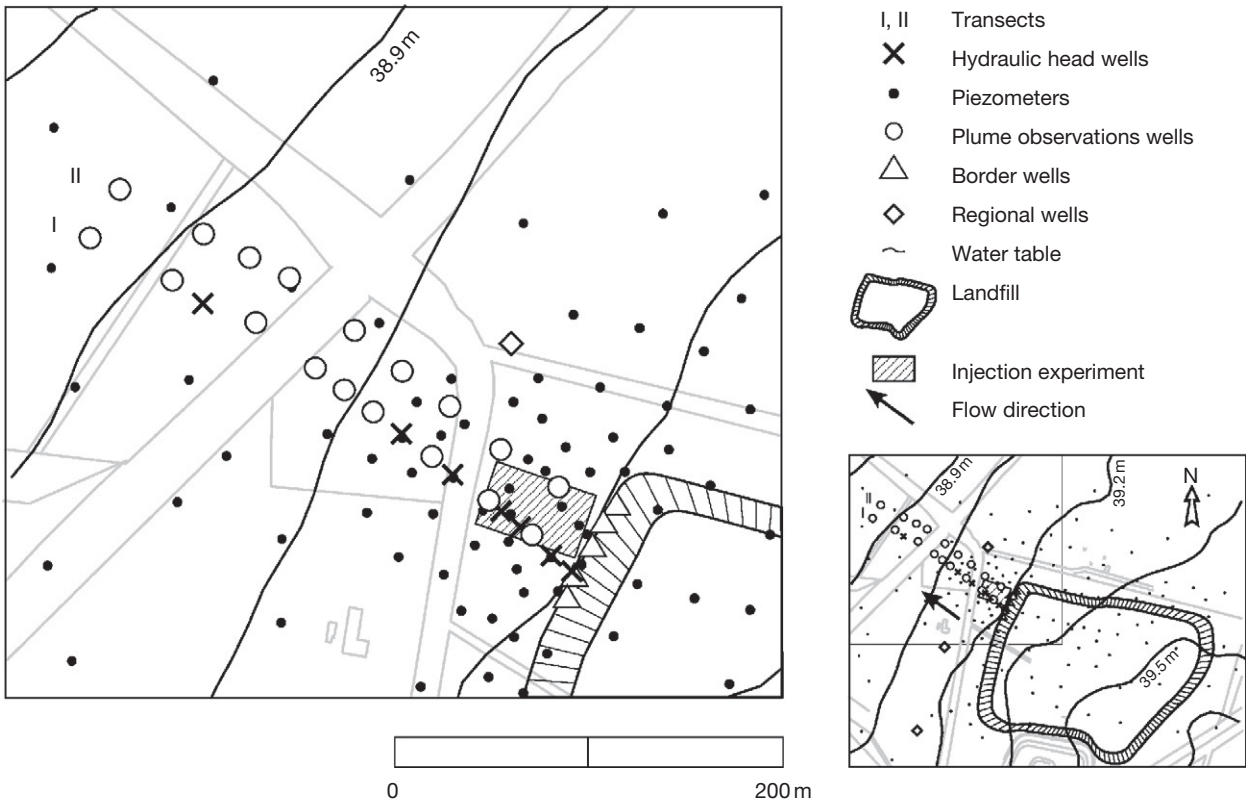

Figure 10 Location of the Grindsted Landfill site (DK), overview of wells and investigated transects.

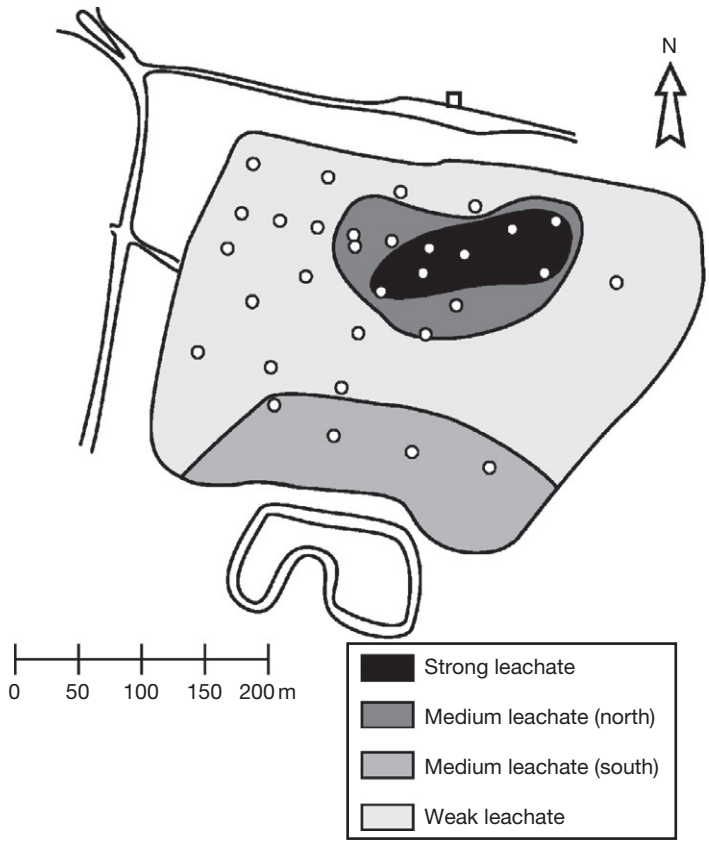

Figure 11 Division of the landfill into four areas with different leachate strength. The division was primarily based on chloride, ammonium, and NVOC (Kjeldsen et al., 1998a).

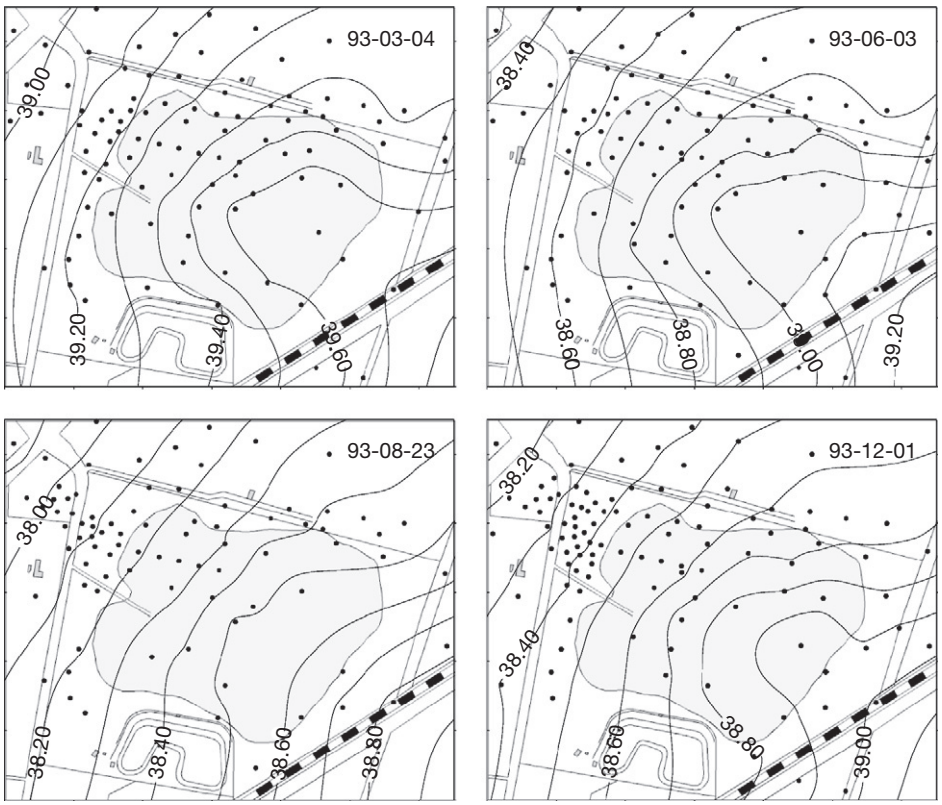

Figure 12 Mounding of the leachate–groundwater table below Grindsted Landfill (DK) shown as isopotential contours for the landfill and surrounding area at four different seasons during 1993. Modified from Kjeldsen P, Bjerg PL, Rügge K, Christensen TH, and Pedersen JK (1998) Characterization of an old municipal landfill (Grindsted, Denmark) as a groundwater pollution source: Landfill hydrology and leachate migration. *Waste Management and Research* 16: 14–22. With permission from Sage Publications.

dioxide; or (3) higher infiltration in the borders of the mounding area. The effects of this local mounding are enhanced lateral spreading of the plume and also downward-directed hydraulic gradients in the groundwater below the landfill. The latter can cause an unexpected vertical spreading pattern, while the enhanced spreading affects the dilution of the plume. Degradation could be increased by enhanced mixing of electron acceptors into the anaerobic parts of the plume. The seasonal variations in the flow field are also important for the design of the monitoring network and interpretation of time series monitoring data.

In order to illustrate the spreading of leachate into the upper aquifer, the groundwater quality along the downgradient border of the landfill was mapped. Figure 13 shows a three-dimensional sketch of the distribution of chloride, ammonium, and NVOC along the northern and western borders of the landfill and the leachate concentrations beneath the landfill.

11.16.7.2 Landfill Leachate Plume

The investigations of the landfill leachate plume at the Grindsted Landfill have been restricted to the upper aquifer (10–12 m) in two transects starting at the western border of the landfill. Transect I (Figure 10) has been characterized in great detail with respect to

- geology and hydrogeology (Bjerg et al., 1995; Heron et al., 1998; Petersen, 2000),
- inorganic and /or redox-sensitive compounds (Bjerg et al., 1995; Jensen et al., 1998),
- hydrogen levels and in situ energetics (Bjerg et al., 1997; Jakobsen et al., 1998),
- aquifer solid composition (Heron et al., 1998),
- microbiology and microbial redox processes (Ludvigsen et al., 1997, 1998, 1999),
- distribution of XOCs (Holm et al., 1995; Rügge et al., 1995), and
- toxicity related to XOCs (Baun et al., 1999, 2000).

Redox environments: At the Grindsted Landfill site, the redox environments were addressed in terms of dissolved redox-sensitive species (Bjerg et al., 1995), aquifer solid compositions (Heron et al., 1998), activity of microorganisms performing each electron-accepting reaction (Ludvigsen et al., 1997), and the concentration of dissolved hydrogen in the groundwater (Jakobsen et al., 1998).

The distribution of dissolved redox-sensitive species (example given in Figure 14) showed that the redox zones were somewhat different in the two parallel vertical transects, separated by only 30 m (Figure 15). The overall sequence was consistent with the one depicted in Figure 3, although the water chemistry of the Grindsted Landfill (DK) leachate plume suggested that several of the redox zones overlapped.

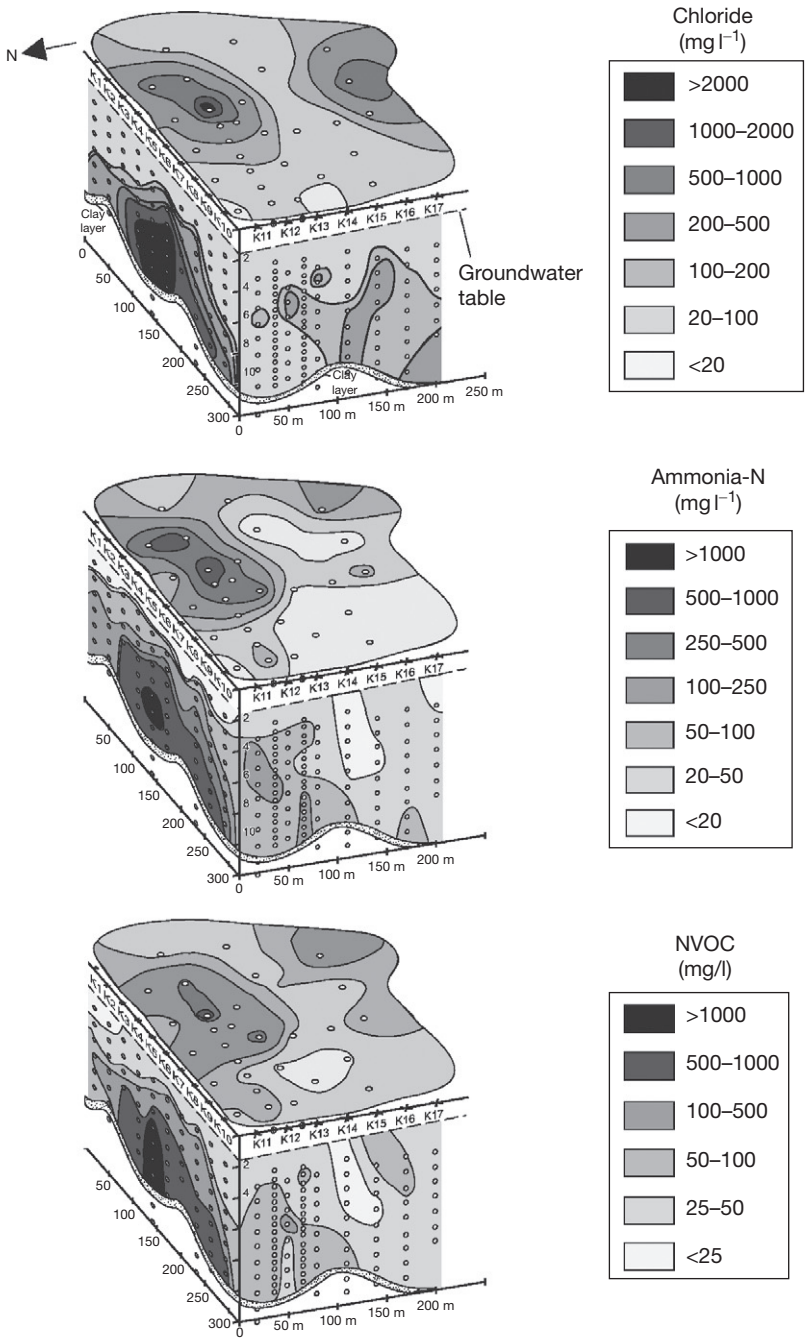

Figure 13 Three-dimensional sketch of leaching pattern for chloride, ammonium, and NVOC from Grindsted Landfill (DK). Reproduced from Kjeldsen P, Bjerg PL, Rügge K, Christensen TH, and Pedersen JK (1998) Characterization of an old municipal landfill (Grindsted, Denmark) as a groundwater pollution source: Landfill hydrology and leachate migration. *Waste Management and Research* 16: 14–22, with permission from Sage Publications.

Certainly, methanogenic and sulfate-reducing zones overlapped (Figure 15). Iron-, manganese-, and nitrate-reducing zones overlapped in some cases but were separate in others. Also, the sizes of the zones varied considerably between neighboring transects (Bjerg et al., 1995), which is interesting in light of the conclusions drawn earlier for sites with much less data. In this, plume methane and ammonium migrate further than dissolved organic matter (Figure 14) and, thus, are the dominant reductants at distances greater than 100–150 m from the landfill.

Detailed geologic and geochemical description of the aquifer sediment resulted in an improved understanding of the distribution of iron species in the plume (Heron et al., 1998). The majority of the aquifer consisted of mineral-poor fine sands, low in organic matter and iron oxides. It was concluded that iron and manganese reduction was less important than

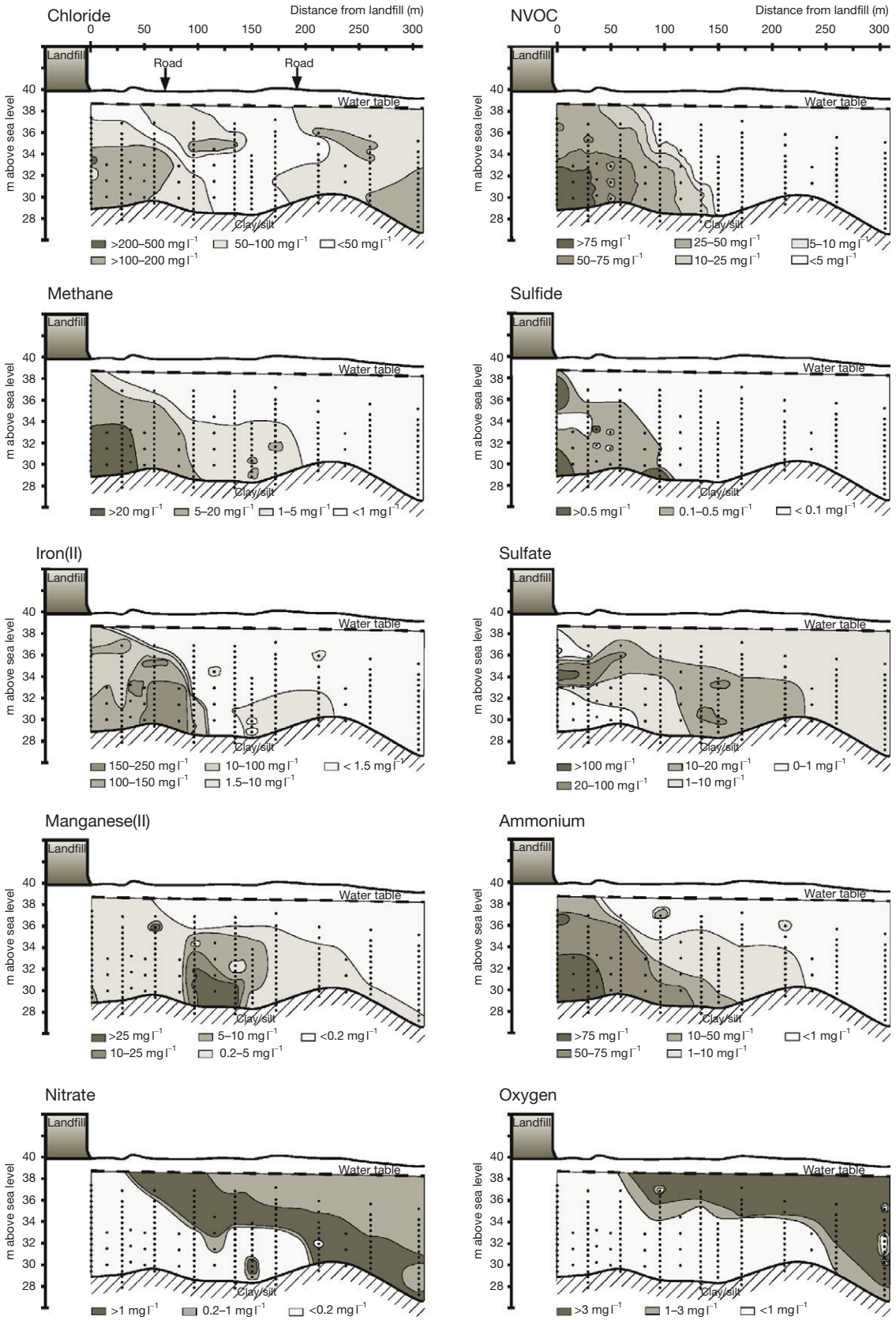

Figure 14 Distribution of Cl^- and dissolved redox-sensitive compounds in Transect I downgradient of Grindsted Landfill (DK). Reproduced from Bjerg PL, Rügge K, Pedersen JK, and Christensen TH (1995) Distribution of redox sensitive groundwater quality parameters downgradient of a landfill (Grindsted, Denmark). *Environmental Science and Technology* 29: 1387–1394, with permission.

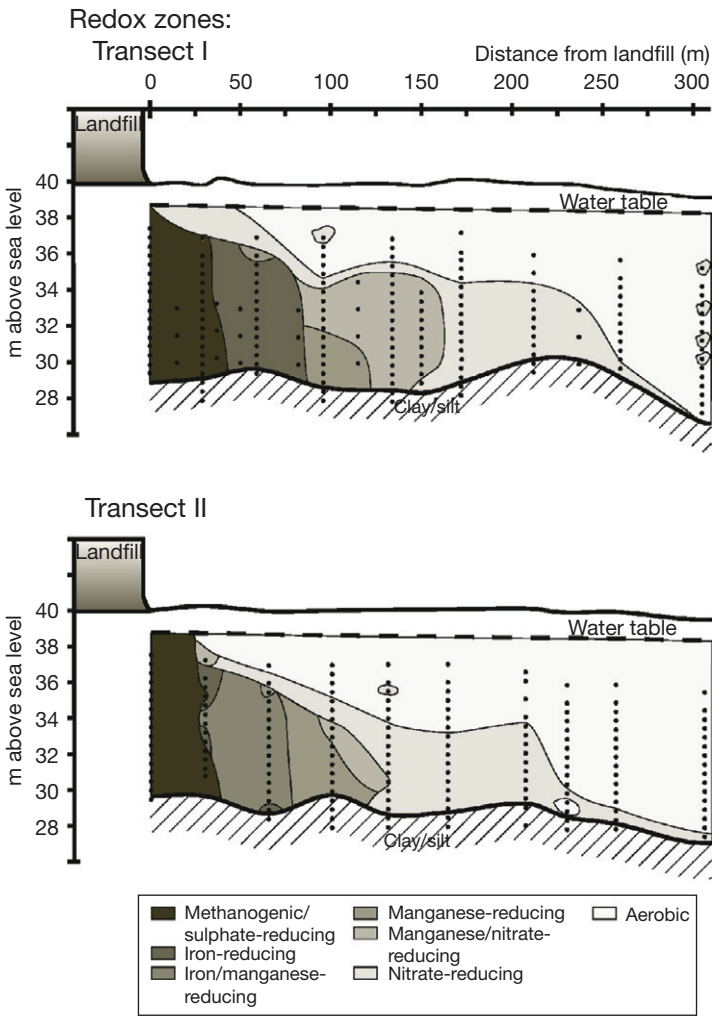

Figure 15 Proposed redox zone distribution in two parallel transects downgradient of Grindsted Landfill (DK) based on the observed groundwater chemistry. Reproduced from Bjerg PL, Rügge K, Pedersen JK, and Christensen TH (1995) Distribution of redox sensitive groundwater quality parameters downgradient of a landfill (Grindsted, Denmark). *Environmental Science and Technology* 29: 1387–1394, with permission.

that at the Vejen Landfill (DK) located in the same geographical area, even though very high concentrations of dissolved Fe^{2+} and Mn^{2+} were observed in the Grindsted Landfill (DK) leachate plume. Both a lower initial iron oxide content and a different iron mineralogy (presumably solid grains of crystal iron oxides) indicated lower iron reactivity.

Bioassays (microbially active and unamended incubations of aquifer solids and groundwater, Ludvigsen et al., 1998) monitored all the redox processes that occurred and allowed for estimating rates of the individual redox processes, as shown in Figure 16. The rates were fairly low for many of the redox processes. The bioassays also showed that in several samples, more than one redox process was significant. However, in most cases, one electron acceptor dominated in terms of equivalent rates of organic matter oxidation, and altogether, the rates balance fairly well the degradation of dissolved organic carbon observed in the plume. However, the rates determined for denitrification exceeded the dissolved carbon available in that part of the plume suggesting that other electron donors also played a role, maybe ammonium. It was furthermore demonstrated that low-permeability layers can lead to unexpected redox activities. This was exemplified by the high sulfate reduction activity 170 m from the landfill caused by localized sulfate and organic matter-rich deposits and not by the leaching from the landfill.

Measurements of dissolved hydrogen have been used to characterize redox levels according to distinct criteria based on competitive exclusion of terminal electron acceptors for hydrogen oxidation (Chapelle et al., 1995; Lovley and Goodwin, 1988). In the Grindsted Landfill plume, the variations in hydrogen concentrations (52 sampling points) were limited, and the values were low (0.004–0.88 nmol l^{-1}) indicating, according to the previous criteria, iron-reducing conditions in most of the anaerobic part of the plume (Jakobsen et al., 1998). This was surprising since the microbial assays and the geochemistry have indicated other active redox processes in the plume (see previous text). This suggested a need for refining the use of hydrogen in identifying terminal electron acceptors in complex plumes. The hydrogen measurements were used along with the measurements of groundwater chemistry in thermodynamic calculations

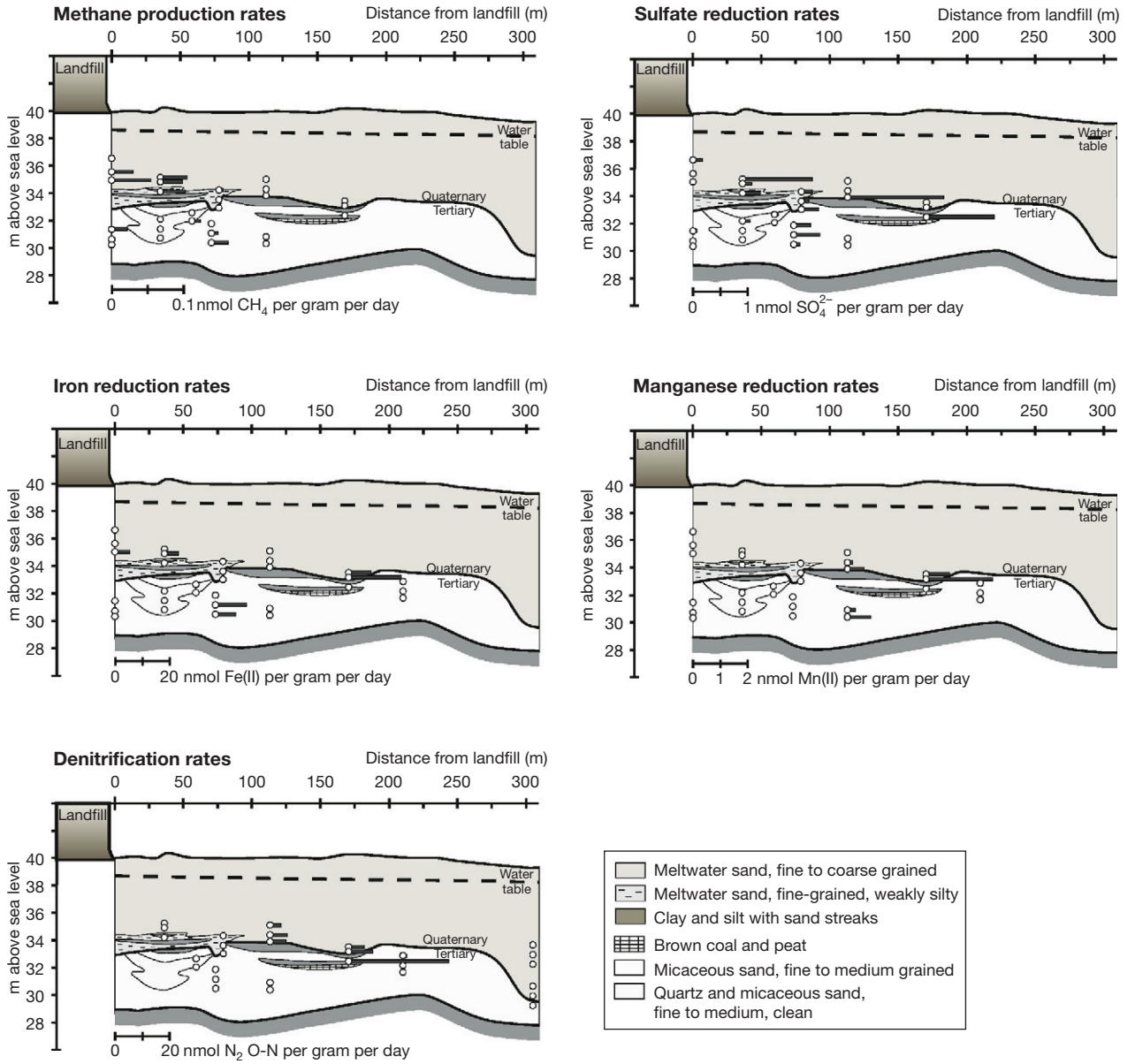

Figure 16 Rates observed by unamended bioassays for individual redox processes at several locations downgradient of Grindsted Landfill (DK). Reproduced from Ludvigsen L, Albrechtsen H-J, Heron G, Bjerg PL, and Christensen TH (1998) Anaerobic microbial redox processes in a landfill leachate contaminated aquifer (Grindsted, Denmark). *Journal of Contaminant Hydrology* 33: 273–291, with permission.

of free energies of the redox reactions at the actual temperature of the plume (11 °C). These calculations showed that both sulfate reduction and iron reduction could occur in the plume, since ΔG_r values for each reaction were below a proposed threshold value of −7 kJ mol^{-1} of H_2 in several places. Methanogenesis (by CO_2 reduction) showed in all samples higher ΔG_r values, suggesting that methanogenesis only occurred in stagnant porewater, where more reducing conditions may prevail. The small differences in calculated ΔG_r values actually suggested that sulfate reduction and iron reduction could take place simultaneously in the same sample.

Overall, this refined use of hydrogen concentrations supported the results of the bioassays and the complex system of redox zones observed from the distribution of dissolved redox-sensitive species. The Grindsted Landfill (DK) plume is host not only to all of the proposed redox reactions but also to secondary oxidation–reduction reactions involving ammonium, methane, manganese oxides, ferrous iron, and sulfides.

Fate of XOCs: The distribution of xenobiotic compounds was mapped in Transect I (Figure 17). More than 15 different organic compounds were identified close to the landfill, with the BTEX compounds dominating. Concentrations of BTEX in the range of 0–222 μg L^{-1} were observed close to the landfill, with single observations of *o*-xylene concentrations up to 1550 μg L^{-1} (Rügge et al., 1995). No chlorinated aliphatic compounds were present in this part of the pollution plume. Most of the XOCs were no longer detectable approximately 60 m from the edge of the landfill site. Since dilution and sorption could not account

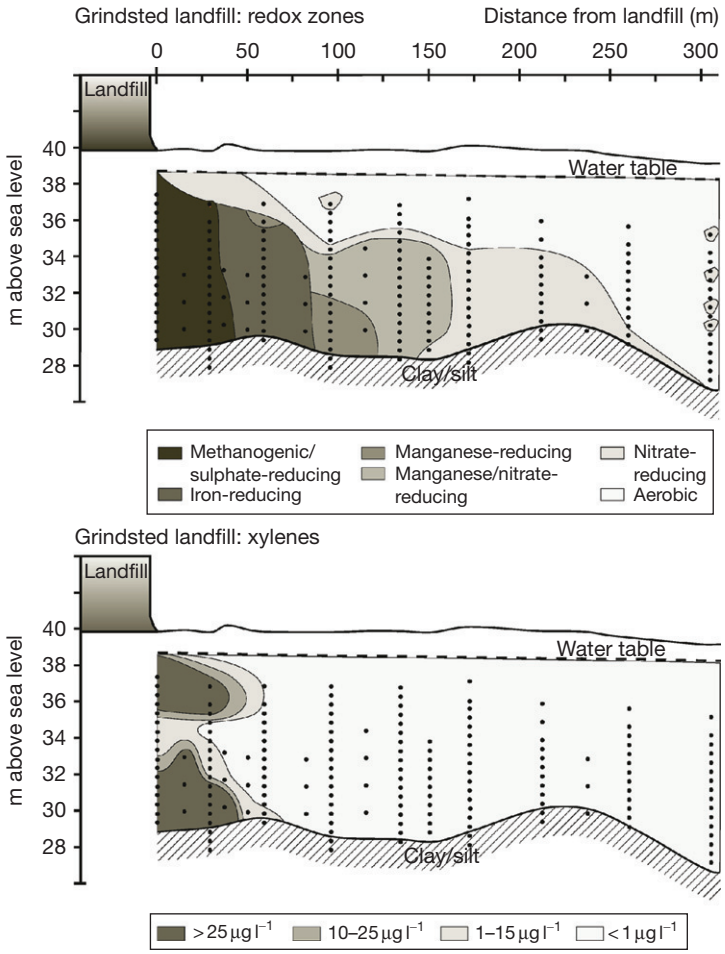

Figure 17 Proposed redox zonation and distribution of xylenes in Transect I at the downgradient of Grindsted Landfill (DK). Modified from Bjerg PL, Rügge K, Pedersen JK, and Christensen TH (1995) Distribution of redox sensitive groundwater quality parameters downgradient of a landfill (Grindsted, Denmark). *Environmental Science and Technology* 29: 1387–1394; Rügge K, Bjerg PL, and Christensen TH (1995) Distribution of organic compounds from municipal solid waste in the groundwater downgradient of a landfill (Grindsted, Denmark). *Environmental Science and Technology* 29: 1395–1400, with permission.

for the disappearance of the xenobiotic compounds, it was proposed that the majority of the xenobiotic compounds in the leachate were transformed under methanogenic/sulfate-reducing or iron-reducing conditions in the aquifer. It should be emphasized that the apparent attenuation close to the landfill was not based on a direct proof but on a comparison of the actual distribution to the leaching period, dilution, and sorption in the plume. This was convincing for a number of compounds and was also supported by reactive solute transport modeling (Lønborg et al., 2006; Petersen, 2000). However, benzene shows a distribution that can indicate recalcitrance in the most reduced parts of the plume but fast disappearance in more oxidized environments (see discussion on benzene in Petersen, 2000). Final conclusions based on field observations may therefore be a difficult task and only feasible where substantial data from different disciplines are available.

The degradation of xenobiotic compounds can also be investigated by microcosm/column experiments and field injection experiments. At the Grindsted Landfill site, the degradation of a mixture of xenobiotic compounds (seven aromatic hydrocarbons, four chlorinated aliphatic hydrocarbons, five nitroaromatic hydrocarbons, and two pesticides) was studied using in situ microcosms (ISM) and laboratory microcosm (LM) (Bjerg et al., 1999; Rügge et al., 1998, 1999a,b). The data from degradation experiments were compared to the field observation data of the aromatic hydrocarbons, and the discussion of these compounds will be limited.

An anaerobic stock solution of the XOCs was injected along with bromide as tracer into five injection wells, installed 15 m downgradient of the landfill. The amount of water injected in the natural gradient experiment was approximately 5% of the groundwater flux passing the injection wells, yielding approximate concentrations of 75–330 $\mu g\,l^{-1}$ of the XOCs and of bromide of 100 $mg\,l^{-1}$ immediately downgradient of the injection wells.

The migration of the compounds was monitored in a dense sampling network consisting of a total of 140 multilevel samplers (1030 sampling points). Over a period of 924 days, samples were collected from approximately 70 discrete sampling points in the central part of the cloud for the determination of breakthrough curves (BTCs). From the BTCs, degradation and sorption could be determined. After the end

of the injection, seven cloud snapshots were established covering approximately 400–700 sampling points each time. From the snapshot, moment analysis provided an evaluation of the mass loss of solute in the system and the spatial distribution of the cloud in the aquifer. The redox conditions in the studied area of the plume were determined by the analysis of water soluble redox-sensitive compounds sampled every 6–8 weeks during the experimental period and by groundwater and sediment characterizations combined with microbial assays conducted on sediment and groundwater sampled 800 days after the start of the injection (Albrechtsen et al., 1999).

In the injection experiment, degradation of toluene was observed as complete mass removal within the most reduced part of the aquifer where iron reduction, sulfate reduction, and methanogenesis occurred. Partial degradation was observed for *o*-xylene. The degradation of *o*-xylene was not initiated before the cloud had reached the part of the aquifer where iron reduction was predominant. Examples of the cloud movement after 649 days are given in **Figure 18**. Benzene was not degraded within the experimental period of 924 days. Due to highly varying background concentrations, it was not possible to determine whether any degradation of the compounds ethylbenzene and *m*-/*p*-xylene occurred.

In parallel with the anaerobic field injection experiment, in situ microcosms were installed at five locations downgradient of the landfill (see Nielsen et al. (1996) for description of this technique). Also, laboratory batch experiments (LBs) were conducted with sediment and groundwater from the corresponding locations. The experimental periods of the ISMs and the LBs were up to 220 and 537 days, respectively. Both systems involved the same mixture of the 18 compounds (Bjerg et al., 1999). For the aromatic compounds, only toluene was degraded in the ISM, while also *o*- and *m*-/*p*-xylene were degraded in the LB. Benzene, ethylbenzene, and naphthalene were not degraded in either the ISM or the LB.

In general, a good accordance was observed between the results obtained in the injection experiment, the ISMs, and the LBs; however, a few differences can be noticed, as shown in **Table 5**. These differences were mainly due to the different experimental periods, namely, 924 days in the injection experiment and up to 210 and 537 days in the ISMs and LBs, respectively. However, also differences between static and flow systems influenced the results. This comparison indicated that the ISM is a good method for studying degradation in the field for compounds with lag periods shorter than 50–100 days. LBs are also a useful and cost-saving approach for studying degradation. The batch setup allows for very long experimental periods. Therefore, the LBs are useful for the mixtures of compounds with both shorter and longer lag periods and for compounds with varying degradation rates. The results on degradation, however, have been obtained for rather simple compounds, and it is not known how well the batch experiments mimic the field situation for more complex compounds.

The experiments carried out in the anaerobic part of the leachate plume indicate that natural attenuation of toluene and *o*-xylene takes place close to landfill. However, the results for ethylbenzene are not in accordance with the plume observations. In the case of benzene, the degradation may take place at larger distance from the landfill in more oxidized environments (see Petersen, 2000).

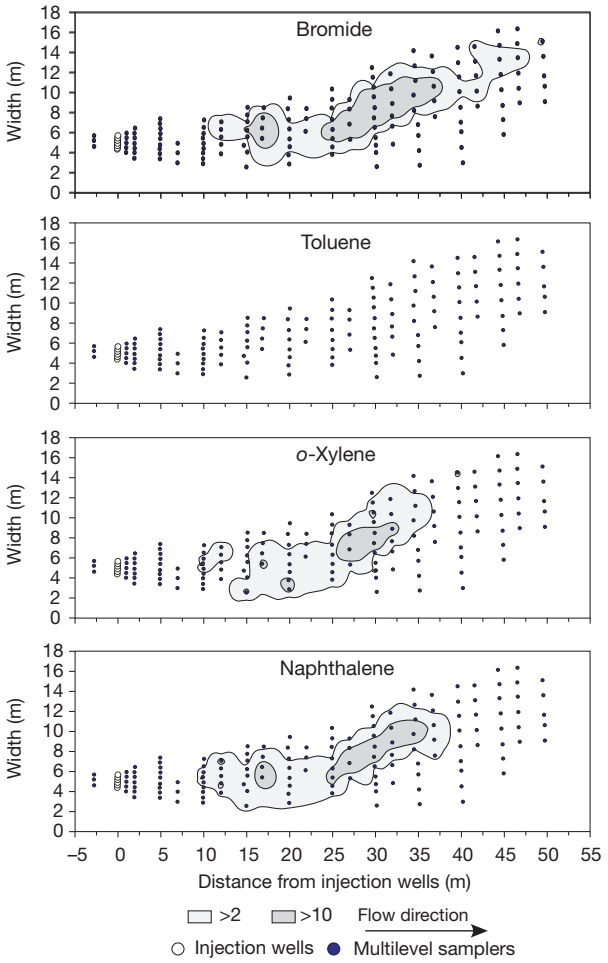

Figure 18 Observed clouds of bromide, toluene, *o*-xylene, naphthalene after 649 days. Bromide in g m^{-2} and xenobiotics in mg m^{-2}. Reproduced from Rügge K, Bjerg PL, Pedersen JK, Mosbæk H, and Christensen TH (1999) An anaerobic field injection experiment in a landfill leachate plume (Grindsted, Denmark), 1. Site description, experimental set up, tracer movement and fate of aromatic and chlorinated aliphatic compounds. *Water Resources Research* 35: 1231–1246, with permission from John Wiley & Sons.

In summary, a description of natural attenuation processes for XOXs in a landfill leachate is not an easy task and may involve different approaches, including field observations, experiments in laboratory and field, and also reactive solute transport modeling. The latter is as an important tool for the integration of data on geology and hydrogeology, redox conditions, distribution of xenobiotic compounds, and degradability/degradation rates.

11.16.8 Monitored Natural Attenuation

Natural attenuation refers to processes that naturally transform contaminants to less harmful forms or immobilize contaminants so that they are less of a threat to the environment; see "Natural Attenuation for Groundwater Remediation" by the

Table 5 Potential for degradation of the aromatic compounds in anaerobic leachate-affected groundwater at Grindsted Landfill (DK)

Grindsted Landfill	*Benzene*	*Toluene*	*Ethylbenzene*	m-/p-*Xylene*	o-*Xylene*	*Naphthalene*
(1) Field injection 15–45 m	−	+	?	?	−	−
(1) Field injection 45–65 m	−	+	?	?	+	−
(2) ISM and LB						
LB (I) 15 m	−	+	−	−	−	−
LB (II) 15 m	−	+	−	−	−	−
LB (II) 25 m	−	+	−	−	−	−
ISM 25 m	−	−	−	−	−	−
LB (II) 35 m	−	−	−	−	−	−
ISM 35 m	−	−	−	−	−	−
LB (II) 45 m	−	+	−	−	−	−
ISM 45 m	−	−	−	−	−	−
LB (II) 55 m	−	+	−	+	−	−
ISM 55 m	−	+	−	+	−	−
LB (I) 60 m	−	+	−	+	+	−

(1) Rügge et al. (1999a) and (2) Bjerg et al. (1999). +, degradation observed; −, no degradation observed; ?, not possible to determine due to highly varying background conditions.

National Research Council (National Research Council, 2000). This includes the following:

- Dispersion/dilution
- Sorption
- Volatilization
- Degradation (abiotic, biotic)

Degradation is the most interesting process because the contaminants can be transformed into less harmful products (carbon dioxide and water). Engineered application of natural attenuation processes as a remedy is termed monitored natural attenuation (MNA, see US EPA). This involves a monitoring component in addition to an evaluation of the natural attenuation processes.

The results from the landfill sites reviewed here indicate a significant potential for natural attenuation of XOCs at landfill sites. There are to date, however, only a few examples, compared to the number of landfill sites around the world, and therefore, additional well-documented field examples are needed. Experience from more landfill sites will also help in developing procedures for the demonstration of natural attenuation, which is not a straightforward procedure. Currently, the experience presented in this chapter and the evaluation of natural attenuation as a remedy at landfill sites by Christensen et al. (2000a) and reviewed by Bjerg et al. (2011) suggest that five points will be critical:

- Local hydrogeological conditions in the landfill area may affect the spreading of the contaminants.
- The size of the landfill and the heterogeneity of the source may create a variable leaching pattern and may be also multiple plumes.
- The complexity of leachate plumes with respect to compounds (inorganic and XOCs) and biogeochemical processes may be an obstacle.
- The time frame for leaching from a landfill site will be very long and call for long-term evaluation of the attenuation capacity.
- Demonstration of natural attenuation in terms of contaminant mass reduction at the field scale is difficult.

The importance of each issue will depend on the actual landfill. It should also be emphasized that even though these problems may be difficult to solve, very few alternatives exist for remediation at landfill sites (see **Section 11.16.9**).

11.16.9 Future Challenges

The number of detailed landfill studies has so far been quite limited. A few sites have been characterized to a high degree (including Banisveld Landfill, Borden Landfill, Grindsted Landfill, Norman Landfill, Vejen Landfill, and Sjoelund Landfill) by the use of multidisciplinary approaches. These studies consistently show the importance of integrated studies in order to understand the biogeochemical processes in landfill leachate plumes. The results presented in this chapter have revealed a number of topics, where future research using similar approaches could be beneficial. Suggestions for future challenges and research topics are listed as follows:

- *Geologic setting.* Most of the work on landfill leachate plumes originates from studies in sandy aquifers. Many landfills are found in such geologic settings, but investigations of landfill leachate plumes in geologic settings with clayey till deposits and fractured consolidated sediments are lacking. In addition, landfills located in former wetlands or leaching into surface water are only studied in few cases.
- *Source and spreading of landfill leachate.* Density flow is most likely at landfill sites, but the current understanding of instability effects and the ability to predict the impact of density flow under field conditions are poor. Also, the reasons for the often observed mounding of the groundwater table beneath landfills are not fully understood and need more attention.
- *Biogeochemical processes*. A good conceptual understanding of the biogeochemical processes in landfill leachate plumes exists, and the overall understanding of redox processes is good. The challenge is to quantify rates and capacity so the relative importance of core processes (e.g., microbial iron RDC) and fringe processes (mixing of electron acceptors)

can be evaluated in order to predict long-term behavior of the plume. Application of stable isotopes and molecular techniques may be useful in such studies.

- *Application of simple model/mass balance approaches or advanced multidimensional reactive solute transport models* are needed in order to integrate flow, transport, and reactive processes. Unfortunately, models are often applied after field investigations are completed instead of as an integrated part of the field investigations. Used as integrative tools, models can be viewed as a quantitative representation of the conceptual model for the landfill leachate plume.
- *Fate of XOC compounds*. Significant degradation of XOC has been demonstrated at most landfill sites, but discrepancies between field observations and experimental work have been observed. Lack of knowledge in terms of the expected fate is mainly related to *new* compounds, such as pesticides, pharmaceuticals, and phthalates. However, the discrepancies also reveal that the methods used for the documentation of natural attenuation processes are poor in landfill leachate plumes. A few studies have applied probe compounds as tracers, degradation products, stable isotopes, and enantiomeric ratios, but these methods all have their limitations, and improvements are needed before they can be applied in practice for the documentation of natural attenuation. Contaminant mass discharges (mass flux) have been suggested for quantification of mass removal for XOCs; however, current applications at landfill sites are few.
- *Risk assessment*. Landfills are difficult to handle as a homogenous contaminant sources, because of the complex composition and large size. Standard risk assessment methodologies often fail or give misleading results when applied at landfill sites. Thus, development of better risk assessment methods in particular at screening level is needed. In addition potential chemical or ecological impact from landfills located in former wetlands or near surface water bodies may deserve attention in future studies.
- *Remediation of landfill leachate plumes* has been performed only in very few cases. The most promising technique is monitored natural attenuation, but guidelines and practical experiences are necessary to ensure a proper implementation. A matter of discussion is the need for monitoring and length of the monitoring period taking the lifetime of a landfill into account.

References

Acton DW and Barker JF (1992) In situ biodegradation potential of aromatic hydrocarbons in anaerobic groundwater. *Journal of Contaminant Hydrology* 9: 325–352.

Adams EE and Gelhar LW (1992) Field study in a heterogeneous aquifer, 2. Spatial moments analysis. *Water Resources Research* 28: 3293–3307.

Albrechtsen H-J, Bjerg PL, Ludvigsen L, Rügge K, and Christensen TH (1999) An anaerobic field injection experiment in a landfill leachate plume (Grindsted, Denmark), 2. Deduction of anaerobic (methanogenic, sulfate- and Fe(III)-reducing) redox conditions. *Water Resources Research* 35: 1247–1256.

Albrechtsen H-J and Christensen TH (1994) Evidence for microbial iron reduction in a landfill leachate-polluted aquifer (Vejen, Denmark). *Applied and Environmental Microbiology* 60: 3920–3925.

Albrechtsen H-J, Mills M, Aamand J, and Bjerg PL (2001) Degradation of herbicides in shallow Danish aquifers – An integrated laboratory and field study. *Pest Management Science* 57: 341–350.

Allen-King RM, Gillham RW, and Barker JF (1996) Fate of dissolved toluene during steady infiltration through unsaturated soil: I. Method emphasizing chloroform as a volatile, sorptive, and recalcitrant tracer. *Journal of Environmental Quality* 25: 279–286.

Arneth J-D, Milde G, Kerndorff H, and Schleyer R (1989) Waste deposit influences on groundwater quality as a tool for waste type and site selection for final storage quality. In: Baccini P (ed.) *The Landfill. Lecture Notes in Earth Sciences*, vol. 20, pp. 399–424. Berlin: Springer.

Assmuth TW and Strandberg T (1993) Ground-water contamination at Finnish landfills. *Water, Air, and Soil Pollution* 69: 179–199.

Báez-Cazull S, McGuire JT, Cozzarelli IM, Raymond A, and Welsh L (2007) Centimeter-scale characterization of biogeochemical gradients at a wetland-aquifer interface using capillary electrophoresis. *Applied Geochemistry* 22(12): 2664–2683. http://dx.doi.org/10.1016/j.apgeochem.2007.06.003.

Barker JF, Tessmann JS, Plotz PE, and Reinhard M (1986) The organic geochemistry of a sanitary landfill leachate plume. *Journal of Contaminant Hydrology* 1: 171–189.

Barnes KK, Christenson SC, Kolpin DW, et al. (2004) Pharmaceuticals and other organic waste water contaminants within a leachate plume downgradient of a municipal landfill. *Ground Water Monitoring and Remediation* 24(2): 119–126.

Baun A, Ask L, Ledin A, Christensen TH, and Bjerg PL (2003) Natural attenuation of xenobiotic organic compounds in a landfill leachate plume (Vejen, Denmark). *Journal of Contaminant Hydrology* 65: 269–291.

Baun A, Jensen SD, Bjerg PL, Christensen TH, and Nyholm N (2000) Toxicity of organic chemical pollution in groundwater downgradient of a landfill (Grindsted, Denmark). *Environmental Science and Technology* 34: 1647–1652.

Baun A, Kløft L, Bjerg PL, and Nyholm N (1999) Toxicity testing of organic chemicals in groundwater polluted with landfill leachate. *Environmental Toxicology and Chemistry* 18: 2046–2056.

Baun A, Ledin A, Reitzel LA, Bjerg PL, and Christensen TH (2004) Xenobiotic organic compounds in leachates from ten Danish MSW landfills – Chemical analysis and toxicity tests. *Water Research* 38: 3845–3858.

Beeman RE and Suflita JM (1987) Microbial ecology of a shallow unconfined ground water aquifer polluted by municipal landfill leachate. *Microbial Ecology* 14: 39–54.

Beeman RE and Suflita JM (1990) Environmental factors influencing methanogenesis in a shallow anoxic aquifer: A field and a laboratory study. *Journal of Industrial Microbiology* 5: 45–58.

Belevi H and Baccini P (1992) Long-term leachate emissions from municipal solid waste landfills. In: Christensen TH, Cossu R, and Stegmann R (eds.) *Landfilling of Waste: Leachate*, pp. 431–440. London: Elsevier Applied Science.

Beller H (2000) Metabolic indicators for detecting in situ anaerobic alkylbenzene degradation. *Biodegradation* 11: 125–139.

Bisdom EBA, Boekestein A, Curmi P, et al. (1983) Submicroscopy and chemistry of heavy metal contaminated precipitates from column experiments simulating conditions in a soil beneath a landfill. *Geoderma* 30: 1–20.

Bjerg PL, Jakobsen R, Bay H, Rasmussen M, Albrechtsen H-J, and Christensen TH (1997) Effects of sampling well construction on H_2 measurements made for characterization of redox conditions in a contaminated aquifer. *Environmental Science and Technology* 31: 3029–3031.

Bjerg PL, Rügge K, Cortsen J, Nielsen PH, and Christensen TH (1999) Degradation of aromatic and chlorinated aliphatic hydrocarbons in the anaerobic part of the Grindsted Landfill leachate plume: In situ microcosm and laboratory batch experiments. *Ground Water* 37: 113–121.

Bjerg PL, Rügge K, Pedersen JK, and Christensen TH (1995) Distribution of redox sensitive groundwater quality parameters downgradient of a landfill (Grindsted, Denmark). *Environmental Science and Technology* 29: 1387–1394.

Bjerg PL, Tuxen N, Reitzel LA, Albrechtsen H-J, and Kjeldsen P (2011) Natural attenuation processes in landfill leachate plumes at three Danish sites. *Ground Water* 49: 688–705.

Bradley PM (2000) Microbial degradation of chloroethenes in groundwater systems. *Hydrogeology Journal* 8: 104–111.

Bradley PM, Chapelle FH, and Löffler F (2008) Anoxic mineralization: Experimental reality or experimental artifact. *Ground Water Monitoring and Remediation* 28(1): 47–49.

Breit GN, Cozzarelli IM, Johnson RD, and Norvell JS (1996) Interaction of alluvial sediments and a leachate plume from a landfill near Norman, Oklahoma. *Geological Society of America Abstracts with Programs* 28(7): A258.

Breit GN, Tuttle MLW, Cozzarelli IM, Berry CJ, Christenson SC, and Jaeschke JB (2008) Results of the chemical and isotopic analyses of sediment and water from alluvium of the Canadian River near a closed municipal landfill, Norman, Oklahoma. U.S. Geological Survey Open-file Report 2008-1134.

Breit GN, Tuttle MLW, Cozzarelli IM, Christenson SC, Jaeschke JB, Fey DL, and Berry CJ (2005) Results of the chemical and isotopic analyses of sediment and water from

alluvium of the Canadian River near a closed municipal landfill, Norman, Oklahoma. U.S. Geological Survey Open-file Report 2005-1091.

Broholm MM, Rügge K, Tuxen N, Højbjerg AL, Mosbæk H, and Bjerg PL (2001) Fate of herbicides in a shallow aerobic aquifer: A continuous field injection experiment (Vejen, Denmark). *Water Resources Research* 37: 3163–3176.

Brun A, Engesgaard P, Christensen TH, and Rosbjerg D (2002) Modelling of transport and biogeochemical processes in pollution plumes: Vejen landfill, Denmark. *Journal of Hydrology* 256: 228–248.

Chapelle FH and Bradley PM (1998) Selecting remediation goals by assessing the natural attenuation capacity of groundwater systems. *Bioremediation Journal* 2: 227–238.

Chapelle FH, McMahon PB, Dubrovsky NM, Fujii RF, Oaksford ET, and Vroblesky DA (1995) Deducing the distribution of terminal electron-accepting processes in hydrologically diverse groundwater systems. *Water Resources Research* 31: 359–371.

Christensen TH, Bjerg PL, Banwart S, Jakobsen R, Heron G, and Albrechtsen H-J (2000a) Characterization of redox conditions in groundwater contaminant plumes. *Journal of Contaminant Hydrology* 45: 165–241.

Christensen TH, Bjerg PL, and Kjeldsen P (2000b) Natural attenuation: A feasible approach to remediation of groundwater pollution at landfills? *Ground Water Monitoring and Remediation* 20(1): 69–77.

Christensen JB, Jensen DL, and Christensen TH (1996) Effect of dissolved organic carbon on the mobility of cadmium, nickel and zinc in leachate polluted groundwater. *Water Research* 30: 3037–3049.

Christensen TH and Kjeldsen P (1989) Basic biochemical processes in landfills. In: Christensen TH, Cossu R, and Stegmann R (eds.) *Sanitary Landfilling: Process, Technology and Environmental Impact*, ch. 2.1, pp. 29–49. London: Academic Press.

Christensen TH, Kjeldsen P, Albrechtsen H-J, et al. (1994) Attenuation of landfill leachate pollutants in aquifers. *Critical Reviews in Environmental Science and Technology* 24: 119–202.

Christensen TH, Kjeldsen P, Bjerg PL, et al. (2001) Biogeochemistry of landfill leachate plumes. *Applied Geochemistry* 16: 659–718.

Cozzarelli IM, Böhlke JK, Masoner J, et al. (2011) Biogeochemical evolution of a landfill leachate plume, Norman, Oklahoma. *Ground Water* 49(5): 663–687.

Cozzarelli IM, Suflita JM, Ulrich GA, Harris SH, Scholl MA, Schlottmann JL, and Jaeschke JB (1999) Biogeochemical processes in a contaminant plume downgradient from a landfill, Norman, Oklahoma. U.S. Geological Survey Water Resources Investigations Report #99-4018C. Reston, VA.

Cozzarelli IM, Suflita JM, Ulrich GA, et al. (2000) Geochemical and microbiological methods for evaluating anaerobic processes in an aquifer contaminated by landfill leachate. *Environmental Science and Technology* 34: 4025–4033.

DeWalle FB and Chian SK (1981) Detection of trace organics in well near solid waste landfill. *Journal of the American Water Works Association* 73: 206–211.

Eganhouse RP, Cozzarelli IM, Scholl MA, and Matthews LL (2001) Natural attenuation of volatile organic compounds (VOCs) in the leachate plume of a municipal landfill: Using alkylbenzenes as a process probe. *Ground Water* 39: 192–202.

Eganhouse RP, Dorsey TF, Phinney CS, and Westcott AM (1996) Processes affecting the fate of monoaromatic hydrocarbons in an aquifer contaminated by crude oil. *Environmental Science and Technology* 30: 3304–3312.

Freeze RA and Cherry JA (1979) *Groundwater*. Englewood Cliffs, NJ: Prentice-Hall.

Gelhar LW, Welty C, and Rehfeldt KR (1992) A critical review of data on field-scale dispersion in aquifers. *Water Resources Research* 28: 1955–1974.

Gossett JM (2010) Sustained aerobic oxidation of vinyl chloride at low oxygen concentrations. *Environmental Science and Technology* 44: 1405–1411.

Grbic-Galic D (1990) Methanogenic transformation of aromatic hydrocarbons and phenols in groundwater aquifers. *Geomicrobiology Journal* 8: 167–200.

Grossman EL, Cifuentes LA, and Cozzarelli IM (2002) Anaerobic methane oxidation in a landfill-leachate plume. *Environmental Science and Technology* 36(11): 2436–2442.

Hackley KC, Liu CL, and Coleman DD (1996) Environmental isotope characteristics of landfill leachates and gases. *Ground Water* 34: 827–836.

Harris SH Jr., Istok JD, and Suflita JM (2006) Changes in organic matter biodegradability influencing sulfate reduction in an aquifer contaminated by landfill leachate. *Microbial Ecology* 51(4): 535–542.

Harris SH, Smith RL, and Suflita JM (2007) In situ hydrogen consumption kinetics as an indicator of subsurface microbial activity. *FEMS Microbiology Ecology* 60: 220–228.

Harris SH, Ulrich GA, and Suflita JM (1999) Dominant terminal electron accepting processes occurring at a landfill leachate-impacted site as indicated by field and laboratory measurements. U.S. Geological Survey Water Resources Investigations Report #99–4018C, Reston, VA.

Heider J, Spormann AM, Beller HR, and Widdel F (1999) Anaerobic bacterial metabolism of hydrocarbons. *FEMS Microbiology Reviews* 22: 459–473.

Heron G (1994) *Redox Buffering in Landfill Leachate Contaminated Aquifers*. PhD Thesis, Department of Environmental Science and Engineering, Technical University of Denmark, Lyngby.

Heron G, Bjerg PL, Gravesen P, Ludvigsen L, and Christensen TH (1998) Geology and sediment geochemistry of a landfill leachate contaminated aquifer (Grindsted, Denmark). *Journal of Contaminant Hydrology* 29: 301–317.

Heron G and Christensen TH (1995) Impact of sediment-bound iron on redox buffering in a landfill leachate polluted aquifer (Vejen, Denmark). *Environmental Science and Technology* 29: 187–192.

Heron G, Christensen TH, and Tjell JC (1994a) Oxidation capacity of aquifer sediments. *Environmental Science and Technology* 28: 153–158.

Heron G, Crouzet C, Bourg ACM, and Christensen TH (1994b) Speciation of Fe(II) and Fe(III) in contaminated aquifer sediments using chemical extraction techniques. *Environmental Science and Technology* 28: 1698–1705.

Holliger C, Wohkfahrt G, and Diekert G (1999) Reductive dechlorination in the energy metabolism of anaerobic bacteria. *FEMS Microbiology Reviews* 22: 383–398.

Holm JV, Rügge K, Bjerg PL, and Christensen TH (1995) Occurrence and distribution of pharmaceutical organic compounds in the groundwater downgradient of a landfill (Grindsted, Denmark). *Environmental Science and Technology* 29: 1415–1420.

Istok JD, Humphrey MD, Schroth MH, Hyman MR, and O'Reilly KT (1997) Single-well. "Push-pull" test for in situ determination of microbial activities. *Ground Water* 35: 619–631.

Jakobsen R, Albrechtsen H-J, Rasmussen M, Bay H, Bjerg PL, and Christensen TH (1998) H_2 concentrations in a landfill leachate plume (Grindsted, Denmark): In situ energetics of terminal electron acceptor processes. *Environmental Science and Technology* 32: 2142–2148.

Jensen KH, Bitsch K, and Bjerg PL (1993) Large-scale dispersion experiments in a sandy aquifer in Denmark: Observed tracer movements and numerical analysis. *Water Resources Research* 29: 673–696.

Jensen DL, Boddum JK, Redemann S, and Christensen TH (1998) Speciation of dissolved iron(II) and manganese(II) in a groundwater pollution plume. *Environmental Science and Technology* 32: 2657–2664.

Jensen DL, Boddum JK, Tjell JC, and Christensen TH (2002) The solubility of rhodochrosite ($MnCO_3$) and siderite ($FeCO_3$) in anaerobic aquatic environments. *Applied Geochemistry* 17: 503–511.

Johnston JJ, Borden RC, and Barlaz MA (1996) Anaerobic biodegradation of alkylbenzene and trichloroetylene in aquifer sediment downgradient of a sanitary landfill. *Journal of Contaminant Hydrology* 23: 263–283.

Jones EJP, Deal A, Lorah MM, Kirshtein JD, and Voytek MA (2002) The effect of Fe(III) on microbial degradation of chlorinated volatile organic compounds in a contaminated freshwater wetland. In: *102nd General Meeting of the American Society for Microbiology*, Salt Lake City, UT, May 19-23, Washington, DC: American Society for Microbiology.

Kehew AE and Passero RN (1990) pH and redox buffering mechanisms in a glacial drift aquifer contaminated by landfill leachate. *Ground Water* 28: 728–737.

Kehew AE, Schwindt FJ, and Brown DJ (1984) Hydrogeochemical interaction between a municipal waste stabilization lagoon and a shallow aquifer. *Ground Water* 22: 746–754.

Kjeldsen P (1986) *Attenuation of Landfill Leachate in Soil and Aquifer Material*. PhD Thesis, Department of Environmental Engineering, Technical University of Denmark, Lyngby.

Kjeldsen P (1993) Groundwater pollution source characterization of an old landfill. *Journal of Hydrology* 142: 349–371.

Kjeldsen P, Barlaz MA, Rooker AP, Baun A, Ledin A, and Christensen TH (2002) Present and long term composition of MSW landfill leachate – A review. *Critical Reviews in Environmental Science and Technology* 32: 297–336.

Kjeldsen P, Bjerg PL, Rügge K, Christensen TH, and Pedersen JK (1998a) Characterization of an old municipal landfill (Grindsted, Denmark) as a groundwater pollution source: Landfill hydrology and leachate migration. *Waste Management and Research* 16: 14–22.

Kjeldsen P and Christophersen M (2001) Composition of leachate from old landfills in Denmark. *Waste Management and Research* 19: 249–256.

Kjeldsen P, Grundtvig A, Winther P, and Andersen JS (1998b) Characterization of an old municipal landfill (Grindsted, Denmark) as a groundwater pollution source: Landfill history and leachate composition. *Waste Management and Research* 16: 3–13.

Kjeldsen P, Kjølholt J, Schultz B, Christensen TH, and Tjell JC (1990) Sorption and degradation of chlorophenols, nitrophenols and organophosphorus pesticides in the subsoil under landfills – Laboratory studies. *Journal of Contaminant Hydrology* 6: 165–184.

Kneeshaw TA, McGuire JT, Smith EW, and Cozzarelli IM (2007) Evaluation of sulfate reduction at experimentally induced mixing interfaces using small-scale push-pull tests in an aquifer-wetland system. *Applied Geochemistry* 22(12): 2618–2629.

Larsen T, Christensen TH, Pfeffer FM, and Enfield CG (1992) Landfill leachate effects on sorption of organic micropollutants onto aquifer materials. *Journal of Contaminant Hydrology* 9: 307–324.

Ledin A, Reitzel LA, and Bjerg PL (2005) Quantitative determination of toluene, ethylbenzene and xylene degradation products in contaminated groundwater by solid phase extraction and in-vial derivatization. *International Journal of Environmental Analytical Chemistry* 85: 1075–1087.

Leenheer JA, Nanny MA, and Mcintyre C (2003) Terpenoids as major precursors of dissolved organic matter in landfill leachates, surface water, and groundwater. *Environmental Science and Technology* 37(11): 2323–2331.

Lønborg MJ, Engesgaard P, Bjerg PL, and Rosbjerg D (2006) A steady state redox zone approach for modeling the transport and degradation of xenobiotic organic compounds from a landfill site. *Journal of Contaminant Hydrology* 87: 191–210.

Lorah MM, Cozzarelli IM, and Böhlke JK (2009) Biogeochemistry at a wetland sediment-alluvial aquifer interface in a landfill leachate plume. *Journal of Contaminant Hydrology* 105(3–4): 99–117.

Lorah MM and Olsen LD (1999a) Degradation of 1,1,2,2-tetrachloroethane in a freshwater tidal wetland: Field and laboratory evidence. *Environmental Science and Technology* 33: 227–234.

Lorah MM and Olsen LD (1999b) Natural attenuation of chlorinated volatile organic compounds in a freshwater tidal wetland: Field evidence of anaerobic biodegradation. *Water Resources Research* 35: 3811–3827.

Lorah MM, Voytek MA, Kirshtein JD, and Jones EJ (2003) Anaerobic degradation of 1,1,2,2-tetrachloroethane and association with microbial communities in a freshwater tidal wetland, Aberdeen Proving Ground, Maryland: Laboratory experiments and comparisons to field data. U.S. Geological Survey Water-Resources Investigations Report 02-4157.

Lovley DR (1991) Dissimilatory Fe(III) and Mn(IV) reduction. *Microbiological Reviews* 55: 259–287.

Lovley DR and Goodwin S (1988) Hydrogen concentrations as an indicator of the predominant terminal electron-accepting reactions in aquatic sediments. *Geochimica et Cosmochimica Acta* 52: 2993–3003.

Ludvigsen L, Albrechtsen H-J, Heron G, Bjerg PL, and Christensen TH (1998) Anaerobic microbial redox processes in a landfill leachate contaminated aquifer (Grindsted, Denmark). *Journal of Contaminant Hydrology* 33: 273–291.

Ludvigsen L, Albrechtsen H-J, Holst H, and Christensen TH (1997) Correlating phospholipid fatty acids (PLFA) in a landfill leachate polluted aquifer with biogeochemical factors by multivariate statistical methods. *FEMS Microbiology Reviews* 20: 447–460.

Ludvigsen L, Albrechtsen H-J, Ringelberg DB, Ekelund F, and Christensen TH (1999) Composition and distribution of microbial biomass in a landfill leachate contaminated aquifer (Grindsted, Denmark). *Microbial Ecology* 37: 197–207.

Lyngkilde J and Christensen TH (1992a) Fate of organic contaminants in the redox zones of a landfill leachate pollution plume (Vejen, Denmark). *Journal of Contaminant Hydrology* 10: 291–307.

Lyngkilde J and Christensen TH (1992b) Redox zones of a landfill leachate pollution plume (Vejen, Denmark). *Journal of Contaminant Hydrology* 10: 273–289.

MacFarlane DS, Cherry JA, Gillham RW, and Sudicky EA (1983) Migration of contaminants in groundwater at a landfill: A case study. 1. Groundwater flow and plume delineation. *Journal of Hydrology* 63: 1–29.

McGuire JT, Long DT, Klug MJ, Haack SK, and Hyndman DW (2002) Evaluating behavior of oxygen, nitrate, and sulfate during recharge and quantifying reduction rates in a contaminated aquifer. *Environmental Science and Technology* 36: 2693–2700.

McGuire JT, Smith EW, Long DT, et al. (2000) Temporal variations in parameters reflecting terminal-electron-accepting processes in an aquifer contaminated with waste fuel and chlorinated solvents. *Chemical Geology* 169: 471–485.

Milosevic N, Qiu S, Elsner M, et al. (2013) Combined isotope and enantiomer analysis to assess the fate of phenoxy acids in a heterogeneous geologic setting at an old landfill. *Water Research* 47(2): 637–649.

Milosevic N, Thomsen NI, Juhler RK, Albrechtsen H-J, and Bjerg PL (2012) Identification of discharge zones and quantification of contaminant mass discharges into a local stream from a landfill in a heterogeneous geologic setting. *Journal of Hydrology* 446–447: 13–23.

Murray J, Rouse JV, and Carpenter AB (1981) Groundwater contamination by sanitary landfill leachate and domestic wastewater in carbonate terrain: Principal source diagnosis, chemical transport characteristics and design implications. *Water Research* 15: 745–757.

Nanny MA and Ratasuk N (2002) Characterization and comparison of hydrophobic neutral and hydrophobic acid dissolved organic carbon isolated from three municipal landfill leachates. *Water Research* 36(6): 1572–1584.

National Research Council (2000) *Natural Attenuation for Groundwater Remediation*, 274 p. Washington, DC: National Academy Press.

Nicholson RV, Cherry JA, and Reardon EJ (1983) Migration of contaminants in groundwater at a landfill: A case study. 6. Hydrogeochemistry. *Journal of Hydrology* 63: 131–176.

Nielsen PH, Albrechtsen H-J, Heron G, and Christensen TH (1995a) In situ and laboratory studies on the fate of specific organic compounds in an anaerobic landfill leachate plume. I: Experimental conditions and fate of phenolic compounds. *Journal of Contaminant Hydrology* 20: 27–50.

Nielsen PH, Bjarnadottir H, Winter PL, and Christensen TH (1995b) In situ and laboratory studies on the fate of specific organic compounds in an anaerobic landfill leachate plume. II: Fate of aromatic and chlorinated aliphatic compounds. *Journal of Contaminant Hydrology* 20: 51–66.

Nielsen PH, Bjerg PL, Nielsen P, Smith P, and Christensen TH (1996) In situ and laboratory determined first-order degradation rate constants of specific organic compounds in an aerobic aquifer. *Environmental Science and Technology* 30: 31–37.

Parkhurst DL, Christenson SC, and Breit GN (1993) Ground-water quality assessment of the Central Oklahoma aquifer, Oklahoma: Geochemical and Geohydrologic Investigations. U.S. Geological Survey Open File Report 92-642. Oklahoma City, OK: U.S. Geological Survey.

Paxeus N (2000) Organic compounds in municipal landfill leachates. *Water Science and Technology* 42(7–8): 323–333.

Pecher K, Haderlein SB, and Schwarzenbach RP (1997) Transformation of polyhalogenated alkanes in suspensions of ferrous iron and iron oxides. In: 213th ASC National Meeting 13–17 April, 1997, pp. 185–187. Washington, DC: ASC Division of Environmental Chemistry.

Petersen MJ (2000) *Modeling of Groundwater Flow and Reactive Transport in a Landfill Leachate Plume*. PhD Thesis, Department of Hydrodynamics and Hydraulic Engineering, Technical University of Denmark, Lyngby (ISVA Series Paper No. 73).

Postma D (1993) The reactivity of iron oxides in sediments: A kinetic approach. *Geochimica et Cosmochimica Acta* 57: 5027–5034.

Prommer H, Tuxen N, and Bjerg PL (2006) Fringe-controlled natural attenuation of phenoxy acids in a landfill plume: Integration of field-scale processes by reactive transport modeling. *Environmental Science and Technology* 40: 4732–4738.

Ravi V, Chen J-S, Wilson JT, Johnson JA, Gierke W, and Murdie L (1998) Evaluation of natural attenuation of benzene and dichloroethane at the KL Landfill. *Bioremediation Journal* 2: 239–258.

Reinhard M, Goodman NL, and Barker JF (1984) Occurrence and distribution of organic chemicals in two landfill leachate plumes. *Environmental Science and Technology* 18: 953–961.

Reitzel LA, Tuxen N, Ledin A, and Bjerg PL (2004) Can degradation products be used as documentation for natural attenuation of phenoxy acids in groundwater? *Environmental Science and Technology* 38: 457–467.

Richnow HH, Meckenstock RU, Ask L, Baun A, Ledin A, and Christensen TH (2003) In situ biodegradation determined by isotope fractionation of aromatic hydrocarbons in an anaerobic landfill leachate plume (Vejen, Denmark). *Journal of Contaminant Hydrology* 64: 59–72.

Röling WFM, van Breukelen BM, Braster M, Groen J, and van Verseveld HW (2000) Analysis of microbial communities in a landfill leachate polluted aquifer using a new method for anaerobic physiological profiling and 16S rDNA based fingerprinting. *Microbial Ecology* 40: 177–188.

Röling WFM, van Breukelen BM, Braster M, Lin B, and van Verseveld HW (2001) Relationship between microbial community structure and hydrochemistry in a landfill leachate-polluted aquifer. *Applied and Environmental Microbiology* 67: 4619–4629.

Rügge K, Bjerg PL, and Christensen TH (1995) Distribution of organic compounds from municipal solid waste in the groundwater downgradient of a landfill (Grindsted, Denmark). *Environmental Science and Technology* 29: 1395–1400.

Rügge K, Bjerg PL, Mosbæk H, and Christensen TH (1999a) Fate of MCPP and atrazine in an anaerobic landfill leachate plume (Grindsted, Denmark). *Water Research* 33: 2455–2458.

Rügge K, Bjerg PL, Pedersen JK, Mosbæk H, and Christensen TH (1999b) An anaerobic field injection experiment in a landfill leachate plume (Grindsted, Denmark), 1. Site description, experimental set-up, tracer movement and fate of aromatic and chlorinated aliphatic compounds. *Water Resources Research* 35: 1231–1246.

Rügge K, Hofstetter TB, Haderlein SB, et al. (1998) Characterization of predominant reductants in an anaerobic leachate-affected aquifer by nitroaromatic probe compounds. *Environmental Science and Technology* 32: 23–31.

Scheutz C, Durant ND, Hansen MH, and Bjerg PL (2011) Natural and enhanced anaerobic degradation of 1,1,1-trichloroethane and its degradation products in the subsurface – A critical review. *Water Research* 45(9): 2701–2723.

Scholl MA and Christenson SC (1998) Spatial variation in hydraulic conductivity determined by slug tests in the Canadian River alluvium near the Norman Landfill, Norman, Oklahoma. U.S. Geological Survey Water-Resources Investigations Report 97-4292, U.S. Oklahoma City, OK.

Scholl MA, Christenson SC, Cozzarelli IM, Ferree DM, and Jaeschke J (2004) Recharge processes in an alluvial aquifer riparian zone, Norman Landfill, Norman, Oklahoma, 1998-2000. U.S. Geological Survey Scientific Investigations Report 2004-5238, p. 54 Oklahoma City, OK.

Scholl MA, Cozzarelli IM, and Christenson SC (2006) Recharge processes drive sulfate reduction in an alluvial aquifer contaminated with landfill leachate. *Journal of Contaminant Hydrology* 86(3–4): 239–261.

Scholl MA, Cozzarelli IM, Christenson SC, Breit GN, and Schlottmann JL (1999) Aquifer heterogeneity at Norman Landfill and its effect on observations of biodegradation processes. *U.S. Geological Survey Toxic Substances Hydrology Program – Proceedings of the Technical Meeting*, Charleston, South Carolina, 8–12 March 1999, In: Morganwalp DW and Buxton HT (eds.) *Subsurface Contamination from Point Sources*, U.S. Geological Survey Water-Resources Investigations Report 99-4018C, West Trenton, NJ, vol. 3, pp. 557–568.

Scholl MA, Cozzarelli IM, Christenson SC, et al. (2001) Measuring variability of in-situ biodegradation rates in a heterogeneous aquifer contaminated by landfill leachate. *Eos, Transactions, American Geophysical Union* 82(20): 146.

Schwarzbauer J, Heim S, Brinker S, and Littke R (2002) Occurrence and alteration of organic contaminants in seepage and leakage water from a waste deposit landfill. *Water Research* 36: 2275–2287.

Scott MJ and Morgan JJ (1990) Energetics and conservative properties of redox systems. *ACS Symposium Series* 416: 368–378.

Senko JM, Istok JD, Suflita JM, and Krumholz LR (2002) In-situ evidence for uranium immobilization and remobilization. *Environmental Science and Technology* 36: 1491–1496.

Suarez MP and Rifai HS (1999) Biodegradation rates for fuel hydrocarbons and chlorinated solvents in groundwater. *Bioremediation Journal* 3: 337–362.

Sykes JF, Soupak S, and Farquhar GJ (1982) Modeling of leachate organic migration in groundwater below sanitary landfills. *Water Resources Research* 18: 135–145.

Thomsen NI, Milosevic N, and Bjerg PL (2012) Application of a mass balance method at an old landfill to assess the impact on surrounding water resources. *Waste Management* 32: 2406–2417.

Thornton SF, Lerner DN, and Banwart SA (2001) Assessing the natural attenuation of organic contaminants in aquifers using plume-scale electron carbon balances: Model development with analysis and parameters sensitivity. *Journal of Contaminant Hydrology* 53: 199–232.

Tuttle MLW, Breit GN, and Cozzarelli IM (2009) Processes affecting $\delta^{34}S$ and $\delta^{18}O$ values of dissolved sulfate in alluvium along the Canadian River, central Oklahoma, USA. *Chemical Geology* 265(3–4): 455–467.

Tuxen N, Albrechtsen H-J, and Bjerg PL (2006) Identification of a reactive degradation zone at a landfill leachate plume fringe using high resolution sampling and incubation techniques. *Journal of Contaminant Hydrology* 85: 179–194.

Tuxen N, Ejlskov P, Albrechtsen H-J, Reitzel LA, Pedersen JK, and Bjerg PL (2003) Application of natural attenuation to ground water contaminated by phenoxy acid herbicides at an old landfill (Sjoelund, Denmark). *Ground Water Monitoring and Remediation* 23(4): 48–58.

Ulrich GA, Breit GN, Cozzarelli IM, and Suflita JM (2003) Sources of sulfate supporting anaerobic metabolism in a contaminated aquifer. *Environmental Science and Technology* 37: 1093–1099.

Ulrich GA, Martino D, Burger K, et al. (1998) Sulfur cycling in the terrestrial subsurface: Commensal interactions, spatial scales, and microbial heterogeneity. *Microbial Ecology* 36: 141–151.

van Duijvenbooden W and Kooper WF (1981) Effects on groundwater flow and groundwater quality of a waste disposal site in Noordwijk, The Netherlands. *Quality of Groundwater. Proceedings of an International Symposium*, Noordwijkerhout, March 1981, *Studies in Environmental Science*, vol. 17, pp. 253–260. Amsterdam: Elsevier.

Vogel TM, Criddle CS, and McCarty PL (1987) Transformations of halogenated aliphatic compounds. *Environmental Science and Technology* 21: 722–736.

Weiss JV, Cozzarelli IM, Lowit MB, and Voytek MA (2005) Biodegradable carbon as a potential control on microbial community structure and function in an aquifer contaminated with landfill leachate. *Geological Society of America 2005 Annual Meeting*, Salt Lake City, UT, 16–19 October. *Geological Society of America Abstracts with Programs,* vol. 37(7), p. 474.


9 780080 959757
9 780080 999791